Environmental Pollution 208 (2016) 395–403

Contents lists available at ScienceDirect

Environmental Pollution

journal homepage: www.elsevier.com/locate/envpol

Reliability of stable Pb isotopes to identify Pb sources and verifying biological fractionation of Pb isotopes in goats and chickens

Hokuto Nakata [a, 1], Shouta M.M. Nakayama [a, 1], John Yabe [b], Allan Liazambi [c], Hazuki Mizukawa [d], Wageh Sobhy Darwish [a, e], Yoshinori Ikenaka [a, f], Mayumi Ishizuka [a, *]

[a] Laboratory of Toxicology, Department of Environmental Veterinary Sciences, Graduate School of Veterinary Medicine, Hokkaido University, Kita 18 Nishi 9, Kita-ku, Sapporo 060-0818, Japan
[b] The University of Zambia, School of Veterinary Medicine, P.O. Box 32379, Lusaka, Zambia
[c] Central Province Veterinary Office, Kabwe, Zambia
[d] Department of Environmental Veterinary Sciences, Graduate School of Veterinary Medicine, Hokkaido University, Kita 18 Nishi 9, Kita-ku, Sapporo 060-0818, Japan
[e] Food Control Department, Faculty of Veterinary Medicine, Zagazig University, Zagazig, Egypt
[f] Water Research Group, School of Environmental Sciences and Development, North-West University, South Africa

ARTICLE INFO

Article history:
Received 30 July 2015
Received in revised form
4 October 2015
Accepted 5 October 2015
Available online 6 November 2015

Keywords:
Biological fractionation
Chicken
Goat
Pb pollution source
Stable Pb isotopes

ABSTRACT

Stable Pb isotope ratios (Pb-IRs) have been recognized as an efficient tool for identifying sources. This study carried out at Kabwe mining area, Zambia, to elucidate the presence or absence of Pb isotope fractionation in goat and chicken, to evaluate the reliability of identifying Pb pollution sources via analysis of Pb-IRs, and to assess whether a threshold for blood Pb levels (Pb-B) for biological fractionation was present. The variation of Pb-IRs in goat decreased with an increase in Pb-B and were fixed at certain values close to those of the dominant source of Pb exposure at Pb-B > 5 μg/dL. However, chickens did not show a clear relationship for Pb-IRs against Pb-B, or a fractionation threshold. Given these, the biological fractionation of Pb isotopes should not occur in chickens but in goats, and the threshold for triggering biological fractionation is at around 5 μg/dL of Pb-B in goats.

1. Introduction

Among metals, lead (Pb) possesses a particularly elevated anthropogenic enrichment factor (Lantzy and Mackenzie, 1979). Widespread pollution has frequently been recorded in regions with long histories of mining and smelting, where high levels of metals contaminate water, soil, sediment, and vegetation (Razo et al., 2004; Ettler et al., 2005; Hudson-Edwards et al., 2008). Nowadays, Pb is not only a local pollutant, but is also a pollutant on a global scale due to its volatile character of Pb (Charalampides and Manoliadis, 2002). The primary sources of Pb exposure, in addition to smelters, are battery recycling, electronics, paint, traditional remedies, and leaded gasoline (Meyer et al., 2008). For animals, Pb is a non-essential and toxic metal. Even at low doses, Pb leads to neurotoxicity in humans, especially in children, due to its ability to compete with calcium (Ca^{2+}) in nerve function (Crosby, 1998). A recent review by Yabe et al. (2010) remarked that toxic metal contamination of the environment and livestock has reached unprecedented levels over the past decade, and that human exposure to toxic metals has become a critical component of the health risk on the African continent. This grave warning was tragically borne out by the Pb poisoning disaster in Zamfara, Nigeria, in which more than 160 people died, mostly children under the age of five (Blacksmith Institute, 2010).

Given these factors, it is necessary not only to consider total concentrations and the chemical/mineralogical position of Pb, but also to precisely determine how multiple sources contribute Pb to the environment. Pb is present in the environment as four main stable isotopes: ^{208}Pb, ^{207}Pb, ^{206}Pb, and ^{204}Pb. Among these isotopes, only ^{204}Pb has no known radiogenic parent, and its abundance in the Earth's crust does not change with time. In contrast, ^{206}Pb, ^{207}Pb, and ^{208}Pb are radiogenic isotopes, and are the products of the radioactive decay of ^{238}U, ^{235}U, and ^{232}Th, respectively.

* Corresponding author.
E-mail address: ishizum@vetmed.hokudai.ac.jp (M. Ishizuka).
[1] Both authors equally contributed to this study.

http://dx.doi.org/10.1016/j.envpol.2015.10.006
0269-7491/

Hence, unlike many other elements whose isotopic abundances have been fixed during cosmological time, the abundance of Pb isotopes in a sample depends strictly on the concentrations of primordial Pb, uranium (U), and thorium (Th) isotopes, and the length of their decay processes (Keinonen, 1992; Sangster et al., 2000). The isotopic composition of Pb can be expressed in several ways. For instance, in the environmental sciences, the Pb isotopic composition is broadly expressed as ratios, with $^{208}Pb/^{206}Pb$ and $^{207}Pb/^{206}Pb$ being the most preferred because these ratios can be measured precisely and analytically, and the abundances of these isotopes are relatively significant. Additionally, it should be emphasized that the isotopic composition of Pb is not affected to a measurable extent by physico-chemical fractionation processes. Stable Pb isotope ratios (Pb-IRs), therefore, can be used as natural tracers, and serve as an efficient tool for identifying sources and pathways of Pb pollution (Bollhöfer and Rosman, 2001; Veysseyre and Bollho, 2001; Charalampides and Manoliadis, 2002). Recently Pb-IRs have been generally used to identify the primary sources of Pb in air and aerosols (Chow and Johnstone, 1965; Chow and Earl, 1972), soil (Gulson et al., 1981; Hansmann and Köppel, 2000), sediments (Shirahata et al., 1980; Petit et al., 1984). Moreover, sources of Pb exposure for wild birds (Scheuhammer and Templeton, 1998) and sea otters (*Enhydra lutris*) (Smith et al., 1990) have been identified using Pb-IRs analysis.

Pb-IRs have been widely assumed to not be as fractionized in biological systems as in the environment (Rabinowitz and Wetherill, 1972; Carlson, 1996). Nevertheless, some earlier studies revealed large differences in the Pb isotopic composition among biological samples within humans (Smith et al., 1996) and within rats (*Rattus norvegicus*) (Wu et al., 2012; Liu et al., 2014). Studies on the distribution of each of the stable Pb isotopes in the living body are still limited. It is thus necessary to clarify whether biological fractionation of Pb isotopes occurs in the body or not in order to verify the accuracy of identifying Pb sources by Pb-IRs analysis. In fact, isotopes of light elements, such as Li (Stokes et al., 1982), C (Tieszen et al., 1983; Gannes et al., 1998), and N (Gannes et al., 1998), have been recognized to be fractionized in biological systems. Isotopic variations of heavier elements, such as Zn (Stenberg et al., 2004), Fe (Walczyk and von Blanckenburg, 2002), and Hg (Epov et al., 2008) in biological systems have also been found in recent years. If isotope fractionation occurs in the body, it should then be determined which tissues most accurately reflect the Pb pollution source and should thus be used to identify the source. As such, the present study was designed to elucidate the presence or absence of Pb isotope fractionation in biological samples, and to evaluate the reliability of identifying Pb pollution sources via analysis of Pb-IRs. Furthermore, Wu et al. (2012) and Liu et al. (2014) have suggested the existence of a threshold for blood Pb levels (Pb-B) for biological fractionation in rats. The current study intended to assess whether such threshold for biological fractionation was present for goats (*Capra hircus*) and chickens (*Gallus gallus*) because these animals are reared and consumed worldwide.

For these purposes, Kabwe, the provincial capital of Zambia's central province, was selected as a study site because it has been well studied, with findings of high levels of Pb accumulation in the environment such as soil (Ikenaka et al., 2010; Nakayama et al., 2011), wild rats (*Rattus rattus*) (Nakayama et al., 2011, 2013), livestock such as cattle and chickens (Yabe et al., 2011, 2013; Ikenaka et al., 2012), and children (Yabe et al., 2015). These studies considered Kabwe to have only one origin for Pb, and so the current study can be considered as a semi-field study on constant Pb exposure. In addition, goats and chickens were chosen as the exposed animals because they are widely bred and consumed in developing countries, including those in Africa. As the Pb exposure route in Kabwe is still unclear, in contrast to the many earlier studies focused merely on the extent of contamination, the current study also aims to identify the Pb source in Kabwe.

2. Materials and methods

2.1. Sampling of animals and environmental samples

This study was conducted in Kabwe, which has no Pb battery-related facilities and is situated 130 km north of Lusaka, the capital and largest city of Zambia (supporting information Fig. S1), and in Chongwe, which is next to Lusaka. The ore in Kabwe contained sphalerite (ZnS) with Cd, galena (PbS), briarite [$Cu_2(Fe,Zn)GeS_4$], and mimetite [$Pb_5(AsO_4)_3Cl$] (Kamona and Friedrich, 2007). The sampling sites were accurately located using a global positioning system (GPS), and are shown in supporting information Fig. S1 and Table S1. Details on samples are also shown in supporting information of Materials and Methods section.

2.2. Sample preparation and analysis of element concentrations

All laboratory materials and instruments used in the heavy metal analysis were washed with 2% nitric acid (HNO_3) and rinsed at least twice with distilled water. We confirmed that there was no metal contamination through the analytical procedures using the regent (digestion) blank measurement. Samples of approximately 0.5 g of liver, kidney, lung, spleen, brain, muscle, heart, feces, stomach contents, gizzard, gizzard contents, adipose, rape, cabbage, onion, or tomato, 0.3 g of maize, 0.05 g of hair, feather, or sugar cane, 0.01 g of soil, or 1.0 mL of blood were dried for 48 h in an oven at 50 °C. The dried samples were placed in pre-washed digestion vessels, followed by acid digestion using 6 mL of nitric acid (atomic absorption spectrometry grade, 60%, Kanto Chemical Corp., Tokyo, Japan) and 1 mL of hydrogen peroxide (Cica reagent, 30%, Kanto Chemical Corp.). 0.1 g of dried bone was placed in the vessels, followed by acid digestion using 6 mL of nitric acid. The digestion vessels were capped and placed onto a 10-position turntable, and subsequently underwent a ramped temperature program in a closed microwave extraction system, the Speed Wave MWS-2 microwave digestion system (Berghof, Germany). After cooling, extracted solutions were transferred into 15 mL plastic tubes and diluted to a final volume of 10 mL with bi-distilled and de-ionized water (Milli-Q). The water samples were simply preserved with nitric acid to obtain acidic conditions. The concentrations of various elements (Pb, Cd, As, Zn, Co, Mn, and Cr) were determined using an inductively coupled plasma-mass spectrometer (ICP-MS: 7700 series, Agilent Technologies, Tokyo, Japan). Analytical quality control was performed using the DORM-3 (fish protein, National Research Council of Canada, Ottawa, Canada) and DOLT-4 (dogfish liver, National Research Council of Canada) certified reference materials. Replicate analysis of these reference materials showed good recoveries (95–105%). The instrument detection limit was 0.001 μg/L.

2.3. Analysis of Pb-IRs

Analyses of the $^{208}Pb/^{206}Pb$ and $^{207}Pb/^{206}Pb$ ratios were conducted using ICP-MS, according to the following procedure (Nakata et al., 2015). Detailed analytical conditions are given in supporting information of Materials and Methods as well as in the Table S2. During the analytical procedure, the following isotopes were measured: ^{204}Pb, ^{206}Pb, ^{207}Pb, and ^{208}Pb. However, only the $^{208}Pb/^{206}Pb$ and $^{207}Pb/^{206}Pb$ ratios are discussed in this study, as they show the most significant differences between the contaminated and natural background materials. Moreover, these ratios have been the most commonly interpreted ratios in previous research (Monna et al., 1998). The ratios of the samples were

corrected every 10 samples using the average value of each isotope ratio obtained by measurement of SRM 981. Each sample was measured in 10 replicates. The standard error for the $^{208}Pb/^{206}Pb$ and $^{207}Pb/^{206}Pb$ measurements was generally <0.5% of RSD (relative standard deviation), except <1.0% of RSD in some of the samples which showed very low Pb concentration. We confirmed that there was no Pb contamination through the analytical procedures using the regent blank measurement.

2.4. Statistical analysis

All the statistical analyses were carried out using JMP 11 (SAS Institute, Cary, NC, USA) in order to evaluate significant differences in the data. The Tukey–Kramer test and Student's *t*-test were used to compare element accumulation levels in the biological samples from the goats and chickens, respectively. Tukey–Kramer test was carried out in each species in order to compare the Pb-IRs among several biological samples from the same sampling site. To determine the relationship between Pb-B and Pb-IRs in the biological samples from the goats and chickens, spline smoothing, a method for fitting a smooth curve to a set of data, was utilized ($\lambda = 0.05$). All of the statistical analyses were performed at the significance level of 0.05 ($p < 0.05$).

3. Results

3.1. Element concentrations in biological samples from goats and chickens

Concentrations of Pb, Cd, As, Zn, Co, Mn, and Cr in the blood, liver, kidney, lung, spleen, brain, muscle, heart, bone, feces, stomach contents, hair, and adipose of the three groups of goats were determined (supporting information Table S3). Levels of these elements in the blood, liver, kidney, lung, spleen, brain, gizzard, gizzard contents, muscle, heart, bone, feces, feather, and adipose of BC and FRC were also determined (supporting information Table S4). Pb levels in the liver, kidney, and lung (equivalent to ≈1.75, 1.98, and 0.86 mg/kg, wet wt., assuming a moisture content of 68.7, 78.7, and 79.5%, respectively) of G0 exceeded the residual limit of 0.5 mg/kg, wet wt. for offal for human consumption (Regulation Council, 2001). As for muscle, 60% of the G0 samples exceeded the 0.1 mg/kg, wet wt. maximum Pb level for human consumption (FAO, 2012). In contrast, the mean level of Cd in all of the goat samples was below the maximum level of 1,000 μg/kg, wet wt (Regulation Council, 2001). For chickens, Pb levels in the liver, kidney, lung, and brain (equivalent to ≈1.25, 3.44, 1.17, and 0.70 mg/kg, wet wt. assuming a moisture content of 71.9, 75.1, 77.4, and 78.9%, respectively) of the FRC exceeded the 0.5 mg/kg maximum Pb level for offal for human consumption (Regulation Council, 2001). Additionally, 20% of the FRC muscle samples exceeded the residual Pb limit of 0.1 mg/kg, wet wt. in muscle for human consumption (FAO, 2012). In contrast to goats, Cd concentrations in liver and kidney (equivalent to ≈1210 and 2620 μg/kg, wet wt., respectively) of the FRC exceeded the maximum level of 1000 μg/kg, wet wt. for offal for human consumption (Regulation Council, 2001).

As indicated in supporting information Table S3, G0 accumulated significantly higher concentrations of Pb in the blood, liver, kidney, lung, spleen, brain, muscle, bone, feces, stomach contents, and hair than the other groups. Significantly higher accumulations of As and Co were also observed in G0 compared with G30 and G150. In contrast, few significant differences in Cd, Zn, Mn, and Cr levels were found between the goat groups. As shown in supporting information Table S4, significantly greater accumulation of Pb was observed in all of the biological samples from the FRC. In contrast to the goat groups, the Cd level in the FRC was significantly higher than in the BC for most of the sample types, except for blood and bone. Significantly higher accumulations of As and Co were also observed in many tissues from the FRC with respect to the BC.

3.2. Concentrations of Pb and Cd in environmental samples

Concentrations of Pb and Cd in the environmental samples are shown in supporting information Table S5. The levels of Pb and Cd in S0 exceeded the benchmark values (USEPA, 2005; Fairbrother et al., 2007). S30, S150, and the sawdust contained lower amounts of Pb and Cd than A0.

The Pb and Cd levels in various vegetables from A0 exceeded or were comparable to food reference values (FAO, 2012). Maize (*Zea mays*) from A0 had higher levels of Pb and Cd than maize from A30 and A150. In contrast to the soil and vegetables, the levels of Pb and Cd in the water samples were lower in A0.

3.3. Pb-IRs in biological samples from goats and chickens

Geographic trends in the Pb-IRs ($^{208}Pb/^{206}Pb$ and $^{207}Pb/^{206}Pb$ ratios) from goats and chickens are shown in Fig. 1, and Fig. 2, respectively. Additionally, mean ± standard deviation (SD) and minimum–maximum values of the Pb-IRs from goats and chickens are shown in supporting information Tables S6 and S7. G150 exhibited large variation in the $^{208}Pb/^{206}Pb$ and $^{207}Pb/^{206}Pb$ ratios among the different tissues, ranged from 1.979 to 2.131 and 0.736 to 0.891, respectively (Fig. 1A). The Pb-IRs in the G30 and G0 tissues ranged from 2.098 to 2.208 and 2.119 to 2.166 for $^{208}Pb/^{206}Pb$ and from 0.846 to 0.890 and 0.873 to 0.886 for $^{207}Pb/^{206}Pb$, respectively (Fig. 1B, C). As the distance to the mining site became shorter, the Pb levels in the goats increased (supporting information Table S3), and the differences in the Pb-IRs among the tissues became smaller (Fig. 1A–C).

The variation in the Pb-IRs in BC was smaller than in G150, ranging from 2.086 to 2.127 and 0.850 to 0.882 for $^{208}Pb/^{206}Pb$ and $^{207}Pb/^{206}Pb$, respectively (Fig. 2A). Additionally, in contrast to G150, the relationship between the $^{208}Pb/^{206}Pb$ and $^{207}Pb/^{206}Pb$ ratios in BC did not indicate a linear trend. FRC, which accumulated higher levels of Pb, showed smaller variation in Pb-IRs than BC, ranging from 2.123 to 2.151 and 0.866 to 0.876 for $^{208}Pb/^{206}Pb$ and $^{207}Pb/^{206}Pb$, respectively (Fig. 2B). The trends in the Pb-IRs for G0 and FRC were quite similar, although the trends for G150 and G30 were different from BC, because of the latter's non-linear appearance.

3.4. Pb-IRs in environmental samples

Pb-IR results for the environmental samples are shown in Fig. 3 and supporting information Table S8. Although the sample size was small, a positive relationship was observed between soil and maize Pb-IRs. Pb-IRs in both soil and maize increased as the distance to the mining site became smaller. Pb-IRs in environmental samples ranged from 2.082 to 2.465 and 0.856 to 0.885 for $^{208}Pb/^{206}Pb$ and $^{207}Pb/^{206}Pb$, respectively. Variation in the Pb-IRs among the environmental samples from A0 was smaller than that for G0 and FRC.

3.5. Relationship between Pb-B and Pb-IRs in various tissues from goats and chickens

In the present study, both the $^{208}Pb/^{206}Pb$ and $^{207}Pb/^{206}Pb$ ratios in the liver, kidney, lung, spleen, brain, blood, muscle, heart, and bone of G30 and G150 showed large variations at ≤1.18 μg/dL of Pb-B, while the Pb-IRs in those tissues of G0 showed limited variation at ≥8.06 μg/dL of Pb-B (Fig. 4 and supporting information Fig. S2).

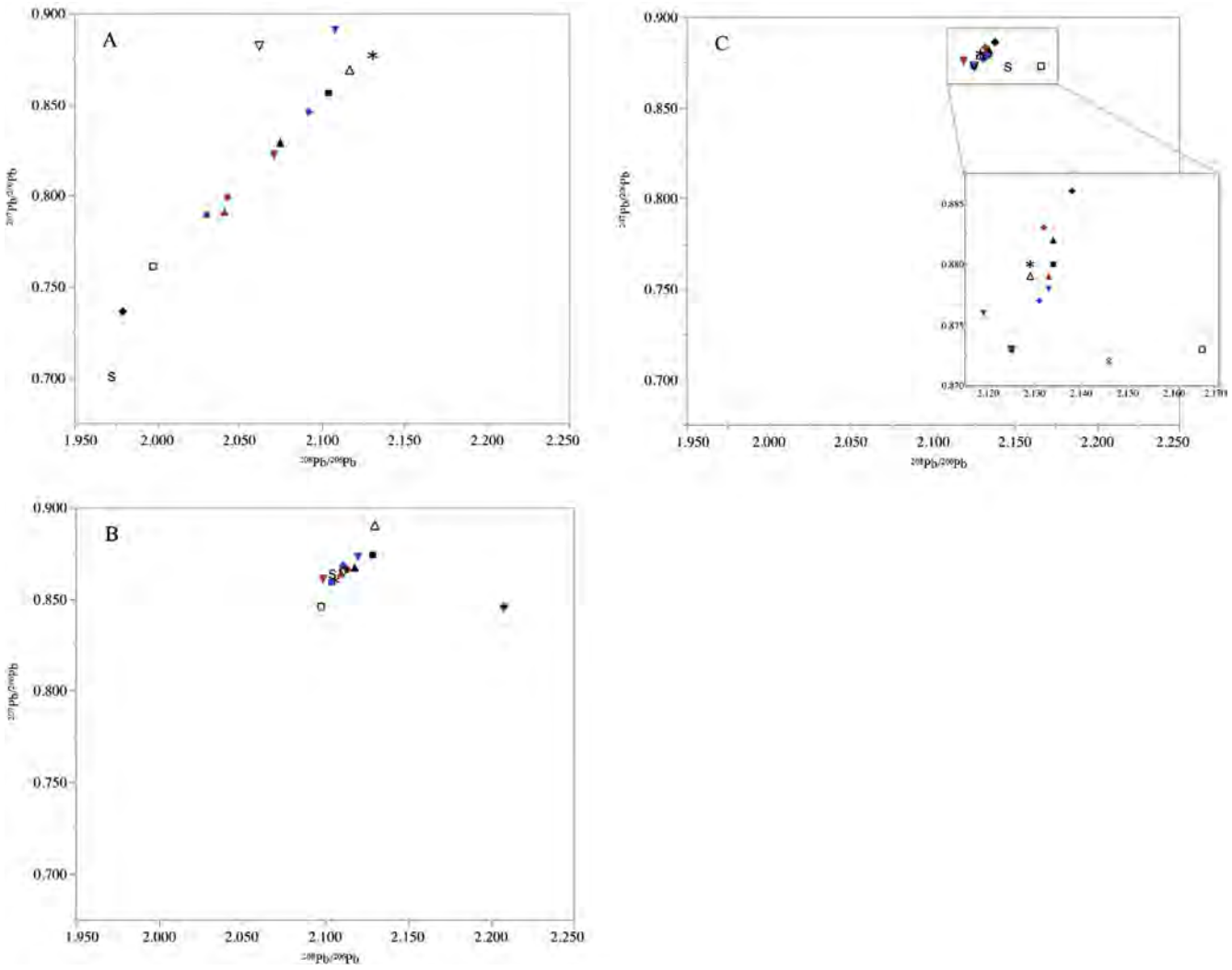

Fig. 1. Pb-IRs ($^{208}Pb/^{206}Pb$ and $^{207}Pb/^{206}Pb$) in G150 and S150 (A), G30 and S30 (B), and G0 and S0 (C). Red diamond = liver, blue circle = kidney, black triangle = lung, white inverted triangle = spleen, blue diamond = brain, asterisk = blood, black square = muscle, white triangle = heart, red inverted triangle = bone, black diamond = feces, white square = stomach contents, red triangle = hair, blue inverted triangle = adipose, S = soil. (For interpretation of the references to color in this figure legend, the reader is referred to the web version of this article.)

In contrast, this trend was not observed in chickens (Fig. 5 and supporting information Fig. S3).

4. Discussion

4.1. High accumulation of metals in goats, chickens, and environmental samples

High accumulations of Pb and Cd in soil (Ikenaka et al., 2010; Nakayama et al., 2011), wild rats (*R. rattus*) (Nakayama et al., 2011, 2013), livestock such as cattle and chickens (Yabe et al., 2011, 2013; Ikenaka et al., 2012), and children (Yabe et al., 2015) from Kabwe have been previously reported. The present study also revealed a high accumulation of Pb and Cd in the edible organs of G0 and FRC (supporting information Table S3 and S4). This study is noteworthy as the first to reveal the extent of metal contamination in goats from Zambia. Goats are a common livestock animal in Zambia, and it was found that Pb concentrations in the liver, kidney, and lung of G0 (supporting information Table S3) exceeded the food reference value (Regulation Council, 2001). What must be heeded is that the breeding period of G0 in the mining site was less than one month. These results should be a grave warning for farmers and consumers living in and around the mining site. There is a clear need to avoid consumption of contaminated goat offal and muscle, as well as to restrict goats from roaming and scavenging for food near mining sites.

As Yabe et al. (2013) previously reported, also in the current study, high levels of Pb and Cd were also observed in FRC (supporting information Table S4), and the Pb and Cd levels in several tissues exceeded the residual limit for human consumption (Regulation Council, 2001; FAO, 2012). However, despite the accumulation of high Pb, the sampled FRC superficially appeared healthy. This is in agreement with findings from previous research, in which adult hens showed tolerance to chronic Pb intoxication (Mazliah et al., 1989). Nonetheless, consumption of Pb-contaminated chicken offal and muscle poses significant health risks to humans, especially children, who are highly susceptible to Pb toxicity (Lockitch, 1993).

High accumulation of Pb and Cd was noted in S0 (supporting information Table S5), as Ikenaka et al. (2010) and Nakayama et al. (2011) previously observed. The levels of Pb and Cd in S0 exceeded benchmark values (USEPA, 2005; Fairbrother et al., 2007). Pb and

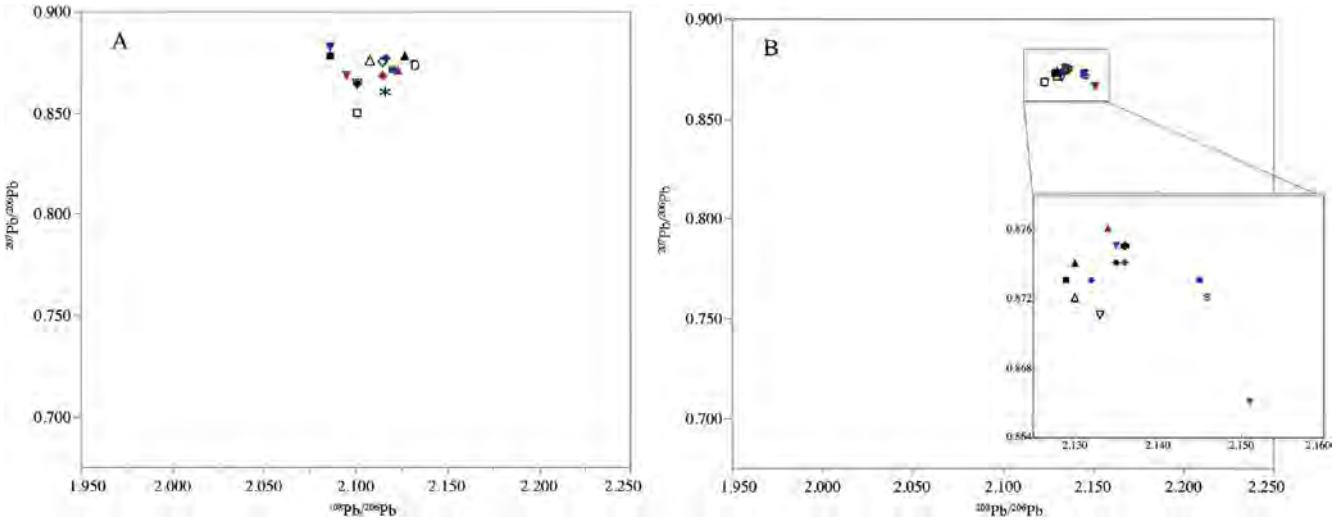

Fig. 2. Pb-IRs ($^{208}Pb/^{206}Pb$ and $^{207}Pb/^{206}Pb$) in BC and sawdust (A), and FRC and S0 (B). Red diamond = liver, blue circle = kidney, black triangle = lung, white inverted triangle = spleen, blue diamond = brain, asterisk = blood, black square = muscle, white triangle = heart, red inverted triangle = bone, black diamond = feces, white diamond = gizzard, white square = gizzard contents, red triangle = feather, blue inverted triangle = adipose, S = S0, D = sawdust. (For interpretation of the references to color in this figure legend, the reader is referred to the web version of this article.)

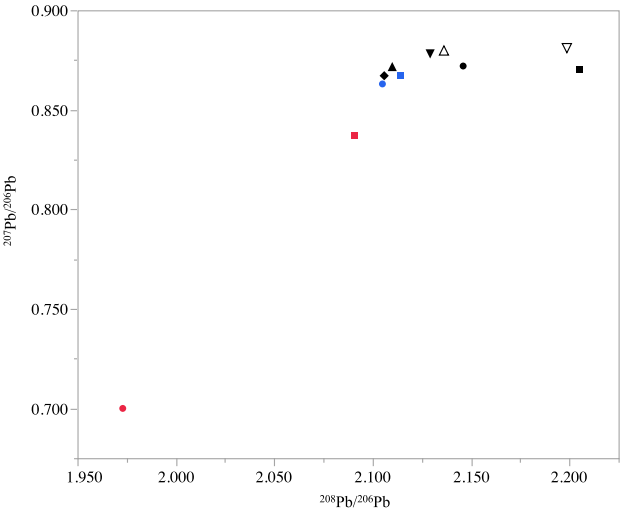

Fig. 3. Pb-IRs ($^{208}Pb/^{206}Pb$ and $^{207}Pb/^{206}Pb$) in the environmental samples. Red circle = S150, blue circle = S30, black circle = S0, red square = maize from A150, blue square = maize from A30, black square = maize from A0, black diamond = rape from A0, black triangle = sugar cane from A0, black inverted triangle = cabbage from A0, white triangle = onion from A0, white inverted triangle = tomato from A0. (For interpretation of the references to color in this figure legend, the reader is referred to the web version of this article.)

Cd are known as toxic pollutants; for instance, renal dysfunction and bone loss have been reported in humans suffering from chronic Cd toxicity (Järup, 2003). It has been previously argued that the source of these toxic metals in the Kabwe area is Pb and Zn mining and smelting activity (Nakayama et al., 2011). The current study revealed that Pb and Cd pollution in the soil around the mining site is still ongoing. Blacksmith Institute (2013) noted that the site still poses an acute health risk that will require further work although the Zambian government has made significant progress in dealing with the issue, particularly through a United States Dollar (USD) 26 millions remediation program funded by World Bank and Nordic Development Fund from 2003 to 2011.

The extent of contamination in the vegetables and water from Kabwe was newly revealed in this study, although the sample size was small (supporting information Table S5). Thus, vegetable consumption can be considered one of the exposure routes of Pb and Cd. In contrast, the levels of Pb and Cd in the water samples were low, even in A0. Therefore, the drinking water was deemed to pose almost no risk to human health.

4.2. Pb exposure route of goats and chickens, and potential health risk of human exposure to Pb

Although previous studies of Kabwe have revealed significant Pb pollution, the actual Pb exposure routes for animals and humans are still unclear. In Kabwe, leaded gasoline has been phased out since March 2008. Additionally, the Pb-IRs detected in biological samples from G0 and FRC in the current study generally differed from those in coals used worldwide in the previous study (1.98–2.12 and 0.81–0.87 for $^{208}Pb/^{206}Pb$ and $^{207}Pb/^{206}Pb$, respectively) (Diaz-Somoano et al., 2009). Hence, leaded gasoline and coal would not be sources of Pb in Kabwe. As shown in Fig. 1C, Pb-IRs in S0 and the biological samples from G0 were quite similar. Additionally, the same trend was observed in S30 and G30 (Fig. 1B). These findings suggest that the Pb-IRs in goat tissues reflect those in soil, indicating that soil is one of the major sources of Pb exposure for goats around the Kabwe mining site. Another interesting point regarding the Pb-IRs is the relationship between S150 and the feces from G150. Liu et al. (2014) previously noted that feces samples are more suitable for tracing Pb sources in case where Pb is detected at low levels in the blood. The results of the current study show a similar trend in the Pb-IRs of feces samples (Fig. 1A).

Incidentally, FRC appeared to show the same tendency as G0 and G30. Moreover, the trend in the Pb-IRs of BC, which were not highly contaminated by Pb, was similar to the corresponding FRC trend (Fig. 2). This result can be explained by the following hypothesis: the sawdust in the poultry house coincidentally had Pb-IRs close to those of S0, and the Pb-IRs of the BC were affected by the sawdust. However, exposure to sawdust does not result in the accumulation of large amounts of Pb. Therefore, while Pb contamination levels indeed differed, the Pb-IRs of the BC and FRC ended up being quite similar.

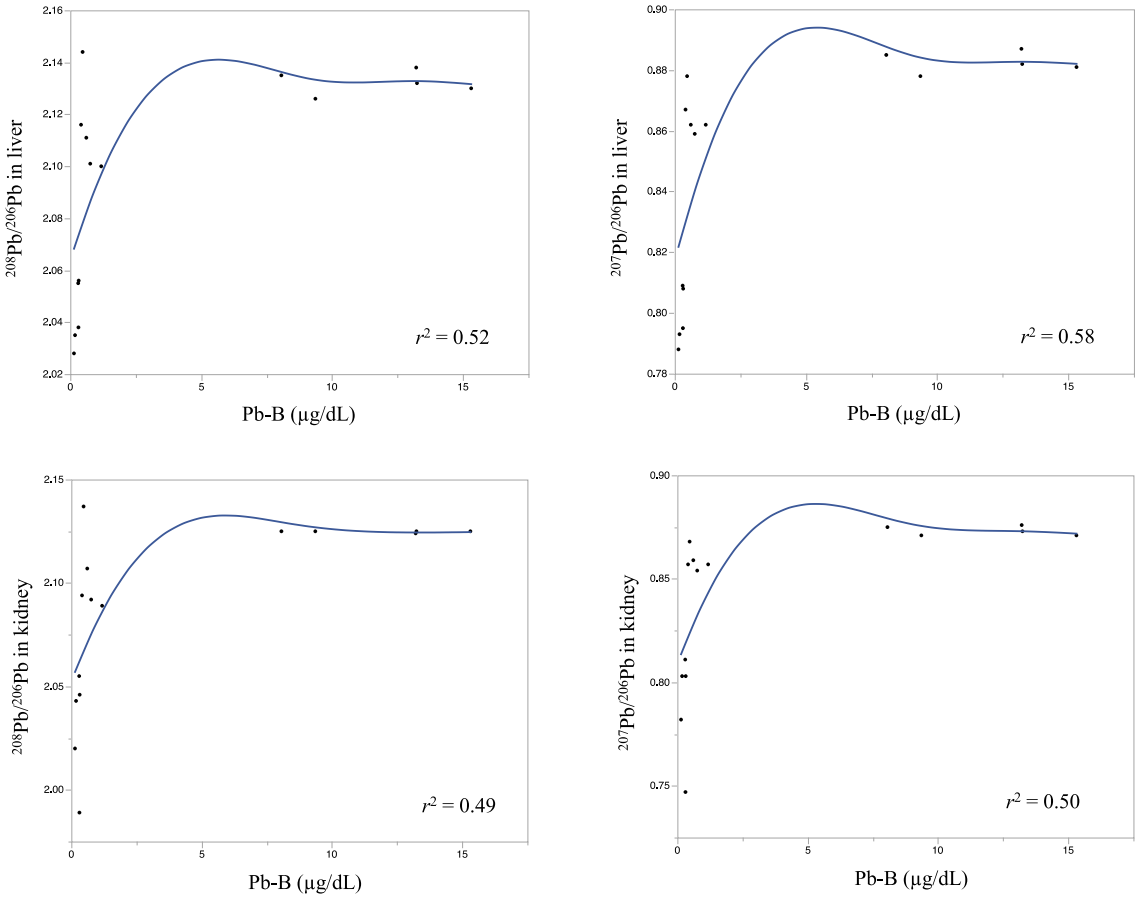

Fig. 4. Pb-B (μg/dL) versus Pb-IRs ($^{208}Pb/^{206}Pb$ and $^{207}Pb/^{206}Pb$) in goat tissues. To determine the relationship between Pb-B and Pb-IRs in the biological samples from the goats, spline smoothing, a method for fitting a smooth curve to a set of data, was utilized ($\lambda = 0.05$).

Since this is the first study to identify Pb exposure routes in Kabwe, the next point of concern is human exposure to Pb. It is well known that Pb is absorbed into the human body mainly through the gastrointestinal and respiratory tracts (Berman, 1966; Neathery and Miller, 1975; Glorennec, 2006). Previous studies (Ikenaka et al., 2010; Nakayama et al., 2011) and the current (supporting information Table S5) study found soil Pb concentration that exceeded benchmark values (USEPA, 2005; Fairbrother et al., 2007), and supposed soil and sawdust could be sources of Pb exposure for goat and chicken, respectively, as described above. Given these considerations, the inhalation of dust or the accidental ingestion of soil, such as by having a meal with unwashed hands, could be a great risk for human exposure to Pb, especially in children. Additionally, the health risks to residents due to contamination of vegetables with heavy metals have been widely reported (Wang et al., 2005; Nabulo et al., 2006; Sharma et al., 2008). In Kabwe, the consumption of vegetables containing high amounts of Pb compared to food reference values (FAO, 2012) could contribute to human exposure to Pb. Furthermore, Farmer and Farmer (2000) previously reported that high levels of toxic metal contamination in livestock as well could be a significant potential risk to human health. As the goats and chickens in Kabwe accumulated high levels of Pb in the current study, there is a clear need to consider the potential risk of human exposure to Pb via this route.

Yabe et al. (2015) recently revealed significant Pb accumulation in the blood of children in Kabwe—all examined children under the age of 7 years had Pb-B exceeding 5 μg/dL—and their great risk for Pb toxicity. Canfield et al. (2003) reported that even a blood Pb level of less than 10 μg/dL can cause neurological abnormalities, such as manifested by a decreased intelligence quotient (IQ), in children. In response to the report, the US Centers for Disease Control and Prevention (CDC, 2012) revised the blood Pb "level of concern" from 10 to 5 μg/dL. Given the pathology and guidelines, it is clear that the residents of Kabwe, especially its children, are at great risk from Pb pollution. Therefore, further studies on the sources of Pb exposure for humans around the Kabwe mining site are imperative.

4.3. Biological fractionation and its threshold for Pb-IRs

It has been well documented that the isotopic composition of Pb is not significantly affected by physico-chemical fractionation processes (Bollhöfer and Rosman, 2001; Veysseyre and Bollho, 2001). Similarly, the high atomic mass of Pb and the slight differences in the mass of Pb isotopes support the notions that no significant degree of fractionation takes place during various metalworking activities (Cheng and Hu, 2010), and that Pb isotopes do not fractionate measurably in biological systems (Rabinowitz and Wetherill, 1972; Carlson, 1996). Therefore, stable Pb isotopes provide an efficient tool for identifying the sources and pathways of Pb pollution. The analysis of stable Pb isotopes is increasingly used in many fields of environmental research (Rabinowitz and Wetherill, 1972; Dolgopolova et al., 2006; Iglesias et al., 2010),

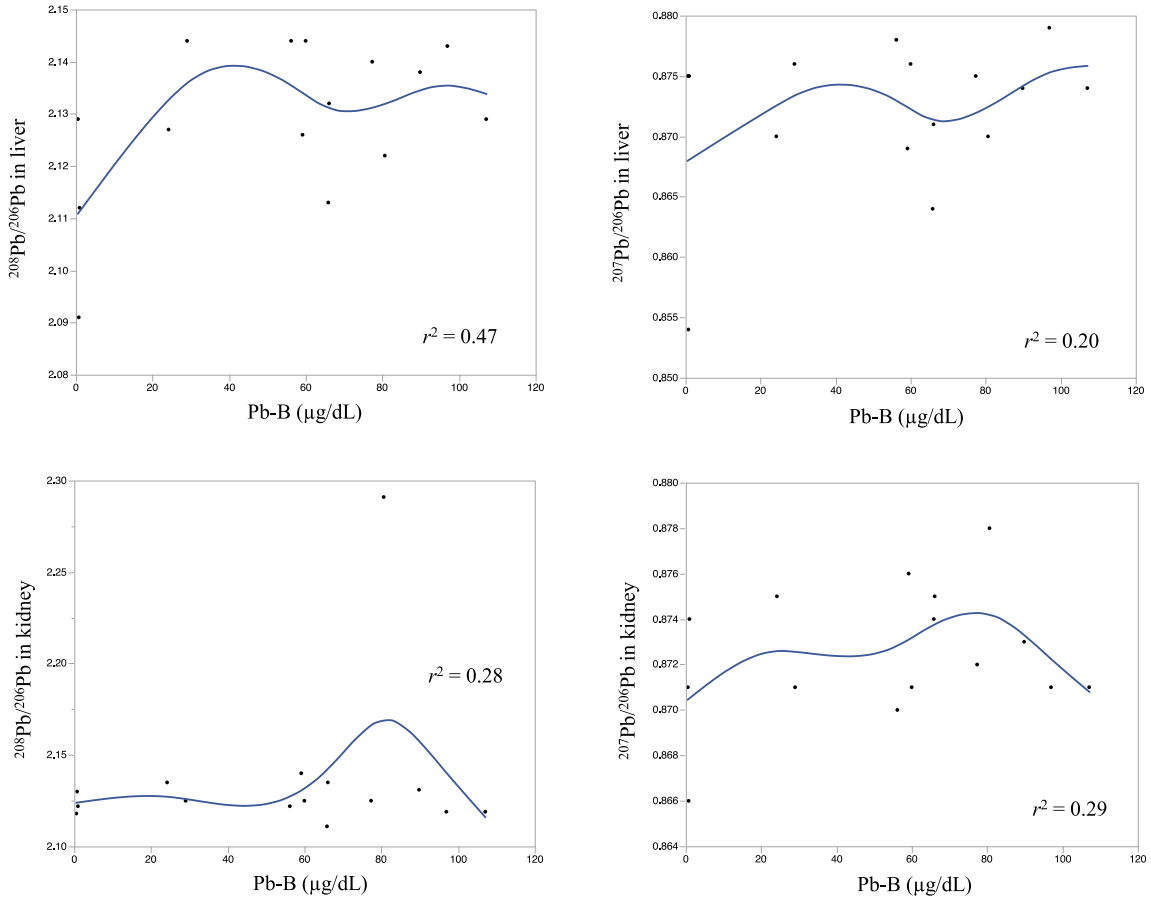

Fig. 5. Pb-B (μg/dL) versus Pb-IRs ($^{208}Pb/^{206}Pb$ and $^{207}Pb/^{206}Pb$) in chicken tissues. To determine the relationship between Pb-B and Pb-IRs in the biological samples from the chickens, spline smoothing, a method for fitting a smooth curve to a set of data, was utilized ($\lambda = 0.05$).

even recently extending to studies of wild animals such as marine mammals (Caurant et al., 2006) and birds (Finkelstein et al., 2010). However, observations of biological fractionation have been documented. Smith et al. (1996) revealed large differences in Pb isotope ratios between paired blood and bone samples from human subjects, and in a recent animal experiment, Wu et al. (2012) and Liu et al. (2014) recorded remarkable differences in Pb isotopic signature between several tissues, blood, urine, and feces of the Sprague–Dawley (SD) rat. These notions suggest there might be biological fractionation of Pb isotopes in different biological samples. Despite these new insights, little is known about the fractionation of Pb isotopes in biological samples from living creatures.

We understand Kabwe to be an area that has only one origin of Pb, namely a mine, a notion supported by the difference of Pb-IRs between in coals from all over the world and in biological samples from G0 and FRC, and the phasing out of leaded gasoline in the past as mentioned above. Hence, the current study can be regarded as a semi-field study on continued exposure to Pb for goats and chickens. As shown in Fig. 1A, G150 exhibited a large variation in its Pb-IRs among different tissues. This result could support the concept of biological fractionation in natural setting. In contrast to G150, the Pb-IRs in the biological samples from G30 and G0, especially G0, were too similar to make such a distinction (Fig. 1B, C). This finding implies that high Pb accumulation in the body might affect biological fractionation, and could also impact the redistribution of Pb isotopes among tissues. The result shown in Fig. 4 and supporting information Fig. S2 revealed that the Pb-IRs in all the goat biological samples are fixed at a certain value (approximately 2.13 for $^{208}Pb/^{206}Pb$ and 0.88 for $^{207}Pb/^{206}Pb$) when the Pb-B exceeds a specific level. This specific level of Pb-B was estimated to be approximately 5 μg/dL, and is considered the threshold for biological fractionation. These findings are quite similar to and support those from a previous study on rats (Liu et al., 2014).

Contrary to goats in the current study and rats in the previous study (Liu et al., 2014), the chicken samples showed a different trend in their Pb-IRs. Although FRC exhibited similar tendencies to G0 and G30 in terms of their Pb-IRs, which showed limited variation and were close to the Pb-IRs of S0 (Fig. 2B), BC showed some small variation in the Pb-IRs of tissues, but seemed to have been primarily affected by the sawdust Pb content (Fig. 2A). These results of only minor variation in Pb-IRs lead to the assumption that chickens might have negligible biological fractionation. Another possibility is that the threshold for the disappearance of biological fractionation might be very low in chickens compared to goats and rats. While the actual reason remains unclear, the trend observed for the Pb-IRs of the chickens clearly differs from that of the mammals. This assumption could be one of the reasons why the relationship between the Pb-B and Pb-IRs in the chickens (Fig. 5 and supporting information Fig. S3) was unexpectedly quite different from that in the goats (Fig. 4 and supporting information Fig. S2). This difference can also be interpreted with the previous finding showing the tolerance of chickens to chronic Pb intoxication (Astrin et al., 1987). Further studies are clearly required to

unravel this interesting species difference in Pb-IR fractionation, as observed among chickens and mammals such as goats and rats.

4.4. Reliability of identifying a Pb pollution source with stable Pb isotope analysis

In evaluating the usefulness of Pb isotope analysis for identifying a Pb pollution source, it should be noted that the Pb-IRs in various tissues from both G0 and FRC were quite similar, and close to those of the soil (Figs. 1C and 2B). In addition, the Pb-IRs in the goat tissues increased up to certain values at around 5 μg/dL of Pb-B, and were constant at >5 μg/dL of Pb-B (Fig. 4 and supporting information Fig. S2). These results were in accordance with the previous findings in rats (Liu et al., 2014). One of the well-known Pb toxicities is hematological toxicity; 5-aminolevulinic acid dehydratase (ALAD) in the blood is generally regarded as an indicator of Pb hematological toxicity (Astrin et al., 1987). The lowest-observed effect concentration (LOEC) for ALAD inhibition in mammals has been reported as 19, 43, 35, and 91 μg/dL for rats (Azar et al., 1972), dogs (Azar et al., 1972), rabbits (Falke and Zwennis, 1990), and calves (Lynch et al., 1976), respectively. For humans, the CDC (2012) recently revised the blood Pb "level of concern" from 10 to 5 μg/dL. Although any Pb isotopic study focusing on the accurate identification of Pb sources must take into account the effect of Pb-B on biological fractionation (Liu et al., 2014), stable Pb isotope analysis can be still regarded as a reliable tool for identifying Pb pollution sources in the case of mammals having a Pb-B exceeding the level of concern (5 μg/dL). Moreover, the observed relationship of the Pb-IRs in S150 and G150 feces (Fig. 2A) implies that feces are the most reliable sample type for the identification of Pb sources at a Pb-B lower than 5 μg/dL. On the other hand, source identification using Pb isotope analysis cannot be regarded as being reliable in chickens. In this study, changes in Pb-IRs did not clearly relate to Pb-B in chickens (Fig. 5 and supporting information Fig. S3), although the actual reason remains uncertain. Moreover, the current study newly demonstrated that for chickens, the values of the natural background Pb-IRs could coincidentally be close to those of a pollution source (Fig. 2). Pb-IRs in both the natural and contaminated sites should be considered when identifying the pollution source.

5. Conclusions

Large variation of Pb-IRs was observed in biological samples from goats and chickens, which had relatively low levels of contamination. The variation in the goats decreased with an increase in Pb-B. Moreover, the Pb-IRs in all goat samples were fixed at certain values close to those of the soil, which can be regarded as the dominant source of Pb exposure at Pb-B >5 μg/dL. The results confirmed that the biological fractionation of Pb isotopes should occur in goats, and that the threshold for triggering biological fractionation is at around 5 μg/dL of Pb-B, as suggested by an earlier study in rats. In addition, feces might be the most reliable sample type for identifying a Pb source at low Pb-B.

In contrast, chickens did not show a clear relationship for Pb-IRs against Pb-B, or a fractionation threshold. Moreover, environmental Pb-IRs in the control and exposure groups of chickens appeared to be similar for reasons unrelated to pollution, and the Pb-IRs of the control group of chickens were also directly affected by environmental Pb-IRs. From these findings, chickens might not be a reliable animal for tracing Pb sources. The results also suggest that Pb-IRs in both the control and polluted area should be taken into account jointly for identification of the Pb source.

Given these, Pb isotope analysis can still be considered a helpful tool for the identification of Pb sources. Nevertheless, further studies should be conducted to clarify the usefulness of Pb isotope analysis for identifying Pb sources more accurately.

Author contribution

H. N., S. M. M. N., J. Y., and M. I. designed research; H. N., S. M. M. N., J. Y., and A. L. performed research; H. N., S. M. M. N., H. M., W. S. D., and Y. I. analyzed data; and H. N., S. M. M. N., and M. I. wrote the paper.

Conflict of interest

The authors declare no conflict of interest.

Acknowledgments

This work was supported by Grants-in-Aid for Scientific Research from the Ministry of Education, Culture, Sports, Science and Technology of Japan awarded to M. Ishizuka (No. 24405004 and No. 24248056) and Y. Ikenaka (No. 26304043, 15H0282505, 15K1221305), and the foundation of JSPS Core to Core Program (AA Science Platforms) and Bilateral Joint Research Project (PG36150002 and PG36150003). We also acknowledge the financial support by The Mitsui & Co., Ltd. Environment Fund and The Nihon Seimei Foundation. We are grateful to Mr. Takahiro Ichise (Laboratory of Toxicology, Graduate School of Veterinary Medicine, Hokkaido University) for technical support with metal concentration analyses using ICP-MS.

Supporting information

Supporting information (details on Materials and Methods, supporting figures and tables) are available free of charge via the Internet at http://pubs.acs.org.

Appendix A. Supplementary data

Supplementary data related to this article can be found at http://dx.doi.org/10.1016/j.envpol.2015.10.006.

References

Astrin, K.H., Bishop, D.F., Wetmur, J.G., Kaul, B., Davidow, B., Desnick, R.J., 1987. δ-aminolevulinic acid dehydratase isozymes and lead toxicity. Ann. N. Y. Acad. Sci. 514 (1), 23–29.

Azar, A., Trochimowicz, H.J., Maxfield, M.E., 1972. Review of lead studies in animals carried out at Haskell Laboratory: two-year feeding study and response to hemorrhage study. Environmental Health Aspects of Lead. In: Proceedings of an International Symposium, pp. 199–210.

Berman, E., 1966. The biochemistry of lead review of the body distribution and methods of lead determination. Clin. Pediatr. 5 (5), 287–291.

Blacksmith Institute, 2010. World's Worst Pollution Problems Report 2010 Top Six Toxic Threats. In: Pap. Annual Reports. http://www.worstpolluted.org/2010-report.html (accessed 21.07.15.).

Blacksmith Institute, 2013. The Worlds Worst 2013: the Top Ten Toxic Threats Cleanup, Progress, and Ongoing Challenges Table. In: Pap. Annu. Reports, pp. 1–19. www.worstpolluted.org/docs/TopTenThreats2013.pdf (accessed 21.07.15.).

Bollhöfer, A., Rosman, K.L.R., 2001. Isotopic source signatures for atmospheric lead: the Northern Hemisphere. Geochim. Cosmochim. Acta 65 (11), 1727–1740.

Canfield, R.L., Henderson Jr., C.R., Cory-Slechta, D.A., Cox, C., Jusko, T.A., Lanphear, B.P., 2003. Intellectual impairment in children with blood lead concentrations below 10 μg per deciliter. N. Engl. J. Med. 348 (16), 1517–1526.

Carlson, A.K., 1996. Lead isotope analysis of human bone for addressing cultural affinity: a case study from Rocky Mountain House, Alberta. J. Archaeol. Sci. 23 (4), 557–567.

Caurant, F., Aubail, A., Lahaye, V., Van Canneyt, O., Rogan, E., López, A., Addink, M., Churlaud, C., Robert, M., Bustamante, P., 2006. Lead contamination of small cetaceans in European waters—the use of stable isotopes for identifying the sources of lead exposure. Mar. Environ. Res. 62 (2), 131–148.

Centers for Disease Control and Prevention, 2012. Low Level Lead Exposure Harms Children : a Renewed Call for Primary Prevention Advisory Committee on Childhood Lead Poisoning Prevention, pp. 1–65.

Cheng, H., Hu, Y., 2010. Lead (Pb) isotopic fingerprinting and its applications in lead pollution studies in China: a review. Environ. Pollut. 158 (5), 1134–1146.
Charalampides, G., Manoliadis, O., 2002. Sr and Pb isotopes as environmental indicators in environmental studies. Environ. Int. 28 (3), 147–151.
Chow, T.J., Johnstone, M.S., 1965. Lead isotopes in gasoline and aerosols of Los Angeles Basin, California. Science 147 (3657), 502–503.
Chow, T.J., Earl, J.L., 1972. Lead isotopes in North American coals. Science. 176 (4034), 510–511.
Crosby, D.G., 1998. Inorganic Toxicants. In: Environ. Toxicol. Chem.. Oxford Univ. Press, New York, pp. 205–224.
Diaz-Somoano, M., Kylander, M.E., Lopez-Anton, M.A., Suarez-Ruiz, I., Martinez-Tarazona, M.R., Ferrat, M., Kober, B., Weiss, D.J., 2009. Stable lead isotope compositions in selected coals from around the world and implications for present day aerosol source tracing. Environ. Sci. Technol. 43 (4), 1078–1085.
Dolgopolova, A., Weiss, D.J., Seltmann, R., Kober, B., Mason, T.F.D., Coles, B., Stanley, C.J., 2006. Use of isotope ratios to assess sources of Pb and Zn dispersed in the environment during mining and ore processing within the Orlovka–-Spokoinoe mining site (Russia). Appl. Geochem. 21 (4), 563–579.
Epov, V.N., Rodriguez-Gonzalez, P., Sonke, J.E., Tessier, E., Amouroux, D., Bourgoin, L.M., Donard, O.X.F., 2008. Simultaneous determination of species-specific isotopic composition of Hg by gas chromatography coupled to multi-collector ICPMS. Anal. Chem. 80 (10), 3530–3538.
Ettler, V., Vaněk, A., Mihaljevič, M., Bezdička, P., 2005. Contrasting lead speciation in forest and tilled soils heavily polluted by lead metallurgy. Chemosphere 58 (10), 1449–1459.
Fairbrother, A., Wenstel, R., Sappington, K., Wood, W., 2007. Framework for metals risk assessment. Ecotoxicol. Environ. Saf. 68 (2), 145–227.
Falke, H.E., Zwennis, W.C.M., 1990. Toxicity of lead acetate to female rabbits after chronic subcutaneous administration. 1. Biochemical and clinical effects. Arch. Toxicol. 64 (7), 522–529.
Farmer, A.A., Farmer, A.M., 2000. Concentrations of cadmium, lead and zinc in livestock feed and organs around a metal production centre in eastern Kazakhstan. Sci. Total Environ. 257 (1), 53–60.
Finkelstein, M.E., George, D., Scherbinski, S., Gwiazda, R., Johnson, M., Burnett, J., Brandt, J., Lawrey, S., Pessier, A.P., Clark, M., 2010. Feather lead concentrations and 207Pb/206Pb ratios reveal lead exposure history of California condors (*Gymnogyps californianus*). Environ. Sci. Technol. 44 (7), 2639–2647.
Food and Agriculture Organization of the United Nations, 2012. Joint FAO/WHO Food Standards Programme, Codex Committee on Contaminants in Foods. Sixth session. CF/6 INF/1, pp. 1–94.
Gannes, L.Z., Del Rio, C.M., Koch, P., 1998. Natural abundance variations in stable isotopes and their potential uses in animal physiological ecology. Comp. Biochem. Physiol. A Mol. Integr. Physiol. 119 (3), 725–737.
Glorennec, P., 2006. Analysis and reduction of the uncertainty of the assessment of children's lead exposure around an old mine. Environ. Res. 100 (2), 150–158.
Gulson, B.L., Tiller, K.G., Mizon, K.J., Merry, R.H., 1981. Use of lead isotopes in soils to identify the source of lead contamination near Adelaide, South Australia. Environ. Sci. Technol. 15 (6), 691–696.
Hansmann, W., Köppel, V., 2000. Lead-isotopes as tracers of pollutants in soils. Chem. Geol. 171 (1), 123–144.
Hudson-Edwards, K.A., Macklin, M.G., Brewer, P.A., Dennis, I.A., 2008. Assessment of Metal Mining-contaminated River Sediments in England and Wales. Environment Agency, pp. 1–64.
Ikenaka, Y., Nakayama, S.M.M., Muzandu, K., Choongo, K., Teraoka, H., Mizuno, N., Ishizuka, M., 2010. Heavy metal contamination of soil and sediment in Zambia. Afr. J. Environ. Sci. Technol. 4 (11), 729–739.
Ikenaka, Y., Nakayama, S.M.M., Muroya, T., Yabe, J., Konnai, S., Darwish, W.S., Muzandu, K., Choongo, K., Mainda, G., Teraoka, H., Umemura, T., Ishizuka, M., 2012. Effects of environmental lead contamination on cattle in a lead/zinc mining area: changes in cattle immune systems on exposure to lead in vivo and in vitro. Environ. Toxicol. Chem. 31 (10), 2300–2305.
Iglesias, M., Sanchez, M., Queralt, I., Hidalgo, M., Margui, E., 2010. Sequential extraction combined with isotopic analysis as a tool for studying lead contamination from mining activity. Int. J. Environ. Waste Manag. 5 (1), 64–78.
Järup, L., 2003. Hazards of heavy metal contamination. Br. Med. Bull. 68 (1), 167–182.
Kamona, A.F., Friedrich, G.H., 2007. Geology, mineralogy and stable isotope geochemistry of the Kabwe carbonate-hosted Pb–Zn deposit, Central Zambia. Ore. Geol. Rev. 30, 217–243.
Keinonen, M., 1992. The isotopic composition of lead in man and the environment in Finland 1966-1987: isotope ratios of lead as indicators of pollutant source. Sci. Total Environ. 113 (3), 251–268.
Lantzy, R.J., Mackenzie, F.T., 1979. Atmospheric trace metals: global cycles and assessment of man's impact. Geochim. Cosmochim. Acta 43, 511–525.
Liu, D., Wu, J., Ouyang, L., Wang, J., 2014. Variations in lead isotopic abundances in Sprague-Dawley rat tissues: possible reason of formation. PLoS One 9 (2), e89805.
Lockitch, G., 1993. Perspectives on lead toxicity. Clin. Biochem. 26, 371–381.
Lynch, G.P., Jackson, E.D., Kiddy, C.A., Smith, D.F., 1976. Responses of young calves to low doses of lead. J. Dairy Sci. 59 (8), 1490–1494.
Mazliah, J., Barron, S., Bental, E., Rogowski, Z., Coleman, R., Silbermann, M., 1989. The effects of long-term lead intoxication on the nervous system of the chicken. Neurosci. Lett. 101 (3), 253–257.
Meyer, P.A., Brown, M.J., Falk, H., 2008. Global approach to reducing lead exposure and poisoning. Mutat. Res. 659 (1), 166–175.
Monna, F., Loizeau, J., Thomas, B.A., Gue, C., Favarger, P., 1998. Pb and Sr isotope measurements by inductively coupled plasma – mass spectrometer : efficient time management for precision improvement. Spectrochim. Acta B. 53, 1317–1333.
Nabulo, G., Oryem-Origa, H., Diamond, M., 2006. Assessment of lead, cadmium, and zinc contamination of roadside soils, surface films, and vegetables in Kampala City, Uganda. Environ. Res. 101 (1), 42–52.
Nakata, H., Nakayama, S.M.M., Ikenaka, Y., Mizukawa, H., Ishii, C., Yohannes, Y.B., Konnai, S., Darwish, W.S., Ishizuka, M., 2015. Metal extent in blood of livestock from Dandora dumping site, Kenya: source identification of Pb exposure by stable isotope analysis. Environ. Pollut. 205, 8–15.
Nakayama, S.M.M., Ikenaka, Y., Hamada, K., Muzandu, K., Choongo, K., Teraoka, H., Mizuno, N., Ishizuka, M., 2011. Metal and metalloid contamination in roadside soil and wild rats around a Pb-Zn mine in Kabwe, Zambia. Environ. Pollut. 159 (1), 175–181.
Nakayama, S.M.M., Ikenaka, Y., Hamada, K., Muzandu, K., Choongo, K., Yabe, J., Umemura, T., Ishizuka, M., 2013. Accumulation and biological effects of metals in wild rats in mining areas of Zambia. Environ. Monit. Assess. 185 (6), 4907–4918.
Neathery, M.W., Miller, W.J., 1975. Metabolism and toxicity of cadmium, mercury, and lead in animals: a review. J. Dairy Sci. 58 (12), 1767–1781.
Petit, D., Mennessier, J.P., Lamberts, L., 1984. Stable lead isotopes in pond sediments as tracer of past and present atmospheric lead pollution in Belgium. Atmos. Environ. 18 (6), 1189–1193.
Rabinowitz, M.B., Wetherill, G.W., 1972. Identifying sources of lead contamination by stable isotope techniques. Environ. Sci. Technol. 6 (8), 705–709.
Razo, I., Carrizales, L., Castro, J., Díaz-Barriga, F., Monroy, M., 2004. Arsenic and heavy metal pollution of soil, water and sediments in a semi-arid climate mining area in Mexico. Water Air Soil. Pollut. 152, 129–152.
Regulation Council, 2001. No 2375/2001 of 29 November 2001 amending Commission Regulation (EC) No 466/2001 setting maximum levels for certain contaminants in foodstuffs. Off. J. Eur. Communities L. 321 (1), 6–12.
Sangster, D.F., Outridge, P.M., Davis, W.J., 2000. Stable lead isotope characteristics of lead ore deposits of environmental significance. Environ. Rev. 8 (2), 115–147.
Scheuhammer, A.M., Templeton, D.M., 1998. Use of stable isotope ratios to distinguish sources of lead exposure in wild birds. Ecotoxicology 7 (1), 37–42.
Sharma, R.K., Agrawal, M., Marshall, F.M., 2008. Heavy metal (Cu, Zn, Cd and Pb) contamination of vegetables in urban India: a case study in Varanasi. Environ. Pollut. 154 (2), 254–263.
Shirahata, H., Elias, R.W., Patterson, C.C., Koide, M., 1980. Chronological variations in concentrations and isotopic compositions of anthropogenic atmospheric lead in sediments of a remote subalpine pond. Geochim. Cosmochim. Acta 44 (2), 149–162.
Smith, D.R., Flegal, A.R., Niemeyer, S., Estes, J.A., 1990. Stable lead isotopes evidence anthropogenic contamination in Alaskan sea otters. Environ. Sci. Technol. 24 (10), 1517–1521.
Smith, D.R., Osterloh, J.D., Flegal, A.R., 1996. Use of endogenous, stable lead isotopes to determine release of lead from the skeleton. Environ. Health Perspect. 104 (1), 60.
Stenberg, A., Andrén, H., Malinovsky, D., Engström, E., Rodushkin, I., Baxter, D.C., 2004. Isotopic variations of Zn in biological materials. Anal. Chem. 76 (14), 3971–3978.
Stokes, P.E., Okamoto, M., Lieberman, K.W., Alexander, G., Triana, E., 1982. Stable isotopes of lithium: in vivo differential distribution between plasma and cerebrospinal fluid. Biol. Psychiatry 17 (4), 413–421.
Tieszen, L.L., Boutton, T.W., Tesdahl, K.G., Slade, N.A., 1983. Fractionation and turnover of stable carbon isotopes in animal tissues: implications for $\delta^{13}C$ analysis of diet. Oecologia 57, 32–37.
United States Environmental Protection Agency, 2005. Guidance for Developing Ecological Soil Screening Levels, pp. 1–85.
Veysseyre, A.M., Bollho, A.F., 2001. Tracing the origin of pollution in French alpine snow and aerosols using lead isotopic ratios. Environ. Sci. Technol. 35 (22), 4463–4469.
Walczyk, T., von Blanckenburg, F., 2002. Natural iron isotope variations in human blood. Science 295 (5562), 2065–2066.
Wang, X., Sato, T., Xing, B., Tao, S., 2005. Health risks of heavy metals to the general public in Tianjin, China via consumption of vegetables and fish. Sci. Total Environ. 350, 28–37.
Wu, J., Liu, D., Xie, Q., Wang, J., 2012. Biological fractionation of lead isotopes in Sprague-Dawley rats lead poisoned via the respiratory tract. PLoS One. 7 (12), e52462.
Yabe, J., Nakayama, S.M.M., Ikenaka, Y., Muzandu, K., Choongo, K., Mainda, G., Kabeta, M., Ishizuka, M., Umemura, T., 2013. Metal distribution in tissues of free-range chickens near a lead-zinc mine in Kabwe, Zambia. Environ. Toxicol. Chem. 32 (1), 189–192.
Yabe, J., Nakayama, S.M.M., Ikenaka, Y., Muzandu, K., Ishizuka, M., Umemura, T., 2011. Uptake of lead, cadmium, and other metals in the liver and kidneys of cattle near a lead-zinc mine in Kabwe, Zambia. Environ. Toxicol. Chem. 30 (8), 1892–1897.
Yabe, J., Ishizuka, M., Umemura, T., 2010. Current levels of heavy metal pollution in Africa. J. Vet. Med. Sci. 72 (10), 1257–1263.
Yabe, J., Nakayama, S.M.M., Ikenaka, Y., Yohannes, Y.B., Bortey-Sam, N., Oroszlany, B., Muzandu, K., Choongo, K., Kabalo, A.N., Ntapisha, J., Mweene, A., Umemura, T., Ishizuka, M., 2015. Lead poisoning in children from townships in the vicinity of a lead-zinc mine in Kabwe, Zambia. Chemosphere. 119, 941–947.

Bull Environ Contam Toxicol (2017) 99:108–116
DOI 10.1007/s00128-017-2089-3

Sediment Metal Contamination in the Kafue River of Zambia and Ecological Risk Assessment

Ethel M'kandawire[1,3] · Kennedy Choongo[1] · John Yabe[1] · Maxwell Mwase[1] · Ngonda Saasa[1] · Shouta M. M. Nakayama[2] · Nesta Bortey-Sam[2] · Claudia A. Blindauer[3]

Received: 24 November 2016 / Accepted: 11 April 2017 / Published online: 22 April 2017

Abstract Zambia's Kafue River receives wastes from various sources, resulting in metal pollution. This study determined the degree of contamination of 13 metals (Al, Cr, Mn, Fe, Co, Ni, Cu, Zn, As, Se, Cd, Hg and Pb) in Kafue River sediment and the associated ecological risks at six sites in three different seasons. The level of contamination for most metals showed significant site and seasonal differences. The contamination factor and pollution load index indicated that concentrations of most metals particularly copper (Cu), cobalt (Co), manganese (Mn) and arsenic (As) were very high at sites within the Copperbelt mining area. The geoaccumulation index showed an absence of anthropogenic enrichment with Cd and Hg at all the study sites and extreme anthropogenic enrichment with Cu at sites in the Copperbelt mining area. Potential ecological risk showed that Cu and As were likely to cause adverse biological effects to aquatic organisms in the Copperbelt mining region of the Kafue River.

Keywords Kafue River sediment · Metals · Copperbelt mining area · Contamination factor · Pollution load index · Geoaccumulation index · Potential ecological risk

✉ Ethel M'kandawire
ethel.mkandawire@unza.zm; ethelmkandawire@yahoo.com

[1] School of Veterinary Medicine, University of Zambia, P.O. Box 32379, Lusaka, Zambia

[2] Laboratory of Toxicology, Department of Environmental Veterinary Sciences, Graduate School of Veterinary Medicine, Hokkaido University, Kita 18, Nishi 9, Kita-ku, Sapporo 060-0818, Japan

[3] Department of Chemistry, University of Warwick, Gibbet Hill road, Coventry CV4 7AL, UK

Metal pollution of water sources has evoked a global interest because metal ions are indestructible and bio-accumulate in aquatic ecosystems such as aquatic plants, invertebrates and fish and humans (Gupta et al. 2009; Solomon 2009). Anthropogenic sources of metals include mining, discharge of untreated domestic and industrial wastes (Khadse et al. 2008) and agricultural run-off (Hatje et al. 1998). Natural sources include weathering of rocks and minerals (Karbassi et al. 2008). Metals released into aquatic bodies may be immobilized within sediment but can be retained or released to the water posing a risk to aquatic life and humans through the food chain (Calmano et al. 1990). Therefore, sediments are important environmental indicators for metal pollution in aquatic bodies (Alaoui et al. 2010). Although metals such as Fe, Zn, Se and Cu are essential to life, they are toxic at high concentrations. Metals like Cd, As, Hg and Pb are non-essential and are toxic at minute concentrations (Fernandes et al. 2008; Mayo et al. 2015). Developing countries including Zambia are plagued by the impact of metal pollution especially from mining (Yabe et al. 2010) with the level of contamination increasing with an increase in industrial activities.

The Kafue River receives large amounts of Cu and Co mining waste from mines in the Copperbelt province (Sracek et al. 2012). The main composition of mineral ores within the Copperbelt mining area include pyrite (FeS_2), chalcopyrite ($CuFeS_2$), bornite (Cu_5FeS_4), chalcocite (CuS_2), digenite (Cu_9S_5), linnaeite (Co_3S_4) and carrolite ($Cu(Co,Ni)_2S_4$) which are embedded in carbonate-rich shales and argillite (Mendelsohn 1961). As the Kafue River passes through this extensive mining region, it receives large volumes of metal effluent. These include waste water discharging from chemical processing plants, erosion and wash out of fine particles from old tailings, mining waste piles, metallurgical slag deposits, and

seepage and overflow of suspensions from active tailing ponds (Sracek et al. 2012). This has resulted in extensive environmental impacts detected in various environmental samples downstream of the mining area (Bäckström 1996; M'kandawire et al. 2012). Studies conducted on the Kafue River sediment have revealed elevated concentrations of Cu. For example, Choongo et al. (2005) reported high levels of this metal in sediment and low coefficient of condition of fish probably due to Cu toxicity. Ikenaka et al. (2010) demonstrated the presence of heavy metals in national parks downstream to the Copperbelt mining area. Total metal contents in sediment showed that the Kafue River was highly enriched with Cu and exceeded the Canadian limit for freshwater sediments (Sracek et al. 2012). However, these previous studies have only examined a few metals in sediment; information which in itself is limiting considering that the river's sediment might be contaminated with many other metals. In addition, there is no information on ecological risk assessment of metal contaminants in the Kafue River. These assessments are essential as they provide policy makers with information on the extent of aquatic ecosystem contamination and are used as early-warning signals of ecological challenges. Therefore, the objective of the study was to determine the degree of contamination of 13 heavy metals in sediment and their associated ecological risk to Kafue River's organisms.

Materials and Methods

A cross sectional study was conducted to determine heavy metal concentrations in sediment along the Kafue River (Fig. 1). The river lies completely within Zambia spanning 1600 Km. From its origin in the North Western Province of Zambia, the river flows through Copperbelt, Central, Southern and Lusaka provinces, before discharging into the Zambezi River. The river drains a catchment of about 157,000 Km^2 accounting for about 20% of the total land area of Zambia (Kambole 2003). Sediment samples (n = 54) were collected from six sites along the river that were selected based on their relative location to the Copperbelt mining area and proximity to fishing camps. The sites were: Chimfunshi (upstream of the Copperbelt mining area, pristine); Chililabombwe, Chingola-Kanyemo and Chingola-Hippo Pool (within Copperbelt mining area); Kafue flats and Kafue town (downstream to Copperbelt mining area). Sediment samples were collected according to the method of Choongo et al. (2005) in 2014 during the warm-rainy (April, n = 18), dry-cold (June, n = 18) and

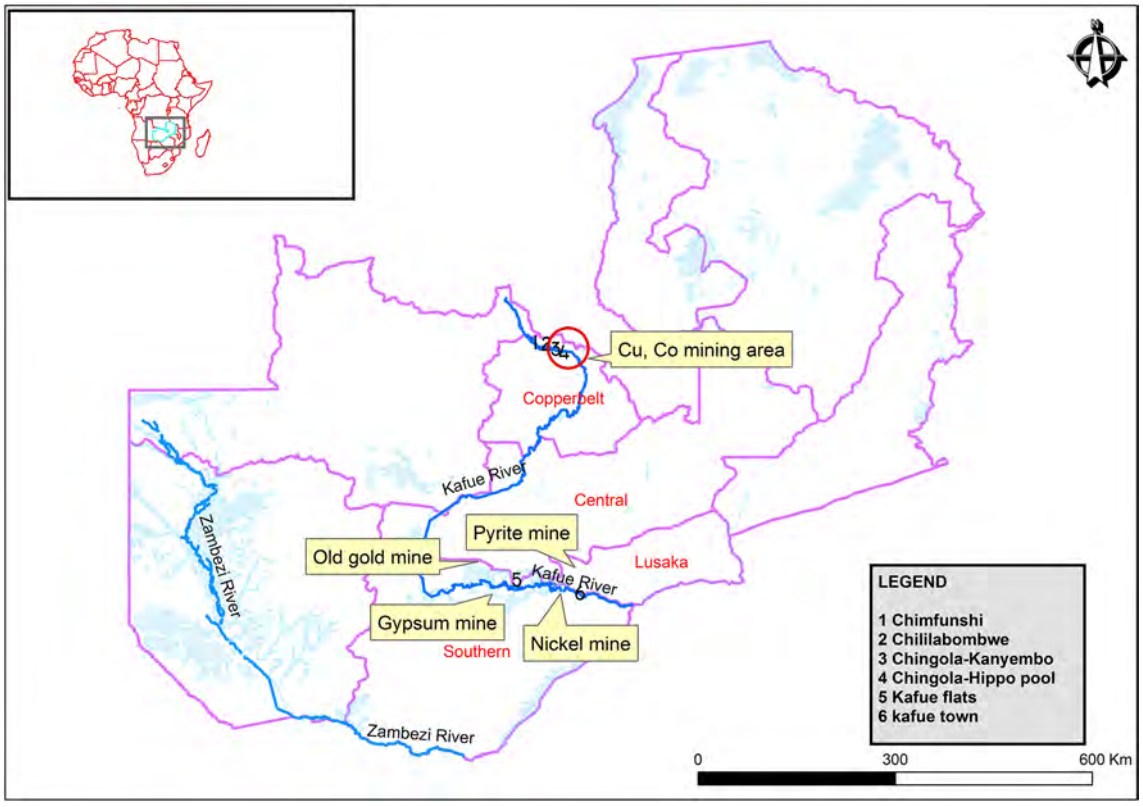

Fig. 1 Map of Zambia showing the location of the mining areas and sampling sites along Kafue River

dry-hot seasons (September, n = 18). Briefly, three surface sediment composite samples were collected in 600 mL polypropylene bottles from each site in each season. Samples were collected from the same location in all seasons. The composite sediment samples were then transported in cooler boxes to the University of Zambia, and stored at 4°C before transportation to the University of Warwick, Department of Chemistry for analysis.

Analytical grade chemicals and ultrapure water (>18 MΩ cm; Millipore Milli-Q) was used for the preparation of all solutions for heavy metal analysis. The sediment samples were oven dried (Status, Thermal Control) at 100°C for two days, ground, homogenized and sieved through a 2 mm mesh. Approximately 0.5 g of each dried sediment sample was acid digested with 7 mL of 72% (v/v) HNO_3 and 1 mL of 30% (v/v) H_2O_2 (Fisher Scientific) using a closed microwave digestion system (Start D, Milestone) for 90 min until the solution was clear and filtered. Solutions from digested sediment samples were analyzed in triplicate for total concentrations of ^{27}Al, ^{53}Cr, ^{55}Mn, ^{56}Fe,^{59}Co, ^{60}Ni, ^{63}Cu, ^{66}Zn, ^{75}As, ^{82}Se, ^{111}Cd, ^{202}Hg and ^{208}Pb using a 7500 series ICP-MS (Agilent Technologies).

A multi-element standard solution IV(4) for inductively coupled plasma (ICP) and a single mercury standard solution for ICP (Fluka Analytical, Buchs) were used to prepare eight multi-element standards to provide suitable calibration curves. Only calibration curves with $R^2 > 0.999$ were accepted for concentration calculations. Erbium (^{166}Er) was used as an internal standard. For quality control, sample triplicates were used to assess precision of the analysis, and reagent blanks and certified reference material (CRM) (CRM015; ISO Guide 34:2009 and ISO/IEC 17,025:2005, fresh water sediment 2) were used to assess method accuracy. Hence, each inductively coupled plasma mass spectrometry (ICP-MS) run included standards and triplicate blanks, triplicate samples and triplicate certified reference material and the results were expressed as the mean. In this study, the measured mean concentrations of each metal in each season at Chimfunshi which is an upstream preindustrial site (Choongo et al. 2005) were used as background concentrations (C_b) (Table 2) to calculate the ecological indicators (contamination factor (CF), pollution load index (PLI), geoaccumulation index (I_{geo}) and potential ecological risk (RI)).

The CF was used to assess the pollution load of the sediments with respect to each heavy metal. CF is a ratio between the content of each metal at a contaminated site (C_c) and the background contents in sediment (C_b) (Loska et al. 2004). It was calculated as follows:

$$CF_{metals} = C_c/C_b \quad (1)$$

The PLI of metals is dependent on the CF and gives an additive indication of the overall level of sediment metal toxicity at a particular site. It was calculated according to Suresh et al. (2011), as:

$$PLI = \left(CF_{metal1} \times CF_{metal2} \times CF_{metal3} \times \ldots CF_n\right)^{1/n} \quad (2)$$

where, CF_{metal} is the contamination factor of each metal, n = number of metals measured.

The I_{geo} value is used to determine the degree of anthropogenic enrichment of heavy metals and hence determines the anthropogenic source of heavy metals and how much they impact the sediment (Loska et al. 2004). It was calculated as follows:

$$I_{geo} = \log_2\left(C_c/1.5C_b\right) \quad (3)$$

where C_c is the measured concentration of each metal at a contaminated site and C_b is the background concentration of each metal (Islam et al. 2014) as determined for the preindustrial site. The factor of 1.5 is introduced to minimize the possible variations in the background values attributed to lithogenic effects (Müller 1969).

The RI value indicates the combined potential ecological risk factors of metals in the monitored sediment and was calculated according to Hakanson (1980) as:

$$RI = \sum Er_{metal}, \text{ where, } Er_{metal} = Tr_{metal}\left(C_c/C_b\right) \quad (4)$$

where Er_{metal} is the potential ecological risk factor for each metal. It considers each heavy metal level in the sediment associating ecological and environmental effects with toxicology, and evaluates metal pollution using comparable and equivalent property index grading method (Qui 2010). Tr_{metal} is the toxic response factor of each selected metal (Hg = 40, Cd = 30, As = 10, Pb = 5, Cu = 5, Cr = 2, Ni = 5, and Zn = 1) (Zhao et al. 2005). The Tr_{metal} reflects the toxicity of each heavy metal and the degree of environment sensitivity of bio-organism to the respective heavy metal. C_c is the content of metal in the samples at the contaminated site, C_b is the background reference sample content for each metal.

Descriptive statistics were calculated using Microsoft Excel® 2013 spreadsheet. Statistical analyses were performed using R statistical software (R Core Team, 2014, Vienna Austria). The data were $\log_{10}$ transformed due to a small sample size and non-normal distribution. One way analysis of variance (ANOVA) was used to test for site and seasonal differences of each metal analyzed in the Kafue River sediment and considered to be significant when $p < 0.05$. Where significant differences were present, the mean values were separated using post-hoc Tukey's HSD pairwise comparison test (Stevens 1999).

Results and Discussion

For quality control and to assess method accuracy, the sediment CRM (CRM15) was analyzed for Al, Cr, Mn, Fe, Co, Ni, Cu, Zn, As, Se, Cd, Hg and Pb. The measured mean ± SD values which were determined by this study (means of replicates), certified values ± SD which are determined values by the manufacturer of the CRM and percent recoveries (measured mean value divided by certified value and expressed as a percentage) of each heavy metal in the sediment certified reference material are reported in Table 1. Results showed that the heavy metal recoveries for the sediment CRM were satisfactory for most heavy metals; although often higher than 100% (with extremely high recoveries for Al and Cr). The detection limits (ppb) for each metal are also shown in Table 1.

Table 2 shows concentrations (mean ± SD) of metals in Kafue River sediment which showed significant site and seasonal differences ($p < 0.05$). Notable observations were that concentrations of Mn, Co, Cu, Zn, As and Pb were found to be higher at sites in the Copperbelt mining area compared to the other sites ($p < 0.05$) (Table 2) probably due to Cu mining and smelting activities in the area that discharge waste into the Kafue River. Contamination with Co and Cu decreased downstream the Kafue River to Kafue flats and Kafue town (Table 2; Fig. 1). This finding is in agreement with previous studies (Choongo et al. 2005; Sracek et al. 2012) that reported concentrations of some metals such as Cu to be higher at sampling sites in Copperbelt mining area than sites downstream and upstream of the Copperbelt mining area. Concentrations of Al, Cr, Fe, Ni, Se, Cd and Hg were observed to be higher at various sites outside the Copperbelt mining area ($p < 0.05$) (Table 2). The differences in metal concentrations among sampling sites suggest diverse sources of metals in the Kafue River sediment rather than one common source. Comparing the results of mean metal concentrations in this study with previous studies (Choongo et al. 2005; Ikenaka et al. 2010; Sracek et al. 2012) showed that the river's sediment was not improving and still under pressure from metal contamination. The present study observed that most metals tended to show higher concentrations in the dry-hot season compared to the other seasons ($p < 0.05$) (Table 2) in agreement with findings by Choongo et al. (2005). Higher levels of most metals in the dry-hot season could be due to the slower movement of water over the sediment and possible higher heavy-metal adsorption ability of the sediment in the dry-hot season (Nwadinigwe et al. 2014). Heavy metal absorption ability is increased in the dry-hot season because of an increase in temperature which enhances efficient sedimentation of metals (Nwadinigwe et al. 2014). High metal discharge into the river and hence availability of metals for adsorption to sediment in the dry-hot season could be another reason why metals were higher in the dry-hot season compared to the other seasons. Apart from temperature, seasonal variations of metal concentrations in sediment are influenced by factors such as salinity (Hatje et al. 2003), organic matter (Peng et al. 2009) and changes in the levels of pollutant discharge over time (Srikanth and Rao 2014).

The CF for most metals in the warm rainy season (Table 3) indicated a moderate degree of contamination, except for Hg and Cd which showed a low degree of contamination at all the sites. CF for Mn, Co and Cu particularly at sites in the Copperbelt mining area showed very high degrees of contamination and this could be attributed to Cu mining and smelting activities in the area. A CF value of 3.18 for As at Chingola-Hippo Pool indicated a considerable degree of contamination which could be due to smelting of As-rich copper concentrates. Similar trends of CFs were observed in the dry-cold and dry-hot seasons

Table 1 Detection limits (ppb, dry-wt.), measured mean ± SD concentrations (ppm dry-wt.) determined by this study, certified values ± uncertainty (ppm dry-wt.) in sediment reference material and percent recoveries of each heavy metal

Heavy metal	Detection limit	Measured mean ± SD	Certified value ± SD	Percent recoveries
^{27}Al	0.773	28,208 ± 296	9200 ± 976	306.61
^{53}Cr	0.02	36.73 ± 1.10	14.3 ± 1.44	256.88
^{55}Mn	0.02	197 ± 9.94	183 ± 4.52	107.46
^{56}Fe	1.346	21,142 ± 91.00	17,100 ± 717	123.64
^{59}Co	0.005	6.41 ± 0.04	6.04 ± 0.142	106.04
^{60}Ni	0.02	19.3 ± 1.01	17.5 ± 0.52	110.42
^{63}Cu	0.1	15.7 ± 0.31	16.1 ± 0.585	97.22
^{66}Zn	0.11	75.3 ± 0.85	69.9 ± 2.82	107.68
^{75}As	0.016	6.29 ± 0.08	6.6 ± 0.433	95.37
^{82}Se	0.597	0.85 ± 0.04	0.8 (non-certified)	106.19
^{111}Cd	0.004	0.35 ± 0.03	0.52 (non-certified)	68.26
^{202}Hg	0.014	0.24 ± 0.04	0.221 ± 0.00619	110.44
^{208}Pb	0.004	14.8 ± 0.08	15 ± 0.539	98.96

Table 2 Concentrations (mean ± SD, ppm, dry-wt.) of the 13 metals in Kafue River sediment at the six study sites in the three seasons

Season	Site		^{27}Al	^{53}Cr	^{55}Mn	^{56}Fe	^{59}Co	^{60}Ni	^{63}Cu	^{66}Zn	^{75}As	^{82}Se	^{111}Cd	^{202}Hg	^{208}Pb
Warm-rainy	Chimfunshi	Mean	29204c	30.3b	128d	10224d	13.9c	16.2c	73.5c	16.8e	1.58b	0.38b	0.03a	0.22a	7.58b
		SD	1334	1.22	3.70	659	0.17	0.30	2.84	0.98	0.11	0.66	0.05	0.19	0.72
	Chililabombwe	Mean	46925b	33.3b	1537a	22433a	394a	21.0b	10671a	58.8a	2.54b	2.82a	0.02a	0.20a	19.8a
		SD	1316	1.68	106	527	19.3	1.38	477	5.57	0.25	0.61	0.03	0.03	0.88
	Chingola-Kanyemo	Mean	24269d	28.8b	489b	18802b	373a	19.6bc	10749a	46.2ab	2.06b	3.21a	0.01a	0.12a	18.3a
		SD	656	2.19	20.2	1624	23.7	1.98	652	4.99	0.83	1.02	0.03	0.02	1.1
	Chingola-Hippo pool	Mean	17311e	21.1e	390c	15304c	205b	16.1c	4962b	43.0bc	6.37a	0.51b	0.01a	0.09a	17.2a
		SD	1472	2.46	23.2	879	9.86	2.00	140	4.72	0.87	0.36	0.02	0.01	0.9
	Kafue flats	Mean	62796a	51.5a	81.8e	21600ab	11.4d	27.4a	29.3e	22.9d	1.64b	0.70b	ND	0.10a	7.54b
		SD	3480	2.60	6.30	1186	0.67	1.54	1.81	1.71	0.15	0.03	ND	0.05	0.83
	Kafue town	Mean	19482e	18.0c	53.4f	9371d	5.08e	8.84d	33.9d	34.4c	2.01b	0.25b	0.01a	0.10a	17.7a
		SD	1991	0.83	1.13	649	0.25	0.18	1.65	4.6	0.58	0.43	0.02	0.03	1.34
Dry-cold	Chimfunshi	Mean	21487c	24.7cd	83.8d	9384d	18.6d	13.8c	78.8d	26.6b	1.62bc	0.27a	0.29a	0.09a	5.47bc
		SD	3143	1.02	2.56	388	0.62	0.56	2.64	2.24	0.12	0.47	0.13	0.03	1.00
	Chililabombwe	Mean	28249b	27.9c	498a	17051ab	248b	18.8b	5660b	57.5a	1.87b	0.77a	0.06b	0.07ab	11.88a
		SD	672	0.79	21.7	2061	5.71	0.60	442	1.79	0.13	0.75	0.07	0.02	1.27
	Chingola-Kanyemo	Mean	18021c	21.4d	460a	16860bc	326a	15.7bc	10131a	39.1ab	1.95b	0.47a	ND	0.07ab	12.9a
		SD	997	1.03	11.2	3988	14.6	0.37	2351	6.79	0.08	0.53	ND	0.01	2.78
	Chingola-Hippo pool	Mean	4852d	6.56e	223b	11,031cd	132c	6.53d	3972c	28.9b	5.17a	ND	ND	0.05ab	9.13ab
		SD	328	0.38	5.51	688	23.1	0.64	253	4.61	1.26	ND	ND	0.01	2.41
	Kafue flats	Mean	60536a	48.9a	108c	25515a	12.3e	23.7a	33.7e	25.9b	1.72bc	ND	ND	0.05ab	7.84abc
		SD	1168	1.71	16.6	3627	0.66	1.02	3.12	2.46	0.01	ND	ND	0.01	1.86
	Kafue town	Mean	27116b	33.4b	64.1e	14649bc	6.45f	17.2b	17.8f	9.75c	1.35c	ND	0.16ab	0.04b	4.42c
		SD	2844	3.05	9.15	3037	0.9	1.84	3.26	3.05	0.03	ND	0.1	0.01	1.91
Dry-hot	Chimfunshi	Mean	30560b	36.0abc	49.2c	11483b	12.4b	22.1b	39.9c	16.0b	0.94c	0.001	0.30a	0.13a	6.17bc
		SD	6986	13.8	17.8	4094	4.12	7.36	13.2	8.35	0.32	0.0003	0.17	0.09	3.65
	Chililabombwe	Mean	16753c	20.6c	603a	16324ab	338a	16.7bc	12037a	44.7a	1.89b	0.76b	0.02b	0.14a	14.6abc
		SD	3202	5.49	143	4015	48	3.1	1810	14.4	0.36	1.32	0.04	0.08	4.88
	Chingola-Kanyemo	Mean	14269c	18.1c	455a	18136ab	357a	10.9c	10416ab	40.5a	1.40bc	2.55ab	0.01b	0.12a	17.6ab
		SD	656	1.46	38	1047	5.99	0.33	202	0.27	0.26	0.37	0.03	0.02	0.11
	Chingola-Hippo pool	Mean	17210c	28.2bc	450a	22675ab	233a	15.9bc	6200b	49.2a	8.23a	6.06a	0.06b	0.13a	22.3a
		SD	2939	6.89	127	6469	35.2	2.52	1177	16.1	1.15	2.25	0.07	0.08	9.04
	Kafue flats	Mean	53101a	47.4ab	141b	25132ab	12.9b	23.2b	40.9c	23.9ab	1.48bc	6.60a	0.01b	0.11a	7.64abc
		SD	2935	11.4	45.3	7687	2.84	4.9	10.4	9.69	0.38	0.2	0.01	0.09	4.12
	Kafue town	Mean	47741b	63.4a	141b	31407a	11.6b	69.8a	23.3c	14.5b	1.37bc	4.49ab	ND	0.09a	4.98c
		SD	9836	19.7	44.5	10,734	3.1	23.7	6.98	7.35	0.28	3.9	ND	0.09	3.28

Each metal level connected by the different letters (a–f) are significantly different ($p < 0.05$)

ND Not detected

Table 3 CF and PLI of metals at study sites in all seasons

Contamination factor (CF)															PLI
Season	Site	Al	Cr	Mn	Fe	Co	Ni	Cu	Zn	As	Se	Cd	Hg	Pb	
Warm-rainy	Chililabombwe	1.61	1.10	12.0	2.19	28.41	1.29	145.22	3.50	1.61	7.37	0.68	0.86	2.61	3.58
	Chingola-Kanyemo	0.83	0.95	3.81	1.84	26.92	1.21	146.00	2.75	1.31	8.41	0.52	0.53	2.41	2.76
	Chingola-Hippo pool	0.59	0.69	3.04	1.50	14.81	0.99	67.63	2.56	4.04	1.34	0.38	0.38	2.27	2.00
	Kafue flats	2.15	1.70	0.64	2.11	0.82	1.69	0.40	1.36	1.04	1.83	ND	0.46	1.00	1.09
	Kafue town	0.67	0.59	0.42	0.92	0.37	0.55	0.46	2.05	1.27	0.65	0.50	0.46	2.34	0.71
Dry-cold	Chililabombwe	1.31	1.13	5.94	1.82	13.33	1.36	71.81	2.16	1.15	2.81	0.22	0.81	2.17	2.32
	Chingola-Kanyemo	0.84	0.87	5.50	1.80	17.51	1.14	129.09	1.47	1.20	1.73	0.01	0.83	2.36	1.68
	Chingola-Hippo pool	0.23	0.27	2.66	1.18	7.13	0.47	50.41	1.09	3.18	ND	0.003	0.60	1.67	0.93
	Kafue flats	2.82	1.98	1.29	2.72	0.66	1.72	0.43	0.97	1.06	ND	ND	0.54	1.43	1.17
	Kafue town	1.26	1.35	0.77	1.56	0.35	1.25	0.23	0.37	0.83	ND	0.54	0.49	0.81	0.72
Dry-hot	Chililabombwe	0.55	0.57	12.30	1.42	27.40	0.76	302.22	2.80	2.00	ND	0.08	1.09	2.37	2.25
	Chingola-Kanyemo	0.47	0.50	9.25	1.58	28.81	0.49	261.35	2.54	1.48	ND	0.05	0.94	2.85	1.96
	Chingola-Hippo pool	0.56	0.78	9.15	1.97	18.93	0.72	156.32	3.08	8.75	ND	0.20	1.04	3.62	2.66
	Kafue flats	1.74	1.32	2.86	2.19	1.05	1.09	1.02	1.50	1.57	ND	0.01	0.83	1.24	0.94
	Kafue town	1.56	1.76	2.87	2.74	0.94	3.16	0.59	0.91	1.45	ND	0.003	0.75	0.81	0.84

ND Not detected. CF (Loska et al. 1997) due to a given metal element: Low degree (CF < 1), Moderate degree (1 ≤ CF < 3), Considerable degree (3 ≤ CF < 6), Very high degree (CF ≥ 6). *PLI* Pollution of a particular site (PLI > 1)

(Table 3), although the actual CF values of most metals (Cu, Mn, Co and As) were higher in the dry-hot season, in agreement with the observed increased concentrations of these metals in this season. The CFs for Ni, Cr and Fe were higher at Kafue town especially in the dry-hot season in agreement with observed increased concentrations of these metals at Kafue town compared to other sites. The high Ni values may be attributed to discharge from a Ni mine near the area. The CF for Cr was higher at Kafue town, probably due to the presence of a tannery that uses chromium sulphate in tanning animal skins.

The PLI > 1 indicates pollution of a particular site (Loska et al. 1997). Results (Table 3) revealed high PLI values at sites in the Copperbelt mining area, with Cu, Co and Mn contributing much to the pollution load. This is consistent with the suggestion that the pollution in these areas is mainly due to mining and smelting activities. Although Kafue flats lies further downstream to the Copperbelt mining sites, results suggest that the site is also polluted. Kafue town showed PLI values of less than one, however, concerns about pollution are likely as PLI values were fairly close to one (Table 3).

The trends of I_{geo} values in the warm-rainy season (Fig. 2) were similar to those in the dry-cold and dry-hot seasons with small variations in values. The I_{geo} is used to estimate anthropogenic enrichment of metal ions in the environment (Müller 1969) and I_{geo} values were interpreted as: $I_{geo} \leq 0$ = practically no anthropogenic enrichment; $0 \leq I_{geo} \leq 1$ = no to moderate anthropogenic enrichment; $1 \leq I_{geo} \leq 2$ = moderate anthropogenic enrichment;

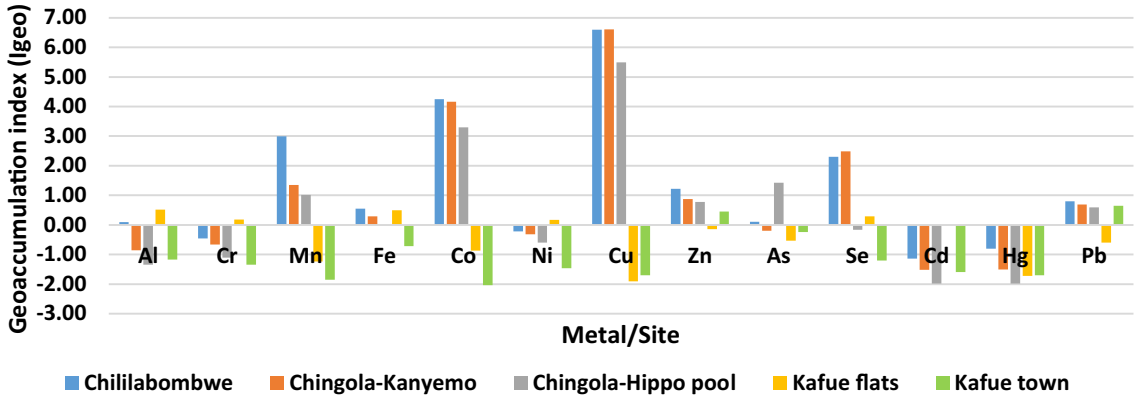

Fig. 2 I_{geo} values of metals at the study sites in the warm-rainy season

$2 \leq I_{geo} \leq 3$ = moderate to heavy anthropogenic enrichment; $3 \leq I_{geo} \leq 4$ = heavy anthropogenic enrichment; $4 \leq I_{geo} \leq 5$ = heavy to extreme anthropogenic enrichment; and $I_{geo} > 5$ = extreme anthropogenic enrichment (Bhuiyan et al. 2010). Results showed variations in anthropogenic enrichment of metal ions at the study sites. In the warm-rainy season (Fig. 2), there was no anthropogenic enrichment to moderate anthropogenic enrichment with Al, Fe, Zn, As, Se and Pb at various sampling sites. Moderate anthropogenic enrichment with Mn, Zn and As was observed at some sites in the Copperbelt mining area. Chililabombwe and Chingola-Kanyemo showed moderate to heavy anthropogenic enrichment with Mn and Se. Heavy to extreme anthropogenic enrichment with Co and extreme anthropogenic enrichment with Cu was observed at all sites in the Copperbelt mining area.

The RI value is the sum of individual metals' potential ecological risk factors (Er_{metal}). RI values of <150, 150–300, 300–600, and >600 represent low, moderate, considerable, and very high levels of potential ecological risk, respectively (Hakanson 1980). Only metals (Hg, Cd, As, Pb, Cu, Cr, Ni and Zn) with available toxic response factors (Tr_{metal}) (Zhao et al. 2005) were used to calculate RI in this study. Results of RI showed site and seasonal variations (Table 4) with a low (RI < 150) to extremely high level (RI > 600) of potential ecological risk. Metals may cause physiological, biochemical, morphological and haematological changes as well as antioxidant responses in various aquatic organisms (Basha and Rani 2003). Metal accumulation within the Kafue River has been associated with various toxicological manifestations. For instance, Mwase et al. (1998) and Norrgren et al. (2000) demonstrated increased fish mortality and decreased aquatic productivity following exposure of caged fish, eggs and fry to water and sediment from Kafue River in the Copperbelt mining area. Choongo et al. (2005) reported high Cu levels in fish at Copperbelt mining area sites along the Kafue River. The fish at these sites also recorded a low coefficient of condition probably as a result of Cu toxicity. Most of the sites in the Copperbelt mining area in the various seasons showed a considerable level of ecological risk (RI = 300–600) to an extremely high level (RI > 600) of potential ecological risk for the river's organisms. Kafue flats and Kafue town in all seasons had RI values which revealed a low potential ecological risk (RI < 150). Of the selected metals used to calculate RI, Cu and As would possibly cause adverse biological effects, especially in the mining areas, because their individual Er_{metal} (Table 4) were moderate (40–80) to significantly high (>320). Mn and Co were also elevated at sites in the mining area and could possibly cause adverse biological effects, however, the Tr_{metal} were not available to calculate their Er_{metal}.

This study has for the first time elaborated the contribution of 13 heavy metals investigated in Kafue River sediment to the ecological risk at various sites. Sediment from the Copperbelt mining area of the Kafue River revealed a high degree of anthropogenic Cu, Co, Mn and As contamination. The highest level of contamination was observed in the dry-hot season. However, the degree of both natural and anthropogenic causes of metal contamination was

Table 4 Er_{metal} and RI of metals at study sites in all seasons

Potential ecological risk factors (Er_{metal})										RI
Season	Site	Cr	Ni	Cu	Zn	As	Cd	Hg	Pb	
Warm-rainy	Chililabombwe	2.19	6.47	726.00	3.50	16.10	20.50	34.40	13.10	822.26
	Chingola-Kanyemo	1.90	6.04	732.00	2.75	13.10	15.80	21.10	12.10	804.79
	Chingola-Hippo Pool	1.39	4.97	338.00	2.56	40.40	11.40	15.20	11.40	425.32
	Kafue flats	3.39	8.46	1.99	1.36	10.40	0.00	18.30	4.98	48.88
	Kafue town	1.18	2.73	2.30	2.05	12.70	14.90	18.40	11.70	65.96
Dry-cold	Chililabombwe	2.26	6.81	359.00	2.16	11.50	6.45	32.40	10.90	431.48
	Chingola-Kanyemo	1.73	5.72	643.00	1.47	12.00	0.23	33.00	11.80	708.95
	Chingola-Hippo Pool	0.53	2.37	252.00	1.09	31.80	0.10	23.80	8.34	320.03
	Kafue flats	3.96	8.61	2.14	0.97	10.60	0.00	21.70	7.17	55.15
	Kafue town	2.70	6.23	1.13	0.37	8.28	16.30	19.60	4.04	58.65
Dry-hot	Chililabombwe	1.15	3.78	1510.00	2.80	20.00	2.35	43.40	11.80	1595.28
	Chingola-Kanyemo	1.01	2.47	1307.00	2.54	14.90	1.48	37.50	14.30	1381.20
	Chingola-Hippo Pool	1.56	3.60	778.00	3.08	87.50	5.95	41.70	18.10	939.49
	Kafue flats	2.64	5.44	5.12	1.50	15.70	0.34	33.30	6.19	70.23
	Kafue town	3.52	15.80	2.93	0.91	14.50	0.10	29.90	4.04	71.70

Er_{metal} (Hakanson 1980): Low (<40), Moderate (40–80), Considerable (80–160), High (160–320), Significantly high (>320)

RI: Low (RI < 150), Moderate (RI 150–300), Considerable (RI 300–600, Very high (RI > 600)

low at sites away from the Copperbelt mining area. The RI showed that Cu, As and possibly Co and Mn at sites in the Copperbelt mining area of the Kafue River were likely to cause harmful biological effects to aquatic organisms. Therefore, a management plan for testing and monitoring for toxic effects of a mixture of these metals in the Copperbelt mining area is proposed. It is recommended that Zambia Environmental Management Agency (ZEMA) should monitor levels of these toxic elements in all the seasons at known or suspected point sources in order to identify erring industries that should be made to control their discharges into the river in line with international limits since Zambia does not have its own regulatory limits. Therefore, regulatory limits should be established and existing environmental regulations should be implemented.

Acknowledgements Authors are grateful to the laboratory technical staff at the University of Warwick (especially Mr. Philip Ashton) and the University of Zambia (Mr. Joseph Ndebe, Mr. Ladsluv Moonga and Mr. John Chilundu). Furthermore, we are grateful to the Commonwealth Scholarship Commission (ZMCN-2013-352), University of Warwick, International Foundation for Science (IFS) number A/5212-1 and University of Zambia for sponsoring this work.

Compliance with Ethical Standards

Conflict of interest The authors declare that they have no conflict of interest.

References

Alaoui AM, Choura M, Maanan M, Zourarah B, Robin M, Conceição MF, Andrade C, Khalid M, Carruesco C (2010) Metal fluxes to the sediments of the Moulay Bousselham lagoon, Morocco. Environ. Earth Sci 61:275–286

Bäckström M (1996) A Sediment Study in the Kafue River, Zambia, Master's Thesis, Luleå University of Technology, Luleå 96

Basha PS, Rani AU (2003) Cadmium-induced antioxidant defense mechanism in freshwater teleost *Oreochromis mossambicus* (Tilapia). Ecotoxicol Environ Saf 56(2):218–221

Bhuiyan MA, Parvez L, Islam MA, Dampare SB, Suzuki S (2010) Heavy metal pollution of coal mine-affected agricultural soils in the northern part of Bangladesh. J Hazard Mater 173:384–392

Calmano W, Ahlf W, Förstner U (1990) Exchange of heavy metals between sediment components and water. Springer, Berlin, pp. 503–522

Choongo KC, Syakalima MS, Mwase M (2005) Coefficient of condition in relation to copper levels in muscle of *serranochromis* fish and sediment from the Kafue river, Zambia. Bull Environ Contam Toxicol 75:645–651

Fernandes C, Fontaínhas-Fernandes A, Cabral D, Salgado MA (2008) Heavy metals in water, sediment and tissues of *Liza saliens* from Esmoriz–Paramos lagoon, Portugal. Environ Monit Assess 36:267–275

Gupta A, Rai DK, Pandey RS, Sharma B (2009) Analysis of some heavy metals in the riverine water, sediments and fish from river Ganges at Allahabad. Environ Monit Assess 157:449–458

Hakanson L (1980) An ecological risk index for aquatic pollution control. A sedimentological approach. Water Res 14:975–1001

Hatje V, Bidone ED, Maddock JL (1998) Estimation of the natural and anthropogenic components of heavy metal fluxes in fresh water Sinos river, Rio Grande do Sul state, SouthBrazil. Environ Technol 19:483–487

Hatje V, Payne TE, Hill DM, McOrist G, Birch GF, Szymczak R (2003) Kinetics of trace element uptake and release by particles in estuarine waters: effects of pH, salinity, and particle loading. Environ Int 29:619–629

Ikenaka Y, Nakayama SM, Muzandu K, Choongo K, Teraoka H, Mizuno N, Ishizuka M (2010) Heavy metal contamination of soil and sediment in Zambia. Afr J Environ Sci Technol 4:729–739

Islam MS, Han S, Ahmed MK, Masunaga S (2014) Assessment of trace metal contamination in water and sediment of some rivers in Bangladesh. J Water Environ Technol 12:109–121

Kambole MS (2003) Managing the water quality of the Kafue River. Phys Chem Earth, Parts A/B/C 28(20):1105–1109

Karbassi AR, Monavari SM, Bidhendi GR, Nouri J, Nematpour K (2008) Metal pollution assessment of sediment and water in the Shur River. Environ Monit Assess 147:107–116

Khadse GK, Patni PM, Kelkar PS, Devotta S (2008) Qualitative evaluation of Kanhan River and its tributaries flowing over central Indian plateau. Environ Monit Assess 147:83–92

Loska K, Cebula J, Pelczar J, Wiechuła D, Kwapuliński J (1997) Use of enrichment, and contamination factors together with geoaccumulation indexes to evaluate the content of Cd, Cu, and Ni in the Rybnik water reservoir in Poland. Water Air Soil Pollut 93:347–365

Loska K, Wiechuła D, Korus I (2004) Metal contamination of farming soils affected by industry. Environ Int 30:159–165

M'kandawire E, Syakalima M, Muzandu K, Pandey G, Simuunza M, Nakayama SM, Kawai YK, Ikenaka Y, Ishizuka M (2012) The nucleotide sequence of metallothioneins (MT) in liver of the Kafue lechwe (*Kobus leche kafuensis*) and their potential as biomarkers of heavy metal pollution of the Kafue River. Gene 506:310–316

Mayo M, Collier ZA, Winton C, Chappell M (2015) Data-driven method to estimate nonlinear chemical equivalence. PLoS ONE 10(7):e0130494

Mendelsohn F (ed) (1961) The geology of the Northern Rhodesian Copperbelt. Macdonald and Co. Ltd, London

Müller G (1969) Index of geoaccumulation in sediments of the Rhine River. Geo J 2:108–118.

Mwase M, Viktor T, Norrgren L (1998) Effects on tropical fish of soil sediments from Kafue River, Zambia. Bull Environ Contam Toxicol 61(1):96–101

Norrgren L, Pettersson URNS, Örn S, Bergqvist PA (2000) Environmental monitoring of the Kafue River, located in the Copperbelt, Zambia. Arch Environ Contam Toxicol 38(3):334–341

Nwadinigwe CA, Udo GJ, Nwadinigwe AO (2014) Seasonal variations of heavy metals concentrations in sediment samples around major tributaries in Ibeno coastal area, Niger delta, Nigeria. IJST 3(11):254–265

Peng JF, Song YH, Yuan P, Cui XY, Qiu GL (2009) The remediation of heavy metals contaminated sediment. J Hazard Mater 161:633–640

Qui H (2010) Studies on the potential ecological risk and homology correlation of heavy metal in the surface soil. JAS 2:194–201

Solomon F (2009) Impacts of copper on aquatic ecosystems and human health. Environ Commun 25–28

Sracek O, Kříbek B, Mihaljevič M, Majer V, Veselovský F, Vencelides Z, Nyambe I (2012) Mining-related contamination of surface water and sediments of the Kafue River drainage system in the Copperbelt district, Zambia: an example of a high neutralization capacity system. J Geochem Explor 112:174–188

Srikanth K, Rao JV (2014) Spatial and seasonal variation of potential toxic elements in *Adocia pigmentifera*, seawater and sediment

from Rameswaram, southeast coast of India. Environ Earth Sci 72(8):2905–2916

Stevens J (1999) Post hoc Tests in ANOVA. Course notes. University of Oregan, Eugene

Suresh G, Ramasamy V, Meenakshisundaram V, Venkatachalapathy R, Ponnusamy V (2011) Influence of mineralogical and heavy metal composition on natural radionuclide concentrations in the river sediments. Appl Radiat Isot 69:1466–1474

Yabe J, Ishizuka M, Umemura T (2010) Current levels of heavy metal pollution in Africa. J Vet Med Sci 72:1257–1263

Zhao QN, Xu QX, Yang K (2005) Application of potential ecological risk index in soil pollution of typical polluting industries. J East China Norm Univ Nat Sci 1:110–115

Multidisciplinary field research in Kabwe, Zambia, towards better understanding of lead contamination of the city - A short report from a field survey

Authors: Yoshitaka Uchida[1)], Kawawa Banda[2)], Imasiku Nyambe[2)], Toru Hamamoto[1)], Yui Yoshii[1)], Kabenuka Munthali[3)], Mukuka Mwansa[3)], Moses Mukuka[2)], Mubanga Mutale[2)], John Yabe[4)], Haruya Toyomaki[5)], Yohannes Yared Beyene[5)], Shouta M. M. Nakayama[5)], Nobuyasu Naruse[6)], Mayumi Ishizuka[5)], Yukihiro Takahashi[7)]

Affiliations: [1)]Faculty of Agriculture, Hokkaido University, Japan [2)]School of Mines, University of Zambia, Zambia [3)]School of Agricultural Sciences, University of Zambia, Zambia [4)]School of Veterinary Medicine, The University of Zambia, Zambia [5)]Laboratory of Toxicology, Graduate School of Veterinary Medicine, Hokkaido University, Japan [6)]Faculty of Medicine, Shiga University of Medical Science, Japan [7)]Space Mission Center (SMC), Creative Research Institution (CRIS), Hokkaido University

Abstract: Heavy metal contamination is a serious issue in many post-mining regions around the world. Kabwe town, Zambia, is known as one of the most polluted cities in the world, where high lead (Pb) levels have been reported in soils, plants, animals and human blood. Multidisciplinary approaches are critically needed to understand the current situation and to remediate the polluted area. In the current research, a large-scale preliminary field survey was performed to understand the current situation in Kabwe and to plan future mitigation approaches. Three aspects were mainly observed; 1) plant communities during the dry season in Kabwe city, 2) spectral images of the land surfaces in various locations in Kabwe and 3) Pb concentrations in soils and water. Overall, >15 different plant species were observed and many of them maintained their green colour even during the dry season. Some tree species, for example, *Caesalpiniaceae* and *Fabaceae* families may be utilised as phytostabilization approaches although their impacts on the soil Pb mobility should be further studied. For the spectral images, we used a handmade portable spectrometer, and our obtained spectral images showed typical curves observed from soils. These data may be used to understand the distribution of different soil types in this area, using aboveground images such as satellite images. For Pb concentrations in soils, extremely high total Pb levels (>1,000 ppm) was observed only within 2 km from the mining site. There was a weak but a positive correlation between the total and soluble Pb thus further study should also focus on the mobility of Pb from soils to plant ecosystems.

Keywords: Pb, spectral images, plant community structures

1. Introduction

There have been many studies done to evaluate the status of heavy metal contamination in Kabwe, Zambia. Due to the history of mining of lead (Pb) and zinc (Zn), it was reported that soils were contaminated with not only by Pb and Zn but also withcopper (Cu) and cadmium (Cd) (Nwankwo & Elinder, 1979; Tembo, Sichilongo, & Cernak, 2006). The contamination of the soils in the area resulted in extensive heavy metal pollution of livestock (Yabe et al., 2011; Yabe et al., 2013), vegetables, and humans (Clark, 1977; Yabe et al., 2015).

Some remediation approaches are needed in this area. Although the number of scientific reports is small, it has been identified that a phytoremediation approach could be used in Kabwe, where plants are used to reduce the risks related to the soil contamination (Reilly & Reilly, 1973; Leteinturier et al. 2001). Plants can remediate heavy metals using different mechanisms, for example, they may be able to extract heavy metals from the soil, and the plants can be taken away from the area to cleanse the contaminated soils. Contrastingly, plants are used to stabilize the heavy metals in soils, preventing them from escaping to other ecosystems (e.g. to groundwater or other soil surfaces as dust). Either way, the societal implementation of the phytoremediation approaches can be efficient when locally available or indigenous species are used.

Thus, a better understanding of the plant community structures for phytoremediation is needed in Kabwe. Earlier intensive surveys that were conducted for plant communities around the mining area in Kabwe recorded nearly 40 species (Leteinturier et al. 2001). However, these previous surveys were performed within the mining site, not extending to the whole Kabwe township. Also, the survey was performed at the end and the beginning of the wet season (April and November), thus not providing information for the driest period of the year (i.e. July–October). We believe that plants surviving in the dry season are critically important regarding their potential use as phytoremediation methods. Plants that become dominant during the dry season might be difficult to efficiently stabilise the Pb-containing soils because it was observed that extensive amount of fine soil particle (dust) is blown off during the dry season and plants may reduce the amount of dust.

Additionally, the adaptation (survival) of plant species and their efficacy regarding soil stabilisation are often influenced by soil types. Thus, detailed soil mapping is very important. Spectral sensing approaches can be an option to differentiate soil types according to their spectral curves and are often used using satellite data (Nanni et al. 2012). Soil properties such as soil moisture contents can also be quantified using the spectral data (Weidong et al. 2002). Also,

the availability (mobility) of Pb in soils is another factor that must be considered to plan efficient phytoremediation approaches. Generally, in soils, Pb that is available to plants is very small when compared to the total Pb in soil. Thus, a better understanding of the amount of available Pb in soils is required not only to investigate the plant survival rates but also to investigate the risk of Pb leaching to water ecosystems (Gleyzes et al. 2002).

Thus, in the present study, plant community structures were investigated as well as land spectral images at various places in Kabwe town. Moreover, some basic information on soil Pb characteristics were studied.

2. Research methods

2.1. Research sites

The field survey was conducted from 5th July to 8th July 2016, in Kabwe town, Zambia. The sites where soil and plant samples were collected are shwn in Fig. 1. From the mine residue damping zone (“022_DUMP”, 14°27′44″S, 28°25′51″E), 0–5 km zones were covered in all the directions. The detailed description of each site is also stated in Table 1. Due to scarce rainfall during this period, most of the sites were dry, but some wetlands were found, particularly in northern part of the town (sites “015_dambo”, “016_dambo”, and “017_dambo_bridge”), where soils were saturated (Photo 1).

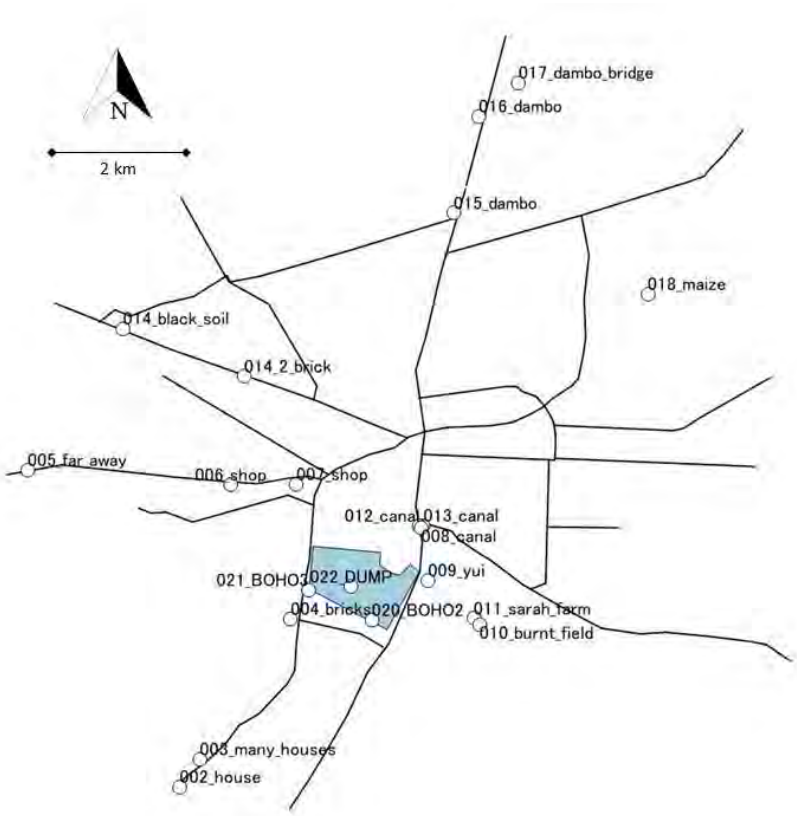

Figure 1. Major roads in Kabwe town, Zambia and our field survey sites (white circles). The shaded area was the mine residue dump site. The centre of the sampling sites, "022_DUMP" was at 14°27′44″S, 28°25′51″E. The map is North on the top, and the 2 km scale bar is indicated.

Table 1. Detailed description of the field survey sites.

Number	Site name	Plant community information	Spectral image data	Soil XRF data	Soluble Pb data	Distance from the mine (m)
1	002_house	No	Yes	Yes	Yes	3,787
2	003_many_houses	No	Yes	Yes	Yes	3,298
3	004_bricks	No	No	Yes	Yes	987
4	005_far_away	No	Yes	Yes	Yes	4,956
5	006_shop	Yes	No	No	No	2,275
6	007_shop	No	No	No	No	1,674
7	008_canal	No	No	Yes	Yes	1,334
8	009_yui	No	No	Yes	Yes	1,112
9	010_burnt_field	Yes	No	Yes	Yes	1,928
10	011_sarah_farm	No	No	Yes	Yes	1,821
11	012_canal	No	No	No	No	1,323
12	013_canal	No	No	Yes	Yes	1,349
13	014_black_soil	Yes	Yes	Yes	Yes	4,954
14	014_2_brick	Yes	Yes	No	No	3,391
15	015_dambo	No	No	No	Yes	5,556
16	016_dambo	Yes	No	No	No	6,903
17	017_dambo_bridge	Yes	No	No	No	7,626
18	018_maize	Yes	Yes	Yes	Yes	5,993
19	020_BOHO2	Yes	No	Yes	No	577
20	021_BOHO3	No	No	Yes	No	613
21	022_DUMP	Yes	No	Yes	No	0

Photo 1. (Left) Dry field (site "018_maize") and (Right) wetland site (site "016_dambo") (taken on July 6th, 2016).

2.2. Plant survey

At each plant survey site (Fig. 1), plant species were visually observed. To identify species, van Wyk and van Wyk (2013) and Pienaar and Smith (2011) were referred to as well as communications with locals.

2.3. Measurement of soil Pb concentrations using X-ray fluorescence approaches (XRF) and a portable colorimetric Pb measurement kits

Approximately 200 g of soils were collected from each soil sampling site. They were placed in plastic bags (Ziploc, Asahi Kasei Home Products Corporation, Japan) and measured for total Pb concentrations using a portable XRF analyser (Innov-X Alpha Series™ Advantages, Innov-X Systems, Inc. USA). Then, the metals in soils were extracted with hot water (80°C, 1 hour, soil:water = 1:10). The supernatant was analysed for the soluble Pb concentrations using a colorimetric kit. Also, some surface and groundwater were analysed for soluble Pb, using the same kit.

2.4. Spectral sensing

A portable spectral sensor was used to investigate the spectrum of land surfaces in different areas in Kabwe. The compact hyperspectral sensor with a USB camera (MCM-4304, Micro Vision Co., Ltd. Japan) was used. The measurement was taken using following approaches: first,

a total reflection at each soil measurement site was obtained by taking a picture of a white filter paper (Tokyo Roshi Kaisha, Ltd. Japan). Then, a soil reflectance was measured without moving the sensor (the sensor was secured on a stand, as shown in Photo 2). Five replicates were taken for each sample.

Photo 2. The compact hyperspectral sensor with a USB camera. The camera was set up at a right angle from the sun to avoid the shadow.

For data analyses, ImageJ software (ver. 1.6.0_24, National Institutes of Health, USA) was used. First, the spectral data was converted to values depending on the strength of white. Then, the X-axis was adjusted for the wavelength using a Hg light value. Spectral data of Hg light has some specific peaks, and these peaks are known as specific wavelengths (Sansonetti et al. 1996). To show the data as reflectance, the data from the soil samples were divided by the spectral data taken from a white filter paper.

3. Research activities and snapshots of the preliminary findings from the field survey in Kabwe

3.1. Observed plant species

The plant communities in Kabwe were recorded in detail by Leteinturier et al. (2001). Most of the plants found in the present study were also reported in the previous report. As shown in Table 1 a total of 20 plant species were identified in the present study. The survey conducted in the current study was not intensive enough to discuss the effect of the mine residue on plant community structures or diversities. On the mine residue, many African fountain grass species (*Pennisetum setaceum*) was observed. According to verbal communication with the landowners, this species has been markedly increasing over the last decades and helped to reduce the dust blowing around the residues. In a wetland site (site 016), totally different plant community structures were observed, including *Phragmites* and *Ipomoea*. This suggests that the availability

of water is probably one of the major factors controlling the plant community structures in Kabwe area. Further studies must focus on plant characteristics regarding the mobility of heavy metals.

Table 1. Plant species observed in Kabwe, Zambia, during the dry season (July 2015). Plant species were visually determined according to Leteinturier et al. (2001), van Wyk and van Wyk (2013) and Pienaar and Smith (2011). The "+" sign means that species were observed at each site. The site names were in the order of distance from the mine (m), from left to right.

	Distance from the mine (m)	0	613	1,112	1,349	2,275	3,391	4,954	5,556	5,993	6,093
Species	Family/Site name	022	020	009	013	005	014_2	014	015	018	016
Ageratum conyzoides L.	Asteraceae								+		
Amaranthus dubius Mart. ex Thell.	Amaranthaceae									+	
Argemone mexicana	Papavaceae			+							
Bauhinia petersiana bolle	Caesalpiniaceae			+	+	+	+				
Bidens oligoflora (Klatt) Wild	Asteraceae						+		+		
Bidens pilosa	Asteraceae							+			
Celosia trigyna	Amaranthaceae	+									
Crotalaria agatiflora	Fabaceae										
Cynodon dactylon (L.) Pers.	Poaceae	+									
Cyperus involucratus Rottb.	Cyperaceae				+						
Flaveria trinerva (Spreng.) Mohr	Asteraceae	+									
Ipomoea cairica (L.) Sweet	Convolvulaceae										+
Lebeckia cytisoides	Fabaceae				+						
Pennisetum setaceum (Forssk.) Chiov.	Poaceae	+	+								
Phragmites mauntianus L.	Poaceae		+								+
Ricinus communis var. *communis*	Euphorbiaceae							+			
Solanum incarnum L.	Solanaceae							+			
Trichodesma zeylanicum (Burm f.) R Br.	Boraginaceae							+			
Tridax procumbens L.	Asteraceae							+		+	
Vernonia erinacea Wild	Asteraceae				+			+			

3.2. Heavy metal concentrations in surface soils

Based on XRF measurements in the current study, the total Pb contents in soils ranged from 20 ppm (site 014_2_brick) to 10,000 ppm (site 008_canal). There was a weak but positive relationship between the total and water soluble Pb contents (Fig. 1a). The water soluble Pb contents ranged from 0 to 4 ppm and it was, in general, less than 1% of the total Pb. We believe that soil characteristics (e.g. parent materials and clay contents) are the major factors controlling the ratio between the total and water soluble Pb. Further research is needed in this area because water soluble Pb can be more mobile and pose a higher risk to plant and animal absorption.

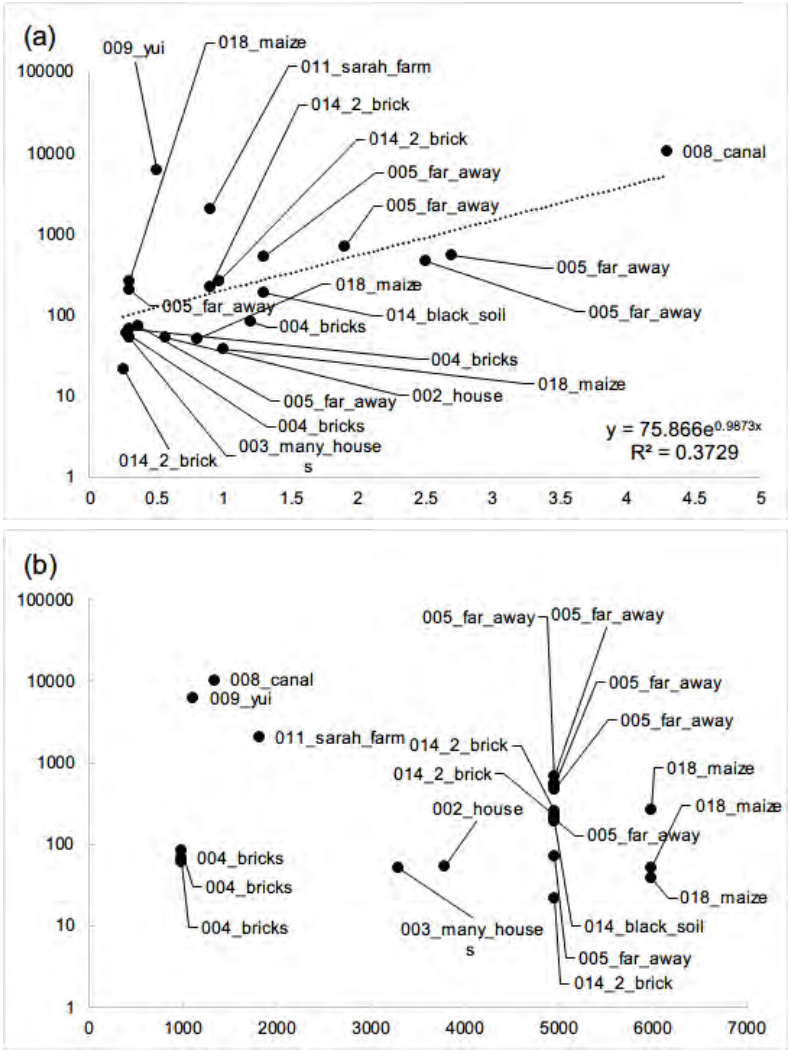

Figure 2. (a) The correlation between water soluble Pb concentration and total Pb concentration and (b) the correlation between the total Pb concentration and the distance from the mine site (site 022). The Y axis were shown as a log-scale. For a detailed description of the site, refer to Fig. 1 and Table 1.

3.3. Spectral characteristics of the site

Fig. 3 shows photos of some soil samples with their reflectance data. The soil from site 005 was brighter in colour and its spectral data shows a marked difference compared with other soils. Moreover, soil samples from site 014 showed a different pattern. Based on personal communications, local people valued this soil as a relatively more fertile soil (called "black soil") and the identification of this soil, when compared with other soils, seemed promising based on preliminary data from the current study. The data below 400 nm or above 900 nm showed large variabilities, but the data between these values (i.e. 400–900 nm) could be used to differentiate the soils. The influence of soil moisture was ignored since the soils were very dry but future analyses should also focus on the effects of soil moisture.

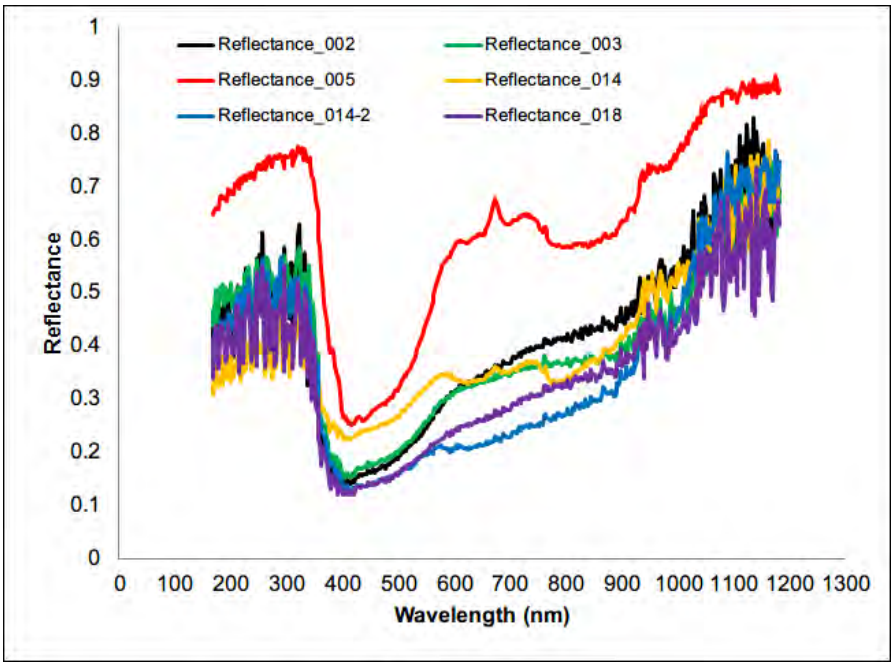

Figure 3. Photos of some of the sampled soils in Kabwe (top) and their reflectance (bottom).

4. Conclusion

The preliminary field survey in the current study clearly indicated that an extensive area within Kabwe was contaminated with Pb. Plant community structure observation revealed that plant species such as *Caesalpiniaceae* and *Fabaceae* families remained viable during the dry season and could potentially be utilised to stabilise the contaminated soils. The percentage of water

soluble Pb in the total soil Pb was < 1 %, but the extreme values were observed within 2 km zone from the mining site. The preliminary taken spectral curves suggested that remote-sensing techniques may be used to differentiate soil types. Further studies should focus on more detailed analyses of plant communities as well as their capacities to stabilise soils and Pb. Also, soil moisture has to be taken into account to further evaluate the potential use of spectral images in the area.

Acknowledgements

We acknowledge the support from Russell Dowling (Pure Earth) and Jack Caravanos (Pure Earth) for XRF measurement. This research was supported by JST/JICA, SATREPS (Science and Technology Research Partnership for Sustainable Development).

References:

Clark, A. R. 1977. Placental transfer of lead and its effects on the newborn. *Postgraduate Medical Journal* 53: 674–678.

Leteinturier, B., Laroche, J., Matera, J. & Malaisse, F. 2001. Reclamation of lead/zinc processing wastes at Kabwe, Zambia: a phytogeochemical approach. *South African Journal of Science* 97: 624-626.

Nanni, M. R., Demattê, J. A., Chicati, M. L., Fiorio, P. R., Cézar, E., & Oliveira, R. B. (2012, 11). Soil surface spectral data from Landsat imagery for soil class discrimination. *Acta Sci. Agron. Acta Scientiarum. Agronomy*, 34(1). doi:10.4025/actasciagron.v34i1.12204

Nwankwo, J. N. & Elinder, C. G. (1979). Cadmium, lead and zinc concentrations in soils and in food grown near a zinc and lead smelter in Zambia. *Bulletin of Environmental Contamination and Toxicology*, 22(1), 625–631. http://doi.org/10.1007/BF02026998

Piennar, K. & Smith, G. F. 2011. The Southern African What Flower Is That? (Fifth edition). Struik Lifestyle (an imprint of Random House Struik (Pty) Ltd), Cape Town, South Africa.

Reilly, A. & Reilly, C. (1973). Zinc, Lead and Copper Tolerance in the Grass Stereochlaena Cameronii (stapf) Clayton. *New Phytologist*, 72(5), 1041–1046. http://doi.org/10.1111/j.1469-8137.1973.tb02080.x

Sansonetti, C.J., Salit, M.L. & Reader, J. (1996). Wavelength of spectral lines in mercury pencil lamps. *Applied Optics*, 35 (1), 74–77.

Tembo, B. D., Sichilongo, K., & Cernak, J. (2006). Distribution of copper, lead, cadmium and zinc concentrations in soils around Kabwe town in Zambia. *Chemosphere*, 63(3), 497–501. http://doi.org/10.1016/j.chemosphere.2005.08.002

Yabe, J., Nakayama, S. M. M., Ikenaka, Y., Muzandu, K., Ishizuka, M., & Umemura, T. (2011). Uptake of lead, cadmium, and other metals in the liver and kidneys of cattle near a lead-zinc mine in Kabwe, Zambia. *Environmental Toxicology and Chemistry*, 30(8), 1892–1897. http://doi.org/10.1002/etc.580

Yabe, J., Nakayama, S. M. M., Ikenaka, Y., Muzandu, K., Choongo, K., Mainda, G., Kabeta, M., Ishizuka, M., & Umemura, T. (2013). Metal distribution in tissues of free-range chickens near a lead-zinc mine in Kabwe, Zambia. *Environmental Toxicology and Chemistry*, 32(1), 189-192.

van Wyk B. and van Wyk P. (2013). Field Guide To Trees of Southern Africa. Struik Nature (an imprint of Penguin Random House (Pty) Ltd). Cape Town, South Africa.

Weidong, L., Baret, F., Xingfa, G., Qingxi, T., Lanfen, Z., & Bing, Z. (2002). Relating soil surface moisture to reflectance. *Remote Sensing of Environment*, 81(2–3), 238–246. doi:10.1016/s0034-4257(01)00347-9

Yabe, J., Nakayama, S. M. M., Ikenaka, Y., Yohannes, Y. B., Bortey-Sam, N., Oroszlany, B., Ishizuka, M. (2015). Lead poisoning in children from townships in the vicinity of a lead–zinc mine in Kabwe, Zambia. *Chemosphere*, 119, 941–947. http://doi.org/10.1016/j.chemosphere.2014.09.028

Chemosphere 202 (2018) 48–55

Contents lists available at ScienceDirect

Chemosphere

journal homepage: www.elsevier.com/locate/chemosphere

Lead and cadmium excretion in feces and urine of children from polluted townships near a lead-zinc mine in Kabwe, Zambia

John Yabe [a], Shouta M.M. Nakayama [b], Yoshinori Ikenaka [b], Yared B. Yohannes [b], Nesta Bortey-Sam [b], Abel Nketani Kabalo [c], John Ntapisha [c], Hazuki Mizukawa [b], Takashi Umemura [b], Mayumi Ishizuka [b, *]

[a] The University of Zambia, School of Veterinary Medicine, P.O. Box 32379, Lusaka, Zambia
[b] Graduate School of Veterinary Medicine, Hokkaido University, Kita 18, Nishi 9, Kita-ku, Sapporo 060-0818, Japan
[c] Ministry of Health, District Health Office, P.O. Box 80735, Kabwe, Zambia

HIGHLIGHTS

- We measured lead and cadmium excretion levels in children near a Pb-Zn mine in Zambia.
- Fecal and urine Pb levels up to 2252 mg/kg and 2914 μg/L, respectively, were very high.
- Cd in fecal (up to 4.49 mg/kg) and urine (up to 18.1 μg/L) samples were elevated.
- Positive correlations were observed between fecal and urinary levels of Pb and Cd.
- Children living near the Pb-Zn mine are at serious risks of Pb and Cd poisoning.

ARTICLE INFO

Article history:
Available online 12 March 2018

Handling Editor: Martine Leermakers

Keywords:
Lead
Cadmium
Excretion
Children's health
Kabwe
Zambia

ABSTRACT

Lead (Pb) and cadmium (Cd) are toxic metals that exist ubiquitously in the environment. Children in polluted areas are particularly vulnerable to metal exposure, where clinical signs and symptoms could be nonspecific. Absorbed metals are excreted primarily in urine and reflect exposure from all sources. We analyzed Pb and Cd concentrations in blood, feces and urine of children from polluted townships near a lead-zinc mine in Kabwe, Zambia, to determine concurrent childhood exposure to the metals. Moreover, the study determined the Pb and Cd relationships among urine, feces and blood as well as accessed the potential of urine and fecal analysis for biomonitoring of Pb and Cd exposure in children. Fecal Pb (up to 2252 mg/kg, dry weight) and urine Pb (up to 2914 μg/L) were extremely high. Concentrations of Cd in blood (Cd-B) of up to 7.7 μg/L, fecal (up to 4.49 mg/kg, dry weight) and urine (up to 18.1 μg/L) samples were elevated. metal levels were higher in younger children (0–3 years old) than older children (4–7). Positive correlations were recorded for Pb and Cd among blood, urine and fecal samples whereas negative correlations were recorded with age. These findings indicate children are exposed to both metals at their current home environment. Moreover, urine and feces could be useful for biomonitoring of metals due to their strong relationships with blood levels. There is need to conduct a clinical evaluation of the affected children to fully appreciate the health impact of these metal exposure.

1. Introduction

Lead (Pb) and cadmium (Cd) are ubiquitous environmental toxicants as a result of contamination from a variety of sources including natural and anthropogenic causes. Children in polluted environments are particularly vulnerable to Pb exposure because of their inclination to ingest soil through pica and to assimilate a relatively greater amount of ingested Pb than adults (Calabrese et al., 1997, Manton et al., 2000; Caravanos et al., 2013). The detrimental effects of low blood lead levels (BLLs) are usually subclinical and may include neurodevelopmental impairment such as decreased IQ in children (Canfield et al., 2003). It has been observed that high BLLs in children can cause abdominal pain, encephalopathy, convulsions, coma and death (Needleman, 2004). Recently,

* Corresponding author.
E-mail address: ishizum@vetmed.hokudai.ac.jp (M. Ishizuka).

https://doi.org/10.1016/j.chemosphere.2018.03.079
0045-6535/

more than 400 children died of Pb poisoning due to artisanal mining activities in Nigeria, where long-term neurological impairment including blindness and deafness were also recorded (Pure Earth, 2014; Dooyema et al., 2012; Lo et al., 2012).

Similarly, Cd toxicity results in a wide range of biochemical and physiological dysfunctions in humans (Ercal et al., 2001). One of the most severe forms of chronic Cd toxicity is *itai itai* disease (a Japanese term meaning "ouch-ouch"), which is characterized by nephrotoxicity, osteoporosis and cardiovascular diseases (Kido et al., 1990; Uno et al., 2005). Cadmium has also been classified as a group I carcinogen as chronic inhalation exposure can produce lung cancer in humans (IARC, 1993). Although the toxic effects of Cd are mainly seen in adults (Kido et al., 1990; Umemura, 2000), exposure to children in even low amounts has associated with neurodevelopmental defects (Ciesielski et al., 2012). Moreover, exposure may have long-term consequences since Cd is a cumulative toxin and has a very long half time in the body.

Major sources of Pb and Cd pollution in many African countries include mining, industrial activities, municipal wastes and agricultural activities (Yabe et al., 2010). In Zambia, the closed Pb-Zn mine that operated from 1902 to 1994 in Kabwe town has contributed to extensive metal pollution in the surrounding residential areas, especially with Pb and Cd that was produced as by-product. Despite closure of the mine, dust emanating from the mine dumps has continued to serve as a source of metal pollution. In earlier studies, extensive Pb and Cd contamination of township soils in the vicinity of the mine were reported and pose a serious health risk to children in these townships (Water Management Consultants Ltd, 2006; Nakayama et al., 2011). Recently, clear evidence of Pb poisoning was reported in children from townships around the mine in Kabwe (Yabe et al., 2015). Using stable Pb isotope analysis, Nakata et al. (2016) revealed that soil was likely the main source of Pb exposure in Kabwe.

Clinical presentations of metal poisoning vary widely depending upon the age at exposure, the amount of exposure and the duration of exposure. Since chronic Pb poisoning in children is asymptomatic and may result in a delay in the appropriate diagnosis, measurement of concentrations in biological samples plays a pivotal role in the diagnosis and management of patients (Lowry, 2010). Currently, Pb concentration in whole blood (Pb-B) is the main biomarker used to monitor exposure and has been widely used in epidemiological studies (CDC, 2012). However, independent of the mode of exposure, absorbed metals such as Pb and Cd are excreted primarily in urine and the biliary-fecal route (Gwiazda et al., 2005; Swaran and Vidhu, 2010). Therefore, Pb and Cd biomonitoring using fecal and urine samples could be useful as they are easy to collect and are non-invasive. Moreover, whereas blood Cd (Cd-B) is the most common marker of recent exposure, urinary Cd (Cd-U) may reflect the kidney burden and is associated with renal health effects (Akerstrom et al., 2013). Evaluating relationships of Pb and Cd among blood, urine and fecal compartments may be useful for understanding exposure patterns. Therefore, the current study measured Pb and Cd concentrations in blood, feces and urine of children with known BLLs (Yabe et al., 2015), from contaminated townships in the vicinity of a Pb-Zn mine in Kabwe, Zambia to determine concurrent childhood exposure. Moreover, the study analysed Pb and Cd relationships in matched feces, urine and blood as well as accessed the potential of urine and fecal analysis for biomonitoring of Pb and Cd exposure in children.

2. Materials and methods

2.1. Sampling sites

Kabwe town, the fourth largest town and the provincial capital of Zambia's Central Province, is located at about 28°26′E and 14°27′S. Kabwe has a long history of open-pit Pb-Zn mining. The mine operated almost continuously from 1902 to 1994 without addressing the potential risks of metal pollution. Cadmium was obtained as a by-product of processing zinc-containing ores. As shown in the survey by Water Management Consultants Ltd (2006), soils in townships in the vicinity of the closed mine and homes downwind from the mine dumps were highly polluted with Pb exceeding acceptable levels for residential areas (Fig. 1). In the current study, fecal and urine samples were collected from children at health centers located in Chowa, Kasanda and Makukulu townships, in May–June of 2012. Matched samples were collected from the same children and townships where extremely high levels of Pb-B were reported by Yabe et al. (2015). More details about the study site and township description, which are in the vicinity of the mine can be obtained from the previous study (Yabe et al., 2015).

2.2. Sample collection

The study was approved by the University of Zambia Research Ethics Committee (UNZAREC) and the Ministry of Health, Zambia. Before sampling commenced, an awareness campaign about the research activities was conducted by community health workers in each township to encourage parents/guardians to take their children under the age of 7 to the selected health centres for sample collection. After informed and written consent was obtained from the children's parents or guardians, paired fecal and urine (morning spot-urine) samples were collected in clean metal-free specimen containers at Chowa, Kasanda and Makululu clinics. Blood samples were collected as described earlier by Yabe et al. (2015). For each child, data on the age, sex, residential area, medical history and past or current metal chelation therapy were recorded. Sample collection and questionnaire administration were done by laboratory technicians and nurses, respectively. In addition to selecting children under the age of 7 years, other inclusion criteria included children that were residing in communities in the vicinity of the Pb-Zn mine. The children must have been born or resided in the selected communities for at least 1 year. Only the children whose parents responded to the awareness campaign and signed the informed consent were selected. Efforts were made to collect urine samples in 50 ml urine containers in the morning of sample collection at the health centres. To avoid sample contamination, all sample collection supplies were kept in plastic ziploc storage bags

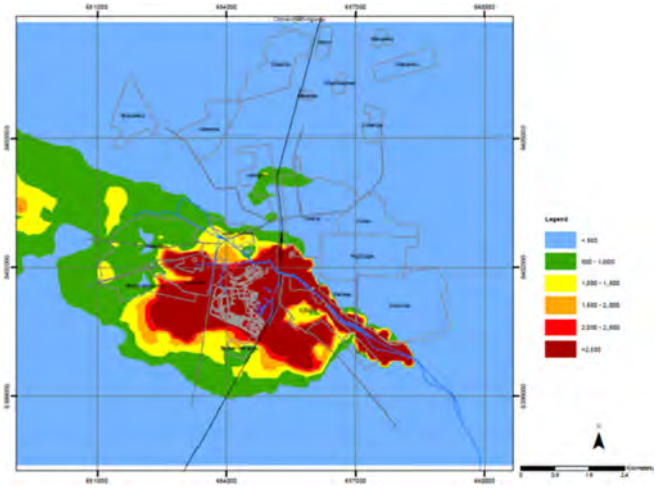

Fig. 1. Map of Kabwe showing distribution of Pb (mg/kg) in township soils around the Pb-Zn mining complex (Water Management Consultants Ltd, 2006).

before sample collection. For fecal samples, parents/guardians were handed 50 ml stool containers equipped with scoops and instructed to let their children deposit their stool on a clean plastic/paper in the morning of the following day. Only the top surface was scooped into a stool container and returned to the health centre the same day to avoid sample storage at home. For infants, fecal samples were scooped from a soiled diaper. After submission, samples were then transferred into 15 ml falcon tubes for storage and transportation. The samples were immediately stored at −20 °C after sampling and then transported in cooler boxes on dry ice to the laboratory of the Kabwe District Health Offices where they were again stored at - 20 °C. After obtaining the material transfer clearance from the Zambia National Health Research Ethics Committee (NHREC), the samples were transported to Japan in cooler boxes on dry ice and analyzed for metal concentrations in the Laboratory of Toxicology, Graduate School of Veterinary Medicine, Hokkaido University.

2.3. Sample preparation and metal extraction

All laboratory materials and instruments used in metal extraction were washed in 2% nitric acid (HNO_3) and oven dried. The metals were extracted in fecal and urine samples using microwave digestion system (Speedwave MWS-2; Berghof) according to the manufacture's instruction and published reports (Fukui et al., 2004; Yabe et al., 2011). Thawed fecal samples were weighed onto heat-resistant tissue drying plates and dried for 24 h in a tissue drying oven at 60 °C while urine samples were just thawed. Briefly, 1 mL of each urine sample and 50 mg of oven-dried fecal sample were separately placed in prewashed microwave digestion flasks. To these samples, 5 mL of 60% nitric acid (Kanto Chemical) and 1 mL of 30% hydrogen peroxide (Kanto Chemical) were added. After digestion in the microwave for 52 min and temperatures of up to 190 °C, the digested samples were each transferred into 15 ml plastic tubes. The volume was then made up to 10 mL with bi-distilled and de-ionized water (Milli-Q).

2.4. Metal analysis

Blood samples for Cd measurements were prepared and analysed as described earlier (Yabe et al., 2015). Fecal and urine metals (Pb and Cd) concentrations were analyzed by Inductively Coupled Plasma-Mass Spectrometer (ICP-MS; 7700 series, Agilent technologies, Tokyo, Japan). The precision and accuracy of the applied analytical method was evaluated by analyzing the recovery rate using digested urine samples and spiking Pb and Cd standard solutions. Using this method, good recoveries of 95% for both Pb and Cd were obtained. Certified Reference Materials, DORM-3 (Fish protein, National Research Council of Canada, Ottawa, Canada) and DOLT-4 (Dogfish liver, National Research Council of Canada, Ottawa, Canada) were used to evaluate recoveries. Replicate analysis of these reference materials also showed good accuracy (relative standard deviation, RSD, $\leq$ 3%) and recovery rates ranged from (95–105%). Using the Certified Reference Materials, the detection limits of Cd and Pb were 0.0005 μg/L and 0.0022 μg/L, respectively (Ogbomida et al., 2018). The instrument detection limit (IDL) was 0.001 μg/L. Replicate urine samples were used at 4 different spike concentrations of 0.01 ppb, 0.1 ppb, 1 ppb and 10 ppb. These yielded detection limits of 0.006 μg/L (Cd) and 0.043 μg/L (Pb) as well as recovery rates of 85.5–99.7% (Cd) and 104.8–107.7% (Pb). To compensate for variations in urine dilution, measured urine-Pb (Pb-U) and urine-Cd (Cd-U) concentrations were adjusted for specific gravity (SG). Urinary SG was measured by a hand refractometer (ATAGO, PAL-095, Tokyo, Japan). Obtained mean SG for Kasanda (1.012) and Makululu (1.021) were used to adjust urinary metal concentrations as illustrated in other studies (Suwazono et al., 2005; Nermell et al., 2008). For example, SG adjusted Pb-U_{SG} was calculated using the obtained mean value of 1.012 and the following formula: Pb-U_{SG} = Pb-U × (1.012−1)/(SG - 1.000) where Pb-U_{SG} is the adjusted value for SG and Pb-U is the measured concentration. The same was done for Pb-U in Makululu as well as Cd-U in Makululu and Kasanda.

2.5. Statistical analysis

Specific gravity-adjusted concentrations of Pb and Cd in urine are presented as Pb-U_{SG} and Cd-U_{SG}, respectively. The data of blood Cd (Cd-B), fecal Pb (Pb-F), Pb-U_{SG}, fecal-Cd (Cd-F) and Cd-U_{SG} were log-transformed to stabilize variances. Statistical analysis was performed using JMP version 10 (SAS Institute, USA). The data are presented as mean, geometric mean (GM), median and minimum-maximum values in mg/kg (feces) and μg/L (urine). Student's *t*-test was used to analyze area differences of metal accumulation. Pearson's correlation was used to analyse associations between Pb and Cd in matched blood, feces and urine. Multiple logistic regression analyses on log-transformed data were used to estimate the influence of area, sex and age on Pb and Cd excretions in feces and urine. Samples from Chowa were not included in the comparisons due to small number of sampled children less than 7 years old compared with Kasanda and Makululu. A p value of less than 0.05 was considered to indicate statistical significance. Data of blood Pb (Pb-B) from the already published results (Yabe et al., 2015) were used (with permission from the journal) for correlations with matched fecal and urine samples.

3. Results

3.1. Sample sizes and characteristics

A total of 190 fecal samples were collected from children, up to 7 years old, at Chowa (n = 8 samples), Kasanda (n = 88) and Makululu (n = 94) health centres. The children were classified as male/female and younger (8 months–3 years)/older (4–7 years) as shown in Table 1. The data on mean age (4.2 years), median (4 years) and ranges (8 months–7 years) are not shown.

3.2. Fecal lead (Pb-F) and urine lead (Pb-U) levels

As shown in Table 2, concentrations of Pb in fecal samples (mg/kg, dry weight) were high in all the sampled children. Similarly, a total of 190 urine samples were collected at Chowa (n = 8 samples), Kasanda (n = 88) and Makululu (n = 94) health centres. The concentrations of Pb in urine (Pb-U_{SG}) were extremely high, with concentration up to 2914 μg/L recorded in Kasanda Township (Table 2). Only five (about 2.6%) of the total sampled children had a history of metal chelation therapy.

3.3. Fecal cadmium (Cd-F), urine cadmium (Cd-U) and blood (Cd-B) levels

As shown in Table 3, concentrations of Cd in fecal samples (mg/kg, dry weight) were elevated in all the sampled children with a maximum concentration of 4.49 mg/kg. The concentrations of Cd in urine (Cd-U_{SG}) were elevated, especially for Kasanda with a mean (GM) of 0.46 μg/L. Similarly, concentrations of Cd in blood were higher in Kasanda, where Cd-B concentrations of up to 7.70 μg/L were recorded.

3.4. Measured Pb-U and Cd-U vs Biomonitoring Equivalents (BE) values

As shown in Table 4, the measured Cd-U_{SG} and Cd-B concentrations were compared with the current BE values that are consistent with established exposure guideline values to evaluate if measured values in the current study were of low, medium, or high priority for risk assessment follow-up of (Hays et al., 2008). The measured Cd-U_{SG} and Cd-B were below the BE values.

3.5. Site, age and sex differences

Multiple logistic regression analyses were performed on log-transformed data to estimate the influence of independent variables (age as continuous variable, sex represented as 0 for girls and 1 for boys, location (area) represented as 0 for Makululu and 1 for Kasanda) on Pb-F. Similar analyses were done on Cd-F, Pb-U_{SG} and Cd-U_{SG} (Table 5). Fecal Pb and Cd as well as urinary Pb concentrations in children from Kasanda were higher than those from Makululu ($p < 0.05$). Children from Kasanda and Makululu had similar concentrations of urinary Cd ($p > 0.05$). Similarly, there was no difference in the concentration of Pb-F and Cd-F between boys and girls. However, girls excreted more urinary Pb and Cd than boys ($p < 0.05$), with the difference in Cd-U being substantial considering an estimated increase of 1.26 μg/L against median concentrations of 0.40 μg/L (female) and 0.31 μg/L (male children). Fecal Pb levels in younger children aged between 8 months and 3 years old were slightly higher than levels in children aged 4–7 years ($p = 0.05$) but not Cd-F. There were urinary Pb and Cd concentration differences between the younger (8 months–3 years) and older (4–7 years) children ($p < 0.05$).

3.6. Pb and Cd correlations

Using Pearson correlation analysis, strong positive correlations were observed between Pb and Cd in feces ($r = 0.81$; $p < 0.0001$) and urine ($r = 0.84$; $p < 0.0001$) of children from Kasanda and Makululu. Lead concentrations also showed positive correlations among blood, feces and urine of children from the polluted townships. Cadmium concentrations showed similar positive associations (Table 6).

When presented by age groups of 8 months–3 years and 4–7 years, Pb concentrations had strong positive associations ($p < 0.05$) among blood, feces and urine (Fig. 2). Correlations of Pb in blood, feces and urine with age were negative but not significant ($p > 0.05$).

4. Discussion

The current study has demonstrated Pb and Cd excretion in urine and feces of children from polluted townships in Zambia's Kabwe mining town. This highlighted concurrent toxic metal exposure, especially in children from Kasanda Township, which is closest to the mine. The study targeted children under the age of 7 years from Kasanda, Makululu and Chowa townships following preliminary studies where extremely elevated Pb-B levels were revealed in the same children by Yabe et al. (2015). All of the sampled children in the current study showed alarming Pb exposure with geometric means up to 35.3 mg/kg (Pb-F) and 67.8 μg/L (Pb-U). The health risk due to Cd was evident as Cd levels up to 4.49 mg/kg (Cd-F), 18.1 μg/L (Cd-U) and 7.70 μg/L (Cd-B) indicated increased exposure. Elevated childhood exposure to Pb could be hazardous as the developing nervous system is sensitive to its neurotoxic effects (Lidsky and Schneider, 2003; Bellinger, 2004). Although Cd toxicity in children is not clear, low-level exposure in children has been implicated with adverse neurodevelopmental outcomes with increasing evidence of learning disabilities and need for special education (Jiang et al., 1990; Ciesielski et al., 2012). Therefore, the findings in the current study are worrisome as simultaneous exposure to Pb and Cd could have detrimental effects on the neurodevelopment of the exposed children given that neurodevelopmental toxicity is dependent on co-exposure to multiple neurotoxicants (Bellinger, 2008).

Biomonitoring methods using fecal and urine metal concentrations may provide alternatives to blood analysis in children from polluted environments (Dos Santosa et al., 2018). As such, measurement of fecal and urine metals have been used to estimate the overall magnitude of metal intake and elimination (Iwao, 1977; Kjellstrom et al., 1978; Moon et al., 1999). According to Gwiazda et al. (2005), fecal Pb content reflects an integrated measure of Pb exposure from all sources, including dietary. Although most of the metals in feces represent the unabsorbed fraction of ingested metals, their presence in feces may also reflect their endogenous

Table 1
Sample sizes and sample characteristics of children from Chowa, Kasanda and Makululu townships near the Pb-Zn in Kabwe, Zambia.

	Chowa	Kasanda	Makululu	Totals
Sample size	8	88	94	190
Males	4	40	39	83
Females	4	48	55	107
Median age	5.9	3.6	4.6	4.2
Younger children (8 months–3 years)	1	42	29	72
Older children (4–7 years)	7	46	65	118

Table 2
Pb-F (mg/kg, dry weight) and Pb-U_{SG} (μg/L, adjusted for SG) concentrations of children from Chowa, Kasanda and Makululu townships near the Pb-Zn mine in Kabwe, Zambia.

Sample	*n*	Mean	GM	Median	Minimum	Maximum	IQR
Pb-F (mg/kg)							
Chowa	8	11.6	9.32	10.3	3.03	92.7	19.9–5.17
Kasanda	88	90.6	35.3	31.9	3.45	1259	71.2–15.4
Makululu	94	67.8	20.3	15.0	2.27	2252	53.3–7.99
Pb-U_{SG} (μg/L)							
Chowa	8	13.4	12.1	13.5	4.62	19.9	17.8–8.88
Kasanda	88	207	67.8	59.6	1.84	2914	117.8–31.2
Makululu	94	81.3	35.1	29.7	2.57	1113	56.4–18.6

Pb-F = fecal Pb; Pb-U = urinary Pb; *n* = number of samples; IQR = Interquartile Range.

Table 3
Cd-F (mg/kg) and Cd-U_{SG} (μg/L, adjusted for SG) concentrations of children from Chowa, Kasanda and Makululu townships in vicinity of the Pb-Zn mine in Kabwe, Zambia.

Sample	*n*	Mean	GM	Median	Minimum	Maximum	IQR
Cd-F (mg/kg)							
Chowa	8	0.18	0.15	0.16	0.07	0.43	0.23–0.09
Kasanda	88	0.54	0.31	0.28	0.04	4.49	0.57–0.15
Makululu	94	0.26	0.18	0.17	0.04	1.58	0.29–0.10
Cd-U_{SG} (μg/L)							
Chowa	8	0.43	0.19	0.13	0.06	1.67	0.93–0.09
Kasanda	88	1.47	0.46	0.38	0.02	18.1	0.79–0.19
Makululu	94	0.71	0.35	0.30	0.03	7.66	0.61–0.17
Cd-B (μg/L)							
Chowa	8	0.69	0.66	0.67	0.46	1.06	0.80–0.51
Kasanda	88	1.10	0.84	0.72	0.24	7.70	1.31–0.40
Makululu	94	0.52	0.44	0.49	0.08	1.56	0.68–0.32

Cd-F = fecal Cd; Cd-U_{SG} = urinary Cd adjusted for SG; Cd-B = blood CD; *n* = number of samples; IQR = Interquartile Range.

Table 4
Comparison between Cd-U and Cd-B concentrations (μg/L) measured in urine and blood samples of children from Chowa, Kasanda and Makululu townships in vicinity of the Pb-Zn mine in Kabwe, Zambia with Biomonitoring Equivalents (BE) values.

Data set	Chowa	Kasanda	Makululu	USEPA (BE value)	ATSDR (BE value)
Cd-U (μg/L)	0.19 μg/L	0.46 μg/L	0.35 μg/L	1.5 μg/L	1.2 μg/L
Cd-B (μg/L)	0.66 μg/L	1.10 μg/L	0.44 μg/L	1.7 μg/L	1.4 μg/L

USEPA and ATSDR Biomonitoring Equivalents (BE) values of blood Cd and creatinine-adjusted urinary Cd (Hays et al., 2008).

Table 5
Log-transformed fecal (Pb and Cd) and urine (Pb and Cd) concentration differences (site, age and sex) multiple logistic regression analyses in children from Kasanda and Makululu townships in Kabwe, Zambia.

	Parameter	Estimate	nDF	SS	F Ratio	*p* value (Prob>F)
Pb-F (mg/kg)	Intercept	1.59	1.00	0.00	0.00	1
	Area {Makululu-Kasanda}	-0.10	1.00	1.75	5.89	**0.016**
	Age	-0.042	1.00	1.14	3.85	0.051
	Sex{M-F}	-0.055	1.00	0.53	1.79	0.183
Cd-F (mg/kg)	Intercept	-0.61	1.00	0.00	0.00	1.00
	Area {Makululu-Kasanda}	-0.123	1.00	2.47	16.09	**0.0001**
	Age	-0.005	1.00	0.01	0.09	0.77
	Sex{M-F}	-0.02	1.00	0.11	0.69	0.41
Pb-U (μg/L)	Intercept	2.05	1.00	0.00	0.00	1.00
	Area {Makululu-Kasanda}	-0.10	1.00	1.76	6.53	**0.01**
	Age	-0.09	1.00	4.90	1821	**0.00003**
	Sex{M-F}	-0.13	1.00	2.74	10.18	**0.00168**
Cd-U (μg/L)	Intercept	-022	1.00	0.00	0.00	1.00
	Area {Makululu-Kasanda}	-0.043	1.00	032	1.16	0.28
	Age	-0.045	1.00	1.28	4.63	**0.03**
	Sex{M-F}	-0.10	1.00	1.89	6.84	**0.01**

Kasanda ($n = 88$) and Makululu ($n = 94$) townships in the vicinity of the Pb-Zn mining area in Kabwe; Age – children between 8 months–3 years ($n = 71$) years old vs children between 4 and 7 ($n = 111$) years; Sex – M ($n = 79$) vs F ($n = 103$); *P* values in bold indicate significant ($p < 0.05$); nDF - number if degrees of freedom for a term; SS - Sequential Sum of Squares.

Table 6
Correlations among Pb concentrations in blood (Pb-B), feces (Pb-F) and urine (Pb-U) as well as Cd in blood (Cd-B), feces (Cd-F) and urine (Cd-U) of children from polluted townships in Kabwe, Zambia.

Township	*r* value	*p* value
Pb (Kasanda and Makululu)		
Pb-B: Pb-U	0.27	= 0.0005
Pb-B: Pb-F	0.36	<0.0001
Pb-U: Pb-F	0.33	<0.0001
Cd (Kasanda and Makululu)		<0.0001
Cd-B: Cd-U	0.26	= 0.0005
Cd-B: Cd-F	0.37	<0.0001
Cd-U: Cd-F	0.21	= 0.007

r = Pearson's correlation coefficient; $n = 182$.

biliary excretion into feces (Hammond et al., 1980; Gregus and Klaassen, 1986; Gwiazda et al., 2005). Mean (GM) concentrations of Pb-F of 9.32 mg/kg (Makululu) and 35.3 mg/kg (Kasanda) in the current study were extremely high and showed that children from the polluted townships in Kabwe are exposed to high levels of Pb. Similarly, Cd-F concentrations of up to 4.49 mg/kg in the current study could raise health concerns in the children from the polluted townships. Since the living space are important sources of environmental exposure for young children (Hornberg and Pauli, 2007), findings of the current study indicate that the current home environment of the children in Kabwe could be the source of metal exposure. This is because young children spend most of their time at home and ingested metals are expected to be eliminated in the feces probably within 24–48 h after exposure (Smith, 2013).

Although fecal metal measurements may be convenient than urinalysis due to difficulties in collecting urine samples in infants, urinary metal biomonitoring is preferred because absorbed Pb and Cd are excreted primarily in urine (Heitland and Koster, 2006). In contrast to blood, urine is equally easy to collect and non-invasive (Zhang et al., 2016). In the current study, recorded mean (GM) Pb-U of 12.1 μg/L (Makululu) and 67.8 μg/L (Kasanda) with levels up to 2914 μg/L were extremely higher than Pb-U_{SG} of 4.08 μg/L recorded in children between 4 and 10 years from a general population in Korea (Moon et al., 2003). Moreover, Pb-U levels in the current study markedly exceeded concentrations of 0.9 μg/L (adjusted for creatinine) recorded in children in USA (Shao et al., 2017). When compared with records in children from the US National Health and Nutrition Examination Survey (NHANES) of 2013–2014, Pb-U levels in the current study extremely exceeded the 0.22 μg/L in US (CDC - Fourth National Report on Human Exposure to Environmental Chemicals, 2017). These findings reveal high Pb exposure among children in Kabwe, Zambia, and could have serious health implications.

Mean (GM) urinary Cd-U_{SG} of 0.19 μg/L (Chowa), 0.35 μg/L (Kasanda) and 0.46 μg/L (Makululu) in the current study were lower than the biomonitoring equivalent values of Hays et al. (2008) for urine Cd according to USEPA (1.5 μg/L) and ATSDR (1.2 μg/L). The current findings were however, similar to median Cd-U_{SG} concentrations of 0.23 μg/L (girls) and 0.22 μg/L (boys) in a cross-sectional study among school children in Belgium (Wang et al., 2017). Although Cd-U concentrations in the current study exceeded the mean (GM) urine level of 0.185 μg/L (adjusted for creatinine) set by ATSDR (2012) in unexposed children, they were of low priority for risk assessment follow-up according to the current health-based exposure guidelines (Hays et al., 2008). However, this should be interpreted with caution given that 23 percent of the 171 sampled children had urinary Cd concentrations exceeding the urine Cd BE values and could be at risk of nephrotoxicity. The means (GM) in the current study also extremely exceeded US children's Cd-U records of 0.057 μg/L in 2009–2010 NHANES (CDC - Fourth National Report on Human Exposure to Environmental Chemicals, 2017). Moreover, 7 percent of the 181 sampled children in the

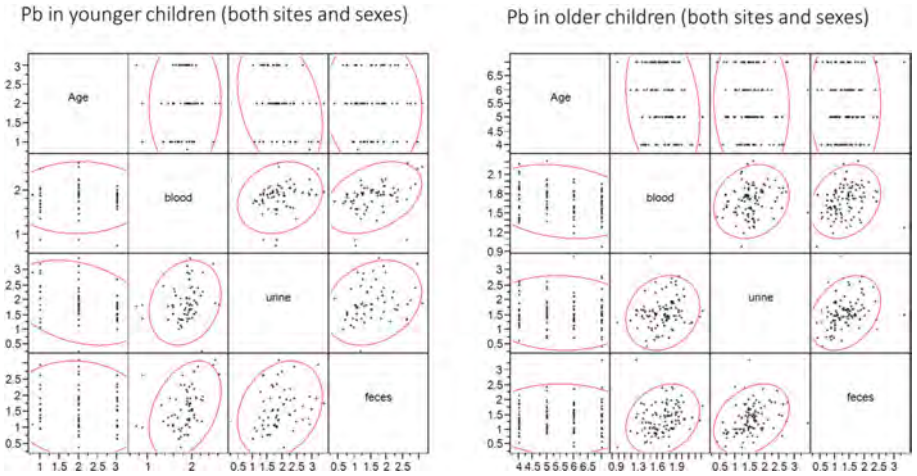

Fig. 2. Positive correlations among Pb concentrations in blood, feces and urine of younger children (8 months–3 years, ($n = 71$)) and older children (4–7 years, ($n = 111$)) from Kasanda and Makululu townships of Kabwe, Zambia. Strong positive correlations were also observed between fecal Pb and Cd ($p = 0.81$, <0.0001) as well as between urinary Pb and Cd ($p = 0.83$, <0.0001).

current study had Cd-B concentrations exceeding the BE values for Cd in blood.

The difference in Pb-U between the two age groups appeared minimal as the concentration of Pb-U marginally increased by 1.23 μg/L (estimate log value = −0.09) in younger children in relation to the higher median of 66.7 μg/L (younger children) and 31.2 μg/L (older children). On the other hand, the Cd-U difference between the two age groups was wide considering an increase estimate of about 1.11 μg/L (estimate log value = −0.045) in relation to the lower median values of 0.38 μg/L (younger children) and 0.31 μg/L (older children). Given that urinary Cd, which reflects body burden increases with age (Hays et al., 2008; Jarup and Akesson, 2009), the higher Cd-U in younger children in the current study could be attributed to behavioural differences as younger children are more exposed to metals due to increased hand-mouth activities. Moreover, the age difference between the two age groups was minimal for the older group to have accumulated more Cd.

Since findings in the current study do not imply that urinary Cd reduces with age, regular biomonitoring of the exposed children up to adulthood in Kabwe need to be conducted, particularly pregnant women as Cd from the placenta may impair fetal development including neurodevelopmental impairment (Ciesielski et al., 2012; Kippler et al., 2010, 2012; Llanos and Ronco, 2009; Salpietro et al., 2002; Zhang et al., 2004). The finding of higher excretion levels of Pb and Cd in the urine of girls compared with boys from both Kasanda and Makululu townships was interesting. More studies need to be conducted to establish gender differences in metal accumulation and excretion in children as the high absorption rate following oral exposures in women is associated with iron deficiency (ATSDR, 2008), which might not be the case in children.

Concurrent exposure to Pb and Cd can result in metal interactions, which may be characterized by alterations in both tissue metal concentrations and toxicity (Mahaffey et al., 1981). In the current study, strong positive correlations were seen between Pb and Cd in both feces and urine of the sampled children, thus indicating concurrent exposure to Pb and Cd. This was not surprising as soils from the selected townships are highly polluted with Pb and Cd (Nakayama et al., 2011). Data on correlations between Pb and Cd levels in feces and urine of children from polluted areas in rare. In a study among adults in the general population in Japan, no close correlations between Pb-U and Cd-U were detected (Fukui et al., 2004). Joint toxicity can result in various effects including greater than additive (synergism and potentiation), additive (no interaction) and less than additive (antagonism and inhibition). However, since additivity is the default assumption for evaluating health effects of multiple chemicals, evaluation of the simultaneous effects of Pb and Cd in Kabwe is needed as it is now known that children from the polluted townships are exposed to both Pb and Cd in their current environment. The current study also revealed positive associations of Pb and Cd concentrations among blood, urine and feces. These findings indicate that either urine or feces could be useful for biomonitoring of Pb and Cd in polluted environments.

5. Conclusions

Childhood Pb and Cd co-exposure in Kabwe poses serious implications on the health of the exposed children and should be given attention. A thorough clinical evaluation of Pb and Cd exposure among children in townships surrounding the Pb-Zn mine in Kabwe is long over-due as it has never been done despite alarming metal exposure. Regular fecal and urine biomonitoring should be considered for prompt remedial measures to avoid irreversible Pb-induced neurological dysfunction. Urgent interventions are required to reduce Pb and Cd exposure in the affected townships. This can be done through community-based programs to educate the affected communities about the health effects of Pb and Cd, sources of the metals and practical ways of reducing exposure in their homes and communities.

Conflict of interest

The authors declare no conflicts of interest.

Acknowledgments

We are highly indebted to the children and their parents for participating in this study. We are also grateful to Chowa, Kasanda and Makululu health services in Kabwe, the Kabwe District Health Office and the Ministry of Health, Zambia, for facilitating the study. We also want to thank all the laboratory technicians and nurses at the health centers for their technical support. This study was supported by Grants-in-Aid for Scientific Research from the Ministry of Education, Culture, Sports, Science and Technology of Japan awarded to M. Ishizuka (No. 16H0177906) and Y. Ikenaka (No. 26304043, 15H0282505, 15K1221305, 17K2003807), and S.M.M. Nakayama

(No. 16K16197), and the foundation of JSPS Core to Core Program (AA Science Platforms) and Bilateral Joint Research Project (PG36150002 and PG36150003). We also acknowledge financial support from The Soroptimist Japan Foundation, The Nakajima Foundation, The Sumitomo foundation and The Nihon Seimei Foundation. This research was supported by JST/JICA, SATREPS (Science and Technology Research Partnership for Sustainable Development). We also acknowledge Mr. Takahiro Ichise, Ms. Mio Yagihashi and Ms. Nagisa Hirano in Graduate School of Veterinary Medicine, Hokkaido University for ICP-MS maintenance and analysis.

References

Agency for Toxic Substances and Disease Registry (ATSDR), 2008. Cadmium Toxicity. What Is the Biological Fate of Cadmium in the Body? Course. WB 1096. Available online: https://www.atsdr.cdc.gov/csem/csem.asp?csem=6&po=9.

Agency for Toxic Substances and Disease Registry (ATSDR), 2012. Toxicological Profile for Cadmim. CAS#: 7440-43-9, Available online: https://www.atsdr.cdc.gov/toxprofiles/tp.asp?id=48&tid=15.

Akerstrom, M., Barregard, L., Lundh, T., Sallsten, G., 2013. The relationship between cadmium in kidney and cadmium in urine and blood in an environmentally exposed population. Toxicol. Appl. Pharmacol. 268, 286–293.

Bellinger, D.C., 2004. Lead. Pediatrics 113, 1016–1022.

Bellinger, D.C., 2008. Very low lead exposures and children's neurodevelopment. Curr. Opin. Pediatr. 2, 172–177.

Calabrese, E.J., Stanek, E.J., James, R.C., Roberts, S.M., 1997. Soil ingestion: a concern for acute toxicity in children. Environ. Health Perspect. 105, 1354–1358.

Canfield, R.L., Henderson Jr., C.R., Cory-Slechta, D.A., Cox, C., Jusko, T.A., Lanphear, B.P., 2003. Intellectual impairment in children with blood lead concentrations below 10 μg per deciliter. N. Engl. J. Med. 348, 1517–1526.

Caravanos, J., Chatham-Stephens, K., Ericson, B., Landrigan, P.J., Fuller, R., 2013. The burden of disease from pediatric lead exposure at hazardous waste sites in 7 Asian countries. Environ. Res. 120, 119–125.

Centers for Disease Control and Prevention (CDC), 2012. Low Level Lead Exposure Harms Children: a Renewed Call for Primary Prevention. Report of the advisory committee on childhood lead poisoning prevention of the Centers for Disease Control and Prevention. Atlanta, Ga. Available online. www.cdc.gov/nceh/lead/acclpp/final_document_030712.pdf.

Centers for Disease Control and Prevention (CDC), 2017. Updated Tables. Fourth National Report on Human Exposure to Environmental Chemicals, vol. 1. Available. https://www.cdc.gov/exposurereport/pdf/FourthReport_UpdatedTables_Volume1_Jan2017.pdf (accessed 09.02.2018).

Ciesielski, T., Weuve, J., Bellinger, D.C., Schwartz, J., Lanphear, B., Wright, R.O., 2012. Cadmium exposure and neurodevelopmental outcomes in U.S. children. Environ. Health Perspect. 120, 758–763.

Dooyema, C.A., Neri, A., Lo, Y.C., Durant, J., Dargan, P.I., Swarthout, T., Biya, O., Gigado, S.O., Haladu, S., Sani-Gwarzo, N., Nguku, P.M., Akpan, H., Idris, S., Bashir, A.M., Brown, M.J., 2012. Outbreak of fatal childhood lead poisoning related to artisanal gold mining in northwestern Nigeria, 2010. Environ. Health Perspect. 120, 601–607.

Dos Santosa, M., Soaresa, M.C.F., Baischa, P.R.M., Baischa, A.L.M., da Silva, R.M.R., 2018. Biomonitoring of trace elements in urine samples of children from a coal-mining region. Chemosphere 197, 622–626. https://doi.org/10.1016/j.chemosphere.2018.01.082.

Ercal, N., Gurer-Orhan, H., Aykin-Burns, N., 2001. Toxic metals and oxidative stress. Part 1. Mechanisms involved in metal-induced oxidative damage. Curr. Top. Med. Chem. 1, 529–539.

Fukui, Y., Ezaki, T., Tsukahara, T., Moriguchi, J., Furuki, K., Okamoto, S., Ukai, H., Ikeda, M., 2004. Lead levels in urine of never-smoking adult women in non-polluted areas in Japan, with references to cadmium levels in urine. Ind. Health 42, 415–423.

Gregus, Z., Klaassen, C.D., 1986. Disposition of metals in rats: a comparative study of fecal, urinary, and biliary excretion and tissue distribution of eighteen metals. Toxicol. Appl. Pharmacol. 85, 24–38.

Gwiazda, R., Campbell, C., Smith, D., 2005. A noninvasive isotopic approach to estimate the bone lead contribution to blood in children: implication for assessing the efficacy of lead abatement. Environ. Health Perspect. 113, 104–110.

Hammond, P.B., Clark, C.S., Gartside, P.S., Berger, O., Walker, A., Michae, L.W., 1980. Fecal lead excretion in young children as related to sources of lead in their environments. Int. Arch. Occup. Environ. Health 46, 191–202.

Hays, S.M., Nordberg, M., Yager, J.W., Aylward, L.L., 2008. Biomonitoring equivalents (BE) dossier for cadmium (Cd). Regul. Toxicol. Pharmacol. 51, S49–S56.

Heitland, P., Koster, H.D., 2006. Biomonitoring of 30 trace elements in urine of children and adults by ICP-MS. Clin. Chim. Acta 365, 310–318.

Hornberg, C., Pauli, A., 2007. Child poverty and environmental justice. Int. J. Hyg. Eviron Health 210, 571–580.

IARC, 1993. Beryllium, Cadmium, Mercury, and Exposures in the Glass Manufacturing Industry. Working Group Views and Expert Opinions, Lyon, France, vol. 58. IARC 508 Monogr Eval Carcinog Risks Hum. Cadmium and cadmium compounds, pp. 41–117.

Iwao, S., 1977. Cadmium, lead, copper and zinc in food, feces and organs of humans. Keio J. Med. 26, 63–78.

Jarup, L., Akesson, A., 2009. Current status of cadmium as an environmental health problem. Toxicol. Appl. Pharmacol. 238, 201–208.

Jiang, H.M., Han, G.A., He, Z.L., 1990. Clinical significance of hair cadmium content in the diagnosis of mental retardation of children. Chin. Med. J. Engl. 103, 331–334.

Kido, T., Nogawa, K., Ishizaki, M., Honda, R., Tsuritani, I., Yamada, Y., Nakagawa, H., 1990. Long-term observation of serum creatinine and arterial blood pressure, and blood pH in persons with cadmium-induced renal dysfunction. Arch. Environ. Health 45, 3–41.

Kippler, M., Hoque, A.M., Raqib, R., Öhrvik, H., Ekström, E.C., Vahter, M., 2010. Accumulation of cadmium in human placenta interacts with the transport of micronutrients to the fetus. Toxicol. Lett. 192, 162–168.

Kippler, M., Tofail, F., Hamadani, J.D., Gardner, R.M., Grantham-McGregor, S.M., Bottai, M., Vahter, M., 2012. Early-life cadmium exposure and child development in 5-year-old girls and boys: a cohort study in rural Bangladesh. Environ. Health Perspect. 120, 1462–1468.

Kjellstrom, T., Borg, K., Lind, B., 1978. Cadmium in feces as an estimator of daily cadmium intake in Sweden. Environ. Res. 15, 242–251.

Lidsky, T.L., Schneider, J.S., 2003. Lead neurotoxicity in children: basic mechanisms and clinical correlates. Brain 126, 5–19.

Llanos, M.N., Ronco, A.M., 2009. Fetal growth restriction is related to placental levels of cadmium, lead and arsenic but not with antioxidant activities. Reprod. Toxicol. 27, 88–92.

Lo, Y.C., Dooyema, C.A., Neri, A., Durant, J., Jefferies, T., Menina-Marino, A., Der avello, L., Throughman, D., Davis, L., Dankoli, R.S., Samson, M.Y., Ibrahim, L.M., Okechukwu, O., Umar-Tsafe, N.T., Dama, A.H., Brown, M.J., 2012. Childhood lead poisoning associated with gold ore processing: a village-level investigation-Zamfara State, Nigeria, October-November 2010. Environ. Health Perspect. 120, 1450–1455.

Lowry, J.A., 2010. Oral Chelation Therapy for Patients with Lead Poisoning. WHO Expert Committee on the Selection and Use of Essential Medicines. Available online. http://www.who.int/selection_medicines/committees/expert/18/applications/4_2_LeadOralChelators.pdf.

Manton, W.I., Angle, C.R., Stanek, K.L., Reese, Y.R., Kuehnemann, T.J., 2000. Acquisition and retention of lead by young children. Environ. Res. 82, 6–80.

Mahaffey, K.R., Capar, S.G., Gladen, B.C., Fowler, B.A., 1981. Concurrent exposure to lead, cadmium, and arsenic. Effects on toxicity and tissue metal concentrations in the rat. J. Lab. Clin. Med. 98, 463–481.

Moon, C.S., Zhang, Z.W., Shimbo, S., Watanabe, T., Lee, C.U., Lee, B.K., Ahn, K.D., Lee, S.H., Ikeda, M., 1999. Evaluation of urinary cadmium and lead as markers of background exposure of middle-aged women in Korea: dietary intake as an influential factor. Toxicol. Lett. 108, 173–178.

Moon, C.S., Paik, J.M., Choi, C.S., Kim, D.H., Ikeda, M., 2003. Lead and cadmium levels in daily foods, blood and urine in children and their mothers in Korea. Int. Arch. Occup. Environ. Health 76, 282–288.

Nakayama, S.M.M., Ikenaka, Y., Hamada, K., Muzandu, K., Choongo, K., Teraoka, H., Mizuno, N., Ishizuka, M., 2011. Metal and metalloid contamination in roadside soil and wild rats around a Pb-Zn mine in Kabwe, Zambia. Environ. Pollut. 159, 175–181.

Nakata, H., Nakayama, S.M., Yabe, J., Liazambi, A., Mizukawa, H., Darwish, W.S., Ikenaka, Y., Ishizuka, M., 2016. Reliability of stable Pb isotopes to identify Pb sources and verifying biological fractionation of Pb isotopes in goats and chickens. Environ. Pollut. 208, 395–403.

Needleman, H., 2004. Lead poisoning. Annu. Rev. Med. 55, 209–222.

Nermell, B., Lindberg, A.L., Rahman, M., Berglund, M., Persson, L.Å., El Arifeen, S., Vahter, M., 2008. Urinary arsenic concentration adjustment factors and malnutrition. Environ. Res. 106, 212–218.

Ogbomida, E.T., Nakayama, S.M.M., Bortey-Sam, N., Oroszlany, B., Tongo, I., Enuneku, A.A., Ozekeke, O., Ainerua, M.O., Fasipe, I.P., Ezemonye, L.I., Mizukawa, H., Ikenaka, Y., Ishizuka, M., 2018. Accumulation patterns and risk assessment of metals and metalloid in muscle and offal of free-range chickens, cattle and goat in Benin city. Ecotoxicol. Environ. Saf. 151, 98–108.

Pure Earth, 2014. Project Completion Report: Nigeria Lead Poisoning Crisis. Available online. http://www.blacksmithinstitute.org/nigerian-lead-poisoning-crisis-blacksmith-report.html.

Salpietro, C.D., Gangemi, S., Minciullo, P.L., Briuglia, S., Merlino, M.V., Stelitano, A., Cristani, M., Trombetta, D., Saija, A., 2002. Cadmium concentration in maternal and cord blood and infant birth weight: a study on healthy non-smoking women. J. Perinat. Med. 30, 395–399.

Shao, W., Liu, Q., He, X., Liu, H., Gu, A., Jiang, Z., 2017. Association between level of urinary trace heavy metals and obesity among children aged 6-19 years: NHANES 1999–2011. Environ. Sci. Pollut. Res. 24, 11573–11581.

Smith, S.W., 2013. The role of chelation in the treatment of other metal poisonings. J. Med. Toxicol. 9, 355–369.

Suwazono, Y., Akesson, A., Alfven, T., Jarup, L., Vahter, M., 2005. Creatinine versus specific gravity-adjusted urinary cadmium concentrations. Biomarkers 10, 117–126.

Swaran, J.S.F., Vidhu, P., 2010. Chelation in metal intoxication. Int. J. Environ. Res. Public Health 7, 2745–2788.

Umemura, T., 2000. Experimental reproduction of itai-itai disease, a chronic cadmium poisoning of humans, in rats and monkeys. Jpn. J. Vet. Res. 48, 15–28.

Uno, T., Kobayashi, E., Suwazono, Y., Okubo, Y., Miura, K., Sakata, K., Okayama, A.,

Ueshima, H., Nakagawa, H., Nogawa, K., 2005. Health effects of cadmium exposure in the general environment in Japan with special reference to the lower limit of the benchmark dose as the threshold level of urinary cadmium. Scand. J. Work Environ. Health 31, 307–315.
Wang, H., Dumont, X., Haufroid, V., Bernard, A., 2017. The physiological determinants of low-level urine cadmium: an assessment in a cross-sectional study among schoolchildren. Environ. Health 16, 99.
Water Management Consultants Ltd, 2006. Copperbelt Environment Project - Kabwe Scoping and Desing Study - Project Synthesis.
Yabe, J., Ishizuka, M., Umemura, T., 2010. Current levels of heavy metal pollution in Africa. J. Vet. Med. Sci. 72, 1257–1263.
Yabe, J., Nakayama, S.M.M., Ikenaka, Y., Muzandu, K., Ishizuka, M., Umemura, T., 2011. Uptake of lead, cadmium, and other metals in the liver and kidneys of cattle near a lead-zinc mine in Kabwe, Zambia. Environ. Toxicol. Chem. 30, 1892–1897.
Yabe, J., Nakayama, S.M.M., Ikenaka, Y., Yohannes, Y.B., Bortey-Sam, N., Oroszlany, B., Muzandu, K., Choongo, K., Kabalo, A.N., Ntapisha, J., Mweene, A., Umemura, T., Ishizuka, M., 2015. Lead poisoning in children from townships in the vicinity of a lead-zinc mine in Kabwe, Zambia. Chemosphere 119, 941–947.
Zhang, Y.L., Zhao, Y.C., Wang, J.X., Zhu, H.D., Liu, Q.F., Fan, Y.G., Wang, N.F., Zhao, J.H., Liu, H.S., Ou-Yang, L., Liu, A.P., Fan, T.Q., 2004. Effect of environmental exposure to cadmium on pregnancy outcome and fetal growth: a study on healthy pregnant women in China. J. Environ. Sci. Health Part A Toxicol. Hazard Subst. Environ. Eng. 39, 2507–2515.
Zhang, X., Cui, X., Lin, C., Ma, J., Liu, X., Zhu, Y., 2016. Reference levels and relationships of nine elements in first-spot morning urine and 24-h urine from 210 Chinese children. Int. J. Hyg. Environ. Health 220, 227–234.

Bull Environ Contam Toxicol (2017) 99:108–116
DOI 10.1007/s00128-017-2089-3

Sediment Metal Contamination in the Kafue River of Zambia and Ecological Risk Assessment

Ethel M'kandawire[1,3] · Kennedy Choongo[1] · John Yabe[1] · Maxwell Mwase[1] · Ngonda Saasa[1] · Shouta M. M. Nakayama[2] · Nesta Bortey-Sam[2] · Claudia A. Blindauer[3]

Received: 24 November 2016 / Accepted: 11 April 2017 / Published online: 22 April 2017

Abstract Zambia's Kafue River receives wastes from various sources, resulting in metal pollution. This study determined the degree of contamination of 13 metals (Al, Cr, Mn, Fe, Co, Ni, Cu, Zn, As, Se, Cd, Hg and Pb) in Kafue River sediment and the associated ecological risks at six sites in three different seasons. The level of contamination for most metals showed significant site and seasonal differences. The contamination factor and pollution load index indicated that concentrations of most metals particularly copper (Cu), cobalt (Co), manganese (Mn) and arsenic (As) were very high at sites within the Copperbelt mining area. The geoaccumulation index showed an absence of anthropogenic enrichment with Cd and Hg at all the study sites and extreme anthropogenic enrichment with Cu at sites in the Copperbelt mining area. Potential ecological risk showed that Cu and As were likely to cause adverse biological effects to aquatic organisms in the Copperbelt mining region of the Kafue River.

Keywords Kafue River sediment · Metals · Copperbelt mining area · Contamination factor · Pollution load index · Geoaccumulation index · Potential ecological risk

✉ Ethel M'kandawire
ethel.mkandawire@unza.zm; ethelmkandawire@yahoo.com

[1] School of Veterinary Medicine, University of Zambia, P.O. Box 32379, Lusaka, Zambia

[2] Laboratory of Toxicology, Department of Environmental Veterinary Sciences, Graduate School of Veterinary Medicine, Hokkaido University, Kita 18, Nishi 9, Kita-ku, Sapporo 060-0818, Japan

[3] Department of Chemistry, University of Warwick, Gibbet Hill road, Coventry CV4 7AL, UK

Metal pollution of water sources has evoked a global interest because metal ions are indestructible and bio-accumulate in aquatic ecosystems such as aquatic plants, invertebrates and fish and humans (Gupta et al. 2009; Solomon 2009). Anthropogenic sources of metals include mining, discharge of untreated domestic and industrial wastes (Khadse et al. 2008) and agricultural run-off (Hatje et al. 1998). Natural sources include weathering of rocks and minerals (Karbassi et al. 2008). Metals released into aquatic bodies may be immobilized within sediment but can be retained or released to the water posing a risk to aquatic life and humans through the food chain (Calmano et al. 1990). Therefore, sediments are important environmental indicators for metal pollution in aquatic bodies (Alaoui et al. 2010). Although metals such as Fe, Zn, Se and Cu are essential to life, they are toxic at high concentrations. Metals like Cd, As, Hg and Pb are non-essential and are toxic at minute concentrations (Fernandes et al. 2008; Mayo et al. 2015). Developing countries including Zambia are plagued by the impact of metal pollution especially from mining (Yabe et al. 2010) with the level of contamination increasing with an increase in industrial activities.

The Kafue River receives large amounts of Cu and Co mining waste from mines in the Copperbelt province (Sracek et al. 2012). The main composition of mineral ores within the Copperbelt mining area include pyrite (FeS_2), chalcopyrite ($CuFeS_2$), bornite (Cu_5FeS_4), chalcocite (CuS_2), digenite (Cu_9S_5), linnaeite (Co_3S_4) and carrolite ($Cu(Co,Ni)_2S_4$) which are embedded in carbonate-rich shales and argillite (Mendelsohn 1961). As the Kafue River passes through this extensive mining region, it receives large volumes of metal effluent. These include waste water discharging from chemical processing plants, erosion and wash out of fine particles from old tailings, mining waste piles, metallurgical slag deposits, and

seepage and overflow of suspensions from active tailing ponds (Sracek et al. 2012). This has resulted in extensive environmental impacts detected in various environmental samples downstream of the mining area (Bäckström 1996; M'kandawire et al. 2012). Studies conducted on the Kafue River sediment have revealed elevated concentrations of Cu. For example, Choongo et al. (2005) reported high levels of this metal in sediment and low coefficient of condition of fish probably due to Cu toxicity. Ikenaka et al. (2010) demonstrated the presence of heavy metals in national parks downstream to the Copperbelt mining area. Total metal contents in sediment showed that the Kafue River was highly enriched with Cu and exceeded the Canadian limit for freshwater sediments (Sracek et al. 2012). However, these previous studies have only examined a few metals in sediment; information which in itself is limiting considering that the river's sediment might be contaminated with many other metals. In addition, there is no information on ecological risk assessment of metal contaminants in the Kafue River. These assessments are essential as they provide policy makers with information on the extent of aquatic ecosystem contamination and are used as early-warning signals of ecological challenges. Therefore, the objective of the study was to determine the degree of contamination of 13 heavy metals in sediment and their associated ecological risk to Kafue River's organisms.

Materials and Methods

A cross sectional study was conducted to determine heavy metal concentrations in sediment along the Kafue River (Fig. 1). The river lies completely within Zambia spanning 1600 Km. From its origin in the North Western Province of Zambia, the river flows through Copperbelt, Central, Southern and Lusaka provinces, before discharging into the Zambezi River. The river drains a catchment of about 157,000 Km^2 accounting for about 20% of the total land area of Zambia (Kambole 2003). Sediment samples (n = 54) were collected from six sites along the river that were selected based on their relative location to the Copperbelt mining area and proximity to fishing camps. The sites were: Chimfunshi (upstream of the Copperbelt mining area, pristine); Chililabombwe, Chingola-Kanyemo and Chingola-Hippo Pool (within Copperbelt mining area); Kafue flats and Kafue town (downstream to Copperbelt mining area). Sediment samples were collected according to the method of Choongo et al. (2005) in 2014 during the warm-rainy (April, n = 18), dry-cold (June, n = 18) and

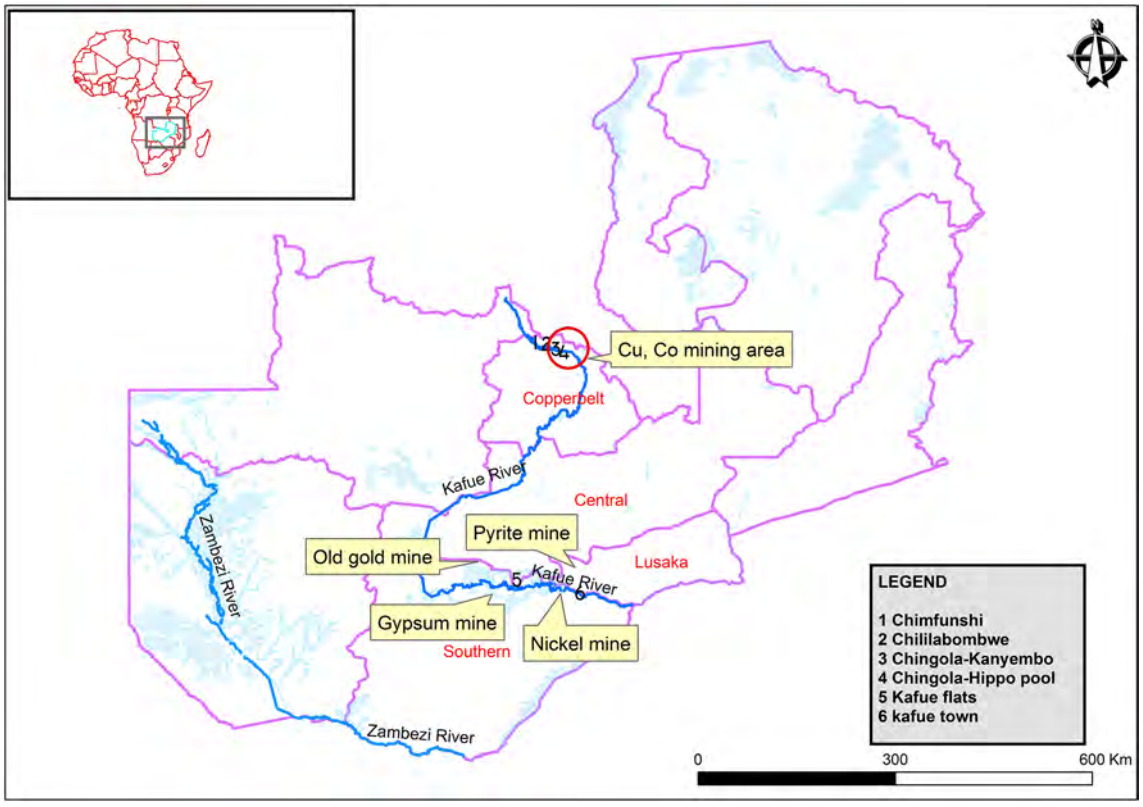

Fig. 1 Map of Zambia showing the location of the mining areas and sampling sites along Kafue River

dry-hot seasons (September, n = 18). Briefly, three surface sediment composite samples were collected in 600 mL polypropylene bottles from each site in each season. Samples were collected from the same location in all seasons. The composite sediment samples were then transported in cooler boxes to the University of Zambia, and stored at 4°C before transportation to the University of Warwick, Department of Chemistry for analysis.

Analytical grade chemicals and ultrapure water (>18 MΩ cm; Millipore Milli-Q) was used for the preparation of all solutions for heavy metal analysis. The sediment samples were oven dried (Status, Thermal Control) at 100°C for two days, ground, homogenized and sieved through a 2 mm mesh. Approximately 0.5 g of each dried sediment sample was acid digested with 7 mL of 72% (v/v) HNO_3 and 1 mL of 30% (v/v) H_2O_2 (Fisher Scientific) using a closed microwave digestion system (Start D, Milestone) for 90 min until the solution was clear and filtered. Solutions from digested sediment samples were analyzed in triplicate for total concentrations of ^{27}Al, ^{53}Cr, ^{55}Mn, ^{56}Fe,^{59}Co, ^{60}Ni, ^{63}Cu, ^{66}Zn, ^{75}As, ^{82}Se, ^{111}Cd, ^{202}Hg and ^{208}Pb using a 7500 series ICP-MS (Agilent Technologies).

A multi-element standard solution IV(4) for inductively coupled plasma (ICP) and a single mercury standard solution for ICP (Fluka Analytical, Buchs) were used to prepare eight multi-element standards to provide suitable calibration curves. Only calibration curves with $R^2 > 0.999$ were accepted for concentration calculations. Erbium (^{166}Er) was used as an internal standard. For quality control, sample triplicates were used to assess precision of the analysis, and reagent blanks and certified reference material (CRM) (CRM015; ISO Guide 34:2009 and ISO/IEC 17,025:2005, fresh water sediment 2) were used to assess method accuracy. Hence, each inductively coupled plasma mass spectrometry (ICP-MS) run included standards and triplicate blanks, triplicate samples and triplicate certified reference material and the results were expressed as the mean. In this study, the measured mean concentrations of each metal in each season at Chimfunshi which is an upstream preindustrial site (Choongo et al. 2005) were used as background concentrations (C_b) (Table 2) to calculate the ecological indicators (contamination factor (CF), pollution load index (PLI), geoaccumulation index (I_{geo}) and potential ecological risk (RI)).

The CF was used to assess the pollution load of the sediments with respect to each heavy metal. CF is a ratio between the content of each metal at a contaminated site (C_c) and the background contents in sediment (C_b) (Loska et al. 2004). It was calculated as follows:

$$CF_{metals} = C_c/C_b \quad (1)$$

The PLI of metals is dependent on the CF and gives an additive indication of the overall level of sediment metal toxicity at a particular site. It was calculated according to Suresh et al. (2011), as:

$$PLI = \left(CF_{metal1} \times CF_{metal2} \times CF_{metal3} \times \ldots CF_n\right)^{1/n} \quad (2)$$

where, CF_{metal} is the contamination factor of each metal, n = number of metals measured.

The I_{geo} value is used to determine the degree of anthropogenic enrichment of heavy metals and hence determines the anthropogenic source of heavy metals and how much they impact the sediment (Loska et al. 2004). It was calculated as follows:

$$I_{geo} = \log_2\left(C_c/1.5C_b\right) \quad (3)$$

where C_c is the measured concentration of each metal at a contaminated site and C_b is the background concentration of each metal (Islam et al. 2014) as determined for the preindustrial site. The factor of 1.5 is introduced to minimize the possible variations in the background values attributed to lithogenic effects (Müller 1969).

The RI value indicates the combined potential ecological risk factors of metals in the monitored sediment and was calculated according to Hakanson (1980) as:

$$RI = \sum Er_{metal}, \text{ where, } Er_{metal} = Tr_{metal}\left(C_c/C_b\right) \quad (4)$$

where Er_{metal} is the potential ecological risk factor for each metal. It considers each heavy metal level in the sediment associating ecological and environmental effects with toxicology, and evaluates metal pollution using comparable and equivalent property index grading method (Qui 2010). Tr_{metal} is the toxic response factor of each selected metal (Hg = 40, Cd = 30, As = 10, Pb = 5, Cu = 5, Cr = 2, Ni = 5, and Zn = 1) (Zhao et al. 2005). The Tr_{metal} reflects the toxicity of each heavy metal and the degree of environment sensitivity of bio-organism to the respective heavy metal. C_c is the content of metal in the samples at the contaminated site, C_b is the background reference sample content for each metal.

Descriptive statistics were calculated using Microsoft Excel® 2013 spreadsheet. Statistical analyses were performed using R statistical software (R Core Team, 2014, Vienna Austria). The data were $\log_{10}$ transformed due to a small sample size and non-normal distribution. One way analysis of variance (ANOVA) was used to test for site and seasonal differences of each metal analyzed in the Kafue River sediment and considered to be significant when $p < 0.05$. Where significant differences were present, the mean values were separated using post-hoc Tukey's HSD pairwise comparison test (Stevens 1999).

Results and Discussion

For quality control and to assess method accuracy, the sediment CRM (CRM15) was analyzed for Al, Cr, Mn, Fe, Co, Ni, Cu, Zn, As, Se, Cd, Hg and Pb. The measured mean ± SD values which were determined by this study (means of replicates), certified values ± SD which are determined values by the manufacturer of the CRM and percent recoveries (measured mean value divided by certified value and expressed as a percentage) of each heavy metal in the sediment certified reference material are reported in Table 1. Results showed that the heavy metal recoveries for the sediment CRM were satisfactory for most heavy metals; although often higher than 100% (with extremely high recoveries for Al and Cr). The detection limits (ppb) for each metal are also shown in Table 1.

Table 2 shows concentrations (mean ± SD) of metals in Kafue River sediment which showed significant site and seasonal differences ($p < 0.05$). Notable observations were that concentrations of Mn, Co, Cu, Zn, As and Pb were found to be higher at sites in the Copperbelt mining area compared to the other sites ($p < 0.05$) (Table 2) probably due to Cu mining and smelting activities in the area that discharge waste into the Kafue River. Contamination with Co and Cu decreased downstream the Kafue River to Kafue flats and Kafue town (Table 2; Fig. 1). This finding is in agreement with previous studies (Choongo et al. 2005; Sracek et al. 2012) that reported concentrations of some metals such as Cu to be higher at sampling sites in Copperbelt mining area than sites downstream and upstream of the Copperbelt mining area. Concentrations of Al, Cr, Fe, Ni, Se, Cd and Hg were observed to be higher at various sites outside the Copperbelt mining area ($p < 0.05$) (Table 2). The differences in metal concentrations among sampling sites suggest diverse sources of metals in the Kafue River sediment rather than one common source. Comparing the results of mean metal concentrations in this study with previous studies (Choongo et al. 2005; Ikenaka et al. 2010; Sracek et al. 2012) showed that the river's sediment was not improving and still under pressure from metal contamination. The present study observed that most metals tended to show higher concentrations in the dry-hot season compared to the other seasons ($p < 0.05$) (Table 2) in agreement with findings by Choongo et al. (2005). Higher levels of most metals in the dry-hot season could be due to the slower movement of water over the sediment and possible higher heavy-metal adsorption ability of the sediment in the dry-hot season (Nwadinigwe et al. 2014). Heavy metal absorption ability is increased in the dry-hot season because of an increase in temperature which enhances efficient sedimentation of metals (Nwadinigwe et al. 2014). High metal discharge into the river and hence availability of metals for adsorption to sediment in the dry-hot season could be another reason why metals were higher in the dry-hot season compared to the other seasons. Apart from temperature, seasonal variations of metal concentrations in sediment are influenced by factors such as salinity (Hatje et al. 2003), organic matter (Peng et al. 2009) and changes in the levels of pollutant discharge over time (Srikanth and Rao 2014).

The CF for most metals in the warm rainy season (Table 3) indicated a moderate degree of contamination, except for Hg and Cd which showed a low degree of contamination at all the sites. CF for Mn, Co and Cu particularly at sites in the Copperbelt mining area showed very high degrees of contamination and this could be attributed to Cu mining and smelting activities in the area. A CF value of 3.18 for As at Chingola-Hippo Pool indicated a considerable degree of contamination which could be due to smelting of As-rich copper concentrates. Similar trends of CFs were observed in the dry-cold and dry-hot seasons

Table 1 Detection limits (ppb, dry-wt.), measured mean ± SD concentrations (ppm dry-wt.) determined by this study, certified values ± uncertainty (ppm dry-wt.) in sediment reference material and percent recoveries of each heavy metal

Heavy metal	Detection limit	Measured mean ± SD	Certified value ± SD	Percent recoveries
^{27}Al	0.773	28,208 ± 296	9200 ± 976	306.61
^{53}Cr	0.02	36.73 ± 1.10	14.3 ± 1.44	256.88
^{55}Mn	0.02	197 ± 9.94	183 ± 4.52	107.46
^{56}Fe	1.346	21,142 ± 91.00	17,100 ± 717	123.64
^{59}Co	0.005	6.41 ± 0.04	6.04 ± 0.142	106.04
^{60}Ni	0.02	19.3 ± 1.01	17.5 ± 0.52	110.42
^{63}Cu	0.1	15.7 ± 0.31	16.1 ± 0.585	97.22
^{66}Zn	0.11	75.3 ± 0.85	69.9 ± 2.82	107.68
^{75}As	0.016	6.29 ± 0.08	6.6 ± 0.433	95.37
^{82}Se	0.597	0.85 ± 0.04	0.8 (non-certified)	106.19
^{111}Cd	0.004	0.35 ± 0.03	0.52 (non-certified)	68.26
^{202}Hg	0.014	0.24 ± 0.04	0.221 ± 0.00619	110.44
^{208}Pb	0.004	14.8 ± 0.08	15 ± 0.539	98.96

Table 2 Concentrations (mean ± SD, ppm, dry-wt.) of the 13 metals in Kafue River sediment at the six study sites in the three seasons

Season	Site		^{27}Al	^{53}Cr	^{55}Mn	^{56}Fe	^{59}Co	^{60}Ni	^{63}Cu	^{66}Zn	^{75}As	^{82}Se	^{111}Cd	^{202}Hg	^{208}Pb
Warm-rainy	Chimfunshi	Mean	29204c	30.3b	128d	10224d	13.9c	16.2c	73.5c	16.8e	1.58b	0.38b	0.03a	0.22a	7.58b
		SD	1334	1.22	3.70	659	0.17	0.30	2.84	0.98	0.11	0.66	0.05	0.19	0.72
	Chililabombwe	Mean	46925b	33.3b	1537a	22433a	394a	21.0b	10671a	58.8a	2.54b	2.82a	0.02a	0.20a	19.8a
		SD	1316	1.68	106	527	19.3	1.38	477	5.57	0.25	0.61	0.03	0.03	0.88
	Chingola-Kanyemo	Mean	24269d	28.8b	489b	18802b	373a	19.6bc	10749a	46.2ab	2.06b	3.21a	0.01a	0.12a	18.3a
		SD	656	2.19	20.2	1624	23.7	1.98	652	4.99	0.83	1.02	0.03	0.02	1.1
	Chingola-Hippo pool	Mean	17311e	21.1e	390c	15304c	205b	16.1c	4962b	43.0bc	6.37a	0.51b	0.01a	0.09a	17.2a
		SD	1472	2.46	23.2	879	9.86	2.00	140	4.72	0.87	0.36	0.02	0.01	0.9
	Kafue flats	Mean	62796a	51.5a	81.8e	21600ab	11.4d	27.4a	29.3e	22.9d	1.64b	0.70b	ND	0.10a	7.54b
		SD	3480	2.60	6.30	1186	0.67	1.54	1.81	1.71	0.15	0.03	ND	0.05	0.83
	Kafue town	Mean	19482e	18.0c	53.4f	9371d	5.08e	8.84d	33.9d	34.4c	2.01b	0.25b	0.01a	0.10a	17.7a
		SD	1991	0.83	1.13	649	0.25	0.18	1.65	4.6	0.58	0.43	0.02	0.03	1.34
Dry-cold	Chimfunshi	Mean	21487c	24.7cd	83.8d	9384d	18.6d	13.8c	78.8d	26.6b	1.62bc	0.27a	0.29a	0.09a	5.47bc
		SD	3143	1.02	2.56	388	0.62	0.56	2.64	2.24	0.12	0.47	0.13	0.03	1.00
	Chililabombwe	Mean	28249b	27.9c	498a	17051ab	248b	18.8b	5660b	57.5a	1.87b	0.77a	0.06b	0.07ab	11.88a
		SD	672	0.79	21.7	2061	5.71	0.60	442	1.79	0.13	0.75	0.07	0.02	1.27
	Chingola-Kanyemo	Mean	18021c	21.4d	460a	16860bc	326a	15.7bc	10131a	39.1ab	1.95b	0.47a	ND	0.07ab	12.9a
		SD	997	1.03	11.2	3988	14.6	0.37	2351	6.79	0.08	0.53	ND	0.01	2.78
	Chingola-Hippo pool	Mean	4852d	6.56e	223b	11,031cd	132c	6.53d	3972c	28.9b	5.17a	ND	ND	0.05ab	9.13ab
		SD	328	0.38	5.51	688	23.1	0.64	253	4.61	1.26	ND	ND	0.01	2.41
	Kafue flats	Mean	60536a	48.9a	108c	25515a	12.3e	23.7a	33.7e	25.9b	1.72bc	ND	ND	0.05ab	7.84abc
		SD	1168	1.71	16.6	3627	0.66	1.02	3.12	2.46	0.01	ND	ND	0.01	1.86
	Kafue town	Mean	27116b	33.4b	64.1e	14649bc	6.45f	17.2b	17.8f	9.75c	1.35c	ND	0.16ab	0.04b	4.42c
		SD	2844	3.05	9.15	3037	0.9	1.84	3.26	3.05	0.03	ND	0.1	0.01	1.91
Dry-hot	Chimfunshi	Mean	30560b	36.0abc	49.2c	11483b	12.4b	22.1b	39.9c	16.0b	0.94c	0.001	0.30a	0.13a	6.17bc
		SD	6986	13.8	17.8	4094	4.12	7.36	13.2	8.35	0.32	0.0003	0.17	0.09	3.65
	Chililabombwe	Mean	16753c	20.6c	603a	16324ab	338a	16.7bc	12037a	44.7a	1.89b	0.76b	0.02b	0.14a	14.6abc
		SD	3202	5.49	143	4015	48	3.1	1810	14.4	0.36	1.32	0.04	0.08	4.88
	Chingola-Kanyemo	Mean	14269c	18.1c	455a	18136ab	357a	10.9c	10416ab	40.5a	1.40bc	2.55ab	0.01b	0.12a	17.6ab
		SD	656	1.46	38	1047	5.99	0.33	202	0.27	0.26	0.37	0.03	0.02	0.11
	Chingola-Hippo pool	Mean	17210c	28.2bc	450a	22675ab	233a	15.9bc	6200b	49.2a	8.23a	6.06a	0.06b	0.13a	22.3a
		SD	2939	6.89	127	6469	35.2	2.52	1177	16.1	1.15	2.25	0.07	0.08	9.04
	Kafue flats	Mean	53101a	47.4ab	141b	25132ab	12.9b	23.2b	40.9c	23.9ab	1.48bc	6.60a	0.01b	0.11a	7.64abc
		SD	2935	11.4	45.3	7687	2.84	4.9	10.4	9.69	0.38	0.2	0.01	0.09	4.12
	Kafue town	Mean	47741b	63.4a	141b	31407a	11.6b	69.8a	23.3c	14.5b	1.37bc	4.49ab	ND	0.09a	4.98c
		SD	9836	19.7	44.5	10,734	3.1	23.7	6.98	7.35	0.28	3.9	ND	0.09	3.28

Each metal level connected by the different letters (a–f) are significantly different ($p < 0.05$)

ND Not detected

Table 3 CF and PLI of metals at study sites in all seasons

Contamination factor (CF)															PLI
Season	Site	Al	Cr	Mn	Fe	Co	Ni	Cu	Zn	As	Se	Cd	Hg	Pb	
Warm-rainy	Chililabombwe	1.61	1.10	12.0	2.19	28.41	1.29	145.22	3.50	1.61	7.37	0.68	0.86	2.61	3.58
	Chingola-Kanyemo	0.83	0.95	3.81	1.84	26.92	1.21	146.00	2.75	1.31	8.41	0.52	0.53	2.41	2.76
	Chingola-Hippo pool	0.59	0.69	3.04	1.50	14.81	0.99	67.63	2.56	4.04	1.34	0.38	0.38	2.27	2.00
	Kafue flats	2.15	1.70	0.64	2.11	0.82	1.69	0.40	1.36	1.04	1.83	ND	0.46	1.00	1.09
	Kafue town	0.67	0.59	0.42	0.92	0.37	0.55	0.46	2.05	1.27	0.65	0.50	0.46	2.34	0.71
Dry-cold	Chililabombwe	1.31	1.13	5.94	1.82	13.33	1.36	71.81	2.16	1.15	2.81	0.22	0.81	2.17	2.32
	Chingola-Kanyemo	0.84	0.87	5.50	1.80	17.51	1.14	129.09	1.47	1.20	1.73	0.01	0.83	2.36	1.68
	Chingola-Hippo pool	0.23	0.27	2.66	1.18	7.13	0.47	50.41	1.09	3.18	ND	0.003	0.60	1.67	0.93
	Kafue flats	2.82	1.98	1.29	2.72	0.66	1.72	0.43	0.97	1.06	ND	ND	0.54	1.43	1.17
	Kafue town	1.26	1.35	0.77	1.56	0.35	1.25	0.23	0.37	0.83	ND	0.54	0.49	0.81	0.72
Dry-hot	Chililabombwe	0.55	0.57	12.30	1.42	27.40	0.76	302.22	2.80	2.00	ND	0.08	1.09	2.37	2.25
	Chingola-Kanyemo	0.47	0.50	9.25	1.58	28.81	0.49	261.35	2.54	1.48	ND	0.05	0.94	2.85	1.96
	Chingola-Hippo pool	0.56	0.78	9.15	1.97	18.93	0.72	156.32	3.08	8.75	ND	0.20	1.04	3.62	2.66
	Kafue flats	1.74	1.32	2.86	2.19	1.05	1.09	1.02	1.50	1.57	ND	0.01	0.83	1.24	0.94
	Kafue town	1.56	1.76	2.87	2.74	0.94	3.16	0.59	0.91	1.45	ND	0.003	0.75	0.81	0.84

ND Not detected. CF (Loska et al. 1997) due to a given metal element: Low degree (CF < 1), Moderate degree (1 ≤ CF < 3), Considerable degree (3 ≤ CF < 6), Very high degree (CF ≥ 6). *PLI* Pollution of a particular site (PLI > 1)

(Table 3), although the actual CF values of most metals (Cu, Mn, Co and As) were higher in the dry-hot season, in agreement with the observed increased concentrations of these metals in this season. The CFs for Ni, Cr and Fe were higher at Kafue town especially in the dry-hot season in agreement with observed increased concentrations of these metals at Kafue town compared to other sites. The high Ni values may be attributed to discharge from a Ni mine near the area. The CF for Cr was higher at Kafue town, probably due to the presence of a tannery that uses chromium sulphate in tanning animal skins.

The PLI > 1 indicates pollution of a particular site (Loska et al. 1997). Results (Table 3) revealed high PLI values at sites in the Copperbelt mining area, with Cu, Co and Mn contributing much to the pollution load. This is consistent with the suggestion that the pollution in these areas is mainly due to mining and smelting activities. Although Kafue flats lies further downstream to the Copperbelt mining sites, results suggest that the site is also polluted. Kafue town showed PLI values of less than one, however, concerns about pollution are likely as PLI values were fairly close to one (Table 3).

The trends of I_{geo} values in the warm-rainy season (Fig. 2) were similar to those in the dry-cold and dry-hot seasons with small variations in values. The I_{geo} is used to estimate anthropogenic enrichment of metal ions in the environment (Müller 1969) and I_{geo} values were interpreted as: $I_{geo} \leq 0$ = practically no anthropogenic enrichment; $0 \leq I_{geo} \leq 1$ = no to moderate anthropogenic enrichment; $1 \leq I_{geo} \leq 2$ = moderate anthropogenic enrichment;

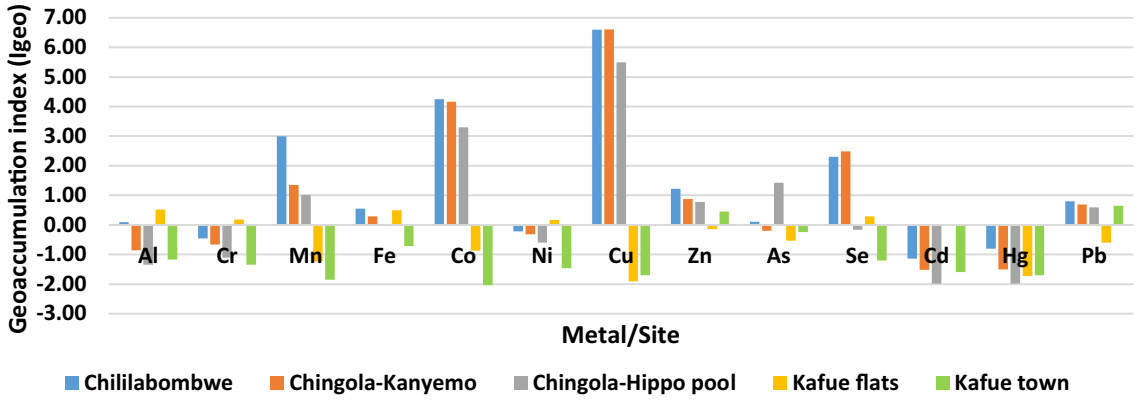

Fig. 2 I_{geo} values of metals at the study sites in the warm-rainy season

$2 \leq I_{geo} \leq 3$ = moderate to heavy anthropogenic enrichment; $3 \leq I_{geo} \leq 4$ = heavy anthropogenic enrichment; $4 \leq I_{geo} \leq 5$ = heavy to extreme anthropogenic enrichment; and $I_{geo} > 5$ = extreme anthropogenic enrichment (Bhuiyan et al. 2010). Results showed variations in anthropogenic enrichment of metal ions at the study sites. In the warm-rainy season (Fig. 2), there was no anthropogenic enrichment to moderate anthropogenic enrichment with Al, Fe, Zn, As, Se and Pb at various sampling sites. Moderate anthropogenic enrichment with Mn, Zn and As was observed at some sites in the Copperbelt mining area. Chililabombwe and Chingola-Kanyemo showed moderate to heavy anthropogenic enrichment with Mn and Se. Heavy to extreme anthropogenic enrichment with Co and extreme anthropogenic enrichment with Cu was observed at all sites in the Copperbelt mining area.

The RI value is the sum of individual metals' potential ecological risk factors (Er_{metal}). RI values of <150, 150–300, 300–600, and >600 represent low, moderate, considerable, and very high levels of potential ecological risk, respectively (Hakanson 1980). Only metals (Hg, Cd, As, Pb, Cu, Cr, Ni and Zn) with available toxic response factors (Tr_{metal}) (Zhao et al. 2005) were used to calculate RI in this study. Results of RI showed site and seasonal variations (Table 4) with a low (RI < 150) to extremely high level (RI > 600) of potential ecological risk. Metals may cause physiological, biochemical, morphological and haematological changes as well as antioxidant responses in various aquatic organisms (Basha and Rani 2003). Metal accumulation within the Kafue River has been associated with various toxicological manifestations. For instance, Mwase et al. (1998) and Norrgren et al. (2000) demonstrated increased fish mortality and decreased aquatic productivity following exposure of caged fish, eggs and fry to water and sediment from Kafue River in the Copperbelt mining area. Choongo et al. (2005) reported high Cu levels in fish at Copperbelt mining area sites along the Kafue River. The fish at these sites also recorded a low coefficient of condition probably as a result of Cu toxicity. Most of the sites in the Copperbelt mining area in the various seasons showed a considerable level of ecological risk (RI = 300–600) to an extremely high level (RI > 600) of potential ecological risk for the river's organisms. Kafue flats and Kafue town in all seasons had RI values which revealed a low potential ecological risk (RI < 150). Of the selected metals used to calculate RI, Cu and As would possibly cause adverse biological effects, especially in the mining areas, because their individual Er_{metal} (Table 4) were moderate (40–80) to significantly high (>320). Mn and Co were also elevated at sites in the mining area and could possibly cause adverse biological effects, however, the Tr_{metal} were not available to calculate their Er_{metal}.

This study has for the first time elaborated the contribution of 13 heavy metals investigated in Kafue River sediment to the ecological risk at various sites. Sediment from the Copperbelt mining area of the Kafue River revealed a high degree of anthropogenic Cu, Co, Mn and As contamination. The highest level of contamination was observed in the dry-hot season. However, the degree of both natural and anthropogenic causes of metal contamination was

Table 4 Er_{metal} and RI of metals at study sites in all seasons

Potential ecological risk factors (Er_{metal})										RI
Season	Site	Cr	Ni	Cu	Zn	As	Cd	Hg	Pb	
Warm-rainy	Chililabombwe	2.19	6.47	726.00	3.50	16.10	20.50	34.40	13.10	822.26
	Chingola-Kanyemo	1.90	6.04	732.00	2.75	13.10	15.80	21.10	12.10	804.79
	Chingola-Hippo Pool	1.39	4.97	338.00	2.56	40.40	11.40	15.20	11.40	425.32
	Kafue flats	3.39	8.46	1.99	1.36	10.40	0.00	18.30	4.98	48.88
	Kafue town	1.18	2.73	2.30	2.05	12.70	14.90	18.40	11.70	65.96
Dry-cold	Chililabombwe	2.26	6.81	359.00	2.16	11.50	6.45	32.40	10.90	431.48
	Chingola-Kanyemo	1.73	5.72	643.00	1.47	12.00	0.23	33.00	11.80	708.95
	Chingola-Hippo Pool	0.53	2.37	252.00	1.09	31.80	0.10	23.80	8.34	320.03
	Kafue flats	3.96	8.61	2.14	0.97	10.60	0.00	21.70	7.17	55.15
	Kafue town	2.70	6.23	1.13	0.37	8.28	16.30	19.60	4.04	58.65
Dry-hot	Chililabombwe	1.15	3.78	1510.00	2.80	20.00	2.35	43.40	11.80	1595.28
	Chingola-Kanyemo	1.01	2.47	1307.00	2.54	14.90	1.48	37.50	14.30	1381.20
	Chingola-Hippo Pool	1.56	3.60	778.00	3.08	87.50	5.95	41.70	18.10	939.49
	Kafue flats	2.64	5.44	5.12	1.50	15.70	0.34	33.30	6.19	70.23
	Kafue town	3.52	15.80	2.93	0.91	14.50	0.10	29.90	4.04	71.70

Er_{metal} (Hakanson 1980): Low (<40), Moderate (40–80), Considerable (80–160), High (160–320), Significantly high (>320)

RI: Low (RI < 150), Moderate (RI 150–300), Considerable (RI 300–600, Very high (RI > 600)

low at sites away from the Copperbelt mining area. The RI showed that Cu, As and possibly Co and Mn at sites in the Copperbelt mining area of the Kafue River were likely to cause harmful biological effects to aquatic organisms. Therefore, a management plan for testing and monitoring for toxic effects of a mixture of these metals in the Copperbelt mining area is proposed. It is recommended that Zambia Environmental Management Agency (ZEMA) should monitor levels of these toxic elements in all the seasons at known or suspected point sources in order to identify erring industries that should be made to control their discharges into the river in line with international limits since Zambia does not have its own regulatory limits. Therefore, regulatory limits should be established and existing environmental regulations should be implemented.

Acknowledgements Authors are grateful to the laboratory technical staff at the University of Warwick (especially Mr. Philip Ashton) and the University of Zambia (Mr. Joseph Ndebe, Mr. Ladsluv Moonga and Mr. John Chilundu). Furthermore, we are grateful to the Commonwealth Scholarship Commission (ZMCN-2013-352), University of Warwick, International Foundation for Science (IFS) number A/5212-1 and University of Zambia for sponsoring this work.

Compliance with Ethical Standards

Conflict of interest The authors declare that they have no conflict of interest.

References

Alaoui AM, Choura M, Maanan M, Zourarah B, Robin M, Conceição MF, Andrade C, Khalid M, Carruesco C (2010) Metal fluxes to the sediments of the Moulay Bousselham lagoon, Morocco. Environ. Earth Sci 61:275–286

Bäckström M (1996) A Sediment Study in the Kafue River, Zambia, Master's Thesis, Luleå University of Technology, Luleå 96

Basha PS, Rani AU (2003) Cadmium-induced antioxidant defense mechanism in freshwater teleost *Oreochromis mossambicus* (Tilapia). Ecotoxicol Environ Saf 56(2):218–221

Bhuiyan MA, Parvez L, Islam MA, Dampare SB, Suzuki S (2010) Heavy metal pollution of coal mine-affected agricultural soils in the northern part of Bangladesh. J Hazard Mater 173:384–392

Calmano W, Ahlf W, Förstner U (1990) Exchange of heavy metals between sediment components and water. Springer, Berlin, pp. 503–522

Choongo KC, Syakalima MS, Mwase M (2005) Coefficient of condition in relation to copper levels in muscle of *serranochromis* fish and sediment from the Kafue river, Zambia. Bull Environ Contam Toxicol 75:645–651

Fernandes C, Fontaínhas-Fernandes A, Cabral D, Salgado MA (2008) Heavy metals in water, sediment and tissues of *Liza saliens* from Esmoriz–Paramos lagoon, Portugal. Environ Monit Assess 36:267–275

Gupta A, Rai DK, Pandey RS, Sharma B (2009) Analysis of some heavy metals in the riverine water, sediments and fish from river Ganges at Allahabad. Environ Monit Assess 157:449–458

Hakanson L (1980) An ecological risk index for aquatic pollution control. A sedimentological approach. Water Res 14:975–1001

Hatje V, Bidone ED, Maddock JL (1998) Estimation of the natural and anthropogenic components of heavy metal fluxes in fresh water Sinos river, Rio Grande do Sul state, SouthBrazil. Environ Technol 19:483–487

Hatje V, Payne TE, Hill DM, McOrist G, Birch GF, Szymczak R (2003) Kinetics of trace element uptake and release by particles in estuarine waters: effects of pH, salinity, and particle loading. Environ Int 29:619–629

Ikenaka Y, Nakayama SM, Muzandu K, Choongo K, Teraoka H, Mizuno N, Ishizuka M (2010) Heavy metal contamination of soil and sediment in Zambia. Afr J Environ Sci Technol 4:729–739

Islam MS, Han S, Ahmed MK, Masunaga S (2014) Assessment of trace metal contamination in water and sediment of some rivers in Bangladesh. J Water Environ Technol 12:109–121

Kambole MS (2003) Managing the water quality of the Kafue River. Phys Chem Earth, Parts A/B/C 28(20):1105–1109

Karbassi AR, Monavari SM, Bidhendi GR, Nouri J, Nematpour K (2008) Metal pollution assessment of sediment and water in the Shur River. Environ Monit Assess 147:107–116

Khadse GK, Patni PM, Kelkar PS, Devotta S (2008) Qualitative evaluation of Kanhan River and its tributaries flowing over central Indian plateau. Environ Monit Assess 147:83–92

Loska K, Cebula J, Pelczar J, Wiechuła D, Kwapuliński J (1997) Use of enrichment, and contamination factors together with geoaccumulation indexes to evaluate the content of Cd, Cu, and Ni in the Rybnik water reservoir in Poland. Water Air Soil Pollut 93:347–365

Loska K, Wiechuła D, Korus I (2004) Metal contamination of farming soils affected by industry. Environ Int 30:159–165

M'kandawire E, Syakalima M, Muzandu K, Pandey G, Simuunza M, Nakayama SM, Kawai YK, Ikenaka Y, Ishizuka M (2012) The nucleotide sequence of metallothioneins (MT) in liver of the Kafue lechwe (*Kobus leche kafuensis*) and their potential as biomarkers of heavy metal pollution of the Kafue River. Gene 506:310–316

Mayo M, Collier ZA, Winton C, Chappell M (2015) Data-driven method to estimate nonlinear chemical equivalence. PLoS ONE 10(7):e0130494

Mendelsohn F (ed) (1961) The geology of the Northern Rhodesian Copperbelt. Macdonald and Co. Ltd, London

Müller G (1969) Index of geoaccumulation in sediments of the Rhine River. Geo J 2:108–118.

Mwase M, Viktor T, Norrgren L (1998) Effects on tropical fish of soil sediments from Kafue River, Zambia. Bull Environ Contam Toxicol 61(1):96–101

Norrgren L, Pettersson URNS, Örn S, Bergqvist PA (2000) Environmental monitoring of the Kafue River, located in the Copperbelt, Zambia. Arch Environ Contam Toxicol 38(3):334–341

Nwadinigwe CA, Udo GJ, Nwadinigwe AO (2014) Seasonal variations of heavy metals concentrations in sediment samples around major tributaries in Ibeno coastal area, Niger delta, Nigeria. IJST 3(11):254–265

Peng JF, Song YH, Yuan P, Cui XY, Qiu GL (2009) The remediation of heavy metals contaminated sediment. J Hazard Mater 161:633–640

Qui H (2010) Studies on the potential ecological risk and homology correlation of heavy metal in the surface soil. JAS 2:194–201

Solomon F (2009) Impacts of copper on aquatic ecosystems and human health. Environ Commun 25–28

Sracek O, Kříbek B, Mihaljevič M, Majer V, Veselovský F, Vencelides Z, Nyambe I (2012) Mining-related contamination of surface water and sediments of the Kafue River drainage system in the Copperbelt district, Zambia: an example of a high neutralization capacity system. J Geochem Explor 112:174–188

Srikanth K, Rao JV (2014) Spatial and seasonal variation of potential toxic elements in *Adocia pigmentifera*, seawater and sediment

from Rameswaram, southeast coast of India. Environ Earth Sci 72(8):2905–2916

Stevens J (1999) Post hoc Tests in ANOVA. Course notes. University of Oregan, Eugene

Suresh G, Ramasamy V, Meenakshisundaram V, Venkatachalapathy R, Ponnusamy V (2011) Influence of mineralogical and heavy metal composition on natural radionuclide concentrations in the river sediments. Appl Radiat Isot 69:1466–1474

Yabe J, Ishizuka M, Umemura T (2010) Current levels of heavy metal pollution in Africa. J Vet Med Sci 72:1257–1263

Zhao QN, Xu QX, Yang K (2005) Application of potential ecological risk index in soil pollution of typical polluting industries. J East China Norm Univ Nat Sci 1:110–115

Ecological Engineering 109 (2017) 57–64

Contents lists available at ScienceDirect

Ecological Engineering

journal homepage: www.elsevier.com/locate/ecoleng

Bioremediation of lead-contaminated mine waste by *Pararhodobacter* sp. based on the microbially induced calcium carbonate precipitation technique and its effects on strength of coarse and fine grained sand

Wilson Mwandira[a], Kazunori Nakashima[b,*], Satoru Kawasaki[b]

[a] Graduate School of Engineering, Hokkaido University, Kita 13, Nishi 8, Kita-ku, Sapporo 060-8628, Japan
[b] Faculty of Engineering, Hokkaido University, Sapporo 060-8628, Japan

ARTICLE INFO

Keywords:
Biomineral
Bioremediation
Microbially induced calcium carbonate precipitation
Lead

ABSTRACT

Lead (Pb^{2+}) is a toxic heavy metal that has a severe negative effect on human health and the environment. Physical, chemical and biological remediation techniques have long been used to remediate lead contamination. However, because of the great danger posed by lead contamination, there is increasing interest to apply eco-friendly and sustainable methods to remediate lead. Therefore, this study was conducted to use the microbially induced calcium carbonate precipitation (MICP) technique in conjunction with the bacterium *Pararhodobacter* sp. to bioremediate lead. Laboratory scale experiments were conducted and complete removal of 1036 mg/L of Pb^{2+} was achieved. These results were further confirmed by scanning electron microscope (SEM) and X-ray diffraction (XRD) analysis, which indicated coprecipitation of calcium carbonate ($CaCO_3$) and lead. The unconfined compressive strength increased with an increase in injection interval with maximum unconfined compressive strength of 1.33 MPa for fine sand, 2.87 MPa for coarse sand and 2.80 MPa for mixed sand. For *Pararhodobacter* sp. to efficiently induce lead immobilisation the bacterial interval required is four times with a calcium and urea concentration of 0.5 M and bacterial concentration of 10^9 cfu/mL. Very few low-cost in situ heavy metal treatment processes for lead bioremediation are available; therefore, bioimmobilization of lead by MICP has the potential for application as a low-cost and eco-friendly method for heavy metal remediation.

1. Introduction

Lead (Pb^{2+}) has been studied extensively worldwide because of its effects on human health and the environment (Yabe et al., 2015; Lin et al., 2009). The main characteristics of lead are that it persists in all parts of the environment, cannot be degraded or destroyed and enters the body through food, drinking water, and air. Lead poisoning results in brain and central nervous system damage, coma, convulsion and even death, mostly in children because they absorb 4–5 times as much lead as adults (Lanphear, 2005). One such area that is heavily contaminated with lead due to mining and smelting is Kabwe Mine, Zambia (Nyambe et al., 2013), which was selected as the study area for this investigation.

The Kabwe mine was a Pb-Zn mine that operated from 1902 to 1994, during which time it caused lead poisoning affecting close to 300,000 people. Despite closure of the mine, its wastes have continued to pollute the soil and water. Plant residue leachate of waste from tailings and thickeners and kiln slag are the major sources of lead, covering an area of approximately 86,600 m^2 and 164,800 m^2, respectively (ZCCM-IH, Zambia Copper and Cobalt Mining-Investment Holding Plc., 2002). In the past, a portion of the coarse kiln slag was used to cover the fine leached plant residue to prevent water erosion and windblown dust.

Several physical, chemical and biological remediation techniques have been used for many years to remediate lead contamination. However, the major challenge of physical-chemical lead remediation technologies involves a huge cost for complete removal or containment of contaminants to prevent them from migrating to surrounding areas. In this study, we seek to investigate the possibility of bioremediation of lead-contaminated mine waste in Kabwe based on microbially induced calcium carbonate precipitation (MICP). This technique involves the hydrolysis of urea into ammonium and carbamate by urease catalysis (Eq. (1)), resulting in $CaCO_3$ formation in the presence of Ca^{2+} ions (Eqs. (2)–(3)) (Whiffin et al., 2007).

$$CO(NH_2)_2 + H_2O \xrightarrow{\text{Urease}} H_2NCOO^- + NH_4^+ \quad (1)$$

$$H_2NCOO^- + H_2O \rightarrow HCO_3^- + NH_3 \quad (2)$$

* Corresponding author.
E-mail address: nakashima@geo-er.eng.hokudai.ac.jp (K. Nakashima).

http://dx.doi.org/10.1016/j.ecoleng.2017.09.011
Received 20 July 2017; Received in revised form 8 September 2017; Accepted 16 September 2017

$$Ca^{2+} + HCO_3^- + NH_3 \rightarrow CaCO_3 + NH_4^+ \quad (3)$$

The role of calcium ion in bioremediation using the MICP technique takes advantage of the incorporation of the Pb^{2+} onto their surfaces through substitution in the calcite lattice (Eq. (4)), after which Pb^{2+} are changed from soluble form to insoluble forms hence detoxifying the toxic lead ions (Anbu et al., 2016). The calcium carbonate formed can either be immobilize or form undissolved substances, with the free ions being attached onto the surfaces of calcium carbonate to yield a chemically stable and non-toxic form (Volodymyr and Viktor, 2017).

$$Pb^{2+} + CO_3^{2-} \rightarrow PbCO_3 \quad (4)$$

Bioremediation using this technique is promising for heavy metals (Cd^{2+}, Ni^{2+}, Pb^{2+} etc.) contaminated soils, sediment and water and has been successfully applied in recent studies (Kang et al., 2014; Zhu et al., 2016; Achal et al., 2012). In this study, we determine for the very first time the use of *Pararhodobacter* sp. for laboratory scale bioremediation of lead. *Pararhodobacter* sp. was selected for investigation because it has shown high urease activity and can maintain the enzyme activity for a long time (Fujita et al., 2017). This characteristic is useful in bioremediation as the bacteria is resilient when injected in the ground and its enzyme activity sustained for a longer period to accomplish biocementation and immobilization of the toxic ions. Previous researchers conducted solidification using *Pararhodobacter* sp. for ground improvement methods for marine (Danjo and Kawasaki, 2016) and land usage purposes (unpublished). However, in this study, *Pararhodobacter* sp. was investigated for both mine waste immobilization and to determine if it exhibits any Pb^{2+} resistance and its applicability for bioremediation. Further investigation on the bacteria would be necessary before possible application of this bacteria in-field.

An improved understanding of this process and mechanism will provide a scientific basis for the development of sound strategies for the provision and sustainable use of ureolytic bacteria for bioremediation of lead contaminated sites such as the Kabwe area in Zambia. The rationale for choosing this technique for mine waste bioremediation is to prevent wind-blown dust from uncovered waste dump sites, as well as to prevent erosion that leads to the transportation of sediments downstream. To achieve this, we determined the solidification and bioremediation conditions necessary for remediation using in vitro experiments by bioaugmentation, then will scale these up for field application via biostimulation (Fig. 1). Studies by Gomez et al., 2017 and Gat et al., 2016 reported that biostimulation offers important economic and environmental benefits through the elimination of expensive nonnative monoclonal bacterial cultivation as well as avoid changes to indigenous microbial population which may be affected to an unknown extent. Thus, the specific objectives of the present study (steps 1 and 2) were to: investigate the effects of lead on urease activity and microbial growth; determine the effectiveness of lead removal by *Pararhodobacter* sp.; determine the effects of varying the injection interval of the bacteria on unconfined compressive strength (UCS) for fine and coarse-grained sand; and evaluate the usefulness of *Pararhodobacter* sp. for lead bioremediation. The results from this study will be used in future studies as outlined in Fig. 1.

2. Materials and methods

2.1. Bacteria, media, and Pb^{2+} stock solution preparation

Pararhodobacter sp., a ureolytic bacterium isolated from the soil near beachrock in Okinawa, Japan, was used in this study (Danjo and Kawasaki, 2013). Cells were cultured in ZoBell2216 medium, which contained 5.0 g/L hipolypeptone (Nihon Seiyaku Co., Ltd., Tokyo, Japan), 1.0 g/L yeast extract (BD Biosciences Advanced Bioprocessing, Miami, FL, USA), and 0.1 g/L $FePO_4$ (Junsei Chemical Co., Ltd., Tokyo, Japan) prepared with artificial seawater with the final solution pH adjusted to 7.6–7.8 using 1 M NaOH (Fujita et al., 2017). Stock solution of lead was prepared using $PbCl_2$ (Wako Pure Chemical Industries Ltd., Tokyo, Japan), which was dissolved in distilled water, sterilized with a 0.22 μm filter and preserved at 4 °C. Different working concentrations of lead were then obtained by serial dilution.

2.2. Effect of lead on microbial growth and urease activity

The tolerance of *Pararhodobacter* sp. to lead was evaluated to elucidate its usefulness in bioremediation. Different concentrations of Pb^{2+} (0 mM, 0.01 mM, and 0.5 mM) were prepared in 100 mL Erlenmeyer flasks containing *Pararhodobacter* sp. and ZoBell2216 culture medium and the time course of cell growth was determined based on the optical density (OD) values at 600 nm by UV–vis spectrophotometry (V-730, Jasco International Co., Ltd., Tokyo, Japan) for 14 days in the presence of Pb^{2+}.

The urease activity of bacterial cells was determined by monitoring ammonium ions generated in urea hydrolysis using the indophenol blue method based on Berthelot's reaction in a water bath maintained at 30 °C (Weatherburn, 1967; Natarajan, 1995). After bacterial cultivation for 48 h, a bacterial suspension (1 mL) (OD_{600} = 1.0) was added to 0.1 M phosphate buffer (100 mL) containing 0.1 M urea. To determine the effects of lead on urease activity, different concentrations of lead (0–0.5 mM) were added. Samples were then collected at intervals of 5 min (0, 5, 10 and 15 min) and passed through a 0.22 μm filter to remove cells. Next, a 2 mL aliquot of the filtered sample was mixed with phenol nitroprusside reagent (4 mL) (0.25 M phenol in 100 mL of deionized water containing 23 μM of sodium nitroprusside) and hypochlorite reagent (4 mL) (0.05 M sodium hydroxide in 100 mL of deionized water containing 7.5 mL bleach (5% NaOCl)). Each reaction mixture was vortexed and then incubated at 50 °C–60 °C for 10 min. The amount of ammonium ion released because of urea hydrolysis was determined by referring to a previously prepared standard curve relating the absorbance at 630 nm to ammonium ion concentration

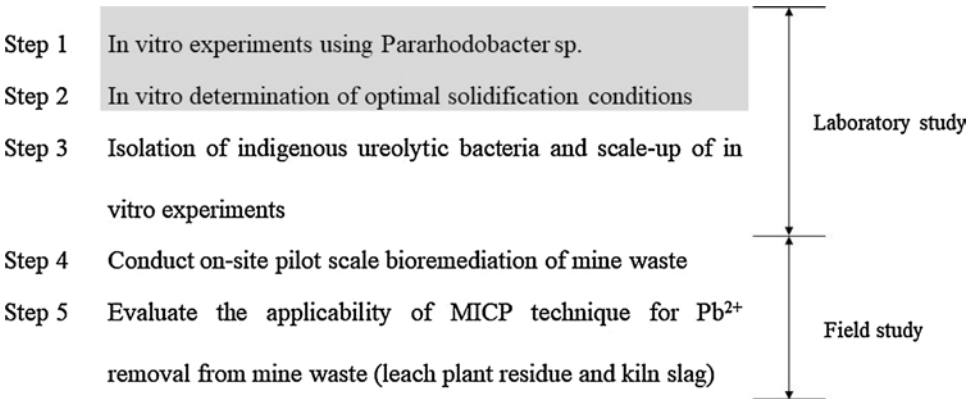

Fig. 1. Flowchart of the study. The steps described in this study are highlighted in grey.

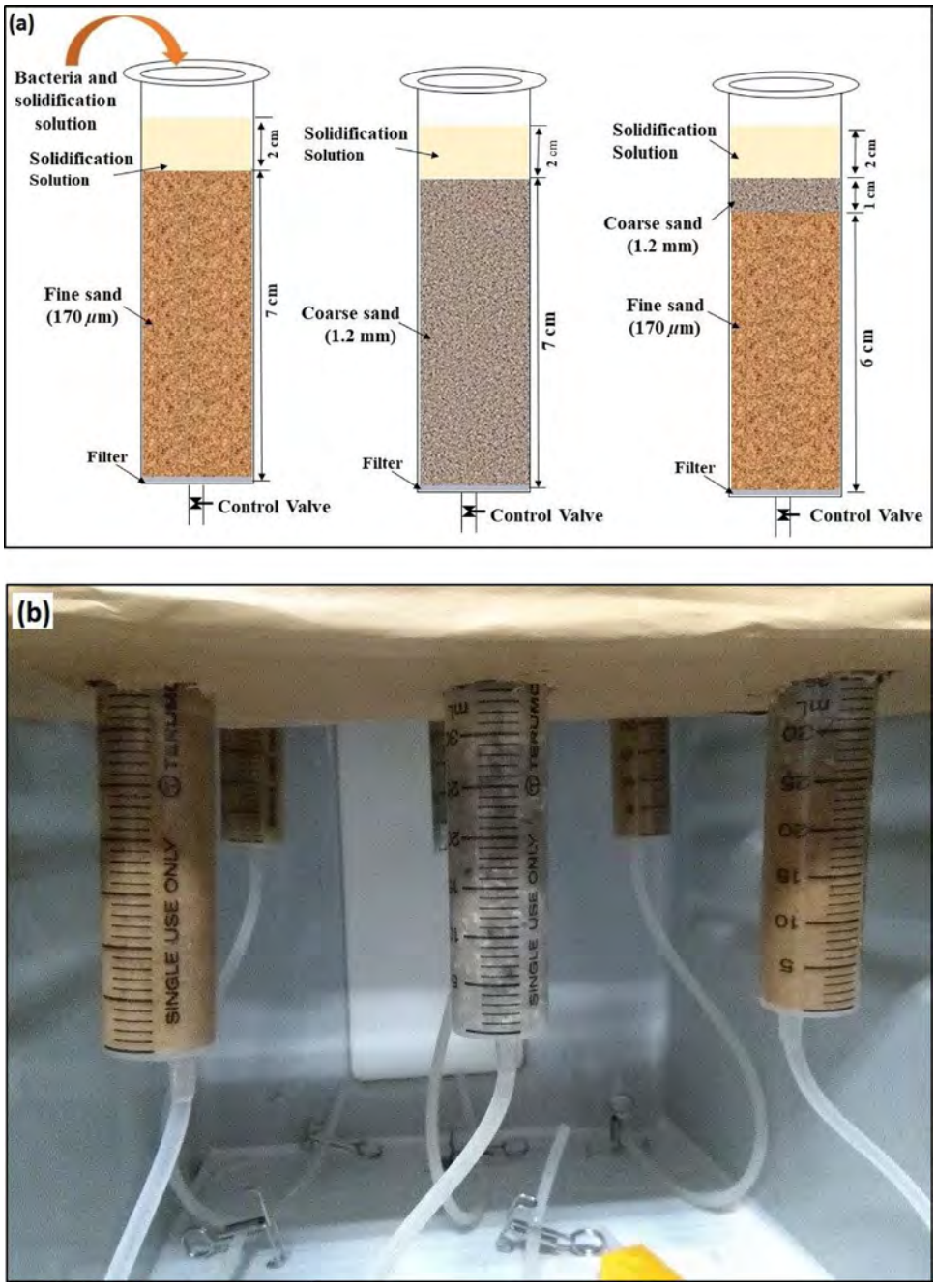

Fig. 2. (a) Conceptual setup and (b) images of the syringe solidification of coarse- and fine-grained sand.

(0–10 mg/L). Using this curve, one unit of urease activity (U) was defined as the amount of enzyme that would hydrolyze 1 μmol of urea per minute. The release of 2 μmol of ammonia is equivalent to the hydrolysis of 1 μmol of urea.

2.3. Bioprecipitation of calcium carbonate and lead

To elucidate the coprecipitation mechanism of lead and calcium, Pb^{2+} bioprecipitation experiments were carried out. Specifically, *Pararhodobacter* sp. was precultured for 24 h in 5 mL ZoBell2216 medium, after which 1 mL of preculture was inoculated into 100 mL of the main culture at 30 °C for 48 h with continuous aeration at 160 rpm. The bacterial suspension (5 mL) was then added to 2 mL calcium chloride (0.5 M) and 2 mL urea (0.5 M), after which different lead final concentrations were added (0 mM, 0.01 mM and 5 mM). The mixture was subsequently incubated for 6 h at 30 °C with shaking (160 rpm) and then further centrifuged (15,000 rpm for 5 min) to collect the precipitate. The concentration of lead in the supernatant was determined by inductively coupled plasma atomic emission spectroscopy (ICP-AES; ICPE-9000, Shimadzu Corporation, Tokyo, Japan), whereas the precipitate was analyzed by XRD/SEM as described in section 2.5. Precipitation experiments were conducted in triplicate.

2.4. Syringe solidification of coarse- and fine-grained sand

The most practical way of remediating a contaminated site is via in situ treatment of a contaminated material facilitated by the injection of microorganisms and nutrients. To understand the optimal injection interval of bacteria, four different injection intervals were tested in syringe solidification experiments. All syringe solidification experiments were conducted in an incubator at 30 °C. A method described by Danjo and Kawasaki was adopted for the syringe solidification

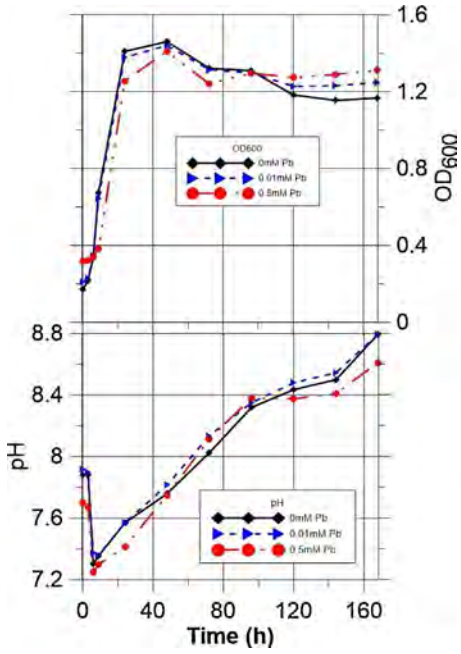

Fig. 3. Effect of lead on *Pararhodobacter* sp. growth curve. Values are averages from two independent experiments.

experiments (Danjo and Kawasaki, 2016). Briefly, 40 g of fine sand (mean diameter, D_{50} = 170 μm) and/or coarse sand (mean diameter, D_{50} = 1.2 mm) was oven dried at 105 °C for 48 h and then placed in a 35 mL syringe (mean diameter, D_{50} = 2.5 cm and height, h = 7 cm) (Fig. 2). The laboratory experiment was designed to mimic the field conditions in Kabwe mine as closely as possible based on grain size, with the very fine and coarse sand representing the plant residue and kiln slag, respectively. The mixed system was selected to mimic slag used to cover leached plant residue to prevent water and wind erosion on site. Bacterial culture (16 mL) (OD_{600} = 1.0 = 10^9 cfu/mL) and 20 mL of solidification solution (0.5 M urea; 0.5 M calcium chloride; 0.02 M sodium hydrogen carbonate; and 0.2 M ammonium chloride and nutrient broth 3 g/L) were sequentially added to the syringe and drained, leaving about 2 mL of solution above the surface of the sand to maintain wet conditions as conceptualized in Fig. 2a. The outlet solution from the syringe was measured for pH and Ca^{2+}. After 14 days of curing, the UCS was estimated using a needle penetration device (SH-70, Maruto Testing Machine Company, Tokyo, Japan).

2.5. XRD and SEM analyses

X-ray diffraction (XRD; MiniFlex™, Rigaku Co., Ltd., Tokyo, Japan) and a scanning electron microscope (SEM; Miniscope TM3000, Hitachi, Tokyo, Japan) were used to qualitatively analyze the MICP precipitate. The sample for XRD was dried at 105 °C and ground into powder using a Multi-beads shocker (Yasui Kikai, Tokyo, Japan). X-ray diffraction was conducted under Ni-filtered Cu1.5406A radiation. Scans were recorded from 5 to 80° 2θ, at a rate of 20°/min. The crystalline phases were identified using the International Centre for Diffraction Data (ICDD) database and MATCH 3.4 (Klaus and Putz, 2017). SEM images were taken under the microscope after mounting on a carbon tape.

3. Results and discussion

3.1. Effect of lead on microbial growth

Pararhodobacter sp. clearly exhibited increased growth following the lag, logarithmic, stationary and retardation phases in lead free media (Fig. 3). In the presence of lead, the logarithmic phase was slightly retarded and an overall decrease in growth was observed. The effects of lead on microbial growth were negligible, whereas no growth was observed for concentrations greater than 1 mM (data not shown). These results indicate that *Pararhodobacter* sp. can be used for bioremediation of lead, even though it was not isolated from a lead contaminated site (Kang et al., 2015). The measured pH of the solution decreased during the logarithmic phase, then increased consistently. It is unclear why a high pH was maintained during incubation; however, this could have occurred because of the release of metabolites in the solution, such as ammonia, by the live cells. The ammonia generation could have originated from amino acids contained in the yeast extract. In many studies, increased pH was only recorded when urea was added to the growth media. These findings are in tandem with those of previous studies, although the effects of lead ions differ for different microorganisms because of different inhibitory concentrations among organisms (Govarthanan et al., 2013; Naik and Dubey, 2013).

3.2. Effect of lead on urease activity

Urease activity of bacterial cells was studied because it serves as a

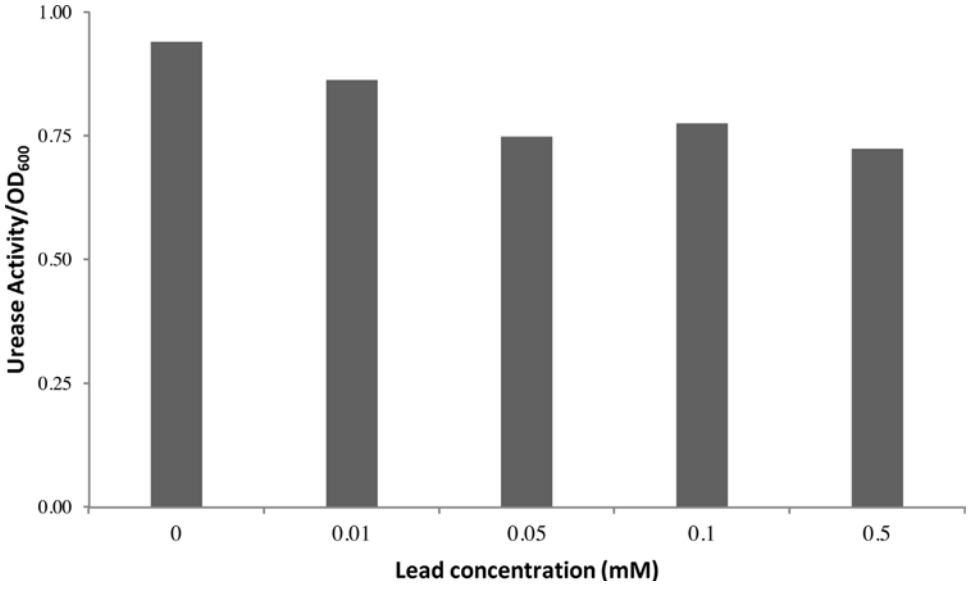

Fig. 4. Effect of lead on urease activity based on the OD_{600} of *Pararhodobacter* sp. Values are averages from two independent experiments.

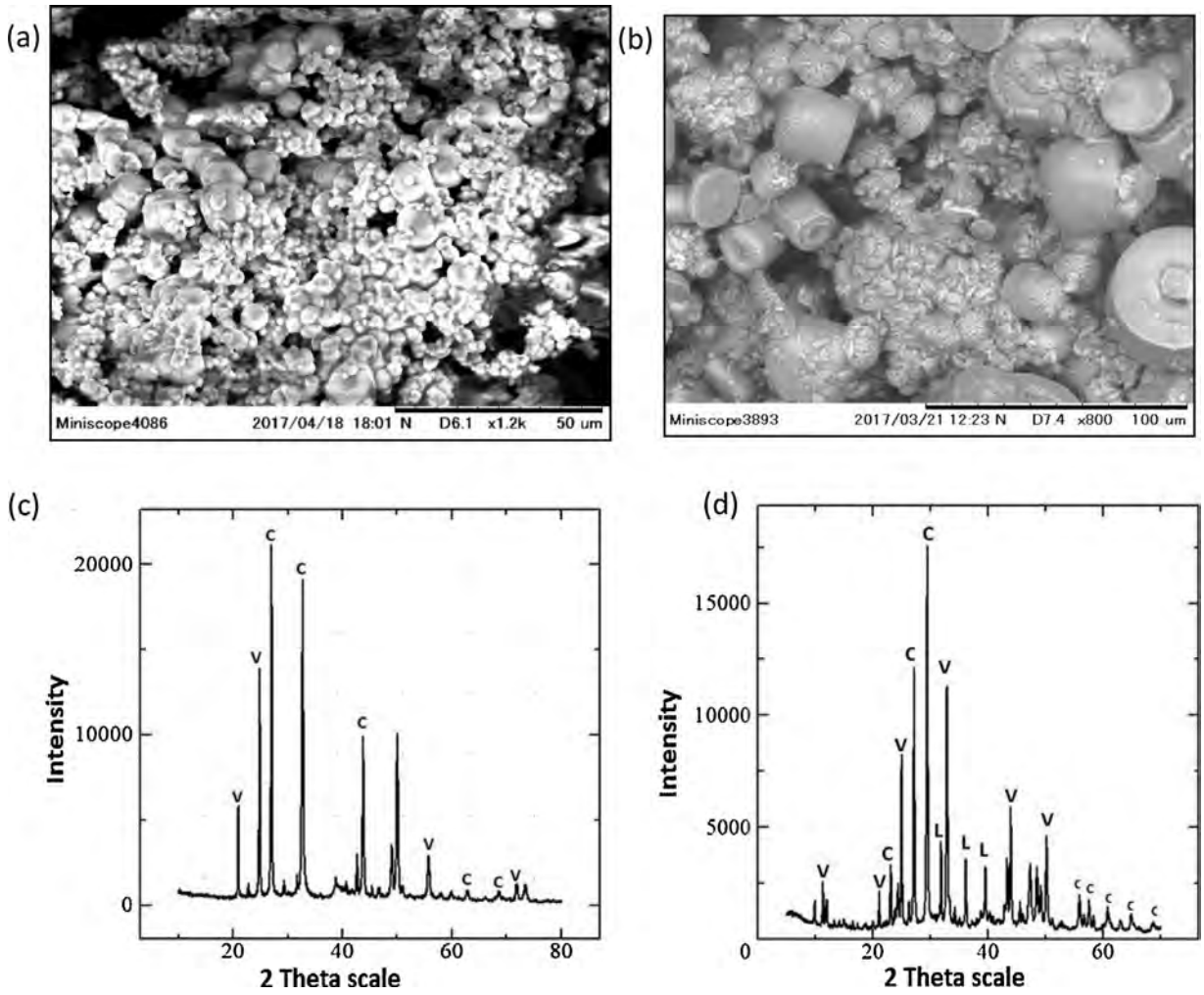

Fig. 5. SEM images (a, b) and XRD data (c, d) of precipitates formed by *Pararhodobacter* sp. in the absence (a, c) and presence of 5 mM Pb^{2+} (b, d). (C = Calcite ($CaCO_3$); V = Vaterite ($CaCO_3$); L = Lead Oxide (PbO)).

good bioindicator of enzyme activity in the MICP bioremediation technique and is used to assess environmental health changes occurring in the environment. As shown in Fig. 4, the urease activity was not significantly affected by lead. This pattern, which was probably because of the effects of lead on enzyme activity, reinforces the findings reported by Fujita et al. (2017), who found that urease accumulated in/on cells of *Pararhodobacter* sp. However, several authors have reported a significant decrease in enzyme activity and microbial activity because of heavy metals pollution of aquatic and soil ecosystems (Sadler and Trudinger, 1967; Nwuche and Ugoji, 2008; Begum et al., 2009). The present study revealed a negligible decreased in urease and microbial activity. These results were probably because of other factors such as synergy of heavy metals as reported by Nwuche and Ugoji (2008), who observed inhibition of soil microbial activities in response to a combination of Cu and Zn.

3.3. Lead bioprecipitation

Pararhodobacter sp. was effective at complete removal of Pb^{2+}. Comparison of the removal percentage of lead during bioprecipitation between this study and previous studies shows comparable figures to other ureolytic bacteria isolated from various sites such as *Rhodobacter spharoides* isolated from an oil field achieved 90.31% (Li et al., 2016); *Enterobacter cloacae* isolated from an abandoned mine achieved 68.1% (Kang et al., 2015); *Sporosarcina pasteurii* achieved 100% (Mugwar and Harbottle, 2016); and *Terrabacter tumescens* achieved 100% (Li et al., 2015). The capability of *Pararhodobacter* to completely remove lead lies in its ability to efficiently hydrolyze urea to generate carbonate ions and elevate the pH to alkaline conditions (8.0–9.1), which promotes precipitation of lead and calcium carbonate.

Fig. 5 shows SEM images and XRD patterns of the control (a, c) and bioremediated (b, d) precipitates. Fig. 6a shows the spherical particles of calcium carbonate precipitated in the absence of lead and confirmed by XRD analysis in Fig. 6c. This finding has been observed from previous studies that reported different polymorphs of calcium carbonate in the form of vaterite and calcite being formed when biomineralization occurs via mediation by bacteria (Park et al., 2010; González-Muñoz et al., 2010). Vaterite does not occur in abundance in the natural environment but is an important precursor in calcite formation of a more stable form of calcium carbonate (Nehrke and Van Cappellen, 2006). Furthermore, Fig. 6b shows the SEM image of precipitate in the presence of lead. In the figure, framboidal aggregates were identified as vaterite, whereas spherical and rhombohedral shaped precipitates were identified as calcite. In the MICP process, calcium carbonate can adsorb or incorporate free toxic ions Pb^{2+} through substitution of the divalent calcium ion in the $CaCO_3$ lattice (Fig. 6d). Detoxification of the lead to insoluble form occurs when the toxic free ion is transformed into a chemically stable and non-toxic form of lead as elucidated in another study by Li et al. (2013).

Fig. 6. Pictorial images of the results of all syringe tests after 14 days while varying the bacterial injection interval to (a) one (b) two (c) four and (d) seven times. Left, fine sand; center, coarse sand; right, mixture of course and fine sand.

Table 1
Solidification conditions of the injection intervals.

	Sand particle size	Bacterial injection times	Solidification solution injection	Bacterial OD_{600}	Temp. (°C)	Timing (Day)	Condition of solidification		
							Top	Middle	Bottom
Case 1	170 μm	Once	Daily	1.0	30	14	Moderately solidified	Not solidified	Not solidified
Case 2	1.2 mm	Once	Daily	1.00	30	14	Solidified	Not solidified	Not solidified
Case 3	170 μm/1.2 mm	Once	Daily	1.00	30	14	Solidified	Not solidified	Not solidified
Case 1	170 μm	Twice	Daily	1.00	30	14	Moderately solidified	Not solidified	Not solidified
Case 2	1.2 mm	Twice	Daily	1.00	30	14	Not solidified	Not solidified	Not solidified
Case 3	170 μm/1.2 mm	Twice	Daily	1.00	30	14	Weakly solidified	Not solidified	Not solidified
Case 4	170 μm	Four times	Daily	1.00	30	14	Solidified	Solidified	Solidified
Case 5	1.2 mm	Four times	Daily	1.00	30	14	Solidified	Not solidified	Not solidified
Case 6	170 μm/1.2 mm	Four times	Daily	1.00	30	14	Moderately Solidified	Solidified	Solidified
Case 4	170 μm	Seven times	Daily	1.00	30	14	Solidified	Solidified	Solidified
Case 5	1.2 mm	Seven times	Daily	1.00	30	14	Solidified	Solidified	Solidified
Case 6	170 μm/1.2 mm	Seven times	Daily	1.00	30	14	Solidified	Solidified	Solidified

3.4. Syringe solidification experiment

Pictorial images of sand samples from all syringe solidification experiments after 14 days are shown in Fig. 6. The UCS comparison of the results obtained after varying the injection interval (once, twice, four and seven times) is summarized in Table 1 and graphically shown in Fig. 7. The classification scheme adopted in this paper was based on that developed by Shafii and Clough (1982), in which weakly cemented

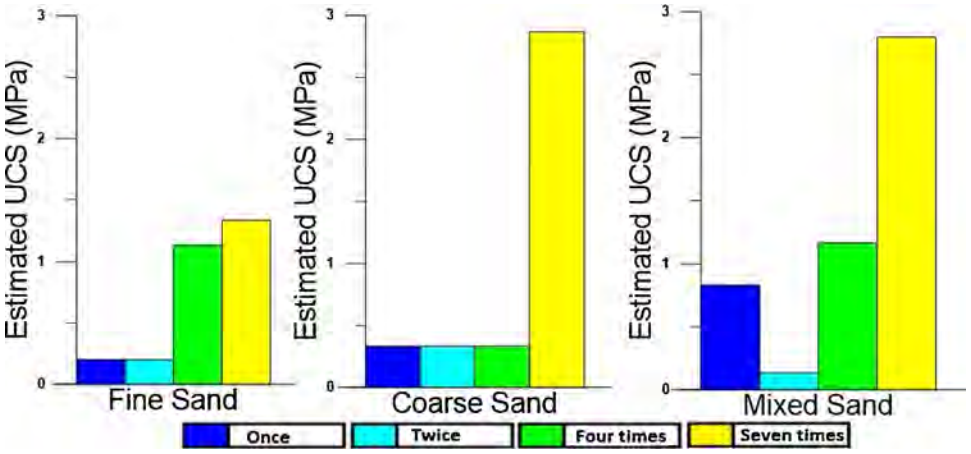

Fig. 7. UCS comparison of the results obtained when varying the bacteria injection for fine, coarse and mixed sand.

sand was defined as having a UCS of less than 0.3 MPa, moderately cemented sand was defined as having a UCS between 0.4 Mpa and 1 MPa and solidified sand was that with greater than 1 MPa (Shafii and Clough, 1982). Generally, UCS increased with increasing injection interval as well as the top part of the sample was solidified more than the bottom. This increase in UCS at the top can be attributed to calcite crystals forming cohesive bonds between sand grains mediated by *Pararhodobacter*, which accumulated at the top of the sample.

Increasing cohesive bonds result in cementation leading to decreased permeability, as was observed during the investigation. Therefore, MICP can both immobilize the lead and induce high resistance of the contaminated materials to erosion. This phenomenon was also observed when conducting a steep slope experiment using *Sporosarcina pasteurii* (Salifu et al., 2016). Overall, the data obtained using the syringe test demonstrated that MICP is a viable option for use in coarse- and fine-grained sand. In syringe experiments, the pH value ranged from 8.0 to 9.5, which is similar to what has been observed in other studies (Stocks-Fischer et al., 1999). The calcium ion concentration was lower in the first 7 days of the experiment, indicating deposition of calcite in the column and a decrease in deposition in the latter half. Clogging of the porous media was greater in coarse sand than in finely graded sand. This clogging was because of the cell growth and calcium carbonate formation that accompany the MICP process.

4. Conclusion

In this study, we demonstrated for the first time that lead (Pb) can be bioremediated by *Pararhodobacter* sp. and that the microorganism was capable of complete removal of 1036 mg/L Pb^{2+} during 6 h of incubation via elevation of the pH to alkaline conditions (8.0–9.1). SEM and XRD further confirmed transformation of toxic free Pb^{2+} ions to a more stable form of lead that bioprecipitated together with calcite or vaterite, which were predominant. Furthermore, syringe experiments revealed that UCS was greater when seven injection were performed as opposed to less injection interval of bacteria. The unconfined compressive strength increased with an increase in injection interval with maximum unconfined compressive strength of 1.33 MPa for fine sand, 2.87 MPa for coarse sand and 2.80 MPa for mixed sand. For *Pararhodobacter* to efficiently induce lead immobilisation the bacterial interval required is four times with a calcium and urea concentration of 0.5 M and bacterial concentration of 10^9 cfu/mL. These results will facilitate the bioremediation of lead in both fine and coarse materials as an eco-friendly and sustainable method of heavy metal remediation.

Acknowledgments

This work was sponsored by JSPS KAKENHI Grant Number JP16H04404 and JST/JICA, SATREPS (Science and Technology Research Partnership for Sustainable Development).

References

Achal, V., Pan, X., Zhang, D., Fu, Q., 2012. Bioremediation of Pb-contaminated soil based on microbially induced calcite precipitation. J. Microbiol. Biotechnol. 22, 244–247. http://dx.doi.org/10.4014/jmb.1108.08033.

Anbu, P., Kang, C.-H., Shin, Y.-J., So, J.-S., 2016. Formations of calcium carbonate minerals by bacteria and its multiple applications. Springerplus 5, 250. http://dx.doi.org/10.1186/s40064-016-1869-2.

Begum, A., Harikrishna, S., Khan, I., 2009. Analysis of heavy metals in water, sediments and fish samples of Madivala lakes of Bangalore, Karnataka. Int. J. Chem. Technol. Res. 1, 245–249.

Danjo, T., Kawasaki, S., 2013. A Study of the Formation Mechanism of Beachrock in Okinawa, Japan: Toward Making Artificial Rock. Int. J. GEOMATE 5 (1), 634–639.

Danjo, T., Kawasaki, S., 2016. Microbially induced sand cementation method using Pararhodobacter sp. strain SO1, inspired by beachrock formation mechanism. Mater. Trans. 57, 428–437. http://dx.doi.org/10.2320/matertrans.M-M2015842.

Fujita, M., Nakashima, K., Achal, V., Kawasaki, S., 2017. Whole-cell evaluation of urease activity of *Pararhodobacter* sp. isolated from peripheral beachrock. Biochem. Eng. J. 124, 1–5. http://dx.doi.org/10.1016/j.bej.2017.04.004.

Gat, D., Ronen, Z., Tsesarsky, M., 2016. Soil bacteria population dynamics following stimulation for ureolytic microbial-induced $CaCO_3$ precipitation. Environ. Sci. Technol. 50, 616–624. http://dx.doi.org/10.1021/acs.est.5b04033.

Gomez, M.G., Anderson, C.M., Graddy, C.M.R., DeJong, J.T., Nelson, D.C., Ginn, T.R., 2017. Large-scale comparison of bioaugmentation and biostimulation approaches for biocementation of sands. J. Geotech. Geoenvironmental Eng. 143, 4016124. http://dx.doi.org/10.1061/(ASCE)GT.1943-5606.0001640.

González-Muñoz, M.T., Rodriguez-Navarro, C., Martínez-Ruiz, F., Arias, J.M., Merroun, M.L., Rodriguez-Gallego, M., 2010. Bacterial biomineralization: new insights from *Myxococcus* – induced mineral precipitation. Geol. Soc. London, Spec. Publ. 336, 31–50. http://dx.doi.org/10.1144/SP336.3.

Govarthanan, M., Lee, K.J., Cho, M., Kim, J.S., Kamala-Kannan, S., Oh, B.T., 2013. Significance of autochthonous *Bacillus* sp. KK1 on biomineralization of lead in mine tailings. Chemosphere 90, 2267–2272. http://dx.doi.org/10.1016/j.chemosphere.2012.10.038.

Kang, C.H., Han, S.H., Shin, Y., Oh, S.J., So, J.S., 2014. Bioremediation of Cd by microbially induced calcite precipitation. Appl. Biochem. Biotechnol. 172, 2907–2915. http://dx.doi.org/10.1007/s12010-014-0737-1.

Kang, C.H., Oh, S.J., Shin, Y., Han, S.H., Nam, I.H., So, J.S., 2015. Bioremediation of lead by ureolytic bacteria isolated from soil at abandoned metal mines in South Korea. Ecol. Eng. 74, 402–407. http://dx.doi.org/10.1016/j.ecoleng.2014.10.009.

Klaus, Putz, H.B., 2017. Match! – Phase Identification from Powder Diffraction, Crystal Impact.

Lanphear, B.P., 2005. Childhood lead poisoning prevention. J. Am. Med. Assoc. 293, 2274. http://dx.doi.org/10.1001/jama.293.18.2274.

Li, M., Cheng, X., Guo, H., 2013. Heavy metal removal by biomineralization of urease producing bacteria isolated from soil. Int. Biodeterior. Biodegradation 76, 81–85. http://dx.doi.org/10.1016/j.ibiod.2012.06.016.

Li, M., Cheng, X., Guo, H., Yang, Z., 2015. Biomineralization of carbonate by *Terrabacter tumescens* for heavy metal removal and biogrouting applications. J. Environ. Eng. http://dx.doi.org/10.1061/(ASCE)EE.1943-7870.0000970. C4015005-C4015005.

Li, X., Peng, W., Jia, Y., Lu, L., Fan, W., 2016. Bioremediation of lead contaminated soil with *Rhodobacter sphaeroides*. Chemosphere 156, 228–235. http://dx.doi.org/10.1016/j.chemosphere.2016.04.098.

Lin, G.Z., Peng, R.F., Chen, Q., Wu, Z.G., Du, L., 2009. Lead in housing paints: an exposure source still not taken seriously for children lead poisoning in China. Environ. Res. 109, 1–5. http://dx.doi.org/10.1016/j.envres.2008.09.003.

Mugwar, A.J., Harbottle, M.J., 2016. Toxicity effects on metal sequestration by microbially-induced carbonate precipitation. J. Hazard. Mater. 314, 237–248. http://dx.doi.org/10.1016/j.jhazmat.2016.04.039.

Naik, M.M., Dubey, S.K., 2013. Lead resistant bacteria: lead resistance mechanisms, their applications in lead bioremediation and biomonitoring. Ecotoxicol. Environ. Saf. 98, 1–7. http://dx.doi.org/10.1016/j.ecoenv.2013.09.039.

Natarajan, K.R., 1995. Kinetic study of the enzyme urease from *Dolichos biflorus*. J. Chem. Educ. 72, 556–557. http://dx.doi.org/10.1021/ed072p556.

Nehrke, G., Van Cappellen, P., 2006. Framboidal vaterite aggregates and their transformation into calcite: a morphological study. J. Cryst. Growth 287, 528–530. http://dx.doi.org/10.1016/j.jcrysgro.2005.11.080.

Nwuche, C.O., Ugoji, E.O., 2008. Effects of heavy metal pollution on the soil microbial activity. Int. J. Environ. Sci. Technol. 5, 409–414. http://dx.doi.org/10.1007/BF03326036.

Nyambe, I.A., Chirwa, M., Chaziya, B., 2013. Impacts of past mining activities on the Ecosystem and on human health in Kabwe Town, Zambia. Workshop on Environmental and Health Impacts of Mining Activities in the Sub-Saharan African Countries (p. 33).

Park, S.J., Park, Y.M., Chun, W.Y., Kim, W.J., Ghim, S.Y., 2010. Calcite-forming bacteria for compressive strength improvement in mortar. J. Microbiol. Biotechnol. 20, 782–788. http://dx.doi.org/10.4014/jmb.0911.11015.

Sadler, W.R., Trudinger, P.A., 1967. The inhibition of microorganisms by heavy metals. Miner. Depos. 2, 158–168. http://dx.doi.org/10.1007/BF00201912.

Salifu, E., MacLachlan, E., Iyer, K.R., Knapp, C.W., Tarantino, A., 2016. Application of microbially induced calcite precipitation in erosion mitigation and stabilisation of sandy soil foreshore slopes: a preliminary investigation. Eng. Geol. 201, 96–105. http://dx.doi.org/10.1016/j.enggeo.2015.12.027.

Shafii, R.-N., Clough, W., 1982. The Influence of Cementation on the Static and Dynamic Behavior of Sands. Stanford, California, California.

Stocks-Fischer, S., Galinat, J.K., Bang, S.S., 1999. Microbiological precipitation of $CaCO_3$. Soil Biol. Biochem. 31, 1563–1571. http://dx.doi.org/10.1016/S0038-0717(99)00082-6.

Volodymyr, Viktor, S.I., 2017. Construction Biotechnology: Biogeochemistry, Microbiology and Biotechnology of Construction Materials and Processes. Springer Nature, Singapore. http://dx.doi.org/10.1007/978-981-10-1445-1.

Weatherburn, M.W., 1967. Phenol-hypochlorite reaction for determination of ammonia. Anal. Chem. 39, 971–974. http://dx.doi.org/10.1021/ac60252a045.

Whiffin, V.S., van Paassen, L.A., Harkes, M.P., 2007. Microbial carbonate precipitation as a soil improvement technique. Geomicrobiol. J. 24, 417–423. http://dx.doi.org/10.1080/01490450701436505.

Yabe, J., Nakayama, S.M.M., Ikenaka, Y., Yohannes, Y.B., Bortey-Sam, N., Oroszlany, B., Muzandu, K., Choongo, K., Kabalo, A.N., Ntapisha, J., Mweene, A., Umemura, T., Ishizuka, M., 2015. Lead poisoning in children from townships in the vicinity of a lead-zinc mine in Kabwe, Zambia. Chemosphere 119, 941–947. http://dx.doi.org/10.1016/j.chemosphere.2014.09.028.

ZCCM-IH – Zambia Copper and Cobalt Mining- Investment Holding Plc, 2002. Environmental Assessment of the Copperbelt and Kabwe Area. Kitwe.

Zhu, X., Li, W., Zhan, L., Huang, M., Zhang, Q., Achal, V., 2016. The large-scale process of microbial carbonate precipitation for nickel remediation from an industrial soil. Environ. Pollut. 219, 149–155. http://dx.doi.org/10.1016/j.envpol.2016.10.047.

Environmental Science and Pollution Research (2019) 26:15653–15664
https://doi.org/10.1007/s11356-019-04984-8

RESEARCH ARTICLE

Efficacy of biocementation of lead mine waste from the Kabwe Mine site evaluated using *Pararhodobacter* sp.

Wilson Mwandira[1] · Kazunori Nakashima[2] · Satoru Kawasaki[2] · Mayumi Ito[2] · Tsutomu Sato[2] · Toshifumi Igarashi[2] · Kawawa Banda[3] · Meki Chirwa[3] · Imasiku Nyambe[3] · Shouta Nakayama[4] · Mayumi Ishizuka[4]

Received: 4 December 2018 / Accepted: 25 March 2019 / Published online: 4 April 2019

Abstract

Biocementation of hazardous waste is used in reducing the mobility of contaminants, but studies on evaluating its efficacy have not been well documented. Therefore, to evaluate the efficacy of this method, physicochemical factors affecting stabilized hazardous products of in situ microbially induced calcium carbonate precipitation (MICP) were determined. The strength and leach resistance were investigated using the bacterium *Pararhodobacter* sp. Pb-contaminated kiln slag (KS) and leach plant residue (LPR) collected from Kabwe, Zambia, were investigated. Biocemented KS and KS/LPR had leachate Pb concentrations below the detection limit of < 0.001 mg/L, resisted slaking, and had maximum unconfined compressive strengths of 8 MPa for KS and 4 MPa for KS/LPR. Furthermore, biocemented KS and KS/LPR exhibited lower water absorption coefficient values, which could potentially reduce the water transportation of Pb^{2+}. The results of this study show that MICP can reduce Pb^{2+} mobility in mine wastes. The improved physicochemical properties of the biocemented materials, therefore, indicates that this technique is an effective tool in stabilizing hazardous mine wastes and, consequently, preventing water and soil contamination.

Keywords Abandoned mine · Solidification · Leaching · Strength · Efficacy

Introduction

Mining and smelting operations generate large quantities of mine wastes that result in contamination of both soil and water resources. The wastes pose a significant risk for biota since they do not undergo biodegradation (Jaishankar et al. 2014). Stabilization or solidification (S/S) is a method commonly used for immobilizing hazardous wastes (Al-Kindi 2019). Recent studies have accomplished S/S using Portland cement (Al-Kindi 2019), fly ash (Tsang et al. 2014), geopolymers (Li et al. 2018), phosphates (Huang et al. 2016), and organic materials (Ashrafi et al. 2015). However, most of these methods are costly and have sub-optimum performance (Jena and Dey 2016). One of the promising techniques for heavy metal remediation is immobilization by microbially induced calcium carbonate precipitation (MICP) using ureolytic bacteria (Ivanov and Stabnikov 2016; Zhang et al. 2016a). Although Achal et al. (2013), Nam et al. (2016), Zhu et al. (2016), Chen et al. (2017), and Kim and Lee (2018) recommended the use of in situ MICP to immobilize hazardous mine waste, they did not evaluate the physicochemical stability of the method. Understanding the physicochemical properties of stabilized mine wastes is essential in evaluating the long-term potential of the technique to prevent water and soil pollution, thus extending the existing knowledge. The effectiveness of stabilized mine wastes is defined by strength and leach resistance (Li et al. 2018; Al-Kindi 2019; Pan et al. 2019). Strength of stabilized mine wastes depend on mechanical strength, slaking, and water absorption, whereas the leaching concentration of an element of concern depends on pH, its mineralogy, and hydraulic conductivity (Fig. 1). In this study, MICP was investigated as a method for stabilizing Pb-contaminated kiln

Responsible editor: Ta Yeong Wu

✉ Kazunori Nakashima
nakashima@geo-er.eng.hokudai.ac.jp

[1] Graduate School of Engineering, Hokkaido University, Kita 13, Nishi 8, Kita-Ku, Sapporo 060-8628, Japan

[2] Faculty of Engineering, Hokkaido University, Kita 13, Nishi 8, Kita-Ku, Sapporo 060-8628, Japan

[3] IWRM Centre/Geology Department, School of Mines, University of Zambia, P.O. Box 32379, Lusaka, Zambia

[4] Graduate School of Veterinary Medicine, Hokkaido University, Kita 18, Nishi 9, Kita-Ku, Sapporo 060-0818, Japan

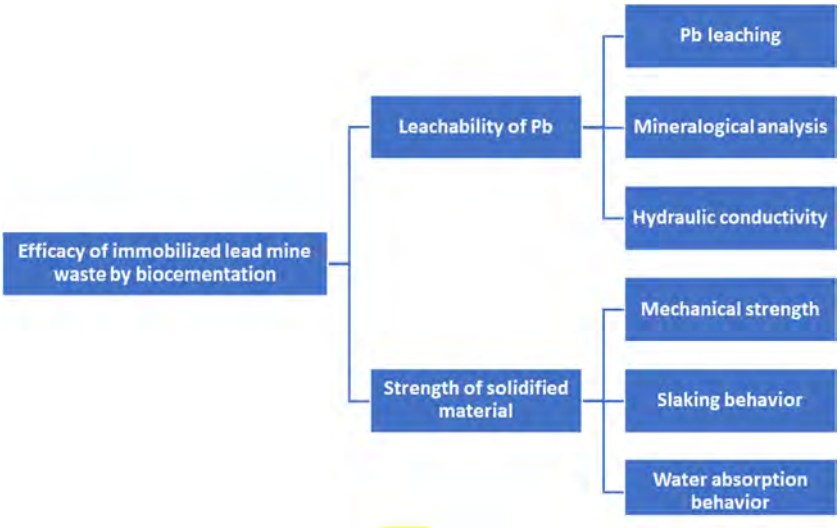

Fig. 1 Flowchart showing the research methodology adopted in this study to evaluate both the leachability and the strength of immobilized mine waste

slag (KS) and leach plant residue (LPR) collected from Kabwe, Zambia. Several researchers have reported Pb contamination general in Kabwe (Blacksmith 2013) and particularly in soils and both surface and groundwater (Kříbek et al. 2019) and in humans (Yabe et al. 2018) and livestock (Yabe et al. 2011). Therefore, stabilization of hazardous materials in Kabwe is critical in both mitigating and controlling pollution in Kabwe. The technique can be extended to other regions where the legacies of closed mines have raised background levels of heavy metals in ecosystems. Biocementation can also be used to mitigate and rehabilitate environments impacted by anthropogenic activities during and after the closure of mining companies.

The objective of this study was to characterize the physical and chemical stability of stabilized mine wastes and, therefore, evaluate the effectiveness of in situ MICP in mitigation and controlling heavy metal pollution. The authors found no previous studies that evaluated the efficacy of in situ MICP for stabilizing mine wastes. Such investigations would be valuable in facilitating the long-term design of bioremediation systems using MICP.

Materials and methods

Mine waste samples

The mine wastes—KS and LPR—used in this study were collected from the abandoned Kabwe Mine of Central Province, Zambia. Figure 2 shows the location of the study area and sampling points for KS (site 1) and LPR (site 2). The mine waste was permitted under approval no. SEP/055/17. KS is granular round ill-sorted pebbles with mean particle diameter size of 1000 μm, density of 2.88 g/cm^3 with bioavailable Pb concentration of 5.40 mg/L, whereas LPR is very fine to fine sand with a mean particle diameter size of 9 μm, density of 2.39 g/cm^3, and bioavailable Pb concentration of 7.87 mg/L.

Culturing of bacteria

Pararhodobacter sp., the biosafety level 1 bacterium used in this study, was cultured in ZoBell 2216 medium. The ZoBell 2216 contained 5.0 g/L hipolypeptone (Nihon Seiyaku Co., Ltd., Tokyo, Japan), 1.0 g/L yeast extract (BD Biosciences Advanced Bioprocessing, Miami, FL, USA), and 0.1 g/L $FePO_4$ (Junsei Chemical Co., Ltd., Tokyo, Japan) prepared with artificial seawater using Aquamarin (Yashima Pure Chemical Co., Ltd.), and the chemical composition is listed in Table 1. The final solution was adjusted to a pH of 7.6–7.8 using 1 M NaOH (Wako Pure Chemical Industries, Ltd., Tokyo, Japan). *Pararhodobacter* sp. was precultured for 24 h in 5 mL of ZoBell 2216 medium. Then, 1 mL of preculture was introduced into 100 mL of the main culture at 30 °C for 48 h with continuous aeration at 160 rpm. This culture was used for subsequent solidification experiments. All supplies and media were sterilized in an autoclave (LSX-500, Tomy Seiko Co., Ltd., Tokyo, Japan) at 121 °C for 20 min.

Biocementation of mine wastes by bacteria

To minimize interferences from antecedent microbes, the LPR and KS samples were oven dried at 110 °C for 48 h. Each dried sample was hand packed into a 35-mL sterile syringe (mean diameter, $D_{50} = 2.5$ cm, and height, $h = 7$ cm). A volume of 16 mL of grown bacteria suspension ($OD_{600} = 4.0$) was initially added. Bacteria fixation was added on days 1, 3, 5, and 7. After 2 h, a flush of 20 mL of cementation solution (0.5 M urea, 0.5 M calcium chloride, 0.02 M sodium hydrogen carbonate, 0.2 M ammonium chloride, and 3 g/L nutrient

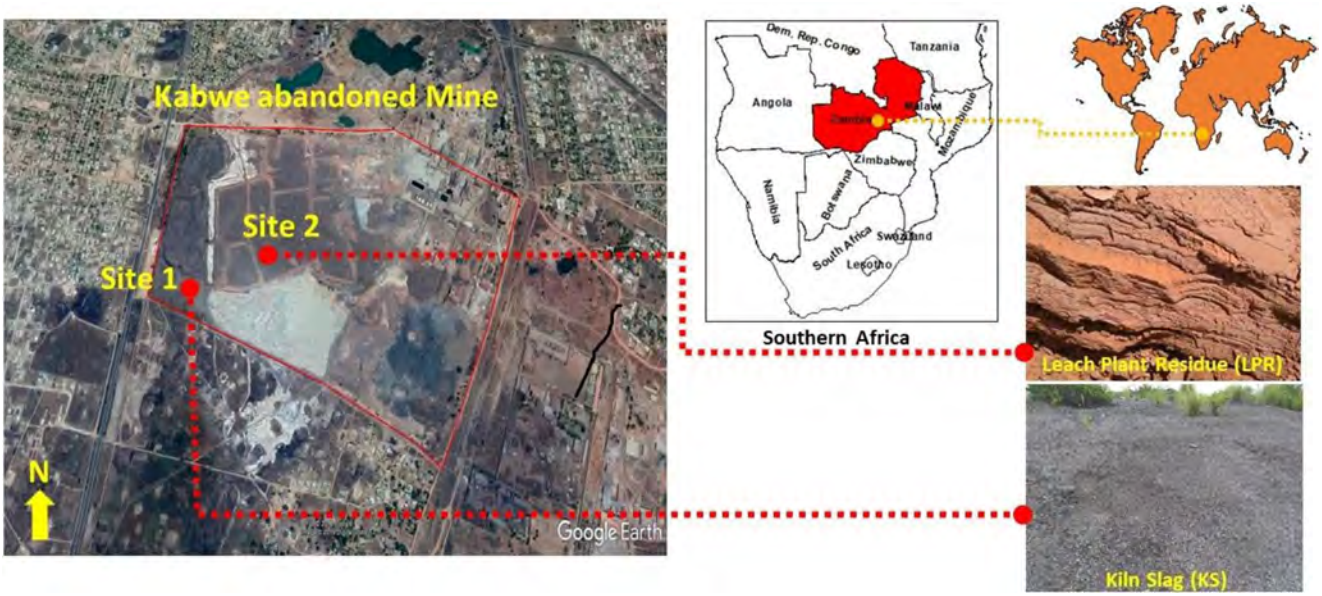

Fig. 2 Location of the study area and sampling sites for KS (site 1) and LPR (site 2)

broth) was added sequentially to the syringe and drained at a constant rate of 2 mL/min for a 14-day period at 30 °C. Two sets of experiments were conducted with procedures formulated to mimic possible conditions for in situ injection of treatment solutions into contaminated ground. The two procedures are illustrated in Fig. 3. In the first set of experiments, 2 mL of cementation solution was left above the surface of the waste to mimic saturated conditions, so this procedure was called the immersed method (Fig. 3a). The second set of experiments was conducted such that solution was added sequentially with all solution drained, so this procedure was called the flow through method (Fig. 3b). Additionally, KS/LPR was an amendment formulated to mimic the mixing of 50% KS and 50% LPR by weight to represent the mix of materials in waste piles at the mine site. In the control, distilled water was used instead of bacterial suspension.

Physical testing procedures

Needle penetration test

Unconfined compressive strength (UCS) was measured using a needle penetration device (SH-70, Maruto Testing Machine Company, Tokyo, Japan) according to ISRM (International Society for Rock Mechanics 2015). To determine the strength of a sample, the needle penetration inclination (N_p) value of each sample was measured using needle penetration device and the UCS was estimated from N_p value. The strength of the sample (N_p value) was calculated using Eq. 1

$$N_p = F/D \quad (1)$$

where F is the penetration load (N) and D is the depth of penetration (mm). The unit of N_p is Newton per millimeter. From the chart of UCS-*N*p correlation, estimated UCS value was determined.

Table 1 Chemical composition of artificial seawater (g/L)

NaCl	$MgCl_2{\cdot}6H_2O$	Na_2SO_4	$CaCl_2{\cdot}2H_2O$	KCl
24.53	11.11	4.094	1.535	0.695
KBr	$SrCl_2$	H_3BO_3	NaF	$NaHCO_3$
0.101	0.043	0.027	0.003	0.201

Capillary water absorption tests

The water absorption tests were conducted in accordance with ASTM C1585-13 (ASTM International 2013). The surface subjected to water absorption was immersed in water (2 ± 1 mm depth) in a shallow tray and covered to prevent air circulation and contact with atmospheric water vapor. The water absorption coefficient (S, kg/(m^2 $h^{0.5}$)) was determined by the slope of the curve of the water absorbed per unit area (kg/m^2) and the square root of the sinking time ($sec^{0.5}$). The tests were conducted on untreated and treated KS and KS/LPR that was prepared by both immersed and flow through methods.

Jar slake test

The jar slake tests were conducted according to ASTM D4644-16 (ASTM International 2016). In brief, samples were oven-dried at 105 °C, cooled, and placed into empty plastic antistatic weighing dishes. Distilled water was poured into the dishes to submerge each sample for 24 h, and the samples

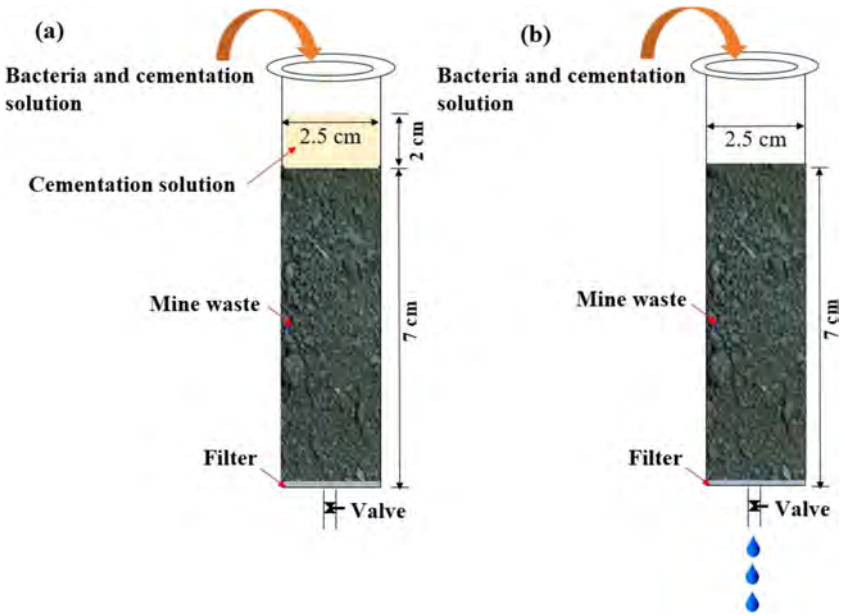

Fig. 3 Experimental setups for **a** immersed and **b** flow through methods for immobilization of mine wastes

were observed and described after 30 min and after 24 h. The samples were classified as 1–6 with corresponding descriptions as follows: (1) degrades to a pile of flakes or mud, (2) breaks rapidly and/or forms many chips, (3) breaks slowly and/or forms few chips, (4) breaks rapidly and/or develops several fractures, (5) breaks slowly and/or develops few fractures, and (6) no change. The tests were conducted on untreated and treated KS and KS/LPR that were prepared by both immersed and flow through methods.

Hydraulic conductivity

A hydraulic conductivity was conducted by the falling head method using a DIK 4000 system (Daiki Rika Kogyo Co., Ltd., Saitama, Japan) according to ASTM D5084-03 (ASTM International 2003). The molds for DIK 4000 were used for solidification of samples which has outside dimension of width 530 mm × diameter 260 mm × height of 380 mm (Fig. 4). To calculate the hydraulic conductivity, Eq. 2 was used.

$$K = \frac{2.3a.L}{A.t} \mathrm{Log}^{10} \frac{h_1}{h_2} \quad (2)$$

where K (m/s) is the hydraulic conductivity, $a = 0.503$ cm^2 cross-sectional area of the scale tube, $L = 5.1$ cm which is thickness of the sample, $A = 19.6$ cm^2 which is the sectional area of sample, $h_1 = 17$ cm, $h_2 = 7$ cm, and t is the time (s) taken for water level to drop from top to bottom of the scale tube.

The methodology described in "Biocementation of mine wastes by bacteria" was used for biocementation, but the bacteria and cementation solutions were scaled up according to the mass of the mine waste in the mold. The samples were saturated and then placed in a desiccator for 48 h before hydraulic conductivity was determined.

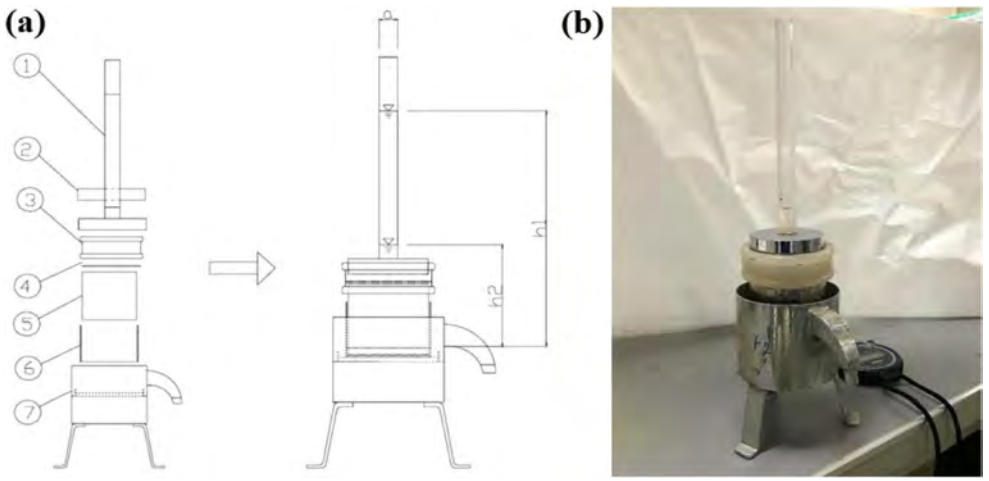

Fig. 4 **a** DIK 4000 system for measuring hydraulic conductivity where 1 = scale tube; 2 = weight for supporting scale tube; 3 = silicon rubber ring; 4 = O ring; 5 = cylindrical sample holder; 6 = casing for sample holder; 7 = water tank. **b** DIK 4000 system used in this study with a stopwatch

Chemical and mineralogical characterization methods

XRD analysis

X-ray diffraction (XRD) analysis (MiniFlex™, Rigaku Co., Ltd., Tokyo, Japan) was conducted using Ni-filtered Cu 1.5406 Å radiation to determine the mineral phases of both the untreated and treated KS and KS/LPR. Scans were recorded from 5 to 80° 2θ at a rate of 20°/min.

SEM and SEM-EDS

The microstructure of fractions of the samples was examined by scanning electron microscopy (SEM) (Miniscope TM3000, Hitachi, Tokyo, Japan) and by energy-dispersive X-ray spectroscopy (EDS) (JSM-IT200, Joel Ltd., Tokyo, Japan). Micrographs and element compositions were acquired under the microscope using samples mounted on carbon tape.

Leaching test of biocemented KS and KS/LPR

USA EPA Method 1315 for mass transfer rates of constituents in monolithic materials using a semi-dynamic tank leaching procedure was used to determine the cumulative release of Pb from the biocemented KS and KS/LPR, as shown in Fig. 5 (U.S. EPA 2017). To determine the rate of release, biocemented KS and KS/LPR samples treated by the flow through method and were immersed in deionized water with the liquid–surface area ratio (L/A) maintained at 9 ± 1 mL/cm^2. Leaching was allowed to continue for 231 days with leachate collected in a sealed high-density polyethylene (HDPE) bucket at defined intervals. Leachate was collected after 8 h, 1 day, 2 days, every 7 days from day 7 to day 49, after 63 days, and every 14 days from day 63 to day 231. Pb^{2+} concentration, pH, and electrical conductivity were measured for the collected leachate at the end of each interval. The leachate was filtered through a 0.45-μm nylon filter into a polypropylene centrifuge tube, acidified, and stored in a refrigerator at 4 °C for analysis by ICP-AES.

Statistical analysis

The data was analyzed by comparing means by independent two-sample t test using R Statistical Package Version 3.5.2 (Team R. Core 2018).

Results and discussion

Physical characterization of the biocemented waste

Needle penetration test

Figure 6 shows untreated and biocemented KS and KS/LPR prepared by the immersed and flow through methods, whereas Table 2 shows the corresponding estimated UCS results. KS, prepared by the immersed method, had a maximum estimated UCS of 8.0 MPa, compared to 5.0 MPa when prepared by the flow through method. KS/LPR, prepared by the immersed method, had a maximum UCS of 4.0 MPa, compared to only 2.8 MPa when prepared by the flow through method. Statistical analysis revealed that there was non-significant difference found between the control and KS treated by immersed method ($p = 0.10$). This result could be due to accumulation of reactants and bacteria at the injection point; hence, only top of the specimen was solidified, whereas comparison between the means of the control and flow through method yielded a significant difference ($p = 0.02$). This further agrees with the results of a previous study that found that the flow through method models environmental conditions and is more

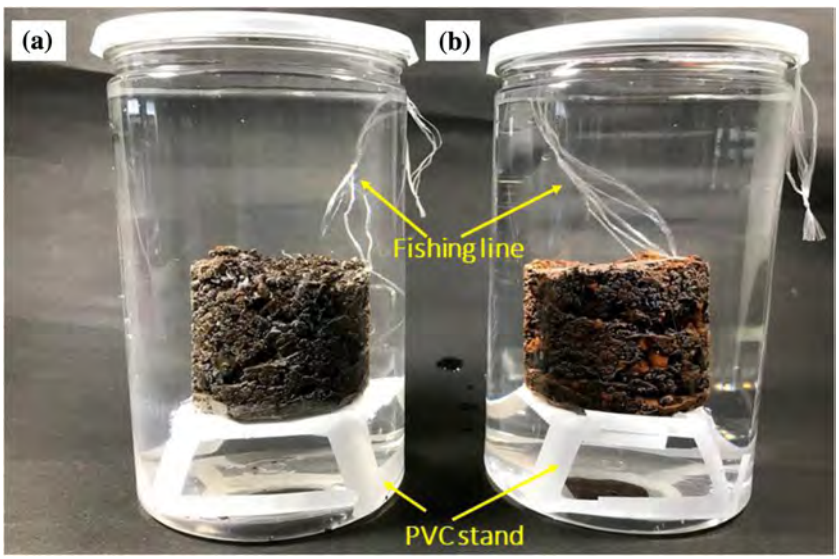

Fig. 5 USA EPA Method 1315 setup of the 3D leaching configuration of **a** biocemented KS and **b** biocemented KS/LPR

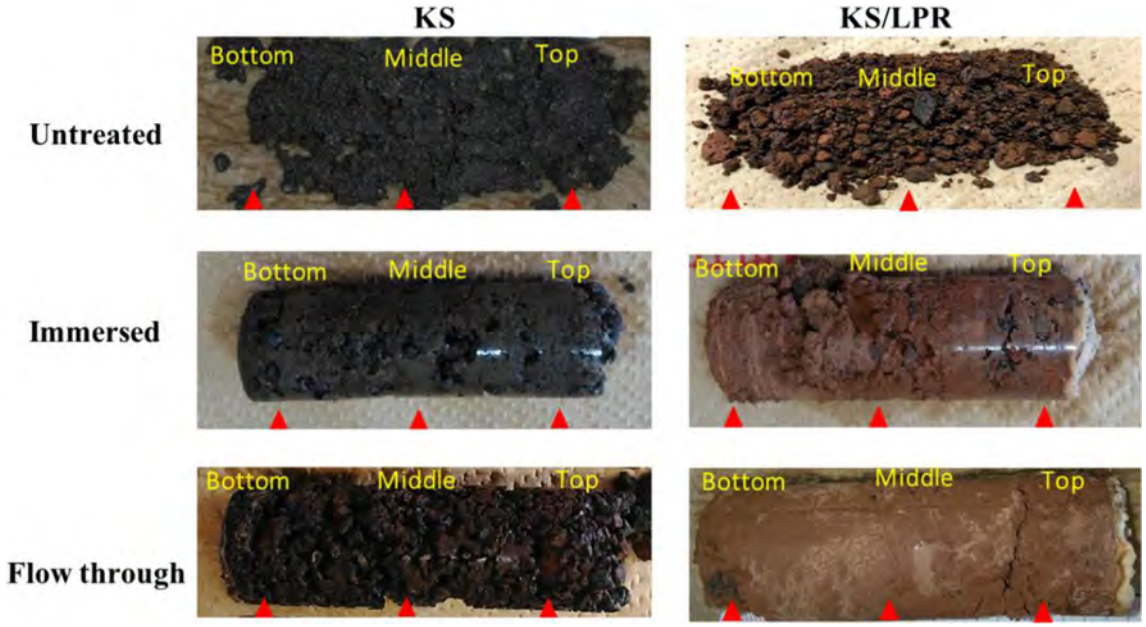

Fig. 6 Comparative view of untreated and treated KS and KS/LPR prepared by the immersed and flow through methods

conducive for effective formation of calcium carbonate ($CaCO_3$) crystals at various degrees of saturation (Cheng et al. 2013). For KS/LPR, statistical analysis revealed that there was no significant difference between the control and both immersed ($p = 0.933$) and flow through ($p = 0.06$) treatment methods. The fine nature of the LPR retards the flow of bacteria down. Therefore, flow through was the most optimal of the two methods. The top of the column closest to the injection point is probably exposed to significantly more reactants than the bottom as described by a previous studies that observed clogging due to accumulation of bacteria and reactants near the injection point (Cheng and Cord-Ruwisch 2014; Eryürük et al. 2015; Dhami et al. 2016). Additionally, it was observed the stabilized products of in situ MICP were not blown by wind. A handheld blower was used to blow on unstabilized and stabilized mine waste at different angles. No dust was observed for biocemented KS and KS/LPR prepared by either the immersed or the flow through methods, while the unstabilized waste was completely dispersed. Similar results were reported in a previous study by Doostmohammadi et al. (2017). The increased particle size resulting from MICP makes the aggregated material less susceptible to being blown by wind, eliminating a current exposure pathway to humans and animals in and around the mine site.

Capillary water absorption

Table 3 shows the water absorption results of untreated KS and KS/LPR, as well as biocemented KS and KS/LPR prepared by the immersed and flow through methods. The water absorption coefficient of unstabilized KS was 3.56 kg m^{-2} $h^{-0.5}$ and that of KS/LPR was 6.56 kg m^{-2} $h^{-0.5}$. The water absorption coefficient for biocemented KS was 1.31 kg m^{-2} $h^{-0.5}$ for the immersed method and 1.96 kg m^{-2} $h^{-0.5}$ for the flow through method, whereas the water absorption coefficient for KS/LPR was 2.42 kg m^{-2} $h^{-0.5}$ for the immersed method and 5.92 kg m^{-2} $h^{-0.5}$ for the flow through method. It was observed that all the treatment methods were statistically significant ($p < 0.05$). The results in this study are similar to those observed in previous studies for materials such as mca20/80 and handmade bricks (Karagiannis et al. 2016) and concrete (Demirci and Sahin 2014). The low water absorption ability of the biocemented mine waste can be attributed to the in situ precipitation of $CaCO_3$ in the pore spaces of the material. This

Table 2 Estimated unconfined compressive strength (UCS) of untreated and biocemented KS and KS/LPR by the immersed and flow through method

Type of treatment	Estimated UCS of KS (MPa)			Estimated UCS of KS/LPR (MPa)		
	Top	Middle	Bottom	Top	Middle	Bottom
Untreated	0	0	0	0	0	0
Biocementation by immersed method	8	1.8	1.7	4	0	0
Biocementation by flow through method	5	4.6	2.5	2.8	2.1	0.5

Table 3 Water absorption results of untreated and biocemented KS and KS/LPR prepared by immersed and flow through methods

Type of material	Untreated	Immersed condition after biocementation (kg m^{-2} $h^{-0.5}$)	Flow through method after biocementation (kg m^{-2} $h^{-0.5}$)	Water absorption of conventional materials (kg m^{-2} $h^{-0.5}$)	Source of results
KS	3.56	1.31	1.96	–	This study
KS/LPR	6.56	2.42	5.92	–	This study
mca20/80 brick	–	–	–	3.2	Karagiannis et al. 2016
Handmade brick	–	–	–	4.5	Karagiannis et al. 2016
Concrete	–	–	–	1.00	Demirci and Sahin, 2014

deposition increased the compressive strength and decreased capillary absorption rate. Possible sources of capillary water include rainfall, runoff from slopes of the mine waste, and capillary rise of groundwater. These results suggest that MICP can bind loose waste material to reduce water absorption, thereby reducing infiltration and increasing runoff, which could prevent water transport of Pb-laden mine wastes into the surrounding water bodies. The findings are in agreement with results reported by Achal et al. (2013) when they stabilized chromium-contaminated slag from China.

Slaking behavior

Slaking tests were conducted to determine the stability of the immobilized mine wastes and to qualitatively predict resistance to erosion. Figure 7 shows the slaking behavior of untreated and treated KS and KS/LPR at 0 min, 30 min, and 24 h. Untreated KS and KS/LPR easily degraded into a pile of mud after the addition of water and were given a classification of 1. These results indicate that untreated KS and KS/LPR cannot resist disruptive forces such as rain or wind and, therefore, will continue to leach Pb^{2+} freely and disperse easily to the surrounding flora and fauna. However, the biocemented KS and KS/LPR, prepared by both immersed and flow through methods, resisted slaking. They were given a classification of 6 since no reaction occurred after immersion in water for 24 h. This observation was further confirmed after five cycles of wetting and drying of the same sample. These results suggest that the biocemented KS and KS/LPR is stable and resist the disruptive forces of wind and rain.

Hydraulic conductivity

It was observed that the unstabilized KS had the hydraulic conductivity of 1.2×10^{-3} m/s while that of unstabilized K/LPR was 8.8×10^{-4} m/s. Results further revealed that treatment by immersed method resulted in a KS stabilized material with a hydraulic conductivity value of 3.9×10^{-5} m/s and also

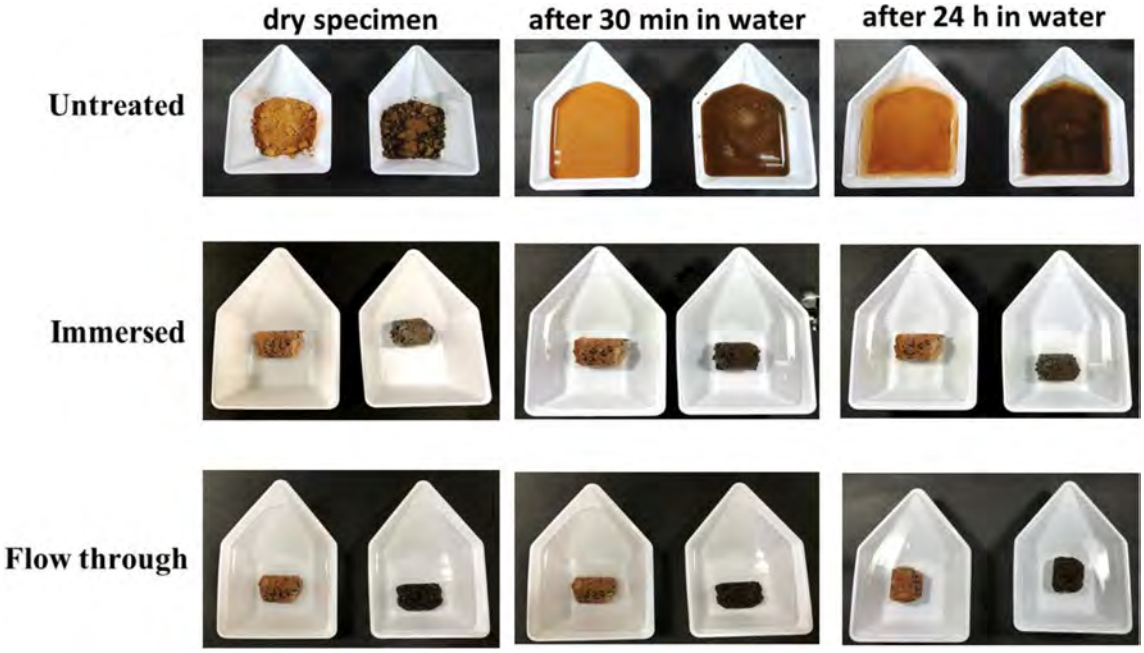

Fig. 7 Slaking test images of untreated KS and KS/LPR and biocemented KS and KS/LPR for dry specimen, 30 min after immersion in water, and 24 h after immersion. Left: KS/LPR. Right: KS

stabilized KS/LPR material with a hydraulic conductivity value of 5.8×10^{-5} m/s, whereas the flow through method showed that KS and KS/LPR had hydraulic conductivity values of 3.2×10^{-4} m/s and 2.1×10^{-6} m/s, a reduction of one and two orders of magnitude respectively. KS had a lower hydraulic conductivity compared to KS/LPR probably due to pore size distribution (Ren and Santamarina 2017). For stabilized hazardous materials, reduced hydraulic conductivity is desired because it reduces the ability of water to contact contaminants and, therefore, reduces contaminant leaching rates.

Chemical testing procedures

XRD

Results obtained from XRD analysis of the untreated waste revealed that the mineral composition of the stabilized mine waste material KS included quartz, hematite, goethite, magnetite, cerussite, and anglesite (Fig. 8). Similar findings were reported by Gutiérrez et al. (2016) and Liu et al. (2018) who noted that the minerals observed in this current study are typical of waste from sites that have the footprints of mining activities. The quartz, hematite, goethite and magnetite mineral components were due to the ore host rock which is characteristic of the geology in Kabwe. The Pb-based minerals identified - cerussite, and anglesite - are associated with sulfide-bearing mine wastes, which are the main source of contamination in and around the Kabwe mine site. The XRD patterns of the biocemented waste were similar to those of the original waste, with calcite as the most abundant mineral components. The precipitated $CaCO_3$ in the voids of the wastes, acted as a binder to the wastes and rendering them less soluble and less likely to cause toxicity to humans, animals and the environment in Kabwe and similar sites.

SEM and EDS

The results of SEM analysis of untreated and biocemented KS are shown in Fig. 9. Figure 9a, b shows that the untreated KS is rough and separated, with no particle bonding. However, the biocemented KS (Fig. 9c, d) had spherical $CaCO_3$ deposited on the surface and between the sand grains. The deposited, spherical $CaCO_3$ caused bridging, which further roughened the surface and decreased the pore space size by filling the voids between particles and causing particle binding. The decrease in pore space size has been reported in a number of previous studies (Ng et al. 2012; Rowshanbakht et al. 2016; Mujah et al. 2017).

The EDS analysis revealed that untreated KS consisted mainly of C, O, S, Mg, Ca, Fe, Si, Zn, and Pb, whereas the biocemented KS and KS/LPR prepared by flow through and immersed methods consisted of C, O, S, Mg, Ca, Fe, Zn, Pb, Si, P, Na, Cl, and Al. This composition is due to the heterogeneous nature of the orebody and

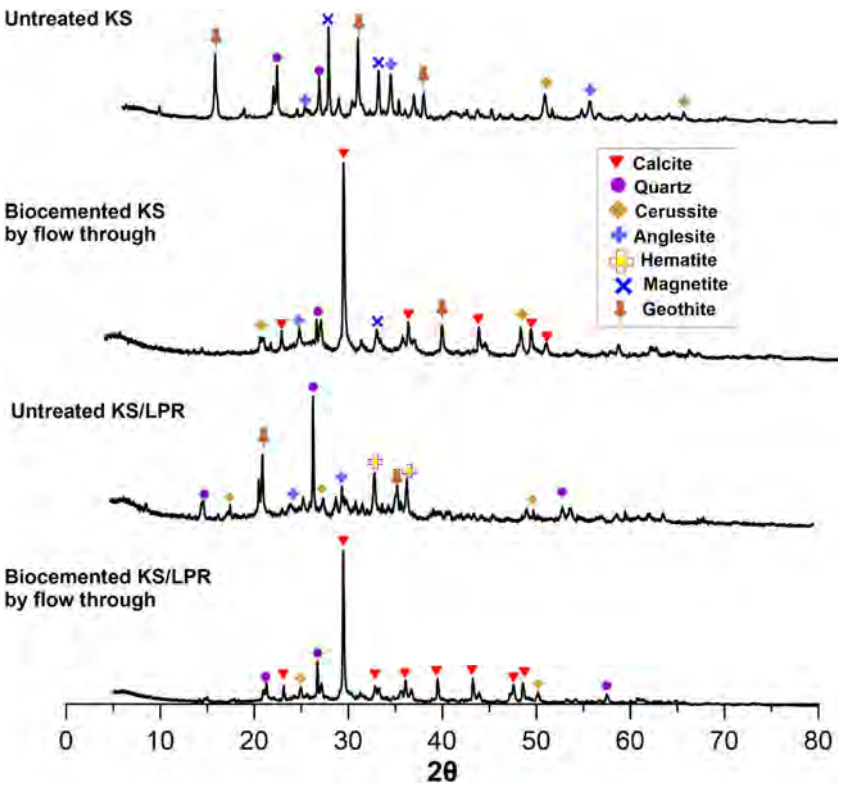

Fig. 8 X-ray diffraction (XRD) patterns of untreated and biocemented KS and KS/LPR

Fig. 9 Scanning electron microscope (SEM) images of **a** untreated KS at × 100 magnification, **b** untreated KS at × 300 magnification, **c** biocemented KS prepared by immersed method at × 100 magnification, and **d** biocemented KS prepared by immersed method at × 300 magnification

subsequent MICP process. The element composition is consistent with the minerals identified by XRD—quartz, hematite, goethite, magnetite, cerussite, and anglesite. Figure 10 shows typical, representative EDS elemental mapping of Pb and Ca in untreated and biocemented KS and KS/LPR prepared by both flow through and immersed methods. The presence of Ca and Pb in treated wastes is evident, which indicates that Pb, after treatment, was immobilized, resulting in the prevention of Pb migration out of the solid phase.

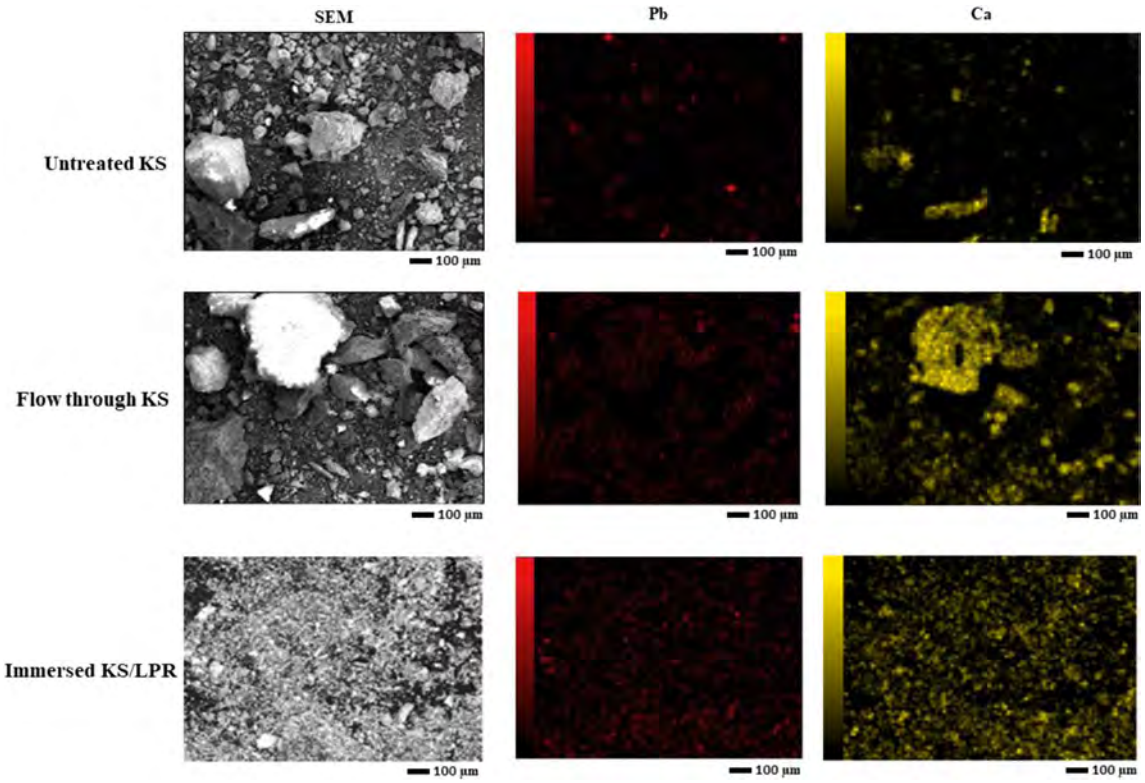

Fig. 10 Scanning electron microscopy (SEM) and energy-dispersive X-ray spectroscopy (EDS) images of untreated and biocemented KS and KS/LPR

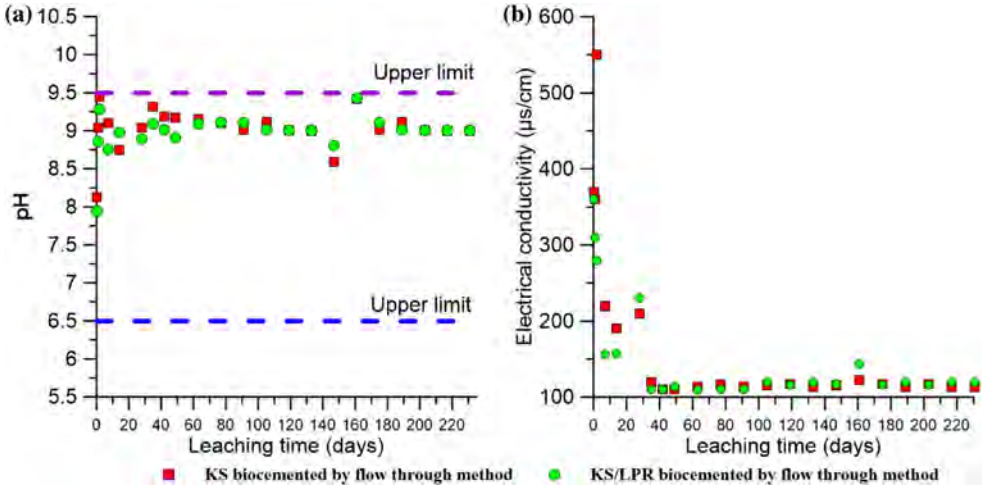

Fig. 11 Results of leaching test for biocemented KS and KS/LPR prepared by flow through method. **a** pH. **b** Hydraulic conductivity

Leaching test results

The results of the leaching stability test results are shown in Fig. 11. After continuous leaching for 231 days, the concentrations of leached Pb^{2+} were below 0.001 mg/L for biocemented KS and KS/LPR prepared by the flow through method. This means that leachability, which is the material's ability to release a contaminant from a solid phase into a contacting liquid, was prevented. Therefore, results of the current study indicate that Pb from the biocemented monolith was negligible. Furthermore, it means that the stabilized mine waste was not influenced by contact with an eluent, binders, and by the solubility of the contaminant (Bates and Hills 2015). These results indicate that Pb release from the biocemented monolith was negligible. Compared with stabilized materials which had a leachability of below 0.001 mg/L, the leachable concentrations of KS of 5.40 mg/L and that of KS/LPR of 7.87 mg/L Pb^{2+} were observed. This further reveals that biocementation can be used to prevent pollution of ecosystems, whereby pollutants like heavy metals cannot be leached into ecosystems to raise background levels of these pollutants. The leachability test results confirm that the Pb^{2+} was effectively immobilized preventing toxic, water-soluble Pb from leaching out of the wastes. The water-soluble fraction of Pb is considered the most toxic fraction due to its potential to contaminate the food chain, surface water, and groundwater (Akbar et al. 2016; Tang et al. 2016; Yutong et al. 2016). The pH values of the leachate from the biocemented KS and KS/LPR are shown in Fig. 11a. The biocemented KS and KS/LPR changed the initial pH of deionized water from pH 6.5 to a maximum pH of 9.5. The increased pH of the leachate, compared to the initial deionized water, could be due to the

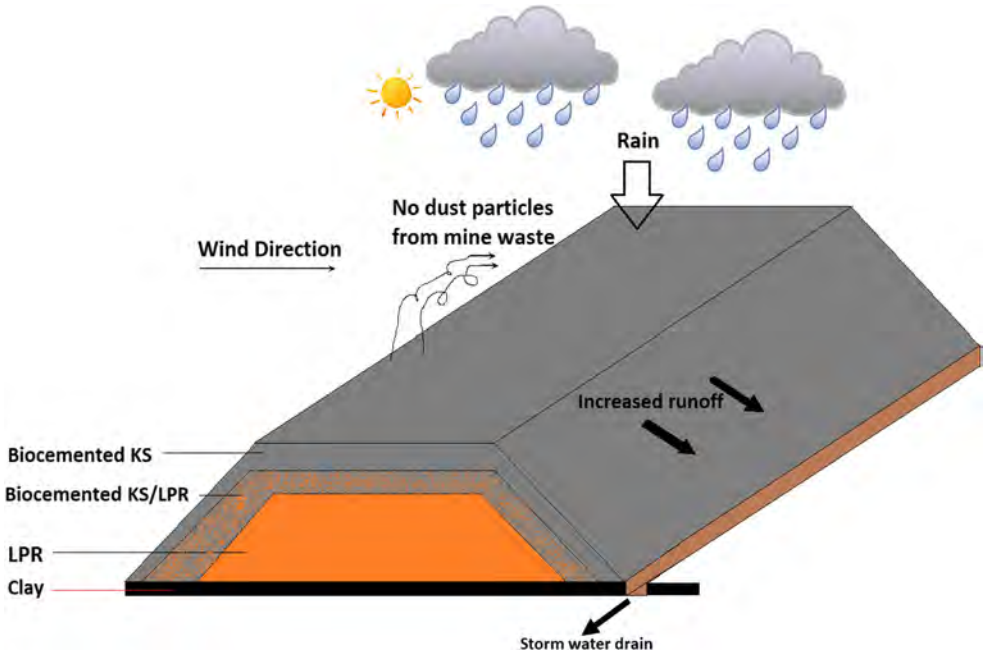

Fig. 12 Conceptual model for immobilization of Pb-contaminated mine wastes at Kabwe Mine site using MICP by *Pararhodobacter* sp.

buffering capacity of the $CaCO_3$ in the biocemented material (Zhang et al. 2016b). The pH of the leachate was weakly alkaline and was within the bounds of the Zambia Environmental Management Agency (ZEMA) guidelines of 6.0 and 9.5 for effluent and wastewater discharge into the environment, indicated by the purple and blue lines in Fig. 11a (ZEMA 2013). The electrical conductivity of the leachate from the KS and KS/LPR is shown in Fig. 11b, ranging from 130 to 550 μS/cm. Schedule III 7(2) of the ZEMA (2013) guidelines for wastewater discharge into the environment is electrical conductivity of less than 4300 μS/cm.

Strategy for immobilization of mine waste in Kabwe

Strength and leach resistance were used to assess the effectiveness of MICP in making stabilized products critical in controlling pollution (Pan et al. 2019). It was observed that biocemented KS had increased strength, with maximum UCS of 8 MPa and KS/LPR had 4 MPa (Table 2). The increased strength is attributed to the hydrolysis of urea and the precipitation of $CaCO_3$, which significantly reduced hydraulic conductivity. Results revealed that leachability of Pb^{2+} was below 0.001 mg/L for both the biocemented KS and KS/LPR. The result was obtained after leaching for 231 days. Furthermore, reduced slaking (Fig. 7) and reduced water absorption capacity (Table 3) of the biocemented samples were noted. This minimizes the mobility of pollutants into lower horizons and consequently and prevents the pollution of aquifers. It was noted that biocemented wastes were not dispersed by a handheld fan. This means that airborne transportation of Pb-contaminated dust particles can be eliminated. Consequently, MICP has potential to reduce the risk of exposure to contaminated particulate matter to living organisms, humans inclusive. The findings of the current study is in agreement with the results of Wang et al. (2018) who reported that MICP can alleviate cracking and wind erosion and can control the diffusion of dust from desert sand. The overall conceptual model for biocementing the Kabwe mine wastes in situ, based on the results of this study, is shown in Fig. 12.

Conclusion

This research promotes the utilization of biocementation as an alternative technique for effectively biocementing mine wastes. The maximum strength value of biocemented KS was observed to be 8 MPa while that of KS/LPR was 4 MPa. The slaking test results revealed that biocemented KS and KS/LPR did not disintegrate and, therefore, are stable and resist erosion by wind and rain. The water absorption coefficient was reduced compared to the unstabilized sample in the treated wastes, which would also improve resistance to water and wind erosion. Finally, leachable Pb^{2+} was below the detection limit after 231 days of continuous leaching. This technique is potentially eco-friendly, easy to manage, and cost-effective because it uses onsite materials. Very few low-cost, in situ heavy metal treatment processes for bioremediation of Pb are available worldwide. Solidification of waste by MICP has the potential for application as a low-cost and eco-friendly method for heavy metal remediation not only at the Kabwe mine but also at other heavy metal–contaminated sites.

Funding information This work was partly supported by Japan International Cooperation Agency (JICA)/Japan Science and Technology Agency (JST), Science and Technology Research Partnership for Sustainable Development (SATREPS), and Japan Society for the Promotion of Science (JSPS) KAKENHI under grant numbers JP18H03395 and JP16H04404.

Compliance with ethical standards

Conflict of interest The authors declare that they have no conflict of interest.

References

Achal V, Pan X, Lee DJ, Kumari D, Zhang D (2013) Remediation of Cr (VI) from chromium slag by biocementation. Chemosphere 93: 1352–1358. https://doi.org/10.1016/j.chemosphere.2013.08.008

Akbar A, Sinegani S, Monsef MJ (2016) Chemical speciation and bioavailability of cadmium in the temperate and semiarid soils treated with wheat residue. Environ Sci Pollut Res 23:9750–9758. https://doi.org/10.1007/s11356-016-6171-x

Al-Kindi G (2019) Evaluation the solidification/stabilization of heavy metals by Portland cement. J Ecol Eng 20:91–100. https://doi.org/10.12911/22998993/99739

Ashrafi M, Mohamad S, Yusoff I, Hamid FS (2015) Immobilization of Pb, Cd, and Zn in a contaminated soil using eggshell and banana stem amendments: metal leachability and a sequential extraction study. Environ Sci Pollut Res 22:223–230. https://doi.org/10.1007/s11356-014-3299-4

ASTM International (2003) ASTM D5084-03 standard test methods for measurement of hydraulic conductivity of saturated porous materials using a flexible wall permeameter

ASTM International (2013) ASTM C1585-13 standard test method for measurement of rate of absorption of water by hydraulic-cement concretes

ASTM International (2016) ASTM D4644-16 standard test method for slake durability of shales and other similar weak rocks

Bates E, Hills C (2015) Stabilization and solidification of contaminated soil and waste: a manual of practice

Blacksmith I (2013) The worlds worst 2013: the top ten toxic threats. Zurich

Chen X, Guo H, Cheng X (2017) Heavy metal immobilisation and particle cementation of tailings by biomineralisation. Environ Geotech: 1–7. https://doi.org/10.1680/jenge.15.00068

Cheng L, Cord-Ruwisch R (2014) Upscaling effects of soil improvement by microbially induced calcite precipitation by surface percolation. Geomicrobiol J 31:396–406. https://doi.org/10.1080/01490451.2013.836579

Cheng L, Cord-Ruwisch R, Shahin MA (2013) Cementation of sand soil by microbially induced calcite precipitation at various degrees of saturation. Can Geotech J 50:81–90. https://doi.org/10.1139/cgj-2012-0023

Demirci EE, Sahin R (2014) Effect of strength class of concrete and curing conditions on capillary water absorption of self-compacting and conventional concrete. Int J Civ Environ Eng 8:1191–1198

Dhami NK, Reddy MS, Mukherjee A (2016) Significant indicators for biomineralisation in sand of varying grain sizes. Constr Build Mater 104:198–207. https://doi.org/10.1016/j.conbuildmat.2015.12.023

Doostmohammadi R, Olfati M, Roodsari FG (2017) Mining pollution control using biogrouting. J Min Sci 53:367–376. https://doi.org/10.1134/S1062739117022248

Eryürük K, Yang S, Suzuki D, Sakaguchi I, Akatsuka T, Tsuchiya T, Katayama A (2015) Reducing hydraulic conductivity of porous media using $CaCO_3$ precipitation induced by *Sporosarcina pasteurii*. J Biosci Bioeng 119:331–336. https://doi.org/10.1016/j.jbiosc.2014.08.009

Gutiérrez M, Mickus K, Camacho LM (2016) Abandoned Pb/Zn mining wastes and their mobility as proxy to toxicity: a review. Sci Total Environ 565:392–400. https://doi.org/10.1016/j.scitotenv.2016.04.143

Huang G, Su X, Rizwan MS, Zhu Y, Hu H (2016) Chemical immobilization of Pb, Cu, and Cd by phosphate materials and calcium carbonate in contaminated soils. Environ Sci Pollut Res 23:16845–16856. https://doi.org/10.1007/s11356-016-6885-9

International Society for Rock Mechanics (2015) The ISRM suggested methods for rock characterization, testing and monitoring: 2007–2014. Springer International Publishing, Cham

Ivanov V, Stabnikov V (2016) Construction biotechnology: biogeochemistry, microbiology and biotechnology of construction materials and processes. Springer

Jaishankar M, Tseten T, Anbalagan N, Mathew BB, Beeregowda KN (2014) Toxicity, mechanism and health effects of some heavy metals. Interdiscip Toxicol 7:60–72. https://doi.org/10.2478/intox-2014-0009

Jena S, Dey SK (2016) Heavy metals. Am J Environ Stud 1:48–60

Karagiannis N, Karoglou M, Bakolas A, Moropoulou A (2016) New approaches to building pathology and durability. New Approaches to Build Pathol Durab 6:27–44. https://doi.org/10.1007/978-981-10-0648-7

Kim JH, Lee JY (2018) An optimum condition of MICP indigenous bacteria with contaminated wastes of heavy metal. J Mater Cycles Waste Manag 21:1–9. https://doi.org/10.1007/s10163-018-0779-5

Kříbek B, Nyambe I, Majer V, Knésl I, Mihaljevič M, Ettler V, Vaněk A, Penížek V, Sracek O (2019) Soil contamination near the Kabwe Pb-Zn smelter in Zambia: environmental impacts and remediation measures proposal. J Geochemical Explor 197:159–173. https://doi.org/10.1016/j.gexplo.2018.11.018

Li D, Zeng L, Jiao B et al (2018) Solidification/stabilization of lead-zinc smelting slag in composite based geopolymer. J Clean Prod 209:1206–1215. https://doi.org/10.1016/j.jclepro.2018.10.265

Liu S, Tian S, Li K, Wang L, Liang T (2018) Heavy metal bioaccessibility and health risks in the contaminated soil of an abandoned, small-scale lead and zinc mine. Environ Sci Pollut Res 25:15044–15056. https://doi.org/10.1007/s11356-018-1660-8

Mujah D, Shahin MA, Cheng L (2017) State-of-the-art review of biocementation by microbially induced calcite precipitation (MICP) for soil stabilization. Geomicrobiol J 34:524–537. https://doi.org/10.1080/01490451.2016.1225866

Nam IH, Roh SB, Park MJ, Chon CM, Kim JG, Jeong SW, Song H, Yoon MH (2016) Immobilization of heavy metal contaminated mine wastes using Canavalia ensiformis extract. Catena 136:53–58. https://doi.org/10.1016/j.catena.2015.07.019

Ng W, Lee M, Hii S (2012) An overview of the factors affecting microbial-induced calcite precipitation and its potential application in soil improvement. World Acad Sci Eng Technol 62:723–729

Pan Y, Rossabi J, Pan C, Xie X (2019) Stabilization/solidification characteristics of organic clay contaminated by lead when using cement. J Hazard Mater 362:132–139. https://doi.org/10.1016/j.jhazmat.2018.09.010

Ren XW, Santamarina JC (2017) The hydraulic conductivity of sediments: a pore size perspective. Eng Geol 233:48–54. https://doi.org/10.1016/j.enggeo.2017.11.022

Rowshanbakht K, Khamehchiyan M, Sajedi RH, Nikudel MR (2016) Effect of injected bacterial suspension volume and relative density on carbonate precipitation resulting from microbial treatment. Ecol Eng 89:49–55. https://doi.org/10.1016/j.ecoleng.2016.01.010

Tang W, Shan B, Zhang H, Zhu X, Li S (2016) Heavy metal speciation, risk, and bioavailability in the sediments of rivers with different pollution sources and intensity. Environ Sci Pollut Res 23:23630–23637. https://doi.org/10.1007/s11356-016-7575-3

Team R. Core (2018) R: a language and environment for statistical computing, p 201

Tsang DCW, Yip ACK, Olds WE, Weber PA (2014) Arsenic and copper stabilisation in a contaminated soil by coal fly ash and green waste compost. Environ Sci Pollut Res 21:10194–10204. https://doi.org/10.1007/s11356-014-3032-3

U.S. EPA (2017) Leaching Environmental Assessment Framework (LEAF) how-to guide understanding the LEAF approach and how and when to use it

Wang Z, Zhang N, Ding J, Lu C, Jin Y (2018) Experimental study on wind erosion resistance and strength of sands treated with microbial-induced calcium carbonate precipitation. Adv Mater Sci Eng 2018:1–10. https://doi.org/10.1155/2018/3463298

Yabe J, Nakayama SMM, Ikenaka Y, Muzandu K, Ishizuka M, Umemura T (2011) Uptake of lead, cadmium, and other metals in the liver and kidneys of cattle near a lead-zinc mine in Kabwe, Zambia. Environ Toxicol Chem 30:1892–1897. https://doi.org/10.1002/etc.580

Yabe J, Nakayama SMM, Ikenaka Y, Yohannes YB, Bortey-Sam N, Kabalo AN, Ntapisha J, Mizukawa H, Umemura T, Ishizuka M (2018) Lead and cadmium excretion in feces and urine of children from polluted townships near a lead-zinc mine in Kabwe, Zambia. Chemosphere 202:48–55. https://doi.org/10.1016/j.chemosphere.2018.03.079

Yutong Z, Qing X, Shenggao L (2016) Distribution, bioavailability, and leachability of heavy metals in soil particle size fractions of urban soils (northeastern China). Environ Sci Pollut Res 23:14600–14607. https://doi.org/10.1007/s11356-016-6652-y

ZEMA (2013) Limits for effluent and wastewater—Licencing Regulations 7(2) Third schedule

Zhang Y, Yao J, Wang T et al (2016a) Bioremediation of Cd by strain GZ-22 isolated from mine soil based on biosorption and microbially induced carbonate precipitation. Environ Sci Pollut Res 24:372–380. https://doi.org/10.1007/s11356-016-7810-y

Zhang Y, Zhang S, Wang R, Cai J, Zhang Y, Li H, Huang S, Jiang Y (2016b) Impacts of fertilization practices on pH and the pH buffering capacity of calcareous soil. Soil Sci Plant Nutr 62:432–439. https://doi.org/10.1080/00380768.2016.1226685

Zhu X, Li W, Zhan L, Huang M, Zhang Q, Achal V (2016) The large-scale process of microbial carbonate precipitation for nickel remediation from an industrial soil. Environ Pollut 219:149–155. https://doi.org/10.1016/j.envpol.2016.10.047

Environmental Pollution 252 (2019) 1267–1276

Contents lists available at ScienceDirect

Environmental Pollution

journal homepage: www.elsevier.com/locate/envpol

One year exposure to Cd- and Pb-contaminated soil causes metal accumulation and alteration of global DNA methylation in rats

Shouta M.M. Nakayama [a, 1], Hokuto Nakata [a, 1], Yoshinori Ikenaka [a, b], John Yabe [c], Balazs Oroszlany [a], Yared B. Yohannes [a, d], Nesta Bortey-Sam [a], Kaampwe Muzandu [c], Kennedy Choongo [c], Takeshi Kuritani [e], Mitsuhiro Nakagawa [e], Mayumi Ishizuka [a, *]

[a] Laboratory of Toxicology, Department of Environmental Veterinary Sciences, Faculty of Veterinary Medicine, Hokkaido University, Kita 18 Nishi 9, Kita-ku, Sapporo, 060-0818, Japan
[b] Water Research Group, School of Environmental Sciences and development, North-West University, South Africa
[c] The University of Zambia, School of Veterinary Medicine, P.O. Box 32379, Lusaka, Zambia
[d] Department of Chemistry, Faculty of Natural and Computational Science, University of Gondar, P.O. Box 196, Gondar, Ethiopia
[e] Graduate School of Science, Hokkaido University, Japan

ARTICLE INFO

Article history:
Received 20 February 2019
Received in revised form
6 May 2019
Accepted 9 May 2019
Available online 9 May 2019

Keywords:
Cd
DNA methylation
Epigenetics
Pb isotope
Soil exposure

ABSTRACT

Metal pollution has been associated with anthropogenic activities, such as effluents and emissions from mines. Soil could be exposure route of wild rats to metals, especially in mining areas. The aim of this study was to verify whether soil exposure under environmentally relevant circumstances results in metal accumulation and epigenetic modifications. Wistar rats were divided to three groups: 1) control without soil exposure, 2) low-metal exposure group exposed to soil containing low metal levels (Pb: 75 mg/kg; Cd: 0.4), and 3) high-metal exposure group exposed to soil (Pb: 3750; Cd: 6). After 1 year of exposure, the metal levels, Pb isotopic values, and molecular indicators were measured. Rats in the high-group showed significantly greater concentrations of Pb and Cd in tissues. Higher accumulation factors (tissue/soil) of Cd than Pb were observed in the liver, kidney, brain, and lung, while the factor of Pb was higher in the tibia. The obtained results of metal accumulation ratios (lung/liver) and stable Pb isotope ratios in the tissues indicated that the respiratory exposure would account for an important share of metal absorption into the body. Genome-wide methylation status and DNA methyltransferase (Dnmt 3a/3b) mRNA expressions in testis were higher in the high-group, suggesting that exposure to soil caused metal accumulation and epigenetic alterations in rats.

1. Introduction

Lead (Pb) and cadmium (Cd) are toxic metals that co-exist ubiquitously in the environment. Mining and smelting activities are among the major sources of these metals, and metal pollution is a matter of worldwide concern. Recently, more than 400 children died of Pb poisoning in Zamfara state, Nigeria, where long-term neurological impairment, including blindness and deafness, were also documented (Blacksmith Institute, 2014; Dooyema et al., 2012; Lo et al., 2012). Children in polluted areas are vulnerable to metal exposure because of their inclination to ingest Pb through pica behavior and to assimilate relatively larger amounts of inhaled and ingested Pb than adults (Calabrese et al., 1997; Manton et al., 2000). With regard to Cd, one of the most severe forms of chronic toxicity is *itai itai* disease (a Japanese term meaning “ouch-ouch”), which is characterized by nephrotoxicity, osteoporosis, and cardiovascular disease (Jarup and Akesson, 2009; Uno et al., 2005).

To evaluate the toxic effects of Cd and Pb exposure and their mechanisms, many laboratory studies have been performed using *in vitro*, *in vivo*, as well as *in silico* techniques in rodent animal models, such as mice and rats. In addition, in field studies, wild rats (e.g., *Rattus norvegicus*, *Rattus rattus*) have frequently been used as sentinel animals to monitor metal pollution around mining areas (Nakayama et al., 2011; Nakayama et al., 2013). These studies showed that fairly high concentrations of metals were accumulated

This paper has been recommended for acceptance by Prof. Wen-Xiong Wang.
* Corresponding author. Laboratory of Toxicology, Department of Environmental Veterinary Sciences, Faculty of Veterinary Medicine, Hokkaido University, N18, W9, Kita-ku, Sapporo 060-0818, Japan.
E-mail address: ishizum@vetmed.hokudai.ac.jp (M. Ishizuka).
[1] Both authors equally contributed to this study.

https://doi.org/10.1016/j.envpol.2019.05.038
0269-7491/

in the tissues of wild rats collected from mining sites compared to those from control sites, resulting in biological reactions such as metallothionein (MT) upregulation. The authors suggested that soil may be major route of exposure to toxic metals in wild rats, especially in mining areas where soil possesses abundant mineral deposits. However, to our knowledge, there have been no reports of laboratory experiments to verify whether soil exposure under environmentally relevant conditions (i.e., not as oral/gavage administration) could result in metal accumulations in rats. As it is difficult to control the experimental conditions in field studies, laboratory soil exposure experiments should be performed to examine this issue. Many studies have been conducted using earthworms as a model animal to characterize metal accumulation patterns and accumulation factors between soil and terrestrial animals (Qiu et al., 2014), but there have been no such laboratory studies in mammals. To provide new knowledge on soil exposure in terrestrial mammals, we used the laboratory rat (*R. norvegicus*) because of the wealth of toxicological knowledge as well as genomics and epigenetics methodological strategies for this species.

We performed prolonged (1-year) exposure of Wistar rats to soil containing Cd and Pb collected in the Kabwe mining area, Zambia (Nakayama et al., 2011), to estimate accumulation factors in tissues of rats. Soil samples from Kabwe were used in this study because high concentrations of Cd and Pb were reported previously in soil, rat, chicken, goat, cattle, and children in this area (Nakata et al., 2016; Nakayama et al., 2011; Yabe et al., 2011; Yabe et al., 2015; Yabe et al., 2018). As inhalation of soil and metal accumulation were expected, we collected lung tissue from rats in addition to tissues known to accumulate Cd and Pb, such as the liver and kidney. Neurological effects, including decreased intelligence quotient (IQ), are serious problems associated with Pb exposure in humans, especially children (Manton et al., 2000). Therefore, brain tissues were also collected. The tibiae were collected as Pb accumulation targets because of the very long half-life of this metal in bone (Gerhardsson et al., 1993).

Pb isotope ratios of the $^{208}Pb/^{206}Pb$ and $^{207}Pb/^{206}Pb$ were also measured to clarify the change of those values by accumulation level and the differences among the tissues. A large number of studies has utilized the method of Pb isotopic analysis since an identification of Pb pollution source is highly required to prevent and mitigate the further Pb exposure from the environment. Pb isotopic compositions which consist of four main stable isotopes: ^{208}Pb, ^{207}Pb, ^{206}Pb, and ^{204}Pb are not affected to a measurable extent by physico-chemical fractionation processes (Bollhöfer and Rosman, 2001; Veysseyre et al., 2001). It is thus well known that isotopic ratios of the $^{208}Pb/^{206}Pb$ and $^{207}Pb/^{206}Pb$ can be used as natural tracers and open up another possibility for tracking the Pb source and pathway. Nevertheless, some previous studies revealed large differences in the isotopic composition of Pb among biological samples within rats (*Rattus norvegicus*), goats and humans (Liu et al., 2014; Nakata et al., 2016; Smith et al., 1996; Wu et al., 2012). It was also suggested the possible biological fractionation system of Pb isotopes and its threshold in the body (Nakata et al., 2016). Given these, we verified the change of Pb isotopic compositions in rat tissues in case of exposure from soil via inhalation.

Biological reactions, such as MT elevation as well as epigenetic alterations regarding global DNA methylation, were examined to provide new insight into epigenetic events associated with chronic metal exposure. This study is significant due to the environmentally relevant soil exposure conditions used to evaluate metal accumulation and biological alterations in rats. In addition, global DNA methylation analysis was performed because DNA 5-methylcytosine (5-mC) modification is increasingly recognized as a key process in the pathogenesis of complex disorders, including cancer, diabetes, and cardiovascular disease (Feinberg, 2010; Ordovas and Smith, 2010). This is another significant point of the present study because a recent review (Ray et al., 2014) noted that there have been few studies to assess associations between DNA methylation and Cd or Pb exposure. Alterations of the DNA methyltransferase (Dnmt) family were also examined because these molecules mediate cytosine methylation through the transfer of a single methyl group from S-adenosine methionine (SAM) to cytosine (Feinberg, 2010; Ordovas and Smith, 2010).

2. Materials and Methods

2.1. Soil sampling

We collected soil samples in Kabwe, Zambia (May 2009), because soil in this area is highly polluted with Pb (9–51188 mg/kg) and Cd (0.01–139 mg/kg) (Nakayama et al., 2011). Soil samples were passed through a 2 mm sieve and transported to the Laboratory of Toxicology, Graduate School of Veterinary Medicine, Hokkaido University, Japan, for laboratory exposure experiments as described in the following section. Details on soil sampling method are mentioned in supporting information of Materials and Methods section.

2.2. Animals and experimental design

All animal experiments were performed under the supervision and with the approval of the Institutional Animal Care and Use Committee of Hokkaido University (approval number 09–0220).

Thirty male Wistar rats (*R. norvegicus*, 7 weeks old) were purchased from Sankyo Labo Service Corporation, Inc. (Tokyo, Japan). The rats (8 weeks of age) were divided into three groups ($n = 10$ for each group): 1) control without soil exposure, 2) low-metal exposure group exposed to soil containing low metal levels (Pb: 75 mg/kg; Cd: 0.4 mg/kg), and 3) high-metal exposure group exposed to soil containing high metal levels (Pb: 3750 mg/kg; Cd: 6 mg/kg) (Supplementary Table S1). Concentrations of Cd and Pb in the test soil samples were determined prior to exposure experiments by atomic absorption spectrometry (AAS) (Z-2010; Hitachi High-Technologies Corporation, Tokyo, Japan) according to the method described previously (Nakayama et al., 2011). Soil samples were spread at the bottom of the cage and rats were exposed to the soil for 1 year (Supplementary Fig. S1). The rats were housed in cages containing either soil for the exposure groups or a bedding of paper chips (Paper Clean; Japan SLC, Hamamatsu, Japan) for the control group (Supplementary Fig. S1). Body weight of the individual rats was measured once every 2 weeks, and no differences were observed among the groups (Tukey's test) during the 1-year exposure period (Supplementary Fig. S2). Details on animal experiment design are also shown in supporting information of Materials and Methods section.

To evaluate the effects of metal exposure, behavioral activity of rats was monitored using a Scanet MV-10 (Matys Co., Tokyo, Japan) before starting exposure (day 0) and after 2, 6, and 12 months of exposure. Rats were placed in a box measuring 480 mm × 480 mm that had infrared ray detectors set 12.5 cm above the floor. Larger (MOVE 1) and smaller (MOVE 2) horizontal movements and vertical movement (rearing) were recorded every 2 min for 20 min (Supplementary Fig. S3). This instrument allowed monitoring of the rat behavior by one examiner without special training. Behavioral experiments were performed at night (20:30–23:00) as rats are nocturnal animals.

After 1 year of soil exposure, rats were euthanized by CO_2 inhalation, and heparinized total blood, liver, kidney, lung, brain, testis, and tibia were collected. Tissue samples other than the tibia

were immediately frozen in liquid nitrogen. Plasma was collected after centrifugation (2000×*g*, 15 min at room temperature) of total blood with heparin for blood biochemistry analysis. The collected samples were stored at −80 °C until analyses.

2.3. Blood biochemistry

A conventional blood chemical analyzer (COBAS Ready; Roche Diagnostic Systems, Basel, Switzerland and Spotchem panels I and II; Arkray, Kyoto, Japan) was used to analyze the levels of alanine aminotransferase (ALT), aspartate aminotransferase (AST), gamma glutamyltranspeptidase (GGT), lactase dehydrogenase (LDH), alkaline phosphatase (ALP), total bilirubin (T-Bil), total protein (TP), blood urea nitrogen (BUN), albumin (Alb), urea acid (UA), and creatinine (Cre).

2.4. Cd and Pb extraction and concentration analysis

Extraction of metals in tissues were performed as described previously (Yabe et al., 2015) with slight modifications. Details on sample digestion and metal extraction procedures are also described in supporting information of Materials and Methods section.

The concentrations of Cd and Pb were determined using an inductively coupled plasma − mass spectrometer (ICP-MS 7700 series; Agilent Technologies, Tokyo, Japan). Analytical quality control was performed using the DORM-3 (fish protein, National Research Council of Canada, Ottawa, Canada) and DOLT-4 (dogfish liver, National Research Council of Canada) certified reference materials. Replicate analysis of these reference materials showed good recoveries (95%–105%). The instrument detection limit was 0.001 μg/L. The accumulation factor for the high-metal exposure group was calculated using the equation: [metal concentration in rat tissue/metal concentration in soil].

2.5. Sample purification and Pb stable isotope analysis

Sample dissolution procedure was similar to the method described by Kuritani and Nakamura (2002). The extracted solutions of liver, kidney, lung, brain, and blood, except for one kidney each of control and low-metal exposure groups whose solution volumes were not enough, were transferred into Teflon tubes after the analyses of Cd and Pb levels. The Pb isotopic data of one kidney sample of each control and low-metal exposure group were not analyzed due to insufficient volume of the solution. Details on sample dissolution and purification procedures are also shown in supporting information of Materials and Methods section.

Pb isotopic ratios of the $^{208}Pb/^{206}Pb$ and $^{207}Pb/^{206}Pb$ were determined on a multiple collector (MC)-ICP-MS (Neptune Plus, Thermo Finnigan, California, USA) in static mode with the Faraday cup configuration. Other general parameters were described in Supplementary Table S2. Details on corrections of fractionation are indicated in supporting information of Materials and Methods section.

2.6. Quantitative reverse transcription polymerase chain reaction (qRT-PCR)

Total RNA was extracted using Nucleospin RNA II kit (Takara Bio, Otsu, Japan) from approximately 100 mg of the liver and kidney according to the manufacturer's instructions. Total RNA concentration was measured using NanoDrop ND-1000 (Thermo-Scientific, Newark, DE). A260/280 and A260/230 were generally ≥2. Total RNA (1 μg) was reverse transcribed using ReverTra Ace (Toyobo, Tokyo, Japan) in a final volume of 40 μL, according to the manufacturer's instructions. Gene-specific qRT-PCR primers for MT-1, MT-2, Dnmt 1, Dnmt 3a, Dnmt 3b, and peptidylprolyl isomerase (cyclophilin) genes (Supplementary Table S3) were synthesized by Sigma-Aldrich (Tokyo, Japan). qRT-PCR was performed using the StepOnePlus Real-Time PCR system (Applied Biosystems, Foster City, CA). The PCR mixtures consisted of Fast SYBR Green Master Mix (Applied Biosystems), forward and reverse primers (200 nM each), and cDNA derived from 10 ng of total RNA in a total volume of 10 μL. Details on PCR profile, primer specificity confirmation, internal control and comparative quantification method are presented in supporting information of Materials and Methods section. Eight rats selected at random from each group were used for the qRT-PCR assay, whereas 10 rats from each group were used for all of the other experiments.

2.7. Genomic DNA extraction and LUminometric methylation (LUMA) assay

Genomic DNA was extracted from the liver, kidney, and testis samples using a GenElute Mammalian Genomic DNA Miniprep kit (Sigma-Aldrich) according to the manufacturer's instructions. DNA concentration was measured spectrophotometrically (NanoDrop ND-1000; Thermo-Scientific). LUminometric Methylation Assay (LUMA) assays were performed according to the method of Pilsner et al. (2009b). Briefly, methylation-sensitive and methylation-insensitive enzymatic digestion of 300 ng genomic DNA at CCGG sites was completely performed using *Hpa*II and *Msp*I restriction enzymes (Invitrogen, Carlsbad, CA), respectively. *Eco*RI (Invitrogen) was also used for complete digestion as an internal control. Annealing buffer (Qiagen, Valencia, CA) was added after digestion, and the products were analyzed using the PyroMark Q96 MD system (Qiagen). The *Msp*I/*Hpa*II ratios were calculated relative to the *Eco*RI control, and the percent methylation of each sample was calculated using the equation: $[1 - (HpaII/EcoRI)/(MspI/EcoRI)] \times 100$.

2.8. Statistical analysis

Tukey's test was used to identify significant differences among the groups and tissues. Principal component analysis (PCA) was performed to characterize the relationships among metal concentrations, methylation status, and mRNA expression of Dnmt 1, Dnmt 3a, and Dnmt 3b in rat testis. JMP ver. 13.0 (SAS Institute Inc., Raleigh, NC) was used for statistical analysis, and $P < 0.05$ was taken to indicate statistical significance.

3. Results

3.1. Blood biochemistry

Significantly elevated levels of ALP and BUN were detected in the rats from the high-metal exposure group compared to the other two groups (Supplementary Table S4).

3.2. Cd and Pb concentrations and accumulation factors

The concentrations of Cd and Pb in rat tissues were determined (Table 1). Significantly higher concentrations of Cd were observed in the blood, testis, lung, liver, and kidney in rats from the high-metal exposure group compared to control and low-metal exposure groups. No significant differences were found in Cd concentrations in the tibia samples. Cd levels in brain samples were below the detection limit (BDL). Significantly higher concentrations of Pb were observed in the blood, testis, brain, lung, liver, kidney, and tibia of rats from the high-metal exposure group compared to the control and low-metal exposure groups.

Table 1
Comparison of Cd and Pb concentrations (mean ± standard deviation) in rat tissues.

Tissue	Group	Cd		Pb	
Blood (μg/dL)	Control	0.005 ± 0.001	b	0.24 ± 0.03	b
	Low	0.005 ± 0.002	b	0.37 ± 0.14	b
	High	0.009 ± 0.002	a	4.22 ± 0.82	a
	Ratio *	1.7		11.3	
Testis (μg/kg)	Control	2.1 ± 0.5	b	19.1 ± 11.3	b
	Low	2.0 ± 0.3	b	13.1 ± 4.9	b
	High	7.2 ± 0.7	a	98.2 ± 79.5	a
	Ratio *	3.6		7.5	
Brain (μg/kg)	Control	BDL		40.2 ± 39.1	b
	Low	BDL		20.8 ± 9.9	b
	High	BDL		128.0 ± 100.4	a
	Ratio *	–		6.1	
Lung (μg/kg)	Control	1.9 ± 1.0	b	4.7 ± 2.3	b
	Low	2.1 ± 1.0	b	6.4 ± 4.8	b
	High	12.1 ± 2.8	a	227.7 ± 132.7	a
	Ratio *	5.9		35.8	
Liver (μg/kg)	Control	5.9 ± 5.0	b	252.1 ± 139.4	b
	Low	13.1 ± 5.2	b	279.7 ± 89.5	b
	High	30.2 ± 16.2	a	527.2 ± 97.0	a
	Ratio *	2.3		1.9	
Kidney (μg/kg)	Control	155.3 ± 19.8	b	833.6 ± 150.3	b
	Low	122.8 ± 16.9	b	1016.5 ± 242.1	b
	High	508.0 ± 88.0	a	2690.7 ± 464.2	a
	Ratio *	4.1		2.6	
Tibia (μg/kg)	Control	5.6 ± 2.0	a	12.6 ± 165	b
	Low	5.0 ± 0.6	a	419.5 ± 56.3	b
	High	5.2 ± 1.5	a	54444 ± 5831	a
	Ratio *	1.0		130	

Note: * and BDL indicate the concentration ratio (High/Low) and the below detection limit, respectively.
Note: Different characters (a, b) indicate significant difference (Tukey's test).

We calculated the accumulation factor between soil and rat tissues (Supplementary Table S5). The unit of blood metal concentration was converted with 1.0 of conveniently set the blood specific gravity. The rank order of accumulation factor ($\times 10^{-4}$) for Cd in rat tissues (except the brain) was as follows: kidney (850) > liver (50) > lung (20) > testis (11) > tibia (8.0) > blood (0.2). The rank order of the accumulation factor ($\times 10^{-4}$) for Pb was as follows: tibia (145) > kidney (7.2) > liver (1.4) > lung (0.6) > brain (0.4) > testis (0.3) > blood (0.1).

3.3. Pb isotopic compositions

Geographical trends and the values of the Pb isotope ratios ($^{208}Pb/^{206}Pb$ and $^{207}Pb/^{206}Pb$ ratios) from various tissues of rats are described in Fig. 1 and Supplementary Table S6, respectively. The tissues of control group which was not exposed to Pb recorded large variation in the mean values of $^{208}Pb/^{206}Pb$ and $^{207}Pb/^{206}Pb$ ratios among the different tissues. The average isotopic ratios of low-metal exposure group exhibited relatively small variety among the tissues compared to control group. Moreover, both ratios of $^{208}Pb/^{206}Pb$ and $^{207}Pb/^{206}Pb$ in the tissues of low-metal exposure group tended to show the values closer to those in Kabwe galena (2.1342 ± 0.0009 of $^{208}Pb/^{206}Pb$ and 0.8731 ± 0.0003 of $^{207}Pb/^{206}Pb$) reported by Kamona et al. (1999). Compared with those two groups, high-metal exposure group indicated surprisingly small differences of the isotopic compositions in the tissues other than liver, with quite similar isotopic values to those in galena from the deposits of Kabwe. The standard deviation values of isotopic ratios in tissues from high-metal exposure group were also quite small, indicating small individual differences of the isotope ratios in the group.

3.4. Behavioral activity

No differences were observed among the groups in MOVE1, MOVE2, or rearing before exposure (Table 2). After 2, 6, and 12 months of exposure, the numbers of horizontal movements (MOVE1 and MOVE2) were significantly reduced in the high-metal

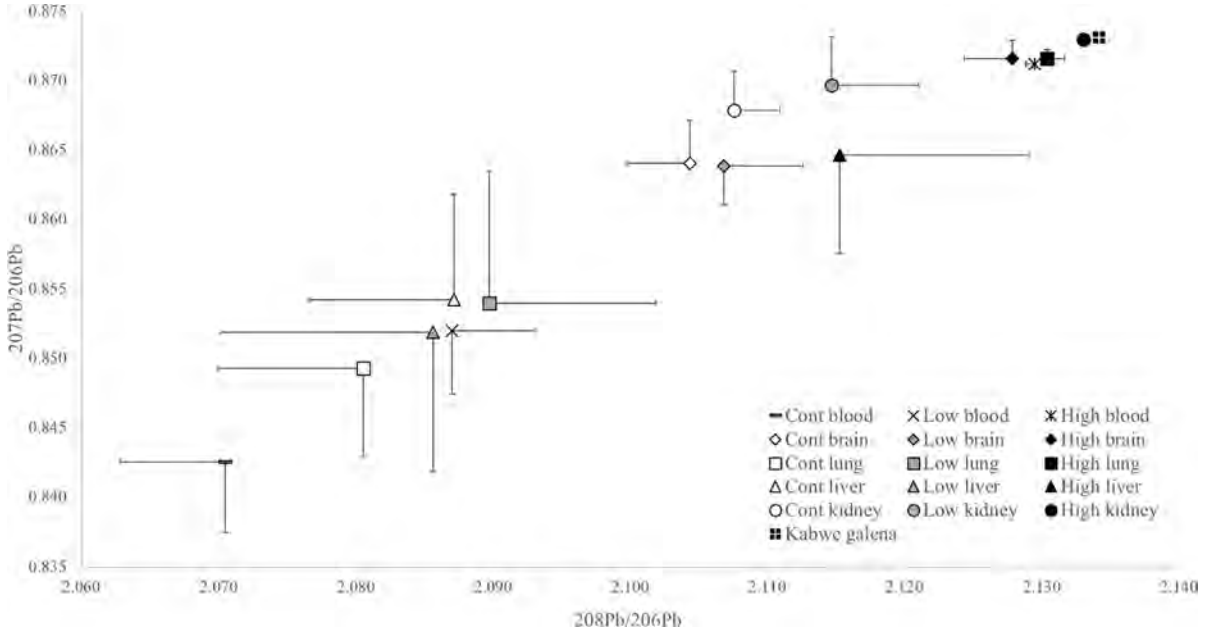

Fig. 1. Analysis of Pb isotope ratios ($^{208}Pb/^{206}Pb$ and $^{207}Pb/^{206}Pb$) in the tissues of rats and Kabwe galena (Kamona et al., 1999). The mean values and SD values are shown with error bars. Bold dash = blood of control group, x mark = blood of low-metal exposure group, astersisk = blood of high-metal exposure group, white diamond = brain of control group, grey diamond = brain of low-metal exposure group, black diamond = brain of high-metal exposure group, white square = lung of control group, grey square = lung of low-metal exposure group, black square = lung of high-metal exposure group, white triangle = liver of control group, grey triangle = liver of low-metal exposure group, black trinagle = liver of high-metal exposure group, white circle = kidney of control group, grey circle = kidney of low-metal exposure group, black circle = kidney of high-metal exposure group, white cross in black square = Kabwe galena.

Table 2
Comparison of behavioral activity (mean ± standard deviation) among the groups.

Period	Group	MOVE 1		MOVE 2		Rearing	
Before exposure	Control	5535 ± 1678	a	3745 ± 1264	a	164 ± 43	a
	Low	5263 ± 1385	a	3557 ± 1022	a	161 ± 42	a
	High	4313 ± 690	a	2861 ± 491	a	159 ± 32	a
2 month	Control	10522 ± 1535	a	6647 ± 1193	a	200 ± 37	a
	Low	7465 ± 1461	b	4795 ± 1036	b	163 ± 24	b
	High	8244 ± 1548	b	5452 ± 1145	ab	203 ± 17	a
6 month	Control	9159 ± 1782	a	5663 ± 1219	a	164 ± 28	a
	Low	7852 ± 989	ab	4852 ± 702	ab	165 ± 10	a
	High	7268 ± 1821	b	4379 ± 1249	b	151 ± 33	a
12 month	Control	6852 ± 1582	a	4281 ± 1174	a	117 ± 24	a
	Low	4894 ± 1755	b	2967 ± 1119	b	98 ± 30	a
	High	4798 ± 1442	b	2928 ± 988	b	104 ± 16	a

Note: MOVE 1 and MOVE 2 indicate large and small horizontal movement, respectively.
Note: Different characters (a, b) indicate significant difference (Tukey's test).

exposure group compared to the other two groups, whereas no differences were observed in the number of rearing behaviors (Table 2).

3.5. MT-1 and MT-2 mRNA expression in the liver and kidney

Metallothionein (MT)-1 and MT-2 mRNA expression in the kidneys from rats in the high-metal exposure group were significantly higher than those in controls (Fig. 2A and B). MT-1 mRNA expression in the kidneys of the high-metal exposure group tended to be higher than that the low-metal exposure group, although the difference was not statistically significant. No significant differences were observed among the three groups in MT-1 or MT-2 mRNA expression in the liver (Fig. 2C and D).

3.6. LUMA assay in the liver, kidney, and testis

Global DNA methylation status was analyzed by LUMA assay. Significantly high methylation level (%) was observed in the testis of the high-metal exposure group compared to the other two groups (Fig. 3A). No significant differences were observed among the groups in the liver or kidney (Fig. 3B and C).

3.7. Dnmt 1, Dnmt 3a, and Dnmt 3b mRNA expression in the testis

Dnmt 1 mRNA expression in the testis did not differ among the groups (Fig. 4A). Dnmt 3a mRNA expression levels in the testis of low- and high-metal exposure groups were significantly higher than those in the control group (Fig. 4B). The high-metal exposure group showed significantly elevated Dnmt 3b mRNA expression compared to the control group and this tended to be higher than that in the low-metal exposure group although the difference was not statistically significant (Fig. 4C).

3.8. PCA

Positive associations between metal concentrations, global DNA methylation level, and methyltransferase (Dnmt 1, Dnmt 3a, and Dnmt 3b) mRNA expression in the testis were observed by PCA (Fig. 5).

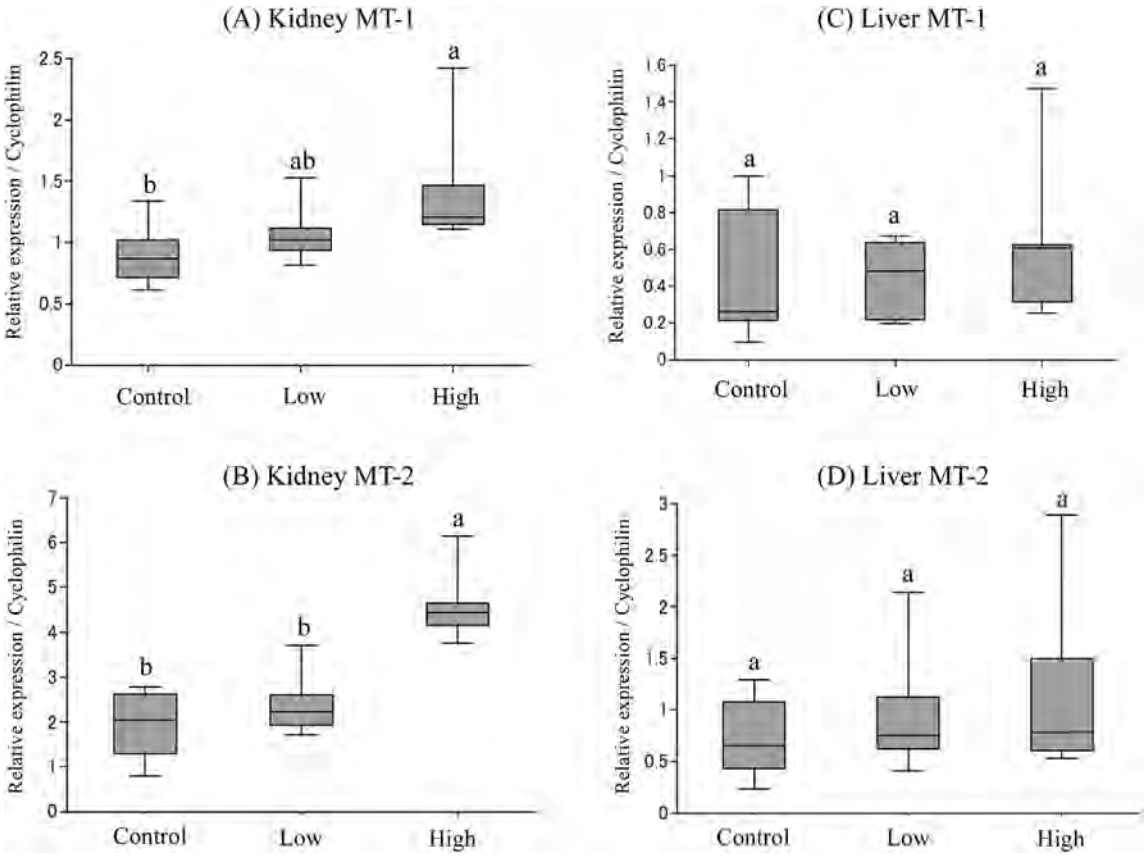

Fig. 2. Analysis of mRNA expression levels ($n = 8$ for each group) for kidney MT-1 (A), kidney MT-2 (B), liver MT-1 (C), and liver MT-2 (D). Data are shown in box and whiskers plots: box limits represent 25 and 75 percentiles; lines within the boxes indicate the medians; whisker ends indicate minimum and maximum values. Different characters (a, b) indicate significant differences (Tukey's test).

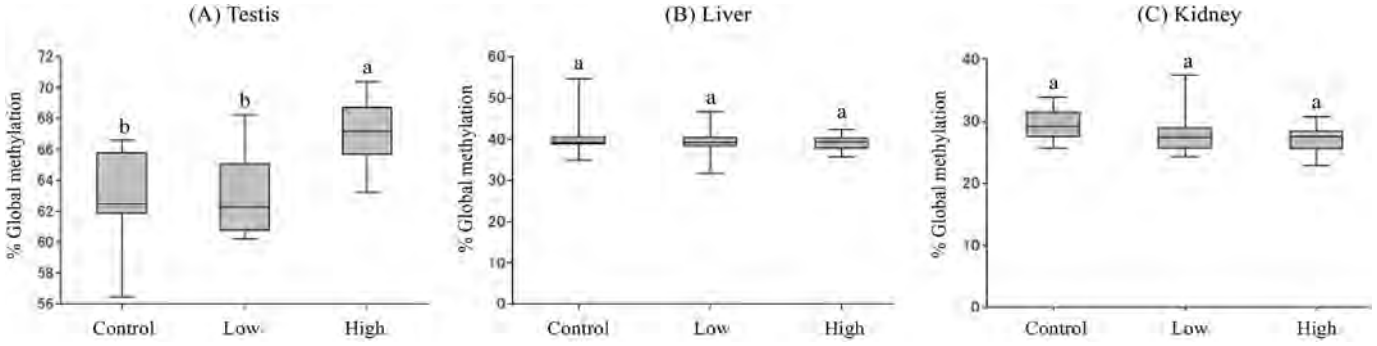

Fig. 3. Analysis of global methylation levels ($n = 10$ for each group) in the testis (A), liver (B), and kidney (C). Data are shown in box and whiskers plots: box limits represent 25 and 75 percentiles; lines within the boxes indicate the medians; whisker ends indicate minimum and maximum values. Different characters (a, b) indicate significant differences (Tukey's test).

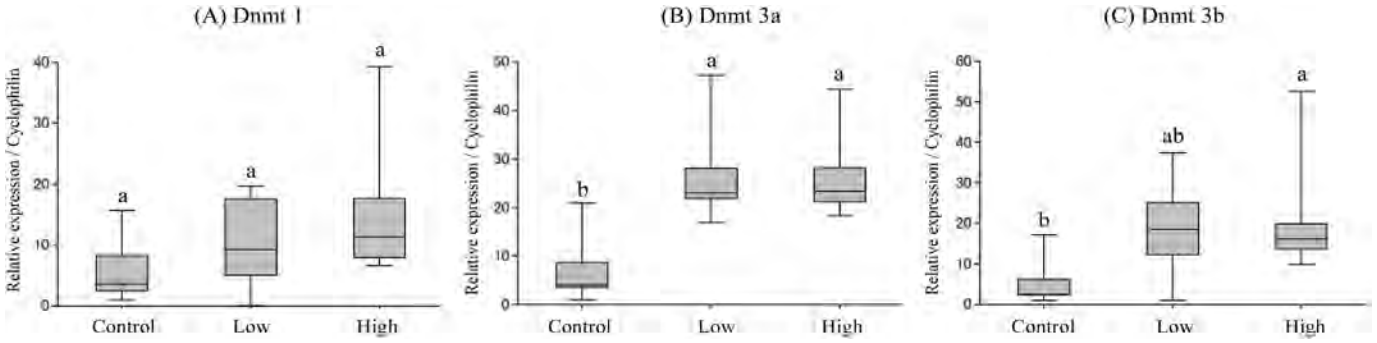

Fig. 4. Analysis of mRNA expression levels ($n = 8$ for each group) of Dnmt 1 (A), Dnmt 3a (B), and Dnmt 3b (C) in the testis. Data are shown in box and whiskers plots: box limits represent 25 and 75 percentiles; lines within the boxes indicate the medians; whisker ends indicate minimum and maximum values. Different characters (a, b) indicate significant differences (Tukey's test).

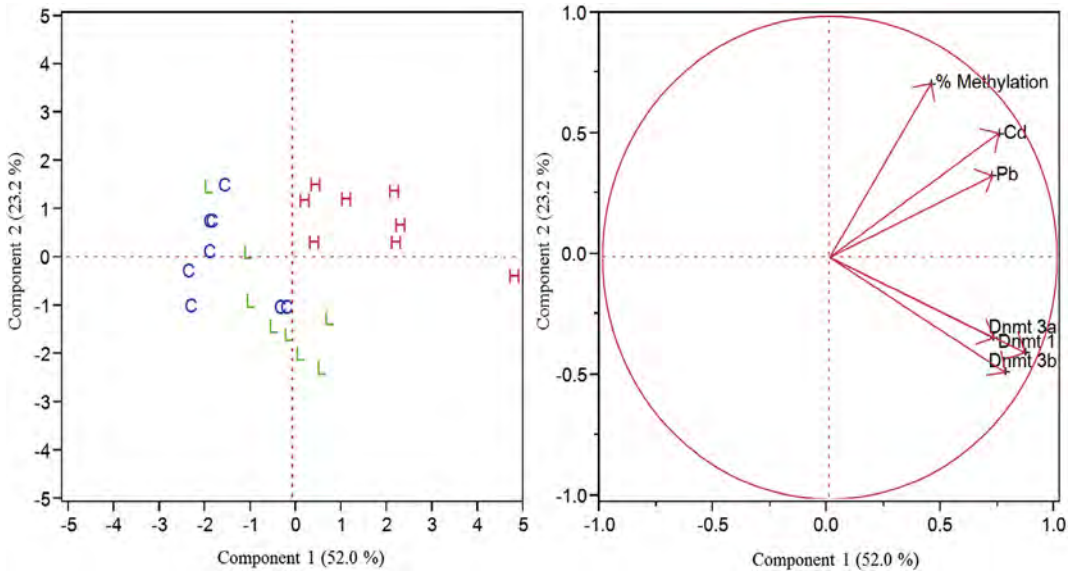

Fig. 5. Principal component analysis among metal concentrations, global DNA methylation, and of Dnmt 1, Dnmt 3a and Dnmt 3b mRNA expression in the rat testis. The letters C, L, and H indicate individual rats of control, low-, and high-metal exposure groups, respectively.

4. Discussion

In the present study, we exposed laboratory rats to soil containing Cd and Pb via inhalation as well as through ingestion (e.g., grooming, soil adsorbed to food) to represent environmentally relevant conditions. Metals were accumulated in the tissues of rats after 1 year of exposure. To our knowledge, this is the first study to estimate the accumulation factor between soil and rat tissues under conditions of natural exposure and to analyze the biological reactions and epigenetic modifications.

Analysis of the tissue distributions of Cd and Pb among the three groups indicated that soil exposure causes metal accumulation in the tissues of rats. As expected, relatively high levels of Cd and Pb were accumulated in the liver and kidneys. The liver and kidneys have been defined as metal accumulating tissues because they express high levels of metal binding proteins (e.g., metallothionein), which play important roles in detoxification of metals and metal elimination (Waalkes and Klaassen, 1985). On the other hand, it is well known that the Cd and Pb accumulation levels in the lung are relatively smaller than those in the liver and kidneys because of the low expression levels of metal binding proteins. A recent research reported that the ratio of Cd and Pb accumulation in the lung as compared to the liver were 0.024 and 0.055, respectively, in case of adult male Wister rat which was exposed to both Cd and Pb with solid feed for 12 weeks (Winiarska-Mieczan, 2014). In the sense of those metal accumulation ratios, our results indicated different trends; namely, the accumulation ratios of Cd and Pb in the lung of high-metal exposure group as compared with the liver were 0.401 and 0.432, respectively, whereas those ratios of low-metal exposure group were 0.158 and 0.023, respectively. These greater ratios in the present study suggested that respiratory exposure would account for a large fraction of Cd and Pb accumulation in rats living at highly contaminated soil environment rather than oral exposure although the distribution of absorbed metals through bloodstream should be taken into consideration as well. In fact, the concentration ratios of low- and high-metal exposure groups for Cd and Pb in the lungs were 5.9 and 35.8 times, respectively, which were higher than the values for other tissues except Pb in the tibia for which a ratio of 130 was observed.

With the intent to consider the exposure route of metals, we also analyzed Pb isotopic ratios of $^{208}Pb/^{206}Pb$ and $^{207}Pb/^{206}Pb$ in rat tissues. The variety of Pb isotope ratios in rat tissues decreased with an increase in Pb accumulation level. Moreover, as greater the Pb level is, as closer the isotopic compositions of tissues to those of Kabwe galena which is considered as the origin of Pb pollution source in Kabwe (Kamona et al., 1999). These findings are quite similar with those which were indicated by previous studies of rat and goat (Liu et al., 2014; Nakata et al., 2016). Among the rat tissues of high-metal exposure group, lung tissues showed the isotopic values closer to those of galena compared with other tissues except for kidney, suggesting the possibility that lung could be the tissue absorbing Pb from outside of the body. After the absorption from lung, the isotopic compositions of Pb could be fractionated during the distribution to other tissues as the former research suggested although the exact mechanism is still unknown (Nakata et al., 2016). These findings also support the hypothesis of a large contribution of inhalation to the Pb absorption which was indicated by the result of metal accumulation ratios of lung to liver. Considering the route of exposure in the present study, the contribution of inhalation of soil particles cannot be neglected. Indeed, Cd was accumulated in the lungs of rats due to inhalation of both soluble and insoluble forms (Takenaka et al., 2004). Our results proposed meteorological factors could play an important role of exposure level via inhalation in the field although the meteorological factor was not verified in the present study of a laboratory experiment. When the amount of precipitation is small and soil moisture level is low, the soil containing Pb could easily scatter. Similarly, the strong wind could also increase the amount of scattered dust. The increased amount of dust would contribute to the increase of Pb exposure via inhalation. On the other hand, the wet surface soil could decrease the exposure level via inhalation. Climate change, which is one of the major concerns in the world in recent years, could also affect the environmental exposure level.

Although Cd was not detected in any individual rat, significantly higher concentrations of Pb were observed in the brain in the high-metal exposure group. Pb is known to pass through the blood/brain barrier and accumulate in the brain (Struzynska et al., 1997), and this phenomenon was also confirmed here in the case of soil exposure.

Among the tissues examined, quite different patterns of accumulation were observed between Cd and Pb in the tibia. Cd in the tibia did not differ among the groups, whereas quite high concentrations of Pb (average: 54.4 mg/kg) were detected. This value was comparable to that reported previously by de Figueiredo et al. (2014) who demonstrated that newborn rats exposed to 30 mg Pb/L in drinking water for 60 days after birth accumulated 43.4 mg/kg of Pb in the tibia (Supplementary Table S7). Similarly, rats exposed to 500 mg Pb/L in drinking water for 84 days had 58.2 mg/kg of Pb in the femur (Li et al., 2013a,b). Notably, in the study by Li et al. (2013a,b), rats showed hippocampal damage associated with Pb exposure. This accumulation pattern in the tibia can be explained by competition of Pb for Ca^{2+} and deposition in the bone as more than 90% of total Pb burden in the body accumulates in bone tissues. The accumulation factor supports this difference between Cd and Pb; i.e., the highest accumulation factor for Pb and the second lowest accumulation factor for Cd were observed in the tibia. The half-life of Pb in the tibia is estimated as 20–30 years in humans (Gerhardsson et al., 1993) and lacteal as well as transplacental transfer is one of the most serious exposure routes in infants (Chen et al., 2014). Although the present study used male rats, similar soil exposure experiments using pregnant females to clarify the effects on neonates would be interest because an earlier study indicated that rat pups of dams exposed to Pb via drinking water showed neurochemical alterations in the cerebellum and striatum (Antonio et al., 2002).

As we found that soil exposure can cause Cd and Pb tissue accumulation, we further analyzed blood biochemistry and behavioral changes in the present study. Some of the items examined suggested that the levels of functional damage in the liver and kidney were not severe. In contrast, decreases in behavioral activity were observed in the soil-exposed groups, suggesting effects of Pb on the central nervous system. In accordance with our study, Pb was reported to cause a significant decrease of locomotor activity in Wistar rats chronically administered 0.5% (v/v) Pb acetate in drinking water for 3 months, with concomitant astrocytic and dopaminergic changes involved in controlling many aspects of brain function (Sansar et al., 2011). Although the molecular mechanism of Pb neurotoxicity is not elucidated well, however some possible pathways such as alterations in genetic regulation and protein synthesis have been reported so far. For instance, the expression, synthesis and conformational maturation of the neuronal cell adhesion molecule (NCAM) are affected by Pb exposure (Breen and Regan, 1988; Davey and Breen, 1998). Additionally, voltage-gated calcium channels, which allow the flow in a number of mono- and polyvalent cations, is also affected by Pb. It was observed that Pb is capable of blocking some types of calcium channels, including potassium currents in neurons (Peng et al., 2002; Dai et al., 2001). Oxidative stress is also associated with neurotoxicity of Pb. The former exposure study of rat discovered higher levels of brain 2-thiobarbituric acid-reactive substances, an indicator of lipid oxidation, and higher activities of glutathione reductase and glutathione peroxidase compared with controls (Adonaylo and Oteiza, 1999). In the exposure study of the rat to Pb which was done by Villeda-Hernandez et al. (2001), revealed Pb accumulation was related with high levels of lipid oxidation products in different brain regions, such as the parietal cortex, striatum, hippocampus, thalamus and cerebellum. Pb is known to be neurotoxic in humans, especially children, because of its ability to compete with Ca^{2+} in nerve functioning (Crosby, 1998). Recently, the Centers for Disease Control and Prevention (CDC, 2012) revised

the blood lead "level of concern" from 10 to 5 μg/dL in response to reports that Pb levels of <10 μg/dL can cause neurological abnormalities, such as decreased IQ in children (Canfield et al., 2003). Therefore, a threshold below which Pb does not result in neurological deficits has not been determined (Needleman et al., 1990). The present results were consistent in that behavioral changes were detected at an earlier stage before tissue dysfunctions were observed. In general, biological responses precede the appearance of tissue damage. Therefore, we analyzed the alterations of MT and confirmed the induction of MT-1 as well as MT-2 mRNA in the kidneys of rats in the high-metal exposure group. On the other hand, no significant difference of MT-1 and MT-2 expression in the liver samples was observed among the groups, supporting the former study which revealed the expression levels of MT-1 and MT-2 expression in the livers of rats from Kabwe, where the soil used in the present study was collected, had no significant difference with those from control site (Nakayama et al., 2013). However, in case of acute exposure, the induction of MT-1 and MT-2 in kidney of Cd-exposed rat was much lower than in the liver (Vasconcelos et al.). The major difference between the current study and the former acute exposure study is the accumulated hepatic metal levels. Our study showed approximately 5 times and 2 times greater levels of Cd and Pb in liver of high-metal exposure group compared with those of control, respectively, whereas almost 100 times elevation of the hepatic Cd level were discovered within 24 h after exposure in the acute exposure experiment. Such the difference of exposure period and accumulation level could be the reason why the significant difference in the hepatic MT expression levels was not observed in our study.

Interestingly, global DNA methylation was altered in the testis in the high-metal exposure group, although no changes were detected in the liver or kidneys in the present study. This finding was supported by the higher mRNA expression levels of *de novo* DNA methyltransferases, Dnmt 3a and Dnmt 3b, in the testis and the positive associations among metals, methylation levels, and methyltransferases characterized by PCA. It is unclear why the only testis showed a significant difference in DNA hypermethylation status; however, one of the possible reasons is the rapid cell division in the testis compared to in other organs. The short cycle of cell division could contribute to the high sensitivity to molecular alteration. Ikeda et al. (2013) reported testis- or germ cell-specific hypomethylated DNA domains with unique epigenetic features on the mouse X chromosome, suggesting the unique molecular character of the testis. Acute exposure (1 week) of TRL 1215 rat liver cells to Cd inhibited DNA methyltransferase activity and induced global DNA hypomethylation, whereas a relatively longer exposure period (10 weeks) resulted in DNA hypermethylation and enhanced DNA methyltransferase activity, suggesting that the effects of prolonged Cd exposure on DNA methylation may be responsible for its carcinogenicity (Arita and Costa, 2009; Takiguchi et al., 2003). Another study also showed that 10-week exposure to Cd induced malignant transformation associated with global DNA hypermethylation, higher Dnmt 3b protein expression, and increased Dnmt activity, without any change in Dnmt 1 (Arita and Costa, 2009; Benbrahim-Tallaa et al., 2007). In fact, previous studies suggested that Dnmt 3a and Dnmt 3b, but not Dnmt 1, are responsible for *de novo* methylation *in vivo*, as embryonic stem (ES) cells of mice lacking Dnmt 1 are still capable of methylating retroviral DNA *de novo* (Lei et al., 1996; Okano et al., 1999). Taken together, our results and those of these previous reports indicate that chronic Cd exposure can cause global DNA hypermethylation in relation to the elevation of Dnmt 3a and Dnmt 3b mRNA expression and activities. It should be noted that Cd induced global DNA hypomethylation, and this could be attributed to the potential facilitator of Cd-stimulated cell proliferation in the chronic myelogenous leukemia K562 cell line (Arita and Costa, 2009; Huang et al., 2008).

In a human epidemiological study, significant associations were observed between urinary Cd concentrations and global DNA methylation as well as between arsenic metabolism (measured as percentage of dimethylarsinate) and global DNA hydroxymethylation (Tellez-Plaza et al., 2014). The major limitation of the present study was that we did not measure hydroxymethylation levels. Histone modification is also one of the key factors of epigenetics while the limited number of studies has reported an effect of Cd and Pb on histone modification. It was suggested that Cd exposure could make heritable change in chromatin structure for rapid transcription activation, resulting the establishment and maintenance of a bivalent chromatin domain at the MT-3 promoter as well as histone modifications (Martinez-Zamudio and Ha, 2011). In Cd-transformed urothelial cells, levels of H3K4me3, H3K27me3 and H3K9me3 occupancy at the MT-3 promoter were increased compared to untransformed cells, indicating chronic Cd exposure may alter transcriptional responses through histone modification (Somji et al., 2011). Relating to Pb, Cantone et al. (2011) reported that the levels of H3K4me2 and H3K9ac on histones from blood leukocytes of steel production plant workers were not significantly associated with the Pb exposure level. Another factor of epigenetic alteration is miRNA expression. After 3 days exposure to particulate matter (PM) containing Cd, the expression of miR-146a in peripheral blood leukocytes from electric furnace steel plant workers was not statistically increased whereas miR-146a was negatively associated with exposure (Bollati et al., 2010). Same research group also reported that miR-222 expression showed a positive association with Pb exposure, while miR-146a expression was negatively correlated with Pb (Bollati et al., 2010). Further studies of the association between metal exposure and hydroxymethylation status, histone modification and miRNA expression are required to reveal the molecular alteration mechanisms.

In contrast to the elevated methylation observed in the present study, the methylation status of Long Interdispersed Nuclear Element 1 (LINE-1) in pheochromocytoma (PC12) cells decreased after acute exposure to 500 nM Pb for 2 and 7 days (Li et al., 2012). In addition, a dose-dependent decrease in global DNA methylation in PC12 cells was observed with decreasing Dnmt 1 mRNA expression (Li et al., 2012). These discrepancies may be explained by differences in exposure duration, as we used 1-year prolonged chronic exposure. Similar phenomena (i.e., hypomethylation with acute exposure and hypermethylation with chronic exposure) observed in the case of Cd exposure were discussed above (Arita and Costa, 2009; Takiguchi et al., 2003). Long-term chronic exposure experiments are necessary to elucidate the effects of Pb on epigenetics.

Another interesting observed in the present study was that we found alterations in DNA methylation in the male testis as a recent study indicated that aberrant DNA methylation of the H19-DMR (differentially methylated region) and the DAZL (deleted in azoospermia-like) gene promoters is associated with defects in sperm production/function in infertile men (Li et al., 2013a,b). Recently, our research team reported severe Pb accumulation in the blood of children in Kabwe mining site, Zambia, from which our soil samples were collected, and all children examined under the age of 7 years ($n = 246$) had blood Pb levels exceeding 5 μg/dL with a maximum of 427.8 μg/dL (Yabe et al., 2015). An earlier report showed that maternal bone Pb levels in humans were inversely associated with cord blood methylation levels in LINE-1 and a short interspersed element (Alu-1), which are frequently analyzed in genomic DNA methylation studies (Pilsner et al., 2009a). However, little is known about the relationship between Pb exposure and DNA methylation (and hydroxymethylation) in humans. Therefore,

the effects of prolonged Pb exposure on epigenetics modifications in children at this site should be examined in future studies.

5. Conclusions

The aim of this study was to verify whether soil exposure under environmentally relevant circumstances results in metal accumulation and epigenetic modifications in the rats. Our present results suggested that soil contaminated with Cd and Pb caused tissue metal accumulation and epigenetic alterations, such as elevation of global DNA methylation, in rats. From the view of metal accumulation ratios (lung/liver) and Pb isotopic ratios in the tissues, it was suggested that the respiratory exposure would make up a significant proportion of metal absorption into the body. Although we found elevation of methylation status in the rat testis, contradictory results have also been documented in the literature. Further studies are required to gain a better understanding of this issue.

Declarations of interest

None.

Acknowledgments

This work was supported by Grants-in-Aid for Scientific Research from the Ministry of Education, Culture, Sports, Science and Technology of Japan awarded to M. Ishizuka (No. 16H0177906, 18K1984708) and Y. Ikenaka (No. 26304043, 15H0282505, 15K1221305, 17K2003807, 18H0413208), and S.M.M. Nakayama (No. 16K16197, 17KK0009), and the foundation of JSPS Core to Core Program (AA Science Platforms), the Environment Research and Technology Development Fund (SII-1/3-2, 4RF-1802/18949907) of the Environmental Restoration and Conservation Agency of Japan. We also acknowledge financial support from The Soroptimist Japan Foundation, The Nakajima Foundation, The Sumitomo Foundation, The Nihon Seimei Foundation and The Japan Prize Foundation. This research was also supported by JST/JICA, SATREPS (Science and Technology Research Partnership for Sustainable Development; No. JPMJSA1501). We are grateful to Mr. Takahiro Ichise and Ms. Nagisa Hirano (Laboratory of Toxicology, Faculty of Veterinary Medicine, Hokkaido University) for technical support with metal concentration and isotope analyses. We are also grateful to Dr. Kazuyuki D. Tanaka, Mr. Kyohei Hamada, and Mr. Taro Muroya for their support in this study.

Appendix A. Supplementary data

Supplementary data to this article can be found online at https://doi.org/10.1016/j.envpol.2019.05.038.

References

Adonaylo, V.N., Oteiza, O.I., 1999. Pb^{2+} promotes lipid oxidation and alterations in membrane physical properties. Toxicology 132 (1), 19–32. PMID: 10199578. https://doi.org/10.1016/S0300-483X(98)00134-6.

Antonio, M.T., Lopez, N., Leret, M.L., 2002. Pb and Cd poisoning during development alters cerebellar and striatal function in rats. Toxicology 176 (1–2), 59–66. PMID: 12062930. https://doi.org/10.1016/S0300-483X(02)00137-3.

Arita, A., Costa, M., 2009. Epigenetics in metal carcinogenesis: nickel, arsenic, chromium and cadmium. Metall 1 (3), 222–228. PMID: 20461219. https://doi.org/10.1039/B903049B.

Benbrahim-Tallaa, L., Waterland, R., Dill, A., Webber, M., Waalkes, M., 2007. Tumorsuppressor gene inactivation during cadmium-induced malignant transformation of human prostate cells correlates with overexpression of de novo DNA methyltransferase. Environ. Health Perspect. 115 (10), 1454–1459. PMID: 17938735. https://doi.org/10.1289/ehp.10207.

Blacksmith Institute, 2014. Project completion report: lead poisoning crisis in Nigeria. Available. https://www.pureearth.org/wp-content/uploads/2014/10/Zamfara_Nigeria_PCR -April-2011.pdf. (Accessed 22 September 2018).

Bollati, V., Marinelli, B., Apostoli, P., Bonzini, M., Nordio, F., Hoxha, M., Pegoraro, V., Motta, V., Tarantini, L., Cantone, L., Schwartz, J., Bertazzi, P.A., Baccarelli, A., 2010. Exposure to metal-rich particulate matter modifies the expression of candidate microRNAs in peripheral blood leukocytes. Environ. Health Perspect. 118 (6), 763–768. PMID: 20061215. https://doi.org/10.1289/ehp.0901300.

Bollhöfer, A., Rosman, K.J.R., 2001. Isotopic source signatures for atmospheric lead: the Northern Hemisphere. Geochem. Cosmochim. Acta 65 (11), 1727–1740. https://doi.org/10.1016/S0016-7037(00)00630-X.

Breen, K.C., Regan, C.M., 1988. Lead stimulates Golgi sialyltransferase at times coincident with the embryonic to adult conversion of the neural cell adhesion molecule, (N-CAM). Toxicology 49, 71-56, PMID: 3376125. https://doi.org/10.1016/0300-483X(88)90176-X.

Calabrese, E.J., Stanek, E., James, R.C., Roberts, S.M., 1997. Soil ingestion: a concern for acute toxicity in children. Environ. Health Perspect. 105 (12), 1354–1358. PMID: 9405323. https://doi.org/10.1289/ehp.971051354.

Canfield, R.L., Henderson Jr., C.R., Cory-Slechta, D.A., Cox, C., Jusko, T.A., Lanphear, B.P., 2003. Intellectual impairment in children with blood lead concentrations below 10 μg per deciliter. N. Engl. J. Med. 348 (16), 1517–1526. PMID: 12700371. https://doi.org/10.1056/NEJMoa022848.

Cantone, L., Nordio, F., Hou, L., Apostoli, P., Bonzini, M., Tarantini, L., Angelici, L., Bollati, V., Zanobetti, A., Schwartz, J., Bertazzi, P.A., Baccarelli, A., 2011. Inhalable metal-rich air particles and histone H3K4 dimethylation and H3K9 acetylation in a cross-sectional study of steel workers. Environ. Health Perspect. 119 (7), 964–969. PMID: 21385672. https://doi.org/10.1289/ehp.1002955.

CDC (Centers for Disease Control and Prevention), 2012. Low Level Lead Exposure Harms Children: a renewed call for primary prevention. Report of the advisory committee on childhood lead poisoning prevention of the Centers for Disease Control and Prevention. Atlanta, Ga. Available. www.cdc.gov/nceh/lead/acclpp/final_document_030712.pdf. (Accessed 22 September 2018).

Chen, Z., Myers, R., Wei, T., Bind, E., Kassim, P., Wang, G., Ji, Y., Hong, X., Caruso, D., Bartell, T., Gong, Y., Strickland, P., Navas-Acien, A., Guallar, E., Wang, X., 2014. Placental transfer and concentrations of cadmium, mercury, lead, and selenium in mothers, newborns, and young children. J Expo Sci Environ 24 (5), 537–544. PMID: 24756102. https://doi.org/10.1038/jes.2014.26.

Crosby, D.G., 1998. Inorganic toxicants. In: Environmental Toxicology and Chemistry. University Press, New York, NY, pp. 205–225. Oxford.

Dai, X., Ruan, D., Chen, J., Wang, M., Cai, L., 2001. The effects of lead on transient outward currents of acutely dissociated rat dorsal root ganglia. Brain Res. 904, 327–340. PMID: 11406131. https://doi.org/10.1016/S0006-8993(01)02505-7.

Davey, F.D., Breen, K.C., 1998. Stimulation of sialyltransferase by subchronic low-level lead exposure in the developing nervous system. Toxicol. Appl. Pharmacol. 151 (1), 16–21. PMID: 9705883. https://doi.org/10.1006/taap.1998.8427.

de Figueiredo, F.A., Gerlach, R.F., da Veiga, M.A., Nakadi, F.V., Ramos, J., Kawakita, E.R., Guerra, C.S., Issa, J.P., 2014. Reduced bone and body mass in young male rats exposed to lead. BioMed Res Int Article ID 571065. PMID: 24800241. https://doi.org/10.1155/2014/571065.

Dooyema, C.A., Neri, A., Lo, Y.C., Durant, J., Dargan, P.I., Swarthout, T., Biya, O., Gigado, S.O., Haladu, S., Sani-Gwarzo, N., Nguku, P.M., Akpan, H., Idris, S., Bashir, A.M., Brown, M.J., 2012. Outbreak of fatal childhood lead poisoning related to artisanal gold mining in northwestern Nigeria, 2010. Environ. Health Perspect. 120 (4), 601–607. PMID: 22186192. https://doi.org/10.1289/ehp.1103965.

Feinberg, A.P., 2010. Genome-scale approaches to the epigenetics of common human disease. Virchows Arch. 456 (1), 13–21. PMID: 19844740. https://doi.org/10.1007/s00428-009-0847-2.

Gerhardsson, L., Attewell, R., Chettle, D.R., Englyst, V., Lundstrom, N.G., Nordberg, G.F., Nyhlin, H., Scott, M.C., Todd, A.C., 1993. In vivo measurements of lead in bone in long-term exposed lead smelter workers. Arch. Environ. Health 48 (3), 147–156. PMID: 8333784. https://doi.org/10.1080/00039896.1993.9940813.

Huang, D., Zhang, Y., Qi, Y., Chen, C., Weihong, J., 2008. Global DNA hypomethylation, rather than reactive oxygen species (ROS), a potential facilitator of cadmium-stimulated K562 cell proliferation. Toxicol. Lett. 179 (1), 43–47. PMID: 18482805. https://doi.org/10.1016/j.toxlet.2008.03.018.

Ikeda, R., Shiura, H., Numata, K., Sugimoto, M., Kondo, M., Mise, N., Suzuki, M., Greally, J.M., Abe, K., 2013. Large, male germ cell-specific hypomethylated DNA domains with unique genomic and epigenomic features on the mouse X chromosome. DNA Res. 20 (6), 549–565. PMID: 23861320. https://doi.org/10.1093/dnares/dst030.

Jarup, L., Akesson, A., 2009. Current status of cadmium as an environmental health problem. Toxicol. Appl. Pharmacol. 238 (3), 201–208. PMID: 19409405. https://doi.org/10.1016/j.taap.2009.04.020.

Kamona, A.F., Leveque, J., Friedrich, G., Haack, U., 1999. Lead isotopes of the carbonate-hosted Kabwe, Tsumeb, and Kipushi Pb-Zn-Cu sulphide deposits in relation to Pan African orogenesis in the Damaran-Lufilian fold belt of Central Africa. Miner. Depos. 34 (3), 273–283.

Kuritani, T., Nakamura, E., 2002. Precise isotope analysis of nanogram-level Pb for natural rock samples without use of double spikes. Chem. Geol. 186 (1–2), 31–43. https://doi.org/10.1016/S0009-2541(02)00004-9.

Lei, H., Oh, S.P., Okano, M., Juttermann, R., Goss, K.A., Jaenisch, R., Li, E., 1996. De novo DNA cytosine methyltransferase activities in mouse embryonic stem cells. Development 122 (10), 3195–3205. PMID: 8898232.

Li, B., Li, J.B., Xiao, X.F., Ma, Y.F., Wang, J., Liang, X.X., Zhao, H.X., Jiang, F., Yao, Y.Q., Wang, X.H., 2013a. Altered DNA methylation patterns of the H19 differentially methylated region and the DAZL gene promoter are associated with defective

human sperm. PLoS One 8 (8), e71215. PMID: 24015185. https://doi.org/10.1371/journal.pone.0071215.

Li, H.W., Deng, J.G., Du, Z.C., Yan, M.S., Long, Z.X., Thi, P.T.P., Yang, K.D., 2013b. Protective effects of mangiferin in subchronic developmental lead-exposed rats. Biol. Trace Elem. Res. 152 (2), 233–242. PMID: 23359033. https://doi.org/10.1007/s12011-013-9610-2.

Li, Y.Y., Chen, T., Wan, Y., Xu, S.Q., 2012. Lead exposure in pheochromocytoma cells induces persistent changes in amyloid precursor protein gene methylation patterns. Environ. Toxicol. 27 (8), 495–502. PMID: 22764079. https://doi.org/10.1002/tox.20666.

Liu, D., Wu, J., Ouyang, L., Wang, J., 2014. Variations in lead isotopic abundances in sprague-dawley rat tissues: possible reason of formation. PLoS One 9 (2), e89805. PMID: 24587048. https://doi.org/10.1371/journal.pone.0089805.

Lo, Y.C., Dooyema, C.A., Neri, A., Durant, J., Jefferies, T., Menina-Marino, A., de Ravello, L., Throughman, D., Davis, L., Dankoli, R.S., Samson, M.Y., Ibrahim, L.M., Okechukwu, O., Umar-Tsafe, N.T., Dama, A.H., Brown, M.J., 2012. Childhood lead poisoning associated with gold ore processing: a village-level investigation-Zamfara State, Nigeria. Environ. Health Perspect. 120 (10), 1450–1455. October-November 2010 PMID: 22766030. https://doi.org/10.1289/ehp.1104793.

Manton, W.I., Angle, C.R., Stanek, K.L., Reese, Y.R., Kuehnemann, T.J., 2000. Acquisition and retention of lead by young children. Environ. Res. 82 (1), 60–80. PMID: 10677147. https://doi.org/10.1006/enrs.1999.4003.

Martinez-Zamudio, R., Ha, H.C., 2011. Environmental epigenetics in metal exposure. Epigenetics 6 (7), 820–827. PMID: 21610324. https://doi.org/10.4161/epi.6.7.16250.

Nakata, H., Nakayama, S.M.M., Yabe, J., Liazambi, A., Mizukawa, H., Darwish, W.S., Ikenaka, Y., Ishizuka, M., 2016. Reliability of stable Pb isotopes to identify Pb sources and verifying biological fractionation of Pb isotopes in goats and chickens. Environ. Pollut. 208, 395–403. PMID: 26549754. https://doi.org/10.1016/j.envpol.2015.10.006.

Nakayama, S.M.M., Ikenaka, Y., Hamada, K., Muzandu, K., Choongo, K., Teraoka, H., Mizuno, N., Ishizuka, M., 2011. Metal and metalloid contamination in roadside soil and wild rats around a Pb-Zn mine in Kabwe, Zambia. Environ. Pollut. 159 (1), 175–181. PMID: 20971538. https://doi.org/10.1016/j.envpol.2010.09.007.

Nakayama, S.M.M., Ikenaka, Y., Hamada, K., Muzandu, K., Choongo, K., Yabe, J., Umemura, T., Ishizuka, M., 2013. Accumulation and biological effects of metals in wild rats in mining areas of Zambia. Environ. Monit. Assess. 185 (6), 4907–4918. PMID: 23054276. https://doi.org/10.1007/s10661-012-2912-6.

Needleman, H.L., Schell, A., Bellinger, D., Leviton, A., Allred, E., 1990. The long-term effects of exposure to low doses of lead in childhood: an 11-year follow-up report. N. Engl. J. Med. 322, 83–88. PMID: 2294437. https://doi.org/10.1056/NEJM199001113220203.

Okano, M., Bell, D.W., Haber, D.A., Li, E., 1999. DNA Methyltransferases Dnmt3a and Dnmt3b are essential for de novo methylation and mammalian development. Cell 99 (3), 247–257. PMID: 10555141. https://doi.org/10.1016/S0092-8674(00)81656-6.

Ordovas, J.M., Smith, C.E., 2010. Epigenetics and cardiovascular disease. Nat. Rev. Cardiol. 7 (9), 510–519. PMID: 20603647. https://doi.org/10.1038/nrcardio.2010.104.

Peng, S., Hajela, R.K., Atchison, W.D., 2002. Characteristics of block by Pb^{2+} of function of human neuronal L-, N-, and R-type Ca^{2+} channels transiently expressed in human embryonic kidney 293 cells. Mol. Pharmacol. 62, 1418–1430. PMID: 12435810. https://doi.org/10.1124/mol.62.6.1418.

Pilsner, J.R., Hu, H., Ettinger, A., Sanchez, B.N., Wright, R.O., Cantonwine, D., Lazarus, A., Lamadrid-Figueroa, H., Mercado-Garcia, A., Tellez-Rojo, M.M., Hernandez-Avila, M., 2009a. Influence of prenatal lead exposure on genomic methylation of cord blood DNA. Environ. Health Perspect. 117 (9), 1466–1471. PMID: 19750115. https://doi.org/10.1289/ehp.0800497.

Pilsner, J.R., Lazarus, A.L., Nam, D.H., Letcher, R.J., Sonne, C., Dietz, R., Basu, N., 2009b. Mercury-associated DNA hypomethylation in polar bear brains via the LUminometric Methylation Assay: a sensitive method to study epigenetics in wildlife. Mol. Ecol. 19 (2), 307–314. PMID: 20002585. https://doi.org/10.1111/j.1365-294X.2009.04452.x.

Qiu, H., Peijnenburg, W.J.G.M., van Gestel, C.A.M., Vijver, M.G., 2014. Can commonly measurable traits explain differences in metal accumulation and toxicity in earthworm species? Ecotoxicology 23 (1), 21–32. PMID: 24193403. https://doi.org/10.1007/s10646-013-1147-9.

Ray, P.D., Yosim, A., Fry, R.C., 2014. Incorporating epigenetic data into the risk assessment process for the toxic metals arsenic, cadmium, chromium, lead, and mercury: strategies and challenges. Front. Genet. 5, 201. PMID: 25076963. https://doi.org/10.3389/fgene.2014.00201.

Sansar, W., Ahboucha, S., Gamrani, H., 2011. Chronic lead intoxication affects glial and neural systems and induces hypoactivity in adult rat. Acta Histochem. 113 (6), 601–607. PMID: 20656334. https://doi.org/10.1016/j.acthis.2010.06.005.

Smith, D.R., Osterloh, J.D., Flegal, A.R., 1996. Use of endogenous, stable lead isotopes to determine release of lead from the skeleton. Environ. Health Perspect. 104 (1), 60–66. PMID: 88344863. https://doi.org/10.1289/ehp.9610460.

Somji, S., Garrelt, S.H., Toni, C., Zhou, X., Zheng, Y., Ajjimaporn, A., Sens, M.A., Sens, D.A., 2011. Differences in the epigenetic regulation of MT-3 gene expression between parental and Cd+ 2 or As+ 3 transformed human urothelial cells. Cancer Cell Int. 11 (1), 2, PMID: 21303554. https://doi.org/10.1186/1475-2867-11-2.

Struzynska, L., Walski, M., Gadamski, R., Dabrowska-Bouta, B., Rafałowska, U., 1997. Lead-induced abnormalities in blood-brain barrier permeability in experimental chronic toxicity. J. Mol. Neurosci. 31 (3), 207–224. PMID: 9336764. https://doi.org/10.1007/BF02815125.

Takenaka, S., Karg, E., Kreyling, W.G., Lentner, B., Schulz, H., Ziesenis, A., Schramel, P., Heyder, J., 2004. Fate and toxic effects of inhaled ultrafine cadmium oxide particles in the rat lung. Inhal. Toxicol. 16 (Suppl. 1), 83–92. PMID: 15204796. https://doi.org/10.1080/08958370490443141.

Takiguchi, M., Achanzar, W., Qu, W., Li, G., Waalkes, M., 2003. Effects of cadmium on DNA-(cytosine-5) methyltransferase activity and DNA methylation status during cadmium induced cellular transformation. Exp. Cell Res. 286 (2), 355–365. PMID: 12749863. https://doi.org/10.1016/S0014-4827(03)00062-4.

Tellez-Plaza, M., Tang, W.Y., Shang, Y., Umans, J.G., Francesconi, K.A., Goessler, W., Ledesma, M., Leon, M., Laclaustra, M., Pollak, J., Guallar, E., Cole, S.A., Fallin, M.D., Navas-Acien, A., 2014. Association of global DNA methylation and global DNA hydroxymethylation with metals and other exposures in human blood DNA samples. Environ. Health Perspect. 122 (9), 946–954. PMID: 24769358. https://doi.org/10.1289/ehp.1306674.

Uno, T., Kobayashi, E., Suwazono, Y., Okubo, Y., Miura, K., Sakata, K., Okayama, A., Ueshima, H., Nakagawa, H., Nogawa, K., 2005. Health effects of cadmium exposure in the general environment in Japan with special reference to the lower limit of the benchmark dose as the threshold level of urinary cadmium. Scand. J. Work. Environ. Health 31 (4), 307–315. PMID: 16161714.

Veysseyre, A.M., Bollhöfer, A.F., Rosman, K.J., Ferrari, C.P., Boutron, C.F., 2001. Tracing the origin of pollution in French Alpine snow and aerosols using lead isotopic ratios. Environ. Sci. Technol. 35 (22), 4463–4469. PMID: 11757602. https://doi.org/10.1021/es0105717.

Villeda-Hernandez, J., Barroso-Moguel, R., Mendez-Armenta, M., Nava-Ruız, C., Huerta-Romero, R., Rıos, C., 2001. Enhanced brain regional lipid peroxidation in developing rats exposed to low level lead acetate. Brain Res. Bull. 55 (2), 247–251. PMID: 11470323. https://doi.org/10.1016/S0361-9230(01)00512-3.

Waalkes, M.P., Klaassen, C.D., 1985. Concentration of metallothionein in major organs of rats after administration of various metals. Toxicol. Sci. 5 (3), 473–477. PMID: 4007305. https://doi.org/10.1016/0272-0590(85)90094-6.

Winiarska-Mieczan, A., 2014. Cumulative rate and distribution of Cd and Pb in the organs of adult male Wistar rats during oral exposure. Environ. Toxicol. Pharmacol. 38 (3), 751–760. PMID: 25305736. https://doi.org/10.1016/j.etap.2014.08.016.

Wu, J., Liu, D., Xie, Q., Wang, J., 2012. Biological fractionation of lead isotopes in sprague-dawley rats lead poisoned via the respiratory tract. PLoS One 7 (12), e52462. PMID: 23300678. https://doi.org/10.1371/journal.pone.0052462.

Yabe, J., Nakayama, S.M.M., Ikenaka, Y., Muzandu, K., Choongo, K., Mainda, G., Kabeta, M., Ishizuka, M., Umemura, T., 2011. Uptake of lead, cadmium, and other metals in the liver and kidneys of cattle near a lead-zinc mine in Kabwe, Zambia. Environ. Toxicol. Chem. 30 (8), 1892–1897. PMID: 21590713. https://doi.org/10.1002/etc.580.

Yabe, J., Nakayama, S.M.M., Ikenaka, Y., Yohannes, Y.B., Bortey-Sam, N., Oroszlany, B., Muzandu, K., Choongo, K., Kabalo, A.N., Ntapisha, J., Mweene, A., Umemura, T., Ishizuka, M., 2015. Lead poisoning in children from townships in the vicinity of a lead-zinc mine in Kabwe, Zambia. Chemosphere 119, 941–947. PMID: 25303652. https://doi.org/10.1016/j.chemosphere.2014.09.028.

Yabe, J., Nakayama, S.M.M., Ikenaka, Y., Yohannes, Y.B., Bortey-Sam, N., Kabalo, A.N., Ntapisha, J., Mizukawa, H., Umemura, T., Ishizuka, M., 2018. Lead and cadmium excretion in feces and urine of children from polluted townships near a lead-zinc mine in Kabwe, Zambia. Chemosphere 202, 48–55. PMID: 29554507. https://doi.org/10.1016/j.chemosphere.2018.03.079.

Chemosphere 228 (2019) 17–25

Contents lists available at ScienceDirect

Chemosphere

journal homepage: www.elsevier.com/locate/chemosphere

Solidification of sand by Pb(II)-tolerant bacteria for capping mine waste to control metallic dust: Case of the abandoned Kabwe Mine, Zambia

Wilson Mwandira [a], Kazunori Nakashima [b, *], Satoru Kawasaki [b], Mayumi Ito [b], Tsutomu Sato [b], Toshifumi Igarashi [b], Meki Chirwa [c], Kawawa Banda [c], Imasiku Nyambe [c], Shouta Nakayama [d], Hokuto Nakata [d], Mayumi Ishizuka [d]

[a] Graduate School of Engineering, Hokkaido University, Kita 13, Nishi 8, Kita-Ku, Sapporo, 060-8628, Japan
[b] Faculty of Engineering, Hokkaido University, Kita 13, Nishi 8, Kita-Ku, Sapporo, 060-8628, Japan
[c] IWRM Centre/Geology Department, School of Mines, University of Zambia, P.O. Box 32379, Zambia
[d] Faculty of Veterinary Medicine, Hokkaido University, Kita 18, Nishi 9, Kita-Ku, Sapporo, 060-0818, Japan

HIGHLIGHTS

- Mine waste dump causing chronic Pb poisoning to humans by inhaling airborne dust.
- Proposed to use biomineralization to prevent the generation of dust.
- Isolated indigenous biomineralization bacteria showing biocementation capability.
- Capping mine waste by biomineralizing bacteria reduces risk to human health.
- Effective, sustainable and novel approach to eliminate Pb poisoning.

GRAPHICAL ABSTRACT

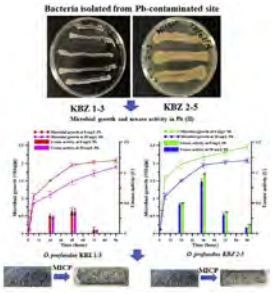

ARTICLE INFO

Article history:
Received 25 January 2019
Received in revised form
8 April 2019
Accepted 14 April 2019
Available online 16 April 2019

Handling Editor: Prof. X. Cao

Keywords:
Kabwe
Mine waste
Capping
Indigenous ureolytic bacteria
Biocementation

ABSTRACT

Environmental impacts resulting from historic lead and zinc mining in Kabwe, Zambia affect human health due to the dust generated from the mine waste that contains lead, a known hazardous pollutant. We employed microbially induced calcium carbonate precipitation (MICP), an alternative capping method, to prevent dust generation and reduce the mobility of contaminants. Pb-resistant Oceanobacillus profundus KBZ 1–3 and O. profundus KBZ 2–5 isolated from Kabwe were used to biocement the sand that would act as a cover to prevent dust and water infiltration. Sand biocemented by KBZ 1–3 and KBZ 2–5 had maximum unconfined compressive strength values of 3.2 MPa and 5.5 MPa, respectively. Additionally, biocemented sand exhibited reduced water permeability values of $9.6 \times 10-8$ m/s and $8.9 \times 10-8$ m/s for O. profundus KBZ 1–3 and KBZ 2–5, respectively, which could potentially limit the entrance of water and oxygen into the dump, hence reducing the leaching of heavy metals. We propose that these isolates represent an option for bioremediating contaminated waste by preventing both metallic dust from becoming airborne and rainwater from infiltrating into the waste. O. profundus KBZ 1–3 and O. profundus KBZ 2–5 isolated form Kabwe represent a novel species that has, for the first time, been applied in a bioremediation study.

* Corresponding author.
E-mail address: nakashima@geo-er.eng.hokudai.ac.jp (K. Nakashima).

https://doi.org/10.1016/j.chemosphere.2019.04.107
0045-6535/

1. Introduction

Kabwe Mine was a lead (Pb) and zinc (Zn) mine that commenced its operations in 1902 until its closure in 1994. Apart from lead and zinc, it also produced silver, manganese, cadmium, vanadium, and titanium in smaller quantities (Mufinda, 2015). Due to the extraction of different minerals, several mineral processing techniques were used, resulting in the production of different types of mine waste dumps (Fig. 1a). Several studies have cited chronic Pb poisoning in humans, and contamination of soil, water, and sediments in the mine and the surrounding areas (Kribek et al., 2009; Tembo et al., 2006; Yabe et al., 2015, 2018). The current blood levels of Pb in children exceeds 45 μg/dL, much higher than the recommended level of 5 μg/dL (Kosnett et al., 2007; Yabe et al., 2015). The predominant reason for this high Pb level in blood is the airborne Pb metallic dusts emanating from the mine waste dump. These dusts are blown by the prevailing winds into the residential areas, and due to their fine particulate nature, are either inhaled or ingested (Yabe et al., 2015). Leach plant residues (LPR) and kiln slag (KS), shown in Fig. 1b, are susceptible to wind and water erosion. These two types of wastes were selected for immobilization because they are deemed to be the most toxic and are distributed over the largest area onsite. In response to the concern of dust emanating from the mine wastes in Kabwe, remediation methods such as the revegetation of the waste dump by metallophytes was proposed and implemented, but subsequently failed because the plants failed to grow (Leteinturier et al., 2001). Additionally, mining waste has not been re-processed due to probably the cost of metal recovery (BMR Group PLC, 2019).

A promising technique to prevent metallic dust from becoming airborne in-situ is the immobilization of these wastes by microbially induced calcium carbonate precipitation (MICP) using ureolytic bacteria (Achal et al., 2013; Chen et al., 2017; Kim and Lee, 2018; Mwandira et al., 2017; Nam et al., 2016; Zhu et al., 2016). MICP involves the hydrolysis of urea into ammonium and carbamate by urease catalysis, which results in $CaCO_3$ formation in the presence of Ca^{2+} ions. The proposed use of MICP to cap mine wastes is expected to eliminate both dust generation and water infiltration, restoring the contaminated site. Related studies have proposed MICP for ground improvement (Salifu et al., 2016), coastal erosion control (Khan et al., 2015), mine waste immobilization (Achal et al., 2013), self-healing concrete (Wiktor and Jonkers, 2011), and wastewater treatment (Torres-Aravena et al., 2018). Although many ureolytic bacteria have been isolated, continued isolation and identification of more novel species, especially those that are indigenous to the area are indispensable. The present study focuses on (i) the isolation of a Pb-resistant ureolytic bacteria from contaminated waste at Kabwe mine site; (ii) the determination of the optimal Ca^{2+}/urea concentration, and (iii) the use of the bacteria to biocement the sand. Such an investigation, involving the isolation and identification of effective microorganisms for biotechnological applications, represents a sustainable approach to remediation, eliminating the current environmental problems without significantly changing the local ecological integrity. In this study, we introduced two new strains of ureolytic bacteria for the MICP process: *Oceanobacillus profundus* KBZ 1–3 and *Oceanobacillus profundus* KBZ 2–5.

2. Materials and methods

2.1. Soil sample collection

Fig. 1a shows the locations of two soil sampling points from the abandoned Kabwe mine site of Central Province, Zambia (15°27′–17°28′ S latitude and 23°06′–25°33′ E longitude). The mine waste was exported from Zambia under approval No. RCT 7686229, and the import was also permitted by Plant Protection Station, Ministry of Agriculture, Forestry and Fisheries, Japan under

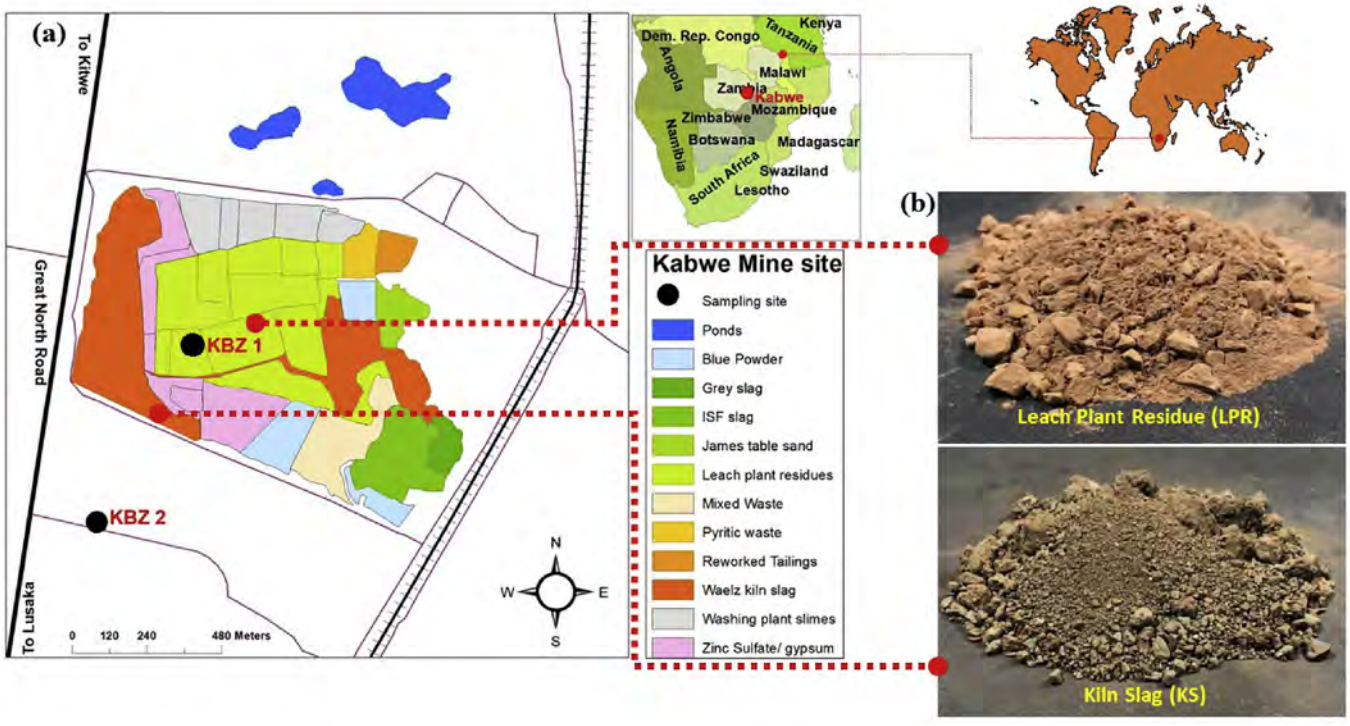

Fig. 1. (a) Location of soil sampling sites and the different mine wastes at the abandoned mine, Kabwe, Zambia (b) Appearance of leach plant residues (LPR) and kiln slag (KS).

the approval No. 29–836. The samples were transported from the site to the Laboratory of Biotechnology for Resources Engineering, Faculty of Engineering, Hokkaido University, Japan.

2.2. Isolation and molecular identification of Pb-resistant bacteria

Bacteria were isolated by placing 1 g of soil in a 15 mL sterile centrifuge tube and adding 10 mL of sterile water, followed by vigorous shaking by hand. Samples were diluted 10- to 10,000-fold using sterile water and plated on NH4 YE agar medium (20 g/L yeast extract; 10 g/L di-ammonium sulfate $(NH_4)_2SO_4$; 0.13 M tris buffer (pH = 8.0); and 20 g/L agar amended with Pb(II)) to isolate Pb-resistant strains. The plates were incubated at 30 °C for 72 h. Urease activity was screened according to a previous study by Danjo and Kawasaki (2015). In brief, the isolated colonies were mixed with 20 mL of cresol red solution (25 g/L urea and 0.4 g/L cresol red) and left standing at 45 °C for 2 h. After 2 h, the samples that changed their color to purple were selected.

The Pb-resistant isolate was identified by 16S rRNA sequence analysis. DNA extracts were amplified using two sets of primers targeting the 16S rRNA region specific for almost all bacterial 16S sequences: primers F9 (5′- GAGTTTGATCCTGGCTCAG -3′) and R1451 (5′- AAGGAGGTGATCCAGCC -3′). The PCR amplification cycle consisted of an initial denaturation step of 5 min at 94 °C, followed by 25 cycles of 1 min at 94 °C, 2 min at 60 °C, and 1 min at 72 °C and a final extension step of 30 min at 72 °C. The amplicons were separated by gel electrophoresis and the resulting DNA bands were extracted and purified using the FastGene™ PCR extraction Kit following the manufacturer's instructions (Nippon Genetics Co. Ltd. Tokyo, Japan). The extracted DNA was sent to Eurofins Genomics laboratory (Eurofins Genomics, Tokyo, Japan) for DNA sequencing. Subsequent phylogenetic analysis was conducted by TechnoSuruga Laboratory (TechnoSuruga Laboratory Company Ltd. Tokyo, Japan), which used the BLAST algorithm to find related sequences in the GeneBank Database, DNA Data Bank of Japan and the European Molecular Biology Laboratory.

2.3. Effects of Pb on microbial growth and urease activity of isolates

Microbial growth and urease activity were measured according to the procedures reported in a previous study (Mwandira et al., 2017). Microbial growth was measured by UV–vis spectrophotometry (V-730, Jasco International Co., Ltd., Tokyo, Japan) that recorded optical density (OD) readings at 600 nm for 96 h in the absence and presence of 50 mg/L Pb(II). Experiments were conducted in triplicate.

2.4. Determination of the optimal Ca^{2+}/urea concentration

Bioprecipitation experiments were carried out to determine the optimal Ca^{2+}/urea concentrations. The bacterial isolate was precultured for 24 h in 5 mL NH4 YE medium, then 1 mL of preculture was inoculated into 100 mL of NH4 YE medium to grow the main culture at 30 °C for 24 h with continuous aeration at 160 rpm. The bacterial suspension was then added to different equimolar concentrations of $CaCl_2$ and urea (0.1, 0.3, 0.5, 0.75, and 1.0 M). The mixtures were subsequently incubated for 24 h at 30 °C with shaking (160 rpm) and then centrifuged (15,000 rpm for 5 min) to collect the precipitate. The precipitate was weighed and then analyzed by XRD. Precipitation experiments were conducted in triplicate.

2.5. Syringe biocementation test

The Mizunami sand used in the experiments is uniformly graded with a mean particle size of 1.2 mm (Fig. S1 Supplementary material). Mizunami sand was used to represent sand that can be obtained locally near the contaminated site. The sand was sterilized, and hand packed into a 35-mL syringe (mean diameter, $D_{50} = 2.5$ cm and height, h = 7 cm), followed by the gentle injection of bacteria and solidification solution as illustrated in Fig. S2 (Supplementary material). Initially bacteria suspension was injected and allowed to stand in the column for 2 h and thereafter solidification solution was injected. This was repeated every 24 h for a period of 14 days. Additionally, two sets of biocementation experiments were conducted using conditions designed to mimic the possible conditions for in-situ injection of treatment solutions. In the first set of experiments, 2 mL of cementation solution was left above the surface of the sand to mimic saturated conditions; this procedure is called the immersed method. The second set of experiments was conducted by sequentially adding solution as the solution was drained; thus, this procedure is called the flow-through method. Control tests were also conducted following the same procedures but without the addition of bacterial cells.

Unconfined compressive strength (UCS) of the cemented samples was measured using a needle penetration device (SH-70, Maruto Testing Machine Company, Tokyo, Japan) to determine the strength of biocemented sand prepared by immersed and flow-through methods.

The $CaCO_3$ contents of the cemented samples were determined by the calcimetric method, which uses 3 M HCl acid and standard grade $CaCO_3$ (Hukue et al., 2001). In brief, 1.5 g solidified sand and 15 mL HCl in plastic vials were placed in a reaction vessel, which was then closed, tightened, zeroed, and sealed with O-rings. The vessel was then shaken to allow HCl to react with the sample, producing CO_2 gas. A digital manometer measured and recorded the CO_2 gas pressure readings. The same procedure was used to generate a calibration curve with known amounts of $CaCO_3$, which was used to quantify the readings from the specimen. The control and top center part of biocemented specimens treated by immersed and flow-through methods were tested.

2.6. Hydraulic conductivity

Hydraulic conductivity was assessed by the falling head method using a DIK 4000 system (Daiki Rika Kogyo Co., Ltd., Saitama, Japan). The samples were saturated with water and placed in a desiccator for 48 h before the measurement of hydraulic conductivity. Hydraulic conductivity was determined in control and biocemented specimens treated by both immersed and flow through methods.

2.7. SEM and XRD analysis

The microstructure of fractions of the biocemented samples was examined by scanning electron microscopy (SEM) (Miniscope TM3000, Hitachi, Tokyo, Japan). Additionally, X-ray diffraction (XRD) analysis (MiniFlex™, Rigaku Co., Ltd., Tokyo, Japan) was conducted using Ni-filtered Cu 1.5406 Å radiation to determine the mineral phases of both the control and biocemented sand. Scans were recorded from 5° to 80° of 2θ at a rate of 20°/min.

3. Results and discussion

3.1. Isolation of ureolytic bacteria

Ureolytic bacteria were isolated based on the color change of the

cresol red solution after urea hydrolysis. Colonies that changed the color of the solution from yellow to purple were selected. Color change is observed due to urea hydrolysis that causes the pH of the medium to rise. Of the thirty-five isolates from Kabwe, only four isolates, identified as *Oceanobacillus profundus* KBZ 1–3, *Psychrobacillus* sp. KBZ 2-2, *Oceanobacillus profundus* KBZ 2–3, and *O. profundus* KBZ 2–5 were found to produce urease and tolerated Pb, and were screened. *O. profundus* KBZ 1–3 and *O. profundus* KBZ 2–5 were selected for subsequent experiments because they were Pb-resistant and capable of biocementation. Supplementary Fig. S3 shows the neighbor-joining phylogenetic tree of *O. profundus* KBZ 1–3 and *O. profundus* KBZ 2–5, which were isolated from the leach plant residue mine waste and near the wastewater pond, respectively. Both *O. profundus* 1–3 and *O. profundus* KBZ 2–5 are gram-positive, motile, aerobic, rod-shaped (0.2–0.4 μm and 0.5–0.6 μm respectively) and are classified as biosafety level 1 bacteria. The genus *Oceanobacillus* has been previously isolated from wastewater (Nam et al., 2008), Korean food (Whon et al., 2010), deep sea sediment core samples (Yu et al., 2014) and human gut (Lagier et al., 2015). To the best of our knowledge, there are no reports indicating their potential application in biotechnology, bioremediation or biosorption. Therefore, *O. profundus* KBZ 1–3 and *O. profundus* KBZ 2–5 isolated from Kabwe waste samples represent a novel *Oceanobacillus* species that is being applied for the first time in a bioremediation study.

3.2. Effects of Pb on microbial growth and urease activity of isolates

Since the isolates are intended to be used in a heavily Pb-contaminated environment, the bacteria were tested for the effect of Pb (II) in aqueous solutions. Fig. 2 shows the effects of Pb on both microbial growth and urease activity of *O. profundus* KBZ 1–3 and *O. profundus* KBZ 2–5. Both bacteria displayed similar growth patterns, i.e., increased growth in Pb-free media and a slight growth retardation in the presence of 50 mg/L Pb (Fig. 2). Therefore, the effects of Pb on microbial growth were minimal, likely because these bacteria were isolated from a Pb-contaminated site with bioavailable concentration of Pb (II) of 7.8 mg/L in LPR whereas KS had 5.4 mg/L bioavailable Pb concentration. The bioavailable fraction determines the potential harm of a contaminant on the receptor (Ng et al., 2015). Similar results have been reported from a previous research where growth retardation was exhibited by a halotolerant bacteria in the presence of Pb isolated from an abandoned mine in South Korea (Kang et al., 2015).

The effects of Pb on urease activity were studied because it is crucial in MICP-mediated bioremediation for the abandoned Kabwe mine site. As shown in Fig. 2, the urease activity *O. profundus* KBZ 2–5 is higher than that of *O. profundus* KBZ 1–3; both bacteria expressed the highest urease activity after 48 h incubation with only appreciable levels at 24 h and 72 h. Only *O. profundus* KBZ 2–5 maintained the enzyme activity until 96 h. The urease activities of both isolates were not significantly affected by Pb, probably because they were isolated from a Pb-contaminated site. Higher urease activity is very important in MICP-mediated processes because it has a significant impact on the rate of carbonate production that consequently precipitates out as $CaCO_3$. The results clearly showed increased growth and urease activity by *O. profundus* KBZ 1–3 and *O. profundus* KBZ 2–5 in the absence and presence of Pb. Overall, both bacteria are suitable for the biocementation of mine waste contaminated with Pb because they are Pb-tolerant, with high growth and urease activities.

3.3. Determination of the optimal Ca^{2+}/urea concentration

Calcium and urea are the two most important ingredients for carrying out the MICP process. The urease enzyme produced from the bacteria hydrolyzes urea ($CO(NH_2)_2$) to ammonium (NH_4^+) and carbonate (CO_3^{2-}) ions, which leads to the precipitation of $CaCO_3$ in the presence of calcium ions (Ca^{2+}). Therefore, the tolerance to and the optimal concentrations of Ca and urea may vary from one bacterial species to another, requiring the determination of optimal conditions for *O. profundus* KBZ 1–3 and *O. profundus* KBZ 2–5. Fig. 3 shows the amount of precipitate formed by both bacteria when the molar concentration ratio of Ca:urea = 1:1; equimolar concentrations were used, according to a previous study (Soga and Qabany, 2013). As shown in Fig. 3, increasing the equimolar Ca and urea concentrations also increased the amount of precipitate. In this study, we used the equimolar concentration of 0.5 M for calcium and urea. Previous studies have indicated that a low equimolar concentration in the solution should be used to ensure

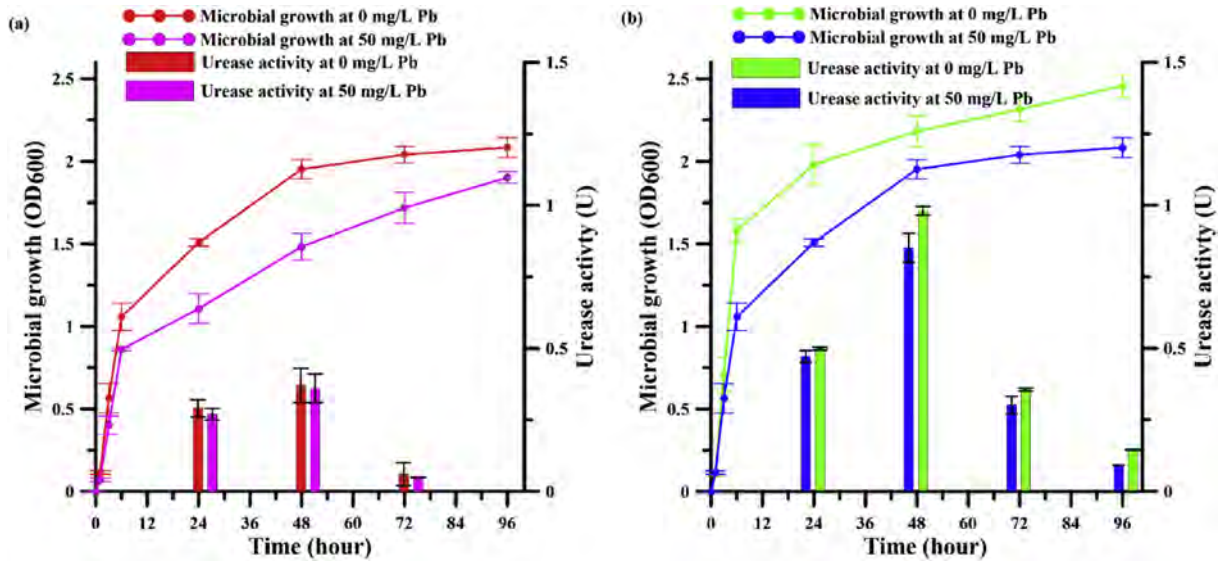

Fig. 2. Microbial growth and urease activity of (a) *O. profundus* KBZ 1–3, and (b) *O. profundus* KBZ 2–5. Error bars indicate standard deviations of three independent replicates. (U = μmol urea hydrolyzed/min).

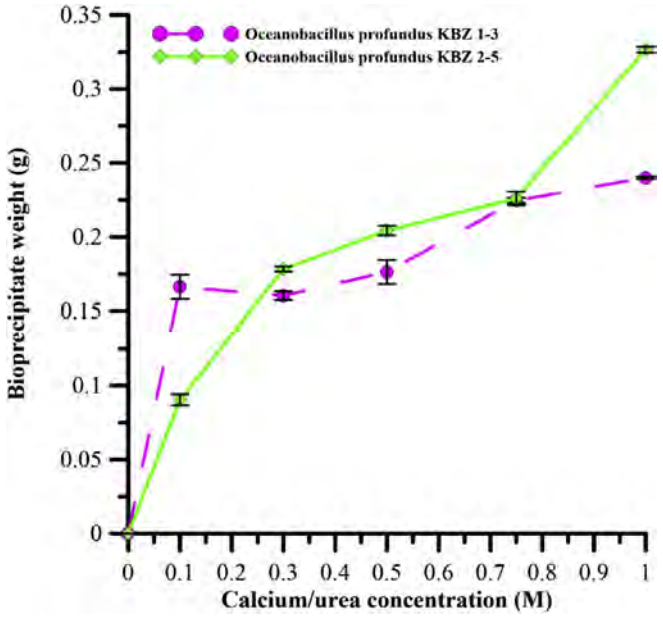

Fig. 3. Weight of $CaCO_3$ bioprecipitated by *O. profundus* KBZ 1–3 and *O. profundus* KBZ 2–5 at different equimolar concentrations of calcium and urea. Error bars indicate the standard deviation of three independent replicates.

uniform $CaCO_3$ precipitation (Mujah et al., 2017). Since a solution with low concentration may produce a more uniform precipitation pattern, even though higher concentrations produce higher amounts of $CaCO_3$ precipitate, a lower concentration was selected. In this study, both *O. profundus* KBZ 1–3 and *O. profundus* KBZ 2–5 produced the precipitation of spherical calcite crystals (Supplementary Fig. S4). Calcite is the preferred form of $CaCO_3$ for biocementation because it is the most stable, compared to the other polymorphic forms such as aragonite and vaterite (Boulos et al., 2014).

The two isolates precipitated $CaCO_3$, which can be used as an inert covering for mine wastes. Capping is advantageous as a treatment technology because it is a permanent remedy that can also eliminate dust, thus addressing chronic risks of Pb poisoning to humans and other ecological receptors (Bellenfant et al., 2013; Johnson et al., 1992; Lottermoser, 2011).

3.4. Strength, SEM and XRD analyses of solidified sand

UCS was measured to characterize the strength of cemented sand. Fig. 4 shows the appearance of the control and biocemented sand, while Table 1 shows the corresponding estimated values of UCS at the top, middle, and bottom parts of the specimens.

The control specimen had no strength while sand biocemented by *O. profundus* KBZ 1–3 under immersed and flow-through conditions had maximum estimated UCS values of 3.2 and 2.0 MPa, respectively. The strength of sand biocemented by *O. profundus* KBZ 2–5 under immersed and flow-through conditions were 5.5 and 3.5 MPa, respectively. Sand biocemented by *O. profundus* KBZ 2–5 was stronger probably because of the higher urease activity (Fig. 2) and greater amount of precipitate formed compared to *O. profundus* KBZ 1–3 (Fig. 3). Since the difference in UCS was marginal, both bacteria may be useful for solidification. Additionally, biocemented sand by both immersed and flow-through cementation methods provided strength. Therefore, both types of injection methods can be used for solidifying sand. The results imply that the increased strength of biocemented sand has the potential to prevent the airborne transport of metallic dust by prevailing winds and to reduce infiltration; these benefits are similar to those of conventional cement, used worldwide for capping mining waste (Batchelor, 2006; Sobiecka, 2013).

To further confirm the role of MICP, biocemented samples were examined by SEM and XRD. Fig. 5 shows typical SEM images and the corresponding XRD patterns of the control (a) and biocemented

Table 1
Estimated UCS values of control and biocemented sand prepared by immersed and flow through methods and mediated by *O. profundus* KBZ 1–3 and *O. profundus* KBZ 2-5.

Specimen	Immersed method			Flow through method		
	Top	Middle	Bottom	Top	Middle	Bottom
Control	0	0	0	0	0	0
KBZ 1-3	3.2	1.8	1.4	2.0	1.4	1.0
KBZ 2-5	5.5	3.0	1.8	3.5	2.0	1.0

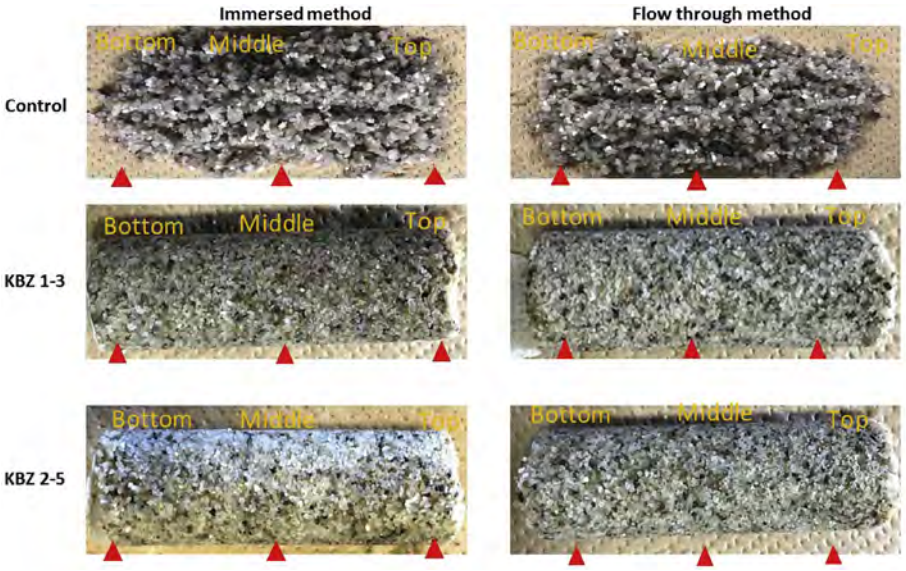

Fig. 4. Comparative view of control and biocemented sand obtained by the immersed and flow-through methods facilitated by *O. profundus* KBZ 1–3 and *O. profundus* KBZ 2–5.

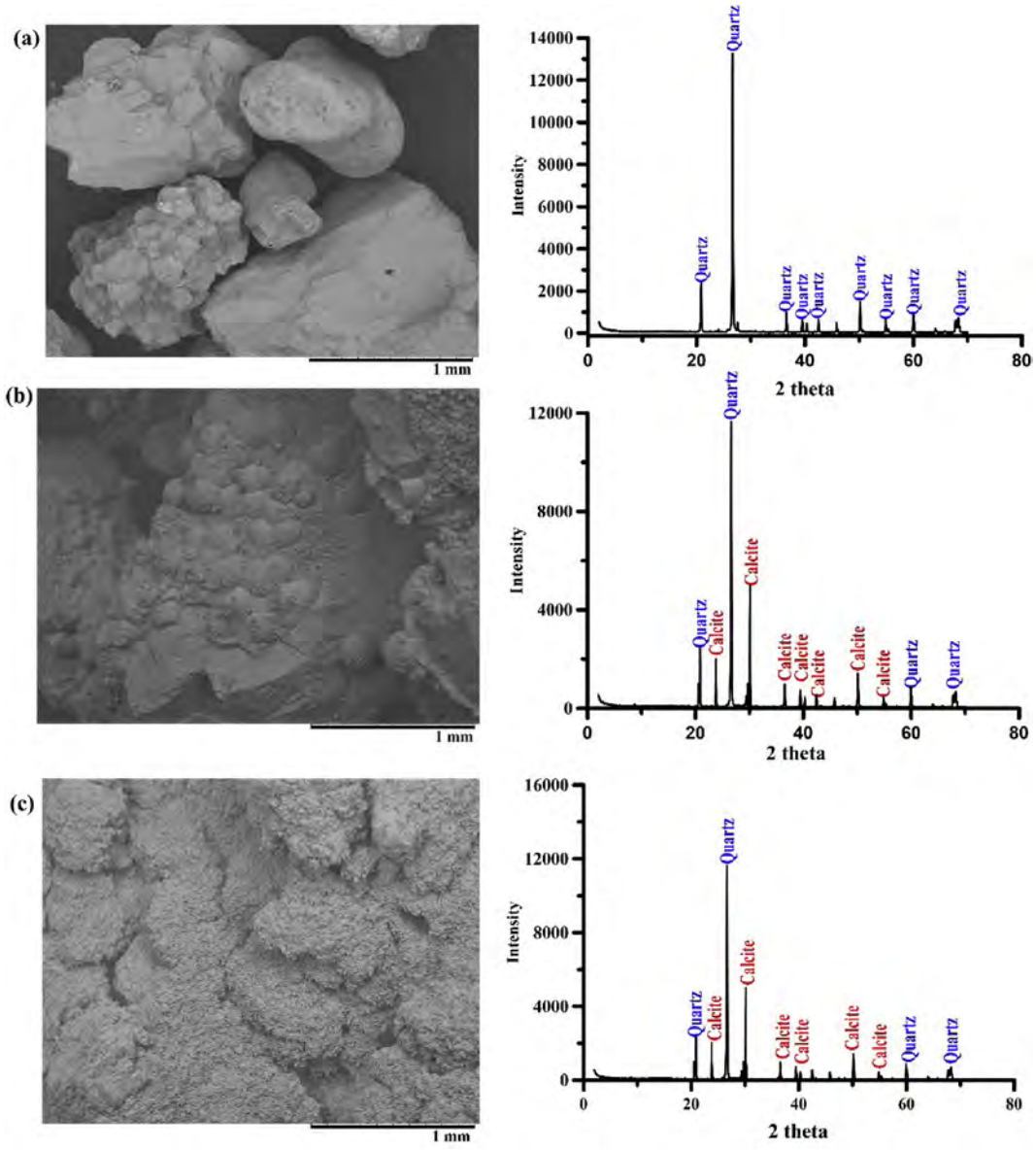

Fig. 5. SEM view and the corresponding XRD analysis comparing (a) control specimen, (b) biocemented sand prepared by the flow-through method using *O. profundus* KBZ 1–3, and (c) biocemented sand prepared by the flow-through method using *O. profundus* KBZ 2–5.

sand (b, c). The control samples presented a typical morphology of sand and appeared as discrete particles, while the biocemented samples showed prominent crystalline deposits on the surface and between sand particles. The SEM micrographs verify the effectiveness of the so-called bridging phenomenon mediated by MICP, i.e. the deposited $CaCO_3$ forms bridges between particles as part of the binding process (Mujah et al., 2017; Ng et al., 2012; Rowshanbakht et al., 2016).

The XRD analysis revealed that the control specimens were composed of only quartz, while the biocemented sand included calcite. This indicated that calcite was formed due to the ureolysis and subsequent precipitation of $CaCO_3$. The XRD results allowed us to conclude that MICP plays an important role in the solidification of sand.

The major pathway for Pb to enter into the blood of humans and animals around the Kabwe mine site is through inhalation and injection of dust particles emanating from the abandoned mine wastes dumps, since the prevailing winds blow mostly from east (the mine site) to west (toward a large residential area) (Tembo et al., 2006; Yabe et al., 2011, 2013, 2015, 2018). Immobilizing the sand via MICP aggregates the sandy material (Fig. 4), making it less susceptible to being blown by wind. This significantly curtails the Pb exposure pathway to humans and animals in and around the mine site. MICP using indigenous bacteria can be immediate and easily implemented because all the required materials such as sand, indigenous bacteria, nutrients, calcium source, and urea are locally available. Some researchers have proposed the use of alternative locally available nutrients and Ca sources such as lactose mother liquor (Achal et al., 2009) and eggshells (Choi et al., 2016), which also demonstrates the flexibility of the process. In a similar way, locally available resources required for capping will be utilized including the indigenous bacteria making the bioremediation process cheap, sustainable, and less likely change the integrity of the local biodiversity.

3.5. $CaCO_3$ content of biocemented sand

To elucidate the strength of the biocement, the content of $CaCO_3$ precipitated between sand grains of specimens was evaluated. Only the top parts of the control and biocemented sand were evaluated. The control contained no $CaCO_3$. On the other hand, sand biocemented by the immersed and flow methods using *O. profundus* KBZ 1–3 had $6.5 \pm 0.10\%$ and $3.0 \pm 0.20\%$ $CaCO_3$, respectively, while sand biocemented by *O. profundus* KBZ 2–5 by the immersed and flow methods had $10.0 \pm 0.20\%$ and $8.0 \pm 0.20\%$ $CaCO_3$, respectively. $CaCO_3$ content is one of the most important engineering factors in MICP-mediated processes. Its relationship with UCS is shown in Fig. 6. As seen in the results, the control contained no $CaCO_3$ and hence had no strength. The UCS of biocemented sand increased with $CaCO_3$ content (indicated by the pink and green circles), which suggests that $CaCO_3$ plays a significant role in the strength of sand, as elucidated by previous studies (Amarakoon and Kawasaki, 2018). Furthermore, more precipitation of $CaCO_3$ occurred in the immersed method probably due to accumulation of reactants and bacteria when the syringe was closed. The findings are in agreement with results reported by Keykha et al. (2019) when they solidified soil and maintained immersed conditions at all times and achieved higher UCS. Similarly, Gomez et al. (2018) reported that the largest $CaCO_3$ contents were observed near the injection, which had higher UCS when they conducted biostimulation and concluded that reductions in $CaCO_3$ content from the top were due to solution mixing and/or urea hydrolysis. In both treatment methods, the mid-top area had higher UCS because the reactants first contacted the mid-top when injected where they were consumed, depleted and less effective, hence the lower UCS in middle and bottom area. The difference in UCS between the treatment methods lies on the contact time of the reactants in the column. In the immersed method, the reactants have more contact time during immersed compared to the flow through method where reactants flow through the column in a shorter time hence the higher UCS in the immersed method compared to the flow through method.

3.6. Hydraulic conductivity

Hydraulic conductivity is a measure of how easily water can pass through a material. During immobilization, reduced hydraulic conductivity is desired because it reduces the ability of water to contact contaminants, and therefore, reduces contaminant leaching rates. Hydraulic conductivity tests were performed for the sand before and after MICP treatment. Before treatment, the hydraulic conductivity was 1.4×10^{-3} m/s. Biocemented sand treated by the immersed and flow-through methods using *O. profundus* KBZ 1–3 reduced the permeability of sand to 9.6×10^{-8} m/s and 2.4×10^{-7} m/s, respectively. Similarly, *O. profundus* KBZ 2–5 reduced the permeability of sand to 8.9×10^{-8} m/s and 2.5×10^{-7} m/s when treated by the immersed and flow-through methods, respectively. In all the cases, the hydraulic conductivity improved by more than three orders of magnitude for both immersed and flow-through methods. The reduced hydraulic conductivity achieved in this study has the potential to limit the entrance of water and oxygen into the dump, and hence reduce the leaching of heavy metals. This reduction in permeability is consistent with results of previous studies (Achal et al., 2013; Eryürük et al., 2015).

Other studies have proposed vegetation cover (Chehregani et al., 2009; Leteinturier et al., 2001) and synthetic cover (Fourie et al., 2010; Mazzieri et al., 2013) to cap mine wastes. Vegetation cover is desirable because like MICP, it reduces surface erosion and because a large proportion of percolating water is lost to the atmosphere through transpiration, reducing the concentrations of soluble heavy metals entering watercourses. However, this method would be difficult to implement in Kabwe, because vegetation growth is not possible at the site due to lack of nutrients and high levels of toxic trace elements at the site (Leteinturier et al., 2001). On the other hand, synthetic covers are uneconomical and expensive, especially compared to the MICP technique. Due to its originality and sustainability, MICP has recently gained much attention from researchers around the world as a replacement for conventional concrete (Seifan et al., 2016). Conventional physicochemical methods have already been tested to clean up the environment. However, most of these methods are costly, perform sub-optimally, and produce secondary sludge, making the cleanup process expensive and unsustainable, requiring large inputs of energy and large quantities of chemical reagents (Jena and Dey, 2016).

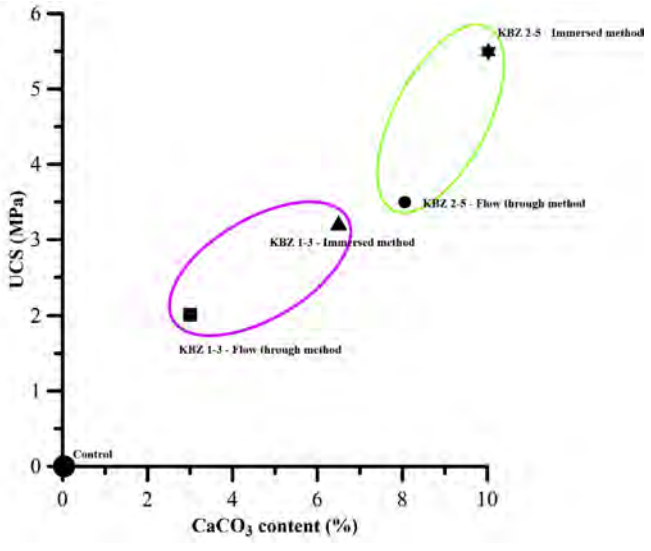

Fig. 6. Relationship between UCS and $CaCO_3$ content of sand biocemented by *O. profundus* KBZ 1–3 and *O. profundus* KBZ 2-5.

4. Conclusions

The abandoned Pb and Zn mine wastes in Kabwe mine continue to pose a serious threat to the quality of human health, water, and soil. We have shown in this study that MICP mediated by indigenous ureolytic bacteria *Oceanobacillus profundus* KBZ 1–3 and KBZ 2–5 can be used to solidify sand, thus preventing dust formation and water infiltration. Both bacteria were able to tolerate Pb and mediate the formation of $CaCO_3$ bioprecipitates, which was confirmed to be calcite by XRD analysis. The biocemented sand achieved maximum unconfined compressive strength values of 3.2 MPa and 5.5 MPa, which are useful enough to prevent Pb dust particles from being blown away by prevailing winds and to prevent water erosion. Combined with reduced hydraulic conductivity of 9.6×10^{-8} m/s and 8.9×10^{-8} m/s mediated by *Oceanobacillus profundus* KBZ 1–3 and KBZ 2–5, respectively, the process is expected to retard heavy metal leaching due to the lack of oxygen and water resulting from reduced infiltration. In a future study, we intend to implement this laboratory-proven procedure in-situ to determine the durability of biocemented materials under field conditions.

Declarations of interest

None.

Acknowledgments

This work was partly supported by JST/JICA, SATREPS (Science and Technology Research Partnership for Sustainable Development) and JSPS KAKENHI under grant numbers JP18H03395 and JP16H04404.

Appendix A. Supplementary data

Supplementary data to this article can be found online at https://doi.org/10.1016/j.chemosphere.2019.04.107.

References

Achal, V., Mukherjee, A., Basu, P.C., Reddy, M.S., 2009. Lactose mother liquor as an alternative nutrient source for microbial concrete production by *Sporosarcina pasteurii*. J. Ind. Microbiol. Biotechnol. 36, 433–438. https://doi.org/10.1007/s10295-008-0514-7.

Achal, V., Pan, X., Lee, D.J., Kumari, D., Zhang, D., 2013. Remediation of Cr(VI) from chromium slag by biocementation. Chemosphere 93, 1352–1358. https://doi.org/10.1016/j.chemosphere.2013.08.008.

Amarakoon, G.G.N.N., Kawasaki, S., 2018. Factors affecting sand solidification using MICP with *Pararhodobacter* sp. Mater. Trans. 59, 72–81. https://doi.org/10.2320/matertrans.M-M2017849.

Batchelor, B., 2006. Overview of waste stabilization with cement. Waste Manag. 26, 689–698. https://doi.org/10.1016/j.wasman.2006.01.020.

Bellenfant, G., Guezennec, Anne-Gwenaëlle Bodénan, F., D'Hugues, P., Cassard, D., 2013. Reprocessing of mining waste: combining environmental management and metal recovery? Mine Clos 571–582.

BMR Group PLC, 2019. Tailings Stockpiles [WWW Document]. http://www.bmrplc.com/tailings_stockpiles.php (accessed 1.25.19).

Boulos, R.A., Zhang, F., Tjandra, E.S., Martin, A.D., Spagnoli, D., Raston, C.L., 2014. Spinning up the polymorphs of calcium carbonate. Sci. Rep. 4, 1–6. https://doi.org/10.1038/srep03616.

Chehregani, A., Noori, M., Yazdi, H.L., 2009. Phytoremediation of heavy-metal-polluted soils: screening for new accumulator plants in Angouran mine (Iran) and evaluation of removal ability. Ecotoxicol. Environ. Saf. 72, 1349–1353. https://doi.org/10.1016/j.ecoenv.2009.02.012.

Chen, X., Guo, H., Cheng, X., 2017. Heavy metal immobilisation and particle cementation of tailings by biomineralisation. Environ. Geotech. 1–7. https://doi.org/10.1680/jenge.15.00068.

Choi, S., Wu, S., Chu, J., 2016. Biocementation for sand using an eggshell as calcium source. J. Geotech. Geoenviron. Eng. 142, 2–5. https://doi.org/10.1061/(ASCE)GT.1943-5606.0001534.

Danjo, T., Kawasaki, S., 2015. Artificial beachrock formation through sand solidification towards the inhibit of coastal erosion. Int. J. Geomater. 9, 1528–1533.

Eryürük, K., Yang, S., Suzuki, D., Sakaguchi, I., Akatsuka, T., Tsuchiya, T., Katayama, A., 2015. Reducing hydraulic conductivity of porous media using CaCO3 precipitation induced by Sporosarcina pasteurii. J. Biosci. Bioeng. 119, 331–336. https://doi.org/10.1016/j.jbiosc.2014.08.009.

Fourie, A.B., Bouazza, A., Lupo, J., 2010. Improving the performance of mining infrastructure through the judicious use of geosynthetics. In: 9th Int. Conf. Geosynth. Brazil.

Gomez, M.G., Graddy, C.M.R., DeJong, J.T., Nelson, D.C., Tsesarsky, M., 2018. Stimulation of native microorganisms for biocementation in samples recovered from field scale treatment depths. J. Geotech. Geoenviron. Eng. 144, 1–13. https://doi.org/10.1061/(ASCE)GT.1943-5606.0001804.

Hukue, M., Kato, Y., Nakamura, T., Moriyama, N., 2001. A method for determining carbonate content for soils and evaluation of the results. Jpn. Geotech. Soc. 49, 2669 (In Japanese).

Jena, S., Dey, S.K., 2016. Heavy metals. Am. J. Environ. Stud. 1, 48–60.

Johnson, M.S., Cooke, J.A., Stevenson, J.K.W., 1992. Revegetation of Metalliferous Wastes and and after Metal Mining, Mining and its Environmental Impact.

Kang, C.H., Oh, S.J., Shin, Y., Han, S.H., Nam, I.H., So, J.S., 2015. Bioremediation of lead by ureolytic bacteria isolated from soil at abandoned metal mines in South Korea. Ecol. Eng. 74, 402–407. https://doi.org/10.1016/j.ecoleng.2014.10.009.

Keykha, H.A., Mohamadzadeh, H., Asadi, A., Kawasaki, S., 2019. Ammonium-free carbonate-producing bacteria as an ecofriendly soil biostabilizer. Geotech. Test J. 42, 20170353. https://doi.org/10.1520/GTJ20170353.

Khan, M.N.H., Amarakoon, G.G.N.N., Shimazaki, S., Kawasaki, S., 2015. Coral sand solidification test based on microbially induced carbonate precipitation using ureolytic bacteria. Mater. Trans. 56, 1725–1732. https://doi.org/10.2320/matertrans.M-M2015820.

Kim, J.H., Lee, J.Y., 2018. An optimum condition of MICP indigenous bacteria with contaminated wastes of heavy metal. J. Mater. Cycles Waste Manag. 1–9. https://doi.org/10.1007/s10163-018-0779-5.

Kosnett, M.J., Wedeen, R.P., Rothenberg, S.J., Hipkins, K.L., Materna, B.L., Schwartz, B.S., Hu, H., Woolf, A., 2007. Recommendations for medical management of adult lead exposure. Environ. Health Perspect. 115, 463–471. https://doi.org/10.1289/ehp.9784.

Kribek, B., Nyambe, I.A., Njamu, F., Chitwa, G., Ziwa, G., 2009. Assessment of Impacts of Mining and Mineral Processing on the Environment and Human Health in Selected Regions of the Central and Copperbelt Provinces of Zambia. Report No. RP/3/2008 for years 2008-2010. Lusaka.

Lagier, J.C., Khelaifia, S., Azhar, E.I., Croce, O., Bibi, F., Jiman-Fatani, A.A., Yasir, M., Helaby, H. Ben, Robert, C., Fournier, P.E., Raoult, D., 2015. Genome sequence of *Oceanobacillus picturae* strain S1, an halophilic bacterium first isolated in human gut. Stand. Genom. Sci. 10, 1–9. https://doi.org/10.1186/s40793-015-0081-2.

Leteinturier, B., Laroche, J., Matera, J., Malaisse, F., 2001. Reclamation of lead/zinc processing wastes at Kabwe, Zambia: a phytogeochemical approach. South Afr. J. Sci. 97, 624–627.

Lottermoser, B.G., 2011. Recycling, reuse and rehabilitation of mine wastes. Elements 7, 405–410. https://doi.org/10.2113/gselements.7.6.405.

Mazzieri, F., Di Emidio, G., Fratalocchi, E., Di Sante, M., Pasqualini, E., 2013. Permeation of two GCLs with an acidic metal-rich synthetic leachate. Geotext. Geomembranes 40, 1–11. https://doi.org/10.1016/j.geotexmem.2013.07.011.

Mufinda, B., 2015. A History of Mining in Broken Hill (Kabwe): 1902-1929. University of the Free State.

Mujah, D., Shahin, M.A., Cheng, L., 2017. State-of-the-art review of biocementation by microbially induced calcite precipitation (MICP) for soil stabilization. Geomicrobiol. J. 34, 524–537. https://doi.org/10.1080/01490451.2016.1225866.

Mwandira, W., Nakashima, K., Kawasaki, S., 2017. Bioremediation of lead-contaminated mine waste by *Pararhodobacter* sp. based on the microbially induced calcium carbonate precipitation technique and its effects on strength of coarse and fine grained sand. Ecol. Eng. 109, 57–64. https://doi.org/10.1016/j.ecoleng.2017.09.011.

Nam, I.H., Roh, S.B., Park, M.J., Chon, C.M., Kim, J.G., Jeong, S.W., Song, H., Yoon, M.H., 2016. Immobilization of heavy metal contaminated mine wastes using Canavalia ensiformis extract. Catena 136, 53–58. https://doi.org/10.1016/j.catena.2015.07.019.

Nam, J.H., Bae, W., Lee, D.H., 2008. *Oceanobacillus caeni* sp. nov., isolated from a Bacillus-dominated wastewater treatment system in Korea. Int. J. Syst. Evol. Microbiol. 58, 1109–1113. https://doi.org/10.1099/ijs.0.65335-0.

Ng, J.C., Juhasz, A., Smith, E., Naidu, R., 2015. Assessing the bioavailability and bioaccessibility of metals and metalloids. Environ. Sci. Pollut. Res. 22, 8802–8825. https://doi.org/10.1007/s11356-013-1820-9.

Ng, W., Lee, M., Hii, S., 2012. An overview of the factors affecting microbial-induced calcite precipitation and its potential application in soil improvement. World Acad. Sci. Eng. Technol. 62, 723–729.

Rowshanbakht, K., Khamehchiyan, M., Sajedi, R.H., Nikudel, M.R., 2016. Effect of injected bacterial suspension volume and relative density on carbonate precipitation resulting from microbial treatment. Ecol. Eng. 89, 49–55. https://doi.org/10.1016/j.ecoleng.2016.01.010.

Salifu, E., MacLachlan, E., Iyer, K.R., Knapp, C.W., Tarantino, A., 2016. Application of microbially induced calcite precipitation in erosion mitigation and stabilisation of sandy soil foreshore slopes: a preliminary investigation. Eng. Geol. 201, 96–105. https://doi.org/10.1016/j.enggeo.2015.12.027.

Seifan, M., Samani, A.K., Berenjian, A., 2016. Bioconcrete: next generation of self-healing concrete. Appl. Microbiol. Biotechnol. 100, 2591–2602. https://doi.org/10.1007/s00253-016-7316-z.

Sobiecka, E., 2013. Investigating the chemical stabilization of hazardous waste material (fly ash) encapsulated in Portland cement. Int. J. Environ. Sci. Technol. 10, 1219–1224. https://doi.org/10.1007/s13762-012-0172-1.

Soga, A.A., Qabany, K., 2013. Effect of chemical treatment used in MICP on engineering properties of cemented soils. Geotechnique 63, 331–339.

Tembo, B.D., Sichilongo, K., Cernak, J., 2006. Distribution of copper, lead, cadmium and zinc concentrations in soils around Kabwe town in Zambia. Chemosphere 63, 497–501. https://doi.org/10.1016/j.chemosphere.2005.08.002.

Torres-Aravena, Á., Duarte-Nass, C., Azócar, L., Mella-Herrera, R., Rivas, M., Jeison, D., 2018. Can microbially induced calcite precipitation (MICP) through a ueolytic pathway be successfully applied for removing heavy metals from wastewaters? Crystals 8, 438. https://doi.org/10.3390/cryst8110438.

Whon, T.W., Jung, M.-J., Roh, S.W., Nam, Y.-D., Park, E.-J., Shin, K.-S., Bae, J.-W., 2010. *Oceanobacillus kimchii* sp nov isolated from a traditional Korean fermented food. J. Microbiol. 48, 862–866. https://doi.org/10.1007/s12275-010-0214-7.

Wiktor, V., Jonkers, H.M., 2011. Quantification of crack-healing in novel bacteria-based self-healing concrete. Cement Concr. Compos. 33, 763–770. https://doi.org/10.1016/j.cemconcomp.2011.03.012.

Yabe, J., Nakayama, S.M.M., Ikenaka, Y., Muzandu, K., Choongo, K., Mainda, G., Kabeta, M., Ishizuka, M., Umemura, T., 2013. Metal distribution in tissues of free-range chickens near a lead-zinc mine in Kabwe, Zambia. Environ. Toxicol. Chem. 32, 189–192. https://doi.org/10.1002/etc.2029.

Yabe, J., Nakayama, S.M.M., Ikenaka, Y., Muzandu, K., Ishizuka, M., Umemura, T., 2011. Uptake of lead, cadmium, and other metals in the liver and kidneys of cattle near a lead-zinc mine in Kabwe, Zambia. Environ. Toxicol. Chem. 30, 1892–1897. https://doi.org/10.1002/etc.580.

Yabe, J., Nakayama, S.M.M., Ikenaka, Y., Yohannes, Y.B., Bortey-Sam, N., Kabalo, A.N., Ntapisha, J., Mizukawa, H., Umemura, T., Ishizuka, M., 2018. Lead and cadmium excretion in feces and urine of children from polluted townships near a lead-zinc mine in Kabwe, Zambia. Chemosphere 202, 48–55. https://doi.org/10.1016/j.chemosphere.2018.03.079.

Yabe, J., Nakayama, S.M.M., Ikenaka, Y., Yohannes, Y.B., Bortey-Sam, N., Oroszlany, B., Muzandu, K., Choongo, K., Kabalo, A.N., Ntapisha, J., Mweene, A., Umemura, T., Ishizuka, M., 2015. Lead poisoning in children from townships in the vicinity of

a lead-zinc mine in Kabwe, Zambia. Chemosphere 119, 941–947. https://doi.org/10.1016/j.chemosphere.2014.09.028.
Yu, C., Yu, S., Zhang, Z., Li, Z., Zhang, X.H., 2014. *Oceanobacillus pacificus* sp. nov., isolated from a deep-sea sediment. Int. J. Syst. Evol. Microbiol. 64, 1278–1283. https://doi.org/10.1099/ijs.0.056481-0.
Zhu, X., Li, W., Zhan, L., Huang, M., Zhang, Q., Achal, V., 2016. The large-scale process of microbial carbonate precipitation for nickel remediation from an industrial soil. Environ. Pollut. 219, 149–155. https://doi.org/10.1016/j.envpol.2016.10.047.

Chemosphere 238 (2020) 124581

Contents lists available at ScienceDirect

Chemosphere

journal homepage: www.elsevier.com/locate/chemosphere

Bioimaging of Pb and STIM1 in mice liver, kidney and brain using Laser Ablation Inductively Coupled Plasma Mass Spectrometry (LA-ICP-MS) and immunohistochemistry

Masao Togao [a, 1], Shouta M.M. Nakayama [a, 1], Yoshinori Ikenaka [a, b], Hazuki Mizukawa [c], Yoshiki Makino [d], Ayano Kubota [e], Takehisa Matsukawa [e], Kazuhito Yokoyama [e], Takafumi Hirata [f], Mayumi Ishizuka [a, *]

[a] Laboratory of Toxicology, Department of Environmental Veterinary Sciences, Graduate School of Veterinary Medicine, Hokkaido University, Kita 18 Nishi 9, Kita-ku, Sapporo, 060-0818, Japan
[b] Water Research Group, School of Environmental Sciences and Development, North-West University, South Africa
[c] Department of Science and Technology for Biological Resources and Environment, Graduate School of Agriculture, Ehime University, Tarumi 3-5-7, Matsuyama, Ehime, 790-8566, Japan
[d] Division of Earth and Planetary Sciences, Kyoto University, Kyoto, Japan
[e] Department of Epidemiology and Environmental Health, Juntendo University Faculty of Medicine, Tokyo, Japan
[f] Graduate School of Science, The University of Tokyo, Tokyo, Japan

HIGHLIGHTS

- Lead acetate (100 mg/L and 1000 mg/L) were given to the BALB/c mice.
- Bioimaging of Pb and STIM1 in liver, kidney and brain was carried out.
- Pb distribution in liver was homogeneous and in kidney and brain was inhomogeneous.
- STIM1 was homogenous in the liver and kidney whereas inhomogeneous in the brain.
- Pb exposure did not induce STIM1 mRNA expression.

GRAPHICAL ABSTRACT

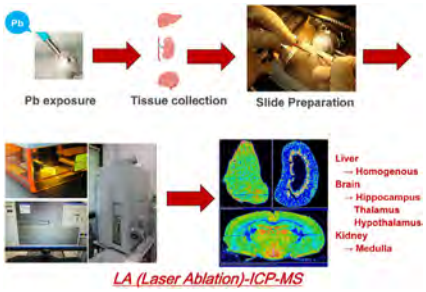

ARTICLE INFO

Article history:
Received 6 May 2019
Received in revised form
10 August 2019
Accepted 12 August 2019
Available online 12 August 2019

Handling Editor: Willie Peijnenburg

Keywords:
Cell entry mechanisms

ABSTRACT

Lead (Pb) pollution is one of the most serious environmental problems and has attracted worldwide attention. Pb causes hematological, central nervous system, as well as renal toxicity, and so on. Although many investigations about Pb in blood to evaluate pollution status and toxic effects have been reported, there are open question about biological behavior of Pb. In order to reveal any toxicological mechanisms or influences, we focused on the local distribution of Pb in mice organs. Lead acetate (100 mg/L and 1000 mg/L) in drinking water were given to the BALB/c mice (male, seven weeks of age, N = 24) for three weeks. Laser Ablation Inductively Coupled Plasma Mass Spectrometry (LA-ICP-MS) analysis revealed a homogenous distribution of Pb in the liver and inhomogeneous distribution in the kidney and brain. The hippocampus, thalamus, and hypothalamus had higher concentrations than other areas such as the white matter. Surprisingly, in the kidney, Pb tended to accumulate in the medulla rather than the cortex,

* Corresponding author. Laboratory of Toxicology, Department of Environmental Veterinary Sciences, Graduate School of Veterinary Medicine, Hokkaido University, N18, W9, Kita-ku, Sapporo, 060-0818, Japan.
E-mail addresses: togamasa12@gmail.com (M. Togao), shouta-nakayama@vetmed.hokudai.ac.jp (S.M.M. Nakayama), y_ikenaka@vetmed.hokudai.ac.jp (Y. Ikenaka), hazuki.mizukawa@vetmed.hokudai.ac.jp (H. Mizukawa), y.makino.kueps@gmail.com (Y. Makino), ay-kubota@juntendo.ac.jp (A. Kubota), tmatsuka@juntendo.ac.jp (T. Matsukawa), kyokoya@juntendo.ac.jp (K. Yokoyama), hrt1@eqchem.s.u-tokyo.ac.jp (T. Hirata), ishizum@vetmed.hokudai.ac.jp (M. Ishizuka).
[1] Both authors equally contributed to this study (Dual first authorship).

https://doi.org/10.1016/j.chemosphere.2019.124581

Laser ablation inductively coupled plasma mass spectrometry (LA-ICP-MS)
Distribution
Pb
Stromal interacting protein 1 (STIM1)

strongly suggesting that high sensitivity areas and high accumulation areas differ. Moreover, distribution of stromal interacting protein 1 (STIM1) which is candidate gene of Pb pathway to the cells was homogenous in the liver and kidney whereas inhomogeneous in the brain. In contrast to our hypothesis, interestingly, Pb exposure under the current condition did not induce mRNA expressions for any candidate channel or transporter genes. Thus, further study should be conducted to elucidate the local distribution of Pb and other toxic metals, and pathway that Pb takes to the cells.

1. Introduction

Elemental analysis of biological samples including internal organs are mainly conducted by atomic absorption spectrometry (AAS; Yabe et al., 2012), Inductively coupled plasma-atomic emission spectrometry (ICP-OES; Rahil-Khazen et al., 2002), and inductively coupled plasma-mass spectrometry (ICP-MS; Nakata et al., 2016). Usually, liquid samples are analyzed by such techniques, therefore organs are acid digested and there is an assumption that they contain a homogeneous distribution of investigated element (Konz et al., 2012). However, it is unknown about distribution patterns of elements such as Pb, Cd and Hg in organs. If they are inhomogeneously distributed, the evaluation of their concentrations in organs should be reconsidered.

Elemental analysis using ICP-MS combined with laser ablation (LA) has been conducted (Pozebon et al., 2014; Noël et al., 2015; Yamashita et al., 2019). A solid surface of sample is ablated by a pulse laser beam in the laser ablation chamber, the ablated material is then analyzed by ICP-MS. Scanning of the surface by LA allows the construction of images of elements distribution (Becker et al., 2010; Yamashita et al., 2019). This method allows direct analysis of solid sample surfaces and is applicable for thin organ slices (Becker, 2005; Becker et al., 2010; Ishii et al., 2018; Limbeck et al., 2015). Numerous studies have used this method to analyze the local distribution of essential elements such as Cu, Fe, and Zn in organs, bones and teeth in human and animals (Becker et al., 2015; Ishii et al., 2018; Johnston et al., 2019; Paul et al., 2015; Urgast et al., 2012). However, with regards to Pb, there is still less published research which investigate distribution in organs and bones (Dobrowolska et al., 2008; Ishii et al., 2018; Johnston et al., 2019). Dobrowolska et al. (2008) showed a homogeneous Pb distribution in brain regions. However, they analyzed the human brain (postmortem from a healthy donor) and found very low Pb levels. Ishii et al. (2018) revealed the distribution of Pb in bone of raptor species. To our best knowledge, there has not yet been any research using Pb administrated laboratory animals (e.g. mice models) to elucidate the local distribution of Pb in internal organs.

Despite various research efforts, the pathway by which Pb enters cells remains unclear; this is still one of the important points concerning Pb toxicity (Chang et al., 2008; Zhang et al., 2014). Pb^{2+} has the ability to mimic Ca^{2+} and other divalent metal ions such as Fe^{2+} and Zn^{2+} (Zhang et al., 2014). Based on this mimicry, Ca^{2+} and other divalent metal channels might be candidates for Pb entry (Godwin, 2001). Two types of Ca^{2+} channels: voltage gated Ca^{2+} channels (VGCCs) and store operated Ca^{2+} channels (SOCs), have been identified as potential routes by which Pb can enter cells (Kerper and Hinkle, 1997). With regards to VGCCs, this would only be feasible for excitable cells. However, Pb may enter not only excitable cells but also other cells such as human embryonic kidney cell 293 (Zhang et al., 2014; Chiu et al., 2009). Thus, VGCCs may still provide a pathway to cells, but there must also be an additional route by which Pb enters the cells in the rest of the body.

Some researchers have proposed that SOCs may play an important role in Pb entry into cells (Chang et al., 2008; Kerper and Hinkle, 1997; Chiu et al., 2009). SOCs are constituted from transient receptor potentials (TRPs) and Orai1 present in the plasma membrane, as well as from stromal interacting protein 1 (STIM1) present in the endoplasmic reticulum (ER) membrane (Chang et al., 2008; Zhang et al., 2014; Chiu et al., 2009).

Researchers have shown that STIM1 can translocate to interact with both Orai1 and TRPC1 during the activation of SOCs (Cheng et al., 2008; Liao et al., 2008). Although some research has indicated that STIM1 may be a key protein by which Pb enters the cell (Chang et al., 2008; Chiu et al., 2009), and may contribute to the localization of STIM1 (Klejman et al., 2009; Skibinska-Kijek et al., 2009), no studies have compared local distribution of Pb with that of STIM1. Additionally, to our knowledge, no studies have yet confirmed whether Pb induces STIM1.

In view of the above, we conducted an experiment using mice to achieve the following aims: (1) to demonstrate the local distribution of Pb in organs; (2) to compare the distribution of STIM1 with that of Pb; and (3) to clarify whether Pb induces STIM1.

2. Materials and methods

2.1. Animals

BALB/c mice (male, seven weeks of age, N = 24) were purchased from Sankyo Labo Service Corporation, Inc. (Tokyo, Japan). The mice were divided into three groups and housed in six polypropylene cages (N = 4 per batch). One batch from each group (control, low, and high) was sampled for ICP-MS, and the other batch from each group for LA-ICP-MS. There was no significant difference in body weight between groups (Supplementary Fig. S1). The animals were allowed to acclimate to the animal facilities at the Graduate School of Veterinary Medicine, Hokkaido University for one week prior to testing. Under these conditions, food (rodent chow, Labo MR Stock, Nosan Corporation, Yokohama, Japan) and distilled water were provided *ad libitum*. After acclimation, two different concentrations of lead acetate: 100 mg/L and 1000 mg/L (Wako Pure Chemical Industries, Osaka, Japan) were given to two of the groups (the low and high dosage groups, respectively) in the drinking water for three more weeks. In our preliminary experiment, dose dependent increase of Pb concentration in blood and organs were observed when we selected 100 mg/L and 1000 mg/L for three weeks of exposure (data not shown). The control groups were provided with distilled water. After three weeks of exposure, mice were anesthetized with sevoflurane and blood and organs (liver, kidney, and brain) were collected via the following methods. For the ICP-MS groups, blood and organ samples were collected in polypropylene tubes, then stored at −80 °C in a deep freezer. For the LA-ICP-MS groups, organ samples were embedded in Tissue-Tec OCT (Sakura Finetek, CA, USA), quickly frozen in isopentane which had been cooled with dry ice, then stored at −80 °C in a deep freezer. Additionally, small pieces of the liver, kidney, and brain samples were collected together with RNAlater Tissue Storage and RNA Stabilization Solution (Sigma-Aldrich, MO, USA) in polypropylene tubes and stored at −80 °C in a deep freezer for real time PCR and

microarray analysis. All experiments using animals were performed under the supervision and with the approval of the Institutional Animal Care and Use Committee of Hokkaido University, Japan (approval number: 16-0017, approval day: 29th March 2016).

2.2. Quantitative analysis by ICP-MS

The ICP-MS groups were used for the quantitative analysis of Pb concentration. In this case, blood, liver, kidney, and brain were acid digested using the method described by Nakata et al. (2016, 2015) with minor modifications. The whole kidney, liver, and brain samples were dried for 48 h in an oven at 50 °C. Then, 0.1 mL of the blood samples and approximately 0.1 g of the dried biological samples were weighted and placed in pre-washed digestion vessels. This was followed by acid digestion using 5 mL of nitric acid (atomic absorption spectrometry grade, 30%; Kanto Chemical, Tokyo, Japan), and 1 mL of hydrogen peroxide (Cica reagent, 30%; Kanto Chemical). The digestion vessels subsequently underwent a ramped temperature program in a closed microwave system (Speed Wave MWS-2 microwave digestion system; Berghof, Eningen, Germany). The operating conditions of microwave system are given in the Supplementary Table S1. After cooling, the sample solutions were transferred into 15 mL polypropylene tubes and diluted to a final volume of 10 mL with bi-distilled and de-ionized water (Milli-Q).

The Pb concentrations determination was performed using the procedure described by Nakata et al. (2016, 2015) with minor modifications. Concentration of Pb was measured by ICP-MS (7700 series; Agilent Technologies, Tokyo, Japan). The operating conditions of ICP-MS are given in the Supplementary Table S2. Quality control was conducted by analysis of DORM-3 (fish protein; National Research Council of Canada, Ottawa, Canada) and DOLT-4 (dogfish liver; National Research Council of Canada) certified reference materials. Replicate analysis of these reference materials showed good recovery rates (95–105%); the instrument detection limit for Pb was 0.001 μg/L.

2.3. Analysis by LA-ICP-MS

Sections of embedded liver, kidney, and brain were cut on a cryostat to a thickness of 20 μm. The native cryosections were then mounted directly onto glass slides. Then, they were analyzed using an LA system (NWR213; esi Japan, Tokyo, Japan) associated with an ICP-MS instrument (8800 series; Agilent Technologies, Tokyo, Japan). The tissue sections were systematically scanned by a focused laser beam (line by line: spot size 100 μm, scan speed 100 μm/s, scan step 100 μm). Measured isotope (dwell time, sec) were as follows; ^{13}C (0.005), ^{25}Mg (0.005), ^{31}P (0.005), ^{43}Ca (0.005), ^{55}Mn (0.005), ^{57}Fe (0.005), ^{65}Cu (0.005), ^{66}Zn (0.005), ^{206}Pb (0.01), ^{207}Pb (0.01), ^{208}Pb (0.01). In this analysis, no quantification of Pb was conducted due to lack of suitable reference materials for calibration, however intensity of Pb (and other elements) was normalized to ^{13}C (carbon) intensity as Wu et al. (2009), Johnston et al. (2019) and others have utilized to normalize the ablation efficiency. Detailed analytical conditions are presented in Supplementary Table S3. From the continuous list of raw pixel values data, elemental images were reconstructed using LA-ICP-MS Image generator house-made software iQquant2 (Kawakami et al., 2016).

2.4. Immunohistochemistry

Immunohistochemistry (IHC) was carried out using the method described by Skibinska-Kijek et al. (2009) and Wang et al. (2010) with minor modifications. Sections of the embedded liver, kidney, and brain samples were cut on a cryostat to a thickness of 20 μm. After fixation with 4% paraformaldehyde phosphate buffer solution and quenching of endogenous peroxidase activity with 0.3% H_2O_2 in methanol, the sections were blocked with goat serum in Phosphate Buffered Saline (PBS). Then, the sections were incubated overnight at 4 °C with antibody recognizing STIM1 (ProteinTech Group Inc., cat no 11565-1-AP, the antibody was raised against an N-terminal fragment of the protein: aa 2-350) diluted 1:200 in PBS. Samples were then washed and incubated with biotinylated secondary antibodies (Vector Laboratories, Burlingame, CA, USA) in PBS for 30 min. After washing, the sections were incubated with Avidin-biotin complex reagent (ABC-Elite kit, Vector Laboratories), following the manufacturers protocol. The immunocomplex was visualized with diaminobenzidine (DAB) (Vector Laboratories), sections were counterstained with haematoxylin (Sigma-Aldrich), and observations were conducted by microscope (BIOREVO BZ-9000 series; KEYENCE, Osaka, Japan).

2.5. Quantitative analysis by real time PCR

Real time PCR was performed using the method described by Skibinska-Kijek et al. (2009) with small modifications. Total RNA was extracted from small pieces of liver, kidney, and brain soaked in RNAlater (Sigma-Aldrich) using Nucleo spin (Takara bio, Shiga, Japan). First-strand cDNA was generated from 600 ng of total RNA in a final volume of 20 μL with ReverTra Ace (Toyobo, Osaka, Japan). This was examined by real time PCR with specific gene primers for *Stim1* (NM_009287; (5′GCTCTCAATGCCATGCCTTCCAAT, 5′TCTAGGCCATGGTTCAACGCCATA), and Fast SYBR Green Master mix (Applied Biosystems). The samples were analyzed using 7000 Sequence Detection System hardware and software (Applied Biosystems). *18S ribosomal RNA* (NR_003278) for normalization was used with the following primers: 5′AACGAACGAGACTCTGGCATG and 5′CGGACATCTAAGGGCATCACA. A relative quantification (RQ) method was used to calculate the relative levels of *Stim1* mRNA. The formula was as follows: $RQ = 2^{-deltaCT}$, where deltaCT = CT(target) − CT(18S). Amplification efficiency was 98.0% for *STIM1* and 100.5% for *18S ribosomal RNA*.

2.6. Microarray analysis

To analyze gene expression profiles, a microarray experiment was performed. Firstly, the total RNA of the liver, kidney, and brain was quantified and qualified using an Agilent 2100 Bioanalyzer series II (Agilent Technologies, Supplementary Table S4). Cyanine 3-labelled cRNA was prepared from 500 ng of total RNA, and amplified using a Low Input Quick Amp Labeling Kit (Agilent Technologies), according to the manufacturer's instructions, followed by RNAeasy column purification (Qiagen, Valencia, CA). Dye incorporation and cRNA yield were checked with the NanoDrop ND-1000 Spectrophotometer the Agilent 2100 Bioanalyzer. Gene Expression (GE) Hybridization Kit (Agilent Technologies) was used for labeling. 600 ng of Cy3-labelled cRNA was fragmented at 60 °C for 30 min following the manufacturer's instructions. On completion of the fragmentation reaction, 25 μL of 2x Agilent hybridization buffer was added to the fragmentation mixture and hybridized to Agilent SurePrint G3 Mouse 8 × 60K ver.2.0 for 17 h at 65 °C in a rotating Agilent hybridization oven. After hybridization, slides were washed 1 min at room temperature with GE Wash Buffer 1 (Agilent) and 1 min with 37 °C GE Wash buffer 2 (Agilent), then air-dried immediately. Slide was scanned immediately after washing on the Agilent DNA Microarray Scanner using one color scan setting (Agilent Technologies, Scan Resolution; 3 μm, TIFF file dynamic range; 20bit). The scanned images were analyzed with Feature Extraction Software 12.0.3.1 (Agilent) using default parameters to

Table 1
Mean ± SD of the Pb concentration in the blood and organs of mice for the three dosage groups.

	Control	Low	High
Blood (μg/dL)	1.8 ± 0.5^{a}	14.9 ± 3.2^{b}	40.8 ± 3.9^{c}
Liver (mg/kg)	0.016 ± 0.001^{a}	4.54 ± 0.59^{b}	16.49 ± 1.58^{c}
Kidney (mg/kg)	0.044 ± 0.002^{a}	11.47 ± 1.48^{a}	56.65 ± 20.20^{b}
Brain (mg/kg)	0.027 ± 0.008^{a}	0.54 ± 0.09^{b}	2.66 ± 0.33^{c}

Note.
Different letters (a, b, and c) between columns indicate a significant difference between dosage groups ($p < 0.05$).

obtain background subtracted and spatially detrended Processed Signal intensities. Normalized (75 Percentile Shift) signal intensity was used for data acquisition. The data for microarray is deposited at the NCBI Gene Expression Omnibus (GEO) database; accession number is "Series GSE93544".

2.7. Statistical analysis

All statistical analyses were carried out using JMP 12 (SAS Institute, Cary, NC, USA). A Tukey-Kramer test was performed to compare body weights, Pb concentration, and gene expression of STIM1 in tissue samples between groups. All statistical analyses were performed at a significance level of 95%.

3. Results

3.1. Pb concentrations in mice organs

Table 1 shows the mean ± standard deviations (SD) of the Pb concentration in the blood, liver, kidney, and brain of the three groups. A dose dependent increase of Pb concentration in the organs was observed and there were significant differences in Pb concentration in the blood and all tissue-types between the control and high Pb dosage groups.

3.2. Pb local distributions in mice organs

The local distribution of Pb in the liver, kidney, and brain of the three mice groups are shown in Figs. 1–3, respectively. A homogeneous distribution of Pb was found in the liver of the low and high dosage groups (Fig. 1). Yet surprisingly, inhomogeneous Pb

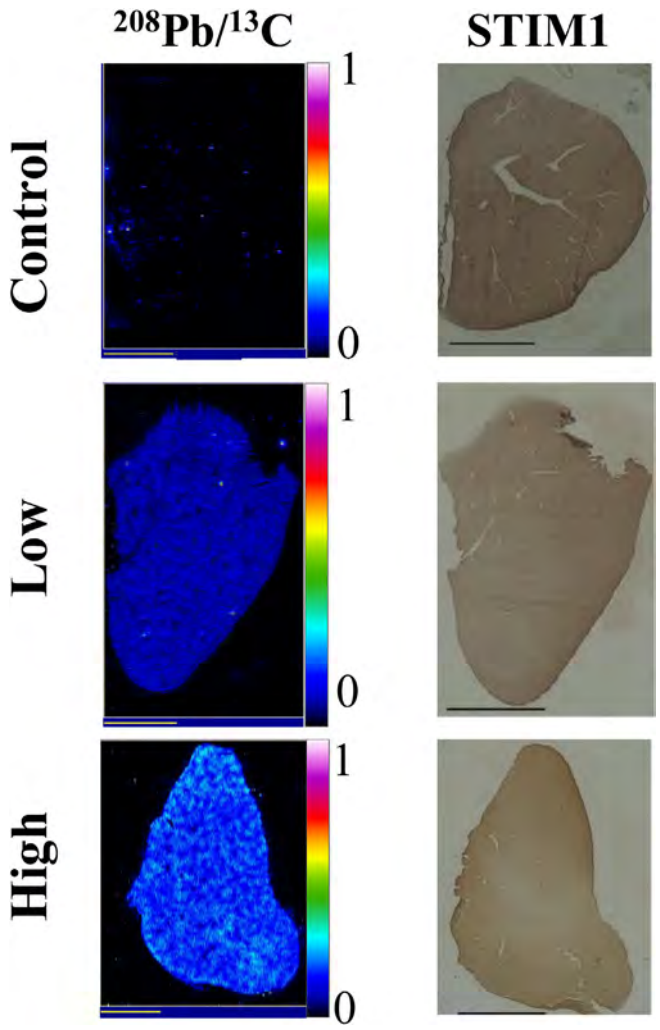

Fig. 1. Distribution of ^{208}Pb and STIM1 in a 20 μm section of liver. Distribution of ^{208}Pb/^{13}C analyzed by LA-ICP-MS (left). STIM1 was analyzed by IHC (right). Scale bar is 3 mm. Among LA-ICP-MS images, the scale bar indicates the ratio of intensity (^{208}Pb/^{13}C).

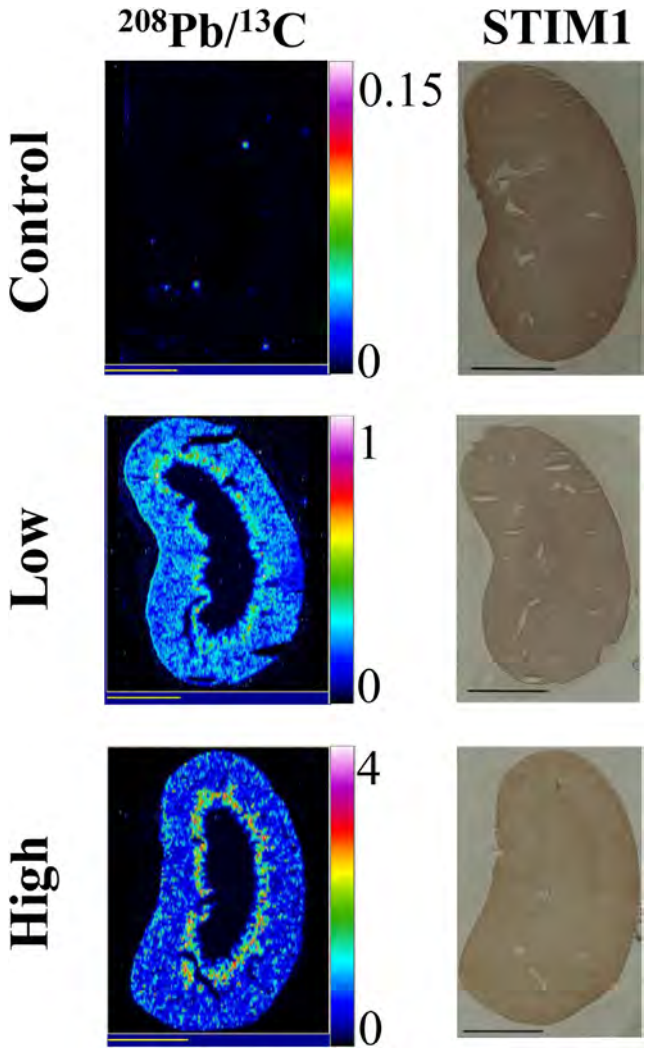

Fig. 2. Distribution of ^{208}Pb and STIM1 in a 20 μm section of kidney. Distribution of ^{208}Pb/^{13}C analyzed by LA-ICP-MS (left). STIM1 was analyzed by IHC (right). Scale bar is 3 mm. Among LA-ICP-MS images, the scale bar indicates the ratio of intensity (^{208}Pb/^{13}C).

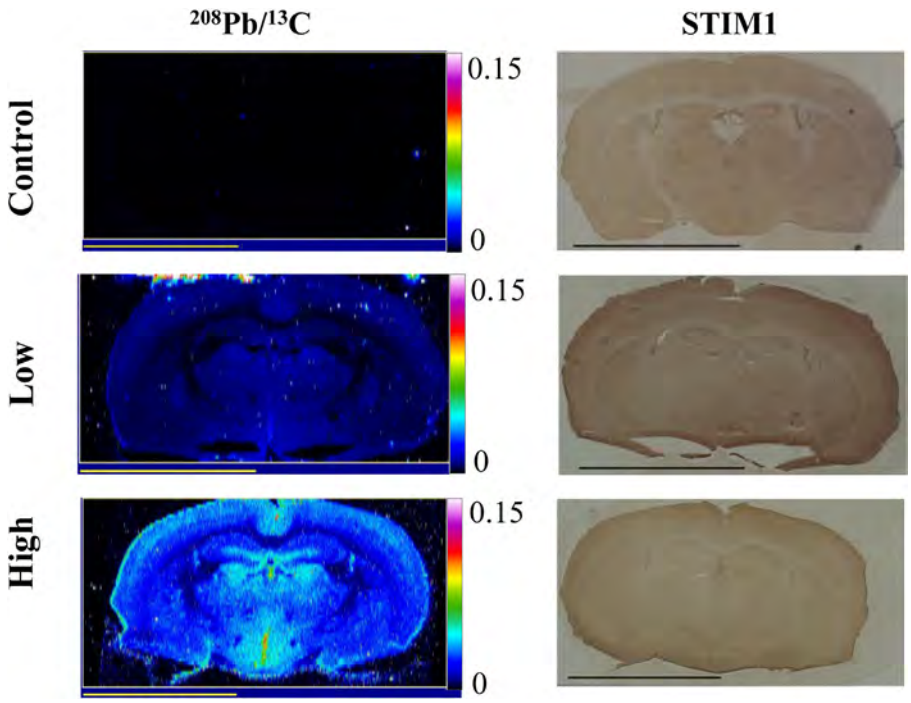

Fig. 3. Distribution of ^{208}Pb and STIM1 in a 20 μm section of brain. Distribution of ^{208}Pb/^{13}C analyzed by LA-ICP-MS (left). STIM1 was analyzed by IHC (right). Scale bar is 5 mm. Among LA-ICP-MS images, the scale bar indicates the ratio of intensity (^{208}Pb/^{13}C).

distribution was discovered in the kidney and brain (Figs. 2 and 3). Within the kidney, in the internal area surrounding the medulla there was a higher regional Pb concentration than in the renal cortex in the low and high dosage groups (Fig. 2). The brain also showed an inhomogeneous distribution; the hippocampus had higher Pb concentration than other areas such as the white matter in high dosage group (Fig. 3). Pb in all tissues of the control group and in the brain of the low dosage group was not detected as count values of ICP-MS were comparable to those of background areas where only glass slide without organs (Fig. 3). Additionally, other elements distribution are shown in Supplementary Fig. S2. For example, Mn tended to accumulate in the renal medulla than cortex (Supplementary Fig. S2 (D, E, F)), while selective accumulation of Zn was observed in the hippocampus of brain (Supplementary Fig. S2 (G, H, I)). These results were in accordance with the previous studies (Becker et al., 2010; Shariatgorji et al., 2016).

3.3. Immuno-localization of STIM1 in mice organs

The reactivity of the primary antibody was confirmed by comparing it with PBS (Supplementary Fig. S3). Figs. 1–3 show the immune-localization of STIM1 in the liver, kidney, and brain of the three groups, respectively. A homogeneous distribution of STIM1 was found in the liver and kidney in all groups (Figs. 1 and 2). However, the brain showed inhomogeneous distribution of STIM1: the gray matter and hippocampus had higher densities than other areas such as the white matter in all groups (Fig. 3).

3.4. Gene induction by Pb in mice organs

Real time PCR was performed to measure the levels of STIM1 mRNA in the liver, kidney, and brain. This confirmed that STIM1 was expressed in all organs (Fig. 4). However, there were no significant differences in gene expression between groups in any of the organs. Additionally, it was examined gene induction of the candidates suspected to be responsible for Pb entry into cells such as STIM1, Orai1, TRP, VGCC, divalent metal transporter 1, and anion exchanger in the liver, kidney, and brain by microarray. However, no significant induction was observed in the liver, kidney, and brain. As a confirmation, the induction of metallothionein, which is known to be induced with Pb exposure, was observed to be two and eight times greater in the liver and kidney, respectively, in the high dosage groups compared with the control group (data not shown).

4. Discussion

4.1. Pb local distribution in organs

The local distribution of Pb and other toxic elements in organs is still unknown. LA-ICP-MS allows direct analysis of thin organ sections (Becker et al., 2010). However, as for Pb, there is little published research regarding bioimaging, especially in the Pb exposed mice model.

In the present study, Pb concentration found in kidney (56.65 mg/kg) and liver (16.49 mg/kg) in high dosage groups were comparable to that for lead-poisoned animals in the previous study (Takano et al., 2015). By analysis using LA-ICP-MS, a homogenous Pb distribution was found in the liver (Fig. 1); however, the kidney and brain showed inhomogeneous distribution of Pb (Figs. 2 and 3) mainly in the kidney. Since it was identified as a target soft tissue for Pb accumulation (Barregard et al., 1999), there has been substantial research published on Pb concentration in animal kidneys (Yabe et al., 2012, 2013; Bortey-Sam et al., 2015; Jarzynska and Falandysz, 2011; Nakayama et al., 2011, 2013; Sedki et al., 2003). These reports were based on the hypothesis that there is a homogenous distribution of Pb in the kidney, and thus did not map the element in this organ. However, the present findings suggest that such mapping should be considered for identifying toxic elements in the kidney. As Pb and other types of toxic elements are mainly observed in the proximal tubule, which is primarily

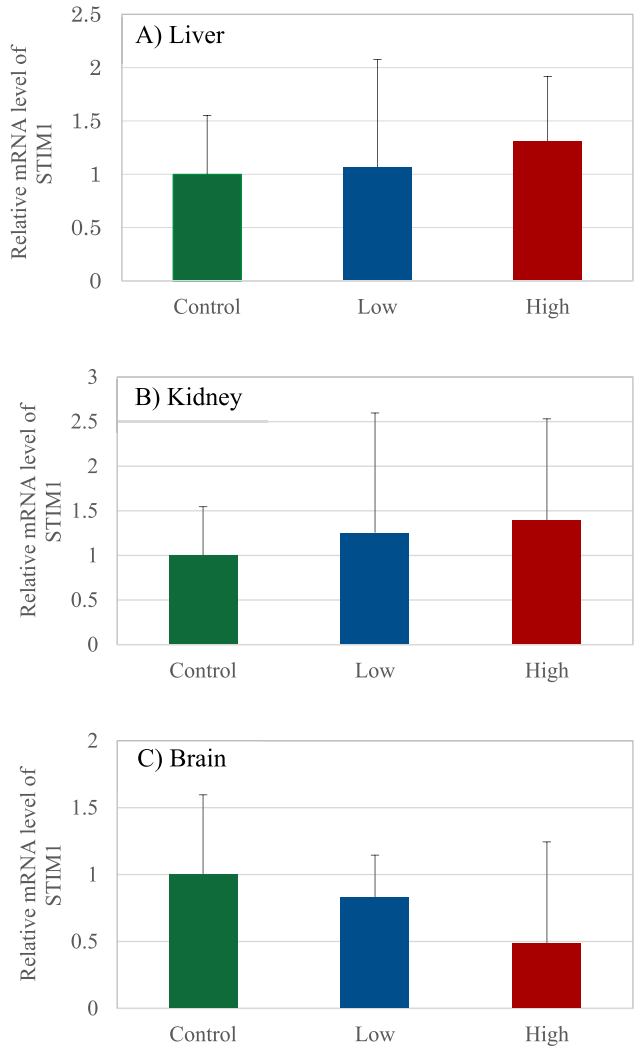

Fig. 4. Mean ± SD of the expression of STIM1 in mice organs in the three dosage groups: (A) liver, (B) kidney, and (C) brain. No significant differences were found between groups.

distributed in the cortex, the proximal tubule was regarded to be the highest accumulation area in the kidney (Sabolic, 2006). Moreover, there are some reports about studies focusing toxic elements distribution in the renal cortex (Smith et al., 1991; Wang et al., 2009; Wlostowski et al., 2006), so, to some extent, it might be reasonable to focus such region. A previous study using LA-ICP-MS to determine Pt in cisplatin (Pt)-administrated rats found that Pt tended to accumulate in the cortex and corticomedullary junction (Moreno-Gordaliza et al., 2011). However, the results of the present study which revealed that Pb tended to accumulate in the medulla rather than the cortex, strongly suggest that high sensitivity areas and high accumulation areas differ. The present study would help to understand mechanism of pathological Pb toxicity.

Differences in Pb distribution among organs may be explained by their individual characteristics. In histological anatomy and physiology, the liver is regarded as a homogenous organ, thus Pb is distributed homogenously. By contrast, the kidneys and brain are regarded as inhomogeneous organs, therefore Pb is distributed inhomogeneously.

In the present study, mice were selected to be the first proof of concept model, yet the method utilized can be applied to other animals. For instance, previous research has shown the tolerance of chickens to chronic Pb intoxication (Mazliah et al., 1989); thus, revealing local distribution of Pb in chicken organs would be interesting.

4.2. Comparison between Pb and STIM1 distribution and gene expression of STIM1

The present study found homogeneous distribution of STIM1, which is the main component of SOCs, in the liver and kidney, whereas there was inhomogeneous distribution in the brain (Figs. 1–3). There was a significant difference between the distribution of Pb and STIM1 in the kidney which suggests that there are alternative mechanisms underlying Pb distribution in the kidney. One explanation is that Pb distribution is due to its reabsorption. In the kidney, Pb is filtered in the glomerulus; however, most of this filtered Pb is reabsorbed by the distal tubule and the collecting duct (Araki et al., 1983, 1978). The distal tubule and the collecting duct are primarily located in the renal medulla, the area which had the highest concentration of Pb compared with the other areas analyzed in the present study. As for channels and transporters, the TRP super family, specifically TRP vanilloid (TRPV) 5, is responsible for transcellular calcium (Ca^{2+}) reabsorption in the distal tubule, connecting tube, and collecting duct of the kidney (Nijenhuis et al., 2005). Moreover, the Na^{+}-Ca^{2+} exchanger (NCX) and plasma membrane Ca^{2+} ATPase (PMCA) are responsible for the extrusion of Ca^{2+} into the blood (Hoenderop et al., 2000). Despite the fact that there have not been any studies revealing linkages between these transporters and Pb distribution, these transporters might also be responsible for Pb^{2+} reabsorption and local distribution in the kidney. Moreover, reabsorption behavior differs between Pb and other toxic metals such as Cd, Hg (Araki et al., 1986); thus further study of transporters and other toxic elements could be a key to support the idea proposed above.

In the brain, STIM1 is mainly distributed in the hippocampus, which is similar with Pb distribution. Therefore, SOCs may be a candidate route for Pb entering brain cells. However, VGCCs in the brain may also be a feasible candidate, as nerve cells are excitable (Davila, 1999; Vassanelli and Fromherz, 1998). Additionally, no induction of STIM1 expression by Pb was observed in the current study, suggesting that Pb enters the cells via other mechanisms.

5. Conclusions

In experimental animals such as mice model, local distribution of Pb was demonstrated for liver, kidney and brain and compared with the distribution of Pb and STIM1 for the first time. Inhomogeneous distribution of Pb was found in the kidney and brain. In the kidney, Pb tended to accumulate in the medulla rather than the cortex. This provides support for the mechanism of Pb toxicity as the proximal tubule is regarded as an area of high accumulation. In this study, however, we did not find evidence supporting that Pb enters the cells via SOCs. Thus, further study should be conducted to elucidate the local distribution of Pb and other toxic elements, and pathway that Pb takes to the cells.

Acknowledgements

The analyses were technically supported by Mr. Takahiro Ichise, Ms. Mio Yagihashi and Ms. Nagisa Hirano. The English in this manuscript was proofread by uni-edit (https://uni-edit.net/usa). This work was supported by Grants-in-Aid for Scientific Research from the Ministry of Education, Culture, Sports, Science and Technology of Japan awarded to M. Ishizuka (No. 16H0177906, 18K1984708, 18KK0287) and Y. Ikenaka (17K2003807,

18H0413208), and S.M.M. Nakayama (No. 16K16197, 17KK0009), and the foundation of JSPS Core to Core Program (AA Science Platforms), the Environment Research and Technology Development Fund (SII-1/3-2, 4RF-1802/18949907) of the Environmental Restoration and Conservation Agency of Japan. We also acknowledge financial support from The Soroptimist Japan Foundation, The Nakajima Foundation, The Sumitomo foundation, The Nihon Seimei Foundation and The Japan Prize Foundation. This research was also supported by JST/JICA, SATREPS (Science and Technology Research Partnership for Sustainable Development).

Appendix A. Supplementary data

Supplementary data to this article can be found online at https://doi.org/10.1016/j.chemosphere.2019.124581.

Conflicts of interest

The authors declare no conflict of interest in this study.

Author contributions

M.T., S.M.M.N., Y.M., Y.I., K.Y., T.H., and M.I. conceived and designed the experiments; M.T., S.M.M.N., Y.M., A.K., and M.T. performed the experiments; M.T., S.M.M.N., and H.M. analyzed the data; M.T., S.M.M.N., Y.M. and M.I. have written the manuscript; all authors have read and approved the final manuscript.

Supplementary material

Detailed information related to this study are available as supplementary material.

References

Araki, S., 1978. The effects of water restriction and water loading on urinary excretion of lead, delta-aminolevulinic acid and coproporphyrin. Br. J. Ind. Med. 35, 312–317.
Araki, S., Aono, H., Yokoyama, K., Murata, K., 1986. Filterable plasma concentration, glomerular filtration, tubular balance and renal clearance of heavy materials and organic substances in metal workers. Arch. Environ. Health 41, 216–221.
Araki, S., Murata, K., Yokoyama, K., Yanagihara, S., Niinuma, Y., Yamamoto, R., Ishihara, N., 1983. Circadian rhythms in the urinary excretion of metals and organic substances in 'healthy' men. Arch. Environ. Health 38, 360–366.
Barregard, L., Svalander, C., Schutz, A., Westberg, G., Sallsten, G., Blohme, I., Molne, J., Attman, P.O., Haglind, P., 1999. Cadmium, mercury, and lead in kidney cortex of the general Swedish population: a study of biopsies from living kidney donors. Environ. Health Perspect. 107, 867–871.
Becker, J.S., 2005. Recent developments in isotope analysis by advanced mass spectrometric techniques Plenary lecture. J. Anal. At. Spectrom. 20, 1173–1184.
Becker, J.S., Breuer, U., Hsieh, H.F., Osterholt, T., Kumtabtim, U., Wu, B., Matusch, A., Caruso, J.A., Qin, Z.Y., 2015. Bioimaging of metals and biomolecules in mouse heart by laser ablation inductively coupled plasma mass spectrometry and secondary ion mass spectrometry. Anal. Chem. 82, 9528–9533.
Becker, J.S., Zoriy, M., Matusch, A., Wu, B., Salber, D., Palm, C., 2010. Bioimaging of metals by laser ablation inductively coupled plasma mass spectrometry (LA-ICP-MS). Mass Spectrom. Rev. 29, 156–175.
Bortey-Sam, N., Nakayama, S.M.M., Ikenaka, Y., Akoto, O., Baidoo, E., Yohannes, Y.B., Mizukawa, H., Ishizuka, M., 2015. Human health risks from metals and metalloid via consumption of food animals near gold mines in Tarkwa, Ghana: estimation of the daily intakes and target hazard quotients (THQs), Ecotoxicol. Environ. Saf. 111, 160–167.
Chang, Y.F., Teng, H.C., Cheng, S.Y., Wang, C.T., Chiou, S.H., Kao, L.S., Kao, F.J., Chiou, A., Yang, D.M., 2008. Orai1-STIM1 formed store-operated Ca2+ channels (SOCs) as the molecular components needed for Pb2+ entry in living cells. Toxicol. Appl. Pharmacol. 227, 430–439.
Cheng, K.T., Liu, X.B., Ong, H.L., Ambudkar, I.S., 2008. Functional requirement for Orai1 in store-operated TRPC1-STIM1 channels. J. Biol. Chem. 283, 12935–12940.
Chiu, T.Y., Teng, H.C., Huang, P.C., Kao, F.J., Yang, D.M., 2009. Dominant role of Orai1 with STIM1 on the cytosolic entry and cytotoxicity of lead ions. Toxicol. Sci. 110, 353–362.
Davila, H.M., 1999. Molecular and functional diversity of voltage-gated calcium channels. Ann. N. Y. Acad. Sci. 868, 102–117.
Dobrowolska, J., Dehnhardt, M., Matusch, A., Zoriy, M., Palomero-Gallagher, N., Koscielniak, P., Zilles, K., Becker, J.S., 2008. Quantitative imaging of zinc, copper and lead in three distinct regions of the human brain by laser ablation inductively coupled plasma mass spectrometry. Talanta 74, 717–723.
Godwin, H.A., 2001. The biological chemistry of lead. Curr. Opin. Chem. Biol. 5, 223–227.
Hoenderop, J.G.J., Hartog, A., Stuiver, M., Doucet, A., Willems, P., Bindels, R.J.M., 2000. Localization of the epithelial Ca2+ channel in rabbit kidney and intestine. J. Am. Soc. Nephrol. 11, 1171–1178.
Ishii, C., Nakayama, S.M.M., Kataba, A., Ikenaka, Y., Saito, K., Watanabe, Y., Makino, Y., Matsukawa, T., Kubota, A., Yokoyama, K., Mizukawa, H., Hirata, T., Ishizuka, M., 2018. Characterization and imaging of lead distribution in bones of lead-exposed birds by ICP-MS and LA-ICP-MS. Chemosphere 212, 994–1001.
Jarzynska, G., Falandysz, J., 2011. Selenium and 17 other largely essential and toxic metals in muscle and organ meats of Red Deer (Cervus elaphus) - consequences to human health. Environ. Int. 37, 882–888.
Johnston, J.E., Franklin, M., Roh, H., Austin, C., 2019. Arora. Lead and arsenic in shed deciduous teeth of children living near a lead-acid battery smelter. Environ. Sci. Technol. 53, 6000–6006.
Kawakami, T., Hokada, T., Sakata, S., Hirata, T., 2016. Possible polymetamorphism and brine infiltration recorded in the garnet-sillimanite gneiss, Skallevik-shalsen, Lutzow-Holm Complex, East Antarctica. J. Mineral. Petrol. Sci. 111, 129–143.
Kerper, L.E., Hinkle, P.M., 1997. Cellular uptake of lead is activated by depletion of intracellular calcium stores. J. Biol. Chem. 272, 8346–8352.
Klejman, M.E., Gruszczynska-Biegala, J., Skibinska-Kijek, A., Wisniewska, M.B., Misztal, K., Blazejczyk, M., Bojarski, L., Kuznicki, J., 2009. Expression of STIM1 in brain and puncta-like co-localization of STIM1 and ORAI1 upon depletion of Ca2+ store in neurons. Neurochem. Int. 54, 49–55.
Konz, I., Fernandez, B., Fernandez, M.L., Pereiro, R., Sanz-Medel, A., 2012. Laser ablation ICP-MS for quantitative biomedical applications. Anal. Bioanal. Chem. 403, 2113–2125.
Liao, Y., Erxleben, C., Abramowitz, J., Flockerzi, V., Zhu, M.X., Armstrong, D.L., Birnbaumer, L., 2008. Functional interactions among Orai1, TRPCs, and STIM1 suggest a STIM-regulated heteromeric Orai/TRPC model for SOCE/Icrac channels. Proc. Natl. Acad. Sci. U.S.A. 105, 2895–2900.
Limbeck, A., Galler, P., Bonta, M., Bauer, G., Nischkauer, W., Vanhaecke, F., 2015. Recent advances in quantitative LA-ICP-MS analysis: challenges and solutions in the life sciences and environmental chemistry. Anal. Bioanal. Chem. 407, 6593–6617.
Mazliah, J., Barron, S., Bental, E., Rogowski, Z., Coleman, R., Silbermann, M., 1989. The effects of long-term lead intoxication on the nervous system of the chicken. Neurosci. Lett. 101, 253–257.
Moreno-Gordaliza, E., Giesen, C., Lazaro, A., Esteban-Fernandez, D., Humanes, B., Canas, B., Panne, U., Tejedor, A., Jakubowski, N., Gomez-Gomez, M.M., 2011. Elemental bioimaging in kidney by LA-ICP-MS as a tool to study nephrotoxicity and renal protective strategies in cisplatin therapies. Anal. Chem. 83, 7933–7940.
Nakata, H., Nakayama, S.M.M., Ikenaka, Y., Mizukawa, H., Ishii, C., Yohannes, Y.B., Konnai, S., Darwish, W.S., Ishizuka, M., 2015. Metal extent in blood of livestock from Dandora dumping site, Kenya: source identification of Pb exposure by stable isotope analysis. Environ. Pollut. 205, 8–15.
Nakata, H., Nakayama, S.M.M., Yabe, J., Liazambi, A., Mizukawa, H., Darwish, W.S., Ikenaka, Y., Ishizuka, M., 2016. Reliability of stable Pb isotopes to identify Pb sources and verifying biological fractionation of Pb isotopes in goats and chickens. Environ. Pollut. 208, 395–403.
Nakayama, S.M.M., Ikenaka, Y., Hamada, K., Muzandu, K., Choongo, K., Teraoka, H., Mizuno, N., Ishizuka, M., 2011. Metal and metalloid contamination in roadside soil and wild rats around a Pb-Zn mine in Kabwe, Zambia. Environ. Pollut. 159, 175–181.
Nakayama, S.M.M., Ikenaka, Y., Hamada, K., Muzandu, K., Choongo, K., Yabe, J., Umemura, T., Ishizuka, M., 2013. Accumulation and biological effects of metals in wild rats in mining areas of Zambia. Environ. Monit. Assess. 185, 4907–4918.
Nijenhuis, T., Hoenderop, J.G.J., Bindels, R.J.M., 2005. TRPV5 and TRPV6 in Ca2+ (re) absorption: regulating Ca2+ entry at the gate. Pflügers Archiv 451, 181–192.
Noël, M., Christensen, J.R., Spence, J., Robbins, C.T., 2015. Using laser ablation inductively coupled plasma mass spectrometry (LA-ICP-MS) to characterize copper, zinc and mercury along grizzly bear hair providing estimate of diet. Sci. Total Environ. 529, 1–9.
Paul, B., Hare, D.J., Bishop, D.P., Paton, C., Nguyen, V.T., Cole, N., Niedwiecki, M.M., Andreozzi, E., Vais, A., Billings, J.L., Bray, L., Bush, A.I., McColl, G., Roberts, B.R., Adlard, P.A., Finkelstein, D.I., Hellstrom, J., Hergt, J.M., Woodhead, J.D., Doble, P.A., 2015. Visualising mouse neuroanatomy and function by metal distribution using laser ablation-inductively coupled plasma-mass spectrometry imaging. Chem. Sci. 6, 5383–5393.
Pozebon, D., Scheffler, G.L., Dressler, V.L., Nunes, M.A., 2014. Review of the applications of laser ablation inductively coupled plasma mass spectrometry (LA-ICP-MS) to the analysis of biological samples. J. Anal. At. Spectrom. 29 (12), 2204–2228.
Rahil-Khazen, R., Bolann, B.J., Myking, A., Ulvik, R.J., 2002. Multi-element analysis of trace element levels in human autopsy tissues by using inductively coupled atomic emission spectrometry technique (ICP-AES). J. Trace Elem. Med. Biol. 16, 15–25.
Sabolic, I., 2006. Common mechanisms in nephropathy induced by toxic metals. Nephron. Physiol. 104, 107–114.
Sedki, A., Lekouch, N., Gamon, S., Pineau, A., 2003. Toxic and essential trace metals in muscle, liver and kidney of bovines from a polluted area of Morocco. Sci. Total Environ. 317, 201–205.

Shariatgorji, M., Nilsson, A., Bonta, M., Gan, J.R., Marklund, N., Clausen, F., Kallback, P., Loden, H., Limbeck, A., Andren, P.E., 2016. Direct imaging of elemental distributions in tissue sections by laser ablation mass spectrometry. Methods 104, 86–92.

Skibinska-Kijek, A., Wisniewska, M.B., Gruszczynska-Biegala, J., Methner, A., Kuznicki, J., 2009. Immunolocalization of STIM1 in the mouse brain. Acta Neurobiol. Exp. 69, 413–428.

Smith, R.M., Griel, L.C., Muller, L.D., Leach, R.M., Baker, D.E., 1991. Effects of dietary cadmium chloride throughout gestation on blood and tissue metabolites of primigravid and neonatal dairy cattle. J. Anim. Sci. 69, 4078–4087.

Takano, T., Okutomi, Y., Mochizuki, M., Ochiai, Y., Yamada, F., Mori, M., Ueda, F., 2015. Biological index of environmental lead pollution: accumulation of lead in liver and kidney in mice. Environ. Monit. Assess. 187, 1–5.

Urgast, D.S., Ou, O., Gordon, M.J., Raab, A., Nixon, G.F., Kwun, I.S., Beattie, J.H., Feldmann, J., 2012. Microanalytical isotope ratio measurements and elemental mapping using laser ablation ICP-MS for tissue thin sections: zinc tracer studies in rats. Anal. Bioanal. Chem. 402, 287–297.

Vassanelli, S., Fromherz, P., 1998. Transistor records of excitable neurons from rat brain. Appl. Phys. Mater. Sci. Process 66, 459–463.

Wang, L., Chen, D.W., Wang, H., Liu, Z.P., 2009. Effects of lead and/or cadmium on the expression of metallothionein in the kidney of rats. Biol. Trace Elem. Res. 129, 190–199.

Wang, L.M., Becker, J.S., Wu, Q., M.F., O., Bliveira, M.F., Bozza, F.A., Schwager, A.L., Hoffman, J.M., Morton, K.A., 2010. Bioimaging of copper alterations in the aging mouse brain by autoradiography, laser ablation inductively coupled plasma mass spectrometry and immunohistochemistry. Metall 2, 348–353.

Wlostowski, T., Bonda, E., Krasowska, A., 2006. Free-ranging European bisons accumulate more cadmium in the liver and kidneys than domestic cattle in north-eastern Poland, Sci. Total Environ 364, 295–300.

Wu, B., Zoriy, M., Chen, Y., Becker, J.S., 2009. Imaging of nutrient elements in the leaves of Elsholtzia splendens by laser ablation inductively coupled plasma mass spectrometry (LA-ICP-MS). Talenta 78, 132–137.

Yabe, J., Nakayama, S.M.M., Ikenaka, Y., Muzandu, K., Choongo, K., Mainda, G., Kabeta, M., Ishizuka, M., Umemura, T., 2013. Metal distribution in tissues of free-range chickens near a lead-zinc mine in Kabwe, Zambia. Environ. Toxicol. Chem. 32, 189–192.

Yabe, J., Nakayama, S.M.M., Ikenaka, Y., Muzandu, K., Ishizuka, M., Umemura, T., 2012. Accumulation of metals in the liver and kidneys of cattle from agricultural areas in Lusaka, Zambia. J. Vet. Med. Sci. 74, 1345–1347.

Yamashita, S., Yoshikuni, Y., Obayashi, H., Suzuki, T., Green, D., Hirata, T., 2019. Simultaneous determination of size and position of silver and gold nanoparticles in onion cells using laser ablation-ICP-MS. Anal. Chem. 91, 4544–4551.

Zhang, H., Li, W., Xue, Y., Zou, F., 2014. TRPC1 is involved in Ca2+ influx and cytotoxicity following Pb2+ exposure in human embryonic kidney cells. Toxicol. Lett. 229, 52–58.

Needleman, H.L., Schnaas, L., Wasserman, G., Graziano, J., Roberts, R., 2005. Low-level environmental lead exposure and children's intellectual function: an international pooled analysis. Environ. Health Perspect. 113, 894–899.
Li, P.J., Sheng, Y.Z., Wang, Q.Y., Gu, L.Y., Wang, Y.L., 2000. Transfer of lead via placenta and breast milk in human. Biomed. Environ. Sci. 13, 85–89.
Lidsky, T.L., Schneider, J.S., 2003. Lead neurotoxicity in children: basic mechanisms and clinical correlates. Brain 126, 5–19.
Lin, S., Hwang, S.A., Marshall, E.G., Marion, D., 1998. Does paternal occupational lead exposure increase the risks of low birth weight or prematurity? Am. J. Epidemiol. 148, 173–181.
Lo, Y.C., Dooyema, C.A., Neri, A., Durant, J., Jefferies, T., Medina-Marino, A., de Ravello, L., Thoroughman, D., Davis, L., Dankoli, R.S., Samson, M.Y., Ibrahim, L.M., Okechukwu, O., Umar-Tsafe, N.T., Dama, A.H., Brown, M.J., 2012. Childhood lead poisoning associated with gold ore processing: a village-level investigation-Zamfara State, Nigeria. Environ. Health Perspect. 120, 1450–1455. October-November 2010.
Manton, W.I., Angle, C.R., Stanek, K.L., Kuntzelman, D., Reese, Y.R., Kuehnemann, T.J., 2003. Release of lead from bone in pregnancy and lactation. Environ. Res. 92, 139–151.
Magellan Industries Inc, 2013. LeadCare II Blood Lead Analyzer User's Guide (V 1.09, Rev 04). Magellan Industries Inc, North Billerica, Mass, USA. http://www.leadcare2.com/Product-Support/Product-Literature-Downloads. (Accessed 20 February 2019).
Miranda, M.L., Kim, D., Galeano, M.A., Paul, C.J., Hull, A.P., Morgan, S.P., 2007. The relationship between early childhood blood lead levels and performance on end-of-grade tests. Environ. Health Perspect. 115, 1242–1247.
Needleman, H., 2004. Lead poisoning. Annu. Rev. Med. 55, 209–222.
Neria, A.J., Royb, J., Jarrettc, J., Panc, Y., Dooyemaa, C., Caldwellc, K., Umar-Tsafed, N.T., Olubiyoe, R., Brownf, M.J., 2014. Analysis of a novel field dilution method for testing samples that exceed the analytic range of point-of-care blood lead analyzers. Int. J. Environ. Health Res. 24, 418–428.
Ogden, T.L., 2010. Handling results below the level of detection. Ann. Occup. Hyg. 54, 255–256.
Ogunseitan, O.A., Smith, T.R., 2007. The Cost of environmental lead (Pb) poisoning in Nigeria. Afr. J. Environ. Sci. Technol. 1, 27–36.
Pearce, J.M., 2007. Burton's line in lead poisoning. Eur. Neurol. 57, 118–119.
Rothenberg, S.J., Khan, F., Manalo, M., Jiang, J., Cuellar, R., Reyes, S., Acosta, S., Jauregui, M., Diaz, M., Sanchez, M., Todd, A.C., Johnson, C., 2000. Maternal bone lead contribution to blood lead during and after pregnancy. Environ. Res. 82, 81–90.
Sadeghniat haghighi, K., Aminian, O., Chavoshi, F., Sadat, B.L., Soltani, S., Rahmati, N.F., 2013. Relationship between blood lead level and male reproductive hormones in male lead exposed workers of a battery factory: a cross-sectional study. Iran. J. Reproductive Med. 11, 673–676.
Sargent, J.D., Brown, M.J., Freeman, J.L., Bailey, A., Goodman, D., Freeman Jr., D.H., 1995. Childhood Pb Poisoning in Massachusetts Communities: it's association with sociodemographic and housing characteristics. Am. J. Public Health 85, 528–534.
Schoeters, G., Den Hond, E., Dhooge, W., van Larebeke, N., Leijs, M., 2008. Endocrine disruptors and abnormalities of pubertal development. Basic Clin. Pharmacol. Toxicol. 102, 168–175.
Sobin, C., Parisi, N., Schaub, T., de la Riva, E., 2011. A Bland-Altman comparison of the lead Care® System and Inductively Coupled Plasma Mass Spectrometry for detecting low-level lead in child whole blood samples. J. Med. Toxicol. 7, 24–32.
Stanton, N.V., Fritsch, T.B.S., 2007. Evaluation of a second-generation portable blood lead analyzer in an occupational setting. Am. J. Ind. Med. 50, 1018–1024.
Téllez-Rojo, M.M., Hernández-Avila, M., González-Cossío, T., Romieu, I., Aro, A., Palazuelos, E., Schwartz, J., Hu, H., 2002. Impact of breast-feeding on the mobilization of lead from bone. Am. J. Epidemiol. 155, 420–428.
Telisman, S., Cvitkovic, P., Juraasovic, J., Pizent, A., Gavella, M., Rocic, B., 2000. Semen quality and reproductive endocrine function in relation to biomarkers of lead, cadmium, zinc and copper in men. Environ. Health Perspect. 108, 45–53.
Thurtle, N., 2014. Description of 3,180 courses of Chelation with Dimercaptosuccinic Acid in Children $\leq$ 5 y with severe lead poisoning in Zamfara, Northern Nigeria: A Retrospective Analysis of Programme Data. PLoS Med 10, 11.
University of Michigan Risk Science Center (UMRSC) and Michigan Network for Children's Environmental Health (MNCEH), 2014. Economic impacts of lead exposure and remediation in Michigan. http://www.mnceh.org/sites/www.mnceh.org/files/mnceh/press-releases/Lead_Cost_Report_MI_2014_smaller.pdf. (Accessed 11 April 2019).
Wani, A.L., Ara, A., Usmani, J.A.H., 2015. Lead toxicity: a review. Interdiscip. Toxicol. 8, 55–64.
Wood, M.D., Beresford, N.A., Copplestone, D., 2011. Limit of detection values in data analysis: do they matter? Radioprotection 46, S85–S90.
World Health Organization, 2010. Childhood Lead Poisoning. WHO Press. http://www.who.int/ceh/publications/leadguidance.pdf. (Accessed 12 February 2019).
World Health Organization, 2018. Lead poisoning and health. https://www.who.int/news-room/fact-sheets/detail/lead-poisoning-and-health. (Accessed 12 February 2019).
Wu, H.M., Lin-Tan, D.T., Wang, M.L., Huang, H.Y., Lee, C.L., Wang, H.S., Soong, Y.K., Lin, J.L., 2012. Lead level in seminal plasma may affect semen quality for men without occupational exposure to lead. Reprod. Biol. Endocrinol. 10, 91.
Yabe, J., Nakayama, S.M.M., Ikenaka, Y., Yohannes, Y.B., Bortey-Sam, N., Oroszlany, B., Muzandu, K., Choongo, K., Kabalo, A.N., Ntapisha, J., Mweene, A., Umemura, T., Ishizuka, M., 2015. Lead poisoning in children from townships in the vicinity of a lead-zinc mine in Kabwe, Zambia. Chemosphere 119, 941–947.
Yabe, J., Nakayama, S.M.M., Ikenaka, Y., Yohannes, Y.B., Bortey-Sam Kabalo, A.N., Ntapisha, J., Mizukawa, H., Umemura, T., Ishizuka, M., 2018. Lead and cadmium excretion in feces and urine of children from polluted townships near a lead-zinc mine in Kabwe, Zambia. Chemosphere 202, 48–55.

Chemosphere 243 (2020) 125412

Contents lists available at ScienceDirect

Chemosphere

journal homepage: www.elsevier.com/locate/chemosphere

Current trends of blood lead levels, distribution patterns and exposure variations among household members in Kabwe, Zambia

John Yabe [a], Shouta MM. Nakayama [b], Hokuto Nakata [b], Haruya Toyomaki [b], Yared B. Yohannes [b], Kaampwe Muzandu [a], Andrew Kataba [a, b], Golden Zyambo [a], Masato Hiwatari [c], Daiju Narita [d], Daichi Yamada [d], Peter Hangoma [e], Nosiku Sipilanyambe Munyinda [e], Tiza Mufune [f], Yoshinori Ikenaka [b], Kennedy Choongo [a], Mayumi Ishizuka [b, *]

[a] The University of Zambia, School of Veterinary Medicine, P.O. Box 32379, Lusaka, Zambia
[b] Faculty of Veterinary Medicine, Hokkaido University, Kita 18, Nishi 9, Kita-ku, Sapporo, 060-0818, Japan
[c] Faculty of Economics & Business, Hokkaido University, Kita 9, Nishi 7, Kita-ku, Sapporo, 060-0809, Japan
[d] Graduate School of Arts and Sciences, University of Tokyo, 3-8-1 Komaba, Meguro-ku, Tokyo, 153-8902, Japan
[e] The University of Zambia, School of Public Health, P.O. Box 32379, Lusaka, Zambia
[f] Ministry of Health, District Health Office, P.O. Box 80735, Kabwe, Zambia

HIGHLIGHTS

- We measured blood lead in household members in Kabwe, which has a history of Pb–Zn mining.
- Blood Lead Levels (BLL) ranged from 1.65 to 162 μg/dL and were highest in children compared to parents.
- LeadCare II analyser provided prompt diagnosis to identify children needing chelation therapy.
- Age, distance from the mine and direction were the main factors influencing Pb exposure.
- Children living near the Pb–Zn mine are at serious risks of Pb and Cd poisoning.

ARTICLE INFO

Article history:
Received 11 August 2019
Received in revised form
5 November 2019
Accepted 18 November 2019
Available online 19 November 2019

Handling Editor: Martine Leermakers

Keywords:
Childhood lead poisoning
LeadCare II analyser
Pb exposure differences
Kabwe

ABSTRACT

Childhood lead (Pb) poisoning has devastating effects on neurodevelopment and causes overt clinical signs including convulsions and coma. Health effects including hypertension and various reproductive problems have been reported in adults. Historical Pb mining in Zambia's Kabwe town left a legacy of environmental pollution and childhood Pb poisoning. The current study aimed at establishing the extent of Pb poisoning and exposure differences among family members in Kabwe as well as determining populations at risk and identify children eligible for chelation therapy. Blood samples were collected in July and August 2017 from 1190 household members and Pb was measured using a portable LeadCare-II analyser. Participants included 291 younger children (3-months to 3-years-old), 271 older children (4-9-years-old), 412 mothers and 216 fathers from 13 townships with diverse levels of Pb contamination. The Blood Lead Levels (BLL) ranged from 1.65 to 162 μg/dL, with residents from Kasanda (mean 45.7 μg/dL) recording the highest BLL while Hamududu residents recorded the lowest (mean 3.3 μg/dL). Of the total number of children sampled (n = 562), 23% exceeded the 45 μg/dL, the threshold required for chelation therapy. A few children (5) exceeded the 100 μg/dL whereas none of the parents exceeded the 100 μg/dL value. Children had higher BLL than parents, with peak BLL-recorded at the age of 2-years-old. Lead exposure differences in Kabwe were attributed to distance and direction from the mine, with younger children at highest risk. Exposure levels in parents were equally alarming. For prompt diagnosis and treatment, a portable point-of-care devise such as a LeadCare-II would be preferable in Kabwe.

* Corresponding author. Graduate School of Veterinary Medicine, Hokkaido University, Kita 18, Nishi 9, Kita-ku, Sapporo, 060-0818, Japan.
E-mail address: ishizum@vetmed.hokudai.ac.jp (M. Ishizuka).

https://doi.org/10.1016/j.chemosphere.2019.125412
0045-6535/

1. Introduction

Lead (Pb) poisoning accounts for about 0.6% of the global burden of disease (WHO, 2010), posing a serious public health concern worldwide. While acute toxicity is related to occupational exposure and is quite uncommon, low level chronic toxicity due to environmental pollution is much more common (ATSDR, 2017). Lead poisoning has devastating effects on neurodevelopment such as mental retardation and lowering of intelligence quotient (IQ) in children, which may further result in poor school performance, lower tertiary education attainment, behavioural disorders and poor lifetime earnings (WHO, 2018; Dapul and Laraque, 2014; Miranda et al., 2007; Canfield et al., 2003; Lidsky and Schneider, 2003). If not treated, Pb poisoning is characterized by persistent vomiting, anaemia, encephalopathy, lethargy, delirium, convulsions, coma and death (WHO, 2018; Flora et al., 2012; Pearce, 2007). The Institute for Health Metrics and Evaluation (IHME, 2017) estimated that in 2016 Pb exposure accounted for 540,000 deaths worldwide. In chronically exposed adults, significant health effects including renal dysfunction, hypertension and various reproductive problems have been shown even at low Pb exposures (Kumar, 2018; Wani et al., 2015). Cases of reduced fertility following chronic exposure have been reported in males (Benoff et al. 2000, 2003; Telisman et al., 2000) as well as miscarriages in pregnant women (Wani et al., 2015). Moreover, childhood Pb exposure poses significant economic losses in affected countries, especially in low- and middle-income countries (Attina and Trasande, 2013).

Clinical presentations of Pb poisoning vary widely depending upon the age, the amount and the duration of exposure, with some individuals seeming well at a blood lead levels (BLLs) that in others results in overt clinical signs (Bellinger, 2004). Given that detrimental effects of chronic Pb exposure are usually subclinical (Yabe et al., 2015, 2018), it may result in a delay in the appropriate diagnosis and chelation therapy, which has been recommended to be initiated at levels $\geq$ 45 μg/dL (CDC 2002; Needleman, 2004). Early diagnosis and chelation therapy are crucial as it has been reported that high BLLs exceeding 100 μg/dL in children can cause encephalopathy, convulsions, coma and death (CDC 2002). Therefore, measurement of BLLs plays a pivotal role in the diagnosis and management of patients as described in Pb poisoned children in Nigeria (Thurtle, 2014). Traditionally, BLLs have been measured using atomic absorption spectrophotometer (AAS), inductively coupled plasma mass spectrometry (ICP-MS), etc. Although highly sensitive to Pb measurement, these equipment are laboratory-based and require trained laboratory technologists. Moreover, they are expensive and would be time-consuming to ship samples to appropriate laboratories.

In a set-up like Kabwe town in Zambia, where historical Pb mining has resulted in alarming Pb poisoning, especially in children from townships in the vicinity of the closed mine and its tailing wastes (Yabe et al., 2018; Bose-O'Reilly et al., 2018; Yabe et al., 2015), prompt diagnosis and immediate chelation therapy would be required. Therefore, a portable point-of-care devise such as a LeadCare II analyser, which can be used on-site in remote medical facilities like Kabwe would be appropriate and preferable. Given that BLL results are read within 3 min, Pb poisoning would be diagnosed and chelation therapy initiated promptly. Therefore, the current study investigated trends of BLL using a LeadCare II Analyser in Kabwe to identify children that required medical management to minimize the toxic effects of Pb. In addition, factors influencing Pb exposure in Kabwe were analyzed and exposure patterns among household members including fathers, mothers and children were evaluated.

2. Materials and methods

2.1. Sampling sites

Kabwe town, with a population of about 230, 000 inhabitants and area size of 1, 547 km^2, is the fourth largest town in Zambia. It is the provincial capital of Zambia's Central Province and is located at about 28°26′E and 14°27′S. Kabwe has a long history of open-pit Pb–Zn mining, from 1902 to 1994. As observed by the Blacksmith Institute (2013), despite closure of the mine, scavenging of metal scraps from the abandoned tailings and wastes stored on the mine has continued to serve as a source of metal pollution, especially dusts emanating from the mine dumps (Fig. 1).

Moreover, some households were within 500 m of the tailings. As shown in Fig. 2, soils in townships in the vicinity of the mine and homes downwind from the tailings were highly polluted with Pb exceeding acceptable levels for residential areas (Bose-O'Reilly et al., 2018). In the current study, blood samples were collected from family members including fathers, mothers and children at health centres around the town of Kabwe, in July and August of 2017. More details about the study site and descriptions of townships that are within the vicinity of the mine can be obtained from the previous study (Yabe et al., 2015).

2.2. Sample collection

The study was approved by the University of Zambia Research Ethics Committee (UNZAREC; REF. No. 012-04-16). Further approvals were granted by the Ministry of Health through the Zambia National Health Research Ethics Board and the Kabwe District Medical Office. The study targeted households from areas diverse in the levels of Pb contamination based on the sample design in a parallel socioeconomic survey under the KAMPAI project (Hiwatari et al., 2018). 1000 target households were randomly chosen in two steps. In the first step, following the sampling frame of Central Statistical Office (CSO), which conducts official census in Zambia and has divided Kabwe town into 384 Standard Enumeration Areas (SEAs). Forty SEAs falling within the catchment area of health facilities were randomly selected (Fig. 3) while 25 households from each SEA were randomly selected in the second stage.

To conduct blood sampling, up to four household members (father, mother, and two children) were invited to local health centres. Younger non-school-going children up to 3 years old and older school-aged children older than 4 years were selected in the study. The age criterion was according to Yabe et al. (2015) who found significant differences BLL in children of the two age groups. Thirteen health centres with catchments areas covering the 40 SEAs were included. These included Kasanda, Chowa, Makululu, Katondo, Railway, Pollen, Mahatma Ghandi, Bwacha, Ngungu, Natuseko, Mpima Prison, Kang'omba and Hamududu with distances between the mine and the health centres ranging from 1.5 to 30 km (Fig. 3). After informed and written consent were obtained

Fig. 1. Figure showing men scavenging for scrape metals at the Kabwe Pb–Zn mine tailings (left) and houses located within 500 m to the tailings (right).

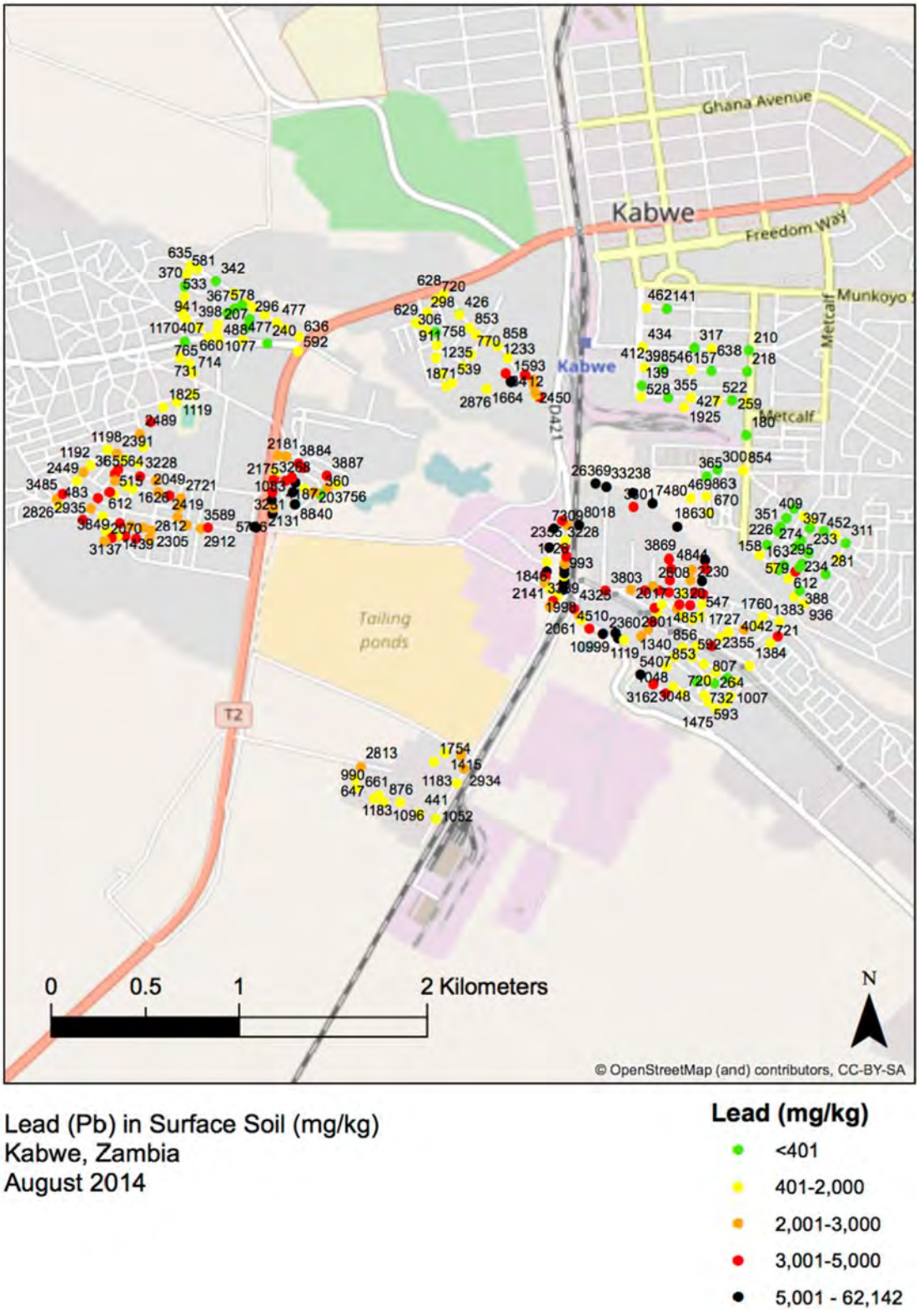

Fig. 2. Map of Kabwe showing distribution of Pb (mg/kg) in township soils around the Pb–Zn mining complex (Bose-O'Reilly et al., 2018).

from household heads, blood samples were collected as described earlier by Yabe et al. (2015). For each of the four family members included in the study, data on the age and sex were recorded. Sample collection and questionnaire administration were done by certified local nurses. In accordance with ethical requirements, confidentiality was upheld in the study.

To avoid sample contamination, all sample collection supplies were kept in plastic ziploc storage bags before sample collection. Moreover, the blood collection site on the arm was thoroughly cleaned and wiped with alcohol swabs before needle pricking to

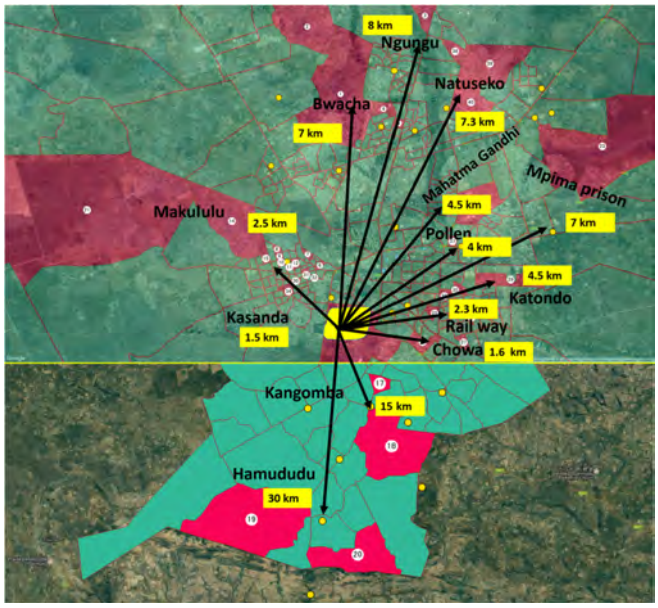

Fig. 3. Map of Kabwe showing the 40 selected SEAs (numbers 1–40 in white circles) widely distributed across the whole Kabwe town and the 13 health centres (yellow blocks) that were included in the study.

minimize contamination from dust. For infants, blood was collected by fingerstick after cleaning the finger with an alcohol swab. A new sterile lancet was used for each infant to penetrate a fingertip. The first drop of blood was wiped off with a clean and dry swab and 50 μL blood sample was collected with a pre-supplied LeadCare II capillary tube and transferred into the LeadCare II reagent vial. After collection, blood samples were immediately analyzed for Pb using a LeadCare© II analyser. The remaining samples were immediately stored at −20 °C at the health centres before being transported in cooler boxes on dry ice to the laboratory of the Kabwe District Health Offices where they were again stored at -20 °C.

2.3. Blood Pb analysis

Lead metal analysis in whole blood samples was done on-site immediately after blood sample collection using a point-of-care blood Pb testing analyser, LeadCare© II (Magellan Diagnostics, USA) according to the manufacturer's instructions. The analyser uses an electrochemical technique called Anodic Stripping Voltammetry (ASV) to determine the amount of Pb in a blood sample (Magellan Industries Inc, 2013). The analyser has been evaluated by several researchers including (Stanton and Fritsch, 2007; Sobin et al., 2011; Neria et al., 2014). Briefly, individual heparinized venous blood samples were drawn using the manufacturer-supplied LeadCare II capillary tubes (approximately 50 μL) and dispensed into labeled vials containing LeadCare II treatment reagent (250 μL of 0.1% of HCl). These were thoroughly mixed by tipping the bottle ten times to enhance red blood cell lysis, which released the bound Pb. About 50 μL of the blood/reagent mixture was then transferred to a sensor using the provided transfer dropper and analyzed for blood Pb concentration. Single analyses were performed with results reflected within 3 min in μg/dL on the analyser's screen. For quality assurance, the instrument was calibrated using a probe before each new lot of test supplies (every 48 tests). Standard controls, one high and one low blood-based controls supplied by the manufacturer were analyzed to assess accuracy, these fell within the manufacturer-specified acceptability limits of 6.9–13.7 μg/dL for the low control and 21.8–32.6 μg/dL for the high control. Since limits of quantitation were 3.3–65 μg/dL as the LeadCare II Analyser can only detect BLL above 3.3 μg/dL. The precise values of BLLs below the 3.3 μg/dL detection limit could not be determined. These BLLs below instrument detection limit were therefore treated as 1.65 μg/dL, the mean of 0 and 3.3 as suggested in other environmental studies (Wood et al., 2011; Ogden, 2010).

For samples above 65 μg/dL, a 3 times dilution was done using 0.1% HCl. Briefly, 50 μL of collected blood was added into 100 μL of 0.1% HCl. Then 50 μL of diluted blood was pipetted into the LeadCare II reagent. This was mixed thoroughly and analyzed in the same way as for undiluted blood. The blood specimens and blood/reagent mixtures were maintained at room temperature throughout the analytical process.

2.4. Statistical analysis

All data were combined into a single electronic database and checked for accuracy and outliers. Statistical analysis was performed using JMP version 10 (SAS Institute, USA). The data are presented as mean, geometric mean (GM), median and minimum-maximum values in μg/dL. Tukey Kramer test was used to analyse BLL differences among family members (younger child, older child, father and mother) as well as area difference. Different letters indicated significant difference. Principal component analysis (PCA) was used to evaluate the relatedness between BLL with age, wind direction and distance from the mine. The data of BLLs (μg/dL) were log-transformed before PCA analysis to stabilize variances.

3. Results

3.1. Subjects and BLL

The current study focused on blood samples that were collected from a total number of 1190 household members including 291 younger children (3 months–3 years old) with an average age of 1.9 years; 271 older children (4–9 years old) with an average age of 6.5 years; 412 mothers with an average age of 39 years and 216 fathers with an average age of 46 years. Participants were drawn from 13 health centres servicing Kasanda, Chowa, Makululu, Katondo, Railway, Pollen, Mahatma Ghandi, Bwacha, Ngungu, Natuseko, Mpima Prison, Kang'omba and Hamududu townships. The recorded BLL ranged from 1.65 to 162 μg/dL (Table 1).

3.2. Critical BLL values among household members

As shown in Table 2, of the 1, 190 participants, 30% had BLL below 5 μg/dL, which is the level of concern. These comprised 57 younger children, 59 older children, 151 mothers and 85 fathers. Of the total number of children sampled ($n = 562$), a total of 130 (23%) exceeded the 45 μg/dL, the threshold required for chelation therapy. A few children (total of 5) exceeded the 100 μg/dL whereas none of the parents exceeded the 100 μg/dL value.

3.3. Pb exposure patterns among household members

Tukey test was performed to analyse age differences in BLL accumulation among family members. Children had significantly higher BLL than parents. However, there was no accumulation difference in BLL between younger children between the ages of 3 months to 3 years and older children aged 4–9 years. Moreover, BLL between fathers and mothers were not different. Similarly, there was no sex difference in blood Pb concentrations as the BLL between boys and girls were not different (data not shown). A positive correlation was seen in the BLL of mothers and their infants (data

Table 1
BLL (μg/dL) exposure characteristics among household members in Kabwe, Zambia.

Category	All	Younger child	Older child	Mother	Father
	$n = 1190$	$n = 291$	$n = 271$	$n = 412$	$n = 216$
Mean	20.8	29.9	24.3	14.8	15.7
Geo. Mean	11.1	17.0	14.2	8.2	8.1
Standard Error	0.62	1.59	1.32	0.74	1.20
Median	13.0	22.0	17.3	10.8	8.6
Standard Deviation	21.4	27.1	21.7	15.0	17.7
Minimum	1.65	1.65	1.65	1.65	1.65
Maximum	162	162	103	86.7	88.2

Table 2
BLL (μg/dL) exposure characteristics among household members in Kabwe, Zambia.

Category BLL ranges	All Number (%)	Young child Number (%)	Child Number (%)	Mother Number (%)	Father Number (%)
BLL < 5 μg/dL	352 (30)	57 (20)	59 (22)	151 (37)	85 (39)
BLL 5–44 μg/dL	666 (56)	154 (53)	162 (60)	239 (58)	111 (51)
BLL 45–99 μg/dL	167 (14)	76 (26)	49 (18)	22 (5.3)	20 (9.3)
BLL > 100 μg/dL	5 (0.4)	4 (1.4)	1 (0.4)	0 (0.0)	0 (0.0)

not shown).

3.4. Relationship between BLL and age

A combined dot plot and box-whisker plot was performed to evaluate the relationship between BLL and age (Fig. 4). In terms of the median BLL, a general trend indicated a high peak in children around the age of 2 years and lower BLL in older children, albeit with fluctuations. Very high BLLs are also more frequently observed among young children although BLL above 45 μg/dL is observed in any age group.

3.5. Pb exposure differences among townships

In order to fully understand the Pb exposure patterns in Kabwe, differences in blood Pb accumulations in residents from the 13 townships were compared. Descriptive statistics of the BLL in residents enrolled at the 13 health centres are shown in Table 3.

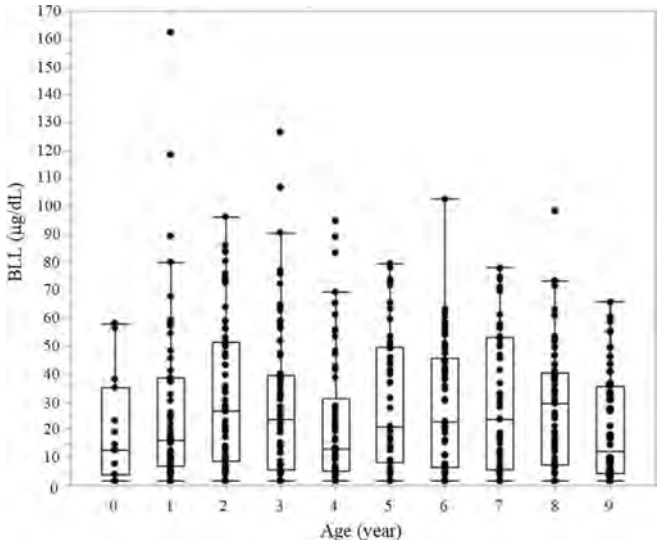

Fig. 4. Figure of combined dot plot and box-whisker plot showing relationship between BLL and age, with peak BLL recorded at 2 years old.

Residents in Kasanda Township, with mean BLL of 45.7 μg/dL accumulated higher BLL than residents in the other 12 locations. Makululu Township had second highest mean BLL (29.3 μg/dL) followed by Chowa and Railway townships. Similar but lower BLL were recorded in residents from Natuseko, Kang'omba, Ngungu, Mpima Prison, Katondo and Mahatma Ghandi followed by Bwacha and Pollen townships. Residents in Hamududu community had the lowest BLL, with a mean value of 3.3 μg/dL.

3.6. Factors contributing to Pb exposure patterns in Kabwe

Principle component analysis (PCA) was performed on log-transformed data to evaluate the relationships among BLL, age, direction and distance from the mine to the township health centres. As shown in Fig. 5, the results of PCA accounted for 44.3% of the variation by the first principal component (PC1) and 26.4% by the second principal component (PC2). Whereas PC1 was positively determined by distance as well as a slight positive influence by age and direction, it was negatively influenced by BLL. On the other hand, PC2 had a strongly positive relationship with age, but rarely with distance and BLL. It was indicated that distance from the mine had a strong and bigger negative relationship with BLL while direction and age had lower negative relationship with BLL.

4. Discussion

A portable LeadCare© II analyser was used and proved to be an effective point of care blood Pb analyser in Kabwe, where alarming childhood Pb poisoning was previously reported (Yabe et al., 2015). Moreover, the LeadCare II analyser is less invasive and suitable for infants as it requires a smaller finger stick blood sample. In an environment like Kabwe where non-specific clinical symptoms of cumulative Pb poisoning can easily be confused with other diseases like malaria, a rapid and appropriate diagnosis of Pb poisoning cannot be overemphasized. The current study analyzed Pb exposure patterns among family members in Kabwe, where household members shared similar risk factors such as area, direction and living conditions. The study revealed that not only children were at risk of the toxic effects of Pb in Kabwe town but women and men as well. Young age was a significant risk factor given that BLL were highest in children, with peak levels recorded at the age of two, in agreement with similar trends in earlier studies (Yabe et al., 2015;

Table 3
Area differences in BLL (μg/dL) among Kabwe residents from 13 health centres.

	Kasanda	Makululu	Chowa	Railway	Natuseko	Bwacha	Ngungu	Pollen	Mahatma Ghandi	Mpima Prison	Katondo	Kang'omba	Hamududu
Mean	45.7	29.3	16.5	11.4	8.58	6.78	5.38	4.70	4.51	5.41	6.51	8.48	3.31
St'd Error	1.64	1.01	1.02	1.97	0.98	1.10	0.59	0.98	0.63	0.59	1.09	1.01	0.41
Median	44.9	24.3	16.6	10.5	6.95	3.90	4.80	1.65	4.60	4.90	3.80	5.40	1.65
Standard Deviation	23.5	19.0	10.5	6.81	6.92	11.1	3.50	4.69	2.36	4.13	7.17	9.94	4.08
Minimum	1.65	1.65	1.65	3.30	1.65	1.65	1.65	1.65	1.65	1.65	1.65	1.65	1.65
Maximum	162	119	48.3	26.2	34.3	94.8	14.2	16.8	9.00	23.3	38.7	63.5	35.6
Count	204	355	105	12	50	103	35	23	14	49	43	96	101

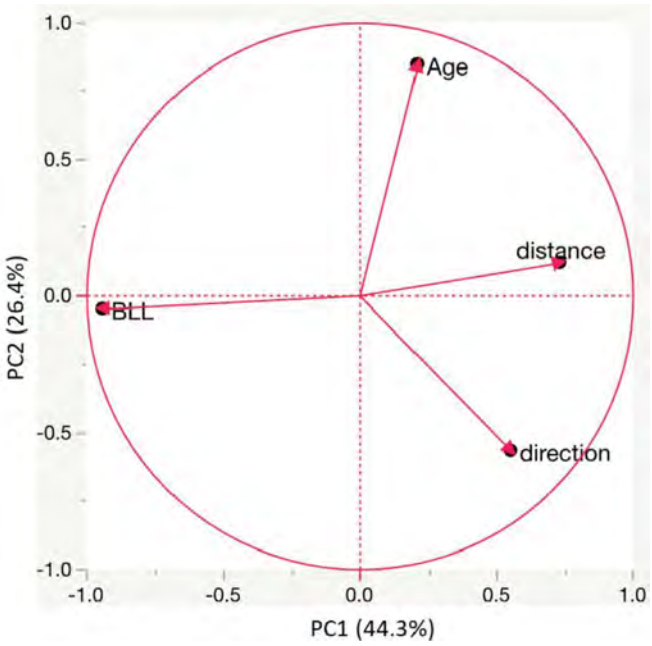

Fig. 5. Principal component analysis on log transformed data showing the influence of age, distance and wind direction on BLL among Kabwe residents.

Koller et al., 2004). This trend could be attributed to the hand-to-mouth or object-to-mouth (pica) behavior of children as they explore their environment after their onset of independent ambulation. In addition to increased exposure, children absorb a greater proportion of ingested Pb from the gastrointestinal tract than adults (Wani et al., 2015). Acute Pb poisoning exceeding 100 μg/dL can be fatal as seen in the Pb poisoning disaster in Nigeria, where more than 400 children died leaving numerous others with long-term neurological impairment (Dooyema et al., 2012; Lo et al., 2012). To minimize the pernicious effects of Pb toxicity in children, chelation therapy is recommended at levels ≥45 μg/dL as clinical symptoms such as abdominal pain, encephalopathy, convulsions, coma and death have been observed in BLLs >60 (CDC, 2002; Needleman, 2004). The current study revealed that of the 556 children, 29% had BLL that exceeded 45 μg/dL and were recommended for chelation therapy. Moreover, the children were followed up for further assessment including neurodevelopmental impairment assessment (data not provided).

For the first time, the current study revealed high BLL in women in some areas in Kabwe, with concentrations up to 86 μg/dL. These findings were similar to BLLs reported in women of child-bearing age in Sub-Saharan Africa where the overall weighted mean BLLs of 24.73 μg/dL was recorded, with the highest mean of 99 μg/dL being recorded in women from Nigeria (Bede-Ojimadu et al., 2018). Most of the mothers that participated in current the study (58%) had BLL ranging between 5 and 44 μg/dL, a few (5%) were above 45 μg/dL with none exceeded 100 μg/dL. Exposure to Pb in the women could be attributed to multiple sources including dust inhalation, ingestion via diet or soil (pica), a habit that is common among pregnant women in Zambia, including Kabwe. Although most studies are focused on childhood Pb exposure, the findings in the current study should be considered carefully as increased BLLs in women of child-bearing age in Sub-Saharan Africa were associated with incidences of preeclampsia and hypertension (Bede-Ojimadu et al., 2018). Delayed puberty due to Pb exposure has also been observed in girls (Schoeters et al., 2008). With a half-life of many years to decades in adults, endogenous exposure to Pb due to increased bone resorption as seen in women during pregnancy and lactation (Rothenberg et al., 2000; Téllez-Rojo et al., 2002; Gulson et al., 2003; Manton et al., 2003) could also not be ruled out in the exposed mothers in Kabwe. When pregnant, blood Pb accumulation in women could pose a threat to the developing fetus given that maternal-fetal transfer is a major source of early life exposure to Pb (Chen et al., 2006; Gardella, 2001; Li et al., 2000; Lin et al., 1998). Additional Pb exposure to the infant can occur via breast milk as breastfeeding is a recognized source of postnatal Pb exposure (Counter et al., 2014). These exposure pathways could explain the alarmingly high BLL in infants in the current study, even before their ambulatory stage. This is critical as pediatric Pb poisoning during a vulnerable period of development can lead to negative neurodevelopmental impacts such as low IQ and cognitive impairments (Lanphear et al., 2005).

Similarly, increased Pb exposure in men from some Kabwe townships was recorded in the current study, with median BLLs of 8.60 μg/dL and maximum levels of 88.2 μg/dL. This is also the first time that Pb exposure is being investigated in men in Kabwe and the sources of exposure could be similar to those of women, with the exception of pica, a practice common especially among expectant mothers. Findings in the current study were similar to reports in Iran where mean BLL of 41.41 μg/dL were reported in male workers at a battery manufacturing plant (Sadeghniat haghighi et al., 2013). Given that chronic low level Pb exposure has been associated with health complications including reduced sperm quality (Wu et al., 2012; Apostoli et al., 1998), the findings of the current study highlight the reproductive health risks that men in Kabwe could be exposed to through chronic Pb exposure. Moreover, Pb exposure has an interactive relationship with socioeconomic factors. While socioeconomic conditions have been established as important predictors of exposure to Pb (Elias et al., 2007; Sargent et al., 1995), health effects of Pb exposure can be the sources of economic losses that can impact families negatively (UMRSC and MNCEH, 2014; Attina and Trasande, 2013; Gould, 2009; Ogunseitan and Smith, 2007). While many studies may place emphasis only on health effects of Pb exposure, the impact of Pb exposure and poisoning in Kabwe could be broad and include healthcare, social, and behavioural costs.

Area differences in BLL exposure patterns among Kabwe residents were established in the current study, where residents from Kasanda Mine Township had the highest BLL followed by Makululu

and Chowa Townships. BLLs in Railway, Natuseko, Katondo, Pollen, Mahatma Ghandi, Bwacha, Ngungu, Mpima Prison, Kang'omba were similar, with residents from Hamududu recording the lowest. These results reveal that severity to Pb poisoning risks among residents of Kabwe was different depending on area of residence. These differences could be attributed to distance from the mine and direction, with distance from the mine exerting the majority influence as seen on PCA analysis. It was shown that townships closest to the mine and lying in the western direction of the mine were affected the most, especially Kasanda, followed by Makululu. Since the wind direction is from east to west in Kabwe, more Pb contaminated dusts emanating from the mine tailings are likely to settle in Kasanda and Makululu than the other townships. Of interest was Natuseko Township, which is located in similar direction with similar distance from the mine as Bwacha and Ngungu Townships but recorded slightly higher BLLs than these two townships. Although not established, this could be attributed to transportation and piling of contaminated soils and stones from the mine in Natuseko Township many years ago (verbal communication from community members).

5. Conclusions

This is the first study that has revealed the true extent of Pb exposure in the whole Kabwe town, which poses a serious public hazard and should be given urgent attention. Exposure to Pb does not only affect children but their parents as well. Factors contributing to Pb exposure included age, distance and direction, with distance playing the major role. Therefore, younger children in townships closer to the mine and lying on the western side of the mine were the most vulnerable. To avert overt Pb toxicity, children with BLL exceeding 45 μg/dL would require chelation therapy. These children were referred to the office of the District Medical Director. Regular BLL monitoring using a portable analyser such as the LeadCare II should be considered for prompt diagnosis and initiation of treatment to avoid the irreversible Pb-induced neurological dysfunction in children. A thorough clinical evaluation of Pb poisoning among the affected children, including neurodevelopmental and cognitive impairments, would reveal the true extend of Pb poisoning in Kabwe. Measuring blood Pb in pregnant women and breast milk will be significant to clarify the exposure pathway from mother to child and recommend appropriate medical management and advice for the mother. Socio-economic factors contributing to Pb exposure and socio-economic impacts of Pb exposure also need to be thoroughly investigated to fully understand the Pb exposure-effect cycle. Moreover, urgent environmental remediation is required to reduce Pb exposure in Kabwe.

Declaration of competing interest

The authors declare no conflicts of interest.

Acknowledgments

We are highly indebted to the families in Kabwe that participated in the study. We are also grateful to the 13 health centres in Kabwe, the Kabwe District Health Office and the Ministry of Health, Zambia, for facilitating the study. We also want to thank all the laboratory technicians and nurses at the health centres for their technical support. This work was supported by Grants-in-Aid for Scientific Research from the Ministry of Education, Culture, Sports, Science and Technology of Japan awarded to M. Ishizuka (No. 16H0177906, 18K1984708) and Y. Ikenaka (17K2003807, 18H0413208), and S.M.M. Nakayama (No. 16K16197, 17KK0009), and the foundation of JSPS Core to Core Program (AA Science Platforms), the Environment Research and Technology Development Fund (SII-1/3—2, 4RF-1802/18949907) of the Environmental Restoration and Conservation Agency of Japan. We also acknowledge financial support from The Soroptimist Japan Foundation, The Nakajima Foundation, The Sumitomo foundation, The Nihon Seimei Foundation and The Japan Prize Foundation. This research was also supported by JST/JICA, SATREPS (Science and Technology Research Partnership for Sustainable Development; No. JPMJSA1501). We also acknowledge the contribution of the Kabwe Municipal Council, especially Mr. Paul Mukuka, the Director of Public Health, for facilitating the study.

References

Agency for Toxic Substances and Disease Registry (ATSDR), 2017. Lead Toxicity. What are possible health effects from lead exposure? Available: https://www.atsdr.cdc.gov/csem/lead/docs/csem-lead_toxicity_508.pdf. (Accessed 21 January 2019).

Apostoli, P., Kiss, P., Porru, S., Bonde, J.P., Vanhoorne, M., 1998. Male reproductive toxicity of lead in animals and humans. Occup. Environ. Med. 55, 364—374.

Attina, T.M., Trasande, L., 2013. Economic costs of childhood Pb exposure in low- and middle-income countries. Environ. Health Perspect. 121, 1097—1102.

Bede-Ojimadu, O., Amadi, C.N., Orisakwe, O.E., 2018. Blood lead levels in women of child-bearing age in sub-Saharan Africa: a systematic review. Front. Public Health 6, 367.

Bellinger, D.C., 2004. Lead. Pediatrics 113, 1016—1022.

Benoff, S., Centola, G.M., Millan, C., Napolitano, B., Marmar, J.L., Hurley, I.R., 2003. Increased seminal plasma lead levels adversely affect the fertility potential of sperm in IVF. Hum. Reprod. 18, 374—383.

Benoff, S., Jacob, A., Hurley, I.R., 2000. Male infertility and environmental exposure to lead and cadmium. Hum. Reprod. Update 6, 107—121.

Blacksmith Institute (PureEarth), 2013. The world's worst 2013: the top ten toxic threats. Available: https://www.worstpolluted.org. (Accessed 29 October 2019).

Bose-O'Reilly, S., Yabe, J., Makumba, J., Schutzmeier, P., Ericson, B., Caravanos, J., 2018. Lead intoxicated children in Kabwe, Zambia. Environ. Res. 168, 420—424.

Canfield, R.L., Henderson Jr., C.R., Cory-Slechta, D.A., Cox, C., Jusko, T.A., Lanphear, B.P., 2003. Intellectual impairment in children with blood lead concentrations below 10 μg per deciliter. N. Engl. J. Med. 348, 1517—1526.

Centers for Disease Control and Prevention (CDC), 2002. Managing elevated blood lead levels among young children: recommendations from the Advisory Committee on Childhood Lead Poisoning prevention. Available: https://stacks.cdc.gov/view/cdc/26980. (Accessed 29 December 2018).

Chen, P.C., Pan, I.J., Wang, J.D., 2006. Parental exposure to lead and small for gestational age births. Am. J. Ind. Med. 49, 417—422.

Counter, S.A., Buchanan, L.H., Ortega, F., Chiriboga, R., Correa, R., Collaguaso, M.A., 2014. Lead levels in the breast milk of nursing Andean mothers living in a lead-contaminated environment. J. Toxicol. Environ. Health A. 77, 993—1003.

Dapul, H., Laraque, D., 2014. Lead poisoning in children. Adv. Pediatr. 61, 313—333.

Dooyema, C.A., Neri, A., Lo, Y.C., Durant, J., Dargan, P.I., Swarthout, T., Biya, O., Gidado, S.O., Haladu, S., Sani-Gwarzo, N., Nguku, P.M., Akpan, H., Idris, S., Bashir, A.M., Brown, M.J., 2012. Outbreak of fatal childhood lead poisoning related to artisanal gold mining in northwestern Nigeria. Environ. Health Perspect. 120, 601—607, 2010.

Elias, S.M., Hashim, Z., Marjan, Z.M., Abdullah, A.S., Hashim, J.H., 2007. Relationship between blood Pb concentration and nutritional status among Malay primary school children in Kuala Lumpur, Malaysia. Asia. Pac. J. Public Health 19, 29—37.

Flora, G., Gupta, D., Tiwari, A., 2012. Toxicity of lead: a review with recent updates. Interdiscip. Toxicol. 5, 47—58.

Gardella, C., 2001. Lead exposure in pregnancy: a review of the literature and argument for routine prenatal screening. Obstet. Gynecol. Surv. 56, 231—238.

Gould, E., 2009. Childhood lead poisoning: conservative estimates of the social and economic benefits of lead hazard control. Environ. Health Perspect. 117, 1162—1167.

Gulson, B.L., Mizon, K.J., Korsch, M.J., Palmer, J.M., Donnelly, J.B., 2003. Mobilization of lead from human bone tissue during pregnancy and lactation - a summary of long-term research. Sci. Total Environ. 303, 79—104.

Hiwatari, M., Yamada, D., Hangoma, P., Narita, D., Mphuka, C., Chitah, B., 2018. Kabwe Household Socioeconomic Survey (KHSS) 2017 Report. Kabwe Mine Pollution Amelioration Initiative (KAMPAI), pp. 1—91 (ISBN978-4-909032-02-7), available at: http://satreps-kampai.vetmed.hokudai.ac.jp/publications/.

Institute for Health Metrics and Evaluation (IHME), 2017. Global Burden of Disease (GBD) Compare. IHME, University of Washington, Seattle, WA. Available: https://vizhub.healthdata.org/gbd-compare/. (Accessed 10 February 2019).

Koller, K., Brown, T., Spurgeon, A., Levy, L., 2004. Recent developments in low-level lead exposure and intellectual impairment in children. Environ. Health Perspect. 112, 987—994.

Kumar, S., 2018. Occupational and environmental exposure to lead and reproductive health impairment: an overview. Indian J. Occup. Environ. Med. 22, 128—137.

Lanphear, B.P., Hornung, R., Khoury, J., Yolton, K., Baghurst, P., Bellinger, D.C., Canfield, R.L., Dietrich, K.N., Bornschein, R., Greene, T., Rothenberg, S.J.,

Needleman, H.L., Schnaas, L., Wasserman, G., Graziano, J., Roberts, R., 2005. Low-level environmental lead exposure and children's intellectual function: an international pooled analysis. Environ. Health Perspect. 113, 894–899.
Li, P.J., Sheng, Y.Z., Wang, Q.Y., Gu, L.Y., Wang, Y.L., 2000. Transfer of lead via placenta and breast milk in human. Biomed. Environ. Sci. 13, 85–89.
Lidsky, T.L., Schneider, J.S., 2003. Lead neurotoxicity in children: basic mechanisms and clinical correlates. Brain 126, 5–19.
Lin, S., Hwang, S.A., Marshall, E.G., Marion, D., 1998. Does paternal occupational lead exposure increase the risks of low birth weight or prematurity? Am. J. Epidemiol. 148, 173–181.
Lo, Y.C., Dooyema, C.A., Neri, A., Durant, J., Jefferies, T., Medina-Marino, A., de Ravello, L., Thoroughman, D., Davis, L., Dankoli, R.S., Samson, M.Y., Ibrahim, L.M., Okechukwu, O., Umar-Tsafe, N.T., Dama, A.H., Brown, M.J., 2012. Childhood lead poisoning associated with gold ore processing: a village-level investigation-Zamfara State, Nigeria. Environ. Health Perspect. 120, 1450–1455. October-November 2010.
Manton, W.I., Angle, C.R., Stanek, K.L., Kuntzelman, D., Reese, Y.R., Kuehnemann, T.J., 2003. Release of lead from bone in pregnancy and lactation. Environ. Res. 92, 139–151.
Magellan Industries Inc, 2013. LeadCare II Blood Lead Analyzer User's Guide (V 1.09, Rev 04). Magellan Industries Inc, North Billerica, Mass, USA. http://www.leadcare2.com/Product-Support/Product-Literature-Downloads. (Accessed 20 February 2019).
Miranda, M.L., Kim, D., Galeano, M.A., Paul, C.J., Hull, A.P., Morgan, S.P., 2007. The relationship between early childhood blood lead levels and performance on end-of-grade tests. Environ. Health Perspect. 115, 1242–1247.
Needleman, H., 2004. Lead poisoning. Annu. Rev. Med. 55, 209–222.
Neria, A.J., Royb, J., Jarrettc, J., Panc, Y., Dooyemaa, C., Caldwellc, K., Umar-Tsafed, N.T., Olubiyoe, R., Brownf, M.J., 2014. Analysis of a novel field dilution method for testing samples that exceed the analytic range of point-of-care blood lead analyzers. Int. J. Environ. Health Res. 24, 418–428.
Ogden, T.L., 2010. Handling results below the level of detection. Ann. Occup. Hyg. 54, 255–256.
Ogunseitan, O.A., Smith, T.R., 2007. The Cost of environmental lead (Pb) poisoning in Nigeria. Afr. J. Environ. Sci. Technol. 1, 27–36.
Pearce, J.M., 2007. Burton's line in lead poisoning. Eur. Neurol. 57, 118–119.
Rothenberg, S.J., Khan, F., Manalo, M., Jiang, J., Cuellar, R., Reyes, S., Acosta, S., Jauregui, M., Diaz, M., Sanchez, M., Todd, A.C., Johnson, C., 2000. Maternal bone lead contribution to blood lead during and after pregnancy. Environ. Res. 82, 81–90.
Sadeghniat haghighi, K., Aminian, O., Chavoshi, F., Sadat, B.L., Soltani, S., Rahmati, N.F., 2013. Relationship between blood lead level and male reproductive hormones in male lead exposed workers of a battery factory: a cross-sectional study. Iran. J. Reproductive Med. 11, 673–676.
Sargent, J.D., Brown, M.J., Freeman, J.L., Bailey, A., Goodman, D., Freeman Jr., D.H., 1995. Childhood Pb Poisoning in Massachusetts Communities: it's association with sociodemographic and housing characteristics. Am. J. Public Health 85, 528–534.
Schoeters, G., Den Hond, E., Dhooge, W., van Larebeke, N., Leijs, M., 2008. Endocrine disruptors and abnormalities of pubertal development. Basic Clin. Pharmacol. Toxicol. 102, 168–175.
Sobin, C., Parisi, N., Schaub, T., de la Riva, E., 2011. A Bland-Altman comparison of the lead Care® System and Inductively Coupled Plasma Mass Spectrometry for detecting low-level lead in child whole blood samples. J. Med. Toxicol. 7, 24–32.
Stanton, N.V., Fritsch, T.B.S., 2007. Evaluation of a second-generation portable blood lead analyzer in an occupational setting. Am. J. Ind. Med. 50, 1018–1024.
Téllez-Rojo, M.M., Hernández-Avila, M., González-Cossío, T., Romieu, I., Aro, A., Palazuelos, E., Schwartz, J., Hu, H., 2002. Impact of breast-feeding on the mobilization of lead from bone. Am. J. Epidemiol. 155, 420–428.
Telisman, S., Cvitkovic, P., Juraasovic, J., Pizent, A., Gavella, M., Rocic, B., 2000. Semen quality and reproductive endocrine function in relation to biomarkers of lead, cadmium, zinc and copper in men. Environ. Health Perspect. 108, 45–53.
Thurtle, N., 2014. Description of 3,180 courses of Chelation with Dimercaptosuccinic Acid in Children $\leq$ 5 y with severe lead poisoning in Zamfara, Northern Nigeria: A Retrospective Analysis of Programme Data. PLoS Med 10, 11.
University of Michigan Risk Science Center (UMRSC) and Michigan Network for Children's Environmental Health (MNCEH), 2014. Economic impacts of lead exposure and remediation in Michigan. http://www.mnceh.org/sites/www.mnceh.org/files/mnceh/press-releases/Lead_Cost_Report_MI_2014_smaller.pdf. (Accessed 11 April 2019).
Wani, A.L., Ara, A., Usmani, J.A.H., 2015. Lead toxicity: a review. Interdiscip. Toxicol. 8, 55–64.
Wood, M.D., Beresford, N.A., Copplestone, D., 2011. Limit of detection values in data analysis: do they matter? Radioprotection 46, S85–S90.
World Health Organization, 2010. Childhood Lead Poisoning. WHO Press. http://www.who.int/ceh/publications/leadguidance.pdf. (Accessed 12 February 2019).
World Health Organization, 2018. Lead poisoning and health. https://www.who.int/news-room/fact-sheets/detail/lead-poisoning-and-health. (Accessed 12 February 2019).
Wu, H.M., Lin-Tan, D.T., Wang, M.L., Huang, H.Y., Lee, C.L., Wang, H.S., Soong, Y.K., Lin, J.L., 2012. Lead level in seminal plasma may affect semen quality for men without occupational exposure to lead. Reprod. Biol. Endocrinol. 10, 91.
Yabe, J., Nakayama, S.M.M., Ikenaka, Y., Yohannes, Y.B., Bortey-Sam, N., Oroszlany, B., Muzandu, K., Choongo, K., Kabalo, A.N., Ntapisha, J., Mweene, A., Umemura, T., Ishizuka, M., 2015. Lead poisoning in children from townships in the vicinity of a lead-zinc mine in Kabwe, Zambia. Chemosphere 119, 941–947.
Yabe, J., Nakayama, S.M.M., Ikenaka, Y., Yohannes, Y.B., Bortey-Sam Kabalo, A.N., Ntapisha, J., Mizukawa, H., Umemura, T., Ishizuka, M., 2018. Lead and cadmium excretion in feces and urine of children from polluted townships near a lead-zinc mine in Kabwe, Zambia. Chemosphere 202, 48–55.

Chemosphere 247 (2020) 125884

Contents lists available at ScienceDirect

Chemosphere

journal homepage: www.elsevier.com/locate/chemosphere

Factors associated with lead (Pb) exposure on dogs around a Pb mining area, Kabwe, Zambia

Haruya Toyomaki [a], John Yabe [b], Shouta M.M. Nakayama [a], Yared B. Yohannes [a, c], Kaampwe Muzandu [b], Allan Liazambi [d], Yoshinori Ikenaka [a, e], Takeshi Kuritani [f], Mitsuhiro Nakagawa [f], Mayumi Ishizuka [a, *]

[a] Department of Environmental Veterinary Sciences, Faculty of Veterinary Medicine, Hokkaido University, Japan
[b] The University of Zambia, School of Veterinary Medicine, Zambia
[c] Department of Chemistry, College of Natural and Computational Science, University of Gondar, Ethiopia
[d] Ministry of Fisheries and Livestock, Central Province Veterinary Office, Kabwe, Zambia
[e] Water Research Group, School of Environmental Sciences and Development, North-West University, South Africa
[f] Department of Earth and Planetary Sciences, Graduate School of Science, Hokkaido University, Sapporo, Japan

HIGHLIGHTS

- Lead (Pb) levels in blood of 120 dogs around a Pb mining area, Kabwe were measured.
- The overall mean of Pb in dog blood in the present study was 271.6 μg/L.
- Pb levels significantly decreased with increasing age and distance from the mine.
- Pb isotope ratios in blood showed values close to those reported for Kabwe galena.
- Dogs could be useful as a sentinel animal of Pb exposure on human in Kabwe.

ARTICLE INFO

Article history:
Received 11 November 2019
Received in revised form
8 January 2020
Accepted 9 January 2020
Available online 13 January 2020

Handling Editor: Willie Peijnenburg

Keywords:
Dog
Sentinel animal
Lead poisoning
Lead stable isotope
Metal
Zambia

ABSTRACT

Lead (Pb)-poisoning is a serious public health concern and dogs have been useful as a sentinel-animal for Pb exposure of humans. In the present study, the blood Pb concentrations (BLC), isotope ratios (208 Pb/206 Pb and 207 Pb/206 Pb), and biochemistry of 120 domestically owned dogs living around a Pb mining area, in Kabwe, Zambia were analyzed to determine factors associated with Pb exposure. The overall mean value of Pb in dog blood in the present study was 271.6 μg/L. The BLC in the dogs from sites near the mine were significantly higher than those in the dogs from a site 4 km from the mine (352.9 ± 205.1 μg/L versus 28.0 ± 13.9 μg/L). BLC significantly decreased with both increasing age of the dogs and distance from the mine. The Pb isotope ratios in the dog that resided near the mine showed values similar to those reported at the galena mine in Kabwe, which is considered to be the source of Pb exposure. In contrast to the high metal exposure that was determined in these dogs, the mean values of most analyzed parameters in the blood biochemical analysis were surprisingly within or close to the standard reference values. Moreover, none of the dogs showed overt signs of Pb-poisoning or other clinical symptoms. The results of analysis of Pb exposure of the dogs obtained in the present study, which are similar to the previously reported results in human in this location, suggest that dogs could be useful as a sentinel animal for Pb exposure of humans in Kabwe.

1. Introduction

Lead (Pb) poisoning is a serious public health concern, that accounted for 0.6% of the Global Burden of Disease (WHO, 2010) and 540,000 deaths worldwide (IHME, 2017). The Agency for Toxic Substances and Disease Registry (ATSDR) listed Pb as the second

* Corresponding author. Laboratory of Toxicology, Department of Environmental Veterinary Sciences, Faculty of Veterinary Medicine, Hokkaido University, Kita 18, Nishi 9, Kita-ku, Sapporo, 060-0818, Japan.
E-mail address: ishizum@vetmed.hokudai.ac.jp (M. Ishizuka).

https://doi.org/10.1016/j.chemosphere.2020.125884
0045-6535/

substance in the Substance Priority List in 2017, which was compiled to determine the most significant potential threat to human health (ATSDR, 2017). Pb exposure primarily occurs via ingestion and inhalation (Calabrese and Stanek, 1995; Schoning et al., 1996). Numerous sources of Pb exposure are known, including gasoline, smelters, battery recycling, paint, and mining (Meyer et al., 2008; Yabe et al., 2010). Eliminating the source of Pb exposure is necessary to reduce and prevent further exposure. Pb has four stable isotopes: ^{208}Pb, ^{207}Pb, ^{206}Pb, and ^{204}Pb. The compositions of these isotopes are not affected to a measurable extent by physicochemical fractionation processes (Bollhöfer and Rosman, 2001; Veysseyre et al., 2001). The ^{208}Pb/^{206}Pb and ^{207}Pb/^{206}Pb isotope ratios are well known to be useful in determining the source of Pb exposure (Binkowski et al., 2016; Cao et al., 2014).

The Pb concentration in whole blood is the main biomarker that is used to monitor the exposure; it has been widely used in epidemiological studies. Symptoms of Pb poisoning are varied, including anemia, vomiting, nephropathy, encephalopathy, and, in the worst case, death (Meyer et al., 2008). At low-level concentrations, Pb exposure can cause neurodevelopmental impairment such as a reduction of the intelligence quotient (IQ) in children. Therefore, the Centers for Disease Control and Prevention (CDC) has set 5 μg/dL of Pb in the whole blood as the blood Pb reference value for Pb exposure (CDC, 2019, 2012).

As in humans, Pb poisoning in companion animals such as dogs and cats has also been reported (Bates, 2018). Lead poisoning in companion animals effects their gastrointestinal and central nervous systems as it does in humans. The concentration of Pb in the whole blood can also be used to confirm exposure of companion animals and a toxic concentration is generally considered to be > 400 μg/L (Bates, 2018). The sources of Pb exposure of animals are similar to those for humans: therefore, the risk of Pb poisoning in animals must also be considered. Companion animals, which share similar risk factors, including the areas of habitation and living conditions with their owners, have been useful as sentinels for toxic substances and infectious diseases (Rabinowitz et al., 2006; Sévère et al., 2015). Thomas et al. (1976) reported an association between high blood Pb concentrations in dogs and children from the same family. Moreover, the socioeconomic characteristics of the dog-owning family were reported to be reliably associated with abnormally high blood Pb concentrations in dogs (Thomas et al., 1975). Dogs have been reported as a useful indicator of Pb exposure for humans. They can be used a feasible, low-cost alternative to a large-scale survey of humans (Kucera, 1988).

The lead-zinc (Zn) mine in Kabwe, Zambia was operational for over 90 years without adequate pollution laws regulating emissions from the mine, and it was closed in 1994. These mining operations have left the city with hazardous concentrations of Pb in the biota and soil. The high accumulation of Pb and other metals in various environmental and biota samples has been reported in Kabwe (Nakayama et al., 2011; Yabe et al., 2013, 2011). High blood Pb concentrations in children near the mine, for whom all samples exceeded the 5 μg/dL blood Pb reference value (CDC, 2019, 2012), were also found (Yabe et al., 2015). Further studies are necessary to determine the scale and impact of Pb poisoning in Kabwe; however, large-scale surveys of humans possess some difficulties such as cost and use of human resources. In Kabwe, guard dogs are commonly owned and could be exposed to a similar amount of Pb as humans. Pb residues in dogs can serve as a potential indicator for predicting the extent of Pb contamination in the environment and Pb exposure of their owners. However, Pb exposure of dogs in Kabwe has not yet been reported.

Therefore, the present study was undertaken to assess the trends of Pb and other metals in the blood of domestic dogs residing in areas around the mine for use as sentinel animals. The factors associated with their exposure to Pb and other metals in Kabwe, Zambia are also discussed. The Pb isotope ratios of ^{208}Pb/^{206}Pb and ^{207}Pb/^{206}Pb in the blood of dogs were analyzed to determine the source of Pb exposure. Moreover, a blood biochemical analysis was conducted to evaluate the health impact of Pb exposure of dogs.

2. Materials and methods

2.1. Sampling sites

Kabwe is the provincial capital of Zambia's Central Province and is located at about 28°26′E and 14°27′S. It is the fourth largest town in Zambia, with a population of about 230, 000 inhabitants and an area of 1, 547 km^2. Kabwe has a long history of open-pit Pb–Zn mining that lasted from 1902 to 1994. Despite the closure of this mine, metal scraps from the abandoned tailings and wastes stored in the mine have continued to serve as sources of metal pollution, especially dusts that emanate from the mine dumps. Moreover, the high Pb exposure of some households within 500 m of the tailings and the residential areas close to the mine could result from these sources of metal pollution.

The present study was conducted in three sites near the mine (Kasanda, Mutwe Wansofu, and Chowa) and one site far from the mine (Lukanga) in June and July of 2016 (Fig. 1).

2.2. Sampling

We conducted a sensitization campaign in which dog owners from the selected townships were requested to take their dogs to designated locations within their townships for free rabies vaccination programs, which acted as part of the recruitment strategy for this study. The rabies vaccinations were performed by government personnel from the Kabwe District Veterinary Office. Only dogs with owners that willingly agreed to participate in the present study were used in the sample collection. The dog owners were also interviewed to obtain necessary information about their dogs such

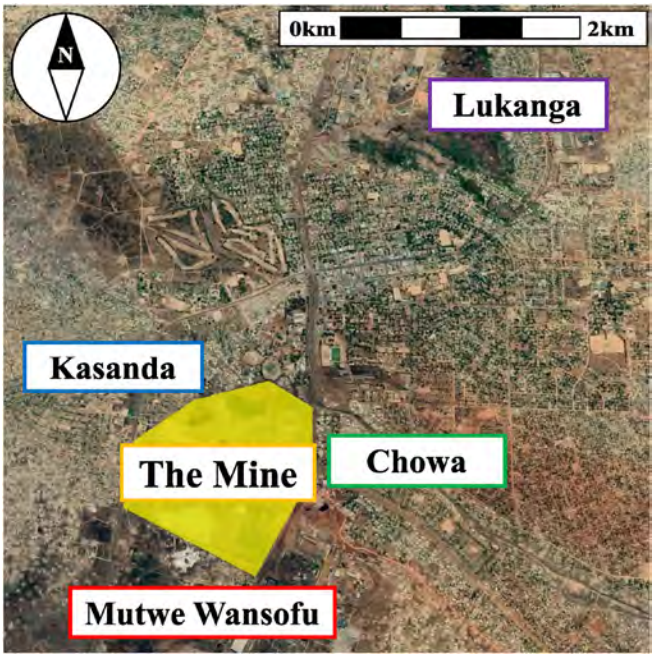

Fig. 1. Map of the sampling areas in Kabwe, Zambia (modified from Google Earth).

as age, sex, and breed.

Blood sample of up to 10 mL were collected from the cephalic veins of each dog into heparinized blood collection tubes for laboratory analysis. To avoid sample contamination, all sample collection supplies were stored in plastic Ziploc storage bags before sampling. The venipuncture site was carefully cleaned and sanitized with an ethanol swab to avoid contamination before sample collection. The blood samples were transported to the laboratory and the plasma samples were separated after they were centrifuged. The processed samples were kept at −20 °C at the University of Zambia, School of Veterinary Medicine, and transported to Japan in temperature-controlled boxes with ice packs. The samples were analyzed in the Toxicology Laboratory at the Faculty of Veterinary Medicine, Hokkaido University, Sapporo, Japan (Approval Number: Vet-17010).

2.3. Pb and metal concentration analysis

The extraction of Pb and other metals (cadmium (Cd), nickel (Ni), chromium (Cr), copper (Cu), zinc (Zn), cobalt (Co), and arsenic (As)) from the whole blood samples was performed. In brief, 1 mL of each blood sample was placed in prewashed digestion vessels, followed by acid digestion using 5 mL of two-fold diluted ultrapure nitric acid (Cica reagent, Specific gravity of 1.38, 60%; Kanto Chemical Corp.) and 1 mL of ultrapure hydrogen peroxide (Cica reagent, 30%; Kanto Chemical Corp.). Microwave digestion was performed using a Speedwave MWS-2 (Berghof) according to the instruction of the manufacturer, as has been described previously (Yabe et al., 2015). The concentrations of Pb and other metals were analyzed by inductively coupled plasma mass spectrometry (ICP-MS, 7700 series; Agilent Technologies, Tokyo, Japan). Analytical quality control was conducted using DORM-3 (fish protein; National Research Council of Canada, Ottawa, Canada) and DOLT-4 (dogfish liver; National Research Council of Canada) certified reference materials. Replicate analyses of these reference materials showed good recovery rates (95–105%) with an instrument detection limit of 0.001 μg/L.

2.4. Stable Pb isotope analysis

The sample dissolution procedure was similar to a previously described method (Kuritani and Nakamura, 2002; Nakayama et al., 2019). The extracted solutions of blood were transferred into Teflon tubes after the Pb concentrations were analyzed. $^{208}Pb/^{206}Pb$ and $^{207}Pb/^{206}Pb$ isotope ratios were determined using a multiple collector (MC)-ICP-MS (Neptune Plus, Thermo Finnigan, California, USA) in static mode with Faraday cup configuration. The other general parameters are provided in Supplementary Table S1.

2.5. Blood biochemical analysis

A conventional blood chemical analyzer (COBAS Ready; Roche Diagnostic Systems, Basel, Switzerland, and Spotchem panels I and II; Arkray, Kyoto, Japan) was used to analyze the concentrations of alanine aminotransferase (ALT), alkaline phosphatase (ALP), aspartate aminotransferase (AST), gamma glutamyl transpeptidase (GGT), lactase dehydrogenase (LDH), total bilirubin (T-Bil), total protein (TP), albumin (Alb), blood urea nitrogen (BUN), creatinine (Cre), and urea acid (UA) in the plasma. The standard reference ranges for each parameter of the Spotchem Series in dogs were provided by Arcray, Kyoto, Japan.

2.6. Statistical analysis

All data from the experiments and questionnaire were combined into a single electronic database and checked for accuracy and outliers. All statistical analyses were performed at a significance level of $p < 0.05$ using R version 3.4.3 and JMP 13.1.0 (SAS Institute, USA). Mean values were indicated in addition to standard deviation (SD) values. The collinearity between factors was analyzed using Spearman's rank correlation test. A Steel–Dwass multiple comparison test was used to compare the differences between the factors among differing areas.

3. Results

3.1. Characteristics of the dogs in the present study

A total of 120 domestic dogs were sampled in the present study, with 90 coming from the three sites near the mine and 30 from Lukanga which is located farther from the mine (Table 1). All of the dogs were crossbreeds with a mean age of 32.0 ± 24.3 months. There was a significant difference in age between the dogs from Kasanda and Chowa ($p < 0.01$). The mean distance between the mine and the location of the dogs was 2.58 ± 1.83 km. There was a significant difference in the distances from the mine between the dogs from sites near the mine (Kasanda, Mutwe Wansofu, and Chowa) and from Lukanga ($p < 0.01$). None of the dogs had overt signs of lead poisoning or other clinical symptoms.

3.2. Concentrations of Pb and other metals in the blood of dogs

The overall mean of Pb concentrations in dog blood in the present study was 271.6 μg/L (Table 1). Of the 120 dogs sampled, 24% (29/120) were above the toxic level for companion animals, which is 400 μg/L (Supplementary Fig. S1). The mean concentration of Pb in the blood of the dogs from Kasanda (525.3 μg/L) was above the toxic level. On the other hand, the mean concentration of Pb in the blood of the dogs from Lukanga was 28.0 μg/L, and all dogs from Lukanga showed concentrations below the toxic level. The mean of all metals in the dogs residing at the three sites near the mine were significantly higher than those in the dogs from Lukanga ($p < 0.01$). Most of the other metal (Cd, Ni, Cr, Co, and As) concentrations in the dogs from Kasanda were significantly higher than those concentrations determined in other areas, except for Pb, Cu, and Zn. In contrast, all metal concentrations in the dogs from Lukanga were significantly lower than those from all other sites, except for Co.

There was no significant difference in the metal concentrations in blood between male and female dogs in all locations as well as in the dogs from sites near the mine. However, the Pb ($p = 0.015$), Cr ($p = 0.015$), and Cu ($p < 0.01$) concentrations in male dogs were significantly higher than those in female dogs from Chowa. The Cd concentrations in male dogs from Mutwe Wansofu ($p = 0.059$), Chowa ($p = 0.09$), and Lukanga ($p = 0.06$) were higher than the concentrations in female dogs, but not significantly. In contrast, the Pb concentrations in female dogs were significantly higher than those in male dogs from Kasanda ($p = 0.047$). The Ni concentrations in female dogs were also higher than those in male dogs from Lukanga ($p = 0.094$).

In all dogs, there were significant positive correlations among all metals (Supplementary Table S2, $p < 0.05$). Most metal concentrations ($p < 0.05$) significantly decreased with increasing age, except for Cu ($p = 0.14$, Spearman's $\rho = -0.13$) and Cd ($p = 0.07$, $\rho = -0.17$). All of the metals concentrations in the dogs significantly decreased with increasing distance between the mine and the location of the dogs ($p < 0.05$). Figs. 2 and 3 respectively show the relationships between the Pb concentrations and the age, and the Pb concentrations and distance from the mine.

In the dogs from sites near the mine, there were also significant positive correlations among all of metals (Supplementary Table S3,

Table 1
Characteristics of dogs and metal concentrations in dog blood (μg/L) in the present study in Kabwe, Zambia; mean ± SD values (minimum-maximum).

Area	Sex, Male:Female	Age, months	Distance between the mine and the location of dogs, km	Pb	Cd	Ni	Cr	Cu	Zn	Co	As
Overall (120)	67:52	32.0 ± 24.3 (3–156)	2.58 ± 1.83 (0.65–7.30)	271.6 ± 226.9 (4.3–1233.5)	1.5 ± 1.6 (0.01–6.1)	86.9 ± 261.8 (2.5–2054.8)	67.2 ± 75.4 (2.0–316.6)	1108.8 ± 634.5 (396.3–3438.0)	6537.1 ± 3509.9 (1976.5–1834.0)	10.5 ± 21.6 (0.2–173.7)	5.2 ± 4.5 (0.6–18.6)
Near the mine (90)	49:40	31.4 ± 22.9 (4–96)	1.53 ± 0.65** (0.65–3.52)	352.9 ± 205.1** (31.2–1233.5)	2.0 ± 1.6** (0.2–6.1)	114.6 ± 298.1** (11.0–2054.8)	88.8 ± 75.9** (11.6–316.6)	1284.3 ± 643.6** (419.5–3438.0)	7494.6 ± 3555.8** (2076.4–18394.0)	12.8 ± 24.6** (0.2–173.7)	6.4 ± 4.6** (0.6–18.6)
Kasanda (27)	15:12	20.7 ± 22.4[a] (4–96)	1.09 ± 0.14[b] (0.87–1.34)	525.3 ± 230.8[a] (189.5–1235.5)	3.4 ± 1.0[a] (1.7–6.1)	213.3 ± 370.0[a] (90.6–2054.8)	175.5 ± 49.9[a] (100.7–316.6)	1802.9 ± 530.8[a] (1043.9–3438.0)	10675.6 ± 3252.9[a] (5055.5–18394.0)	16.6 ± 7.9[a] (5.4–44.0)	11.5 ± 2.3[a] (6.9–18.6)
Mutwe Wansofu (14)	5:9	32.1 ± 18.4[a,b] (4–60)	0.85 ± 0.11[a] (0.65–1.03)	392.3 ± 112.0[a] (253.0–652.8)	2.9 ± 0.4[b] (2.2–3.4)	199.5 ± 521.4[b] (37.9–2007.6)	74.3 ± 19.6[b] (54.0–127.2)	1571.1 ± 146.4[a] (1246.8–1780.0)	9158.9 ± 1109.7[a] (7394.9–11245.7)	8.4 ± 5.1[b] (4.3–24.2)	9.2 ± 1.9[b] (7.3–12.6)
Chowa (49)	29:19	37.2 ± 22.6[b] (4–96)	2.00 ± 0.55[c] (1.34–3.52)	246.5 ± 130.6[b] (31.2–530.0)	0.9 ± 1.3[c] (0.2–5.0)	34.3 ± 34.1[c] (11.0–160.4)	44.2 ± 53.7[c] (11.6–294.4)	908.9 ± 539.2[b] (419.5–2782.3)	5219.9 ± 2357.3[b] (2076.4–12633.4)	12.0 ± 32.8[b, c] (0.2–173.7)	2.7 ± 2.3[c] (0.6–8.6)
Lukanga (30)	18:12	33.8 ± 28.6[a,b] (3–156)	5.44 ± 0.55[d] (4.67–7.30)	28.0 ± 13.9[c] (4.3–53.0)	0.03 ± 0.01[d] (0.01–0.08)	5.0 ± 1.4[d] (2.5–8.6)	3.4 ± 1.1[d] (2.0–6.8)	588.0 ± 79.8[c] (396.3–742.6)	3696.4 ± 774.1[c] (1976.5–5196.5)	3.5 ± 2.7[c] (1.0–12.4)	1.5 ± 0.8[d] (0.6–3.9)

Note: ** indicates a significant difference ($p < 0.01$) between sites near the mine and Lukanga. Different letters indicate a significant difference among areas ($p < 0.05$). In Chowa, the following data was not recorded: the age of one dog, the sex of one dog, and the locations of three dogs (home address).

$p < 0.05$). The concentrations of all metals in the dogs significantly decreased with increasing age and distance from the mine ($p < 0.05$). There was a significantly positive correlation between the age of the dog and distance from the mine ($p < 0.05$, $\rho = 0.21$).

In the dogs from Lukanga, there were significant positive correlations between Pb and Zn ($p < 0.01$, $\rho = 0.50$), as well as between Ni and Cr ($p < 0.01$, $\rho = 0.60$) (Supplementary Table S4). The As concentrations were found to be nearly significantly correlated with Co ($p = 0.09$, $\rho = 0.31$) and Zn ($p = 0.09$, $\rho = -0.31$) concentrations. The Cd concentrations were almost significantly correlated with Cr ($p = 0.07$, $\rho = 0.33$) and Co ($p = 0.07$, $\rho = 0.34$) concentrations. The Pb concentrations decreased with the age of the dog, but not significantly ($p = 0.052$, $\rho = -0.36$). The concentrations of Pb ($p < 0.05$, $\rho = -0.42$) and Cu ($p < 0.05$, $\rho = -0.42$) were significantly correlated with the distance from the mine. The Ni concentrations increased with the distance, but not significantly ($p = 0.059$, $\rho = 0.35$).

3.3. Pb isotope ratio analysis

The mean values of the $^{208}Pb/^{206}Pb$ and $^{207}Pb/^{206}Pb$ ratios in the blood of all dogs were 2.129 ± 0.006 and 0.8727 ± 0.003, respectively (Table 2). Both Pb isotope ratios in the blood of the dogs from sites near the mine ($^{208}Pb/^{206}Pb$: 2.131 ± 0.003 and $^{207}Pb/^{206}Pb$: 0.8734 ± 0.0014) were significantly different from those of the dogs from Lukanga ($^{208}Pb/^{206}Pb$: 2.122 ± 0.007 and $^{207}Pb/^{206}Pb$: 0.8708 ± 0.0047, $p < 0.05$). The SD values of the isotope ratios of the dogs from sites near the mine were smaller than those of the dogs from Lukanga, indicating small individual differences in the isotope ratios of the dogs from sites near the mine. Both ratios in the blood of the dogs from sites near the mine (Fig. 4 and Supplementary Figs. S2 and S3), especially from Kasanda ($^{208}Pb/^{206}Pb$: 2.133 and $^{207}Pb/^{206}Pb$: 0.8735) showed values similar to those reported for Kabwe galena ($^{208}Pb/^{206}Pb$: 2.134 and $^{207}Pb/^{206}Pb$: 0.8731, Kamona et al., 1999).

3.4. Blood biochemical analysis

Table 3 shows the mean values of the blood biochemical analysis. The means values of all parameters in the dogs in the present study were within the reference range or slightly higher. The LDH

Fig. 2. Relationship between the blood Pb concentrations in the dogs and their age (months). The blue, red, green, and violet circles indicate samples from Kasanda, Mutwe Wansofu, Chowa, and Lukanga, respectively. (For interpretation of the references to colour in this figure legend, the reader is referred to the Web version of this article.)

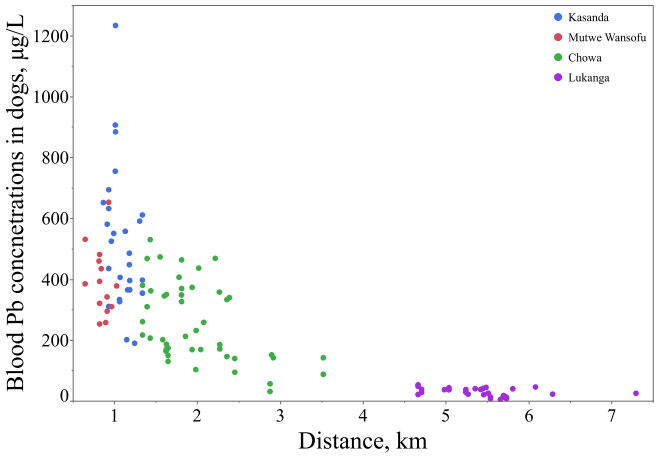

Fig. 3. Relationship between the blood Pb concentrations in the dogs and the distance between the mine and the location of the dogs (km). The blue, red, green, and violet circles indicate samples from Kasanda, Mutwe Wansofu, Chowa, and Lukanga, respectively. (For interpretation of the references to colour in this figure legend, the reader is referred to the Web version of this article.)

Table 2
Mean ± SD values of the Pb isotope ratios.

Area	$^{208}Pb/^{206}Pb$	$^{207}Pb/^{206}Pb$
Overall (119)	2.129 ± 0.006	0.8727 ± 0.003
Near the mine (89)	2.131 ± 0.003**	0.8734 ± 0.0014**
Kasanda (27)	2.133 ± 0.001[a]	0.8735 ± 0.0003[a]
Mutwe Wansofu (14)	2.130 ± 0.002[b]	0.8747 ± 0.0009[b]
Chowa (48)	2.130 ± 0.003[b]	0.8729 ± 0.0017[c]
Lukanga (30)	2.122 ± 0.007[c]	0.8708 ± 0.0047[d]
Kabwe galena (Kamona et al., 1999)	2.134 ± 0.0009	0.8731 ± 0.0003

Note: ** indicates a significant difference ($p < 0.01$) between sites near the mine and Lukanga. Different letters indicate a significant difference among areas.

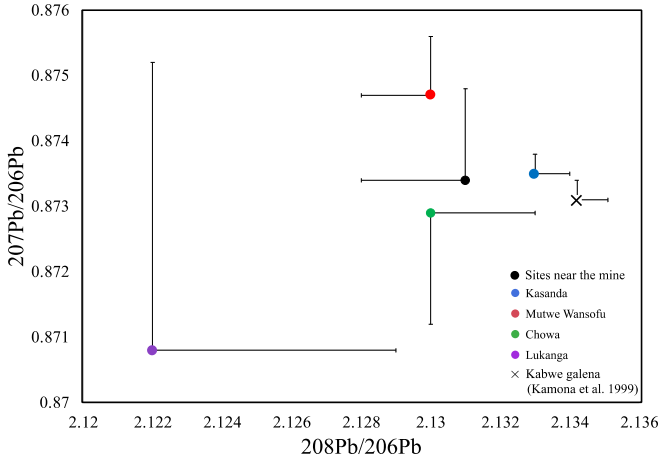

Fig. 4. Pb isotope ratios ($^{208}Pb/^{206}Pb$ and $^{207}Pb/^{206}Pb$) in the blood of the dogs residing in different areas. The mean values are shown with error bars indicating the SD. The blue, red, green, and violet circles indicate samples from Kasanda, Mutwe Wansofu, Chowa, and Lukanga, respectively. The black circle indicates the mean values of samples from three sites near the mine (Kasanda, Mutwe Wansofu, and Chowa). The reference value of Kabwe galena was obtained from a report by Kamona et al. (1999) and is indicated by a cross mark. (For interpretation of the references to colour in this figure legend, the reader is referred to the Web version of this article.)

concentrations in the dogs from Lukanga (279.9 IU/L) was significantly higher than that in the dogs from sites near the mine (192.0 IU/L, $p < 0.01$). The GGT ($p = 0.08$) and Alb ($p = 0.052$) concentrations in the dogs from Lukanga were higher than those in the dogs from sites near the mine, although these differences were not significant. There was no significant difference in the blood biochemistry parameters between male and female dogs.

In all dogs in the present study, there was a significant positive correlation between Pb and ALP concentrations (Supplementary Table S5, $p = 0.047$, $\rho = 0.18$). The LDH ($p = 0.08$, $\rho = -0.16$), BUN ($p = 0.08$, $\rho = -0.16$), and Cre ($p = 0.07$, $\rho = -0.17$) concentrations decreased as the Pb concentrations increased, but not significantly.

In the dogs from sites near the mine, the Pb concentrations were significantly associated with increased ALT ($p < 0.01$, $\rho = 0.29$), ALP ($p < 0.01$, $\rho = 0.29$), and AST ($p = 0.014$, $\rho = 0.29$) concentrations. On the other hand, a significant negative correlation between Pb and BUN concentrations ($p < 0.05$, $\rho = -0.26$) was observed. The Cre ($p = 0.07$, $\rho = -0.20$) and UA ($p = 0.099$, $\rho = -0.20$) concentrations almost significantly decreased as Pb concentrations increased.

In the dogs from Lukanga, the ALP concentrations almost significantly increased with Pb concentrations ($p = 0.06$, $\rho = 0.35$), as was found in other groups. There was also a significantly negative correlation between Pb and TP ($p < 0.05$, $\rho = -0.39$) in the dogs from this area, while BUN ($p = 0.06$, $\rho = -0.36$) and Cre ($p = 0.09$, $\rho = -0.32$) appeared to decrease with Pb concentrations increased, but not significantly.

4. Discussion

In the present study, high blood Pb concentrations (271.6 μg/L) have been recorded in dogs in townships around the mine in Kabwe, wherein cases of Pb poisoning in animals and humans have been reported (Nakayama et al., 2011; Yabe et al., 2015, 2013, 2011). Of all dogs that were surveyed, 24% (29/120) had Pb concentrations in their blood that are above the toxic level (400 μg/L) for Pb exposure in companion animals (Bates, 2018). The Pb concentrations in the dogs from sites near the mine that were determined in a present study (352.9 μg/L) were similar to or higher than the blood Pb concentrations in polluted sites in other countries where the concentrations ranged from 28.3 to 262 μg/L (Balagangatharathilagar et al., 2006; Brownie et al., 2009; Thomas et al., 1975). In the present study, elevated Pb concentrations in the blood were found in the dogs from Kasanda, with the highest concentration being 1233.5 μg/L. Several studies have reported severe clinical cases of Pb poisoning due to elevated blood Pb concentrations in dogs, such as those found in Kasanda in the present study (Hamir et al., 1985; King, 2016; Langlois et al., 2017). These findings suggest that Pb exposure of the dogs residing in sites near the mine in Kabwe, Zambia, is a serious health risk. On the other hand, the dogs from Lukanga had lower mean blood Pb concentrations (28.0 μg/L), which agree with the results obtained for dogs from unpolluted areas in previous reports (Balagangatharathilagar et al., 2006; Brownie et al., 2009; Thomas et al., 1975).

The present study found different trends of Pb and other metals concentrations in the blood of dogs among the different observed areas in Kabwe. The mean blood Pb concentrations in the dogs from Kasanda (525.3 μg/L), was higher than that in the dogs from Mutwe Wansofu (392.3 μg/L), whereas the locations of the dogs from Mutwe Wansofu (0.85 km from the mine) were closer to the mine than those of the dogs from Kasanda (1.09 km from the mine). Kasanda is located on the western side of the mine, which is in the direction of the prevailing winds. The accumulation of metal in the dogs from Chowa (2.00 km from the mine) were lower than those in the dogs from the other two sites that were located near the mine. A similar trend was also found in a previous study of the children in these arears, in which the mean blood Pb concentration in the children in Kasanda (822 μg/L) was higher than that in Chowa

Table 3
Mean ± SD values (minimum-maximum) of the blood biochemical analysis of the dogs.

Factors	Overall (115)	Near the mine (86)	Lukanga (29)	Reference range
ALT, IU/L	15.3 ± 23.9 (5–214)	13.5 ± 16.2 (5–103)	20.8 ± 38.5 (5–214)	0–113
ALP, IU/L	126.2 ± 129.9 (25–747)	126.7 ± 128.7 (25–747)	124.8 ± 135.7 (25–745)	0–132
AST, IU/L	16.6 ± 12.9 (5–106)	16.3 ± 13.3 (5–106)	17.8 ± 12.0 (5–73)	0–47
GGT, IU/L	19.6 ± 26.3 (5–170)	18.16 ± 26.8 (5–170)	23.8 ± 24.6 (5–105)	0–20
LDH, IU/L**	214.1 ± 132.5 (15–704)	192.0 ± 120.9 (15–704)	279.9 ± 145.2 (57–632)	0–201
T-Bil, mg/dL	0.4 ± 0.3 (0.1–2.3)	0.4 ± 0.4 (0.1–2.3)	0.4 ± 0.3 (0.1–1.2)	0–0.3
TP, g/dL	7.2 ± 1.4 (4.2–9.8)	7.2 ± 1.5 (4.3–9.8)	7.1 ± 1.3 (4.2–9.4)	4.7–7.3
Alb, g/dL	2.1 ± 0.4 (0.5–3.1)	2.1 ± 0.4 (0.5–2.9)	2.3 ± 0.4 (1.1–3.1)	1.8–3.1
BUN, mg/dL	12.7 ± 7.4 (3.0–53.0)	13.1 ± 7.7 (3.0–53.0)	12.6 ± 6.9 (3.0–34.0)	0–29
Cre, mg/dL	1.4 ± 0.4 (0.5–2.3)	1.3 ± 0.4 (0.5–2.3)	1.4 ± 0.4 (0.6–2.2)	0–1.6
UA, mg/dL	1.2 ± 0.3 (0.5–2.2)	1.2 ± 0.3 (0.5–2.2)	1.3 ± 0.2 (1.0–2.0)	0–1.0

Note: ** indicates $p < 0.01$ between sites near the mine and Lukanga.

(390 μg/L, Yabe et al., 2015). In the present study, the Pb concentrations in dog blood significantly decreased with increasing distance from the mine, as did the concentrations of other metals. These trends agree with those determined in studies by Tembo et al. (2006) and Nakayama et al. (2011), who reported similar trends in the soil in Kabwe. Therefore, these trends suggest that the location of the townships in the relation to the wind direction and distance from the mine are key factors that influenc the severity of the exposure to Pb and other metals in dogs in Kabwe. The obtained results also suggest that the exposure to Pb and other metals in dogs remarkably decreased about 5 km away from the mine. Therefore, severe metal exposure in Kabwe may only occur in areas near the mine.

The significant positive correlations between Pb and other metals in the blood of the dogs analyzed in the current study agreed with the findings of previous studies that reported high concentrations of Pb and other metals in both soil and animal samples in Kabwe (Nakata et al., 2016; Nakayama et al., 2011; Tembo et al., 2006; Yabe et al., 2013, 2011). Moreover, Kamona and Friedrich (2007) reported that the ore in Kabwe contained sphalerite (ZnS) with Cd, galena (PbS), briarite [Cu2(Fe,Zn)GeS4], and mimetite [Pb5(AsO4)3Cl]. These findings suggest that in addition to Pb, other toxic metal contaminants including As and Cd, may spread into the environment and pose a health risk to humans and animals. However, the toxicity of other metals in dogs is unknown, although many studies concerning Pb poisoning in dogs have been reported. Therefore, the health risks associated with the exposure of dogs in Kabwe to other metals should be further investigated.

The mean Pb concentrations in the blood of dogs from Kasanda and Chowa in the present study were 525.3 and 246.5 μg/L, respectively. The concentrations were lower than the findings of a previous study examining children in the same township which reported the mean blood Pb concentrations in children from Kasanda and Chowa as 822 and 390 μg/L, respectively (Yabe et al., 2015). This result agrees with the findings of Thomas et al. (1976) who reported higher blood Pb concentrations in children than those in dogs from the same household environment. Therefore, children may be more vulnerable to Pb exposure than dogs are. Thomas et al. (1976) also reported that an abnormally high blood Pb concentration in a family dog increase by six-fold the probability that at least one child in that family would also have an abnormally high blood Pb concentration. Therefore, children from households with dogs that have high blood Pb concentrations should be examined for Pb exposure.

Significant negative correlations between the blood Pb concentrations and age of the dogs were found, indicating that the concentrations of blood Pb reduced as the dog age. Langlois et al. (2017) reported a similar trend in the Pb poisoning outbreak in Flint, Michigan, wherein the blood Pb concentrations in young dogs (≤2 years of age) were higher than those in older dogs (≥6 years of age). This trend was similar to that found in humans, as significant negative correlations were observed between the blood Pb concentrations and ages of children in Kabwe (Yabe et al., 2015). The hand-to-mouth or object-to-mouth (pica) behavior of children are known to be factors related to high Pb exposure. In addition, children absorb a greater proportion of ingested Pb from the gastrointestinal tract than adults do (Wani et al., 2015). Therefore, similar behaviors and high absorbances from the gastrointestinal tracts of young dogs may also be attributed to high Pb exposure of young dogs compared with older dogs. Pb poisoning during a vulnerable period of development can lead to negative neurodevelopmental impacts such as a low IQ and cognitive impairments in humans (ATSDR, 2007; Lanphear et al., 2005). Mielke and Zahran (2012) found a strong association between air Pb concentrations and the latent aggravated assault rate at the scale of city. This finding provides insight into latent behavioral effects resulting from environmental Pb exposure of children that were subjected to lead dust during their most sensitive developmental years. Pb exposure of dogs might also results in negative developmental and behavioral impacts such as increased aggression. On the other hand, Schoning et al. (1996) reported that the lung dust concentrations of substances including silicate and other metals increased linearly with age in dogs. High Pb accumulation in the organs of adult dogs might occurred even with low blood Pb concentrations, especially when dogs are chronically exposed to Pb because Pb is deposited in bone and has a long half-life.

In the present study, blood Pb concentrations were significantly higher in male dogs than in female dogs from Chowa, but this trend was reversed in dogs from Kasanda. It was also previously determined that the blood Pb concentrations in boys were significantly higher than those in girls in Makululu Township, which is located on the western side of the mine (Yabe et al., 2015). Yabe et al. (2015) suggested that the different behaviors between boys and girls could be one of the factors contributing to this difference, as boys are more likely than girls to wander farther from home and play near the mine dumps. Considering studies other locations, Koh and Bidge (1986) reported blood Pb concentrations in male dogs that are significantly higher than those in female dogs at four different locations in Australia. On the other hand, several studies did not report any such association between sex and Pb exposure or accumulation (Balagangatharathilagar et al., 2006; Esposito et al., 2019; Serpe et al., 2012; Tomza-Marciniak et al., 2012). The differences in the behaviors of dogs due to differing sex may influence their exposure to Pb, especially in mature male dogs that are likely to travel across wide areas to find female dogs for reproduction, while female dogs do not move around so freely as they need to care for their offspring. However, the sex of dogs might not be strongly associated with exposure to Pb and other metals in the

present study.

The $^{208}Pb/^{206}Pb$ and $^{207}Pb/^{206}Pb$ isotope ratios in dog blood were analyzed in the present study to determine the source of Pb exposure of the dogs. There were significant differences in the Pb isotope ratios in the dogs between the sites near the mine ($^{208}Pb/^{206}Pb$: 2.131 and $^{207}Pb/^{206}Pb$: 0.8734) and Lukanga ($^{208}Pb/^{206}Pb$: 2.122 and $^{207}Pb/^{206}Pb$: 0.8708). Moreover, the isotope ratios in the dogs from Kasanda ($^{208}Pb/^{206}Pb$: 2.133 and $^{207}Pb/^{206}Pb$: 0.8735) were significantly different from those in the dogs from Mutwe Wansofu ($^{208}Pb/^{206}Pb$: 2.130 and $^{207}Pb/^{206}Pb$: 0.8747) and Chowa ($^{208}Pb/^{206}Pb$: 2.130 and $^{207}Pb/^{206}Pb$: 0.8729). With increasing blood Pb concentrations, the variance of the Pb isotope ratios decreased and approached those of the Kabwe galena ($^{208}Pb/^{206}Pb$: 2.134 and $^{207}Pb/^{206}Pb$: 0.8731), which is considered to be the exposure source (Kamona et al., 1999). Similar trends were found in a previous study of goats and chicken located in Kabwe (Nakata et al., 2016). Moreover, a Pb exposure study on rats that used soils from Kabwe revealed that the Pb isotope ratios in the biological samples of high exposure groups were more similar to those in Kabwe galena (Kamona et al., 1999), than to those of the control and low exposure groups (Nakayama et al., 2019). These results suggest that the source of Pb exposure of dogs in Kabwe could be the galena from the mine. Understanding the route of Pb exposure in dogs is required to minimize their exposure. Future studies should include environmental and biological samples that relate to the various routes of exposure, such as lung and feces sample, for further clarification.

The blood biochemical profiles of the plasma of the dogs in Kabwe were analyzed in the present study. In contrast to the high metal exposure of these dogs, the mean values of most analyzed parameters were surprisingly within or close to the standard reference values. This indicates that Pb exposure in the dogs in Kabwe did not significantly impact their health, as was observed during sampling, in which all sampled dogs appeared healthy. Only the LDH values in the dogs from Lukanga were significantly higher than those of the dogs from sites near the mine; therefore this could not be attributed to Pb exposure related to distance from the mine. However, the ALP concentrations in all dogs as well as the dogs from sites near the mine significantly increased as the blood Pb concentrations increased. There were significant positive correlations between ALT and Pb concentrations, as well as AST and Pb concentrations in the dogs from sites near the mine. These relationships were also almost significant when the dogs from all locations were considered. These results suggest that Pb exposure in dogs may have caused some mild liver damage. Of course, it is difficult to exclude the possibility of other factors or diseases since a detailed questionnaire survey or medical check-up was not performed in the present study. On the other hand, the BUN and Cre concentrations which are indicators of kidney functions, were not elevated and negatively related to blood Pb concentrations in the dogs. High Pb exposure is known to cause kidney damage in conjunction with an increase the selected biomarkers. However, King (2016) reported that two dogs with elevated blood Pb concentrations had glucosuria and proteinuria in their urinalysis that was consistent with damage to the proximal renal tubules, whereas the BUN and Cre concentrations in the dogs were within the reference range. There is therefore a possibility that Pb exposure could damage and disrupt kidney functions without increasing the BUN and Cre concentrations. The reasoning behind these antithetical results could not be established and would require further studies of dogs using both blood biochemical analysis and urinalysis.

The findings of Pb exposure of dogs obtained in the present study, which were similar to the results of previous studies of humans in Kabwe, suggest that dogs could be a useful sentinel animal for Pb exposure. Although similar trends were seen in humans, a direct relationship between the Pb exposure in dogs and their owners was not determined in the present study. Berny et al. (1995) reported the likelihood of finding one person with a blood Pb concentrations of greater than above 10 was significantly increased when there was one pet with a high blood Pb concentration in the same household. Further studies should focus on the relationship between Pb exposure of dogs and their owners. The present study revealed large individual differences in Pb exposures observed in sites near the mine. A similar trend was seen in the blood Pb concentrations in children in Kabwe (Yabe et al., 2015). Determining the factors that influence the differing exposures to Pb would be helpful in reducing the Pb exposures observed in this area. Because most dogs in Kabwe roam freely, the difference in exposure levels could be attributed to their different activities. As opposed to humans monitoring, the monitoring of animals has become popular with the development of new monitoring techniques such as GPS. Therefore, future studies may focus on the relationship between Pb exposure of dogs and their behaviors by using a GPS monitoring system.

5. Conclusion

The present study is the first report to reveal high exposures of dogs in Kabwe to Pb and other metals. The locations of the dogs and their ages were related to their Pb and metal exposures. The trends of the exposures of dogs were shown to be largely similar to those previously reported for humans, although some differences between dogs and humans were found. These results suggest that dogs could be useful as sentinel animals for Pb exposure of human residing in Kabwe. Moreover, different trends of exposure among individual dogs were found, and the trends were previously found in humans. The factors contributing to the individual differences of Pb exposure must be investigated to reduce Pb exposure. The source of Pb exposure of dogs was determined to result from the galena in mine in Kabwe. The findings of this study suggest that environmental remediation is urgently needed to reduce Pb exposure in Kabwe.

Declaration of competing interest

The authors declare no conflicts of interest.

CRediT authorship contribution statement

Haruya Toyomaki: Writing - original draft, Conceptualization, Data curation. **John Yabe:** Writing - review & editing, Supervision, Investigation. **Shouta M.M. Nakayama:** Supervision, Investigation. **Yared B. Yohannes:** Writing - review & editing, Investigation. **Kaampwe Muzandu:** Writing - review & editing, Investigation. **Allan Liazambi:** Investigation. **Yoshinori Ikenaka:** Writing - review & editing. **Takeshi Kuritani:** Methodology. **Mitsuhiro Nakagawa:** Methodology. **Mayumi Ishizuka:** Writing - review & editing, Supervision, Project administration.

Acknowledgement

We are grateful to the dogs and their owners for participating in this study. This work was supported by the Grants-in-Aid for Scientific Research from the Ministry of Education, Culture, Sports, Science and Technology of Japan awarded to M. Ishizuka (No. 16H0177906, 18KK0287 and 18K1984708), Y. Ikenaka (No. 26304043, 15H0282505, 15K1221305, 17K2003807, and

18H0413208), and S.M.M. Nakayama (No. 16K16197 and 17KK0009), as well as by the foundation of the JSPS Core to Core Program (AA Science Platforms) and the Environment Research and Technology Development Fund (SII-1/3–2, 4RF-1802/18949907) of the Environmental Restoration and Conservation Agency of Japan. We also acknowledge financial support from the Program for Leading Graduate Schools "Fostering Global Leaders in Veterinary Science for Contributing to One Health" (F01), Grant-in-Aid for JSPS Research Fellow (17J05756), the Soroptimist Japan Foundation, the Nakajima Foundation, the Sumitomo foundation, the Nihon Seimei Foundation, and the Japan Prize Foundation. This research was also supported by JST/JICA, SATREPS (Science and Technology Research Partnership for Sustainable Development; No. JPMJSA1501). We are grateful to Mr. Takahiro Ichise and Ms. Nagisa Hirano (Laboratory of Toxicology, Faculty of Veterinary Medicine, Hokkaido University) for technical support with metal concentration and isotope analyses. The English was proofread by Uni-edit (https://uni-edit.net/usa).

Appendix A. Supplementary data

Supplementary data to this article can be found online at https://doi.org/10.1016/j.chemosphere.2020.125884.

References

Agency for Toxic Substances and Disease Registry (ATSDR), 2007. Toxicological profile for lead. Available. https://www.atsdr.cdc.gov/toxprofiles/tp13.pdf. (Accessed 13 December 2019). accessed.

Agency for Toxic Substances and Disease Registry (ATSDR), 2017. 2017 substance priority list. Available. https://www.atsdr.cdc.gov/SPL/#2017spl. (Accessed 13 December 2019). accessed.

Balagangatharathilagar, M., Swarup, D., Patra, R.C., Dwivedi, S.K., 2006. Blood lead level in dogs from urban and rural areas of India and its relation to animal and environmental variables. Sci. Total Environ. 359, 130–134. https://doi.org/10.1016/j.scitotenv.2005.09.063.

Bates, N., 2018. Lead toxicosis in cats and dogs. Companion Animal 23, 674–682. https://doi.org/10.12968/coan.2018.23.12.674.

Berny, P.J., Côté, L.M., Buck, W.B., 1995. Can household pets be used as reliable monitors of lead exposure to humans? Sci. Total Environ. 172, 163–173. https://doi.org/10.1016/0048-9697(95)04787-5.

Binkowski, Ł.J., Meissner, W., Trzeciak, M., Izevbekhai, K., Barker, J., 2016. Lead isotope ratio measurements as indicators for the source of lead poisoning in Mute swans (Cygnus olor) wintering in Puck Bay (northern Poland). Chemosphere 164, 436–442. https://doi:10.1016/j.chemosphere.2016.08.120.

Bollhöfer, A., Rosman, K.J., 2001. Isotopic source signatures for atmospheric lead: the Northern Hemisphere. Geochem. Cosmochim. Acta 65, 1727–1740. https://doi.org/10.1016/s0016-7037(00)00630-x.

Brownie, C.F., Brownie, C., Lopez, V., Cadogan, P., 2009. Dogs and goats as sentinels for environmental lead burden in Caribbean basin islands: Jamaica West Indies. West Indian Veterinary Journal 9 (2), 17–20.

Calabrese, E.J., Stanek, E.J., 1995. A Dog's tale: soil ingestion by a canine. Ecotoxicol. Environ. Saf. 32, 93–95. https://doi.org/10.1006/eesa.1995.1090.

Cao, S., Duan, X., Zhao, X., Wang, B., Ma, J., Fan, D., Sun, C., He, B., Wei, F., Jiang, G., 2014. Isotopic ratio based source apportionment of children's blood lead around coking plant area. Environ. Int. 73, 158–166. https://doi:10.1016/j.envint.2014.07.015.

Centers for Disease Control and Prevention (CDC), 2012. Low level lead exposure harms children: a renewed call for primary prevention. Report of the advisory committee on childhood lead poisoning prevention of the Centers for disease control and prevention. Available. https://www.cdc.gov/nceh/lead/ACCLPP/Final_Document_030712.pdf. (Accessed 13 December 2019). accessed.

Centers for Disease Control and Prevention (CDC), 2019. CDC - lead - blood lead levels in children. Available. https://www.cdc.gov/nceh/lead/prevention/blood-lead-levels.htm. (Accessed 13 December 2019). accessed.

Esposito, M., De Roma, A., Maglio, P., Sansone, D., Picazio, G., Bianco, R., De Martinis, C., Rosato, G., Baldi, L., Gallo, P., 2019. Heavy metals in organs of stray dogs and cats from the city of Naples and its surroundings (Southern Italy). Environ. Sci. Pollut. Res. 26, 3473–3478. https://doi.org/10.1007/s11356-018-3838-5.

Hamir, A., Sulivan, N., Handson, P., Barr, S., 1985. An outbreak of lead poisoning in dogs. Aust. Vet. J. 62, 21–23. https://doi.org/10.1111/j.1751-0813.1985.tb06034.x.

Institute for Health Metrics and Evaluation (IHME), 2017. Global burden of disease (GBD) compare. Available. https://vizhub.healthdata.org/gbd-compare/. (Accessed 13 December 2019). accessed.

Kamona, A.F., Friedrich, G.H., 2007. Geology, mineralogy and stable isotope geochemistry of the Kabwe carbonate-hosted Pb–Zn deposit, Central Zambia. Ore Geol. Rev. 30, 217–243. https://doi.org/10.1016/j.oregeorev.2006.02.003.

Kamona, A., Lévêque, J., Friedrich, G., Haack, U., 1999. Lead isotopes of the carbonate-hosted Kabwe, tsumeb, and kipushi Pb-Zn-Cu sulphide deposits in relation to Pan african orogenesis in the damaran-lufilian fold belt of central africa. Miner. Depos. 34, 273–283. https://doi.org/10.1007/s001260050203.

King, J., 2016. Proximal tubular nephropathy in two dogs diagnosed with lead toxicity. Aust. Vet. J. 94, 280–284. https://doi.org/10.1111/avj.12463.

Koh, T., Bidge, P., 1986. A comparison of blood lead levels in dogs from a lead-mining, lead-smelting, urban and rural island environment. Aust. Vet. J. 63, 282–285. https://doi.org/10.1111/j.1751-0813.1986.tb08067.x.

Kucera, E., 1988. Dogs as indicators of urban lead distribution. Environ. Monit. Assess. 10, 51–57. https://doi.org/10.1007/bf00394256.

Kuritani, T., Nakamura, E., 2002. Precise isotope analysis of nanogram-level Pb for natural rock samples without use of double spikes. Chem. Geol. 186, 31–43. https://doi.org/10.1016/s0009-2541(02)00004-9.

Langlois, D.K., Kaneene, J.B., Yuzbasiyan-Gurkan, V., Daniels, B.L., Mejia-Abreu, H., Frank, N.A., Buchweitz, J.P., 2017. Investigation of blood lead concentrations in dogs living in Flint, Michigan. J. Am. Vet. Med. Assoc. 251, 912–921. https://doi.org/10.2460/javma.251.8.912.

Lanphear, B.P., Hornung, R., Khoury, J., Yolton, K., Baghurst, P., Bellinger, D.C., Canfield, R.L., Dietrich, K.N., Bornschein, R., Greene, T., Rothenberg, S.J., Needleman, H.L., Schnaas, L., Wasserman, G., Graziano, J., Roberts, R., 2005. Low-level environmental lead exposure and children's intellectual function: an international pooled analysis. Environ. Health Perspect. 113, 894–899. https://doi.org/10.1289/ehp.7688.

Meyer, P.A., Brown, M., Falk, H., 2008. Global approach to reducing lead exposure and poisoning. Mutat. Res. Rev. Mutat. Res. 659, 166–175. https://doi.org/10.1016/j.mrrev.2008.03.003.

Mielke, H.W., Zahran, S., 2012. The urban rise and fall of air lead (Pb) and the latent surge and retreat of societal violence. Environ. Int. 43, 48–55. https://doi.org/10.1016/j.envint.2012.03.005.

Nakata, H., Nakayama, S., Yabe, J., Liazambi, A., Mizukawa, H., Darwish, W., Ikenaka, Y., Ishizuka, M., 2016. Reliability of stable Pb isotopes to identify Pb sources and verifying biological fractionation of Pb isotopes in goats and chickens. Environ. Pollut. 208, 395–403. https://doi.org/10.1016/j.envpol.2015.10.006.

Nakayama, S., Ikenaka, Y., Hamada, K., Muzandu, K., Choongo, K., Teraoka, H., Mizuno, N., Ishizuka, M., 2011. Metal and metalloid contamination in roadside soil and wild rats around a Pb–Zn mine in Kabwe, Zambia. Environ. Pollut. 159, 175–181. https://doi.org/10.1016/j.envpol.2010.09.007.

Nakayama, S., Nakata, H., Ikenaka, Y., Yabe, J., Oroszlany, B., Yohannes, Y.B., Bortey-Sam, N., Muzandu, K., Choongo, K., Kuritani, T., Nakagawa, M., Ishizuka, M., 2019. One year exposure to Cd- and Pb-contaminated soil causes metal accumulation and alteration of global DNA methylation in rats. Environ. Pollut. 252, 1267–1276. https://doi.org/10.1016/j.envpol.2019.05.038.

Rabinowitz, P., Gordon, Z., Chudnov, D., Wilcox, M., Odofin, L., Liu, A., Dein, J., 2006. Animals as sentinels of bioterrorism agents. Emerg. Infect. Dis. 12, 647–652. https://doi.org/10.3201/eid1204.051120.

Schoning, P., Abraham, J., Burnett, B., 1996. Silicate and metal dust in lungs of Greyhounds. Am. J. Vet. Res. 57, 1006–1009.

Serpe, F., Russo, R., Simone, D.A., Florio, S., Esposito, M., Severino, L., 2012. Levels of heavy metals in liver and kidney of dogs from urban environment. Open Vet. J. 2, 15–18.

Sévère, S., Marchand, P., Guiffard, I., Morio, F., Venisseau, A., Veyrand, B., Bizec, B., Antignac, J.-P., Abadie, J., 2015. Pollutants in pet dogs: a model for environmental links to breast cancer. SpringerPlus 4, 27. https://doi.org/10.1186/s40064-015-0790-4.

Tembo, B.D., Sichilongo, K., Cernak, J., 2006. Distribution of copper, lead, cadmium and zinc concentrations in soils around Kabwe town in Zambia. Chemosphere 63, 497–501. https://doi.org/10.1016/j.chemosphere.2005.08.002.

Thomas, C., Rising, J., Moore, J., 1975. Blood lead concentrations in three groups of dogs from a suburban Illinois community. J. Am. Vet. Med. Assoc. 167, 995–999.

Thomas, C., Rising, J., Moore, J., 1976. Blood lead concentrations of children and dogs from 83 Illinois families. J. Am. Vet. Med. Assoc. 169, 1237–1240.

Tomza-Marciniak, A., Pilarczyk, B., Bąkowska, M., Ligocki, M., Gaik, M., 2012. Lead, cadmium and other metals in serum of pet dogs from an urban area of NW Poland. Biol. Trace Elem. Res. 149, 345–351. https://doi.org/10.1007/s12011-012-9433-6.

Veysseyre, A.M., Bollhöfer, A.F., Rosman, K.J., Ferrari, C.P., Boutron, C.F., 2001. Tracing the origin of pollution in French alpine snow and aerosols using lead isotopic ratios. Environ. Sci. Technol. 35, 4463–4469. https://doi.org/10.1021/es0105717.

Wani, A., Ara, A., Usmani, J., 2015. Lead toxicity: a review. Interdiscip. Toxicol. 8, 55–64. https://doi.org/10.1515/intox-2015-0009.

World Health Organization (WHO), 2010. Childhood lead poisoning. Available. https://www.who.int/ceh/publications/leadguidance.pdf. (Accessed 13 December 2019). accessed.

Yabe, J., Ishizuka, M., Umemura, T., 2010. Current levels of heavy metal pollution in africa. J. Vet. Med. Sci. 72, 1257–1263. https://doi.org/10.1292/jvms.10-0058.

Yabe, J., Nakayama, S., Ikenaka, Y., Muzandu, K., Ishizuka, M., Umemura, T., 2011. Uptake of lead, cadmium, and other metals in the liver and kidneys of cattle near a lead-zinc mine in Kabwe, Zambia. Environ. Toxicol. Chem. 30, 1892–1897. https://doi.org/10.1002/etc.580.

Yabe, J., Nakayama, S., Ikenaka, Y., Muzandu, K., Choongo, K., Mainda, G., Kabeta, M., Ishizuka, M., Umemura, T., 2013. Metal distribution in tissues of free-range chickens near a lead–zinc mine in Kabwe, Zambia. Environ. Toxicol. Chem. 32,

189–192. https://doi.org/10.1002/etc.2029.
Yabe, J., Nakayama, S., Ikenaka, Y., Yohannes, Y.B., Bortey-Sam, N., Oroszlany, B., Muzandu, K., Choongo, K., Kabalo, A., Ntapisha, J., Mweene, A., Umemura, T., Ishizuka, M., 2015. Lead poisoning in children from townships in the vicinity of a lead–zinc mine in Kabwe, Zambia. Chemosphere 119, 941–947. https://doi.org/10.1016/j.chemosphere.2014.09.028.

metals

MDPI

Article

Recovery of Lead and Zinc from Zinc Plant Leach Residues by Concurrent Dissolution-Cementation Using Zero-Valent Aluminum in Chloride Medium

Marthias Silwamba [1,2,*], Mayumi Ito [3], Naoki Hiroyoshi [3], Carlito Baltazar Tabelin [4], Ryota Hashizume [1], Tomoki Fukushima [1], Ilhwan Park [3], Sanghee Jeon [3], Toshifumi Igarashi [3], Tsutomu Sato [3], Meki Chirwa [5], Kawawa Banda [5], Imasiku Nyambe [5], Hokuto Nakata [6], Shouta Nakayama [6] and Mayumi Ishizuka [6]

1 Division of Sustainable Resources Engineering, Graduate School of Engineering, Hokkaido University, Sapporo 060-8628, Japan
2 Department of Metallurgy and Mineral Processing, School of Mines, The University of Zambia, Lusaka P.O. Box 32379, Zambia
3 Division of Sustainable Resources Engineering, Faculty of Engineering, Hokkaido University, Sapporo 060-8628, Japan
4 School of Minerals and Energy Resources Engineering, The University of New South Wales, Sydney NSW 2052, Australia
5 IWRM Centre/Geology Department, School of Mines, The University of Zambia, Lusaka P.O. Box 32379, Zambia
6 Faculty of Veterinary Medicine, Hokkaido University, Kita 18, Nishi 9, Kita-Ku, Sapporo 060-0818, Japan
* Correspondence: smarthias11@gmail.com or marthias.silwamba@unza.zm; Tel.: +81-80-8745-1805

Received: 2 April 2020; Accepted: 18 April 2020; Published: 20 April 2020

Abstract: Zinc plant leach residues (ZPLRs) contain significant amounts of metal compounds of lead (Pb), zinc (Zn), iron (Fe), etc., hence, they are considered as a secondary source of metals. On the other hand, ZPLRs are regarded as hazardous materials because they contain heavy metals that pollute the environment. Resources and environmental concerns of ZPLRs were addressed in this study by removing/recovering Pb and Zn using a concurrent dissolution and cementation technique. To cement the dissolved Pb and Zn in leaching pulp, zero-valent aluminum (ZVAl) was added during ZPLRs leaching in the hydrochloric (HCl)–sodium chloride (NaCl) solution. The resulting cemented metals were agglomerated and separated by sieving. Lead removal increased with increasing both NaCl and HCl concentrations. However, when ZVAl was added, significant Pb removal was achieved at a low concentration. Zinc was not cemented out of the pulp using ZVAl and its recovery from ZPLRs was dependent on the HCl concentration only. By applying a concurrent dissolution and cementation technique, both Pb and Zn were removed using a low concentration of NaCl, and most importantly Pb—the most toxic metal in ZPLRs—was captured and separated before the solid-liquid separation, hence, eliminating the need for extensive washing of the generated residues to remove the inherent residual solution.

Keywords: lead; zinc; zinc plant leach residues; zero-valent aluminum; leaching; cementation

1. Introduction

Explosive population growth and its associated economic activities such as massive construction projects to modernize and improve communication, transportation, and agricultural sectors have in recent years led to high demands for metals [1–4]. To keep up with demands, mining and metals production have also increased at unprecedented levels. Enormous amounts of solid wastes are also

generated as a result of more extensive mining, mineral processing, and metal extraction operations by metallurgical processes [5–7]. For example, zinc (Zn) metal production via hydrometallurgical processes (i.e., leaching of calcine or zinc oxide minerals followed by electrowinning of Zn) generates huge amounts of zinc plant leach residues (ZPLRs) [8,9], which are stockpiled and often abandoned after closure of mining/processing operations.

With the rapid depletion of high-grade ores, ZPLRs are now considered as secondary resources because they still contain substantial amounts of residual Zn, copper (Cu), lead (Pb), and iron (Fe) [10–13]. From an environmental point of view, ZPLRs are considered hazardous wastes because they contain hazardous heavy metals such as Pb, Cu, and Zn. Pb, for example, is extremely toxic to babies and children and is known to cause various disorders of the reproductive organs, central nervous system, and kidneys [14–16]. Therefore, the reprocessing of ZPLRs for metal removal/recovery could address both environmental and resource concerns associated with these waste materials.

Pyrometallurgical [17,18] and hydrometallurgical [19,20] techniques can be employed to recover valuable metals from ZPLRs. When appropriate, the latter approach is preferred because it is less energy-intensive and generates wastes (e.g., solid residues) that may cause less or no secondary environmental pollution. Numerous studies have been published to process metallurgical wastes using conventional hydrometallurgical processes that follow the sequence of leaching, solid-liquid separation, and recovery of dissolved metals (usually Cu, Pb, and Zn) from pregnant leach solutions [9,11,20–23]. Although effective, there are two serious drawbacks of conventional approaches for Pb and Zn extraction-recovery from ZPLRs. Firstly, leaching approaches require highly concentrated reagents to extract the target metals [10,20]. Secondly, leaching residues contain a heavy metal-rich residual solution due to difficulties and inherently incomplete solid-liquid separation partly exacerbated by silica gel formation and the presence of very fine particles in ZPLRs [24,25]. To remove residual solutions from generated solid residues after solid-liquid separation, extensive washing or stabilization before disposal should be carried out, requiring complex treatment processes that increase operating costs.

To address these limitations of conventional hydrometallurgical techniques for Pb and Zn recovery from ZPLRs, this study used a technique combining Pb and Zn dissolution from ZPLRs with the recovery of these metals directly in one reaction reactor without solid-liquid separation (i.e., concurrent dissolution-cementation). Since dissolved metals are sequestered (i.e., recovered) in the leaching pulp, it follows that a low concentrated solution can be used to achieve high removal/recovery as the solution would not be saturated with dissolved metals. Additionally, heavy metals are removed before solid-liquid separation, so the need for extensive washing to remove the residual heavy metal-rich solution is eliminated.

In this study, concurrent dissolution-cementation was applied to extract and recover Pb and Zn removal from historic abandoned ZPLRs obtained from Kabwe, Zambia. To dissolve Pb and Zn from ZPLRs, acidified chloride (HCl–NaCl) solutions of various concentrations were used. The chloride solution was used due to the complexation capability of chloride with Pb. The dissolved amounts Pb and Zn were quantified by inductively coupled plasma atomic emission spectroscopy (ICP-AES). The recovery of dissolved Pb and Zn from leaching pulp was achieved by cementation using the zero-valent aluminum (ZVAl) powder. Cementation products were characterized by the scanning electron microscopy equipped with an energy dispersive X-ray spectroscopy (SEM-EDX) and X-ray powder diffraction (XRD). To evaluate whether the solid residues generated by concurrent dissolution-cementation meets environmental standards, the toxicity characteristic leaching procedure (TCLP) was carried out.

2. Materials and Methods

2.1. Materials

ZPLR samples were collected from the historic dumpsite of Pb-Zn mine wastes in Kabwe, Zambia (Figure 1). The samples were air-dried for 30 days in the laboratory, lightly pulverized with an agate

mortar and pestle, and then dry-sieved using stainless steel sieves to obtain sample with particles passing 106 μm fraction. Chemical characterization of the ZPLR samples was carried out using both X-ray fluorescence spectroscopy (XRF, EDXL 300, Rigaku Corporation, Tokyo, Japan) and ICP-AES (ICPE-9820, Shimadzu Corporation, Kyoto, Japan) after aqua regia (3 HCl:1 HNO_3 v/v) digestion in a microwave-assisted acid digestion system (Ethos Advanced Microwave Lab station, Milestone Inc., Sorisole, Italy). The amounts of Pb and Zn in ZPLR samples were as high as 6.19% and 2.53%, respectively (Table 1). ZPLR samples also contained significant amounts of other elements such as Si, Fe, Ca, S, Cu, and other elements, as shown in Table 1. The mineralogical composition of ZPLRs was determined by XRD (MultiFlex, Rigaku Corporation, Tokyo, Japan) and crystalline minerals were identified using a full package of the Crystallography Open Database (COD) and MATCH 3.4. The crystalline Pb and Zn minerals in ZPLRs that were detected included anglesite ($PbSO_4$), cerussite ($PbCO_3$), esperite ($PbCa_2Zn_3(SiO_4)_3$), and zinkosite ($ZnSO_4$), as illustrated in Figure 2. Other minerals detected in the samples are quartz (SiO_2), gypsum ($CaSO_4{\cdot}2H_2O$), hematite (Fe_2O_3), and goethite (FeOOH). The particle size distributions of lightly pulverized ZPLRs were analyzed using Laser diffraction (Microtrac® MT3300SX, Nikkiso Co. Ltd., Osaka, Japan) and were found to have a median size (D_{50}) of around 9.6 μm (Figure 3a).

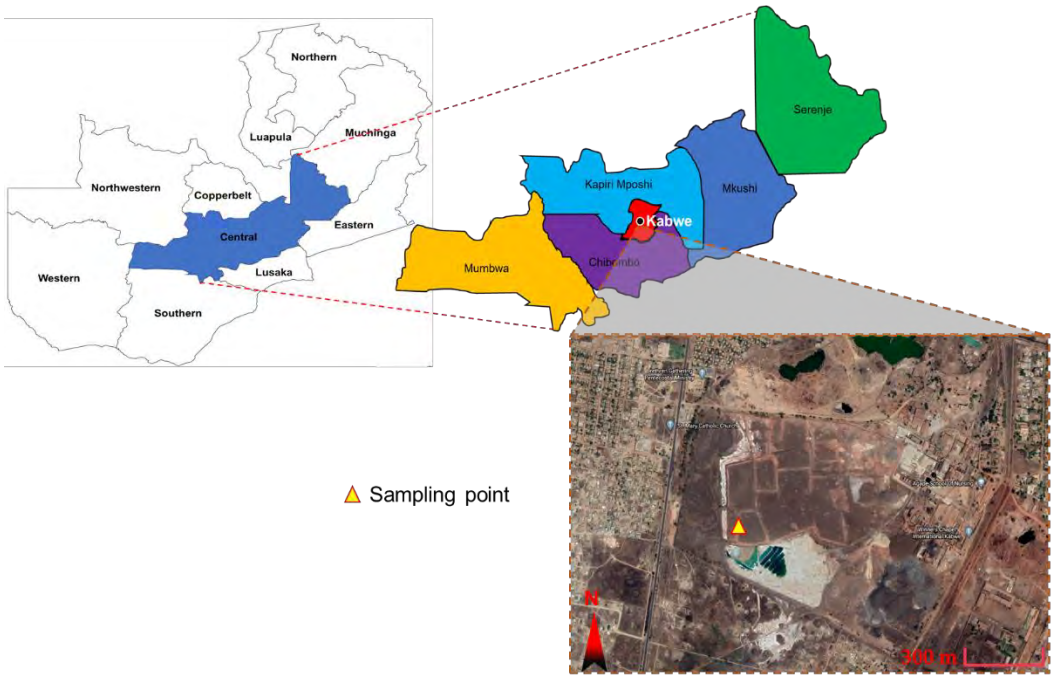

Figure 1. Schematic geographic map of Zambia superimposed with the location of Kabwe and historic Pb-Zn mine wastes.

Table 1. Chemical composition of zinc plant leach residues from Pb-Zn mine wastes from Kabwe, Zambia.

Elements/Oxides	Pb *	Zn *	Fe *	Cu *	CaO	SiO_2	Al_2O_3	SO_3	V_2O_5	MnO	Others
Mass %	6.2	2.5	17.0	0.2	10.6	31.4	2.9	18.2	0.7	0.3	1.1

* Elemental composition was determined by the inductively coupled plasma atomic emission spectroscopy (ICP-AES) after aqua regia digestion. Elemental oxides were determined by XRF.

Reagent grade NaCl and HCl (Wako Pure Chemical Industries, Ltd., Osaka, Japan) were used to prepare the leaching solutions of different concentrations by dissolution and dilution using deionized (DI) water (18 MΩ·cm, Milli-Q® Integral Water Purification System, Merck Millipore, Burlington, Vermont, USA). To simultaneously precipitate reductively (cement) the dissolved Pb^{2+} and Zn^{2+} in leaching pulp, ultra-pure ZVAl powder (>99.99%, 50–150 μm, Wako Pure Chemical Industries, Ltd.,

Osaka, Japan) was used (the median particle size (D_{50}) of ZVAl was 126.8 µm). The particle size distribution is shown in Figure 3b. A stainless steel sieve with 150 µm aperture size was used to separate cemented and agglomerated Pb and Zn from the leaching pulp. The sieve size was selected by taking into consideration the particles size ranges of both ZPLRs and ZVAl. In other words, this sieve could only retain cemented and agglomerated particles while passing particles of unreacted ZVAl and particles of undissolved minerals particles of ZPLRs.

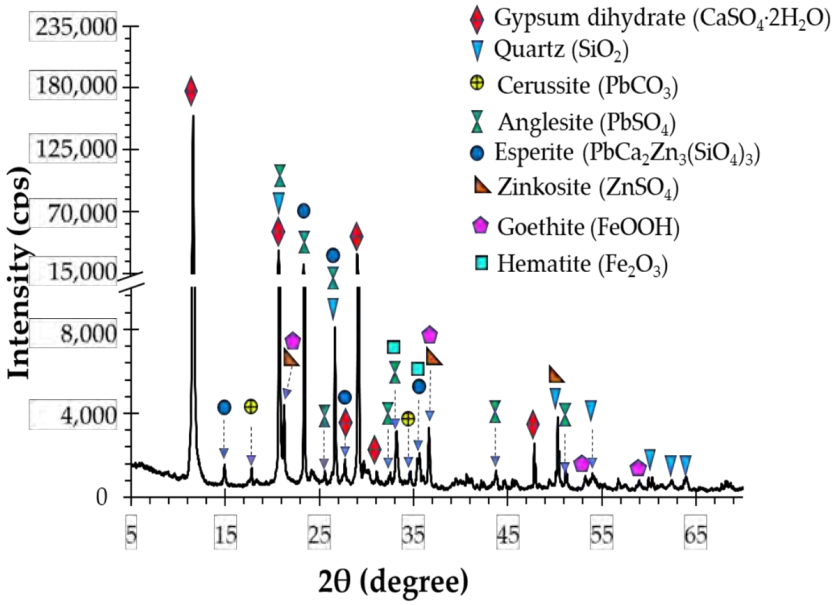

Figure 2. XRD pattern of the zinc plant leach residues from Kabwe, Zambia.

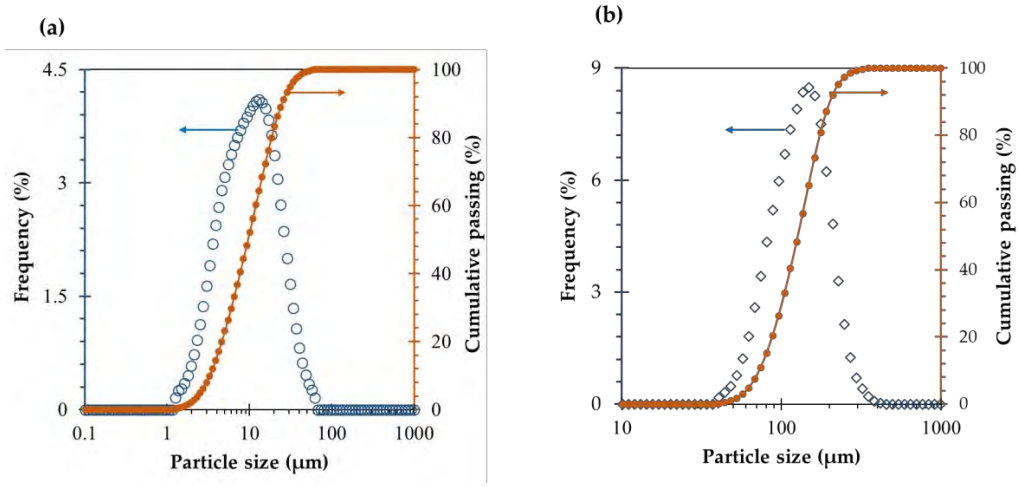

Figure 3. The particle size distribution of (**a**) zinc plant leach residues and (**b**) zero-valent aluminum.

2.2. Methods

2.2.1. Leaching-Cementation Experiments in Chloride Solution

Batch leaching experiments for the extraction of Pb and Zn from ZPLRs with and without ZVAl additions were conducted using a 200-mL Erlenmeyer flask. The volume of the leaching solution was at 50 mL for all experiments. Concentrations of NaCl (0–3 M) were varied and acidified with different HCl concentrations (0–0.1 M) to obtain required leaching solutions. Fifty milliliters (50 mL) of leaching solution of a given concentration was initially poured in an Erlenmeyer flask and nitrogen (N_2) was purged for 10 min to remove dissolved oxygen (DO). Nitrogen gas (N_2) purging was again carried out

for 2 min after the addition of 2.5 g ZPLRs with and without 0.1 g ZVAl that were added before sealing the flask using silicon stoppers and parafilm®. The flask was then shaken at 4 cm amplitude and 120 min^{-1} shaking frequency in a water-bath shaker maintained at 25 °C for a predetermined length of time. At the end of the predetermined shaking time, the leaching pulp was carefully collected, and solid-liquid separation was carried out by filtering the collected leaching pulp using a syringe-driven membrane filter—pore size of 0.20 µm— (LMS Co., Ltd. Tokyo, Japan). The filtrate was then analyzed for dissolved Pb and Zn using ICP-AES. In the case where ZVAl was added during ZPLR leaching, additional steps—the separation of cemented and agglomerated product from the leaching pulp by screening using a sieve of aperture size of 150 µm—were carried out. The +150 µm particles (cemented and agglomerated) were thoroughly washed with deionized (DI) water before drying in a vacuum oven at 40 °C for 24 h. Dried +150 µm particles were then digested in aqua regia using a microwave-assisted acid digestion system and the leachate was analyzed for Pb and Zn using ICP-EAS. Furthermore, the +150 µm particles obtained were examined by both XRD and SEM-EDX (JSM-IT200, JEOL Ltd., Tokyo, Japan). All the experimental tests were carried out twice and the average was reported here.

The Pb and Zn removal ($R_{Pb,Zn}$) from ZPLRs without and with ZVAl were quantified using Equations (1) and (2), respectively.

$$R_{Pb,Zn} = \frac{V * C_{Pb,Zn}}{W_S * M_s} * 100 \quad (1)$$

$$R_{Pb,Zn} = \frac{\left(V * C_{Pb,Zn}\right) + \left(W_{cg} * M_{cg}\right)}{W_S * M_s} * 100 \quad (2)$$

where $C_{Pb,Zn}$ is the concentration (g/L) of Pb and Zn, V is the volume (L) of leaching solution, W_S is the weight percent (%) of either Pb and Zn, M_s is the mass (g) of leached ZPLRs, M_{cg} is the mass (g) of cemented and agglomerated particles, and W_{cg} is the weight percent (%) of cemented and agglomerated particles calculated based on the digested fraction of M_{cg} in aqua regia and analysis of the solution by ICP-AES.

2.2.2. Leachability of Lead and Zinc after Concurrent Dissolution-Cementation

To evaluate the leachability of Pb and Zn from before and after concurrent dissolution-cementation, leachability experiments were conducted according to the toxicity characteristic leaching procedure (TCLP) [26]. For TCLP, 1 g of vacuum-dried treated and untreated residues were equilibrated with 20 mL of acetic acid solution (pH 2.89) in a centrifuge tube shaken at 30 rpm on a rotary tumbler for 18 h. After the predetermined leaching time, the leachate was filtered through 0.20 µm syringe-driven membrane filters and the filtrate was analyzed for dissolved Pb and Zn using ICP-AES.

3. Results and Discussion

3.1. Concurrent Dissolution-Cementation of Pb and Zn from Zinc Plant Leach Residues

The concentrations of Pb and Zn as a function of time when 2.5 g of ZPLRs were leached in a solution composed of 3 M NaCl and 0.05 M HCl with and without the addition of 0.1 g ZVAl is shown in Figure 4a,b. The concentration of Pb when ZPLRs were leached without ZVAl reached an apparent equilibrium of around 8.5 mM (which represents 59% of total Pb) after just 15 min (Figure 4a). Pb dissolution from ZPLRs involves the formation of lead-chloride complexes as explained by Equations (3) and (4) [20,27–29]:

$$PbSO_4 + xCl^- = PbCl_x^{(2-x)} + SO_4^{2-} \quad (3)$$

$$PbCO_3 + 2H^+ + xCl^- = PbCl_x^{(2-x)} + CO_2 + H_2O \quad (4)$$

where $PbCl_x^{(2-x)}$ and x are lead-chloride complex(es) and integers from 1 to 4, respectively, all of which depended on the chloride concentration.

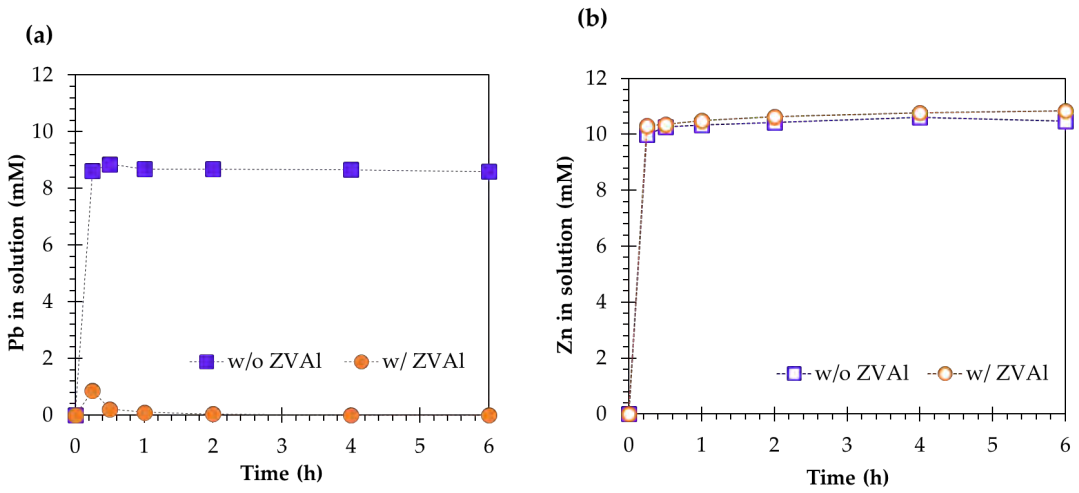

Figure 4. Concentration of (**a**) Pb and (**b**) Zn dissolved in the leaching solution as a function of time when zinc plant leach residues (ZPLRs) were leached without and with zero-valent aluminum (ZVAl).

The concentration of dissolved Pb when ZVAl was added was 10-fold lower than when only ZPLRs were leached in the same solution. The dissolved concentration of Pb decreased further with increasing the treatment time and reached below 0.048 mM (i.e., 0.1 mg/L) with ZVAl after 4 h. The dramatically lower dissolved concentration of Pb after 15 min and its continued decrease to below 0.1 mg/L with ZVAl could be attributed to its sequestration from the solution via cementation. In other words, an additional chemical reaction—cementation described by the overall reaction (Equation (7)) which is the sum of two half-reactions (i.e., Equations (5) and (6))—occurred concurrently with dissolution reactions, as previously described.

$$Al^{3+} + 3e^- = Al^0 E^0 = -1.66\ V \quad (5)$$

$$Pb^{2+} + 2e^- = Pb^0 \quad E^0 = -0.126\ V \quad (6)$$

$$3Pb^{2+} + 2Al^0 = 3Pb^0 + 2Al^{3+} \quad (7)$$

The overall reaction potential, ΔE^0, is calculated by subtracting the standard electrode potential of Equation (5) from Equation (6), that is, $\Delta E^0 - 0.126 - (-1.66) = 1.534\ V$. The standard Gibbs free energy change, ΔG^0 (i.e., $\Delta G^0 = -nF\Delta E^0$, n number of electrons transferred, F is Faraday's constant, and ΔE^0 is the galvanic cell potential), of Equation (7) is negative (−888.047 kJ/mol) because ΔE^0 is positive indicating that cementation of dissolved Pb^{2+} from ZPLRs by ZVAl is thermodynamically spontaneous. In addition, the Al_2O_3 layer which was inherently present on the surface of ZVAl and passivated the cementation is removed at the acidified chloride solution [30,31]. Hence, simultaneous cementation of dissolved Pb^{2+} from ZPLRs occurred, which could explain why Pb^{2+} was comparatively lower and was even below 0.1 mg/L with ZVAl during ZPLRs leaching.

Meanwhile, the concentration of dissolved Zn reached an apparent equilibrium after 15 min at around 10.3 mM (i.e., equivalent to around 52% of total Zn) for without and with ZVAl (Figure 4b). This implied that dissolved Zn from ZPLRs was not cemented on ZVAl as described by Equation (10) (i.e., the summation of two half-cell reactions Equations (8) and (9)) though it is thermodynamically feasible due to negative ΔG^0 (i.e., −519.282 kJ/mol).

$$Al^{3+} + 3e^- = Al^0 \quad E^0 = -1.660\ V \quad (8)$$

$$Zn^{2+} + 2e^{-} = Zn^{0} \quad E^{0} = -0.763\ V \tag{9}$$

$$3Zn^{2+} + 2Al^{0} = 3Zn^{0} + 2Al^{3+} \tag{10}$$

The cementation product that was obtained as +150 µm particles were characterized by SEM-EDX and XRD. Figure 5 shows that Pb was cemented on ZVAl and agglomerated. However, Zn was not detected, which confirms that dissolved Zn was not cemented by ZVAl. Further characterization of the cementation product by XRD (Figure 6) showed that cemented Pb was mainly in a zero-valent Pb (metallic Pb) form and a small amount of oxidized metallic Pb as PbO, which supports the chemical reaction expressed in Equation (7).

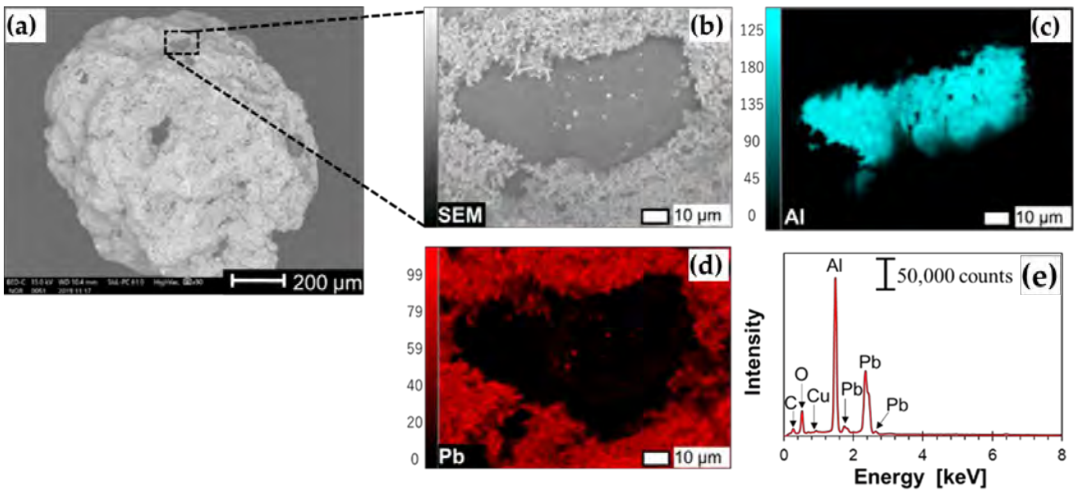

Figure 5. SEM-EDX of ZVAl "coated" with Pb from the +150 µm particles obtained after sieving the leaching pulp when ZVAl was added during leaching of ZPLRs: (**a**) SEM image of +150 µm particles, (**b**) zoomed SEM image, EDX elemental mapping of (**c**) Al and (**d**) Pb, as well as (**e**) EDX spectra.

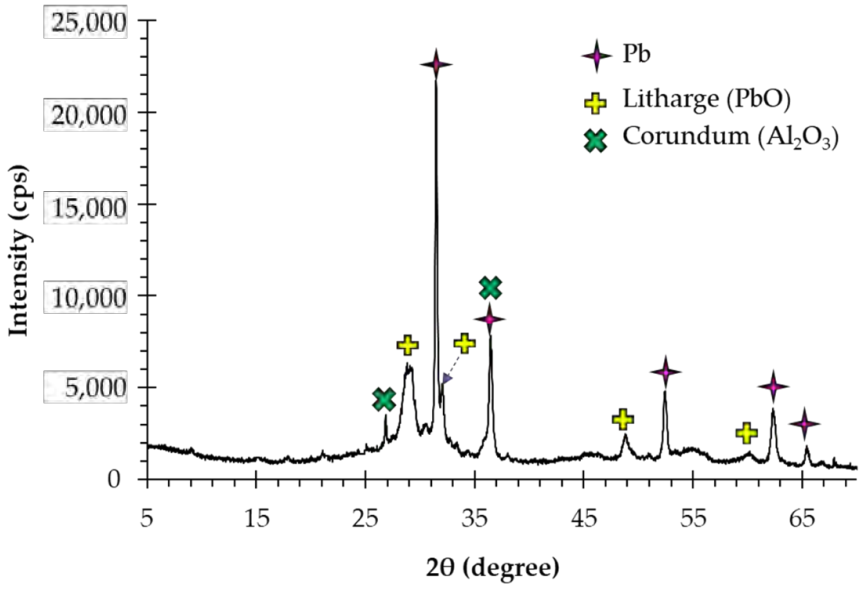

Figure 6. XRD pattern of the +150 µm fraction obtained after sieving the leaching residue in the experiments with ZVAl.

The explanation to why Zn could not be cemented by ZVAl in the leaching solution could be (a) the dissolution of cemented Zn by the proton (H^+) (Equation (11)) and (b) the reduction of H^+ to H_2 on ZVAl, which competes with the reduction of Zn^{2+} to Zn^0 (Equation (12)).

$$6\,H^+ + 3Zn \rightarrow 3H_2 + 3Zn^{2+} \quad (11)$$

$$6\,H^+ + 2Al \rightarrow 3H_2 + 2Al^{3+} \quad (12)$$

In an acidic region, the redox potential of H^+/H_2 redox pair is higher than that of Zn^{2+}/Zn redox pair, indicating that the reaction in Equation (11) ($\Delta G^0 = -6121.203$ kJ/mol) occurs, and Zn once cemented on the ZVAl surface would be dissolved [32]. Similarly, since the redox potential of H^+/H_2 redox pair is higher than that of Al^{3+}/Al redox pair, the reaction as shown in Equation (12) ($\Delta G^0 = -8168.614$ kJ/mol) also takes place. This reaction consumes the electron supplied from ZVAl and competes with Zn^{2+} reduction to Zn (Equation (10)). As a result, these reactions suppress the Zn cementation on ZVAl. The rates and equilibrium of these reactions (Equations (11) and (12)) depend on the H^+ concentration, hence, suppression of Zn cementation on ZVAl would decrease at higher pH.

To investigate the effects of H^+ concentration on cementation of Zn^{2+} from the solution using ZVAl, simulated (model) acidic and alkaline solutions containing both 8 mM Pb^{2+} and 10 mM Zn^{2+}, and to mimic the composition similar to what would be obtained by leaching ZPLRs, were prepared by dissolving $ZnCl_2$ and $PbCl_2$ (Wako Pure Chemical Industries, Ltd., Japan) in an acidified chloride solution (3 M NaCl and 0.05 M HCl, initial pH = 0.82) and alkaline solution (3 M NaOH, initial pH = 14.5), respectively. To cement both Pb and Zn, 0.15 g of ZVAl was added after N_2 purging.

Figure 7a shows the percentage of cemented Pb and Zn from the simulated acidified chloride solution. Only Pb (around 99.7% after 30 min) was cemented out leaving Zn in the solution, which is in line with the results obtained when ZVAl was added during ZPLRs leaching. However, in the alkaline solution around 99.8% of both Pb and Zn were cemented out of the solution (Figure 7b). The SEM-EDX analysis and mapping results showed that both Pb and Zn were deposited on the ZVAl surface (Figure 8). The results confirm the suppression of Zn cementation, which depends on pH. In the acidic region, Zn cementation is strongly suppressed by the reactions shown in Equations (11) and (12), while in the alkaline region the suppressive effects become negligible because of low H^+ concentrations.

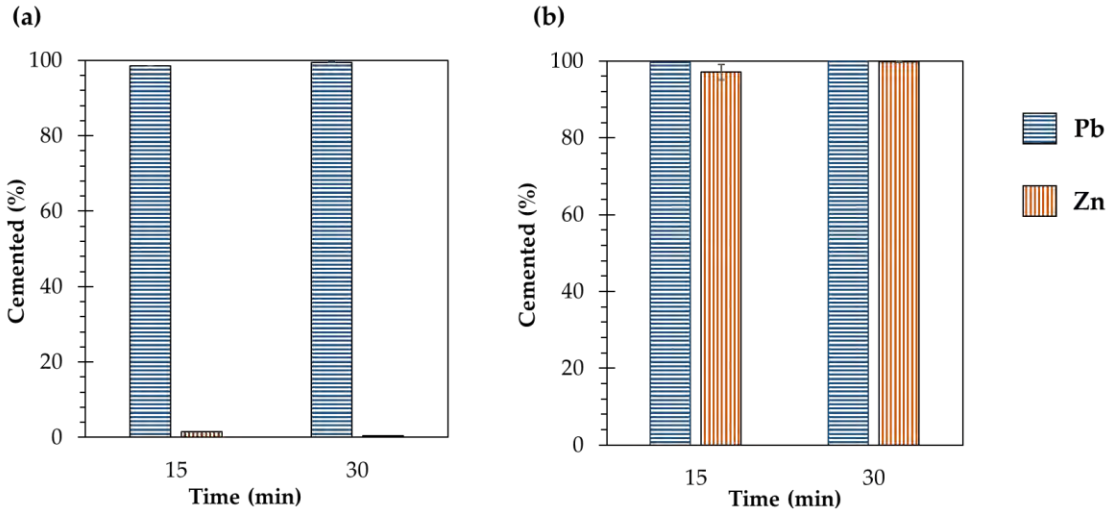

Figure 7. Amount of Pb and Zn cemented out using ZVAl in model experiments under (**a**) the simulated acidic chloride and (**b**) simulated alkaline solutions.

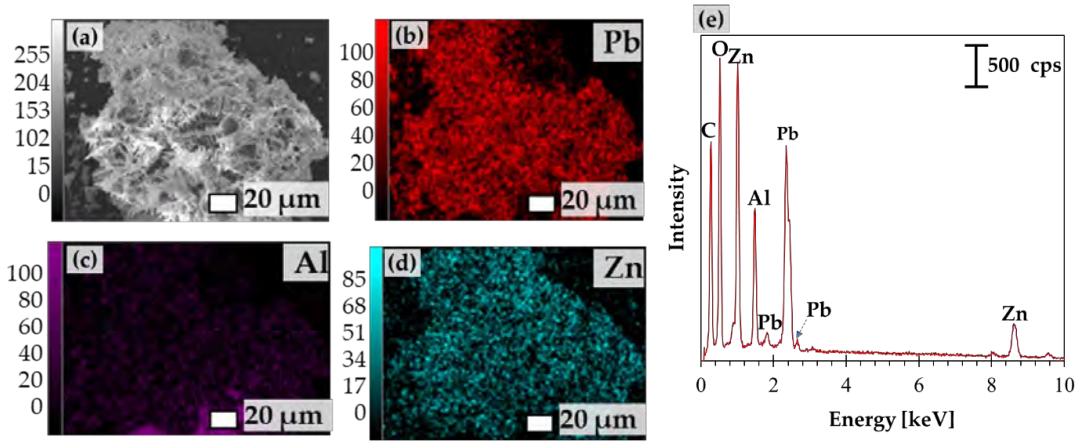

Figure 8. SEM-EDX of cementation product of Pb and Zn by ZVAl from the alkaline simulated solution: (**a**) SEM image, EDX elemental mapping of (**b**) Pb, (**c**) Al, (**d**) Zn, and (**e**) EDX spectra.

3.2. *Effects of Solution Composition on Pb and Zn Removal from Zinc Plant Leach Residues*

Lead and Zn removal from ZPLRs was evaluated for different solution compositions and compared with the removal efficiencies when ZPLRs was leached with and without ZVAl addition. When ZVAl was added during ZPLRs leaching, Pb was extracted into a leaching solution and concurrently cemented and agglomerated. The Pb distribution among the solution (i.e., extracted but uncemented Pb), +150 µm particles (i.e., cementation and agglomerated product), and −150 µm particles (unextracted Pb in residues). Since the amount of Pb that remained in the solution was negligible (in most cases below 0.1 mg/L), Pb removal in a case when ZVAl was added during ZPLRs leaching is referred to as Pb that was extracted, cemented, and separated as +150 µm particles. However, in the case when ZPLRs were leached without the addition of ZVAl, Pb removal is referred to as the Pb that was extracted into a leaching solution. The same definition was also applied to Zn removal with and without ZVAl addition since it was not cemented from the leaching solution, as discussed previously.

Lead removal when ZPLRs were leached without the addition of ZVAl increased with increasing both HCl and NaCl concentrations, as shown in Figure 9. Pb removal steadily increased from around 0% to 28%, 0.5% to 58%, and 0.5% to 72% for 0.01, 0.05, and 0.1 M HCl, respectively, when NaCl increased from 0 to 3 M, respectively. Lead dissolution from anglesite ($PbSO_4$) depends on (1) Cl^- concentration, (2) SO_4^{2-} concentration, and (3) solution pH (Figure 10). For example, for a 1:1 ratio of Pb concentration to SO_4^{2-} concentration (i.e., assuming the source of SO_4^{2-} in the leaching system is from $PbSO_4$) Pb dissolution depends on the Cl^- concentration only to form Pb-Cl complexes and not on pH (Equation (3)) (Figure 10a,b). However, even in this case, some Pb from $PbSO_4$ would remain in solid form as $PbCl_2$(s) depending on the Cl^- concentration. The sample used in our study contains $CaSO_4{\cdot}2H_2O$ and $ZnSO_4$ and these minerals contribute SO_4^{2-} in the system. At high SO_4^{2-} concentration, Pb dissolution from $PbSO_4$ depends on pH (Figure 10c). As the pH increases (i.e., H^+ concentration decreases) HSO_4^- speciates to form SO_4^{2-}, which then reacts with dissolved lead in the leaching system to form $PbSO_4$ (Figure 10c,d). Meaning at high SO_4^{2-} concentration, the $PbSO_4$ dissolution is limited at high pH. Meanwhile, the release of Pb from other Pb-minerals such as cerussite ($PbCO_3$) in ZPLRs requires an H^+ attack in addition to the Cl^- concentration, as previously described in Equation (4) (Supplementary Information, Figure S1). This is the possible reason why Pb removal increased when NaCl and HCl concentrations were increased. The semi-quantitative analysis of the residues obtained after treating ZPLRs in a 3 M NaCl and 0.05 M HCl solution with the addition of ZVAl by XRD show the disappearance/decrease of peaks of anglesite, cerussite, gypsum, and other minerals (Supplementary Figure S2).

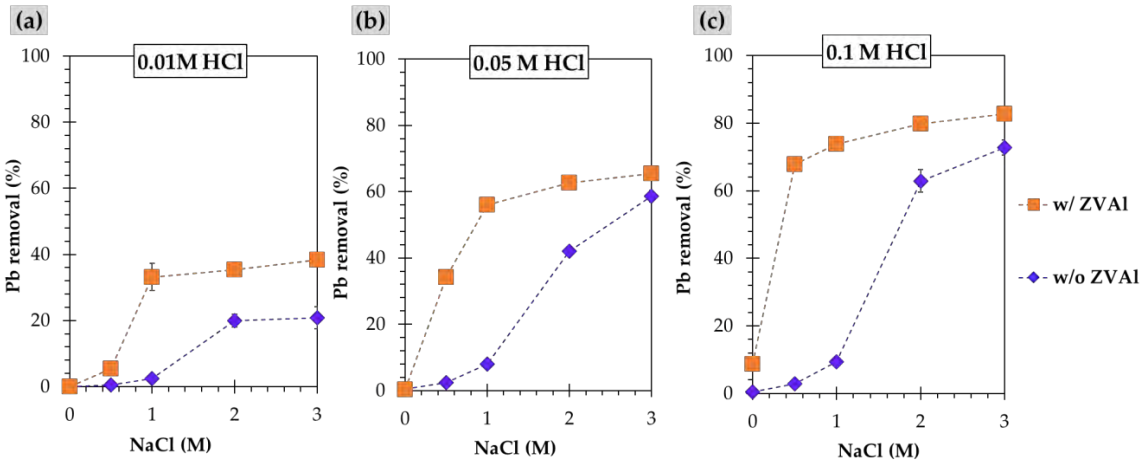

Figure 9. Effects of solution compositions on Pb removal from ZPLRs with and without ZVAl addition: (**a**) 0.01 M HCl and 0–3 M NaCl, (**b**) 0.05 M HCl and 0–3 M NaCl, and (**c**) 0.1 M HCl and 0–3 M NaCl.

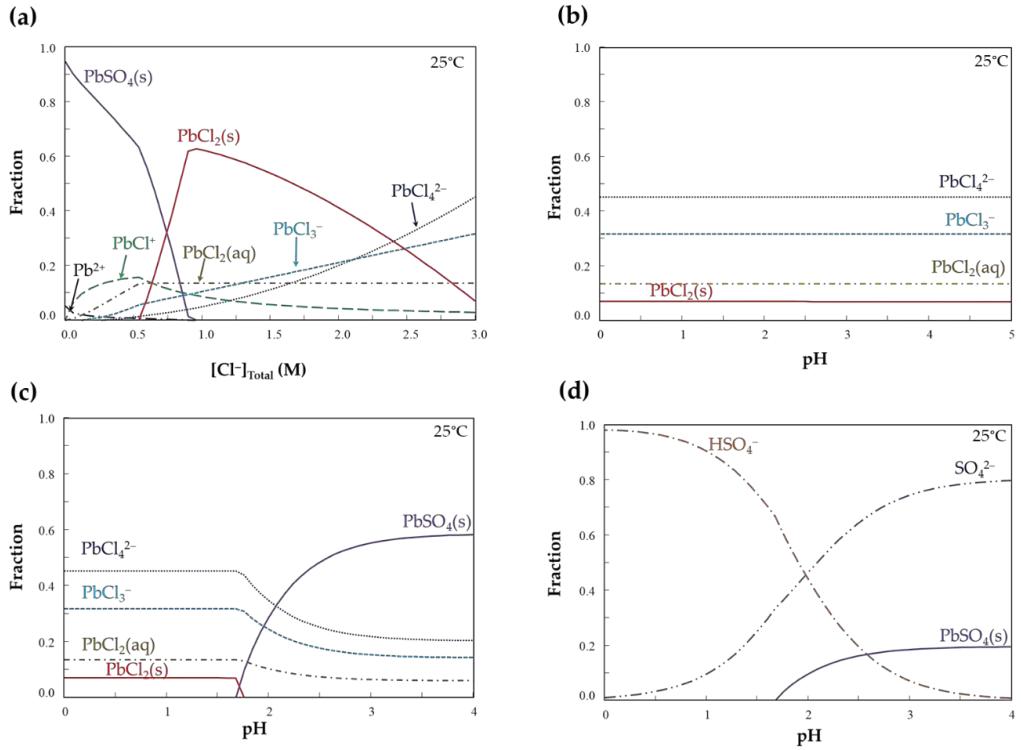

Figure 10. Thermodynamic calculation of dissolution of $PbSO_4$, speciation of Pb-Cl complexes, and SO_4^{2-} at (**a**) Pb^{2+} = 8 mM, SO_4^{2-} = 8 mM, pH = 1, (**b**) Pb^{2+} = 8 mM, SO_4^{2-} = 8 mM, Cl^- = 3 M, (**c**) Pb^{2+} = 8 mM, SO_4^{2-} = 24 mM, Cl^- = 3 M, and (**d**) Pb^{2+} = 8 mM, SO_4^{2-} = 12 mM, Cl^- = 3 M (created using the MEDUSA Ver. 1 software [33]).

The addition of ZVAl during leaching of ZPLRs significantly increased the Pb removal even at low NaCl concentration especially when HCl was increased from 0.01 to 0.05 and 0.1 M (Figure 9). For example, while maintaining HCl at 0.05 M, the addition of ZVAl during ZPLRs leaching increased the Pb removal from 2.5% to 35.5% and 8% to 57% for 0.5 and 1 M NaCl concentration, respectively. Meanwhile, for 0.1 M HCl, the addition of ZVAl during ZPLRs leaching increased the Pb removal from 3% to 69% and 9% to 72% for 0.5 and 1 M NaCl concentration, respectively. The dramatic increase of Pb removal at low NaCl concentration is attributed to the leaching solution not attaining saturated with dissolved Pb^{2+} and Pb-Cl complexes. In other words, when ZVAl was added during ZPLRs leaching, dissolved soluble Pb^{2+} and Pb-Cl complexes were simultaneously sequestered from the

solution by cementation, hence, more Pb could dissolve from the host minerals (e.g., $PbSO_4$), as well as the conversion of intermediate sparingly soluble solid, $PbCl_2$, to more Pb-Cl complexes (Figure 11a,b).

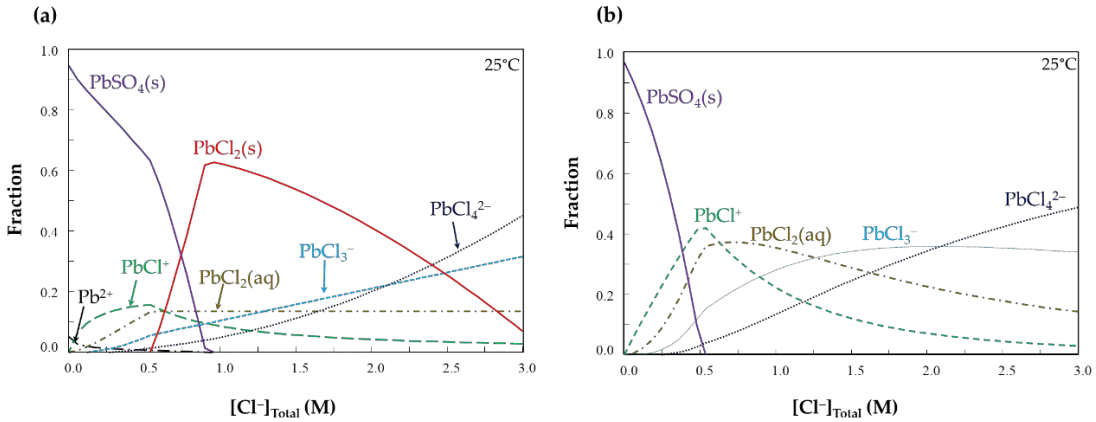

Figure 11. Effects of Pb^{2+} concentration on solubility and speciation of Pb^{2+} and Pb-Cl complexes in the lead-chloride-sulfate-water system under the condition (**a**) Pb^{2+} = 8 mM, SO_4^{2-} = 8 mM, pH = 1, and (**b**) Pb^{2+} = 1 mM, SO_4^{2-} = 8 mM, pH = 1.

Zinc removal was, however, independent of the increase of NaCl concentration, as well as the addition of ZVAl but it increased when the HCl concentration increased, as shown in Figure 12. When HCl increased from 0.01 to 0.05 and 0.1 M, Zn removal increased from around 27% to 60% and 70%, respectively. Increasing HCl concentration increased the H^+ concentration, which in turn increased Zn solubilization from minerals in ZPLRs by an H^+ attack mechanism (e.g., dissolution of Zn associated with amorphous iron oxyhydroxide phase fraction as determined elsewhere [34]). Zinc removal was not affected by the NaCl concentration. Unlike Pb that forms an intermediate solid ($PbCl_2$) at low chloride concentration and dissolves as the chloride concentration increases, Zn does form solid Zn-Cl species, and it does not complex strongly with chloride. Additionally, Zn removal was not affected by the addition of ZVAl because it was not sequestered (remained in solution) from the solution, as previously discussed. Since Zn was not be recovered by cementation using ZVAl from the leaching pulp, methods such as precipitation as ZnS [35] or electrowinning [36] can be employed to recover Zn from the solution. Unfortunately, these methods are beyond the scope of this study.

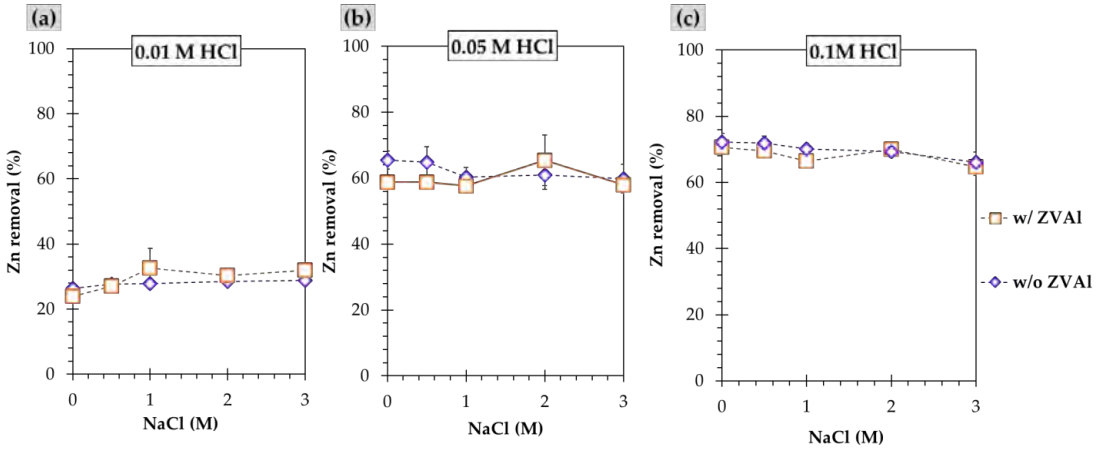

Figure 12. Effects of solution compositions on Zn removal from ZPLRs with and without ZVAl addition: (**a**) 0.01 M HCl and 0–3 M NaCl, (**b**) 0.05 M HCl and 0–3 M NaCl, and (**c**) 0.1 M HCl and 0–3 M NaCl.

3.3. Leachability of Lead and Zinc after Concurrent Dissolution-Cementation

To evaluate if the solid residues generated after treatment by concurrent dissolution-cementation meet environmental standards, the leachability of Pb and Zn using TCLP was examined out. The amounts of Pb and Zn leached before (untreated ZPLRs) and after treatment (treated by combined dissolution-cementation technique under the conditions 0.1 M HCl, 2 M NaCl, and 0.1 g ZVAl) were compared with the regulatory thresholds. As illustrated in Table 2, the levels of Pb and Zn that leached from untreated ZPLRs were substantially high: Pb was higher than environmental standards. In contrast, the amounts of Pb and Zn that leached from the residues after treatment by the concurrent dissolution-cementation method were dramatically lower. Leachable Pb (which was about 0.12 mg/L) was lower than the regulatory threshold, which entails the detoxification of ZPLRs.

Table 2. Toxicity characteristic leaching procedure (TCLP) leachability tests of untreated ZPLRs and treated residues after concurrent dissolution and cementation treatment.

Element	Untreated ZPLRs	Treated Residues	Threshold (USEPA)
Pb	12.95 mg/L	0.12 mg/L	5 mg/L
Zn	473.5 mg/L	21.5 mg/L	–*

* No Zn TCLP regulatory threshold.

3.4. Conceptual Flowsheet

Based on the results obtained in this study, the conceptual flowsheet for ZPLRs treatment by a concurrent dissolution-cementation technique to remove/recover Pb and Zn by using the HCl–NaCl solution with ZVAl is proposed (Figure 13). The flowsheet involves the removal of Pb—more toxic heavy metal to human beings than Zn—by cementation using ZVAl before solid-liquid separation. The Zn that remains in a solution can be recovered by precipitation or electrowinning. High removal of Pb and Zn can be achieved using a less concentrated NaCl (even as low as 1 M) solution acidified with 0.1 M HCl by the addition of ZVAl. The generated solid residues may not necessarily need to be washed because the most toxic metal that remains in the solution as a result of the inherent incomplete solid-liquid separation is negligible. In addition, this approach shortens and simplifies the treatment of ZPLRs compared to the conventional approach (i.e., leach, solid-liquid separation, and finally recovery of dissolved metals).

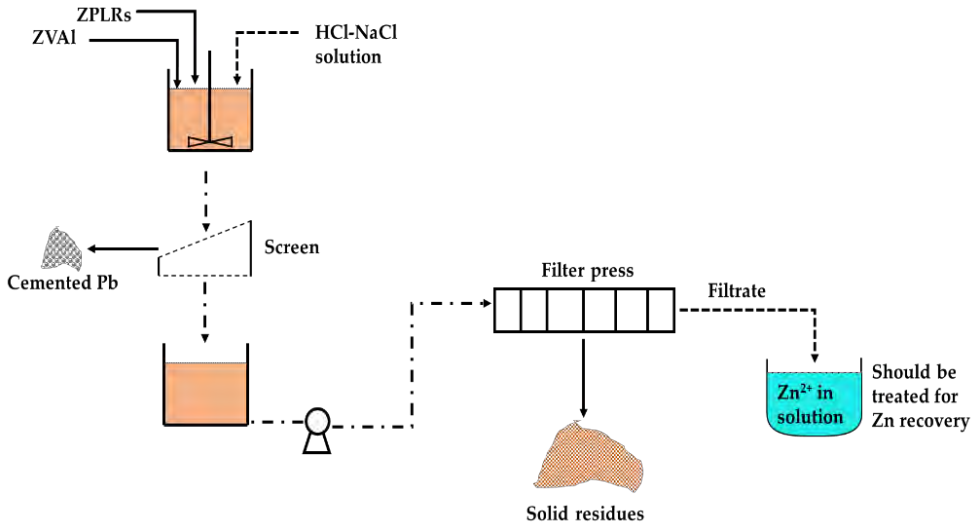

Figure 13. A conceptual flowsheet of the treatment of ZPLRs using the concurrent dissolution-cementation technique.

4. Conclusions

This study investigated Pb and Zn removal from ZPLRs using a concurrent dissolution-cementation technique in acidified chloride solution. The following is a summary of the findings:

1. Zinc removal from ZPLRs increased with increasing the HCl concentration (i.e., increased from 27% to 60% and 70% when the HCl concentration increased from 0.01 to 0.05 and 0.1 M, respectively) but it was neither affected by the increase of NaCl concentration nor the addition of ZVAl during leaching;
2. Zinc was not to be sequestered from the acidified chloride leaching pulp by cementation using ZVAl and was attributed to the dissolution of cemented Zn or preferential reduction of H^+ to H_2 by ZVAl over Zn^{2+} to Zn;
3. Lead removal from ZPLRs without the addition of ZVAl increased with increasing NaCl and HCl concentrations. Pb removal steadily increased from around 0% to 28%, 0.5% to 58%, and 0.5% to 72% for 0.01, 0.05, and 0.1 M HCl, respectively, when NaCl increased from 0 to 3 M, respectively. The increase of Pb removal with HCl concentration was attributed to an H^+ attack to dissolve Pb from carbonates, as well as fixing free SO_4^{2-} as HSO_4^-, thereby, limiting the precipitation/formation of solid $PbSO_4$. Meanwhile, Pb removal increased at higher NaCl concentrations because of the formation of more soluble Pb-Cl complexes;
4. The addition of ZVAl during ZPLRs leaching (concurrent dissolution-cementation technique) dramatically increased the Pb removal even at low chloride concentration. Pb removal at 0.05 M HCl increased from 2.5% to 35.5% and 8% to 57% for 0.5 and 1 M NaCl concentration, respectively. Meanwhile, for 0.1 M HCl, the addition of ZVAl during ZPLRs leaching increased the Pb removal from 3% to 69% and 9% to 72% for 0.5 and 1 M NaCl concentration, respectively. The increase was attributed to shifting the equilibrium as the result of sequestration of dissolved Pb, thereby, enhancing dissolution of lead host minerals and dissolution of intermediate sparling soluble solid, $PbCl_2$; and
5. The most toxic metal, Pb, from ZPLRs was recovered and separated before solid-liquid separation, which simplifies the treatment flowsheet, as well as eliminates the need for extensive washing of the solid residues generated.

Supplementary Materials: The following are available online at http://www.mdpi.com/2075-4701/10/4/531/s1, Figure S1: log–log activity of Pb^{2+} and Cl^- at 25 °C, 1.013 bars, and $CO_3^{2-} = 10^{-5}$ M for (a) pH 4, (b) pH 2, and (c) pH 1 for 0.01, 0.05, and 0.1 M HCl (created using the Geochemist's Workbench® with the MINTEQ database). Figure S2: XRD pattern of (a) ZPLRs before being treated and (b) the residues obtained after treating ZPLRs by the concurrent dissolution-cementation technique in the solution composed of 3 M NaCl and 0.05 M HCl.

Author Contributions: Conceptualization, M.S.; methodology, M.S., T.F., and R.H.; formal analysis, M.S., M.I. (Mayumi Ito), N.H., S.J., I.P., and C.B.T.; investigation, M.S.; writing—original draft preparation, M.S.; writing—review and editing, M.S., M.I. (Mayumi Ito), N.H., C.B.T., S.J., I.P., K.B., M.C., I.N., T.S., and T.I.; supervision, M.I. (Mayumi Ito) and N.H.; project administration, M.I. (Mayumi Ishizuka), S.N., and H.N.; funding acquisition, M.I. (Mayumi Ishizuka), S.N., and H.N. All authors have read and agreed to the published version of the manuscript.

Funding: This work was supported partly by the Japan Science and Technology Agency (JST), and Science and Technology Research Partnership for Sustainable Development (SATREPS), under grant number JPMJSA1505.

Conflicts of Interest: The authors declare no conflict of interest.

References

1. Backman, C.-M. Global Supply and Demand of Metals in the Future. *J. Toxicol. Environ. Health Part A* **2008**, *71*, 1244–1253. [CrossRef]
2. Halada, K.; Shimada, M.; Ijima, K. Forecasting the Consumption of Metals up to 2050. *J. Jpn. Inst. Met.* **2007**, *71*, 831–839. [CrossRef]
3. Tabelin, C.B.; Igarashi, T.; Villacorte-Tabelin, M.; Park, I.; Opiso, E.M.; Ito, M.; Hiroyoshi, N. Arsenic, selenium, boron, lead, cadmium, copper, and zinc in naturally contaminated rocks: A review of their sources, modes

of enrichment, mechanisms of release, and mitigation strategies. *Sci. Total Environ.* **2018**, *645*, 1522–1553. [CrossRef]
4. Mohr, S.; Giurco, D.; Retamal, M.; Mason, L.; Mudd, G. Global Projection of Lead-Zinc Supply from Known Resources. *Resources* **2018**, *7*, 17. [CrossRef]
5. Park, I.; Tabelin, C.B.; Jeon, S.; Li, X.; Seno, K.; Ito, M.; Hiroyoshi, N. A review of recent strategies for acid mine drainage prevention and mine tailings recycling. *Chemosphere* **2019**, *219*, 588–606. [CrossRef]
6. Igarashi, T.; Herrera, P.S.; Uchiyama, H.; Iyatomi, N.; Hashimoto, K.; Tabelin, C.B. The two-step neutralization ferrite-formation process for sustainable acid mine drainage treatment: Removal of copper, zinc and arsenic, and the influence of coexisting ions on ferritization. *Sci. Total Environ.* **2020**, *715*, 136877. [CrossRef]
7. Aikawa, K.; Ito, M.; Segawa, T.; Jeon, S.; Park, I.; Tabelin, C.B.; Hiroyoshi, N. Depression of lead-activated sphalerite by pyrite via galvanic interactions: Implications to the selective flotation of complex sulfide ores. *Miner. Eng.* **2020**, *152*, 106367. [CrossRef]
8. Behnajady, B.; Moghaddam, J.; Behnajady, M.A.; Rashchi, F. Determination of the optimum conditions for the leaching of lead from zinc plant residues in NaCl–H_2SO_4–$Ca(OH)_2$ media by the Taguchi method. *Ind. Eng. Chem. Res.* **2012**, *51*, 3887–3894. [CrossRef]
9. Hyk, W.; Kitka, K.; Rudnicki, D. Selective recovery of zinc from metallurgical waste materials from processing zinc and lead ores. *Molecules* **2019**, *24*, 2275. [CrossRef]
10. Guo, Z.; Pan, F.; Xiao, X.; Zhang, L.; Jiang, K. Optimization of brine leaching of metals from hydrometallurgical residue. *Trans. Nonferr. Met. Soc. China* **2010**, *20*, 2000–2005. [CrossRef]
11. Sethurajan, M.; Huguenot, D.; Jain, R.; Lens, P.N.L.; Horn, H.A.; Figueiredo, L.H.A.; van Hullebusch, E.D. Leaching and selective zinc recovery from acidic leachates of zinc metallurgical leach residues. *J. Hazard. Mater.* **2017**, *324*, 71–82. [CrossRef] [PubMed]
12. Ruşen, A.; Sunkar, A.S.; Topkaya, Y.A. Zinc and lead extraction from Çinkur leach residues by using hydrometallurgical method. *Hydrometallurgy* **2008**, *93*, 45–50. [CrossRef]
13. Ru, Z.; Pan, C.; Liu, G.; Wang, X.; Dou, G.; Zhu, K. Leaching and recovery of zinc from leaching residue of zinc calcine based on membrane filter press. *Trans. Nonferr. Met. Soc. China* **2015**, *25*, 622–627. [CrossRef]
14. Tabelin, C.B.; Hashimoto, A.; Igarashi, T.; Yoneda, T. Leaching of boron, arsenic and selenium from sedimentary rocks: I. Effects of contact time, mixing speed and liquid-to-solid ratio. *Sci. Total Environ.* **2014**, *472*, 620–629. [CrossRef]
15. Needleman, H. Lead poisoning. *Annu. Rev. Med.* **2004**, *55*, 209–222. [CrossRef]
16. Tabelin, C.B.; Igarashi, T.; Tamoto, S.; Takahashi, R. The roles of pyrite and calcite in the mobilization of arsenic and lead from hydrothermally altered rocks excavated in Hokkaido, Japan. *J. Geochem. Explor.* **2012**, *119*, 17–31. [CrossRef]
17. Li, Y.; Yang, S.; Lin, W.; Taskinen, P.; He, J.; Wang, Y.; Chen, Y.; Tang, C.; Jokilaakso, A. Cleaner extraction of lead from complex lead-containing wastes by reductive sulfur-fixing smelting with low SO_2 emission. *Minerals* **2019**, *9*, 119. [CrossRef]
18. Rämä, M.; Nurmi, S.; Jokilaakso, A.; Klemettinen, L.; Taskinen, P.; Salminen, J. Thermal processing of jarosite leach residue for a safe disposable slag and valuable metals recovery. *Metals* **2018**, *8*, 744. [CrossRef]
19. Yang, S.; Zhao, D.; Jie, Y.; Tang, C.; He, J.; Chen, Y. Hydrometallurgical process for zinc recovery from C.Z.O. generated by the steelmaking industry with ammonia–ammonium chloride solution. *Metals* **2019**, *9*, 83. [CrossRef]
20. Farahmand, F.; Moradkhani, D.; Safarzadeh, M.S.; Rashchi, F. Brine leaching of lead-bearing zinc plant residues: Process optimization using orthogonal array design methodology. *Hydrometallurgy* **2009**, *95*, 316–324. [CrossRef]
21. Thao, N.T.; Tsuji, S.; Jeon, S.; Park, I.; Ito, M.; Hiroyoshi, M. Redox potential-dependent chalcopyrite leaching in acidic ferric chloride solutions: Leaching experiments. *Hydrometallurgy* **2020**. [CrossRef]
22. Choi, S.; Yoo, K.; Alorro, R.D.; Tabelin, C.B. Cementation of Co ion in leach solution using Zn powder followed by magnetic separation of cementation-precipitate for recovery of unreacted Zn powder. *Miner. Eng.* **2020**, *145*, 106061. [CrossRef]
23. Calderon, A.R.M.; Alorro, R.D.; Tadesse, B.; Yoo, K.; Tabelin, C.B. Evaluation of maghemite-rich iron oxide composite prepared from magnetite as adsorbent for gold from chloride solution. *JOM* **2019**, *71*, 4639–4646. [CrossRef]

24. Bodas, M.G. Hydrometallurgical treatment of zinc silicate ore from Thailand. *Hydrometallurgy* **1996**, *40*, 37–49. [CrossRef]
25. He, S.; Wang, J.; Yan, J. Pressure leaching of synthetic zinc silicate in sulfuric acid medium. *Hydrometallurgy* **2011**, *108*, 171–176. [CrossRef]
26. United States Environmental Protection Agency (U.S. EPA). *Toxicity Characteristic Leaching Procedure (TCLP), Test Method 1311- TCLP*; US Environmental Protection Agency: Washington, DC, USA, 1991.
27. Feng, Q.; Wen, S.; Wang, Y.; Zhao, W.; Liu, J. Dissolution kinetics of cerussite in acidic sodium chloride solutions. *Bull. Korean Chem. Soc.* **2015**, *36*, 1100–1107.
28. Liu, W.; Yang, T.; Xia, X. Behavior of silver and lead in selective chlorination leaching process of gold-antimony alloy. *Trans. Nonferr. Met. Soc. China* **2010**, *20*, 322–329. [CrossRef]
29. Xie, H.; Zhang, L.; Li, H.; Li, H.; Koppala, S.; Yin, S.; Li, S.; Yang, K.; Zhu, F. Efficient recycling of Pb from zinc leaching residues by using the hydrometallurgical method. *Mater. Res. Express* **2019**, *6*, 075505. [CrossRef]
30. Seng, S.; Tabelin, C.B.; Kojima, M.; Hiroyoshi, N.; Ito, M. Galvanic microencapsulation (GME) using zero-valent aluminum and zero-valent iron to suppress pyrite oxidation. *Mater. Trans.* **2019**, *60*, 277–286. [CrossRef]
31. Jeon, S.; Tabelin, C.B.; Takahashi, H.; Park, I.; Ito, M.; Hiroyoshi, N. Enhanced cementation of gold via galvanic interactions using activated carbon and zero-valent aluminum: A novel approach to recover gold ions from ammonium thiosulfate medium. *Hydrometallurgy* **2020**, *191*, 105165. [CrossRef]
32. St-Pierre, J.; Piron, D.L. Electrowinning of zinc from alkaline solutions. *J. Appl. Electrochem.* **1986**, *16*, 447–456. [CrossRef]
33. Puigdomenech, I. *Make Equilibrium Diagrams Using Sophisticated Algorithms (MEDUSA), Inorganic Chemistry*; Royal Institute of Technology: Stockholm, Sweden, 2010.
34. Silwamba, M.; Ito, M.; Fukushima, T.; Tabelin, C.B.; Takakuwa, S.; Hiroyoshi, N.; Chirwa, M.; Banda, K.; Nyambe, I. Characterization of zinc leaching residue in Kabwe area, Zambia. In Proceedings of the 2nd International Kabwe Mine Pollution Amelioration Initiative (KAMPAI)/JST, Lusaka, Zambia, 12 August 2018; p. 22.
35. Ye, M.; Li, G.; Yan, P.; Zheng, L.; Sun, S.; Huang, S.; Li, H.; Chen, Y.; Yang, L.; Huang, J. Production of lead concentrate from bioleached residue tailings by brine leaching followed by sulfide precipitation. *Sep. Purif. Technol.* **2017**, *183*, 366–372. [CrossRef]
36. Tuffrey, N.E.; Jiricny, V.; Evans, J.W. Fluidized bed electrowinning of zinc from chloride electrolytes. *Hydrometallurgy* **1985**, *15*, 33–54. [CrossRef]

Environmental Research 188 (2020) 109759

Contents lists available at ScienceDirect

Environmental Research

journal homepage: www.elsevier.com/locate/envres

Blood lead levels and aberrant DNA methylation of the ALAD and p16 gene promoters in children exposed to environmental-lead

Yared B. Yohannes[a,b], Shouta MM. Nakayama[a], John Yabe[c], Hokuto Nakata[a], Haruya Toyomaki[a], Andrew Kataba[a,c], Kaampwe Muzandu[c], Yoshinori Ikenaka[a], Kennedy Choongo[c], Mayumi Ishizuka[a,*]

[a] Laboratory of Toxicology, Department of Environmental Veterinary Sciences, Faculty of Veterinary Medicine, Hokkaido University, Sapporo, Japan
[b] Department of Chemistry, College of Natural and Computational Science, University of Gondar, Gondar, Ethiopia
[c] School of Veterinary Medicine, The University of Zambia, Lusaka, Zambia

ARTICLE INFO

Keywords:
Lead
DNA methylation
ALAD
p16
Children

ABSTRACT

Background: Lead (Pb) is a well-known toxic heavy metal which can have serious public health hazards. As of today, there is no safe threshold for Pb exposure, especially for children. Lead exposure has been associated with adverse health outcomes involving epigenetic mechanisms, such as aberrant DNA methylation. The objective of the present study was to elucidate the associations between blood lead levels (BLLs) and gene-specific promoter DNA methylation status in environmental Pb-exposed children from Kabwe, Zambia.

Methods: A cross-sectional study was conducted using 2 to 10-year-old children from high Pb exposed area (N = 102) and low Pb exposed area (N = 38). We measured BLLs using a LeadCare II analyzer and investigated the methylation status of the ALAD and p16 gene promoters by methylation–specific PCR.

Results: The mean BLLs were 23.7 μg/dL and 7.9 μg/dL in high Pb exposed and low Pb exposed children, respectively. Pb exposure was correlated with increased methylation of the ALAD and p16 genes. The promoter methylation rates of ALAD and p16 in high Pb exposed children were 84.3% and 67.7%, and 42.1% and 44.7% in low Pb exposed children, respectively. Significantly increased methylation was found in both genes in high Pb exposed children compared with low Pb exposed children ($p < 0.05$). Children with methylated ALAD and p16 genes showed an increased risk of Pb poisoning (odd ratio > 1) compared to the unmethylated status.

Conclusions: This study for the first time tries to correlate promoter methylation status of the ALAD and p16 genes in environmental Pb-exposed children from Kabwe, Zambia as a representative. The result suggests that Pb exposure increases aberrations in ALAD and p16 gene methylation, which may be involved in the mechanism of Pb toxicity.

1. Introduction

Lead (Pb) is one of the predominant environmental pollutants with no threshold level for its health effects (Vorvolakos et al., 2016). Lead does not have any essential physiological role in the human body and exposure to it can have a wide range of health effects such as cancer (Steenland and Boffeta, 2000), permanent damage to children's cognitive functioning (Canfield et al., 2003) and toxic effects on the hematopoietic, cardiovascular and renal system (Flora et al., 2012). Lead poisoning contributed to about 0.6% of the global burden of disease and childhood Pb exposure is still a significant public health problem, especially in developing countries (WHO, 2010). Several studies showed that children with blood lead levels (BLLs) < 10 μg/dL, which was previously thought to be safe, are at risk of decreased brain volume, reduced cognitive functioning and low IQ scores that persist into adulthood (Cecil et al., 2008; Canfield et al., 2003; Lanphear et al., 2005). Thus, in 2012 the Centers for Disease Control and Prevention set a blood Pb reference value of 5 μg/dL (CDC, 2012). Besides, there are evidences on both *in vitro* and *in vivo* studies that suggested epigenetics might mediate Pb toxicity by the alteration of the DNA methylation profile of the genome (Cortessis et al., 2012; Nye et al., 2015).

DNA methylation is the most widely studied epigenetic modification that involves in transcription regulation, and genomic stability (Jaenisch and Bird, 2003). Previous studies in humans have shown that

* Corresponding author. Laboratory of Toxicology, Department of Environmental Veterinary Sciences, Faculty of Veterinary Medicine, Hokkaido University, Kita 18, Nishi 9, Kita-ku, Sapporo, 060-0818, Japan.
E-mail address: ishizum@vetmed.hokudai.ac.jp (M. Ishizuka).

https://doi.org/10.1016/j.envres.2020.109759
Received 11 February 2020; Received in revised form 23 May 2020; Accepted 27 May 2020
Available online 05 June 2020
0013-9351/

environmental exposure can alter DNA methylation, which is linked to impacts on human health (Martin and Fry, 2018; Martinez-Zamudio and Ha, 2011). Especially in early life, the developing brain and nervous system are supposed to be more sensitive to toxic effects than the mature one (Cecil et al., 2008; Rice and Barone, 2000). Aberrant DNA methylation comprises gene-specific hypermethylation, which is associated with gene repression and global hypomethylation, a prelude to structural changes in chromosomes (Baylin and Ohm, 2006; Ushijima et al., 2006). Lead, a "probable" human carcinogen (IARC, 2006), is a prevalent toxic metal that can alter both global and gene-specific DNA methylation (Kovatsi et al., 2010; Li et al., 2011, 2014; Pilsner et al., 2009; Wright et al., 2010).

Hematopoietic system is one of the targets of Pb poisoning since most of the Pb accumulates in erythrocytes (Onalaja and Claudio, 2000). Lead can inhibit the δ-aminolevulinic acid dehydratase (ALAD) activity in heme synthesis and results in the accumulation of δ-aminolevulinic acid (ALA), which is associated with oxidative damage by causing formation of reactive oxygen species (Ahamed et al., 2006; Martinez et al., 2013). Thus, ALAD activity is considered as a valuable indicator for early Pb effect and a biomarker of oxidative stress in the Pb-exposed hematological system (Gurer-Orhan et al., 2004). To date, there is only one study that showed an association between ALAD CpG hypermethylation with an increased risk of Pb poisoning in Pb-exposed workers (Li et al., 2011). Another gene that is affected by Pb is the tumor suppressor gene p16. It is one of the most extensively studied genes due to its critical roles in cell cycle progression (Sherr and Roberts, 2004) and development of cancers in humans (Herman et al., 1995).

Kabwe town is the capital of the Zambian Central Province with a population estimated at 230,000. The town is ranked among "The 10 World's most polluted places" (Blacksmith Institute, 2013) due to the long history of Pb–Zn mine that operated without adequate environmental pollution regulations for almost a century. However, despite the mine being closed over 25 years ago, the site left the city with alarming concentrations of toxic Pb in the soil. Recent studies have shown evidence of childhood Pb poisoning in Kabwe, with up to 427 μg/dL (Yabe et al., 2015, 2020). However, to date, no data exist regarding the influence of environmental Pb exposure on DNA methylation levels in children from Kabwe.

Therefore, this cross-sectional study analyzed BLLs and its association with the promoter methylation of ALAD and p16 genes in children exposed to environmental Pb in Kabwe, Zambia. The association of promoter methylation of these genes with reported Pb-related clinical symptoms was also evaluated.

2. Material and methods

2.1. Study participants

The study was a community-based cross-sectional design that was undertaken in July 2016. Children, aged 2–10 years, were randomly chosen from five townships in Kabwe, Zambia, and invited to their respective local health centers (Fig. 1). Before sampling commenced, an awareness campaign about the research activities was conducted by community health workers in their catchment areas around the health centers. The parents or guardians of all children provided written informed consent. All parents/guardians were interviewed a short set of questions concerning a child's age, gender, place of residence, and Pb-related clinical symptoms such as anemia, insomnia, pain in joints, headache, fatigue, abdominal pain and memory problems.

The population used in this study consisted of 140 children from five townships and divided into 2 groups. Of the total number of children, 102 children resided near the closed mine; Chowa, Kasanda and Makululu townships (2–3 km from mine tailings) categorized as "high Pb exposed" children and 38 children living far from the mine; Bwacha and Nakoli townships (6–7 km from mine tailings) categorized as "low Pb exposed" children. Trained nurses performed the collection of children's blood samples. Approximately 3 mL of venous blood samples was collected from each child at their respective health centers.

2.2. Analysis of lead

BLLs were analyzed immediately up on collection using a LeadCare II analyzer (Magellan Diagnostics, USA) per manufacturer's instructions. The instrument was calibrated before each new lot of test supplies (every 48 tests). Two levels of blood Pb quality control samples, "level 1" and "level 2" were run to assess accuracy. Results of control samples were within the target ranges given by the manufacturer of 6.9–13.7 μg/dL for the level 1 (low) control and 21.8–32.6 μg/dL for the level 2 (high) control. The limits of detection for LeadCare II are 3.3–65 μg/dL. Thus, BLLs below 3.3 μg/dL (3/38 samples from low Pb exposed groups) were treated as 1.65 μg/dL for statistics. Blood samples were immediately stored at −20 °C after Pb analysis and the frozen samples were transported to Japan for biological analysis after obtaining a material transfer agreement (MTA, Approval No. E00417) from the Ministry of Health, Zambia.

2.3. DNA extraction, bisulfite modification, and methylation-specific polymerase chain reaction (MSP)

DNA extraction, bisulfite modification, and MSP were performed in the Laboratory of Toxicology, Faculty of Veterinary Medicine, Hokkaido University, Japan. Genomic DNA was extracted from 200 μL of blood using the NucleoSpin Blood Kit (Macherey-Nagel, Duren, Germany). Bisulfite modification of genomic DNA (1 μg) was performed using the EpiTect Bisulfite Kit (Qiagen, Hilden, Germany). Bisulfite conversion of DNA changes unmethylated cytosine to uracil whereas methylated cytosines remain intact.

The methylation analysis was conducted by the MSP assay. The bisulfite-modified DNA was amplified with two primer pairs specific for methylated (M) and unmethylated (U) alleles. The primers for the ALAD gene were designed using MethPrimer (Li and Dahiya, 2002). M primers: 5′-ATAGCGGTGATAGGAGTAGCGGTC-3' (forward) and 5′-AAACGCACAACA CAATCTAAAAACG-3' (reverse); U primers: 5′-GGAGATAGTGGTGATAGGAGTAGT GGTT-3' (forward) and 5′-CAA ACACACAACACAATCTAAAAACA-3' (reverse). The primer sequences for p16 were as described previously (Herman et al., 1996). M primers: 5′-TTATTAGAGGGTGGGGCGGATCGC-3' (forward) and 5′-GACCCCGA ACCGCGACCG TAA-3′ (reverse); U primers: 5′-TTATTAGAGGGTGGG GTGGATTGT-3' (forward) and 5′-CAACCCCAAACCACAACCATAA-3' (reverse). MSP was performed with EpiScope MSP Kit (TaKaRa Bio, Tokyo, Japan). The PCR conditions were as follows: initial denature at 95 °C for 30 s, followed by 40 cycles of denaturation at 98 °C for 5 s, annealing at 60 °C for ALAD-M & -U; 62 °C for p16-M & -U for 30 s, and extension at 72 °C for 1 min. CpGenome universal methylated DNA (S7821) was used as a positive control for methylation while water used as a negative control. After amplification, PCR products were loaded onto a 2% agarose gel and visualized under UV elimination. Samples demonstrating methylation for each gene were repeated to confirm the results.

2.4. Statistical analysis

All statistical analyses were performed using JMP pro 14 (SAS Institute, Cary, NC, USA). Continuous variables were reported as means ± standard deviation (SD) while nominal data were expressed as percentages. The variable's distribution was assessed by Shapiro-wilk test and Levene's test was performed to assess the homogeneity of variance. Continuous variables were compared using the student *t*-test. The differences of the ALAD and p16 genes promoter methylation status between high Pb exposed and low Pb exposed groups were analyzed using a Pearson chi-square exact test. Crude and adjusted odds ratios

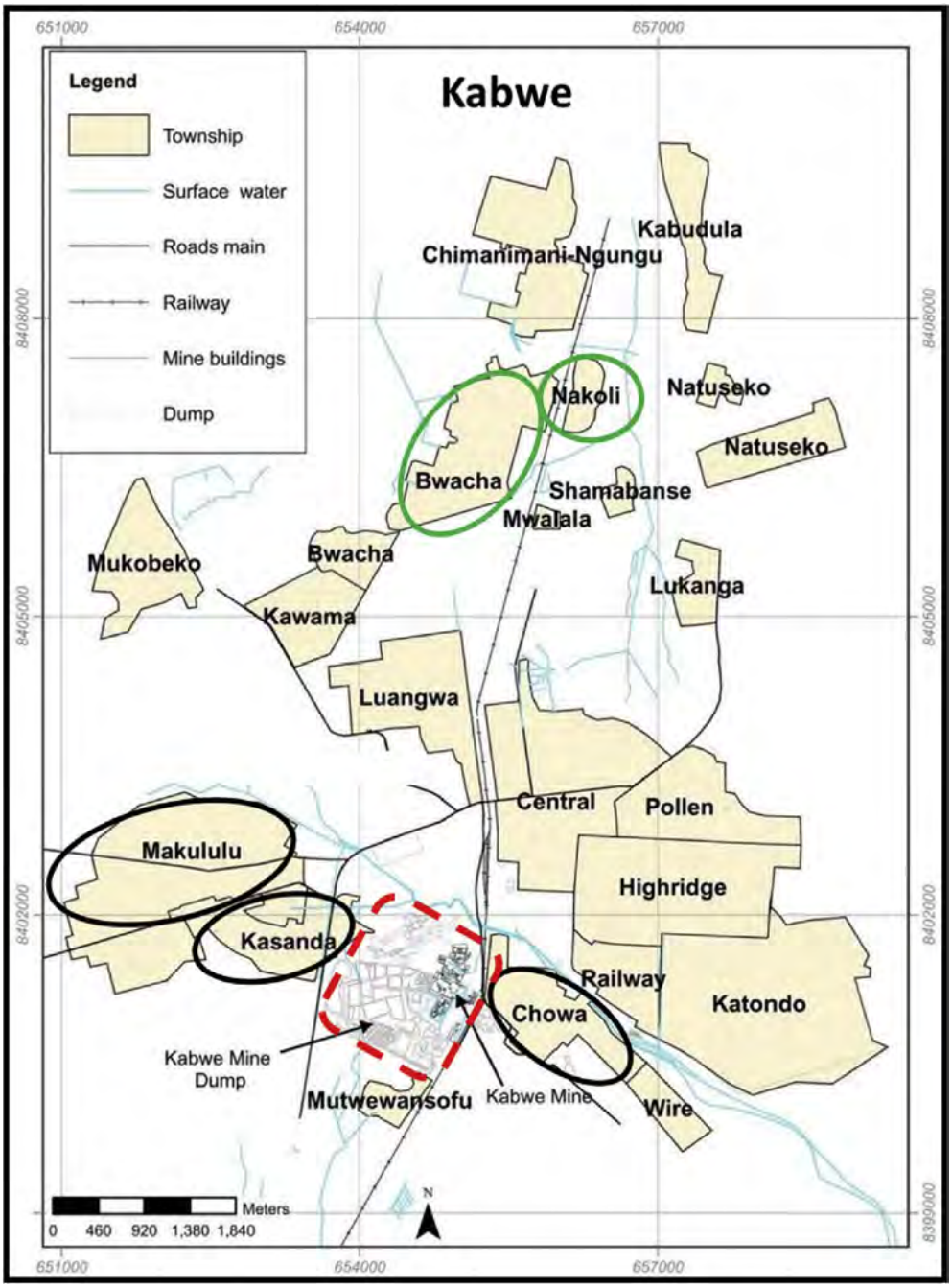

Fig. 1. Location of the Pb–Zn mine (in red color) and sampling townships in Kabwe, Zambia (Source: Joseph Makumba/ZCCM-IH). (For interpretation of the references to color in this figure legend, the reader is referred to the Web version of this article.)

(ORs) with their corresponding 95% confidence intervals (95% CIs) were obtained to assess the association of ALAD and p16 gene promoters hypermethylation with the risk of Pb poisoning using the logistic regression model stratified by residential area and adjusted for age and sex. BLLs were divided into quartiles [quartile 1 (Q1): $x \leq 10$ μg/dL; quartile 2 (Q2):$10 < x \leq 19$ μg/dL; quartile 3 (Q3): $19 < x \leq 25$ μg/dL; quartile 1 (Q4): $x > 25$ μg/dL] and the influence of Pb exposure level on ALAD and p16 genes promoter methylation status was assessed using chi-square test. Then we conducted a non-parametric pairwise multiple comparison between BLLs quartiles and methylation status using the first quartile as a reference value. ORs and their 95% CIs were estimated as a measure of association of ALAD and p16 genes promoter methylation status with reported Pb-related clinical symptoms without Chowa samples (N = 32), which had incomplete questionnaire data. In all analysis, $p < 0.05$ was considered to indicate a statistically significant difference.

3. Results

3.1. Characteristics of the study participants and BLL

Table 1 provides demographic and biological characteristics of the children. A total of one hundred and forty children, 65 females and 75 males in the relative age between 2 and 10 years, were recruited for this study. There is no significant difference in sex distribution between the two groups. Most of the children are born in Kabwe and resided in their respective townships for most of their lifetime. The average ages of the participants were 5.9 ± 1.88 and 5.1 ± 1.68 years in high exposed

Table 1
Characteristics and BLLs of children by area.

Variables[c]	Participants in high exposed area*	p[a]	Participants in low exposed area*	p[a]	p[b]
Total participants (N)	102		38		
Age (mean ± SD, years) [range]	5.9 ± 1.88 [2–10] <		5.1 ± 1.68 [2–8]		
Sex Male [N (%)]	53 (51.9)		21 (55.2)		
Female [N (%)]	49 (48.1)		17 (44.8)		
BLLs (mean ± SD, μg/dL) [range]	23.7 ± 9.01 [7.80–60.8]		7.9 ± 4.51 [1.65–22.5]		< 0.001
BLLs by sex Male	22.3 ± 6.75	0.132	8.34 ± 4.49	0.563	
Female	25.4 ± 10.8		7.47 ± 4.61		

$p < 0.05$ is considered statistically significant.
*High exposed area: Chowa, Kasanda and Makululu townships; Low exposed area: Bwacha and Nakoli townships.
[a] p value for difference in BLL between male and female in the same area.
[b] p value for difference in BLL between high Pb exposed area and low Pb exposed area.
[c] Continuous variables are expressed as mean ± SD [range].

children (Chowa, Kasanda and Makululu townships; near the closed mine) and low exposed children (Bwacha and Nakoli townships; far from the closed mine), respectively.

The BLLs among the study children ranged from 1.65 to 60.8 μg/dL as shown in Table 1. A significantly higher BLL (23.7 ± 9.01 μg/dL) was observed in the high Pb exposed children as compared to the low Pb exposed children (7.9 ± 4.51 μg/dL). All blood samples in high Pb exposed children exceeded the CDC blood Pb reference value of 5 μg/dL. There was no gender difference in BLLs between boys and girls in the same area, showing equal exposure extent.

3.2. Methylation status of ALAD and p16 genes among the study subjects

MSP was employed to assess ALAD and p16 promoter hypermethylation. The methylation frequencies of ALAD and p16 genes and their association with the risk of Pb poisoning are summarized in Table 2. The methylation frequencies for both genes showed a significant difference between the areas. Aberrant methylation of the ALAD gene observed in 86 out of 102 (84.3%) high Pb exposed children while the incidence of hypermethylation in low Pb exposed children was 42.1% (16 of 38). This result demonstrates that the ALAD gene was significantly hypermethylated in high Pb exposed children compared to low Pb exposed children ($p < 0.001$). The methylated ALAD gene was associated with an increased risk of Pb poisoning (Adjusted OR = 7.84, 95% CI: 3.22–19.07; $p < 0.001$) compared with the unmethylated status.

A statistically significant (p = 0.015) difference in the hypermethylation of the p16 gene was also observed (Table 2). The profile of p16 methylation showed that 69 out 102 children (67.7%) in high Pb exposed area and 17 out of 38 children (44.7%) from low Pb exposed area presented hypermethylation of the gene. Moreover, the methylated p16 gene was associated with an increased risk of Pb poisoning (p16: OR = 2.58, 95% CI: 1.20–5.53; $p = 0.015$).

3.3. Correlation between quartiles of BLLs and methylation status

Fig. 2 illustrates the potential effect of Pb levels on the extent of methylation. The relationships of ALAD and p16 genes methylation status with quartiles of BLLs were examined. There was a strong evidence for statistically significant association of the ALAD gene methylation with the quartiles of BLLs (chi-square test: $X^2 = 22.9$, df = 3, $p < 0.001$). Methylation frequency of the ALAD gene ranged from 42% in Q1 children with BLLs < 10 μg/dL to 90% in Q4 children with BLLs > 25 μg/dL regardless of their age and sex. Moreover, the effect of Pb exposure level using the Q1 as a reference value was investigated. The result showed that the ALAD gene methylation status was markedly increased as the quartiles of BLLs increased in a dose-dependent manner ($p < 0.001$). For the p16 gene, it showed an increment in methylation frequencies (48% in Q1 children with BLLs < 10 μg/dL to 72% in Q3 groups) as quartiles of BLLs increase, but not statistically significant (chi-square test: $X^2 = 3.22$, df = 3, $p = 0.358$).

3.4. Methylation status vs lead-related clinical symptoms

Moreover, we investigated associations between the methylation status of the target genes and reported Pb-related clinical symptoms (anemia, insomnia, pain in joints, headache, fatigue, abdominal pain and memory problems) (Fig. 3). We found odds ratio (OR) greater than 1 for some factors even though none of the variables displayed statistically significant association with either gene methylation. In the ALAD gene (Fig. 3a), anemia (OR = 4.12) and insomnia (OR = 3.72) showed high OR value with higher methylation of this gene, while headache (OR = 1.12) and memory problem (OR = 1.55) showed a marginal association. Analysis of the p16 gene showed a marginal association with anemia (OR = 1.41), pain in joints (OR = 1.19) and memory loss (OR = 1.33) (Fig. 3b).

Table 2
Methylation status of ALAD and p16 genes promoter in the study groups and their associations with the risk of lead poisoning.

Gene	Methylation status	High Pb exposed* (N = 102)		Low Pb exposed* (N = 38)		P#	Crude OR (95% CI)	p	Adjusted OR (95% CI)[a]	p
		N	%	N	%					
ALAD	Unmethylated	16	15.7	22	57.9	< 0.001	1.00	< 0.001	1.00	< 0.001
	Methylated	86	84.3	16	42.1		6.64 (2.88–15.27)		7.84 (3.22–19.07)	
p16	Unmethylated	33	32.3	21	55.3	0.015	1.00	0.015	1.00	0.044
	Methylated	69	67.7	17	44.7		2.58 (1.20–5.53)		2.24 (1.02–4.91)	
BLL (Mean ± SD)		23.7 ± 9.01		7.90 ± 4.51		< 0.001				

$P < 0.05$ is considered statistically significant.
N: sample number in each group; OR: odds ratio; CI: confidence interval.
*High Pb exposed: Chowa, Kasanda and Makululu townships; Low Pb exposed: Bwacha and Nakoli townships.
#Pearson Chi-square ($\chi 2$) exact test for methylation distribution frequency.
[a] Obtained from logistic regression models with adjustment for sex and age.

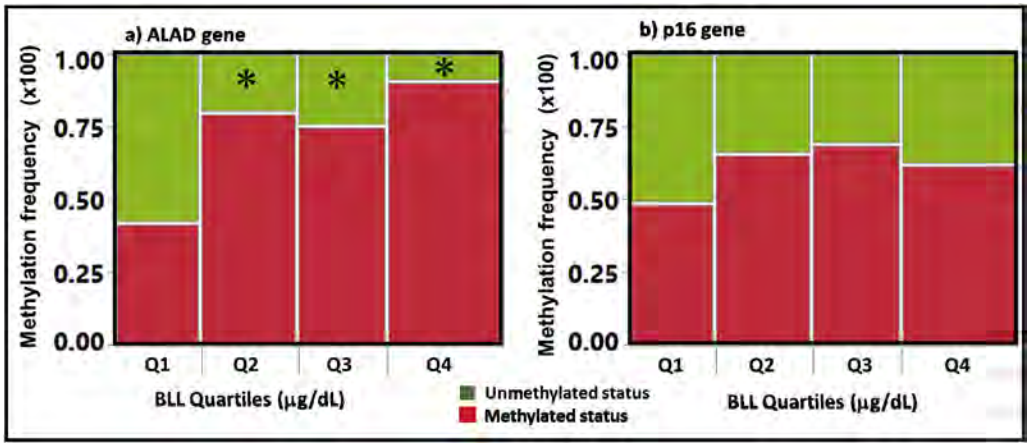

Fig. 2. Mosaic plots for ALAD and p16 genes methylation status with BLL quartiles (Q1: x ≤ 10 µg/dL; Q2:10 < x ≤ 19 µg/dL; Q3: 19 < x ≤ 25 µg/dL; Q4: x > 25 µg/dL). *p < 0.01: Dunn's nonparametric multiple comparison test using Q1 as a reference category.

4. Discussion

The toxicology of Pb has been widely studied for centuries and the issue of Pb carcinogenicity is of great current interest in science and public health policy (Wani et al., 2015). Despite laws and significant efforts to eliminate Pb in the environment, toxic levels of Pb are still a big concern, especially in developing countries. Increasing epidemiologic and experimental evidence indicates that Pb exposure is associated with DNA methylation and affects health outcomes. However, to date, few studies have assessed the associations between DNA methylation and Pb exposure. If available, most studies have been conducted on global genomic methylation, such as measuring Alu or long interspersed nuclear elements-1 (LINE-1) (Pilsner et al., 2009; Wright et al., 2010). To our knowledge, this is the first study evaluating the association between BLLs and aberrant ALAD and p16 genes methylation status in environmental Pb-exposed children.

The BLL was high in the three townships near the mine and reached a maximum level of 60.8 µg/dL. There was no gender difference in BLLs between boys and girls, which shows an equal exposure extent. Compared to the CDC concern of level i.e., 5 µg/dL, 92% of the participants had exceeded this value. To date, only a few studies have been undertaken on Pb exposure in the Kabwe population. In a group of children under the age of 7 years, BLL up to 427 µg/dL was recorded and almost all the sampled children had BLLs exceeding 10 µg/dL (Yabe et al., 2015). Another study from the same area showed that BLLs in children ranged from 1.65 to 162 µg/dL and about 80% of the children had a BLL greater the concern level (Yabe et al., 2020). These incidents showed that Pb poisoning among children in Kabwe is extensive. Thus, urgent interventions should be required to reduce Pb exposure in the affected townships.

Aberrant DNA methylation patterns of CpG islands are associated with gene inactivation and play vital roles in the development of diseases (Jin and Liu, 2018). The present study showed a significant increase in ALAD and p16 CpG methylation levels in children from high Pb exposed areas relative to the low Pb exposed areas. It is well known that ALAD activity can be inhibited by Pb, and this inhibition has become one of the most sensitive diagnostic indicators of Pb exposure (Gurer-Orhan et al., 2004; Sakai and Morita, 1996). Lead inhibition of ALAD activity results in the accumulation of δ-aminolevulinic acid, which is associated with oxidative DNA damage through the formation of reactive oxygen species (Ahamed et al., 2006; Martinez et al., 2013). Although genetic susceptibility related to ALAD polymorphism is a possible mechanism for the toxicity of Pb, no correlation of epigenetic changes in the ALAD gene and environmental Pb exposure has yet been elucidated. To our knowledge, no other study has examined ALAD methylation in environmental Pb-exposed children. In this study, the methylated ALAD gene showed a significant risk of Pb poisoning (OR = 7.84, 95% CI, 3.22–19.07) compared to unmethylated status. In a previous case-control study based on occupational Pb exposure, a significant increase in ALAD CpG methylation levels was detected in adult exposed workers relative to unexposed workers (Li et al., 2011). Furthermore, in the same study, they confirmed that the CpG methylation of the ALAD promoter plays a functional role in regulating ALAD transcription. These results suggest that besides inhibiting ALAD enzyme activity, Pb could result in cell toxicity by increasing the level of ALAD methylation and thus decreasing the level of ALAD gene transcription.

The p16 gene is a key factor involved in the early stages of

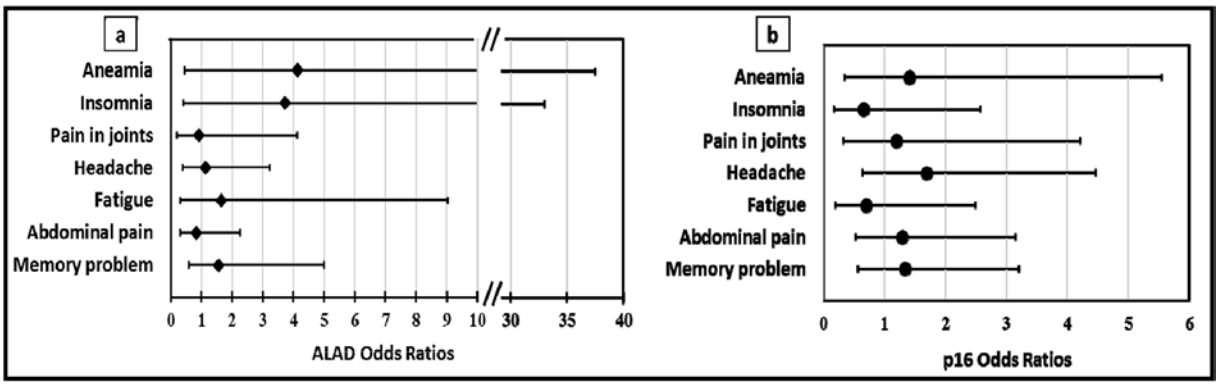

Fig. 3. Forest plot showing the odds ratios with 95% confidence intervals for the association of reported lead-related clinical symptoms with DNA promoter methylation a) ALAD gene; b) p16 gene. Dots represent odds ratios for each reported lead-related clinical symptom.

carcinogenesis and one of the most extensively studied genes in cancer, including epigenetic alterations. It is implicated in a variety of human cancers and is frequently silenced in human tumors through DNA hypermethylation (Inoue and Fry, 2018). A population-based data in the US indicated a significant association between BLLs > 20 μg/dL and increased risks of premature mortality, primarily due to increased deaths due to cancer and heart disease (Lustberg and Silbergeld, 2002). As of 2006, inorganic Pb and Pb compounds belong to Group 2 A (probably carcinogenic to humans) in the IARC monographs (IARC, 2006). In this study, the promoter region of the tumor suppressor gene p16 was highly methylated in children from the three townships near the closed mine compared to the other two townships (67.7% vs 44.7%; $p = 0.015$). Thus, this hypermethylation can lead to the down-regulation of the p16 gene in the environmental Pb-exposed children and could result in cancer via the dysregulation of cell cycle progression (Sherr and Roberts, 2004). Moreover, the methylated p16 gene was associated with an increased risk of Pb poisoning (OR = 2.58, 95% CI, 1.20–5.53) compared to unmethylated status. In the previous study based on Pb-exposed workers, which employed in a production line using Pb, the level of p16 CpG methylation was frequent and extensive, suggesting that DNA methylation could be involved in the mechanism of Pb toxicity (Kovatsi et al., 2010).

Epidemiological studies have suggested a significant dose-response relationship between Pb toxicity and cumulative Pb exposure (Weuve et al., 2013; Wu et al., 2016). Thus, to elucidate the potential effect of Pb exposure more on methylation status, a nonparametric pairwise multiple comparison was performed using Q1 BLL as a referent. The result showed that the three quartiles; Q2, Q3, and Q4 BLLs showed a significant increased level in the ALAD methylation status compared to Q1 level in a dose-dependent manner ($p < 0.001$). In a previous cultured-cell model study by Li et al. (2011), the level of ALAD CpG methylation status for the HepG2 cell line exposed with 100 μM lead acetate was increased significantly relative to that of lead-free cells. These results suggested that Pb may exert its harmful effects through epigenetic mechanisms by DNA hypermethylation in the CpG islands of gene promoters and/or it could result in cell toxicity by inhibition of enzymatic activities. In the case of the p16 gene, there was no significant difference on the extent of methylation as BLLs increases. As Pb-related symptoms based on questionnaire data are concerned, we found an OR value of greater than 1 for some features. However, there was no significant association between the promoter hypermethylation of both genes and the clinical symptoms. Overall in the current study, we present that children exposed to environmental Pb are significantly more likely to have ALAD and p16 DNA hypermethylation.

The primary strength of the present study is the use children and all the subjects residing in the same urban area. Secondly, it is the first study to investigate the influence of environmental Pb exposure in children, especially in Kabwe which is among the top polluted places in the world (Blacksmith Institute, 2013). This study also has some limitations: (i) small numbers of samples used in low Pb exposed areas compared to high Pb exposed areas and (ii) the use of MSP analysis which may be prone to false-positive results. Thus, additional larger cohort population-based studies are warranted based on whether Pb exposure influences gene-specific DNA methylation profiles as well as epigenome-wide DNA methylation patterning in Kabwe, Zambia.

In conclusion, we found a relationship between BLLs and aberrant DNA methylation in an environmentally Pb exposed population. Our study demonstrates that environmental Pb exposure is associated with promoter regions of ALAD and p16 DNA hypermethylation, leading to epigenetic silencing, in children from Kabwe, Zambia. This result suggests that this aberrant DNA methylation may be involved in the mechanism of Pb toxicity. Based on these observations, besides genetic variations like polymorphisms, epigenetic modifications might act as biomarkers in identifying Pb exposure susceptibility.

Funding

This work was supported by Grants-in-Aid for Scientific Research from the Ministry of Education, Culture, Sports, Science and Technology of Japan awarded to M. Ishizuka (No. 16H0177906, 18KK0287) and Y. Ikenaka (17K2003807, 18H0413208) and S.M.M. Nakayama (No. 16K16197, 17KK0009), and the foundation of JSPS Bilateral Open Partnership Joint Research Projects (JPJSBP120209902), the Environment Research and Technology Development Fund (SII-1/3–2, 4RF-1802/18,949,907) of the Environmental Restoration and Conservation Agency of Japan. This research was also supported by JST/JICA and SATREPS (Science and Technology Research Partnership for Sustainable Development; No. JPMJSA1501).as well as aXis (Accelerating Social Implementation for SDGs Achievement) funded by JST.

Ethical approval

The study was approved by the University of Zambia Research Ethics Committee (UNZAREC; REF. No. 012-04-16) and permission was granted by the Ministry of Health through the Zambia National Health Research Ethics Board and the Kabwe District Medical Office.

CRediT authorship contribution statement

Yared B. Yohannes: Conceptualization, Data curation, Formal analysis, Methodology, Writing - original draft, Writing - review & editing. **Shouta MM. Nakayama:** Funding acquisition, Investigation, Writing - review & editing. **John Yabe:** Investigation, Writing - review & editing. **Hokuto Nakata:** Investigation, Writing - review & editing. **Haruya Toyomaki:** Investigation, Writing - review & editing. **Andrew Kataba:** Investigation, Writing - review & editing. **Kaampwe Muzandu:** Investigation, Writing - review & editing. **Yoshinori Ikenaka:** Funding acquisition, Investigation, Writing - review & editing. **Kennedy Choongo:** Supervision, Writing - review & editing. **Mayumi Ishizuka:** Funding acquisition, Project administration, Supervision, Writing - review & editing.

Declaration of competing interest

Authors declare no conflicts of interest.

Acknowledgments

We are highly indebted to the children and families in Kabwe that participated in the study. We are also grateful to the laboratory technicians and nurses at the five health centers in Kabwe, the Kabwe District Health Office and the Zambian Ministry of Health for facilitating the study. We also acknowledge the contribution of the Kabwe Municipal Council, especially Mr. Paul Mukuka, the Director of Public Health, for facilitating the study.

References

Ahamed, M., Verma, S., Kumar, A., Siddiqui, M.K., 2006. Delta-aminolevulinic acid dehydratase inhibition and oxidative stress in relation to blood lead among urban adolescents. Hum. Exp. Toxicol. 25 (9), 547–553. https://doi.org/10.1191/0960327106het657oa.

Baylin, S.B., Ohm, J.E., 2006. Epigenetic gene silencing in cancer - a mechanism for early oncogenic pathway addiction? Nat. Rev. Canc. 6 (2), 107–116. https://doi.org/10.1038/nrc1799.

Blacksmith Institute, 2013. The World's Worst 2013: the Top Ten Toxic Threats. Cleanup, Progress, and Ongoing Challenges. New York Blacksmith Institute Available. http://www.worstpolluted.org/docs/TopTenThreats2013.pdf, Accessed date: 12 December 2019.

Canfield, R.L., Henderson, C.R., Cory-Slechta, D.A., Cox, C., Jusko, T.A., Lanphear, B.P., 2003. Intellectual impairment in children with blood lead concentrations below 10 micrograms per deciliter. N. Engl. J. Med. 348, 1517–1526. https://doi.org/10.1056/NEJMoa022848.

CDC (Centers for Disease Control and Prevention), 2012. Low Level Lead Exposure Harms Children: a Renewed Call for Primary Prevention - Report of the Advisory Committee on Childhood Lead Poisoning Prevention of the Centers for Disease Control and Prevention. Atlanta, GA. Available. http://www.cdc.gov/nceh/lead/acclpp/final_document_010412.pdf, Accessed date: 12 December 2019.

Cecil, K.M., Brubaker, C.J., Adler, C.M., Dietrich, K.N., Altaye, M., Egelhoff, J.C., Wessel, S., Elangovan, I., Hornung, R., Jarvis, K., Lanphear, B.P., 2008. Decreased brain volume in adults with childhood lead exposure. PLoS Med. 5 (5), e112. https://doi.org/10.1371/journal.pmed.0050112.

Cortessis, V.K., Thomas, D.C., Levine, A.J., Breton, C.V., Mack, T.M., Siegmund, K.D., Haile, R.W., Laird, P.W., 2012. Environmental epigenetics: prospects for studying epigenetic mediation of exposure-response relationships. Hum. Genet. 131, 1565–1589. https://doi.org/10.1007/s00439-012-1189-8.

Li, L.C., Dahiya, R., 2002. MethPrimer: designing primers for methylation PCRS. Bioinformatics 18, 1427–1431. https://doi.org/10.1093/bioinformatics/18.11.1427.

Flora, G., Gupta, D., Tiwari, A., 2012. Toxicity of lead: a review with recent updates. Interdiscipl. Toxicol. 5, 47–58. https://doi.org/10.2478/v10102-012-0009-2.

Gurer-Orhan, H., Sabir, H.U., Ozgünes, H., 2004. Correlation between clinical indicators of lead poisoning and oxidative stress parameters in controls and lead-exposed workers. Toxicology 195 (2–3), 147–154. https://doi.org/10.1016/j.tox.2003.09.009.

Herman, J.G., Merlo, A., Mao, L., Lapidus, R.G., Issa, J.P., Davidson, N.E., Sidransky, D., Baylin, S.B., 1995. Inactivation of the CDKN2/p16/MTS1 gene is frequently associated with aberrant DNA methylation in all common human cancers. Canc. Res. 55, 4525–4530.

Herman, J.G., Graff, J.R., Myöhänen, S., Nelkin, B.D., Baylin, S.B., 1996. Methylation specific PCR: a novel PCR assay for methylation status of CpG islands. Proc. Natl. Acad. Sci. U.S.A. 93, 9821–9826. https://doi.org/10.1073/pnas.93.18.9821.

IARC (International Agency for Research on Cancer), 2006. Monographs on the Evaluation of Carcinogenic Risks to Humans, vol. 87 Inorganic and organic lead compounds, Lyon, France 2006.

Inoue, K., Fry, E.A., 2018. Aberrant Expression of ARF in human cancer - a new biomarker? Cancer Rep. Rev. 2 (2). https://doi.org/10.15761/CRR.1000145.

Jaenisch, R., Bird, A., 2003. Epigenetic regulation of gene expression: how the genome integrates intrinsic and environmental signals. Nat. Genet. 33 (Suppl. l.), 245–254. https://doi.org/10.1038/ng1089.

Jin, Z., Liu, Y., 2018. DNA methylation in human diseases. Genes Dis 5 (1), 1–8. https://doi.org/10.1016/j.gendis.2018.01.002.

Kovatsi, L., Georgiou, E., Ioannou, A., Haitoglou, C., Tzimagiorgis, G., Tsoukali, H., kouidou, S., 2010. p16 promoter methylation in Pb2+-exposed individuals. Clin. Toxicol. 48, 124–128. https://doi.org/10.3109/15563650903567091.

Lanphear, B.P., Hornung, R., Khoury, J., Yolton, K., Baghurst, P., et al., 2005. Low-level environmental lead exposure and children's intellectual function: an international pooled analysis. Environ. Health Perspect. 113, 894–899. https://doi.org/10.1289/ehp.7688.

Li, C., Xu, M., Wang, S., Yand, X., Zhou, S., Zhang, J., Liu, Q., Sun, Y., 2011. Lead exposure suppressed ALAD transcription by increasing methylation level of the promoter CpG islands. Toxicol. Lett. (Shannon) 203, 48–53. https://doi.org/10.1016/j.toxlet.2011.03.002.

Li, C., Yang, X., Xu, M., Zhang, J., Sun, N., 2014. Association between GSTP1 CpG methylation and the early phase of lead exposure. Toxicol. Mech. Methods 24 (2), 111–115. https://doi.org/10.3109/15376516.2013.859195.

Lustberg, M., Silbergeld, E., 2002. Blood lead levels and mortality. Arch. Intern. Med. 162 (21), 2443–2449. https://doi.org/10.1001/archinte.162.21.2443.

Martin, E.M., Fry, R.C., 2018. Environmental influences on the epigenome: exposure-associated DNA methylation in human populations. Annu. Rev. Publ. Health 39, 309–333. https://doi.org/10.1146/annurev-publhealth-040617-014629.

Martínez, S.A., Simonella, L., Hansen, C., Rivolta, S., Cancela, L.M., Virgolini, M.B., 2013. Blood lead levels and enzymatic biomarkers of environmental lead exposure in children in Cordoba, Argentina, after the ban of leaded gasoline. Hum. Exp. Toxicol. 32 (5), 449–463. https://doi.org/10.1177/0960327112454893.

Martinez-Zamudio, R., Ha, H., 2011. Environmental epigenetics in metal exposure. Epigenetics 6, 820–827. https://doi.org/10.4161/epi.6.7.16250.

Nye, M.D., Hoyo, C., Murphy, S.K., 2015. In vitro lead exposure changes DNA methylation and expression of IGF2 and PEG1/MEST. Toxicol. Vitro 29 (3), 544–550. https://doi.org/10.1016/j.tiv.2015.01.002.

Onalaja, A.O., Claudio, L., 2000. Genetic susceptibility to lead poisoning. Environ. Health Perspect. 108 (Suppl. 1), 23–28. https://doi.org/10.1289/ehp.00108s123.

Pilsner, J.R., Hu, H., Ettinger, A., Sánchez, B.N., Wright, R.O., Cantonwine, D., et al., 2009. Influence of prenatal lead exposure on genomic methylation of cord blood DNA. Environ. Health Perspect. 117 (9), 1466–1471. https://doi.org/10.1289/ehp.0800497.

Rice, D., Barone Jr., S., 2000. Critical periods of vulnerability for the developing nervous system: evidence from humans and animal models. Environ. Health Perspect. 108 (Suppl. 3), 511–533. https://doi.org/10.1289/ehp.00108s3511.

Sakai, T., Morita, Y., 1996. δ-Aminolevulinic acid in plasma or whole blood as a sensitive indicator of lead effects, and its relation to the other heme-related parameters. Int. Arch. Occup. Environ. Health 68, 126–132. https://doi.org/10.1007/bf00381245.

Sherr, C.J., Roberts, J.M., 2004. Living with or without cyclins and cyclin-dependent kinases. Genes Dev. 18, 2699–2711. https://doi.org/10.1101/gad.1256504.

Steenland, K., Boffetta, P., 2000. Lead and cancer in humans: where are we now? Am. J. Ind. Med. 38, 295–299 doi.org/10.1002/1097-0274(200009)38:3 < 295::AID-AJIM8 > 3.0.CO;2-L.

Ushijima, T., Nakajima, T., Maekita, T., 2006. DNA methylation as a marker for the past and future. J. Gastroenterol. 41, 401–407. https://doi.org/10.1007/s00535-006-1846-6.

Vorvolakos, T., Arseniou, S., Samakouri, M., 2016. There is no safe threshold for lead exposure: A literature review. Psychiatriki 27, 204–214. https://doi.org/10.22365/jpsych.2016.273.204.

Wani, A.L., Ara, A., Usmani, J.A., 2015. Lead toxicity: a review. Interdiscipl. Toxicol. 8, 55–64. https://doi.org/10.1515/intox-2015-0009.

Weuve, J., Press, D.Z., Grodstein, F., Wright, R.O., Hu, H., Weisskopf, M.G., 2013. Cumulative exposure to lead and cognition in persons with Parkinson's disease. Mov. Disord. 28, 176–182. https://doi.org/10.1002/mds.25247.

WHO (World Health Organization), 2010. Childhood Lead Poisoning. 2010. Geneva, Switzerland. Available. https://www.who.int/ceh/publications/leadguidance.pdf, Accessed date: 14 December 2019.

Wright, R.O., Schwartz, J., Wright, R.J., Bollati, V., Tarantini, L., Park, S.K., et al., 2010. Biomarkers of lead exposure and DNA methylation within retrotransposons. Environ. Health Perspect. 118 (6), 790–795. https://doi.org/10.1289/ehp.0901429.

Wu, Y., Gu, J.M., Huang, Y., Duan, Y.Y., Huang, R.X., Hu, J.A., 2016. Dose-response relationship between cumulative occupational lead exposure and the associated health damages: a 20-year cohort study of a smelter in China. Int. J. Environ. Res. Publ. Health 13 (3). https://doi.org/10.3390/ijerph13030328.

Yabe, J., Nakayama, S.M.M., Ikenaka, Y., Yohannes, Y.B., Bortey-Sam, N., Oroszlany, B., Muzandu, K., Choongo, K., Kabalo, A.N., Ntapisha, J., Mweene, A., Umemura, T., Ishizuka, M., 2015. Lead poisoning in children from townships in the vicinity of a lead-zinc mine in Kabwe, Zambia. Chemosphere 119, 941–947. https://doi.org/10.1016/j.chemosphere.2014.09.028.

Yabe, J., Nakayama, S.M.M., Nakata, H., Toyomaki, H., Yohannes, Y.B., Muzandu, K., Kataba, A., Zyambo, G., Hiwatari, M., Narita, D., Yamada, D., Hangoma, P., Muntinda, N.S., Mufune, T., Ikenaka, Y., Choongo, K., Ishizuka, M., 2020. Current trends of blood lead levels, distribution patterns and exposure variations among household members in Kabwe, Zambia. Chemosphere 243, 125412. https://doi.org/10.1016/j.chemosphere.2019.125412.

Environmental Science & Technology

pubs.acs.org/est

Article

Land Use in Habitats Affects Metal Concentrations in Wild Lizards Around a Former Lead Mining Site

Rio Doya,[#] Shouta M. M. Nakayama,[#] Hokuto Nakata, Haruya Toyomaki, John Yabe, Kaampwe Muzandu, Yared B. Yohannes, Andrew Kataba, Golden Zyambo, Takahiro Ogawa, Yoshitaka Uchida, Yoshinori Ikenaka, and Mayumi Ishizuka*

Cite This: https://dx.doi.org/10.1021/acs.est.0c00150

Read Online

ACCESS | Metrics & More | Article Recommendations | Supporting Information

ABSTRACT: We investigated the potential effects of different land use and other environmental factors on animals living in a contaminated environment. The study site in Kabwe, Zambia, is currently undergoing urban expansion, while lead contamination from former mining activities is still prevalent. We focused on a habitat generalist lizards (*Trachylepis wahlbergii*). The livers, lungs, blood, and stomach contents of 224 lizards were analyzed for their lead, zinc, cadmium, copper, nickel, and arsenic concentrations. Habitat types were categorized based on vegetation data obtained from satellite images. Multiple regression analysis revealed that land use categories of habitats and three other factors significantly affected lead concentrations in the lizards. Further investigation suggested that the lead concentrations in lizards living in bare fields were higher than expected based on the distance from the contaminant source, while those in lizards living in green fields were lower than expected. In addition, the lead concentration of lungs was higher than that of the liver in 19% of the lizards, implying direct exposure to lead via dust inhalation besides digestive exposure. Since vegetation reduces the production of dust from surface soil, it is plausible that dust from the mine is one of the contamination sources and that vegetation can reduce exposure to this.

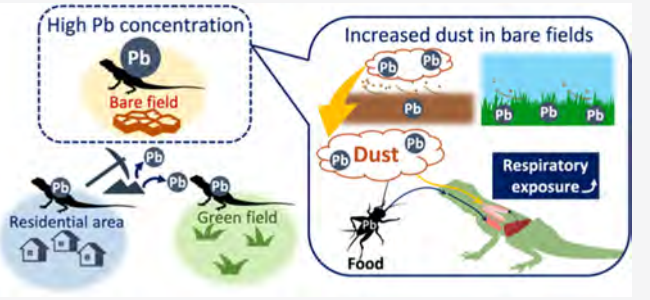

1. INTRODUCTION

Several studies have described environmental hazards preceding city development. Examples are environmental contamination in developing countries that is caused by poorly managed electronic waste-recycling facilities, dumping grounds, and mining sites.[1−5] Since diversification of land use is one of the characteristics of urbanization,[6] the status of long-standing contamination and how the effects thereof differ between different land use patterns should be understood before cities are developed in regions where environmental pollution has already occurred. Existing studies have examined the effects of different land uses on environmental contamination status only by describing the existence of pollution sources, such as intensive crop fields, various industries, power plants, and heavy traffic.[6−9] In contrast, we have considered land use as one of the environmental factors controlling exposure to and accumulation of contaminants in living organisms. Such insight is necessary for creating proper methodologies for city development that can minimize the potential negative environmental and health effects. Although environmental remediation is the most fundamental solution for heavily contaminated regions, it costs an enormous amount of money and is not always feasible for addressing problems in widely spread populations.[10,11] Until remediation is complete, humans and animals continue to be exposed to toxic substances. Moreover, even if the environment is not suitable for people to live in since contamination sources often correspond with local economic drivers, social communities and economic activities continue to flourish and fuel urbanization regardless. Therefore, appropriate city planning should be conducted before mass construction begins, so that people can receive the benefits of urbanization while their exposure to environmental pollutants is mitigated.

Kabwe, in the Republic of Zambia, is a remarkable example of a city undergoing urban expansion in an environment that has long been contaminated.[12] In Kabwe, the primary contamination source is a lead (Pb) and zinc (Zn) mine. After the mine closed in 1993, slags were deposited in the open environment on the premises (S14°27′44″, E28°25′51″).[13] Even though the official operation had stopped, high concentrations of Pb, Zn, copper (Cu), cadmium (Cd), and arsenic (As) were detected in the soil around the mine in 2009.[14] Leaded gasoline has been eliminated from fuel

Received: January 8, 2020
Revised: June 2, 2020
Accepted: June 3, 2020
Published: June 3, 2020

distribution in Zambia since 2008, and the majority of electricity powering of Kabwe is provided by hydroelectric plants. There is no major heavy industry in Kabwe. Considering these points, the mining site is regarded as the predominant contaminant source in Kabwe. Samples from humans and animals (chicken, cattle, goats, rats, and dogs) in Kabwe have revealed accumulation of high concentrations of metals in the blood, liver, kidneys, and muscles.[5,12,14−18]

The Pb contamination in Kabwe has been intensively analyzed, due to the high toxicity of Pb and the associated health risk to animals. Pb is a nonessential element and can cause various toxic effects, including neurodevelopmental and cardiovascular disorders, renal failure, and hypochromic anemia.[19] Recent guidelines require exposure to Pb to be minimized as much as possible.[20,21] To achieve this goal, it is necessary to understand the exposure pathways and factors that affect the amount of exposure.

Reptiles are the least-studied group in ecotoxicology;[22] however, lizards are increasingly regarded as important in ecotoxicological field research. There are increasing reports on field research, which feature lizards, including some geckoes, as a bioindicator of pollutants.[23−25] These studies take advantage of the species' insect-based feeding habits in estimating the quantities of contaminants entering into the vertebrate food web from the invertebrate level. In addition, some species of lizards are abundant throughout a region, while the areas of individual habitats tend to be small. There are also increasing numbers of laboratory studies using lizards as model species or investigating contaminant kinetics in lizards.[26,27] In this study, the lizard *Trachylepis wahlbergii* (Wahlberg's striped skink; Scincidae) was selected as the target species in an investigation of the relationship between land use and Pb exposure. *T. wahlbergii* is a diurnal lizard with a snout−vent length (SVL) of around 10 cm. This species is common and widespread throughout southern and eastern Africa and is a habitat generalist. The lizards are terrestrial, arboreal, or rock-living. They have also become habituated themselves to humans and settle in houses.[28] Therefore, this species can be used to monitor a wide range of geographic areas. In addition, its home range is thought to be less than 500 m^2,[29] which is relatively small compared to its body size,[30] so it can be used to compare the status of locations that are close to each other. This is important because few other species have such small home ranges. The lizards eat a variety of insects, such as beetles, flies, and grasshoppers. They forage actively but also bask in a strategic position so that they can dart forward to catch the passing prey.[28] Although they may sometimes accidentally eat soil or small stones, their main source of contaminants via oral exposure is assumed to be the insects they eat. This feature is optimal for identifying exposure sources. Together, these characteristics make *T. wahlbergii* an ideal species for investigating differences in metal accumulation among individual animals living in different environments.

The objective of this study is to explore the environmental factors affecting the contamination status of living organisms by comparing metal (Pb, Zn, Cd, Cu, nickel [Ni]) and As concentrations in lizards inhabiting various locations and a range of environments.

2. MATERIALS AND METHODS

2.1. Sampling. The primary ore mineral assemblage and metal production history in Kabwe are described in the Supporting Information (SI1).

The sampling of lizards and soil was conducted in the vicinity of the Kabwe Pb−Zn mine from May to September 2017, which corresponded to the dry season in the region (Figure S1, SI2). The distance from the mine to the sampling sites ranged from 0.26 to 21.2 km (Figure S2, SI2). The sampling sites were accurately located using global positioning system (GPS) coordinates. The sampling took place under a permit from the Zambian Ministry of Fisheries and Livestock, as well as the Faculty of Veterinary Medicine, Hokkaido University, Sapporo, Japan (approval number: Vet-17010). A total of 224 lizards were captured by hand or using adhesive traps, and their body weight (BW) and SVL were measured. Juveniles were assigned to the "unknown sex" category since it was difficult to sex them. The lizards were carried in ventilated plastic cases to a laboratory in the Central Province Veterinary Office of the Ministry of Fisheries and Livestock in Kabwe and dissected after being euthanized with isoflurane (Isotroy, Troikaa Pharmaceuticals, Gujarat, India). First, blood was collected from the heart with a 27-gauge needle and syringe, which had been flushed with heparin (Mochida Pharmaceutical, Tokyo, Japan). Subsequently, the livers, lungs, and stomach contents were placed in sampling tubes and stored at −20 °C until metal analysis. A small portion of the heart was preserved in RNAlater (Sigma-Aldrich, St. Louis) for species identification. Kidneys were not collected because they were too small to be differentiated. Surface soils (n = 29) were collected from each sampling site and stored at −20 °C until analysis. Biological samples and soils were transported to the Laboratory of Toxicology, Faculty of Veterinary Medicine, Hokkaido University, Sapporo, Japan, under permits from both the Zambian and the Japanese governments, for the following analyses.

2.2. Species Identification. Whole genomic DNA was extracted from the hearts using the Wizard Genomic DNA Purification Kit (Promega, Fitchburg). The 12S rRNA region was amplified via polymerase chain reaction (PCR) using Tks Gflex DNA Polymerase (Takara Bio, Kyoto, Japan). The primers and PCR conditions are shown in Table S1, SI3. After purification, PCR products were sequenced using the same primers. All nucleotide sequences were confirmed by the Fasmac sequencing service (Kanagawa, Japan). Sequences were aligned, and the phylogenetic tree was constructed using MEGA7 software (Molecular Evolutionary Genetics Analysis version 6.0).[31,32] Information on the 12S rRNA genes used in the phylogenetic analysis is shown in Table S2, SI3.

2.3. Metal and As Analysis. Metal and As analysis was conducted based on an existing method[5] with minor modifications. After being dried at 50 °C for 48 h, the 29 soil samples were sieved to eliminate particles larger than a diameter of 2 mm. The average dry weight used for analysis was 51.0 mg. With the lizard tissue samples, parts of organs or whole organs were analyzed. The average wet weight of samples was 82.7 mg for the liver and 51.5 mg for the lung. Whole volumes of blood and stomach contents were used in the analysis. The mean wet weight of blood was 68.0 mg, while that of stomach contents was 182.3 mg. Samples were dried in an oven at 50 °C for 48 h. For stomach content samples whose dry weight exceeded 100 mg, the dried samples were homogenized, and a dry weight of approximately 50 mg was used. Dried samples were placed in prewashed digesting vessels with 5 mL of 30% HNO_3 (nitric acid for atomic absorption spectrometry, 60%, Kanto Chemical, Tokyo, Japan) in distilled deionized water (DDW) and 1 mL of 30% H_2O_2 (hydrogen

https://dx.doi.org/10.1021/acs.est.0c00150
Environ. Sci. Technol. XXXX, XXX, XXX−XXX

peroxide for atomic absorption spectrometry, 30%, Kanto Chemical, Tokyo, Japan) and digested in a microwave digestion system (Speed Wave MWS-2, Berghof, Eningen, Germany). Parameters for digestion are shown in Table S3, SI4.

Analysis of Pb, Zn, Cd, Cu, Ni, and As contents was performed using inductively coupled plasma mass spectrometry (ICP-MS 7700 series, Agilent Technologies, Tokyo, Japan). Detailed operating conditions are shown in Table S4, SI4. The procedure for verifying analytical quality is described in SI5. All concentrations are expressed in micrograms per gram on a dry-weight (μg/g DW) basis in the following results.

2.4. Categorization of Land Use. Land use was categorized based on the analysis of satellite images taken in the rainy season (January−March; Figure S1, SI2) in QGIS 2.14.14 Essen (QGIS Development Team, 2016). Data sets of spectral reflectance were obtained from the Sentinel-2 (European Space Agency) database via the EO browser (https://apps.sentinel-hub.com/eo-browser/?lat=41.9000&lng=12.5000&zoom=10). Satellite images with cloud coverage of less than 10% were selected. Data sets containing bands 3 (green), 4 (visible red), and 8A (near-infrared) were imported to QGIS and merged to create new raster graphics, which indicate the status of vegetation. By comparing these with true-color images, which are also created in QGIS from data sets containing bands 2 (blue), 3, and 4, the coloration of the merged band images was linked to the actual land use pattern (Figure 1). Changes in the surface land cover during the rainy season were compared to categorize land use into the following four groups: bare field (no vegetation cover throughout the rainy season), green field (vegetation cover present throughout the rainy season), open field (vegetation cover present for part of the rainy season), and residential area (several buildings present).

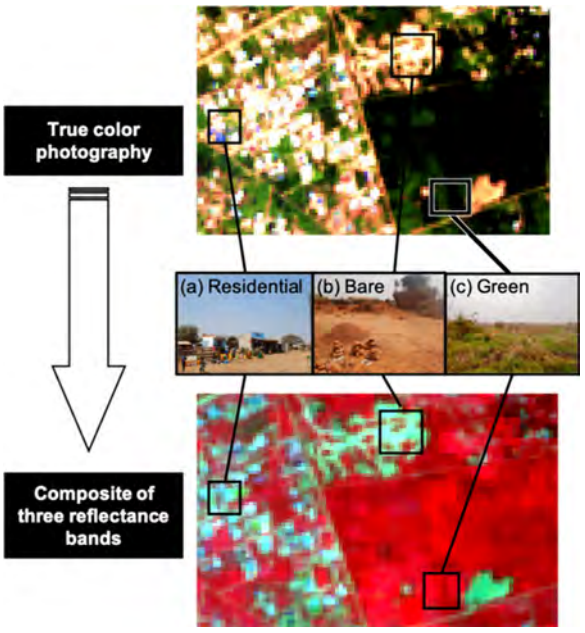

Figure 1. Process of land use categorization. Composite images were created from three reflectance band images that had been separately colored and categorized. Photographs are representative of (a) residential areas, (b) bare fields, and (c) green fields. They contain modified Copernicus Sentinel data [2017].

2.5. Calculation of the Normalized Difference Vegetation Index (NDVI). The normalized difference vegetation index (NDVI) indicates the amount of vegetation by measuring the activity of photosynthetic pigments. Calculation of the NDVI is based on the aerial imagery of spectral reflectance in the visible red (665 nm) and the near-infrared (865 nm) wavelengths, as shown in SI6.

2.6. Defining the Angle toward the Prevailing Wind. Since the prevailing wind in Kabwe is from the east-southeast (ESE), the angle of the sampling sites from the mine with respect to the ESE wind direction was calculated to investigate the effect of wind, as shown in SI7.

2.7. Measurement of Soil pH. Soil pH was measured according to an existing method,[33] as shown in SI8.

2.8. Statistical Analysis. All statistical analyses were conducted using JMP Pro 14 software (SAS Institute, NC). Spearman's rank correlation test was used to determine the relationships between the distance from the mine and the metal/As concentrations in the soil (Figure S8, SI10) and Pb concentrations among biological samples (Table S9, SI11). Multiple regression analysis was used to investigate the effects of various environmental factors on the Pb concentrations in lizard's organ (Table 1). To examine the confounding effect of the distance from the mine to the sampling site, we used the residuals between the measured liver Pb concentration and the concentrations modeled based on the distance from the mine (Figure 3). The estimated Pb concentration was calculated with least-squares method between the measured liver Pb concentration and the distance from the mine (Figure S10, SI12). The Steel−Dwass test was used to evaluate the differences among the above-mentioned residuals (Figure 3), metal concentrations (Figure S9, SI11 and Figure S11, SI12), and NDVI annual averages (Figure S12, SI12).

Table 1. Association between Liver Pb Concentration and Environmental Parameters[a]

	β	t	p
distance from the mine	−0.382	−3.20	0.0018
bare field	0.450	5.00	<0.0001
green field	−0.427	−4.02	0.0001
open field	−0.028	−0.29	0.7735
residential area	−0.002	0.09	0.9317
soil Pb	0.287	2.63	0.0098
soil pH	−0.165	−2.06	0.0414
angle from ESE	0.020	0.24	0.8118
average annual NDVI	0.019	0.21	0.8337

[a]Standardized partial regression coefficient (β) and t-values (β divided by the standard error of each parameter) were obtained from multiple regression analysis (least-squares method). ESE, east-southeast; NDVI, normalized difference vegetation index.

3. RESULTS AND DISCUSSION

3.1. Species Identification. A total of 224 lizards captured in Kabwe were identified as *T. wahlbergii* (Wahlberg's striped skink; Scincidae) based on coloration, distribution,[34] and phylogenetic analysis of their 12S rRNA (Figure S3, SI3). Sex distribution and SVLs are shown in Table S6, SI9. The median SVL of captured lizards was 8 cm, and there was no significant difference in SVL between males and females.

3.2. Metal and As Concentrations in the Soil. The concentrations of the elements (Pb, Zn, Cd, Cu, Ni, and As) in

https://dx.doi.org/10.1021/acs.est.0c00150
Environ. Sci. Technol. XXXX, XXX, XXX−XXX

the soil samples (median and range, μg/g DW) are shown in Table S7, SI10, alongside the values for Zambian soils obtained from other studies, as well as the ecological soil-screening levels (Eco-SSLs) for birds and mammals suggested by the U.S. Environmental Protection Agency (EPA).[14,35−40] The medians of the Pb, Zn, and Cd concentrations were higher than the U.S. EPA Eco-SSL values for both birds and mammals. Although the median concentration of Cu was lower than the Eco-SSL for mammals, the maximum value exceeded the Eco-SSL. These patterns of accumulation in the soil were in agreement with the previous research,[14,41] which means that soil contamination is still a cause for concern in Kabwe. In contrast, even the maximum concentrations of Ni and As were lower than the Eco-SSL values. As shown in Figure S8, SI10, concentrations of Pb, Zn, Cd, Cu, and As in the soil were negatively correlated with the distance from the mine ($p < 0.0001$). Therefore, the mine can be identified as the primary metal contamination source in Kabwe. For Ni, however, the concentrations in the soil were low, and this was the only element that did not show a significant correlation with the distance from the mine. Thus, of the six elements investigated, only Ni can be excluded as a potential metal contaminant originating from the Kabwe mine. There were no significant differences in the concentrations of any of the elements among the land use categories.

3.3. Metal and As Concentrations in Lizards. The metal and As concentrations in the livers, lungs, blood, and stomach contents of lizards in the current study are shown in Table S8, SI11, along with the concentrations reported in previous studies for other animals collected in Kabwe (μg/g DW).[12,14,16] Box-and-whisker plots are shown in Figure S9, SI11. Liver concentrations of Pb, Cd, and Cu showed the widest variability among the tissue samples. The liver samples that displayed the highest concentrations of Pb, Zn, Cd, and Cu were all taken from lizards living inside the mine. The wide range of Pb concentrations could be a consequence of the broad coverage and differences in the habitats of the analyzed lizards. Although further investigation of the biological and toxicological aspects of lizards is required, the current results highlight the potential for lizards to be indicators of pollution status in a range of environments.

Pb concentrations in the livers, lungs, blood, and stomach contents showed significant positive correlations with each other, as shown in Table S9, SI11 ($p < 0.0001$). The strongest correlations were between livers and blood and between lungs and blood (both $\rho = 0.91$, $p < 0.0001$). Therefore, it is reasonable to assume that the accumulation of Pb in livers and lungs reflects the blood Pb levels. Due to the limited number of blood samples ($n = 102$), liver Pb levels were used as an indicator of systemic contamination in the following analyses.

3.4. Effects of Environmental Parameters on Metal and As Exposure. As shown in Figure S11, SI12, lizards living in Hamududu, which is 21.2 km away from the mine, had accumulated significantly lower concentrations of Pb than lizards living near the mine ($p < 0.01$). Therefore, Hamududu could be considered not polluted by the mine. In contrast, liver Pb concentrations of lizards captured inside the mine site were significantly higher than those of lizards captured at other sites ($p < 0.01$). Since extremely low or high contamination levels may conceal other underlying factors, the results from lizards from Hamududu and inside the mine were excluded from the following analyses.

Figure 2 demonstrates the distribution of sampling sites together with the mean liver Pb concentrations and sample

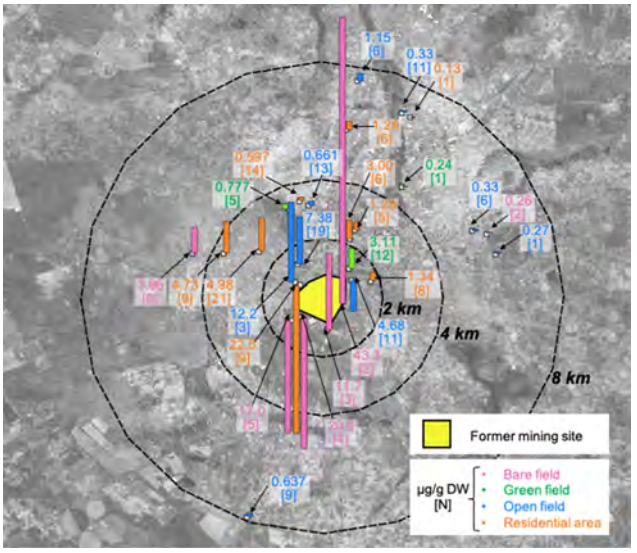

Figure 2. Mean liver Pb concentration (μg/g DW) with sample sizes indicated in brackets. Bars and texts are colored according to land use categories (pink, bare field; green, green field; blue, open field; orange, residential area); bar length is proportional to the Pb concentration. This figure contains modified Copernicus Sentinel data [2020] processed by Sentinel Hub.

sizes. The height of each bar represents the mean concentration, and its color indicates the land use category. It is clear that the mean Pb concentrations in lizards were higher in the areas closer to the mine. In addition, sites categorized as bare fields also tended to show high Pb concentrations.

To evaluate the effects of possible environmental factors (land use category, distance from the mine, wind direction, average annual NDVI, and soil Pb concentration and pH), multiple regression analysis was performed (Table 1). Land use category affected the liver Pb concentration, especially bare fields and green fields, which were positively ($t = 5.00$) and negatively ($t = -4.02$) associated with the Pb concentration, respectively. The absolute values of t for these two categories were the largest among all of the potential environmental factors. Therefore, it is assumed that lizards living in a bare field accumulate more Pb than lizards living in other habitats, while those living in green fields accumulate less Pb. In addition, the distance from the mine negatively affected the liver Pb concentration, and the soil Pb concentration was positively correlated with the liver Pb concentrations ($t = -3.20$ and 2.63, respectively; $p < 0.01$). These results show that Pb accumulation is enhanced in surface soils adjacent to the mine, which results in a higher Pb concentration in the lizards inhabiting these areas.

The pH values of most of the soil samples were close to neutral (median 7.56), as shown in Figure S7, SI8, although one sample exhibited an extremely high pH (11.5). This might have been caused by fire since high temperatures and ash promote alkalization of soil.[42,43] In fact, controlled burns are commonly used in Kabwe as a way of reducing the growth of wild plants. Since alkaline conditions suppress metal mobility,[44] it is reasonable that the high soil pH value would

https://dx.doi.org/10.1021/acs.est.0c00150
Environ. Sci. Technol. XXXX, XXX, XXX−XXX

negatively affect the liver Pb concentration, as shown in Table 1.

The frequency distribution of the angle of the sites between the mine and ESE, and the prevailing wind direction is shown in Figure S6, SI7. The distribution indicated that 64% of all sampling sites were located downwind of the mine (angle from ESE > 90°). Although Figure 2 suggests that lizards on the west side of the mine showed higher concentrations of Pb than those living on the east side, there was no significant effect of wind direction (angle from ESE in Table 1).

Figure 2 also suggests that bare fields tend to be located near the mine. To further assess the effect of land use while controlling the effect of the distance from the mine, the residuals between the measured liver Pb concentrations and the concentrations predicted by a model based on the distance from the mine were compared among land use categories (Figure 3). These residuals were positive for bare fields and

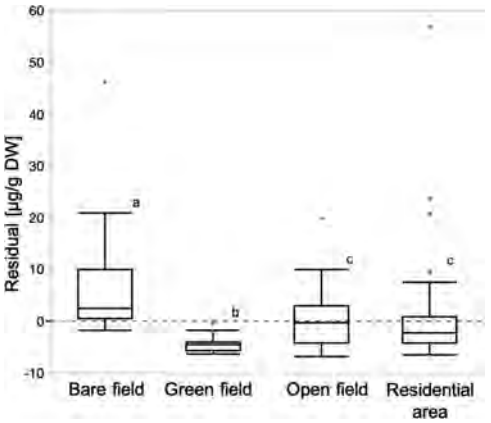

Figure 3. Box-and-whisker plots of the residuals obtained by subtracting the liver Pb concentration predicted based on the distance from the mine from the measured values. The upper and lower boundaries of the box and the line inside each box indicate the upper and lower quartiles and the median, respectively. The whiskers extend to the maximum and minimum values observed, excluding outliers. Significant differences between groups are indicated by different letters (Steel−Dwass test, $p < 0.01$).

negative for green fields. This suggests that the lizards living in bare fields accumulated more Pb than expected based on the location of their habitat, while those living in green fields accumulated less. Since the median values of the residuals of open fields and residential areas were almost zero and there were no significant differences between these two categories, the extent of accumulation in these areas was assumed to be intermediate between the extent observed for bare and green fields. This result suggests that vegetation status is an important factor affecting Pb accumulation in living organisms, supporting the result shown in Table 1. Previous reports have concluded that both distance and direction from the source of pollution are important factors affecting Pb accumulation in terms of dust scattering.[11,12] The present findings support these results since vegetation can suppress both the production and the remobilization of dust.[45] In regions that have long dry seasons, like Kabwe, the role of dust both in spreading pollutants from the pollution source to the surrounding areas and in allowing pollutants to travel through the air even when distant from the source cannot be dismissed.

The median NDVI value was 0.315, and the range was from 0.050 to 0.486 (Figure S4, SI6). To confirm the validity of the link between vegetation status and the land use categories defined in this study, the NDVI value was compared among different land use categories (Figure S12, SI12). The NDVI value increased in the following order: bare fields ≈ residential areas < open fields < green fields ($p < 0.05$). There was no significant difference between bare fields and residential areas. Since the average annual NDVI was consistent with the land use categories, we attempted to use it as a parameter to describe land use. However, despite the significant differences in the effects of different land use categories on liver Pb concentrations (Table 1 and Figure 3), the effect of NDVI was not significant (Table 1). This striking difference between the effects of the land use categories used in this study and that of NDVI can be explained by the fact that the calculation of NDVI does not reflect the existence of houses. Thus, it is possible that not only the amount of vegetation but also human activities, such as the construction of buildings or frequent traffic on unpaved roads, affect the contamination status of the animals inhabiting those areas. In fact, the variation in the residuals between the measured and predicted liver Pb concentrations shown in Figure 3 was the largest in the residential areas. This implies that there are other potential factors affecting the accumulation of Pb in this type of habitat. Therefore, to further investigate the effect of land use on contamination status, additional parameters that reflect these differences should be developed and used.

3.5. Pathway of Exposure of Lizards to Pb. Among the four biological sample types, the concentrations of most elements (except for Cu) were highest in the stomach contents (Table S8 and Figure S9, SI11). Stomach content concentrations can be considered to reflect the quantity of ingested contaminants. To compare the present results with the in vivo studies in which the dosage is expressed as μg/g body weight (BW), our Pb concentrations in the stomach content samples were converted to μg/g BW. The results are shown in Figure S13, SI13. Generally, the stomach contents contained <10 μg/g BW Pb. The highest Pb concentration (1478 μg/g DW) was equivalent to 32.9 μg/g BW. Since the Pb concentration of the stomach contents was positively correlated with that of the livers (Table S9, SI11), ingestion may be an important Pb exposure pathway. Salice et al. performed toxicity tests of inorganic Pb administered via oral exposure in *Sceloporus occidentalis* (Western fence lizard).[46] They reported that the approximate lethal dose was >2000 μg/g BW, with subacute effects, such as weight loss, seen in the 62.5 μg/(g BW day) group and subchronic effects, such as decreased hematocrit, in the 10 μg/(g BW day) group. Holem et al. also conducted acute toxicity tests on *S. occidentalis*.[47] After a single administration of 1000 μg/g BW Pb via gavage, 30% of the lizards died within 24 h and 50% of the surviving lizards exhibited a significant increase in skin pigmentation (they became darker). Dark coloration was also seen in the acute exposure test conducted by Salice et al.,[46] although its biological meaning remains unknown. In the current study, only two individuals had >10 μg/g BW Pb in their stomach contents (Figure S13). In fact, a small fragment with a stonelike structure was found in the stomach of the lizard that had the highest Pb concentration in its stomach contents (32.9 μg/g BW). That fragment was removed prior to the analysis, but the Pb concentration was nevertheless high. The Pb concentrations in the tissues of this lizard were not especially

https://dx.doi.org/10.1021/acs.est.0c00150
Environ. Sci. Technol. XXXX, XXX, XXX−XXX

high compared to those of other lizards captured at the same site. It should be noted that while the Pb concentration of stomach contents can be considered to represent the oral exposure levels, they capture only a limited time frame. Although these Pb concentrations overall tended to be much lower than the reported toxicity levels, they should not be disregarded, particularly because there has been limited research on the consequences of chronic exposure to such levels of Pb for lizards.

In the case of oral exposure, Pb is absorbed from the digestive tract, enters systematic circulation, and is subsequently delivered to every organ, including the lungs. Generally, Pb accumulation in the lungs via blood circulation is subtle. Winiarska-Mieczan and Kwiecień have reported the distribution of Pb among the organs of rats after subacute oral exposure.[48,49] In their studies, the concentration of Pb in the lungs was only 4% of that in the livers. However, in the present results, the median ratio of the lung Pb concentration to liver Pb concentration was 0.6 (Figure 4). Remarkably, 19% of the

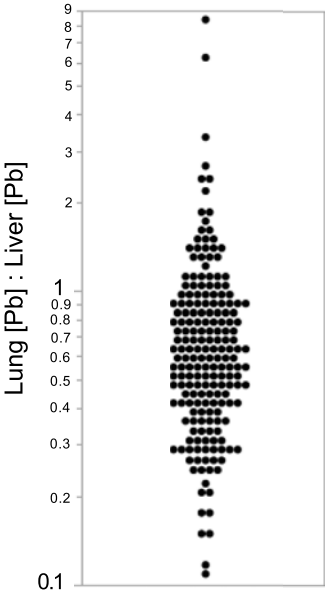

Figure 4. Distribution of the ratios of the lung Pb concentration to liver Pb concentration (N = 207).

lizards had accumulated higher concentrations of Pb in their lungs than in their livers (i.e., ratios of the lung Pb concentration to liver Pb concentration >1). Similar patterns have been reported for goats and chickens in Kabwe (Table S8, SI11).[12] If exposure via ingestion were the only pathway of Pb exposure in Kabwe, the concentration of Pb in the lungs would be much lower than that in the liver. Therefore, it is suspected that not only distribution via blood circulation but also direct exposure to Pb via dust inhalation is responsible for the high accumulation of Pb in the lungs of lizards in Kabwe. In fact, a prolonged (1 year) study on the exposure of rats to Pb-contaminated soil has shown that Pb can accumulate in tissues without exposure via food sources.[50] In that study, the Pb accumulation ratio of lungs to livers was also found to be high (0.432). Studies in the field of occupational exposure show that the absorption rate of Pb from the lungs is 40−50% after the Pb reaches the alveolar region,[51] while that from the digestive tract is only 10%.[52] Considering the high absorption rate from the lungs, Pb exposure via dust inhalation should be considered an important pathway, in addition to digestive exposure.

In rapidly developing countries, land use patterns are altered and diversified through urbanization. Topsoil is often exposed to the wind at construction sites or along temporary roads. Our results suggest that these bare lands produce dust that is contaminated with metals from pollution sources, thus increasing Pb exposure via inhalation. Apart from dust generation, several studies have reported that changes in land use can affect soil properties, altering the leaching rate and bioavailability of pollutants.[53,54] In these studies, both vegetation cover and the type of vegetation, which was not considered in this study, affected the transfer of trace elements from the environment to organisms. Overall, the influence of land use and vegetation patterns on exposure to contaminant warrants further research. Moreover, to take effective measures to mitigate the impact of contaminated land on organisms in the course of city development, exposure pathways should be well understood and taken into account from the planning phase onwards. Our results contribute to both of these needs by demonstrating the significance of land use categorization in a contaminant study and indicating the implications of respiratory exposure to metal contaminants.

■ ASSOCIATED CONTENT

Supporting Information

The Supporting Information is available free of charge at https://pubs.acs.org/doi/10.1021/acs.est.0c00150.

Detailed description of the sampling period and site locations; analytical methods; analytical results for each trace element; and the determination methods and distributions of environmental parameters (PDF)

■ AUTHOR INFORMATION

Corresponding Author

Mayumi Ishizuka − *Laboratory of Toxicology, Faculty of Veterinary Medicine, Hokkaido University, Sapporo, Hokkaido 060-0818, Japan*; orcid.org/0000-0001-5486-5745; Email: ishizum@vetmed.hokudai.ac.jp

Authors

Rio Doya − *Laboratory of Toxicology, Faculty of Veterinary Medicine, Hokkaido University, Sapporo, Hokkaido 060-0818, Japan*

Shouta M. M. Nakayama − *Laboratory of Toxicology, Faculty of Veterinary Medicine, Hokkaido University, Sapporo, Hokkaido 060-0818, Japan*

Hokuto Nakata − *Laboratory of Toxicology, Faculty of Veterinary Medicine, Hokkaido University, Sapporo, Hokkaido 060-0818, Japan*

Haruya Toyomaki − *Laboratory of Toxicology, Faculty of Veterinary Medicine, Hokkaido University, Sapporo, Hokkaido 060-0818, Japan*

John Yabe − *School of Veterinary Medicine, The University of Zambia, Lusaka, Zambia*

Kaampwe Muzandu − *School of Veterinary Medicine, The University of Zambia, Lusaka, Zambia*

Yared B. Yohannes − *Laboratory of Toxicology, Faculty of Veterinary Medicine, Hokkaido University, Sapporo, Hokkaido 060-0818, Japan*

https://dx.doi.org/10.1021/acs.est.0c00150
Environ. Sci. Technol. XXXX, XXX, XXX−XXX

Andrew Kataba − *Laboratory of Toxicology, Faculty of Veterinary Medicine, Hokkaido University, Sapporo, Hokkaido 060-0818, Japan*
Golden Zyambo − *School of Veterinary Medicine, The University of Zambia, Lusaka, Zambia*
Takahiro Ogawa − *Faculty of Information Science and Technology, Hokkaido University, Sapporo 060-0814, Japan*
Yoshitaka Uchida − *Research Faculty of Agriculture, Hokkaido University, Sapporo, Hokkaido 060-8589, Japan*
Yoshinori Ikenaka − *Laboratory of Toxicology, Faculty of Veterinary Medicine, Hokkaido University, Sapporo, Hokkaido 060-0818, Japan; Water Research Group, School of Environmental Sciences and Development, NorthWest University, Potchefstroom 2520, South Africa*

Complete contact information is available at: https://pubs.acs.org/10.1021/acs.est.0c00150

Author Contributions

#R.D. and S.M.M.N. contributed equally to this study (co-first authorship).

Notes

The authors declare no competing financial interest.

■ ACKNOWLEDGMENTS

This work was supported by the Grants-in-Aid for Scientific Research from the Ministry of Education, Culture, Sports, Science, and Technology of Japan awarded to M.I. (nos. 16H0177906, 18K1984708, and 18KK0287), Y.I. (18H0413208), and S.M.M.N. (nos. 17KK0009 and 20K20633). This work was also the result of using research equipment shared in the MEXT Project for promoting public utilization of advanced research infrastructure (Program for supporting introduction of the new sharing system) Grant no. JPMXS0420100619. This work was also supported by the foundation of JSPS Bilateral Open Partnership Joint Research Projects (JPJSBP120209902) and the Environment Research and Technology Development Fund (SII-1/3-2, 4RF-1802/18949907) of the Environmental Restoration and Conservation Agency of Japan. The authors also acknowledge financial support from the Soroptimist Japan Foundation, the Nakajima Foundation, the Sumitomo Foundation, the Nihon Seimei Foundation, and the Japan Prize Foundation. This research was also supported by JST/JICA, the Science and Technology Research Partnership for Sustainable Development (SATREPS; no. JPMJSA1501), JST aXis (Accelerating Social Implementation for SDGs Achievement no. JPMJAS2001) and the Program for supporting introduction of the new sharing system (JPMXS0420100619). Takahiro Ichise and Nagisa Hirano provided support for the technical analyses. The English in this manuscript was proofread by Uni-edit (https://uni-edit.net/usa). The authors gratefully acknowledge the contributions of Dr. Ramiro Pastorinho (Department of Biology, University of Évora, Portugal) and Dr. Ana Catarina Almeida Sousa (CICECO, Department of Chemistry, University of Aveiro, Portugal) in active discussions. The authors also wish to thank the residents of Kabwe who offered their kind help during the sampling process.

■ REFERENCES

(1) Ackah, M. Informal E-Waste Recycling in Developing Countries: Review of Metal(Loid)s Pollution, Environmental Impacts and Transport Pathways. *Environ. Sci. Pollut. Res.* **2017**, *24*, 24092−24101.
(2) Gottesfeld, P.; Were, F. H.; Adogame, L.; Gharbi, S.; San, D.; Nota, M. M.; Kuepouo, G. Soil Contamination from Lead Battery Manufacturing and Recycling in Seven African Countries. *Environ. Res.* **2018**, *161*, 609−614.
(3) Nakata, H.; Nakayama, S. M. M.; Ikenaka, Y.; Mizukawa, H.; Ishii, C.; Yohannes, Y. B.; Konnai, S.; Darwish, W. S.; Ishizuka, M. Metal Extent in Blood of Livestock from Dandora Dumping Site, Kenya: Source Identification of Pb Exposure by Stable Isotope Analysis. *Environ. Pollut.* **2015**, *205*, 8−15.
(4) Cabral, M.; Dieme, D.; Verdin, A.; Garçon, G.; Fall, M.; Bouhsina, S.; Dewaele, D.; Cazier, F.; Tall-Dia, A.; Diouf, A.; Shirali, P. Low-Level Environmental Exposure to Lead and Renal Adverse Effects: A Cross-Sectional Study in the Population of Children Bordering the Mbeubeuss Landfill near Dakar, Senegal. *Hum. Exp. Toxicol.* **2012**, *31*, 1280−1291.
(5) Yabe, J.; Nakayama, S. M. M.; Ikenaka, Y.; Yohannes, Y. B.; Bortey-Sam, N.; Oroszlany, B.; Muzandu, K.; Choongo, K.; Kabalo, A. N.; Ntapisha, J.; Mweene, A.; Umemura, T.; Ishizuka, M. Lead Poisoning in Children from Townships in the Vicinity of a Lead−Zinc Mine in Kabwe, Zambia. *Chemosphere* **2015**, *119*, 941−947.
(6) Lin, Y.-P.; Teng, T.-P.; Chang, T.-K. Multivariate Analysis of Soil Heavy Metal Pollution and Landscape Pattern in Changhua County in Taiwan. *Landscape Urban Plann.* **2002**, *62*, 19−35.
(7) Lee, C. S.-l.; Li, X.; Shi, W.; Cheung, S.; Thornton, I. Metal Contamination in Urban, Suburban, and Country Park Soils of Hong Kong: A Study Based on GIS and Multivariate Statistics. *Sci. Total Environ.* **2006**, *356*, 45−61.
(8) Xia, X.; Chen, X.; Liu, R.; Liu, H. Heavy Metals in Urban Soils with Various Types of Land Use in Beijing, China. *J. Hazard. Mater.* **2011**, *186*, 2043−2050.
(9) Luo, W.; Lu, Y.; Giesy, J. P.; Wang, T.; Shi, Y.; Wang, G.; Xing, Y. Effects of Land Use on Concentrations of Metals in Surface Soils and Ecological Risk around Guanting Reservoir, China. *Environ. Geochem. Health* **2007**, *29*, 459−471.
(10) Madejón, P.; Domínguez, M. T.; Madejón, E.; Cabrera, F.; Marañón, T.; Murillo, J. M. Soil-Plant Relationships and Contamination by Trace Elements: A Review of Twenty Years of Experimentation and Monitoring after the Aznalcóllar (SW Spain) Mine Accident. *Sci. Total Environ.* **2018**, *625*, 50−63.
(11) Scheckel, K. G.; Diamond, G. L.; Burgess, M. F.; Klotzbach, J. M. Amending Soils With Phosphate As Means To Mitigate Soil Lead Hazard: A Critical Review Of The State Of The Science. *J. Toxicol. Environ. Health, Part B* **2013**, 337−380.
(12) Nakata, H.; Nakayama, S. M. M.; Yabe, J.; Liazambi, A.; Mizukawa, H.; Darwish, W. S.; Ikenaka, Y.; Ishizuka, M. Reliability of Stable Pb Isotopes to Identify Pb Sources and Verifying Biological Fractionation of Pb Isotopes in Goats and Chickens. *Environ. Pollut.* **2016**, *208*, 395−403.
(13) Uchida, Y.; Banda, K.; Nyambe, I.; Hamamoto, T.; Yoshii, Y.; Munthali, K.; Mwansa, M.; Mukuka, M.; Mutale, M.; Yabe, J.; Toyomaki, H.; Beyene, Y. Y.; Nakayama, S. M. M.; Naruse, N.; Takahashi, Y. Multidisciplinary Field Research in Kabwe, Zambia, towards Better Understanding of Lead Contamination of the City - A Short Report from a Field Survey. *bioRxiv* **2017**, 1−13.
(14) Nakayama, S. M. M.; Ikenaka, Y.; Hamada, K.; Muzandu, K.; Choongo, K.; Teraoka, H.; Mizuno, N.; Ishizuka, M. Metal and Metalloid Contamination in Roadside Soil and Wild Rats around a Pb−Zn Mine in Kabwe, Zambia. *Environ. Pollut.* **2011**, *159*, 175−181.
(15) Yabe, J.; Nakayama, S. M. M.; Ikenaka, Y.; Muzandu, K.; Choongo, K.; Mainda, G.; Kabeta, M.; Ishizuka, M.; Umemura, T. Metal Distribution in Tissues of Free-Range Chickens near a Lead-Zinc Mine in Kabwe, Zambia. *Environ. Toxicol. Chem.* **2013**, *32*, 189−192.
(16) Yabe, J.; Nakayama, S. M. M.; Ikenaka, Y.; Muzandu, K.; Ishizuka, M.; Umemura, T. Uptake of Lead, Cadmium, and Other Metals in the Liver and Kidneys of Cattle near a Lead-Zinc Mine in Kabwe, Zambia. *Environ. Toxicol. Chem.* **2011**, *30*, 1892−1897.
(17) Yabe, J.; Mm, S.; Nakata, H.; Toyomaki, H.; Yohannes, Y. B.; Muzandu, K.; Kataba, A.; Zyambo, G.; Hiwatari, M.; Narita, D.;

Yamada, D.; Hangoma, P.; Sipilanyambe, N.; Mufune, T.; Ikenaka, Y.; Choongo, K.; Ishizuka, M. Current Trends of Blood Lead Levels, Distribution Patterns and Exposure Variations among Household Members in Kabwe, Zambia. *Chemosphere* **2020**, *243*, No. 125412.
(18) Toyomaki, H.; Yabe, J.; Nakayama, S. M. M.; Yohannes, Y. B.; Muzandu, K.; Liazambi, A.; Ikenaka, Y.; Kuritani, T.; Nakagawa, M.; Ishizuka, M. Factors Associated with Lead (Pb) Exposure on Dogs around a Pb Mining Area, Kabwe, Zambia. *Chemosphere* **2020**, *247*, No. 125884.
(19) Menon, A. V.; Chang, J.; Kim, J. Mechanisms of Divalent Metal Toxicity in Affective Disorders. *Toxicology* **2016**, *339*, 58−72.
(20) American Academy of Pediatrics. Prevention of Childhood Lead Toxicity. *Pediatrics* **2016**, *138*, No. e20161493.
(21) Centers for Disease Control and Prevention. *Interpreting and Managing Blood Lead Levels <10 μg/dL in Children and Reducing Childhood Exposures to Lead*, Recommendations of CDC's Advisory Committee on Childhood Lead Poisoning Prevention; CDC, 2007.
(22) Hopkins, W. A. Reptile Toxicology: Challenges and Opportunities on the Last Frontier in Vertebrate Ecotoxicology. *Environ. Toxicol. Chem.* **2000**, *19*, 2391−2393.
(23) Fletcher, D. E.; Hopkins, W. A.; Saldaña, T.; Baionno, J. A.; Arribas, C.; Standora, M. M.; Fernández-Delgado, C. Geckos as Indicators of Mining Pollution. *Environ. Toxicol. Chem.* **2006**, *25*, 2432−2445.
(24) Marsili, L.; Casini, S.; Mori, G.; Ancora, S.; Bianchi, N.; D'Agostino, A.; Ferraro, M.; Fossi, M. C. The Italian Wall Lizard (*Podarcis sicula*) as a Bioindicator of Oil Field Activity. *Sci. Total Environ.* **2009**, *407*, 3597−3604.
(25) Nasri, I.; Hammouda, A.; Hamza, F.; Zrig, A.; Selmi, S. Heavy Metal Accumulation in Lizards Living near a Phosphate Treatment Plant: Possible Transfer of Contaminants from Aquatic to Terrestrial Food Webs. *Environ. Sci. Pollut. Res.* **2017**, *24*, 12009−12014.
(26) Talent, L. G.; Dumont, J. N.; Bantle, J.; Janz, D. M.; Talent, S. G. Evaluation of Western Fence Lizards (*Sceloporus occidentalis*) and Eastern Fence Lizards (*Sceloporus undulatus*) as Laboratory Reptile Models for Toxicological Investigations. *Environ. Toxicol. Chem.* **2002**, *21*, 899.
(27) Mann, R. M.; Sánchez-Hernández, J. C.; Serra, E. A.; Soares, A. M. V. M. Bioaccumulation of Cd by a European Lacertid Lizard after Chronic Exposure to Cd-Contaminated Food. *Chemosphere* **2007**, *68*, 1525−1534.
(28) Alexander, G.; Marais, J. *A Guide to the Reptiles of Southern Africa*; Struik Nature, 2007; Vol. *1*.
(29) Verwaijen, D.; Van Damme, R. Wide Home Ranges for Widely Foraging Lizards. *Zoology* **2008**, *111*, 37−47.
(30) Perry, G.; Garland, T., Jr. Lizard Home Ranges Revisited: Effects of Sex, Body Size, Diet, Habitat, and Phylogeny. *Ecology* **2002**, *83*, 1870−1885.
(31) Tamura, K.; Nei, M. Estimation of the Number of Nucleotide Substitutions in the Control Region of Mitochondrial DNA in Humans and Chimpanzees. *Mol. Biol. Evol.* **1993**, *10*, 512−526.
(32) Kumar, S.; Stecher, G.; Tamura, K. MEGA7: Molecular Evolutionary Genetics Analysis Version 7.0 for Bigger Datasets. *Mol. Biol. Evol.* **2016**, *33*, 1870−1874.
(33) Kabała, C.; Musztyfaga, E.; Gałka, B.; Łabuńska, D.; Mańczyńska, P. Conversion of Soil PH 1:2.5 KCl and 1:2.5 H_2O to 1:5 H_2O: Conclusions for Soil Management, Environmental Monitoring, and International Soil Databases. *Pol. J. Environ. Stud.* **2016**, *25*, 647−653.
(34) Castiglia, R.; Corti, M.; Annesi, F. Molecular and Karyological Homogeneityin *Trachylepis striata* (Peters 1844) and *T. wahlbergii* (Peters 1869) (*Scincidae reptilia*). *Trop. Zool.* **2006**, *19*, 119−128.
(35) U.S. Environmental Protection Agency. *Ecological Soil Screening Levels for Nickel*; EPA, 2007.
(36) U.S. Environmental Protection Agency. *Ecological Soil Screening Levels for Zinc*; EPA, 2007.
(37) U.S. Environmental Protection Agency. *Ecological Soil Screening Levels for Arsenic*; EPA, 2005.
(38) U.S. Environmental Protection Agency. *Ecological Soil Screening Levels for Cadmium*; EPA, 2005.
(39) U.S. Environmental Protection Agency. *Ecological Soil Screening Levels for Lead*; EPA, 2005.
(40) U.S. Environmental Protection Agency. *Ecological Soil Screening Levels for Copper*; EPA, 2007.
(41) Tembo, B. D.; Sichilongo, K.; Cernak, J. Distribution of Copper, Lead, Cadmium and Zinc Concentrations in Soils around Kabwe Town in Zambia. *Chemosphere* **2006**, *63*, 497−501.
(42) Certini, G. Effects of Fire on Properties of Forest Soils: A Review. *Oecologia* **2005**, *143*, 1−10.
(43) Raison, R. J.; McGarity, J. W. Some Effects of Plant Ash on the Chemical Properties of Soils and Aqueous Suspensions. *Plant Soil* **1980**, *55*, 339−352.
(44) Zheng, R.; Zhao, J.; Zhou, X.; Ma, C.; Wang, L.; Gao, X. Land Use Effects on the Distribution and Speciation of Heavy Metals and Arsenic in Coastal Soils on Chongming Island in the Yangtze River Estuary, China. *Pedosphere* **2016**, *26*, 74−84.
(45) Gil-Loaiza, J.; Field, J. P.; White, S. A.; Csavina, J.; Felix, O.; Betterton, E. A.; Sáez, A. E.; Maier, R. M. Phytoremediation Reduces Dust Emissions from Metal(Loid)-Contaminated Mine Tailings. *Environ. Sci. Technol.* **2018**, *52*, 5851−5858.
(46) Salice, C. J.; Suski, J. G.; Bazar, M. A.; Talent, L. G. Effects of Inorganic Lead on Western Fence Lizards (*Sceloporus occidentalis*). *Environ. Pollut.* **2009**, *157*, 3457−3464.
(47) Holem, R. R.; Hopkins, W. A.; Talent, L. G. Effect of Acute Exposure to Malathion and Lead on Sprint Performance of the Western Fence Lizard (*Sceloporus occidentalis*). *Arch. Environ. Contam. Toxicol.* **2006**, *51*, 111−116.
(48) Winiarska-Mieczan, A.; Kwiecień, M. The Effect of Exposure to Cd and Pb in the Form of a Drinking Water or Feed on the Accumulation and Distribution of These Metals in the Organs of Growing Wistar Rats. *Biol. Trace Elem. Res.* **2016**, *169*, 230−236.
(49) Winiarska-Mieczan, A. Cumulative Rate and Distribution of Cd and Pb in the Organs of Adult Male Wistar Rats during Oral Exposure. *Environ. Toxicol. Pharmacol.* **2014**, *38*, 751−760.
(50) Nakayama, S. M. M.; Nakata, H.; Ikenaka, Y.; Yabe, J.; Oroszlany, B.; Yohannes, Y. B.; Bortey-Sam, N.; Muzandu, K.; Choongo, K.; Kuritani, T.; Nakagawa, M.; Ishizuka, M. One Year Exposure to Cd- and Pb-Contaminated Soil Causes Metal Accumulation and Alteration of Global DNA Methylation in Rats. *Environ. Pollut.* **2019**, *252*, 1267−1276.
(51) Chamberlain, A. C.; Clough, W. S.; Heard, M. J.; Newton, D.; Stott, A. N.; Wells, A. C. Uptake of Inhaled Lead from Motor Exhaust. *Postgrad. Med. J.* **1975**, *51*, 790−794.
(52) United Nations Environment Programme; International Labour Organization; World Health Organization; International Program on Chemical Safety. *Inorganic Lead*; World Health Organization, 1995.
(53) Yan, K.; Dong, Z.; Wijayawardena, M. A. A.; Liu, Y.; Naidu, R.; Semple, K. Measurement of Soil Lead Bioavailability and Influence of Soil Types and Properties: A Review. *Chemosphere* **2017**, *184*, 27−42.
(54) Tian, H.; Fang, L.; Duan, C.; Wang, Y.; Wu, H. Dominant Factor Affecting Pb Speciation and the Leaching Risk among Land-Use Types around Pb-Zn Mine. *Geoderma* **2018**, *326*, 123−132.

https://dx.doi.org/10.1021/acs.est.0c00150
Environ. Sci. Technol. XXXX, XXX, XXX−XXX

Journal of Environmental Chemical Engineering 8 (2020) 104197

Contents lists available at ScienceDirect

Journal of Environmental Chemical Engineering

journal homepage: www.elsevier.com/locate/jece

Detoxification of lead-bearing zinc plant leach residues from Kabwe, Zambia by coupled extraction-cementation method

Marthias Silwamba[a,b,*], Mayumi Ito[c], Naoki Hiroyoshi[c], Carlito Baltazar Tabelin[d], Tomoki Fukushima[a], Ilhwan Park[c], Sanghee Jeon[c], Toshifumi Igarashi[c], Tsutomu Sato[c], Imasiku Nyambe[e], Meki Chirwa[e], Kawawa Banda[e], Hokuto Nakata[f], Shouta Nakayama[f], Mayumi Ishizuka[f]

[a] Division of Sustainable Resources Engineering, Graduate School of Engineering, Hokkaido University, Sapporo, 060-8628, Japan
[b] Department of Metallurgy and Mineral Processing, School of Mines, The University of Zambia, P.O. Box 32379, Lusaka, Zambia
[c] Division of Sustainable Resources Engineering, Faculty of Engineering, Hokkaido University, Sapporo, 060-8628, Japan
[d] School of Minerals and Energy Resources Engineering, The University of New South Wales, Sydney, NSW 2052, Australia
[e] IWRM Centre/Geology Department, School of Mines, University of Zambia, P.O. Box 32379, Zambia
[f] Faculty of Veterinary Medicine, Hokkaido University, Kita 18, Nishi 9, Kita-Ku, Sapporo, 060-0818, Japan

ARTICLE INFO

Editor: Z. Wen

Keywords:
Lead
Zinc plant leach residues
Zero-valent iron
Extraction
Cementation

ABSTRACT

Zinc plant leach residues (ZPLRs) are hazardous solid wastes generated from zinc metal production owing to their substantial contents of lead (Pb), a toxic heavy metal. This study investigated the detoxification of historic ZPLRs from Kabwe, Zambia by removing Pb using a coupled extraction-cementation method in chloride media. For the coupled extraction-cementation method, micro-scale zero-valent iron (mZVI) was added during ZPLRs leaching in acidified chloride solution. Cemented Pb on the surface of mZVI was recovered easily from the leaching pulp by magnetic separation. Pb removal was evaluated in different solution compositions (NaCl:1–5.13 M, HCl: 0–0.1 M) with and without the addition of mZVI. The addition of mZVI during ZPLRs leaching (i.e., coupled extraction-cementation) increased Pb removal from 3% to 24%, 1.3% to 27.5%, 5.2% to 34.9%, and 6.5% to 55.8% when NaCl concentration was fixed at 0.86 M and HCl concentrations were 0 M, 0.01 M, 0.05 M and 0.1 M, respectively. When NaCl concentration was increased above 3.42 M and HCl maintained at 0.1 M HCl, Pb removal increased to 80%. Analysis of the Pb-loaded mZVI (magnetic fraction) by scanning electron microscopy with energy dispersive X-ray spectroscopy (SEM-EDX) and X-ray photoelectron spectroscopy (XPS) revealed that Pb was recovered during leaching via cementation as Pb°. The toxicity characteristic leaching procedure (TCLP) and in vitro solubility and bioavailability research consortium gastric phase (SBRC-G) tests for Pb of ZPLRs before and after treatment decreased drastically from 11.3 to 3.5 mg/L (below 5 mg/L threshold) and 12 300 to 2 840 mg/Kg, respectively.

1. Introduction

The rapid degradation of the environment due to heavy metal pollution is one of the most pressing global environmental concerns as highlighted by the United Nation's Sustainable Development Goals [1,2]. Anthropogenic activities such as underground space development [3–8] and mining, mineral processing and extractive metallurgy [9–13], as well as the rapid generation of municipal solid wastes and electronic wastes [14–16], including industrial and traffic emissions [17,18], are largely to blame for this degradation. Among the heavy metals of concern, lead (Pb) is one of the most problematic because of its deleterious effects on human health even at very low amounts (i.e., 0.01 mg/L levels) [3]. It is notorious for causing irreversible brain damage and severe neurological disorders in infants and children, liver and kidney diseases in both children and adults, cardiovascular diseases like anemia and various types of cancers [19,20].

Lead pollutions of the air, water, and soil are three of the biggest environmental challenges in developing countries, particularly in several African countries [21–24]. For example, Kabwe town—the capital of Central Province, Zambia (Supplementary Fig. S1a) —is one of the world's most Pb-polluted areas where the topsoil of residential areas had alarmingly high Pb content of over 2000 mg/kg [25,26]. A recent

* Corresponding author at: Division of Sustainable Resources Engineering, Graduate School of Engineering, Hokkaido University, Sapporo, 060-8628, Japan.
E-mail address: marthias.silwamba@unza.zm (M. Silwamba).

https://doi.org/10.1016/j.jece.2020.104197
Received 30 April 2020; Received in revised form 15 June 2020; Accepted 15 June 2020
Available online 18 June 2020

study on the extent of Pb poisoning in children from the residential areas of Kabwe showed blood Pb levels (BLL) as high as 4.28 mg/L [27,28], which are almost 100-fold higher than the 0.05 mg/L level recommended by the Centers for Diseases Control and Prevention [29]. The bioaccumulation of Pb in animals such as cattle, free-range chickens, goats, and wild rats has also been reported by other authors [30–32]. The excessively high Pb levels in the topsoil of residential areas in Kabwe, including its bioaccumulation in animals and humans, is partly because of the mining solid wastes generated and dumped between 1902 and 1994 when the area had a large lead-zinc (Pb-Zn) mining and processing industry. These mining solid wastes—most notably zinc plant leach residues (ZPLRs) (Supplementary Fig. S1b)—continue to pollute the area via the groundwater and/or wind dispersion as they still contain substantial amounts of Pb [25,33].

Several techniques such as immobilization of Pb by solidification/stabilization [34–36], phytoextraction/phytostabilization [37,38], and chemical extraction of Pb from ZPLRs [39–41] have been proposed as potential strategies to limit the Pb pollution problem from ZPLRs. Stabilization/solidification is, however, not a lasting detoxification approach for ZPLRs because Pb and other toxic heavy metals are only 'stored' and not permanently removed [42]. Meanwhile, phytoextraction/phytostabilization of Pb, typically requires a very long time for detoxification and suffers from serious challenges in terms of plant growth [43]. To date, solidification using bacteria and phytostabilization have been applied to stabilize Pb in ZPLRs in Kabwe [36,44]. Unfortunately, the long-term evaluation and monitoring of Pb stability after solidification have not been carried out while stunted plant growth during phytostabilization remains a critical problem.

To achieve the rapid and permanent detoxification of ZPLRs, chemical extraction of Pb may be considered as one of the best options. In hydrometallurgy, conventional chemical extraction typically follows this order [39–41,45]: leaching→solid-liquid separation→recovery. One serious drawback of this approach is the generation of residues containing residual Pb-rich solution due to the incomplete solid-liquid separation typically encountered with very fine particles like ZPLRs. A common approach to remove this residual solution from the residues after solid-liquid separation is via extensive washing or stabilization prior to disposal but both require subsequent complex treatment of the resulting waste stream. One innovative approach around this problem is the detoxification of ZPLRs via coupled extraction-cementation—a process whereby Pb from the pulp is recovered as soon as it is extracted during the leaching stage via cementation onto magnetic materials—prior to solid-liquid separation. Cementation (i.e., reductive precipitation) is a process well-known in hydrometallurgy for the recovery of redox-active metal ions and metal-complexes like those of gold, silver, copper, cobalt, and nickel [46–49]. This approach has three advantages over the previously discussed decontamination techniques: (1) Pb is removed from ZPLRs, (2) Pb is recovered for other applications, and (3) the residual solution after filtration is relatively free of dissolved Pb, so the final residue could be disposed of without the need for additional treatment. Although similar techniques have been applied to treat municipal solid waste molten fly ash [50], the applicability of coupled extraction-cementation for the detoxification of materials containing very high Pb and relatively insoluble Pb-bearing phases like those encountered in historic ZPLRs remains unknown.

In this study, detoxification of ZPLRs obtained from Kabwe via coupled extraction-cementation process using magnetic micro-scale zero-valent iron (mZVI) in chloride medium is proposed. Specifically, the objectives of this study are as follows: (1) to characterize the chemical and mineralogical properties of ZPLRs, (2) to identify the solid-phase partitioning of Pb, (3) to remove Pb from ZPLRs using the proposed technique, and (4) evaluate Pb leachability of the final residue. The first and second objectives were achieved using X-ray fluorescence spectroscopy (XRF), inductively coupled plasma atomic emission spectroscopy (ICP-AES), X-ray powder diffraction (XRD), and sequential extraction. For the third objective, coupled batch extraction-cementation experiments were carried out and the loaded mZVI was characterized by scanning electron microscopy with energy dispersive X-ray spectroscopy (SEM-EDX) and X-ray photoelectron spectroscopy (XPS). Finally, the fourth objective was accomplished by evaluating the leachability and bio-accessibility of Pb from ZPLRs before and after treatment using the toxicity characteristic leaching procedure (TCLP) and in vitro solubility and bioavailability research consortium gastric phase (SBRC-G), respectively.

2. Materials and methods

2.1. Materials

The ZPLRs samples were collected from the dump site and air-dried for 30 days in the laboratory. The samples contained compact and agglomerated particles, hence, they were lightly crushed with an agate mortar and pestle, then dry-sieved using stainless steel sieves to obtain −106 µm fraction. Light crushing to −106 µm was necessary to improve the leaching and recovery of metals. The chemical and mineralogical compositions of the ZPLRs samples have been reported in previous studies of the authors [51,52]. The ZPLRs sample is composed of 6.19 wt% Pb, 2.53 wt% Zn, 17.0 wt% Fe, 7.3 wt% Ca, and 31.4 wt% Si. The ZPLRs also contain small amounts of Cu (0.21 wt %), V (0.72 wt %) and other elements. The Pb-bearing mineral in ZPLRs include anglesite ($PbSO_4$), cerussite ($PbCO_3$), and esperite ($PbCa_2Zn_3(SiO_4)_3$). Other minerals identified in ZPLRs include gypsum ($CaSO_4{\cdot}2H_2O$), zinc sulfate dihydrate ($ZnSO_4{\cdot}2H_2O$), quartz (SiO_2), goethite (FeOOH), and hematite (Fe_2O_3).

All chemicals used for the experiments were reagent grades (Wako Pure Chemical Industries, Ltd., Osaka, Japan). Leaching solutions of different concentrations were prepared from these chemicals by dissolving them or diluting them with deionized (DI) water (18 MΩ cm, Milli-Q® Integral Water Purification System, Merck Millipore, Burlington, Vermont, USA). Ultrapure micro-scale zero-valent iron (mZVI) (> 99.9%, −150 µm, Wako Pure Chemical Industries, Ltd., Osaka, Japan) was selected as the reductant of extracted Pb^{2+} because it has a lower standard redox potential than Pb and could be collected from the pulp my magnetic separation.

2.2. Methods

2.2.1. Solid-phase fractionation of lead, zinc, and iron in zinc plant leach residues

Solid-phase fractionation of Pb, Zn, and Fe in ZPLRs was investigated by the sequential extraction procedure developed by Dold [53] for mine tailings. This was carried out to gain insights into the fraction of Pb-bearing solid phases in ZPLRs amenable to non-oxidative acidic leaching. Table S1 (Supplementary information) summarizes the different lixiviants and experimental conditions applied in each extraction step including their target solid phases. In the first step, 3 g of ZPLRs was mixed with 120 mL of deionized water in a 300-mL Erlenmeyer flask agitated using a magnetic stirrer at 200 rpm for 4 h. After equilibration, solid-liquid separation was done by centrifugation of suspensions at 3000 rpm for 20 min.. The supernatant was decanted and filtered through 0.20 µm syringe-driven membrane filters (Sartoris AG, Göttingen, Germany) and the filtrates were analyzed for Pb, as well as Zn and Fe by ICP-AES (ICPE-9820, Shimadzu Corporation, Kyoto, Japan). The solid residues were washed with 20 mL DI water before subjecting it to the next extraction step. The same procedure was repeated for all the extraction steps except for the last one (5th step). In the 5th step, the residue was dissolved in aqua regia using a microwave-assisted acid digestion system (Ethos Advanced Microwave Lab station, Milestone Inc., Sorisole, Italy) prior to ICP-AES analysis.

2.2.2. Leachability and gastric bio-accessibility tests

To assess the mobility and bio-accessibility of Pb from ZPLRs before

and after the coupled extraction-cementation procedure proposed in this study, the toxicity characteristics leaching procedure (TCLP) [54] and in vitro solubility and bioavailability research consortium gastric phase (SBRC-G) [55] leaching tests were carried out. For the TCLP, 1 g of untreated ZPLRs or treated ZPLRs was mixed with 20 mL of acetic acid solution (pH 2.89) in a centrifuge tube shaken at 30 rpm on a rotary tumbler for 18 h. After each batch leachability test, the leachate was filtered through 0.20 µm syringe-driven membrane filters and analyzed for Pb concentration using ICP-AES. To evaluate Pb solubilization in the gastric fluid of a fasting human (bio-accessibility), 1 g of sample was added in a 300 mL Erlenmeyer flask containing 100 mL solution composed of 0.4 M glycine with pH of 1.5 ± 0.05 (pH adjusted using concentrated HCl). Each flask was tightly capped using a silicon stopper and lightly shaken at 40 rpm in a thermostat water bath shaker maintained at 37 ± 0.5 °C for 1 h. After each test, the leachate was filtered through 0.20 µm syringe-driven membrane filters and analyzed for Pb concentration using ICP-AES

2.2.3. Lead removal from zinc plant leach residues by leaching in chloride solution

Batch experiments with and without coupled extraction-cementation treatment of ZPLRs were carried out using 200 mL Erlenmeyer flasks and the solution volume was fixed at 50 mL for all experiments. Solutions containing different concentrations of NaCl and HCl were added in the flasks and purged with N_2 gas for 10 min. prior to samples addition. 2.5 g of ZPLRs (i.e., solid to liquid ratio of 1:20) with and without mZVI were added in the flasks containing the leaching solutions. N_2 purging of the pulp after sample addition was carried out for 5 min. before completely sealing the flasks with silicon stoppers and parafilm®. The flasks were then shaken in a thermostat water bath shaker maintained at 25 ± 0.5 °C at a shaking speed of 120 strokes/min and amplitude of 40 mm. After the predetermined time, the suspension was collected, filtered through 0.20 µm syringe-driven membrane filters, and analyzed for Pb and Zn concentration using ICP-AES. After the coupled extraction-cementation treatment of ZPLRs, Pb-loaded mZVI was recovered from the pulp using a handheld 0.6 T permanent magnet. The magnetic fractions were then thoroughly washed with DI water and dried in a vacuum drying oven at 40 °C for 24 h. After drying, the magnetic fractions were digested using aqua regia in a microwave-assisted acid digestion system and the leachates were analyzed for Pb by ICP-AES. In addition, the magnetic fractions were analyzed by SEM-EDX (JSM-IT200, JEOL Ltd., Tokyo, Japan) and XPS (JPS-9200, JEOL Ltd., Tokyo, Japan). For the XPS analysis, a monochromatic Al Kα X-ray source operating at 140 W (voltage, 14 kV; current, 10 mA) was used to analyze the sample in a chamber maintained under ultrahigh vacuum conditions ($\sim 10^{-7}$ Pa). High-resolution narrow scan spectra of $Pb4f_{7/2}$, $Fe2p_{3/2}$, and O1 s were obtained and calibrated using the binding energy of adventitious carbon (C1 s) (285.0 eV) for charge correction. Deconvolution of the XPS spectra was done using XPSPEAK version 4.1 by applying an 80% Gaussian–20% Lorentzian peak model and a true Shirley background [56–59].

Lead removal efficiency from ZPLRs after treatment was calculated according to Eq. (1):

$$\text{Pb removal}\ (\%) = (M_m{*}W_m + C_{sol} * V_{sol})/(M_s * W_s)\,\text{x}\,100 \quad (1)$$

where M_s is the mass of ZPLRs (g), M_m is the mass of magnetic fraction (g), W_s is the weight percent of Pb in ZPLRs (%), W_m is the weight percent of Pb in magnetic fraction, C_{sol} is the Pb concentration in solution (g/L) and V_{sol} is the volume of leach solution (L). When ZPLRs were leached without the addition of mZVI, the Pb removal efficiency was calculated using Eq. (2):

$$\text{Pb removal}\ (\%) = (C_{sol} * V_{sol})/(M_s * W_s)\,\text{x}\,100 \quad (2)$$

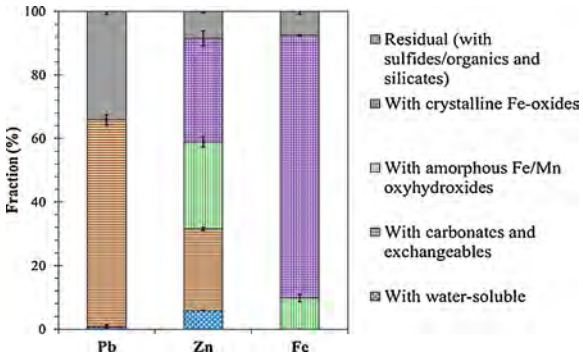

Fig. 1. Solid-phase fractionation of Pb, Zn, and Fe in zinc plant leach residues (ZPLRs).

3. Results and discussion

3.1. Solid-phase fractionation of lead, zinc, and iron in zinc plant leach residues

Solid-phase fractionation of Pb as well Zn and Fe were carried out to understand the chemical forms and solid-phase fraction amenable to non-oxidative acid leaching. Fig. 1 shows the solid-phase fractionation of Pb, Zn, and Fe in ZPLRs. Pb was mainly associated with three solid-phase fractions: 1.3% with water-soluble, 63.5% with exchangeable and carbonates, and 35.2% partitioned with the residual (in this study, residual denotes Pb associated with sulfides/organic and silicates). The results indicate up to 65% of Pb (i.e. around 65% which is the summation of water, exchangeable, and carbonates fractions) can readily dissolve from the ZPLRs and pollute the environment under slightly acidic condition. High amounts of Pb associated with exchangeable and carbonates fractions in ZPLRs may be attributed to anglesite ($PbSO_4$) and cerussite ($PbCO_3$) [51,52] that are slightly soluble in water and more soluble in acetate solution as the result of the formation of lead-acetate complexes [60,61].

Unlike Pb which was mainly partitioned in three of the five solid-phase fractions, Zn was distributed in all solid-phases in the following order: crystalline Fe-oxides > amorphous Fe/Mn oxyhydroxides ≈ carbonates > residual > water-soluble. High amounts of Zn associated with the reducible fraction (i.e., 27% at amorphous Fe/Mn oxyhydroxides and 33% crystalline Fe-oxides stages) have also been reported by Sethurajan et al. [62], Iavazzo et al. [63], and Anju and Banerjee [64] in 30-year-old ZPLRs from Brazil, abandoned mine wastes from Morocco, and soil contaminated by mining activities of Pb and Zn in India, respectively. The possible reason for Zn association with reducible fractions can be due to isomorphic substitution of Fe and co-precipitation with Fe-oxyhydroxide [65,66].

3.2. Leachability and gastric bio-accessibility of Pb from zinc plant leach residues

The leachability and gastric bio-accessibility of Pb from historic ZPLRs was evaluated by TCLP and SBRC-G. The amount of Pb leached from the ZPLRs using TCLP was around 11.3 mg/L which exceeded the allowable threshold (i.e., 5 mg/L) by over 6 mg/L. Furthermore, the SBRC-G leaching results showed that Pb of around 12 300 mg/kg (19.8% of the total Pb) could dissolve from ZLRs in gastric fluid especially for a fasting human being. The TCLP and SBRC-G leaching results indicate that Pb in ZPLRs is easily mobilized, which makes them potentially hazardous to the surrounding ecosystem and health of people living nearby.

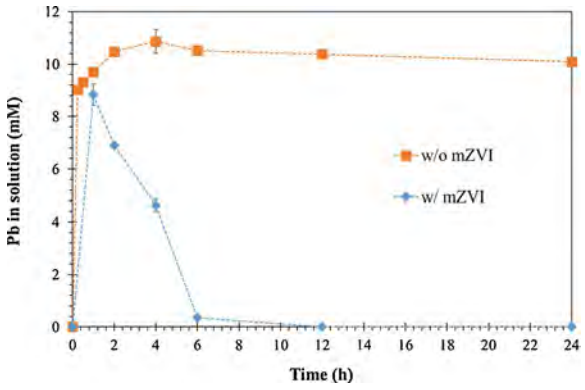

Fig. 2. The concentration of dissolved Pb from zinc plant leach residues (ZPLRs) as a function of time with and without micro-scale zero-valent iron (mZVI).

3.3. Detoxification zinc plant leach residues by removal of Pb using the coupled extraction-cementation method

3.3.1. Effects of micro-scale zero valent iron addition

The concentration of dissolved Pb from ZPLRs (2.5 g) leached in a 50 mL solution composed of 5.13 M (300 g/L) NaCl and 0.05 M HCl with and without addition 0.5 g mZVI (Fig. 2). In the absence of mZVI, the concentration of dissolved Pb increased rapidly with time, stabilizing at around 10.4 mM after 2 h. Considering the two Pb-bearing minerals —$PbSO_4$ and $PbCO_3$— that were detected in ZPLRs, Pb dissolution can be explained by the following chemical reactions [39,67]:

$$PbSO_{4(s)} + Cl^- = PbCl^+ + SO_4^{2-} \quad (3)$$

$$PbCO_{3(s)} + 2H^+ + Cl^- = PbCl^+ + H_2O + CO_2 \quad (4)$$

$$PbCl^+ + Cl^- = PbCl_{2(s)} \quad (5)$$

$$PbCl_{2(s)} + Cl^- = PbCl_3^- \quad (6)$$

$$PbCl_3^- + Cl^- = PbCl_4^{2-} \quad (7)$$

The chemical reaction depicted by Eq. (5) shows the formation of sparingly soluble $PbCl_{2(s)}$ intermediate phase (solubility of $PbCl_{2(s)}$ in water at 25 °C is 0.99 g/L). The solubilization of $PbCl_{2(s)}$ can increase by either increasing the reaction temperature [68,69] or increasing the chloride concentration to form soluble Pb-chloride complexes as depicted by Eqs. (6) and (7) [70].

When mZVI was added during ZPLRs leaching, the concentration of dissolved Pb reached a maximum of around 8.8 mM after 1 h. After this, it decreased dramatically with time to around 0.35 and $< 1 \times 10^{-6}$ mM (0.1 mg/L) after 6 and 12 h, respectively. The dissolved Pb concentration decrease after 1 h suggests that soluble Pb-Cl complexes were sequestered by mZVI, probably due to cementation (e.g., Eq. (8)).

$$PbCl_4^{2-} + Fe \rightarrow Pb + Fe^{2+} + 4Cl^- \quad (8)$$

The magnetic fraction collected after 12 h of coupled extraction-cementation treatment of ZPLRs was analyzed by SEM-EDX. The SEM photomicrograph, EDX elemental maps, and EDX spectra showed Pb cemented on the surface of mZVI particles (Fig. 3). Further analysis of the magnetic fraction was carried out to identify the elemental forms of Pb observed on the surface of mZVI by XPS analysis. The XPS spectra of Pb4f (i.e., $Pb4f_{7/2}$ and $Pb4f_{5/2}$), $Fe2p_{3/2}$, and O1s are shown in Fig. 4 and the corresponding curve fitting parameters are summarized in Table 1. The Pb4f spectrum (Fig. 4a) imply that Pb on mZVI was present in two valent forms: (1) as zero-valent lead (Pb°) at binding energy 136.59 eV ($Pbf_{7/2}$) and 141.45 eV ($Pbf_{5/2}$) [71–73], and (2) as divalent lead (Pb(II)) attributed to PbO at binding energy 138.50 eV ($Pbf_{7/2}$) and 143.32 eV ($Pbf_{5/2}$) [71,74]. The spectrum of $Fe2p_{3/2}$ (Fig. 4b) shows peaks of oxidized Fe at binding energies of 708.3 and 709.75 eV that are attributed to FeO while the peaks at binding energies at 711.1, 712.2, and 713.2 eV are attributed to goethite (α–FeOOH) [10,75]. The formation of PbO, FeO and α–FeOOH was also corroborated by the spectrum of O1s (Fig. 4c), the deconvolution of which identified several peaks at different binding energies: (1) binding energies at 529.2 and 530.1 eV are attributed to lattice oxygen (O^{2-}), (2) binding energies at 531.3 and 532.3 eV are attributed to hydroxyl oxygen (OH–), and (3) peak at binding energy at 533.4 eV is attributed to the adsorbed water (≡H_2O) [74,75]. Based on the XPS results, Pb recovered on mZVI was primarily because of the cementation of extracted Pb^{2+} on mZVI as Pb° (Eq. 8). Moreover, the presence of oxidation products of mZVI (FeO and α–FeOOH) and Pb° (PbO) could be attributed to the oxidation of mZVI and Pb° during the experiments, storage and drying because these two metals are known to readily react with oxygenated water and moist air [73,76]

The concentration of dissolved Zn when ZPLRs were leached with and without mZVI are shown in Supplementary Fig. S2. In these experiments, Zn dissolution reached 10.5 mM after 15 min but remained almost constant even after 24 h in the presence of mZVI. These results suggest that mZVI is ineffective in the recovery of dissolved Zn leached from ZPLRs via cementation, which is to be expected because dissolved Zn cementation onto mZVI is thermodynamically unfavorable because Zn^{2+}/Zn (–0.763 V vs SHE) is more electronegative than Fe^{2+}/Fe (–0.44 V vs SHE)). To recover dissolved Zn in solution, techniques such as electrowinning [78,79] or precipitation [80] may be applied but these techniques are beyond the scope of this study. From this point forward, only the results and discussion of Pb removal are presented.

3.3.2. Effects of solution composition on lead distribution in solution, mZVI, and treated residues

The experimental conditions on the study of the effects of solution composition were based on our preliminary experimental results (Supplementary Fig. S3) and previous results (Fig. 2), thus the solid-to-liquid ratio, mZVI dosage and treatment time were fixed at 1:20, 0.35 g and 12 h, respectively. During the coupled extraction-cementation treatment of ZPLRs, Pb was expected to distribute into three fractions: (1) extracted and cemented Pb on mZVI, (2), extracted Pb but remain in solution, and (3) unextracted Pb remaining in the residues.

Fig. 5 shows the effects of solution composition (i.e., NaCl and HCl concentrations) on the distribution of Pb in the three defined fractions. The distribution of Pb to mZVI was independent of NaCl when HCl concentration in the system was 0.01 M or less (Fig. 5a and b). Pb recovered on mZVI fraction was around 28% of the total Pb in ZPLRs at 0.86 M (50 g/L) NaCl solution and an insignificant increase was obtained even after increasing the NaCl concentration 6-fold to 5.13 M. At higher HCl concentrations (i.e., 0.05 M and 0.1 M), however, the partitioning of Pb to mZVI became more extensive as the NaCl concentration increased. Pb recovered by mZVI in 0.05 M and 0.1 M HCl increased from 32% to 65% and from 55% to 80% as the NaCl increased from 0.86 M to 5.13 M, respectively (Fig. 5c and d). The percentage of Pb remaining in the solution for almost all the solution compositions was almost zero except for 0.1 M HCl and 5.13 M NaCl solution composition as around 5 % (0.2 mg/L) of Pb remained in solution. This means that almost all extracted Pb was cemented out of the leaching solution for almost all the solution compositions.

The amounts of Pb removed from ZPLRs when leached with and without the addition of mZVI in different leaching solution compositions were compared. As defined in Eq. (2), Pb removal without mZVI addition during ZPLRs leaching is referred to as %Pb distributed in solution, whereas when mZVI was added Pb removal corresponds to the summation of %Pb distributed to the solution and mZVI (Eq. (1)). Because Pb remaining in solution was almost 0% in the presence of mZVI, it is reasonable to assume that Pb removal by mZVI is approximately equal to %Pb distributed to mZVI. When ZPLRs were leached without the addition of mZVI, Pb removal increased with increasing NaCl and HCl concentrations (Fig. 6a–c). However, the dependence of Pb removal

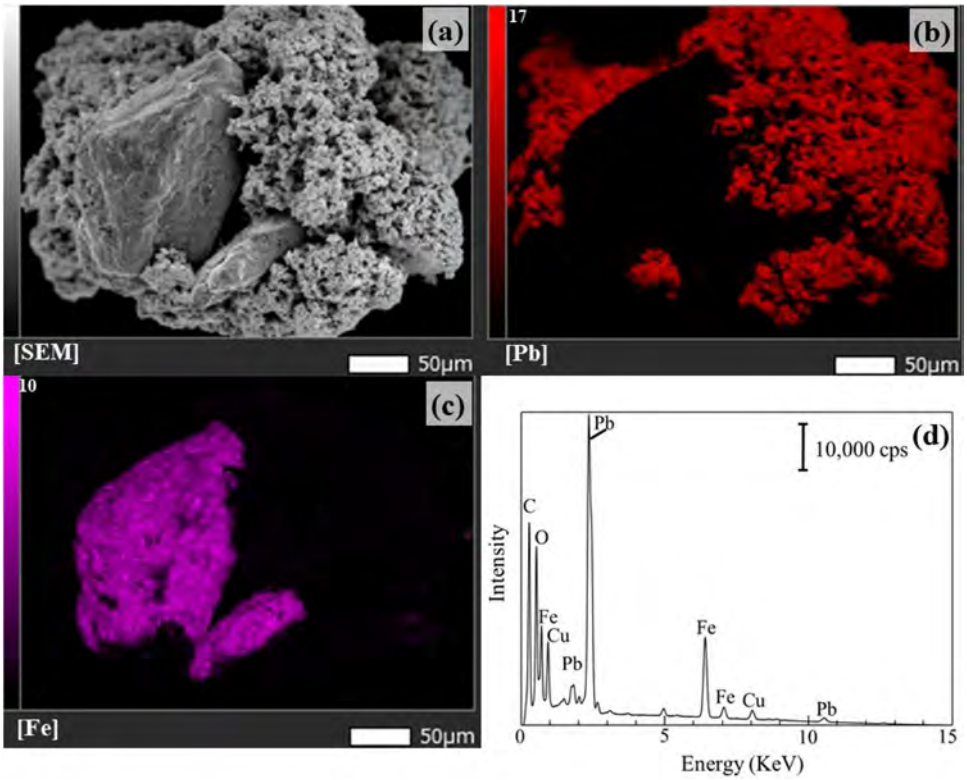

Fig. 3. SEM-EDX of the magnetic fraction obtained when mZVI was added during ZPLRs leaching for 12 h: (a) SEM microphotograph image, (b) EDX elemental mapping of Pb, (c) EDX elemental mapping of Fe, and (d) EDX spectra of the whole area.

from ZPLRs on NaCl concentration was insignificant when HCl was < 0.05 M (Fig. 6a&b). For example, for 0 and 0.01 M HCl increasing NaCl to 5.13 M removed Pb of around 16% and 32%, respectively. When HCl concentration was increased to 0.05 M and 0.1 M, Pb removal increased with increasing NaCl concentration (Fig. 6c&d). For the former case, the maximum Pb removal was around 70% at the highest NaCl concentration of 5.13 M while for the latter the removal was around 80% when NaCl concentration was 5.13 M.

The addition of mZVI during ZPLRs leaching (i.e., the coupled extraction-cementation technique) favored Pb removal at low NaCl concentrations (Fig. 6a–c). For example, when NaCl concentration was fixed at 0.86 M and HCl concentrations were 0, 0.01, 0.05 and 0.1 M, Pb removal increased from 3 to 24 %, 1.3 to 27.5 %, 5.2 to 34.9 %, and 6.5 to 55.8 %, respectively. It is also noteworthy that the highest Pb removal obtained was around 80% of the total Pb in ZPLRs when HCl and NaCl concentrations were 0.1 M HCl and above 3.42 M, respectively. This was higher than the amount of Pb amenable to acid leaching as determined by sequential extraction (65 %), which may be attributed to the dissolution of Pb associated with sulfide/organics. Cl– in acidic solutions typically enhances the non-oxidative dissolution of sulfide minerals (i.e. galena) [81–83].

The increase of Pb removal as NaCl concentration increased was attributed to the formation of soluble Pb-Cl complexes (i.e., $PbCl_3^-$ and $PbCl_4^{2-}$) as previous explained in chemical reactions in Eq. (5)–(7) and depicted in Supplementary Fig. S4. Additionally, the concentration of sulfate (SO_4^{2-}) in the leaching system determines the required concentration of chloride (Cl–) for chemical reaction represented by Eq. (3) to move forward to its completion. Furthermore, SO_4^{2-} and Cl–

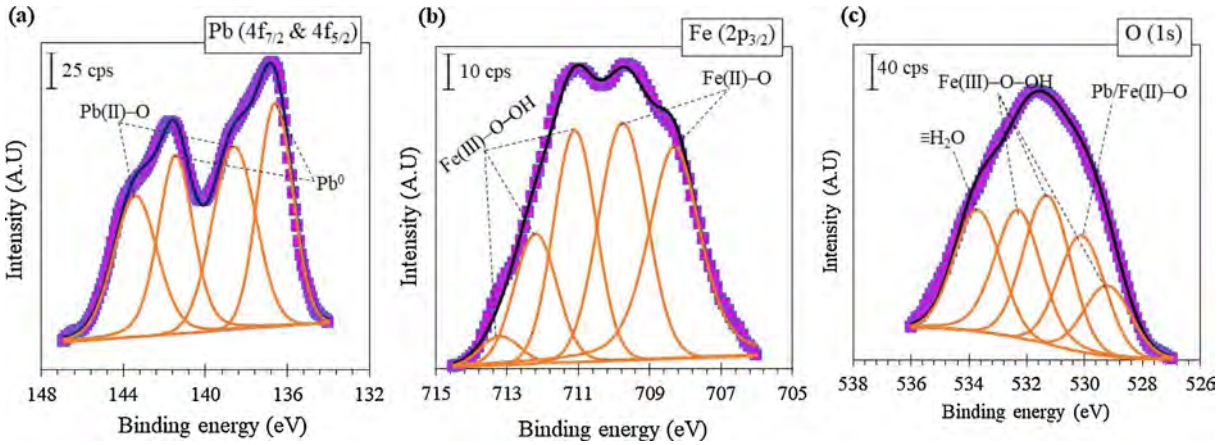

Fig. 4. XPS of the magnetic fraction obtained when mZVI was added during ZPLRs leaching for 12 h: (a) $Pb4f_{7/2\&5/2}$, (b) $Fe2p_{5/2}$, and (c) O1 s. Data points are represented by squares, fitted results are referred to by the dark blue lines, and deconvoluted peaks are denoted by orange lines. (For interpretation of the references to color in this figure legend, the reader is referred to the web version of this article.)

Table 1
XPS peak parameters and chemical state of Pb $4f_{7/2\&5/2}$, $Fe2p_{5/2}$, and O1 s spectra.

Spectra Peak	Binding Energy (eV) This study	Reference	FWHM This study	Reference	Comments (chemical state)
$Pb4f_{7/2}$	136.56	136.6[a]	2.01	–	Zero-valent lead (Pb^0)
$Pb4f_{5/2}$	141.45	141.5[a]	2.01	–	Zero-valent lead (Pb^0)
$Pb4f_{7/2}$	138.5	137.8[a]	2.5	–	Lead oxide (Pb(II)–O)
$Pb4f_{5/2}$	143.32	142.7[a]	2.5	–	Lead oxide (Pb(II)–O)
$Fe2p_{3/2}$	708.3	708.4[b]	1.65	1.4[b]	Iron oxide (Fe(II)–O)
$Fe2p_{3/2}$	709.75	709.7[b]	1.65	1.6[b]	Iron oxide (Fe(II)–O)
$Fe2p_{3/2}$	711.1	711.2[b]	1.4	1.2[b]	Iron hydroxide (α–Fe(III)–O–OH)
$Fe2p_{3/2}$	712.2	712.1[b]	1.4	1.4[b]	Iron hydroxide (α–Fe(III)–O–OH)
$Fe2p_{3/2}$	713.2	713.2[b]	1.4	1.4[b]	Iron hydroxide (α–Fe(III)–O–OH)
O1 s	529.2	529.9[b]	1.9	–	Hydroxyl oxygen in Fe hydroxide (O^{2-})
O1 s	530.1	530.0[c]	1.9	–	Lattice oxygen in Pb and Fe oxide (O^{2-})
O1 s	531.3	531.2[e]	1.9	1.6[e]	Hydroxyl oxygen in Fe hydroxide (OH–)
O1 s	532.3	532.3[e]	1.9	1.6[e]	Hydroxyl oxygen in Fe hydroxide (OH–)
O1 s	533.7	533.2[e]	1.9	1.6[e]	Adsorbed water (≡H_2O)

[a] [72]; [b] [75]; [c] [77]; [e] [57]. Note "-" means "not reported".

concentration in the leaching system affect dissolved Pb^{2+} resulting from $PbCO_3$ leaching (depicted in Eq. (4)) from precipitating as $PbSO_4$. In our leaching system, the source of SO_4^{2-} is not only $PbSO_4$ but also $CaSO_4{\cdot}2H_2O$ and $ZnSO_4{\cdot}2H_2O$, hence the need of high NaCl concentration to attain high Pb removal. Furthermore, proton (H^+) concentration (i.e., pH) also plays crucial role in release of Pb from both $PbSO_4$ and $PbCO_3$ minerals. Pb dissolution as function of H^+ concentration for the former mineral is indirect in the sense that it involves the speciation of SO_4^{2-}. At low pH SO_4^{2-} speciate as bisulfate (HSO_4^-) [84], meaning high H^+ concentration lowers the free SO_4^{2-} concentration in the leaching system that would hinder the chemical reaction depicted in Eq. (3) going in the forward direction (right direction), that is, promotes precipitation of $PbSO_4$.

Meanwhile, the enhancement of Pb removal from ZPLRs at low chloride (NaCl) concentration when mZVI was added during leaching can be attributed to shifting the equilibrium between the dissolved Pb (i.e., Pb^{2+} and $PbCl^+$) and sparingly soluble solid $PbCl_{2(s)}$ as well as Pb host minerals—$PbSO_4$ and $PbCO_3$. The addition of mZVI consumes Pb^{2+} and $PbCl^+$ by reductive precipitation (Eq. (8)), so more $PbSO_4$(s) dissolves by the shift of equilibria in Eqs. (3)–(5). This could be one possible reason for the enhanced removal of Pb from ZPLRs when mZVI was added.

3.4. Leachability and gastric bio-accessibility of Pb from treated residues

The leachability (TCLP leaching test) and bio-accessibility (SBRC-G leaching test) of Pb from the residues after coupled extraction-cementation treatment (conditions: 5.13 M NaCl and 0.1 M HCl with addition of 0.35 g of mZVI) showed significant decrease from 11.3 (untreated ZPLRs) to 3.5 mg/L (below 5 mg/L which is the regulatory threshold [54]) and 12 300 (untreated ZPLRs) to 2840 mg/kg, respectively. These results suggest that detoxification of ZPLRs by coupled extraction-cementation using mZVI is effective. The coupled extraction-cemntation eliminated not only the need to extensively wash the generated residues to remove residual leaching solution but also the treatment of the contaminated solution after washing. Finally, the recovered Pb may be reprocessed for other applications. The technique may also be extended to the decontamination of soils containing toxic

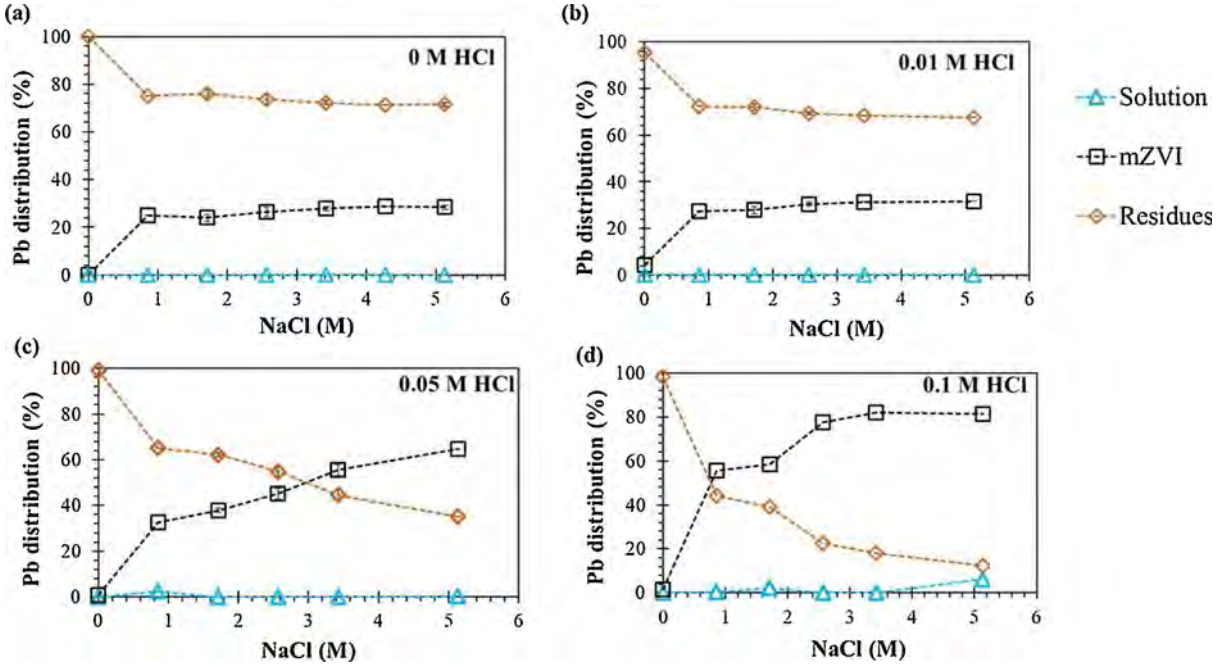

Fig. 5. Effects of solution composition on distribution of Pb in three solution, mZVI and residues: (a) 0 M HCl and 0–5.13 M NaCl, (b) 0.01 M HCl and 0–5.13 M NaCl, (c) 0.05 M HCl and 0–5.13 M NaCl, and (d) 0.1 M HCl and 0–5.13 M NaCl.

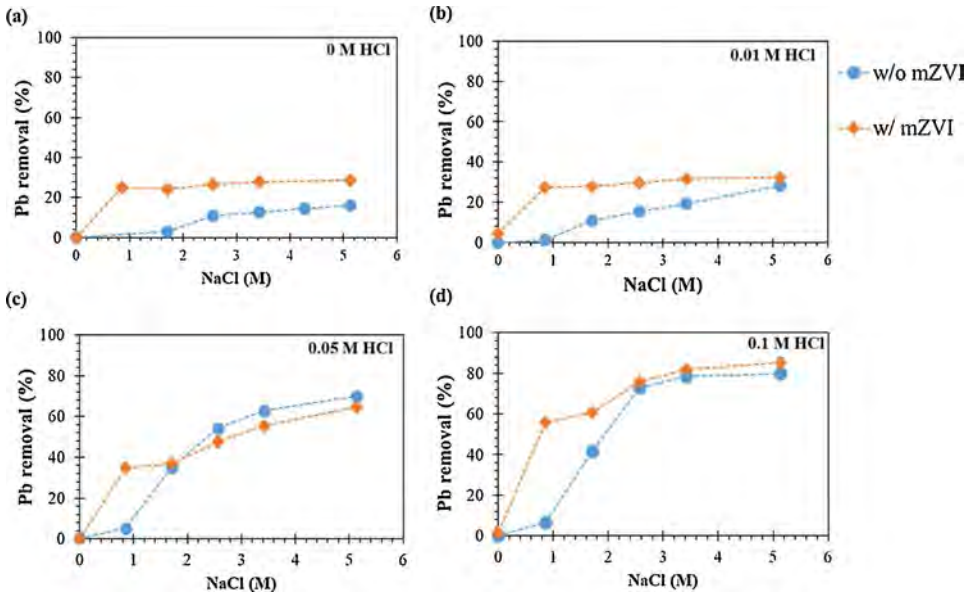

Fig. 6. Effects of solution composition on Pb removal from ZPLRs with and without addition of mZVI: (a) 0 M HCl and 0–5.13 M NaCl, (b) 0.01 M HCl and 0–5.13 M NaCl, (c) 0.05 M HCl and 0–5.13 M NaCl, and (d) 0.1 M HCl and 0–5.13 M NaCl.

and hazardous elements like mercury (Hg) from small-scale mining operations as well as the recovery of valuable elements like palladium (Pd) and gold (Au) from wastes.

4. Conclusions

This study investigated the detoxification of historic ZPLRs from Kabwe, Zambia by removing Pb using the coupled extraction-cementation method using mZVI in chloride media. Pb removal was investigated under different solution compositions and the detoxification efficacy of the method was evaluated using TCLP and SBRC-G. The findings are summarized as follows:

1) Concentration Pb^{2+} in the leaching solution was < 0.1 mg/L at the end of the treatment of ZPLRs by the coupled extraction-cementation method, so treated residues may not need extensive washing for the removal of a residual solution after solid-liquid separation;
2) Lead removal was low especially at low NaCl and HCl concentration (i.e. Pb removal 6.5% at 0.86 M NaCl and 0.1 M HCl) when ZPLRs were leached without the addition of mZVI, which could be attributed to the leaching solution reaching saturation with dissolved Pb^{2+};
3) The coupled extraction-cementation method significantly enhanced Pb removal even at low NaCl and HCl concentration (i.e. Pb removal from 6.5 to 55.8% when mZVI was added at 0.86 M NaCl and 0.1 M HCl), which was ascribed to shifting of equilibrium between dissolved Pb (i.e., Pb^{2+} and $PbCl^{+}$) and the Pb host minerals (i.e., $PbSO_4$ and $PbCO_3$) as well as sparingly intermediate solid product $PbCl_2$(s);
4) Lead removal increased to around 80% when NaCl concentration was above 3.42 M in 0.1 M HCl solution; and
5) Leachability of Pb from ZPLRs before and after treatment by the coupled extraction-cementation method drastically decreased from 11.3 to 3.5 mg/L, which was below the regulatory threshold of 5 mg/L. Similarly, the bio-accessibility of Pb from the untreated and treated ZPLRs decreased from 12 300 to 2 840 mg/kg.

CRediT authorship contribution statement

Marthias Silwamba: Conceptualization, Methodology, Investigation, Writing - original draft, Writing - review & editing, Project administration. **Mayumi Ito:** Conceptualization, Methodology, Supervision, Writing - original draft, Project administration. **Naoki Hiroyoshi:** Conceptualization, Methodology, Formal analysis, Writing - original draft, Project administration. **Carlito Baltazar Tabelin:** Writing - original draft, Project administration. **Tomoki Fukushima:** Investigation. **Ilhwan Park:** Writing - original draft, Project administration. **Sanghee Jeon:** Writing - original draft, Project administration. **Toshifumi Igarashi:** Project administration. **Tsutomu Sato:** Project administration. **Imasiku Nyambe:** Project administration. **Meki Chirwa:** Project administration. **Kawawa Banda:** Project administration. **Hokuto Nakata:** Funding acquisition. **Shouta Nakayama:** Funding acquisition. **Mayumi Ishizuka:** Project administration, Funding acquisition.

Declaration of Competing Interest

The authors declare that they have no known competing financial interests or personal relationships that could have appeared to influence the work reported in this paper.

Acknowledgments

This work was supported partly by the Japan Science and Technology Agency (JST), and Science and Technology Research Partnership for Sustainable Development (SATREPS) under grant number JPMJSA1505.

Appendix A. Supplementary data

Supplementary material related to this article can be found, in the online version, at doi:https://doi.org/10.1016/j.jece.2020.104197.

References

[1] A. Farmer, Tackling Pollution Is Essential for Meeting SDG Poverty Objectives, London: Institute for European Environmental Policy, 2017.
[2] U.N. Nation Sustainable Development Goals, (2018).
[3] C.B. Tabelin, T. Igarashi, M. Villacorte-Tabelin, I. Park, E.M. Opiso, M. Ito, N. Hiroyoshi, Arsenic, selenium, boron, lead, cadmium, copper, and zinc in naturally contaminated rocks: A review of their sources, modes of enrichment, mechanisms of release, and mitigation strategies, Sci. Total Environ. 645 (2018) 1522–1553, https://doi.org/10.1016/j.scitotenv.2018.07.103.

[4] C. Tabelin, R. Sasaki, T. Igarashi, I. Park, S. Tamoto, T. Arima, M. Ito, N. Hiroyoshi, Simultaneous leaching of arsenite, arsenate, selenite and selenate, and their migration in tunnel-excavated sedimentary rocks: I. Column experiments under intermittent and unsaturated flow, Chemosphere. 186 (2017) 558–569, https://doi.org/10.1016/j.chemosphere.2017.07.145.
[5] C.B. Tabelin, A. Hashimoto, T. Igarashi, T. Yoneda, Leaching of boron, arsenic and selenium from sedimentary rocks: I. Effects of contact time, mixing speed and liquid-to-solid ratio, Sci. Total Environ. 472 (2014) 620–629, https://doi.org/10.1016/j.scitotenv.2013.11.006.
[6] C.B. Tabelin, T. Igarashi, S. Tamoto, R. Takahashi, The roles of pyrite and calcite in the mobilization of arsenic and lead from hydrothermally altered rocks excavated in Hokkaido, Japan, J. Geochem. Explor. 119–120 (2012) 17–31, https://doi.org/10.1016/j.gexplo.2012.06.003.
[7] S. Tamoto, C.B. Tabelin, T. Igarashi, M. Ito, N. Hiroyoshi, Short and long term release mechanisms of arsenic, selenium and boron from a tunnel-excavated sedimentary rock under in situ conditions, J. Contam. Hydrol. 175–176 (2015) 60–71, https://doi.org/10.1016/j.jconhyd.2015.01.003.
[8] T. Tatsuhara, T. Arima, T. Igarashi, C.B. Tabelin, Combined neutralization–adsorption system for the disposal of hydrothermally altered excavated rock producing acidic leachate with hazardous elements, Eng. Geol. 139–140 (2012) 76–84, https://doi.org/10.1016/j.enggeo.2012.04.006.
[9] I. Park, C.B. Tabelin, S. Jeon, X. Li, K. Seno, M. Ito, N. Hiroyoshi, A review of recent strategies for acid mine drainage prevention and mine tailings recycling, Chemosphere 219 (2019) 588–606, https://doi.org/10.1016/j.chemosphere.2018.11.053.
[10] C.B. Tabelin, R.D. Corpuz, T. Igarashi, M. Villacorte-Tabelin, M. Ito, N. Hiroyoshi, Hematite-catalysed scorodite formation as a novel arsenic immobilisation strategy under ambient conditions, Chemosphere 233 (2019) 946–953, https://doi.org/10.1016/j.chemosphere.2019.06.020.
[11] S. Tomiyama, T. Igarashi, C.B. Tabelin, P. Tangviroon, H. Ii, Acid mine drainage sources and hydrogeochemistry at the Yatani mine, Yamagata, Japan: A geochemical and isotopic study, J. Contam. Hydrol. 225 (2019) 103502, https://doi.org/10.1016/j.jconhyd.2019.103502.
[12] C. Lei, B. Yan, T. Chen, S.-X. Quan, X.-M. Xiao, Comprehensive utilization of lead–zinc tailings, part 1: pollution characteristics and resource recovery of sulfur, J. Environ. Chem. Eng. 3 (2015) 862–869, https://doi.org/10.1016/j.jece.2015.03.015.
[13] G.S. Simate, S. Ndlovu, Acid mine drainage: challenges and opportunities, J. Environ. Chem. Eng. 2 (2014) 1785–1803, https://doi.org/10.1016/j.jece.2014.07.021.
[14] M. Ito, M. Takeuchi, A. Saito, N. Murase, T. Phengsaart, C.B. Tabelin, N. Hiroyoshi, Improvement of hybrid jig separation efficiency using wetting agents for the recycling of mixed-plastic wastes, J. Mater Cycles Waste Manag. 21 (2019) 1376–1383, https://doi.org/10.1007/s10163-019-00890-w.
[15] S. Jeon, M. Ito, C.B. Tabelin, R. Pongsumrankul, S. Tanaka, N. Kitajima, A. Saito, I. Park, N. Hiroyoshi, A physical separation scheme to improve ammonium thiosulfate leaching of gold by separation of base metals in crushed mobile phones, Miner. Eng. 138 (2019) 168–177, https://doi.org/10.1016/j.mineng.2019.04.025.
[16] T. Phengsaart, M. Ito, N. Hamaya, C.B. Tabelin, N. Hiroyoshi, Improvement of jig efficiency by shape separation, and a novel method to estimate the separation efficiency of metal wires in crushed electronic wastes using bending behavior and “entanglement factor”, Miner. Eng. 129 (2018) 54–62, https://doi.org/10.1016/j.mineng.2018.09.015.
[17] C.L.S. Wiseman, F. Zereini, W. Püttmann, Traffic-related trace element fate and uptake by plants cultivated in roadside soils in Toronto, Canada, Sci. Total Environ. 442 (2013) 86–95, https://doi.org/10.1016/j.scitotenv.2012.10.051.
[18] G. Yan, L. Mao, S. Liu, Y. Mao, H. Ye, T. Huang, F. Li, L. Chen, Enrichment and sources of trace metals in roadside soils in Shanghai, China: a case study of two urban/rural roads, Sci. Total Environ. 631–632 (2018) 942–950, https://doi.org/10.1016/j.scitotenv.2018.02.340.
[19] M. Jaishankar, T. Tseten, N. Anbalagan, B.B. Mathew, K.N. Beeregowda, Toxicity, mechanism and health effects of some heavy metals, Interdiscip, Toxicol. 7 (2014) 60–72, https://doi.org/10.2478/intox-2014-0009.
[20] H. Needleman, Lead poisoning, Annu. Rev. Med. 55 (2004) 209–222, https://doi.org/10.1146/annurev.med.55.091902.103653.
[21] S.A.M.S. Eqani, R. Khalid, N. Bostan, Z. Saqib, J. Mohmand, M. Rehan, N. Ali, I.A. Katsoyiannis, H. Shen, Human lead (Pb) exposure via dust from different land use settings of Pakistan: A case study from two urban mountainous cities, Chemosphere 155 (2016) 259–265, https://doi.org/10.1016/j.chemosphere.2016.04.036.
[22] G. Ngueta, R. Ndjaboue, Blood lead concentrations in sub-Saharan African children below 6 years: systematic review, Trop. Med. Int. Health 18 (2013) 1283–1291, https://doi.org/10.1111/tmi.12179.
[23] O.C. Nweke, W.H. Sanders, Modern environmental health hazards: a public health issue of increasing significance in Africa, Environ. Health Perspect. 117 (2009) 863–870, https://doi.org/10.1289/ehp.0800126.
[24] D.J. Oyedele, I.B. Obioh, J.A. Adejumo, A.F. Oluwole, P.O. Aina, O.I. Asubiojo, Lead contamination of soils and vegetation in the vicinity of a lead smelter in Nigeria, Sci. Total Environ. 172 (1995) 189–195, https://doi.org/10.1016/0048-9697(95)04810-3.
[25] B. Kříbek, I. Nyambe, V. Majer, I. Knésl, M. Mihaljevič, V. Ettler, A. Vaněk, V. Penížek, O. Sracek, Soil contamination near the Kabwe Pb-Zn smelter in Zambia: Environmental impacts and remediation measures proposal, J. Geochem. Explor. 197 (2019) 159–173, https://doi.org/10.1016/j.gexplo.2018.11.018.
[26] B.D. Tembo, K. Sichilongo, J. Cernak, Distribution of copper, lead, cadmium and zinc concentrations in soils around Kabwe town in Zambia, Chemosphere 63 (2006) 497–501, https://doi.org/10.1016/j.chemosphere.2005.08.002.
[27] J. Yabe, S.M.M. Nakayama, H. Nakata, H. Toyomaki, Y.B. Yohannes, K. Muzandu, A. Kataba, G. Zyambo, M. Hiwatari, D. Narita, D. Yamada, P. Hangoma, N.S. Munyinda, T. Mufune, Y. Ikenaka, K. Choongo, M. Ishizuka, Current Trends of Blood Lead Levels, Distribution Patterns and Exposure Variations among Household Members in Kabwe, Zambia, Chemosphere (2019) 125412, https://doi.org/10.1016/j.chemosphere.2019.125412.
[28] J. Yabe, S.M.M. Nakayama, Y. Ikenaka, Y.B. Yohannes, N. Bortey-Sam, B. Oroszlany, K. Muzandu, K. Choongo, A.N. Kabalo, J. Ntapisha, A. Mweene, T. Umemura, M. Ishizuka, Lead poisoning in children from townships in the vicinity of a lead–zinc mine in Kabwe, Zambia, Chemosphere 119 (2015) 941–947, https://doi.org/10.1016/j.chemosphere.2014.09.028.
[29] CDC, Low Level Lead Exposure Harms Children: a Renewed Call for Primary Prevention. Report of the Advisory Committee on Childhood Lead Poisoning Prevention of the Centers for Disease Control and Prevention, Atlanta (2012).
[30] S.M.M. Nakayama, Y. Ikenaka, K. Hamada, K. Muzandu, K. Choongo, H. Teraoka, N. Mizuno, M. Ishizuka, Metal and metalloid contamination in roadside soil and wild rats around a Pb–Zn mine in Kabwe, Zambia, Environ. Pollut. 159 (2011) 175–181, https://doi.org/10.1016/j.envpol.2010.09.007.
[31] J. Yabe, S.M.M. Nakayama, Y. Ikenaka, K. Muzandu, K. Choongo, G. Mainda, M. Kabeta, M. Ishizuka, T. Umemura, Metal distribution in tissues of free-range chickens near a lead–zinc mine in Kabwe, Zambia, Environ. Toxicol. Chem. 32 (2013) 189–192, https://doi.org/10.1002/etc.2029.
[32] J. Yabe, S.M.M. Nakayama, Y. Ikenaka, K. Muzandu, M. Ishizuka, T. Umemura, Uptake of lead, cadmium, and other metals in the liver and kidneys of cattle near a lead-zinc mine in Kabwe, Zambia, Environ. Toxicol. Chem. 30 (2011) 1892–1897, https://doi.org/10.1002/etc.580.
[33] ZCCM-IH, Environmental assessment of the copperbelt and Kabwe Area, Zambia Consolidated Copper Mines Investment Holdings, (2002).
[34] G. Demır, S. Çoruh, O.N. Ergun, Leaching behavior and immobilization of heavy metals in zinc leach residue before and after thermal treatment, Environ. Prog. 27 (2008) 479–486, https://doi.org/10.1002/ep.10302.
[35] M. Erdem, A. Özverdi, Environmental risk assessment and stabilization/solidification of zinc extraction residue: II. Stabilization/solidification, Hydrometallurgy 105 (2011) 270–276, https://doi.org/10.1016/j.hydromet.2010.10.014.
[36] W. Mwandira, K. Nakashima, S. Kawasaki, M. Ito, T. Sato, T. Igarashi, M. Chirwa, K. Banda, I. Nyambe, S. Nakayama, H. Nakata, M. Ishizuka, Solidification of sand by Pb(II)-tolerant bacteria for capping mine waste to control metallic dust: Case of the abandoned Kabwe Mine, Zambia, Chemosphere 228 (2019) 17–25, https://doi.org/10.1016/j.chemosphere.2019.04.107.
[37] P.B.A.N. Kumar, V. Dushenkov, H. Motto, I. Raskin, Phytoextraction: The use of plants to remove heavy metals from soils, Environ. Sci. Technol. 29 (1995) 1232–1238, https://doi.org/10.1021/es00005a014.
[38] B. Lorestani, N. Yousefi, M. Cheraghi, A. Farmany, Phytoextraction and phytostabilization potential of plants grown in the vicinity of heavy metal-contaminated soils: a case study at an industrial town site, Environ. Monit. Assess. 185 (2013) 10217–10223, https://doi.org/10.1007/s10661-013-3326-9.
[39] F. Farahmand, D. Moradkhani, M.S. Safarzadeh, F. Rashchi, Brine leaching of lead-bearing zinc plant residues: process optimization using orthogonal array design methodology, Hydrometallurgy 95 (2009) 316–324, https://doi.org/10.1016/j.hydromet.2008.07.012.
[40] A. Ruşen, A.S. Sunkar, Y.A. Topkaya, Zinc and lead extraction from Çinkur leach residues by using hydrometallurgical method, Hydrometallurgy 93 (2008) 45–50, https://doi.org/10.1016/j.hydromet.2008.02.018.
[41] M.D. Turan, H.S. Altundoğan, F. Tümen, Recovery of zinc and lead from zinc plant residue, Hydrometallurgy 75 (2004) 69–76, https://doi.org/10.1016/j.hydromet.2004.07.008.
[42] L. Tiruta-Barna, A. Imyim, R. Barna, Long-term prediction of the leaching behavior of pollutants from solidified wastes, Adv. Environ. Res. 8 (2004) 697–711, https://doi.org/10.1016/S1093-0191(03)00042-X.
[43] S.D. Cunningham, W.R. Berti, Phytoextraction and phytostabilization: technical, economic, and regulatory considerations of the Soil–Lead issue, Phytoremediation of Contaminated Soil and Water, Lewis Publishers, Boca Raton, 2000, pp. 359–379.
[44] B. Leteinturier, J. Laroche, J. Matera, F. Malaisse, Reclamation of lead / zinc processing wastes at Kabwe, Zambia: a phytogeochemical approach, S. Afr. J. Sci. 97 (2001) 624–627.
[45] F. Farahmand, D. Moradkhani, S.M. Safarzadeh, F. Rashchi, Optimization and kinetics of the cementation of lead with aluminum powder, Hydrometallurgy 98 (2009) 81–85, https://doi.org/10.1016/j.hydromet.2009.04.001.
[46] S. Choi, K. Yoo, R.D. Alorro, C.B. Tabelin, Cementation of Co ion in leach solution using Zn powder followed by magnetic separation of cementation-precipitate for recovery of unreacted Zn powder, Miner. Eng. 145 (2020) 106061, https://doi.org/10.1016/j.mineng.2019.106061.
[47] N. Demirkıran, A. Ekmekyapar, A. Künkül, A. Baysar, A kinetic study of copper cementation with zinc in aqueous solutions, Int. J. Miner. Process. 82 (2007) 80–85, https://doi.org/10.1016/j.minpro.2006.10.005.
[48] S. Jeon, C.B. Tabelin, H. Takahashi, I. Park, M. Ito, N. Hiroyoshi, Enhanced cementation of gold via galvanic interactions using activated carbon and zero-valent aluminum: a novel approach to recover gold ions from ammonium thiosulfate medium, Hydrometallurgy 191 (2020) 105165, , https://doi.org/10.1016/j.hydromet.2019.105165.
[49] S. Jeon, C.B. Tabelin, I. Park, Y. Nagata, M. Ito, N. Hiroyoshi, Ammonium thiosulfate extraction of gold from printed circuit boards (PCBs) of end-of-life mobile phones and its recovery from pregnant leach solution by cementation, Hydrometallurgy 191 (2020) 105214, , https://doi.org/10.1016/j.hydromet.2019.105214.

[50] R.D. Alorro, S. Mitani, N. Hiroyoshi, M. Ito, M. Tsunekawa, Recovery of heavy metals from MSW molten fly ash by carrier-in-pulp method: Fe powder as carrier, Miner. Eng. 21 (2008) 1094–10101, https://doi.org/10.1016/j.mineng.2008.02.005.

[51] M. Silwamba, M. Ito, N. Hiroyoshi, C.B. Tabelin, R. Hashizume, T. Fukushima, I. Park, S. Jeon, T. Igarashi, T. Sato, M. Chirwa, K. Banda, I. Nyambe, H. Nakata, S. Nakayama, M. Ishizuka, Recovery of lead and zinc from zinc plant leach residues by concurrent dissolution-cementation using zero-valent aluminum in chloride medium, Metals 10 (2020) 531, https://doi.org/10.3390/met10040531.

[52] M. Silwamba, M. Ito, T. Fukushima, C.B. Tabelin, S. Takakuwa, N. Hiroyoshi, et al., Characterization of zinc leaching residue in Kabwe area, Zambia, Proceedings of the 2nd International Kabwe Mine Pollution Amelioration Initiative (KAMPAI)/JST, Lusaka, Zambia. 12 August, 2019, p. 22.

[53] B. Dold, Speciation of the most soluble phases in a sequential extraction procedure adapted for geochemical studies of copper sulfide mine waste, J. Geochem. Explor. 80 (2003) 55–68, https://doi.org/10.1016/S0375-6742(03)00182-1.

[54] U.S. EPA, Toxicity Characteristic Leaching Procedure (TCLP), Test Method 1311-TCLP, (1991).

[55] U.S. EPA, Estimation of Relative Bioaccessibility of Lead in Soil and Soil-like Materials Using in Vivo and in Vitro Methods, (2007).

[56] H.W. Nesbitt, I.J. Muir, X-ray photoelectron spectroscopic study of a pristine pyrite surface reacted with water vapour and air, Geochim. Cosmochim. Acta 58 (1994) 4667–4679, https://doi.org/10.1016/0016-7037(94)90199-6.

[57] I. Park, C.B. Tabelin, K. Seno, S. Jeon, H. Inano, M. Ito, N. Hiroyoshi, Carrier-microencapsulation of arsenopyrite using Al-catecholate complex: nature of oxidation products, effects on anodic and cathodic reactions, and coating stability under simulated weathering conditions, Heliyon 6 (2020) e03189, , https://doi.org/10.1016/j.heliyon.2020.e03189.

[58] C.B. Tabelin, R.D. Corpuz, T. Igarashi, M. Villacorte-Tabelin, R.D. Alorro, K. Yoo, S. Raval, M. Ito, N. Hiroyoshi, Acid mine drainage formation and arsenic mobility under strongly acidic conditions: Importance of soluble phases, iron oxyhydroxides/oxides and nature of oxidation layer on pyrite, J. Hazard. Mater. 399 (2020) 122844, , https://doi.org/10.1016/j.jhazmat.2020.122844.

[59] J.B. Zoleta, G.B. Itao, V.J.T. Resabal, A.A. Lubguban, R.D. Corpuz, M. Ito, N. Hiroyoshi, Improved pyrolysis behavior of ammonium polyphosphate-melamine-expandable (APP-MEL-EG) intumescent fire retardant coating system using ceria and dolomite as additives for I-beam steel application, Heliyon 6 (2020) e03119, , https://doi.org/10.1016/j.heliyon.2019.e03119.

[60] T.H. Giordano, Anglesite (PbSO4) solubility in acetate solutions: the determination of stability constants for lead acetate complexes to 85°C, Geochim. Cosmochim. Acta 53 (1989) 359–366, https://doi.org/10.1016/0016-7037(89)90387-6.

[61] R.W. Leinz, S.J. Sutley, G.A. Desborough, P.H. Briggs, An investigation of the partitioning of metals in Mine wastes using sequential extractions, Proceedings from the 5th International Conference on Acid Rock Drainage, Vol. 2, Colorado USA: Society for Mining, Metallurgy, and Exploration, 2000, pp. 1489–1499.

[62] M. Sethurajan, D. Huguenot, P.N.L. Lens, H.A. Horn, L.H.A. Figueiredo, E.D. van Hullebusch, Fractionation and leachability of heavy metals from aged and recent Zn metallurgical leach residues from the Três Marias zinc plant (Minas Gerais, Brazil), Environ. Sci. Pollut. Res. 23 (2016) 7504–7516, https://doi.org/10.1007/s11356-015-6014-1.

[63] P. Iavazzo, P. Adamo, M. Boni, S. Hillier, M. Zampella, Mineralogy and chemical forms of lead and zinc in abandoned mine wastes and soils: an example from Morocco, J. Geochem. Explor. 113 (2012) 56–67, https://doi.org/10.1016/j.gexplo.2011.06.001.

[64] M. Anju, D.K. Banerjee, Associations of cadmium, zinc, and lead in soils from a lead and zinc mining area as studied by single and sequential extractions, Environ. Monit. Assess. 176 (2011) 67–85, https://doi.org/10.1007/s10661-010-1567-4.

[65] R.B. Herbert, Metal retention by iron oxide precipitation from acidic ground water in Dalarna, Sweden, Appl. Geochem. 11 (1996) 229–235, https://doi.org/10.1016/0883-2927(95)00070-4.

[66] T. Igarashi, P.S. Herrera, H. Uchiyama, H. Miyamae, N. Iyatomi, K. Hashimoto, C.B. Tabelin, The two-step neutralization ferrite-formation process for sustainable acid mine drainage treatment: Removal of copper, zinc and arsenic, and the influence of coexisting ions on ferritization, Sci. Total Environ. 715 (2020) 136877, , https://doi.org/10.1016/j.scitotenv.2020.136877.

[67] D. Sinadinović, Ž. Kamberović, A. Šutić, Leaching kinetics of lead from lead (II) sulphate in aqueous calcium chloride and magnesium chloride solutions, Hydrometallurgy 47 (1997) 137–147, https://doi.org/10.1016/S0304-386X(97)00041-8.

[68] S. Choi, K. Yoo, R.D. Alorro, Hydrochloric acid leaching behavior of metals from non-magnetic fraction of Pb dross, Geosystem Eng. 22 (2019) 347–354, https://doi.org/10.1080/12269328.2019.1681301.

[69] G. Moon, K. Yoo, Separation of Cu, Sn, Pb from photovoltaic ribbon by hydrochloric acid leaching with stannic ion followed by solvent extraction, Hydrometallurgy 171 (2017) 123–127, https://doi.org/10.1016/j.hydromet.2017.05.003.

[70] F. Farahmand, D. Moradkhani, M.S. Safarzadeh, F. Rashchi, Brine leaching of lead-bearing zinc plant residues: process optimization using orthogonal array design methodology, Hydrometallurgy 95 (2009) 316–324, https://doi.org/10.1016/j.hydromet.2008.07.012.

[71] H. Abdel-Samad, P.R. Watson, An XPS study of the adsorption of lead on goethite (α-FeOOH), Appl. Surf. Sci. 136 (1998) 46–54, https://doi.org/10.1016/S0169-4332(98)00337-7.

[72] L.P. Pederson, Two-dimensional chemical-state plot for lead using XPS, J. Electron Spectros. Relat. Phenomena 28 (1982) 203–209, https://doi.org/10.1016/0368-2048(82)85043-3.

[73] J.A. Taylor, An x-ray photoelectron and electron energy loss study of the oxidation of lead, Journal of Vacuum Science & Technology A. 2 (1984) 771–774, https://doi.org/10.1116/1.572569.

[74] J.M. Thomas, M.J. Tricker, Electronic structure of the oxides of lead. Part 2.-An XPS Study of Bulk Rhombic PbO, Tetragonal PbO, β-PbO_2 and Pb_3O_4, J. Chem. Soc., Faraday Trans. 2 (71) (1975) 313–328, https://doi.org/10.1039/F29757100313.

[75] A.P. Grosvenor, B.A. Kobe, M.C. Biesinger, N.S. McIntyre, Investigation of multiplet splitting of Fe 2p XPS spectra and bonding in iron compounds, Surf. Interface Anal. 36 (2004) 1564–1574, https://doi.org/10.1002/sia.1984.

[76] Y. Xi, M. Mallavarapu, R. Naidu, Reduction and adsorption of Pb^{2+} in aqueous solution by nano-zero-valent iron—A SEM, TEM and XPS study, Mater. Res. Bull. 45 (2010) 1361–1367, https://doi.org/10.1016/j.materresbull.2010.06.046.

[77] M. Ding, B.H.W.S. de Jong, Chapter 30 characterizing the surface chemistry of oxides with X-ray photoelectron spectroscopy: assessment regarding surface oxygen valence charge and acid–base properties, in: D. Sarkar, R. Datta, R. Hannigan (Eds.), Developments in Environmental Science, vol. 5, Elsevier, 2007, pp. 665–683, , https://doi.org/10.1016/S1474-8177(07)05030-9.

[78] K. Kashida, S. Oue, H. Nakano, Effect of Chloride Ions in Electrowinning Solutions on Zinc Deposition Behavior and Crystal Texture, Mater. Trans. 58 (2017) 1418–1426, https://doi.org/10.2320/matertrans.M-M2017827.

[79] N.E. Tuffrey, V. Jiricny, J.W. Evans, Fluidized bed electrowinning of zinc from chloride electrolytes, Hydrometallurgy 15 (1985) 33–54, https://doi.org/10.1016/0304-386X(85)90065-9.

[80] M. Sethurajan, D. Huguenot, R. Jain, P.N.L. Lens, H.A. Horn, L.H.A. Figueiredo, E.D. van Hullebusch, Leaching and selective zinc recovery from acidic leachates of zinc metallurgical leach residues, J. Hazard. Mater. 324 (2017) 71–82, https://doi.org/10.1016/j.jhazmat.2016.01.028.

[81] Y. Awakura, S. Kamei, H. Majima, A kinetic study of nonoxidative dissolution of galena in aqueous acid solution, Metallurgical Transaction B. 11 (1980) 377–381, https://doi.org/10.1007/BF02676882.

[82] A.A. Baba, F.A. Adekola, A study of dissolution kinetics of a Nigerian galena ore in hydrochloric acid, J. Saudi Chem. Soc. 16 (2012) 377–386, https://doi.org/10.1016/j.jscs.2011.02.005.

[83] T.N. Thao, S. Tsuji, S. Jeon, I. Park, C.B. Tabelin, M. Ito, N. Hiroyoshi, Redox potential-dependent chalcopyrite leaching in acidic ferric chloride solutions: leaching experiments, Hydrometallurgy (2020) 105299, https://doi.org/10.1016/j.hydromet.2020.105299.

[84] J.M. Casas, F. Alvarez, L. Cifuentes, Aqueous speciation of sulfuric acid–cupric sulfate solutions, Chem. Eng. Sci. 55 (2000) 6223–6234, https://doi.org/10.1016/S0009-2509(00)00421-8.

South African Journal of Plant and Soil 2020: 01–10
Printed in South Africa — All rights reserved

SOUTH AFRICAN JOURNAL OF
PLANT AND SOIL
ISSN 0257-1862 EISSN 2167-034X
https://doi.org/10.1080/02571862.2020.1772386

Evaluation of phytoremediation effects of chicken manure, urea and lemongrass on remediating a lead contaminated soil in Kabwe, Zambia

Yui Yoshii[1], Isabell von Rein[2], Kabenuka Munthali[3], Mukuka Mwansa[4], Hokuto Nakata[5], Shota Nakayama[5], Mayumi Ishizuka[5] and Yoshitaka Uchida[6,7*]

[1] *Department of Social and Preventive Epidemiology, School of Public Health, University of Tokyo, Japan*
[2] *Soil and Water Systems, University of Idaho, Moscow, USA*
[3] *Zambia Agriculture Research Institute, Agriculture, Chilanga, Zambia*
[4] *Zambia Ministry of Agriculture and Cooperatives, Agriculture, Shiwang'andu, Zambia*
[5] *School of Veterinary Medicine, Hokkaido University, Japan*
[6] *Research Faculty of Agriculture, Hokkaido University, Japan*
[7] *Global Institution for Collaborative Research and Education, Global Station for Food, Land and Water Resources, Hokkaido University, Japan*
**Corresponding author, email: uchiday@chem.agr.hokudai.ac.jp*

High levels of lead (Pb) in the soil is a serious issue in the city of Kabwe, Zambia. Phytoremediation is an effective approach to revive the life-supporting functions of the soils. Locally available soil amendments, such as chicken manure, can strengthen phytoremediation. This study aims to find an appropriate combination of a locally available Pb hyperaccumulator, lemongrass (*Cymbopogon citratus* (DC.) Stapf.), and soil amendments, to minimize the Pb pollution. After a short-term (78 day) pot experiment with lemongrass and three soil amendments (chicken manure, biochar of chicken manure, and urea) on a Pb-contaminated soil in Kabwe, an edible crop, dent corn (*Zea mays var. indentata* (Sturtev.) L.H.Bailey), was grown for two weeks. Chicken manure combined with lemongrass had the most beneficial impact, reducing the Pb level in dent corn by 19%, compared to the Pb in dent corn grown on the control soil. By growing lemongrass in the Kabwe soil with chicken manure, the exchangeable soil Pb was reduced by 70%. The growth of lemongrass without chicken manure reduced the exchangeable soil Pb by 20%. In conclusion, lemongrass successfully reduced Pb levels, in combination with chicken manure. Soil amendments must be chosen carefully by considering the soil properties and environmental conditions for an optimized Pb reduction.

Keywords: chicken manure, dent corn, Kabwe, lead-contaminated soil, lemongrass, phytoremediation

Online supplementary material: Supplementary data for this article are available at https://doi.org/10.1080/02571862.2020.1772386

Introduction

Phytoremediation is a promising phytotechnology for the remediation of metals from contaminated soils whereby living plants are used to remove, transfer, or stabilize the soil contaminants (Burges et al. 2018). Plants can (i) extract metals from contaminated soil (phytoextraction) and/or (ii) immobilize them through sorption by roots, precipitation, complexation or metal reduction in the rhizosphere (phytostabilisation) (Raskin et al. 1997; Ali et al. 2013; Burges et al. 2018).

Within the approaches relating to phytoremediation, phytoextraction or phytomining is the process of planting hyperaccumulators (i.e. plants that can accumulate high concentrations of contaminants in their above-ground biomass) (Yang et al. 2005) and then harvesting them to remove the contaminant (Ali et al. 2016; Burges et al. 2018). A limitation of phytoextraction is the extensive time required to effectively extract metals from soils (Burges et al. 2018), particularly in highly contaminated sites (Zhao et al. 2000). However, if the aim of the phytoextraction strategy is only to remove the bioavailable metal fraction (i.e. the fraction of the total contaminants in the soil solution and soil particles that is available to the receptor organism) from soil (Naidu et al. 2008), and not to reach the total metal removal, the time for successfully completing the task can be considerably shorter (Vangronsveld et al. 2009).

Phytostabilisation is another phytoremediation approach and was developed to reduce the bioavailability of contaminants in soils and to prevent the pollution from spreading further to surrounding areas (Raskin et al. 1994). This technique can also be used to re-establish the vegetation cover at sites where natural vegetation fails to survive due to high metal concentrations (Pilon-Smits 2005). The vegetation cover can then help minimizing the wind dispersion of heavy metals and water migration through the soil resulting from evaporation (Arienzo et al. 2004).

The efficiency of phytoremediation depends on the type of contaminant, its bioavailability, and the soil properties (Cunningham and Ow 1996). For phytoextraction, the low biomass and slow growth of most hyperaccumulators often limit their efficiency. To overcome this issue, fertilizers are

often used to increase hyperaccumulators' biomass yield, thus enabling the plants to access and deplete larger pools of bioavailable metals, as a consequence of root proliferation (Robinson et al. 1997; Kayser et al. 2000; Schwartz et al. 2003; Barrutia et al. 2009; Salomon et al. 2012; Bani et al. 2015; Deng et al. 2016). For example, chicken manure has been shown to successfully reduce contamination effects of Pb. Adams et al. (2018) applied chicken manure to contaminated soil from the Niger-Delta region of Nigeria, which had traces of copper, nickel, zinc, and lead (0.1840, 0.0820, 0.4120, and 0.0198 mg/g, respectively). They found that vegetation on the soil treated with chicken manure showed more heavy metal removal efficiency (82.8%) compared to untreated soil (69.7%).

With regard to phytostabilisation, previous studies have shown that soil amendments can increase its effectiveness. For example, organic amendments such as chicken manure, which contains a high level of humified organic matter (OM), can decrease the bioavailability of heavy metals in soil (Walker et al. 2003). Biochar, or charred materials made of biomass, is also known to help achieve phytostabilisation (Park et al. 2011). Thus, these widely available organic materials (i.e. chicken manure and biochar) should be tested in more detail in heavily contaminated soils, especially where the application of expensive approaches (e.g. the physical removal of soils or surface-sealing using solid-materials) is difficult.

In this study, we targeted contaminated soils sampled in the city of Kabwe, Zambia. Kabwe is known as one of the most polluted cities in the world with high lead (Pb) levels reported in soils, water, plants, animals, and human blood samples because of previous mining activities (Yabe et al. 2010, 2011, 2013, 2015). However, many residents still grow vegetable crops in their gardens around the mine area. Thus, it is essential to minimize the Pb transfer from soils to crops by simple measures that local people can easily apply. When locally available species are used, the societal implementation of this technology can easily be carried out by the residents. According to previous studies, lemongrass (*Cymbopogon citratus* (DC.) Stapf.) has a relatively high ability to accumulate heavy metals in its biomass, compared to other plants (Obiora et al. 2016). Thus, this plant has the potential to be used as an approach to remediate the heavy metal contaminated soils, although there also needs to be a strategy to deal with the harvested plant biomass which has a high heavy metal content. An example of this would be recovery of the heavy metals from plant biomass using an engineering approach. Soil amendments such as chicken manure, urea, and biochar made from chicken manure are readily available in Kabwe. Thus, this study aims to find the most effective combination of lemongrass and these locally available soil amendments to minimize the Pb concentration of edible crops such as dent corn in Kabwe.

Our hypotheses are as follows:

1. The transfer of Pb from contaminated Kabwe soil to crops can be reduced by growing lemongrass before planting the vegetable crops.
2. One of three organic sources i.e. chicken manure, biochar from chicken manure, and urea will strengthen the phytoremediation potential of lemongrass.

Materials and methods

Soil

The soil (pH 8.14, total Pb concentration: 2.85 g kg^{-}) used in this experiment was a Sandveldt type collected (0–10 cm depth) from local farmland at Kabwe, Zambia (14°28′08.1″ S; 28°26′05.2″ E, 546 m above sea level) in October 2015. Soils were sieved through 2 mm, air-dried, and packed into polyethylene bottles. Sandveldt soil is one of the major soil types in Zambia. The topsoil textures range from sand to sandy loam. The total carbon (C) and nitrogen (N) contents of the soil were 24.8 ± 1.2 and 2.0 ± 0.1 g kg^{-1}, respectively. Sandveldt is characterized as being low in exchangeable bases and has a low organic matter content (Clayton 1962).

Experimental design

Two experiments were conducted in the current study. The first experiment was conducted to investigate the ability of lemongrass to reduce soil Pb concentrations (experiment 1) and the second experiment was performed to measure the combined effects of lemongrass and soil amendments on reducing the contamination risk of an edible crop (dent corn) (experiment 2).

For experiment 1, the soils were placed in small square pots (length 60 mm × width 60 mm × height 52 mm), holding 80 g of air-dry soil each. The soil was loosely packed to one cm below the height of the pot (the bulk density of the soil was 0.53 g cm^{-3}). The experiment consisted of two treatments; no lemongrass (control) and lemongrass. One stump of lemongrass was planted per pot for the lemongrass treatment. The pot experiment was carried out in the laboratory with LED light (HOME GROWN, World Trading Co., Ltd, LED Ratio: 630 nm:460 nm = 165:60) turned on between 08:00−20:00 from February to April of 2016 for six weeks. The air temperature of the laboratory was kept at 25°C throughout the experimental period. The soils were supplied with 10 ml Milli-Q water daily for the duration of the experiment. Loss of water from the bottom of the pot was not observed. The Pb concentration for each fraction in soils before and after growing lemongrass for six weeks was measured using a sequential extraction procedure (as described below). The total Pb concentration of the soil was also measured. From each pot, approximately 5 g of fresh soil was sampled before and after growing lemongrass (i.e. 0 days and 42 days after the start of experiment) and oven-dried (105°C for 24 hours) for the analyses.

Experiment 2 was performed using the same pot and lighting parameters as described for experiment 1. This experiment consisted of eight treatments with three to four replicates as shown in Table 1. Lemongrass was grown in the soil from July to September 2016 (100 g of air-dry soil per pot) with one of three organic amendments (chicken manure, biochar from chicken manure, or urea) for ten weeks, and then the lemongrass was harvested from the pots. The Pb level of the chicken manure (obtained from Clean Alpha Co., Ltd., Japan) used in our experiment was negligible. The concentration of Pb in the chicken manure has to be less than 100 mg Pb kg^{-1} to be sold as a commercial product in Japan, based on the guideline produced by the Ministry of Agriculture and Fishery, Japan and our experiment did

Table 1: Summary of the treatment structures, used soil amendments, application rates, and replicate numbers for experiment 2.

Treatment	Soil amendment	Lemongrass	Replicates
N-L	No soil amendment	No lemongrass	3
C-L	Chicken manure (total N 26.9 ± 0.1 g kg^{-1}, total C 167 ± 0.3 g kg^{-1}, total P 50 g kg^{-1}, total K 28 g kg^{-1}, water content 247 ± 13 g kg^{-1}) *The application rate per application was 7.44 g kg^{-1} (equivalent of 200 mg N kg^{-1}) and it was added to the soil before planting.	No lemongrass	4
B-L	Biochar made from chicken manure (total N 25.3 ± 3.3 g kg^{-1}, total C 473 ± 58.8 g kg^{-1}, total P 84 g kg^{-1}, total K 49 g kg^{-1}, water content 26.3 ± 1.8 g kg^{-1}) *The application rate per application was 7.91 g kg^{-1} (equivalent of 200 mg N kg^{-1}) and it was added to the soil before planting.	No lemongrass	4
U-L	Urea *The application rate per application was 20 mg N kg^{-1} and it was applied in 10 ml of water, weekly, for 10 weeks..	No lemongrass	4
N+L	No soil amendment	Lemongrass	3
C+L	Chicken manure	Lemongrass	4
B+L	Biochar made from chicken manure *added to the soil before planting	Lemongrass	4
U+L	Urea	Lemongrass	4

not show any increase in soil Pb after the application of the chicken manure. Dent corn (*Zea mays* var. *indentata* (Sturtev.) L.H.Bailey) was grown for two weeks after being planted in the same soil in which lemongrass had been grown. Soils without the lemongrass but with the same organic amendment types (−L) were also prepared to study the single effect of organic amendments. The control treatments (no organic amendment) were prepared with (N+L) and without lemongrass (N−L). The pots were watered with 10 ml Milli-Q water daily for the experiment duration. The leaching of added water through the pots was negligible.

Measurement of Pb content – sequential extraction procedure

The Tessier method sequential extraction procedure has been used to investigate the fate of Pb in soils (Tessier et al. 1979; Hamzenejad Taghlidabad and Sepehr 2018). The method partitions elements into five operationally-defined geochemical fractions, including 1) exchangeable; 2) carbonates (acid-soluble); 3) iron (Fe) and manganese (Mn) oxides (reducible); 4) organic matter (oxidizable) and 5) the residual. The different reagents used for these purposes are as follows:

Exchangeable Pb (representing the water-soluble and exchangeable fraction): 0.32 g of oven-dried soil was extracted at room temperature for 1h with 8 ml of 1 M $MgCl_2$ (pH 7.0) with continuous agitation.

Carbonate (acid-soluble) bound Pb (representing the inorganically bound fraction): the soil residue from (i) is extracted at room temperature for over 5 h with 8 ml of 1 M NaOAc adjusted to pH 5.0 with HOAc with continuous agitation.

Fe and Mn oxides (reducible) bound Pb (representing iron and manganese oxides existing as nodules, concretions, cement between particles, or just as a coating on particles): the soil residue from (ii) was extracted at 96 ± 3°C for over 5 h with 20 ml of 0.04 M NH_2OH-HCl in 25% (v/v) HOAc with occasional agitation.

Organic matter (oxidisable) bound Pb (representing various forms of organic matter including living organisms, detritus and coatings on mineral particles): the soil residues from (iii) were extracted at 85 ± 2°C for 2 h with 3 ml of 0.02 M HNO_3 and 5 ml of 30% H_2O_2 adjusted to pH 2 with HNO_3 with occasional agitation. A second 3-ml aliquot of 30% H_2O_2 (pH 2 with HNO_3) was then added, and the sample was again heated to 85 ± 2°C for 3 h with intermittent agitation. After cooling, 5 ml of 3.2 M NH_4OAc in 20% (v/v) HNO_3 was added, and the sample was diluted to 20 ml and agitated continuously for 30 min.

Residual: Once the four fractions (above) have been extracted, the residual solid should contain mainly primary and secondary minerals, which may hold trace metals within their crystal structures. To obtain this value, the sum of the Pb concentrations of the four fractions above was subtracted from the total Pb concentration. The method used to obtain the total Pb is explained in the next section.

Each soil suspension was filtered using filter paper (0.22 µm) (Toyo Roshi Kaisha No. 5C filter paper, Toyo Roshi Kaisha, Ltd., Tokyo, Japan). The concentration of Pb in the extracts was determined using an Inductively Coupled Plasma-Mass Spectrometer (ICP-MS; 7700 series, Agilent Technologies, Tokyo, Japan). The Pb of dent corn was measured as described in the next section and calculated as a concentration (mg Pb/kg soil), and as an amount (µg Pb/pot or plant).

Measurements total Pb concentrations by using microwave and ICP-MS

For the preparation of both soil and plant samples, 5 ml of 30% HNO_3 and 1 ml of H_2O_2 were added to approximately 0.3 g of the sample. This solution was digested in 10 ml vessels made of TFM™-PTFE in a Speedwave microwave oven (Berghof, Germany). The optimized digestion program includes heating for 5 min at 160°C, 20 min at 190 °C, 20 min at 200 °C, and 5 min at 100 °C. The digested samples were transferred into plastic tubes. The volume was then adjusted to 10 ml with Milli-Q water. The concentrations of Pb in the digested samples were determined using an Inductively Coupled Plasma-Mass Spectrometer (ICP-MS; 7700 series, Agilent Technologies, Tokyo, Japan).

Measurements of soil and plant characteristics – Experiment 1

After growing lemongrass, the soils were sampled and the first to fourth fraction Pb concentrations were measured following the Tessier method Sequential extraction procedure for Pb.

Soil pH was determined using 5 g of air-dried soil mixed with 12.5 ml of 10% Milli-Q water and shaken for 30 min followed by measurement using a pH sensor (AS800, AS ONE Co., Osaka, Japan).

Measurements of soil and plant characteristics – Experiment 2

After growing lemongrass, the total Pb concentration of the lemongrass plants was measured. We carefully removed the whole plants from the soil in each pot, washed them, particularly the roots, and then the shoots and roots were separated using scissors. They were carefully washed with deionized water and oven-dried at 80°C for over 24 hours.

The soils were also subsampled and the first and second fraction Pb concentrations were measured, as well as other soil properties including pH, NO_3^--N and NH_4^+-N concentrations, and total C and N contents. In order to measure the NO_3^--N and NH_4^+-N concentrations, 5 g of each soil was placed in a polyethylene bottle, and 25 ml of 10% KCl was added. After shaking for 30 minutes, the eluate was filtered through a filter paper (0.22 µm) (Toyo Roshi Kaisha No.5C filter paper, Toyo Roshi Kaisha, Ltd., Tokyo, Japan). The NO_3^--N and NH_4^+-N concentrations of the filtrate were measured using a colorimetric method with a flow injection analyzer (AQLA-700, Aqualab Co., Ltd., Japan) (Hamamoto and Uchida, 2015). Total C contents (TC) and Total N (TN) were measured using oven dried and finely ground soils with an organic elemental analyzer (2400 Series II CHNS/O Elemental Analysis, PerkinElmer Co., Waltham, US) (Mogi et al. 2017).

The remaining soil was used for growing dent corn. Each pot contained 50 g of air-dry soil. The pots were watered with 5 ml MilliQ-water daily for the duration of the experiment. The leaching of added water through the pots was negligible. Dent corn was grown from September to October 2016 for two weeks after germination. After growing dent corn, the same sampling procedures and measurements, as previously described for lemongrass, were carried out.

Statistical analysis

All measurements, including the total Pb concentrations of plant and soil, the Pb concentrations for each fraction in soil, NO_3^--N and NH_4^+-N concentrations, and total C and N contents, were obtained from triplicates or quadruplicates of each treatment. Statistical significance of the experimental data was analyzed using R Studio Version 1.0.15 software (2009–2017 R Studio, Inc.) at a significance level of $p < 0.05$. The comparisons between with/without lemongrass in the same fertilizer treatments were performed using a Welch Two Sample *t*-test, because of no evidence of homoscedasticity. The comparisons among treatments were performed using a two-way ANOVA (with the lemongrass and the organic amendment treatments as two factors) and a Tukey method for multiple comparisons.

Results

Original soil Pb concentration for each fraction

Before growing lemongrass, the total Pb concentration in the soil was 2 846 ± 323 mg kg^{-1}. Within the total soil, Pb occurred as 1.5% as exchangeable forms (first fraction), 24% as a form bound to carbonate (second fraction), 38.6% as Fe-Mn oxide (third fraction), 21.8% as organic matter (fourth fraction) and 14.1% remained in the residual form (fifth fraction) (Figure 1). The presence of lemongrass significantly decreased the first (Figure 1a: exchangeable Pb) and the second fractions (Figure 1b: bound to carbonates Pb) ($p < 0.001$ and $p < 0.01$, respectively) in the

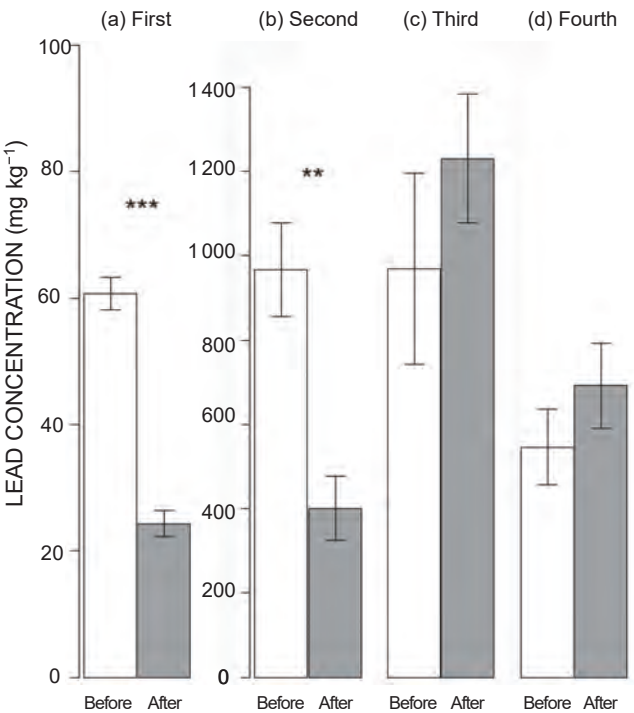

Figure 1: Soil Pb concentration reduction by lemongrass for first (a: exchangeable Pb), second (b: bound to carbonates Pb), third (c: bound to Fe-Mn oxides Pb), and fourth fraction (d: bound to organic matter). The error bars indicate standard errors ($n \geq 3$). Asterisks indicate significant differences (**$p < 0.01$, ***$p < 0.001$).

soil. However, it did not have a significant effect on the third and fourth fractions (Figures 1c and d).

Lemongrass and soil Pb concentrations after growing lemongrass

After growing in the Pb contaminated soil for ten weeks without any soil amendments, the lemongrass root and leaf Pb concentrations were 739 and 498 mg kg^{-1}, respectively, averaged across the soil amendment treatments. The growth of lemongrass leaves was slightly improved by chicken manure, compared to other treatments, while the root biomass was the largest in the control treatment (Figure S1, supplementary file). The bioaccumulation factor (plant Pb/soil Pb) was less than 0.25 (the total Pb concentration in soil was 2846 mg kg^{-1}), on average. Regarding the lemongrass root Pb concentrations, soil amendments had no significant impact. In contrast, the application of urea significantly decreased Pb concentrations in lemongrass leaves compared to the control treatment (Figure 2).

Analysis of soils in which lemongrass had been grown showed that the presence of lemongrass significantly reduced soil exchangeable Pb concentration (first fraction), when averaged across the soil amendment treatments (Figure 3a). When averaged across the lemongrass treatments, chicken manure treated soils showed higher exchangeable Pb concentrations (first fraction), when compared to the control soils. For the Pb bound to carbonate concentration (second fraction), there was no influence of lemongrass or soil amendments (Figure 3b). The mass balance calculation (based on the weight of Pb per pot) suggested that the decrease of fraction one Pb in the soil due to the presence of lemongrass was larger than the actual uptake of Pb by lemongrass (Figure S2, supplementary file).

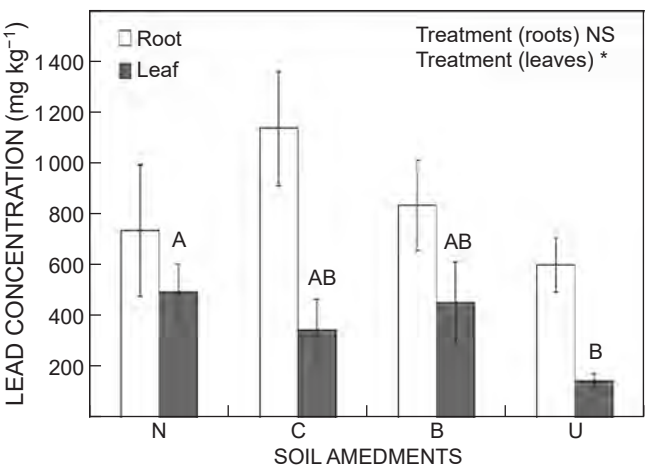

Figure 2: Total Pb concentration in the lemongrass roots (white bars) and leaves (grey bars) after growth in a Pb contaminated soil with different soil amendments for ten weeks (N: No soil amendment, C: Chicken manure, B: Biochar made from chicken manure, U: Urea). The error bars indicate standard errors ($n \geq 3$). The capital letters indicate significant differences regarding the lemongrass leaves within each treatment. Asterisk indicates a significant difference ($^*p < 0.05$).

Dent corn and soil Pb concentration after growing dent corn

There was an interaction between the fertilizer treatments and the lemongrass treatments for fraction one Pb in the soils after the growth of the dent corn (Figure 4a). For the soils in which lemongrass had not been grown, the chicken manure treated soils showed the lowest levels of fraction one Pb. For the soils in which lemongrass had been grown, treatments with chicken manure and urea showed relatively lower fraction one Pb contents than the other treatments. In contrast, the prior presence of lemongrass did not significantly reduce the carbonate (acid-soluble) bound Pb concentration in the soil after growing dent corn (Figure 4b).

For the Pb concentrations in the dent corn, there was no significant effect of the organic amendments and the previous lemongrass treatment. However, within the chicken manure treated soils, prior growth of lemongrass resulted in a decrease in the dent corn Pb concentration compared to the plants grown in soils treated with chicken manure without lemongrass treatment (Figure 5). There

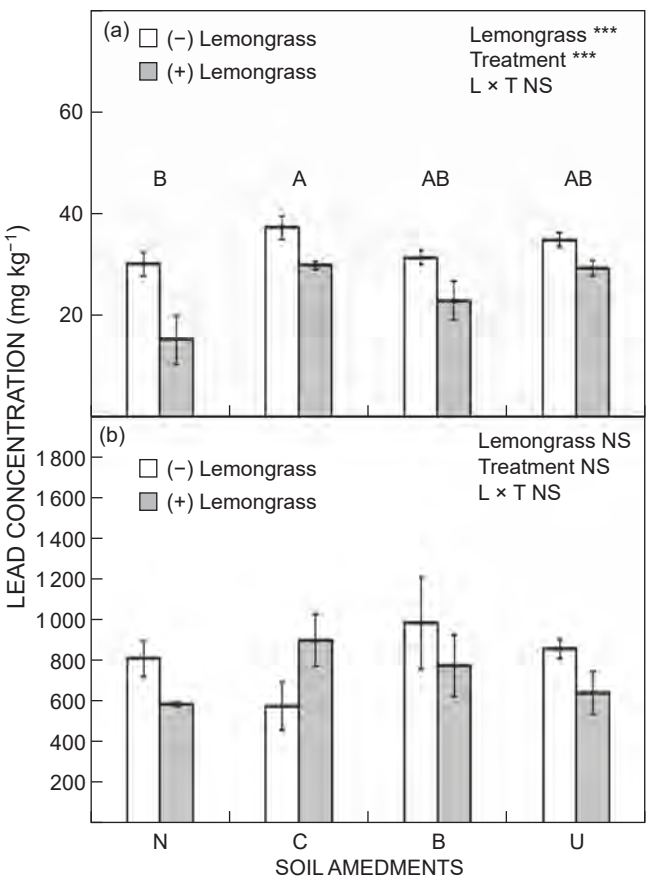

Figure 3: Soil Pb concentration for first (a: exchangeable Pb) and second fraction (b: bound to carbonates Pb), with (white bars) and without (grey bars) the growth of lemongrass with different soil amendments (N: No soil amendment, C: Chicken manure, B: Biochar made from chicken manure, U: Urea) after growing lemongrass. The error bars indicate standard errors ($n \geq 3$). Asterisk indicates a significant difference ($^{***}p < 0.001$).

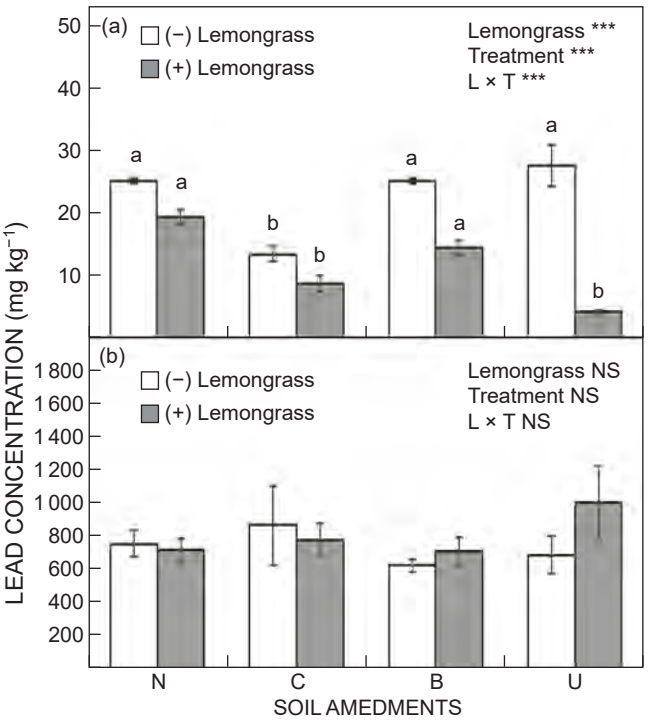

Figure 4: Soil Pb concentration for first (a: exchangeable Pb) and second fraction (b: bound to carbonates Pb), with (white bars) and without (grey bars) the growth of lemongrass with different soil amendments (N: No soil amendment, C: Chicken manure, B: Biochar made from chicken manure, U: Urea) after growing dent corn. The error bars indicate standard errors ($n \geq 3$). Asterisks indicate a significant differences (*$p < 0.05$; ***$p < 0.001$). Because there was an interaction between the lemongrass and fertilizer treatments in fig. (a), we have performed a multiple comparison for the group without lemongrass (white bars) and the group with lemongrass (gray bars). For each comparison, the statistical differences were shown as alphabets on each bar.

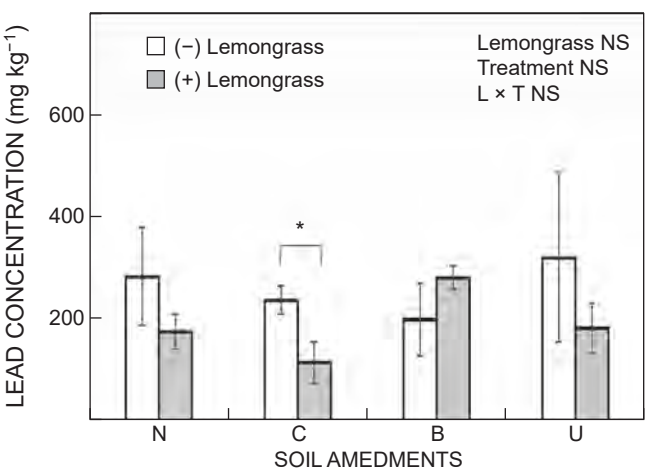

Figure 5: Total Pb concentration in dent corn after growing on the Pb-contaminated soil with (white bars) and without (grey bars) prior growth of lemongrass with different soil amendments (N: No soil amendment, C: Chicken manure, B: Biochar made from chicken manure, U: Urea). The error bars indicate standard errors ($n \geq 3$). Asterisk indicates significant differences (*$p < 0.05$).

was no clear influence of the soil amendments on the dent corn biomass (per pot), and the dent corn biomass was markedly smaller than lemongrass (Figure S1). The actual mass of Pb accumulated in the dent corn biomass (per pot) was also much smaller than Pb accumulated in the lemongrass (Figure S2).

Soil nutrition conditions

Growing lemongrass significantly decreased soil pH and NO_3^--N, regardless of the organic amendment treatments. Levels of NH_4^+-N, total N and C in the soils were not significantly decreased by lemongrass. Soil pH in the biochar treatment was significantly higher than the other treatments, when averaged across the lemongrass treatments. Urea significantly increased the NO_3^--N levels compared to the other amendment treatments (Table 2).

Discussion

The effects of lemongrass on bioavailable Pb in Kabwe soils

The results of experiment 1 show that the growth of lemongrass significantly reduced the exchangeable Pb (first fraction), and Pb bound to carbonate (second fraction) in soils, when averaged across all the soil amendment treatments (Figure 1a). The lemongrass growth also decreased soil pH in the current study (Table 2). When the soil pH decreases, Pb^{2+} concentrations in soil solution normally increase due to the release of Pb, which may be bound to carbonate species, such as $PbCO_3$ or $Pb_3(CO_3)_2(OH)_2$. Thus, the solubilized Pb^{2+} was absorbed by the lemongrass and this resulted in the decrease of both first and second fraction Pb, in the current study.

Having grown lemongrass in the soil did not decrease the second fraction pool of Pb in experiment 2, when averaged across the soil amendment treatments (Figure 3b). This was because the soil amendment treatments hindered the impact of lemongrass on the second fraction soil Pb in experiment 2. For the control treatment (without any fertilizer inputs) in experiment 2, the second fraction was reduced, similar to the experiment 1, but when there was an input of organic amendments (chicken manure and biochar chicken manure), the effect of the lemongrass on Pb fraction two became unclear. This was because these organic amendments increased the variability of data (Figure 3b). These organic amendments were solid materials and probably increased the heterogeneity of the soils.

Overall, the amount of Pb absorbed by the lemongrass relative to the total soil Pb observed in the current study was relatively small compared to the previous studies. Lemongrass was reported to be able to absorb Pb efficiently, and some studies report that lemongrass Pb concentration equalized soil Pb concentrations. For example, Yashim (2015) reported that lemongrass Pb concentrations were 40–45 mg/kg in contaminated soil containing 40–45mg/kg Pb in field experiments. Using a pot experimental setup, Dawle et al. (2014) reported that Pb concentrations of lemongrass increased up to 200–300 mg Pb/kg in a soil contaminated at a level of 200–300 mg/kg Pb. In the current experiment,

Table 2: Characteristics (pH, nitrate (NO_3^--N), ammonium (NH_4^+-N), total carbon (C) and nitrogen (N)) in the soils with and without lemongrass with variable soil amendments (N: No soil amendment, C: Chicken manure, B: Biochar made from chicken manure, U: Urea). The significance based on the two-way ANOVA ($p < 0.001$: ***, $p < 0.01$: **, $p < 0.05$: * and $p < 0.1$) for each characteristic is shown below the data.

	pH	NO_3^--N (mg kg^{-1})	NH_4^+-N (mg kg^{-1})	Total C (g kg^{-1})	Total N (g kg^{-1})
N without lemongrass	8.18 ± 0.09	12.01 ± 6.80	2.94 ± 0.24	24.8 ± 1.2	2.6 ± 0.1
N with lemongrass	7.97 ± 0.09	6.03 ± 2.04	2.32 ± 0.22	24.1 ± 2.2	3.3 ± 0.7
C without lemongrass	8.36 ± 0.04	12.59 ± 6.70	2.27 ± 0.14	25.1 ± 2.0	3.4 ± 0.8
C with lemongrass	7.97 ± 0.07	5.77 ± 3.68	2.56 ± 0.17	27.7 ± 2.3	5.0 ± 0.8
B without lemongrass	8.72 ± 0.13	3.54 ± 1.31	2.33 ± 0.09	25.9 ± 1.0	2.5 ± 0.6
B with lemongrass	8.47 ± 0.04	2.97 ± 0.77	2.68 ± 0.16	24.7 ± 2.1	2.4 ± 0.6
U without lemongrass	7.98 ± 0.10	51.4 ± 13.7	2.56 ± 0.08	28.7 ± 2.4	3.9 ± 0.6
U with lemongrass	7.60 ± 0.14	28.4 ± 10.8	2.37 ± 0.28	20.9 ± 0.4	4.5 ± 0.7
Significance					
Treatment	*	*	NS	*	*
Lemongrass	***	*	NS	NS	NS
Interaction	NS	*	.	NS	NS

lemongrass Pb concentrations were much lower than the Pb concentration in the soil. However, the first fraction Pb in soils was reduced by 10–40%, due to the presence of lemongrass, based on the mass balance calculation, and this decrease was higher than the Pb contents in the lemongrass biomass (Figure S2). This suggested that in our experiment, the lemongrass markedly impacted and reduced the soluble fraction (the first fraction) of Pb in the soil but the impacts of plants and soil amendments on other fractions, which were less available and soluble, were not clear.

The effects of chicken manure soil amendments

This study suggested that growing and harvesting lemongrass with chicken manure could lower Pb concentrations in edible crops (dent corn) planted afterwards (Figure 5). According to previous studies, chicken manure has two contrasting influences on exchangeable metal in soil: decreasing exchangeable Pb through the complexing of heavy metals (Tordoff et al. 2000) or increasing exchangeable Pb through increasing dissolved organic carbon (DOC) (Bolan et al. 2011). In this study, the chicken manure treatment temporarily increased the exchangeable Pb concentration in the soil, when compared to the control treatment, when averaged across the lemongrass treatment (Figure 3a). This increase of the exchangeable Pb might be through increasing DOC (Bolan et al. 2011), and it could lead to a higher efficiency of phytoextraction by lemongrass. An increase of the exchangeable Pb could lead to higher Pb concentrations in plants. Thus, when a hyperaccumulator such as lemongrass is used with chicken manure, our study suggests that it could increase the Pb accumulation capacity of the plants, leading to the reduction in levels of Pb contamination in the soil. However, when chicken manure is used as a fertilizer for edible crops (rather than for the non-edible plants used for phytoextraction), it needs to be used with caution, since it could increase the Pb levels in the edible crops planted afterwards.

After growing the dent corn, chicken manure significantly decreased the soil exchangeable Pb concentration, when compared to the control treatment, when averaged across the lemongrass treatment (Figure 4a). The decrease of the exchangeable Pb might be through complexing of heavy metals (Tordoff et al. 2000), and it could lead to a higher efficiency of phytostabilisation for dent corn. Since the exchangeable Pb could also easily be absorbed by edible crops such as dent corn, a decrease of this fraction could minimize Pb contamination for the edible crop.

Also, the previous presence of lemongrass with chicken manure significantly decreased the Pb concentration in dent corn planted afterwards (Figure 5). The decrease in Pb in the dent corn was because of the dilution due to larger biomass of dent corn, when it was grown after lemongrass. This suggests that chicken manure with lemongrass could improve soil properties for the growth of dent corn.

In conclusion, the effect of chicken manure on the plant uptake of Pb can differ depending on the physiology of plants. Lemongrass could uptake a relatively larger amount of Pb into the biomass, whereas the dent corn's ability to accumulate Pb in its biomass was relatively lower, when compared per pot (Figure S2). For lemongrass, the chicken manure positively impacted the production of leaf biomass (Fig. S1b) and the Pb concentration within the leaves (Fig. 2). However, for dent corn, these positive impacts of chicken manure on plant activities (leaf growth and its Pb concentration) were not observed. These differences might be due to the fact that the lemongrass is a hyperaccumulator of heavy metals and can generally actively grow in soils with high heavy metal levels (Gautam et al. 2016). More studies are needed to determine how chicken manure and other organic amendments influence the ability of different plants to uptake or modify Pb in soils.

The effects of urea on soil and plant Pb levels

The application of urea significantly decreased the Pb concentration in lemongrass leaves, compared to those grown without any amendment (Fig. 2). This suggests that urea reduced the translocation of Pb from roots to leaves. In some cases, plants were used to remove the heavy metals from soils by harvesting their aboveground biomass (Environmental Protection Agency, 2000). Thus,

the reduction of the translocation of Pb from roots to leaves can be a negative aspect if the plants are used to remove the Pb from soils. The TF (Translocation Factor = plant leaf/plant root metal concentration) of the urea treatment (0.12) was significantly smaller than that of the control treatment (0.76). In contrast, Hadi et al. (2014) reported that urea increased the Pb-TF of *Cannabis sativa* from 0.535 to 0.577. However, urea decreased the Cd-TF of *Cannabis sativa* from 0.308 to 0.194. This suggests that the effect of urea on the TF depends on the combination of soil type, plant species and metal under investigation. In the current experiment, the aboveground biomass of the lemongrass was not increased by the urea application, compared to the other treatments (Fig. S1). If the urea increased the biomass of plants, the heavy metal concentration per unit weight of the plant (e.g. per gram plant tissue) could be decreased even when the plant adsorbed the same amount of the heavy metal per whole plant, when compared to a plant with a relatively smaller biomass. Thus, the dilution of the Pb in the leaves was not the reason for the relatively lower Pb contents in the lemongrass leaves with urea. Other possible reasons can be an increase of microbial biomass Pb, because urea-N is readily available for microbes and it might have increased microbial biomass (Zhang et al. 2019). Soil microbes might have absorbed Pb, preventing plants from taking up excess Pb. Also, both Pb and N are transported from roots to shoot via xylem (Brennan and Shelley 1999). Thus, there is a possibility that the addition of urea-N changed the root metabolism and prevented the transport of Pb to leaves due to changes in the balance between different ions within the xylem. Both Pb and ammonium-N (products of urea hydrolysis) are present in soils as protons and the balance between different types of protons is a known factor controlling the activity of xylem transport of nutrients from roots to shoots (van Beusichem and Neeteson 1982). The possibilities stated above are also related to the fact that prior growing of lemongrass combined with urea significantly decreased the exchangeable Pb concentration in the soil after growing dent corn (Fig. 4a). Although the urea did not decrease the dent corn Pb contents in the current study (Fig. 5), we note that the urea has a potential to reduce the soil's available Pb (the fraction one), when used with the lemongrass and dent corn (Fig. 4a). Because of the limited data, we could only suggest possible reasons behind this, as above. Further experiments are clearly needed in this area.

The effects of soil amendments - biochar made from chicken manure

Compared to the control treatment, the biochar treatment without lemongrass did not reduce the soil exchangeable Pb after growing dent corn, in this study (Fig. 4a). A review paper by Paz-Ferreiro et al. (2014) stated that the impact of biochar on the availability of Pb in soils was dependent on the source of biochar, pyrolysis conditions and soil types. For example, chicken manure pyrolyzed at 350°C had a higher Pb stabilizing capacity when compared to the same chicken manure pyrolyzed at 650°C, according to a previous study (Uchimiya et al. 2012), thus the pyrolysis condition for the chicken manure biochar used in the current study might not have been optimal. Also, the presence of lemongrass decreased the available soil N in the chicken manure biochar treatment compared to the other treatments (e.g. NO_3^--N, Table 2), thus the changes in soil nutrient status may influence the behavior of Pb in soils with biochar (e.g. adsorption of Pb^{2+} to organic matter or precipitation of Pb^{2+}). These phenomena may explain why the biochar reduced soil exchangeable Pb after growing dent corn only in soils in which lemongrass had previously been grown (Fig. 4a). The above mentioned review paper (Paz-Ferreiro et al. 2014) stated that there were few studies which observed the effects of the combined use of phytoremediation (the use of plants) and biochar, thus the current study added important information regarding the interaction between plants and biochar in reducing the Pb availability in soils.

Conclusion

In our study, the presence of lemongrass significantly decreased the exchangeable Pb in soils. When dent corn was planted in the Pb contaminated soil after growing lemongrass with chicken manure, the concentration of Pb in the dent corn was significantly reduced, when compared to the dent corn grown with chicken manure without prior lemongrass treatment. The presence of lemongrass enhanced the beneficial effects of the chicken manure, in terms of reducing the availability of Pb in the soil. Other tested soil amendments (urea and chicken manure biochar) reduced the exchangeable Pb in soils but did not have an impact on dent corn Pb levels. Overall, we found that the combined use of lemongrass and chicken manure (both are locally available resources across sub-Saharan Africa) provided benefits in Pb-contaminated soils regarding the reduction of Pb uptake risks for human beings, through consuming dent corn grown on the soils. Further studies are needed to investigate the applicability of this technique to other soil types and the mechanisms behind the reduction of Pb uptake by dent corn when lemongrass and chicken manure are used to condition the soils.

Geolocation

The study area is Kabwe, Zambia, located at 14°28′08.1″ S; 28°26′05.2″ E, 546 m above sea level.

Acknowledgements — This research was also supported by JST/JICA, SATREPS (Science and Technology Research Partnership for Sustainable Development; No. JPMJSA1501). We also thank Mr. Ichise and Ms. Hirano at Research Faculty of Veterinary Medicine, Hokkaido University, Japan for technical support.

ORCIDs

Hokuto Nakata – https://orcid.org/0000-0003-1161-7164
Shota Nakayama – https://orcid.org/0000-0003-1635-2898
Yoshitaka Uchida – https://orcid.org/0000-0003-4354-7842

References

Adams FV, Awode MF, Agboola BO. 2018. Effectiveness of Sorghum Husk and Chicken Manure in Bioremediation of

Crude Oil Contaminated Soil. *Advances in Bioremediation and Phytoremediation*. https://doi.org/10.5772/intechopen.71832
Ali H, Khan E, Sajad MA. 2013. Phytoremediation of heavy metals-Concepts and applications. *Chemosphere* 91(7): 869–881.
Ali SY, Banerjee SN, Chaudhury S. 2016. Phytoextraction of cadmium and lead by three vegetable-crop plants. *Plant Science Today* 3(3): 298. https://doi.org/10.14719/pst.2016.3.3.247
Arienzo M, Adamo P, Cozzolino V. 2004. The potential of *Lolium perenne* for revegetation of contaminated soil from a metallurgical site. *Science of the Total Environment* 319(1–3): 13–25. 2
Bani A, Echevarria G, Sulçe S, Morel JL. 2015. Improving the Agronomy of *Alyssum murale* for Extensive Phytomining: A Five-Year Field Study. *International Journal of Phytoremediation* 17(2): 117–127.
Barrutia O, Epelde L, García-Plazaola JI, Garbisu C, Becerril JM. 2009. Phytoextraction potential of two *Rumex acetosa* L. accessions collected from metalliferous and non-metalliferous sites: Effect of fertilization. *Chemosphere* 74(2): 259–264.
Bolan NS, Adriano DC, Kunhikrishnan A, James T, McDowell R, Senesi N. 2011. Dissolved Organic Matter. Biogeochemistry, Dynamics, and Environmental Significance in Soils. *Advances in Agronomy* 110. https://doi.org/10.1016/B978-0-12-385531-2.00001-3
Brennan MA, Shelley ML. 1999. A model of the uptake , translocation , and accumulation of lead (Pb) by maize for the purpose of phytoextraction. *Ecological Engineering* 12(3–4): 271–297.
Burges A, Alkorta I, Epelde L, Garbisu C. 2018. From phytoremediation of soil contaminants to phytomanagement of ecosystem services in metal contaminated sites. *International Journal of Phytoremediation* 20(4): 384–397.
Clayton DB. 1968. Investigations into the nature and distribution of the sandveldt soils of the central province of Zambia with observations on their land use potential. Masters thesis. Durham University. Durham, UK.
Cunningham SD, Ow DW. 1996. Promises and Prospects of Phytoremediation. *Plant Physiology* 110(3): 715–719.
Dawle N, Patil PV, Panhekar D. 2014. Screening of Plants for Phytoremediation of Lead (Pb) on soils contaminated with Fly Ash. *International Journal of Advances Reserch* 2(3): 692–700.
Deng L, Li Z, Wang J, Liu H, Li N, Wu L, Hu P, Luo Y, Christie P. 2016. Long-term field phytoextraction of zinc/cadmium contaminated soil by *Sedum plumbizincicola* under different agronomic strategies. *International Journal of Phytoremediation* 18(2): 134–140.
Enviromental Protection Agency. 2000. Introduction to Phytoremediation. U.S. Environmental Protection Agency, February 1–72.
Gautam M, Pandey D, Agrawal M. 2016. Phytoremediation of metals using lemongrass (*Cymbopogon citratus* (D.C.) Stapf.) grown under different levels of red mud in soil amended with biowastes. *International Journal of Phytoremediation* 19(6): 555–562.
Hadi F, Hussain F, Hussain M, Ahmad A, Ur Rahman S, Ali N. 2014. Phytoextraction of Pb and Cd; the effect of Urea and EDTA on Cannabis sativa growth under metals stress. *International Journal of Agronomy and Agricultural Research* 5(3): 30–39.
Hamzenejad Taghlidabad R, Sepehr E. 2018. Heavy metals immobilization in contaminated soil by grape-pruning-residue biochar. *Archives of Agronomy and Soil Science* 64(8): 1041–1052.
Kayser A, Wenger K, Keller A, Attinger W, Felix HR, Gupta SK, Schulin R. 2000. Enhancement of phytoextraction of Zn, Cd, and Cu from calcareous soil: The use of NTA and sulfur amendments. *Environmental Science and Technology* 34(9): 1778–1783.
Naidu R, Semple KT, Megharaj M, Juhasz AL, Bolan NS, Gupta SK, Clothier BE, Schulin R. 2008. Bioavailability: Definition, assessment and implications for risk assessment. *Developments in Soil Science* 32: 39–51.
Obiora SC, Chukwu A, Davies TC. 2016. Heavy metals and health risk assessment of arable soils and food crops around Pb-Zn mining localities in Enyigba, southeastern Nigeria. *Journal of African Earth Sciences* 116: 182–189.
Park JH, Choppala GK, Bolan NS, Chung JW, Chuasavathi T. 2011. Biochar reduces the bioavailability and phytotoxicity of heavy metals. *Plant and Soil* 348(1–2): 439–451.
Paz-Ferreiro J, Lu H, Fu S, Méndez A, Gascó G. 2014. Use of phytoremediation and biochar to remediate heavy metal polluted soils: A review. *Solid Earth* 5(1): 65–75.
Pilon-Smits E. 2005. Phytoremediation. *Annual Review of Plant Biology* 56(1): 15–39.
Raskin I, Kumar PN, Dushenkov S, Salt DE. 1994. Bioconcentration of heavy metals by plants. *Current Opinion in Biotechnology* 5(3): 285–290.
Raskin I, Smith RD, Salt DE. 1997. Phytoremediation of metals: Using plants to remove pollutants from the environment. *Current Opinion in Biotechnology* 8(2): 221–226.
Robinson BH, Chiarucci A, Brooks RR, Petit D, Kirkman JH, Gregg PEH, De Dominicis,V. 1997. The nickel hyperaccumulator plant *Alyssum bertolonii* as a potential agent for phytoremediation and phytomining of nickel. *Journal of Geochemical Exploration* 59(2): 75–86.
Salomon JA, Wang H, Freeman MK, Vos T, Flaxman AD, Lopez AD, Murray CJL. 2012. Healthy life expectancy for 187 countries, 1990-2010: A systematic analysis for the Global Burden Disease Study 2010. *The Lancet* 380(9859): 2144–2162.
Schwartz C, Echevarria G, Morel JL. 2003. Phytoextraction of cadmium with Thlaspi caerulescens. *Plant and Soil* 249(1): 27–35.
Tessier A, Campbell PGC, Bisson M. 1979. Sequential Extraction Procedure for the Speciation of Particulate Trace Metals. *Analytical Chemistry* 51(7): 844–851.
Tordoff GM, Baker AJM, Willis AJ. 2000. Current approaches to the revegetation and reclamation of metalliferous mine wastes. *Chemosphere* 41(1–2): 219–228.
Uchimiya M, Bannon DI, Wartelle LH, Lima IM, Klasson KT. 2012. Lead retention by broiler litter biochars in small arms range soil: Impact of pyrolysis temperature. *Journal of Agricultural and Food Chemistry* 60(20): 5035–5044.
van Beusichem ML, Neeteson JJ. 1982. Urea Nutrition of Young Maize and Sugar-Beet Plants with Emphasis on Ionic Balance and Vascular Transport of Nitrogenous Compounds. *Netherlands Journal of Agricultural Science* 30(4): 317–330.
Vangronsveld J, Herzig R, Weyens N, Boulet J, Adriaensen K, Ruttens A, Thewys T, Vassilev A, Meers E, Nehnevajova E, van der Lelie D, Mench M. 2009. Phytoremediation of contaminated soils and groundwater: Lessons from the field. *Environmental Science and Pollution Research* 16(7): 765–794.
Walker DJ, Clemente R, Roig A, Bernal MP. 2003. The effects of soil amendments on heavy metal bioavailability in two contaminated Mediterranean soils. *Environmental Pollution* 122(2) 303–312.
Yabe J, Ishizuka M, Umemura T. 2010. Current levels of heavy metal pollution in Africa. *The Journal of Veterinary Medical Science / the Japanese Society of Veterinary Science* 72(10) 1257–1263.
Yabe J, Nakayama SMM, Ikenaka Y, Muzandu K, Choongo K, Mainda G, Kabeta M, Ishizuka M, Umemura T. 2013. Metal distribution in tissues of free-range chickens near a lead-zinc mine in Kabwe, Zambia. *Environmental Toxicology and Chemistry* 32(1): 189–192.

Yabe J, Nakayama SMM, Ikenaka Y, Muzandu K, Ishizuka M, Umemura T. 2011. Uptake of lead, cadmium, and other metals in the liver and kidneys of cattle near a lead-zinc mine in Kabwe, Zambia. *Environmental Toxicology and Chemistry* 30(8): 1892–1897.

Yabe J, Nakayama SMM, Ikenaka Y, Yohannes YB, Bortey-Sam N, Oroszlany B, Muzandu K, Choongo K, Kabalo AN, Ntapisha J, Mweene A, Umemura T, Ishizuka M. 2015. Lead poisoning in children from townships in the vicinity of a lead-zinc mine in Kabwe, Zambia. *Chemosphere* 119: 941–947.

Yang X, Feng Y, He Z, Stoffella PJ. 2005. Molecular mechanisms of heavy metal hyperaccumulation and phytoremediation. *Journal of Trace Elements in Medicine and Biology* 18(4): 339–353.

Yashim ZI. 2015. Phytoextraction of Heavy Metals by *Vetivera zizanioides*, *Cymbopogon citrates* and *Helianthus annuus*. *American Journal of Applied Chemistry* 3(1): 1.

Zhang C, Song Z, Zhuang D, Wang J, Xie S, Liu G. 2019. Urea fertilization decreases soil bacterial diversity, but improves microbial biomass, respiration, and N-cycling potential in a semiarid grassland. *Biology and Fertility of Soils* 55(3): 229–242.

Zhao FJ, Lombi E, Breedon T, McGrath SP. 2000. Zinc hyperaccumulation and cellular distribution in *Arabidopsis halleri*. *Plant, Cell and Environment* 23(5): 507–514.

Chemosphere 262 (2021) 127788

Contents lists available at ScienceDirect

Chemosphere

journal homepage: www.elsevier.com/locate/chemosphere

Clinical biochemical parameters associated with the exposure to multiple environmental metals in residents from Kabwe, Zambia

Hokuto Nakata [a, 1], Shouta M.M. Nakayama [a, 1], John Yabe [b], Kaampwe Muzandu [b], Haruya Toyomaki [a], Yared Beyene Yohannes [a, c], Andrew Kataba [a, b], Golden Zyambo [b], Yoshinori Ikenaka [a, d], Kennedy Choongo [b, e], Mayumi Ishizuka [a, *]

[a] Laboratory of Toxicology, Department of Environmental Veterinary Sciences, Faculty of Veterinary Medicine, Hokkaido University, Kita 18 Nishi 9, Kita-ku, Sapporo, 060-0818, Japan
[b] The University of Zambia, School of Veterinary Medicine, P.O. Box 32379, Lusaka, Zambia
[c] Department of Chemistry, College of Natural and Computational Science, University of Gondar, Ethiopia
[d] Water Research Group, School of Environmental Sciences and Development, North-West University, South Africa
[e] Fiji National University, College of Agriculture, Fisheries & Forestry, School of Animal and Veterinary Sciences, Koronivia Campus, Suva, Fiji

HIGHLIGHTS

- Cross-sectional study with representative 504 residents in closed mine site.
- Significant elevation of blood lead and cadmium levels at areas near mine.
- Increase of hepatic and renal parameters in 20–50% of target adult population.
- Inhibition of δ-aminolevulinic acid dehydratase activity due to Pb exposure.
- Negative association between Cd level and estimated glomerular filtration rate.

ARTICLE INFO

Article history:
Received 16 April 2020
Received in revised form
27 June 2020
Accepted 20 July 2020
Available online 17 August 2020

Handling Editor: A. Gies

Keywords:
Liver function
Kidney function
ALAD activity
Lead
Cadmium
Mining site

ABSTRACT

Lead (Pb) interferes with various bodily functions. Although high blood Pb (Pb–B) levels in residents from Kabwe, Zambia have been reported, the accumulation pattern of other metals remains unknown. The study was designed to determine the Pb–B, blood cadmium (Cd–B), and zinc (Zn–B) values of 504 representative samples from Kabwe, as well as the potential associated adverse health effects. The Pb–B level ranged from 0.79 to 154.75 μg/dL and generally increased in areas near the mine. A significant elevation of Cd–B was observed in two areas (0.37 ± 0.26 and 0.32 ± 0.30 μg/L) where the two highest mean Pb–B levels were recorded. By contrast, the Zn–B values did not differ greatly with respect to area. Some blood biochemical parameters relating to hepatic and renal functions were out of the normal range in approximately 20–50% of studied adult participants. The δ-aminolevulinic acid dehydratase (δ-ALAD) activity was significantly inhibited in the two areas contaminated by Pb and Cd. A significant negative relationship was observed between metal levels and clinical parameters, e.g., between Pb–B and δ-ALAD for all the age categories and between Cd–B and the estimated glomerular filtration rate for all the age categories except 0–4 years. The elevated Cd–B in areas near the mine relative to the other areas suggested the potential adverse health effects of Cd and/or the interaction of Pb and Cd. A significant association of metal levels with clinical parameters also indicated the effects of metal exposure on hematopoietic, hepatic, and renal systems.

1. Introduction

Lead (Pb) poisoning has been recognized as a major public health risk. According to the World Health Organization (WHO), Pb poisoning accounts for 0.6% of the global disease burden, which is

* Corresponding author.
E-mail address: ishizum@vetmed.hokudai.ac.jp (M. Ishizuka).
[1] Both authors equally contributed to this study.

https://doi.org/10.1016/j.chemosphere.2020.127788
0045-6535/

highest in developing countries (WHO, 2009). Lead is a persistent toxic substance that impacts human health through inhalation and ingestion pathways. Human exposure to Pb generally occurs via various sources, such as leaded gasoline, Pb-based paints, Pb-containing water pipes, battery recycling, and industrial processes including smelting and mining. The blood lead level (Pb–B) is used as the main bioindicator to monitor the current exposure level. The Center for Disease Control and Prevention (CDC) defined the blood reference value as 5 μg/dL in their new guidelines for assessing children's Pb–B (CDC, 2012). Chronic environmental Pb poisoning with approximately 40–60 μg/dL of Pb–B has been widely reported (Bede-Ojimadu et al., 2018; Li et al., 2014; Tuakuila et al., 2013), whereas acute poisoning is relatively uncommon.

Lead is known to interfere with a number of bodily functions including nervous, hematopoietic, hepatic, and renal systems (Lockitch, 1993). Exposure to Pb causes hematotoxicity through the restriction of hemoglobin synthesis by inhibiting key enzymes, such as δ-aminolevulinic acid dehydratase (δ-ALAD), and shortening the life span of circulating erythrocytes (Gonick, 2011). Anemia, which is caused by these processes, is one of the most well-known toxicities of Pb. Renal toxicity occurs at Pb–B > 60 μg/dL (Wang et al., 2002); however, even at lower levels, toxic effects appear (Harari et al., 2018). Chronic nephropathy causes functional and morphological changes, resulting in renal breakdown and hypertension (Rastogi, 2008). Lead intoxication also causes hepatic injury, namely, hepatic hyperplasia, and high serum levels of hepatic enzymes, such as alkaline phosphatase (ALP) (Mudipalli, 2007).

Kabwe is the fourth largest town and the administrative capital of Zambia's central province, with a long history of Pb and zinc (Zn) mining activity, which operated for nearly a century until 1994. Despite the end of the mining operation, some activities have continued, such as the smelting of the mineral ores that were left in the mine dump or transported from outside the town. Artisanal mining at the closed mine tailing dams and the use of Pb-contaminated soil to make bricks are other activities commonly seen at the site. Earlier observational studies reported serious Pb contamination in soil (Nakata et al., 2016; Nakayama et al., 2011), wild rats (Nakayama et al., 2013), goats (Nakata et al., 2016), chickens (Nakata et al., 2016), dogs (Toyomaki et al., 2020), wild lizards (Doya et al., 2020) and even humans (Yabe et al., 2015, 2018, 2020). Moreover, a recent cross-sectional study with the sample size of 1190 using a LeadCare® II instrument, which enables on-the-spot testing of Pb–B, revealed that Pb contamination has spread to wide areas of Kabwe (Yabe et al., 2020). Among the tested people of all ages, 70% had higher Pb–B than the reference level of 5 μg/dL although the reference level was determined for not all age group, but children ages 1–5 years old (CDC, 2012). The Pb–B level of approximately 15% of the people exceeded 45 μg/dL, which is the threshold in children ages 1–5 years old required for chelation therapy (CDC, 2002). With the wide spread of Pb poisoning across age groups in Kabwe, the accompanying adverse effects of Pb are anticipated; however, no clinical observation has been conducted. Given these factors, the current study aimed to assess the possible health effect of Pb poisoning in Kabwe. Furthermore, we also targeted blood cadmium (Cd) and Zn levels, as high concentrations of Cd in rats (N = 20) (Nakayama et al., 2013), free range chickens (N = 10) (Nakata et al., 2016) and children (N = 190) (Yabe et al., 2018) as well as that of Zn in soil (N = 101) (Nakayama et al., 2011) have also been recorded in Kabwe. Cadmium exhibits nephrotoxic activity, with a reduction in the estimated glomerular filtration rate (eGFR) and albumin (Alb) loss in urine (ATSDR, 2012). An observational study reported a significant relationship between low-level environmental Cd exposure and renal dysfunction (Ferraro et al., 2010). Additionally, according to both observational and experimental studies, various adverse health effects can occur due to the co-exposure to Pb and Cd (Hambach et al., 2013; Ni et al., 2014; Pan et al., 2018; Nakayama et al., 2019). In contrast to Pb- and Cd-related diseases, disease relating to Zn excess is not common. Rather, a protective effect of Zn on Pb and Cd intoxication has been suggested by experimental studies using laboratory rats (Saxena et al., 1989; Soussi et al., 2018).

In this study, we targeted the inhibition of δ-ALAD as a marker of hematotoxicity as well as various hepatic and renal function parameters. Studies focusing on the exact impact of metal poisoning on human health are limited. To the best of our knowledge, this is the first study that reports the widespread association of exposure to multiple metals with clinical screening parameters for humans on the African continent where serious Pb poisoning cases exist (Yabe et al., 2010). The present study was designed to clarify the exact health impact in Kabwe and to facilitate the implementation of possible countermeasures that can help us to overcome this type of pollution.

2. Methods

2.1. Sample collection and plasma preparation

The study was approved by the University of Zambia Research Ethics Committee (UNZAREC; REF. No. 012-04-16) and the Ministry of Health through the Zambia National Health Research Ethics Board as well as the Kabwe District Medical Office. The sampling was done in Kabwe, which is located approximately 130 km north of Lusaka, the capital city of Zambia. Kabwe has a population of approximately 230,000 residents and an area of 1547 km^2. The study was designed to select 1000 households from across Kabwe using two-stage random selection. After informed and written consent was obtained from household heads, the data and samples were collected. Further details of sample selection and collection have been described in recent papers (Hiwatari et al., 2019; Yabe et al., 2020). Heparinized blood was dispensed and immediately centrifuged for 10 min at 1500×g, after which the plasma was stored at −20 °C. Analysis was performed at the KAbwe Mine Pollution Amelioration Initiative (KAMPAI) project monitoring laboratory in the Department of Biomedical Sciences, School of Veterinary Medicine, the University of Zambia. The remaining whole blood samples were transported to Japan in cooler boxes after obtaining a material transfer agreement (MTA) from the Ministry of Health, Zambia, through the National Health Research Ethics Committee (No. E03618) and analyzed in the Laboratory of Toxicology, Faculty of Veterinary Medicine, Hokkaido University, Japan. After sample collection, we randomly ranked the 40 standard enumeration areas (SEAs) and selected them in sequential order until the total sample size of the selected SEAs exceeded 500. Consequently, 504 samples from 20 SEAs were chosen for laboratory analysis in the current study. Supplementary Figure S1 shows the locations of the selected SEAs.

2.2. Data collection and physical measurement

We asked the participants their age and measured their height and body weight at the same time as blood collection. Data were recorded using Survey Solutions (version 5.22.20, the latest version at the time of our survey), developed by the World Bank. Body mass index (BMI) was calculated using the following formula:

$$\mathrm{BMI} = \mathrm{body\ weight\ (kg)/height\ (m)\text{^}2}$$

The BMI z-score for participants with the age between 5 and 17 years old was also determined with reference to sex- and age-

specific mean BMI values and distributions using the charts and tables provided by WHO (2007) because the z-score gives a relative measure of adiposity adjusted for sex and age.

2.3. Whole blood digestion and metal extraction

Blood digestion and metal extraction were performed as described previously (Nakata et al., 2016) with minor modifications. All laboratory materials and instruments used in the metal extraction were washed in 2% nitric acid (HNO_3) and rinsed at least twice with distilled water. Two hundred microliters of whole blood were placed in pre-washed digestion vessels, followed by acid digestion using 5 mL of twofold diluted ultrapure nitric acid (Cica reagent, specific gravity of 1.38, 60%; Kanto Chemical Corp., Tokyo, Japan) and 1 mL of ultrapure hydrogen peroxide (Cica reagent, 30%; Kanto Chemical Corp.). The digestion and metal extraction were conducted using a microwave digestion system (Speed Wave MWS-2; Berghof, Eningen, Germany) following the manufacturer's instruction. After cooling, extracted solutions were transferred into 15-mL plastic tubes and diluted to a final volume of 10 mL with double distilled and deionized water (Milli-Q; Millipore, Bedford, MA).

2.4. Metal analysis

The concentrations of metals (Pb, Cd, and Zn) were determined using Inductively Coupled Plasma − Mass Spectrometer (ICP-MS) (7700 series; Agilent Technologies, Tokyo, Japan). Detailed operating conditions are shown in Supplementary Table S1. Analytical quality control was performed using the certified reference material, Seronorm™ Trace Elements Whole Blood L-2 (Sero, Billingstad, Norway). Replicate analysis of these reference materials showed good accuracy (relative standard deviation (RSD) was less than 3%) and recoveries (95–105%). The instrument detection limit was 0.001 μg/L.

2.5. Blood biochemical analysis

A conventional blood biochemical analyzer (Spotchem EZ SP-4430, Arkray Inc., Kyoto, Japan) was used to analyze the levels of plasma total bilirubin (T-bil), aspartate aminotransferase (AST), alanine aminotransferase (ALT), lactase dehydrogenase (LDH), γ-glutamyltranspeptidase (GGT), ALP, total protein (T-pro), Alb, blood urea nitrogen (BUN), urea acid (UA), and creatinine (Cre) in all participants. The analyses were done following the manufacturer's instructions. Normal ranges of the parameters for participants with the age of 18 years and above were presented in the manufacturer's manual. The BUN/Cre ratio was determined because it is widely used to assess renal function. The eGFR Modification of Diet in Renal Disease ($eGFR_{MDRD}$) value was also calculated for participants older than or equal to 18 years for renal function screening using the following formulas (Levey et al., 2006). A value < 60 mL/min/1.73 m^2 is considered normal (Levey et al., 2009).

$$eGFR_{MDRD} = 175 \times (Cre\text{^} - 1.154) \times (age\ \ (y)\text{^} - 0.203) \times 1.212 \times 0.742\ \ (for\ females)$$

$$eGFR_{MDRD} = 175 \times (Cre\text{^} - 1.154) \times (age\ \ (y)\text{^} - 0.203) \times 1.212\ \ (for\ males)$$

The following formula was used to calculate $eGFR_{MDRD}$ for children and adolescents aged below 18 years old (Schwartz et al., 2009). The value below 75 mL/min/1.73 m^2 is considered normal (National Institute of Diabetes and Digestive and Kidney Disease).

$$eGFR_{MDRD} = 0.413 \times height\ \ (cm)/Cre$$

In cases where the T-bil level was below the limit of detection (LOD) of 0.2 mg/dL, the data were adjusted to the LOD value divided by the square root of 2 (0.14 mg/dL) for statistical analysis (Hornung and Reed, 1990). Similarly, the AST, ALT, and GGT levels lower than the LOD of 10 international unit (IU)/L were adjusted to 7.07 IU/L. Furthermore, BUN values below the detection limit of 5 mg/dL were adjusted to 3.54 mg/dL. These changes were made to minimize the effect on statistical analysis where the exact distribution of values below the detection limit was unknown.

2.6. δ-ALAD activity assay

Enzymatic activity and the ratio between non-activated and *in vitro*-activated enzymes were measured as described in previous studies (Espín et al., 2015; Scheuhammer, 1987) with slight modifications. Three aliquots of 20 μL of whole blood of each participant were separated to measure non-activated δ-ALAD activity, reactivated δ-ALAD activity, and the activity of the matrix. For the non-activated enzyme activity assay, 80 μL of 0.1% Triton X-100 (Sigma–Aldrich, MO, USA) was added to the blood as a lysate. Then, 100 μL of 0.5-M phosphate-buffered saline (PBS) (pH 6.8), 50 μL of 60-mM 5-aminolevulinic acid (ALA) hydrochloride (Sigma–Aldrich) solution in PBS, and 50 μL of distilled water (DW) were added. For the reactivated activity assay, 0.1% Triton X-100, 0.5-M PBS, and 60-mM ALA hydrochloride were added to the sample with the same volume of each solution used in the non-activated enzyme activity assay. Then, 25 μL of 0.8-mM Zn acetate (Himedia Laboratories Pvt. Ltd., Mumbai, India) and 25 μL of 1-M dithiothreitol (DTT) (Himedia Laboratories Pvt. Ltd.) were added. For the matrix blank assay, 80 μL of Triton X-100, 150 μL of PBS, and 50 μL of DW were added, followed by 200 μL of 0.4-M trichloroacetic acid (TCA) (Merck, Darmstadt, Germany)/60-mM mercury chloride ($HgCl_2$) (Himedia Laboratories Pvt. Ltd.) as a stop solution. After a 60-min incubation and termination of the reaction by $HgCl_2$ in both the non-activated and reactivated activity assays, all samples were centrifuged at 10,000 g for 5 min. Supernatants were transferred to new tubes and mixed with 750 μL of modified Ehrlich's reagent, which consisted of dimethylaminobenzaldehyde (Nacalai tesque, Kyoto, Japan) in acetic acid (glacial; 99.6%, Himedia Laboratories Pvt. Ltd.) and perchloric acid (Merck KGaA, Darmstadt, Germany). After 10 min, the absorbance was read at 555 nm against the appropriate blank using a UV spectrophotometer (Shimadzu UV-2600, Shimadzu Inc., Kyoto, Japan). The activity was expressed as μmol porphobilinogen (PBG)/h/L red blood cells using the equation provided by Scheuhammer (1987). Then, the ratio between the non-activated and the *in vitro* reactivated enzymes was calculated.

2.7. Statistical analysis

IBM SPSS Statistics 26 (IBM Corporation, Armonk, NY, USA) was used to evaluate significant differences in the data in all statistical analyses except principal component analysis (PCA), which was carried out using JMP Pro version 14 (SAS Institute, NC, USA). The data were log-transformed and fitted a normal distribution. The Tukey–Kramer test was used to compare age, height, body weight, BMI, blood metal levels, blood biochemical parameters, δ-ALAD enzyme activity, and the δ-ALAD activity ratio among areas in Kabwe as well as groups categorized by age or Pb–B. Pearson's product–moment correlation (r) was used to analyze the relationship between blood metal levels, blood biochemical parameters, and the δ-ALAD activity ratio. PCA was performed with blood

metal levels, age, BMI, and the δ-ALAD activity ratio. All statistical analyses were performed at the significance level of 0.05 ($p < 0.05$).

3. Results

3.1. General outcomes of the randomly selected subjects

In the random selection, subjects were drawn from people who were tested at the following eight health centers: Kasanda, Makululu, Chowa, Natuseko, Bwacha, Mpima prison, Kang'omba, and Hamududu (Supplementary Figure S1). The age of the 504 selected Kabwe residents ranged from 0 to 96 years (Supplementary Table S2). The mean and median ages of all tested people were 28.1 and 27 years, respectively, and their mean and median heights were 144.9 and 156.0 cm, respectively. Their body weight ranged from 7 to 154 kg, with mean and median values of 47.8 and 53.0 kg, respectively. For adults 18 years or older, the mean and median BMI values were 24.0 and 22.6, respectively, whereas the mean and median BMI values for all age groups were 21.0 and 20.4, respectively.

Significant area differences in age, height, body weight, and BMI for all age groups were recorded. The age, height, and body weight of people in Makululu were significantly higher than those in Natuseko and Mpima prison. Similarly, the age, height and body weight of people in Kasanda were significantly higher than those in Natuseko. Significantly higher BMI values were recorded in Makululu and Bwacha compared to those recorded in Mpima prison for all age groups.

The distribution patterns of BMI z-score for children and adolescents with the age between 5 and 17 years old were summarized in Supplementary Table S3 and S4. Generally, approximately 75% of both girl and boy showed the value of z-score between −1 and 1, which are the values considered normal. The 16% of girls and 18% of boys had the z-score below −2, indicating thinness, whereas 9% of girls and 4% of boys recorded the z-score above 2 which means obesity. There was no clear area trend and relationship with Pb−B.

3.2. Metal levels in blood

Levels of Pb−B, Cd−B, and Zn−B in the whole blood samples are shown in Table 1. The minimum, maximum, mean, and median Pb−B levels of all subjects were 0.79, 154.75, 14.62, and 10.75 μg/dL, respectively. Values of Pb−B and Cd−B for all age groups in Kasanda were significantly higher than those in other areas except for Cd−B in a comparison between Kasanda and Makululu. The highest Pb−B level was measured in Kasanda. All people tested in Kasanda had Pb−B levels higher than the 5 μg/dL reference level. In Kang'omba and Hamududu, which are far from the mine site, the mean Pb−B values for all age groups were lower than the reference level although the values for children and adolescents in Kang'omba with the age below 18 were slightly greater than the reference level. The Zn−B level showed less variation among areas, and significant differences for all age groups were observed only between Kasanda and Natuseko and between Kasanda and Kang'omba.

In comparison among age groups, Pb−B for the group with the age between 0 and 4 in Kasanda was remarkably greater than that for the other age groups. In general, the group with age between 5 and 17 years had significantly elevated Pb−B than adult female and male groups. Contrary to Pb−B, Cd−B and Zn−B showed higher values in participants with the age of 18 and above compared to children and adolescent groups.

3.3. Blood biochemical parameters

The values of the blood biochemical parameters in 8 areas of Kabwe are presented in Supplementary Table S5. The T-bil value recorded in Natuseko was significantly higher than that recorded in Makululu and Kang'omba. Kasanda also showed a significantly higher level of T-bil compared with Makululu. Hanududu had significantly higher AST value than Makululu and Kang'omba. The LDH level in Chowa was significantly higher than those in Makululu, Mpima prison, Kang'omba and Hamududu. Bwacha recorded the highest mean value of GGT with statistical significant difference compared to Kang'omba. A significantly lower Alb value was measured in Makululu compared to those in Kasanda and Chowa. The significant increase of Cre was observed in Chowa compared to Makululu, Mpima prison and Hamududu. The $eGFR_{MDRD}$ value in Kasanda was significantly lower than those in Makululu and Hamududu. ALT, BUN and BUN/Cre did not show any significant area difference.

The distribution pattern of the parameters by age and Pb−B range is presented in Supplementary Table S6. Moreover, the comparison of parameters with normal levels for the participants with the age of 18 and above is summarized in Fig. 1. Most of the participants had T-bil values in the normal range or below, whereas only 1.5% of adult female and 0.9% adult male participants had a value higher than the normal range. Adult male participants recorded significantly greater T-bil level compared to other categories although there was no significant difference of T-bil level by Pb−B range in adult male group. Similarly, two major hepatic parameters, AST and ALT, were within the normal range for most of the participants. In addition, those two parameters in adult male group was significantly higher than those in other three categories as same as T-bil. However, the LDH, GGT, and ALP levels exceeded the normal values in approximately 20−70% of the adult participants. The highest values of LDH, GGT, and ALP were 1176, 390, and 1660 IU/L, respectively, which are approximately 5−10 times higher than the upper limit of the normal range. For the LDH and ALP, adult female and male groups recorded significantly lower values compared with other two age categories while GGT in these two adult groups were significantly higher than that in two younger age categories. The T-pro and Alb levels were lower than the normal range in approximately 30% of the adult participants. The significantly higher T-pro and Alb levels were shown in adult female and male groups than other two groups except the relationship of Alb value between the group with age of 5−17 years and the adult female group. There was no Pb−B effect on T-pro and Alb. Approximately 20% of the tested adult female and male participants had values higher than the normal range for UA, whereas Cre levels of approximately 60% of female and 30% male participants exceeded the normal range. The BUN/Cre ratio was lower than the normal range for almost half of the adults. By contrast, BUN and $eGFR_{MDRD}$ were mostly in the normal range. The significant effect of Pb−B on these parameters relating to renal function were rarely recorded. Generally, male aduly group showed significantly greater values of BUN, UA, Cre, BUN/Cre and $eGFR_{MDRD}$.

3.4. δ-ALAD activity

The δ-ALAD activities recorded in the matrix blank and non-activated and reactivated assays are shown in Supplementary Table S7 together with the activity ratio. Significantly lower ratios were recorded in Kasanda and Makululu compared with those recorded in the six other areas. The maximum ratio of 0.85 occurred in Kang'omba and Hamududu, whereas the two minimum ratios, 0.29 and 0.30, occurred in Makululu and Kasanda, respectively. The values of the non-activated and reactivated assays in Hamududu were significantly the highest across the areas followed by those in Kang'omba, while no significant area difference was found for the value of the matrix blank assay.

Table 1
Blood Pb, Cd and Zn levels in whole blood among the 504 representative Kabwe residents from 8 areas by age (Mean ± SD, minimum − maximum).

Area	Kasanda	Makululu	Chowa	Natuseko	Bwacha	Mpima prison	Kangomba	Hamududu	All area	
Pb−B (μg/dL)										
all age	31.74 ± 19.05 (9.90−154.75) a	16.38 ± 9.67 (3.29−65.9) b	8.10 ± 7.72 (1.47−33.44) c	8.20 ± 7.07 (1.30 −35.58) c	6.28 ± 6.71 (1.26 −27.89) cd	5.31 ± 3.85 (1.67 −21.58) cd	3.99 ± 3.34 (0.95 −17.06) de	2.99 ± 2.01 (0.79 −12.61) e	14.62 ± 14.40 (0.79 −154.75)	
0 - 4	85.61 ± 48.04 (43.55 −154.75)	24.55 ± 13.25 (6.06−43.43)	8.46 (6.82, 10.09)	11.68 ± 7.52 (3.94 −31.32)	23.70 (19.50, 27.89)	5.60 ± 3.56 (2.30 −13.35)	6.76 ± 5.37 (2.50 −14.55)	3.67 ± 1.64 (1.73−7.36)	16.84 ± 26.35 (1.73 −154.75)	AB
5 - 17	31.97 ± 12.16 (12.31−66.89)	25.17 ± 11.54 (9.74−65.94)	14.42 ± 13.56 (3.24−33.44)	6.74 ± 3.82 (2.78 −15.35)	6.44 ± 1.69 (5.23−8.90)	5.68 ± 3.30 (2.69 −15.11)	5.47 ± 4.76 (1.78 −17.06)	3.10 ± 1.57 (1.62−5.77)	19.63 ± 14.64 (1.62−66.89)	A
18 -, female	25.47 ± 12.91 (9.90−57.87)	12.93 ± 6.10 (4.53−49.87)	3.62 ± 1.41 (1.47−4.92)	6.95 ± 8.16 (1.30 −35.58)	3.28 ± 1.36 (1.66−6.31)	4.72 ± 4.90 (1.67 −21.58)	3.00 ± 1.52 (1.11−6.34)	2.58 ± 2.77 (0.79 −12.61)	11.63 ± 10.32 (0.79−57.87)	B
18 -, male	31.31 ± 12.84 (10.41−63.63)	13.00 ± 6.00 (3.29−26.80)	7.20 ± 7.15 (5.62−8.90)	6.37 ± 3.77 (2.43 −11.39)	4.49 ± 4.67 (1.26−9.85)	5.53 ± 2.99 (3.32 −10.64)	2.80 ± 1.15 (0.95−4.80)	3.04 ± 1.31 (1.18−6.36)	13.23 ± 12.07 (0.95−63.63)	B
Cd−B (μg/L)										
all age	0.37 ± 0.26 (0.12−1.38) a	0.32 ± 0.30 (0.04−2.27) ab	0.16 ± 0.08 (0.06−0.33) cde	0.17 ± 0.11 (0.05−0.52) cde	0.12 ± 0.06 (0.05−0.26) de	0.26 ± 0.26 (0.04−1.30) bc	0.19 ± 0.11 (0.06−0.56) cd	0.13 ± 0.14 (0.02−0.99) e	0.27 ± 0.26 (0.02−2.27)	
0 - 4	0.30 ± 0.16 (0.14−0.52)	0.16 ± 0.15 (0.04−0.38)	0.09 (0.08, 0.10)	0.11 ± 0.05 (0.05−0.25)	0.06 (0.05, 0.07)	0.15 ± 0.13 (0.04−0.43)	0.15 ± 0.01 (0.13−0.16)	0.06 ± 0.03 (0.02−0.11)	0.13 ± 0.11 (0.02−0.52)	A
5 - 17	0.27 ± 0.17 (0.12−1.04)	0.21 ± 0.10 (0.05−0.52)	0.13 ± 0.09 (0.06−0.26)	0.14 ± 0.08 (0.06−0.31)	0.08 ± 0.01 (0.07−0.10)	0.19 ± 0.13 (0.05−0.40)	0.14 ± 0.03 (0.10−0.19)	0.07 ± 0.03 (0.05−0.12)	0.20 ± 0.13 (0.05−1.04)	B
18 -, female	0.38 ± 0.17 (0.14−0.72)	0.39 ± 0.36 (0.08−2.27)	0.21 ± 0.10 (0.08−0.33)	0.21 ± 0.13 (0.08−0.52)	0.16 ± 0.07 (0.07−0.26)	0.24 ± 0.16 (0.08−0.52)	0.19 ± 0.06 (0.09−0.30)	0.11 ± 0.07 (0.03−0.25)	0.31 ± 0.28 (0.03−2.27)	C
18 -, male	0.51 ± 0.39 (0.18−1.38)	0.34 ± 0.30 (0.07−1.46)	0.16 ± 0.05 (0.11−0.21)	0.23 ± 0.17 (0.13−0.48)	0.11 ± 0.07 (0.05−0.19)	0.70 ± 0.49 (0.19−1.30)	0.23 ± 0.19 (0.06−0.56)	0.21 ± 0.22 (0.05−0.99)	0.34 ± 0.32 (0.05−1.46)	C
Zn−B (mg/L)										
all age	5.92 ± 1.37 (3.45−10.20) a	5.52 ± 1.25 (2.30−10.06) ab	5.14 ± 1.05 (3.53−7.02) ab	5.01 ± 1.11 (2.95−7.53) b	5.49 ± 1.13 (3.72−7.36) ab	5.80 ± 1.46 (2.99−9.27) ab	5.04 ± 1.09 (3.05−6.85) b	5.37 ± 1.38 (2.78−8.53) ab	5.51 ± 1.30 (2.30−10.20)	
0 - 4	5.31 ± 1.18 (4.17−6.84)	3.84 ± 1.15 (2.30−5.14)	4.55 (4.29, 4.81)	4.49 ± 0.82 (2.95−5.96)	4.16 (3.72, 4.60)	4.50 ± 0.84 (2.99−5.93)	4.26 ± 0.73 (3.46−4.91)	3.99 ± 1.58 (2.78−7.75)	4.36 ± 1.06 (2.30−7.75)	A
5 - 17	4.95 ± 0.95 (3.45−7.34)	4.95 ± 0.95 (3.45−7.34)	4.48 ± 0.90 (3.53−5.69)	4.51 ± 0.85 (3.40−5.88)	5.27 ± 1.20 (4.27−6.70)	5.04 ± 0.98 (3.40−6.79)	4.19 ± 0.94 (3.05−6.19)	4.94 ± 1.24 (3.40−6.93)	4.71 ± 1.02 (3.03−9.70)	A
18 -, female	6.22 ± 1.13 (4.61−8.84)	5.67 ± 1.00 (3.48−8.82)	5.59 ± 1.16 (4.36−6.82)	5.49 ± 1.04 (3.05−7.53)	5.78 ± 0.94 (4.45−7.36)	6.78 ± 1.27 (4.93−9.27)	5.54 ± 1.00 (3.93−6.83)	5.33 ± 0.94 (3.16−7.09)	5.79 ± 1.09 (3.05−9.27)	B
18 -, male	6.97 ± 1.32 (4.94−10.20)	6.44 ± 1.02 (4.64−10.06)	5.52 ± 1.06 (4.57−7.02)	5.71 ± 1.70 (4.00−7.24)	5.69 ± 1.68 (3.92−7.26)	7.17 ± 0.81 (6.25−8.06)	5.48 ± 0.84 (3.66−6.85)	6.36 ± 1.03 (4.61−8.53)	6.40 ± 1.17 (3.66−10.20)	C

Note: Different small letters (a, b, c, d and e) between columns indicate a significant difference among areas. Different capital letters (A, B and C) indicate a significant difference among age categories.

Additionally, the comparison of the δ-ALAD activity ratios by age and Pb−B was summarized in Table 2. In comparison of different Pb−B categories in the group with the age from 0 to 4 years, two categories with Pb−B of 20.0 μg/dL and above had significantly lower δ-ALAD activity ratios than other two categories with Pb−B below 20.0 μg/dL. Similar trend was observed in the age groups of 5−17 years as well as 18 years and above. There was no significant difference among different age groups.

3.5. Association among blood metal levels and other factors

The association between Pb−B and the δ-ALAD activity ratio is shown in Fig. 2. Within the group of all Kabwe residents who were randomly selected in the current study, the Pb−B level and δ-ALAD activity ratio were negatively correlated, with an r^2 value of 0.288 ($p < 0.0001$). Correlation coefficients between blood metal levels and blood biochemical parameters, as well as the δ-ALAD activity ratio, are shown in Table 3. The Pb−B and Cd−B were positively correlated with statistical significance for all the age categories. A significant positive correlation between Pb−B and UA was recorded for all the age categories except the category of 0−4 years, whereas there was a significant negative correlation between the Pb−B level and T-bil, as well as the δ-ALAD activity ratio, for the category of all age. The Pb−B andδ-ALAD activity ratio showed a strong negative correlation with a statistical significance for all the age categories as Fig. 2 drew the statistical negative significance for the category of all age. The Cd−B level showed significant positive or negative correlations with most of the parameters other than T-bil, AST and $eGFR_{MDRD}$. However, those significant association with Cd−B did not appear for all the categorized age groups while UA andδ-ALAD activity ratio were positively and negatively correlated with Cd−B for the age categories of 5−17 years as well as 18 years and above, respectively. Similarly, Zn−B value was significantly correlated with most of the parameters for the category of all age whereas no significant association was observed for the age categories of 0−4 years as well as 5−17 years. PCA was performed on log-transformed data to evaluate the relationship between blood metal levels, age, BMI, and the δ-ALAD activity ratio for the category of all age (Fig. 3). The results showed that the first principal component (PC1) accounted for 37.2% of the variation, and the second principal component (PC2) accounted for 28.8%. The Zn−B level was the factor that most positively contributed to PC1 followed by the Cd−B level, age, and BMI. PC2 had a strongly positive relationship with the δ-ALAD activity ratio and a negative relationship with Pb−B. The Pb−B level and δ-ALAD activity ratio had the strongest negative relationship.

4. Discussion

Although environmental metal pollution remains a significant

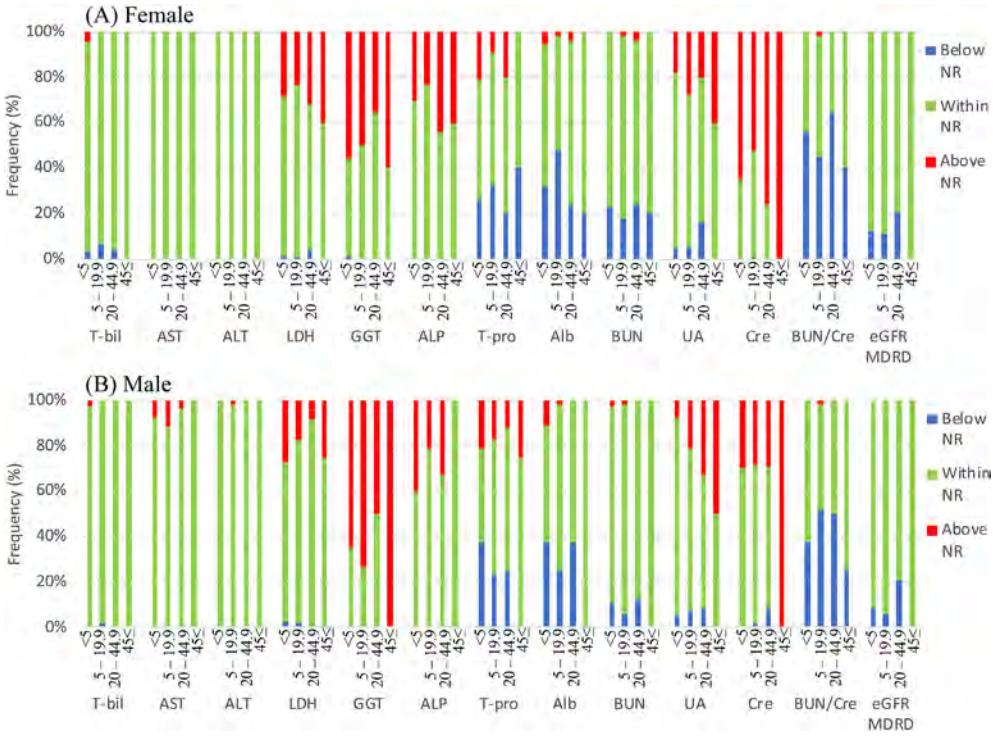

Fig. 1. Comparison of blood biochemical parameters in plasma of adult female (A) and male (B) with normal range (NR) by Pb–B range (0–4.9, 5–19.9, 20–44.9, 45≤ μg/dL).

Table 2
The δ-ALAD activity ratio in whole blood in Kabwe residents by groups categorized by age and Pb–B range (0–4.9, 5–19.9, 20–44.9, 45≤ μg/dL).

age group	Pb–B range	min	25% quartile	median	75% quartile	max	mean	SD	SE		
all age	all Pb–B	0.294	0.490	0.581	0.667	0.850	0.577	0.122	0.006		
0–4	all Pb–B	0.333	0.532	0.629	0.686	0.773	0.596	0.126	0.022	A	
	<5	0.463	0.633	0.646	0.679	0.742	0.643	0.072	0.020		a
	5–19.9	0.483	0.565	0.619	0.706	0.758	0.636	0.092	0.028		a
	20.0–44.9	0.333	0.388	0.486	0.542	0.773	0.499	0.158	0.065		b
	45≤	0.351	0.354	0.356	0.358	0.360	0.356	0.006	0.004		b
5–17	all Pb–B	0.303	0.462	0.560	0.634	0.850	0.558	0.125	0.011	A	
	<5	0.553	0.613	0.678	0.759	0.850	0.686	0.090	0.019		a
	5–19.9	0.355	0.532	0.595	0.669	0.800	0.590	0.108	0.016		b
	20.0–44.9	0.313	0.411	0.500	0.558	0.714	0.496	0.099	0.013		c
	45≤	0.303	0.401	0.431	0.445	0.463	0.411	0.058	0.024		c
18 -	all Pb–B	0.294	0.500	0.587	0.667	0.849	0.583	0.120	0.007	A	
	<5	0.364	0.594	0.667	0.727	0.849	0.659	0.097	0.010		a
	5–19.9	0.333	0.469	0.564	0.633	0.847	0.560	0.115	0.009		b
	20.0–44.9	0.294	0.481	0.533	0.600	0.755	0.526	0.091	0.014		b
	45≤	0.308	0.333	0.393	0.484	0.545	0.412	0.093	0.031		c

Note: Only one capital letter (A) indicate that there was no significant difference among age groups. Different small letters (a, b and c) indicate a significant difference among Pb–B range categories.

risk factor for human health all over the world, many serious pollution cases associated with industrial activities have been recently reported especially in Africa where a rapid economic growth is being achieved (Dooyema et al., 2012; Olewe et al., 2009; Tuakuila et al., 2013; Yabe et al., 2010). However, exact effect on human health due to metal exposure remains unknown despite the big effort to evaluate metal accumulation status in the past studies. Assessment of adverse health effect would be a key to quantify the impact of pollution and to move toward resolution. In this sense, it is vitally important that our cross-sectional study of clinical screening relating to the exposure to multiple metals indicated the effect on hematopoietic, hepatic and renal functions.

Dispersibility of areas in Kabwe was maintained after the random selection of SEAs to choose 504 individuals in terms of the direction and distance from the mine, which are key factors that determine the Pb contamination level (Nakayama et al., 2011; Yabe et al., 2020). The selected subjects were considered representative of the Kabwe region. Kasanda and Makululu are seriously contaminated by Pb. This result agrees with previous reports of Pb contamination in children's blood (Yabe et al., 2015), feces, and urine (Yabe et al., 2018). Similarly, the result of higher Pb–B of younger generation in some areas including Kasanda, Natuseko and Bwacha supported the previous findings that children had greater Pb–B than adults (Yabe et al., 2020) although such a trend was not

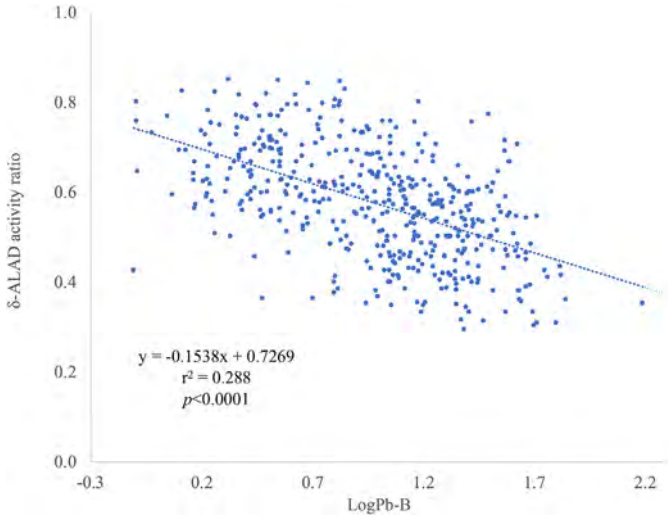

Fig. 2. Relationship between logPb-B and δ-ALAD activity ratio of the 504 representative Kabwe residents.

clearly shown in general. Chowa and Natuseko followed Kasanda and Makululu, with mean values close to 10 μg/dL. It should also be emphasized that some residents had Pb–B values above the reference level of 5 μg/dL, even in rural areas away from the mine, such as Mpima prison, Kang'omba, and Hamududu. Considering the possibility that the reference level may be revised to 3.48 μg/dL based on the 2011–2014 National Health and Nutrition Examination Survey (NHANES) (Caldwell et al., 2017), observed mean Pb–B levels below 5 μg/dL in Kang'omba and Hamududu should also be carefully considered. Compared with the results concerning other African countries, the Pb–B levels recorded in the current study were higher, although elevated Pb–B values have been reported in northwestern Nigeria where more than 400 children died because of Pb poisoning caused by artisanal mining activities; the values ranged from 36.5 to 445 μg/dL in 86 children <5 years of age (Dooyema et al., 2012; Pure Earth, 2014). In a cross-sectional study in Kinshasa, Democratic Republic of Congo, where leaded gasoline was still used at the time, Pb–B levels in 275 representative residents ranged from 2.9 to 49.3 μg/dL, with a median value of 9.9 μg/dL (Tuakuila et al., 2013). In Kibera slum, Nairobi, Kenya, a mean Pb–B level of 6.0 μg/dL with a range of 3.3–24.7 μg/dL was recorded in a cross-sectional study targeting 387 children aged 6–59 months (Olewe et al., 2009). Mean Pb–B values of 5.85 (N = 618) and 5.66 (N = 1546) μg/dL at birth and the age of 13 years, respectively, were reported in a cohort study conducted in the Johannesburg–Soweto metropolitan area (Naicker et al., 2010). The elevated Pb–B level in Kabwe relative to that in other countries has sounded the alarm due to the serious effects on human health.

Elevated fecal and urine Cd levels in Kasanda and Makululu residents have been reported (Yabe et al., 2018), and supportive results were obtained in our blood analysis study. A significantly higher Cd–B level was detected in Kasanda than in other areas except Makululu. A similar significantly high level of Cd–B was also recorded in Makululu compared with those recorded in the other areas except Mpima prison. In comparison of Cd–B by age, it was found that adults accumulated greater level of Cd in their blood than children and adolescents on the contrary to Pb accumulation pattern. Although the exact Cd–B threshold that would cause adverse health effects is unclear, the mean values for all residents in Kasanda and Makululu were markedly higher than those reported for children in Koprivnica (Croatia), i.e., 0.17 μg/L

Table 3
Correlation coefficients (r^2) between blood metal levels, biochemical parameters and δ-ALAD activity ratio by age.

Age category	Pb–B								Cd–B								Zn–B							
	all age		0–4		5–17		18 -		all age		0–4		5–17		18 -		all age		0–4		5–17		18 -	
	r2	p	r2	p	r2	p	r2	p	r2	p	r2	p	r2	p	r2	p	r2	p	r2	p	r2	p	r2	p
Pb–B	–	–	–	–	–	–	–	–	0.46	**<.0001**	0.48	**<.01**	0.56	**<.0001**	0.56	**<.0001**	0.03	0.47	0.27	0.15	0.03	0.74	0.19	**<.001**
Cd–B	0.46	**<.0001**	0.48	**<.01**	0.56	**<.0001**	0.56	**<.0001**	–	–	–	–	–	–	–	–	0.32	**<.0001**	0.35	0.07	0.12	0.19	0.16	**<.005**
Zn–B	0.03	0.47	0.27	0.15	0.03	0.74	0.19	**<.001**	0.32	**<.0001**	0.35	0.07	0.12	0.19	0.16	**<.005**	–	–	–	–	–	–	–	–
T-bil	−0.12	**<.05**	0.08	0.68	−0.22	**<.05**	−0.04	0.44	0.06	0.22	0.11	0.57	−0.07	0.43	−0.04	0.46	0.23	**<.0001**	0.09	0.63	−0.04	0.65	0.19	**<.001**
AST	0.04	0.35	0.28	0.14	−0.02	0.84	0.01	0.80	0.00	0.98	0.21	0.29	0.01	0.94	0.07	0.23	−0.02	0.74	0.14	0.46	−0.13	0.16	0.15	**<.01**
ALT	−0.05	0.27	0.30	0.11	0.00	0.97	−0.02	0.69	0.14	**<.005**	0.13	0.49	0.08	0.39	0.06	0.25	0.20	**<.0001**	0.08	0.67	−0.06	0.53	0.11	**<.05**
LDH	0.09	0.05	0.41	**<.05**	0.01	0.91	−0.03	0.58	−0.12	**<.01**	0.21	0.28	−0.06	0.52	0.00	0.93	−0.23	**<.0001**	0.24	0.20	−0.15	0.09	−0.03	0.65
GGT	−0.08	0.09	0.31	0.11	−0.03	0.71	−0.01	0.87	0.14	**<.005**	0.20	0.30	−0.03	0.74	0.00	0.93	0.30	**<.0001**	0.11	0.58	0.04	0.68	0.11	0.05
ALP	0.16	**<.001**	−0.05	0.79	−0.04	0.66	0.00	0.93	−0.24	**<.0001**	−0.10	0.61	0.06	0.53	0.05	0.37	−0.44	**<.0001**	0.09	0.66	−0.04	0.63	0.02	0.79
T-pro	−0.06	0.23	−0.20	0.29	−0.11	0.20	0.07	0.22	0.15	**<.005**	0.13	0.49	−0.10	0.28	0.08	0.14	0.20	**<.0001**	−0.05	0.78	−0.05	0.58	0.11	**<.05**
Alb	−0.07	0.12	−0.09	0.66	−0.15	0.10	0.00	0.94	0.10	**<.05**	0.24	0.21	−0.05	0.56	0.00	0.94	0.22	**<.0001**	0.00	0.98	−0.03	0.74	0.21	**<.0005**
BUN	0.00	0.95	−0.08	0.67	−0.03	0.70	0.08	0.14	0.12	**<.05**	0.14	0.45	−0.10	0.27	0.08	0.14	0.18	**<.0001**	0.02	0.92	0.14	0.13	0.07	0.19
UA	0.11	**<.05**	0.22	0.25	0.24	**<.01**	0.19	**<.005**	0.29	**<.0001**	0.23	0.22	0.18	**<.05**	0.18	**<.005**	0.35	**<.0001**	0.12	0.55	0.10	0.28	0.23	**<.0001**
Cre	−0.07	0.12	0.13	0.51	−0.13	0.15	0.08	0.15	0.28	**<.0001**	0.37	**<.05**	−0.01	0.88	0.05	0.34	0.44	**<.0001**	0.15	0.44	0.12	0.20	0.17	**<.01**
BUN/Cre	0.07	0.15	−0.14	0.46	0.11	0.22	0.02	0.79	−0.12	**<.01**	−0.16	0.40	−0.06	0.54	0.03	0.60	−0.20	**<.0001**	−0.15	0.45	0.03	0.70	−0.04	0.52
$eGFR_{MDRD}$	−0.10	**<.05**	−0.17	0.37	0.14	0.12	−0.10	0.07	0.03	0.53	−0.27	0.15	0.04	0.63	−0.13	**<.05**	0.13	**<.005**	−0.02	0.90	−0.08	0.35	−0.09	0.10
δ-ALAD activity ratio	−0.53	**<.0001**	−0.63	**<.0005**	−0.61	**<.0001**	−0.48	**<.0001**	−0.25	**<.0001**	−0.25	0.20	−0.33	**<.0005**	−0.26	**<.0001**	−0.02	0.60	−0.04	0.82	0.02	0.86	−0.11	0.05

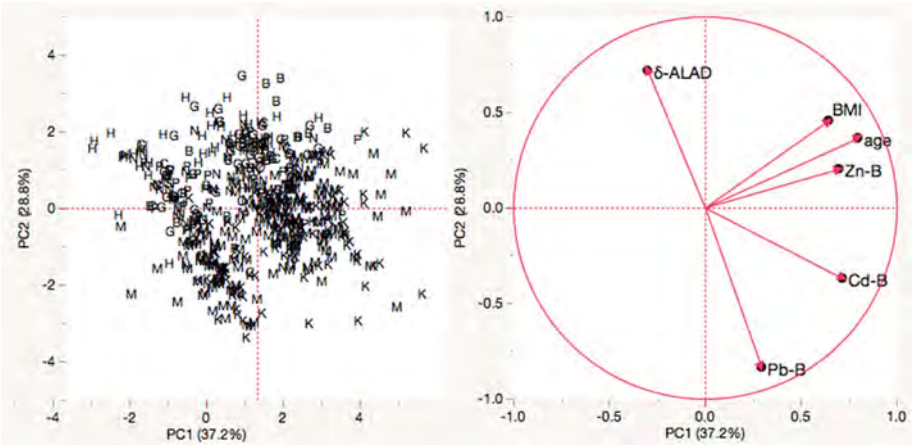

Fig. 3. Principal component analysis on log-transformed data of the 504 representative Kabwe residents showing the relationship among blood metal levels, age, BMI and δ-ALAD activity ratio. K = Kasanda, M = Makululu, C = Chowa, N = Natuseko, B = Bwacha, P = Mpima Prison, G = Kang'omba, H = Hamududu.

(N = 46), Prague (Czech Republic), i.e., 0.13 μg/L (N = 8), Wroclaw (Poland), i.e., 0.15 μg/L (N = 27), Ban (Slovakia), i.e., 0.14 μg/L (N = 57), Landskrona (Sweden), i.e., 0.11 μg/L (N = 41), Camilo Ponce Enríquez (Ecuador), i.e., 0.26 μg/L (N = 69), and Fez (Morocco), i.e., 0.21 μg/L (N = 39) (Hrubá et al., 2012). By contrast, higher Cd–B values have been reported in Asian countries where the dietary intake of rice and vegetables could be the major sources of Cd in the general population. Mean Cd–B levels of 1.57 (N = 955) and 1.49 (N = 954) μg/L have been reported in South Korean men and women, respectively (Hwangbo et al., 2011), compared with 1.05 μg/L in 289 pregnant Taiwanese women (Lin et al., 2011). However, in addition to the well-known fact that Cd is a nephrotoxin at high exposure levels (Järup et al., 1995), Cd-related nephrotoxicity at relatively low exposure levels has also been revealed (Åkesson et al., 2005; Ferrano et al., 2010; Thomas et al., 2008). Thus, the potential health effect of Cd should be carefully observed in Kabwe. In contrast to Pb–B and Cd–B, variation in Zn–B was small among areas, whereas some significant differences that cannot be clearly explained were detected. Similarly, no elevation of Zn–B was previously reported for goats and chickens in Kabwe (Nakata et al., 2016) or for Zn levels in rat organs (Nakayama et al., 2013), although soil Zn concentrations increased around the Kabwe mine area (Nakayama et al., 2011).

Analyzed blood biochemical parameters for adult participants were compared with normal ranges which were presented in manual supplied by the manufacturer of the instrument. However, the values for children and adolescents could not compare with the manual's normal range because the physiological normal values of biochemical parameters usually differ by age (Adeli et al., 2015). Besides, although the reference values for the younger generation which were derived from developed countries are often used for the African population, the normal values differ by race especially for the younger generation (Dosoo et al., 2014; Quintó et al., 2006). Unfortunately, there is no reference values specifically for Zambian children. These are common challenge and limitation of this kind of study. Thus, we compare the results of blood biochemical parameters for children and adolescents by Pb–B to evaluate the effect of Pb exposure. Additionally, Pearson product-moment correlation analysis was applied to assess the correlation between blood metal levels and blood biochemical parameters.

Among the hepatic function parameters, most of the adult participants were within the normal range of T-bil, AST and ALT despite some significant area differences for T-bil and AST. The reason for the unexpected high LDH levels in Chowa and Bwacha as well as GGT in Bwacha is unclear; however, the small sample size of Chowa and Bwacha may have played a role. Although approximately 25–60% of the tested adult participants showed the values of LDH, GGT and ALP above normal ranges, the frequencies of abnormal values for these parameters were not Pb–B level-dependent. Analysis of T-pro, Alb, UA, Cre and $eGFR_{MDRD}$ for renal function screening showed significant area differences. Interestingly, most of the observed area differences did not reflect the ranking of the metal levels. The low Alb value in Makululu, as well as that of Cre in Makululu and Hamududu, could be attributed to poverty and malnutrition in these areas (Hiwatari et al., 2019). The $eGFR_{MDRD}$ value was lowest in Kasanda, indicating the inhibition of glomerular filtration function by Pb and Cd exposure. The activity of δ-ALAD, an enzyme involved in heme biosynthesis that catalyzes the condensation of two molecules of δ-aminolevulinic acid (δ-ALA) to form porphobilinogen (PBG) (Sakai and Morita, 1996), was also significantly inhibited in Kasanda and Makululu. Inhibition of δ-ALAD leads to hemoglobin oxidation, which directly causes red blood cell (RBC) hemolysis. The δ-ALAD assay results are indicative of both Pb-induced hematological disorder and oxidative stress (Ahamed et al., 2006; Gurer-Orhan et al., 2004), suggesting that δ-ALAD inhibition may imply other health effects in Kasanda and Makululu in addition to hematotoxicity.

Some significant area differences were detected in the residents' characteristics, such as age, height, body weight, and BMI. Thus, the statistical relationship among blood metal levels and other factors was evaluated as one group without distinguishing between areas. It should be emphasized that this is the first report about clinical outcomes affected by metal exposure in Africa. Most of the blood biochemical parameters had a statistically significant relationship with Cd–B and Zn–B for the category of all age. These significant association would be understood by the fact that adult participants generally recorded greater Cd–B, Zn–B and some biochemical parameters such as T-bil, ALT, GGT, T-pro, Alb, UA, Cre and $eGFR_{MDRD}$ than the age groups of 0–4 years as well as 5–17 years. Conversely, adult participants had lower parameters including LDH, ALP and BUN/Cre. These higher or lower biochemical parameters in adults compared to children and adolescents are well-studied and known fact as physiologically normal (Adeli et al., 2015). It should be also noted that some biochemical parameters did not significantly correlate with Cd–B and Zn–B at comparison within each age category. Taken together, the change of parameters which significantly correlated with Cd–B and Zn–B only for the category of all age, but not for each age category, should not be considered as the

effect of Cd or Zn. No statistical correlation with blood metal levels was observed for LDH, GGT, and ALP, whereas approximately 25–60% of tested subjects had elevated values compared with the normal range. An increase in LDH, GGT, and ALP normally suggests disorder of the liver or biliary system. However, the two major hepatic enzymes, AST and ALT, were within the normal range in most of the subjects. It should be also remembered that the increases of LDH, GGT and ALP were not Pb–B level-dependent. Taken together, our results suggested that biliary system disease is a common health issue in Kabwe due to reasons other than metal exposure. T-pro and Alb had significant positive correlations with Zn–B for the adult participants and were below normal levels in approximately 30% of the studied population. This finding suggests that people with insufficient Zn have lower amounts of blood protein. This is reasonable, as malnutrition is usually linked to a shortage of both blood protein and Zn. Another possible reason for a lower amount of blood protein is an increase in kidney Alb excretion due to renal dysfunction, which was suspected due to the elevated UA and Cre levels. In the statistical comparison, UA had a significant and positive correlation with Pb–B, Cd–B, and Zn–B for the adult participants. Although it is known that Pb and Cd exhibit dose-dependent renal toxicity (ATSDR, 2012; 2017; Bernard, 2008), the reason for the significant relationship between Zn–B and UA is unclear. The inverse correlation between $eGFR_{MDRD}$ and Cd–B for the adult participants in the current study is in agreement with earlier reports (Buser et al., 2016; Hwangbo et al., 2011). High r^2 value was recorded between Pb–B and the δ-ALAD activity ratio, which is widely considered a sensitive indicator of early Pb exposure (Fontanellas et al., 2002). While a significant negative association was also observed between Cd–B and the δ-ALAD activity ratio, the PCA and Pearson product-moment correlation analysis results indicated that the reduction in the δ-ALAD activity ratio was caused mainly by increased Pb–B rather than increased Cd–B. In addition, the confounding relationship between Pb–B and Cd–B affected the association between Cd–B and the δ-ALAD activity ratio. In fact, an inverse effect of Pb exposure on δ-ALAD has been widely reported (Fontanellas et al., 2002; Mani et al., 2018), contrary to that observed for Cd. The relationship between BMI and age based on PCA agrees with a finding reported in Lusaka, the capital city of Zambia (Rudatsikira et al., 2012). The association of Zn–B with BMI can also be explained by the nutrition status, similar to that mentioned above for blood protein.

5. Conclusion

The current study provides new insights into the accumulation status of Pb, Cd, and Zn in Kabwe. It is noteworthy that Cd–B and Zn–B are reported for the first time, as it is important to consider interactions between metals. In addition to the elevated Pb–B levels in a wide area of Kabwe, an increase in Cd–B was also recorded in Kasanda and Makululu where high Pb–B levels were measured, whereas Zn–B had lower variation among areas. This is also the first clinical evaluation for hemato-, hepato-, and renal toxicity screening related to the exposure to multiple metals on the African continent. Significant correlations were found between blood metal levels and clinical parameters especially for adult participants, indicating potential adverse health effects due to metal exposure in Kabwe. Based on the observed scientific evidences in our study, immediate treatment of affected people and remediation of polluted environments are strongly recommended in addition to further studies to reveal exposure pathways and other toxic effects, such as neurodevelopmental disorders.

Author statement

Hokuto Nakata: Conceptualization, Methodology, Formal analysis, Investigation, Writing - original draft, Visualization. Shouta M.M. Nakayama: Conceptualization, Investigation, Writing - review & editing. John Yabe: Conceptualization, Investigation, Writing - review & editing. Kaampwe Muzandu: Conceptualization, Investigation, Writing - review & editing. Haruya Toyomaki: Investigation, Data curation, Writing - review & editing, Yared Beyene Yohannes: Validation, Investigation, Writing - review & editing. Andrew Kataba: Validation, Investigation, Writing - review & editing. Golden Zyambo: Investigation, Writing - review & editing, Yoshinori Ikenaka: Resources, Writing - review & editing, Kennedy Choongo: Conceptualization, Resources, Writing - review & editing, Supervision, Project administration, Mayumi Ishizuka: Conceptualization, Resources, Writing - review & editing, Supervision, Project administration, Funding acquisition

Declaration of competing interest

The authors declare that they have no known competing financial interests or personal relationships that could have appeared to influence the work reported in this paper.

Acknowledgements

This work was supported by Grants-in-Aid for Scientific Research from the Ministry of Education, Culture, Sports, Science, and Technology of Japan awarded to M. Ishizuka (No. 16H0177906, 18KK0287), Y. Ikenaka (No. 17K2003807, 18H0413208), S.M.M. Nakayama (No. 16K16197, 17KK0009), and H. Nakata (No. 19K2047209) and the foundation of JSPS Bilateral Open Partnership Joint Research Projects (JPJSBP120209902), and the Environment Research and Technology Development Fund (SII-1/3–2, 4RF-1802/18949907) of the Environmental Restoration and Conservation Agency of Japan. We also acknowledge financial support from The Soroptimist Japan Foundation, The Nakajima Foundation, The Sumitomo foundation, The Nihon Seimei Foundation, The Japan Prize Foundation, and The Akiyama Life Science Foundation. This research was also supported by JST/JICA, SATREPS (Science and Technology Research Partnership for Sustainable Development; No. JPMJSA1501), and Accelerating Social Implementation for SDGs achievement (aXis) and Program for supporting introduction of the new sharing system (JPMXS0420100619) by JST. We are highly indebted to the communities that participated in this study. We are also grateful to the health centers in Kabwe, the Kabwe District Health Office, Kabwe Municipal Council, and the Ministry of Health, Zambia, for facilitating our work. We also want to thank all of the laboratory technicians and nurses at the health centers for their technical support. Our appreciation is extended to Mr. Hisao Odagiri, Ms. Michiko Nyanga, and Mr. Susumu Makino for their coordination, Ms. Sayako Yamamoto for her assistance, as well as Mr. Takahiro Ichise and Ms. Nagisa Hirano for their technical support.

Appendix A. Supplementary data

Supplementary data to this article can be found online at https://doi.org/10.1016/j.chemosphere.2020.127788.

References

Adeli, K., Higgins, V., Nieuwesteeg, M., Raizman, J.E., Chen, Y., Wong, S.L., Blais, D., 2015. Biochemical marker reference values across pediatric, adult, and geriatric ages: establishment of robust pediatric and adult reference intervals on the basis of the Canadian Health Measures Survey. Clin. Chem. 61 (8), 1049–1062. https://doi.org/10.1373/clinchem.2015.240515. PMID: 26044506.

Agency for Toxic Substances and Disease Registry (ATSDR), 2012. Toxicological Profile for Cadmium. U.S. Department of Health and Human Services, Public Health Service, Atlanta, GA. Available: https://www.atsdr.cdc.gov/toxprofiles/tp5.pdf. (Accessed 27 January 2020).

Agency for Toxic Substances and Disease Registry (ATSDR), 2017. Lead Toxicity. What Are Possible Health Effects from Lead Exposure? Available: https://www.atsdr.cdc.gov/csem/lead/docs/csem-lead_toxicity_508.pdf. (Accessed 27 January 2020).

Ahamed, M., Verma, S., Kumar, A., Siddiqui, M.K., 2006. Delta-aminolevulinic acid dehydratase inhibition and oxidative stress in relation to blood lead among urban adolescents. Hum. Exp. Toxicol. 25 (9), 547–553. https://doi.org/10.1191/0960327106het657oa. PMID: 17017008.

Åkesson, A., Lundh, T., Vahter, M., Bjellerup, P., Lidfeldt, J., Nerbrand, C., Samsioe, G., Strömberg, U., Skerfving, S., 2005. Tubular and glomerular kidney effects in Swedish women with low environmental cadmium exposure. Environ. Health Perspect. 113 (11), 1627–1631. https://doi.org/10.1289/ehp.8033. PMID: 16263522.

Bede-Ojimadu, O., Amadi, C.N., Orisakwe, O.E., 2018. Blood lead levels in women of child-bearing age in Sub-Saharan Africa: a systematic review. Frontiers in public health 6, 367. https://doi.org/10.3389/fpubh.2018.00367. PMID: 30619808.

Bernard, A., 2008. Cadmium & its adverse effects on human health. Indian J. Med. Res. 128 (4), 557.

Buser, M.C., Ingber, S.Z., Raines, N., Fowler, D.A., Scinicariello, F., 2016. Urinary and blood cadmium and lead and kidney function: NHANES 2007–2012. Int. J. Hyg Environ. Health 219 (3), 261–267. https://doi.org/10.1016/j.ijheh.2016.01.005.

Caldwell, K.L., Cheng, P.Y., Jarrett, J.M., Makhmudov, A., Vance, K., Ward, C.D., Jones, R.L., Mortensen, M.E., 2017. Measurement challenges at low blood lead levels. Pediatrics 140 (2), e20170272. https://doi.org/10.1542/peds.2017-0272. PMID: 28771411.

Centers for Disease Control and Prevention (CDC), 2002. Managing Elevated Blood Lead Levels Among Young Children: Recommendations from the Advisory Committee on Childhood Lead Poisoning Prevention. Available: https://stacks.cdc.gov/view/cdc/26980. (Accessed 27 January 2020).

Centers for Disease Control and Prevention (CDC), 2012. Low Level Lead Exposure Harms Children: A Renewed Call for Primary Prevention. Available: https://www.cdc.gov/nceh/lead/acclpp/Final_Document_030712.pdf. (Accessed 27 January 2020).

Dooyema, C.A., Neri, A., Lo, Y.C., Durant, J., Dargan, P.I., Swarthout, T., Biya, O., Gidado, S.O., Haladu, S., Sani-Gwarzo, N., Nguku, P.M., Akpan, H., Idris, S., Bashir, A.M., Brown, M.J., 2012. Outbreak of fatal childhood lead poisoning related to artisanal gold mining in northwestern Nigeria, 2010. Environ. Health Perspect. 120 (4), 601–607. https://doi.org/10.1289/ehp.1103965.

Dosoo, D.K., Asante, K.P., Kayan, K., Adu-Gyasi, D., Osei-Kwakye, K., Mahama, E., Danso, S., Amenga-Etego, S., Bilson, P., Koram, K.A., Owusu-Agyei, S., 2014. Biochemical and hematologic parameters for children in the middle belt of Ghana. Am. J. Trop. Med. Hyg. 90 (4), 767–773. https://doi.org/10.4269/ajtmh.13-0098. PMID: 24591437.

Doya, R., Nakayama, S.M., Nakata, H., Toyomaki, H., Yabe, J., Muzandu, K., Yohannes, Y.B., Kataba, A., Zyambo, G., Ogawa, T., Uchida, Y., Ikenaka, Y., Ishizuka, M., 2020. Land use in habitat affects metal concentrations in wild lizards around a former lead mining site. Environ. Sci. Technol. https://doi.org/10.1021/acs.est.0c00150. PMID: 32490671.

Espín, S., Martínez-López, E., Jiménez, P., María-Mojica, P., García-Fernández, A.J., 2015. Delta-aminolevulinic acid dehydratase (δALAD) activity in four free-living bird species exposed to different levels of lead under natural conditions. Environ. Res. 137, 185–198. https://doi.org/10.1016/j.envres.2014.12.017. PMID: 25569843.

Ferraro, P.M., Costanzi, S., Naticchia, A., Sturniolo, A., Gambaro, G., 2010. Low level exposure to cadmium increases the risk of chronic kidney disease: analysis of the NHANES 1999-2006. BMC Publ. Health 10 (1), 304. https://doi.org/10.1186/1471-2458-10-304. PMID: 20525263.

Fontanellas, A., Navarro, S., Morán-Jiménez, M.J., Sánchez-Fructuoso, A.I., Vegh, I., Barrientos, A., de Salamanca, R.E., 2002. Erythrocyte aminolevulinate dehydratase activity as a lead marker in patients with chronic renal failure. Am. J. Kidney Dis. 40 (1), 43–50. https://doi.org/10.1053/ajkd.2002.33912. PMID: 12087560.

Gonick, H.C., 2011. Lead-binding proteins: a review, 2011 J. Toxicol.. https://doi.org/10.1155/2011/686050. PMID: 21941540.

Gurer-Orhan, H., Sabır, H.U., Özgüneş, H., 2004. Correlation between clinical indicators of lead poisoning and oxidative stress parameters in controls and lead-exposed workers. Toxicology 195 (2–3), 147–154. https://doi.org/10.1016/j.tox.2003.09.009. PMID: 14751670.

Hambach, R., Lison, D., D'haese, P.C., Weyler, J., De Graef, E., De Schryver, A., Lamberts, L.V., van Sprundel, M., 2013. Co-exposure to lead increases the renal response to low levels of cadmium in metallurgy workers. Toxicol. Lett. 222 (2), 233–238. https://doi.org/10.1016/j.toxlet.2013.06.218. PMID: 23806787.

Harari, F., Sallsten, G., Christensson, A., Petkovic, M., Hedblad, B., Forsgard, N., Melander, O., Nilsson, P.M., Borné, Y., Engström, G., Barregard, L., 2018. Blood lead levels and decreased kidney function in a population-based cohort. Am. J. Kidney Dis. 72 (3), 381–389. https://doi.org/10.1053/j.ajkd.2018.02.358. PMID: 29699886.

Hiwatari, M., Yamada, D., Hangoma, P., Narita, D., Mphuka, C., Chitah, B., Yabe, J., Nakayama, S.M., Nakata, H., Choongo, K., Ishizuka, M., 2019. Assessing the population-wide exposure to lead pollution in Kabwe, Zambia: blood lead level estimation based on survey data. Discussion Paper, Series A 338, 1–28.

Hornung, R.W., Reed, L.D., 1990. Estimation of average concentration in the presence of nondetectable values. Appl. Occup. Environ. Hyg 5 (1), 46–51. https://doi.org/10.1080/1047322X.1990.10389587.

Hrubá, F., Strömberg, U., Černá, M., Chen, C., Harari, F., Harari, R., Horvat, M., Koppová, K., Kos, A., Krsková, A., Krsnik, M., Laamech, J., Li, Y., Löfmark, L., Lundh, T., Lundström, N., Lyoussi, B., Mazej, D., Osredkar, J., Pawlas, K., Pawlas, N., Prokopowicz, A., Rentschler, G., Spěváčková, V., Spiric, Z., Tratnik, J., Skerfving, S., Bergdahl, I.A., 2012. Blood cadmium, mercury, and lead in children: an international comparison of cities in six European countries, and China, Ecuador, and Morocco. Environ. Int. 41, 29–34. https://doi.org/10.1016/j.envint.2011.12.001. PMID: 22257910.

Hwangbo, Y., Weaver, V.M., Tellez-Plaza, M., Guallar, E., Lee, B.K., Navas-Acien, A., 2011. Blood cadmium and estimated glomerular filtration rate in Korean adults. Environ. Health Perspect. 119 (12), 1800–1805. https://doi.org/10.1289/ehp.1003054. PMID: 21835726.

Järup, L., Persson, B., Elinder, C.G., 1995. Decreased glomerular filtration rate in solderers exposed to cadmium. Occup. Environ. Med. 52 (12), 818–822. https://doi.org/10.1136/oem.52.12.818. PMID: 8563845.

Levey, A.S., Coresh, J., Greene, T., Stevens, L.A., Zhang, Y.L., Hendriksen, S., Kusek, J.W., Lente, F.V., 2006. Using standardized serum creatinine values in the modification of diet in renal disease study equation for estimating glomerular filtration rate. Ann. Intern. Med. 145 (4), 247–254. https://doi.org/10.7326/0003-4819-145-4-200608150-00004. PMID: 16908915.

Levey, A.S., Stevens, L.A., Schmid, C.H., Zhang, Y.L., Castro, A.F., Feldman, H.I., Kusek, J.W., Eggers, P., van Lente, F., Greene, T., Coresh, J., 2009. A new equation to estimate glomerular filtration rate. Ann. Intern. Med. 150 (9), 604–612. https://doi.org/10.7326/0003-4819-150-9-200905050-00006. PMID: 19414839.

Li, M.M., Cao, J., Xu, J., Cai, S.Z., Shen, X.M., Yan, C.H., 2014. The national trend of blood lead levels among Chinese children aged 0–18 years old, 1990–2012. Environ. Int. 71, 109–117. https://doi.org/10.1016/j.envint.2014.06.005. PMID: 25000556.

Lin, C.M., Doyle, P., Wang, D., Hwang, Y.H., Chen, P.C., 2011. Does prenatal cadmium exposure affect fetal and child growth? Occup. Environ. Med. 68 (9), 641–646. https://doi.org/10.1136/oem.2010.059758. PMID: 21186202.

Lockitch, G., 1993. Perspectives on lead toxicity. Clin. Biochem. 26 (5), 371–381. https://doi.org/10.1016/0009-9120(93)90113-k. PMID: 8299207.

Mani, M.S., Kunnathully, V., Rao, C., Kabekkodu, S.P., Joshi, M.B., D'Souza, H.S., 2018. Modifying effects of δ-Aminolevulinate dehydratase polymorphism on blood lead levels and ALAD activity. Toxicol. Lett. 295, 351–356. https://doi.org/10.1016/j.toxlet.2018.07.014. PMID: 30025905.

Mudipalli, A., 2007. Lead hepatotoxicity & potential health effects. Indian J. Med. Res. 126 (6), 518. PMID: 18219078.

Naicker, N., Norris, S.A., Mathee, A., von Schirnding, Y.E., Richter, L., 2010. Prenatal and adolescent blood lead levels in South Africa: child, maternal and household risk factors in the Birth to Twenty cohort. Environ. Res. 110 (4), 355–362. https://doi.org/10.1016/j.envres.2010.02.006, 20226441.

Nakata, H., Nakayama, S.M., Yabe, J., Liazambi, A., Mizukawa, H., Darwish, W.S., Ikenaka, Y., Ishizuka, M., 2016. Reliability of stable Pb isotopes to identify Pb sources and verifying biological fractionation of Pb isotopes in goats and chickens. Environ. Pollut. 208, 395–403. https://doi.org/10.1016/j.envpol.2015.10.006. PMID: 26549754.

Nakayama, S.M., Ikenaka, Y., Hamada, K., Muzandu, K., Choongo, K., Teraoka, H., Mizuno, H., Ishizuka, M., 2011. Metal and metalloid contamination in roadside soil and wild rats around a Pb–Zn mine in Kabwe, Zambia. Environ. Pollut. 159 (1), 175–181. https://doi.org/10.1016/j.envpol.2010.09.007. PMID: 20971538.

Nakayama, S.M., Ikenaka, Y., Hamada, K., Muzandu, K., Choongo, K., Yabe, J., Umemura, T., Ishizuka, M., 2013. Accumulation and biological effects of metals in wild rats in mining areas of Zambia. Environ. Monit. Assess. 185 (6), 4907–4918. https://doi.org/10.1007/s10661-012-2912-6. PMID: 23054276,.

Nakayama, S.M., Nakata, H., Ikenaka, Y., Yabe, J., Oroszlany, B., Yohannes, Y.B., Bortey-Sam, N., Muzandu, K., Choongo, K., Kuritani, T., Nakagawa, M., Ishizuka, M., 2019. One year exposure to Cd-and Pb-contaminated soil causes metal accumulation and alteration of global DNA methylation in rats. Environ. Pollut. 252, 1267–1276. https://doi.org/10.1016/j.envpol.2019.05.038. PMID: 31252124.

Ni, W., Huang, Y., Wang, X., Zhang, J., Wu, K., 2014. Associations of neonatal lead, cadmium, chromium and nickel co-exposure with DNA oxidative damage in an electronic waste recycling town. Sci. Total Environ. 472, 354–362. https://doi.org/10.1016/j.scitotenv.2013.11.032. PMID: 24295751.

National Institute of Diabetes and Digestive and Kidney Disease. Glomerular Filtration Rate (GFR) Calculators, for children (Conventional Units). Available: https://www.niddk.nih.gov/health-information/professionals/clinical-tools-patient-management/kidney-disease/laboratory-evaluation/glomerular-filtration-rate-calculators/children-conventional-units [accessed 15 June 2020]..

Olewe, T.M., Mwanthi, M.A., Wang'ombe, J.K., Griffiths, J.K., 2009. Blood lead levels and potental environmental exposures among children under five years in Kibera slums, Nairobi. East Afr. J. Publ. Health 6 (1). https://doi.org/10.4314/eajph.v6i1.45734. PMID: 20000055.

Pan, S., Lin, L., Zeng, F., Zhang, J., Dong, G., Yang, B., Jung, Y., Chen, S., Zhang, G., Yu, Z., Sheng, G., Ma, H., 2018. Effects of lead, cadmium, arsenic, and mercury co-exposure on children's intelligence quotient in an industrialized area of southern China. Environ. Pollut. 235, 47–54. https://doi.org/10.1016/j.envpol.2017.12.044. PMID: 29274537.

Pure Earth, 2014. Project Completion Report: Nigeria Lead Poisoning Crisis. Available: https://www.pureearth.org/wp-content/uploads/2014/10/Zamfara_Nigeria_PCR-April-2011.pdf. (Accessed 27 January 2020).

Quintó, L., Aponte, J.J., Sacarlal, J., Espasa, M., Aide, P., Mandomando, I., Guinovart, C., Macete, E., Navia, M.M., Thompson, R., Menéndez, C., Alonso, P.L., 2006. Haematological and biochemical indices in young African children: in search of reference intervals. Trop. Med. Int. Health 11 (11), 1741–1748. https://doi.org/10.1111/j.1365-3156.2006.01764.x. PMID: 17054755.

Rastogi, S.K., 2008. Renal effects of environmental and occupational lead exposure. Indian J. Occup. Environ. Med. 12 (3), 103. https://doi.org/10.4103/0019-5278.44689. PMID: 20040966.

Rudatsikira, E., Muula, A.S., Mulenga, D., Siziya, S., 2012. Prevalence and correlates of obesity among Lusaka residents, Zambia: a population-based survey. Int. Arch. Med. 5 (1), 14. https://doi.org/10.1186/1755-7682-5-14. PMID: 22551418.

Sakai, T., Morita, Y., 1996. δ-Aminolevulinic acid in plasma or whole blood as a sensitive indicator of lead effects, and its relation to the other home-related parameters. Int. Arch. Occup. Environ. Health 68 (2), 126–132. https://doi.org/10.1007/bf00381245. PMID: 8720283.

Saxena, D.K., Murthy, R.C., Singh, C., Chandra, S.V., 1989. Zinc protects testicular injury induced by concurrent exposure to cadmium and lead in rats. Res. Commun. Chem. Pathol. Pharmacol. 64 (2), 317–329. PMID: 2740621.

Scheuhammer, A.M., 1987. Erythrocyte δ-aminolevulinic acid dehydratase in birds. I. The effects of lead and other metals in vitro. Toxicology 45 (2), 155–163. https://doi.org/10.1016/0300-483X(87)90101-6. PMID: 3603581.

Schwartz, G.J., Munoz, A., Schneider, M.F., Mak, R.H., Kaskel, F., Warady, B.A., Furth, S.L., 2009. New equations to estimate GFR in children with CKD. J. Am. Soc. Nephrol. 20 (3), 629–637. https://doi.org/10.1681/ASN.2008030287. PMID: 19158356.

Soussi, A., Gargouri, M., El Feki, A., 2018. Effects of co-exposure to lead and zinc on redox status, kidney variables, and histopathology in adult albino rats. Toxicol. Ind. Health 34 (7), 469–480. https://doi.org/10.1177/0748233718770293. PMID: 29702030,.

Thomas, L.D., Hodgson, S., Nieuwenhuijsen, M., Jarup, L., 2008. Early kidney damage in a population exposed to cadmium and other heavy metals. Environ. Health Perspect. 117 (2), 181–184. https://doi.org/10.1289/ehp.11641. PMID: 19270785.

Toyomaki, H., Yabe, J., Nakayama, S.M., Yohannes, Y.B., Muzandu, K., Liazambi, A., Ikenaka, Y., Kuritani, T., Nakagawa, M., Ishizuka, M., 2020. Factors associated with lead (Pb) exposure on dogs around a Pb mining area, Kabwe, Zambia. Chemosphere 125884. https://doi.org/10.1016/j.chemosphere.2020.125884.

Tuakuila, J., Lison, D., Mbuyi, F., Haufroid, V., Hoet, P., 2013. Elevated blood lead levels and sources of exposure in the population of Kinshasa, the capital of the Democratic Republic of Congo. J. Expo. Sci. Environ. Epidemiol. 23 (1), 81–87. https://doi.org/10.1038/jes.2012.49. PMID: 22617721.

Wang, V.S., Lee, M.T., Chiou, J.Y., Guu, C.F., Wu, C.C., Wu, T.N., Lai, J.S., 2002. Relationship between blood lead levels and renal function in lead battery workers. Int. Arch. Occup. Environ. Health 75 (8), 569–575. https://doi.org/10.1007/s00420-002-0362-0. PMID: 12373319.

World Health Organization (WHO), 2007. Growth Reference 5-19 Years Old, BMI-For-Age (5-19 Years). Available: https://www.who.int/growthref/who2007_bmi_for_age/en/. (Accessed 26 May 2020).

World Health Organization (WHO), 2009. Global Health Risks: Mortality and Burden of Disease Attributable to Selected Major Risks. Available: http://whqlibdoc.who.int/publications/2009/9789241563871_eng.pdf. (Accessed 24 May 2020).

Yabe, J., Ishizuka, M., Umemura, T., 2010. Current levels of heavy metal pollution in Africa. J. Vet. Med. Sci. 72 (10), 1257–1263. https://doi.org/10.1292/jvms.10-0058. PMID: 20519853.

Yabe, J., Nakayama, S.M., Ikenaka, Y., Yohannes, Y.B., Bortey-Sam, N., Oroszlany, B., Muzandu, K., Choongo, K., Kabalo, A.N., Ntapisha, J., Mweene, A., Umemura, T., Ishizuka, M., 2015. Lead poisoning in children from townships in the vicinity of a lead–zinc mine in Kabwe, Zambia. Chemosphere 119, 941–947. https://doi.org/10.1016/j.chemosphere.2014.09.028. PMID: 25303652.

Yabe, J., Nakayama, S.M., Ikenaka, Y., Yohannes, Y.B., Bortey-Sam, N., Kabalo, A.N., Ntapisha, J., Mizukawa, H., Umemura, T., Ishizuka, M., 2018. Lead and cadmium excretion in feces and urine of children from polluted townships near a lead-zinc mine in Kabwe, Zambia. Chemosphere 202, 48–55. https://doi.org/10.1016/j.chemosphere.2018.03.079. PMID: 29554507.

Yabe, J., Nakayama, S.M., Nakata, H., Toyomaki, H., Yohannes, Y.B., Muzandu, K., Kataba, A., Zyambo, G., Hiwatari, M., Narita, D., Yamada, D., Hangoma, P., Munyinda, N.S., Mufune, T., Ikenaka, Y., Choongo, K., Ishizuka, M., 2020. Current trends of blood lead levels, distribution patterns and exposure variations among household members in Kabwe, Zambia. Chemosphere 243, 125412. https://doi.org/10.1016/j.chemosphere.2019.125412. PMID: 31995873.

Aquatic Toxicology 227 (2020) 105607

Contents lists available at ScienceDirect

Aquatic Toxicology

journal homepage: www.elsevier.com/locate/aqtox

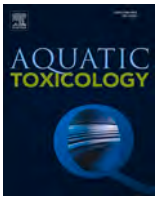

Acute exposure to environmentally relevant lead levels induces oxidative stress and neurobehavioral alterations in larval zebrafish (*Danio rerio*)

Andrew Kataba [a,b], Tarryn L. Botha [a,c], Shouta M.M. Nakayama [a], Yared B. Yohannes [a,d], Yoshinori Ikenaka [a,c], Victor Wepener [a,c], Mayumi Ishizuka [a,*]

[a] Laboratory of Toxicology, Department of Environmental Veterinary Sciences, Faculty of Veterinary Medicine, Hokkaido University, Kita 18, Nishi 9, Kita-ku, Sapporo, Hokkaido 060-0818, Japan
[b] Department of Biomedical Sciences, School of Veterinary Medicine, The University of Zambia, P. O. Box 32379, Lusaka, Zambia
[c] Water Research Group, Unit for Environmental Sciences and Management, North-West University, Private Bag X6001, Potchefstroom, South Africa
[d] Department of Chemistry, College of Natural and Computational Science, University of Gondar, P. O. Box 196, Gondar, Ethiopia

ARTICLE INFO

Keywords:
Lead
Zebrafish larvae
Behavioral toxicology
Hormesis
Hyperactivity

ABSTRACT

The ubiquitous contamination of environmental lead (Pb) remains a worldwide threat. Improper Pb mine waste disposal from an abandoned lead-zinc mine has recently unearthed widespread Pb poisoning in children in Kabwe Zambia. Although the adverse effects of Pb on human health have begun to receive attention, the ecotoxicological effects on aquatic vertebrates still need further investigation. In addition, there is paucity in the knowledge on the behavioural and molecular subcellular responses in larval zebrafish exposed to Pb within the range of environmental relevant concentration (average 3 μg/L with maximum of 94 μg/L) on aquatic organisms such as zebrafish. The adverse effects of environmentally relevant levels of Pb on larval zebrafish was evaluated by measuring swimming behaviour under alternating dark and light conditions. Larval zebrafish acutely exposed to environmentally relevant Pb exhibited neuro-behavioural alteration including enhanced hyperactivity under light conditions evidenced by increased distanced covered and speed compared to the control. The alteration of entire behavioral profiles was further associated with the disturbed expression patterns of mRNA level of key genes associated with antioxidant (HO-1, Ucp-2 and CoxI), proapoptotic gene (TP53), and antiapoptotic gene (Bcl-2). To our knowledge, this is the first report on the effects of environmentally relevant Pb levels from Kabwe, Zambia and their adverse neurobehavioural effects and subcellular molecular oxidative responses in larval zebrafish acutely exposed within a 30 min period. The current results would be beneficial in our understanding of the effects of low Pb levels acutely discharged into an aquatic environment and the life of aquatic organisms.

1. Introduction

Lead (Pb) has been reported as the most abundant toxic metal element in the environment and is generally found in trace amounts in soils, plants, and water (Cheng and Hu, 2010; Wani et al., 2015). Although Pb is ubiquitous in aquatic environments, high levels of Pb could be attributed to anthropogenic activities including the manufacture of batteries, paint, cement, as well as mining and smelting (Kim and Kang, 2017). Because of its valuable use historically, lead was extensively mined, and very large piles of leaded soil waste tailings are still found in some parts of the world. One of the most well-known cases is a now closed lead-zinc mine that operated for over 90 years in Kabwe (Zambia) without any Pb waste management system (Ikenaka et al., 2010; Nakayama et al., 2011). Dispersion of the contaminated soils in the form of dust particles, by strong winds and occasional flooding, has led to the pollution of the city and eventual contamination of children; leaving the majority of them with blood Pb levels above the 5 μg/dL level of concern as set by by the Centers for Disease Control and Prevention (Bose-O'Reilly et al., 2017; Yabe et al., 2020, 2015). Samples from domestic animals like cattle, goats, free range chickens and wild rodents within the vicinity of the closed mine had substantial Pb accumulation in their tissues (Nakata et al., 2016; Nakayama et al., 2011; Yabe et al., 2013, 2011). On the other hand, Pb levels in natural water bodies and ground water drawn from boreholes in the area were found to have the highest concentration of 94 μg/L from a given site with the average concentration of 3 μg/L. The average concentration was below

* Corresponding author.
E-mail address: ishizum@vetmed.hokudai.ac.jp (M. Ishizuka).

https://doi.org/10.1016/j.aquatox.2020.105607
Received 1 May 2020; Received in revised form 11 August 2020; Accepted 12 August 2020
Available online 19 August 2020

the Pb permissible values of 50 μg/L by the Zambia Bureau of Standards (Nachiyunde et al., 2013).

Lead is known to be deleterious to almost all living organisms even in smaller amounts (Pokras and Kneeland, 2008). In humans, especially children, deficits in cognitive and academic skills have been reported in blood Pb concentrations lower than 5 μg /dL (Lanphear et al., 2000). In both young animals and humans, the nervous system, especially the brain, has been widely reported as the most vulnerable to Pb toxicosis due to its rapid growth that may incorporate Pb and the immature blood brain barrier (Flora et al., 2012). Furthermore, associations between subclinical Pb toxicosis and altered behaviour such as delinquent, antisocial and aggressive behaviours in humans have been reported in several studies (Nevin, 2000; Olympio et al., 2010; Sciarillo et al., 1992). Zebrafish are increasingly being used as a model organism due to their close homology (71 %) with the human genome (Howe et al., 2014). In zebrafish, Pb exposure to various levels and at different stages of the zebrafish development has been known to induce an array of neurobehavioral derangements such as memory deficit, altered colour preferences, altered responses to environmental stimuli such as locomotor activity patterns under light and dark illumination and sensorimotor responses among others (Chen et al., 2012; Dou and Zhang, 2011; Fraysse et al., 2006; Lefauve and Connaughton, 2017; Xu et al., 2016; Zhao et al., 2019). This neurotoxicity is suggested to arise due to direct damage to the nervous tissue through oxidative stress or alteration on the neurotransmitters and or their receptors (Lee and Freeman, 2014a; Tu et al., 2018; Weber et al., 1997). For example, Pb^{2+} arouses Ca^{2+} and calmodulin to stimulate and modulate the release of neurotransmitters in neurons (Zhong et al., 2017). In addition, Pb exposure disturbs the balance of pro-oxidants and antioxidants, causing oxidative stress and Pb poisoning (Kim and Kang, 2017). In vivo studies have suggested that Pb exposure might induce increases in antioxidant responses in fish through the production of reactive oxygen species (ROS) (Kim and Kang, 2017; Maiti et al., 2010). Lead exposure in fish also has toxic effects on membrane structure and function owing to its high affinity to red blood cells, which increases susceptibility to oxidative stresses (Gurer and Ercal, 2000).

Environmental Pb exposure at low levels have been linked to wildlife mortality by hindering the complex mental processes and social behaviours required in general (Pokras and Kneeland, 2008). In zebrafish a subset of low Pb level studies affecting developmental and behaviours in embryos and adult fish in particular (Chen et al., 2012; Lee and Freeman, 2014a, 2014b; Lefauve and Connaughton, 2017; Li et al., 2019a, 2019b; Tu et al., 2018; Weber et al., 1997; Zhao et al., 2019) have been reported. However, no studies have examined the effects of very-low acute Pb exposure on the larval zebrafish neurobehavioural and oxidative stress responses. A paucity of information on the adverse effects of the reported Pb levels from water samples obtained from Kabwe, Zambia on aquatic life formed the background of the present study. To this end, the following questions were asked: Do acute exposure to levels of Pb, as they occur in Kabwe, causes locomotor pattern activity change under dark/light illumination? If so, are the resulting neurobehavioural changes accompanied by oxidative stress responses?

2. Materials and methods

2.1. Fish husbandry and larviculture

Adult wild-type zebrafish strain specifically kept as a breeding stock were used. Fish were maintained at 26 – 28 °C on a 14 -h light and 10 -h dark cycle in a ZebTec (Tecniplast, Italy) flow-through, reconstituted water system in the National Aquatic Bioassay Facility (NABF) at North -West University, South Africa. All experimental procedures were conducted in accordance and adherence to guidelines approved by the North–West University AnimCare Ethics Committee (Ethics number NWU-00269-16-A5). Zebrafish were bred in a 60 L iSpawn breeding tank with a 1/8″ nylon mesh false bottom to protect fertilized eggs from being consumed by the adults. Eggs were collected ≤ 2 h post fertilization (hpf), counted, and placed into Pb-free, glass culture dishes containing an embryo development medium (E3 medium: each litre contains 0.875 g NaCl, 0.038 g KCl, 0.120 g $MgSO_4$, 0.021 g KH_2PO_4, and 0.006 g Na_2HPO_4). The unfertilized embryos were sorted out under a Zeiss stemi microscope and the viable embryos were kept in an incubator at 28 °C in Pb-free embryo media. After 24 hpf again the embryos were examined under the stemi microscope to remove any coagulated embryos. Half of the embryo medium (E3 medium) was replaced daily with freshly oxygenated medium until the test started at 120 h post fertilization (hpf). The zebrafish larvae were not fed throughout the test.

2.2. Lead (Pb) stock solution and exposure protocols

Lead acetate trihydrate (PbAc; Purity 99.5 %) was purchased from Fluka chemika (Sigma-Aldrich), Buchs, Switzerland. A Pb stock solution of 10 mg/L was prepared from PbAc in ultrapure water and stored at 4 °C. The exposure doses of Pb were prepared from the stock after appropriately diluting with Pb-free embryo media to 3 μg/L, 91 μg/L and 250 μg/L Pb concentrations, respectively. The 3 μg/L was based on the average Pb levels in water and 91 μg/L was estimated based on the maximum Pb sampled nearest to the point source (Nachiyunde et al., 2013) and 250 μg/L was the included as highest level of exposure approximately three times the maximum Pb level in Kabwe water bodies.

2.3. Acute Pb exposure, recording and analysis of locomotor behaviour in 120 hpf old larval zebrafish

Larval zebrafish, 120 hpf, reared in Pb-free embryo media were exposed to Pb at three concentrations (3 μg/L, 91 μg/L and 250 μg/L) and a control group (0 μg/L). The choice of the age of the zebrafish larvae (120 hpf) was based on standard protocol that recommends that all behaviour studies are done between day 5–7 days post fertilization when fish are free swimming but feeding on the yolk sac (Strähle et al., 2012). The experimental design consisted of a negative control (n = 12) and exposure concentrations; 3 μg/L (n = 12), 91 μg/L (n = 12) and 250 μg/L (n = 12). One larva per well was transferred to the 12 well testing plate using a plastic pipette with each well containing 3 mL of the respective exposure solution. The acute exposure was replicated four times in order to achieve twelve replicates (n = 3 per group per run). The 12-well plate was placed in a Noldus DanioVision chamber (Wageningen, Netherlands) and recorded at 25 frames per second. Experiments were performed at 28 °C in embryo media at a 10-minute light: dark cycle intervals for a total time of 30 min. We excluded the first 2 min as habituation, and selected the 5th minute under the first dark phase and 15 min time point in the light phase as the statistical behaviour reference point as previously described by Li et al. (2019a). In addition, zones (center and outer) within each well were setup by digitally dissecting zones per plate using Noldus EthoVision XT15 software. The exposure and recording were repeated four times while changing the position of each treatment to minimize the effect of positioning of the larvae in the DanioVision chamber. Thereafter, the larval zebrafish were sacrificed in cold ice water as approved by the North West University ethics committee and immediately preserved in 1.5 mL Eppendorf tubes with cold RNAlater® (Ambion, South Africa). To obtain adequate pooled samples (5–10 larvae) for RNA extraction based on our pre-experimental trials, additional exposures were carried out across the groups (n = 24) using same conditions and concentrations of test compound. The samples were stored at −80 °C prior to RNA extraction.

2.4. RNA extraction and real-time PCR analysis

An RNA isolation protocol was used where 5–10 pooled larvae samples were homogenized in TRI Reagent® with a zirconia bead using a tissue lyser; chloroform was added, and samples were vortexed and

then centrifuged at 13,000*g* for twenty minutes at 4 °C. The supernatant was then mixed with 350 µL of 70 % ethanol and then placed in the FastGene® RNA binding column. Afterwards, the standard FastGene® RNA Basic kits protocol was followed for the rest of the steps. The RNA was eluted from the membrane using RNase free ultrapure MilliQ water. The RNA quality was assessed by spectrophotometry (OD 260:280 ratio) using a NanoDrop 1000A Spectrophotometer (Delaware, USA). The first strand cDNA synthesis kit ReverTra Ace-α (Toyobo) was used for cDNA synthesis according to manufacturer instructions.

The real-time quantitative reverse transcription polymerase chain reaction (RT-qPCR) analysis (StepOnePlus Real-Time PCR System, Applied Biosystems, USA) was performed using a 10 µL PCR reaction mixture containing 5 µL of Fast SYBR Green Master Mix (Applied Biosystems, USA), 0.4 µL of 5 µM forward and reverse primers (Thermo Fisher Scientific, Life Technologies Japan Ltd., Japan), 20 ng of cDNA of each pooled zebrafish larvae samples, and 2.2 µL of distilled water. The qRT-PCR condition for all target genes was 95 °C for 20 s, followed by 40 cycles of 95 °C for 3 s, and 60 °C, 62 °C or 65 °C for 30 s depending on the annealing temperature of a given primer set as shown in Table 1. Most of the primers used were obtained from published works (Jin et al., 2010; Shi and Zhou, 2010; Stancová et al., 2015) and some were generated using the NCBI and Primer3 tools. The gene expressions of various oxidative stress related genes were quantified according to the relative absolute method using tubulin 1a (Tuba1) as a house keeping reference gene (Table 1). The choice of Tuba I as a housekeeping gene was based on its stability and constant expressions in both control and Pb exposed groups after preliminary validation when compared with beta actin, which is in agreement with (Mccurley and Callard, 2008) in zebrafish at various developmental stages following chemical treatment. The primer efficiency range was from 96.5%–100.4%.

2.5. Measurement of Pb in exposure test solutions

The Pb in exposure media were measured for verification purposes. Freshly constituted Pb exposure dose solutions using 99.5 % lead acetate trihydrate and the actual Pb exposure solutions that remained in wells after sacrificing the zebrafish larvae during the study were collected and analyzed. After acidification, concentration of Pb was measured using the inductively coupled plasma mass spectrometry (ICP-MS, 7700 series; Agilent Technologies, Tokyo, Japan). The instrument detection limit for Pb was 0.001 µg/L.

2.6. Data analysis

The larval locomotor behaviour data and gene expression data were analysed using GraphPad Prism software (Prism 7 for Windows; Version 5.02, California USA). The data were reported as mean and SEM (standard error of the mean). Data were tested for criteria of normality using the Kolmogorov–Smirnov test and homogeneity of variance using Levene's test. If data were normally distributed an analysis of variance (one-way ANOVA) was performed and the differences among test groups were assessed with the Tukey's test. For non-parametric data the Kruskal–Wallis test and Dunn's Multiple Comparison test or Mann-Whitney *U* test was used. In our experiment the difference between groups was assessed to be significant at $P < 0.05$ (*) and $P < 0.01$ (**).

3. Results

3.1. Concentration of Pb in exposure test solutions

The nominal Pb dose represents the theoretical doses upon which the exposure solutions were prepared (0, 3, 91 and 250 µg/L) using pure grade 99.5 % lead acetate trihydrate. The actual Pb concentrations detected by ICP-MS (100 – 106.7 % recovery) in the exposure solutions were within an 8% range (0, 3.2, 93 and 252.6 µg/L, respectively).

3.1.1. Effect of acute Pb exposure on locomotor behaviour and molecular subcellular responses in larval zebrafish (120 hpf old Danio rerio larvae)

Under locomotor behaviour, we investigated the mean distance covered, the mean speed, cumulative mobility, cumulative immobility, mobile frequency, immobile frequency, durations (time) spent in the center/outer of the plate (Fig. 1), dark/light illumination related locomotor behaviour with emphasis on the distance covered and speed as shown in Figs. 2 and 3.

3.1.2. Pb effects on the mean distance covered and speed of larval zebrafish

The mean total distance travelled across the exposed group was significantly higher (Tukey test, $p < 0.01$) than that of the control group. The mean distance for the control, 3 µg/L, 91 µg/L and 250 µg/L were 51,891 ± 3054 mm,77,857 ± 5108 mm, 88,623 ± 4737 mm and 85,287 ± 3545 mm, respectively as shown in Fig. 1A. However, there was no significant difference in the mean distance covered among the Pb exposed groups. Regarding the mean swimming speed, we observed similar trend with the pattern of the mean distance covered. The

Table 1
Primers used for real-time qPCR with annealing temperatures used and PCR product lengths.

Target gene	Primer Sequence (5′-3′)	Annealing Temperature (°C)	Product length (bp)	Reference
Tubulin alpha I (Tuba I)	**F:** TTTGTGCACTGGTACGTGGG **R:** CCACACTCTCAGCTCCAACCTC	60	112	a
Glutathione-S-transferase (GST)	**F:** ACAACCTGTTCGATCTCCTGCTGA **R:** GTTGCCGTTGATGGGCAGTTTCTT	60	161	(Jin et al., 2010)
Superoxidase dismutase (SOD2)	**F:** CGCATGTTCCCAGACATCTA **R:** GAGCGGAAGATTGAGGATTG	60	100	(Stancová et al., 2015)
Catalase (CAT)	**F:** AGTGCTCCTGACGTCCAGCCA **R:** TGAAGAACGTGCGCACCTGGG	65	115	(Jin et al., 2010)
Glutathione Peroxidase (GPX 4b)	**F:** GGACGATCCAAGCGTGGTGGA **R:** CAGCCGTCACACGTCTGGGC	60	148	(Stancová et al., 2015)
Uncoupling protein 2 (Ucp-2)	**F:** TGGCTCAACCCACTGATGTA **R:** CAATGGTCCGATATGCGTC	62	102	(Jin et al., 2010)
Heme Oxygenase 1 (HO-1)	**F:** GGAAGAGCTGGACAGAAACG **R:** CGAAGAAGTGCTCCAAGTCC	62	107	(Shi and Zhou, 2010)
B-cell lymphoma 2 (Bcl2)	**F:** AGGAAAATGGAGGTTGGGATG **R:** TGTTAGGTATGAAAACGGGTGGA	62	83	(Jin et al., 2010)
Tumour protein p53 (TP53)	**F:** CCCAGGTGGTGGCTCTTGCT **R:** GAGTGGATGGCTGAGGCTGTTCT	62	113	a
Nuclear factor erythroid 2 (Nrf2)	**F:** GACAAAATCGGCGACAAAAT **R:** TTAGGCCATGTCCACACGTA	65	165	(Shi and Zhou, 2010)
Cytochrome c oxidase subunit I (COXI)	**F:** GGATTTGGAAACTGACTTGTG **R:** AAGAAGAAATGAGGGTGGAAG	60	105	(Jin et al., 2010)

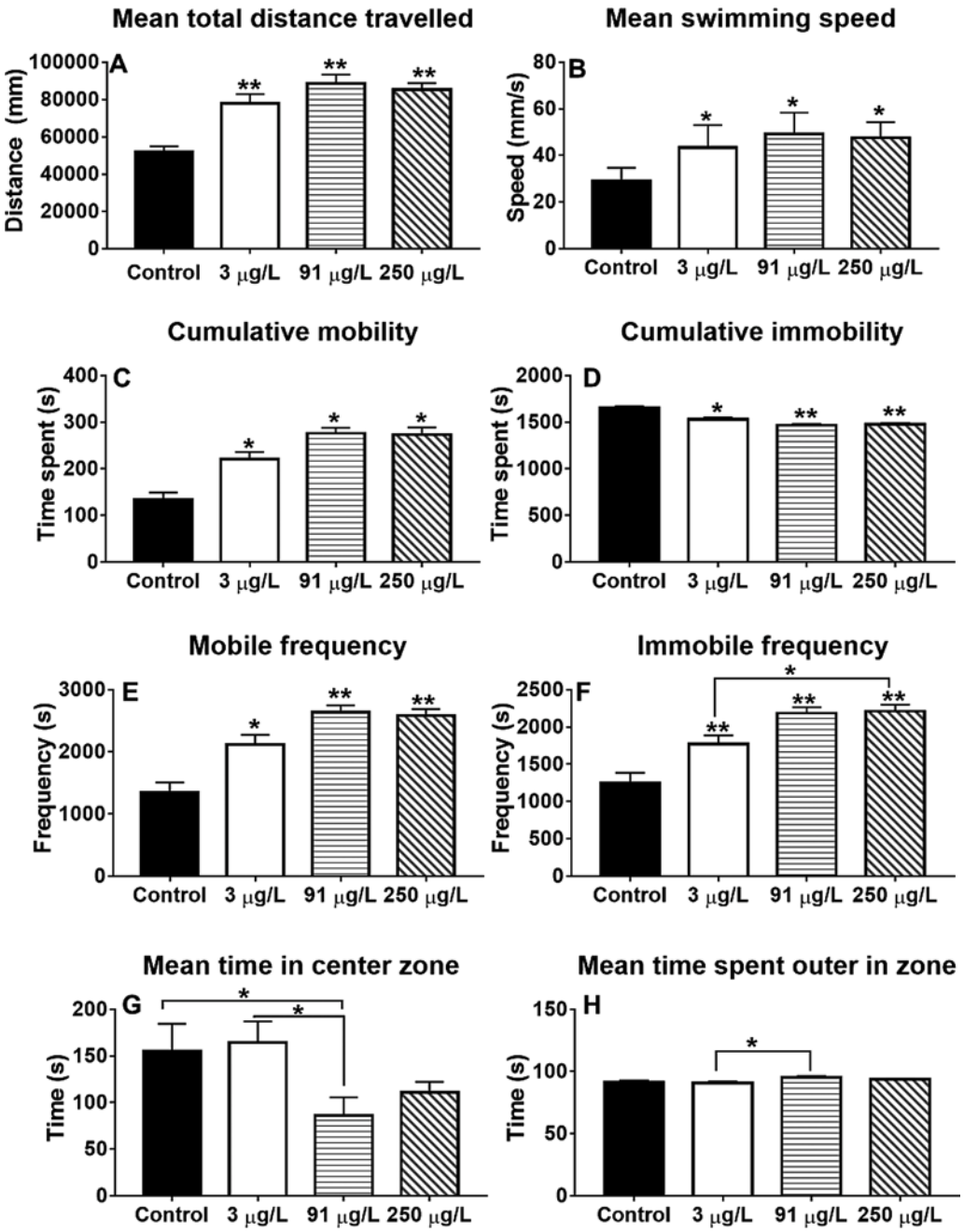

Fig. 1. Locomotor behaviour of larval zebrafish (120 hpf) exposed to 3 µg/L, 91 µg/L and 250 µg/L concentrations of Pb for 30 min during the test. For each exposure treatment n = 12. Significance was regarded at $p < 0.05$* and at $p < 0.01$**.

exposed groups had significantly higher speed implying faster speed compared with that of the control (Tukey test, $p < 0.01$). The mean speed for the control, 3 µg/L, 91 µg/L and 250 µg/L were 28.8 ± 1.7 mm/s, 43.3 ± 2.8 mm/s, 49.3 ± 2.6 mm/s and 47.4 ± 2 mm/s, respectively (Fig. 1B).

3.1.3. *Pb effects on the cumulative mobility time*

Significant differences in cumulative mobility (Dunn's multiple comparison test, $p < 0.001$) were observed in the control (133.6 ± 15.4 s) versus 91 µg/L (275.9 ± 11.9 s) and 250 µg/L (273.4 ± 15.3 s) as shown in Fig. 1C. Among the exposed groups compared with that of the control we observed a reduction in the time spent immobile by the larval zebrafish during the behavioural assessment period. The control spent statistically significant less time being immobile with mean of 1652 ± 17.9 s while the larval zebrafish in the 3 µg/L, 91 µg/L and 250 µg/L spent 1531 ± 21.8 s, 1466 ± 17.4 s and 1478 ± 16.3 s respectively, as shown in Fig. 1D.

3.1.4. *Pb effects on the mean mobile and immobile frequency*

The total number of times the larval zebrafish spent mobile were significantly higher in the exposed groups compared to the control. The average mean frequencies were 1348 ± 158.1 s; 2115 ± 157.3 s; 2638 ± 11.9 s and 2580 ± 107.8 s for the control, 3 µg/L, 91 µg/L and 250 µg/L, respectively (Fig. 1E). Regarding the immobility frequency, the control group recorded a significantly lower frequency of 1247 ± 139 s when compared to the exposed groups namely; 3 µg/L which recorded 1770 ± 118.2 s; 91 µg/L with 2184 ± 82.8 s and 250 µg/L with 2210 ± 90 s. Among the exposed groups, there was an increased pattern in the immobility frequency with an increased in Pb exposure dose. A significant difference was seen between 3 µg/L and 250 µg/L immobility

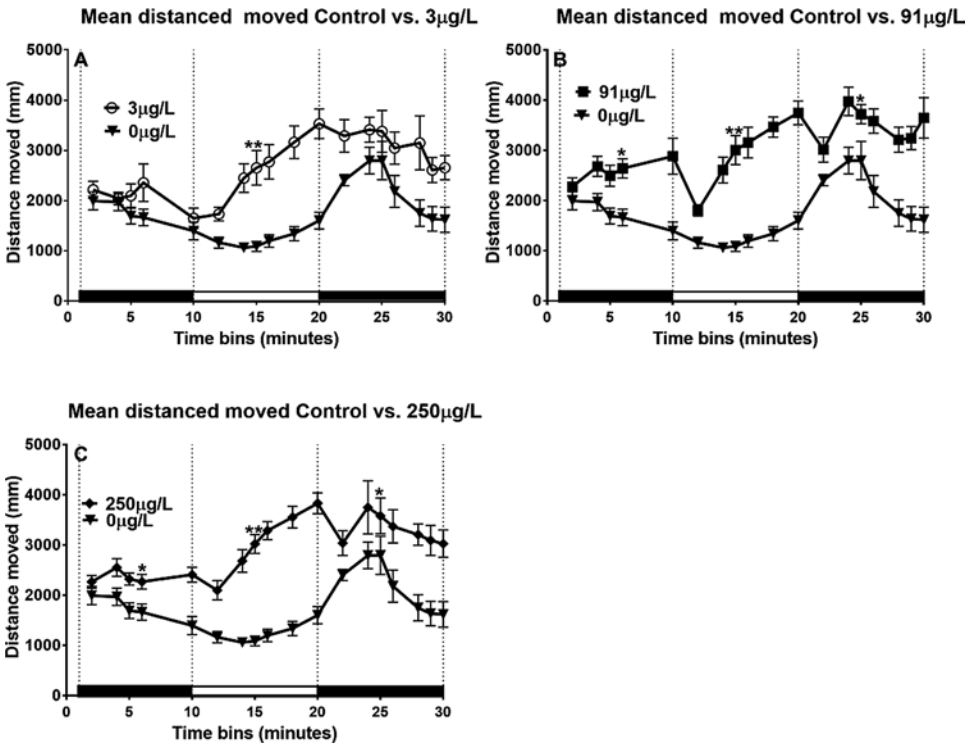

Fig. 2. Locomotor behaviour of larval Zebrafish (120 hpf) distance moved for exposed to 3 μg/L(A), 91 μg/L(B) and 250 μg/L (C) Pb concentrations and control for 30 min under dark/light transition illumination (515 and 25 min) during the test. The dark and white bar represents dark and light phases, respectively. For each exposure treatment n = 12 Significance was regarded at $p < 0.05$* and at $p < 0.01$**.

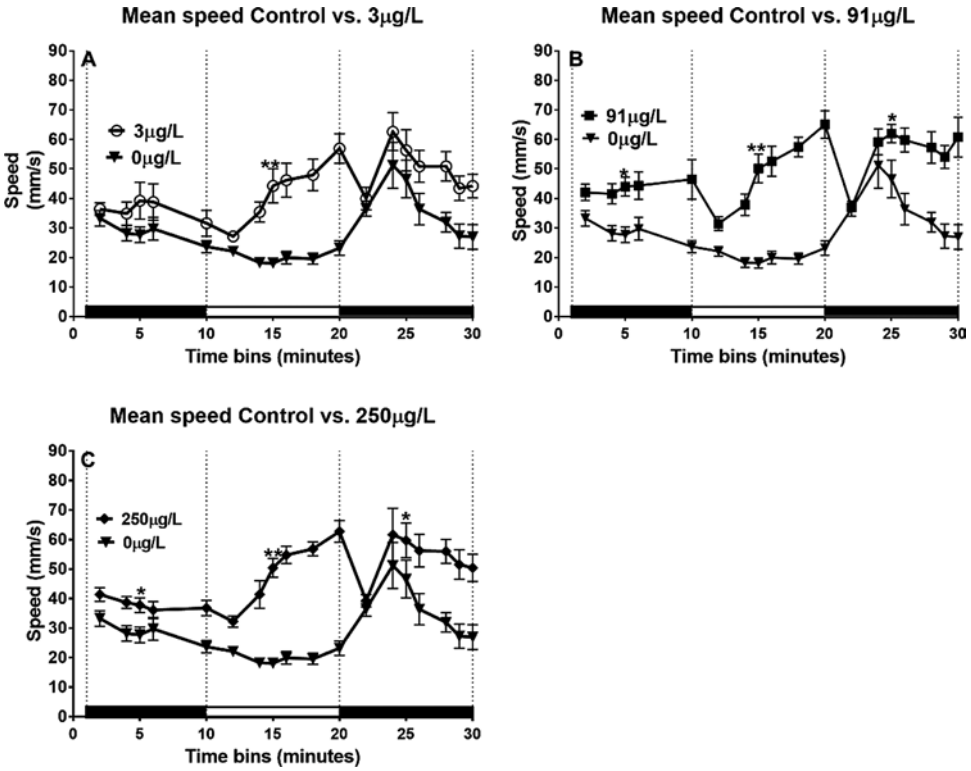

Fig. 3. Locomotor behaviour of larval Zebrafish (120 hpf) speed for exposed to 3 μg/L(A), 91 μg/L (B) and 250 μg/L (C) Pb concentrations and control for 30 min under dark/light transition illumination (515 and 25 min) during the test. The dark and white bar represents dark and light phases, respectively. For each exposure treatment n = 12. Significance was regarded at $p < 0.05$* and at $p < 0.01$**.

frequencies (Fig. 1F).

3.1.5. Pb effects on the time spent by larval zebrafish in the centre/outer zones

At the lowest level of exposure (3 μg/L - mean time was 164.6 ± 22.5 s) no difference in the centre zone preferences to that of the control group (155.7 ± 29 s) were recorded. However, a significant reduction in the time spent in the center zones was observed at 91 μg/L (86.4 ± 19.3 s) compared to the control group (Fig. 1G). The exposure groups spent more time in the outer zones of the well although not statistically significant when compared to the control group. Among the exposed groups a significant ($p < 0.05$) outer zones preference between 3 μg/L (90.9 ± 1.6 s) and 91 μg/L (95.2 ± 1.1 s) was recorded with the of the larval zebrafish spending more time in the outer zone at 91 μg/L (Fig. 1H).

3.2. Pb effects on the distance covered and speed of larval zebrafish in the dark/light phases

In general, the exposed groups covered longer distances in both the dark and light phase compared to that of the control group (Fig. 2). Mean distance recorded at 5 min during the first dark phase was significantly higher in 91 μg/L (2642 ± 193.1 mm) than that of the control (1655 ± 163.7 mm). Under the light phase, the control group (1199 ± 126.2 mm) had covered significantly lower ($p < 0.01$) distance at 15 min time bin compared to the 3 μg/L (2773 ± 177.6 mm), 91 μg/L (3156 ± 305.4 mm) and 250 μg/L (3289 ± 177.6 mm) as shown in Fig. 2 (A–C), respectively. During the second dark phase, the distance covered

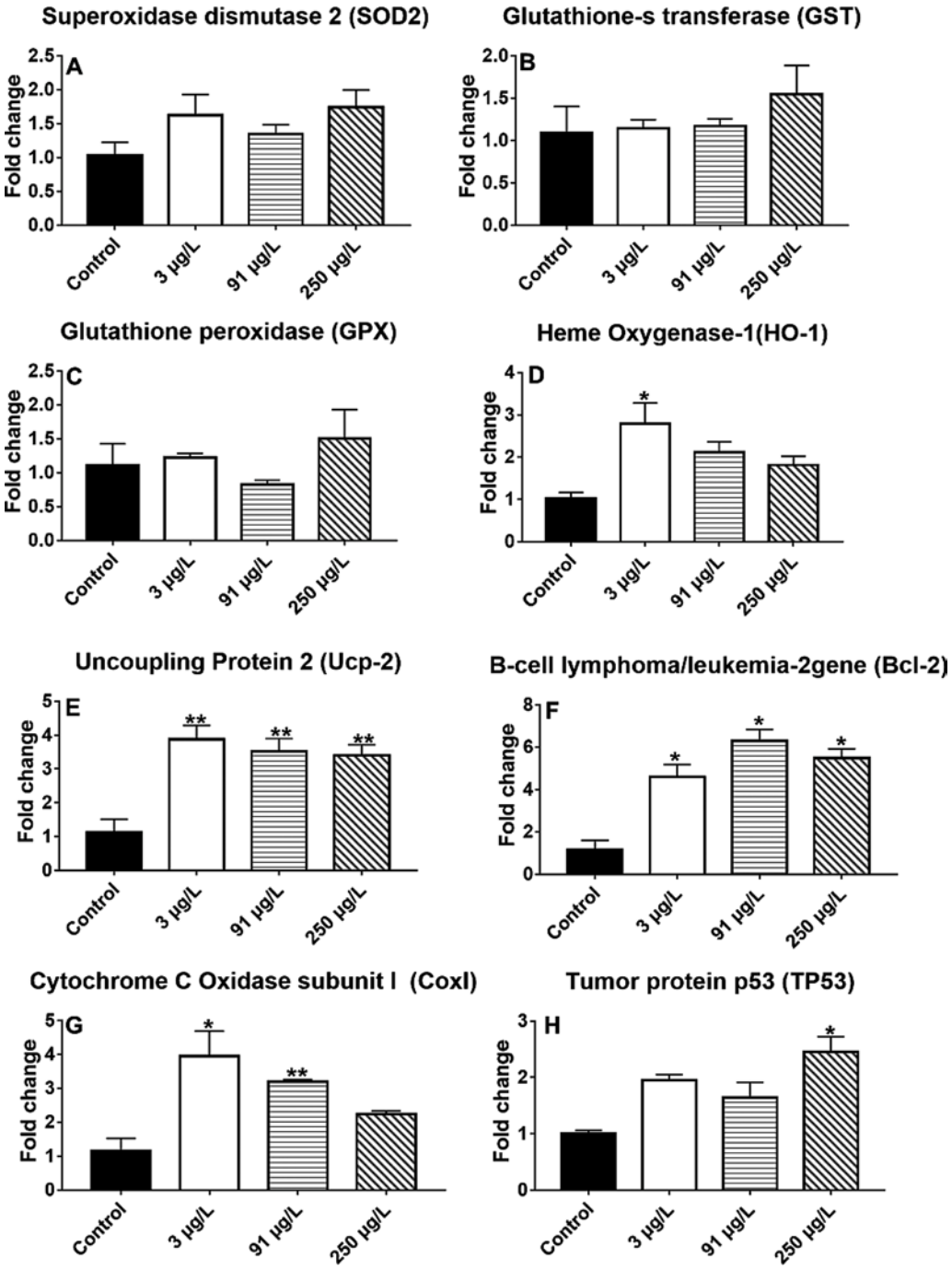

Fig. 4. Expression of SOD2, GST, GPX, HO-1, Ucp-2, TP53, COX1 and Bcl-2 (A, B, C, D,E,F,H and G) in the pooled samples from the larval zebrafish after the acute Pb 30 min dark/light illuminations (120 hpf old larval zebrafish) groups at 3 μg/L Pb, 91 μg/L Pb and 250 μg/L Pb concentrations and control. Values normalized against Tubulin alpha-1A (used as house-keeping gene) and represent the mean mRNA expression value ± SEM (n = 3 pooled samples) relative to those of the controls. The asterisk represents a statistically significant difference when compared with the controls *at $p < 0.05$ and **at $p < 0.01$ levels.

by the control group (2182 ± 318.5 mm) was lower than the exposed groups and the difference was significant in the 91 μg/L group (3585 ± 242.7 mm) and 250 μg/L group (3396 ± 328.6 mm) at 25 min time bin (Fig. 2B and C), respectively.

For swimming speed, the trend was similar as observed with the distance covered. At 5 min time bin, the speed of the 91 μg/L group (44 ± 3.2 mm/s) was significantly faster ($p < 0.05$) than that of the control group (27.8 ± 2.7 mm/s) as shown in Fig. 3B. At the 15 min time bin of the light phase, the larval zebrafish exposed to Pb were significantly faster than the control group ($p < 0.01$). The mean speeds at 15 min time bin were 20 ± 2.1 mm/s, 46.2 ± 5.8 mm/s, 52.6 ± 5.1 mm/s and 54.8 ± 3 mm/s for the control, 3 μg/L, 91 μg/L and 250 μg/L, respectively (Fig. 3B and C).

3.3. Pb effects on the subcellular oxidative stress responses in larval zebrafish

The messenger ribonucleic acid (mRNA) level of SOD2 in the larval zebrafish samples showed a slight increased level of expression in the exposed groups with 1.6-fold change at 3 μg/L, 1.3-fold change at 91 μg/L and 1.7-fold change at 250 μg/L levels of exposure though not statistically significant (Fig. 4A). On the other hand, acute effect of Pb was not accompanied by statistically significant GST mRNA across the exposed groups though a slight increase in the mRNA levels was seen at 250 μg/L with 1.5-fold change (Fig. 4B). Similarly, the mRNA for GPX expression levels showed a slight increase at 3 μg/L of 1.2-fold change and at 250 μg/L of 1.5-fold change though not statistically significant. At 91 μg/L, we observed a slight decrease in the mRNA levels of GPX of 0.8-fold change which was not statistically significant (Fig. 4C). Additionally, we observed that the mRNA levels of HO-1 were upregulated in exposed groups when compared to the control with 2.8-fold change, 2.1-fold change and 1.8-fold change for the 3 μg/L Pb, 91 μg/L Pb and 250 μg/L Pb, respectively. The upregulation was statistically significant in the 3 μg/L exposed group compared to the control (Fig. 3D).

The mRNA levels of Ucp-2 were significantly upregulated ($p < 0.05$) in exposed groups when compared to the control with 3.9-fold change, 3.5-fold change and 3.4-fold change for the 3 μg/L, 91 μg/L and 250 μg/L, respectively (Fig. 4E). The expression of the mRNA levels for the Bcl-2 gene were significantly upregulated following the Pb exposure across the exposed groups. The fold changes were 4.6-fold change, 6.3-fold change and 5.5-fold change at 3 μg/L Pb, 91 μg/L Pb and 250 μg/L Pb, respectively (Fig. 4F). In addition, the expression of CoxI which is involved in the mitochondrial respiratory chain and ATP synthesis was significantly upregulated in 3 μg/L Pb and 91 μg/L Pb groups when compared to the control with 3.9-fold change and 3.2-fold change, respectively (Fig. 4G). The expression of the mRNA levels for the TP53 gene were slightly upregulated following the Pb exposure across the exposed groups. However, only the mRNA levels in 250 μg/L Pb group with a 2.5-fold (Fig. 4H) change were statistically significant when compared to the control ($p < 0.05$).

4. Discussion

In this study, we investigated the effects of environmentally relevant levels of Pb (as reported in Kabwe town and Zambia (Nachiyunde et al., 2013) on ensuing subcellular oxidative stress responses of the primary antioxidant, pro-apoptotic and anti-apoptotic genes and locomotor behaviour of larval zebrafish. Acute Pb exposure to larval zebrafish for 30 min induced hyperactivity characterised by significant increases in distance covered, swimming speed and mobile frequency as well as increased distance covered and speed under light illumination. We observed that the hyperactivity was significantly increased in exposed groups under light conditions when the zebrafish are reported to assume relaxed state (Lee and Freeman, 2014b) indicating Pb's potentiating neurobehavioural effects. Our results were similar to the activity of zebrafish larval that were exposed as embryos to low Pb of 25 μg/L (Chen et al., 2012) and contrary to findings reported in other studies where they observed hypoactivity (Dou and Zhang, 2011; Lefauve and Connaughton, 2017; Li et al., 2019a). The difference between some of the foregoing studies and the present study could have been related to the dose of Pb, the duration of exposure and the developmental stages of the zebrafish. For instance Li et al. (2019a) reported a concentration dependent reduction in locomotion of adult zebrafish exposed Pb over a 14 day period to 1 μg/L, 10 μg/L and 100 μg/L Pb, respectively. Dose and duration effects in Pb exposure in fish have been reported in the Mirror carp exposed to 50 μg/L of Pb over a 30 day period with hyperactivity reported in the first week and last week of exposure (Shafiq-ur-Rehman, 2003). Other neuroactive chemicals such an cholinesterase inhibitor, paraoxon showed hyperactivity in a lower exposure range and hypoactive with a 100-fold increase in exposure concentration (Yozzo et al., 2013). This study confirms the responses that were obtained using the mammalian models, humans and rodents, exposed to chronic low Pb concentrations where hyperactivity was been reported as the neurobehavioural end point (Ma et al., 1999); thereby showing the application value of the zebrafish model to assess Pb exposure responses. While our experimental design was not aimed at elucidating the mechanism behind this behaviour, our results demonstrated alterations in free locomotor activity manifested by hyperactivity, a recognized effect of Pb neurotoxicity (Atchison et al., 1987). In Mirror carp that exhibited Pb induced hyperactivity, a positive correlation between enhanced lipid peroxidation, a marker of oxidative damage in the brain and increased behavioural activity was reported (Shafiq-ur-Rehman, 2003). The abnormal behaviour of increased locomotor activity in larval zebrafish during daylight phases has potential ecological implications in the form of increased predation vulnerability. South et al. (2019) linked increased locomotion to reduced anti-predator behaviour in mosquito larvae following exposure to low levels of the insecticide.

In case of the mRNA responses to acute exposure of environmentally relevant Pb in larval zebrafish, we observed a non-significant induction of the primary antioxidant enzymes apart from HO-1 that was significantly upregulated at 3 μg/L. Functionally, HO-1 catabolize free heme, that is, iron (Fe) protoporphyrin (IX), into equimolar amounts of Fe^{2+}, carbon monoxide (CO), and biliverdin (Gozzelino et al., 2010). In our study, the upregulation of HO-1 at 3 μg/L Pb and its accompanying lack of significant upregulation at high levels (91 and 250 μg/L Pb) may have been a protective response against acute Pb exposure or a hormetic response (Calabrese et al., 2012). Heme oxygenase (HO-1) gene has been classified among the vitagene family exhibiting hormetic responses (Calabrese et al., 2004). According to the hormetic principles, low doses of drugs, toxicants, and natural substances may elicit a positive response in terms of adaptation to or protection from the stressor, whereas at higher concentration the toxic effect prevails (Calabrese et al., 2008). The hormetic dose – response can occur through different mechanisms: as a direct stimulatory response; after an initial disruption in homeostasis followed by the modest overcompensation response; or as a response to an "adapting" or "preconditioning" dose that is followed by a more challenging dose (Piantadosi, 2008). Furthermore, we observed significant upregulation of the Ucp-2 gene and Bcl-2 across the exposed group. The upregulation of CoxI and the proapoptotic TP53 genes seem to suggest an acute upregulation of ROS that led to an enhanced mobilization of the Ucp-2 and Bcl2 genes to quail the ROS production as an initial protective mechanism (Craig et al., 2007). Ucp-2 functions by an incompletely defined mechanism to reduce the production of reactive oxygen species during mitochondrial electron transport (Giardina et al., 2008), while Bcl-2 works to counter the effect of the TP53 elevated gene expression and has been said to be an indicator of a conspicuous increase in ROS (Kowaltowski and Fiskum, 2005). Similarly, the significant upregulation of CoxI expression in the acutely Pb exposed larval zebrafish points to the acute requirement for cellular responses to the generated ROS following exposure (Bourens et al., 2013).

While Pb has been reported as a neurotoxic element that causes

behavioural dysfunction in fishes within days of exposure to sublethal concentrations (Weber et al., 1997), our study has demonstrated that effects in zebrafish larvae manifest within a very short period following exposure to environmentally relevant Pb levels. Taken together, our results showed that the lowest average Pb level of 3 μg/L Pb as found in Kabwe, Zambia may have deleterious effects to the same degree as higher exposure concentrations (91 μg/L and 250 μg/L) on aquatic life triggering a surge in ROS generation and hyperactive swimming behaviour as observed in the larval zebrafish.

The following limitations of using toxicogenomics in this study were identified. There is a long-standing debate as to what fold change in gene expression can be considered to be biologically significant (Mccarthy and Smyth, 2009). In this study we regarded a significant difference from the control to reflect those genes that are differentially expressed. It is however acknowledged that there is a threshold for minimum fold gene change below which differential expression is unlikely to be of any biological interest for a particular gene. Therefore, this ad hoc approach probably provides an over estimation of the effects likely to occur following exposure to low levels of Pb. It is further acknowledged that the use of gene expression profiling as an indicator of sub-cellular changes needs to be verified through assessment of molecular and biochemical to reveal and confirm precise mechanisms of action (Fielden and Zacharewski, 2001). Due to the small sample volume we were not able to verify increased antioxidant responses through analyses of enzymatic (e.g. SOD and catalase) and non-enzymatic (lipid peroxidase and protein carbonyl) compounds. However, based on the studies (Ahmadifar et al., 2019; Parolini et al., 2017; and Safari et al., 2017) where similar fold changes were accompanied by significant biochemical changes, seem to support that the gene expression (i.e. upregulation of the anti-oxidant genes) results in increase of the enzymes thereby combatting ROS formation. It is then this premise that we use to postulate that the gene expression maybe a good indicator (biomarker) of antioxidant responses against ROS formation.

5. Conclusion

Environmentally relevant concentrations of Pb as they occur in Kabwe could be detrimental to aquatic life especially in larval fish. Acute exposure to the environmentally relevant Pb levels attenuated larval zebrafish behaviour by inducing hyperactivity under dark/light illumination. This locomotor activity pattern alteration could be linked to altered neurobehavior via neurotoxicity mediated by oxidative stress or direct Pb neuro-intoxication due to lack of fully formed brain blood barrier. This has potential ecological ramifications through alterations in predator-prey interactions. However, the degree to which these observed effects following an acute exposure period to low Pb levels will persist during prolonged exposure needs to be investigated further.

Ethical statement

All experimental procedures were approved by the AnimCare animal research ethics committee (NHREC reg. number AREC-130913-015) of the North-West University. All animals were maintained, and procedures performed in accordance with the code of ethics in research, training and testing of drugs in South Africa and complied with national legislation (ethics approval number: NWU-00269-16-A5).

Note: a: Primers designed by the authors using NCBI and Primer3 tools. F and R represents forward primer and reverse primer sequences, respectively.

CRediT authorship contribution statement

Andrew Kataba: Conceptualization, Methodology, Formal analysis, Writing - original draft, Visualization. **Tarryn L. Botha:** Conceptualization, Validation, Investigation, Writing - review & editing. **Shouta M. M. Nakayama:** Conceptualization, Investigation, Writing - review & editing. **Yared B. Yohannes:** Validation, Writing - review & editing. **Yoshinori Ikenaka:** Resources, Writing - review & editing. **Victor Wepener:** Conceptualization, Resources, Writing - review & editing, Supervision, Project administration. **Mayumi Ishizuka:** Conceptualization, Resources, Writing - review & editing, Supervision, Project administration, Funding acquisition.

Declaration of Competing Interest

The authors report no declarations of interest.

Acknowledgements

This work was supported by the Grants-in-Aid for Scientific Research from the Ministry of Education, Culture, Sports, Science and Technology of Japan awarded to M. Ishizuka (No. 16H0177906, 18K1984708, and 18KK028708), Y. Ikenaka (18H0413208), and S.M.M. Nakayama (No. 17KK0009). This work was also supported by the foundation of JSPS Bilateral Open Partnership Joint Research Projects (JPJSBP120209902) and the Environment Research and Technology Development Fund of the Environmental Restoration and Conservation Agency of Japan (SII-1/3-2, 4RF-1802/18949907). We also acknowledge financial support from the Soroptimist Japan Foundation, the Nakajima Foundation, the Sumitomo Foundation, the Nihon Seimei Foundation, and the Japan Prize Foundation. This research was also supported by JST/JICA, SATREPS (Science and Technology Research Partnership for Sustainable Development); No. JPMJSA1501 and the Hokkaido University Faculty of Veterinary Medicine Wise/Leading Travel and Subsistence grant. Bioassays were conducted in the National Aquatic Bioassay Facility at North-West University, South Africa (NRF Grant UID99024). This is publication number 474 of the Water Research Group, NWU.

References

Ahmadifar, E., Sheikhzadeh, N., Roshanaei, K., Dargahi, N., 2019. Can dietary ginger (Zingiber officinale) alter biochemical and immunological parameters and gene expression related to growth, immunity and antioxidant system in zebra fi sh (Danio rerio)? Aquaculture 507, 341–348. https://doi.org/10.1016/j.aquaculture.2019.04.049.

Atchison, G.J., Henry, M.G., Sandheinrich, M.B., 1987. Effects of metals on fish behavior: a review. Environ. Biol. Fishes 18, 11–25. https://doi.org/10.1007/BF00002324.

Bose-O'Reilly, S., Yabe, J., Makumba, J., Schutzmeier, P., Ericson, B., Caravanos, J., 2017. Lead intoxicated children in Kabwe, Zambia. Environ. Res. 0–1. https://doi.org/10.1016/j.envres.2017.10.024.

Bourens, M., Fontanesi, F., Soto, I.C., Liu, J., Barrientos, A., 2013. Redox and reactive oxygen species regulation of mitochondrial cytochrome C oxidase biogenesis. Antioxidants Redox Signal. 19, 1940–1952. https://doi.org/10.1089/ars.2012.4847.

Calabrese, V., Boyd-Kimball, D., Scapagnini, G., Butterfield, D.A., 2004. Nitric oxide and cellular stress response in brain aging and neurodegenerative disorders: the role of vitagenes. In Vivo (Brooklyn). 18, 245–268.

Calabrese, V., Cornelius, C., Mancuso, C., Pennisi, G., Calafato, S., Bellia, F., Bates, T.E., Giuffrida Stella, A.M., Schapira, T., Dinkova Kostova, A.T., Rizzarelli, E., 2008. Cellular stress response: a novel target for chemoprevention and nutritional neuroprotection in aging, neurodegenerative disorders and longevity. Neurochem. Res. 33, 2444–2471. https://doi.org/10.1007/s11064-008-9775-9.

Calabrese, V., Cornelius, C., Dinkova-Kostova, A.T., Iavicoli, I., Di Paola, R., Koverech, A., Cuzzocrea, S., Rizzarelli, E., Calabrese, E.J., 2012. Cellular stress responses, hormetic phytochemicals and vitagenes in aging and longevity. Biochim. Biophys. Acta - Mol. Basis Dis. 1822, 753–783. https://doi.org/10.1016/j.bbadis.2011.11.002.

Chen, J., Chen, Y., Liu, W., Bai, C., Liu, X., Liu, K., Li, R., Zhu, J.H., Huang, C., 2012. Developmental lead acetate exposure induces embryonic toxicity and memory deficit in adult zebrafish. Neurotoxicol. Teratol. 34, 581–586. https://doi.org/10.1016/j.ntt.2012.09.001.

Cheng, H., Hu, Y., 2010. Lead (Pb) isotopic fingerprinting and its applications in lead pollution studies in China: a review. Environ. Pollut. 158, 1134–1146. https://doi.org/10.1016/j.envpol.2009.12.028.

Craig, P.M., Wood, C.M., McClelland, G.B., 2007. Oxidative stress response and gene expression with acute zebrafish (Danio rerio). Am. J. Physiol. - Regul. Integr. Comp. Physiol. 293, 1882–1892. https://doi.org/10.1152/ajpregu.00383.2007.

Dou, C., Zhang, J., 2011. Effects of lead on neurogenesis during zebrafish embryonic brain development. J. Hazard. Mater. 194, 277–282. https://doi.org/10.1016/j.jhazmat.2011.07.106.

Fielden, M.R., Zacharewski, T.R., 2001. Challenges and limitations of gene expression profiling in mechanistic and predictive toxicology. Toxicol. Sci. 60, 6–10.

Flora, G., Gupta, D., Tiwari, A., 2012. Toxicity of lead: a review with recent updates. Interdiscip. Toxicol. 5, 47–58. https://doi.org/10.2478/v10102-012-0009-2.
Fraysse, B., Mons, R., Garric, J., 2006. Development of a zebrafish 4-day embryo-larval bioassay to assess toxicity of chemicals. Ecotoxicol. Environ. Saf. 63, 253–267. https://doi.org/10.1016/j.ecoenv.2004.10.015.
Gozzelino, R., Jeney, V., Soares, M.P., 2010. Mechanisms of cell protection by heme Oxygenase-1. Annu. Rev. Pharmacol. Toxicol. 50, 323–354. https://doi.org/10.1146/annurev.pharmtox.010909.105600.
Gurer, H., Ercal, N., 2000. Can antioxidants be beneficial in the treatment of lead poisoning? Free Radic. Biol. Med. 29, 927–945. https://doi.org/10.1016/S0891-5849(00)00413-5.
Howe, K., Clark, M.D., Torroja, C.F., Torrance, J., Muffato, M., Collins, J.E., et al., 2014. The Zebrafish Reference Genome Sequence, 496, pp. 498–503. https://doi.org/10.1038/nature12111.The.
Ikenaka, Y., Nakayama, S.M.M., Muzandu, K., Choongo, K., Teraoka, H., Mizuno, N., Ishizuka, M., 2010. Heavy metal contamination of soil and sediment in Zambia. African J. Environ. Sci. Technol. 4, 729–739. https://doi.org/10.4314/ajest.v4i11.71339.
Jin, Y., Zhang, X., Shu, L., Chen, L., Sun, L., Qian, H., Liu, W., Fu, Z., 2010. Oxidative stress response and gene expression with atrazine exposure in adult female zebrafish (Danio rerio). Chemosphere 78, 846–852. https://doi.org/10.1016/j.chemosphere.2009.11.044.
Kim, J.H., Kang, J.C., 2017. Effects of sub-chronic exposure to lead (Pb) and ascorbic acid in juvenile rockfish: antioxidant responses, MT gene expression, and neurotransmitters. Chemosphere 171, 520–527. https://doi.org/10.1016/j.chemosphere.2016.12.094.
Kowaltowski, A.J., Fiskum, G., 2005. Redox mechanisms of cytoprotection by Bcl-2. Antioxidants Redox Signal. 7, 508–514. https://doi.org/10.1089/ars.2005.7.508.
Lanphear, B.P., Dietrich, K., Auinger, P., Cox, C., 2000. Cognitive deficits associated with blood lead concentrations < 10 μg/dL in US children and adolescents. Public Health Rep. 115, 521–529. https://doi.org/10.1093/phr/115.6.521.
Lee, J., Freeman, J.L., 2014a. Zebrafish as a model for investigating developmental lead (Pb) neurotoxicity as a risk factor in adult neurodegenerative disease: a mini-review. Neurotoxicology 43, 57–64. https://doi.org/10.1016/j.neuro.2014.03.008.
Lee, J., Freeman, J.L., 2014b. Zebrafish as a model for developmental neurotoxicity assessment: the Application of the zebrafish in defining the effects of arsenic, methylmercury, or lead on early neurodevelopment. Toxics 2, 464–495. https://doi.org/10.3390/toxics2030464.
Lefauve, M.K., Connaughton, V.P., 2017. Developmental exposure to heavy metals alters visually-guided behaviors in zebrafish. Curr. Zool. 63, 221–227. https://doi.org/10.1093/cz/zox017.
Li, X., Kong, H., Ji, X., Gao, Y., Jin, M., 2019a. Zebrafish behavioral phenomics applied for phenotyping aquatic neurotoxicity induced by lead contaminants of environmentally relevant level. Chemosphere 224, 445–454. https://doi.org/10.1016/j.chemosphere.2019.02.174.
Li, X., Zhang, B., Li, N., Ji, X., Liu, K., Jin, M., 2019b. Zebrafish neurobehavioral phenomics applied as the behavioral warning methods for fingerprinting endocrine disrupting effect by lead exposure at environmentally relevant level. Chemosphere 231, 315–325. https://doi.org/10.1016/j.chemosphere.2019.05.146.
Ma, T., Chen, H.H., Ho, I.K., 1999. Effects of chronic lead (Pb) exposure on neurobehavioral function and dopaminergic neurotransmitter receptors in rats. Toxicol. Lett. 105, 111–121. https://doi.org/10.1016/S0378-4274(98)00388-9.
Maiti, A.K., Saha, N.C., Paul, G., 2010. Effect of lead on oxidative stress, Na +K +ATPase activity and mitochondrial electron transport chain activity of the brain of clarias batrachus L. Bull. Environ. Contam. Toxicol. 84, 672–676. https://doi.org/10.1007/s00128-010-9997-9.
Mccarthy, D.J., Smyth, G.K., 2009. Testing significance relative to a fold-change threshold is a TREAT. Bioinformatics 25, 765–771. https://doi.org/10.1093/bioinformatics/btp053.
Mccurley, A.T., Callard, G.V., 2008. Characterization of housekeeping genes in zebrafish: male-female differences and effects of tissue type, developmental stage and chemical treatment. BMC Mol. Biol. 12, 1–12. https://doi.org/10.1186/1471-2199-9-102.
Nachiyunde, K., Ikeda, H., Okuda, T., Nishijima, W., 2013. Assessment of dissolved heavy metal pollution in five provinces of Zambia. J. Environ. Prot. (Irvine, Calif.) 04, 80–85. https://doi.org/10.4236/jep.2013.41b015.
Nakata, H., Nakayama, S.M.M., Yabe, J., Liazambi, A., Mizukawa, H., Darwish, W.S., Ikenaka, Y., Ishizuka, M., 2016. Reliability of stable Pb isotopes to identify Pb sources and verifying biological fractionation of Pb isotopes in goats and chickens. Environ. Pollut. 208, 395–403. https://doi.org/10.1016/j.envpol.2015.10.006.
Nakayama, Shouta M.M., Ikenaka, Y., Hamada, K., Muzandu, K., Choongo, K., Teraoka, H., Mizuno, N., Ishizuka, M., 2011. Metal and metalloid contamination in roadside soil and wild rats around a Pb-Zn mine in Kabwe, Zambia. Environ. Pollut. 159, 175–181. https://doi.org/10.1016/j.envpol.2010.09.007.
Nevin, R., 2000. How lead exposure relates to temporal changes in IQ, violent crime, and unwed pregnancy how lead exposure relates to temporal changes in IQ, violent crime, and unwed pregnancy. Environ. Res. 83, 1–22.
Olympio, K.P.K., Oliveira, P.V., Naozuka, J., Cardoso, M.R.A., Marques, A.F., Günther, W.M.R., Bechara, E.J.H., 2010. Surface dental enamel lead levels and antisocial behavior in Brazilian adolescents. Neurotoxicol. Teratol. 32, 273–279. https://doi.org/10.1016/j.ntt.2009.12.003.
Parolini, M., Ghilardi, A., Della Torre, C., Magni, S., Prosperi, L., Calvagno, M., Del Giacco, L., Binelli, A., 2017. Environmental concentrations of cocaine and its main metabolites modulated antioxidant response and caused cyto-genotoxic effects in zebra fi sh embryo cells *. Environ. Pollut. 226, 504–514. https://doi.org/10.1016/j.envpol.2017.04.046.
Piantadosi, C.A., 2008. Carbon monoxide, reactive oxygen signaling, and oxidative stress. Free Radic. Biol. Med. 45, 562–569. https://doi.org/10.1016/j.freeradbiomed.2008.05.013.
Pokras, M.A., Kneeland, M.R., 2008. Lead poisoning: using transdisciplinary approaches to solve an ancient problem. Ecohealth 5, 379–385. https://doi.org/10.1007/s10393-008-0177-x.
Safari, R., Hossein, S., Van Doan, H., Dadar, M., 2017. The effects of dietary Myrtle (Myrtus communis) on skin mucus immune parameters and mRNA levels of growth, antioxidant and immune related genes in zebra fi sh (Danio rerio). Fish Shellfish Immunol. 66, 264–269. https://doi.org/10.1016/j.fsi.2017.05.007.
Sciarillo, W.G., Alexander, G., Farrell, K.P., 1992. Lead exposure and child behavior. Am. J. Public Health 82, 1356–1360. https://doi.org/10.2105/AJPH.82.10.1356.
Shafiq-ur-Rehman, 2003. Lead-exposed increase in movement behavior and brain lipid peroxidation in fish. J. Environ. Sci. Heal. - Part A Toxic/Hazardous Subst. Environ. Eng. 38, 631–643. https://doi.org/10.1081/ESE-120016928.
Shi, X., Zhou, B., 2010. The role of Nrf2 and MAPK pathways in PFOS-induced oxidative stress in zebrafish embryos. Toxicol. Sci. 115, 391–400. https://doi.org/10.1093/toxsci/kfq066.
Stancová, V., Ziková, A., Svobodová, Z., Kloas, W., 2015. Effects of the non-steroidal anti-inflammatory drug(NSAID) naproxen on gene expression of antioxidant enzymes in zebrafish (Danio rerio). Environ. Toxicol. Pharmacol. 40, 343–348. https://doi.org/10.1016/j.etap.2015.07.009.
Strähle, U., Scholz, S., Geisler, R., Greiner, P., Hollert, H., Rastegar, S., Schumacher, A., Selderslaghs, I., Weiss, C., Witters, H., Braunbeck, T., 2012. Zebrafish embryos as an alternative to animal experiments-a commentary on the definition of the onset of protected life stages in animal welfare regulations. Reprod. Toxicol. 33, 128–132. https://doi.org/10.1016/j.reprotox.2011.06.121.
Tu, H., Peng, T., Liu, J., Chen, X., Fan, C., Huang, Z., Zhang, Y., Zou, F., Meng, X., 2018. Role of neurexin2a in lead-induced locomotor defect in developing zebrafish. Aquat. Toxicol. 194, 167–175. https://doi.org/10.1016/j.aquatox.2017.11.011.
Wani, A.L., Ara, A., Usmani, J.A., 2015. Lead toxicity: a review. Interdiscip. Toxicol. 8, 55–64. https://doi.org/10.1515/intox-2015-0009.
Weber, D.N., Dingel, W.M., Panos, J.J., Steinpreis, R.E., 1997. Alterations in neurobehavioral responses in fishes exposed to lead and lead-chelating agents. Am. Zool. 37, 354–362. https://doi.org/10.1093/icb/37.4.354.
Xu, X., Weber, D., Burge, R., VanAmberg, K., 2016. Neurobehavioral impairments produced by developmental lead exposure persisted for generations in zebrafish (Danio rerio). Neurotoxicology 52, 176–185. https://doi.org/10.1016/j.neuro.2015.12.009.
Yabe, J., Nakayama, S.M.M., Ikenaka, Y., Muzandu, K., Ishizuka, M., Umemura, T., 2011. Uptake of lead, cadmium, and other metals in the liver and kidneys of cattle near a lead-zinc mine in Kabwe, Zambia. Environ. Toxicol. Chem. 30, 1892–1897. https://doi.org/10.1002/etc.580.
Yabe, J., Nakayama, S.M.M., Ikenaka, Y., Muzandu, K., Choongo, K., Mainda, G., Kabeta, M., Ishizuka, M., Umemura, T., 2013. Metal distribution in tissues of free-range chickens near a lead-zinc mine in Kabwe, Zambia. Environ. Toxicol. Chem. 32, 189–192. https://doi.org/10.1002/etc.2029.
Yabe, J., Nakayama, S.M.M., Ikenaka, Y., Yohannes, Y.B., Bortey-Sam, N., Oroszlany, B., Muzandu, K., Choongo, K., Kabalo, A.N., Ntapisha, J., Mweene, A., Umemura, T., Ishizuka, M., 2015. Lead poisoning in children from townships in the vicinity of a lead-zinc mine in Kabwe, Zambia. Chemosphere 119, 941–947. https://doi.org/10.1016/j.chemosphere.2014.09.028.
Yabe, J., Nakayama, S.M., Nakata, H., Toyomaki, H., Yohannes, Y.B., Muzandu, K., Kataba, A., Zyambo, G., Hiwatari, M., Narita, D., Yamada, D., Hangoma, P., Munyinda, N.S., Mufune, T., Ikenaka, Y., Choongo, K., Ishizuka, M., 2020. Current trends of blood lead levels, distribution patterns and exposure variations among household members in Kabwe, Zambia. Chemosphere 243, 125412. https://doi.org/10.1016/j.chemosphere.2019.125412.
Yozzo, K.L., McGee, S.P., Volz, D.C., 2013. Adverse outcome pathways during zebrafish embryogenesis: a case study with paraoxon. Aquat. Toxicol. 126, 346–354. https://doi.org/10.1016/j.aquatox.2012.09.008.
Zhao, J., Zhang, Q., Zhang, B., Xu, T., Yin, D., Gu, W., Bai, J., 2019. Developmental exposure to lead at environmentally relevant concentrations impaired neurobehavior and NMDAR-dependent BDNF signaling in zebrafish larvae. Environ. Pollut. 113627. https://doi.org/10.1016/j.envpol.2019.113627.
Zhong, B., Wang, X., Mao, H., Wan, Y., Liu, Y., Zhang, T., Hu, C., 2017. A mechanism underlies fish GRP78 protection against Pb2+ toxicity. Fish Shellfish Immunol. 66, 185–188. https://doi.org/10.1016/j.fsi.2017.03.056.

SCIENTIFIC REPORTS
nature research

OPEN

Assessing the population-wide exposure to lead pollution in Kabwe, Zambia: an econometric estimation based on survey data

Daichi Yamada[1]✉, Masato Hiwatari[2], Peter Hangoma[3], Daiju Narita[1], Chrispin Mphuka[4], Bona Chitah[4], John Yabe[5], Shouta M. M. Nakayama[6], Hokuto Nakata[6], Kennedy Choongo[5] & Mayumi Ishizuka[6]

This study quantitatively assessed the population-wide lead poisoning conditions in Kabwe, Zambia, a town with severe lead pollution. While existing data have reported concerning blood lead levels (BLLs) of residents in pollution hotspots, the data representing the entire population are lacking. Further, selection bias is a concern. Given the lack of compulsory testing schemes, BLLs have been observed from voluntary participants in blood sampling surveys, but such data can represent higher or lower BLLs than the population average because of factors simultaneously affecting participation and BLLs. To illustrate the lead poisoning conditions of the population, we expanded the focus of our surveys and then econometrically estimated the BLLs of individuals representing the population, including those not participating in blood sampling, using background geographic, demographic, and socioeconomic information. The estimated population mean BLL was 11.9 µg/dL (11.6–12.1, 95% CI), lower than existing data because of our wide focus and correction of selection bias. However, the scale of lead poisoning remained immense and 74.9% of residents had BLLs greater than 5 µg/dL, the standard reference level for lead poisoning. Our estimates provide a deeper understanding of the problem and a foundation for policy intervention designs.

Lead poisoning is one of the most serious and harmful consequences of environmental pollution. High levels of lead intake adversely affect the functioning of the circulatory and nervous systems, which can be fatal in extreme cases, whereas low-level exposure can also reduce cognitive ability and cause developmental disorders[1–4]. The adverse health effects can further result in poor school performance, lowered educational attainment and lifetime earning, and behavioural disorders[5–8]. While the use of lead in certain products, such as gasoline and paints, has been globally banned or reduced, lead poisoning remains imposing considerable costs to society, particularly in low- and middle-income countries, owing to the continued use of lead in various products, mining and smelting activities, and the lack of remediation for contaminated environments[4,9,10].

Kabwe, Zambia, provides a devastating example of lead pollution. The fourth largest town with a population of approximately 200,000 as of 2010 was once the site of prominent lead and zinc mining activities, and the pollution problem has received attention since the 1970s[11]. Although the mine was formally closed in 1994, mining residues were abandoned in a dumping site adjacent to residential areas, locally known as Black Mountain, and continued to contaminate surrounding areas through the flow of wind and water[12–15]. Presently, Kabwe is listed as one of the ten most polluted sites in the world and the health conditions of the residents are concerning[16,17]. Lead poisoning is often measured by blood lead levels (BLLs). Recent standards, such as the one adopted by the Centers for Disease Control and Prevention (CDC) of the United States[18], often regard 5 µg/dL as a reference level for lead poisoning, and chelation therapy is recommended for those with BLLs above 45 µg/dL. We also

[1]Graduate School of Arts and Sciences, The University of Tokyo, Tokyo 153-8902, Japan. [2]Faculty of Economics and Business, Hokkaido University, Sapporo, Hokkaido 060-0809, Japan. [3]School of Public Health, The University of Zambia, Lusaka, Zambia. [4]School of Humanity and Social Sciences, The University of Zambia, Lusaka, Zambia. [5]School of Veterinary Medicine, The University of Zambia, Lusaka, Zambia. [6]Faculty of Veterinary Medicine, Hokkaido University, Sapporo, Hokkaido 060-0818, Japan. ✉email: dyamada@global.c.u-tokyo.ac.jp

adopt these levels for reference—although health damages have been reported for BLLs below 5 μg/dL[1,4], and we do not imply that BLLs below 5 μg/dL are safe. Previous studies on Kabwe have reported BLLs exceeding 45 μg/dL, including the levels normally considered fatal[15,19–22]. The scale of the problem is also large. According to the Toxic Sites Identification Program (TSIP)[23], Kabwe's lead contamination affects the largest number of people, with 120,000, among all the confirmed cases of lead contamination around the world.

Despite these alarming reports, representative data of the extent of lead poisoning among the entire population of Kabwe are lacking. This can be attributed to two issues related to data collection. First, most previous surveys have primarily focused on a small sample of data collected from children residing in areas around the mining sites. Although the pollution problem is the most acute in these areas, and children are generally at the highest risk of lead poisoning[4,18], the data coverage has been far from representative. Second, while BLL data were obtained from those who voluntarily participated in studies, given the lack of public mechanisms for formal and compulsory blood lead testing, there could be selection bias in the data, a problem widely recognised in the medical, statistical, public health, and economics literature[24–28]. Data from voluntary (or self-selected) participants in studies generally can fail to reflect the conditions of the population if certain factors simultaneously affect participation decisions and the outcomes of interest. In the context of our study, the residents voluntarily participating in the blood sampling can be those particularly concerned about or suspected to have lead poisoning, and their BLLs can be lower or higher than the population average. Various background characteristics, including both observable (e.g. education, age, employment and living standards) and unobservable ones (e.g. health preferences), can also form their willingness and constraints to participate and directly affect BLLs. As the demographic composition, socioeconomic conditions and pollution levels are diverse in Kabwe, data reflecting these diversities and correcting for potential selection bias are essential.

The purpose of this study is to quantitatively assess the prevalence of lead poisoning among the entire population of Kabwe (administratively, the district of Kabwe). Our methodology to accomplish this purpose is twofold. First, we chose our sample individuals based on random sampling covering the entire Kabwe district. Although we could obtain BLL data from the subset of the chosen individuals who voluntarily participated in blood sampling, this expanded our focus beyond that of previous studies and helped define the target samples representing the population. Quick results of the blood sampling survey are available elsewhere[22]. Second, we employed econometric models to estimate BLLs for the representative sample individuals. Concurrently with the blood sampling survey, we conducted a household survey to obtain background socioeconomic, demographic, and geographic information for the sample individuals, including those who did not participate in the blood sampling survey. We then used these data to econometrically estimate the equation to determine BLLs and, finally, calculated the BLLs of the entire sample individuals. We paid attention to the potential differences in both observable and unobservable characteristics between the participants and non-participants under two econometric methods: ordinary least squares (OLS) and Heckman's sample selection model[24].

The contributions of our study are twofold. First, this study illustrates the severity and diversity of the lead pollution problem in Kabwe and help policymakers design remedial measures. This study is the first attempt to systematically obtain representative estimates of the lead poisoning conditions of residents in the entire Kabwe district. The estimated mean BLL was 11.9 μg/dL and 74.9% of residents had BLLs above the standard reference level of 5 μg/dL. Data representing the population are important to fully understand the pollution problem in Kabwe. Representative data can also serve as a foundation for a policy intervention design and cost–benefit analysis. Further, our estimates shed light on the extent of risks facing low- and middle-income countries, contributing to studies quantifying the global burden of general and pollution-related diseases[29–32]. Despite the substantial impact of lead poisoning on the global disease burden, there remain gaps in the literature, and existing data do not precisely depict the burden of diseases at contaminated sites[31].

The second contribution is methodological and refers to the management of selection bias. Health surveys are often subject to selection bias analogous to our data, which can lead to biased conclusions[27,28]. The methodology adopted not only is consequential for bias mitigation in the current study. Although the details of our specifications would need modifications, our approach is applicable to many other cases where formal and compulsory testing for a disease is lacking.

Methods

Data collection and potential selection bias. We conducted two joint surveys from July to September 2017 in Kabwe: the Kabwe Household Socioeconomic Survey (KHSS) 2017 conducted by the Central Statistical Office of Zambia and University of Zambia under the supervision of the authors, and a BLL survey performed by the authors. The surveys were approved by the University of Zambia Research Ethics Committee (UNZAREC; REF. No. 012-04-16). Further approvals were granted by the Ministry of Health through the Zambia National Health Research Ethics Board and the Kabwe District Medical Office. The data were collected in accordance to the Declaration of Helsinki, and the informed consent was obtained from all the study participants including the parents/legal guardian of the minor subjects for participating in the study.

The two surveys were designed consistently and targeted the same sample households selected in the following two-step approach. In the first step, utilising the Zambia's national census frame which divides the Kabwe district into 384 standard enumeration areas (SEAs), we randomly selected 40 SEAs across the entire district. In the second step, we randomly selected 25 households (and a few replacements) from each sampled SEA. The sampling weights were generated to account for population differences across the SEAs.

The KHSS 2017 conducted interviews with 895 households (4,900 individuals) at houses and collected data on socioeconomic, demographic and geographic information. The response rate was 88.2%, and we could regard the data adjusted by the sampling weights as representative of the entire Kabwe population (for more details of the survey, see the report[33]).

To obtain BLL data, we conducted a blood sampling survey concurrently with the KHSS 2017. For hygiene and ethical considerations, we selected 13 local clinics to perform the blood sampling, instead of collecting blood at houses. We invited up to four members (two children aged 10 years or younger and their parents or guardians) from each sample household for the blood sampling. We prioritised young children over children older than 10 years old. The invitations were made sequentially. We assigned identical venues and dates for households from the same SEAs. The typical assigned dates had a 3-day window from the day after the invitation. However, we allowed for some flexibility and sampled the blood of those who visited the clinic even after the assigned time window, as long as the clinic was operational for households from other SEAs. Therefore, the window for blood sampling was effectively the number of days from the day after the invitation until the pre-set blood sampling period in each clinic was over, which had a substantial variation across households from 3 days to a month. We revisit this feature of the survey window when setting up our econometric model later. A total of 372 households (41.6%) participated in the blood sampling and, on average, 2.2 members from the participating households provided blood samples.

We performed blood digestion and metal extraction as described by our previous study[34] with minor modifications and measured BLLs using an Inductively Coupled Plasma-Mass Spectrometer (ICP-MS). In addition, we also measured BLLs with a portable analyser, LeadCare II, to obtain quick results[22]. However, we in this study focus on the ICP-MS data, considering their general accuracy. See the Supplementary Material Section S1 for details on the methods used to measure BLLs and the difference in the data between the two analysers.

Regardless of the accuracy of the techniques, however, we further need to account for the risk of selection bias in the BLL data. In the absence of formal and compulsory testing mechanisms, we relied on individuals' voluntary (self-selected) visits to the clinics. However, the participants in blood sampling could have traits leading to higher or lower BLLs than the population. Such traits can include education, gender, age and living standards. The survey design did not prioritise children aged 11 years or older, and this could also contribute to the deviation of characteristics, although a small number of such children attended clinics. Moreover, certain unobservable characteristics affecting BLLs can further differ between the participants and non-participants. For example, those with greater preferences for health possibly had low BLLs but tended to participate in the blood sampling surveys, whereas those with a high innate physiological capacity for lead excretion possibly tended not to participate because they had low BLLs and did not perceive symptoms of lead poisoning. These issues can lead to selection bias, and the raw data observed from the voluntary participants can fail to illustrate the lead poisoning conditions of the population.

BLL estimation approach. To correct for potential selection bias, we first estimated the equations to explain BLLs of children aged 0–10 years and adults aged 19 years or above. Then, using the estimated equations, we calculated BLLs for all individuals, including children aged 11–18 years and those in the other age groups who did not participate in the blood sampling.

BLLs generally depend on the ambient pollution level, the opportunities of exposure to pollution, the physiological capacity of lead absorption and excretion, and the knowledge and technologies used to prevent lead poisoning. We controlled for ambient pollution levels by including the distance, direction, and altitude of household location—the first two variables are with respect to the mine waste dumping site (Black Mountain). The remaining factors were measured by age and various other individual and household characteristics denoted by $\boldsymbol{X}_i$. Data for these variables are available regardless of participation in blood sampling. We assumed the following equation for BLL:

$$\begin{aligned}\log BLL_i = {} & \beta_{dis} \log distance_i + \beta_{dir1} direction_i + \beta_{dir2} direction_i^2 \\ & + \beta_{alt} altitude_i + f\left(age_i\right) + \boldsymbol{X}_i \boldsymbol{\gamma}' + \varepsilon_i.\end{aligned} \tag{1}$$

The logarithmic form for BLL adjusts its distribution to approximately normal—BLL is bounded from below and has a skewed distribution—and allows the factors on the right-hand side to have proportional effects rather than level effects. ε_i is the independent and identically distributed error term that captures noise, such as casual fluctuations and measurement errors in BLLs, and the effects of unobservable factors. While we presented a single equation above, we assumed different equations for children aged 0–10 years and adults aged 19 years or above.

Below, we discuss our specification in detail.

Geographic factors. Existing studies have examined the relationship between the geographic location and ambient pollution level[12–14]. Since lead is transported from the mine waste dumping site through the flow of wind and water, the distance from the site is negatively correlated with ambient lead levels. The soil lead contamination spreads to the western side of the site, particularly towards the west-northwest (WNW), which corresponds to the direction of the prevailing local wind. The contamination also slightly extends to the low-elevation south-eastern side, reflecting pollution transported by water. The northern and southern sides are the least contaminated.

We defined $distance_i$ as the distance between the mine waste dumping site and the location of i's household, with $\beta_{dis} < 0$ expected. Also, we assumed that the WNW is the most contaminated and, accordingly, we defined $direction_i$ as the radian of the acute angle passing through WNW, the mine waste dumping site, and the location of i's household. That is, the household location is WNW at $direction_i = 0$, either north-northeast or south-southwest at $\pi/2$, and east-southeast (ESE) at π. We employed a quadratic specification in Eq. (1), which allows BLLs to have two peaks at WNW and ESE if $\beta_{dir1} < 0$, $\beta_{dir2} > 0$ and $-\beta_{dir1}/(2\beta_{dir2}) < \pi$. We statistically assessed the appropriateness of the specification for direction in Supplementary Material Section S2. We also

used altitude in metres, $altitude_i$, considering that elevated areas can be less exposed to dust and water flows, although the general tendency of land elevation can be absorbed by the direction variables.

Age and other covariates. For children, we assumed a non-linear relationship between their ages and BLLs and defined the following functional form:

$$f(age_i) = \left[\phi_0 + \phi_1 mage_i + \phi_2 mage_i^2\right] \times I(age_i < 2) + \phi_3 age_i \times I(age_i \geq 2). \quad (2)$$

$I(\cdot)$ is an indicator function that takes the value of 1 if the argument condition is satisfied, and $mage_i$ denotes age in months. The functional form reflects the findings in the literature. Young children are generally at a high risk of lead poisoning. Playing outside and age-appropriate hand-to-mouth behaviours expose them to lead, and their gastrointestinal absorption of lead is high[4]. Foetuses and infants born to exposed mothers absorb lead in utero and through breastfeeding[35]. Consequently, BLLs often reach a peak at or before the age of 24 months and then decrease as children grow older, reflecting their physical and behavioural growth[1,36]. Thus, we employed a specification that allows an inverted U-shaped relationship between the logarithmic BLL and age up to 23 months, but assume a linearly decreasing relationship between the two factors for children aged 2 years or above.

For adults, the physiological foundation of the BLL-age relationship is not clear, but age-related changes in metabolism and lifestyle can affect BLLs. We simply assumed a log linear relationship between BLL and age for adults.

In addition, we used the following individual and household characteristics, denoted as $\boldsymbol{X}_i$, for children: a dummy variable for female; the mothers' education level (grades), which reflects their general, health-related and lead-related knowledge; a dummy variable for children whose mothers were absent (the mothers' education level was set at zero for such children); a dummy variable for female-headed households; household size; dependency ratio (the proportion of household members aged 0–15 years and 65 years or above); and the log of per capita household expenditure, which measures living standards. We also used dummy variables for household location: urban areas, small-scale farming areas, large-scale farming areas, and the Makululu compound—an area of informal settlement where public services are poorly delivered. We set urban area as the base category.

For adults, we continued to use the dummy variables for female and household location, household size and dependency ratio but dropped the variables related to mothers and household heads. The per capita household expenditure was not used, either, because it is not exogenous for adults. Instead, we used their own education level, which reflects living conditions to certain extent as well as knowledge levels. We also used a dummy variable for marital status, which takes the value of one for either married or co-habiting individuals, and the duration of residence in Kabwe (in years) to account for the effects of long-term lead exposure.

Econometric methods to estimate BLL equation. We considered two methods to estimate Eq. (1). The first one is OLS, which directly estimates Eq. (1) from the data of the participants in the blood sampling survey. If the bias in BLLs are attributable to the difference in observable factors between the participants and non-participants, then the OLS estimate of Eq. (1) is unbiased and can be used to obtain estimates representing the population. However, as previously mentioned, unobservable characteristics can also affect both BLLs and participation decisions. This can disrupt the error term distribution and bias the OLS estimate of Eq. (1).

To account for this risk, we also adopted Heckman's sample selection model[24]. This model corrects for the bias in unobservable factors by simultaneously estimating the probability of participation (selection equation) for the entire sample, including non-participants. Specifically, we considered the following selection equation:

$$\begin{aligned}\Pr(i\ participates) = \Psi\{&\delta_{dis}\log distance_i + \delta_{dir1} direction_i + \delta_{dir2} direction_i^2 \\ &+ \delta_{alt} altitude_i + g(age_i) + \boldsymbol{X}_i\boldsymbol{\xi}' + \zeta\, window_i\},\end{aligned} \quad (3)$$

where Ψ is the normal distribution function with the probability density function of ψ, $\boldsymbol{X}_i$ is the same as in Eq. (1), and $g(age_i)$ has the functional forms identical to $f(age_i)$. The bias in Eq. (1) can be fixed by estimating Eq. (1) with the inverse Mills ratio, ψ/Ψ.

In the sample selection model, the use of an exclusion restriction variable, which affects the probability of participation but not BLL, is preferable. We used the number of days of the blood sampling window denoted by $window_i$ as an exclusion restriction. As described above, the blood sampling window was effectively the number of days that the assigned clinic remained operational for blood sampling after the day following the invitation. Other factors being equal, households that received early invitations and had longer time windows would more easily manage to attend clinics and would have higher probabilities of participation. The exogenous nature of the blood sampling window renders it irrelevant for BLLs.

Estimation of the representative BLLs. After obtaining the BLL equations, we estimated the BLLs of the representative sample individuals by inputting their characteristics on the right-hand side of the equations. We applied the survey's sampling weights when aggregating the estimated BLLs.

To estimate the BLLs of adolescents aged 11–18 years, who were basically not covered in our BLL survey and thus not used in the BLL equation estimations, we used the equation for children aged 0–10 years, assuming that age-BLL trend, which we expected to be negative, would hold up to the age of 18 years.

Next, we calculated the number of the residents with BLLs above 5 μg/dL by interacting the estimated proportion of those with such BLLs and the total population. Considering the population growth, we used the population estimates of our own[33] and the Central Statistical Office of Zambia[37], both as of 2017, instead of 200,000 as of 2010.

	All	Male	Female	0–5 years	6–10 years	11–18 years	19 years or above
Panel A: BLLs (μg/dL)							
Mean	15.9	17.5	14.7	22.9	21.0	14.6	11.3
(95% CI)	(14.9, 17.0)	(15.7, 19.2)	(13.4, 16.0)	(19.8, 26.0)	(18.7, 23.3)	(9.2, 20.0)	(10.4, 12.3)
25 percentile	4.6	5.3	3.9	5.9	6.8	5.3	3.6
50 percentile	11.3	11.9	11.0	18.5	20.7	10.2	9.2
75 percentile	22.4	24.2	20.0	31.6	30.1	23.8	15.2
Panel B: percentage of those with the following BLLs							
< 5 μg/dL	27.5	24.0	30.2	22.4	16.8	23.8	33.6
5–45 μg/dL	67.1	70.2	64.8	63.4	78.1	76.2	64.4
> 45 μg/dL	5.3	5.7	5.0	14.2	5.2	0.0	2.0
Observations	806	349	457	183	154	21	447

Table 1. Observed blood lead levels (BLLs) of participants. Based on surveys in Jul–Sep 2017. *CI* confidence interval.

Further, we present two graphical results. The first one is an in-depth examination of the mean BLLs across age groups. In the second one, we simulated the geographic variation of the mean BLLs. We divided the entire Kabwe district into 1 km × 1 km grids, and estimated the mean BLL in each grid cell. Distance and direction were measured for each cell and other independent variables were measured by the means in the ward—official inner-district division—to which the cell corresponds (we provide additional technical notes before showing results).

All estimations were performed using Stata 15 software.

Results

Observed BLL data. The observed mean BLL among the participants in the blood sampling survey was 15.9 μg/dL, in which we did not make econometric adjustments (Table 1). The 50 percentile (median) BLL was 11.3 μg/dL, indicating a skewed distribution. Male BLLs tended to be higher than female ones. BLLs were generally negatively associated with age. Overall, approximately 5.3% of the participants reported BLLs exceeding 45 μg/dL. This proportion was 14.2% among children aged 0–5 years, but only nine adults (2.0%) reported such high BLLs. The observation size for those aged 11–18 years were small.

Characteristics of blood sampling participants and non-participants. The characteristics of the participants and non-participants in blood sampling were not identical. Among children aged 0–10 years, the two groups significantly differed in terms of household location, size and living standards, with *P* values below 0.10 (Table 2). Among adults, the characteristics of the two groups were more clearly distinct, with *P* values mostly below 0.01 (Table 3). Therefore, the participants in blood sampling were not a random subset of our study target. Their BLLs (Table 1) can fail to represent the lead poisoning conditions of the population.

Estimated BLL equation for children. In the BLL equation estimation based on OLS (Table 4, column I), the coefficients of the distance and direction variables had expected signs with *P* values below 0.01. BLL was decreasing in the distance, whereas the relationship between BLL and direction was U-shaped, with the highest peak at WNW, the lowest peaks at northeast and south ($direction_i \approx 5\pi/8$), and a small peak at ESE. The explanatory powers of distance and direction were so large that R^2 remained at 0.67 even after dropping other independent variables. Considering the strong powers of these factors and given that the values of these variables were similar among neighbouring households, we clustered standard errors for SEAs (in all the subsequent estimations as well). Altitude did not have a significant effect.

Age also had a significant effect. BLL peaked at 16.5 months, which is close to the average age of children to stop breastfeeding in Kabwe, 15.8 months[33]. This suggests a role of lead transfer through breastfeeding. BLL decreased by approximately 5% per year from the age of two years.

Among other factors, the dependency ratio raised BLLs, albeit with a marginally significant *P* value of 0.07. This suggests the possibility that parents in households with high dependency ratios failed to take sufficient precautionary measures for lead exposure. Mothers' education reported a negative coefficient but its effect was insignificant with a *P* value of 0.10. Similarly, the per capita household expenditure did not have a significant coefficient.

Under Heckman's sample selection model, the probability of participation significantly depended on age and household size (Table 4, column II). Although household income per capita reported significantly different means between the participants and non-participants (Table 2), its effect on participation was insignificant after other factors were controlled for. Conversely, while the mean age was almost identical between the two groups (Table 2), age had a significant non-linear effect on the probability of participation. The exclusion restriction, the duration of blood sampling window, had a significant effect with a *P* value below 0.01. However, the resulting BLL equation was similar to the OLS estimate (Table 4, column III). The inverse Mills ratio did not have a significant effect on BLLs with the *P* value of selection bias greater than 0.10. Therefore, selection bias was limited in terms of unobservable factors and the OLS estimate of the BLL equation was not significantly biased.

	Participants	Non-participants	
	Mean ± SD	Mean ± SD	*P* value
Distance	6.25 ± 6.03	6.07 ± 5.31	0.60
Direction	1.12 ± 0.85	1.32 ± 0.85	< 0.01
Altitude	1,185 ± 9.78	1,185 ± 8.97	0.83
Age	5.16 ± 2.88	5.21 ± 3.20	0.81
Female	0.46 ± 0.50	0.49 ± 0.50	0.33
Household size	6.45 ± 2.57	6.98 ± 2.72	< 0.01
Dependency ratio	0.54 ± 0.14	0.54 ± 0.15	0.86
Mothers' education	6.37 ± 4.36	6.39 ± 4.77	0.93
Mother absent	0.17 ± 0.37	0.19 ± 0.40	0.26
Female head	0.23 ± 0.42	0.22 ± 0.41	0.62
Household expenditure per capita[a]	414 ± 416	505 ± 777	0.04
Urban area	0.31 ± 0.46	0.36 ± 0.48	0.08
Small-scale farming area	0.27 ± 0.43	0.20 ± 0.40	0.08
Large-scale farming area	0.13 ± 0.34	0.19 ± 0.39	0.02
Makululu compound	0.31 ± 0.46	0.25 ± 0.43	0.02
Blood sampling window	11.2 ± 9.88	9.26 ± 8.36	< 0.01
Observations	338	1,176	

Table 2. Summary statistics for the characteristics of children aged 0–10 years. *P* values of *t* tests on the null hypothesis of identical mean. [a]Monthly values in local currency, Zambian kwacha. Based on surveys in Jul–Sep 2017.

	Participants	Non-participants	
	Mean ± SD	Mean ± SD	*P* value
Distance	6.64 ± 6.36	5.23 ± 4.68	< 0.01
Direction	1.13 ± 0.81	1.38 ± 0.90	< 0.01
Altitude	1,185 ± 10.3	1,187 ± 8.65	0.01
Age	41.7 ± 14.8	35.6 ± 14.8	< 0.01
Female	0.64 ± 0.48	0.51 ± 0.50	< 0.01
Own education	8.02 ± 3.91	9.86 ± 4.06	< 0.01
Married	0.77 ± 0.42	0.51 ± 0.11	< 0.01
Duration of residence in Kabwe	26.2 ± 15.3	21.7 ± 13.8	< 0.01
Household size	5.68 ± 2.51	6.46 ± 2.94	< 0.01
Dependency ratio	0.46 ± 0.21	0.40 ± 0.21	< 0.01
Urban areas	0.31 ± 0.46	0.48 ± 0.11	< 0.01
Small-scale farming areas	0.27 ± 0.45	0.15 ± 0.35	< 0.01
Large-scale farming areas	0.13 ± 0.33	0.16 ± 0.37	0.07
Makululu compound	0.29 ± 0.46	0.22 ± 0.41	< 0.01
Blood sampling window	10.8 ± 9.33	9.29 ± 7.72	< 0.01
Observations	447	1,923	

Table 3. Summary statistics for the characteristics of adults aged 19 years or above. *P* values of *t* tests on the null hypothesis of identical mean. Based on surveys in Jul–Sep 2017.

Estimated BLL equation for adults. Under OLS, the effects of distance and direction were similar to those for children: BLL decreased with distance and had a U-shape relationship with direction, reaching the lowest levels in the northeast and south (Table 5, column I). Altitude had a negative coefficient, but was not significant with a *P* value above 0.10. Age and being female had significantly negative effects, although the marginal effect of age was moderate compared to that for children, approximately 0.5% per year. Own education also had a significantly negative effect on BLL, suggesting that knowledge or living conditions indicated by education levels affected adult BLLs. Duration of residence in Kabwe significantly increased BLLs.

The remaining columns show the results under Heckman's sample selection model. The participation decisions of adults depended on various individual and household characteristics. Those with high levels of education and from large households were less likely to participate, whereas older adults, women, and those either married or co-habiting, having resided in Kabwe for a prolonged period, and from households with high dependency

	(I) OLS BLL		(II) Heckman selection		(III) Heckman BLL	
Log distance	−0.755	(<0.01)	−0.0397	(0.78)	−0.753	(<0.01)
Direction	−1.08	(<0.01)	−0.485	(0.13)	−1.07	(<0.01)
Direction squared	0.294	(<0.01)	0.123	(0.21)	0.293	(<0.01)
Altitude	0.0053	(0.44)	−0.0038	(0.55)	0.0053	(0.41)
Being < 2 years old	−2.23	(0.04)	−1.48	(<0.01)	−2.21	(0.03)
Monthly age, < 2 years old	0.308	(0.05)	0.122	(0.07)	0.307	(0.03)
Monthly age squared, < 2 years old	−0.0093	(0.07)	−0.0037	(0.14)	−0.0093	(0.05)
Yearly age, ≥2 years old	−0.0507	(<0.01)	−0.0511	(<0.01)	−0.0500	(<0.01)
Female	−0.0188	(0.68)	−0.0618	(0.42)	−0.0179	(0.68)
Mothers' education	−0.0212	(0.10)	−0.0007	(0.95)	−0.0212	(0.09)
Mother absent	0.0145	(0.92)	−0.144	(0.28)	0.0164	(0.90)
Female head	−0.0226	(0.75)	0.0619	(0.54)	−0.0241	(0.72)
Household size	−0.0202	(0.11)	−0.0464	(<0.01)	−0.0194	(0.08)
Dependency ratio	0.469	(0.07)	−0.413	(0.24)	0.474	(0.06)
Log per capita household expenditure	0.0181	(0.75)	−0.0438	(0.55)	0.0188	(0.73)
Large-scale farming area	−0.0050	(0.99)	0.363	(0.14)	−0.0101	(0.97)
Small-scale farming area	0.116	(0.59)	−0.0107	(0.96)	0.115	(0.57)
Makululu compound	0.149	(0.26)	−0.189	(0.37)	0.149	(0.24)
Blood sampling window			0.0202	(<0.01)		
Inverse Mills ratio					−0.0193	(0.90)
Constant	−1.71	(0.84)	5.07	(0.50)	−1.77	(0.82)
Observations	338		1,514			
R-squared	0.742					

Table 4. Estimation results of the blood lead level (BLL) and selection equations for children aged 0–10 years. *P* values are in parentheses and calculated based on standard errors clustered for the standard enumeration areas (SEAs), the survey's primary sampling unit. Based on surveys in Jul–Sep 2017. *OLS* ordinary least squares.

	(I) OLS BLL		(II) Heckman selection		(III) Heckman BLL	
Log distance	−0.926	(<0.01)	−0.0214	(0.91)	−0.910	(<0.01)
Direction	−1.39	(<0.01)	0.0134	(0.97)	−1.40	(<0.01)
Direction squared	0.386	(<0.01)	−0.0484	(0.68)	0.399	(<0.01)
Altitude	−0.0074	(0.11)	−0.0017	(0.83)	−0.0072	(0.09)
Age	−0.0047	(0.02)	0.0085	(<0.01)	−0.0062	(0.01)
Female	−0.245	(<0.01)	0.388	(<0.01)	−0.307	(<0.01)
Own education	−0.0200	(0.01)	−0.0296	(<0.01)	−0.0155	(0.06)
Married	0.0650	(0.25)	0.617	(<0.01)	−0.0384	(0.63)
Duration of residence	0.0042	(0.04)	0.0058	(0.04)	0.0033	(0.11)
Household size	0.0000	(0.99)	−0.0702	(<0.01)	0.0112	(0.35)
Dependency ratio	0.121	(0.28)	0.401	(0.03)	0.0492	(0.68)
Large-scale farming area	0.516	(0.01)	0.523	(0.13)	0.436	(0.01)
Small-scale farming area	0.470	(<0.01)	0.0157	(0.95)	0.465	(<0.01)
Makululu compound	−0.160	(0.07)	−0.0286	(0.85)	−0.184	(0.07)
Blood sampling window			0.0176	(0.01)		
Inverse Mills ratio					−0.214	(0.15)
Constant	13.2	(0.02)	0.416	(0.97)	13.3	(0.01)
Observations	447		2,370			
R-squared	0.697					

Table 5. Estimation results of the blood lead level (BLL) and selection equation for adults aged 19 years or above. *P* values are in parentheses and calculated based on standard errors clustered for the standard enumeration areas (SEAs), the survey's primary sampling unit. Based on surveys in Jul–Sep 2017. *OLS* ordinary least squares.

	All	Male	Female	0–5 years	6–10 years	11–18 years	19 years or above
Panel A: BLLs (μg/dL)							
Mean	11.9	12.6	11.2	18.2	15.4	11.2	8.9
(95% CI)	(11.6, 12.1)	(12.2, 13.0)	(10.8, 11.5)	(17.3, 19.2)	(14.7, 16.1)	(10.7, 11.6)	(8.6, 9.1)
25 percentile	5.0	5.5	4.6	7.9	6.8	4.9	4.2
50 percentile	8.7	9.5	7.9	12.7	11.8	8.2	6.8
75 percentile	16.1	17.4	14.9	28.1	24.2	17.1	12.0
Panel B: percentage of those with the following BLLs							
< 5 μg/dL	25.1	21.5	28.6	9.6	9.8	26.0	34.9
5–45 μg/dL	74.1	77.7	70.5	85.8	89.9	74.0	65.1
> 45 μg/dL	0.8	0.8	0.8	4.6	0.3	0.0	0.0
Observations	4,898	2,380	2,518	768	746	1,014	2,370

Table 6. Estimated blood lead levels (BLLs) representative of Kabwe population. The survey's population weights were applied. Based on surveys in Jul–Sep 2017. *CI* confidence interval.

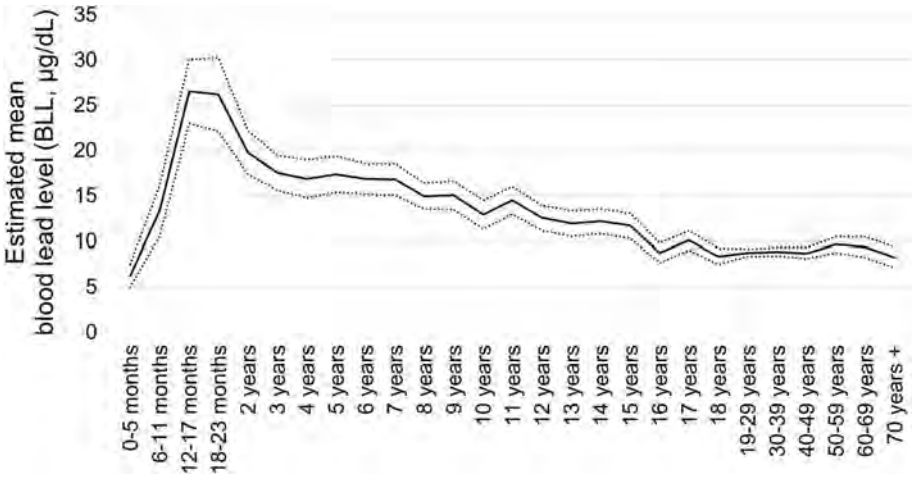

Figure 1. Estimated blood lead levels (BLLs) and age. Solid line: mean. Dotted lines: 95% confidence interval. Based on surveys in Jul–Sep 2017.

ratios were more likely to participate. The duration of the blood sampling window significantly increased the probability of participation. However, similar to the results for children, the inverse Mills ratio did not have a significant effect with *P* value above 0.10.

Representative estimates of lead poisoning conditions. We estimated the BLLs of 4,898 individuals, all but two sample individuals who had missing information, that represent the lead poisoning conditions of the entire population (Table 6). Since the selection bias in terms of unobservable factors was not significantly observed (Tables 4, 5), we used the BLL equations obtained under OLS. All figures hereafter were weighted by the survey's population weights.

The representative mean BLL was 11.9 μg/dL, with a 95% confidence interval of 11.6–12.1 μg/dL, which is 2.4 times higher than the standard reference level of 5 μg/dL. 74.9% of the residents had BLLs above 5 μg/dL. This proportion, as of 2017, corresponds to approximately 202,500 individuals based on our population estimate, 270,389 individuals[33], and to approximately 170,400 individuals based on the relatively moderate population projection of 227,551 individuals by the Central Statistical Office of Zambia[37]. The 50 percentile (median) was 8.7 μg/dL. Men had significantly higher BLLs than women (the *P* value for zero difference is below 0.01). Notably, only 9.6% of children aged 0–5 years and 9.8% of children aged 6–10 years had BLLs below 5 μg/dL, although this study expanded the focus beyond the immediate neighbourhood of the mine waste dumping site. 4.6% of children aged 0–5 years had BLLs above 45 μg/dL, but our estimates did not predict such high BLLs for adolescents aged 11–18 years and adults.

Figure 1 depicts the in-depth relationship between the estimated BLLs and age. After peaking within the ages of 12–23 months, BLLs for children demonstrated a declining trend with age, albeit with fluctuations. Note that the BLLs of those aged 18 years and 19–29 years were continuously connected. This suggests that we successfully estimated the BLLs of those aged 11–18 years from the equation for children aged 0–10 years.

Figure 2 illustrates the simulated geographic distributions of BLLs, separately for children (a) and adults (b). To obtain the figure for children, we set age at 16 months, when BLL reaches the maximum. Thus, the figure for

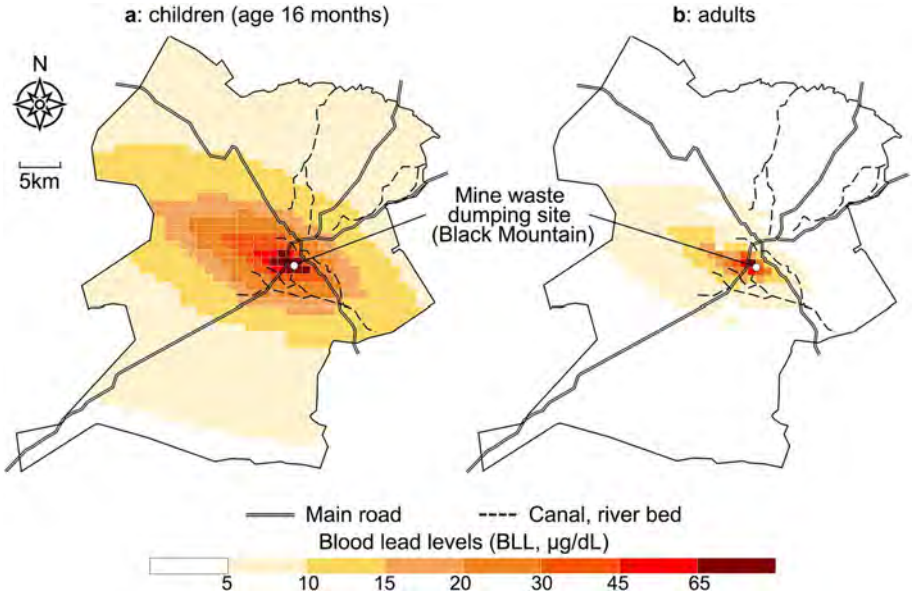

Figure 2. Geographic distribution of estimated blood lead levels (BLLs). (**a**) Children (age 16 months). (**b**) Adults. Based on surveys in Jul–Sep 2017.

children can be considered the geographic distribution of the maximum BLL that a child with average traits is expected to report. Age is set at the local mean for adults, approximately 34–38 years.

For both children and adults, BLLs were high in WNW and ESE. BLLs greater than 45 µg/dL were found in the neighbourhood of the mine waste dumping site. BLLs tended to decrease with distance. However, the BLLs of children, at the maximum, exceeded 5 µg/dL throughout most areas.

Discussion

This study estimated BLLs representative of the lead poisoning conditions among the entire population of Kabwe, Zambia, using the combined dataset of the ICP-MS measures of BLLs and a socioeconomic household survey. As in the previous studies on Kabwe and other health surveys in general, we were faced with the risk of selection bias in the BLL data in terms of both observable and unobservable factors, owing to non-random participation in the blood sampling survey. To overcome this problem, we employed econometric methods that controlled for differences in observable and unobservable factors between participants and non-participants in the blood sampling survey.

Our estimates showed that the mean BLL for the population was 11.9 µg/dL (Table 6), which is 25.2% lower than the mean of the observed BLLs of the participants (15.9 µg/dL, Table 1). While unobservable factors reported a minor bias (Tables 4, 5), the observable factors were not identical between the participants and non-participants (Tables 2, 3). In particular, the participants (or their parents) tended to have lower education levels and resided in Kabwe for a prolonged period, which were factors positively associated with BLLs. The age composition and household location were also different. These differences led to higher BLLs among the participants. Our estimate of the mean BLL was also lower than the ones in existing studies[15,19–21], mainly because their focus was placed mostly on pollution hotspots, but their data could be faced by selection bias similar to our observed data. Further, both our estimated and observed mean BLLs were lower than our early results based on LeadCare II analyser[22]. Although LeadCare II analyser is considered fairly accurate, our samples included higher BLLs than ones to which LeadCare II is often applied, and this apparently led to overestimation of BLLs (see the Supplementary Material Section S2).

Nevertheless, our results illustrate the devastating lead poisoning problems in Kabwe. We confirmed critically high BLLs among children residing in the most contaminated areas. Further, the mean BLL of our estimates was considerably higher than the standard reference level of 5 µg/dL, and the proportion of those with BLLs above this level amounted to 74.9%. Based on our population estimate as of 2017[33], this proportion corresponds to 202,500 individuals (or 170,400 based on another population estimate[37]), which is greater than an existing estimate of 120,000 in the TSIP[23].

These estimates provide a foundation for policy intervention designs. Since lead poisoning was widespread across the entire Kabwe district, interventions that span across the entire population are required. Thus, although immediate interventions, such as chelation therapy proposed under a World Bank project[38], could focus on pollution hotspots, interventions to reduce lead transportation, such as capping the mine waste dumping site with concrete or clean soil, would be of fundamental importance. Our estimates also provide grounds for proper cost–benefit evaluations of interventions. For large-scale interventions, the benefits for the entire population, not only the residents in hotspots, need to be accounted for, and this requires population-level data. Proper cost–benefit evaluations are important for sustainability of interventions as they require large costs and long-term commitment (e.g. monitoring and maintenance).

Our methodology has an implication for other cases of health studies. Medical and clinical data collected through voluntary participation in testing can be subject to analogous selection bias problems to ours, particularly in cases in which formal and compulsory testing schemes are lacking. The extent of disruptions caused by selection bias can vary by case, and our econometric specifications would require modifications if applied to other cases. Nevertheless, the principle of our approach—collection of background data from the representative sample individuals, including those who did not participate in the medical testing, and correction of deviation in the characteristics of the participants—is applicable to various cases in which selection bias is a concern.

Finally we address the limitations of our study. First, our methodology was not employed to perfectly predict the BLL of each individual. Our estimates reflected variations of BLLs by gender, age groups, areas within Kabwe and various other factors but did not fully reflect idiosyncratic variations. Certain individuals with particular idiosyncratic factors can have high or low BLLs even if their traits and residential locations are associated with low or high BLLs. The second limitation, related to the first one, is the general difficulty to econometrically predict extreme outcomes. Such outcomes are scarce and idiosyncratic factors prevail over systematic ones. In our case, a small proportion of adults did report such BLLs, but our estimates did not predict such BLLs for adults. Finally, while we employed BLL as the measure, a comparison with alternative measures would improve the understandings of the lead poisoning problem in Kabwe. For example, bone and tooth conditions would reflect the effects of long-term lead exposure better, and clinical conditions would reflect idiosyncratic variations in the sensitivity to lead intake. Analysing these alternative measures could be the topic for further research.

Data availability

The datasets used in the current study are not publicly available based on the ethical approvals from the University of Zambia Research Ethics Committee, the Ministry of Health of Zambia and the Kabwe District Medical Office.

Received: 2 April 2020; Accepted: 24 August 2020
Published online: 15 September 2020

References

1. Canfield, R. L. *et al.* Intellectual impairment in children with blood lead concentrations below 10 μg per deciliter. *N. Engl. J. Med.* **348**, 1517–1526 (2003).
2. Dapul, H. & Laraque, D. Lead poisoning in children. *Adv. Pediatr.* **61**, 313–333 (2014).
3. Meyer, P. A., Brown, M. J. & Falk, H. Global approach to reducing lead exposure and poisoning. *Mutat. Res.* **659**, 166–175 (2008).
4. World Health Organization (WHO). *Childhood Lead Poisoning* (WHO Press, Geneva, 2010).
5. Aizer, A., Currie, J., Simon, P. & Vivier, P. Do low levels of blood lead reduce children's future test scores?. *Am. Econ. J. Appl. Econ.* **10**, 1–36 (2018).
6. Aizer, A. & Currie, J. Lead and juvenile delinquency: new evidence from linked birth, school and juvenile detention records. *Rev. Econ. Stat.* **101**, 575–587 (2019).
7. Miranda, M. L. *et al.* The relationship between early childhood blood lead levels and performance on end-of-grade tests. *Environ. Health Persp.* **115**, 1242–1247 (2007).
8. Needleman, H. Lead poisoning. *Annu. Rev. Med.* **55**, 209–222 (2004).
9. Attina, T. M. & Trasande, L. Economic costs of childhood lead exposure in low- and middle-income countries. *Environ. Health Perspect.* **121**, 1097–1102 (2013).
10. Dooyema, C. A. *et al.* Outbreak of fatal childhood lead poisoning related to artisanal gold mining in northwestern Nigeria, 2010. *Environ. Health Perspect.* **120**, 601–607 (2012).
11. Clark, A. R. L. Placental transfer of lead and its effects on the newborn. *Postgrad. Med. J.* **53**, 674–678 (1977).
12. Kříbek, B. *et al.* Soil contamination near the Kabwe Pb-Zn smelter in Zambia: environmental impacts and remediation measures proposal. *J. Geochem. Explor.* **197**, 159–173 (2019).
13. Nakayama, S. M. M. *et al.* Metal and metalloid contamination in roadside soil and wild rats around a Pb–Zn mine in Kabwe, Zambia. *Environ. Pollut.* **159**, 175–181 (2011).
14. Tembo, B. D., Sichilongo, K. & Cernak, J. Distribution of copper, lead, cadmium and zinc concentrations in soils around Kabwe town in Zambia. *Chemosphere* **63**, 497–501 (2006).
15. Yabe, J. *et al.* Lead poisoning in children from townships in the vicinity of a lead–zinc mine in Kabwe, Zambia. *Chemosphere* **119**, 941–947 (2015).
16. Blacksmith Institute & Green Cross Switzerland. *The World's Worst 2013: Top Ten Toxic Threats*. https://www.worstpolluted.org/docs/TopTenThreats2013.pdf (Pure Earth, 2013).
17. Human Rights Watch. *We Have to Be Worried: The Impact of Lead Contamination on Children's Rights in Kabwe, Zambia*. https://www.hrw.org/report/2019/08/23/we-have-be-worried/impact-lead-contamination-childrens-rights-kabwe-zambia (2019).
18. Centers for Disease Control and Prevention (CDC). *Low Level Lead Exposure Harms Children: A Renewed Call for Primary Prevention* (CDC, Atlanta, 2012).
19. Bose-O'Reilly, S. *et al.* Lead intoxicated children in Kabwe, Zambia. *Environ. Res.* **165**, 420–424 (2018).
20. Caravanos, J., Fuller, R. & Robinson, S. Notes from the field: severe environmental contamination and elevated blood lead levels among children—Zambia, 2014. *Morb. Mortal. Wkly. Rep.* **63**, 1013 (2014).
21. Mbewe, A., Muneku, E., Michelo, C. & Siulapwa, Y. Blood lead levels and likely adverse health outcomes in under five children in Kabwe, Zambia. *Int. J. Sci. Basic Appl. Res.* **24**(5), 171–183 (2015).
22. Yabe, J. *et al.* Current trends of blood lead levels, distribution patterns and exposure variations among household members in Kabwe, Zambia. *Chemosphere* **243**, 125412 (2020).
23. Toxic Sites Identification Program (TSIP). https://www.pureearth.org/projects/toxic-sites-identification-program-tsip/ (Pure Earth).
24. Heckman, J. J. Sample selection bias as a specification error. *Econometrica* **47**, 153–161 (1979).
25. Rosenbaum, P. R. & Rubin, D. B. The central role of the propensity score in observational studies for causal effects. *Biometrika* **70**, 41–55 (1983).
26. Duflo, E., Glennerster, R. & Kremer, M. Using randomization in development economics research: a toolkit. In *Handbook of Development Economics*, Vol. 4 (eds Schultz, T. P. & Strauss, J. A.) 3895–3962 (Elsevier, Amsterdam, 2007).
27. Gluud, L. L. Bias in clinical intervention research. *Am. J. Epidemiol.* **163**, 495–501 (2006).
28. Tripepi, G., Jager, K. J., Dekker, F. W. & Zoccali, C. Selection bias and information bias in clinical research. *Nephron Clin. Pract.* **115**, c94–c99 (2010).
29. The Lancet. *Global Burden of Disease Study*. https://www.thelancet.com/gbd (2020).

30. Landrigan, P. J. & Fuller, R. Environmental pollution: an enormous and invisible burden on health systems in low-and middle-income counties. *World Hosp. Health Serv.* **50**(4), 35–40 (2012).
31. Landrigan, P. J. *et al.* The Lancet commission on pollution and health. *The Lancet* **391**, 462–512 (2018).
32. Prüss-Ustün, A., Vickers, C., Haefliger, P. & Bertollini, R. Knowns and unknowns on burden of disease due to chemicals: a systematic review. *Environ. Health* **10**(9), 1–15 (2011).
33. Hiwatari, M. *et al. Kabwe Household Socioeconomic Survey (KHSS) 2017 Report* (KAbwe Mine Pollution Amelioration Initiative, 2018). On-line version available at https://satreps-kampai.vetmed.hokudai.ac.jp/images/publications/2018/The%20Kabwe%20Household%20Socioeconomic%20Survey%20(KHSS)%20Report%20(WEB).pdf.
34. Nakata, H. *et al.* Reliability of stable Pb isotopes to identify Pb sources and verifying biological fractionation of Pb isotopes in goats and chickens. *Environ. Pollut.* **208**, 395–403 (2016).
35. Centers for Disease Control and Prevention (CDC). *Guidelines for the Identification and Management of Lead Exposure in Pregnant and Lactating Women* (CDC, Atlanta, 2010).
36. Dietrich, K. N., Berger, O. G., Succop, P. A., Hammond, P. B. & Bornschein, R. L. The developmental consequences of low to moderate prenatal and postnatal lead exposure: intellectual attainment in the Cincinnati Lead Study cohort following school entry. *Neurotoxocol. Teratol.* **15**, 37–44 (1993).
37. Central Statistical Office of Zambia. *Population and Demographic Projections 2011–2035* (Central Statistical Office, Lusaka, Zambia, 2013).
38. World Bank. *Zambia—Mining and Environmental Remediation and Improvement Project*. https://projects.worldbank.org/en/projects-operations/project-detail/P154683 (2020).

Acknowledgements

We are indebted to participants in our surveys in Kabwe. We are also grateful to the Central Statistical Office and Ministry of Health of Zambia, the Kabwe District Health Office, and laboratory technicians and nurses at health clinics in Kabwe. The study of this paper was conducted as a part of KAbwe Mine Pollution Amelioration Initiative (KAMPAI) project supported by Science and Technology Research Partnership for Sustainable Development (SATREPS; No. JPMJSA1501), a collaboration between Japan Science and Technology Agency (JST) and Japan International Cooperation Agency (JICA). This paper was also supported by Grants-in-Aid for Scientific Research from the Ministry of Education, Culture, Sports, Science and Technology of Japan awarded to D. Y., M. H., D. N. (No. 19KK0040), S. N. (Nos. 16K16197, 17KK0009) and M. I. (Nos. 16H0177906, 18K1984708).

Author contributions

All authors made contribution in data collection. J.Y., S.N. and H.N. analysed blood samples and D.Y., M.H., P.H., D.N., C.M. and B.C. conducted data curation and analysis. The study was conceptualised by K.C. and M.I., supervised by M.H., C.M., J.Y. and S.N. and administrated by H.N. The manuscript was drafted by D.Y. and M.H., edited by P.H. and D.N., and critically revised and approved by all authors.

Competing interests

The authors declare no competing interests.

Additional information

Supplementary information is available for this paper at https://doi.org/10.1038/s41598-020-71998-5.

Correspondence and requests for materials should be addressed to D.Y.

Reprints and permissions information is available at www.nature.com/reprints.

Publisher's note Springer Nature remains neutral with regard to jurisdictional claims in published maps and institutional affiliations.

minerals

MDPI

Article

Immobilization of Lead and Zinc Leached from Mining Residual Materials in Kabwe, Zambia: Possibility of Chemical Immobilization by Dolomite, Calcined Dolomite, and Magnesium Oxide

Pawit Tangviroon [1,*], Kenta Noto [2], Toshifumi Igarashi [1], Takeshi Kawashima [3], Mayumi Ito [1], Tsutomu Sato [1], Walubita Mufalo [2], Meki Chirwa [4], Imasiku Nyambe [4], Hokuto Nakata [5], Shouta Nakayama [5] and Mayumi Ishizuka [5]

1 Division of Sustainable Resources Engineering, Faculty of Engineering, Hokkaido University, Sapporo 060-8628, Japan; tosifumi@eng.hokudai.ac.jp (T.I.); itomayu@eng.hokudai.ac.jp (M.I.); tomsato@eng.hokudai.ac.jp (T.S.)
2 Division of Sustainable Resources Engineering, Graduate School of Engineering, Hokkaido University, Sapporo 060-8628, Japan; kn1855@docon.jp (K.N.); wmufalo@gmail.com (W.M.)
3 Yoshizawa Lime Industry Co., LTD., Libra Bldg, 3-2 Nihonbashi-Kobuncho, Chuo-Ku, Tokyo 103-0024, Japan; tkawashi@yoshizawa.co.jp
4 IWRM Centre/Geology Department, School of Mines, The University of Zambia, Lusaka 32379, Zambia; meki.chirwa@gmail.com (M.C.); inyambe@gmail.com (I.N.)
5 Faculty of Veterinary Medicine, Hokkaido University, Kita 18, Nishi 9, Kita-Ku, Sapporo 060-0818, Japan; hokuto.nakata@vetmed.hokudai.ac.jp (H.N.); shouta-nakayama@vetmed.hokudai.ac.jp (S.N.); ishizum@vetmed.hokudai.ac.jp (M.I.)
* Correspondence: tangviroon.p@eng.hokudai.ac.jp or tangviroon.p@gmail.com; Tel.: +81-90-6217-0676

Received: 22 July 2020; Accepted: 24 August 2020; Published: 28 August 2020

Abstract: Massive amount of highly contaminated mining residual materials (MRM) has been left unattended and has leached heavy metals, particularly lead (Pb) and zinc (Zn) to the surrounding environments. Thus, the performance of three immobilizers, raw dolomite (RD), calcined dolomite (CD), and magnesium oxide (MO), was evaluated using batch experiments to determine their ability to immobilize Pb and Zn, leached from MRM. The addition of immobilizers increased the leachate pH and decreased the amounts of dissolved Pb and Zn to different extents. The performance of immobilizers to immobilize Pb and Zn followed the following trend: MO > CD > RD. pH played an important role in immobilizing Pb and Zn. Dolomite in RD could slightly raise the pH of the MRM leachate. Therefore, the addition of RD immobilized Pb and Zn via adsorption and co-precipitation, and up to 10% of RD addition did not reduce the concentrations of Pb and Zn to be lower than the effluent standards in Zambia. In contrast, the presence of magnesia in CD and MO significantly contributed to the rise of leachate pH to the value where it was sufficient to precipitate hydroxides of Pb and Zn and decrease their leaching concentrations below the regulated values. Even though MO outperformed CD, by considering the local availability of RD to produce CD, CD could be a potential immobilizer to be implemented in Zambia.

Keywords: mine waste; contamination; batch experiments; lead; zinc; immobilization; remediation; Kabwe; Zambia

1. Introduction

Kabwe District was one of the most important mining regions in Zambia for almost a century (1902–1994). It was regarded as Southern Africa's principal lead (Pb)-zinc (Zn) producer, producing

over 1.8 and 0.8 Mt of Zn and Pb, respectively [1]. While in operation, no pollution laws were enforced to regulate the discharge from wastes of the mine; therefore, operations of the mine have left Kabwe with a massive amount of unattended mining residual materials (MRM), which still contain elevated amounts of heavy metals, particularly Zn, Pb, and iron (Fe). Weathering of MRM causes heavy metals to transport from the contaminated sites to the surrounding environments (groundwater, surface water, and soil) [2]. In particular, the redistribution of heavy metals through solute transport processes has been reported to be one of the most dangerous pathways, which invokes harmful effects on water sources of nearby ecosystems and health-threatening to the nearby residents [3–9]. Therefore, the remediation of heavy metals in and around the mine is necessary.

In our recent studies, several potential remediation techniques have been investigated to remediate the contaminated site in Kabwe. Silwamba et al. (2020) [10,11] have proposed the concurrent dissolution and cementation method. The method shows promising results in terms of Pb removal and recovery. However, Zn could not be effectively recovered from the extraction solution, and further investigation is needed. Biocementation by locally available bacteria has been studied by Mwandira et al. (2019) [12,13]. The results indicate that the biocemented material can be effectively used as a covering layer to prevent airborne contamination of metallic dust and infiltration of water into the waste. In the present study, chemical immobilization is introduced as an alternative and practical method to remediate the site.

Remediation techniques for heavy metals polluted sites can be classified into two main categories, in-situ and ex-situ. In general, ex-situ treatment has high efficiency; however, it is less cost-effective than in-situ remediation due significantly to the costs for excavation and transport of large quantities of contaminated materials. In-situ remediation avoids the excavation and transportation costs because of on-site treatments of contaminants. Various kinds of in-situ remediation techniques have been developed to immobilize or extract the heavy metals in the contaminated sites. Among them, chemical immobilization is cheap, easy to implement, and quick in execution [14,15]. Thus, this is the most promising technique, especially to be applied in one of the developing countries.

In in-situ chemical immobilization, the leaching potential of heavy metals from contaminated soils is reduced via sorption and/or precipitation processes by adding chemical agent (immobilizer) into the contaminated area. The performance of a variety of immobilizers, including carbonates, phosphates, alkaline agents, clay, iron-containing minerals, and organic matters, has been evaluated [14–23]. However, most of the studies have been conducted to remediate contaminated soil samples in which they generally contain much lesser metals contents than those in MRM. Moreover, because of the complex interactions between solutes and immobilizers, the definite efficiency of the immobilizer remains site-specific. In other words, there is no guarantee on the effectiveness of a particular immobilizer implemented on different contaminated sites. Therefore, the objective of this study was to evaluate and compare the performance of selected potential immobilizers (e.g., locally available, low-cost) to reduce the mobility of Pb and Zn leached from the highly contaminated sample (MRM).

It is necessary to apply immobilizers that is low cost and abundant in nature for remediating contaminated areas. Hence, in this study, raw dolomite (RD) was selected as one of the potential candidates because it is naturally available in a large quantity in Zambia [24]. It is a carbonate mineral; therefore, it can increase and buffer pH of MRM, leading to more adsorption and precipitation of cationic heavy metal ions [25–27]. In the present study, calcined dolomite (CD) was also used as an immobilizer. The heat treatment was performed to change the carbonate property of dolomite to be more alkaline [28]. As a result, the immobilizer was expected to strongly increase the pH of MRM, favoring the immobilization of heavy metals by hydroxide precipitation in addition to adsorption and precipitation of other secondary minerals. At the same time, commercially available alkaline-based agent, magnesium oxide (MO), was also tested to compare the ability of RD and CD on immobilizing heavy metals in MRM. The current study will provide meaningful information for the development of chemical immobilization to remediate heavy metals contaminated sites in Zambia.

2. Materials and Methods

2.1. Solid Sample Collection, Preparation, and Characterization

MRM was collected from the dumping site of Pb-Zn mine wastes in Kabwe, Zambia. The sampling was done using shovels at random points within the area shown in Figure 1. This leaching residual was selected as one of the representative wastes because the leaching concentrations of Zn and Pb from the waste were higher compared with the other wastes. Moreover, the storage size of this waste occupies more than 50% of the total dumping area. The sample was stored in vacuum bags and transported to the laboratory in Japan with permission by the Ministry of Agriculture, Forestry, and Fisheries of Japan. In preparation, it was air-dried under ambient conditions, lightly crushed, sieved using a 2 mm aperture screen, and kept in a polypropylene bottle before use. Particle sizes of less than 2 mm were chosen to follow the Japanese standard for the leaching test of contaminated soils [29].

Figure 1. Dumping site in Kabwe; (□) sampling area (top left: 14°27′39″ South, 28°25′42″ East; down right: 14°27′55″ South, 28°26′16″ East).

Three types of immobilizing agents were selected to immobilize Zn and Pb in the waste: raw dolomite, calcined dolomite, and magnesium oxide denoted as RD, CD, and MO, respectively. RD was taken from a dolomite quarry source near the MRM storage site, while CD was prepared by burning RD with particle sizes of less than 2 mm in a furnace at 700 °C for 2 h. MO was commercially available, purchased from Ube Industry, Japan. The same preparation procedure as that for MRM was also applied to these materials.

Chemical and mineralogical properties of all solid samples were characterized on the pressed powder of finely crushed samples (<50 µm) using an X-ray fluorescence spectrometer (XRF) (Spectro Xepos, Rigaku Corporation, Tokyo, Japan) and X-ray diffractometer (XRD) (MultiFlex, Rigaku Corporation, Tokyo, Japan), respectively. Sequential extraction was conducted to evaluate solid-phase heavy metals speciation of MRM. The procedure used in this study was modified from two well-known procedures, Tessier et al. (1979) [30] and Clevenger (1990) [31]. The modification was done by Marumo et al. (2003) [32], and it was widely used to extract the tailings sample, mineral processing wastes, and leaching residues [10,33–36]. The process can divide solid-phase heavy metals bounded to solid into five different phases, including exchangeable, carbonates, Fe-Mn oxides, sulfide/organic matter, and residual. The details of the extraction procedure are summarized in Table 1. The extraction was done on 1 g of the <2 mm MRM sample. Between each step, the extractant solution of the previous step was retrieved by centrifugation of the suspension at 3000 rpm for 40 min to separate the residue out of the leachate. The residual was then washed with 20 mL of deionized water. Finally, the washing and extractant solutions were mixed, diluted to 50 mL, filtrated through 0.45-µm Millex® filters, and kept in polypropylene bottles prior to chemical analysis.

Table 1. Sequential extraction for heavy metals speciation.

Step	Extractant	pH	Liquid to Solid Ratio (mL/g)	Temperature (°C)	Duration (h)	Mixing Speed (rpm)	Extracted Phase
1	1 M $MgCl_2$	7	20/1	25	1	120	Exchangeable
2	1 M CH_3COONa	5	20/1	25	5	120	Carbonates
3	0.04 M $NH_2OH{\cdot}HCl$ in 25% acetic acid		20/1	50	5	120	Reducible
4	0.04 M $NH_2OH{\cdot}HCl$ in 25% acetic acid; 30% H_2O_2; 0.02 M HNO_3		36/1	85	5	120	Oxidizable
5	Calculated						Residual

2.2. Batch Leaching Experiments

Batch leaching experiments were performed using 250 mL polypropylene Erlenmeyer flasks with a lateral reciprocating shaker (EYELA Multi Shaker MMS, Tokyo Rikakikai Co., Ltd., Tokyo, Japan). All batches were conducted under ambient conditions by mixing 15 g of solid sample to 150 mL of deionized water (1:10 solid-to-liquid ratio) at 200 rpm for 6 h. Five replications of the leaching tests of MRM were conducted, while a single run of every immobilization experiment was done. The reason is that in immobilization tests, we adjusted the addition of immobilizers and did not control the pH of the suspension. In other words, pH is determined by the complex chemical and physical interactions between immobilizer and MRM. Thus, a variation of pH can be easily observed even though the same mixing ratio between MRM and immobilizer and the conditions is employed. To avoid the uncertainty of the variation of pH at the same immobilizer:MRM mixing ratio, we varied the immobilizer:MRM mixing ratios at 1:100, 3:100, 1:20, and 1:10 to evaluate the performance of immobilizers. After 6 h of shaking, the pH, electrical conductivity (EC), redox potential (ORP), and temperature were immediately measured. The leachates were collected by first centrifuging the mixtures at 3000 rpm for 40 min to separate the suspended particles. The supernatants were then filtered with 0.45-µm Millex® filters (Merck Millipore, Burlington, MA, USA) and kept in air-tight polypropylene bottles prior to chemical analysis.

2.3. Chemical Analysis of Liquid Samples

Inductively coupled plasma atomic emission spectrometer (ICP-AES) (ICPE-9000, Shimadzu Corporation, Kyoto, Japan) and inductively coupled plasma atomic emission mass spectrometry (ICP-MS) (ICAP Qc, Thermo Fisher Scientific, Waltham, MA, USA) were used to quantify the dissolved concentrations of heavy metals and coexisting ions. The analyses were performed on the pretreated liquid samples in which 1% by volume of 60% nitric acid (HNO_3) was added to the liquid samples. The acidification was done to make sure that all target elements were in a dissolved form. The non-acidified samples, on the other hand, were used to determine alkalinity or acid resistivity. This parameter is generally reported as bicarbonate concentration (meq/L), quantified by titration of a known volume of sample with 0.01 M sulfuric acid (H_2SO_4) until pH 4.8. All chemicals used were reagent-grade.

2.4. Geochemical Modeling

An aqueous geochemical modeling program, PHREEQC (Version 3, U.S. Geological Survey, Sunrise Valley Drive Reston, VA, USA) [37], was used to aid in the interpretation of the experimental results. The program can determine the parameters that may affect the mobility of heavy metals from MRM, such as stability of minerals and chemical species. The input data included temperature, pH, ORP, and concentrations of heavy metals and other coexisting ions. Thermodynamic properties were taken from the WATEQ4F database.

3. Results and Discussion

3.1. Properties of Solid Samples

The mineralogical and chemical compositions of MRM and immobilizers, including RD, CD, and MO, are listed in Tables 2 and 3, respectively. MRM was composed of anglesite ($PbSO_4$) as a primary mineral; zinkosite ($ZnSO_4$) and quartz (SiO_2) as the second-highest; and goethite (FeOOH), hematite (Fe_2O_3), and gypsum ($CaSO_4{\cdot}2H_2O$) as the miner minerals. Anglesite and zinkosite are commonly found as the weathering products of Pb- and Zn-sulfides under natural oxygenated environments [38,39]. Therefore, the presence of these two minerals indicates that MRM has already been exposed to the surface environment for a long time before the sampling was done. It can also be expected that other than goethite and hematite, MRM also contained amorphous iron-(hydr)oxides and iron-sulfate salts (e.g., melanterite, coquimbite) since goethite and hematite were found as the miner minerals but Fe_2O_3 content was the highest among all compositions detected. The contents of Pb and Zn in MRM were 10.9% and 8.1%, respectively. The values of both metals were extremely high and exceeded the permissible limit in soil, 600 mg/kg for Pb and 1500 mg/kg for Zn [40]. However, this does not guarantee that MRM can release significant amounts of Pb and Zn since their mobility also depends significantly on the chemical speciation. Sequential extraction was then performed, and the result showed that around 40% of the total contents of Pb and Zn were in mobile fractions (exchangeable, carbonates, and oxidizable) under surface environments (Figure 2). This confirms that MRM could be a potential source contaminating the surrounding environment with Pb and Zn.

Table 2. Mineralogical composition of solid samples.

	MRM	RD	CD	MO
Quartz	++	-	-	-
Gypsum	+	-	-	-
Anglesite	+++	-	-	-
Zinkosite	++	-	-	-
Hematite	+	-	-	-
Goethite	+	-	-	-
Dolomite	-	+++	+++	-
Calcite	-	-	+	-
Magnesia	-	-	+	+++

+++: Strong; ++: Moderate; +: Weak; -: None.

Table 3. Chemical composition of solid samples (the unit is in wt%).

	MRM	RD	CD	MO
SiO_2	20.9	0.39	0.37	<0.01
TiO_2	0.35	<0.01	<0.01	<0.01
Al_2O_3	1.91	0.24	0.11	<0.01
Fe_2O_3	45.8	0.52	0.68	<0.01
MnO	1.59	0.46	0.43	<0.01
MgO	<0.01	36.9	33.3	100
CaO	4.64	60.7	62.4	<0.01
Na_2O	<0.01	<0.01	<0.01	<0.01
K_2O	<0.01	0.15	0.16	<0.01
P_2O_5	<0.01	0.14	<0.01	<0.01
SO_3	2.71	0.15	0.2	<0.01
Pb	10.9	<0.01	<0.01	<0.01
Zn	8.1	<0.01	<0.01	<0.01

The most dominant mineral found in RD was dolomite ($CaMg(CO_3)_2$). Magnesium (Mg) and calcium (Ca) oxides contents accounted for more than 95% with a molar ratio of Ca to Mg of 1.2.

This indicates that RD adequately consisted of pure dolomite. Burning RD at 700 °C for 2 h generated the new type of immobilizer, CD. Calcite ($CaCO_3$) and magnesia (MgO) were detected in addition to dolomite. With almost the same molar ratio of Ca to Mg in CD compared with that in RD, it clearly indicates that the calcination process transformed dolomite into calcite and magnesia. MO composed only of magnesia with 100% MgO content, which shows pure magnesia.

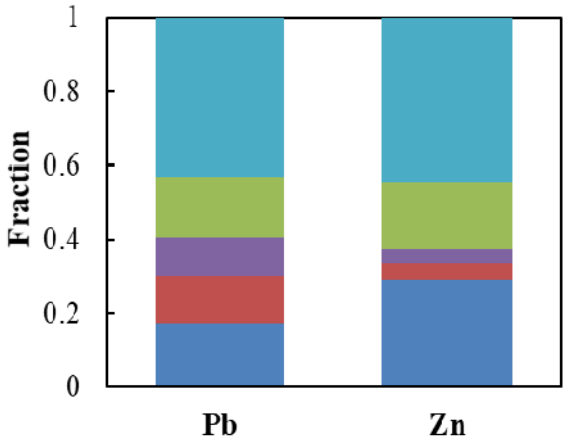

Figure 2. Solid-phase Pb and Zn speciation of mining residual materials (MRM); (□) exchangeable, (□) carbonates, (□) sulfide/organic matter, (□) Fe-Mn oxides, and (□) residual.

3.2. Leaching Characteristic of MRM

Table 4 shows the leaching characteristic of MRM. The experimental values were reproducible with high precision since the standard deviations of all parameters were quite small. Four heavy metals, Pb, Zn, cadmium (Cd), and copper (Cu), were leached at the concentrations falling within the instrument detection limits of ICP-AES and -MS. Among these heavy metals, the leaching concentrations of only Pb (2.1 mg/L) and Zn (365 mg/L) exceeded the effluent standard in Zambia (0.5 mg/L for Pb and 1 mg/L for Zn) [41]. Therefore, this study focused only on the mobility of these two metals. PHREEQC simulation on the saturation indices of all possible Pb- and Zn-minerals showed that with the given conditions and components in MRM leachate, only saturation index of anglesite fell within a common error interval used to indicate saturation equilibrium (±0.2) (Table 5). The result indicates that the low solubility of anglesite restricted the dissolved concentration of Pb, while no restriction by means of precipitation was observed on the leaching of Zn. This can explain why 4.51% of the total Zn content was leached from MRM, while only 0.02% was observed in the case of Pb leaching.

Table 4. Leaching characteristic of MRM (n = 5).

	MRM	Reg. Value * (mg/L)
pH	5.26 ± 0.04	-
ORP (mv)	300 ± 36	-
EC (mS/cm)	2.7 ± 0.09	-
Pb (mg/L)	2.1 ± 0.008	0.5
Zn (mg/L)	365 ± 18	1
Cd (mg/L)	0.21 ± 0.009	0.5
Cu (mg/L)	0.08 ± 0.01	1.5
Ca^{2+} (mg/L)	547 ± 48.2	-
Mg^{2+} (mg/L)	27.7 ± 3.1	-
SO_4^{2-} (mg/L)	1907 ± 36.8	-
Si (mg/L)	13 ± 0.5	-

* Regulated value in mg/L specified by the Environment Management Act (2013) [40].

Table 5. Calculated saturation indices of possible Pb- and Zn-minerals in MRM leachate.

Mineral	Saturation Index
Anglesite	−0.2
Cerussite	−2.25
$Pb(OH)_2$	−3.4
Smithsonite	−2.45
Willemite	−3.62
$Zn(OH)_2$	−3.82
Hydrocerussite	−8.41
Hydrozincite	−3.08

Calcium ion (Ca^{2+}) and sulfate ion ($SO_4{}^{2-}$) were the major ions in the leachate, accounting for more than 85% of the total dissolved ions. These ions were likely to be enriched by the dissolution of soluble phase minerals, such as gypsum and zinkosite [42,43]. However, the dissolution of these two minerals might not only be the sources of $SO_4{}^{2-}$ since the molar ratio of Ca^{2+} and Zn to $SO_4{}^{2-}$ was lower than one. The sulfide fractions of both metals in MRM (Figure 2), together with the slightly acidic pH (5.2) and positive ORP (300 mV) of the leachate, suggest that the oxidation of sulfide minerals (e.g., pyrite, galena, sphalerite) and dissolution of iron-sulfate salts (e.g., melanterite, coquimbite) also occurred and attributed to the enrichment of $SO_4{}^{2-}$, even though they were not detected by XRD. This could also partly contribute to the enrichment of Pb and Zn in the leachate.

3.3. Potential of Immobilizers

3.3.1. Effects of Addition of Immobilizers on pH and Coexisting Ions

Changes in the pH of the leachate as a function of the amounts of addition of RD, CD, and MO are shown in Figure 3. The pH increased from 5.2 to 6.7, 8.2, and 9.8 with increasing RD, CD, and MO addition from 0 to 10%. When the same amount of immobilizer was added, the performance of the immobilizers to increase the leachate pH followed the order: MO > CD > RD. The results clearly showed the improvement of the alkaline property of CD over RD. The variation in pH could mainly be attributed to the liming effect(s) of dolomite (Equation (1)) in RD treatments, of dolomite (Equation (1)), of calcite (Equation (2)), and of magnesia (Equation (3)) in CD treatments, and of magnesia (Equation (3)) in MO treatments [44–47].

$$CaMg(CO_3)_2 + 2\,H^+ \Leftrightarrow Ca^{2+} + Mg^{2+} + 2HCO_3{}^-, \quad (1)$$

$$CaCO_3 + H^+ \Leftrightarrow Ca^{2+} + HCO_3{}^-, \quad (2)$$

$$MgO + H_2O \Leftrightarrow Mg(OH)_2 \Leftrightarrow Mg^{2+} + 2OH^-. \quad (3)$$

Figure 4a–c illustrates the leaching concentrations of major coexisting ions, Ca^{2+}, magnesium (Mg^{2+}), and $SO_4{}^{2-}$, as a function of the amount of immobilizer added. The dissolved concentrations of Ca^{2+} and Mg^{2+} in RD treatments were higher than those in MRM and increased with the increasing addition of RD, indicating the simultaneous leaching of Ca^{2+} and Mg^{2+} from the dissolution of dolomite (Equation (1)). In CD treatments, Ca^{2+} and Mg^{2+} were also leached at higher concentrations than those in MRM leachate. At the same amount of CD and RD addition, the leaching concentration of Mg^{2+} in CD treatment was higher than that in RD treatment, while almost the same dissolved concentration of Ca^{2+} was observed in both treatments. This, together with the result that CD contained less dolomite and more calcite compared to those in RD, suggest the occurrence of hydration of magnesia (Equation (3)) in addition to the dissolution of carbonate minerals (Equations (1) and (2)) in CD treatments. Moreover, the difference in the leaching concentration of Mg^{2+} between CD and RD treatments became more significant as the addition of immobilizers increased, which indicates that as pH increased, the hydration of magnesia (Equation (3)) played a more important role in controlling

pH. In MO treatments, the concentration of Mg^{2+} increased with higher addition of MO, while almost no change in the concentration of Ca^{2+} from that in MRM was observed. This result suggests the occurrence of hydration of magnesia (Equation (3)) in MO treatments.

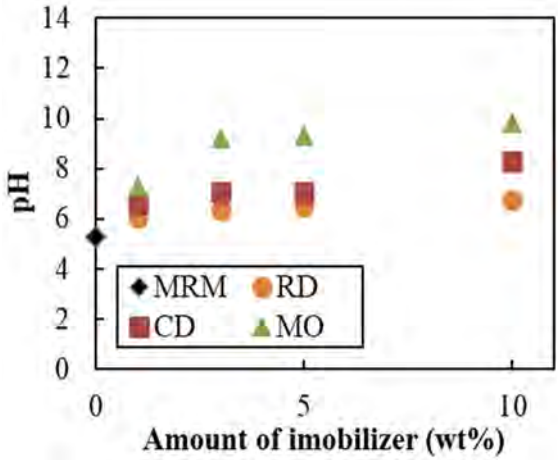

Figure 3. pH of leachate upon addition of immobilizers.

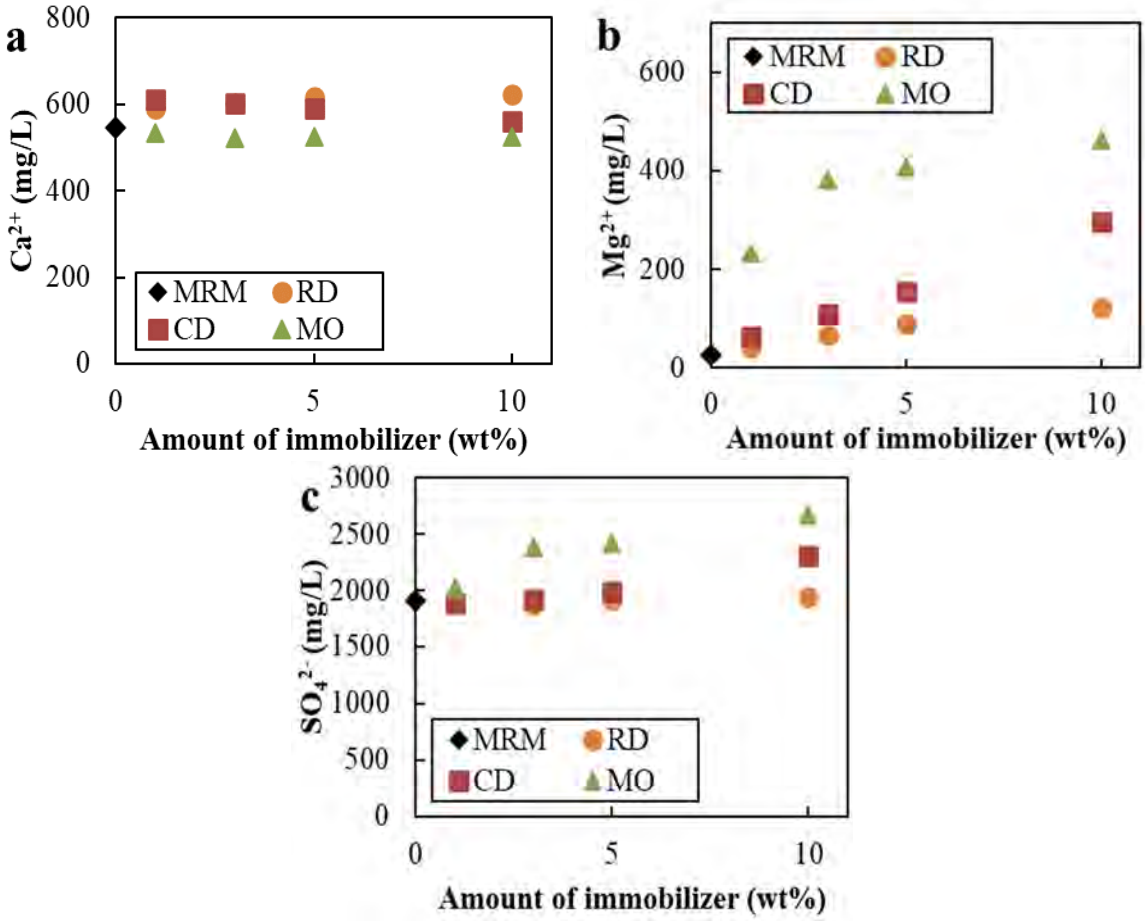

Figure 4. Leaching concentrations of major ions upon addition of immobilizers: (**a**) Ca^{2+}, (**b**) Mg^{2+}, and (**c**) SO_4^{2-}.

At the same amount of immobilizer added, the leaching concentration of SO_4^{2-} was the highest when treating MRM with MO, followed by CD and RD (Figure 4c). In consideration of the trace amount of SO_3 content in all immobilizers, the results suggest that MRM should be the source of SO_4^{2-}, and the leaching of SO_4^{2-} might be caused by the change in the parameter(s) of the leachate, triggered

by the addition of immobilizer. Figure 5 illustrates the correlation between the leaching concentration of SO_4^{2-} vs. pH. The SO_4^{2-} concentration exhibited a strong positive correlation with pH (correlation coefficient (r) = 0.92, $p < 0.01$), suggesting that SO_4^{2-} level could mainly be influenced by pH due possibly to the following mechanisms: (1) desorption, (2) production by oxidation of sulfide minerals, (3) common-ion of between calcite, dolomite, and gypsum, and (4) dissolution of anglesite. The pH increase led to a higher negative surface potential of MRM, thereby decreasing the affinity of SO_4^{2-} toward the surface of MRM. However, Tabatabai (1987) [48] reported that since the adsorption of SO_4^{2-} was only flavored under strongly acidic conditions, the amount of adsorbed SO_4^{2-} became almost negligible under weakly acidic pH. This means that the desorption might not be a viable explanation in this study since all leachates' pH ranged from weakly acidic (5.2) to moderately alkaline (9.8). Therefore, the fact that the oxidation rate of sulfide minerals, such as pyrite and galena, increases with pH becomes the potential reason contributing to the higher leaching concentration of SO_4^{2-} [49,50]. However, the enrichment of SO_4^{2-} could be restricted by the solubility of gypsum because the saturation index of gypsum was within the equilibrium condition range of ±0.2 in all leachates. This could explain why the leaching concentration of SO_4^{2-} slightly increased with pH at lower pH region where the dissolution of dolomite containing in RD and calcite and dolomite containing in and CD tended to control the pH (Equations (1) and (2)). In other words, Ca^{2+} produced from the dissolution of calcite and dolomite precipitated with SO_4^{2-} to form gypsum, thereby restricting SO_4^{2-} concentration. Meanwhile, as pH became more alkaline, the concentration of SO_4^{2-} increased rapidly. This could be attributed to the less contribution of calcite and dolomite dissolution (Equations (1) and (2)) to control the leachate pH in the case of CD addition, conjointly in MO treatments, only hydration of magnesia (no production of Ca^{2+}) (Equation (3)) was found to control the pH of the leachates. The pH-dependent solubility of anglesite could also be attributed to the rapid increase of SO_4^{2-} concentration under alkaline conditions since anglesite was originally contained in MRM and is unstable under alkaline pH [51].

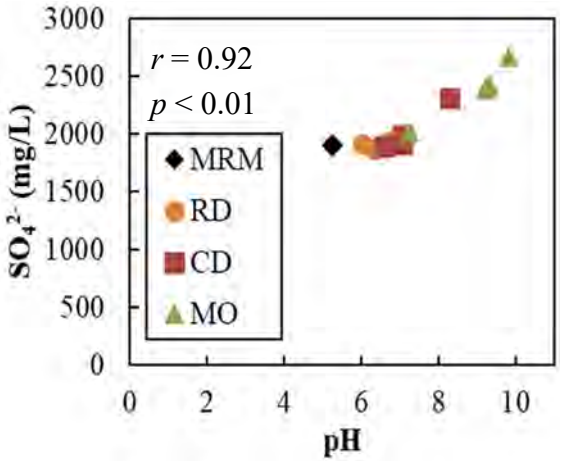

Figure 5. Leaching concentration of SO_4^{2-} vs. pH.

3.3.2. Effects of the Addition of Immobilizers on Mobility of Heavy Metals

In this study, the performance of immobilizers was evaluated based on the solubility of Pb and Zn. Figure 6a,b shows the changes in Pb and Zn concentrations as a function of the amount of addition of immobilizers. In general, the leaching concentrations of Pb and Zn exponentially decreased with an increase in the dose of immobilizers. Figure 7a,b illustrates the correlation between leaching concentrations of Pb and Zn vs. pH. The mobility of heavy metals was strongly influenced by pH, indicated by significant negative correlations of Pb-pH (r = −0.92) and Zn-pH (r = −0.87) at the 0.01 significance level (2-tailed). Coupled with the results of the leaching concentration of SO_4^{2-} and the characteristic of immobilizers, as well as the leaching condition used in the current study, the major modes of Pb and Zn attenuation could be either one or more of the following

mechanisms: precipitations of metal-sulfate, -carbonate, and/or -hydroxide, co-precipitation of metal with iron-(oxy)hydroxides, and metal ion adsorption to immobilizer. The formation of low soluble anglesite under acidic conditions was expected since the leaching concentration of SO_4^{2-} was high and increased with pH (Figure 5) [52,53]. The carbonate property of RD and CD might result in the precipitation of cerussite ($PbCO_3$), hydrocerussite ($Pb_3(CO_3)_2(OH)_2$), smithsonite ($ZnCO_3$), and hydrozincite ($Zn_3(CO_3)_2(OH)_2$) [35,54–56]. The carbonate precipitations of Pb and Zn are also expected to occur in MO treatments since the experiments were done under atmospheric conditions in which carbon dioxide (CO_2) in the atmosphere was freely dissolved [57]. However, the simulation results by PHREEQC showed that except hydrozincite in 3% addition of MO treatment, the precipitations of anglesite, cerussite, hydrocerussite, smithsonite, and hydrozincite were thermodynamically unfavorable (saturation index < −0.2) regardless of the type and amount of immobilizer added (Table 6). Therefore, the possible immobilization mechanisms of Pb and Zn in all types of immobilizers could be narrowed down to the hydroxide precipitation, adsorption, and co-precipitation.

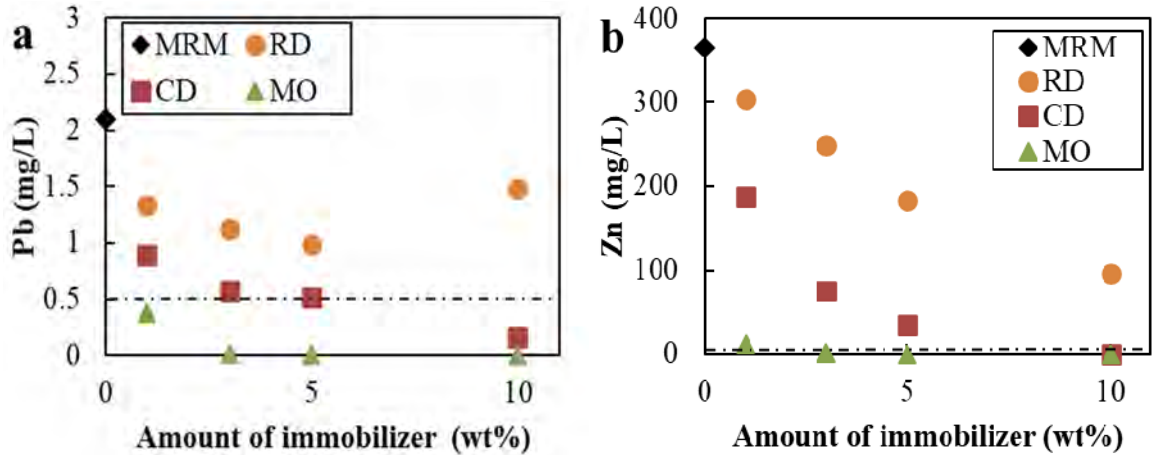

Figure 6. Leaching concentrations of heavy metals upon addition of immobilizers: (**a**) Pb and (**b**) Zn (dashed lines represent the effluent standards of Pb and Zn in Zambia).

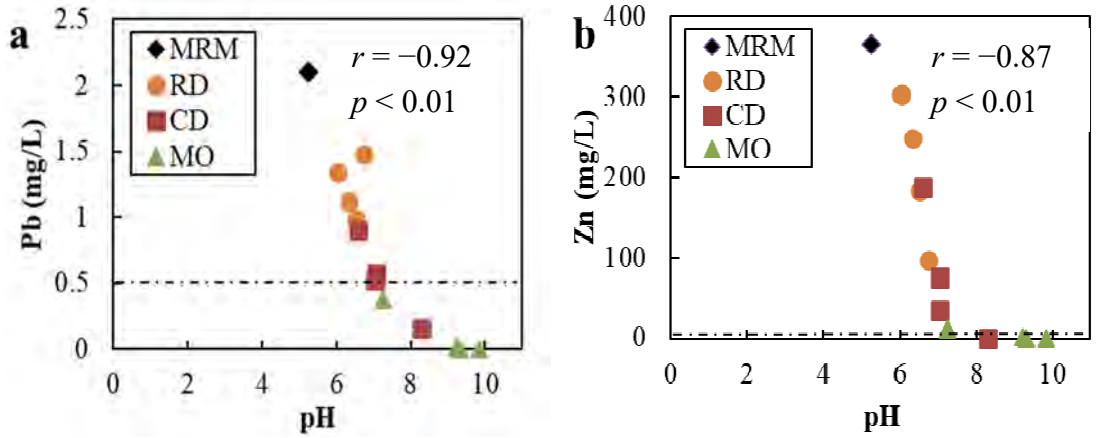

Figure 7. Leaching concentrations of heavy metals vs. pH: (**a**) Pb vs. pH and (**b**) Zn vs. pH (dash lines represent the effluent standards of Pb and Zn in Zambia).

To verify the dominant mechanism(s), pH-dependent solubility diagrams of Pb- and Zn-hydroxides were plotted (Figure 8a,b). Points in the figures represent the relationship between the logarithmic activity of divalent heavy metal and pH in each batch test. The solid lines demonstrate the solubility of heavy metal hydroxides. Therefore, any point located on or close to the line implies the hydroxide precipitation-controlled sequestration process.

Table 6. Calculated saturation indices of anglesite, cerussite, hydrocerussite, smithsonite, and hydrozincite in leachates with the addition of RD, CD, and MO.

Treatment		Saturation Index				
		Anglesite	Cerussite	Smithsonite	Hydrocerussite	Hydrozincite
RD treatments	1%	−0.4	−1.15	−1.63	−5.63	−1.82
	3%	−0.49	−1.13	−1.21	−4.28	−1.35
	5%	−0.55	−0.98	−1.13	−3.68	−1.17
	10%	−0.41	−0.48	−1.01	−2.11	−1.01
CD treatments	1%	−0.6	−0.78	−0.87	−3.19	−0.98
	3%	−0.92	−0.27	−0.44	−1.56	−0.48
	5%	−0.99	−0.23	−0.66	−1.58	−0.79
	10%	−2.39	−0.3	−1.24	−0.64	−0.64
MO treatments	1%	−1.13	−0.38	−1.16	−1.57	−1
	3%	−4.36	−1.6	−1.16	−3.31	0.22
	5%	−4.72	−1.86	−2.19	−4.05	−0.78
	10%	−5.49	−2.52	−2.99	−5.16	−1.02

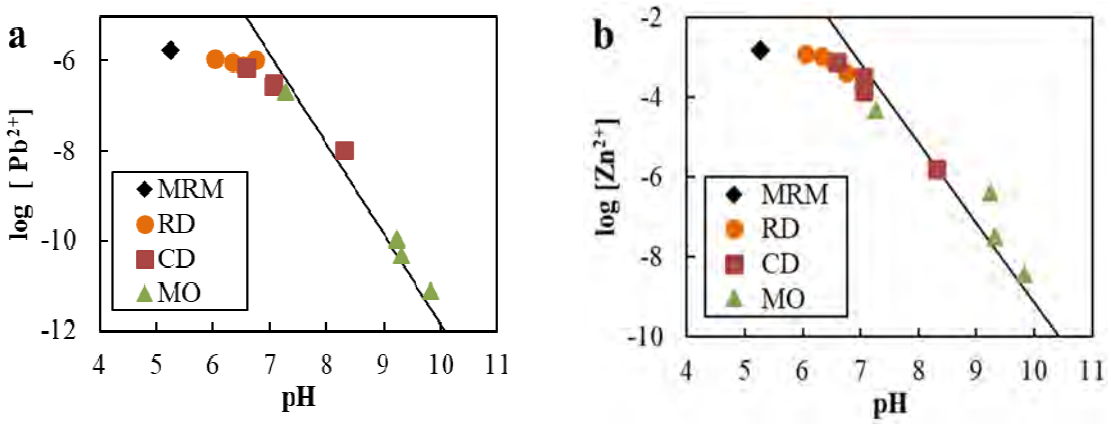

Figure 8. pH-dependent solubility diagrams of (**a**) Pb-hydroxide and (**b**) Zn-hydroxide ([ ] represents activity).

In the case of RD addition, a discrepancy from the equilibrium line for Pb and Zn was observed. This means that at pH from weekly acid to neutral, hydroxide precipitation was not the main mechanism controlling the mobility of Pb and Zn. Therefore, Pb and Zn were suspected to be immobilized by sorption and co-precipitation with iron-(oxy)hydroxides. The sorption was likely to occur since dolomite, major mineral in the immobilizer, can adsorb Pb and Zn [58,59]. Besides, adding more of this immobilizer induced the leachate pH increase. This could change the surface charge of goethite, hematite, and iron-(hydr)oxide compounds in MRM to more negative, thereby increasing their adsorption ability against cationic divalent Pb and Zn [58–63]. During the neutralization process under ambient conditions, iron-(oxy)hydroxides precipitate from the oxidative dissolution of pyrite and dissolution of iron-bearing salts [63–66]. The precipitations of iron-(oxy)hydroxides have been reported by many studies to induce co-precipitation of divalent metals, including Pb(II) and Zn(II) [50,67,68], and thus the co-precipitation of Pb and Zn with iron-(oxy)hydroxides was also expected in RD treatments. From the above explanations, adding more RD should reduce the leaching concentration of both metals. However, leaching concentration of Pb increased from 0.98 mg/L to 1.4 mg/L when RD rose from 5% to 10% (Figure 6a). This could be attributed to the stability of Pb(II) species as a function of pH. Theoretically, as pH increases under acidic region, more of free Pb(II) ion tends to complex with OH^- and CO_3^{2-}, generating larger ion with lower charge ($Pb(OH)^+$ and $PbCO_3$), which lowers the affinity of Pb to the surface of the potential adsorbents and inhibits the co-precipitation [69–71].

On the other hand, adding CD and MO made most of the logarithmic leaching activities of Pb^{2+} and Zn^{2+} to approach their solubility product lines. This means that hydroxide precipitation is the dominant mechanism of attenuating Pb and Zn. Regardless of the type of immobilizer, at low pH, the logarithmic activities of both metals were slightly lower than their equilibrium lines and then tended to stay on or be slightly higher than the lines afterward. This probably indicates that at low pH, adsorption and co-precipitation with iron-(oxy)hydroxides also occurred in addition to the precipitation, but as pH got higher, they diminished. There are two probable explanations for this phenomenon as follows: (1) competition with strong competing ion (Mg^{2+}) and (2) change in specification of the dissolved metals. The pH alteration mechanisms of CD and MO appeared to generate Mg^{2+} as a by-product (Equations (1) and (3)). Because of this, the concentration of Mg^{2+} significantly increased with pH with a correlation coefficient of 0.97, $p < 0.01$(Figure 9). Therefore, as pH increased, high concentration of Mg^{2+} could compete for Pb and Zn for adsorption sites and for co-precipitation with iron-(oxy)hydroxides, attributing to the less contribution of the adsorption and co-precipitation on the immobilization process. Increasing pH could also result in the redistributions of Pb(II) and Zn(II) species. The fraction of free Pb(II) and Zn(II) reduces as pH increases since they are thermodynamically preferable to be hydrolyzed forming $-(OH)^{+}$, $-(OH)_2$, and $-(OH)_3^{-}$ [69–72]. Moreover, since the systems contained high dissolved carbonate, the formation of carbonate complexes of Pb(II) and Zn(II) was also expected [69,73]. Once these complexes are formed, their abilities to get adsorbed and co-precipitated are inhibited by the larger size and lower positive potential they become.

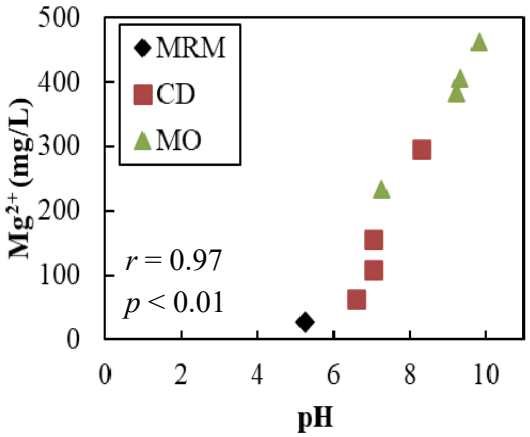

Figure 9. Leaching concentration of Mg^{2+} vs. pH.

3.3.3. Performance of Immobilizers

When the same amount of immobilizer was added, the dissolved concentrations of Pb and Zn were the highest in RD treatment, second highest in CD treatment, and the lowest in MO treatment (Figure 6a,b). As previously mentioned, adsorption, co-precipitation, and hydroxide precipitation were the major sink of Pb and Zn, and their mobilities depended strongly on pH. Because of the carbonate property of dolomite, RD could not raise the pH of MRM leachate to the value favoring the precipitations of Pb- and Zn-hydroxides. Therefore, RD treatments remediated Pb and Zn by adsorption and co-precipitation in which it was insufficient to reduce the leaching concentrations of Pb and Zn down below their regulated values. On the other hand, magnesia in CD and MO played a significant role in increasing the leachate pH of MRM into the alkaline region. Lead and Zn were then mainly immobilized by precipitation as hydroxides. Thus, metal concentrations as high as 368 mg/L for Zn and 2.1 mg/L for Pb released from MRM were reduced to the values below their regulated concentrations. Efficiency-wise, MO was the most effective immobilizer in immobilizing Pb and Zn since it contained the highest MgO content. However, CD could be the immobilizer of choice since it can be produced from the naturally abundant material in Zambia (RD), and its performance was almost the same as that of MO.

4. Conclusions

The leachate of MRM was slightly acidic (pH 5.2) and contained high concentrations of Pb (2.1 mg/L) and Zn (365 mg/L), exceeding those of Zambian regulation. When immobilizers were introduced, the leachate pH increased, and the leaching concentrations of Pb and Zn decreased. Lead and Zn immobilized by RD were interpreted by the adsorption and co-precipitation mechanisms. On the contrary, chemical immobilization using CD and MO suppressed Pb and Zn leaching mainly by the hydroxide precipitation. Of the immobilizers investigated, only CD and MO decreased the dissolved Pb and Zn concentrations to below their regulated values, in which MO had a higher performance than CD. The results show that heat treatment on RD to produce CD drastically improved the immobilizing performance of Pb and Zn. Even though MO provided the highest efficiency, Pb and Zn could also be effectively immobilized by giving an adequate amount of CD. Therefore, by considering the availability of CD in the local area, CD could be the most promising chemical agent to be implemented in Zambia.

Author Contributions: Conceptualization, P.T.; methodology, P.T., K.N., T.I., and T.K.; formal analysis, P.T. and T.I.; writing—original draft preparation, P.T.; writing—review and editing, P.T., T.I., M.I. (Mayumi Ito), T.S., W.M., M.C., and I.N.; supervision, P.T. and T.I.; project administration, M.I. (Mayumi Ishizuka), S.N., and H.N.; funding acquisition, M.I. (Mayumi Ishizuka), S.N., and H.N.; All authors have read and agreed to the published version of the manuscript.

Funding: This research was supported by JST/JICA SATREPS (Science and Technology Research Partnership for Sustainable Development; No. JPMJSA1501) and aXis (Accelerating Social Implementation for SDGs Achievement; No. JPMJAS2001) funded by JST.

Acknowledgments: The authors would like to acknowledge JST/JICA SATREPS (Science and Technology Research Partnership for Sustainable Development; No. JPMJSA1501) and aXis (Accelerating Social Implementation for SDGs Achievement; No. JPMJAS2001) funded by JST for the financial support.

Conflicts of Interest: The authors declare no conflict of interest.

References

1. Kamona, A.F.; Friedrich, G.H. Geology, mineralogy, and stable isotope geochemistry of the Kabwe carbonate-hosted Pb-Zn deposit, Central Zambia. *Ore Geol. Rev.* **2007**, *30*, 217–243. [CrossRef]
2. Kříbek, B.; Nyambe, I.; Majer, V.; Knésl, I.; Mihaljevič, M.; Ettler, V.; Vaněk, A.; Penížek, V.; Sracek, O. Soil contamination near the Kabwe Pb-Zn smelter in Zambia: Environmental impacts and remediation measures proposal. *J. Geochem. Explor.* **2019**, *197*, 159–173. [CrossRef]
3. Fuge, R.; Pearce, M.F.; Pearce, N.J.G.; Perkins, W.T. Geochemistry of Cd in the secondary environment near abandoned metalliferous mines, Wales. *J. Appl. Geochem.* **1993**, *8*, 29–35. [CrossRef]
4. Paulson, A.J. The transport and fate of Fe, Mn, Cu, Zn, Cd, Pb and SO4 in a groundwater plume and in downstream surface waters in the Coeur d'Alene Mining District, Idaho, U.S.A. *J. Appl.* **1997**, *12*, 447–464. [CrossRef]
5. Yabe, J.; Nakayama, S.M.M.; Ikenaka, Y.; Muzandu, K.; Ishizuka, M.; Umemura, T. Uptake of lead, cadmium, and other metals in the liver and kidneys of cattle near a lead-zinc mine in Kabwe, Zambia. *Environ. Toxicol. Chem.* **2011**, *30*, 1892–1897. [CrossRef]
6. Yabe, J.; Nakayama, S.M.M.; Ikenaka, Y.; Muzandu, K.; Choongo, K.; Mainda, G.; Kabeta, M.; Ishizuka, M.; Umemura, T. Metal distribution in tissues of free-range chickens near a lead-zinc mine in Kabwe, Zambia. *Environ. Toxicol. Chem.* **2013**, *32*, 189–192. [CrossRef]
7. Yabe, J.; Nakayama, S.M.M.; Ikenaka, Y.; Yohannes, Y.B.; Bortey-Sam, N.; Oroszlany, B.; Muzandu, K.; Choongo, K.; Kabalo, A.N.; Ntapisha, J.; et al. Lead poisoning in children from townships in the vicinity of a lead-zinc mine in Kabwe, Zambia. *Chemosphere* **2015**, *119*, 941–947. [CrossRef]
8. Yabe, J.; Nakayama, S.M.M.; Ikenaka, Y.; Yohannes, Y.B.; Bortey-Sam, N.; Kabalo, A.N.; Ntapisha, J.; Mizukawa, H.; Umemura, T.; Ishizuka, M. Lead and cadmium excretion in feces and urine of children from polluted townships near a lead-zinc mine in Kabwe, Zambia. *Chemosphere* **2018**, *202*, 48–55. [CrossRef]
9. Basta, N.T.; McGowen, S.L. Evaluation of chemical immobilization treatments for reducing heavy metal transport in a smelter-contaminated soil. *Environ. Pollut.* **2004**, *127*, 73–82. [CrossRef]

10. Silwamba, M.; Ito, M.; Hiroyoshi, N.; Tabelin, C.B.; Hashizume, R.; Fukushima, T.; Park, I.; Jeon, S.; Igarashi, T.; Sato, T.; et al. Recovery of lead and zinc from zinc plant leach residues by concurrent dissolution-cementation using zero-valent aluminum in chloride medium. *Metals* **2020**, *10*, 531. [CrossRef]
11. Silwamba, M.; Ito, M.; Hiroyoshi, N.; Tabelin, C.B.; Fukushima, T.; Park, I.; Jeon, S.; Igarashi, T.; Sato, T.; Nyambe, I.; et al. Detoxification of lead-bearing zinc plant leach residues from Kabwe, Zambia by coupled extraction-cementation method. *J. Environ. Chem. Eng.* **2020**, *8*, 104197. [CrossRef]
12. Mwandira, W.; Nakashima, K.; Kawasaki, S.; Ito, M.; Sato, T.; Igarashi, T.; Banda, K.; Chirwa, M.; Nyambe, I.; Nakayama, S.; et al. Efficacy of biocementation of lead mine waste from the Kabwe Mine site evaluated using Pararhodobacter sp. *Environ. Sci. Pollut. Res.* **2019**, *26*, 15653–15664. [CrossRef] [PubMed]
13. Mwandira, W.; Nakashima, K.; Kawasaki, S.; Ito, M.; Sato, T.; Igarashi, T.; Chirwa, M.; Banda, K.; Nyambe, I.; Nakayama, S.; et al. Solidification of sand by Pb(II)-tolerant bacteria for capping mine waste to control metallic dust: Case of the abandoned Kabwe Mine, Zambia. *Chemosphere* **2019**, *228*, 17–25. [CrossRef] [PubMed]
14. Liu, L.; Li, W.; Song, W.; Guo, M. Remediation techniques for heavy metal-contaminated soils: Principles and applicability. *Sci. Total Environ.* **2018**, *633*, 206–219. [CrossRef]
15. Gray, C.W.; Dunham, S.J.; Dennis, P.G.; Zhao, F.J.; McGrath, S.P. Field evaluation of in situ remediation of a heavy metal contaminated soil using lime and red-mud. *Environ. Pollut.* **2006**, *142*, 530–539. [CrossRef]
16. Kumpiene, J.; Lagerkvist, A.; Maurice, C. Stabilization of As, Cr, Cu, Pb and Zn in soil using amendments—A review. *J. Waste Manag.* **2008**, *28*, 215–225. [CrossRef]
17. Farrell, M.; Jones, D.L. Use of composts in the remediation of heavy metal contaminated soil. *J. Hazard. Mater.* **2010**, *175*, 575–582. [CrossRef]
18. He, M.; Shi, H.; Zhao, X.; Yu, Y.; Qu, B. Immobilization of Pb and Cd in contaminated soil using nano-crystallite hydroxyapatite. *Procedia Environ. Sci.* **2013**, *18*, 657–665. [CrossRef]
19. Bolan, N.; Kunhikrishnan, A.; Thangarajan, R.; Kumpiene, J.; Park, J.; Makino, T.; Kirkham, M.B.; Scheckel, K. Remediation of heavy metal(loid)s contaminated soils—To mobilize or to immobilize? *J. Hazard. Mater.* **2014**, *266*, 141–166. [CrossRef]
20. Mahar, A.; Wang, P.; Li, R.; Zhang, Z. Immobilization of lead and cadmium in contaminated soil using amendments: A review. *Pedosphere* **2015**, *25*, 555–568. [CrossRef]
21. Ali, A.; Guo, D.; Zhang, Y.; Sun, X.; Jiang, S.; Guo, Z.; Huang, H.; Liang, W.; Li, R.; Zhang, Z. Using bamboo biochar with compost for the stabilization and phytotoxicity reduction of heavy metals in mine-contaminated soils of China. *Sci. Rep.* **2017**, *7*, 2690. [PubMed]
22. Seshadri, B.; Bolan, N.S.; Choppala, G.; Kunhikrishnan, A.; Sanderson, P.; Wang, H.; Currie, L.D.; Tsang, D.C.W.; Ok, Y.S.; Kim, G. Potential value of phosphate compounds in enhancing immobilization and reducing bioavailability of mixed heavy metal contaminants in shooting range soil. *Chemosphere* **2017**, *184*, 197–206. [CrossRef]
23. Andrunik, M.; Wołowiec, M.; Wojnarski, D.; Zelek-Pogudz, S.; Bajda, T. Transformation of Pb, Cd, and Zn minerals using phosphates. *Minerals* **2020**, *10*, 342. [CrossRef]
24. Southwood, M.; Cairncross, B.; Rumsey, M.S. Minerals of the Kabwe ("Broken Hill") mine, central province, Zambia. *Rocks Miner.* **2019**, *94*, 114–149. [CrossRef]
25. Trakal, L.; Neuberg, M.; Tlustoš, P.; Száková, J.; Tejnecký, V.; Drábek, O. Dolomite limestone application as a chemical immobilization of metal-contaminated soil. *Plant Soil Environ.* **2011**, *4*, 173–179.
26. Deer, W.A.; Howie, R.A.; Zussman, J. *An Introduction to The Rock Forming Minerals*, 2nd ed.; Longmans: London, UK, 1966; pp. 489–493.
27. Krauskopf, K.B.; Bird, D.K. *Introduction to Geochemistry*, 3rd ed.; McGraw-Hill: New York, NY, USA, 1995.
28. Salameh, Y.; Albadarin, A.B.; Allen, S.; Walker, G.; Ahmad, M.N.M. Arsenic (III,V) adsorption onto charred dolomite: Charring optimization and batch studies. *Chem. Eng. J.* **2015**, *259*, 663–671. [CrossRef]
29. JLT-13. Departmental notification No. 13 on leaching test method for landfill wastes. *Jap. Environ. Agcy.* **1973**. Available online: http://www.env.go.jp/hourei/11/000178.html (accessed on 26 August 2020).
30. Tessier, A.; Campbell, G.C.; Bisson, M. Sequential extraction procedure for the speciation of particulate trace metals. *Anal. Chem.* **1979**, *51*, 844–850.
31. Clevenger, T.E. Use of sequential extraction to evaluate the heavy metals in mining wastes. *Water Air Soil Pollut.* **1990**, *50*, 241–253.

32. Marumo, K.; Ebashi, T.; Ujiie, T. Heavy metal concentrations, leachabilities and lead isotope ratios of Japanese soils. *Shigen Chihsitsu* **2003**, *53*, 125–146. (In Japanese)
33. Dang, Z.; Liu, C.; Haigh, M.J. Mobility of heavy metals associated with the natural weathering of coal mine spoils. *Environ. Pollut.* **2002**, *118*, 419–426. [CrossRef]
34. Anju, M.; Banerjee, D.K. Comparison of two sequential extraction procedures for heavy metal partitioning in mine tailings. *Chemosphere* **2010**, *78*, 1393–1402. [CrossRef] [PubMed]
35. Tabelin, C.B.; Silwamba, M.; Paglinawan, F.C.; Mondejar, A.J.S.; Duc, H.G.; Resabal, N.J.; Opiso, E.M.; Igarashi, T.; Tomiyama, S.; Ito, M.; et al. Solid-phase partitioning and release-retention mechanisms of copper, lead, zinc and arsenic in soils impacted by artisanal and small-scale gold mining (ASGM) activities. *Chemosphere* **2020**, *260*, 127574. [CrossRef] [PubMed]
36. Khoeurn, K.; Sasaki, A.; Tomiyama, S.; Igarashi, T. Distribution of zinc, copper, and iron in the tailings dam of an abandoned mine in Shimokawa, Hokkaido, Japan. *Mine Water Environ.* **2018**, *38*, 119–129. [CrossRef]
37. Parkhurst, D.L.; Appelo, C.A.J. User's guide to PHREEQC (Version 2): A computer program for speciation, batch-reaction, one-dimensional transport, and inverse geochemical calculations. *Water Resour. Investig. Rep.* **1999**, *99*, 312.
38. Blowes, D.W.; Jambor, J.L.; Alpers, C.N. The environmental geochemistry of sulfide mine-wastes. *Mineral. Assoc. Can.* **1994**, *22*, 59–102.
39. Hayes, S.M.; White, S.A.; Thompson, T.L.; Maier, R.M.; Chorover, J. Changes in lead and zinc lability during weathering-induced acidification of desert mine tailings: Coupling chemical and micro-scale analyses. *Appl. Geochem.* **2009**, *42*, 2234–2245. [CrossRef]
40. Wuana, R.A.; Okieimen, F.E. Heavy metals in contaminated soils: A review of sources, chemistry, risks and best available strategies for remediation. *ISRN Ecol.* **2011**, *2011*, 20. [CrossRef]
41. The Environment Management Act. The environment management (licensing) regulations. *SI Govt. Zambia* **2013**, *112*, 737–858.
42. Klimchouk, A.B. The dissolution and conversion of gypsum and anhydrite. *Speleolog* **1996**, *25*, 21–36. [CrossRef]
43. Hester, R.E.; Harrison, R.M. *Contaminated Land and Its Reclamation*, 1st ed.; Royal Society of Chemistry: London, UK, 1997.
44. Lui, Z.; Dreybrodt, W. Dissolution kinetics of calcium carbonate minerals in H_2O-CO_2 solutions in turbulent flow: The role of the diffusion boundary layer and the slow reaction $H_2O + CO_2 \leftrightarrow H^+ + HCO_3^-$. *Geochem. Cosmochim. Acta* **1997**, *61*, 2879–2889.
45. Pokrovsky, O.S.; Schott, J.N. Kinetics and mechanism of dolomite dissolution in neutral to alkaline solutions revisited. *Am. J. Sci.* **2001**, *301*, 597–626. [CrossRef]
46. Fu, J.; He, Q.; Miedziak, P.J.; Brett, G.L.; Huang, X.; Pattisson, S.; Douthwaite, M.; Hutchings, G.J. The role of $Mg(OH)_2$ in the so-called "base-free" oxidation of glycerol with Au Pd catalysts. *Chemistry* **2018**, *24*, 2396–2402. [CrossRef]
47. Xing, Z.; Bai, L.; Ma, Y.; Wang, D.; Li, M. Mechanism of magnesium oxide hydration based on the multi-rate model. *Materials* **2018**, *11*, 1835. [CrossRef] [PubMed]
48. Tabatabai, M.A. Physicochemical fate of sulfate in soils. *JAPCA* **1987**, *37*, 34–38. [CrossRef]
49. Evangelou, V.P. *Pyrite Oxidation and Its Control*, 1st ed.; CRC Press: New York, NY, USA, 1995.
50. Tabelin, C.B.; Igarashi, T.; Tabelin, M.V.; Park, I.; Opiso, E.M.; Ito, M.; Hiroyoshi, N. Arsenic, selenium, boron, lead, cadmium, copper, and zinc in naturally contaminated rocks: A review of their sources, modes of enrichment, mechanisms of release, and mitigation strategies. *Sci. Total Environ.* **2018**, *645*, 1522–1553. [CrossRef]
51. Cappuyns, V.; Alian, V.; Vassilieva, E.; Swennen, R. pH dependent leaching behavior of Zn, Cd, Pb, Cu and as from mining wastes and slags: Kinetics and mineralogical control. *Waste Biomass Valor.* **2014**, *5*, 355–368. [CrossRef]
52. Lindsay, W.L. *Chemical Equilibria in Soils*, 1st ed.; Wiley: Hoboken, NJ, USA, 1979.
53. Tatsuhara, T.; Arima, T.; Igarashi, T.; Tabelin, C.B. Combined neutralization-adsorption system for the disposal of hydrothermally altered excavated rock producing acidic leachate with hazardous elements. *Eng. Geol.* **2012**, *139*, 76–84. [CrossRef]
54. McBride, M.B. Reactions controlling heavy metal solubility in soils. *Adv. Soil Sci.* **1989**, *10*, 1–56.

55. Mench, M.J.; Didier, V.L.; Leoffler, M.; Gomez, A.; Pierre, M. A mimicked in-situ remediation study of metal-contaminated soils with emphasis on cadmium and lead. *J. Environ. Qual.* **1994**, *23*, 58–63. [CrossRef]
56. Chlopecka, A.; Adriano, D.C. Mimicked in-situ stabilization of metals in a cropped soil: Bioavailability and chemical form of zinc. *Environ. Sci. Technol.* **1996**, *30*, 3294–3303. [CrossRef]
57. Carbonate Equilibria in Natural Waters. Available online: https://www.fkit.unizg.hr/_download/repository/CO2_ravnoteza%5B1%5D.pdf (accessed on 20 July 2020).
58. Tozsin, G. Inhibition of acid mine drainage and immobilization of heavy metals from copper flotation tailings using marble cutting waste. *Int. J. Min. Met. Mater.* **2016**, *23*, 1–6. [CrossRef]
59. Gruszecka-Kosowska, A.; Baran, P.; Wdowin, M.; Franus, W. Waste dolomite powder as an waste dolomite powder as an adsorbent of Cd, Pb(II), and Zn from aqueous solutions. *Environ. Earth. Sci.* **2017**, *79*, 521. [CrossRef]
60. Gadde, R.R.; Laitinen, H.A. Studies of heavy metal adsorption by hydrous iron and manganese oxides. *Anal. Chem.* **1974**, *46*, 2022–2026. [CrossRef]
61. Millward, G.E.; Moore, R.M. The adsorption of Cu, Mn and Zn by iron oxyhydroxide in model estuarine solutions. *Water Res.* **1982**, *16*, 981–985. [CrossRef]
62. Tangviroon, P.; Endo, Y.; Fujinaga, R.; Kobayashi, M.; Igarashi, T.; Yamamoto, T. Change in arsenic leaching from silty soil by adding slag cement. *Water Air Soil Pollut.* **2020**, *231*, 259. [CrossRef]
63. Marove, C.A.; Tangviroon, P.; Tabelin, C.B.; Igarashi, T. Leaching of hazardous elements from Mozambican coal and coal ash. *J. Afr. Earth Sci.* **2020**, *168*, 103861. [CrossRef]
64. Tangviroon, P.; Hayashi, R.; Igarashi, T. Effects of additional layer(s) on the mobility of arsenic from hydrothermally altered rock in laboratory column experiments. *Water Air Soil Pollut.* **2017**, *228*, 191. [CrossRef]
65. Tangviroon, P.; Igarashi, T. Modeling and evaluating the performance of river sediment on immobilizing arsenic from hydrothermally altered rock in laboratory column experiments with Hydrus-1D. *Water Air Soil Pollut.* **2017**, *228*, 465. [CrossRef]
66. Huyen, D.T.; Tabelin, C.B.; Thuan, H.M.; Dang, D.H.; Truong, P.T.; Vongphuthone, B.; Kobayashi, M.; Igarashi, T. The solid-phase partitioning of arsenic in unconsolidated sediments of the Mekong Delta, Vietnam and its modes of release under various conditions. *Chemosphere* **2019**, *233*, 512–523. [CrossRef]
67. Igarashi, T.; Herrera, P.S.; Uchiyama, H.; Miyamae, H.; Iyatomi, N.; Hashimoto, K.; Tabelin, C.B. The two-step neutralization ferrite-formation process for sustainable acid mine drainage treatment: Removal of copper, zinc and arsenic, and the influence of coexisting ions on ferritization. *Sci. Total Environ.* **2020**, *715*, 136877. [CrossRef] [PubMed]
68. HoungAloune, S.; Kawaai, T.; Hiroyoshi, N.; Ito, M. Study on schwertmannite production from copper heap leach solutions and its efficiency in arsenic removal from acidic sulfate solutions. *Hydrometallurgy* **2014**, *147*, 30–40. [CrossRef]
69. Powell, K.J.; Brown, P.L.; Byrne, R.H.; Gajda, T.; Hefter, G.; Leuz, A.K.; Sjöberg, S.; Wanner, H. Chemical speciation of environmentally significant metals with inorganic ligands, Part 3. The Pb^{2+}, OH^-, Cl^-, CO_3^{2-}, SO_4^{2-}, and PO_4^{3-} systems. IUPAC Technical Report. *Pure Appl. Chem.* **2009**, *81*, 2425–2476. [CrossRef]
70. Badawy, S.H.; Helal, M.I.D.; Chaudri, A.M.; Lawlor, K.; McGrath, S.P. Heavy metals in the environment. Soil solid-phase controls lead activity in soil solution. *J. Environ. Qual.* **2002**, *31*, 162–167. [CrossRef]
71. Namieśnik, J.; Rabajczyk, A. The speciation and physicochemical forms of metals in surface waters and sediments. *Chem. Speciat. Bioavailab.* **2010**, *22*, 1–24. [CrossRef]
72. Masliy, A.N.; Shapnik, M.S.; Kuznetsov, A.M. Quantum-chemical investigation of electrochemical processes. Part I. Investigation of the mechanism of Zn(II) complex electroreduction from alkaline water solutions. Quantum chemical simulation, chemistry, and computational simulation. *Butlerov. Commun.* **2000**, *3*, 1–6.
73. Fouillac, C.; Criaud, A. Carbonate and bicarbonate trace metal complexes: Critical reevaluation of stability constants. *Geochem. J.* **1984**, *18*, 297–303. [CrossRef]

scientific reports

Check for updates

OPEN

Biosorption of Pb (II) and Zn (II) from aqueous solution by *Oceanobacillus profundus* isolated from an abandoned mine

Wilson Mwandira[1,2], Kazunori Nakashima[1]✉, Satoru Kawasaki[1], Allison Arabelo[3], Kawawa Banda[2], Imasiku Nyambe[2], Meki Chirwa[2], Mayumi Ito[1], Tsutomu Sato[1], Toshifumi Igarashi[1], Hokuto Nakata[4], Shouta Nakayama[4] & Mayumi Ishizuka[4]

The present study investigated biosorption of Pb (II) and Zn (II) using a heavy metal tolerant bacterium *Oceanobacillus profundus* KBZ 3-2 isolated from a contaminated site. The effects of process parameters such as effect on bacterial growth, pH and initial lead ion concentration were studied. The results showed that the maximum removal percentage for Pb (II) was 97% at an initial concentration of 50 mg/L whereas maximum removal percentage for Zn (II) was at 54% at an initial concentration of 2 mg/L obtained at pH 6 and 30 °C. The isolated bacteria were found to sequester both Pb (II) and Zn (II) in the extracellular polymeric substance (EPS). The EPS facilitates ion exchange and metal chelation-complexation by virtue of the existence of ionizable functional groups such as carboxyl, sulfate, and phosphate present in the protein and polysaccharides. Therefore, the use of indigenous bacteria in the remediation of contaminated water is an eco-friendly way of solving anthropogenic contamination.

The contamination of water bodies by heavy metals has resulted in increased research on how to remove such toxic pollutants from the environment. The most investigated heavy metals include chromium (Cr), cadmium (Cd), zinc (Zn), mercury (Hg), lead (Pb), nickel (Ni), and arsenic (As) because of the significant public health and environmental risks that they pose[1]. These heavy metals are introduced into the environment by human activities such as mining and agriculture[2]. Reverse osmosis, ion exchange, precipitation, and solvent extraction have been used to decontaminate wastewater before release into the natural environment; however, these technologies are either extremely expensive or not sufficiently effective[3]. The removal of heavy metals using biological materials has emerged as one of the most promising alternatives, as it does not induce secondary pollution and is cost-effective by avoiding the need for sludge disposal systems[4]. Biological materials employed for the removal of heavy metals from aqueous solutions include bacteria[5], yeast[6], algae[7], fungi[8], agricultural waste[4] or wood waste[9]. The isolation and identification of many indigenously available biological materials are indispensable in sites heavily contaminated with heavy metals.

Heavy metal bioremediation can be classified as either bioaccumulation, a metabolically controlled process that requires the active uptake of heavy metal ions by living biomass, or biosorption, a non-metabolic process that passively binds metal cations onto non-living biomass[4]. Bioaccumulation requires energy for the uptake of metal ions and typically occurs through the interaction of metal ions and the cell wall. The second step is intracellular uptake, wherein metal ions penetrate the cell membrane and enter the cell to bind on the active sites provided by polysaccharides and proteins. Biosorption relies on the presence of functional groups in the cell wall and/or metabolites exported to the external area. Mechanisms of biosorption include ion exchange, complexation, precipitation, reduction, and chelation[10].

Under harsh conditions in the presence of toxic heavy metals and antibiotics, bacteria commonly produce extracellular polymeric substances (EPS) as a protective response. Bacterial EPS are natural polymers of high molecular weight secreted by microorganisms into their environment[11]. Bacterial EPS typically contains

[1]Faculty of Engineering, Hokkaido University, Kita 13, Nishi 8, Kita-Ku, Sapporo 060-8628, Japan. [2]IWRM Centre/Geology Department, School of Mines, University of Zambia, P.O. Box 32379, Lusaka, Zambia. [3]Department of Mining, Metallurgical, and Materials Engineering, University of the Philippines Diliman, Quezon City, Philippines. [4]Graduate School of Veterinary Medicine, Hokkaido University, Kita 18, Nishi 9, Kita-Ku, Sapporo 060-0818, Japan. ✉email: k.naka@eng.hokudai.ac.jp

polysaccharides with ionizable functional groups such as carboxyl, sulfate, and phosphate. These functional groups can be deprotonated to anionic species, which interact with cationic metal ions through electrostatic interactions, resulting in the immobilization of heavy metals within the EPS[12]. Biosorption through EPS has been extensively studied because of its efficient sequestration of toxic metals[10,13,14]. The metabolism-independent process of biosorption within the EPS is typically more favorable than bioaccumulation within the cell, which is metabolism-dependent[12]. Biosorption has thus received significant research attention. Despite the isolation of various types of bacteria, the isolation and characterization of indigenous bacteria are indispensable since they are environmentally acceptable and preserve the ecosystem in their locality as evidenced by studies that have used metal tolerant bacteria from industrial effluent[15]. The local population, soil, water, and food are contaminated with Pb (II) and Zn (II) in the study area at Kabwe Mine, Zambia, Africa, leading Kabwe to be labeled as one of the 10 most polluted places on Earth in 2013[16].

Therefore, this study aims to assess the heavy metal removal by *Oceanobacillus profundus* KBZ 3-2, a strain isolated by our research group at the Kabwe Mine site, Zambia, Africa[17]. This bacterium was isolated when we investigated the biocementation of mine waste by immobilization using ureolytic bacteria by microbially induced calcium carbonate precipitation. The results from the investigation showed that mine waste was stabilized by indigenous bacteria. Additionally, during the characterizing of the bacteria isolated from the site, we found out that *O. profundus* KBZ 3-2 had a higher biosorption capacity and was worth investigation for heavy metal removal. This study investigated the removal of heavy metals by isolated bacteria in single metal ion batch experiments in a solution prepared to imitate the environment at the abandoned lead–zinc mine at Kabwe, Zambia. The Pb (II) and Zn (II) metal ions were selected for investigation because both pollutants have caused significant health problems to communities near the site[18]. Moreover, the mechanism of biosorption was discussed and especially focused on the dominant factor affecting biosorption.

Materials and methods

Bacterial strain and chemical reagents. The mine waste was exported from the abandoned Kabwe Mine, Zambia under approval No. RCT 7686229, and the import was permitted by Plant Protection Station, Ministry of Agriculture, Forestry and Fisheries, Japan under the approval No. 29-836. The bacterial strain *O. profundus* KBZ 3-2 used in this study was isolated from the mine waste when screening for ureolytic bacteria for the solidification of sand[17]. The same methodology described in our previous study was used to screen the bacterium[17]. Chemical reagents used in this study were obtained from Wako Pure Chemical Industries Ltd., Tokyo, Japan, otherwise mentioned.

Growth of bacteria in the presence of Pb (II)/Zn (II). After preculturing *O. profundus* KBZ 3-2, the bacteria were cultured in 100 mL of LB medium containing $PbCl_2$ or $ZnCl_2$ with different concentrations ranging from 0–50 mg/L for 24 h. Cell growth was monitored by checking the turbidity of the culture with a UV–vis spectrophotometer at 600 nm (OD_{600}).

Effect of pH on biosorption of Pb (II)/Zn (II). The bacteria were inoculated in a 100 mL LB medium containing 20 mg/L of $PbCl_2$ or 2 mg/L of $ZnCl_2$ at different pH ranging from 2 to 9 and adjusted by HNO_3 or NaOH. After cultivation at 30 °C at 160 rpm for 24 h, the cell culture was centrifuged at 8000 × *g* at 4 °C for 10 min to separate the supernatant and precipitate. The heavy metal concentrations of Pb or Zn in the supernatant were measured by inductively coupled plasma atomic emission spectroscopy (ICP-AES) (ICPE-9820, Shimadzu Corporation, Kyoto, Japan). The biosorption efficiency of heavy metals by the bacteria was calculated as $(C_i - C_f)/C_i \times 100$ (%), where C_i is the initial concentration, and C_f is the final concentration of metal ions.

Localization of Pb (II) and Zn (II) in bacterial cells. The localization of Pb (II) and Zn (II) in cellular parts was determined according to the methodology reported by Sheng, et al.[19] with some modifications and has been illustrated in Scheme 1. Briefly, cells were cultured in 100 mL of LB medium containing 20 mg/L of Pb or 2 mg/L of Zn at 30 °C at 160 rpm for 24 h and were harvested by centrifuge at 8000 × *g* for 10 min. The supernatant was filtered by a 0.45 µm membrane filter, where EPS and EPS-bound metal ions were trapped and free metal ions passed through. The concentration of Pb (II) or Zn (II) in the filtrate was measured by ICP-AES. The cell pellets were ultrasonicated at 30 kHz for 5 min (Vibra-Cell VCX 130, Sonics & Materials, Inc., Newtown, USA) in 5 mL Tris–HCl (10 mM, pH 8.0), followed by centrifugation at 8000 × *g* for 10 min to separate the supernatant (cell-free extract: cytoplasm) and precipitate (cell debris: cell wall/membrane). The supernatant was thereafter collected for analysis to determine the cytoplasmic water-soluble Pb (II) or Zn (II). The precipitate, cell debris, was then suspended in protein extracting solution (5% Sodium Dodecyl Sulfate: SDS, 10 mM Tris–HCl, pH 8), followed by centrifugation at 8000 × *g* for 10 min. The resulting supernatant was used for the determination of metal ions accumulated in cell wall/membrane proteins, and the obtained precipitate was digested by 65% nitric acid to quantify the Pb (II) or Zn (II) accumulated in cell wall/membrane components. The concentration of Pb (II) or Zn (II) accumulated in EPS was calculated by subtracting the metal concentration in the other factions from the initial concentration. Meanwhile, protein and carbohydrate contents in a supernatant (soluble fraction) after 24 h cell cultivation were measured. The protein content in the supernatant was determined by the Bradford protein assay with bovine serum albumin as the standard, and the total carbohydrate content was determined by the phenol sulfuric acid method as previously described[20].

Confocal laser scanning microscopy (CLSM) analysis. The bacteria cells were cultured in 100 mL LB medium for 24 h in the presence of 20 mg/L of Pb (II) and collected by centrifuge at 8000 × *g* for 10 min, followed by suspension in saline buffer. Three different staining dyes were sequentially added to the cell suspension to

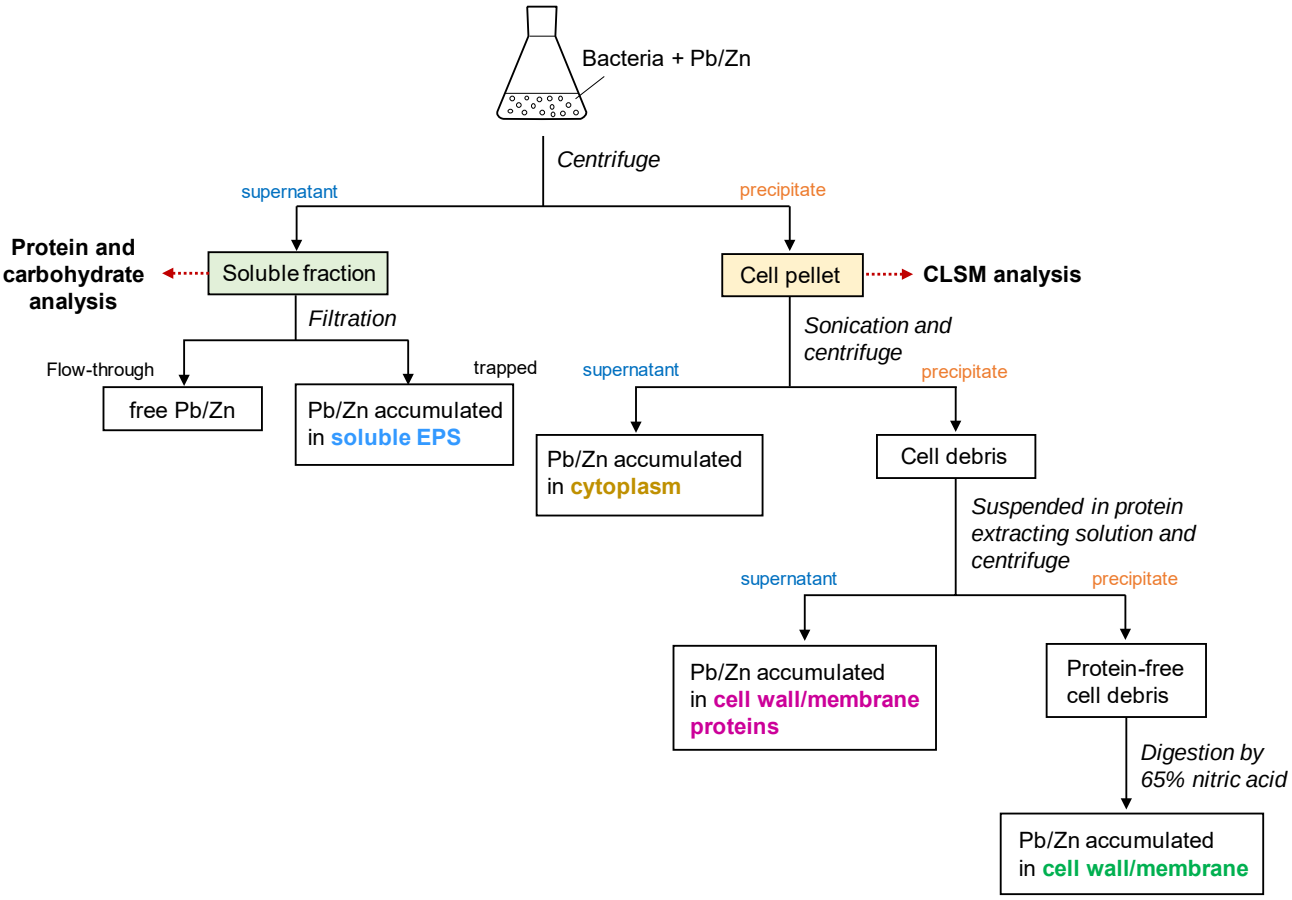

Scheme 1. Flowchart for the analytical procedure for the determination of the distribution of heavy metal in different cellar parts.

stain the DNA (DAPI Nucleic Acid Stain, Molecular probes, Invitrogen), EPS (Wheat Germ Agglutinin, Alexa Fluor 633 Conjugate, Molecular Probes, Invitrogen), and Pb (II) (Leadmium Green AM Dye, Molecular Probes, Invitrogen). The samples were analyzed with a CLSM (Nikon A1 and Ti-E) equipped with a Plan Apo VC × 60 objective lens (NA 1.40, Nikon).

Results and discussion

Effect of Pb (II) and Zn (II) on bacterial growth. Bacterial growth under exposure to the heavy metal ions of interest was assessed to gauge the applicability of the strain for bioremediation. Figure 1 shows the effect of Pb (II) and Zn (II) on the growth of *O. profundus* KBZ 3-2 in different concentrations. The bacterial cells grew well in all the tested concentrations of Pb (II), demonstrating resistance to Pb (II) contamination up to 50 mg/L. However, the bacteria were less tolerant of Zn (II), displaying growth only in 2 mg/L Zn (II). This result indicates that the bacteria can be used for bioremediation of Pb (II) and Zn (II), albeit at a lower concentration for the latter. Inefficient biosorption of Zn (II) at higher Zn(II) concentrations occurs because Zn (II) is a trace element required for the growth of heterotrophic bacteria[21], such as *O. profundus*. However, at higher concentrations, Zn (II) hinders the survival of the bacteria; this is consistent with previous results that Zn (II) is a highly reactive divalent metal ion and that it would readily displace metal ions required for bacterial growth[22]. Moreover, Zn (II) is a known antibacterial agent because it is a strong oxidative agent that causes cell membrane disruption, leading to cell death[22].

Effect of pH on adsorption. The pH of the solution is among the most important parameters in biosorption because the initial pH of the solution is a key factor that affects the metal speciation, metal solubility, and the dissociation of the functional groups[23,24]. Figure 2 shows the effect of pH on heavy metal removal efficiency. The removal percentage of metal ions was as low as 18% for Pb (II) and 12% for Zn (II) at pH 2. The maximum removal percentage for Pb (II) was 97% at an initial concentration of 50 mg/L whereas maximum removal percentage for Zn (II) was 54% at an initial concentration of 2 mg/L obtained at pH 6. This low removal percentage at low pH was attributed to the protonation of functional groups, which were responsible for metal ion adsorption[22]. Similar findings by earlier investigators have also attributed lower biosorption efficiency to protonation or poor ionization of functional groups at low pH, resulting in a weak complex affinity of the metal ions[25,26]. On the other hand, at higher pH values, the binding efficiency increased because the functional groups

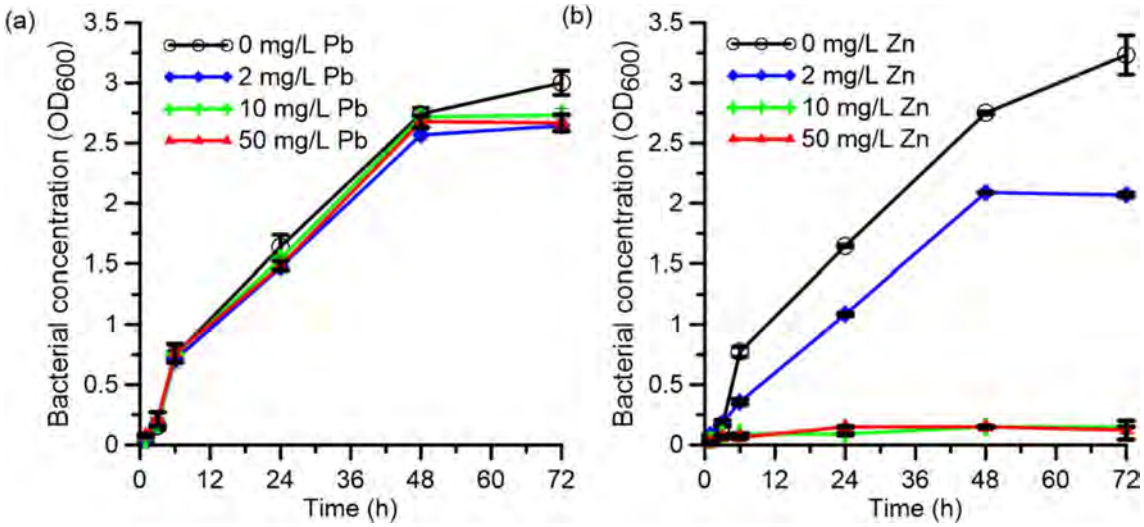

Figure 1. Microbial growth of *O. profundus* KBZ 3-2 in the presence of **(a)** Pb (II) and **(b)** Zn (II) with different concentrations.

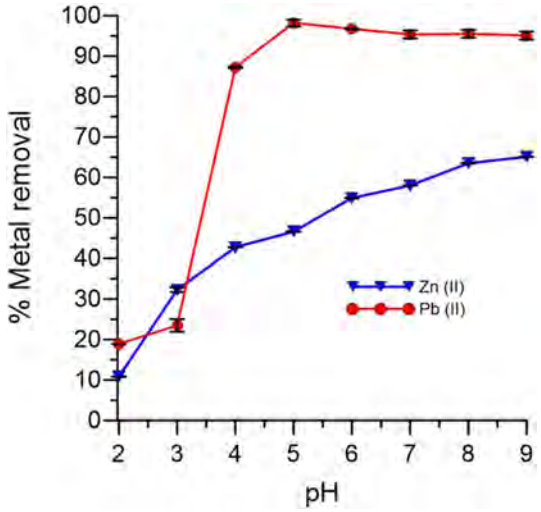

Figure 2. Effect of pH on biosorption by *O. profundus* KBZ 3-2.

were negatively charged, thereby facilitating biosorption of the metal cations through ion exchange and metal chelation complexation. Additionally, the resulting effective pH for biosorption is consistent with the data obtained from bacteria in the Bacillaceae family, which showed an effective pH range of 5–9[22]. A sharp increase in biosorption was observed in Pb and a gradual increase for Zn was probably caused by the gradual exhaustion of active sites for the biosorption of zinc ions. This trend has been observed in previous investigation[5]. Table 1 represents a comparison between *O. profundus* KBZ 3-2 with other biosorbent materials. The results show the *O. profundus* KBZ 3-2 can be used as an effective biosorbent.

Localization of Pb (II) and Zn (II) in a cell. We found there was no Pb/Zn left in the filtrate after filtration of the supernatant of cell culture added with Pb/Zn, which indicates heavy metal ions were totally trapped by the bacteria. The localization of metal ions in the different cellular parts of the bacteria was investigated to understand the possible mechanism of Pb (II) and Zn (II) accumulation in the bacteria cells. The percentages of metal ions in (1) soluble EPS, (2) the cytoplasm, (3) cell wall/membrane proteins, and (4) the cell wall/membrane of *O. profundus* KBZ 3-2 are shown in Fig. 3. The highest concentration for both elements was in soluble EPS (87%), which is produced in the soluble phase by bacteria as a defense mechanism against heavy metal contamination[22]. Pb (II) accumulation in other parts was determined in the cytoplasm (1%), cell wall/membrane proteins (2%), and the cell wall/membrane (10%). Zn (II) was found in the cytoplasm (6%), cell membrane/wall proteins (3%), and the cell wall/membrane (4%). For both heavy metals, biosorption would predominantly be metabolism-independent since it primarily occurred on the exterior of the cell, EPS. We can conclude that metabolism-dependent biosorption has a minor role[30].

Metal ion	Biosorbent	Metal ion conc	Adsorption efficiency (%)	Ref
Pb	*Pseudomonas* sp.	1 mg/L	87.9	[27]
	S. maltophilia	39.6 mg/L	96	[28]
	B. iodium	100 mg/L	87	[29]
	O. profundus KBZ 3–2	50 mg/L	97	This study
Zn	*S. maltophilia*	20.6 mg/L	96	[28]
	Pseudomonas sp.	1 mg/L	49.8	[27]
	Zinc sequestering bacterium VMSDCM	0.21 mol/g of biomass		[5]
	O. profundus KBZ 3–2	2 mg/L	54	This study

Table 1. Comparison between *O. profundus* KBZ 3-2 with other biosorbents.

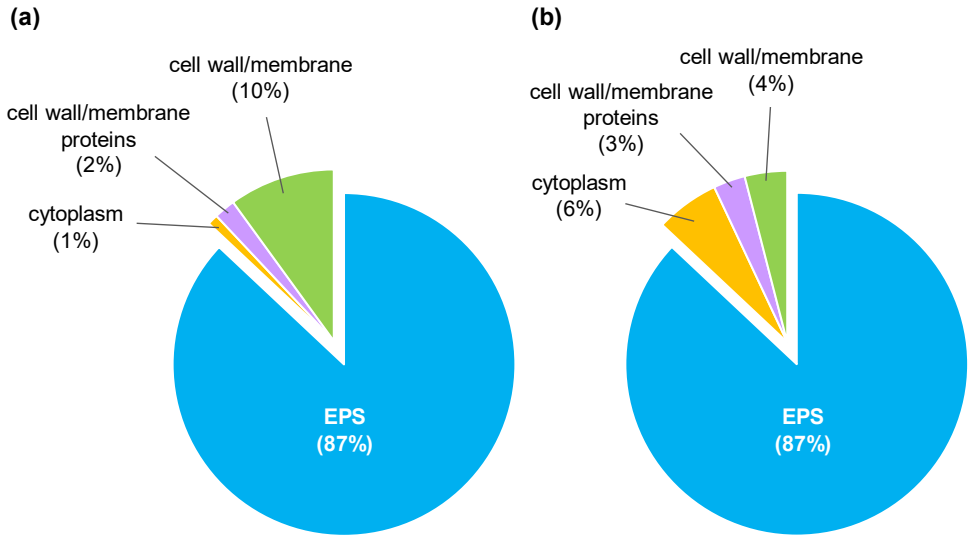

Figure 3. Distribution of **(a)** Pb(II) and **(b)** Zn(II) in different cellular parts of *O. profundus* KBZ 3-2.

The amount of cytoplasmic Zn (II) in Fig. 3b was higher than that of Pb (II) in Fig. 3a, probably because Zn (II) is used for microbial metabolic processes in trace amounts. The formation of EPS-Pb could have prevented the entry of Pb into the cell; hence a small amount of Pb (II) was detected inside the cell. EPS contains different carbohydrates and their derivatives[31], which are usually polyanionic because of the functional groups. This allows biosorption through mechanisms such as ion exchange and metal complexation[32]. Thus, we propose that the dominant mechanism of Pb (II) and Zn (II) biosorption by *O. profundus* KBZ 3-2 occurs by soluble EPS being actively secreted by a bacterium to defend itself from toxic ions, thereby binding Pb (II) and Zn (II) ions from solutions through metal chelation-complexation and consequently removing Pb (II) and Zn (II) through metabolism-independent process biosorption. Bioaccumulation also occurred, albeit at a significantly lesser degree, as evidenced by the presence of heavy metals within the cell.

Composition of EPS released by the bacteria. Figure 4a shows the photo of a centrifuged bacterial suspension-cultured for 24 h in the presence of 20 mg/L Pb. We observed the supernatant containing soluble EPS and the precipitates containing bacterial cells. The composition of soluble EPS was analyzed over time in terms of proteins and carbohydrates (Fig. 4b), because it is the main component responsible for metal sequestration. Typically, EPS consists of water, protein, polysaccharides, nucleic acid, uronic acid, and humic acid[33–35]. The EPS had 105 µg/L of protein and 679 µg/L of carbohydrates; these components are primarily responsible for the biosorption of Pb (II) and Zn (II) through metal chelation-complexation because they contribute to the negatively charged carboxyl group ($-COO^-$), sulfate group ($-SO_3^-$), and phosphate group ($-PO_3^-$). This result is consistent with the characteristic of a bacterium having defensive mechanisms for Pb (II). Previous studies have also shown that bacterium can survive in the conditions with high heavy metal exposure by developing resistance and could be isolated and used for the bioremediation of Zn (II), Cd (II), Cu (II), and Pb (II)[27,31,32]. A representative diagram for the bacterial biosorption mechanism is depicted in Fig. 5.

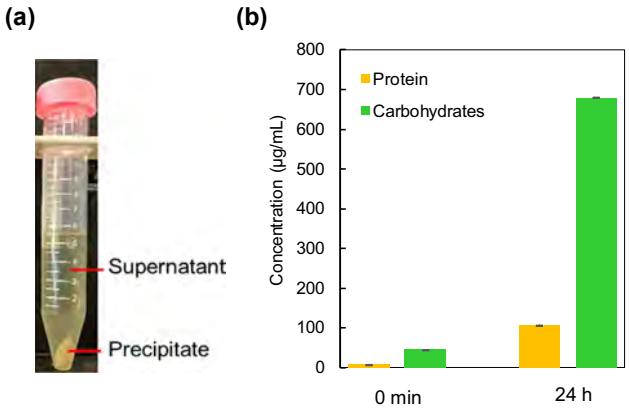

Figure 4. Analysis of *O. profundus* KBZ 3-2 cultured in 20 mg/L Pb for 24 h; **(a)** image of centrifuged culture, **(b)** quantitative determination of proteins and carbohydrates in soluble EPS.

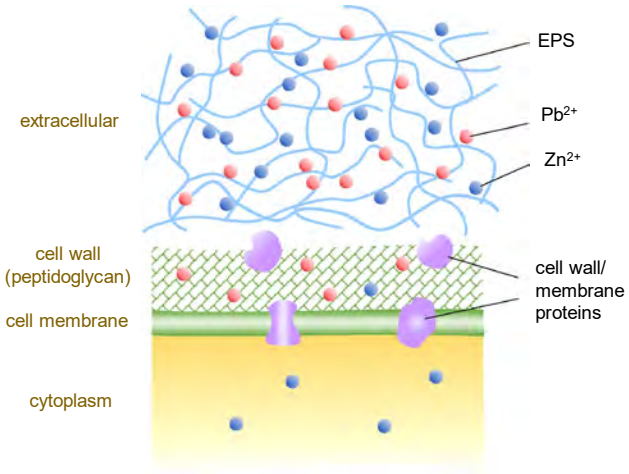

Figure 5. Representative diagram for biosorption mechanism for Pb(II) and Zn(II).

CLSM analysis. As indicated in the study methods, we conducted a CLSM analysis of grown cells in the presence of 20 mg/L Pb (II) to further confirm the native associations of cell-EPS-metal ion aggregates. Most of the EPS was found in the supernatant after centrifugation, some EPS would be staying around the cells. Figure 6 shows the CSLM images of the bacterial suspension, showing the bright-field image (a), the bacterial cells (b, in blue), EPS (c, in red), and Pb (II) (d, in green). The correlation and visualization of each component (bacterial cells, EPS, and Pb (II)) confirm the adsorption of Pb ions onto the cells and their surroundings. Since the cells were surrounded by the remaining EPS, which was secreted by cells, the protein and carbohydrates in EPS would be responsible for the heavy metal detoxification via complexation with metal ions. Consequently, EPS has an important role in the adsorption of different toxic heavy metals, which is consistent with the previous report[13].

Conclusion

The study demonstrated that *O. profundus* KBZ 3-2 isolated from Pb–Zn contaminated soil at the Kabwe Mine site in Zambia was capable of removing Pb (II) and Zn (II) from water. The proposed mechanism of biosorption was through chelation-complexation on the present functional groups of EPS excreted by the bacteria. *O. profundus* KBZ 3-2 was a highly efficient biosorbent and had high potential in upscaling its biosorption purpose for bioremediation at Kabwe Mine site as an eco-friendly solution to contaminated site restoration. This is recommended for the cleaning of contaminated water from the mine site.

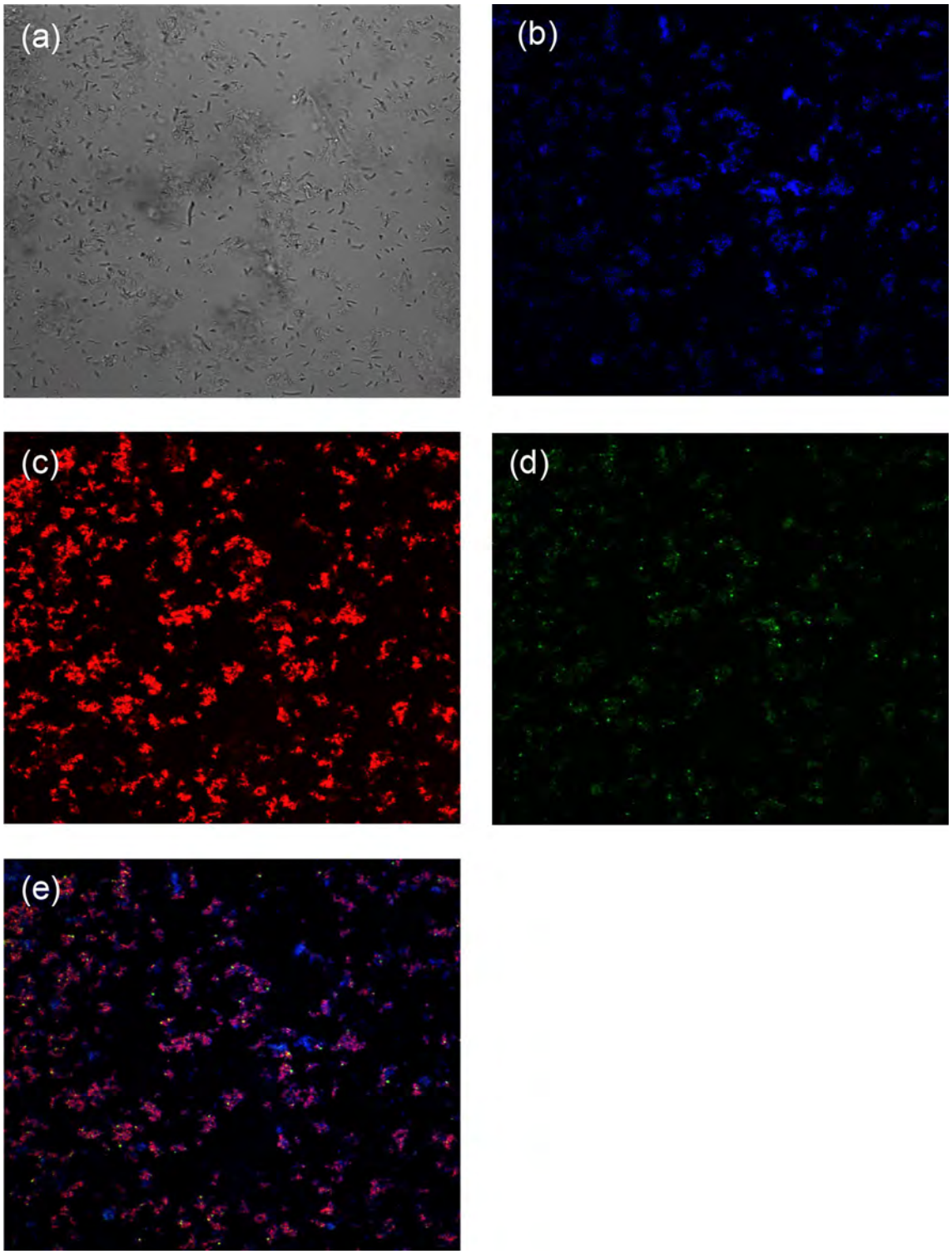

Figure 6. Confocal images of *O. profundus* KBZ 3-2 cultured in 20 mg/L Pb for 24 h; **(a)** bright-field image, **(b)** bacterial cells stained by DAPI (blue), **(c)** EPS stained by Alexa Fluor 633-conjugated agglutinin (red), **(d)** Pb (II) stained by Leadmium Green AM Dye (green), **(e)** overlay image of **(b–d)**.

Received: 20 May 2020; Accepted: 19 November 2020
Published online: 03 December 2020

References

1. Tchounwou, P. B., Yedjou, C. G., Patlolla, A. K. & Sutton, D. J. Heavy metal toxicity and the environment. *Exp. Suppl.* **101**, 133–164 (2012).
2. Jena, S. & Dey, S. K. Heavy metals. *Am. J. Environ. Stud.* **1**, 48–60 (2016).
3. Ayangbenro, A. S. & Babalola, O. O. A new strategy for heavy metal polluted environments: A review of microbial biosorbents. *Int. J. Environ. Res. Public Health* **14**, 1–16 (2017).
4. Abdi, O. & Kazemi, M. A review study of biosorption of heavy metals and comparison between different biosorbents. *J. Mater. Environ. Sci.* **6**, 1386–1399 (2015).
5. Vishal, M., Shail, D. & Chandrajit, B. Optimization of physical parameters for batch mode Zn (II) ion removal from liquid phase: A potential biosorption study. *Environ. Prog. Sustain. Energy* **32**, 213–222 (2013).
6. Rodríguez, I. A. *et al*. Biosorption of heavy metals by *Candida albicans*. *Adv. Bioremediat. Phytoremediat.* 43–63, https://doi.org/10.5772/intechopen.72454 (2018).
7. Anastopoulos, I. & Kyzas, G. Z. Progress in batch biosorption of heavy metals onto algae. *J. Mol. Liq.* **209**, 77–86 (2015).
8. Prasad, A. S. A., Varatharaju, G., Anushri, C. & Dhivyasree, S. Biosorption of lead by *Pleurotus florida* and *Trichoderma viride*. *Br. Biotechnol. J.* **3**, 66–78 (2013).
9. Mishra, V., Balomajumder, C. & Agarwal, V. K. Design and optimization of simultaneous biosorption and bioaccumulation (SBB) system: A potential method for removal of Zn(II) ion from liquid phase. *Desalin. Water Treat.* **51**, 3179–3188 (2013).
10. Vishan, I., Laha, A. & Kalamdhad, A. Biosorption of Pb(II) by *Bacillus badius* AK strain originating from rotary drum compost of water hyacinth. *Water Sci. Technol.* **75**, 1071–1083 (2017).
11. Caruso, C. *et al.* Extracellular polymeric substances with metal adsorption capacity produced by *Pseudoalteromonas* sp. MER144 from Antarctic seawater. *Environ. Sci. Pollut. Res.* **25**, 4667–4677 (2018).
12. Saba, Rehman, Y., Ahmed, M. & Sabri, A. N. Potential role of bacterial extracellular polymeric substances as biosorbent material for arsenic bioremediation. *Bioremediat. J.* **23**, 72–81 (2019).
13. More, T. T., Yadav, J. S. S., Yan, S., Tyagi, R. D. & Surampalli, R. Y. Extracellular polymeric substances of bacteria and their potential environmental applications. *J. Environ. Manag.* **144**, 1–25 (2014).
14. Shameer, S. Biosorption of lead , copper and cadmium using the extracellular polysaccharides (EPS) of *Bacillus* sp ., from solar salterns. *3 Biotech* **6**, 1–10 (2016).
15. Mishra, V., Balomajumder, C. & Agarwal, V. K. Biological removal of heavy metal zinc from industrial effluent by zinc sequestering bacterium VMSDCM. *Clean Technol. Environ. Policy* **16**, 555–568 (2013).
16. Blacksmith, I. The worlds worst 2013: The top ten toxic threats. https://doi.org/10.1017/CBO9781107415324.004 (2013).
17. Mwandira, W. *et al.* Solidification of sand by Pb(II)-tolerant bacteria for capping mine waste to control metallic dust: Case of the abandoned Kabwe Mine, Zambia. *Chemosphere* **228**, 17–25 (2019).
18. Yabe, J. *et al.* Lead poisoning in children from townships in the vicinity of a lead-zinc mine in Kabwe, Zambia. *Chemosphere* **119**, 941–947 (2015).
19. Sheng, Y. et al. Cadmium tolerant characteristic of a newly isolated *Lactococcus lactis* subsp. lactis. *Environ. Toxicol. Pharmacol.* **48**, 183–190 (2016).
20. Dubois, M., Gilles, K. A., Hamilton, J. K., Rebers, P. A. & Smith, F. Colorimetric method for determination of sugars and related substances. *Anal. Chem.* **28**, 350–356 (1956).
21. Bong, C. W., Alfatti, F. M., Zam, F. A., Obayashi, Y. & Suzuki, S. The effect of zinc exposure on the bacteria abundance and proteolytic activity in seawater. *Interdiscip. Stud. Environ. Chem. Responses Contam.* 57–63 (2010).
22. Capdevila, D. A., Wang, J. & Giedroc, D. P. Bacterial strategies to maintain zinc metallostasis at the host-pathogen interface. *J. Biol. Chem.* **291**, 20858–20868 (2016).
23. Lu, W. Bin, Shi, J. J., Wang, C. H. & Chang, J. S. Biosorption of lead, copper and cadmium by an indigenous isolate *Enterobacter* sp. J1 possessing high heavy-metal resistance. *J. Hazard. Mater.* **134**, 80–86 (2006).
24. Kalita, D. & Joshi, S. R. Study on bioremediation of lead by exopolysaccharide producing metallophilic bacterium isolated from extreme habitat. *Biotechnol. Rep.* **16**, 48–57 (2017).
25. Jnr, M. H. & Harcourt, P. Studies on the effect of pH on the sorption of Pb^{2+} and Cd^{2+} ions from aqueous solutions by *Caladium bicolor* (Wild Cocoyam) biomass. *Electron. J. Biotechnol.* **7**, 313–323 (2004).
26. Pehlivan, E., Altun, T. & Parlayici, S. Modified barley straw as a potential biosorbent for removal of copper ions from aqueous solution. *Food Chem.* **135**, 2229–2234 (2012).
27. Sundaramanickam, A. A comparative study of physico-chemical investigation along Parangipettai and Cuddalore coast. *J. Environ. Sci. Technol.* 1–10, https://doi.org/10.3923/jest.2008.1.10 (2008).
28. Wierzba, S. Biosorption of lead(II), zinc(II) and nickel(II) from industrial wastewater by *Stenotrophomonas maltophilia* and *Bacillus subtilis*. *Polish J. Chem. Technol.* **17**, 79–87 (2015).
29. De, J., Ramaiah, N. & Vardanyan, L. Detoxification of toxic heavy metals by marine bacteria highly resistant to mercury. *Mar. Biotechnol.* **10**, 471–477 (2008).
30. Muthu, M., Wu, H. F., Gopal, J., Sivanesan, I. & Chun, S. Exploiting microbial polysaccharides for biosorption of trace elements in aqueous environments—Scope for expansion via nanomaterial intervention. *Polymers (Basel).* **9**, 1–12 (2017).
31. Shameer, S. Biosorption of lead, copper and cadmium using the extracellular polysaccharides (EPS) of *Bacillus* sp., from solar salterns. *3 Biotech* **6**, 1–10 (2016).
32. Igiri, B. E. *et al.* Toxicity and bioremediation of heavy metals contaminated ecosystem from tannery wastewater: A review. *J. Toxicol.* **2018**, 1–16 (2018).
33. Tourney, J. & Ngwenya, B. T. The role of bacterial extracellular polymeric substances in geomicrobiology. *Chem. Geol.* **386**, 115–132 (2014).
34. Shi, Y. *et al.* Exploiting extracellular polymeric substances (EPS) controlling strategies for performance enhancement of biological wastewater treatments: An overview. *Chemosphere* **180**, 396–411 (2017).
35. Nouha, K., Kumar, R. S., Balasubramanian, S. & Tyagi, R. D. Critical review of EPS production, synthesis and composition for sludge flocculation. *J. Environ. Sci. (China)* **66**, 225–245 (2018).

Acknowledgements

This work was supported by JSPS KAKENHI under Grant Number JP18H03395, JST/JICA SATREPS (Science and Technology Research Partnership for Sustainable Development; No. JPMJSA1501), and JST aXis (Accelerating Social Implementation for SDGs Achievement; No. JPMJAS2001). We are grateful to Dr. K. Kobayashi and the Nikon Imaging Center at Hokkaido University for being very helpful with confocal microscopy, image acquisition, and analysis.

Author contributions

W.M., K.N. and S.K. designed the research. K.B., I.N. and M.C. provided the samples that made the study possible. W.M. and A.A. performed the experiments and analyzed the data. W.M. and K.N. wrote the manuscript, and K.B., I.N., and T.I. carefully read to edit the manuscript. M.It., T.S., H.N., S.N., and M.Is. participated in discussions of this work. All authors reviewed the manuscript.

Competing interests

The authors declare no competing interests.

Additional information

Correspondence and requests for materials should be addressed to K.N.

Reprints and permissions information is available at www.nature.com/reprints.

Publisher's note Springer Nature remains neutral with regard to jurisdictional claims in published maps and institutional affiliations.

International Journal of
Environmental Research and Public Health

MDPI

Article

Lead, Zinc and Cadmium Accumulation, and Associated Health Risks, in Maize Grown Near the Kabwe Mine in Zambia in Response to Organic and Inorganic Soil Amendments

Patricia N. Mwilola [1], Ikabongo Mukumbuta [1,2,*], Victor Shitumbanuma [1], Benson H. Chishala [1], Yoshitaka Uchida [3], Hokuto Nakata [2], Shouta Nakayama [2] and Mayumi Ishizuka [2]

1 Department of Soil Science, School of Agricultural Sciences, University of Zambia, Lusaka P.O. Box 32379, Zambia; mwilolanalishebo@gmail.com (P.N.M.); vshitumbanuma@unza.zm (V.S.); bchishala@unza.zm (B.H.C.)
2 Faculty of Veterinary Medicine, Hokkaido University, Kita 18, Nishi 9, Kita-Ku, Sapporo 060-0809, Japan; hokuto.nakata@vetmed.hokudai.ac.jp (H.N.); shouta-nakayama@vetmed.hokudai.ac.jp (S.N.); ishizum@vetmed.hokudai.ac.jp (M.I.)
3 Research Faculty of Agriculture, Hokkaido University, Kita 9, Nishi 9, Kita-ku, Sapporo 060-8589, Japan; uchiday@chem.agr.hokudai.ac.jp
* Correspondence: ikabongo1@gmail.com; Tel.: +260-961-486-377

Received: 29 September 2020; Accepted: 1 December 2020; Published: 4 December 2020

Abstract: Health risks due to heavy metal (HM) contamination is of global concern. Despite concerns of high levels of HMs in soils near Kabwe mine in Zambia, edible crop production is common, posing potential health risks. This study assessed the potential of chicken manure (CM), triple superphosphate (TSP) and a blended fertilizer (BF; consisting of Nitrogen, Phosphorous and Potassium (NPK) fertilizer and composted chicken manure) to reduce lead (Pb), zinc (Zn) and cadmium (Cd) in soils and their accumulation in maize grown near the Kabwe mine. Maize was grown to maturity and its HM concentrations and associated health risk indices were calculated. All soil amendments decreased bioavailable soil Pb concentrations by 29–36%, but only CM decreased Zn, while the amendments increased or had no effect on Cd concentrations compared to the control. The amendments reduced Pb (>25%) and Zn concentrations (>18%) in the maize stover and grain. However, Cd concentrations in maize grain increased in the BF and TSP treatments. Bioaccumulation factors showed that Cd had the highest mobility from the soil into maize stover and grain, indicating the need for greater attention on Cd in Kabwe despite its apparently lower soil concentration compared to Pb and Zn. The hazard quotients for Pb and Cd were much greater than one, indicating a high risk of possible exposure to toxic levels by people consuming maize grain grown in this area. This study demonstrated the significant potential of manure and phosphate-based amendments to reduce Pb and Zn, and to some extent Cd, uptake in maize grain and consequently reduce associated health risks.

Keywords: legacy mining; heavy metals; soil amendments; maize; health risks

1. Introduction

Contamination of the environment due to heavy metals (HMs) from mining and other industrial activities is of major concern globally due to their effect on water and food quality and the resulting effect on human healthy [1–3]. Heavy metals accumulate in soils following the disposal of tailings, dust emission, through water transport or pesticide use [4–8]. Food crops can accumulate high

amounts of HMs through soil-plant uptake, leading to food contamination and significant human health risks [8–12]. Food crop consumption has been reported as one of the major pathways for human exposure to HMs [11]. Furthermore, due to being non-biodegradable, HMs can accumulate in the human body even when their concentrations in the ingested food are low.

Heavy metals pose a significant effect on the health of soils, plants, animals and humans [4,8,13]. Among the HMs, lead (Pb) and cadmium (Cd) have serious adverse effects on plant growth, and human and animal health when ingested. Cd is reported to be carcinogenic and highly toxic to humans and animals [14] and leads to reduced germination and growth of plants [15]. Pb affects neurodevelopment of humans especially children [14,16] and inhibits plant growth. Unlike Pb and Cd, Zinc (Zn) is an essential plant nutrient but at elevated concentrations it has adverse effects on soil microorganisms, plants and animal health [5,15] and decreases soil quality [17].

Different strategies such as soil inversion or replacement [18], phytoremediation [19], use of raised garden beds [20], use of specific plants/crops [21] and addition of soil amendments [22–24], have been used to minimize accumulation of HMs in food crops and the resulting human exposure. However, phytoremediation takes long to show positive effects [25] and other methods such as soil replacement are very costly [26]. Soil amendments, such as manure and phosphate-fertilizers can be both effective and cheaper [20,26] and therefore more suited for poorer countries. Soil amendments such as manure, compost and phosphorous-based fertilizers have been proposed and shown to immobilize HMs in soil and reduce plant uptake [4,22–24,27,28]. Organic amendments such as animal manure immobilize HMs through chelation, formation of insoluble complexes, adsorption on charged functional groups and cation exchange [4,22,29]. Phosphate amendments immobilize HMs by formation of insoluble compounds such as pyromorphite [22,24].

In Kabwe, a town in central Zambia, mining was the main economic activity for several years but despite the closure of the mine, small-scale mining, including scavenging by local residents, is still widespread [30,31]. These activities, combined with poor environmental management have resulted in high levels of HMs such as Pb, Cd and Zn in many parts of the town [30,32]. Gardening and food crop production in the areas close to the mine is common and therefore, posing a high risk of human exposure to toxic levels of these HMs through food crop consumption. To date, there is limited information on the extent of this risk and on possible management and mitigation measures to remedy the problem [30]. Although inorganic and organic amendments, such as phosphate and manure, have shown potential to mitigate the accumulation of HMs in food crops [4,20,22–24], there is still lack of site-specific information in many African countries like Zambia [20,33]. In-situ field studies like this one are therefore still very crucial to fully understand the interaction between soil amendments and HMs in diverse settings and locations [20]. Furthermore, to the best of our knowledge, there haven't been in-situ field experiments in the vicinity of the Kabwe mine to assess the extent of the human health risks through maize consumption and potential mitigation measures.

The main goals of this study were to: (i) assess the levels of accumulation of Pb, Zn and Cd in the roots, stover and grain of maize (Zea mays), a crop widely grown and consumed in the study area, and the associated health risks, based on the joint United Nations Food and Agricultural Organization (FAO) and World Health Organization (WHO) limits for human health, and (ii) evaluate the effect of phosphate-bearing organic and inorganic soil amendments: chicken manure, triple super phosphate and an NPK fertilizer mixed with chicken manure on the bioavailable concentrations of Pb, Zn and Cd in the soil and their uptake by maize. We hypothesized that although the maize could be contaminated due to proximity to the mine, the HM concentrations and the health risks of consuming the maize can be significantly reduced after applying amendments to the soils.

2. Materials and Methods

2.1. Study Site

This study was conducted on a field located within 500 m from the former Pb/Zn mine in Kabwe town, central Zambia (14°27′28.3″ S, 28°27′37″ E). Before this study, this field had been used for

growing maize and other crops by local residents. The permission to use the land for this study was granted by the Kabwe municipal council.

This area receives an average of 900 mm rainfall annually with a mean annual temperature of 20.2 °C [30]. The soils at this site are classified as Chromic Haplic Lixisol [34]. The main properties of the soil and amendments are shown in Table 1.

Table 1. Soil and amendment characteristics.

Parameter	Soil	Manure	BF	TSP
Total Pb (mg kg^{-1})	8810 ± 310	-	-	-
Total Zn (mg kg^{-1})	1102 ± 203	-	-	-
Total Cd (mg kg^{-1})	260 ± 17	-	-	-
Total P	21.0 mg kg^{-1}	1.2%	20%	46%
Total carbon (%)	3.7			
Total nitrogen (%)	0.28	3.0	10	0
pH	5.7			
CEC (cmol + kg^{-1})	5.2			

CEC is cation exchange capcity; P is phosphorous; BF is blended fertilizer (a mixture of NPK fertilizer and chicken manure; TSP is triple super phosphate.

2.2. Experimental Design

This study examined the effects of raw chicken manure (CM), triple super phosphate (TSP), and blended fertilizer (BF)—a mixture of inorganic NPK fertilizer (10:20:10) and chicken manure on Pb, Zn and Cd immobilization in the soil and uptake in maize. These amendments were chosen in part due to ease of use, high availability in the study site and relatively low cost. Chicken manure was used its raw form as this is the common practice among gardeners in Zambia. Including the un-amended control (CT), there were a total of 16 plots each 4 × 4 m in size. Each of the four treatments was replicated four times and arranged in a Latin square design with a space of 0.5 m left between the plots. The field was ploughed to ~20 cm depth before application of the amendments. The amount of each amendment applied was aimed at supplying enough phosphate (PO_4) to immobilize the Pb within the top 20 cm soil by converting it to pyromorphite ($Pb_5(PO_4)_3C/$) at 5:3 Pb:phosphorous (P) ratio [4,35]. Although the soil contains different HMs, the amendments were applied based on the concentration of Pb, the metal of highest concern in the area [30]. The P contents in CM, BF and TSP were 1.2%, 20% and 46% respectively, resulting in the application of 82 kg CM, 5 kg BF and 3.2 kg TSP per plot. The applied amendments were equivalent to 50 ton, 6 ton and 0.9 ton ha^{-1} CM, BF and TSP respectively. These application rates of the amendments were similar to those used in other studies [4,23]. Nitrogen equal to that applied in the BF treatment (300 g plot^{-1}, 187 kg N ha^{-1}) was applied in the TSP and CT plots. The amendments were incorporated into the soil to the rooting depth of 20 cm [36,37].

The maize was planted at 20 and 40 cm intra- and inter-row spacing. At physiologic maturity, about 125 days after planting, maize plants were harvested and separated into roots, stover and grain. To determine total maize biomass production, maize plants in each plot were weighed and then 10 plants selected for drying used for determination of the moisture content and HM concentration. After drying (at 70 °C) the roots, stover and grains were ground and homogenized. The HM concentrations in the different plant parts were extracted in 1 M HNO_3 after dry ashing [38] and analyzed using a Flame Atomic Adsorption Spectrophotometer (FAAS; AA-6300, Shimadzu, Kyoto, Japan). The FAAS was run using acetylene gas and air as an oxidant at 2.5 mL min^{-1}. The detection limit for the FAAS was 0.01, 0.002 and 0.0004 mg L^{-1} for Pb, Zn and Cd respectively.

2.3. Determination of Total and Bioavailable Pb, Zn and Cd in Soils

Soil samples (0–20 cm depth) were collected prior to starting the experiment at 10 points within a 50 × 50 m field, and in each plot at the end of the experiment. The soils were air-dried, homogenized and then passed through a 2 mm sieve. The soils were analyzed for total Pb,

Zn and Cd contents extracted using aqua-regia solution (a mixture of nitric acid and hydrochloric acid in 1:3 ratio), and potentially-plant available Pb, Zn and Cd concentrations extracted using diethylentriaminopentanacetic acid triethanolamine (DTPA-TEA) solution buffered at pH 7.3 according to Lindsay and Norvell [39]. The DTPA-TEA extractable HMs are considered as bioavailable for plant uptake in this study [40]. Both the total and potentially-plant available soil Pb, Zn and Cd concentrations were determined using a FAAS.

For quality control, standard reference materials (SRM) 1573a (dried tomato leaves) and 2710a (Montana soil) were used. Additionally, all reagents used for both plant and soil extractions were analytical grade. For every set of sample analysis, a blank, with only the extracting reagent, was run during both the digestion and analysis throughout the experiment, and additionally, all containers were thoroughly washed, immersed in diluted HNO_3 for 24 h and subsequently rinsed with deionized water before use. Standard solutions were used to precondition the FAAS during each analysis. All plant and soil analyses were replicated four times.

2.4. Determination of Bioaccumulation Factors for Pb, Zn and Cd in Maize Stover and Grain

The bioaccumulation factor (BAF) is an important index that shows the transfer of HMs and other hazardous materials from the soil into plants [8]. In this study, the BAFs were determined separately for transfer of HMs from soil into the maize stover and from the soil into the maize grain using Equation (1).

$$\text{BAF} = \text{HM concentration in stover (or grain)/Soil HM concentration} \quad (1)$$

2.5. Pb and Cd Dietary Intake and Health Risk Assessment

The Joint United Nations Food and Agricultural Organization (FAO)/WHO Codex Alimentarius Commission (2018) [41] maximum tolerable intake limits were used as critical values to check the extent to which maize grown in soils near the Kabwe mine pose a risk to the local people. The hazard quotient (HQ) was used to assess the potential risk to human health resulting from maize consumption and was calculated as follows:

$$\text{HQ} = \text{EI/TI} \quad (2)$$

$$\text{EI} = \text{HM concentration in grain} * \text{Df} * \text{Y/HBW} \quad (3)$$

where: EI is the estimated metal intake (weekly for Pb and monthly for Cd) through maize grain consumption; TI represents the safe level of metal exposure through food crop consumption (weekly for Pb and monthly for Cd) [41]; Df is the average daily consumption of maize grain for an adult in Zambia; HBW is the average human body weight of an adult; Y is the number of days in a week or month.

In this study, 350 g was used as the Df [42], 70 kg as HBW [43] and 0.025 mg kg^{-1} HBW as the monthly Cd and weekly Pb TI values [41].

HQ values greater than 1 indicate significant risk to human health, while values less than 1 are considered safer for human health [10,40].

The TI value for Zn has not been established yet [41,43] and therefore EI and HQ values were not calculated for Zn in this study.

2.6. Data Analysis

All statistical analyses were performed using STATA 13 (Stata Corporation, College Station, TX, USA). The effect of soil amendments on bioavailable Pb, Zn and Cd concentrations in soils, and Pb, Zn and Cd concentrations in maize roots, stover and grain were evaluated using one-way ANOVA. Differences among the amendments were tested using Tukey's significance test. Pearson's correlation analysis was used to establish relationships among the bioavailable Pb, Zn and Cd concentrations in soils, Pb, Zn and Cd concentrations in maize roots, stover and grain with maize biomass

3. Results

3.1. Effect of Soil Amendments on Potentially-Plant Available Pb, Zn and Cd and Maize Biomass Production

The DTPA-TEA extractable Pb concentrations in the soil decreased by 30%, 36% and 29% in the CM, TSP and BF treatments respectively, compared to the unamended control plots (Figure 1). In contrast to results for Pb, TSP and BF did not decrease DTPA-TEA extractable Zn or Cd compared to the un-amended soil (Figure 1). Chicken manure on the other hand decreased concentrations of DTPA-TEA extractable Zn by 19% but increased those of Cd by 10% compared to the control.

Relative to the control treatment, the maize biomass production significantly increased in the CM and BF amended plots (Table 2). Maize biomass in the TSP plot was higher than that in the control although not statistically significant.

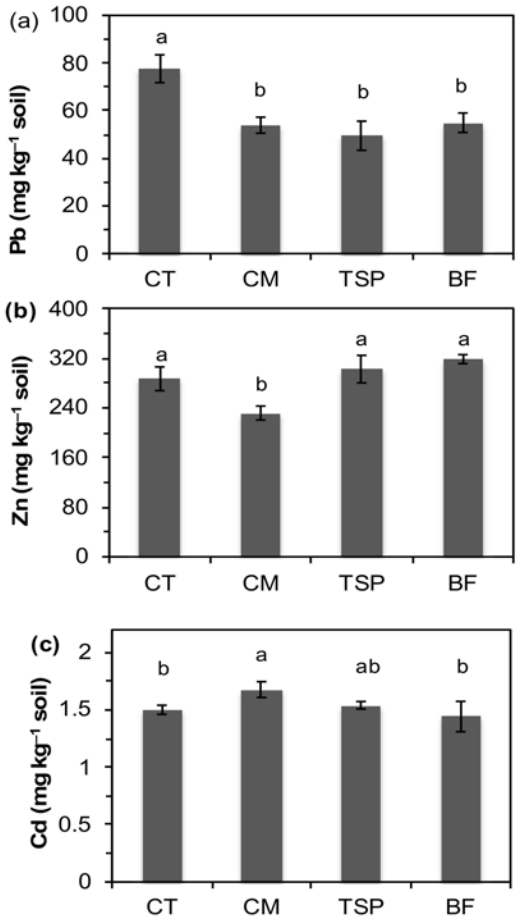

Figure 1. Concentrations of bioavailable: (**a**) lead (Pb); (**b**) zinc (Zn); (**c**) cadmium (Cd) in the soil at the end of the experiment. CT is the control, CM is chicken manure, TSP is triple superphosphate, BF is blended fertilizer (a mixture of NPK fertilizer and chicken manure). Bars with different letters are significantly different ($p < 0.05$).

Table 2. Mean maize biomass yield (±standard error) for different treatments.

	CT	CM	TSP	BF
Biomass Yield (kg plot^{-1})	0.9 ± 0.2 ^{b}	22.7 ± 2.2 ^{a}	5.2 ± 0.4 ^{b}	22.5 ± 3.7 ^{a}
Biomass Yield (kg ha^{-1})	1164 ± 310 ^{b}	28,438 ± 2830 ^{a}	6578 ± 529 ^{b}	28,092 ± 4726 ^{a}

CT is the control, CM is chicken manure, TSP is triple superphosphate, BF is blended fertilizer (mixture of NPK fertilizer and chicken manure) treatments. Values with different superscripts within a row indicate significantly different treatment means at $p < 0.05$.

3.2. Effect Soil Amendments on Pb, Zn and Cd Accumulation in Maize

Lead concentrations were highest in roots and lowest in the maize grain (Figure 2). Application of TSP and BF decreased Pb concentration in roots by more than 75% with root Pb concentration averaging 156.2 and 157.1 mg kg^{-1} in TSP and BF treatments compared to 743.3 mg kg^{-1} in the control plot. Manure application on the other hand did not decrease root Pb concentrations and instead resulted in a slight increase. Unlike the concentrations of Pb in roots, all three soil amendments significantly ($p < 0.01$) reduced Pb concentrations in the maize stover from 554 mg kg^{-1} to below 130 mg kg^{-1}, on average, representing a reduction of more than 75% (Figure 2). In the maize grain, Pb concentration decreased by 27%, 76% and 83% in the treatments TSP, BF and CM, respectively, compared to the control (Figure 2). The maize grain Pb concentrations ranged from 27.3–29.0, 3.1–5.3, 20.6–21.6 and 5.8–8.4 mg kg^{-1} in the un-amended control, CM, TSP and BF treatments, respectively. The Pb concentrations in the maize grain, from all treatments, were higher than the joint FAO/WHO maximum permissible limit of 0.2 mg kg^{-1} for human health safety.

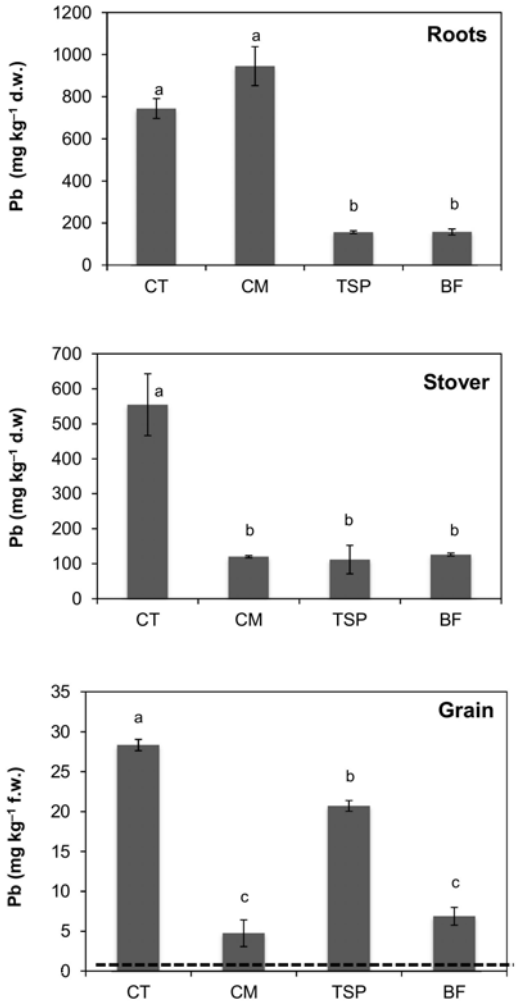

Figure 2. Concentrations of lead (Pb) in maize roots, stover and grain in plots amended with chicken manure (CM), triple superphosphate (TSP) and blended fertilizer (BF; a mixture of NPK fertilizer and chicken manure) compared to the control (CT). The horizontal broken line indicates the FAO/WHO maximum allowable limit of 0.2 mg Pb kg^{-1} maize grain for human health. Concentrations in roots and stover are on dry matter weight (d.w) basis, but on fresh weight (f.w) basis in grain. Bars with different letters are significantly different ($p < 0.05$).

Zinc concentrations in different maize parts generally decreased with soil amendment application (Figure 3). In the roots, the Zn concentration in the amended soils ranged from 3100–3400 mg kg^{-1} compared to an average of over 4600 mg kg^{-1} in the un-amended soils, representing a 26–33% decrease (Figure 3). Chicken manure and TSP significantly ($p < 0.01$) decreased Zn concentration in the stover. A significant reduction of 18–29% in maize grain Zn concentration was observed in all three soil amendments compared to the control, but there was no significant difference among the three amendments. The maize grain Zn concentrations ranged from 62.4–71.9, 45.2–55.3, 50.9–58.5 and 45.7–49.9 mg kg^{-1} in the un-amended control, CM, TSP and BF treatments, respectively.

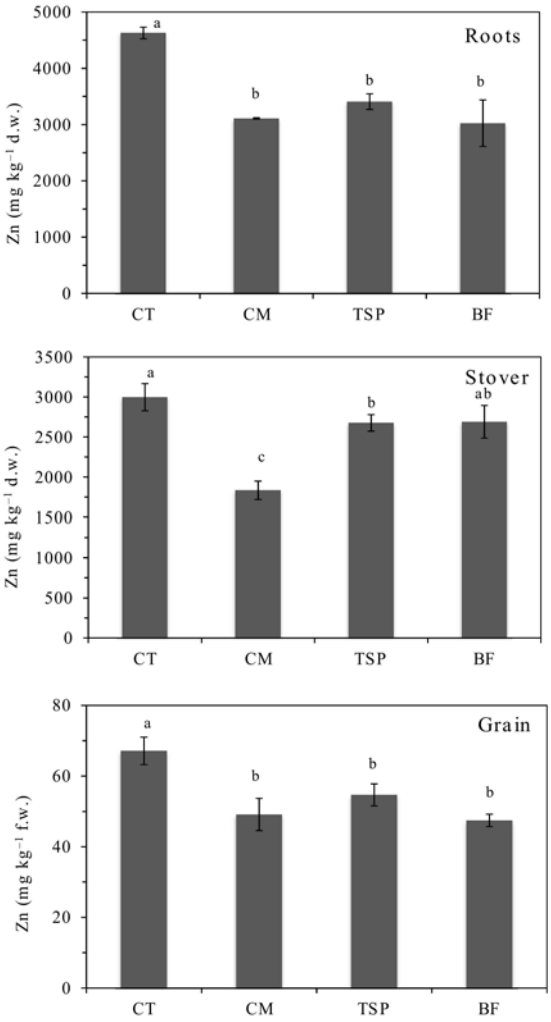

Figure 3. Concentrations of zinc (Zn), in maize roots, stover and grain in plots amended with chicken manure (CM), triple superphosphate (TSP) and blended fertilizer (BF; a mixture of NPK fertilizer and chicken manure) compared to the control (CT). Concentrations in roots and stover are on dry matter weight (d.w) basis, but on fresh weight (f.w) basis in grain. Bars with different letters are significantly different ($p < 0.05$).

Chicken manure and TSP significantly increased Cd concentrations in the roots, while all the soil amendments decreased Cd concentrations in the stover compared to the control (Figure 4). Cadmium concentrations in maize grain were significantly higher ($p < 0.05$) in TSP amended plots than other amendments including the control. The maize grain Cd concentrations ranged from 1.7–2.4, 0.8–1.5, 2.4–5.6 and 1.8–2.9 mg kg^{-1} in the un-amended control, CM, TSP and BF treatments, respectively. Cadmium accumulation in maize grain in CM, BF and control was not significantly different, but the

mean maize grain Cd concentration in CM was lower than that in the control. Cadmium concentrations in the grain were 20, 11, 41 and 23 times higher than the joint FAO/WHO maximum limit of 0.1 mg kg^{-1} in the control, CM, TSP and BF treatments respectively.

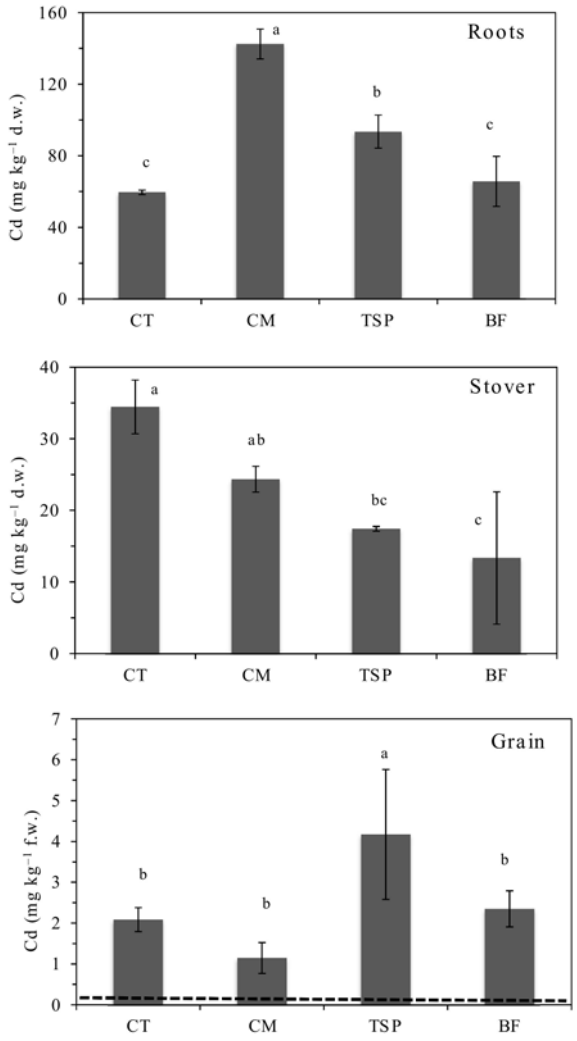

Figure 4. Concentrations of cadmium (Cd), in maize roots, stover and grain in plots amended with chicken manure (CM), triple superphosphate (TSP) and blended fertilizer (BF; a mixture of NPK and chicken manure). The horizontal broken line indicates the FAO/WHO maximum allowable limit of 0.1 mg Cd kg^{-1} maize grain for human health. Concentrations in roots and stover are on dry matter weight (d.w) basis, but on fresh weight (f.w) basis in grain. Bars with different letters are significantly different ($p < 0.05$).

Lead concentrations in maize grain were positively correlated with Pb concentrations in soil and stover, but not with Pb concentrations in roots (Table 3). There was no correlation between Zn concentrations in maize grain and Zn concentrations in soil, but Zn concentrations in the roots had positive correlations with Zn in the stover. The biomass production was negatively correlated with Zn and Pb concentrations in the stover and grain, but only weakly, and not statistically significant, correlated with HM concentrations in the soil (Table 3).

Table 3. Correlations between metal concentrations in soil and plant parts and biomass yield.

	Pb Grain	**Yield**
Pb soil	0.59 *	−0.45
Pb roots	−0.03 ^{ns}	0.06 ^{ns}
Pb stover	0.74 **	−0.61 *
Pb grain	1	−0.92 ***
	Zn Grain	**Yield**
Zn soil	0.04 ^{ns}	−0.26 ^{ns}
Zn roots	0.86 ***	−0.66 **
Zn stover	0.60 *	−0.66 **
Zn grain	1	−0.75 ***
	Cd Grain	**Yield**
Cd soil	−0.30 ^{ns}	0.18 ^{ns}
Cd roots	−0.28 ^{ns}	0.38 ^{ns}
Cd stover	−0.33 ^{ns}	−0.41 ^{ns}
Cd grain	1	−0.47 ^{ns}

* p <0.05; ** p < 0.01; *** p < 0.001, ns not significant.

3.3. Effect of Soil Amendments on Bioaccumulation Factors of Pb, Zn and Cd

The bioaccumulation factors (BAF) of the stover and grain, which indicate the transfer of HMs from soil into above-ground plant parts, are shown in Figure 5. There was a 6-fold reduction in the BAF_{Pb} of maize stover with the application of soil amendments. Chicken manure and BF resulted in 8- and 5-fold reductions in the BAF_{Pb} in the maize grain, while TSP had a 19% reduction compared to the control. Soil amendments significantly decreased the BAF_{Zn} of the stover and grain, except for TSP in stover (Figure 5). The soil amendments significantly decreased the BAF_{Cd} in maize stover, but TSP increased the BAF_{Cd} in the maize grain. Overall, the BAF values were in the order Zn ≥ Cd > Pb.

3.4. Estimated Dietary Intake and Hazard Quotient Assessment of Pb and Cd

A preliminary hazard assessment for human Pb and Cd ingestion through consumption of maize grain is shown in Table 4. The assessment was based on the assumption that daily intake of maize grain for an average adult Zambian weighing 70 kg is 350 g day^{-1} [42]. The estimated weekly Pb ingestion from maize consumption was highest in the un-amended control soils and lowest from soils amended with chicken manure. Although higher than the joint FAO/WHO maximum tolerable Pb weekly intake of 0.025 mg kg^{-1} human body weight (HBW), estimated weekly Pb ingestion decreased by 83%, 27% and 75% with application of CM, TSP and BF, respectively.

The estimated monthly Cd ingestion from maize grain consumption increased by 100% with the application of TSP compared to the control. Chicken manure reduced the estimated monthly Cd ingestion by 40% compared to the control. This difference was however not statistically significant. The monthly Cd ingestion in all treatments was higher than the joint FAO/WHO maximum tolerable limit of 0.025 mg Cd kg^{-1} HBW.

The HQ values for both Pb and Cd in all treatments were much greater than 1, indicating that the maize grain grown in these soils was not safe for human consumption (Table 4). However, the HQ values for Pb were significantly reduced in plots with CM and BF. Plots with TSP had the highest HQ values for Cd.

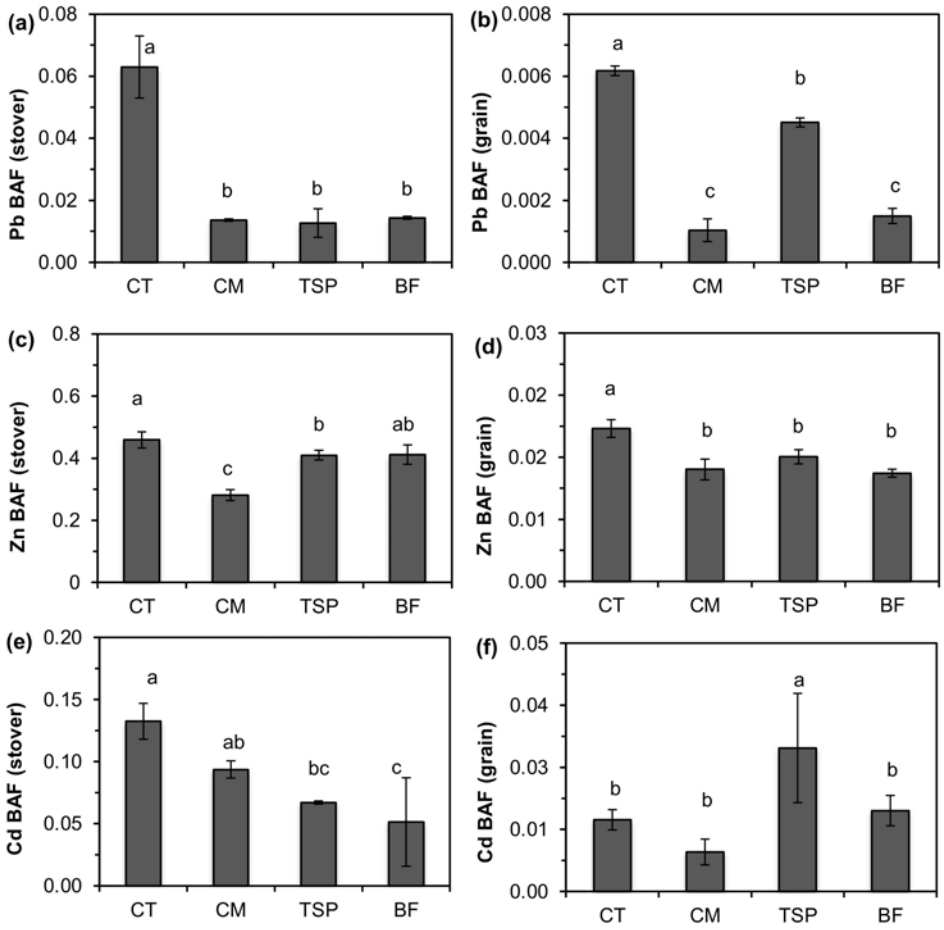

Figure 5. Bioaccumulation values for (**a**,**b**) Pb; (**c**,**d**) Zn; (**e**,**f**) Cd of maize stover and grain in plots amended with chicken manure (CM), triple superphosphate (TSP) and blended fertilizer (BF; a mixture of NPK fertilizer and chicken manure) and the control (CT). Bars with different letters are significantly different ($p < 0.05$).

Table 4. Estimated weekly Pb and monthly Cd intakes (EI) and hazard quotient (HQ) for raw uncooked maize grain grown in plots with different soil amendments compared to joint United Nations Food and Agricultural Organization (FAO)/WHO food tolerable intake limits [41].

	CT †	CM	TSP	BF	FAO/WHO Limit
EI_{Pb} (mg/kg HBW/week)	0.99 ± 0.02 ^{a}	0.16 ± 0.05 ^{b}	0.72 ± 0.02 ^{a}	0.24 ± 0.04 ^{b}	0.025
EI_{Cd} (mg/kg HBW/month)	0.31 ± 0.04 ^{b}	0.17 ± 0.05 ^{b}	0.62 ± 0.23 ^{a}	0.35 ± 0.06 ^{b}	0.025
HQ_{Pb}	39.6 ± 1.0 ^{a}	6.6 ± 2.3 ^{b}	28.9 ± 0.9 ^{a}	9.6 ± 1.5 ^{b}	
HQ_{Cd}	12.5 ± 1.7 ^{b}	6.8 ± 2.3 ^{b}	25.0 ± 9.5 ^{a}	14.1 ± 2.6 ^{b}	

† CT is the control, CM is chicken manure, TSP is triple superphosphate, BF is blended fertilizer (mixture of NPK fertilizer and chicken manure) treatments. Means with different superscripts within each row are significantly different at $p < 0.05$.

4. Discussion

4.1. Effects of Soil Amendments on Heavy Metal Bioavailability and Plant Uptake

The reduction in bioavailable HMs in the soil after application of manure and P based amendments has been reported by other studies [4,22–24]. Contrary to other studies (e.g., Putwattana et al., 2015), no significant reduction in bioavailable Cd and Zn concentrations were observed after applying inorganic P amendments in this study. This finding is in agreement with that of a laboratory study by Bohdan et al. (2019) who reported that inorganic P amendment decreased concentrations of

bioavailable Pb but not Zn, and that humate application did not affect bioavailable Zn and Cd in Kabwe soils. Unlike the findings of Bohdan et al. (2019), in this study bioavailable (DTPA-TEA extractable) Cd did not decrease after applying inorganic P amendments. Results of this study suggest that a single amendment was unlikely to decrease the bioavailability of all the three HMs of concern in Kabwe, and therefore future studies should look at different combinations of these amendments.

The decreased uptake of Pb and Zn in the maize in the amended soils was likely due to their immobilization in the soil through the formation of insoluble precipitates or complexes [23,24], or due to fixation to organic matter functional groups [9], or ion exchange due to increased soil surface charge [23] following application of organic amendments like CM and BF. Despite increasing Pb concentration in plant roots, the phosphate and organic amendments reduced Pb translocation from the roots to shoots. This could be due to the formation of pyromorphite-like minerals on the root membrane surface [24] or to inhibited metal transfer within the plant [23].

The reduction of HM concentrations in maize stover and grain in plots amended with CM, TSP and BF (Figures 2–4) could also have been due to the "growth dilution effect" [4,23] following higher biomass production compared to the control. In this study, the maize biomass yield in plots amended with CM and BF was 25 times higher, while the biomass in the plots with TSP was 6 times higher than that in the control (Table 2). Increased plant growth, which likely resulted from the increased availability of plant nutrients in the soil and decreased plant stress due to reduced soil HM bioavailability, could have reduced the concentration of the HMs in the aboveground plant parts. The observed higher Cd concentrations in the maize grain from plots with TSP and BF amended soils than that in the control (Figure 4) was likely due to the reported increased solubility of Cd in the presence of phosphate compounds [22]. Some Cd-phosphate complexes are reported to have relatively high solubility in the presence of high phosphate [22], making the Cd more mobile.

Other studies have suggested that inorganic phosphate fertilizers increase Cd uptake in plants due to the introduction Cd to the soil by fertilizers [14,22]. Studies have shown that inorganic phosphate fertilizers tend to increase Cd concentrations in soils [14,22], because some rock phosphates used to produce phosphate fertilizers contain high levels of Cd. It is unlikely that increased Cd the maize grain could have resulted from the fertilizers because the Cd concentrations in all three amendments were below the detection limit in the current study. However, this cannot be ruled out completely.

The soil-to-plant bioaccumulation factors of all three HMs were higher for maize stover than for grain, indicating a possible defense mechanism against the translocation of excess HMs into grains [40]. The general trend was that Zn showed the highest bioaccumulation factors while Pb had the lowest. However, in the maize grain, the bioaccumulation factors for Cd were either of similar magnitude or even higher than those for Zn. This suggests that once in the plant, Cd had a higher ability for translocation than both Zn and Cd. High Cd mobility in plants has been reported by Bi et al. [10].

4.2. Health Risk Assessment

The concentrations of Pb and Cd in the maize grain (Figures 2 and 4) were higher than the Joint FAO/WHO Codex Alimentarius Commission [41] limits for food safety. In the un-amended soil, the Pb concentrations in the maize grain were more than 100 times higher than the joint FAO/WHO maximum permissible limit of 0.2 mg kg^{-1} for health safety but decreased significantly (only 24 times higher) in the chicken manure amended plots. High Pb and Cd concentrations in maize in Kabwe was previously reported by Nakata et al. [44]. These high concentrations resulted in high estimated intake (EI) values as well as hazard quotients (HQ). The HQ values were higher than 1 (Table 4), indicating significant human health risk. Higher HQ values near former mining sites have been reported by other studies [5,10,40]. Despite relatively low Cd concentrations in the soils, Cd concentrations in the maize grain were high. This could be due to the reported high mobility and transfer of Cd from soil into plants [5].

Maize is widely grown and consumed in areas surrounding the old Kabwe mine and throughout Zambia. Results of this study have shown that the concentrations of Pb and Cd in maize grain grown

on soils near the former Kabwe Pb/Zn mine were higher than the maximum tolerable limits for food safety and human health. It is therefore clear, from this study, that the risk of human exposure to toxic levels of Pb and Cd by consuming maize grown in areas surrounding the mine is very high. This study also demonstrated that there is a high potential to reduce this risk by applying amendments such as chicken manure and phosphate-based fertilizers to these soils. Because this study was conducted at a site within 500 m from the old Pb-Zn mine with very high HM concentrations [30], it is possible that on sites much further away from the mine, the application of amendments tested in this study could potentially decrease HM concentrations to below the maximum tolerable limits and further reduce the hazard quotients. Additionally, these results are useful to various parts of Zambia and the world at large, where contamination exists either from mining or other sources such as pesticide use [4]. Compared to phosphate fertilizer, chicken manure is relatively widely available and cheaper for most local residents in low-income mining townships in Zambia where backyard gardening is widely practiced. Hence using chicken manure could not only reduce the HM accumulation in edible crops but also to increase productivity and is a potentially low-cost management option.

The observed high health risk of Cd requires that serious attention be paid to the problem of Cd pollution, which has currently been overshadowed by that of Pb, owing to the higher concentrations of Pb than Cd in Kabwe soils. Therefore, while Pb receives its due attention by researchers, health and civic authorities and the public at large, the problems posed by Cd in the environment should equally be of concern in Kabwe.

5. Conclusions

All three soil amendments (chicken manure, triple superphosphate and NPK fertilizer mixed with chicken manure) decreased bioavailable soil Pb concentrations, but only chicken manure decreased Zn and Cd in soil compared to the control. The soil amendments reduced Pb and Zn concentrations in the maize stover and grain. Amendments containing inorganic phosphate increased Cd concentrations in maize grain. The health risk assessment reviewed that Pb and Cd concentrations in maize, and the resulting estimated weekly and monthly metal intakes exceeded the FAO/WHO limits. The hazard quotients for Pb and Cd indicated that there is a high health risk to people who consume maize grain grown on the soils in the study area. Results of this study have demonstrated that the use of chicken manure and phosphate-based soil amendments have significant potential to reduce the concentrations of Pb, Zn and Cd in maize grown in the study area and consequently reduce related health risks associated with the consumption of the maize.

Author Contributions: Conceptualization, I.M. and P.N.M.; formal analysis, P.N.M. and I.M.; investigation, P.N.M. and I.M.; data curation, I.M., P.N.M. and Y.U.; writing—original draft preparation, I.M.; writing—review and editing, I.M., V.S., Y.U., B.H.C., H.N., S.N.; visualization, I.M.; supervision, Y.U., B.H.C., V.S.; project administration, M.I., H.N., S.N.; funding acquisition, M.I. All authors have read and agreed to the published version of the manuscript.

Funding: This study was financially supported by Japan Science and Technology Agency (JST) and Japan International Cooperation Agency (JICA), Science and Technology Research Partnership for Sustainable Development (SATREPS), No. JPMJSA1501, and JST aXis (Accelerating Social Implementation for Sustainable Development Goals (SDGs) Achievement; No. JPMJAS2001).

Acknowledgments: The authors are thankful to the Kabwe Municipal Council for their support to this study.

Conflicts of Interest: The authors declare no conflict of interest. The funders had no role in the design of the study; in the collection, analyses, or interpretation of data; in the writing of the manuscript, or in the decision to publish the results.

References

1. Puga, P.A.; Melo, C.L.A.; Abreu, A.C.; Coscione, R.A.; Paz-ferreiro, J. Leaching and fractionation of heavy metals in mining soils amended with biochar. *Soil Tillage Res.* **2016**, *164*, 25–33. [CrossRef]
2. Tóth, G.; Hermann, T.; Da Silva, M.R.; Montanarella, L. Heavy metals in agricultural soils of the European Union with implications for food safety. *Environ. Int.* **2016**, *88*, 299–309. [CrossRef] [PubMed]

3. Shi, G.; Chen, Z.; Xu, S.; Zhang, J.; Wang, L.; Bi, C.; Teng, J. Potentially toxic metal contamination of urban soils and roadside dust in Shanghai, China. *Environ. Pollut.* **2008**, *156*, 251–260. [CrossRef] [PubMed]
4. Paltseva, A.; Cheng, Z.; Deeb, M.; Groffman, P.M.; Shaw, R.K.; Maddaloni, M. Accumulation of arsenic and lead in garden-grown vegetables: Factors and mitigation strategies. *Sci. Total Environ.* **2018**, *640*, 273–283. [CrossRef] [PubMed]
5. Zhuang, P.; Mcbride, M.B.; Xia, H.; Li, N.; Li, Z. Health risk from heavy metals via consumption of food crops in the vicinity of Dabaoshan mine, South China. *Sci. Total Environ.* **2009**, *407*, 1551–1561. [CrossRef] [PubMed]
6. Cai, Q.; Long, M.; Zhu, M.; Zhou, Q.; Zhang, L.; Liu, J. Food chain transfer of cadmium and lead to cattle in a lead–zinc smelter in Guizhou, China. *Environ. Pollut.* **2009**, *157*, 3078–3082. [CrossRef]
7. Luo, L.; Ma, Y.; Zhang, S.; Wei, D.; Zhu, Y. An inventory of trace element inputs to agricultural soils in China. *J. Environ. Manag.* **2009**, *90*, 2524–2530. [CrossRef]
8. Rai, K.P.; Sang, L.S.; Zhang, M.; Tsang, F.Y.; Kim, K. Heavy metals in food crops: Health risks, fate, mechanisms, and management. *Environ. Int.* **2019**, *125*, 365–385. [CrossRef]
9. Khan, A.; Khan, S.; Khan, M.A.; Qamar, Z.; Waqas, M. The uptake and bioaccumulation of heavy metals by food plants, their effects on plants nutrients, and associated health risk: A review. *Environ. Sci. Pollut. Res.* **2015**, *22*, 13772–13799. [CrossRef]
10. Bi, C.; Zhou, Y.; Chen, Z.; Jia, J.; Bao, X. Heavy metals and lead isotopes in soils, road dust and leafy vegetables and health risks via vegetable consumption in the industrial areas of Shanghai, China. *Sci. Total Environ.* **2018**, *619–620*, 1349–1357. [CrossRef]
11. Abbas, Q.; Yousaf, B.; Liu, G.; Zia-ur-rehman, M.; Ali, M.U.; Munir, M.A.M.; Hussain, S.A. Evaluating the health risks of potentially toxic elements through wheat consumption in multi-industrial metropolis of Faisalabad, Pakistan. *Environ. Sci. Pollut. Res.* **2017**, *24*, 26646–26657. [CrossRef] [PubMed]
12. Adejumo, S.A.; Ogundiran, M.B.; Togun, A.O. Soil amendment with compost and crop growth stages influenced heavy metal uptake and distribution in maize crop grown on lead-acid battery waste contaminated soil. *J. Environ. Chem. Eng.* **2018**, *6*, 4809–4819. [CrossRef]
13. Oka, M.; Uchida, Y. Heavy metals in slag affect inorganic N dynamics and soil bacterial community structure and function. *Environ. Pollut.* **2018**, *243*, 713–722. [CrossRef] [PubMed]
14. UNEP. Environmental Risks and Challenges of Anthropogenic Metals Flows and Cycles. In *A Report of the Working Group on the Global Metal Flows to the International Resource Panel*; van der Voeat, E., Salminen, R., Eckelman, M., Mudd, G., Norgate, T., Hischier, R., Eds.; UNEP: Nairobi, Kenya, 2013.
15. Chibuike, G.U.; Obiora, S.C. Heavy Metal Polluted Soils: Effect on Plants and Bioremediation Methods. *Appl. Environ. Soil Sci.* **2014**, *2014*, 243–254. [CrossRef]
16. Caravanos, J.; Kevin, C.; Bret, E.; Landrigan, P.J.; Richard, F. The burden of disease from pediatric lead exposure at hazardous waste sites in 7 Asian countries. *Environ. Res.* **2013**, *120*, 119–125. [CrossRef]
17. Voegelin, A.; Tokpa, G.; Jacquat, O.; Barmettler, K.; Kretzschmar, R. Zinc Fractionation in Contaminated Soils by Sequential and Single Extractions: Influence of Soil Properties and Zinc Content. *J. Environ. Qual.* **2008**, *37*, 1190–1200. [CrossRef]
18. Spliethoff, H.M.; Mitchell, R.G.; Shayler, H.; Marquez-bravo, L.G.; Russell-Anelli, J.; Ferenz, G.; Mcbride, M. Estimated lead (Pb) exposures for a population of urban community gardeners. *Environ. Geochem. Health* **2017**, *38*, 955–971. [CrossRef]
19. Suelee, A.L.; Hasan, S.N.S.M.; Kusin, F.M.; Yusuff, F.M.; Ibrahim, Z.Z. Phytoremediation Potential of Vetiver Grass (*Vetiveria zizanioides*) for Treatment of Metal-Contaminated Water. *Water Air Soil Pollut.* **2017**, *228*, 158. [CrossRef]
20. Paltseva, A.A.; Cheng, Z.; Egendorf, S.P.; Groffman, P.M. Remediation of an Urban Garden with Elevated Levels of Soil Contamination. *Sci. Total Environ.* **2020**, *722*, 137965. [CrossRef]
21. Mcbride, M.B.; Richards, B.K.; Steenhuis, T. Bioavailability and crop uptake of trace elements in soil columns amended with sewage sludge products. *Plant. Soil* **2004**, *262*, 71–84. [CrossRef]
22. Mahar, A.; Wang, P.; Li, R.; Zhang, Z. Immobilization of Lead and Cadmium in Contaminated Soil Using Amendments: A Review. *Pedosphere* **2015**, *25*, 555–568. [CrossRef]
23. Gao, W.; Zhao, P.; Sui, F.; Liu, H.; Fu, H. Influence of Soil Amendments on Uptake and Accumulation of Cd and Pb in Maize (*Zea mays* L.). *Environ. Eng. Sci.* **2018**, *35*, 194–202. [CrossRef]

24. Cao, R.X.; Ma, L.Q.; Chen, M.; Singh, S.P.; Harris, W.G. Phosphate-induced metal immobilization in a contaminated site. *Environ. Pollut.* **2003**, *122*, 19–28. [CrossRef]
25. Bernardino, C.A.R.; Mahler, C.F.; Preussler, K.H.; Novo, L.A. State of the Art of Phytoremediation in Brazil—Review and Perspectives. *Water Air Soil Pollut.* **2016**, *227*, 272. [CrossRef]
26. Osmond, G.; Hamon, R.E. Remediation of polluted soils. In *Encyclopedia of Soils in the Environment*; Hillel, D., Ed.; Elsevier: Amsterdam, The Netherlands, 2004; pp. 379–385.
27. Munir, M.A.M.; Liu, G.; Yousaf, B.; Mian, M.; ALi, U.M.; Ahmed, R.; Cheema, I.A.; Naushad, M. Contrasting effects of biochar and hydrothermally treated coal gangue on leachability, bioavailability, speciation and accumulation of heavy metals by rapeseed in copper mine tailings. *Ecotoxicol. Environ. Saf.* **2020**, *191*, 110244. [CrossRef]
28. Adejumo, S.A.; Togun, A.O.; Adediran, A.J.; Ogundiran, M.B. Field Assessment of Progressive Remediation of Soil Contaminated with Lead-acid Battery Waste in Response to Compost Application. *Pedologist* **2011**, *54*, 182–193.
29. Putwattana, N.; Kruatrachue, M.; Kumsopa, A.; Pokethitiyook, P. Evaluation of Organic and Inorganic Amendments on Maize Growth and Uptake of Cd and Zn from Contaminated Paddy Soils. *Int. J. Phytoremediat.* **2015**, *17*, 165–174. [CrossRef]
30. Bohdan, K.; Nyambe, I.; Majer, V.; Knésl, I.; Mihaljevi, M.; Pení, V.; Sracek, O. Soil contamination near the Kabwe Pb-Zn smelter in Zambia: Environmental impacts and remediation measures proposal. *J. Geochemical Explor.* **2019**, *197*, 159–173.
31. Yabe, J.; Nakayama, S.M.M.; Ikenaka, Y.; Yohannes, Y.B.; Bortey-sam, N.; Nketani, A.; Ntapisha, J.; Mizukawa, H.; Umemura, T.; Ishizuka, M. Lead and cadmium excretion in feces and urine of children from polluted townships near a lead-zinc mine in Kabwe, Zambia. *Chemosphere* **2018**, *202*, 48–55. [CrossRef]
32. Yabe, J.; Nakayama, S.M.M.; Ikenaka, Y.; Yohannes, Y.B.; Bortey-sam, N.; Oroszlany, B.; Muzandu, K.; Choongo, K.; Nketani, A.; Ntapisha, J.; et al. Lead poisoning in children from townships in the vicinity of a lead—Zinc mine in Kabwe, Zambia. *Chemosphere* **2015**, *119*, 941–947. [CrossRef]
33. Cachada, A.; Rocha-santos, T.; Duarte, A.C. *Soil and Pollution: An Introduction to the Main Issues*; Duarte, A.C., Cachada, A., Rocha-Santos, T., Eds.; Academic Press: Cambridge, MA, USA, 2018.
34. Ministry of Agriculture. *Exploratory Soil Map of Zambia. Scale 1: 1,000,000*; Ministry of Agriculture: Lusaka, Zambia, 1991.
35. Hettiarachchi, G.M.; Pierzynski, G.M. Soil Lead Bioavailability and in Situ Remediation of Lead-Contaminated Soils: A Review. *Environ. Prog.* **2004**, *23*, 78–93. [CrossRef]
36. TerAvest, D.; Carpenter-Boggs, L.; Thierfelder, C.; Reganold, J.P. Crop production and soil water management in conservation agriculture, no-till, and conventional tillage systems in Malawi. *Agric. Ecosyst. Environ.* **2015**, *212*, 285–296. [CrossRef]
37. Clark, H.F.; Hausladen, D.M.; Brabander, D.J. Urban gardens: Lead exposure, recontamination mechanisms, and implications for remediation design. *Environ. Res.* **2008**, *107*, 312–319. [CrossRef] [PubMed]
38. Roy, R.N.; Finck, A.; Blair, G.J.; Tandon, H.L.S. *Plant Nutrition for Food Security: FAO Fertilizer and Plant Nutrition Bulletin 16*; United Nations Food and Agricultural Organization (FAO): Rome, Italy, 2006.
39. Lindsay, W.; Norvell, W. Development of a DTPA Soil Test for Zinc, Iron, Manganese, and Copper. *Soil Sci. Soc. Am. J.* **1978**, *42*, 421–428. [CrossRef]
40. Antoniadis, V.; Golia, E.E.; Liu, Y.; Wang, S.; Shaheen, S.M.; Rinklebe, J. Soil and maize contamination by trace elements and associated health risk assessment in the industrial area of Volos, Greece. *Environ. Int.* **2019**, *124*, 79–88. [CrossRef] [PubMed]
41. Joint FAO/WHO. *Codex Alimentarius Commission General Standard for Contaminants and Toxins in Food and Feed (CXS 193-1995)*; FAO: Rome, Italy, 2018.
42. Alaofe, H.; Kohler, L.; Taren, D.; Mofu, M.J.; Chileshe, J.; Kalungwana, N. *Zambia Food Consumption and Nutrition Survey Report*; National Food and Nutrition Commission: Lusaka, Zambia, 2014.
43. Kribek, B.; Majer, V.; Knésl, I.; Nyambe, I.; Mihaljevic, M.; Ettler, V.; Sracek, O. Concentrations of arsenic, copper, cobalt, lead and zinc in cassava (*Manihot esculenta* Crantz) growing on uncontaminated and contaminated soils of the Zambian Copperbelt. *J. Afr. Earth Sci.* **2014**, *99*, 713–723. [CrossRef]

44. Nakata, H.; Nakayama, S.M.M.; Yabe, J.; Liazambi, A.; Mizukawa, H.; Darwish, W.S.; Ikenaka, Y.; Ishizuka, M. Reliability of stable Pb isotopes to identify Pb sources and verifying biological fractionation of Pb isotopes in goats and chickens. *Environ. Pollut.* **2016**, *208*, 395–403. [CrossRef]

Meta Gene 27 (2021) 100838

Contents lists available at ScienceDirect

Meta Gene

journal homepage: www.elsevier.com/locate/mgene

Delta-aminolevulinic acid dehydratase (ALAD) and vitamin D receptor (VDR) genes polymorphisms in children residing in an abandoned lead-zinc mine area in Kabwe, Zambia

Yared B. Yohannes [a,b], Shouta M.M. Nakayama [a,*], John Yabe [c], Haruya Toyomaki [a], Andrew Kataba [a,c], Hokuto Nakata [a], Kaampwe Muzandu [c], Yoshinori Ikenaka [a], Kennedy Choongo [c,d], Mayumi Ishizuka [a,*]

[a] Laboratory of Toxicology, Department of Environmental Veterinary Sciences, Faculty of Veterinary Medicine, Hokkaido University, Sapporo, Japan
[b] Department of Chemistry, College of Natural and Computational Science, University of Gondar, Gondar, Ethiopia
[c] School of Veterinary Medicine, The University of Zambia, Lusaka, Zambia
[d] Fiji National University, College of Agriculture, Fisheries & Forestry, School of Animal and Veterinary Sciences, Koronivia Campus, Suva, Fiji

ARTICLE INFO

Keywords:
Lead
Gene polymorphism
ALAD
VDR
Children

ABSTRACT

Lead is a ubiquitous environmental pollutant that poses serious health problems to humans, especially to children. However, genetic variability in individuals varies their susceptibility to lead poisoning. One possible factor is genetic polymorphism. Thus, this study aimed to investigate the association between blood lead level (BLL), and polymorphisms in the delta-aminolevulinic acid dehydratase (ALAD) *MspI* (rs1800435) and vitamin D receptor (VDR) *FokI* (rs19735810), *BsmI* (rs15444410), *ApaI* (rs7975232) and *TaqI* (rs731236) genes in children exposed to lead. A total of 140 children (aged 2–10 years) were recruited in areas living closer to and far away from an abandoned lead-zinc mine in Kabwe, Zambia. Blood samples were collected from each child for BLLs and polymorphisms analysis.

All children were homozygous for the ALAD 1 allele, indicating there might be bioavailable lead in the children's blood which can transfer to the soft tissues and the brain. The distribution of the VDR gene polymorphisms showed major alleles prevalence's of 81%, 80%, 68%, and 75% for *FokI*, *BsmI*, *ApaI*, and *TaqI* polymorphisms, respectively. The aa genotype of VDR *ApaI* showed significantly higher BLL compared to other genotypes of the VDRs polymorphism. The *TaqI* - TT genotype was associated with an increase of lead exposure risk in female children (OR = 2.06; 95% CI:1.04–4.06, $p = 0.03$). The haplotype analysis showed 10 haplotypes with a frequency above 1%, and the *FbAt* haplotype showed a protective role against lead toxicity. In conclusion, the children, especially female children, which exposed to lead mainly from the abandoned lead-zinc mine might be at a higher risk of developing lead poisoning. Further, larger scale sample sizes are needed to corroborate the role of ALAD and VDR genetic variants on the implications of lead toxicity in the general population, particularly in children.

1. Introduction

Lead is a ubiquitous environmental contaminant that caused adverse health problems and widespread environmental contamination. To date, no safe blood lead-exposure threshold has been identified. Children compared to adults are particularly susceptible, and at a greater risk to the neurotoxic effects of lead (Sanders et al., 2010). Lead can cause damage to children's cognitive functioning that persist into adulthood and in some cases irreversible neurological damage (Flora et al. 2012; Lanphear et al. 2005;). There is an inter-individual variation in susceptibility to the adverse health effects of lead and molecular evidence has indicated that genetic factors such as gene polymorphism can modify lead toxicity or might be protective from lead poisoning (Kim et al. 2014). The delta-aminolevulinic acid dehydratase (δ-ALAD) and

* Corresponding authors at: Laboratory of Toxicology, Department of Environmental Veterinary Sciences, Faculty of Veterinary Medicine, Hokkaido University, Kita 18, Nishi 9, Kita-ku, Sapporo 060-0818, Japan.
E-mail addresses: shoutanakayama0219@gmail.com (S.M.M. Nakayama), ishizum@vetmed.hokudai.ac.jp (M. Ishizuka).

https://doi.org/10.1016/j.mgene.2020.100838
Received 17 September 2020; Received in revised form 17 November 2020; Accepted 3 December 2020
Available online 7 December 2020

vitamin D receptor (VDR) have shown potential as candidate genes for lead susceptibility in humans (Onalaja and Claudio 2000).

Aminolevulinic acid dehydratase, the second enzyme in the heme biosynthesis, is a polymorphic enzyme with two codominant alleles called ALAD 1 and ALAD 2 (Wetmur et al. 1991a). The difference between these two polypeptides is a single nucleotide polymorphism (SNP) results in the substitution of neutral asparagine for positively charged lysine at position 177 of the coding region (rs1800435). The biological explanation to this substitution makes the ALAD 2 enzyme more electronegative than the ALAD 1 and may have a greater affinity for lead ions (Battistuzzi et al., 1981; Wetmur et al. 1991a). Several studies reported higher blood lead concentrations in the ALAD 2 allele carriers than the ALAD 1 allele carriers (Montenegro et al. 2006; Wetmur et al. 1991b), suggesting the individual variation in susceptibility to lead exposure.

Lead can substitute calcium in many biological systems since both are divalent cations. Thus, lead can exert toxic effects by mimicking the actions of calcium and interact with proteins (Tchounwou et al. 2012). The high binding capacity of lead to calcium-binding proteins suggested that at low calcium intake lead absorption can increase in our body. Bruening et al. (1999) reported significantly lower dietary calcium intake in children with elevated blood lead levels. The vitamin D endocrine system and the VDR are vital parts for calcium homeostasis. And in humans, several VDR SNPs have been identified (Uitterlinden et al. 2004). Among these several SNPs, the *ApaI* - rs7975232, *BsmI* - rs1544410, *FokI* - rs2228570, and *TaqI* - rs731236 were investigated intensively for their association with altered calcium metabolism and human traits (Uitterlinden, 2004, Valdivielso and Fernandez 2006).

Lead exposure represents a significant contributor to adverse health effects in developing countries. Children's deaths due to lead poisoning were reported from the recycling of used lead-acid battery in Senegal (Haefliger et al., 2009) and artisanal gold mining in Nigeria (Dooyema, 2010). Because of the abandoned lead-zinc mine in the town which operated for almost a century, Kabwe - Zambia present in a list of the top ten world's most polluted places (Blacksmith Institute 2013). Yabe et al. (2015) has reported blood lead levels up to 427.8 μg/dL in children residing close to the closed mine in Kabwe. Besides, previous studies reported very high lead concentrations in different biological and environmental matrices (Nakayama et al. 2011; Toyomaki et al. 2020; Yabe et al. 2011, 2013, 2020;). However, regardless of the high burden of lead exposure in Kabwe town, gaps still exist in the knowledge of lead exposure and its impact on children. To our knowledge, there is only one study that investigated the methylation status of ALAD and p16 genes in children exposed to environmental lead from Kabwe, Zambia (Yohannes et al. 2020). Nevertheless, no data exist concerning the impacts of lead on genetic variants among the people from Kabwe.

In this study, we aimed to investigate the associations of ALAD *MspI* (rs1800435), VDR - *ApaI* (rs7975232), *BsmI* (rs1544410), *FokI* (rs2228570), and *TaqI* (rs731236) polymorphisms with blood lead concentration in children living closer to or/and distance away from an abandoned lead-zinc mine in Kabwe, Zambia. As there is no information about gene polymorphism in association with the lead exposure in Kabwe, the present study is one of the first efforts and the result of this study will serve as baseline information for future researches.

2. Materials and methods

2.1. Study subjects and sampling

The sampling area information and demographic data of the recruited children have been published in our previous study (Yohannes et al. 2020). Participation in this study was voluntary. The study recruited a total of 140 randomly chosen children from five townships called Bwacha, Chowa, Kasanda, Makululu, and Nakoli in Kabwe town, Zambia. The children's parents or guardians signed written informed consent forms before the enrollment.

The study was conducted in July 2016. From each child, 3 mL of the venous blood sample was collected into vacuum tubes containing heparin. The BLLs were measured using a portable LeadCare II analyzer after blood collection that same day as described by Yohannes et al. (2020). For genetic analysis, the blood samples were immediately stored at −20 °C after lead analysis. After obtaining a material transfer agreement (MTA, Approval No. E00417) from the Ministry of Health, Zambia, the frozen samples were transported to Japan. All the genetic analyses were carried out in the Laboratory of Toxicology, Faculty of Veterinary Medicine, Hokkaido University, Japan.

2.2. Genetic analyses

Genomic DNA was isolated from whole blood using the NucleoSpin Blood Kit (Macherey-Nagel, Duren, Germany) according to the manufacturer's instructions. The concentration and quality of genomic DNA were assessed using a NanoDrop 1000 UV/Vis Spectrophotometer (Thermo Fisher Scientific Inc., USA). The purified DNA was kept at −20 °C until genotyping was conducted.

Polymerase chain reaction-restriction fragment length polymorphism (PCR-RFLP) was performed for the genotyping of ALAD - *MspI* (G/C), VDR - *BsmI* (G/A), *FokI* (T/C), *ApaI* (G/T), and *TaqI* (T/C). The ALAD polymorphism (917 bp) was performed using primers: 5′-AGACAGACATTAGCTCAGTAGAGG-3′ and 5′-GGCAAAGACCACGTCCATTCAC-3′. Genomics for the *BsmI* polymorphism (831 bp) was determined using primers: 5′-GACCTGTGGCAACCAAGACT-3′ and 5′-AACCAGCGGAAGAGGTCAAG-3′; *FokI* polymorphism (267 bp) using primers: 5′-AGCTGGCCCTGGCACTGACTCTGGCT-3′ and 5′-ATGGAAACACCTTGCTTCTTCTCCCTC-3′; and *ApaI* and *TaqI* polymorphisms (832 bp) using primers: 5′-CAGAGCATGGACAGGGAGCAA-3′ and 5′-AGGCAGCGGTGGAGGCATCTCT-3′. PCR reaction was performed in a 20 μL reaction mixture containing 0.3 μmol/L of each primer, 500 ng of genomic DNA and 10 μL EmeraldAmp PCR Master Mix (2× premix, TaKaRa Bio, Japan). PCR conditions consisted of an initial denaturation at 94 °C for 2 min, followed by 35 cycles of denaturation at 94 °C for 30 s, annealing at 62 °C for ALAD and *BsmI*, and 68 °C for *FokI*, *ApaI* and *TaqI* for 30 s and extension at 72 °C for 1 min, and a final extension at 72 °C for 7 min. The DNA bands were visualized under a Blue-LED transilluminator system and photographed.

The resulting amplified products were subjected to restriction digestion using their respective enzymes obtained from New England Biolabs (NEB). The samples were incubated for 4 h at 65 °C for *BsmI* and *TaqI*, and heat inhibited for 20 min at 80 °C; incubated for 4 h at 37 °C for *ApaI* and *FokI*, and heat inhibited for 20 min at 65 °C; incubated for 4 h at 37 °C for *MspI* (ALAD) with no heat inactivation step. Digestion of the ALAD amplified product by *MspI* produces fragments of 584 bp and 158 bp for the ALAD 1–1, 584 bp, 513 bp and 158 bp for ALAD 1–2, and 513 and 158 bp for the ALAD 2–2 genotypes. The VDR Alleles were designated by capital letters A, B, F, and T in the absence of restriction site and by small letters a, b, f, and t for the presence of restriction site for *ApaI*, *BsmI*, *FokI*, and *TaqI* polymorphisms, respectively. The genotypes and fragment lengths were 832 bp for AA, 832 bp, 615 bp and 217 bp for Aa, and 615 bp and 217 bp for aa genotypes; 831 bp for BB, 831 bp, 655 bp and 176 bp for Bb, and 655 bp and 176 bp for bb genotypes; 267 bp for FF, 267 bp, 197 bp and 70 bp for Ff, and 197 bp and 70 bp for ff genotypes; 494 bp and 338 bp for TT, 498 bp, 338 bp, 293 bp and 201 bp for tt, and 338 bp, 293 bp and 201 bp for tt genotypes. The details of nucleotide sequence, primer sets, and genotypes with fragment sizes after RFLP are presented as **Supplementary Material**. Digested products were visualized after agarose gel electrophoresis under a Blue-LED transilluminator system. Gel electrophoresis showed the identification of genotypes of each VDR SNPs has been presented in Fig. 1.

2.3. Statistical analysis

The JMP Pro 14 (SAS Institute, Cary, NC, USA) software was used for

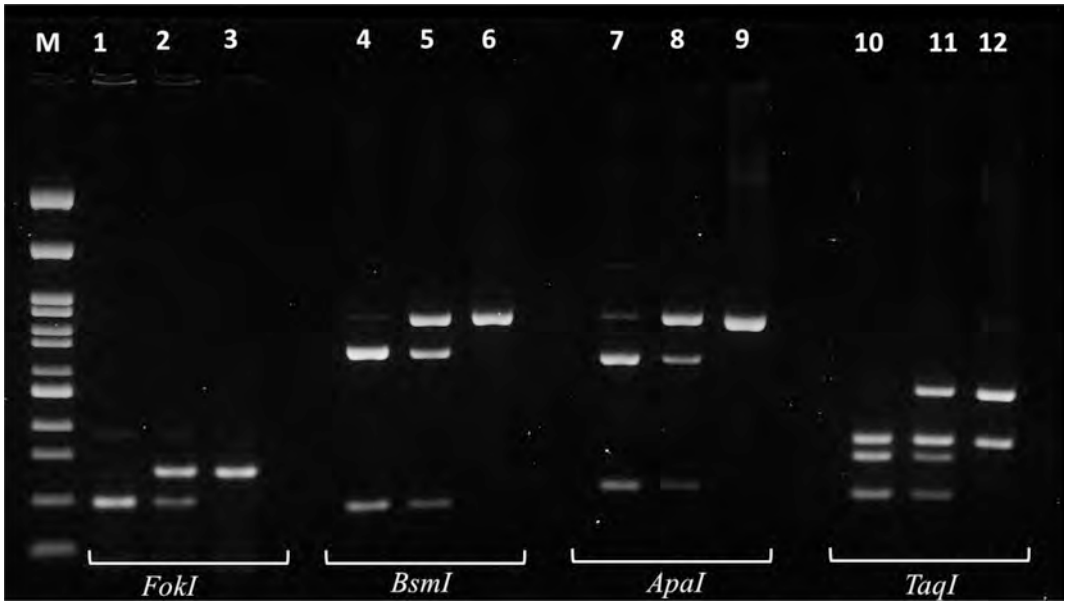

Fig. 1. PCR-RFLP analysis for VDR gene- *Fok*I, *Bsm*I, *Apa*I and TaqI polymorphisms. M: 100 bp DNA marker; Lane 1: ff homozygote, Lane 2: Ff heterozygote, Lane 3: FF homozygote; Lane 4: bb homozygote, Lane 5: Bb heterozygote, Lane 6: BB homozygote; Lane 7: aa homozygote, Lane 8: Aa heterozygote, Lane 9: AA homozygote; Lane 10: tt homozygote, Lane 11: Tt heterozygote, Lane 12: TT homozygote.

statistical analysis, and a p-value <0.05 was considered significant. The distribution of genotypes and allele frequencies among the studied children was analyzed for Hardy-Weinberg equilibrium (HWE) by the chi-square test ($\chi 2$), and the genotype and allele frequencies were compared in relative to BLL quartiles. The comparison of allele frequencies between the studied subjects and other studies with different populations was performed by pairwise chi-square test. The odds ratios (ORs) with 95% confidence interval (CI) were calculated to compare the risk of lead toxicity in low and high BLL level based on the first quartile BLL, and between females and males. Due to low frequencies of aa, BB, ff, and tt genotypes, we grouped *ApaI* genotype as AA and (Aa + aa) groups; *BsmI* genotype as (BB + Bb) and bb groups; *FokI* genotype as FF and (Ff + ff) groups, and *TaqI* genotype as TT and (Tt + tt) groups. SNPStats software (available online at http://bioinfo.iconcologia.net/SNPstats).was used to perform haplotype analysis and analyze the association with BLL.

Table 1
Genotype and allele frequency of ALAD and VDR polymorphisms (*BsmI, FokI, ApaI and TaqI*) in children from Kabwe, Zambia in comparison with quartiles of BLLs.

Gene	Genotype	N (%)	HWE equation [a]	Quartiles of BLL [b]				
			$\chi 2$, p-value	Q1, N (%)	Q2, N (%)	Q3, N (%)	Q4, N (%)	p-Value *
ALAD	ALAD 1–1	140 (100)		31 (22.1)	36 (25.7)	32 (22.9)	41 (29.3)	
	ALAD 1–2	0						
	ALAD 2–2	0						
	G	1						
	C	0						
FokI	FF (CC)	92 (65.7)	0.001, 0.99	20 (64.5)	24 (66.7)	21 (65.6)	27 (65.8)	NS
T > C	Ff (CT)	43 (30.7)		10 (32.3)	12 (33.3)	9 (28.1)	12 (29.3)	
	ff (TT)	5 (3.6)		1 (3.2)	0	2 (6.3)	2 (4.9)	
	F (C)	81						
	f (T)	19						
BsmI	BB (AA)	3 (2.1)	1.88, 0.17	1 (3.2)	1 (2.8)	0	1 (2.4)	NS
G > A	Bb (AG)	50 (35.7)		9 (29.1)	14 (38.9)	13 (40.6)	14 (34.1)	
	bb (GG)	87 (62.1)		21 (67.7)	21 (58.3)	19 (59.4)	26 (63.4)	
	B (A)	20						
	b (G)	80						
ApaI	AA (TT)	63 (45.0)	0.09, 0.76	12 (38.7)	16 (44.4)	17 (53.1)	18 (43.9)	0.01*
G > T	Aa (TG)	63 (45.0)		19 (61.3)	18 (50.0)	12 (37.5)	14 (34.1)	
	aa (GG)	14 (10.0)		0	2 (5.6)	3 (9.4)	9 (22.0)	
	A (T)	68		69	69	72	61	
	a (G)	32		31	31	28	39	
TaqI	TT (TT)	75 (53.6)	2.85, 0.09	14 (45.2)	20 (55.6)	13 40.6)	28 (68.3)	NS
T > C	Tt (TC)	60 (42.8)		16 (51.6)	14 (38.9)	18 (56.3)	12 (29.3)	
	tt (CC)	5 (3.6)		1 (3.2)	2 (5.5)	1 (3.1)	1 (2.4)	
	T (T)	75						
	t (C)	25						

N: number; HWE: Hardy-Weinberg equilibrium.
* Chi-square test.
[a] HWE equation: $\chi 2$ (chi-squared test) < 3.841 and/or p-value >0.05 indicates no deviation from HWE.
[b] BLL quartiles (Q1: x ≤ 10 μg/dL; Q2:10 < x ≤ 19 μg/dL; Q3: 19 < x ≤ 25 μg/dL; Q4: x > 25 μg/dL).

3. Results

A total of 140 children, 75 males and 65 females aged between 2 and 10 years, were engaged in the present study (Yohannes et al. 2020). The mean ages of children were 5.7 ± 1.78 years for females and 5.6 ± 1.88 years for males. The average BLL was 19.4 ± 10.6 μg/dL and ranged from 1.65 to 60.8 μg/dL among the children. There was no significant difference in BLL between sexes ($p = 0.236$) with mean values of 20.5 ± 12.4 μg/dL and 18.4 ± 8.82 μg/dL in female and male children, respectively.

3.1. Prevalence of ALAD and VDR SNPs, and haplotype frequencies of VDR genes

The alleles and genotypes frequencies (%) of ALAD and VDR genes SNPs among the studied children from Kabwe, Zambia are summarized in Table 1. All loci follow the Hardy-Weinberg equilibrium ($p > 0.05$). Molecular analysis revealed that all the children tested for the ALAD genotype were 100% ALAD 1–1. The overall prevalence of the VDR SNPs allele frequencies of A/a, B/b, F/f, and T/t for the *ApaI*, *BsmI*, *FokI*, and *TaqI* polymorphisms were 0.68/0.32, 0.20/0.80, 0.81/0.19, and 0.75/0.25, respectively. For VDR-*ApaI*, a significantly higher percentage of allele a (39%) was observed at the Q4 group with BLL > 25 μg/dL (Table 1).

3.2. Evaluation of VDR SNPs genotypes distribution between this study children and other studied populations

The distribution of the four VDR SNPs data was available from other studies and the International HapMap project populations (http://hapmap.ncbi.nlm.nih.gov/). A pairwise chi-square test was conducted to compare the alleles frequencies of the present study with different populations. The distribution of VDR SNPs alleles showed no significant difference between the present studied subjects and the black race population. On the other hand, the white race population and Chinese people showed significant differences in the allele frequencies of the VDR SNPs compared to the present study as shown in Table 2.

3.3. BLLs among the four VDR SNPs

Fig. 2 shows the association between VDR SNPs and BLLs among the studied children. The *ApaI* polymorphism exhibited a higher mean BLL (25.9 μg/dL) in aa genotype and a lower BLL (16.9 μg/dL) in the Aa genotype ($\chi 2 = 11.3$, DF = 2, $p = 0.003$). No variations were observed in BLLs in *TaqI*, *BsmI*, and *FokI* SNP genotypes (Fig. 2). Further, we examined the different VDR SNPs genotype combinations and revealed the highest mean BLL (37.8 ± 14.9 μg/dL) in AA/TT/bb/Ff combination (Table S1). The highest BLL (60.8 μg/dL) was also observed in this group (Fig. 2).

3.4. Association between VDR SNPs and susceptibility to lead toxicity

To examine the impact of BLLs on the VDR genotyping frequency and their association with risk of lead toxicity, we categorized the subjects based on the lowest quartile of blood lead (Q1) into two groups as low BLL children (BLL ≤10 μg/dL) and high BLL children (BLL >10 μg/dL). Table 3 shows the associations of VDR SNPs genotype distributions with the risk of lead toxicity in low and high BLL groups.

Results showed that the only *ApaI* genotype distributions were different in the two studied groups ($\chi^2 = 6.68$, $p = 0.03$). Significantly higher aa genotype among high BLL children was found compared to low BLL children. The frequencies of *ApaI* genotypes determined from low BLL children were 100% for (AA + Aa) and 0% for aa genotype while in high BLL children the frequency of (AA + Aa) and aa was present in a percentage of 87% and 13%, respectively. No statistically significant correlation was observed between the VDR genotypes and susceptibility to lead toxicity. However, the BB + Bb (OR = 1.36), FF (OR = 1.07), AA (OR = 1.44) and TT (OR = 1.54) genotypes showed an OR value of greater than 1 (Table 3). This result suggests the possibility of a higher risk of lead toxicity to children with high frequencies of TT, AA, BB, and FF genotypes than the tt, aa, bb, and ff genotypes carrier children, respectively.

Table 4 shows VDR genotype distributions and the risk of lead toxicity in association with gender. Genotypic frequencies of 63% and 29% in females and 45% and 55% in males were observed for TT and Tt genotypes, respectively. On the contrary, the tt genotype was found only in females with a frequency of 8%. The *TaqI* genotype distribution between female and male subjects was statistically different ($\chi^2 = 13.0$, $p = 0.001$). We found that the TT groups for *TaqI* SNP showed an increased risk of lead toxicity in female children (OR = 2.06, 95% CI:1.04–4.06, $p = 0.03$). For the other VDR SNPs, we did not observe a significant association but, an OR > 1 in the presence of one or mixed alleles was observed.

3.5. haplotype analysis of VDR genes

Haplotype analysis performed in the four-marker haplotype alleles (VDR-*FokI*, *BsmI*, *ApaI*, and *TaqI*) was presented in Table 5. It was observed 10 haplotypes with a frequency above 1% in our analysis. The three most represented haplotype were *FbaT* (28.7%), followed by *FbAT* (25.7%) and *FbAt* (12.1%). Compared between the children, the frequency of *FbAt* was significantly higher in low BLL children (21.9%) compared to children with high BLL (9.9%). The association analysis between the haplotype and susceptibility to lead toxicity showed that the *FbAt* haplotype was associated with a statistically decrease risk of lead toxicity (OR = 0.33, 95% CI:0.11–1.00, $p = 0.04$), indicating a protective role against lead toxicity.

4. Discussion

Lead exposure can cause adverse health effects, particularly in

Table 2
Comparison of VDR SNPs allele frequencies between Zambian children and different populations.

Population	*FokI* (rs2228570) C/T	*BsmI* (rs1544410) G/A	*ApaI* (rs7975232) T/G	*TaqI* (rs731236) T/C	Reference
Zambian children	0.81/0.19	0.80/0.20	0.68/0.32	0.75/0.25	This study
African ancestry	0.83/0.17	0.71/0.29	0.62/0.38	0.75/0.25	Lins et al. 2011
European ancestry	0.52/0.48***	0.52/0.48***	0.57/0.43	0.52/0.48**	〃
Asian ancestry	0.64/0.36**	0.92/0.08**	0.35/0.65***	0.93/0.07***	〃
Brazil	0.67/0.33*	0.60/0.40**	0.54/0.46*	0.62/0.38	〃
Black South Africans	0.84/0.16	0.74/0.26	0.76/0.24	0.66/0.34	Meyer et al. 2017
White South Africans	0.54/0.46***	0.62/0.38**	0.54/0.46*	0.61/0.39*	〃
African American	0.77/0.23	0.63/0.37**	0.70/0.30	0.73/0.27	Sarkissyan et al. 2014
China	0.60/0.40**	0.91/0.08**	0.35/0.65***	0.90/0.10***	Yu et al. 2017

* = p < 0.05; ** = p < 0.01; *** = $p < 0.001$; Two-tailed Fisher's exact test and chi square test was done using Zambian children as reference value.

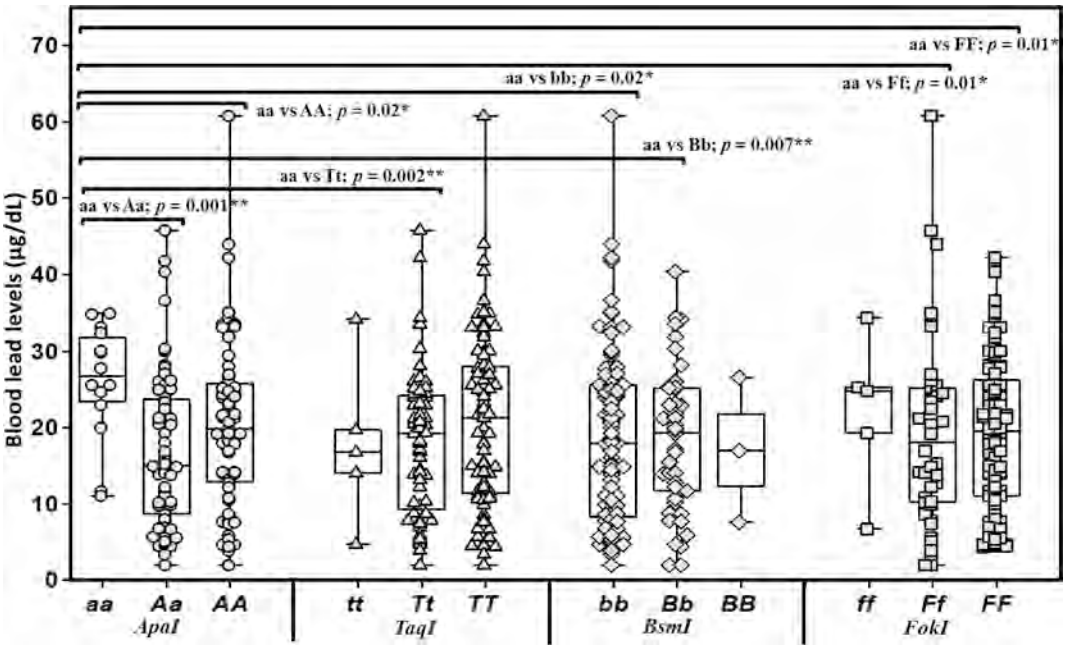

Fig. 2. Blood lead levels for all genotypes of VDR gene polymorphic variants (*BsmI*, *FokI*, *ApaI* and *TaqI*) in environmental lead exposed children (* = $p < 0.05$; ** = $p < 0.01$; nonparametric Wilcoxon / Kruskal-Wallis tests between aa genotype and other genotypes).

Table 3
Distribution of VDR genotypes in low vs high BLL subjects and associations with lead toxicity.

SNP	Genotype / Allele	High BLL children[#] ($N = 109$)		Low BLL children[#] ($N = 31$)		HWE equation	OR [95% CI], *p*-value
		N	%	N	%	X^2, *p*	
BsmI	BB	2	1.8	1	3.2	0.91, 0.63	(BB + Bb) vs bb
	Bb	41	37.6	9	29		1.36 [0.58–3.18], 0.46
	bb	66	60.6	21	67.7		
FokI	FF	72	66.0	20	64.5	0.05, 0.97	FF vs (Ff + ff)
	Ff	33	30.3	10	32.3		1.07 [0.46–2.46], 0.87
	ff	4	3.7	1	3.2		
ApaI	AA	52	46.8	12	38.7	6.68, 0.03*	AA vs (Aa + aa)
	Aa	43	40.4	19	61.3		1.44 [0.64–3.26], 0.37
	aa	14	12.8	0	0		
TaqI	TT	61	56.0	14	45.2	1.25, 0.54	TT vs (Tt + tt)
	Tt	44	40.4	16	51.6		1.54 [0.69–3.44], 0.28
	tt	4	3.6	1	3.2		

N: Number of children; %: Frequency; BLL: Blood lead level; HWE: Hardy-Weinberg equilibrium.
OR: Odds ratios; 95% CI: 95% Confidence interval.
[#] Low BLL children: BLL ≤ 10 µg/dL; High BLL children: BLL > 10 µg/dL.
* Result is significant at $p < 0.05$.

children. To our knowledge, this is the first study to investigate the ALAD and VDR genes SNPs in association with lead toxicity in children living closer to or/and far away from an abandoned lead-zinc mine in Kabwe, Zambia. Considering 5 µg/dL, the current CDC blood reference value, 92% of the children's blood samples exceeded this value in the present study. Thus, the findings from this study may have some implications for lead toxicity and support the ongoing efforts to reduce childhood lead exposure in a region where only levels of lead in human

Table 4
Genotype frequencies of VDR SNPs and association with gender.

SNP/ Genotype		All children		HWE equation χ^2, *p*	OR [95% CI], *p*-value
		Female N (%)	Male N (%)		Female vs Male
BsmI	BB	1 (1.5)	2 (3)	0.26, 0.87	(BB + Bb) vs bb
	Bb	24 (37)	26 (34)		1.04 [0.54–2.08], 0.89
	bb	40 (61.5)	47 (63)		
FokI	FF	44 (68)	48 (64)	4.51, 0.11	FF Vs (Ff + ff)
	Ff	21 (32)	22 (29)		1.17 [0.58–2.38], 0.64
	ff	0 (0)	5 (7)		
ApaI	AA	29 (45)	34 (45)	0.11, 0.94	AA vs (Aa + aa)
	Aa	30 (46)	33 (44)		0.92 [0.47–1.79], 0.81
	aa	6 (9)	8 (11)		
TaqI	TT	41 (63)	34 (45)	13.0, 0.001**	TT vs (Tt + tt)
	Tt	19 (29)	41 (55)		2.06 [1.04–4.06], 0.03*
	tt	5 (8)	0 (0)		

N: Number of children; %: Frequency; HWE: Hardy-Weinberg equilibrium.
OR: Odds ratios; 95% CI: 95% Confidence interval.
* Result is significant at $p < 0.05$.

and biota samples were investigated without any further genetic analysis. Thus, in the current study, we aimed to assess the impact of lead exposure in children through the biomarkers of susceptibility genes such as ALAD and VDR genes polymorphisms (Sakai 2000).

In the current study, we found all children were ALAD 1–1 genotypes. This finding was in accordance with other African population studies from Liberian populations (Benkmann et al. 1983), Ghanaian, Ovambos (Bantusin of Namibia), and Xhosas (Cape Town of South Africa) (Fujihara et al. 2009) that showed 100% ALAD 1–1 genotype, with neither ALAD 1–2 nor ALAD 2–2 genotypes. Although the more electronegative ALAD 2 allele could bind more lead easily and maintain higher BLLs than the ALAD 1 allele, the latter allele could be more prone to the detrimental effects of lead because of the easy transfer of the bioavailable lead from blood to the soft and hard tissues (Kelada et al. 2001). Previous studies reported that individuals with ALAD 1–1 genotypes had higher bone lead levels, which suggested higher body burdens of lead and could be at greater risk of the long-term health

Table 5
Haplotypes frequency of vitamin D receptor gene polymorphisms in high and low BLL children.

FokI	*BsmI*	*ApaI*	*TaqI*	Total	High BLL children[#]	Low BLL children[#]	OR (95% CI)
F	*b*	*a*	*T*	0.287	0.295	0.258	1
F	*b*	*A*	*T*	0.257	0.274	0.188	1.58 (0.60–4.13)
F	*b*	*A*	*t*	0.121	0.099	0.219	0.33 (0.11–1.00) *
F	*B*	*A*	*T*	0.083	0.079	0.069	1.29 (0.29–5.68)
f	*b*	*A*	*T*	0.071	0.064	0.108	0.41 (0.10–1.61)
F	*B*	*A*	*t*	0.065	0.068	0.071	0.76 (0.17–3.46)
f	*b*	*a*	*T*	0.034	0.030	0.048	0.73 (0.10–5.37)
f	*B*	*A*	*T*	0.030	0.036	0.036	0.62 (0.06–6.19)
f	*b*	*A*	*t*	0.028	0.029	0	
f	*B*	*A*	*t*	0.020	0.022	0	

[#] Low BLL children: BLL $\leq$ 10 μg/dL; High BLL children: BLL $>$ 10 μg/dL.
* Result is significant at $p < 0.05$.

effects of lead (Wan et al. 2014; Yang et al. 2012). Kim et al. (2004) also reported higher hematological effects of lead for ALAD 1 homozygote subjects and they are more likely to be anemic. Another study on male Japanese lead workers by Sakai et al. (2000) showed high amino-levulinic acid (ALA), which is neurotoxic to the brain, in plasma for ALAD 1–1 genotype. These results suggest that the ALAD 1 homozygotes may be at greater risk due to the bioavailable lead in the blood that can transfer and accumulate in the tissues and brain. Also, we reported significant hypermethylation of the ALAD gene in these lead-exposed children with an odd ration of greater than one for anemia (Yohannes et al. 2020). Thus, the people, particularly infants and children in Kabwe might be at high risk of lead poisoning.

The genetic variants of VDR have been identified as potential factors to influence the lead toxicokinetic in the human body, and the effects of VDR SNPs such as *FokI*, *BsmI*, *ApaI*, and *TaqI* have been reported (Onalaja and Claudio 2000; Rezende et al. 2008). In the present study, the observed genotype frequencies of the four VDR SNPs are conformed to the Hardy-Weinberg equilibrium. The A, b, F, and T alleles were the dominant alleles with incidences of 68%, 80%, 81%, and 75% in *ApaI*, *BsmI*, *FokI*, and *TaqI* polymorphisms, respectively. The most common genotype for each polymorphism was bb (62.1%) for *BsmI*, FF (65.7%) for *FokI*, both AA and Aa (45%) for *ApaI*, and TT (53.6%) for *TaqI*. The general distributions of these VDR SNPs were consistent with other population studies of black South Africans (Meyer et al. 2017), African Americans (Sarkissyan et al. 2014), and African ancestry studies (Lins et al. 2011). On the contrary, there were significant differences in allele distribution between this study subjects and white South Africans (Meyer et al. 2017), European ancestry, Asian ancestry and Brazilians (Lins et al. 2011), and Chinese population (Yu et al., 2017). So, our results offered additional evidence to the distribution specificity of VDR gene polymorphisms based on ethnicity.

In the present study, we found an association of high BLLs in *ApaI* polymorphism variants. The prevalence of aa genotype increases from 0% (Q1) to 22% (Q4), and the aa genotype of ApaI variants had significantly increased mean blood lead levels than those of the other genotypes (aa vs AA, $p = 0.02$; aa vs Aa $p = 0.001$). This finding corroborates with previous studies reported that *ApaI* aa genotype had higher BLLs than the Aa and AA genotypes in workers exposed to lead due to their workplace (Chuang et al. 2004; Himani et al., 2020). Further analysis among the SNPs showed that the aa genotype had significantly higher BLL than FF, Ff, Bb, bb, and Tt genotypes ($p < 0.05$). No significant associations of BLLs within *BsmI*, *FokI*, and *TaqI* variants were observed.

The influences of VDR SNPs to different traits have been investigated in adults with occupational lead exposure (Chuang et al. 2004; Himani et al., 2020; Shaik et al. 2019; Wananukul et al. 2012) or patients with different types of diseases such as cancer (Kostner et al., 2009), diabetes (Ahmed et al. 2019) and autism (Cie'sli'nska et al., 2017). In the current study, we investigated the correlation between the VDR SNPs and environmental lead exposure in children. The results showed no statistical associations between the genotypes at the VDR polymorphic sites and susceptibility to lead toxicity. Nevertheless, the BB + Bb, FF, AA, and TT genotypes showed OR values of greater than one, but not statistically significant. Previous studies showed the association of these VDR genotypes with bone mineral density. Haynes et al. (2003) showed increased bone density in the VDR-*FokI* FF genotype while the AA genotype in *ApaI* and BB genotype in *BsmI* were associated with lower bone mineral density (Li et al. 2012). In another study by Pawlas et al. (2012), the *BsmI* B allele showed an inverse correlation against cognitive function with a steeper slope ($\beta = -0.08$), suggesting that lead has a negative influence on children's performance IQ. In the present study, the highest BLL (60.8 μg/dL) was detected in these genotypes. Thus, children with high frequencies of those genotypes might be at higher risk of calcium absorption and IQ problem. We also found an association between gender and *TaqI* polymorphism. In the present study, female children with TT genotypes showed higher susceptibility to lead toxicity (OR = 2.06, $p = 0.03$) than males. Chakraborty et al. (2008) examined the effect of lead on the neuromotor response in association with *TaqI* genotypes in 82 children and observed adverse effects of lead exposure on postural balance response in association with genetic polymorphisms of VDR at the *TaqI* site. A study from the National Health and Nutrition Examination Survey also investigated the relationship between the children's cognitive function and blood lead concentration in association with VDR SNPs and suggested that the *TaqI* variants can alter the children's central nervous system toxicity of lead (Krieg Jr et al. 2010). These results suggest that the children in Kabwe might be at higher risk for the biological effects of lead. In the current study, haplotype structure revealed 10 haplotypes with >1% frequency. There was a trend of increased frequency of *FbAt* haplotype in low BLL children compared to High BLL children, suggesting that this haplotype could be protective against lead toxicity.

There are limitations to our study. First, this study is a cross-sectional study that collected samples at a single point in time, and thus it is difficult to determine incidence. Second, the small sample size may weaken the statistical power. Third, the current study depends on lead levels using blood samples at which the half-life of lead is about 35 days in blood, which may inevitably affect the result to some degree. Reliable bone lead measurements are needed. Thus, our findings need to be replicated in other long-term follow-up studies with large scale samples among the population exposed to both environmental and occupational lead, and bone lead measurement with the prevalence of disease as VDR SNPs have been linked to human traits.

5. Conclusions

This study provides insight into the association of ALAD and VDR polymorphic variants in association with BLL in children exposed to environmental lead. Our finding suggests that all subjects were ALAD 1 homozygotes at which they might be at risk due to the bioavailable lead in the blood that can transit to soft tissues and the brain. Regarding the

VDR SNPs, the *ApaI* homozygous mutant genotype showed association with BLLs in environmentally lead-exposed children. The TT-genotype in *TaqI* (rs731236) site was allied with lead toxicity in female children. In haplotype analysis, the haplotype *FbAt* showed a protective role against lead toxicity compared to the most frequent haplotype (*FbaT*). Overall, further larger-scale samples alongside bone lead measurements are warranted to assess the ALAD and VDR SNPs in association with their implications on lead toxicity manifestations in the general population.

Funding

This work was supported by Grants-in-Aid for Scientific Research from the Ministry of Education, Culture, Sports, Science and Technology of Japan awarded to M. Ishizuka (No. 16H01779, 18K19847, 18KK0287), Y. Ikenaka (18H04132) and S.M.M. Nakayama (No. 17KK0009, 20K20633), and the foundation of JSPS Bilateral Open Partnership Joint Research Projects (JPJSBP120209902), the Japan Prize Foundation and Hokkaido University SOUSEI Support Program for Young Researchers in FY2020 (SMMN). This research was also supported by JST/JICA and SATREPS (Science and Technology Research Partnership for Sustainable Development; No. JPMJSA1501), aXis (Accelerating Social Implementation for SDGs Achievement) funded by JST as well as Program for supporting introduction of the new sharing system (JPMXS0420100619).

Ethical approval

The study protocol was approved by the University of Zambia Research Ethics Committee (UNZAREC; REF. No. 012–04-16), and permission was granted by the Ministry of Health through the Zambia National Health Research Ethics Board and the Kabwe District Medical Office.

Declaration of Competing Interest

None.

Acknowledgments

We would like to thank the children and families that participated in this study and many thanks to the laboratory technicians and nurses at the five health centers in Kabwe, the Ministry of Health Zambia, and the Kabwe District Health Office for facilitating the study.

Appendix A. Supplementary data

Supplementary data to this article can be found online at https://doi.org/10.1016/j.mgene.2020.100838.

References

Cie'sli'nska, A., et al., 2017. Vitamin D receptor gene polymorphisms associated with childhood autism. Brain Sci 7, 115.
Himani, et al., 2020. Association of vitamin D receptor (VDR) gene polymorphism with blood lead levels in occupationally lead-exposed male battery workers in Delhi – national capital region. India. Indian J. Biochem. & Biophy. 57, 236–244.
Ahmed, A.E.A., et al., 2019. Vitamin D receptor rs797523, rs731236 and rs1544410 single nucleotide polymorphisms, and 25-hydroxyvitamin D levels in Egyptian children with type 1 diabetes mellitus: effect of vitamin D co-therapy. Diabetes Metab. Syndr. Obes. 12, 703–716.
Benkmann, H.G., et al., 1983. Polymorphism of delta-aminolevulinic acid dehydratase in various populations. Hum. Hered. 33, 62–64.
Blacksmith Institute, 2013. The World's Worst 2013: The Top Ten Toxic Threats. Cleanup, Progress, and Ongoing Challenges. New York Blacksmith Institute. Available. http://www.worstpolluted.org/docs/TopTenThreats2013.pdf.
Bruening, K., et al., 1999. Dietary calcium intakes of urban children at risk of lead poisoning. Environ. Health Perspect. 107 (6), 431–435.
Chakraborty, B.M., et al., 2008. Low dose effect of chronic lead exposure on neuromotor response impairment in children is moderated by genetic polymorphisms. J. Hum. Ecol. 23, 183–194.
Chuang, H.Y., et al., 2004. Investigations of vitamin D receptor polymorphism affecting workers' susceptibility to lead. J. Occup. Health 2004 (46), 316–322.
Dooyema, C.A., 2010. Outbreak of fatal childhood lead poisoning related to artisanal gold mining in northwestern Nigeria. 2010. Environ. Health Perspect. 120 (4), 601–607.
Flora, G., et al., 2012. Toxicity of lead: a review with recent updates. Interdiscip. Toxicol. 5, 47–58.
Fujihara, J., et al., 2009. Ethnic variation in genotype frequencies of delta-aminolevulinic acid dehydratase (ALAD). Toxicol. Lett. 91 (2–3), 236–239.
Haefliger, P., et al., 2009. Mass lead intoxication from informal used lead-acid battery recycling in Dakar, Senegal. Environ. Health Perspect. 117, 1535–1540.
Haynes, E.N., et al., 2003. Vitamin D receptor Fok1 polymorphism and blood Lead concentration in children. Environ. Health Perspect. 111, 1665–1669.
Kelada, S.N., et al., 2001. δ-Aminolevulinic acid dehydratase genotype and lead toxicity: a huge review. Am. J. Epidemiol. 154, 1–13.
Kim, H.S., et al., 2004. The protective effect of δ-aminolevulinic acid dehydratase 1-2 and 2-2 isozymes against blood lead with higher hematologic parameters. Environ. Health Perspect. 112, 538–541.
Kim, J., et al., 2014. Environmental exposure to lead (Pb) and variations in its susceptibility. J Environ. Sci. Health C Environ. Carcinog. Ecotoxicol. Rev. 32, 159–185.
Kostner, K., et al., 2009. The relevance of vitamin D receptor (VDR) gene polymorphisms for cancer: a review of the literature. Anticancer Res. 29, 3511–3536.
Krieg Jr., E.F., et al., 2010. Lead and cognitive function in VDR genotypes in the third National Health and nutrition examination survey. Neurotoxicol. Teratol. 32, 262–272.
Lanphear, B.P., et al., 2005. Low-level environmental lead exposure and children's intellectual function: an international pooled analysis. Environ. Health Perspect. 113, 894–899.
Li, Y., et al., 2012. Association between vitamin D receptor gene polymorphisms and bone mineral density in Chinese women. Mol. Biol. Rep. 39 (5), 5709–5717.
Lins, T.C., et al., 2011. Population analysis of vitamin D receptor polymorphisms and the role of genetic ancestry in an admixed population. Genet. Mol. Biol. 34, 377–385.
Meyer, V., et al., 2017. Methylation of the vitamin D receptor (VDR) gene, together with genetic variation, race, and environment influence the signaling efficacy of the toll like receptor 2/1-VDR pathway. Front. Immunol. 8, 1048.
Montenegro, M.F., et al., 2006. A polymorphism in the delta-aminolevulinic acid dehydratase gene modifies plasma/whole blood lead ratio. Arch. Toxicol. 80, 394–398.
Nakayama, S., et al., 2011. Metal and metalloid contamination in roadside soil and wild rats around a Pb-Zn mine in Kabwe, Zambia. Environ. Pollut. 159, 175–181.
Onalaja, A.O., Claudio, L., 2000. Genetic susceptibility to lead poisoning. Environ. Health Perspect. 108 (Suppl. 1), 23–28.
Pawlas, N., et al., 2012. Modification by the genes ALAD and VDR of lead-inducedcognitive effects in children. Neurotoxicology 33, 37–44.
Rezende, V.B., et al., 2008. Haplotypes of vitamin D receptor modulate the circulating levels of lead in exposed subjects. Arch. Toxicol. 82, 29–36.
Sakai, T., 2000. Biomarkers of lead exposure: a review article. Ind. Health 38, 127–142.
Sakai, T., et al., 2000. Relationship between aminolevulinic acid dehydratase genotypes and heme precursors in lead workers. Am. J. Ind. Med. 38, 355–360.
Sanders, T., et al., 2010. Neurotoxic effects and biomarkers of lead exposure: A review. Rev. Environ. Health 24 (1), 15–45.
Sarkissyan, M., et al., 2014. Vitamin D receptor FokI gene polymorphisms may be associated with colorectal cancer among African American and Hispanic participants. Cancer 120, 1387–1393.
Shaik, A.P., et al., 2019. Vitamin D receptor FokI, ApaI, and TaqI polymorphisms in lead exposed subjects from Saudi Arabia. Front. Genet. 10, 388.
Tchounwou, P.B., et al., 2012. Heavy metals toxicity and the environment. Mol. Clin. Environ. Toxicol. 101, 133–164.
Toyomaki, H., et al., 2020. Factors associated with lead (Pb) exposure on dogs around a Pb mining area, Kabwe, Zambia. Chemosphere 247, 125884.
Uitterlinden, A.G., 2004. Vitamin D receptor gene polymorphisms in relation to vitamin D related disease states. J. Steroid Biochem. Mol. Biol. 89-90, 187–193.
Uitterlinden, A.G., et al., 2004. Genetics and biology of vitamin D receptor polymorphisms. Gene 338, 143–156.
Valdivielso, J.M., Fernandez, E., 2006. Vitamin D receptor polymorphisms and diseases. Clin. Chim. Acta 371, 1–12.
Wan, H., et al., 2014. Investigation of delta-aminolevulinic acid dehydratase polymorphism affecting hematopoietic, hepatic and renal toxicity from lead in Han subjects of southwestern China. Acta Physiol. Hung. 101 (1), 59–66.
Wananukul, W., et al., 2012. Impact of vitamin D receptor gene polymorphisms on blood lead levels in Thai lead exposed workers. Asian Biomed. 6, 43–50.
Wetmur, J.G., et al., 1991a. Molecular characterization of the human δ-aminolevulinate dehydratase 2 (ALAD2) allele: implications for molecular screening of individuals for genetic susceptibility to lead poisoning. Am. J. Hum. Genet. 49, 757–763.
Wetmur, J.G., et al., 1991b. The delta-aminolevulinate dehydratase polymorphism: higher blood lead levels in lead workers and environmentally exposed children with the 1-2 and 2-2 isozymes. Environ. Res. 56, 109–119.
Yabe, J., et al., 2011. Uptake of lead, cadmium, and other metals in the liver and kidneys of cattle near a lead-zinc mine in Kabwe, Zambia. Environ. Toxicol. Chem. 30, 1892–1897.
Yabe, J., et al., 2013. Metal distribution in tissues of free-range chickens near a lead-zinc mine in Kabwe, Zambia. Environ. Toxicol. Chem. 32, 189–192.

Yabe, J., et al., 2015. Lead poisoning in children from townships in the vicinity of a lead-zinc mine in Kabwe, Zambia. Chemosphere 119, 941–947.
Yabe, J., et al., 2020. Current trends of blood lead levels, distribution patterns and exposure variations among household members in Kabwe. Zambia. Chemosphere 243, 125412.
Yang, Y., et al., 2012. Effects of delta-aminolevulinic acid dehydratase polymorphisms on susceptibility to lead in Han subjects from southwestern China. Int. J. Environ. Res. Public Health 9 (7), 2326–2338.
Yohannes, Y.B., et al., 2020. Blood lead levels and aberrant DNA methylation of the ALAD and p16 gene promoters in children exposed to environmental-lead. Environ. Res. 188, 109759.
Yu, M., et al., 2017. Association between single nucleotide polymorphisms in vitamin d receptor gene polymorphisms and permanent tooth caries susceptibility to permanent tooth caries in Chinese adolescent. Biomed. Res. Int. 40, 31–36.

Journal of Functional Foods 77 (2021) 104344

Contents lists available at ScienceDirect

Journal of Functional Foods

journal homepage: www.elsevier.com/locate/jff

Evaluation of the ameliorative effect of Spirulina (*Arthrospira platensis*) supplementation on parameters relating to lead poisoning and obesity in C57BL/6J mice

Hokuto Nakata [a], Shouta M.M. Nakayama [a], Andrew Kataba [a,b], Yared Beyene Yohannes [a,c], Yoshinori Ikenaka [a,d], Mayumi Ishizuka [a,*]

[a] *Laboratory of Toxicology, Department of Environmental Veterinary Sciences, Faculty of Veterinary Medicine, Hokkaido University, Kita 18 Nishi 9, Kita-ku, Sapporo 060-0818, Japan*
[b] *The University of Zambia, School of Veterinary Medicine, P.O. Box 32379, Lusaka, Zambia*
[c] *Department of Chemistry, College of Natural and Computational Science, University of Gondar, Ethiopia*
[d] *Water Research Group, School of Environmental Sciences and Development, North-West University, South Africa*

ARTICLE INFO

Keywords:
Lead poisoning
Obesity prevention
Spirulina
Cost-effective
C57BL/6J

ABSTRACT

The current study aimed to validate the possible ameliorative effects of Spirulina (*Arthrospira platensis*) on lead poisoning and obesity using C57BL/6J mice. After a treatment period, we performed metal analyses, as well as hematocrit and plasma biochemical parameter measurements, and assayed oxidative stress markers and erythrocyte δ-aminolevulinic acid dehydratase (ALAD) activity. Our results highlighted the effectiveness of Spirulina in improving anemia status with the normalization of hematocrit levels and ALAD activity ratios, even in mice that exhibited obesity in addition to lead poisoning. Spirulina treatment also decreased epididymal white adipose tissue weight and increased plasma high-density lipoprotein levels, which are normally reduced after lead exposure. However, most of the studied plasma biochemical parameters and oxidative stress markers did not show large changes after treatment, likely because of the short duration of treatment. Further studies with longer-term exposures are required to validate the usefulness of Spirulina suggested in the present study.

1. Introduction

Lead (Pb) is a non-essential element that occurs ubiquitously in the environment, although anthropogenic Pb sources generally cause Pb pollution. The World Health Organization (WHO) reported that Pb accounts for 0.6% of the global disease burden, which is highest in developing countries (WHO, 2009). Elevation of blood Pb levels has been reported in humans from several developing countries (Dooyema et al., 2012; Nakata et al., 2020; Parnia et al., 2018). Additionally, low-income communities tend to be more susceptible to pollution (Miranda, Edwards, Keating, & Paul, 2011). Lead has been implicated in many adverse health outcomes, such as kidney disorders (Sabath and Robles-Osorio, 2012) and anemia, as Pb inhibits δ-aminolevulinic acid dehydratase (ALAD) (Gonick, 2011). One of the important mechanisms underlying Pb toxicity is oxidative-stress induction resulting from the generation of reactive species and/or depletion of the antioxidant defensive system (Matović, Buha, Đukić-Ćosić, & Bulat, 2015).

Being overweight or obese are also common health issues and are major risk factors for chronic non-communicable diseases (NCDs), including cardiovascular diseases and type 2 diabetes (WHO, 2011). Nearly 80% of NCD deaths occur in low- and middle-income countries (WHO, 2011). Drewnowski and Specter (2004) reported that the highest rates of obesity occur among population groups with the highest poverty rates. They also stated in linear programming models that a reduction in diet costs leads to energy-dense diets, which consist of refined grains or fats and are similar in composition to the diets of people with low incomes. Similarly, economic deprivation leads people to choose cheaper foods, namely, food high in fats and carbohydrates, rather than foods high in protein (Hruschka, 2012). Hence, the poor in the developing world generally take more calories from fats and carbohydrates instead of protein and are likely to suffer from both Pb poisoning and obesity.

Spirulina (*Arthrospira platensis*) is the general name of a filamentous cyanobacterium (blue-green algae). Spirulina exists in tropical and subtropical lakes in Africa, Asia, and South and Central America. Although

* Corresponding author.
E-mail address: ishizum@vetmed.hokudai.ac.jp (M. Ishizuka).

https://doi.org/10.1016/j.jff.2020.104344
Received 5 September 2020; Received in revised form 3 December 2020; Accepted 14 December 2020

it has been used as a traditional medicine and as a food source in some areas, Spirulina has recently attracted greater attention because of its potential use in nutritional and medical applications (FAO/IOC 2011). It has high protein content, approximately 50%–70% of its dry weight (Hoseini, Khosravi-Darani, & Mozafari, 2013), and is rich in essential minerals, including iron (Fe), which results in significantly higher hemoglobin (Hb) content (Campanella, Crescentini, & Avino, 1999). Further, *A. platensis* provides antioxidant protection due to the antioxidant activity of the vitamins it contains, such as β-carotene and tocopherols, as well as phycocyanin (Estrada, Bescós, & Del Fresno, 2001; Miranda, Cintra, Barros, & Mancini-Filho, 1998). Upasani and Balaraman (2003) reported that the administration of *A. platensis* to Pb-exposed rats significantly inhibited lipid peroxidation (LPO) and restored the levels of endogenous antioxidants, including superoxide dismutase (SOD), catalase, and glutathione (GSH), in various organs. It was indicated that co-administration of *A. platensis* and Pb acetate minimized the increased levels of LPO and other oxidative stress markers (Khalil, Elhady, Elewa, Abd El-Hameed, & Ali, 2018). The antioxidative property of *A. platensis* was also demonstrated in subchronically Pb-exposed rabbits (Aladaileh et al., 2020). Moreover, *A. platensis* has a protective effect against obesity-related metabolic disorders (Yousefi, Mottaghi, & Saidpour, 2018) and anemia (Selmi et al., 2011). Zhao et al. (2019) recently reported that the protein hydrolysate of *A. platensis* exhibited good anti-obesity effects with modulation of gene expression.

On the basis of this available data, we hypothesized that Spirulina (*A. platensis*) supplementation may play a role in ameliorating Pb poisoning and obesity. Because both Pb poisoning and obesity are common health concerns in developing countries, people in these regions may be considered doubly affected. However, to the best of our knowledge, there have been no studies examining the possible mitigative effects of Spirulina on this combination of conditions. To investigate this possibility, we designed a laboratory exposure experiment using mice. We assessed hematotoxicity-related parameters including erythrocyte ALAD activity, which can be induced by Pb exposure. As kidney damage is also a common clinical effect of Pb, we assayed several plasma markers including clusterin, cystatin C, and neutrophil gelatinase-associated lipocalin (NGAL) which have recently attracted attention because of their sensitivity and their characteristic of being unaffected by other factors (Vinken et al., 2012; Zhang, Lu, Sheng, & Jin, 2011). Moreover, two markers in liver were measured to assess the oxidative stress status of the mice. To assess obesity, we measured epididymal white adipose tissue (eWAT) weight, as well as plasma parameters. As Spirulina is cultivated and exists naturally worldwide, Spirulina supplementation has great potential as a cost-effective solution for Pb poisoning and obesity.

2. Materials and methods

2.1. Animals and experimental design

All animal experiments were performed with the approval and supervision of the Institutional Animal Care and Use Committee of Hokkaido University (approval number 19–0119), Japan. Forty-two male C57BL/6J mice (*Mus musculus*, 7 weeks old) were purchased from Sankyo Labo Service Corporation, Inc. (Tokyo, Japan) and Hokudo Co., Ltd. (Hokkaido, Japan). Food (rodent chow, Labo MR Stock; Nosan Corporation, Yokohama, Japan) and distilled water were provided *ad libitum* during the one-week acclimation period at the Faculty of Veterinary Medicine, Hokkaido University. After acclimation, the mice (8 weeks of age) were divided into seven groups ($n = 6$ for each group) and treated for ten days as follows: 1) given no treatment (control, NC), 2) given special diet (SD), 3) given 1,000 mg/L lead acetate (Wako Pure Chemical Industries, Osaka, Japan) in water (PB), 4) given Spirulina powder (1,000 mg/kg body weight/day) (SP), (5) given special diet and Spirulina powder (SD-SP), (6) given lead acetate water and Spirulina powder (PB-SP), and (7) given a special diet, lead acetate water, and Spirulina powder (SD-PB-SP). A control diet (D12450H, Research Diets, Inc., NJ, USA) was given to the groups, which were not given the special diet during the treatment period. The special diet (modified D12451, Research Diets, Inc.) contained more fats and carbohydrates, as well as lower protein compared to the control diet, with a calorie-based formulation under the premise that mice eat for calories and adjust their overall intake in food weight to achieve a certain caloric intake (Bullen et al., 2004). The detailed blending ratios of ingredients are shown in Supplementary Table S1. Purified Spirulina (*A. platensis*) powder (DIC Lifetec Co., Ltd., Tokyo, Japan) was mixed with distilled water, then the suspension was given orally to mice everyday using sonde. The suspension was prepared at time of use for each animal to ensure the same concentration. The compositions of the Spirulina product were reported by the previous study (Okamoto et al., 2019). Both control and special diets were given *ad libitum*. Prepared lead acetate as given in the drinking water *ad libitum*. The mice in the Pb-exposed group had an average of 5.0 mL/day/animal of water to drink, indicating the animals ingested 5.0 mg/day/animal of lead acetate in average. The mice were housed under a 12 h light–12 h dark cycle throughout the acclimation and treatment periods.

2.2. Sample collection

After the treatment period, mice were euthanized by carbon dioxide (CO_2) gas inhalation. Heparinized whole blood was then collected from the postcava using syringe and needle, as well as feces, liver, kidneys, and eWAT. The collected eWAT was immediately weighed. Plasma was collected after centrifugation (10 min at 2,000 × *g* at room temperature) of heparinized whole blood for further analyses. The collected samples were stored at −20 °C prior to the analyses.

2.3. Sample digestion and metal extraction

Sample digestion and metal extraction were performed as previously described (Nakata et al., 2016) with minor modifications. Fifty microliters of whole blood were placed in pre-washed digestion vessels, followed by acid digestion using 5 mL of two-fold diluted nitric acid (atomic absorption spectrometry grade, 60%; Kanto Chemical Co., Tokyo, Japan) and 1 mL of hydrogen peroxide (Cica reagent, 30%; Kanto Chemical Co.). Similarly, approximately 0.1 g of dried liver and kidney, as well as 50 mg of dried feces, were treated using the same volume of nitric acid and hydrogen peroxide as the blood sample. The digestion and metal extraction were conducted using a microwave digestion system (Speed Wave MWS-2; Berghof, Eningen, Germany) following the manufacturer's instruction. The operating conditions of the microwave system are given in Supplementary Table S2. After cooling, the sample solutions were transferred into 15 mL polypropylene tubes and diluted to a final volume of 10 mL with double distilled and deionized water (Milli-Q; Millipore, Bedford, MA, USA).

2.4. Metal analysis

The concentrations of the metals (Pb and Fe) were determined using an inductively coupled plasma-mass spectrometer (ICP-MS) (7700 Series; Agilent Technologies, Tokyo, Japan). Detailed operating conditions are shown in Supplementary Table S3. Analytical quality control was performed using the following certified reference materials: Seronorm™ Trace Elements Whole Blood L-2 (Sero, Billingstad, Norway), DORM-3 (fish protein; National Research Council of Canada, Ottawa, Canada), and DOLT-4 (dogfish liver; National Research Council of Canada). A replicate analysis of these reference materials showed good accuracy (a relative standard deviation of less than 3%) and recoveries (95%–105%). The instrument detection limit was 0.001 μg/L.

2.5. Hct and plasma biomarker analyses

Hct values were measured using an Hct centrifuge (Kubota 3220; Kubota Corp., Osaka, Japan). A conventional blood biochemical analyzer (Spotchem EZ SP-4430; Arkray Inc., Kyoto, Japan) was used to analyze the levels of plasma high-density lipoprotein (HDL-C), triglyceride (TG), glucose (Glu), and total cholesterol (T-Cho). Another conventional blood biochemical analyzer (Fuji Drichem 7000 V; Fujifilm Corporation, Tokyo, Japan) was used to analyze plasma total protein (TP), albumin (Alb), blood urea nitrogen (BUN), uric acid (UA), and creatinine (Cre) levels. The analyses were done following the manufacturer's instructions.

A Milliplex MAP Mouse Kidney Injury Magnetic Bead Panel 2 Kit (EMD, Millipore Corporation, Billerca, MA, USA) was used with a Bio-Plex 200 System (Bio-Rad, Hercules, CA, USA) and Bio-Plex Manager software version 6.0 (Bio-Rad) to measure clusterin, cystatin C, and NGAL. Five mice were selected at random from each group for the Milliplex MAP assay, unlike in the other experiments.

2.6. Oxidative-stress marker analysis

Genomic DNA was extracted from the liver with the sodium iodide method using a DNA Extractor WB Kit (Fujifilm Wako Pure Chemical Corporation, Tokyo, Japan) according to the manufacturer's manual. The DNA concentration was measured spectrophotometrically using a NanoDrop spectrophotometer (ND-1000; Thermo Scientific, Newark, DE) and diluted to 100–200 ng/μL. The EpiQuik One-Step DNA Hydrolysis Kit (Epigentek Group Inc., NY, USA) was used to hydrolyze DNA according to the manufacturer's protocol. Afterward, the 8-hydroxy-2′-deoxyguanosine (8-OHdG) assay was done using the highly sensitive 8-OHdG Check ELISA Kit (KOG-HS10/E, Japan Institute for the Control of Aging, Nikken Seil Co., Ltd., Shizuoka, Japan).

The extraction of protein carbonyls from the liver was performed as described previously (Augustyniak et al., 2015) with minor modifications. Approximately 0.4 g of liver tissue was homogenized in ice-cold phosphate-buffered saline (PBS; pH 7.4) at 2:1 PBS/tissue ratio using a rotor stator homogenizer. Phenylmethylsulphonyl fluoride (Nacalai Tesque, Kyoto, Japan) was added as a protease inhibitor at a final concentration of 1 mM immediately before homogenization. The homogenate was then centrifuged (600 × *g*, 5 min at 4 °C). The collected supernatant was re-centrifuged (3,000 × *g*, 20 min at 4 °C). The supernatant was collected again and re-centrifuged using an ultracentrifuge (100,000 × *g*, 4 h at 4 °C), after which the supernatant containing soluble proteins was collected. Protein concentration in the collected supernatant was measured using a Pierce BCA Protein Assay Kit (Thermo Scientific, IL, USA) following the manufacturer's instructions. Finally, the protein carbonyl assay was carried out with 250 μg of protein using a Protein Carbonyl ELISA Kit (ALX-850-312-KI01; Enzo Life Sciences, NY, USA).

2.7. ALAD activity assay

Erythrocyte enzymatic activity and the ratio between non-activated and enzymes activated *in vitro* were measured as described in a previous study (Nakata et al., 2020), which was slightly modified from the original method (Espín, Martínez-López, Jiménez, María-Mojica, & García-Fernández, 2015; Scheuhammer, 1987). Three aliquots (20 μL each) of erythrocytes from each mouse were separated to measure non-activated ALAD activity, reactivated ALAD activity, and the activity of the matrix. For the non-activated enzyme activity assay, 80 μL of 0.1% Triton X-100 (Sigma–Aldrich, MO, USA) was added to the erythrocytes to form a lysate. Subsequently, 100 μL of 0.5 M PBS (pH 6.8), 50 μL of 60 mM 5-aminolevulinic acid (ALA) hydrochloride (Sigma–Aldrich) solution in PBS, and 50 μL of distilled water were added. For the reactivated-activity assay, 0.1% Triton X-100, 0.5 M PBS, and 60 mM ALA hydrochloride were added to the sample with the same volume of each solution as used in the non-activated enzyme activity assay. Subsequently, 25 μL of 0.8 mM zinc acetate (Kishida Chemical Co., Ltd., Osaka, Japan) and 25 μL of 1 M dithiothreitol (Fujifilm Wako Pure Chemical Corporation) were added. For the matrix blank assay, 80 μL of Triton X-100, 150 μL of PBS, and 50 μL of distilled water were added, followed by 200 μL of 0.4 M trichloroacetic acid (Fujifilm Wako Pure Chemical Corporation)/60 mM mercury chloride ($HgCl_2$) (Kanto Chemical Co.) as a stop solution. After 60 min incubation and termination of the reaction by $HgCl_2$ in both the non-activated and reactivated activity assays, all samples were centrifuged at 10,000 rpm for 5 min. Supernatants were transferred to new tubes and mixed with 750 μL of modified Ehrlich's reagent, which consisted of dimethylaminobenzaldehyde (Nacalai Tesque) in acetic acid (glacial; 99.7%, Thermo Fisher Scientific, Lancashire, UK) and perchloric acid (Kanto Chemical Co.). After 10 min, the absorbance was read at 555 nm against the appropriate blank using a UV spectrophotometer (Shimadzu UV-2600; Shimadzu Inc., Kyoto, Japan). The activity was expressed as μmol porphobilinogen/h/L red blood cells using the equation provided by Scheuhammer (1987). The ratio between the non-activated and the *in vitro* reactivated enzymes was then calculated.

2.8. Statistical analysis

IBM SPSS Statistics 26 (IBM Corporation, Armonk, NY, USA) was used to evaluate significant differences in the data in all statistical analyses. The data were log-transformed and fitted with a normal distribution. The Tukey–Kramer test was used to compare food and water consumption, body and eWAT weight, Hct values, blood biochemical parameters, renal function parameters, oxidative stress markers, and ALAD activity among groups. All statistical analyses were performed with a significance level of 0.05 ($p < 0.05$).

3. Results

3.1. Metal concentrations in mice tissues and feces

The sample size for the SP and PB-SP groups decreased by one in each because of deaths during the treatment period attributed to Spirulina powder aspiration. The remainder of the samples ($n = 5$ for SP and PB-SP, $n = 6$ for other groups) were used in the laboratory experiments. There were no significant differences in body weight or in food and water consumption rates among groups throughout the experiment period.

The Pb and Fe levels in the blood, liver, kidney, and feces of the mice were analyzed and are summarized in Table 1 and Table 2, respectively. The blood and liver Pb levels of the Pb-administered groups (PB, PB-SP, and SD-PB-SP) were within the range of 11.74–22.51 μg/dL and 1.23–4.22 mg/kg, respectively, significantly higher than those of groups that were not given Pb. The kidney and feces Pb concentrations of the PB, PB-SP, and SD-PB-SP groups similarly showed significant elevation compared to those of other groups. However, the kidney Pb level of the SD-PB-SP group was significantly lower than that of the PB group. The SD-PB-SP group also showed a significant reduction of Pb concentration in their feces compared with the PB-SP group.

In contrast to Pb level, blood and liver Fe levels did not differ statistically among groups, although the SD-SP group showed a significant increase in kidney Fe concentration compared with the NC group. The ranges of blood and liver Fe for all groups were 311.90–524.04 μg/mL and 202.88–797.50 mg/kg, respectively. The excreted Fe levels in the feces of the SD, SD-SP, and PB-SP groups were also greater than those of the NC group.

3.2. Adipose weight, Hct, and blood biochemical parameters

The values of eWAT weight and Hct, as well as plasma HDL-C, TG, Glu, and T-Cho, were measured (Fig. 1, Table 3). A significant increase

Table 1
Pb levels in blood, liver, kidney, and feces samples by group (control group and treated groups with sole or combination of special diet, lead acetate and spirulina powder).

Pb level	Blood (μg/dL)		Liver (mg/kg)		Kidney (mg/kg)		Feces (mg/kg)	
NC	0.69 ± 0.14	a	0.01 ± 0.00	a	0.01 ± 0.00	a	0.04 ± 0.01	a
	(0.52–0.88)		(0.01–0.01)		(0.01–0.02)		(0.03–0.05)	
SD	0.71 ± 0.12	a	0.01 ± 0.00	a	0.01 ± 0.00	a	0.11 ± 0.04	a
	(0.56–0.89)		(0.01–0.01)		(0.01–0.01)		(0.06–0.19)	
PB	19.25 ± 2.51	b	2.06 ± 0.62	b	13.20 ± 1.86	c	705.83 ± 252.26	bc
	(14.98–22.06)		(1.23–3.16)		(11.11–15.54)		(360.34–1008.95)	
SP	0.55 ± 0.18	a	0.01 ± 0.00	a	0.01 ± 0.00	a	0.17 ± 0.07	a
	(0.44–0.87)		(0.01–0.01)		(0.01–0.01)		(0.08–0.27)	
SD-SP	0.55 ± 0.08	a	0.01 ± 0.00	a	0.01 ± 0.00	a	0.20 ± 0.16	a
	(0.43–0.66)		(0.00–0.02)		(0.01–0.02)		(0.07–0.49)	
PB-SP	16.94 ± 3.05	b	1.96 ± 0.43	b	11.42 ± 1.60	bc	948.41 ± 494.33	c
	(12.57–21.07)		(1.30–2.40)		(9.77–13.93)		(481.76–1654.53)	
SD-PB-SP	16.48 ± 3.48	b	2.90 ± 1.14	b	10.62 ± 2.15	b	431.37 ± 85.14	b
	(11.74–22.51)		(1.31–4.22)		(7.83–13.96)		(277.06–520.25)	

Note: Mean ± standard deviation in the upper row, and range in the lower row.
Note: Different small letters (a, b and c) between columns indicate significant differences among groups.

Table 2
Fe levels in blood, liver, kidney, and feces samples by group (control group and treated groups with sole or combination of special diet, lead acetate and spirulina powder).

Fe level	Blood (μg/mL)		Liver (mg/kg)		Kidney (mg/kg)		Feces (mg/kg)	
NC (N = 6)	472.29 ± 36.50	a	246.41 ± 40.76	a	337.45 ± 40.60	b	224.65 ± 57.57	b
	(414.46–521.30)		(208.49–298.00)		(297.07–385.82)		(159.53–294.09)	
SD (N = 6)	490.97 ± 11.87	a	281.56 ± 50.31	a	373.83 ± 54.00	ab	441.75 ± 97.31	a
	(479.78–507.28)		(213.59–336.73)		(291.79–434.19)		(371.04–633.12)	
PB (N = 6)	484.86 ± 16.62	a	268.07 ± 40.03	a	361.53 ± 34.04	ab	335.68 ± 77.74	ab
	(466.96–511.18)		(202.88–324.50)		(335.54–414.48)		(214.44–418.90)	
SP (N = 5)	468.25 ± 30.68	a	301.78 ± 40.37	a	397.30 ± 25.34	ab	341.47 ± 51.55	ab
	(424.65–493.66)		(262.26–366.62)		(361.86–422.15)		(271.46–389.67)	
SD-SP (N = 6)	429.91 ± 59.49	a	417.73 ± 156.22	a	426.44 ± 36.23	a	455.54 ± 161.21	a
	(311.90–477.18)		(275.30–627.99)		(379.61–470.19)		(230.04–729.87)	
PB-SP (N = 5)	422.96 ± 15.02	a	394.28 ± 228.07	a	398.94 ± 32.93	ab	445.43 ± 194.22	a
	(402.66–441.69)		(243.50–797.50)		(362.29–446.30)		(289.33–749.04)	
SD-PB-SP (N = 6)	449.34 ± 49.80	a	348.55 ± 61.07	a	387.47 ± 18.75	ab	380.88 ± 85.07	ab
	(389.03–524.04)		(278.88–457.22)		(359.12–415.16)		(287.49–484.82)	

Note: Mean ± standard deviation in the upper row, and range in the lower row.
Note: Different small letters (a and b) between columns indicate significant differences among groups.

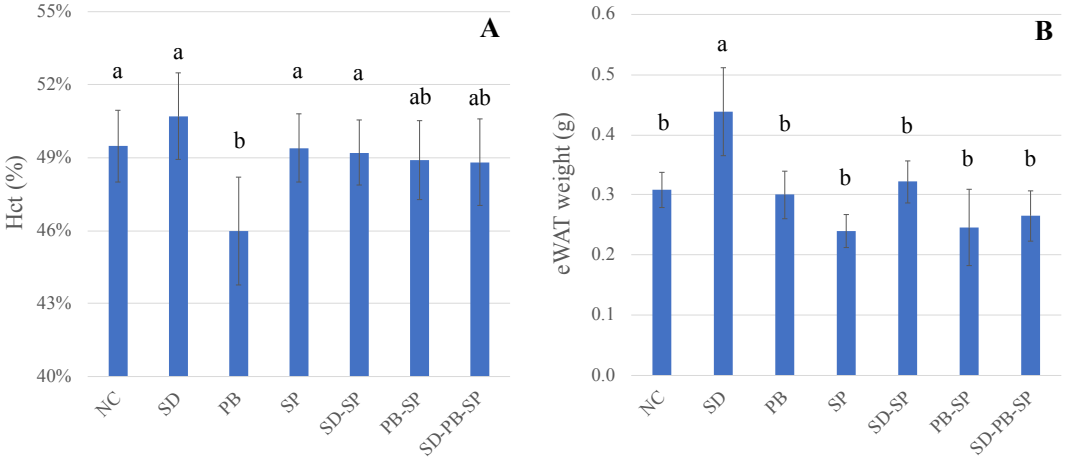

Fig. 1. Means and standard deviation values (error bars) of blood Hct (A) and eWAT weight (B) by groups. Different small letters (a and b) indicate significant differences among groups. NC = control without any treatment, SD = given special diet, PB = given 1,000 mg/L Pb acetate, SP = given Spirulina powder (1,000 mg/kg body weight/day), SD-SP = given special diet and Spirulina powder, PB-SP = given Pb acetate and Spirulina powder, SD-PB-SP = given special diet, Pb acetate and Spirulina powder.

in eWAT weight was recorded in the SD group, with a mean increase and standard deviation of 0.44 ± 0.07 g over the eWAT weight of other groups. The Hct of the PB group (46.0 ± 2.2%) was significantly lower than that of the NC, SD, SP, and SD-SP groups. The SD group showed significantly elevated HDL-C compared with the PB-SP and SD-PB-SP groups, and there was no significant difference in TG, Glu, or T-Cho

Table 3
Values of plasma biochemical parameters relating to obesity assessment by group (control group and treated groups with sole or combination of special diet, lead acetate and spirulina powder).

	HDL-C (mg/dL)		TG (mg/dL)		Glu (mg/dL)		T-Cho (mg/dL)	
NC	51.2 ± 9.4 (40–66)	ab	103.3 ± 17.4 (90–137)	a	271.5 ± 66.8 (193–367)	a	104.5 ± 19.4 (71–127)	a
SD	61.5 ± 6.2 (56–71)	a	110.0 ± 14.8 (85–130)	a	324.3 ± 51.9 (249–384)	a	114.0 ± 7.3 (102–124)	a
PB	48.7 ± 2.6 (44–51)	ab	118.3 ± 23.0 (96–147)	a	324.3 ± 44.1 (275–396)	a	116.3 ± 9.1 (109–128)	a
SP	49.6 ± 9.7 (40–66)	ab	116.6 ± 12.4 (100–134)	a	356.4 ± 52.1 (289–407)	a	114.4 ± 4.6 (110–122)	a
SD-SP	54.0 ± 5.2 (48–62)	ab	111.2 ± 6.2 (103–118)	a	353.8 ± 17.1 (335–380)	a	116.5 ± 8.4 (105–125)	a
PB-SP	38.0 ± 14.1 (17–54)	b	121.8 ± 11.5 (112–139)	a	344.4 ± 39.5 (298–387)	a	107.2 ± 15.5 (85–124)	a
SD-PB-SP	38.8 ± 10.9 (21–51)	b	113.0 ± 13.7 (92–127)	a	352.2 ± 37.7 (290–401)	a	106.7 ± 14.0 (81–119)	a

Note: Mean ± standard deviation in the upper row, and range in the lower row.
Note: Different small letters (a and b) between columns indicate significant differences among groups.

among groups.

3.3. Renal function parameters

The analyzed data for renal function parameters, including TP, Alb, BUN, UA, Cre, clusterin, cystatin C, and NGAL, are summarized in Table 4. Significant elevations of TP and Alb for the SD group as compared with the NC, PB, SP, and SD-PB-SP groups were recorded. The SD, SP, SD-SP, and SD-PB-SP groups showed significantly BUN lower than those of the NC group. A significant increase in UA was observed for the Spirulina-administrated groups (SP, SD-SP, PB-SP, and SD-PB-SP) as compared with the NC group. No significant differences were found for the other four target plasma parameters.

3.4. Oxidative-stress parameters

The 8-OHdG value ranged from 0.05 to 0.24 ng/mL, and the protein carbonyl level ranged from 0.12 to 0.84 nmol/mg for all groups. No statistically significant differences were observed among groups for either 8-OHdG or protein carbonyl (Table 5).

3.5. ALAD activity

The SP group showed the highest ALAD activity ratio with statistical significance, followed by the SD, SD-SP, and NC groups (Fig. 2, Supplementary Table S4). The ALAD activity ratio of the PB group was significantly reduced compared with the other groups. There were no significant differences in assays other than the non-activated assay.

4. Discussion

In the current study, a Spirulina solution was administrated to mice that had been exposed to either Pb acetate, a special diet high in fats and carbohydrates, or a combination of both to elucidate the potential ameliorative effect of Spirulina on Pb poisoning and obesity. However, because of the unfortunate deaths of two mice during the experimental period, we had to discontinue administration after 10 days, which is a major limitation of this study.

The Pb concentrations in all of the studied tissues and feces of Pb-exposed groups (PB, PB-SP, and SD-PB-SP) were significantly elevated relative to those of the other groups (NC, SP, SD, and SD-SP). Spirulina administration did not significantly change Pb levels in the blood, liver, and feces, but the kidney Pb level in the SD-PB-SP group was significantly lower than that of the PB group. Although the reason for the reduction in the renal Pb concentration in the SD-PB-SP group was unclear, these results suggest that Spirulina supplementation does not affect Pb deposition in tissues or excretion through the feces. This is in agreement with a previous laboratory-exposure study that used Wistar rats (Upasani and Balaraman, 2003). On the other hand, Khalil, Elhady, Elewa, Abd El-Hameed, & Ali. (2018) found the significant reduction of Pb accumulation levels in blood and liver by Spirulina supplementation in their exposure study albeit the longer treatment period (30 days) and lower dose of the intraperitoneally administrated Pb acetate (50 mg/kg body weight).

The previous study administered Spirulina to healthy Wistar rats for 30 days and did not record a change in serum Fe concentration (Nasirian, Dadkhah, Moradi-kor, & Obeidavi, 2018), supporting our results showing no change in blood Fe levels after Spirulina treatment. According to Simsek, Karadeniz, & Karaca (2007), erythrocyte formation and Hb synthesis were stimulated by Spirulina administration in rats. Moreover, in a previous study on humans, Spirulina supplementation increased the mean corpuscular volume, mean corpuscular Hb, and mean corpuscular Hb concentration (Selmi et al., 2011). In our study, a protective effect of Spirulina supplementation was observed in two indicators of Pb hematotoxicity. The Hct value dropped significantly in the PB group compared with the groups not exposed to Pb, however the Hct value was restored by Spirulina treatment. Similarly, the reduction of the ALAD activity ratio observed in the PB group was significantly ameliorated in the PB-SP and SD-PB-SP groups. Furthermore, the SP group exhibited the highest ALAD activity ratio among groups, indicating a promotive effect of Spirulina on ALAD activity. Simsek, Karadeniz, Kalkan, Keles, & Unal (2009) also reported that Spirulina treatments in rats improved red blood cell counts and Hb concentrations, as well as improved Hct values reduced by Pb administration. The results in the current and previous studies support Spirulina having an ameliorative effect on anemia. It should also be emphasized that the same extent of restoration in the Hct value and ALAD activity ratio were seen in the SD-PB-SP group as in the PB-SP group; this suggests that Spirulina supplementation improves anemia status even in mice fed a high-fat, low-protein diet.

Regarding the renal injury assessment, the three plasma proteins (clusterin, cystatin C, and NGAL), which are preferred for detecting changes in renal function at an early stage over traditional parameters (Vinken et al., 2012; Zhang et al., 2011), did not differ among the groups in our study, contrary to our expectations. Although Poręba, Gać, Poręba, Antonowicz-Juchniewicz, & Andrzejak (2011) reported a significant association between blood Pb and serum cystatin C levels in humans, the short duration of exposure period in our study could have resulted in the lack of observed kidney injury. On the other hand, for some traditional parameters, significant differences among the groups were recorded. The increase in Alb in the SD group is especially interesting because the special diet contains less protein than the control diet.

Table 4
Values of plasma biochemical parameters relating to kidney injury assessment by group (control group and treated groups with sole or combination of special diet, lead acetate and spirulina powder).

	TP (g/dL)		Alb (g/dL)		BUN (mg/dL)		UA (mg/dL)		Cre (mg/dL)		Clusterin (μg/mL)		Cystatin C (μg/mL)		NGAL (μg/mL)	
NC	2.0 ± 0.3 (1.7–2.5)	a	0.6 ± 0.2 (0.4–0.8)	a	8.0 ± 0.6 (7.4–9.1)	a	0.9 ± 0.4 (0.3–1.3)	a	0.27 ± 0.03 (0.24–0.31)	a	72.32 ± 7.80 (59.50–78.50)	a	0.45 ± 0.07 (0.36–0.53)	a	0.17 ± 0.03 (0.14–0.21)	a
SD	2.6 ± 0.3 (2.2–2.9)	b	1.1 ± 0.2 (0.8–1.3)	b	4.8 ± 0.4 (4.2–5.4)	c	1.6 ± 0.4 (0.9–2.2)	abc	0.25 ± 0.04 (0.19–0.29)	a	74.31 ± 5.64 (64.62–79.17)	a	0.49 ± 0.07 (0.41–0.58)	a	0.33 ± 0.17 (0.21–0.60)	a
PB	2.1 ± 0.1 (1.9–2.3)	a	0.7 ± 0.1 (0.6–0.8)	a	7.6 ± 0.8 (6.4–8.8)	ab	1.4 ± 0.2 (1.1–1.7)	ab	0.25 ± 0.03 (0.22–0.29)	a	80.49 ± 15.93 (67.94–105.44)	a	0.44 ± 0.06 (0.36–0.53)	a	0.14 ± 0.02 (0.12–0.16)	a
SP	2.1 ± 0.1 (2.0–2.3)	a	0.7 ± 0.1 (0.6–0.9)	a	6.1 ± 1.1 (4.2–6.9)	bc	2.0 ± 0.5 (1.5–2.7)	bc	0.26 ± 0.03 (0.24–0.30)	a	93.38 ± 26.96 (59.66–133.35)	a	0.53 ± 0.12 (0.40–0.72)	a	0.26 ± 0.10 (0.15–0.41)	a
SD-SP	2.5 ± 0.3 (2.1–3.0)	ab	0.8 ± 0.3 (0.4–1.3)	ab	4.7 ± 0.4 (4.3–5.5)	c	2.0 ± 0.3 (1.6–2.5)	bc	0.24 ± 0.02 (0.21–0.26)	a	94.90 ± 17.69 (64.18–107.57)	a	0.55 ± 0.08 (0.45–0.64)	a	0.22 ± 0.05 (0.14–0.28)	a
PB-SP	2.2 ± 0.2 (2.0–2.5)	ab	0.8 ± 0.1 (0.6–1.0)	ab	7.3 ± 1.4 (5.1–8.7)	ab	2.3 ± 0.7 (1.1–2.9)	c	0.26 ± 0.01 (0.25–0.27)	a	106.85 ± 29.68 (80.41–151.99)	a	0.56 ± 0.04 (0.51–0.61)	a	0.98 ± 1.46 (0.22–3.58)	a
SD-PB-SP	2.2 ± 0.3 (1.9–2.6)	a	0.8 ± 0.2 (0.6–1.1)	a	4.5 ± 1.0 (3.1–5.9)	c	2.2 ± 0.5 (1.6–2.9)	c	0.25 ± 0.01 (0.24–0.27)	a	93.41 ± 13.45 (71.76–107.79)	a	0.54 ± 0.04 (0.50–0.61)	a	1.38 ± 2.62 (0.15–6.06)	a

Note: Mean ± standard deviation in the upper row, and range in the lower row.
Note: Different small letters (a, b and c) between columns indicate significant differences among groups.

Table 5
Values of oxidative-stress markers by group (control group and treated groups with sole or combination of special diet, lead acetate and spirulina powder).

	8-OHdG (ng/mL)		Protein carbonyl (nmol/mg)	
NC	0.11 ± 0.02 (0.09–0.13)	a	0.18 ± 0.05 (0.13–0.27)	a
SD	0.12 ± 0.02 (0.09–0.14)	a	0.26 ± 0.09 (0.12–0.40)	a
PB	0.08 ± 0.03 (0.05–0.13)	a	0.17 ± 0.05 (0.12–0.25)	a
SP	0.10 ± 0.03 (0.06–0.12)	a	0.18 ± 0.04 (0.12–0.24)	a
SD-SP	0.12 ± 0.04 (0.08–0.18)	a	0.34 ± 0.27 (0.14–0.84)	a
PB-SP	0.12 ± 0.07 (0.08–0.24)	a	0.29 ± 0.15 (0.15–0.55)	a
SD-PB-SP	0.12 ± 0.03 (0.08–0.15)	a	0.40 ± 0.20 (0.22–0.74)	a

Note: Mean ± standard deviation in the upper row, and range in the lower row.
Note: One small letter of a indicates no significant difference among groups.

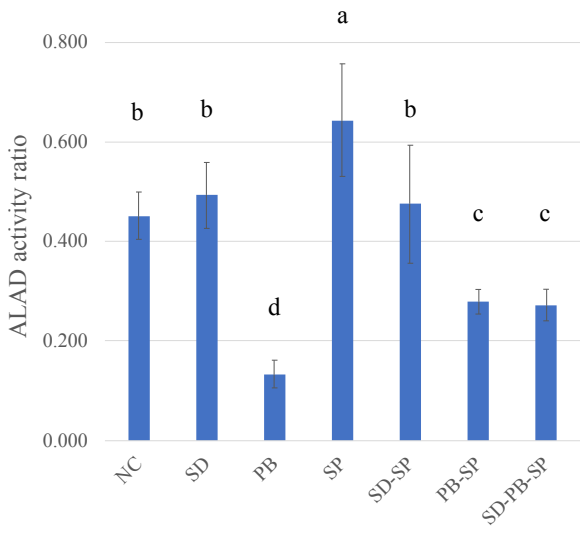

Fig. 2. Means and standard deviation values (error bars) of erythrocyte δ-aminolevulinic acid dehydratase activity ratio by groups. Different small letters (a, b, c and d) indicate significant differences among groups. NC = control without any treatment, SD = given special diet, PB = given 1,000 mg/L Pb acetate, SP = given Spirulina powder (1,000 mg/kg body weight/day), SD-SP = given special diet and Spirulina powder, PB-SP = given Pb acetate and Spirulina powder, SD-PB-SP = given special diet, Pb acetate and Spirulina powder.

Although to the best of our knowledge, there have been no studies reporting Alb increases due to a low protein diet, it could be hypothesized that more lipid was used for energy metabolism instead of Alb because of the high-fat diet; this results in the temporal plasma Alb increase on day 10 of treatment. In our study, feeding mice the special diet, which had low levels of protein, also caused the decline of plasma BUN. This phenomenon is well-known and can be explained by the theory that low protein intake suppresses protein metabolism, resulting in low BUN synthesis in the liver (Boulay, Scott, Conly, Stevenson, & Koski, 1998). Another interesting finding is the increase in UA in mice fed Spirulina. Considering the fact that high UA is usually caused by a high intake of dietary purines, the purine-rich alkaloids in Spirulina (Kata et al., 2018) would have enhanced purine metabolism in liver and increased the UA metabolite. It is also generally known that changes in these indices can result from renal dysfunction; however, the absence of changes in parameters such as clusterin, cystatin C, and NGAL suggests that renal disorders did not occur in the present study.

The plasma HDL-C, TG, Glu, and T-Cho levels were assessed to evaluate obesity status. A previous study showed that type 2 diabetes mellitus patients who took Spirulina supplements for two months had decreased blood TG, Glu, and T-Cho, coupled with a marginal increase in HDL-C (Parikh, Mani, & Iyer, 2001). Likewise, a study using CD-1 mice with experimental diabetes demonstrated the elevation of HDL-C after four weeks of Spirulina administration (Rodrıguez-Hernández, Ble-Castillo, Juarez-Oropeza, & Dıaz-Zagoya, 2001). Serban et al. (2016) concluded that Spirulina supplementation reduced plasma concentrations of TG and T-Cho and elevated those of HDL-C. In our study, however, such phenomenon was not observed; the plasma parameters did not differ greatly among groups. The meta-analysis study explained this unexpected result with the finding of significant associations between Spirulina supplementation duration and plasma HDL-C, TG, and T-Cho concentration changes (Serban et al., 2016). In contrast to the other parameters, HDL-C in the SD group was significantly greater than that of the PB-SP and SD-PB-SP groups. The observed increase in HDL-C in C57BL/6J mice due to the high-fat diet was in agreement with a previous study (Yang, Du, Hosokawa, & Miyashita, 2020). A former exposure study on lead acetate in rats revealed a significant reduction in blood HDL-C in, the Pb-exposed group (Abdel-Moneim et al., 2015). Similarly, decreases in serum and liver HDL-C levels in Pb-exposed rats have also been reported (Newairy and Abdou, 2009). Taken together, these suggest the HDL-C decline in the PB-SP and SD-PB-SP groups was caused by the Pb administration. In fact, HDL-C in the PB group also marginally decreased relative to the NC group. Additionally, the comparison of the PB group with the PB-SP and SD-PB-SP groups supports the hypothesis that Spirulina treatment induces the reductive effect Pb has on plasma HDL-C.

The eWAT weight results, which are widely used as an indicator of obesity status in mice (Pham et al., 2019; Yang, Du, Hosokawa, & Miyashita, 2020), showed a clear trend. The significant increase in eWAT weight in the SD group was observed to be similar to that in a previous study on C57BL/6J mice on a 21-weeks high-fat diet (Duval et al., 2010). In the comparison of the SD group with the SD-SP and SD-PB-SP groups, the increase of eWAT weight due to the high-fat diet was significantly decreased upon Spirulina supplementation, indicating the mitigative effect Spirulina has on eWAT accumulation. Moreover, the SP group showed the lowest mean eWAT weight, followed by PB-SP, although the difference between these two groups was not statistically significant. A similarly significant reduction of total white adipose tissue (WAT) and mesenteric WAT weights of C57BL6/J mice by Spirulina has been reported, albeit there was no significant difference in eWAT weight (Yang, Du, Hosokawa, & Miyashita, 2020). But in contrast to our study, Pham et al. (2019) treated C57BL6/J mice with a high-fat/high-sucrose diet (34%/38%, w/w) for 20 weeks and found that dietary Spirulina supplementation (2%, w/w) did not affect eWAT weight. Considering the fact that our study used a diet containing a relatively low weight ratio of fat and sucrose (24%/20%) compared with the study by Pham et al. (2019), it can be hypothesized that Spirulina supplementation is not effective in reducing WAT weight after fat and sucrose intakes exceed a certain level.

Unlike the other parameters that showed significant changes with treatment, there were no significant differences between the groups in terms of oxidative-stress status on either of the two studied indices. Given that increases of reactive oxygen species, antioxidant capacity, and reactive oxygen metabolites due to Pb exposure are commonly known (Matović et al., 2015), the most likely explanation is the short exposure period, similar to the reason behind the absence of renal damage. Thus, further studies with longer treatment periods are considered necessary.

5. Conclusion

We examined the potential mitigative effects of Spirulina on Pb poisoning and obesity using a mouse model. While Spirulina treatment did not greatly affect the Pb and Fe accumulation patterns, probably because of the short duration of the experimental period, the anemia caused by Pb administration was improved by Spirulina, as shown through the Hct values and ALAD activity ratios, even for mice fed a high-fat low-protein diet. Regarding obesity-related indicators, Spirulina supplementation aided in decreasing eWAT weight, although the plasma biochemical parameters for obesity assessment did not greatly change in mice fed a high-fat diet. However, Spirulina treatment may have normalized the plasma HDL-C, which otherwise declines after Pb administration. No changes in any of the studied oxidative-stress-related indices were recorded in the current study. In summary, our study provided some positive insights into the efficacy of Spirulina; however, further validations are needed.

Ethics statements

All animal experiments were performed with the approval and supervision of the Institutional Animal Care and Use Committee of Hokkaido University (approval number 19-0119), Japan. The institute of Faculty of Veterinary Medicine, Hokkaido University has been accredited by The European Association of Establishments for Veterinary Education (EAEVE) and regulated under the EU Directive 2010/63/EU, and all animal experiments are reviewed by AAALAC International.

CRediT authorship contribution statement

Hokuto Nakata: Conceptualization, Data curation, Formal analysis, Funding acquisition, Investigation, Methodology, Validation, Visualization, Writing - original draft. **Shouta M.M. Nakayama:** Funding acquisition, Investigation, Methodology, Supervision, Writing - review & editing. **Andrew Kataba:** Investigation, Methodology, Validation, Writing - review & editing. **Yared Beyene Yohannes:** Investigation, Methodology, Validation, Writing - review & editing. **Yoshinori Ikenaka:** Funding acquisition, Resources, Supervision, Writing - review & editing. **Mayumi Ishizuka:** Funding acquisition, Project administration, Supervision, Writing - review & editing.

Declaration of Competing Interest

The authors declare that they have no known competing financial interests or personal relationships that could have appeared to influence the work reported in this paper.

Acknowledgements

This work was supported by Grants-in-Aid for Scientific Research from the Ministry of Education, Culture, Sports, Science, and Technology of Japan awarded to M. Ishizuka (No. 16H01779, 18KK0287), Y. Ikenaka (No. 17K20038, 18H04132), S.M.M. Nakayama (No. 17KK0009, 20K20633), and H. Nakata (No. 19K20472) and the foundation of JSPS Bilateral Open Partnership Joint Research Projects (JPJSBP120209902), and the Environment Research and Technology Development Fund (SII-1/3-2, 4RF-1802/18949907) of the Environmental Restoration and Conservation Agency of Japan. We also acknowledge financial support from The Soroptimist Japan Foundation, The Nakajima Foundation, The Sumitomo foundation, The Nihon Seimei Foundation, The Japan Prize Foundation, The Akiyama Life Science Foundation, and Hokkaido University SOUSEI Support Program for Young Researchers in FY2020 (SMMN). This research was also supported by JST/JICA, SATREPS (Science and Technology Research Partnership for Sustainable Development; No. JPMJSA1501), JST aXis (Accelerating Social Implementation for SDGs Achievement; No. JPMJAS2001) and Program for supporting introduction of the new sharing system (JPMXS0420100619). Our appreciation is extended to Sayako Yamamoto, Yumi Miyabe and Ami Matsuno for their assistance, as well as Takahiro Ichise and Nagisa Hirano for their technical support.

Appendix A. Supplementary material

Supplementary data to this article can be found online at https://doi.org/10.1016/j.jff.2020.104344.

References

Abdel-Moneim, A. M., El-Toweissy, M. Y., Ali, A. M., Allah, A. A. M. A., Darwish, H. S., & Sadek, I. A. (2015). Curcumin ameliorates lead (Pb 2+)-induced hemato-biochemical alterations and renal oxidative damage in a rat model. Biological trace element research, 168(1), 206-220. PMID: 25947936, https://doi.org/10.1007/s12011-015-0360-1.

Aladaileh, S. H., Khafaga, A. F., Abd El-Hack, M. E., Al-Gabri, N. A., Abukhalil, M. H., Alfwuaires, M. A., … Abdelnour, S. (2020). Spirulina platensis ameliorates the sub chronic toxicities of lead in rabbits via anti-oxidative, anti-inflammatory, and immune stimulatory properties. Science of The Total Environment, 701, 134879. PMID: 31734488, https://doi.org/10.1016/j.scitotenv.2019.134879.

Augustyniak, E., Adam, A., Wojdyla, K., Rogowska-Wrzesinska, A., Willetts, R., Korkmaz, A., …, Griffiths, H. R. (2015). Validation of protein carbonyl measurement: a multi-centre study. Redox Biology, 4, 149-157. PMID: 25560243, https://doi.org/10.1016/j.redox.2014.12.014.

Boulay, M., Scott, M. E., Conly, S. L., Stevenson, M. M., & Koski, K. G. (1998). Dietary protein and zinc restrictions independently modify a Heligmosomoides polygyrus (Nematoda) infection in mice. Parasitology, 116(5), 449-462. PMID: 9614328, https://doi.org/10.1017/s0031182098002431.

Bullen Jr, J. W., Ziotopoulou, M., Ungsunan, L., Misra, J., Alevizos, I., Kokkotou, E., …, Mantzoros, C. S. (2004). Short-term resistance to diet-induced obesity in A/J mice is not associated with regulation of hypothalamic neuropeptides. American Journal of Physiology-Endocrinology and Metabolism, 287(4), E662-E670. PMID: 15361355, https://doi.org/10.1152/ajpendo.00114.2004.

Campanella, L., Crescentini, G., & Avino, P. (1999). Chemical composition and nutritional evaluation of some natural and commercial food products based on Spirulina. *Analusis, 27*(6), 533–540. https://doi.org/10.1051/analusis:1999130.

Dooyema, C. A., Neri, A., Lo, Y. C., Durant, J., Dargan, P. I., Swarthout, T., … Brown, M. J. (2012). Outbreak of fatal childhood lead poisoning related to artisanal gold mining in northwestern Nigeria, 2010. *Environmental Health Perspectives, 120*(4), 601–607. https://doi.org/10.1289/ehp.1103965.

Drewnowski, A., & Specter, S. E. (2004). Poverty and obesity: the role of energy density and energy costs. The American Journal of Clinical Nutrition, 79(1), 6-16. PMID: 14684391, https://doi.org/10.1093/ajcn/79.1.6.

Duval, C., Thissen, U., Keshtkar, S., Accart, B., Stienstra, R., Boekschoten, M. V., Roskams, T., Kersten, S., & Müller, M. (2010). Adipose tissue dysfunction signals progression of hepatic steatosis towards nonalcoholic steatohepatitis in C57BL/6 mice. Diabetes, 59(12), 3181-3191. PMID: 20858684, https://doi.org/10.2337/db10-0224.

Estrada, J. P., Bescós, P. B., & Del Fresno, A. V. (2001). Antioxidant activity of different fractions of Spirulina platensis protean extract. Il farmaco, 56(5-7), 497-500. PMID: 11482785, https://doi.org/10.1016/s0014-827x(01)01084-9.

Espín, S., Martínez-López, E., Jiménez, P., María-Mojica, P., & García-Fernández, A. J. (2015). Delta-aminolevulinic acid dehydratase (δALAD) activity in four free-living bird species exposed to different levels of lead under natural conditions. Environmental research, 137, 185-198. PMID: 25569843, https://doi.org/10.1016/j.envres.2014.12.017.

FAO and IOC (2011). Spirulina: a livehood and a business venture. Available: http://www.fao.org/3/a-az386e.pdf [accessed 20 April 2020].

Gonick, H. C. (2011). Lead-binding proteins: a review. Journal of Toxicology, 2011. PMID: 21941540, https://doi.org/10.1155/2011/686050.

Hoseini, S. M., Khosravi-Darani, K., & Mozafari, M. R. (2013). Nutritional and medical applications of spirulina microalgae. Mini Reviews in Medicinal Chemistry, 13(8), 1231-1237. PMID: 23544470, https://doi.org/10.2174/1389557511313080009.

Hruschka, D. J. (2012). Do economic constraints on food choice make people fat? A critical review of two hypotheses for the poverty–obesity paradox. American Journal of Human Biology, 24(3), 277-285. PMID: 22345082, https://doi.org/10.1002/ajhb.22231.

Kata, F. S., Athbi, A. M., Manwar, E. Q., Al-Ashoor, A., Abdel-Daim, M. M., & Aleya, L. (2018). Therapeutic effect of the alkaloid extract of the cyanobacterium Spirulina platensis on the lipid profile of hypercholesterolemic male rabbits. Environmental Science and Pollution Research, 25(20), 19635-19642. PMID: 29736642, https://doi.org/10.1007/s11356-018-2170-4.

Khalil, S. R., Elhady, W. M., Elewa, Y. H., Abd El-Hameed, N. E., & Ali, S. A. (2018). Possible role of Arthrospira platensis in reversing oxidative stress-mediated liver damage in rats exposed to lead. Biomedicine & Pharmacotherapy, 97, 1259-1268. PMID: 29145152, https://doi.org/10.1016/j.biopha.2017.11.045.

Matović, V., Buha, A., Đukić-Ćosić, D., & Bulat, Z. (2015). Insight into the oxidative stress induced by lead and/or cadmium in blood, liver and kidneys. Food and Chemical Toxicology, 78, 130-140. PMID: 25681546, https://doi.org/10.1016/j.fct.2015.02.011.

Miranda, M. S., Cintra, R. G., Barros, S. B. D. M., & Mancini-Filho, J. (1998). Antioxidant activity of the microalga Spirulina maxima. Brazilian Journal of Medical and biological research, 31(8), 1075-1079. PMID: 9777014, https://doi.org/10.1590/s0100-879x1998000800007.

Miranda, M. L., Edwards, S. E., Keating, M. H., & Paul, C. J. (2011). Making the environmental justice grade: the relative burden of air pollution exposure in the United States. International Journal of Environmental Research and Public Health, 8(6), 1755-1771. PMID: 21776200, https://doi.org/10.3390/ijerph8061755.

Nakata, H., Nakayama, S. M., Yabe, J., Liazambi, A., Mizukawa, H., Darwish, W. S., Ikenaka, Y., & Ishizuka, M. (2016). Reliability of stable Pb isotopes to identify Pb sources and verifying biological fractionation of Pb isotopes in goats and chickens. Environmental Pollution, 208, 395-403. PMID: 26549754, https://doi.org/10.1016/j.envpol.2015.10.006.

Nakata, H., Nakayama, S. M., Yabe, J., Muzandu, K., Toyomaki, H., Yohannes, Y. B., … Ishizuka, M. (2020). Clinical biochemical parameters associated with the exposure to multiple environmental metals in residents from Kabwe, Zambia. *Chemosphere, 127788*. https://doi.org/10.1016/j.chemosphere.2020.127788.

Nasirian, F., Dadkhah, M., Moradi-kor, N., & Obeidavi, Z. (2018). Effects of Spirulina platensis microalgae on antioxidant and anti-inflammatory factors in diabetic rats. Diabetes, Metabolic Syndrome and Obesity: Targets and Therapy, 11, 375-380. PMID: 30104892, https://doi.org/10.2147/DMSO.S172104.

Newairy, A. S. A., & Abdou, H. M. (2009). Protective role of flax lignans against lead acetate induced oxidative damage and hyperlipidemia in rats. Food and Chemical Toxicology, 47(4), 813-818. PMID: 19271316, https://doi.org/10.1016/j.fct.2009.01.012.

Okamoto, T., Kawashima, H., Osada, H., Toda, E., Homma, K., Nagai, N., …, Ozawa, Y. (2019). Dietary spirulina supplementation protects visual function from photostress by suppressing retinal neurodegeneration in mice. Translational Vision Science & Technology, 8(6), 20-20. PMID: 31788349, https://doi.org/10.1167/tvst.8.6.20.

Parikh, P., Mani, U., & Iyer, U. (2001). Role of Spirulina in the control of glycemia and lipidemia in type 2 diabetes mellitus. Journal of Medicinal Food, 4(4), 193-199. PMID: 12639401, https://doi.org/10.1089/10966200152744463.

Parnia, A., Chakravartty, D., Wiseman, C. L., Archbold, J., Copes, R., Zawar, N., …, Cole, D. C. (2018). Environmental factors associated with blood lead among newcomer women from South and East Asia in the Greater Toronto Area. Science of the Total Environment, 624, 558-566. PMID: 29268227, https://doi.org/10.1016/j.scitotenv.2017.11.336.

Pham, T. X., Lee, Y., Bae, M., Hu, S., Kang, H., Kim, M. B., …, Lee, J. Y. (2019). Spirulina supplementation in a mouse model of diet-induced liver fibrosis reduced the pro-inflammatory response of splenocytes. British Journal of Nutrition, 121(7), 748-755. PMID: 30806344, https://doi.org/10.1017/S0007114519000126.

Poręba, R., Gać, P., Poręba, M., Antonowicz-Juchniewicz, J., & Andrzejak, R. (2011). Relation between occupational exposure to lead, cadmium, arsenic and concentration of cystatin C. Toxicology, 283(2-3), 88-95. PMID: 21356263, https://doi.org/10.1016/j.tox.2011.02.008.

Rodrıguez-Hernández, A., Ble-Castillo, J. L., Juarez-Oropeza, M. A., & Dıaz-Zagoya, J. C. (2001). Spirulina maxima prevents fatty liver formation in CD-1 male and female mice with experimental diabetes. Life Sciences, 69(9), 1029-1037. PMID: 11508645, https://doi.org/10.1016/s0024-3205(01)01185-7.

Sabath, E., & Robles-Osorio, M. L. (2012). Renal health and the environment: heavy metal nephrotoxicity. Nefrología (English Edition), 32(3), 279-286. PMID: 22508139, https://doi.org/10.3265/Nefrologia.pre2012.Jan.10928.

Scheuhammer, A. M. (1987). Erythrocyte δ-aminolevulinic acid dehydratase in birds. I. The effects of lead and other metals in vitro. Toxicology, 45(2), 155-163. PMID: 3603581, https://doi.org/10.1016/0300-483X(87)90101-6.

Selmi, C., Leung, P. S., Fischer, L., German, B., Yang, C. Y., Kenny, T. P., …, Gershwin, M. E. (2011). The effects of Spirulina on anemia and immune function in senior citizens. Cellular & Molecular Immunology, 8(3), 248. PMID: 21278762, https://doi.org/10.1038/cmi.2010.76.

Serban, M. C., Sahebkar, A., Dragan, S., Stoichescu-Hogea, G., Ursoniu, S., Andrica, F., & Banach, M. (2016). A systematic review and meta-analysis of the impact of Spirulina supplementation on plasma lipid concentrations. Clinical Nutrition, 35(4), 842-851. PMID: 26433766, https://doi.org/10.1016/j.clnu.2015.09.007.

Simsek, N., Karadeniz, A., & Karaca, T. (2007). Effects of the Spirulina platensis and Panax ginseng oral supplementation on peripheral. *Revue Méd. Vét, 158*(10), 483–488.

Simsek, N., Karadeniz, A., Kalkan, Y., Keles, O. N., & Unal, B. (2009). Spirulina platensis feeding inhibited the anemia-and leucopenia-induced lead and cadmium in rats. Journal of Hazardous Materials, 164(2-3), 1304-1309. PMID: 18976856, https://doi.org/10.1016/j.jhazmat.2008.09.041.

Upasani, C. D., & Balaraman, R. (2003). Protective effect of Spirulina on lead induced deleterious changes in the lipid peroxidation and endogenous antioxidants in rats. Phytotherapy Research: An International Journal Devoted to Pharmacological and Toxicological Evaluation of Natural Product Derivatives, 17(4), 330-334. PMID: 12722134, https://doi.org/10.1002/ptr.1135.

Vinken, P., Starckx, S., Barale-Thomas, E., Looszova, A., Sonee, M., Goeminne, N., …, Lampo, A. (2012). Tissue Kim-1 and urinary clusterin as early indicators of cisplatin-induced acute kidney injury in rats. Toxicologic Pathology, 40(7), 1049-1062. PMID: 22581811, https://doi.org/10.1177/0192623312444765.

World Health Organization (WHO), 2009. Global health risks: mortality and burden of disease attributable to selected major risks. Available: http://whqlibdoc.who.int/publications/2009/9789241563871_eng.pdf [accessed 24 May 2020].

World Health Organization, 2011. Global status report on noncommunicable diseases 2010. Available: https://apps.who.int/iris/bitstream/handle/10665/44579/9789240686458_eng.pdf;jsessionid=8C88471C98B5D9640B654D832C983F8C?sequence=1 [accessed 20 April 2020].

Yang, Y., Du, L., Hosokawa, M., & Miyashita, K. (2020). Effect of Spirulina lipids on high-fat and high-sucrose diet induced obesity and hepatic lipid accumulation in C57BL/6J mice. *Journal of Functional Foods, 65*, Article 103741. https://doi.org/10.1016/j.jff.2019.103741.

Yousefi, R., Mottaghi, A., & Saidpour, A. (2018). Spirulina platensis effectively ameliorates anthropometric measurements and obesity-related metabolic disorders

in obese or overweight healthy individuals: A randomized controlled trial. Complementary Therapies in Medicine, 40, 106-112. PMID: 30219433, https://doi.org/10.1016/j.ctim.2018.08.003.

Zhang, Z., Lu, B., Sheng, X., & Jin, N. (2011). Cystatin C in prediction of acute kidney injury: a systemic review and meta-analysis. American Journal of Kidney Diseases, 58(3), 356-365. PMID: 21601330, https://doi.org/10.1053/j.ajkd.2011.02.389.

Zhao, B., Cui, Y., Fan, X., Qi, P., Liu, C., Zhou, X., & Zhang, X. (2019). Anti-obesity effects of Spirulina platensis protein hydrolysate by modulating brain-liver axis in high-fat diet fed mice. PloS One, 14(6), e0218543. PMID: 31220177, https://doi.org/10.1371/journal.pone.0218543.

International Journal of
Environmental Research and Public Health

MDPI

Article

An Investigation of the Wild Rat Crown Incisor as an Indicator of Lead (Pb) Exposure Using Inductively Couple Plasma Mass Spectrometry (ICP-MS) and Laser Ablation ICP-MS

Andrew Kataba [1,2], Shouta M. M. Nakayama [1,*], Hokuto Nakata [1], Haruya Toyomaki [1], Yared B. Yohannes [1,3], John Yabe [2], Kaampwe Muzandu [2], Golden Zyambo [2], Ayano Kubota [4], Takehisa Matsukawa [4], Kazuhito Yokoyama [4], Yoshinori Ikenaka [1,5] and Mayumi Ishizuka [1,*]

1 Laboratory of Toxicology, Department of Environmental Veterinary Sciences, Faculty of Veterinary Medicine, Hokkaido University, Kita 18 Nishi 9, Kita-ku, Sapporo 060-0818, Japan; andrewkataba@gmail.com (A.K.); hokuto.nakata@vetmed.hokudai.ac.jp (H.N.); yahahuhru@gmail.com (H.T.); ybyared@gmail.com (Y.B.Y.); y_ikenaka@vetmed.hokudai.ac.jp (Y.I.)
2 School of Veterinary Medicine, The University of Zambia, P.O. Box 32379, Lusaka 10101, Zambia; mjyabe@yahoo.co.uk (J.Y.); kmuzandu@yahoo.com (K.M.); goldzgambo@gmail.com (G.Z.)
3 Department of Chemistry, College of Natural and Computational Science, University of Gondar, P.O. Box 196, Gondar 6200, Ethiopia
4 Department of Epidemiology and Environmental Health, Faculty of Medicine, Juntendo University, 2-1-1 Hongo, Bunkyo-ku, Tokyo 113-8421, Japan; ay-kubota@juntendo.ac.jp (A.K.); tmatsuka@juntendo.ac.jp (T.M.); kyokoya@juntendo.ac.jp (K.Y.)
5 Water Research Group, School of Environmental Sciences and Development, North-West University, Private Bag X6001, Potchefstroom 2531, South Africa
* Correspondence: shoutanakayama0219@gmail.com (S.M.M.N.); ishizum@vetmed.hokudai.ac.jp (M.I.); Tel./Fax: +81-11-706-5105 (S.M.M.N.)

Abstract: Lead (Pb) is a metal toxicant of great public health concern. The present study investigated the applicability of the rat incisor in Pb exposure screening. The levels of lead in teeth (Pb-T) in the crown and root of incisors in laboratory Pb-exposed Sprague Dawley rats were quantified using inductively coupled plasma mass spectrometry (ICP-MS). The crown accumulated much Pb-T than the root of the Sprague Dawley rat incisor. The levels of lead in blood (Pb-B) were positively correlated with the Pb-T in the crown and root incisors of the Sprague Dawley rats. As an application of the Pb-T crown results in experimental rats, we subsequently analyzed the Pb-T in the crown incisors of Pb-exposed wild rats (*Rattus rattus*) sampled from residential sites within varying distances from an abandoned lead–zinc mine. The Pb-T accumulation in the crown of incisors of *R. rattus* rats decreased with increased distance away from the Pb–Zn mine. Furthermore, the Pb-T was strongly correlated ($r = 0.85$) with the Pb levels in the blood. Laser ablation ICP-MS Pb-T mappings revealed a homogenous distribution of Pb in the incisor with an increased intensity of Pb-T localized in the tip of the incisor crown bearing an enamel surface in both Sprague Dawley and *R. rattus* rats. These findings suggest that Pb-T in the crown incisor may be reflective of the rat's environmental habitat, thus a possible indicator of Pb exposure.

Keywords: lead; incisor; biomarker; sentinel; wild rodent

Citation: Kataba, A.; Nakayama, S.M.M.; Nakata, H.; Toyomaki, H.; Yohannes, Y.B.; Yabe, J.; Muzandu, K.; Zyambo, G.; Kubota, A.; Matsukawa, T.; et al. An Investigation of the Wild Rat Crown Incisor as an Indicator of Lead (Pb) Exposure Using Inductively Couple Plasma Mass Spectrometry (ICP-MS) and Laser Ablation ICP-MS. *Int. J. Environ. Res. Public Health* **2021**, *18*, 767. https://doi.org/10.3390/ijerph18020767

Received: 24 November 2020
Accepted: 13 January 2021
Published: 18 January 2021

1. Introduction

Lead (Pb) is a toxic metal known to cause a number of physiological and biochemical dysfunctions in animals and humans [1]. Although Pb poisoning has considerably receded in developed countries [2], chronic exposure to low levels of Pb remains a perennial phenomenon in some developing countries. A case in point is Kabwe town in Zambia, with a lead–zinc mine history legacy characterized by an alarming Pb poisoning in adults and children living near the closed lead–zinc mine [3–5]. Moreover, acute fatal cases of Pb poisoning in over 400 children in Nigeria [6] and 18 children in Dakar, Senegal [7] linked

to anthropogenic activities have been reported. Even at low non-fatal levels, Pb exposure causes cognitive impairments in children exposed in early life stages [2]. In adults, low cumulative Pb exposure has been linked to renal, cardiovascular, and reproductive-system-related disorders [8,9]. Bellinger et al. [8] further revealed that early stage Pb exposure in children led to disadvantaged adult outcomes such as poor academic performance and low income. Thus, biomarkers of Pb exposure that are reliable and easy to obtain from humans and sentinel animals that share habitats with humans are required [10].

Traditionally, Pb in blood (Pb-B) has been widely used as a biomarker for Pb exposure in humans [11,12]. However, Pb-B poses a short mean biological life of only around 30–40 days and may only reflect primarily both ongoing steady-state exposures and relatively recent exposures [10]. Moreover, changing the conditions of exposure causes a Pb-B variation and typically the blood Pb level reverts to normal once the exposure ceases [13]. In contrast, the concentration of Pb in teeth (Pb-T) is a cumulative function of earlier exposure which allows for the identification of historic undetected cases of Pb exposure even after the other indices have returned to normal [14]. Although the Pb-T in the whole tooth has been considered as a biomarker of Pb exposure in children [15] and rodents [16], the distribution Pb within is not even. The uneven distribution of Pb in teeth may be due to different dental structures and the level of calcification of the dental parts [12].

The use of laser ablation inductively coupled plasma mass spectrometry (LA-ICP-MS) as a technique has been applied to estimate the distribution patterns of metals in the dentine and enamel parts of the teeth [17–19]. However, there are limited reports on the distribution or mapping of Pb in rodent incisor teeth of wild or laboratory rats exposed to Pb. Therefore, further investigations using techniques for advanced mapping of distribution Pb in teeth such as LA-ICP-MS are needed.

Wild rodents have been used as sentinel animals and biomonitors of environmental-related pollution assessments of pesticides [20], asbestos [21], and heavy metal pollution [22]. In the present study, the rodent incisor tooth was investigated in laboratory and wild rodents as an indicator of Pb exposure. We hypothesized that Pb accumulates differently within the incisor teeth and that the part with much accumulation may be sampled as a biomarker of Pb exposure. To the best of our knowledge, the quantification of Pb-T in the root and crown subdivisions of incisor teeth in Pb-exposed laboratory rats and the use of the incisor crown of wild rats as an indicator of Pb exposure has never been reported. Lead distribution mappings were performed using LA-ICP-MS in both laboratory and wild rats exposed to Pb to augment the Pb-T quantification done using ICP-MS and ascertain the distribution of Pb in rodent incisor. The purpose of this study was to evaluate the accumulation pattern of lead in the crown and root incisor teeth of laboratory rats following lead exposure. Based on the laboratory rat results that showed high levels of Pb in the crown incisor, the study explored the use of the wild rat crown incisor as an indicator of lead exposure in a field situation. Furthermore, the distribution pattern of lead in rodent incisor using laser ablation inductively coupled plasma mass spectrometry was evaluated.

2. Materials and Methods

2.1. Laboratory Animals and Exposure

Animal experiments were performed at the Faculty of Veterinary Medicine, Hokkaido University under the supervision and with the endorsement of the Institutional Animal Care and Use Committee of Hokkaido University, Sapporo, Japan (approval number: 16-0017). Male Sprague Dawley rats (n = 18) aged seven weeks were purchased from Sankyo Labo Service Corporation, Inc. (Tokyo, Japan). The rats were kept in six lead-free polypropylene cages in community housing of three rats (n = 3 per cage). The animals were acclimated to the animal facility for one week prior to Pb exposure with access to lead-free food (rodent chow, Labo MR Stock, Nosan Corporation, Yokohama, Japan) and distilled water *ad libitum*. There were no significant body weight differences among all the groups. Two cages with six (n = 6) rats were randomly assigned to the three

exposure levels (control, low, and high dosage exposure). Two different concentrations of Pb acetate, 100 mg/L and 1000 mg/L Pb (Wako Pure Chemical Industries, Osaka, Japan), were given through drinking water for eight weeks to the low and high dosage groups, respectively. The control group received only distilled water for the same period. The choice of Pb levels of exposure for the current study was based on the previous study in mice that had a dose-dependent Pb tissue accumulation at 100 mg/L and 1000 mg/L lead acetate concentrations [23]. At the end of the exposure period, rats were euthanized under carbon dioxide with sevoflurane. Blood and incisors teeth (upper and lower) were collected following extraction. For uniformity, we assigned the upper and lower incisors on the left side of the jaws for quantitative Pb analysis using inductively coupled plasma mass spectrometry (ICP-MS), and those on the right side were assigned for qualitative Pb mapping using LA-ICP-MS for each individual rat across all the groups. The blood and teeth samples were collected in lead-free polypropylene tubes and were kept at −80 °C and −20 °C prior to analysis, respectively.

2.2. Wild Rat Sampling and Species Identification

The sampling was done with permission and strict adherence to the guidelines from the Zambian Ministry of Fisheries and Livestock, as well as the Faculty of Veterinary Medicine, Hokkaido University, Sapporo, Japan (approval number: Vet-17010). Wild rats were collected from Kabwe, Zambia, a town known for extensive Pb environmental contamination [4,5,24,25] between June and July 2017. Kabwe is situated at approximately 142°70′ S and 28°260′ E. Four residential townships in Kabwe, namely, Lukanga (LK), Makululu (MK), Chowa (CH), and Mutwe Wansofu (MW) were used as sampling sites for wild rats based on their relative distances to the closed lead–zinc (Pb–Zn) mine. Six (n = 6) wild rats were captured using live traps as previously described by our research group [25] from each of the four sites within varying distance from the closed Pb–Zn mine. The furthest distance away from the closed mine in Lukanga (LK; 5.90 km) was used as the control site. The other sites closer to the closed mine were taken as exposed sites, namely, Makululu (MK; 2.11 km), Chowa (CH; 0.86 km), and Mutwe Wansofu (MW; 0.81 km), respectively. The sampling sites were located and identified (Figure 1) using a global positioning system (GPS). The rats were euthanized with sevoflurane and blood and incisors teeth (lower) were collected following extraction. The samples were then immediately stored at –20 °C before being transported to the Faculty of Veterinary Medicine, Hokkaido University Sapporo, Japan under the cold chain systems. The transportation of samples was done in accordance with the international sample passage certificate from the Ministry of Fisheries and Livestock, Zambia (No. 11614). At Hokkaido University, the blood and teeth samples were stored at −80 °C and −20 °C in a deep freezer, respectively, until analysis. The species of the wild rats were identified using the genomic DNA sequencing method previously described by Robins et al. [26], and only rats that were of *Rattus rattus* species (Supplementary Materials, Table S1) were used in the current study. After the exclusion of the non-*R. rattus* rat species from the six (n = 6) rats trapped from each site, the final sample sizes were n = 2 (LK), n = 5 (CH), n = 5 (MK), and n = 3 (MW), respectively. A detailed description of the methods of species identification can be found in Appendix A.

Figure 1. Sampling sites for wild rats. Mutwe Wansofu (MW; $n = 6$), Chowa (CH; $n = 6$), Makululu (MK; $n = 6$), and Lukanga (LK; $n = 6$). The closed Pb–Zn mine is shown with a "yellow" shape.

2.3. Digestion and Quantitative Analysis of Lead in Blood and Teeth Subdivisions

The Pb concentration in the blood and incisors teeth collected from the laboratory exposed Sprague Dawley rats and the *R. rattus* rats from Kabwe, Zambia were quantified. In the current study, blood and teeth were digested using the microwave acid method previously described by Nakata et al. [27,28] with minor modifications. To minimize surface contamination and remove excess blood, the teeth were firstly cleaned using an ultrasonic bath method as described by Ishii et al. [29] with some modifications. Briefly, the teeth samples were placed in an ultrasonic bath of L-cysteine (Cica reagent, 100 mg/L; Kanto Chemical, Tokyo, Japan) for 5 min followed by rinsing in an ultrasonic bath of distilled water for 10 min prior to drying. The samples were then dried in an oven at 54 °C for 48 h. Each tooth was divided into two subdivisions using the yellow-orange pigmentation of enamel on the crown part of the labial surface of the tooth [30] as a distinguishing reference mark as illustrated in Figure 2. Each lower (L) incisor was divided into two subdivisions, namely, L1 (root) and L2 (crown). The L1 is a part of the tooth that is embedded in the jawbone and L2 for the part tooth visible in the oral cavity. Similarly, the upper (U) incisor was divided into two subdivisions, namely, U1 (root) for the upper part of the tooth embedded in the jawbone and U2 (crown) for the part tooth visible in the oral cavity in live rodents as shown in Figure 2. In the case of the blood sample digestion, 0.1 mL of the blood were measured and put in pre-washed digestion vessels. To the vessels was added 5 mL of nitric acid (atomic absorption spectrometry grade, 30%; Kanto Chemical, Tokyo, Japan), and 1 mL of hydrogen peroxide (Cica reagent, 30%; Kanto Chemical, Tokyo, Japan) in readiness for digestion. The sample digestion was done using a ramped temperature program in a closed microwave system (Speed Wave MWS-2 microwave digestion system; Berghof, Eningen, Germany). The microwave system operating conditions used are given in the Supplementary Materials Table S2. Following cooling, the sample solutions were transferred into 15 mL polypropylene tubes and diluted to a final volume of 10 mL with ultra-distilled and de-ionized water.

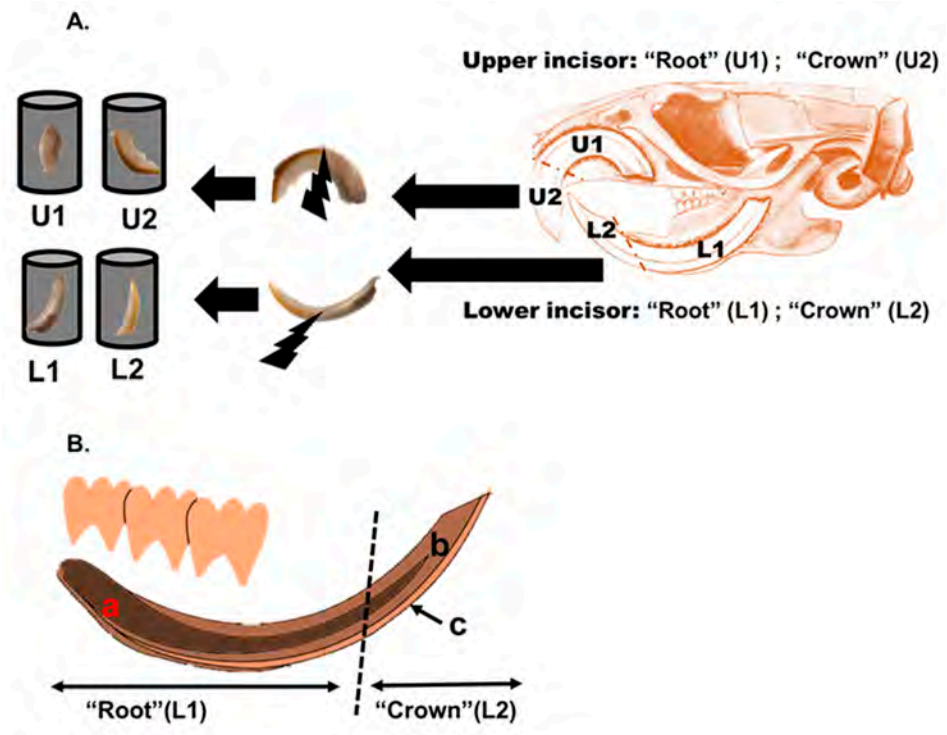

Figure 2. Divisions of the incisor teeth and schematic illustration of the longitudinal section of the incisor tooth. (**A**) Lower and upper incisor tooth divisions based on the yellow-orange enamel for microwave acid digestion. For upper incisors, the root (U1) part is anchored in the maxillary bone, and the crown (U2) part of the tooth is seen externally. Similarly, for lower incisors, the root (L1) part is anchored in the mandibular bone, and the crown (L2) part of the tooth is seen externally. (**B**) Illustrated schematic longitudinal section modified from Park et al. [31] of lower incisor tooth as was sectioned for direct LA-ICP-MS analysis. Furthermore, the three major parts of the incisor tooth are seen—(a) dental pulp, (b) dentine, and (c) enamel running only in the front part of the tooth. The dotted line is the imaginary division line used based on the obvious discoloration of enamel on the crown part of the tooth.

The Pb concentration quantification was performed using the ICP-MS (7700 series; Agilent Technologies, Tokyo, Japan), as described by Nakata et al. [28,29] with minor modifications. The operating conditions of ICP-MS were as given in the Supplementary Table S3. The quality control was performed by analysis of DOLT-4 (dogfish liver) (National Research Council of Canada, Ottawa, Canada) certified reference material. Replicate analysis of the reference material gave good recovery rates ranging from 95% to 105%. The detection limit for Pb was 0.001 mg/L.

2.4. Laser Ablation Inductively Coupled Plasma Mass Spectrometry (LA-ICP-MS) Analysis of Incisor Teeth of Sprague Dawley and R. rattus Rats

The incisor teeth samples from laboratory and x Pb-exposed wild rats were processed and analyzed according to the method previously described by Ishii et al. [29] with some minor modifications. Briefly, excess tissues and surface contamination of the teeth were cleaned using an ultrasonic bath of L-cysteine for 5 min followed by cleaning in an ultrasonic bath of distilled water and drying at 54 °C for 48 h. Samples were sliced into ~40 µm sections along the longitudinal axis with a diamond blade and polished. The teeth sections were systematically scanned by a focused laser beam with the following parameters—spot diameter: 100 µm, scan speed: 70 µm/sec using LA (NWR213; ESI, Portland, OR, USA)-ICP-QQQ-MS (8800 series; Agilent Technologies) (Agilent Technologies, Inc., Santa Clara, CA, USA). Detailed analytical conditions are presented in Table S4. We reconstructed two-dimensional images from time-resolved analysis data of LA-ICP-MS by iQuant2, as

described by Suzuki et al. [32], an in-house developed software. This software shows the localization of elements.

2.5. Data Analysis

The data analysis was performed using GraphPad Prism software (Prism 7 for Windows; Version 5.02, GraphPad Software, Inc., CA, USA) and reported as mean and standard deviation (SD). The data were first tested for normality using Kolmogorov–Smirnov test. The data was not normally distributed. We log-transformed the data for statistical analyses and retained the original values in the results and figures for easier interpretation and comparisons with other studies. We applied one analysis of variance (ANOVA) and multiple Tukey's comparison test as post hoc tests. In the present study, the difference between groups was deemed to be significant at $p < 0.05$ (*) and highly significant at $p < 0.01$ (**). Log transformation of Pb concentrations was also done for the Pearson's correlations analysis between Pb-B concentration and Pb-T levels. The graphical representations were compiled using GraphPad Prism software.

3. Results

3.1. Lead in Blood (Pb-B) and Incisors Subdivisions of Laboratory-Exposed Sprague Dawley Rats

The Pb-B levels increased significantly with the increase in the dose of Pb given through water with the high Pb group having the highest mean concentration of 39.63 ± 8.09 µg/dL, followed by the low Pb group, which had a mean of 9.90 ± 1.71 µg/dL and the control had lowest with 4.01 ± 0.86 µg/dL (Figure 3A). Both the high Pb and low Pb groups accumulated significantly higher Pb levels ($p < 0.01$) when compared to the control (Figure 3A). Further, the Pb-B levels between the low and high groups were also significantly different ($p < 0.05$).

The accumulation of Pb in the teeth subdivisions (Pb-T) in L1 and L2 of lower and U1 and U2 upper incisors are shown in Figure 3B,C, respectively. The accumulation Pb-T in both subdivisions of the lower incisors was in a Pb dose-dependent manner with the high Pb group accumulating higher Pb-T than the low Pb group and the control. The Pb-T in the L2 was significantly higher (Tukey test, $p < 0.01$) than that of L1 for both low Pb and high Pb groups. At low Pb, the Pb-T in L1 was 4.72 ± 2.10 mg/kg, and L2 had 90.17 ± 13.57 mg/kg. At high Pb exposure, L1 had 33.07 ± 15.51 mg/kg, and L2 had 132.40 ± 47.33 mg/kg Pb-T, respectively. Similarly, Pb-T accumulation in the upper incisors and their subdivisions accumulated in Pb dose-dependent manner. The Pb-T in the U1 (6.79 ± 2.03 mg/kg) was significantly lower ($p < 0.01$) than U2 (42.44 ± 16.58 mg/kg) in the low Pb group. Likewise, in the high Pb group, the U1 (26.13 ± 11.63 mg/kg) accumulated lower Pb-T than U2 (63.32 ± 24.89 mg/kg). In addition, we observed that L2 or U2 at lower exposure accumulated significantly higher Pb-T than the L1 or U1 at high exposure (Figure 3B,C).

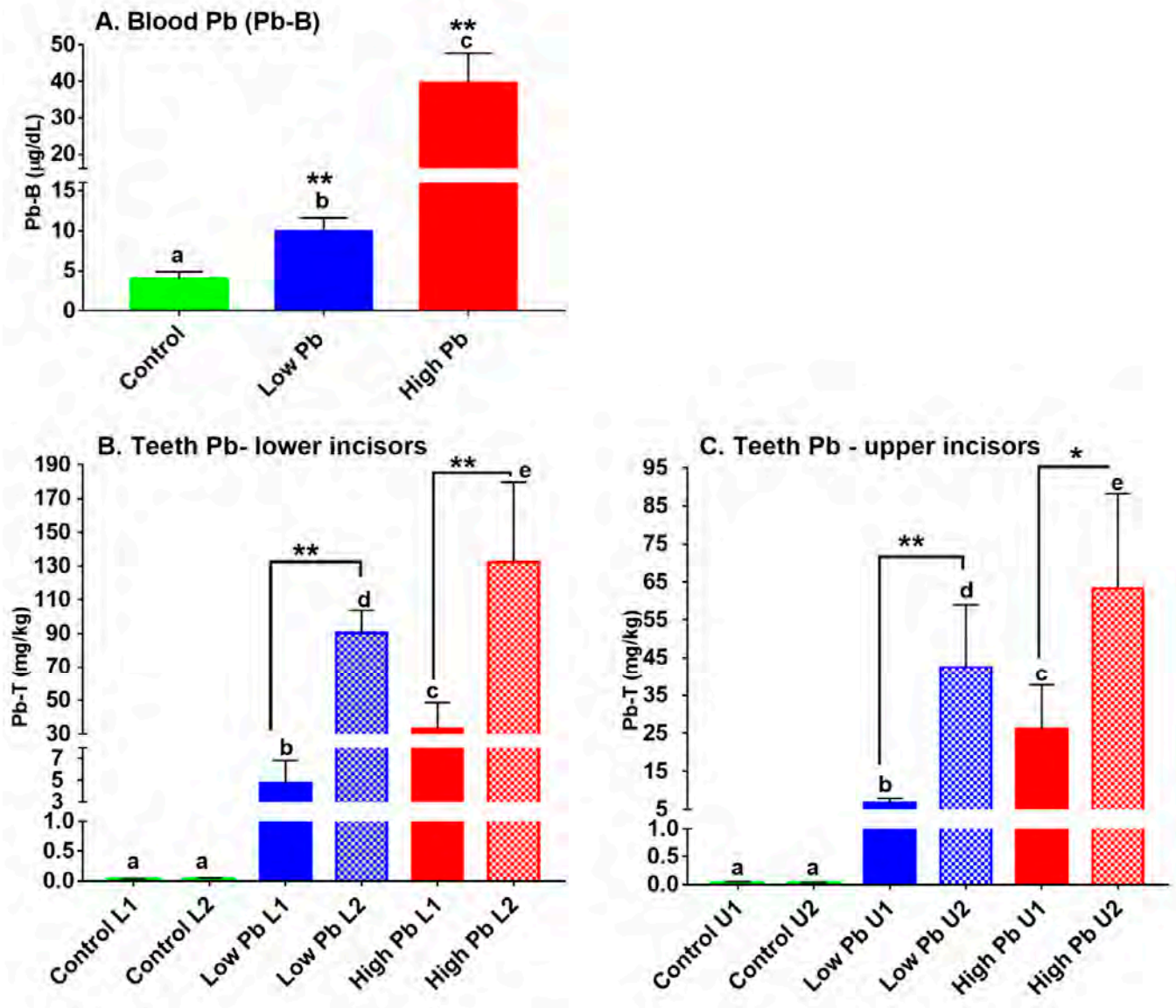

Figure 3. Mean ± SD of Pb-B and Pb-T of laboratory Pb exposed Sprague Dawley rats. (**A**) Pb-B in control (n = 6), low Pb (100 mg/L Pb; n = 6), and high Pb (1000 mg/L Pb; n = 6); (**B**) Pb-T in the lower incisor divisions (L1 and L2) and; (**C**) Pb-T in the upper incisor divisions (U1 and U2). The lower-case letters a, b, c, d, and e represent significant differences among the groups using Tukey's multiple comparison test ($p < 0.05$). For the Pb-B, ** at $p < 0.01$ represents a significant difference between the control and exposure groups, and for the Pb-T, * at $p < 0.05$ and ** at $p < 0.01$ represent a significant difference between the crown and root of incisor teeth in each group Turkey's test.

3.2. Relationship between Incisor Teeth Parts Pb and Blood Pb in the Laboratory Exposed Sprague Dawley Rats

Figure 4 shows the relationship between the Pb-T in the lower and upper incisors root and crown subdivisions with the Pb-B concentration in the laboratory Sprague Dawley rats. In the present study, positive log-transformed Pearson's correlations between the Pb-B and Pb-T across all the exposed groups in the root and crown of the lower and upper incisors were observed. Much stronger correlations between Pb-T and Pb-B were recorded in the root of both lower and upper incisors than in the crown. The correlations were significant, namely, lower incisor (L1) Pb-T versus Pb-B (r = 0.91, $p < 0.01$), lower incisor (L2) Pb-T versus Pb-B (r = 0.82, $p < 0.01$), upper incisor (U1) Pb-T versus Pb-B (r = 0.91, $p < 0.01$), and upper incisor (U2) Pb-T versus Pb-B (r = 0.85, $p < 0.01$), as shown in Figure 4A–D.

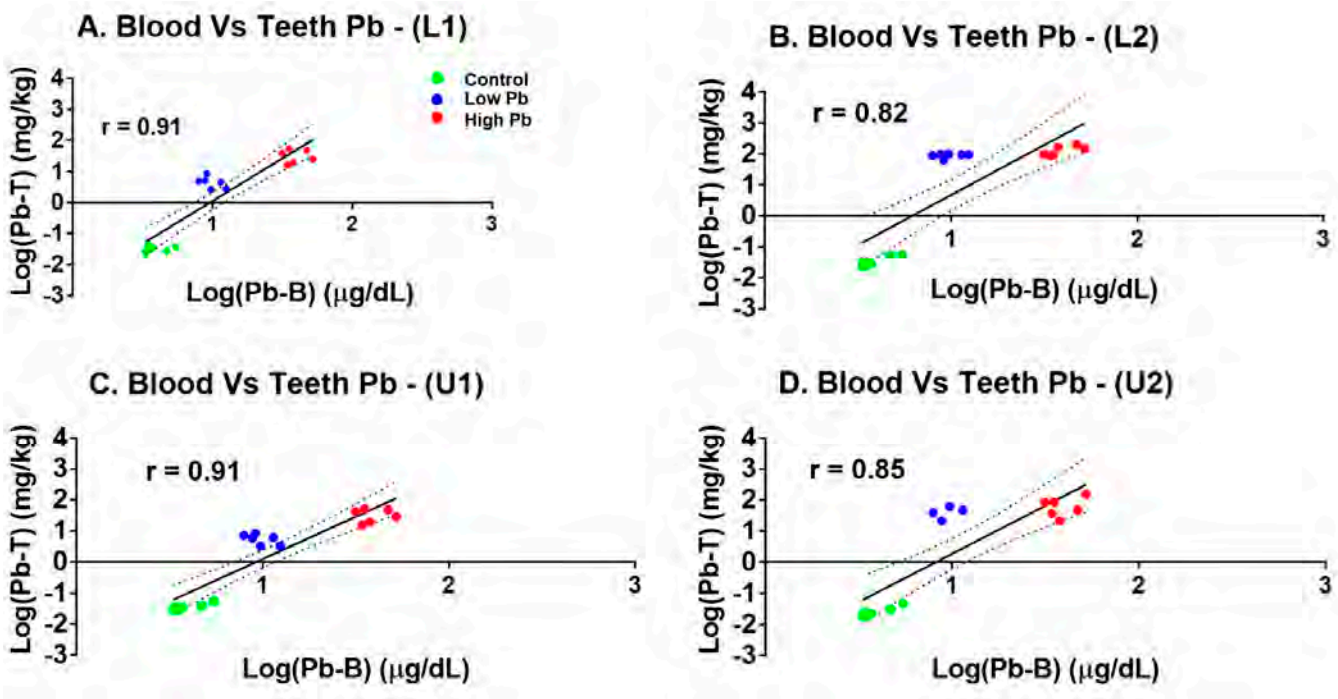

Figure 4. Pearson's correlations showing the relationship between log-transformed Pb-B and Pb-T crown and root of the lower and upper incisors in the laboratory Pb-exposed Sprague Dawley rats. (**A**) lower incisor (L1) Pb-B versus Pb-T ($r = 0.91$, $p < 0.01$); (**B**) lower incisor (L2) Pb-B versus Pb-T ($r = 0.82$, $p < 0.01$); (**C**) upper incisor (U1) Pb-B versus Pb-T ($r = 0.91$, $p < 0.01$) and (**D**) upper incisor (U2) Pb-B Vs Pb-T ($r = 0.85$, $p < 0.01$).

3.3. Lead in Blood and Teeth and Their Relationship in the Lead-Exposed R. rattus Rats

Figure 5A shows the Pb-B in wild rats sampled from different sites within varying distances from the closed Pb–Zn mine as a reference point as shown in Figure 1. The accumulation of Pb-B differed significantly among the sites with the highest Pb-B levels seen in rat samples captured closer to the old mine and lowest in rat samples collected furthest from the mine (Figure 5A). Quantitatively, the CH site group had a mean Pb-B of 245.40 ± 161.90 µg/dL, the MW site group had 213.20 ± 14.22 µg/dL, the MK site group had 40.11 ± 15.56 µg/dL and the LK site group had 15.60 ± 0.99 µg/dL. Furthermore, in reference to the control site sample (LK), the Pb-B levels in known contaminated sites were significantly higher in MK ($p < 0.05$), MW ($p < 0.01$), and CH ($p < 0.01$) groups. No difference in Pb-B levels in the CH and MW groups was observed (Figure 5A).

Figure 5B shows the accumulation pattern of Pb-T in the crown part of the lower incisor (L2) of *R. rattus* rats exposed to Pb in their natural environment. Because an application of our laboratory results showed a higher Pb level in the L2 section compared to the L1 section of incisors (Figure 3B,C), only L2 Pb levels in *R. rattus* rats are shown. The accumulation Pb-T was higher in the rats that were captured closer to the closed Pb–Zn mine had higher Pb-T levels than those captured further away from the closed Pb–Zn mine. Quantitatively, the CH group had the highest levels with Pb-T of 383.60 ± 144.10 mg/kg, followed by MW group with Pb-T of 102.60 ± 91.60 mg/kg, MK with 32.66 ± 8.02 mg/kg, and the least Pb-T was in the LK group with 3.17 ± 1.69 mg/kg. The Pb-T concentrations among the groups were statistically significant ($p < 0.05$), as shown by lower case letters (Figure 5B). In addition, the exposed groups were significantly different from the assigned control (LK) group ($p < 0.01$). In the present study, the Pearson's correlation analysis between Pb-B and Pb-T of log-transformed data in the crown of lower incisors in wild rats exposed to Pb was positive ($r = 0.85$, $p < 0.01$), as shown (Figure 5C).

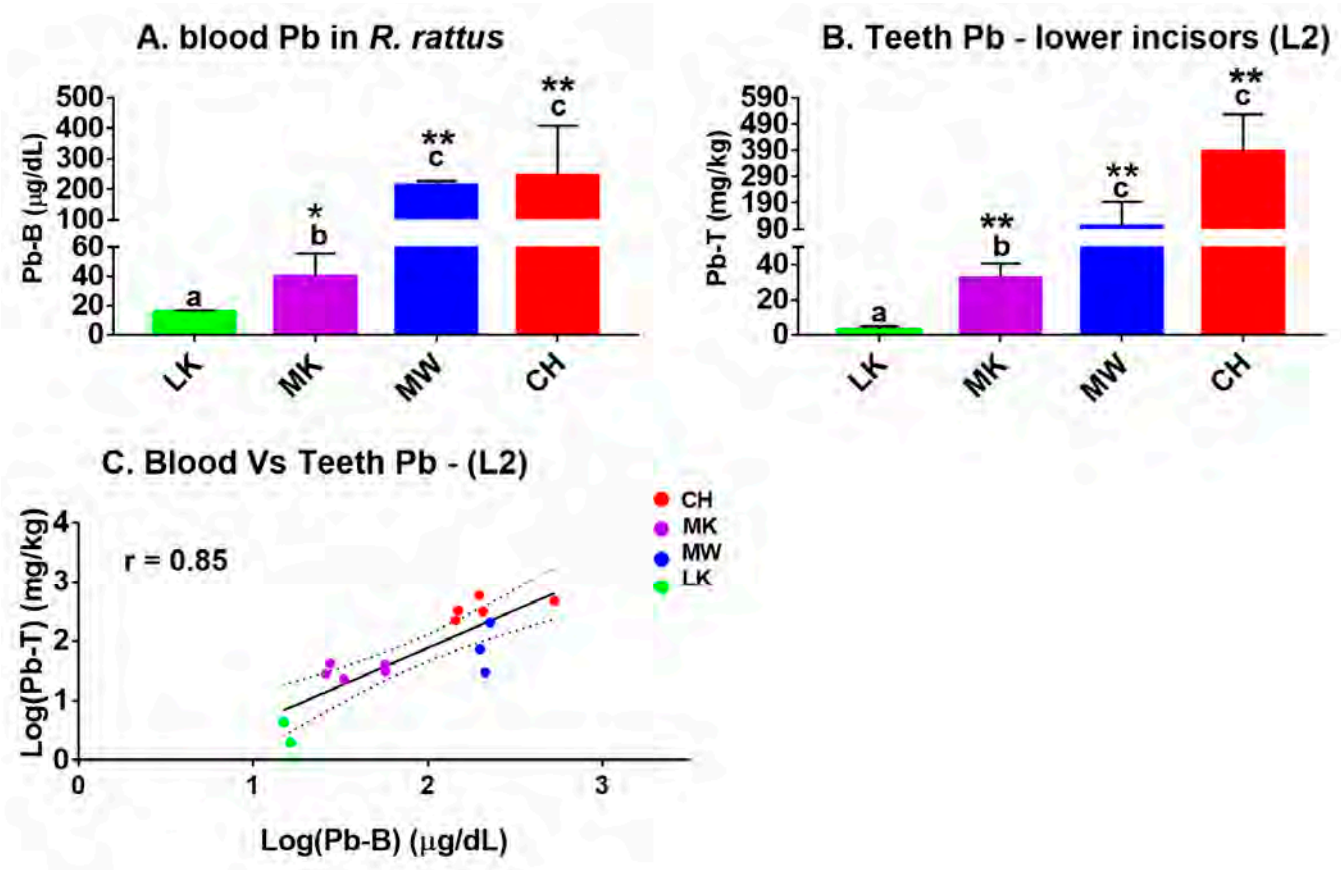

Figure 5. Mean ± SD of Pb-B and Pb-T of Pb-exposed *R. rattus* rats. (**A**) Pb-B from rats sampled from Lukanga (LK; $n = 2$); Makululu (MK; $n = 5$); Mutwe Wansofu (MW; $n = 3$) and Chowa (CH; $n = 5$). (**B**) Pb-T from rats sampled from LK ($n = 2$); MK ($n = 5$); MW ($n = 3$), and CH ($n = 5$); The lower case letters a, b, and c represent significant differences among the groups using the Tukey's multiple comparison test ($p < 0.05$). For the both Pb-B and the Pb-T, * at $p < 0.05$ and ** at $p < 0.01$ represent significant difference between the LK site (control group) and other groups sampled closer to the former Pb–Zn mine using the Turkey's test. (**C**) Log-transformed Pearson's correlations of Pb-B versus Pb-T in *R. rattus* rats ($r = 0.85$, $p < 0.01$).

3.4. Lead Distribution in the Incisor Teeth of the Lead-Exposed Laboratory Sprague Dawley and Wild R. rattus Rats Using LA-ICP-MS

The local distribution of the Pb mappings using LA-ICP-MS in the incisor teeth of both laboratory and wild rats exposed to Pb is shown in Figure 6A,B, respectively. A homogenous distribution of Pb was observed in the greater portion of the tooth from the root extending to the pulp and the dentine in both laboratory and wild rodent teeth samples (Figure 6A,B). On the other hand, an inhomogeneous distribution of Pb was found in the surface enamel near the tip of the incisor crown having an intense localized distribution of Pb. The distribution of Pb in both laboratory and wild rodent teeth was similar (Figure 6A,B).

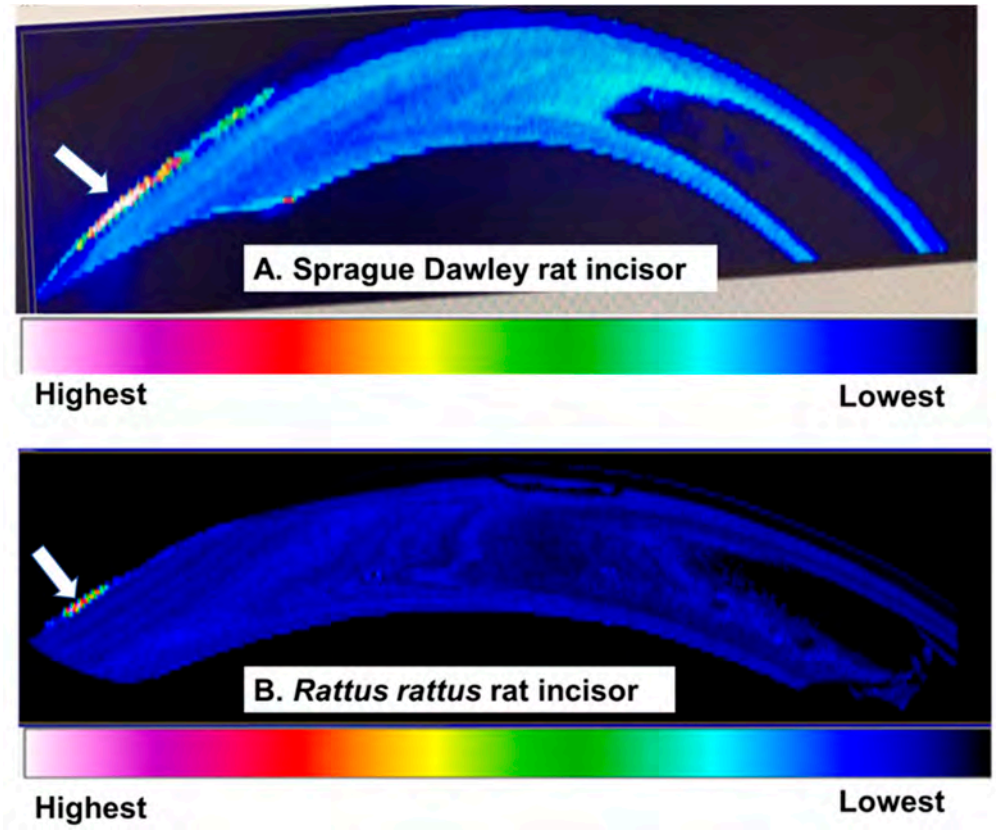

Figure 6. Pb distribution in the incisor teeth of the lead-exposed laboratory Sprague Dawley and wild exposed (*R. rattus)* rats using LA-ICP-MS. Homogenous distribution of Pb in the pulp and dentine of the with inhomogeneous distribution of Pb-T characterized by intense deposits of Pb in the exterior enamel (arrow). (**A**) Sprague Dawley and (**B**) *R. rattus* rats in incisors.

4. Discussion

The present study focused on Pb quantities in the rodent incisor tooth as a biomarker of Pb and its applicability in Pb exposure screening. The most striking observation was the high accumulation of Pb-T in the crown of the upper and lower incisor teeth than the roots across all levels of exposure in laboratory Pb-exposed Sprague Dawley rats. The inherent incisor tooth structural variations between the root and crown due to the larger part of the dental root pulp and higher dentine crown mass, as well as dentine-enamel ratio, could be the key factors in the accumulation of Pb-T differences [33]. The rodent incisors are predominantly dentine with a thin layer of enamel located only in the front part of the tooth [30]. The influence of the presence of the large dentine mass in the crown of incisor teeth may have been one of the contributing factors behind the L2 or U2 in the low Pb group accumulating much Pb than the L1 or U1 in the high Pb exposure group. The current findings seem to agree with other studies that demonstrated that Pb is highly accumulated in the dentine part of the teeth [14,34–36].

The Pb-T in both the root and the crown of the lower incisors and upper incisor teeth and the Pb-B accumulation in the Sprague Dawley rats following laboratory exposure were in a Pb dose-dependent pattern. These findings suggest that rodent incisors could be a useful indicator of exposure to Pb, as was reported in goats [34] and rats [16]. Furthermore, strong positive correlations between Pb-B and Pb-T were found in the Pb-exposed laboratory rats, similar to what has been reported in humans [33,37]. Taken together, our results in the laboratory Pb-exposed Sprague Dawley rats showed that Pb-T in the crown incisor analysis may provide some advantages in assessing Pb exposure.

In the *R. rattus* rat species that were used as sentinel animals around the closed Pb–Zn mine in Kabwe, Zambia, the accumulation of Pb-T in L2 and Pb-B were linked to the

distance in reference to the point source. Moreover, there was a strong positive correlation between Pb-T in L2 and Pb-B in the wild of rats, suggesting that the incisor crown would be a good predictor of Pb exposure just like Pb in blood. This was in agreement with the pattern of Pb-T accumulation reported in deciduous teeth of children living near a lead-acid battery smelter [38]. Comparatively, our results were also in tandem with surface enamel Pb-T in children, where much Pb-T accumulation was reported in polluted areas than in less polluted areas [39]. Furthermore, the Pb-T in the crown of the sentinel rats in the present study corroborated the findings of Pb concentrations in soils [25], and Pb-B in free-roaming dogs [40] and free-range chickens [41] sampled within the vicinity of the former Pb–Zn mine. Taken together, the current findings indicate that the rodent tooth incisor crown may be a useful tool for environmental Pb exposure monitoring.

The Pb-T in the crown incisors were relatively higher than the Pb-B, corroborating reports that indicated that Pb-T were better indicator exposure and cumulative Pb body burden than Pb-B [42]. The high Pb-B levels observed in wild rats were however not surprising because they were recorded from the Chowa and Mutwe Wansofu sampling sites that were near to the mine where children with very high Pb-B were previously reported [4]. On the other hand, we observed that the lower the Pb-B level, the lower the Pb-T, which adds further merits to the use of L2 sample as a biomarker of exposure. While the duration of exposure in wild rats *(R. rattus)* may not be clearly known, findings in the laboratory Pb exposed rats that were exposed for eight weeks suggest that the teeth may be useful both for chronic Pb exposure and in sub-chronic conditions exposure where blood levels are elevated.

The Pb-T distribution mapping using LA-ICP-MS in the lower incisors of the Pb-exposed laboratory and wild rats was performed for the first time. Interestingly, the distribution of Pb-T was homogeneously distributed in the dental pulp, dentine, and the greater part of enamel except on the front tip part of the incisor crown with enamel in both laboratory and wild rats. The intense Pb localization seen on the tip of the incisor crown with an enamel surface was in contrast to other studies that demonstrated that calcified tissue layers in direct contact or in proximity to vascular tissues accumulated much more Pb than those further away in bones [29] and teeth around the circumpulpal dentine [18,34,43]. However, the present findings agreed in part with a report in human incisor teeth samples where most of the Pb were primarily deposited in the secondary dentine region close to the pulp, and secondarily, at surface enamel [12]. Moreover, the observed high intensities of Pb in the outer part of incisors were only on the front side, the only side bearing enamel in rodent incisors [30]. This phenomenon has been demonstrated in both erupted and non-erupted teeth that highly accumulated Pb in the outer enamel surface and with a gradual reduction of Pb in the deeper layers of the enamel [19,39,44,45]. Taken together, the characteristic enamel surface Pb accumulation in the crown incisors further supports the use of the crown incisor as an alternative biomarker of Pb exposure screening in wild and laboratory rats, with the former having merits for use as a sentinel marker of exposure.

The current study limitation bordered around wild rats sampling. The small number of samples for the LK (n = 2) and MW (n = 3) after the exclusion of other species after genomic sequencing except the *R. rattus* species is the notable limitation. The logistics and travel restrictions could not permit re-sampling to increase the sample size of the *R. rattus*. Further validation of the rat incisor crown as a suitable alternative biomarker to blood-Pb for environmental Pb exposure assessment with a much larger sample size is recommended. Notwithstanding, the current study has revealed that the crown subdivision of the incisor rodents could be a suitable biomarker of Pb exposure. The use of the incisor crown subdivision has merits because it is easy to extract and is stable for preservation purposes [10]. Besides, the inherent advantage of teeth over the blood sample matrix in its ability to retain Pb after a month or more after the source is removed makes it an attractive alternative biomarker of Pb exposure. In the current study, wild rodents were trapped from residential areas, and sometimes in houses, making them suitable sentinel markers for

human exposure, especially children with hand-to-mouth activities. Furthermore, targeting the crown incisor for Pb exposure assessment without targeting the whole incisor tooth will maximize time, resources, and increase the chances of detection of Pb in sentinel wild rats.

5. Conclusions

The crown and the root of both lower and upper incisor teeth Pb-T in laboratory Pb-exposed Sprague Dawley rats accumulated Pb in a dose-dependent manner with the crown accumulating much more Pb-T than the root, suggesting that the crown may be a superior marker of Pb exposure than the root. Furthermore, the Pb-T accumulation in the crown of the lower incisors (L2) of wild rats discriminated the varying distances of sampling sites in relation to the Pb–Zn mine point source in Pb exposed *R. rattus* rats. In addition, the strong positive correlations between Pb-B and Pb-T observed in both laboratory and wild rats exposed to Pb support the possibility of rodent teeth as a useful tool for environmental assessment of Pb exposure. The high Pb-T in the crown compared to the root and the highly localized distribution of Pb in the incisor crown bearing enamel, as observed from the LA-ICP-MS mapping, indicate that the crown subdivision of the incisor tooth may be adequate for its use in sentinel rodents for Pb exposure assessment. Further studies are required to validate the rat incisor crown as a suitable alternative biomarker to blood-Pb for environmental Pb exposure assessment.

Supplementary Materials: The following are available online at https://www.mdpi.com/1660-4601/18/2/767/s1, Table S1: Wild rat species, Table S2: Microwave operating conditions for teeth and blood digestion, Table S3: Detailed analytical conditions of ICP-MS, Table S4: Detailed analytical conditions of LA-ICP-MS.

Author Contributions: Conceptualization, A.K. (Andrew Kataba) and S.M.M.N.; methodology, A.K. (Andrew Kataba)., H.T. and S.M.M.N.; software, A.K. (Ayano Kubota) and T.M.; validation, A.K. (Andrew Kataba)., H.T. and S.M.M.N.; formal analysis A.K. (Andrew Kataba); investigation, A.K. (Andrew Kataba), S.M.M.N., H.N., H.T., Y.B.Y., J.Y., K.M. and G.Z.; resources, S.M.M.N., K.Y., Y.I. and M.I.; data curation, A.K. (Andrew Kataba), A.K. (Ayano Kubota) and T.M.; writing—original draft preparation, A.K. (Andrew Kataba); writing—review and editing, S.M.M.N., H.N., H.T., Y.B.Y., J.Y., K.M. and G.Z.; visualization, A.K. (Andrew Kataba), A.K. (Ayano Kubota) and T.M.; supervision, S.M.M.N., K.Y., Y.I. and M.I.; project administration, K.Y. and M.I.; funding acquisition, S.M.M.N., K.Y., Y.I. and M.I. All authors have read and agreed to the published version of the manuscript.

Funding: The current work was supported by Grants-in-Aid for Scientific Research from the Ministry of Education, Culture, Sports, Science and Technology of Japan awarded to M. Ishizuka (No. 16H01779, 18K19847, 18KK0287) and Y. Ikenaka (17K20038, 18H04132) and S.M.M. Nakayama (No. 17KK0009, 20K20633) and K. Yokoyama (19H01081), and the foundation of JSPS Bilateral Open Partnership Joint Research Projects (JPJSBP120209902), the Japan Prize Foundation and Hokkaido University SOUSEI Support Program for Young Researchers in FY2020 (SMMN). This research was equally supported by JST/JICA SATREPS (Science and Technology Research Partnership for Sustainable Development; No. JPMJSA1501), aXis (Accelerating Social Implementation for SDGs Achievement No. JPMJAS2001) funded by JST as well as Program for supporting introduction of the new sharing system (JPMXS0420100619).

Institutional Review Board Statement: "Not applicable" for studies not involving humans or animals.

Informed Consent Statement: "Not applicable" for studies not involving humans.

Data Availability Statement: The datasets generated and analyzed during the current study are are available from the corresponding author on reasonable request.

Acknowledgments: The analyses were technically supported by Takahiro Ichise and Nagisa Hirano (Faculty of Veterinary Medicine, Hokkaido University) as well as by Kosuke Nakamura and Hidehiko Nomura (Faculty of Science, Hokkaido University).

Conflicts of Interest: The authors declare no conflict of interest.

Appendix A. Wild Rat Species Identification

The species of the wild rats sampled were identified using genomic DNA sequencing. Genomic DNA was extracted from liver samples of wild rodents with Wizard® Genomic DNA Purification Kit (Promega Corporation Madison, WI, USA). Species discrimination was done following a slight modification of the method described by Robins et al. [24]. To amplify Cytochrome b, 762 bp (*Cyt-b)* gene with accession number: JX887164.1, the primers used were Forward primer (5′-GGTGAAGGCTTCAACGCCAACCCTA-3′) and Reverse primer (5′-TAGAATATCAGCTTTGGGTGTTGATGG-3′). The polymerase chain reaction (PCR) thermal regime for all amplifications was one initial denaturation step of 94 °C for 2 min and 35 cycles of denaturation at 94 °C for 30 min, annealing at 60 °C for 30 min and extension at 72 °C for 1 min; and a final extension step of 72 °C for 6 min with a thermal cycler (iCycler, Bio-Rad, Hercules, CA, USA) and EmeraldAmp MAX PCR Master Mix (Takara Bio Inc., Shiga, Japan). The volume of PCR mix was 10 µL containing in 50 ng genomic DNA, 5 µL of EmeraldAmp MAX PCR Master Mix and 0.2 µM of each forward and reverse primer. The amplified products were purified by QIAquick® PCR Purification kit (Qiagen, Hilden, Germany). The sequence reaction was done by Fasmac Co. Ltd. (Kanagawa, Japan). From these sequences done by Fasmac Co. Ltd., the rat species were identified through blast analysis using the National Center for Biotechology Information (NCBI) website. Based on the results 15 *Rattus rattus* rats in total were identified and used for the study. And from each sampling site, the following numbers of paired blood and lower incisors teeth of *R. rattus* rats in brackets were included in the study, namely, Lukanga (LK) (n = 2); Mutwe Wansofu (MW) (n = 3); Chowa (CH) (n = 5); and Makululu (MK) (n = 5), respectively (Table S1).

References

1. Galal, M.K.; Elleithy, E.M.; Abdrabou, M.I.; Yasin, N.A.; Shaheen, Y.M. Modulation of caspase-3 gene expression and protective effects of garlic and spirulina against CNS neurotoxicity induced by lead exposure in male rats. *NeuroToxicology* **2019**, *72*, 15–28. [CrossRef] [PubMed]
2. Dapul, H.; Laraque, D. Lead Poisoning in Children. *Adv. Pediatr.* **2014**, *61*, 313–333. [CrossRef] [PubMed]
3. Bose-O'Reilly, S.; Yabe, J.; Makumba, J.; Schutzmeier, P.; Ericson, B.; Caravanos, J. Lead intoxicated children in Kabwe, Zambia. *Environ. Res.* **2018**, *165*, 420–424. [CrossRef] [PubMed]
4. Yabe, J.; Nakayama, S.; Ikenaka, Y.; Yohannes, Y.B.; Bortey-Sam, N.; Oroszlany, B.; Muzandu, K.; Choongo, K.; Kabalo, A.N.; Ntapisha, J.; et al. Lead poisoning in children from townships in the vicinity of a lead–zinc mine in Kabwe, Zambia. *Chemosphere* **2015**, *119*, 941–947. [CrossRef]
5. Yabe, J.; Nakayama, S.M.; Nakata, H.; Toyomaki, H.; Yohannes, Y.B.; Muzandu, K.; Kataba, A.; Zyambo, G.; Hiwatari, M.; Narita, D.; et al. Current trends of blood lead levels, distribution patterns and exposure variations among household members in Kabwe, Zambia. *Chemosphere* **2020**, *243*, 125412. [CrossRef]
6. Dooyema, C.A.; Neri, A.; Lo, Y.; Durant, J.; Dargan, P.I.; Swarthout, T.; Biya, O.; Gidado, S.O.; Haladu, S.; Sani-Gwarzo, N.; et al. Outbreak of Fatal Childhood Lead Poisoning Related to Artisanal Gold Mining in Northwestern Nigeria, 2010. *Environ. Health Perspect.* **2012**, *120*, 601–607. [CrossRef]
7. Haeflinger, P.; Mathieu-Nolf, M.; Lociciro, S.; Ndiaye, C.; Coly, M.; Diouf, A.; Faye, L.A.; Sow, A.; Tempowski, J.; Pronczuk, J.; et al. Mass Lead Intoxication from Informal Used Lead-Acid Battery Recycling in Darkar, Senegal. *Environ. Health Perspect.* **2009**, *117*. [CrossRef]
8. Bellinger, D.C. Childhood Lead Exposure and Adult Outcomes. *JAMA* **2017**, *317*, 1219–1220. [CrossRef]
9. Chang, S.-H.; Cheng, B.-H.; Lee, S.-L.; Chuang, H.-Y.; Yang, C.-Y.; Sung, F.-C.; Wu, T.-N. Low blood lead concentration in association with infertility in women. *Environ. Res.* **2006**, *101*, 380–386. [CrossRef]
10. Barbosa, F.; Tanus-Santos, J.E.; Gerlach, R.F.; Parsons, P.J. A Critical Review of Biomarkers Used for Monitoring Human Exposure to Lead: Advantages, Limitations, and Future Needs. *Environ. Health Perspect.* **2005**, *113*, 1669–1674. [CrossRef]
11. De Figueiredo, F.A.T.; Ramos, J.; Kawakita, E.R.H.; Bilal, A.S.; De Sousa, F.B.; Swaim, W.D.; Issa, J.P.M.; Gerlach, R.F. Lead line in rodents: An old sign of lead intoxication turned into a new method for environmental surveillance. *Environ. Sci. Pollut. Res.* **2016**, *23*, 21475–21484. [CrossRef] [PubMed]
12. Wang, Y.; Specht, A.J.; Liu, Y.; Finney, L.; Maxey, E.; Vogt, S.; Zheng, W.; Weisskopf, M.; Nie, L.H. Microdistribution of lead in human teeth using microbeam synchrotron radiation X-ray fluorescence (µ-SRXRF). *X-ray Spectrom.* **2016**, *46*, 19–26. [CrossRef] [PubMed]
13. Rossi, E. Low Level Environmental Lead Exposure—A Continuing Challenge. *Clin. Biochem. Rev.* **2008**, *29*, 63–70. [PubMed]
14. Steenhout, A.; Pourtois, M. Lead accumulation in teeth as a function of age with different exposures. *Occup. Environ. Med.* **1981**, *38*, 297–303. [CrossRef] [PubMed]

15. Winneke, G.; Hrdina, K.-G.; Brockhaus, A. Neuropsychological studies in children with elevated tooth-lead concentrations. *Int. Arch. Occup. Environ. Health* **1982**, *51*, 169–183. [CrossRef]
16. Arora, M.; Hare, D.J. Tooth lead levels as an estimate of lead body burden in rats following pre- and neonatal exposure. *RSC Adv.* **2015**, *5*, 67308–67314. [CrossRef]
17. Evans, R.D.; Richner, P.; Outridge, P.M. Micro-spatial variations of heavy metals in the teeth of walrus as determined by laser ablation ICP-MS: The potential for reconstructing a history of metal exposure. *Arch. Environ. Contam. Toxicol.* **1995**, *28*, 55–60. [CrossRef]
18. Cox, A.; Keenan, F.; Cooke, M.; Appleton, J. Trace element profiling of dental tissues using laser ablation-inductively coupled plasma-mass spectrometry. *Anal. Bioanal. Chem.* **1996**, *354*, 254–258. [CrossRef]
19. Uryu, T.; Yoshinaga, J.; Yanagisawa, Y.; Endo, M.; Takahashi, J. Analysis of Lead in Tooth Enamel by Laser Ablation-Inductively Coupled Plasma-Mass Spectrometry. *Anal. Sci.* **2003**, *19*, 1413–1416. [CrossRef]
20. Yohannes, Y.B.; Ikenaka, Y.; Ito, G.; Nakayama, S.M.M.; Mizukawa, H.; Wepener, V.; Smit, N.J.; Van Vuren, J.H.J.; Ishizuka, M. Assessment of DDT contamination in house rat as a possible bioindicator in DDT-sprayed areas from Ethiopia and South Africa. *Environ. Sci. Pollut. Res.* **2017**, *24*, 23763–23770. [CrossRef]
21. Ardizzone, M.; Vizio, C.; Bozzetta, E.; Pezzolato, M.; Meistro, S.; Dondo, A.; Giorgi, I.; Seghesio, A.; Mirabelli, D.; Capella, S.; et al. The wild rat as sentinel animal in the environmental risk assessment of asbestos pollution: A pilot study. *Sci. Total Environ.* **2014**, *479*, 31–38. [CrossRef]
22. Martiniakova, M.; Omelka, R.; Jančová, A.; Stawarz, R.; Formicki, G. Concentrations of Selected Heavy Metals in Bones and Femoral Bone Structure of Bank (*Myodes glareolus*) and Common (*Microtus arvalis*) Voles from Different Polluted Biotopes in Slovakia. *Arch. Environ. Contam. Toxicol.* **2011**, *60*, 524–532. [CrossRef]
23. Togao, M.; Nakayama, S.; Ikenaka, Y.; Mizukawa, H.; Makino, Y.; Kubota, A.; Matsukawa, T.; Yokoyama, K.; Hirata, T.; Ishizuka, M. Bioimaging of Pb and STIM1 in mice liver, kidney and brain using Laser Ablation Inductively Coupled Plasma Mass Spectrometry (LA-ICP-MS) and immunohistochemistry. *Chemosphere* **2020**, *238*, 124581. [CrossRef]
24. Ikenaka, Y.; Nakayama, S.M.M.; Muzandu, K.; Choongo, K.; Teraoka, H.; Mizuno, N.; Ishizuka, M. Heavy Metal Contamination of Soil and Sediment in Zambia. *Afr. J. Environ. Sci. Technol.* **2010**, *4*, 729–739.
25. Nakayama, S.; Ikenaka, Y.; Hamada, K.; Muzandu, K.; Choongo, K.; Teraoka, H.; Mizuno, N.; Ishizuka, M. Metal and metalloid contamination in roadside soil and wild rats around a Pb–Zn mine in Kabwe, Zambia. *Environ. Pollut.* **2011**, *159*, 175–181. [CrossRef]
26. Robins, J.H.; Hingston, M.; Matisoo-Smith, E.; Ross, H.A. Identifying Rattus species using mitochondrial DNA. *Mol. Ecol. Notes* **2007**, *7*, 717–729. [CrossRef]
27. Nakata, H.; Nakayama, S.; Yabe, J.; Liazambi, A.; Mizukawa, H.; Darwish, W.S.; Ikenaka, Y.; Ishizuka, M. Reliability of stable Pb isotopes to identify Pb sources and verifying biological fractionation of Pb isotopes in goats and chickens. *Environ. Pollut.* **2016**, *208*, 395–403. [CrossRef]
28. Nakata, H.; Nakayama, S.M.M.; Oroszlany, B.; Ikenaka, Y.; Mizukawa, H.; Tanaka, K.; Harunari, T.; Tanikawa, T.; Darwish, W.S.; Yohannes, Y.B.; et al. Monitoring Lead (Pb) Pollution and Identifying Pb Pollution Sources in Japan Using Stable Pb Isotope Analysis with Kidneys of Wild Rats. *Int. J. Environ. Res. Public Health* **2017**, *14*, 56. [CrossRef]
29. Ishii, C.; Nakayama, S.M.; Kataba, A.; Ikenaka, Y.; Saito, K.; Watanabe, Y.; Makino, Y.; Matsukawa, T.; Kubota, A.; Yokoyama, K.; et al. Characterization and imaging of lead distribution in bones of lead-exposed birds by ICP-MS and LA-ICP-MS. *Chemosphere* **2018**, *212*, 994–1001. [CrossRef]
30. Mancinelli, E.; Capello, V. Anatomy and Disorders of the Oral Cavity of Rat-like and Squirrel-like Rodents. *Veter- Clin. North Am. Exot. Anim. Pr.* **2016**, *19*, 871–900. [CrossRef]
31. Park, M.K.; Min, S.-Y.; Song, J.S.; Lee, J.-H.; Jung, H.-S.; Kim, S.-O. Estimated Time of Biomineralization in Developing Rat Incisors. *J. Korean Acad. Pedtatric Dent.* **2017**, *44*, 138–146. [CrossRef]
32. Suzuki, T.; Sakata, S.; Makino, Y.; Obayashi, H.; Ohara, S.; Hattori, K.; Hirata, T. iQuant2: Software for Rapid and Quantitative Imaging Using Laser Ablation-ICP Mass Spectrometry. *Mass Spectrom.* **2018**, *7*, A0065. [CrossRef]
33. Rabinowitz, M. Relating tooth and blood lead levels in children. *Bull. Environ. Contam. Toxicol.* **1995**, *55*, 853–857. [CrossRef]
34. Bellis, D.J.; Hetter, K.M.; Jones, J.; Amarasiriwardena, D.; Parsons, P.J. Lead in teeth from lead-dosed goats: Microdistribution and relationship to the cumulative lead dose. *Environ. Res.* **2008**, *106*, 34–41. [CrossRef]
35. Grobler, S.; Theunissen, F.S.; Kotze, T. The relation between lead concentrations in human dental tissues and in blood. *Arch. Oral Biol.* **2000**, *45*, 607–609. [CrossRef]
36. Teeth as Indicators of Environmental Pollution with Lead. *J. Environ. Anal. Toxicol.* **2012**, *2*, 1–5. [CrossRef]
37. Barton, H.J. Advantages of the Use of Deciduous Teeth, Hair, and Blood Analysis for Lead and Cadmium Bio-Monitoring in Children. A Study of 6-Year-Old Children from Krakow (Poland). *Biol. Trace Element Res.* **2010**, *143*, 637–658. [CrossRef]
38. Johnston, J.E.; Franklin, M.; Roh, H.; Austin, C.; Arora, M. Lead and Arsenic in Shed Deciduous Teeth of Children Living Near a Lead-Acid Battery Smelter. *Environ. Sci. Technol.* **2019**, *53*, 6000–6006. [CrossRef] [PubMed]
39. De Almeida, G.R.C.; Saraiva, M.; Barbosa, F.; Krug, F.J.; Cury, J.A.; Sousa, M.D.L.R.D.; Buzalaf, M.A.R.; Gerlach, R.F. Lead contents in the surface enamel of deciduous teeth sampled in vivo from children in uncontaminated and in lead-contaminated areas. *Environ. Res.* **2007**, *104*, 337–345. [CrossRef] [PubMed]

40. Toyomaki, H.; Yabe, J.; Nakayama, S.M.; Yohannes, Y.B.; Muzandu, K.; Liazambi, A.; Ikenaka, Y.; Kuritani, T.; Nakagawa, M.; Ishizuka, M. Factors associated with lead (Pb) exposure on dogs around a Pb mining area, Kabwe, Zambia. *Chemosphere* **2020**, *247*, 125884. [CrossRef] [PubMed]
41. Yabe, J.; Nakayama, S.; Ikenaka, Y.; Muzandu, K.; Choongo, K.; Mainda, G.; Kabeta, M.; Ishizuka, M.; Umemura, T. Metal distribution in tissues of free-range chickens near a lead-zinc mine in Kabwe, Zambia. *Environ. Toxicol. Chem.* **2012**, *32*, 189–192. [CrossRef]
42. Hegde, S.; Sridhar, M.; Bolar, D.R.; Bhaskar, S.A.; Sanghavi, M.B. Relating tooth- and blood-lead levels in children residing near a zinc-lead smelter in India. *Int. J. Paediatr. Dent.* **2010**, *20*, 186–192. [CrossRef]
43. Hare, D.J.; Austin, C.; Doble, P.; Arora, M. Elemental bio-imaging of trace elements in teeth using laser ablation-inductively coupled plasma-mass spectrometry. *J. Dent.* **2011**, *39*, 397–403. [CrossRef]
44. Olympio, K.; Huila, M.F.; Cardoso, C.D.A.B.; Ferreira, A.P.S.D.S.; Ortiz, A.G.; Toma, H.E.; Da Silva, R.H.A.; Luz, M.S.; Cardoso, M.R.A.; Kelmer, G.A.R.; et al. Can in vivo surface dental enamelmicrobiopsies be used to measure remote lead exposure? *Environ. Sci. Pollut. Res.* **2017**, *25*, 9322–9329. [CrossRef] [PubMed]
45. Cleymaet, R.; Collys, K.; Retief, D.H.; Michotte, Y.; Slop, D.; Taghon, E.; Maex, W.; Coomans, D. Relation between lead in surface tooth enamel, blood, and saliva from children residing in the vicinity of a non-ferrous metal plant in Belgium. *Occup. Environ. Med.* **1991**, *48*, 702–709. [CrossRef] [PubMed]

Chemosphere 271 (2021) 129832

Contents lists available at ScienceDirect

Chemosphere

journal homepage: www.elsevier.com/locate/chemosphere

Assessment of LeadCare® II analysis for testing of a wide range of blood lead levels in comparison with ICP–MS analysis

Hokuto Nakata [a, 1], Shouta M.M. Nakayama [a, *, 1], John Yabe [b], Kaampwe Muzandu [b], Haruya Toyomaki [a], Yared Beyene Yohannes [a, c], Andrew Kataba [a, b], Golden Zyambo [b], Yoshinori Ikenaka [a, d], Kennedy Choongo [b, e], Mayumi Ishizuka [a, **]

[a] Laboratory of Toxicology, Department of Environmental Veterinary Sciences, Faculty of Veterinary Medicine, Hokkaido University, Kita 18 Nishi 9, Kita-ku, Sapporo, 060-0818, Japan
[b] The University of Zambia, School of Veterinary Medicine, P.O. Box 32379, Lusaka, Zambia
[c] Department of Chemistry, College of Natural and Computational Science, University of Gondar, Ethiopia
[d] Water Research Group, School of Environmental Sciences and Development, North-West University, South Africa
[e] Fiji National University, College of Agriculture, Fisheries & Forestry, School of Animal and Veterinary Sciences, Koronivia Campus, Suva, Fiji

HIGHLIGHTS

- Comparison between blood lead levels measured by LeadCare II and ICP-MS.
- 994 venous blood samples compared by three different statistical comparison methods.
- Large positive bias of LeadCare II compared to ICP-MS at the levels above 45 μg/dL.
- No intermetallic interferences of blood copper, cadmium and iron.
- Conversion or retesting using a laboratory machine is recommended at a higher level.

ARTICLE INFO

Article history:
Received 6 November 2020
Received in revised form
26 January 2021
Accepted 28 January 2021
Available online 2 February 2021

Handling Editor: Myrto Petreas

Keywords:
LeadCare
ICP-MS
Bias
Bland–altman analysis
Passing–bablok regression
Deming regression

ABSTRACT

The LeadCare® testing system, which utilizes anodic stripping voltammetry (ASV) methodology, has been widely used worldwide for cost-effective blood lead level (BLL) screening. However, some concerns have recently been issued regarding inaccurate results obtained using LeadCare®. Hence, we aimed to evaluate the accuracy of BLL measured by LeadCare® II (BLL_{LC}) by comparison with ICP-MS (BLL_{IM}) by the Passing–Bablok regression, Deming regression, and Bland–Altman analyses by using 994 venous blood samples. BLL_{LC} ranged from 3.3 to 162.3 μg/dL, while BLL_{IM} ranged from 0.8 to 154.8 μg/dL. Although BLL_{LC} and BLL_{IM} exhibited a strong and positive correlation, BLL_{LC} values were generally greater than BLL_{IM} values, indicative of the overestimation of the LeadCare® analysis. A large positive bias of 19.15 ± 8.26 μg/dL and 29.25 ± 14.04 μg/dL for BLL_{LC} compared with BLL_{IM} were recorded in the BLL_{LC} range of 45.0–64.9 μg/dL and for ≥65.0 μg/dL, respectively. In contrast, a bias of ≤0.3 μg/dL was observed at a BLL_{LC} of less than 10.0 μg/dL. Blood copper, cadmium, and iron levels did not exhibit an effect on the bias of BLL_{LC}, indicative of the minimal potential interferences of the metals; these interferences are a cause for concern with the ASV method. In conclusion, LeadCare® analysis is thought to be a good tool for screening purposes at a lower BLL around the reference level of 5 μg/dL in the initial stage; however, conversion or retesting using a laboratory analyzer is recommended at a higher BLL for appropriate clinical evaluation and research.

1. Introduction

Environmental exposure to lead (Pb) still remains a public health concern. Pb poisoning occurs because of the current anthropogenic sources and historic air Pb emissions, including

* Corresponding author.
** Corresponding author.
E-mail addresses: shouta-nakayama@vetmed.hokudai.ac.jp (S.M.M. Nakayama), ishizum@vetmed.hokudai.ac.jp (M. Ishizuka).
[1] Both authors equally contributed to this study.

https://doi.org/10.1016/j.chemosphere.2021.129832
0045-6535/

those of gasoline and from industries and mining operations (ATSDR, 2010). The Pb concentration of the bone reflects long-term exposure and body burden, while the blood Pb level (BLL) reflects more recent exposure. BLL is currently used widely as an indicator of Pb exposure (Barbosa et al., 2005). Although the Center for Disease Control and Prevention (CDC) stipulated an action level of 60 μg/dL for BLL in the 1960s, the action level for BLL has dramatically and gradually decreased. In 2012, the CDC has issued new guidelines for assessing children's BLL with its reference level of 5 μg/dL (Centers for Disease Control and Prevention, 2012). On the basis of scientific evidence, chelation therapy is currently highly recommended at a BLL of greater than or equal to 45 μg/dL (CDC, 2002; Needleman, 2004).

Because of the demand for a rapid and inexpensive method for screening and monitoring BLL, some early instruments that utilize anodic stripping voltammetry (ASV) have been developed. However, potential interference by copper (Cu) was a major concern since it may affect the BLL result from the ASV method (Roda et al., 1988). In a recent review by Borrill et al. (2019), interferences of intermetallic compounds on solid electrodes are problematic because preconcentration occurs only on the electrode surface where interactions are likely to occur between different metals. Cadmium (Cd)−Pb (Zhao and Liu, 2018) and iron (Fe)−Pb (Chau and Lum-Shue-Chan, 1974) are additional examples of problematic intermetallic compounds at solid electrodes. Currently, only LeadCare® testing systems from Magellan Diagnostics Inc. (North Billerica, MA, USA) are commercially available and widely utilized in developed countries (Green et al., 2017; Sobin et al., 2011) and developing countries (Dooyema et al., 2011; Safi et al., 2019; Yabe et al., 2020). However, recently, the United States Food and Drug Administration (FDA) has issued a Class I recall, the most serious type, for the LeadCare® testing system (US FDA, 2017; 2018a). The US FDA has warned that LeadCare® testing systems may underestimate BLL for the processing of venous blood samples. In addition, in late 2018, the US FDA has concluded that there is a significant chance of obtaining incorrect results by using the LeadCare® system in cases where venous blood is collected in certain blood tubes containing a chemical called thiuram (US FDA, 2018b). The suspected tubes manufactured by Becton Dickinson & Company (NJ, USA) include BD Vacutainer® Lithium Heparin Green Top, which was used in our study before the FDA announcement. Thiuram in the rubber stopper of the tube can release reactive gases, carbon disulfide (CS_2), and carbonyl sulfide which can dissolve into the blood and tightly bind to Pb particles. Similarly, the CDC also has issued concerns regarding the inaccurate results obtained by using the LeadCare® instrument (Centers for Disease Control and Prevention, 2018). Taken together, these indicate that careful consideration and further scientific investigation of the LeadCare® analyzer's validity are required.

To the best of our knowledge, only two studies comparing BLL measured using the LeadCare® analyzer (BLL_{LC}) and inductively coupled plasma−mass spectrometry (ICP−MS, BLL_{IM}) at around the reference value of 5 μg/dL have been reported (Johnson et al., 2019; Sobin et al., 2011). In those studies, which were conducted in the laboratory or a primary school in the USA, the LeadCare® analyzer was deemed to provide an acceptable screening result. For the field study, Neri et al. (2014) reported that the dilution method using human blood, which is verified to have a BLL below the lower detection limit of 3.3 μg/dL for the LeadCare® II analyzer, can give an adequate result for BLL greater than 65 μg/dL, corresponding to the upper detection limit of LeadCare® II. In addition, in the same study, the BLL_{LC} consistency overestimated BLL_{IM} by twofold or greater, and the concordance correlation coefficient was quite low (0.423) when blood was diluted with saline. However, a study investigating the suitability of the LeadCare® system for field analysis in a wide range of BLL values has not been reported thus far. Moreover, there is a high demand for a portable instrument for rapid analysis, such as LeadCare® testing systems, especially in rural areas of developing countries with limited applicable resources.

As a core mining area, Kabwe Town in the Republic of Zambia has been in operation for almost a century. Despite the closure of the mine in 1994, alarming concentrations of Pb have been reported in the environment (Nakayama et al., 2011) and animals (Doya et al., 2020; Nakata et al., 2016; Toyomaki et al., 2020; Yabe et al., 2013). Recently, our study investigating human BLL_{LC} reported an increased BLL in Kabwe in the range of 1.65−162 μg/dL for 1190 participants, although the dilution was performed using hydrochloric acid (HCl) and not uncontaminated blood. The results below the lower detection limit of 3.3 μg/dL were adjusted to half their value of 1.65 μg/dL (Yabe et al., 2020). A similar elevated trend of BLL_{IM} in the range of 0.79−154.75 μg/dL was also reported for 504 representatives from Kabwe (Nakata et al., 2020).

From the above discussion, LeadCare® II analysis was compared with ICP−MS analysis in terms of validity in this study. To obtain a better picture, the maximum available number of samples collected in Kabwe was compared, whereas some blood samples were excluded from the analysis of two earlier studies (Nakata et al., 2020; Yabe et al., 2020) because of the research design and limited budget for further clinical assessment. As LeadCare® series demonstrates immense potential for field analysis due to its unique and convenient characteristics, the evaluation in this study is significant for the monitoring and control of global Pb pollution.

2. Methods

2.1. Venous blood sample collection

The study was approved by the University of Zambia Research Ethics Committee (UNZAREC; ref. no. 012-04-16) and the Ministry of Health through the Zambia National Health Research Ethics Committee and the Kabwe District Medical Office. After two-stage random selection to capture the representative data of this area, blood sampling was performed in Kabwe in July and August 2017. Geographical information including the distance between the mine and each sampling point are shown in Supplementary Figure S1. The details of sample selection were described in a recent paper (Yamada et al., 2020). For blood collection in clinics, all collection items were placed in plastic Ziploc® storage bags until use to avoid contamination as described in a previous study (Nakata et al., 2020). After the cleaning and wiping of the collection site on the arm with alcohol swabs to eliminate environmental contaminants, blood was collected from the cubital vein. The collected samples were then immediately subjected to LeadCare II (Magellan Diagnostics, North Billerica, MA, USA) analysis as described below. Additionally, 200 μL of blood were separated into 1.5 mL plastic tubes immediately after blood collection for metal extraction and ICP-MS analysis. The separated blood samples and the remainder of the blood samples were stored at −20 °C until transportation. After the Material Transfer Agreement (MTA) was granted by the Zambian Ministry of Health through the National Health Research Ethics Committee (approval no. E03618), the samples were packed in cooler boxes and transported to the Laboratory of Toxicology, Faculty of Veterinary Medicine, Hokkaido University, Japan, for laboratory analysis by ICP−MS.

2.2. LeadCare II analysis

Analysis was performed according to the manufacturer's instructions and as recently described (Yabe et al., 2020). In brief,

50 μL of venous blood from a heparinized tube (BD Vacutainer® Lithium Heparin Green Top (Becton, Dickinson and Company, Franklin Lakes, NJ, USA)) was transferred into a vial containing the LeadCare II treatment reagent (250 μL of 0.1% HCl) for hemolysis and for the release of Pb into the solution. The mixed solution was then applied onto the electrochemical sensor for single analysis. For quality assurance, the instrument was calibrated using a calibration probe assigned to a specific reagent kit box (48 tests) by the manufacturer. In addition, analyses of standard control reagents supplied by the manufacturer were performed as per the manufacturer's instruction to confirm the accuracy. Those samples with a BLL_{LC} above the detection limit of 65 μg/dL were diluted for reanalysis. Next, 50 μL of blood was added into 100 μL of 0.1% HCl for three times dilution. Subsequently, 50 μL of the mixed solution was transferred into a vial in the same way as that performed for undiluted blood.

2.3. Blood digestion and metal extraction

Blood digestion and metal extraction were performed as described recently (Nakata et al., 2020). First, 200 μL of whole blood was digested with 5 mL of twofold diluted ultrapure nitric acid (Cica reagent, specific gravity of 1.38, 60%; Kanto Chemical Corp., Tokyo, Japan) and 1 mL of ultrapure hydrogen peroxide (Cica reagent, 30%; Kanto Chemical Corp.) using a microwave digestion system (Speed Wave MWS-2; Berghof, Eningen, Germany). The extracted solutions were then transferred into 15 mL plastic tubes and diluted to a final volume of 10 mL with double-distilled and deionized water (Milli-Q; Millipore, Bedford, MA). Supplementary Table S1 summarizes the detailed heating program of the microwave digestion system.

2.4. Blood Pb, Cu, Cd, and Fe analysis using ICP–MS

Levels of BLL_{IM} as well as blood Cu (BCuL), Cd (BCdL), and Fe (BFL) were determined by ICP–MS (7700 series, Agilent Technologies, Tokyo, Japan) as reported by Nakata et al. (2020). Supplementary Table S2 summarizes the detailed operating conditions. Analytical quality control was performed using the certified reference material of Seronorm™ Trace Elements Whole Blood L-2 (Sero, Billingstad, Norway). Replicate analysis of these reference materials revealed good accuracy (relative standard deviation (RSD) of less than 3%) and recoveries (95–105%). The instrument detection limit was 0.001 μg/L for all the targeted metals. The limits of detection (LOD) of the extracted sample analysis were 0.048, 0.024, 0.008, and 11.65 μg/L for Pb, Cu, Cd, and Fe, respectively.

2.5. Statistical analysis

JMP Pro version 14 (SAS Institute, NC, USA) was employed for all statistical analyses, except the Passing–Bablok regression analysis, which was carried out using Analyze-it Method Validation Edition version 5.65.3 (Analyze-it Software, Ltd., Leeds, UK). Following lack of normality in the BLL data distribution based on the Shapiro-Wilk test, the data were log-transformed. The log-transformed data fitted a normal distribution for statistical analysis as was confirmed by the Shapiro-Wilk test. However, the results for the actual and log-transformed numbers were recorded in this study for easy comparison with other studies. Those samples with a BLL_{LC} below the detection limit of 3.3 μg/dL were excluded from the analysis and comparison. The Passing–Bablok regression analysis and Deming regression analysis were performed to assess the correlation between BLL_{LC} and BLL_{IM} in real and log-transformed data, respectively. In addition, Bland–Altman tests were conducted to evaluate comparability across BLL measurement methods. The Pearson correlation coefficient was utilized to assess the relationship of log-transformed BCuL with log-transformed BLL_{LC}, BLL_{IM}, and the bias (log-transformed BLL_{LC} − log-transformed BLL_{IM}); log-transformed BCdL with log-transformed BLL_{LC}, BLL_{IM}, and the bias; as well as log-transformed BFL with log-transformed BLL_{LC}, BLL_{IM}, and the bias. Statistical analyses were performed at a significance level of 0.05 ($p < 0.05$).

3. Results

3.1. Overall trend of BLL_{LC} and BLL_{IM}

In total, 1208 venous blood samples were analyzed using the LeadCare II analyzer and ICP–MS. Supplementary Table S3 provides the characteristics of the studied population by area. Among 1208 blood samples, 214 samples (17.7%) exhibited a BLL_{LC} below the detection limit of 3.3 μg/dL; hence, these samples were excluded from the study, and the remaining 994 samples were used for data analysis and comparison. Table 1 summarizes the statistical distribution of the obtained BLL_{LC} and BLL_{IM}, and Fig. 1 shows the corresponding analysis using the box-and-whisker plot. The BLL_{LC} ranged from its lower detection limit of 3.3–162.3 μg/dL with a mean ± standard deviation (SD) of 25.9 ± 21.8 μg/dL. In contrast, the range and mean ± SD of BLL_{IM} were 0.8–154.8 μg/dL and 18.1 ± 14.8 μg/dL, respectively. The BLL_{LC} values were greater than the BLL_{IM} values for all descriptive statistical values, including the mean, 95% confidence interval (CI), SD, and minimum and maximum values, as well as percentiles.

3.2. Comparability between BLL_{LC} and BLL_{IM}

Strong and positive correlations between BLL_{LC} and BLL_{IM}, as well as between log BLL_{LC} and log BLL_{IM}, with correlation coefficients (r^2) of 0.904 and 0.903, respectively, were observed (Fig. 2, Supplementary Figure S2; Supplementary Figure S3). A regression-line slope of <1 indicated that BLL_{LC} is generally greater than BLL_{IM}. The Bland–Altman analysis was performed to assess the bias of BLL_{LC} as compared with BLL_{IM}, as well as that of log BLL_{LC} against log BLL_{IM} (Fig. 3). Overall, the mean bias of BLL_{LC} was 7.76 μg/dL, with a CI of 7.103–8.412 μg/dL. The lower and upper limits of agreement were −12.87 and 28.39 μg/dL, respectively. The increasing tendency of bias at a higher Pb level was observed rather than constant bias. Compared with the log-transformed data, logBLL_{LC} exhibited a positive mean bias of 0.129 with a CI of 0.119–0.140. The lower and upper limit of agreement were −0.207 and 0.465, respectively. Table 2 summarizes the mean and SD of the bias in the different BLL_{LC} range groups calculated by the Bland–Altman analysis. Compared with that observed for BLL_{IM}, large positive biases of 19.15 ± 8.26 μg/dL and 29.25 ± 14.04 μg/dL for BLL_{LC} were recorded in the range of 45.0–64.9 μg/dL and at ≥65.0 μg/dL, respectively. On the other hand, the bias was within 0.3 μg/dL in the ranges of 3.3–4.9 μg/dL and 5.0–9.9 μg/dL. Generally, the higher was the BLL_{LC}, the higher was the bias.

3.3. Distribution of BCuL, BCdL, and BFL, as well as the associations with BLL_{LC} and BLL_{IM}

Table 1 summarizes the BCuL, BCdL, and BFL distributions. The recorded BCuL ranged from 0.27 to 3.06 mg/L, with a mean of 1.15 ± 0.24 mg/L. The comparison of the log-transformed values for BLL_{LC} and BLL_{IM} revealed significant positive associations ($p < 0.0001$ and $p < 0.0001$, respectively) for BCuL despite the low r^2 values of 0.13 and 0.17, respectively (Table 3). On the other hand, a statistical relationship was not observed between log BCuL and the BLL measurement bias ($p = 0.06$). BCdL and BFL were within the

Table 1
Statistical distributions of BLL_{LC}, BLL_{IM}, BCuL, BCdL, and BFL.

	BLL_{LC} (μg/dL)	BLL_{IM} (μg/dL)	BCuL (mg/L)	BCdL (μg/L)	BFL (mg/mL)
mean	25.9	18.1	1.15	0.25	0.47
95% CI	24.6–27.3	17.2–19.1	1.14–1.16	0.24–0.26	0.46–0.47
SD	21.8	14.8	0.24	0.24	0.08
minimum	3.3	0.8	0.27	0.02	0.07
maximum	162.3	154.8	3.06	2.27	0.91
Percentiles					
0.5	3.3	1.3	0.67	0.03	0.21
2.5	3.6	2.6	0.80	0.05	0.30
10	4.6	4.2	0.91	0.07	0.37
25	8.3	7.2	1.00	0.11	0.42
50	19.1	13.9	1.11	0.18	0.47
75	38.1	24.8	1.26	0.31	0.52
90	56.7	39.2	1.44	0.48	0.57
97.5	78.0	54.7	1.72	0.93	0.61
99.5	106.9	74.1	2.18	1.60	0.73

Note: Part of BLLLC data was reported in an earlier paper [14], similarly for BLLIM and BCdL [26].

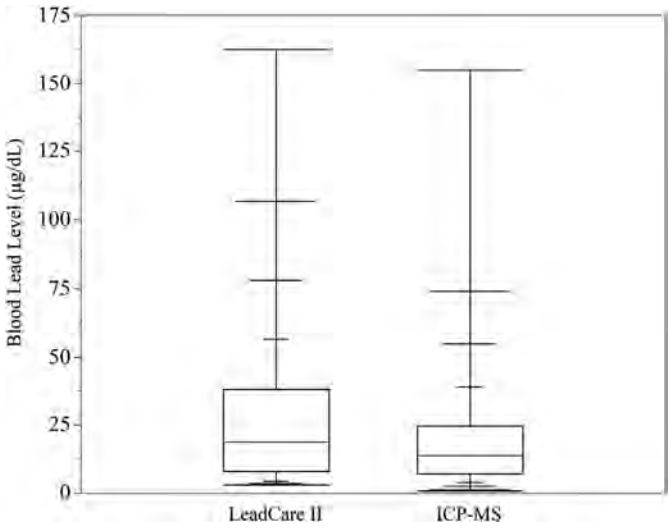

Fig. 1. Box-and-whisker plot of BLL_{LC} and BLL_{IM}. Percentile lines represent 0, 0.5, 2.5, 10, 25, 50, 75, 90, 97.5, and 99.5% percentiles from the bottom to top. Parts of BLL_{LC} (Yabe et al., 2020) and BLL_{IM} (Nakata et al., 2020) data were reported in earlier papers and cited.

range of 0.02–2.27 μg/L and 0.07–0.91 mg/mL, with mean values of 0.25 ± 0.24 μg/L and 0.47 ± 0.08 mg/mL, respectively. Compared with the BLL measurement bias, BCdL did not exhibit a statistically significant association ($p = 0.43$). The significant relationship between BLL measurement bias and BFL ($p < 0.01$) was observed albeit the low r^2 value of −0.09.

4. Discussion

A portable LeadCare® testing system has been widely considered as a good tool for screening the Pb exposure level because of its convenient characteristics. However, the US FDA and CDC have expressed concerns related to the possible inaccurate results of BLL_{LC} (Centers for Disease Control and Prevention, 2018; US FDA, 2017; 2018a; 2018b). Even before these reports, Bossarte et al. (2007) raised concerns that LeadCare may provide a falsely low BLL result. On the basis of this concern, several earlier studies were carried out to assess the suitability of LeadCare® analysis compared with a laboratory metal analyzer such as ICP–MS in a specific range of BLL. In this study, the comparison between the 994 pairs of BLL_{LC} and BLL_{IM} was done with a wide range of BLL and a larger sample size as compared with previous investigations to further verify the validity of LeadCare® II analysis. For this purpose, three statistical

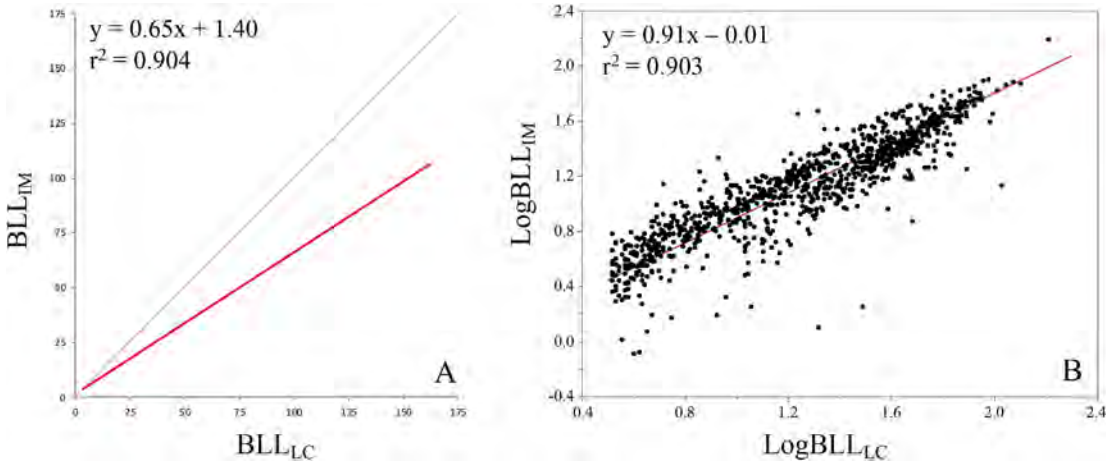

Fig. 2. Passing–Bablok regression analysis between BLL_{LC} and BLL_{IM} (A), as well as Deming regression analysis between log BLL_{LC} and log BLL_{IM} (B). Parts of BLL_{LC} (Yabe et al., 2020) and BLL_{IM} (Nakata et al., 2020) data were reported in earlier papers and cited.

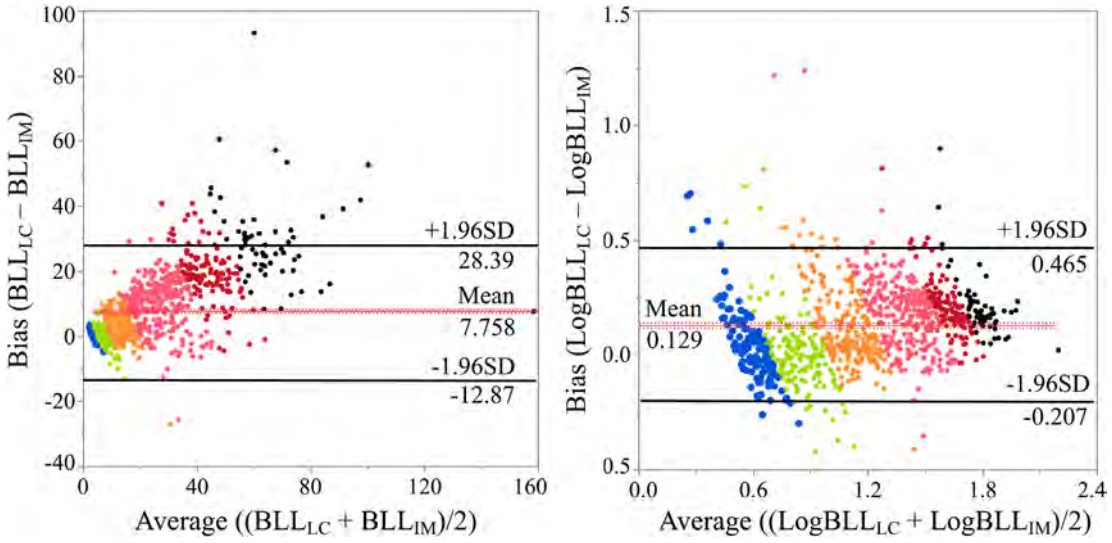

Fig. 3. Bland–Altman plot of differences between BLL_{LC} and BLL_{IM} (left) and between log BLL_{LC} and log BLL_{IM} (right). Mean difference is indicated by a red line, with a 95% confidence interval indicated by the red dotted line. Black lines show upper and lower limits of agreement of Bland–Altman analysis (±1.96 × standard deviation). Blue = sample whose BLL_{LC} ranges from 3.3 to 4.9, light green = sample whose BLL_{LC} ranges from 5.0 to 9.9, orange = sample whose BLL_{LC} ranges from 10.0 to 19.9, pink = sample whose BLL_{LC} ranges from 20.0 to 44.9, red = sample whose BLL_{LC} ranges from 45.0 to 64.9, and black = sample whose BLL_{LC} is ≥ 65.0. (For interpretation of the references to colour in this figure legend, the reader is referred to the Web version of this article.)

Table 2
Bias of BLL_{LC} relative to BLL_{IM} calculated using the Bland–Altman analysis, as well as the regression equation with a correlation coefficient calculated using the Passing–Bablok regression analysis.

BLL_{LC} range (μg/dL)	Sample size	Bland-Altman analysis					Passing-Bablok regression analysis	
		Mean BLL_{LC} (μg/dL)	Mean BLL_{IM} (μg/dL)	Mean bias (μg/dL) (BLL_{LC} - BLL_{IM})	SD of bias (μg/dL)	Lower and upper limits of agreement	Regression equation (x = BLL_{LC}, y = BLL_{IM})	Correlation coefficient
3.3–4.9	129	4.12	3.95	0.17	1.29	−0.05, 0.39	y = 3.74x − 11.48	0.41
5.0–9.9	156	7.07	7.37	−0.30	2.56	−0.72, 0.1	y = 1.89x − 6.21	0.46
10.0–19.9	227	14.57	11.73	2.84	4.21	2.29, 3.39	y = 1.50x − 9.32	0.45
20.0–44.9	297	31.18	21.31	9.87	7.35	9.04, 10.71	y = 0.97x − 10.41	0.54
45.0–64.9	124	53.38	34.23	19.15	8.26	17.70, 20.6	y = 1.78x − 59.75	0.53
65.0 -	61	80.85	51.57	29.25	14.04	25.72, 32.77	y = 1.38x − 56.99	0.71
Overall	994	25.91	18.15	7.76	10.53	7.10, 8.41	y = 0.65x + 1.40	0.90

Table 3
Pearson's coefficients of correlation (r^2) between BCuL with BLL_{LC}, BLL_{IM}, and the bias; BCdL with BLL_{LC}, BLL_{IM}, and the bias; and BFL with BLL_{LC}, BLL_{IM}, and the bias.

	BCuL		BCdL		BFL	
	r^2	p	r^2	p	r^2	p
BLL_{LC}	0.13	<.0001	0.26	<.0001	−0.08	<.01
BLL_{IM}	0.17	<.0001	0.30	<.0001	−0.05	.1168
Bias	−0.06	0.06	−0.03	0.43	−0.09	<.01

comparative methods were applied although the Passing-Bablok regression does not account for random variation between the two analytical methods.

Our results revealed a good correlation between BLL_{LC} and BLL_{IM} when compared in the overall BLL_{LC} range of 3.3–162.3 μg/dL. In contrast, the overestimation of LeadCare® measurement was indicated by regression analyses and Bland–Altman analysis, with an overall positive bias of 7.76 μg/dL. However, the comparison of different BLL_{LC} ranges revealed a small bias in the BLL_{LC} ranges of 3.3–4.9 μg/dL and 5.0–9.9 μg/dL, indicating the validity of BLL_{LC} in a lower BLL range. This trend is similar to that previously reported for the bias of mainly around 5 μg/dL for children's BLL (Johnson et al., 2019; Sobin et al., 2011). In addition, a small positive bias of 0.45 μg/dL was reported for a Pb-exposed employee's BLL of less than 10 μg/dL upon comparison of the LeadCare® instrument with graphite furnace atomic absorption spectrometry (GFAAS) (Taylor et al., 2001). For fresh blood samples of the Scandinavian brown bear (*Ursus arctos*), the BLL_{IM} of which ranged from 3.3 to 17.3 μg/dL, a bias of 0.225 in log-transformed data the real number of which is described by the unit μg/L (equivalent to 0.17 μg/dL for a real number) was recently recorded (Boesen et al., 2019). As a BLL of 5 μg/dL is considered as a reference value (Centers for Disease Control and Prevention, 2012), the LeadCare® analyzer can be considered as a good tool for primary screening. In the BLL_{LC} range of 10.0–19.9 μg/dL, a higher positive bias of 2.84 μg/dL was detected, while a slight negative bias (−0.8 μg/dL) was previously reported for the samples for which BLL mostly ranged from 10 to 20 μg/dL (Johnson et al., 2019).

On the other hand, a strong positive bias were detected at a higher BLL_{LC} range of >20 μg/dL. A previous study investigating the suitability of the LeadCare® analyzer for raptor venous blood reported an adverse bias of −1.12 μg/dL for blood samples for which BLL_{IM} ranged from 10 to 80 μg/dL (González et al., 2019). Pineau et al. (2002) performed recovery tests using pooled blood (3.68 ± 0.21 μg/dL) and additive blood, the BLL of which is 22 μg/dL.

The LeadCare® analyzer returned a mean value of 27.1 ± 1.8 μg/dL, in contrast to that of 24.9 ± 0.35 μg/dL by GFAAS and indicative of 2.2 μg/dL overestimation of LeadCare analysis as compared with GFAAS. Compared with earlier observations, a higher bias was observed herein for the BLL_{LC} range of 20.0–44.9 μg/dL and between 45.0 and 64.9 μg/dL. As chelation therapy is recommended at a BLL of ≥45 μg/dL (CDC, 2002; Needleman, 2004), the observed large bias at around the threshold for treatment would be crucial. Although the bias did not exhibit a statistically significant relationship with BCuL, BCdL, and BFL, one of the possible reasons for this large bias is the interference of intermetallic compounds, which are concerns reported previously (Borrill et al., 2019; Chau and Lum-Shue-Chan, 1974; Zhao and Liu, 2018). In addition to Cu, Cd, and Fe, which were verified in this study, the elevated concentration of some metals (such as cobalt, nickel, and chromium) and a metalloid (arsenic) in the environment (Nakayama et al., 2011) and animals (Doya et al., 2020; Nakata et al., 2016; Toyomaki et al., 2020; Yabe et al., 2013) has been previously reported for the examined area of Kabwe. Borrill et al. (2019) reported that Pb speciation is another factor that should be carefully considered. To the best of our knowledge, data have not been reported about Pb speciation in humans or any other animals in Kabwe. Cerussite ($PbCO_3$) and anglesite ($PbSO_4$) are the two main crystalline states of Pb in leached residues from the Kabwe mine (Silwamba et al., 2020a, 2020b). Further investigation should be performed to answer this inexplicable large bias.

At a BLL of greater than 65 μg/dL, at which blood samples need to be diluted for LeadCare® measurement because of the exceeding upper detection limit, the mean bias was extremely high (29.25 μg/dL). A limitation of this study was possibly the dilution medium used for readings that were above the detection limit. In this study, use of the LeadCare® II treatment reagent of 0.1% HCl for dilution was done instead of the recommended dilution protocol using "unpolluted blood" (Neri et al., 2014) because of the practical challenge in the investigated area considerably contaminated with Pb.

BCuL, BCdL, and BFL exhibited significant positive relationships with BLL_{LC} and BLL_{IM}, whereas correlation coefficients were small. This result is in agreement with the elevated Cu, Cd, and Fe levels in soil (Nakayama et al., 2011) and animals (Doya et al., 2020; Nakata et al., 2016; Toyomaki et al., 2020; Yabe et al., 2013) around the mine area, along with that observed for Pb. However, the recorded range of BCuL was comparable to the formerly reported normal values of 1.4 ± 0.32 and 1.5 ± 0.38 mg/L for men and women, respectively, with ages between 46 and 60 years (Kazi et al., 2008). This result could be explained by the function of Cu in homeostasis in the body; it is an essential metal for the human body (Araya et al., 2006). On the other hand, the comparison with previously reported normal values of BFL for men (0.71 ± 0.05 mg/mL) and women (0.70 ± 0.06 mg/mL) suggested that the observed BFL in this study is relatively lower (Kazi et al., 2008). In contrast to the correlation with BLL_{LC} and BLL_{IM}, the associations of BCuL, BCdL, and BFL with the bias of BLL_{LC} against BLL_{IM} were not significant. On the other hand, intermetallic interference has been suggested as one of the potential factors that may affect the BLL result from the ASV method (Borrill et al., 2019; Chau and Lum-Shue-Chan, 1974; Roda et al., 1988; Zhao and Liu, 2018). Interferences such as Cu, Cd, or Fe were not observed in this study using the modern LeadCare® testing system.

A recent FDA recall suggested the potential falsely underestimated BLL in venous blood when using the LeadCare® analyzer (FDA, 2017). In addition, the FDA again reported that a chemical compound of thiuram in the rubber stopper of certain blood collection tubes can result in a negative bias for the result (FDA, 2018b). Unfortunately, as these suspected tubes are common, they were used in this study before the FDA announcement. With respect to specimen collection, it was not practically possible to collect blood samples twice from one person, one from a capillary by using the pricking method for LeadCare® analysis only, and the other from the vein using a blood collection needle for ICP–MS analysis and subsequent laboratory analysis, because of ethical reasons and limited field capacity. Because this study was not originally designed to assess the potential falsely low Pb levels due to thiuram as pointed out by the FDA, a clear answer was unfortunately not obtained although the observed bias was found to be generally positive.

However, it should be emphasized that the results obtained herein suggest that the LeadCare® testing system is appropriate and acceptable for screening with a BLL cut-off of 5 μg/dL, as recently concluded (Johnson et al., 2019). At higher range, greater than 10 μg/dL, converting from BLL_{LC} to BLL_{IM} or simple retesting using a laboratory metal analyzer such as ICP–MS for data confirmation would be recommended as proposed before (Boesen et al., 2019; Sobin et al., 2011), although a positive bias should be preferred than a negative bias in terms of risk management. Our results are also in agreement with the suggestion of Sobin et al. (2011) that LeadCare® measurement is not recommended for investigating the threshold for health effects or any other associated factors. In contrast, the statistically strong positive association between BLL_{LC} and BLL_{IM} indicates that the LeadCare® system is applicable to the assessment of concentration-dependent effect of Pb on the associated factors. In addition, LeadCare® analysis is beneficial to determining the pollution status in the initial stage in the field.

5. Limitations

There are some limitations in the current study. First, we used the LeadCare® II treatment reagent of 0.1% HCl for dilution of blood samples whose BLL_{LC} at initial measurement were above the detection limit of 65 μg/dL. This is because it was realistically difficult to follow the recommended dilution protocols using "unpolluted blood" (Neri et al., 2014) due to the capacity issue. Second, venous blood samples were used for LeadCare® measurement instead of capillary blood because of the ethical reasons and limited capacity in the field. The venous blood samples may have caused an underestimation of BLL measured by the LeadCare® instrument as the US FDA suggested (US FDA, 2017). Finally, the blood collection tubes with thiuram-contained rubber stoppers were used for venous blood collection. The US FDA reported that there is a possibility of obtaining inaccurate results of BLL because thiuram can release chemical compounds which can interfere with Pb particles (US FDA, 2018b).

6. Conclusions

A possibility of underestimation or overestimation of the BLL following LeadCare® analysis exists. The observed bias differed considerably between the low and high concentration ranges. Our results suggest that LeadCare® analysis is a good screening method for Pb exposure at a lower BLL at around the current reference level of 5 μg/dL. However, conversion or retesting using laboratory analyzers, such as ICP–MS, is recommended at a higher BLL of greater than 10 μg/dL for the adequate clinical evaluation of exposure status, albeit the good correlations between BLL_{LC} and BLL_{IM} even at ≥10 μg/dL. Moreover, the use of the LeadCare® instrument to determine the threshold for any factor should be carefully considered because of the analytical bias with ICP–MS.

Declaration of competing interest

The authors declare that they have no known competing financial interests or personal relationships that could have appeared to influence the work reported in this paper.

Acknowledgements

This work was supported by Grants-in-Aid for Scientific Research from the Ministry of Education, Culture, Sports, Science and Technology of Japan awarded to M. Ishizuka (No. 16H01779, 18K19847, and 18KK0287), Y. Ikenaka (No. 17K20038, 18H04132), S.M.M. Nakayama (No. 17KK0009, 20K20633), and H. Nakata (No. 19K20472) and the foundation of JSPS (Japan Society for the Promotion of Science) Bilateral Open Partnership Joint Research Projects (JPJSBP120209902). We also acknowledge financial support from The Japan Prize Foundation and The Akiyama Life Science Foundation. This research was also supported by JST (Japan Science and Technology Agency)/JICA (Japan International Cooperation Agency) SATREPS (Science and Technology Research Partnership for Sustainable Development; No. JPMJSA1501), JST aXis (Accelerating Social Implementation for SDGs Achievement No. JPMJAS2001) and Program for supporting introduction of the new sharing system (JPMXS0420100619). We are highly indebted to the communities that participated in the study. We are also grateful to the health centers in Kabwe, the Kabwe District Health Office, Kabwe Municipal Council and the Ministry of Health, Zambia, for facilitating our work. We also want to thank all the laboratory technicians and nurses at the health centers for their technical support. Our appreciation is extended to Hisao Odagiri, Michiko Nyanga and Susumu Makino for their coordination, Sayako Yamamoto for her assistance as well as Takahiro Ichise and Nagisa Hirano for their technical support.

Appendix A. Supplementary data

Supplementary data to this article can be found online at https://doi.org/10.1016/j.chemosphere.2021.129832.

Credit Author statement

Hokuto Nakata: Conceptualization, Methodology, Formal analysis, Investigation, Writing – original draft, Visualization, Shouta M.M. Nakayama: Conceptualization, Investigation, Writing – review & editing, John Yabe: Conceptualization, Investigation, Writing – review & editing, Kaampwe Muzandu: Conceptualization, Investigation, Writing – review & editing, Haruya Toyomaki: Investigation, Data curation, Writing – review & editing, Yared Beyene Yohannes: Validation, Investigation, Writing – review & editing, Andrew Kataba: Validation, Investigation, Writing – review & editing, Golden Zyambo: Investigation, Writing – review & editing, Yoshinori Ikenaka: Resources, Writing – review & editing, Kennedy Choongo: Conceptualization, Resources, Writing – review & editing, Supervision, Project administration, Mayumi Ishizuka: Conceptualization, Resources, Writing – review & editing, Supervision, Project administration, Funding acquisition.

References

Araya, M., Pizarro, F., Olivares, M., Arredondo, M., Gonzalez, M., Méndez, M., 2006. Understanding copper homeostasis in humans and copper effects on health. Biol. Res. 39 (1), 183–187. https://doi.org/10.4067/s0716-97602006000100020. PMID: 16629178.

Agency for Toxic Substances and Disease Registry (ATSDR), 2010. Case Studies in Environmental Medicine: Lead Toxicity. http://www.atsdr.cdc.gov/csem/lead/docs/lead.pdf. (Accessed 14 February 2020).

Barbosa Jr., F., Tanus-Santos, J.E., Gerlach, R.F., Parsons, P.J., 2005. A critical review of biomarkers used for monitoring human exposure to lead: advantages, limitations, and future needs. Environ. Health Perspect. 113 (12), 1669–1674. https://doi.org/10.1289/ehp.7917. PMID: 16330345.

Boesen, A.H., Thiel, A., Fuchs, B., Evans, A.L., Bertelsen, M.F., Rodushkin, I., Arnemo, J.M., 2019. Assessment of the LeadCare® plus for use on scandinavian Brown bears (Ursus arctos). Frontiers in veterinary science 6, 285. https://doi.org/10.3389/fvets.2019.00285. PMID: 31552279.

Borrill, A.J., Reily, N.E., Macpherson, J.V., 2019. Addressing the practicalities of anodic stripping voltammetry for heavy metal detection: a tutorial review. Analyst 144 (23), 6834–6849. https://doi.org/10.1039/c9an01437c. PMID: 31657380.

Bossarte, R.M., Brown, M.J., Jones, R.L., 2007. Blood lead misclassification due to defective LeadCare® blood lead testing equipment. Clin. Chem. 53 (5), 994–995. https://doi.org/10.1373/clinchem.2006.082404. PMID: 17468412.

Centers for Disease Control and Prevention (CDC), 2002. Managing elevated blood lead levels among young children: recommendations from the Advisory Committee on Childhood Lead Poisoning prevention. https://stacks.cdc.gov/view/cdc/26980. (Accessed 12 February 2020).

Centers for Disease Control and Prevention, 2012. Low Level Lead Exposure Harms Children: a Renewed Call of Primary Prevention. CDC, Atlanta, GA. https://www.cdc.gov/nceh/lead/acclpp/final_document_030712.pdf. (Accessed 12 February 2020).

Centers for Disease Control and Prevention, 2018. Emergency preparedness and response potential for falsely low blood lead test results from LeadCare analyzers. Available: https://emergency.cdc.gov/han/han00403.asp. (Accessed 14 February 2020).

Chau, Y.K., Lum-Shue-Chan, K., 1974. Determination of labile and strongly bound metals in lake water. Water Res. 8 (6), 383–388. https://doi.org/10.1016/0043-1354(74)90052-9.

Dooyema, C.A., Neri, A., Lo, Y.C., Durant, J., Dargan, P.I., Swarthout, T., Biya, O., Gidado, S.O., Haladu, S., Sani-Gwarzo, N., Nguku, P.M., Akpan, H., Idris, S., Bashir, A.M., Brown, M.J., 2011. Outbreak of fatal childhood lead poisoning related to artisanal gold mining in northwestern Nigeria, 2010. Environ. Health Perspect. 120 (4), 601–607. https://doi.org/10.1289/ehp.1103965. PMID: 22186192.

Doya, R., Nakayama, S.M., Nakata, H., Toyomaki, H., Yabe, J., Muzandu, K., Yohannes, Y.B., Kataba, A., Zyambo, G., Ogawa, T., Uchida, Y., Ikenaka, Y., Ishizuka, M., 2020. Land use in habitat affects metal concentrations in wild lizards around a former lead mining site. Environ. Sci. Technol. https://doi.org/10.1021/acs.est.0c00150. PMID: 32490671.

González, F., Camacho, M., Tiburón, N.P., Peña, M.Z., Rueda, L.R., Luzardo, O.P., 2019. Suitability of anodic stripping voltammetry for routine analysis of venous blood from raptors. Environ. Toxicol. Chem. 38 (4), 737–747. https://doi.org/10.1002/etc.4339. PMID: 30556155.

Green, D., Sullivan, M., Cooper, N., Dean, A., Marquez, C., 2017. A pilot study of children's blood lead levels in Mount Isa, Queensland. Int. J. Environ. Res. Publ. Health 14 (12), 1567. https://doi.org/10.3390/ijerph14121567. PMID: 29236077.

Johnson, L.M., Lynch, M., Johnson, C., Karger, A.B., 2019. Evaluation of LeadCare Ultra® as an initial screen for elevated blood lead levels. Clin. Biochem. 66, 95–99. https://doi.org/10.1016/j.clinbiochem.2019.02.010. PMID: 30790543.

Kazi, T.G., Afridi, H.I., Kazi, N., Jamali, M.K., Arain, M.B., Jalbani, N., Kandhro, G.A., 2008. Copper, chromium, manganese, iron, nickel, and zinc levels in biological samples of diabetes mellitus patients. Biol. Trace Elem. Res. 122 (1), 1–18. https://doi.org/10.1007/s12011-007-8062-y. PMID: 18193174.

Nakata, H., Nakayama, S.M., Yabe, J., Liazambi, A., Mizukawa, H., Darwish, W.S., Ikenaka, Y., Ishizuka, M., 2016. Reliability of stable Pb isotopes to identify Pb sources and verifying biological fractionation of Pb isotopes in goats and chickens. Environ. Pollut. 208, 395–403. https://doi.org/10.1016/j.envpol.2015.10.006. PMID: 26549754.

Nakata, H., Nakayama, S.M., Yabe, J., Muzandu, K., Toyomaki, H., Yohannes, Y.B., Kataba, A., Zyambo, G., Ikenaka, Y., Choongo, K., Ishizuka, M., 2020. Clinical biochemical parameters associated with the exposure to multiple environmental metals in residents from Kabwe, Zambia. Chemosphere 262, 127788. https://doi.org/10.1016/j.chemosphere.2020.127788.

Nakayama, S.M., Ikenaka, Y., Hamada, K., Muzandu, K., Choongo, K., Teraoka, H., Mizuno, H., Ishizuka, M., 2011. Metal and metalloid contamination in roadside soil and wild rats around a Pb–Zn mine in Kabwe, Zambia. Environ. Pollut. 159 (1), 175–181. https://doi.org/10.1016/j.envpol.2010.09.007. PMID: 20971538.

Needleman, H., 2004. Lead poisoning. Annu. Rev. Med. 55 (209e222) https://doi.org/10.1146/annurev.med.55.091902.103653. PMID: 14746518.

Neri, A.J., Roy, J., Jarrett, J., Pan, Y., Dooyema, C., Caldwell, K., Umar-Tsafe, N.T., Olubiyo, R., Brown, M.J., 2014. Analysis of a novel field dilution method for testing samples that exceed the analytic range of point-of-care blood lead analyzers. Int. J. Environ. Health Res. 24 (5), 418–428. https://doi.org/10.1080/09603123.2013.857390. PMID: 24266724,.

Pineau, A., Fauconneau, B., Rafael, M., Viallefont, A., Guillard, O., 2002. Determination of lead in whole blood: comparison of the LeadCare blood lead testing system with Zeeman longitudinal electrothermal atomic absorption spectrometry. J. Trace Elem. Med. Biol. 16 (2), 113–117. https://doi.org/10.1016/S0946-672X(02)80037-2. PMID: 12195725.

Roda, S.M., Greenland, R.D., Bornschein, R.L., Hammond, P.B., 1988. Anodic stripping voltammetry procedure modified for improved accuracy of blood lead analysis. Clin. Chem. 34 (3), 563–567. PMID: 3280164.

Safi, J.M., Yassin, M.M., El-Nahhal, Y.Z., Abed, Y.A., Safi, M.J., Suleiman, H.D., 2019.

Childhood lead poisoning in gaza strip, the Palestinian Authority. J. Trace Elem. Med. Biol. 54, 118–125. https://doi.org/10.1016/j.jtemb.2019.04.004. PMID: 31109601.

Silwamba, M., Ito, M., Hiroyoshi, N., Tabelin, C.B., Hashizume, R., Fukushima, T., Park, I., Jeon, S., Igarashi, T., Sato, T., Chirwa, M., Banda, K., Nyambe, I., Nakata, H., Nakayama, S., Ishizuka, M., 2020a. Recovery of lead and zinc from zinc plant leach residues by concurrent dissolution-cementation using zero-valent aluminum in chloride medium. Metals 10 (4), 531. https://doi.org/10.3390/met10040531.

Silwamba, M., Ito, M., Hiroyoshi, N., Tabelin, C.B., Fukushima, T., Park, I., Jeon, S., Igarashi, T., Sato, T., Nyambe, I., Chirwa, M., Banda, K., Nakata, H., Nakayama, S., Ishizuka, M., 2020b. Detoxification of lead-bearing zinc plant leach residues from Kabwe, Zambia by coupled extraction-cementation method. Journal of Environmental Chemical Engineering. https://doi.org/10.1016/j.jece.2020.104197, 104197.

Sobin, C., Parisi, N., Schaub, T., de la Riva, E., 2011. A Bland–Altman comparison of the Lead Care® System and inductively coupled plasma mass spectrometry for detecting low-level lead in child whole blood samples. J. Med. Toxicol. 7 (1), 24–32. https://doi.org/10.1007/s13181-010-0113-7. PMID: 20886381.

Taylor, L., Jones, R.L., Kwan, L., Deddens, J.A., Ashley, K., Sanderson, W.T., 2001. Evaluation of a portable blood lead analyzer with occupationally exposed populations. Am. J. Ind. Med. 40 (4), 354–362. https://doi.org/10.1002/ajim.1109. PMID: 11598984.

Toyomaki, H., Yabe, J., Nakayama, S.M., Yohannes, Y.B., Muzandu, K., Liazambi, A., Ikenaka, Y., Kuritani, T., Nakagawa, M., Ishizuka, M., 2020. Factors associated with lead (Pb) exposure on dogs around a Pb mining area, Kabwe, Zambia. Chemosphere 125884. https://doi.org/10.1016/j.chemosphere.2020.125884. PMID: 31978655.

US Food and Drug Administration, 2017. FDA warns against using magellan Diagnostics LeadCare testing systems with blood obtained from a vein: FDA safety communication. Available: https://www.fda.gov/medical-devices/safety-communications/fda-warns-against-using-magellan-diagnostics-leadcare-testing-systems-blood-obtained-vein-fda-safety. (Accessed 14 February 2020).

US Food and Drug Administration, 2018a. Magellan Diagnostics Inc. Expands recall for LeadCare testing systems due to inaccurate test results. Available: https://www.fda.gov/medical-devices/medical-device-recalls/magellan-diagnostics-inc-expands-recall-leadcare-testing-systems-due-inaccurate-test-results. (Accessed 14 February 2020).

US Food and Drug Administration, 2018b. Safety issue on magellan Diagnostics LeadCare testing systems. Available: https://www.fda.gov/medical-devices/tests-used-clinical-care/safety-issue-magellan-diagnostics-leadcare-testing-systems. (Accessed 14 February 2020).

Yabe, J., Nakayama, S.M., Ikenaka, Y., Muzandu, K., Choongo, K., Mainda, G., Kabeta, M., Ishizuka, M., Umemura, T., 2013. Metal distribution in tissues of free-range chickens near a lead–zinc mine in Kabwe, Zambia. Environ. Toxicol. Chem. 32 (1), 189–192.

Yabe, J., Nakayama, S.M., Nakata, H., Toyomaki, H., Yohannes, Y.B., Muzandu, K., Kataba, A., Zyambo, G., Hiwatari, M., Narita, D., Yamada, D., Hangoma, P., Munyinda, N.S., Mufune, T., Ikenaka, Y., Choongo, K., Ishizuka, M., 2020. Current trends of blood lead levels, distribution patterns and exposure variations among household members in Kabwe, Zambia. Chemosphere 243, 125412. https://doi.org/10.1016/j.chemosphere.2019.125412. PMID: 31995873.

Yamada, D., Hiwatari, M., Hangoma, P., Narita, D., Mphuka, C., Chitah, B., Yabe, J., Nakayama, S.M., Nakata, H., Choongo, K., Ishizuka, M., 2020. Assessing the population-wide exposure to lead pollution in Kabwe, Zambia: an econometric estimation based on survey data. Sci. Rep. 10 (1), 1–11. https://doi.org/10.1038/s41598-020-71998-5.

Zhao, G., Liu, G., 2018. A portable electrochemical system for the on-site detection of heavy metals in farmland soil based on electrochemical sensors. IEEE Sensor. J. 18 (14), 5645–5655. https://doi.org/10.1109/JSEN.2018.2845306.

Chemosphere 246 (2020) 125733

Contents lists available at ScienceDirect

Chemosphere

journal homepage: www.elsevier.com/locate/chemosphere

Cellulose-metallothionein biosorbent for removal of Pb(II) and Zn(II) from polluted water

Wilson Mwandira [a], Kazunori Nakashima [b, *], Yuki Togo [a], Tsutomu Sato [b], Satoru Kawasaki [b]

[a] Graduate School of Engineering, Hokkaido University, Kita 13, Nishi 8, Kita-Ku, Sapporo, 060-8628, Japan
[b] Faculty of Engineering, Hokkaido University, Kita 13, Nishi 8, Kita-Ku, Sapporo, 060-8628, Japan

HIGHLIGHTS

- Metallothionein/cellulose biosorbent was designed for heavy metal removal.
- The biosorbents was found to be very efficient in removal of heavy metals.
- The biosorbent showed regeneration and recyclability for seven times.
- Effective metal ion removal was achieved when applied in real mine wastewater.

GRAPHICAL ABSTRACT

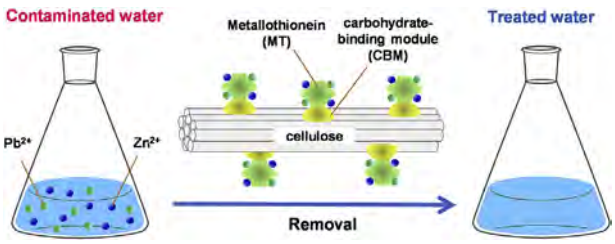

ARTICLE INFO

Article history:
Received 24 September 2019
Received in revised form
20 December 2019
Accepted 22 December 2019
Available online 26 December 2019

Handling Editor: Y Yeomin Yoon

Keywords:
Metallothionein
Cellulose
Biosorbent
Adsorption
Metal ions
Mine wastewater

ABSTRACT

Intake of toxic trace elements in drinking water can lead to adverse health effects. To remove toxic trace elements from water, we developed a novel biosorbent composed of cellulose and a fusion protein. The fusion protein was constructed from metallothionein (MT) and a carbohydrate-binding module (CBM), where CBM can bind to cellulose while MT can capture heavy metal ions in solution. In a batch experiment, the biosorbent had maximum biosorption capacities for Pb(II) and Zn(II) ions of 39.02 mg/g and 29.28 mg/g, respectively. Furthermore, the biosorbent could be used in a semi-continuous system and showed good regeneration and recyclability. Both cellulose and the MT-CBM are environmentally friendly and renewable materials, and this biosorbent has great potential for efficient removal of toxic trace elements from polluted water.

1. Introduction

Heavy metals have become a predominant contaminant of water because of constant growth in industrialization and urbanization (Chen et al., 2018). Once toxic heavy metals, such as lead (Pb) and zinc (Zn), enter the human body, they accumulate and cause various health problems. Lead has no known beneficial effects on human health, whereas Zn is essential (Zoroddu et al., 2019). However, Zn is toxic at high concentrations (Baran et al., 2018). Lead causes neurodevelopment disorders and Zn imparts an undesirable astringent taste to water, and both should be removed from drinking water (World Health Organization, 2017).

To date, toxic trace elements have been removed by

* Corresponding author.
E-mail address: nakashima@geo-er.eng.hokudai.ac.jp (K. Nakashima).

https://doi.org/10.1016/j.chemosphere.2019.125733
0045-6535/

conventional water treatment methods which include coagulation, flocculation, clarification, and filtration, and followed by disinfection (Gitis and Hankins, 2018; Singh et al., 2018). However, many of these techniques are suboptimal. Biosorption has emerged as an alternative method that is efficient, simple, and specific (Singh et al., 2018). The biosorption process involves interaction of a solid phase (biosorbent) with a liquid phase (water) containing the dissolved species to be adsorbed (metal ions). Biosorbents effectively remove heavy metals from water (Fakhre and Ibrahim, 2018). Cellulose is attractive as a biosorbent because it is stable, inert, and the most abundant polymer on Earth (Abouzeid et al., 2019). However, natural cellulose has not been used as a biosorbent because of its low metal-ion adsorption capacity (Hokkanen et al., 2016). To address this challenge, we have developed a functional cellulose modified with metallothionein (MT), which adsorbs metal ions, by using a carbohydrate-binding module (CBM) as a binder.

In this research, we constructed a biosorbent by fusion protein of MT from *Synechococcus elongatus* and CBM from *Clostridium thermocellum* (Fig. 1). MTs are a group of well-conserved proteins that act as antioxidants. They are found in all living organisms and contain a sulfhydryl group that bind to heavy metals (Chaudhary et al., 2018; Mekawy et al., 2018). However, MT would not be easy to recover after dispersion. To address this, we investigated modifying MT by fusing it with CBM. Because CBM binds to cellulose by hydrophobic interaction (Chang et al., 2018), the cellulose-MT-CBM biosorbent would be stable and easily recycled (Yunus and Tsai, 2015). Although peptide-based biosorbents have been previously suggested for water treatment (Xu et al., 2002), our biosorbent is unique in that it can be prepared in a single-step without protein purification by using cellulose-binding ability of CBM. The MT can adsorb various toxic trace elements that may be present in polluted water. We have investigated the removal of toxic metal ions, which are contained in real mine wastewater, by using a novel biosorbent.

2. Materials and methods

2.1. Plasmid construction and protein expression

The gene for MT from *S. elongatus* PCC7942 (Shi et al., 1992) was synthesized by Eurofins Genomics (Tokyo, Japan). Genomic DNA from *C. thermocellum* NBRC 103400 was obtained from NBRC (Kisarazu, Japan). The polymerase chain reaction (PCR) was performed using PrimeSTAR® HS DNA polymerase (Takara Bio Inc., Otsu, Japan) with the oligonucleotide primers (Eurofins Genomics) listed in Table S1. The gene for MT was amplified from the vector containing the synthesized MT gene using primers MT-F and MT-R.

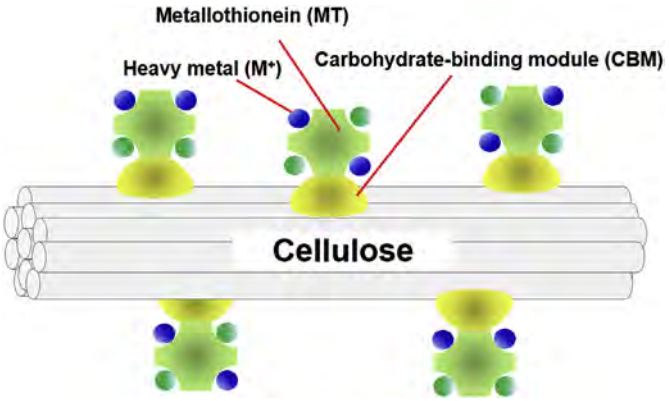

Fig. 1. Illustration of cellulose-MT-CBM.

The gene for CBM 3 (Hong et al., 2007) was cloned from genomic DNA of *C. thermocellum* using the primers CBM-F and CBM-R. The genes of MT and CBM were fused by overlap PCR using the primers OL-F, OL-R, IF-F, and IF-R. The amplified gene was inserted into pET-15b vector (Merck Biosciences GmbH, Schwalbach Ts., Germany), which was cut by *Nco* I and *Xho* I, using an In-Fusion HD Cloning Kit to obtain the pET-MT-CBM vector (Fig. S1). The nucleotide sequence of the MT-CBM fusion gene (648 bp) was verified by DNA sequencing (Eurofins Genomics).

To express the target protein, *Escherichia coli* BL21(DE3) strain (Nippon Gene Co. Ltd, Toyama, Japan) was transformed with the pET-MT-CBM vector. The transformant was grown at 37 °C in Luria-Bertani (LB) medium containing 100 μg/mL ampicillin. When the optical density of the culture medium measured at a wavelength of 600 nm (OD_{600}) reached 0.45, the expression of the protein was induced by adding isopropyl β-D-1- thiogalactopyranoside (IPTG, final concentration of 1 mM) to the medium and culturing at 15 °C for 24 h. The bacterial cells expressing the proteins were harvested by centrifugation at 8000×*g* for 10 min and lysed by ultrasonication at 30 kHz for 5 min (Vibra-Cell™ VCX 130, Sonics & Materials, Inc., Newtown, USA). After centrifugation of the cell lysate at 8000×*g* for 10 min, the supernatant was recovered and used directly in biosorption studies.

2.2. Preparation of the cellulose-MT-CBM biosorbent

Biosorption of the protein onto cellulose is illustrated in Fig. 2. To immobilize the MT-CBM fusion protein on cellulose and obtain the cellulose-MT-CBM biosorbent, Whatman filter paper No. 1 was cut into rectangular pieces (1 g) and then suspended in 5 mL of the crude protein mixture (protein concentration of 250 μg/mL) obtained in Section 2.1 for 2 h at 25 °C. The filter paper and cellulose-MT-CBM biosorbent were analyzed by using attenuated total reflectance Fourier transform infrared (ATR-FTIR) (JASCO 360 FTIR Spectrometer, JASCO, Japan). The point of zero charge (pzc) for the cellulose-MT-CBM was determined by the pH drift method (Bakatula et al., 2018).

2.3. Metal ion adsorption experiments

A metal ion stock solution was prepared using $PbCl_2$ and $ZnCl_2$ (Wako Pure Chemical Industries Ltd, Tokyo, Japan), which were dissolved in distilled water. Solutions with different final concentrations of the metal ions were obtained by dilution of the stock solution. Metal adsorption was investigated in batch experiments. The effect of pH (2.0–9.0) on the removal of Pb(II) and Zn(II) was investigated by mixing 1 g of the prepared biosorbent with 100 mL of a 20 mg/L metal solution in a 250 mL Erlenmeyer flask. Then, the flasks were placed on a shaker at 100 rpm for 1 h. The adsorbent was recovered by centrifugation at 8000×*g* for 10 min and the supernatant was filtered through a 0.45-μm filter. The metal ion concentration in the supernatant was measured by inductively coupled plasma atomic emission spectroscopy (ICP-AES) (ICPE-9820, Shimadzu Corporation, Kyoto, Japan). The effect of the contact time (0–60 min) was studied by varying this while keeping all other parameters fixed.

Biosorption was analyzed using the Langmuir isotherm model:

$$Q_{eq} = \frac{Q_{max} \cdot K \cdot C_{eq}}{1 + K \cdot C_{eq}}, \quad (1)$$

where Q_{eq} is the quantity adsorbed (mg/g), C_{eq} is the equilibrium concentration of the adsorbate (mg/L), Q_{max} is the saturation adsorption capacity (mg/g), and K is the equilibrium constant.

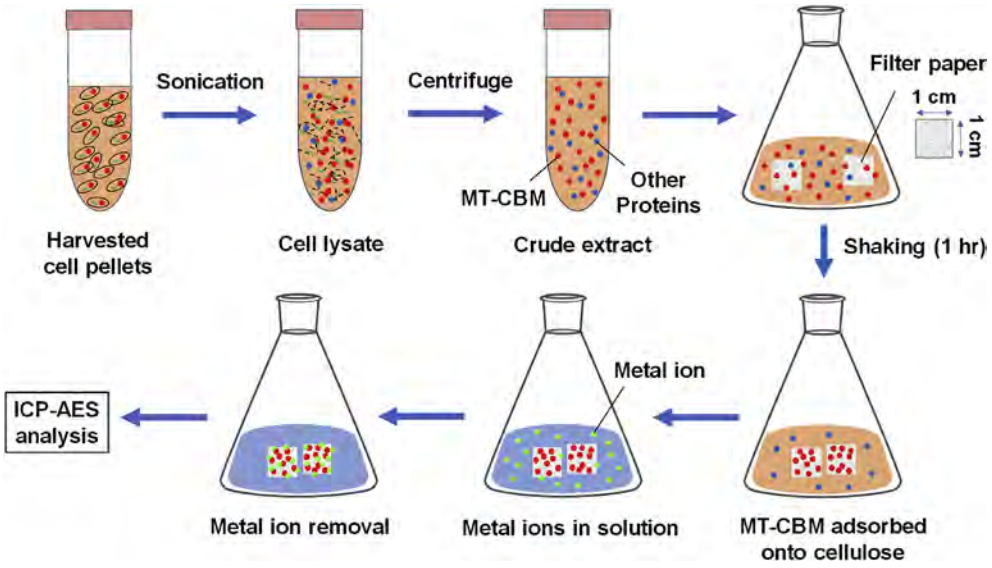

Fig. 2. The process of immobilization of the MT-CBM protein on cellulose.

2.4. Semi-continuous adsorption system and recyclability of the cellulose-MT-CBM biosorbent

The reusability of the adsorbent in a semi-continuous system was tested seven times with the experimental setup illustrated in Fig. 3. To determine the recoverability and reusability of the biosorbent, a column (syringe of mean diameter, D_{50} = 2.5 cm and height, h = 7 cm) was prepared by placing 2 g of cellulose in a 30-mL syringe. Then, 10 mL of crude extract containing overexpressed MT-CBM protein (total protein concentration: 250 μg/mL) was added to be adsorbed onto the cellulose, and the column was kept at 25 °C in an incubator for 1 h. After washing three times with deionized water, a Pb(II) or Zn(II) aqueous solution was allowed to percolate through the column. The filtrate was collected for metal analysis. A valve was used to regulate the flow rate of the filtrate from the column. To desorb the adsorbed metal ions, 10 mL of 20 mM EDTA buffer (pH 8) was added to the column. To regenerate the column, 10 mL of fresh MT-CBM protein was added. A column containing only cellulose was used for control experiments. Treatment of actual mine wastewater collected from Chingola, Copperbelt, Zambia was investigated using the column.

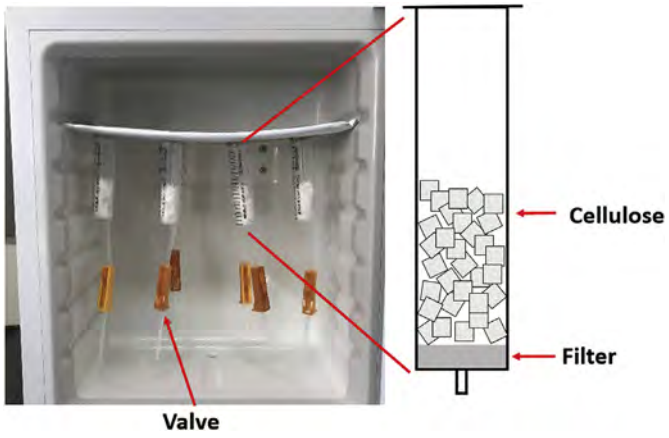

Fig. 3. Setup for the cellulose-MT-CBM biosorbent regeneration experiments.

2.5. X-ray photoelectron spectroscopy analysis

X-ray photoelectron spectroscopy (XPS) measurements were performed by using a JPS-9200 spectrometer (JEOL Ltd, Tokyo, Japan) to explore the electronic states of Pb and Zn on the biosorbent using monochromatic Mg Kα radiation. To compensate for surface charge effects, the binding energies were calibrated using C 1s at 284.80 eV.

3. Results and discussion

3.1. Verification of plasmid construction, protein expression, and protein binding ability to cellulose

Fig. 4 shows the results of SDS-PAGE analysis for the protein expressed in *E. coli* BL21(DE3) and biosorption of the protein to cellulose. Fig. 4(a) shows the supernatant of the cell lysate of *E. coli* expressing MT-CBM. We found that the MT-CBM was successfully expressed in a soluble form with a molecular weight of 23.1 kDa. To

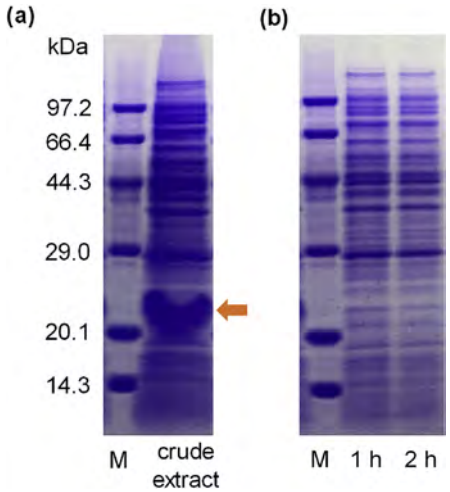

Fig. 4. SDS-PAGE of (a) crude extract after expression of MT-CBM and (b) after addition of filter paper to crude extract (1 h and 2 h). M: protein marker.

verify the binding ability of the MT-CBM on cellulose, filter papers were added to the cell lysate. After 1 h, the band for MT-CBM disappeared, indicating that the MT-CBM in the cell lysate was adsorbed on cellulose (Fig. 4(b)). This result showed that MT-CBM could be purified using cellulose in a single step. This result is consistent with previous studies where CBM was observed to bind to cellulosic material (Hong et al., 2007). We then used the cellulose-based biosorbent (cellulose-MT-CBM) for further studies. The FTIR spectra are obtained for pure cellulose and cellulose-MT-CBM (Fig. S2). The results showed that the pure cellulose had no distinguishable functional groups compared with the cellulose-MT-CBM, where broad and strong bands at 3251 cm^{-1} (amine (-NH)), 1625 cm^{-1} (amide group (C=O), and 1302 cm^{-1} (C—O stretching) confirmed the presence of bound protein on the cellulose.

3.2. Metal ion adsorption experiments

3.2.1. The effect of contact time

Contact time is an important factor affecting the efficiency of biosorption because it provides valuable information on how fast the removal process occurs. Time course of metal ion adsorption is shown in Fig. S3. Equilibrium of the biosorption of Pb(II) and Zn(II) on the cellulose-MT-CBM reached equilibrium within 10 min. This rapid metal sorption is highly desirable for biosorbents for practical applications.

3.2.2. Effect of pH on metal ion adsorption

The effect of the initial pH of the solution on metal ion adsorption on cellulose-MT-CBM and untreated cellulose (control) is shown in Fig. 5(a). The influence of pH on the biosorption of Pb(II) and Zn(II) indicated that the biosorption increased with pH. From pH 2.0 to 7.0, the percentage of Pb(II) removed increased from 0.8% to 94%, and that of Zn(II) increased from 52% to 60%. The slightly lower biosorption yield observed for Zn(II) could be attributed to the possible inert nature of one of the MT binding sites to Zn as reported previously (Harrison et al., 2002).

At lower pH values, the binding sites are protonated and the metal ions are in solution because they cannot access the binding sites on the cellulose-MT-CBM. At higher pH values, the binding sites are deprotonated, negatively charged, and more favorable for adsorption. The control had negligible biosorption capacity at all pH values because of a lack of binding ability. The percentages of Pb(II) and Zn(II) removed increased significantly at pH 6.5. This higher adsorption could be related to the pzc of the cellulose-MT-CBM (Fig. 5(b)). At pH > pzc, the biosorption of Pb(II) and Zn(II) to the biosorbent is favorable because of the presence of negatively charged functional groups of the protein (Bakatula et al., 2018). Therefore, negatively charged functional groups at pH 6.5 would be able to attract and sequester positively charged metal ions.

3.2.3. Biosorption capacity

The adsorption isotherm was studied to understand the equilibrium distribution of Pb(II) and Zn(II) between the aqueous phase and surface of the biosorbent. The Langmuir isotherm model was suitable for the experimental data as shown by a good fit with model data (Fig. S4). This indicates that the biosorption of Pb(II) and Zn(II) onto the cellulose-MT-CBM takes place via a monolayer mechanism. The maximum biosorption capacities for Pb(II) and Zn(II) were higher than those obtained with other cellulose-based biosorbents. For Pb (II), Dhir and Kumar (2010) found a Q_{max} value of 41.84 mg/g for wheat straw compared with 39.02 mg/g for the cellulose-MT-CBM in the present study. For Zn (II), Tian et al. (2017) found a Q_{max} value of 5.38 mg/g on a cellulose nanofibril aerogel compared with 29.28 mg/g on the cellulose-MT-CBM in the present study. These results indicate that the cellulose-MT-CBM biosorbent can be used for the removal of heavy metals from water.

3.3. Recyclability of the cellulose-MT-CBM biosorbent

Recyclability of the cellulose-MT-CBM biosorbent was examined because waste has a huge negative impact on the natural environment. The results for the biosorbent recyclability experiments are shown in Fig. 6. The cellulose-MT-CBM was regenerated seven times and the bound metal ion was desorbed by 20 mM EDTA. In cycle 4, the adsorption ability slightly decreased. The adsorption ability could be restored by addition of MT-CBM to the cellulose, which resulted in an increase in the metal biosorption. These results show that the biosorbent could be used for multiple metal sorption/desorption cycles without any significant loss in its efficiency.

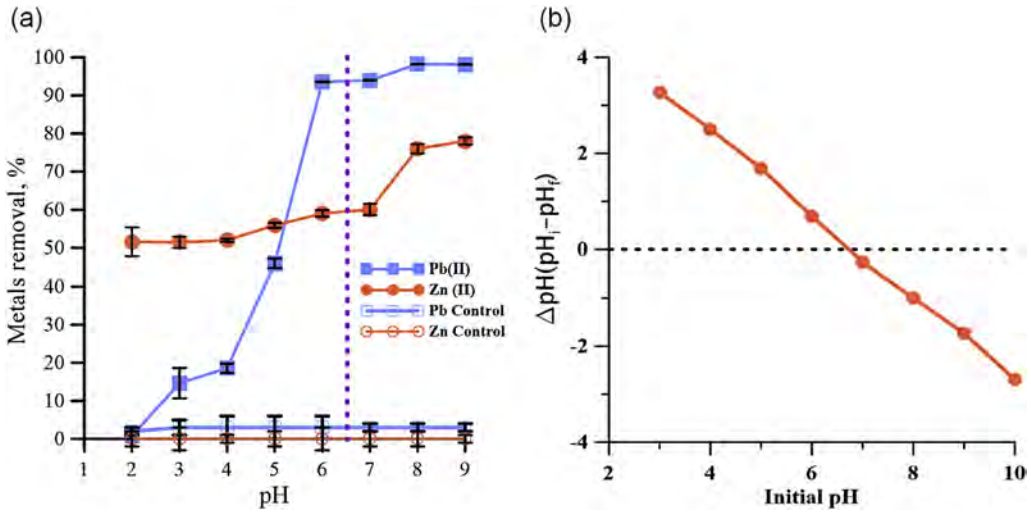

Fig. 5. (a) Effect of pH on the adsorption of Pb(II) and Zn(II) on cellulose-MT-CBM (biomass dosage: 10 g/L, initial metal ion concentration: 20 mg/L, temperature: room temperature; the purple dotted line indicates the pzc of the biosorbent) and (b) pzc of the cellulose-MT-CBM biosorbent. (For interpretation of the references to colour in this figure legend, the reader is referred to the Web version of this article.)

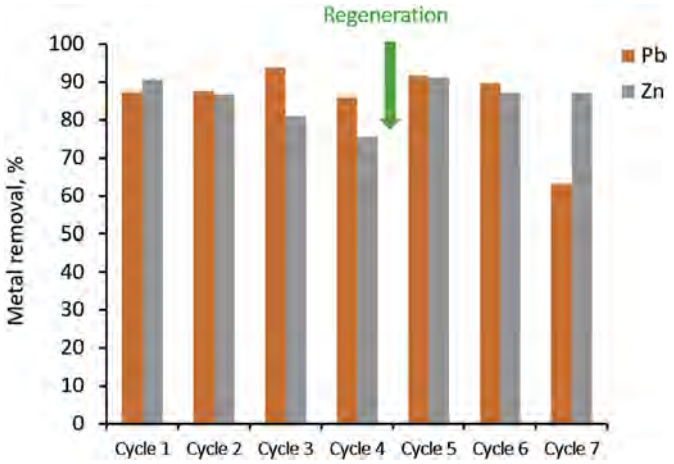

Fig. 6. Pb(II) and Zn(II) removal efficiencies of the cellulose-MT-CBM biosorbent for different cycles (initial metal ion concentration: 20 mg/L, pH: 6.5, temperature: room temperature).

3.4. XPS analysis

XPS measurements of cellulose-MT-CBM after metal adsorption were performed to confirm the electronic state(s) of Pb(II) and Zn(II) on the biosorbent. XPS wide scan spectra of cellulose-MT-CBM before and after Pb(II) and Zn(II) adsorption depicted core levels of C 1s, O 1s, N 1s, Pb 4d, and Zn 2p (Fig. 7). Two new peaks at 141 and 136 eV appeared after Pb (II) adsorption, which were attributed to the Pb 4f orbital (Qiao et al., 2019). One new peak at 1022 eV was attributed to the Zn 2p orbital (Zhou et al., 2016). These results indicate that Pb(II) and Zn(II) are adsorbed on the biosorbent. The source of N 1s is the MT-CBM protein bound on the cellulose.

Metal adsorption by cellulose-MT-CBM could be attributed to the formation of N: Pb^{2+} and N: Zn^{2+} complexes, in which a lone pair of electrons from the N atom in $-NH_2$ group is donated to a shared bond between the nitrogen atom and Pb^{2+} or Zn^{2+}. Additionally, the oxygen atom could be responsible for heavy metal removal via ionic interactions with Pb^{2+} and Zn^{2+}. The O 1s peak at 532.29 eV was modeled after curve fitting and attributed to the oxygen-rich functional groups such as −COOH group, which interact with heavy metals to form O: Pb^{2+} or O: Zn^{2+}. The XPS results confirm the FTIR data that identified organic functional groups such as $-NH_2$ and −COOH groups on the biosorbent (Fig. S2). Furthermore, the removal of heavy metals by the cellulose-MT-CBM occurs via heavy metal complexation with the thiol group of cysteine-rich MTs (Diep et al., 2018) and ion exchange with the O atom in the biosorbent as previously reported (Jana et al., 2016).

3.5. Treatment of actual mine wastewater by the cellulose-MT-CBM biosorbent

To demonstrate industrial application of the cellulose-MT-CBM, the biosorbent was used to treat contaminated surface water from an industrial source. The Mushishima stream in Chingola, Zambia, which flows into the Kafue River, is affected by effluent from the active Nchanga Mine (Sracek et al., 2012). It is essential to evaluate the performance of the biosorbent in a multi-metal system that reflects real effluent as opposed to simulated metal ion solutions. Table 1 shows the water quality data obtained before and after treatment with the cellulose-MT-CBM using the setup illustrated in

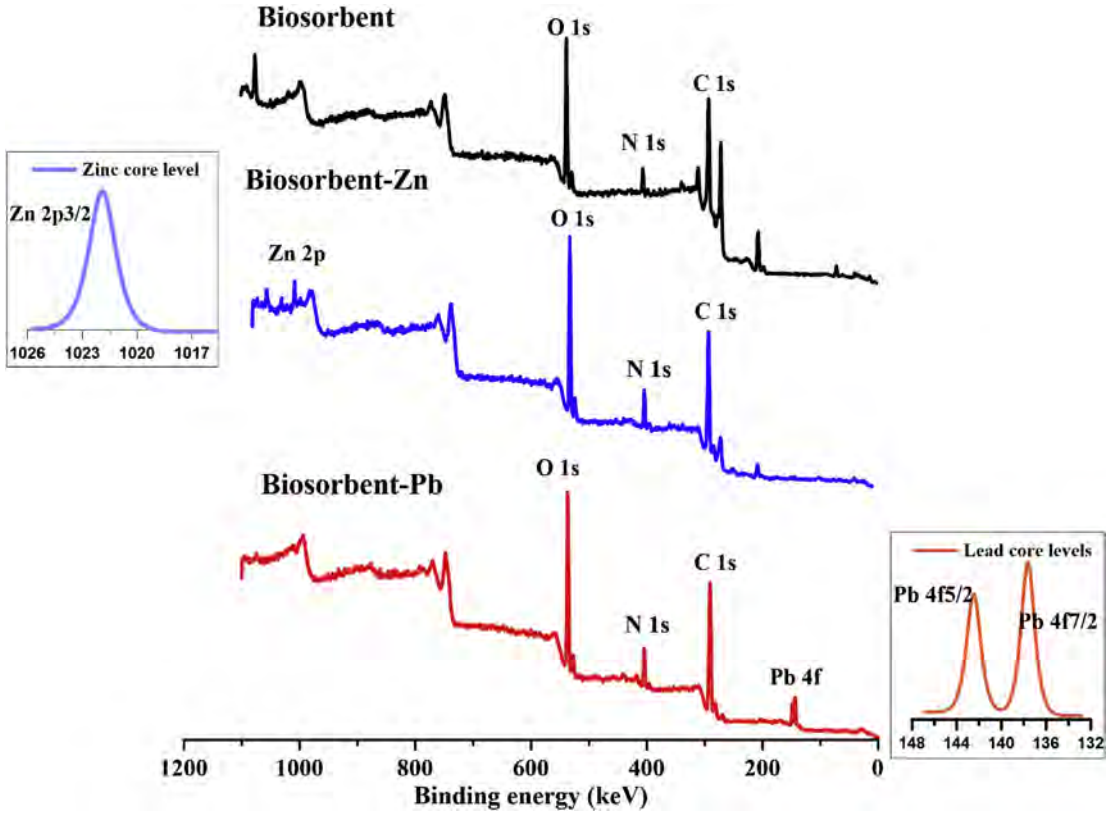

Fig. 7. Typical XPS wide scan spectra of the cellulose-MT-CBM before and after Pb(II) and Zn(II) adsorption.

Table 1
Concentrations of metal ions in mine wastewater before and after treatment with the cellulose-MT-CBM biosorbent.

Toxic trace elements of concern	Before (mg/L)	After (mg/L)	WHO acceptable Limit (mg/L)
Pb	0.19	<0.001	0.01
Cu	14.56	<0.001	2.00
Ni	7.74	<0.001	0.07
Cd	0.34	<0.001	0.10

Fig. 3. Treated water from the site showed complete removal of toxic elements with below the detection limit of ICP-AES. These results show that the cellulose-MT-CBM is effective and be applied in the mining industry as a clean-up technique.

4. Conclusion

In this study we developed a novel biosorbent composed of cellulose and a fusion protein. The fusion protein was constructed from metallothionein (MT) and a carbohydrate-binding module (CBM), where CBM binds to cellulose and MT captures heavy metal ions in solution. The biosorbent had maximum biosorption capacities of 39.02 mg/g for Pb(II) and 29.28 mg/g for Zn(II) ions. The resulted cellulose-MT-CBM biosorbent showed regeneration and reusability after repeated using seven times in a semi-continuous system. The biosorbent was applied to purify multiparameter contaminated real mining wastewater and showed complete removal of Pb(II), Cu(II), Ni(II), and Cd(II) to below detection limit. Because of these capabilities, this biosorbent has great potential for efficient removal of toxic trace elements from polluted water.

Declaration of competing interest

None.

CRediT authorship contribution statement

Wilson Mwandira: Conceptualization, Investigation, Methodology, Writing - original draft. **Kazunori Nakashima:** Conceptualization, Funding acquisition, Investigation, Methodology, Project administration, Writing - review & editing. **Yuki Togo:** Methodology, Writing - review & editing. **Tsutomu Sato:** Investigation, Writing - review & editing. **Satoru Kawasaki:** Funding acquisition, Supervision, Writing - review & editing.

Acknowledgments

This work was partly supported by Japan Society for the Promotion of Science (JSPS) KAKENHI (grant number JP18H03395) and Japan Science and Technology Agency (JST), Japan International Cooperation Agency (JICA), and Science and Technology Research Partnership for Sustainable Development (SATREPS). We thank the Laboratory of XPS analysis, Joint-use facilities, Hokkaido University, supported by the Material Analysis and Structure Analysis Open Unit (MASAOU) for XPS analysis.

Appendix A. Supplementary data

Supplementary data to this article can be found online at https://doi.org/10.1016/j.chemosphere.2019.125733.

References

Abouzeid, R.E., Khiari, R., El-Wakil, N., Dufresne, A., 2019. Current state and new trends in the use of cellulose nanomaterials for wastewater treatment. Biomacromolecules 20, 573–597. https://doi.org/10.1021/acs.biomac.8b00839.
Bakatula, E.N., Richard, D., Neculita, C.M., Zagury, G.J., 2018. Determination of point of zero charge of natural organic materials. Environ. Sci. Pollut. Res. 25, 7823–7833. https://doi.org/10.1007/s11356-017-1115-7.
Baran, A., Wieczorek, J., Mazurek, R., Urban, K., Klimkowicz-pawlas, A., 2018. Potential Ecological Risk Assessment and Predicting Zinc Accumulation in Soils, pp. 435–450. https://doi.org/10.1007/s10653-017-9924-7.
Chang, F., Xue, S., Xie, X., Fang, W., Fang, Z., Xiao, Y., 2018. Carbohydrate-binding module assisted purification and immobilization of β-glucosidase onto cellulose and application in hydrolysis of soybean isoflavone glycosides. J. Biosci. Bioeng. 125, 185–191. https://doi.org/10.1016/J.JBIOSC.2017.09.001.
Chaudhary, K., Agarwal, S., Khan, S., 2018. Role of phytochelatins (PCs), metallothioneins (MTs), and heavy metal ATPase (HMA) genes in heavy metal tolerance. In: Mycoremediation and Environmental Sustainability. Springer, Cham, pp. 39–60. https://doi.org/10.1007/978-3-319-77386-5_2.
Chen, L., Zhou, S., Shi, Y., Wang, C., Li, B., Li, Y., Wu, S., 2018. Heavy metals in food crops , soil , and water in the Lihe River Watershed of the Taihu Region and their potential health risks when ingested. Sci. Total Environ. 615, 141–149. https://doi.org/10.1016/j.scitotenv.2017.09.230.
Dhir, B., Kumar, R., 2010. Adsorption of heavy metals by salvinia biomass and agricultural residues. Int. J. Environ. Res. 4, 427–432.
Diep, P., Mahadevan, R., Yakunin, A.F., 2018. Heavy metal removal by bioaccumulation using genetically engineered microorganisms. Front. Bioeng. Biotechnol. 6, 157. https://doi.org/10.3389/fbioe.2018.00157.
Fakhre, N.A., Ibrahim, B.M., 2018. The use of new chemically modified cellulose for heavy metal ion adsorption. J. Hazard Mater. 343, 324–331. https://doi.org/10.1016/j.jhazmat.2017.08.043.
Gitis, V., Hankins, N., 2018. Water treatment chemicals. Trends and challenges 25, 34–38. https://doi.org/10.1016/j.jwpe.2018.06.003.
Harrison, M.D., Sadler, P.J., Robinson, A.K., Robinson, N.J., Parkinson, J.A., Cavet, J.S., Blindauer, C.A., 2002. A metallothionein containing a zinc finger within a four-metal cluster protects a bacterium from zinc toxicity. Proc. Natl. Acad. Sci. 98, 9593–9598. https://doi.org/10.1073/pnas.171120098.
Hokkanen, S., Bhatnagar, A., Sillanpää, M., 2016. A review on modification methods to cellulose-based adsorbents to improve adsorption capacity. Water Res. 91, 156–173. https://doi.org/10.1016/j.watres.2016.01.008.
Hong, J., Ye, X., Zhang, Y.H.P., 2007. Quantitative determination of cellulose accessibility to cellulase based on adsorption of a nonhydrolytic fusion protein containing CBM and GFP with its applications. Langmuir 23, 12535–12540. https://doi.org/10.1021/la7025686.
Jana, A., Bhattacharya, P., Sarkar, S., Majumdar, S., Ghosh, S., 2016. An ecofriendly approach towards remediation of high lead containing toxic industrial effluent by a combined biosorption and microfiltration process: a total reuse prospect. Desalin. Water Treat. 57, 5498–5513. https://doi.org/10.1080/19443994.2015.1004596.
Mekawy, A.M.M., Assaha, D.V.M., Munehiro, R., Kohnishi, E., Nagaoka, T., Ueda, A., Saneoka, H., 2018. Characterization of type 3 metallothionein-like gene (OsMT-3a) from rice, revealed its ability to confer tolerance to salinity and heavy metal stresses. Environ. Exp. Bot. 147, 157–166. https://doi.org/10.1016/j.envexpbot.2017.12.002.
Qiao, W., Zhang, Y., Xia, H., Luo, Y., Liu, S., Wang, S., Wang, W., 2019. Bioimmobilization of lead by Bacillus subtilis X3 biomass isolated from lead mine soil under promotion of multiple adsorption mechanisms. R. Soc. Open Sci. 6 https://doi.org/10.1098/rsos.181701.
Shi, J., Lindsay, W.P., Huckle, J.W., Morby, A.P., Robinson, N.J., 1992. Cyanobacterial metallothionein gene expressed in Escherichia coli Metal-binding properties of the expressed protein. FEBS Lett. 303, 159–163. https://doi.org/10.1016/0014-5793(92)80509-F.
Singh, N.B., Nagpal, G., Agrawal, S., Rachna, 2018. Water purification by using adsorbents: a review. Environ. Technol. Innov. 11, 187–240. https://doi.org/10.1016/j.eti.2018.05.006.
Sracek, O., Kříbek, B., Mihaljevič, M., Majer, V., Veselovský, F., Vencelides, Z., Nyambe, I., 2012. Mining-related contamination of surface water and sediments of the Kafue River drainage system in the Copperbelt district, Zambia: an example of a high neutralization capacity system. J. Geochem. Explor. 112, 174–188. https://doi.org/10.1016/j.gexplo.2011.08.007.
Tian, C., Qing, Y., Luo, S., Wu, Q., She, J., Wu, Y., 2017. Reusable and cross-linked cellulose nanofibrils aerogel for the removal of heavy metal ions. Polym. Compos. 39, 4442–4451. https://doi.org/10.1002/pc.24536.
World Health Organization, 2017. Guidelines for Drinking-Water Quality. https://doi.org/10.1016/S1462-0758(00)00006-6.
Xu, Z., Bae, W., Mulchandani, A., Mehra, R.K., Chen, W., 2002. Heavy metal removal by novel CBD-EC20 sorbents immobilized on cellulose. Biomacromolecules 3, 462–465. https://doi.org/10.1021/bm015631f.
Yunus, I.S., Tsai, S.-L., 2015. Designed biomolecule–cellulose complexes for

palladium recovery and detoxification. RSC Adv. 5, 20276–20282. https://doi.org/10.1039/C4RA16200E.
Zhou, Y., Zhang, Z., Zhang, J., Xia, S., 2016. New insight into adsorption characteristics and mechanisms of the biosorbent from waste activated sludge for heavy metals. J. Environ. Sci. (China) 45, 248–256. https://doi.org/10.1016/j.jes.2016.03.007.
Zoroddu, M.A., Aaseth, J., Crisponi, G., Peana, M., Nurchi, V.M., 2019. The essential metals for humans: a brief overview Maria. J. Inorg. Biochem. #pagerange#. https://doi.org/10.1016/j.jinorgbio.2019.03.013.

Chemosphere 279 (2021) 130490

Contents lists available at ScienceDirect

Chemosphere

journal homepage: www.elsevier.com/locate/chemosphere

The impact of elevated blood lead levels in children on maternal health-related quality of life

Hokuto Nakata [a], Harukazu Tohyama [b, *], Wakako Fujita [b, c], Shouta M.M. Nakayama [a], Mayumi Ishizuka [a], John Yabe [d], Nosiku S. Munyinda [e], Doreen Sakala [f], Kennedy Choongo [d, g], Shojiro Yamasaki [b], Natsumi Nagai [b], Takahiko Yoshida [h], Takeshi Saito [b]

[a] Laboratory of Toxicology, Department of Environmental Veterinary Sciences, Faculty of Veterinary Medicine, Hokkaido University, Japan
[b] Faculty of Health Sciences, Hokkaido University, Japan
[c] Institute of Biomedical Sciences, Nagasaki University, Japan
[d] The University of Zambia, School of Veterinary Medicine, Zambia
[e] The University of Zambia, School of Public Health, Zambia
[f] Ministry of Health, Zambia
[g] Fiji National University, College of Agriculture, Fisheries & Forestry, School of Animal and Veterinary Sciences, Koronivia Campus, Suva, Fiji
[h] Department of Social Medicine, Asahikawa Medical University, Japan

HIGHLIGHTS

- Impact assessment of childhood lead poisoning to maternal health-related QoL.
- Significant positive correlation between lead levels of mothers and children.
- Negative associaton of children's lead level with mothers' vitality and mental health scores.
- Negative association of mothers' lead level and social role functioning score.
- Contribution of socio-economic factors to mothers' QoL scores.

ARTICLE INFO

Article history:
Received 14 February 2021
Received in revised form
28 March 2021
Accepted 2 April 2021
Available online 15 April 2021

Handling Editor: A. Gies

Keywords:
Lead poisoning
Short-form 36
Health-related quality of life
Mother
Stepwise
Multiple linear regression analysis

ABSTRACT

Kabwe is a mining town in Zambia that has been ranked among "the ten most polluted places in the world" with previous findings of serious lead (Pb) pollution. In this study, we aim to examine the impact of childhood Pb poisoning on the health-related quality of life (HRQoL) of mothers in Kabwe. The HRQoL was assessed using the Short-Form 36 survey for 404 mothers coming from residences in 40 randomly selected standard enumeration areas (SEAs). Blood lead levels (BLLs) of the household members including the mothers themselves were measured. We found a significant positive correlation between the BLLs of the mothers and their children ($R = 0.6385$, $p < 0.0001$), while the BLLs of preschool-aged and school-aged children were significantly higher than those of their mothers and fathers. Using the data sets containing the BLLs of the household members, the age of the mothers, the household income, and the household SEA, we performed stepwise multiple linear regression analyses. The results showed significant negative associations between the representative BLL of household children and the BLL of preschool-aged children with the vitality and mental health scores of their mothers. Additionally, the BLL of school-aged children was only significantly associated with the mental health score of their mothers. By contrast, there was a significant negative association between the BLLs of the mothers with the social role functioning score. This suggests that elevated BLLs in children have a negative impact on the mental health conditions of their mothers regardless of the mothers' BLL.

* Corresponding author. Faculty of Health Sciences, Hokkaido University, Kita 12 Nishi 5, Kita-ku, Sapporo, 060-0812, Japan.
E-mail address: tohyama@med.hokudai.ac.jp (H. Tohyama).

https://doi.org/10.1016/j.chemosphere.2021.130490

1. Introduction

Lead (Pb) poisoning is one of the most common and preventable pediatric health problems of environmental origin (World Health Organization, 2010). Infants and children are at a higher risk for Pb exposure than are adults since they are smaller in size, ingest a proportionately larger dose of toxins, spend more time in proximity to ground dirt and indoor dust, display oral exploratory and pica (hand-to-mouth) behaviors, and ingest a proportionately larger daily intake of water and milk (Abelsohn and Sanborn 2010; Hauptman et al., 2017). In addition, the Centers for Disease Control and Prevention (CDC) has reported that children absorb a greater percentage of Pb from the gastrointestinal tract than do adults (Centers for Disease Control (CDC), 1985). Fasting, iron deficiency, and calcium deficiency may further increase the gastrointestinal absorption of lead (Centers for Disease Control (CDC), 1985). Exposure to Pb affects multiple organ systems, resulting in numerous morphological, biochemical, and physiological changes (Dapul and Laraque 2014). Fatigue, problems with sleep, headaches, stupor, and anemia have been associated with chronic Pb poisoning (Kim et al., 2015; Yassin and Lubbad 2013).

Kabwe, the fourth largest town in Zambia, has a history of Pb–zinc (Zn) mining, which occurred between 1902 and 1994. Despite the closure of the mine, people in Kabwe continue to scavenge for metal scraps in abandoned tailings and waste sites (Blacksmith Institute, 2013). These operations serves as a continued source of metal pollution. Soils in townships near the mine and homes downwind from the tailings were highly polluted with Pb (Nakayama et al., 2011). Lead toxicity in the children of Kabwe is widespread, especially in townships near the mine (Yabe et al., 2020). In a recent study, we revealed a statistically significant association between blood lead levels (BLLs) and plasma biochemical parameters relating to hepatic and renal functions (Nakata et al., 2021). However, clinical signs and symptoms of Pb poisoning are nonspecific, though symptoms usually begin with loss of appetite and abdominal pain (Yassin and Lubbad 2013). It is therefore difficult to evaluate the whole impact of elevated BLLs only from clinical tests.

As mothers are strongly affected by their children's health, functioning, and social environment (World Health Organization, 2007), it is important that the health of the mothers be considered in the comprehensive context of the family system. Health-related quality of life (HRQoL) consists of multiple dimensions of health status and well-being (Ware Jr. and Sherbourne 1992); it encompasses both physical and mental health and refers to the impacts of health, illness, and the treatment of illness on quality of life (Ferrans et al., 2005). Because it represents specific health aspects of well-being, HRQoL has been used to assess how an individual's well-being may be influenced by a disease, disability, or disorder (Bullinger 2003).

Previous studies have shown that the HRQoL of mothers reflects the physical and psychological conditions in their children (Edelstein et al., 2019; Rousseau et al., 2019). However, little is known about the impact of childhood Pb poisoning on the HRQoL scores of mothers. Therefore, we hypothesized that Pb poisoning in children in Kabwe can deteriorate the HRQoL of their mothers. The present study is a cross-sectional analysis with the aim of evaluating the impact of childhood Pb poisoning on the HRQoL of mothers in Kabwe. We expected to find a negative correlation between higher BLLs in children in Kabwe and their mothers' lower HRQoL scores. Secondly, we aimed to explore a possible association between the HRQoL of the mothers and their age and household income.

2. Materials and methods

2.1. Subjects

The study was approved by the University of Zambia Research Ethics Committee (UNZAREC; REF. No. 012-04-16). The Ministry of Health through the Zambia National Health Research Ethics Board and the Kabwe District Medical Office also granted approval for this work. In this study, the HRQoL data were obtained through interviews with the mothers. We collected blood samples from family members, including children, mothers, and fathers, at 13 health centers around the town of Kabwe in July and August of 2017. The study targeted households from specific areas based on the sample design presented in a parallel socioeconomic survey called the Kabwe Household Socioeconomic Survey (KHSS) 2017 (Yamada et al., 2020). Following the sampling frame of the Central Statistical Office (CSO) in Zambia, we divided Kabwe into 384 Standard Enumeration Areas (SEAs). In the first stage, 40 SEAs were randomly selected. In the second stage, we randomly selected 25 households from each SEA. Up to four household members (two children, the mother, and the father) were invited to local health centers for blood sampling and the HRQoL survey. Thirteen health centers that served the 40 SEAs were included. These included Kasanda (SEA 16, 30–34), Chowa (SEA 22, 27), Makululu (SEA 6–15, 21), Katondo (SEA 26, 28, 29, 35), Railway (SEA 24, 25), Pollen (SEA 37), Mahatma Ghandi (SEA 36), Bwacha (1, 4, 5), Ngungu (SEA 2, 3), Natuseko (SEA 38–40), Mpima Prison (SEA 23), Kang'omba (SEA 17, 18), and Hamududu (SEA 19, 20). The distance between the mine and each health center ranged from approximately 1.5 to 30 km (Fig. 1). Some of the participants in this study came to the health centers voluntarily to join the study as a part of the targeted SEAs and were not a part of the KHSS 2017 study. However, the blood collection and questionnaire were administered according to the same protocol.

2.2. The HRQoL questionnaire survey

The Medical Outcome Study (MOS) Short-Form 36-Item Health Survey (SF-36) questionnaire survey was given simultaneously at 13 health centers using Computer-Assisted Personal Interviewing (CAPI) through the Survey Solutions application (version 5.22.20, the latest version at the time of the survey), developed by the World Bank. Although the questionnaire was prepared in English, the interviews were also conducted in local languages, such as Bemba, Nyanja and Tonga. The SF-36 is a standardized, multipurpose, multi-item scale used to assess the health of the general population or individual patients across eight health categories. These categories include vitality, physical functioning, bodily pain, general health perceptions, role limitation due to physical health problems (physical role functioning), role limitation due to personal or emotional problems (emotional role functioning), social role functioning, and general mental health (Ware and Sherbourne, 1992). These eight subscales each consisted of 2–10 items, and they were scored using a 0–100 scale according to the RAND 36-Item Health Survey version 1.0 scoring procedure. A high value for any of these eight subscales indicates that the participant has a favorable or good self-perceived health status, while lower scores indicate poorer health status.

2.3. Blood collection and Pb concentration analysis

After obtaining informed and written consent, laboratory technicians or nurses collected blood samples and administered the

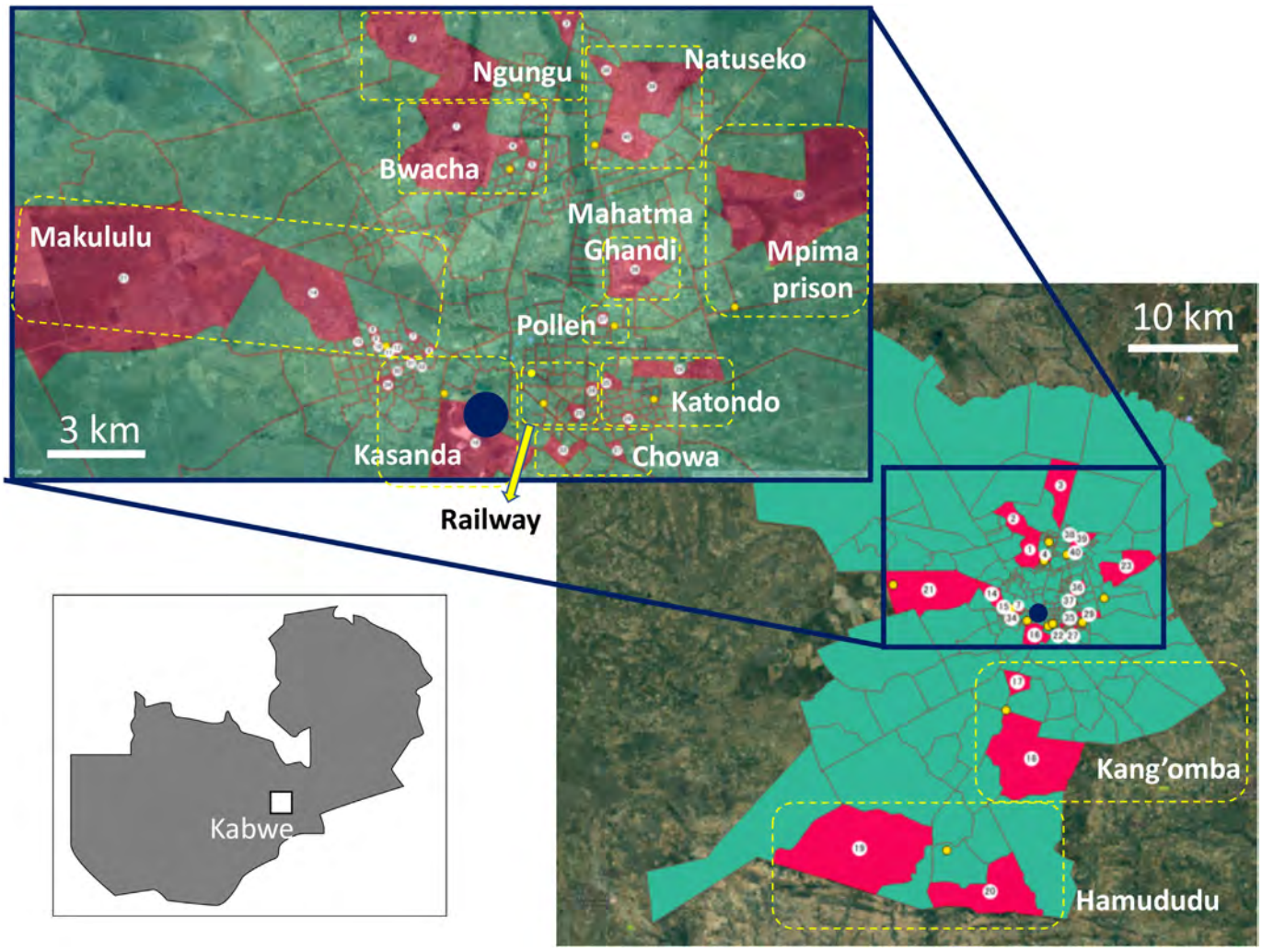

Fig. 1. Map of Kabwe showing 13 selected areas (clinics indicated by yellow circles) and 40 SEAs (shown in red, with numbers 1–40 written in white circles). (For interpretation of the references to colour in this figure legend, the reader is referred to the Web version of this article.)

questionnaires mentioned above. The blood collection method and procedure were conducted according to a previously described method (Nakata et al., 2021). Blood sample digestion and Pb concentration analysis using the ICP-MS (7700 series, Agilent technologies, Tokyo, Japan) were performed according to a protocol described by Nakata et al. (2021). Analytical quality control was performed using the certified reference material, Seronorm™ Trace Elements Whole Blood L-2 (Sero, Billingstad, Norway). Details of sample treatment and analytical quality control are shown in Supplementary Material.

2.4. Household income data

In this study, we also used the data of monthly household income from the KHSS 2017 study (Yamada et al., 2020). The KHSS 2017 conducted interview-based surveys with 895 households (4900 individuals), including 385 households that were invited to participate in the BLL and HRQoL surveys. We conducted the fieldwork for KHSS 2017 over three weeks from late August to early September 2017, using CAPI and the same application as in the HRQoL investigation. Interviews were conducted mostly at the houses of the sampled households. The survey included questions about monthly wage income and income from non-agricultural business during the month preceding the survey. Income from sources other than monthly wage and non-agricultural business was included in the survey as yearly earnings, but the amount was rescaled to a monthly equivalent. All the monetary terms were expressed in Kwacha (abbreviated as K), the national currency of Zambia.

2.5. Data analysis

Descriptive univariate analyses are presented as frequencies and percentages for categorical variables and as means and standard deviations (SD) for continuous variables. First, we compared the BLLs of different family members (infants [<12 months old], preschool-aged children [1–5 years old], school-aged children [6–12 years old], adolescents [>13 years old], mothers, and fathers) using one-way ANOVA with Bonferroni's post-hoc multiple comparison test. Second, we performed a linear regression analysis to examine the associations between the BLLs of the children and fathers in each household and those of the mother. If we collected blood samples from two children in the same household, we averaged this data and used the representative BLL as the value for the household children. Third, we determined the effects of the SEA on the mothers' BLL, HRQoL score, and household income using

one-way ANOVA. Finally, we conducted stepwise multiple linear regression analyses that incorporated dummy independent variables for the SEAs to control for the confounding effects of covariates using the following five sets of household data: 1) the households with complete data for monthly household income, the age of the mothers, and the BLLs of the mothers; 2) the households with complete data for monthly household income, the age of the mothers, and the BLLs of the mothers and their children; 3) the households with complete data for monthly household income, the age of the mothers, and the BLLs of mothers as well as their preschool-aged children; 4) the households with complete data for monthly household income, the age of the mothers, and the BLLs of mothers as well as their school-aged children; and 5) the households with complete data for monthly household income, the age of the mothers, and the BLLs of both the mothers and fathers. The data analysis was performed using IBM SPSS Statistics version 26.0 (IBM Corporation, Armonk, NY, USA), and $p < 0.05$ was considered to be statistically significant. We also investigated floor and/or ceiling effects for each HRQoL score reported by the mothers according to the methods presented by Terwee et al. (2007). According to this method, floor or ceiling effects were considered to be present if more than 15% of respondents achieved the lowest or highest possible score, respectively.

3. Results

3.1. BLLs of children, mothers, and fathers

We collected blood samples of family members from 404 households in 13 health clinics. The data included SF-36 scores for all mothers, and we collected blood samples from 404 mothers, 13 infants, 219 preschool-aged children, 208 school-aged children, 6 adolescents and 125 fathers. The average BLLs for mothers, infants, preschool-aged children, school-aged children, adolescents, and fathers were 10.6, 15.4, 23.6, 19.7, 24.5, and 11.6 μg/dL, respectively (Table 1). The one-way ANOVA test with Bonferroni's post-hoc multiple comparison showed that the BLLs of preschool and school-age children were significantly higher than those of mothers and fathers ($F = 30.339$, $p < 0.0001$). We found a significant positive correlation between the BLL of the mothers and their children ($R = 0.6385$, $p < 0.0001$) (Fig. 2a). We also found a significant positive correlation between the BLLs of the mothers and fathers ($R = 0.6899$, $p < 0.0001$) (Fig. 2b). The one-way ANOVA analyses showed significant differences between the BLLs of each household member across different SEAs (mothers: $F = 15.79$, $p < 0.0001$; children: $F = 7.78$, $p < 0.0001$; fathers: $F = 4.76$, $p < 0.0001$).

3.2. Scores of HRQoL sections

For the HRQoL of the mothers, the average scores of the SF-36 questionnaire (0–100 scale) were 64.1, 84.2, 72.3, 65.7, 66.5, 66.0, 75.8, and 52.6 points for the measures of vitality, physical functioning, bodily pain, general health perceptions, physical role functioning, emotional role functioning, social role functioning, and mental health, respectively. Ceiling effects, which were identified if more than 15% of the respondents achieved the highest possible score, were detected for the physical functioning, bodily pain, physical role functioning, emotional-role functioning, and social-role functioning scales. In addition, floor effects, which were identified if more than 15% of the respondents achieved the lowest possible score, were also observed for the physical role functioning and emotional role functioning scales (Table 2). The influence of household SEA on HRQoL scores of the mothers was investigated using one-way ANOVA analyses, which demonstrated significant differences between the SF-36 scores according to the SEAs for the following categories: vitality ($p = 0.002$), general health

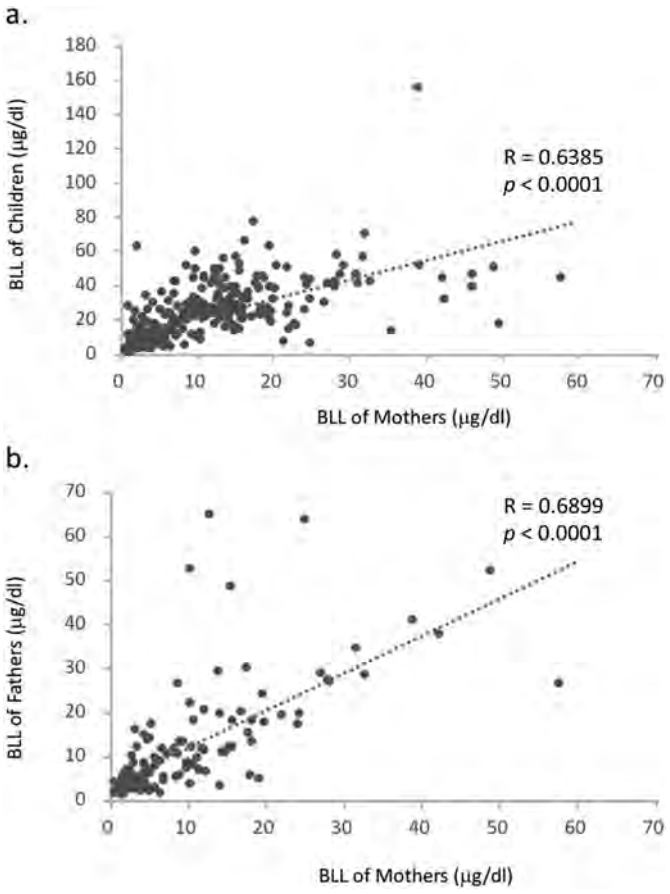

Fig. 2. Linear regression analysis for the BLLs of mothers and other family members (A. mothers vs. household children; B. mothers vs. fathers).

Table 1
Demographic characteristics of the subjects.

	Mothers	Fathers	Infants (−12 months old)	Preschool-aged children (1–5 years old)	School-aged children (6–12 years old)	Adolescents (13 years old−)
N (female: male)	404	125	13 (8: 5)	219 (102: 117)	208 (93: 115)	6 (3: 3)
Age (year)	37.8 ± 12.7	44.4 ± 13.7	0.6 ± 0.2	2.9 ± 1.3	7.8 ± 1.4	16.0 ± 3.2
Height (cm)	158.8 ± 6.5	169.0 ± 7.4	66.4 ± 4.5	94.0 ± 54.5	122.0 ± 14.5	153.0 ± 18.8
Weight (kg)	63.4 ± 13.8	65.6 ± 13.4	7.6 ± 1.2	13.9 ± 7.4	24.3 ± 11.0	46.6 ± 17.7
BLL (μg/dL)[1]	10.6 ± 9.3	11.6 ± 12.5	15.4 ± 13.5	23.6 ± 20.2*,#	19.7 ± 14.3*,#	24.5 ± 22.8

BLL: blood lead level; mean ± SD.
1: One-way ANOVA showed a significant difference in BLLs among family members ($F = 30.339$, $p < 0.0001$). Bonferroni's post-hoc multiple comparison: *$p < 0.0001$ (vs mother), #$p < 0.0001$ (vs. father).

Table 2
Summary of Short-Form 36 scores for each health category (n = 404).

	Vitality	Physical functioning	Bodily pain	General health perception	Physical role functioning	Emotional role functioning	Social role functioning	Mental health
Mean ± SD	64.1 ± 17.9	84.2 ± 23.5	72.3 ± 26.2	65.7 ± 18.8	66.5 ± 44.8	66.0 ± 45.5	75.8 ± 22.7	52.6 ± 13.3
Median (Min, Max)	65 (10, 100)	95 (0, 100)	72 (0, 100)	67 (15, 100)	100 (0, 100)	100 (0, 100)	75 (0, 100)	50 (16.6, 80.0)
Ceiling effect: Number of the respondents achieved the highest possible score (%)	17/404 (4.2%)	201/404 (49.7%)	153/404 (37.8%)	7/404 (1.7%)	264/404 (65.3%)	251/404 (62.1%)	142/404 (35.1%)	0/404 (0%)
Floor effect: Number of the respondents achieved the lowest possible score (%)	0/404 (0%)	3/404 (0.7%)	2/404 (0.4%)	0/404 (0%)	117/404 (28.9%)	122/404 (30.1%)	2/404 (0.4%)	0/404 (0%)

perceptions ($p < 0.0001$), physical role functioning ($p < 0.0001$), emotional role functioning ($p < 0.0001$), social role functioning ($p = 0.002$), and mental health ($p < 0.0001$). We also found significant differences in the household incomes between SEAs ($F = 2.593$, $p < 0.0001$).

3.3. Association of HRQoL scores and the factors

To investigate the statistical association between the BLL of the mothers and the HRQoL scores, we performed stepwise multiple linear regression analyses. According to the analysis of 319 households with complete data for monthly household income, the age of the mothers, and the BLLs of the mothers, there was no significant association between the mothers' BLL and their HRQoL scores, except for the social-role functioning score ($p < 0.05$) (Supplementary Table S1). There were significant negative associations between the mothers' ages and their HRQoL scores, except for the emotional-role functioning score. We did not detect a significant association between the household income and the HRQoL scores except for the social-role functioning score ($p < 0.05$). The maximum variance inflation factor (VIF) of the multiple linear regression analysis ranged between 1.010 and 1.448 for this analysis.

For the dataset containing 252 households with complete data for monthly household income, the age of the mothers, and BLLs of the mothers and their children in any age category, we found negatively significant correlations between the representative BLL of the children with the mothers' vitality (coefficients: 0.191 points/μg/dL, $p = 0.004$) and mental health scores (coefficients: 0.202 points/μg/dL, $p = 0.001$). There were significant negative relationships between the BLL of the mother and the social-role functioning score (coefficients: 0.339 points/μg/dL, $p = 0.028$) (Table 3). Additionally, there were significant negative associations between the mother's age and her HRQoL scores except for the emotional-role functioning score. We did not detect a significant relationship between household income and any of the HRQoL scores of the mothers. The maximum VIF ranged between 1.026 and 1.512 for this dataset.

For the dataset containing 130 households with the complete data for monthly household income, the age of the mothers, and the BLLs of the mothers and their preschool-aged children, we found significant negative associations between the BLL of the preschool-aged children and the vitality and mental health scores of the mothers. However, there were no significant relationships between the mother's BLL and their HRQoL scores (Table 4). The age of the mother was negatively correlated with the physical functioning ($p = 0.002$), general health perceptions ($p = 0.001$), physical-role functioning ($p = 0.015$), and social-role functioning ($p = 0.001$) scores. There were significant positive correlations between the household monthly income and vitality ($p = 0.010$), general health perceptions ($p = 0.007$), physical-role functioning ($p = 0.041$), and mental health scores ($p = 0.015$). The maximum VIF of the multiple linear regression analysis ranged between 1.004 and 1.137 for this dataset.

To statistically analyze the relationship between the BLLs of the school-aged children and the HRQoL scores of their mothers, we investigated a dataset containing 206 households. We found a significant negative correlation between the BLL of the school-aged children and the mental health score of their mothers ($p = 0.016$). There was also a significant negative association between the BLL of the mother and the social-role functioning score ($p = 0.024$) (Table 5). The mother's age was negatively correlated with vitality ($p = 0.035$), physical functioning ($p = 0.002$), bodily pain ($p = 0.001$), and general health perceptions ($p = 0.001$). There were no significant associations between the household income and any of HRQoL scores of the mothers. The maximum VIF of the multiple linear regression analysis ranged between 1.001 and 1.374 for this dataset.

For a dataset containing 101 households with the complete data for the monthly household income, the age of the mothers, and the BLLs of the mothers and fathers, the analysis showed no significant relationship between the BLL of the mothers or fathers and any of the mother's HRQoL scores (Supplementary Table S2). However, there were significant negative relationships between the age of the mothers and all HRQoL scores except for the mental health score. We found a significant positive correlation between the household income and the mental health scores ($p = 0.004$). The maximum VIF of the multiple linear regression analysis ranged from 1.000 to 1.314.

4. Discussion

In this study, we aimed to evaluate the impact of childhood Pb poisoning on the HRQoL of mothers in Kabwe, Zambia, where the serious Pb contamination of soil (Nakayama et al., 2011) and human (Nakata et al., 2021) have been reported, using the SF-36 questionnaire. As pointed out by da Silva e al. (2020), the soil Pb level is closely related to human Pb exposure. Kabwe is considered to be a typical Pb contaminated area and appropriate site for this study. As a result, we demonstrated significant negative associations between the BLL of the children in Kabwe and the vitality and mental-health scores of their mothers. We also found that the BLLs of preschool and school-aged children in Kabwe were significantly higher than those of their parents in spite of the significant positive correlation between the BLLs of the mothers and their children. These findings are valuable for understanding the negative impacts of childhood Pb poisoning on the lives of women in polluted townships near a lead–zinc mine, since our data suggested that the elevation of BLLs in children deteriorated the vitality and mental health of the mothers.

The SF-36 was originally designed as an HRQoL assessment tool for populations with chronic medical conditions (Ware and Gandek 1998; McHorney et al., 1994). A particular concern in our study was the potential for ceiling effects in a population of the relatively

Table 3
The results of the stepwise multiple linear regression analyses using the data set containing the following: the BLLs of children and mothers, the age of the mothers, the household income, and the SEA of their household (n = 252).

	Adjusted R-squared	Intercept (point)	Coefficients of mothers' BLL (point/μg/dl)	Coefficients of children' BLL (point/μg/dl)	Coefficients of mother's age (point/year)	Coefficients of household income (point/K)	SEAs having a negative association with QoL sore	SEAs having a positive association with QoL sore	Maximum VIF
Vitality	0.1375***	75.5		−0.1913***	−0.2287*		SEAs 31, 36*	SEAs 16***, 22**, 24	1.264
Physical functioning	0.0936***	100.8			−0.3712***	0.0005	SEAs 10*, 13, 17, 31, 33, 34		1.081
Bodily pain	0.0980***	89.0			−0.4166**		SEAs 20, 36, 39*	SEAs16*,22, 40	1.038
General health perceptions	0.2582***	85.8			−0.4230***		SEAs 2, 10*, 11*, 17**, 20**, 26, 31***, 36**	SEAs 16*, 34*	1.044
Physical role functioning	0.1531***	95.5			−0.4429*		SEAs 2*, 5**, 6*, 7, 17***, 20***, 32, 36*		1.039
Emotional role functioning	0.1213***	65.0					SEAs 17*, 31*, 32*	SEAs 9*, 12*, 14*, 19*, 21, 30, 39	1.026
Social role functioning	0.1748***	90.0	−0.3391*		−0.2511*		SEAs 8, 17**, 26**, 36***	SEAs 14*, 16**, 21*, 22*	1.492
Mental health	0.2579***	59.0		−0.2024***	−0.1716*	0.0003	SEAs 17, 36***	SEAs 3*, 4, 14**, 15*, 16***, 19, 21*, 22***, 23*, 24*, 30**, 34, 40	1.512

*p < 0.05, **p < 0.01, ***p < 0.005.

young mothers without any particular diseases (McHorney et al., 1994). We assumed that floor and ceiling effects occurred if >15% of the population scored 0 or 100, respectively, for each category of the questionnaire (Terwee et al., 2007). We discovered substantial ceiling effects for the categories of physical functioning, bodily pain, physical-role functioning, emotional-role functioning, and social-role functioning. This is consistent with a study on the HRQoL of women in urban Ghana, which reported similar ceiling effects for the same five scales in the SF-36 (Frempong-Ainguah et al., 2018). Therefore, it is possible that we underestimated the associations between independent variables and the HRQoL scores for those five scales. However, our analyses showed a significant negative association between the mother's BLL and the social-role functioning score. On the other hand, the vitality, general health perceptions, and mental health categories presented neither floor nor ceiling effects.

Another concern is that multicollinearity may have had an adverse impact on our multiple regression analyses, since we observed a significant positive correlation between the BLLs of the mothers and their children. We also showed significant differences in the BLLs of household members, household incomes, and HRQoL scores among the 40 SEAs. We therefore aimed to reduce multicollinearity using stepwise multiple linear regression analysis that incorporated dummy independents for the SEAs and assessed the multicollinearity of each analysis using a VIF. If the VIF is greater than 5 then we can assume the existence of multicollinearity (Kutner et al., 2004). The VIFs in this study ranged from 1.000 to 1.512, suggesting that multicollinearity was insignificant in our multiple regression analyses.

Multiple linear regression analysis showed that the BLL of children had significant negative effects on the vitality and the mental health scores of their mothers. To analyze the responsiveness of the children's BLL to the HRQoL scores of the mother, we calculated the coefficients of the children's BLL for the vitality and the mental health scores, which were −0.191 and −0.202 points/μg/dL, respectively. A review aimed at developing minimal clinically important differences (MCIDs) reported that the MCID for all SF-36 scales ranged from 3 to 5 points (Samsa et al., 1999). From these values, we estimate that increases of 15–25 μg/dL in the BLL of children could induce clinically important changes in the vitality and mental health conditions of their mothers. Our previous study revealed that the mean BLLs of children between the ages of 0–4 years and 5–17 years in areas near the mine were 85.61 and 31.97 μg/dL, respectively (Nakata et al., 2021). The CDC recommends chelation therapy for children with BLLs of 45 μg/dL or above (Centers for Disease Control (CDC), 2002); therefore, medical management of high BLLs in children in Kabwe could improve the HRQoLs of their mothers.

We showed that the BLL of preschool-aged children was negatively associated with the vitality score of their mothers; however, there was no statistically significant relationship between the BLL of school-aged children and the vitality scores of their mothers. Baker et al. (2005) reported that behavioral problems in preschool-aged children (3–5 years) were strongly correlated with the depression scores of their mothers, while developmental delays in preschool-aged children were not significantly associated with higher depression scores in their mothers. A previous study that considered African–American children ages 2 to 5 described detrimental effects of Pb poisoning on child behavior (Sciarillo et al., 1992). This suggests that Pb exposure may cause behavioral problems in children, which can then affect the vitality of their mothers. In addition, 45% of mothers of children with intellectual disabilities had elevated depression scores, whereas the fathers of the same children showed normal depression scores (Olsson and Hwang 2001).

Table 4
The results of the stepwise multiple linear regression analyses using the data set containing the following: the BLLs of preschool-aged children and mothers, the age of the mothers, the household income, and the SEA of their household (n = 130).

	Adjusted R-squared	Intercept (point)	Coefficients of mothers' BLL (point/μg/dL)	Coefficients of preschool children' BLL (point/μg/dL)	Coefficients of mother's age (point/year)	Coefficients of Household income (point/K)	SEAs having a negative association with QoL sore	SEAs having a positive association with QoL sore	Maximum VIF
Vitality	0.1212***	67.0		−0.1731*		0.0009*		SEAs 16***	1.137
Physical functioning	0.1367***	106.7			−0.4856***		SEAs 10*, 13*, 17		1.028
Bodily pain	0.0763**	76.6					SEAs 20*, 36*	SEAs16*, 34	1.009
General health perceptions	0.2460***	84.8			−0.4334***	0.0008**	SEAs 10**, 17**, 19*, 20**, 26, 36*		1.032
Physical role functioning	0.2389***	97.9			−0.7987*	0.0016*	SEAs 17***, 20***	SEAs 4, 12*	1.186
Emotional role functioning	0.0319*	70.7					SEAs 17	SEAs 9	1.004
Social role functioning	0.2236***	98.3			−0.5465***		SEAs 10*, 17**, 26**, 36*	SEAs 14, 21	1.028
Mental health	0.2154***	56.7		−0.1526*		0.0006*	SEAs 11, 13, 17, 20*, 36**	SEAs 14, 16**	1.128

*p < 0.05, **p < 0.01, ***p < 0.005.

Our stepwise multiple linear regression analyses showed negative associations between the age of the mothers and the QoL scores, except for the emotional role functioning score. A study by Okekunle et al. (2015) assessed the QoL of premenopausal women in Nigeria, a sub-Saharan African country, and found that the proportion of respondents with good QoL was significantly higher for women aged <20 years compared with older women. Additionally, teenage participants were almost ten times more likely to have good social relationships than were participants over the age of 35. A recent study that investigated the general population in Pakistan reported that participants that were female and older were more likely to have lower physical, psychological, and relationship scores (Lodhi et al., 2019). Another study investigating QoL and its associated factors among women in rural districts of Iran showed that participants with lower age, satisfaction with their family income, lower level of education, higher BMI, and lower diastolic blood pressure had higher scores for psychological health (Keshavarzi et al., 2013). The same study also concluded that participants with higher age, satisfaction with family income, higher levels of education, lower number of pregnancies, and lower age at menarche were more likely to have higher scores in the social relationships domain of QoL (Keshavarzi et al., 2013). The findings of these studies suggest that older mothers are more likely to have lower QoLs. However, for this study, mothers aged <20 years accounted for only 5% of all mothers in the present study.

In a multiple linear regression analysis using data sets from this study, we did not find a significant association between the household income and the mother's HRQoL scores except for the social-role functioning scores in the dataset without children BLLs and HRQoL scores in the dataset with preschool-aged children BLLs. However, there were significant associations between the HRQoL scores and the age of the mothers, the BLL of the children, and the SEA the household belonged to SEAs. Kim and Kim (2020) reported that the QoL of married women was influenced by other factors when their income was above a certain level. In our study, it is possible that the positive associations between household income and the QoL of the mothers may be weakened by other factors, including the age of the mothers, the BLLs of their children, and their residence area.

In our study, the SEAs of the participants' residence was incorporated into stepwise multiple linear regression analyses as dummy independents, since there is a possibility that the SEAs could introduce cofounding factors. The SEAs are associated with the level of exposure; therefore, the BLLs of the participants are likely to be influenced by the location of their residence (Yabe et al., 2020). The SEA is also associated with the outcome of the studies because certain environmental factors in the SEAs could impact on the mothers' HRQoL. Many previous studies have shown that the location of residences affects the QoL of women (Esmaeilzadeh et al., 2013; Okekunle et al., 2015; Paulose and Kamath 2018). In fact, we found significant correlations between the HRQoL of mothers and certain SEAs. For example, participants living at SEA 36 were more likely to have lower HRQoL scores for general health perceptions, social-role functioning, and mental health, for all datasets, irrespective of the BLLs of other household members, the household income, and the age of the mother. Therefore, the socio-economic factors pertaining to specific SEAs that contribute to the HRQoL of mothers must be thoroughly investigated.

In summary, this study found a significant negative correlation between children's BLL and the vitality and the mental health scores of their mothers although the impacts of socio-economic factors in certain SEAs and maternal age was also observed. This correlation would be interpreted by the previously reported detrimental effects of Pb poisoning on behavior of children (Sciarillo et al., 1992) and the strong association between children's

Table 5
The results of the stepwise multiple linear regression analyses using the data set containing the following: the BLLs of school-aged children and mothers, the age of the mothers, the household income, and the SEA of their household (n = 206).

	Adjusted R-squared	Intercept (point)	Coefficients of mothers' BLL (point/μg/dl)	Coefficients of school-age children' BLL (point/μg/dl)	Coefficients of mother's age (point/year)	Coefficients of household income (point/K)	SEAs having a negative association with QoL sore	SEAs having a positive association with QoL sore	Maximum VIF
Vitality	0.1696***	75.3			−0.2293*		SEAs 6*, 7*, 10*, 11*, 12, 13, 31*, 36*, 38	SEAs 16, 22*	1.069
Physical functioning	0.0519**	102.1			−0.4078***		SEA 10*		1.001
Bodily pain	0.0897***	93.4			−0.5299***		SEA 39**	SEAs16*, 40	1.032
General health perceptions	0.2795***	87.7			−0.4689***		SEAs 2*, 10*, 11*, 17**, 20**, 31***, 36**	SEAs 16*, 34*	1.052
Physical role functioning	0.1398***	97.1			−0.4587		SEAs 2*, 5**, 6*, 7*, 9, 17**, 18*, 20**, 32		1.045
Emotional role functioning	0.1217***	77.4					SEAs 7, 13, 18, 20, 27, 31**, 32**, 34*, 36*		1.013
Social role functioning	0.1355***	79.8	−0.3822*				SEAs 17*, 26, 36**	SEAs 14**, 16*, 21**, 22*	1.374
Mental health	0.2810***	59.8		−0.1218*			SEAs 6*, 7**, 8*, 9**, 10**, 11***, 12**, 13*, 17**, 18*, 20*, 36***	SEA 22**	1.171

*p < 0.05, **p < 0.01, ***p < 0.005.

behavioral problems and maternal depression (Baker et al., 2005). The present study demonstrated our hypothesized effects of child Pb poisoning on maternal HRQoL. On the other hand, we identified the following limitations in our study. First, although we had originally invited 1000 households from 40 SEAs to participate in the investigation, we analyzed the data from 404 households. Thus, the HRQoL scores of the mothers who did not visit the health center could differ from those of the mothers who visited. Second, the blood samples for the BLL measurements were collected from a maximum of two children per household. An average value of the BLLs of two children was defined as a BLL of the household children if two children from the same household visited our clinics. Therefore, the BLL of the household children did not represent the BLL values of all children in each household. Third, we individually analyzed five different data sets for the stepwise multiple linear regression analyses. Because only 71 households had complete datasets from HRQoL score, household income, and BLLs for all mothers, fathers, and children, we used separate datasets according to the available information for data analysis. Fourth, the causal relationships between variables could not be easily evaluated because of the cross-sectional study design. Therefore, we recommend a longitudinal study in the future that would assess the mothers' HRQoL scores before and after medical intervention in which children in Kabwe with high BLLs receive chelation therapy.

5. Conclusions

This is the first study that has evaluated the impact of childhood Pb poisoning on the HRQoL of the children's mothers in Kabwe, Zambia. The results revealed significant negative associations between the BLL of children and the vitality and mental-health scores of their mothers. Therefore, we hypothesize that urgent medical intervention for the children with high BLL and environmental remediation in Kabwe could improve the HRQoL of mothers in addition to the health status of children. Moreover, the socio-economic factors associated with certain SEAs that contributed to differences in the HRQoL scores of mothers should be thoroughly investigated.

Declaration of competing interest

The authors declare that they have no known competing financial interests or personal relationships that could have appeared to influence the work reported in this paper.

Acknowledgements

This work was supported by the Grants-in-Aid for Scientific Research from the Ministry of Education, Culture, Sports, Science, and Technology of Japan, awarded to M. Ishizuka (No. 18KK0287), S.M.M. Nakayama (No. 17KK0009, 20K20633), and H. Nakata (No. 19K20472), and by the JSPS Bilateral Open Partnership Joint Research Projects foundation (JPJSBP120209902). We also acknowledge financial support from JST/JICA SATREPS (Science and Technology Research Partnership for Sustainable Development; No. JPMJSA1501), a program created to support the introduction of the new sharing system (JPMXS0420100619), The Japan Prize Foundation, and Hokkaido University SOUSEI Support Program for Young Researchers in FY2020 (SMMN). We are highly indebted to the communities that participated in this study. We are also grateful to the health centers in Kabwe, the Kabwe District Health Office, the Kabwe Municipal Council, and the Ministry of Health, Zambia, for facilitating our work. We also want to thank all of the laboratory technicians and nurses at the health centers for their technical support. Our appreciation is extended to Hisao Odagiri,

Michiko Nyanga, and Susumu Makino for their coordination, Sayako Yamamoto for her assistance, and Takahiro Ichise and Nagisa Hirano for their technical support.

Appendix A. Supplementary data

Supplementary data to this article can be found online at https://doi.org/10.1016/j.chemosphere.2021.130490.

Credit author statement

Hokuto Nakata: Investigation, Data curation, Formal analysis, Visualization, Validation, Writing – original draft, **Harukazu Tohyama:** Conceptualization, Methodology, Investigation, Supervision, Formal analysis, Writing – original draft, **Wakako Fujita:** Conceptualization, Investigation, Supervision, Writing – Review&Editing, **Shouta M.M. Nakayama:** Conceptualization, Investigation, Project administration, Writing – Review&Editing, **Mayumi Ishizuka:** Conceptualization, Resources, Supervision, Project administration, Funding acquisition, Writing – Review&Editing, **John Yabe:** Conceptualization, Investigation, Writing – Review&Editing, **Nosiku S. Munyinda:** Conceptualization, Investigation, Writing – Review&Editing, **Doreen Sakala:** Conceptualization, Investigation, Writing – Review&Editing, **Kennedy Choongo:** Conceptualization, Resources, Supervision, Project administration, Writing – Review&Editing, **Shojiro Yamasaki:** Investigation, Writing – Review&Editing, **Natsumi Nagai:** Investigation, Writing – Review&Editing, **Takahiko Yoshida:** Conceptualization, Writing – Review&Editing, **Takeshi Saito:** Conceptualization, Writing – Review&Editing.

References

Abelsohn, A.R., Sanborn, M., 2010. Lead and children: clinical management for family physicians. Can. Fam. Physician 56 (6), 531–535. PMID: 20547517.

Baker, B.L., Blacher, J., Olsson, M.B., 2005. Preschool children with and without developmental delay: behaviour problems, parents' optimism and well-being. J. Intellect. Disabil. Res. 49 (Pt 8), 575–590. https://doi.org/10.1111/j.1365-2788.2005.00691.x. PMID: 16011551.

Blacksmith Institute (PureEarth), 2013. The World's Worst 2013: the Top Ten Toxic Threats. Available: https://www.worstpolluted.org/docs/TopTenThreats2013.pdf. (Accessed 25 July 2020).

Bullinger, M., 2003. Measuring health related quality of life. An international perspective Advances in Experimental Medicine and Biology 528, 113–122.

Centers for Disease Control and Prevention (CDC), 2002. Managing elevated blood lead levels among young children: recommendations from the Advisory Committee on Childhood Lead Poisoning Prevention. Available: https://stacks.cdc.gov/view/cdc/26980. (Accessed 25 July 2020).

Centers for Disease Control (CDC), 1985. Preventing lead poisoning in young children—United States, 73 MMWR Morb. Mortal. Wkly. Rep. 34 (5), 66–68. PMID: 2982087.

da Silva, E.B., Gao, P., Xu, M., Guan, D., Tang, X., Ma, L.Q., 2020. Background concentrations of trace metals As, Ba, Cd, Co, Cu, Ni, Pb, Se, and Zn in 214 Florida urban soils: different cities and land uses. Environ. Pollut. 264, 114737. https://doi.org/10.1016/j.envpol.2020.114737. PMID: 32559860.

Dapul, H., Laraque, D., 2014. Lead poisoning in children. Adv. Pediatr. 61 (1), 313–333. https://doi.org/10.1016/j.yapd.2014.04.004. PMID: 25037135.

Edelstein, O.E., Shorer, T., Shorer, Z., Bachner, Y.G., 2019. Correlates of quality of life in mothers of children with diagnosed epilepsy. Epilepsy Behav. 93, 80–86. https://doi.org/10.1016/j.yebeh.2019.01.039. PMID: 30831406.

Esmaeilzadeh, S., Delavar, M.A., Delavar, M.H., 2013. Assess quality of life among Iranian married women residing in rural places, 4 Global J. Health Sci. 13 (5), 182–188. https://doi.org/10.5539/gjhs.v5n4p182. PMID: 23777734.

Ferrans, C.E., Zerwic, J.J., Wilbur, J.E., Larson, J.L., 2005. Conceptual model of health-related quality of life. J. Nurs. Scholarsh. 37 (4), 336–342. https://doi.org/10.1111/j.1547-5069.2005.00058.x. PMID: 16396406.

Frempong-Ainguah, F., Bailey, C.E., Hill, A.G., 2018. Women's health status in urban Ghana: dimensions and differentials using short form 36, 74 Health Qual. Life Outcome 24 (1), 16. https://doi.org/10.1186/s12955-018-0894-y. PMID: 29690865.

Hauptman, M., Bruccoleri, R., Woolf, A.D., 2017. An update on childhood lead poisoning. Clin. Pediatr. Emerg. Med. 18 (3), 181–192. https://doi.org/10.1016/j.cpem.2017.07.010. PMID: 29056870.

Keshavarzi, S., Ayatollahi, S.M., Zare, N., Sharif, F., 2013. Quality of life of childbearing age women and its associated factors: an application of seemingly unrelated regression (SUR) models. Qual. Life Res. 22 (6), 1255–1263. https://doi.org/10.1007/s11136-012-0250-3. PMID: 22903633.

Kim, G.E., Kim, E.J., 2020. Factors affecting the quality of life of single mothers compared to married mothers, 169 BMC Psychiatr. 15 (1), 20. https://doi.org/10.1186/s12888-020-02586-0. PMID: 32295559.

Kim, H.C., Jang, T.W., Chae, H.J., Choi, W.J., Ha, M.N., Ye, B.J., Kim, B.G., Jeon, M.J., Kim, S.Y., Hong, Y.S., 2015. Evaluation and management of lead exposure. Ann Occup Environ Med 27, 30. https://doi.org/10.1186/s40557-015-0085-9. PMID: 26677413.

Kutner, M., Nachtsheim, C., Neter, J., 2004. Applied Linear Statistical Models, 4th. McGraw-Hill, Irwin.

Lodhi, F.S., Montazeri, A., Nedjat, S., Mahmoodi, M., Farooq, U., Yaseri, M., Kasaeian, A., Holakouie-Naieni, K., 2019. Assessing the quality of life among Pakistani general population and their associated factors by using the World Health Organization's quality of life instrument (WHOQOL-BREF): a population based cross-sectional study. Health Qual. Life Outcome 14 (1), 17. https://doi.org/10.1186/s12955-018-1065-x, 9. PMID: 30642360.

McHorney, C.A., Ware Jr., J.E., Lu, J.F., Sherbourne, C.D., 1994. The MOS 36-item Short-Form Health Survey (SF-36): III. Tests of data quality, scaling assumptions, and reliability across diverse patient groups. Med. Care 32 (1), 40–66. https://doi.org/10.1097/00005650-199401000-00004. PMID: 8277801.

Nakata, H., Nakayama, S.M., Yabe, J., Muzandu, K., Toyomaki, H., Yohannes, Y.B., Kataba, A., Zyambo, G., Ikenaka, Y., Choongo, K., Ishizuka, M., 2021. Clinical biochemical parameters associated with the exposure to multiple environmental metals in residents from Kabwe, Zambia. Chemosphere 262, 127788. https://doi.org/10.1016/j.chemosphere.2020.127788. PMID: 33182082.

Nakayama, S.M., Ikenaka, Y., Hamada, K., Muzandu, K., Choongo, K., Teraoka, H., Mizuno, N., Ishizuka, M., 2011. Metal and metalloid contamination in roadside soil and wild rats around a Pb–Zn mine in Kabwe, Zambia. Environ. Pollut. 159 (1), 175–181. https://doi.org/10.1016/j.envpol.2010.09.007. PMID: 20971538.

Okekunle, A.P., Akpa, O.M., Akinyele, I.O., 2015. Sociodemographic factors related to quality of life among premenopausal women in ibadan, Nigeria. Women Health 55 (6), 646–662. https://doi.org/10.1080/03630242.2015.1039179. PMID: 26020293.

Olsson, M.B., Hwang, C.P., 2001. Depression in mothers and fathers of children with intellectual disability. J. Intellect. Disabil. Res. 45 (Pt 6), 535–543. https://doi.org/10.1046/j.1365-2788.2001.00372.x. PMID: 11737541.

Paulose, B., Kamath, N., 2018. Quality of life of postmenopausal women in urban and rural communities. J Menopausal Med 24 (2), 87–91. https://doi.org/10.6118/jmm.2018.24.2.87. PMID: 30202757.

Rousseau, M.C., Baumstarck, K., Khaldi-Cherif, S., Brisse, C., Felce, A., Moheng, B., Loundou, A., Billette de Villemeur, T., Auquier, P., French Polyhandicap Group, 2019. Impact of severe polyhandicap on parents' quality of life: a large French cross-sectional study, 2 PloS One 4 (14), e0211640. https://doi.org/10.1371/journal.pone.0211640. PMID: 30716093.

Samsa, G., Edelman, D., Rothman, M.L., Williams, G.R., Lipscomb, J., Matchar, D., 1999. Determining clinically important differences in health status measures: a general approach with illustration to the Health Utilities Index Mark II. Pharmacoeconomics 15 (2), 141–155. https://doi.org/10.2165/00019053-199915020-00003. PMID: 10351188.

Sciarillo, W.G., Alexander, G., Farrell, K.P., 1992. Lead exposure and child behavior. Am. J. Publ. Health 82 (10), 1356–1360. https://doi.org/10.2105/ajph.82.10.1356. PMID: 1415859.

Terwee, C.B., Bot, S.D., de Boer, M.R., van der Windt, D.A., Knol, D.L., Dekker, J., Bouter, L.M., de Vet, H.C., 2007. Quality criteria were proposed for measurement properties of health status questionnaires. J. Clin. Epidemiol. 60 (1), 34–42. https://doi.org/10.1016/j.jclinepi.2006.03.012. PMID: 17161752.

Ware Jr., J.E., Gandek, B., 1998. Overview of the SF-36 health survey and the international quality of life assessment (IQOLA) Project. J. Clin. Epidemiol. 51 (11), 903–912. https://doi.org/10.1016/s0895-4356(98)00081-x. PMID: 9817107.

Ware Jr., J.E., Sherbourne, C.D., 1992. The MOS 36-item short-form health survey (SF-36): I. Conceptual framework and item selection. Med. Care 30 (6), 473–483. PMID: 1593914.

World Health Organization, 2007. International Classification of Functioning, Disability and Health: Children and Youth Version. Available: http://www.who.int/iris/handle/10665/43737. (Accessed 25 July 2020).

World Health Organization, 2010. Childhood Lead Poisoning. WHO Press. http://www.who.int/ceh/publications/leadguidance.pdf. (Accessed 25 July 2020).

Yabe, J., Nakayama, S.M., Nakata, H., Toyomaki, H., Yohannes, Y.B., Muzandu, K., Kataba, A., Zyambo, G., Hiwatari, M., Narita, D., Yamada, D., Hangoma, P., Munyinda, N.S., Mufune, T., Ikenaka, Y., Choongo, K., Ishizuka, M., 2020. Current trends of blood lead levels, distribution patterns and exposure variations among household members in Kabwe, Zambia. Chemosphere 243, 125412. https://doi.org/10.1016/j.chemosphere.2019.125412. PMID: 31995873.

Yamada, D., Hiwatari, M., Hangoma, P., Narita, D., Mphuka, C., Chitah, B., Yabe, J., Nakayama, S.M.M., Nakata, H., Choongo, K., Ishizuka, M., 2020. Assessing the population-wide exposure to lead pollution in Kabwe, Zambia: an econometric estimation based on survey data. Sci. Rep. 10 (1), 1–11. https://doi.org/10.1038/s41598-020-71998-5. PMID: 32934309.

Yassin, M.M., Lubbad, A.M., 2013. Blood lead level in relation to awareness and self reported symptoms among gasoline station workers in the Gaza Strip. J. Med. 14, 135–142.

Environmental Pollution 286 (2021) 117229

Contents lists available at ScienceDirect

Environmental Pollution

journal homepage: www.elsevier.com/locate/envpol

Genome-wide DNA methylation analysis of dogs with high lead exposure living near a lead mining area in Kabwe, Zambia☆

Jumpei Yamazaki [a,f], Haruya Toyomaki [b], Shouta M.M. Nakayama [b,*], John Yabe [c,h], Kaampwe Muzandu [c], Jaroslav Jelinek [d], Shoko Yokoyama [e], Yoshinori Ikenaka [a,b,f,g], Mitsuyoshi Takiguchi [e], Mayumi Ishizuka [b]

[a] Translational Research Unit, Veterinary Teaching Hospital, Faculty of Veterinary Medicine, Hokkaido University, Sapporo, 060-0818, Japan
[b] Laboratory of Toxicology, Faculty of Veterinary Medicine, Hokkaido University, Japan
[c] School of Veterinary Medicine, The University of Zambia, P.O. Box 32379, Lusaka, Zambia
[d] Coriell Institute for Medical Research, Camden, NJ, USA
[e] Veterinary Teaching Hospital, Faculty of Veterinary Medicine, Hokkaido University, Sapporo, 060-0818, Japan
[f] One Health Research Center, Hokkaido University, Japan
[g] Water Research Group, Unit for Environmental Sciences and Management, North-West University, Potchefstroom, South Africa
[h] Dept of Pathobiology, Faculty of Agriculture & Natural Resources, School of Veterinary Medicine, University of Namibia, Windhoek, Namibia

ARTICLE INFO

Keywords:
DREAM
DNA methylation
Epigenetics
Lead exposure
Dogs

ABSTRACT

Lead (Pb) is a heavy metal that has been proven to be toxic to both animals and humans. Genom-wide DNA methylation in domestic dogs exposed to high levels of Pb in Kabwe, Zambia was analyzed in this study. Using next-generation sequencing on samples from 20 domestic dogs (mean blood Pb concentration: 43.6 μg/dL and 7.2 μg/dL in the high and low exposure groups), a digital restriction enzyme analysis of methylation was performed to identify the genomic locations of differentially methylated CpG sites. A validation study on an additional 20 dogs followed (blood Pb concentration: 4.9–29.7 μg/dL). The cluster analysis resolved two broad clusters indicating high and low Pb exposure. The study identified 827 (1.2%) CpG sites with differences in methylation (101 CpG sites were hypermethylated in the low exposure group and 726 were hypermethylated in the high exposure group). The sites corresponded to 26 genes with differentially methylated CpG sites at their promoter regions, including the *NGF* gene. The methylation of four CpG sites was validated using bisulfite pyrosequencing. The results indicate that aberrant hypermethylation is prevalent in dogs exposed to Pb. The altered DNA methylation of the genes identified in this study contributes to a greater understanding of the epigenetic changes caused by Pb exposure and highlights novel biomarker discoveries across species.

1. Introduction

Variability in gene expression can result from epigenetic changes, which are heritable through mitosis but do not alter the genetic sequence. Such epigenetic processes are critical in embryonic development. They determine cellular lineage commitment (Meissner et al., 2008), inactivation of an X chromosome in women (Heard et al., 1997), and imprinting (Barlow, 1995; Ferguson-Smith, 2011). The results of epigenetic changes can be as significant as DNA sequence mutations. However, epigenetic marks are reversible and responsive to the environment, unlike DNA mutations (Baccarelli and Bollati, 2009). DNA methylation is an epigenetic mechanism wherein cytosine is converted to 5-methylcytosine at cytosine-guanine (CpG) dinucleotides. This biological process causes structural changes that affect DNA–protein interactions. DNA methylation is generally observed in cytosines within CpG repeat sequences, also known as CpG islands (CGIs). CGIs are found in gene promoter regions in mammals. High levels of DNA methylation are generally inversely correlated with gene expression (Jones and Wolffe, 1999).

As environmental pollutants, metals have been associated with numerous diseases, such as neurological disorders, cancer, cardiovascular diseases, and autoimmune diseases (Hemdan et al., 2007). There is

☆ This paper has been recommended for acceptance by Christian Sonne.

* Corresponding author.
E-mail addresses: shouta-nakayama@vetmed.hokudai.ac.jp, shoutanakayama0219@gmail.com (S.M.M. Nakayama).

https://doi.org/10.1016/j.envpol.2021.117229
Received 1 March 2021; Received in revised form 12 April 2021; Accepted 22 April 2021
Available online 3 May 2021

a growing body of research on the role of molecular factors in the etiology of diseases caused by heavy metals (Salnikow and Zhitkovich, 2008). Metal ions produce reactive oxygen species (ROS), and thus generate free radicals (Galaris and Evangelou, 2002). Lead (Pb) exposure produces several disease symptoms, such as anemia and nephropathy, and can even cause fatalities among humans and companion animals (Meyer et al., 2008). Even at low levels, Pb exposure can impair pediatric neurodevelopment, and reduced intelligence quotient (IQ) has been reported as a consequence (Canfield et al., 2003).

Exposure to metals may contribute to epigenetic modifications as studies have shown that cells exposed to environmental metals display *de novo* hypermethylation (Reichard et al., 2007; Sciandrello et al., 2004; Takiguchi et al., 2003). The accumulation of ROS also impacts epigenetic factors (Monks et al., 2006). In addition, global methylation is thought to indicate changes in environment-based responses and chemical exposure (Hou et al., 2012), thus suggesting a crucial role of DNA methylation in the mechanisms of diseases caused by environmental pollutants. In fact, high Pb levels in the patella were found to lead to indications of reduced global DNA methylation of LINE-1 in peripheral blood leukocytes (Wright et al., 2010). Exposure to Pb in childhood has been reported to affect differentially methylated regions (DMRs), which control the monoallelic expression of imprinted genes in adulthood (Li et al., 2016). A recent genome-wide screen for DNA methylation revealed that environmental agents, such as smoking and Pb exposure, induce differential methylation (Joubert et al., 2012; Sen et al., 2015).

Kabwe's lead-zinc mine in Zambia operated for more than 90 years without adequate pollution and emissions laws before it was shut down in 1994. Detection of hazardous concentrations of Pb continues throughout the city. Humans and animals (particularly chickens, cattle, rats, and lizards) are exposed to high levels of Pb in Kabwe (Doya et al., 2020; Nakayama et al., 2011; Yabe et al., 2011, 2013, 2015). Our previous study found that higher levels of Pb in the blood of Kabwe's domestic dogs (range; 3.1–123.4 μg/dL), which exceeded the toxic level of 40 μg/dL (Toyomaki et al., 2020). Dogs are sentinels for toxic substances and share risk factors with their owners, such as areas of habitation and living conditions (Severe et al., 2015; Thomas et al., 1975, 1976). Thus, dogs could be useful in the determination of the extent of Pb exposure among Kabwe residents. As epigenetic profiling of target tissues in model organisms exposed to chemical compounds can reveal an underlying mode of action (Groh et al., 2015), high Pb exposure in dogs (Pb $\geq$ 10 μg/dL) in Kabwe is hypothesized to produce prominent changes in the DNA methylation of key metabolic and neuronal genes. Accordingly, this study aims to examine a genome-wide analysis of DNA methylation in domestic dogs with high Pb exposure in Kabwe, Zambia.

2. Materials and methods

2.1. Dog blood samples

A door-to-door campaign offering free rabies vaccinations for domestic dogs in the township of Kasanda in Kabwe, Zambia, in April and May 2017 was conducted. The campaign was part of a recruitment strategy for the study. Government personnel from the Kabwe District Veterinary Office administered the rabies vaccinations. Samples were collected only from dogs whose owners were willing to participate in the present study. In addition, interviews were conducted with the dog owners to gain information about their dogs (age, sex, and breed). All dogs in the sample were crossbreeds, and their mean age was 3.4 years. No explicit signs of Pb poisoning or related clinical symptoms were observed in any dog.

An ethanol swab was used to clean and sanitize the venipuncture site over the cephalic vein. A maximum of 5 mL was taken from each dog and collected into heparinized blood collection tubes. The blood sample tubes were stored in plastic Ziploc storage bags to prevent the contamination of the samples. All processed samples were stored at −20 °C at the University of Zambia, School of Veterinary Medicine, and transported to Japan in temperature-controlled boxes containing ice packs. The samples were examined at the Faculty of Veterinary Medicine, Hokkaido University, in Sapporo, Japan (Approval Number: Vet-17010).

2.2. Pb concentration analysis

The Pb extraction and concentration analysis of whole blood samples were conducted following the protocols in a previous study (Toyomaki et al., 2020). One mL of the blood sample was transferred into a pre-washed digestion vessel. Acid digestion was then performed with 5 mL of two-fold diluted ultrapure nitric acid (Cica reagent, specific gravity of 1.38, 60%; Kanto Chemical Corp., Tokyo, Japan) and 1 mL of ultrapure hydrogen peroxide (Cica reagent, 30%; Kanto Chemical Corp.). Then a Speedwave MWS-2 (Berghof, Germany) was used to conduct microwave digestion; manufacturer instructions were followed for the procedure (Toyomaki et al., 2020). Pb and other metal concentrations were examined using inductively coupled plasma mass spectrometry (ICP-MS, 7700 series; Agilent Technologies, Tokyo, Japan). Finally, analytical quality control was conducted using certified reference materials (DORM-3 [fish protein; National Research Council of Canada, Ottawa, Canada] and DOLT-4 [dogfish liver; National Research Council of Canada]). Replicate analyses on the reference materials indicated recovery rates of 95%–105% with an instrument detection limit of 0.001 μg/L.

2.3. Digital restriction enzyme analysis of methylation in dogs (Canine DREAM)

For Canine DREAM, dogs with blood Pb levels above 30 μg/dL (mean 43.6 μg/dL) were classified as the high exposure group (N = 10) and those with Pb levels below 10 μg/dL (mean 7.2 μg/dL) as the low exposure group (N = 10) (Table 1). Each group comprised five male and five female dogs. A genome-wide DNA methylation analysis was performed on the blood samples using next-generation sequencing (Yamazaki et al., 2018). Briefly, genomic DNA (1 μg) extracted from the samples was mixed with 2 pg of a set of artificial methylation standards. These mixes were digested with SmaI and XmaI endonuclease (New England Biolabs) followed by filling in and 3′-dA tails by Klenow DNA polymerase lacking 3′-to-5′ exonuclease activity (New England Biolabs). Illumina paired-end sequencing adaptors were ligated using T4 DNA ligase (New England Biolabs), the ligation mix was size-selected by Agencourt AMPure XP to obtain DNA fragments ranging from 250 bp to 450 bp in size. Purified DNA was amplified using KAPA Hifi HotStart ReadyMix (Kapa Biosystems) and 11 cycles of amplification followed by sequencing on an Illumina HiSeq 2000 (Illumina). The reads were then mapped to SmaI and XmaI sites in the dog genome (canFam3.1). For CpG islands, the definition proposed by the University of California, Santa Cruz (UCSC): GC content $\geq$ 50%, length $>$ 200 bp, and a ratio $>$ 0.6 of the observed number of CG dinucleotides to the expected number based on the amount of Gs and Cs in the segment was utilized (Gardiner-Garden and Frommer, 1987). Promoter regions were defined as being those located within 1 kb upstream from the transcription start sites (TSS) of genes in the Ensembl database (Flicek et al., 2014).

2.4. Bisulfite pyrosequencing

Bisulfite pyrosequencing was used to quantitatively assess DNA methylation (Colella et al., 2003) for the promoter regions of canine NGF, ZGPAT, and GALNT6, and the gene body of canine GRIK5 in additionally selected dogs with blood lead levels greater than 24 μg/dL (N = 9, of which 8 were male and 1 female) and less than 13 μg/dL (N = 11, 3 male and 8 female, Table 2). These dogs differed from those in the samples used to conduct the Canine DREAM analysis. Bisulfite conversion was performed on genomic DNA (500 ng) from the samples using

Table 1
Sex, age (year), the lead (Pb) concentration detected in blood (μg/dL) and classification of blood Pb concentrations, as well as number of unique useable reads and CpG sites with more than 20 reads per sample for DNA methylation analysis using Canine DREAM.

Samples	Sex	Age (year)	Pb concentrations in blood (μg/dL)	Classification	Number of reads	Number of CpG sites covered
PbHF19	Female	3	32.6	High	7,123,624	107,776
PbHF48	Female	3	81.8	High	7,983,853	112,484
PbHF551	Female	2	39.2	High	7,163,124	109,457
PbHF552	Female	5	38.2	High	8,075,213	112,684
PbHF66	Female	3	32.7	High	8,150,005	116,715
PbHM19	Male	6	60.8	High	7,963,651	111,682
PbHM39	Male	4	33.5	High	8,579,236	114,188
PbHM542	Male	4	36.4	High	10,160,619	123,773
PbHM55	Male	3	42.6	High	7,060,760	106,271
PbHM60	Male	5	38.1	High	7,438,844	106,774
PbLF101	Female	4	5.3	Low	7,988,403	114,667
PbLF105	Female	5	4.0	Low	18,968,226	152,574
PbLF78	Female	2	8.5	Low	7,456,237	108,694
PbLF891	Female	3	8.8	Low	9,886,315	125,853
PbLF892	Female	3	9.5	Low	7,543,150	109,002
PbLM104	Male	3	6.8	Low	7,973,392	112,083
PbLM21	Male	2	7.3	Low	6,166,367	100,420
PbLM47	Male	3	9.0	Low	5,990,726	99,365
PbLM98	Male	4	4.5	Low	6,429,206	102,885
PbLM99	Male	2	8.1	Low	6,826,275	105,596

(In sample names: H = High exposure group, L = Low exposure group, F = Female, M = Male).

Table 2
Sex, age (year), the lead (Pb) concentration detected in blood (μg/dL) and classification of blood Pb concentrations for pyrosequencing analysis.

Samples	Sex	Age (year)	Pb concentrations in blood (μg/dL)	Classification
F207-2	Female	6	6.1	Low
F25	Female	3	11.6	Intermediate
M56	Male	3	29.7	High
F102	Female	6	4.9	Low
F103	Female	4	8.1	Low
M40	Male	2	29.1	High
F212	Female	4	7.0	Low
F56-2	Female	2	26.5	High
M112	Male	4	11.3	Intermediate
M63	Male	4	26.5	High
M108	Male	4	9.5	Low
M95	Male	3	24.6	High
F206	Female	4	12.1	Intermediate
M62	Male	2	25.2	High
M26-2	Male	2	25.0	High
F16	Female	3	12.0	Intermediate
F24	Female	2	10.4	Intermediate
M18	Male	3	25.0	High
M92	Male	3	9.0	Low
M51	Male	3	26.0	High

the innuCONVERT Bisulfite Basic Kit (Analytika yena); manufacturer instructions were followed for the procedure. The Canine DREAM analysis identified fragments with differentially methylated CpG sites. These fragments were amplified. Supplementary Table 1 lists the primer sequences and PCR conditions. DNA methylation was estimated as a percentage of bisulfite-resistant cytosines at CpG sites with pyrosequencing. The pyrosequencing was performed using a PSQ24 system with the Pyro-Gold Reagents Kit (QIAGEN) and PyroMark Q24 software (QIAGEN) to examine the results.

2.5. Statistical analysis and data visualization

DNA methylation levels between the groups were compared using the Student's *t*-test. Adjustment for multiple-testing in Canine DREAM was performed with the procedure of Benjamini and Hochberg (1995) to identify differential methylation at FDR of 10%. A pairplot was drawn and visualized with Seaborn on Python 3.7 (Michael Waskom and The seaborn development team, 2020). Pearson's correlation coefficient was calculated for associations between DNA methylation levels of all CpG sites analyzed for each pair of the samples. Hierarchical clustering analysis was performed with the agglomeration method 'ward' where the distance was calculated with the Euclidean.

3. Results

3.1. Genome-wide DNA methylation analysis

To determine the genomic locations of differentially methylated CpG sites in dogs exposed to Pb, Canine DREAM was conducted in this study where 6–19 million unique useable reads were successfully generated from the 20 samples (high and low groups; N = 10 per group) after conservative filtering (quality-based filtered and alignment with the dog genome). CpG sites with more than 20 reads were selected to ensure quantitative ability and obtained DNA methylation data for approximately 100,000 CpG sites. Table 1 contains the data and analyses.

Fig. 1 is a heat map for the correlation coefficients for all comparisons conducted within the sample. First, the study revealed that all comparisons reported relatively high consistencies ($R^2 = 0.913–0.977$), indicating subtle changes, if any, in DNA methylation for the dogs exposed to Pb. However, after excluding four samples, the analysis showed two separate clusters: one with dogs with high Pb exposure (seven out of nine samples in the cluster) and the other comprising dogs with low Pb exposure (six out of seven samples in the cluster). The other four samples were on the borderline between the two groups (Fig. 1).

Next, 70,211 CpG sites (those with greater than 20 reads in the 20 samples) were analyzed to determine differences in DNA methylation between dogs with high and low Pb exposure. Of these, 26,557 sites are in CGIs and 43,654 sites in non-CGIs. The average DNA methylation for each CpG sites in dogs with high and low Pb exposure was calculated. By comparison of the averages of DNA methylation in dogs with high and low Pb, differential methylation (using the criteria of >10%, $p < 0.05$, false discovery rate 10%) were identified at 827 CpG sites (1.2% of analyzed sites) of which 101 CpG sites were hypermethylated in the low Pb exposure group and 726 were hypermethylated in the high Pb exposure group (Fig. 2).

To derive deeper insights into differential CpG sites and their characteristics, the genomic coordinates of the differential CpG sites was examined to explore the biological relevance of studying DNA methylation in dogs exposed to high Pb levels. Hypermethylated CpG sites were compared between dogs with high and low Pb exposure and assessed for

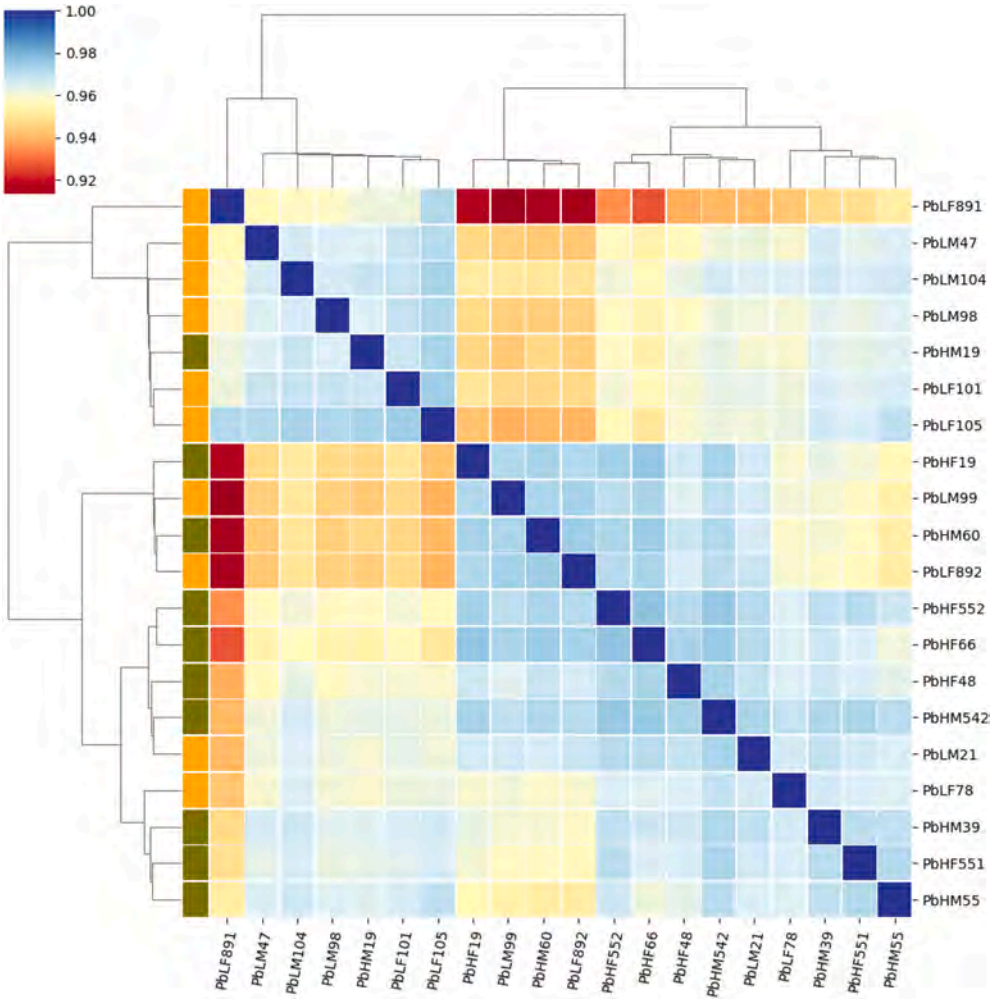

Fig. 1. Pairplot for correlation scores of DNA methylation levels for all CpG sites analyzed using Canine DREAM. Samples with low lead (Pb) exposure (<10 μg/dL) and high Pb exposure (>30 μg/dL) are highlighted in orange and green in the column to the extreme left. (For interpretation of the references to colour in this figure legend, the reader is referred to the Web version of this article.)

genomic localization using the UCSC browser (Fig. 3). Two of the CpGs that could be analyzed in this study, chr1:1593290 and chr1:1593637, are close to each other and showed DNA methylation levels of 56.1% and 52.5% in the high exposure group and 30.5% and 27.0% in the low exposure group. However, the functional relevance of this gain in DNA methylation in dogs after high Pb exposure is unclear, as these sites were not located close to any genes (Fig. 3A). It is well known that hypermethylation at the promoter region of genes correlates with gene expression silencing. Therefore, the CpG sites at promoter regions (within 1000 bp upstream of the transcription start site of genes) that showed differential methylation between the high and low Pb exposure groups were selected for the following analyses. As a result, 26 differentially methylated CpG sites were identified to be located at promoter regions of genes annotated by the Ensembl database (Flicek et al., 2014). Table 3 is a complete list of the differentially methylated genes. Select CpG sites were analyzed in this study. Two of the CpGs that could be analyzed, chr32:24352693 and chr32:24353037, were close to each other and showed a similar trend in DNA methylation (31.6% and 36.4% in the high exposure group and 14.2% and 16.3% in the low exposure group; Fig. 3B). Interestingly, both sites are located in the promoter region of *SLC9B1*, indicating a possible relationship between high Pb exposure and gene expression silencing by the aberrant hypermethylation. Another example of a hypermethylated CpG site in dogs with high Pb exposure is chr17:52902166, located in the promoter region of the *NGF* gene; the site showed 42.9% and 32.8% DNA methylation in the high and low Pb exposure groups (Fig. 3C).

3.2. *Bisulfite pyrosequencing to validate differentially methylated CpG sites*

To validate the findings of Canine DREAM, bisulfite pyrosequencing was performed to measure the DNA methylation levels of the differentially methylated CpG sites for a different sample of 20 dogs living in Kabwe. Pb concentrations in the dogs' blood ranged between 4.9 μg/dL and 29.7 μg/dL. Of the 827 differentially methylated CpG sites at promoter regions, the DNA methylation levels at the CpG sites in the promoter regions of canine *NGF*, *ZGPAT*, and *GALNT6* and the gene body region of canine *GRIK5* were analyzed for the following reasons: (1) higher DNA methylation levels were reported in dogs with high Pb exposure, (2) concordant results for DNA methylation level were observed for the nearest CpG sites analyzed in Canine DREAM, (3) the primers for bisulfite pyrosequencing were confirmed to amplify the fragment as a single band in gel electrophoresis, and (4) relevance to Pb poisoning was assumed from the gene function. Since the samples with intermediate levels of Pb concentration (10.4–12.1 μg/dL) observed in 5 out of 20 dogs in this validation set could not be classified as low or high in Canine DREAM, a hierarchical clustering analysis with the four CpG sites was utilized. Four samples with low Pb concentration (<8.1 μg/dL) were clustered along with one intermediate and two high samples, while the remaining 13 samples (two low, four intermediate, and seven high)

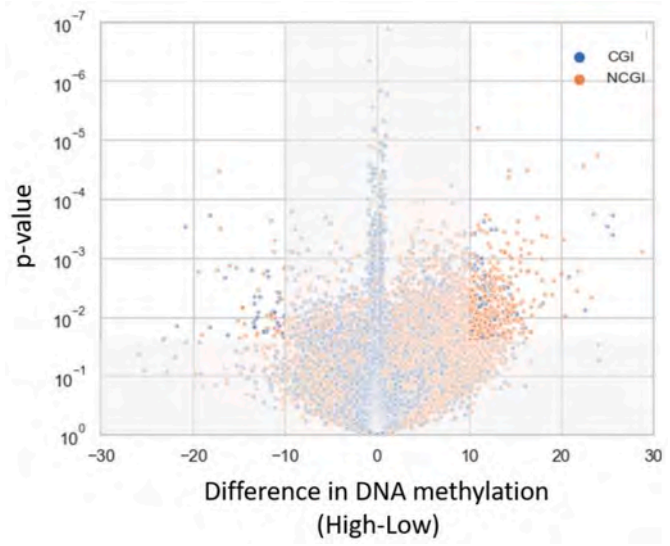

Fig. 2. Comparison of DNA methylation levels between high and low lead (Pb) exposure groups. Volcano plots with differences between the averages of high and low Pb exposure are on the x-axis, and the unadjusted p-value for each site is on the y-axis for sites in CpG islands (blue) and non-CpG islands. (For interpretation of the references to colour in this figure legend, the reader is referred to the Web version of this article.)

formed another cluster (Fig. 4). Importantly, the DNA methylation levels of the samples in the former cluster were lower than those in the other clusters. In other words, the four differentially methylated CpG sites identified using Canine DREAM suggested low levels of DNA methylation in dogs with low Pb exposure, and this was confirmed in the validation set analyzed using bisulfite pyrosequencing.

4. Discussion

The unique characteristics of our approach — that is, the high stability and the ease with which the samples could be obtained — facilitated the smooth execution of the DNA methylation analysis. In addition, using models where the results are applicable to humans is essential, considering that environment-based responses and the associated challenges may be species-specific. This study integrated two novel research strategies. A unique field sample set of dogs who resided around a Pb mine in Kabwe, Zambia, with high and low Pb exposure levels were used to conduct a genome-wide DNA methylation analysis using next-generation sequencing (Yamazaki et al., 2018). This approach produced unique useable reads for a quantitative DNA methylation analysis, which also allowed for an examination of more than 100,000 common CpG sites in dogs with high and low Pb exposure. These numbers are comparable with those in previous studies (Yamazaki et al., 2018).

The correlation coefficient for every pairwise combination of 20 blood samples revealed differences in global DNA methylation patterns between dogs with high and low Pb exposure, although these differences were not perfect. These findings are consistent with those of the Pb exposure reports, as well as the changes in global DNA methylation in human blood (Wright et al., 2010) and umbilical cord blood (Pilsner et al., 2009). In other words, the distribution of cytosine methylation is perturbed in the blood samples of dogs exposed to Pb. The genome-wide DNA methylation analysis allowed us to determine 827 differentially methylated CpG sites between dogs with high and low Pb exposure. In addition, the number of CpG sites that showed a increase in DNA methylation was significantly higher in dogs with high Pb exposure than in those with low Pb exposure (101 CpG sites in the low Pb exposure group compared with 726 in the high Pb exposure group). A validation study with bisulfite pyrosequencing on four hypermethylated CpG sites was condcuted to confirm the DNA methylation levels using additional samples and confirmed that dogs with low Pb exposure had lower levels of DNA methylation. These results indicate that aberrant hypermethylation is a dominant event under Pb exposure, as has been indicated for other metals such as nickel (Lee et al., 1995) and chromium (Takiguchi et al., 2003). This finding is also supported by the fact that

Table 3
Genes with differentially methylated CpG sites in the high and low Pb exposure groups. Underlined genes denote hypermethylation in the low Pb exposure group.

JCAD	F10	WDR91
SLC9B1	ZGPAT	ENPP7
ALYREF	SPDEF	ZGPAT
KRTCAP3	GALNT6	PRSS33
LPIN1	SNRNP27	SDC1
NGF	PDCD2L	HAPLN3
SORCS2	CAPZB	ITGAV
RAB17	ZBTB7A	GRB7
TMEM259	AMOTL1	

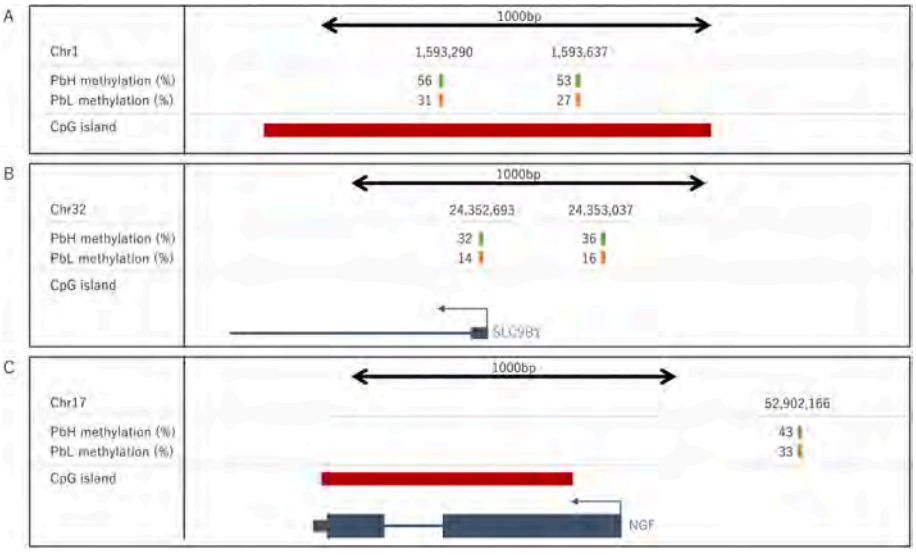

Fig. 3. Representative genomic landscapes for differentially methylated CpG sites (A = chromosome 1, B = chromosome 32, C = chromosome 17). Images are adopted from the UCSC browser (http://genome.ucsc.edu/cgi-bin/hgGateway). The black bars in each image denote the sequence of CCCGGG, which is a recognition site for SmaI and XmaI. The average DNA methylation levels for the analyzed sites are labeled with numbers for the high (PbH) and low (PbL) lead exposure groups. The red bar indicates the CpG island region. The middle (B) and lower (C) panels show SLC9B1 and NGF close to the differentially methylated CpG sites. (For interpretation of the references to colour in this figure legend, the reader is referred to the Web version of this article.)

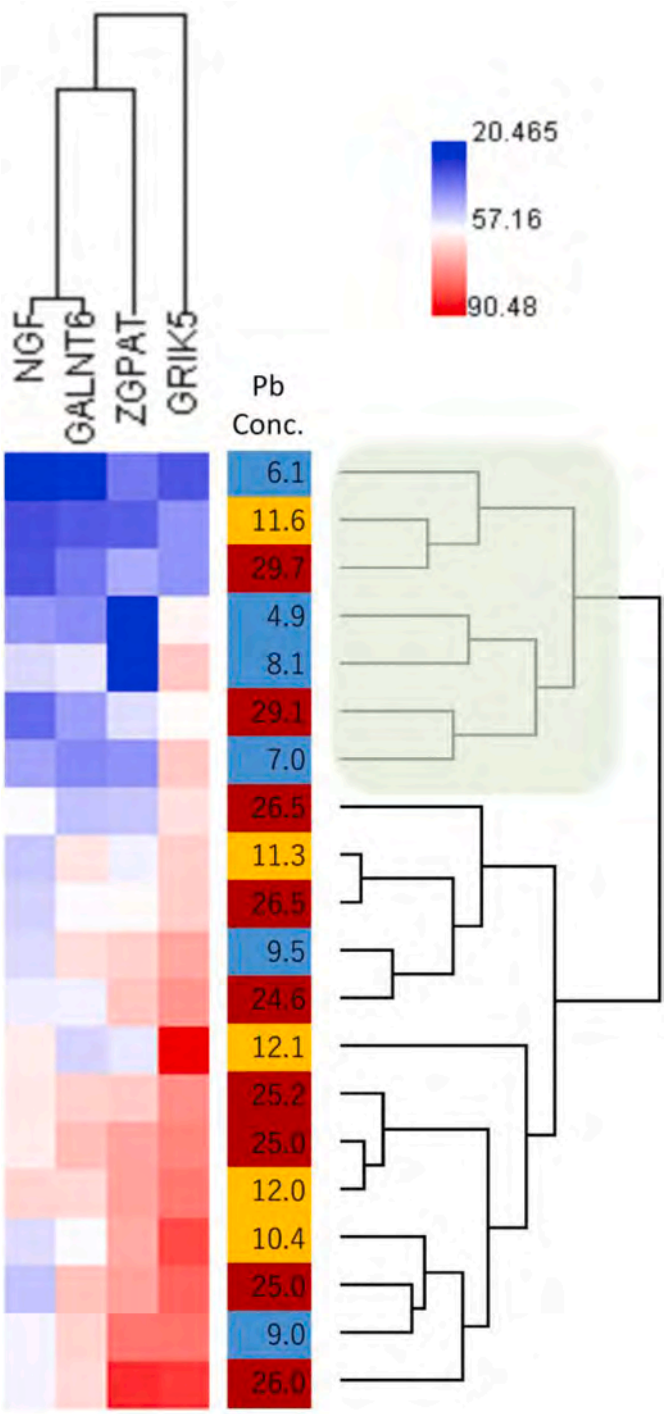

Fig. 4. Unsupervised hierarchical clustering analysis on DNA methylation levels using bisulfite pyrosequencing for four differentially methylated CpG sites. Lead (Pb) concentration levels are classified as low (blue), intermediate (yellow), and high (red). All low Pb exposure samples are clustered (in green), with some exceptions. Details of sample ID, sex, age, lead (Pb) concentration detected in blood (μg/dL) and classification of blood Pb concentrations were also shown in Table 2. (For interpretation of the references to colour in this figure legend, the reader is referred to the Web version of this article.)

early exposure to Pb results in the predominant repression of a small subset of genes alongside an upregulation of even fewer genes in a primate model (Bihaqi et al., 2011). A rodent model revealed a repression of a subset of genes that were upregulated in the normal aging process (Dosunmu et al., 2012). Importantly, studies have found more hypermethylated CpG sites in children with early exposure to Pb (Sen et al., 2015). Our previous studies indicated that both dogs and humans in Kabwe are chronically exposed to Pb (Toyomaki et al., 2020; Yabe et al., 2020). Given these findings based on our data on dogs, the effects of Pb exposure on DNA methylation and gene expression changes seem to be similar across species.

The validation study on the samples from dogs with intermediate blood Pb concentrations (10.4–12.1 μg/dL) showed DNA methylation patterns similar to those observed for high Pb concentrations (>24.6 μg/dL), which was different from dogs with low blood Pb concentrations (<9.5 μg/dL). This result suggests that a Pb concentration of approximately 10 μg/dL could be a threshold to differentiate the effect of aberrant DNA methylation caused by Pb exposure in the dog samples. Further studies with more samples are warranted to confirm this finding.

As it is well known that DNA methylation in the promoter region of genes represses gene transcription, DNA methylation status of CpG sites in the promoter regions was analyzed. Of the 746 CpG sites hypermethylated in the high Pb exposure group, 26 genes were identified to have hypermethylated CpG sites at their promoter regions. One of the identified genes, *SLC9B1*, is known to be expressed only in the testis in humans (Donowitz et al., 2013) and methylated in the fetal intolerance of labor (Knight et al., 2018). It would be insightful to research the relationships among Pb accumulation, *SLC9B1* methylation status, and *SLC9B1* gene expression levels in the testis of dogs around the Kabwe mining sites. The findings could clarify a possible link between the methylation of this gene and Pb poisoning since the other SLC family genes, including *SLC22A23* and *SLC6A2*, were observed to mediate the association between prenatal arsenic exposure and gestational age at birth (Bozack et al., 2018).

ZGPAT is a zinc finger transcription factor protein that represses transcription by recruiting the nucleosome remodeling and deacetylase (NuRD) complex to the promoter region (Sun et al., 2011). Changes in ZGPAT hippocampal gene expression are common in individuals addicted to both cocaine and alcohol, and may reflect similar neuronal adaptations (Zhou et al., 2011). A similar mechanism might be observed through the DNA methylation changes induced by high Pb exposure.

NGF is crucial in neuronal development and the functioning of the nervous system of mammals. NGF decreases with age, which may also contribute to declining cognitive function contingent on age, including that of Alzheimer's disease (Budni et al., 2015). Recent studies have reported the downregulation of NGF induced by maternal Pb exposure in the hippocampus of mouse pups (Li et al., 2017; Sanchez-Martin et al., 2013). This suggests a link between Pb poisoning and the hypermethylation of these sites. Furthermore, DNA methylation studies using the Illumina HumanMethylation450 BeadChip on Pb-treated human embryonic stem cells (hESCs) demonstrated that exposure to Pb caused changes in the methylation status of genes in neurogenetic signaling pathways (Senut et al., 2014). However, our study did not examine the gene expression levels in the same samples to confirm if gene silencing was caused by the hypermethylation in the dogs. Gene expression silencing accompanied by the hypermethylation of neurogenic genes could be associated with various symptoms caused by Pb exposure across species, including humans, mice, and dogs.

Numerous reports have demonstrated a relationship between chemical and environmental agents and abnormal DNA methylation. Most studies examining epigenetic responses have adopted highly targeted approaches including the p16 and p53 genes, which are hypermethylated by arsenic, nickel, and chromium (Chanda et al., 2006). In contrast, a screening approach to identify CpG sites with differential DNA methylation was conducted, followed by a validation step that used bisulfite pyrosequencing. The results revealed 26 differentially methylated genes between the high and low Pb exposure groups, which were subsequently validated by bisulfite pyrosequencing. This number is comparable to the findings of a screening study that examined DNA methylation in children exposed to Pb and identified 113 differentially methylated CpG sites using human array-based methods, which could

analyze 450,000 CpG sites (Sen et al., 2015). The DNA methylation of the genes identified in this study should be further analyzed under different exposure conditions that allow for a comprehensive examination of epigenetic changes. Such a study will help identify critically sensitive biological pathways involved in Pb exposure and allow for the establishment of appropriate risk assessments.

This study is subject to the following limitations. First, peripheral blood was used for the DNA methylation analysis. It is conceivable that epigenetic alterations could be tissue-specific (Minard et al., 2009). Epigenetic changes may differ in response to the same environmental pollutant, and this holds true for both different tissues and different cell types. Measuring DNA methylation in a target organ such as the brain would be ideal; however, obtaining such samples from either humans or dogs is not possible. Nevertheless, a high level of Pb in the patella, which can be used as a marker of cumulative exposure, correlated with a decline in global DNA methylation seen in LINE-1 assayed from blood samples (Wright et al., 2010). In addition, researchers have shown significant hypermethylation of the p16 gene promoter in DNA using peripheral blood lymphocytes of subjects exposed to arsenic-contaminated water (Chanda et al., 2006). Further research is needed to determine the role of white blood cell DNA methylation in Pb poisoning. Finally, this study only focused on one epigenetic mark, that is, DNA methylation. However, epigenetic marks have an intricate series of interactions that control gene expression through additional epigenetic mechanisms, such as histone modifications or miRNA expression (Fuks, 2005). The application of multiple integrated epigenetic marks and genetic profiling of mechanisms for Pb exposure will enable an enhanced interpretation of the mechanisms and the novel discovery of biomarkers.

5. Conclusion

In conclusion, the results indicate that aberrant hypermethylation is prevalent in dogs exposed to Pb. The altered DNA methylation of the genes identified in this study contributes to a greater understanding of the epigenetic changes caused by Pb exposure and highlights novel biomarker discoveries across species.

Declaration of competing interest

The authors declare that they have no known competing financial interests or personal relationships that could have appeared to influence the work reported in this paper.

Acknowledgements

We thank the dog owners for participating in this study. This work was supported by Grants-in-Aid for Scientific Research by the Ministry of Education, Culture, Sports, Science and Technology (MEXT) of Japan awarded to M. Ishizuka (No. 16H01779, 18K19847, 18KK0287, 21H04919), Y. Ikenaka (18H04132), J. Yamazaki (No. 18K05964, 21H02351), and S.M.M. Nakayama (No. 17KK0009, 20K20633) and the JSPS Bilateral Open Partnership Joint Research Projects (JPJSBP120209902). This work was also supported by the Kurita Water and Environment Foundation (J. Yamazaki). This work was also supported by JSPS CORE to CORE program (MI). We acknowledge financial support from the Program for Leading Graduate Schools, "Fostering Global Leaders in Veterinary Science for Contributing to One Health" (F01) and the World-leading Innovative and Smart Education (WISE) Program (1801); MEXT's Grant-in-Aid for JSPS Research Fellow (17J05756; HT); The Japan Prize Foundation; and Hokkaido University's SOUSEI Support Program for Young Researchers in FY2020 (SMMN); Hokkaido University Specific Research Projects (MI). This research was also supported by the Japan Science and Technology Agency (JST) and the Japan International Cooperation Agency's (JICA) Science and Technology Research Partnership for Sustainable Development (SATREPS; No. JPMJSA1501), JST's Accelerating Social Implementation for SDGs Achievement (aXis; No. JPMJAS2001), the Program for supporting introduction of the new sharing system (JPMXS0420100619) and JST's AJ-CORE (Africa-Japan Collaborative Research, MI). We are grateful to Takahiro Ichise and Nagisa Hirano (Laboratory of Toxicology, Faculty of Veterinary Medicine, Hokkaido University) for the technical support offered for the metal concentration analyses. The authors also thank Dr. Chihiro Miyashita for the opportunity to perform bisulfite pyrosequencing.

Appendix A. Supplementary data

Supplementary data to this article can be found online at https://doi.org/10.1016/j.envpol.2021.117229.

Author statement

Jumpei Yamazakia: Conceptualization, Methodology, Data curation, Formal analysis, Software, Writing – original draft. Haruya Toyomaki: Investigation, Methodology, Data curation, Software, Writing – review. Shouta M.M. Nakayama: Funding acquisition, Project administration, Writing – review & editing. John Yabe: Investigation, Writing – review. Kaampwe Muzandu: Investigation, Writing – review. Jaroslav Jelinek: Investigation, Writing – review. Shoko Yokoyama: Investigation. Yoshinori Ikenaka: Funding acquisition, Supervision. Mitsuyoshi Takiguchi: Supervision. Mayumi Ishizuka: Funding acquisition, Project administration, Writing – review & editing.

References

Baccarelli, A., Bollati, V., 2009. Epigenetics and environmental chemicals. Curr. Opin. Pediatr. 21, 243–251.
Barlow, D.P., 1995. Gametic imprinting in mammals. Science 270, 1610–1613.
Benjamini, Yoav, Hochberg, Yosef, 1995. Controlling the false discovery rate: a practical and powerful approach to multiple testing. J. Roy. Stat. Soc. B 57, 289–300.
Bihaqi, S.W., Huang, H., Wu, J., Zawia, N.H., 2011. Infant exposure to lead (Pb) and epigenetic modifications in the aging primate brain: implications for Alzheimer's disease. J. Alzheim. Dis. 27, 819–833.
Bozack, A.K., Cardenas, A., Quamruzzaman, Q., Rahman, M., Mostofa, G., Christiani, D. C., Kile, M.L., 2018. DNA methylation in cord blood as mediator of the association between prenatal arsenic exposure and gestational age. Epigenetics 13, 923–940.
Budni, J., Bellettini-Santos, T., Mina, F., Garcez, M.L., Zugno, A.I., 2015. The involvement of BDNF, NGF and GDNF in aging and Alzheimer's disease. Aging and Disease 6, 331–341.
Canfield, R.L., Henderson Jr., C.R., Cory-Slechta, D.A., Cox, C., Jusko, T.A., Lanphear, B. P., 2003. Intellectual impairment in children with blood lead concentrations below 10 microg per deciliter. N. Engl. J. Med. 348, 1517–1526.
Chanda, S., Dasgupta, U.B., Guhamazumder, D., Gupta, M., Chaudhuri, U., Lahiri, S., Das, S., Ghosh, N., Chatterjee, D., 2006. DNA hypermethylation of promoter of gene p53 and p16 in arsenic-exposed people with and without malignancy. Toxicol. Sci. 89, 431–437.
Colella, S., Shen, L., Baggerly, K.A., Issa, J.P., Krahe, R., 2003. Sensitive and quantitative universal Pyrosequencing methylation analysis of CpG sites. Biotechniques 35, 146–150.
Donowitz, M., Ming Tse, C., Fuster, D., 2013. SLC9/NHE gene family, a plasma membrane and organellar family of Na(+)/H(+) exchangers. Mol. Aspect. Med. 34, 236–251.
Dosunmu, R., Alashwal, H., Zawia, N.H., 2012. Genome-wide expression and methylation profiling in the aged rodent brain due to early-life Pb exposure and its relevance to aging. Mech. Ageing Dev. 133, 435–443.
Doya, R., Nakayama, S.M.M., Nakata, H., Toyomaki, H., Yabe, J., Muzandu, K., Yohannes, Y.B., Kataba, A., Zyambo, G., Ogawa, T., Uchida, Y., Ikenaka, Y., Ishizuka, M., 2020. Land use in habitats affects metal concentrations in wild lizards around a former lead mining site. Environ. Sci. Technol. 54 (22), 14474–14481. https://doi.org/10.1021/acs.est.0c00150.
Ferguson-Smith, A.C., 2011. Genomic imprinting: the emergence of an epigenetic paradigm. Nat. Rev. Genet. 12, 565–575.
Flicek, P., Amode, M.R., Barrell, D., Beal, K., Billis, K., Brent, S., Carvalho-Silva, D., Clapham, P., Coates, G., Fitzgerald, S., Gil, L., Giron, C.G., Gordon, L., Hourlier, T., Hunt, S., Johnson, N., Juettemann, T., Kahari, A.K., Keenan, S., Kulesha, E., Martin, F.J., Maurel, T., McLaren, W.M., Murphy, D.N., Nag, R., Overduin, B., Pignatelli, M., Pritchard, B., Pritchard, E., Riat, H.S., Ruffier, M., Sheppard, D., Taylor, K., Thormann, A., Trevanion, S.J., Vullo, A., Wilder, S.P., Wilson, M., Zadissa, A., Aken, B.L., Birney, E., Cunningham, F., Harrow, J., Herrero, J., Hubbard, T.J., Kinsella, R., Muffato, M., Parker, A., Spudich, G., Yates, A., Zerbino, D.R., Searle, S.M., 2014. Ensembl 2014. Nucleic Acids Res. 42, D749–D755.
Fuks, F., 2005. DNA methylation and histone modifications: teaming up to silence genes. Curr. Opin. Genet. Dev. 15, 490–495.

Galaris, D., Evangelou, A., 2002. The role of oxidative stress in mechanisms of metal-induced carcinogenesis. Crit. Rev. Oncol. Hematol. 42, 93–103.
Gardiner-Garden, M., Frommer, M., 1987. CpG islands in vertebrate genomes. J. Mol. Biol. 196, 261–282.
Groh, K.J., Carvalho, R.N., Chipman, J.K., Denslow, N.D., Halder, M., Murphy, C.A., Roelofs, D., Rolaki, A., Schirmer, K., Watanabe, K.H., 2015. Development and application of the adverse outcome pathway framework for understanding and predicting chronic toxicity: I. Challenges and research needs in ecotoxicology. Chemosphere 120, 764–777.
Heard, E., Clerc, P., Avner, P., 1997. X-chromosome inactivation in mammals. Annu. Rev. Genet. 31, 571–610.
Hemdan, N.Y., Emmrich, F., Faber, S., Lehmann, J., Sack, U., 2007. Alterations of TH1/TH2 reactivity by heavy metals: possible consequences include induction of autoimmune diseases. Ann. N. Y. Acad. Sci. 1109, 129–137.
Hou, L., Zhang, X., Wang, D., Baccarelli, A., 2012. Environmental chemical exposures and human epigenetics. Int. J. Epidemiol. 41, 79–105.
Jones, P.L., Wolffe, A.P., 1999. Relationships between chromatin organization and DNA methylation in determining gene expression. Semin. Canc. Biol. 9, 339–347.
Joubert, B.R., Haberg, S.E., Nilsen, R.M., Wang, X., Vollset, S.E., Murphy, S.K., Huang, Z., Hoyo, C., Midttun, O., Cupul-Uicab, L.A., Ueland, P.M., Wu, M.C., Nystad, W., Bell, D.A., Peddada, S.D., London, S.J., 2012. 450K epigenome-wide scan identifies differential DNA methylation in newborns related to maternal smoking during pregnancy. Environ. Health Perspect. 120, 1425–1431.
Knight, A.K., Conneely, K.N., Kilaru, V., Cobb, D., Payne, J.L., Meilman, S., Corwin, E.J., Kaminsky, Z.A., Dunlop, A.L., Smith, A.K., 2018. SLC9B1 methylation predicts fetal intolerance of labor. Epigenetics 13, 33–39.
Lee, Y.W., Klein, C.B., Kargacin, B., Salnikow, K., Kitahara, J., Dowjat, K., Zhitkovich, A., Christie, N.T., Costa, M., 1995. Carcinogenic nickel silences gene expression by chromatin condensation and DNA methylation: a new model for epigenetic carcinogens. Mol. Cell Biol. 15, 2547–2557.
Li, Y., Xie, C., Murphy, S.K., Skaar, D., Nye, M., Vidal, A.C., Cecil, K.M., Dietrich, K.N., Puga, A., Jirtle, R.L., Hoyo, C., 2016. Lead exposure during early human development and DNA methylation of imprinted gene regulatory elements in adulthood. Environ. Health Perspect. 124, 666–673.
Li, X., Li, N., Sun, H.L., Yin, J., Tao, Y.C., Mao, Z.X., Yu, Z.L., Li, W.J., Bogden, J.D., 2017. Maternal lead exposure induces down-regulation of hippocampal insulin-degrading enzyme and nerve growth factor expression in mouse pups. Biomed. Environ. Sci. 30, 215–219.
Meissner, A., Mikkelsen, T.S., Gu, H., Wernig, M., Hanna, J., Sivachenko, A., Zhang, X., Bernstein, B.E., Nusbaum, C., Jaffe, D.B., Gnirke, A., Jaenisch, R., Lander, E.S., 2008. Genome-scale DNA methylation maps of pluripotent and differentiated cells. Nature 454, 766–770.
Meyer, P.A., Brown, M.J., Falk, H., 2008. Global approach to reducing lead exposure and poisoning. Mutat. Res. 659, 166–175.
Michael Waskom and The seaborn development team, 2020. mwaskom/seaborn. Series. https://doi.org/10.5281/zenodo.592845.
Minard, M.E., Jain, A.K., Barton, M.C., 2009. Analysis of epigenetic alterations to chromatin during development. Genesis 47, 559–572.
Monks, T.J., Xie, R., Tikoo, K., Lau, S.S., 2006. Ros-induced histone modifications and their role in cell survival and cell death. Drug Metabol. Rev. 38, 755–767.
Nakayama, S.M.M., Ikenaka, Y., Hamada, K., Muzandu, K., Choongo, K., Teraoka, H., Mizuno, N., Ishizuka, M., 2011. Metal and metalloid contamination in roadside soil and wild rats around a Pb-Zn mine in Kabwe, Zambia. Environ. Pollut. 159, 175–181.
Pilsner, J.R., Hu, H., Ettinger, A., Sanchez, B.N., Wright, R.O., Cantonwine, D., Lazarus, A., Lamadrid-Figueroa, H., Mercado-Garcia, A., Tellez-Rojo, M.M., Hernandez-Avila, M., 2009. Influence of prenatal lead exposure on genomic methylation of cord blood DNA. Environ. Health Perspect. 117, 1466–1471.
Reichard, J.F., Schnekenburger, M., Puga, A., 2007. Long term low-dose arsenic exposure induces loss of DNA methylation. Biochem. Biophys. Res. Commun. 352, 188–192.
Salnikow, K., Zhitkovich, A., 2008. Genetic and epigenetic mechanisms in metal carcinogenesis and cocarcinogenesis: nickel, arsenic, and chromium. Chem. Res. Toxicol. 21, 28–44.
Sanchez-Martin, F.J., Fan, Y., Lindquist, D.M., Xia, Y., Puga, A., 2013. Lead induces similar gene expression changes in brains of gestationally exposed adult mice and in neurons differentiated from mouse embryonic stem cells. PloS One 8, e80558.
Sciandrello, G., Caradonna, F., Mauro, M., Barbata, G., 2004. Arsenic-induced DNA hypomethylation affects chromosomal instability in mammalian cells. Carcinogenesis 25, 413–417.
Sen, A., Heredia, N., Senut, M.C., Hess, M., Land, S., Qu, W., Hollacher, K., Dereski, M.O., Ruden, D.M., 2015. Early life lead exposure causes gender-specific changes in the DNA methylation profile of DNA extracted from dried blood spots. Epigenomics 7, 379–393.
Senut, M.C., Sen, A., Cingolani, P., Shaik, A., Land, S.J., Ruden, D.M., 2014. Lead exposure disrupts global DNA methylation in human embryonic stem cells and alters their neuronal differentiation. Toxicol. Sci. 139, 142–161.
Severe, S., Marchand, P., Guiffard, I., Morio, F., Venisseau, A., Veyrand, B., Le Bizec, B., Antignac, J.P., Abadie, J., 2015. Pollutants in pet dogs: a model for environmental links to breast cancer. SpringerPlus 4, 27.
Sun, L.D., Xiao, F.L., Li, Y., Zhou, W.M., Tang, H.Y., Tang, X.F., Zhang, H., Schaarschmidt, H., Zuo, X.B., Foelster-Holst, R., He, S.M., Shi, M., Liu, Q., Lv, Y.M., Chen, X.L., Zhu, K.J., Guo, Y.F., Hu, D.Y., Li, M., Li, M., Zhang, Y.H., Zhang, X., Tang, J.P., Guo, B.R., Wang, H., Liu, Y., Zou, X.Y., Zhou, F.S., Liu, X.Y., Chen, G., Ma, L., Zhang, S.M., Jiang, A.P., Zheng, X.D., Gao, X.H., Li, P., Tu, C.X., Yin, X.Y., Han, X.P., Ren, Y.Q., Song, S.P., Lu, Z.Y., Zhang, X.L., Cui, Y., Chang, J., Gao, M., Luo, X.Y., Wang, P.G., Dai, X., Su, W., Li, H., Shen, C.P., Liu, S.X., Feng, X.B., Yang, C.J., Lin, G.S., Wang, Z.X., Huang, J.Q., Fan, X., Wang, Y., Bao, Y.X., Yang, S., Liu, J.J., Franke, A., Weidinger, S., Yao, Z.R., Zhang, X.J., 2011. Genome-wide association study identifies two new susceptibility loci for atopic dermatitis in the Chinese Han population. Nat. Genet. 43, 690–694.
Takiguchi, M., Achanzar, W.E., Qu, W., Li, G., Waalkes, M.P., 2003. Effects of cadmium on DNA-(Cytosine-5) methyltransferase activity and DNA methylation status during cadmium-induced cellular transformation. Exp. Cell Res. 286, 355–365.
Thomas, C.W., Rising, J.L., Moore, J.K., 1975. Blood lead concentrations in three groups of dogs from a suburban Illinois community. J. Am. Vet. Med. Assoc. 167, 995–999.
Thomas, C.W., Rising, J.L., Moore, J.K., 1976. Blood lead concentrations of children and dogs from 83 Illinois families. J. Am. Vet. Med. Assoc. 169, 1237–1240.
Toyomaki, H., Yabe, J., Nakayama, S.M.M., Yohannes, Y.B., Muzandu, K., Liazambi, A., Ikenaka, Y., Kuritani, T., Nakagawa, M., Ishizuka, M., 2020. Factors associated with lead (Pb) exposure on dogs around a Pb mining area, Kabwe, Zambia. Chemosphere 247, 125884.
Wright, R.O., Schwartz, J., Wright, R.J., Bollati, V., Tarantini, L., Park, S.K., Hu, H., Sparrow, D., Vokonas, P., Baccarelli, A., 2010. Biomarkers of lead exposure and DNA methylation within retrotransposons. Environ. Health Perspect. 118, 790–795.
Yabe, J., Nakayama, S.M., Ikenaka, Y., Muzandu, K., Ishizuka, M., Umemura, T., 2011. Uptake of lead, cadmium, and other metals in the liver and kidneys of cattle near a lead-zinc mine in Kabwe, Zambia. Environ. Toxicol. Chem. 30, 1892–1897.
Yabe, J., Nakayama, S.M., Ikenaka, Y., Muzandu, K., Choongo, K., Mainda, G., Kabeta, M., Ishizuka, M., Umemura, T., 2013. Metal distribution in tissues of free-range chickens near a lead-zinc mine in Kabwe, Zambia. Environ. Toxicol. Chem. 32, 189–192.
Yabe, J., Nakayama, S.M.M., Ikenaka, Y., Yohannes, Y.B., Bortey-Sam, N., Oroszlany, B., Muzandu, K., Choongo, K., Kabalo, A.N., Ntapisha, J., Mweene, A., Umemura, T., Ishizuka, M., 2015. Lead poisoning in children from townships in the vicinity of a lead-zinc mine in Kabwe, Zambia. Chemosphere 119, 941–947.
Yabe, J., Nakayama, S.M., Nakata, H., Toyomaki, H., Yohannes, Y.B., Muzandu, K., Kataba, A., Zyambo, G., Hiwatari, M., Narita, D., Yamada, D., Hangoma, P., Munyinda, N.S., Mufune, T., Ikenaka, Y., Choongo, K., Ishizuka, M., 2020. Current trends of blood lead levels, distribution patterns and exposure variations among household members in Kabwe, Zambia. Chemosphere 243, 125412.
Yamazaki, J., Jelinek, J., Hisamoto, S., Tsukamoto, A., Inaba, M., 2018. Dynamic changes in DNA methylation patterns in canine lymphoma cell lines demonstrated by genome-wide quantitative DNA methylation analysis. Vet. J. 231, 48–54.
Zhou, Z., Yuan, Q., Mash, D.C., Goldman, D., 2011. Substance-specific and shared transcription and epigenetic changes in the human hippocampus chronically exposed to cocaine and alcohol. Proc. Natl. Acad. Sci. U. S. A 108, 6626–6631.

Environmental Pollution 286 (2021) 117456

Contents lists available at ScienceDirect

Environmental Pollution

journal homepage: www.elsevier.com/locate/envpol

Lead concentrations and isotope ratios in blood, breastmilk and feces: contribution of both lactation and soil/dust exposure to infants in a lead mining area, Kabwe, Zambia☆

Haruya Toyomaki [a], John Yabe [b,h], Shouta M.M. Nakayama [a,*], Yared B. Yohannes [a,c], Kaampwe Muzandu [a,b], Tiza Mufune [d], Hokuto Nakata [a], Yoshinori Ikenaka [a,e,i,j], Takeshi Kuritani [f], Mitsuhiro Nakagawa [f], Kennedy Choongo [b,g], Mayumi Ishizuka [a]

[a] Laboratory of Toxicology, Department of Environmental Veterinary Sciences, Faculty of Veterinary Medicine, Hokkaido University, Japan
[b] The University of Zambia, School of Veterinary Medicine, Zambia
[c] Department of Chemistry, College of Natural and Computational Science, University of Gondar, Ethiopia
[d] Ministry of Health, District Health Office, Kabwe, Zambia
[e] Water Research Group, School of Environmental Sciences and Development, North-West University, South Africa
[f] Department of Earth and Planetary Sciences, Graduate School of Science, Hokkaido University, Sapporo, Japan
[g] Fiji National University, College of Agriculture, Fisheries & Forestry, School of Animal and Veterinary Sciences, Koronivia Campus, Suva, Fiji
[h] Department of Pathobiology, School of Veterinary Medicine, University of Namibia, Windhoek, Namibia
[i] Translational Research Unit, Veterinary Teaching Hospital, Faculty of Veterinary Medicine, Hokkaido University, Sapporo, 060-0818, Japan
[j] One Health Research Center, Hokkaido University, Japan

ARTICLE INFO

Keywords:
Lead poisoning
Infant
Mother
Breastmilk
Lead stable isotope

ABSTRACT

Lead (Pb) poses a serious public health concern. Breastmilk may be a possible source of Pb exposure in infants, as Pb can be transferred from the maternal blood to breastmilk. The present study was undertaken to determine the Pb exposure and the contribution of lactation as one of the exposure pathways to infants in a Pb mining area, Kabwe, Zambia. Blood, breastmilk and infants' feces were collected from 418 pairs of infants and mothers. The Pb concentrations, isotope ratios in the samples, and biochemistry in mothers' plasma were analyzed. The overall mean of blood lead levels (BLLs) in infants and mothers were 18.0 and 11.3 μg/dL, respectively. High Pb concentration in breastmilk (range: 0.4–51.9, mean: 5.3 μg/L) above the WHO acceptable level between 2 and 5 μg/L were found and could be one of the sources of Pb exposure in infants. The Pb isotope ratios in infants' feces were the most similar to Pb ratios in the soil samples. The results suggest that infants are also exposed to Pb from the environment. Pb exposure in infants through breastfeeding and soil ingestion could potentially exceed daily intake of Pb which causes neurodevelopmental toxicity. In contrast to the high BLLs in mothers, the plasma biochemical profiles of most analyzed parameters were interestingly within, or close to, the standard reference values. Our data suggest that environmental remediation is urgently needed to reduce the Pb exposure in infants and mothers from the environment in Kabwe in parallel with chelation therapy.

1. Introduction

Lead (Pb) poses a serious public health concern, accounting for 0.6% of the global burden of disease (World Health Organization, 2010). Serious cases of Pb exposure have been reported in both developed and developing countries (Ajumobi et al., 2014; Haefliger et al., 2009; Ruckart et al., 2019). Lead poisoning causes various symptoms, including anemia, nephropathy, and death (Meyer et al., 2008). Children, especially infants are more vulnerable to Pb, compared to adults. To measure exposure to Pb, blood lead level (BLL) has been widely used. In the blood, Pb has a short half-life of 30–40 days (Barbosa et al., 2005). Even at low levels, Pb exposure can cause pediatric neurodevelopmental

☆ This paper has been recommended for acceptance by Wen-Xiong Wang.

* Corresponding author. Laboratory of Toxicology, Department of Environmental Veterinary Sciences, Faculty of Veterinary Medicine, Hokkaido University, Kita 18, Nishi 9, Kita-ku, Sapporo, 060-0818, Japan.
E-mail addresses: shouta-nakayama@vetmed.hokudai.ac.jp, shoutanakayama0219@gmail.com (S.M.M. Nakayama).

https://doi.org/10.1016/j.envpol.2021.117456
Received 16 September 2020; Received in revised form 18 May 2021; Accepted 22 May 2021
Available online 24 May 2021

impairments, such as a reduction in intelligence quotient (IQ) (Canfield et al., 2003). Due to this, the blood Pb reference value for Pb exposure has been set to 5 μg/dL (Centers for Disease Control and Prevention, 2019; 2012). A BLL above 45 μg/dL is considered the level where treatment is required (CDC, 2012; 2002; Needleman, 2004), and a BLL above 100 μg/dL is considered a fatal level in children, which causes serious clinical symptoms such as encephalopathy, even in adults (Meyer et al., 2008; National Academy of Science, 1972). The European Food Safety Authority (EFSA) observed that Pb dietary intake of 0.5 μg/kg body weight (bw)/day would be associated with developmental neurotoxicity in young children (European Food Safety Authority, 2010).

Breastmilk is vital for infants, to ensure normal development and to prevent infectious diseases. However, breastmilk may be a possible source of Pb exposure in infants, as Pb can be transferred from the maternal blood to breastmilk. As a result, BLLs in mothers should be monitored to prevent Pb exposure in infants via breastfeeding. Therefore, to minimize Pb exposure in infants through breastmilk, World Health Organization (1989) has set the acceptable level of breastmilk Pb concentration to be between 2 and 5 μg/L. Mothers with confirmed BLLs above 40 μg/dL should pump and discard their breastmilk (Centers for Disease Control and Prevention, 2010).

Lead exposure primarily occurs via ingestion and inhalation, and can be traced to numerous sources, including battery recycling, gasoline, paint, as well as mining (Calabrese and Stanek, 1995; Meyer et al., 2008; Schoning et al., 1996; Yabe et al., 2010). Identifying the source of Pb exposure is important to prevent exposure. One such method for identifying sources is the use of Pb isotopic tracing (Komárek et al., 2008; Gulson, 2008). Lead is present in the environment as four main isotopes: ^{208}Pb (52%), ^{207}Pb (23%), ^{206}Pb (24%), and ^{204}Pb (1%) (Komárek et al., 2008). The compositions of these isotopes are not affected to a measurable extent by physicochemical fractionation processes (Bollhöfer and Rosman, 2001; Veysseyre et al., 2001).

The Zambian town of Kabwe accommodates a Pb-zinc (Zn) mining area which, up until its closure in 1994, was operated without adequate pollution laws to regulate mining emissions. Elevated BLLs and Pb concentrations in the feces and urine of children near the mine have been reported, all of which exceeded the 5 μg/dL blood Pb reference value (Yabe et al., 2018, 2015). Yabe et al. (2015) found that BLLs in children between the ages of one and two years old were higher compared with those in children between the ages of four and seven years old in Kabwe, as has been observed in many other studies. It is necessary to reduce and prevent Pb exposure in children. This is especially important in infants, who are more vulnerable to Pb poisoning. Moreover, a more recent study has revealed a high Pb exposure also in mothers, where approximately 5% of mothers were found to have a BLL above 45 μg/dL which indicated that treatment was required (Yabe et al., 2020; Nakata et al., 2021). The breastfeeding practices of mothers with high BLLs are a possible source of Pb exposure for infants in Kabwe. However, the precise sources and routes of Pb exposure in infants have not yet been determined. Furthermore, no clinical studies of Pb poisoning have been done in Kabwe, despite high BLLs being reported in the local people. Some previous studies have reported that metallothionein concentrations, which is a cysteine-rich protein that binds and detoxifies toxic metals, increase as metal concentrations in the blood increase (Bizoń and Milnerowicz, 2014; Kowalska et al., 2015). Metallothionein may therefore play an important role in reducing Pb toxicity in the people of Kabwe.

The current study aimed to determine the Pb exposure and the contribution of lactation as one of the exposure pathways to infants in a lead mining area, Kabwe, Zambia. Pb concentrations in mothers' breastmilk, infants' feces, and both infants' and mothers' blood, were analyzed. Daily intake of Pb in infants through breastfeeding and soil ingestion was calculated to estimate the burden of routes of Pb exposure. The Pb isotope ratios in samples were analyzed in a limited number of samples to determine the source of Pb exposure. Furthermore, a plasma biochemical analysis including metallothionein concentrations was conducted in the mothers to evaluate the health impact of Pb exposure in this population.

2. Materials and methods

2.1. Sampling sites

The town of Kabwe is located at about 28°26′E and 14°27′S, and is the provincial capital of Zambia's Central Province. It is the fourth largest town in Zambia, with a population of about 230,000 inhabitants and an area of 1547 km^2. In Kabwe, metallic residues from abandoned tailings and waste stored in the mine have continued to serve as potential sources of metal pollution even after the closure of the mine. Dust emanates from the mine dumps, and residents in townships close to the mine may be exposed to high levels of Pb in contaminated dust and soil.

The present study was conducted at health centers in four sites near the mine (Kasanda, Makululu, Chowa and Katondo) and one site far from the mine (Bwacha) in the rainy season from January to March of 2017 (Fig. 1). Kasanda, Makululu, Chowa, Katondo, and Bwacha health centers were located about 0.9, 2.6, 1.4, 4.5, and 6.1 km from the mine, respectively. Kasanda and Makululu are located on the western side of the mine and in the direction of prevailing winds.

2.2. Sampling

This study was approved by the University of Zambia Research Ethics Committee (UNZAREC; REF. No. 012-04-16). Further approvals were granted by the Ministry of Health through the Zambia National Health Research Ethics Board and the Kabwe District Health Office.

A sensitization campaign about the research activities was conducted by community health workers before sampling in their catchment areas around the health centers. Mothers and guardians were encouraged to participate in the study, and were asked to take their breastfed infants under the age of 1 year and 6 months to the selected health centers for sample collection. Only infants with mothers/guardians that willingly agreed to participate and signed the informed consent were included in the present study. After informed and written consent were obtained from the mothers/guardians, blood samples were collected as described by Yabe et al. (2015). The mothers/guardians were also interviewed to obtain necessary personal details about themselves and their infants, such as age and sex. Sample collection and questionnaire administration were undertaken by certified local nurses. In accordance with ethical requirements, confidentiality was upheld in the study.

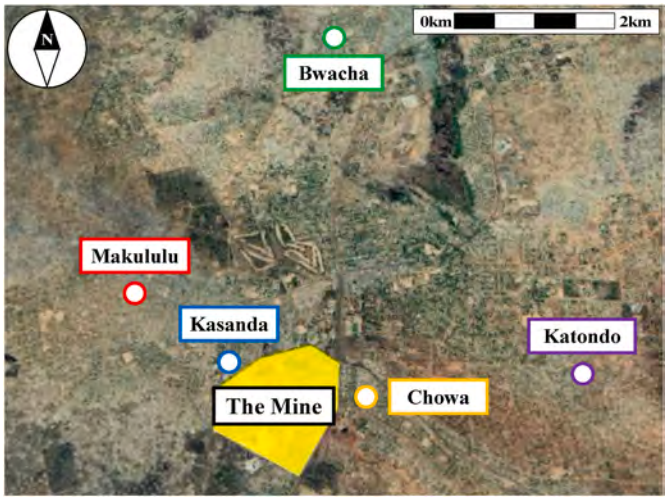

Fig. 1. Map of the sampling sites in Kabwe, Zambia (image modified from Google Earth).

Blood samples up to 2 mL and 5 mL were collected from the cephalic veins of each infant and mother, respectively, and were placed into heparinized blood collection tubes. Breastmilk samples from mothers were collected in clean sample cups by gentle compression of the breast and transferred to 2 mL sample tubes for storage and transportation. To avoid contamination, the hands as well as venipuncture and breast sites were cleaned and sanitized with an ethanol swab before the sample collection. Plasma samples were separated only from the mothers' blood after centrifugation. For infants' fecal samples, mothers/guardians were handed 30 mL stool containers equipped with scoops and were instructed to scoop feces into the container from a used diaper in the morning of the following day. Household soil samples were collected in June 2016 from Kasanda (n = 12) and Makululu (n = 20) as a reference of environmental samples for Pb stable isotope analysis.

The processed samples were transported to the laboratory of The University of Zambia, School of Veterinary Medicine, Zambia, and stored at −20 °C. The material transfer agreement (MTA) for human samples from the Zambia National Health Research Ethics Committee (approval No. E00417) was obtained before transportation. Similarly, the phytosanitary certificate from plant quarantine and phytosanitary service, Zambia Ministry of Agriculture, and import permission by plant protection station, Japanese Ministry of Agriculture, Forestry and Fisheries (approval No. 28–313) was also granted for soil samples. The human samples were transported in temperature-controlled boxes with ice packs, and the soil samples in temperature-controlled boxes, for further analysis at Hokkaido University, Japan.

2.3. Pb and metal concentration analysis

Pb and other metals (iron (Fe), copper (Cu), Zn, and silver (Ag) were extracted from the samples. Thawed fecal and bulk soil samples were weighed on heat-resistant tissue drying plates and dried for 48 h in a tissue drying oven at 60 °C, whereas whole blood and breastmilk samples were only thawed. Each blood and breastmilk sample (1 mL) and 50 mg of each dried fecal and soil sample were analyzed. Detailed method was described in the supplementary materials.

2.4. Calculation of daily intake of Pb in infants through breastfeeding and soil ingestion

Daily intake of Pb in infants through breastfeeding and soil ingestion was calculated. The calculation was conducted using the maximum, mean, and minimum Pb concentrations in breastmilk and soil samples in the present study using the formulas below. The amounts of daily breastmilk intake and soil ingestion in infants were set as 0.78 L/day and 30 mg/day reported by Costa et al. (2010) and United States Environmental Protection Agency (US EPA, 2011), respectively.

Daily intake of Pb = (Pb concentrations in breastmilk × Amount of daily breastmilk intake) + (Pb concentrations in soil × amount of daily soil ingestion).

In the present study, 0.5 μg/kg bw/day was used as the reference value as the limit of daily intake of Pb for infants (European Food Safety Authority, 2010).

2.5. Stable Pb isotope analysis

Only 26 sample sets with high Pb concentrations of infants' and mothers' blood, breastmilk, and infants' feces from Kasanda and Makululu, were chosen and analyzed during Pb isotope analysis as well as 32 soil samples. As mentioned above, these soil samples were collected at the preliminary survey in 2016. The sampling area between blood and soil are same, but not all the locations were exactly from the same household. The sample dissolution procedure was similar to previously described methods (Kuritani and Nakamura, 2002; Nakayama et al., 2019). The detailed methods of the high precision isotope analysis were described in the supplementary materials. We have measured duplicates of breastmilk samples and the results of Pb isotope ratios had the similar trends. As sample amounts decrease, the uncertainty of ion beam intensity measurements for the minor isotope ^{204}Pb tends to increase, and the accuracy and precision of the isotopic ratios involving ^{204}Pb decrease (^{204}Pb error; Hamelin et al., 1985). Therefore, the isotopic composition of Pb is commonly expressed as ratios of ^{208}Pb, ^{207}Pb, and ^{206}Pb. However, since normalization to ^{204}Pb yields the largest variability between reservoirs (Komárek et al., 2008), we included ^{204}Pb data with correction (Kuritani and Nakamura, 2003; 2002). This was done in order to observe the detail variability of isotope ratio among the breastmilk, blood, feces and soil samples in this study.

2.6. Plasma biochemical analysis and metallothionein ELISA

A conventional blood biochemical analyzer (FUJI DRICHEM 7000V; FUJIFILM corporation, Tokyo, Japan) was used to analyze the concentrations of alanine aminotransferase (ALT), alkaline phosphatase (ALP), aspartate aminotransferase (AST), gamma glutamyl transpeptidase (GGT), lactase dehydrogenase (LDH), total bilirubin (T-Bil), total protein (TP), albumin (Alb), blood urea nitrogen (BUN), creatinine (Cre), and urea acid (UA) in mothers' plasma samples. Metallothionein in mothers' plasma samples was measured by ELISA using an antibody against iso-Metallothionein I and II (Metallothionein ELISA kit; Frontier Institute Co., Ltd., Hokkaido, Japan). The standard reference ranges for each parameter in humans were provided by the kit manufacturers.

2.7. Statistical analysis

All data from the experiments and questionnaires were combined into a single electronic database and checked for accuracy and outliers. All statistical analyses were performed at a significance level of $p < 0.05$ using JMP 13.1.0 (SAS Institute, USA). Mean values were indicated in addition to standard deviation (SD) values. The collinearity between factors was analyzed using Spearman's rank correlation test. A Steel–Dwass multiple comparisons test was used to compare the differences between the factors among areas and samples.

3. Results

3.1. Characteristics of the infants and mothers

A total of 418 pairs of infants and mothers participated in this study. Of these, 333 participants came from four sites near the mine, and 85 came from Bwacha, which is located about 6 km from the mine (Table 1; Fig. 1). None of the infants and mothers had overt signs of Pb poisoning. Infants from Chowa were younger than those from other areas, except for Bwacha ($p < 0.05$). In regard to height, infants from Chowa were significantly shorter and infants from Katondo were significantly taller than infants from other areas ($p < 0.05$). Body weight of the infants from Chowa was significantly lower than that of the infants from other areas ($p < 0.05$).

The overall height of boys was greater than that of girls overall ($p < 0.01$), with boys found to be significantly taller in the four areas near the mine considered together ($p < 0.01$) and in Makululu alone ($p < 0.01$, Supplementary Table S3). In Katondo, the height of boys tended to be greater than that of girls, but no significant difference was recorded ($p = 0.09$). The weight of boys was significantly higher than that of girls when considering all infants ($p < 0.01$), and for infants from near the mine ($p < 0.01$), and infants in Kasanda ($p < 0.05$), Makululu ($p < 0.01$), Katondo ($p < 0.01$), and Bwacha ($p < 0.045$) alone.

3.2. Pb and other metals concentrations in blood, breastmilk, infants' feces, and soil

The overall mean of Pb concentrations in the soil samples (n = 32) was 1048 ± 1470 mg/kg (dry weight) and ranged from 346 to 6327 mg/

Table 1
General characteristics of infants and mothers, as well as Pb concentrations in blood, breastmilk and fecal samples in Kabwe, Zambia; mean ± SD values (sample size, minimum–maximum).

Area (N)	Sex of infants, boy:girl	Age of infants, months	Height, Cm	Weight, kg	Age of mothers, years	BLLs in infants, μg/dL	BLLs in mothers, μg/dL	Pb in breastmilk, μg/L	Pb in infants' feces, mg/kg dry weight
Overall (418)	221:197	7.1 ± 3.8 (417, 0.1–16.8)	64.2 ± 7.7 (361, 45.0–95.0)	7.3 ± 1.7 (411, 1.9–12.1)	26.1 ± 6.5 (412, 16.3–46.1)	18.0 ± 18.1 ^{A} (406, 0.8–93.4)	11.3 ± 9.2 ^{B} (417, 1.5–82.6)	5.3 ± 7.0 ^{C} (407, 0.4–51.9)	39.2 ± 217.7 ^{D} (212, 0.08–3002.7)
Near the mine (333)	171:162	7.2 ± 4.0 (332, 0.1–16.8)	64.5 ± 8.0 (280, 45.0–95.0)	7.2 ± 1.7 (329, 1.9–12.1)	26.1 ± 6.6 (329, 16.3–46.1)	21.4 ± 18.9 **, ^{A} (321, 1.6–93.4)	13.0 ± 9.5 **, ^{B} (333, 1.9–82.6)	6.1 ± 7.5 **, ^{C} (324, 0.4–51.9)	49.2 ± 248.0 **, ^{D} (162, 0.09–3002.7)
Kasanda (82)	43:39	7.3 ± 3.8 ^{a} (82, 0.6–16.7)	64.5 ± 8.4 ^{a} (74, 49.0–95.0)	7.6 ± 1.5 ^{a} (79, 4.0–12.1)	27.1 ± 6.7 (82, 17.4–45.4)	24.8 ± 20.9 ^{a,} ^{A} (80, 3.7–93.4)	15.8 ± 10.6 ^{a,} ^{B} (82, 2.3–82.6)	9.2 ± 8.9 ^{a,} ^{C} (79, 1.9–50.4)	38.8 ± 88.9 ^{ab,} ^{D} (28, 0.6–451.0)
Makululu (102)	44:58	7.7 ± 3.7 ^{a} (102, 1.5–16.7)	63.0 ± 7.0 ^{a} (102, 45.0–85.0)	7.4 ± 1.4 ^{a} (101, 4.1–11.9)	26.2 ± 7.0 (102, 16.6–45.9)	30.8 ± 19.4 ^{b,} ^{A} (102, 5.6–82.7)	17.6 ± 10.1 ^{a,} ^{B} (102, 3.3–67.3)	7.1 ± 7.1 ^{ab,} ^{C} (100, 1.1–40.2)	82.4 ± 362.7 ^{a,} ^{D} (69, 1.1–3002.7)
Chowa (58)	35:23	5.3 ± 3.9 ^{b} (58, 0.1–15.2)	56.2 ± 7.1 ^{b} (13, 49.0–67.0)	5.6 ± 1.4 ^{b} (58, 3.5–8.7)	26.9 ± 6.3 (58, 17.6–41.8)	15.7 ± 15.5 ^{c,} ^{A} (49, 3.2–62.3)	11.2 ± 6.1 ^{b,} ^{A} (58, 3.0–36.2)	5.6 ± 6.5 ^{b,} ^{B} (57, 1.4–42.1)	33.7 ± 139.4 ^{bc,} ^{C} (31, 0.09–780.4)
Katondo (91)	49:42	7.7 ± 4.3 ^{a} (90, 0.9–16.8)	67.5 ± 7.6 ^{c} (91, 48.0–94.0)	7.8 ± 1.7 ^{a} (91, 1.9–11.1)	24.6 ± 5.9 (87, 16.3–46.1)	10.9 ± 9.9 ^{c,} ^{A} (90, 1.6–51.0)	6.3 ± 3.5 ^{c,} ^{B} (91, 1.9–21.6)	2.3 ± 5.5 ^{c,} ^{C} (88, 0.4–51.9)	4.4 ± 5.1 ^{c,} ^{D} (34, 0.1–19.4)
Bwacha (85)	50:35	6.9 ± 3.2 ^{ab} (85, 1.6–13.5)	63.0 ± 6.6 ^{a} (81, 51.0–86.0)	7.6 ± 1.6 ^{a} (82, 4.6–11.4)	26.2 ± 5.9 (83, 16.6–43.3)	5.2 ± 4.1 ^{d,} ^{A} (85, 0.8–22.0)	4.7 ± 3.4 ^{d,} ^{A} (84, 1.5–23.1)	2.3 ± 2.9 ^{c,} ^{B} (83, 0.5–17.9)	6.9 ± 27.6 ^{d,} ^{C} (50, 0.08–184.0)

Note: ** indicates a significant difference ($p < 0.01$) between sites near the mine and Bwacha. Various small letters indicate a significant difference among areas ($p < 0.05$). Various capital letters indicate a significant difference among infants' and mothers' blood, breastmilk, and infants' feces ($p < 0.05$).

kg.

The overall mean values of BLLs in infants and mothers were 18.0 ± 18.1 and 11.3 ± 9.2 μg/dL, respectively (Table 1 and Fig. 2a). We found 76.8% of infants (312/406) and 73.6% of mothers (307/417) had BLLs above the reference value for Pb exposure (5 μg/dL; Centers for Disease Control and Prevention, 2019; 2012). Moreover, BLLs in 8.9% of infants (36/406) and 1.2% of mothers (5/417) were above 45 μg/dL, the recommended threshold BLL for chelation therapy (Meyer et al., 2008). No infants or mothers had BLLs above the lethal level for Pb exposure (100 μg/dL), however, the highest BLL in an infant in the present study was 93.4 μg/dL. The overall mean of Pb concentrations in breastmilk and infants' feces were 5.3 ± 7.0 μg/L and 39.2 ± 217.7 mg/kg (dry weight), respectively (Fig. 2b and c). Overall, 30.0% of breastmilk samples (122/407) had Pb concentrations of more than 5 μg/L, which is above the accepted level for breastfeeding (World Health Organization, 1989).

There were significant differences in Pb concentrations among sample types in the samples from all sites: infants' feces > infants' blood > mothers' blood > breastmilk ($p < 0.05$). Among the samples from Chowa and Bwacha, there were no significant differences in Pb concentrations between infants' and mothers' blood. Pb concentrations in infants' blood were 1.8 ± 1.5 and 60.2 ± 67.6 times higher than those in the mothers' blood and Pb concentrations in breastmilk, respectively (Supplementary Table S4). On the other hand, Pb concentrations in infants' blood were 5.3 ± 7.4% of the Pb concentrations in infants' feces.

Pb concentrations in infants' and mothers' blood, breastmilk, and infants' feces from sites near the mine (Kasanda, Makululu, Chowa, and Katondo) were significantly higher than the concentrations in samples from Bwacha. Among sites, the mean of Pb concentrations in each sample type from Makululu were the highest, except in breastmilk. Pb concentrations in samples from Bwacha were significantly lower than those from other sites ($p < 0.05$), except in breastmilk.

BLLs in boys were significantly higher than those in girls ($p = 0.04$) in Makululu, and higher in Bwacha ($p = 0.06$, Supplementary Table S5). Pb concentrations in infants' feces of boys were significantly higher than those of girls in Chowa ($p < 0.01$). The same trend was found in all infants, although the association was not statistically significant ($p = 0.08$).

Supplementary Tables S6, S7, S8, and S9 show Fe, Cu, Zn, and Ag concentrations in the samples, respectively. Fe concentrations in infants' blood and Fe, Cu, Zn, and Ag concentrations in mothers' blood from sites near the mine were significantly lower than the concentrations in samples from Bwacha. On the other hand, Fe concentrations in breastmilk from sites near the mine were significantly higher than the concentrations in samples from Bwacha.

3.3. Relationships among samples and factors

In the samples from all areas, significant positive correlations existed among infants in the factors of age, height, and weight (Table 2, $p < 0.001$). There were significant positive correlations of Pb concentrations among all sample types ($p < 0.001$, Supplementary Fig. S2). BLLs in infants and Pb concentrations in infants' feces had a significant positive correlation with the age (Supplementary Fig. S3), height, and weight of infants ($p < 0.001$).

In all samples from sites near the mine, the same trend was found (Supplementary Table S10). Moreover, the height of infants had a significant negative correlation with BLLs in mothers ($p < 0.01$, $\rho = -0.19$) and Pb concentrations in breastmilk ($p < 0.05$, $\rho = -0.13$). In the samples from Bwacha, the same trend was found as in the samples from all other sites, except for the relationship between Pb concentrations in breastmilk and other samples, and the BLLs in mothers and Pb concentrations in infants' feces (Supplementary Table S11). Supplementary Tables S12, 13, and 14 show the relationships among Pb and other metals in the samples from all areas, from sites near the mine, and Bwacha, respectively. In the samples from all areas, Pb concentrations in infants' blood significantly increased as Cu ($p < 0.001$, $\rho = 0.34$) and Ag ($p < 0.001$, $\rho = 0.28$) concentrations in infants' blood. There were significant negative correlations between Pb and Fe concentrations in infants' blood as well as in mothers' blood.

3.4. Daily intake of Pb in infants through breastfeeding and soil ingestion

Table 3 shows the results of daily intake of Pb in infants through breastfeeding and soil ingestion. The results ranged from 0.3 to 40.5 μg/day through breastfeeding and from 10.4 to 189.8 μg/day through soil ingestion depending on Pb concentrations in the samples. Daily intake of Pb through combined breastfeeding and soil ingestion ranged from 10.7 to 230.3 μg/day. The reference value of daily intake of Pb which would

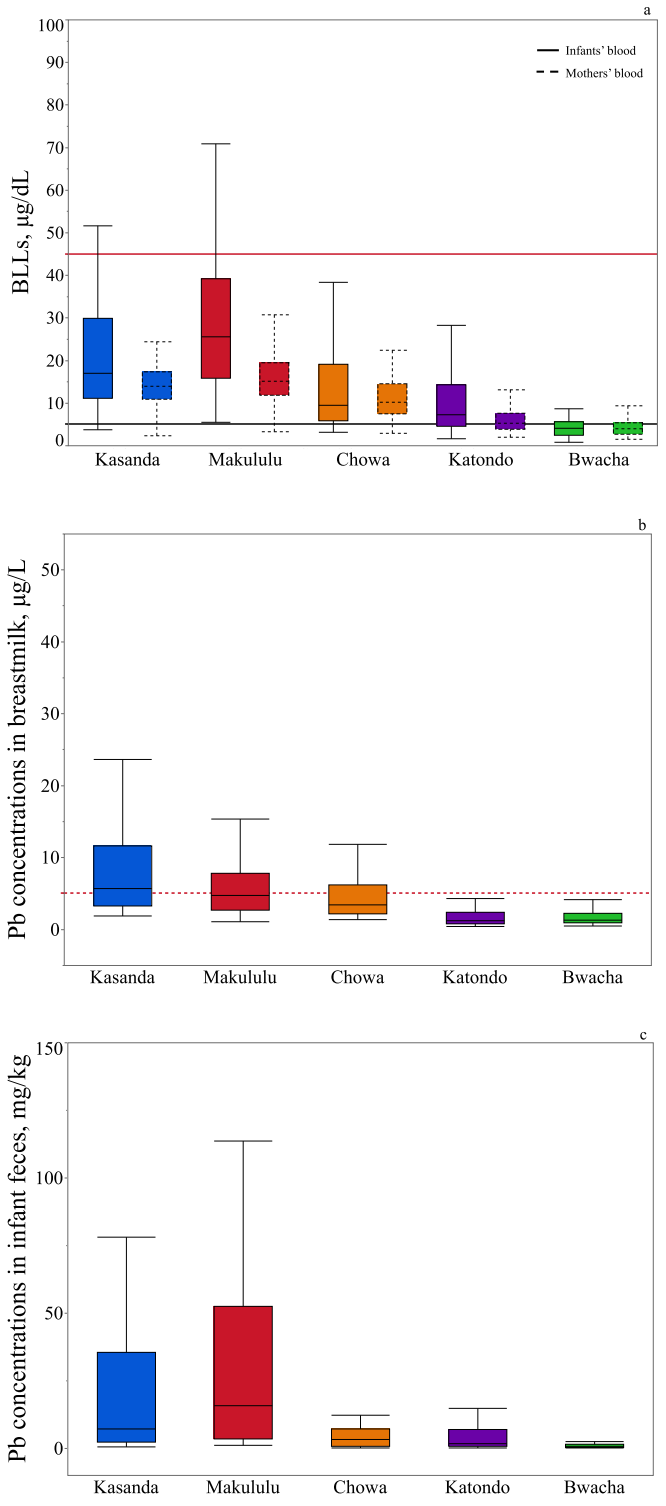

Fig. 2. BLLs in infants and mothers (2a), Pb concentrations in breastmilk (2b), and infants' feces (2c) among areas. The blue, red, orange, violet, and green colors indicate samples from Kasanda, Makululu, Chowa, Katondo, and Bwacha, respectively. Solid and dot box plots in Fig. 2a indicate BLLs in infants and mothers, respectively. Red and black lines in Fig. 2a indicate 45 and 5 μg/dL, respectively. The red dotted line in Fig. 2b indicates the 5 μg/L level. (For interpretation of the references to color in this figure legend, the reader is referred to the Web version of this article.)

be associated with developmental neurotoxicity in infants in the present study was 3.7 μg/day (the mean bw: 7.3 kg) and ranged from 1.0 μg/day (the minimum bw: 1.9 kg) to 6.1 μg/day (the maximum bw: 12.1) based on the EFSA's reference value (0.5 μg/kg bw/day) (European Food Safety Authority, 2010). The minimum of calculated daily intake of Pb even only through soil ingestion exceeded the maximum of the limit.

3.5. Pb isotope ratio analysis

Table 4 shows the mean values of the $^{208}Pb/^{206}Pb$, $^{207}Pb/^{206}Pb$, $^{208}Pb/^{204}Pb$, and $^{207}Pb/^{204}Pb$ ratios in the samples. The $^{208}Pb/^{206}$ Pb Pb isotope ratios in mothers' blood (2.127 ± 0.006) were significantly different from those in infants' blood and feces and the soil (2.129 ± 0.006, 2.130 ± 0.004, and 2.131 ± 0.002, respectively, $p < 0.05$). On the other hand, there was no significant difference in $^{207}Pb/^{206}Pb$ ratios between infants' and mothers' blood. Both $^{208}Pb/^{204}Pb$, and $^{207}Pb/^{204}Pb$ ratios in mothers' blood were significantly different from those in other samples ($p < 0.05$), except for those in breastmilk. Pb isotope ratios in soil samples were similar to those reported for Kabwe galena (Kamona et al., 1999).

Pb isotope ratios in infants' and mothers' blood, and infants' feces were closer to those reported for Kabwe galena (Kamona et al., 1999) as the reciprocal of Pb concentrations decreased (Supplementary Fig. S4).

The $^{208}Pb/^{204}Pb$ and $^{207}Pb/^{204}Pb$ ratios (Fig. 3b) clearly show trends of samples compared to $^{208}Pb/^{206}Pb$ and $^{207}Pb/^{206}Pb$ ratios (Fig. 3a and Supplementary Fig. S5).

3.6. Plasma biochemical analysis

Supplementary Table S15 shows the mean values of the plasma biochemical analysis on mothers' plasma. The mean values of all parameters in mothers were within the reference range or slightly higher, except for ALP. The ALT and ALP concentrations in the mothers from sites near the mine were significantly higher than those in the mothers from Bwacha ($p < 0.05$). On the other hand, LDH ($p < 0.05$), Alb ($p = 0.049$), and metallothionein ($p < 0.001$) concentrations in the mothers from Bwacha were significantly higher than those in mothers from sites near the mine. T-Bil concentrations in the mothers from Bwacha were higher than those in the mothers from sites near the mine, although this difference was not significant.

In all mothers, there was a significant positive correlation between the Pb and AST concentrations (Supplementary Table S16, $p < 0.05$, $\rho = 0.16$), and Fe and metallothionein concentrations (Supplementary Table S17, $p < 0.05$, $\rho = 0.17$). The ALT concentrations displayed an almost significant increase as Pb concentrations increased ($p = 0.08$, $\rho = 0.13$). The Alb ($p < 0.05$, $\rho = -0.14$) and metallothionein concentrations ($p < 0.001$, $\rho = -0.53$) significantly decreased as the Pb concentrations increased.

In the mothers from sites near the mine, the Pb concentrations were significantly associated with increased AST ($p < 0.05$, $\rho = 0.17$) and LDH ($p < 0.05$, $\rho = 0.19$) concentrations. On the other hand, the BUN ($p < 0.05$, $\rho = -0.26$) and metallothionein concentrations ($p < 0.001$, $\rho = -0.43$) significantly decreased as Pb concentrations increased. Moreover, the metallothionein concentrations significantly associated with decreased Cu concentrations ($p < 0.05$, $\rho = -0.21$). In the mothers from Bwacha, there were no significant correlations between Pb and plasma biochemical factors.

4. Discussion

To the authors' knowledge, the present study undertook the first ever analysis of Pb in breastmilk of mothers from the sites around the mine in Kabwe. The overall mean Pb concentration in breastmilk was 5.3 μg/L, which was marginally above the acceptable level of 2–5 μg/L for breastfeeding (World Health Organization, 1989), and 30.0% of breastmilk samples contained Pb levels above the acceptable level.

Table 2
Correlation coefficients (R^2) among factors and Pb concentrations in samples in all infants and mothers in the present study.

	Age of infants	Height	Weight	Age of mothers	BLLs in infants	BLLs in mothers	Pb in breastmilk	Pb in infants' feces
Age of infants		0.64***	0.59***	NS	0.46***	NS	NS	0.44***
Height			0.76***	NS	0.36***	NS	NS	0.27***
Weight				NS	0.32***	NS	NS	0.28***
Age of mothers					NS	NS	NS	NS
BLLs in infants						0.68***	0.52***	0.83***
BLLs in mothers							0.58***	0.57***
Pb in breastmilk								0.46***
Pb in infants' feces								

Note: *** indicates $p < 0.001$. BLL, blood lead level; NS, not significant.

Table 3
Sum of possible daily intake of Pb (μg/day) through breastfeeding and soil ingestion.

			Daily intake of Pb through soil ingestion (30 mg/day)		
			Maximum Pb (6326.7 mg/kg)	Mean Pb (1047.6 mg/kg)	Minimum Pb (345.7 mg/kg)
			189.8 μg/day	31.4 μg/day	10.4 μg/day
Daily intake of Pb through breastmilk (0.78 L/day)	Maximum Pb (51.9 μg/L)	40.5 μg/day	230.3	71.9	50.8
	Mean Pb (5.3 μg/L)	4.1 μg/day	193.9	35.5	14.5
	Minimum Pb (0.4 μg//L)	0.3 μg/day	190.1	31.8	10.7

Note: The reference value of daily intake Pb in the present study was 3.7 μg (the mean bw: 7.3 kg) ranged from 1.0 μg (the minimum bw: 1.9 kg) to 6.1 μg (the maximum bw: 12.1) based on the EFSA's reference value (0.5 μg/kg bw/day) (European Food Safety Authority, 2010).

Compared with previous studies that reported elevated Pb concentrations in breastmilk ranged from 8.8 to 35.4 μg/L (Isaac et al., 2012; Turan et al., 2001), Pb concentrations in the breastmilk of mothers from sites near the mine were comparable or even lower. On the other hand, the mean values of Pb concentrations in breastmilk of mothers from Katondo and Bwacha (2.3 μg/L) were within the acceptable level, which agrees with the results obtained in unpolluted areas in other reports (Ettinger et al., 2014; Klein et al., 2017), although the highest individual Pb breastmilk concentration in this study was found in Katondo (51.9 μg/L). Pb in breastmilk may be one of the sources of Pb exposure in infants. Pb concentrations in breastmilk in this study were 5.6% of Pb concentrations in maternal blood. This result agreed with previous studies reporting breastmilk/mothers' blood ratios between 1% and 10% (Anastácio et al., 2004; Ettinger et al., 2005; Koyashiki et al., 2010a, 2010b; Koyashiki et al., 2010; Gulson et al., 1998a, 1998b). In an evaluation of breastmilk/mothers' blood relationships, Gulson et al. (1998a, 1998b) suggested that a ratio of Pb concentration in breastmilk to the concentration of Pb in maternal blood greater than 15% should be treated with caution, higher values than this arising probably from sampling and/or analytical contamination.

High overall mean Pb concentration in infants' feces (39.2 mg/kg) was recorded in the present study. The highest Pb concentration in infants' feces was 3002 mg/kg. These results are in agreement with a previous study conducted in Kabwe (Yabe et al., 2018). Even in Bwacha, which is far from the mine, high Pb concentrations were found in infants' feces. This suggests that infants in Kabwe were exposed to Pb via ingestion.

Among sample types, Pb concentrations in infants' feces were significantly higher than in blood and breastmilk. There were significant positive correlations among samples. BLLs in infants significantly increased with BLLs in mothers ($p < 0.001$, $\rho = 0.68$), Pb concentrations in breastmilk ($p < 0.001$, $\rho = 0.43$), and infants' feces ($p < 0.001$, $\rho = 0.82$). These results suggest that mothers, as well as infants, are exposed to Pb from the environment, as they share the same living conditions. Pb concentrations in infants' feces may be a useful indicator of Pb exposure in infants, in addition to BLLs.

The present study found different trends of Pb exposure in infants and mothers among the studied areas in Kabwe. The mean BLL in infants and mothers from Makululu, which is further from the mine than Kasanda, were the highest among the area. Following Makululu, those from Kasanda and Chowa were the second and the third highest, respectively. Yabe et al. (2015) reported a similar trend for BLLs in children under seven years old, but the highest BLL mean was found in Kasanda, among the three sites. Since most areas in Makululu are dusty and unpaved compared to Kasanda, residents could easily come in to contact with polluted soils or dusts in the area. Pb exposure in infants and mothers from Kasanda and Makululu, which are located on the western side of the mine and in the direction of prevailing winds, could be higher than that in Chowa, which lies in the opposite direction. Pb concentrations in breastmilk and infants' feces showed similar trends to BLLs in infants and mothers. These trends agreed with those determined in earlier studies by Tembo et al. (2006) and Nakayama et al. (2011), who reported similar trends in the soils in Kabwe. Toyomaki et al. (2020) reported that Pb concentrations in dog blood decreased with the distance from the mine in Kabwe, and that the exposure to Pb in dogs remarkably decreased about 5 km away from the mine. These findings

Table 4
Mean ± SD values of the Pb isotope ratios in different samples from Kasanda and Makululu.

Samples (N)	$^{208}Pb/^{206}Pb$	$^{207}Pb/^{206}Pb$	$^{208}Pb/^{204}Pb$	$^{207}Pb/^{204}Pb$	$^{206}Pb/^{204}Pb$
Infants' blood (26)	2.129 ± 0.006 ^{ac}	0.8724 ± 0.003 ^{ac}	38.271 ± 0.063 ^{acd}	15.691 ± 0.012 ^{a}	17.997 ± 0.062 ^{ab}
Mothers' blood (26)	2.127 ± 0.006 ^{b}	0.8726 ± 0.002 ^{a}	38.223 ± 0.080 ^{bc}	15.680 ± 0.015 ^{b}	17.970 ± 0.059 ^{a}
Breastmilk (26)	2.129 ± 0.001 ^{bc}	0.8729 ± 0.0005 ^{b}	38.271 ± 0.046 ^{c}	15.691 ± 0.010 ^{b}	17.972 ± 0.018 ^{a}
Infants' feces (26)	2.130 ± 0.004 ^{ac}	0.8725 ± 0.002 ^{c}	38.349 ± 0.067 ^{d}	15.709 ± 0.012 ^{a}	18.005 ± 0.048 ^{b}
Soil (32)	2.131 ± 0.002 ^{a}	0.8724 ± 0.001 ^{d}	38.407 ± 0.036 ^{e}	15.723 ± 0.005 ^{c}	18.022 ± 0.027 ^{c}
Kabwe galena (Kamona et al., 1999)	2.134 ± 0.0009	0.8731 ± 0.0003	38.410 ± 0.033	15.713 ± 0.010	17.997 ± 0.007

Note: Various small letters indicate a significant difference among areas ($p < 0.05$).
Note: The number of significant digits in each ratio value were adjusted with those of the reference (Kamona et al., 1999).

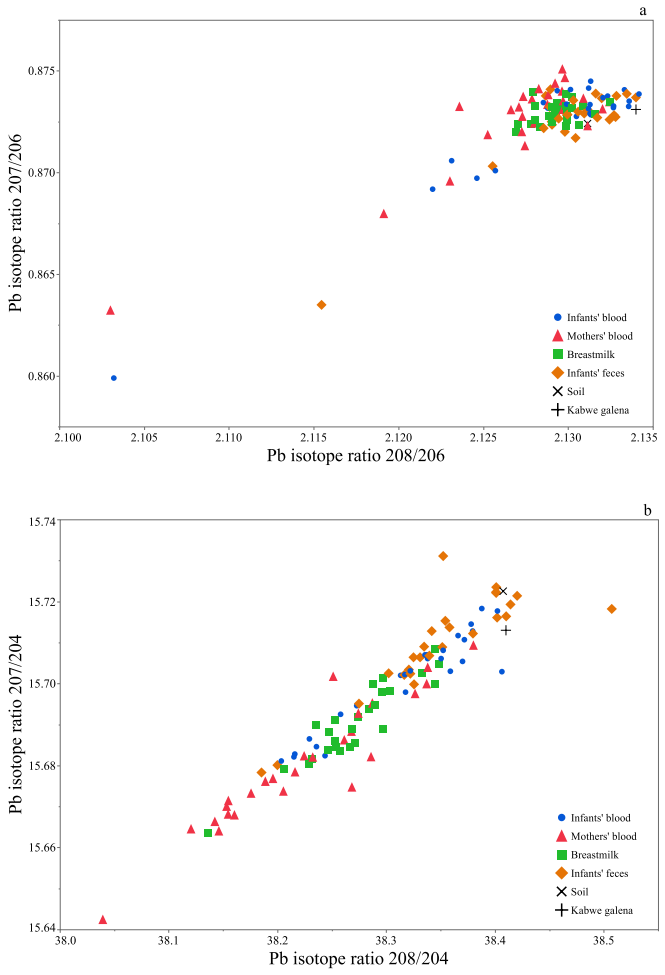

Fig. 3. Pb isotope ratios of individual sample (3a: $^{208}Pb/^{206}Pb$ and $^{207}Pb/^{206}Pb$ and 3b: $^{208}Pb/^{204}Pb$ and $^{207}Pb/^{204}Pb$) in different samples from Kasanda and Makululu. The blue circle, red triangle, green square, orange rhombus, and black cross markers indicate infants' blood, mothers' blood, breastmilk, infants' fecal, and soil samples, respectively. The reference value of Kabwe galena was obtained from a report by Kamona et al. (1999) and is indicated by a plus sign. (For interpretation of the references to color in this figure legend, the reader is referred to the Web version of this article.)

suggested that location of the townships in the relation to the wind direction and distance from the mine influence the extent of the exposure to Pb in infants and mothers in Kabwe, as has been shown in other studies (Soto-Jiménez and Flegal, 2011; Yun et al., 2018).

In the present study, Fe, Cu, Zn and Ag were also analyzed. In contrast to Pb, the concentrations of Fe, Cu, Zn and Ag in the blood of infants and mothers tended to be lower in areas surrounding the mine area than in Bwacha. Given that Pb poisoning is known to cause anemia, the negative correlation between Pb and Fe concentrations suggested that the higher Pb concentrations negatively affected Fe metabolism, especially absorption (Hegazy et al., 2010; Chen et al., 2019). Positive correlations were found between Pb and Cu, Zn, as well as Ag. These positive co-exposures could be attributed to the presence of Pb, Zn and Ag in the galena in Kabwe as confirmed in previous studies (Nakayama et al., 2011).

Blood lead levels in boys were significantly higher than those in girls in Makululu. The same trend for children under seven years old in the same township was previously reported (Yabe et al., 2015). Moreover, Pb concentrations in infants' feces of boys were significantly higher than those of girls in Chowa. This difference could be attributed to differences in breastmilk consumptions as reported by Costa et al. (2010) were boys consumed breastmilk 0.05 kg/d more than girls. These results suggest that boys are more exposed to Pb via ingestion than girls.

Significant positive correlations between BLLs in infants and age of the infants were found. The hand-to-mouth or object-to-mouth (pica) behavior of children, and high absorbance of ingested Pb from the gastrointestinal tract are well known factors attributed to high Pb exposure in children (Wani et al., 2015). However, younger infants who are not ambulatory could display less hand-to-mouth behaviors, as they are under the care of their mothers or guardians although inhalation may be an important pathway for very young children in windy environments (Gulson et al., 2009). Given that BLLs in infants increases from birth to around two years of age in Kabwe, it is important to pay more attention to activities of infants during this period. Moreover, cleaning floors in the house where infants spend most of the time and the kitchen where food could be contaminated by house dust would be important to reduce Pb exposure in infants. On the other hand, only BLLs in mothers from Bwacha significantly decreased as the age of mothers increased. Adults in Bwacha, which is farthest from the mine, could be less exposed to Pb, thus, Pb in the blood of adults may mainly occur from redistribution of endogenous bone-derived Pb (Gulson et al., 1998; Manton et al., 2003). From this point of view, adults even from sites far from the mine in Kabwe could be chronically exposed to Pb via endogenous exposure.

The Pb isotope ratios in infants' samples, especially feces, were almost identical to those in the soil samples. The soil samples exhibited Pb isotope ratios similar to those in Kabwe galena (Kamona et al., 1999). Furthermore, a Pb exposure study on rats exposed to lead in the Kabwe soil revealed that the Pb isotope ratios in these biological samples were also similar to those in Kabwe galena (Kamona et al., 1999; Nakayama et al., 2019). These results suggest that contaminated soil or dust from the mine could be one of the important sources of Pb exposure in infants of Kabwe as well as breastmilk. Understanding which infant behaviors and activities are related to their Pb exposure is required to determine the routes and to minimize the exposure. Pb isotope ratios in infants' blood were similar to those in mothers' blood as infants could be exposed to Pb through breastfeeding and through the placenta before birth. On the other hand, Pb isotope ratios in mothers' samples, especially blood were different from those in infants' feces and the soil samples. Pb isotope ratios in chicken, goats, and vegetables in Kabwe reported by Nakata et al. (2016) were similar to the results in the present study, suggesting that consuming contaminated food could be an important route of Pb exposure in mothers. In the present study, both ^{206}Pb and ^{204}Pb ratios were used to compare the differences of Pb isotope ratios among sample types. Both results were similar, but ^{204}Pb-based ratios displayed clear differences among sample types. Therefore, ^{204}Pb ratios could be more useful than ^{206}Pb ratios to elucidate the source of Pb exposure as recommended by Gulson (2008).

Daily intake of Pb in infants through breastfeeding and soil ingestion was calculated to estimate the burden of the possible routes of Pb exposure. Given that Pb exposure can cause pediatric neurodevelopmental impairments even at low level (Canfield et al., 2003), the reference value 0.5 μg/kg bw/day was used (US EPA, 2011). From the results obtained in the present study, daily intake of Pb even through soil ingestion alone highly exceeded the reference value. Although the bioavailability of Pb in galena is known to be minimal (Rasmussen et al., 2011), Pb exposure through soil ingestion could be the important source due to the high concentrations. Moreover, the results of daily intake of Pb through breastfeeding using the maximum Pb concentrations were larger than the reference value. These results suggest that both Pb though breastfeeding and soil ingestion are important sources of Pb exposure in infants. In the present study, the daily intake of Pb from the environment was only calculated from soil ingestion. However, US EPA (2011) estimated the same amount (30 mg/day) of dust ingestion in parallel with soil ingestion. This implies that the actual daily intake in the field could be underestimated in the present study. Thus, future studies need to evaluate the detail of Pb exposure in infants as well as

mothers in Kabwe including other routes, such as dust ingestion.

In contrast to the high BLLs in mothers, the plasma biochemical profiles of most analyzed parameters were interestingly within, or close to, the standard reference values, except in the case of ALP. These results indicate that Pb exposure in Kabwe mothers did not significantly impact their health, as was observed during sampling, where all sampled mothers appeared healthy. More specifically, the ALT and ALP values in the mothers from sites near the mine were significantly higher than those in the mothers from Bwacha although these values were not significantly correlated with BLLs in mothers. Therefore, these results could not only be attributed to Pb exposure, but also other factors. On the other hand, LDH and AST, which are indicators of liver function, significantly increased as BLLs increased. These results suggest that Pb exposure in mothers may have caused some mild liver damage. High Pb exposure is known to cause kidney damage in conjunction with an increase in BUN and a decrease in Alb. However, both biomarkers significantly decreased as BLLs increased in mothers. During a previous study on Pb poisoning in refugee children in the United States, the CDC reported chronic and acute malnutrition as risk factors for Pb poisoning (Centers for Disease Control and Prevention, 2005). Further studies in Kabwe should therefore focus on the relationship between Pb exposure and nutrition status. In our study, metallothionein concentrations significantly decreased as BLLs increased. A previous study by Mustonen et al. (2014) found constant metallothionein expression in earthworms from a contaminated site, and therefore suggested that the inducibility of the metallothionein response could be lost in earthworms with a history of metal exposure. It is probable that local people in the sites near the mine may be chronically exposed to metals, including Pb, over a long period of time compared to people in sites far from the mine, such as Bwacha. Therefore, metallothionein expression in people residing near the mine was lower than that in people residing far from the mine. Further studies should focus on both metallothionein concentrations and gene expression. In the present study, it is difficult to exclude the possibility of other factors or diseases since a detailed questionnaire survey or medical check-ups were not performed.

The findings in the present study suggest that one of the important sources of Pb exposure in infants could be Pb from the environment, especially from soils. Daily intake of Pb in infants through soil ingestion could be enough to exceed the EFSA's reference value of daily intake of Pb. It is important to minimize Pb exposure in infants from soil and dust.. Thus, remediation of the environment in Kabwe is urgently needed to reduce Pb exposure. High BLLs in mothers could also be one of the important sources of Pb exposure in infants via breastfeeding. Also, high BLLs in mothers may cause their fetus to be exposed to Pb during pregnancy. In the current situation, chelation therapy for Pb poisoning is prioritized more in children than in adults, as children are more vulnerable to Pb. However, in utero exposure to environmental lead may be adversely associated with neurodevelopment at two years of age (Lin et al., 2013). Pilsner et al. (2009) reported that the epigenome of the developing fetus can be influenced by the maternal cumulative lead burden, which may influence long-term epigenetic programming and disease susceptibility throughout a child's life. Reducing the Pb exposure in mothers is important to reduce Pb exposure in fetuses via the placenta, as well as Pb exposure in infants, via breastfeeding. Thus, it is necessary that mothers with high BLLs are treated with chelation therapy, as well as their children.

5. Conclusions

High Pb concentrations in breastmilk, which were above the WHO acceptable level for breastfeeding, could be one of the important sources of Pb exposure in infants. The results of the isotope ratio analysis suggest that Pb from the environment, such as contaminated soil is one of the important sources of Pb exposure in infants. Moreover, Pb exposure in infants through breastfeeding and soil ingestion potentially exceeded the EFSA's reference value of daily intake of Pb. Therefore, environmental remediation, in parallel with chelation therapy, is urgently needed to reduce the Pb exposure in infants and mothers in Kabwe. Moreover, mothers with high BLLs in Kabwe should be treated with chelation therapy to reduce the Pb exposure of their infants via breastfeeding.

Declaration of competing interest

The authors declare that they have no known competing financial interests or personal relationships that could have appeared to influence the work reported in this paper.

Acknowledgements

We are grateful to the infants and mothers who participated in this study. We are also grateful to Takahiro Ichise and Nagisa Hirano (Laboratory of Toxicology, Faculty of Veterinary Medicine, Hokkaido University) for technical support with metal concentrations and isotope analyses. This work was supported by the Grants-in-Aid for Scientific Research from the Ministry of Education, Culture, Sports, Science and Technology of Japan awarded to M. Ishizuka (No. 16H0177906, 18K1984708, 18KK028708, 21H02351), Ikenaka (18H0413208), and S. M.M. Nakayama (No. 17KK0009 and 20K20633). This work was also supported by the foundation of JSPS Bilateral Open Partnership Joint Research Projects (JPJSBP120209902). This work was also supported by JSPS CORE to CORE program (MI),The Japan Prize Foundation; and Hokkaido University's SOUSEI Support Program for Young Researchers in FY2020 (SMMN); Hokkaido University Specific Research Projects (MI). We also acknowledge financial support from the Program for Leading Graduate Schools "Fostering Global Leaders in Veterinary Science for Contributing to One Health" (F01), Grant-in-Aid for JSPS Research Fellow (17J05756), "Global Leadership Training Programme in Africa (GLTP)" of United Nations University, as well as the Japan Prize Foundation. This research was also supported by JST/JICA, SATREPS (Science and Technology Research Partnership for Sustainable Development; No. JPMJSA1501) and aXis (Accelerating Social Implementation for SDGs Achievement; No. JPMJAS2001) funded by JST as well as Program for supporting introduction of the new sharing system (JPMXS0420100619). The English was proofread by Uni-edit (https://uni-edit.net/usa).

Appendix A. Supplementary data

Supplementary data to this article can be found online at https://doi.org/10.1016/j.envpol.2021.117456.

Author statement

Haruya Toyomaki: Conceptualization, Methodology, Data curation, Formal analysis, Software, Writing – original draft. John Yabe: Investigation, Conceptualization, Methodology, Data curation, Software, Writing – review & editing, Shouta M.M. Nakayama: Conceptualization, Methodology, Funding acquisition, Project administration, Writing – review & editing. Yared B. Yohannes: Investigation, Writing - review, Kaampwe Muzandu: Investigation, Writing – review, Tiza Mufune: Investigation, Writing – review, Hokuto Nakata: Investigation, Writing – review, Yoshinori Ikenaka: Funding acquisition, Supervision, Takeshi Kuritani: Investigation, Writing – review, Mitsuhiro Nakagawa: Investigation, Writing – review, Kennedy Choongo: Supervision, Mayumi Ishizuka: Funding acquisition, Project administration, Writing – review & editing.

References

Ajumobi, O.O., Tsofo, A., Yango, M., Aworh, M.K., Anagbogu, I.N., Mohammed, A., Umar-Tsafe, N., Mohammed, S., Abdullahi, M., Davis, L., Idris, S., Poggensee, G.,

Nguku, P., Gitta, S., Nsubuga, P., 2014. High concentration of blood lead levels among young children in Bagega community, Zamfara – Nigeria and the potential risk factor. Pan Afr Medical J 18, 14. https://doi.org/10.11694/pamj.supp.2014.18.1.4264.

Anastácio, A. da S., Silveira, C.L.P. da, Miekeley, N., Donangelo, C.M., 2004. Distribution of lead in human milk fractions: relationship with essential minerals and maternal blood lead. Biol. Trace Elem. Res. 102 https://doi.org/10.1385/bter:102:1-3:027, 027–038.

Barbosa, F., Tanus-Santos, J.E., Gerlach, R.F., Parsons, P.J., 2005. A critical review of biomarkers used for monitoring human exposure to lead: advantages, limitations, and future needs. Environ. Health Perspect. 113, 1669–1674. https://doi.org/10.1289/ehp.7917.

Bizoń, A., Milnerowicz, H., 2014. Participation of metallothionein and superoxide dismutase in the blood of smoking smelters. Int J Occup Med Env 27, 326–334. https://doi.org/10.2478/s13382-014-0258-8.

Bollhöfer, A., Rosman, K.J.R., 2001. Isotopic source signatures for atmospheric lead: the Northern Hemisphere. Geochem. Cosmochim. Acta 65, 1727–1740. https://doi.org/10.1016/s0016-7037(00)00630-x.

Calabrese, E.J., Stanek, E.J., 1995. A Dog's tale: soil ingestion by a canine. Ecotoxicol. Environ. Saf. 32, 93–95. https://doi.org/10.1006/eesa.1995.1090.

Canfield, R.L., Henderson, C.R., Cory-Slechta, D.A., Cox, C., Jusko, T.A., Lanphear, B.P., 2003. Intellectual impairment in children with blood lead concentrations below 10 μg per deciliter. N. Engl. J. Med. 348, 1517–1526. https://doi.org/10.1056/nejmoa022848.

Centers for Disease Control and Prevention, 2019. CDC - lead - blood lead levels in children. Available: https://www.cdc.gov/nceh/lead/prevention/blood-lead-levels.htm. (Accessed 20 February 2020).

Centers for Disease Control and Prevention, 2012. CDC response to advisory committee on childhood lead poisoning prevention recommendations in "low level lead exposure harms children: a renewed call of primary prevention.". Available: https://www.cdc.gov/nceh/lead/ACCLPP/Final_Document_030712.pdf. (Accessed 20 February 2020).

Centers for Disease Control and Prevention, 2010. Guidelines for the identification and management of lead exposure in pregnant and lactating women. Available: https://www.cdc.gov/nceh/lead/publications/leadandpregnancy2010.pdf. (Accessed 19 February 2020).

Centers for Disease Control and Prevention, 2005. Elevated blood lead levels in refugee children–New Hampshire, 2003-2004. MMWR Morb. Mortal. Wkly. Rep. 54, 42–46.

Centers for Disease Control and Prevention, 2002. Managing elevated blood lead levels among young children: recommendations from the Advisory Committee on Childhood Lead Poisoning Prevention. Available: https://www.cdc.gov/nceh/lead/casemanagement/managingEBLLs.pdf. (Accessed 19 February 2020).

Chen, C.-J., Lin, T.-Y., Wang, C.-L., Ho, C.-K., Chuang, H.-Y., Yu, H.-S., 2019. Interactive effects between chronic lead exposure and the homeostatic iron regulator transport HFE polymorphism on the human red blood cell mean corpuscular volume (MCV). Int. J. Environ. Res. Publ. Health 16 (3), 354. https://doi.org/10.3390/ijerph16030354.

Costa, T.H.M. da, Haisma, H., Wells, J.C.K., Mander, A.P., Whitehead, R.G., Bluck, L.J.C., 2010. How much human milk do infants consume? Data from 12 countries using a standardized stable isotope methodology. J. Nutr. 140, 2227–2232. https://doi.org/10.3945/jn.110.123489.

Ettinger, A.S., Roy, A., Amarasiriwardena, C.J., Smith, D., Lupoli, N., Mercado-García, A., Lamadrid-Figueroa, H., Tellez-Rojo, M.M., Hu, H., Hernández-Avila, M., 2014. Maternal blood, plasma, and breast milk lead: lactational transfer and contribution to infant exposure. Environ. Health Perspect. 122, 87–92. https://doi.org/10.1289/ehp.1307187.

Ettinger, A.S., Téllez-Rojo, M.M., Amarasiriwardena, C., Peterson, K.E., Schwartz, J., Aro, A., Hu, H., Hernández-Avila, M., 2005. Influence of maternal bone lead burden and calcium intake on levels of lead in breast milk over the course of lactation. Am. J. Epidemiol. 163, 48–56. https://doi.org/10.1093/aje/kwj010.

European Food Safety Authority, 2010. Scientific opinion on lead in food. Efsa J 8, 1570. https://doi.org/10.2903/j.efsa.2010.1570.

Gulson, B., 2008. Stable lead isotopes in environmental health with emphasis on human investigations. Sci. Total Environ. 400, 75–92. https://doi.org/10.1016/j.scitotenv.2008.06.059.

Gulson, B., Korsch, M., Matisons, M., Douglas, C., Gillam, L., McLaughlin, V., 2009. Windblown lead carbonate as the main source of lead in blood of children from a seaside community: an example of local birds as "canaries in the mine. Environ. Health Perspect. 117, 148–154. https://doi.org/10.1289/ehp.11577.

Gulson, B.L., Jameson, C.W., Mahaffey, K.R., Mizon, K.J., Patison, N., Law, A.J., Korsch, M.J., Salter, M.A., 1998a. Relationships of lead in breast milk to lead in blood, urine, and diet of the infant and mother. Environ. Health Perspect. 106, 667–674. https://doi.org/10.1289/ehp.98106667.

Gulson, B.L., Mahaffey, K.R., Jameson, C.W., Mizon, K.J., Korsch, M.J., Cameron, M.A., Eisman, J.A., 1998b. Mobilization of lead from the skeleton during the postnatal period is larger than during pregnancy. J. Lab. Clin. Med. 131, 324–329. https://doi.org/10.1016/s0022-2143(98)90182-2.

Haefliger, P., Mathieu-Nolf, M., Lociciro, S., Ndiaye, C., Coly, M., Diouf, A., Faye, A.L., Sow, A., Tempowski, J., Pronczuk, J., Junior, A.P.F., Bertollini, R., Neira, M., 2009. Mass lead intoxication from informal used lead-acid battery recycling in dakar, Senegal. Environ. Health Perspect. 117, 1535–1540. https://doi.org/10.1289/ehp.0900696.

Hamelin, B., Manhes, G., Albarede, F., Allègre, C.J., 1985. Precise lead isotope measurements by the double spike technique: a reconsideration. Geochem. Cosmochim. Acta 49, 173–182.

Hegazy, A.A., Zaher, M.M., Abd El-Hafez, M.A., Morsy, A.A., Saleh, R.A., 2010 May 12. Relation between anemia and blood levels of lead, copper, zinc and iron among children. BMC Res. Notes 3, 133. https://doi.org/10.1186/1756-0500-3-133. PMID: 20459857; PMCID: PMC2887903.

Isaac, C.P.J., Sivakumar, A., Kumar, C.R.P., 2012. Lead levels in breast milk, blood plasma and intelligence quotient: a health hazard for women and infants. Bull. Environ. Contam. Toxicol. 88, 145–149. https://doi.org/10.1007/s00128-011-0475-9.

Kamona, A.F., Lévêque, J., Friedrich, G., Haack, U., 1999. Lead isotopes of the carbonate-hosted Kabwe, tsumeb, and kipushi Pb-Zn-Cu sulphide deposits in relation to Pan african orogenesis in the damaran-lufilian fold belt of central Africa. Miner. Deposita 34, 273–283. https://doi.org/10.1007/s001260050203.

Klein, L.D., Breakey, A.A., Scelza, B., Valeggia, C., Jasienska, G., Hinde, K., 2017. Concentrations of trace elements in human milk: comparisons among women in Argentina, Namibia, Poland, and the United States. PloS One 12, e0183367. https://doi.org/10.1371/journal.pone.0183367.

Komárek, M., Ettler, V., Chrastný, V., Mihaljevič, M., 2008. Lead isotopes in environmental sciences: a review. Environ. Int. 34, 562–577. https://doi.org/10.1016/j.envint.2007.10.005. K., Bizoń, A., Zalewska, M., Milnerowicz, H., 2015. The influence of biological and environmental factors on metallothionein concentration in the blood. J Trace Elem Med Bio 29, 99–103. https://doi.org/10.1016/j.jtemb.2014.05.001.

Koyashiki, G.A.K., Paoliello, M.M.B., Matsuo, T., Oliveira, M.M.B. de, Mezzaroba, L., Carvalho, M. de F., Sakuma, A.M., Turini, C., Vannuchi, M.T.O., Barbosa, C.S.D., 2010a. Lead levels in milk and blood from donors to the breast milk bank in southern Brazil. Environ. Res. 110, 265–271. https://doi.org/10.1016/j.envres.2009.12.001.

Koyashiki, G.A.K., Paoliello, M.M.B., Tchounwou, P.B., 2010b. Lead levels in human milk and children's health risk: a systematic review. Rev. Environ. Health 25, 243–254. https://doi.org/10.1515/reveh.2010.25.3.243.

Kuritani, T., Nakamura, E., 2003. Highly precise and accurate isotopic analysis of small amounts of Pb using 205 Pb– 204 Pb and 207 Pb- 204 Pb, two double spikes. J Anal Spectrom 18, 1464–1470. https://doi.org/10.1039/b310294g.

Kuritani, T., Nakamura, E., 2002. Precise isotope analysis of nanogram-level Pb for natural rock samples without use of double spikes. Chem. Geol. 186, 31–43. https://doi.org/10.1016/s0009-2541(02)00004-9.

Lin, C.-C., Chen, Y.-C., Su, F.-C., Lin, C.-M., Liao, H.-F., Hwang, Y.-H., Hsieh, W.-S., Jeng, S.-F., Su, Y.-N., Chen, P.-C., 2013. In utero exposure to environmental lead and manganese and neurodevelopment at 2 years of age. Environ. Res. 123, 52–57. https://doi.org/10.1016/j.envres.2013.03.003.

Manton, W.I., Angle, C.R., Stanek, K.L., Kuntzelman, D., Reese, Y.R., Kuehnemann, T.J., 2003. Release of lead from bone in pregnancy and lactation. Environ. Res. 92, 139–151. https://doi.org/10.1016/s0013-9351(03)00020-3.

Meyer, P.A., Brown, M.J., Falk, H., 2008. Global approach to reducing lead exposure and poisoning. Mutat. Res. Rev. Mutat. Res. 659, 166–175. https://doi.org/10.1016/j.mrrev.2008.03.003.

Mustonen, M., Haimi, J., Väisänen, A., Knott, K.E., 2014. Metallothionein gene expression differs in earthworm populations with different exposure history. Ecotoxicology 23, 1732–1743. https://doi.org/10.1007/s10646-014-1338-z.

Nakata, H., Nakayama, S.M.M., Yabe, J., Liazambi, A., Mizukawa, H., Darwish, W.S., Ikenaka, Y., Ishizuka, M., 2016. Reliability of stable Pb isotopes to identify Pb sources and verifying biological fractionation of Pb isotopes in goats and chickens. Environ. Pollut. 208, 395e403. PMID: 26549754. https://doi.org/10. 1016/j.envpol.2015.10.006.

Nakata, H., Nakayama, S.M.M., Yabe, J., Muzandu, K., Toyomaki, H., Yohannes, Y.B., Kataba, A., Zyambo, G., Ikenaka, Y., Choongo, K., Ishizuka, M., 2021. Assessment of LeadCare® II analysis for testing of a wide range of blood lead levels in comparison with ICP–MS analysis. Chemosphere 129832. https://doi.org/10.1016/j.chemosphere.2021.129832.

Nakayama, S.M.M., Ikenaka, Y., Hamada, K., Muzandu, K., Choongo, K., Teraoka, H., Mizuno, N., Ishizuka, M., 2011. Metal and metalloid contamination in roadside soil and wild rats around a Pb–Zn mine in Kabwe, Zambia. Environ. Pollut. 159, 175–181. https://doi.org/10.1016/j.envpol.2010.09.007.

Nakayama, S.M.M., Nakata, H., Ikenaka, Y., Yabe, J., Oroszlany, B., Yohannes, Y.B., Bortey-Sam, N., Muzandu, K., Choongo, K., Kuritani, T., Nakagawa, M., Ishizuka, M., 2019. One year exposure to Cd- and Pb-contaminated soil causes metal accumulation and alteration of global DNA methylation in rats. Environ. Pollut. 252, 1267–1276. https://doi.org/10.1016/j.envpol.2019.05.038.

National Academy of Science, 1972. Lead: Airborne Lead in Perspective: Biological Effects of Atmospheric Pollutants, vols. 71–177. National Academy of Sciences, Washington, DC, pp. 281–313.

Needleman, H., 2004. Lead poisoning. Annu. Rev. Med. 55, 209–222. https://doi.org/10.1146/annurev.med.55.091902.103653.

Pilsner, J.R., Hu, H., Ettinger, A., Sánchez, B.N., Wright, R.O., Cantonwine, D., Lazarus, A., Lamadrid-Figueroa, H., Mercado-García, A., Téllez-Rojo, M.M., Hernández-Avila, M., 2009. Influence of prenatal lead exposure on genomic methylation of cord blood DNA. Environ. Health Perspect. 117, 1466–1471. https://doi.org/10.1289/ehp.0800497.

Rasmussen, P.E., Beauchemin, S., Chénier, M., Levesque, C., MacLean, L.C.W., Marro, L., Jones-Otazo, H., Petrovic, S., McDonald, L.T., Gardner, H.D., 2011. Canadian house dust study: lead bioaccessibility and speciation. Environ. Sci. Technol. 45, 4959–4965. https://doi.org/10.1021/es104056m.

Ruckart, P.Z., Ettinger, A.S., Hanna-Attisha, M., Jones, N., Davis, S.I., Breysse, P.N., 2019. The flint water crisis. J. Publ. Health Med. 25, S84–S90. https://doi.org/10.1097/phh.0000000000000871.

Schoning, P., Abraham, J., Burnett, B., 1996. Silicate and metal dust in lungs of Greyhounds. Am. J. Vet. Res. 57, 1006–1009.

Soto-Jiménez, M.F., Flegal, A.R., 2011. Childhood lead poisoning from the smelter in Torreón, México. Environ. Res. 111, 590–596. https://doi.org/10.1016/j.envres.2011.01.020.

Tembo, B.D., Sichilongo, K., Cernak, J., 2006. Distribution of copper, lead, cadmium and zinc concentrations in soils around Kabwe town in Zambia. Chemosphere 63, 497–501. https://doi.org/10.1016/j.chemosphere.2005.08.002.

Toyomaki, H., Yabe, J., Nakayama, S.M.M., Yohannes, Y.B., Muzandu, K., Liazambi, A., Ikenaka, Y., Kuritani, T., Nakagawa, M., Ishizuka, M., 2020. Factors associated with lead (Pb) exposure on dogs around a Pb mining area, Kabwe, Zambia. Chemosphere 125884. https://doi.org/10.1016/j.chemosphere.2020.125884.

Turan, S., Saygi, Ş., Kiliç, Z., Acar, O., 2001. Determination of heavy metal contents in human colostrum samples by electrothermal atomic absorption spectrophotometry. J. Trop. Pediatr. 47, 81–85. https://doi.org/10.1093/tropej/47.2.81.

United States Environmental Protection Agency, 2011. Exposure Factors Handbook 2011 Edition (Final Report). U.S. Environmental Protection Agency, Washington, DC. EPA/600/R-09/052F.

Veysseyre, A.M., Bollhöfer, A.F., Rosman, K.J.R., Ferrari, C.P., Boutron, C.F., 2001. Tracing the origin of pollution in French alpine snow and aerosols using lead isotopic ratios. Environ. Sci. Technol. 35, 4463–4469. https://doi.org/10.1021/es0105717.

Wani, A., Ara, A., Usmani, J., 2015. Lead toxicity: a review. Interdiscipl. Toxicol. 8, 55–64. https://doi.org/10.1515/intox-2015-0009.

World Health Organization, 2010. Childhood lead poisoning. Available: https://www.who.int/ceh/publications/leadguidance.pdf. (Accessed 19 February 2020).

World Health Organization, 1989. Minor and Trace Elements in Human Milk. World Health Organization, Geneva, Switz. Available: https://apps.who.int/iris/bitstream/handle/10665/39678/9241561211.pdf?sequence=1. (Accessed 19 February 2020).

Yabe, J., Ishizuka, M., Umemura, T., 2010. Current levels of heavy metal pollution in Africa. J. Vet. Med. Sci. 72, 1257–1263. https://doi.org/10.1292/jvms.10-0058.

Yabe, J., Nakayama, S., Ikenaka, Y., Yohannes, Y.B., Bortey-Sam, N., Oroszlany, B., Muzandu, K., Choongo, K., Kabalo, A., Ntapisha, J., Mweene, A., Umemura, T., Ishizuka, M., 2015. Lead poisoning in children from townships in the vicinity of a lead–zinc mine in Kabwe, Zambia. Chemosphere 119, 941–947. https://doi.org/10.1016/j.chemosphere.2014.09.028.

Yabe, J., Nakayama, S.M., Nakata, H., Toyomaki, H., Yohannes, Y.B., Muzandu, K., Kataba, A., Zyambo, G., Hiwatari, M., Narita, D., Yamada, D., Hangoma, P., Munyinda, N.S., Mufune, T., Ikenaka, Y., Choongo, K., Ishizuka, M., 2020. Current trends of blood lead levels, distribution patterns and exposure variations among household members in Kabwe, Zambia. Chemosphere 243, 125412. https://doi.org/10.1016/j.chemosphere.2019.125412.

Yabe, J., Nakayama, S.M.M., Ikenaka, Y., Yohannes, Y.B., Bortey-Sam, N., Kabalo, A.N., Ntapisha, J., Mizukawa, H., Umemura, T., Ishizuka, M., 2018. Lead and cadmium excretion in feces and urine of children from polluted townships near a lead-zinc mine in Kabwe, Zambia. Chemosphere 202, 48–55. https://doi.org/10.1016/j.chemosphere.2018.03.079.

Yun, S.-W., Baveye, P.C., Kim, D.-H., Kang, D.-H., Lee, S.-Y., Kong, M.-J., Park, C.-G., Kim, H.-D., Son, J., Yu, C., 2018. Analysis of metal(loid)s contamination and their continuous input in soils around a zinc smelter: development of methodology and a case study in South Korea. Environ. Pollut. 238, 140–149. https://doi.org/10.1016/j.envpol.2018.03.020.

minerals

MDPI

Article

Evaluation of Dispersion of Lead-Bearing Mine Wastes in Kabwe District, Zambia

Shinsaku Nakamura [1,2,*], Toshifumi Igarashi [3], Yoshitaka Uchida [4], Mayumi Ito [3], Kazuyo Hirose [2], Tsutomu Sato [3], Walubita Mufalo [1], Meki Chirwa [5], Imasiku Nyambe [5], Hokuto Nakata [6], Shouta Nakayama [6] and Mayumi Ishizuka [6]

1 Division of Sustainable Resources Engineering, Graduate School of Engineering, Hokkaido University, Sapporo 060-8628, Japan; wmufalo@gmail.com
2 International Cooperation Department, Japan Space Systems, Tokyo 105-0011, Japan; Hirose-Kazuyo@jspacesystems.or.jp
3 Division of Sustainable Resources Engineering, Faculty of Engineering, Hokkaido University, Sapporo 060-8628, Japan; tosifumi@eng.hokudai.ac.jp (T.I.); itomayu@eng.hokudai.ac.jp (M.I.); tomsato@eng.hokudai.ac.jp (T.S.)
4 Research Faculty of Agriculture, Hokkaido University, Sapporo 060-8589, Japan; uchiday@chem.agr.hokudai.ac.jp
5 IWRM Centre/Geology Department, School of Mines, The University of Zambia, Lusaka 32379, Zambia; meki.chirwa@gmail.com (M.C.); inyambe@gmail.com (I.N.)
6 Faculty of Veterinary Medicine, Hokkaido University, Kita 18, Nishi 9, Kita-ku, Sapporo 060-0818, Japan; hokuto.nakata@vetmed.hokudai.ac.jp (H.N.); shouta-nakayama@vetmed.hokudai.ac.jp (S.N.); ishizum@vetmed.hokudai.ac.jp (M.I.)
* Correspondence: Nakamura-Shinsaku@jspacesystems.or.jp; Tel.: +81-3-6435-6945

Abstract: Dispersion of lead (Pb) in mine wastes was simulated for reproducing Pb contamination of soil in Kabwe District, Zambia. Local weather data of year 2019 were monitored in situ and used for the simulations. The plume model, weak puff model, and no puff model were adopted for calculation of Pb dispersion under different wind conditions. The results showed that Pb dispersion from the Kabwe mine was directly affected by wind directions and speeds in the dry season, although it was not appreciably affected in the rainy season. This may be because the source strength is lower in the rainy season due to higher water content of the surface. This indicates that Pb dispersion patterns depend on the season. In addition, the distribution of the amount of deposited Pb-bearing soils around the mine corresponded to the distribution of Pb contents in soils. These results suggest that Pb contamination in soils primarily results from dispersion of fine mine wastes.

Keywords: mine wastes; contamination; lead; dispersion; weather conditions; wind; Kabwe; Zambia

Citation: Nakamura, S.; Igarashi, T.; Uchida, Y.; Ito, M.; Hirose, K.; Sato, T.; Mufalo, W.; Chirwa, M.; Nyambe, I.; Nakata, H.; et al. Evaluation of Dispersion of Lead-Bearing Mine Wastes in Kabwe District, Zambia. *Minerals* **2021**, *11*, 901. https://doi.org/10.3390/min11080901

Academic Editor: Pierfranco Lattanzi

Received: 13 July 2021
Accepted: 17 August 2021
Published: 20 August 2021

1. Introduction

Heavy metals and metalloids from mining and smelting activities have huge impacts on environmental pollution [1,2]. Environmental as well as human health issues are increased by heavy metal contaminations from such activities [3]. The impacts of the pollution appear for the workers of mine companies and people living around the mines through incidental dust ingestion and inhalation [4]. In particular, soil pollution by heavy metals from mine areas in arid countries is one of the serious issues to be solved.

Mining is the key industry in Zambia. Mineral resources, such as lead (Pb), zinc (Zn), cobalt (Co) and copper (Cu) had been mined and smelted for over 90 years between 1902 and 1994 in Kabwe, Zambia [5]. Unrefined mining wastes have been dumped at the mine like a hill, and they have been exposed to the environment until today. For this reason, Kabwe was ranked as one of the worst polluted areas in the world [6]. The dumping site in Kabwe is thought to be the source of contamination, and the waste is dispersed by winds around the mine. Thus, the heavy metals contained in the wastes directly induce environmental and health problems. Nakayama et al. [7] indicated that soil samples from

roadsides in Kabwe had higher concentrations of Pb than benchmark values. Results of spectral measurements and satellite data around the dumping site indicated high Pb contents (>1000 mg/kg as total) in the soils within 2 km from the site [8]. The mean blood Pb levels of the population in Kabwe were estimated at 11.9 μg/dL (11.6–12.1 μg/dL) by blood sampling from volunteers with backgrounds with geographic, demographic, and socioeconomic information [9]. Moreover, Pb contamination has influenced children's health: about 50% of children took in an intolerable daily intake [10]. For mitigation and remediation of this environmental issue, immobilization techniques by dolomite, calcined dolomite, and magnesium oxide were performed [11], and concurrent dissolution and cementation methods were proposed [12]. Although Pb contamination and its impacts on the environment and human health have been unveiled and mitigated by multilateral approaches in Kabwe, the mechanisms of heavy metal dispersion from the mine are not quantitatively evaluated.

The purpose of this study is to understand Pb dispersion mechanism and to quantify Pb contamination of soil in Kabwe, Zambia by simulating dispersion of Pb contained in the mine wastes with local weather data of year 2019, and then comparing the simulated results with measured Pb content in soils. Lead was selected as a target material for the simulation because Pb seriously affects the health of children in Kabwe and the solubility of Pb is lower than the other heavy metals like Zn and Cu. Mufalo et al. [13] characterized surface soils at eight playgrounds in Kabwe, and the measured results were compared with the simulated results of Pb dispersion in this study to verify the simulation model.

2. Materials and Methods

2.1. Study Site

A dumping site of Pb-Zn mine wastes in Kabwe, Zambia (Figure 1) was selected as the source of contaminants for simulating Pb dispersion because the wastes are stacked as a small hill, named Black Mountain, and causes fine waste particles to be swirled up by winds [14]. The height of the source was estimated at the same height of the slag hill, and it was calculated with shuttle radar topography model (SRTM) with 30 m spatial resolution. Although a single point, such as the location of a chimney in industrial factories, was used for the simulation [15], the source was adopted as a bundle of point sources in this study. The area of the source was estimated at 46,110 m^2. Twelve points were selected as Pb source in the mine based on the topographical condition. Pb dispersion was calculated and compared with the results of Pb content in surrounding surface soils. The collected soils were located in the northwest of the dumping site by considering the wind direction.

2.2. Lead Dispersion Simulation Models

Dispersion of soils and mine wastes depends on particle size. Mufalo et al. [13] measured the particle size distribution of collected soils and Zn leaching residue, and they showed that 50% of the collected soils had a diameter less than 50 μm. On the other hand, the dumping site that is the source of Pb dispersion simulation is covered by slags. The slag samples located at Black Mountain were also collected, and the particle size of the slags was measured. The results showed that 6% of the slag was less than 150 μm. Figure 2 shows the particle size distribution of the slag. Sieves with different pore sizes were used for the particles larger than 0.15 mm whereas the particle size less than 0.15 mm was measured by the particle size analyzer based on laser diffraction. Siciliano et al. [16] suggest that slags less than 45 μm have risks of oral bioaccessibility in human beings. The particle size less than 10 μm is regarded as an air pollution source and the formula of dispersion depends on wind speed [17,18]. Thus, the target particle sizes of soils/mine wastes were classified into 10, 15, 20, 25, 30, 35, 40, 45, and 50 μm.

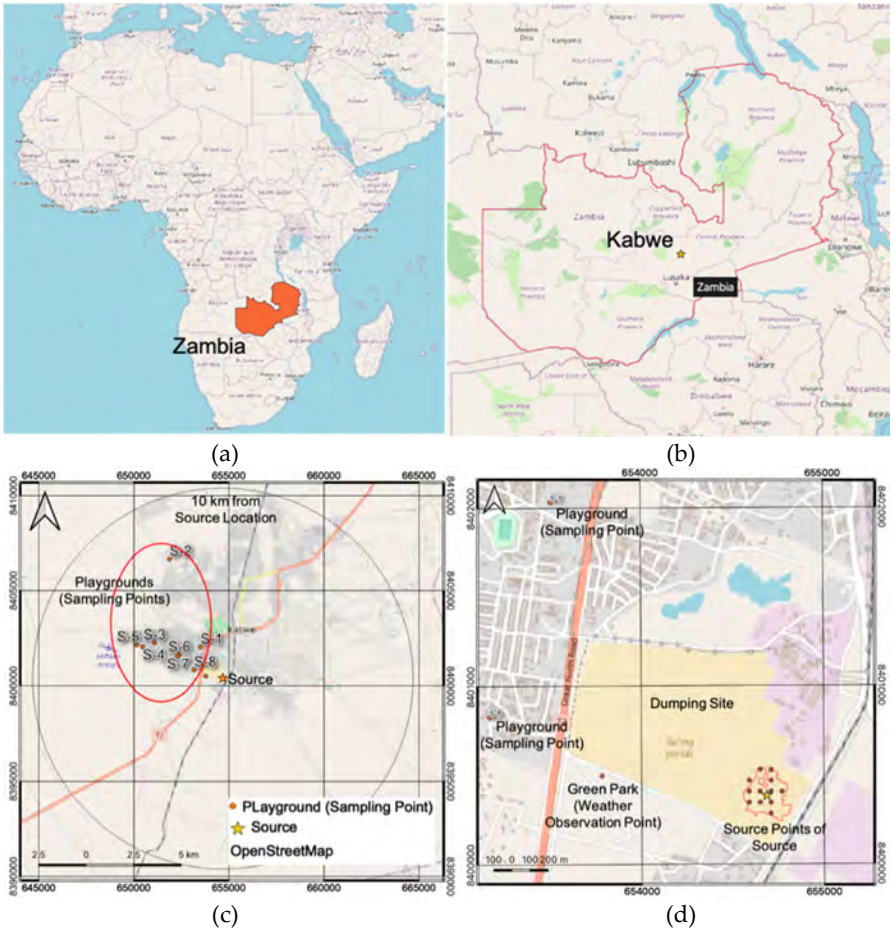

Figure 1. Source location and sampling points in Kabwe, Zambia: (**a**) territory of Zambia; (**b**) location of Kabwe; (**c**) locations of dumping site (source) and playgrounds (sampling points; S-1 to S-8); (**d**) source location and Green Park where weather data were collected.

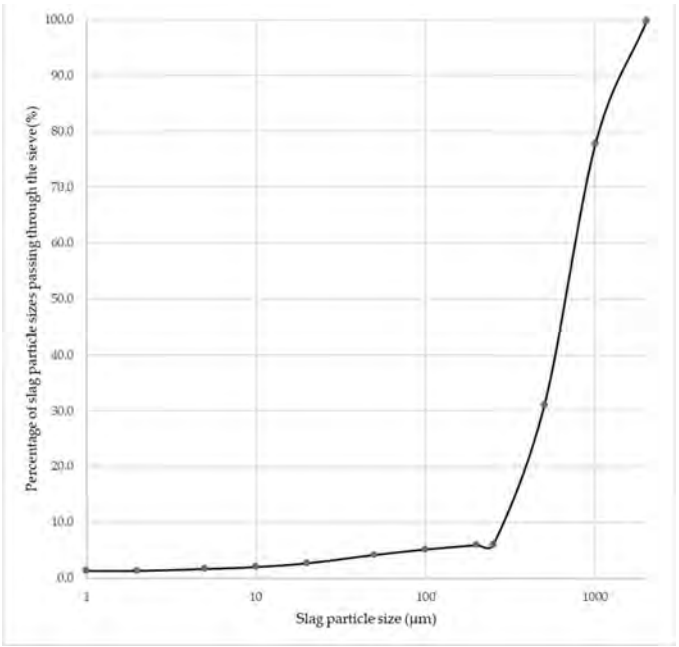

Figure 2. Measured particle-size distribution of the slag sample.

Three models of Pb dispersion and a model of redispersion, depending on wind directions and speeds, were constructed in this study. The plume model was used in the case of wind speed over 1.0 m/s. The weak puff model was used in the case of wind speed lower than 1.0 m/s and higher than 0.4 m/s. The no puff model was used in the case of wind speed lower than 0.4 m/s [19–22]. The models are expressed by the following equations.

Plume model:

$$C = \frac{Q}{\sqrt{2\pi}(\pi/8)R\sigma_z u}\left\{exp\left[\frac{(z-He)^2}{2{\sigma_z}^2}\right] + exp\left[\frac{(z+He)^2}{2{\sigma_z}^2}\right]\right\}, \quad (1)$$

where,

C: Concentration (mg/m^2)

Q: Source strength (estimated at 0.025 m^3/s and 0.0025 m^3/s for the dry and rainy seasons, respectively)

R: Distance from source (= $(x^2 + y^2 + z^2)^{1/2}$)

x: Downwind distance along wind direction (m)

y: Horizontal distance perpendicular to x (m)

z: Elevation at simulating point (m)

σ_z: Diffusion width (m)

u: Wind speed (m/s)

He: Elevation of source (m)

Weak puff model:

$$C = \frac{Q}{\sqrt{2\pi}(\pi/8)\gamma}\left\{\frac{1}{{\eta_-}^2}exp\left[-\frac{u^2(z-He)^2}{2\alpha^2{\eta_-}^2}\right] + \frac{1}{{\eta_+}^2}exp\left[-\frac{u^2(z+He)^2}{2\alpha^2{\eta_+}^2}\right]\right\}, \quad (2)$$

In this equation

${\eta_-}^2 = x^2 + y^2 + (\alpha^2/\gamma^2) \times (z - He)^2$

${\eta_+}^2 = x^2 + y^2 + (\alpha^2/\gamma^2) \times (z + He)^2$

where

α: Dispersivity with respect to horizontal direction

γ: Dispersivity with respect to vertical direction

No puff model:

$$C = \frac{Q}{\sqrt{2\pi}(\pi/8)R\gamma}\left\{\frac{1}{{\eta_-}^2} + \frac{1}{{\eta_+}^2}\right\}, \quad (3)$$

$R = (x^2 + y^2)^{1/2}$.

${\eta_-}^2 = x^2 + y^2 + (\alpha^2/\gamma^2) \times (z - He)^2$.

${\eta_+}^2 = x^2 + y^2 + (\alpha^2/\gamma^2) \times (z + He)^2$.

The source strength (Q) is a key parameter to simulate Pb dispersion and redispersion. Here, a total of 1 m^3 of the slag per one second was assumed to be dispersed. However, only finer particles (<50 μm) are transported to a further distance. Thus, the finer fraction of 2.5% of the slag was assumed to be dispersed (0.025 m^3/s) as a source strength for the dry season. Rain is another factor to restrain soil dispersion by winds. For the rainy season, the source strength of Pb dispersion by each model was set at 0.0025 m^3/s, 1/10 of the value of the dry season, because the higher water content of the surface restricts the dispersion.

The dispersion of the slag with less than 50 μm was simulated every hour, and the accumulated amount of precipitated slag with Pb was calculated by considering the particle sizes and weather conditions. The amounts of deposition of slag depending on the particle size at each playground were summed up in the rainy and dry seasons in 2019 and throughout the year 2019.

Redispersion is related to particle sizes of soils and slags and wind speed at the deposited locations. Target particle sizes were between 10 μm and 50 μm in this study. So, these particle sizes are similar to the size of cedar pollen (mean diameter: 30 μm). Nakatani and Nakane [23] developed and simulated pollen retransport behavior. By applying the

following model, particles of soils and slags on the ground have five forces: gravity, static friction force, drag force, Saffman lift force, and adhesion force. The particles are able to be retransported when the drag force is larger than the friction force and Saffman lift force is larger than the gravity plus vertical adhesion forces. Therefore, redispersion at the deposited locations was calculated by Equation (4).

Redispersion:

$$R = P_R \times C1 \times \left[F_D - F_f + F_s - g\right], \quad (4)$$

where,

R: Redispersion (mg)

P_R: Percentage of redispersion

$C1$: Amount of dispersed soils/mine wastes (mg/m^2)

F_D: Drag force (= $\frac{1}{2}\rho_a u^2 C_D \frac{\pi d^2}{4}$)

ρ_a: Fluid density (1.2250 kg/m^3, standard atmospheric density)

u: Wind speed (m/s)

C_D: Drag coefficient (= 0.6, particle was estimated at elliptical pillar)

d: Particle size (μm)

F_f: Friction force (= $\mu \times N$)

μ: Friction coefficient (estimated at 0.52)

N: Normal force (= density of slag (3.45, the average values between 3.3 and 3.6) × volume of particle)

F_S: Saffman lift (= $6.46 \times \left(\frac{d}{2}\right)^2 u\sqrt{\rho_a \mu}$)

g: Gravity (= density of slag (3.45, the average values between 3.3 and 3.6) × volume of particle)

Value of drag coefficient (C_D) for estimating drag force for the redispersion calculation depends on the shape of the particle. The target soils and slags have various shapes: sphere, angled cube, cylinder, etc. Here, a spheroid shape with the value of 0.6 between sphere and angled cube was selected.

At the playgrounds, various particle sizes and minerals of soils are mixed, and various conditions, such as human activities and weather, change every moment throughout the year. By referring to the previous studies [24,25], the friction coefficient (μ) was set at 0.52 with considerations of the environmental conditions under which soils were easily swirled and dispersed Pb-bearing soils were redispersed by winds and flushed by rains after depositing immediately.

2.3. Weather Data Collection

Weather information for year 2019 was used to simulate Pb dispersion at and around the mine because all required data were collected in situ or in Lusaka. The weather information consists of six items as Pb dispersion parameters: wind direction, wind speed, solar radiation, barometric pressure, humidity, and air temperature [26]. However, due to machine troubles and errors of the data collection system, the data of August 2019 were not collected.

Wind direction and wind speed were collected at Green Park, which is located at the southwest of the mine about 900 m away from the source, and it was prepared for monitoring heavy metals absorbed by plants (Figure 1). In addition, a small-sized meteorological instrument named POTEKA (Meisei Electric Co., Ltd., Tokyo, Japan) collected hourly data. Thus, wind speed and direction data have been monitored at Green Park.

Solar radiation, barometric pressure, humidity, and air temperature data were collected at the test site of the University of Zambia, Lusaka. Although Lusaka, the capital city of Zambia, is about 100 km south of Kabwe, the measured solar radiation, barometric pressure, humidity, and air temperature were collected and applied to the simulation. Thus, the weather data obtained at the two cities were used for simulation.

Values of wind speed and direction were used as parameters of Pb dispersion and redispersion simulation directly. Solar radiation, barometric pressure, humidity, and air

temperature were used to determine coefficients of horizontal and vertical dispersivities for the plume, weak puff, and no puff models.

2.4. Comparison with Field Survey Results

Results of Pb dispersion simulations were compared with results of measured Pb contents by Mufalo et al. [13] (Table 1). They collected samples at eight playgrounds within 10 km radius from the dumping site. They took topsoil samples (5 cm depth) by mixing 3–4 soils for each sample and analyzing the total contents of Pb in the soils. Their data are appropriate for comparison with the simulated deposition of Pb because the playground is not influenced by change in land use.

Table 1. Pb contents of soil samples (XRF-chemical composition) by Mufalo et al. [13].

Playground	Pb (mg/kg)
S-1	3320
S-2	1080
S-3	1070
S-4	265
S-5	633
S-6	863
S-7	1770
S-8	3170

3. Results

3.1. Results of Weather Data Collection

Weather condition sensitively affects Pb dispersion. Winds in Kabwe tended to blow from the east-southeast side (annual frequency was 10.95%) (Figure 3). The frequency of wind from the west was 10.94%, and from the southeast was 9.78% throughout the year of 2019. On the other hand, the wind speed was 2.47 m/s from the west whereas 2.19 m/s and 1.50 m/s of winds blew from the east and the south, respectively. The annual average of solar radiation was 0.20 kW/m^2, the annual average of barometric pressure was 874.99 hPa, the annual average of humidity was 58.07%, and the annual average of temperature was 21.83 °C.

During the rainy season (January to April and November to December) in Kabwe, the frequent wind directions were from the west (11.79%), the north (10.45%), and the east-southeast (7.78%). Strong winds came from the west (2.45 m/s), the east (1.77 m/s), and the west-southwest (1.59 m/s). The average of solar radiation was 0.22 kW/m^2, the average of barometric pressure was 872.62 hPa, the average of humidity was 68.65%, and the average of temperature was 23.08 °C.

During the dry season (May to October, August not included) in Kabwe, the frequent wind directions were from the east-southeast (14.71%), the southeast (14.08%), and the south-southeast (11.08%). Strong winds blew from the east (2.72 m/s), the west (2.49 m/s), and the south-southwest (1.85 m/s). The average of solar radiation was 0.19 kW/m^2, the average of barometric pressure was 877.79 hPa, the average of humidity was 45.54%, and the average of temperature was 20.34 °C.

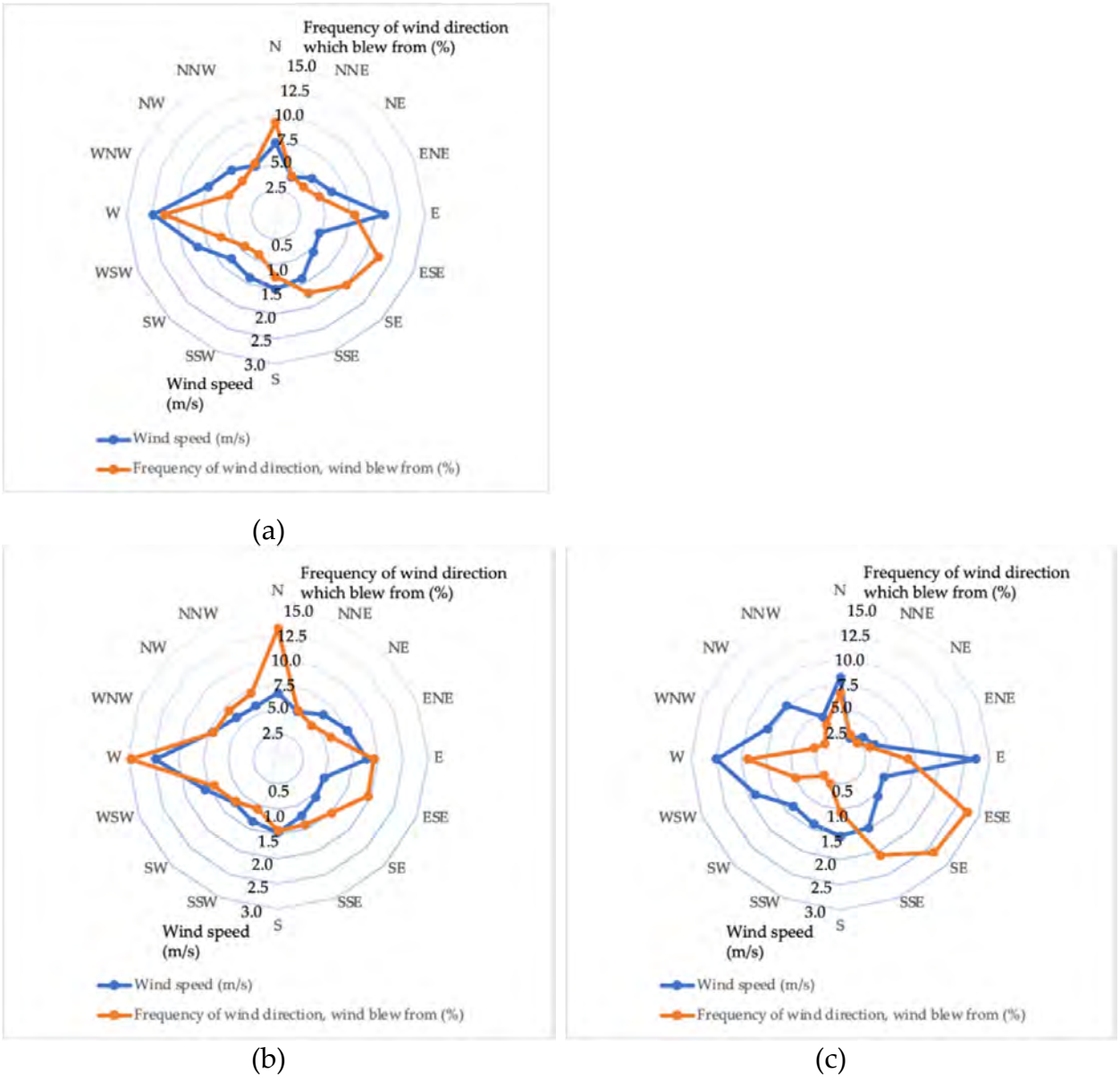

Figure 3. Results of the measured wind conditions in Kabwe in 2019: (**a**) wind condition throughout the year; (**b**) wind condition in the rainy season; (**c**) wind condition in the dry season. Orange plots in these charts show frequencies of wind directions from which wind blew, and the axis was set at 15.0%, 12.5%, 10.0%, 7.5%, 5.0%, and 2.5% from outside to inside, respectively. Blue plots in these charts show wind speeds, and the axis was set at 3.0, 2.5, 2.0, 1.5, 1.0, and 0.5 m/s from outside to inside, respectively.

3.2. Results of Lead Dispersion Simulations

The deposition of Pb-bearing mine wastes at eight playgrounds from the dumping site by dispersion was calculated seasonally; during the rainy season (January to April and November to December), during the dry season (May to October, August not included), and throughout the year (January to December, but August not included). Calculated seasonal deposition rates at each playground were accumulated. The results for S-2, located 6904.1 m away from the dumping site (the farthest distance), S-3, located 4042.2 m (the middle distance), and S-8, located 1577.4 m (the nearest distance) were compared. The accumulated deposition rates throughout the year by simulation were compared with results of Pb content in soil samples by Mufalo et al. [13].

Figure 4 shows the simulated results of the accumulated amount deposited at S-2 located on the north-northwest direction (335.05°) and 6904.1 m from the source. In the rainy season, the accumulated amount deposited was lower when the winds blew from the east side compared to the winds from the west. The dispersion in the rainy season was not significantly affected by winds from the east even though S-2 is in the north-northwest direction from the source. The total amount deposited by winds from the east and the east-southeast was 0.00014 mg/m^2. The total amount deposited by winds from the northwest, the north-northwest, and the north was 0.00100 mg/m^2. These results indicate that the amount deposited was affected by the lower wind speed from the east-southeast to the south-southeast directions at S-2. In the dry season, the accumulated amount deposited was higher when the winds blew from the east and the south compared to the winds from the west. The total amount deposited by winds from the east-southeast and the southeast was 0.00684 mg/m^2. The total amount deposited by winds from the west was 0.00067 mg/m^2. Dispersion simulations indicate that deposition was affected by the frequency of winds from the east-southeast and the southeast because of low humidity and ignorance of the effects of rain.

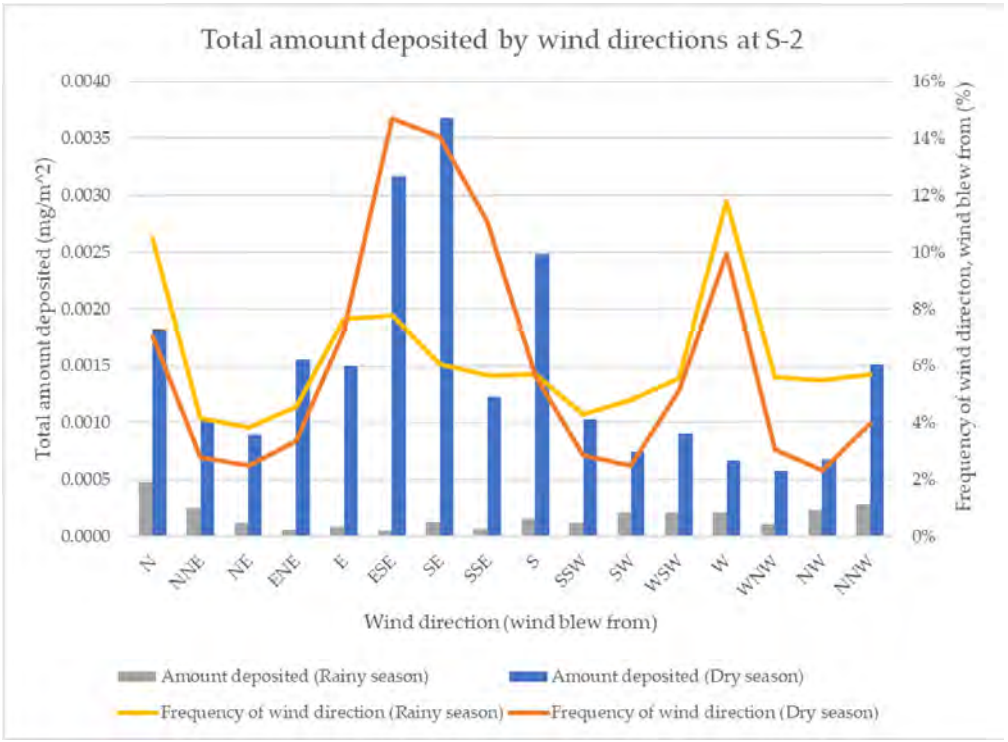

Figure 4. Total amount deposited by the wind directions at S-2: gray and blue bars show total amount deposited by wind directions from which wind blew in the rainy and dry seasons, respectively. Yellow and orange lines show frequencies of wind directions from which wind blew in the rainy and dry seasons, respectively.

Figure 5 shows the simulated results of the accumulated amount deposited at S-3 located on the west-northwest direction (296.64°) and 4042.2 m from the source. In the rainy season, the accumulated amount deposited was lower when the winds blew from the east compared to the winds from the west. The dispersion in the rainy season was not affected by winds from the east even though S-3 is on the north-northwest direction from the source. The total amount deposited by winds from the east and the east-southeast was 0.00034 mg/m^2 whereas the total amount deposited by winds from the west was 0.00066 mg/m^2. The amount deposited was negative (−0.00123 mg/m^2) when the winds blew from the west-southwest. This is due to the net effects of deposition and redispersion by winds from the west-southwest. In the dry season, the accumulated amount deposited

was higher when the winds blew from the east and the south compared to the winds from the west. The amount deposited was affected by winds from the east-southeast and the southeast. The total amount deposited by winds from the east-southeast and the southeast was 0.02124 mg/m^2 whereas the total amount deposited by winds from the west was 0.00188 mg/m^2. The results indicate that deposition was affected by the winds from the east-southeast and the southeast because of low humidity and no rain.

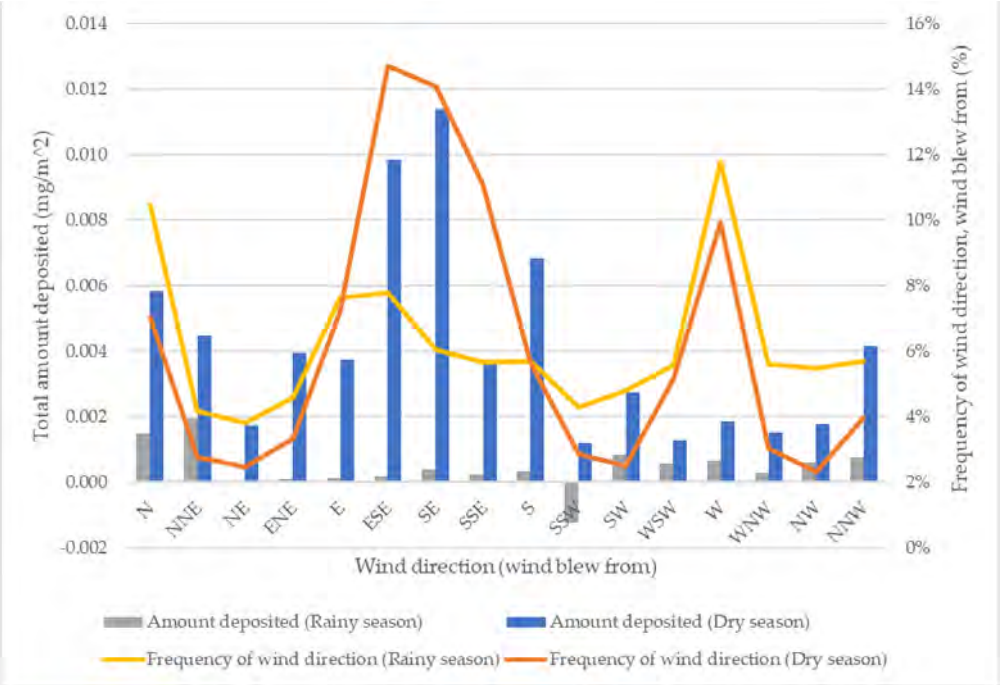

Figure 5. Total amount deposited by wind directions at S-3: gray and blue bars show total amount deposited by wind directions from which wind blew in the rainy and dry seasons, respectively. Yellow and orange lines show frequencies of wind directions from which wind blew in the rainy and dry seasons, respectively.

Figure 6 shows the simulated results of the accumulated amount deposited at S-8 located on the west-northwest direction (285.89°) and 1577.4 m from the source. In the rainy season, the accumulated amount deposited was lower when the winds blew from the east compared to the winds from the west. The results indicate that dispersion in the rainy season was not affected by winds, and that humidity and rain might flush the deposits at the location. The total amount deposited by winds from the east and the east-southeast was 0.00423 mg/m^2. The total amount deposited by winds from the west was 0.00306 mg/m^2. In the dry season, the amount deposited was higher when the winds blew from the east and the south compared to the winds from the west. These results indicate that the amount deposited was affected by the winds from the east-northeast and the south because of low humidity and almost no rain. The total amount deposited by winds from the east-southeast and the southeast was 0.16561 mg/m^2. The total amount deposited by winds from the west was 0.01075 mg/m^2.

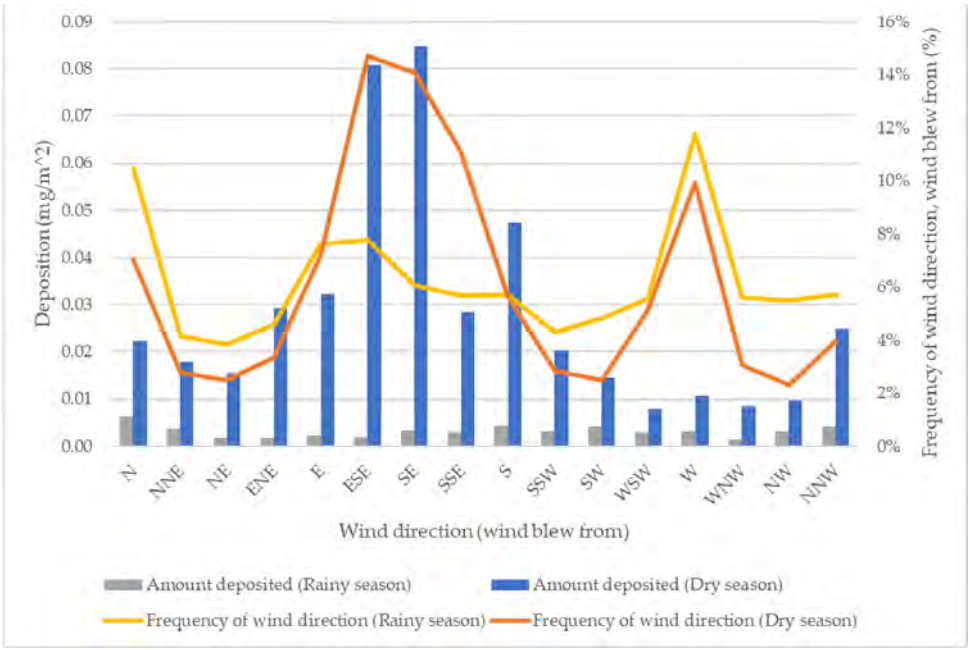

Figure 6. Total amount deposited by wind directions at S-8: gray and blue bars show total amount deposited by wind directions from which wind blew in the rainy and dry seasons, respectively. Yellow and orange lines show frequencies of wind directions from which wind blew in the rainy and dry seasons, respectively.

4. Discussion

In the rainy season, the amount deposited was affected by higher humidity and rain, and the correlation between winds and the amount deposited was not clearly observed at each playground. On the other hand, in the dry season, the amount deposited at each playground was affected by winds from the east-southeast and the southeast, and winds were found to be a sensitive factor of Pb dispersion from the source.

Simulated results for amounts deposited of mine wastes containing Pb were compared with Pb contents in playground soils for their verification. Figure 7 shows the relationship between measured Pb content in soil and simulated amount of deposition. The contents of Pb generally increased with the amount deposited. However, when the amount deposited was lower than 0.1 mg/m^2, the Pb content decreased with the amount deposited. This indicates that not only dispersion by wind but also other factors affect the distribution of Pb.

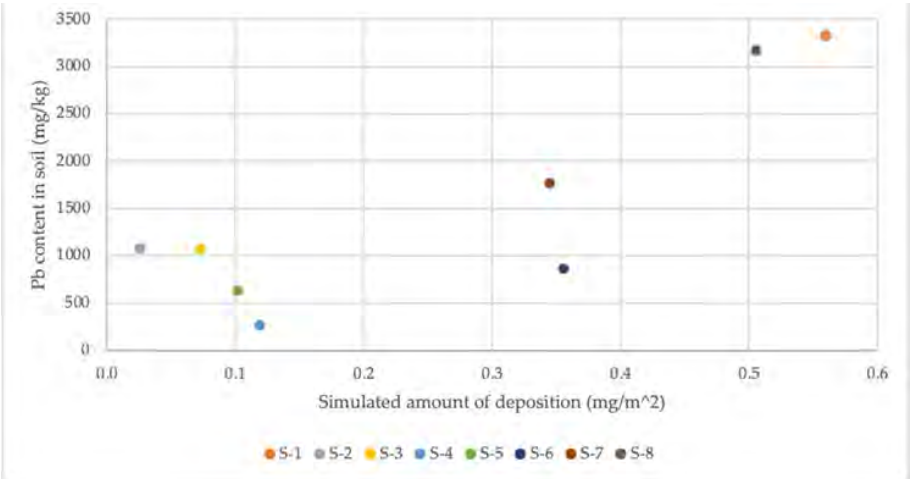

Figure 7. Relationship between measured Pb content in soil and simulated amount of deposition.

Figure 8 shows the simulated amount of deposition and Pb content in soil vs. distance from the source. Both the Pb content and the simulated amount of deposition decreased with distance from the source. This indicates that the dispersion model used here can well express the dispersion of mine wastes from the dumping site. This means that Pb dispersion is mainly caused by dispersion by winds from the dumping site.

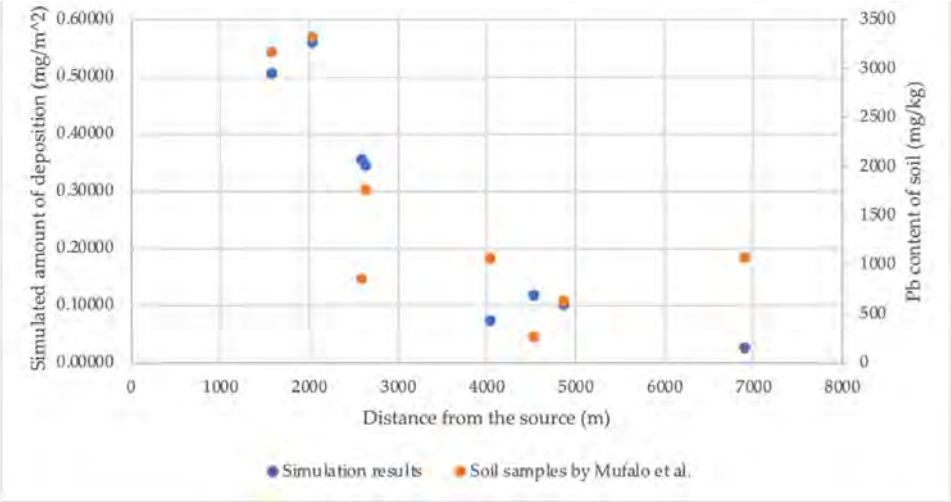

Figure 8. Simulated amount of deposition and Pb content in soil vs. distance from the source.

Figure 9 shows the simulated amount of dispersion depending on particle sizes of Pb-bearing soil at S-2, S-3, and S-8 throughout the year 2019. Although the simulated amount of dispersion decreased with distance, the particles are dispersed within a restricted distance whereas the finer particles are dispersed for a longer distance. In addition, the finer particles are easily redistributed because the fraction of finer particles decreased at any location.

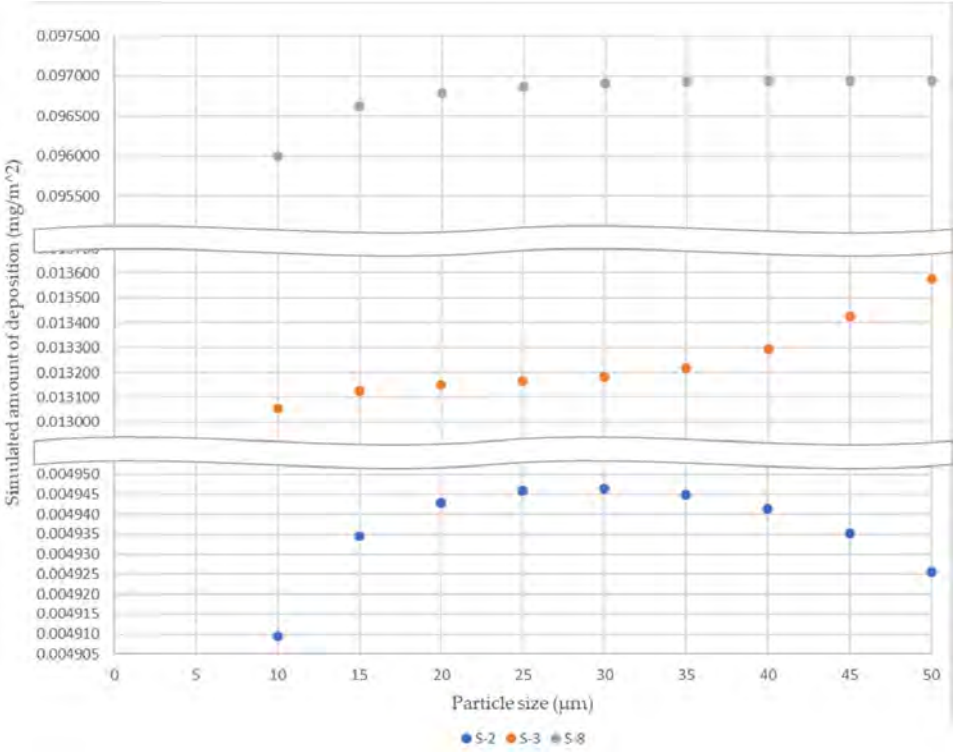

Figure 9. Simulated amount of deposition depending on particle sizes of Pb-bearing soil at S-2, S-3, and S-8.

The dispersion model of fine particles of mine wastes explained the measured results of Pb contents in soils and qualitatively expressed the dependency of particle size on dispersion. Thus, the obtained results imply that the model used in this study may be applicable to the phenomenon of aerial dispersion of contaminants. However, the applicability of this model should be evaluated by using data of the other year and other sites.

5. Conclusions

Lead dispersion simulations using terrain data and local weather data of year 2019 were conducted and compared with the Pb contents in soils around the dumping site of Kabwe, Zambia. The following results were found.

1. Wind direction and speed and humidity, including rain, sensitively affected dispersion of soils/mine wastes containing Pb.
2. The simulated amount deposition decreased with distance from the source and agreed with the calculation of Pb contents of soils.
3. Winds dispersed the smaller sizes of particles farther and dispersed the larger sizes near the source, and easily redispersed the smaller sizes, according to the dispersion simulation, depending on particle sizes.
4. The above results indicate that Pb content in soils is significantly affected by dispersion of mine wastes. In other words, Pb contamination of soils is primarily caused by dispersion of mine wastes by winds.

Based on the obtained results, effective countermeasures against Pb dispersion and remediation of soil contamination should be proposed by considering Pb dispersion calculations after remediation of the dumping site and surrounding ground surfaces.

Author Contributions: Conceptualization, S.N. (Shinsaku Nakamura); methodology, S.N. (Shinsaku Nakamura), and T.I.; formal analysis, S.N. (Shinsaku Nakamura) and T.I.; writing—original draft preparation, S.N. (Shinsaku Nakamura); writing—review and editing, S.N. (Shinsaku Nakamura), T.I., Y.U., M.I. (Mayumi Ito), K.H., T.S., W.M., M.C., and I.N.; supervision, S.N. (Shinsaku Nakamura) and T.I.; project administration, M.I. (Mayumi Ishizuka), S.N. (Shouta Nakayama), and H.N.; funding acquisition, M.I. (Mayumi Ishizuka), S.N. (Shouta Nakayama), and H.N. All authors have read and agreed to the published version of the manuscript.

Funding: The research was supported by JST/JICA SATREPS (Science and Technology Research Partnership for Sustainable Development; No. JPMJSA1501) and aXis (Accelerating Social Implementation for SDGs Achievement: No. JPMJAS2001).

Data Availability Statement: Data are available on request to the authors.

Acknowledgments: The authors would like to acknowledge JST/JICA SATREPS (Science and Technology Research Partnership for Sustainable Development; No. JPMJSA1501) and aXis (Accelerating Social Implementation for SDGs Achievement; No. JPMJAS2001) funded by JST for the financial support.

Conflicts of Interest: The authors declare no conflict of interest.

References

1. Etter, V. Soil contamination near non-ferrous metal smelters: A review. *Appl. Geochem.* **2016**, *64*, 56–74. [CrossRef]
2. Nriagu, J.O. A History of Global Metal Pollution. *Science* **1996**, *272*, 223. [CrossRef]
3. Tchounwou, P.B.; Yedjou, C.G.; Patlolla, A.K.; Sutton, D.J. Heavy Metal Toxicity and the Environment. *Mol. Clin. Environ. Toxicol.* **2012**, *101*, 133–164. [CrossRef]
4. Ettler, V.; Vítková, M.; Mihaljevič, M.; Šebek, O.; Klementová, M.; Veselovský, F.; Vybíral, P.; Kříbek, B. Dust from Zambian smelters: Mineralogy and contaminant bioaccessibility. *Environ. Geochem. Health* **2014**, *36*, 919–933. [CrossRef] [PubMed]
5. Entwistle, J.A.; Hursthouse, A.S.; Reis, P.A.M.; Stewart, A.G. Metalliferous Mine Dust: Human Health Impacts and the Potential Determinants of Disease in Mining Communities. *Curr. Pollut. Rep.* **2019**, *5*, 67–83. [CrossRef]
6. Ettler, V.; Štěpánek, D.; Mihaljevič, M.; Drahota, P.; Jedlicka, R.; Kříbek, B.; Vaněk, A.; Penížek, V.; Sracek, O.; Nyambe, I. Slag dusts from Kabwe (Zambia): Contaminant mineralogy and oral bioaccessibility. *Chemosphere* **2020**, *260*, 127642. [CrossRef]
7. Nakayama, S.M.; Ikenaka, Y.; Hamada, K.; Muzandu, K.; Choongo, K.; Teraoka, H.; Mizuno, N.; Ishizuka, M. Metal and metalloid contamination in roadside soil and wild rats around a Pb–Zn mine in Kabwe, Zambia. *Environ. Pollut.* **2011**, *159*, 175–181. [CrossRef] [PubMed]

8. Uchida, Y.; Banda, K.; Nyambe, I.; Hamamoto, T.; Yoshii, Y.; Munthali, K.; Mwansa, M.; Mukuka, M.; Mutale, M.; Yabe, J.; et al. Multidisciplinary field research in Kabwe, Zambia, towards better understanding of lead contamination of the city—A short report from a field survey. *bioRxiv* **2017**. Available online: https://www.biorxiv.org/content/10.1101/096164v2.full.pdf (accessed on 28 October 2020).
9. Yamada, D.; Hiwatari, M.; Hangoma, P.; Narita, D.; Mphuka, C.; Chitah, B.; Yabe, J.; Nakayama, S.M.M.; Nakata, H.; Choongo, K.; et al. Assessing the population-wide exposure to lead pollution in Kabwe, Zambia: An econometric estimation based on survey data. *Sci. Rep.* **2020**, *10*, 1–11. [CrossRef]
10. Kříbek, B.; Nyambe, I.; Majer, V.; Knésl, I.; Mihaljevic, M.; Ettler, V.; Vanek, A.; Penížek, V.; Sracek, O. Soil contamination near the Kabwe Pb-Zn smelter in Zambia: Environmental impacts and remediation measures proposal. *J. Geochem. Explor.* **2018**, *197*, 159–173. [CrossRef]
11. Tangviroon, P.; Noto, K.; Igarashi, T.; Kawashima, T.; Ito, M.; Sato, T.; Mufalo, W.; Chirwa, M.; Nyambe, I.; Nakata, H.; et al. Immobilization of Lead and Zinc Leached from Mining Residual Materials in Kabwe, Zambia: Possibility of Chemical Immobilization by Dolomite, Calcined Dolomite, and Magnesium Oxide. *Minerals* **2020**, *10*, 763. [CrossRef]
12. Silwamba, M.; Ito, M.; Hiroyoshi, N.; Tabelin, C.B.; Hashizume, R.; Fukushima, T.; Park, I.; Jeon, S.; Igarashi, T.; Sato, T.; et al. Recovery of Lead and Zinc from Zinc Plant Leach Residues by Concurrent Dissolution-Cementation Using Zero-Valent Aluminum in Chloride Medium. *Metals* **2020**, *10*, 531. [CrossRef]
13. Mufalo, W.; Tangviroon, P.; Igarashi, T.; Ito, M.; Sato, T.; Chirwa, M.; Nyambe, I.; Nakata, H.; Nakayama, S.; Ishizuka, M. Characterization and leaching behavior of playground soils in Kabwe, Zambia. In Proceedings of the International Symposium on Earth Science and Technology, Fukuoka, Japan, 26–27 November 2020; pp. 154–157.
14. Kataoka, H.; Tabata, Y. *Numerical Prediction Method for Snowdrift Dust Dispersion*; Report of Obayashi Corporation Technical Research Institute: Tokyo, Japan, 2010; Volume 74.
15. Japan Environmental Management Association for Industry; Ministry of Economy, Trade and Industry. Low Rise Industrial Source Dispersion MODEL. 2021. Available online: http://www.jemai.or.jp/tech/meti-lis/detailobj-6117-attachment.pdf (accessed on 28 October 2020).
16. Siciliano, S.D.; James, K.; Zhang, G.; Schafer, A.N.; Peak, J.D. Adhesion and Enrichment of Metals on Human Hands from Contaminated Soil at an Arctic Urban Brownfield. *Environ. Sci. Technol.* **2009**, *43*, 6385–6390. [CrossRef] [PubMed]
17. Tada, K.; Hazama, H.; Kobayashi, K.; Okamoto, S. Development and evaluation of a diffusion model for particle matter—Application to Kashima area. *J. Japan Soc. Air Pollut.* **1989**, *24*, 64–73.
18. Matsusaka, S.; Masuda, H. Reentrainment Phenomena of Fine Particles. *J. Soc. Powder Technol. Jpn.* **1992**, *29*, 530–538. [CrossRef]
19. Sherman, C.A. A Mass-Consistent Model for Wind Fields over Complex Terrain. *J. Appl. Meteorol.* **1978**, *17*, 312–319. [CrossRef]
20. Fukuyama, T.; Izumi, K.; Utiyama, M. Dry deposition of atmospheric aerosols—A browse on recent papers. *J. Aerosol Res.* **2004**, *19*, 245–253.
21. Ministry of Economy, Trade and Industry of Japan. Technical Manual of Ministry of Economy, Trade and Industry Low rise Industrial Source dispersion model (METI-LIS) ver. 3.02, March 2012. Available online: https://www.jemai.or.jp/tech/meti-lis/detailobj-6117-attachment.pdf (accessed on 30 May 2019).
22. Luhar, A.K. Analytical puff modelling of light-wind dispersion in stable and unstable conditions. *Atmos. Environ.* **2011**, *45*, 357–368. [CrossRef]
23. Nakatani, N.; Nakane, I. A study of pollen re-transportation in urban environment by using physical model and numerical simulation. *Jpn. Soc. Comput. Methods Eng.* **2017**, *17*, 171215.
24. Fuller, D.D. *Coefficient of Friction*; Columbia University: New York, NY, USA; pp. 2-42–2-48. Available online: https://web.mit.edu/8.13/8.13c/references-fall/aip/aip-handbook-section2d.pdf (accessed on 6 May 2020).
25. Nabeel, M.; Karasev, A.; Jönsson, P.G. Friction Forces and Mechanical Dust Generation in an Iron Ore Pellet Bed Subjected to Varied Applied Loads. *ISIJ Int.* **2017**, *57*, 656–664. [CrossRef]
26. Klingmuller, K.; Metzger, S.; Abdelkader, M.; Karydis, V.A.; Stenchikkov, G.L.; Pozzer, A.; Lelievbeld, J. Revised mineral dust emission in the atmospheric chemistry-climate model EMAC (MESSy 2.52 DU_Astithal KKDU2017 patch). *Geosci. Model Dev.* **2018**, *11*, 989–1008. [CrossRef]

Environmental Science and Pollution Research
https://doi.org/10.1007/s11356-021-16098-1

RESEARCH ARTICLE

Glutathione S-transferase gene polymorphisms in association with susceptibility to lead toxicity in lead- and cadmium-exposed children near an abandoned lead-zinc mining area in Kabwe, Zambia

Yared Beyene Yohannes[1,2] · Shouta M. M. Nakayama[1] · John Yabe[3,4] · Haruya Toyomaki[1] · Andrew Kataba[1,3] · Hokuto Nakata[1] · Kaampwe Muzandu[3] · Yoshinori Ikenaka[1,5,6,7] · Kennedy Choongo[3,8] · Mayumi Ishizuka[1]

Received: 16 June 2021 / Accepted: 18 August 2021

Abstract

Interindividual genetic variations determine human's susceptibility to heavy metal-induced toxicity. Thus, we analyzed blood concentrations of lead (Pb) and cadmium (Cd) in 140 lead-exposed children. Genotyping of the glutathione S-transferase (GST) genes, *GSTM1*, *GSTT1*, and *GSTP1* genes, was carried out to investigate their possible association with heavy metal concentrations and the risk of susceptibility to Pb toxicity. Exposure to both heavy metals was prevalent among the children. The blood Pb level ranged from 3.30 to 74.0 μg dL^{-1} with an average value of 26.8 μg dL^{-1} that is five times above its reference level. The average Cd level (0.22 μg L^{-1}) was below its reference level. The metal-gene interaction showed positive correlation between *GSTT1* null genotype and Pb and Cd levels ($\beta = 0.11$; $p = 0.02$ and $\beta = 0.10$; $p = 0.01$, respectively). More pronounced effects ($\beta = 0.19$; $p < 0.01$ and $\beta = 0.25$; $p = 0.04$) were found for the mixture of the three putative genes with blood Pb concentration. The susceptibility analysis using 10 μg dL^{-1} as blood Pb cutoff level showed a high risk of Pb toxicity (OR = 2.54; 95% CI: 1.02-6.32, $p = 0.04$) for children carrying the *GSTP1 Ile/Val* genotype. Further, the combined effect of *GSTP1 Ile/Val* with *GSTT1* null genotype was more pronounced and showed an increased risk of susceptibility to Pb toxicity (OR = 11.7; 95% CI: 1.36-102.1, $p = 0.02$). In summary, this study suggests that *GSTT1* null and *GSTP1 Ile/Val* genotypes are the main genetic factors, and individual and specific combinations of *GSTP1 Ile/Val* with *GSTM1* and *GSTT1* GST polymorphisms are associated with susceptibility to Pb toxicity.

Keywords Blood · Children · Lead · Cadmium · *GST* · Polymorphism · Kabwe

Responsible Editor: Lotfi Aleya

Yared Beyene Yohannes and Shouta M.M. Nakayama are equally contributed to the work

✉ Shouta M. M. Nakayama
shouta-nakayama@vetmed.hokudai.ac.jp;
shoutanakayama0219@gmail.com

✉ Mayumi Ishizuka
ishizum@vetmed.hokudai.ac.jp

[1] Laboratory of Toxicology, Department of Environmental Veterinary Sciences, Faculty of Veterinary Medicine, Hokkaido University, Kita 18 Nishi 9, Kita-Ku, Sapporo 060-0818, Japan

[2] Department of Chemistry, College of Natural and Computational Science, University of Gondar, P.O. Box 196, Gondar, Ethiopia

[3] School of Veterinary Medicine, The University of Zambia, P.O. Box 32379, Lusaka, Zambia

[4] Department of Veterinary Para-Clinical Studies, School of Veterinary Medicine, University of Namibia, Windhoek, Namibia

[5] Water Research Group, Unit for Environmental Sciences and Development, North-West University, Potchefstroom, South Africa

[6] Translational Research Unit, Veterinary Teaching Hospital, Faculty of Veterinary Medicine, Hokkaido University, Sapporo 060-0818, Japan

[7] One Health Research Center, Hokkaido University, Sapporo, Japan

[8] College of Agriculture, Fisheries & Forestry, School of Animal and Veterinary Sciences, Fiji National University, Koronivia Campus, Suva, Fiji

Published online: 28 August 2021

Introduction

Heavy metals like lead (Pb) and cadmium (Cd) have no known biological roles in living organisms and are considered toxic metals. According to the International Agency for Research on Cancer (IARC), Pb and Cd are classified as probable carcinogenic (group 2A) and known carcinogenic (group 1) compounds, respectively (IARC 2021). Once inside the body, either from natural or anthropogenic sources, they can interact metabolically with essential metals and displace them from their specific cell constituent sites (Jan et al. 2015; Godwill et al. 2019). Generally, heavy metal exposure can cause multiple organ dysfunctions that led to toxicity and oxidative stress (Tchounwou et al. 2012; Jan et al. 2015; Godwill et al. 2019). Owing to their developing bodies, children are more prone to numerous adverse effects of heavy metals such as cognitive impairments and central nervous system functional deficits that persist into older age (Jaishankar et al. 2014).

Glutathione-S-transferases (GST), recognized as oxidative stress-related genes, are vital defense enzymes engaged in metal biotransformation and detoxification of reactive oxygen species (Hayes et al. 2005). It catalyzes the conjugations of hydrophobic and electrophilic compounds with reduced glutathione (GSH) and excreted via feces and urine after GSH-metal conjugate formation (Jozefczak et al. 2012). The GST superfamily comprises eight polymorphic genes, and of these, polymorphic variants of the GST-mu 1 (*GSTM1*), theta 1 (*GSTT1*), and pi (*GSTP1*) are the most studied and reported globally (Sharma et al. 2014; Saitou and Ishida 2015). Genetic variations in these genes (deletion in *GSTM1* and *GSTT1* genes and polymorphism in *GSTP1*) contribute to interindividual differences in susceptibility to xenobiotic toxicity (Hollman et al. 2016). Previous studies reported an absence or decreased detoxification ability of GST enzymes (Kasperczyk et al. 2004) and linked it with oxidative stress and health outcomes in different polymorphic GST gene carriers. Individuals with *GSTP1* variant alleles and double-null genotypes of *GSTM1* and *GSTT1* were associated with the induction of oxidative stress (Sirivarasai et al. 2013). In another study, individuals with the *GSTM1* null genotype and *GSTP1* wild allele had lower GSH levels and be at increased risk from exposure to toxicants (Hunaiti and Soud 2000; Khansakorn et al. 2011). Pregnant mothers with combined *GSTM1* and *GSTT1* genetic variants showed an inverse association of blood Pb and birth weight (Lamichhane et al. 2018). However, polymorphisms in these functional genes vary by race and ethnicity (Sharma et al. 2014; Saitou and Ishida 2015).

Kabwe, a capital town of the Central Province of Zambia, has a long history of Pb-zinc (Zn) mining that operated from 1902 to 1994 without adequate pollution regulations. Thus, the town is one of the most polluted places in the world. Even though the mine is inactive, the residue left a legacy of contaminated soil with Pb, Zn, and other byproducts like cadmium (Cd). Moreover, illegal mining activities are still ongoing. These create wide-contaminated surroundings and an environment that poses a significant health risk. Recent studies involving a population-wide screening on Pb poisoning in this town reported that approximately 75% of the residents had BLLs higher than 5 μg dL^{-1} (Yabe et al. 2020; Yamada et al. 2020). Nevertheless, only one study investigated gene polymorphism on candidate Pb biomarkers of effect genes delta-aminolevulinic acid dehydratase (ALAD) and vitamin D receptor (VDR) genes in Kabwe (Yohannes et al. 2021).

Thus, this study (i) assessed the burden of Pb and Cd concentrations in children blood; (ii) investigated the genetic polymorphism in the GST family, *GSTM1*, *GSTT1*, and *GSTP1* polymorphisms; and (iii) examined the effect of the GST polymorphic variants on blood heavy metal levels and the influence on the risk of susceptibility to Pb toxicity in children living near an abandoned Pb-Zn mining area. We also reported Zn concentration. Thus, the data generated here provide reference data for future studies.

Materials and methods

Study subjects and sampling

A total of 140 healthy children, aged 2-10 years, were recruited from five townships (Chowa, Kasanda, Makululu, Bwacha, and Nakoli townships) in Kabwe, Zambia. Among these children, 102 children live in three townships near the abandoned mine, and 38 children from two townships live far away from the mine (Fig. 1). Children were invited to health centers, and parents were asked a short questionnaire on demography and Pb-related clinical symptoms. No evidence or any sign and symptoms of neurotoxicity among the children. Venous blood samples (≈ 3 mL) were obtained from each child by trained nurses into heparinized blood collection tubes in July 2016 (Yohannes et al. 2020). A 500 μL blood sample was kept in a 1.5-mL tube for heavy metal analysis and stored all samples at −20 °C. All analyses were done in the Laboratory of Toxicology, Faculty of Veterinary Medicine, Hokkaido University, Japan.

Heavy metal analysis

Blood sample digestion and heavy metal analyses were done as described by Yohannes et al. (2017). Briefly, the 500 μL blood sample was digested with 5 mL 61% HNO_3 and 1 mL 30% H_2O_2 in a speedwave MWS-2 microwave system. Then, samples were made to a final volume of 10 mL using Milli-Q water in a 15-mL tube. Blood Pb, Cd, and Zn concentrations were measured using inductively coupled plasma mass

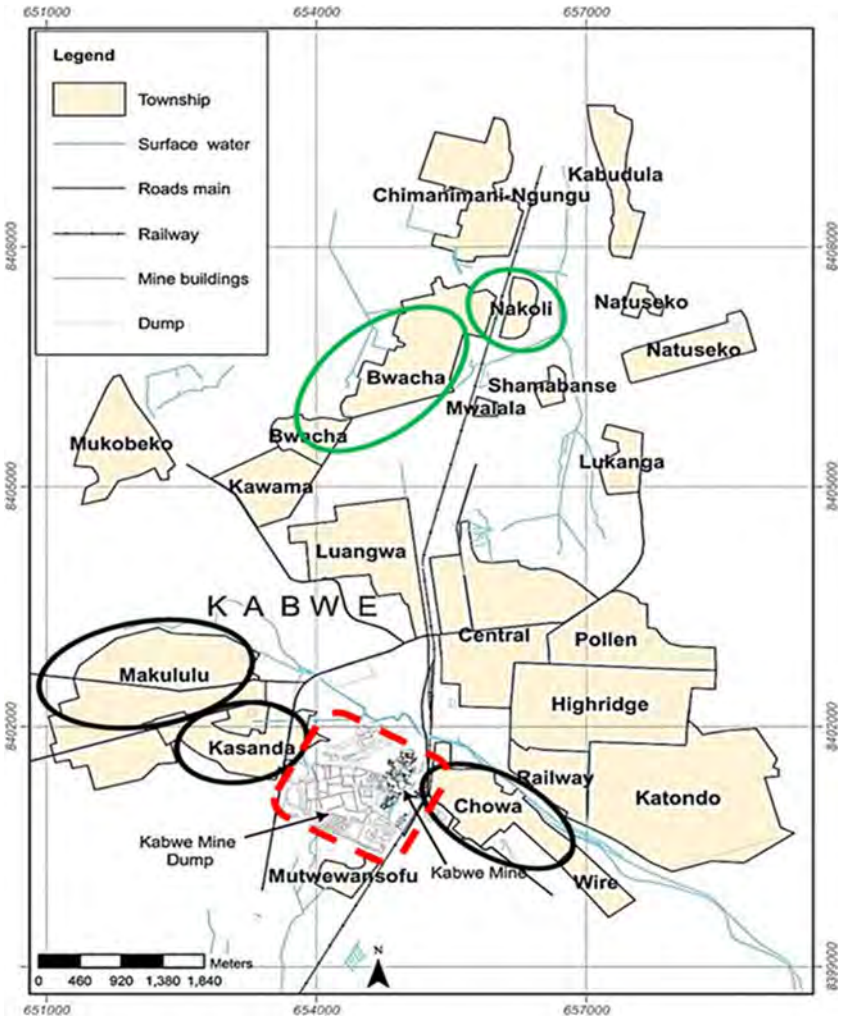

Fig. 1 Location of the Pb-Zn mine (in red dotted color) and sampling townships (black ovals, near the mine site and green ovals, far away from mine site) in Kabwe, Zambia (Yohannes et al. 2020)

spectrometry (ICP-MS 7700 series). Seronorm™ Trace Elements Whole Blood L-2 certified reference material (Sero AS, Norway) was used as quality control. Replicate analyses of this reference material showed recovery rates ranging from 90 to 105% with a detection limit of 0.01 μg L^{-1} for the measured heavy metals.

GST genotyping

Genomic DNA was isolated from whole blood using a NucleoSpin Blood Kit (Macherey-Nagel) and kept at –25 °C until genotyping analysis. A multiplex polymerase chain reaction (PCR) was used for *GSTM1* and *GSTT1* genotyping to detect the presence or absence of the genes with the CYP 1A1 gene as a positive control. A PCR-restriction fragment length polymorphism (PCR–RFLP) method was carried out for *GSTP1 Ile105Val* (rs1695; A > G) polymorphism. PCR was done to a mixture containing 1 μL DNA (>20 ng), 1x PCR buffer, 2.0 mM $MgCl_2$, 200 μM of each dNTP, 0.25 μM of each primer, and 1 U Taq polymerase in a total volume of 10 μL. The sequences of primers and the PCR amplification conditions are displayed in Table 1.

The presence of *GSTM1*, *GSTT1*, and *CYP 1A1* genes were identified by the bands at 219 bp, 480 bp, and 312 bp, respectively. The absence of the band describes the gene deletion referred to as null genotype. For *GSTP1* genotyping, the resulting 433 bp PCR product was digested at 55 °C for 4 h with the restriction enzyme *BsmAI* (5 U). The corresponding fragmented product bands were visible with 328 bp and 105 bp fragments (*Ile/Ile* genotype); 328 bp, 222 bp, and 105 bp fragments (*Ile/Val* genotype); and 222 bp and 105 bp fragments (*Val/Val* genotype). The PCR fragments were electrophoresed in a 2% agarose gel with Midori Green direct and visualized under a Blue-LED transilluminator system. Representative gel electrophoresis showed that the genotypes of *GSTM1*, *GSTT1*, and *GSTP1* are presented in Fig. 2. For ensuring quality control, random samples (10%) were genotyped twice, and no contamination was confirmed using no-template control samples.

Table 1 Primer pairs and PCR amplification conditions for amplifying genomic DNA

Gene	Sense	Antisense	Size (bp)
GSTM1	5′-GAACTCCCTGAAAAGCTAAAGC-3′	5′-GTTGGGCTCAAATATACGGTGG-3′	219
GSTT1	5′-TTCCTTACTGGTCCTCACATCTC-3′	5′-TCACCGGATCATGGCCAGCA-3′	480
CYP 1A1	5′-GAACTGCCACTTCAGCTGTCT-3′	5′-CAGCTGCATTTGGAAGTGCTC-3′	312
GSTP1	5′-GTAGTTTGCCCAAGGTCAAG-3′	5′-AGCCACCTGAGGGGTAAG-3′	433

Amplification condition: initial denaturation at 94 °C for 3 min, then 35 cycles of denaturation at 94 °C for 30 s, annealing for 30 s at 60 °C, extension at 72 °C for 1 min, and a final extension for 7 min at 72 °C

Statistical analysis

To improve normality and homogeneity of variance of heavy metal concentrations, data were log-transformed before statistical analysis. Blood heavy metals were expressed as mean ± standard deviation and analyzed by the non-parametric Kruskal-Wallis test. Deviation of *GSTP1* genotype distribution from Hardy-Weinberg equilibrium (HWE) was assessed using Pearson's chi-square (χ^2) test. Comparisons of the observed *GSTM1* and *GSTT1* null genotypes and *GSTP1 Val* allele frequencies between this study and global studies were examined using the χ^2 test. We checked the effect of covariates (age and sex) on the statistical analysis, and no significant association was found. Thus, linear regression analysis was performed for assessing the association between polymorphic variants of GST genes and log-transformed blood heavy metal concentrations. Next, crude odds ratios (ORs) and 95% confidence intervals (CIs) were calculated to examine associations between the GST gene genotypes and susceptibility to Pb toxicity using 10 μg/dL as a cutoff level. A $p \leq 0.05$ was considered statistically significant, and a p between 0.051 and 0.100 was marginally significant (Amrhein et al. 2019). The JMP 14.0 software (SAS Institute, Cary, NC, USA) was used to perform all analyses.

Results and discussion

Blood Pb, Cd, and Zn concentrations

The subjects of the current study were 65 females and 75 male children with mean ages of 5.72 and 5.69 years, respectively. The majority of children have lived in their respective townships for most of their lifetime. The descriptive statistics of heavy metal concentrations are given in Table 2. The blood Pb concentrations among participants ranged from 3.30 to 74.0 μg dL^{-1} with the mean and median concentrations of 26.8 and 26.3 μg dL^{-1} (interquartile range: 13.6-36.6 μg dL^{-1}), respectively. These mean and median Pb levels were 5 times higher than the blood Pb reference

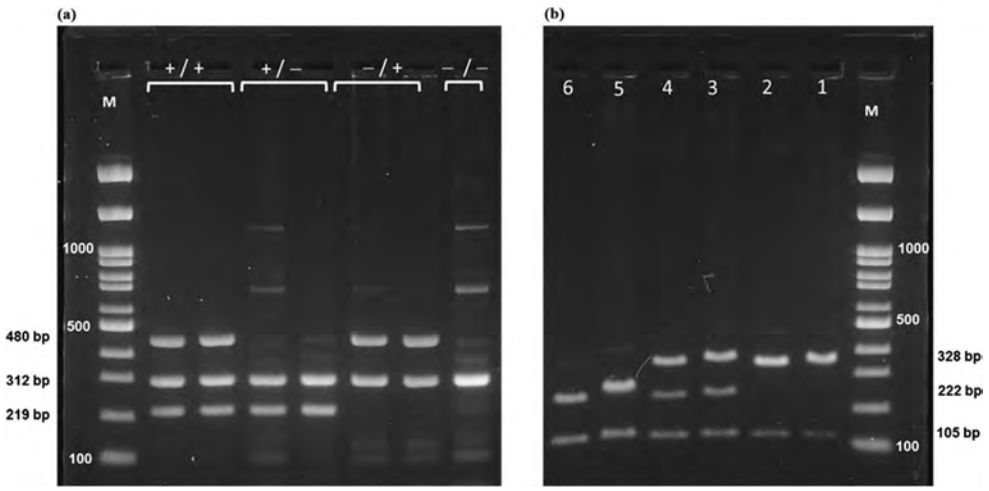

Fig. 2 Representative agarose gel electrophoresis for identification of **a** a multiplex PCR amplification of *GSTM1* (219 bp), *GSTT1* (480 bp), and CYP1A1 (312 bp) genes (+/+, presence of GSTM1 and GSTT1 genes; +/-, presence of *GSTM1* and absence of *GSTT1*genes; -/+, absence of *GSTM1* and presence of *GSTT1* genes; -/-, absence of *GSTM1* and *GSTT1* genes; M, 100 bp DNA ladder). **b** PCR-RFLP product of *GSTP1* gene (lanes 1 and 2, *Ile/Ile* genotypes (328 bp and 105 bp); lanes 3 and 4, *Ile/Val* genotypes (328 bp, 222 bp, and 105 bp); lanes 5 and 6, *Val/Val* genotypes (222 bp and 105 bp); M, 100 bp DNA ladder)

value of 5 μg dL^{-1} (CDC, 2012). Among the 140 participants, 131 (93.5%) children exceeded this blood Pb reference value. The mean/median concentrations of Cd and Zn were 0.22/0.18 μg L^{-1} and 4135/4167 μg L^{-1}, respectively. These concentration values were below their respective reference values (Table 2).

In addition, the measured heavy metals demonstrated some correlations among them and showed Spearman's correlation coefficients $\rho = 0.497$ for Pb-Cd and $\rho = 0.400$ for Pb-Zn. These correlations imply that these elements share the same sources of exposure and children are exposed to both toxic metals. The closed mine is still a source of pollution. As shown in Table 2, the concentrations of the measured heavy metals near the mine site were significantly higher than far from the mine site. There were no significant differences between blood heavy metal concentrations and sex, showing equal exposure regardless of sex (data not shown). Owing to their immature defense mechanisms, children are more vulnerable to heavy metal toxicity. Thus, appropriate measures should be taken to prevent or minimize exposure for reducing the toxic effects of Pb and Cd on the community.

GST polymorphism and blood Pb, Cd, and Zn concentrations by GST polymorphic variants

Table 3 shows the distribution rate of *GSTM1*, *GSTT1*, and *GSTP1* genotypes. We found *GSTM1* present genotype as the most prevalent genotype with a frequency of 76.4%, followed by the *GSTT1* present genotype (65.0%) and then the *GSTP1 Ile/Val* genotype (59.3%). The null genotype prevalence was 23.6% and 35.0% for *GSTM1* and *GSTT1*, respectively. The combined polymorphic variants of *GSTM1* and *GSTT1* were 8.6% for null/null, 41.4% for null/present, and 50.0% for present/present genotypes. Regarding the *GSTP1* polymorphism, 40 children (28.6%) were *Ile/Ile* homozygous, 83 children (59.3%) were heterozygous *Ile/Val*, and 17 children (12.1%) were *Val/Val* homozygous genotypes (Table 3). The distribution of *GSTP1 Ile*105*Val* showed significant deviation from HWE ($\chi^2 = 6.69$; $p < 0.05$). The analysis revealed an excess number of heterozygous *Ile/Val* genotypes (observed = 83 children vs expected = 68 children). The prevalence of *GSTP1 Ile* and *Val* allele frequencies were 58% and 42%, respectively.

The blood heavy metal concentrations per *GSTM1*, *GSTT1*, and *GSTP1* genotypes are depicted in Table 3. None of the measured heavy metals showed significant differences between the genotypes of *GSTM1* and *GSTP1* genes, whereas the *GSTT1* null group showed significantly higher blood levels for Pb and Cd (Table 3).

GST gene polymorphisms have been studied in various human races with pervasive existence (Fig. 3). Globally, the *GSTM1* null genotype frequency ranged from 20 to 46% in Africans, 42–55% in Europeans, 36–52% in Americans, and 41–60% in Asians (Fig. 3a) (Palma-Cano et al. 2017). The distribution frequency of *GSTT1* null genotype ranged from 30 to 50% for Asians followed by Africans (20–47%), then Europeans and Americans (11–26%) (Fig. 3a) (Palma-Cano et al. 2017). Thus, our study *GSTM1* null genotype prevalence rate of 23.6% was found in the lower range in the Africans and lower than the levels reported from other continents. The 35%

Table 2 Summary statistics of Pb, Cd, and Zn concentrations in whole blood samples and by area

	Mean ± SD	GM	Median	Minimum	Maximum	IQR	RV
All children ($N = 140$)							
Pb (μg dL^{-1})	26.8 ± 15.8	21.2	26.3	3.30	74.0	13.6–36.6	5[a]
Cd (μg L^{-1})	0.22 ± 0. 13	0.18	0.18	0.04	0.72	0.13–0.28	1.4[b]
Zn (μg L^{-1})	4135 ± 875	4035	4167	1479	6429	3612–4703	6265[c,d]
Children near the mine area ($N = 102$)							
Pb (μg dL^{-1})	33.7[e] ± 12.6	31.4	33.1	13.1	74.0	24.8–40.5	
Cd (μg L^{-1})	0.24[f] ± 0.12	0.21	0.22	0.06	0.72	0.15–0.31	
Zn (μg L^{-1})	4280[g] ± 891	4179	4361	1479	6429	3716–4803	
Children far from the mine area ($N = 38$)							
Pb (μg dL^{-1})	8.36 ± 4.68	7.37	6.18	3.27	25.5	5.07–10.7	
Cd (μg L^{-1})	0.15 ± 0.13	0.12	0.11	0.04	0.52	0.07–0.17	
Zn (μg L^{-1})	3746 ± 704	3674	3892	2257	4903	3408–4185	

SD standard deviation, *GM* geometric mean, *IQR* interquartile range, *RV* reference values

[a] CDC, 2012

[b] Hays et al. 2008

[c] Poddalgoda et al. 2019

[d] ATSDR chronic MRL toxicity value

[e,f,g] p value < 0.05, nonparametric Wilcoxon test comparing the Pb, Cd, and Zn concentrations between children near the mine area and far from mine area, respectively

Table 3 Distribution of the *GSTM1*, *GSTT1*, and *GSTP1* polymorphisms and blood heavy metal concentrations (mean ± standard deviation) by GST polymorphisms

	Genotype distribution			Blood concentrations		
		Number	%	Pb (μg dL^{-1})	Cd (μg L^{-1})	Zn (μg L^{-1})
GSTM1	Present (+)	107	76.4	26.7 ± 16.1	0.22 ± 0.14	4115 ± 858
	Null (-)	33	23.6	27.4 ± 15.1	0.22 ± 0.11	4200 ± 939
GSTT1	Present	91	65	24.5 ± 14.3[a]	0.20 ± 0.13[b]	4084 ± 884
	Null	49	35	31.5 ± 17.5	0.25 ± 0.13	4230 ± 858
GSTM1 and *GSTT1*	+/+	70	50	24.5 ± 14.2	0.20 ± 0.14	4103 ± 876
	-/+ and +/-	58	41.4	28.9 ± 17.4	0.22 ± 0.12	4095 ± 863
	-/-	12	8.6	31.9 ± 15.1	0.27 ± 0.10	4515 ± 908
GSTP1[#]	*Ile/Ile*	40	28.6	23.1 ± 15.8	0.22 ± 0.12	4151 ± 710
	Ile/Val	83	59.3	28.7 ± 16.3	0.21 ± 0.14	4185 ± 962
	Val/Val	17	12.1	27.2 ± 11.9	0.22 ± 0.10	3855 ± 763

[#] HWE test; significant difference for *GSTP1* ($\chi^2 = 6.69$; $p < 0.05$)

[a] p value = 0.036, compared the Pb level between *GSTT1* present and null genotypes

[b] p value < 0.01, compared the Cd level between *GSTT1* present and null genotypes

prevalence rate for the *GSTT1* null genotype in the current study was significantly higher than those reported from European and American countries. Comparing our study GSTP1 *Val* allele frequency (42%) with global *Val* allele frequency based on the new Allele Frequency Aggregator (ALFA) dataset (https://www.ncbi.nlm.nih.gov/snp/rs1695#frequency_tab), we observed apparent variation of the *Val* allele frequencies between Africans and Asians (Fig. 3b). The *Val* allele was more frequent in the Latin American individuals with mostly European and Native American Ancestry (49.7%), followed by Africans (42%), Europeans (32.6%), and then Asians (18.9–28.9%). The chi-square statistical analysis showed clear out variation between this study and Asians ($p < 0.05$).

In respect to metal-gene interactions, the effect of the three putative genes on blood heavy metal levels showed both direct and inverse significant effects. The regression analysis coefficient for genetic variants of GST genes in association with blood heavy metals is shown in Table 4. Logistic regression analysis using log-transformed concentration as a dependent variable confirmed a positive significant association for the *GSTT1* null genotype with blood Pb ($\beta = 0.11$, $p = 0.02$) and Cd ($\beta = 0.10$, $p = 0.01$) levels. In the combined analysis, the result showed direct association of blood Pb level with *GSTT1* null/*GSTP1 Ile/Val* genotypes ($\beta = 0.19$, $p = 0.002$), with *GSTM1* present/*GSTT1* null/*GSTP1 Ile/Val* genotypes ($\beta = 0.16$, $p = 0.03$), and with *GSTM1* null/*GSTT1* null/*GSTP1 Ile/Val* genotypes ($\beta = 0.25$, $p = 0.04$). For Cd, the double-null genotypes showed a significant higher association with beta coefficient of 0.11 ($p = 0.05$). On the other hand, the *GSTP1 Ile/Ile* genotype showed an inverse association with blood Pb level ($\beta = -0.10$, $p = 0.04$), suggesting a protective role of this genotype. The combined effect of this genotype with others also showed negative beta estimates, *GSTP1 Ile/Ile/GSTT1* null ($\beta = -0.17$, $p = 0.03$), *GSTP1 Ile/Ile/GSTM1* present/*GSTT1* null ($\beta = -0.28$, $p = 0.01$), and *GSTP1 Ile/Ile/GSTM1* null/*GSTT1* present ($\beta = -0.32$, $p = 0.03$) in relation with blood Pb levels.

To our knowledge, most of the studies on the impact of GST polymorphism are based on case-control studies, and only a few had available on healthy people (Khansakorn et al. 2011, 2012). In nonoccupationally exposed populations, Khansakorn et al. (2011) reported an association between GST polymorphism and the level of Cd in blood. The result revealed higher Cd levels for subjects with the *GSTP1 Val/Val* genotype than their counterparts. The combination of *GSTP1* with *GSTM1* and *GSTT1* also showed an association with increased blood Cd levels. In our study, the metal-to-gene interaction showed significant associations between GST polymorphism and blood heavy metal concentrations. The study revealed that individual and combined GST gene variants could play substantial roles in heavy metal accumulation in our bodies. The result showed direct positive associations between gene deletion of *GSTT1* and blood Pb and Cd concentration. Moreover, *GSTP1* polymorphism (substitution of *Ile* →*Val*) coupled with the *GSTT1* null genotype showed a higher association with blood Pb concentration. This incidence can reduce the GST enzyme activity and as a result reduce Pb- and Cd-GSH conjugates and excretion. Thus, these toxic metals can accumulate in blood and tissues (Jozefczak et al. 2012). It is known that Pb and Cd can replace essential elements such as calcium, copper, iron, and zinc in several major biological processes and mimic the actions of essential elements (Tchounwou et al.

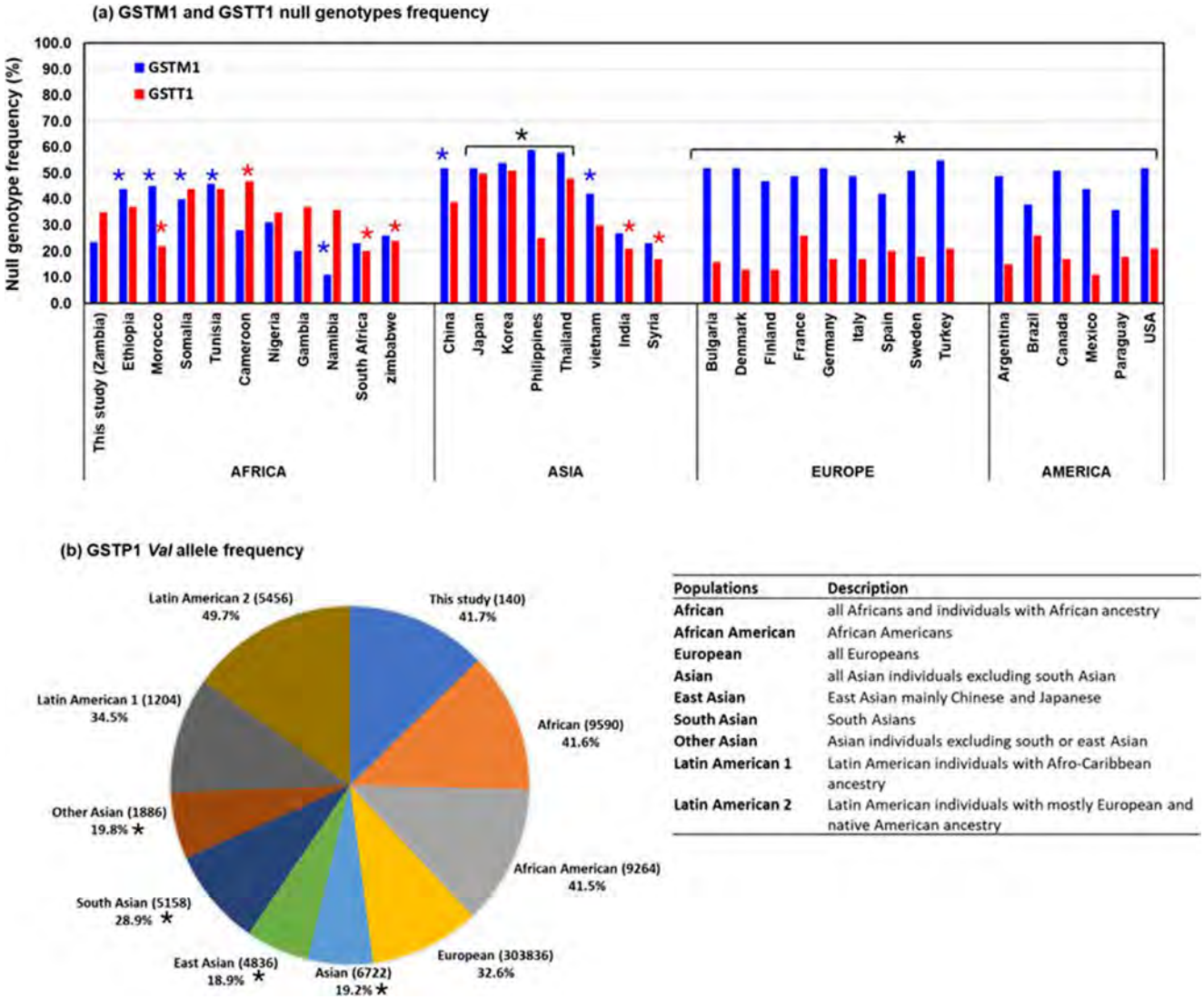

Populations	Description
African	all Africans and individuals with African ancestry
African American	African Americans
European	all Europeans
Asian	all Asian individuals excluding south Asian
East Asian	East Asian mainly Chinese and Japanese
South Asian	South Asians
Other Asian	Asian individuals excluding south or east Asian
Latin American 1	Latin American individuals with Afro-Caribbean ancestry
Latin American 2	Latin American individuals with mostly European and native American ancestry

Fig. 3 Comparison of current study *GSTs* genotypes frequency result with global population. **a** *GSTM1* and *GSTT1* null genotypes frequency compared with 33 countries populations from 4 continents (*$p < 0.05$; blue is for *GSTM1*, red for *GSTT1*, and black for both). **b** The *GSTP1 Val* allele frequency compared with global populations based on the ALFA dataset. (https://www.ncbi.nlm.nih.gov/snp/docs/gsr/data_inclusion/#population. Accessed on 30 April 2021) (number in bracket indicates sample size; *$p < 0.05$).

2012). Overall, the combined effect of *GSTP1* polymorphism with *GSTM1* and *GSTT1* gene deletions could affect the levels of Pb and Cd in children living around the closed mine.

The effect of GST genotypes on susceptibility to lead toxicity

The GST genetic variant's impact on susceptibility to Pb toxicity was investigated using a blood Pb level of 10 μg dL^{-1} as a cutoff point. Thus, we categorized the subjects as low-exposed (≤ 10 μg dL^{-1}) and high-exposed (> 10 μg dL^{-1}) children. The frequencies of the GST genotypes in these groups are depicted in Table 5. The prevalence of *GSTM1* null in high-exposed (23.7%) and low-exposed (23.1%) groups were similar, and susceptibility analysis showed no association between *GSTM1* polymorphism and susceptibility to Pb toxicity (OR = 1.03; 95% CI: 0.38-2.84, $p = 0.94$). For the *GSTT1* polymorphism, the null genotype was marginally higher in the highly exposed group (35.6%) than the low-exposed group (19.2%) ($\chi^2 = 3.49$; $p = 0.06$). Analysis of susceptibility to Pb toxicity also showed a marginal association between the *GSTT1* null genotype and risk of lead toxicity (OR = 2.64; 95% CI: 0.92-7.51, $p = 0.06$), suggesting that individuals with *GSTT1* null genotype are at higher risk of susceptibility to Pb toxicity. The combined effects of *GSTM1* present/*GSTT1* null, *GSTM1* null/*GSTT1* present,

Table 4 Effect of GST polymorphic variants on blood heavy metal concentrations

GST polymorphic variants				β (95% CI)	*t ratio*	*p**
Pb			*GSTT1* null	0.11 (0.03, 0.21)	2.24	0.02
Cd			*GSTT1* null	0.10 (0.01, 0.18)	2.55	0.01
Pb			*Ile/Ile*	–0.10 (–0.18, –0.003)	–2.04	0.04
GSTM1 and *GSTT1*						
Cd		Present	Present	–0.06 (–0.13, 0.001)	–1.95	0.05
		Null	Null	0.11 (–0.003, 0.23)	1.92	0.05
GSTT1 and *GSTP1*						
Pb		Null	*Ile/Ile*	–0.17 (–0.33, –0.01)	–2.15	0.03
		Null	*Ile/Val*	0.19 (0.07, 0.30)	3.19	<0.01
Cd		Present	*Ile/Val*	–0.10 (–0.17, –0.01)	–2.34	0.02
Zn		Present	*Val/Val*	–0.05 (–0.10, 0.003)	–1.86	0.06
GSTM1, *GSTT1*, and *GSTP1*						
Pb	Present	Null	*Ile/Ile*	–0.28 (–0.52, –0.05)	–2.43	0.01
	Present	Null	*Ile/Val*	0.16 (0.01, 0.30)	2.18	0.03
	Null	Present	*Ile/Ile*	–0.32 (–0.62, –0.02)	–2.11	0.03
	Null	Null	*Ile/Val*	0.25 (–0.02, 0.52)	1.83	0.04
Cd	Present	Present	*Ile/Val*	–0.09 (–0.19, 0.006)	–1.87	0.06
Zn	Null	Present	*Val/Val*	–0.11 (–0.22, –0.01)	–2.13	0.03
	Null	Null	*Val/Val*	0.15 (–0.02, 0.34)	1.74	0.08

Results showed beta coefficients for significant associations

β beta coefficient, *CI* confidence interval

*$p \leq 0.05$, significant association; $0.05 < p < 0.1$, marginal association

and *GSTM1* null/*GSTT1* null genotypes were not associated with Pb toxicity (p = 0.12, 0.56, and 0.23, respectively).

The *GSTP1* polymorphism deviated from HWE for the high-exposed group (χ^2 = 7.83; p = 0.005) (Table 5). The *Ile/Val* genotypes showed a higher prevalence of 62.3% in the high-exposed group compared with 46.2% in the low-exposed group. The *Ile* and *Val* allele percentages were 56% and 44% in the high-exposed group, while 67.7% and 32.3% in the low-exposed group. These allele frequency differences showed marginal differences (χ^2 = 3.18, p = 0.07) between the groups. This result implies that living in precarious conditions might affect the genetic variants. The genetic impact of *GSTP1* on susceptibility to Pb toxicity revealed a significant association of the *GSTP1 Ile/Val* genotype with the susceptibility to Pb toxicity. Individuals with this genotype were at a 2.54-fold higher risk of Pb toxicity (OR = 2.54; 95% CI: 1.02-6.32, p = 0.04) than individuals carrying the *Ile/Ile* genotype. As for the wild *Val/Val* genotype, the OR was greater than one (OR = 3.21) but not significant (p = 0.15). The combination of the heterozygous *Ile/Val* and mutant homozygous *Val/Val* genotypes showed a risk of susceptibility to Pb toxicity increased up to 2.63 (p = 0.02) times compared with the wild homozygous *Ile/Ile* genotype. The combined effect of all three putative genes showed associations on susceptibility to Pb toxicity. The combination of the *GSTP1 Ile/Val* with *GSTT1* null showed a risk factor of 11.7 (95% CI: 1.36-102.1, p = 0.02), while *GSTP1 Ile/Val* with *GSTM1* present and the combination of *GSTP1 Ile/Val*/*GSTM1* present/*GSTT1* null genotypes showed marginal associations with Pb susceptibility (OR = 2.62, 95% CI: 0.91-7.50, p = 0.07 and OR = 8.12, 95% CI: 0.89-73.8, p = 0.06, respectively) compared to their non-risk genotype counterparts (Table 5). In general, the high prevalence of the Ile/Val genotype might play the main role in Pb susceptibility.

Studies have reported an increased health risk with occupational or environmental Pb exposure among adults with GST polymorphisms. The *GSTM1* and *GSTT1* null genotypes with increased levels on oxidative stress biomarkers such as malondialdehyde and high-sensitivity C-reactive protein (Khansakorn et al. 2011; Sirivarasai et al. 2013), *GSTT1* present genotype with increased Pb-related hypertension (Lee et al. 2012), and *GSTP1* risk genotypes (*Ile/Val* and *Val/Val*) with the increasing effect of Pb on amyotrophic lateral sclerosis disease (Eum et al. 2015) were reported. In another study, a 15 μg g^{-1} tibia Pb concentration was associated with weak cognitive function (a decrement of Mini-Mental State Exam score by 0.24 point) on men with *GSTP1* risk genotype (Eum et al. 2013). In our study, the genetic variants on

Table 5 Association of *GSTM1*, *GSTT1*, and *GSTP1* genotype distributions in low and high blood lead level (BLL) children with the risk of susceptibility to lead toxicity

Gene	Polymorphism	High BLL[#] ($N = 114$)[$] N (%)	Low BLL[#] ($N = 26$) N (%)	χ^2, p	OR (95% CI), p
GSTM1	Present (+)	87 (76.3)	20 (76.9)	0.004	1
	Null (-)	27 (23.7)	6 (23.1)		1.03 (0.38–2.84)
GSTT1	Present (+)	70 (61.4)	21 (80.8)	3.49, *	1
	Null (-)	44 (35.6)	5 (19.2)		2.64 (0.92–7.51) *
GSTM1 and *GSTT1*	+/+	54 (47.4)	16 (61.5)		1
	+/-	33 (28.9)	4 (15.4)		2.44 (0.75–7.94)
	-/+	16 (14.0)	5 (19.2)		0.95 (0.30–2.99)
	-/-	11 (9.6)	1 (3.8)		3.26 (0.39–27.2)
GSTP1 Genotype	*Ile/Ile*	28 (24.6)	12 (46.2)	4.90, *	1
	Ile/Val	71 (62.3)	12 (46.2)		2.54 (1.02–6.32) **
	Val/Val	15 (13.1)	2 (7.6)		3.21 (0.63–16.3)
	Ile/Val and *Val/Val*	86 (75.4)	14 (53.8)		2.63 (1.09–6.35) **
Allele	*Ile*	127 (56)	36 (67.7)	3.18, *	1
	Val	101 (44)	16 (32.3)		1.78 (0.93–3.41) *
Combined genes	*Ile/Ile/GSTM1+*	21 (18.4)	9 (34.6)		1
	Ile/Val/GSTM1+	55 (48.2)	9 (34.6)		2.62 (0.91–7.50) *
	Ile/Ile/GSTT1+	19 (16.79	8 (30.8)		1
	Ile/Val/GSTT1-	28 (24.6)	1 (3.8)		11.7 (1.36–102.1) **
	Ile/Ile/GSTM1+/GSTT1+	17 (14.9)	6 (23.1)		1
	Ile/Val/GSTM1+/GSTT1-	23 (20.2)	1 (3.8)		8.12 (0.89–73.8) *

N number, % frequency, *OR* odds ratio, *CI* confidence interval

[#] High BLL, >10 μg dL^{-1} ; low BLL, ≤10 μg dL^{-1}

[$] Significant difference for *GSTP1* Hardy-Weinberg equilibrium test ($\chi^2 = 7.83$; $p = 0.005$)

**$p \leq 0.05$ (significant association); *$p < 0.1$ (marginal association)

susceptibility to Pb toxicity showed significant associations with *GSTT1* null and *GSTP1* risk genotypes (*Ile/Val* and *Val/Val* genotypes). The logistic regression analysis showed a risk of > 1 for *GSTT1* null, *GSTP1* risk genotypes. Moreover, the combined effect of *GSTP1 Ile/Val* and *GSTT1* null showed a more pronounced risk of 11.7 times compared with the non-risk genotypes. Overall, these results indicated that children with deletions of the *GSTT1* gene and *GSTP1 Ile/Val* and *Val/Val* genotypes are at higher risk of Pb susceptibility due to high blood Pb levels. Our findings stress continued prevention programs on lead exposure in younger populations as lead exposure at early ages has harmful impacts on cognitive functions and impairs development that can continue throughout the lifespan (Sanders et al. 2009).

We noticed that there are some limitations to this study: (i) the small number (26 out of 140) in the low-exposed group (< 10 μg dL^{-1}), (ii) heavy metal levels were measured at a single point blood sample at which the half-life of heavy metals in the blood is short (especially Pb) compared to bone, and (iii) no epidemiological or clinical data for the study subjects. All these factors might inevitably alter determining a true effect incidence and weakened the statistical power on the outcome result. This study, however, still contributes to the understanding of the GSTs' involvement in the development of childhood Pb toxicity in children. Second, in this study, we measured the levels of other heavy metals to highlight their burden on the children residing near the abandoned Pb mine site.

Conclusions

Our results stress the significance of genetic factors in determining individual differences in blood heavy metal concentrations. We found a direct association between *GSTT1* null genotype and blood Pb and Cd concentrations. Furthermore, *GSTT1* null genotype and *GSTP1* risk genotypes (*Ile/Val* and *Val/Val*) play more significant roles in modifying the blood Pb and Cd and, as a result, be risk factors associated with Pb susceptibility. Owing to

GST's potential role in detoxifying toxic metals, children with more copies of the *GSTP1 Val* allele and gene deletion of *GSTT1* are at higher risk of Pb toxicity. These results suggest that the exposure of heavy metals, especially Pb, may be influenced by genotypic variants of the GST genes. As a preliminary study, the results generated will be used as baseline data for future studies. However, replication of this finding using population-based research is warranted.

Acknowledgements We are very grateful to the children that participated in this study and the laboratory technicians and nurses at the five health centers in Kabwe. We are also grateful to the Kabwe District Health Office, Kabwe Municipal Council and the Ministry of Health, Zambia, for facilitating our work. Our appreciation is extended to Takahiro Ichise and Nagisa Hirano for their technical support.

Author contribution YBY: Responsible for conceptualization, data analysis, investigation, methodology, and writing both drafting the original paper and reviewing.

SMMN: Responsible for conceptualization, analysis, funding acquisition, investigation, and writing and corresponding author.

JY, HN, HT, AK and KM: Participate in sample collection, material preparation, and reviewing the manuscript.

YK: Funding acquisition and supervision.

KC: Supervision.

MI: Responsible for project administration, funding acquisition, supervision, and reviewing the manuscript and corresponding author.

Funding This work was supported by the Grants-in-Aid for Scientific Research from the Ministry of Education, Culture, Sports, Science and Technology of Japan awarded to M. Ishizuka (Nos. 16H0177906, 18K1984708, 18KK028708, 21H02351), Ikenaka (18H0413208), and S.M.M. Nakayama (Nos. 17KK0009 and 20K20633). This work was also supported by the foundation of JSPS Bilateral Open Partnership Joint Research Projects (JPJSBP120209902; SMMN). This work was also supported by JSPS CORE to CORE program (MI), The Japan Prize Foundation; Hokkaido University's SOUSEI Support Program for Young Researchers in FY2020 (SMMN); and Hokkaido University Specific Research Projects (MI). This research was also supported by JST/JICA, SATREPS (Science and Technology Research Partnership for Sustainable Development; No. JPMJSA1501) and aXis (Accelerating Social Implementation for SDGs Achievement; No. JPMJAS2001) funded by JST as well as Program for supporting introduction of the new sharing system (JPMXS0420100619).

Data availability Not applicable.

Declarations

Ethics approval Study protocol approval and permission to conduct the research were obtained from the University of Zambia Research Ethics Committee (UNZAREC; REF. No. 012-04-16) and the Ministry of Health Zambia, respectively. Material transfer agreement (MTA, Approval No. E00417) has been issued from the Ministry of Health, Zambia, for transporting frozen samples to Japan.

Consent to participate Participation in this study was voluntary, and participants enrolled after getting signed informed consent from the parents.

Consent for publication Children's parent signed informed consent before participation and be aware regarding publishing the data. All the coauthors have read the manuscript and agreed for publication.

Competing interests The authors declare no competing interests.

References

Amrhein V, Greenland S, McShane B (2019) Scientists rise up against statistical significance. Nature 567:305–307. https://doi.org/10.1038/d41586-019-00857-9

Centers for Disease Control and Prevention (CDC) (2012) Update on BLLs in children. Available online at http://www.cdc.gov/nceh/lead/ACCLPP/blood_lead_levels.htm. Accessed 1 June 2020

Eum KD, Wang FT, Schwartz J, Hersh CP, Kelsey K, Wright RO, Spiro A, Sparrow D, Hu H, Weisskopf MG (2013) Modifying roles of glutathione S-transferase polymorphisms on the association between cumulative lead exposure and cognitive function. Neurotoxicology 39:65–71. https://doi.org/10.1016/j.neuro.2013.08.002

Eum KD, Seal RM, Taylor KM, Grespin M, Umbach DM, Hu H, Sandler DP, Kamel F, Weisskopf MG (2015) Modification of the association between lead exposure and amyotrophic lateral sclerosis by iron and oxidative stress related gene polymorphisms. Amyotroph Lateral Scler Frontotemporal Degener 16(1-2):72–79. https://doi.org/10.3109/21678421.2014.964259

Godwill EA, Ferdinand PU, Nwalo FN, Unachukwu MN (2019) Mechanism and health effects of heavy metal toxicity in humans. In: Poisoning in the modern world - new tricks for an old dog? Intechopen. https://doi.org/10.5772/intechopen.82511

Hayes JD, Flanagan JU, Jowsey IR (2005) Glutathione transferases. Annu Rev Pharmacol Toxicol 45:51–88. https://doi.org/10.1146/annurev.pharmtox.45.120403.095857

Hays SM, Nordberg M, Yager JW, Aylward LL (2008) Biomonitoring equivalents (BE) dossier for cadmium (Cd) (CAS No. 7440-43-9). Regul Toxicol Pharmacol 51(3):S49–S56. https://doi.org/10.1016/j.yrtph.2008.05.008

Hollman AL, Tchounwou PB, Huang HC (2016) The association between gene-environment interactions and diseases involving the human GST superfamily with SNP variants. Int J Environ Res Public Health 13(4):379. https://doi.org/10.3390/ijerph13040379

Hunaiti AA, Soud M (2000) Effect of lead concentration on the level of glutathione, glutathione S-transferase, reductase and peroxidase in human blood. Sci Total Environ 248:45–50. https://doi.org/10.1016/s0048-9697(99)00548-3

International Agency for Research on Cancer (IARC) (2021) IARC monographs on the identification of carcinogenic hazards to humans. List of classifications. Agents classified by the IARC Monographs, 1–129. https://monographs.iarc.who.int/list-of-classifications. Accessed 20 March 2021

Jaishankar M, Tseten T, Anbalagan N, Mathew BB, Berregowda NK (2014) Toxicity, mechanism and health effects of some heavy metals. Interdiscip Toxicol 7(2):60–72. https://doi.org/10.2478/intox-2014-0009

Jan AT, Azam M, Siddiqui K, Ali A, Choi I, Rizwanul Haq QM (2015) Heavy metals and human health: mechanistic insight into toxicity and counter defense system of antioxidants. Int J Mol Sci 16(12):29592–29630. https://doi.org/10.3390/ijms161226183

Jozefczak M, Remans T, Vangronsveld J, Cuypers A (2012) Glutathione is a key player in metal-induced oxidative stress defenses. Int J Mol Sci 13(3):3145–3175. https://doi.org/10.3390/ijms13033145

Kasperczyk S, Kasperczyk A, Ostalowska A, Dziwisz M, Birkner E (2004) Activity of glutathione peroxidase, glutathione reductase,

and lipid peroxidation in erythrocytes in workers exposed to lead. Biol Trace Elem Res 102:61–72. https://doi.org/10.1385/bter:102:1-3:061

Khansakorn N, Wongwit W, Tharnpoophasiam P, Hengprasith B, Suwannathon L, Pethchpoung K, Yoovathaworn K, Chanprasertyothin S, Sura T, Kaojarern S, Sritara P, Sirivarasai J (2011) Impact of *GSTM1*, *GSTT1*, *GSTP1* polymorphism and environmental lead exposure on oxidative stress biomarkers. Sci Res Essays 6(31):6540–6547. https://doi.org/10.5897/SRE11.1519

Khansakorn N, Wongwit W, Tharnpoophasiam P, Hengprasith B, Suwannathon L, Chanprasertyothin S, Sura T, Kaojarern S, Sritara P, Sirivarasai J (2012) Genetic variations of glutathione S-transferase influence on blood cadmium concentration. J Toxicol 2012:356126–356126. https://doi.org/10.1155/2012/356126

Lamichhane DK, Leem JH, Park CS, Ha M, Ha EH, Kim HC, Lee JY, Ko JK, Kim Y, Hong YC (2018) Associations between prenatal lead exposure and birth outcomes: modification by sex and *GSTM1*/*GSTT1* polymorphism. Sci Total Environ 619–620:176–184. https://doi.org/10.1016/j.scitotenv.2017.09.159

Lee BK, Lee SJ, Joo JS, Cho KS, Kim NS, Kim HJ (2012) Association of glutathione S-transferase genes (*GSTM1* and *GSTT1*) polymorphisms with hypertension in lead-exposed workers. Mol Cell Toxicol 8:203–208. https://doi.org/10.1007/s13273-012-0025-5

Palma-Cano LE, Córdova EJ, Orozco L, Martinez-Hernandez A, Cid M, Leal-Berumen I, Licón-Trillo A, Lechuga-Valles R, González-Ponce M, González-Rodríguez E, Moreno-Brito V (2017) *GSTT1* and GSTM1 null variants in Mestizo and Amerindian populations from northwestern Mexico and a literature review. Genet Mol Biol 40(4):727–735. https://doi.org/10.1590/1678-4685-GMB-2016-0142

Poddalgoda D, Macey K, Hancock S (2019) Derivation of biomonitoring equivalents (BE values) for zinc. Regul Toxicol Pharmacol 106:178–176. https://doi.org/10.1016/j.yrtph.2019.04.018

Saitou M, Ishida T (2015) Distributions of the *GSTM1* and *GSTT1* null genotypes worldwide are characterized by latitudinal clines. Asian Pac J Cancer Prev 16:355–361. https://doi.org/10.7314/apjcp.2015.16.1.355

Sanders T, Liu Y, Buchner V, Tchounwou PB (2009) Neurotoxic effects and biomarkers of lead exposure-Review. Rev Environ Health 24(1):15–45. https://doi.org/10.1515/reveh.2009.24.1.15

Sharma A, Pandey A, Sharma S, Chatterjee I, Mehrotra R, Sehgal A, Sharma JK (2014) Genetic polymorphism of glutathione S-transferase P1 (*GSTP1*) in Delhi population and comparison with other global populations. Meta Gene 2:134–142. https://doi.org/10.1016/j.mgene.2013.12.003

Sirivarasai J, Wananukul W, Kaojarern S, Chanprasertyothin S, Thongmung N, Ratanachaiwong W, Sura T, Sritara P (2013) Association between inflammatory marker, environmental lead exposure, and glutathione S-transferase gene. Biomed Res Int 2013:474963–474966. https://doi.org/10.1155/2013/474963

Tchounwou PB, Yedjou CG, Patlolla AK, Sutton DJ (2012) Heavy metals toxicity and the environment. EXS 101:133–164. https://doi.org/10.1007/978-3-7643-8340-4_6

Yabe J, Nakayama SMM, Nakata H, Toyomaki H, Yohannes YB, Muzandu M, Kataba A, Zyambo G, Hiwatari M, Narita D, Yamada D, Hangoma P, Munyinda NS, Mufune T, Ikenaka Y, Choongo K, Ishizuka M (2020) Current trends of blood lead levels, distribution patterns and exposure variations among household members in Kabwe, Zambia. Chemosphere 243:125412. https://doi.org/10.1016/j.chemosphere.2019.125412

Yamada D, Hiwatari M, Hangoma P, Narita D, Mphuka C, Chitah B, Yabe J, Nakayama SMM, Nakata H, Choongo K, Ishizuka M (2020) Assessing the population-wide exposure to lead pollution in Kabwe, Zambia: an econometric estimation based on survey data. Sci Rep 10:15092. https://doi.org/10.1038/s41598-020-71998-5

Yohannes YB, Yoshinori Y, Nakayama SMM, Mizukawa H, Ishizuka M (2017) Trace element contamination in tissues of four bird species from the Rift Valley Region, Ethiopia. Bull Environ Contam Toxicol 98:172–177. https://doi.org/10.1007/s00128-016-2011-4

Yohannes YB, Nakayama SMM, Yabe J, Nakata H, Toyomaki H, Kataba A, Muzandu K, Ikenaka Y, Choongo K, Ishizuka M (2020) Blead lead levels and aberrant DNA methylation of the ALAD and p16 gene promoters in children exposed to environmental-lead. Environ Res 188:109759. https://doi.org/10.1016/j.envres.2020.109759

Yohannes YB, Nakayama SMM, Yabe J, Toyomaki H, Kataba A, Nakata H, Muzandu K, Ikenaka Y, Choongo K, Ishizuka M (2021) Delta-aminolevulinic acid dehydratase (ALAD) and vitamin D receptor (VDR) genes polymorphisms in children residing in an abandoned lead-zinc mine area in Kabwe, Zambia. Meta Gene 27:100838. https://doi.org/10.1016/j.mgene.2020.100838

toxics

MDPI

Article

Solid-Phase Partitioning and Leaching Behavior of Pb and Zn from Playground Soils in Kabwe, Zambia

Walubita Mufalo [1,*], Pawit Tangviroon [2], Toshifumi Igarashi [2], Mayumi Ito [2], Tsutomu Sato [2], Meki Chirwa [3], Imasiku Nyambe [3], Hokuto Nakata [4], Shouta Nakayama [4] and Mayumi Ishizuka [4]

1 Division of Sustainable Resources Engineering, Graduate School of Engineering, Hokkaido University, Sapporo 060-8628, Japan
2 Division of Sustainable Resources Engineering, Faculty of Engineering, Hokkaido University, Sapporo 060-8628, Japan; tangviroon.p@gmail.com (P.T.); tosifumi@eng.hokudai.ac.jp (T.I.); itomayu@eng.hokudai.ac.jp (M.I.); tomsato@eng.hokudai.ac.jp (T.S.)
3 IWRM Centre/Geology Department, School of Mines, The University of Zambia, Lusaka 32379, Zambia; meki.chirwa@gmail.com (M.C.); inyambe@gmail.com (I.N.)
4 Faculty of Veterinary Medicine, Hokkaido University, Kita 18, Nishi 9, Kita-Ku, Sapporo 060-0818, Japan; hokuto.nakata@vetmed.hokudai.ac.jp (H.N.); shouta-nakayama@vetmed.hokudai.ac.jp (S.N.); ishizum@vetmed.hokudai.ac.jp (M.I.)
* Correspondence: walubita.mufalo.u6@elms.hokudai.ac.jp; Tel.: +81-080-8851-6452

Abstract: Zambia's Kabwe mine wastes (KMWs) are responsible for contaminating the surrounding soil and dust in the Kabwe district. Unfortunately, these wastes arise from the historical mining activities of lead (Pb) and Zinc (Zn), which lacked adequate waste management strategies. As a result, potentially toxic elements (PTEs) (Pb and Zn) spread across the Kabwe district. To assess the soil pollution derived from previous mining activities, we studied topsoil samples (n = 8) from the school playground soils (SPs). In this study, the degree of contamination, geochemical partitioning, and leachability, coupled with the release and retention of Pb and Zn, were studied. The SPs were classified as extremely enriched (EF > 40) and contaminated with Pb (I_{geo} > 5). On average, Pb (up to 89%) and Zn (up to 69%) were bound with exchangeable, weak acid-soluble, reducible and oxidizable phases, which are considered as 'geochemically mobile' phases in the environment. The leachates from the soils (n = 5) exceeded the Zambian standard (ZS: 190:2010) for Pb in potable drinking water (Pb < 0.01 mg/L). Furthermore, the spatial distribution of Pb and Zn showed a significant reduction in contents of Pb and Zn with the distance from the mine area.

Keywords: contamination; lead; zinc; bio-accessibility; leaching; Kabwe; Zambia

Citation: Mufalo, W.; Tangviroon, P.; Igarashi, T.; Ito, M.; Sato, T.; Chirwa, M.; Nyambe, I.; Nakata, H.; Nakayama, S.; Ishizuka, M. Solid-Phase Partitioning and Leaching Behavior of Pb and Zn from Playground Soils in Kabwe, Zambia. *Toxics* **2021**, *9*, 248. https://doi.org/10.3390/toxics9100248

Academic Editor: Manfred Sager

Received: 30 August 2021
Accepted: 30 September 2021
Published: 4 October 2021

1. Introduction

Kabwe is a district in the central province of Zambia, which has geology dominated by carbonate-hosted Pb-Zn deposits [1]. Kabwe town is considered one of the most polluted cities globally due to the historical mining of lead (Pb) and Zinc (Zn) [2]. Mining activities between 1902 and 1994 produced approximately 0.8 Mt and 1.8 Mt of Pb and Zn, respectively [3]. The deposits are composed of massive sulfides ore bodies surrounded by secondary mineralization oxide zones of silicate ore (willemite; Zn_2SiO_4), cerussite ($PbCO_3$), quartz (SiO_2), smithsonite ($ZnCO_3$), goethite (FeOOH), hematite (Fe_2O_3), and metal-bearing; vanadates, phosphates, carbonates of Zn, Pb, and V [1,3]. After nearly 90 years of mining without any environmental regulations, mining activities ceased in 1994 due to the depletion of the mineral resources. As a result, huge stockpiles of Kabwe Mine Wastes (KMWs) were disposed of and left unattended after decommissioning the mines in 1994. The profound KMWs consist of Zinc leach plant residues (ZLPRs) [4] and slag heaps [5].

Kabwe town has a semi-arid/barren topography. Thus, dust generation and transportation of potentially toxic elements (PTEs) from KMWs to the surrounding environment

is high. Although many researchers have proposed immobilization techniques to reduce contamination in the town [6–8], pollution of the surrounding soils with PTEs is inevitable because of the dust dispersion from KMWs [9]. Generally, PTEs are bioaccessible through inhalation, intentional/accidental ingestion of contaminated soil, or dust [10,11]. Depending on age groups, pica behavior is higher in children than adults because of their hand-to-mouth etiquette [11,12]. The U.S Environmental Protection Agency (EPA) estimates that a typical child up to 84 months can swallow 100 mg of contaminated soil/day [13]. Moreover, a recent study in Kabwe revealed high Pb contents in the infant's feces with an overall average value of 39.2 mg/kg, ranging from 0 to 256.7 mg/kg (dry weight) [14]. In addition, the children within the vicinity of the mine area of Kabwe have constantly recorded high blood lead levels (BLL) (BLL > 5 μg/dL) [15,16].

Since children are the most affected, one potential exposure source of Pb intoxication are school playgrounds soils (SPs). Most of the playfields for the children in Zambia are characterized by bare land and insufficient lawn maintenance. Thus, play activities are depicted by the substantial generation of dust from the soil. Since children are typically fond of playing in the SPs, there are several exposure pathways in which the PTEs can enter the body, i.e., ingestion or inhalation of soil settled on play equipment or dust adhered to hands, fingers, or clothes [17,18]. Prolonged exposure to this environment may lead to the uptake of PTEs into the respiratory and digestive systems. Consequently, elevated blood Pb is detrimental to human health and may cause severe nervous system problems, retardation, behavioral disorders [11], and formation of porous bones due to substitutions (Pb apatite's) inside the bones.

Previous research works on Kabwe have reported high contents of Pb (>20,000 mg/kg) in the topsoils of the former smelter and processing plant for Pb and Zn [6]. However, detecting high contents of PTEs in the soil, in particular, Pb and Zn, does not necessarily mean the high risk of contaminants in the environment or bioavailability into the body. Instead, this depends on the leachability of the heavy metals under various environmental conditions [19]. Furthermore, the bioaccessible and bioavailable Pb and Zn in the soil depends on the binding and mineralogical forms in which they exist in [20,21]. Thus, understanding their specific characteristics in the binding states leads to their bio-accessibility in the soil because the release and retention mechanisms of heavy metals in the soils are influenced by the solubility-controlling mineral phases [22].

Therefore, the purpose of this study was to determine the extent of pollution, leachability, and the solid-phase partitioning of Pb and Zn in the SPs, because the playgrounds may be potential sources of PTEs for the children in Kabwe.

2. Materials and Methods

2.1. Site Description and Ssampling Location

Figure 1 shows the location of Kabwe and the sampling points of the SPs. The soil samples were collected in the dry season from the west and northwest of the KMWs. The prevailing winds are usually downwind of the KMWs, to the west-northwest direction [6]. A total of 8 soil samples were collected from a community ground in Kasanda area (S1), Makululu primary school (S2), Malumbo community ground (S3), Makululu day secondary (S4), Makululu day secondary garden (S5), David Ramushu secondary school (S6), David Ramushu secondary school garden (S7), and Kebar Christian academy (S8). All the sampling points were approximately within a radius of 10 km from the mine area. Using a stainless-steel hand shovel, soil samples were collected from topsoil (about 5 cm depths) with 3 to 4 mixing points for each sample. These samples were stored in airtight vacuum bags and then shipped to Hokkaido University, Japan. The soil samples were then dried at room temperature before characterization, sequential extraction, and leaching experiments.

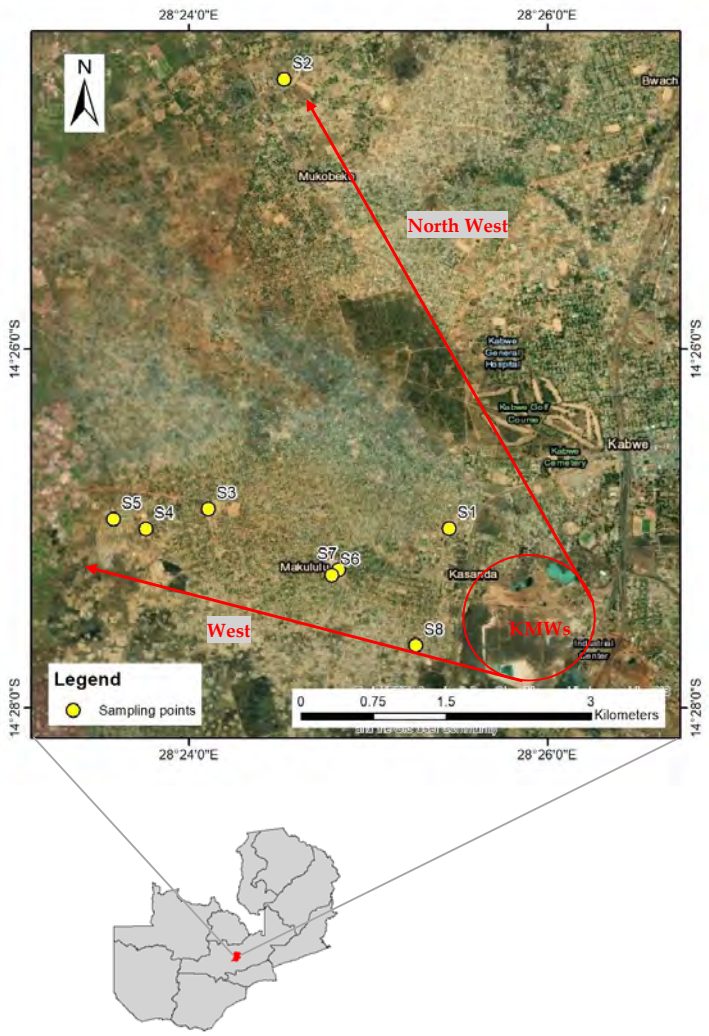

Figure 1. A map of Zambia with the sampling locations of Kabwe school playground soils (SPs): northwest direction (S1 and S2) and the west direction (S3, S4, S5, S6, S7, and S8) of Kabwe Mine Wastes (KMWs).

2.2. Soil Characterization

Mineralogical and chemical properties of the soils were conducted using pressed powders of the SPs (<50 µm) and analysed using X-ray diffractometer (XRD) (MultiFlex, Rigaku Corporation, Tokyo, Japan) and X-ray fluorescence spectrometer (XRF) (Spectro Xepos, Rigaku Corporation, Tokyo, Japan) respectively. The SPs' particle size distribution was analyzed using the laser diffraction (Microtrac® MT3300SX, Nikkiso Co. Ltd., Osaka, Japan). The total organic carbon content was calculated by the difference between total carbon content and inorganic carbon content measured by a total carbon analyzer with a solid sample combustion unit (TOC-VCSH-SSM-5000A, Shimadzu Corporation, Kyoto, Japan).

2.3. Determination of Pollution Indices

Two pollution indices were employed to calculate the extent of contamination in the SPs, i.e., geo-accumulation index (I_{geo}) and enrichment factor (EF). The I_{geo} quantifies the degree of anthropogenic contamination. The index was introduced by Muller [23], given by the following equation.

$$I_{geo} = \log_2(C_n/1.5B_n) \quad (1)$$

where, C_n is the content of an examined element in the SPs and B_n is the background value of the element in the studied area. This study selected the median soil background values

in Sub-Sahara Africa [24] because it gives a more representative extent of pollution. The value of 1.5 is a constant introduced to normalize the variances in background levels. Seven categories based on the level of contamination are classified as: class 0,uncontaminated ($I_{geo} < 0$); Class 1, uncontaminated to moderately contaminated ($0 < I_{geo} < 1$); Class 2, moderately contaminated ($1 < I_{geo} < 2$); Class 3, moderately to heavily contaminated ($2 < I_{geo} < 3$); Class 4, heavily contaminated ($3 < I_{geo} < 4$); Class 5, heavily to extremely contaminated ($4 < I_{geo} < 5$); and Class 6, extremely contaminated ($I_{geo} > 5$).

The EF differentiates between metals originating from human activities and natural processes. The EF was calculated as the ratio of the content of the metal in the sample to the content of the same metal in the earth crust using the modified formula from Buat-Menard and Chesselet [25], as shown below:

$$EF = (M_x * Ti_b)/(M_b * Ti_x) \quad (2)$$

where, M_x is the content of the measured sample, Ti_b is the background content of titanium (Ti) in the earth crust, here we chose Ti as a reference element for normalization because it is conservative; historic mining activities may not influence Ti in the SPs compared to Al or Fe. Meanwhile, M_b is the background content of the targeted element in the earth crust, while T_x is the measured content of the reference value in the sample. The earth crust content values were taken from Turekian and Wedepohl [26]. The calculated values were based on the classification of enrichment as: deficiency to minimal enrichment ($EF < 2$); moderate enrichment ($2 < EF < 5$); significant enrichment ($5 < EF < 20$); very high enrichment ($20 < EF < 40$); and extremely high enrichment ($EF > 40$) [27].

2.4. Geochemical Modeling and Multivariant Statistical Analysis

PHREEQC; Version 3, United states, Geological Survey, Sunrise Valley Drive Reston, USA, was used to calculate the saturation indices (*SIs*) for the possible mineral phases controlling the release and retention of Pb and Zn in the SPs [28]. The thermodynamic properties were taken from the MINTEQ.V4.DAT database. Principal component analysis (PCA) was used for finding the correlations between the metal content or metal ion concentration and several environmental leaching conditions.

2.5. Batch Leaching Experiments

The batch leaching experiments were conducted by mixing 15 g of soil sample and 150 mL of deionized (DI) water in a 300-mL Erlenmeyer flask followed by lateral reciprocating shaking speed of 200 rpm for 6 h. After the predetermined shaking time, the pH, oxidation-reduction potential (ORP) and electrical conductivity (EC) were measured followed by centrifugation of the suspension using a centrifuge (Sigma 3K30 laboratory centrifuge, Osterode, Germany) for 30 min at a speed of 3500 rpm. The leachates from the experiments were collected by filtration through 0.45 Millex® filters (Merck Millipore, Burlington, MA, USA). The leachates were preserved by 1% nitric acid (HNO_3) before chemical analysis to maintain the target elements in dissolved forms. For accuracy and precision, all batches were performed in triplicates. The concentrations of major ions were then analyzed by inductively coupled plasma atomic emission spectroscopy (ICP-AES) (ICPE-9000, Shimadzu Corporation, Kyoto, Japan) (margin of error = ± 2~3%, determination limit 0.01–0.001 mg/L). All the chemicals used for conducting the experiments were reagent grade (Wako Pure Chemical Industries Ltd, Osaka, Japan).

2.6. Sequential Extraction

The sequential extraction experiment was based on the earlier works of Tessier et al. [29] and modifications of the procedure by Marumo et al. [30]. The procedure partitions Pb and Zn into five phases: (1) exchangeable, (2) carbonates, (3) iron and manganese oxides, (4) organic matter and sulfide minerals, and (5) residual. The extraction procedure is summarized in Table 1.

Table 1. Procedure for the Determination of the Solid-Phase Partitioning of Pb and Zn.

Phase	Extractant	L/S Ratio (mL/g)	Temperature (°C)	Duration (h)	Speed (rpm)	Extracted Phase
1	1 M $MgCl_2$ at pH 7	20/1	25	1	200	Exchangeable
2	1 M CH_3COONa at pH 5	20/1	25	5	200	Carbonates
3	0.04 M $NH_2OH{\cdot}HCl$ in 25% acetic acid	20/1	80	5	120	Reducible
4	0.04 M $NH_2OH{\cdot}HCl$ in 25% acetic acid; 30% H_2O_2; 0.02 M HNO_3	36/1	80	5	120	Oxidizable
5	60% HNO_3	20/1	120	1		Residue

The extraction was performed on 1g of the SPs sample (<2mm) mixed with a predetermined volume of the extractant for each step. The leachate was separated from the residue by centrifugation of the suspension at 3000 rpm for 30 min. Between each step, the residue was washed with 20 mL of DI water, which was combined with the leachate of the extraction step and diluted to 50 mL. The diluted solution was filtrated through 0.45 Millex® filters, and kept in polypropylene bottles before chemical analysis. The samples were analyzed using inductively coupled plasma atomic emission mass spectrometry (ICP-MS) (ICAP Qc, Thermo Fisher Scientific, Waltham, MA, USA).

3. Results

3.1. Chemical Composition and Mineralogy of SPs

Table 2 illustrates the major chemical composition, total organic carbon (TOC) and trace elements (Pb and Zn) of the SPs. The samples were mainly dominated with SiO_2 (56.1–83.7 wt%), Al_2O_3 (6.4–29.7 wt%), and Fe_2O_3 (2.2–7.6 wt%). The TOC for the samples ranged from 0.3 to 5 wt%. The SPs were classified according to the United States Department of Agriculture (USDA) soil classification, as either sandy loam (S1, S5, S6, and S7), silt loam (S3, S4, and S8), or loam (S2) (Table S1). High contents of trace elements of Pb (265–3320 mg/kg) and Zn (359–2600 mg/kg) were recorded. Although XRD did not detect Pb-and Zn-bearing minerals, the possible mineral phases might be attributed to anglesite ($PbSO_4$), and zinkosite ($ZnSO_4$) [7]. The contents of Pb and Zn are much higher than the average background contents in Sub-Sahara Africa; Pb (37 mg/kg) and Zn (29 mg/kg) [24].

Figure S1 shows XRD patterns of the SPs. Quartz (SiO_2) is the primary mineral in all the SPs. Noticeable kaolinite peaks ($Al_2SiO_5(OH)$) were detected in samples S1, S2, S3, S4, and S5. This is consistent with the high content of Al_2O_3 (Table 1) and the clay fractions in the samples (S1, S2, S3, S4, and S5) (Table S1).

Table 3 shows PCA multivariant correlations in the SPs using variables in Table 1. PCA 1, PCA 2, and PCA 3 accounted for 82% of the total chemical composition of the SPs. PCA 1 showed that the Pb and Zn were associated with TOC and S with a 42% variance. This means that Pb and Zn had a close relationship with these chemical components in the SPs. PCA 2 and PCA 3 accounted for 21 and 19%, respectively. The high loadings of Zn and Al_2O_3 from PCA 2 indicate Zn's associations with the phyllosilicate minerals present in deposited material from old smelting activities and dust dispersion from KMWs. PCA 3 is mainly attributed to the geogenic chemical components (CaO, Fe_2O_3, and MnO) controlling the characteristics of the SPs such as pH, and release, and retention of Pb and Zn.

Table 2. Chemical Composition of the Major Components and the Trace Elements in the School Playground Soils (SPs).

	SPs							
	S1	**S2**	**S3**	**S4**	**S5**	**S6**	**S7**	**S8**
SiO_2 (wt%)	56.4	56.1	72.2	67.7	60.7	69.9	75.4	83.7
TiO_2 (wt%)	0.9	1.6	0.8	1.4	1.0	1.0	1.3	1.0
Al_2O_3 (wt%)	22.8	29.7	16.6	23.9	15.9	8.5	15.2	6.4
Fe_2O_3 (wt%)	7.2	4	7.6	6.2	6.9	6.2	4	2.2
MnO (wt%)	0.54	0.10	0.10	0.06	0.24	0.17	0.11	0.09
MgO (wt%)	0.8	1.9	1.2	2.8	2.3	0.9	1	0.6
CaO (wt%)	0.3	0.6	1.2	0.1	2.2	2	0.7	0.8
Na_2O (wt%)	<0.1	<0.1	<0.1	<0.1	<0.1	<0.1	<0.1	<0.1
K_2O (wt%)	0.9	0.8	1.1	1.1	0.7	0.7	1.5	0.7
P_2O_5 (wt%)	0.26	0.14	0.17	0.08	0.06	0.12	0.26	0.24
S (wt%)	0.2	0.07	0.07	0.05	0.06	0.2	0.15	0.93
TOC (wt%)	2.46	1.86	2.79	0.52	0.33	0.77	1.55	5.02
Pb (mg/kg)	3320	1080	1070	265	633	863	1770	3170
Zn (mg/kg)	2600	1990	750	359	399	1370	1840	090

Table 3. Principal Component Analysis (PCA) for the Chemical Composition of the SPs, Including Total Variance, Eigenvalue, and Cumulative Frequency.

	PCA1	**PCA2**	**PCA3**
SiO_2 (wt%)	0.24	−0.35	−0.31
Al_2O_3 (wt%)	−0.22	**0.49**	−0.04
Fe_2O_3 (wt%)	−0.24	−0.01	**0.44**
MnO (wt%)	0.07	0.25	**0.55**
MgO (wt%)	−0.37	0.04	−0.17
CaO (wt%)	−0.09	−0.47	0.25
K_2O (wt%)	−0.02	0.21	−0.25
P_2O_5 (wt%)	0.37	0.23	0.02
S (wt%)	**0.36**	−0.18	−0.12
TOC (wt%)	**0.37**	−0.01	−0.07
Pb (mg/kg)	**0.39**	0.19	0.16
Zn (mg/kg)	**0.32**	**0.33**	0.08
Eigenvalue	5.47	2.68	2.45
Variance (%)	42.0	20.6	18.8
Cumulative	42.0	62.6	81.5

Bold values indicate high loading of the chemical components.

Table S2 shows the Pearson correlation matrix for the chemical composition of the SPs. The results indicated a significant correlation between TOC and S ($r = 0.8$, $p < 0.05$). Pb showed high correlations with TOC ($r = 0.8$, $p < 0.05$) and S ($r = 0.7$, $p < 0.05$). On the other hand, Zn showed lower correlation with TOC ($r = 0.6$, $p > 0.05$) and S ($r = 0.4$, $p < 0.05$). This maybe because zinc sulfide (ZnS) oxidizes faster on air than galena (PbS); a problem known from the sediments of the Wadden sea in Germany.

3.2. The Extent of Pollution and Particle Size Distribution of the SPs

Table S3 summarizes I_{geo} and EF. The SPs from S1, S3, S7 and S8 showed 'extremely high enrichment' of Pb (EF > 40). Meanwhile, S2, S5 and S6 had 'very high enrichment' of Pb (20 < EF < 40). The SPs (S4) had the lowest enrichment of Pb (5 < EF < 20, indicating a significant enrichment). However, only (S1) showed 'very high enrichment' for Zn (20 < EF < 40), while S2, S3, S6 and S7 indicated 'significant enrichment' of Zn (5 < EF < 20). The order of enrichment followed S1 > S8 > S3 > S7 > S6 > S2 > S5 > S4 for Pb and S1 > S8 > S7 > S6 > S2 > S3 > S5 > S4 for Zn.

The I_{geo} for SPs indicated that S1, S2, S3, S6, S7, and S8 were 'extremely contaminated' with Pb ($I_{geo} > 5$). The S4 and S5 were (heavily:$3 < I_{geo} < 4$) and (heavily to extremely: $4 < I_{geo} < 5$) contaminated with Pb respectively. Meanwhile, S1, S2, S6, S7 and S8 were 'extremely contaminated' with Zn. The order of contamination followed S1, S8 > S7 > S3, S2 > S6 > S5 > S4 for Pb and S1 > S8, S2 > S7 > S6 > S3 > S5 > S4 for Zn. The pollution indices shows that the SPs were highly enriched and contaminated with PTEs.

Figure 2 shows the particle size distribution of the SPs and predominate KMWs, i.e., ZLPRs. The residues had fine particles (<6 µm is a 10% effective diameter (D_{10})). Kabwe is characterized by bare land and a windy, dry season [6]. Therefore, particles (<20 µm) are likely to become aerosol from the KMWs; consequently, finer particles are transported further [31]. Moreover, S2, the furthest site from the KMWs had 'very high enrichment' of Pb. The simulation results at S2 by Nakamura et al. [9] suggest that prevailing winds in the northwest, north-northwest, and north direction from the KMWs might have influenced the deposition of smaller particles to the area.

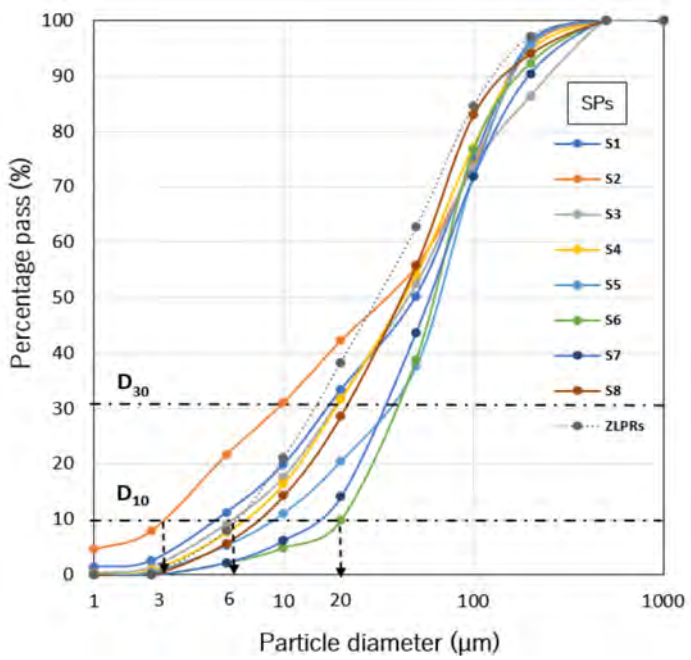

Figure 2. Particle size distribution of SPs and the zinc leach plant residues (ZLPRs) with their 10% and 30% diameters D_{10} and D_{30}.

3.3. Leaching Characteristics of SPs

Figure 3 shows the leachate characteristics of the SPs based on the standard leaching tests. The leachates were compared with the Zambia Bureau of standards for drinking water quality (ZS.190.2010). The quality prescribes requirements for drinking water suitable for human consumption. The SPs from S4, S5, and S6 had no leachable Pb, while S1, S2, S3, S7, and S8 had leaching concentrations of Pb above the permissible limit for drinking water in Zambia (Pb < 0.01 mg/L) (Figure 3a). Meanwhile, Zn was within the tolerable limit for all the SPs (Zn < 3 mg/L). The pH of all the SPs ranged from slightly acidic to alkaline conditions (pH 6.2–8.2). The pH values of the leachates from S1, S4, S5, and S6 exceeded the Zambian drinking water standard (pH 6.5–8.0), while those from S2, S3, S7, and S8 were within the permissible limits (Figure 3b).

Table 4 shows the results from PCA analysis using the leachate concentration. PCA 1 and PCA 2 accounted for 79% of the total variance, with high loadings of Al, Si, Fe, Pb, SO_4^{2-}, pH, EC, Eh, Mg and Zn. The PCA loadings of alkalinity, positive pH, and Ca in PCA 3 (17% variance) indicates the chemical components controlling the buffering effects of the SPs. This is consistent with geogenic CaO in PCA 3 from the chemical composition

of the SPs. The high loadings of SO_4^{2-}, Mg, EC, and Eh in PCA 2 accounted for 27% of the co-existing ions controlling the EC of the leachate in SPs.

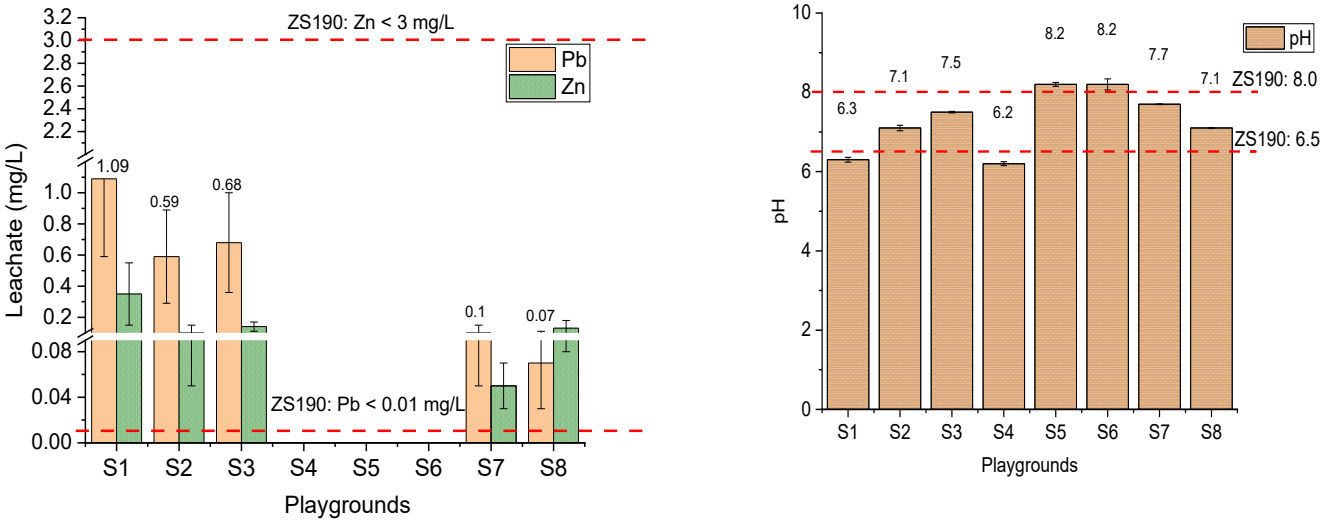

(**a**) (**b**)

Figure 3. Leachate characteristics for the SPs: (**a**) water-soluble Pb and Zn (**b**) pH. The dotted line represents permissible limits for drinking water standards in Zambia (ZS190.2010).

Table 4. Principal Component Analysis (PCA) for Water-Soluble Pb and Zn, including Total Variance, Eigenvalue, and Cumulative Frequency.

	PCA 1	PCA 2	PCA 3
pH	−0.24	**−0.31**	**0.38**
Eh (mV)	0.2	**0.42**	−0.29
EC (mS/cm)	−0.27	**0.36**	0.24
alkalinity	−0.24	−0.29	**0.38**
Ca (mg/L)	−0.34	0.12	**0.32**
Si (mg/L)	0.36	−0.02	0.29
Fe (mg/L)	**0.34**	−0.03	**0.32**
Al (mg/L)	**0.35**	−0.04	**0.31**
SO_4^{2-} (mg/L)	−0.2	**0.46**	0.16
Pb (mg/L)	**0.36**	0.09	0.25
Zn (mg/L)	**0.28**	0.29	0.25
Mg (mg/L)	−0.19	**0.44**	0.19
Eigenvalue	6.19	3.26	2.01
Variance (%)	52	27	17
Cumulative	52	79	96

Bold values indicate high loading of the chemical components.

3.4. Partitioning of Pb and Zn in the SPs

The sequential extraction patterns of Pb and Zn are shown in Figure 4. The solid-phase partitioning of Pb in the SPs ranged from 0.3 to 21% for the exchangeable fraction, weak acid soluble (17 to 42%), reducible (20 to 43%), oxidizable (16 to 33%), and residue (4 to 20%) (Figure 4a). Meanwhile for Zn, exchangeable (0.4 to 23%), weak acid soluble (13 to 33%), reducible (13 to 45%), oxidizable (9 to 23%) and residue (10 to 51%) (Figure 4b).The Pb in the SPs was mainly bound with carbonates, reducible and oxidizable phases while Zn showed strong association with reducible and residue fractions.

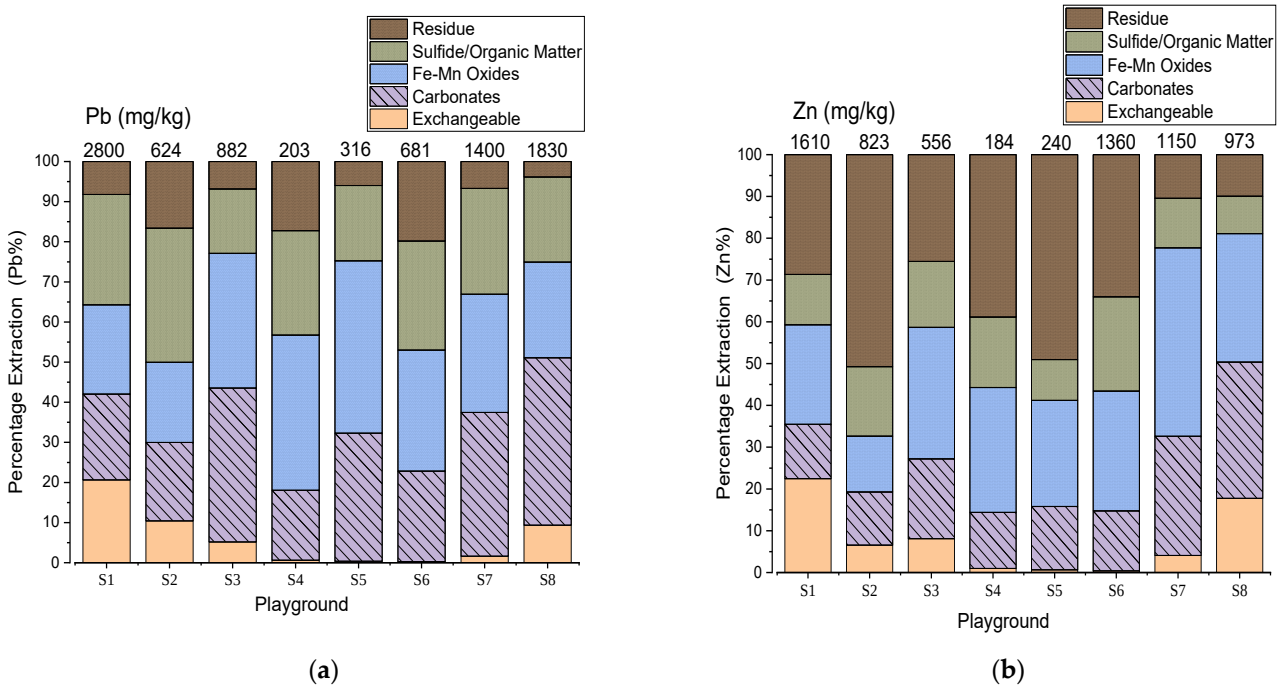

(**a**) (**b**)

Figure 4. Solid-phase partitioning of Pb (**a**) and Zn (**b**) in SPs. The values on top of each sample represent the total content (mg/kg) from the extraction of the five phases. The phases are expressed in percentage of the total content.

The SPs of S4, S5, and S6 with the undetected water-soluble Pb corresponded to the exchangeable phase; 0.6% (S4), 0.4% (S5) and 0.3% (S6) (Table S4). On the other hand, Zn was mainly in the reducible phase of 30% (S4), 25% (S5), and 29% (S6), and the residue phase of 39% (S4), 49% (S5), and 34% (S6) (Table S5). The highest partitioning for Pb in the SPs (S4, S5, and S6) was with the Fe and Mn oxides.

Table S6 shows the labile phases (Phase 1; exchangeable + Phase 2; carbonates + Phase 3; Fe/Mn oxides) for Pb and Zn. The labile phases for Pb added up to 50 to 77%. Those for Zn added up to 33 to 81%. The results indicate that the mobile fractions were notably high for all the SPs.

Figures S2 and S3 illustrate the leachable water-soluble (Pb and Zn) relationship with the exchangeable, labile phases and the total content. The water-soluble Pb showed a strong correlation with exchangeable phase (r = 0.8), labile phase (r = 0.6), and a lower correlation with the total content (r = 0.5). Meanwhile, the correlation for the water-soluble Zn showed (r = 0.9) with the exchangeable phase, (r = 0.5) with the labile phase and (r = 0.6) with the total content. The correlations certainly indicate the close relationship between the water-soluble Pb and Zn with the exchangeable phase.

3.5. The Distance of SPs from the KMWs

Figure 5 shows the trend for the total content, exchangeable phase, and the water-soluble Pb and Zn for each SPs site with the distance from the KMWs. The S1 and S8 are the nearest sites to the KMWs. Consequently, they had the highest contents of Pb and Zn, with S1 having 3320 mg/kg for Pb and 2600 mg/kg for Zn, while S8 records 3170 mg/kg for Pb and 2090 mg/kg for Zn (Figure 5a). The trend was similar to water-soluble and exchangeable phases (Figure 5b,c). There was a noticeable decrease as moving away from the KMWs.

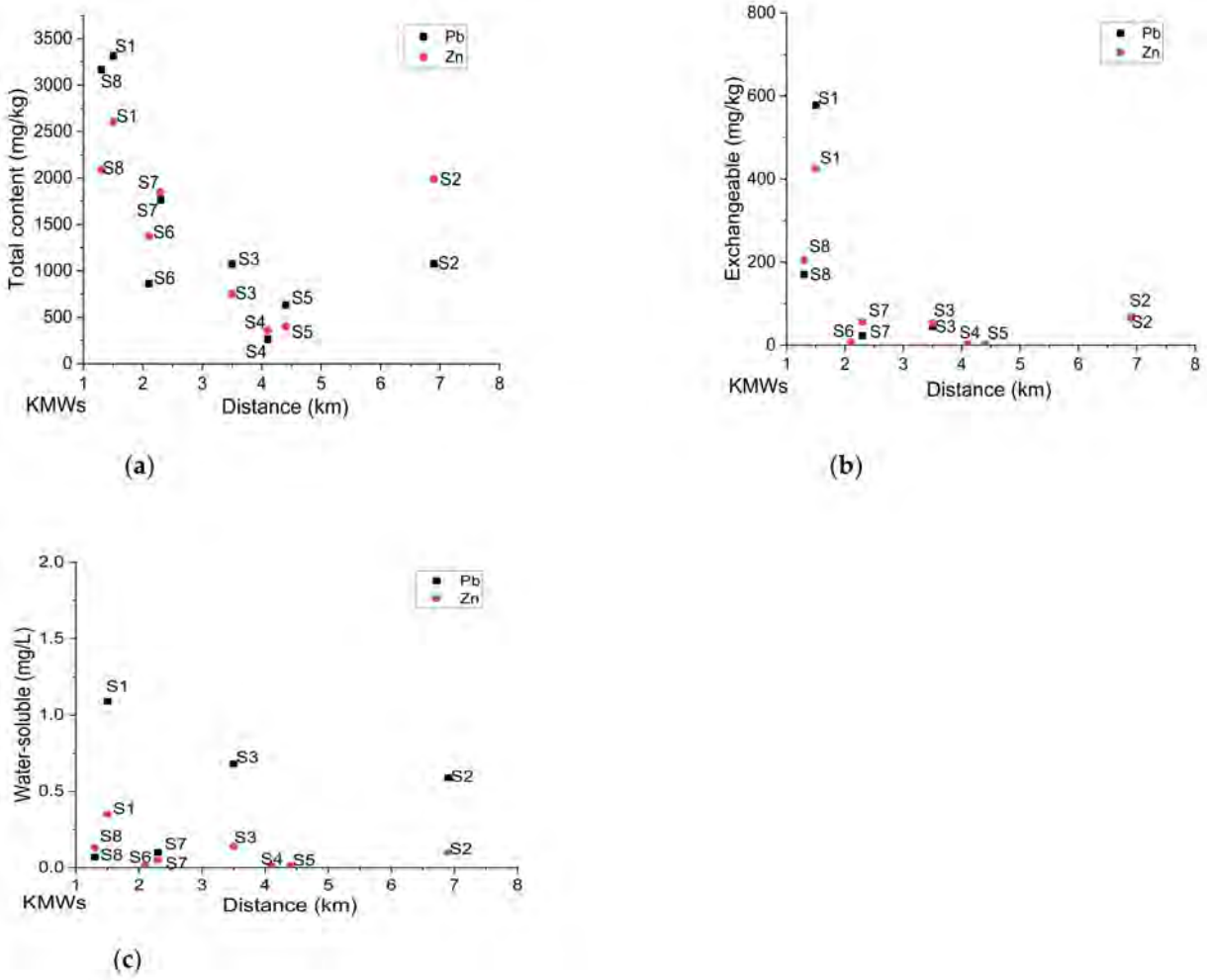

Figure 5. The distribution of Pb and Zn with the distance of each playground from Kabwe Mine Wastes (KMWs): (**a**) contents (XRF), (**b**) exchangeable and (**c**) water-soluble.

4. Discussion

The SPs have exceptionally high contents of Pb and Zn. Soil contamination in the SPs might be attributed to the deposition of aerosol particles to surrounding soils from the KMWs. Nakamura et al. [9] confirmed that the contents of Pb generally increased with the amount deposited; also, the Pb content in the SPs and the simulated amount of deposition decreased with distance from the source. This is consistent with the high enrichment and contamination of Pb in the soils near the mine area (S1 and S8). The results of the substantial enrichment in S1 and S8 were consistent with the profound intensity of contamination in the SPs near the KMWs.

However, the discrepancies in the contents and leaching of Pb and Zn in the SPs might be attributed to the volume of aerosols deposited, particle size distribution and environmental conditions controlling the mobilities of the PTEs. Moreover, the mobility of PTEs such as Pb and Zn in groundwater, mine tailings, and contaminated soils are extensively influenced by the pH, precipitation, redox conditions, and adsorption/desorption reactions [32]. Regardless, the enrichment of Pb was exceptionally higher than Zn in all the SPs. In comparison with other playgrounds for different cities in the world, the contents of Pb and Zn from Kabwe SPs were higher than those of Warsaw and Bydgoszcz, Poland (Pb up to 167 mg/kg, Zn up to 57.4 mg/kg [33], Beijing, China (Pb up to 207.5 mg/kg, Zn, up to 196.9 mg/kg [34], Ibadan, Nigeria (Pb up to 58 mg/kg, Zn up to 460 mg/kg [35] and Hong Kong, country parks (Pb up to 124 mg/kg, Zn up to 136 mg/kg [36].

Figure 3a showed that the Pb in the leachates from S1, S2, S3, S7, and S8 were above the permissible limit for drinking water in Zambia. Water consumption from such an environment may be detrimental to human health because some communities in Kabwe rely on groundwater from boreholes. The release of Pb into the environment may be attributed to sulfide oxidation [21]. This is explained by the SO_4^{2-} in PCA 2 for the leachate concentration. The high loadings of SO_4^{2-}, EC, and Eh suggest the sulfide minerals oxidation in the SPs. Moreover, Silwamba et al. [4] pointed out that in the leaching system for ZLPR, the SO_4^{2-} was attributed to the soluble minerals phases, anglesite ($PbSO_4$), zinkosite ($ZnSO_4$), and gypsum $CaSO_4{\cdot}2H_2O$.

Table S7 shows the PHREEQC simulation for the possible mineral phases that could affect the release and retention of PTEs in the SPs. The results shows that the *SIs* for $CaSO_4{\cdot}2H_2O$ (−3.45 to −1.55) and $PbSO_4$ (−2.41 to −1.43) implied the dissolution of these mineral phases. Consequently, suggesting that the release Pb in the SPs may be from the dissolution of $PbSO_4$. However, the *SIs* of goethite ($Fe(OH)_3$; 4.6 to 7.94) and those of ferrihydrite (FeOOH; 1.85 to 5.22) showed that precipitation was thermodynamically favored after leaching. This explains why no leachable Pb, and Zn were detected in S4, S5 and S6, meaning that the available PTEs in the SPs might have been redistributed and adsorbed with hydrous ferric oxides (HFOs). Moreover, HFOs have an excellent affinity for PTEs such as Pb, Cu, Cd, Zn, Ni, and metal oxyanions such as Cr, Sb, and As [37,38]. This is consistent with batch leaching results; no Fe was detected in the S4, S5, and S6 (Table S8).

Fractionation of Pb by sequential extraction confirmed the strong associations between Pb with the Fe/Mn oxides and sulfide/organic phases. This means that Pb was relatively stable after deposition [39]. Therefore, the Pb in the Fe/Mn phase might have been attributed to weathering of PbS. The Pb bound to the oxidizable (sulfide/organic) phases was higher than Zn, which is consistent with the high correlation of Pb and S for the chemical composition of the soils. Although the SPs were characterized by bare land and little vegetative cover, the strong correlations of Pb with TOC suggest that some of the Pb might be retained with the organic phases [40]. Agnieszka et al. [41] also highlighted the strong correlations of Pb, Cu, Ni, and Cr with TOC in the organic phase.

The mobile fractions for the labile phases (exchangeable + carbonates + Fe/Mn oxides) for Pb and Zn were notably high for all the SPs. Generally, it is typically assumed that the greater the labile percentage, the greater the potential for bioavailability in the body [42]. Therefore, the high bioaccessible fractions of PTEs in the labile phases significantly increase the bioaccessibility of the ingested PTEs, thereby posing a serious threat to the respiratory and digestive systems for the children because a substantial amount of PTEs might be absorbed into the bloodstream.

The correlations between the leachable water-soluble Pb and Zn with the exchangeable, labile phases and the total content suggests that the release of Pb and Zn into the environment from the SPs was mainly attributed to the exchangeable phase and not so much from the total content of Pb and Zn (Figures S2 and S3). In addition, the Pb bound to carbonate phase is usually influenced by the pH of the environment; for example, under gastric conditions, cerussite ($PbCO_3$) might significantly dissolve in the acidic conditions [43], which increases the bioaccessibility of ingested PTEs. However, the present study could not identify the host minerals for the PTEs; electron microprobe analysis might be a possible approach to identifying the mineral phases [44].

5. Conclusions

The leachability, solid-phase partitioning and contamination assessment of the SPs were conducted in Kabwe SPs near the mine area. The anthropogenic contamination and enrichment of Pb and Zn in the SPs can be traced back to the old mining activities. The SPs were extremely enriched with PTEs. The Pb and Zn in the SPs were mainly bound with the carbonates, reducible and oxidizable phases. The bioaccessible fractions of the PTEs for the labile phases were exceptionally high for all the SPs.

Thus, the SPs are potential sources of PTEs for the children in Kabwe. In general, the human health risk associated with inhalation/ingestion of PTEs from the SPs is high. Therefore, revegetation, soil turning, and watering the SPs to suppress dust generation could be some short-term measures to reduce the high bioaccessibility of PTEs in the SPs.

Supplementary Materials: The following are available online at https://www.mdpi.com/article/10.3390/toxics9100248/s1, Table S1: A brief description of the type of soil samples collected, Figure S1: XRD patterns showing the major minerals found in the SPs, Table S2: Pearson correlation matrix for chemical composition for the soil samples. Marked correlation is significant at $p < 0.05$, Table S3: Pollution indices with the total average value across the SPs. Table S4 and Table S5: Solid-phase partitioning of Pb and Zn: mean content for each phase (mg/kg), standard deviation (SD), and percentage (%) partitioning for each phase in the SPs, Table S6: Labile % (Phase 1;exchangeable + Phase 2;carbonates + Phase 3;Fe/Mn oxides) for the SPs, Figure S2 and S3: Relationship between water-soluble Pb and Zn with (a) exchangeable phase, (b) labile Phases 1 + 2 + 3 and (c) total content, Table S7: Saturation indices (*SI*) of selected mineral phases controlling the release and retention of Pb and Zn in the selected SPs. Table S8: Leachate characteristics of the SPs, including other dissolved minerals.

Author Contributions: Conceptualization, W.M.; formal analysis, W.M., T.I. and P.T.; writing—original draft preparation, W.M.; writing—review and editing, investigation, methodology, W.M., P.T., T.I., M.I. (Mayumi Ito), T.S., M.C., I.N. and H.N.; resources, M.I. (Mayumi Ito), T.S., M.C., I.N., M.I. (Mayumi Ishizuka) and S.N.; project administration, M.I. (Mayumi Ishizuka), H.N. and S.N.; supervision, T.I. and S.N.; funding acquisition, M.I. (Mayumi Ishizuka). All authors have read and agreed to the published version of the manuscript.

Funding: This research was supported by JST/JICA SATREPS (Science and Technology Research Partnership for Sustainable Development; No. JPMJSA1501) and aXis (Accelerating Social Implementation for SDGs Achievement; No. JPMJAS2001) funded by JST.

Institutional Review Board Statement: Not applicable.

Data Availability Statement: Not applicable.

Acknowledgments: The authors would like to acknowledge JST/JICA SATREPS (Science and Technology Research Partnership for Sustainable Development; No. JPMJSA1501) and aXis (Accelerating Social Implementation for SDGs Achievement; No. JPMJAS2001) funded by JST for the financial support.

Conflicts of Interest: The authors declare no conflict of interest.

References

1. Kamona, A.F.; Friedrich, G.H. Geology, mineralogy and stable isotope geochemistry of the Kabwe carbonate-hosted Pb–Zn deposit, Central Zambia. *Ore Geol. Rev.* **2007**, *30*, 217–243. [CrossRef]
2. Blacksmith Institute and Green Cross Switzerland. 2013. Available online: https://www.worstpolluted.org/docs/TopTenThreats.pdf (accessed on 11 September 2021).
3. Southwood, M.; Cairncross, B.; Rumsey, M.S. Minerals of the Kabwe ("Broken Hill") mine, central province, Zambia. *Rocks Miner.* **2019**, *94*, 114–149. [CrossRef]
4. Silwamba, M.; Ito, M.; Hiroyoshi, N.; Tabelin, C.B.; Fukushima, T.; Park, I.; Jeon, S.; Igarashi, T.; Sato, T.; Nyambe, I.; et al. Detoxification of lead-bearing zinc plant leach residues from Kabwe, Zambia by coupled extraction-cementation method. *J. Environ. Chem. Eng.* **2020**, *8*, 104197. [CrossRef]
5. Ettler, V.; Štěpánek, D.; Mihaljevič, M.; Drahota, P.; Jedlicka, R.; Kříbek, B.; Nyambe, I. Slag dusts from Kabwe (Zambia): Contaminant mineralogy and oral bioaccessibility. *Chemosphere* **2020**, *260*, 127642. [CrossRef]
6. Kříbek, B.; Nyambe, I.; Majer, V.; Knésl, I.; Mihaljevič, M.; Ettler, V.; Sracek, O. Soil contamination near the Kabwe Pb-Zn smelter in Zambia: Environmental impacts and remediation measures proposal. *J. Geochem. Explor.* **2019**, *197*, 159–173. [CrossRef]
7. Tangviroon, P.; Noto, K.; Igarashi, T.; Kawashima, T.; Ito, M.; Sato, T.; Mufalo, W.; Chirwa, M.; Nyambe, I.; Nakata, H.; et al. Immobilization of lead and zinc leached from mining residual materials in Kabwe, Zambia: Possibility of chemical immobilization by dolomite, calcined dolomite, and magnesium oxide. *Minerals* **2020**, *10*, 763. [CrossRef]
8. Mwandira, W.; Nakashima, K.; Kawasaki, S.; Ito, M.; Sato, T.; Igarashi, T.; Chirwa, M.; Banda, K.; Nyambe, I.; Nakayama, S.; et al. Solidification of sand by Pb (II)-tolerant bacteria for capping mine waste to control metallic dust: Case of the abandoned Kabwe Mine, Zambia. *Chemosphere* **2019**, *228*, 17–25. [CrossRef]

9. Nakamura, S.; Igarashi, T.; Uchida, Y.; Ito, M.; Hirose, K.; Sato, T.; Mufalo, W.; Chirwa, M.; Nyambe, I.; Nakata, H.; et al. Evaluation of Dispersion of Lead-bearing Mine wastes in Kabwe District, Zambia. *Minerals* **2021**, *11*, 901. [CrossRef]
10. Bello, O.; Naidu, R.; Rahman, M.M.; Liu, Y.; Dong, Z. Lead concentration in the blood of the general population living near a lead-zinc mine site, Nigeria: Exposure pathways. *Sci. Total Environ.* **2016**, *542*, 908–914. [CrossRef]
11. Yabe, J.; Nakayama, S.M.; Ikenaka, Y.; Yohannes, Y.B.; Bortey-Sam, N.; Oroszlany, B.; Ishizuka, M. Lead poisoning in children from townships in the vicinity of a lead-zinc mine in Kabwe, Zambia. *Chemosphere* **2015**, *119*, 941–947. [CrossRef]
12. Ljung, K.; Selinus, O.; Otabbong, E. Metals in soils of children's urban environments in the small northern European city of Uppsala. *Sci. Total Environ.* **2006**, *366*, 749–759. [CrossRef]
13. EPA, US. *A Review of the Reference Dose and Reference Concentration Processes. Risk Assessment Forum, U*; The Environmental Protection Agency: Washington, DC, USA, 2002.
14. Toyomaki, H.; Yabe, J.; Nakayama, S.M.; Yohannes, Y.B.; Muzandu, K.; Mufune, T.; Nakata, H.; Ikenaka, Y.; Kuritani, T.; Nakagawa, M.; et al. Lead concentrations and isotope ratios in blood, breastmilk and feces: Contribution of both lactation and soil/dust exposure to infants in a lead mining area, Kabwe, Zambia. *Environ. Pollut.* **2021**, *286*, 117456. [CrossRef]
15. Yabe, J.; Nakayama, S.M.; Nakata, H.; Toyomaki, H.; Yohannes, Y.B.; Muzandu, K.; Ishizuka, M. Current trends of blood lead levels, distribution patterns and exposure variations among household members in Kabwe, Zambia. *Chemosphere* **2020**, *243*, 125412. [CrossRef]
16. Bose-O'Reilly, S.; Yabe, J.; Makumba, J.; Schutzmeier, P.; Ericson, B.; Caravanos, J. Lead intoxicated children in Kabwe, Zambia. *Environ. Res.* **2018**, *165*, 420–424. [CrossRef]
17. Jin, Y.; O'Connor, D.; Ok, Y.S.; Tsang, D.C.; Liu, A.; Hou, D. Assessment of sources of heavy metals in soil and dust at children's playgrounds in Beijing using GIS and multivariate statistical analysis. *Environ. Int.* **2019**, *124*, 320–328. [CrossRef]
18. Peng, T.; O'Connor, D.; Zhao, B.; Jin, Y.; Zhang, Y.; Tian, L.; Hou, D. Spatial distribution of lead contamination in soil and equipment dust at children's playgrounds in Beijing, China. *Environ. Pollut.* **2019**, *245*, 363–370. [CrossRef]
19. Yan, B.; Xu, D.M.; Chen, T.; Yan, Z.A.; Li, L.L.; Wang, M.H. Leachability characteristic of heavy metals and associated health risk study in typical copper mining-impacted sediments. *Chemosphere* **2020**, *239*, 124748. [CrossRef]
20. Huyen, D.T.; Tabelin, C.B.; Thuan, H.M.; Dang, D.H.; Truong, P.T.; Vongphuthone, B.; Igarashi, T. The solid-phase partitioning of arsenic in unconsolidated sediments of the Mekong Delta, Vietnam and its modes of release under various conditions. *Chemosphere* **2019**, *233*, 512–523. [CrossRef]
21. Tabelin, C.B.; Silwamba, M.; Paglinawan, F.C.; Mondejar, A.J.S.; Duc, H.G.; Resabal, V.J.; Opiso, E.M.; Igarashi, T.; Tomiyama, S.; Ito, M.; et al. Solid-phase partitioning and release-retention mechanisms of copper, lead, zinc and arsenic in soils impacted by artisanal and small-scale gold mining (ASGM) activities. *Chemosphere* **2020**, *260*, 127574. [CrossRef]
22. Tabelin, C.B.; Igarashi, T.; Villacorte-Tabelin, M.; Park, I.; Opiso, E.M.; Ito, M.; Hiroyoshi, N. Arsenic, selenium, boron, lead, cadmium, copper, and zinc in naturally contaminated rocks: A review of their sources, modes of enrichment, mechanisms of release, and mitigation strategies. *Sci. Total Environ.* **2018**, *645*, 1522–1553. [CrossRef]
23. Muller, G. Index of geo-accumulation in sediments of the Rhine River. *GeoJournal* **1969**, *2*, 108–118.
24. Towett, E.K.; Shepherd, K.D.; Tondoh, J.E.; Winowiecki, L.A.; Lulseged, T.; Nyambura, M.; Cadisch, G. Total elemental composition of soils in Sub-Saharan Africa and relationship with soil-forming factors. *Geoderma Reg.* **2015**, *5*, 157–168. [CrossRef]
25. Buat-Menard, P.; Chesselet, R. Variable influence of the atmospheric flux on the trace metal chemistry of oceanic suspended matter. *Earth Planet Sci. Lett.* **1979**, *42*, 399–411. [CrossRef]
26. Turekian, K.; Wedepohl, K. Distribution of the elements in some major units of the earth's crust. *Geol. Soc. Am. Bull.* **1961**, *72*, 175–192. [CrossRef]
27. Sutherland, R.A.; Tolosa, C.A.; Tack, F.M.G.; Verloo, M.G. Characterization of selected element concentrations and enrichment ratios in background and anthropogenically impacted roadside areas. *Arch. Environ. Contam. Toxicol.* **2000**, *38*, 428–438. [CrossRef]
28. Parkhurst, D.L.; Appelo, C.A.J. *User's guide to PHREEQ (Version 2)—A Computer Program for Speciation, Batch Reaction, One-Dimensional Transport, and Inverse Geochemical Calculations*; Department of the Interior and U.S. Geological Survey: Denver, CO, USA, 1999; pp. 99–4259.
29. Tessier, A.; Campbell, G.C.; Bisson, M. Sequential extraction procedure for the speciation of particulate trace metals. *Anal. Chem.* **1979**, *51*, 844–851. [CrossRef]
30. Marumo, K.; Ebashi, T.; Ujiie, T. Heavy metal concentrations, leachabilities, and lead isotope ratios of Japanese soils. *Shigen-Chihsitsu* **2003**, *53*, 125–146.
31. Kok, J.F.; Parteli, E.J.; Michaels, T.I.; Karam, D.B. The physics of wind-blown sand and dust. *Rep. Prog. Phys.* **2012**, *75*, 106901. [CrossRef]
32. Tabelin, C.B.; Igarashi, T. Mechanisms of arsenic and lead release from hydrothermally altered rock. *J. Hazard. Mater.* **2009**, *169*, 980–990. [CrossRef]
33. Różański, S.Ł.; Kwasowski, W.; Castejón, J.M.P.; Hardy, A. Heavy metal content and mobility in urban soils of public playgrounds and sport facility areas, Poland. *Chemosphere* **2018**, *212*, 456–466. [CrossRef]
34. Chen, T.B.; Zheng, Y.M.; Lei, M.; Huang, Z.C.; Wu, H.T.; Chen, H.; Tian, Q.Z. Assessment of heavy metal pollution in surface soils of urban parks in Beijing, China. *Chemosphere* **2005**, *60*, 542–551. [CrossRef] [PubMed]

35. Akinwunmi, F.; Akinhanmi, T.F.; Atobatele, Z.A.; Adewole, O.; Odekunle, K.; Arogundade, L.A.; Ademuyiwa, O. Heavy metal burdens of public primary school children related to playground soils and classroom dusts in Ibadan North-West local government area, Nigeria. *Environ. Toxicol. Pharmacol.* **2017**, *49*, 21–26. [CrossRef] [PubMed]
36. Lee, C.S.L.; Li, X.; Shi, W.; Cheung, S.C.N.; Thornton, I. Metal contamination in urban, suburban, and country park soils of Hong Kong: A study based on GIS and multivariate statistics. *Sci. Total Environ.* **2006**, *356*, 45–61. [CrossRef] [PubMed]
37. Shi, M.; Min, X.; Ke, Y.; Lin, Z.; Yang, Z.; Wang, S.; Wei, Y. Recent progress in understanding the mechanism of heavy metals retention by iron (oxyhydr) oxides. *Sci. Total Environ.* **2020**, *752*, 141930. [CrossRef]
38. Trivedi, P.; Dyer, J.A.; Sparks, D.L.; Pandya, K. Mechanistic and thermodynamic interpretations of zinc sorption onto ferrihydrite. *J. Colloid Interface Sci.* **2004**, *270*, 77–85. [CrossRef]
39. Prathumratana, L.; Kim, R.; Kim, K.W. Lead contamination of the mining and smelting district in Mitrovica, Kosovo. *Environ. Geochem. Health* **2020**, *42*, 1033–1044. [CrossRef]
40. Khan, B.; Ullah, H.; Khan, S.; Aamir, M.; Khan, A.; Khan, W. Sources and contamination of heavy metals in sediments of Kabul River: The role of organic matter in metals retention and accumulation. *Soil Sediment Contam. An Int. J.* **2016**, *25*, 891–904. [CrossRef]
41. Baran, A.; Mierzwa-Hersztek, M.; Gondek, K.; Tarnawski, M.; Szara, M.; Gorczyca, O.; Koniarz, T. The influence of the quantity and quality of sediment organic matter on the potential mobility and toxicity of trace elements in bottom sediment. *Environ. Geochem. Health* **2019**, *41*, 2893–2910. [CrossRef]
42. Sethurajan, M.; Huguenot, D.; Lens, P.N.; Horn, H.A.; Figueiredo, L.H.; Van Hullebusch, E.D. Fractionation and leachability of heavy metals from aged and recent Zn metallurgical leach residues from the Três Marias zinc plant (Minas Gerais, Brazil). *Environ. Sci. Pollut. Res.* **2016**, *23*, 7504–7516. [CrossRef]
43. Helser, J.; Cappuyns, V. Trace elements leaching from pbzn mine waste (plombières, belgium) and environmental implications. *J. Geochem. Explor.* **2021**, *220*, 106659. [CrossRef]
44. Vollprecht, D.; Riegler, C.; Ahr, F.; Stuhlpfarrer, S.; Wellacher, M. Sequential chemical extraction and mineralogical bonding of metals from Styrian soils. *Int. J. Environ. Sci. Technol.* **2020**, *17*, 3663–3676. [CrossRef]

Comparative Biochemistry and Physiology, Part C 252 (2022) 109215

Contents lists available at ScienceDirect

Comparative Biochemistry and Physiology, Part C

journal homepage: www.elsevier.com/locate/cbpc

Research article

Environmentally relevant lead (Pb) water concentration induce toxicity in zebrafish (*Danio rerio*) larvae

Andrew Kataba [a,b], Tarryn L. Botha [a,c,d], Shouta M.M. Nakayama [a], Yared B. Yohannes [a,e], Yoshinori Ikenaka [a,c,f,g], Victor Wepener [a,c], Mayumi Ishizuka [a,*]

[a] Laboratory of Toxicology, Department of Environmental Veterinary Sciences, Faculty of Veterinary Medicine, Hokkaido University, Kita18, Nishi 9, Kita-ku, Sapporo, Hokkaido 060-0818, Japan
[b] Department of Biomedical Sciences, School of Veterinary Medicine, The University of Zambia, Box 32379, Lusaka, Zambia
[c] Water Research Group, Unit for Environmental Sciences and Management, North-West University, Private Bag X6001, Potchefstroom, South Africa
[d] Institute for Nanotechnology and Water Sustainability, College of Science, Engineering and Technology, University of South Africa, Florida Science Campus, P/Bag X6, Roodepoort 1709, South Africa
[e] Department of Chemistry, College of Natural and Computational Science, University of Gondar, P. O. Box 196, Gondar, Ethiopia
[f] Translational Research Unit, Veterinary Teaching Hospital, Faculty of Veterinary Medicine, Hokkaido University, Sapporo 060-0818, Japan
[g] One Health Research Center, Hokkaido University, Japan

ARTICLE INFO

Editor: Martin Grosell

Keywords:
Zebrafish
Lead
Cardiovascular
Apoptosis
Twitching
Fish Embryo Test (FET)

ABSTRACT

Early developmental stages of aquatic organisms including fish are inherently vulnerable to lead (Pb) and other water metal contaminants. However, reports on the deleterious effects of environmentally relevant Pb levels are limited. To this end, we exposed 2.5 h post fertilization (hpf) old zebrafish (*Danio rerio*) embryos to a range of Pb concentrations encompassing environmentally relevant levels (1, 10, 25, 50 and 100 μg/L Pb) until 96 hpf. Exposure negatively impacted the development and survival of zebrafish embryos by inducing embryo coagulation related mortalities in a concentration-dependent manner. At 24 hpf, the highest level of exposure (100 μg/L Pb) had impaired embryo activity characterized by reduced burst activity and the number of movements per minute made by embryos. At 72 hpf, newly hatched larvae exhibited adverse cardiovascular effects (100 μg/L Pb group) and neuromuscular effects (50 and 100 μg/L Pb groups). The antioxidant system dysregulation evidenced by downregulation of catalase, and upregulation of mRNA expression of glutathione S-transferase and cytochrome oxidase subunit I were observed. The pro-apoptotic tumour protein P53 (*TP53*) and the anti-apoptotic B cell lymphoma −2 (*Bcl-2*) mRNA expression levels were also affected. The former was downregulated across exposed groups and the latter was upregulated and downregulated in the groups with Pb concentrations less than 50 μg/L Pb and downregulated in 50 μg/L Pb, respectively. These findings suggest that Pb within environmentally relevant levels may be deleterious to developing zebrafish.

1. Introduction

Lead (Pb) is a metal that naturally occurs in small amounts in the environment (Hailegnaw et al., 2015). High quantities of Pb in the environment are traceable to anthropogenic activities such as mining, Pb products production processes and their use (Komárek et al., 2008). An example of a heavily Pb polluted town with mining activities as a source is Kabwe, Zambia following 9 decades of unregulated waste management at the now closed lead-zinc mine (Yabe et al., 2018). The extensive Pb pollution of the Kabwe town has plunged the majority of its residents into chronic Pb poisoning especially children having blood Pb levels above the minimum Pb reference value of 5 μg/dL (Yabe et al., 2015, 2020). Domesticated animals, free-range chickens including free-roaming dogs around the region of the closed mine have been found with remarkable Pb levels in blood (Nakayama et al., 2011; Toyomaki et al., 2020; Yabe et al., 2011, 2013). Moreover, water sampled from natural water bodies and boreholes inside the region of the closed mine was found to have a Pb concentration range of 0.1–94 μg/L against the country's regulatory limit of 50 μg/L Pb in water (Nachiyunde et al., 2013).

* Corresponding author at: Laboratory of Toxicology, Department of Environmental Veterinary Sciences, Faculty of Veterinary Medicine, Hokkaido University, Kita 18 Nishi 9, Kita-ku, Sapporo 060-0818, Japan.
E-mail address: ishizum@vetmed.hokudai.ac.jp (M. Ishizuka).

https://doi.org/10.1016/j.cbpc.2021.109215
Received 17 June 2021; Received in revised form 8 October 2021; Accepted 14 October 2021
Available online 18 October 2021

Lead exposure to developing fish embryos has been linked to undesirable effects including delayed hatching, premature hatching, and malformations of larvae, which leads to mortalities (Jezierska et al., 2009). In addition, Pb poisoning causes an imbalance of the antioxidants and eventual dysregulation of the antioxidant system (Kim and Kang, 2017). Studies have demonstrated that the antioxidant system dysregulation through increased generation of reactive oxygen species (ROS) is the major cause of oxidative-induced damage in fish exposed to Pb (Kim and Kang, 2017). A review paper citing Pb exposure studies revealed that early developmental stages of fish are more sensitive to Pb-induced toxicity (Sfakianakis et al., 2015). However, the Pb exposure concentrations in most of the cited studies ranged from 100 to 10,000 μg/L (Sfakianakis et al., 2015), which may not reflect the real prevailing environmental Pb levels.

Altered swimming behaviour accompanied by an increased oxidative stress response in larval zebrafish following acute exposure to water Pb concentrations in Kabwe, Zambia has been reported (Kataba et al., 2020). However, a dearth of data on the impacts of these Pb levels on the cardiovascular, neuromuscular and ROS-induced toxicity on the early developmental stages of fish exists. Moreover, to the best of our knowledge, the environmentally relevant Pb-induced neuromuscular toxicity in hatched embryos from the 50 and 100 μg/L Pb level of exposure has never been reported before. To bridge this information gap, we investigated the undesirable effects of the Kabwe water Pb levels on fish health by means of the zebrafish embryo toxicity testing (FET) protocol. Zebrafish (*Danio rerio*) has been known to be an ideal model for toxicological investigations owing to its morphological, biochemical and physiological data that is obtainable in early life stages such as embryos (Hill et al., 2005). Furthermore, the zebrafish lifecycle that can be managed in a laboratory environment, the embryo's ability to absorb compounds in water (Yin et al., 2017) and the shared sensitivity range with other fish species endemic to Africa (Botha et al., 2015) made the zebrafish embryos a choice model for the present study. The FET test was employed to investigate: 1) how safe are the water Pb levels reported from Kabwe, Zambia (range 0.1–94 μg/L Pb) on early developing stages of fish?; and 2) is the country's regulatory limit for Pb in water (50 μg/L) as reported by Nachiyunde et al. (2013) conducive to support early developmental stages of fish?

2. Materials and methods

2.1. Fish husbandry and embryo collection

Wild-type zebrafish breeding stock kept at 26–28 °C on a 14-h light and 10-h dark cycle in a ZebTec (Tecniplast, Italy) system at the North-West University's National Aquatic Bioassay Facility (NABF), South Africa were used to breed fertilized embryos. All the experiments conducted following and in strict adherence to research guidelines mandated by the North-West University AnimCare Ethics Committee (Approval number NWU-00269-16-A5). The breeding process and the collection of embryos were carried out as previously described by Kataba et al. (2020).

2.2. Lead (Pb) stock solution preparation and concentrations selection

A 10 mg/L Pb stock solution was prepared using pure grade (99.5%) lead acetate trihydrate in lead-free ultrapure water. From the Pb stock solution, five dilutions (1, 10, 25, 50, and 100 μg/L) were prepared using the embryo development medium (each litre contains 0.875 g NaCl, 0.038 g KCl, 0.120 g $MgSO_4$, 0.021 g KH_2PO_4, and 0.006 g Na_2HPO_4) constituted in deionized water (pH 8.2). The selections of the first four exposure concentrations (1–50 μg/L) were chosen to reflect the range reported in water samples from Kabwe, Zambia and the permissible water Pb level by the national authority body (Nachiyunde et al., 2013). The 100 μg/L Pb concentration was included in adherence with the Fish Embryo toxicity (FET) test protocol recommended by the Organisation for Economic Co-operation and Development (OECD) test guidelines (TG 236) for the testing of Chemicals (Busquet et al., 2014).

2.3. Fish Embryo Toxicity (FET) test and embryo activity analysis

Fertilized zebrafish embryos (2.5 hpf old) within an early developmental stage, following sorting under a Zeiss stemi microscope, were assigned to 5 concentrations of Pb at selected concentrations (0, 1, 10, 25, 50, and 100 μg/L) diluted with the embryo media in plastic 6-well plates (total volume 5000 μL/ well). A positive control with 3,4-dichloroaniline test solution was prepared. Six well plate replicates ($n = 5$ embryos per well plate) for the control with 30 total embryos, five replicates of total 25 embryos per treatment (1-100 μg/L) were performed without renewal of the treatment solutions. The plates were covered with self-adhesive, oxygen-permeable sealing film (BRAND®, Sigma Alrich) to prevent evaporation of the test solution. The embryos were incubated at 28 °C for 96 h and their morphological condition was monitored every 24 h interval. Normal embryo morphology referencing was as described by Kimmel et al. (1995) and any dead or coagulated embryos were recorded and removed from the test plate. The six control replicates numbers (30 embryos) used were in line with the OECD guidelines (TG 236) for the testing of chemicals (Busquet et al., 2014).

2.4. Sub-lethal embryo activity, cardiology and twitching

A non-invasive video recording technique of assessing embryos within their chorions or hatched larvae was used. To assess embryo activity at 24 hpf, movements of embryos within test solutions were recorded for 1 min using a remote-controlled stereomicroscope (Zeiss, Germany) connected to a camera. Videos from 8 randomly selected individual embryos per replicates were assessed using DanioScope V1 software (Zeiss, Germany).

The burst activity and the burst count/min were computed as a representation of embryo activity. The mean burst activity represents the percentage of time (from total measurement duration) the embryo was moving, and the burst count/per minute represents the number of movements per minute.

At 72 hpf, blood flow and heart rate were assessed using 6 newly hatched larvae per group ($n = 6$) that were randomly selected using video recording followed by analysis. Individual zebrafish larvae were picked with a pipette and placed in a drop of the exposure media on a glass slide and videos were taken using a stereomicroscope (Zeiss, Germany) using a remote-controlled microscope camera. Heart rate videos were taken for 30 s with the heart in view while the larvae lay in lateral recumbence in the exposure media in a temperature-controlled room at the same used during the exposure period. The videos were imported in DanioScope and automatically the numbers of beats per minute (BPM) were calculated. The blood flow analysis video recordings were taken by focusing on the caudal artery caudal to the anal pore in view for 30 s. The blood flow was presented as an activity percentage.

The muscular activity of the larvae was assessed using video recordings which were later analyzed as an indicator of twitching movements. The full video was used, and movements were confirmed by watching the video as well as action potential output graphs. A peak of the action potential indicated a twitch count, and the action potential peak width represented the duration of the twitch over the 60 s time interval. The raw data was exported and used for time scale determinations (DanioScope V1 Software, Noldus Information Technology, Wageningen, Netherlands). In the present study, only action potentials with an amplitude of 5% and above were classified as muscular twitches (Fig. 3 C - H). Normal swimming or pectoral fin movement of larval zebrafish was not considered as twitch activity. Fig. SV1 shows the representative larvae video recordings for each Pb exposure level that were included in the current study.

2.5. RNA extraction and real-time PCR analysis

At the end of the exposure period (96 hpf), hatched embryos (larvae) from the different groups were sacrificed using ice-cold embryo media and 5–10 larvae were collected as a pooled sample and immediately preserved in RNA Later solution (SIGMA Life Science, St. Louis, MO, USA) at −80 °C prior to their transportation to Hokkaido University, Japan. Following the sample transportation using a cold chain system on dry ice to the Laboratory of Toxicology, Faculty of Veterinary Medicine, Hokkaido University the samples were stored at −80 °C until RNA extraction. The total RNA was extracted from 5 to 10 pooled zebrafish hatched embryos and the cDNA synthesis was done using the TOYOBO cDNA kit (TOYOBO Co., Ltd., Life Science Department, Osaka, Japan). The quantitative reverse transcription polymerase chain reaction conditions used were as previously described by Kataba et al. (2020). The primer sets used shown in Table S1 and all primers underwent validation and were obtained as described by Kataba et al. (2020). The normalization and the mRNA expression levels calculations was done using the comparative ($2^{-\Delta\Delta Ct}$) method.

2.6. Verification of Pb in exposure concentrations

The nominal exposure concentrations that were prepared (0, 1, 10, 25, 50, and 100 μg/L) and used in the current study were verified using the inductively coupled plasma mass spectrometry (ICP-MS). Aliquots of freshly prepared Pb exposure concentrations in which zebrafish embryos and larvae were reared during the exposure period were used for verification by two independent analysts. The sample treatment and analysis were done as previously described by Kataba et al. (2020). Recoveries from freshly prepared Pb solutions ranged from 97 to 110% with actual concentrations of 0, 1.1, 9.7, 25.2, 49.6, and 100.7 μg/L Pb, respectively.

2.7. Data analysis

The FET test data statistics were generated from the TOXRAT® software. GraphPad Prism software (Prism 7 for Windows; Version 5.02, California USA) was used to perform the rest of the data analysis including embryo activity, blood flow, heart rate, twitching and gene expression. The data were first tested for normality using Kolmogorov–Smirnov test. For normally distributed data, an analysis of variance (one-way ANOVA) and the differences among test groups were assessed using Tukey's test. A non-parametric Kruskal–Wallis test followed by a Mann–Whitney test (all other comparisons) was applied for non-normally distributed data were used. The data were reported as mean and standard error of the mean (SEM). The hatching and overall survival rates proportions differences between the exposed and control groups were analyzed by MedCalc® which uses the "N-1" Chi-squared test (Campel, 2007). The difference between groups was considered at two levels of significance and was marked at $p < 0.05$ (*) and at $p < 0.01$ (**). The graphical presentation of data was done using GraphPad Prism software (Prism 7 for Windows; Version 5.02, California, USA).

3. Results

3.1. Lead induced developmental toxicity in zebrafish embryo toxicity

The overall survival in the present study is defined as the total number of embryos that survived prior to hatching and those that hatched at 72 hpf. All the embryos that died during the exposure period were removed from testing plates. Hatching rates in the control and exposed groups are shown in Table 1. Lead exposure reduced the overall survival rate of exposed zebrafish embryos in a concentration-dependent manner; from 84% in the 1.0 μg/L to 52% in the 100 μg/L Pb. Lead-induced coagulation embryo mortalities that increased with the increase in Pb exposure concentration (Table 1) were recorded between 24 and 72 hpf. All surviving embryos hatched in all treatments by 72 hpf. No mortalities were observed in hatched larvae between 72 and 96 hpf periods.

3.2. Lead exposure attenuated zebrafish embryo activity

Lead exposure affected the burst activity (Fig. 1A) and the burst count per minute (Fig. 1B) of zebrafish embryos at 24 hpf. Only the 100 μg/L Pb group (0.10 ± 0.05%) recorded significant ($p < 0.01$) lower burst activity compared to the control group (0.62 ± 0.13%). The burst count per minute was significantly lower ($p < 0.01$) in the 100 μg/L Pb group (0.24 ± 0.16 burst/min) relative to the control group (1.00 ± 0.19 burst/min). The embryo activity data retrieved for two concentrations namely; 25 and 50 μg/L Pb at 24 hpf from the video recordings were not sufficient for data analysis.

3.3. Lead exposure induced cardiovascular dysfunction

Lead exposure caused changes in cardiovascular responses of 72 hpf zebrafish for heart rate (Fig. 2A) and blood flow (Fig. 2B). The heart rate was significantly lower in the 100 μg/L Pb compared to the control ($p < 0.05$). No differences were observed in heart rate in exposed groups with Pb concentrations less than 100 μg/L. The blood flow at the 100 μg/L Pb exposure concentration was significantly elevated when compared to the control groups ($p < 0.05$).

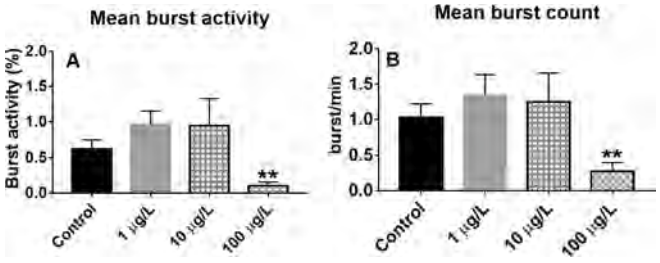

Fig. 1. Embryo activity at 24 hpf ($n = 8$) (A) mean burst activity (B) Burst count per minute. Values are presented as mean ± SEM. The asterisk (*) represents significant differences between exposed and the control group based on the Mann-Whitney test (**$p < 0.01$).

Table 1
Overall survival and hatching rates of embryos.

Treatment (μg/L)	Total introduced	Mortality 24–72 hpf	Mortality (%)	Hatched 72 hpf	Hatch 72 hpf (%)	Overall survival rate (%)
Control	30	2	6.7	28	93.3	93.3
1.0	25	4	16	21	84.0	84.0
10	25	13	52	12	48.0**	48.0
25	25	8	32	17	68.0*	68.0
50	25	8	32	17	68.0*	68.0
100	25	12	48	13	52.0**	52.0

(* $p < 0.05$ and ** $p < 0.01$ between exposure groups and the control group).

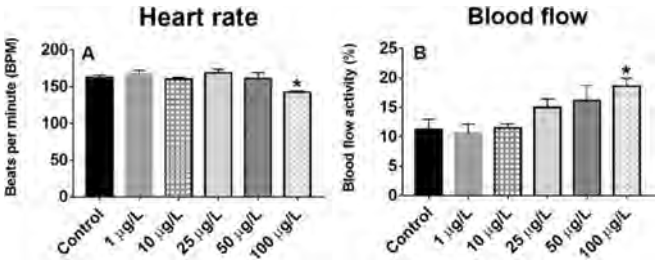

Fig. 2. Effects of Pb on the cardiovascular system of larvae (72 hpf). (A) Heart rate in beats per minute ($n = 6$). (B). Blood flow (n = 6 for all groups). Values are presented as mean ± SEM. The asterisk represents significant differences from the control using Mann-Whitney test ($^*p < 0.05$).

3.4. Lead exposure induced muscular twitching

In the present study, muscular twitches were observed in zebrafish larvae in the 50 and 100 µg/L Pb exposed groups. The muscular twitching effects were absent in zebrafish larvae in exposed groups with less than 50 µg/L Pb concentration and the control group (Fig. 3). The twitching increased from 3.5 ± 1.4 twitches per min in the 50 µg/L exposure group to 17.0 ± 3.3 twitches per minute in the 100 µg/L Pb exposed group (Fig. 3A). The muscular twitch durations were 0.55 ± 0.16 and 0.51 ± 0.06 s in the 50 µg/L Pb and the 100 µg/L Pb groups, respectively (Fig. 3B).

3.5. Lead exposure affected mRNA expression

Changes in the mRNA expression levels of antioxidant enzymes (CAT, GPX, SOD, GST, HO-1 and Nrf2) following exposure to different Pb concentrations are shown in Fig. 4. Lead induced significant down regulation of CAT mRNA expression in 50 µg/L Pb group (0.6-fold change) in relation to the control (Fig. 4A). The mRNA expression levels of GPX, SOD and Nrf2 enzymes across the exposed groups remained

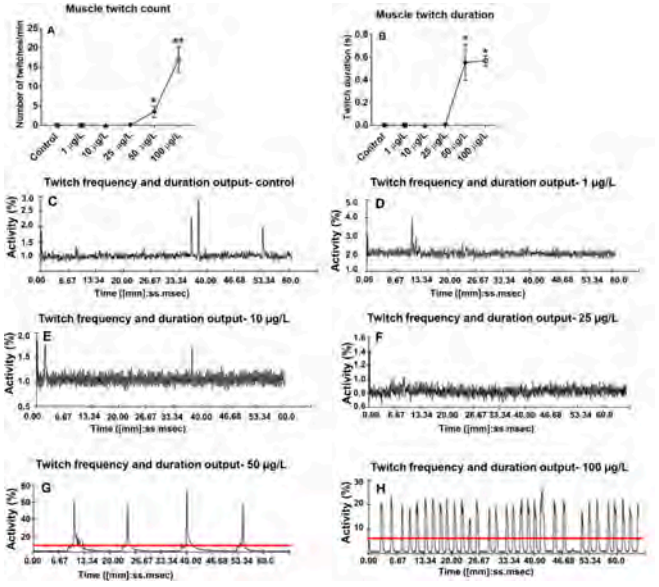

Fig. 3. Lead induced involuntary muscular twitching ($n = 6$): A. Muscle twitching (number of twitches/min); B. Twitch durations (s) Values are presented as mean ± SEM. The asterisk represents significant difference from the control using Mann-Whitney test ($^*p < 0.05$; $^{**}p < 0.01$); C, D, E, F, G and H. Representative outputs files indicating twitch frequency and duration. The red line represents the 5% activity used as a cut-off point mark. Activity of less than 5% in a larva fish was considered a normal muscular activity and above 5% represented muscular twitching. (For interpretation of the references to colour in this figure legend, the reader is referred to the web version of this article.)

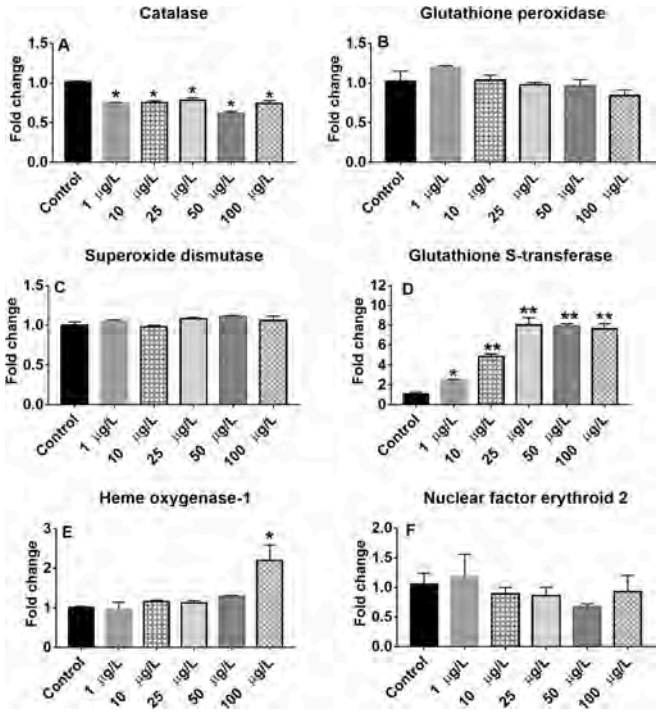

Fig. 4. Expression of mRNA in the pooled samples ($n = 4$). Values were normalized against Tubulin alpha-1A (used as house-keeping gene) and represent the mean mRNA expression value ± SEM relative to those of the controls. The asterisk represents significant difference when compared with the controls ($^*p < 0.05$ and $^{**}p < 0.01$; Mann-Whitney test).

unchanged when compared with the control (Fig. 4 B, C and F). The mRNA levels of GST were upregulated significantly in comparison with the control. The GST expression levels followed a concentration-dependent pattern, i.e. 1 µg/L Pb (2.5-fold change), 10 µg/L Pb (4.9-fold change), 25 µg/L Pb (8.0-fold change), 50 µg/L Pb (7.9-fold change) and 100 µg/L Pb (7.6-fold change), respectively (Fig. 4D). Furthermore, Pb exposure induced significant upregulation of HO-1 mRNA levels at 100 µg/L Pb with 2.2-fold change (Fig. 4E).

3.6. Lead exposure affected mRNA expression of pro-apoptotic and anti-apoptotic enzymes

Mitochondrial related electron transport reactive oxygen species (ROS) associated oxidative stress response enzymes namely uncoupling protein-2 (*Ucp-2*) and cytochrome *c* oxidase subunit I (*CoxI*) mRNA levels were investigated. Lead exposure did not induce *Ucp-2* mRNA expression changes across the exposed groups (Fig. 5A). On the other hand, *CoxI* mRNA levels were significantly upregulated across all the exposed groups with 7.8-fold change (1 µg/L Pb), 5.9-fold change (10 µg/L Pb), 5.9-fold change (25 µg/L Pb), 5.4-fold change (50 µg/L Pb) and 7.3-fold change (100 µg/L Pb) compared to the control (Fig. 5B.)

The expression of the mRNA levels of the pro-apoptotic encoding protein tumour protein p53 (*TP53*) was significantly downregulated across all the exposure groups except in the 100 µg/L treatment when compared to the control (Fig. 5C). The B cell lymphoma-2 (*Bcl-2*) mRNA expression was significantly upregulated with 2-fold change (1 µg/L Pb), 1.8-fold change (10 µg/L Pb) and 1.7-fold change (25 µg/L Pb) when compared to the control. A significant downregulation of *TP53* mRNA expression with 0.8-fold at 50 µg/L Pb concentration was observed (Fig. 5D).

4. Discussion

The current study sheds light on the negative effects of the

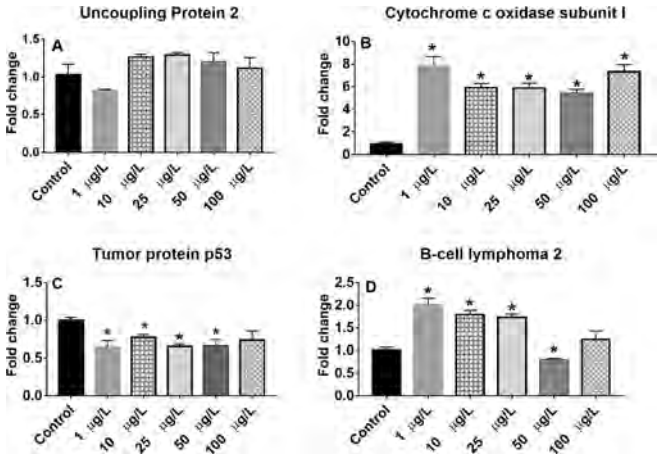

Fig. 5. Expression of mRNA of mitochondrial related enzymes (A, B, C and D) in the pooled samples ($n = 4$). Values normalized against Tubulin alpha-1A (used as house-keeping gene) and represent the mean mRNA expression value ± SEM (n = 4 pooled samples) relative to those of the controls. The asterisk represents a statistically significant difference when compared with the controls ($^*p < 0.05$; Mann-Whitney test).

environmental Pb water levels including the permissible value of 50 µg/L that were reported by Nachiyunde et al. (2013) in Kabwe, Zambia on aquatic life. The permissible dissolved Pb in water Kabwe was comparable to the acute toxic criteria limit for dissolved Pb of 54.1 µg/L at a hardness of 85 mg/L (as $CaCO_3$) as set by the United States Environmental Protection Agency (USEPA) as recently reported by DeForest et al. (2017). However, regulatory institutions around the globe seem not to have common criteria for dissolved Pb in water to ensure good water quality to support aquatic life (Li et al., 2019). For instance, the action level for dissolved Pb in water delivered to users for public consumption according to the Comprehensive Environmental Response Compensation and Liability Act (CERCLA), USA is 15 µg/L (DeForest et al., 2017).

The present study showed that varying Pb concentrations induced toxicity in zebrafish embryos between 1 and 100 µg/L Pb. The deleterious effects of Pb exposure in the development and survival of zebrafish embryos were observed within environmentally relevant and regulatory Pb concentrations. Neuromuscular, cardiovascular and antioxidant system effects due to Pb exposure with similar to what has been reported in studies which had higher Pb concentrations (Chen et al., 2012; Zhao et al., 2019) are discussed.

In developmental toxicity studies involving zebrafish embryos, mortality and hatching of embryos are widely regarded as endpoints that influence the overall survival rate of zebrafish (Hallare et al., 2006). In this study, none of the surviving embryos failed to hatch at 72 hpf across all the exposed groups, pre-hatched embryo mortalities were observed with highest concentration having the highest percentage of the mortalties. All the mortalities were recorded between 24 and 72 hpf, a feature that was consistent with reports that indicated that the early embryonic stages after fertilization are more vulnerable to metal intoxication (Jezierska et al., 2009). The high permeability of the embryo membrane to metal ions and rapid organogenesis accounts for the high sensitivity and vulnerability of embryos during the early stages (Fraysse et al., 2006). The permeability of the embryo membrane or chorion imply that the concentration Pb in the exposure solution influences the level Pb ion that accumulates in the body of the embryo to cause residual toxicity. Although the mechanisms of accumulated Pb-induced toxicity in embryos may be complex, an indirect connection between survival rates and neuromuscular effects was observed in the present study suggesting Pb cumulative toxicity. For instance 50 and 100 µg/L Pb concentrations with larvae that had neuromuscular toxicity, the former that exhibited mild effects had 68% survival rate, and the latter with much pronounced effects had 52% survival rate.

Muscular twitching has been suggested as neuromuscular toxic effects of Pb (Van Den Avyle et al., 1989). In the present study, the 100 µg/L Pb group which had decreased embryo activity at 24 hpf had pronounced muscular twitching at 72 hpf suggestive of early onset of Pb-induced neuromuscular toxicity. Although altered spontaneous movements in zebrafish larvae have been reported at 1000 µg/L Pb (Chen et al., 2012), the neuromuscular toxicity being reported in our study at 50 µg/L Pb suggest that zebrafish embryos may be vulnerable to Pb-induced toxicity even in low Pb concentrations. The lack of the mature functional blood-brain barrier and rapid growth that incorporates Pb into cellular processes due to the high affinity of Pb^{2+} for Ca^{2+} dependent processes could be among the reasons low Pb concentrations in the present study elicited similar effects with studies that employed high Pb concentrations.

Lead induced cardiovascular toxicity was observed at 100 μg/L Pb level of exposure characterized by reduced heart rate and increased blood flow in the present study. These findings were in tandem with previously reported cardiovascular toxicity in zebrafish embryos exposed to much higher concentrations of Pb (3000, 6000 and 12,000 µg/L Pb) than our study (Yin et al., 2017). The reduced heart rate may be linked to the antagonism between Pb and Ca and the ability of Pb^{2+} ions to block calcium channels causing impaired Ca availability for optimum heart function (Mattos et al., 2017). The increase in blood flow observed in the 100 µg/L Pb exposed group corroborated evidence indicating that Pb may induce increased blood flow. Although the mechanisms that accounting for Pb-induced blood flow increase are complex, impaired nitric oxide system, inhibition of endothelial cell growth, oxidative stress and altered cellular Ca^{2+} tracking have been implicated in Pb-induced hypertension (ATSDR, 2019). Moreover, the Pb concentration at which the cardiovascular toxicity observed in the present study was close to the upper limit of the environmentally reported water Pb concentration (94 µg/L Pb) in Kabwe, Zambia (Nachiyunde et al., 2013).

Lead induced oxidative stress is one of the mechanisms by which Pb exposure induces toxicity in animals including fish (Kim and Kang, 2017). Therefore, mRNA expression of the antioxidant system and related genes were analyzed in the present study. The major antioxidant gene coding enzymes were dysregulated in the Pb exposed zebrafish larvae with the groups that showed cardiovascular and neuromuscular toxicity having enhanced dysregulation in some cases. For instance, catalase enzyme mRNA expression was downregulated in all exposed groups. Catalase enzyme gene downregulation is associated with the inhibition of catalase enzyme activity (Craig et al., 2007). Catalase offers cellular protection against oxidative damage due to its involvement in the detoxification and elimination of hydrogen peroxide generated from reactive oxygen species (Stancová et al., 2015). Hence the downregulation of the catalase transcripts observed in the current study could be a reflection of an overwhelmed antioxidant response due to excessive generation of non-radical hydrogen peroxide molecules. The other two key antioxidant encoding genes, heme oxygenase- 1 (*HO-1*) and glutathione-S-transferase (*GST*) mRNA expression levels were upregulated with the latter following a Pb concentration response. The *GST* enzyme is a vital metabolic and antioxidant enzyme whose gene expression pattern suggests an enhanced response in an attempt to decrease Pb toxicity through conjugation of Pb to glutathione to facilitate elimination (He et al., 2011).

It has been elucidated that ROS generation is linked to the activity of the mitochondria through the electron transport chain (Flora et al., 2012). Thus, we analyzed vital mitochondrial cytochrome *c* oxidase I (*CoxI*) and uncoupling protein-2 (*Ucp-2*) enzymes gene expression levels. *CoxI* is a terminal electron acceptor of the mitochondrial respiratory chain related to the generation of superoxide anion and *Ucp-2* mitigates against the impact of mitochondrial superoxide anion (Sohal et al., 2008). In the present study, *CoxI* was upregulated across all exposed groups without an accompanying upregulation of *Ucp-2* mRNA expression. This was in contrast to previous findings in larval zebrafish

exposed to acute environmentally relevant Pb levels (Kataba et al., 2020). The difference observed in the expression of the *CoxI* and *Ucp-2* mRNA expression in Kataba et al. (2020) and the current study may be due to the differences in the Pb exposure duration as well as the age of the zebrafish at the beginning of the exposure. The younger, the fish, the more susceptible it is to waterborne toxicants (Jezierska et al., 2009). This upregulation of *CoxI* without the concurrent upregulation of *Ucp-2* may explain the Pb-induced toxic effects observed in zebrafish embryos as *Ucp-2* activity tend to neutralize the impact of *CoxI* (Kataba et al., 2020). Moreover, increased superoxide anion and disruption of the *Ucp-2* levels have been linked to neuronal oxidative damages and sustained neuronal oxidative damage causes neuronal apoptosis (Wu et al., 2010). The neuronal apoptosis may manifest as neurotoxicity a probable mechanism behind the neuromuscular toxicity observed in the present study.

In aquatic organisms, oxidative stress has been linked to enhanced apoptosis (Livingstone, 2001). In the current study, we used the B-cell lymphoma 2 (*Bcl-2*) and tumour protein p53 (*TP53*) genes as transcriptional markers related to the apoptosis signaling processes (Jin et al., 2011). The *Bcl-2* mRNA expression levels in Pb exposure concentrations less than 50 μg/L (1–25 μg/L Pb) were upregulated and downregulated in Pb exposure concentrations equal to or greater than 50 μg/L. The upregulation of the Bcl-2 mRNA expression in Pb concentrations less than 50 μg/L Pb could be an indirect compensatory and protective response against Pb-induced apoptotic elements (Bonneau et al., 2013). Whereas, the downregulation of *Bcl-2* mRNA expression levels at 50 μg/L Pb could be a reflection of an exhausted Bcl-2 protein compensatory mechanism due to the high presence of Pb (Jin et al., 2010). On the other hand, Pb exposure seemed to have triggered the downregulation of *TP53* mRNA expression across exposed groups. The *Bcl-2* gene encodes for protein that is a member of the Bcl-2 family that regulates, suppresses and prevents aberrant apoptosis (Jin et al., 2010). The prevention is achieved by neutralization of the pro-apoptotic proteins (p53) by Bcl-2 proteins (Pyati et al., 2007). Notwithstanding the striking non-Pb concentration-dependent mRNA expression of the anti-apoptosis and proapoptosis genes, the mRNA expression pattern of these genes suggested that apoptosis could have been among the possible contributors to the neuromuscular twitching observed. Moreover, the significant downregulation of anti-apoptotic and pro-apoptotic gene transcripts at 50 μg/L Pb and non-significant downregulation at 100 μg/L Pb reflects a hormetic response, a feature that has been reported in larval zebrafish (Kataba et al., 2020). Overall, the study has demonstrated the deleterious effects of the water Pb levels in Kabwe on zebrafish embryos and larvae including cardiovascular and neuromuscular toxicity.

There are limitations to our study. The lack of accompanying enzymatic assays and non-enzymatic such as lipid peroxidase or protein carbonyl compound analyses and antioxidant tissue levels analyses are among the major limitations to support the gene expression effects thus observed (Mccarthy and Smyth, 2009). The non-retrieval of the embryo activity data at 24 hpf for 25 and 50 μg/L Pb poses another limitation on the comparison of the embryo activity and neuromuscular toxicity at these levels of exposure. Furthermore, in the light of anti-apoptotic and pro-apoptotic genes, mRNA dysregulation observed without accompanying apoptosis assays such as acridine orange staining limits the interpretation of our results. Notwithstanding, the present study has demonstrated that environmentally relevant Pb levels could affect the overall survival rates of zebrafish embryos through or accompanied by cardiovascular, neuromuscular, and antioxidant system aberrations.

5. Conclusions

Lead dissolved in water poses a threat to aquatic life even in lowest quantifiable amounts. Water Pb concentrations that are below and within the “permissible limit” (10 to 50 μg/L Pb) could be detrimental to zebrafish life especially at early developmental stages as evidenced by embryonic coagulation linked mortalities. Furthermore, our FET test concentrations provided additional insights on the Kabwe Pb water concentrations. Lead water concentrations of 50 to above 100 μg/L could even be more detrimental to developing fish embryos with a myriad Pb linked toxicities. Embryonic activity aberrations, cardiovascular toxicity (reduced heart rate, increased blood flow activity), oxidative stress system imbalance, antiapoptotic and proapoptotic balance and the neuromuscular toxicity (muscle twitching) are among the deleterious effects of environmentally relevant Pb levels. Further investigations on the impact of environmentally relevant water Pb concentrations and the permissible (regulatory) water Pb levels on reproduction, development and health of locally available fish species are needed.

6. Ethical statement

All experimental procedures were done with the due approval by the AnimCare animal research ethics committee (ethics approval number: NWU-00269-16-A5) at the North-West University. All animals were maintained, and procedures carried out in adherence with the code of ethics in research, training and testing of drugs in South Africa and complied with national legislation (NHREC reg. Number AREC-130913-015).

Supplementary data to this article can be found online at https://doi.org/10.1016/j.cbpc.2021.109215.

CRediT authorship contribution statement

Andrew Kataba: Conceptualization, Data curation, Formal analysis, Methodology, Writing – original draft, Writing – review & editing. **Tarryn L. Botha:** Validation, Methodology, Software, Writing – review & editing. **Shouta M.M. Nakayama:** Funding acquisition, Resources, Writing – review & editing. **Yared B. Yohannes:** Validation, Methodology, Software, Writing – review & editing. **Yoshinori Ikenaka:** Funding acquisition, Resources, Writing – review & editing. **Victor Wepener:** Funding acquisition, Resources, Supervision, Writing – review & editing. **Mayumi Ishizuka:** Funding acquisition, Resources, Supervision, Writing – review & editing.

Declaration of competing interest

The authors declare that they have no known competing financial interests or personal relationships that could have appeared to influence the work reported in this paper.

Acknowledgements

The chemical analyses were technically supported by Mr. Takahiro Ichise and Ms. Nagisa Hirano.at Hokkaido University, Faculty of Veterinary Medicine and; Dr. Hannes Erasmus at the North-West University, South Africa. This work was supported by the Grants-in-Aid for Scientific Research from the Ministry of Education, Culture, Sports, Science and Technology of Japan awarded to M. Ishizuka (No. 16H0177906, 18K1984708, 18KK028708, 21H02351), Ikenaka (18H0413208), and S. M.M. Nakayama (No. 17KK0009 and 20K20633). This work was also supported by the foundation of JSPS Bilateral Open Partnership Joint Research Projects (JPJSBP120209902; SMMN). This work was also supported by JSPS CORE to CORE program (MI), The Japan Prize Foundation; and Hokkaido University’s SOUSEI Support Program for Young Researchers in FY2020 (SMMN); Hokkaido University Specific Research Projects (MI). This research was also supported by JST/JICA, SATREPS (Science and Technology Research Partnership for Sustainable Development; No. JPMJSA1501) and aXis (Accelerating Social Implementation for SDGs Achievement; No. JPMJAS2001) funded by JST as well as Program for supporting introduction of the new sharing system (JPMXS0420100619) and the Hokkaido University Faculty of

Veterinary Medicine Wise/Leading Travel and Subsistence grant.

Bioassays were conducted in the National Aquatic Bioassay Facility at North-West University, South Africa (NRF Grant UID99024). This is publication number 555 of the Water Research Group, North-West University.

References

ATSDR, A.for T.S.and D.R., 2019. Toxicological Profile for lead (draft for public comment). ATSDR's Toxicol. Profiles. https://doi.org/10.1201/9781420061888_ch106.

Bonneau, B., Prudent, J., Popgeorgiev, N., Gillet, G., 2013. Non-apoptotic roles of Bcl-2 family: the calcium connection. Biochim. Biophys. Acta - Mol. Cell Res. 1833, 1755–1765. https://doi.org/10.1016/j.bbamcr.2013.01.021.

Botha, T.L., James, T.E., Wepener, V., 2015. Comparative aquatic toxicity of gold nanoparticles and ionic gold using a species sensitivity distribution approach. J. Nanomater. 2015 https://doi.org/10.1155/2015/986902.

Busquet, F., Strecker, R., Rawlings, J.M., Belanger, S.E., Braunbeck, T., Carr, G.J., Cenijn, P., Fochtman, P., Gourmelon, A., Hübler, N., Kleensang, A., Knöbel, M., Kussatz, C., Legler, J., Lillicrap, A., Martínez-jerónimo, F., Polleichtner, C., Rzodeczko, H., Salinas, E., Schneider, K.E., Scholz, S., Brandhof, E.Van, Den, Ven, Van Der, L.T.M., Walter-rohde, S., Weigt, S., Witters, H., Halder, M., 2014. OECD validation study to assess intra- and inter-laboratory reproducibility of the zebrafish embryo toxicity test for acute aquatic toxicity testing. Regul. Toxicol. Pharmacol. 69, 496–511. https://doi.org/10.1016/j.yrtph.2014.05.018.

Campel, I., 2007. Chi-squared and Fisher-Irwin tests of two-by-two tables with small sample recommendations. Stat. Med. 26, 3661–3675. https://doi.org/10.1002/sim.2832.

Chen, J., Chen, Y., Liu, W., Bai, C., Liu, X., Liu, K., Li, R., Zhu, J.H., Huang, C., 2012. Developmental lead acetate exposure induces embryonic toxicity and memory deficit in adult zebrafish. Neurotoxicol. Teratol. 34, 581–586. https://doi.org/10.1016/j.ntt.2012.09.001.

Craig, P.M., Wood, C.M., Mcclelland, G.B., 2007. Oxidative stress response and gene expression with acute copper exposure in zebrafish (Danio rerio). Am. J. Phys. Regul. Integr. Comp. Phys. 5, 1882–1892. https://doi.org/10.1152/ajpregu.00383.2007.

DeForest, D.K., Santore, R.C., Ryan, A.C., Church, B.G., Chowdry, J.M., Brix, Kevin, V., 2017. Development of biotic ligand model–based freshwater aquatic life criteria for lead following us environmental protection agency guidelines. Environ. Toxicol. Chem. 36, 2965–2973. https://doi.org/10.1002/etc.3861.

Flora, G., Gupta, D., Tiwari, A., 2012. Toxicity of lead: a review with recent updates. Interdiscip. Toxicol. 5, 47–58. https://doi.org/10.2478/v10102-012-0009-2.

Fraysse, B., Mons, R., Garric, J., 2006. Development of a zebrafish 4-day embryo-larval bioassay to assess toxicity of chemicals. Ecotoxicol. Environ. Saf. 63, 253–267. https://doi.org/10.1016/j.ecoenv.2004.10.015.

Hailegnaw, B., Kirmayer, S., Edri, E., Hodes, G., Cahen, D., 2015. Rain on methylammonium Lead iodide based perovskites: possible environmental E ff ects of perovskite solar cells. J. Phys. Chem. https://doi.org/10.1021/acs.jpclett.5b00504.

Hallare, A., Nagel, K., Köhler, H.R., Triebskorn, R., 2006. Comparative embryotoxicity and proteotoxicity of three carrier solvents to zebrafish (Danio rerio) embryos. Ecotoxicol. Environ. Saf. 63, 378–388. https://doi.org/10.1016/j.ecoenv.2005.07.006.

He, X., Nie, X., Wang, Z., Cheng, Z., Li, K., Li, G., Hung Wong, M., Liang, X., Tsui, M.T.K., 2011. Assessment of typical pollutants in waterborne by combining active biomonitoring and integrated biomarkers response. Chemosphere 84, 1422–1431. https://doi.org/10.1016/j.chemosphere.2011.04.054.

Hill, A.J., Teraoka, H., Heideman, W., Peterson, R.E., 2005. Zebrafish as a model vertebrate for investigating chemical toxicity. Toxicol. Sci. 86, 6–19. https://doi.org/10.1093/toxsci/kfi110.

Jezierska, B., Ługowska, K., Witeska, M., 2009. The effects of heavy metals on embryonic development of fish (a review). Fish Physiol. Biochem. 35, 625–640. https://doi.org/10.1007/s10695-008-9284-4.

Jin, Y., Zhang, X., Shu, L., Chen, L., Sun, L., Qian, H., Liu, W., Fu, Z., 2010. Oxidative stress response and gene expression with atrazine exposure in adult female zebrafish (Danio rerio). Chemosphere 78, 846–852. https://doi.org/10.1016/j.chemosphere.2009.11.044.

Jin, Y., Zheng, S., Pu, Y., Shu, L., Sun, L., Liu, W., Fu, Z., 2011. Cypermethrin has the potential to induce hepatic oxidative stress, DNA damage and apoptosis in adult zebrafish (Danio rerio). Chemosphere 82, 398–404. https://doi.org/10.1016/j.chemosphere.2010.09.072.

Kataba, A., Botha, T.L., Nakayama, S.M.M., Yohannes, Y.B., Ikenaka, Y., Wepener, V., Ishizuka, M., 2020. Acute exposure to environmentally relevant lead levels induces oxidative stress and neurobehavioral alterations in larval zebrafish (Danio rerio). Aquat. Toxicol. 227, 105607 https://doi.org/10.1016/j.aquatox.2020.105607.

Kim, J., Kang, J., 2017. Chemosphere effects of sub-chronic exposure to lead (pb) and ascorbic acid in juvenile rock fi sh : antioxidant responses, MT gene expression, and neurotransmitters. Chemosphere 171, 520–527. https://doi.org/10.1016/j.chemosphere.2016.12.094.

Kimmel, C.B., Ballard, W.W., Kimmel, S.R., Ullmann, B., Schilling, T.F., 1995. Stages of embryonic development of the zebrafish. Dev. Dyn. 203, 253–310. https://doi.org/10.1002/aja.1002030302.

Komárek, M., Chrastný, V., Mihaljevi, M., 2008. Lead isotopes in environmental sciences : a review. Environ. Int. 34, 562–577. https://doi.org/10.1016/j.envint.2007.10.005.

Li, X., Kong, H., Ji, X., Gao, Y., Jin, M., 2019. Zebrafish behavioral phenomics applied for phenotyping aquatic neurotoxicity induced by lead contaminants of environmentally relevant level. Chemosphere 224, 445–454. https://doi.org/10.1016/j.chemosphere.2019.02.174.

Livingstone, D.R., 2001. Contaminant-stimulated reactive oxygen species production and oxidative damage in aquatic organisms. Mar. Pollut. Bull. 42, 656–666. https://doi.org/10.1016/S0025-326X(01)00060-1.

Mattos, G.F.De, Costa, C., Savio, F., Alonso, M., Nicolson, G.L., 2017. Lead poisoning: Acute exposure of the heart to lead ions promotes changes in cardiac function and Cav1. 2 ion channels. Biophys. Rev. 807, 825. https://doi.org/10.1007/s12551-017-0303-5.

Mccarthy, D.J., Smyth, G.K., 2009. Testing significance relative to a fold-change threshold is a TREAT. Bioinformatics 25, 765–771. https://doi.org/10.1093/bioinformatics/btp053.

Nachiyunde, K., Ikeda, H., Okuda, T., Nishijima, W., 2013. Assessment of dissolved heavy metal pollution in five provinces of Zambia. J. Environ. Prot. (Irvine, Calif) 04, 80–85. https://doi.org/10.4236/jep.2013.41b015.

Nakayama, Shouta M.M., Ikenaka, Y., Hamada, K., Muzandu, K., Choongo, K., Teraoka, H., Mizuno, N., Ishizuka, M., 2011. Metal and metalloid contamination in roadside soil and wild rats around a Pb-Zn mine in Kabwe, Zambia. Environ. Pollut. 159, 175–181. https://doi.org/10.1016/j.envpol.2010.09.007.

Pyati, U.J., Look, A.T., Hammerschmidt, M., 2007. Zebrafish as a powerful vertebrate model system for in vivo studies of cell death. Semin. Cancer Biol. 17, 154–165. https://doi.org/10.1016/j.semcancer.2006.11.007.

Sfakianakis, D.G., Renieri, E., Kentouri, M., Tsatsakis, A.M., 2015. Effect of heavy metals on fish larvae deformities: a review. Environ. Res. 137, 246–255. https://doi.org/10.1016/j.envres.2014.12.014.

Sohal, R.S., Toroser, D., Brégère, C., Mockett, R.J., Orr, W.C., 2008. Age-related decrease in expression of mitochondrial DNA encoded subunits of cytochrome c oxidase in Drosophila melanogaster. Mech. Ageing Dev. 129, 558–561. https://doi.org/10.1016/j.mad.2008.04.006.

Stancová, V., Ziková, A., Svobodová, Z., Kloas, W., 2015. Effects of the non-steroidal anti-inflammatory drug(NSAID) naproxen on gene expression of antioxidant enzymes in zebrafish (Danio rerio). Environ. Toxicol. Pharmacol. 40, 343–348. https://doi.org/10.1016/j.etap.2015.07.009.

Toyomaki, H., Yabe, J., Nakayama, S.M.M., Yohannes, Y.B., Muzandu, K., Liazambi, A., Ikenaka, Y., Kuritani, T., Nakagawa, M., Ishizuka, M., 2020. Factors associated with lead (Pb) exposure on dogs around a Pb mining area, Kabwe, Zambia. Chemosphere 247, 125884. https://doi.org/10.1016/j.chemosphere.2020.125884.

Van Den Avyle, M.J., Garvick, S.J., Blazer, V.S., Hamilton, S.J., Brumbaugh, W.G., 1989. Skeletal deformities in smallmouth bass, Micropterus dolomieui, from southern appalachian reservoirs. Arch. Environ. Contam. Toxicol. 18, 688–696. https://doi.org/10.1007/BF01225007.

Wu, Z., Zhao, Y., Zhao, B., 2010. Superoxide anion, uncoupling proteins and Alzheimer's disease. J. Clin. Biochem. Nutr. 46, 187–194. https://doi.org/10.3164/jcbn.09-104-2.

Yabe, J., Nakayama, S.M.M., Ikenaka, Y., Muzandu, K., Ishizuka, M., Umemura, T., 2011. Uptake of lead, cadmium, and other metals in the liver and kidneys of cattle near a lead-zinc mine in Kabwe, Zambia. Environ. Toxicol. Chem. 30, 1892–1897. https://doi.org/10.1002/etc.580.

Yabe, J., Nakayama, S.M.M., Ikenaka, Y., Muzandu, K., Choongo, K., Mainda, G., Kabeta, M., Ishizuka, M., Umemura, T., 2013. Metal distribution in tissues of free-range chickens near a lead-zinc mine in Kabwe, Zambia. Environ. Toxicol. Chem. 32, 189–192. https://doi.org/10.1002/etc.2029.

Yabe, J., Nakayama, S.M.M., Ikenaka, Y., Yohannes, Y.B., Bortey-Sam, N., Oroszlany, B., Muzandu, K., Choongo, K., Kabalo, A.N., Ntapisha, J., Mweene, A., Umemura, T., Ishizuka, M., 2015. Lead poisoning in children from townships in the vicinity of a lead-zinc mine in Kabwe, Zambia. Chemosphere 119, 941–947. https://doi.org/10.1016/j.chemosphere.2014.09.028.

Yabe, J., Nakayama, S.M.M., Ikenaka, Y., Yohannes, Y.B., Bortey-sam, N., Nketani, A., Ntapisha, J., Mizukawa, H., Umemura, T., Ishizuka, M., 2018. Chemosphere Lead and cadmium excretion in feces and urine of children from polluted townships near a lead-zinc mine in Kabwe, Zambia. Chemosphere 202, 48–55. https://doi.org/10.1016/j.chemosphere.2018.03.079.

Yabe, J., Nakayama, S.M., Nakata, H., Toyomaki, H., Yohannes, Y.B., Muzandu, K., Kataba, A., Zyambo, G., Hiwatari, M., Narita, D., Yamada, D., Hangoma, P., Munyinda, N.S., Mufune, T., Ikenaka, Y., Choongo, K., Ishizuka, M., 2020. Current trends of blood lead levels, distribution patterns and exposure variations among household members in Kabwe, Zambia. Chemosphere 243, 125412. https://doi.org/10.1016/j.chemosphere.2019.125412.

Yin, J., Wang, A.P., Li, W.F., Shi, R., Jin, H.T., Wei, J.F., 2017. Sensitive biomarkers identification for differentiating cd and pb induced toxicity on zebrafish embryos. Environ. Toxicol. Pharmacol. 56, 340–349. https://doi.org/10.1016/j.etap.2017.10.010.

Zhao, J., Zhang, Q., Zhang, B., Xu, T., Yin, D., Gu, W., Bai, J., 2019. Developmental exposure to lead at environmentally relevant concentrations impaired neurobehavior and NMDAR-dependent BDNF signaling in zebrafish larvae. Environ. Pollut. 113627 https://doi.org/10.1016/j.envpol.2019.113627.

Chemosphere 144 (2016) 1365–1371

Contents lists available at ScienceDirect

Chemosphere

journal homepage: www.elsevier.com/locate/chemosphere

Distribution and health risk assessment of organochlorine pesticides (OCPs) residue in edible cattle tissues from northeastern part of Egypt: High accumulation level of OCPs in tongue

Abdallah Fikry A. Mahmoud[a,b], Yoshinori Ikenaka[b,c], Yared B. Yohannes[b], Wageh S. Darwish[a], Elsaid A. Eldaly[a], Alaa Eldin M.A. Morshdy[a], Shouta M.M. Nakayama[b], Hazuki Mizukawa[d], Mayumi Ishizuka[b,*]

[a] Food Control Department, Faculty of Veterinary Medicine, Zagazig University, Zagazig, 44519, Egypt
[b] Laboratory of Toxicology, Department of Environmental Veterinary Sciences, Graduate School of Veterinary Medicine, Hokkaido University, Kita 18, Nishi 9, Kita-ku, Sapporo, 060-0818, Japan
[c] Water Research Group, Unit for Environmental Sciences and Management, North-West University, Potchefstroom, South Africa
[d] Department of Environmental Veterinary Science, Graduate School of Veterinary Medicine, Hokkaido University, N18, W9, Kita-ku, Sapporo, 060-0818, Japan

HIGHLIGHTS

- We measured OCPs in edible cattle tissues from Egypt.
- HCHs, DDTs, Drins, chlordanes, heptachlors, and HCB were investigated.
- HCHs were the predominant contaminant.
- EDIs of OCPs were significantly lower than ADIs.
- Hazard ratios of HCHs showed a potential health concern.

ARTICLE INFO

Article history:
Received 28 August 2014
Received in revised form 11 September 2015
Accepted 4 October 2015
Available online 23 October 2015

Handling editor: Andreas Sjodin

Keywords:
Organochlorine pesticides
Liver
Kidney
Tongue
Risk assessment
Egypt

ABSTRACT

Food consumption is an important route of human exposure to organochlorine pesticides (OCPs). In order to assess the potential human health risks associated with OCPs, edible cattle tissues (liver, kidney and tongue) were collected from three slaughter houses in Mansoura, Zagazig and Ismailia cities, Egypt. Levels of 22 OCPs such as hexachlorocyclohexanes (HCHs), dichlorodiphenyltrichloroethanes (DDTs), aldrin, dieldrin and endrin (Drins), chlordanes (CHLs), heptachlors (HPTs) and hexachlorobenzene (HCB) residues were investigated. Among the investigated OCPs, HCHs represented the most dominant group with high proportions of γ–HCH isomer (53–91% of total HCHs). Mansoura city had the highest OCPs contamination load ranged from 0.1 to 2827 ng g^{-1} lw (lipid weight). Surprisingly, tongue samples collected from Mansoura showed the highest concentration of HCHs (448 ng g^{-1} lw) in comparison to liver (152 ng g^{-1} lw) and kidney (266 ng g^{-1} lw). Generally, contamination pattern of OCPs was in the order of HCHs > Drins > CHLs > DDTs ≅ HCB and HPTs. Estimated daily intakes (EDIs) through dietary consumption of cattle tissues were lower than the recommended acceptable daily intakes (ADIs) established by FAO/WHO. However, the hazard ratios (HRs) based on cancer risk were greater than 1.0 for HCHs based on the average and 95th centile concentrations, indicating carcinogenic effects to consumers through cattle tissues consumption.

1. Introduction

Organochlorine pesticides (OCPs) have been produced and used for agricultural and industrial purposes for a long time and on a large scale throughout the world because of exceptional

* Corresponding author.
E-mail address: ishizum@vetmed.hokudai.ac.jp (M. Ishizuka).

http://dx.doi.org/10.1016/j.chemosphere.2015.10.016
0045-6535/

insecticidal and fungicidal properties (Xu et al., 2010). OCPs have emerging environmental issues and received considerable attention during the past decades because of their persistence, long-range atmospheric transport, bioaccumulation ability and potential toxicity (El-Shahawi et al., 2010). These chemicals tend to bioconcentrate and bio-magnify in the food chains, causing a variety of reproductive, carcinogenic, immunological, neurological and other adverse effects for both animals and humans (Kalyoncu et al., 2009).

Egypt is a large agricultural country. Agricultural activities account for 28% of total national income, and nearly half of the country's work force is dependent on the agricultural subsector for its livelihood. An increase in environmental contamination by various chemicals such as OCPs is anticipated along the Nile Delta, which is referred to as "Green Lungs of Egypt" (Mansour, 2004). Furthermore, Egypt is rapidly industrializing and is using chemicals extensively in a wide spectrum of industrial sectors. The reported major OCPs used in Egypt during a 30-year period were 45,000 Mt (metric tons) of toxaphene (1955–1961), endrin 10,500 Mt (1961–1981), DDT 13,500 Mt (1952–1971) and lindane 11,300 Mt (1952–1978), with the continuous shifting from one compound to another (El-Sebae et al., 1993). Consequently, pesticides residues in water, plants and grasses may be ingested by herbivorous animals and eventually find their way into tissues (WHO, 1990). Thus, data about presence and distribution of organic contaminants in food are of paramount importance not only for ecological considerations, but also in terms of human health.

The main objective of this study was to investigate the accumulation levels of OCPs in cattle liver, kidney, and tongue tissues collected from Mansoura, Zagazig and Ismailia cities, and to assess the potential risks to human health posed through dietary consumption of the tissues.

2. Materials and methods

2.1. Study area and sample collection

Tissue samples were collected from Mansoura, Zagazig and Ismailia, in the northeastern part of Egypt. The study focused on this part because majority of 85 million inhabitants of Egypt live along the narrow green strip of land beside the River Nile, and its northern Delta around the capital, Cairo. Mansoura and Zagazig cities are close to Nile Delta, where agricultural activities, raising of farm animals and industries are predominant. While Ismailia is a desert area located near the Delta but with low agricultural and industrial activities. Between 1952 (beginning of pesticide evolution in Egypt) and 2003, about one million metric tons of commercial OCPs were used in the environment in this densely populated area (Mansour, 2004).

A total of 135 random samples of livers, kidneys and tongues were collected from male cattle (native breed) in three locations (45 samples for each location divided as 15 for each tissues) from October 2010 to June 2011 directly after inspection at Mansoura, Zagazig and Ismailia slaughter houses. The collected samples were shipped from Egypt to Japan with permission from the Ministries of Agriculture and animal quarantine departments of both countries. The collected samples (a slice taken from each tissue ~200 g) were stored in labeled plastic bags in a deep freezer unit (−20 °C) and then the frozen samples were transported to Japan for analysis.

2.2. Analysis of OCPs residues

Samples were processed and analyzed using a method described by (Yohannes et al., 2013) with minor modifications. Briefly, approximately 10 g sample was finely chopped with scissors, homogenized with anhydrous sodium sulfate and spiked with internal standard solution of 2,4,5,6-tetrachloro-*m*-xylene (TC*m*X). Extraction was carried out with 150 mL hexane:acetone (3:1, v/v) in a Soxhlet S306AK Automatic Extractor System (Gerhardt, Germany) in hot extraction mode for 6 h. The extract was concentrated to approximately 2 mL using rotary evaporator, which then diluted to 10 mL with hexane. The lipid content was determined gravimetrically using an aliquot (20%) of the extract, and the rest was subjected for clean-up process after solvent evaporation on a column filled with ~6 g activated florisil (activated at 150 °C overnight) and eluted with 100 mL hexane:dichloromethane (7:3, v/v). The eluate was concentrated on rotary evaporator, and then to near dryness under gentle nitrogen flow. The extract was redissolved in 100 μL n-decane and transferred to GC-vials for analysis.

Analysis of twenty two OCPs namely hexachlorocyclohexanes (HCHs; *α*−, *β*−, *γ*− and *δ*−HCH), dichlorodiphenyltrichloroethanes (DDTs; *o,p′*−DDT, *p,p′*−DDT, *o,p′*−DDE, *p,p′*−DDE, *o,p′*−DDD and *p,p′*−DDD), heptachlors (HPTs; heptachlor, *cis*− and *trans*−heptachlor epoxide), chlordanes (CHLs; *cis*− and *trans*−chlordane, *cis*− and *trans*−nonachlor and oxychlordane), Drins (aldrin, dieldrin and endrin) and hexachlorobenzene (HCB) were carried out with a gas-chromatography equipped with ^{63}Ni electron capture detector (GC-ECD: Shimadzu GC-2014, Kyoto, Japan). An ENV-8MS capillary column (30 m × 0.25 mm i.d., 0.25 μm film thickness) with splitless injection was used for separation. One μL of each sample was injected. The GC oven temperature was programmed from 100 °C for 1 min; ramp at 12 °C min^{-1} to 180 °C; 4 °C min^{-1} to 240 °C, and finally at 10 °C min^{-1} to 270 °C (5 min hold). The injector and detector temperatures were 250 °C and 310 °C, respectively. Helium at a flow rate of 1.0 mL min^{-1} was used as the carrier gas and nitrogen as the make-up gas at 45 mL min^{-1}.

2.3. Quality control and quality assurance (QA/QC)

OCPs were identified by comparing their retention time with reference to the corresponding standard using external standard method. Multi-level calibration curves were created for the quantification and linearity ($r^2 \geq 0.995$) was achieved. The quality control was performed by analysis of procedural blanks and spiked blanks for every 10 samples. Results showed that no target analytes were detected in blank samples and recoveries for spiked blanks ranged from 90% to 105%. To check for the validity of the method used for the extraction and analysis of the samples, the standard reference material, SRM 1947 (Lake Michigan Fish Tissue) was analyzed during the analysis of samples and recoveries ranged from 85 to 105% with RSD < 9% were obtained. The values reported here were not corrected for recoveries. Detection limits based on 3:1 signal to noise ratio (S/N) ranged from 0.08 to 0.12 ng g^{-1}, 0.04–0.20 ng g^{-1}, 0.08–0.15 ng g^{-1}, 0.10 ng g^{-1}, 0.06–0.15 ng g^{-1}, and 0.16 ng g^{-1} for HCHS, DDTs, HPTs, CHLs, Drins, and HCB respectively.

2.4. Human risk assessment

In the present study, risks of OCPs to human health were evaluated by using two main guidelines recommended by the (USEPA, 2012). Firstly, the estimated daily intakes (EDIs) of OCPs through bovine tissues consumption was calculated using Eq. (1):

$$EDI = Ca \times F \times Fi \quad (1)$$

where C_a is the average concentration of chemical contaminants (ng/g lipid weight), F is the fat content (%) in the tissue samples, and F_i is the average daily consumption rate of edible bovine tissues per person (g kg^{-1} bw d^{-1}). The body weight was assumed to

be 60 kg (WHO, 2009). The amount of regional daily consumption of cattle's liver, kidney and tongue was derived from the Global Environment Monitoring System/Food Contamination Monitoring and Assessment Programme (GEMS/Food Regional Diets) (WHO, 2003). The F_i was estimated at 0.1 g d^{-1} per person. The EDIs were compared with the acceptable daily intake (ADI) recommended by (FAO/WHO, 2009) to estimate the human health risk from food consumption.

Secondly, the non-cancer and cancer risk assessment were conducted using hazard ratio (HR). The hazard ratios were assessed by the Eq. (2). A hazard ratio greater than one indicates that there could be potential human health risks (Dougherty et al., 2000; Jiang et al., 2005).

$$\mathrm{HRs} = \frac{\mathrm{EDI}}{\mathrm{BMC}} \quad (2)$$

The benchmark concentration (BMC) for carcinogenic effects was derived from cancer slope factor (CSF) and for non-carcinogenic effects was based on the oral reference dose (RfD). Both cancer slope factors and the oral reference doses were obtained from the United States Environmental Protection Agency (USEPA) Integrated Risk Information System (IRIS) (http://www.epa.gov/IRIS/). A benchmark concentration represents a daily concentration below which there is a high probability of no adverse health effect. For carcinogenic effects, CBC (cancer benchmark concentration) calculated by using Eq. (3) below: where RL is the maximum acceptable risk level (1×10^{-6}), CSF is the cancer slope factor (mg kg^{-1} d^{-1}), BW is the average body weight (kg) and CR is the tissue consumption rate (g d^{-1}).

$$\mathrm{CBC} = \frac{(\mathrm{RL}/\mathrm{CSF}) \times \mathrm{BW}}{\mathrm{CR}} \quad (3)$$

To assess the potential cancer risk, HRs at two exposure concentrations were estimated. The mean and 95th percentile measured concentrations were used (Jiang et al., 2005; USEPA, 2009).

2.5. Statistical analysis

All the statistical analyses were done using JMP 9 (SAS Institute, Cary, NC, USA). The value below the limit of detection (LOD) was set to be zero (<LOD = 0). The data collected were presented as mean and standard deviation. Statistical differences in concentrations of organochlorines among the different areas and different tissues analyzed were evaluated by one-way analysis of variance (ANOVA) accompanied with Tukey–Kramer HSD test if necessary. All the statistical analyses were performed at the significance level of 0.05 ($p < 0.05$).

3. Results and discussion

3.1. Concentrations of OCPs residues

The average concentrations of OCPs in the edible cattle tissues based on lipid weight are summarized in Table 1. In general, the mean concentrations of OCPs ranged from 0.1 to 2827 ng g^{-1} lw in Mansoura, 1–2203 ng g^{-1} lw in Zagazig and ND to 852 ng g^{-1} lw in Ismailia. However, there was no significant differences for all OCPs concentrations among the sampling locations ($p > 0.05$). Among the OCPs analyzed, HCHs represented the predominant group. Relatively small concentrations of Drins, CHLs, DDTs, HCB and HPTs were found in different tissues samples from different locations. This dominance of HCHs in meat has also been documented in previous studies from Egypt (Sallam and Morshedy, 2008; Mahmoud et al., 2013) and from Jordan (Ahmad et al., 2010).

3.1.1. HCHs

The concentrations of HCHs in the cattle tissues samples analyzed were found at moderate levels by a large range in measured concentrations among different locations ranged from 1 to 2827 ng g^{-1} lw. The detection frequency of ΣHCHs in cattle tissue samples was 91% in Mansoura, 93% in Zagazig and 90% in Ismailia. The mean concentration of ΣHCHs varied among tissues samples, and was greatest in tongue samples in all three locations as they recorded 478 ng g^{-1} lw in Mansoura, 390 ng g^{-1} lw in Zagazig and 147 ng g^{-1} lw in Ismailia, respectively (Table 1). However, ΣHCHs concentration did not exhibit significant differences by locations ($p > 0.05$). The tongue samples from Mansoura city showed the highest content of HCHs as compared to kidney and liver. Similar finding was reported in the Egyptian buffalo meats (Mahmoud et al., 2013), which might be attributed to the fact that cattle chew their food several times in order to digest it properly, and spend nearly 8 h per day chewing their cud. According to Darwish et al. (2010), the tongues of camel showed the highest cytochrome P450 1A1 mRNA expression compared with the kidney and liver. Additionally, the farming system can potentially influence exposure because cattle can consume pesticides sorbed from the atmosphere and from soil onto grass surface (Lorber et al., 1994). The possible reasons for the presence of high level of HCHs in both Mansoura and Zagazig (mainly agricultural areas of high animal breeding activities), might be due to continuous usage of lindane (γ–HCH) for agricultural and public health purposes (Mansour, 2008). The higher concentrations of HCHs in Egypt could be explained by the shift in favor of HCHs over the other organochlorines for agricultural purposes due to its low cost and powerful elimination of pests, coupled with a lack of law enforcement (Nasr et al., 2009). The concentrations of HCHs in this study are comparable with the data reported for HCHs in meat from Mexico (Pardío et al., 2012) and Jordan (Ahmad et al., 2010), however higher levels were reported in meat from India (Kannan et al., 1992b).

HCHs are available in two formulations: technical HCH (mixture of different isomers) usually contains 55–80% α–HCH, 5–15% β–HCH, 8–15% γ–HCH and 2–16% δ–HCH (Lee et al., 2001), and technical lindane contains more than 99% γ–HCH. The proportions of HCH isomers in the examined tissues samples serves as evidence of the preferential usage of pure γ–HCH (lindane) than the technical mixture of HCHs (Fig. 1). Therefore, the predominance of γ–HCH in all tissues reflects the recent use of lindane around the investigated areas.

3.1.2. Other OCPs

In comparison to HCHs, other OCPs had lower concentrations (Table 1). For Drins, the detection frequency was 56% in Mansoura, 56% in Zagazig and 42% in Ismailia. Total Drins concentration exhibited significant differences among the tissues collected from Mansoura ($p < 0.05$). The tongue samples collected from Mansoura city showed the highest residual levels of Drins with a mean value (87 ng g^{-1} lw) followed by kidney (30 ng g^{-1} lw) and liver (16 ng g^{-1} lw), respectively. However, higher mean concentrations were seen for Zagazig samples as they recorded 32, 57 and 55 ng g^{-1} lw in liver, kidney and tongue. The residual contents of Drins were the lowest in the collected samples from Ismailia city with a mean value of 5, 7 and 6 ng g^{-1} lw in livers, kidneys and tongues, respectively. In addition, ΣDrins concentration did not exhibit significant differences among the tissues collected from Zagazig and Ismailia ($p > 0.05$). The mean concentration of Drins in the samples analyzed in this study is approximately similar to that reported in meat from Vietnam (Kannan et al., 1992a) and also in meat and tissues from Egypt (Sallam and Morshedy, 2008; Mahmoud et al., 2013). However, higher concentrations had been

Table 1
Concentrations [(Median) Mean ± SD (range) in ng g^{-1} lipid weight] of OCPs in the edible cattle tissues slaughtered in Egypt.

Locations/ Tissues	Lipid %	*n*	ΣHCHs	HCB	ΣHPTs	ΣDrins	ΣCHLs	ΣDDTs	ΣOCPs
Mansoura		*	91%	38%	38%	56%	56%	60%	
Liver	3.01 ± 0.19	15	(47.88) 152 ± 204 (4–549)	(ND) 3 ± 6 (0.4–20)	(ND) 4 ± 8 (0.1–28)	(ND) 16 ± 21[c] (3–58)	(2.27) 14 ± 32 (0.5–125)	(7.84) 19 ± 21 (1–72)	207 ± 292 (0.1–549)
Kidney	2.31 ± 0.14	15	(236.72) 266 ± 261 (6–881)	(ND) 22 ± 35 (6–105)	(ND) 6 ± 10 (5–29)	(6.68) 29 ± 38[b] (7–108)	(3.90) 13 ± 18 (4–56)	(5.11) 25 ± 32 (5–91)	351 ± 394 (4–881)
Tongue	2.18 ± 0.57	15	(142.81) 448 ± 759 (9–2827)	(ND) 21 ± 50 (4–162)	(ND) 18 ± 35 (1–101)	(42.12) 87 ± 104[a] (5–271)	(ND) 35 ± 52 (5–152)	(4) 70 ± 107 (4–308)	678 ± 1107 (1–2827)
Zagazig		*	93%	40%	58%	56%	44%	51%	
Liver	3.60 ± 0.54	15	(24.97) 124 ± 221 (1–841)	(ND) 7 ± 11 (ND) 7 ± 12	(6.32) 12 ± 22 (ND) 13 ± 18	(4.35) 32 ± 75 (17.4) 57 ± 122	(ND) 18 ± 48 (ND) 32 ± 55	(5.83) 15 ± 25 (8.1) 26 ± 49	208 ± 402 371 ± 753
Kidney	2.61 ± 0.24	15	(122.35) 235 ± 497 (5–1987)	(5–35) (ND) 6 ± 15	(7–52) (9.99) 23 ± 26	(6–470) (7.14) 55 ± 108	(8–194) (ND) 39 ± 89	(8–147) (ND) 35 ± 54	(5–1987) 547 ± 905
Tongue	2.23 ± 0.42	15	(99.77) 390 ± 615 (3–2203)	(3–54) 27%	(7–74) 0%	(7–364) 42%	(5–277) 36%	(8–134) 60%	(3–2203)
Ismailia		*	90%	(ND) 2 ± 3	(ND) ND	(ND) 5 ± 9	(ND) 4 ± 6	(7.62) 8 ± 7	72 ± 97
Liver	3.21 ± 0.15	15	(36.76) 53 ± 71 (3–292)	(3–10) (ND) 4 ± 8	(ND) ND	(2–33) (ND) 7 ± 14	(2–19) (ND) 9 ± 24	(3–22) (ND) 12 ± 19	(ND – 292) 144 ± 271
Kidney	2.42 ± 0.18	15	(47.98) 111 ± 207 (5–815)	(5–27) (ND) 6 ± 15	(ND) ND	(6–79) (ND) 6 ± 11	(6–90) (ND) 10 ± 24	(4–56) (7.95) 20 ± 17	(ND – 815) 189 ± 322
Tongue	2.07 ± 0.35	15	(10.77) 147 ± 255 (2–852)	(3–48)		(4–35)	(4–92)	(3–117)	(ND – 852)

n = number of samples * = detection frequency SD = Standard deviationND indicates not detected or results were lower than the limit of detection.Values with different letters (a, b, c) within a column are significantly different at $p < 0.05$ level (Tukey test is applied).

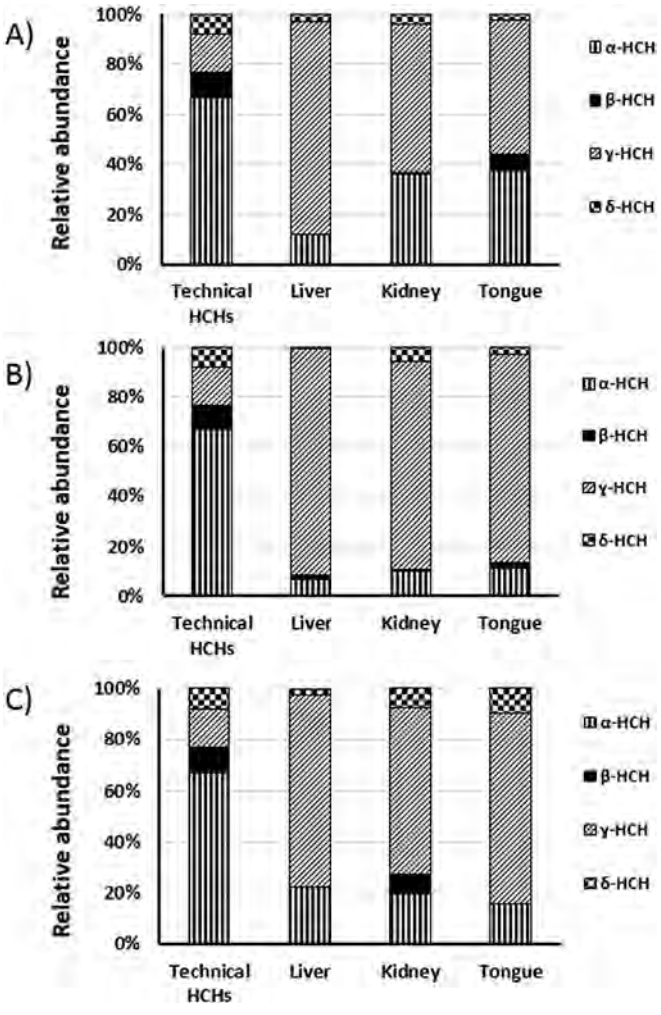

Fig. 1. Percentage of HCH isomers in technical product and cattle tissues in the investigated areas. (A- Mansoura; B- Zagazig and C-Ismailia).

detected in meat and tissues from Nigeria (Osibanjo and Adeyeye, 1997). Additionally, the concentration of aldrin found in this work is lower than the recommended maximal limit (200 ng g^{-1}) set by (FAO/WHO, 2008) and Egyptian Organization for Standardization (EOS, 1992b).

CHLs were detected in 56%, 44% and 36% of cattle tissue samples collected from Mansoura, Zagazig and Ismailia, respectively (Table 1). Tongue samples from both Zagazig (39 ng g^{-1} lw) and Mansoura (35 ng g^{-1} lw) revealed higher concentration of CHLs compared to Ismailia (10 ng g^{-1} lw). In the present study, concentrations of CHLs in the samples corresponds with that reported by (Sallam and Morshedy, 2008; Mahmoud et al., 2013). Higher concentration of chlordane was however reported in meat and fat from Australia (Kannan et al., 1994).

DDTs concentrations were found at low levels ranged from 6 to 147 ng g^{-1} lw, and 3–117 ng g^{-1} lw in Zagazig and Ismailia cities, respectively. Meanwhile, Mansoura city showed the highest DDTs residual level ranged from 1 to 308 ng g^{-1} lw. The detection frequency of DDTs in cattle tissues was 60% in Mansoura, 51% in Zagazig and 60% in Ismailia. The highest mean concentration of DDTs was found in tongue samples collected from Mansoura (70 ng g^{-1} lw) followed by Zagazig (35 ng g^{-1} lw), Ismailia (20 ng g^{-1} lw). Like most developing countries, cattle are raised on grass and crop residues. The differences in DDT levels among tissues analyzed could be related to feeding and farming system. Cattle raised outdoors on pasture could also ingest soil, which has been contaminated with pesticides deposited from the atmosphere (Sharpe and Livesey, 2005). Nonetheless, the residual contents of DDTs in the samples were below the maximal permissible levels (5 mg kg^{-1} fat) recommended by (FAO/WHO, 2008) and (EOS, 1992a). Additionally, the obtained results revealed that there has been no recent input of DDT into the environment. Our findings are comparable with those reported in meat and tissues from Mexico (Pardío et al., 2012). On the other hand, much higher DDT concentration had been detected in meat analyzed from Vietnam (Kannan et al., 1992a), Nigeria (Osibanjo and Adeyeye, 1997).

HCB and HPTs were detected in most of the samples analyzed but at lower concentrations. The residual HCB levels in the examined samples from Mansoura (15 ng g^{-1} lw) were the

highest, followed by Zagazig (7 ng g^{-1} lw), while the analyzed samples from Ismailia were the lowest (4 ng g^{-1} lw). The detection frequency of HCB was 38%, 40% and 27% in Mansoura, Zagazig and Ismailia, respectively. HPTs could not be detected in the collected samples from Ismailia but detected in 38% and 58% of the samples collected from Zagazig and Mansoura with a mean concentration value of 16 ng g^{-1} lw and 9 ng g^{-1} lw, respectively. The highest residual levels of HPTs were found in tongue samples from Zagazig (23 ng g^{-1} lw) and Mansoura (18 ng g^{-1} lw). The levels of HCB and HPTs in this study were comparable with previous studies in muscle and tissue samples from Egypt (Sallam and Morshedy, 2008; Mahmoud et al., 2013).

3.2. Human health risk assessment

3.2.1. Estimated daily intakes (EDIs) of OCPs through consumption of cattle tissues

The EDIs of OCPs through cattle liver, kidney and tongue consumption from Mansoura, Zagazig and Ismailia cities are summarized in Table 2. Among tissues analyzed, consumer exposure to pesticide residues through consumption of tongue showed the highest contributions to dietary exposure. Dietary intakes from Mansoura and Zagazig cities were higher than exposures from Ismailia city. The EDIs of all OCPs through consumption of tissues were far below the recommended ADIs (FAO/WHO, 2009), indicating minimum risk caused by these pollutants.

Generally, HCHs and DDTs represent the most common kinds of OCPs highly distributed in Egypt in the past several years (Mansour, 2008). Studies had been done in Egypt for determining OCPs residual levels in meat and meat products (Abou-Arab, 2002; Sallam and Morshedy, 2008) and in aquatic environment including water, sediment and fish (El-Mekkawi et al., 2009). These different studies revealed the dominance of HCHs and DDTs among the most frequently detectable pesticides in Egypt. Comparing the mean residual levels of ΣHCHs (1070 and 644 ng g^{-1} lw) and ΣDDTs (1327 and 702 ng g^{-1} lw) in liver and kidney tissues from Sharkia province (Sallam and Morshedy, 2008) with our study, a different trend was noted in last few years. The EDI of ΣHCHs in liver and kidney from the study by Sallam and Morshedy (2008) decreased from (7.68 and 5.55 ng kg^{-1} bw d^{-1}) to (0.74 and 1.02 ng kg^{-1} bw d^{-1}) in the present study representing a reduction of 10.4 and 5.4 times. Meanwhile ΣDDTs estimated intakes in liver and kidney (9.53 and 6.05 ng kg^{-1} bw d^{-1}) by Sallam and Morshedy (2008) decreased to (0.10 and 0.11 ng kg^{-1} bw d^{-1}) in the present study, which means a considerable decline (95.3% and 55% for liver and kidneys tissues, respectively) with respect to the past estimated intakes. The decrease of ΣHCH and ΣDDTs intakes may be related to restriction in using these pesticides in Egypt.

3.2.2. Risk characterization

The analyzed OCPs in the current study have both cancer and non-cancer risks (ATSDR, 2005). Two HRs based on average and 95th centile exposure concentration were estimated to assess the potential health risks for OCPs (Jiang et al., 2005). The oral RfD and CSF values obtained from (USEPA's Integrated Risk Information System (IRIS) (USEPA IRIS, 2012) and cancer benchmark concentrations for OCPs are summarized in Table 3. An evaluation of the non-cancer and cancer risks to human health associated with the consumption of cattle tissues was performed and the results were shown in Table 4. The HRs of non-cancer risk based on both percentile concentrations were all less than one. However, the HRs for cancer risk based on the average and 95th centile concentrations of HCHs were greater than one in all tissue samples from Mansoura, and Zagazig. Meanwhile, in Ismailia only 95th centile concentrations of HCHs were greater than one. The results suggested that daily exposure to these compounds due to consumption of cattle tissues could yield a lifetime cancer risk greater than one in a million inhabitants. The HRs of cancer risk to 95th centile daily consumption through the tongue from Mansoura for HCHs were 1.2 and 2.8 times higher than HRs estimated for exposures from Zagazig and Ismailia, respectively (Fig. 2). Similarly, cancer HR values greater than one were observed in bovine tissues from Veracruz, Mexico (Pardío et al., 2012). From these findings, there is increased risk for those who consume large quantities of cattle meat, especially tongue. The results indicate that HCHs are of particular concern because of their high levels, and they are still in use.

4. Conclusion

To the best of our knowledge, this is the first study reporting on the accumulation level of OCPs in different edible tissues of cattle from northeastern part of Egypt. Our results indicated the presence of HCHs, Drins, CHLs, DDTs, HPTs and HCB with varying concentrations among the studied areas. Interestingly, Mansoura city showed the highest contamination level while tongue samples showed the highest content of HCHs, Drins and DDTs. The Overall residual concentrations of OCPs detected in all of the samples analyzed from the three sites were below the respective maximal permissible limits stated by local or international organizations. The HRs based on non-cancer risk for all OCPs were less than one, while the HRs based on cancer risk of HCHs based on the average and 95th centile concentrations was greater than one. This indicated that there could be carcinogenic effects caused by these compounds through consumption of cattle tissue. However, in this study only liver, kidney and tongue tissues of cattle and some OCPs were investigated to assess the risk. The consumption of water, vegetable, animal meat, and the levels of other environmental pollutants were not considered. Therefore, the actual health risk for local people through dietary intake could be higher.

Table 2
Estimated Daily intakes (EDI) (ng kg^{-1} bw d^{-1}) of OCPs through cattle tissues consumption from different studied areas.

Compounds	ADIs[a]	Mansoura			Zagazig			Ismailia		
		Liver	Kidney	Tongue	Liver	Kidney	Tongue	Liver	Kidney	Tongue
HCHs	5000	0.76	1.02	1.63	0.74	1.02	1.45	0.28	0.45	0.51
HPTs	100	0.02	0.02	0.06	0.07	0.06	0.09	0.00	0.00	0.00
Drins	100	0.08	0.11	0.32	0.19	0.25	0.20	0.03	0.03	0.02
CHLs	500	0.07	0.05	0.13	0.11	0.14	0.14	0.02	0.04	0.03
HCB	600	0.02	0.08	0.08	0.04	0.03	0.02	0.01	0.02	0.02
DDTs	10,000	0.09	0.09	0.25	0.09	0.11	0.13	0.04	0.05	0.04

ADIs = Acceptable daily intakes (ng kg^{-1} d^{-1}).
[a] FAO/WHO, 2009.

Table 3
Reference values for organochlorine pesticides and benchmark concentrations for daily consumption of cattle tissues.

Contaminants	Oral reference dose (mg/kg day)[d]	Cancer slope factor (mg/kg day)$^{-1}$ [d]	Cancer benchmark concentration (ng/kg/day)[e]	Cancer benchmark concentration for liver, kidney and tongue (ng/kg/day)
HCHs[f]	3.0E−4[a]	1.1[a]	0.91	0.545
HCB[f]	8.0E−4	1.6	0.63	0.133
HPTs[f]	5.0E−4[b]	4.5[b]	0.22	0.035
Drins	3.0E−5[c]	17[c]	0.06	1.714
CHLs[f]	5.0E−4	0.35	2.86	0.375
DDTs[f]	5.0E−4	0.34	2.94	1.764

[a] For γ-HCH.
[b] For heptachlor.
[c] For aldrin.
[d] USEPA IRIS, 2012.
[e] Benchmark concentration for carcinogenic effects equals 10^{-6} divided by the cancer slope factor and represents the exposure concentration at which lifetime cancer risk is one in one million (Dougherty et al., 2000).
[f] Possibly carcinogenic to humans (group 2B) – based on (WHO, 2011).

Table 4
Non-cancer and Cancer Hazard Ratios (HRs) for daily consumption of OCPs in cattle tissues from studied areas.

Compound	Non-cancer HR			Cancer HR(Average concentrations)			Cancer HR(95th centile concentrations)		
	Liver	Kidney	Tongue	Liver	Kidney	Tongue	Liver	Kidney	Tongue
Mansoura									
HCHs	0.00254	0.00341	0.00543	1.40	1.88	2.99	4.72	5.15	12.00
HPTs	0.00004	0.00005	0.00013	0.14	0.17	0.48	0.58	0.80	2.64
CHLs	0.00014	0.00010	0.00025	0.04	0.03	0.07	0.17	0.11	0.27
HCB	0.00002	0.00010	0.00010	0.04	0.22	0.20	0.21	0.89	1.29
DDTs	0.00019	0.00019	0.00051	0.05	0.05	0.14	0.15	0.19	0.52
Zagazig									
HCHs	0.00247	0.00341	0.00482	1.36	1.87	2.65	5.10	6.47	10.74
HPTs	0.00015	0.00011	0.00017	0.55	0.43	0.65	1.99	1.67	1.81
CHLs	0.00022	0.00028	0.00029	0.06	0.08	0.08	0.26	0.32	0.53
HCB	0.00005	0.00004	0.00003	0.11	0.08	0.05	0.39	0.41	0.31
DDTs	0.00018	0.00023	0.00026	0.05	0.06	0.07	0.17	0.36	0.26
Ismailia									
HCHs	0.00095	0.00149	0.00169	0.52	0.82	0.93	1.56	3.20	4.25
HPTs	0.00000	0.00000	0.00000	0.00	0.00	0.00	0.00	0.00	0.00
CHLs	0.00004	0.00007	0.00007	0.01	0.02	0.02	0.04	0.11	0.09
HCB	0.00001	0.00002	0.00003	0.03	0.05	0.05	0.12	0.18	0.37
DDTs	0.00008	0.00010	0.00008	0.02	0.03	0.02	0.06	0.11	0.10

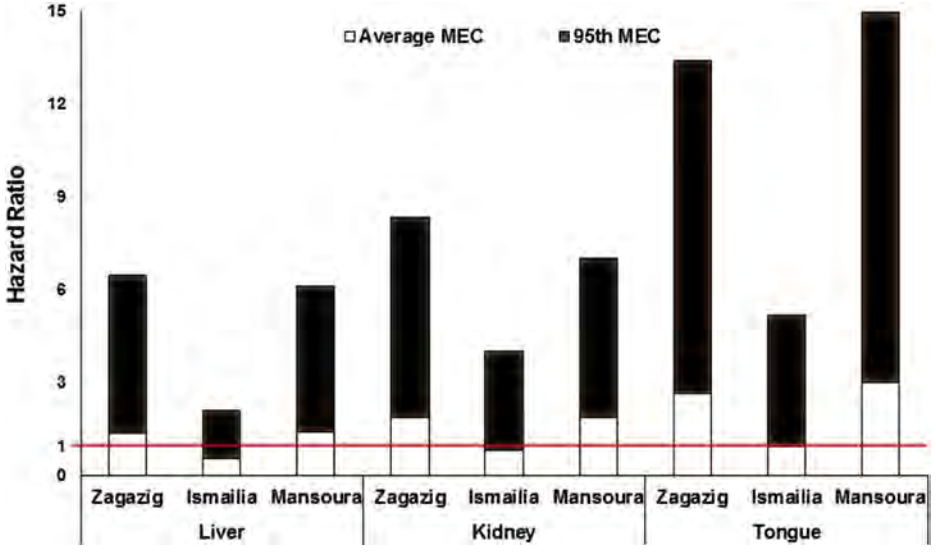

Fig. 2. Cancer hazard ratios for daily cattle tissues consumption of HCHs by people in the three studied areas, based on average and 95th centile cancer risk. MEC, measured concentration. (The horizontal red line represents the hazard ratio of >1, and any ratio higher than that indicates a risk). (For interpretation of the references to colour in this figure legend, the reader is referred to the web version of this article.)

Conflicts of interest

No conflict of interest among the authors.

Acknowledgments

This work was supported in part by Grants-in-Aid for Scientific Research from the Ministry of Education, Culture, Sports, Science and Technology of Japan, which was awarded to M Ishizuka (No. 24248056, 24405004 and Core to Core program) and from Ministry of Higher Education and Scientific Research, Egypt, which was awarded to Abdallah. F. A. Mahmoud. We gratefully acknowledge Dr. Mohamed A. M. Hussein, Dr. Waleed R. El-Ghareeb and Dr. Mohamed Tharwat El-Abbasy for their kind indeed help in every aspect during sample collection.

References

Abou-Arab, A.A., 2002. Degradation of organochlorine pesticides by meat starter in liquid media and fermented sausage. Food Chem. Toxicol. 40, 33–41.

Ahmad, R., Salem, N.M., Estaitieh, H., 2010. Occurrence of organochlorine pesticide residues in eggs, chicken and meat in Jordan. Chemosphere 78, 667–671.

ATSDR (Agency for Toxic Substances and Disease Registry), 2005. Toxicological Profiles of Toxic Substances. US Department of Health and Human Services. Public Health Service, Atlanta, GA Available at: http://www.atsdr.cdc.gov .

Darwish, W.S., Morshdy, A.E., Ikenaka, Y., Ibrahim, Z.S., Fujita, S., Ishizuka, M., 2010. Expression and sequence of CYP1A1 in camel. J. Vet. Med. Sci. 72, 221–224.

Dougherty, C.P., Henricks Holtz, S., Reinert, J.C., Panyacosit, L., Axelrad, D.A., Woodruff, T.J., 2000. Dietary exposures to food contaminants across the United States. Environ. Res. 84, 170–185.

El-Mekkawi, H., Diab, M., Zaki, M., Hassan, A., 2009. Determination of chlorinated organic pesticide residues in water, sediments, and fish from private fish farms at Abbassa and Sahl Al-Husainia, Shakia Governorate. Aust. J. Basic Appl. Sci. 3, 4376–4383.

El-Sebae, A.H., Abou Zeid, M., Saleh, M.A., 1993. Status and environmental impact of toxaphene in the third World—A case study of African agriculture. Chemosphere 27, 2063–2072.

El-Shahawi, M.S., Hamza, A., Bashammakh, A.S., Al-Saggaf, W.T., 2010. An overview on the accumulation, distribution, transformations, toxicity and analytical methods for the monitoring of persistent organic pollutants. Talanta 80, 1587–1597.

EOS., 1992a. Maximum Limits for Pesticide Residues in Meat Paper No. 2081. DDT. Egyptian Organization for Standardization and Quality Control, Cairo, Egypt.

EOS., 1992b. Maximum Limits for Pesticide Residues in Meat Paper No. 2078. Aldrin and dieldrin. Egyptian Organization for Standardization and Quality Control, Cairo, Egypt.

FAO/WHO, 2008. CODEX Alimentarius, pesticide residues in food. http://www.codexalimentarius.net.

FAO/WHO, 2009. Pesticide Residues in Food. Joint FAO/WHO Meeting on Pesticide Residues Report of the Joint meeting of the FAO Panel of Experts on Pesticide Residues in Food and the Environment and the WHO Core Assessment Group on Pesticide Residues. World Health Organization, Food and Agriculture Organization of the United Nations, Rome.

Jiang, Q.T., Lee, T.K., Chen, K., Wong, H.L., Zheng, J.S., Giesy, J.P., Lo, K.K., Yamashita, N., Lam, P.K., 2005. Human health risk assessment of organochlorines associated with fish consumption in a coastal city in China. Environ. Pollut. 136, 155–165.

Kalyoncu, L., Agca, I., Aktumsek, A., 2009. Some organochlorine pesticide residues in fish species in Konya, Turkey. Chemosphere 74, 885–889.

Kannan, K., Tanabe, S., Quynh, H.T., Hue, N.D., Tatsukawa, R., 1992a. Residue pattern and dietary intake of persistent organochlorine compounds in foodstuffs from Vietnam. Arch. Environ. Con. Tox 22, 367–374.

Kannan, K., Tanabe, S., Ramesh, A., Subramanian, A., Tatsukawa, R., 1992b. Persistent organochlorine residues in foodstuffs from India and their implications on human dietary exposure. J. Agr. Food. Chem. 40, 518–524.

Kannan, K., Tanabe, S., Williams, R.J., Tatsukawa, R., 1994. Persistent organochlorine residues in foodstuffs from Australia, Papua New Guinea and the Solomon Islands: contamination levels and human dietary exposure. Sci. Total Environ. 153, 29–49.

Lee, K.T., Tanabe, S., Koh, C.H., 2001. Distribution of organochlorine pesticides in sediments from Kyeonggi Bay and nearby areas, Korea. Environ. Pollut. 114, 207–213.

Lorber, M., Cleverly, D., Schaum, J., Phillips, L., Schweer, G., Leighton, T., 1994. Development and validation of an air-to-beef food chain model for dioxin-like compounds. Sci. Total Environ. 156, 39–65.

Mahmoud, A.F., Darwish, W.S., Morshdy, A.E., Eldaly, E.A., Ikenaka, Y., Ishizuka, M., 2013. Determination of organochlorine pesticides (OCPs) in the edible offal of Egyptian buffalo. Jpn. J. Vet. Res. 61, S58–S63.

Mansour, S.A., 2004. Pesticide exposure–Egyptian scene. Toxicology 198, 91–115.

Mansour, S.A., 2008. Environmental impact of pesticides in Egypt. Rev. Environ. Contam. Toxicol. 196, 1–51.

Nasr, N., Arief, M., Abdel-Aleem, A., Malhat, F., 2009. Persistent organic pollutants (POPs) in Egyptian aquatic environment. J. Appl. Sci. Res. 5, 1929–1940.

Osibanjo, O., Adeyeye, A., 1997. Organochlorine pesticide residues in foodstuffs of animal origin in Nigeria. B. Environ. Contam. Tox 58, 206–212.

Pardío, V., Martínez, D., Flores, A., Romero, D., Suárez, V., Lopez, K., Uscanga, R., 2012. Human health risk of dietary intake of organochlorine pesticide residues in bovine meat and tissues from Veracruz, Mexico. Food Chem. 135, 1873–1893.

Sallam, K.I., Morshedy, A.E., 2008. Organochlorine pesticide residues in camel, cattle and sheep carcasses slaughtered in Sharkia Province. Egypt. Food Chem. 108, 154–164.

Sharpe, R.T., Livesey, C.T., 2005. Surveillance of suspect animal toxicoses with potential food safety implications in England and Wales between 1990 and 2002. Vet. Rec. 157, 465–469.

United States Environmental Protection Agency (USEPA), 2009. Risk-based Concentration Table Environmental Protection Agency (Philadelphia PA, Washington DC, United States).

USEPA's Integrated Risk Information System (USEPA IRIS), 2012. Human Health Risk Assessment; Risk Based Screening Table (accessed 21.04.13.). http://www.epa.gov/reg3hwmd/risk/human/pdf/NOV_2012_FISH.pdf.

WHO, 1990. Public Health Impact of Pesticides Used in Agriculture WHO in collaboration with the UNEP. World Health Organization, Geneva.

WHO, 2003. Food Safety Issues GEMS/Food Regional Diets Regional per capita consumption of raw and semi-processed agricultural commodities prepared by the Global Environment Monitoring System/Food Contamination Monitoring and Assessment Programme (GEMS/Food). Food Safety Department WHO, Geneva, Switzerland.

WHO, 2009. Dietary Exposure Assessment of Chemicals in Food (Chapter 6). Principles and methods for the risk assessment of chemicals in food. Environmental Health Criteria 240. FAO/WHO. International Programme on Chemical Safety (IPCS). WHO, Geneva Available at: http://www.who.int/ipcs/food/principles/en/index.html.

WHO, 2011. Agents Classified by the IARC Monographs, Volumes 1–101 Available at: http://monographs.iarc.fr/ENG/Classification/index.php (accessed 30.10 2013.).

Xu, X., Dailey, A.B., Talbott, E.O., Ilacqua, V.A., Kearney, G., Asal, N.R., 2010. Associations of serum concentrations of organochlorine pesticides with breast cancer and prostate cancer in U.S. adults. Environ. Health Persp 118, 60–66.

Yohannes, Y.B., Ikenaka, Y., Nakayama, S.M., Saengtienchai, A., Watanabe, K., Ishizuka, M., 2013. Organochlorine pesticides and heavy metals in fish from Lake Awassa, Ethiopia: Insights from stable isotope analysis. Chemosphere 91, 857–863.

Science of the Total Environment 550 (2016) 522–533

Contents lists available at ScienceDirect

Science of the Total Environment

journal homepage: www.elsevier.com/locate/scitotenv

Bioaccumulation and human health risk assessment of DDT and other organochlorine pesticides in an apex aquatic predator from a premier conservation area

Ruan Gerber [a,*], Nico J. Smit [b], Johan H.J. Van Vuren [a], Shouta M.M. Nakayama [c], Yared B. Yohannes [c], Yoshinori Ikenaka [b,c], Mayumi Ishizuka [c], Victor Wepener [b]

[a] Department of Zoology, Kingsway Campus, University of Johannesburg, PO Box 524, Auckland Park 2006, South Africa
[b] Water Research Group, Unit for Environmental Sciences and Management, Potchefstroom Campus, North-West University, Private Bag X6001, Potchefstroom, South Africa
[c] Laboratory of Toxicology, Department of Environmental Veterinary Sciences, Graduate school of Veterinary Medicine, Hokkaido University, Kita 18, Nishi 9, Kita-ku, Sapporo 060-0818, Japan

HIGHLIGHTS

- First record of OCPs in top predator tigerfish from rivers in Kruger National Park
- Pesticides used for vector control bioaccumulate at very high levels in fish from conservation areas
- Both rivers flowing through the Kruger National Park are polluted by OCPs originating from the catchment.
- OCP bioaccumulation is the highest reported for Africa.
- Significant human cancer risk is associated with the consumption of fish from these rivers.

GRAPHICAL ABSTRACT

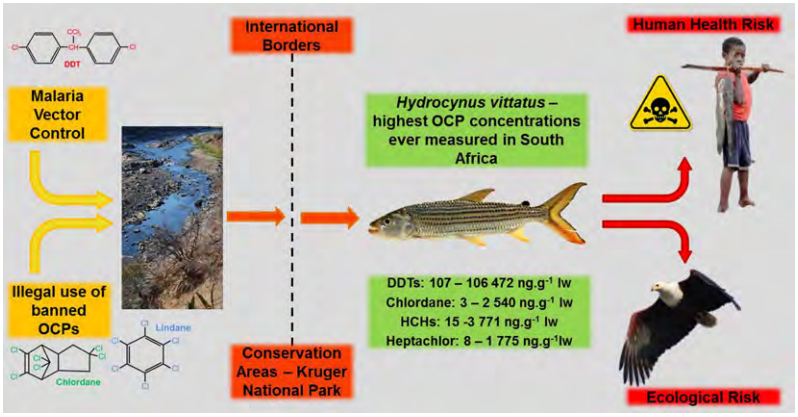

ARTICLE INFO

Article history:
Received 30 September 2015
Received in revised form 21 January 2016
Accepted 21 January 2016
Available online 1 February 2016

Editor: Adrian Covaci

Keywords:
Chlordane
DDE
HCH
Kruger National Park
Lindane

ABSTRACT

With the second highest gross domestic product in Africa, South Africa is known to have a high pesticide usage, including the highly persistent and banned group of organochlorine pesticides (OCPs). South Africa is also one of few countries to still actively spray DDT as malaria vector control. The aim of the study was to determine the degree to which aquatic biota in selected rivers of the world renowned Kruger National Park (KNP) are exposed to by use of OCPs in the catchments outside the KNP and how this exposure relates to human health. Tigerfish (*Hydrocynus vittatus*) are economically important apex predators and was selected as bioindicator for this study. Fish were sampled from the KNP sections of the Luvuvhu, Letaba and Olifants rivers during the high and low flow periods from 2010 to 2011 within the KNP and 19 OCPs were determined in muscle tissue using GC-ECD techniques. Significant flow related and spatial OCP bioaccumulation was observed. Tigerfish from the Luvuvhu River displayed the highest OCP bioaccumulation. Concentrations of the majority of the OCPs including the DDTs were the highest levels ever recorded from South African freshwater systems and in many cases the concentrations were higher than most contaminated areas from around the world. The concentrations found in *H. vittatus* muscle also exceeded maximum residue levels in edible fat as set by the European Union. The health

* Corresponding author at: Department of Zoology, Kingsway Campus, University of Johannesburg, PO Box 524, Auckland Park 2006, South Africa.
E-mail address: gerberrjl@gmail.com (R. Gerber).

http://dx.doi.org/10.1016/j.scitotenv.2016.01.129

Multivariate analysis
Tigerfish

risk assessment also demonstrated that the levels of OCPs pose very high cancer risks to the local populations consuming tigerfish, as high as 2 in 10 increased risk factor. This is of concern not only when managing the water resources of the conservation area but also for surrounding communities consuming freshwater fish. Contaminants enter the park from outside the borders and pose potential risks to the mandated conservation of aquatic biota within the KNP.

1. Introduction

South Africa has the second highest gross domestic product in Africa and is also one of the top four pesticide importers in Africa (Quinn et al., 2011). These pesticides include the highly persistent and lipophilic group of hydrocarbon compounds known as organochlorine pesticides (OCPs) which are used extensively in industry as well as agriculture throughout the world (Dallaire et al., 2013). Environmental contaminants such as OCPs are known to be ubiquitous anthropogenic pollutants in aquatic ecosystems (Sarkar et al., 2008) and because of their high persistence and the fact that they are highly lipophilic, OCPs are known to bioaccumulate in the fatty tissues of aquatic organisms (Dallaire et al., 2013), specifically those of fish. Organochlorine pesticides are known to have deleterious effects on aquatic ecosystems, and as such monitoring the bioaccumulation of these pollutants is essential for the assessment of potential impacts (Wepener et al., 2011; Yohannes et al., 2013a, b).

Tigerfish (*Hydrocynus vittatus*) were selected as the indicator organism as they are an important freshwater fish species due to their high economic value and role in sustaining the livelihoods of many communities (Smit et al., 2009). They are abundant and widely distributed within the sampling area, easy to sample and target, occupy the top position in the aquatic food chain (McHugh et al., 2011) and relatively long lived (up to 20 years, Gerber et al., 2009; Soekoe et al., 2013). As apex predators they have been shown to accumulate pollutants, which include DDTs, various heavy metals and organohalogens (Bouwman et al., 1990; Du Preez and Steyn, 1992; Mhlanga, 2000; Wepener et al., 2012).

Notwithstanding the high volume of pesticide use in South Africa (Dabrowski et al., 2014), there is limited reporting of bioaccumulation data. By virtue of its position on the western border of South Africa, the rivers that flow through the Kruger National Park (KNP) transport pollutants from the industrial and agricultural heartland (Gerber et al., 2015a) into this premier conservation area. Various studies have shown that rainfall and therefore seasonal runoff has a very strong influence on the water and sediment quality of rivers in the KNP (Wepener et al., 2000; Gerber et al., 2015a). The previous assessment of OCPs in the KNP was by Heath and Claassen (1999), who recorded low concentrations of various OCPs in a number of fish species sampled from the various rivers during the period 1992 to 1993. Recent studies in upstream reaches of the Olifants and Luvuvhu rivers adjacent to the KNP have, however, highlighted that concentrations of a number of OCPs in both abiotic (Gerber et al., 2015b) and biotic (Barnhoorn et al., 2009, 2010) compartments are at concerning levels. This is of concern to conservation managers but also to local communities bordering the KNP and its rivers. Inland water bodies throughout central and southern Africa are considered to be important sources of artisanal fisheries (Andrew et al., 2000) with rural communities relying on rivers where large inland lakes are not available (Coetzee et al., 2015). The threats of OCPs especially DDTs to human health in the region have been highlighted in other studies outside the KNP (Barnhoorn et al., 2009; Bornman et al., 2010). The consumption of potentially contaminated freshwater fish could be a primary source of human exposure to OCPs in the area.

The aim of this study was to evaluate the distribution and current levels of various OCPs, including DDTs in *H. vittatus* tissue from selected rivers of the KNP by describing the temporal changes in OCP bioaccumulation related to abiotic concentrations during different flow periods in the rivers. This paper further investigates the potential risks posed to the human health of local rural communities by OCPs and provides a baseline for managers to make informed decisions and thereby take effective measures aimed at mitigating the potential ecological and health risks posed by the OCPs.

2. Materials and methods

2.1. Study area and sampling

Sampling of tigerfish was undertaken between May 2010 to June 2011 at sampling sites along the Olifants, Letaba and Luvuvhu rivers within the KNP (Fig. 1). The Letaba River site was included for comparative purposes to assess whether the Letaba River may act as a refuge for the large *H. vittatus* population found at Olifants River Gorge in the Olifants River. Tigerfish were sampled in the Olifants River Gorge S23° 59′ 25.2″ E31° 49′ 33.3″ located at the confluence of the Olifants and Letaba rivers, the Letaba River site (S23° 56′ 32.9″ E31° 43′ 53.5″) located in the Letaba River before its confluence with the Olifants River. The Luvuvhu River site (S22° 27′ 04.3″ E31° 04′ 47.7″) is located downstream of the confluence of the Mutale and Luvuvhu rivers and before the confluence of the Luvuvhu and the Limpopo rivers (Fig. 1).

Tigerfish were sampled using standard angling techniques. Following capture, fish were sacrificed by severing the spinal cord just behind the head. Fish were weighed (g) and measured (mm) for standard length (SL) and axial muscle sample was removed, placed in aluminium and frozen at −20 °C until further analysis. Tigerfish were sampled at the end of alternating low (LF) and high flow (HF) periods between 2010 and 2011. During these surveys the top 5- to 10 cm of inundated surface sediments were collected using an Eckman grab sampler for OCP analysis. The uppermost sediments were collected as it is considered that these sediments have been recently deposited are closely associated with the water column and therefore pose the most direct significant risk to the aquatic biota at the selected sites. For detailed sampling and treatment methods refer to Gerber et al. (2015b).

2.2. OCP bioaccumulation

2.2.1. Materials

Pesticide grade organic solvents (diethyl ether, acetone and *n*-hexane), anhydrous sodium sulphate and florisil (60–100 mesh) were obtained from Kanto Chemical Corp. (Tokyo, Japan). The florisil was activated in an oven at 130 °C for 12 h. A standard mixture (DDTs, HCHs, chlordanes, drins, heptachlors and hexachlorobenzene (HCB) at 10 μg mL^{-1} was purchased from Dr. Ehrenstorfer GmbH, Germany.

2.2.2. Analysis of OCPs

2.2.2.1. Muscle tissue. Muscle tissue analyses were done following the method of Yohannes et al. (2013a). Acetone/hexane pre-washed extraction thimbles were filled with 10 g of fish fillet which was homogenised together with anhydrous sodium sulphate. The sample was extracted for 6 h with 150 mL mixture of hexane:acetone (3:1 *v*/*v*) in a Soxtherm apparatus (S306AK Automatic Extractor, Gerhardt, Germany). The extract was concentrated to approximately 2 mL using a rotary vacuum evaporator, and diluted to 10 mL using hexane. Gravimetric lipid determination was done using an aliquot of 20% of the extract and the remaining 80% was subjected to a clean-up process after more of the

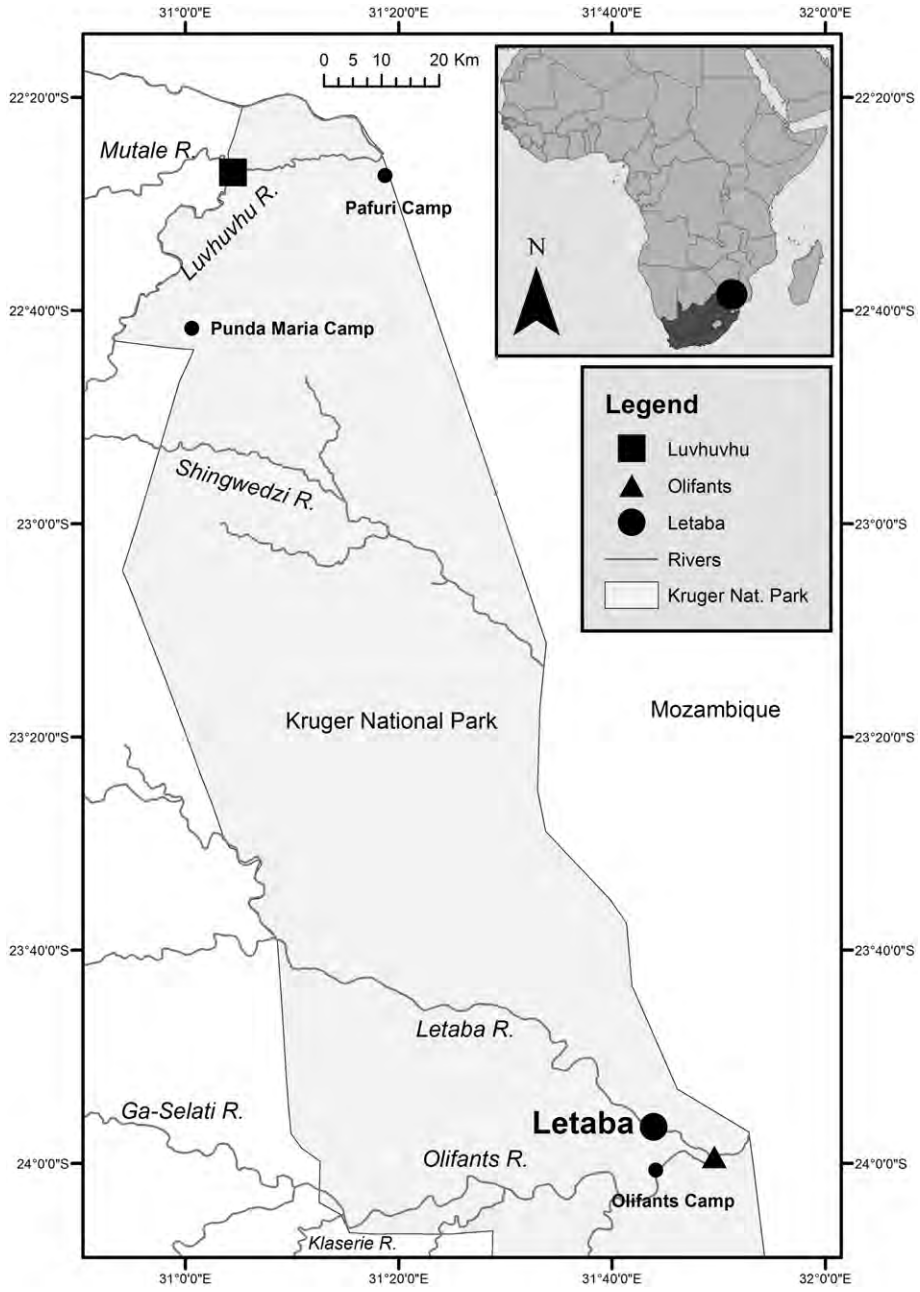

Fig. 1. Position of sampling sites on the Olifants, Letaba and Luvuvhu rivers, Kruger National Park, South Africa.

solvent had been evaporated. The clean-up process was performed on a glass column packed with 6 g of activated florisil topped with anhydrous sodium sulphate. Elution was carried out with 80 mL of hexane containing 25% diethyl ether. The resulting effluent was concentrated to about 2 mL and then under gentle nitrogen flow it was concentrated further; to near dryness. The extract was redissolved in 100 μL *n*-decane and transferred to GC-vials for analysis.

2.2.2.2. Sediments. The analytical and quality control procedures of OCP analysis of surface sediments are described in detail in Gerber et al. (2015b) and are done according to Yohannes et al. (2013b) and are briefly discussed below.

Samples were air dried (5 g) and 15 g of sodium sulphate added, where after they were sonicated (twice) with 30 mL hexane/acetone (1:1, *v*/*v*) in an ultrasonic bath for 20 min with 2,4,5,6-tetrachloro-*m*-xylene (TCmX) added as surrogate standard. The resultant extracts were concentrated on a rotary vacuum evaporator and solvent exchanged to hexane. Desulphurisation was achieved with activated copper powder and samples were cleaned up with a silica gel column containing 5 g of 5% deactivated silica gel topped with anhydrous sodium sulphate. Elution of the column was done with 100 mL hexane/dichloromethane (7:3, *v*/*v*). Gentle nitrogen flow was used to reduce the eluate to about 2 mL and then to near dryness before redissolving in 100 μL *n*-decane and transferring to GC vials for analysis. A known amount of pentachloronitrobenzene was added as an internal standard prior to analysis.

2.2.2.3. Gas-chromatography analysis of OCPs. Analysis of the various OCPs including DDTs (*o*,*p*′-DDT, *p*,*p*′-DDT, *o*,*p*′-DDE, *p*,*p*′-DDE, *o*,*p*′-DDD, *p*,*p*′-DDD; the sum expressed as Σ-DDTs), hexachlorocyclohexanes (HCHs; α-, β-, γ- and δ-HCH; the sum expressed as Σ-HCHs), heptachlors (HPTs; heptachlor, *cis*- and *trans*-heptachlor epoxide; the sum expressed as Σ-HPTs), chlordanes (CHLs; *cis*- and *trans*-chlordane, *cis*- and *trans*-nonachlor and oxychlordane; the sum expressed as Σ-CHLs) and

hexachlorobenzene (HCB) was carried out with a gas-chromatograph equipped with ^{63}Ni electron capture detector (GC-ECD: Shimadzu GC-2014, Kyoto, Japan). Separation was achieved using an ENV-8MS capillary column (30 m × 0.25 mm i.d., 0.25 μm film thickness). One microlitre of each sample was injected in splitless mode. The GC oven temperature was programmed from 100 °C (1 min hold); ramp at 12 °C min^{-1} to 180 °C; 4 °C min^{-1} to 240 °C, and finally at 10 °C min^{-1} to 270 °C (5 min hold). The temperatures of the injector and detector were 250 °C and 320 °C, respectively. Helium was used as the carrier gas with a flow rate of 1.0 mL min^{-1} and nitrogen as the make-up gas at a flow rate of 45 mL min^{-1}.

2.2.3. Quality assurance and quality control

Analytical and quality control procedures of OCPs in tigerfish muscle and sediments were done according to Yohannes et al. (2013a, b). The OCPs were identified by comparing their retention time with reference to the corresponding standard. The concentrations of the target analytes were quantified from the peak area of the sample to that of the standard peak area. The correlation coefficients (r^2) for the calibration curves were all greater than 0.995. For each set of 10 samples, a procedural blank and spiked blank were run to check for interference and cross-contamination. The mean recovery of OCPs for the spiked blanks was 90 ± 11%.

2.2.3.1. Muscle tissue. Spiking experiments using fortified samples, *Oreochromis niloticus* at 5 ng g^{-1} of the composite standards, showed recovery ranged from 70 to 110% for all OCPs. To further test the precision and accuracy of the analytical method, the standard reference material SRM 1947 (Lake Michigan Fish Tissue) was analysed using the same procedures. Accepted recoveries ranged from 75% to 110% with RSD less than 12% were obtained. Limits of detection based on 3:1 signal to noise ratio (S/N) were between 0.05 and 0.1 ng g^{-1} for all OCPs.

2.2.3.2. Sediments. The procedural performance was monitored using TCmX as a surrogate standard and recoveries ranged from 82% to 110%. The quality assurance of the analytical method was done using the SRM 1944 (New York/New Jersey Waterway Sediment) and average recoveries of the DDTs ranged from 90% to 110%. Limits of detection based on 3:1 signal to noise ratio (S/N) was 0.05 ng g^{-1} for all OCPs.

2.3. Risk assessment

A range of standards and instructions estimating potential risks to human health from fish contaminated with environmental pollutants have been established by various international organisations (USEPA, 2013). Straight forward risk assessments can be performed by comparing levels with laws and guidelines, these assessments do not however consider factors such as eating habits and consumption rates. Therefore in this study the health risk assessment was performed at both the 50th and 95th percentile of measured concentrations. This was done in order to provide a comprehensive evaluation of potential health risks posed by the consumption of OCP contaminated fish from the area (Yohannes et al., 2014).

2.3.1. Estimated daily intake (EDI)

The estimated daily dietary intakes of groups of OCPs from tigerfish consumption were calculated as follows:

$$EDI = \frac{C \times DR}{BW}$$

where C is the measured OCP concentration (ng·g^{-1} ww), DR is the estimated daily consumption rate of fish (g·d^{-1}) and BW is the estimated average body weight (kg) of people in the area. The BW was set at 60 kg (WHO, 2010), and the estimated daily consumption rate was conservatively assumed to be 30 g·d^{-1} per person.

2.3.2. Potential carcinogenic risks

In order to assess the potential carcinogenic risks posed by OCPs through contaminated fish consumption, both cancer risk estimates and hazard ratios were calculated according to USEPA guidelines and Dougherty et al. (2000) and Jiang et al. (2005) respectively. The cancer risks (CR) associated with OCPs were estimated using the following equation:

$$CR = EDI \times CSF$$

where CSF is the cancer slope factor taken from USEPA (2012) and the equation from USEPA (2005). Results are interpreted as follows: $<10^6$ is considered acceptable, between 10^6 and 10^4 is considered to be an area of concern and carcinogenic risks $>10^4$ are considered unacceptable (USEPA, 2005).

Hazard ratios (HR) for both non-carcinogenic and carcinogenic effects were calculated following Jiang et al. (2005):

$$HR = \frac{EDI}{BMC}$$

where the BMC refers to the Benchmark calculation. The BMC for cancer effects was derived from the USEPA cancer slope factor (CSF) obtained from the USEPA Integrated Risk Information System (IRIS). The BMC is calculated as follows:

$$\text{Cancer BMC} = \frac{\text{Risk} \times \text{BW}}{\text{Fish consumption} \times \text{CSF}}$$

where the risk is set to a one in a million chance due to a lifetime of exposure and the fish consumption is the amount of fish consumed per kg body weight of the individual per day i.e. g·kg^{-1}·d^{-1}. A hazard ratio greater than one indicates that there is a potential risk to human health (Dougherty et al., 2000).

2.4. Data analysis

All relevant data, OCP concentrations, length, weight, and lipid content were log transformed and a one way analysis of variance performed using SPSS version 18 (PASW Statistics, IBM, USA). Significant differences between the groups (i.e. the different sampling periods on each of the rivers) were determined a priori using Tukey–Kramer post hoc analyses. Significance was set at $p < 0.05$. In this study a redundancy analysis (RDA) assessment was carried out to investigate relationships in OCP concentrations in *H. vittatus* muscle and OCP concentrations reported in the sediments from the study area by Gerber et al. (2015b). An RDA is a derivative of a PCA with one additional feature which allows for the selection of the driving variables which are intended to be overlaid onto the PCA. The values entered into the RDA analysis are not the original data but the best-fit values estimated from a multiple linear regression between each variable in turn and a second matrix of complementary biological or environmental data. The RDA plots are interpreted through 2-dimensional bi-plots that present the (dis)similarities between the samples analysed (Shaw, 2003). The bi-plots were interpreted according to Ter Braak and Smilauer (2004), where the ordination of the surveys from the different rivers is related to the environmental variables and the angles between these variables. Where an angle closer to 0° indicates that variables are positively correlated, an angle close to 90° indicates that variables are uncorrelated and an angle close to 180° indicates that variables are negatively correlated. A further Spearman-Rho linear regression analysis (two tailed) using SPSS version 18 (PASW Statistics, IBM, USA) was done to determine whether any significant relationships occur between the biotic and abiotic OCP concentrations.

3. Results

Sampled fish (Table 1) were of comparable size with no significant differences in length or weight. Significant differences were observed for the lipid content of the sampled muscle tissue. Lipid content in tigerfish from the Olifants River was higher than in tigerfish from the other rivers. Lipid content in tigerfish sampled in the Luvuvhu River during the HF2011 survey were however comparable to the tigerfish sampled from the Olifants River during the LF2010 and HF2011 surveys.

3.1. OCP concentrations: temporal, spatial and flow related variation

The concentrations of OCPs are expressed as $ng \cdot g^{-1}$ lipid weight in muscle tissue of *H. vittatus* (Table 2a) and as $ng \cdot g^{-1}$ dry weight in sediments (Table 2b). The OCPs show clear spatial and temporal related differences. The fewest number of OCPs were detected in *H. vittatus* and sediments sampled from the Olifants River HF2010 survey, i.e. of the total of 19 OCPs analysed for, only 10 were detected in tissue. The number of OCPs detected in Olifants River tigerfish however increased during successive surveys; 17/19 for the LF2010 and 18/19 for the HF2011 surveys respectively. The same pattern was seen in the aforementioned surveys with two and 13 detected in the sediments respectively. This was in contrast to the number of OCPs detected in tigerfish muscle from the Luvuvhu River, which decreased from 19/19 during the LF2010 survey to 16/19 for the HF2011 survey. The sediments reflected the same pattern with 16/19 and 8/19 detected respectively. Eighteen of the 19 OCPs analysed for were found in the muscle tissue of *H. vittatus* and 3/19 detected from sediments sampled from the Letaba River. There were distinct flow-related differences in OCP bioaccumulation with the low flow periods displaying significantly higher concentrations. The Luvuvhu River surveys tended to have significantly higher concentrations of OCPs when compared to the respective flow periods of the Olifants and Letaba Rivers.

The Σ-DDTs (*o,p′*- and *p,p′*-DDE, DDD, DDT) were the most abundant OCPs (Fig. 2a) and all of the samples had measurable concentrations of the DDT isomers, which were in the order of DDE > DDT > DDD in all of the rivers during all of the surveys (Fig. 2a). There were clear flow-related influences on the DDT bioaccumulation. The Letaba River and HF2011 and LF2010 surveys in the Olifants River had high DDE/DDT ratios (>4) whilst the HF2010 surveys of the Olifants River and both surveys on the Luvuvhu River had low DDE/DDT ratios (≤ 2). The *o,p′*-/*p,p′*-DDT ratios ranged between 0.11 and 1.48, the Letaba River had the highest *o,p′*-/*p,p′*-DDT ratio whilst the Luvuvhu River surveys had the lowest *o,p′*-/*p,p′*-DDT ratios (Table 2a). The Σ-HCHs were the next highest OCPs (Fig. 2a) and the isomers showed clear flow related trends, namely; the γ-isomer making up the largest fraction of the Σ-HCHs during the high flow periods and low flow periods having an almost even mix of all the isomers (Fig. 3a). The third highest group of OCPs present was chlordane (Fig. 2a). Tigerfish sampled from the Luvuvhu and Letaba Rivers contained all of the chlordane isomers analysed for (Fig. 3b) of which there were high concentrations of *trans*-chlordane present in the Luvuvhu River tigerfish. The number of chlordane isomers present in tigerfish muscle from the Olifants River increased with successive surveys. The chlordanes were followed closely by heptachlor (Fig. 2a) and its isomers (Fig. 3c). The least abundant OCP was HCB (Fig. 2a).

3.2. Relationships between biotic and abiotic OCP concentrations

The redundancy analysis triplot (Fig. 4) explains 81.9% of the variation in the accumulation and sediment OCP data with 58.2% on the first axis and 23.7% on the second axis. The ordination confirmed the flow related variation in the OCP data and revealed that high flow periods were associated with lower muscle tissue concentrations and higher sediment concentrations and vice versa for the low flow periods. The triplot seems to suggest that there are no or very weak correlations between environmental concentrations and the subsequent accumulated concentrations.

Table 1
Mean ± 1 standard error and range values of biometric data, and lipid content of *H. vittatus* sampled during the various high flow (HF) and low flow (LF) surveys to the Olifants (OLI), Letaba (LET) and Luvuvhu (LUV) rivers, Kruger National Park. Within rows, values with common superscripts indicate no significant difference.

N	OLI HF2010	OLI LF2010	OLI HF2011	LET LF2010	LUV LF2010	LUV HF2011
	6	11	16	7	16	16
Standard Length (mm)	316 ± 14 (270–375)	348 ± 18 (264–443)	314 ± 15 (233–456)	259 ± 9 (220–280)	290 ± 22 (205–430)	340 ± 22 (221–509)
Weight (g)	490 ± 79 (280–860)	887 ± 213 (206–2400)	553 ± 120 (160–1840)	223 ± 18 (160–280)	488 ± 120 (120–1240)	698 ± 140 (140–1840)
Lipid (%)	^{a}4.06 ± 0.577 (2.01–6.36)	^{ab}3.25 ± 0.823 (0.555–8.14)	^{ab}2.40 ± 0.289 (0.845–2.4)	^{c}0.535 ± 0.081 (0.192–0.925)	^{c}0.960 ± 0.253 (0.025–0.51)	^{bc}1.52 ± 0.571 (0.215–2.07)

Table 2a
Mean ± 1 standard error and range of organochlorine pesticides (ng g^{-1} lipid) in *H. vittatus* muscle tissue sampled during the various high flow (HF) and low flow (LF) surveys to the Olifants (OLI), Letaba (LET) and Luvuvhu (LUV) rivers, Kruger National Park. Common superscripts within rows indicate no significant differences ($p > 0.05$). BD represents OCP below detection limits. Values are compared to maximum residue limits (MRL) as set by the European Union (EU) (EC, 2005).

	EU MRL ng g^{-1} fat	OLI HF2010	OLI LF2010	OLI HF2011	LET LF2010	LUV LF2010	LUV HF2011
α-HCH	200	^{ab}**16.97 ± 3.53** (4.47–25.59)	^{a}**84.64 ± 28.84** (13.07–288.30)	BD	^{ab}**44.39 ± 16.73** (32.93–131.51)	^{b}**100.87 ± 53.48** (45.53–871.57)	^{ab}**36.17 ± 6.42** (4.91–101.88)
β-HCH	100	BD	^{bc}**83.98 ± 56.37** (55.01–624.26)	^{b}**12.40 ± 4.24** (6.38–52.81)	^{a}**57.17 ± 7.31** (37.85–96.35)	^{a}**120.38 ± 45.21** (18.63–775.57)	BD
γ-HCH	20	^{ab}**71.06 ± 12.57** (14.63–106.33)	^{c}**115.71 ± 89.42** (32.14–998.23)	^{bc}**37.29 ± 14.13** (11.28–241.06)	^{ab}**135.59 ± 11.94** (104.95–197.01)	^{bc}**156.39 ± 80.88** (44.74–1328.60)	^{a}**370.87 ± 62.96** (7.12–919.99)
δ-HCH		BD	^{b}**22.77 ± 11.34** (8.12–120.84)	^{b}**13.30 ± 5.26** (7.73–58.40)	^{a}**70.91 ± 13.54** (32.82–143.62)	^{a}**122.86 ± 46.23** (21.50–795.97)	^{b}**18.38 ± 6.45** (9.10–81.24)
Σ-HCH's		^{ab}**88.08 ± 14.40** (19.10–114.12)	^{a}**307.09 ± 106.36** (26.93–1081.04)	^{b}**63.01 ± 15.55** (14.72–241.06)	^{a}**308.06 ± 36.13** (208.56–498.18)	^{a}**500.50 ± 222.05** (46.94–3771.71)	^{a}**425.44 ± 70.64** (12.03–1103.11)
Heptachlor		BD	**10.49 ± 5.78** (21.85–51.61)	**2.09 ± 1.14** (7.97–13.99)	BD	**42.82 ± 34.35** (32.68–553.75)	^{a}**54.15 ± 10.98** (10.97–176.80)
cis-Hep-epoxide		BD	^{b}**16.15 ± 7.71** (24.19–66.36)	^{b}**18.08 ± 4.91** (6.35–76.78)	^{a}**92.74 ± 14.76** (47.90–156.61)	^{a}**112.13 ± 34.56** (19.14–585.42)	BD
trans-Hep-epoxide		BD	BD	^{b}**8.52 ± 4.59** (5.10–70.12)	^{a}**98.75 ± 14.61** (54.03–157.89)	^{a}**121.77 ± 35.38** (19.38–615.37)	BD
Σ-HPT's	200	BD	^{c}**26.66 ± 8.79** (21.85–66.36)	^{bc}**28.70 ± 8.84** (8.07–146.90)	^{a}**191.51 ± 28.95** (101.92–300.63)	^{a}**276.73 ± 101.85** (38.52–1754.55)	^{ab}**54.20 ± 10.98** (10.97–176.80)
oxy-Chlordane		BD	^{ab}**58.27 ± 25.12** (9.88–290.04)	^{bc}**11.65 ± 4.79** (5.42–70.42)	^{a}**93.09 ± 12.28** (59.24–146.65)	^{a}**94.36 ± 24.70** (12.05–412.25)	^{c}**3.60 ± 2.10** (13.45–29.87)
cis-Chlordane		BD	BD	^{ab}**12.14 ± 3.38** (5.31–44.41)	^{a}**123.57 ± 44.18** (22.89–292.67)	^{ab}**76.20 ± 36.29** (19.31–546.07)	^{bc}**15.18 ± 4.78** (6.81–67.21)
trans-chlordane		^{b}**14.85 ± 6.98** (7.36–39.16)	^{a}**123.73 ± 63.33** (49.54–627.22)	^{b}**8.01 ± 3.46** (5.61–42.16)	^{a}**59.43 ± 17.45** (26.37–141.20)	^{a}**152.43 ± 33.71** (19.48–533.01)	^{b}**28.34 ± 10.76** (15.65–156.49)
cis-Nonachlor		BD	^{a}**191.97 ± 84.78** (7.17–945.10)	^{b}**5.32 ± 3.37** (8.32–47.78)	^{a}**41.21 ± 28.04** (35.32–202.87)	^{a}**72.12 ± 33.82** (53.23–556.47)	^{b}**6.81 ± 2.50** (6.77–36.60)
trans-Nonachlor		^{cd}**9.91 ± 6.27** (9.24–39.65)	^{c}**74.98 ± 35.63** (11.84–332.53)	^{bc}**12.68 ± 2.68** (3.02–36.14)	^{ab}**82.17 ± 17.18** (41.26–175.87)	^{a}**119.61 ± 29.26** (21.85–492.54)	^{d}**4.30 ± 3.62** (10.69–57.71)
Σ-CHL's	50	^{b}**24.84 ± 11.98** (16.60–78.81)	^{a}**448.98 ± 166.43** (15.75–1532.80)	^{b}**49.81 ± 14.86** (3.02–203.04)	^{a}**399.45 ± 83.94** (156.98–789.03)	^{a}**514.72 ± 144.23** (82.83–2540.35)	^{b}**58.23 ± 14.25** (13.58–238.39)
HCB	200	BD	^{b}**2.62 ± 1.45** (3.36–15.84)	^{ab}**3.19 ± 1.07** (0.55–18.04)	^{a}**9.88 ± 1.86** (5.93–19.21)	^{a}**26.37 ± 11.16** (4.99–185.34)	^{a}**7.37 ± 1.65** (0.93–25.79)
o,p′-DDE		^{ab}**29.93 ± 6.75** (9.97–49.64)	^{ab}**201.38 ± 78.32** (12.53–749.38)	^{b}**12.66 ± 3.76** (8.12–38.88)	^{a}**125.03 ± 30.15** (22.43–249.81)	^{ab}**102.21 ± 35.02** (36.54–543.78)	^{a}**78.64 ± 15.83** (7.91–248.87)
p,p′-DDE		^{cd}**181.71 ± 97.99** (48.83–668.38)	^{ab}**4359.55 ± 1923.82** (546.11–22,996.50)	^{d}**474.66 ± 229.10** (52.12–3799.22)	^{ab}**4745.26 ± 1645.48** (1131.91–11,647.06)	^{a}**16,184.23 ± 5026.47** (1541.67–72,117.65)	^{bc}**2342.58 ± 945.66** (49.46–12,046.94)
o,p′-DDD		^{ab}**49.16 ± 35.18** (13.59–222.87)	^{ab}**361.30 ± 266.28** (22.90–2993.39)	^{b}**17.97 ± 5.63** (5.08–79.77)	^{a}**512.85 ± 262.07** (79.81–1977.31)	^{a}**258.66 ± 68.36** (58.28–1051.48)	^{ab}**64.48 ± 11.33** (5.57–152.18)
p,p′-DDD		^{cd}**85.62 ± 28.41** (24.93–214.81)	^{abc}**978.02 ± 333.29** (81.84–3262.79)	^{d}**62.59 ± 13.46** (12.48–184.09)	^{ab}**1205.75 ± 390.20** (295.39–2863.13)	^{a}**3411.15 ± 1106.75** (581.47–15,529.41)	^{bc}**451.45 ± 171.08** (15.77–2081.79)
o,p′-DDT		**34.97 ± 15.91** (8.17–104.25)	**970.09 ± 516.66** (16.98–4777.84)	**29.31 ± 9.71** (6.68–133.57)	**1465.48 ± 892.38** (107.05–6565.90)	**476.61 ± 135.39** (100.16–1638.81)	**122.39 ± 31.44** (24.98–474.39)
p,p′-DDT		^{cd}**116.27 ± 56.57** (53.33–386.89)	^{ab}**2166.83 ± 1128.08** (143.65–12,816.08)	^{d}**49.68 ± 17.39** (11.93–250.35)	^{ab}**1382.89 ± 248.33** (743.43–2237.55)	^{a}**11,934.22 ± 2860.89** (406.70–35,453.74)	^{bc}**1189.45 ± 554.89** (27.76–8366.29)
Σ-DDT	**1000**	^{cd}**497.66 ± 200.93** (121.98–1409.52)	^{ab}**9037.17 ± 3221.60** (898.04–33,833.60)	^{d}**646.86 ± 260.49** (95.95–4354.52)	^{ab}**9437.27 ± 2395.55** (2667.08–17,651.35)	^{a}**32,367.07 ± 8031.88** (2725.73–106,752.15)	^{bc}**4248.99 ± 1680.02** (106.47–21,610.19)
o,p′-DDT/*p,p′*-DDT		**0.35 ± 0.13** (0.14–0.84)	**0.61 ± 0.27** (0.1–1.91)	**0.62 ± 0.12** (0.00–1.54)	**1.48 ± 0.02** (0.07–8.42)	**0.11 ± 0.02** (0.02–0.25)	**0.28 ± 0.04** (0.06–0.49)
DDE/DDT		**1.37 ± 0.17** (0.79–3.24)	**4.80 ± 1.33** (0.12–17.07)	**7.47 ± 1.30** (1.76–15.09)	**4.55 ± 2.03** (0.54–15.67)	**1.75 ± 0.32** (0.61–4.11)	**2.25 ± 0.16** (1.44–3.64)

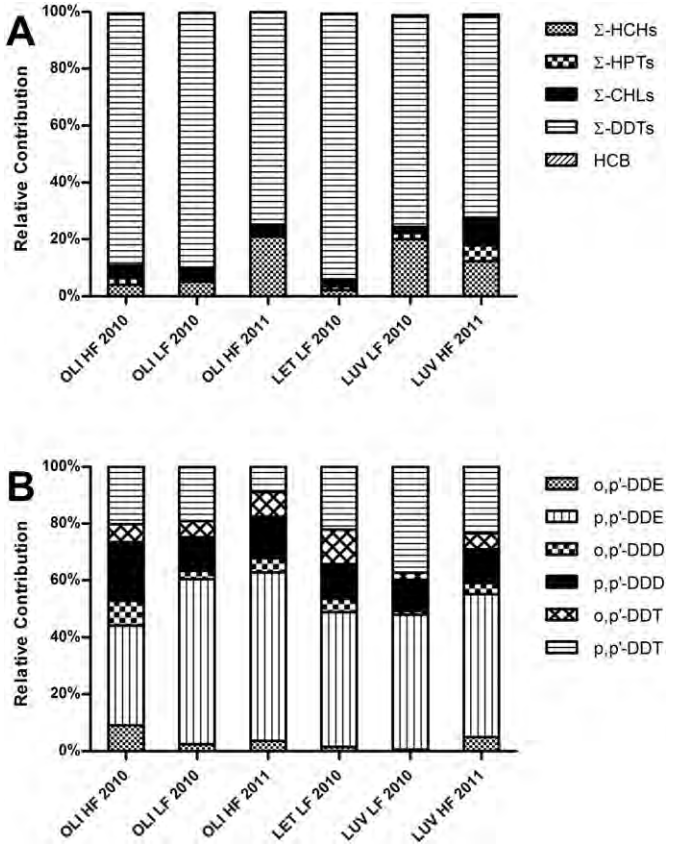

Fig. 2. (a) The relative contribution of the various groups of organochlorine pesticides to (Σ-OCPs) and (b) Relative contribution of individual DDT components (to Σ-DDT) in *H. vittatus* muscle tissue sampled during the various high flow (HF) and low flow (LF) surveys to the Olifants (OLI), Letaba (LET) and Luvuvhu (LUV) rivers, in the Kruger National Park.

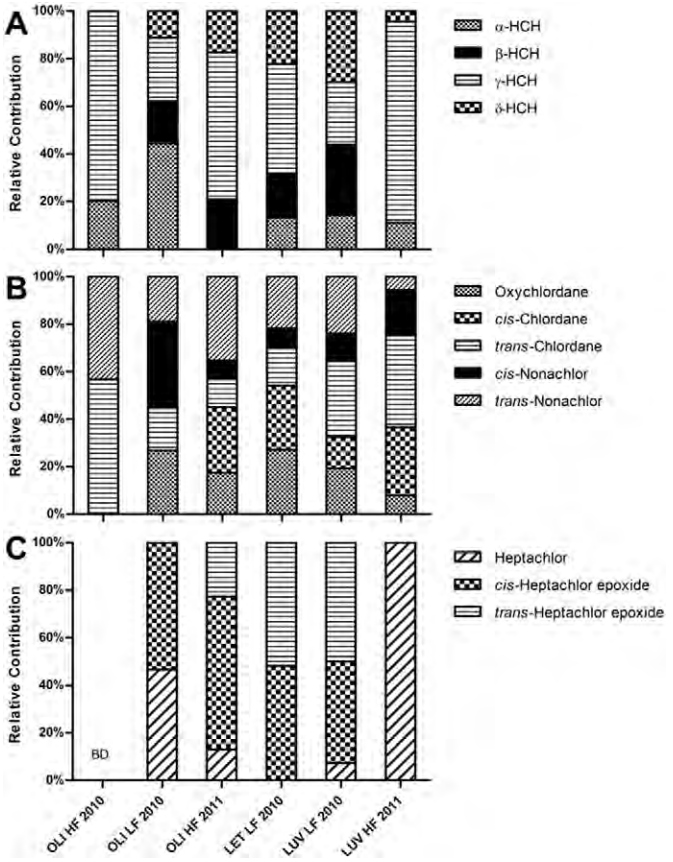

Fig. 3. Relative contribution of individual (a) hexachlorocyclohexane, (b) chlordane and (c) heptachlor components to Σ-HCH, Σ-CHL and Σ-HPT respectively in *H. vittatus* muscle tissue sampled during the various high flow (HF) and low flow (LF) surveys to the Olifants (OLI), Letaba (LET) and Luvuvhu (LUV) rivers, in the Kruger National Park. BD represents OCP below detection limits.

Table 2b
Mean concentrations of organochlorine pesticides (ng g^{-1} dry weight) in sediment samples from selected sites on the Olifants, Letaba and Luvuvhu Rivers, Kruger National Park, adapted from Gerber et al. (2015b). BD represents OCP below detection.

	Olifants River		Letaba River	Luvuvhu River	
	LF 2010	HF 2011	LF 2010	LF 2010	HF 2011
α-HCH	BD	0.20	0.17	0.21	BD
β-HCH	BD	0.19	BD	0.29	BD
γ-HCH	BD	0.07	BD	0.10	1.56
δ-HCH	BD	BD	BD	0.24	BD
Σ-HCHs	*BD*	*0.46*	*0.17*	*0.84*	*1.56*
Heptachlor	0.24	0.24	BD	BD	BD
cis-Hep-epoxide	BD	BD	BD	0.19	0.63
trans-Hep-epoxide	BD	0.18	BD	0.18	1.43
Σ-HPTs	*0.24*	*0.42*	*BD*	*0.37*	*2.06*
oxy-Chlordane	BD	0.12	BD	0.19	0.62
cis-Chlordane	0.17	0.15	BD	0.15	BD
trans-Chlordane	BD	BD	BD	BD	BD
cis-Nonachlor	BD	0.29	BD	0.54	0.67
trans-Nonachlor	BD	0.18	BD	0.19	0.63
Σ-CHLs	*0.17*	*0.74*	*BD*	*1.07*	*1.92*
o,p′-DDE	BD	0.24	BD	0.23	1.25
p,p′-DDE	BD	0.23	0.31	0.51	1.56
o,p′-DDD	BD	0.19	BD	0.34	BD
p,p′-DDD	BD	0.07	0.26	0.14	BD
o,p′-DDT	BD	BD	BD	BD	BD
p,p′-DDT	BD	BD	BD	0.55	BD
Σ-DDTs	*BD*	*0.73*	*0.57*	*1.77*	*2.81*
HCB	BD	BD	BD	0.02	BD

The Spearman-Rho linear regression analysis confirmed that this was true for many of the OCP isomers, however significant positive correlations ($p < 0.01$) were found for the following isomers: α-HCH, γ-HCH, δ-HCH, *cis*-chlordane, HCB, *o,p′*-DDD and *p,p′*-DDT.

3.3. Human health risk assessment

The average EDI and the subsequent health risk assessment in terms of HRs and the cancer risk estimates of groups of OCPs from each of the rivers are shown in Table 3. The results are shown for both the 50th and 95th percentiles. The results show that although the EDIs in each of the rivers are far below the acceptable/tolerable daily intakes, the OCPs in tigerfish tissues pose a very large risk to humans consuming them, as indicated by the HRs and cancer risk estimates at both the 50th and 95th percentiles. The DDTs from each of the rivers pose the greatest risk of all the different OCPs. The HPTs and CHLs pose the least risk when considering the HRs and cancer risk estimates respectively. The 50th percentile HPT concentrations in each of the rivers indicated no risk whereas the 95th percentile concentrations did. All other OCP groups at both the 50th and 95th percentile indicated a very high risk to humans. The cancer risk for all OCP groups at both the 50th and 95th percentile indicated unacceptable cancer risks to humans through a lifetime exposure.

4. Discussion

Measurement of organic chemicals in abiotic compartments is limited in reliability, as such living organisms are used as indicators of environmental exposure through bioaccumulation (Smolders et al., 2003). According to Chapman (1997) and Rainbow (2007), bioaccumulation

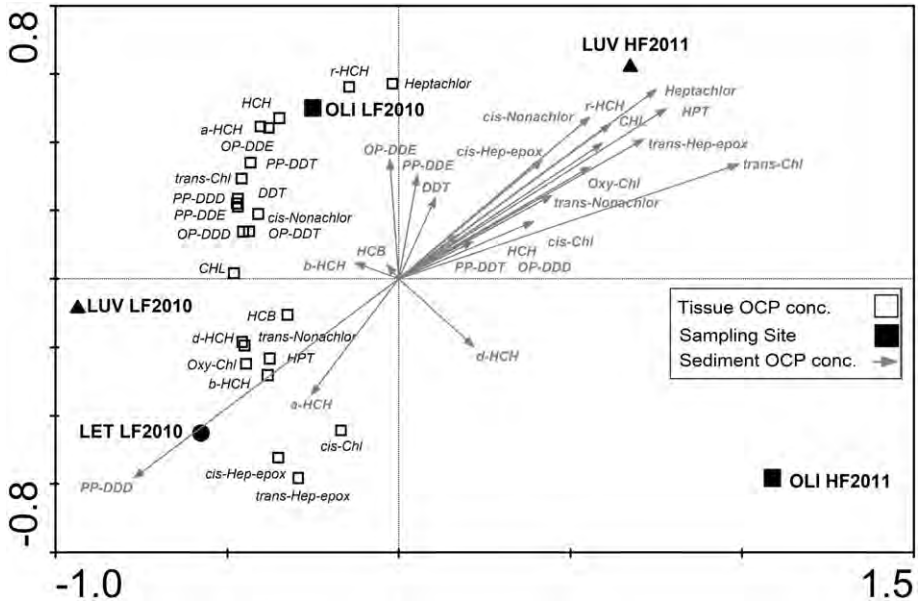

Fig. 4. Redundancy analysis (RDA) triplot of organochlorine pesticide (OCP) concentrations in *H. vittatus* muscle during the low flow (LF) 2010 and high flow (HF) 2011 surveys to the Olifants (OLI) and Luvuvhu (LUV) rivers. Sediment OCP concentrations are overlayed. The ordination explains 81.9% of the variance in the data with 58.2% on the first axis and 23.7% on the second axis.

studies provide information on contaminant-specific bioavailability, assist in identifying possible causative agent(s) of toxicity, and relate body burdens to food chain accumulation values. However, caution should be practised when interpreting the results of bioaccumulation monitoring studies. Too often residue levels in tissues of aquatic organisms are used to make assumptions on potential toxicity due to the presence of the toxicants. Bioaccumulation results that are presented should therefore be seen as a biological measure of OCP bioavailability within the study area and reflect potential concentrations of OCPs which humans may be exposed to through ingestion of tigerfish.

4.1. OCP bioaccumulation

Organochlorine pesticides are known to be lipophilic (Dallaire et al., 2013) and the accumulation of OCPs are highly influenced by the lipid content of the organism (Deribe et al., 2011; Gewurtz et al., 2006). There were no significant differences in the lipid content of the muscle tissue between the different flows on the selected rivers. Therefore the temporal OCP bioaccumulation patterns reflect the OCP usage and run-off patterns of each of the catchments and the bioaccumulation of OCPs in tigerfish is thus rather a function of the bioavailability of these pollutants, either directly from the environment or through the food web. The measured OCP concentrations varied between the various surveys to the rivers studied and OCP concentrations were generally higher in the Luvuvhu River > Olifants River = Letaba River, although the Olifants and Letaba rivers had differences in certain OCPs, where some were higher in Olifants River *H. vittatus* and vice versa. This is indicative of the different types of anthropogenic activities occurring in the catchments even though these rivers are relatively close to each other. The majority of the measured OCPs are significantly higher during the LF periods in both the Olifants and Luvuvhu rivers, suggesting that input from diffuse sources has a longer residence time in the environment (i.e. reduced sediment transport) with ensuing bioaccumulation. Wepener et al. (2012) attributed the differences in OCP levels in *H. vittatus* from Lake Pongolapoort in Northern KwaZulu-Natal, South Africa, to lipid content rather than changes in run off. However, increased concentrations of OCPs in *H. vittatus* from the sampled rivers are attributed to additional inputs of OCPs rather than changes in the lipid reserve status of the sampled fish. Comparisons between the current study and other studies should be made with caution due to the fact that many studies on OCP levels in fish are expressed in wet weight and this study in lipid weight. However, since OCP concentrations were recorded for both lipid content and wet tissue mass, comparisons may be made.

Numerous studies in both African and international aquatic freshwater systems have found Σ-DDTs to be the most abundant of the OCPs measured in freshwater fish with *p,p′* DDE the most abundant and persistent of the congeners measured (Barnhoorn et al., 2009; Covaci et al., 2006; Kaur et al., 2008; Van Ael et al., 2012; Wepener et al., 2012; Yohannes et al., 2013a, 2013b). The high levels and abnormal accumulation of *p,p′* DDE in fish species can be attributed to the induced dechlorination of *p,p′* DDT to *p,p′* DDE by mixed function oxidases (Schmitt et al., 1990). The internal biotransformation of DDT to DDE was also proposed by Wepener et al. (2012) behind the higher levels of *p,p′* DDE in *H. vittatus* from Lake Pongolapoort. The Σ-DDTs measured in *H. vittatus* from the Olifants and Letaba during LFs and from the Luvuvhu River during HF2011 were similar to *H. vittatus* from Lake Pongolapoort (6443.9 ± 2635 $ng \cdot g^{-1}$ lw) (Wepener et al., 2012). The Σ-DDTs, however, far exceeded those found by Covaci et al. (2006) for several fish species in the Danube Delta, Romania (178–4829 $ng \cdot g^{-1}$ lw). The high levels of DDT can be attributed to the application of DDT for malaria vector control in the upper catchment of the Luvuvhu River (van Dyk et al., 2010). The spraying of DDTs specifically for malaria vector control commenced in South Africa during the 1940s and continued up until 1996, where after pyrethroids were applied up until 2000 and then DDT was once again applied due to the discovery of pyrethroid resistant mosquitoes (Mabaso et al., 2004). The ratios of DDE and DDT are useful and indicate whether contamination is recent or historic, with low ratios indicating the recent contamination. The low DDE:DDT ratio in specifically *H. vittatus* and sediments from the Luvuvhu River indicates that the DDT exposure is a mixture of recent DDT application and historical levels. The DDT levels in *H. vittatus* from both the Olifants and Letaba rivers can be ascribed to long range transport and subsequent deposition of this pesticide from areas where DDT spraying occurs, its persistent nature and illegal use within the catchments.

The isomeric composition of technical grade HCH is considered to have an α/γ ratio of between 3 and 7 and be comprised of 60–70% α, 5–12% β, 10–12% γ and 6–10% δ (Saadati et al., 2012). Considering the bioaccumulation of HCH isomers ($\alpha < \gamma < \beta$) and current results ($\alpha/\gamma < 1$), it is evident that the HCH inputs into all three rivers are a mixture of technical HCH and more importantly pure γ-HCH (lindane), the most

Table 3
Average concentrations of OCPs (wet weight), estimated exposure, benchmark concentrations, carcinogenic hazard ratios and estimated cancer risks for tigerfish consumed from the Letaba, Olifants and Luvuvhu rivers from the Kruger National Park.

	Letaba River				Olifants River				Luvuvhu River			
	Σ-HCH	Σ-HPT	Σ-CHL	Σ-DDT	Σ-HCH	Σ-HPT	Σ-CHL	Σ-DDT	Σ-HCH	Σ-HPT	Σ-CHL	Σ-DDT
Cancer slope factor[b] ($mg \cdot kg^{-1} \cdot d^{-1}$)	1.1[a]	4.5	0.35	0.34	1.1[a]	4.5	0.35	0.34	1.1[a]	4.5	0.35	0.34
Cancer benchmark concentration ($\mu g \cdot kg^{-1} \cdot d^{-1}$)	0.132	0.54	0.042	0.0408	0.132	0.54	0.042	0.0408	0.132	0.54	0.042	0.0408
ADI[c] ($ng \cdot kg^{-1} \cdot bw \cdot d^{-1}$)	5000[a]	100	500	10,000	5000	100	500	10,000	5000	100	500	10,000
TDI[d] ($ng \cdot kg^{-1}$ bw $\cdot d^{-1}$)	3000[a]	500	500	2000	3000	500	500	2000	3000	500	500	2000
50th (95th) percentile measured concentrations ($ng \cdot g^{-1}$) ww	1.46 (1.90)	0.93 (1.33)	1.51 (3.59)	35.18 (79.79)	2.25 (8.99)	0.34 (2.41)	0.81 (12.22)	12.34 (279.81)	1.98 (9.73)	0.42 (3.88)	0.77 (9.05)	32.02 (1071)
50th (95th) percentile estimated daily intakes ($ng \cdot kg^{-1}$ bw $\cdot d^{-1}$)	0.73 (0.95)	0.46 (0.67)	0.76 (1.79)	17.59 (39.90)	1.13 (4.49)	0.17 (1.2)	0.41 (6.11)	6.17 (139.9)	0.99 (4.86)	0.21 (1.94)	0.39 (4.52)	16.01 (535.26)
50th (95th) percentile carcinogenic hazard ratios[e]	5.5 (7.2)	0.9 (1.2)	18 (42.7)	431 (978)	8.5 (34)	0.3 (2.2)	9.7 (145.4)	151 (3429)	7.5 (36.8)	0.4 (3.6)	9.2 (107.7)	392 (13,119)
50th (95th) percentile cancer risk estimates ($\times 10^4$)[f]	8.03 (10.47)	20.84 (30.03)	2.64 (6.28)	59.8 (135.7)	12.38 (49.43)	7.65 (54.22)	1.43 (21.38)	20.98 (475.7)	10.87 (53.5)	9.36 (87.2)	1.35 (15.83)	54.43 (1820)

[a] For γ-HCH.
[b] Cancer slope factors from USEPA (2013).
[c] ADI – Acceptable daily intake; from WHO (2010).
[d] TDI – Tolerable daily intake; from Australian Government Department of Health Office of Chemical Safety (AGDHOCS) (2014).
[e] Any ratio > 1 indicates a risk.
[f] Risks > 10^4 are unacceptable.

toxicologically active of the HCH isomers. The extent to which these pesticides are being used in the respective catchments can be seen when compared to the much lower concentrations of individual isomers and Σ-HCHs found in *H. vittatus* by Wepener et al. (2012) from Lake Pongolapoort (Σ-HCH – 15.75 ± 11.43 $ng \cdot g^{-1}$ lw) and several fish species analysed by Covaci et al. (2006) in the Danube Delta; α-HCH (32–97 $ng \cdot g^{-1}$ lw), γ-HCH (13–108 $ng \cdot g^{-1}$ lw) and Σ-HCHs (56–319 $ng \cdot g^{-1}$ lw). The predominance of the γ-HCH isomer can only be attributed to the constant and renewed input of lindane into the systems and is clearly demonstrated by the fact that γ-HCH is easily degraded in soils and sediments by microorganisms and is isomerised to the α isomer photochemically (Malik et al., 2007).

Chlordane is a mixture of many related chemicals, as seen by the numerous components found in *H. vittatus* from this study. The Σ-CHL found in *H. vittatus* from the respective rivers during LF periods were hundreds of times greater than those found by Wepener et al. (2012) (3.8 ± 1.61 $ng \cdot g^{-1}$ lw). Wet mass concentrations of the chlordanes were similar and in some cases higher than the maximum concentrations found all around the U.S.A. during the period 1976–1984 (<0.6 $\mu g \cdot g^{-1}$ ww) (Schmitt et al., 1990). This clearly demonstrates the high levels of exposure and thus bioaccumulation in *H. vittatus* in this study. The results show an equally high usage of chlordanes within each of the catchments of the selected rivers. Heptachlor is one of the minor components of chlordane, but is discussed on its own due to its highly toxic nature (ATSDR, 1994). Heptachlor epoxide concentrations measured in *H. vittatus* from the respective systems were higher than concentrations of heptachlor, an occurrence also found in fish from the Gomti River, India (Malik et al., 2007). This is expected as the more stable heptachlor epoxides are metabolised from heptachlor in sediments, plants and animals in aquatic systems (Malik et al., 2007). Wet mass concentrations of heptachlor were similar and in some cases higher than the maximum concentrations found in several fish species sampled from all around the U.S.A. during the period 1976–1984 (<0.1 $\mu g \cdot g^{-1}$ ww) (Schmitt et al., 1990). When compared to concentrations in fish from the Gomti River, India (BD – 3.5 $ng \cdot g^{-1}$ ww) (Malik et al., 2007), both heptachlor and its metabolites are similar in tigerfish from all of the selected systems during the present study. The relatively high levels are due to both persistence as well as limited use of heptachlor still being allowed in South Africa (Bouwman, 2003) but may also be a metabolite of chlordane use in these systems as chlordane levels were also relatively high. Concentrations of Σ-CHL and Σ-HPT are quite similar during the respective surveys to the sampled rivers as their use goes hand in hand in the control of insects (ATSDR, 1994).

Hexachlorobenzene (HCB) concentrations were the lowest of all the OCPs measured. The use of this fungicide has been banned in South Africa since 1983 (Bouwman, 2003) and the limited use of HCB within the catchments of the study area is clearly demonstrated by the low levels found compared to *H. vittatus* from Lake Pongolapoort (355.5 ± 230 $ng \cdot g^{-1}$ lw) (Wepener et al., 2012) and *Labeo capensis* from the Vaal River, South Africa (588.3 ± 442.6 $ng \cdot g^{-1}$ lw) (Wepener et al., 2011). Concentrations of HCB found during the present study are, however, similar to concentrations in several different fish species from the Danube Delta (1.6–33 $ng \cdot g^{-1}$ lw) (Covaci et al., 2006).

The higher OCP exposure and subsequent bioaccumulation in the Luvuvhu River is reflected in the higher sediment and muscle tissue concentrations compared to the Olifants River. The association of OCP concentrations in the sediments with OCP concentration in *H. vittatus* tissue from the selected rivers were corroborated by the order of dominance of the individual OCPs. In the sediments the order was; DDT > CHL > HCH > HPT > HCB (Gerber et al., 2015b), whilst in tissue it was; DDT > HCH > CHL > HPT > HCB. Continued inputs of lindane and DDT are evident in each of the systems. The OCP concentrations in *H. vittatus* muscle showed clear flow related variation, with concentrations being significantly higher during LF than HF periods. However, the concentrations of these pollutants increased in the abiotic compartments during HF periods. Therefore the concentrations in the abiotic

and biotic compartments in each of the rivers do not correlate. This finding rather suggests that the bioaccumulation of these pollutants is a function of exposure time and that the increased concentrations in the abiotic compartments of the aquatic environment are only reflected in the biota at a later stage. Luvuvhu River sediments contained a greater diversity and higher concentrations of OCPs compared to the Letaba and Olifants River sediments reflecting the bioaccumulation patterns in the *H. vittatus* from the respective rivers. Biomagnification of OCPs is highly likely in the studied systems because of the low concentrations found in sediments (Gerber et al., 2015b), versus the extremely high concentrations found in *H. vittatus*.

Organochlorines have been shown to biomagnify in food webs throughout the world i.e. DDTs (ATSDR, 2002; Covaci et al., 2006; McIntyre and Beauchamp, 2007; Yohannes et al., 2013a, b), HPTs (López-Martin et al., 1995), CHLs (ATSDR, 1994; McIntyre and Beauchamp, 2007), as well as HCB (ATSDR, 2013). Wepener et al. (2012) proposed that the high level of OCPs accumulated by *H. vittatus* from Lake Pongolapoort was due to biomagnification processes. Further Verheart et al. (2013) showed trophic transfer of persistent organic pollutants through the aquatic food webs of selected sites in the tropical system of the Congo River Basin. Biomagnification was not determined during this study but is an important factor to take into account, as *H. vittatus* are apex predators and are therefore at risk of accumulating high pollutant loads (Barnhoorn et al., 2009; McIntyre and Beauchamp, 2007). The high levels do not only pose a threat to aquatic organisms in the study area but also to the bird populations in the area as shown by Bouwman et al. (2013) in terms of Σ-DDTs. These authors found that there was a relationship between egg shell thinning and DDTs in eggs of the Grey heron (*Ardea cinerea*) and African darter (*Anhinga rufa*) from the Luvuvhu catchment. Although they were not able to demonstrate a causal relationship with decreased bird populations other studies showed threats of DDTs in Bald eagles (*Haliaeetus leucocephalus*) from the Great Lakes area of North America (Bowerman et al., 1998; Fry, 1995).

4.2. Human health risk assessment

The comprehensive risk evaluation at both the 50th and 95th percentiles revealed that OCP concentrations did not exceed the acceptable daily intake (ADI) or the tolerable daily intake (TDI) according to the World Health Organisation and Australian Government guidelines respectively (AGDHOCS, 2014; WHO, 2010). The concentrations of many of the OCP metabolite and isomer concentrations measured during this study did however exceed the maximum residue levels in edible fat as set by the European Union (EC, 2005).The evaluation of the cancer risks to human health associated with the consumption of fish containing OCP contaminants further demonstrated that there is an unacceptable cancer risk to local rural communities when consuming tigerfish daily over a lifetime. The results demonstrated that Σ-DDTs are of particular concern, albeit that all groups of OCPs posed a very high risk. According to Jiang et al. (2005) the use of both the 50th and 95th percentile to calculate HRs provides a simple way of screening chemicals that might require more detailed analysis. Where if only the 95th percentile HR is >1 a refined risk assessment should be conducted to ascertain the real risk. When both the 50th and 95th percentile HRs are >1 the initiation of appropriate management strategies should be considered. The results from this study indicate that appropriate management strategies should be put in place in all three of the rivers studied with regards to Σ-DDTs, Σ-HCHs and Σ-CHLs. When calculating the benchmark concentration, the use of a cancer risk of one in a million may lead to an over-conservative assessment of risk (Dougherty et al., 2000). Thus the risks posed by Σ-HPTs may also warrant managerial concern.

Although it is believed that using such a conservative approach provides an appropriate means for the initial screening of potential risks (Jiang et al., 2005). Each of the individual OCPs posed risks greater than 1 in 1,000,000 of getting cancer over and above the 1 in 4 cancer risk as indicated by the South African National Cancer Association (Albrecht, 2006), but these chemicals occur as mixtures and therefore potentially pose an even greater cancer risk to the consumers in the region. For example the additional risk of getting cancer is increased by 8 in 1000 chance at the 50th percentile and a 2 in 10 chance at the 95th percentile from eating OCP contaminated tigerfish from the Luvuvhu River. The risk estimates indicate similar albeit slightly lower risk from contaminated fish consumption from the Letaba and Olifants rivers. The potential risks posed by freshwater fish consumption demonstrated in this study were several magnitudes greater than those found by Barnhoorn et al. (2015) for other freshwater systems in South Africa. The OCPs however not only pose cancer risks but also numerous non-cancer risks as listed in Table 4, including such mechanisms as immune suppression, central nervous system effects, various reproductive effects and liver alterations and damage as discussed by Barnhoorn et al. (2015).

Similar to Jiang et al. (2005) there are however a number of limitations in this study; firstly we did not consider the potentially different risks associated with separate age groups, secondly the possible interactions of these toxic chemicals were not considered and thirdly no formal assessment was made as to the exact frequency of fish consumption by locals in the region, providing a better reflection of the certainty of the risks identified. However in a study done by Coetzee et al. (2015) in the Ndumo region of South Africa, tigerfish were found to be consumed by up to 47% of the local subsistence fishermen, which consumed up to three tigerfish per week. The authors suggested that tigerfish was an acquired taste as the longer fishermen had lived in the area the more likely they were to consume tigerfish. This potentially indicates that people local to our study area are at the greatest risk from consuming contaminated fish. The current assessment despite the listed limitations indicates a potentially very high cancer risk associated with eating contaminated tigerfish from all of the rivers. The study further provides an important evaluation and understanding of the human health risks associated with OCP exposure through freshwater fish consumption in the surrounding communities of the KNP.

5. Conclusions

This is the first study reporting on the OCP contaminant concentrations in the aquatic biota of the selected rivers within the KNP. It was demonstrated that *H. vittatus* accumulates OCPs and that bioaccumulation in this species was flow dependant. The flow related variation in pollutant accumulation can be attributed to the increased bioavailability of the selected contaminants. The wide-scale application of OCPs in the catchment of the study area is evident from the high chlordane, lindane, and DDTs. The OCP concentrations found in *H. vittatus* from both the Olifants and Luvuvhu rivers was alarmingly high, more so when considering the Luvuvhu River *H. vittatus*. Concentrations of the majority of the OCPs measured were the highest levels ever recorded in South African freshwater biota, these include; DDT and its metabolites, HCH and all of its various isomers, CHL and its isomers, as well as HPT and its isomers

Table 4
Non-cancer effects of organochlorine pesticides. Adapted from Huang et al. (2006).

Non-cancer effects	Contaminants			
	HCH — lindane	HPT	CHL	DDT
Immune suppression	X		X	X
Decrements in IQ/central nervous system effects	X	X	X	X
Fetotoxicity	X			X
Reproductive effects	X	X		X
Musculoskeletal		X		
Liver	X	X	X	X
Kidney	X			
Cardiovascular or haematological effects		X	X	X
Endocrine dysfunction			X	X

(Ansara-Ross et al., 2012). Additionally, many of these OCP metabolite and isomer concentrations measured during this study exceeded the maximum residue levels in edible fat as set by the European Union. This is worrying as most of these chemicals have been banned, not only due to their persistent nature but due to the effects these OCPs have on the natural environment. The presence of these contaminants indicates the need for continual monitoring of these systems and results in a dilemma for managers and conservationists as upstream human activities are impacting upon these aquatic ecosystems even though they are situated within a premier conservation area. This is of concern when managing the water resources of the conservation area since the contaminants pose potential risks to the mandated conservation of aquatic biota within the KNP. This is the first study to assess the potential health risks posed to the health of rural communities by OCPs through fish consumption and results show that real concern should be shown. The ingestion of other products such as water, vegetables, and animal meat, and the levels of other environmental pollutants were however not considered. Therefore, the actual health risk for local people through dietary intake could be significantly higher, especially considering that chicken and beef products are also consumed in rural areas.

Acknowledgements

The authors would like to thank the Water Research Commission (WRC) of South Africa (Project K5-1922, N.J. Smit, PI) for the financial support of this study. Views expressed are those of the authors and not those of the WRC. The financial assistance of the National Research Foundation (NRF) towards this research is hereby acknowledged (Bilateral project no. PG36150002). Opinions expressed and conclusions arrived at, are those of the authors and are not necessarily to be attributed to the NRF. This study was supported in part by a Grant-in-Aid for Scientific Research from the Ministry of Education, Culture, Sports, Science, and Technology of Japan awarded to M. Ishizuka (No. 24248056) and Y. Ikenaka (Nos. 26304043 and 15H02825) as well as a foundation of the JSPS Core to Core Program (AA Science Platforms PG36150001), and the Bilateral Joint Research Project (PG36150002). The authors also wish to thank the Scientific Services of the South African National Parks Board (SANParks) for logistical support during the study and Dr. Wynand Malherbe, North-West University, for generating the study site map.

References

van Ael, E., Covaci, A., Blust, R., Bervoets, L., 2012. Persistent organic pollutants in the Scheldt estuary: environmental distribution and bioaccumulation. Environ. Int. 48, 17–27.

Agency for Toxic Substances and Disease Registry (ATSDR), 1994. Toxicological Profile for Chlordane. US Department of Health and Human Services, Public Health Service, Atlanta, GA.

Agency for Toxic Substances and Disease Registry (ATSDR), 2002. Toxicological Profile for DDT, DDE and DDD. US Department of Health and Human Services, Public Health Service, Atlanta, GA.

Agency for Toxic Substances and Disease Registry (ATSDR), 2013. Toxicological Profile for Hexachlorobenzene. US Department of Health and Human Services, Public Health Service, Atlanta, GA.

Albrecht, C., 2006. Overview of the South African cancer research environment as a basis for discussions concerning the activation of CARISA (Cancer Research Initiative of South Africa) report of the South African cancer association. Available from http://www.drcarlalbrecht.com/documents/2013/Cancer_Research_Initiative_of_South_Africa.pdf. Accessed December 2015.

Andrew, T.G., Rouhani, Q.A., Seti, S.J., 2000. Can small-scale fisheries contribute to poverty alleviation in traditionally non-fishing communities ins South Africa? Afr. J. Aquat. Sci. 25, 49–55.

Ansara-Ross, T.M., Wepener, V., Van den Brink, P.J., Ross, M.J., 2012. Pesticides in South African freshwaters. Afr. J. Aquat. Sci. 37, 1–16.

Australian Government Department of Health Office of Chemical safety (AGDHOCS), 2014. ADI List: Acceptable Daily intakes for agricultural and veterinary chemicals. Available from http://www.health.gov.au/internet/main/publishing.nsf/content/ocs-adi-list.htm. Accessed December 2015.

Barnhoorn, I.E.J., Bornman, M.S., Jansen van Rensburg, C., Bouwman, H., 2009. DDT residues in water, sediment, domestic and indigenous biota from a currently DDT-sprayed area. Chemosphere 77, 1236–1241.

Barnhoorn, I.E.J., van Dyk, J.C., Genthe, B., Harding, W.R., Wagenaar, G.M., Bornman, M.S., 2015. Organochlorine pesticide levels in *Clarias gariepinus* from polluted freshwater impoundments in South Africa and associated human health risks. Chemosphere 120, 391–397.

Barnhoorn, I.E.J., van Dyk, J.C., Pieterse, G.M., Bornman, M.S., 2010. Intersex in feral indigenous freshwater *Oreochromis mossambicus*, from various parts in the Luvuvhu River, Limpopo province, South Africa. Ecotoxicol. Environ. Saf. 73, 1537–1542.

Bornman, M.S., Barnhoorn, I.E.J., Genthe, B., 2010. DDT for malaria control: effects in indicators and health risk. WRC Report No. 1674/1/09. Water Research Commission, Pretoria.

Bouwman, H., 2003. Pops in Southern Africa. In: Fiedler, H. (Ed.), The Handbook of Environmental Chemistry Volume 3 part 30 — Persistent Organic Pollutants. Springer-Verlag, Heidelberg, Berlin, pp. 297–320.

Bouwman, H., Coetzee, A., Schutte, C.H.J., 1990. Environmental and health implications of DDT contaminated fish from the Pongolo flood plain. J. Afr. Zool. 104, 275–286.

Bouwman, H., Viljoen, I.M., Quinn, L.P., Polder, A., 2013. Halogenated pollutants in terrestrial and aquatic bird eggs: converging patterns of pollutant profiles, and impacts and risks from high levels. Environ. Res. 126, 240–253.

Bowerman, W.W., Best, D.A., Grubb, T.G., Zimmerman, G.M., Giesy, J.P., 1998. Trends of contaminants and effects in bald eagles of the Great lakes basin. Environ. Monit. Assess. 53, 197–212.

Chapman, P.M., 1997. Is bioaccumulation useful for predicting impacts? Mar. Pollut. Bull. 34, 282–283.

Coetzee, H.C., Nell, W., van Eeden, E., de Crom, N., 2015. Artisanal fisheries in the Ndumo area of the lower Phongolo River Floodplain, South Africa. Koedoe 57, 1248.

Covaci, A., Gheorghe, A., Hulea, O., Schepens, P., 2006. Levels and distribution of organochlorine pesticides, polychlorinated biphenyls and polybrominated diphenyl ethers in sediments and biota from the Danube Delta, Romania. Environ. Pollut. 140, 136–149.

Dabrowski, J.M., Shadung, J.M., Wepener, V., 2014. Prioritizing agricultural pesticides used in South Africa based on their environmental mobility and potential human health effects. Environ. Int. 62, 31–40.

Dallaire, R., Dewailly, E., Ayotte, P., Forget-Dubois, N., Jacobson, S.W., Jacobson, J.L., Muckle, G., 2013. Exposure to organochlorines and mercury through fish and marine mammal consumption: associations with growth and duration of gestation among Inuit newborns. Environ. Int. 54, 85–91.

Deribe, E., Rosseland, B.O., Borgstrom, R., Salbu, B., Gebremariam, Z., Dadebo, E., Norli, H.R., Eklo, O.M., 2011. Bioaccumulation of persistent organic pollutants (POPs) in fish species from Lake Koka, Ethiopia: the influence of lipid content and trophic position. Sci. Total Environ. 410, 136–145.

Dougherty, C.P., Holtz, S.H., Reinert, J.C., Panyocosit, L., Axelrad, D.A., Woodruff, T.J., 2000. Dietary exposures to food contaminants across the United States. Environ. Res. 84, 170–185.

Du Preez, H.H., Steyn, G.J., 1992. A preliminary investigation of the concentration of selected metals in the tissues and organs of tigerfish (*Hydrocynus vittatus*) from the Olifants River, Kruger National Park, South Africa. Water SA 18, 131–136.

EC, 2005. Regulation (EC) No 396/2005 of the European parliament and the council of 23 February 2005 on maximum residue levels of pesticides in or on food and feed of plant and animal origin and amending council directive 91/414/EEC. OJ.L 70, 16.3.2005, p 1. Available via Dialog http://eurlex.europa.eu/LexUriServ.do?uri=CONSLEG:2005R0396:20080410:EN:PDF (Accessed August 2015).

Fry, D.M., 1995. Reproductive effects in birds exposed to pesticides and industrial chemicals. Environ. Health Perspect. 103, 165–171.

Gerber, R.J.L., Smit, N.J., Pieterse, G.M., Durholtz, D., 2009. Age estimation, growth rate and size at sexual maturity of tigerfish *Hydrocynus vittatus* from the Okavango Delta, Botswana. Afr. J. Aquat. Sci. 34, 239–247.

Gerber, R., Smit, N.J., van Vuren, J.H.J., Nakayama, S.M.M., Yohannes, Y.B., Ikenaka, Y.B., Ishizuka, M., Wepener, V., 2015a. Application of multivariate statistics and toxicity indices to evaluate the water quality suitability for fish of three rivers in the Kruger National Park. Afr. J. Aquat. Sci. 40, 247–259.

Gerber, R., Smit, N.J., van Vuren, J.H.J., Nakayama, S.M.M., Yohannes, Y.B., Ikenaka, Y.B., Ishizuka, M., Wepener, V., 2015b. Application of a sediment quality index for the assessment and monitoring of metals and organochlorines in a premier conservation area. Environ. Sci. Pollut. Res. 22, 19971–19989.

Gewurtz, S.B., Laposa, R., Gandhi, N., Christensen, G.N., Evenset, A., Gregor, D., Diamond, M.L., 2006. A comparison of contaminant dynamics in arctic and temperate fish: a modelling approach. Chemosphere 63, 1328–1341.

Heath, R.G.M., Claassen, M., 1999. An Overview of the Pesticide and Metal Levels Present in Populations of the Larger Indigenous Fish Species Selected in South African rivers. Water Research Commission (WRC), Pretoria (Report no:428/1/99).

Huang, X., Hites, R.A., Foran, J.A., Hamilton, C., Knuth, B.A., Schwager, S.J., Carpenter, D.O., 2006. Consumption advisories for salmon based on risk of cancer and noncancer health effects. Environ. Res. 101, 263–274.

Jiang, Q.T., Lee, T.K., Chen, K., Wong, H.L., Zheng, J.S., Giesy, J.P., Lo, K.K., Yamashita, N., Lam, P.K., 2005. Human health risk assessment of organochlorines associated with fish consumption in a coastal city in China. Environ. Pollut. 136, 155–165.

Kaur, M., Sharma, J.K., Gill, J.P., Aulakh, R.S., Bedi, J.S., Joia, B.S., 2008. Determination of organochlorine pesticide residues in freshwater fish species in Punjab, India. Bull. Environ. Contam. Toxicol. 80, 154–157.

López-Martin, J.M., Ruis-Olmo, J., Borrell, A., 1995. Levels of organochlorine compounds in freshwater fish from Catalonia, N.E. Spain. Chemosphere 31, 3523–3535.

Mabaso, M.L.H., Sharp, B., Lengeler, C., 2004. Historical review of malarial control in southern African with emphasis on the use of indoor residual house-spraying. Tropical Med. Int. Health 9, 846–856.

Malik, A., Singh, K.P., Ojha, P., 2007. Residues of organochlorine pesticides in fish from the Gomti River, India. Bull. Environ. Contam. Toxicol. 78, 335–340.

McHugh, K.J., Smit, N.J., van Vuren, J.H.J., van Dyk, J.C., Bervoets, L., Covaci, A., Wepener, V., 2011. A histology-based fish health assessment of the tigerfish, *Hydrocynus vittatus* from a DDT-affected area. Phys. Chem. Earth 36, 895–904.

McIntyre, J.K., Beauchamp, D.A., 2007. Age and trophic position dominate bioaccumulation of mercury and organochlorines in the food web of Lake Washington. Sci. Total Environ. 372, 571–584.

Mhlanga, W., 2000. Mercury in tigerfish (*Hydrocynus vittatus*, Castelnau), green happy (*Sargochromis codringtonii*, Boulenger) and kapenta (*Limnothrissa miodon*, Boulenger) from Lake Kariba, Zimbabwe. Afr. J. Ecol. 38, 224–229.

Quinn, L.P., de Vos, B.J., Fernandes-Whaley, M., Roos, C., Bouwman, H., Kylin, H., Pieters, R., van den Berg, J., 2011. Pesticide use in South Africa: one of the largest importers of pesticides in Africa. In: Stoytcheva, M. (Ed.), Pesticides in the Modern World — Pesticides Use and Management. Intech open, Rijeka, Croatia, pp. 49–96.

Rainbow, P.S., 2007. Trace metal concentrations in aquatic invertebrates: why and so what? Environ. Pollut. 120, 497–507.

Saadati, N., Abdullah, M.D.P., Zakaria, Z., Rezayi, M., Hosseinizare, N., 2012. Distribution and fate of HCH isomers and DDT metabolites in a tropical environment—case study Cameron Highlands—Malaysia. Chem. Cent. J. 6, 130–144.

Sarkar, S.K., Bhattacharya, B.D., Chatterjee, M., Alam, A., Satpathy, K.K., Jonathan, M.P., 2008. Occurrence, distribution and possible sources of organochlorine pesticide residues in tropical coastal environment of India: an overview. Environ. Int. 34, 1062–1071.

Schmitt, C.J., Zajicek, J.L., Peterman, P.H., 1990. National Contaminant Biomonitoring Program: residues of organochlorine chemicals in U.S. freshwater fish, 1976–1984. Arch. Environ. Contam. Toxicol. 19, 748–781.

Shaw, P.J.A., 2003. Multivariate Statistics for the Environmental Science. Arnold Publishers, London.

Smit, N.J., Howatson, G., Greenfield, R., 2009. Blood lactate levels as a biomarker for angling-induced stress in tigerfish, *Hydrocynus vittatus*, from the Okavango Delta, Botswana. Afr. J. Aquat. Sci. 34, 255–259.

Smolders, R., De Boeck, G., Blust, R., 2003. Changes in cellular energy budget as a measure of whole effluent toxicity in zebrafish (*Danio rerio*). Environ. Toxicol. Chem. 22, 890–899.

Soekoe, M., van der Bank, F.H., Smit, N.J., 2013. Determining the most suitable method of otolith preparation for estimating the age of tigerfish, *Hydrocynus vittatus* in the Pongolapoort Dam, South Africa. Afr. Zool. 48, 187–192.

Ter Braak, C.J., Smilauer, F., 2004. Canoco for Windows Version 4.53. Biometrics — Plant Research International, Wageningen.

United States Environmental Protection Agency (USEPA), 2005. Guidelines for carcinogen risk assessment. http://www.epa.gov/cancerguidelines/2005 (Accessed December 2015).

United States Environmental Protection Agency (USEPA), 2012. Human health risk assessment: risk based screening table. http://www.epa.gov/reg3hwmd/risk/human/pdf/NOV_2012_FISH.pdf (Accessed December 2015).

United States Environmental Protection Agency (USEPA), 2013. Food safety. http://www.epa.gov/oecaagct/tfsy.html (Accessed December 2015).

van Dyk, J.C., Bouwman, H., Barnhoorn, I.E.J., Bornman, M.S., 2010. DDT contamination from indoor residual spraying for malaria control. Sci. Total Environ. 408, 2745–2752.

Verheart, V., Covaci, A., Bouillon, S., Abrantes, K., Musibono, D., Bervoets, L., Verheyen, E., Blust, R., 2013. Baseline levels and trophic transfer of persistent organic pollutants in sediments and biota from the Congo River Basin (DR Congo). Environ. Int. 59, 290–302.

Wepener, V., Smit, N.J., Covaci, A., Dyke, S., Bervoets, L., 2012. Seasonal bioaccumulation of organohalogens in tigerfish *Hydrocynus vittatus* Castelnau, from Lake Pongolapoort South Africa. Bull. Environ. Contam. Toxicol. 88, 277–282.

Wepener, V., van Dyk, C., Bervoets, L., O'Brien, G., Covaci, A., Cloete, Y., 2011. An assessment of the influence of multiple stressors on the Vaal River, South Africa. Phys. Chem. Earth 36, 949–962.

Wepener, V., Van Vuren, J.H.J., Du Preez, H.H., 2000. Application of the equilibrium partitioning method to derive copper and zinc quality criteria for water and sediment: a South African perspective. Water SA 26, 97–104.

World Health Organisation (WHO), 2010. Inventory of ICPS and other WHO pesticide evaluations and summary of toxicological evaluations performed by the joint meeting on pesticide residues (JMPRs) through 2010. http://www.who.int/foodsafety/chem/jmpr_pesticide/en/index.html (Accessed December 2015).

Yohannes, Y.B., Ikenaka, Y., Nakayama, S.M.M., Saengtienchai, A., Watanabe, K., Ishizuka, M., 2013a. Organochlorine pesticides and heavy metals in fish from Lake Awassa, Ethiopia: insights from stable isotope analysis. Chemosphere 91, 857–863.

Yohannes, Y.B., Ikenaka, Y., Saengtienchai, A., Watanabe, K.P., Nakayama, S.M.M., Ishizuka, M., 2013b. Occurrence, distribution, and ecological risk assessment of DDts and heavy metals in surface sediments from Lake Awassa — Ethiopian Rift Valley Lake. Environ. Sci. Pollut. Res. 20, 8663–8671.

Yohannes, Y.B., Ikenake, Y., Saengtienchai, A., Watanabe, K.P., Nakayama, S.M.M., Ishizuka, M., 2014. Concentrations and human health risk assessment of organochlorine pesticides in edible fish species from a Rift Valley lake — Lake Ziway, Ethiopia. Ecotoxicol. Environ. Saf. 106, 95–101.

academicJournals

Vol. 8(7), pp. 58-68, July, 2016
DOI:10.5897/JECE2016.0374
Article Number: D44277B59394
ISSN 2141-226X

http://www.academicjournals.org/JECE

Journal of Environmental Chemistry and Ecotoxicology

Full Length Research Paper

Heavy metals and metalloid accumulation in livers and kidneys of wild rats around gold-mining communities in Tarkwa, Ghana

Nesta Bortey-Sam[1], Shouta M. M. Nakayama[1], Yoshinori Ikenaka[1], Osei Akoto[2], Elvis Baidoo[2], Hazuki Mizukawa[1] and Mayumi Ishizuka[1]*

[1]Laboratory of Toxicology, Department of Environmental Veterinary Sciences, Graduate School of Veterinary Medicine, Hokkaido University, Japan.
[2]Department of Chemistry, Kwame Nkrumah University of Science and Technology, Kumasi, Ghana.

Received 25 February, 2016; Accepted 27 May, 2016

Previous studies revealed high levels of metals in soils, drinking water, foodstuffs and food animals in several communities in Tarkwa, Ghana. Therefore wild rats were trapped from 16 communities in Tarkwa to estimate the environmental pollution state of metals; determine differences in sex in metal accumulation; and assess the potential risks involved. Concentrations of arsenic (As), cadmium (Cd), cobalt (Co), chromium (Cr), copper (Cu), manganese (Mn), nickel (Ni), lead (Pb) and zinc (Zn) were measured in the livers and kidneys of wild rats; and livers accumulated higher levels of As than kidneys but the reverse was for Cd and Pb. In both organs, As, Cd and Zn levels were higher in female than the male rats. There was a strong positive correlation between body weight and Cd concentrations in livers and kidneys of wild rats which reflects a mechanism of protection against the development of osteopenia, although a biological effect remains a concern. Pb levels in the kidneys could cause intra nuclear inclusion bodies and karyocytomegaly in the proximal tubular cells in 29% of wild rats in Tarkwa and structural and functional kidney damage in 6%. Concentrations of As in kidneys of these wild rats could cause glomerular swelling in 9% of rats. Principal component analysis of the results showed that wild rats in Tarkwa were exposed to heavy metals and a metalloid through borehole drinking water and soils.

Key words: Wild rats, heavy metal, metalloid, liver, kidney, Ghana.

INTRODUCTION

Anthropogenic activities including artisanal and small-scale gold mining have caused elevated levels of heavy metal and metalloids in the environment (Naccari et al., 2009; Licata et al., 2010). This activity could lead to spillage and run-off into rivers, ponds, streams, wells, and borehole drinking water (Obiri, 2007), and further result in

*Corresponding author. E-mail: ishizum@vetmed.hokudai.ac.jp. Tel: +81–11–706–6949. Fax: +81–11–706–5105.

heavy metal and/or metalloid exposure to humans and animals through various pathways. Heavy metals and metalloids have a wide range of health effects including mutagenicity, carcinogenicity, teratogenicity, immunosuppression, poor body condition, and impaired reproduction in humans and animals (Scheuhammer, 1987; Florea and Busselberg, 2006). All of these make them a serious threat to living organisms (Battaglia et al., 2005; López-Alonso et al., 2007; Naccari et al., 2009).

Tarkwa (05°18′00″N; 01°59′00″W) is a town in the southwest of Ghana, with a population of 90,477 (Ghana Statistical Service, 2010). It is a noted centre for gold and manganese mining. Tarkwa mine, which is a large open-cast gold mine, is situated to the northwest of the town, and Nsuta manganese mine is situated to the east. Tarkwa has nearly a century of gold mining history and the largest concentration of mining companies in a single district in Ghana and the West African sub-region (Akabzaa and Darimani, 2001).

Studies conducted by Asante et al. (2007), Bortey-Sam et al. (2015a, b, c, d) and Hayford et al. (2008) on the impact of gold mining in soil, drinking water, foodstuffs and food animals (free-range chickens, goat and sheep) collected around mining communities in Tarkwa showed high levels of some toxic metals including arsenic (As) and mecury (Hg) than maximum levels by European Commission (EC) (2006), World Health Organization (WHO) (1996; 2011) and United States Environmental Protection Agency (USEPA) (2004; 2012). Bortey-Sam et al. (2015a) indicated that the concentrations of some heavy metals/metalloid in agricultural soils in some communities in Tarkwa exceeded the ecological-soil screening levels (USEPA, 2004) recommended for mammalian wildlife, which includes wild rats and mice. However, levels of metals (0.24 [Hg] to 72 mg/kg dw [Zn]) detected in soils collected from the University of Mines and Technology (uMaT) campus (reference site) were low compared to world range for unpolluted soils by Kabata-Pendias and Pendias (1992).

Although wildlife is rich and diverse, with a large number of mammals, reptiles and insects in the study area, rats were used as sentinels to measure the environmental pollution state because they are mammals that share many processes with humans and are appropriate for use to answer many research questions. They tend to pick food and water from the ground which could be contaminated with various pollutants including metals. In studies by Nakayama et al. (2011, 2013), wild rats in mining areas in Zambia were used as sentinels for heavy metal accumulation, and results showed that rats accumulated metals had likely originated from mining activities. Similarly, Guerrero-Castilla et al. (2014) used wild mice around coal mining areas in Columbia to study the exposure and health effects of heavy metals from the mining processes.

Despite the wide and numerous studies of heavy metals concentrations in various samples in Tarkwa, Ghana, there is limited or no data from literature on its accumulation in wild rats. The objectives of this study were to determine the accumulation of heavy metals and a metalloid in livers and kidneys of wild rats in Tarkwa; to determine sex differences in heavy metals and metalloid accumulation; to examine the relationship between body weight of rats and metal; to identify the possible exposure route of these metals to wild rats in Tarkwa; and to examine the potential risks heavy metals could pose to wild rats.

MATERIALS AND METHODS

Sampling

All procedures used in this experiment were according to the guidelines of the Hokkaido University Institutional Animal Care and Use Committee and the local veterinarian policy of the study area. In June, 2012, live wild rats (*Rattus norvegicus* or *R. rattus*) were captured using gauze cage traps with food as bait, in residential, commercial and farming areas (within 16 communities) in Tarkwa (n = 46). Rat species were morphologically identified. Some of the sampled communities were 2 (Samahu), 3.4 (Abekuase) and 5.2 (T-Tamso) km away from the mines, respectively (Figure 1). After anesthesia overdose, rats were euthanized, and body weight and sex were determined (25 females and 21 males). The livers and kidneys are target organs for monitoring metal contamination in animals because both organs function in removing toxic metals from the body (Abou-Arab, 2001; Husain et al., 1996). Studies of three animal species (free-range chickens, goat and sheep) in Tarkwa showed that the livers and kidneys contained the highest levels of metals (Bortey-Sam et al., 2015d). For these reasons, livers and kidneys were collected from each rat and stored at −20°C. Samples were kept in a freezer at the Chemistry Department of the Kwame Nkrumah University of Science and Technology, KNUST, Ghana and later transported to the Laboratory of Toxicology, Graduate School of Veterinary Medicine, Hokkaido University, Japan where they were stored in -30°C until analysis.

Sample preparation and metal analysis

Preparations and digestion of liver and kidney samples for heavy metals and metalloid analysis were done according to method described by Bortey-Sam et al. (2015d). Approximately 0.5 g of individual samples were dried in an oven at 40°C and placed in prewashed digestion vessels. Samples were digested (for 52 min) (Speed Wave MWS-2 microwave digestion, Berghof, Germany) using 5 ml of (65%) nitric acid, HNO_3 (Kanto Chemical Corp., Tokyo, Japan) and 1 ml of (30%) hydrogen peroxide, H_2O_2 (Kanto Chemical Corp., Tokyo, Japan). After digestion, cooled samples were transferred into corning tubes (Corning Incorporated, New York, USA) and diluted to a final volume of 10 ml with milli Q water. A reagent blank was prepared using the same procedure.

An inductively coupled plasma-mass spectrometer (ICP-MS; 7700 series, Agilent technologies, Tokyo, Japan) was used for quantification. The instrument was calibrated using standard solutions of the respective metals (to establish standard curves before metal analysis). All chemicals and standard stock solutions were of analytical reagent grade (Wako Pure Chemicals, Osaka, Japan). The detection limits (ng/g) of chromium (Cr), manganese (Mn), iron (Fe), cobalt (Co), nickel (Ni), copper (Cu), zinc (Zn),

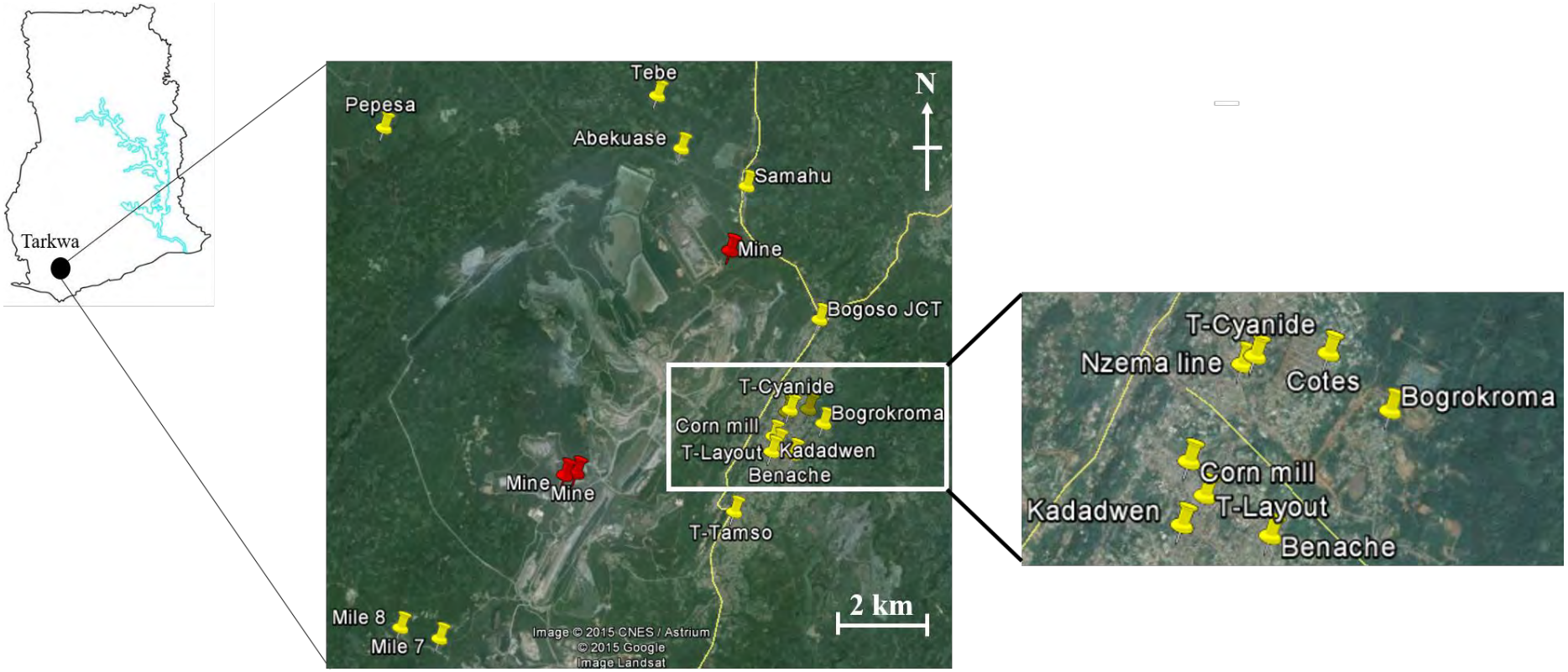

Figure 1. Map showing wild rats sample locations in Tarkwa, Ghana (yellow and red and pins indicate sampled communities and gold mines, respectively).

arsenic (As), cadmium (Cd), and lead (Pb) were 0.003, 0.025, 0.154, 0.0004, 0.024, 0.007, 0.226, 0.002, 0.001 and 0.001, respectively. Concentrations of metals were expressed in mg/kg dry weight (mg/kg dw).

Quality assurance and quality control

For heavy metals and metalloid, replicate blanks and reference materials, DORM-3 (Fish protein, The National Research Council, Canada) and DOLT-4 (Dogfish liver, The National Research Council, Canada) were used for method validation and quality control. Replicate analysis of these reference materials showed good accuracy (relative standard deviation, RSD, ≤ 3%) and recovery rates ranged from 80 to 115%.

Statistical analysis

Statistical analyses were performed using SPSS 20.0 (IBM SPSS Inc., Chicago, USA). Kolmogorov-Smirnov (K-S) and Shapiro-Wilk's (S-W) tests were used to determine the normality of data and was considered statistically significant if p value was less than 0.05. Statistical analyses were carried out after data were log transformed (normalized). Student's T-test was used to compare distribution of metals between livers and kidneys, and differences were considered statistically significant with p value < 0.05. Pearson's correlations were used to determine the relationship between concentrations of metals and body weight, and significant level was p value less than 0.05. Principal component analysis (PCA) based on log transformed data was done to determine the distribution pattern and possible route of heavy metals exposure to wild rats, using JMP statistical software v. 10

Table 1. Mean concentrations (± SD) and ranges of heavy metals and a metalloid (mg/kg dw) in the livers and kidneys of wild rats in Tarkwa, Ghana.

Samples		n	As	Cd	Co	Cr	Cu	Mn	Ni	Pb	Zn
Liver	Mean	46	2.59[a]	0.198[a]	0.198[a]	0.147[a]	18.9[a]	5.50[a]	0.869[a]	1.05[a]	263[a]
	SD		2.81	0.321	0.207	0.0908	14.0	2.86	0.522	2.23	95.2
	Minimum		0.0699	0.0213	0.0784	0.0166	7.59	2.54	0.219	0.0532	112
	Maximum		12.6	1.45	1.21	0.406	71.8	19.1	2.11	10.7	524
Kidney	Mean	46	1.91[a]	1.41[b]	0.382[b]	0.375[b]	14.3[a]	4.09[b]	2.02[b]	3.97[b]	117[b]
	SD		2.33	3.57	0.333	0.327	4.57	2.79	1.85	8.15	41.7
	Minimum		0.102	0.0039	0.0741	0.0773	9.17	1.53	0.172	0.044	64.3
	Maximum		14.0	21.1	1.62	1.72	39.5	16.8	7.85	41.6	284

n: number of samples; SD: standard deviation; different letters (a and b) between groups indicates significant difference (Student's T-Test; $p < 0.05$.

(SAS Institute). The principal components were extracted with eigenvalues > 1.

RESULTS AND DISCUSSION

Levels of heavy metals and a metalloid

Mean concentrations of heavy metals and a metalloid in livers of wild rats in Tarkwa decreased in the order; Zn > Cu > Mn > As > Pb > Ni > Cr > Co = Cd; and the order in the kidney was Zn > Cu > Mn > Pb > Ni > As > Cd > Co = Cr (Table 1). All metals measured were detected in 100% of liver and kidney samples. K-S and S-W's tests for normality showed a significant variation ($p < 0.001$) in metal distribution in livers and kidneys of wild rats in Tarkwa. Distribution of Cd, Co, Cr, Mn, Ni, Pb, and Zn between livers and kidneys differed significantly (Student's T-test; $p < 0.05$) (Table 1). The following paragraphs discusses As, Pb and Cd which were classified as the first, second and seventh most hazardous substances (Agency for Toxic Substances and Disease Registry (ATSDR), 2013), and Mn because Tarkwa is also noted for Mn mining.

Mean concentration of As was higher in livers (2.59 ± 2.81 mg/kg dw) than kidneys (1.91 ± 2.33 mg/kg dw) (Table 1). The liver is a major target organ of As carcinogenesis (Waalkes et al., 2003) and could be the reason for the higher As levels. As is toxic and most hazardous substance (ATSDR, 2013) and due to its non-biodegradable nature, it could accumulate in soil, food and water (Amonoo-Neizer et al., 1995), through which wild rats could be exposed since they pick food and water mainly from the ground. Levels of As in soils, drinking water and organs of free-range chickens raised health risk concerns for both humans and animals in some communities in Tarkwa with food and water picking being the dominant sources in chicken (Bortey-Sam et al., 2015a, b, d). The levels were attributed to processing of the ore which involves roasting, and this result in the production of arsenic trioxide gas which is distributed throughout the study area by air current (Amonoo-Neizer et al., 1995).

As shown in Table 1, the mean levels of Cd in the kidneys (1.42 ± 3.57) was seven times higher ($p < 0.05$) compared to the liver (0.198 ± 0.321) of wild rats in Tarkwa. There have been suggestions that animals exposed to Cd accumulate it in their kidneys because of the presence of free protein-thiol groups which leads to a strong fixation of the metal (Pompe-Gotal and Crnic, 2002). Cd concentrations in blood, urine and kidney have been recognized as good indicators of exposure (Brzoska et al., 2004). Cd could increase excretion of calcium and reduce the generation of active vitamin D in kidney. Consequently, calcium uptake and absorption in gastrointestinal gut are decreased (Chen et al., 2013). Bone lesions, apart from kidney damage, are the main health consequences of chronic exposure to Cd. Osteopenia, osteomalacia and osteoporosis with pathological fractures have been reported in Cd-exposed humans (Jarup, 2002; Alfven et al., 2000; Honda et al., 2003) and experimental animals (Whelton et al., 1997; Uriu et al., 2000).

Levels of Pb were higher ($p < 0.05$) in kidneys (3.97 ± 8.15 mg/kg dw) than livers (1.05 ± 2.23 mg/kg dw) (Table 1). In previous studies, high levels of Pb was found in *Manihot esculenta* (cassava), soils and chickens from some communities around mining areas in Tarkwa, which could cause health risk to residents and especially children (Bortey-Sam et al., 2015a, c, d). The levels of Pb in organs of free-range chickens in Tarkwa emanated from contamination of soil, feeds and/or water sources (Bortey-Sam et al., 2015d), and these could be the same route through which wild rats were exposed.

Livers (5.50 ± 2.86) accumulated higher ($p < 0.05$) levels of Mn than kidneys (4.09 ± 2.79) (Table 1). This is because, the liver is key for maintaining Mn homeostasis (Finley, 1998), and among organs with highest Mn levels (Dorman et al., 2006) as it produces two of the main

Table 2. Sex differences in accumulation of heavy metals and a metalloid (mg/kg dw) in the livers and kidneys of wild rats in Tarkwa, Ghana.

Organ	Sex		As	Cd	Co	Cr	Cu	Mn	Ni	Pb	Zn
Livers	Male	Mean	0.573[a]	0.066[a]	0.132[a]	0.185[a]	19.8[a]	5.45[a]	0.921[a]	0.237[a]	256[a]
		SD	0.586	0.027	0.045	0.078	23.2	6.65	0.607	0.217	103
		Minimum	0.070	0.021	0.088	0.071	8.95	2.54	0.219	0.053	164
		Maximum	1.92	0.098	0.210	0.294	71.8	19.1	1.72	0.666	433
	Female	Mean	1.08[a]	0.117[a]	0.163[a]	0.198[a]	15.3[a]	4.60[a]	0.894[a]	0.292[a]	301[a]
		SD	2.53	0.181	0.194	0.106	7.27	1.21	0.605	1.34	111
		Minimum	0.113	0.040	0.078	0.094	7.59	2.60	0.269	0.093	177
		Maximum	12.6	1.45	1.21	0.406	30.9	6.66	2.12	10.7	524
Kidneys	Male	Mean	0.645[a]	0.292[a]	0.332[a]	0.410[a]	18.1[a]	5.21[a]	4.82[a]	1.24[a]	122[a]
		SD	0.603	0.283	0.316	0.247	9.55	3.53	1.99	1.69	68.7
		Minimum	0.103	0.004	0.074	0.128	11.6	1.53	1.82	0.044	64.3
		Maximum	1.89	0.867	1.62	0.816	39.5	16.8	7.85	5.17	284
	Female	Mean	0.905[a]	0.650[a]	0.244[a]	0.513[a]	13.7[a]	4.32[a]	2.52[b]	1.53[a]	140[a]
		SD	1.32	1.15	0.172	0.508	1.85	1.70	1.33	2.69	45.6
		Minimum	0.159	0.107	0.082	0.077	10.2	2.29	0.939	0.305	81.6
		Maximum	14.0	21.1	0.519	1.72	16.4	6.89	5.03	41.6	284

SD: standard deviation; different letters (a and b) between male and female rats within the same organ indicates significant difference (Student's T-Test; $p < 0.05$).

plasma transport proteins of Mn-albumin and transferrin (Crossgrove and Zheng, 2004). Excess Mn causes neurotoxicity, production of reactive oxygen species and disturbance of mitochondrial dynamics (Barhoumi et al., 2004; Martinez-Finley et al., 2013). In the offal and muscles of free-range chickens, goat and sheep in Tarkwa, the mean concentrations of Mn were above the WHO (1996) maximum levels (0.5 mg/kg) except in chicken muscle, and levels were attributed to proximity of the sample sites to the Mn mine (Bortey-Sam et al., 2015d).

Sex differences in heavy metal and metalloid accumulation

Bio-accumulation of heavy metals in animals vary according their sex, size and/or age (Hunter et al., 1989; Sawicka-Kapusta et al., 1995; Damek-Poprawa and Sawicka-Kapusta, 2004). Although, we could not determine the ages of wild rats in this study, the results of sex differences in the accumulation of metals showed no statistical variation ($p > 0.05$) except Ni in kidneys (Table 2). However, levels of As, Cd and Zn were higher in the livers of female rats compared to males, while in livers of male rats, Cu and Mn were higher ($p > 0.05$). Co, Cr, Ni and Pb levels were similar in livers of both sexes (Table 2). This trend was similar for the kidneys except for Ni which was higher in male rats compared to females (Table 2). Study of Blagojevic et al. (2012) in skull of mice from two localities in Serbia revealed that no gender dependent variation was detected for Fe, Mn, Co, Cd, Zn, Ni, Pb and Cu.

Although not significant ($p > 0.05$), average Cd levels in livers (0.12 mg/kg dw) and kidneys (0.65 mg/kg dw) of females were two times higher than in males (liver [0.07 mg/kg dw] and kidney [0.29 mg/kg dw]), respectively. Absorption of Cd is through the gastrointestinal tract (GIT), however this can be affected by several factors, such as age, sex, nutritional status, and preceding Cd burden. Among these, young age, iron deficiency, and being female are reported to accelerate the absorption of Cd through the GIT in both humans and animals (Berglund et al., 1994; Flanagan et al., 1978; Hamilton and Valberg, 1974; Kowel, 1988; Taguchi and Suzuki, 1981) and these could be the reasons why Cd levels were higher in females than males.

Heavy metals correlation with body weight of wild rats

Levels of Ni in the livers and kidneys negatively correlated ($p < 0.05$) with body weight of rats (Table 3). Ni is a carcinogen and overexposure could cause decreased body weight and damage to the heart and liver (Homady et al., 2002). On the other hand, body weights

Table 3. Pearson's correlation between heavy metals and body weight of wild rats in Tarkwa, Ghana.

Metal	As	Cd	Co	Cr	Cu	Mn	Ni	Pb	Zn	Body weight/g
As	1	**0.518***	**0.516***	**-0.003**	**0.152**	**0.215**	**-0.553***	**0.531***	**0.704****	**0.318**
Cd	0.333	1	**0.393**	**0.167**	**-0.195**	**0.255**	**-0.631****	**0.704****	**0.480**	**0.599***
Co	0.225	0.531*	1	**0.355**	**0.553***	**0.066**	**-0.166**	**0.112**	**0.394**	**0.444**
Cr	0.398	0.058	0.511*	1	**0.204**	**0.562***	**0.313**	**0.128**	**0.097**	**-0.315**
Cu	0.324	-0.153	0.217	0.328	1	**0.298**	**0.283**	**0.004**	**0.305**	**0.045**
Mn	0.420	-0.506*	0.045	0.359	0.733**	1	**0.219**	**0.590***	**0.395**	**-0.374**
Ni	-0.349	-0.526*	0.199	0.212	0.319	0.380	1	**-0.418**	**-0.469**	**-0.725****
Pb	-0.061	-0.049	0.167	-0.264	-0.017	0.064	0.090	1	**0.653****	**0.253**
Zn	0.076	0.075	-0.394	-0.357	0.032	-0.068	-0.022	-0.236	1	**0.449**
body weight/g	0.350	0.864**	0.538*	0.076	-0.149	-0.391	-0.580*	0.078	-0.047	1

*: Correlation is significant at the 0.05 level.**: Correlation is significant at the 0.01 level. Bold indicates correlations between heavy metals and body weight in kidneys of wild rats otherwise for livers.

correlated positively ($p < 0.05$) with Cd (both livers and kidneys) and Co (livers only). In exposure studies of Brzoska et al. (2004) and Chen et al. (2013), increase in the body weights of rats was noted when exposed to Cd. Wronski et al. (1987) demonstrated that increased body weight provides a partial protection against the development of osteopenia in the long bones of ovariectomized (OVX) rats. Nevertheless, the protective effect of obesity against osteopenia in OVX rats is only partial and that marked osteopenia develops in the long bones of OVX rats regardless of body weight. This trend suggests that the increased body weight of obese OVX rats may have provided an additional stimulus for bone formation in the weight-bearing long bones (Wronski et al., 1987). The findings of Wronski et al. (1987) were consistent with reports of diminished bone loss in obese postmenopausal women (Saville and Nilsson, 1966; Daniell, 1976; Lindsay et al., 1984). These trends could explain the significant positive correlation ($p < 0.05$) between Cd levels in livers and kidneys and body weight of rats.

Possible sources of heavy metal and metalloid in wild rats

PCA was used to trace the possible route of heavy metals and a metalloid exposure to wild rats in Tarkwa. Soil, bore hole drinking water and foodstuff (cassava and *Musa paradisiaca* [plantain]) data on heavy metals in communities in Tarkwa, used for PCA was obtained from Bortey-Sam et al. (2015a, b, c). As shown in Figure 2, component 1 (PC1) makes up 40% of the PCA and score plot has high loadings of livers, kidneys (of wild rats), soils and borehole drinking water, with some highly associated with all the studied metals. This suggests that exposure of wild rats to metals were through soils and borehole drinking water, which is similar to conclusion of Bortey-Sam et al. (2015d) on the sources of metals in free-range chickens in Tarkwa. This is obvious because like chickens, these wild rats also pick food and water from the ground which contains heavy metals and/or metalloids. There was a strong association between the livers and kidneys with borehole drinking water from Tarkwa, which was also highly associated with Cu, Cd and Zn (Figure 2).

Toxicological significance

The levels of heavy metals and metalloid in this study were compared with studies by Nakayama et al. (2013), Soewu et al. (2014) and Guerrero-Castilla et al. (2014) on the accumulation and biological effects (oxidative stress) of metals in wild rats and mice around mining and industrial communities in Zambia, Nigeria and Colombia, respectively. Among the livers and kidneys, levels of As, Ni, Zn and Cd (observed only in kidneys) were higher in this study compared to studies by Soewu et al. (2014), Nakayama et al. (2013) and Guerrero-Castilla et al. (2014) (Table 4). Exposure of wild rats to Ni, Zn and Cd in Tarkwa could have resulted from mining/smelting, municipal waste and/or the use and sometimes abuse of phosphate fertilizers and organic manures. Other sources may include leachates from Ni-Cd based batteries and Cd plated items which are so carelessly discarded by battery chargers and users in Ghana as indicated by Bortey-Sam et al. (2015a, d). Recently, electronic wastes are disposed and often burnt at refuse dumps.

Nakayama et al. (2013) studied heavy metals in wild rats and reported to cause toxicological effects, since the accumulated metals caused induction of metallothionein (MT) in the livers and kidneys. Similarly, levels of metals in exposed mice from coal mining areas in Colombia

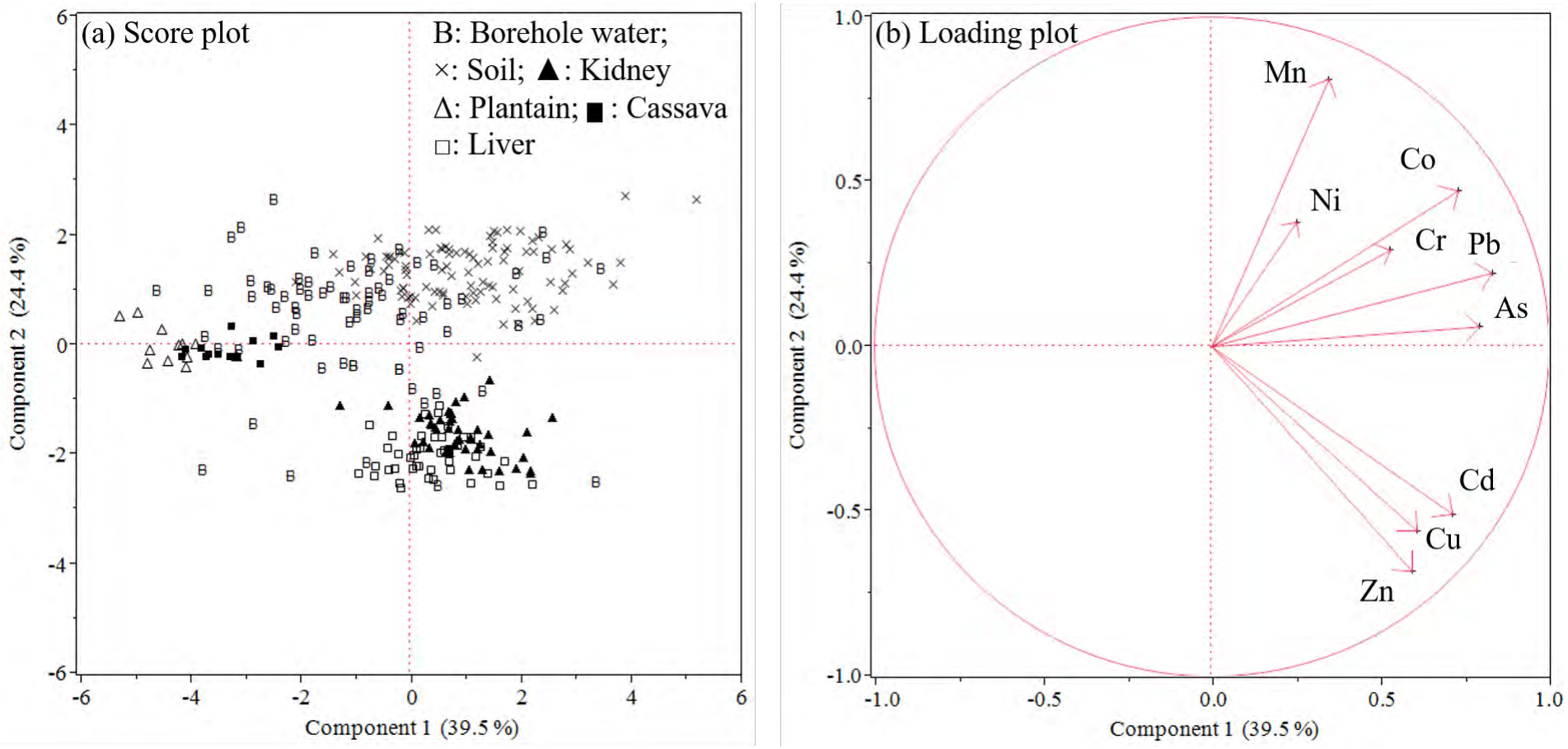

Figure 2. Distribution pattern of heavy metals and a metalloid in cassava, plantain, borehole drinking water, soils, livers and kidneys of wild rats in Tarkwa characterized by PCA.

caused a significant increase ($p < 0.05$) in mRNA expression of genes related to oxidative stress, metal transport and DNA damage (Guerrero-Castilla et al., 2014).

Concentrations of Cd in both organs of this study were below the critical renal intoxication level (119 mg/kg dw) which leads to subclinical symptoms for small mammals (Tohyama et al., 1987; Ma et al., 1991). Similarly, a critical liver concentration of 20 to 30 mg/kg leads to hepatocyte damage (Godowicz, 1988; Swiergosz-Kowalewska, 2001). The toxicity of As in mammals was found to be related with levels above 3 mg/kg in the liver and kidney(Gupta, 1998) and animal data suggest that As exposure may have chronic effects on the kidneys (WHO, 1981). Liu et al. (2000) recorded that glomerular swelling is one of the degenerative changes that

Table 4. Comparison of mean concentrations (mg/kg dw) of heavy metal and a metalloid with other studies.

Organ	Sample site/country	Site description	n	As	Cd	Co	Cr	Cu	Mn	Ni	Pb	Zn
Livers	Tarkwa, Ghana (This study)	Gold and Mn mining	46	2.59	0.198	0.198	0.147	23.0	5.50	0.869	1.05	263
	Kabwe, Zambia*	Pb and Zn mining	20	0.5	0.12	0.22	0.28	10.2		0.11	1.19	151
	Chingola, Zambia*	Co and Cu mining	13	0.07	0.05	1.72	0.15	29.5		0.05	0.41	115
	Lusaka, Zambia*	University campus	18	0.57	0.03	0.37	0.78	14		0.69	0.14	141
	La Jagua, Colombia#	Coal mining		0.35	2.36			22.2			0.18	2.2
	La Loma, Colombia#	Coal mining		0.24	0.55			13.8			0.35	16.7
	Omo forest, Nigeria*#	Undisturbed site	4		0.00		0.77	8.55	6.16		0.77	103
	Mosinmi ecotome*#	Oil and gas industries	4		0.58		0.00	8.05	16.2		0.00	87.1
	Ibese ecotome*#		4		0.00		2.16	11.9	8.64		0.00	77.1
	Agbara ecotome*#	Industrial	4		0.00		0.80	11.9	11.5		0.00	114
Kidneys	Tarkwa, Ghana (This study)	Gold and Mn mining	46	1.91	1.41	0.382	0.375	14.3	4.09	2.02	3.97	117
	Kabwe, Zambia*	Pb and Zn mining	20	0.52	0.64	0.26	0.93	11.5		0.64	5	91
	Chingola, Zambia*	Co and Cu mining	13	0.28	0.71	1.88	0.82	23		0.63	2.85	109
	Lusaka, Zambia*	University campus	18	1.72	0.14	0.98	0.75	14		0.59	0.39	0.39
	Omo forest, Nigeria*#	Undisturbed site	4		0.00		1.44	13.5	5.76		1.45	93.2
	Mosinmi ecotome*#	Oil and gas industries	4		0.00		1.08	13.8	11.0		0.96	95.7
	Ibese ecotome*#		4		0.00		2.04	13.9	6.72		0.00	86.4
	Agbara ecotome*#	Industrial	4		0.32		2.16	15.3	5.76		0.00	97.0

n: number of samples; * indicates study by Nakayama et al. 2013 in wild rats; # indicates study by Guerrero-Castilla et al. 2014 in wild house mice and concentrations were in mg/kg fresh weight; *# indicates study by Soewu et al. 2014 in cane rats (wild grass cutters).

usually occur in mice chronically exposed to As. These changes were also observed in livers and kidneys of mice at concentrations of 1.79 ± 0.946 and 3.89 ± 0.817 mg/kg dw, respectively (Pereira et al., 2006). In the present study, concentrations of As in both organs were higher in 47 and 9% of livers and kidneys, respectively, compared with levels observed by Pereira et al. (2006) and could cause glomerular swelling in 9% of rats.

Levels of Pb in the livers and kidneys of wild rats in this study were higher than study by Guerrero-Castilla et al. (2014) but comparable with levels in Kabwe, Zambia, which was a Pb-Zn mine area (Nakayama et al., 2013) (Table 4). Ma (2011) reported that kidney Pb level >15 mg/kg dw caused structural and functional kidney damage, while concentrations >120 mg/kg dw caused body weight loss in adults rats. In histopathological studies, changes in the kidney, such as Pb intranuclear inclusion bodies and karyocytomegaly in the proximal tubular cells were detected in wild brown rat (*R. norvegicus*) at kidney Pb concentrations > 2.5 mg/kg dw (Ceruti et al., 2002). In this study, the average concentration of Pb in kidneys (3.97 mg/kg dw) exceeded this histopathological threshold (2.5 mg/kg dw) and was higher in 29% of wild rats in Tarkwa. Moreover, 3 kidney samples (6%) exceeded the structural and functional kidney damage level (> 15 mg/kg dw) (Ma, 2011). The high levels of metals detected in the livers and kidneys of wild rats in Tarkwa could cause health risk to mammalian wild life.

Conclusions

Wild rats in Tarkwa, a mining community in Ghana, have been exposed to heavy metals and a metalloid through borehole drinking water and

soils; and livers accumulated higher levels of As than kidneys but the reverse was for Cd and Pb. In both organs As, Cd and Zn levels were higher in female than the male rats. The strong positive correlation between body weight and concentrations of Cd in livers and kidneys of wild rats reflects a mechanism of protection against the development of osteopenia in the long bones, although biological effects remain a concern. Concentration of Pb in kidneys caused intranuclear inclusion bodies and karyocytomegaly in the proximal tubular cells in 29% of wild rats in Tarkwa; and structural and functional kidney damage in 6%. Concentrations of As in kidneys of these wild rats caused glomerular swelling in 9% of rats. With the rapid increase in mining in Ghana and high concentrations and possible risk of metals to wild life, it is recommended that the government considers the following:

1. Educate the public on environmental pollution and management.
2. Continuous screening and monitoring of heavy metals and metalloids in the study area.
3. Set policies to curb the rate of metal pollution in Ghana.

Conflict of Interests

The authors have not declared any conflict of interests.

ACKNOWLEDGEMENTS

This work was supported by Grants-in-Aid for Scientific Research from the Ministry of Education, Culture, Sports, Science and Technology of Japan awarded to M. Ishizuka (No. 24405004 and No. 24248056) and Y. Ikenaka (No. 26304043, 15H0282505, 15K1221305), and the foundation of JSPS Core to Core Program (AA Science Platforms) and Bilateral Joint Research Project (PG36150002 and PG36150003). The financial support by The Mitsui & Co., Ltd. Environment Fund and The Nihon Seimei Foundation is also acknowledged. We are grateful to Mr. Takahiro Ichise (Laboratory of Toxicology, Graduate School of Veterinary Medicine, Hokkaido University) for technical support. We also express our sincere gratitude to Mr. Joseph Prah, and Mr. Joseph Addae who in various ways assisted to carry out this research.

REFERENCES

Abou-Arab AAK (2001). Heavy metal contents in Egyptian meat and the role of detergent washing on their levels. Food Chem. Toxicol. 39(6):593-599.

Akabzaa T, Darimani A (2001). Impact of mining sector investment in Ghana: a study of the Tarkwa mining region. Health Impacts 6(4):60.

Alfven T, Elinder CG, Carlsson MD, Grubb A, Hellstrom L, Persson B, Pettersson C, Spång G, Schütz A, Järup L(2000). Low-level cadmium exposure and osteoporosis. J. Bone Miner. Res. 15:1579-1586.

Amonoo-Neizer EH, Nyamah D, Bakiamoh SB (1995). Mercury and arsenic pollution in soil and biological samples around mining towns if Obuasi, Ghana. Water Air Soil Pollut. 91:363-373.

Asante KA, Agusa T, Subramanian A, Ansa-Asare OD, Biney CA, Tanabe S (2007). Contamination status of arsenic and other trace elements in drinking water and residents from Tarkwa, a historic mining township in Ghana. Chemosphere 66:1513-1522.

ATSDR (2013). Agency for Toxic Substances and Disease Registry. Minimum risk levels (MRLs). Available online at http://www.atsdr.cdc.gov/mrls/pdfs/atsdr_mrls_february_2012.pdf

Barhoumi R, Faske J, Liu X, Tjalkens RB (2004). Manganese potentiates lipopolysaccharide-induced expression of NOS2 in C6 glioma cells through mitochondrial-dependent activation of nuclear factor kappaB. Mol. Brain Res. 122:167-179.

Battaglia A, Ghidini S, Campanini G, Spaggiari R (2005). Heavy metal contamination in little owl (Athene noctua) and common buzzard (Buteo buteo) from northern Italy. Ecotoxicol. Environ. Saf. 60:61-66.

Berglund M, Akesson A, Nermell B, Vahter M (1994). Intestinal absorption of dietary cadmium in women depends on body iron stores and fiber intake. Environ. Health Perspect. 102:1058-1066.

Blagojevic J, Jovanović V, Stamenković G, Jojić V, Bugarski-Stanojević V, Adnađević T, Vujošević M (2012). Age differences in bioaccumulation of heavy metals in populations of the black-striped field mouse, Apodemusagrarius (Rodentia, Mammalia). Int. J. Environ. Res. 6(4):1045-1052.

Bortey-Sam N, Nakayama SM, Akoto O, Ikenaka Y, Baidoo E, Mizukawa H, Ishizuka M (2015a). Ecological Risk of Heavy Metals and a Metalloid in Agricultural Soils in Tarkwa, Ghana. Int. J. Environ. Res. Public Health 12(9):11448-11465.

Bortey-Sam N, Nakayama SM, Akoto O, Ikenaka Y, Fobil JN, Baidoo E, Mizukawa H, Ishizuka M (2015c). Accumulation of heavy metals and metalloid in foodstuffs from agricultural soils around Tarkwa area in Ghana, and associated human health risks. Int. J. Environ. Res. Public Health 12(8):8811-8827.

Bortey-Sam N, Nakayama SM, Ikenaka Y, Akoto O, Baidoo E, Mizukawa H, Ishizuka M (2015b). Health risk assessment of heavy metals and metalloid in drinking water from communities near gold mines in Tarkwa, Ghana. Environ. Monit. Assess. 187(7):1-12.

Bortey-Sam N, Nakayama SM, Ikenaka Y, Akoto O, Baidoo E, Yohannes YB, Mizukawa H, Ishizuka M (2015d). Human health risks from metals and metalloid via consumption of food animals near gold mines in Tarkwa, Ghana: Estimation of the daily intakes and target hazard quotients (THQs). Ecotoxicol. Environ. Saf. 111:160-167.

Brzoska MM, Majewska K, Moniuszko-Jakoniuk J (2004). Mineral status and mechanical properties of lumbar spine of female rats chronically exposed to various levels of cadmium. Bone 34(3):517-526.

Ceruti R, Ghisleni G, Ferretti E, Cammarata S, Sonzogni O, Scanziani E (2002). Wild rats as monitors of environmental lead contamination in the urban area of Milan, Italy. Environ. Pollut. 117:255-259.

Chen X, Wang G, Li X, Gan C, Zhu G, Jin T, Wang Z (2013). Environmental level of cadmium exposure stimulates osteoclasts formation in male rats. Food Chem. Toxicol. 60:530-535.

Crossgrove J, Zheng W (2004). Manganese toxicity upon overexposure. NMR Biomed. 17:544-553.

Damek-Poprawa M, Sawicka-Kapusta K (2004). Histopathological changes in the liver, kidneys, and testes of bank voles environmentally exposed to heavy metal emissions from the steelworks and zinc smelter in Poland. Environ. Res. 92:72-78.

Daniell HW (1976). Osteoporosis of the slender smoker. Obstet. Gynecol. Surv. 31(11):808-810.

Dorman DC, Struve MF, Marshall MW, Parkinson CU, James RA, Wong BA (2006). Tissue manganese concentrations in young male rhesus monkeys following subchronic manganese sulfate inhalation. Toxicol. Sci. 92:201-210.

EC (2006). European Commission Regulation (EC) No 1881/2006 of 19 December 2006 setting maximum levels for certain contaminants in

foodstuff. Off. J. Eur. Union.
Finley JW (1998). Manganese uptake and release by cultured human hepato-carcinoma (Hep-G2) cells. Biol. Trace Elem. Res. 64:101-118.
Flanagan PR, McLellan JS, Haist J, Cherian MG, Chamberlain MJ, Valberg LS (1978). Increased dietary cadmium absorption in mice and human subjects with iron deficiency. Gastroenterology 74:841–846.
Florea AM, Busselberg D (2006). Occurrence, use and potential toxic effects of metals and metal compounds. Biometals 19(4):419-427.
Ghana Statistical Service (2010). Population and Housing census. https://www.google.co.uk/#q=Ghana+Statistical+Service%2C+2010.+Population+and+Housing+census+ P 93.
Godowicz B (1988). Cadmium-induced liver and spleen damage in inbred mouse strains. Folia Biol. 36:47-52.
Guerrero-Castilla A, Olivero-Verbel J, Marrugo-Negrete J (2014). Heavy metals in wild house mice from coal-mining areas of Colombia and expression of genes related to oxidative stress, DNA damage and exposure to metals. Mutat. Res Gen. Tox. Environ. 762:24-29.
Gupta UC (1998). Trace element toxicity relationships to crop production and livestock and human health: implications for management. Commun. Soil Sci. Plan. 29:1491-1522.
Hamilton DL, Valberg LS (1974). Relationship between cadmium and iron absorption. Am. J. Physiol. 227:1033–1037.
Hayford EK, Amin A, Osae EK, Kutu J (2008). Impact of gold mining on soil and some staple foods collected from selected mining communities in and around Tarkwa Prestea Area. West African J. Appl. Ecol. 14:1-12.
Homady M, Helmi H, Jiries A, Mahasneh A, AlNasir F, Khleifat K (2002). Survey of some heavy metals in sediments from vehicular service stations in Jordan and their effects on social aggression in prepubertal male mice. Environ. Res. 8 (1):43-49.
Honda R, Tsuritani I, Noborisaka Y, Suzuki H, Ishizaki M (2003). Urinary cadmium excretion is correlated with calcaneal bone mass in Japanese women living in an urban area. Environ. Res. 91:63-70.
Hunter BA, Johnson MS, Thompson DJ (1989). Ecotoxicology of copper and cadmium in contaminated grassland ecosystem. 4. Tissue distribution and age accumulation in small mammals. J. Appl. Ecol. 26:89–99.
Husain A, Al-Rashdan A, Al-Awadhi A, Mahgoub B, Al-Amiri H (1996). Toxic metals in food products originating from locally reared animals in Kuwait. Bull. Environ. Contam. Toxicol. 57:549-555.
Jarup L (2002). Cadmium overload and toxicity. Nephrol. Dial Transplant 17(2):35-39.
Kabata-Pendias A, Pendias H (1992). Trace Elements in Soils and Plants, second ed. CRC Press, London, P 413.
Kowel NE (1988). Urinary cadmium and beta2-microglobulin: correlation with nutrition and smoking history. J. Toxicol. Environ. Health 25:179–183.
Licata P, Naccari F, Lo Turco V, Rando R, Di Bella G, Dugo G (2010). Levels of Cd (II), Mn (II), Pb (II), Cu (II), and Zn (II) in Common Buzzard (Buteo buteo) from Sicily (Italy) by Derivative Stripping Potentiometry. Int. J. Ecol. 1-7.
Lindsay R, Dempster DW, Clemens T, Herrington BS, Wilt S (1984). Incidence, cost, and risk factors of fracture of the proximal femur in the USA. Osteoporosis 1:311-315.
Liu J, Liu Y, Goyer RA, Achanzar W, Waalkes MP (2000). Metallothionein-I/II null mice are more sensitive than wild-type mice to the hepatotoxic and nephrotoxic effects of chronic oral or injected inorganic arsenicals. Toxicol. Sci. 55:460-467.
López-Alonso M, Miranda M, García-Partida P, Cantero F, Hernández J, Benedito JL (2007). Use of dogs as indicators of metal exposure in rural and urban habitats in NW Spain. Sci. Total Environ. 372:668-675.
Ma WC (2011). Lead in mammals. In Beyer & Meador (Eds.), Environmental contaminants in biota: interpreting tissue concentrations (2nd ed.). New York: CRC Press pp. 595-607.
Ma WC, Denneman W, Faber J (1991). Hazardous exposure of ground living small mammals to cadmium and lead in contaminated terrestrial ecosystem. Arch. Environ. Contam. Toxicol. 20:266-270.
Martinez-Finley EJ, Gavin CE, Aschner M, Gunter TE (2013). Manganese neurotoxicity and the role of reactive oxygen species. Free Radic. Biol. Med. 62:65-75.
Naccari C, Cristani M, Cimino F, Arcoraci T, Trombetta D (2009). Common buzzards (Buteo buteo) bio-indicators of heavy metals pollution in Sicily (Italy). Environ. Int. 35:594-598.
Nakayama SM, Ikenaka Y, Hamada K, Muzandu K, Choongo K, Teraoka H, Mizuno N, Ishizuka M (2011). Metal and metalloid contamination in roadside soil and wild rats around a Pb–Zn mine in Kabwe, Zambia. Environ. Pollut. 159(1):175-181.
Nakayama SM, Ikenaka Y, Hamada K, Muzandu K, Choongo K, Yabe J, Umemura T, Ishizuka M (2013). Accumulation and biological effects of metals in wild rats in mining areas of Zambia. Environ. Monit. Assess. 185(6):4907-4918.
Obiri S (2007). Determination of heavy metals in water from boreholes in Dumasi in the Wassa West District of the Western Region of the Republic of Ghana. Environ. Monit. Assess. 130:455-463.
Pereira R, Pereira ML, Ribeiro R, Gonçalves F (2006). Tissues and hair residues and histopathology in wild rats (*Rattus rattus* L.) and Algerian mice (*Mus spretus* Lataste) from an abandoned mine area (Southeast Portugal). Environ. Pollut. 139:561-575.
Pompe-Gotal J, Crnic AP (2002). Cadmium in tissue of roe deer (*Capreolus capreolus*) in Croatia. Vet. Arh. 72:303-310.
Saville PD, Nilsson BE (1966). Height and weight in symptomatic postmenopausal osteoporosis. Clin. Orthop. Relat. Res. 45:49-54.
Sawicka-Kapusta K, Zakrzewska M, Kowalska A, Lenda B, Skrobacz M (1995). Heavy metal concentrations in small mammals from Borecka forest. Arch. Ochr. Środ. 3(4):229-234.
Scheuhammer AM (1987). The chronic toxicity of aluminium, cadmium, mercury, and lead in birds: A review. Environ. Pollut. 46:263-295.
Soewu DA, Agbolade OM, Oladunjoye RY, Ayodele IA (2014). Bioaccumulation of heavy metals in cane rat (Thryonomys swinderianus) in Ogun State, Nigeria. J.Toxicol. Environ. Health Sci. 6(8):154-160.
Swiergosz R (2001). Cadmium distribution and toxicity in tissues of small rodents. Microsc. Res. Tech. 55:208-222.
Taguchi T, Suzuki S (1981). Influence of sex and age on the biological half-life of cadmium in mice. J. Toxicol. Environ. Health 7:239–249.
Tohyama C, Sugihira N, Saito H (1987). Critical concentration of cadmium for renal toxicity in rats. J. Toxicol. Environ. Health 22:255-259.
Uriu K, Morimoto I, Kai K, Okazaki Y, Okada Y, Qie YL, et al. (2000). Uncoupling between bone formation and resorption in ovariectomized rats with chronic cadmium exposure. Toxicol. Appl. Pharmacol. 164:264-272.
USEPA (United States Environmental Protection Agency) (2004). Framework for Inorganic Metals Risk Assessment; USEPA: Washington, DC, USA.
USEPA (United States Environmental Protection Agency) (2012). Ground water and drinking water http://www.water.epa.gov/drink
Waalkes MP, Ward JM, Liu J, Diwan BA (2003). Transplacental carcinogenicity of inorganic arsenic in the drinking water: induction of hepatic, ovarian, pulmonary, and adrenal tumors in mice. Toxicol. Appl. Pharmacol. 186:7-17.
Whelton BD, Peterson DP, Moretti ES, Dare H, Bhattacharyya MH (1997). Skeletal changes in multiparous, nulliparous and ovariectomized mice fed either a nutrient-sufficient or -deficient diet containing cadmium. Toxicology 119:103-121.
WHO (World Health Organization) (1981). Environmental Health Criteria 18. Arsenic. International Programme on Chemical Safety.World Health Organization, Finland.
WHO (World Health Organization) (1996). Trace Elements in Human Nutrition and Health. Geneva.
WHO (World Health Organization) (2011). Guidelines for drinking-water quality (4th ed., http://www.whqlibdoc.who.int/publications/2011/9789241548151_eng.pdf). Geneva

Wronski TJ, Schenk PA, Cintron M, Walsh CC (1987). Effect of body weight on osteopenia in ovariectomized rats. Calcif. Tissue Int. 40(3):155-159.

Environmental Pollution 218 (2016) 331–337

Contents lists available at ScienceDirect

Environmental Pollution

journal homepage: www.elsevier.com/locate/envpol

Excretion of polycyclic aromatic hydrocarbon metabolites (OH-PAHs) in cattle urine in Ghana☆

Nesta Bortey-Sam [a], Yoshinori Ikenaka [a, b], Osei Akoto [c], Shouta M.M. Nakayama [a], Jemima Marfo [a], Aksorn Saengtienchai [a, d], Hazuki Mizukawa [e], Mayumi Ishizuka [a, *]

[a] Laboratory of Toxicology, Department of Environmental Veterinary Science, Graduate School of Veterinary Medicine, Hokkaido University, Kita 18, Nishi 9, Kita ku, Sapporo 060-0818, Japan
[b] Water Research Group, Unit for Environmental Sciences and Management, North-West University, Potchefstroom, South Africa
[c] Department of Chemistry, Kwame Nkrumah University of Science and Technology, Kumasi, Ghana
[d] Department of Pharmacology, Faculty of Veterinary Medicine, Kasetsart University, Bangkok, Thailand
[e] Department of Environmental Veterinary Science, Graduate School of Veterinary Medicine, Hokkaido University, Kita 18, Nishi 9, Kita ku, Sapporo 060-0818, Japan

ARTICLE INFO

Article history:
Received 21 February 2016
Received in revised form
3 July 2016
Accepted 3 July 2016
Available online 15 July 2016

Keywords:
OH-PAHs
Kumasi
Metabolites
Cattle
Urine

ABSTRACT

Previous studies of polycyclic aromatic hydrocarbons (PAHs) in particulate matter, soils and livers of wild rats indicated that the city centre of Kumasi, Ghana has been severely polluted with high cancer potency. Cattle urine were therefore collected from Kumasi (urban) and Offinso (rural), Ghana: to determine concentrations of urinary PAH metabolites (OH-PAHs); and find their association with sex; and to estimate exposure of cattle to PAHs from the different sites. From the results, geometric mean concentrations (adjusted by specific gravity), GM_{SG}, showed that 2-OHNaphthalene (2-OHNap) was the most abundant OH-PAH in cattle urine from all study sites, and naphthalene-containing-mothballs might have contributed significantly to the levels. There was no significant difference between urinary OH-PAHs concentrations in cattle from urban and rural sites except for 2-OHPhe and 4-OHPhe, and similar to urban areas, rural sites could also be polluted with PAHs. GM_{SG} of 2-OHNap in cattle urine in Kokote (21.9 ± 6.51 ng/mL; a rural area), was significantly higher compared to the other sites followed by Oforikrom (4.15 ± 4.37 ng/mL; urban). The GM_{SG} concentration (ng/mL) of the sum of OH-PAHs decreased in the order, Kokote (44.7) > Oforikrom (7.87) > Saboa (6.98) > Santasi (6.68) > and Twumasen Estate (5.23). The high concentrations of urinary 2-OHNap, 2-3-OHFlu, 2-OHPhe, 3-OHPhe and 4-OHPhe in Kokote indicated high PAHs exposure to cattle in this area or different/specific source of PAHs exposure. GM_{SG} of 2-OHNap was significantly higher in male cattle compared to females while 1-9-OHPhe was significantly higher in females.

1. Introduction

Polycyclic aromatic hydrocarbons (PAHs) are pollutants formed during incomplete combustion of organic materials. They are found in vehicle exhaust, wood and cigarette smoke, and also in grilled foods. Human and animal exposure to PAHs occur mainly through inhalation of contaminated air or ingestion of soil, food and/or drinking contaminated water (Barranco et al., 2004; Dissanayake and Galloway, 2004). According to the Agency for Toxic Substances and Disease Registry's (ATSDR, 2013) priority list of hazardous chemicals, PAHs were classified as the 9th most hazardous chemical. In humans and animals, PAHs are metabolized by cytochrome P450 enzymes and excreted in urine. One of the major metabolites is monohydroxylated PAH (OH-PAHs) (Burczynski et al., 1998) and urinary levels of 1-hydroxypyrene has been used as biomarker of PAHs exposure (Bouchard and Viau, 1999; Jongeneelen, 2001). However, since ratios of different PAHs may vary depending on the source and personal enzymatic capacity, concentration profiles of multiple OH-PAHs biomarkers are necessary and required to assess the environmental exposure risk. Urinary metabolites of naphthalene, fluorene and phenanthrene are also commonly used as biomarkers to assess the exposure level and

☆ This paper has been recommended for acceptance by Chen Da.

* Corresponding author.
E-mail address: ishizum@vetmed.hokudai.ac.jp (M. Ishizuka).

http://dx.doi.org/10.1016/j.envpol.2016.07.008
0269-7491/

environmental risk (Li et al., 2008; Fan et al., 2012a; 2012b).

The assessment of health risk to humans exposed to PAHs is primarily based on results from animal studies, which indicated that PAHs can produce carcinogenic and mutagenic effects. Recent studies also indicated that some PAH metabolites have strong correlation with atherosclerosis and cardiovascular diseases (Xu et al., 2010), and exposure of rats and mice to naphthalene caused nasal and bronchiolar tumors, respectively (NTP, 1992; 2000).

As a developing country, the economic and population growth rates in Ghana have seen tremendous increases over the past few years. The growing rate of industrialization is gradually leading to contamination and deterioration of the environment and pollution is likely to reach disturbing levels (Bortey-Sam et al., 2014). Studies by Bortey-Sam et al. (2013; 2014; 2015a) in particulate matter (PM10) and soils indicated that the city centre of Kumasi, Ghana has been polluted with PAHs when compared with recommended levels, and fuel and wood/grass combustion were the dominant sources. The total benzo(a)pyrene equivalent concentration and estimated carcinogenicity of PAHs in PM10 and soil from the city centre was approximately 18 and 150 times higher, respectively, as compared to a pristine site. Rats were therefore used as sentinels to measure the environmental pollution state, and higher levels of PAHs were detected in the livers of wild rats in the city centre of Kumasi. Naphthalene was detected in 80% of those samples, and levels of phenanthrene and pyrene (the first and second most abundant, respectively) were significantly higher than other PAHs measured (Bortey-Sam et al., 2015b).

Based on the high levels and cancer potency of PAHs in PM10, soils and the levels found in livers of wild rats (Bortey-Sam et al., 2013, 2014; 2015a, 2015b), cattle urine was collected because cattle is known to excrete large amount of PAH metabolites due to high intake of the parent compound through feed or inhalation (Saengtienchai et al., 2014). PAHs in the atmosphere are known to settle in soil (Rey-Salgueiro et al., 2008) and this could increase the levels of exposure in Kumasi, Ghana, because these free-range cattle also pick food and/or water from the ground. Urinary levels of PAHs could be widely used as biological indicator of exposure (Jongeneelen, 2001), and there is limited/no data from literature that addresses the excretory levels of OH-PAHs in cattle in Ghana. The objectives of the present study were therefore: to determine the concentrations of OH-PAHs in cattle urine in Kumasi (urban) and Offinso (rural), Ghana; find the association between urinary OH-PAHs concentrations and sex; and to estimate cattle's exposure to PAHs from the different sites.

2. Materials and methods

2.1. Sampling

In August 2014, urine samples of healthy cattle (West African Shorthorn) were randomly collected from 5 communities in Kumasi and Offinso, both in the Ashanti Region of Ghana. Offinso is about 33 km from the city centre of Kumasi (Fig. 1). Samples were collected from Oforikrom and Santasi in Kumasi (urban), which are 5.1 and 3.5 km from the city centre, respectively (Fig. 1), where previous studies reported high levels of PAHs in PM10, soils and livers of wild rats (Bortey-Sam et al., 2013, 2014, 2015a, 2015b). On the other hand, the three sites in Offinso (Twumasen Estate, Saboa and Kokote) selected for cattle urine sampling (Fig. 1) are in rural and agricultural areas where bush burning is rampant and the use and sometimes abuse of pesticides such as carbaryl (1-naphthyl-*N*-methylcarbamate), which could be metabolized to 1-hydroxy naphthalene, was possible (Meeker et al., 2007; Orjuela et al., 2012). In addition, due to the lack of background urine and interferences during OH-PAHs quantification, 500 mL of cattle urine (blank stock) was collected from Hokkaido University School farm. Hokkaido University is a public university located in Sapporo, Japan, and because of the low vehicular movement and industrial activities around the farm, PAHs exposure from point sources were assumed to be negligible. However, because cattle could be exposed to PAHs through feed and/or inhalation the sample collected was measured several times to confirm levels of OH-PAHs.

From the sample sites in Ghana, spot urine ($n = 95$; with 30 males and 65 females) were collected, transferred into labelled corning tubes (Corning Incorporated, New York, USA) and stored at −20 °C in the Department of Chemistry, Kwame Nkrumah University Science and Technology (KNUST), Ghana. Of the 5 sites, only ages of some cattle in 2 sites (Twumasen Estate and Saboa) were obtained from the herdsmen. The average ages (ranges) of cattle were 2.9 ± 1.0 years (1–4.5years) in Twumasen Estate and 4.2 ± 2.9 years (1–12 years) in Saboa, respectively. Samples were later transported to the Laboratory of Toxicology, Graduate School of Veterinary Medicine, Hokkaido University, Japan where they were stored at −30 °C until analysis (quarantine number for importing is 26 douken 383).

2.2. Sample extraction and analysis

20 μL each of β-glucuronidase (bovine liver, type B-1; 1240 U/mg; Sigma Aldrich) and arylsulfatase (limpets Type V; 34 units/mg; Sigma Aldrich) enzymes, and 5 mL of 0.1 M sodium acetate buffer (pH 5.6) were added to 5 mL urine sample after spiking with three PAH internal standards (13C6-2-OHFluorene, 3-OHPhenanthrene-d9, and 13C6-1OHPyrene). The pH of sample was adjusted to 5.5 using 1 M acetic acid (Wako Pure Chemicals, Osaka, Japan) and incubated overnight at 37 °C. The sample was diluted with 4 mL of Milli-Q water and extracted twice (liquid-liquid extraction) with 10 mL each of *n*-pentane (Kanto Chemical Corp., Tokyo, Japan) by shaking for 1 h. To reduce the interference of sulfur metabolites, the combined extracts were washed with 2 mL of 1 N $AgNO_3$ solution (Wako Pure Chemicals, Osaka, Japan), concentrated to 50–100 μL, redissolved to 0.5 mL using methanol and filtered (0.20 μm DISMIC-13JP membrane filter, ADVANTEC, Toyo Roshi Kaisha Ltd., Japan) prior to instrumental analysis. All sample preparation steps were performed in darkness (by covering tubes completely with aluminum foil) to avoid possible photodegradation of target analytes. A total of 13 OH-PAHs; 2-hydroxynaphthalene (2-OHNap), 2-hydroxyfluorene (2-OHFlu), 3-hydroxyfluorene (3-OHFlu), 9-hydroxyfluorene (9-OHFlu), 1-hydroxyphenanthrene (1-OHPhe), 2-hydroxyphenanthrene (2-OHPhe), 3-hydroxyphenanthrene (3-OHPhe), 4-hydroxyphenanthrene (4-OHPhe), 9-hydroxyphenanthrene (9-OHPhe), 1-hydroxypyrene (1-OHPyr), 6-hydroxychrysene (6-OHChry), 3-hydroxybenzo(e)pyrene (3-OHBeP) and 9-hydroxybenzo(a)pyrene (9-OHBaP), were analyzed in each sample. The standards (purity ≥ 98%) were purchased from Cambridge Isotope Laboratories Inc. (Andover, MA, USA) and Toronto Research Chemical Inc. (Brisbane Road, North York, Canada). Difficulties were often associated with the separation of 1-OHPhe and 9-OHPhe, for this reason, the sum of these isomers was used as an abbreviation, 1-9-OHPhe. Similarly, 2-3-OHFlu was used as sum of 2-OHFlu and 3-OHFlu. All results were adjusted by specific gravity and expressed in ng/mL.

A Shimadzu 8030 triple quadrupole mass spectrometer, upgraded to 8040 with UF lens, (ESI MS-MS; Shimadzu, Kyoto, Japan), equipped with a Prominence UFLC system (Shimadzu, Kyoto, Japan) was used for analysis. Chromatographic separation was achieved using an Agilent Eclipse PAH column (150 mm × 2.1 mm, 3.5 μm). The mobile phases were methanol:water (2:3, v:v) (A) and methanol (B), pumped at a flow rate of 250 μL/min. The mobile phase

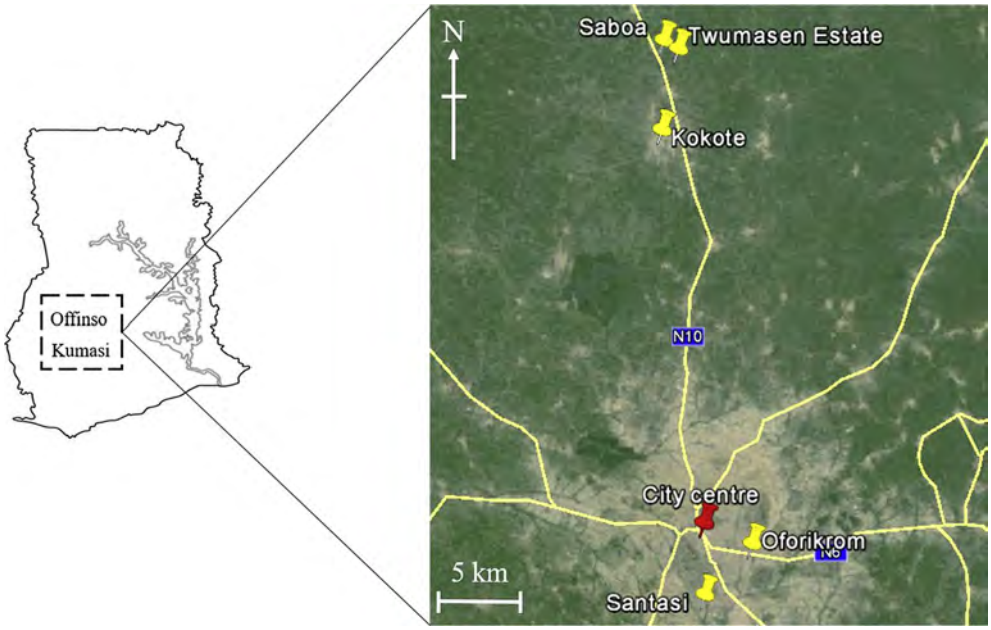

Fig. 1. Map showing cattle urine sampling locations in the Ashanti Region, Ghana (yellow pins indicate sampled locations and red pin indicate city centre in Kumasi). (For interpretation of the references to colour in this figure legend, the reader is referred to the web version of this article.)

gradient was maintained as follows: 0.0–2.0 min, 5% B; 2.0–20 min, 40% B; 20–25 min, 40% B; 25–30 min, 95% B; 30–35 min, 95% B; 35–35.01 min, 5% B. Target compounds were determined by multiple-reaction monitoring (MRM) in the negative ionization mode.

2.3. Specific gravity (SG) of cattle urine

To compensate for variations in urine dilution, urinary OH-PAH concentrations were adjusted by specific gravity (SG). Urinary SG was measured by a hand refractometer (ATAGO, PAL-095, Tokyo, Japan). Obtained mean and ranges of SG in urine of cattle in Oforikrom (1.013; [1.004–1.029]), Santasi (1.035; [1.03–1.041]), Twumasen Estate (1.035; [1.028–1.04]), Saboa (1.036; [1.026–1.049]) and Kokote (1.037; [1.029–1.042]) were used to adjust urinary OH-PAHs concentrations as illustrated by Nermell et al. (2008). The correction formula applied to each urine concentration was as follows:

$$\text{SG\_corrected concentration} = \text{urinary OH} - \text{PAH concentration} \times \frac{(SG_{target} - 1.0)}{(SG_{sample} - 1.0)}$$

where, SG_{target} is the mean specific gravity of cattle urine per community; SG_{sample} is the specific gravity of a particular sample.

2.4. Quality control and quality assurance

A mixture of three 13C-isotopically labelled OH-PAHs (13C6-2-OHFlu, 3-OHPhe-d9, and 13C6-1-OHPyr) was spiked into urine samples as internal standard prior to sample preparation and extraction. 13C6-2-OHFlu was used for quantification of metabolite of naphthalene and three metabolites of fluorene. 3-OHPhe-d9 was used for quantification of the five metabolites of phenanthrene and 13C6-1-OHPyr was used for quantification of 1OHPyr, 6-OHChry, 3-OHBeP and 9-OHBaP.

Quantitation was performed using internal standard method (five–point calibration; 1, 5, 10, 50 and 100 ng/mL), and average correlation coefficients (r^2) for the calibration curves in cattle urine were greater or equal to 0.99. The standard solutions (spiked with internal standards) for the calibration curves were prepared in urine in order to normalize differences in interferences between standards and samples. Concentrations of OH-PAHs in urine sample used for this purpose were below the limits of detection (LOD) and differences between this and sample concentration was used in this study. Analytical methods were checked for precision and accuracy. Limits of quantification (LOQs) were calculated based on 10SD/S (SD is the standard deviation of the response of seven replicate standard solution measurements and S is the slope of the calibration curve). LOQs (ng/mL) of OH-PAHs were, 0.29 (2-OHNap), 0.24 (2-3-OHFlu), 0.60 (9-OHFlu), 0.23 (2-OHPhe), 0.71 (1-9-OHPhe), 1.16 (3-OHPhe), 0.15 (4-OHPhe), 0.87 (1-OHPyr), 0.73 (6-OHChry), 0.54 (3-OHBeP) and 0.32 (9-OHBeP), respectively. Internal standard recoveries (13C6-2OHFlu, 3-OHPhe-d9, and 13C6-1-OHPyr) ranged from 89 ± 5.8–96 ± 11.4% (Table 1).

For every batch of 10 samples, a solvent blank, a spiked solvent blank (internal standards spiked into solvent), a matrix spike (internal standards spiked into blank urine), and duplicate sample were analyzed. The average recoveries in spiked solvents blanks ranged from 92 ± 4.6–98 ± 8.3%, and that for matrix spikes was 85 ± 9.1–96 ± 7.1%. Blanks were run periodically and contained no detectable amount of target analyte. The coefficients of variation of OH-PAH in duplicate samples were less than 15%.

2.5. Data analysis

Data analysis was performed using IBM SPSS v 20 for windows (SPSS Inc., Illinois, USA). Kolmogorov–Smirnov (K–S) and Shapiro-Wilks tests were used to determine the normality of data and were considered statistically significant if p value was less than 0.05. Concentrations of OH-PAH below their respective LOQs were replaced with a value of LOQ/2. Geometric mean concentrations were used to represent the central tendency of OHPAH in this study (Wayne, 1990). ANOVA and Tukey analyses of log transformed data

Table 1
Quality assurance and control (QA/QC) for OH-PAHs analysis in cattle urine.

Compound name	LOD (ng/mL)	LOQ (ng/mL)	ISTD Recovery (%)	Spiked solvent blanks (%)	Matrix spikes (%)
2-OHNaphthelene	0.0898	0.295			
9-OHFluorene	0.181	0.603			
2-3-OHFluorene	0.0745	0.248			
13C6-2-OHFluorene			94	96	96
1-9-OHPhenanthrene	0.214	0.714			
2-OHPhenanthrene	0.0696	0.232			
3-OHPhenanthrene	0.348	1.16			
4-OHPhenanthrene	0.0437	0.145			
3-OHPhenanthrene-d9			96	98	95
1-OHPyrene	0.259	0.865			
13C6-1-OHPyrene			89	92	85
6-OHChrysene	0.220	0.733			
3-OHBenzo(e)Pyrene	0.162	0.542			
9-OHBenzo(a)Pyrene	0.0959	0.319			

Italicized compounds are internal standards (ISTD); LOD: Limit of detection; LOQ: Limit of quantification.

were used to compare concentrations of OH-PAH in cattle urine from the study areas and differences were considered statistically significant with p value < 0.05. Student's t-test was also used to compare distribution of OH-PAHs between male and female cattle; and, urban and rural sites.

3. Results and discussion

3.1. Excretory levels of OH-PAH in cattle urine

As shown in Table 2, there was no significant difference ($p > 0.05$) between urinary OH-PAHs concentrations in cattle from urban and rural sites except for 2-OHPhe and 4-OHPhe. Data for 3-OHPhe was not included because concentrations from urban sites and 2 rural sites were below the LOQ (Table 3). The significant differences ($p < 0.05$) could indicate differences in cattle's exposure to PAHs from urban and rural sites. Table 3 shows the distribution of OH-PAHs in cattle urine from the 5 sample sites. From the results, 2-OHNap, 2-3-OHFlu, 1-9-OHPhe, 2-OHPhe, 3-OHPhe, 4-OHPhe and 1-OHPyr were detected. 9-OHFlu and the high molecular weight, HMW ($\geq$4 rings) PAHs (6-OHChry, 3-OHB(e)P and 9-OHB(a)P) were however not detected in the cattle urine and could be due to low detection sensitivity (Campo et al., 2008) and/or because the HMW PAHs, such as BaP, are mainly excreted through feces (Burgaz et al., 1992; Li et al., 2008).

Specific gravity adjusted geometric mean concentrations (GM_{SG}) showed that 2-OHNap (2.77 ± 5.91 ng/mL; $p < 0.01$) was the most abundant OH-PAH in cattle urine from all study sites followed by 1-9-OHPhe (2.02 ± 1.16 ng/mL) > 4-OHPhe (1.74 ± 1.87 ng/mL) > 1-OHPyr (1.22 ± 0.87 ng/mL) > 2-3-OHFlu (1.08 ± 1.75 ng/mL) > 2-OHPhe (0.489 ± 0.555 ng/mL) > and 3-OHPhe (0.278 ± 0.553 ng/mL) (Fig. 2). The GM_{SG} concentration (ng/mL) of the sum of OH-PAHs (2-OHNap, 2-3-OHFlu, 1-9OHPhe, 2-OHPhe, 3-OHPhe, 4-OHPhe and 1-OHPyr) decreased in the order, Kokote (44.7 ± 10.4) > Oforikrom (7.87 ± 7.41) > Saboa (6.98 ± 3.86) > Santasi (6.68 ± 2.701) > and Twumasen Estate (5.23 ± 1.55). High urinary concentrations of 2-OHNap, 2-3-OHFlu, 2-OHPhe, 3-OHPhe and 4-OHPhe were detected in Kokote (Table 3) indicating high exposure of cattle to the parent PAHs within the sample site. Kokote is a rural area filled with many farmlands, with high agricultural and burning activities compared to the other sites, and the levels of OH-PAHs could mean that there were different or specific sources of PAHs exposure to cattle in the area.

3.2. 2-OHNaphthalene

The GM_{SG} of 2-OHNap in cattle urine in Kokote (21.9 ± 6.51 ng/mL) was significantly higher ($p < 0.05$) compared to the other sites followed by Oforikrom (4.15 ± 4.37 ng/mL).

(Table 3). However, the least GM_{SG} concentration for 2-OHNap was recorded in Santasi (0.61 ± 0.23 ng/mL). Although 1-OHNap could be derived from both naphthalene and carbaryl, 2-OHNap is derived only from naphthalene (Orjuela et al., 2012). The high levels of 2-OHNap could be due to exposure through ingestion and/or inhalation, although it has been proposed as a biomarker of inhalation (Kim et al., 2000). Naphthalene is ubiquitous in ambient air with high volumes in vehicular traffic, cigarette smoke (ATSDR, 2005) and is elevated when mothballs or stoves burning biomass fuels are used (Griego et al., 2008; Riojas-Rodriguez et al., 2011). Urinary levels of 2-OHNap are markers of vehicular traffic (Li et al., 2010) and mothball exposure (Owa et al., 1993). Naphthalene is most likely the primary ingredient of mothballs in Ghana (Soghoian et al., 2012), and is frequently used in driving away insects both in and outdoors. This practice could also contribute to 2-OHNap being the most abundant metabolite in cattle urine since exposure through ambient air was also possible because of its volatile nature.

3.3. 1-OHPyrene

The highest GM_{SG} concentration of 1-OHPyr were detected in cattle in Kokote (2.29 ± 1.28 ng/mL) and Oforikrom (1.37 ± 1.18 ng/mL). Levels in Kokote were significantly higher ($p < 0.05$) compared

Table 2
Specific gravity adjusted urinary OH-PAHs concentrations (ng/mL) in cattle from urban and rural sites in Kumasi and Offinso, Ghana.

Site	n	2-OHNap (GM_{SG} ± SD)	2-3-OHFlu (GM_{SG} ± SD)	2-OHPhe (GM_{SG} ± SD)	1-9-OHPhe (GM_{SG} ± SD)	4-OHPhe (GM_{SG} ± SD)	1-OHPyr (GM_{SG} ± SD)
Urban	17	2.29 ± 3.40[a]	0.919 ± 0.462[a]	0.245 ± 0.171[a]	1.96 ± 1.14[a]	1.09 ± 0.841[a]	1.52 ± 0.873[a]
Rural	78	2.91 ± 6.37[a]	1.24 ± 1.97[a]	0.552 ± 0.598[b]	2.03 ± 1.17[a]	1.88 ± 2.01[b]	1.27 ± 0.824[a]

n: number of samples; GM_{SG}: geometric mean concentration adjusted by specific gravity; SD: standard deviation; different letters (a and b) within a column indicate significant differences (Student's t-test; $p < 0.05$).

Table 3
Specific gravity adjusted OH-PAHs concentrations (ng/mL) in cattle urine.

Sample site	n	Location	2-OHNap (GM_{SG} ± SD)	2-3-OHFlu (GM_{SG} ± SD)	1-9-OHPhe (GM_{SG} ± SD)	2-OHPhe (GM_{SG} ± SD)	3-OHPhe (GM_{SG} ± SD)	4-OHPhe (GM_{SG} ± SD)	1-OHPyr (GM_{SG} ± SD)
Oforikrom	8	urban	4.15 ± 4.37^{b}	0.99 ± 0.62^{b}	1.67 ± 1.21^{b}	0.17 ± 0.10^{c}	nd	0.73 ± 0.41^{c}	1.37 ± 1.18^{ab}
Santasi	9	urban	0.61 ± 0.23^{cd}	0.75 ± 0.35^{b}	2.26 ± 1.14^{ab}	0.32 ± 0.20^{bc}	nd	1.14 ± 0.33^{bc}	1.33 ± 0.80^{ab}
Twumasen Estate	31	rural	0.69 ± 0.57^{d}	0.31 ± 0.13^{c}	1.73 ± 0.58^{ab}	0.29 ± 0.26^{c}	nd	1.50 ± 0.86^{b}	0.99 ± 0.73^{b}
Saboa	40	rural	1.24 ± 0.67^{c}	0.80 ± 0.79^{b}	2.07 ± 1.43^{ab}	0.41 ± 0.16^{b}	nd	1.27 ± 0.91^{bc}	1.16 ± 0.74^{b}
Kokote	7	rural	21.9 ± 6.51^{a}	6.74 ± 1.41^{a}	3.12 ± 0.79^{a}	2.26 ± 0.51^{a}	2.1 ± 0.57	7.49 ± 1.73^{a}	2.29 ± 1.28^{a}

n: number of samples; nd: below limits of quantification (LOQ); different letter (a, b, c and d) within a column indicate significant difference ($p < 0.05$) among communities; GM_{SG}: geometric mean concentration adjusted by specific gravity; SD: standard deviation.

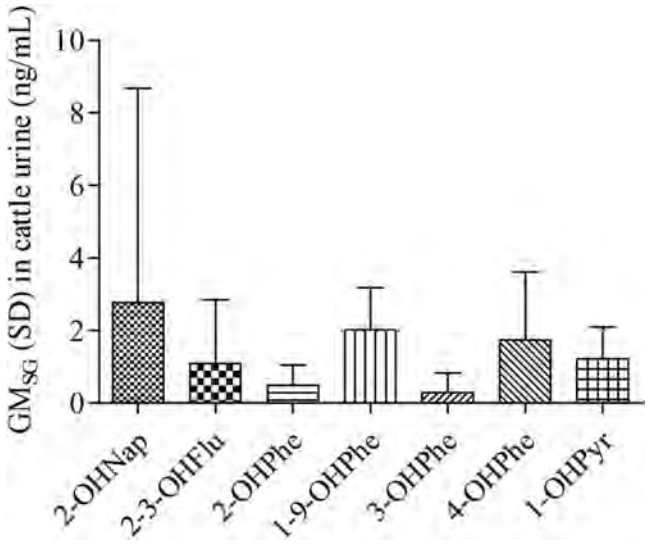

Fig. 2. Geometric mean concentrations (adjusted by specific gravity) of OH-PAHs in cattle urine from 5 sample sites in Kumasi and Offinso, Ghana.

to other sites except Oforikrom and Santasi (Table 3). GM concentrations (not adjusted by SG) of 1-OHPyr in this study (1.02 ng/mL [Twumasen Estate] to 2.41 ng/mL [Kokote]) were generally higher compared to study by Saengtienchai et al. (2014) using cattle from Japan and Thailand (non-adjusted). A study by Ferrari et al. (2002) on determination of 1-OHPyr in bovine urine from three farms located near rural and urban areas recorded non-adjusted average concentrations of 0.66 ng/mL (urban area); 1.52 ng/mL (rural) and 5.09 ng/mL (highway). Similar to the present study, Ferrari et al. (2002) indicated higher levels of 1-OHPyr in rural areas compared to urban and suggested that other important sources besides traffic could contribute to the PAHs burden of animals. Results of non-adjusted 1-OHPyr concentrations from the present study was higher compared to study by Ferrari et al. (2002) except for levels recorded in cattle raised on farms located in the vicinity of a highway (5.09 ng/mL).

The levels in the present study could be due to vehicular activities or traffic. At high temperature combustion (that is during vehicular emissions) the HMW PAH compounds are dominant (Laflamme and Hites, 1978). Previous studies by Bortey-Sam et al. (2014; 2015a) in PM10 and soils indicated pyrene as the eighth and second most abundant PAH in Kumasi, respectively, and combustion of fuel (74%) and wood/grass (23%) were the dominant sources in the region. In Ghana, some farms are generally located close to major roads with high vehicular activities or traffic (Tay and Biney, 2013), and exposure to domestic and grazing animals could be through inhalation, or picking food or water from the ground.

3.4. OHPhenanthrenes and OHFluorenes

The distribution of 2-OHPhe, 4-OHPhe and 2-3-OHFlu were significantly higher ($p < 0.05$) in Kokote than the other sites (Table 3). Urinary levels of 1-9-OHPhe in Kokote was however significantly higher ($p < 0.05$) than levels found in Oforikrom. 3-OHPhe levels in cattle urine from all sites were below the LOQ except Kokote (Table 3). In this study, the most dominant OHPhe isomer from all sites was 1-9-OHPhe, which is similar to results obtained by Fan et al. (2012a) in humans. However, in Kokote, 4-OHPhe was most abundant (Table 3). In human urine, Thai et al. (2016) and Levine et al. (2015) found 1-OHPhe as most dominant while Guo et al., 2013 also reported 3-OHPhe as the most dominant of four phenanthrene metabolites. These variations could be due to differences in metabolic pathway among species. The possible source of phenanthrene and fluorene exposure to cattle in Kokote could be due to inhalation during combustion at low temperatures such as wood or grass combustion since the low molecular weight, LMW (< 4 rings) PAH compounds are abundant during low temperature combustion (Lake et al., 1979). Because Kokote is mainly agricultural area with many farmlands, resident farmers frequently practice bush burning. Another possible source could be due to ingestion of soil or water since the cattle graze freely and the soil from which they pick food or water may be bound to PAHs from burning activities. Previous study by Tay and Biney (2013) indicated that agricultural soils in Accra, Ghana were dominated by LMW PAHs through which domestic animals could be exposed. PAHs tend to adsorb tightly to organic matter in soil rendering them less susceptible to biological and chemical degradation (Hatzinger and Alexander, 1997) and in general, LMW PAHs are more water soluble than HMW PAHs (Nam et al., 2008).

3.5. Association between urinary OH-PAHs concentrations and sex

Gender differences have been used in various studies to predict

Table 4
Specific gravity adjusted urinary OH-PAHs concentrations (ng/mL) in male and female cattle in Kumasi and Offinso, Ghana.

Sex	2-OHNap (GM_{SG} ± SD)	2-3-OHFlu (GM_{SG} ± SD)	1-9-OHPhe (GM_{SG} ± SD)	2-OHPhe (GM_{SG} ± SD)	3-OHPhe (GM_{SG} ± SD)	4-OHPhe (GM_{SG} ± SD)	1-OHPyr (GM_{SG} ± SD)	∑OHPAHs (GM_{SG} ± SD)
Male	4.43 ± 7.16^{a}	1.36 ± 1.94^{a}	1.71 ± 1.07^{a}	0.534 ± 0.650^{a}	0.364 ± 0.658^{a}	1.91 ± 2.22^{a}	1.19 ± 0.981 ^{a}	11.5 ± 14.6^{a}
Female	2.01 ± 5.11^{b}	0.950 ± 1.65 ^{a}	2.16 ± 1.18^{b}	0.468 ± 0.510^{a}	0.237 ± 0.499^{a}	1.65 ± 1.69^{a}	1.22 ± 0.827^{a}	8.71 ± 10.0^{a}

GM_{SG}: geometric mean concentration adjusted by specific gravity; SD: standard deviation; ∑OHPAHs: sum of OHPAHs; different letters (a and b) within a column indicate significant differences (Student's *t*-test; $p < 0.05$).

differences in OH-PAHs concentrations in human (Sul et al., 2012; Levine et al., 2015; Bartolomé et al., 2015; CDC, 2015). Study by Thai et al. (2016) in human urine showed no association between sex and urinary OH-PAHs concentrations. In this study, 2-OHNap was significantly higher ($p < 0.05$) in male cattle ($GM_{SG} = 4.43 \pm 7.16$ ng/mL) compared to females ($GM_{SG} = 2.01 \pm 5.12$ ng/mL) (Table 4). Kim et al. (2013) suggested that rates of intake, accumulation, and excretion of chemicals differ in male and female cattle, although ADME (absorption, distribution, metabolism, and excretion) data would be needed to support that assertion. Differences could also be due to different rearing systems from the various sites.

Several non pharmacogenetic factors such as age, gender, species, disease factors or exposure to environmental pollutants might contribute to the expression and regulation of hepatic P450 in man, laboratory species and domestic animals (Guengerich, 2002; Nebbia, 2001). In a study by Dacasto et al. (2005), male piedmontese cattle showed significantly higher CYP3A-dependent drug metabolizing enzymes, erythromycin *N*-demethylase (ERDEM), ethylmorphine *N*-demethylation (ETDEM) and testosterone 6ß-hydroxylation (6ß-OHT), activities compared to females, with the exception of testosterone 2ß-hydroxylase, 2ß-OHT, (whose enzymatic activity was yet lower in females). On the other hand, no gender-difference was noticed in limousin cattle.

In human, Sul et al. (2012) observed significantly higher levels of urinary 2-OHNap in men than females, and suggested that gender were predictors of urinary 2-OHNap concentrations. 1-9-OHPhe on the other hand was significantly higher in female cattle ($GM_{SG} = 2.17 \pm 1.18$ ng/mL) than males ($GM_{SG} = 1.71 \pm 1.07$ ng/mL) (Table 4), while ∑OHPhes in women were low compared to men (Bartolomé et al., 2015). These differences could be due to variations in metabolism, levels and route of exposure to PAHs. The urinary levels of 1-OHNap, 2-OHNap, ∑OHNap, 1-OHPhe, 9-OHPhe, ∑OHPhe, 1-OHPyr, and ∑OHPAHs among women were all significantly or marginally higher than those among men workers (Guo et al., 2014). In consistency, Guo et al. (2014) found that, when exposed to similar levels of PAHs, women had significantly higher micronuclei frequencies than men. Emerging evidence also indicates that women may be at greater risk of lung cancer than men, probably because the elevated activity of CYP1A1 enzymes in women can produce higher levels of DNA adducts, and women have lower DNA repair capacity than men (Mollerup et al., 2006; Uppstad et al., 2011).

4. Conclusions

Cattle urine samples were collected from both urban (Kumasi) and rural (Offinso) sites in the Ashanti Region, Ghana, and GM_{SG} concentration of OH-PAHs indicated that, 2-OHNap was the most abundant followed by; 1-9-OHPhe > 4-OHPhe > 1-OHPyr > 2-3OHFlu > 2-OHPhe > 3-OHPhe. The results of the present study showed that cattle in Kokote (rural area) were exposed to significantly higher levels of PAHs than the other sites, and naphthalene-containing-mothballs might have contributed significantly to 2-OHNap levels detected in cattle urine. There was no significant difference between urinary OH-PAHs concentrations in cattle in urban and rural sites except for 2-OHPhe and 4-OHPhe and similar to urban areas, rural sites could also be polluted with PAHs. Levels of 2-OHNap was significantly higher in male cattle compared to females, while the opposite was for 1-9-OHPhe.

Acknowledgements

This work was supported by Grants-in-Aid for Scientific Research from the Ministry of Education, Culture, Sports, Science and Technology of Japan awarded to M. Ishizuka (No. 16H0177906), Y. Ikenaka (No. 26304043, 15H0282505, 15K1221305), S. Nakayama (16K16197), and the foundations of Sumitomo and JSPS Core to Core Program (AA Science Platforms) and Bilateral Joint Research Project (PG36150002 and PG36150003). We also acknowledge the financial support by The Mitsui & Co., Ltd. Environment Fund, the Soroptimist Japan Foundation and the Nakajima Foundation. We are grateful to Mr. Takahiro Ichise (Laboratory of Toxicology, Graduate School of Veterinary Medicine, Hokkaido University) for technical support.

References

Agency for Toxic Substances, Disease Registry (ATSDR), 2005. Toxicological Profile for Naphthalene, 1-Methylnaphthalene, and 2-Methylnaphthalene.

Agency for Toxic Substances, Disease Registry (ATSDR), 2013. Detailed Data for 2013 Priority List of Hazardous Substances. Public Health Service, ATSDR, Division of Toxicology and Environmental Medicine.

Barranco, A., Alonso-Salces, R.M., Crespo, I., Burreta, L.A., Gallo, B., Vicente, F., Sarobe, M., 2004. Polycyclic aromatic hydrocarbon content in commercial Spanish fatty foods. J. Food Prot. 67, 2786–2971.

Bartolomé, M., Ramos, J.J., Cutanda, F., Huetos, O., Esteban, M., Ruiz-Moraga, M., Calvo, E., Pérez-Gómez, B., González, O., Castaño, A., 2015. Urinary polycyclic aromatic hydrocarbon metabolites levels in a representative sample of the Spanish adult population: the BIOAMBIENT.ES project. Chemosphere 135, 436–446.

Bortey-Sam, N., Akoto, O., Ikenaka, Y., Nakayama, S.M., Ishizuka, M., 2013. Determination of benzo[a]pyrene levels in ambient air and the source of polycyclic aromatic hydrocarbons using a diagnostic ratio method in Ghana. Jpn. J. Vet. Res. 61, S72–S74.

Bortey-Sam, N., Ikenaka, Y., Nakayama, S.M., Akoto, O., Yohannes, Y.B., Baidoo, E., Mizukawa, H., Ishizuka, M., 2014. Occurrence, distribution, sources and toxic potential of polycyclic aromatic hydrocarbons (PAHs) in surface soils from the Kumasi Metropolis, Ghana. Sci. Total Environ. 496, 471–478.

Bortey-Sam, N., Ikenaka, Y., Akoto, O., Nakayama, S.M., Yohannes, Y.B., Baidoo, E., Mizukawa, H., Ishizuka, M., 2015a. Levels, potential sources and human health risk of polycyclic aromatic hydrocarbons (PAHs) in particulate matter (PM10) in Kumasi, Ghana. Environ. Sci. Pollut. Res. 22, 9658–9667.

Bortey-Sam, N., Ikenaka, Y., Akoto, O., Nakayama, S.M., Yohannes, Y.B., Baidoo, E., Saengtienchai, A., Mizukawa, H., Ishizuka, M., 2015b. Exposure levels of polycyclic aromatic hydrocarbons (PAHs) and heavy metals in wild rats in Kumasi, Ghana. In: Proceedings of the 7th International Toxicology Symposium in Africa, Johannesburg, South Africa. 31st August, 2015, pp. 67–68. Available online: http://aa.vetmed.hokudai.ac.jp/en/uploads/2015/10/7th_International_Toxicology_Sym posium_in_Africa.pdf.

Bouchard, M., Viau, C., 1999. Urinary 1-hydroxypyrene as a biomarker of exposure to polycyclic aromatic hydrocarbons: biological monitoring strategies and methodology for determining biological exposure indices for various work environments. Biomarkers 4, 159–187.

Burczynski, M.E., Harvey, R.G., Penning, T.M., 1998. Expression and characterization of four recombinant human dihydrodiol dehydrogenase isoforms: oxidation of trans7,8-Dihydroxy-7,8-dihydrobenzo[a]pyrene to the activated o-quinone metabolite benzo[a]pyrene-7,8-dione. Biochemistry 37, 6781–6790.

Burgaz, S., Borm, P.J.A., Jongeneelen, F.J., 1992. Evaluation of excretion of 1hydroxypyrene and thioethers in workers exposed to bitumen fumes. Int. Arch. Occup. Environ. Health 63, 397–401.

Campo, L., Rossella, F., Fustinoni, S., 2008. Development of a gas chromatography/mass spectrometry method to quantify several urinary monohydroxy metabolites of polycyclic aromatic hydrocarbons in occupationally exposed subjects. J. Chromatogr. B 875, 531–540.

CDC, 2015. Fourth National Report on Human Exposure to Environmental Chemicals, Updated Tables, February 2015 (last accessed 22.12.15.). http://www.cdc.gov/exposurereport/.

Dacasto, M., Eeckhoutte, C., Capolongoa, F., Dupuy, J., Carletti, M., Calléja, C., Nebbia, C., Alvinerie, M., Galtier, P., 2005. Effect of breed and gender on bovine liver cytochrome P450 3A (CYP3A) expression and inter-species comparison with other domestic ruminants. Vet. Res. 36 (2), 179–190.

Dissanayake, A., Galloway, T.S., 2004. Evaluation of fixed wavelength fluorescence and synchronous fluorescence spectrophotometry as a biomonitoring tool of environmental contamination. Mar. Environ. Res. 58, 281–285.

Fan, R., Ramage, R., Wang, D., Zhou, J., She, J., 2012a. Determination of ten monohydroxylated polycyclic aromatic hydrocarbons by liquid–liquid extraction and liquid chromatography/tandem mass spectrometry. Talanta 93, 383–391.

Fan, R., Wang, D., Mao, C., Ou, S., Lian, Z., Huang, S., Lin, Q., Ding, R., She, J., 2012b. Preliminary study of children's exposure to PAHs and its association with 8-hydroxy2′-deoxyguanosine in Guangzhou, China. Environ. Int. 42, 53–58.

Ferrari, S., Mandel, F., Berset, J.D., 2002. Quantitative determination of 1-hydroxypyrene in bovine urine samples using high-performance liquid chromatography with fluorescence and mass spectrometric detection. Chemosphere 47 (2), 173–182.

Griego, F.Y., Bogen, K.T., Price, P.S., Weed, D.L., 2008. Exposure, epidemiology and

human cancer incidence of naphthalene. Regul. Toxicol. Pharmacol. 51 (2), S22–S26.
Guengerich, F.P., 2002. Cytochrome P450. In: Ioannides, C. (Ed.), Enzyme Systems that Metabolise Drugs and Other Xenobiotics. John Wiley & Sons Inc., New York, pp. 33–65.
Guo, H., Huang, K., Zhang, X., Zhang, W., Guan, L., Kuang, D., Deng, Q., Deng, H., Zhang, X., He, M., Christiani, D., 2014. Women are more susceptible than men to oxidative stress and chromosome damage caused by polycyclic aromatic hydrocarbons exposure. Environ. Mol. Mutagen. 55 (6), 472–481.
Guo, Y., Senthilkumar, K., Alomirah, H., Moon, H.B., Minh, T.B., Mohd, M.A., Kannan, K., 2013. Concentrations and profiles of urinary polycyclic aromatic hydrocarbon metabolites (OH-PAHs) in several Asian countries. Environ. Sci. Technol. 47 (6), 2932–2938.
Hatzinger, P.B., Alexander, M., 1997. Biodegradation of organic compounds sequestered in organic solids or in nanopores within silica particles. Environ. Toxicol. Chem. 16 (11), 2215–2221.
Jongeneelen, F.J., 2001. Benchmark guideline for urinary 1- hydroxypyrene as biomarker of occupational exposure to polycyclic aromatic hydrocarbons. Ann. Occup. Hyg. 45 (1), 3–13.
Kim, H., Cho, S.H., Kang, J.W., Kim, Y.D., Nan, H.M., Lee, C.H., Lee, H., Kawamoto, T., 2000. Urinary 1-hydroxypyrene and 2-naphthol concentrations in male Koreans. Int. Arch. Occ. Environ. Health 74 (1), 59–62.
Kim, M., Kim, D.G., Bong, Y.H., Jang, J.H., Son, S.W., 2013. Concentrations of PCDD/Fs, dioxin-like PCBs, PBDEs, and hexachlorobenzene in fat samples from cattle of different ages and gender in Korea. Food Chem. 138 (2), 1786–1791.
Laflamme, R.E., Hites, R.A., 1978. The global distribution of polyaromatic hydrocarbons in recent sediments. Geochim. Cosmochim. Acta 42, 289–303.
Lake, J.L., Norwood, C., Dimock, C., Bowen, R., 1979. Origins of polycyclic aromatic hydrocarbons in estuarine sediments. Geochim. Cosmochim. Acta 43, 1847–1854.
Levine, H., Berman, T., Goldsmith, R., Göen, T., Spungen, J., Novack, L., Amitai, Y., Shohat, T., Grotto, I., 2015. Urinary concentrations of polycyclic aromatic hydrocarbons in Israeli adults: demographic and life-style predictors. Int. J. Hyg. Environ. Health 218 (1), 123–131.
Li, Z., Mulholland, J.A., Romanoff, L.C., Pittman, E.N., Trinidad, D.A., Lewin, M.D., et al., 2010. Assessment of non-occupational exposure to polycyclic aromatic hydrocarbons through personal air sampling and urinary biomonitoring. J. Environ. Monit. 12, 1110–1118.
Li, Z., Sandau, C.D., Romanoff, L.C., Caudill, S.P., Sjodin, A., Needham, L.L., Patterson Jr., D.G., 2008. Concentration and profile of 22 urinary polycyclic aromatic hydrocarbon metabolites in the US population. Environ. Res. 107, 320–331.
Meeker, J.D., Barr, D.B., Serdar, B., Rappaport, S.M., Hauser, R., 2007. Utility of urinary 1-naphthol and 2-naphthol levels to assess environmental carbaryl and naphthalene exposure in an epidemiology study. J. Expo. Sci. Environ. Epidemiol. 17 (4), 314–320.
Mollerup, S., Berge, G., Baera, R., Skaug, V., Hewer, A., Phillips, D.H., Stangeland, L., Haugen, A., 2006. Sex differences in risk of lung cancer: expression of genes in the PAH bioactivation pathway in relation to smoking and bulky DNA adducts. Int. J. Cancer 119, 741–744.
Nam, J.J., Thomas, G.O., Jaward, F.M., Steinnes, E., Gustafsson, O., Jones, K.C., 2008. PAHs in background soils from Western Europe: influence of atmospheric deposition and soil organic matter. Chemosphere 70 (9), 1596–1602.
Nebbia, C., 2001. Biotranformation enzymes as determinants of xenobiotic toxicity in domestic animals. Vet. J. 161, 238–252.
Nermell, B., Lindberg, A.L., Rahman, M., Berglund, M., Persson, L.A., El Arifeen, S., Vahter, M., 2008. Urinary arsenic concentration adjustment factors and malnutrition. Environ. Res. 106, 212–218.
National Toxicology Program, NTP, 1992. Toxicology and carcinogenesis study of naphthalene in B6C3F1 mice (inhalation studies). Research Triangle Park, NC.
National Toxicology Program, NTP, 2000. Toxicology and Carcinogenesis Study of Naphthalene in F344/N Rats (Inhalation Studies). Research Triangle Park, NC.
Orjuela, M.A., Liu, X., Miller, R.L., Warburton, D., Tang, D., Jobanputra, V., Perera, F.P., 2012. Urinary naphthol metabolites and chromosomal aberrations in 5-year-old children. Cancer Epidemiol. Biomarkers Prev. 21 (7), 1191–1202.
Owa, J.A., Izedonmwen, O.E., Ogundaini, A.O., Ogungbamila, F.O., 1993. Quantitative analysis of 1-naphthol in urine of neonates exposed to mothballs: the value in infants with unexplained anaemia. Afr. J. Med. Med. Sci. 22 (1), 71–76.
Rey-Salgueiro, L., Martínez-Carballo, E., García-Falcón, M.S., Simal-Gándara, J., 2008. Effects of a chemical company fire on the occurrence of polycyclic aromatic hydrocarbons in plant foods. Food Chem. 108, 347–353.
Riojas-Rodriguez, H., Schilmann, A., Marron-Mares, A.T., Masera, O., Li, Z., Romanoff, L., et al., 2011. Impact of the improved patsari biomass stove on urinary polycyclic aromatic hydrocarbon biomarkers and carbon monoxide exposures in rural Mexican women. Environ. Health Perspect. 119 (9), 1301–1307.
Saengtienchai, A., Ikenaka, Y., Nakayama, S.M., Mizukawa, H., Kakehi, M., Bortey-Sam, N., Darwish, W.S., Tsubota, T., Terasaki, M., Poapolathep, A., Ishizuka, M., 2014. Identification of interspecific differences in phase II reactions: determination of metabolites in the urine of 16 mammalian species exposed to environmental pyrene. Environ. Toxicol. Chem. 33 (9), 2062–2069.
Soghoian, S., Nyadedzor, C., Ed Nignpense, B., Clarke, E.E.K., Hoffman, R.S., 2012. Health risks of using mothballs in Greater Accra, Ghana. Trop. Med. Int. Health 17 (1), 135–138.
Sul, D., Ahn, R., Im, H., Oh, E., Kim, J.H., Kim, J.G., Kim, P., et al., 2012. Korea National Survey for Environmental Pollutants in the human body 2008: 1-hydroxypyrene, 2- naphthol, and cotinine in urine of the Korean population. Environ. Res. 118, 25–30.
Tay, C.K., Biney, C.A., 2013. Levels and sources of polycyclic aromatic hydrocarbons (PAHs) in selected irrigated urban agricultural soils in Accra, Ghana. Environ. Earth Sci. 68, 1773–1782.
Thai, P.K., Heffernan, A.L., Toms, L.M.L., Li, Z., Calafat, A.M., Hobson, P., Broomhall, S., Mueller, J.F., 2016. Monitoring exposure to polycyclic aromatic hydrocarbons in an Australian population using pooled urine samples. Environ. Int. 88, 30–35.
Uppstad, H., Osnes, G.H., Cole, K.J., Phillips, D.H., Haugen, A., Mollerup, S., 2011. Sex differences in susceptibility to PAHs is an intrinsic property of human lung adenocarcinoma cells. Lung Cancer 71, 264–270.
Wayne, R.O., 1990. A physical explanation of the lognormality of pollutant concentrations. J. Air Manag. Assoc. 40, 1378–1383.
Xu, X., Cook, R.L., Ilacqua, V.A., Kan, H., Talbott, E.O., Kearney, G., 2010. Studying associations between urinary metabolites of polycyclic aromatic hydrocarbons (PAHs) and cardiovascular diseases in the United States. Sci. Total Environ. 408, 4943–4948.

Science of the Total Environment 574 (2017) 1389–1395

Contents lists available at ScienceDirect

Science of the Total Environment

journal homepage: www.elsevier.com/locate/scitotenv

DDTs and other organochlorine pesticides in tissues of four bird species from the Rift Valley region, Ethiopia

Yared Beyene Yohannes [a,b,1], Yoshinori Ikenaka [a,d,1], Shouta M.M. Nakayama [a], Hazuki Mizukawa [c], Mayumi Ishizuka [a,*]

[a] Laboratory of Toxicology, Department of Environmental Veterinary Sciences, Graduate School of Veterinary Medicine, Hokkaido University, Kita 18, Nishi 9, Kita-ku, Sapporo 060-0818, Japan
[b] Department of Chemistry, College of Natural and Computational Science, University of Gondar, P.O. Box 196, Gondar, Ethiopia
[c] Department of Environmental Veterinary Sciences, Graduate School of Veterinary Medicine, Hokkaido University, Kita 18, Nishi 9, Kita-ku, Sapporo 060-0818, Japan
[d] Water Research Group, Unit for Environmental Sciences and Management, North-West University, Potchefstroom 2520, South Africa

HIGHLIGHTS

- Indoor residual spraying and indiscriminate pesticide usage underlines relevance of this study.
- 22 OCPs in different tissues of 4 bird species were monitored.
- List ParagraphPotential ecological risk to birds associated with exposure to *p,p*'-DDE.
- Further ecotoxicological study using a wide range of species and sample size is necessary.

GRAPHICAL ABSTRACT

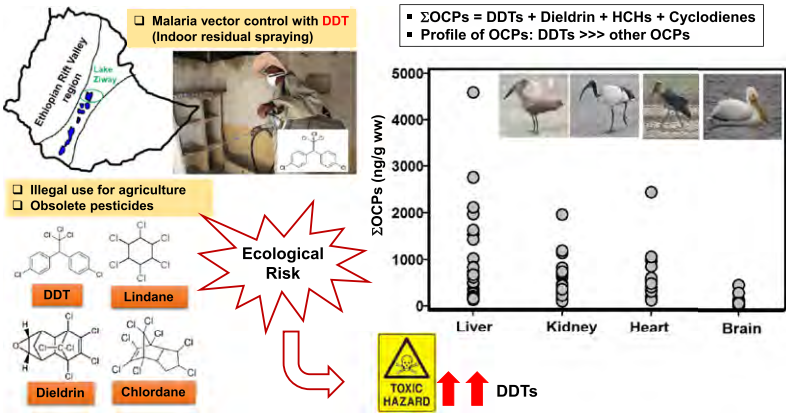

ARTICLE INFO

Article history:
Received 8 April 2016
Received in revised form 7 August 2016
Accepted 7 August 2016
Available online 15 August 2016

Editor: D. Barcelo

Keywords:
DDT
Organochlorine pesticides
Bird
Risk evaluation
Rift valley
Ethiopia

ABSTRACT

Despite the presence of a wide variety and number of birds, there is exceedingly little data on organochlorine pesticide (OCP) residues in birds inhabiting in Africa. In the present study, concentrations of dichlorodiphenyltrichloroethanes (DDTs), hexachlorocyclohexanes, drins, cyclodienes, and hexachlorobenzene were measured in liver, kidney, heart and brain of 4 bird species from the Rift Valley region, Ethiopia. Indoor residual spraying of DDT for malaria vector control, and indiscriminate and illegal use of pesticides underline the relevance of this study. Levels of ΣOCPs ranged from 1.87 to 4586 ng/g wet weight, and the scavenger bird species *Leptoptilos crumeniferus* had the highest level in liver. In all tissues, contamination profiles of OCPs within the species were similar, with DDTs ≫ other OCPs. Among the DDTs, *p,p*'-DDE was the most abundant compound and had significantly a higher burden in all tissues. The risk characterization demonstrated potential risks to the studied birds associated with DDE exposure. Maximum hepatic levels of *p,p*'-DDE exceeded the levels reported to trigger adverse effects. The detection of *p,p*'-DDT in all bird tissues suggests the release of fresh DDT to the environment. This is the first study to assay OCPs in different tissues of birds from the Ethiopian Rift Valley region, and henceforth the data will serve as a reference data for future studies.

* Corresponding author.
E-mail address: ishizum@vetmed.hokudai.ac.jp (M. Ishizuka).
[1] Both authors contributed equally in this manuscript.

http://dx.doi.org/10.1016/j.scitotenv.2016.08.056
0048-9697/

1. Introduction

Organochlorine pesticides (OCPs) are ubiquitous pollutants characterized by their environmental persistence and lipophilicity. The release of these pollutants into the environment is of great concern because of their bioaccumulative potential and chronic adverse effects on both humans and wildlife (Walker et al., 2001). Thus, OCPs are currently banned or restricted from use, and therefore their levels are generally declining in developed countries. However, they are still in use for agriculture and public health purposes in some African countries. Especially, dichlorodiphenyltrichloroethane (DDT) has been extensively used for malaria vector control (Sadasivaiah et al., 2007; van den Berg, 2009). Ethiopia is one of the many African countries which have implemented indoor residual spraying (IRS) with DDT for malaria vector control, and is still the insecticide of choice (Cid et al., 2007; Hamusse et al., 2012). In addition, the country is burdened by illegal usage of pesticides on food crops, and leaching from obsolete pesticide stocks. Thus, due to their bioaccumulative and biomagnification potential, high concentrations of OCPs can be found in top predators including birds, potentially leading to detrimental health effect in these organisms.

Birds have been widely used as sentinel species to monitor exposure and effects of pollution in the environment owing to their high trophic position, widespread distribution, and sensitivity to environmental changes (Furness, 1993; Jaspers et al., 2006). Adverse effects of OCPs on birds include reduced reproductive success, impaired reproductive behavior, and alteration of liver metabolic activities (Giesy et al., 2003; Mineau and Whiteside, 2013; Mitra et al., 2011). One of the well-known sub-lethal effects caused by DDTs, particularly *p,p*'-DDE, is the eggshell thinning, which leads to breeding failure (Blus, 2011; Lundholm, 1997; Ratcliffe, 1967). Thus, monitoring levels of organic pollutants such as OCPs, polychlorinated biphenyls, polybrominated diphenyl ethers, etc. in wildlife including avian species can yield information about the bioavailability, and biomagnification of pollutants to prevent potential risks to living beings. Regrettably, in Africa there are only a few studies from South Africa (Bouwman et al., 2008, 2013; van Wyk et al., 2001) and one study from Ethiopia (Yohannes et al., 2014a) which investigated the levels, and risks of organohalogenated pesticides in blood, egg, and tissues of different bird species. Most studies have been carried out on birds inhabiting other continents (Lam et al., 2008; van Drooge et al., 2008; Yordy et al., 2013).

The Ethiopian Rift Valley (ERV) region which encompasses seven lakes is a densely populated area with various agricultural activities and flower farms in close proximity. The region serves as a breeding and wintering ground, and as a migration stopover habitat for several bird species (Birdlife International, 2013). However, the indiscriminate usage of pesticides, especially DDTs, has resulted in the occurrence of OCPs residues in biotic (Deribe et al., 2014; Yohannes et al., 2013a, 2014b) and abiotic (Yohannes et al., 2013b) compartments of the ERV region. In general, the African environments have not received adequate attention on ecological impacts of environmental pollutants in birds to date even though the presence of a wide variety and number of birds. Thus, it is expected that the data generated in this study will serve as a reference and a baseline data for future studies.

Therefore, the aims of this study were: (1) to assess concentrations of 22 OCPs in liver, kidney, heart and brain samples of four bird species from the Ethiopian Rift Valley region, and (2) to compare hepatic concentrations of OCPs to avian toxic effects thresholds for assessing any potential risk to the avifauna at the study site.

2. Materials and methods

2.1. Study site and sampling

Fig. 1 shows the ERV region lakes and the sampling spot at the shore of Lake Ziway for this study. The wet land of Lake Ziway supports over 20,000 water birds (Birdlife International, 2013). It provides a foraging and breeding ground for many resident and migrant bird species. Lake Ziway is one of the best sites in Ethiopia to see a diversity of bird species such as *Haliaeetus vocifer* (African fish eagle), *Pelecanus onocrotalus* (great white pelican), *Phalacrocorax lucidus* (white-breasted cormorant), *Scopus umbretta* (hamerkop), *Chroicocephalus cirrocephalus* (grey-headed gull), *Threskiornis aethiopicus* (African sacred ibis), *Chlidonias leucopterus* (white-winged black tern), *Leptoptilos crumeniferus* (marabou stork), etc. However, the lake faces several anthropogenic threats from untreated industrial and domestic wastes. Moreover, the expansion of intensive agricultures (producing fruits, vegetables and flowers) and the IRS for malaria vector control programme have introduced pesticides into the ecosystem. In recent years, a decline in water birds and fish species compositions has been noted (Birdlife International, 2013; Mengesha et al., 2014).

A total of 23 birds belonging to *Scopus umbretta* (Hamerkop, $N = 5$), *Threskiornis aethiopicus* (African sacred ibis, $N = 7$), *Leptoptilos crumeniferus* (Marabou stork, $N = 6$), and *Pelecanus onocrotalus* (Great white pelican, $N = 5$) were captured in 2012 at the shore of Lake Ziway (Fig. 1). These birds are almost sedentary species and widely distributed in the ERV ecosystems, and thus can be considered as potential bio-monitoring species for environmental contamination. 19 males and 4 females were sampled by chance. Feeding and habitat information about the species is summarized in Table 1. Each bird was euthanized (using ether after capture) and excised. Samples of liver, kidney, heart and brain were collected and stored at −20 °C. The frozen samples were then transported to the Laboratory of Toxicology, Graduate School of Veterinary Medicine, Hokkaido University, Japan for analysis. Permission for capturing and sacrificing the aforementioned birds has been granted from the Ethiopian Wildlife Conservation Authority (Permission No. DA/31/284/012).

2.2. Reagents and chemicals

All solvents and reagents used were specific for pesticide residue analysis, and purchased from Kanto Chemical Corp. (Tokyo, Japan). Florisil (60–100 mesh) was activated at 130 °C overnight before use. Standards of OCPs, surrogate (2,4,5,6-tetrachloro-*m*-xylene) and internal (PCB 209) standards were purchased from Dr. Ehrenstorfer (Augsburg, Germany). The analytes of interest are: DDTs (*o,p*'-DDT, *p,p*'-DDT, *o,p*'-DDE, *p,p*'-DDE, *o,p*'-DDD and *p,p*'-DDD), hexachlorocyclohexanes (HCHs; α-, β-, γ- and δ-HCH), cyclodienes (CYLs; heptachlor, *cis*- and *trans*-heptachlor epoxide, *cis*-, *trans*-and *oxy*-chlordane, and *cis*- and *trans*-nonachlor), drins (aldrin, dieldrin and endrin) and hexachlorobenzene (HCB). Stock solutions of each compound at 10 mg/L were prepared in *n*-decane and stored at 4 °C.

2.3. Chemical analysis

The protocol for analysis was performed as described by Yohannes et al. (2014a) with minor modifications. Briefly, wet tissue (1 g for liver; 2 g for kidney, 2 g for heart and brain) was homogenized with anhydrous Na_2SO_4 and spiked with a surrogate standard (2,4,5,6-tetrachloro-*m*-xylene). Extraction was carried out with 150 mL hexane/acetone (3:1, *v*/*v*) in a Soxtherm apparatus (S306AK Automatic Extractor, Gerhardt, Germany) in hot extraction mode (180 °C) for 4 h. The lipid content was determined gravimetrically on an aliquot of the extract, while the rest of the extract was cleaned up on a column filled with 6 g activated florisil and eluted with 100 mL hexane:dichloromethane (7:3, *v*/*v*). The eluate was concentrated to near dryness under a gentle stream of nitrogen, and redissolved in 100 μL *n*-decane. Finally, an internal standard (100 μg/L PCB 209) was added to all extracts prior to instrumental analysis.

OCPs were analyzed with a Shimadzu Model 2014 gas chromatography equipped with a ^{63}Ni μ-electron capture detector (Shimadzu, Kyoto, Japan) and an ENV−8MS capillary column (30 m × 0.25 mm i.d. with film thickness 0.25 μm). The oven temperature began at 100 °C (1 min

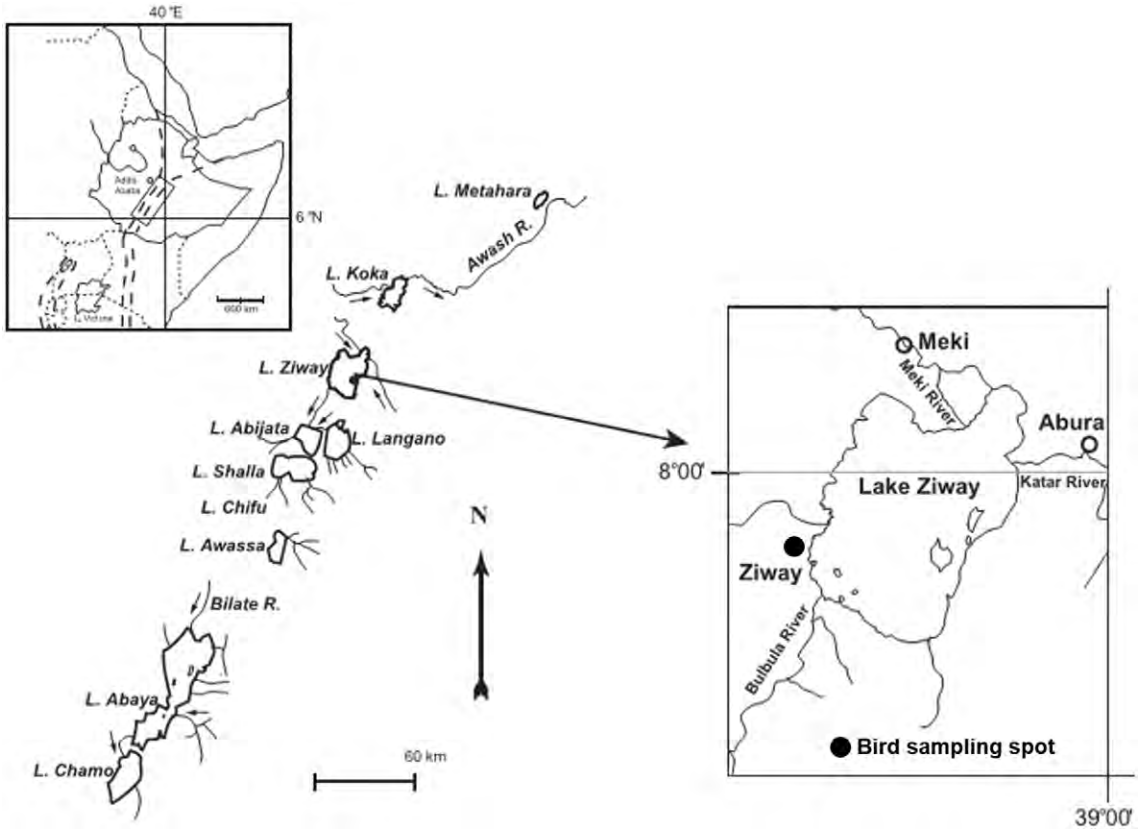

Fig. 1. Ethiopian Rift Valley lakes and location where birds were collected at the shore of Lake Ziway.

hold time), ramped at 20 °C/min to 200 °C, then raised at 3 °C/min to 280 °C with a 10 min hold time. Injector and detector temperatures were maintained at 250 °C and 310 °C, respectively. Helium at a flow rate of 1.0 mL/min and nitrogen at 45 mL/min were used as carrier gas and make-up gas, respectively. 1 μL of each sample was injected in splitless mode.

2.4. Quality assurance/quality control (QA/QC)

OCPs were identified by a comparison of its relative retention time with the calibration standards. Confirmation of residues on representative samples was performed using a Thermo Scientific DSQ II single stage quadrupole GC–MS system. Standard solutions were used to calibrate the instrument, and multi-level calibration curves in the linear response interval of the detector were created for the quantification and good correlation ($r^2 > 0.995$) was achieved. The quality control and quality assurance were performed by analyses of procedural blanks, spiked blanks and blind duplicate samples, and consisted in daily check of calibration curves. Recoveries for individual OCPs were between 80% and 105%, and average recovery for the surrogate standard, 2,4,5,6-tetrachloro-*m*-xylene, was 85 ± 9%. A standard reference material SRM 1947 (Lake Michigan Fish Tissue) was also used to test the method accuracy. Obtained values were in agreement with the certified values, not deviating >10%. The limit of detection (LOD) was set at a signal-to-noise ratio (S/N) of 3. LODs were 0.1 ng/g, 0.08–0.22 ng/g, 0.1–0.6 ng/g, 0.05–0.3 ng/g, and 0.05–0.2 ng/g for HCB, HCHs, drins, CYLs, and DDTs, respectively.

2.5. Statistical analysis

The concentrations of OCPs showed skewed distribution so geometric means were reported. Data were, therefore, log transformed to

Table 1
Sample information and feeding habits of the species under study.

Scientific name (common name)	Habitat and breeding[a]	Feeding habit[a]
Scopus umbretta (hamerkop)	Mainly terrestrial. Breeds in a fork of a tree overhanging water, on cliff ledges, rock columns	Predominantly of amphibians and small fish as well as crustaceans, worms and insects
Threskiornis aethiopicus (African sacred ibis)	Mainly terrestrial. Breeds colonially in trees near water	Insectivorous and other small prey. Feeds opportunistically on plowed lands. Also eats small prey such as worms, molluscs, fish, frogs, lizards, small mammals, eggs of birds and crocodiles, and organic material from rubish heaps or at sewerage plants.
Leptoptilos crumeniferus (marabou stork)	Mainly terrestrial. Breeds colonially in trees, on cliffs, or on buildings in towns and villages	Scavenger: predominantly of carrion and scraps of fish discarded by humans as well as live fish, termites, locusts, frogs, lizards, snakes, rats, mice and birds.
Pelecanus onocrotalus (great white pelican)	Aquatic. Breeds colonially on the ground either on a pile of sticks and vegetation or in a simple shallow scrape	Entirely piscivorous, preferentially taking fish

[a] References: birdlife International species factsheet. (http://www.birdlife.org).

reduce the skewness and kurtosis of the raw data prior to statistical comparisons. One-way analysis of variance (ANOVA) with a post hoc test (Tukey's HSD test) was used for interspecies comparisons of contaminant levels to find significant differences among the species with sample size ≥3. Samples with concentrations below the detection limits were assigned a value of one-half of the detection limits. All the statistical analyses were performed using JMP 10 (SAS Institute, Cary, NC, USA) and the level of significance throughout the study was set at $p < 0.05$. For comparison, liver residue levels of OCPs reported in other bird species were referred due to the absence of residues level data in same species and matrices.

3. Results and discussion

3.1. Accumulation pattern of OCPs

OCPs were detected in all species and tissues of the analyzed birds. The geometric means and range of concentrations for individual OCPs in liver, kidney, heart and brain of the studied 4 bird species are presented in Table 2. Levels of individual OCPs quantified in all tissues ranged from ND to 4578 ng/g ww, indicating low to high levels of OCPs. The highest ΣOCPs geometric mean concentration was found in *L. crumeniferus* (1098 ng/g ww), followed by *P. onocrotalus* (953 ng/g ww). Likewise, a large variability of ΣOCPs levels was observed among and within the studied bird species in all tissues (Fig. 2). This variation in the magnitude of pollutants could be associated with feeding ecology, trophic level, age, birds' body condition, metabolic capabilities, and duration of contamination (Jaspers et al., 2006; Walker et al., 2001). However, interspecies differences in tissue levels of ΣOCPs exhibited no significant differences ($p > 0.05$) among bird species except in brain (F-ratio = 6.24; $p = 0.01$). Other studies on birds having different dietary habits from Argentina (Cid et al., 2007) and Italy (Naso et al., 2003) also showed no significant differences for total OCP accumulation. In muscle tissue of these bird species, levels of ΣOCPs were ranged from 3.7 to 148.7 μg/g lipid (Yohannes et al., 2014a).

The accumulation profiles of OCPs showed the highest concentrations in liver, and this was followed by kidney and heart tissues. This tissue distribution can probably be attributed to the lipid distribution and tissue-specific accumulation abilities. It can be seen that lipid contents in the liver were generally higher than those in the kidney and heart (Table 2). Moreover, liver is an active site for biotransformation and accumulation of contaminants. However, although lipid content of brain is significantly higher than the other tissues, accumulation of OCPs was low in brain. This result shows the protective role of the blood-brain barrier, which limits access of xenobiotics to the cerebral compartment (Tebourbi et al., 2006). Generally, concentrations of ΣOCPs in the liver were significantly higher than those in the brain (F-ratio = 12.5; $p = 0.001$).

It is important to investigate tissue distribution of OCPs within the studied bird species for more information on the extent of exposure to pesticides. Fig. 3 shows percentage contribution of DDTs, dieldrin, HCHs, and CYLs in liver and kidney tissues (heart and brain exhibited similar OCPs distribution, data not shown). The OCP profile in tissues of all species was clearly dominated by DDTs, accounting for 94 to 99% in liver and 91 to 95% in kidney. The dominance of DDTs in total OCPs indicates a high degree of exposure to DDTs in biota from the ERV

Table 2
Geometric mean concentrations and range (ng/g wet weight [ng/g lipid weight]) of DDT metabolites and organochlorine pesticides in different tissues of 4 bird species from the Rift Valley region, Ethiopia.

Tissue	Bird species (N,n[a])	Lipid (%)	*pp*'-DDE	*pp*'-DDD	*pp*'-DDT	ΣDDT	Dieldrin	ΣHCH	ΣCYL
Liver	*Scopus umbretta*	4.44	451	15	1.23	569 [15,598]	8.5 [127]	15.9 [239]	4.91 [73]
	(5,5)	(4.03–4.75)	(105–1958)	(3–180)	(ND–21.6)	(242–1962)	(2.2–39.2)	(8.55–27.2)	(1.89–17.2)
	Threskiornis aethiopicus	4.83	249	2.56	0.05	254 [8359]	0.83 [69]	5.68 [94]	1.07 [17]
	(7,7)	(4.03–4.75)	(100–1535)	(0.91–8.30)	(ND–1.44)	(103–1537)	(0.10–8.7)	(1.03–56.4)	0.53–1.47)
	Leptoptilos crumeniferus	4.15	1003	36	0.40	1088 [40,317]	1.96 [38]	2.21 [42]	1.51 [29]
	(6,6)	(3.44–4.83)	(108–4498)	(11.1–64.3)	(ND–14.7)	(151–4578)	(0.89–7.23)	(0.74–6.40)	(0.54–3.95)
	Pelecanus onocrotalus	5.47	784	104	0.47	895 [24,565]	1.36 [19]	9.43 [137]	43.1 [628]
	(5,5)	(4.99–5.84)	(454–1423)	(79–137)	(ND–1.64)	(558–1562)	(0.74–2.77)	(4.28–17.5)	(33.2–58.3)
Kidney	*Scopus umbretta*	2.32	448	2.24	0.21	451 [19,585]	36.2 [1561]	1.94 [83]	0.95 [40]
	(5,2[a])	(2.15, 2.52)	(340, 590)	(1.86, 2.70)	(0.10, 0.43)	(344, 592)	(20.7, 63.1)	(1.80, 2.09)	(0.90, 0.99)
	Threskiornis aethiopicus	2.76	242	3.75	0.22	251 [6742]	11.4 [306]	0.23 [6.2]	1.13 [30]
	(7,7)	(2.47–3.95)	(101–776)	(0.84–19.28)	(ND–1.29)	(108–779)	(5.61–39.0)	(ND-0.54)	(0.16–3.34)
	Leptoptilos crumeniferus	1.78	482	0.88	0.10	484 [27,184]	8.71 [488]	0.20 [11]	0.15 [8.3]
	(6,6)	(1.14–3.03)	(95–1962)	(0.29–4.69)	(ND–3.0)	(95–1965)	(0.16–115)	(0.12–0.23)	(0.02–0.69)
	Pelecanus onocrotalus	1.37	348	54	1.20	406 [29,366]	18.9 [1369]	0.20 [14]	3.64 [263]
	(5,5)	(0.87–2.05)	(167–1029)	(39.3–123)	(ND–2.54)	(211–1155)	(8.91–30.4)	(0.10–0.22)	(1.99–5.17)
Heart	*Scopus umbretta*	-	-	-	-	-	-	-	-
	(5,0)								
	Threskiornis aethiopicus	1.87	188	3.10	1.90	194 [9901]	4.75 [345]	0.70 [36.9]	1.18 [62]
	(7,3[a])	(1.84–1.96)	(129–285)	(2.60–4.34)	(1.20–4.56)	(138–289)	(0.16–34.2)	(0.51–0.84)	(0.84–2.12)
	Leptoptilos crumeniferus	1.64	495	2.81	1.72	500 [30,339]	39.8 [2432]	0.27 [16.4]	0.50 [30]
	(6,5)	(1.00–2.11)	(111–2214)	(0.45–15.3)	(0.53–7.66)	(112–2237)	(3.91–208.4)	(0.15–0.48)	(0.11–1.13)
	Pelecanus onocrotalus	2.31	520	71	18.9	614 [27,575]	13.2 [694]	0.63 [27.3]	6.39 [2375]
	(5,5)	(1.86–3.04)	(299–912)	(52.1–92.8)	(16.2–24.8)	(384–1030)	(12.7–13.7)	(0.47–0.93)	(3.41–10.6)
Brain	*Scopus umbretta*	8.66	192	2.56	1.05	198 [2282]	21.1 [242]	ND	1.20 [14]
	(5,2[a])	(7.78, 9.65)	(89, 412)	(1.70, 3.84)	(0.67, 1.63)	(94, 415)	(11.8, 37.7)		(1.10, 1.30)
	Threskiornis aethiopicus	6.67	7	0.17	0.11	7.46 [111]	1.25 [17]	ND	0.13 [2.2]
	(7,6)	(5.08–8.87)	(1–15)	(ND–1.00)	(ND–0.52)	(1.73–16)	(ND-1.29)		(0.10–0.17)
	Leptoptilos crumeniferus	7.64	84	0.32	0.51	85 [1115]	6.38 [144]	ND	0.10 [2.2]
	(6,4)	(6.71–8.97)	(15–266)	(ND–1.70)	(0.30–0.84)	(15–268)	(0.65–18.9)		(0.07–0.13)
	Pelecanus onocrotalus	8.10	51	0.67	0.20	52 [638]	3.13 [71]	ND	0.29 [6.6]
	(5,5)	(6.89–9.97)	(39–65)	(0.49–0.91)	(0.12–0.39)	(39–67)	(2.59–3.98)		(0.14–0.55)

N: number of birds captured; n: number of samples analyzed.
-: no sample available.
ND: below detection limit.
ΣDDT: *p,p*'-DDT + *p,p*'-DDE + *p,p*'-DDD.
ΣHCH: α-HCH + β-HCH + γ-HCH.
ΣCYL: *cis*-heptachlor epoxide + *trans*-chlordane + *trans*-nonachlor + *oxy*-chlordane.
[a] Pooled samples.

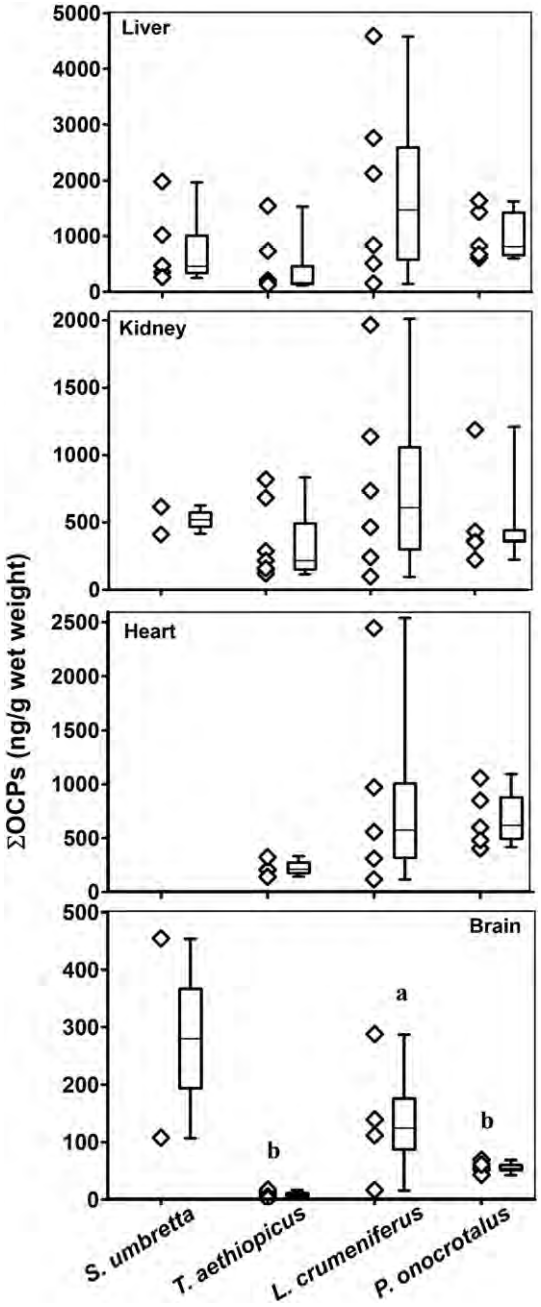

Fig. 2. Box and whisker plots of ∑OCPs concentrations in liver, kidney, heart, and brain tissues of 4 bird species from the Rift Valley region, Ethiopia. The line of the box plot represents 5th, 25th, 50th, 75th, and 95th percentiles of the distribution. ΣOCPs: ΣDDT + ΣHCH + Dieldrin + ΣCYL.

region. This result could be explained most likely due to the recent use of DDT in IRS for vector control like mosquitoes in the region (van den Berg, 2009; WHO, 2007), as well as from illegal usage for agriculture, and contamination from past usage. Even though sample sizes were small and making definite conclusions premature, birds living in the study area exhibited moderate to high levels of DDTs, suggesting that DDTs are ubiquitous in the biosphere of Ethiopia. For brevity, mostly liver concentrations are discussed, unless otherwise noted.

3.2. Concentrations of DDTs

Levels of DDTs measured in tissues of birds reflect the widespread occurrence of these compounds in the environment. Concentrations of ΣDDT in liver, kidney, heart and brain ranged from 103 to 4578 ng/g ww, 95 to 1965 ng/g ww, 112 to 2237 ng/g ww and 1.73 to 415 ng/g ww, respectively (Table 2). The highest geometric mean ΣDDT concentration was observed in *L. crumeniferus* (1088 ng/g ww), followed by *P. onocrotalus* (895 ng/g ww). Ecological and feeding habits of these bird species may be a plausible explanation for elevated DDTs (Table 1). The *L. crumeniferus* species is a scavenger, eating whatever it finds and has a wide range of feeding habits from both mainly terrestrial and aquatic food webs. This bird species often occurs close to human settlements where DDT is sprayed for malaria vector control in addition to sewage ponds and agricultural areas. The aquatic bird species, *P. onocrotalus* is entirely piscivorous that prefers eating fish, and eats the prey as a whole (Table 1). As a consequence, this bird species could be exposed to the entire body burden of its prey. This species is also found at a higher trophic level than the other studied bird species (Yohannes et al., 2014a).

The *p,p*'-DDT, DDE and DDD isomers were the most abundant compounds; whereas concentrations of *o,p*'-isomers (*o,p*'-DDT, DDD, and DDE) were seldom higher than the LOD. Levels of *p,p*'-isomer metabolites ranged from ND (below detection limit) to 4498 ng/g ww. The metabolite present at the highest concentration was *p,p*'-DDE, with geometric means ranged from 7 to 1003 ng/g ww (Table 2). The maximum load of *p,p*'-DDE is detected in the liver tissue of *L. crumeniferus* (4498 ng/g ww). In agreement with other studies (Minh et al., 2002; Naso et al., 2003; van Drooge et al., 2008; Zhang et al., 2011), *p,p*'-DDE made up the bulk of ΣDDT and concentrations of *p,p*'-DDE were 1–3 orders of magnitude higher than those of *p,p*'-DDD, and *p,p*'-DDT. This result suggests the persistence of *p,p*'-DDE in the environment and living organisms, with resistance against degradation and elimination from the body (Minh et al., 2002; Naso et al., 2003). Generally, the accumulation profile of DDTs i.e., DDE ≫ DDD > DDT, and the mean ratios of *p,p*'-DDT/*p,p*'-DDE < 1.0, suggesting historical input of DDT rather than contribution from recent sources. However, this hypothesis may not apply in the study area since the Ethiopian government has decided to continue using DDT because of high incidence of malaria and corresponding fatalities in addition to its illegal use for agriculture. Moreover, *p,p*'-DDT was detected in all tissue samples of the bird species (Table 2), indicating a fresh release of DDT into the environment.

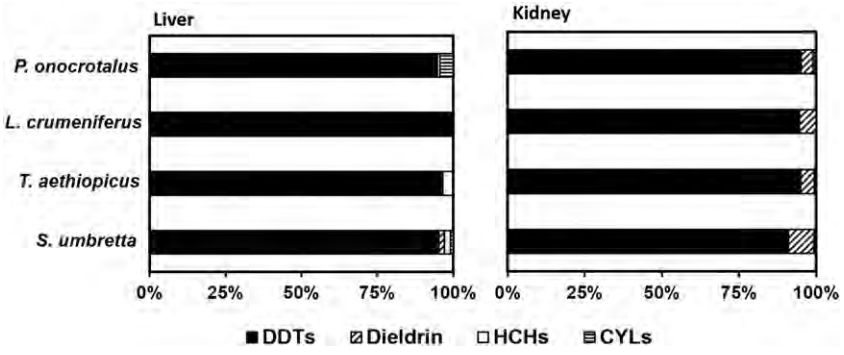

Fig. 3. Percentage contributions of DDTs, dieldrin, HCHs, and CYLs in liver and kidney tissues of 4 bird species from the Rift Valley region, Ethiopia.

ΣDDT in liver tissues in the present study (103 to 4578 ng/g ww or 4.4 to 195 μg/g lw) are higher than the concentration levels in birds from a contaminated region in South China (1.6 to 370 ng/g ww) (Zhang et al., 2011), birds collected from Chilika Lake, Orissa, India (37 to 1987 ng/g ww) (Dhananjayan, 2012), and from Ahmedabad, India (3.0 to 520 ng/g ww) (Dhananjayan, 2013) where DDT is still in use. A similar concentration values ranged from 17.4 to 4064 ng/g ww was observed in liver tissues of short toed eagle (*Ciraetus galicus*) from Greece (Hela et al., 2006). On the other hand, ΣDDT levels in the present study are lower than those reported in predatory birds from Belgium (0.06 to 510 μg/g lw) (Jaspers et al., 2006), Canary islands, Spain (30.7 to 24,772 ng/g ww) (Luzardo et al., 2014), Spain (8.0 to 87,138 ng/g ww for *p,p'*-DDE) (van Drooge et al., 2008), and Falconidae birds from Greece (32 to 19,607 ng/g ww) (Hela et al., 2006) as the usage of OCPs in developed countries ceased in the early 1980s. High levels of DDTs in these countries could be explained either by the migratory habits of predator birds with close proximity to the African continent where DDT is still in use or by the extreme environmental persistence of DDE. Enzymatic metabolisms of these predator birds could also be the reason for high levels of DDTs. Predator birds are excellent bioaccumulators of organic pollutants because of their low hepatic P450 activity, leading to weak detoxification systems (Walker and Ronis, 1989).

3.3. Other OCPs

Among the drins, dieldrin was the compound detected in all tissues, and the geometric mean concentration ranged from 0.83 to 39.8 ng/g ww in all tissues (Table 2) (aldrin and endrin were not detected). This could be an indication that aldrin degraded to dieldrin, and also that dieldrin is resistant to degradation and biological metabolism (ATSDR, 2002). The levels of dieldrin in the present study are lower than those reported in predatory bird species from the Canary Islands, Spain (18 to 1423 ng/g ww) (Luzardo et al., 2014), and birds collected from Chilika Lake, India (ND to 70.8 ng/g ww) (Dhananjayan, 2012), but similar to those in liver of Barrow's Goldeneyes (*Bucephala islandica*) from St. Lawrence Marine Ecosystem, Eastern Canada (mean value: from 1.7 ± 1.9 to 5.4 ± 3.3 ng/g ww) (Ouellet et al., 2012).

The α-, γ-, and β-HCH isomers were the most detectable isomers forms, whereas δ-HCH was rarely encountered. β-HCH constituted the highest contribution of ΣHCH, which indicates the relative stability of this isomer against enzymatic degradation in birds. The highest level of ∑HCH was found in the liver of *T. aethiopicus* with a concentration of 56.4 ng/g ww followed by *S. umbretta* (27.2 ng/g ww) (Table 2). HCH concentrations in liver tissue of birds (0.74 to 56.4 ng/g ww or 15 to 647 ng/g lw) in the present study are in the same range with those observed in liver tissue of different bird species from a contaminated region in South China (2.4 to 99 ng/g ww) (Zhang et al., 2011), but are lower than what has been observed in various bird species from northern China (90 to 37,500 ng/g lw) (Chen et al., 2009) and predatory birds from the Canary Islands, Spain (14 to 1228 ng/g ww) (Luzardo et al., 2014).

Cyclodiene insecticides (heptachlors and chlordanes) were also detected in tissues of bird species with varying concentrations. Generally, the geometric concentration of CYLs ranged from 0.1 to 43 ng/g ww (Table 2), with *trans*-chlordane followed by *oxy*-chlordane as the most abundant and dominant contributors to total CYLs. Significantly (F-ratio = 61.6; $p < 0.001$) high CYLs concentrations ranged from 33.2 to 58.3 ng/g ww (median: 616 ng/g lw) were detected in liver of *P. onocrotalus*. Compared to other aquatic bird species, the median is higher than the concentrations reported in great crested grebe (*Podiceps cristatus*) (28 ng/g lw), but comparable to the grey heron (*Ardea cinerea*) (630 ng/g lw) from Belgium (Jaspers et al., 2006). HCB was not detected in any of the samples (below detection limit).

3.4. Risk evaluation

OCPs are toxic, persistent, can be biomagnified along the food chain and may adversely affect the health, survival and reproduction of birds (Walker et al., 2001). High concentrations of OCPs affect reproduction in birds, with effects such as feminization in males, embryotoxicity and diminishing or even impeding reproduction (Blus, 2011; Connell et al., 2003; Elliott and Bishop, 2011). In the present study, risk assessment on the birds of interest was determined by comparing concentrations of OCP residues in liver samples to toxicity reference values. Mean hepatic levels of ∑DDT residues ranged from 1 to 35 μg/g ww (Blus, 2011) and average concentrations of *p,p'*-DDE of 20 to 1000 μg/g lw (Tanabe et al., 1998) were considered to pose a threat to individual bird reproduction and therefore on the population as a whole. The experimental study by Henny et al. (1983) concluded that heptachlor epoxide residues >1.5 μg/g ww were associated with decreased reproduction rates in avian species. As far as dieldrin is concerned, 1 μg/g ww dieldrin in brain is potentially associated with threshold value, and above which reported with cessation of feeding (Elliott and Bishop, 2011).

Except for *p,p'*-DDE, the residue levels for most of the OCPs in the present study were below values reported to be harmful to birds. The maximum of levels of *p,p'*-DDE (ranged from 1423 to 4498 ng/g ww; 41 to 195 μg/g lw) in liver tissues of the studied bird species may have an impact on the breeding success of many bird species. High levels of *p,p'*-DDE have been associated with an inhibition of carbonic anhydrase activity and lowering the levels of calcium, which in turn leads to eggshell thinning and breakage (Blus, 2011; Lundholm, 1997; Peakall, 1994). Previous study on the muscle of these bird species also showed high levels of *p,p'*-DDE up to 138 μg/g lw (Yohannes et al., 2014a). Therefore, there are indications that levels of ∑DDT, in particular *p,p'*-DDE, in the current study might pose a threat in terms of toxicity (i.e., eggshell thinning and survival of young birds) to the bird species resides in the Rift Valley region since DDT is still using in the region. Assuming a transfer rate of 20% of maternal DDTs to eggs (Barron et al., 1995), the maximum levels of DDTs reported in this study may be a concern for the studied bird species. Moreover, even low concentrations of toxicants may harm organisms by interacting and/or synergizing with other compounds besides to no species-specific toxic assays for the studied bird species. Generally, in Africa there are few reports assessing the potential ecological risk of organic pollutants applied into the environment. The lack of sufficient information stresses the urgent need to continue monitoring the aquatic and terrestrial ecosystems to the state of living for both humans and wildlife.

4. Conclusions

To the authors' knowledge, this study is the first report of OCPs contamination in different tissues of birds from Ethiopia. Despite the small sample size, all four bird species exhibited high variability of OCPs level in the order of ∑DDT ≫ dieldrin > ∑HCH ≅ ∑CYL. The main DDT metabolite, *p,p'*-DDE was by far the most abundant in all tissues. The maximum *p,p'*-DDE concentrations might have been enough to cause eggshell thinning, and have an impact on survival and breeding success of the bird species in the Rift Valley region. The detection of *p,p'*-DDT in all tissues suggests a release of fresh DDT into the environment because DDT is still in use. Generally, the status of contamination by OCPs (especially DDTs) investigated in this study could be an invitation for future researches, and the data will serve as a baseline for future references to managing avian populations from Ethiopia, in general Africa. Furthermore, detail efforts are needed so that a wide range of avian species and large sample size including bird eggs would be analyzed for more ecotoxicological consequences of persistent organic pollutants in the African ecosystem.

Acknowledgments

This study was funded by Grants-in-Aid for Scientific Research from the Ministry of Education, Culture, Sports, Science and Technology of Japan (MEXT) awarded to M. Ishizuka (No. 16H0177906) and Y. Ikenaka (No. 26304043, 15H0282505, 15K1221305), and S.M.M. Nakayama (No. 16 K16197), and the foundation of JSPS Core to Core Program (AA Science Platforms) and Bilateral Joint Research Project (PG36150002 and PG36150003). We also acknowledge the financial support by The Mitsui & Co., Ltd. Environment Fund. The authors sincerely gratitude to the Ethiopian Wildlife Conservation Authority (EWCA) especially to Mr. Yeneneh Teka (EWCA, director) and Dr. Fekede Regassa (EWCA, Wildlife veterinary senior expert) for the permission and their collaboration with the collection of samples. Finally we would like to thank Mr. Lemma Abera, Director of the Institute of Ziway Fisheries Resources Research Center laboratory for allowing us to perform dissections in the laboratory, as well as Mr. Takahiro Ichise (Laboratory of Toxicology, Graduate School of Veterinary Medicine, Hokkaido University) for the technically support.

References

ATSDR (Agency for Toxic Substances and Disease Registry), 2002. Toxicological Profile for Aldrin/Dieldrin. http://www.atsdr.cdc.gov/toxprofiles/tp1.pdf.

Barron, M.G., Galbraith, H., Beltman, D., 1995. Comparative reproductive and developmental toxicology of PCB in birds. Comp. Biochem. Physiol. C 112, 1–14.

Birdlife International, 2013. Country Profile: Ethiopia. http://www.birdlife.org/datazone/userfiles/file/IBAs/AfricaCntryPDFs/Ethiopia.pdf.

Blus, J.L., 2011. DDT, DDD and DDE in birds. In: Beyer, W.N., Meador, J.P. (Eds.), Environmental Contaminants in Biota-Interpreting Tissue Concentrations. CRC Press, New York, NY, USA, pp. 425–443.

Bouwman, H., Polder, A., Venter, B., Skaare, J.U., 2008. Organochlorine contaminants in cormorant, darter, egret, and ibis eggs from South Africa. Chemosphere 71, 227–241.

Bouwman, H., Viljoen, I.M., Quinn, L.P., Polder, A., 2013. Halogenated pollutants in terrestrial and aquatic bird eggs: converging patterns of pollutant profiles, and impacts and risks from high levels. Environ. Res. 126, 240–253.

Chen, D., Zhang, X., Mai, B., Sun, Q., Song, J., Luo, X., Zheng, E.Y., Hale, R.C., 2009. Polychlorinated biphenyls and organochlorine pesticides in various bird species from northern China. Environ. Pollut. 157, 2023–2029.

Cid, F.D., Antón, R.I., Caviedes-Vidal, E., 2007. Organochlorine pesticide contamination in three bird species of the Embalse La Florida water reservoir in the semiarid midwest of Argentina. Sci. Total Environ. 385, 86–96.

Connell, D.W., Fung, C.N., Minh, T.B., Tanabe, S., Lam, P.K.S., Wong, B.S.F., Lam, M.H.W., Wong, L.C., Wu, R.S.S., Richardson, B.J., 2003. Risk to breeding success of fish-eating ardeids due to persistent organic contaminants in Hong Kong: evidence from organochlorine compounds in eggs. Water Res. 37, 459–467.

Deribe, E., Rosseland, B.O., Borgstrøm, R., Salbu, B., Gebremariam, Z., Dadebo, E., Skipperud, L., Eklo, O.M., 2014. Organochlorine pesticides and polychlorinated biphenyls in fish from Lake Awassa in the Ethiopian Rift Valley: human health risks. Bull. Environ. Contam. Toxicol. 93, 238–244.

Dhananjayan, V., 2012. Accumulation pattern of persistent organochlorine pesticides in liver tissues of various species of birds from India. Environ. Sci. Pollut. Res. 20, 3149–3156.

Dhananjayan, V., 2013. Organochlorine pesticides and polychlorinated biphenyls in various tissues of waterbirds in Nalabana bird sanctuary, Chilika Lake, Orissa, India. Bull. Environ. Contam. Toxicol. 89, 197–201.

Elliott, J.E., Bishop, C.A., 2011. Cyclodienes and other organochlorine pesticides in birds. In: Beyer, W.N., Meador, J.P. (Eds.), Environmental Contaminants in Biota-Interpreting Tissue Concentrations. CRC Press, New York, NY, USA, pp. 447–475.

Furness, R.W., 1993. Birds as monitors of pollutants. In: Furness, R.W., Greenwood, J.J.D. (Eds.), Birds as Monitors of Environmental Change. Chapman and Hall, London, pp. 86–143.

Giesy, J.P., Feyk, L.A., Jones, P.D., Kannan, K., Sanderson, T., 2003. Review of the effects of endocrine-disrupting chemicals in birds. Pure Appl. Chem. 75, 2287–2303.

Hamusse, S.D., Balcha, T.T., Belachew, T., 2012. The impact of indoor residual spraying on malaria incidence in East Shoa Zone, Ethiopia. Glob. Health Action 5, 11619.

Hela, D.G., Konstantinou, I.K., Sakellarides, T.M., Lambropoulou, D.A., Akriotis, T., Albanis, T.A., 2006. Persistent organochlorine contaminants in liver and fat of birds of prey from Greece. Arch. Environ. Contam. Toxicol. 50, 603–613.

Henny, C.J., Blus, L.J., Stafford, C.J., 1983. Effects of heptachlor on American kestrels in the Columbia basin, Oregon. J. Wildl. Manag. 47, 1080–1087.

Jaspers, V.L.B., Covaci, A., Voorspoels, S., Dauwe, T., Eens, M., Schepens, P., 2006. Brominated flame retardants and organochlorine pollutants in aquatic and terrestrial predatory birds of Belgium: levels, patterns, tissue distribution and condition factors. Environ. Pollut. 13, 340–352.

Lam, J.C.W., Murphy, M.B., Wang, Y., Tanabe, S., Giesy, J.P., Lam, P.K.S., 2008. Risk assessment of organohalogenated compounds in water bird eggs from South China. Environ. Sci. Technol. 42, 6296–6302.

Lundholm, C.E., 1997. DDE-induced eggshell thinning in birds: effects of *p,p'*-DDE on the calcium and prostaglandin metabolism of the eggshell gland. Comp. Biochem. Physiol. C Pharmacol. Toxicol. Endocrinol. 118, 113–128.

Luzardo, O.P., Ruiz-Suárez, N., Henríquez-Hernández, L.A., Valerón, P.F., Camacho, M., Zumbado, M., Boada, L.D., 2014. Assessment of the exposure to organochlorine pesticides, PCBs and PAHs in six species of predatory birds of the Canary Islands, Spain. Sci. Total Environ. 472, 146–153.

Mengesha, G., Bekele, A., Fraser, G., Mamo, Y., 2014. Land use, land cover and climate change impacts on the bird community in and around Lake Zeway, Ethiopia. Int. J. Biodivers. Conserv. 6, 256–270.

Mineau, P., Whiteside, M., 2013. Pesticide acute toxicity is a better correlate of U.S. grassland bird declines than agricultural intensification. PLoS One 8 (2), e57457.

Minh, T.B., Kunisue, T., Yen, N.T.H., Watanabe, M., Tanabe, S., 2002. Persistent organochlorine residues and their bioaccumulation profiles in resident and migratory birds from North Vietnam. Environ. Toxicol. Chem. 21, 2108–2118.

Mitra, A., Chatterjee, C., Mandal, F.B., 2011. Synthetic chemical pesticides and their effects on birds. Res. J. Environ. Toxicol. 5, 81–96.

Naso, B., Perrone, D., Ferrante, M.C., Zaccaroni, A., Lucisano, A., 2003. Persistent organochlorine pollutants in liver of birds of different trophic levels from coastal areas of Campania, Italy. Arch. Environ. Contam. Tox. 45, 407–411.

Ouellet, J.F., Champoux, L., Robert, M., 2012. Metals, trace elements, polychlorinated biphenyls, organochlorine pesticides, and brominated flame retardants in tissues of Barrow's goldeneyes (*Bucephala islandica*) wintering in the St. Lawrence marine ecosystem, eastern Canada. Arch. Environ. Contam. Toxicol. 63, 429–436.

Peakall, D.B., 1994. DDE-induced eggshell thinning: an environmental detective story. Environ. Rev. 1, 13–20.

Ratcliffe, D.A., 1967. Decrease in eggshell weight in certain birds of prey. Nature 215, 208–210.

Sadasivaiah, S., Tozan, Y., Breman, J.G., 2007. Dichlorodiphenyltrichloroethane (DDT) for indoor residual spraying in Africa: how can it be used for malaria control? Am.J.Trop. Med. Hyg. 77, 249–263.

Tanabe, S., Senthilkumar, K., Kannan, K., Subramanian, A.N., 1998. Accumulation features of polychlorinated biphenyls and organochlorine pesticides in resident and migratory birds from South India. Arch. Environ. Contam. Toxicol. 34, 387–397.

Tebourbi, O., Driss, M.R., Sakly, M., Rhouma, K.B., 2006. Metabolism of DDT in different tissues of young rats. J. Environ. Sci. Health B 41, 167–176.

van den Berg, H., 2009. Global status of DDT and its alternatives for use in vector control to prevent disease. Environ. Health Perspect. 117, 1656–1663.

van Drooge, B., Mateo, R., Vives, I., Cardiel, I., Guitart, R., 2008. Organochlorine residue levels in livers of birds of prey from Spain: inter-species comparison in relation with diet and migratory patterns. Environ. Pollut. 153, 84–91.

van Wyk, E., Bouwman, H., van der Bank, H., Verdoorn, G.H., Hofmann, D., 2001. Persistent organochlorine pesticides detected in blood and tissue samples of vultures from different localities in South Africa. Comp. Biochem. Phys. C 129, 243–264.

Walker, C.H., Hopkin, S.P., Sibly, R.M., Peakall, D.B., 2001. Principles of Ecotoxicology. second ed. CRC press (Taylor & Francis), Glasgow.

Walker, C.H., Ronis, M.J.J., 1989. The monooxygenases of birds, reptiles and amphibians. Xenobiotica 19, 1111–1121.

WHO (World Health Organization), 2007. Implementation of Indoor Residual Spraying of Praying of Insecticides for Malaria Control in the Who African Region Report: Irs Report 2007. pp. 20–22.

Yohannes, Y.B., Ikenaka, Y., Nakayama, S.M.M., Saengtienchai, A., Watanabe, K.P., Ishizuka, M., 2013a. Organochlorine pesticides and heavy metals in fish from Lake Awassa; Ethiopia: insights from stable isotope analysis. Chemosphere 91, 857–863.

Yohannes, Y.B., Ikenaka, Y., Nakayama, S.M.M., Ishizuka, M., 2014a. Bioaccumulation features of organochlorine pesticide residues in bird species and their prey from the Rift Valley Region, Ethiopia. Environ. Pollut. 192, 121–128.

Yohannes, Y.B., Ikenaka, Y., Saengtienchai, A., Watanabe, K.P., Nakayama, S.M.M., Ishizuka, M., 2013b. Occurrence, distribution, and ecological risk assessment of DDTs and heavy metals in surface sediments from Lake Awassa–Ethiopian Rift Valley Lake. Environ. Sci. Pollut. Res. 20, 8663–8671.

Yohannes, Y.B., Ikenaka, Y., Saengtienchai, A., Watanabe, K.P., Nakayama, S.M.M., Ishizuka, M., 2014b. Concentrations and human health risk assessment of organochlorine pesticides in edible fish species from a Rift Valley lake-Lake Ziway, Ethiopia. Ecotoxicol. Environ. Safe 106, 95–101.

Yordy, J.E., Rossman, S., Ostrom, P.H., Reiner, J.L., Bargnesi, K., Hughes, S., Elliot, J.D., 2013. Levels of chlorinated, brominated, and perfluorinated contaminants in birds of prey spanning multiple trophic levels. J. Wildl. Dis. 49, 347–354.

Zhang, X.L., Luo, X.J., Liu, J., Luo, Y., Chen, S.J., Mai, B.X., 2011. Polychlorinated biphenyls and organochlorinated pesticides in birds from a contaminated region in South China: association with trophic level, tissue distribution and risk assessment. Environ. Sci. Pollut. Res. 18, 556–565.

Bull Environ Contam Toxicol (2017) 98:172–177
DOI 10.1007/s00128-016-2011-4

Trace Element Contamination in Tissues of Four Bird Species from the Rift Valley Region, Ethiopia

Yared Beyene Yohannes[1,2] · Yoshinori Ikenaka[1,4] · Shouta M. M. Nakayama[1] · Hazuki Mizukawa[3] · Mayumi Ishizuka[1]

Received: 20 April 2016 / Accepted: 15 December 2016 / Published online: 29 December 2016

Abstract Concentrations of ten trace elements (Hg, As, Cd, Pb, Co, Cr, Cu, Ni, Se and Zn) were determined in different tissues (liver, kidney, muscle, heart and brain) of African sacred ibis (*Threskiornis aethiopicus*), Hamerkop (*Scopus umbretta*), marabou stork (*Leptoptilos crumeniferus*) and great white pelican (*Pelecanus onocrotalus*) inhabiting the Ethiopian Rift Valley region. There were differences in trace element patterns among the bird species. Significantly ($p < 0.05$) higher concentrations of Cd (5.53 μg/g dw ± 2.94) in kidney and Hg (0.75 μg/g ww ± 0.30) in liver were observed in the great white pelican compared to the other species, and liver concentrations of these two elements showed positive correlations with trophic level. Concentrations of toxic elements (As, Cd, Pb and Hg) in liver were below their respective toxicological thresholds, indicating that the data may provide baseline information for future studies.

Keywords Bird · Tissue · Trace element · Ecological risk assessment · Ethiopian rift valley

Trace elements are highly persistent, have bioaccumulation and/or biomagnification potential along the food web, and depending upon their concentrations may be toxic to humans and wildlife. Owing to their wide distribution, feeding at different trophic levels and sensitivity to environmental changes, birds have been recognized as sentinel species for heavy metal contamination (Furness 1993; Zhang and Ma 2011). In particular, top-level piscivorous birds are liable to consume prey containing high level of pollutants, and can accumulate higher levels of contaminants than birds that are lower on the food chain (Burger and Gochfeld 2002). Chronic metal exposures can result in detrimental effects on growth, development, reproduction, behavior and physiological mechanisms (Scheuhammer 1987; Snoeijs et al. 2004). For example, lead (Pb) impairs the growth and survival of nestlings and causes haemolytic anaemia in wild Pb-poisoned birds (Mateo et al. 2007; Scheuhammer 1987). Mercury (Hg) correlates with decreased reproductive success (Varian-Ramos et al. 2014), and at high doses essential elements such as zinc (Zn) and selenium (Se) may have toxic effects on kidneys and impair reproduction, respectively (Carpenter et al. 2004; Heinz 1996). In general, effects of exposure to trace elements have been associated with declines in bird populations [http://www.birdlife.org]. However, despite the presence of the great biodiversity and numbers of birds, the African environment has received little attention from researchers in reference to environmental contamination up to the present day. As a consequence, there is a paucity of information about the contamination status and ecological impacts of pollutants like trace elements in birds inhabiting Africa. Thus, monitoring levels of

✉ Mayumi Ishizuka
ishizum@vetmed.hokudai.ac.jp

1 Laboratory of Toxicology, Department of Environmental Veterinary Sciences, Graduate School of Veterinary Medicine, Hokkaido University, Kita 18, Nishi 9, Kita-ku, Sapporo 060-0818, Japan

2 Department of Chemistry, College of Natural and Computational Sciences, University of Gondar, P.O. Box 196, Gondar, Ethiopia

3 Department of Environmental Veterinary Sciences, Graduate School of Veterinary Medicine, Hokkaido University, Kita 18, Nishi 9, Kita-ku, Sapporo 060-0818, Japan

4 Water Research Group, Unit for Environmental Sciences and Management, North-West University, Potchefstroom 2520, South Africa

environment pollutants in avian species may be of crucial importance in preventing potential risks to living beings.

The Ethiopian Rift Valley comprises seven principal lakes in a closed water basin. It is a highly productive agricultural region, and a major tourism attraction area for bird watching in the country. The region provides ideal habitat for a variety of avian species and wildlife. It serves as a breeding, and wintering ground, and as a migration stopover area for several resident and migratory bird species. Lake Ziway is one of the best sites in Ethiopia to see a diversity of bird species such as marabou stork, African fish eagle (*Haliaeetus vocifer*), white-breasted cormorant (*Phalacrocorax lucidus*), African sacred ibis and great white pelican. The wetland supports over 20,000 water birds (Bird life international 2013). However, in recent years it has been noted that the lake faces several anthropogenic threats from industrial and domestic wastewater, solid waste, and agricultural runoff. These pressures may adversely affect the lake ecosystem, potentially reducing populations of various fish, invertebrate and bird species. Nevertheless, no research has been performed on the potential ecological effects of trace elements in different bird species inhabiting the Ethiopian Rift Valley region. Thus, it is expected that the data generated here will serve as reference values and baseline data for future studies.

Therefore, this work was intended to (1) assess the bioaccumulation levels of ten elements (Hg, As, Cd, Pb, Co, Cr, Cu, Ni, Se, and Zn) in liver, kidney, muscle, heart and brain of four bird species, and (2) investigate potential ecological risks in birds to delineate the bird species at risk. The information will henceforth be highly useful for conservation research on avian species.

Materials and Methods

Detailed information about the studied bird species is described elsewhere (Yohannes et al. 2014). With the help of the local people, a total of 23 birds comprising four species; African sacred ibis (N = 7), hamerkop (N = 5), marabou stork (N = 6), and great white pelican (N = 5) were captured alive using nets in May 2012 at the shore of Lake Ziway (7°59′19″N; 38°50′30″E, surface area: 400 km^2, elevation: 1638 m). These bird species are widely distributed in the African ecosystems, and can be considered as potential bio-monitoring species for environmental contamination. Each bird was euthanized (using ether after capture) and necropsied. Samples of liver, kidney, muscle, heart and brain were placed in polyethylene bags and stored at −20°C. The frozen samples were then transported to Japan for trace element and stable isotope analyses. All analyses were carried out in the Laboratory of Toxicology, Graduate School of Veterinary Medicine, Hokkaido University, Japan. Permission was granted from the Ethiopian Wildlife Conservation Authority (EWCA) (Permission No. DA/31/284/012) for capturing and sacrificing the birds.

Levels of nine elements (As, Cd, Pb, Co, Cr, Cu, Ni, Se, and Zn) were analyzed using an inductively coupled plasma-mass spectrometer (ICP-MS; 7700 series, Agilent technologies, Tokyo, JP) in liver, kidney, muscle, heart and brain tissues. Briefly, approximately 1.0 g of individual samples were dried at 40°C, and digested using 70% (v/v) HNO_3 (5 mL) and 30% (v/v) H_2O_2 (1 mL) in a microwave system (Speed Wave MWS-2, Berghof, DE). After cooling, each mixture was transferred into a numbered plastic tube and topped to 10 mL with Milli Q-water. Analytical blanks were run in the same way as the samples. Total mercury (Hg) was determined directly without any pre-treatment using a fully automated thermal vaporization mercury analyzer (MA-3000, Nippon Instrument Corp., Osaka, JP).

The certified reference material, DOLT-4 (dogfish liver, National Research Council of Canada, Ottawa, CA) was used for method validation and quality control/quality assurance. Replicate analysis of DOLT-4 showed good recoveries ranging from 90% to 110%. The measured dry weight (dw) values were converted to wet weight (ww) for the threshold levels comparison based on their respective average water content, 68% ± 1.4% for liver and 74% ± 1.1% for kidney samples.

Stable nitrogen isotope analysis ($\delta^{15}N$) was analyzed using a Fisons NA1500 elemental analyzer (Fisons Instruments SpA, Strada Rivoltana, IT) coupled to a Finnigan MAT 252 mass spectrometer (Finnigan MAT GmbH, Bremen, DE) using dried and ground muscle subsamples. The procedure for the assessment of isotopic ratio was described in our previous study (Yohannes et al. 2014).

Statistical analyses were performed using JMP 9 (SAS Institute, Cary, NC, USA), and the level of significance was set at $p < 0.05$. Concentrations of trace elements in each tissue were used for analysis and presented as mean ± standard deviation. Data were log transformed to obtain normal distributions that satisfied the homogeneity of variance. Statistical differences in trace element concentrations in each tissue among the bird species were evaluated by one-way analysis of variance (ANOVA) followed by the Tukey HSD test. Linear regression analysis was employed to analyze relations between log-transformed liver concentrations of trace elements and $\delta^{15}N$.

Results and Discussion

Limited information is currently available for trace element concentrations in tissues of birds from Africa. This is the first study reporting on the levels and toxicity assessment of trace elements in birds from Ethiopia. Elemental

concentrations in each of the five analyzed tissues of the four bird species are presented in Table 1. Of the ten elements tested, Zn followed by Cu were found at higher concentrations than the other trace elements in all bird tissues. Although concentrations were low, trace element concentrations showed significant differences ($p < 0.05$) among the bird species in at least two tissues, indicating differences in tissue-specific accumulation of these elements. Hg and Pb in all tissues, Co in liver, heart and brain, Cr in heart, Cu in muscle and heart, Ni in liver and heart, Se in brain, and Zn in kidney and muscle showed significant differences ($p < 0.05$) among the studied bird species. This might be caused by variations in diet, body condition, metabolic capacity, and detoxification ability among the bird species.

Essential elements such as Co, Cu, Ni, Se and Zn are of particular importance in cell metabolism because hundreds of known enzymes require these metals for their catalytic activities (Goyer 1997). Concentrations of Zn, Se, and Cu were higher than the non-essential elements (Hg, As, Pb, and Cd). Among the essential elements, concentrations of Ni and Co were much lower than the others. Higher concentrations of Hg, Pb, Cu, and Zn were found in liver; As and Cd in the kidney; Cr in the heart and Ni in the muscle. Element concentrations were generally higher in liver and kidney than in other tissues, which might be associated with normal homeostatic mechanisms, and which typically are found bound to metallothioneins for storage (Lucia et al. 2012).

Kidney, followed by liver, was the main organ for Cd accumulation in all bird species. The high Cd accumulation in these two internal organs demonstrates the role of these organs in the detoxification process and storage of nonessential elements (Lucia et al. 2012). Concentrations of Cd in kidney tissue of the great white pelican were high compared with other tissues, and significantly (F-ratio = 8.34, $p = 0.001$) higher than the other studied bird species. The highest level of Cd (5.53 µg/g dw ± 2.94) was observed in the great white pelican, an aquatic bird species, followed by marabou stork (1.57 µg/g dw ± 1.07) (Table 1). Similar patterns of Cd accumulation in kidneys of aquatic birds were reported elsewhere (Kojadinovic et al. 2007; Lucia et al. 2010; Nam et al. 2005).

Mercury was most highly accumulated in the liver in all four species, followed by the kidney. The great white pelican exhibited the highest level of Hg (0.75 µg/g ww ± 0.30) compared to the other bird species (F-ratio = 8.63, $p < 0.001$). This is in accordance with the findings of other authors that Hg predominantly accumulates in liver (Nam et al. 2005; Skoric et al. 2012). Birds demethylate organic Hg in tissues such as the liver and kidney, and store a large portion of their Hg burdens in inorganic form (Kim et al. 1996). The accumulation of this toxic element in the aquatic white pelican species might be related to diet and trophic levels. The pelican is a piscivorous bird which feeds primarily on fish and eats their prey whole, and fish are known to be a source of Hg contamination for aquatic birds.

Pb accumulated differently in the tissues and showed significant difference in kidney (F-ratio = 7.32, $p = 0.001$), muscle (F-ratio = 4.05, $p = 0.02$) and heart (F-ratio = 3.16, $p = 0.04$) among the bird species (Table 1). In the present study, mean Pb levels in the liver ranged from 0.01 to 0.09 µg/g dw, and the marabou stork had the highest mean hepatic level, followed by the African sacred ibis. Ecological and feeding habitats of these bird species might be a plausible explanation for elevated Pb levels. They feed on a wide variety of food and their eating habits may have led them into urban areas to access garbage and waste from abattoirs and food waste from humans. With regard to As, there were no significant differences ($p > 0.05$) among the studied bird species in all tissues. The highest level of As was observed in kidney. Nevertheless, all the bird species exhibited low As levels (<0.1 µg/g dw) (Table 1).

In this study, significantly high ($p < 0.05$) concentrations of Cr ranging from 6.6 µg/g dw to 130.3 µg/g dw were observed in great while pelican heart samples (F-ratio = 4.78, $p = 0.01$). Even though the source of elevated Cr in pelican heart samples could not be identified, further study is needed to speciate Cr and address concerns regarding this element; Cr(VI) is known to be highly toxic, while Cr(III) is an essential trace element (Levina et al. 2003). Nonetheless, Cr levels in liver and kidney of the studied bird species do not reach the level of adverse effects for internal tissues (Eisler 1986). Selenium presented the highest levels in kidney (ranged from 10.7 to 12.8 µg/g dw), followed by liver tissue (ranged from 6.28 to 7.03 µg/g dw) (Table 1). These levels of Se in liver and kidney observed in the present study were less than the accepted threshold levels for adverse biological effects in birds (Heinz 1996). Thus, this level of Se is probably beneficial, considering its importance in detoxification processes of other toxic elements (Ikemoto et al. 2004).

Exposure to trace elements is a hypothesis proposed to explain the decline in birds. At high concentrations, Cd can cause kidney damage, suppression of egg production, and testicular damage (Furness 1996; Lucia et al. 2009). Mercury disturbs the nervous system and may have a negative impact on growth, development, and reproduction (Scheuhammer 1987; Scheuhammer et al. 2007; Varian-Ramos et al. 2014). Lead can affect the brain and nervous system, and cause adverse effects on reproduction, such as decreased plasma calcium and egg production; and also cause behavioral impairments (Burger and Gochfeld 2000; Clark and Scheuhammer 2003). Arsenic, in its inorganic forms, may act as an endocrine disruptor, bring about the death of an individual, produce sublethal

Table 1 Trace element concentrations (mean ± SD, µg/g dry weight) in different tissues of four bird species from Ethiopia

Tissue	Species	Hg[§]	As	Cd	Pb	Co	Cr	Cu	Ni	Se	Zn
Liver	African sacred ibis	0.21 ± 0.10^{b}	0.07 ± 0.02	0.11 ± 0.17^{b}	0.05 ± 0.04	0.12 ± 0.04^{a}	0.03 ± 0.02	32.4 ± 23.8	0.02 ± 0.004^{ab}	6.71 ± 0.63	118 ± 43
	Hamerkop	0.26 ± 0.04^{b}	0.03 ± 0.009	0.14 ± 0.09^{b}	0.01 ± 0.003	0.06 ± 0.01^{b}	0.02 ± 0.003	11.4 ± 3.82	0.01 ± 0.003^{b}	7.03 ± 0.80	98 ± 39
	Marabou stork	0.44 ± 0.23^{ab}	0.04 ± 0.01	0.19 ± 0.04^{b}	0.09 ± 0.08	0.11 ± 0.03^{ab}	0.07 ± 0.06	46.6 ± 47.7	0.05 ± 0.04^{a}	6.28 ± 0.88	153 ± 84
	Great white pelican	0.75 ± 0.30^{a}	0.05 ± 0.01	1.04 ± 0.08^{a}	0.01 ± 0.005	0.09 ± 0.02^{ab}	0.02 ± 0.004	31.2 ± 14.2	0.02 ± 0.007^{ab}	6.44 ± 1.61	144 ± 33
Kidney	African sacred ibis	0.10 ± 0.08^{b}	0.09 ± 0.03	0.99 ± 1.55^{b}	0.05 ± 0.01^{ab}	1.59 ± 1.89	0.04 ± 0.01	13.3 ± 1.28	0.07 ± 0.007	10.7 ± 2.79	94 ± 8^{b}
	Hamerkop	0.19 ± 0.07^{b}	0.07 ± 0.02	0.98 ± 0.78^{b}	0.03 ± 0.01^{b}	0.39 ± 0.15	0.04 ± 0.02	13.1 ± 1.90	0.06 ± 0.02	12.8 ± 1.46	84 ± 4^{b}
	Marabou stork	0.28 ± 0.14^{ab}	0.06 ± 0.02	1.57 ± 1.07^{b}	0.07 ± 0.03^{a}	0.39 ± 0.11	0.22 ± 0.21	16.9 ± 3.31	0.07 ± 0.04	11.4 ± 1.14	113 ± 13^{a}
	Great white pelican	0.47 ± 0.22^{a}	0.08 ± 0.02	5.53 ± 2.94^{a}	0.03 ± 0.01^{b}	0.64 ± 0.42	0.13 ± 0.14	13.8 ± 2.43	0.10 ± 0.04	11.9 ± 1.96	97 ± 15^{ab}
Muscle	African sacred ibis	0.06 ± 0.04^{b}	0.03 ± 0.02	0.01 ± 0.02^{b}	0.02 ± 0.01^{a}	0.06 ± 0.04	0.54 ± 1.22	6.63 ± 2.99^{b}	0.23 ± 0.52	2.52 ± 0.46	45 ± 12^{ab}
	Hamerkop	0.12 ± 0.01^{b}	0.01 ± 0.005	0.005 ± 0.003^{b}	0.01 ± 0.002^{ab}	0.03 ± 0.006	0.14 ± 0.09	10.1 ± 1.53^{b}	0.03 ± 0.01	2.70 ± 0.39	42 ± 9^{b}
	Marabou stork	0.11 ± 0.05^{b}	0.02 ± 0.006	0.005 ± 0.003^{b}	0.01 ± 0.01^{ab}	0.03 ± 0.01	0.10 ± 0.03	10.3 ± 3.24^{b}	0.08 ± 0.05	2.45 ± 0.25	44 ± 11^{b}
	Great white pelican	0.41 ± 0.12^{a}	0.03 ± 0.02	0.04 ± 0.01^{a}	0.01 ± 0.002^{b}	0.03 ± 0.006	0.16 ± 0.08	19.9 ± 2.81^{a}	0.10 ± 0.05	2.77 ± 0.11	63 ± 10^{a}
Heart	African sacred ibis	0.07 ± 0.05^{b}	0.05 ± 0.03	0.003 ± 0.003^{b}	0.01 ± 0.008^{ab}	0.16 ± 0.03^{ab}	0.04 ± 0.01^{b}	21.2 ± 2.37^{a}	0.02 ± 0.01^{b}	4.13 ± 1.04	116 ± 15
	Hamerkop	0.10 ± 0.02^{b}	0.02 ± 0.006	0.003 ± 0.002^{b}	0.01 ± 0.003^{b}	0.09 ± 0.01^{b}	0.08 ± 0.04^{b}	20.7 ± 2.07^{ab}	0.02 ± 0.01^{b}	4.22 ± 0.44	99 ± 9
	Marabou stork	0.09 ± 0.04^{b}	0.01 ± 0.004	0.003 ± 0.002^{b}	0.01 ± 0.01^{ab}	0.21 ± 0.07^{a}	0.86 ± 0.72^{b}	17.7 ± 1.24^{ab}	0.02 ± 0.01^{b}	3.67 ± 0.26	133 ± 12
	Great white pelican	0.27 ± 0.06^{a}	0.06 ± 0.03	0.01 ± 0.008^{a}	0.02 ± 0.007^{a}	0.13 ± 0.06^{ab}	50.2 ± 54.9^{a}	16.0 ± 5.19^{b}	0.36 ± 0.33^{a}	3.49 ± 0.53	102 ± 39
Brain	African sacred ibis	0.02 ± 0.01^{b}	0.03 ± 0.02	0.005 ± 0.007^{b}	0.03 ± 0.01	0.06 ± 0.01^{a}	0.05 ± 0.01	12.2 ± 1.70	0.02 ± 0.01	2.90 ± 0.23^{b}	61 ± 13
	Hamerkop	0.04 ± 0.01^{b}	0.01 ± 0.005	0.001 ± 0.001^{b}	0.01 ± 0.002	0.05 ± 0.02^{ab}	0.35 ± 0.65	9.65 ± 0.79	0.02 ± 0.01	3.35 ± 0.31^{a}	53 ± 4
	Marabou stork	0.04 ± 0.01^{b}	0.01 ± 0.002	0.001 ± 0.001^{b}	0.03 ± 0.04	0.05 ± 0.007^{ab}	0.10 ± 0.07	14.0 ± 2.70	0.02 ± 0.005	3.01 ± 0.08^{ab}	62 ± 5
	Great white pelican	0.12 ± 0.02^{a}	0.01 ± 0.006	0.01 ± 0.001^{a}	0.01 ± 0.005	0.03 ± 0.008^{b}	0.09 ± 0.02	14.4 ± 11.8	0.01 ± 0.004	2.63 ± 0.20^{b}	47 ± 12
Toxicity thresholds*	Background levels			<5.0[d]	<2.0[e]						
	Reproductive impairment									>3.0[g]	
	Sublethal effects	>4.0[f]	>5.0[h]	>40.0[d]	>6.0[e]		>4.0[i]			>10.0[g]	
Instrumental detection limit[c]		0.002 ng/g	0.002 µg/L	0.001 µg/L	0.001 µg/L	0.001 µg/L	0.003 µg/L	0.07 µg/L	0.01 µg/L	0.02 µg/L	0.02 µg/L

In each tissue, means not sharing the same letters (a, b) among the bird species are significantly different (ANOVA and Tukey HSD test; $p < 0.05$)

*Toxicity thresholds—based on the clinical signs implicated in waterfowl, corresponding to liver concentrations (µg/g ww)

[§]Concentration expressed as µg/g wet weight

[c]Instrumental detection limit—calculated as three times the standard deviation of ten blank sample measurements divided by the slope of the calibration curve

[d]Furness (1996)

[e]Pain et al. (1995)

[f]Eisler (1987)

[g]Heinz (1996)

[h]Eisler (1994)

[i]Eisler (1986)

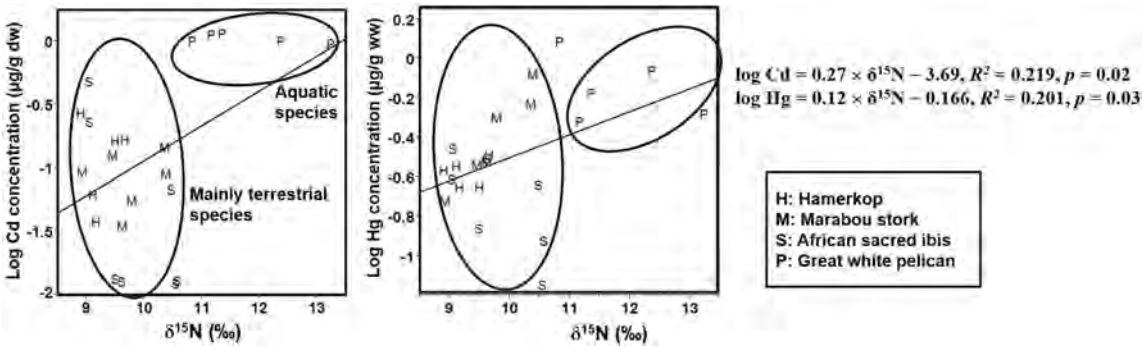

Fig. 1 Relationships between stable nitrogen signatures and log-transformed liver concentrations of Cd and Hg in four bird species from Ethiopia

effects (such as decreased body weight and feed intake), or disrupt reproduction (Eisler 1994; Kunito et al. 2008).

In the present study, the hepatic element concentrations were below the threshold values reported for waterfowl (Table 1). Concentrations of Cd ranged from 0.005 to 5.53 µg/g dw, and mean hepatic Hg concentrations ranged from 0.21 to 0.75 µg/g (ww) (~0.65 to 2.34 µg/g dw), revealing low exposure of these elements. Moreover, in this study the hepatic–Cd/renal–Cd concentration ratio was <1 (ranged from 0.03 to 0.44), indicating a low level of Cd exposure (Scheuhammer 1987). Meanwhile, hepatic Pb levels ranged from 0.01 to 0.09 µg/g dw and levels of As <0.1 µg/g dw were lower than their respective threshold limits.

At high exposure, Se and Hg can be individually toxic. However, because of the high binding affinity between Hg and Se, direct Hg sequestration by Se has often been assumed to be the mechanism for the protective effect of Se against Hg toxicity (Ralston et al. 2007). The existence of Se:Hg at 1:1 molar ratio suggests that detoxification might occur in the liver by forming insoluble mercury selenide (Ikemoto et al. 2004). In this study, molar ratios were always above one. Consequently, birds are protected against Hg toxicity, but the excess hepatic Se concentrations support a possible toxicity of this element for the studied bird species. Levels of Se in liver >3 µg/g ww are proposed to cause reproductive impairment (Heinz 1996).

Stable nitrogen isotope analysis can be used to establish trophic relationships and trophic transfer of environmental pollutants in both freshwater and marine ecosystems (Cabana and Rasmussen 1994). Thus, relationships between the $\delta^{15}N$ and the log-transformed concentrations of trace elements were examined to investigate the trophic level-dependent accumulation of trace elements (Fig. 1). The stable nitrogen isotope ($\delta^{15}N$) signatures ranged from 8.90‰ to 13.3‰, with the great white pelican showing a significantly higher $\delta^{15}N$ value (11.8‰ ± 1.0‰) compared to other bird species (F-ratio = 13.8, $p < 0.001$). There were significant correlations of $\delta^{15}N$ with Cd and Hg but not with other elements (data not shown). Concentrations of Cd and Hg increased with increasing $\delta^{15}N$ (Fig. 1). This relationship suggests that food intake may play an important part in Cd and Hg trophic transfer for the analyzed species, and the bioaccumulation potential of these two trace elements in the aquatic environment could be apparent, and related to trophic level.

In conclusion, our results give a first insight into the contamination of wild birds inhabiting the Ethiopian Rift Valley region. Meta-analyses using data from this study suggested that metal concentrations of the studied bird species were relatively low and below the toxic levels. Thus the data may serve as baseline data to facilitate management guidelines and conservation measures with the goal to ensure a healthy environment for all species in the Rift Valley region. However, even low concentrations of toxicants may harm the organisms by interacting and/or synergizing with other compounds. Thus, given the bioaccumulation potential of trace elements, and the importance of the wetland habitat for this region for breeding, wintering and migration stopovers of birds, future studies seem necessary for continued ecological risk assessment so that the region continues its role in global bird conservation.

Acknowledgements This study was supported by a Grant-in-Aid for Scientific Research from the Ministry of Education, Culture, Sports, Science, and Technology of Japan awarded to M. Ishizuka (No. 16H01779, Core to Core), Y. Ikenaka (No. 26304043) and S. Nakayama (No. 16K16197). We would also like to acknowledge the financial support of the Soroptimist Japan Foundation and the Nakajima Foundation. The authors are grateful to EWCA senior experts, Mr. Yeneneh Teka and Dr. Fekede Regassa, for their assistance with bird sampling. We also appreciate Mr. Lemma Abera for his kind help during sampling, as well as Mr. Takahiro Ichise for his technical input.

References

Birdlife International (2013) Country profile: Ethiopia http://www.birdlife.org/datazone/userfiles/file/IBAs/AfricaCntryPDFs/Ethiopia.pdf

Burger J, Gochfeld M (2000) Effects of lead on birds (Laridae): a review of laboratory and field studies. J Toxicol Environ Health B Crit Rev 3:59–78

Burger J, Gochfeld M (2002) Effects of chemicals and pollution on seabirds. In: Schreiber EA, Burger J (eds) Biology of marine birds. CRC, NewYork, pp 492–525

Cabana G, Rasmussen JB (1994) Modelling food chain structure and contaminant bioaccumulation using stable nitrogen isotopes. Nature 372:255–257

Carpenter JW, Andrews GA, Nelson Beyer W (2004) Zinc toxicosis in a free-flying trumpeter swan (*Cygnus buccinator*). J Wildl Dis 40:769–774

Clark AJ, Scheuhammer AM (2003) Lead poisoning in upland foraging birds of prey in Canada. Ecotoxicology 12:23–30

Eisler R (1986) Chromium hazards to fish, wildlife and invertebrates: a synoptic review. Biological report 85 (1.6). U.S. Fish and Wildlife Service, Washington

Eisler R (1987) Mercury hazards to fish, wildlife and invertebrates: a synoptic review. Biological report 85 (1.10). U.S. Fish and Wildlife Service, Washington

Eisler R (1994) A review of arsenic hazards to plants and animals with emphasis on fishery and wildlife resources. In: Nriagu JO, Simmons MS (eds) Arsenic in the environment. Part II: human health and ecosystem effects. Wiley, New York, pp 185–259

Furness RW (1993) Birds as monitors of pollutants. In: Furness RW, Greenwood JJD (eds) Birds as monitors of environmental change. Chapman and Hall, London, pp 86–143

Furness RW (1996) Cadmium in birds. In: Beyer WN, Heinz GH, Redmon-Norwood AW (eds) Environmental contaminants in wildlife: interpreting tissue concentrations. Lewis Press, Boca Raton, pp 389–404

Goyer AR (1997) Toxic and essential metal interactions. Ann Rev Nutr 17:37–50

Heinz GH (1996) Selenium in birds. In: Beyer WN, Heinz GH, Redmon-Norwood AW (eds) Environmental contaminants in wildlife: interpreting tissue concentrations. Lewis Press, Boca Raton, pp 447–458

Ikemoto T, Kunito T, Tanaka H, Baba N, Miyazaki N, Tanabe S (2004) Detoxification mechanism of heavy metals in marine mammals and seabirds: interaction of selenium with mercury, silver, copper, zinc, and cadmium in liver. Arch Environ Contam Toxicol 47:402–413

Kim EY, Murakami T, Saeki K, Tatsukawa R (1996) Mercury levels and its chemical form in tissues and organs of seabirds. Arch Environ Contam Toxicol 30:259–266

Kojadinovic J, Le Corre M, Cosson RP, Bustamante P (2007) Trace elements in three marine birds breeding on Reunion Island (Western Indian Ocean) part 1: factors influencing their bioaccumulation. Arch Environ Contam Toxicol 52:418–430

Kunito T, Kubota R, Fujihara J, Agusa T, Tanabe S (2008) Arsenic in marine mammals, seabirds, and sea turtles. Rev Environ Contam Toxicol 195:31–69

Levina A, Codd R, Dillon CT, Lay PA (2003) Chromium in biology: nutritional aspects and toxicology. Prog Inorg Chem 51:145–250

Lucia M, André JM, Gonzalez P, Baudrimont M, Gontier K, Maury-Brachet R, Davail S (2009) Impact of cadmium on aquatic bird *Cairina moschata*. Biometals 22:843–845

Lucia M, André JM, Gontier K, Diot N, Veiga J, Davail S (2010) Trace element concentrations (mercury, cadmium, copper, zinc, lead, aluminium, nickel, arsenic, and selenium) in some aquatic birds of the Southwest Atlantic Coast of France. Arch Environ Contam Toxicol 58:844–853

Lucia M, Bocher P, Cosson RP, Churlaud C, Bustamante P (2012) Evidence of species-specific detoxification processes for trace elements in shorebirds. Ecotoxicology 21:2349–2362

Mateo R, Green AJ, Lefranc H, Baos R, Figuerola J (2007) Lead poisoning in wild birds from southern Spain: a comparative study of wetland areas and species affected, and trends over time. Ecotoxicol Environ Saf 66:119–126

Nam DH, Anan Y, Ikemoto T, Tanabe S (2005) Multielemental accumulation and its intracellular distribution in tissues of some aquatic birds. Mar Pollut Bull 50:1347–1362

Pain D, Sears J, Newton I (1995) Lead concentrations in birds of prey in Britain. Environ Pollut 87:173–180

Ralston NVC, Blackwell JL, Raymond LJ (2007) Importance of molar ratios in selenium dependent protection against methylmercury toxicity. Biol Trace Elem Res 119:255–268

Scheuhammer AM (1987) The chronic toxicity of aluminium, cadmium, mercury, and lead in birds: a review. Environ Pollut 46:263–295

Scheuhammer AM, Meyer MW, Sandheinrich MB, Murray MW (2007) Effects of environmental methylmercury on the health of wild birds, mammals, and fish. Ambio 36:12–18

Skoric S, Visnjic-Jeftic Z, Jaric I, Djikanovic V, Mickovic B, Nikcevica M, Lenhardt M (2012) Accumulation of 20 elements in great cormorant (*Phalacrocorax carbo*) and its main prey, common carp (*Cyprinus carpio*) and Prussian carp (*Carassius gibelio*). Ecotoxicol Environ Saf 80:244–251

Snoeijs T, Dauwe T, Pinxten R, Vandesande F, Eens M (2004) Heavy metal exposure affects the humoral immune response in a free-living small songbird, the great tit (*Parus major*). Arch Environ Contam Toxicol 46:399–404

Varian-Ramos CW, Swaddle JP, Cristol DA (2014) Mercury reduces avian reproductive success and imposes selection: an experimental study with adult- or lifetime-exposure in zebra finch. PLoS ONE 9(4):e95674. doi:10.1371/journal.pone.0095674

Yohannes YB, Ikenaka Y, Nakayama SMM, Ishizuka M (2014) Organochlorine pesticides in bird species and their prey (fish) from the Ethiopian Rift Valley region, Ethiopia. Environ Pollut 192:121–128

Zhang WW, Ma JZ (2011) Waterbirds as bioindicators of wetland heavy metal pollution. Procedia Environ Sci 10:2769–2774

International Journal of
Environmental Research and Public Health

MDPI

Article

Monitoring Lead (Pb) Pollution and Identifying Pb Pollution Sources in Japan Using Stable Pb Isotope Analysis with Kidneys of Wild Rats

Hokuto Nakata [1,†], Shouta M. M. Nakayama [1,†], Balazs Oroszlany [1], Yoshinori Ikenaka [1,2], Hazuki Mizukawa [3], Kazuyuki Tanaka [4], Tsunehito Harunari [4], Tsutomu Tanikawa [4], Wageh Sobhy Darwish [1,5], Yared B. Yohannes [1,6], Aksorn Saengtienchai [1,7] and Mayumi Ishizuka [1,*]

1 Laboratory of Toxicology, Department of Environmental Veterinary Sciences, Graduate School of Veterinary Medicine, Hokkaido University, Kita 18 Nishi 9, Kita-ku, Sapporo 060-0818, Japan; big.dipper.7v@gmail.com (H.N.); shoutanakayama0219@gmail.com (S.M.M.N.); rorimack@gmail.com (B.O.); y_ikenaka@vetmed.hokudai.ac.jp (Y.I.); wagehdarwish@yahoo.ca (W.S.D.); ybyared@gmail.com (Y.B.Y.); aksornvet64@hotmail.com (A.S.)

2 Water Research Group, Unit for Environmental Sciences and Management, North-West University, Potchefstroom 2520, South Africa

3 Department of Environmental Veterinary Sciences, Graduate School of Veterinary Medicine, Hokkaido University, Sapporo 060-0818, Japan; hazuki.mizukawa@vetmed.hokudai.ac.jp

4 Technical Research Laboratory, Ikari Corporation, Chiba 260-0844, Japan; kazuyuki-tanaka@ikari.co.jp (K.T.); giken@ikari.co.jp (T.H.); tanikawa@ikari.co.jp (T.T.)

5 Food Control Department, Faculty of Veterinary Medicine, Zagazig University, Zagazig 44519, Egypt

6 Department of Chemistry, College of Natural and Computational Science, University of Gondar, P.O. Box 196, Gondar, Ethiopia

7 Department of Pharmacology, Faculty of Veterinary Medicine, Kasetsart University, Bangkok 10900, Thailand

* Correspondence: ishizum@vetmed.hokudai.ac.jp; Tel.: +81-11-706-6949; Fax: +81-11-706-5105

† These authors contributed equally to this study.

Academic Editor: José G. Dórea
Received: 23 November 2016; Accepted: 6 January 2017; Published: 10 January 2017

Abstract: Although Japan has been considered to have little lead (Pb) pollution in modern times, the actual pollution situation is unclear. The present study aims to investigate the extent of Pb pollution and to identify the pollution sources in Japan using stable Pb isotope analysis with kidneys of wild rats. Wild brown (*Rattus norvegicus*, n = 43) and black (*R. rattus*, n = 98) rats were trapped from various sites in Japan. Mean Pb concentrations in the kidneys of rats from Okinawa (15.58 mg/kg, dry weight), Aichi (10.83), Niigata (10.62), Fukuoka (8.09), Ibaraki (5.06), Kyoto (4.58), Osaka (4.57), Kanagawa (3.42), and Tokyo (3.40) were above the threshold (2.50) for histological kidney changes. Similarly, compared with the previous report, it was regarded that even structural and functional kidney damage as well as neurotoxicity have spread among rats in Japan. Additionally, the possibility of human exposure to a high level of Pb was assumed. In regard to stable Pb isotope analysis, distinctive values of stable Pb isotope ratios (Pb-IRs) were detected in some kidney samples with Pb levels above 5.0 mg/kg. This result indicated that composite factors are involved in Pb pollution. However, the identification of a concrete pollution source has not been accomplished due to limited differences among previously reported values of Pb isotope composition in circulating Pb products. Namely, the current study established the limit of Pb isotope analysis for source identification. Further detailed research about monitoring Pb pollution in Japan and the demonstration of a novel method to identify Pb sources are needed.

Keywords: metal contamination; wild rodent; stable Pb isotope; source identification; developed country

1. Introduction

Among toxic metals, lead (Pb) exhibits a particularly elevated anthropogenic enrichment factor [1]. Pb moves into the environment during use (including batteries and paint), recycling, and disposal of Pb compounds; metal production processes (mining and smelting activities); combustion of fossil fuels (coal, former use of leaded gasoline); and sewage sludge applications [2–4]. Although leaded gasoline has been strictly regulated all over the world, the use of Pb-based products has increased greatly since the Industrial Revolution. As a result, Pb pollution does not only occur locally but also worldwide due to its volatile character [5]. Additionally, Pb is a proven non-essential and toxic metal for humans and animals [6–9]. For humans, Pb is known to be neurotoxic, especially to children because of its ability to compete with calcium (Ca^{2+}) in nerve functioning [10]. Moreover, it has been thoroughly studied that Pb poisoning progresses from biochemical and subclinical abnormalities, such as gastrointestinal problems, stunted growth, and cognition problems, to death [9]. These types of Pb poisoning cases have been reported in humans worldwide. For instance, more than 160 people, mainly children under the age of five, died in the Pb poisoning disaster in Zamfara, Nigeria [11].

In addition to considering the total levels and chemical/mineralogy composition of Pb, the contribution of Pb to the environment from multiple sources should be accurately determined. Among the natural abundance of four stable isotopes of Pb, i.e., ^{208}Pb, ^{207}Pb, ^{206}Pb, and ^{204}Pb, only ^{204}Pb is not radiogenic. The abundance of ^{204}Pb in the Earth's crust has remained since the Earth solidified. On the other hand, ^{208}Pb, ^{207}Pb, and ^{206}Pb are radiogenic isotopes, and are the products of the radioactive decay of ^{232}Th, ^{235}U, and ^{238}U, respectively. The abundance of Pb isotopes in a sample, therefore, strictly depends on the concentrations of primordial Pb, uranium (U), and thorium (Th) isotopes, and the length of their decay processes [12]. In addition, the isotopic Pb composition is not significantly affected by physico-chemical fractionation processes [13,14]. Hence, identifying the Pb pollution source using stable Pb isotope ratios (Pb-IRs) has been widely carried out in many fields of environmental research, including in air and aerosols [15], soil [16], birds [17], and marine mammals [18].

It has been reported that people in pre-industrialized Japan were highly contaminated with Pb of domestic origin [19]. By contrast, after industrialization, which was accompanied by the import of foreign Pb-containing materials including leaded gasoline, pollution with foreign Pb, Pb-IRs of which differ from domestic materials, occurred [19,20]. Recent studies focused on the contemporary Pb level in Japanese human samples reported relatively low concentrations of Pb in cord blood [21], children's blood [22], and women's hair [20]. However, the maximum weekly intake per kg body weight (bw) for a five-year-old Japanese child was surprisingly revealed to be 26 μg/kg bw [23]. This value is higher compared to the provisional tolerable weekly intake (PTWI) for Pb of 25 μg/kg bw, which is recommended by the Joint Food and Agriculture Organization (FAO)/World Health Organization (WHO) Expert Committee in Food Additives (JECFA) [24]. Furthermore, high levels of Pb were previously confirmed in montane soil [25], public playground soil [26], and road-side dust and sediment [27]. Besides, Bellis et al. [28] provided evidence of the long-range transport of Pb from continental Asia to Japan. For these reasons, environmental monitoring of Pb pollution is necessary to prevent risking human health in Japan.

To evaluate the biological effects of Pb in detail, a model based on a living organism is needed. Inherent and external factors, such as size, sensitivity, physiological characteristics, position in the food chain, migration, abundance, and ability to propagate in captivity, were widely regarded as criteria for a good sentinel [29]. From these standpoints, the wild rat is large enough as a sentinel, and they actually have been used as mammalian sentinels for terrestrial metal pollution [30–33]. Besides, a

previous report revealed that Pb-IRs in the rat kidney comparatively accurately reflect those of the Pb source, although biological fractionation of Pb isotopes was speculated [34]. Thus, it is likely that a Pb pollution source could be identified using Pb isotope analysis of rat kidneys as mentioned above. As a consequence, the current study aims to elucidate the extent of Pb contamination and to identify Pb sources in Japan using kidneys of wild rats. To the best of our knowledge, this is the first study that focuses on Pb-IRs in wild rats.

2. Materials and Methods

2.1. Sampling of Wild Rats

Wild rats, including brown (*Rattus norvegicus*, n = 43) and black rats (*R. rattus*, n = 98) were collected from various sampling sites in Japan (Figure 1) from July 2004 to November 2013 using gauze cage traps with food. Rat species were morphologically identified. Kidney samples were collected from both *R. norvegicus* and *R. rattus*, and kept at −20 °C until further use.

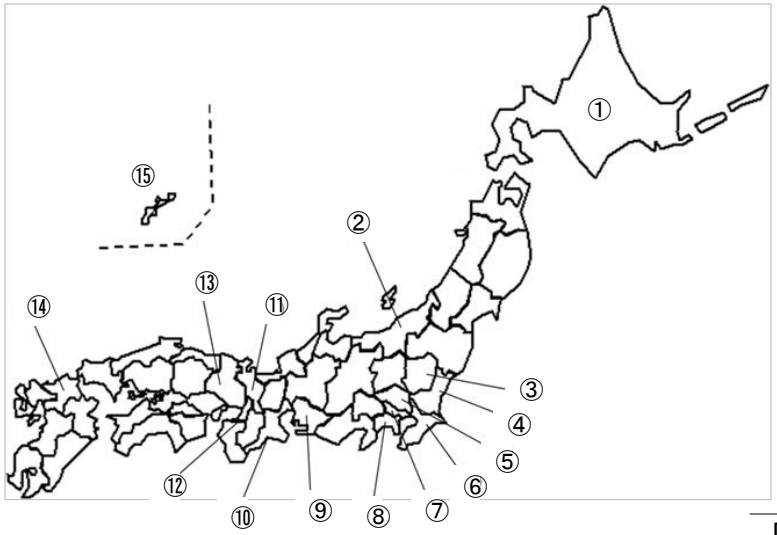

①	Hokkaido	15
②	Niigata	22
③	Tochigi	2
④	Ibaraki	12
⑤	Saitama	4
⑥	Chiba	34
⑦	Tokyo	7
⑧	Kanagawa	23
⑨	Aichi	7
⑩	Mie	1
⑪	Kyoto	3
⑫	Osaka	4
⑬	Hyogo	4
⑭	Fukuoka	2
⑮	Okinawa	1
□	Total:	141

Figure 1. Distribution and number of rat samples by region.

2.2. Sample Preparations and Extraction

All laboratory materials and instruments used in the current study were washed with 2% nitric acid (HNO_3, atomic absorption spectrometry grade, Kanto Chemical Corp., Tokyo, Japan) and rinsed at least twice with distilled water. For acid digestion, a dry thermal unit was used following methodology modified from Nakayama et al. [33]. Kidney samples (1.0 g or available amount) were dried in heat resistant glass tubes for 48 h. The dry weight was calculated, and the dried samples were then digested in 5 mL of 60% HNO_3 for 48 h in a dry thermal unit. The temperature was increased gradually to 140 °C, and after complete digestion, the acid was evaporated at 160 °C to reduce the volume to 0.5 mL. The cooled samples were transferred into 15 mL plastic tubes, followed by dilution to 10 mL with 2% HNO_3. The resulting samples were stored at room temperature in preparation for spectrophotometry analysis. Replicate blanks and the certified reference material DOLT-4 (dogfish liver, National Research Council of Canada: Ottawa, ON, Canada) were used for method validation and quality control. Replicate analysis of these reference materials showed good accuracy, with recovery rates of 90% ± 3.5%.

2.3. Analysis of Pb Concentration

The Pb concentration was determined with a flame/flame-less atomic absorption spectrophotometer (AAS, Z-2010, Hitachi High-Technologies Corporation, Tokyo, Japan) equipped with a Zeeman graphite furnace or an inductively coupled plasma–mass spectrometer (ICP-MS: 7700 series, Agilent Technologies, Tokyo, Japan). The instrument was calibrated using standard stock solutions (Kanto Chemical Corp.). A flame-less method with argon gas was used for measuring the Pb concentration.

2.4. Analysis of Pb-IRs

Analyses of the Pb-IRs ($^{208}Pb/^{206}Pb$ and $^{207}Pb/^{206}Pb$) were conducted using ICP-MS, according Nakata et al. [35]. For precise analysis, the extracted solutions from the kidney samples were diluted so that Pb concentration in the solutions became less than 40 μg/L. In order to correct for mass bias and dead-time effects, standard reference material (SRM) 981 (National Institute of Standards and Technology; NIST, Gaithersburg, MD, USA) was measured at every 10 samples. During the analytical procedure, the following isotopes were measured: ^{204}Pb, ^{206}Pb, ^{207}Pb, and ^{208}Pb. However, only the $^{208}Pb/^{206}Pb$ and $^{207}Pb/^{206}Pb$ ratios are discussed in this study, as these ratios have been commonly interpreted in previous research [36]. The ratios of the samples were corrected at every 10 samples using the average value of each isotope ratio obtained from the SRM 981 measurement. The standard error for the $^{208}Pb/^{206}Pb$ and $^{207}Pb/^{206}Pb$ measurements was <0.4% of relative standard deviation (RSD). There was no metal contamination through the analytical procedures using the reagent (digestion) blank measurement.

2.5. Statistical Analysis

The Pb concentration data were log-transformed to stabilize the variances. All statistical analyses were carried out using JMP 12 (SAS Institute, Cary, NC, USA). Significant difference in the Pb concentrations of the kidney between *R. norvegicus* and *R. rattus* were evaluated by the Student's *t*-test. Significant differences in the Pb concentrations and Pb-IRs of the kidney among various regions were analyzed by the Tukey-Kramer test, except for Okinawa, Fukuoka, Tochigi, and Mie of which sample sizes are small. All the statistical analyses were performed at a significance level of 0.05 ($\alpha = 0.05$, $p < 0.05$).

3. Results

3.1. Pb Concentrations in Kidneys of Wild Rats

The Pb concentrations in the kidneys of wild rats were determined (Table 1). No significant difference was observed in the pattern of Pb accumulation between *R. norvegicus* and *R. rattus*. In addition, it has been reported that the accumulation pattern of metals in *R. norvegicus* and *R. rattus* shows limited differences [37]. Therefore, the rats were not distinguished in the present study.

As shown in Table 1, rats from Aichi accumulated significantly higher concentrations of Pb in their kidneys compared with rats from Chiba and Hokkaido. Similarly, a significantly higher level of Pb was observed in the rat kidneys from Niigata than those from Kanagawa, Chiba, and Hokkaido. Additionally, the Pb concentrations in the kidneys of the rats from Ibaraki were significantly higher compared with those of the rats from Hokkaido. A high variability in the Pb level was observed in the kidney samples from every location (Table 1).

Table 1. Pb concentration (mg/kg, dry weight) in kidneys of wild rats from various regions in Japan.

Regions	No. of Samples	Mean ± SD	Median	Range
Okinawa	total (n = 1)	15.58	NA	NA
	RN (n = 0)	-	-	-
	RR (n = 1)	15.58	NA	NA
Aichi [a,b]	total (n = 7)	10.83 ± 12.58	NA	NA
	RN (n = 0)	-	-	-
	RR (n = 7)	10.83 ± 12.58	NA	NA
Niigata [a]	total (n = 22)	10.62 ± 11.08	5.51	0.40–42.63
	RN (n = 2)	0.79, 30.70	NA	NA
	RR (n = 20)	10.95 ± 11.38	5.51	0.40–42.63
Fukuoka	total (n = 2)	2.50, 13.68	NA	NA
	RN (n = 0)	-	-	-
	RR (n = 2)	2.50, 13.68	NA	NA
Ibaraki [a,b,c]	total (n = 12)	5.06 ± 6.68	1.90	1.07–22.80
	RN (n = 0)	-	-	-
	RR (n = 12)	5.06 ± 6.68	1.90	1.07–22.80
Kyoto [a,b,c,d]	total (n = 3)	4.58 ± 3.33	4.34	1.37 ± 8.02
	RN (n = 2)	1.37, 4.34	NA	NA
	RR (n = 1)	8.02	NA	NA
Osaka [a,b,c,d]	total (n = 4)	4.57 ± 4.03	3.83	0.49–10.13
	RN (n = 2)	3.71, 10.13	NA	NA
	RR (n = 2)	0.49, 3.96	NA	NA
Kanagawa [b,c,d]	total (n = 23)	3.42 ± 5.29	1.03	0.26–20.56
	RN (n = 19)	3.04 ± 5.64	0.86	0.26–20.56
	RR (n = 4)	4.09 ± 2.73	4.55	0.49–6.78
Tokyo [a,b,c,d]	total (n = 7)	3.40 ± 3.81	1.86	1.09–11.78
	RN (n = 3)	5.60 ± 5.53	3.93	1.09–11.78
	RR (n = 4)	1.75 ± 0.27	1.75	1.44–2.05
Tochigi	total (n = 2)	0.98, 3.81	NA	NA
	RN (n = 0)	-	-	-
	RR (n = 2)	0.98, 3.81	NA	NA
Hyogo [a,b,c,d]	total (n = 4)	2.30 ± 2.81	1.07	0.58–6.50
	RN (n = 3)	2.78 ± 3.24	1.26	0.57–6.50
	RR (n = 1)	0.87	NA	NA
Saitama [a,b,c,d]	total (n = 4)	2.16 ± 1.47	2.43	0.23–3.55
	RN (n = 1)	0.23	NA	NA
	RR (n = 3)	2.80 ± 0.87	3.02	1.84, 3.55
Chiba [c,d]	total (n = 34)	1.88 ± 2.57	1.11	0.02–10.26
	RN (n = 7)	3.66 ± 3.02	1.83	1.16–8.32
	RR (n = 27)	1.42 ± 2.28	0.59	0.02–10.26
Hokkaido [d]	total (n = 15)	0.69–0.41	0.65	0.09–1.59
	RN (n = 3)	0.48 ± 0.32	0.65	0.11–0.68
	RR (n = 12)	0.74 ± 0.42	0.69	0.09–1.59
Mie	total (n = 1)	0.09	NA	NA
	RN (n = 1)	0.09	NA	NA
	RR (n = 0)	-	-	-

RN = *R. norvegicus*. RR = *R. rattus*. Different lowercase letters (a, b, c, and d) indicate a significant difference among regions. No significance test was conducted for Okinawa, Fukuoka, Tochigi, and Mie, due to small sample size. NA means not analyzed due to small sample size.

3.2. Pb-IRs in the Kidneys of Wild Rats

Geographic trends of the kidney Pb-IRs are shown in Figure 2, and the trends classified by the Pb level in the kidney (Pb < 2.5 mg/kg (dry weight, Figure 3a), 2.5 mg/kg ≤ Pb < 5.0 mg/kg (Figure 3b), 5.0 mg/kg ≤ Pb < 15.0 mg/kg (Figure 3c), 15.0 mg/kg ≤ Pb (Figure 3d)) are shown in Figure 3. These separation values of 2.5 mg/kg and 15.0 mg/kg for the classification were chosen following the previous reported threshold values for the detection of histological kidney changes [30] and structural as well as functional kidney damage [38], respectively. Another separation value of 5.0 mg/kg was set because a different tendency was observed at the Pb concentration ≥5.0 mg/kg as described below. Mean ± SD, median, and minimum-maximum values of the Pb-IRs are shown in Table 2.

Table 2. Pb-IRs in kidneys of wild rats from various regions in Japan.

Regions (No. of Samples)	$^{208}Pb/^{206}Pb$			$^{207}Pb/^{206}Pb$		
	Mean ± SD	Median	Range	Mean ± SD	Median	Range
Okinawa (n = 1)	2.109	NA	NA	0.867	NA	NA
Aichi (n = 7) [a,b]	2.120 ± 0.011	2.120	2.102–2.133	0.871 ± 0.006	0.872	0.861–0.876
Niigata (n = 22) [b]	2.105 ± 0.013	2.106	2.079–2.126	0.862 ± 0.005	0.862	0.849–0.871
Fukuoka (n = 2)	2.093, 2.110	NA	NA	0.859, 0.865	NA	NA
Ibaraki (n = 12) [a,b]	2.113 ± 0.026	2.116	2.076–2.175	0.866 ± 0.020	0.866	0.843–0.922
Kyoto (n = 3) [a,b]	2.122 ± 0.004	2.120	2.119–2.126	0.871 ± 0.002	0.872	0.870–0.873
Osaka (n = 4) [a,b]	2.109 ± 0.012	2.107	2.098–2.124	0.863 ± 0.009	0.860	0.855–0.876
Kanagawa (n = 23) [a,b]	2.105 ± 0.018	2.104	2.056–2.138	0.865 ± 0.012	0.866	0.825–0.884
Tokyo (n = 7) [a,b]	2.119 ± 0.009	2.119	2.104–2.132	0.873 ± 0.006	0.873	0.863–0.880
Tochigi (n = 2)	2.098, 2.117	NA	NA	0.859, 0.872	NA	NA
Hyogo (n = 4) [a,b]	2.107 ± 0.011	2.106	2.096–2.120	0.865 ± 0.006	0.865	0.858–0.872
Saitama (n = 4) [a,b]	2.114 ± 0.004	2.114	2.109–2.119	0.866 ± 0.003	0.867	0.861–0.868
Chiba (n = 34) [a]	2.120 ± 0.011	2.121	2.101–2.162	0.874 ± 0.007	0.873	0.865–0.909
Hokkaido (n = 15) [a,b]	2.110 ± 0.009	2.109	2.098–2.129	0.867 ± 0.005	0.867	0.858–0.875
Mie (n = 1)	2.104	NA	NA	0.861	NA	NA

Different lowercase letters (a and b) indicate a significant difference in both $^{208}Pb/^{206}Pb$ and $^{207}Pb/^{206}Pb$ among regions. No significance test was conducted for Okinawa, Fukuoka, Tochigi, and Mie, due to small sample size. NA means not analyzed due to small sample size.

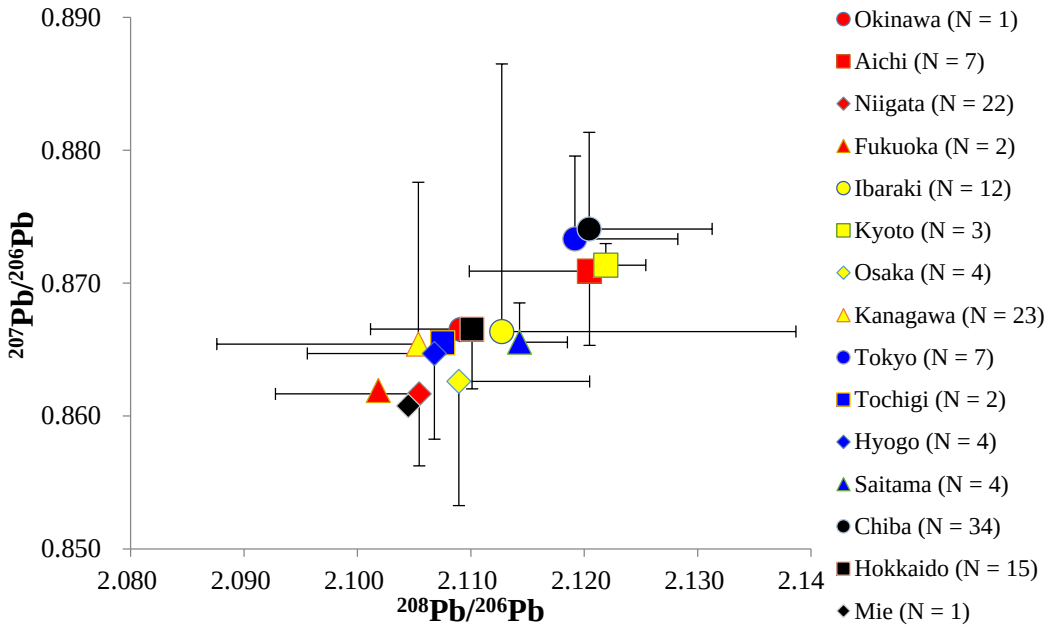

Figure 2. Pb-IRs ($^{208}Pb/^{206}Pb$ and $^{207}Pb/^{206}Pb$) in kidneys of wild rats from various regions in Japan.

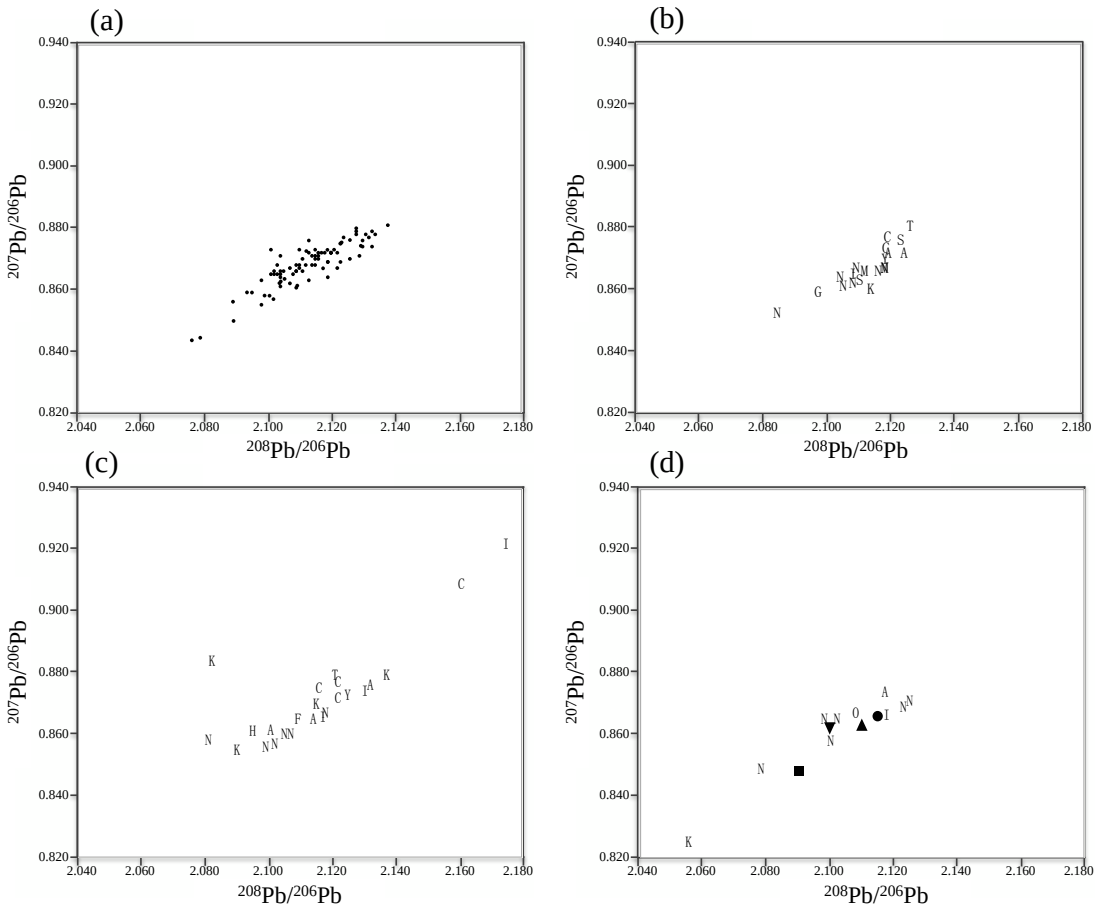

Figure 3. Pb-IRs in kidneys of wild rat from various regions in Japan. Pb level in kidney < 2.5 mg/kg (**a**); 2.5 ≤ Pb level in kidney < 5.0 (**b**); 5.0 ≤ Pb level in kidney < 15.0 (**c**); 15.0 ≤ Pb level in kidney (**d**). A = Aichi, C = Chiba, F = Fukuoka, G = Tochigi, H = Hyogo, I = Ibaraki, K = Kanagawa, M = Saitama, N = Niigata, O = Okinawa, S = Osaka, T = Tokyo, Y = Kyoto. Circle = solder circulated in Japan [39], square = paint [39], triangle = battery [40], inverted triangle = airborne particulate matter [39]. Figure 3a was shown with simple dots due to too many individuals.

The ratios of both $^{208}Pb/^{206}Pb$ and $^{207}Pb/^{206}Pb$ in the kidneys of the rats from Chiba were significantly higher compared with those ratios in the kidneys of the rats from Niigata; however, the mean values of Pb-IRs in the kidneys of rats from each region generally converged closely at around approximately 2.100 to 2.120 ($^{208}Pb/^{206}Pb$) and 0.860 to 0.875 ($^{207}Pb/^{206}Pb$), and showed slight variations (Figure 2, Table 2). Likewise, a small variability in the Pb-IRs was observed (approximately 2.080–2.140 in $^{208}Pb/^{206}Pb$, 0.840–0.880 in $^{207}Pb/^{206}Pb$) across most of the individual samples. In addition, the Pb-IRs in most of the rat kidneys generally showed a linear relationship. On the other hand, the individuals from Ibaraki (2.175 and 0.922 for $^{208}Pb/^{206}Pb$ and $^{207}Pb/^{206}Pb$, respectively), Kanagawa (2.083, 0.884 and 2.056, 0.825), and Chiba (2.162, 0.909), whose concentrations of Pb in the kidneys were higher than 5.0 mg/kg, showed characteristic Pb-IR values (Figure 3).

4. Discussion

4.1. Comparison of Pb Concentrations in Japanese Rats with International Rodent Data

Pb accumulation levels in the kidneys of rats from various regions in Japan showed a large variation. Rats from some regions, such as Okinawa, Aichi, Niigata, and Fukuoka, accumulated higher levels of Pb in their kidneys as compared with other regions (Table 1). Consequently, it is necessary to clarify whether the present Pb levels in Japanese rats are comparable to other countries or are above the international average. However, few studies comparing biological contamination with Pb in terrestrial

animals between Japan and other countries have been carried out. Furthermore, data before 1990 should be excluded because of extremely elevated Pb levels owing to the high utilization of leaded gasoline, which might distort the comparison with the current data. Due to these reasons and the small number of previous reports on Pb contamination in wild rats, the renal Pb levels found in the present study were compared with previously reported levels in Rodentia (small carnivores and lagomorphs were not included) from Italy [30], Poland [32], Belgium [41], and Zambia [33] (Figure 4).

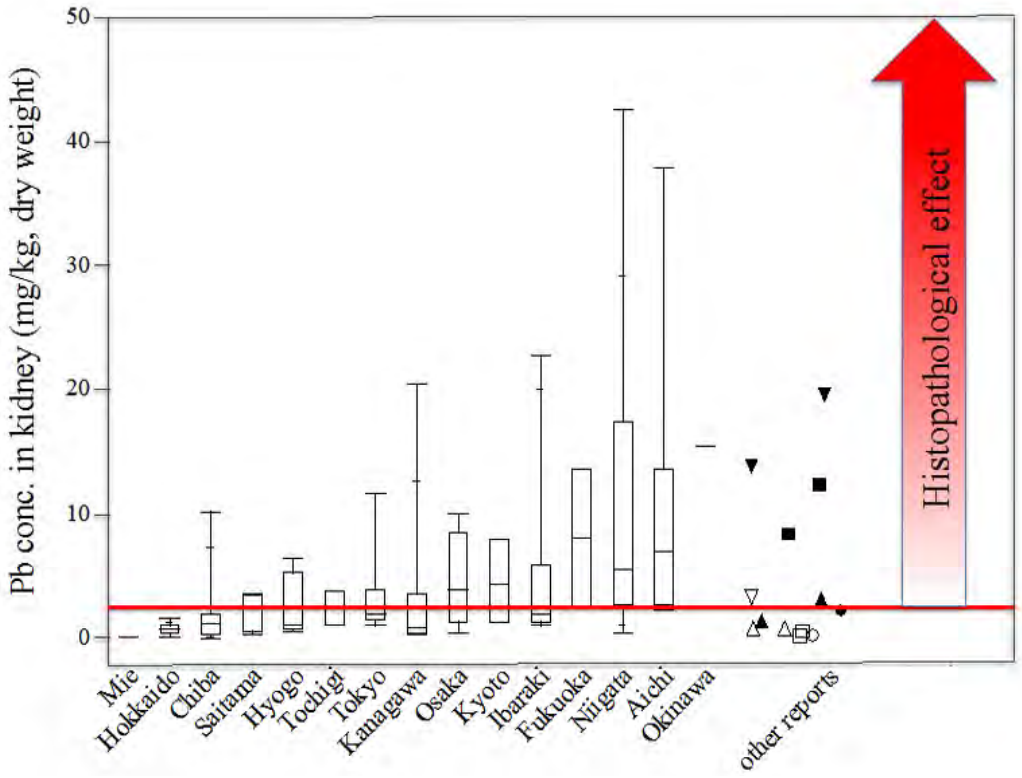

Figure 4. Pb levels (mg/kg, dry weight) in kidneys of wild rats from various regions in Japan and other countries. Data are shown in box and whisker plots: box limits represent 25th and 75th percentiles; lines within the boxes indicate the medians; whisker ends indicate minimum and maximum values. The red line indicates the previously reported renal Pb level (2.5 mg/kg) above which histopathological changes should be expected. Black and white inverted triangle = rats from polluted and control area in Poland [32], black and white square = rats from polluted and control area in Italy [30], black and white triangle = rats from polluted and control area in Belgium [41], black and white circle = rats from polluted and control area in Zambia [33].

Previous studies on wild brown rats (*R. norvegicus*) indicated a renal Pb concentration of 0.6 mg/kg wet weight (equivalent to ≈ 2.50 mg/kg dry weight) as a threshold for the detection of histological kidney changes, such as karyocytomegaly in proximal tubular cells and Pb intranuclear inclusion bodies [30]. Renal Pb levels exceeding the threshold, i.e., 19.55 mg/kg and 13.89 mg/kg dry weight, were previously revealed in wild bank voles (*Clethrionomys glareolus*) from two areas located 2.5 km and 6.5 km, respectively, from a smelter in Poland [32]. Similarly, several wild black rats (*R. rattus* and *R. tanezumi*) from a mining area in Zambia had accumulated higher levels of Pb in their kidneys (up to 22.1 mg/kg dry weight) compared to the threshold [33]. In addition, values from wild brown rats (*R. norvegicus*) from urban areas (8.37–12.38 mg/kg) in Italy [30], and wood mice (*Apodemus sylvaticus*) from two areas situated 200–600 m (3.03 mg/kg) from a non-ferrous smelter in Belgium [41] have been reported (Figure 4). Although the sample size was small in some regions, a mean Pb level above the threshold of 2.50 mg/kg was found in the kidneys of the rats from Okinawa, Aichi, Niigata, Fukuoka,

Ibaraki, Kyoto, Osaka, Kanagawa, and Tokyo (Table 1). Even in other regions of which mean levels of Pb were lower than the threshold, a portion of individuals accumulated higher concentrations of Pb in their kidneys compared to the threshold. As a whole, approximately 38% of the individuals in the present study surprisingly accumulated higher Pb levels in the kidneys compared to the threshold.

Ma [38] reported that a kidney Pb concentration exceeding 15 mg/kg dry weight caused structural and functional kidney damage in adult rats. Interestingly, several of the renal Pb levels in rats from Okinawa, Aichi, Niigata, Ibaraki, and Kanagawa were higher than the threshold of 15 mg/kg (Table 1). Further, it has been reported that Pb accumulates in the brain with a half-life of two years and causes neurotoxicity [42]. Similarly, disorders in memory and learning as well as in spatial and visual recognition of 0.4–0.7 mg/kg dry weight in the brain have been previously confirmed [38]. Some brains of rats from the mining area in Zambia were within this range [43]. Considering that the Pb concentrations in kidneys of rats in the present study were generally comparable to those of rats from Zambia, neurotoxicity might spread among rats in Japan, although brain samples were not collected in the current study.

Because of an early and complete abandonment of leaded gasoline and a relatively low Pb content in the soil, Japan has generally been regarded as one of the least risk-prone countries regarding Pb pollution [20–23]. Thus, the importance of the current findings on relatively high Pb levels in wild rats cannot be over-emphasized. Furthermore, it can be assumed that the pathological kidney changes, structural and functional damage in the kidneys, and neurotoxicity exist in the rat population throughout Japan, although these investigations were not suitable because of the condition of the samples in the present study. Furthermore, it could be possible that humans have been exposed to Pb at a high concentration because wild rats are widely regarded to share their living environment with humans.

4.2. Pb-IRs in the Kidney of Wild Rats and Identification of Pb Pollution Sources in Japan

Pb-IRs in rat kidneys of which the Pb level was <5.0 mg/kg converged closely at around approximately 2.080–2.140 ($^{208}Pb/^{206}Pb$) and 0.840–0.880 ($^{207}Pb/^{206}Pb$), and generally showed positive linear relationship (Figure 3a,b). These values of Pb-IRs were very similar to the previously reported values in sediment and roadside dust from Tokyo, Osaka, and Kyoto (2.109–2.126, 0.862–0.876) [27], soil from a residential area in Tokyo (2.104, 0.863) [26], airborne particulate matter from several regions including Fukuoka, Ibaraki, and Tokyo (2.099, 0.863) [39], precipitation in Niigata (approximately 2.090–2.160, 0.860–0.880) [28], solder circulated in Japan (2.115, 0.866) [39], paint (yellow line on a road) (2.090, 0.848) [39], and batteries (2.110, 0.863) [40]. The close match of the Pb-IRs implies that these values can be regarded as the baseline values for Japan. Although Pb-IRs in rat kidneys of which the Pb concentration was ≥5.0 mg/kg recorded generally similar values with those in rat kidneys of which the Pb level was <5.0 mg/kg, some individuals whose Pb concentration was greater than 5.0 mg/kg from Ibaraki (2.175, 0.922), Kanagawa (2,083, 0.884 and 2.056, 0.825), and Chiba (2.162, 0.909) showed distinctive values (Figure 3). However, it is difficult to estimate or identify exact Pb pollution sources due to the absence of previous reports about Pb-IRs close to these values in natural or anthropogenic Pb from Japan, and due to the absence of environmental samples from habitats of rats in the current study.

In the case of Pb pollution caused by a single source such as leaded gasoline or mining activity, Pb-IRs in the living body reflect those in the pollution source comparatively accurately; therefore, the exact pollution source could be identified [44]. Unlike such a case with a single pollution source, it is widely considered that Japan has no single major source of Pb after the discontinuance of leaded gasoline in 1975. Many types of Pb seem to be used in complex ways in Japan. Additionally, Pb-IRs of the Pb products circulated in Japan have no clear difference as described above. For these reasons, it is unfortunately difficult to identify specific sources of Pb in the current study even using Pb-IRs, although solder, paint, and batteries may have the potential to be some of the Pb pollution sources in Japan [39,40]. That is, the present study demonstrated the limitation of Pb isotope analysis for the

identification of the sources. In other words, alternative methods or factors are needed to identify the sources more accurately in the case of multiple sources. With this objective, the isotope ratios of other elements might be available with the coupled use of Pb-IRs. For instance, Simonetti et al. [45] drew an inference on the source of metals using Pb and strontium (Sr) isotopic compositions of a snowpack. The isotope composition of Sr ($^{87}Sr/^{86}Sr$) is also useful, as well as that of nitrogen ($\delta^{15}N$), oxygen ($\delta^{18}O$), and sulfur ($\delta^{34}S$), to trace the contamination of fertilizer, which contains Pb [46]. Similarly, sulfur (S) isotope analysis might have a great potential because Pb generally exists as galena (lead sulfide, PbS) in mines. As an example, Mukai et al. [47] previously focused on S isotopic compositions ($\delta^{34}S$) and Pb-IRs to reveal regional sources' characteristics in the atmosphere. In addition, the isotope composition of titanium (Ti) and tin (Sn) should be considered because electronic materials and solder, which are common Pb products, contain Ti and Sn as alloys with Pb, respectively. Turning back to the identification of the Pb sources in the current study, it should be taken into account that composite factors are involved in Pb pollution in Japan considering the wide range of activity of rats and their omnivorous. Further, the results of Pb-IRs in the present study were also similar to the previously reported results of Pb-IRs in the hair of Japanese subjects (2.115, 0.869) [20]. Although the concrete identification of Pb exposure sources is a challenge in the present study, as noted above, it is noteworthy that a high level of Pb was observed in the kidneys of wild rats from various regions in Japan. It might be considered from the current results and previous reports that even humans might be exposed to high levels of Pb in Japan; therefore, more exhaustive research on the status of Pb exposure in humans and wildlife should be conducted to evaluate the impact on human health.

5. Conclusions

The present study revealed that Pb pollution has occurred in several regions in Japan, including Okinawa, Aichi, Niigata, Fukuoka, Ibaraki, Kyoto, Osaka, Kanagawa, and Tokyo, unlike the prevailing view that Japan has had little Pb pollution in recent years. Moreover, it could be considered that histological changes and functional damage have been caused in rat kidneys as well as neurotoxicity in rat brains, and that human also have been exposed to a high level of Pb. However, specific pollution sources and exposure routes of Pb have not been identified since Pb products that are used in Japan have unclear differences of Pb-IRs. Our results suggested that Pb-IR analysis does not always identify the exact Pb pollution source in cases of multiple sources. Further studies focusing on revealing the situation of Pb pollution in Japan and the establishment of a method to identify Pb sources, alongside the existing Pb isotope analysis, are essential.

Acknowledgments: This work was supported by Grants-in-Aid for Scientific Research from the Ministry of Education, Culture, Sports, Science and Technology of Japan awarded to Mayumi Ishizuka (No. 16H0177906), Yoshinori Ikenaka (No. 26304043, 15H0282505, 15K1221305), Shouta M. M. Nakayama (16K16197), and the foundations of the Sumitomo and JSPS Core to Core Program (AA Science Platforms) and the Bilateral Joint Research Project (PG36150002 and PG36150003). We also acknowledge the financial support by the Nihon Seimei Foundation, the Soroptimist Japan Foundation, and the Nakajima Foundation. This research was supported by JST/JICA, SATREPS (Science and Technology Research Partnership for Sustainable Development). The analyses were technically supported by Takahiro Ichise, Mio Yagihashi and Nagisa Hirano.

Author Contributions: Hokuto Nakata, Shouta M. M. Nakayama, Balazs Oroszlany, Yoshinori Ikenaka, Kazuyuki Tanaka, and Mayumi Ishizuka designed the research. Shouta M. M. Nakayama, Balazs Oroszlany, Yoshinori Ikenaka, Kazuyuki Tanaka, Tsunehito Harunari, and Tsutomu Tanikawa conducted the field work. Hokuto Nakata, Shouta M. M. Nakayama, Balazs Oroszlany, and Kazuyuki Tanaka performed the experiment. Hokuto Nakata, Shouta M. M. Nakayama, Balazs Oroszlany, Hazuki Mizukawa, Kazuyuki Tanaka, Wageh Sobhy Darwish, Yared B. Yohannes, and Aksorn Saengtienchai analyzed the data. Hokuto Nakata, Shouta M. M. Nakayama, Balazs Oroszlany, and Mayumi Ishizuka wrote the paper.

Conflicts of Interest: The authors declare no conflict of interest.

References

1. Lantzy, R.J.; Mackenzie, F.T. Atmospheric trace metals: Global cycles and assessment of man's impact. *Geochim. Cosmochim. Acta* **1979**, *43*, 511–525. [CrossRef]

2. Rieuwerts, J.S.; Farago, M.; Cikrt, M.; Bencko, V. Heavy metal concentrations in and around households near a secondary lead smelter. *Environ. Monit. Assess.* **1999**, *58*, 317–335. [CrossRef]
3. Adriano, D.C. *Trace Elements in Terrestrial Environments: Biogeochemistry, Bioavailability, and Risks of Metals*, 2nd ed.; Springer: New York, NY, USA, 2001; pp. 315–348.
4. Ahlberg, G.; Gustafsson, O.; Wedel, P. Leaching of metals from sewage sludge during one year and their relationship to particle size. *Environ. Pollut.* **2006**, *144*, 545–553. [CrossRef] [PubMed]
5. Charalampides, G.; Manoliadis, O. Sr and Pb isotopes as environmental indicators in environmental studies. *Environ. Int.* **2002**, *28*, 147–151. [CrossRef]
6. Demayo, A.; Taylor, M.C.; Taylor, K.W.; Hodson, P.V.; Hammond, P.B. Toxic effects of lead and lead compounds on human health, aquatic life, wildlife plants, and livestock. *Crit. Rev. Environ. Sci. Technol.* **1982**, *12*, 257–305. [CrossRef]
7. Goering, P.L. Lead-protein interactions as a basis for lead toxicity. *Neurotoxicology* **1992**, *14*, 45–60.
8. Domingo, J.L. Metal-induced developmental toxicity in mammals: A review. *J. Toxicol. Environ. Health Part A* **1994**, *42*, 123–141. [CrossRef] [PubMed]
9. Duruibe, J.O.; Ogwuegbu, M.O.C.; Egwurugwu, J.N. Heavy metal pollution and human biotoxic effects. *Int. J. Phys. Sci.* **2007**, *2*, 112–118.
10. Lidsky, T.I.; Schneider, J.S. Lead neurotoxicity in children: Basic mechanisms and clinical correlates. *Brain* **2003**, *126*, 5–19. [CrossRef] [PubMed]
11. Blacksmith Institute's World's Worst Pollution Problems Report 2010 Top Six Toxic Threats. Available online: http://www.cricouncil.com/wp-content/uploads/2011/03/Worst-polluting-chemicals.pdf (accessed on 23 September 2016).
12. Komárek, M.; Ettler, V.; Chrastný, V.; Mihaljevič, M. Lead isotopes in environmental sciences: A review. *Environ. Int.* **2008**, *34*, 562–577. [CrossRef] [PubMed]
13. Bollhöfer, A.; Rosman, K.J.R. Isotopic source signatures for atmospheric lead: The Northern Hemisphere. *Geochim. Cosmochim. Acta* **2001**, *65*, 1727–1740. [CrossRef]
14. Veysseyre, A.M.; Bollhöfer, A.F.; Rosman, K.J.; Ferrari, C.P.; Boutron, C.F. Tracing the origin of pollution in French Alpine snow and aerosols using lead isotopic ratios. *Environ. Sci. Technol.* **2001**, *35*, 4463–4469. [CrossRef] [PubMed]
15. Chow, T.J.; Johnstone, M.S. Lead isotopes in gasoline and aerosols of Los Angeles basin, California. *Science* **1965**, *147*, 502–503. [CrossRef] [PubMed]
16. Hansmann, W.; Köppel, V. Lead-isotopes as tracers of pollutants in soils. *Chem. Geol.* **2000**, *171*, 123–144. [CrossRef]
17. Scheuhammer, A.M.; Templeton, D.M. Use of stable isotope ratios to distinguish sources of lead exposure in wild birds. *Ecotoxicology* **1998**, *7*, 37–42. [CrossRef]
18. Smith, D.R.; Flegal, A.R.; Niemeyer, S.; Estes, J.A. Stable lead isotopes evidence anthropogenic contamination in Alaskan sea otters. *Environ. Sci. Technol.* **1990**, *24*, 1517–1521. [CrossRef]
19. Yoshinaga, J.; Yoneda, M.; Morita, M.; Suzuki, T. Lead in prehistoric, historic and contemporary Japanese: Stable isotopic study by ICP mass spectrometry. *Appl. Geochem.* **1998**, *13*, 403–413. [CrossRef]
20. Matsumoto, M.; Yoshinaga, J. Isotope ratios of lead in Japanese women's hair of the twentieth century. *Environ. Sci. Pollut. Res.* **2010**, *17*, 643–649. [CrossRef] [PubMed]
21. Iijima, K.; Otake, T.; Yoshinaga, J.; Ikegami, M.; Suzuki, E.; Naruse, H.; Yamanaka, T.; Shibuya, N.; Yasumizu, T.; Kato, N. Cadmium, lead, and selenium in cord blood and thyroid hormone status of newborns. *Biol. Trace Elem. Res.* **2007**, *119*, 10–18. [CrossRef] [PubMed]
22. Yoshinaga, J.; Takagi, M.; Yamasaki, K.; Tamiya, S.; Watanabe, C.; Kaji, M. Blood lead levels of contemporary Japanese children. *Environ. Health Prev. Med.* **2012**, *17*, 27–33. [CrossRef] [PubMed]
23. Aung, N.N.; Yoshinaga, J.; Takahashi, J.I. Exposure assessment of lead among Japanese children. *Environ. Health Prev. Med.* **2004**, *9*, 257–261. [CrossRef] [PubMed]
24. Joint FAO/WHO Expert Committee on Food Additives (JECFA). *Evaluation of Certain Food Additives and Contaminants*; World Health Organization: Geneva, Switzerland, 2011.
25. Takamatsu, T.; Watanabe, M.; Koshikawa, M.K.; Murata, T.; Yamamura, S.; Hayashi, S. Pollution of montane soil with Cu, Zn, As, Sb, Pb, and nitrate in Kanto, Japan. *Sci. Total Environ.* **2010**, *408*, 1932–1942. [CrossRef] [PubMed]

26. Takaoka, M.; Yoshinaga, J.; Tanaka, A. Influence of paint chips on lead concentration in the soil of public playgrounds in Tokyo. *J. Environ. Monit.* **2006**, *8*, 393–398. [CrossRef] [PubMed]
27. Wijaya, A.R.; Ouchi, A.K.; Tanaka, K.; Shinjo, R.; Ohde, S. Metal contents and Pb isotopes in road-side dust and sediment of Japan. *J. Geochem. Explor.* **2012**, *118*, 68–76. [CrossRef]
28. Bellis, D.J.; Satake, K.; Inagaki, M.; Zeng, J.; Oizumi, T. Seasonal and long-term change in lead deposition in central Japan: Evidence for atmospheric transport from continental Asia. *Sci. Total Environ.* **2005**, *341*, 149–158. [CrossRef] [PubMed]
29. O'Brien, D.J.; Kaneene, J.B.; Poppenga, R.H. The use of mammals as sentinels for human exposure to toxic contaminants in the environment. *Environ. Health Persp.* **1993**, *99*, 351–368. [CrossRef]
30. Ceruti, R.; Ghisleni, G.; Ferretti, E.; Cammarata, S.; Sonzogni, O.; Scanziani, E. Wild rats as monitors of environmental lead contamination in the urban area of Milan, Italy. *Environ. Pollut.* **2002**, *117*, 255–259. [CrossRef]
31. Pereira, R.; Pereira, M.L.; Ribeiro, R.; Gonçalves, F. Tissues and hair residues and histopathology in wild rats (*Rattus rattus* L.) and Algerian mice (*Mus spretus* Lataste) from an abandoned mine area (Southeast Portugal). *Environ. Pollut.* **2006**, *139*, 561–575. [CrossRef] [PubMed]
32. Swiergosz-Kowalewska, R.; Bednarska, A.; Callaghan, A. Expression of metallothionein genes I and II in bank vole *Clethrionomys glareolus* populations chronically exposed in situ to heavy metals. *Environ. Sci. Technol.* **2007**, *41*, 1032–1037. [CrossRef] [PubMed]
33. Nakayama, S.M.; Ikenaka, Y.; Hamada, K.; Muzandu, K.; Choongo, K.; Teraoka, H.; Mizuno, N.; Ishizuka, M. Metal and metalloid contamination in roadside soil and wild rats around a Pb–Zn mine in Kabwe, Zambia. *Environ. Pollut.* **2011**, *159*, 175–181. [CrossRef] [PubMed]
34. Liu, D.; Wu, J.; Ouyang, L.; Wang, J. Variations in lead isotopic abundances in sprague-dawley rat tissues: Possible reason of formation. *PLoS ONE* **2014**, *9*, e89805. [CrossRef] [PubMed]
35. Nakata, H.; Nakayama, S.M.; Ikenaka, Y.; Mizukawa, H.; Ishii, C.; Yohannes, Y.B.; Konnai, S.; Darwish, W.S.; Ishizuka, M. Metal extent in blood of livestock from Dandora dumping site, Kenya: Source identification of Pb exposure by stable isotope analysis. *Environ. Pollut.* **2015**, *205*, 8–15. [CrossRef] [PubMed]
36. Monna, F.; Loizeau, J.L.; Thomas, B.A.; Guéguen, C.; Favarger, P.Y. Pb and Sr isotope measurements by inductively coupled plasma–mass spectrometer: Efficient time management for precision improvement. *Spectrochim. Acta B* **1998**, *53*, 1317–1333. [CrossRef]
37. McLean, C.M.; Koller, C.E.; Rodger, J.C.; MacFarlane, G.R. Mammalian hair as an accumulative bioindicator of metal bioavailability in Australian terrestrial environments. *Sci. Total Environ.* **2009**, *407*, 3588–3596. [CrossRef] [PubMed]
38. Ma, W.C. Lead in mammals. In *Environmental Contaminants in Biota: Interpreting Tissue Concentrations*, 2nd ed.; CRC Press: New York, NY, USA, 2011; pp. 595–607.
39. Mukai, H.; Furuta, N.; Fujii, T.; Ambe, Y.; Sakamoto, K.; Hashimoto, Y. Characterization of sources of lead in the urban air of Asia using ratios of stable lead isotopes. *Environ. Sci. Technol.* **1993**, *27*, 1347–1356. [CrossRef]
40. Research and Statistics Department, Ministry of International Trade and Industry (MITI). *Yearbook of Energy Production: Supply and Demand Statistics*; Ministry of International Trade and Industry (MITI): Tokyo, Japan, 1984.
41. Beernaert, J.; Scheirs, J.; Leirs, H.; Blust, R.; Verhagen, R. Non-destructive pollution exposure assessment by means of wood mice hair. *Environ. Pollut.* **2007**, *145*, 443–451. [CrossRef] [PubMed]
42. Barry, P.S. A comparison of concentrations of lead in human tissues. *Br. J. Ind. Med.* **1975**, *32*, 119–139. [CrossRef] [PubMed]
43. Nakayama, S.M.; Ikenaka, Y.; Hamada, K.; Muzandu, K.; Choongo, K.; Yabe, J.; Umemura, T.; Ishizuka, M. Accumulation and biological effects of metals in wild rats in mining areas of Zambia. *Environ. Monit. Assess.* **2013**, *185*, 4907–4918. [CrossRef] [PubMed]
44. Nakata, H.; Nakayama, S.M.; Yabe, J.; Liazambi, A.; Mizukawa, H.; Darwish, W.S.; Ikenaka, Y.; Ishizuka, M. Reliability of stable Pb isotopes to identify Pb sources and verifying biological fractionation of Pb isotopes in goats and chickens. *Environ. Pollut.* **2016**, *208*, 395–403. [CrossRef] [PubMed]
45. Simonetti, A.; Gariépy, C.; Carignan, J. Pb and Sr isotopic compositions of snowpack from Québec, Canada: Inferences on the sources and deposition budgets of atmospheric heavy metals. *Geochim. Cosmochim. Acta* **2000**, *64*, 5–20. [CrossRef]

46. Vitòria, L.; Otero, N.; Soler, A.; Canals, À. Fertilizer characterization: Isotopic data (N, S, O, C, and Sr). *Environ. Sci. Technol.* **2004**, *38*, 3254–3262. [PubMed]
47. Mukai, H.; Tanaka, A.; Fujii, T.; Zeng, Y.; Hong, Y.; Tang, J.; Guo, S.; Xue, H.; Sun, Z.; Zhou, J.; et al. Regional characteristics of sulfur and lead isotope ratios in the atmosphere at several Chinese urban sites. *Environ. Sci. Technol.* **2001**, *35*, 1064–1071. [CrossRef] [PubMed]

Ecological Engineering 109 (2017) 57–64

Contents lists available at ScienceDirect

Ecological Engineering

journal homepage: www.elsevier.com/locate/ecoleng

Bioremediation of lead-contaminated mine waste by *Pararhodobacter* sp. based on the microbially induced calcium carbonate precipitation technique and its effects on strength of coarse and fine grained sand

Wilson Mwandira[a], Kazunori Nakashima[b,*], Satoru Kawasaki[b]

[a] Graduate School of Engineering, Hokkaido University, Kita 13, Nishi 8, Kita-ku, Sapporo 060-8628, Japan
[b] Faculty of Engineering, Hokkaido University, Sapporo 060-8628, Japan

ARTICLE INFO

Keywords:
Biomineral
Bioremediation
Microbially induced calcium carbonate precipitation
Lead

ABSTRACT

Lead (Pb^{2+}) is a toxic heavy metal that has a severe negative effect on human health and the environment. Physical, chemical and biological remediation techniques have long been used to remediate lead contamination. However, because of the great danger posed by lead contamination, there is increasing interest to apply eco-friendly and sustainable methods to remediate lead. Therefore, this study was conducted to use the microbially induced calcium carbonate precipitation (MICP) technique in conjunction with the bacterium *Pararhodobacter* sp. to bioremediate lead. Laboratory scale experiments were conducted and complete removal of 1036 mg/L of Pb^{2+} was achieved. These results were further confirmed by scanning electron microscope (SEM) and X-ray diffraction (XRD) analysis, which indicated coprecipitation of calcium carbonate ($CaCO_3$) and lead. The unconfined compressive strength increased with an increase in injection interval with maximum unconfined compressive strength of 1.33 MPa for fine sand, 2.87 MPa for coarse sand and 2.80 MPa for mixed sand. For *Pararhodobacter* sp. to efficiently induce lead immobilisation the bacterial interval required is four times with a calcium and urea concentration of 0.5 M and bacterial concentration of 10^9 cfu/mL. Very few low-cost in situ heavy metal treatment processes for lead bioremediation are available; therefore, bioimmobilization of lead by MICP has the potential for application as a low-cost and eco-friendly method for heavy metal remediation.

1. Introduction

Lead (Pb^{2+}) has been studied extensively worldwide because of its effects on human health and the environment (Yabe et al., 2015; Lin et al., 2009). The main characteristics of lead are that it persists in all parts of the environment, cannot be degraded or destroyed and enters the body through food, drinking water, and air. Lead poisoning results in brain and central nervous system damage, coma, convulsion and even death, mostly in children because they absorb 4–5 times as much lead as adults (Lanphear, 2005). One such area that is heavily contaminated with lead due to mining and smelting is Kabwe Mine, Zambia (Nyambe et al., 2013), which was selected as the study area for this investigation.

The Kabwe mine was a Pb-Zn mine that operated from 1902 to 1994, during which time it caused lead poisoning affecting close to 300,000 people. Despite closure of the mine, its wastes have continued to pollute the soil and water. Plant residue leachate of waste from tailings and thickeners and kiln slag are the major sources of lead, covering an area of approximately 86,600 m^2 and 164,800 m^2, respectively (ZCCM-IH, Zambia Copper and Cobalt Mining-Investment Holding Plc., 2002). In the past, a portion of the coarse kiln slag was used to cover the fine leached plant residue to prevent water erosion and windblown dust.

Several physical, chemical and biological remediation techniques have been used for many years to remediate lead contamination. However, the major challenge of physical-chemical lead remediation technologies involves a huge cost for complete removal or containment of contaminants to prevent them from migrating to surrounding areas. In this study, we seek to investigate the possibility of bioremediation of lead-contaminated mine waste in Kabwe based on microbially induced calcium carbonate precipitation (MICP). This technique involves the hydrolysis of urea into ammonium and carbamate by urease catalysis (Eq. (1)), resulting in $CaCO_3$ formation in the presence of Ca^{2+} ions (Eqs. (2)–(3)) (Whiffin et al., 2007).

$$CO(NH_2)_2 + H_2O \xrightarrow{\text{Urease}} H_2NCOO^- + NH_4^+ \quad (1)$$

$$H_2NCOO^- + H_2O \rightarrow HCO_3^- + NH_3 \quad (2)$$

* Corresponding author.
E-mail address: nakashima@geo-er.eng.hokudai.ac.jp (K. Nakashima).

http://dx.doi.org/10.1016/j.ecoleng.2017.09.011
Received 20 July 2017; Received in revised form 8 September 2017; Accepted 16 September 2017
Available online 22 September 2017
0925-8574/

$$Ca^{2+} + HCO_3^- + NH_3 \rightarrow CaCO_3 + NH_4^+ \quad (3)$$

The role of calcium ion in bioremediation using the MICP technique takes advantage of the incorporation of the Pb^{2+} onto their surfaces through substitution in the calcite lattice (Eq. (4)), after which Pb^{2+} are changed from soluble form to insoluble forms hence detoxifying the toxic lead ions (Anbu et al., 2016). The calcium carbonate formed can either be immobilize or form undissolved substances, with the free ions being attached onto the surfaces of calcium carbonate to yield a chemically stable and non-toxic form (Volodymyr and Viktor, 2017).

$$Pb^{2+} + CO_3^{2-} \rightarrow PbCO_3 \quad (4)$$

Bioremediation using this technique is promising for heavy metals (Cd^{2+}, Ni^{2+}, Pb^{2+} etc.) contaminated soils, sediment and water and has been successfully applied in recent studies (Kang et al., 2014; Zhu et al., 2016; Achal et al., 2012). In this study, we determine for the very first time the use of *Pararhodobacter* sp. for laboratory scale bioremediation of lead. *Pararhodobacter* sp. was selected for investigation because it has shown high urease activity and can maintain the enzyme activity for a long time (Fujita et al., 2017). This characteristic is useful in bioremediation as the bacteria is resilient when injected in the ground and its enzyme activity sustained for a longer period to accomplish biocementation and immobilization of the toxic ions. Previous researchers conducted solidification using *Pararhodobacter* sp. for ground improvement methods for marine (Danjo and Kawasaki, 2016) and land usage purposes (unpublished). However, in this study, *Pararhodobacter* sp. was investigated for both mine waste immobilization and to determine if it exhibits any Pb^{2+} resistance and its applicability for bioremediation. Further investigation on the bacteria would be necessary before possible application of this bacteria in-field.

An improved understanding of this process and mechanism will provide a scientific basis for the development of sound strategies for the provision and sustainable use of ureolytic bacteria for bioremediation of lead contaminated sites such as the Kabwe area in Zambia. The rationale for choosing this technique for mine waste bioremediation is to prevent wind-blown dust from uncovered waste dump sites, as well as to prevent erosion that leads to the transportation of sediments downstream. To achieve this, we determined the solidification and bioremediation conditions necessary for remediation using in vitro experiments by bioaugmentation, then will scale these up for field application via biostimulation (Fig. 1). Studies by Gomez et al., 2017 and Gat et al., 2016 reported that biostimulation offers important economic and environmental benefits through the elimination of expensive nonnative monoclonal bacterial cultivation as well as avoid changes to indigenous microbial population which may be affected to an unknown extent. Thus, the specific objectives of the present study (steps 1 and 2) were to: investigate the effects of lead on urease activity and microbial growth; determine the effectiveness of lead removal by *Pararhodobacter* sp.; determine the effects of varying the injection interval of the bacteria on unconfined compressive strength (UCS) for fine and coarse-grained sand; and evaluate the usefulness of *Pararhodobacter* sp. for lead bioremediation. The results from this study will be used in future studies as outlined in Fig. 1.

2. Materials and methods

2.1. Bacteria, media, and Pb^{2+} stock solution preparation

Pararhodobacter sp., a ureolytic bacterium isolated from the soil near beachrock in Okinawa, Japan, was used in this study (Danjo and Kawasaki, 2013). Cells were cultured in ZoBell2216 medium, which contained 5.0 g/L hipolypeptone (Nihon Seiyaku Co., Ltd., Tokyo, Japan), 1.0 g/L yeast extract (BD Biosciences Advanced Bioprocessing, Miami, FL, USA), and 0.1 g/L $FePO_4$ (Junsei Chemical Co., Ltd., Tokyo, Japan) prepared with artificial seawater with the final solution pH adjusted to 7.6–7.8 using 1 M NaOH (Fujita et al., 2017). Stock solution of lead was prepared using $PbCl_2$ (Wako Pure Chemical Industries Ltd., Tokyo, Japan), which was dissolved in distilled water, sterilized with a 0.22 μm filter and preserved at 4 °C. Different working concentrations of lead were then obtained by serial dilution.

2.2. Effect of lead on microbial growth and urease activity

The tolerance of *Pararhodobacter* sp. to lead was evaluated to elucidate its usefulness in bioremediation. Different concentrations of Pb^{2+} (0 mM, 0.01 mM, and 0.5 mM) were prepared in 100 mL Erlenmeyer flasks containing *Pararhodobacter* sp. and ZoBell2216 culture medium and the time course of cell growth was determined based on the optical density (OD) values at 600 nm by UV–vis spectrophotometry (V-730, Jasco International Co., Ltd., Tokyo, Japan) for 14 days in the presence of Pb^{2+}.

The urease activity of bacterial cells was determined by monitoring ammonium ions generated in urea hydrolysis using the indophenol blue method based on Berthelot's reaction in a water bath maintained at 30 °C (Weatherburn, 1967; Natarajan, 1995). After bacterial cultivation for 48 h, a bacterial suspension (1 mL) (OD_{600} = 1.0) was added to 0.1 M phosphate buffer (100 mL) containing 0.1 M urea. To determine the effects of lead on urease activity, different concentrations of lead (0–0.5 mM) were added. Samples were then collected at intervals of 5 min (0, 5, 10 and 15 min) and passed through a 0.22 μm filter to remove cells. Next, a 2 mL aliquot of the filtered sample was mixed with phenol nitroprusside reagent (4 mL) (0.25 M phenol in 100 mL of deionized water containing 23 μM of sodium nitroprusside) and hypochlorite reagent (4 mL) (0.05 M sodium hydroxide in 100 mL of deionized water containing 7.5 mL bleach (5% NaOCl)). Each reaction mixture was vortexed and then incubated at 50 °C–60 °C for 10 min. The amount of ammonium ion released because of urea hydrolysis was determined by referring to a previously prepared standard curve relating the absorbance at 630 nm to ammonium ion concentration

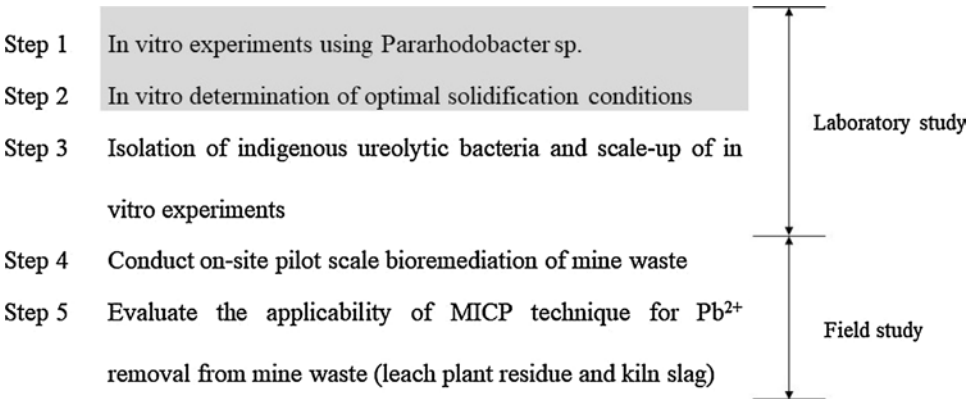

Fig. 1. Flowchart of the study. The steps described in this study are highlighted in grey.

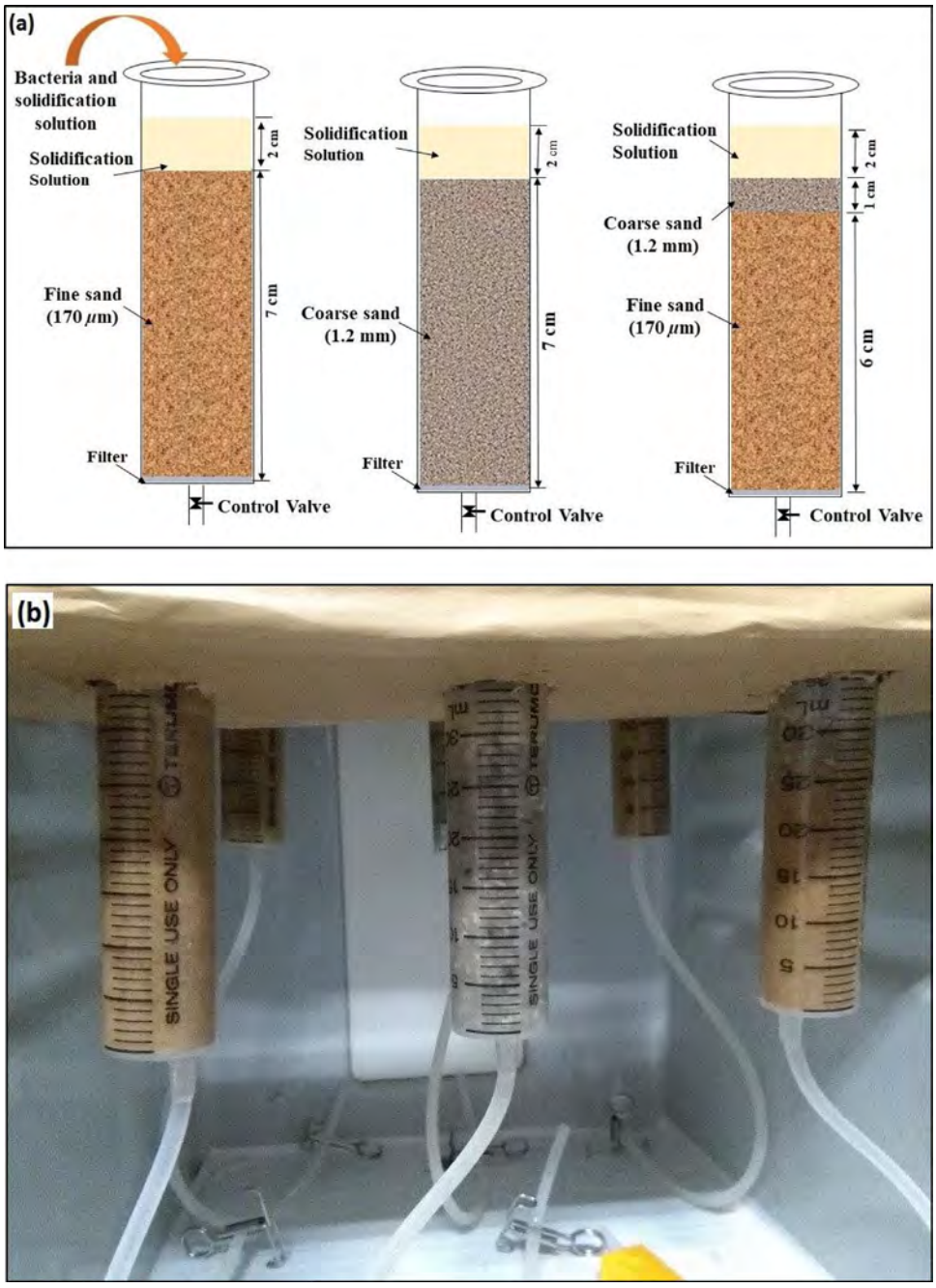

Fig. 2. (a) Conceptual setup and (b) images of the syringe solidification of coarse- and fine-grained sand.

(0–10 mg/L). Using this curve, one unit of urease activity (U) was defined as the amount of enzyme that would hydrolyze 1 μmol of urea per minute. The release of 2 μmol of ammonia is equivalent to the hydrolysis of 1 μmol of urea.

2.3. Bioprecipitation of calcium carbonate and lead

To elucidate the coprecipitation mechanism of lead and calcium, Pb^{2+} bioprecipitation experiments were carried out. Specifically, *Pararhodobacter* sp. was precultured for 24 h in 5 mL ZoBell2216 medium, after which 1 mL of preculture was inoculated into 100 mL of the main culture at 30 °C for 48 h with continuous aeration at 160 rpm. The bacterial suspension (5 mL) was then added to 2 mL calcium chloride (0.5 M) and 2 mL urea (0.5 M), after which different lead final concentrations were added (0 mM, 0.01 mM and 5 mM). The mixture was subsequently incubated for 6 h at 30 °C with shaking (160 rpm) and then further centrifuged (15,000 rpm for 5 min) to collect the precipitate. The concentration of lead in the supernatant was determined by inductively coupled plasma atomic emission spectroscopy (ICP-AES; ICPE-9000, Shimadzu Corporation, Tokyo, Japan), whereas the precipitate was analyzed by XRD/SEM as described in section 2.5. Precipitation experiments were conducted in triplicate.

2.4. Syringe solidification of coarse- and fine-grained sand

The most practical way of remediating a contaminated site is via in situ treatment of a contaminated material facilitated by the injection of microorganisms and nutrients. To understand the optimal injection interval of bacteria, four different injection intervals were tested in syringe solidification experiments. All syringe solidification experiments were conducted in an incubator at 30 °C. A method described by Danjo and Kawasaki was adopted for the syringe solidification

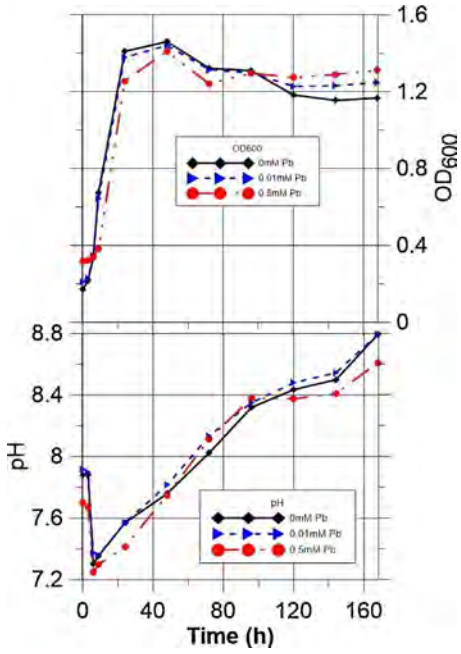

Fig. 3. Effect of lead on *Pararhodobacter* sp. growth curve. Values are averages from two independent experiments.

experiments (Danjo and Kawasaki, 2016). Briefly, 40 g of fine sand (mean diameter, D_{50} = 170 μm) and/or coarse sand (mean diameter, D_{50} = 1.2 mm) was oven dried at 105 °C for 48 h and then placed in a 35 mL syringe (mean diameter, D_{50} = 2.5 cm and height, h = 7 cm) (Fig. 2). The laboratory experiment was designed to mimic the field conditions in Kabwe mine as closely as possible based on grain size, with the very fine and coarse sand representing the plant residue and kiln slag, respectively. The mixed system was selected to mimic slag used to cover leached plant residue to prevent water and wind erosion on site. Bacterial culture (16 mL) (OD_{600} = 1.0 = 10^9 cfu/mL) and 20 mL of solidification solution (0.5 M urea; 0.5 M calcium chloride; 0.02 M sodium hydrogen carbonate; and 0.2 M ammonium chloride and nutrient broth 3 g/L) were sequentially added to the syringe and drained, leaving about 2 mL of solution above the surface of the sand to maintain wet conditions as conceptualized in Fig. 2a. The outlet solution from the syringe was measured for pH and Ca^{2+}. After 14 days of curing, the UCS was estimated using a needle penetration device (SH-70, Maruto Testing Machine Company, Tokyo, Japan).

2.5. XRD and SEM analyses

X-ray diffraction (XRD; MiniFlex™, Rigaku Co., Ltd., Tokyo, Japan) and a scanning electron microscope (SEM; Miniscope TM3000, Hitachi, Tokyo, Japan) were used to qualitatively analyze the MICP precipitate. The sample for XRD was dried at 105 °C and ground into powder using a Multi-beads shocker (Yasui Kikai, Tokyo, Japan). X-ray diffraction was conducted under Ni-filtered Cu1.5406A radiation. Scans were recorded from 5 to 80° 2θ, at a rate of 20°/min. The crystalline phases were identified using the International Centre for Diffraction Data (ICDD) database and MATCH 3.4 (Klaus and Putz, 2017). SEM images were taken under the microscope after mounting on a carbon tape.

3. Results and discussion

3.1. Effect of lead on microbial growth

Pararhodobacter sp. clearly exhibited increased growth following the lag, logarithmic, stationary and retardation phases in lead free media (Fig. 3). In the presence of lead, the logarithmic phase was slightly retarded and an overall decrease in growth was observed. The effects of lead on microbial growth were negligible, whereas no growth was observed for concentrations greater than 1 mM (data not shown). These results indicate that *Pararhodobacter* sp. can be used for bioremediation of lead, even though it was not isolated from a lead contaminated site (Kang et al., 2015). The measured pH of the solution decreased during the logarithmic phase, then increased consistently. It is unclear why a high pH was maintained during incubation; however, this could have occurred because of the release of metabolites in the solution, such as ammonia, by the live cells. The ammonia generation could have originated from amino acids contained in the yeast extract. In many studies, increased pH was only recorded when urea was added to the growth media. These findings are in tandem with those of previous studies, although the effects of lead ions differ for different microorganisms because of different inhibitory concentrations among organisms (Govarthanan et al., 2013; Naik and Dubey, 2013).

3.2. Effect of lead on urease activity

Urease activity of bacterial cells was studied because it serves as a

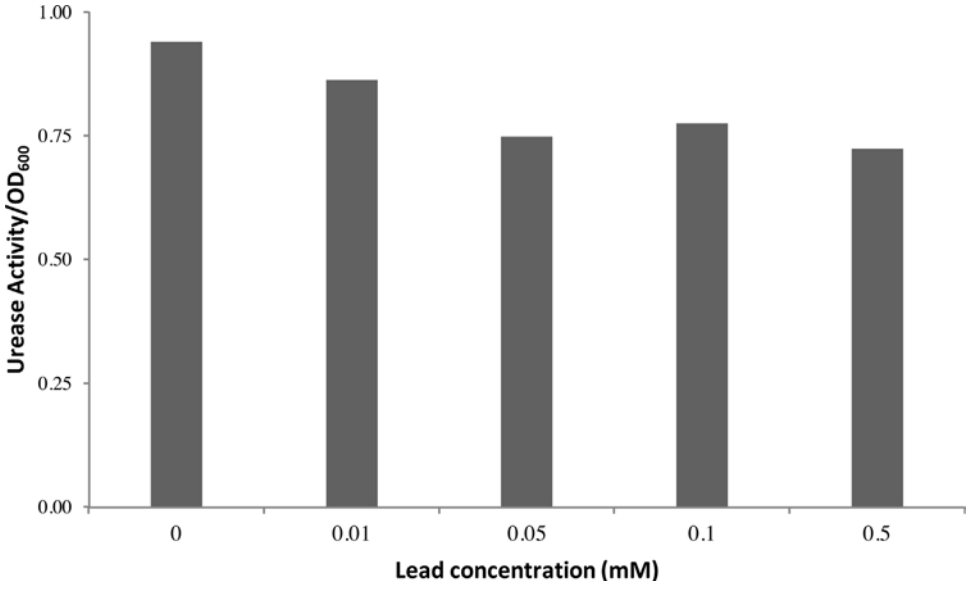

Fig. 4. Effect of lead on urease activity based on the OD_{600} of *Pararhodobacter* sp. Values are averages from two independent experiments.

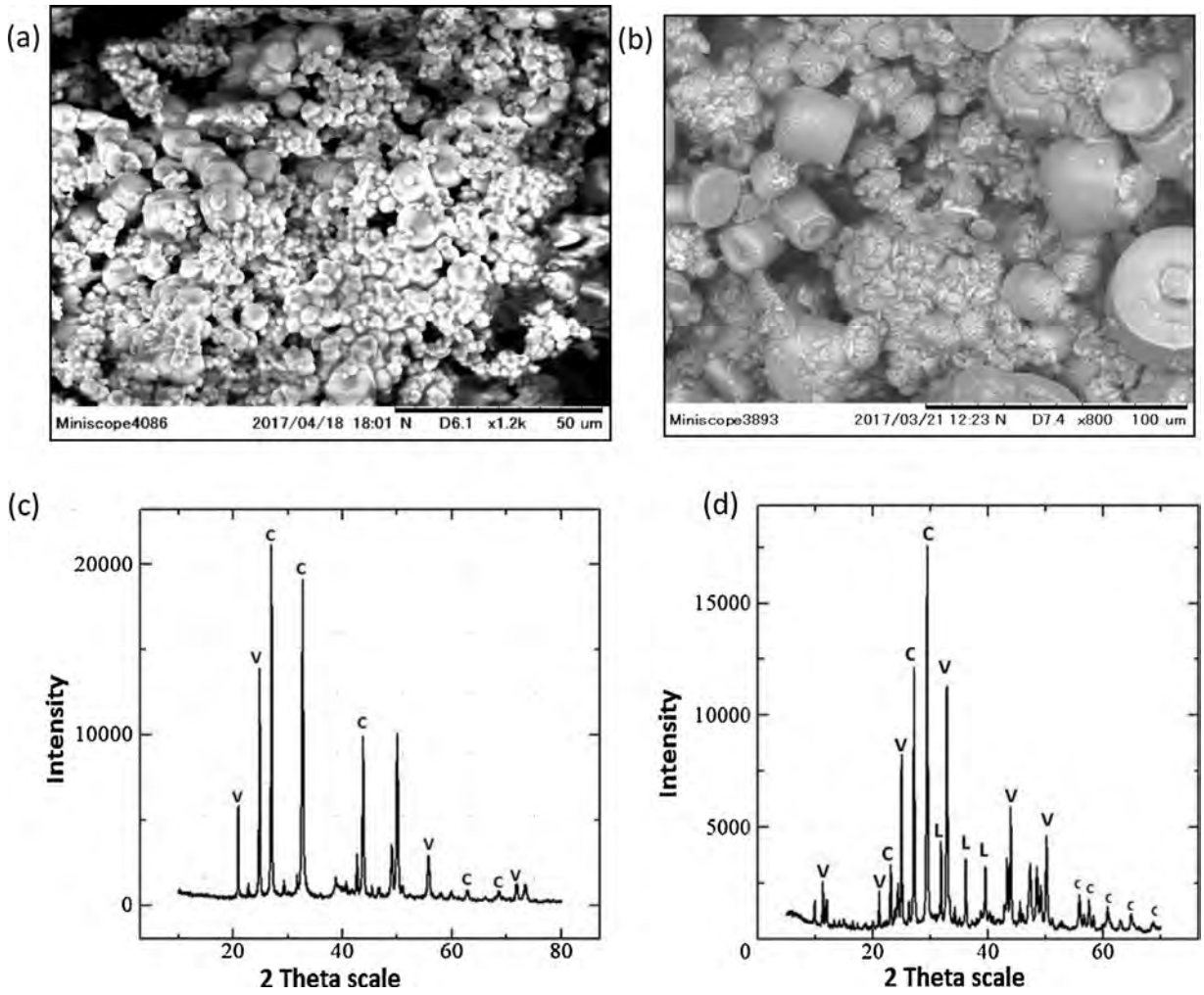

Fig. 5. SEM images (a, b) and XRD data (c, d) of precipitates formed by *Pararhodobacter* sp. in the absence (a, c) and presence of 5 mM Pb^{2+} (b, d). (C = Calcite ($CaCO_3$); V = Vaterite ($CaCO_3$); L = Lead Oxide (PbO)).

good bioindicator of enzyme activity in the MICP bioremediation technique and is used to assess environmental health changes occurring in the environment. As shown in Fig. 4, the urease activity was not significantly affected by lead. This pattern, which was probably because of the effects of lead on enzyme activity, reinforces the findings reported by Fujita et al. (2017), who found that urease accumulated in/on cells of *Pararhodobacter* sp. However, several authors have reported a significant decrease in enzyme activity and microbial activity because of heavy metals pollution of aquatic and soil ecosystems (Sadler and Trudinger, 1967; Nwuche and Ugoji, 2008; Begum et al., 2009). The present study revealed a negligible decreased in urease and microbial activity. These results were probably because of other factors such as synergy of heavy metals as reported by Nwuche and Ugoji (2008), who observed inhibition of soil microbial activities in response to a combination of Cu and Zn.

3.3. Lead bioprecipitation

Pararhodobacter sp. was effective at complete removal of Pb^{2+}. Comparison of the removal percentage of lead during bioprecipitation between this study and previous studies shows comparable figures to other ureolytic bacteria isolated from various sites such as *Rhodobacter spharoides* isolated from an oil field achieved 90.31% (Li et al., 2016); *Enterobacter cloacae* isolated from an abandoned mine achieved 68.1% (Kang et al., 2015); *Sporosarcina pasteurii* achieved 100% (Mugwar and Harbottle, 2016); and *Terrabacter tumescens* achieved 100% (Li et al., 2015). The capability of *Pararhodobacter* to completely remove lead lies in its ability to efficiently hydrolyze urea to generate carbonate ions and elevate the pH to alkaline conditions (8.0–9.1), which promotes precipitation of lead and calcium carbonate.

Fig. 5 shows SEM images and XRD patterns of the control (a, c) and bioremediated (b, d) precipitates. Fig. 6a shows the spherical particles of calcium carbonate precipitated in the absence of lead and confirmed by XRD analysis in Fig. 6c. This finding has been observed from previous studies that reported different polymorphs of calcium carbonate in the form of vaterite and calcite being formed when biomineralization occurs via mediation by bacteria (Park et al., 2010; González-Muñoz et al., 2010). Vaterite does not occur in abundance in the natural environment but is an important precursor in calcite formation of a more stable form of calcium carbonate (Nehrke and Van Cappellen, 2006). Furthermore, Fig. 6b shows the SEM image of precipitate in the presence of lead. In the figure, framboidal aggregates were identified as vaterite, whereas spherical and rhombohedral shaped precipitates were identified as calcite. In the MICP process, calcium carbonate can adsorb or incorporate free toxic ions Pb^{2+} through substitution of the divalent calcium ion in the $CaCO_3$ lattice (Fig. 6d). Detoxification of the lead to insoluble form occurs when the toxic free ion is transformed into a chemically stable and non-toxic form of lead as elucidated in another study by Li et al. (2013).

Fig. 6. Pictorial images of the results of all syringe tests after 14 days while varying the bacterial injection interval to (a) one (b) two (c) four and (d) seven times. Left, fine sand; center, coarse sand; right, mixture of course and fine sand.

Table 1
Solidification conditions of the injection intervals.

	Sand particle size	Bacterial injection times	Solidification solution injection	Bacterial OD_{600}	Temp. (°C)	Timing (Day)	Condition of solidification		
							Top	Middle	Bottom
Case 1	170 μm	Once	Daily	1.0	30	14	Moderately solidified	Not solidified	Not solidified
Case 2	1.2 mm	Once	Daily	1.00	30	14	Solidified	Not solidified	Not solidified
Case 3	170 μm/1.2 mm	Once	Daily	1.00	30	14	Solidified	Not solidified	Not solidified
Case 1	170 μm	Twice	Daily	1.00	30	14	Moderately solidified	Not solidified	Not solidified
Case 2	1.2 mm	Twice	Daily	1.00	30	14	Not solidified	Not solidified	Not solidified
Case 3	170 μm/1.2 mm	Twice	Daily	1.00	30	14	Weakly solidified	Not solidified	Not solidified
Case 4	170 μm	Four times	Daily	1.00	30	14	Solidified	Solidified	Solidified
Case 5	1.2 mm	Four times	Daily	1.00	30	14	Solidified	Not solidified	Not solidified
Case 6	170 μm/1.2 mm	Four times	Daily	1.00	30	14	Moderately Solidified	Solidified	Solidified
Case 4	170 μm	Seven times	Daily	1.00	30	14	Solidified	Solidified	Solidified
Case 5	1.2 mm	Seven times	Daily	1.00	30	14	Solidified	Solidified	Solidified
Case 6	170 μm/1.2 mm	Seven times	Daily	1.00	30	14	Solidified	Solidified	Solidified

3.4. Syringe solidification experiment

Pictorial images of sand samples from all syringe solidification experiments after 14 days are shown in Fig. 6. The UCS comparison of the results obtained after varying the injection interval (once, twice, four and seven times) is summarized in Table 1 and graphically shown in Fig. 7. The classification scheme adopted in this paper was based on that developed by Shafii and Clough (1982), in which weakly cemented

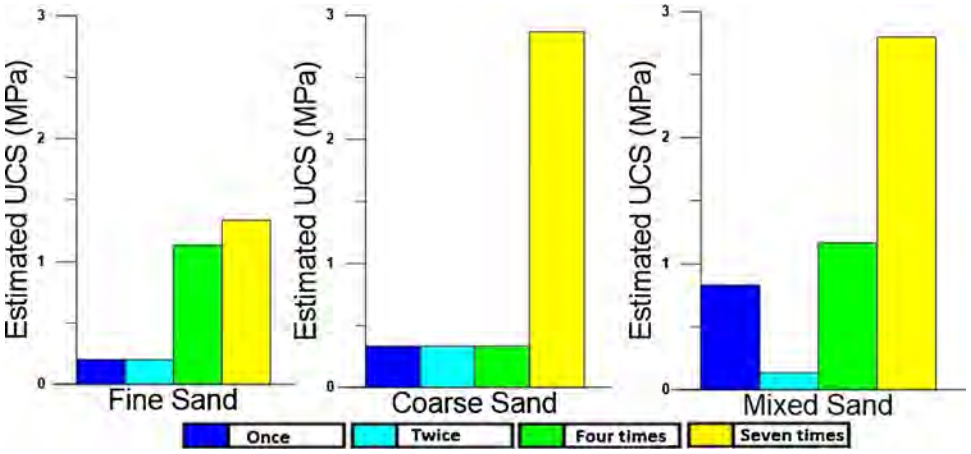

Fig. 7. UCS comparison of the results obtained when varying the bacteria injection for fine, coarse and mixed sand.

sand was defined as having a UCS of less than 0.3 MPa, moderately cemented sand was defined as having a UCS between 0.4 Mpa and 1 MPa and solidified sand was that with greater than 1 MPa (Shafii and Clough, 1982). Generally, UCS increased with increasing injection interval as well as the top part of the sample was solidified more than the bottom. This increase in UCS at the top can be attributed to calcite crystals forming cohesive bonds between sand grains mediated by *Pararhodobacter*, which accumulated at the top of the sample.

Increasing cohesive bonds result in cementation leading to decreased permeability, as was observed during the investigation. Therefore, MICP can both immobilize the lead and induce high resistance of the contaminated materials to erosion. This phenomenon was also observed when conducting a steep slope experiment using *Sporosarcina pasteurii* (Salifu et al., 2016). Overall, the data obtained using the syringe test demonstrated that MICP is a viable option for use in coarse- and fine-grained sand. In syringe experiments, the pH value ranged from 8.0 to 9.5, which is similar to what has been observed in other studies (Stocks-Fischer et al., 1999). The calcium ion concentration was lower in the first 7 days of the experiment, indicating deposition of calcite in the column and a decrease in deposition in the latter half. Clogging of the porous media was greater in coarse sand than in finely graded sand. This clogging was because of the cell growth and calcium carbonate formation that accompany the MICP process.

4. Conclusion

In this study, we demonstrated for the first time that lead (Pb) can be bioremediated by *Pararhodobacter* sp. and that the microorganism was capable of complete removal of 1036 mg/L Pb^{2+} during 6 h of incubation via elevation of the pH to alkaline conditions (8.0–9.1). SEM and XRD further confirmed transformation of toxic free Pb^{2+} ions to a more stable form of lead that bioprecipitated together with calcite or vaterite, which were predominant. Furthermore, syringe experiments revealed that UCS was greater when seven injection were performed as opposed to less injection interval of bacteria. The unconfined compressive strength increased with an increase in injection interval with maximum unconfined compressive strength of 1.33 MPa for fine sand, 2.87 MPa for coarse sand and 2.80 MPa for mixed sand. For *Pararhodobacter* to efficiently induce lead immobilisation the bacterial interval required is four times with a calcium and urea concentration of 0.5 M and bacterial concentration of 10^9 cfu/mL. These results will facilitate the bioremediation of lead in both fine and coarse materials as an eco-friendly and sustainable method of heavy metal remediation.

Acknowledgments

This work was sponsored by JSPS KAKENHI Grant Number JP16H04404 and JST/JICA, SATREPS (Science and Technology Research Partnership for Sustainable Development).

References

Achal, V., Pan, X., Zhang, D., Fu, Q., 2012. Bioremediation of Pb-contaminated soil based on microbially induced calcite precipitation. J. Microbiol. Biotechnol. 22, 244–247. http://dx.doi.org/10.4014/jmb.1108.08033.

Anbu, P., Kang, C.-H., Shin, Y.-J., So, J.-S., 2016. Formations of calcium carbonate minerals by bacteria and its multiple applications. Springerplus 5, 250. http://dx.doi.org/10.1186/s40064-016-1869-2.

Begum, A., Harikrishna, S., Khan, I., 2009. Analysis of heavy metals in water, sediments and fish samples of Madivala lakes of Bangalore, Karnataka. Int. J. Chem. Technol. Res. 1, 245–249.

Danjo, T., Kawasaki, S., 2013. A Study of the Formation Mechanism of Beachrock in Okinawa, Japan: Toward Making Artificial Rock. Int. J. GEOMATE 5 (1), 634–639.

Danjo, T., Kawasaki, S., 2016. Microbially induced sand cementation method using Pararhodobacter sp. strain SO1, inspired by beachrock formation mechanism. Mater. Trans. 57, 428–437. http://dx.doi.org/10.2320/matertrans.M-M2015842.

Fujita, M., Nakashima, K., Achal, V., Kawasaki, S., 2017. Whole-cell evaluation of urease activity of *Pararhodobacter* sp. isolated from peripheral beachrock. Biochem. Eng. J. 124, 1–5. http://dx.doi.org/10.1016/j.bej.2017.04.004.

Gat, D., Ronen, Z., Tsesarsky, M., 2016. Soil bacteria population dynamics following stimulation for ureolytic microbial-induced $CaCO_3$ precipitation. Environ. Sci. Technol. 50, 616–624. http://dx.doi.org/10.1021/acs.est.5b04033.

Gomez, M.G., Anderson, C.M., Graddy, C.M.R., DeJong, J.T., Nelson, D.C., Ginn, T.R., 2017. Large-scale comparison of bioaugmentation and biostimulation approaches for biocementation of sands. J. Geotech. Geoenvironmental Eng. 143, 4016124. http://dx.doi.org/10.1061/(ASCE)GT.1943-5606.0001640.

González-Muñoz, M.T., Rodriguez-Navarro, C., Martínez-Ruiz, F., Arias, J.M., Merroun, M.L., Rodriguez-Gallego, M., 2010. Bacterial biomineralization: new insights from *Myxococcus* – induced mineral precipitation. Geol. Soc. London, Spec. Publ. 336, 31–50. http://dx.doi.org/10.1144/SP336.3.

Govarthanan, M., Lee, K.J., Cho, M., Kim, J.S., Kamala-Kannan, S., Oh, B.T., 2013. Significance of autochthonous *Bacillus* sp. KK1 on biomineralization of lead in mine tailings. Chemosphere 90, 2267–2272. http://dx.doi.org/10.1016/j.chemosphere.2012.10.038.

Kang, C.H., Han, S.H., Shin, Y., Oh, S.J., So, J.S., 2014. Bioremediation of Cd by microbially induced calcite precipitation. Appl. Biochem. Biotechnol. 172, 2907–2915. http://dx.doi.org/10.1007/s12010-014-0737-1.

Kang, C.H., Oh, S.J., Shin, Y., Han, S.H., Nam, I.H., So, J.S., 2015. Bioremediation of lead by ureolytic bacteria isolated from soil at abandoned metal mines in South Korea. Ecol. Eng. 74, 402–407. http://dx.doi.org/10.1016/j.ecoleng.2014.10.009.

Klaus, Putz, H.B., 2017. Match! – Phase Identification from Powder Diffraction, Crystal Impact.

Lanphear, B.P., 2005. Childhood lead poisoning prevention. J. Am. Med. Assoc. 293, 2274. http://dx.doi.org/10.1001/jama.293.18.2274.

Li, M., Cheng, X., Guo, H., 2013. Heavy metal removal by biomineralization of urease producing bacteria isolated from soil. Int. Biodeterior. Biodegradation 76, 81–85. http://dx.doi.org/10.1016/j.ibiod.2012.06.016.

Li, M., Cheng, X., Guo, H., Yang, Z., 2015. Biomineralization of carbonate by *Terrabacter tumescens* for heavy metal removal and biogrouting applications. J. Environ. Eng. http://dx.doi.org/10.1061/(ASCE)EE.1943-7870.0000970. C4015005-C4015005.

Li, X., Peng, W., Jia, Y., Lu, L., Fan, W., 2016. Bioremediation of lead contaminated soil with *Rhodobacter sphaeroides*. Chemosphere 156, 228–235. http://dx.doi.org/10.1016/j.chemosphere.2016.04.098.

Lin, G.Z., Peng, R.F., Chen, Q., Wu, Z.G., Du, L., 2009. Lead in housing paints: an exposure source still not taken seriously for children lead poisoning in China. Environ. Res. 109, 1–5. http://dx.doi.org/10.1016/j.envres.2008.09.003.

Mugwar, A.J., Harbottle, M.J., 2016. Toxicity effects on metal sequestration by microbially-induced carbonate precipitation. J. Hazard. Mater. 314, 237–248. http://dx.doi.org/10.1016/j.jhazmat.2016.04.039.

Naik, M.M., Dubey, S.K., 2013. Lead resistant bacteria: lead resistance mechanisms, their applications in lead bioremediation and biomonitoring. Ecotoxicol. Environ. Saf. 98, 1–7. http://dx.doi.org/10.1016/j.ecoenv.2013.09.039.

Natarajan, K.R., 1995. Kinetic study of the enzyme urease from *Dolichos biflorus*. J. Chem. Educ. 72, 556–557. http://dx.doi.org/10.1021/ed072p556.

Nehrke, G., Van Cappellen, P., 2006. Framboidal vaterite aggregates and their transformation into calcite: a morphological study. J. Cryst. Growth 287, 528–530. http://dx.doi.org/10.1016/j.jcrysgro.2005.11.080.

Nwuche, C.O., Ugoji, E.O., 2008. Effects of heavy metal pollution on the soil microbial activity. Int. J. Environ. Sci. Technol. 5, 409–414. http://dx.doi.org/10.1007/BF03326036.

Nyambe, I.A., Chirwa, M., Chaziya, B., 2013. Impacts of past mining activities on the Ecosystem and on human health in Kabwe Town, Zambia. Workshop on Environmental and Health Impacts of Mining Activities in the Sub-Saharan African Countries (p. 33).

Park, S.J., Park, Y.M., Chun, W.Y., Kim, W.J., Ghim, S.Y., 2010. Calcite-forming bacteria for compressive strength improvement in mortar. J. Microbiol. Biotechnol. 20, 782–788. http://dx.doi.org/10.4014/jmb.0911.11015.

Sadler, W.R., Trudinger, P.A., 1967. The inhibition of microorganisms by heavy metals. Miner. Depos. 2, 158–168. http://dx.doi.org/10.1007/BF00201912.

Salifu, E., MacLachlan, E., Iyer, K.R., Knapp, C.W., Tarantino, A., 2016. Application of microbially induced calcite precipitation in erosion mitigation and stabilisation of sandy soil foreshore slopes: a preliminary investigation. Eng. Geol. 201, 96–105. http://dx.doi.org/10.1016/j.enggeo.2015.12.027.

Shafii, R.-N., Clough, W., 1982. The Influence of Cementation on the Static and Dynamic Behavior of Sands. Stanford, California, California.

Stocks-Fischer, S., Galinat, J.K., Bang, S.S., 1999. Microbiological precipitation of $CaCO_3$. Soil Biol. Biochem. 31, 1563–1571. http://dx.doi.org/10.1016/S0038-0717(99)00082-6.

Volodymyr, Viktor, S.I., 2017. Construction Biotechnology: Biogeochemistry, Microbiology and Biotechnology of Construction Materials and Processes. Springer Nature, Singapore. http://dx.doi.org/10.1007/978-981-10-1445-1.

Weatherburn, M.W., 1967. Phenol-hypochlorite reaction for determination of ammonia. Anal. Chem. 39, 971–974. http://dx.doi.org/10.1021/ac60252a045.

Whiffin, V.S., van Paassen, L.A., Harkes, M.P., 2007. Microbial carbonate precipitation as a soil improvement technique. Geomicrobiol. J. 24, 417–423. http://dx.doi.org/10.1080/01490450701436505.

Yabe, J., Nakayama, S.M.M., Ikenaka, Y., Yohannes, Y.B., Bortey-Sam, N., Oroszlany, B., Muzandu, K., Choongo, K., Kabalo, A.N., Ntapisha, J., Mweene, A., Umemura, T., Ishizuka, M., 2015. Lead poisoning in children from townships in the vicinity of a lead-zinc mine in Kabwe, Zambia. Chemosphere 119, 941–947. http://dx.doi.org/10.1016/j.chemosphere.2014.09.028.

ZCCM-IH – Zambia Copper and Cobalt Mining- Investment Holding Plc, 2002. Environmental Assessment of the Copperbelt and Kabwe Area. Kitwe.

Zhu, X., Li, W., Zhan, L., Huang, M., Zhang, Q., Achal, V., 2016. The large-scale process of microbial carbonate precipitation for nickel remediation from an industrial soil. Environ. Pollut. 219, 149–155. http://dx.doi.org/10.1016/j.envpol.2016.10.047.

Environ Sci Pollut Res (2017) 24:23763–23770
DOI 10.1007/s11356-017-9911-7

RESEARCH ARTICLE

Assessment of DDT contamination in house rat as a possible bioindicator in DDT-sprayed areas from Ethiopia and South Africa

Yared Beyene Yohannes[1,2] · Yoshinori Ikenaka[1,3] · Gengo Ito[1] · Shouta M. M. Nakayama[1] · Hazuki Mizukawa[4] · Victor Wepener[3] · Nico J. Smit[3] · Johan H. J. Van Vuren[5] · Mayumi Ishizuka[1]

Received: 11 April 2017 / Accepted: 3 August 2017 / Published online: 1 September 2017

Abstract Ethiopia and South Africa are among the few countries to still implement indoor residual spraying with dichloro-diphenyl-trichloroethane (DDT) for malaria vector control. In this study, we investigated the levels and ecological risks of DDT and its metabolites in liver tissues of house rat, as a sentinel animal, for providing an early warning system for public health and wildlife intervention from Ethiopia and South Africa. The results showed that ΣDDT concentration ranged from 127 to 9155 μg/kg wet weight, and the distribution order of DDT and its metabolites in the analyzed liver samples was *p,p′*-DDD > *p,p′*-DDE >> *p,p′*-DDT, o,*p′*-DDT, and o,*p′*-DDD. The risk assessment indicated a potential adverse impact on humans, especially for pregnant women and children, because they spend majority of their time in a DDT-sprayed house. The ecological assessment also showed a concern for birds of prey and amphibians like frogs. This study is the first report on DDT contamination in liver tissues of house rats from Ethiopia and South Africa, and henceforth, the data will serve as a reference data for future studies.

Keywords DDT · House rat · Liver · Risk assessment · Ethiopia · South Africa

Responsible editor: Hongwen Sun

✉ Mayumi Ishizuka
ishizum@vetmed.hokudai.ac.jp

[1] Laboratory of Toxicology, Department of Environmental Veterinary Sciences, Graduate School of Veterinary Medicine, Hokkaido University, Kita 18, Nishi 9, Kita-ku, Sapporo 060-0818, Japan

[2] Department of Chemistry, College of Natural and Computational Science, University of Gondar, P.O. Box 196, Gondar, Ethiopia

[3] Water Research Group, Unit for Environmental Sciences and Management, Potchefstroom Campus, North-West University, Private Bag X6001, Potchefstroom, South Africa

[4] Department of Environmental Veterinary Sciences, Graduate School of Veterinary Medicine, Hokkaido University, Kita 18, Nishi 9, Kita-ku, Sapporo 060-0818, Japan

[5] Department of Zoology, Kingsway Campus, University of Johannesburg, PO Box 524, Auckland Park 2006, South Africa

Introduction

Rachel Carson's book "*Silent Spring*" first drew attention to the effects of the widespread extensive use of pesticides, especially dichloro-diphenyl-trichloroethane (DDT), on the environment and human health (Carson 1962). Due to their high persistence and lipophilicity, DDTs tend to bioaccumulate in fatty tissues of living organisms and are toxic to humans and wildlife. Exposure to DDT and its metabolites has been associated with both estrogenic potentials and anti-androgenic effects (Crews et al. 2000). Both *p,p′*-DDT and *o,p′*-DDT promote estrogenic activity (Bhatia et al. 2005), while *p,p′*-DDE is a potent androgen receptor antagonist (You 2000). The effects of DDT-induced endocrine disruption such as infertility, and reduced reproductive success in birds and wildlife, are also documented (Fisk et al. 2005; Giesy et al. 2003; Tyler et al. 1998). Thus, the necessity for continual monitoring and surveillance of DDTs in natural surroundings has been recognized.

Humans and wildlife can expose to DDT either through direct contact or through secondary exposure via ingesting and inhalation. House rat, also called as the black rat or roof rat, is a good indicator of human exposure to environmental chemicals, because they live in proximity and exposed to many of the same influences as human beings (Ardizzone et al. 2014; Ishizuka et al. 2005). They are potential sinks

for accumulation of indoor pesticides from the food supply and/or inhalation of pesticides while used for vector control indoors and outdoors. They are also food for a lot of natural predators, like foxes and cats just to name a few, including birds of prey. Therefore, the knowledge on the contamination status in house rat is not only to estimate the magnitude of environmental pollution but also to predict human health and wildlife risks.

Currently, DDT is produced in India and exported as a pure or as a commercially formulated product to other, mostly African, countries (UNEP 2016). South Africa formulated DDT with the technical product and exports the formulated product to other African countries. In Ethiopia, the Adami Tulu Pesticide Processing Plant has been operating since 1992 in the formulation of pesticides, including DDT. The plant imports technical grade material and has been supplying formulated DDT to the Ministry of Health since 2001 (UNEP 2016). Ethiopia and South Africa are among the others African countries which have used DDT for indoor residual spraying (IRS) for malaria vector control and is still the insecticide of choice (Van den Berg 2009; WHO 2011). As a consequence, DDT residues have been measured at concerning levels in biotic including humans (Gerber et al. 2016; Van Dyk et al. 2010; Yohannes et al. 2014a, b, 2017) and abiotic compartments (Barnhoorn et al. 2009; Yohannes et al. 2013) in these two countries.

With this in mind, the aim of this study was to investigate the levels of DDT and its metabolites in liver tissues of house rats from Ethiopia and South Africa. This study further investigates the potential human and ecological risks pose by the DDTs. To the authors' knowledge, this is the first report on DDT contamination in house rats from Africa and to document house rats as sentinel of DDT contamination in indoor residual spraying environment.

Materials and methods

Sampling site

The sample stations were Ziway town from Ethiopia and Pongola river basin in South Africa (Fig. 1). Both sampling areas are known for having high incidence of malaria.

Ziway town is located 165 km from south of Addis Ababa, the capital city of Ethiopia. It is a town with a population of about 50,000 and lies on the western side of Lake Ziway. The communities are engaged in mixed farming, fishing, rearing livestock, and meet their daily water needs from the lake. The Ziway area is known for its irrigation practice where smallholder horticulture farmers and large-scale flower growing companies are located around the lake, with the use of pesticides and chemical fertilizers. The irrigation scheme, subsequently suitable habitats for vector mosquitoes, resulted in increased malaria transmission in communities throughout most of the year.

The Pongola River, with a catchment of 7000 km^2 at the eastern extent of South Africa, passes through a narrow gorge between the Lebombo and the Ubombo mountains, where the Pongolapoort Dam is now situated on the border between Swaziland and South Africa. The catchment area is under large-scale agricultural activities, dominated by sugar cane, cotton, irrigated fruits, and vegetables. The surrounding area of the impoundment is classified as an malaria endemic area, and vector control has been done through indoor spraying of DDT in dwellings. Vector control based on IRS has been applied indoors on walls, ceilings, and outdoors with 75% DDT wettable powder at a dosage of 2 g active ingredient per square meter.

Collection of house rat and sample preparation

House rats were captured using gauze cage traps with food as bait in residential areas from Ziway town ($n = 21$), Ethiopia, in February 2013 and from KwaZulu-Natal, Pongola river basin ($n = 24$), South Africa, in April 2014. The traps were set indoors in the evening and collected in the next morning. Rats were euthanized, and body weight and sex were determined. Liver samples were collected from each rat and kept at − 20 °C. The frozen samples were then transported to the Laboratory of Toxicology, Graduate School of Veterinary Medicine, Hokkaido University, Japan, for analysis. All the experiments were performed using the rule approved by the Institutional Animal Care and Use Committee of Hokkaido University.

Reagents and chemicals

Mixture of DDTs (*o,p′*-DDT, *p,p′*-DDT, *o,p′*-DDE, *p,p′*-DDE, *o,p′*-DDD, and *p,p′*-DDD) was obtained from Dr. Ehrenstorfer GmbH (Augsburg, Germany). Surrogate standard 3,3′,4,4′-tetrachlorobiphenyl (PCB 77) and syringe spike 2,4,5,6-tetrachloro-*m*-xylene (TC*m*X) solutions were purchased from Sigma-Aldrich (Tokyo, Japan) and AccuStandard, Inc. (New Haven, CT, USA), respectively. Solvents and reagents used were analytical grade and purchased from Kanto Chemical Corp. (Tokyo, Japan).

Analysis of DDT

The protocol for analysis was performed as described by Yohannes et al. (2014b). Briefly, about 2-g liver tissue was homogenized with anhydrous sodium sulfate and spiked with surrogate standard (PCB 77). Extraction was carried out with 150 mL hexane/acetone (3:1, *v*/*v*) in a Soxtherm apparatus (S306AK Automatic Extractor, Gerhardt, Germany) in hot extraction mode for 4 h. The lipid content was determined gravimetrically on an aliquot of the extract, and the remaining

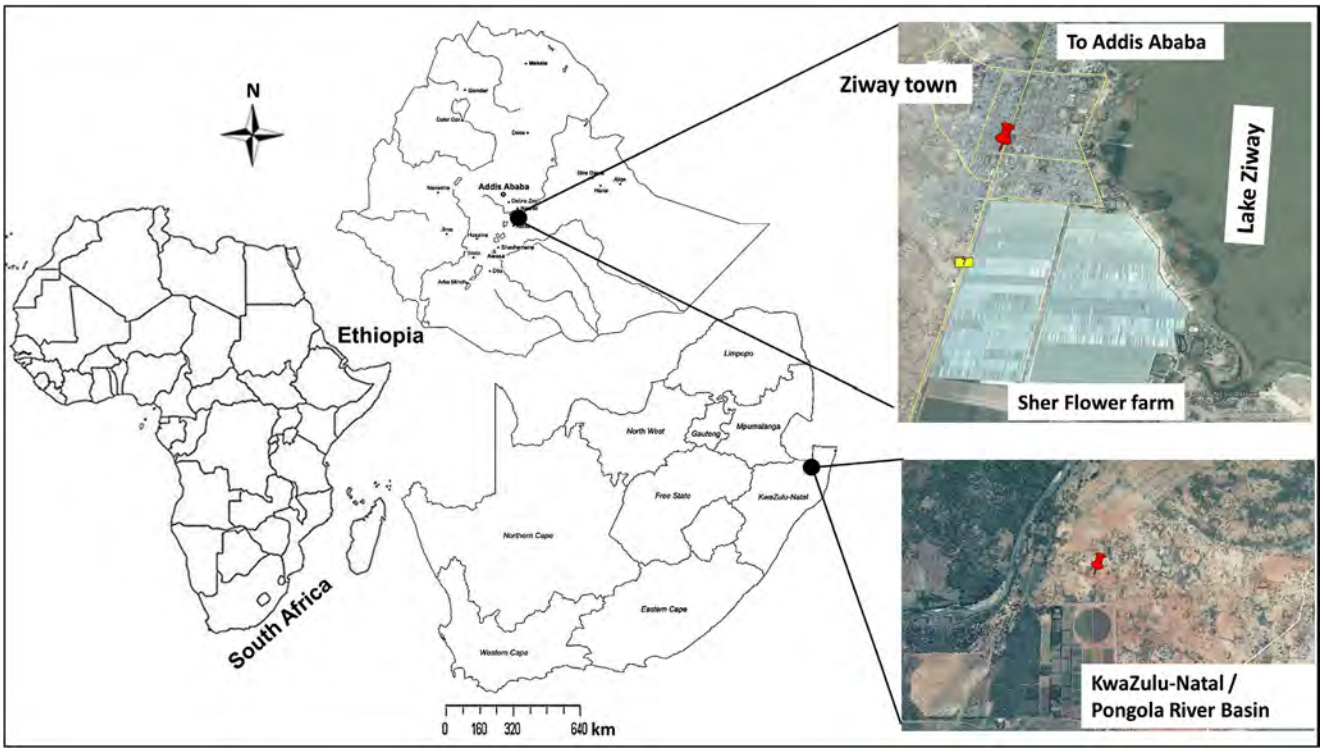

Fig. 1 Map of the study area with sample locations indicated from Google Earth map

extract was cleaned up on a column packed with 5 g activated Florisil and topped with 1 g of anhydrous sodium sulfate. The extract was eluted with 100 mL hexane/dichloromethane (7:3, *v*/*v*). The eluate was finally concentrated to near dryness and redissolved in 100 μL *n*-decane. A known amount of TC*m*X as a syringe spike standard was added to all extracts prior to instrumental analyses.

The samples were analyzed on a Shimadzu gas chromatography equipped with a ^{63}Ni μ–electron capture detector (GC-ECD: Shimadzu GC 2014, Kyoto, Japan). An ENV-8MS capillary column (30 m × 0.25 mm × 0.25 μm) was used for separation. The oven initial temperature was 100 °C (1 min hold), raised to 200 °C at a rate of 20 °C/min and then at 3 °C/min to 260 °C (10 min hold). Injector and detector temperatures were 250 and 310 °C, respectively. Helium at a flow rate of 1 mL/min and nitrogen at a flow rate of 45 mL/min were used as carrier and make-up gases, respectively. A 1-μL volume of samples was injected in splitless mode.

Quality assurance/quality control

DDT and its metabolites were identified by a comparison of their retention time to the peaks from the calibration standards. Multiple-level calibration curves were created for the quantification, and good linearity ($r^2 > 0.995$) was achieved. QC and QA were performed by analyses of procedural blanks, spiked blanks, and blind duplicate samples and consisted in daily calibration curves check. Recoveries for individual DDTs in spiked blanks were between 90 and 105%, and average recovery for PCB 77 was 90 ± 9%. The limit of detection (LOD) calculated as three times the signal-to-noise ratio was < 0.1 μg/kg for all DDTs. Confirmation of residues on representative samples using an ENV-8MS capillary column was carried on a Thermo Scientific DSQ II single stage quadrupole GC–MS system.

Statistical analysis

Concentrations of DDTs were tested for homogeneity of variance and log transformed to approximate a normal distribution of the data. As few samples had undetectable values for *op*′-DDD, *op*′, and *pp*′-DDT, geometrical mean calculation was impossible. Therefore, samples with concentrations below the detection limits were assigned a value of one half of the detection limit for statistical analysis (Croghan and Egeghy 2003). Student's *t* test was used for determining differences in the concentrations of DDTs between both sites and sexes. The significant level was set at 0.05. All statistical analyses were performed with the JMP software version 12.0 (SAS Institute, Cary, NC, USA).

Results and discussion

Table 1 shows basic parameters of the samples. The house rats (n = 21) from Ziway area, Ethiopia, weighed between 33 and

Table 1 DDT residues (μg/kg wet weight [μg/kg lipid weight]) in liver tissues of house rats from Ethiopia and South Africa

Country	Sex	*N*		BW (g)	Lipid (%)	*pp*′-DDE	*op*′-DDD	*pp*′-DDD	*op*′-DDT	*pp*′-DDT	ΣDDTs
Ethiopia	Male	7	Geo-Mean	75	4.3	623 [18802]	17 [508]	973 [35564]	3 [324]	110 [3056]	1875 [58116]
			Range	35–197	2.8–6.7	206–1666	ND–70	343–7005	ND–33	49–413	667–9155
			Median	65	4.1	737	18	752	3	98	1289
	Female	14	Geo-Mean	93	3.4	931 [32130]	10 [1475]	1268 [35219]	2 [336]	191 [7163]	2657 [75735]
			Range	33–160	1.8–7.9	216–3746	ND–259	365–5268	ND–20	24–1165	817–7066
			Median	109	3.2	914	16	1249	1.5	168	2440
South Africa	Male	12	Geo-Mean	59	4.1	410 [25480]	5 [416]	432 [28408]	42 [1504]	37 [4977]	1379 [64054]
			Range	19–190	3.0–6.8	67–4427	ND–55	42–4733	12–165	ND–1278	173–5777
			Median	52	3.7	399	8	246	36	51	2131
	Female	12	Geo-Mean	90	4.2	306 [15630]	1 [121]	613 [38934]	35 [988]	72 [8768]	1389 [65380]
			Range	47–187	1.8–12.0	14–2296	ND–27	42–4828	14–79	24–1165	127–7334
			Median	82	4.4	610	ND	882	32	74	2470

N number of samples, *BW* body weight, *ND* below detection limit

197 g with a geometric mean of 86 g and had a fat content between 1.8 and 7.9% (geometric mean 3.7%). The house rats ($n = 24$) from Pongola area, South Africa, weighed from 19 to 190 g (geometric mean 73 g) and with fat content between 1.8 and 12% (geometric mean 4.1%). Of the 45 house rats, 14 from Ziway area and 12 from Pongola area were females. The female rats were generally larger than the males, while their lipid content were comparable with those of the males (Table 1). There were no significance differences ($p > 0.05$) in both body weight and lipid content between both sites and sexes.

Concentrations of DDTs

DDT and its metabolites residues were detected in all liver samples of rats in the present study. Concentrations of total DDTs (ΣDDTs) ranged from 127 to 9155 μg/kg wet weight (ww) (1775 to 215,748 μg/kg lipid weight (lw)) (Fig. 2). Median concentration ΣDDTs were comparable between the two sites, and concentrations were 2121 and 2214 μg/kg wet weight from Ethiopia and South Africa, respectively. In both sampling sites, high dispersion, in the levels of ΣDDTs, ranged from 667 to 9155 μg/kg ww in Ethiopia and from 127 to 7334 μg/kg ww in South Africa, was exhibited within the studied rat samples. This high variation on the magnitude of pollutants could be associated with age, metabolic capabilities, and duration of contamination. However, there was no significant difference in concentration of ΣDDTs between sites ($p > 0.05$).

Detailed statistical information such as geometrical mean, median, and range values of ΣDDT concentrations (based on wet weight) in the liver tissues is presented in Table 1. In both sites, female rats had higher geometrical mean concentrations of ΣDDTs than the males. This apparently contradicts the usual pattern observed in other mammals, where mature females are less polluted than males of comparable age due to the lactation transfer of lipophilic xenobiotics from mothers to offspring (Berghe et al. 2012; Lailson-Brito et al. 2012; Sørmo

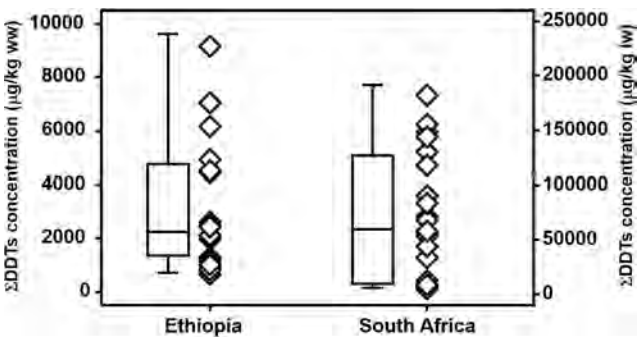

Fig. 2 Box and whisker plot (horizontal lines are fifth, 25th, 50th, 75th, and 95th percentiles) of ∑DDTs in liver tissues of house rats from Ethiopia and South Africa

et al. 2003). Although the female rats had higher geometric mean/median concentrations of ΣDDTs than male in both sites, no significant difference in ΣDDT concentration was found between sexes in both sampling site ($p > 0.05$). Overall, the accumulation of DDTs in the studied house rats reflects widespread DDT contamination within indoor and outdoor environment in these two countries.

Lipid content and body weight are important variable for explaining the concentrations of organochlorine compounds like DDTs in the ecosystem. In this study, lipid content instead of body weight was used to avoid bias due to the increased body weight of the pregnant rats and the variation in gut fullness. Thus, log-transformed values of each DDT concentrations were regressed against lipid content (%). With all data pooled for both sites, no significant relationships ($p > 0.05$) between the lipid levels (%) and log-transformed DDTs (μg/kg ww) were found, even within genders (data not shown). The lack of this significant relationship and sex-related differences in the present study might be due to the great variability of the individual DDT loads detected caused by the current use of DDT for IRS in the sampling places and reduced sample size.

Composition of DDTs

Basic descriptive statistics of DDT and its metabolite concentrations in rat liver are presented in Table 1. *p,p′*-isomers of DDT, DDE, and DDD and *o,p′*-isomers of DDT and DDD were detected in the investigated samples. The metabolite present at the highest concentration in the liver of the studied rat samples was *p,p′*-DDD with geometric mean concentration of 1268 μg/kg ww followed by *p,p′*-DDE (931 μg/kg ww) in female rats from Ethiopia (Table 1). In other studies, DDE is the main metabolite of DDT found in the liver and adipose tissues of mammals and birds (Lailson-Brito et al. 2012; Sørmo et al. 2003; Tomza-Marciniak et al. 2014; Yohannes et al. 2014b, 2017).

In the environment and in vivo, DDT can be degraded to DDE and DDD. Thus, the DDT profiles or composition index in biota may provide information on input (sources) in the ecosystem or metabolism of DDT in biota. Figure 3 shows the relative (%) distribution of DDT, DDD, and DDE in liver tissues of both sexes. The profile of DDTs in the studied livers was clearly dominated by *p,p′*-DDD, accounting for 45 to 66%, followed by *p,p′*-DDE (Fig. 3). The dominance of *p,p′*-DDD can be explained by a rapid metabolism of *p,p′*-DDT to *p,p′*-DDD in the rat liver tissue. An exposure study by Kitamura et al. (2002) has demonstrated that the metabolism of *p,p′*-DDT to *p,p′*-DDD in rat liver was favored through two processes: (i) mainly reductive, catalyzed by the microsomal CYP system in the presence of NADPH or NADH under anaerobic conditions; and (ii) via the catalytic action of the heme group of

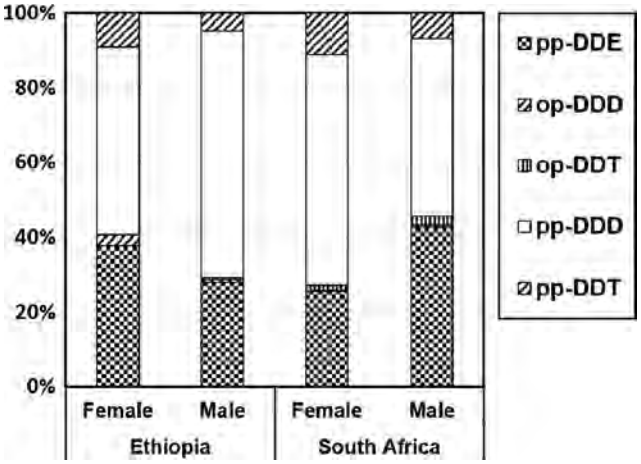

Fig. 3 Percentage distribution of individual DDT metabolites in liver tissues of house rats from Ethiopia and South Africa

hemoproteins in the liver microsomes of rats, it can also be reduced to *p,p′*-DDD in a non-enzymatically manner.

Generally, the accumulation profile of DDTs, i.e., DDD ≅ DDE >> DDT, highlighting the fact that *p,p′*-DDD and *p,p′*-DDE are resistance against degradation and elimination from the body of the rats, thus accumulated in the liver tissues. Nevertheless, *p,p′*-DDT was detected in almost all liver samples of the house rats, indicating the presence of fresh DDT source in these countries. Although internationally banned by the Stockholm Convention on Persistent Organic Pollutants, DDT use is exempted for IRS because of high incidence of malaria and corresponding fatalities in some African countries including Ethiopia and South Africa (WHO 2015), in addition to its unrestricted agricultural use.

Comparison with other wild terrestrial mammals

The present study data are important, because they represent, to the best of our knowledge, the first report of DDT residues in house rats from Ethiopia and South Africa, in general from Africa. The absence of data concerning residue levels in liver samples of rats rendered direct analogies extremely difficult. Thus, the residue levels of DDTs reported in other animals elsewhere in the world, and in birds and domestic chicken from the current sampling sites, are referred (Table 2). However, the species are different and interpretation should also be carefully done, as the usage of DDTs, species, nature of the sampled tissues, environment, dates, matrixes, and ecosystems differs widely. Some terrestrial animals have a great capacity to metabolize and eliminate DDTs. Recent literature data show the levels from Europe, where DDTs in wild animals (boar, badger, mongoose, etc.) are mostly detected. Concentrations of DDTs in liver tissues of house rats detected in the present study are higher than the concentrations reported in various wild mammals from Poland (2.13–1116 μg/kg ww) (Cholewa et al. 2015; Tomza-

Table 2 Comparison of DDT residues (range, μg/kg ww) in wild mammals and birds with the current study

Location	Species[a]	Sample	*pp*′-DDE	*pp*′-DDD	*pp*′-DDT	ΣDDTs	References
Ethiopia	Wild rat	Liver[c]	206–3746 3179–131,116	343–7005 4397–108,478	24–1165 1113–42,243	667–9155 12,755–215,748	This study
South Africa		Liver[c]	14–4427 396–120,186	42–4828 411–114,132	ND–1154 ND–38,702	127–7334 1775–156,804	This study
Poland	Coypu (river rat)	Liver	3				Cholewa et al. (2015)
Poland	Wild mammals[a]	Liver[c]	0.39–897.6	0.30–28.3	0.21–20.8	2.13–1116	Tomza-Marciniak et al. (2014)
Spain	Carnivores[a]	Liver[b]	5–2736	< 0.01–72.3			Mateo et al. (2012)
		Adipose tissue[b,c]	506–63,297	< 0.01–13.9	< 0.01–30.1		
Ethiopia	Wild bird[a]	Liver	100–4498	0.9–180	ND–21.6	103–4578	Yohannes et al. (2017)
South Africa	Wild bird[a]	Egg	3.2–870	ND–1.4	ND–4.2	3.2–870	Bouwman et al. (2008)
	Domestic chicken	Fat[c]	5000–12,000	2100–21,000	3500–12,000		Barnhoorn et al. (2009)
	Chicken	Egg	2600–31,000	ND–17	2300–17,000	5200–48,000	Bouwman et al. (2015)

ND below detection limit

[a] Species: *Poland*: raccoon dog (14), European badger (11), and wild boar (19); *Spain*: Iberian lynx (6), feral cat (2), red fox (16), Egyptian mongoose (10), common genet (4), and European badger (1); *Ethiopia*: hamerkop (5), African sacred ibis (7), marabou stork (5), and great white pelican (5); *South Africa*: cattle egret (20), African darter (14), reed cormorant (3), and African sacred ibis (2)

[b] Units were expressed as range of maximum values

[c] Values were expressed as μg/kg lw

Marciniak et al. 2014) and Spain (liver: < 0.01–2736 μg/kg ww; adipose tissue: < 0.01–63,297 μg/kg lw) (Mateo et al. 2012) (Table 2). Even comparing with other high trophic level predators, levels of DDTs in the present study are higher than the levels of DDTs found in the wild birds' liver from Ethiopia (Yohannes et al. 2017) and in egg samples of wild birds and chicken fat from South Africa (Bouwman et al. 2008; Barnhoorn et al. 2009). On the other hand, ΣDDT levels in the present study are lower than the levels of DDTs detected from domestic chicken egg (Bouwman et al. 2015) in a DDT-sprayed area from South Africa (Table 2). Care should also be taken to egg samples compared with liver, as the former samples have a higher lipid content, and also, there is transformation of DDT from liver to egg. Overall, the total DDT burden in the liver tissues of the house rats revealed that the sampling regions are contaminated more with DDT.

Potential ecological risks

House rats share the same environment with humans, where DDT is sprayed. Thus, the exposure data measured on rats can be (in)directly applied for risk assessment because many toxicological studies use rodent models. Toxic effects of DDT and its analogues, such as increment of liver weight, pathological alterations of liver, changes in serum estradiol and progesterone levels, and induction of liver cytochrome enzymes, have been studied in rats (Hojo et al. 2006; Li et al. 1995). The health of human and wildlife is relevant due to the process of bioaccumulation and biomagnification of organic pollutants through the predator–prey cycle.

Because of their persistence and excessive use in the past and the present, DDTs continue to be of serious environmental concern worldwide. In the present study, levels of DDTs ranged from 127 to 9155 μg/kg ww in the liver tissues of the house rats suggest that IRS may result in high DDT exposure in the entire population. Previous studies reported high concentrations of DDT and DDE in blood and breast milk from people residing in IRS houses (Aneck-Hahn et al. 2007; Bouwman et al. 2006; Röllin et al. 2009). Thus, the detection of high levels of DDTs in the present study provides additional input for monitoring health risk of human, in particular for pregnant women and children because they spend more time in and around the DDT-sprayed house. On the other hand, the hepatic levels of ∑DDT residues ranged from 1 to 35 μg/g reported to pose a threat to individual bird reproduction and therefore on the population (Blus 2011). Thus, it should be emphasized that birds of prey could be at high risk when preying on these rats with high levels of organic pollutants like DDTs. Wildlife and domestic animals that feed around the sprayed areas and agricultural areas could also be at risk, since DDTs can bioaccumulate and biomagnify through the predator–prey behavior on the food chain. In addition, DDT levels at a range of 5.5 to 910 ng/g ww, which is by far less than from the present study, showed a significant asymmetric testicular morphology in frogs from DDT-sprayed areas in South Africa (Viljoen et al. 2016). Generally, the DDTs that we found in the liver tissues of house rats may have contributed to DDT loads higher up in the food web. This finding supports the need to reduce and eventually terminate the use of DDT in malaria control program and to control its unrestricted agricultural use.

Conclusion

To the best of our knowledge, this is the first report on DDT and its metabolites levels in liver tissues of house rats from Ethiopia and South Africa. Although sample size was limited, the data in the present study clearly indicate the ubiquitous pollution of DDTs in the ecosystems of Ethiopia and South Africa. It stresses the need for further investigations and continuous monitoring of persistent organic pollutants such as OCPs, PCBs, and PBDEs. Even though IRS application has been regarded as an environmentally safer option in malaria vector control, the current result showed a concern for humans and wildlife. In addition, the domesticated animals kept near the homestead where DDT is applied could also be affected by the DDT used in IRS. Due to their importance for the ecosystems and their protection status, it is difficult to perform invasive tissue analyses in humans and wildlife. Thus, monitoring environmental health by using house rats as sentinels could be useful for inferring the state of higher organisms.

Acknowledgements This work was supported by Grants-in-Aid for Scientific Research from the Ministry of Education, Culture, Sports, Science and Technology of Japan awarded to M. Ishizuka (no. 16H0177906), Y. Ikenaka (no. 26304043, 15H0282505, 15K1221305), S. Nakayama (16K16197), and the foundations of JSPS Core to Core Program (AA Science Platforms) and the Bilateral Joint Research Project (PG36150002 and PG36150003). We also acknowledge the financial support by the Mitsui & Co., Ltd. Environment Fund; the Sumitomo foundation for Environmental Research Projects; the Soroptimist Japan Foundation; the Nakajima Foundation; and the Inui Memorial Trust for Research on Animal Science. The authors are grateful to thank the local people for allowing us to catch the house rats and Mr. Takahiro Ichise, Ms. Mio Yagihashi, and Ms. Nagisa Hirano for their technical support and great input throughout the research work.

Compliance with ethical standards All the experiments were performed in accordance with the guidelines approved by the Institutional Animal Care and Use Committee of Hokkaido University.

Conflict of interest The authors declare that they have no conflict of interest.

References

Aneck-Hahn NH, Schulenburg GW, Bornman MS, Farias P, de Jager C (2007) Impaired semen quality associated with environmental DDT

exposure in young men living in a malaria area in the Limpopo Province, South Africa. J Androl 28:423–434

Ardizzone M, Vizio C, Bozzetta E, Pezzolato M, Meistro S, Dondo A, Giorgi I, Seghesio A, Mirabelli D, Capella S, Vigliaturo R, Belluso E (2014) The wild rat as sentinel animal in the environmental risk assessment of asbestos pollution: a pilot study. Sci Total Environ 479-480:31–38

Barnhoorn IEJ, Bornman MS, Jansen van Rensburg C, Bouwman H (2009) DDT residues in water, sediment, domestic and indigenous biota from a currently DDT-sprayed area. Chemosphere 77:1236–1241

Berghe MV, Weijs L, Habran S, Das K, Bugli C, Rees JF, Pomeroy P, Cocaci A, Debier C (2012) Selective transfer of persistent organic pollutants and their metabolites in grey seals during lactation. Environ Int 46:6–15

Bhatia R, Shiau R, Petreas M, Weintraub JM, Farhang L, Eskenazi B (2005) Organochlorine pesticides and male genital anomalies in the child health and development studies. Environ Health Perspect 113(2):220–224

Blus JL (2011) DDT, DDD and DDE in birds. In: Beyer WN, Meador JP (eds) Environmental contaminants in biota-interpreting tissue concentrations. CRC Press, New York, pp 425–443

Bouwman H, Sereda B, Meinhardt HM (2006) Simultaneous presence of DDT and pyrethroid residues in human breast milk from a malaria endemic area in South Africa. Environ Pollut 144:602–917

Bouwman H, Polder A, Venter B, Skaare JU (2008) Organochlorine contaminants in cormorant, darter, egret, and ibis eggs from South Africa. Chemosphere 71:227–241

Bouwman H, Bornman R, Van Dyk C, Barnhoorn I (2015) First report of the concentrations and implications of DDT residues in chicken eggs from a malaria-controlled area. Chemosphere 137:174–177

Carson R (1962) Silent spring. Houghton Mifflin, Boston

Cholewa R, Beutling D, Budzyk J, Pietrzak M, Walorczyk S (2015) Persistent organochlorine pesticides in internal organs of coypu, *Myocastor coypus*. J Environ Sci Health B 50:590–594

Crews D, Willingham E, Skipper JK (2000) Endocrine disruptors: present issues, future directions. Q Rev Biol 75:243–260

Croghan C, Egeghy PP (2003) Methods of dealing with values below the limit of detection using SAS. Available online: http://analytics.ncsu.edu/sesug/2003/SD08-Croghan.pdf. (Accessed 16 July 2017)

Fisk AT, de Wit CA, Wayland M, Kuzyk ZZ, Burgess N, Letcher R, Braune B, Norstrom R, Blum SP, Sandau C, Lie E, Larsen HJS, Skaar JU, Muir DCG (2005) An assessment of the toxicological significance of anthropogenic contaminants in Canadian arctic wildlife. Sci Total Environ 351–352:57–93

Gerber R, Smit NJ, van Vuren JHJ, Nakayama SMM, Yohannes YB, Ikenaka Y, Ishizuka M, Wepener V (2016) Bioaccumulation and human health risk assessment of DDT and other organochlorine pesticides in an apex aquatic predator from a premier conservation area. Sci Total Environ 550:522–533

Giesy JP, Feyk LA, Jones PD, Kannan K, Sanderson T (2003) Review of the effects of endocrine-disrupting chemical in birds. Pure Appl Chem 75:2287–2303

Hojo H, Aoyama H, Takahashi KL, Shimizu N, Araki M, Takizawa Y, Sakasai K, Kuwahara M, Saka M, Teramoto S (2006) Two-generation reproduction toxicity study in rats with 1,1,1-trichloro-2,2-bis(4-chlorophenyl)ethane (*p,p′*-DDT). Congenit Anom Kyoto 46:105–114

Ishizuka M, Takasuga T, Senthil Kumar K, Tanikawa T, Fujita S (2005) Accumulation of persistent organochlorine pollutants and polybrominated diphenyl ether in wild rats, and toxicogenomic analyses of their effects. Organohalogen Compd 67:2435–2436

Kitamura S, Shimizu Y, Shiraga Y, Yoshida M, Sugihara K, Ohta S (2002) Reductive metabolism of *p,p′*-DDT and *o,p′*-DDT by rat liver cytochrome P450. Drug Metab Dispos 30:113–118

Lailson-Brito J, Dorneles PR, Azevedo-Silva CE, Bisi TL, Vidal LG, Legat LN, Azevedo AF, Torres JPM, Malm O (2012) Organochlorine compound accumulation in delphinids from Rio de Janeiro State, southeastern Brazilian coast. Sci Total Environ 433:123–131

Li HC, Dehal SS, Kupfer D (1995) Induction of the hepatic CYP2B and CYP3A enzymes by the proestrogenic pesticide methoxychlor and by DDT in the rat. Effects on methoxychlor metabolism. J Biochem Toxicol 10:51–61

Mateo R, Millán J, Rodríguez-Estival J, Camarero PR, Palomares F, Ortiz-Santaliestra ME (2012) Levels of organochlorine pesticides and polychlorinated biphenyls in the critically endangered Iberian lynx and other sympatric carnivores in Spain. Chemosphere 86:691–700

Röllin HB, Sandanger TM, Hansen L, Channa K, Odland JØ (2009) Concentration of selected persistent organic pollutants in blood from delivering women in South Africa. Sci Total Environ 408:146–152

Sørmo E, Skaare J, Lydersen C, Kovacs K, Hammill M, Jenssen B (2003) Partitioning of persistent organic pollutants in grey seal (*Halichoerus grypus*) mother–pup pairs. Sci Total Environ 302:145–155

Tomza-Marciniak A, Marciniak A, Pilarczyk B, Prokulewicz A, Bakowska M (2014) Interspecies comparison of chlorinated contaminant concentrations and profiles in wild terrestrial mammals from Northwest Poland. Arch Environ Contam Toxicol 66:491–503

Tyler CR, Jobling S, Sumpter JP (1998) Endocrine disruption in wildlife: a critical review of the evidence. Crit Rev Toxicol 28:319–361

UNEP (United Nations Environment Programme) (2016) Report of the DDT expert group on the assessment of the production and use of DDT and its alternatives for disease vector control. Sixth expert group meeting on DDT, 9 November 2016 Geneva, Switzerland. UNEP/POPS/DDT/EG.6/5

Van den Berg H (2009) Global status of DOT and its alternatives for use in vector control to prevent disease. Environ Health Perspect 17:1656–1663

Van Dyk JC, Bouwman H, Barnhoorn IEJ, Bornman MS (2010) DDT contamination from indoor residual spraying for malaria control. Sci Total Environ 408:2745–2752

Viljoen IM, Bornman R, Bouwman H (2016) DDT exposure of frogs: a case study from Limpopo Province, South Africa. Chemosphere 159:335–341

WHO (World Health Organization) (2011) The use of DDT in malaria vector control: WHO position statement. Geneva, Switzerland

WHO (World Health Organization) (2015) World Health Organization. World malaria report. Geneva

Yohannes YB, Ikenaka Y, Saengtienchai A, Watanabe KP, Nakayama SMM, Ishizuka M (2013) Occurrence, distribution, and ecological risk assessment of DDTs and heavy metals in surface sediments from Lake Awassa—Ethiopian Rift Valley Lake. Environ Sci Pollut Res 20:8663–8671

Yohannes YB, Ikenaka Y, Nakayama SMM, Ishizuka M (2014a) Concentrations and human health risk assessment of organochlorine pesticides in edible fish species from a Rift Valley lake—Lake Ziway, Ethiopia. Ecotoxicol Environ Saf 106:95–101

Yohannes YB, Ikenaka Y, Nakayama SMM, Ishizuka M (2014b) Organochlorine pesticides in bird species and their prey (fish) from the Ethiopian Rift Valley region, Ethiopia. Environ Pollut 192:121–128

Yohannes YB, Ikenaka Y, Nakayama SMM, Mizukawa H, Ishizuka M (2017) DDTs and other organochlorine pesticides in tissues of four bird species from the Rift Valley region, Ethiopia. Sci Total Environ 574:1389–1395

You L (2000) *p,p′*-DDE: an endocrine-active compound with the potential of multiple mechanisms of action. CIIT Activ 20:1–9

Chemosphere 186 (2017) 367–373

Contents lists available at ScienceDirect

Chemosphere

journal homepage: www.elsevier.com/locate/chemosphere

Lead exposure in raptors from Japan and source identification using Pb stable isotope ratios

Chihiro Ishii [a], Shouta M.M. Nakayama [a], Yoshinori Ikenaka [a, b], Hokuto Nakata [a], Keisuke Saito [c], Yukiko Watanabe [c], Hazuki Mizukawa [d], Shinsuke Tanabe [e], Kei Nomiyama [e], Terutake Hayashi [f], Mayumi Ishizuka [a, *]

[a] Laboratory of Toxicology, Department of Environmental Veterinary Sciences, Graduate School of Veterinary Medicine, Hokkaido University, Kita18, Nishi9, Kita-ku, Sapporo, Hokkaido, 060-0818, Japan
[b] Water Research Group, Unit for Environmental Sciences and Management, North-West University, Potchefstroom, South Africa
[c] Institute for Raptor Biomedicine Japan, 2-2101, Hokuto, Kushiro-shi, Hokkaido, 084-0922, Japan
[d] Department of Environmental Veterinary Sciences, Graduate School of Veterinary Medicine, Hokkaido University, Kita 18 Nishi 9, Kita-ku, Sapporo, Hokkaido, 060-0818, Japan
[e] Center for Marine Environmental Studies (CMES), Ehime University, Bunkyo-cho 2-5, Matsuyama, 790-8577, Japan
[f] Tochigi Prefectural Museum, 2-2, Mutsumi-cho, Utsunomiya, Tochigi, 320-0865, Japan

HIGHLIGHTS

- In Hokkaido, one quarter of sea eagles showed a high Pb concentration, suggesting exposure to abnormally high Pb levels.
- Pb isotope ratios indicated that sea eagles in Hokkaido were poisoned by Pb ammunition that were likely used illegally.
- Pb poisoning is still a serious problem in raptors in various areas of Japan due to accidental ingestion of Pb ammunition.

ARTICLE INFO

Article history:
Received 11 April 2017
Received in revised form
26 July 2017
Accepted 27 July 2017
Available online 28 July 2017

Handling Editor: Petra Petra Krystek

Keywords:
Pb poisoning
Raptor
Japan
Pb isotope ratios

ABSTRACT

Lead (Pb) poisoning is widespread among raptors and water birds. In Japan, fragments of Pb ammunition are still found in endangered eagles although more than 10 years have passed since legislation regarding use of Pb ammunition was introduced. This study was performed to investigate Pb exposure in raptors from various locations in Japan. We measured hepatic and renal Pb concentrations and hepatic Pb isotope ratios of Steller's sea eagles (*Haliaeetus pelagicus*), white-tailed sea eagles (*Haliaeetus albicilla*), golden eagles (*Aquila chrysaetos*), and 13 other species (total 177 individuals) that were found dead, as well as blood samples from three eagles found in a weakened state during 1993–2015 from Hokkaido (northern part), Honshu (the main island), and Shikoku (a southern island) of Japan. In the present study in Hokkaido, one quarter of the sea eagles showed a high Pb concentration, suggesting exposure to abnormally high Pb levels and Pb poisoning. Pb isotope ratios indicated that endangered Steller's sea eagle and white-tailed sea eagle were poisoned by Pb ammunition that was used illegally in Hokkaido. In other areas of Japan, both surveillance and regulations were less extensive than in Hokkaido, but Pb poisoning in raptors was also noted. Therefore, Pb poisoning is still a serious problem in raptors in various areas of Japan due to accidental ingestion of materials containing Pb, especially Pb ammunition.

1. Introduction

Lead (Pb) poisoning has been widespread among raptors and water birds (Fisher et al., 2006; Kendall et al., 1996; Kim et al., 1999; Kurosawa, 2000; Saito, 2009) since the 1870s (Rattner, 2009). Raptors mainly ingest fragments of Pb rifle bullets or shot pellets when consuming animals killed by hunters. Pb is dissolved rapidly

* Corresponding author. Laboratory of Toxicology, Department of Environmental Veterinary Sciences, Graduate School of Veterinary Medicine, Hokkaido University, N18, W9, Kita-ku, Sapporo, 060-0818, Japan.
E-mail address: ishizum@vetmed.hokudai.ac.jp (M. Ishizuka).

http://dx.doi.org/10.1016/j.chemosphere.2017.07.143
0045-6535/

in the stomach of raptors by the low-pH gastric acid and subsequently absorbed (Saito, 2009), exposing raptors to high Pb concentrations. Water birds also tend to accidentally ingest Pb from shot pellets or fishing sinkers when they swallow pebbles as gastroliths (Martinez-Haro et al., 2011; Pain et al., 2007).

Pb exposure causes neurological dysfunction, hematopoietic system dysfunction, immune suppression, reproductive impairment, and with accumulation of Pb at very high levels, it eventually leads to death. Even at low levels, Pb exposure deprives birds of bodily strength (Haig et al., 2014; Kendall et al., 1996; Saito, 2009). Poor health condition increases susceptibility to illness, making it difficult to accomplish migration. Pb exposure at non-lethal levels has been linked to other causes of death, such as traffic accidents (Saito, 2009). A significant positive association has been found between collision/electrocution/trauma and Pb contamination in raptors (Berny et al., 2015), and Pb exposure effects on reproduction in an avian model (Vallverdú-Coll et al., 2016). Therefore, Pb poisoning may be one of the causes for the decline in raptor populations mainly due to the death of raptors, and also poisoning inhibits their breeding activities and success.

Various types of wildlife—including endangered species—inhabit the six national parks in, Hokkaido, the northernmost island of Japan (Fig. S1 in Supplementary data). The world's Steller's sea eagle (*Haliaeetus pelagicus*) population is only 4600–5100, and white-tailed sea eagle (*Haliaeetus albicilla*) population is approximately 20300–39600 (IUCN, 2015). In Japan, 1400–1700 of Steller's sea eagles and 700–900 of white-tailed sea eagles migrate to Hokkaido to spend the winter (Ministry of the Environment, Japan, 2016, *in Japanese*). Both types of sea eagle are protected with the "Act on Conservation of Endangered Species of Wild Fauna and Flora" in Japan from 1993 (Ministry of the Environment, Japan).

In Hokkaido, the population of sika deer (*Cervus nippon yesoensis*) has been increasing, and the government encourages people to control the number of deer. Hunters have used Pb rifle bullets to hunt sika deer, as a consequence raptors have been exposed to Pb by consuming deer carcasses containing Pb fragments (Iwata et al., 2000; Kim et al., 1999; Kurosawa, 2000). It is reported that Pb poisoning accounted for 79% of all deaths of these types of eagles in winter 1998–1999 (26 of 33 cases) (Saito, 2009). Therefore, Pb rifle bullets and shot pellets for hunting sika deer have been prohibited since 2000 and 2001, respectively. After the regulation, hunters were required to use much less toxic material, such as copper (Cu) instead of Pb ammunition. However, the incidence of Pb poisoning in the total number of raptor deaths remained high (69% in winter 2001–2002, 11 of 16 cases reported by Wildlife Preservation Bureau of Hokkaido Corporation, and Saito (2009)). In 2004, an extended ban was implemented in Hokkaido, which prohibited the use of any type of Pb containing ammunition for hunting of large-sized animal species.

In other areas of Japan, such as Honshu (the main island) and Shikoku (a southern island), there are few regulations regarding the use of Pb containing ammunition and the current situation of Pb poisoning is unknown. Moreover, Pb ammunition is still used in these areas. The golden eagle (*Aquila chrysaetos*), which inhabits Honshu, is an endangered species with a population of only 500 in Japan (Kyodo, 2015).

Pb poisoning in wild birds is still being reported worldwide (Haig et al., 2014; Langner et al., 2015; Madry et al., 2015), even though some countries, such as the USA and Denmark, have introduced regulations to curb the incidence of such poisoning (Finkelstein et al., 2014; Mateo, 2009). Therefore, it is necessary to accurately determine the occurrence of Pb poisoning in raptors to develop appropriate regulations for their conservation.

There are many sources of Pb poisoning, and Pb isotope ratios (Pb isotope ratios; $^{207}Pb/^{206}Pb$, and $^{208}Pb/^{206}Pb$ values) are useful for identifying possible exposure sources (Church et al., 2006; Komárek et al., 2008; Pain et al., 2007; Scheuhammer and Templeton, 1998). There are four stable isotopes of Pb: ^{204}Pb, ^{206}Pb, ^{207}Pb, and ^{208}Pb. The combination of $^{208}Pb/^{206}Pb$ and $^{207}Pb/^{206}Pb$ ratios differs depending on the original source of Pb.

This study was performed to investigate the occurrence of Pb exposure in raptors from various locations in Japan and to identify the sources of Pb by using stable isotope ratios. We measured hepatic and renal Pb concentrations and hepatic Pb isotope ratios of Steller's sea eagles, white-tailed sea eagles, golden eagles, and 13 other species (total 177 individuals) that were found dead, as well as blood samples from three eagles found in a weakened state during 1993–2015 in Hokkaido, Honshu, and Shikoku in Japan.

2. Materials and methods

2.1. Sampling

Samples of birds that died in nature, in medical centers for wild birds, and carcasses kept in museums or universities were collected from various areas in Japan for analysis of Pb concentration and Pb isotope ratios. The liver and kidney samples of white-tailed sea eagle ($n = 51$), Steller's sea eagle ($n = 47$), Blakiston's fish owl (*Ketupa blakistoni*) ($n = 13$), mountain hawk eagle (*Spizaetus nipalensis*) ($n = 7$), northern goshawk (*Accipiter gentilis*) ($n = 6$), sparrow hawk (*Accipiter nisus*) ($n = 2$), peregrine falcon (*Falco peregrinus*) ($n = 1$), and black kite (*Milvus migrans*) ($n = 1$), as well as blood samples from a mountain hawk eagle ($n = 1$) and a white-tailed sea eagle ($n = 1$), were collected by the Institute for Raptor Biomedicine Japan and Shiretoko Museum in the eastern part of Hokkaido, Japan, from 1998 to 2015. From Honshu and Shikoku, liver samples of golden eagle ($n = 13$), northern goshawk ($n = 9$), black kite ($n = 9$), ural owl (*Strix uralensis*) ($n = 4$), sparrow hawk ($n = 2$), brown hawk owl (*Ninox scutulata*) ($n = 2$), mountain hawk eagle ($n = 1$), peregrine falcon ($n = 1$), osprey (*Pandion haliaetus*) ($n = 1$), grey-faced buzzard (*Butastur indicus*) ($n = 1$), Japanese sparrow hawk (*Accipiter gularis*) ($n = 1$), common kestrel (*Falco tinnunculus*) ($n = 1$), and Sunda scops owl (*Otus lempiji*) ($n = 1$), as well as a blood sample from a golden eagle ($n = 1$), were collected by the Environmental Specimen Bank (*es*-BANK) of Ehime University, Tochigi Prefectural Museum, and the Institute for Raptor Biomedicine Japan from 1993 to 2015. Blood samples were collected from three eagles (mountain hawk eagle, and white-tailed sea eagle from Hokkaido, and golden eagle from Honshu) that were found in a weakened state and were treated at the animal hospital. Samples were transported to the Graduate School of Veterinary Medicine, Hokkaido University, Sapporo, Japan. All samples were preserved −20 °C until analysis. The age of raptors was estimated by the morphological characteristics, such as the development of the gonad and the feather, and the color of their feather and the iris. The condition of their molting was also determined to estimate their age.

As Pb ammunition; three shot pellets (one is from a hunter, and the other two are from the carcasses of birds), three rifle bullets (one is silver chip from the hunter, and the others are unknown from the stomach of raptors), three slugs (one is produced by Federal, another one is unknown that was found in the stomach of raptor, and the other is from the ground), and one air gun bullet (from the ground) and one sinker (from a fisherman) were also collected to compare Pb isotope ratios with the raptor tissues.

2.2. Pb analysis

Pb concentrations were analyzed according to the method of

Yabe et al. (2015). Samples of 100–300 mg of soft tissues were used for the analysis. Subsequently, samples were digested with 5 mL of 30% nitric acid (Kanto Chemical Corporation, Tokyo, Japan) and 1 mL of 30% hydrogen peroxide (Kanto Chemical Corporation) in a microwave digestion system (Speed wave Two; Berghof, Eningen, Germany), after which the volume was brought to 10 mL with 2% nitric acid. Digestion was performed under the following conditions: 180 °C for 15 min, 200 °C for 20 min, and 100 °C for 20 min. Concentration and isotope ratios of Pb were measured with an inductively coupled plasma–mass spectrometer (ICP-MS) (7700 series; Agilent Technology, Tokyo, Japan). The instrument was calibrated using ICP-MS Calibration Standards (Agilent Technology) to establish standard curves before analysis. Standard solutions (0, 10, 50, 100, 250, 500 μg/L) were prepared with 2% nitric acid and the R^2 value of the linear regression line was 0.998. All chemicals and standard stock solutions were of analytical reagent grade (Wako Pure Chemicals Industries, Osaka, Japan). Water was distilled and deionized (Milli-Q; Merck Millipore, Billerica, MA). Analytical quality control was performed using DOLT-4 (dogfish liver) and DORM-3 (fish protein) certified reference material (National Research Council of Canada, Ottawa, Canada). Replicate analysis of these reference materials showed good recoveries (95%–105%). The limit of detection for Pb was 0.01 μg/kg. For the analysis of Pb concentration, Thallium (^{205}Tl) was used as internal standard, but not for the isotope ratio analyses.

Analysis of Pb isotope ratios was performed according to the method of Nakata et al. (2015). Dissolved samples were diluted to Pb concentration <25 μg/L with 2% nitric acid. NIST SRM 981 (National Institute of Standards and Technology, Gaithersburg, MD) was used as a standard reference material for the external standardization of Pb isotopes. Detailed analytical conditions are shown in Table S1. The relative standard deviation (RSD) of the ratios was found to be <0.5% for both ^{207}Pb/^{206}Pb and ^{208}Pb/^{207}Pb. Samples where the RSD value exceeded 0.5% were excluded from the analysis. Standard solutions were measured every 10 samples to correct calibration.

2.3. Assessment of Pb exposure

Various thresholds for Pb toxicity in birds have been reported in the literature (Fisher et al., 2006; Kendall et al., 1996; Kim et al., 1999; Kurosawa, 2000; Saito, 2009). Background level of Pb in the liver of avian is generally <2 mg/kg wet weight (6–7 mg/kg dry weight) or < 1 mg/kg wet weight (3 mg/kg dry weight). The level of >6 mg/kg dry weight indicates abnormally high exposure to Pb and >20 mg/kg dry weight indicates acute exposure and absorption, resulting in Pb poisoning (Pain et al., 1995; Pain and Amiardtriquet, 1993). The categories used in Japan are as follows; hepatic Pb concentration in wet weight: < 0.2 mg/kg, normal range; 0.2–2 mg/kg, high level of Pb exposure; and >2 mg/kg, Pb poisoning. In the blood, Pb concentration in raptors by wet weight is used: < 0.1 mg/kg, normal range; 0.1–0.6 mg/kg, high level of Pb exposure; and >0.6 mg/kg, Pb poisoning (Saito, 2009).

2.4. Statistics

For comparison of Pb concentrations among species, sexes, and ages of Steller's sea eagles and white-tailed sea eagles, data were analyzed using the Mann–Whitney *U* test (for species, and sexes) or Steel-Dwass test (for ages) with a significance level at $p < 0.05$. Statistical analyses were performed in JMP Pro 11 (SAS Institute, Cary, NC).

3. Results

3.1. Pb concentrations in the liver, kidney, and blood samples of raptors from Hokkaido

Table 1 shows the median hepatic Pb concentrations in the studied raptors from Hokkaido. The results indicated that Pb accumulation in 42% of Steller's sea eagles (18 of 43 cases) and 24% of white-tailed sea eagles (12 of 50 cases) from Hokkaido exceeded the level of Pb poisoning (>2 mg/kg wet weight in liver). They were collected after the regulation was introduced in 2004, which prohibited the use of any type of Pb ammunition for hunting of large-sized animal species. The Steller's sea eagle had a higher ratio of Pb poisoning than the white-tailed sea eagle, although their Pb levels were not significantly different. Data regarding age, sex, and Pb concentrations (liver, kidney, and blood) are shown in Table S2. In these raptors, renal Pb levels were also high. Blood samples collected after the regulation from one mountain hawk eagle and one white-tailed sea eagle also showed high Pb concentrations (0.38 and 0.16 mg/kg wet weight, respectively). The hepatic Pb levels in the present study were comparable to previous data obtained from 1995 to 1998 (Table S3).

One Steller's sea eagle that died in 2013 was examined by postmortem radiography (Fig. 1), and the slightly large and pointed fragment that indicated a rifle bullet was found in the stomach. Measurements of metal concentrations showed that the bullet fragment was almost entirely (>90%) composed of Pb. Hepatic Pb level (36.3 mg/kg, wet weight) showed that this raptor died due to Pb poisoning. Pb concentration in the kidney was also high (Table S2). Furthermore, hair of sika deer was found in the stomach of the eagle, indicating this bird ate sika deer.

The ratio of Pb poisoning in adults and sub-adults was significantly higher than in juveniles of the Steller's sea eagle (Table 2). The white-tailed sea eagle showed similar pattern of Pb accumulation depending on their ages, although not statistically significant. There were no significant differences between males and females ($p = 0.42$) in either the Steller's sea eagle or the white-tailed sea eagle (data not shown).

3.2. Pb concentrations in the liver, kidney, and blood samples s of raptors from Honshu and Shikoku

The liver sample of one golden eagle exceeded the level of Pb poisoning (Table 3). Hepatic Pb concentration of another golden eagle, one black kite, and one northern goshawk, and the blood Pb concentration of one golden eagle (0.14 mg/kg, wet weight) showed accumulation of high Pb concentrations, indicating Pb exposure. Although the number of kidney samples was limited, Pb level was almost the same between liver and kidney. Data regarding age, sex, and Pb concentrations (liver, kidney, and blood) are shown in Table S2.

3.3. Pb isotope ratios

The distributions of Pb isotope ratios (^{208}Pb/^{206}Pb, ^{207}Pb/^{206}Pb) in various types of rifle bullets (1.90–2.10, 0.75–0.88), shot pellets (2.07–2.14, 0.85–0.87), and sinkers (2.08–2.20, 0.84–0.90), which were obtained from the shops in Japan, were reported in 2002. These materials had been purchased or collected from the carcasses or birds until 2001. It was confirmed that Pb isotope ratios of Pb rifle bullets, shot pellets and fishing sinkers used in 2015 by hunters or fishers in Japan were comparable (Fig. 2). Although it is difficult to distinguish between Pb shot pellets, slugs, hollow-point, air gun bullets, and sinkers due to the close distribution of Pb isotope ratios between them, Pb ratios from rifle bullets were almost distinct

Table 1
Hepatic Pb levels (mg/kg, wet weight, range) and the assesments of Pb exposure in raptors from Hokkaido after the regulation.

Species	Sample size	Pb concentration in liver	Assessments		
		mg/kg, wet wt, median, (range)	Pb poisoning (>2.0 mg kg)	High Pb exposure (0.2–2.0 mg/kg)	Non toxic (<0.2 mg/kg)
Steller's sea eagle	43	0.12 (ND - 36.6)	18	2	23
White-tailed sea eagle	50	0.06 (ND - 56.4)	12	4	34
Blakiston's fish owl	13	0.01 (ND - 0.04)	0	0	13
Mountain hawk eagle	7	0.01 (ND - 0.09)	0	0	7
Northern goshawk	6	0.01 (ND - 0.04)	0	0	6
Sparrowhawk	2	-(ND - 0.04)	0	0	2
Peregrine falcon, Black kite	1, each species	0.07 (0.01–0.12)	0	0	2

ND: non detectable (The limit of detection for Pb was 0.01 μg/L in digested solution.).

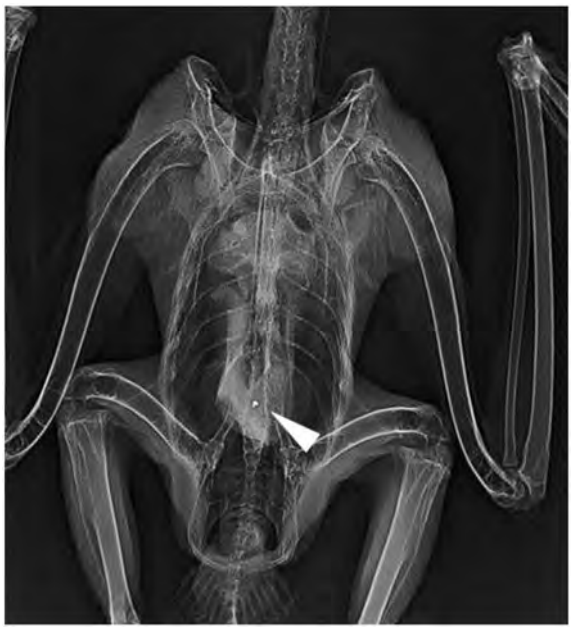

Fig. 1. A X-ray photograph (ventrodorsal) of 1 the Steller's sea eagle specimen that died in 2013 (provided by the Institute for Raptor Biomedicine Japan (IRBJ)). The stomach contained a bullet fragment as indicated with the white arrow.

among ammunition. Pb isotope ratios of slugs were different among three specimens, suggesting that the original source regions for the Pb present in these slugs were different.

Table 2
Hepatic concentrations of Pb depending on age in Steller's sea eagle and White-tailed sea eagle.

Species	Age	Sample size	Pb concentration in liver
			mg/kg, wet wt, median, (range)
Steller's sea eagle	ad.	22	2.5 (ND –36.6) †
	sub.	8	17.2 (0.02–23.8) ‡
	juv.	13	0.01 (ND –3.7)†, ‡
	unk.	0	
White-tailed sea eagle	ad.	18	0.1 (0.01–53.7)
	sub.	19	0.1 (ND –56.4)
	juv.	10	0.02 (ND –10.8)
	unk.	3	0.1 (ND –0.24)

ad.: adult; sub.: sub-adult; juv.: juvenile; unk.: unknown; ND: non detectable (The limit of detection for Pb was 0.01 μg/L in digested solution.).
Steel-Dwass test for each age was used.
†: Significantly ($p < 0.01$) different between adults and juvenile in Steller's sea eagle.
‡: Significantly ($p < 0.01$) different between sub-adults and juvenile in Steller's sea eagle.

We determined the Pb isotope ratios in the liver and the rifle bullets/shot pellets found in the stomach of the same individual ($n = 4$). In three sea eagles, Pb isotope ratios in the liver and the ammunition inside the stomach were comparable (Fig. 3), whereas one eagle showed different Pb isotope ratios between the liver and the ammunition (indicated in green, triangle). Fig. 4 shows the Pb isotope ratios in the liver of poisoned raptors.

The result shows that Steller's sea eagles were mainly poisoned by Pb rifle bullets, white-tailed sea eagles were poisoned by various types of ammunition or sinkers. Golden eagles were poisoned by Pb rifle bullets and other ammunition or sinkers, and black kite and northern goshawk were poisoned by Pb shot pellets, slugs, small rifle bullets, or sinkers (all data including normal Pb levels are shown in Fig. S2).

4. Discussion

In the present study, one quarter of the sea eagles from Hokkaido showed high Pb concentration of >2 mg/kg wet weight in the liver, suggesting that these birds had been exposed to abnormally high Pb levels and suffered from Pb poisoning (Table 1). In addition, the Steller's sea eagle death in 2013 was suspected to be from Pb poisoning because X-ray and post-mortem examination showed that the stomach contained a rifle bullet fragment (Fig. 1). This eagle accumulated high Pb levels in both the liver and the kidney, indicating that these tissues would have had severe damage due to Pb exposure. Although more than 10 years have passed since the legislation regarding Pb ammunition was introduced, some hunters are still using Pb containing ammunition because they believe that Pb ammunition has stronger power than other types of ammunition, or the price of Pb ammunition is slightly inexpensive.

Pb poisoning in adults and sub-adults was higher than in juveniles of sea eagles (Table 2) because adults begin to consume their prey prior to juveniles. It means that adults have more opportunities to ingest Pb fragments, as they eat at locations on the carcasses of animals killed by Pb containing ammunition. Furthermore, Steller's sea eagles had a higher ratio of Pb poisoning than white-tailed sea eagles. This result may be due to several factors. First, although the sea eagles naturally consume fish, they have changed their major food source to deer carcasses in Hokkaido (Saito, 2009), and this tendency is particularly strong in the Steller's sea eagle. Second, as the body size of Steller's sea eagle is larger than that of the white-tailed sea eagle, it probably out-competes the white-tailed sea eagle at carcasses. This trend might be a reason for a higher risk of ingesting Pb ammunition in Steller's sea eagle compared to the other species. Naturally, sea eagles consume fish, they have opportunities to eat sika deer carcasses in Hokkaido, because hunters leave carcasses or the deer are killed by trains (Saito, 2009). It is prohibited to leave the carcasses on the ground. However, some hunters take only a small portion of muscle to eat

Table 3
Hepatic Pb levels (mg/kg, wet weight, range) and the assesments of Pb exposure in raptors from Honshu and Shikoku.

Species	Sample size	Pb concentration in liver	Assessments		
		mg/kg, wet wt, median, (range)	Pb poisoning (>2.0 mg kg)	High Pb exposure (0.2 −2.0 mg/kg)	Non toxic (<0.2 mg/kg)
Golden eagle	13	0.04 (0.01−2.3)	1	1	11
Northern goshawk	9	0.02 (0.01−0.35)	0	1	8
Black kite	9	0.05 (0.02−0.42)	0	1	8
Ural owl	4	0.02 (0.01−0.03)	0	0	4
Sparrowhawk	2	0.04 (0.02−0.06)	0	0	2
Brown hawk owl	2	0.08 (0.02−0.13)	0	0	2
Mountain hawk eagle, Peregrine falcon, Osprey, Grey-faced buzzard, Japanese sparrowhawk, Common kestrel, Sunda scops owl	1, each species	0.01 (ND - 0.04)	0	0	7

ND: non detectable (The limit of detection for Pb was 0.01 μg/L in digested solution.).

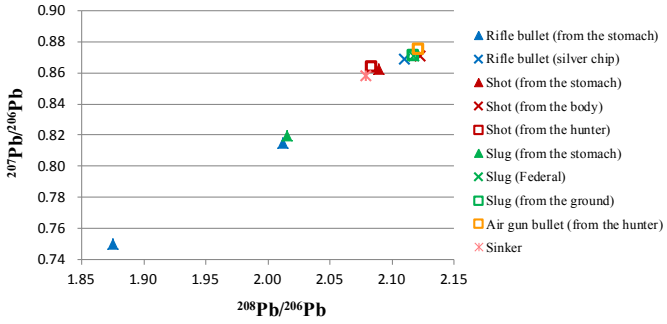

Fig. 2. Pb isotope ratios in ammunition currently being used.

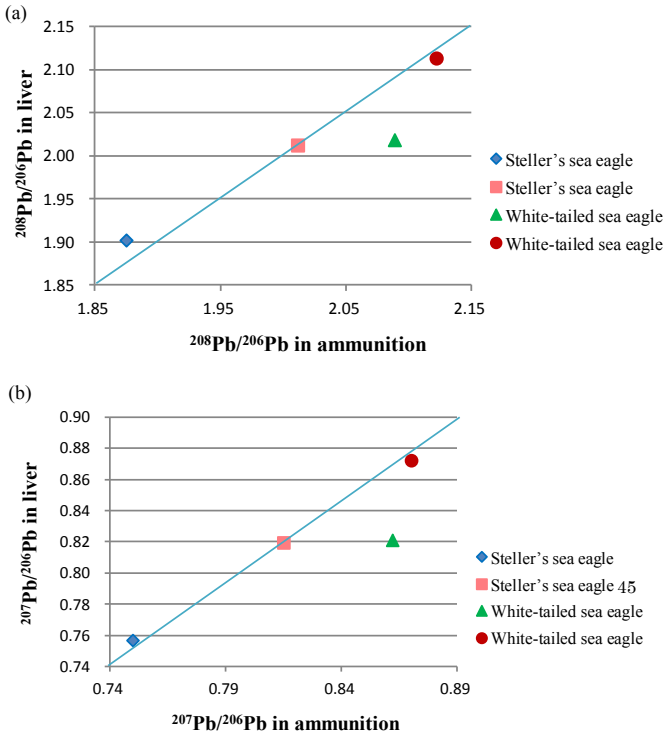

Fig. 3. Comparison of Pb isotope ratios of $^{208}Pb/^{206}$ Pb (a) or $^{207}Pb/^{206}Pb$ (b) between the liver and the ammunition found in the stomach from the same individual of raptors.

and leave the rest. Others take only one carcass and leave other carcasses due to limited human labor or a space in a light truck, although most hunters follow the regulation. Several cities give grants to hunters for culling harmful beasts. Therefore, hunters try to hunt sika deer as many as possible. There are also several hunters who think that it could be enough if they reduce the number of harmful beasts to protect farm products, and trees, and they leave the carcasses.

In 2014, the regulation was enforced in Hokkaido that prohibited the possession of Pb rifle bullets, slugs, or large shot pellets for hunting. Prior to this regulation, it was not illegal for hunters to keep Pb ammunition, but they were punished if they were found to use such ammunition. The new regulation aimed to improve this situation. However, the livers of four sea eagles showed high Pb concentrations at fatal levels and the blood of one mountain hawk eagle accumulated high concentration of Pb in 2015 (Table S2), indicating that the regulations are not yet effective or another path of Pb ingestion is possible.

The results from Honshu and Shikoku showed that Pb exposure in raptors also occurred in these areas (Table 3). The golden eagle, black kite, and most northern goshawks are resident birds. The results suggest that there is wider raptor Pb exposure in Japan. Many hunters use Pb ammunition for hunting wild animals, such as wild boar (*Sus scrofa*) or waterfowl. In Honshu, the Japanese black bear (*Ursus thibetanus japonicas*) was reported to accumulate high Pb concentrations, which suggests that they ingested Pb bullet or shot pellet fragments from their prey (Sato et al., 2007).

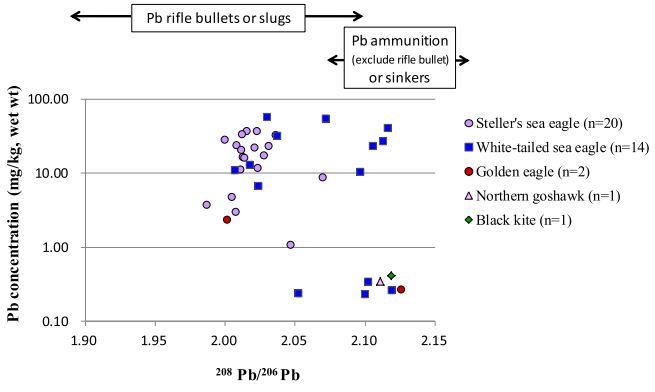

Fig. 4. Comparison of Pb levels and Pb isotope ratio ($^{208}Pb/^{206}Pb$, RSD < 0.5) in the liver of raptors that had high Pb concentration (> 0.2 mg/kg, wet weight). Comparison of Pb levels and $^{208}Pb/^{206}Pb$ or $^{207}Pb/^{206}$ Pb of all samples including normal Pb levels are shown in Fig. S2.

In Honshu and Shikoku, the use of Pb ammunition was restricted in certain locations, such as a wetland designated by the Ramsar Convention and its surrounding area. Moreover, Japan has conducted only a few studies of Pb poisoning of birds in these islands. Our results may only represent a fraction of the actual number of cases of Pb poisoning. The prevalence of Pb poisoning is not well known due to the shortage of data. Therefore, it is crucial to conduct further analyses of Pb concentrations in raptors and to determine the present state of Pb pollution, both in Hokkaido and in other parts of Japan.

Pb isotope ratios in the liver and the ammunition found in the stomach of the same individual showed that isotope ratios in liver would reflect those of ingested ammunition itself. One eagle had different Pb isotope ratios between the liver and ammunition (Fig. 3, indicated in green and triangle), indicated that this eagle had been exposed to Pb from one source (e.g. rifle bullets) and then subsequently ingested Pb from another source (e.g. shot pellets). Although Pb isotope ratios in the liver do not always indicate recently ingested ammunition, those in liver can be used to indicate the source of Pb exposure in many cases.

From the results of Pb isotope ratios in the liver of poisoned raptors, sea eagles were still contaminated by illegal Pb ammunition in Hokkaido (Fig. 4). The black kite also eats large animals, so it is also possible they were poisoned by rifle bullets. Therefore, all Pb ammunition and sinkers have a risk of causing Pb poisoning in all parts of Japan.

Some areas, such as California, have legislations against using Pb shot pellets as a means of combating Pb poisoning. Nevertheless, Pb poisoning persisted in the population of California condors (*Gymnogyps californianus*) despite a ban on Pb ammunition introduced in 2008 in some regions where condors had been reintroduced (Finkelstein et al., 2012). Therefore, an expanded legislation that requires hunters to use non-lead ammunition was signed into law by the governor of California on October 11, 2013, for implementation no later than July 2019. As an alternative, Pb-free ammunition, such as Cu bullets, have almost the same efficiency for hunting as Pb ammunition (Knott et al., 2009; Thomas, 2013; Trinogga et al., 2013) and is less toxic to raptors (Franson et al., 2012). The modern international trend in hunting to use monolithic Cu or brass rifle bullets for large animals will likely take a long time to replace Pb rifle bullets due to higher cost.

5. Conclusions

In the present study, one quarter of the sea eagles from Hokkaido showed high Pb concentrations, suggesting that these birds were exposed to abnormally high Pb levels and suffered from Pb poisoning although more than 10 years have passed since the regulation was introduced. In other areas of Japan, both surveillance and regulation were less strict than in Hokkaido, and there was also Pb exposure in raptors in these areas. In addition, Pb isotope ratios showed that about half of Pb-poisoned raptors, mainly endangered Steller's sea eagles and white-tailed sea eagles, were exposed to the possible illegal use of Pb rifle bullets in Hokkaido. The number of identified cases of Pb poisoning in raptors found dead could be only a fraction of the actual cases because of the wildlife behavior. Therefore, it is necessary to accurately determine the situation to develop appropriate regulations for the conservation of wild birds.

Acknowledgments

We would like to express our appreciation to Yasushi Masuda, Kazuo Jin, and Kentaro Q Sakamoto for the provision of samples. This work was supported by Grants-in-Aid for Scientific Research from the Ministry of Education, Culture, Sports, Science and Technology of Japan awarded to M. Ishizuka (No. 16H0177906), Y. Ikenaka (No. 26304043, 15H0282505, 15K1221305), S. Nakayama (16K16197), and the foundations of Sumitomo and JSPS Core to Core Program (AA Science Platforms) and Bilateral Joint Research Project (PG36150002 and PG36150003). We also acknowledge the financial support by the Nihon Seimei Foundation, the Soroptimist Japan Foundation, the Nakajima Foundation, and the Inui Memorial Trust for Research on Animal Science. One of the authors (C. Ishii) is a Research Fellow of the Japan Society for the Promotion of Science (No. 15J01937). This research was also supported by JST/JICA, SATREPS (Science and Technology Research Partnership for Sustainable Development), and the Ministry of Education, Culture, Sports, Science and Technology, Japan (MEXT) to a project on Center of Excellence for Cooperative and Collaborative Studies – Leading Academia in Marine and Environmental Research (LaMer), Ehime University. We are grateful to Takahiro Ichise, Mio Yagihashi, and Nagisa Hirano for their technical support.

Appendix A. Supplementary data

Supplementary data related to this article can be found at http://dx.doi.org/10.1016/j.chemosphere.2017.07.143.

References

Berny, P., Vilagines, L., Cugnasse, J.-M., Mastain, O., Chollet, J.-Y., Joncour, G., Razin, M., 2015. Vigilance poison: illegal poisoning and lead intoxication are the main factors affecting avian scavenger survival in the Pyrenees (France). Ecotoxicol. Environ. Saf. 118, 71–82.

Church, M.E., Gwiazda, R., Risebrough, R.W., Sorenson, K., Chamberlain, C.P., Farry, S., Heinrich, W., Rideout, B.A., Smith, D.R., 2006. Ammunition is the principal source of lead accumulated by California condors re-introduced to the wild. Environ. Sci. Technol. 40, 6143–6150.

Finkelstein, M.E., Doak, D.F., George, D., Burnett, J., Brandt, J., Church, M., Grantham, J., Smith, D.R., 2012. Lead poisoning and the deceptive recovery of the critically endangered California condor. Proc. Natl. Acad. Sci. http://dx.doi.org/10.1073/pnas.1203141109.

Finkelstein, M.E., Kuspa, Z.E., Welch, A., Eng, C., Clark, M., Burnett, J., Smith, D.R., 2014. Linking cases of illegal shootings of the endangered California condor using stable lead isotope analysis. Environ. Res. 134, 270–279.

Fisher, I.J., Pain, D.J., Thomas, V.G., 2006. A review of lead poisoning from ammunition sources in terrestrial birds. Biol. Conserv. 131, 421–432. http://dx.doi.org/10.1016/j.biocon.2006.02.018.

Franson, J.C., Lahner, L.L., Meteyer, C.U., Rattner, B.A., 2012. Copper pellets simulating oral exposure to copper ammunition: absence of toxicity in American kestrels (Falco sparverius). Arch. Environ. Contam. Toxicol. 62, 145–153.

Haig, S.M., D'Elia, J., Eagles-Smith, C., Fair, J.M., Gervais, J., Herring, G., Rivers, J.W., Schulz, J.H., 2014. The persistent problem of lead poisoning in birds from ammunition and fishing tackle. Condor 116, 408–428. http://dx.doi.org/10.1650/CONDOR-14-36.1.

Iwata, H., Watanabe, M., Kim, E.-Y., Gotoh, R., Yasunaga, G., Tanabe, S., Masuda, Y., Fujita, S., 2000. Contamination by chlorinated hydrocarbons and lead in Steller's sea eagle and white-tailed sea eagle from Hokkaido, Japan. In: First Symposium on Stellar's and White-Tailed Sea Eagles in East Asia. Wild Bird Society of Japan, Tokyo, pp. 91–106.

Kendall, R.J., Lacker, T.E., Bunck, C., Daniel, B., Driver, C., Grue, C.E., Leighton, F., Stansley, W., Watanabe, P.G., Whitworth, M., 1996. An ecological risk assessment of lead shot exposure in non-waterfowl avian species: upland game birds and raptors. Environ. Toxicol. Chem. 15, 4–20. http://dx.doi.org/10.1002/etc.5620150103.

Kim, E.-Y., Goto, R., Iwata, H., Masuda, Y., Tanabe, S., Fujita, S., 1999. Preliminary survey of lead poisoning of Steller's sea eagle (Haliaeetus pelagicus) and white-tailed sea eagle (Haliaeetus albicilla) in Hokkaido. Jpn. Environ. Toxicol. Chem. 18, 448–451. http://dx.doi.org/10.1002/etc.5620180312.

Knott, J., Gilbert, J., Green, R.E., Hoccom, D.G., 2009. Comparison of the lethality of lead and copper bullets in deer control operations to reduce incidental lead poisoning; field trials in England and Scotland. Conserv. Evid. 6, 71–78.

Komárek, M., Ettler, V., Chrastný, V., Mihaljevič, M., 2008. Lead isotopes in environmental sciences: a review. Environ. Int. 34, 562–577.

Kurosawa, N., 2000. Lead poisoning in Steller's sea eagles and white-tailed sea eagles. In: First Symposium on Stellar's and White-Tailed Sea Eagles in East Asia. Wild Bird Society of Japan, Tokyo, pp. 107–109.

Kyodo, 2015. The Japan Times NEWS Website; http://www.japantimes.co.jp/news/2015/03/16/national/japanese-golden-eagles-face-extinction-as-numbers-dive [WWW Document]. Japan Times NEWS Website. URL http://www.japantimes.co.jp/news/2015/03/16/national/japanese-golden-eagles-face-extinction-as-

numbers-dive/.
Langner, H.W., Domenech, R., Slabe, V.A., Sullivan, S.P., 2015. Lead and mercury in fall migrant golden eagles from western north America. Arch. Environ. Contam. Toxicol. 1–8.
Madry, M.M., Kraemer, T., Kupper, J., Naegeli, H., Jenny, H., Jenni, L., Jenny, D., 2015. Excessive lead burden among golden eagles in the Swiss Alps. Environ. Res. Lett. 10, 34003.
Martinez-Haro, M., Taggart, M.A., Martín-Doimeadiós, R.R.C., Green, A.J., Mateo, R., 2011. Identifying sources of Pb exposure in waterbirds and effects on porphyrin metabolism using noninvasive fecal sampling. Environ. Sci. Technol. 45, 6153–6159. http://dx.doi.org/10.1021/es2009242.
Mateo, R., 2009. Lead poisoning in wild birds in Europe and the regulations adopted by different countries. Ingestion lead from spent Ammunit. Implic. Wildl. Humans 2009, 71–98.
Nakata, H., Nakayama, S.M.M., Ikenaka, Y., Mizukawa, H., Ishii, C., Yohannes, Y.B., Konnai, S., Darwish, W.S., Ishizuka, M., 2015. Metal extent in blood of livestock from Dandora dumping site, Kenya: source identification of Pb exposure by stable isotope analysis. Environ. Pollut. 205, 8–15.
Pain, D.J., Amiardtriquet, C., 1993. Lead poisoning of raptors in France and elsewhere. Ecotoxicol. Environ. Saf. 25, 183–192. http://dx.doi.org/10.1006/eesa.1993.1017.
Pain, D.J., Carter, I., Sainsbury, A.W., Shore, R.F., Eden, P., Taggart, M.A., Konstantinos, S., Walker, L.A., Meharg, A.A., Raab, A., 2007. Lead contamination and associated disease in captive and reintroduced red kites Milvus milvus in England. Sci. Total Environ. 376, 116–127.
Pain, D.J., Sears, J., Newton, I., 1995. Lead concentrations in birds of prey in Britain. Environ. Pollut. 87, 173–180. http://dx.doi.org/10.1016/0269-7491(94)P2604-8.
Rattner, B.A., 2009. History of wildlife toxicology. Ecotoxicology 18, 773–783.
Saito, K., 2009. Lead poisoning of Steller's Sea-Eagle (Haliaeetus pelagicus) and Whitetailed Eagle (Haliaeetus albicilla) caused by the ingestion of lead bullets and slugs. Hokkaido Japan. In: Watson, R.T., Fuller, M., Pokras, M., Hunt, W.G. (Eds.), Ingestion Lead from Spent Ammunit. Implic. Wildl. Humans. Peregrine Fund, Boise, Idaho, USA.
Sato, I., Tsujimoto, T., Yamashita, T., Saita, E., Watanabe, G., Taya, K., Sera, K., Tsuda, S., 2007. A survey on contamination with cadmium, Thallium and lead in wild Fauna. J. Jpn. Vet. Med. Assoc. 60, 733–737. http://dx.doi.org/10.12935/jvma1951.60.733.
Scheuhammer, A.M., Templeton, D.M., 1998. Use of stable isotope ratios to distinguish sources of lead exposure in wild birds. Ecotoxicology 7, 37–42.
Thomas, V.G., 2013. Lead-free hunting rifle ammunition: product availability, price, effectiveness, and role in global wildlife conservation. Ambio 42, 737–745. http://dx.doi.org/10.1007/s13280-012-0361-7.
Trinogga, A., Fritsch, G., Hofer, H., Krone, O., 2013. Are lead-free hunting rifle bullets as effective at killing wildlife as conventional lead bullets? A comparison based on wound size and morphology. Sci. Total Environ. 443, 226–232.
Vallverdú-Coll, N., Mougeot, F., Ortiz-Santaliestra, M.E., Castaño, C., Santiago-Moreno, J., Mateo, R., 2016. Effects of lead exposure on sperm quality and reproductive success in an avian model. Environ. Sci. Technol. 50, 12484–12492.
Yabe, J., Nakayama, S.M.M., Ikenaka, Y., Yohannes, Y.B., Bortey-Sam, N., Oroszlany, B., Muzandu, K., Choongo, K., Kabalo, A.N., Ntapisha, J., Mweene, A., Umemura, T., Ishizuka, M., 2015. Lead poisoning in children from townships in the vicinity of a lead-zinc mine in Kabwe, Zambia. Chemosphere 119, 941–947. http://dx.doi.org/10.1016/j.chemosphere.2014.09.028.

FOOD ADDITIVES & CONTAMINANTS: PART A, 2017
VOL. 34, NO. 11, 1959–1969
https://doi.org/10.1080/19440049.2017.1357209

Taylor & Francis
Taylor & Francis Group

Concentrations and human health risk assessment of DDT and its metabolites in free-range and commercial chicken products from KwaZulu-Natal, South Africa

L. A. Thompson[a], Y. Ikenaka[a,b], Y. B. Yohannes[a,c], J. J. van Vuren[b,d], V. Wepener[b], N. J. Smit[b], W. S. Darwish[a,e], S. M. M. Nakayama[a], H. Mizukawa[f] and M. Ishizuka[a]

[a]Laboratory of Toxicology, Department of Environmental Veterinary Sciences, Graduate School of Veterinary Medicine, Hokkaido University, Sapporo, Japan; [b]Water Research Group, Unit for Environmental Sciences and Management, North-West University, Potchefstroom, South Africa; [c]Department of Chemistry, College of Natural and Computational Science, University of Gondar, Gondar, Ethiopia; [d]Department of Zoology, University of Johannesburg, Johannesburg, South Africa; [e]Food Control Department, Faculty of Veterinary Medicine, Zagazig University, Zagazig, Egypt; [f]Department of Environmental Veterinary Sciences, Graduate School of Veterinary Medicine, Hokkaido University, Sapporo, Japan

ABSTRACT

Organochlorine pesticides such as dichlorodiphenyltrichloroethane (DDT) have been used in agriculture and for disease control purposes over many decades. Reports suggest that DDT exposure may result in a number of adverse effects in humans. In the KwaZulu-Natal Province of South Africa, DDT is sprayed annually in homes (indoor residual spraying) to control the mosquito vector of malaria. In the northern part of the Province, samples of free-range chicken meat (n = 48) and eggs (n = 13), and commercially produced chicken meat (n = 6) and eggs (n = 11), were collected and analysed. Of the free-range chicken meat samples, 94% (45/48) contained DDTs (ΣDDTs median 6.1 ng/g wet weight [ww], maximum 79.1 ng/g ww). Chicken egg contents were also contaminated (ΣDDTs in free-range eggs median 9544 ng/g ww, maximum 96.666 ng/g ww; and in commercial eggs median 1.3 ng/g ww, maximum 4.6 ng/g ww). The predominant DDT congener detected was p,p′-DDE in both free-range meat (>63%) and eggs (>66%), followed by p,p′-DDT and then p,p′-DDD. Based on estimated daily intake values, calculated human risk ratio (carcinogenic) values were >1 for DDTs detected in both free-range chicken products. Consumption of free-range eggs poses a particularly high health risk.

ARTICLE HISTORY
Received 9 May 2017
Accepted 27 June 2017

KEYWORDS
Dichlorodiphenyltrichloroethane; chicken; egg; human health risk; KwaZulu-Natal

Introduction

Dichlorodiphenyltrichloroethane (DDT) became popular in the 1950s as an agricultural pesticide, but associated toxic effects were soon seen, initially as population declines in wild avian species. DDT use is now permitted only under advisement by the WHO, with special exemption from the Stockholm Convention for approved disease vector control (Stockholm Convention 2008). Although originally thought to be relatively safe in humans, reports have shown bioaccumulation to occur and suggested exposure may result in neurotoxic, carcinogenic, immunotoxic and reproductive effects (van den Berg 2009). DDT is now classed by the International Agency for Research on Cancer as a Group 2A agent, probably carcinogenic to humans (IARC 2017).

In South Africa, malaria is caused mostly by the *Plasmodium falciparum* parasite and spread mainly by *Anopheles arabiensis* and *A. funestus* mosquitoes (WHO 2016c). According to WHO estimates, there were 12,000 cases of malaria in the country in 2015, with 160 deaths (WHO 2016a); 10% of the population lives in a malaria-endemic area. Malaria is endemic in three provinces – KwaZulu-Natal (KZN), Limpopo and Mpumalanga (Maharaj et al. 2012, 2013). Health reports show that the uMkhanyakude district is the hotspot of malaria cases in the KZN Province, with 696 new cases (fatality rate of 1.7%) in the period 2013–14, an incidence of 1.09 per 1000 population at risk (KZN Health 2014). In the region, the mainstay of disease control is annual application in buildings (indoor residual spraying [IRS]) of long-acting insecticides such as DDT (Wepener et al. 2012). With interventions, KZN has shown the greatest reduction in both cases and number of deaths due to malaria since an outbreak in 2000 that resulted in over 40,000 cases

CONTACT M. Ishizuka ishizum@vetmed.hokudai.ac.jp Laboratory of Toxicology, Department of Environmental Veterinary Sciences, Graduate School of Veterinary Medicine, Hokkaido University, Sapporo 060-0818, Japan

and 100 deaths (KZN Health 2006; Moonasar et al. 2012; Maharaj et al. 2013).

Although DDT is sanctioned for use only in malaria control programmes, other possible sources of the pesticide exist. Previously applied DDT residues may persist for up to 30 years in the environment, and obsolete chemicals accumulated prior to the ban may be being used without licence (ATSDR 2002). Exposure to DDT and its metabolites (DDTs) is a potential health risk for people in the area.

A common source of xenobiotic exposure is through ingestion, such as consumption of contaminated livestock products. The primary objective of this study was thus to investigate the presence of DDTs in chickens reared for consumption in an area of KZN where this chemical is currently used routinely to control malaria vectors, including an assessment of any ensuing potential health risk to people from consuming such free-range chicken meat or eggs.

Materials and methods

Study area

The study area is located in the north-eastern corner of South Africa, bordered to the north by Mozambique and to the west by Swaziland (Figure 1). Sampling locations were within the Jozini (3442 km^2 area) and uMhlabuyalingana (3964 km^2) local municipalities, in uMkhanyakude District Municipality of KZN Province. Malaria is endemic in this district (KZN 2014). Significant portions of this subtropical valley bushveld region are poorly developed rural areas, with a high level of poverty and poor service provision (Morgenthal et al. 2006). Industrial hubs in the province are in the more southerly urban areas, while the study region has no significant industry. The estimated population density in the two local municipalities from which samples were collected is a mere 46 people per km^2, with unemployment between 44 and 47% (Statistics South Africa 2011a, 2011b). As such, products from home-reared chickens offer a relatively cheap and accessible option for nutrition in the local population.

Malaria control in KZN is by IRS, predominantly using DDT. In the spraying season prior to sampling, 4.8 metric tons of DDT were applied to households by Jozini Health officials (official data). Spray coverage of households in KZN in 2013–14 was 85% – down from the previous year due to factors such as use of temporary spray operators for spraying and surveillance, but still above the 80% coverage of premises as recommended by WHO (WHO 2006; KZN 2014). Spraying of DDT for malaria control in the area is undertaken by staff who work under the guidance and central control of the Jozini Health Office. Living conditions for people and animals were similar in homesteads across the sampling area.

Sampling

Sampling was conducted in October 2014 during the dry season, just before spray teams commenced the annual IRS application. Representative rural homesteads were selected within five areas covered by health centres under overall control of the Jozini Health Office – namely Mamfene, Shemula, Mzondi (also known as Mlambo Ngwenya), Makanis and Ndumo (Figure 1 and Table 1). Traditional buildings are thatch-roof huts with

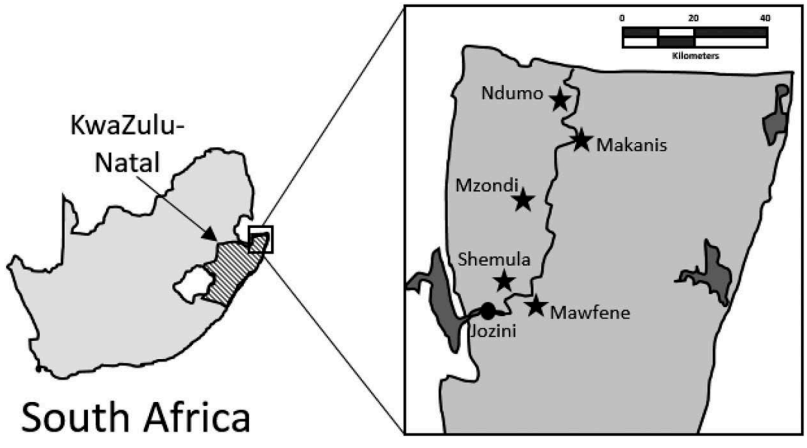

Figure 1. Map of region showing sampling sites in northern KwaZulu-Natal Province, South Africa.

Table 1. Biometric data for samples in this study from KwaZulu-Natal.

	Free range	Commercially produced
Chickens		
Estimated age (months)[a]	7–30, mean 13 ± 7	N/K
Weight (kg)[b]	0.9–2.8, mean 1.5 ± 0.4	1.3–1.8, mean 1.5 ± 0.2
Body condition score (0–4)[c]	0–3, mean 2 ± 0.7	4 (in all)
Sex	22 male, 26 female	3 male, 3 N/K
Supplied diet[d]	Maize (home-grown or shop-bought), leftovers, rice, bread, fresh vegetables	Commercial feed
Lipid content of meat (%)	0.004–1.4, mean 0.3 ± 0.3	0.4–2.0, mean 1.5 ± 0.6
Source (*n*)[e]	Mamfene (8), Shemula (12), Mzondi (10), Makanis (10), Ndumo (8)	Jozini town, Jozini (*n* = 4), Ephondweni, uMhlabuyalingana (*n* = 2)
Eggs		
Supplied diet[d]	Maize (home-grown or shop-bought), leftovers, rice, bread, fresh vegetables	Commercial feed
Eggshell thickness (mm)	2.6–3.5, mean 3.0 ± 0.3	3.1–4.0, mean 3.6 ± 0.3
Lipid content of eggs (%)	7.8–13.1, mean 10.0 ± 1.5	7.9–21.2, mean 10.6 ± 3.5
Source (*n*)[f]	Mamfene (1), Shemula (1), Mzondi (7), Makanis (2), Ndumo (2)	Jozini (n = 8), Ephondweni (*n* = 3)

N/K, not known.
[a]Age estimation by owner at time of purchase.
[b]Body weights for free-ranging chickens are ante-mortem. Those for commercial chickens are as prepared for purchase, thus were eviscerated and excluded feathers/feet/head/neck.
[c]Based on Gregory and Robins (1998) 0–3 scale for layer hens, with an additional score of 4 for individuals with concave breast muscle development resulting in difficulty palpating the keel.
[d]Diet supplied by owner in addition to chickens foraging around the homestead.
[e]Commercial chickens were from three different companies (*n* = 2 of each). Source listed is purchase location.
[f]Commercial chicken eggs were from two different companies. Source listed is purchase location.

walls of mud/cement and floors of mud. Alternative buildings are constructed of concrete blocks with corrugated metal roofs. During IRS, inner walls are sprayed with pesticide, as are the outside eaves of thatched roofs, with DDT being used on unpainted surfaces. The surrounding ground that chickens inhabit within the homestead boundary is soil.

Muscle tissues of recently slaughtered free-ranging chickens living in the homesteads were purchased for DDT analysis (total *n* = 48; see Table 1 for biometric details). In the case of eggs, contents from free-range eggs (total *n* = 13) were analysed (Table 1). Commercially produced and slaughtered chickens (*n* = 6) and chicken eggs (*n* = 11) were also purchased from local shops and sampled for comparative analysis. Each sample was individually stored in clean plastic vessels, transported to the laboratory in Hokkaido University, and maintained at −20°C until chemical analysis. After egg contents were collected, shell thickness was measured, using a micrometer gauge, at the equator of cleaned, dried eggs according to Kamata et al. (2013).

DDT analysis

A standard mixture of DDTs (Dr Ehrenstorfer GmbH, Germany), pesticide grade organic solvents and reagents (Kanto Chemical Corp., Tokyo, Japan) were purchased. The DDTs analysed were: o,p′-DDT, p,p′-DDT, o,p′-DDD, p,p′-DDD, o,p′-DDE and p,p′-DDE.

Sample analysis was performed using a slightly modified version of the method previously described by Yohannes et al. (2014). In brief, a sample of approximately 5 g of muscle or 1 g of egg contents was homogenised with anhydrous sodium sulphate. After automatic extraction for 3.5 h with a mixture of hexane:acetone (3:1 v/v) in a Soxhlet extractor (SOX416 macro SOXTHERM unit, Gerhardt, Germany), the sample was spiked with the surrogate standard 3,3′,4,4′-tetrachlorobiphenyl (polychlorinated biphenyl [PCB], congener 77). The extract was concentrated and an aliquot separated for gravimetric lipid determination. Egg samples were then additionally subjected to gel permeation chromatography (GPC) packed with S-X3 Bio-Beads in a 500 × 25 mm glass column eluted with hexane: dichloromethane (1:1 v/v) for lipid removal. All samples underwent clean-up in a glass column packed with florisil (Kanto Chemical Corp., Tokyo, Japan) (activated at 180°C for 8 h, and then 5% deactivated with distilled water) topped with anhydrous sodium sulphate and eluted with hexane:dichloromethane (7:3 v/v). The resultant extract was concentrated to near dryness, before redissolution in n-decane. The internal standard 2,3,5,6-tetrachloro-m-xylene was added to the sample prior to instrumental analysis using a gas-chromatograph coupled with ^{63}Ni electron capture detector (Shimadzu GC-2014, Kyoto, Japan).

Quality control and quality assurance

Chemicals were identified by comparing retention times with those of corresponding standards, and concentrations were quantified from sample peak area compared to that of the internal standard. Correction coefficients (R^2) for multilevel calibration curves were all >0.99. Based on a signal-to-noise ratio of 3:1, detection limits were between 0.16 and 0.45 ng/g for all DDTs.

Risk assessment

Potential risk to human health through consumption of chicken products was assessed in two ways. Firstly, daily intake of DDTs in foods were calculated and compared with published guidelines for acceptable levels. Secondly, cancer risk due to consumption was estimated.

Estimated daily intake

The estimated daily intake (EDI) was calculated using the detected concentrations of DDTs in chicken meat and eggs. In samples with concentrations below the LOD, a value equivalent to half of the LOD was used for this calculation. As risk analysis is dependent on wet weight (ww) consumed, concentrations of DDTs detected are expressed on a ww basis.

$$\mathrm{EDI} = (\mathrm{C} \times \mathrm{DR})/\mathrm{BW}$$

where C is the measured concentration of DDTs (ng/g ww), DR is the average daily consumption rate of chicken product (g/d) and BW is body weight (kg), which was set at 60 kg. EDIs were calculated based on the DR derived from annual national poultry meat and egg consumption values (SAPA 2015a, 2015b). In South Africa, the national reported daily chicken meat consumption is 103 g/d and chicken egg consumption is 24 g/d per person.

Estimation of the risk of non-carcinogenic effects from consumption of chicken meat was made by comparing these calculated EDIs with published reference doses: WHO provisional tolerable daily intake (PTDI) of DDTs of 0.01 mg/kg bw/d, and the US Environmental Protection Agency (EPA) reference dose for chronic oral exposure (reference dose [RfD]) for p,p′-DDT of 0.0005 mg/kg bw/d (IRIS 1987; JECFA 2010).

Potential carcinogenic risks

US EPA guidelines were used to assess potential carcinogenic public health risks from consumption of chicken meat and eggs containing DDT residues. Cancer risk estimates and hazard ratios (HR) were calculated.

The cancer benchmark concentration (CBC) for carcinogenic effects represents the lifetime exposure concentration at which the acceptable lifetime cancer risk is set at one in a million, i.e. $10^{-}6$. A risk level between 10^{-6} and 10^{-4} is considered to be of concern, while a level $>10^{-4}$ is considered an unacceptable risk. The CBC was calculated as the cancer risk divided by the cancer slope factor:

$$\mathrm{CBC} = 10^{-6}/\,\mathrm{slope\ factor}$$

The cancer slope factor for DDTs was set to 0.34 per mg/kg/d, obtained from the IRIS database (IRIS 1987). Comparison of EDI with the CBC for carcinogenic effects was used to assess the HR for cancer risk:

$$\mathrm{HR} = \mathrm{EDI}\,/\,\mathrm{CBC}$$

Using the above definition of CBC, a one in a million lifetime cancer risk results in a HR of 1. Thus a HR value >1 indicates a potentially increased human health risk over that considered acceptable in the general population (Dougherty et al. 2000).

Statistical analysis

Data were processed and statistically analysed using Microsoft Excel 2014 and JMP® Pro 12 (SAS Institute Inc., Cary, NC, USA). One-way analysis of variance (ANOVA) was used to produce descriptive statistics to characterise DDT levels in chicken samples. Tukey's HSD *post hoc* test was used for multiple comparisons among sample sites. The significance level was set at $p < 0.05$.

Results and discussion

The fresh weight of the free-ranging chickens ranged from 0.9 to 2.8 kg, and the dead weight of commercial chicken carcasses from 1.3 to 1.8 kg (Table 1). The mean lipid (%) of chicken muscle was 0.3 ± 0.3 for free-range and 1.5 ± 0.6 for commercially reared chickens (Table 1). The mean lipid (%) of egg contents was 10.0 ± 1.5 for free-range and 10.6 ± 3.5 for commercially produced eggs (Table 1).

Levels of DDTs

Chicken meat

In muscle samples from free-ranging chickens in KwaZulu-Natal, varying concentrations of DDTs were detected. DDTs were not detected in muscle samples from commercially produced chickens.

Concentrations of DDTs (values of p,p′-DDE, p,p′-DDD and p,p′-DDT) detected in chicken meat in each area sampled in the region are shown in Table 2. The congeners o,p′-DDE, o,p′-DDD and o,p′-DDT were not detected in any meat samples. DDTs were detected in 93.8% (45/48) of free-range chicken muscle samples but were below the LOD in all commercial samples. Summed DDT concentrations in free-range samples ranged up to a maximum of 79.1 ng/g ww, being highest in Makanis (median 29.6 ng/g ww) and lowest in Shemula (median 1.3 ng/g ww). In these samples, the predominant chemical detected was the p,p′-DDE metabolite (median 6.0 ng/g ww, maximum 60.2 ng/g ww). The most likely reason for such high levels of DDTs is past and current use of DDT in IRS within homesteads, resulting in contamination of the local environment, although illegal usage or contamination from obsolete pesticides cannot be ruled out. These results indicate that free-ranging chickens in the sample area are subject to a high degree of DDT exposure, likely associated with the regular use of the chemical in IRS for malaria control in the region.

Composition profiles of DDTs in chicken meat are shown in Figure 2A. The predominant metabolite congener detected was p,p′-DDE, at 73.6% (range 29.5–98.3%), followed by p,p′-DDT (16.0%) and p,p′-DDD (10.3%). The predominant congener in technical grade DDT is p,p′-DDT, which is then degraded to the other two congeners, with p,p′-DDE the most persistent in biological organisms. In 50% (24/48) of free-range chicken samples, p,p′-DDE was the sole DDT congener detected (>LOD). Most samples contained either none or only a small percentage of the p,p′-DDD congener, but notably a higher proportion was detected in samples from Mamfene (maximum 37%). Between areas, Makanis contained the highest percentages of p,p′-DDT (14.1–61.0%). In this area, the ratio of p,p′-DDT to p,p′-DDE was >1 in a single sample, suggesting the possibility of recent exposure to the parent chemical.

Comparison of different sampling sites showed a significant difference between concentrations of total

Table 2. Levels of DDT and metabolites in chicken products from KwaZulu-Natal.

Chicken meat (uncooked breast meat), ng/g ww								
	Free range[a]							
	Mamfene	Shemula	Mzondi	Makanis	Ndumo	*Mean*	*Median (max)*	Commercially produced[a]
p,p′-DDE	6.9 ± 4.9 (7/8)	4.3 ± 6.2 (10/12)	6.8 ± 9.6 (10/10)	21.7 ± 16.3 (10/10)	11.7 ± 18.6 (8/8)	*10.1 ± 13.6 (45/48)*	*6.0 (60.2)*	<LOD
p,p′-DDD	2.4 ± 2.9 (5/8)	0.5 ± 0.8 (3/12)	0.2 (1/10)	1.6 ± 1.9 (8/10)	0.6 (1/8)	*1.0 ± 1.8 (18/48)*	*(6.7)*	<LOD
p,p′-DDT	1.4 ± 1.6 (6/8)	0.3 ± 0.5 (2/12)	0.18 (1/10)	9.4 ± 8.0 (10/10)	0.63 (1/8)	*2.4 ± 5.2 (20/48)*	*(26.2)*	<LOD
ΣDDTs	**10.8 ± 7.3 (7/8)**	**5.0 ± 7.0 (10/12)**	**7.2 ± 10.1 (10/10)**	**32.6 ± 25.5 (10/10)**	**12.9 ± 21.3 (8/8)**	***13.5 ± 18. 9 (45/48)***	***6.1 (79.1)***	**<LOD**
Chicken egg contents (uncooked), ng/g ww								
	Free range [a]					Commercially produced[a]		
	Mean ± SD (number of samples)			*Median (maximum)*		Mean ± SD (number of samples)		*Median (maximum)*
o,p′-DDE	1.1 ± 1.8 (6/13)			*0.3 (5.1)*		0.8 ± 0.5 (5/11)		*0.7 (1.5)*
p,p′-DDE	12,079 ± 16,245 (13/13)			*6819 (59,966)*		0.8 ± 0.7 (8/11)		*0.5 (2.2)*
o,p′-DDD	3.1 ± 3.9 (11/13)			*1.9 (11.3)*		<LOD		*<LOD*
o,p′-DDT	6.8 ± 8.5 (13/13)			*4.0 (32.4)*		1.0 (1/11)		*1*
p,p′-DDD	506.9 ± 760.3 (13/13)			*289.4 (2870)*		0.3 ± 0.3 (8/11)		*0.2 (0.9)*
p,p′-DDT	5485 ± 9573 (13/13)			*1918 (33,782)*		0.5 ± 0.2 (7/11)		*0.5 (0.9)*
ΣDDTs	**18,081 ± 25,879 (13/13)**			*9544 (96,666)*		**1.5 ± 1.3 (11/11)**		***1.3 (4.6)***

LOD, limit of detection.
[a] Mean ± standard deviation (SD) (number of samples > LOD/total number of samples in group).

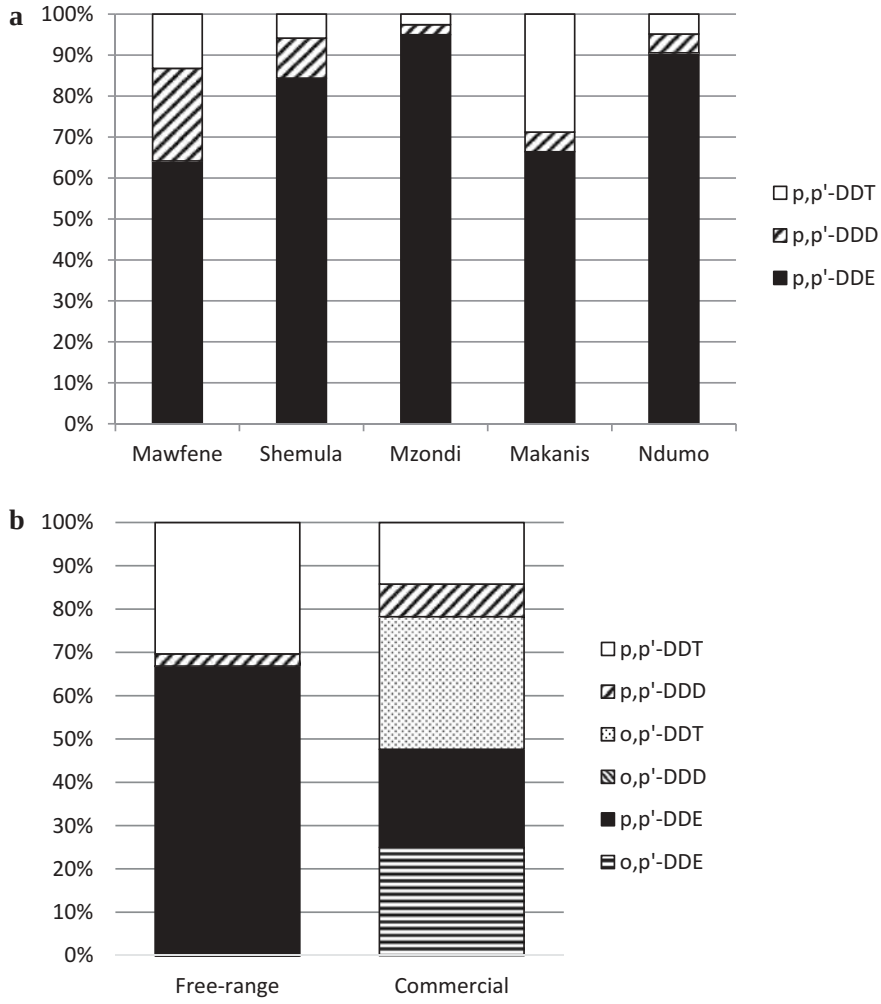

Figure 2. Relative abundance of individual DDT components in free-range chickens from KwaZulu-Natal: (a) Chicken meat samples; (b) Chicken egg contents.

DDTs at Makanis and Shemula (p = 0.0036) and Makanis and Mzondi (p = 0.0126). No significant association was shown between DDT concentrations and parameters such as body weight, body condition score, estimated age, or sex. Concentrations of p,p′-DDE were significantly higher in Makanis (mean 21.6 ± 16.3 ng/g ww) than in Shemula (mean 4.3 ± 6.2 ng/g ww, p = 0.0212) and p,p′-DDT significantly higher in Makanis (mean 9.4 ± 8.0 ng/g ww) than in all other sites ($p < 0.001$ for Shemula and Mzondi, $p = 0.0003$ for Ndumo and $p = 0.0011$ for Mamfene).

Concentrations of DDTs in chicken meat in this study (mean 13.5 ± 18.9 ng/g ww, maximum 79.1 ng/g ww) were lower than those detected in a smaller study on chickens in the Limpopo Province of South Africa in 2008, another IRS-using province (mean 500 ± 400 ng/g ww, with a maximum of 1400 ng/g ww meat) (Van Dyk et al. 2010). This difference may in part be attributed to the fact that sampling was performed soon after IRS in the Limpopo study. In the current KZN study, sampling was performed just before IRS, with the most recent spraying in homesteads 9 months prior to sampling.

Chicken eggs

DDTs were also detected in chicken egg contents, although differences were seen between free-range and commercial samples.

Concentrations of DDTs (values of o,p′-DDE, p,p′-DDE, o,p′-DDD, p,p′-DDD, o,p′-DDT and p,p′-DDT) detected in chicken egg contents sampled in the region are shown in Table 2. DDT and its metabolites were detected in 100% of free-range (13/13) and commercial (11/11) egg samples. Summed DDT concentrations in free-range samples ranged from 807.6 to 96,666 ng/g ww (median 9544 ng/g ww). By comparison, summed DDTs in commercial samples ranged from <LOD to 4.6 ng/g

ww (median 1.3 ng/g ww). In these samples, the predominant chemical detected was again the p,p′-DDE metabolite (median 6819 ng/g ww in free-range samples and 0.5 ng/g ww in commercial samples). These results not only support the evidence for high levels of DDTs exposure to free-range chickens, but show that commercially reared birds are also exposed to, albeit much lower, levels of contamination.

Composition profiles of DDTs in chicken eggs are shown in Figure 2B. The predominant metabolite congener detected was p,p′-DDE, median presence in samples of 75.7% (range 48.0–92.1%), followed by p,p′-DDT (22.0%) and p,p′-DDD (3.0%) in free-range samples. Contribution by o,p′ congeners was <1% in total. However, in commercial eggs, p,p′-DDT predominated, at a median presence of 21.3% (range <LOD to 75.8%). The pattern of remaining congeners was of a varied composition: p,p′-DDE (19.4%) > p,p′-DDE (6.7%), and o,p′-congeners <1.0%. This difference may indicate a different source of DDTs in these birds. Again, the ratio of p,p′-DDT to p,p′-DDE exceeded one in a single free-range sample from Makanis.

A study of DDT contamination in eggs collected in 2008 in Limpopo just after IRS application reported a median level of 11,000 ng/g ww and a maximum of 48,000 ng/g ww (Bouwman et al. 2015). Contamination levels in eggs obtained in this KZN study had a lower median value (9544 ng/g ww), but the maximum was more than double that in Limpopo (96,666 ng/g ww). Another study in Limpopo detected a mean concentration of 1600 ng/g in chicken liver samples, higher than levels in KZN chicken meat (mean 13.5 ng/g ww) but lower than those in KZN eggs (mean 18,081 ng/g ww) (Van Dyk et al. 2010). There may be a temporal shift in body distribution pattern of DDTs in chickens, initially with higher concentrations in the animal's organs but taking time for metabolites to pass to egg contents.

Mechanisms of DDT toxicity in humans are poorly understood. The most abundant DDT detected in this KZN study was p,p′-DDE. This congener is commonly associated with fertility problems in many wild avian species (Gómez-Ramírez et al. 2012). Laboratory studies also show effects in chickens, with reduced fertility and hatchability when exposed to DDT in feed (Sauter and Steele 1972). Reduced fertility in the chickens was not reported by owners, and *post mortem* examination did not reveal any gross abnormalities. Eggshell thickness was not significantly reduced by DDTs in these samples (Table 1). The presence of p,p′-DDT is an indicator of recent release of DDT into the environment, although homestead IRS record cards indicated that the most recent application for properties was 9 months prior to sampling.

Human health risk assessment

The study area is a low economic region, and many homesteads rear free-range chickens to provide a readily available source of nutrition. Coetzee et al. (2015) reported that chicken is the most common form of protein consumption in the study area. Consumption of meat or eggs from these may pose a risk to human health if DDTs accumulate in livestock from contaminants in the environment. DDT concentrations from the current study were evaluated against existing international limits. In order to evaluate risk exposure through consumption of chicken products, EDIs were calculated at 25th, 50th, 75th and 95th percentiles of DDT concentrations, expressed as nanogram per kilogram body weight per day (ng/kg/bw/d) (Table 3). EDI values were then compared with the WHO and US EPA published limits for non-cancer effects.

Table 3. Estimated daily intake values (ng/kg bw/d) in people of DDTs from the studied chickens. Values are given at the 25th, 50th, 75th and 95th percentile measured concentrations.

Percentile	25th	50th	75th	95th
Chicken meat				
p,p′-DDE	2.3	11.2	21.1	72.8
p,p′-DDD	0.2	0.2	2.7	11.0
p,p′-DDT	0.2	0.4	3.5	19.6
ΣDDTs	**2.8**	**12.1**	**32.4**	**111.0**
Chicken egg contents				
Free range				
o,p′-DDE	0.003	0.004	0.1	0.9
p,p′-DDE	479.6	2727	7440	16,204
o,p′-DDD	0.1	0.7	0.9	4.4
o,p′-DDT	0.6	1.6	3.3	8.9
p,p′-DDD	18.8	115.7	177.0	756.9
p,p′-DDT	91.8	767.3	1314	9945
ΣDDTs	**525.7**	**3818**	**11,803**	**24,775**
Commercially produced				
o,p′-DDE	0.00	0.003	0.2	0.6
p,p′-DDE	0.02	0.1	0.3	0.8
o,p′-DDD	0.002	0.002	0.002	0.003
o,p′-DDT	0.002	0.002	0.002	0.2
p,p′-DDD	0.01	0.05	0.1	0.3
p,p′-DDT	0.002	0.1	0.2	0.3
ΣDDTs	**0.2**	**0.5**	**0.9**	**1.4**

Table 4. Cancer risk estimates (hazard ratio[a]) for DDTs. Values are given at the 25th, 50th, 75th and 95th percentile measured concentrations (based on national consumption rates).

Percentile	25th	50th	75th	95th
Chicken meat				
p,p′-DDE	0.8	3.5	5.9	23.6
p,p′-DDD	0.1	0.1	0.5	3.4
p,p′-DDT	0.1	0.1	1.2	6.5
ΣDDTs	**0.9**	**3.6**	**10.5**	**34.9**
Chicken egg contents				
Free range				
o,p′-DDE	0.001	0.001	0.04	0.3
p,p′-DDE	163.1	927.3	2529	5509
o,p′-DDD	0.0	0.2	0.3	1.5
o,p′-DDT	0.2	0.5	1.1	3.0
p,p′-DDD	6.4	39.4	60.2	257.4
p,p′-DDT	31.2	260.9	446.8	3381
ΣDDTs	**178.7**	**1298.0**	**4013**	**8423**
Commercially produced				
o,p′-DDE	0.001	0.001	0.1	0.2
p,p′-DDE	0.01	0.03	0.1	0.3
o,p′-DDD	0.001	0.001	0.001	0.001
o,p′-DDT	0.001	0.001	0.001	0.1
p,p′-DDD	0.002	0.02	0.03	0.1
p,p′-DDT	0.001	0.05	0.1	0.1
ΣDDTs	**0.1**	**0.2**	**0.3**	**0.5**

[a] A value >1 indicates a potential health risk.

For chicken meat and commercial egg samples, these were at exposure levels below the WHO provisional tolerable daily intake (PTDI) of DDTs of 0.01 mg/kg bw/d, and the US EPA RfD of 0.0005 mg/kg bw/d (IRIS 1987; JECFA 2010). However, at the 75th percentile and above, these levels were breached in free-range egg samples, due to contributions from high levels of p,p′-DDE and p,p′-DDT.

Further calculations assessed the carcinogenic risk of DDTs, using cancer risk estimates and HRs for the above percentile concentrations (Table 4). Based on published daily consumption values for chicken meat (103 g/person/d) and eggs (24 g/person/d) in South Africa, calculated HR values were much greater than 1 for DDTs detected in free-range chicken meat and eggs (Schonfeldt and Hall 2013).

Using the national consumption values, the calculated cancer risk for DDTs through consumption of free-range chicken meat ranged from 0.7×10^{-4} in the Shemula area to 17.2×10^{-4} in Makanis (at the 50th percentiles), suggesting a 0.7–17.2 chance in 10,000 of developing cancer due to the DDTs present in chicken meat. These risks increased, relatively, to 10.7 and 43.9×10^{-4} at the 95th exposure level (10.7–43.9 chance in 10,000) – risks considered unacceptable for human health. Considering concentrations of all free-range meat samples together, cancer risk estimates for DDTs ranged from 3.6 at 50th to 34.9×10^{-4} at 95th exposure levels (3.6–34.9 chance in 10,000). Again, compared to a target risk of less than 1×10^{-4}, these risk estimates are considered above an acceptable level and should be of concern.

In commercial egg samples, calculations resulted in HR values <1 (0.5×10^{-4} at the 95th percentile), indicating no associated increase in cancer risk through consumption. Much higher concentrations of DDTs detected in free-range egg samples contributed to higher HRs. Even at the 25th percentile, HR was 178.7×10^{-4}, ranging up to 8423×10^{-4} at the 95th percentile level (178.7–8423 chance in 10,000). Of great concern is the finding in KZN that levels high enough to be potentially detrimental to human health were present in chicken eggs many months after DDT spraying occurred.

Calculated risk values for human health may be overestimated in this study for two main reasons. In this area of lower economic status, consumption of meat products may be lower than the national average. Also, in the region, commercially produced chicken products are eaten as well as free-range animal products. In this study, levels in commercially reared chicken meat purchased locally were below the limit of detection, and levels in commercial eggs much lower than in free-range eggs. A study in Beijing, China, showed low levels of DDTs in farmed chicken meat (0.05 ng/g ww) and eggs (2.4 ng/g ww) (Tao et al. 2009). These concentrations were lower than samples from the KZN free-range chickens. Higher levels (30 ng/g ww) were detected in farmed chicken meat in India several decades ago (Kaphalia et al. 1981). The lower level of DDTs in recent commercial products gives a correspondingly lower adjusted risk value from consumption.

Cumulative consumption of both free-range chicken meat and eggs at current detected contamination levels in the KZN study area have been shown by hazard risk analysis to yield a lifetime cancer risk of greater than one in a million, indicating a relatively high risk to human health, particularly from consumption of free-range eggs. WHO estimates cancer mortality in South Africa to be 6.8% of all deaths (WHO 2014). Concern is not only due to continued use of DDT in the region but also due to the prolonged persistence of the DDT and its metabolites in the environment. However, other studies have shown that cooking

(including boiling) of chicken meat reduces total DDT compounds by ~25% (Morgan et al. 1972). Of the total DDT compounds remaining after cooking, 80% are found in the broth and 20% remain in the meat (except for DDD isomers, of which 60% remain in the meat). As such, local people should be advised against regular consumption of free-range chicken products, particularly eggs, even if they are cooked. Discarding the broth after boiling meat appears to significantly reduce available DDTs and may be a simple option to reduce exposure. Based on discussions with local residents about their diet, the local consumption of chicken products is likely lower than the national *per capita* level (Schonfeldt and Hall 2013). The risks therefore reported may be overestimations, but if local chicken consumption increased in line with the average South African, the associated risk from DDTs may become greater. These risk estimates do not include contamination in other food sources. For example, DDTs in leafy vegetables from the IRS-using Limpopo area in South Africa contained 43.0 ng/g of DDTs (Van Dyk et al. 2010). Although ingestion is the main route of DDTs exposure in people, other additional sources of exposure are inhalation and dermal contact (Yu et al. 2012). These are a concern, particularly for the family members who spend most time in the home – usually women and infants.

KZN Province's Department of Health has a strategic objective to maintain preventative strategies to reduce and maintain malaria incidence at less than 1 per 1000 population, but cites various reasons for deviation from this planned target including difficulties in performing IRS due to furniture in homes, and poor acceptance of spraying. Resistance by vectors to pesticides (including DDT) and therapeutic agents have been recorded in many malaria areas. It is also reported that DDT has recently become more expensive to purchase in South Africa (KZN 2014). The benefits of using this chemical may soon be outweighed by the costs – financially, to health, and to the environment – and research developing viable alternatives to DDT for malaria control is ongoing, but requires validation and implementation. It is likely that the solution will be a combination of different methods (WHO 2016a, 2016b). The South African government has a goal of eliminating malaria by 2018 (WHO 2015).

This study shows that free-range chickens in homesteads are contaminated with DDTs. It would be useful for future studies to analyse feed for both free-range and commercially reared chickens in the region to clarify the source of contamination. Although they do not live so intimately with people as chickens, other livestock such as goats and cattle are also susceptible to exposure from environmental contamination and therefore are a source of DDTs if consumed. The Jozini and uMhlabuyalingana local municipalities encompass the Ndumo Game Reserve, with rich biodiversity and home to over 400 bird species. Except for research on fish (McHugh et al. 2011), the potential risks from DDTs to wildlife in this region have not yet been fully ascertained, but there is concern that environmental contamination by DDT near such an area may affect wildlife, particularly the abundant bird species for which the reserve is renowned (Smit et al. 2016). The effects of chronic DDT exposure on people are still uncertain. Several studies have suggested effects on body systems including immunological function, neurodevelopment and reproductive success, but others have shown weak or no statistically proven correlation (Bornman et al. 2010; Ouyang et al. 2014; Cohn et al. 2015; Gaspar et al. 2015; Jusko et al. 2016; Perry et al. 2016).

Conclusion

This is the first study reporting levels and human risk assessment of DDTs in food products from free-ranging chickens in the northern area of KwaZulu-Natal. Chemicals used on buildings as part of malaria vector-control strategies make their way into the adjacent environment and thence to livestock living there. This study based on recent sampling confirms the presence of high levels of the parent DDT compound and its metabolites in products from free-ranging chickens. The persistence of DDT in the environment ensures that its detrimental effects will be seen for some time to come on the environment and organisms, including humans, their livestock and wildlife.

Acknowledgments

We gratefully acknowledge contacts in the KZN region of South Africa, without whom it would not have been possible to collect samples and perform questionnaires. In particular,

thanks to Samwel Menyuka and Nelson Nkwanyana for guiding and interpreting, and Dr Ntantiso at Jozini Agriculture Office. From the KwaZula-Natal Health Department, Bruce Margot, Bheki Owabe, Phineas Zikhali and various guides to health camps facilitated this study greatly. Laboratory assistance given by Takahiro Ichise in Hokkaido University is appreciated. This is contribution number 210 from the NWU-Water Research Group.

Disclosure statement

No potential conflict of interest was reported by the authors.

Funding

This study was supported in part by the Leading Program at Hokkaido University, and in part by the Japan Society for the Promotion of Science (JSPS KAKENHI Grant Number 16J02013). Support was also received from Grants-in-Aid for Scientific Research from the Ministry of Education, Culture, Sports, Science and Technology of Japan (No. 16H01779, 24248056, 26304043, 15H0282505 and 15K1221305), the foundation of JSPS Core-to-Core Program (AA Science Platforms) and Bilateral Program, and the Soroptimist Japan Foundation, the Nakajima Foundation and the Sumitomo Foundation Grant for Environmental Research Projects.

References

[ATSDR] Agency for Toxic Substances and Disease Registry. 2002. Toxicological profile for DDT, DDE, and DDD. U.S. Department of Health and Human Services, Public Health Service, Agency for Toxic Substances and Disease Registry; [accessed 2017 Jan 18]. https://www.atsdr.cdc.gov/toxprofiles/tp35.pdf

Bornman R, De Jager C, Worku Z, Farias P, Reif S. 2010. DDT and urogenital malformations in newborn boys in a malarial area. BJU Int. 106(3):405–411.

Bouwman H, Bornman R, Van Dyk C, Barnhoorn I. 2015. First report of the concentrations and implications of DDT residues in chicken eggs from a malaria-controlled area. Chemosphere. 137:174–177.

Coetzee HC, Nell W, Van Eeden ES, De Crom EP. 2015. Artisanal fisheries in the Ndumo area of the lower Phongolo River Floodplain, South Africa. Koedoe. 57(1): Art. #1248.

Cohn BA, La Merrill M, Krigbaum NY, Yeh G, Park J-S, Zimmermann L, Cirillo PM. 2015. DDT exposure in utero and breast cancer. J Clin Endocrinol Metabol. 100 (8):2865–2872.

Dougherty CP, Holtz SH, Reinert JC, Panyacosit L, Axelrad DA, Woodruff TJ. 2000. Dietary exposures to food contaminants across the United States. Environ Res. 84 (2):170–185.

Gaspar FW, Harley KG, Kogut K, Chevrier J, Mora AM, Sjödin A, Eskenazi B. 2015. Prenatal DDT and DDE exposure and child IQ in the CHAMACOS cohort. Environ Int. 85:206–212.

Gómez-Ramírez P, Martínez-López E, García-Fernández AJ, Zweers AJ, Van Den Brink NW. 2012. Organohalogen exposure in a Eurasian Eagle owl (Bubo bubo) population from Southeastern Spain: temporal–spatial trends and risk assessment. Chemosphere. 88(8):903–911.

Gregory NG, Robins JK. 1998. A body condition scoring system for layer hens. N Z J Agric Res. 41(4):555–559.

[IARC] International Agency for Research on Cancer. 2017. IARC Monographs on the Evaluation of Carcinogenic Risks to Humans, list of classifications, volumes 1–117. International Agency for Research on Cancer; accessed 2017 Jan 18. http://monographs.iarc.fr/ENG/Classification/latest_classif.php

[IRIS] Integrated Risk Information System. 1987. U.S. Environmental Protection Agency; [accessed 2016 Jan 18]. https://cfpub.epa.gov/ncea/iris/iris_documents/documents/subst/0147_summary.pdf

[JECFA] Joint FAO/WHO Expert Committee on Food Additives. 2010. Evaluations of the Joint FAO/WHO Expert Committee on Food Additives (JECFA). DDT; [accessed 2017 Mar 12]. http://apps.who.int/food-additives-contaminants-jecfa-database/chemical.aspx?chemID=3183

Jusko TA, De Roos AJ, Lee SY, Thevenet-Morrison K, Schwartz SM, Verner MA, Murinova LP, Drobná B, Kocan A, Fabisiková A, et al. 2016. A birth cohort study of maternal and infant serum PCB-153 and DDE concentrations and responses to infant tuberculosis vaccination. Environ Health Perspect. 124(6):813.

Kamata R, Shiraishi F, Takahashi S, Shimizu A, Nakajima D, Kageyama S, Sasaki T, Temma K. 2013. The effects of transovarian exposure to p, p'-DDT and p, p'-DDE on avian reproduction using Japanese quails. J Toxicol Sci. 38(6):903–912.

Kaphalia BS, Husain MM, Seth TD, Kumar A, Murti CR. 1981. Organochlorine pesticide residues in some Indian wild birds. Pestic Monit J. 15(1):9–13.

[KZN] KwaZulu-Natal Health. 2006. Health statistics available for KwaZulu-Natal; [accessed 2017 Jan 13]. http://www.kznhealth.gov.za/healthstatistics.htm

[KZN] KwaZulu-Natal Health. 2014. KwaZulu-Natal Department of Health Annual Report 2013–2014; Part B: programme 3: emergency Medical Services; [accessed 2017 Mar 16]. http://www.kznhealth.gov.za/AnnualReport/2013_2014.pdf

Maharaj R, Morris N, Seocharan I, Kruger P, Moonasar D, Mabuza A, Raswiswi E, Raman J. 2012. The feasibility of malaria elimination in South Africa. Malar J. 11(1):423.

Maharaj R, Raman J, Morris N, Moonasar D, Durrheim DN, Seocharan I, Kruger P, Shandukani B, Kleinschmidt I. 2013. Epidemiology of malaria in South Africa: from control to elimination. SAMJ. 103(10):779–783.

McHugh KJ, Smit NJ, van Vuren JHJ, van Dyk JC, Bervoets L, Covaci A, Wepener V. 2011. A histology-based fish

health assessment of the tigerfish, *Hydrocynus vittatus* from a DDT-affected area. Phys Chem Earth Parts A/B/C. 36:895–904.

Moonasar D, Nuthulaganti T, Kruger PS, Mabuza A, Rasiswi ES, Benson FG, Maharaj R. 2012. Malaria control in South Africa 2000–2010: beyond MDG6. Malar J. 11(1):294.

Morgan KJ, Zabik ME, Funk K. 1972. Lindane, dieldrin and DDT residues in raw and cooked chicken and chicken broth. Poult Sci. 51(2):470–475.

Morgenthal TL, Kellner K, Van Rensburg L, Newby TS, Van der Merwe JPA. 2006. Vegetation and habitat types of the Umkhanyakude Node. S Afr J Bot. 72(1):1–10.

Ouyang F, Longnecker MP, Venners SA, Johnson S, Korrick S, Zhang J, Xu X, Christian P, Wang M-C, Wang X. 2014. Preconception serum 1, 1, 1-trichloro-2, 2, bis (p-chlorophenyl) ethane and B-vitamin status: independent and joint effects on women's reproductive outcomes. Am J Clin Nutr. 100(6):1470–1478.

Perry MJ, Young HA, Grandjean P, Halling J, Petersen MS, Martenies SE, Karimi P, Weihe P. 2016. Sperm aneuploidy in Faroese men with lifetime exposure to dichlorodiphenyldichloroethylene (*p, p'*-DDE) and polychlorinated biphenyl (PCB) pollutants. Environ Health Perspect. 124(7):951.

[SAPA] South African Poultry Association. 2015a. Egg industry stats summary for 2015; [accessed 2016 Feb 25]. http://www.sapoultry.co.za/pdf-statistics/Egg-industry-stats-summary.pdf

[SAPA] South African Poultry Association. 2015b. South African Poultry Association 2014 Industry Profile; [accessed 2017 Jan 16]. Available from: http://www.sapoultry.co.za/pdf-docs/sapa-industry-profile.pdf

Sauter EA, Steele EE. 1972. The effect of low level pesticide feeding on the fertility and hatchability of chicken eggs. Poult Sci. 51(1):71–76.

Schonfeldt HC, Hall N. 2013. "Fish, chicken, lean meat and eggs can be eaten daily": a food-based dietary guideline for South Africa. S Afr J Clin Nutr. 26(3):S66–S76.

Smit NJ, Vlok W, van Vuren JHJ, Du Preez LH, Van Eeden E, O'Brien GC, Wepener V. 2016. Socio-ecological system management of the lower phongolo river and floodplain using relative risk methodology. Pretoria, p. 456. Water Research Commission (WRC) Project K5-2185.

Statistics South Africa. 2011a. Jozini municipality; [accessed 2017 Mar 17]. http://www.statssa.gov.za/?page_id=993&id=jozini-municipality

Statistics South Africa. 2011b. Umhlabuyalingana municipality; [accessed 2017 Mar 17]. http://www.statssa.gov.za/?page_id=993&id=umhlabuyalingana-municipality

Stockholm Convention. 2008. Listing of POPs in the Stockholm convention; [accessed 2017 Jan 19]. http://chm.pops.int/TheConvention/ThePOPs/ListingofPOPs/tabid/2509/Default.aspx

Tao S, Liu WX, Li XQ, Zhou DX, Li X, Yang YF, Yue DP, Coveney RM. 2009. Organochlorine pesticide residuals in chickens and eggs at a poultry farm in Beijing, China. Environ Pollut. 157(2):497–502.

van den Berg H. 2009. Global status of DDT and its alternatives for use in vector control to prevent disease. Environ Health Perspect. 117(11):1656–1663.

Van Dyk JC, Bouwman H, Barnhoorn IEJ, Bornman MS. 2010. DDT contamination from indoor residual spraying for malaria control. Sci Total Environ. 408(13):2745–2752.

Wepener V, Smit NJ, Covaci A, Dyke S, Bervoets L. 2012. Seasonal bioaccumulation of organohalogens in tigerfish, *Hydrocynus vittatus* Castelnau, from Lake Pongolapoort, South Africa. Bull Environ Contam Toxicol. 88:277–282.

[WHO] World Health Organization. 2006. Malaria vector control and personal protection. WHO Technical Report Series, 936; [accessed 2017 Mar 17]. http://www.who.int/malaria/publications/atoz/who_trs_936/en/

[WHO] World Health Organization. 2014. Cancer country profiles 2014; [accessed 2017 Mar 17]. http://www.who.int/cancer/country-profiles/en/#S

[WHO] World Health Organization. 2015. Malaria Strategic Plan 2012–2018: mid-term Review; [accessed 2017 Mar 17]. http://www.afro.who.int/en/south-africa/press-materials/item/7978-malaria-strategic-plan-2012-2018-mid-term-review.html

[WHO] World Health Organization. 2016a. World Malaria Report 2016; [accessed 2017 Jan 19]. http://apps.who.int/iris/bitstream/10665/252038/1/9789241511711-eng.pdf?ua=1

[WHO] World Health Organization. 2016b. "WHO welcomes global health funding for malaria vaccine" News release, 17 November 2016; [accessed 2017 Jan 19]. http://www.who.int/mediacentre/news/releases/2016/funding-malaria-vaccine/en/

[WHO] World Health Organization. 2016c. South Africa country malaria profile; [accessed 2017 Jan 13]. http://www.who.int/malaria/publications/country-profiles/profile_zaf_en.pdf

Yohannes YB, Ikenaka Y, Saengtienchai A, Watanabe KP, Nakayama SM, Ishizuka M. 2014. Concentrations and human health risk assessment of organochlorine pesticides in edible fish species from a Rift Valley lake—lake Ziway, Ethiopia. Ecotoxicol Environ Saf. 106:95–101.

Yu Y, Li C, Zhang X, Zhang X, Pang Y, Zhang S, Fu J. 2012. Route-specific daily uptake of organochlorine pesticides in food, dust, and air by Shanghai residents, China. Environ Int. 50:31–37.

Contamination Levels and Sources of Heavy Metals and a Metalloid in Surface Soils in the Kumasi Metropolis, Ghana

Osei Akoto,[1] Nesta Bortey-Sam,[2] Yoshinori Ikenaka,[2] Shouta M.M. Nakayama,[2] Elvis Baidoo,[1] Yared Beyene Yohannes,[2] Mayumi Ishizuka[2]

1 Department of Chemistry, Kwame Nkrumah University of Science and Technology, Kumasi, Ghana
2 Laboratory of Toxicology, Graduate School of Veterinary Medicine, Hokkaido University, Kita 18, Nishi 9, Kita ku, Sapporo 060-0818, Japan

Corresponding Author:
Mayumi Ishizuka
Tel. +81-11-706-6949
Fax +81-11-706-5105
ishizum@vetmed.hokudai.ac.jp

Background. Environmental contamination with heavy metals and metalloids due to industrial, smelting and mining activities have become common in large and growing cities. Kumasi is one of the most industrialized cities in Ghana and experiences metal pollution due to recent and past activities. Although metals are naturally abundant in the area, their accumulation in soils could potentially lead to adverse effects on local ecosystems.
Objectives. The aims of this study were to determine the distribution, enrichment, geo-accumulation and sources of metals in Kumasi soils and to estimate the contamination factor (CF) and pollution load index (PLI) of these metals in soils.
Methods. Concentrations of eight heavy metals and a metalloid were determined in 112 soil samples randomly collected from 31 sampling sites in the area. In addition, 5 soil samples were collected from a pristine site (Kwame Nkrumah University of Science and Technology Botanical Gardens) for data comparison, to determine the local background values for metal concentrations and to evaluate the extent of metal pollution in the study area.
Results. Heavy metals such as zinc (Zn), lead (Pb), cadmium (Cd) and chromium (Cr) were enriched in 65, 32, 58 and 93% of the sampling sites, respectively, and geo-accumulation indexes for Cr, Zn, Cd, mercury (Hg) and Pb showed moderate to extreme contamination in 100, 97, 77, 65 and 45% of the sampling sites, respectively. Principal component and cluster analyses revealed that industrial activities including mining were the major sources of metals in Kumasi soils with high metal input in the community of Suame. Distribution maps revealed hotspots of Cd, nickel (Ni), arsenic (As), cobalt (Co), copper (Cu) and Pb in Suame. The highest CFs for Cu, Cd, Ni, As, Co and Pb highlighted anthropogenic inputs in Suame, while Hg was highest in Mbrom, Zn in Suntreso, and Cr in Aboabo.
Conclusions. The PLI of metals revealed Suame as the most polluted study site, while Anomangye and Bomso were the least polluted.
Competing Interests. The authors declare no competing financial interests.
Keywords. heavy metals; metalloid; Kumasi; contamination factor; pollution load index
Received March 20, 2017. Accepted June 29, 2017.
J Health Pollution 15: 28–39 (2017)

Introduction

Contamination of soil with heavy metal and metalloids results mainly from anthropogenic activities including mining, smelting, tanning, draining of sewage and dumping of wastes. Although metals occur naturally in the environment, chemical and metallurgical industries are the most important sources of metal contamination.[1] Heavy metals/metalloids cannot be easily degraded and are continuously being deposited into soil, water and sediment, causing pollution.[2] Metal concentrations are greatest near towns, indicating their urban/industrial origins. Apart from destabilizing the ecosystem, accumulation of these toxic metals in the food web is a threat to public health and their potential long-term impact on the ecosystem cannot be ignored.[3]

Kumasi (6° 40'00" N 1° 37'00" W) is the capital city of the Ashanti Region and covers a land area of 254 km^2 (98 sq miles). It is the second largest city in Ghana with over 2.5 million inhabitants. The land is dominated by middle Precambrian rocks and the major soil type is forest Ochrosols.[4] On the basis of land use, the study area can be divided into a number of categories: agriculture, human settlement, vegetation cover, water bodies, and industrial. The human population and number of cars have drastically increased during the past few years. In addition, many gas/fuel stations, auto-mechanic/repair workshops, metals fabricators, tanning industries, mining operations (including illegal mining operations popularly known as galamsey), stone quarrying and sand mining industries are located in this region. These and many other anthropogenic factors have led to the release of heavy metals and

metalloids into the environment.[4,5]

There have been a limited number of studies assessing the enrichment/pollution levels and sources of heavy metals and metalloids in the Kumasi metropolis. The objectives of the present study were to determine the concentrations of heavy metals and a metalloid in Kumasi soils, determine the levels of metal accumulation compared to a pristine site using enrichment factor and geo-accumulation index, develop distribution maps of heavy metals/metalloid throughout the sample site using geographic information system (GIS), identify the possible sources of metals by multivariate analysis, and evaluate the extent of metal pollution in Kumasi soils using contamination factor and pollution load index.

Abbreviations

CF	Contamination factor	*KNUST*	Kwame Nkrumah University of Science and Technology
EF	Enrichment factor	*PC*	Principal component
GM	Geometric mean	*PLI*	Pollution load index
I_{geo}	Geoaccumulation index	*USEPA*	United States Environmental Protection Agency

Methods

Sampling

Soil samples were randomly collected from 31 communities (sample sites) in the Kumasi metropolis. A map showing the sampling sites is presented in Figure 1. The sites were selected to represent a wide area of the town and global positioning system was used to locate the sampling positions. Sampling was done in May, 2011 and a total of 112 soils (0-10 cm top layer) were collected using

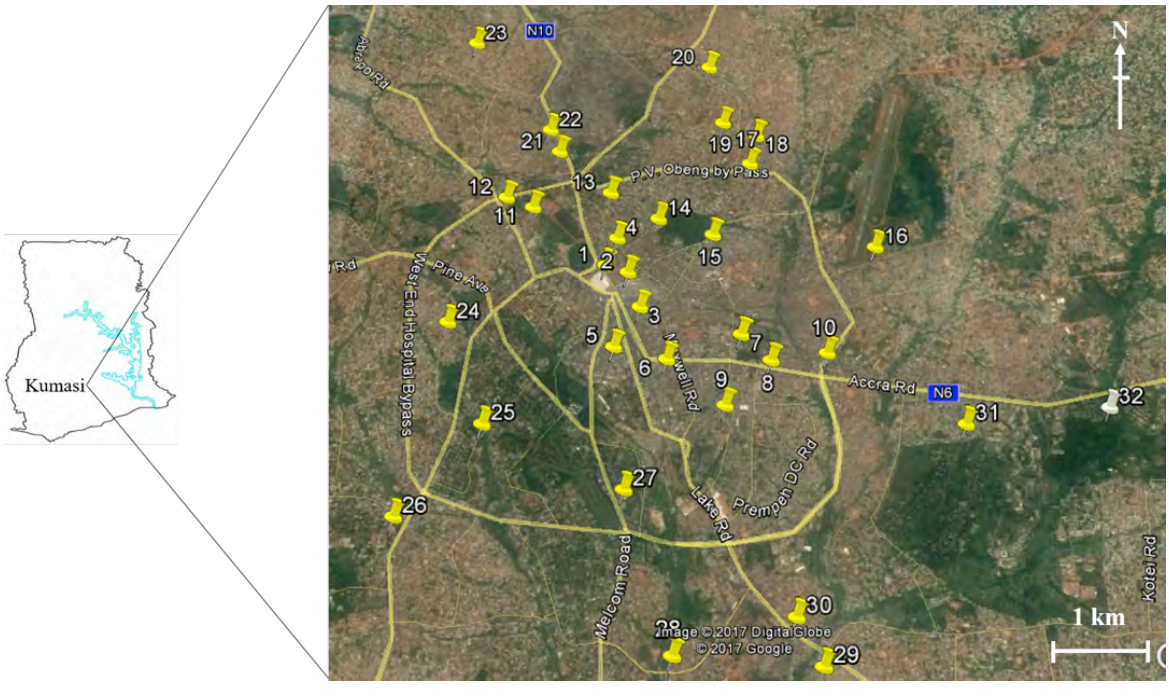

Figure 1 — Sampling area/sites (yellow pins indicate sampled communities and white pin indicates reference site, KNUST Botanical Gardens). 1: Kejetia; 2: Central market; 3: Romanhill; 4: Mbrom; 5: Adum; 6: Asafo; 7: Amakom; 8: Afunkwanta; 9: Asokwa; 10: Oforikrom; 11: Racecourse; 12: Bantama; 13: Ashtown; 14: Manhyia; 15: Asawase; 16: Aboabo; 17: Dichemso; 18: Yennyawoso; 19: Tafo Nhyiaso; 20: Tafo; 21: New Suame; 22: Suame; 23: Anomangye; 24: Suntreso; 25: Danyame; 26: Patasi, 27: Ahodwo, 28: Kaase; 29: Atonsu; 30: Ahinsan; 31: Bomso and 32: KNUST Botanical Gardens.

a stainless steel scoop and stored in labeled Corning tubes (Corning Incorporated, New York, USA). In addition, due to the lack of known background soil concentrations in Ghana, 5 soil samples were collected from the Botanical Gardens of Kwame Nkrumah University of Science and Technology (KNUST) for data comparison (reference values), and to evaluate the extent of metal pollution and enrichment in the study samples. KNUST is a university located in Kumasi, Ghana, and because it experiences low vehicular traffic with no industrial (mining) activities, heavy metals from point sources were assumed to be negligible. Heavy metals and metalloid levels in KNUST Botanical Gardens soil were low compared to the world range for unpolluted soils.[6] In addition, KNUST was used as a reference site for determination of polycyclic aromatic hydrocarbons in particulate matter and soils.[7-9]

All samples were stored at −20°C in the Department of Chemistry, KNUST, Ghana and later transported to the Laboratory of Toxicology, Graduate School of Veterinary Medicine, Hokkaido University, Japan, where they were stored at −30°C until analysis.

Chemical Analysis

Prior to chemical analysis, soil samples were air-dried at room temperature and passed through a 2 mm sieve to remove the coarse soil fraction. Briefly, 1 g of dried soil was weighed into pre-washed digestion vessels and digested (Speed Wave MWS-2, Berghof, Germany) using 10.0 mL of 60% nitric acid, (atomic absorption spectrometry grade; Kanto Chemical Corporation, Tokyo, Japan). The microwave unit was calibrated to a temperature of 200°C and digestion was allowed for 45 minutes at 180 psi. After digestion, the solutions were allowed to cool, filtered using ashless filter paper 5B (Advantec, Tokyo, Japan) into Corning tubes (Corning Incorporated, New York, USA). Lanthanum chloride (1 mL, atomic absorption spectrometry grade, 100 g La/L solution, Wako Pure Chemical Industries Ltd., Osaka, Japan) was added to prevent ionization/interference during metal analysis. Samples were diluted to 50 mL with 2% nitric acid prepared with Milli-Q water. Concentrations of heavy metals and metalloids were determined by atomic absorption spectrophotometry (AAS) (Z-2010, Hitachi High Technologies Corporation, Tokyo, Japan) after preparation of calibration standards. Cadmium (Cd), chromium (Cr), nickel (Ni), lead (Pb) and arsenic (As) were analyzed by graphite furnace AAS (argon gas) with Zeeman background correction. Copper and zinc (Zn) were analyzed by flame AAS (acetylene flame) with deuterium background correction.

In addition, total mercury (Hg) was measured by thermal decomposition, gold amalgamation and atomic absorption spectrophotometry (mercury analyzer, MA–3000, Nippon Instruments Corporation, Tokyo, Japan), after preparation of calibration standards. Blanks were prepared using the same procedure.

The water content (WC) of each sample was measured after 12 h of oven drying at 105°C. Organic matter (OM) content was determined by loss of weight on ignition at an oven temperature of 600°C for 5 hours. Then pH was measured in a soil deionized water suspension (soil: water, 1:2.5 by volume) with a calibrated pH meter.

Quality Control and Quality Assurance

For quality control, blanks were analyzed after every 10 samples. The instrument was calibrated using standard solutions of the respective metals (to establish standard curves before metal analysis). The detection limits (mg/kg) were 0.5 for Cr, 0.5 for cobalt (Co), 1.0 for copper (Cu), 0.1 for Zn, 0.2 for Cd, 1.0 for Pb, 0.5 for Ni and 2.0 for As. Reference materials, Standard Reference Material 1944 (New York/New Jersey Waterway Sediment) and BCR–320 (Channel Sediment, Institute for Reference Materials and Measurements, Belgium) were used for method validation. Replicate analyses of these reference materials showed good accuracy and recovery rates ranged from 80% to 115%. Recovery rates (%) of Hg for these certified reference materials (BCR–320R and Standard Reference Material 1944) ranged from 92–103. The detection limit of Hg in soil samples was 2.0 pg total Hg.

Data Analysis

Enrichment Factor

A common approach to estimating the anthropogenic impact on soil is to calculate the enrichment factor (EF) for metal concentrations above uncontaminated background levels. The EF method normalizes the measured metal content with respect to a reference metal.[10] The reference material would then represent a benchmark to which the metal concentrations in the polluted samples are compared and measured. Pollution, in this case, will be measured as the amount (or ratio) of the sample metal enrichment above the concentrations present in the reference sample. Similar to the approach by Matthai and Birch, Co was considered a normalizing element for determining anthropogenic pollution sources in this study.[11] The EF was calculated according to Equation 1:

Equation 1

$$EF = (M_{sample} \times Co_{ref})/(M_{ref} \times Co_{sample})$$

where M_{sample} is the geometric mean (GM) concentration of metal in soil, Co_{ref} is the GM of Co in the reference sample (KNUST Botanical Gardens), Mref is the GM of metal in reference sample and Co_{sample} is the GM of Co in the sample. Classification of EF by Chen et al. was adopted in this study and has been provided in Supplemental Material 1.[12]

Geoaccumulation Index

This method assesses the degree of metal pollution in terms of seven enrichment classes based on the increasing numerical values of the index. Geoaccumulation index (I_{geo}) is calculated using Equation 2:

Equation 2

$$I_{geo} = log_2 (C_n|1.5Bn)$$

Where C_n is the GM concentration of the element in the enriched samples, and Bn is the background or pristine value of the element (KNUST Botanical Gardens). A factor of 1.5 was introduced to minimize the effect of possible variations in the background values which may be attributed to lithologic variations.[13] Classification of I_{geo} by Muller was used (*Supplemental Material 1*).[14]

Contamination Factor

Contamination factor (CF) reflects the anthropogenic input in elemental pollution and is widely used as a measure of overall contamination of soil. CF was calculated using Equation 3:

Equation 3

$$CF = C_i/B_i$$

Where C_i and B_i are GM concentrations of the examined metal, i, in sample and reference (KNUST Botanical Gardens), respectively.[15] The contamination grades in an increasing order are rated from 1 to 6 (0 = none, 1 = none to medium, 2 = moderate, 3 = moderate to strong, 4 = strongly polluted, 5 = strong to very strong, 6 = very strong).[16]

Pollution Load Index

The pollution load index (PLI) for a set of "n" polluting elements is defined as a value calculated from the GM of the contamination factors of those elements. PLI was calculated by the following expression given by Tomlinson et al:[17]

$$PLI = (CF1 \times CF2 \times CF3 \times ...CFn)^{1/n}$$

A PLI value higher than unity suggests pollution, while values lower than 1 indicate no pollution load.

Statistical Analysis

Statistical analyses were performed using SPSS 20.0 (IBM SPSS Inc., Chicago, USA). Kolmogorov–Smirnov and Shapiro–Wilk's tests were used to determine the normality of data and data were considered statistically significant if the *p* value was less than 0.05. Statistical analyses were carried out after data were log transformed (normalized). Spatial distributions were performed using Arc-GIS 9.3 (ESRI Co., Redlands, USA). Kriging was adopted for the interpolation of geographical data. Geographic Information System coordinates and concentrations of metals obtained in soil were used to create the distribution maps. In order to identify the important parameters that affect the chemistry of soil, Pearson's correlation matrix was used (at a significance level (p) less than 0.05). Principal component analysis and cluster analysis were carried out to describe the degree of association/possible sources of metals in Kumasi soils. The principal components based on log transformed data were extracted with eigenvalues > 1 through a varimax rotation. Cluster analysis was also performed based on Euclidean distance using Ward's clustering method.

Results

Heavy Metals and Metalloid Concentrations in Kumasi Soils

Concentrations of eight heavy metals and a metalloid (As) were measured in Kumasi soils and results are shown in Table 1. The metal concentrations from some sample sites exceeded the recommended levels by Kabata-Pendias and Pendias (unpolluted soils), the United States Environmental Protection Agency (USEPA) and the reference site (KNUST Botanical Gardens).[6,18] Kolmogorov-Smirnov tests for normality showed a significant variation ($p < 0.01$) in metal distribution in Kumasi soils (*Table 1*). As shown in Table 1, Zn was the most abundant metal (107 ± 64.6 mg/kg dry weight (dw)), followed by Cr (97.0 ± 43.7 mg/kg dw) and Pb (52.8 ± 37.9 mg/kg dw). Concentrations of Hg (0.05 ± 0.0363 mg/kg dw) and Cd (0.147 ± 0.159 mg/kg dw) were the lowest.

Enrichment Factor and Geoaccumulation Index

The results of EF revealed that 65, 32, 58 and 93% of soils from the sample sites were moderately to extremely high enriched with Zn, Pb, Cd and Cr, respectively (*Supplemental Material 2*), suggesting anthropogenic inputs. As shown in Table 2, Yennyawoso and Anomangye were extremely highly enriched with Cd (24.6) and Cr (21.1), respectively, and revealed extreme contamination (I_{geo}; *Supplemental Material 3*) in these areas. The I_{geo} values for Cr, Zn, Cd, Hg and Pb indicated moderate to extreme contamination (I_{geo} classes 3 to 6) in 100, 97, 77, 65 and 45% of the sample

Sample Site	n	pH	WC	OM	Hg	Zn	Cu	Cd	Ni	As	Co	Cr	Pb
Kejetia	4	7.88	11.2	7.8	0.15	**217**	38.7	0.34	31.0	1.11	5.21	44.6	**112**
Ahinsan	3	8.47	7.69	4.8	0.05	81.6	28.3	0.11	19.1	1.37	4.25	71.4	23.9
Ahodwo	3	8.74	7.75	3.37	0.01	51.7	24.8	0.05	16.3	1.21	3.78	95.2	23.4
Danyame	3	7.8	9.69	5.61	0.04	69.3	33.8	0.08	27.3	1.92	4.58	113	51.1
Asawase	4	8.44	4.49	3.93	0.04	104	36.5	0.21	12.8	1.03	3.66	113	80.1
Atonsu	3	8.13	9.05	3.96	0.03	79.6	18.9	0.09	11.7	0.73	2.18	29.6	45.1
Mbrom	4	8.4	7.56	4.39	0.20	81.4	33.5	0.15	25.9	1.47	5.02	106	58.5
Bantama	3	8.66	3.7	3.29	0.02	58.0	24.7	0.14	8.28	1.04	2.94	49.2	66.5
Ashtown	4	8.63	5.13	5.53	0.05	**160**	26.1	0.19	11.4	0.75	2.51	102	61.6
Racecourse	4	8.65	8.5	6.21	0.05	**158**	**99.8**	0.15	25.7	1.14	5.42	114	**74.8**
Yennyawoso	3	8.78	0.93	4.34	0.06	60.5	37.0	0.64	23.5	1.94	3.73	**146**	**140**
Kaasi	3	8.98	7.81	4.46	0.02	**127**	33.3	0.09	17.1	2.68	3.05	109	24.5
Aboabo	5	7.98	1.97	5.32	0.04	81.0	40.2	0.09	26.1	1.11	6.02	**249**	55.1
Romanhill	3	9.11	3.1	5.55	0.04	**128**	**68.3**	0.17	9.72	0.93	1.88	86.9	38.5
Dichemso	3	8.88	2.96	4.07	0.14	54.3	24.0	0.07	18.6	1.58	2.65	81.1	26.1
Anomangye	3	8.76	3.35	2.71	0.02	48.2	23.2	0.03	10.1	0.88	2.28	**173**	19.1
Asokwa	4	8.62	5.53	8.2	0.04	71.2	23.3	0.05	9.75	0.91	1.94	58.8	22.3
Afunkwanta	3	8.66	3.84	3.24	0.05	58.9	23.5	0.05	8.38	0.69	2.12	49.9	24.3
Suame	6	8.74	3.1	4.69	0.06	**229**	**278**	0.66	73.9	7.35	14.6	107	**171**
Tafo	6	8.47	6.03	4.41	0.03	108	38.3	0.08	19.6	0.94	3.77	106	**93.3**
Adum	4	8.23	6.34	7.56	0.05	**174**	46.8	0.42	13.4	1.22	3.17	47.7	55.2
New Suame	3	8.6	8.48	4.52	0.16	63.5	29.3	0.07	16.4	1.25	3.67	101	26.7
Central market	4	8.11	5.21	5.98	0.08	119	54.7	0.08	35.9	1.14	5.16	95.9	23.6
Oforikrom	3	7.85	12.3	7.43	0.04	60.6	34.3	0.03	54.6	0.94	6.51	**144**	49.8
Asafo	5	8.69	5.09	3.37	0.05	**212**	46.7	0.17	12.1	1.52	3.24	55.0	**105**
Suntreso	4	9.09	7.83	3.97	0.03	**309**	33.4	0.06	15.4	2.36	3.38	**122**	20.7
Tafo Nhyiaso	3	8.61	6.58	5.57	0.05	62.5	34.2	0.07	22.1	1.73	4.46	98.8	24.3
Patasi	3	8.55	4.85	4.73	0.03	62.9	30.7	0.05	24.8	1.88	5.24	100	31.4
Manhyia	3	8.11	3.58	4.17	0.06	123	27.5	0.06	10.6	1.37	3.27	117	25.7
Amakom	3	8.18	5.55	3.42	0.03	78.1	22.7	0.08	8.22	1.35	1.87	75.2	41.6
Bomso	3	8.89	6.84	3.09	0.03	40.6	22.3	0.04	11.87	1.39	2.36	50.3	21.5
GM		8.50	6.00	4.82	0.0506	107	43.1	0.147	20.4	1.51	3.98	97.4	52.8
Minimum		7.8	0.93	2.71	0.01	40.6	18.9	0.03	8.22	0.69	1.87	29.6	19.1
Maximum		9.11	12.3	8.2	0.16	309	278	0.66	73.9	7.35	14.6	249	171
CV		4.22	44.7	29.9	71.7	59.9	107	108	68.8	78.1	59.0	44.8	71.7
K-S					< 0.01	< 0.01	< 0.01	< 0.01	< 0.01	< 0.01	< 0.01	< 0.01	< 0.01
Reference[#]		5.01	6.14	4.18	0.005	7.49	12.6	0.01	4.28	0.3	1.29	4.67	7.91
USEPA[b]					32	17-125	6-60	0.07-1.1	1-200	1-15	0.1-20	5-120	10-70
World range[c]					-	50-120	70	1.6	30-200	18	-	240	120

Abbreviations: n, number of samples; USEPA[b], USEPA Ecological-Soil Screening Levels;[18] World range[c], world range of metals in unpolluted soils;[6] Reference#, reference values (KNUST Botanical Gardens); nd, not detected; K-S, Kolmogorov-Smirnov test; WC, water content; OM, organic matter; GM, geometric mean; dw, dry weight.

Bold values indicate concentrations higher than limits of the USEPA[18] and/or Kabata–Pendias and Pendias[6]

Table 1 — Geometric Mean Concentrations (mg/kg dw) of Heavy Metals and Metalloid in Soils in Kumasi, Ghana

	Contamination Factor									PLI
Sample Site	Hg	Zn	Cu	Cd	Ni	As	Co	Cr	Pb	
Kejetia	**30.0**	**29.0**	**3.06**	**37.4**	**7.25**	**3.66**	**3.86**	**9.57**	**14.1**	**10.3**
Ahinsan	**10.0**	**10.9**	**2.24**	**11.7**	**4.48**	**4.49**	**3.28**	**15.3**	**3.03**	**5.90**
Ahodwo	**2.00**	**6.92**	1.96	**5.48**	**3.81**	**3.98**	**2.92**	**20.4**	**2.97**	**4.18**
Danyame	**6.00**	**9.26**	**2.67**	**8.65**	**6.40**	**6.31**	**3.54**	**24.4**	**6.46**	**6.74**
Asawase	**8.00**	**14.0**	**2.88**	**23.1**	**2.99**	**3.40**	**2.83**	**24.4**	**10.1**	**7.21**
Atonsu	**6.00**	**10.6**	1.49	**10.1**	**2.74**	**2.40**	1.69	**6.36**	**5.71**	**4.18**
Mbrom	**40.0**	**10.8**	**2.65**	**16.4**	**6.06**	**4.85**	**3.88**	**22.7**	**7.40**	**8.93**
Bantama	**4.00**	**7.74**	1.95	**15.1**	1.94	**3.41**	**2.27**	**10.5**	**8.41**	**4.74**
Ashtown	**10.0**	**21.4**	**2.06**	**20.8**	**2.67**	**2.47**	1.94	**21.8**	**7.79**	**6.47**
Racecourse	**10.0**	**21.2**	**7.87**	**16.8**	**6.02**	**3.75**	**4.19**	**24.5**	**9.46**	**9.47**
Yennyawoso	**12.0**	**8.08**	**2.92**	**71.1**	**5.50**	**6.38**	**2.88**	**31.4**	**17.7**	**10.1**
Kaasi	**4.00**	**17.0**	**2.62**	**10.3**	**4.01**	**8.81**	**2.36**	**23.3**	**3.10**	**6.06**
Aboabo	**8.00**	**10.8**	**3.17**	**10.5**	**6.11**	**3.66**	**4.66**	**53.4**	**6.97**	**7.84**
Romanhill	**8.00**	**17.1**	**5.38**	**18.8**	**2.27**	**3.07**	1.46	**18.6**	**4.88**	**6.16**
Dichemso	**28.0**	**7.26**	1.89	**7.31**	**4.35**	**5.20**	**2.05**	**17.3**	**3.31**	**5.8**
Anomangye	**4.00**	**6.44**	1.83	**2.97**	**2.36**	**2.91**	1.76	**37.2**	**2.42**	**3.77**
Asokwa	**8.00**	**9.52**	1.84	**6.07**	2.28	**2.99**	1.50	**12.6**	**2.83**	**4.07**
Afunkwanta	**10.0**	**7.86**	1.85	**6.04**	1.96	**2.28**	1.64	**10.7**	**3.07**	**3.90**
Suame	**12.0**	**30.6**	**21.9**	**73.5**	**17.2**	**24.1**	**11.3**	**23.1**	**21.6**	**22.3**
Tafo	**6.00**	**14.4**	**3.02**	**8.48**	**4.58**	**2.97**	**2.92**	**22.8**	**11.8**	**6.60**
Adum	**10.0**	**23.2**	**3.69**	**47.1**	**3.13**	**3.95**	**2.40**	**10.2**	**6.99**	**7.60**
New Suame	**32.0**	**8.48**	**2.31**	**7.90**	**3.84**	**4.10**	**2.84**	**21.6**	**3.38**	**6.32**
Central market	**16.0**	**15.9**	**4.32**	**8.85**	**8.41**	**3.63**	**3.95**	**20.5**	**2.99**	**7.46**
Oforikrom	**8.00**	**8.10**	**2.71**	**3.69**	**12.7**	**3.08**	**5.03**	**30.9**	**6.30**	**6.63**
Asafo	**10.0**	**28.3**	**3.68**	**18.5**	**2.83**	**4.93**	**2.51**	**11.7**	**13.3**	**7.79**
Suntreso	**6.00**	**41.2**	**2.64**	**7.01**	**3.62**	**7.77**	**2.61**	**26.2**	**2.62**	**6.58**
Tafo Nhyiaso	**10.0**	**8.35**	**2.70**	**7.54**	**5.18**	**5.68**	**3.45**	**21.1**	**3.08**	**6.07**
Patasi	**6.00**	**8.41**	**2.42**	**5.07**	**5.81**	**6.19**	**4.05**	**21.4**	**3.97**	**5.82**
Manhyia	**12.0**	**16.4**	**2.17**	**7.10**	**2.48**	**4.51**	**2.53**	**25.1**	**3.25**	**5.76**
Amakom	**6.00**	**10.4**	1.79	**9.17**	1.92	**4.44**	1.44	**16.1**	**5.26**	**4.67**
Bomso	**6.00**	**5.43**	1.76	**4.01**	**2.77**	**4.59**	1.83	**10.7**	**2.72**	**3.77**
Average	11.2	14.3	3.40	16.3	4.77	4.97	3.08	20.8	6.68	6.89
SD	8.97	8.63	3.67	17.7	3.28	3.88	1.82	9.36	4.79	3.38
Minimum	2.00	5.43	1.49	2.97	1.92	2.28	1.44	6.36	2.42	3.77
Maximum	40.0	41.2	21.9	73.5	17.2	24.1	11.3	53.4	21.6	22.3

Abbreviations: PLI, pollution load index; SD, standard deviation

Bold contamination factor indicates moderate to very strong contamination; Bold PLI indicates values greater than 1 and signifies pollution

Table 2 — Contamination Factor and Pollution Load Index of Heavy Metals in Soils in Kumasi, Ghana

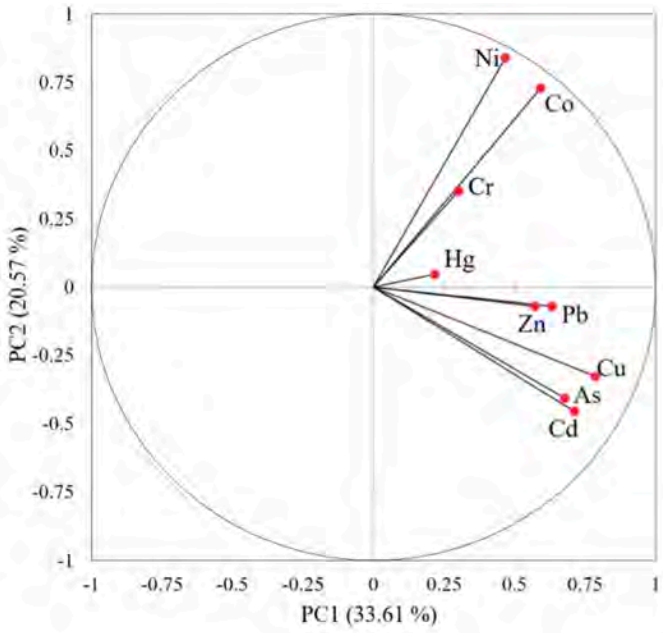

Figure 2 — Source characterization of heavy metals and metalloid concentrations by principal component analysis

sites, respectively, (*Supplemental Material 3*) when compared the reference site. In Suame, all the studied metals showed moderate to extreme contamination with I_{geo} ranging from 2.92 (Co) to 5.62 (Cd) (*Supplemental Material 3*).

Sources Characterization by Multivariate Analysis

Principal Component Analysis

Principal component (PC) analysis was used to characterize sources of metals in Kumasi soils. From the results, three principal components (PC1, PC2, and PC3) were extracted and accounted for 66.9% of the total variance. As shown in Figure 2, PC1 explained 33.6% of the total variance and was characterized by high loadings of Cu, Pb, Cd, As and Zn. PC2 explained 20.6% of the total variance (*Figure 2*) and was dominated by high loadings

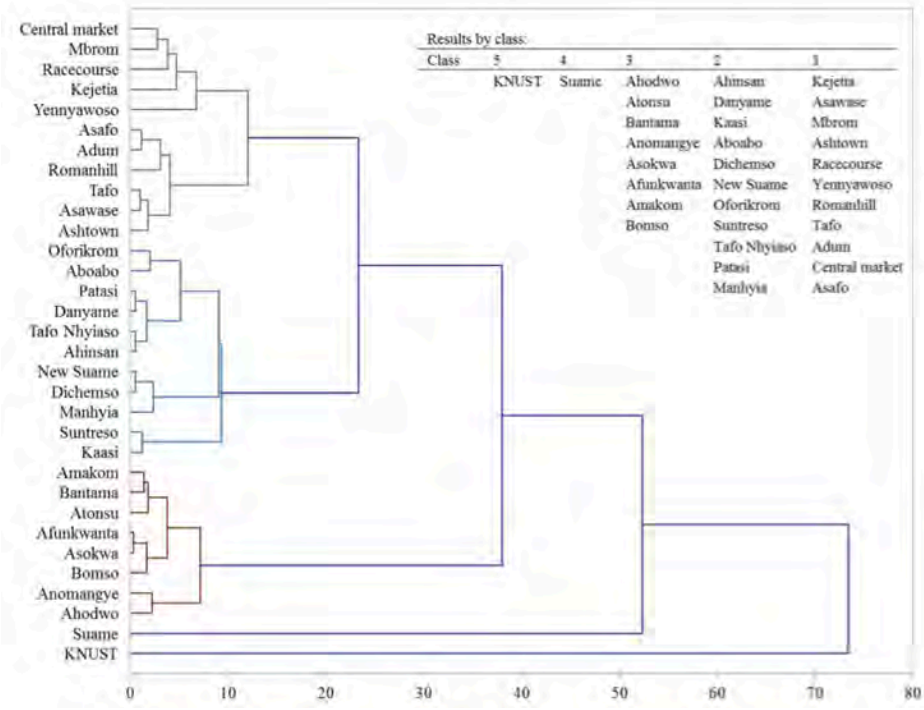

Figure 3 — Hierarchical dendrogram of heavy metals and metalloid concentrations from the sample sites obtained using Ward's clustering method

of Ni, Co, and Cr, while PC3 (Hg) explained 12.7% of the total variance.

Cluster Analysis

Hierarchical cluster analysis was used in this study to identify the degree of association and/or accumulation pattern of heavy metals from the sample sites (*Figure 3*). The dendrogram revealed five classes with Suame and KNUST Botanical Gardens in different clusters (*Figure 3*). Kejetia, Asawase, Mbrom, Ashtown, Racecourse, Yennyawoso, Romanhill, Tafo, Adum, Central market and Asafo were in class 1 of the dendrogram (*Figure 3*), indicating a strong association between metal levels, sources or distribution in soils at these sites.

Correlation Between Metals and Soil Properties

The physico-chemical parameters determined in Kumasi soils were soil pH, organic matter and water content. Mean pH values ranged from 7.88 ± 0.49 (Kejetia) to 9.11 ± 0.5 (Romanhill) (*Table 1*). pH influences the rate of adsorption, retention and the transfer/migration of heavy metals in soil.[19] The organic matter content ranged from 2.71 (Anomangye) to 8.2% (Asokwa) (*Table 1*). In the present study, concentrations of metals did not correlate with either pH or organic matter (*Supplemental Material 4*), similar to the results of a previous study.[20]

Distribution Maps of Heavy Metals and a Metalloid

The distribution maps of Cd, Ni, As, Co, Cu and Pb highlighted Suame (*22 on Figure 1*) as hotspot zone, indicating high metal concentrations (*Figures 1 and 4*). The hotspots identified from the geochemical map for Zn, Cr and Hg indicated high concentrations of these metals in Suntreso, Aboabo/ Yennyawoso and Mbrom/Kejetia/New Suame, respectively.

Contamination Factor and Pollution Load Index

Table 2 shows the CF and PLI of metals in soils from the sample sites. The average CF for all the studied metals were greater than 3, indicating moderate to very strong contamination in Kumasi soils. The highest CF for Cu, Cd, Ni, As, Co and Pb were in Suame, while the highest CF for Hg was in Mbrom, Zn (Suntreso), and Cr in Aboabo (*Table 2)*. In this study, the PLI of heavy metals and a metalloid revealed Suame (22.3) as the sample site most polluted with metals, followed by Kejetia (10.3) ≥ Yennyawoso (10.1) > Racecourse (9.47) > Mbrom (8.93) > Aboabo (7.84) ≥ Asafo (7.79) ≥ Adum (7.60) ≥ Central market (7.46) > …, Afunkwanta (3.90) ≥ Bomso (3.77) = Anomangye (3.77). The study showed that all study sites (average PLI = 6.89 ± 3.38; range: 3.77 to 22.3) were polluted with metals when compared to KNUST Botanical Gardens (*Table 2*).

Discussion

Metal Enrichment and Accumulation in Kumasi Soils

The concentrations, EF and I_{geo} of heavy metals and a metalloid from some sample sites within the Kumasi metropolis were higher and this could be due to the fact that the sampling sites in Kumasi were located within an area with heavy vehicular movement/traffic and industrialization. In addition, the high soil metal enrichment could be attributed to differences in the magnitude of input for each metal and/or differences in the removal rate from soil.[5] The moderate to extreme metal contamination in Suame could have resulted from the many auto mechanical/repair workshops and vehicles in the area.

Principal Component Analysis

As shown in Figure 2, PC1 showed an association with Cu, Pb, Cd, As and Zn and inputs of these metals and metalloid could have resulted from industrial activities and discharges such as mining and smelting processes.[21] Cd is soft, ductile and is obtained as a by-product from the smelting of Zn ores. In mining contexts, Cd can also be found in the form of the greenockite mineral, cadmium sulfide. Cadmium in soils from the study area may come from the mining and processing of Zn and chalcophilic metals.[22] The presence of Zn in the environment is associated with mining and smelting, which pollutes the air, water and soil and ultimately undergoes oxidation to release Zn^{2+} ions into water bodies.[22]

Processing ore after blasting gold bearing rock involves roasting, and this results in the production of arsenic trioxide gas which is distributed throughout the study area by air currents. Arsenic is toxic and could accumulate in surface soils because of its non-biodegradable nature.[23] Cadmium and As concentrations could also be associated with industrial activities/discharges, sewage sludge and municipal solid waste.[24]

Large amounts of vehicular/industrial emissions and improper disposal of wastes could have contributed to the Cu, Pb, and Zn levels in Kumasi. Although no longer in use, previous use of leaded fuel could have accounted for the levels of Pb in soils. Lead is considered immobile in sub-surface soil and generally gets accumulated and remains strongly bound to soil mineral or organic components when deposited.[25]

Ni, Co and Cr were grouped in the same principal component. The high EF and I_{geo} from the sample sites, especially for Cr, suggest an

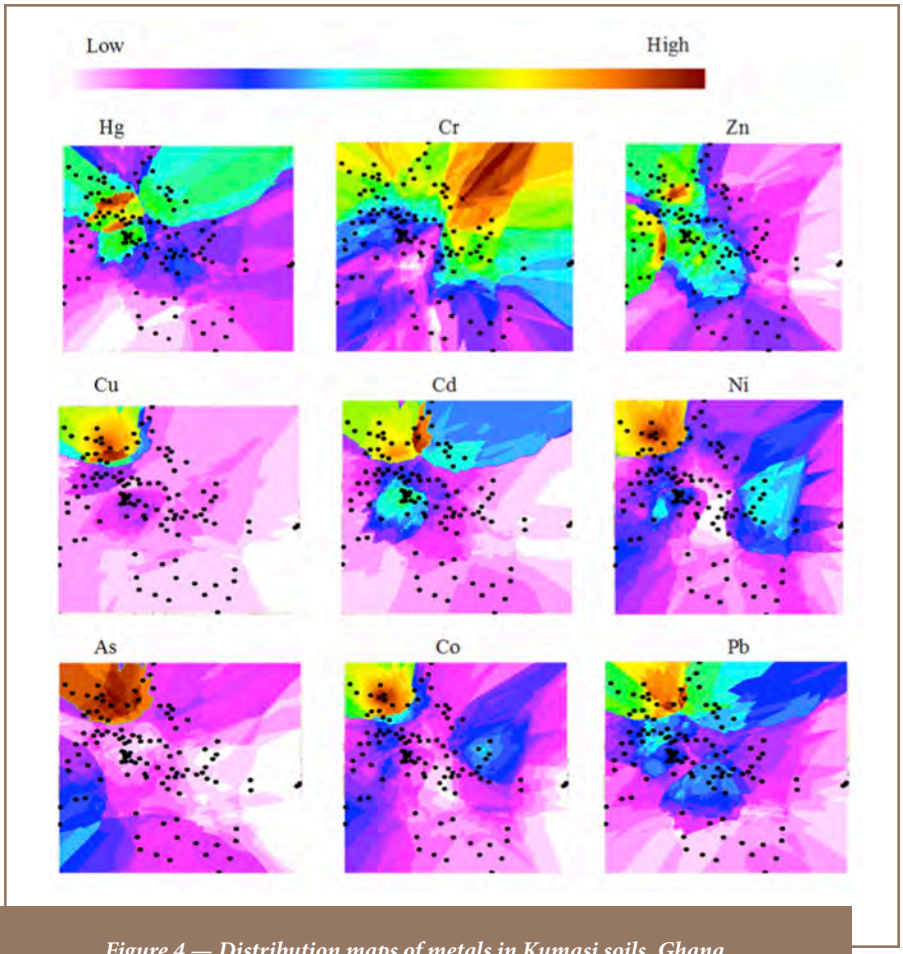

Figure 4 — Distribution maps of metals in Kumasi soils, Ghana

anthropogenic input from industrial sources.[26] Ghana, including the Kumasi metropolis, is filled with many tanning industries where animal skin is converted into leather, a practice considered to be an environmental threat. During this process, a variety of chemicals are used along with large volumes of water which are discharged as effluents containing liquid and solid wastes, and a significant amount of Cr.[27] An average tannery uses approximately 65,000 tons of chemicals, including Cr (as chromium sulfate), annually, only to be discharged as effluents.[28] The processes involved in the treatment of skin/hides are highly associated with sodium, potassium, magnesium and Co in effluents. Similarly, tanning processes are highly associated with Cr in soil.[27]

Artisanal and small-scale gold mining, production of cement and non-ferrous metals (including Cu, Pb, Zn, aluminum and large-scale gold production) and disposal of Hg wastes are some of the main sources of environmental Hg contamination.[29] Artisanal and small-scale mining is highly practiced in some sample sites in Kumasi, and during this process Hg is used to amalgamate gold.[23,30] This practice, although simple and inexpensive, could contribute to the concentrations of metals, including Hg levels, in the environment. Other sources of Hg in Kumasi soils could include discarded thermometers, batteries and fluorescent lamps, as these accounted for 40% of Hg emissions in North America. In addition, the use of barometers releases Hg into the environment.[31] In agricultural systems, pesticides, fertilizers, sewage sludge and irrigation water were some of the main sources of Hg contamination.[32]

Cluster Analysis

KNUST Botanical Gardens (reference site) was grouped in a different cluster of the dendrogram (*Figure 3*) and this trend could be attributed to the low metal concentrations compared to other sites and the world range for unpolluted soils.[6] This trend, again, suggests that metals detected in KNUST Botanical Garden soils originated from natural/geological processes. On the other hand, high levels of metals were detected in Suame (*Table 1*) which was in class 4 of the dendrogram (*Figure 3*) and, EF and I_{geo} indicated moderate to extreme contamination at this site (*Supplemental Material 1 and 3*). Differences in metal sources or the higher level of soil metal contamination could have contributed significantly to the present results.

Sampling sites such as Kejetia, Asawase, Mbrom, Ashtown, Racecourse, Yennyawoso, Romanhill, Tafo, Adum, Central market and Asafo were grouped in class 1 of the dendrogram (*Figure 3*), implying a similar/single source of metal pollution at these sites. Sources of metals in Mbrom and Central market, and Adum and Asafo were closely related and showed a strong association with metals levels in Racecourse, Kejetia and Yennyawoso (*Figure 3*). As shown in Figure 1, the sampling sites grouped in class 1 are

close together, with the exception of Yennyawoso (site # 18) and Tafo (site # 20), which are about 1.3 km apart. This trend could possibly be due to effects of artisanal and small-scale gold mining in some sample sites.

Correlation Between Metals and Soil Properties

Lack of significant correlation between soil properties and heavy metals could be attributed to a continuous input, since the release and transport of heavy metals are governed by complex processes.[33,34] Another possible reason could be variations in soil type within the sampled area.[33,34]

Distribution Maps of Heavy Metals and a Metalloid

As shown in the distribution maps (*Figure 4*), the high metal concentrations in Suame could also be due to heavy vehicle traffic and the large amount of metal scrap in the area. The "Suame Magazine" is one of Africa's largest light-industrial clusters. It is a 200 hectare area filled with polluted industrial waste, auto-mechanic workshops and saw mills, with frequent burning of tires generating a significant amount of waste.[35] The hotspots identified from the distribution maps for Zn (Suntreso), Cr (Aboabo and Yennyawoso) and Hg (Mbrom, Kejetia and New Suame) could be due to the fact that some of these sampling sites are densely populated with vehicles and light (small scale) industries, including many tanneries.

Conclusions

Concentrations of heavy metals and a metalloid were studied in Kumasi soils and Zn, Pb, Cd and Cr were found to be enriched in some of the sample sites, suggesting anthropogenic inputs. Based on the obtained I_{geo} values, Cr, Zn, Cd, Hg and Pb showed moderate to extreme contamination in 100, 97, 77, 65 and 45% of the sample sites, respectively. Distribution maps and pollution load index values highlighted Suame as the most significantly polluted site, followed by Kejetia ≥ Yennyawoso > Racecourse > Mbrom > Aboabo ≥ Asafo ≥ Adum ≥ Central market > …, Afunkwanta ≥ Bomso = Anomangye. Finally, the present study indicates that industrial activities, including mining, are the major sources of metals in Kumasi soils, as observed at the most contaminated site of Suame.

Acknowledgements

This work was supported by Grants-in-Aid for Scientific Research from the Ministry of Education, Culture, Sports, Science and Technology of Japan awarded to M. Ishizuka (No. 24405004 and No. 24248056) and Y. Ikenaka (No. 26304043, 15H0282505, 15K1221305), and the foundation of JSPS Core to Core Program (AA Science Platforms) and Bilateral Joint Research Project (PG36150002 and PG36150003). We also acknowledge the financial support by The Mitsui & Co., Ltd. Environment Fund. We are grateful to Mr. Takahiro Ichise (Laboratory of Toxicology, Graduate School of Veterinary Medicine, Hokkaido University) for technical support.

References

1. **Navarro MC, Perez-Sirvent C, Martinez-Sanchez MJ, Vidal J, Tovar PJ, Bech J**. Abandoned mine sites as a source of contamination by heavy metals: a case study in a semi-arid zone. *J Geochem Explor* [Internet]. 2008 Feb-Mar [cited 2016 Oct 12];96(2-3):183-93. Available from: http://www.sciencedirect.com/science/article/pii/S0375674207000519 Subscription required to view.

2. **Linnik PM, Zubenko IB**. Role of bottom sediments in the secondary pollution of aquatic environments by heavy metal compounds. *Lake Reserv: Res Manag* [Internet]. 2000 Mar [cited 2016 Oct 12];5(1):11-21. Available from: http://onlinelibrary.wiley.com/doi/10.1046/j.1440-1770.2000.00094.x/full Subscription required to view.

3. **Ogoyi DO, Mwita CJ, Nguu1 EK, Shiundu PM**. Determination of heavy metal content in water, sediment and microalgae from Lake Victoria, East Africa. *Open Environ Eng J* [Internet]. 2011 [cited 2016 Oct 12];4:156-61. Available from: http://erepository.uonbi.ac.ke/bitstream/handle/11295/40017/Main%20Article?sequence=1&isAllowed=y

4. **2010 population and housing census** [Internet]. Accra, Ghana: Ghana Statistical Service; 2012 May [cited 2016 Oct 12]. 117 p. Available from: http://www.statsghana.gov.gh/docfiles/2010phc/Census2010_Summary_report_of_final_results.pdf

5. **Akoto O, Ephraim JH, Darko G**. Heavy metals pollution in surface soils in the vicinity of abundant railway servicing workshop in Kumasi, Ghana. *Int J Environ Res* [Internet]. 2008 Autumn [cited 2016 Oct 12];2(4):359-64. Available from: https://tspace.library.utoronto.ca/bitstream/1807/49403/1/er08047.pdf

6. **Kabata-Pendias A, Pendias H**. Trace elements in soils and plants. 2nd ed. Boca Raton, Florida: CRC Press; 1991 Dec 7. 384 p.

7. **Bortey-Sam N, Akoto O, Ikenaka Y, Nakayama SM, Ishizuka M**. Determination of benzo [a] pyrene levels in ambient air and the source of polycyclic aromatic hydrocarbons using a diagnostic ratio method in Ghana. *Jpn J Vet Res* [Internet]. 2013 Feb 1 [cited 2016 Oct 12];61 Suppl:S72-4. Available from: http://europepmc.org/abstract/med/23631159 Subscription required to view.

8. **Bortey-Sam N, Ikenaka Y, Nakayama SM, Akoto O, Yohannes YB, Baidoo E, Mizukawa H, Ishizuka M.** Occurrence, distribution, sources and toxic potential of polycyclic aromatic hydrocarbons (PAHs) in surface soils from the Kumasi Metropolis, Ghana. *Sci Total Environ* [Internet]. 2014 Oct 15 [cited 2016 Oct 12];496:471-8. Available from: http://dx.doi.org/10.1016/j.scitotenv.2014.07.071 Subscription required to view.

9. **Bortey-Sam N, Ikenaka Y, Akoto O, Nakayama SM, Yohannes YB, Baidoo E, Mizukawa H, Ishizuka**

M. Levels, potential sources and human health risk of polycyclic aromatic hydrocarbons (PAHs) in particulate matter (PM10) in Kumasi, Ghana. *Environ Sci Pollut Res* [Internet]. 2015 Jul [cited 2016 Oct 12];22(13):9658-67. Available from: https://link.springer.com/article/10.1007%2Fs11356-014-4022-1 Subscription required to view.

10. **Ravichandran M, Baskaran M, Santschi PH, Bianchi T. History of trace metal pollution in Sabine-Neches Estuary, Beaumont, Texas.** *Environ Sci Technol* [Internet]. 1995 Jun [cited 2016 Oct 12];29(6):1495-503. Available from: http://pubs.acs.org/doi/abs/10.1021/es00006a010 Subscription required to view.

11. **Matthai C, Birch G. Detection of anthropogenic Cu, Pb, and Zn in continental shelf sediments off Sydney, Australia – a new approach using normalization with cobalt.** *Marine Poll Bull* [Internet]. 2001 Nov [cited 2016 Oct 12];42(11):1055-63. Available from: http://www.sciencedirect.com/science/article/pii/S0025326X01000686 Subscription required to view.

12. **Chen CW, Kao CM, Chen CF, Dong CD. Distribution and accumulation of heavy metals in the sediments of Kaohsiung Harbor, Taiwan.** *Chemosphere* [Internet]. 2007 Jan [cited 2016 Oct 12];66(8):1431-40. Available from: http://dx.doi.org/10.1016/j.chemosphere.2006.09.030 Subscription required to view.

13. **Stoffers P, Glasby GP, Wilson CJ, Davis KR, Walter P. Heavy metal pollution in Wellington Harbour.** *N.Z. J Marine Freshwater Res* [Internet]. 1986 Dec [cited 2016 Oct 12];20(3):495-512. Available from: http://www.tandfonline.com/doi/abs/10.1080/00288330.1986.9516169

14. **Muller G. Index of geoaccumulation in sediments of the Rhine River.** *Geol J.* 1969;2(3):109-18.

15. **Hakanson L. An ecological risk index for aquatic pollution control. a sedimentological approach.** *Water Res* [Internet]. 1980 Apr [cited 2016 Oct 12];14(8):975-1001. Available from: http://www.sciencedirect.com/science/article/pii/0043135480901438 Subscription required to view.

16. **Varol M. Assessment of heavy metal contamination in sediments of the Tigris River (Turkey) using pollution indices and multivariate statistical techniques.** *J Hazard Mater* [Internet]. 2011 Nov [cited 2016 Oct 12];195:355-64. Available from: http://www.sciencedirect.com/science/article/pii/S0304389411010697 Subscription required to view.

17. **Tomlinson DL, Wilson JG, Harris CR, Jeffrey DW. Problems in the assessment of heavy-metal levels in estuaries and the formation of a pollution index.** *Helgol Meeresunters* [Internet]. 1980 [cited 2016 Oct 12];33:566-75. Available from: http://hmr.biomedcentral.com/articles/10.1007/BF02414780

18. **Guidance for developing ecological soil screening levels: OSWER-directive 9285.7-55** [Internet]. Washington, D.C.: United States Environmental Protection Agency; 2003 Nov [revised 2005 Feb; cited 2016 Oct 12]. 85 p. Available from: https://www.epa.gov/chemical-research/guidance-developing-ecological-soil-screening-levels

19. **de Matos AT, Fontes MPF, da Costa LM, Martinez MA. Mobility of heavy metals as related to soil chemical and mineralogical characteristics of Brazilian soils.** *Environ Pollut* [Internet]. 2001 Oct [cited 2016 Oct 12];111(3):429-35. Available from: http://dx.doi.org/10.1016/S0269-7491(00)00088-9 Subscription required to view.

20. **Al–Khashman OA, Shawabkeh RA. Metals distribution in soils around the cement factory in southern Jordan.** *Environ Pollut* [Internet]. 2006 April [cited 2016 Oct 12];140(3):387-94. Available from: http://dx.doi.org/10.1016/j.envpol.2005.08.023 Subscription required to view.

21. **Bortey-Sam N, Nakayama SM, Akoto O, Ikenaka Y, Baidoo E, Mizukawa H, Ishizuka M. Ecological risk of heavy metals and a metalloid in agricultural soils in Tarkwa, Ghana.** *Int J Environ Res Public Health* [Internet]. 2015 Sep [cited 2016 Oct 12];12(9):11448-65. Available from: http://www.mdpi.com/1660-4601/12/9/11448/htm

22. **Obiri S. Determination of heavy metals in water from boreholes in Dumasi in the Wassa west district of the western region of the Republic of Ghana.** *Environ Monit Assess* [Internet]. 2007 Jul [cited 2016 Oct 12];130(1-3):455-63. Available from: http://link.springer.com/article/10.1007/s10661-006-9435-y Subscription required to view.

23. **Amonoo–Neizer EH, Nyamah D, Bakiamoh SB. Mercury and arsenic pollution in soil and biological samples around mining towns of Obuasi, Ghana.** *Water Air Soil Poll* [Internet]. 1996 Oct [cited 2016 Oct 12];91(3-4):363-73. Available from: https://link.springer.com/article/10.1007/BF00666270 Subscription required to view

24. **Zhao L, Xu Y, Hou H, Shangguan Y, Li F. Source identification and health risk assessment of metals in urban soils around the Tanggu chemical industrial district, Tianjin, China.** *Sci Total Environ* [Internet]. 2014 Jan [cited 2016 Oct 12];468-469:654-62. Available from: http://www.sciencedirect.com/science/article/pii/S0048969713010218 Subscription required to view.

25. **McLean JE, Bledsoe BE. Behavior of metals in soil. In: Ground water issue** [Internet]. Washington, D.C.: United States Environmental Protection Agency; 1992 Oct [cited 2016 Oct 12]. 25 p. Available from: https://nepis.epa.gov/Exe/ZyPURL.cgi?Dockey=10002DSF.TXT

26. **Bai J, Xiao R, Cui B, Zhang K, Wang Q, Liu X, Gao H, Huang L. Assessment of heavy metal pollution in wetland soils from the young and old reclaimed regions in the Pearl River Estuary, South China.** *Environ Pollut* [Internet]. 2011 Mar [cited 2016 Oct 12];159(3):817-24. Available from: http://dx.doi.org/10.1016/j.envpol.2010.11.004 Subscription required to view.

27. **Tariq SR, Shah MH, Shaheen N, Khalique A, Manzoor S, Jaffar M. Multivariate analysis of selected metals in tannery effluents and related soil.** *J Hazard Mater* [Internet]. 2005 Jun 30 [cited 2016 Oct 12];122(1-2):17-22. Available from: http://www.sciencedirect.com/science/article/pii/S0304389405001238 Subscription required to view.

28. **Landgrave J. A pilot plant for removing chromium from residual water of tanneries.** *Environ Health Perspect* [Internet]. 1995 Feb [cited 2016 Oct 12];103(Suppl 1):63-5. Available from: https://www.ncbi.nlm.nih.gov/pmc/articles/PMC1519324/

29. **Mason RP, Choi AL, Fitzgerald WF, Hammerschmidt CR, Lamborg CH, Soerensen AL, Sunderland EM. Mercury biogeochemical cycling in the ocean and policy implications.** *Environ Res* [Internet]. 2012 Nov [cited 2016 Oct 12];119:101-17. Available from: http://www.sciencedirect.com/science/article/pii/S0013935112001132 Subscription required to view.

30. **Rajaee M, Long RN, Renne EP, Basu N. Mercury exposure assessment and spatial distribution in a Ghanaian small-scale gold mining community.** *Int J Environ Res Public Health* [Internet]. 2015 Sep [cited 2016 Oct 12];12(9):10755-82. Available from: http://www.mdpi.com/1660-4601/12/9/10755/htm

31. **Hutchison AR, Atwood DA. Mercury pollution and remediation: the chemist's response to a global crisis.** *J Chem Crystallogr* [Internet]. 2003 Aug [cited 2016 Oct 12];33(8):631-45. Available from: http://link.springer.com/article/10.1023/A:1024906212586 Subscription required to view.

32. **Hseu ZY, Su SW, Lai HY, Guo HY, Chen TC, Chen ZS. Remediation techniques and heavy metal uptake by different rice varieties in metal-contaminated soils of Taiwan: new aspects for food safety regulation and sustainable agriculture.**

Soil Sci Plant Nutr [Internet]. 2010 [cited 2016 Oct 12];56(1):31-52. Available from: http://dx.doi.org/10.1111/j.1747-0765.2009.00442.x Subscription required to view.

33. **Lu AX, Wang JH, Qin XY, Wang KY, Han P, Zhang SZ**. Multivariate and geostatistical analyses of the spatial distribution and origin of heavy metals in the agricultural soils in Shunyi, Beijing, China. *Sci Total Environ* [Internet]. 2012 May 15 [cited 2016 Oct 12];425:66-74. Available from: http://www.sciencedirect.com/science/article/pii/S0048969712003348 Subscription required to view.

34. **Grant C, Sheppard S.** Fertilizer impacts on cadmium availability in agricultural soils and crops. *Hum Ecol Risk Assess* [Internet]. 2008 Apr [cited 2016 Oct 12];14(2):210-28. Available from: http://dx.doi.org/10.1080/10807030801934895 Subscription required to view.

35. **Dartey E, Adimado AA, Agyarko K**. Evaluation of airborne lead levels in storage battery workshops and some welding environments in Kumasi metropolis in Ghana. *Environ Monit Assess* [Internet]. 2010 May [cited 2016 Oct 12];164(1-4):1-8. Available from: https://www.ncbi.nlm.nih.gov/pubmed/19357980 Subscription required to view.

Science of the Total Environment 628–629 (2018) 517–527

Contents lists available at ScienceDirect

Science of the Total Environment

journal homepage: www.elsevier.com/locate/scitotenv

Fish consumption from urban impoundments: What are the health risks associated with DDTs and other organochlorine pesticides in fish to township residents of a major inland city

Wihan Pheiffer [a,*], Nico J. Wolmarans [a], Ruan Gerber [a], Yared B. Yohannes [b,c], Yoshinori Ikenaka [a,b], Mayumi Ishizuka [b], Nico J. Smit [a], Victor Wepener [a], Rialet Pieters [a]

[a] Water Research Group, Unit for Environmental Science and Management, North-West University, Private Bag X6001, Potchefstroom 2520, South Africa
[b] Laboratory of Toxicology, Department of Environmental Veterinary Science, Faculty of Veterinary Medicine, Hokkaido University, Kita 18, Nishi 9, Kita ku, Sapporo 060–0818, Japan
[c] Department of Chemistry, College of Natural and Computational Science, University of Gondar, P.O. Box 196, Gondar, Ethiopia

HIGHLIGHTS

- Organochlorine pesticides (OCPs) found in urban area
- *Clarias gariepinus* accumulated OCPs in muscle tissue.
- The cancer risk associated with consumption was greater than acceptable levels.
- Non-cancerous risk was up to a 1000 times that what is considered safe.

GRAPHICAL ABSTRACT

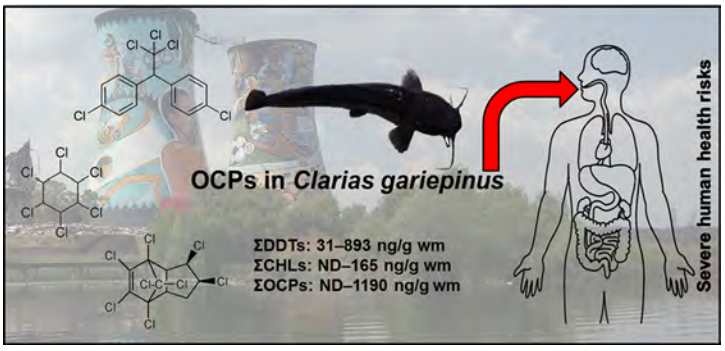

ARTICLE INFO

Article history:
Received 10 November 2017
Received in revised form 1 February 2018
Accepted 7 February 2018
Available online 13 February 2018

Editor: Adrian Covaci

Keywords:
Chlordane
Clarias gariepinus
DDT
Human health risk
Soweto

ABSTRACT

Organochlorine pesticides (OCPs) in South Africa have for the most part been banned, except dichlorodiphenyltrichloroethane (DDT) which is still used as malaria vector control. The aim of this study was to determine OCP residues in the aquatic fauna of one of South Africa's most populated areas, Soweto. Risk to human health through OCP exposure via fish consumption was investigated. *Clarias gariepinus* was chosen as bioindicator because it is an apex predator that is in abundance, but is also a valued food source. Dichlorodiphenyltrichloroethanes (DDTs), hexachlorocyclohexanes (HCHs), and chlordanes (CHLs) were detected in the fish tissue with the DDTs being the most prevalent at all sites. Of the three locations, Fleurhof, Orlando, and Lenasia, the latter location's fish had the highest ΣOCP load, ranging between 81 and 1190 ng/g wm. The DDTs were determined to be from historic use, whereas the CHL levels indicated more recent inputs. Although the possibility of illegal use cannot be excluded completely, the presence of OCPs outside of their allowed areas of use indicate that these compounds not only stay in the aquatic systems long term, but may be of concern in areas previously not considered high risk areas. The OCP residues in *C. gariepinus* from the study area pose an extremely high risk to human health when consumed, and has a cancer risk as high as 1 in 10. This potential problem should be kept in consideration when developing national health and conservation strategies.

* Corresponding author.
E-mail address: wihan.pheiffer@nwu.ac.za (W. Pheiffer).

https://doi.org/10.1016/j.scitotenv.2018.02.075
0048-9697/

1. Introduction

The unregulated use of organochlorine pesticides (OCPs) in South Africa was banned in 2002 as per the Stockholm Convention (Bouwman, 2004). However the ban on one of these, namely DDT (dichlorodiphenyltrichloroethane), was lifted for the use of malaria vector control (MVC) by indoor residual spraying (IRS), under strict legislation, overseen by provincial government. A detailed overview on malaria vector control in South Africa is described by Brooke et al. (2013). There have been an increasing number of reports on the accumulation of DDT and other organochlorine pesticides (OCPs) in the aquatic wildlife (Barnhoorn et al., 2009; Gerber et al., 2016; Viljoen et al., 2016). Aquatic ecosystems are especially at risk as most OCPs are more stable in sediments, therefore increasing its persistence (Doong et al., 2002; Yohannes et al., 2013a). OCPs are transferred from the sediment via different mechanisms into aquatic organisms and magnify up the food chain (Van der Oost et al., 2003). High bioaccumulation of these OCPs have been reported in aquatic predators at the top of the food chain, such as the tigerfish (*Hydrocynus vittatus* Castelnau, 1861) (McHugh et al., 2011; Wepener et al., 2012; Gerber et al., 2016) and sharptooth catfish (*Clarias gariepinus* (Burchell, 1822)) (Barnhoorn et al., 2009, 2015). These aforementioned studies were all in subtropical areas of South Africa, where spraying of DDT for MVC is still allowed and results showed very high concentrations of not only DDTs, but also various other banned OCPs, such as chlordane and HCHs, in the tissues of these species. The study areas were of a rural nature and included important conservation areas and their surroundings with low human population densities. In the present study we determined the levels of OCPs in aquatic organisms in ecosystems within surrounding densely populated areas of South Africa. The demographic includes many unemployed people that rely on subsistence fishing to supplement their diet.

The study area is in the urban area of Soweto (South Western Townships), one of South Africa's most densely populated areas (6400 people/km^2) (StatsSA, 2011). Soweto is found south west of the city of Johannesburg and is South Africa's largest township with a high unemployment rate with some people reliant on subsistence fishing as a means of obtaining food. There is no direct spraying of OCPs, particularly DDT in this area. However, the fact that long range air transport of OCPs is well documented (Gong et al., 2015; Pozo et al., 2006), it could potentially result in the exposure of this region to these persistent pollutants. The study area is also relatively close to sources where OCPs were manufactured in the past. The production of DDT and other OCPs in Gauteng occurred in the Wadeville and Chloorkop areas, and in the neighbouring North West province, at the town of Brits (DEA, 2011). These locations are approximately 35 (east), 40 (north east) and 75 km (north) from the selected study area, respectively. Manufacturing of various OCPs, such as lindane, heptachlor, aldrin, dieldrin, endrin and DDT was discontinued in South Africa in the 1980s and the formulation of DDT in 2010 (DEA, 2011). In addition, a study of the middle Vaal River, into which our study area drains, reported surprisingly high levels of OCPs in fish species (Wepener et al., 2011).

Clarias gariepinus was chosen as an indicator species because it is abundant in South Africa, it is resilient, it is the apex aquatic predator in the sampling area, and most importantly, is a valued food source (Rouhani and Britz, 2011). They are targeted by local fishermen not only in rural areas but are specifically targeted by fisherman in the study area (personal communication: W Pheiffer). Their position on the food web and preference for bottom dwelling in the aquatic systems makes it ideal to study exposure to pollutants, as well as the bioaccumulation and bio-magnification of organic chemical pollutants, allowing for investigation into possible transfer of pollutants to humans.

The aim of this study was to determine DDT and other OCP residues in *C. gariepinus* muscle tissue from impoundments in the urban area of Soweto, South Africa post the cessation of use and formulation. These findings are compared to other African studies on *C. gariepinus* or relevant apex predators. This paper most importantly investigates the potential risk posed to health of the local human population through consumption of OCP contaminated *C. gariepinus*.

2. Materials and methods

2.1. Study area and sampling

Clarias gariepinus was sampled during Austral summer (October) of 2013 from three impoundments in the upper Klip River catchment (Fig. 1) in Soweto and Lenasia. The Klip River drains the Witwatersrand area in the Gauteng province of South Africa. It is the largest tributary of the Vaal River. These rivers together supply >12 million people of potable water in Gauteng (DWAS, 2004). Fleurhof Dam (26°12′03.49″S 27°54′31.87″E) is the most northern site, representing the upper region of the study area. Orlando Dam (26°15′21.63″S 27°55′18.97″E) is located in the centre of Soweto, and Lenasia Dam (26°18′8.33″S 27°50′10.8″E) is located in the southern stretches of the Klip River. The fish were caught using fyke and gill nets (110 mm mesh). Nets were left in for 5 h and checked periodically every half hour. Fish weighing less than 1 kg were released. Following capture, fish were euthanized by severing the spinal cord behind the head (NWU Ethics approval: AREC-130913-015). The mass (g) and standard length (SL; mm) of each fish were recorded. Epaxial muscle samples were removed, placed in pre-cleaned (acetone/hexane) aluminium foil, and kept frozen at −20 °C. Epaxial muscle was selected for consistency in sampling between specimens and because the epaxial muscle is the part of the fish primarily consumed by humans. For comparative purposes a group of ten fish from the Mooi River system in the North West province (part of different catchment as the study area) were depurated for half a year at the Water Research Group's aquarium at the North-West University (Potchefstroom Campus). Fish were kept under standard aquarium conditions (CCAC, 2005). These reference fish were processed in the same manner as the experimental fish.

2.2. Organochlorine pesticide determination

2.2.1. Materials

An OCP standard reference mixture (all isomers of chlordane and nonachlor, oxychlordane (collectively CHLs); all isomers of DDT, DDD and DDE (collectively DDTs; group referred to as DDx when DDT is excluded); dieldrin, endrin and aldrin (collectively drins); hexachlorobenzene (HCB); hexachlorocyclohexanes (α-, β-, γ-, δ-isomers, collectively HCHs); and all isomers of heptachlor and heptachlor-epoxide (collectively heptachlors)) were obtained from Dr. Ehrenstorfer GmbH (Germany). Analytical grade organic solvents (acetone, hexane, and dichloromethane), and anhydrous sodium sulphate (pesticide residue and PCB analysis grade) were obtained from Kanto Chemical Corp. (Tokyo, Japan). Florisil (60–100 mesh) from Kanto Chemical Corp. (Tokyo, Japan) was activated in an oven at 180 °C for 8 h.

2.2.2. Extraction of OCPs in muscle

Analysis of OCPs in muscle samples followed an adapted version of the method by Yohannes et al. (2013b). Sample (10 g wet mass; wm) was homogenized with anhydrous sodium sulphate and placed in pre-cleaned (acetone/hexane) cellulose extraction thimbles. Samples were spiked with PCB#77 as internal standard. Extraction was carried out with 150 mL hexane:acetone (3:1 v/v) for 6 h using a Soxtherm (S306AK Automatic Extractor, Gerhardt, Germany). Extracts were concentrated to approximately 2 mL using a rotary evaporator and diluted to 10 mL with hexane. Lipid content was determined gravimetrically using an air dried 10% aliquot of the extract. The remaining extract after concentrated to 5 mL was passed through gel permeation chromatography columns (Waka Gel Bio-Rad) with dichloromethane (DCM): hexane (1:1 v/v) as mobile phase, collecting only the fraction containing the OCPs. The fraction collected was concentrated and cleaned-up on a glass column packed with 6 g 5% activated Florisil, and eluted with

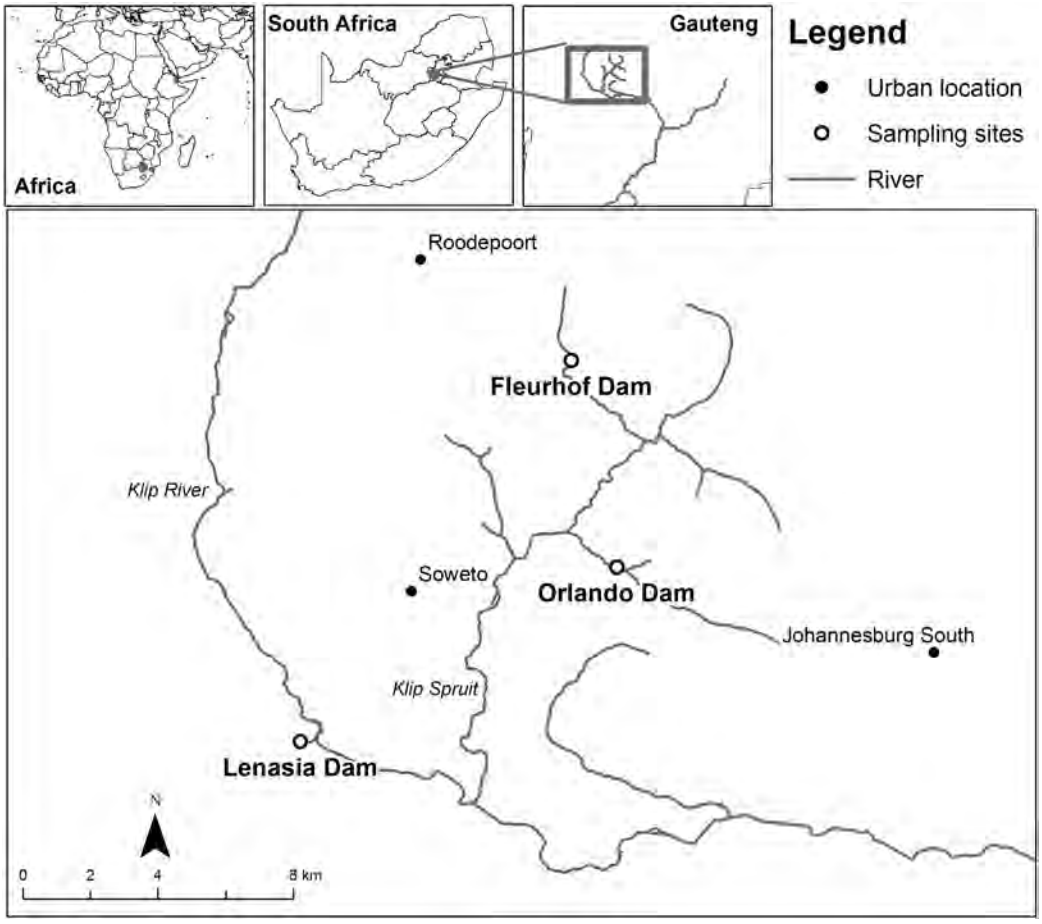

Fig. 1. *Clarias gariepinus* were sampled for organochlorine pesticide residue analysis from three impoundments (Lenasia Dam, Fleurhof Dam and Orlando Dam) in the Klip River catchment, Soweto in October 2013.

120 mL DCM:hexane (3,7 v/v). The eluate was concentrated to near dryness under gentle flow of nitrogen and resuspended in 100 μL *n*-decane (containing surrogate standard, tetrachloro-*m*-xylene) for analysis.

2.2.3. Analysis of OCPs in muscle

OCP analysis was performed as described by Yohannes et al. (2013b) on a gas-chromatograph coupled to an electron capture detector (GC-ECD, Shimadzu GC-2014, Kyoto, Japan). Separation was achieved with a Mighty Cap™ ENV-8MS capillary column (30 m × 0.25 mm, I.D, 0.25 um df; Kanto Chemical Corp. Tokyo, Japan). Samples were injected (1 μL) in splitless mode. Helium was used as carrier gas at a flow-rate of 1.0 mL/min and nitrogen as the make-up gas at a flow rate of 45 mL/min. The GC oven temperature was programmed from 100 °C (1 min hold), ramp at 12 °C/min to 180 °C; 4 °C/min to 240 °C, and finally at 10 °C/min to 270 °C (5 min hold). The temperatures of the detector and injector were 320 °C and 250 °C, respectively.

2.2.4. Quality assurance and quality control

The OCPs were identified based on their retention times relative to corresponding standards. Concentrations of the target compounds were quantified based on the ratio of the sample's peak area to that of the standard peak area. The coefficient of variance (R^2) for all calibration curves was >0.995. A blank and reference standards were run after each set of 10 samples, to check for interferences and cross-contamination. Initially an internal standard (PCB#77) was spiked to monitor procedural performance. However, quantification showed all recoveries above 110%, indicating the unexpected presence of environmental PCB 77 in the samples. The data reported is thus not adjusted according to recoveries of the internal standard, but only in terms of the surrogate marker, tetrachloro-*m*-xylene (TmX). The mean recovery was 81.5% ± 12.6. To evaluate the accuracy and precision of the analytical method the standard reference material (SRM 1947) was analysed in the same manner as the samples. The recoveries of the SRM ranged between 74 and 108% with a coefficient of variance <11%. Limit of detection (LOD) and limit of quantification (LOQ) was calculated using the standard deviation of the residuals ($S_{y/x}$). The LOD was defined as three times the standard deviation of $S_{y/x}$ and the LOQ was defined as ten times the standard deviation of $S_{y/x}$. Detection limits ranged between 0.38 and 30 ng/g, and the LOQ ranged between 13 and 100 ng/g, for all OCPs.

2.3. Human health risk assessment

The human health risk was calculated for the consumption of *Clarias gariepinus* only, not including any of the other edible fish species that might occur in the area. Doing this created a worst-case scenario. In order to consider factors such as eating habits and consumption rates, both the 50th and 95th percentiles of measured concentrations were included in the risk assessment. This allows for a more comprehensive evaluation of health risk associated with the consumption of OCP contaminated fish from the study area (Gerber et al., 2016; Yohannes et al., 2014a). The health risk assessment firstly calculated the maximum safe consumption limit, which indicates the maximum amount of fish that can be consumed per day without posing an acute health risk. Secondly, the estimated dietary intakes (EDI) of OCPs were determined and subsequently the carcinogenic risks after lifetime exposure to the OCPs were calculated.

2.3.1. Maximum safe consumption limit

The maximum amount of fish that can be safely consumed without potential human health risk can be determined by using the minimal risk levels (MRLs) for oral intake, set by the Agency of Toxic Substances and Disease Registry (ATSDR). Maximum safe consumption limit was calculated according to Verhaert et al. (2017), following the formulae:

$$Y = BM \times MRL \quad (1)$$

where Y is the maximum amount (ng/day) of OCPs a 60 kg person may consume without health risk. BM is the average body mass (bm) set at 60 kg (WHO, 2010), and MRL is the minimal risk levels (ng/kg BM per day). The MRLs for ΣHCH, ΣCHL, and ΣDDT are 600, 600, and 500 ng/kg BM per day, respectively (ATSDR, 2017b).

$$Q = (Y/C)/1000 \quad (2)$$

where Q is the maximum amount (kg) of fish that can be consumed safely without health risk, C is the concentration of the OCP (ng/g wm), and 1000 is for the conversion from gram to kilogram. It is important to note that the lowest value calculated is considered as the maximum safe consumption limit.

2.3.2. Estimated daily intake (EDI)

The estimated daily dietary intake of OCPs from *C. gariepinus* consumption was calculated using the following equation:

$$EDI = (C \times DR)/BM \quad (3)$$

where C is the concentration of the OCP (ng/g wet mass; wm), DR is the daily consumption of fish (g/day) and BM is the average body mass (bm) set at 60 kg (WHO, 2010). We chose to use the 60 kg of the WHO and not the 80 kg of the USEPA because it enabled comparison of our data to others who also used the 60 kg body mass. Additionally, the average body mass of South Africans is 66.5 kg according to Puoane et al. (2002). The estimated daily consumption rate was conservatively set at 30 g/day per person (Gerber et al., 2016). EDI was compared with the allowable daily intake (ADI) set by the WHO (2010). These ADIs (ng/kg bm per day) are 5000, 500, and 100,000 for ΣHCH, ΣCHL, and ΣDDT respectively.

2.3.3. Carcinogenic risk

Both cancer risk (CR) and hazard ratios (HR) were calculated according to the USEPA (2005) and Jiang et al. (2005). The CR was calculated as:

$$CR = EDI \times CSF \quad (4)$$

where the CSF is the cancer slope factor of the congener (USEPA, 2012). If the CR is $>10^6$ it is considered 'acceptable risk', between 10^6 and 10^4 are considered 'levels of concern' and a CR smaller than 10^4 is deemed 'unacceptable risk' (USEPA, 2005). The CSFs (mg/kg per day) for ΣHCH (as γ-HCH), ΣCHL, and ΣDDT are 1.1, 0.35, and 0.34 respectively.

The hazard ratios for both non-carcinogenic and carcinogenic effects were calculated according to Jiang et al. (2005):

$$HR = EDI/BMC \quad (5)$$

where the BMC is the benchmark concentration, derived from the USEPA CSF:

$$BMC = (Risk \times BM)/(Fish\ consumption \times CSF) \quad (6)$$

where the risk is set at one in a million chance for lifetime exposure, and fish consumption is the amount of fish consumed per day relative to body mass (g/kg per day). An HR greater than one indicates a potential risk to human health (Dougherty et al., 2000).

2.4. Statistical analysis

Chemical analysis results were grouped based on the congener classes (ΣHCHs, ΣCHLs, ΣDDTs, and ΣOCPs). The data sets were tested for normality using the D'Agostino-Pearson omnibus test. The data sets were found to be non-parametric and thus significant differences were tested using the Kruskal-Wallis test with Dunn's multiple comparison-test as post-hoc test. Unpaired *t*-tests were used to compare means from literature with our results provided that results from literature were reported as means and standard deviations. Significant differences ($p < 0.05$) are indicated by common superscripts in the tables and figures.

Discriminant function analysis (DFA) is similar to multivariate ANOVAs but indicate the similarity/dissimilarity of datasets (OCP accumulation profiles). Datapoints below LOD were replaced with the frequency of detection multiplied by the LOQ (Wepener et al., 2012; Verheart et al., 2013). This DFA was performed using PASW Statistics 18. Fisher's functional coefficient was used as a posteriori test.

3. Results

3.1. OCP tissue residues

The OCP residues quantified in the muscle of *C. gariepinus* (ng/g wet mass) from the study area are reported in Table 1. Of the 22 compounds analysed two were detected in the reference fish (n = 10), 50% from fish at Orlando Dam (n = 9), 60% in fish from Lenasia Dam (n = 11), and 55% from fish at Fleurhof Dam (n = 10). The lipid content, fish mass and fish lengths are presented in Table S1. Significant differences were found between the lipid percentages ($p < 0.05$) of fish from the different sites (Table S1). However, there were no significant differences between the sizes (both mass and length) of the fish between the sites ($p > 0.05$) (Table S1). For accurate comparison, concentration in terms of wet mass were reported, however lipid mass concentrations

Table 1
Means, standard deviation, and ranges of organochlorine pesticides (ng/g wet mass) in *Clarias gariepinus* muscle tissue sampled during October 2013 from impoundments in the upper Klip River catchment, namely Orlando, Lenasia and Fleurhof Dams, and a reference group. Common superscripts within rows denote significant differences ($p < 0.05$). ND indicates that OCPs were not detected.

OCP	Reference (n = 10)	Orlando (n = 9)	Lenasia (n = 11)	Fleurhof (n = 10)
HCB	ND	22 ± 6	30 ± 19	8.2*
α-HCH	ND	ND	9	ND
γ-HCH	ND	ND	ND	6.9 ± 1.8
ΣHCHs	ND	ND	[a]9*	[a]6.9 ± 1.8
Range			ND–9	4.9–11
trans-Heptachlor-epoxide	ND	ND	10 ± 12	6.5*
trans-Chlordane	ND	20 ± 14	13 ± 5.8	17 ± 9.9
trans-Nonachlor	ND	21 ± 13	28 ± 22	15 ± 7.4
cis-Chlordane	ND	18 ± 10	19 ± 14	14 ± 9.1
cis-Nonachlor	ND	ND	8.8 ± 1.2	12 ± 6.3
ΣCHLs	ND	29 ± 39	49 ± 44	47 ± 33
Range		ND–124	ND–165	8.6–133
Dieldrin	ND	18 ± 12	13 ± 7.4	13 ± 9.4
o,p′-DDE	ND	37*	ND	ND
p,p′-DDE	5.6 ± 1.4	76 ± 73	138 ± 120	80 ± 36
o,p′-DDD	ND	19 ± 15	48 ± 45	9.4 ± 3.7
p,p′-DDD	5.0 ± 2.6	37 ± 36	55 ± 57	17 ± 10
o,p′-DDT	ND	7 ± 2.2	7.4 ± 4.0	ND
p,p′-DDT	88*	15 ± 14	7.4 ± 5.5	12 ± 5.0
ΣDDTs	[abc]12.7 ± 28	[a]145 ± 141	[b]256 ± 231	[c]117 ± 97
Range	ND–97.4	31–683	73–893	69–264
ΣDDT/ΣDDxa	0	0.13	0.06	0.11
ΣOCPs	[abc]12.7 ± 28	[a]193 ± 190	[b]335 ± 315	[c]183 ± 100
Range	ND–97.4	32–683	81–1190	105–458

* Indicates data for single fish (N = 1).

were also recorded and were only used when comparative literature lacked wet mass concentration values.

Among the DDTs, *p,p′*-DDE, *p,p′*-DDD, and *p,p′*-DDT were detected in the fish from the reference group but the ΣDDTs in these fish was significantly lower than all the environmental sites despite the unexpected high *p,p′*-DDT found in only one specimen. The ΣOCPs of the reference site were also significantly less than the other sites. The only site that had α-HCH in fish was Lenasia. Similarly, Fleurhof was the only site with fish that had γ-HCH residues. *trans*-Heptachlor epoxide was detected at Lenasia and Fleurhof only. Concentrations of ΣCHLs were similar among sites (no significant differences, $p > 0.05$). The fish from Lenasia had the widest range of ΣCHLs, ranging between ND and 165 ng/g wm. Dieldrin was the only drin detected in the fish from all the sites, with similar residue levels. The DDTs were the most prevalent class across the sites. All targeted DDTs were present at Orlando and almost all were detected at Fleurhof and Lenasia. Only *o,p′*-DDE was not detected at Fleurhof and Lenasia. The ΣDDTs were the greatest at Lenasia and ranged between 73 and 893 ng/g wm. Lenasia had the greatest ΣOCPs with a range of 81 to 1190 ng/g wm.

3.2. OCP compositions

The compositions of the different congeners per OCP class are shown in Fig. 2. The composition of ΣHCHs differed between the sites. The ΣHCH compositions were dominated by α-HCH in fish from Lenasia and γ-HCH in the fish from Fleurhof.

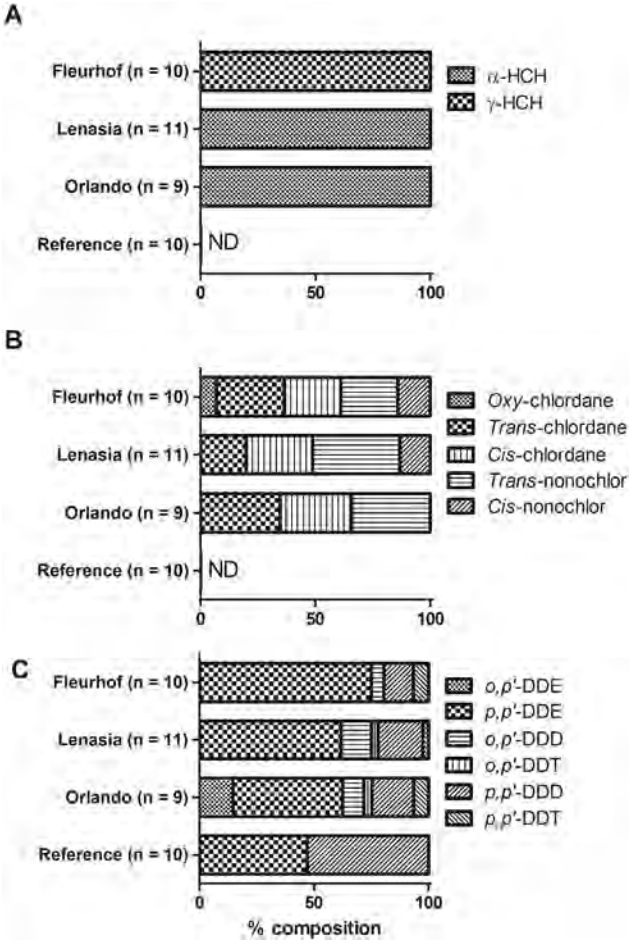

Fig. 2. Composition of organochlorine pesticides residues in *Clarias gariepinus* from a reference group and individuals sampled from three impoundments (Lenasia Dam, Fleurhof Dam and Orlando Dam) in the Klip River catchment A) hexachlorocyclohexanes (HCHs); B) chlordanes (CHLs); and C) DDTs.

The ΣCHLs at Fleurhof were divided between nonachlor (47%) and chlordane (53%). The contributions made to the ΣCHLs at Lenasia were dominated by the *trans* isomer of nonachlor and *cis* isomer of chlordane. The two chlordane isomers made up more than half of the CHLs at Orlando.

The most dominant DDT congener in the reference fish was *p,p′*-DDT. Overall, *p,p′*-DDE was the dominant congener at the environmental sites, contributing 68% at Fleurhof, 54% at Lenasia, and 40% at Orlando. *p,p′*-DDD was the second most prevalent congener at these sites.

The discriminant function analysis on OCP accumulation data explained 92.5% of the variation in the data (Fig. 3). Function 1 along the x-axis accounted for 79.4% of the total variation whilst function 2 along the y-axis accounted for 13.1%. Based on the structure matrix of the analysis (Table S2) γ-HCH and *cis*-nonachlor loads in the fish were the main factors for separation along the x-axis with dieldrin, *p,p′*-DDE and *trans*-chlordane driving y-axis separation. Reclassification of the data resulted in 100% of the data points reclassified into their respective original site classifications (Table S3). The ordination in Fig. 3 and the reclassification results indicate that the accumulated concentrations of OCPs in *C. gariepinus* from the various sites are distinct. In order to confirm site differences a discriminant function analysis (DFA) was performed on the OCP results. This analysis classifies samples based on their unique combination of variable values (in this case the combination of concentration and composition of OCPs) in order to determine statistical difference between the sample sets (sites). Fleurhof separated from all the other sites along the first function mainly in terms of γ-HCH load whereas differences between the other sites were along the y-axis attributing the separation to the driving factors along that function, i.e. Lenasia Dam had the highest OCP concentrations and greatest diversity of OCPs detected, and separated from all the other surveys along the second function.

3.3. Human health risk from consumption of fish tissue

The maximum safe consumption limit, EDI, HR and CR from fish consumption from the study sites are shown in Table 2. The maximum amount of fish that can be safely consumed per day was deemed the smallest for the ΣDDTs at all the sites, followed by that for ΣCHLs (Table 2). The HR for HCH at Fleurhof was >1 (50th percentile) but was not calculated for the other two sites because HCH was not detected

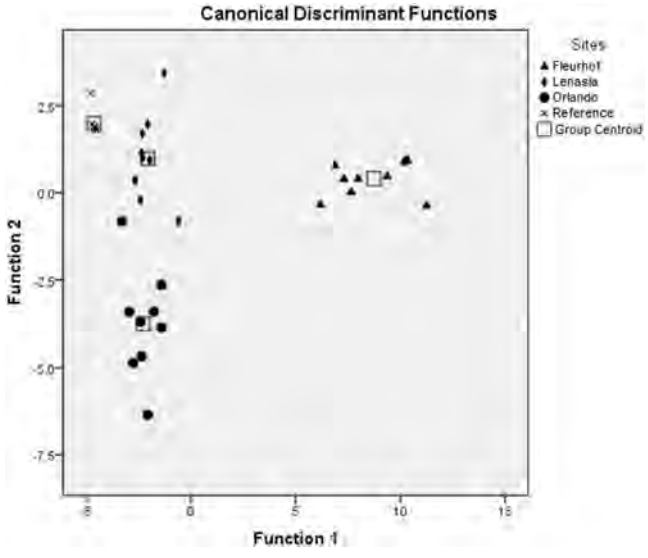

Fig. 3. Discriminant function analysis of organochlorine pesticides residues in *Clarias gariepinus* from a reference group and individuals sampled from three impoundments (Lenasia Dam, Fleurhof Dam and Orlando Dam) in the Klip River catchment. Function 1 (79.4%) and 2 (13.1%) refer to the first two canonical functions of a multivariate data set and collectively explain 92.5% of the variation in the accumulation data.

Table 2
The 50th and 95th (in parentheses) percentile wet mass OCP concentrations, estimated daily intakes, cancer hazard ratio and risks for consuming *Clarias gariepinus* from Orlando, Lenasia and Fleurhof Dams in the upper Klip River catchment compared to Yohannes et al. (2014a) and Gerber et al. (2016). Exposure parameters included in subscript.

	Orlando *Clarias gariepinus*			Lenasia *Clarias gariepinus*			Fleurhof *Clarias gariepinus*			Yohannes et al., 2014a, 2014bLake Ziway *Clarias gariepinus*			Gerber et al., 2016 Luvuvhu River *Hydrocynus vitattus*			Gerber et al., 2016 Olifants River *Hydrocynus vitattus*		
	ΣHCH	ΣCHL	ΣDDT	ΣHCH	ΣCHL	ΣDDT	ΣHCH	ΣCHL	ΣDDT	ΣHCH	ΣCHL	ΣDDT	ΣHCH	ΣCHL	ΣDDT	ΣHCH	ΣCHL	ΣDDT
50th(95th) concentrations (ng/g wm)	0 (0)	5.3 (94)	113 (367)	0 (4.6)	28 (123)	148 (650)	6.6 (10)	35 (106)	101 (211)	0.54 (1.53)	0.85 (1.41)	4.91 (21.21)	1.98 (9.73)	0.77 (9.05)	32.02 (1071)	2.25 (8.99)	0.81 (12.22)	12.34 (279.81)
50th(95th) maximum safe consumption limit (kg per day)	–	6.7 (0.4)	0.3 (0.08)	– (7.8)	1.3 (0.3)	0.2 (0.04)	5.5 (3.5)	1.0 (0.3)	0.3 (0.1)									
50th(95th) estimated daily intake(ng/kg body mass per day)	0 (0)	2.7 (47)	56 (184)	0 (2.3)	14 (62)	74 (325)	3.3 (5.1)	18 (53)	50 (106)	0.27 (0.77)	0.42 (0.72)	2.46 (10.61)	0.99 (4.86)	0.39 (4.52)	16.01 (535.26)	1.13 (4.49)	0.41 (6.11)	6.17 (139.9)
50th(95th) hazard ratio	0 (0)	64 (1119)	1379 (4500)	0 (17)	337 (1467)	1810 (7966)	25 (39)	417 (1260)	1237 (2587)				7.5 (36.8)	9.2 (107.7)	392 (13,119)	8.5 (34)	9.7 (145.4)	151 (3429)
50th(95th) cancer risk ($\times 10^4$)	0 (0)	9 (164)	191 (624)	0 (25)	50 (216)	251 (1105)	36 (56)	61 (185)	172 (359)	2.9 (8.4)	1.5 (2.5)	8.4 (36)	10.87 (53.5)	1.35 (15.83)	54.43 (1820)	12.38 (49.43)	1.43 (21.38)	20.98 (475.7)

Cancer slope factors: ΣHCH (1.1); ΣCHL (0.35); ΣDDT (0.34) [USEPA, 2000].
Benchmark concentration (μg/kg per day): ΣHCH (0.132); ΣCHL (0.042); ΣDDT (0.0408).
Allowable daily intake g/kg per day): ΣHCH (5000); ΣCHL (500); ΣDDT (10,000) (WHO, 2010).
Safety action levels: ΣCHL (300 ng/g); ΣDDT (5000 ng/g) (FDA, 2011).
Minimal risk level: ΣHCH (600); ΣCHL (600); ΣDDT (500) (ATSDR, 2017b).

Table 3
Mean ± SD of organochlorine pesticide concentrations (ng/g wet mass and ng/g lipid mass in bold) in epaxial muscle tissue of *Clarias gariepinus* from three impoundments, Orlando, Lenasia and Fleurhof, from the Klip River catchment South Africa. Results are compared to other studies across South Africa and Africa as well as compared to another apex predator.

	Sites	*trans*-Chlordane	*trans*-Nonachlor	*cis*-Chlordane	*cis*-Nonachlor	ΣCHLs	*o,p′* -DDE	*p,p′*-DDE	*o,p′* -DDD	*p,p′* -DDD	*o,p′* -DDT	*p,p′*-DDT	ΣDDTs	DDT/DDx	References
Clarias gariepinus	Orlando Dam, South Africa	20 ± 14 **49 ± 104**	21 ± 13 **42 ± 98**	18 ± 10 **35 ± 81**	–	29 ± 39 **127 ± 285**	37 **152**	76 ± 73 **345 ± 561**	19 ± 15 **75 ± 116**	37 ± 36 **176 ± 291**	7 ± 2.2 **8.2 ± 16**	15 ± 14 **57 ± 108**	145 ± 141 **680 ± 1069**	**0.13**	This study
	Lenasia Dam, South Africa	13 ± 5.8 **20 ± 42**	28 ± 22 **102 ± 138**	19 ± 14 **63 ± 90**	8.08 ± 1.2 **12 ± 28**	49 ± 44 **198 ± 268**	–	138 ± 120 **581 ± 741**	48 ± 45 **200 ± 270**	55 ± 57 **230 ± 351**	7.4 ± 4.0 **24 ± 29**	7.4 ± 5.5 **33 ± 36**	256 ± 231 **1070 ± 1423**	**0.06**	
	Fleurhof dam, South Africa	17 ± 9.9 **297 ± 189**	15 ± 7.4 **512 ± 430**	14 ± 9.1 **322 ± 158**	12 ± 6.3 **137 ± 264**	47 ± 33 **1270 ± 689**	–	80 ± 36 **3593 ± 4570**	9.4 ± 3.7 **377 ± 415**	17 ± 10 **531 ± 355**	–	12 ± 5.0 **257 ± 142**	117 ± 97 **4760 ± 5284**	**0.11**	
	Xikundu Weir, South Africa[a]	–	–	–	–	–	50	63,500	440	8500	2500	6600	81,000	1.01	Barnhoorn et al., 2009
	Nanondi Dam, South Africa[a]	–	–	–	–	–	–	2100 ± 1000	30 ± 20	500 ± 300	–	–	2600 ± 1300		Barnhoorn et al., 2009
	Roodeplaat Dam, South Africa	–	–	–	–	–	–	138 ± 95	–	113	–	168	151 ± 88	0.67	Barnhoorn et al., 2015
	Rietvlei Dam, South Africa	–	–	–	–	–	–	212 ± 13	–	127 ± 86	–	198 ± 77	336 ± 263	0.58	Barnhoorn et al., 2015
	Okavango Delta (MVC),Botswana	–	–	–	–	–	–	–	–	–	–	–	16 ± 7.2	–	Mbongwe et al., 2003
	Okavango Delta (Tsetse fly control), Botswana	–	–	–	–	–	–	–	–	–	–	–	3.0 ± 1.6	–	Mbongwe et al., 2003
	Lake Ziway, Ethiopia	0.29 ± 0.1	0.35 ± 0.23	0.16 ± 0.05	–	0.90 ± 0.25	0.1 ± 0.1	6.9 ± 11	–	0.8 ± 0.7	0.4 ± 0.1	0.6 ± 0.4	9.0 ± 11	0.13	Yohannes et al., 2014a
	Lakes Volta & Weija, Ghana	**0.63–2.7**	**0.42–1.4**	**0.62–1.6**	**0.23–0.58**	**1.9–6.28**	–	–	–	–	–	–	–	–	Adu-Kumi et al., 2010
	Mamba Weir, South Africa	–	–	–	–	<LOQ	–	–	–	–	–	–	13 ± 7.2	–	Verhaert et al., 2017
	Olifants River Gorge, South Africa	–	–	–	–	<LOQ	–	–	–	–	–	–	21 ± 17	–	Verhaert et al., 2017
Hydrocynus vittatus	Pongolapoort Dam, South Africa	–	–	–	**1.05 ± 0.65**	**3.8 ± 1.61**	**7.1 ± 2.7**	**5600 ± 2499**	**20 ± 3.5**	**245 ± 46**	**36 ± 7.9**	**536 ± 113**	**6444 ± 2635**	0.10	Wepener et al., 2012
	Olifants River, South Africa	**8 ± 3.5**	**13 ± 2.7**	**12 ± 3.4**	**5.3 ± 3.4**	**50 ± 15**	**13 ± 3.7**	**475 ± 229**	**18 ± 5.6**	**63 ± 13**	**29 ± 9.7**	**50 ± 17**	**647 ± 260**	0.14	Gerber et al., 2016
	Luvuvhu River, South Africa	**28.3 ± 11**	**4.3 ± 3.6**	**15 ± 4. 8**	**6.8 ± 2.5**	**58 ± 14**	**79 ± 16**	**2342 ± 945**	**64 ± 11**	**451 ± 171**	**122 ± 31**	**1189 ± 555**	**4249 ± 1680**	0.45	Gerber et al., 2016

[a] Study determined OCPs in fat samples only.

in fish from those sites. The greatest HR values were for the DDTs ranging from 1237 to 1810 for the 50th percentile (Table 2). Hazard risk could be determined for all 95th percentiles across all compound classes except for ΣHCHs at Orlando because they were not detected. The risk at the 95th percentile was very high for both the chlordanes and the DDTs, with maximum HR values of 1467 and 7966 respectively, both at Lenasia (Table 2). The carcinogenic risk (CR) calculated for those with detected concentrations were the greatest for DDT for both the 50th and 95th percentiles. The greatest DDT CR was at Lenasia (1105) followed by Orlando (624) (Table 2). The CR for chlordane (216) was also the greatest at Lenasia (Table 2). A Monte-Carlo simulation (Oracle Crystal Ball) with a 1000 iterations was applied to quantify the uncertainties of the effect of BM (60–80 kg) on the final CR. The results showed a maximum variation of 9% in the final cancer risk calculated.

4. Discussion

This paper reports the residue levels of DDT and other OCPs in epaxial muscle tissue of *C. gariepinus* from impoundments in an urban area where the poor and unemployed make use of fish as a source of protein. This paper further compares to levels found in other studies (Table 3) and extrapolates findings to potential human health risks from fish consumption in the study area. For accurate comparison, concentrations in terms of wet mass were used. The fact that *C. gariepinus* is the top predator in the study area, apart from piscivorous water birds, makes the species comparable to other apex predators from other African systems e.g. tigerfish (*Hydrocynus vittatus*). For those findings in literature where ng/g lipid was used, we converted our results to ng/g lipid for comparison (Table 3). The OCP concentrations in fish from the different sites were in the order of Lenasia > Orlando > Fleurhof. There were no statistical significant differences ($p > 0.05$) in composition of OCPs in the fish among the different sites (Fig. 2). This indicates towards shared sources of OCPs between the sites. Only the HCHs differed statistically ($p < 0.05$) between the sites. The dissimilarities in OCP concentrations (Table 1) supported by the DFA results (Fig. 3) indicate that the extent of OCP input, rather than the type of input, is the major difference between the sites. A study of the catchment (Fig. 1) shows different sub-catchment sizes of each impoundment, which may be the main attributing factor to the OCP input differences.

Chlordanes were one of the most prominent OCP classes in fish from the present study. Oxychlordane mostly, nonachlor, and to a lesser extent heptachlor-epoxide are all bio-accumulating metabolites of chlordane (Bondy et al., 2000). Heptachlor-epoxide, in the absence of other stable chlordane metabolites, is generally considered to have originated from heptachlor itself (ATSDR, 2007). The detection of only nonachlor and trace amounts of *trans*-heptachlor-epoxide could indicate a recent uptake and that chlordane had not been converted into oxychlordane yet. Historic exposure would only leave oxychlordane, as it is the dominant bio-accumulating metabolite (Hirasawa and Takizawa, 1989; Sasaki et al., 1992). Chlordane and its metabolites have the ability to irreversibly bind to cellular macromolecules and are considered epigenetic carcinogens, causing liver cancer in mice (ATSDR, 1994). The *trans*-isomer of both nonachlor and chlordane were higher at Fleurhof and Orlando, than its *cis*-counterpart, and so more toxic effects are expected in the fish from these sites as the *trans*-isomers are regarded as more toxic (Bondy et al., 2000). The individual CHL isomers reported by Yohannes et al. (2014a) were significantly lower ($p < 0.05$) than the lowest detected values in our study (Table 3). The ΣCHLs reported by Wepener et al. (2012) and Adu-Kumi et al. (2010) were significantly lower ($p < 0.05$) than the ΣCHLs in the fish from Fleurhof, and all our sites, respectively. Gerber et al. (2016) reported significantly lower ($p < 0.05$) ΣCHLs (in ng/g lipid) from the Olifants- and Luvuvhu Rivers during a high flow survey that was roughly half of what is reported at Orlando and Lenasia, and 20 times lower than Fleurhof (Table 3). The higher levels found in the present study, indicate a recent input event. The lack of oxychlordane indicates that the trace *trans*-heptachlor-epoxide detected might be from historic use of heptachlor only (ATSDR, 2007). However, the similar levels of both chlordane to nonachlor indicate a possible recent input event only for chlordane.

In the case of drins the expected result for historic input would be dieldrin as the major accumulating metabolite. This is because aldrin breaks down faster in the environment into dieldrin, which readily accumulates in lipid tissue where it is highly stable (ATSDR, 2002). In this study, dieldrin was the only drin detected. Therefore there is no evidence of recent drin input, except if only dieldrin itself was introduced.

As with many other studies the most prevalent congener measured was *p,p′*-DDE (Barnhoorn et al., 2009; Wepener et al., 2012; Yohannes et al., 2014a; Gerber et al., 2016). Higher metabolite levels (DDE and DDD) show historic use of DDT, but a higher *p,p′*-DDE residue level may also be indicative of internal bio-transformation of DDT ingested with prey (Ssebugere et al., 2009; Wepener et al., 2012). When compared to the ΣDDTs in *C. gariepinus* from a South African DDT sprayed area, the residue levels found in the fish from our study were considerably lower than what was quantified in *C. gariepinus* from Xikunndu Weir and Nanondi Dam (Barnhoorn et al., 2009) (Table 3). The ΣDDTs in fish from Orlando and Fleurhof were statistically lower ($p < 0.05$) than Nanondi Dam. Apart from being in an active MVC area, the ΣDDTs reported by Barnhoorn et al. (2009) were not quantified in the muscle tissue (as in the present study) but in the fat—where these lipophilic pollutants bio-accumulate (Jones and De Voogt, 1999). Mbongwe et al. (2003) reported ΣDDT values in *C. gariepinus* from areas in Botswana sprayed for mosquito and tsetse fly control. These levels were between 20 and 100 times lower than the greatest concentrations (Lenasia and Fleurhof) of the present study (Table 3). Similarly, *C. gariepinus* from Lake Ziway in Ethiopia where DDT is actively used, had ΣDDT concentrations 11 times lower (significantly, $p < 0.05$) (Yohannes et al., 2014a) (Table 3). Due to the lack of information on OCPs in *C. gariepinus* in South African systems in general, we compared our results to that of another apex predator, *H. vittatus* in South African systems. The DDT and its metabolites in *H. vittatus* from South Africa were more comparable to those found in *C. gariepinus* from Soweto and Lenasia (Table 3). The ΣDDTs in Pongolapoort Dam *H. vittatus* were greater than Lenasia (significantly, $p < 0.05$) and Fleurhof, whereas Gerber et al. (2016) reported lower values in tigerfish from the Olifants River (high flow) in the Kruger National Park—which is similar to what was found in the fish from Orlando (Table 3). However, in the same study by Gerber et al. (2016), the ΣDDTs in the *H. vittatus* from the Luvuvhu River (high flow) was 4248 ± 1680 ng/g lipid, which is similar to what was found in the Orlando fish. It must be mentioned that these authors reported ΣDDT concentrations double (Olifants River) and 6.7 times (Luvuvhu River) greater than the greatest concentrations of the current study, during the low flow season (2010). This was attributed to additional OCP inputs rather than lipid reserves (Gerber et al., 2016). In contrast to the high ΣDDTs in the tigerfish from the Olifants River, Verhaert et al. (2017) reported lower levels of ΣDDTs in *C. gariepinus* from the same study area (Olifants River). These results were 12 times lower than what was found in the fish from Lenasia (Table 3). In *C. gariepinus* from Roodeplaat and Rietvlei Dams, which are not in the South African MVC area (Barnhoorn et al., 2015), ΣDDTs levels were similar (not significantly different) to our results (Table 3).

The occurrence of OCPs in this urban area is of concern as it is not an MVC area. An explanation of possible sources could be illegal use (Rother et al., 2008) or from the historic production and formulation of these pesticides within the province/larger area surrounding the study area (DEA, 2011). The ratio between metabolites and parent compounds was calculated to indicate recent or historic use of DDT (Strandberg and Hites, 2001). DDT breaks down into DDD or DDE in the environment. The mechanisms of breakdown in different substrates are explained in the toxicological profile of DDT (ATSDR, 2002). Both DDD and DDE are more persistent in an aquatic environment (USEPA, 1979). In light of these differences in breakdown rates and differences

in metabolism and excretion rates between DDT and its metabolites in animals the ratio of DDT/DDx is used as an indication of recent DDT introduction. A ratio larger than 1 provides evidence that DDT has been recently introduced however Strandberg and Hites (2001) do not allude to a specific timeframe. This is difficult to do as breakdown can be influenced by a number of abiotic and biotic factors as evident from the ATSDR (2002) report. The ratios of ΣDDT/ΣDDx were all below one indicating historic use of DDT. Other studies in South Africa had similar results (Table 3) with the exception of Xikundu Weir, which is located in an active MVC area (Barnhoorn et al., 2009). The result of the present study is not surprising, since DDT is not actively used in the study area. The DDT inputs can only be attributed to historic use/production in the area or long range air transport from MVC areas.

Other OCP groups such as the heptachlors and chlordanes can also give an indication as to how recent inputs occurred, to a certain extent, when compared to their breakdown products as previously discussed. This is however, less accurate than for DDT, because these compounds are generally less persistent. Looking at the evidence that chlordane might be the only OCP recently introduced into the system illegal use of pesticides arises as a potential source. The applications of chlordane include termite control and as a broad spectrum agro-insecticide (Stockholm Convention, 2008). The study area is an urban area and not a prominent agricultural area. Thus illegal use in the immediate area is not likely and a more probable source would be long range transport. Barnhoorn et al. (2015) indicated the presence of OCPs in *C. gariepinus* at sites outside MVC areas also indicating long range transport possibilities. OCPs have been found in areas as far as the Arctic Circle (Halsall, 2004; Kallenborn et al., 2007). This implies that organisms from an environment with no direct input of a specific contaminant can present low- to mid-level bio-accumulation concentrations of that contaminant.

The relatively high OCP levels is of concern as one would expect the residue levels to be lower in urban areas than in areas such as actively DDT sprayed zones. This suggests major overall input in the Klip River system. The relatively high residues in the fish can also be attributed to bio-magnification through the food web. Even though it was not determined in the present study, it is an important factor to consider when making interpretations, as OCPs have been shown to bio-magnify in fish (Kidd et al., 2001; Verheart et al., 2013). *Clarias gariepinus* specifically is expected to have higher accumulation as it is a bottom-dwelling fish and associated with the sediments—where most of these lipophilic compounds accumulate in the aquatic environment (Yohannes et al., 2013a). Other than the fish, aquatic birds which are higher in the food web are also at risk. OCPs have been reported in African birds: in non-piscivorous birds such as ducks (Evans and Bouwman, 1993), egrets and ibises (Bouwman et al., 2008); small piscivorous birds like kingfishers (Evans and Bouwman, 2000) and hamerkop (Yohannes et al., 2014b, 2017); and large piscivorous birds like cormorant (Bouwman et al., 2008), and pelican (Yohannes et al., 2014b, 2017). Since this catchment is not within major agricultural land, the levels of agricultural pesticides at high enough concentrations to cause unacceptable human health risk are alarming.

Humans who are consuming contaminated fish are at risk of both acute and chronic effects health effects (Du Preez et al., 2003). The MRLs used in the maximum safe consumption limit calculations are based on non-carcinogenic effects only (ATSDR, 2017a). More specifically the MRLs of HCH, chlordane, and DDT were derived from acute (1–14 days) and intermediate (14–364 days) exposure data, which measured developmental, hepatic, and neurological end-points (ATSDR, 2017b). The maximum safe consumption limit results show that if a person (weighing 60 kg) consumes >40 g of *C. gariepinus* from Lenasia per day, they may be at risk of acute health effects associated with OCPs. Similarly, consuming 80 g and 100 g of fish from Orlando and Fleurhof respectively, persons would also be at risk for acute health effects. These maximum consuming limits are very conservative and only serve as an indication of limits not to be exceeded to prevent acute toxicity. The EDI at each site were well below the allowable daily intake set by the WHO (2010), as well as the action safety levels in edible fish by the United States Food and Drug Administration (FDA, 2011) (Table 2).

The current study used the same parameters to calculate health risk as Yohannes et al. (2014a) and Gerber et al. (2016) and therefore the EDIs and lifetime cancer risks can be compared. The EDIs of ΣHCHs for the present study were lower than literature (Table 2). In contrast, the ΣCHLs of all three sites (both 50th and 95th percentiles) were greater than EDIs reported by Yohannes et al. (2014a) and Gerber et al. (2016). For the ΣDDT 95th percentile the EDI of the Luvuvhu River (Gerber et al., 2016) was 1.6 times greater than the Lenasia EDI (Table 2). After Lenasia, the third greatest EDI was calculated for Orlando, followed by the Olifants River and finally Lake Ziway (Table 2). Based on these results it is apparent that the potential intake of OCPs in this urban study area is similar and even greater than areas where active use of pesticides occurs.

The HR and cancer risk estimates show that the OCP residues in the muscle of *C. gariepinus* pose a severe risk to human health if consumed. The threshold for allowable risk using the HR is set at one (Dougherty et al., 2000). All the calculated HR values for the present study exceeded this allowable threshold (Table 2). In most cases the HRs were in the thousands and were comparable to the HR values calculated by Gerber et al. (2016) for ΣDDTs (Table 2). Acceptable risk, when applying cancer risk estimations, is set at 1 in 10,000 (USEPA, 2005). All those sites with detected concentrations of any OCP had cancer risk. The health risk calculated by Barnhoorn et al. (2015) for fish from non-MVC areas were considerably lower than what was surmised in the present study. The most notable risks were calculated for the ΣDDTs, with an 1100 in 10,000 risk at Lenasia (95th percentile) and a 620 in 10,000 risk (95th percentile) at Orlando. These high health risks were similar to what Gerber et al. (2016) reported for the Luvuvhu River ΣDDT cancer risks. Background cancer rates for South Africa projected by the National Cancer Registry of South Africa are estimated as one in eight for men and one in nine for women (CANSA, 2015). This translates to 1250 in 10,000 for men and 1110 in 10,000 for women. The results of the present study are below this background rate, except for Lenasia where the 95th percentile value is similar to the background value for women. Although our health risk assessment was conservatively calculated for adults, it must be mentioned that infants and children are considered to be high risk groups. Because OCPs accumulate in breast milk (Bouwman and Kylin, 2009; Landigran et al., 2002), nursing infants are exposed to these pollutants and are also at risk. The USEPA (2017) reports an extra safety factor of ten (×10) when calculating risk for infants and children.

Overall, the data suggest that OCPs in fish from this area potentially make a low contribution to cancer cases in the study area. However, a few factors have to be considered when interpreting these risk values: The calculations made regarding human health risk assessments are based on assumptions regarding lifetime exposure parameters. Other toxic and carcinogenic compounds not targeted in the present study may very well be present in these fish that would also contribute to the health risk to consumers. The data arises from a model species which is not necessarily the only species of fish consumed in the area. With all of these limitations considered, the maximum safe consumption limit was calculated to be 40 g of fish per day and this would protect the consumer from acute health risks. However, the cancer risk assessment demonstrated that there is an unacceptable risk when consuming 30 g of fish per day over a lifetime.

5. Conclusion

This study found unexpected high levels of apparently redundant OCPs in a highly populated urban area. DDTs were the most detected OCP group. Their presence is most likely attributed to long distance transport and historic production and formulation of OCPs in the areas

surrounding the study site. The concentrations of OCPs in the fish pose great risk to human health, even higher than international acceptable levels using standard risk assessment parameters. With the record unemployment rate (StatsSA, 2017a) and increasing poverty among South Africans (StatsSA, 2017b) citizens resorting to urban fisheries for food may be a reality. The results obtained through the present study should be considered by national authorities to be incorporated into management plans for the Klip River, to decrease the potential risk of these pollutants to human and wildlife health.

Acknowledgements

The authors acknowledge the reviewers for their valued inputs into improving the manuscript. This study was funded by the Water Research Commission of South Africa (WRC, K2/2242/1/16), and the National Research Foundation (Innovation student bursary SF1208219521, and Grant No. 103487) with no conflict of interest. Opinions expressed and conclusions arrived at are those of the authors only, and are not necessarily to be attributed to the NRF. This work was supported by Grants-in-Aid for Scientific Research from the Ministry of Education, Culture, Sports, Science and Technology of Japan awarded to M. Ishizuka (No. 16H0177906), Y. Ikenaka (No. 26304043, 15H0282505, 15K1221305), and the Sumitomo Foundation (PK361791) and JSPS Core to Core Program (AA Science Platforms) and Bilateral Joint Research Project (PG36150002 and PG36150003). We are grateful to Natasha Vogt for generating the map and Takahiro Ichise for technical support. This is contribution number 219 from the NWU-Water Research Group.

Appendix A. Supplementary data

Supplementary data to this article can be found online at https://doi.org/10.1016/j.scitotenv.2018.02.075.

References

Adu-Kumi, S., Kawano, M., Shiki, Y., Yeboah, P.O., Carboo, D., Pwamang, J., Morita, M., Suzuki, N., 2010. Organochlorine pesticides (OCPs), dioxin-like polychlorinated biphenyls (dl-PCBs), polychlorinated dibenzo-*p*-dioxins and polychlorinated dibenzo furans (PCDD/Fs) in edible fish from Lake Volta, Lake Bosumtwi and Weija Lake in Ghana. Chemosphere 81, 675–684.

ATSDR, Agency for Toxic Substances and Disease Registry, 1994. Toxicological profile for chlordane. https://www.atsdr.cdc.gov/toxprofiles/tp31.pdf, Accessed date: 11 January 2017.

ATSDR, Agency for Toxic Substances and Disease Registry, 2002. Toxicological profile for aldrin/dieldrin. https://www.atsdr.cdc.gov/toxprofiles/tp1.pdf, Accessed date: 11 January 2017.

ATSDR, Agency for Toxic Substances and Disease Registry, 2007. Toxicological profile for heptachlor and heptachlor epoxide. https://www.atsdr.cdc.gov/toxprofiles/tp12.pdf, Accessed date: 11 January 2017.

ATSDR, Agency for Toxic Substances and Disease Registry, 2017a. Minimum risk levels (MRLs). https://www.atsdr.cdc.gov/mrls/index.asp, Accessed date: 11 January 2017.

ATSDR, Agency for Toxic Substances and Disease Registry, 2017b. Minimum risk levels (MRLs). https://www.atsdr.cdc.gov/mrls/pdfs/atsdr_mrls.pdf, Accessed date: 11 January 2017.

Barnhoorn, I.E.J., Bornman, M.S., Jansen van Rensburg, C., Bouwman, H., 2009. DDT residues in water, sediment, domestic and indigenous biota from a currently DDT-sprayed area. Chemosphere 77, 1236–1241.

Barnhoorn, I.E.J., Van Dyk, J.C., Genthe, B., Harding, W.R., Wagenaar, G.M., Bornman, M.S., 2015. Organochlorine pesticide levels in *Clarias gariepinus* from polluted freshwater impoundments in South Africa and the associated human health risks. Chemosphere 120, 391–397.

Bondy, G.S., Newsome, W.H., Armstrong, C.L., Suzuki, A.M., Doucet, J., Fernie, S., Hierlihy, S.L., Feeley, M.M., Baker, M.G., 2000. *trans*-Nonachlor and *cis*-nonachlor toxicity in Sprague-Dawley rats: comparison with technical chlordane. Toxicol. Sci. 58, 386–398.

Bouwman, H., 2004. South Africa and the Stockholm Convention on persistent organic pollutants. S. Afr. J. Sci. 100, 323–328.

Bouwman, H., Kylin, H., 2009. Malaria control insecticide residues in breast milk: the need to consider infant health risks. Environ. Health Perspect. 117, 1477–1480.

Bouwman, H., Polder, A., Venter, B., Skaare, J.U., 2008. Organochlorine contaminants in cormorant, darter, egret and ibis eggs from South Africa. Chemosphere 71, 227–241.

Brooke, B., Koekemoer, L., Kruger, P., Urbach, J., Misiani, E., Coetzee, M., 2013. Malaria vector control in South Africa. S. Afr. Med. J. 103, 784–788.

CANSA, Cancer Association of South Africa, 2015. Fact sheet on the top ten cancers per population group. http://www.cansa.org.za/files/2015/09/Fact-Sheet-Top-Ten-Cancers-per-Population-Group-Sept-2015.pdf, Accessed date: 6 May 2017.

CCAC, Canadian Council on Animal Care, 2005. Guidelines on: the care and use of fish in research, teaching and testing. http://www.ccac.ca/Documents/Standards/Guidelines/Fish.pdf, Accessed date: 5 December 2017.

DEA, Department of Environmental Affairs, 2011. National implementation plan for the Stockholm Convention in persistent organic pollutants. https://www.environment.gov.za/sites/default/files/docs/national_implementation_plaun_organic_pollutants.pdf, Accessed date: 30 March 2017.

Doong, R.-A., Sun, Y.-C., Liao, P.-L., Peng, C.-K., Wu, S.-C., 2002. Distribution and fate of organochlorine pesticide residues in sediments from selected rivers in Taiwan. Chemosphere 48, 237–246.

Dougherty, C.P., Holtz, S.H., Reinert, J.C., Panyocosit, L., Axelrad, D.A., Woodruff, T.J., 2000. Dietary exposures to food contaminants across the United States. Environ. Res. 84, 170–185.

Du Preez, H.H., Heath, R.G.M., Sandham, L.A., Genthe, B., 2003. Methodology for the assessment of human health risks associated with the consumption of chemical contaminated freshwater fish in South Africa. Water SA 29, 69–90.

DWAS, Department of Water Affairs and Sanitation, 2004. Upper Vaal Water Management Area: internal strategic perspective. https://www.dwaf.gov.za/Documents/Other/WMA/Upper_Vaal_ISP.pdf, Accessed date: 5 December 2017.

Evans, S.W., Bouwman, H., 1993. Levels of DDT in the liver tissue of two duck species from the Pongolo floodplain. Ostrich 64, 46–47.

Evans, S.W., Bouwman, H., 2000. The geographic variation and potential risk of DDT in the blood of pied kingfishers from northern KwaZulu-Natal, South Africa. Ostrich 71, 351–354.

FDA, Food and Drug Administration, 2011. FDA and EPA safety levels in regulation and guidance. Fish and Fishery Products: Hazards and Control Guidance :pp. 439–454. https://www.fda.gov/downloads/food/guidanceregulation/ucm251970.pdf, Accessed date: 10 April 2017.

Gerber, R., Smit, N.J., Van Vuren, J.H.J., Nakayama, S.M.M., Yohannes, Y.B., Ikenaka, Y., Ishizuka, M., Wepener, V., 2016. Bioaccumulation and human health risk assessment of DDT and other organochlorine pesticides in an apex aquatic predator from a premier conservation area. Sci. Total Environ. 550, 522–533.

Gong, P., Wang, X., Xue, Y., Sheng, J., Gao, S., Tian, L., Yao, T., 2015. Influence of atmospheric circulation on the long-range transport of organochlorine pesticides to the western Tibetan Plateau. Atmos. Res. 166, 157–164.

Halsall, C.J., 2004. Investigating the occurrence of persistent organic pollutants (POPs) in the arctic: their atmospheric behaviour and interaction with the seasonal snow pack. Environ. Pollut. 128, 163–175.

Hirasawa, F., Takizawa, Y., 1989. Accumulation and declination of chlordane congeners in mice. Toxicol. Lett. 47, 109–117.

Jiang, Q.T., Lee, T.K., Chen, K., Wong, H.L., Zheng, J.S., Giesy, J.P., Lo, K.K., Yamashita, N., Lam, P.K., 2005. Human health risk assessment of organochlorines associated with fish consumption in a coastal city in China. Environ. Pollut. 136, 155–165.

Jones, K.C., De Voogt, P., 1999. Persistent organic pollutants (POPs): state of the science. Environ. Pollut. 100, 209–221.

Kallenborn, R., Christensen, G., Evenset, A., Schlabach, M., Stohl, A., 2007. Atmospheric transport of persistent organic pollutants (POPs) to Bjørnøya (Bear Island). J. Environ. Monit. 9, 1082–1091.

Kidd, K.S., Bootsma, H.A., Hesslein, R.H., 2001. Biomagnification of DDT through the benthic and pelagic food webs of Lake Malawi, East Africa: importance of trophic level and carbon source. Environ. Sci. Technol. 35, 14–20.

Landigran, P.J., Sonawane, B., Mattison, D., McCally, M., Garg, A., 2002. Chemical contaminants in breast milk and their impacts on children's health: an overview. Environ. Health Perspect. 110, A313–A315.

Mbongwe, B., Legrand, M., Blais, J.M., Kimpe, L.E., Ridal, J., Lean, D.R.S., 2003. Dichlorodiphenyltrichloroethane in aquatic ecosystem of the Okavango Delta, Botswana, South Africa. Environ. Toxicol. Chem. 22, 7–19.

McHugh, K.J., Smit, N.J., Van Vuren, J.H.J., Van Dyk, J.C., Bervoets, L., Covaci, A., Wepener, V., 2011. A histology-based fish health assessment of the tigerfish, *Hydrocynus vittatus* from a DDT-affected area. Phys. Chem. Earth 36 (985-904).

Pozo, K., Harner, T., Wania, F., Muir, D.C.G., Jones, K.C., Barrie, L.A., 2006. Towards a global network for persistent organic pollutants in air: results from the GAPS study. Environ. Sci. Technol. 40, 4867–4873.

Puoane, T., Steyn, K., Bradshaw, D., Laubscher, R., Fourie, J., Lambert, V., Mbananga, N., 2002. Obesity in South Africa: the South African demographic and health survey. Obes. Res. 10, 1038–1048.

Rother, H.A., Hall, R., London, L., 2008. Pesticide use among emerging farmers in South Africa: contributing factors and stakeholder perspectives. Dev. South. Afr. 25, 399–424.

Rouhani, Q., Britz, P.J., 2011. Participatory development of provincial aquaculture programmes for improved rural food security and livelihood alternatives. Water Research Commission Report TT 502/11 (Pretoria).

Sasaki, K., Kawasaki, Y., Sekita, K., Ochiai, T., Takeda, M., Uchiyama, M., 1992. Disposition of β-hexachlorocyclohexane, *p,p′*-DDT, and *trans*-chlordane administered subcutaneously to monkeys (*Macaca fascicularis*). Arch. Environ. Contam. Toxicol. 22, 25–29.

Ssebugere, P., Kiremire, B.T., Kishimba, M., Wandiga, S.O., Nyanzi, S.A., Wasswa, J., 2009. DDT and metabolites in fish from Lake Edward, Uganda. Chemosphere 76, 212–215.

Statistics South Africa (StatsSA), 2011. Statistics by place. http://www.statssa.gov.za/?page_id=993&id=city-of-johannesburg-municipality, Accessed date: 4 December 2017.

Statistics South Africa (StatsSA), 2017. Statistical release P0211 quarterly labour force survey quarter 2: 2017. http://www.statssa.gov.za/publications/P0211/P02112ndQuarter2017.pdf, Accessed date: 4 December 2017.

Statistics South Africa (StatsSA), 2017b. Poverty trends in South Africa: an examination of absolute poverty between 2006 & 2015. http://www.statssa.gov.za/?p=10341, Accessed date: 8 August 2017.
Stockholm Convention, 2008. All POPs listed in the Stockholm Convention. http://www.pops.int/TheConvention/ThePOPs/AllPOPs/tabid/2509/Default.aspx, Accessed date: 9 December 2017.
Strandberg, B., Hites, R.A., 2001. Concentration of organochlorine pesticides in wine corks. Chemosphere 44, 729–735.
USEPA, United States Environmental Protection Agency, 1979. Water-related environmental fate of 129 priority pollutants. Introduction and Technical Background, Metals and Inorganics, Pesticides and PCBs. vol. I . https://nepis.epa.gov/EPA/html/DLwait.htm?url=/Exe/ZyPDF.cgi/P100K7FH.PDF?Dockey=P100K7FH.PDF, Accessed date: 26 January 2018.
USEPA, United States Environmental Protection Agency, 2005. Guidelines for carcinogen risk assessment. http://www.epa.gov/cancerguidelines/2005, Accessed date: 13 August 2017.
USEPA United States Environmental Protection Agency, 2000. Guidance for assessing chemical contaminant data for use in fish advisories volume 2 risk assessment and fish consumption limits third edition. https://www.epa.gov/sites/production/files/2015-06/documents/volume2.pdf, Accessed date: 8 February 2018.
USEPA, United States Environmental Protection Agency, 2012. Human health risk assessment: risk based screening table. http://www.epa.gov/reg3hwmd/risk/human/pdf/NOV_2012_FISH.pdf, Accessed date: 13 August 2017.
USEPA, United States Environmental Protection Agency, 2017. Assessing human health risk from pesticides. https://www.epa.gov/pesticide-science-and-assessing-pesticide-risks/assessing-human-health-risk-pesticides#safety, Accessed date: 12 December 2017.
Van der Oost, R., Beyer, J., Vermeulen, N.P.E., 2003. Fish bioaccumulation and biomarkers in environmental risk assessment: a review. Environ. Toxicol. Pharmacol. 13, 57–149.
Verhaert, V., Newmark, N., D'Hollander, W., Covaci, A., Vlok, W., Wepener, V., Addo-Bediako, A., Jooste, A., Teuchies, J., Blust, R., Bervoets, L., 2017. Persistent organic pollutants in the Olifants River Basin, South Africa: bioaccumulation and trophic transfer through a subtropical aquatic food web. Sci. Total Environ. 586, 792–806.
Verheart, V., Covaci, A., Bouillon, S., Abrantes, K., Musibono, D., Bervoets, L., Verheyen, E., Blust, R., 2013. Baseline levels and trophic transfer of persistent organic pollutants in sediments and biota from the Congo River Basin (DR Congo). Environ. Int. 59, 290–302.
Viljoen, I.M., Bornman, R., Bouwman, H., 2016. DDT exposure of frogs: a case study from Limpopo Province, South Africa. Chemosphere 159, 335–341.
Wepener, V., Van Dyk, C., Bervoets, L., O'Brien, G., Covaci, A., Cloete, Y., 2011. An assessment of the influence of multiple stressors on the Vaal River, South Africa. Phys. Chem. Earth 36, 949–962.
Wepener, V., Smit, N., Covaci, A., Dyke, S., Bervoets, L., 2012. Seasonal bioaccumulation of organohalogens in tigerfish *Hydrocynus vittatus* Castelnau, from Lake Pongolapoort, South Africa. Bull. Environ. Contam. Toxicol. 88, 277–282.
WHO, World Health Organisation, 2010. Human health risk assessment toolkit. World Health Organisation, Geneva, Switzerlandhttp://apps.who.int/iris/bitstream/10665/44458/1/9789241548076_eng.pdf, Accessed date: 25 October 2017.
Yohannes, Y.B., Ikenaka, Y., Saengtienchai, A., Watanabe, K.P., Nakayama, S.M.M., Ishizuka, M., 2013a. Occurrence, distribution, and ecological risk assessment of DDTs and heavy metals in surface sediments from Lake Awassa–Ethiopian Rift Valley Lake. Environ. Sci. Pollut. Res. 20, 8663–8671.
Yohannes, Y.B., Ikenaka, Y., Nakayama, S.M.M., Saengtienchai, A., Watanabe, K., Ishizuka, M., 2013b. Organochlorine pesticides and heavy metals in fish from Lake Awassa, Ethiopia: insights from stable isotope analysis. Chemosphere 91, 857–863.
Yohannes, Y.B., Ikenaka, Y., Saengtienchai, A., Watanabe, K.P., Nakayama, S.M.M., Ishizuka, M., 2014a. Concentrations and human health risk assessment of organochlorine pesticides in edible fish species from a Rift Valley Lake–Lake Ziway, Ethiopia. Ecotoxicol. Environ. Saf. 106, 95–101.
Yohannes, Y.B., Ikenaka, Y., Nakayama, S.M.M., Ishizuka, M., 2014b. Organochlorine pesticides in bird species and their prey (fish) from the Ethiopian Rift Valley region, Ethiopia. Environ. Pollut. 192, 121–128.
Yohannes, Y.B., Ikenaka, Y., Nakayama, S.M.M., Ishizuka, M., 2017. DDTs and other organochlorine pesticides in tissues of four bird species from the Rift valley region, Ethiopia. Sci. Total Environ. 574, 1389–1395.

Environmental Pollution 235 (2018) 163–170

Contents lists available at ScienceDirect

Environmental Pollution

journal homepage: www.elsevier.com/locate/envpol

Association between human exposure to heavy metals/metalloid and occurrences of respiratory diseases, lipid peroxidation and DNA damage in Kumasi, Ghana☆

Nesta Bortey-Sam [a], Yoshinori Ikenaka [a, b], Osei Akoto [c], Shouta M.M. Nakayama [a], Kwadwo A. Asante [d], Elvis Baidoo [c], Christian Obirikorang [e], Hazuki Mizukawa [a], Mayumi Ishizuka [a, *]

[a] Laboratory of Toxicology, Department of Environmental Veterinary Science, Graduate School of Veterinary Medicine, Hokkaido University, Kita 18, Nishi 9, Kita Ku, Sapporo, 060–0818, Japan
[b] Water Research Group, Unit for Environmental Sciences and Management, North-West University, Potchefstroom, South Africa
[c] Department of Chemistry, Kwame Nkrumah University of Science and Technology, Kumasi, Ghana
[d] CSIR Water Research Institute, P. O. Box AH 38, Achimota, Accra, Ghana
[e] Department of Molecular Medicine, School of Medical Sciences, Kwame Nkrumah University of Science & Technology, Kumasi, Ghana

ARTICLE INFO

Article history:
Received 12 May 2017
Received in revised form
2 November 2017
Accepted 3 December 2017
Available online 27 December 2017

Keywords:
Metals
Urine
Kumasi
Asthma
DNA damage

ABSTRACT

Heavy metals and metalloids contamination in soils, water, food and livers of wild rats have been studied in Kumasi, Ghana and despite the estimated risks to residents, there is no epidemiological study to ascertain these projections. In addition, the World Health Organization and International Agency for Research on Cancer have reported an increase in respiratory diseases and cancers, in Ghana. The study's purpose was therefore to explore the potential associations between metal exposure and occurrences of respiratory diseases, lipid peroxidation and/or DNA damage to different age groups and sexes in Kumasi. Human urine was collected from the general population in urban and control sites in Kumasi and nine metals were measured in each sample. Results showed that although Zn was the most abundant total urinary As concentration was higher in 83% of samples compared to reference values. Urinary concentrations of metals, malondialdehyde (MDA) and 8-hydroxy-2-deoxy-guanosine (8-OHdG) were higher in urban sites compared to the control site. Based on the results obtained, there was no significant correlation between urinary metals and age. However, urinary Cd and MDA were highest in age groups 61–85 and 3–20 years, respectively. Significantly higher levels of urinary Co, As and Cd were detected in female participants. The study revealed that exposure to As was significantly associated with increased odds of asthma (odds ratio (OR) = 2.76; CI: 1.11–6.83) and tachycardia (OR = 3.93; CI: 1.01–15.4). Significant association was observed between urinary metals and MDA and 8-OHdG indicating possibility of lipid peroxidation and/or DNA damage in Kumasi residents.

1. Introduction

Heavy metals and metalloids are among the most toxic substances (ATSDR, 2015) and despite their natural abundance, they are formed mainly from human activities such as mining, smelting, combustion, tannery or fertilizer applications. Humans and animals could be exposed to metals via inhalation, consumption and/or dermal contact (Saoudi et al., 2012). Despite the importance metals (iron, zinc, copper and manganese) play in maintaining normal physiological functions, excessive intake could result in health implications (Magge et al., 2013). In addition, exposure to cadmium, nickel, lead and arsenic could generate reactive oxygen species (ROS) leading to modifications of DNA and lipids (Stohs and Bagchi, 1995). These modifications have been reported to contributes to the incidence of cancers and cardiovascular diseases (Shi et al., 2004). Indicators of DNA damage, oxidative stress and lipid peroxidation

☆ This paper has been recommended for acceptance by David Carpenter.

* Corresponding author. Laboratory of Toxicology, Department of Environmental Veterinary Sciences, Graduate School of Veterinary Medicine, Hokkaido University, N18, W9, Kita–ku, Sapporo, 060–0818, Japan.
E-mail address: ishizum@vetmed.hokudai.ac.jp (M. Ishizuka).

https://doi.org/10.1016/j.envpol.2017.12.005
0269-7491/

such as 8-hydroxy-2-deoxyguanosine (8-OHdG) and malondialdehyde (MDA) have widely been used to determine the health effects of human exposure to metals (Chen et al., 2005).

Besides DNA damage and lipid peroxidation, various epidemiological studies have also found and reported associations between heavy metal/metalloid (including arsenic, cadmium, copper, manganese, nickel, lead) exposure and the occurrence of respiratory effects such as asthma, rhinitis, wheeze, bronchitis, and allergies (Gehring et al., 2015; Huang et al., 2016).

The growing rate of industrialization (including mining), and resulting increases in economic activity and population growth in Kumasi, Ghana, has led to increased pollution of the environment (Bortey-Sam et al., 2014). Studies of environmental contamination and possible health risks due to metal exposure via medicinal herbs (Nkansah et al., 2016a), geophagic white clay (Nkansah et al., 2016b), food (Nkansah et al., 2016c), dust (Nkansah et al., 2015), soils (Akoto et al., 2016, 2017) and streams (Akoto et al., 2010) within Kumasi metropolis have been reported. Furthermore, levels of zinc, arsenic, copper and nickel in livers of wild rats sampled in Kumasi (Bortey-Sam et al., 2015a) were higher compared to the levels in wild rats sampled around mining sites in Kabwe, Zambia (Nakayama et al., 2013). Despite these reports and estimated risks, there is no study to assess the impact of metal exposure to Kumasi residents.

In Ghana, there are an estimated 16,000 cancer cases annually and also an increase in occurrence of respiratory disease (GLOBACAN, 2008; WHO, 2011). In 2012, the estimated cancer incidence in Kumasi was 11.9 per 100,000 and was higher in females (15.7 per 100,000) than males (7.3 per 100,000) (Laryea et al., 2014). Due to the high cancer incidence and respiratory symptoms in Kumasi (GLOBACAN, 2008; Laryea et al., 2014; WHO, 2011), and unavailability of research on the epidemiology and risks of metal exposure to residents, the objectives of this study were to: explore the potential associations between metal exposure and occurrence of respiratory diseases; assess the relationship between metal exposure and incidence of oxidative stress; find the association between urinary concentrations of metals, MDA, 8-OHdG with age and sex.

2. Materials and methods

2.1. Sampling

Urine is considered the main excretory pathway for metals and a better medium for biomonitoring metal exposure (Smolders et al., 2014). Heavy metals and metalloid concentrations in urine could be an indication of both long and short term exposures (Crinnion, 2010). In view of this, human urine (n = 190; 57 males and 133 females) was collected in the morning from the general population of three urban sites (Atonsu, Manhyia and Tafo) in Kumasi (Fig. 1). Samples were collected into corning tubes (Corning Incorporated, New York, USA) in January to February of 2015. Manhyia is in close proximity to Kejetia (1.1 km apart), Adum (1.5 km apart) and Romanhill (1.2 km apart), where soils were polluted with metals (Akoto et al., 2017). In previous studies, concentrations of metals were highest in the livers of wild rats trapped in Adum compared to other sites in Kumasi (Bortey-Sam et al., 2015a). Tafo is also 2.3 and 2.6 km from Suame and Mbrom, respectively, whose soils were polluted with metals (Akoto et al., 2017).

Moreover, 12 human urine samples (7 males and 5 females) were collected from Kwame Nkrumah University of Science and Technology campus (KNUST) and used as reference/control samples, even though metal exposure via consumption or inhalation was possible. KNUST, a university in Kumasi, has minimal vehicular motion and no industrial activities. In previous studies, heavy metals and metalloid levels in KNUST soils were low compared to recommended levels (Akoto et al., 2016, 2017). In addition, particulate matter and soil samples from KNUST have been used as controls in previous studies of environmental contaminants (Bortey-Sam et al., 2013, 2014; Bortey-Sam et al., 2015b).

For quality control purposes, urine was collected from 4 children in residential areas of KNUST to form a composite. Composite samples were used to give a more representative measure and also to account for any variabilities in heavy metals and metalloid concentrations. Since humans could be exposed to metals through various sources, the sample was measured several times to confirm the concentration.

During the sampling process, participant's information, including age, gender, body weight, height, place of residence, occupation, and personal lifestyle including smoker/non-smoker, were obtained through face-to-face interviews. Further, information on respiratory symptoms related to metals such as asthma, wheeze, tachycardia, bronchitis and rhinitis (Gehring et al., 2015; Huang et al., 2016) were collected. The Ethical/Institutional Review Board of Ghana Health Service (GHS) and Council for Scientific and Industrial Research (CSIR), Accra, Ghana, approved this study. Written and informed consent was obtained from each participant and parents gave consent and completed questionnaires on behalf of their children. The samples collected were kept frozen at the Department of Chemistry, KNUST, Ghana. Later the samples were transported to the Toxicology laboratory of the Graduate School of Veterinary Medicine, Hokkaido University, Japan, and stored at −30 °C until analysis.

2.2. Sample extraction and analysis

2.2.1. Heavy metals and a metalloid

Method described by Yabe et al., (2015) was used for the extraction of heavy metals and a metalloid from the urine samples collected. Briefly, 1 mL of each urine was transferred into a digestion vessel and 5 mL of 60% nitric acid (Kanto Chemical) and 1 mL of 30% hydrogen peroxide (Kanto Chemical) were added. Sample digestion (Speedwave MWS-2; Berghof) was for 52 min and up to 190 °C. The digested samples were transferred into corning tubes and diluted to 10 mL with de-ionized water (Milli-Q). Concentrations of arsenic (As), cadmium (Cd), cobalt (Co), chromium (Cr), copper (Cu), lead (Pb), manganese (Mn), nickel (Ni) and zinc (Zn) in each urine were measured by Inductively Coupled Plasma-Mass Spectrometer (ICP-MS; 7700 series, Agilent technologies, Tokyo, Japan).

2.2.2. Malondialdehyde, MDA (elisa kit)

Concentrations of urinary MDA were measured (based on instructions from manufacturer) using a UV-VIS Spectrophotometer (UV-2600 Shimadzu Corporation, Kyoto, Japan). Briefly, 10 μL of butylated hydroxytoluene (BHT) reagent was transferred into a vial and 250 μL of calibrator (0, 1, 2, 3 and 4 μM) or urine was added. After the addition of 250 μL each of 1 M phosphoric acid and 2-thiobarbituric acid (TBA) reagent, the solution was vortexed vigorously and incubated at 60 °C for 1 h. The mixture was transferred into a cuvette and spectra was recorded from 400 to 700 nm after it was centrifuged at 10,000×*g* for 2–3 min. 3rd derivative analysis was performed at 514 nm.

2.2.3. 8-Hydroxy-2-deoxy-guanosine (8-OHdG)

Extraction and analysis of urine sample for 8-OHdG followed the method described by Bortey-Sam et al., (2017). Briefly, urine (1 mL) was diluted with HPLC grade water (2 mL) after spiking with 25 ng/mL of (15N5) 8-OHdG (internal standard). Prior to sample loading, the Oasis HLB cartridge (3 cc, 60 mg; Waters Corporation, Milford, MA, USA) was primed with I mL each of methanol and water. The solid-phase extraction cartridge was then washed with 3 mL of water and the target analyte (8-OHdG) eluted with 3 mL of water:

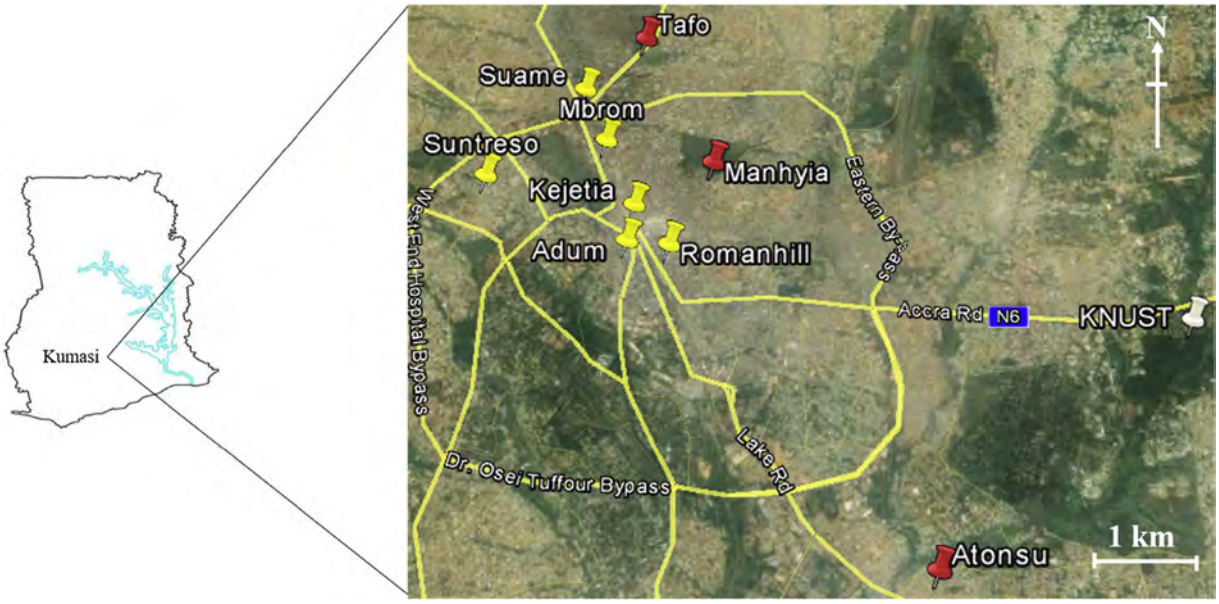

Fig. 1. Map showing human urine sampling locations in Kumasi, Ghana (yellow pins indicate city centre and environs contaminated with metals; red pins indicate human urine sites; white pin indicate KNUST campus). Obtained from (Bortey-Sam et al., 2017). (For interpretation of the references to colour in this figure legend, the reader is referred to the Web version of this article.)

acetonitrile (1:1, v/v). The eluate was evaporated to near dryness under nitrogen gas. The residue was re-dissolved in water (100 μL), and 10 μL injected into the LC–MS/MS. A Phenomenex Gemini 3u C18 110A column (150 mm × 2 mm i.d., 4 μm, Phenomenex, California, USA) with a guard column was used for the separation of 8-OHdG and (15N5) 8-OHdG in urine. Gradient elution was as follows: 0.0–1.0 min, 5% B; 1.01–3.00 min, 50% B; 3.01–6.00 min, 5% B. Multiple reaction monitoring (MRM) in negative ionization mode was used to identify the target analytes at a column temperature of 40 °C. Mobile phases A (0.1% formic acid) and B (100% methanol) were pumped at a flow rate of 250 μL/min (Bortey-Sam et al., 2017).

2.3. Creatinine concentrations in human urine

To compensate for variations in urine dilution, urinary creatinine was used to adjust concentrations of metals, MDA and 8-OHdG. Concentrations of creatinine in urine were determined based on the manufacturer's instructions (Arbor Assays, Michigan, USA). Briefly, 100 μL of DetectX® Creatinine Reagent (Arbor Assays, Michigan, USA) was added to 50 μL of sample, blank (water), or standards into clear plate wells. Prior to 30 min incubation (at room temperature), the sides of the plate was tapped for adequate mixing and the plate was covered with a plate sealer and pressed to seal adequately. The optical density produced from the plate reader well (Muiltiskan GO, Thermo Scientific, Vantaa, Finland) was read at 490 nm. To calculate the creatinine concentrations, a 4PLC built-in software was used and results expressed in g/L. Obtained creatinine concentrations (g/L) (mean; [range]) in human urine in Atonsu (1.57 ± 0.969; [0.0398–4.35]), Manhyia (1.76 ± 1.33; [0.202–5.96]), Tafo (2.30 ± 1.59; [0.0185–7.43]) and KNUST (2.71 ± 1.45; [1.46–5.58]) were used to adjust the respective urinary metal concentrations.

2.4. Quality control and quality assurance

2.4.1. Heavy metals and a metalloid

After every 10 sample analyses, blanks and duplicates were analysed and the Relative Standard Deviation (RSD) obtained for duplicate runs was ≤4%. Calibration curves using standard solutions were run and the linearity obtained for each metal was greater than 0.999. Analytical-reagent grade chemicals and standard stock solutions were used (Wako Pure Chemicals). The detection limits (μg/L) were 0.009 (As), 0.001 (Cd), 0.003 (Co), 0.003 (Cr), 0.008 (Cu), 0.002 (Pb), 0.034 (Mn), 0.003 (Ni) and 0.019 (Zn). Heavy metals and metalloid concentrations in human urine were expressed in μg/g creatinine.

The urine samples of children collected from residential areas of KNUST was used for quality control and recovery tests. The samples were spiked with standard solutions of metals and digested using the method described. The recovery rates of the spiked urine ranged from 95 (Pb) - 98% (Cd). Concentrations of metals in urine sample used for this purpose were below the respective limits of detection (LODs) and differences between concentrations before and after spiking was used to calculate the recoveries.

2.4.2. MDA and 8-OHdG

For 8-OHdG, (15N5) 8-OHdG was used as internal standard and spiked into urine prior to sample preparation and extraction. Internal standard method with a five-point calibration (1, 5, 10, 50 and 100 ng/mL) was used for quantification. The average linearity of the calibration standards for both MDA and 8-OHdG were greater than 0.99. The LOD and limit of quantification (LOQ) for 8-OHdG were 0.0196 and 0.6 ng/mL, respectively, and average recovery ([15N5] 8-OHdG) was 86 ± 9.8%. After every 10 samples, spiked solvent blanks (with 8-OHdG only) and duplicate samples were analysed and average internal standard recovery for spiked solvents blanks was 104 ± 8.7%. The %RSD for duplicate samples were less than or equal to 10% (MDA and 8-OHdG). LOD and LOQ for MDA were 0.205 and 0.63 μM, respectively.

2.4.3. Creatinine

Quantitation was performed based on a seven–point calibration (0.3125, 0.625, 1.25, 2.5, 5, 10, and 20 mg/dL) and the average linearity of the calibration standard was greater or equal to 0.9996. LODs and LOQs were calculated based on 3SD/S and 10SD/S, respectively (SD is the standard deviation of five replicate

measurements of the target analyte and S is the slope of the calibration curve). LOD and LOQ of creatinine were 0.00151 and 0.00505 g/L, respectively. Duplicate samples were run after every batch of 10 samples and the %RSD was 2.99 ± 2.30. Blank samples were also run after every 11 samples.

2.5. Data analysis

IBM SPSS v 20 (SPSS Inc., Illinois, USA) was used for statistical analyses and the normality of the data was tested using Kolmogorov–Smirnov (K–S) and Shapiro-Wilks tests. A value of LOD/2 was assigned to metals/metalloid concentrations below their respective LODs. The central tendency of the analyte concentrations was illustrated with the geometric mean concentrations (Ott, 1990). To compare urinary concentrations of metals from the study areas, ANOVA and Tukey tests were performed, after data was normalized by log transformation, and a p value less than 0.05 was considered significant. Pearson's correlation of logged data was used to determine the association between metals, MDA, 8-OHdG and age. The distribution of metals/metalloid, MDA and 8-OHdG between male and female participants was done using Student's T-Test and statistical significance was at p less than 0.05. Odds ratios (ORs) at 95% confidence interval (CI) was used to determine the association between exposure to As and occurrences of respiratory symptoms. This was derived using logistic regression model. Arsenic was treated as a continuous variable in the logistic regression. Regression models were adjusted for covariates such as age and sex. Statistical significance was set at $p < .05$ and performed with JMP 10 statistical software (SAS Institute).

3. Results and discussion

3.1. Urinary levels of heavy metals and a metalloid

The order of the geometric mean concentrations (adjusted by urinary creatinine; GM_{creat}) of heavy metal and metalloid from all study sites in Kumasi was Zn (335 ± 340) > As (49.8 ± 52.2) > Cu (14.7 ± 28.9) > Ni (2.36 ± 6.33) > Cr (0.825 ± 7.32) > Pb (0.716 ± 7.59) ≥ Co (0.712 ± 3.57) > Mn (0.276 ± 2.35) ≥ and Cd (0.240 ± 2.22) μg/g creatinine. The urinary concentrations of all metals measured varied significantly (p <0.01) (K-S and S-W's tests). The results of GM_{creat} indicated that Co, Cu, Zn and As were detected in all samples (100%) while the detection rate for urinary Cr was 78%, Mn (89%), Ni (79%), Cd (99%), Pb (76%), MDA (95%) and 8-OHdG (59%).

Urinary concentrations of Ni and Cr (except Manhyia) were significantly higher (p = .0002–.0145) in participants who lived in Atonsu compared to other sites including KNUST (Table 1). Additionally, urinary concentrations of As and Cd in participants who lived in urban sites were significantly higher (p = .0001–.01) compared to KNUST participants (Table 1). Although not significant (p = .0798–.838), concentrations of Mn, Co and Cd (significantly lower in KNUST) in urine were higher in Atonsu participants while highest levels of Pb and Cu (significantly lower in KNUST) were detected in Tafo participants. The high urinary metals could be due to high metal exposure to residents. Previous studies reported that although metal concentrations in Atonsu soils were below recommended levels, the soils were enriched with Zn, Cd, Cr and Pb (Akoto et al., 2017). Tafo on the other hand is close to communities (Suame and Mbrom) polluted with metals and filled with light scale industries (Akoto et al., 2017).

Metals and metalloid concentrations detected in urine of participant's from the present study were compared to studies conducted in the US (Caldwell et al., 2009; CDC, 2005), Czech Republic (Benes et al., 2002), Spain (Aguilera et al., 2010), France (de Burbure et al., 2006), Italy (Alimonti et al., 2000) China (Huang et al., 2016; Lu et al., 2016) and Democratic Republic of Congo (Banza et al., 2009) (Table S1). The results (Table S1) showed that all metal measured in this study were comparable or lower than previous studies with the exception of urinary As concentrations which were higher in this study. From Table S2, the unadjusted urinary concentrations (ng/mL) of metals (except Co) from all sites were on the average (11.3 (Zn) - 83.3% (As)) higher compared to the unadjusted reference values suggested by the Canadian Health Measure (Saravanabhavan et al., 2016); Fourth National Report on Human Environmental Chemicals, USA (Crinnion, 2010) and Human Biomonitoring Commission, Germany (Schulz et al., 2009).

In addition to water and food consumption, soil and dust are other possible ways of exposure to metals/metalloids especially children via hand-to-mouth practices (Berglund et al., 2011). Residents of various countries including Ghana, consume large amounts of geophagic white clay for religious, cultural, nutritional, and medicinal reasons as well as in response to famine and pregnancy-related cravings (Mathee et al., 2014; Nkansah et al., 2016b). Also, exposure to metals could be through the intake of medicinal herbs (Nkansah et al., 2016a) frequently used in the treatment of various ailments. Lower levels of urinary metals in KNUST participants could be due to the low vehicular movement and industrial activities, and point source of metal pollution was low.

The high levels of urinary As in participants could be attributed to the gold mining activities in some parts of Kumasi. Residents could be exposed because of the composition of the ore containing the gold. After blasting the gold bearing rock, miners roast the ore and this leads to the production and distribution of arsenic trioxide gas (Amonoo-Neizer et al., 1996). In addition, exposure to organic As was associated with consumption of sea foods such as shellfish (Aguilera et al., 2010), although the recommended total urinary As concentration was estimated to be 27 ng/mL by the Canadaian Health Measures (Saravanabhavan et al., 2016). Highest urinary concentrations of As (336, 297 and 234 μg/g creatinine) were detected in urine of participants who complained of asthma, diabetes, rhinitis and tachycardia, symptoms which have been associated with As exposure (Maull et al., 2012; Parvez et al., 2008, 2010, 2011; Saha et al., 1999).

3.2. Association between urinary metals, MDA, 8-OHdG with age

As shown in Table 2, there was no significant association (p = .424–.928) between urinary metal concentrations and age from KNUST participants and participants who lived in urban areas. Previous studies reported a positive correlation between urinary Cd levels and age while a negative association was observed between other metals and age (Banza et al., 2009). Results of this study further showed that urinary MDA was highest in age group 3–20 years. The effects of metal exposure is more pronounced in children than adults because their immune and nervous systems are not fully developed (Olsen, 2000). Moreover, the breathing rate of children is higher and their consumption rate per body weight is also higher than adults (Schwartz, 2004).

Although significant correlation (p = .443) between age and urinary Cd concentrations was not observed (Table 2), levels were highest in ages 61–85 years compared to the other age groups (Table 3). This is possibly because concentrations of Cd in urine indicates long-term accumulation and consequently higher in the elderly (Paschal et al., 2000).

3.3. Association between urinary metals, MDA, 8-OHdG with sex

As shown in Table 4, significantly higher levels (p = .0089–.017) of Co, As and Cd were detected in urine of female participants

Table 1
Creatinine adjusted metal concentrations (μg/g creatinine) in human urine, collected in 2015, from four sites in Kumasi, Ghana.

Sample site	n		Cr	Mn	Co	Ni	Cu	Zn	As	Cd	Pb	MDA	8-OHdG
Atonsu	82	GM_{creat}	1.50^{a}	0.375^{a}	0.855^{a}	4.20^{a}	15.7^{a}	386^{a}	67.3^{a}	0.289^{a}	0.615^{a}	54.9^{a}	1.02^{a}
		SD	2.21	2.94	4.00	6.30	25.6	291	61.1	0.980	8.27	68.2	1.99
Manhyia	51	GM_{creat}	0.961^{ab}	0.220^{a}	0.734^{a}	1.19^{b}	16.1^{a}	350^{a}	43.5^{b}	0.227^{a}	0.636^{a}	40.1^{ab}	0.876^{a}
		SD	1.17	2.01	1.17	5.66	13.6	409	31.6	0.254	0.897	55.9	1.82
Tafo	57	GM_{creat}	0.442^{c}	0.259^{a}	0.569^{a}	1.76^{b}	16.7^{a}	290^{a}	42.8^{b}	0.231^{a}	0.962^{a}	32.7^{b}	0.911^{a}
		SD	3.84	1.45	4.36	6.58	23.2	357	45.5	3.861	9.601	48.7	3.78
KNUST	12	GM_{creat}	0.180^{bc}	0.115^{a}	0.481^{a}	0.524^{b}	5.67^{b}	180^{a}	15.9^{c}	0.074^{b}	0.312^{a}	23.7^{ab}	0.779^{a}
		SD	0.132	0.310	0.359	0.970	2.88	80.9	18.1	0.046	0.302	11.9	0.270

n: number of samples; GM_{creat}: geometric mean concentration adjusted by creatinine; SD: standard deviation; different letters (a, b and c) within a column indicates significant differences ($p < 0.05$).

Table 2
Correlation analysis between urinary concentrations (μg/g creatinine) of metals, MDA, 8-OHdG and age of participants in Kumasi, Ghana.

Variables	Age/years	Cr	Mn	Co	Ni	Cu	Zn	As	Cd	Pb	MDA	8-OHdG
Urban sites												
Age/years	1	−0.0643	−0.0585	-0.337^{*}	−0.0174	0.0698	0.0493	0.0466	0.11	−0.0314		
MDA	−0.181	0.532^{**}	0.381^{**}	0.669^{**}	0.592^{**}	0.660^{**}	0.585^{**}	0.777^{**}	0.593^{**}	0.586^{**}	1	
8-OHdG	0.0812	0.171	0.217	0.218	0.223	0.360^{*}	0.224	0.488^{**}	0.267	0.108	0.453^{**}	1
KNUST (Control site)												
Age/years	1	0.0352	−0.142	−0.305	−0.077	−0.250	−0.205	−0.217	−0.254	−0.707		
MDA	0.0451	0.357	0.339	0.271	0.311	0.332	0.348	0.371	0.263	0.182	1	
8-OHdG	−0.567	0.490	−0.013	0.411	0.077	0.340	0.242	0.270	0.224	0.221	0.340	1

*: Indicates significance at $p < .05$.
** : Indicates significance at $p < .01$.

Table 3
Age differences in urinary concentrations (μg/g creatinine) of metals, MDA, and 8-OHdG among participants in Kumasi, Ghana.

Age groups	n		Cr	Mn	Co	Ni	Cu	Zn	As	Cd	Pb	MDA	8-OHdG
3–20	36	GM_{creat}	1.66^{a}	0.400^{a}	1.24^{a}	3.26^{a}	20.3^{a}	425^{a}	51.6^{a}	0.296^{a}	1.18^{a}	50.5^{a}	0.557^{a}
		SD	1.02	0.43	4.59	4.74	17.2	572	51.2	0.619	8.18	98.9	0.558
21–40	102	GM_{creat}	0.801^{a}	0.249^{a}	0.700^{ab}	2.36^{a}	14.2^{a}	297^{a}	49.3^{a}	0.224^{a}	0.664^{a}	43.0^{a}	1.07^{a}
		SD	3.39	2.75	2.82	5.61	24.9	256	51.1	3.08	7.87	48.2	3.48
41–60	33	GM_{creat}	0.554^{a}	0.279^{a}	0.472^{b}	2.99^{a}	17.4^{a}	336^{a}	63.9^{a}	0.299^{a}	0.758^{a}	42.2^{a}	1.12^{a}
		SD	2.57	0.653	0.414	7.12	27.3	238	57.8	0.269	1.39	70.3	2.21
61–85	31	GM_{creat}	1.25^{a}	0.421^{a}	0.572^{ab}	2.59^{a}	17.6^{a}	528^{a}	82.7^{a}	0.400^{a}	0.728^{a}	47.9^{a}	0.604^{a}
		SD	1.76	0.330	8.69	5.93	6.93	291	36.6	2.02	16.7	36.9	0.539

n: number of samples; GM_{creat}: geometric mean concentration adjusted by creatinine; SD: standard deviation; different letters (a and b) within a column indicates significant differences ($p < .05$) among age groups.

compared to males. However, urinary MDA and 8-OHdG were comparable (Table 4) and this is similar to outcomes obtained by Lu et al., (2016). Although not significant ($p = .054–.383$), urinary concentrations of Cr, Mn, Cu and Zn were also higher in females than males which is similar to results obtained by Banza et al., (2009). The significantly higher urinary Cd in females was similar to results obtained in other studies (Berglund et al., 2011; Castano et al., 2012; Paschal et al., 2000; Vahter et al., 2007). Iron deficiency has mainly been related to gender differences in urinary Cd excretion. This influences high levels of duodenal divalent transporter which results in the rise in transport and absorption of Cd (Berglund et al., 2011; Paschal et al., 2000; Vahter et al., 2007).

Sex differences in Cu levels have been reported and females recorded higher concentrations than males (Benes et al., 2002). The higher urinary Cu levels in women could be attributed to hormonal changes that occur in puberty (Wapnir, 1998). Additionally, significantly higher urinary Mn was detected in women than men and this trend could be attributed to biological differences in the way females

Table 4
Sex differences in urinary metal, MDA and 8-OHdG concentrations (μg/g creatinine) in Kumasi, Ghana.

Sex	n		Cr	Mn	Co	Ni	Cu	Zn	As	Cd	Pb	MDA	8-OHdG
Female	138	GM_{creat}	0.903^{a}	0.331^{a}	0.812^{a}	2.24^{a}	16.5^{a}	362^{a}	56.1^{a}	0.283^{a}	0.687^{a}	42.3^{a}	0.962^{a}
		SD	2.84	2.67	3.92	11.5	22.6	334	57.9	2.692	8.46	60.1	2.86
Male	64	GM_{creat}	0.678^{a}	0.187^{a}	0.547^{b}	3.00^{a}	14.2^{a}	291^{a}	40.8^{b}	0.175^{b}	0.838^{a}	45.0^{a}	0.910^{a}
		SD	2.13	0.529	2.80	7.63	21.5	215	36.3	0.314	5.08	59.4	2.33

n: number of samples; GM_{creat}: geometric mean concentration adjusted by creatinine; SD: standard deviation; different letters (a and b) within a column indicate significant differences (Student's T-Test; $p < 0.05$).

and males handle Mn (Berglund et al., 2011). Lindberg et al. reported that women had significantly higher dimethylarsinic acid (DMA) concentrations than men, because they (women) can more efficiently methylate arsenic than men (Lindberg et al., 2008). Although not significant ($p = .371$), urinary concentrations of Pb were higher in males than females. In a study by Berglund et al., higher levels of Pb were detected in urine of men than women (Berglund et al., 2011). This results was opposite from previous studies where women excreted higher urinary Pb than men (Castano et al., 2012). These in addition to other factors (such as differences in exposure levels, lifestyle etc.) could explain the sex difference in urinary excretion of metals although the mechanisms underlying these sex differences remain unknown (Howe et al., 2016).

3.4. Association between metal exposure and occurrence of respiratory symptoms

OR was performed for all metals, however, the study focused on As since it was the most toxic substance (ATSDR, 2015) and the second most abundant metal detected in human urine in Kumasi. In addition, concentrations of urinary As in this study was higher than previously conducted studies in China, Congo, Spain and USA (Table S1). Moreover, urinary As was on average 83% higher (from all study sites) compared to recommended values.

The study revealed that exposure to As was significantly ($p = .041–.043$) associated with increased odds of asthma (OR = 2.76, CI: 1.11–6.83) and tachycardia (OR = 3.93, CI: 1.01–15.4) in Kumasi residents (Table 5). In a study by Huang et al., urinary concentrations of As were significantly and positively associated with the occurrence of asthma when the metalloid was considered as a continuous variable and when divided into quantiles (Huang et al., 2016). Similarly, As exposure has been associated with (i) occurrence of lung dysfunction (ii) increased mortality due to respiratory diseases (Parvez et al., 2011). Additionally, inhalation of As dust or fumes during milling of ores or mining (which is a common practice in Kumasi) often resulted in chronic cough, laryngitis, bronchitis and rhinitis (Saha et al., 1999). In other cohort studies, chronic cough, chest sounds, shortness of breath, blood in sputum and other respiratory symptoms were observed due to As exposure (Parvez et al., 2010). Additionally, positive association between urinary As and serum Clara cell protein (CC16; a novel biomarker of respiratory illness) was found, with urinary As levels inversely related with lung function (Parvez et al., 2008).

Environmental factors have been associated with the occurrence of asthma (Huang et al., 2016) and as a results, living in metal contaminated areas could increase the risks of respiratory disease among residents.

3.5. Human health risk implications

As shown in Table 2, there was no association ($p = .180–.972$) between urinary concentrations of metals, MDA and 8-OHdG in KNUST participants. However, in urine of participants at urban sites, significant association ($p = <0.0001–0.0063$) was noted between metals and MDA. Additionally, concentrations of urinary As also correlated significantly ($p = .0003$) with 8-OHdG. This trend indicates the possibility of lipid peroxidation or DNA damage although these products have also been associated with the presence of cardiovascular diseases, atherosclerosis, diabetes and cancers (Wu et al., 2004). Aflanie et al. concluded that human exposure to As and Cd could increase MDA levels and cause oxidative stress and inflammation (Aflanie et al., 2015). Lu et al. also reported a correlation between As and 8-OHdG (Lu et al., 2016). Arsenic could bind to thiols and this has been considered crucial in increasing 8-OHdG levels (Valko et al., 2007). In previous reports, urinary As was associated with diabetes (Maull et al., 2012). Several metals (e.g. As, Cd, Pb) are also known to impair kidney function and increase different cancer risks, while others could affect the nervous and cardiovascular systems (e.g., As, Cd, Mn, Pb) (EFSA, 2011; Straif et al., 2009; WHO, 2008). In previous studies, oxidative stress correlated with allergic inflammatory diseases (Bartsch and Nair, 2004), obesity and atherosclerosis (Kobayashi et al., 2011; Wu et al., 2004) and these were some symptoms participants complained of during the face-to-face interview. 10% of participants in this study were diabetics and 2% had arthritis. Of the 33 participants whose body mass indexes were calculated, 11 were overweight and 7 were obese.

Table 5
Adjusted odds ratios (OR; 95% CI) for the presence or absence of respiratory symptoms in Kumasi residents due to arsenic exposure.

Metalloid	Clinical symptom	OR	CI		*p* value
As	Asthma	2.76	1.11	6.83	.043
	RTI	2.42	0.075	7.86	.618
	Tachycardia	3.93	1.01	15.4	.041
	Rhinitis	0.848	0.145	4.97	.855
	Dyspnea	1.09	0.344	3.47	.880

OR: Odds ratio; CI: 95% Confidence Interval; RTI: respiratory tract infection; The models were adjusted for age and sex.

3.6. Limitations of the study

The major limitation to this study was the small sample size which could have resulted in wide CI in the regression analysis. Additionally, participants were not medically examined and this could have resulted in false information.

4. Conclusions

Urinary metal/metalloid concentrations were studied in Kumasi residents, and although Zn was the most abundant, urinary As was higher in 83% of participants compared to reference values. The study revealed that urinary concentrations of metals, MDA and 8-OHdG were higher in urban sites participants compared to the control site. Females excreted significantly higher levels of Co, As and Cd than males. As exposure was significantly associated with increased odds of asthma and tachycardia. Although no relationship was found between urinary metals and age, Cd and MDA levels were highest in age groups 61–85 and 3–20 years, respectively. Exposure of Kumasi residents to heavy metals and a metalloid increased the occurrences of lipid peroxidation and/or DNA damage.

Acknowledgements

We are highly grateful to all the participants, hospital administration and staff, the Ghana Health Service and Council for Scientific and Industrial Research, Ghana, for facilitating this study. This work was supported by Grants-in-Aid for Scientific Research from the Ministry of Education, Culture, Sports, Science and Technology of Japan awarded to M. Ishizuka (No. 24405004 and No. 24248056), Y. Ikenaka (No. 26304043, 15H0282505, 15K1221305), S. Nakayama, H. Mizukawa and the foundation of JSPS Core to Core Program (AA Science Platforms) and Bilateral Joint Research Project (PG36150002 and PG36150003). We also acknowledge the financial support by The Mitsui & Co., Ltd. Environment Fund and Sumitomo, and Soroptimist Japan Foundation We are grateful to Mr. Takahiro Ichise and Ms. Mio Yagihashi (Laboratory of Toxicology, Graduate School of Veterinary Medicine, Hokkaido University) for technical support.

Appendix A. Supplementary data

Supplementary data related to this article can be found at https://doi.org/10.1016/j.envpol.2017.12.005.

References

Aflanie, I., Muhyi, R., Suhartono, E., 2015. Effect of heavy metal on malondialdehyde and advanced oxidation protein produtcs concentration: a focus on arsenic, cadmium, and mercury. J. Med. Biogr. 4, 332–337.

Aguilera, I., Daponte, A., Gil, F., Hernandez, A.F., Godoy, P., Pla, A., et al., 2010. Urinary levels of arsenic and heavy metals in children and adolescents living in the industrialised area of ria of huelva (sw Spain). Environ. Int. 36, 563–569.

Akoto, O., Bruce, T.N., Darko, G., 2010. Chemical and biological characteristics of streams in the owabi watershed. Environ. Monit. Assess. 161, 413–422.

Akoto, O., Nimako, C., Asante, J., Bailey, D., 2016. Heavy metals enrichment in surface soil from abandoned waste disposal sites in a hot and wet tropical area. Environ. Prog. 3, 747–761.

Akoto, O., Bortey-Sam, N., Ikenaka, Y., Nakayama, S.M.M., Baidoo, E., Yohannes, Y.B., et al., 2017. Contamination levels and sources of heavy metals and metalloid in surface soils in the kumasi metropolis, Ghana. J. Health Pollut. 7, 28–39.

Alimonti, A., Petrucci, F., Krachler, M., Bocca, B., Caroli, S., 2000. Reference values for chromium, nickel and vanadium in urine of youngsters from the urban area of rome. J. Environ. Monit.: JEM 2, 351–354.

Amonoo-Neizer, E., Nyamah, D., Bakiamoh, S., 1996. Mercury and arsenic pollution in soil and biological samples around the mining town of obuasi, Ghana. Water Air Soil Pollut. 91, 363–373.

ATSDR, 2015. Priority List of Hazardous Substances. ATSDR (Agency for Toxic Substance and Disease Registry), Division Of Toxicology & Human Health Sciences.

Banza, C.L., Nawrot, T.S., Haufroid, V., Decree, S., De Putter, T., Smolders, E., et al., 2009. High human exposure to cobalt and other metals in katanga, a mining area of the democratic republic of Congo. Environ. Res. 109, 745–752.

Bartsch, H., Nair, J., 2004. Oxidative stress and lipid peroxidation-derived DNA-lesions in inflammation driven carcinogenesis. Canc. Detect. Prev. 28, 385–391.

Benes, B., Spevackova, V., Smid, J., Cejchanova, M., Kaplanova, E., Cerna, M., et al., 2002. Determination of normal concentration levels of cd, pb, hg, cu, zn and se in urine of the population in the Czech Republic. Cent. Eur. J. Publ. Health 10, 3–5.

Berglund, M., Lindberg, A.L., Rahman, M., Yunus, M., Grander, M., Lonnerdal, B., et al., 2011. Gender and age differences in mixed metal exposure and urinary excretion. Environ. Res. 111, 1271–1279.

Bortey-Sam, Ikenaka, Y., Akoto, O., Nakayama, S.M.M., Yohannes, Y.B., Baidoo, E., et al., 2015a. Exposure levels of polycyclic aromatic hydrocarbons (pahs) and heavy metals in wild rats in kumasi, Ghana. 7th Int. Toxicol. Symp. Afr. 2.

Bortey-Sam, N., Ikenaka, Y., Akoto, O., Nakayama, S.M.M., Yohannes, Y.B., Baidoo, E., et al., 2015b. Levels, potential sources and human health risk of polycyclic aromatic hydrocarbons (pahs) in particulate matter (pm10) in kumasi, Ghana. Environ. Sci. Pollut. Res. 22, 9658–9667.

Bortey-Sam, N., Akoto, O., Ikenaka, Y., Nakayama, S.M.M., Ishizuka, M., 2013. Determination of benzo[a]pyrene levels in ambient air and the source of polycyclic aromatic hydrocarbons using a diagnostic ratio method in Ghana. Jpn. J. Vet. Res. 61, S72–S74.

Bortey-Sam, N., Ikenaka, Y., Nakayama, S.M., Akoto, O., Yohannes, Y.B., Baidoo, E., et al., 2014. Occurrence, distribution, sources and toxic potential of polycyclic aromatic hydrocarbons (pahs) in surface soils from the kumasi metropolis, Ghana. Sci. Total Environ. 496, 471–478.

Bortey-Sam, N., Ikenaka, Y., Akoto, O., Nakayama, S.M.M., Asante, K.A., Baidoo, E., et al., 2017. Oxidative stress and respiratory symptoms due to human exposure to polycyclic aromatic hydrocarbons (pahs) in kumasi, Ghana. Environ. Pol. 228, 311–320.

Caldwell, K.L., Jones, R.L., Verdon, C.P., Jarrett, J.M., Caudill, S.P., Osterloh, J.D., 2009. Levels of urinary total and speciated arsenic in the us population: national health and nutrition examination survey 2003-2004. J. Expo. Sci. Environ. Epidemiol. 19, 59–68.

Castano, A., Sanchez-Rodriguez, J.E., Canas, A., Esteban, M., Navarro, C., Rodriguez-Garcia, A.C., et al., 2012. Mercury, lead and cadmium levels in the urine of 170 Spanish adults: a pilot human biomonitoring study. Int. J. Hyg Environ. Health 215, 191–195.

CDC, 2005. National Center for Environmental Health. Third National Report on Human Exposure to Environmental Chemicals. Nceh pub, Atlanta, ga. No. 05-0570; 2005.

Chen, C.Y., Qu, L.Y., Li, B., Xing, L., Jia, G., Wang, T.C., et al., 2005. Increased oxidative DNA damage, as assessed by urinary 8-hydroxy-2 '-deoxyguanosine concentrations, and serum redox status in persons exposed to mercury. Clin. Chem. 51, 759–767.

Crinnion, W.J., 2010. The cdc fourth national report on human exposure to environmental chemicals: what it tells us about our toxic burden and how it assists environmental medicine physicians. Alternative Med. Rev. 15, 101–108.

de Burbure, C., Buchet, J.P., Leroyer, A., Nisse, C., Haguenoer, J.M., Mutti, A., et al., 2006. Renal and neurologic effects of cadmium, lead, mercury, and arsenic in children: evidence of early effects and multiple interactions at environmental exposure levels. Environ. Health Perspect. 114, 584–590.

EFSA, 2011. Statement on tolerable weekly intake for cadmium. Efsa j 9 (2), 1975.

Gehring, U., Beelen, R., Eeftens, M., Hoek, G., de Hoogh, K., de Jongste, J.C., et al., 2015. Particulate matter composition and respiratory health: the piama birth cohort study. Epidemiology 26, 300–309.

GLOBACAN, 2008. Country Fast Stats, Ghana. Lyon, France: Iarc; 2008. International Agency for Research on Cancers.

Howe, C.G., Liu, X.H., Hall, M.N., Slavkovich, V., Ilievski, V., Parvez, F., et al., 2016. Associations between blood and urine arsenic concentrations and global levels of post-translational histone modifications in bangladeshi men and women. Environ. Health Perspect. 124, 1234–1240.

Huang, X.J., Xie, J.G., Cui, X.Q., Zhou, Y., Wu, X.J., Lu, W., et al., 2016. Association between concentrations of metals in urine and adult asthma: a case-control study in wuhan, China. PLoS One 11.

Kobayashi, S., Susa, T., Tanaka, T., Wada, Y., Okuda, S., Doi, M., et al., 2011. Urinary 8-hydroxy-2'-deoxyguanosine reflects symptomatic status and severity of systolic dysfunction in patients with chronic heart failure. Eur. J. Heart Fail. 13, 29–36.

Laryea, D.O., Awuah, B., Amoako, Y.A., Osei-Bonsu, E., Dogbe, J., Larsen-Reindorf, R., et al., 2014. Cancer incidence in Ghana, 2012: evidence from a population-based cancer registry. BMC Canc. 14, 362.

Lindberg, A.L., Ekstrom, E.C., Nermell, B., Rahman, M., Lonnerdal, B., Persson, L.A., et al., 2008. Gender and age differences in the metabolism of inorganic arsenic in a highly exposed population in Bangladesh. Environ. Res. 106, 110–120.

Lu, S.Y., Ren, L., Fang, J.Z., Ji, J.J., Liu, G.H., Zhang, J.Q., et al., 2016. Trace elements are associated with urinary 8-hydroxy-2'-deoxyguanosine level: a case study of college students in guangzhou, China. Environ. Sci. Pollut. Res. 23, 8484–8491.

Magge, H., Sprinz, P., Adams, W.G., Drainoni, M.L., Meyers, A., 2013. Zinc protoporphyrin and iron deficiency screening: trends and therapeutic response in an urban pediatric center. J. Pediatr. 167, 361–367.

Mathee, A., Naicker, N., Kootbodien, T., Mahuma, T., Nkomo, P., Naik, I., et al., 2014. A cross-sectional analytical study of geophagia practices and blood metal concentrations in pregnant women in johannesburg, South Africa. SAMJ: S. Afr. Med. J. 104, 568–573.

Maull, E.A., Ahsan, H., Edwards, J., Longnecker, M.P., Navas-Acien, A., Pi, J.B., et al., 2012. Evaluation of the association between arsenic and diabetes: a national toxicology program workshop review. Environ. Health Perspect. 120, 1658–1670.

Nakayama, S.M.M., Ikenaka, Y., Hamada, K., Muzandu, K., Choongo, K., Yabe, J., et al., 2013. Accumulation and biological effects of metals in wild rats in mining areas of Zambia. Environ. Monit. Assess. 185, 4907–4918.

Nkansah, M.A., Fianko, J.R., Mensah, S., Debrah, M., Francis, G.W., Slawin, A.M.Z., 2015. Determination of heavy metals in dust from selected nursery and kindergarten classrooms within the kumasi metropolis of Ghana. Coke Chem. 1.

Nkansah, M.A., Hayford, S.T., Borquaye, L.S., Ephraim, J.H., Ng, C.A., 2016a. Heavy metal contents of some medicinal herbs from kumasi, Ghana. Cogent Environ. Sci. 2.

Nkansah, M.A., Korankye, M., Darko, G., Dodd, M., 2016b. Heavy metal content and potential health risk of geophagic white clay from the kumasi metropolis in Ghana. Toxicol. Rev. 3, 644–651.

Nkansah, M.A., Opoku, F., Ackumey, A.A., 2016c. Risk assessment of mineral and heavy metal content of selected tea products from the ghanaian market. Environ. Monit. Assess. 188, 1–11.

Olsen, J., 2000. Prenatal exposures and long-term health effects. Epidemiol. Rev. 22, 76–81.

Ott, W.R., 1990. A physical explanation of the lognormality of pollutant concentrations. J. Air Waste Manag. Assoc. 40, 1378–1383.

Parvez, F., Chen, Y., Brandt-Rauf, P.W., Bernard, A., Dumont, X., Slavkovich, V., et al., 2008. Nonmalignant respiratory effects of chronic arsenic exposure from drinking water among never-smokers in Bangladesh. Environ. Health Perspect. 116, 190–195.

Parvez, F., Chen, Y., Brandt-Rauf, P.W., Slavkovich, V., Islam, T., Ahmed, A., et al., 2010. A prospective study of respiratory symptoms associated with chronic arsenic exposure in Bangladesh: findings from the health effects of arsenic longitudinal study (heals). Thorax 65, 528–533.

Parvez, F., Chen, Y., Yunus, M., Zaman, R.U., Ahmed, A., Islam, T., et al., 2011. Associations of arsenic exposure with impaired lung function and mortality from diseases of the respiratory system: findings from the health effects of arsenic longitudinal study (heals). Epidemiology 22, S179.

Paschal, D.C., Burt, V., Caudill, S.P., Gunter, E.W., Pirkle, J.L., Sampson, E.J., et al., 2000. Exposure of the u.S. Population aged 6 years and older to cadmium: 1988-1994. Arch. Environ. Contam. Toxicol. 38, 377–383.

Saha, J., Dikshit, A., Bandyopadhyay, M., Saha, K., 1999. A review of arsenic poisoning and its effects on human health. Crit. Rev. Environ. Sci. Technol. 29, 281–313.

Saoudi, A., Zeghnoun, A., Bidondo, M.L., Garnier, R., Cirimele, V., Persoons, R., et al., 2012. Urinary arsenic levels in the French adult population: the French national nutrition and health study, 2006-2007. Sci. Total Environ. 433, 206–215.

Saravanabhavan, G., Werry, K., Walker, M., Haines, D., Malowany, M., Khoury, C., 2016. Human biomonitoring reference values for metals and trace elements in blood and urine derived from the canadian health measures survey 2007-2013. Int. J. Hyg Environ. Health 220, 189–200.

Schulz, C., Angerer, J., Ewers, U., Heudorf, U., Wilhelm, M., Human Biomonitoring Commission of the German Federal Environment A, 2009. Revised and new reference values for environmental pollutants in urine or blood of children in Germany derived from the German environmental survey on children 2003-2006 (geres iv). Int. J. Hyg Environ. Health 212, 637–647.

Schwartz, J., 2004. Air pollution and children's health. Pediatrics 113, 1037–1043.

Shi, H., Hudson, L.G., Liu, K.J., 2004. Oxidative stress and apoptosis in metal ion-induced carcinogenesis. Free Radic. Biol. Med. 37, 582–593.

Smolders, R., Koch, H.M., Moos, R.K., Cocker, J., Jones, K., Warren, N., et al., 2014. Inter- and intra-individual variation in urinary biomarker concentrations over a 6-day sampling period. Part 1: Metals. Toxicol. Lett. 231, 249–260.
Stohs, S.J., Bagchi, D., 1995. Oxidative mechanisms in the toxicity of metal ions. Free Radic. Biol. Med. 18, 321–336.
Straif, K., Benbrahim-Tallaa, L., Baan, R., Grosse, Y., Secretan, B., El Ghissassi, F., et al., 2009. A review of human carcinogens-part c: metals, arsenic, dusts, and fibres. Lancet Oncol. 10, 453–454.
Vahter, M., Akesson, A., Liden, C., Ceccatelli, S., Berglund, M., 2007. Gender differences in the disposition and toxicity of metals. Environ. Res. 104, 85–95.
Valko, M., Leibfritz, D., Moncol, J., Cronin, M.T., Mazur, M., Telser, J., 2007. Free radicals and antioxidants in normal physiological functions and human disease. Int. J. Biochem. Cell Biol. 39, 44–84.
Wapnir, R.A., 1998. Copper absorption and bioavailability. Am. J. Clin. Nutr. 67, 1054S–1060S.
WHO, 2008. Guidelines for Drinking Water Quality, Recommendations (Web Version), vol. 1. World health organization.
WHO, 2011. Noncommunicable diseases country profiles. Behav. Environ. Risk Factor.
Wu, L.L., Chiou, C.C., Chang, P.Y., Wu, J.T., 2004. Urinary 8-ohdg: a marker of oxidative stress to DNA and a risk factor for cancer, atherosclerosis and diabetics. Clin. Chim. Acta J. Int. Fed. Clin. Chem. 339, 1–9.
Yabe, J., Nakayama, S.M., Ikenaka, Y., Yohannes, Y.B., Bortey-Sam, N., Oroszlany, B., et al., 2015. Lead poisoning in children from townships in the vicinity of a lead-zinc mine in kabwe, Zambia. Chemosphere 119, 941–947.

Ecotoxicology and Environmental Safety 151 (2018) 98–108

Contents lists available at ScienceDirect

Ecotoxicology and Environmental Safety

journal homepage: www.elsevier.com/locate/ecoenv

Accumulation patterns and risk assessment of metals and metalloid in muscle and offal of free-range chickens, cattle and goat in Benin City, Nigeria

Emmanuel Temiotan Ogbomida[a], Shouta M.M. Nakayama[b], Nesta Bortey-Sam[b], Balazs Oroszlany[b], Isioma Tongo[c], Alex Ajeh Enuneku[c], Ogbeide Ozekeke[c], Martins Oshioriamhe Ainerua[c], Iriagbonse Priscillia Fasipe[a], Lawrence Ikechukwu Ezemonye[c], Hazuki Mizukawa[b], Yoshinori Ikenaka[b,d], Mayumi Ishizuka[b,*]

[a] Ecotoxicology and Environmental Forensic Unit, National Centre for Energy and Environment, Energy Commission of Nigeria, University of Benin, P.M.B 1154, Benin City, Nigeria
[b] Laboratory of Toxicology, Department of Environmental Veterinary Sciences, Graduate School of Veterinary Medicine, Hokkaido University, Kita 18, Nishi 9, Kita ku, Sapporo 0600818, Japan
[c] Department of Animal and Environmental Biology (AEB), University of Benin, P.M.B 1154, Benin City, Nigeria
[d] Water Research Group, Unit for Environmental Sciences and Management, North-West University, Potchefstroom, South Africa

ARTICLE INFO

Keywords:
Heavy metals
Offal
Muscles
Hazard Quotient
Hazard Index

ABSTRACT

The use of free range animals for monitoring environmental health offers opportunities to detect exposure and assess the toxicological effects of pollutants in terrestrial ecosystems. Potential human health risk of dietary intake of metals and metalloid via consumption of offal and muscle of free range chicken, cattle and goats by the urban population in Benin City was evaluated. Muscle, gizzard, liver and kidney samples were analyzed for Cr, Mn, Fe, Co, Ni, Cu, Zn, As, Cd, and Pb concentrations using inductively coupled plasma mass spectrometer (ICP-MS) while Hg was determined using Hg analyzer. Mean concentrations of metals (mg/kg ww) varied significantly depending upon the tissues and animal species. Human health risk estimations for children and adults showed estimated daily intake (EDI) values of tissues below oral reference dose (RfD) threshold for non essential metals Cd, As, Pb and Hg thus strongly indicating no possible health risk via consumption of animal based food. Calculated Hazard quotient (THQ) was less than 1 (< 1) for all the metals analyzed for both adult and children. However, Cd and As had the highest value of THQ suggestive of possible health risk associated with continuous consumption of Cd and As contaminated animal based foods. Hazard Index (HI) for additive effect of metals was higher in chicken liver and gizzard for children and chicken liver for adults. Thus, HI indicated that chicken liver and gizzard may contribute significantly to adult and children dietary exposure to heavy metals. Principal component analysis (PCA) showed a clear species difference in metal accumulation between chickens and the ruminants. This study provides baseline data for future studies and also valuable evidence of anthropogenic impacts necessary to initiate national and international policies for control of heavy metal and metalloid content in food items.

1. Introduction

Heavy metals and metalloids are pollutants that pose a great potential threat to the environment and human health on a global scale. They are intrinsic, natural constituents of the environment (Simone et al., 2012) and humans may promote their pollution through anthropogenic activities (Gall et al., 2015) such as extensive application of fertilizers or sewage sludge and pesticides in agriculture, waste disposal, atmospheric deposition, burning of fossil fuels, smelting, mining operations, electroplating, and discharge of wastewater from manufacturing industries including textile industry (Gall et al., 2015).

Heavy metals are widespread and highly persistent in the ecosystems due to their stability and non-degradable properties (Ali et al., 2013). They can enter the food chain via anthropogenic or natural

* Correspondence to: Laboratory of Toxicology, Department of Environmental Veterinary Sciences, Graduate School of Veterinary Medicine, Hokkaido University, N18, W9, Kita–ku, Sapporo 060–0818, Japan.
E-mail address: ishizum@vetmed.hokudai.ac.jp (M. Ishizuka).

https://doi.org/10.1016/j.ecoenv.2017.12.069
Received 3 February 2017; Received in revised form 28 December 2017; Accepted 30 December 2017
Available online 09 January 2018
0147-6513/

contaminations of air, water or soil and accumulate in animals at the top of the food chain through bio-magnification effects to pose chronic toxicity and serious health risk to man. Heavy metal toxicity in man can diminish mental and central nervous system function, elicit damage to blood composition, as well as the kidneys, lungs, and liver, and reduces energy levels (Amirah et al., 2013). Long-term exposure may result in slow progressive physical, muscular and neurological degeneration that mimics Alzheimer's disease, Parkinson's disease, muscular dystrophy and multiple sclerosis (Amirah et al., 2013).

In recent years, human exposures to heavy metals in Africa have risen as a result of an exponential increase in industrialization, urbanization, municipal solid waste generation and agricultural processes. Also uncontrolled illegal mining activities have added to the enormous amount of heavy metal contamination. The impact of these heavy metals on the environment can be a serious threats to the stability of the ecosystem and human health especially the African children as vulnerable group. In Sub-Sahara Africa environmental pollution by heavy metals has become a serious problem due to non-compliance and enforcement of existing environmental laws and regulations, inadequate monitoring capabilities, weak institutional structures and poor legal framework. In March 2010 large scale of lead poisoning due to artisanal/illegal gold mining activities occurred in Anka and Bukkuyum local government area of Zamfara state North-Western Nigeria leading to 163 deaths of which 111 were children under 5 years of age (Médecins Sans Frontières (MSF), 2010). Similarly, in May 2015, 28 children also died in Angwan Maijero and Angwan Karo, Madaka district of Rafi local government area of Niger State, Nigeria as a result of lead poisoning (Ministry of Mines and Steel Development MMSD, 2015).

Contamination of the environment and dietary intake of contaminated meat and meat products from food chain has been the most common and principal pathways of human exposure to heavy metals. Animals at the top of food chain may generally accumulate a large amount of heavy metals in their tissue, according to their age, size and feeding habits (Mahmood et al., 2012). In Nigeria, traditional rural animal production systems are mainly based on free-range (FMAWR, 2008). These animals could potentially pick heavy metals through grazing pesticide treated vegetation land, scavenging in open waste dumps for fodder, drinking polluted water from drains and streams and exposure to atmospheric depositions especially from automobile fumes and open burning of solid waste. These heavy metals can accumulate in organs and other fatty tissues, thus providing a major route for human exposure upon consumption. A recent study conducted by Bortey-Sam et al. (2015) evaluated human health risks from metals and metalloid via consumption of food animals in Tarkwa municipality in the western region of Ghana, an area predominantly known for artisanal gold mining activities. They indicated accumulation and distribution of heavy metals and metalloid in offal and muscles of chicken, goat and sheep with sufficient emphasis on species sensitivity and public health risk through consumption of these animal based foods. The study shows evidence of metal transfer from artisanal gold mining sites to free range animals thus, leading to accumulation of different metals in offal and muscles (Cd, Cr, Cu, Ni, Pb and Zn). They observed that metal accumulation was more pronounced in the liver and kidney of chicken than in muscles. This signifies sensitivity of chicken to heavy metals accumulation and the unique role of animal based food play in metals and metalloid transfer to man with possible health risks. While Bortey-Sam et al. (2015) succinctly compare health risks of metals and metalloid via intake of offal and muscles of free range animals from Tarkwa artisanal gold mining sites, recent studies in Nigeria focused mainly on human health risk assessment of some selected heavy metals via drinking water (Maigari et al., 2016), consumption of fishes (Orosun et al., 2016), cow meat (Ihedioha and Okoye, 2013), and illegal gold mining site (Olujimi et al., 2015). However, potential health impacts of municipal solid waste (MSW) in urban areas with specific reference to free range animals reared in proximity to dumpsites have not been fully evaluated. Causal linkages between exposure to waste and health outcomes for some particular types waste are well established, but the impacts of MSW on free range animals still remain unclear or not prioritized as public health issues. MSW is a growing major challenge to many rapidly urbanizing Africa countries. Furthermore, the full extent of the burden of ill health attributable to exposure of free range animals and the consumption of their muscles and offal has not also be elucidated.

The present study address health risks of metals and metalloid of offal and muscles of free range animals from municipal solid waste sites in Benin City Nigeria, a major environmental problem of urbanization, population growth and economic development. Free range animals are important in heavy metal studies as bio-indicators of the general environmental pollution status (Roggeman et al., 2013). Therefore, comprehensive study of heavy metal levels in tissues and offal of free range animals are needed to document the safety of meat and meat products in Nigeria. Although heavy metal contamination have been documented in literatures, information concerning human health risk via consumption of meat and meat products contaminated with heavy metal in Benin City, Edo State still remain very scarce. Therefore, this study describes and compares accumulation, distribution and species sensitivity to heavy metals under different land use pattern. The accumulation of metals and metalloid in free range animals from different locations and ecological regions present a clear picture of environmental pollution status. The distribution pattern of metals in different organs using principal component analysis (PCA) showed species sensitivity to metal and possible human exposure through dietary intake. The outcome of this study will aid in the development of sustainable environmental management options of municipal solid wastes and health intervention policies for affected areas and many other developing countries.

2. Materials and methods

2.1. Study area

The study was conducted in Benin City, Edo State around markets, abattoirs and dumpsite areas (Fig. 1). Benin City is located 6.3176°N, 5.6145°E and is the capital and largest City of Edo State in Southern Nigeria. The city has a total area of 1225 km^2 with an estimated human population of 1147,188 (National Population Commission (NPC), 2006). The city is a commercial centre strategically positioned as the gateway to the northern, eastern and western states of Nigeria. The notable economic activities include breweries, wood carving, traditional brass and bronze casting, wood and timber processing, printing and publishing. Major markets located within the city are Oba, New Benin, Oliha, Uselu, Agbado and Edaiken markets. Domestic and industrial wastes are often generated and discharged into the environment causing public health nuisances. Heaps of solid wastes are often seen littering the streets and market places. The disposal sites are capable of releasing large amounts of harmful chemicals such as heavy metals into the soil which easily found their ways into the food chain.

2.2. Sample collection

This study was carried out between August 2013 to March 2014 in Benin City, Edo State of Nigeria. Samples were collected from six locations in the three Local Government Areas which includes Ovia North-East Local Government Area (Oluku abattoir), Egor Local Government Area (Benin Technical College Road abattoir, Uselu market, University of Benin residential quarters, Ekiuwa market) and Oredo Local Government Area (Oliha market) of Edo State (Fig. 1). Fresh samples of kidney, liver and muscle of free-range goats (*Capra hircus*) and cattle (*Bos taurus*) were collected from the abattoirs while kidney, liver and muscle of free-range chickens (*Gallus gallus domesticus*) were collected from live adult chickens after exsanguination and dissection in the laboratory. Samples were kept frozen in labelled

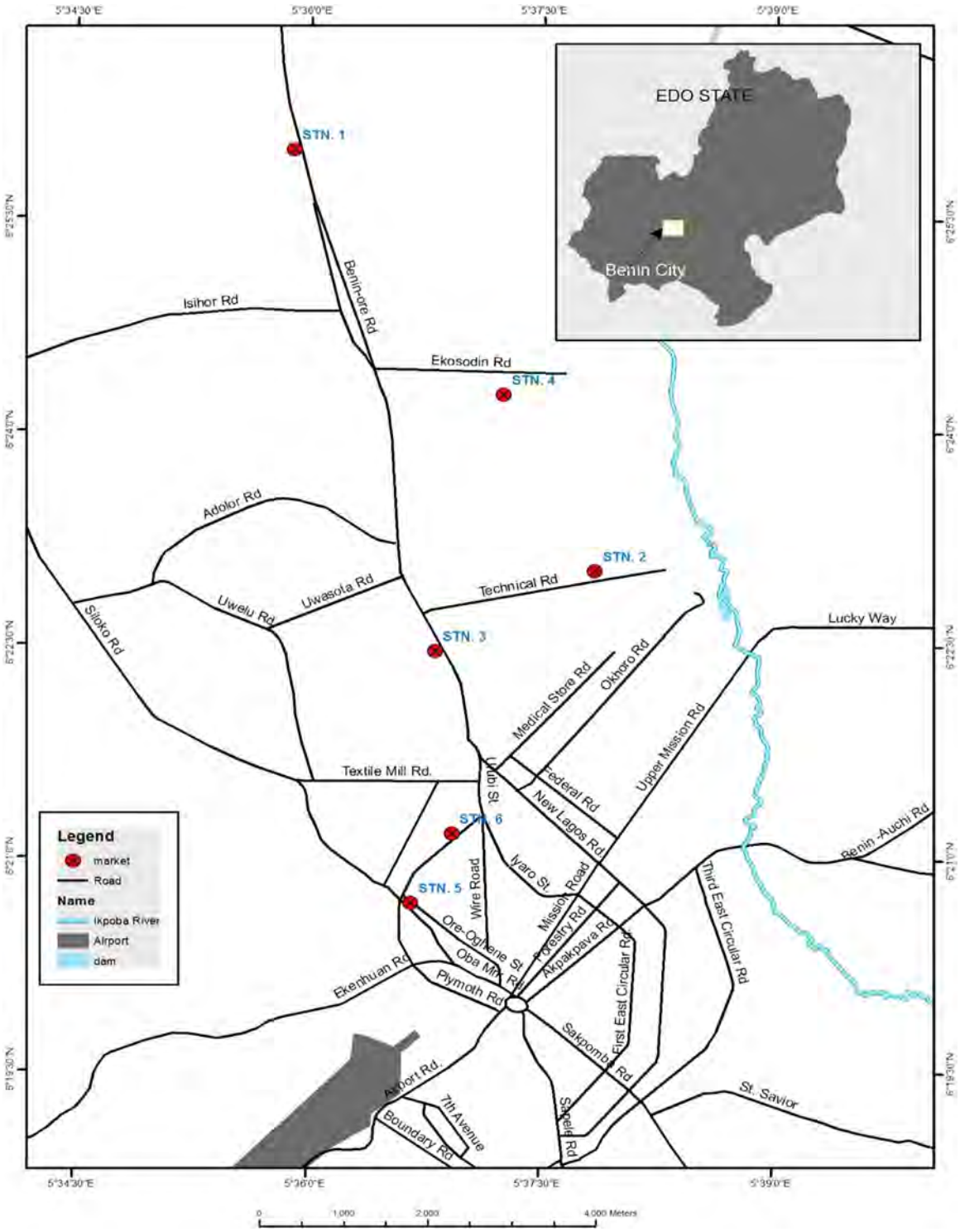

Fig. 1. Map of Benin City showing sampling locations.

plastic bags in the National Centre for Energy and Environment laboratory, University of Benin and were later tansported to the Laboratory of Toxicology, Graduate School of Veterinary Medicine, Hokkaido University, Japan and stored in − 20 °C until analysis. All procedures used in this experiment were performed according to the guidelines of the Committee of Animal Care and Use, University of Benin.

2.3. Sample preparation and metal extraction

All materials and instruments used in metal extraction were washed in 2% nitric acid (HNO_3) and rinsed at least twice with distilled water. Metals were extracted from liver, kidney and muscle by acid digestion using a closed microwave digestion system (Speed wave MWS-2; Berghof, Germany) according to the method of Nakayama et al. (2011). Briefly, 0.5 g of thawed liver, kidney and muscle samples each were placed in a prewashed DAP-60K digestion vessel. 5 ml of 65% HNO_3 (Kanto Chemical Corp., Tokyo, Japan) and 1 ml of (30%) hydrogen

peroxide, H_2O_2 (Kanto Chemical Corp., Tokyo, Japan) spectrometry grade were added. The digestion vessels were capped and placed into a 10-position turntable conditions followed by a ramped temperature program: ramp to 160 °C (5 min hold); and increase to 190 °C (15 min hold). After digestion in the microwave for 52 min, the samples were cooled and transferred into plastic tubes and diluted to final volume of 10 ml with distilled deionized water (Milli-Q water). A reagent blank was also prepared using the same procedure.

2.4. Metal analysis

The quantification of metals in the digested samples were determined using an Inductive Coupled Plasma-Mass Spectrometer (ICP-MS) model 7700 series, Agilent technologies, Tokyo, Japan). The instrument was calibrated using standard solutions of respective metals to establish standard curves before metal analysis. All chemicals and standard stock solutions were analytical reagent–grade (Wako Pure Chemicals, Osaka, Japan), while the water was bi distilled and deionized (Milli-Q; Merck Millipore). The detection limits (μg/L) of chromium (Cr), manganese (Mn), Iron (Fe), cobalt (Co), nickel (Ni), copper (Cu), zinc (Zn), arsenic (As), cadmium (Cd), and lead (Pb) were 0.0024, 0.0118, 0.0187, 0.0008, 0.0081, 0.0042, 0.0161, 0.0022, 0.0005 and 0.0022 respectively. Concentrations of metals were expressed in mg/kg wet weight (mg/kg ww).

2.4.1. Total mercury analysis

The concentration of total mercury (Hg) was measured by thermal decomposition, gold amalgamation and atomic absorption spectrophotometry (Mercury Analyzer, MA-3000; Nippon Instruments Corporation, Tokyo, Japan), after preparation of calibration standards. Recovery rates of Hg for the certified reference material, DOLT-4 (Dogfish liver, the National Research Council, Canada) ranged from 92% to 103% (94.3 ± 4.2%). The detection limit of total mercury (Hg) was 2.0 pg.

2.5. Quality assurance and quality control

All analytes were subjected to stringent quality control methods. Before sample analysis, appropriate quality assurance procedures and precautions were carried out to ensure reliability of the results. Double distilled deionized water was used throughout the study. Glassware were properly cleaned, and reagents were of analytical grade. Reagents blank determinations were used to correct the instrument readings. Replicate blanks and standard reference materials (SRM), DORM-3 (Fish protein, the National Research Council, Canada) and DOLT-4 (Dogfish liver, the National Research Council, Canada) were used for method validation and quality control. Replicate analysis of these reference materials showed good accuracy (relative standard deviation, RSD, ≤ 3%) and recovery rates ranged from 80% to 115%.

2.6. Human health risk assessment

Risk assessment was done based on the mean concentrations of carcinogenic and non-carcinogenic metals determined in the meat samples using United States Environment Protection Agency (USEPA, 2015) human health risk assessment models. It was assumed that the ingested dose is equal to the adsorbed contaminant dose and that cooking has no effect on the toxicity of heavy metal (Copat et al., 2013). Health risk estimates for heavy metals concentrations in cattle, goat and chicken tissues were computed using three basic standard indices: Estimated Daily Intake (EDI), Hazard Quotient (THQ) and Hazards index (HI). Two hypothetical age/weight categories were used. 30 kg was assumed for children and 60 kg for adults (Ihedioha and Okoye, 2013).

2.7. Data analysis

2.7.1. Estimated daily intake (EDI) of toxic metals

The estimated daily intakes (EDI) of heavy metals (Cr, Mn, Fe, Co, Ni, Cu, Zn, As, Cd, Hg and Pb) was expressed as mg/kg/day and was dependent on both the concentration of heavy metals in offal or muscle and the amount of consumption. The EDI of metals for children and adults were determined by the following equation according to Bortey-Sam (et al. (2015).

$$\mathrm{EDI} = \frac{MC \times FDC}{BW} \quad (1)$$

Where MC is average concentration of metal in food (μg/g, on fresh weight basis); FDC represents the average offal/muscle daily consumption in this region (g/person/d); BW is the average body weight. It was assumed that local inhabitants consumed an average liver, muscle and gizzard of 150 and 100 g/day for adult (60 kg in BW) and children (30 kg in BW) respectively (Bortey-Sam, et al., 2015). For kidney, it was assumed that inhabitants consumed 10 and 8 g/day for adults and children respectively (Ihedioha and Okoye, 2013), because the size of kidneys are relatively smaller and is not the favorite compared with liver, muscle, or gizzard. The metal intakes were compared with the tolerable daily intakes for metals recommended by FAO/WHO (2010).

2.7.2. Target Hazard Quotient (THQ)

The Target Hazard Quotient (THQ) was used to assess risk associated with non-carcinogenic and carcinogenic health effect. The health risks from consumption of offal and muscle of chicken, goat and cattle by the local inhabitants were assessed based on the THQ. The THQ is a ratio of determined dose of a pollutant to a reference dose level. If the ratio is less than 1, the exposed population is unlikely to experience obvious adverse effects. The method of estimating risk using THQ was provided in the USEPA Region III risk-based concentration table (USEPA, 2007), and is based on the equation below:

$$\mathrm{THQ} = \frac{EFr \times ED \times FIR \times MC}{RfD \times BW \times AT} \times 10^{-3} \quad (2)$$

Where THQ is target hazard quotient; EFr is exposure frequency (365 days/year); ED is exposure duration (70 years); FIR is food ingestion rate (g/person/d); MC is average concentration of metal in food (μg/g, on fresh weight basis); RfD is the oral reference dose (mg/kg/d); BW is the average body weight, adult (60 kg); children (30 kg); AT is the average exposure time (365 days/year number of exposure years, assuming 70 years in this study). Oral reference doses (RfD) were based on 3E-04, 1E-03, 5E-04, 4E-03, 3E-01, 4E-02, 1.4E-01, 2E-02, 7E-01, 15E-1 mg/kg/d for As, Cd, Hg, Pb, Zn, Cu, Mn, Ni, Fe, Cr respectively (USEPA IRIS, 2007). There is no consensus about the RfD for Co, However, the RfD for Co was estimated as 4.3E-02 (Food and Nutrition Board, 2004).

2.7.3. Hazardous index (HI)

To estimate the human health risk for more than one heavy metal, the hazard index (HI) was calculated by the summation of the target hazard quotients for all heavy metals in the Equation below.

$$\mathrm{HI} = \sum \mathrm{THQ_n} \quad (3)$$

It assumes that the magnitude of the adverse effect will be proportional to the sum of multiple metal exposures. It also assumes similar working mechanisms that linearly affect the target organ. When HI is equal to or less than one (HI ≤ 1), it indicates no appreciable health risk, while if HI > 1, then it indicates a reason for health concern (Cao et al., 2015). Hence, HI < 1 means no hazard; 1 > HI < 10 means moderate hazard while greater than 10 means high hazard or risk (Ukoha et al., 2014).

Table 1
Mean concentrations (mg/kg ww) of heavy metal in different tissues of free range chicken (*Gallus gallus domesticus*), Cattle (*Bos taurus*) and Goat (*Capra hircus*).

		Cr	Mn	Fe	Co	Ni	Cu	Zn	As	Cd	Pb	Hg
CL	Mean ± SD	0.064 ± 0.014	2.785 ± 0.440*	91.935 ± 20.228	0.054 ± 0.023	0.019 ± 0.003	88.016 ± 36.349	46.704 ± 5.400	0.006 ± 0.003	0.044 ± 0.013	0.036 ± 0.018	0.001 ± 0.000*
CHL	Mean ± SD	0.077 ± 0.053	3.607 ± 1.198*	305.484 ± 187.966	0.049 ± 0.026	0.018 ± 0.009	4.362 ± 1.017	43.363 ± 13.084	0.069 ± 0.091*	0.291 ± 0.338*	0.171 ± 0.193*	0.034 ± 0.036*
GL	Mean ± SD	0.051 ± 0.030	1.656 ± 0.526*	65.328 ± 27.470	0.033 ± 0.030	0.013 ± 0.005	11.883 ± 8.118	22.731 ± 3.197	0.005 ± 0.005*	0.023 ± 0.009*	0.044 ± 0.032*	0.003 ± 0.002*
CK	Mean ± SD	0.051 ± 0.017	1.109 ± 0.137*	82.850 ± 16.001	0.030 ± 0.008	0.030 ± 0.020	4.187 ± 0.400	30.463 ± 11.204	0.008 ± 0.004*	0.238 ± 0.065	0.052 ± 0.002	0.006 ± 0.003
CHK	Mean ± SD	0.089 ± 0.076	2.468 ± 0.565*	101.521 ± 28.623*	0.049 ± 0.028	0.020 ± 0.004	2.904 ± 0.326	24.700 ± 3.368	0.081 ± 0.073*	0.890 ± 1.035*	0.588 ± 0.703*	0.030 ± 0.031
GK	Mean ± SD	0.060 ± 0.097	0.821 ± 0.302	80.520 ± 22.191*	0.025 ± 0.012	0.028 ± 0.020	2.765 ± 0.298	15.232 ± 2.026	0.008 ± 0.011*	0.123 ± 0.158*	0.072 ± 0.066*	0.019 ± 0.012
CM	Mean ± SD	0.261 ± 0.216	0.163 ± 0.067	28.918 ± 8.863	0.004 ± 0.002	0.023 ± 0.008	0.978 ± 0.312	40.658 ± 20.102	0.007 ± 0.011*	0.001 ± 0.000	0.013 ± 0.010	ND*
CHM	Mean ± SD	0.148 ± 0.166	0.130 ± 0.037*	10.349 ± 5.706	0.004 ± 0.002	0.035 ± 0.032	0.499 ± 0.156	4.430 ± 0.673	0.023 ± 0.018*	0.003 ± 0.003*	0.024 ± 0.029*	0.004 ± 0.003*
GM	Mean ± SD	0.106 ± 0.159	0.187 ± 0.050*	24.792 ± 6.287	0.006 ± 0.006	0.017 ± 0.011	0.825 ± 0.137	24.541 ± 6.737	0.007 ± 0.011*	0.001 ± 0.001*	0.009 ± 0.006*	0.001 ± 0.002*
CHG	Mean ± SD	0.286 ± 0.131	0.547 ± 0.204	80.856 ± 36.112	0.010 ± 0.006	0.049 ± 0.037	3.069 ± 1.412	24.690 ± 4.774	0.047 ± 0.026	0.126 ± 0.111	0.239 ± 0.327	0.003 ± 0.003

CL: Cattle liver; CHL: Chicken Liver; GL: Goat Liver; CK: Cattle kidney; CHK: Chicken kidney; GK: Goat kidney; CM: Cattle muscle; CHM: Chicken muscle; GM: Goat muscle. Letter (*) between columns in the same organ indicates statistical difference (Tukey's test; $p < 0.05$).
ND = Not detectable.

2.7.4. Statistical analysis

Statistical analyses were performed using SPSS version 16.0 statistical software (SPSS Inc., Illinois, USA) after data were normalized by log transformation. To analyze differences in the distribution of metals in tissues of free-range chickens, cattle and goats, analysis of variance (ANOVA) and Tukey was done and differences were considered statistically significant with p value < 0.05. Principal component analysis (PCA) based on log transformed data was done to determine the distribution pattern of metals in organs, using JMP statistical software v.10 (SAS Institute). The principal components were extracted with eigen values > 1. Statistical differences between the different organs (liver, muscle, gizzard and kidney) were determined by one-way analysis of variance (ANOVA). The limit of significant level was accepted at $p < 0.05$.

3. Results and discussion

3.1. Concentration of metals and metalloid in offal and muscle

The mean concentrations of these metals in offal and muscle of free-range chickens, cattle and goats from Benin city are presented in Table 1. The composition profile of the metals in the three animal food species are Cr (0.050-0.29), Mn (0.13-3.6), Fe (10-310), Co (0.0040-0.054), Ni (0.013-0.049), Cu (0.50-88), Zn (4.4-47), As (0.0040-0.081), Cd (0.0010-0.89), Pb (0.0090-0.59) and Hg (nd-0.019) mg/kg ww. The results showed that chicken liver accumulated the highest levels of Fe, Mn and Hg, chicken kidney (Pb, Cd and As) and chicken gizzard (Ni and Cr) while cattle liver accumulated Co, Cu and Zn. This findings comform with Demirezen and Uruc (2006) who reported that the primary site of heavy metals are the liver and kidney due to exposure and physiological responses of animals to detoxify the system. The reason for high accumulation of metals in the gizzard could be attributed to the function of the gizzard which is the primary reservoir of food materials and organ for grinding up food partilces. Free range local chickens according to Nesheim et al. (1979) have been found to harbour the greatest pollutants in their body system as they have no oral discrimination for food hence pick whatever they find edible in the environment. In this study free-range chicken accumulated more metals than the cattle and goat which can be attributed to their foraging dietary habits. The high levels of Pb, Cd, Hg, As, Ni, Cr, Mn and Fe in the offal of the chickens could have come from anthropogenic activities in the environment and feeds fed on by the chickens. Several studies have shown that diet is the primary pathway for metal accumulation in animals and man. For example, toxicological investigations on bovines, ducks and poultry have shown a direct correlation between metal concentrations in animal feed and animal tissues accumulation (Sedki et al., 2003; Kim and Koo, 2007). Also, it has been reported that rice and vegetables grown in mining areas contaminated by heavy metals have posed a great potential health risk for consumers, who suffered from serious cancers (Zhuang et al., 2009). Plants uptake from soil contribute to the circulation of heavy metal in the food chain through their active and passive absorption, accumulation in tissues as well as subsequent grazing by animals that depends on them for nutrients or consumption by man. This reflect that metal-rich diets lead to high tissue metal accumulation. Metal accumulation in liver and kidney also reflect short-term exposure and are most appropriate target organ to test metals.

3.1.1. Human essential metals

The 11 elements of highest concern within the European Community are: As, Cd, Co, Cr, Cu, Hg, Mn, Fe, Zn, Ni, and Pb (Stankovic and Stankovic, 2013). Some of these elements are actually necessary for humans in trace amounts (Co, Cu, Cr, Mn, Ni), while more than necessary amounts of these trace elements and some others are carcinogenic or toxic, affecting among others, the central nervous system (Hg, Pb, As, Mn), the kidneys or liver (Hg, Pb, Cd, Cu) or skin,

bones, or teeth (Ni, Cd, Cu, Cr) (Rai and Pal, 2002; Chen et al., 2008; Lavery et al., 2009; Jovic et al., 2012; Stankovic and Jovic, 2012; Markovic et al., 2012). Essential metals are significant to humans because they are important in various metabolic enzymes and constituents of cells (Maret, 2016). The frequent consumption of animal based food contaminated with heavy metals could increase the level in humans. Large doses of essential metals can damage living organisms or in some cases results in toxic effects (Nagajyoti et al., 2010).

Cu is a component of various enzymes (Amaral et al., 2008; Osredkar and Sustar, 2011). It is involved in collagen synthesis and in the normal development of connective tissues, nerves and immune system (Amaral et al., 2008). High intake has been recognized to cause adverse health problems such as liver and kidney damage (Amaral et al., 2008). Concentration of Cu was highest in cattle and chicken liver (Table 1). This is because the liver act as the primary storage organ for Cu and maintains Cu homeostasis for animal. In the present study the results shows that the average concentration of Cu in cattle liver (88.016 ± 36.349 mg/kg ww) is higher than the permissible limits of 20 mg/kg set by USDA (2006) and European Commission Regulation (ECR) (2006) and also 30 mg/day maximum limit set by WHO (1996).

Mn is an essential element for both animals and plants; its deficiency results in severe skeletal and reproductive abnormalities in mammals (Sivaperumal et al., 2007). Mn concentration was found to be high in livers and kidneys of chicken and cattle liver. The mean concentrations of Mn ranged from 0.130 ± 0.037 (chicken muscle) to 3.607 ± 1.198 mg/kg ww (chicken liver). Mn levels in chicken liver, kidney and cattle liver and were above the WHO (1996) reference standard of 0.5 mg/kg. Mn has been found to be toxic in excess; in brain it can cause a Parkinson-type syndrome (Aschner, 2000).

Fe is one of the most abundant transition element, and probably the most well known metal in biologic systems participating in a wide variety of metabolic processes, including oxygen transport, DNA synthesis, and electron transport. High levels of iron may lead to tissue damage, as a result of the formation of free radicals. The concentration of Fe in this study was highest in chicken liver and kidney. The mean concentration of Fe ranged from 10.349 mg/kg ww in cattle muscle to 305.484 mg/kg ww in chicken liver (wet weight). This result reflect the dominance of Fe concentration observed in other animal based foods by Medeiros et al. (2012). The most serious forms of Fe overload is acute poisoning while chronic Fe intoxication is associated with genetic and metabolic diseases leading to repeated blood transfusions (Fraga and Oteiza, 2002).

Zn is the most abundant intracellular component which is needed to maintain some important biological functions such as genetic stability, gene expression, DNA repair and programmed cell death (Hussein and Khaled, 2014). High levels of zinc can cause pancreatitis, anemia, muscle pain, and acute renal failure (Pais and Benton Jones, 1997). In this study the mean concentration of Zn ranged from 4.430 mg/kg ww in chicken muscle to 46.704 mg/kg ww in cattle liver. This result conform with Okoye and Ugwu (2010) who reported elevated zinc levels in goats bred in Nigeria. The high concentrations of Zn in animal based food can be attributed to food chain transfer. The values of zinc reported in this study were below the Codex Alimentarium Commission maximum permissible limit of 50 mg/kg for muscle and 80 mg/kg for edible offals (Codex, 1995).

Cr is an important element known to enhance the action of insulin in man (Mertz, 1998), a hormone critical to the metabolism and storage of carbohydrate, fat, and protein in the body (Porte et al., 2003). The mean concentrations of Cr in this study ranged from 0.051 (chicken kidney) to 0.286 mg/kg ww (chicken gizzard). Our data is similar to Iwegbue et al. (2008) who reported 0.33 ± 0.14 mg/kg in chicken meat consumed in southern Nigeria. Cr detected in the gizzard of chicken could be attributed to chicken diet.

Ni plays an important role in the biology of plants and animals. Overexposure to Ni can cause decreased body weight, heart and liver damage and skin irritation (Homady et al., 2002). The average concentration of Ni observed in this study ranged from (0.017 ± 0.011–0.049 ± 0.037 mg/kg ww) in chicken (0.019 ± 0.003 - 0.030 ± 0.020 mg/kg ww) in cattle and (0.013 ± 0.005 - 0.028 ± 0.020 mg/kg ww) in goat. The levels of Ni in the kidneys of chicken, cattle and goat showed no significant difference ($P > 0.05$) while the livers and muscles of cattle showed significant difference when compared with chicken and goat. Chicken gizzard and muscle had the highest value of Ni. The observed levels in this study were below the 0.5 mg/kg maximum permissible limit of Ni in food according to FAO/WHO (2000).

3.1.2. Human non-essential metals

Human non essential metals Cd, As, Pb and Hg have no biological role in living organisms but are tolerated at very low concentration and also inhibit metabolic activity at higher concentrations (Pandey and Madhuri, 2014). They are potentially toxic to living organisms. Animals are contantly exposed to these toxicant through dietary intake. As shown in Table 1 the concentration of Cd ranged from 0.890 ± 1.035 mg/kg ww in chicken kidney to 0.001 ± 0.00 mg/kg ww in muscle of cattle and goat.

The range of Cd level in this study is lower than result obtained by Ihedioha and Okoye (2013) in swine and broiler chicken (ND-40.14 mg/kg ww). The levels of Cd observed in free range chicken kidney were below the maximum permissible limit of 1.0 mg/kg (FAO/WHO, 2000). However, Doganoc (1996) observed higher levels of Cd in the liver and kidney of chicken which exceeded the official tolerance levels. The ability of liver and kidney to accumulate high concentration of Cd is a common feature of chickens and many other animals and may be due to the detoxification function of the organs (Stoyke et al., 1995). Similar levels of Cd has also been reported by Okoye and Ugwu (2010) in liver (0.35 mg/kg) and kidney (0.83 mg/kg) of goats from Nigeria. Cd is presently listed as number 7 of 275 of the most hazardous substances in the environment, behind As, Pb and Hg (Agency for Toxic Substances and Diseases Registry ATSDR, 2013). Chronic Cd poisoning impair calcium metabolism leading to softening of bones, fractures, and skeletal deformations (Stankovic et al., 2011). Liver and kidney tissues are the two main sites of Cd storage and these organs accumulate considerable amounts of Cd, about 40-80% of the body burden (WHO, 2007).

Pb is the second element (after arsenic) on the ASTDR's top 20 list of the most poisoning heavy metals (ASTDR, 2013). Its target organs are bones, brain, blood, kidneys, reproductive and cardiovascular systems, and thyroid gland (Homady et al., 2002). The levels of Pb in the offal and muscle of free range cattle, goat and chicken ranged from 0.58826 mg/kg ww in chicken kidney to 0.009 mg/kg ww in goat muscle (Table 1). Pb is the most frequently reported causes of accidental poisoning in domestic animals, with cattle as the most commonly affected species because they are very inquisitive and commonly 'taste test' new finds (Khalafalla et al., 2015). Absorbed Pb is stored mainly in the liver and kidney, and like Cd, it accumulates in tissues of animals (Khalafalla et al., 2015). However, there was significant differences when the concentration of Pb in chicken kidney and liver were compared with goat kidney and liver (Tukey test: $p < 0.05$) Table 1. Similarly, the level of Pb in the muscles were statistically different (Tukey test: $p < 0.05$). Apart from the chicken kidney, the gizzard was second highest in the accumulation of Pb. This could be attributed to the feeding pattern of chicken. In this study, concentration of Pb in the kidney (0.588 ± 0.703 mg/kg ww), and gizzard (0.239 ± 0.327 mg/kg ww) of free range chicken were slightly above the recommended limits of 0.5 and 0.1 mg/kg ww for offal and muscle by European Commission Regulation(ECR) (2006) and USDA (2006) respectively.

The result of this study indicated that the highest concentration of Hg was found in chicken liver (0.034 ± 0.036 mg/kg ww) and kidney (0.030 ± 0.031 mg/kg ww) while the lowest concentrations was found in cattle liver (0.001 ± 0.000) and goat muscle (0.0010 ± 0.002) mg/kg ww respectively. This is in conformity with Landis et al. (2010) that

birds accumulate Hg in the kidney and liver with less in the muscle. The concentrations of Hg in the kidney of free-range chicken, cattle and goat were not statistically different (Tukey test; $p > 0.05$) However, levels of Hg in chicken liver were significantly different ($P < 0.05$) when compared with the levels in the livers of cattle and goat. In the muscle, the levels were significantly different ($p < 0.05$) with high value in chicken muscle. In this study the values of Hg in offal and muscles were below the permissible limit of 0.05 mg/kg established by European Commission Regulation(ECR) (2006) and USDA (2006).

The metalloid As was detected in all the tissues and offal samples of the three animal foods. Concentrations of As in muscle and offal of free-range chicken, goat and cattle ranged from (0.040 ± 0.034–0.081 ± 0.073 mg/kg ww), (0.007 ± 0.011-0.008 ± 0.011 mg/kg ww) and (0.007 ± 0.011 − 0.008 ± 0.004 mg/kg ww) respectively (Table 1). The distribution of As in liver, kidney, gizzard and muscle of chicken was found to be higher than that of goat and cattle ($p < 0.05$). Mean concentration of 0.08 mg/kg ww in the kidney of free-range chicken in Benin City was found to be higher than the USDA (2006), European Commission Regulation(ECR) (2006) and SAC/MOHC (2005) standard of 0.05 mg/kg.

3.1.3. Principal component analysis (PCA) of metals distribution

Principal component analysis (PCA) of heavy metals and metalloid distribution in offal and muscle samples of animal based food was performed and the results are presented in Fig. 2 and Table 3. PCA was used to determine the multivariate structure of the data, to highlight the possible trend and to further identify the potential source of heavy metals contamination. In the interpretation of PCA patterns, factor loadings greater than 0.71 are typically consider excellent while those less than 0.32 are regarded as very poor (Nowak, 1998). Factor loading determine the relationships between the variables and each factor. The first principal component (PC1) of metals and metalloid in liver of cattle (Fig. 2) showed 38.7% of the total variance with the loading of the variables Mn, Fe, Ni, Zn and Pb. Fe and Zn in PC1 which were highly associated, displaying high factor loading values (0.827 and 0.843) suggesting metals may have come from the same source. Also, zinc and iron share common dietary sources. The second component (PC2) accounts for 14.7% of the total variance of heavy metals in the chicken liver and dominated by Co, As and Cd while the third component PC3 accounts for 12.5% of the total variance in goat liver with a positive loading for Cu. The first principal component which explains 38.7% may be controlled by a long term anthropic activity such as municipal solid waste found to be seriously contaminated by toxic metals from electronic waste (Naveedullah et al., 2013) in the area for a long period of time in agreement with the clustering of variables in Group I. Also metallic zinc and iron are used in a wide variety of applications but when exposed to the atmosphere may be subject to corrosion that may result in the slow release of small amounts of zinc and iron into the environment. The PCA results also showed a clear separation between chicken (F) grouped on one side and the ruminants; goat (G) and cattle (C) clustered on the other side. The results obtained from PCA of kidney of the three animal based foods Fig. 2 and Table 3 indicates that Mn, Co, As, Cd and Pb are associated with high factor loadings of 0.857, 0.823 and 0.776 (Co, Cd and As) in cattle kidney. This association strongly suggests that these variables have a similar source and may be attributed to cattle grazing in polluted environment or drinking wastewater with heavy metals. The first PC which explains 33.5% of the total variance and loads in the cattle kidney confirm the interpretation of their anthropogenic origin. The occurrence of Cd and Hg likely reflects the increased use of nickel-cadmium batteries in electronic items and a variety of Hg-containing devices and lamps such

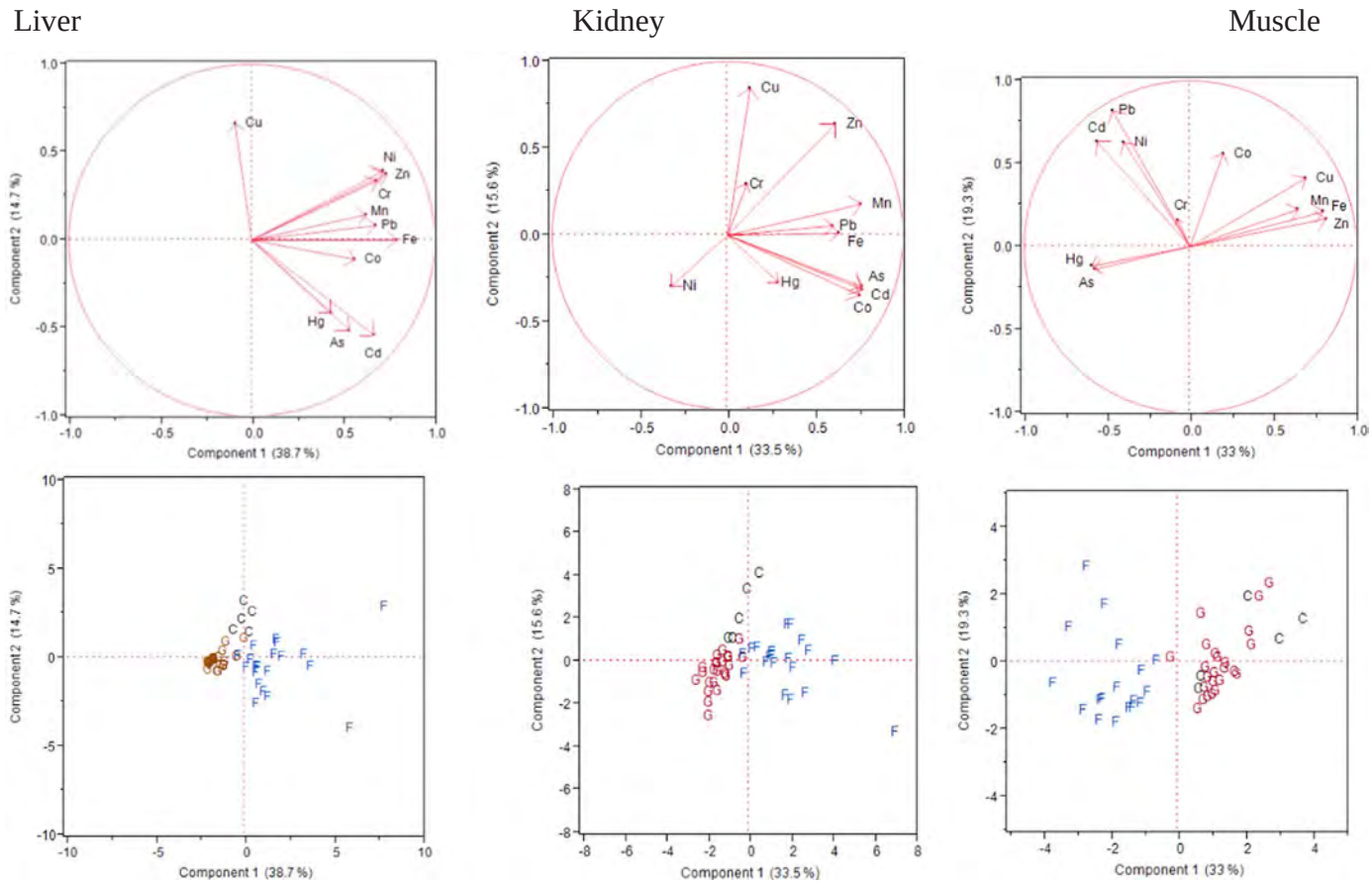

Fig. 2. Distribution patterns of heavy metals in tissues of free range chicken (*Gallus gallus domesticus*), Cattle (*Bos taurus*) and Goat (*Capra hircus*) characterized by PCA (C: Cattle; F: Chicken; G: Goat).

Table 2
Estimated daily intake (μg/kg bw/day) of heavy metals.

Sample name		Cr	Mn	Fe	Co	Ni	Cu	Zn	As	Cd	Pb	Hg
Cattle Liver	Adult	0.161	6.962	229.838	0.135	0.048	220.041	116.760	0.014	0.109	0.089	0.002
	Child	0.214	9.282	306.451	0.180	0.065	293.388	155.681	0.018	0.145	0.119	0.002
Cattle Muscle	Adult	0.653	0.408	72.296	0.011	0.057	2.445	101.644	0.009	0.002	0.034	0
	Child	0.871	0.545	96.394	0.015	0.076	3.260	135.526	0.012	0.003	0.045	0
Cattle Kidney	Adult	0.008	0.185	13.808	0.005	0.005	0.698	5.077	0.001	0.040	0.009	0.001
	Child	0.013	0.296	22.093	0.008	0.008	1.117	8.123	0.002	0.063	0.014	0.002
Chicken Liver	Adult	0.192	9.018	763.710	0.122	0.045	10.905	108.409	0.172	0.728	0.427	0.085
	Child	0.257	12.024	1018.281	0.163	0.060	14.540	144.545	0.229	0.970	0.569	0.113
Chicken Muscle	Adult	0.369	0.326	25.874	0.010	0.088	1.248	11.076	0.057	0.007	0.061	0.009
	Child	0.492	0.434	34.498	0.014	0.117	1.664	14.768	0.076	0.009	0.081	0.013
Chicken Kidney	Adult	0.015	0.411	16.920	0.008	0.003	0.484	4.117	0.014	0.148	0.098	0.005
	Child	0.024	0.658	27.072	0.013	0.005	0.774	6.587	0.022	0.237	0.157	0.008
Chicken Gizzard	Adult	0.716	1.367	202.140	0.026	0.123	7.673	61.725	0.117	0.314	0.596	0.008
	Child	0.954	1.823	269.520	0.034	0.164	10.231	82.300	0.156	0.419	0.795	0.010
Goat Liver	Adult	0.127	4.140	163.320	0.083	0.032	29.707	56.828	0.012	0.058	0.111	0.007
	Child	0.169	5.521	217.760	0.111	0.043	39.610	75.771	0.016	0.077	0.147	0.009
Goat Muscle	Adult	0.264	0.468	61.980	0.014	0.044	2.063	61.353	0.018	0.002	0.022	0.003
	Child	0.352	0.624	82.640	0.018	0.058	2.750	81.804	0.024	0.003	0.030	0.003
Goat Kidney	Adult	0.025	0.342	33.550	0.010	0.012	1.152	6.347	0.003	0.051	0.030	0.008
	Child	0.040	0.547	53.680	0.017	0.019	1.843	10.155	0.005	0.082	0.048	0.012

as compact florescence lamps (CFLs) which are usually disposed in municipal solid waste. The second component (PC2) showed 15.6% total variance of heavy metals in chicken kidney which contributes Cu and Zn with factor loading of 0.840 and 0.784. Cu and Zn may be controlled by a long-term anthropic activity such as pesticides usage (Yang et al., 2014). Copper is usually considered as a marker element of environmental waste dumps, domestic waste water, combustion of fossil fuels and wastes, wood production, phosphate fertilizer production, and natural sources. The third component (PC3) alone explains 11.6% of the variance of Cr and Ni in the goat kidney while Hg showed negative loadings. In the cattle muscle the first component (PC1) with 33% of variance comprises positive factor loading of Mn, Fe, Cu and Zn which could be linked to anthropogenic and natural sources with some contributions from the municipal waste system. The second component (PC2) explains 19.3% of the total variation, which exhibited a high positive factor loading of 0.755, 0.815 and 0.955 on Ni, Cd and Pb. These are significant environmental pollutants with anthropogenic origin especially from industry, production of lead-acid batteries, metal products (solder and pipes) and poor urban waste management system which are common in developing countries. The third component (PC3) showed a high positive factor loading with 14% variance of As and Hg. This suggest that levels of these toxic metals can be primarily attributed to anthropogenic influences. Animals are constantly exposed to As and Hg through contaminated drinking water, feedstuff, grasses, vegetables etc. However, arsenic has been one of the most common causes of inorganic chemical poisoning in farm animals and also a main threat to human health. Africa today is becoming a dumping ground for electronic waste especially used computers, mobile phones etc from developed countries which contains hazardous metals such as lead, cadmium and mercury. All these electronic wastes subsequently end up in municipal waste dump sites which consists of a mix of combustible and non-combustible materials and subsequently over time contribute to increased environmental problem.

3.2. Human health risk assessment

3.2.1. Estimated dietary intake of metals

The Estimated Daily Intakes (EDI) of metals and metalloid taken by an adult or children per day through the consumption of free range chicken, cattle and goat offal and tissue are presented in Table 2. Meat and edible offal are considered a significant part of most diet in Nigeria. They serve as major sources of animal derived protein, vitamins, essential trace elements and fatty acids. However, meat and edible offal consumption had been identified as an important pathway of human exposure to pollutants. The degree of heavy metal toxicity to human population depends upon their daily intake. The EDI values for human non essential metals Cd, As, Pb and Hg for adults person of 60 kg body weight show that chicken liver had the highest EDI value. The EDI values obtained were generally lower than the respective oral reference dose (RfD) threshold for human non essential metals Cd, As and Pb except in Hg. Our results strongly indicate no possible health risk associated with animal based food consumed by the local population of Benin city. The RfD threshold dose or intake is an estimate of a daily exposure to the human population that is likely to be without an appreciable adverse risk of deleterious noncancer effects when exposure is long-term (lifetime) intake. If the predicted intake is less than the oral reference dose (THQ < 0.1), it indicates almost no possibility of an adverse health effects. However if the intake exceeds the reference dose (THQ > 0.1) does not necessarily imply that adverse health effects are expected only that a conservative reference oral dose (RfDo) is exceeded. The results of this study are similar to those obtained in an earlier study on offal and muscles of sheep, goat and chicken (Bortey-Sam et al., 2015) where they reported low daily intakes of As, Cd, Hg, Pb and Mn in food animals compared to the provisional tolerable daily intake guidelines. Chronic exposure to low doses of Cd, As, Pb and Hg above their safe threshold in humans and animals could therefore result to many non- carcinogenic hazards such as neurologic involvement, headache and liver malfunctions. For human essential heavy metals Co, Cr, Cu, Mn, Fe, Zn and Ni, the estimated daily intake of Co, Cr, Cu, Mn, Fe, Zn and Ni in this study ranged from 0.005–0.135, 0.008–0.716, 0.698–220.041, 0.185–9.018, 13.808–229.838, 4.117–116.760 and 0.005–0.123 μg/kg bw/day respectively. Based on this values, the EDI is lower than the RfD guidelines which strongly showed that there is no serious health risk via consumption of these food based animals. The calculated EDIs of As, Cd, Hg, Pb and Mn in offal and muscle samples of the three food animals from Benin city were below the WHO (2000), FSA (2006) and FAO/WHO (2010) tolerable daily intakes (Table 2). However, the EDI values in children were higher than the adult values. Therefore, children are especially more vulnerable to acute, sub-acute and chronic effects of ingestion of chemical pollutants, since they (children) consume more (twice of the amount) of food per unit of body weight as adults (European Environment and Health Information System ENHIS, 2007). As a result, intakes of these toxic metals through food could be higher for children in Benin city. The EDI values from other studies agreed with our findings. Specifically, the findings of Tongo and Ezemonye (2015) on predicted EDI values for children

Table 3
Rotated component matrix of heavy metal distribution in tissues of cattle, chicken and goat.

Metals	Liver			Kidney			Muscle		
	Factor 1	Factor 2	Factor 3	Factor 1	Factor 2	Factor 3	Factor 1	Factor 2	Factor 3
Cr	0.57295	0.442054	0.3478	0.125716	0.171982	0.586742	0.322429	0.076322	0.560515
Mn	0.746037	0.006849	− 0.16617	0.634222	0.451342	− 0.13242	0.788645	− 0.16787	0.019669
Fe	0.826638	0.164758	− 0.30036	0.597652	0.21665	− 0.02082	0.860973	− 0.23712	− 0.11556
Co	0.152608	0.787065	0.167181	0.857003	− 0.07441	0.03258	0.563319	0.349646	0.119911
Ni	0.601517	0.471661	0.41585	− 0.08658	− 0.52952	0.525105	− 0.07011	0.754954	0.005269
Cu	0.014404	− 0.0496	0.761673	− 0.15836	0.839743	0.129631	0.647074	0.065516	− 0.49891
Zn	0.843317	0.115863	0.118478	0.385707	0.784202	0.149639	0.702072	− 0.23161	− 0.39122
As	0.063011	0.784748	− 0.27553	0.775946	0.027437	− 0.2946	− 0.19852	0.069948	0.832405
Cd	0.220286	0.782195	− 0.38159	0.823136	− 0.0745	− 0.10271	− 0.1393	0.81524	0.170016
Pb	0.683165	0.19457	− 0.12312	0.618564	0.168359	0.287615	− 0.03435	0.955143	0.012434
Hg	0.324645	0.200308	− 0.54916	0.223473	0.005372	− 0.69775	− 0.22616	0.055939	0.769395

associated with residual pesticide levels in edible tissues of slaughtered cattle in Benin City conform with our current findings. Also, Onwukeme et al. (2014) and Oforka et al. (2012) predicted the risk of heavy metals via consumption of cow meat and offal in Enugu and chicken meat in Port-Harcourt, Nigeria. However, our findings in this study regarding metals contents in meat and offal suggest that their consumption are not free of risks as they may present detrimental health concerns through a lifetime. Due to interspecific differences however, the EDI levels of heavy metals were higher in chicken than other species.

3.2.2. Target hazard quotient (THQ)

Estimated health risk from consumption of offal and muscle from chicken, cattle and goat were assessed based on the THQ. A THQ value greater than 1 would indicate that a potential health risk may exist. THQ value in this study was less than 1 which means the exposed population is unlikely to experience any obvious adverse effects (USEPA, 2000) from the intake of individual metals through the consumption of offal and muscle (Fig. 3). Generally, consumption of muscle tissue poses less health risk to man compared to kidney and liver because it accumulates low level of metal. However, muscle tissue seldom come in direct contact with metals as it is totally covered externally by the skin that in many ways prevent the penetration of metals. It is also not an active site for detoxification, and therefore, transport of metals from other tissues to muscle does not seem to arise (Elnabris et al., 2013). Our findings also indicates that the severity of metals and metalloids are more in liver and kidney. THQ for Cd and As were highest in chicken liver and gizzard but less than 1 in both adults and children. This may indicate potential significant health risk associated with continuous consumption of chicken liver and gizzard. Therefore, some attention should be paid for Cd and As content in chicken because their THQ values for adults and children are not far below the threshold value of 1. The higher levels of cadmium shown in chicken liver relative to other tissues may be attributed to the high coordination of metallothionein protein with cadmium. In addition, the liver act as the principal organ responsible for detoxification, transportation, and storage of toxic substances. Also, feed habits and composition can influence retention of heavy metals in the liver. Therefore continuous consumption of chicken liver may lead to biomagnification suggesting possible significant risk to man. The muscle of the three animal based food showed lowest values of THQ an indication that there might be no public health risk from the consumption of muscle of free-range chicken, cattle and goats. Our findings agrees with Tyokumbur (2016) and Ihedioha and Okoye (2013) who reported THQ value less than 1 for chicken and cow meat. The essential metals Cu, Zn, Fe and Mn were also clearly below all the permissible limits for human consumption.

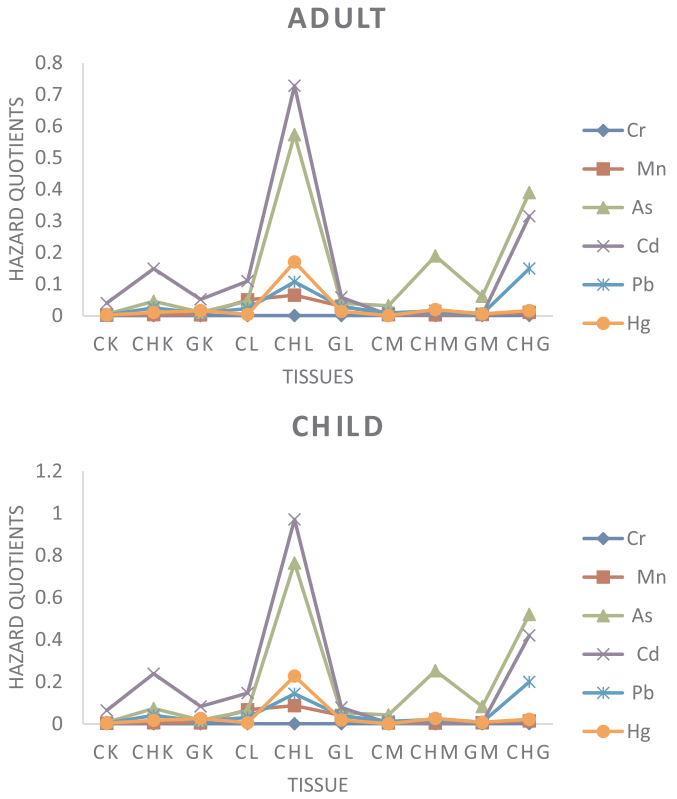

Fig. 3. Hazard quotient (THQ) of heavy metals (Cr, Mn, As, Cd, Pb and Hg) in children and adults via consumption of cattle liver CL, chicken liver CHL, goat liver GL, cattle kidney CK, chicken kidney CHK, goat kidney GK, cattle muscle CM, chicken muscle CHM, goat muscle GM, chicken gizzard CHG.

3.2.3. Estimated hazard index (HI)

The hazard index (HI) of the mixture of different non-essential metals Cd, As, Pb and Hg was calculated by adding together all the component hazard quotients (THQ). The potential health effects of the mixture were further analyzed and investigated if the HI value is equal to or greater than 1. Hence, HI < 1 means no hazard; 1 > HI < 10 means moderate hazard while greater than 10 means high hazard or risk (Ukoha et al., 2014). This approach assumes that all components have similar joint action for residents ingesting metals via consumption of tissues and offal of free range chicken, cattle and goat. The calculated HI values for both adults and children are given in Fig. 4. The HI for human non essential metals Cd, As, Pb and Hg revealed that chicken liver (2.19) and chicken gizzard (1.17) for children were greater than 1. This suggests that there is overtly adverse health effects from the consumption of chicken liver and gizzard. In adult, HI value showed that chicken liver (1.64) and gizzard (0.88) suggests higher health risk from the consumption of chicken liver than chicken gizzard. This implies that when metals combined they pose a greater health risk than any lone metal. All heavy metals analyzed had a hazard quotient of less than one

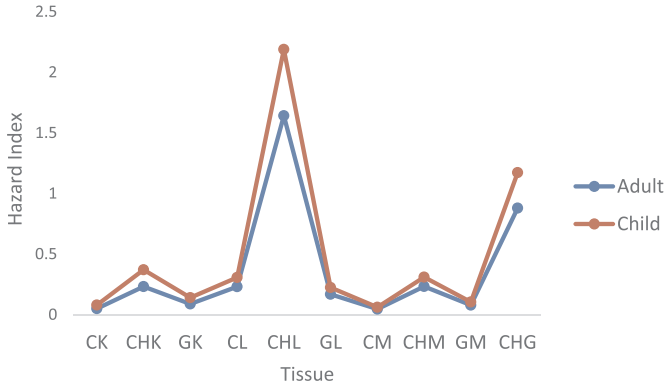

Fig. 4. Hazard Index (HI) for children and adults through the consumption of offal and muscle.

(THQ < 1). The greater the value of (THQ) and (HI) (if > 1), the greater the level of risk associated with offal and muscle consumption. Our results agreed with MahMoud et al. (2015) that reported HI greater than 1 for Cd indicating high potential risk to the Egyptian consumers.

4. Conclusion

This study was developed to provide baseline information on heavy metals and metalloid concentration in free range animals; chicken, cattle and goats sampled in Benin City, Edo State, Nigeria. As expected, metal concentrations showed a great variability. The levels of metals in the offal and muscle suggested that significant differences existed in the concentrations of elements across offal and muscles of animal species. It was observed that free-range chickens reared in Benin City accumulated large quantities of Cd above maximum permissible limits compared to cattle and goats. This may be largely related to the organism mobility, food preferences, or other factors with respect to environment pollution most likely from dumpsites. The estimation of risk showed that adverse health effect may occur from prolonged consumption of chicken liver with high concentrations of Cd and may lead to accumulation in the human body thereby causing metal toxicity. Overall, our findings show that consumption of chicken liver and gizzard present more health risk than muscle tissue especially to children. Contamination is due mainly to environmental pollution as the animals are free ranging. Therefore, it is strongly recommended that appropriate steps should be taken to identify ways to reduce the health risk via consumption of contaminated chicken offal especially the gizzard and liver as well as restrict chickens from roaming and scavenging for food in dumpsites in order to safeguard the food chain. Further research is required to investigate the dietary intake of heavy metals and possible health risks from other communities where animal free ranging is predominant. This will help to provide consumption advisories to the public about the risks of eating contaminated leaner meat products in an effort to avoid the dangers of high cholesterol.

Acknowledgments

This work was supported by Grants-in-Aid for Scientific Research from the Ministry of Education, Culture, Sports, Science and Technology of Japan awarded to M. Ishizuka (No. 24405004 and No. 24248056) and Y. Ikenaka (No. 26304043, 15H0282505, 15K1221305), S.M.M. Nakayama (No. 16K16197) and the Foundation of JSPS Core to Core Program (AA Science Platforms) and Bilateral Joint Research Project (PG36150002 and PG36150003). We also acknowledge financial support from The Soroptimist Japan Foundation, The Nakajima Foundation, The Sumitomo Foundation and The Nihon Seimei Foundation. This research was supported by JST/JICA, SATREPS (Science and Technology Research Partnership for Sustainable Development). We are grateful to Mr. Takahiro Ichise (Laboratory of Toxicology, Graduate School of Veterinary Medicine, Hokkaido University) for technical support. We acknowledged the National Centre for Energy and Environment (Energy Commission of Nigeria), University of Benin, Benin City, Edo State Nigeria for support and provision of its ancillary facilities used in the preparation and preservation of samples. We gratefully appreciate the assistance of Prof Lawrence N I Ezemonye and staff of the National Centre for Energy and Environment during field sampling.

References

Agency for Toxic Substances and Diseases Registry (ATSDR), 2013. The Priority List of Hazardous Substances that will be the subject of toxicological profiles. 〈http://www.atsdr.cdc.gov/SPL/index.html〉.

Ali, H., Khan, E., Sajad, M.A., 2013. Phytoremediation of heavy metals-concepts and applications. Chemosphere 91, 869–881.

Amaral, A.F.S., Arruda, M., Cabral, S., Rodrigues, A.S., 2008. Essential and non-essential trace metals in scalp hair of men chronically exposed to volcanogenic metals in the Azores, Portugal. Environ. Int. 34, 1104–1108.

Amirah, M.N., Afiza, A.S., Faizal, W.I.W., Nurliyana, M.H., Laili, S., 2013. Human health risk assessment of metal contamination through consumption of fish. J. Environ. Pollut. Human. Health 1 (1), 1–5.

Aschner, M., 2000. Manganese: brain transport and emerging research needs. Environ. Health Perspect. 108 (3), 429–432.

Bortey-Sam, N., Nakayama, S.M.M., Ikenaka, Y., Akoto, O., Baidoo, E., Yohannes, Y.B., Mizukawa, H., Ishizuka, M., 2015. Human health risks from metals and metalloid via consumption of food animals near gold mines in Tarkwa, Ghana: estimation of the daily intakes and target hazard quotients (THQTHQs). Ecotoxicol. Environ. Saf. 111, 160–167.

Cao, L.L., Yang, J., Wang, P., Wang, L., Tian, H.T., Zou, M.K., Xie, J., 2015. Potentially toxic metal and metalloid fractionation contamination in sediments of Daya Bay, South China Sea. Kem. Ind. 64 (5–6), 255–262.

Chen, Y.C., Serrell, N., Evers, C.D., Fleishman, J.B., Lambert, F.K., Weiss, J., Mason, R.P., Bank, S.M., 2008. Methylmercury in marine ecosystems - from sources to seafood consumers. Environ. Health Perspect. 116 (12), 1706–1712.

Codex, 1995. Alimentarius Commission (CAC) Doc. no. CX/FAC 96/17. Joint FAO/WHO food standards programme. Codex general standard for contaminants and toxins in foods.

Copat, C., Conti, G.O., Signorelli, C., Marmiroli, S., Sciacca, S., Vinceti, M., Ferrante, M., 2013. Risk assessment for metals and PAHs by Mediterranean seafood. Food Nutr. Sci. 4, 10–13.

Demirezen, D., Uruc, K., 2006. Comparative study of trace elements in certain fish, meat and meat products. Food Chem. 32, 215–222. http://dx.doi.org/10.1016/j.meatsci.2006.03.012.

Doganoc, D.Z., 1996. Lead and cadmium concentrations in meat, liver and kidney of Slovenian cattle and pigs from 1989–1993. Food Addit. Contam. 13, 237–241.

Elnabris, K.J., Muzyed, S.K., El-Ashgar, N.M., 2013. Heavy metal concentrations in some commercially important fishes and their contribution to heavy metals exposure in Palestinian people of Gaza Strip (Palestine). J. Assoc. Arab Univ. Basic Appl. Sci. 13, 44–51.

European Commission Regulation(ECR), 2006. Setting maximum levels for certain contaminants in foodstuff (No 1881/2006). Off. J. Eur. Union L 364, 5–24.

European Environment and Health Information System (ENHIS)., 2007. Exposure of children to chemical hazards in food. Fact Sheet No.4.4, CODE: RPG4-Food-EX1. World Health Organization.

FAO/WHO, 2010. Summary Report of the Seventy-third Meeting of JECFA. Joint FAO/WHO Expert Committee on Food Additives, Geneva.

FAO/WHO, 2000. Report of the 32nd Session of the codex committee of the food additives Contaminants. Beijing People's Republic of China, 20–24 March.

FMAWR, 2008. National Programme for Food Security. Federal Ministry of Agriculture and Water Resources (FMA&WR), pp. 107.

Food and Nutrition Board, 2004. Dietary Reference Intakes [DRIs]: recommended Intakes for Individuals. National Academy of Sciences, Washington, DC, USA.

Fraga, C.G., Oteiza, P.I., 2002. Iron toxicity and antioxidant nutrients. Toxicology 180, 23–32.

Gall, J.E., Boyd, R.S., Rajakaruna, N., 2015. Transfer of heavy metals through terrestrial food webs: a review. Environ. Monit. Assess. 187 (4), 201–222.

Homady, M., Hussein, H., Jiries, A., Mahasneh, A., Al-Nasir, F., Khleifat, K., 2002. Survey of some heavy metals in sediments from vehicular service stations in Jordan and their effects on social aggression in prepubertal male mice. Environ. Res. 89, 43–49.

Hussein, A., Khaled, A., 2014. Determination of Metals in Tuna Species and Bivalves from Alexandria, Egypt. Egypt. J. Aquat. Res. 40, 9–17. http://dx.doi.org/10.1016/j.ejar.2014.02.003.

Ihedioha, J.N., Okoye, C.O.B., 2013. Dietary intake and health risk assessment of lead and cadmium via consumption of cow meat for an urban population in Enugu State, Nigeria. Ecotoxicol. Environ. Saf. 93, 101–106.

Iwegbue, C.M.A., Nwajei, G.E., Iyoha, E.H., 2008. Heavy metal residues of chicken meat and gizzard and turkey meat consumed in Southern Nigeria. Bulg. J. Vet. Med. 11 (4), 275–280.

Jovic, M., Onjia, A., Stankovic, S., 2012. Toxic metal health risk by mussel consumption. Environ. Chem. Lett. 1, 69–77.

Khalafalla, F.A., Abdel-Atty, N.S., Abd-El- Wahab, M.A., Ali, O.I., Rofaida, B.A., 2015. Assessment of heavy metal residues in retail meat and offals. J. Am. Sci. 11 (5), 50–54.
Kim, J., Koo, T.H., 2007. Heavy metal concentrations in diet and livers of black-crowned night heron Nycticorax nycticorax and grey heron Ardea cinereal chicks from Pyeongtaek, Korea. Ecotoxicology 16, 411–416.
Landis, W., Sofield, R., Yu, M.H., Landis, W.G., Sofield, R.M., 2010. Introduction to Environmental Toxicology: Molecular Substructures to Ecological Landscapes, Fourth Ed. (542 pages).
Lavery, J.T., Kemper, M.C., Sanderson, K., Schultz, G.C., Coyle, P., James, G., Mitchell, G.J., Seuront, L., 2009. Heavy metal toxicity of kidney and bone tissues in South Australian adult bottlenose dolphins (Tursiops aduncus). Mar. Environ. Res. 67, 1–7.
Mahmood, Q., Rashid, A., Ahmad S.S., Azim, M.R., Bilal, M., 2012.Current status of toxic metals addition to environment and its consequences. In: Anjum NA, et al., editors. The Plant Family Brassicaceae: Contribution Towards Phytoremediation, Environmental Pollution.
Mahmoud, M.A.M., Abdel-Mohsein, H.S., 2015. Health risk assessment of heavy metals for Egyptian population via consumption of poultry edibles. Adv. Anim. Vet. Sci. 3 (1), 58–70.
Maigari, A.U., Ekanem, E.O., Garba, I.H., Harami, A., Akan, J.C., 2016. Health risk assessment for exposure to some selected heavy metals via drinking water from Dadinkowa Dam and River Gombe Abba in Gombe State, Northeast Nigeria. World J. Anal. Chem. 4 (1), 1–5.
Maret, W., 2016. The metals in the biological periodic system of the elements: concepts and conjectures. Int. J. Mol. Sci. 17 (1), 66. http://dx.doi.org/10.3390/ijms17010066.
Markovic, J., Joksimovic, D., Stankovic, S., 2012. Trace elements concentrations determined in collected wild mussels in the coastal area of southeastern Adriatic, Montenegro. Arch. Biol. Sci. Belgrade 64 (1), 265–275.
Médecins Sans Frontières (MSF), 2010. Field News; Lead Poisoning In Zamfara State, Nigeria; Nigeria 16.07.10. Available from corresponding website; ⟨http://www.msf.org.au/from-the-field/fieldnews/field-news/article/lead-poisoning-inzamfara-state-igeria.html⟩.
Medeiros, R.J., dos Santos, L.M.G., Freire, A.S., Santelli, R.E., Braga, A.M.C.B., Krauss, T.M., Jacob, S.C., 2012. Determination of inorganic trace elements in edible marine fish from Rio de Janeiro State, Brazil. Food Control 23, 535–541.
Mertz, W., 1998. Interaction of chromium with insulin: a progress report. Nutr. Rev. 56, 174–177.
Ministry of Mines and Steel Development (MMSD), 2015. Lead poisoning in Angwan Maijero and Angwan Karo, Madaka districts of Rafi LGA, Niger State, Nigeria. A report by the Federal Ministry of Mines and Steel Development.
Nagajyoti, C.P., Lee, D.K., Sreekanth, M.V.T., 2010. Heavy metals, occurrence and toxicity for plants: a review. Environ. Chem. Lett. 8, 199–216.
Nakayama, S.M.M., Ikenaka, Y., Hamada, K., Muzandu, K., Choongo, K., Teraoka, H., Mizuno, N., Ishizuka, M., 2011. Metal and metalloid contamination in roadside soil and wild rats around a Pb–Zn mine in Kabwe, Zambia. Environ. Pollut. 159, 175–181.
National Population Commission (NPC), 2006. The Report of National Population Commission on the Census Conducted in Nigeria.
Naveedullah, M.Z.H., Yu, C., Shen, H., Duan, D., Shen, C., Lou, L., Chen, Y., 2013. Risk assessment of heavy metals pollution in agricultural soils of Siling Reservoir Watershed in Zhejiang Province. China BioMed. Res. Int. 2013. http://dx.doi.org/10.1155/2013/590306.
Nesheim, M.C., Austic, R.E., Cand, L., 1979. Poultry Production, 12th ed. Lea and Febiger, Philadelphia, pp. 123–125.
Nowak, B., 1998. Contents and relationship of elements in human hair for a non-industrialised population in Poland. Sci. Total Environ. 209 (1), 59–68.
Oforka, N.C., Osuji, L.C., Onwuachu, U.I., 2012. Estimation of Dietary intake of Cadmium, Lead, Manganese, Zinc and Nickel due to consumption of chicken meat by inhabitants of Port-Harcourt Metropolis, Nigeria. Arch. Appl. Sci. Res. 4 (1), 675–684.
Okoye, C.O.B., Ugwu, J.N., 2010. Impact of environmental cadmium, lead, copper and zinc on quality of goat meat in Nigeria. Bull. Chem. Soc. Ethiop. 24 (1), 133–138.
Olujimi, O.O., Oputu, O., Fatoki, O., Opatoyinbo, O.E., Aroyewun, O.A., Baruani, J., 2015. Heavy metals speciation and human health risk assessment at an illegal gold mining site in Igun, Osun State, Nigeria. J. Health Pollut. 8, 19–32.
Onwukeme, V.I., Nwako, P.M., Mgbemena, M.N., Onuoha, M.U., 2014. Dietary exposure to heavy metals via consumption of some vegetables and parts of cow meat by adults in Awka, Nigeria. IOSR J. Environ. Sci., Toxicol. Food Technol. (IOSR-JESTFT) 8 (5), 01–06.
Orosun, M.M., Tchokossa, P., Orosun, R.O., Akinyose, F.C., Ige, S.O., Oduh, V.O., 2016. Determination of selected heavy metals and human health risk assessment in fishes from Kiri Dam and River Gongola, North eastern Nigeria. J. Phys. Chem. Biophys. 6, 229. http://dx.doi.org/10.4172/2161-0398.1000229.
Osredkar, J., Sustar, N., 2011. Copper and zinc, biological role and significance of copper/zinc imbalance. J. Clin. Toxicol. S3, 001. http://dx.doi.org/10.4172/2161-0495.S3-001.
Pais, I., Benton Jones Jr., J., 1997. The Handbook of Trace Elements. Saint Lucie Press, Boca Raton, Florida (223p).
Pandey, G., Madhuri, S., 2014. Heavy metals causing toxicity in animals and fishes. Res. J. Anim. Vet. Fish. Sci. 2 (2), 17–23.
Porte Jr., D., Sherwin, R.S., Baron, A., 2003. Ellengerg and Rifkin's Diabetes Mellitus, 6th ed. McGraw-Hill, New York.
Rai, N., Pal, A., 2002. Health hazards of heavy metals. EnviroNews ISEB India vol 8 No. 1. International conference on plants and environmental pollution (ICPEP-2). In: Proceedings of the 2nd International Conference on Plants and Environmental Pollution, Lucknow, India, 4–9 Feb 2002. ⟨http://isebindia.com/issuewise.html⟩.
Roggeman, S., Van Den Brink, N., Van Praet, N., Blust, R., Bervoets, L., 2013. Metal exposure and accumulation patterns in free-range cows (Bos taurus) in a contaminated natural area: influence of spatial and social behaviour. Environ. Pollut. 172, 186–199.
SAC/MOHC, 2005. (The Standardization Administration China/Ministry of Health, China). Maximum levels of contaminants in foods (GB2762-2005). Beijing.
Sedki, A., Lekouch, N., Gamon, S., Pineau, A., 2003. Toxic and essential trace metals in muscle, liver and kidney of bovines from a polluted area of Morocco. Sci. Total Environ. 317, 201–205.
Simone, M., Fernando, G.C., Maria, L.P., 2012. Heavy Metals and Human Health, Environmental Health - Emerging Issues and Practice. In Tech, pp. 227–246 (Prof. Jacques Oosthuizen (Ed.), ISBN: 978-953-307-854-0).
Sivaperumal, P., Sankar, T.V., Viswanathan Nair, P.G., 2007. Heavy metal concentrations in fish, shellfish and fish products from internal markets of India vis-a-vis international standards. Food Chem. 102, 612–620.
Stankovic, S., Jovic, M., 2012. Health risks of heavy metals in the Mediterranean mussels as seafood. Environ. Chem. Lett. 2, 119–130.
Stankovic, S., Stankovic, A.R., 2013. Bioindicators of toxic metals. In: In: Lichtfouse, E. (Ed.), Green Materials for Energy, Products and Depollution. Environmental Chemistry for a Sustainable World 3. pp. 151–228.
Stankovic, S., Jovic, M., Stankovic, R.A., Katsikas, L., 2011. Heavy metalsin seafood mussels. Risks for human health. In: 64. In: Lichtfouse, E. (Ed.), Environmental Chemistry for a Sustainable World 1. pp. 311–375.
Stoyke, M., Doberschutz, K.D., Lusky, K., 1995. Heavy metal contents (cadmium, lead and mercury) in selected feedstuff, organs and tissue in cattle found different sites of Brandenburg. Mengen. Spureneler. Arb. 15, 269–276.
Tongo, I., Ezemonye, L., 2015. Human health risks associated with residual pesticide levels in edible tissues of slaughtered cattle in Benin City, Southern Nigeria. Toxicol. Rep. 2, 1117–1135.
Tyokumbur, E.T., 2016. Evaluation of cadmium (Cd) in domestic chicken meat and offal and associated health risk assessment in Ibadan. Int. J. Pure Appl. Zool. 4 (2), 155–160.
Ukoha, P.O., Ekere, N.R., Udeogu, U.V., Agbazue, V.E., 2014. Potential health risk assessment of heavy metals concentrations in some imported frozen fish species consumed in Nigeria. Int. J. Chem. Sci. 12 (2), 366–374.
USDA, 2006. Foreign Agricultural Service GAIN Report Global Agriculture Information Network Voluntary Report-public distribution GAIN Report Number CH 6064, China Peoples Republic of FAIRS Product. Specific maximum levels of contaminants in foods, Jim Butterworth and Wu Bugang.
USEPA, 2000. Risk-based Concentration Table. Philadelphia PA: United States Environmental Protection Agency, Washington DC.
USEPA, 2007. Integrated Risk Information System-Database (IRIS), Philadelphia PA; Washington, DC.
USEPA, 2015. Integrated Risk Information System. Available online: ⟨http://www.epa.gov/iris/rfd.htm⟩.
WHO, 1996. Trace Elements in Human Nutrition and Health. Geneva.
WHO, 2007. Health risks of heavy metals from long-range transboundary air pollution. World Health Organization 2007. WHO Regional Office for Europe Copenhagen, Denmark (ISBN 978 92 890 7179 6).
Yang, P., Yang, M., Mao, R., Shao, H., 2014. Multivariate-statistical assessment of heavy metals for agricultural soils in Northern China. Sci. World J. 2014. http://dx.doi.org/10.1155/2014/517020.
Zhuang, P., Zou, B., Li, N.Y., Li, Z.A., 2009. Heavy metal contamination in soils and food crops around Dabaoshan mine in Guangdong, China: implication for human health. Environ. Geochem. Health 31. pp. 707–715.

Comparative Biochemistry and Physiology, Part C 214 (2018) 28–35

Contents lists available at ScienceDirect

Comparative Biochemistry and Physiology, Part C

journal homepage: www.elsevier.com/locate/cbpc

Comparison of xenobiotic metabolism in phase I oxidation and phase II conjugation between rats and bird species

Aksorn Saengtienchai[a,b], Yoshinori Ikenaka[a,c,*], Minami Kawata[a], Yusuke Kawai[d], Kazuki Takeda[a], Takamitsu Kondo[a], Nesta Bortey-Sam[a], Shouta M.M. Nakayama[a], Hazuki Mizukawa[e], Mayumi Ishizuka[a]

[a] Laboratory of Toxicology, Department of Environmental Veterinary Sciences, Graduate School of Veterinary Medicine, Hokkaido University, N18 W9, Kita-ku, Sapporo 060-0818, Japan
[b] Department of Pharmacology, Faculty of Veterinary Medicine, Kasetsart University, 50 Ngam Wong Wan Rd, Lat Yao, Chatuchak, Bangkok 10900, Thailand
[c] Water Research Group, Unit for Environmental Sciences and Management, North-West University, Potchefstroom, South Africa
[d] Department of Animal and Food Hygiene, Obihiro University of Agriculture and Veterinary Medicine, Inada-cho, Obihiro, Hokkaido 080-8555, Japan
[e] Department of Environmental Veterinary Sciences, Graduate School of Veterinary Medicine, Hokkaido University, N18 W9, Kita-ku, Sapporo 060-0818, Japan

ARTICLE INFO

Keywords:
Birds
Species differences
Pyrene
Conjugated metabolites
Kinetics

ABSTRACT

There have been many reports regarding toxic chemicals in birds. Chemicals are mainly metabolized in the liver through phase I oxidation by cytochrome P450 (CYP) and phase II conjugation by conjugated enzymes, such as UDP-glucuronosyltransferase (UGT), sulfotransferase (SULT), glutathione-S-transferase (GST), *etc*. Xenobiotic metabolism differs among bird species, but little detailed information is available. In the present study, the four-ring polycyclic aromatic hydrocarbon (PAH), pyrene, was used as a model xenobiotic to clarify the characteristics of xenobiotic metabolism in birds compared with laboratory animals by *in vivo* and *in vitro* studies. Plasma, bile, and excreta (urine and feces) were collected after oral administration of pyrene and analyzed to clarify xenobiotic metabolism ability in chickens and quails. Interestingly, pyrenediol-glucuronide sulfate (PYDOGS) and pyrenediol-diglucuronide (PYDOGG) were present in chickens and quails but not in rats. In addition, the area under the curve (AUC), maximum plasma concentration (C_{max}), and time to maximum plasma concentration (T_{max}) of pyrene-1-sulfate (PYOS) were higher than those of the parent molecule, pyrene, while the elimination half-life ($t_{1/2}$) and mean residence time (MRT) were faster than those of the parent pyrene. With regard to sulfation of 1-hydroxypyrene (PYOH), the maximum velocity (V_{max}) and Michaelis constant (K_m) of rat liver cytosol were greater than those of chicken and quail liver cytosol. Furthermore, V_{max}/K_m of UGT activity in rat liver microsomes was also greater than those of chicken and quail liver microsomes. Characterization of xenobiotic metabolism revealed species differences between birds and mammals, raising concerns about exposure to various xenobiotics in the environment.

1. Introduction

Since the 1950s, there have been increasing reports of injuries to wild birds worldwide due to the influence of various xenobiotics, such as dichlorodiphenyltrichloroethane (DDT), coumarin-derived anticoagulant rodenticides, and non-steroidal anti-inflammation drugs (NSAIDs), such as diclofenac (Bowerman et al., 1995; Elliott et al., 1988; Erickson and Urban, 2004; Norstrom and Hebert, 2006; Prakash et al., 2007). These xenobiotics cause secondary poisoning that could affect and damage the reproductive system, liver, and kidney in scavenging and raptorial birds (Albers et al., 2003; Albert et al., 2010; Erickson and Urban, 2004; Prakash et al., 2007).

Polycyclic aromatic hydrocarbons (PAHs) are a ubiquitous group of several chemically related compounds produced naturally and by human activities. They also persist in the environment and show varied toxic effects on organisms through various actions causing carcinogenic and mutagenic effects. Generally, PAHs enter the environment and animal bodies through various routes, and are usually found as mixtures containing two or more of these compounds (Armstrong et al., 2004). In birds, the mechanism of toxicity is considered to involve interference with the function of cellular membranes as well as with enzyme systems associated with the cell membrane. Toxic effects have

* Corresponding author at: Laboratory of Toxicology, Department of Environmental Veterinary Sciences, Graduate School of Veterinary Medicine, Hokkaido University, N18 W9, Kita-ku, Sapporo 060-0818, Japan.
E-mail address: y_ikenaka@vetmed.hokudai.ac.jp (Y. Ikenaka).

https://doi.org/10.1016/j.cbpc.2018.08.007
Received 11 January 2018; Received in revised form 14 March 2018; Accepted 28 August 2018
Available online 31 August 2018

been documented mostly in embryos, young birds, and adult birds. There have also been reports of reduced egg production, hatching, and growth (Albers et al., 2003). Although PAHs influence absorption to organic material or degradation in the environment, some are persistent and bioaccumulate in the food chain (Jiang et al., 2011). Wild and domestic birds may be exposed to PAHs and accumulate them in their bodies. Xenobiotics, including PAHs, are generally absorbed and distributed in the body, and are metabolized based by phase I oxidation (mainly enzymes as cytochrome P450s) and phase II conjugation enzymes, such as UDP-glucuronosyltransferase (UGT), sulfotransferase (SULT), and glutathione-S-transferase (GST). The more water-soluble metabolites are excreted in the urine and feces. However, there have been reports of interspecies differences in xenobiotic metabolic activity among bird species *in vitro* (Watanabe et al., 2010). However, insufficient information is available to clarify the xenobiotic metabolism ability in phase I oxidation and phase II conjugation in bird species *in vivo*, especially with regard to their kinetic parameters.

Pyrene, a four-ring PAH, was selected as a xenobiotic model to observe the metabolic activity in birds in comparison with laboratory animals following *in vivo* and *in vitro* studies. In addition, pyrene and it metabolites are typical phenolic xenobiotic models. To understand xenobiotic metabolism in bird species, we used pyrene as a xenobiotic model and analyzed pyrene metabolites in urine. The excretion of urine containing pyrene metabolites is useful to characterize differences in phase II xenobiotic conjugation reactions between species (Saengtienchai et al., 2016).

To clarify the roles of phase I oxidation and phase II conjugation reactions of pyrene in bird species in comparison with laboratory animals, an *in vivo* exposure study was performed. An important factor in pharmacokinetics of pyrene and its conjugated metabolites were observed to complete the absorption, distribution, metabolism, and excretion in birds. To assess the efficiency of phase II conjugation enzymes *in vitro*, 1-hydroxypyrene (PYOH) was chosen as a substrate to measure UGT-dependent and SULT-dependent activities.

2. Materials and methods

2.1. Animals

Nine-week-old male Wistar rats (*Rattus norvegicus*) ($n = 3$) were obtained from SLP (Hamamatsu, Japan). Eight-week-old male White Leghorn chickens (*Gallus gallus*) ($n = 3$) were obtained from Hokudo Co., Ltd. (Sapporo, Japan). One-year-old quails (*Coturnix japonica*) (male, $n = 1$; female, $n = 2$) were obtained from a local commercial supplier in Sapporo, Japan. The animals were acclimated for one week in the laboratory and kept under conditions of 40% – 70% humidity at 23 °C ± 2 °C in a temperature-controlled room with a 12-h light/dark cycle. They were given laboratory food and clean water *ad libitum*. All animal experiments were performed under supervision and with the approval of the Institutional Animal Care and Use Committee of Hokkaido University (approval no. 100067), in accordance with the Association for Assessment and Accreditation of Laboratory Animal Care International (AAALAC).

2.2. Chemicals

Pyrene, PYOH, 3′-phosphoadenosine 5′-phosphoslfate (PAPS), sulfatase (from limpet Type V; 34 U/mg), β-glucuronidase (from bovine liver, Type B-1; 1240 U/mg), β-glucosidase (from almond; 3.4 U/mg), and bovine serum albumin were obtained from Sigma-Aldrich Co. (St. Louis, MO). Methanol, acetonitrile, acetic acid, and ammonium acetate were purchased from Kanto Chemical Co., Inc. (Tokyo, Japan). Pyrene-1-sulfate (PYOS) was obtained from TOPU Bio (Toyama, Japan). Uridine-diphosphate-glucuronic acid (UDP-GA) was purchased from Wako (Osaka, Japan). All chemicals used for high-performance liquid chromatography (HPLC) and mass spectrometry (MS) were of HPLC or MS grade, respectively, and were obtained from Kanto Chemical Co. Inc.

2.3. Pyrene exposure and sample collection

Chickens, quails, and rats were fasted for 24 h before exposure to pyrene as the test chemical. Pyrene was dissolved in corn oil and administered orally at a dose of 4 mg/kg body weight. Plasma was collected from chickens at 0, 1, 2, 3, 6, 9, 12, 24, and 48 h after pyrene exposure for pharmacokinetic analysis. In rats, plasma samples were collected at 24 h after oral administration of pyrene. In the case of quails, plasma samples were collected after 2 h exposure, which showed a high distribution of pyrene metabolites. The excreta, such as urine, feces, urine-feces mixed (in chickens and quails), bile (in chickens), and urine contained in the ureter (in chickens) were obtained from chickens, quails, and rats after 24 h of pyrene exposure. Samples were kept at −20 °C until analysis. Animals were then sacrificed by carbon dioxide inhalation at 48 h after pyrene exposure. The livers were removed and perfused with cold 1.15% potassium chloride to remove blood, and samples were immediately placed in liquid nitrogen and kept at −80 °C.

2.4. Extraction of pyrene metabolites in samples from in vivo study

The method of Boocock et al. (2007) was used in this study. Briefly, aliquots of 10 μL of plasma from each animal species were extracted with 90 μL of 100% methanol. The mixed samples were stored at −20 °C for 50 min to precipitate protein. After melting at room temperature, samples were centrifuged at 13,000*g* for 15 min at room temperature. Aliquots of 10 μL of the supernatant were subjected to HPLC with fluorescence detection (FD).

Urine and feces samples were extracted and cleaned up according to the protocol described by Saengtienchai et al. (2015). Briefly, 1 mL of urine was extracted with the same amount of 70% methanol (50:50, v:v). The mixtures were extracted by vortexing for 1 min and centrifugation at 9000*g* for 10 min at room temperature. The supernatants were then filtered with a 0.2-μm syringe filter (SupraPure; Recenttec, Tokyo, Japan). Aliquots of 1 μL of the filtrates were subjected to HPLC/FD.

Samples of approximately 1 g of feces or urine-feces mixture were homogenized with 20 mL of 70% methanol. The mixtures were then extracted by sonication for 20 min and centrifuged at 9000*g* for 10 min at room temperature. The supernatants were transferred into 50-mL Falcon tubes. The residual samples were extracted again. The pooled supernatants were filtered with a 0.2-μm syringe filter and kept at −20 °C until analysis. Then, 5 μL of each pooled supernatant was subjected to HPLC/FD.

Aliquots of bile samples were diluted 400-fold with 70% methanol. The samples were then centrifuged at 10,000*g* for 5 min at room temperature. Then 5 μL of each supernatant was subjected to HPLC/FD.

The urine contained in the ureter samples were extracted with 500 μL of 70% methanol. The mixtures were then extracted by sonication for 20 min and centrifuged at 10,000*g* for 5 min at room temperature. Then, 5 μL of each supernatant was analyzed by HPLC/FD.

2.5. Analysis and identification of pyrene metabolites

The supernatant was then injected into the HPLC/FD system (pump: LC-20AD, auto sampler: SIL-20A, column oven: CTO-20A, controller: CEM-20A; Shimadzu) equipped with an ODS column (ODS-120T 4.6 mm × 300 mm; Tosoh, Tokyo, Japan). HPLC was performed according to the method of Beach et al. (2010) with slight modifications. Mobile phase A consisted of a mixture of 10 mM ammonium acetate buffer (pH 5) and mobile phase B (9:1, v/v). A mixture of methanol:acetonitrile:water (38:57:5, v/v/v) was used as mobile phase B. The solvent gradient was 100% mobile phase A at 0 min, followed by a

linear gradient to 100% of mobile phase B from 0 to 35 min. The gradient was held at 100% of mobile phase B for 5 min until 40 min. Then, the gradient was held at 100% of mobile phase A from 40.1 to 47 min. The solvent flow rate was set at 0.5 mL/min, and a column temperature of 45 °C was used throughout. The excitation and emission wavelengths for fluorescence detection were 343 and 385 nm, respectively. Furthermore, each separated peak was identified by electrospray ionization ion-trap mass spectrometry (ESI/ion-trap/MS, LTQ XL; Thermo Fisher Scientific, Waltham, MA). The ESI conditions were fully scanned (*m/z* 80–800) in negative mode, with an ion source voltage and temperature of −4.2 kV and 420 °C, respectively.

2.6. Deconjugation of pyrene metabolites

Deconjugation was performed using the method described by Ikenaka et al. (2007). Briefly, the enzymes sulfatase, β-glucuronidase, and β-glucosidase were dissolved in 0.1 M sodium acetate buffer and the pH was adjusted to 5.0 with acetic acid. The enzyme concentrations were 10, 4000, and 17 U/mL, respectively. Aliquots of 30 μL of urine sample extracts containing pyrene metabolites were mixed with 270 μL of buffer, and each deconjugation enzyme (200 μL) was added. As a control, the same quantity of bovine serum albumin (1 mg/mL) was added, and reactions were performed under the same conditions as used for the deconjugation enzymes. All samples were incubated at 37 °C for 8 h. The reaction was stopped by adding 500 μL of methanol. The deconjugation solutions were analyzed by HPLC/FD.

2.7. Preparation of liver microsomal and cytosolic fractions

Liver microsomal and cytosolic fractions were prepared according to the method of Omura and Sato (1964). The liver samples were homogenized in potassium phosphate buffer (KPB; 0.1 M, pH 7.4) on ice. The homogenates were transferred to tubes and centrifuged at 9000*g* for 20 min at 4 °C. The supernatants (S9 fraction) were decanted into ultracentrifugation tubes and centrifuged at 105,000*g*, 4 °C for 70 min. Each homogenate consisted of two parts, with the supernatant containing the cytosolic fraction. The pellets were homogenized on ice with KPB and washed by centrifugation at 105,000*g*, 4 °C for 70 min. The microsomal pellets were homogenized with KPB again. The microsomal and cytosolic fractions were transferred to 1.5-mL tubes and stored at −80 °C. The cytosolic fractions were used to measure SULT activity; microsomal fractions were used to determine UGT activities. The protein concentrations in the microsomes and cytosol were determined using the method of Lowry et al. (1951).

2.8. UGT-dependent PYOH glucuronidation activity

UGT activity of PYOH was assessed using the method described by Ueda et al. (2011) with slight modifications. Initially, microsomes were diluted to 4 mg/mL protein with 0.1 M phosphate buffer (pH 7.4), and then 2.5 μL of 1% sodium cholate solution was added and incubated on ice for 30 min. After treatment, 50 μL of microsome solution was mixed with 41.5 μL of buffer, 5 μL of 100 mM $MgCl_2$, and 1 μL of PYOH. The final concentrations of PYOH were 10, 20, 25, 38, 50, 100, and 200 μM. Samples were preincubated at 37 °C for 5 min. The reaction was started with 2.5 μL of a 50 mM UDP-GA in a final volume of 100 μL. The reaction was allowed to proceed for 10 min, and 400 μL of ice-cold methanol was added to stop the reaction. The reaction solutions were placed on ice for 20 min, and then centrifuged at 1600*g* for 15 min. The supernatants were transferred to HPLC vials and subjected to HPLC/FD (Shimadzu). Samples were analyzed with an Inertsil ODS-3 column (2.1 mm × 150 mm; GL Sciences). Mobile phase A was 10 mM ammonium acetate buffer (pH 5) and mobile phase B consisted of methanol:acetonitrile:water (38:57:5, v/v/v). The linear gradient was 17 min in length with 90% phase B. injection volume was 10 μL, the flow rate was 0.5 mL/min, and the column temperature was 45 °C. Excitation and emission wavelengths were 343 and 385 nm, respectively. Kinetic parameters, including maximal velocity (V_{max}), Michaelis – Menten constant (K_m), and V_{max}/K_m ratio (enzyme efficiency), were determined by the Michaelis – Menten equation using GraphPad Prism version 5.01 for Windows (GraphPad Software, San Diego, CA).

2.9. SULT-dependent PYOH sulfation activity

The SULT activity for PYOH was determined using a modification of the method of Ueda et al. (2011). The final protein concentration in the liver cytosol was 250 μg protein/mL, which was adjusted with 100 mM Tris-HCl buffer (pH 7.4). Then, 50 μL of cytosol solution was mixed with 10 μL of 100 mM $MgCl_2$, 10 μL of 50 mM Na_2SO_3, and 1 μL of 1-hydroxypyrene. Tris-HCl buffer (100 mM, pH 7.4) was added to make up the volume to 97.5 μL. The final concentrations of 1-hydroxypyrene were 0.005, 0.01, 0.02, 0.05, 0.1, 0.2, and 0.5 μM. The mixtures were preincubated at 37 °C for 5 min. The reaction was initiated by adding 2.5 μL of 1 mM PAPS and the final volume was 100 μL. After 10 min of incubation, 400 μL of ice-cold methanol was added to stop the reaction. The samples were placed on ice for 20 min, and then centrifuged at 1600*g* for 15 min. The supernatants were transferred into HPLC vials and subjected to HPLC/FD (Shimadzu). Samples were analyzed with an Inertsil ODS-3 column (2.1 mm × 150 mm: GL Sciences, Inc.). Mobile phase A was 10 mM ammonium acetate buffer (pH 5) and mobile phase B consisted of methanol:acetonitrile:water (38:57:5, v/v/v). The linear gradient was 17 min with 90% phase B. Injection volume was 10 μL, the flow rate was 0.5 mL/min, and the column temperature was 45 °C. Excitation and emission wavelengths were 343 and 385 nm, respectively. Kinetic parameters were determined using the Michaelis – Menten equation, as described above.

2.10. Statistical analysis

The results were subjected to Tukey's HSD test (JMP 7.0; SAS Institute Inc., Raleigh, NC). All kinetic parameters (Michaelis–Menten equation) were analyzed using GraphPad Prism Version 5.01. In all analyses, $p < 0.05$ was taken to indicate statistical significance.

3. Results

3.1. Identification of pyrene metabolites in chicken

The chromatograms of pyrene metabolites in chicken bile are shown in Fig. 1. A total of six pyrene metabolites were detected, peak-a to peak-f, with retention times (RT) of 11.6, 14.8, 15.0, 17.4, 22.9, and 25.9 min, respectively. Table 1 presents a summary of each RT, results of deconjugation enzymes treatment, and estimated metabolites. PYOH and pyrene were eluted at RT of 36 and 41.8 min, respectively. The other unidentified peaks were determined by LC/MS/MS. The ESI negative mass spectra of peak-a (RT 11.6 min) had a parent ion of mass to charge ratio (*m/z*) 489 (MS) and MS^2 of *m/z* 409 (M-80; considered as sulfate moiety), 313 (M-176; glucuronide moiety), and 233 (M-256; both sulfate and glucuronide moieties). Peak-b eluted at 14.8 min and contained a major ion at *m/z* 585 (MS) with MS^2 of *m/z* 409 (M-176; glucuronide moiety). Peak-c was eluted at RT 15.0 min and had *m/z* 393 (MS) including MS^2 of *m/z* 313 (M-80; sulfate moiety) and 233 (M-160; di-sulfate moieties). The metabolite from peak-d (RT 17.4 min) consisted of an ion at *m/z* 313 (MS) and MS^2 at *m/z* 233 (M-80; sulfate moiety). Peak-e eluted at 22.9 min with parent ion at *m/z* 393 (MS) and MS^2 at *m/z* 217 (M-176; glucuronide moiety) it was pyrene-1-glucuronide (PYOG). Furthermore, peak-f was eluted at 25.9 min with *m/z* of 297 (MS) and MS^2 217 (M-80; sulfate moiety) and it was suspected to be PYOS. These results suggested that pyrenediol (PYDOH) (*m/z* 233) could be a conjugation product of peak-a, c, and d. In addition, peak-e and f also had PYOH (*m/z* 217) as a conjugation product. Interestingly, the conjugation product of peak-b seemed to differ from the other

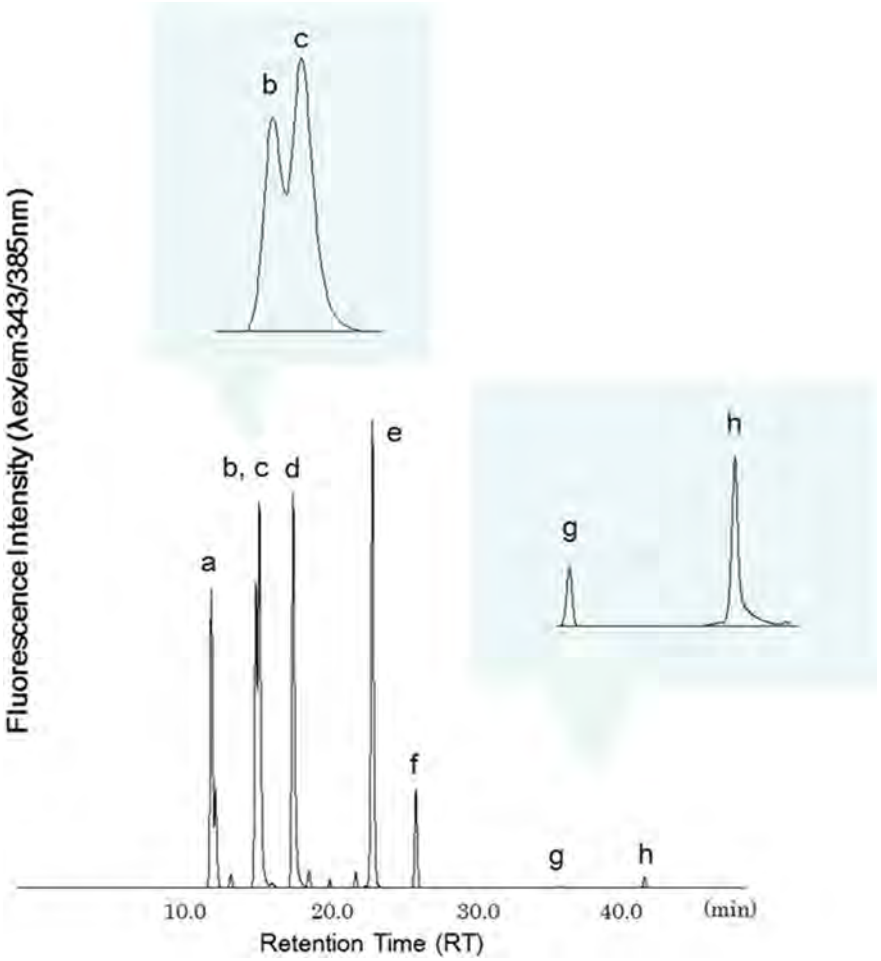

Fig. 1. Chromatograms of pyrene metabolites in chicken bile after oral administration and analysis by HPLC/FD. Peak-a, b, c, d, e, and f represent the pyrene metabolites detected, and included PYOH (peak-g) and pyrene (peak-h). Peak-a was a PYDOGS, peak-b was a PYDOGG, peak-c was a PYDOSS, peak-d was a PYDOS, peak-e was a PYOG, and peak-f was a PYOS. Excitation (Ex) and emission (Em) wavelengths for FD were 343 and 385 nm, respectively.

Table 1
Pyrene and its metabolites under MS, MS/MS, and deconjugation conditions in chicken bile.

				Deconjugation reaction		Metabolites
	RT (min)	MS (m/z)	MS^2 (m/z)	Sulfatase	β-Glucuronidase	
Peak-a	11.6	489	409	+ +	+ +	PYDOGS
			313			
			233			
Peak-b	14.8	585	409	−	+ +	PYDOGG
Peak-c	15.0	393	313	+ +	−	PYDOSS
			233			
Peak-d	17.4	313	233	+ +	−	PYDOS
Peak-e	22.9	393	217	−	+	PYOG
Peak-f	25.9	297	217	+ +	−	PYOS
PYOH	36.0		217	–	–	
Pyrene	41.8			–	–	

–: no change.
+: peak reduction 10%.
+ +: peak disappearance.

peaks. The ion of m/z 409 may have been similar to PYDOG.

Deconjugation conditions were used to identify each pyrene metabolite peak (peak-a to peak-f) in chicken bile after collection of each peak by fraction collectors. The fractions were treated with the specific enzymes used to digest the conjugated metabolites. Sulfatase, β-glucuronidase, and β-glucosidase were used for deconjugation (Table 1). Peak-a, c, d, and f disappeared after sulfatase treatment. In the case of β-glucuronidase treatment, peak-a disappeared completely, while this enzyme reduced peak-e by about 10%. However, all six peaks did not respond to β-glucosidase treatment. These results indicated that peak-a to peak-f were pyrene conjugated metabolites in chicken bile. Peak-a was suspected to be a PYDOGS, peak-b to be a PYDOGG, peak-c to be a PYDOSS, peak-d to be a PYDOS, peak-e, to be a PYOG, and peak-f, to be a PYOS.

3.2. Qualification and distribution ratio of pyrene metabolites in chickens, quails, and rats

Chickens, quails, and rats were exposed to pyrene, and plasma was collected at 24 h after oral administration. In chicken and quail plasma, the conjugated metabolites detected were PYDOGS, PYDOGG, PYDOSS, PYDOS, PYOG, and PYOS (Fig. 2). Although these three-species had similar types of conjugated pyrene metabolites, the composition of pyrene metabolites which are derived from PYDOH (such as PYDOSS and PYDOS) were seemed to be higher in rat plasma than that in chicken and quail. On the other hand, > 90% of pyrene metabolites in both chicken and quail plasma were PYOS, while a smaller proportion of glucuronide conjugation was detected. Interestingly, sulfate conjugates were the main metabolites present in plasma of both bird species and rats. In addition, only PYDOGG and PYDOGS were detected in bird plasma but not in rat plasma.

The type of conjugated metabolites in the excreta (urine and feces) in both chicken and quail, such as PYDOSS, PYDOS, PYDOGS, PYDOGG,

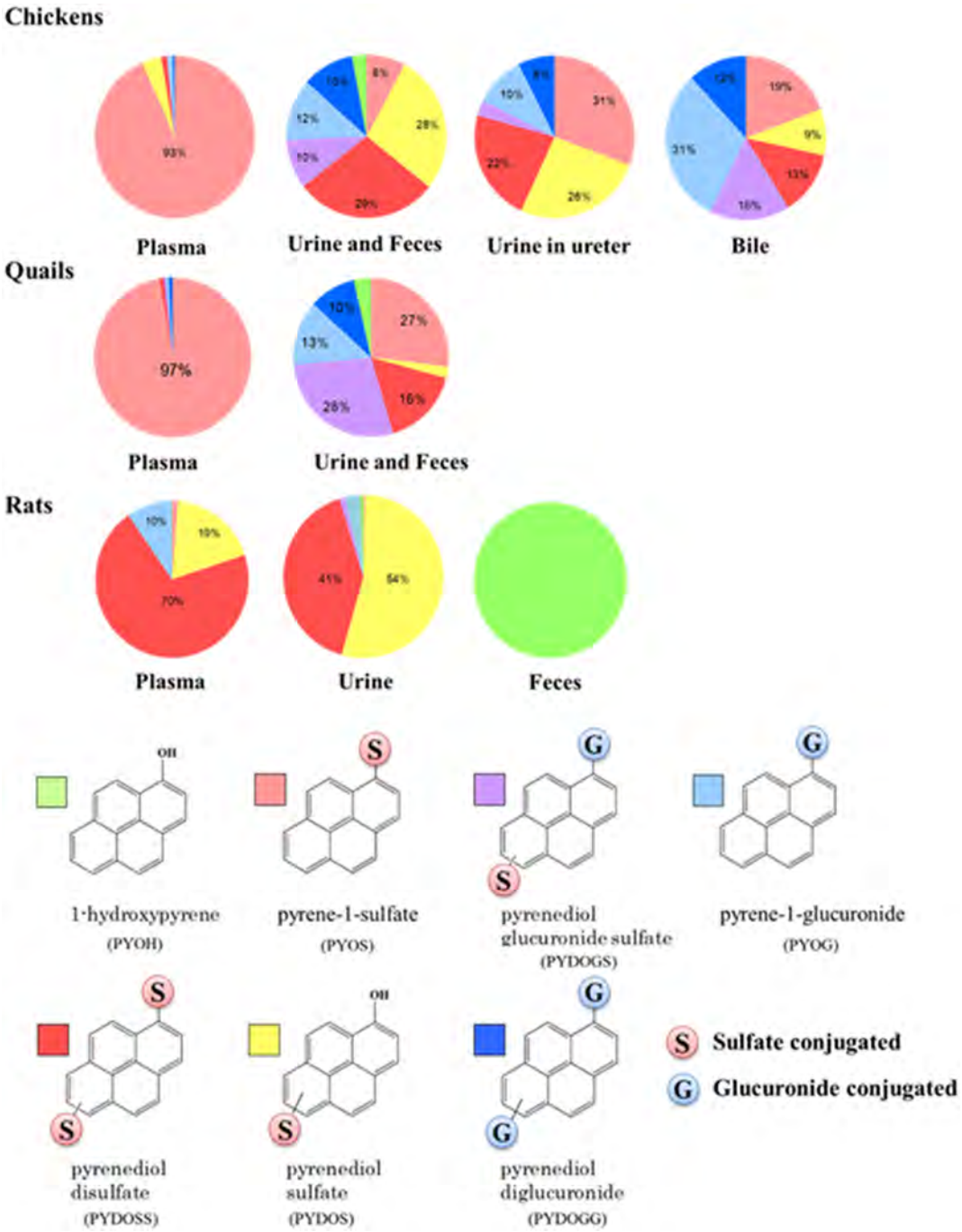

Fig. 2. Percentages of each pyrene metabolite in plasma, excreta, bile, and urine contained in the ureter in chickens ($n = 3$); plasma and excreta in quails ($n = 3$); plasma, urine, and feces in rats ($n = 3$). These percentages were obtained from the area of each metabolite peak detected by HPLC/FD. Each pyrene metabolite structure is indicated in color.

PYOS, and PYOG, were similar as observed in plasma. On the other hand, the proportion of pyrene metabolites between plasma and excreta in chicken and quail were different (Fig. 2). Although > 90% of the conjugated metabolites were found as PYOS in plasma, various types of the metabolites were equally detected in excreta. Interestingly, only PYOH was present in rat feces.

Moreover, bile and urine in the ureter from chickens were collected to examine pyrene metabolites. The results are summarized in Fig. 2. These samples showed similar conjugated pyrene metabolites present as sulfate and glucuronide conjugates. Only PYOH was present in bird excreta but not in plasma, bile, or urine contained in the ureter. The order for percentages of PYDOSS and PYDOS was as follows: excreta > urine contained in the ureter > bile and plasma. PYOS was mainly present in chicken samples in the order: plasma > urine contained in the ureter > bile and excreta. In addition, PYDOS, PYDOGG, and PYOG were detected at high levels in bile, excreta, urine contained in the ureter, and plasma, respectively.

3.3. Pharmacokinetic evaluation in chickens

The distributions of each peak area of pyrene metabolite-time profiles of pyrene following a single oral administration are shown in Fig. 3. Both glucuronide and sulfate conjugated metabolites were detected, and PYOS was the dominant metabolite among all conjugated

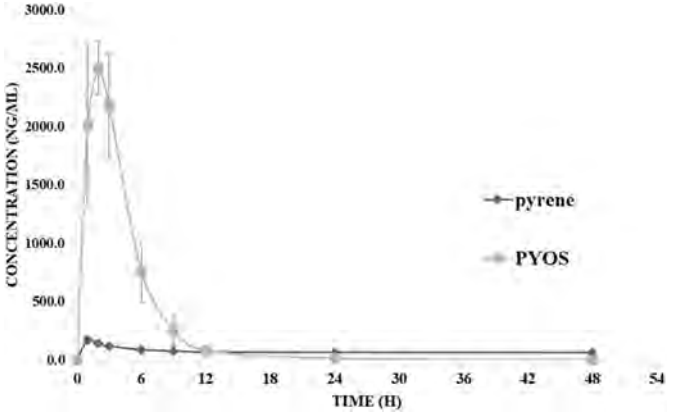

Fig. 3. Distribution profiles between pyrene and PYOS and time (h) in chicken plasma. Each point represents the average peak area ± SD, $n = 3$.

Table 2
Pharmacokinetic parameters of pyrene and PYOS after oral administration of pyrene (4 mg/kg) in chickens (mean ± SD), $n = 3$.

Parameters	Pyrene	PYOS
AUC (ng*h/mL)	3375 ± 84	12,677 ± 799
C_{max} (ng/mL)	169 ± 28	2524 ± 265
T_{max} (h)	–	1.7 ± 0.6
$t_{1/2}$ (h)	91.2 ± 68.2	3.6 ± 0.9
MRT (h)	134.5 ± 94.4	4.2 ± 0.8
CL/F (L/h)	0.3 ± 0.1	0.2 ± 0.01

AUC, area under the curve; C_{max}, maximum plasma concentration; T_{max}, time to maximum plasma concentration; $t_{1/2,}$ elimination half-life; MRT, mean residence time; CL/F, total clearance of the drug from plasma after oral administration.

pyrene metabolites. Corresponding exposure data in terms of area under the curve (AUC), maximum plasma concentration (C_{max}), time to maximum plasma concentration (T_{max}), elimination half-life ($t_{1/2}$), mean residence time (MRT), and total clearance of the drug from plasma after oral administration (CL/F) of pyrene and its metabolite, PYOS, in chicken plasma are summarized in Table 2. Pyrene was rapidly absorbed after oral administration, the peak concentration occurring faster than 1 h, whereas the peak concentration of PYOS (C_{max}, 2524 ± 265 ng/mL) was observed at 1.7 ± 0.6 h. Furthermore, the AUC of PYOS was also larger than that of pyrene (12,677 ± 799 and 3375 ± 84 ng*h/mL, respectively). The $t_{1/2}$ of pyrene was longer than that of its metabolite, PYOS (91.2 ± 68.2 and 3.6 ± 0.9 h, respectively). However, MRT (4.2 ± 0.8 h) and CL/F (0.2 ± 0.01 L/h) of PYOS were shorter than those of the parent compound, pyrene (MRT, 134.5 ± 94.4 h; CL/F, 0.3 ± 0.1 L/h).

3.4. Comparison of pyrene metabolizing ability among bird species and rats

The enzyme kinetics activities were examined by *in vitro* study to observe sulfation (in cytosol) and glucuronidation (in microsome) activities in chickens, quails, and rats using PYOH as a substrate. The results for sulfotransferase activity are presented in Fig. 4A and Table 3. The hepatic intrinsic clearance (V_{max}/K_m), the maximum reaction rate (V_{max}), and the Michaelis constant (K_m) were examined to estimate conjugated enzyme affinities. The sulfotransferase activity of PYOH was detected in both chicken and quail cytosols. Interestingly, interspecies differences between rats and bird species were found, with V_{max} and K_m of rat cytosol being significantly greater than those of chicken and quail cytosols. Although, the V_{max}/K_m in quail cytosol was greater than those in chicken and rat cytosols (830 ± 352, 608 ± 472, and 429 ± 51.1 μL/min/mg protein, respectively), the differences among species were not significant. Furthermore, UGT activity of PYOH is also

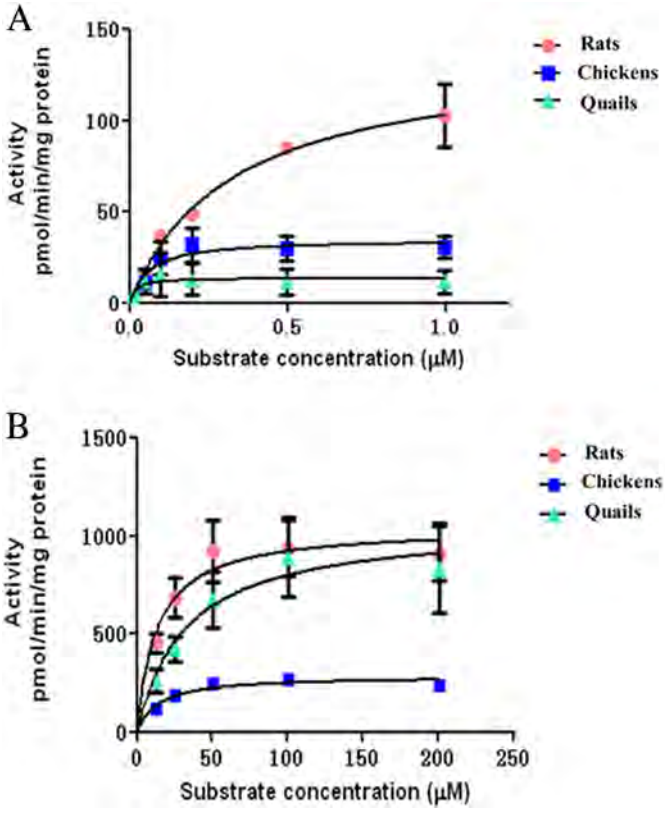

Fig. 4. Enzyme kinetics of SULT activity (4A) and UGT activity (4B) in rats and bird species. The Michaelis–Menten equation was fitted and compared between rats, chickens, and quails. Plots show the average ± SD, $n = 3$, each species.

Table 3
Kinetic analysis of hepatic cytosol sulfotransferase activity toward PYOH in rats, chickens, and quails.

	V_{max} (pmol/min/mg protein)	K_m (μM)	V_{max}/K_m (μL/min/mg protein)
Rats	136 ± 30.8[a]	0.32 ± 0.11[a]	429 ± 51.1[a]
Chickens	34.9 ± 8.04[b]	0.057 ± 0.03[b]	608 ± 472[a]
Quails	13.9 ± 8.89[b]	0.017 ± 0.004[b]	830 ± 352[a]

Mean ± SD, $n = 3$.
[a,b]Tukey's HSD, $p < 0.05$.
V_{max} = maximum velocity (pmol/min/mg protein); K_m = Michaelis constant (μM); V_{max}/K_m (μL/min/mg protein).

Table 4
Kinetic analysis of hepatic microsome UDP-glucuronosyltransferase activity toward PYOH in rats, chickens, and quails.

	V_{max} (pmol/min/mg protein)	K_m (μM)	V_{max}/K_m (μL/min/mg protein)
Rats	1044 ± 175[a]	13.1 ± 5.57[b]	80.8 ± 25.6[a]
Chickens	287 ± 11.6[b]	13.5 ± 0.92[b]	21.2 ± 1.39[b]
Quails	1057 ± 308[a]	31.9 ± 9.46[a]	33.1 ± 7.76[b]

Mean ± SD, $n = 3$.
[a,b]Tukey's HSD, $p < 0.05$.
V_{max} = maximum velocity (pmol/min/mg protein); K_m = Michaelis constant (μM); V_{max}/K_m (μL/min/mg protein).

shown in Fig. 4B and Table 4. The V_{max} of rat and quail microsomes were similar and were significantly higher than that of chicken microsomes. Surprisingly, the K_m of quail microsomes was significantly faster than those of rats and chicken. Moreover, the V_{max}/K_m of chicken and quail microsomes were significantly lower than that of rat

microsome (21.2 ± 1.39, 33.1 ± 7.76, and 80.8 ± 25.6 μL/min/mg protein, respectively).

4. Discussion

Glucuronide and sulfate conjugated metabolites of pyrene were identified and detected in the plasma and their excreta, including bile, of birds. The main conjugated metabolites were PYOG and PYOS, which were detected at levels similar to those in various mammals, fish, reptiles, amphibians, and marine snails (Beach et al., 2010; Ikenaka et al., 2013; Oroszlany et al., 2013; Saengtienchai et al., 2014; Ueda et al., 2011). Interestingly, PYDOGG and PYDOGS were detected in excreta and bile of birds, but not in urine or feces of rats. Although there have been reports of glucuronide and sulfate conjugates of 1,6-PYDOH and 1,8-PYDOH, and *trans*-4,5-PYDOH in urine of rats, rabbits, fish, reptiles, amphibians, and marine snails treated with pyrene (Beach et al., 2010; Boyland and Sims, 1964; Ikenaka et al., 2013; Oroszlany et al., 2013; Saengtienchai et al., 2014; Ueda et al., 2011), PYDOGG and PYDOGS were first reported in birds. It has been reported that genetic polymorphism of conjugated enzymes, such as UGT1A isoforms, differed among birds and mammals (Kakehi et al., 2015; Hong et al., 2007). The present study showed interspecies differences in pyrene metabolites.

Furthermore, the portion of pyrene conjugated metabolites in plasma, excreta, and bile showed interspecies differences between birds and rats. In plasma, sulfate conjugated metabolites were mainly detected in both birds and rats. However, > 90% of sulfate conjugated metabolites observed in birds was the sulfate conjugate for PYOH, whereas the around 90% of the metabolites observed from rats were for PYDOH. These results seemed to parallel those of the *in vitro* study indicating that V_{max}/K_m of PYOH sulfation in hepatic cytosol of birds was higher than that of rats.

In urine and feces, conjugated metabolites of pyrene had various forms and unique characteristics among species, including birds. Glucuronide conjugated metabolites were mainly detected in the excreta of birds, whereas sulfate conjugated metabolites and PYOH were mostly excreted into urine and feces of rats, respectively. In contrast, the V_{max}/K_m of PYOH glucuronidation in hepatic microsomes of birds was lower than that of rats *in vitro*. This discrepancy may be explained by the potentially divergent biotransformation in birds and rats due to differences in the pattern of xenobiotic elimination. With regard to xenobiotic metabolism, the metabolizing organs above the liver, such as the kidney, lung, and intestines, also showed phase II conjugation reactions with rapid passage of xenobiotics and/or their metabolites from the circulation into the tissues (Saengtienchai et al., 2015). Moreover, the ability of the transporters expressed in various tissues, such as multidrug resistance protein 2 and breast cancer resistance protein, may be other factors that could drive excretion of sulfate and glucuronide conjugate into urine and feces (Fink-Gremmels, 2009). On the other hand, differences in biliary excretion could also explain the observed species-related differences in xenobiotic metabolism, and the molecular weight has been suggested as an important factor in biliary excretion (Abou-El-Makaren et al., 1967; Hirom et al., 1972). High molecular weight compounds (in the range > 355–550) could cause an apparent increase in excretion through biliary excretion in rats, dogs, guinea pigs, rabbits, hen, and turkeys (Abou-El-Makaren et al., 1967; Hirom et al., 1972; Smith et al., 1995; Smith et al., 2000). Meanwhile, the conjugated metabolites with higher molecular weights were present in the bile of birds. However, the percentage of conjugated pyrene metabolites was altered in the excreta associated with biodegradation of pyrene conjugated metabolites by normal flora in the intestine (Kanaly and Harayama, 2000; Saengtienchai et al., 2015). Conjugated pyrene metabolites present in urine and feces of rats were markedly different from those in birds. Furthermore, Watanabe et al. (2010, 2015) previously reported a large interspecies difference in CYP-mediated metabolism in phase I oxidation following treatment with warfarin. This may be because birds have unique xenobiotic metabolism occurring in both phase I oxidation and phase II conjugation.

The pharmacokinetics findings provided an understanding of the influence of a single pyrene exposure in chickens on absorption, metabolism, and elimination. In addition, the $t_{1/2}$ of pyrene in chickens was longer than that of its metabolite, PYOS. The results of the present study indicated a longer $t_{1/2}$ of pyrene than that reported in rats (4.9 h) (Bouchard et al., 1998; Withey et al., 1991). This may have been because pyrene showed persistence in plasma with prolongation of MRT and CL/F. Therefore, pyrene could be accumulated in various tissues and its metabolism may also occur in these tissues (Saengtienchai et al., 2015). Meanwhile, PYOS was produced rapidly and was eliminated with less residue in the chicken body. Moreover, Watanabe et al. (2015) reported that the $t_{1/2}$ of warfarin in chickens was longer than in mammalian species. The results of the present study indicated that xenobiotics seemed to accumulate in bird tissues following a single exposure, which could be sufficient to cause toxicity.

5. Conclusions

In the present study, interspecies differences in xenobiotic metabolism were clarified among bird and mammalian species. Pyrene was readily metabolized with conjugated enzymes from birds upon single exposure, although pyrene itself had a longer elimination half-life in birds than in rats. Moreover, conjugated metabolites, such as PYDOGG and PYDOGS, were first reported in the present study. Further studies are required regarding the bioaccumulation of xenobiotics. This may be related to the decreases in bird populations and may affect the ecosystem in the near future.

Acknowledgments

This work was supported by Grants-in-Aid for Scientific Research from the Ministry of Education, Culture, Sports, Science and Technology of Japan awarded to M. Ishizuka (No. 16H0177906), Y. Ikenaka (15H0282505, 17K2003807), S. Nakayama (16K16197), and the foundations of the JSPS Core to Core Program (AA Science Platforms) and the Bilateral Joint Research Project (PG36150002 and PG36150003). We also acknowledge the financial support of Mitsui & Co., Ltd. Environment Fund, the Sumitomo Foundation for Environmental Research Projects, the Soroptimist Japan Foundation, the Nakajima Foundation, and the Inui Memorial Trust for Research on Animal Science. The authors are grateful to thank Mr. Takahiro Ichise, Ms. Mio Yagihashi, and Ms. Nagisa Hirano for their technical support and input throughout this research.

References

Abou-El-Makaren, M.M., Millburn, P., Smith, R.L., Williams, R.T., 1967. Biliary excretion of foreign compounds: species differences in biliary excretion. Biochem. J. 105, 1289–1293.

Albers, P.H., Hoffman, D.J., Rattner, B.A., Burton, G.A., Cairns, J., 2003. Petroleum and individual polycyclic aromatic hydrocarbons. In: Handbook of Ecotoxicology, second ed. Lewis Publishers, Boca Raton, FL, pp. 341–371 Chapter 14.

Albert, C.A., Wilson, L.K., Mineau, P., Trudeau, S., Elliott, J.E., 2010. Anticoagulant rodenticides in three owl species from Western Canada, 1983–2003. Arch. Environ. Contam. Toxicol. 58, 451–459.

Armstrong, B.G., Hutchinson, E., Unwin, J., Fletcher, T., 2004. Lung cancer risk after exposure to polycyclic aromatic hydrocarbons: a review and meta-analysis. Environ. Health Perspect. 112, 970–978.

Beach, D.G., Quilliam, M.A., Rouleau, C., Croll, R.P., Hellou, J., 2010. Bioaccumulation and biotransformation of pyrene and 1-hydroxypyrene by the marine whelk *Buccinum undatum*. Environ. Toxicol. Chem. 29, 779–788.

Boocock, D.J., Patel, K.R., Faust, G.E.S., Normolle, D.P., Marczylo, T.H., Crowell, J.A., Brenner, D.E., Booth, T.D., Gescher, A., Steward, W.P., 2007. Quantitation of trans-resveratrol and detection of its metabolites in human plasma and urine by high performance liquid chromatography. J. Chromatogr. B 848, 182–187.

Bouchard, M., Krishnan, K., Viau, C., 1998. Kinetics of tissue distribution and elimination of pyrene and 1-hydroxypyrene following intravenous administration of [^{14}C]pyrene in rats. Toxicol. Sci. 46, 11–20.

Bowerman, W.W., Giesy, J.P., Best, D.A., Krame, V.J., 1995. A review of factors affecting

productivity of bald eagles in the Great Lakes Region: implications for recovery. Environ. Health Perspect. 103, 51–59.
Boyland, E., Sims, P., 1964. Metabolism of polycyclic compounds. 23. The metabolism of pyrene in rats and rabbits. Biochem. J. 90, 391–398.
Elliott, J.E., Norstrom, R.J., Keith, J.A., 1988. Organochlorines and eggshell thinning in northern gannets (*Sula bassanus*) from Eastern Canada, 1968–1984. Environ. Pollut. 52, 81–102.
Erickson, W., Urban, D., 2004. Potential Risks of Nine Rodenticides to Birds and Nontarget Mammals: A Comparative Approach. Environmental Protection Agency Office of Prevention, Pesticides and Toxic Substances, Washington, D.C., USA.
Fink-Gremmels, J., 2009. Defense mechanisms against toxic phytochemicals in the diet of domestic animals. Mol. Nutr. Food Res. 54, 249–258.
Hirom, P.C., Millburn, P., Smith, R.L., Williams, R.T., 1972. Species variations in the threshold molecular-weight factor for the biliary excretion of organic anions. Biochem. J. 129, 1071–1077.
Hong, A., Huo, D., Kim, H., Niu, Q., Fackenthal, D., Cummings, S., John, E., West, D., Whittemore, A., Das, S., Ol, Olopade, 2007. UDP-glucuronosyltransferase 1A1 gene polymorphisms and total bilirubin levels in an ethnically diverse cohort of women. Drug Metab. Dispos. 35, 1254–1261.
Ikenaka, Y., Ishizaka, M., Eun, H., Miyabara, Y., 2007. Glucose–sulfate conjugates as a new phase II metabolite formed by aquatic crustaceans. Biochem. Biophys. Res. Commun. 360, 490–495.
Ikenaka, Y., Oguri, M., Saengtienchai, A., Nakayama, S.M.M., Ijiri, S., Ishizuka, M., 2013. Characterization of phase-II conjugation reaction of polycyclic aromatic hydrocarbons in fish species: unique pyrene metabolism and species specificity observed in fish species. Environ. Toxicol. Pharmacol. 36, 567–578.
Jiang, Y.F., Wang, X.T., Wu, M.H., Sheng, G.Y., Fu, J.M., 2011. Contamination, source identification, and risk assessment of polycyclic aromatic hydrocarbons in agricultural soil of Shanghai, China. Environ. Monit. Assess. 183, 139–150.
Kakehi, M., Ikenaka, Y., Nakayama, M.M.S., Kawai, Y., Watanabe, K., Mizukawa, H., Nomiyama, K., Tanabe, S., Ishizuka, M., 2015. Uridine Diphosphate-Glucuronosyltransferase (UGT) xenobiotic metabolizing activity and genetic evolution in pinniped species. Toxicol. Sci. 147, 360–369.
Kanaly, R.A., Harayama, S., 2000. Biodegradation of high-molecular-weight polycyclic aromatic hydrocarbons by bacteria. J. Bacteriol. 182, 2059–2067.
Lowry, O.H., Rosebrough, N.J., Farr, A.L., Randall, R.J., 1951. Protein measurement with the Folin phenol reagent. J. Biol. Chem. 193, 265–275.
Norstrom, R., Hebert, C.E., 2006. Comprehensive re-analysis of archived herring gull eggs reconstructs historical temporal trends in chlorinated hydrocarbon contamination in Lake Ontario and Green Bay, Lake Michigan, 1971–1982. J. Environ. Monit. 8, 835–847.
Omura, T., Sato, R., 1964. The carbon monoxide-binding pigment of liver microsomes. J. Biol. Chem. 239, 2370–2378.
Oroszlany, B., Ikenaka, Y., Saengtienchai, A., Oguri, M., Nakayama, S.M.M., Ishizuka, M., 2013. Metabolism of pyrene, a polycyclic aromatic hydrocarbon in freshwater turtles. Jpn. J. Vet. Res. 61, S62–S63.
Prakash, V., Green, R.E., Pain, D.J., Ranade, S.P., Saravanan, S., Prakash, N., Venkitachalam, R., Cuthbert, R., Rahmani, A.R., Cunningham, A.A., 2007. Recent changes in populations of resident Gyps vultures in India. J. Bombay Nat. Hist. Soc. 104, 129–135.
Saengtienchai, A., Ikenaka, Y., Nakayama, S.M.M., Mizukawa, H., Kakehi, M., Bortey-Sam, N., Darwish, W.S., Tsubota, T., Terasaki, M., Poapolathep, A., Ishizuka, M., 2014. Identification of interspecific differences in phase II reactions: determination of metabolites in the urine of 16 mammalian species exposed to environmental pyrene. Environ. Toxicol. Chem. 33, 2062–2069.
Saengtienchai, A., Ikenaka, Y., Darwish, W.S., Nakayama, S.M.M., Mizukawa, H., Ishizuka, M., 2015. Characterization and tissue distribution of conjugated metabolites of pyrene in the rat. J. Vet. Med. Sci. 77, 1261–1267.
Saengtienchai, A., Ikenaka, Y., Bortey-Sam, N., Jermnark, U., Mizukawa, H., Kawai, Y.K., Nakayama, S.M.M., Ishizuka, M., 2016. The African hedgehog (*Atelerix albiventris*): low phase I and phase II metabolism activities. Comp. Biochem. Physiol. C Toxicol. Pharmacol. 190, 38–47.
Smith, D.J., Giddings, J.M., Feil, V.J., Paulson, G.D., 1995. Identification of ractopamine hydrochloride metabolites excreted in rat bile. Xenobiotica 25, 511–520.
Smith, D.J., Feil, V.J., Paulson, G.D., 2000. Identification of turkey biliary metabolites of ractopamine hydrochloride and the metabolism and distribution of synthetic[14C] ractopamine glucuronides in the turkey. Xenobiotica 30, 427–440.
Ueda, H., Ikenaka, Y., Nakayama, S.M.M., Tanaka-Ueno, T., Ishizuka, M., 2011. Phase-II conjugation ability for PAH metabolism in amphibians: characteristics and interspecies differences. Aquat. Toxicol. 105, 337–343.
Watanabe, K.P., Saengtienchai, A., Tanaka, K.D., Ikenaka, Y., Ishizuka, M., 2010. Comparison of warfarin sensitivity between rat and bird species. Comp. Biochem. Physiol. C Toxicol. Pharmacol. 152, 114–119.
Watanabe, K.P., Kawata, M., Ikenaka, Y., Nakayama, S.M.M., Ishii, C., Darwish, W.S., Saengtienchai, A., Mizukawa, H., Ishizuka, M., 2015. Cytochrome P450-mediared metabolic ability is not a critical determinant of warfarin sensitivity in avian species: in vitro assays in several birds and in vivo assays in chicken. Environ. Toxicol. Chem. 34, 2328–2334.
Withey, J.R., Law, F.C., Endrenyi, L., 1991. Pharmacokinetics and bioavailability of pyrene in the rat. J. Toxicol. Environ. Health 32, 429–447.

Bulletin of Environmental Contamination and Toxicology (2018) 100:672–676
https://doi.org/10.1007/s00128-018-2323-7

Human Health Risk from Consumption of Marine Fish Contaminated with DDT and Its Metabolites in Maputo Bay, Mozambique

L. A. Thompson[1] · Y. Ikenaka[1,2] · Y. B. Yohannes[1,3] · T. Ichise[1] · G. Ito[1] · N. Bortey-Sam[1] · J. J. van Vuren[2] · V. Wepener[2] · N. J. Smit[2] · W. S. Darwish[1,4] · S. M. M. Nakayama[1] · H. Mizukawa[5] · M. Ishizuka[1]

Received: 22 September 2017 / Accepted: 12 March 2018 / Published online: 15 March 2018

Abstract

Many countries with incidence of malaria, including those surrounding Maputo Bay, use dichloro-diphenyl-trichloroethane (DDT) to reduce mosquitoes. This study is the first to estimate the human health risk associated with consumption of marine fish from Maputo Bay contaminated with DDTs. The median for ∑DDTs was 3.8 ng/g ww (maximum 280.9 ng/g ww). The overall hazard ratio for samples was 1.5 at the 75th percentile concentration and 28.2 at the 95th percentile. These calculations show increased potential cancer risks due to contamination by DDTs, data which will help policy makers perform a risk–benefit analysis of DDT use in malaria control programs in the region.

Keywords Marine fish · Contamination · Food safety · Maputo Bay

Some 90% of global malaria cases occur in the African Region, necessitating control measures (WHO 2016). Indoor residual spraying (IRS) with pesticides such as dichloro-diphenyl-trichloroethane (DDT) is commonly used under WHO recommendation to control mosquito vectors in many countries. This pesticide contaminates the environment and is persistent for many years. The ecological risk of DDTs on fish and other wildlife has been common knowledge for over seven decades (Cottam and Higgins 1946). Although the mechanisms of toxicity are still unclear, DDT has now been classed by the International Agency for Research on Cancer as Group 2A, an agent probably carcinogenic to humans (IARC 2017).

Maputo Bay is an important environmental site as water originating from the Phongolo/Maputo River Basin in three countries – Mozambique, Swaziland and South Africa – enters the Indian Ocean here. During the rainy season, mosquito populations and malaria cases increase. Thus DDT is applied annually just before commencement of the rainy summer season (WHO 2016). DDTs are hydrophobic, but travel within waterways either adsorbed to sediment or within biota. Previous studies have confirmed contamination of freshwater fish within the Phongolo flood plain, without significant seasonal variation (Bouwman et al. 1990; McHugh et al. 2011). Despite the use of IRS for malaria control in these countries, there is limited information from literature assessing the impacts on the environment and residents (Blumberg and Frean 2007). The objective of this study was therefore to estimate the human health risk associated with consumption of marine fish from Maputo Bay contaminated with DDT and its metabolites.

✉ M. Ishizuka
ishizum@vetmed.hokudai.ac.jp

1 Laboratory of Toxicology, Department of Environmental Veterinary Sciences, Graduate School of Veterinary Medicine, Hokkaido University, Sapporo, Japan

2 Water Research Group, Unit for Environmental Sciences and Management, North-West University, Potchefstroom, South Africa

3 Department of Chemistry, College of Natural and Computational Science, University of Gondar, Gondar, Ethiopia

4 Food Control Department, Faculty of Veterinary Medicine, Zagazig University, Zagazig, Egypt

5 Department of Environmental Veterinary Sciences, Graduate School of Veterinary Medicine, Hokkaido University, Sapporo, Japan

Materials and Methods

Marine species caught by fishermen in Maputo Bay were purchased from local markets on Inhaca Island, Mozambique (Fig. 1). The species were mainly reef fish, with various dietary behaviours (Heemstra and Heemstra 2004). Samples included: rockcod (*Epinephelus* spp., n = 7), blacktip kingfish (*Caranx heberi*, n = 5), spadefish (*Tripterodon orbis*, n = 4), delagoa threadfin bream (*Nemipterus bipunctatus*, n = 3), blue-lined barenose (*Gymnocranius grandoculis*, n = 2) and great barracuda (*Sphyraena barracuda*, n = 2). Muscle samples were collected from each fish, placed into clean plastic containers, and transported to the Laboratory of Toxicology, Graduate School of Veterinary Medicine, Hokkaido University, Japan. They were stored at − 20°C in a deep freezer until analysis.

DDTs were extracted and analysed using a modified protocol (Yohannes et al. 2013). Approximately 5 g muscle sample was homogenized with anhydrous sodium sulfate, before extraction with hexane:acetone (3:1 *v*/*v*) in

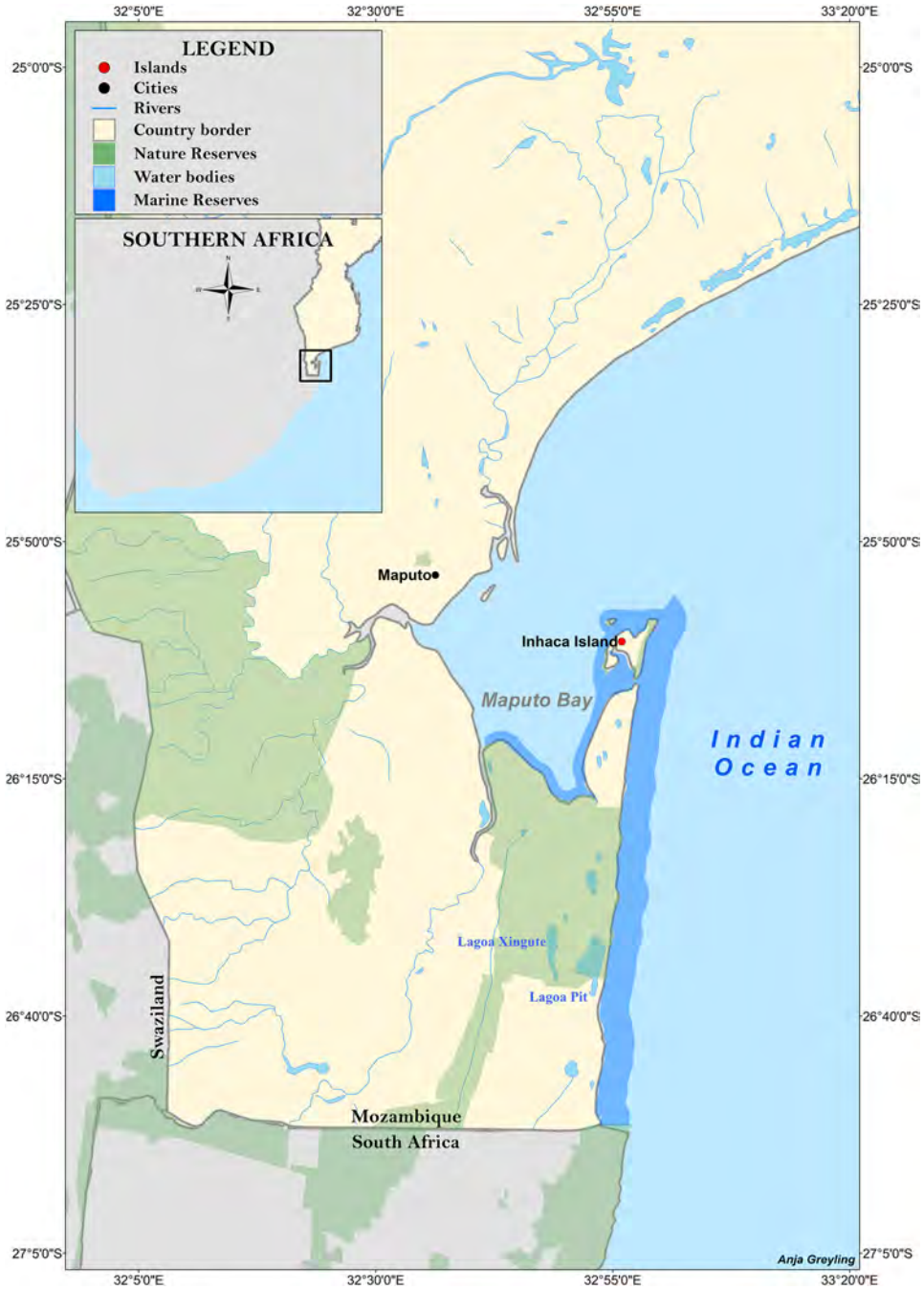

Fig. 1 Map showing Maputo Bay sampling region in southern Mozambique

a Soxhlet extractor (SOX416 macro SOXTHERM unit, Gerhardt, Germany). An aliquot of extract was used for gravimetric lipid determination. The surrogate standard 3,3′,4,4′-tetrachlorobiphenyl (PCB 77) was used to spike the sample; then the extract was concentrated prior to clean-up in a glass column packed with activated florisil and eluted with hexane:dichloromethane (7:3 *v/v*). After further concentration, 2,4,5,6-tetrachloro-*m*-xylene was added as a syringe spike. Final analysis was conducted using a gas-chromatograph with ^{63}Ni electron capture detector (GC-ECD: Shimadzu GC-2014, Kyoto, Japan). Chemical identification in samples was performed by comparison of retention times with those of standards (Dr Ehrenstorfer GmbH, Germany), quantifying concentrations in samples from peak areas compared to the internal standard. Multi-level calibration curves had correction coefficients (R^2) greater than 0.99. Detection limits were between 0.16 and 0.45 ng/g, based on a signal to noise ratio (S/N) of 3:1. In order to assess precision and accuracy, a standard reference material (SRM 1947 Lake Michigan Fish Tissue) was analysed with the same method; recoveries were between 85% and 105% with RSD < 12%.

Potential human health risk from consumption of fish meat was assessed. Using detected concentrations (C, ng/g ww) of DDTs, the estimated daily intake (EDI) was calculated using Eq. (1). DR is the average daily consumption of fish (23.3 g/d), according to published national consumption values (FAO 2013). BW is body weight (kg), set at 60 kg. EDIs were calculated at 25th, 50th, 75th and 95th percentiles of DDT concentrations, expressed as nanogram per kilogram body weight per day (ng/kg/bw/d). Then cancer risk estimates and hazard ratios (HR) were calculated using US EPA guidelines. For an acceptable lifetime cancer risk set at one in a million, i.e. 10^{-6}, the cancer benchmark concentration (CBC) for carcinogenic effects represents the lifetime exposure concentration. A risk level greater than 10^{-4} is considered unacceptable, while the area of concern is set between 10^{-4} and 10^{-6}. The cancer slope factor (CSF) for DDTs is set according to the Integrated Risk Information System (IRIS) database to 0.34 per mg/kg/d (IRIS 1987), and CBC calculated using Eq. (2). The HR for cancer risks was calculated by comparing EDI with CBC [Eq. (3)]. With this definition, an HR of greater than one implies a greater than one in a million lifetime cancer risk (Dougherty et al. 2000).

$$\mathrm{EDI} = (\mathrm{C} \times \mathrm{DR})/\mathrm{BW} \quad (1)$$

$$\mathrm{CBC} = 10^{-6}/\text{slope factor} \quad (2)$$

$$\mathrm{HR} = \mathrm{EDI}/\mathrm{CBC} \quad (3)$$

Statistical analysis was performed using JMP Pro software, Version 12 (SAS Institute). Concentration of DDTs data are shown as median and range values in ng/g wet weight (ww) of tissue.

Results and Discussion

Contamination levels differed among fish species. The median ∑DDTs by species ranged from 2.35 ng/g ww in *T. orbis* to 11.62 ng/g ww in *Epinephelus* spp. (Table 1). The highest value of ∑DDTs detected in an *Epinephelus* sample was 280.91 ng/g ww. Previously it has been shown that biota at higher trophic levels have higher accumulation of DDTs due to bioaccumulation and biomagnification effects (Yohannes et al. 2013). There is a diet overlap in fish analysed for this study (Heemstra and Heemstra 2004). Further fish and environmental samples should be analysed to investigate this relationship in the study area. Considering all samples, the median ∑DDTs was 3.77 ng/g ww. A previous study on freshwater tigerfish (*Hydrocynus vittatus*) from Lake Pongolapoort, which feeds into the Phonogolo River, showed contamination by DDTs of 5400–6000 ng/g lipid weight (Wepener et al. 2012). Although a few (4/23) samples in this study from Maputo Bay exceeded that level of contamination, the median for all fish was 922.7 ng/g lipid weight.

Of the DDT congeners analysed (*o,p′*-DDT, *p,p′*-DDT, *o,p′*-DDE, *p,p′*-DDE, *o,p′*-DDD and *p,p′*-DDD), *o,p′*-DDD was detected in only two fish samples, and *o,p′*-DDE in none. The most common congeners detected were *p,p′*-DDT (in *N. bipunctatus* and *G. grandoculis*), *p,p′*-DDE (*C. heberi, T. orbis* and *S. barracuda*), and *p,p′*-DDD (*Epinephelus* spp.) (Fig. 2). The highest concentration of *p,p′*-DDD, 210.8 ng/g ww, was detected in an *Epinephelus* sp sample. This species is a major predator, and thus relatively higher contamination levels are expected. Based on concentrations, the order of magnitude for abundance of congeners detected is: DDE > DDT > DDD. DDT is rapidly degraded both biotically and abiotically (Boul 1995). DDE is the most common metabolite of DDT detected in many species, and has

Table 1 ∑DDTs (ng/g wet weight) detected in muscle from marine fish in Maputo Bay

Species (n)	Median	Minimum	Maximum
Epinephelus spp. (7)	11.6	ND	280.9
Gymnocranius grandoculis (2)	9.0	6.8	11.2
Sphyraena barracuda (2)	3.3	2.9	3.8
Nemipterus bipunctatus (3)	7.8	1.5	13.0
Caranx heberi (5)	2.4	ND	95.1
Tripterodon orbis (4)	2.4	ND	11.5
All samples (23)	3.8	ND	280.9

n number of samples, *ND* below level of detection

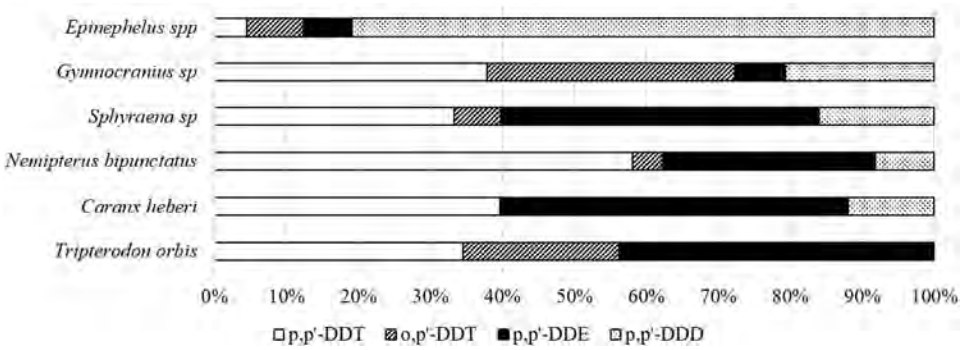

Fig. 2 Relative abundance of DDT congeners in marine fish from Maputo Bay, Mozambique

been linked to toxic side effects including testicular tumors, eggshell thinning, and impaired neurodevelopment (Mrema et al. 2013). The *p,p′*-DDT congener was present in all but two fish samples, and the DDT/DDE ratio greater than one in nine samples, suggesting recent exposure to the parent DDT compound.

When all samples were considered and EDIs calculated, HR greater than one were found above the 75th percentile (HR of 1.5 at 75th and 28.2 at 95th percentile) (Table 2). These equate to 1.5 to 28.2×10^{-4} (1.5–28.2 chances in 10,000 people) risk of cancer associated with consumption of the fish. Calculations for *S. barracuda* alone did not show an increased risk. As expected, the greatest risk was associated with consumption of *Epinephelus* spp. (HR of 1.5 at 50% and 34.9 at 95% percentile, or 1.5–34.9 chances in 10,000 people).

Fish is a very important part of the diet for many local people around Maputo Bay. As contamination and congener profiles vary between fish species, it is necessary to consider not only how much fish is consumed but also the species. All species sampled are fished for consumption, but discussions with Inhaca locals suggested they were more likely to consume smaller fish species. Official reports by parties for the Stockholm Convention show annual use of DDT in 2014 of 12 metric tons of active ingredient applied in Mozambique and 18 metric tons in South Africa. Also not recently reported, independent data sources indicate that DDT has been used in Swaziland (Van Den Berg et al. 2017). Unregulated use of obsolete or illegal stockpiles may occur.

In summary, findings from this study suggest that historical and ongoing use of DDT results in contamination of the environment and biota contained therein. Thus, we investigated concentrations of DDTs in marine fish species in Maputo Bay, Mozambique, and assessed the possible health risk through consumption. Results revealed concentrations of DDTs ranging from ND to 280.9 ng/g ww. Albeit from a small sample size, results confirmed contamination of marine species that are a potential health risk not only for wildlife but also people. Assessment of human health risk from consumption of fish meat shows that people eating *Epinephelus* spp. in particular should be made aware of higher contamination and thus greater potential health risk from regular consumption of this species. This data will help policy makers perform a risk–benefit analysis of DDT use in malaria control programs in the region. Future research should focus on alternatives to DDT use in vector control programs, as well as remediation methods for DDT and its metabolites in the environment and biota.

Table 2 Estimated daily intake values (EDI, ng/kg bw/d) of ∑DDTs in people from consumption of fish sampled, with corresponding cancer risk estimates (HR)

Species	EDI (ng/kg bw/d)				Cancer risk estimates (HR)			
	25th	50th	75th	95th	25th	50th	75th	95th
Epinephelus spp.	0.6	4.5	46.9	102.7	0.2	1.5	16.0	34.9
Gymnocranius grandoculis	3.1	3.5	3.9	4.3	1.0	1.2	1.3	1.4
Sphyraena barracuda	1.2	1.3	1.4	1.4	0.4	0.4	0.5	0.5
Nemipterus bipunctatus	1.8	3.0	4.0	4.9	0.6	1.0	1.4	1.7
Caranx heberi	0.6	0.9	1.7	29.9	0.2	0.3	0.6	10.2
Tripterodon orbis	0.6	0.9	1.9	3.9	0.2	0.3	0.7	1.3
All species	0.7	1.5	4.5	82.9	0.2	0.5	1.5	28.2

Values presented correspond to 25th, 50th, 75th and 95th percentile measured concentrations. An HR value greater than one indicates a potential health risk

Acknowledgements This study was supported by the Leading Program at Hokkaido University and the Japan Society for the Promotion of Science (JSPS KAKENHI Grant Number 16J02013). Also thanks to Grants-in-Aid for Scientific Research from the Ministry of Education, Culture, Sports, Science and Technology of Japan (Nos. 16H0177906, 15H0282505 and 15K1221305), and the foundation of the Soroptimist Japan, the Nakajima, the Sumitomo, and JSPS Core-to-Core Program (AA Science Platforms) and Bilateral Program.

References

[FAO] Food and Agriculture Organization of the United Nations (2013) National Aquaculture Sector Overview: Mozambique. http://www.fao.org/fishery/countrysector/naso_mozambique/en Accessed 1 May 2017

[IARC] International Agency for Research on Cancer (2017) IARC Monographs on the Evaluation of Carcinogenic Risks to Humans, list of classifications, volumes 1-117. International Agency for Research on Cancer. http://monographs.iarc.fr/ENG/Classification/latest_classif.php. Accessed 18 Jan 2017

[IRIS] Integrated Risk Information System (1987) U.S. Environmental Protection Agency. https://cfpub.epa.gov/ncea/iris/iris_documents/documents/subst/ 0147_summary.pdf. Accessed 18 Jan 2016

Blumberg L, Frean J (2007) Malaria control in South Africa-challenges and successes. S Afr Med J 97(11):1193–1197

Boul HL (1995) DDT residues in the environment—a review with a New Zealand perspective. N Z J Agric Res 38(2):257–277

Bouwman H, Coetzee A, Schutte CHJ (1990) Environmental and health implications of DDT-contaminated fish from the Pongolo flood plain. J Afr Zool 104(4):275–286

Cottam C, Higgins E (1946) DDT and its effect on fish and wildlife. J Econ Entom 39(1):44–52

Dougherty CP, Holtz SH, Reinert JC, Panyacosit L, Axelrad DA, Woodruff TJ (2000) Dietary exposures to food contaminants across the United States. Environ Res 84(2):170–185

Heemstra PC, Heemstra E (2004) Coastal fishes of southern Africa. NISC (PTY) LTD, Grahamstown

McHugh KJ, Smit NJ, Van Vuren JHJ, Van Dyk JC, Bervoets L, Covaci A, Wepener V (2011) A histology-based fish health assessment of the tigerfish, *Hydrocynus vittatus* from a DDT-affected area. Phys Chem Earth 36(14):895–904

Mrema EJ, Rubino FM, Brambilla G, Moretto A, Tsatsakis AM, Colosio C (2013) Persistent organochlorinated pesticides and mechanisms of their toxicity. Toxicology 307:74–88

Van Den Berg H, Manuweera G, Konradsen F (2017) Global trends in the production and use of DDT for control of malaria and other vector-borne diseases. Malaria J 16(1):401

Wepener V, Smit N, Covaci A, Dyke S, Bervoets L (2012) Seasonal bioaccumulation of organohalogens in tigerfish, Hydrocynus vittatus Castelnau, from Lake Pongolapoort, South Africa. Bull Environ Contam Toxicol 88(2):277–282

WHO (2016) World Malaria Report 2016. http://apps.who.int/iris/ bitstream/10665/252038/1/9789241511711-eng.pdf?ua = 1. Accessed 19 Jan 2017

Yohannes YB, Ikenaka Y, Nakayama SM, Saengtienchai A, Watanabe K, Ishizuka M (2013) Organochlorine pesticides and heavy metals in fish from Lake Awassa, Ethiopia: insights from stable isotope analysis. Chemosphere 91(6):857–863

A glycomics approach to discover novel renal biomarkers in birds by administration of cisplatin and diclofenac to chickens

C. Ishii,[*] Y. Ikenaka,[*,†] O. Ichii,[‡] S. M. M. Nakayama,[*] S.-I. Nishimura,[§] T. Ohashi,[#] M. Tanaka,[#] H. Mizukawa,[‖] and M. Ishizuka[*,1]

[*]*Laboratory of Toxicology, Department of Environmental Veterinary Sciences, Graduate School of Veterinary Medicine, Hokkaido University, Kita18, Nishi9, Kita-ku, Sapporo, Hokkaido 060–0818, Japan;* [†]*Water Research Group, Unit for Environmental Sciences and Management, North-West University, Potchefstroom, South Africa;* [‡]*Laboratory of Anatomy, Department of Biomedical Sciences, Graduate School of Veterinary Medicine, Hokkaido University, Kita 18-Nishi 9, Kita-ku, Sapporo, Hokkaido 060–0818, Japan;* [§]*Faculty of Advanced Life Science, Hokkaido University, Kita21, Nishi11, Kita-ku, Sapporo, Hokkaido 001–0021, Japan;* [#]*Medicinal Chemistry Pharmaceuticals, Co., Ltd., Corabo-Hokkaido, Kita21 Nishi12, Kita-ku, Sapporo, Hokkaido 001–0021, Japan; and* [‖]*Department of Environmental Veterinary Sciences, Graduate School of Veterinary Medicine, Hokkaido University, Kita 18 Nishi 9, Kita-ku, Sapporo, Hokkaido 060–0818, Japan*

ABSTRACT Avian species have a unique renal structure and abundant blood flow into the kidneys. Although many birds die due to nephrotoxicity caused by chemicals, there are no early biomarkers for renal lesions. Uric acid level in blood, which is generally used as a renal biomarker, is altered when the kidney function is damaged by over 70%. Therefore, early biomarkers for kidney injury in birds are needed. In humans, glycomics has been at the forefront of biological and medical sciences, and glycans are used as biomarkers of diseases, such as carcinoma. In this study, a glycomics approach was used to screen for renal biomarkers in chicken. First, a chicken model of kidney damage was generated by injection of diclofenac or cisplatin, which cause acute interstitial nephritis (AIN) and acute tubular necrosis (ATN), respectively. The nephrotoxicity levels were determined by a blood chemical test and histopathological analysis. The plasma *N*-glycans were then analyzed to discover renal biomarkers in birds. Levels of 14 glycans increased between pre- and post administration in kidney-damaged chickens in the diclofenac group, and some of these glycans had the same presumptive composition as those in human renal carcinoma patients. Glycan levels did not change remarkably in the cisplatin group. It is possible that there are changes in glycan expression due to AIN, but they do not reflect ATN. Although further research is needed in other species of birds, glycans are potentially useful biomarkers for AIN in avian species.

Key words: acute interstitial nephritis, acute tubular necrosis, bird, glycan, renal biomarker

2018 Poultry Science 97:1722–1729
http://dx.doi.org/10.3382/ps/pey016

INTRODUCTION

Avian species have a unique kidney structure with abundant blood flow into the kidneys (Harr, 2002) because of the renal portal veins. This system does not exist in mammals (Lierz, 2003), and the avian kidney is vulnerable to various chemicals from the blood.

Indeed, many birds die due to nephrotoxicity caused by chemicals. In the Indian subcontinent, over 90% of 3 vulture species were killed by the non-steroidal anti-inflammatory drug (**NSAID**), diclofenac (Green et al., 2004; Swan et al., 2006). Diclofenac was used for the medical treatment of cattle, and the drug was accidentally ingested by vultures when they consumed cattle carcasses (Oaks et al., 2004). It has been reported that primary cultures of avian kidney cells were much more susceptible to diclofenac than mammalian cell cultures (Naidoo and Swan, 2009). In addition, other NSAID, such as ketoprofen, cause renal lesions in birds as a side effect (Mohan et al., 2012). Furthermore, lead (**Pb**), mercury (**Hg**), and other therapeutic agents, such as anticancer drugs and antifungal agents, cause renal toxicity in birds (Johnson, 1998; Wolfe et al., 1998; Joseph, 2000; Filippich et al., 2001). In the case of humans, drug-induced kidney injury is a serious problem in clinical practice and accounts for 19 to 26% of cases of acute kidney injury (**AKI**) among hospitalized patients (Hosohata, 2016). In avian species, there have been many reports of renal damage in both wild birds and companion birds.

Received September 4, 2017.
Accepted January 11, 2018.
[1]Corresponding author: ishizum@vetmed.hokudai.ac.jp

The diagnosis of kidney disease in birds is challenging. Generally, uric acid (**UA**) level in blood is used as a renal biomarker in birds. However, UA is not an early biomarker because its levels can be altered when the kidney function is damaged by >70% (Lierz, 2003). The end product of protein metabolism in birds is UA, and because most of the UA in the urine is in an insoluble form, it does not have an osmotic effect (Styles and Phalen, 1998). Furthermore, as most UA is secreted from the proximal tubules and not filtered, blood UA levels will not be affected by moderate changes in the glomerular filtration rate (**GFR**) (Styles and Phalen, 1998). Even in the event of extensive tubular disease, polyuria and resultant polydipsia and the resulting increase in glomerular filtration can maintain UA levels within the normal range. Therefore, UA concentrations may not reflect glomerular disease, and widespread tubular disease also may be present long before UA levels rise above normal. Diagnosis of kidney disease is further complicated in that it is difficult to obtain urine samples from birds because the ureter opens into the cloaca, and the urine is stored in the cloaca or intestine until defecation of a semisolid mixture of urine and feces (Skadhauge, 1968). The level of phosphorus is not changed commonly in all species of birds although the concentration increases due to renal lesions in some avian species (Tully et al., 2009). Therefore, discovery and identification of novel biomarkers for kidney injury in birds are required.

Genomics and proteomics approaches are generally used for the discovery of biomarkers. Glycomics is also a useful tool to identify biomarkers (Adamczyk et al., 2012). Glycosylation is a frequent co-/posttranslational modification of proteins, which modulates a variety of biological functions (Dall'Olio et al., 2013). Glycan structures on newly synthesized glycoproteins are crucial for protein secretion (Moremen et al., 2012). Over 50% of proteins are glycosylated in humans, and the effects of disease states on glycan biosynthesis can be more evident than those on proteins (Adamczyk et al., 2012). It has been reported that glycans in humans may potentially be used as biomarkers of renal carcinoma (Hatakeyama et al., 2014). Therefore, it is possible that glycans would be useful as biomarkers in birds.

The present study was performed to identify novel renal biomarkers in avian species for the conservation and to develop cures for wild birds as well as companion birds. First, a model of kidney damage was generated in chickens by injection of diclofenac or cisplatin, and renal biomarkers were examined. Acute kidney injury includes acute interstitial nephritis (**AIN**) and acute tubular necrosis (**ATN**) (Hosohata, 2016); diclofenac causes AIN, whereas cisplatin causes ATN. Diclofenac caused severe nephrotoxicity in birds as mentioned above, and the anticancer drug, cisplatin, induces renal lesions as a side effect and is used to make models of kidney injury in rats (Pinches et al., 2012). The kidney shows greater accumulation of cisplatin than other organs, and the kidney is the major route for its excretion (Yao et al., 2007). To our knowledge, this is the first study to use glycomics to discover biomarkers in birds. Plasma *N*-glycans in chicken were analyzed by glycoblotting, which can be used for high-throughput analysis of biological samples (Hirose et al., 2011), along with matrix-assisted laser desorption ionization, time-of-flight mass spectrometry (**MALDI-TOF MS**), and they were profiled to discover novel biomarkers for kidney injury in avian species.

MATERIALS AND METHODS

Animal Experiments

All experimental protocols were approved by the Laboratory Animal Care and Use Committee of Graduate School of Veterinary Medicine, Hokkaido University, Japan. The animal experiments were performed in accordance with the Guide for the Care and Use of Laboratory Animals, which conforms to the Association for the Assessment and Accreditation of Laboratory Animal Care International (**AAALAC**) (approval number: 14–0119). The endpoints were weight loss >20% compared to pre-injection, or severe clinical symptoms. Euthanasia was carried out by carbon dioxide inhalation under anesthesia by an overdose of isoflurane (Abbott Laboratories, Chicago, IL) after fasting for over 12 hours. The animals were monitored twice per d during the administration period to check their health. Their body weight was measured from pre-administration to the final d of the experiment. A 27 G needle was used for injection to reduce pain and stress.

Experimental Design

Male white leghorn chickens (*Gallus gallus domesticus*) ($n = 15$, 10 wk old, body weight: 1.2 to 1.4 kg) were purchased from Hokudo Co., Ltd. (Tokyo, Japan) and were housed under conditions of constant temperature (20 ± 2°C) and humidity (40 ± 10%), with a 12:12 h light: dark cycle and given food and water ad libitum. They were allowed to acclimatize to the environment for one wk before commencement of the experiment. Animals were divided into the following 4 groups: (1) control group (injection of 20% DMSO, $n = 3$: Cont. −1, −2, −3); (2) diclofenac sodium group A (1.5 mg/kg body weight, $n = 4$: A-1, -2, -3, -4); (3) diclofenac sodium group B (2.0 mg/kg body weight, $n = 4$: B-1, -2, -3, -4); and (4) cisplatin group (3.5 mg/kg body weight, $n = 4$: C-1, -2, -3, -4). Injection doses were considered according to reference papers of diclofenac treatments (Naidoo et al., 2007; Jain et al., 2009; Mohan et al., 2012) or cisplatin administrations (Cacini and Fink, 1995; Filippich et al., 2001).

Pre-administration plasma was collected one wk after arrival. Administration was started after a further one week. The control group received injection of 20% dimethyl sulfoxide (**DMSO**) (Nacalai Tesque, Kyoto,

Japan) diluted in saline once daily in the morning for 4 consecutive days. The treatment groups received administration of diclofenac sodium diluted in 20% DMSO into the pectoral muscle once daily in the morning for 4 consecutive d, or a single dose of cisplatin (Wako Pure Chemical Industries, Osaka, Japan) diluted in saline into the basilic vein. Control and diclofenac groups were euthanized on d 5 after the first administration, whereas the cisplatin group was euthanized on d 3 because of the endpoint of clinical signs.

Blood Collection

Blood collection (6 mL) from the basilic vein was carried out pre- and post injection in the morning (from 9:00 a.m.) using a 23 G or 24 G needle and heparin-containing syringe. Regarding the post injection, administration was started just after the blood collection. Whole blood was stored on ice after collection, and plasma was prepared by centrifugation within 2 h after collection. Centrifugation was performed at 1630 $\times$ g for 20 min at 4°C. Plasma specimens were immediately frozen in liquid nitrogen and stored at –80°C.

Tissue Sample Collection

Chickens were euthanized with an overdose of isoflurane (Abbott Laboratories) and carbon dioxide. After euthanasia, the kidneys, liver, lungs, and heart were collected. The weights of the whole body, liver, and kidney were measured. The excised tissues were cut into small pieces and stored in 10% neutral buffered formalin for histopathological analysis.

Blood Tests

Aspartate aminotransferase (**AST**), total plasma protein (**TPP**), lactate dehydrogenase (**LDH**), creatine phosphokinase (**CK**), inorganic phosphate (**P**), and calcium (**Ca**) levels were determined using Cobas Ready® (Roche Diagnostics K.K., Basel, Switzerland). The upper detection limit of UA by COBAS is 20 mg/dL, and UA in birds with high degrees of kidney damage exceeds this level. Therefore, UA level was analyzed by high-performance liquid chromatography separation and ultraviolet detection (**HPLC-UV**, 20A series; Shimadzu, Kyoto, Japan). The significance of each test is shown in the Supporting Information (Text S1 in Supporting Information).

For measurement of hematocrit (**Ht**), 200 μL of whole blood was collected from the basilic vein before dissection using a 24 G needle without heparin and immediately moved into tubes containing ethylenediaminetetraacetic acid (**EDTA**). Ht level was measured using a microhematocrit centrifuge (Kubota 3220; Kubota Corporation, Tokyo, Japan) at 15,000 $\times$ g for 5 minutes.

Uric Acid Analysis by HPLC

Analyses were performed by HPLC-UV (20A series; Shimadzu), and the improved HPLC method of the Japan Society of Clinical Chemistry (**JSCC**) was used for measurement of UA. Briefly, 25-μL aliquots of plasma specimens or standard solution were mixed with 225 μL of 0.3 mol/L perchloric acid and cooled on ice for 30 minutes. The samples were mixed again by vortexing and centrifuged at 750 $\times$ g for 10 min at 4°C. Aliquots of 150 μL of the supernatants were collected and centrifuged again at 750 $\times$ g for 10 min at 4°C. Then, 50-μL aliquots of the supernatants were collected and moved to HPLC vials, followed by addition of 50 μL of 10 mM ammonium acetate. For HPLC calibration, 100.3 mg of UA (Wako Pure Chemical Industries) were dissolved in 0.01 mol/L lithium carbonate and made up to 100 mL (1 g/L). Standard solutions (1.25, 2.5, 5, 10, 25, and 50 mg/L) were diluted with deionized distilled water. A UV detector set at 284 nm was used to monitor the effluent. Mobile phase A consisted of 10 mM ammonium acetate (pH 4.8), and phase B consisted of 100% methanol. An Inertsil ODS-3 column (2.1 mm $\times$ 150 mm: GL Sciences, Inc., Tokyo, Japan) was used for separation at a flow rate of 0.2 mL/min, and the injection volume was 5 μL. The R^2 value of the linear regression line was 0.998.

Histopathological Analysis

Paraffin-embedded kidney sections were stained with periodic acid-Schiff, and liver, heart, and lung sections were stained with hematoxylin and eosin.

Glycoblotting-based Plasma Glycomics

Analyses of *N*-glycans were performed according to the methods of Kamiyama et al. (Kamiyama et al., 2013). Plasma specimens were pretreated for release of *N*-glycans and subjected to glycoblotting for enrichment and quantification of *N*-glycans prior to MALDI-TOF/MS. Briefly, pretreatment of plasma glycoproteins was performed to release whole *N*-glycans using PNGase F. Glycans were selectively captured by glycoblotting using BlotGlyco® beads. Methyl esterification of sialic acid residues and transiminization reaction to tag *N*-glycans with benzyloxyamine (**BOA**) were carried out on the beads. BOA-tagged *N*-glycans were subjected to MALDI-TOF/MS analysis. More details regarding pretreatment, glycoblotting, mass spectrometry, and data analysis are presented in S2 Text. Expression levels of each glycan were expressed by the ratio with the plasma mixture of healthy chickens.

Statistical Analysis

To compare the results of biochemical analyses between pre- and post administration, the weight of

Table 1. Plasma concentrations of UA (uric acid), P (inorganic phosphate), Ca (calcium), AST (aspartate aminotransferase), LDH (lactate dehydrogenase), CK (creatine phosphokinase), and TPP (total protein) in diclofenac- or cisplatin-treated and control chickens.

		Pre-injection	24 h	48 h	72 h	96 h
Cont. (n = 3)	UA (mg/dL)	5.0 ± 0.5	3.2 ± 0.3	2.4 ± 1.0	2.7 ± 0.6	2.9 ± 0.6
	P (mg/dL)	7.1 ± 0.5	6.2 ± 0.4	6.4 ± 0.6	6.1 ± 0.0	6.1 ± 0.9
	Ca (mg/dL)	9.7 ± 0.5	9.6 ± 0.5	9.8 ± 0.5	10.1 ± 0.2	10.3 ± 0.5
	AST (IU/L)	132 ± 8	142 ± 5	168 ± 18	164 ± 17	149 ± 18
	LDH (IU/L)	706 ± 358	575 ± 164	639 ± 99	497 ± 48	514 ± 171
	CK (IU/I)	1110 ± 468	844 ± 107 *2	1290 *1	1437 ± 191 *2	514 ± 171
	TPP (g/dL)	2.9 ± 0.1	2.7 ± 0.3	2.9 ± 0.3	2.9 ± 0.3	2.6 ± 0.5
Diclofenac A (1.5 mg/kg, n = 4)	UA (mg/dL)	4.4 ± 1.0	3.7 ± 1.0	3.8 ± 1.2	72.9 ± 117.8	48.8 ± 78.6
	P (mg/dL)	7.5 ± 0.3	6.8 ± 0.7	7.0 ± 0.4	8.1 ± 1.4	8.8 ± 3.2
	Ca (mg/dL)	9.9 ± 0.2	9.7 ± 0.2	9.3 ± 0.1	9.3 ± 0.2	9.1 ± 1.2
	AST (IU/L)	132 ± 5.9	198 ± 10.1	250 ± 16.1	304 ± 69.6	302 ± 88.1
	LDH (IU/L)	433 ± 43	1490 ± 234	1967 ± 639	1710 ± 1002	941 ± 202 *3
	CK (IU/I)	1134 ± 284	>2000	>2000	>2000	>2000
	TPP (g/dL)	3.0 ± 0.3	2.9 ± 0.2	3.1 ± 0.2	3.1 ± 0.2	2.8 ± 0.3
Diclofenac B (2.0 mg/kg, n = 4)	UA (mg/dL)	3.7 ± 0.5	52.6 ± 64.5	74.5 ± 103.9	12.0 ± 6.6 *3	6.7 ± 3.3 *3
	P (mg/dL)	7.9 ± 0.7	7.2 ± 0.8	7.3 ± 0.9 *3	7.9 ± 1.2 *3	6.1 ± 1.1 *3
	Ca (mg/dL)	9.8 ± 0.3	9.7 ± 0.1	9.2 ± 0.6	9.6 ± 0.4 *3	9.5 ± 0.2 *3
	AST (IU/L)	130 ± 14	228 ± 67	287 ± 22	282 ± 12 *3	258 ± 12 *3
	LDH (IU/L)	492 ± 132	1596 ± 672	2437 ± 978 *3	2032 ± 984 *3	985 ± 313 *3
	CK (IU/I)	1340 ± 423	>2000	>2000	>2000	>2000
	TPP (g/dL)	2.9 ± 0.2	2.9 ± 0.3	2.9 ± 0.3	3.1 ± 0.6 *3	2.8 ± 0.4 *3
Cisplatin (3.5 mg/kg, n = 4)	UA (mg/dL)	3.5 ± 0.3	8.0 ± 1.0	77.0 ± 16.2	—	—
	P (mg/dL)	4.7 ± 0.4	6.3 ± 0.2	8.0 ± 1.0	—	—
	Ca (mg/dL)	10.5 ± 0.5	10.9 ± 0.3	11.6 ± 1.5	—	—
	AST (IU/L)	137 ± 8	170 ± 8	246 ± 19	—	—
	LDH (IU/L)	425 ± 74	370 ± 71	870 ± 302	—	—
	CK (IU/I)	870 ± 69	1069 ± 70 *3	1020 ± 169	—	—
	TPP (g/dL)	3.4 ± 0.2	3.8 ± 0.0	3.3 ± 0.6	—	—

*The values were calculated from one chicken*1, 2 chickens*2, or 3 chickens*3, because the others exceeded the detection limit (LDH: 3937 IU/L, CK: 2000 IU/L).

In diclofenac group B, one chicken died on the third d of administration.

There were no significant differences between pre- and post administration (Steel's test, $P < 0.05$).

the body and tissues between controls and treatment groups were analyzed by Steel's test. For comparison of renal damage scores and glycan levels among chickens, data were analyzed using Spearman's rank correlation coefficient. Statistical analyses were performed using JMP Pro 13 (SAS Institute, Cary, NC). In all analyses, $P < 0.05$ was taken to indicate statistical significance.

RESULTS

Clinical Signs

In the diclofenac-treated group, chicken B-1 showed depressed activity and polyuria from the second d of administration and was dead on the third day. Therefore, regarding chicken B-1, blood samples were collected until the third day. Chicken A-1 also showed weakness from the fourth day. All 4 cisplatin-treated chickens had polyuria and depressed activity from the second day. The other chickens generally appeared normal. The control group did not show any symptoms.

Biochemical Analysis

The plasma concentrations of UA, P, Ca, AST, LDH, CK, and TPP as indicators of various tissues are shown in Table 1. The normal UA concentration in chickens ranges from 2.5 to 8.1 mg/dL (Miller and Fowler, 2014). Although there were no significant differences between pre- and post administration in any of the groups, several chickens in the treatment groups showed high levels of UA. In the diclofenac group, chicken A-1 exceeded the normal UA level 72 h after injection. Chickens B-1 and B-2 showed high levels of UA after 24 h, and the level in chicken B-4 increased after 72 hours. However, the UA level in chickens B-2 and B-4 recovered after 96 hours. In the cisplatin group, UA level was high in all chickens 48 h after the injection, and markedly exceeded the reference level. As other indicators of renal lesions, P concentration was also elevated in some of these chickens; the reference level in chicken is 6.2 to 7.9 mg/dL (Miller and Fowler, 2014). Although AST level of chickens in the treatment group increased, the levels were within the normal range for turkeys of 255 to 499 IU/L, and the LDH level exceeded the reference level for turkeys of 420 to 1338 IU/L (Miller and Fowler, 2014).

Gross Pathology

All cisplatin-treated chickens, and chickens A-1, B-1, and B-2 in the diclofenac group showed pale kidneys compared with the controls (Fig. 1). Kidneys in these chickens were enlarged, although there were no significant differences in kidney weight between controls and each exposure group (Table S1). The control group and the other chickens in the treatment groups did not show any gross pathological changes. The liver specimens in all chickens had no lesions, and there were no significant differences in tissue weight (Table S1).

Histopathological Analysis

All cisplatin-treated chickens and 4 diclofenac-treated chickens showed renal damage (Fig. 2). Although they commonly showed degenerative and necrotic lesions in the proximal and distal tubules, and sometimes glomeruli, and the shape of nuclei in the proximal tubules became unclear, the histology was different between diclofenac and cisplatin groups. Diclofenac-treated chickens showed the infiltration of leukocytes such as heterophils in interstitium. In the cisplatin group, necrosis of tubules was shown, and many proteinaceous casts in the tubular lumen also were found. In addition, tubular epithelial cells were detached from the basement membrane of some tubules in chickens A-1 and B-1 in the diclofenac group and all cisplatin-treated chickens. Chickens B-2 and B-4 in the diclofenac group showed mild degenerative lesions, such as slight dilation of proximal and distal tubular lumens. Chickens A-2, A-3, A-4, and B-3 appeared normal.

According to the histopathological changes, renal lesions were given scores from K0 (no lesions) to K5 (most severe). For scoring, the ratio of outer/lumen area at the cross section of tubules was measured using Axiovision Rel 4.8 software (Zeiss, Germany). In addition, 3 stages of histopathological alterations of kidney (Salamat et al., 2014) were used as a reference. Damage scores are as follows: K0, no lesions (the median of outer/lumen area was >10); K1, mild damage, such as infiltration of heterophils and cells in the proximal tubular lumens in a very limited area (the median of outer/lumen area was 8 to 9); K2, moderate damage, such as infiltration of heterophils and cells in proximal tubular lumens, and dilation of distal tubular lumens in a large area (the median of outer/lumen area was 5 to 7); K3, severe damage, such as infiltration of heterophils and cells in the proximal tubular lumens, dilation of tubular lumens, and proteinaceous casts (the median of outer/lumen area was approximately 4); K4, severe damage with unclear structure of renal tubules and glomeruli, and several proteinaceous casts (the median of outer/lumen area was approximately 3); or K5, severe damage with many necrotic cells, and proteinaceous casts (the median of outer/lumen area was 1 to 2, and most tubules were disintegrated). The damage levels of each chicken were as follows: K0 (control); K1 (B-4); K2 (B-2); K3 (C-2); K4 (A-1, C-4); K5 (B-1, C-1, C-3). In the exposure group, chickens A-2, A-3, A-4, and B-3 did not show histopathological changes, and they were ranked K0.

The livers in chicken B-1 and all cisplatin-treated chickens showed mild hyperemia (Fig. S1). There were no lesions in the heart or lung in any of the chickens, and the control group did not show histopathological changes in any tissues.

Glycomics Analysis

For glycomics analysis, 10 chickens (Cont.-1, -2, A-1, B-1, B-2, B-4, C-1, -2, -3, and -4) were selected according to the results of histopathological analysis and biochemical analysis, and plasma *N*-glycans were measured. A total of 40 plasma *N*-glycans were detected, and the levels of each glycan are shown by the ratio with glycan expression of plasma mix from the controls and pre-injection chickens (Table S2). The control group did not show any significant differences due to injection. Fourteen glycans were increased in the diclofenac-treated kidney damaged chickens (Fig. 3, Table S3).

In the cisplatin group, glycan levels did not change significantly according to kidney injury, although the renal lesions were severe, and UA concentrations were high.

DISCUSSION

In the present study, we succeeded to cause various stages of nephrotoxicity in chickens after cisplatin (3.5 mg/kg) or 2 doses of diclofenac (1.5 to 2.0 mg/kg) treatments. The results of biochemical analyses indicated that UA, P, and LDH levels exceeded the respective normal ranges in several chickens. Both UA and P indicate severe renal lesions in chickens, but UA level was altered earlier than P level. According to the UA level, kidney function in the cisplatin group (C-1, -2, -3, and -4) would be markedly damaged 48 h after injection. In the diclofenac group, chicken A-1 had severe renal injury from 72 h after injection. The kidneys of chickens B-1 and B-2 were impaired with heavy renal failure after 24 h, and chicken B-1 died due to nephrotoxicity. Although LDH level increased in the treatment groups, it was difficult to identify the cause, because elevation of LDH is nonspecific, and is found in skeletal and cardiac muscle, liver, kidney, bone, and erythrocytes (Tully et al., 2009).

Histopathological analysis of the kidney, liver, heart, and lung showed that chickens A-1, B-1, B-2, and B-4 and all cisplatin-treated chickens had damage almost specific to the kidney. Furthermore, the histology of the kidney might indicate that diclofenac caused AIN and cisplatin induced ATN in chicken, although the infiltration of leukocytes in interstitial in diclofenac-treated chickens was not so severe compared to AIN in humans. In the case of diclofenac exposure, renal

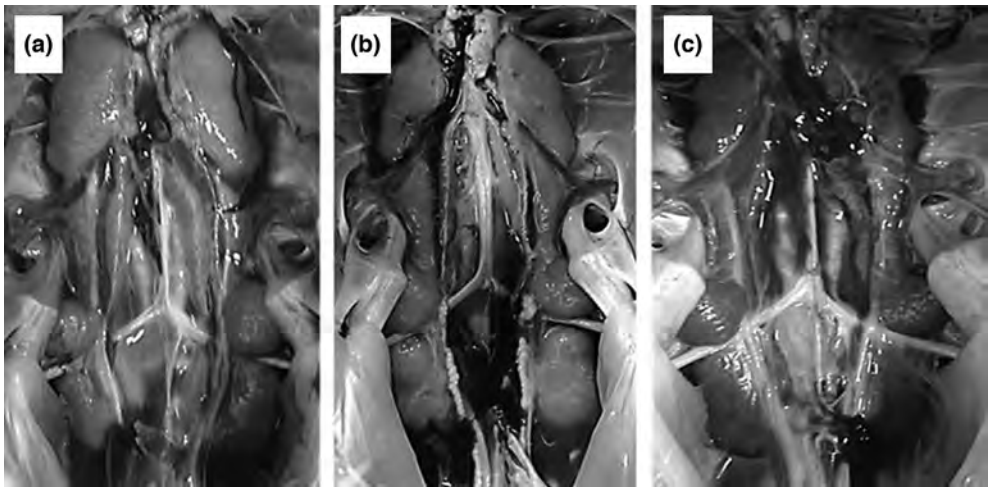

Figure 1. Gross pathological features of kidneys in diclofenac- or cisplatin-treated and control chickens. The chickens treated with diclofenac (a) or cisplatin (b) showed pale and enlarged kidneys compared with the controls (c). The kidney weights are shown in Table S2.

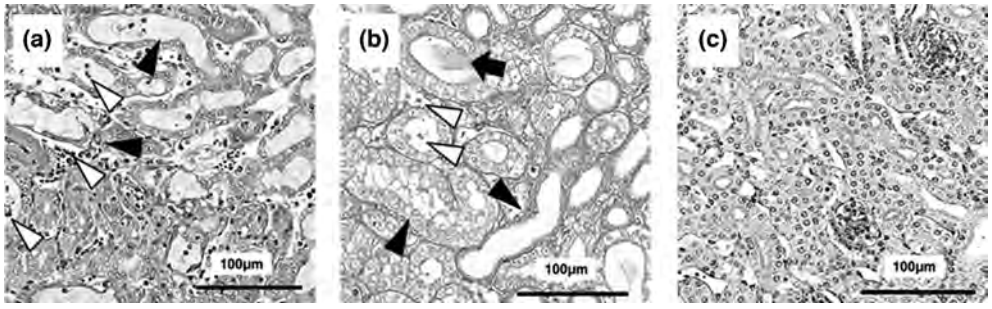

Figure 2. Histopathological features of the kidneys in diclofenac- or cisplatin-treated and control chickens. Chickens treated with diclofenac (a) or cisplatin (b) showed severe renal lesions compared with controls (c). Briefly, there were degenerative and necrotic lesions, such as proteinaceous casts (arrowheads), heterophil infiltration into the tubulointerstitium and dead cells in the proximal tubular lumens (white arrows), and dilation of proximal and distal tubular lumens (black arrows). Diclofenac-treated chickens showed much infiltration of heterophils, and cisplatin-treated chickens had a large number of proteinaceous casts. The controls showed normal renal structures.

damage levels were completely different depending on the individual, and this tendency also was described in the reports mentioned above. There may be large differences in sensitivity even within a species. Therefore, the renal damage was shown by scores for comparison with other analyses.

Glycomics analysis showed that a high degree of kidney damage was associated with increased levels of both sialylated and non-fucosylated glycans in diclofenac-treated chickens. Although not applicable to 6 glycans (No. 9, 22, 24, 26, 34, and 37), this tendency was seen for the remaining 34 glycans. The synthesis pathway of *N*-linked glycans starts from the cytosolic surface of the endoplasmic reticulum membrane by addition of sugars, and in the early secretory pathway, the glycans have important roles in protein folding, oligomerization, quality control, sorting, and transport (Helenius and Aebi, 2001). The glycans acquire more complex structures and new functions in the Golgi complex (Helenius and Aebi, 2001). The *trans* compartment elaborates additional branching and capping reactions on complex *N*-glycans, and capping reactions are continued in the *trans*-Golgi network (Moremen et al., 2012). Therefore, the final synthesis pathway, where sialic acids are attached, could be disturbed, or glycoproteins that have these glycans may be susceptible to the effects of kidney injury.

In cisplatin-treated chickens, there is no relation between glycan expression and kidney damage. Therefore, the glycans that increased in the diclofenac group may indicate the effects of diclofenac injection, rather than kidney injury itself. Another possibility is that glycans may have reflected parts of kidney injury, and not all types of renal damage.

With regard to AIN and ATN, although the mechanism underlying AIN is underestimated even in humans, it is generally accepted that the pathogenesis is based on an immunologic reaction against endogenous nephritogenic antigens or exogenous antigens processed by tubular cells, with cell-mediated immunity having a major pathogenic role (Praga and González, 2010). In avian species, there is less information. However, it is reported that diclofenac causes nephrotoxicity due to reduction of UA transport by interfering with p-aminohippuric acid (**PAH**) channels in the chicken (Naidoo and Swan, 2009). The mechanism of diclofenac-induced renal failure in oriental white-backed vultures has been proposed to be through

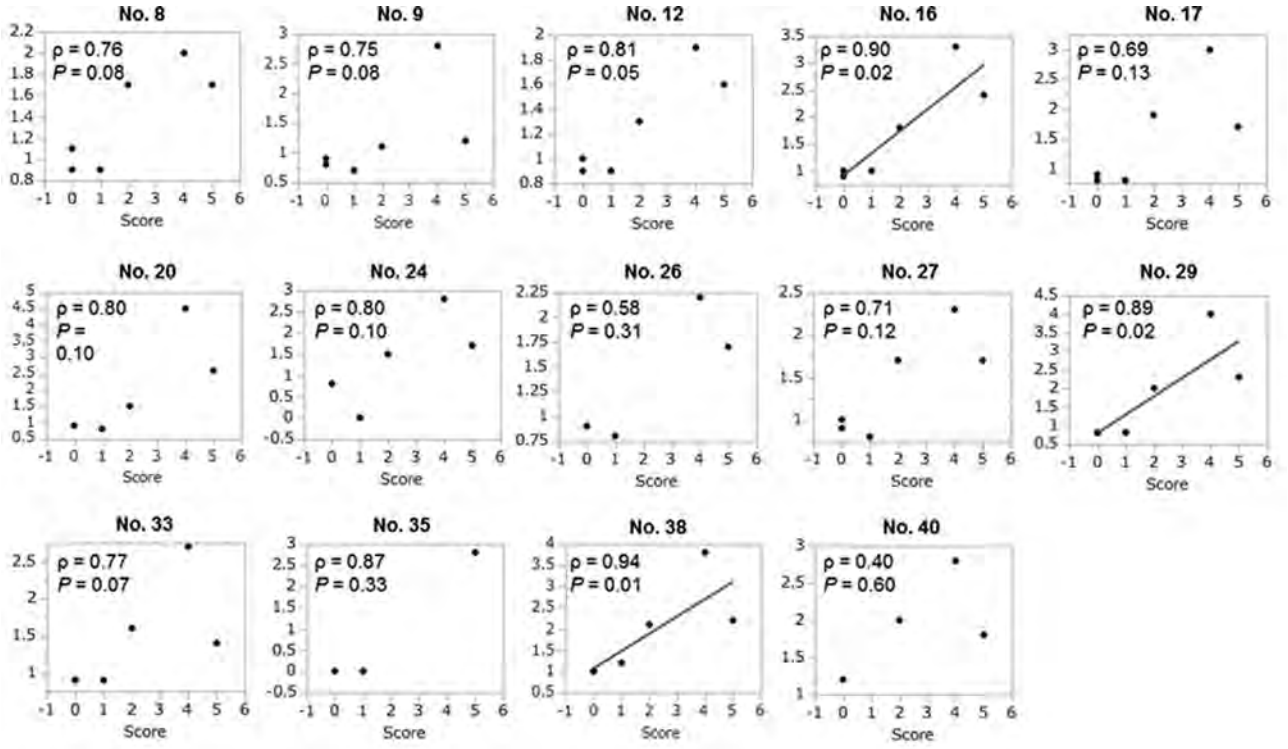

Figure 3. Spearman's rank correlation coefficients of expression levels for 14 increased *N*-glycans (μM) on the final d and renal damage score in the diclofenac-treated group. No. 16, 29, and 38 had significant correlation, and lines show the linear approximation.

inhibition of the modulating effect of prostaglandin on angiotensin II-mediated adrenergic stimulation (Jain et al., 2009). Cisplatin induces DNA damage, either necrotic or apoptotic cell death, formation of reactive oxygen species, mitochondrial dysfunction, and caspase activation (Ramesh and Reeves, 2002). These events cause both acute and chronic kidney injury, and the nephrotoxicity is characterized by activation of both proinflammatory cytokines and chemokines (Havasi and Borkan, 2016).

The mechanisms of metabolism of diclofenac and cisplatin are different. Therefore, it is possible that glycans reflect the limited pathway of kidney injury, and glycan expression profiles change due to AIN but do not reflect ATN. Although further studies including investigation of species differences are needed, glycans have the potential to be useful biomarkers for AIN in avian species. The glycan expression profile may reflect some types of kidney injury, and these molecules have the potential for use as biomarkers for the evaluation of functional disorders in birds.

SUPPLEMENTARY DATA

Supplementary data are available at *Poultry Science* online.

Figure S1. Histopathological features of the liver in diclofenac- or cisplatin-treated and control chickens.
Table S1. Weights of the body, liver, and kidney after exposure in chickens
Table S2. Ratios of all detected *N*-glycans (μM) on the final day/pre-administration
Table S3. Ratios of increased *N*-glycans (μM) on the final day/pre-administration in diclofenac-treated group

ACKNOWLEDGMENTS

This work was supported by Grants-in-Aid for Scientific Research from the Ministry of Education, Culture, Sports, Science, and Technology of Japan awarded to M. Ishizuka (No. 16H0177907), Y. Ikenaka (No. 26304043, 15H0282505, 15K1221305), S. Nakayama (16K16197), and the foundations of Sumitomo and JSPS Core to Core Program (AA Science Platforms) and Bilateral Joint Research Project (PG36150002 and PG36150003). We also acknowledge the financial support by the Nihon Seimei Foundation, the Soroptimist Japan Foundation, the Nakajima Foundation, and the Inui Memorial Trust for Research on Animal Science. One of the authors (C. Ishii) is a Research Fellow of the Japan Society for the Promotion of Science (No. 15J01937). This research was also supported by JST/JICA, SATREPS (Science and Technology Research Partnership for Sustainable Development). We are grateful to Takahiro Ichise, So Shinya, Kazuki Takeda, Ayuko Morita, Misaki Maehara, Takamitsu Kondo, Masao Togao, Kodai Motohira, Mio Yagihashi, and Nagisa Hirano (Graduate School of Veterinary Medicine, Hokkaido University) for their technical support. The English in this manuscript was proofread by the Dolphin Corporation.

REFERENCES

Adamczyk, B., T. Tharmalingam, and P. M. Rudd. 2012. Glycans as cancer biomarkers. Biochim. Biophys. Acta (BBA)-General Subj. 1820:1347–1353.

Cacini, W., and I. M. Fink. 1995. Toxicity and excretion of cisplatin in the avian kidney. Comp. Biochem. Physiol. Part C Pharmacol. Toxicol. Endocrinol. 111:343–350.

Dall'Olio, F., V. Vanhooren, C. C. Chen, P. E. Slagboom, M. Wuhrer, and C. Franceschi. 2013. N-glycomic biomarkers of biological aging and longevity: A link with inflammaging. Ageing Res. Rev. 12:685–698.

Filippich, L. J., A. M. Bucher, B. G. Charles, and R. H. Sutton. 2001. Intravenous cisplatin administration in sulphur-crested cockatoos (Cacatua galerita): Clinical and pathologic observations. J. Avian Med. Surg. 15:23–30.

Green, R. E., I. A. N. Newton, S. Shultz, A. A. Cunningham, M. Gilbert, D. J. Pain, and V. Prakash. 2004. Diclofenac poisoning as a cause of vulture population declines across the Indian subcontinent. J. Appl. Ecol. 41:793–800.

Harr, K. E. 2002. Clinical chemistry of companion avian species: A review. Vet. Clin. Pathol. 31:140–151.

Hatakeyama, S., M. Amano, Y. Tobisawa, T. Yoneyama, N. Tsuchiya, T. Habuchi, S.-I. Nishimura, and C. Ohyama. 2014. Serum N-glycan alteration associated with renal cell carcinoma detected by high throughput glycan analysis. J. Urol. 191:805–813.

Havasi, A., and S. C. Borkan. 2016. Apoptosis and acute kidney injury. Kidney Int. 80:29–40 Available at http://dx.doi.org/10.1038/ki.2011.120.

Helenius, A., and M. Aebi. 2001. Intracellular functions of N-ninked glycans. Sci. 291:2364–2369 Available at http://www.sciencemag.org/content/291/5512/2364.abstract.

Hirose, K., M. Amano, R. Hashimoto, Y. C. Lee, and S.-I. Nishimura. 2011. Insight into glycan diversity and evolutionary lineage based on comparative avio-N-glycomics and sialic acid analysis of 88 egg whites of Galloanserae. Biochemistry 50:4757–4774.

Hosohata, K. 2016. Role of oxidative stress in drug-induced kidney injury. Int. J. Mol. Sci. 17:1826.

Jain, T., K. M. Koley, V. P. Vadlamudi, R. C. Ghosh, S. Roy, S. Tiwari, and U. Sahu. 2009. Diclofenac-induced biochemical and histopathological changes in white leghorn birds (Gallus domesticus). Indian J. Pharmacol. 41:237–241 Available at http://www.ncbi.nlm.nih.gov/pmc/articles/PMC2812785/.

Johnson, F. M. 1998. The genetic effects of environmental lead. Mutat. Res. Mutat. Res. 410:123–140.

Joseph, V. 2000. Aspergillosis in raptors. Pages 66–74 in Seminars in avian and exotic pet medicine. Elsevier.

Kamiyama, T., H. Yokoo, J. Furukawa, M. Kurogochi, T. Togashi, N. Miura, K. Nakanishi, H. Kamachi, T. Kakisaka, and Y. Tsuruga. 2013. Identification of novel serum biomarkers of hepatocellular carcinoma using glycomic analysis. Hepatology 57: 2314–2325.

Lierz, M. 2003. Avian renal disease: Pathogenesis, diagnosis, and therapy. Vet. Clin. North Am. Exot. Anim. Pract. 6: 29–55.

Miller, R. E., and M. E. Fowler. 2014. Fowler's zoo and wild animal medicine. Elsevier Health Sciences.

Mohan, K., K. Jayakumar, H. D. Narayanaswamy, M. Manafi, and B. H. Pavithra. 2012. An initial safety assessment of hepatotoxic and nephrotoxic potential of intramuscular ketoprofen at single repetitive dose level in broiler chickens. Poult. Sci. 91:1308–1314.

Moremen, K. W., M. Tiemeyer, and A. V Nairn. 2012. Vertebrate protein glycosylation: Diversity, synthesis and function. Nat Rev Mol Cell Biol 13:448–462 Available at http://dx.doi.org/10.1038/nrm3383.

Naidoo, V., N. Duncan, L. Bekker, and G. Swan. 2007. Validating the domestic fowl as a model to investigate the pathophysiology of diclofenac in Gyps vultures. Environ. Toxicol. Pharmacol. 24:260–266.

Naidoo, V., and G. E. Swan. 2009. Diclofenac toxicity in Gyps vulture is associated with decreased uric acid excretion and not renal portal vasoconstriction. Comp. Biochem. Physiol. Part C Toxicol. Pharmacol. 149:269–274.

Oaks, J. L., M. Gilbert, M. Z. Virani, R. T. Watson, C. U. Meteyer, B. A. Rideout, H. L. Shivaprasad, S. Ahmed, M. J. Iqbal Chaudhry, M. Arshad, S. Mahmood, A. Ali, and A. Ahmed Khan. 2004. Diclofenac residues as the cause of vulture population decline in Pakistan. Nature 427:630–633 Available at http://dx.doi.org/10.1038/nature02317.

Pinches, M., C. Betts, S. Bickerton, L. Burdett, H. Thomas, N. Derbyshire, H. B. Jones, and M. Moores. 2012. Evaluation of novel renal biomarkers with a cisplatin model of kidney injury: Gender and dosage differences. Toxicol. Pathol. 40: 522–533.

Praga, M., and E. González. 2010. Acute interstitial nephritis. Kidney Int. 77:956–961.

Ramesh, G., and W. B. Reeves. 2002. TNF-α mediates chemokine and cytokine expression and renal injury in cisplatin nephrotoxicity. J. Clin. Invest. 110:835–842 Available at https://doi.org/10.1172/JCI15606.

Salamat, N., E. Etemadi-Deylami, A. Movahedinia, and Y. Mohammadi. 2014. Heavy metals in selected tissues and histopathological changes in liver and kidney of common moorhen (Gallinula chloropus) from Anzali Wetland, the south Caspian Sea, Iran. Ecotoxicol. Environ. Saf. 110:298–307.

Skadhauge, E. 1968. The cloacal storage of urine in the rooster. Comp. Biochem. Physiol. 24:7–18.

Styles, D. K., and D. N. Phalen. 1998. Clinical avian urology. Pages 104–113 in Seminars in avian and exotic pet medicine. Elsevier.

Swan, G. E., R. Cuthbert, M. Quevedo, R. E. Green, D. J. Pain, P. Bartels, A. A. Cunningham, N. Duncan, A. A. Meharg, and J. L. Oaks. 2006. Toxicity of diclofenac to Gyps vultures. Biol. Lett. 2:279–282.

Tully, T. N., G. M. Dorrestein, and A. K. Jones. 2009. Handbook of Avian Medicine. Elsevier/Saunders.

Wolfe, M. F., S. Schwarzbach, and R. A. Sulaiman. 1998. Effects of mercury on wildlife: A comprehensive review. Environ. Toxicol. Chem. 17:146–160 Available at http://dx.doi.org/10.1002/etc.5620170203.

Yao, X., K. Panichpisal, and N. Kurtzman 2007. Cisplatin nephrotoxicity: A review. Am J Med Sci 334:115–124.

Science of the Total Environment 628–629 (2018) 517–527

Contents lists available at ScienceDirect

Science of the Total Environment

journal homepage: www.elsevier.com/locate/scitotenv

Fish consumption from urban impoundments: What are the health risks associated with DDTs and other organochlorine pesticides in fish to township residents of a major inland city

Wihan Pheiffer [a,*], Nico J. Wolmarans [a], Ruan Gerber [a], Yared B. Yohannes [b,c], Yoshinori Ikenaka [a,b], Mayumi Ishizuka [b], Nico J. Smit [a], Victor Wepener [a], Rialet Pieters [a]

[a] Water Research Group, Unit for Environmental Science and Management, North-West University, Private Bag X6001, Potchefstroom 2520, South Africa
[b] Laboratory of Toxicology, Department of Environmental Veterinary Science, Faculty of Veterinary Medicine, Hokkaido University, Kita 18, Nishi 9, Kita ku, Sapporo 060–0818, Japan
[c] Department of Chemistry, College of Natural and Computational Science, University of Gondar, P.O. Box 196, Gondar, Ethiopia

HIGHLIGHTS

- Organochlorine pesticides (OCPs) found in urban area
- *Clarias gariepinus* accumulated OCPs in muscle tissue.
- The cancer risk associated with consumption was greater than acceptable levels.
- Non-cancerous risk was up to a 1000 times that what is considered safe.

GRAPHICAL ABSTRACT

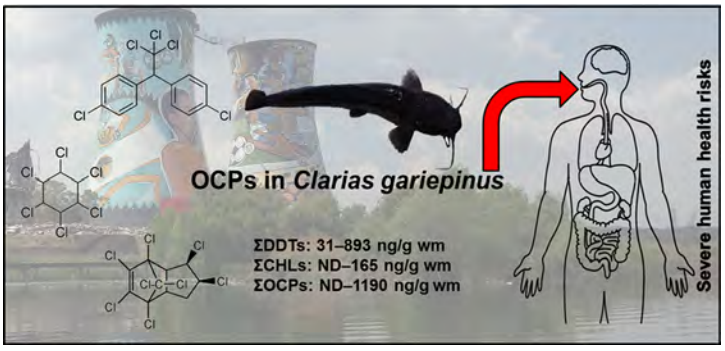

ARTICLE INFO

Article history:
Received 10 November 2017
Received in revised form 1 February 2018
Accepted 7 February 2018
Available online 13 February 2018

Editor: Adrian Covaci

Keywords:
Chlordane
Clarias gariepinus
DDT
Human health risk
Soweto

ABSTRACT

Organochlorine pesticides (OCPs) in South Africa have for the most part been banned, except dichlorodiphenyltrichloroethane (DDT) which is still used as malaria vector control. The aim of this study was to determine OCP residues in the aquatic fauna of one of South Africa's most populated areas, Soweto. Risk to human health through OCP exposure via fish consumption was investigated. *Clarias gariepinus* was chosen as bioindicator because it is an apex predator that is in abundance, but is also a valued food source. Dichlorodiphenyltrichloroethanes (DDTs), hexachlorocyclohexanes (HCHs), and chlordanes (CHLs) were detected in the fish tissue with the DDTs being the most prevalent at all sites. Of the three locations, Fleurhof, Orlando, and Lenasia, the latter location's fish had the highest ΣOCP load, ranging between 81 and 1190 ng/g wm. The DDTs were determined to be from historic use, whereas the CHL levels indicated more recent inputs. Although the possibility of illegal use cannot be excluded completely, the presence of OCPs outside of their allowed areas of use indicate that these compounds not only stay in the aquatic systems long term, but may be of concern in areas previously not considered high risk areas. The OCP residues in *C. gariepinus* from the study area pose an extremely high risk to human health when consumed, and has a cancer risk as high as 1 in 10. This potential problem should be kept in consideration when developing national health and conservation strategies.

* Corresponding author.
E-mail address: wihan.pheiffer@nwu.ac.za (W. Pheiffer).

https://doi.org/10.1016/j.scitotenv.2018.02.075
0048-9697/

1. Introduction

The unregulated use of organochlorine pesticides (OCPs) in South Africa was banned in 2002 as per the Stockholm Convention (Bouwman, 2004). However the ban on one of these, namely DDT (dichlorodiphenyltrichloroethane), was lifted for the use of malaria vector control (MVC) by indoor residual spraying (IRS), under strict legislation, overseen by provincial government. A detailed overview on malaria vector control in South Africa is described by Brooke et al. (2013). There have been an increasing number of reports on the accumulation of DDT and other organochlorine pesticides (OCPs) in the aquatic wildlife (Barnhoorn et al., 2009; Gerber et al., 2016; Viljoen et al., 2016). Aquatic ecosystems are especially at risk as most OCPs are more stable in sediments, therefore increasing its persistence (Doong et al., 2002; Yohannes et al., 2013a). OCPs are transferred from the sediment via different mechanisms into aquatic organisms and magnify up the food chain (Van der Oost et al., 2003). High bioaccumulation of these OCPs have been reported in aquatic predators at the top of the food chain, such as the tigerfish (*Hydrocynus vittatus* Castelnau, 1861) (McHugh et al., 2011; Wepener et al., 2012; Gerber et al., 2016) and sharptooth catfish (*Clarias gariepinus* (Burchell, 1822)) (Barnhoorn et al., 2009, 2015). These aforementioned studies were all in subtropical areas of South Africa, where spraying of DDT for MVC is still allowed and results showed very high concentrations of not only DDTs, but also various other banned OCPs, such as chlordane and HCHs, in the tissues of these species. The study areas were of a rural nature and included important conservation areas and their surroundings with low human population densities. In the present study we determined the levels of OCPs in aquatic organisms in ecosystems within surrounding densely populated areas of South Africa. The demographic includes many unemployed people that rely on subsistence fishing to supplement their diet.

The study area is in the urban area of Soweto (South Western Townships), one of South Africa's most densely populated areas (6400 people/km^2) (StatsSA, 2011). Soweto is found south west of the city of Johannesburg and is South Africa's largest township with a high unemployment rate with some people reliant on subsistence fishing as a means of obtaining food. There is no direct spraying of OCPs, particularly DDT in this area. However, the fact that long range air transport of OCPs is well documented (Gong et al., 2015; Pozo et al., 2006), it could potentially result in the exposure of this region to these persistent pollutants. The study area is also relatively close to sources where OCPs were manufactured in the past. The production of DDT and other OCPs in Gauteng occurred in the Wadeville and Chloorkop areas, and in the neighbouring North West province, at the town of Brits (DEA, 2011). These locations are approximately 35 (east), 40 (north east) and 75 km (north) from the selected study area, respectively. Manufacturing of various OCPs, such as lindane, heptachlor, aldrin, dieldrin, endrin and DDT was discontinued in South Africa in the 1980s and the formulation of DDT in 2010 (DEA, 2011). In addition, a study of the middle Vaal River, into which our study area drains, reported surprisingly high levels of OCPs in fish species (Wepener et al., 2011).

Clarias gariepinus was chosen as an indicator species because it is abundant in South Africa, it is resilient, it is the apex aquatic predator in the sampling area, and most importantly, is a valued food source (Rouhani and Britz, 2011). They are targeted by local fishermen not only in rural areas but are specifically targeted by fisherman in the study area (personal communication: W Pheiffer). Their position on the food web and preference for bottom dwelling in the aquatic systems makes it ideal to study exposure to pollutants, as well as the bioaccumulation and bio-magnification of organic chemical pollutants, allowing for investigation into possible transfer of pollutants to humans.

The aim of this study was to determine DDT and other OCP residues in *C. gariepinus* muscle tissue from impoundments in the urban area of Soweto, South Africa post the cessation of use and formulation. These findings are compared to other African studies on *C. gariepinus* or relevant apex predators. This paper most importantly investigates the potential risk posed to health of the local human population through consumption of OCP contaminated *C. gariepinus*.

2. Materials and methods

2.1. Study area and sampling

Clarias gariepinus was sampled during Austral summer (October) of 2013 from three impoundments in the upper Klip River catchment (Fig. 1) in Soweto and Lenasia. The Klip River drains the Witwatersrand area in the Gauteng province of South Africa. It is the largest tributary of the Vaal River. These rivers together supply >12 million people of potable water in Gauteng (DWAS, 2004). Fleurhof Dam (26°12′03.49″S 27°54′31.87″E) is the most northern site, representing the upper region of the study area. Orlando Dam (26°15′21.63″S 27°55′18.97″E) is located in the centre of Soweto, and Lenasia Dam (26°18′8.33″S 27°50′10.8″E) is located in the southern stretches of the Klip River. The fish were caught using fyke and gill nets (110 mm mesh). Nets were left in for 5 h and checked periodically every half hour. Fish weighing less than 1 kg were released. Following capture, fish were euthanized by severing the spinal cord behind the head (NWU Ethics approval: AREC-130913-015). The mass (g) and standard length (SL; mm) of each fish were recorded. Epaxial muscle samples were removed, placed in pre-cleaned (acetone/hexane) aluminium foil, and kept frozen at −20 °C. Epaxial muscle was selected for consistency in sampling between specimens and because the epaxial muscle is the part of the fish primarily consumed by humans. For comparative purposes a group of ten fish from the Mooi River system in the North West province (part of different catchment as the study area) were depurated for half a year at the Water Research Group's aquarium at the North-West University (Potchefstroom Campus). Fish were kept under standard aquarium conditions (CCAC, 2005). These reference fish were processed in the same manner as the experimental fish.

2.2. Organochlorine pesticide determination

2.2.1. Materials

An OCP standard reference mixture (all isomers of chlordane and nonachlor, oxychlordane (collectively CHLs); all isomers of DDT, DDD and DDE (collectively DDTs; group referred to as DDx when DDT is excluded); dieldrin, endrin and aldrin (collectively drins); hexachlorobenzene (HCB); hexachlorocyclohexanes (α-, β-, γ-, δ-isomers, collectively HCHs); and all isomers of heptachlor and heptachlor-epoxide (collectively heptachlors)) were obtained from Dr. Ehrenstorfer GmbH (Germany). Analytical grade organic solvents (acetone, hexane, and dichloromethane), and anhydrous sodium sulphate (pesticide residue and PCB analysis grade) were obtained from Kanto Chemical Corp. (Tokyo, Japan). Florisil (60–100 mesh) from Kanto Chemical Corp. (Tokyo, Japan) was activated in an oven at 180 °C for 8 h.

2.2.2. Extraction of OCPs in muscle

Analysis of OCPs in muscle samples followed an adapted version of the method by Yohannes et al. (2013b). Sample (10 g wet mass; wm) was homogenized with anhydrous sodium sulphate and placed in pre-cleaned (acetone/hexane) cellulose extraction thimbles. Samples were spiked with PCB#77 as internal standard. Extraction was carried out with 150 mL hexane:acetone (3:1 v/v) for 6 h using a Soxtherm (S306AK Automatic Extractor, Gerhardt, Germany). Extracts were concentrated to approximately 2 mL using a rotary evaporator and diluted to 10 mL with hexane. Lipid content was determined gravimetrically using an air dried 10% aliquot of the extract. The remaining extract after concentrated to 5 mL was passed through gel permeation chromatography columns (Waka Gel Bio-Rad) with dichloromethane (DCM): hexane (1:1 v/v) as mobile phase, collecting only the fraction containing the OCPs. The fraction collected was concentrated and cleaned-up on a glass column packed with 6 g 5% activated Florisil, and eluted with

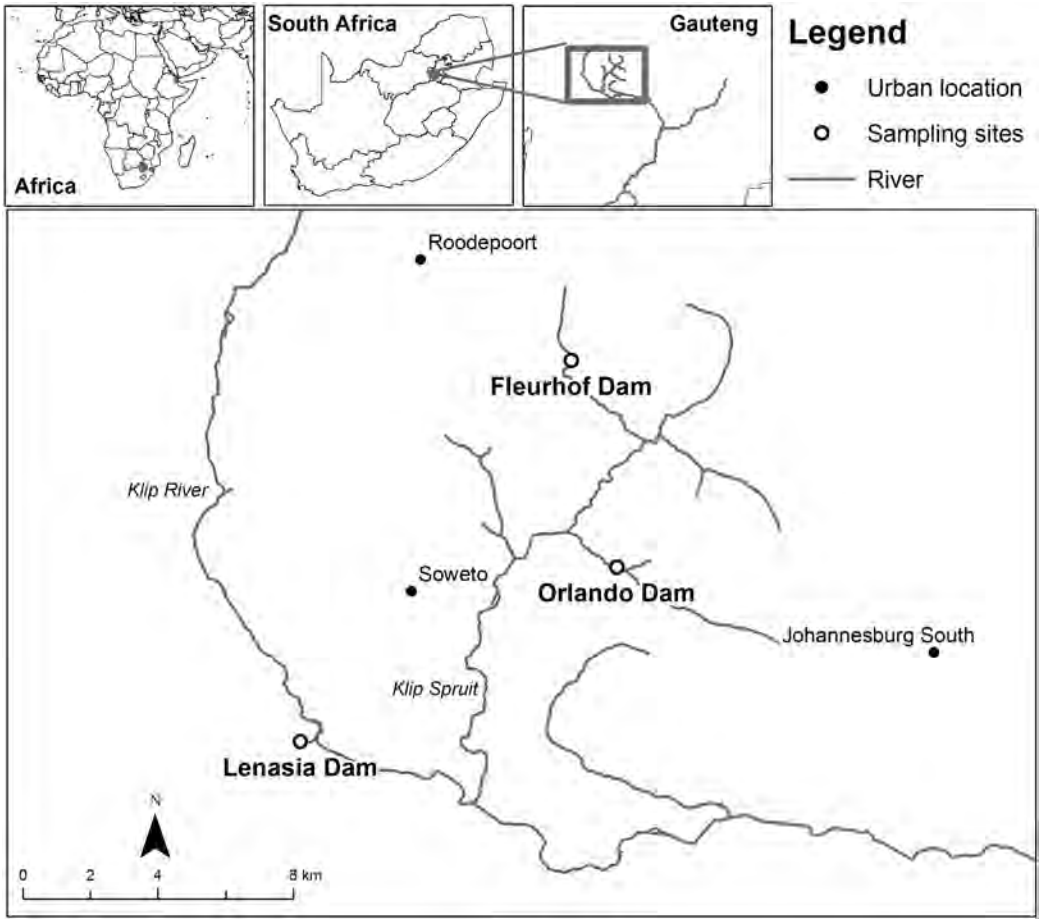

Fig. 1. *Clarias gariepinus* were sampled for organochlorine pesticide residue analysis from three impoundments (Lenasia Dam, Fleurhof Dam and Orlando Dam) in the Klip River catchment, Soweto in October 2013.

120 mL DCM:hexane (3,7 v/v). The eluate was concentrated to near dryness under gentle flow of nitrogen and resuspended in 100 μL *n*-decane (containing surrogate standard, tetrachloro-*m*-xylene) for analysis.

2.2.3. Analysis of OCPs in muscle

OCP analysis was performed as described by Yohannes et al. (2013b) on a gas-chromatograph coupled to an electron capture detector (GC-ECD, Shimadzu GC-2014, Kyoto, Japan). Separation was achieved with a Mighty Cap™ ENV-8MS capillary column (30 m × 0.25 mm, I.D, 0.25 um df; Kanto Chemical Corp. Tokyo, Japan). Samples were injected (1 μL) in splitless mode. Helium was used as carrier gas at a flow-rate of 1.0 mL/min and nitrogen as the make-up gas at a flow rate of 45 mL/min. The GC oven temperature was programmed from 100 °C (1 min hold), ramp at 12 °C/min to 180 °C; 4 °C/min to 240 °C, and finally at 10 °C/min to 270 °C (5 min hold). The temperatures of the detector and injector were 320 °C and 250 °C, respectively.

2.2.4. Quality assurance and quality control

The OCPs were identified based on their retention times relative to corresponding standards. Concentrations of the target compounds were quantified based on the ratio of the sample's peak area to that of the standard peak area. The coefficient of variance (R^2) for all calibration curves was >0.995. A blank and reference standards were run after each set of 10 samples, to check for interferences and cross-contamination. Initially an internal standard (PCB#77) was spiked to monitor procedural performance. However, quantification showed all recoveries above 110%, indicating the unexpected presence of environmental PCB 77 in the samples. The data reported is thus not adjusted according to recoveries of the internal standard, but only in terms of the surrogate marker, tetrachloro-*m*-xylene (TmX). The mean recovery was 81.5% ± 12.6. To evaluate the accuracy and precision of the analytical method the standard reference material (SRM 1947) was analysed in the same manner as the samples. The recoveries of the SRM ranged between 74 and 108% with a coefficient of variance <11%. Limit of detection (LOD) and limit of quantification (LOQ) was calculated using the standard deviation of the residuals ($S_{y/x}$). The LOD was defined as three times the standard deviation of $S_{y/x}$ and the LOQ was defined as ten times the standard deviation of $S_{y/x}$. Detection limits ranged between 0.38 and 30 ng/g, and the LOQ ranged between 13 and 100 ng/g, for all OCPs.

2.3. Human health risk assessment

The human health risk was calculated for the consumption of *Clarias gariepinus* only, not including any of the other edible fish species that might occur in the area. Doing this created a worst-case scenario. In order to consider factors such as eating habits and consumption rates, both the 50th and 95th percentiles of measured concentrations were included in the risk assessment. This allows for a more comprehensive evaluation of health risk associated with the consumption of OCP contaminated fish from the study area (Gerber et al., 2016; Yohannes et al., 2014a). The health risk assessment firstly calculated the maximum safe consumption limit, which indicates the maximum amount of fish that can be consumed per day without posing an acute health risk. Secondly, the estimated dietary intakes (EDI) of OCPs were determined and subsequently the carcinogenic risks after lifetime exposure to the OCPs were calculated.

2.3.1. Maximum safe consumption limit

The maximum amount of fish that can be safely consumed without potential human health risk can be determined by using the minimal risk levels (MRLs) for oral intake, set by the Agency of Toxic Substances and Disease Registry (ATSDR). Maximum safe consumption limit was calculated according to Verhaert et al. (2017), following the formulae:

$$Y = BM \times MRL \quad (1)$$

where Y is the maximum amount (ng/day) of OCPs a 60 kg person may consume without health risk. BM is the average body mass (bm) set at 60 kg (WHO, 2010), and MRL is the minimal risk levels (ng/kg BM per day). The MRLs for ΣHCH, ΣCHL, and ΣDDT are 600, 600, and 500 ng/kg BM per day, respectively (ATSDR, 2017b).

$$Q = (Y/C)/1000 \quad (2)$$

where Q is the maximum amount (kg) of fish that can be consumed safely without health risk, C is the concentration of the OCP (ng/g wm), and 1000 is for the conversion from gram to kilogram. It is important to note that the lowest value calculated is considered as the maximum safe consumption limit.

2.3.2. Estimated daily intake (EDI)

The estimated daily dietary intake of OCPs from *C. gariepinus* consumption was calculated using the following equation:

$$EDI = (C \times DR)/BM \quad (3)$$

where C is the concentration of the OCP (ng/g wet mass; wm), DR is the daily consumption of fish (g/day) and BM is the average body mass (bm) set at 60 kg (WHO, 2010). We chose to use the 60 kg of the WHO and not the 80 kg of the USEPA because it enabled comparison of our data to others who also used the 60 kg body mass. Additionally, the average body mass of South Africans is 66.5 kg according to Puoane et al. (2002). The estimated daily consumption rate was conservatively set at 30 g/day per person (Gerber et al., 2016). EDI was compared with the allowable daily intake (ADI) set by the WHO (2010). These ADIs (ng/kg bm per day) are 5000, 500, and 100,000 for ΣHCH, ΣCHL, and ΣDDT respectively.

2.3.3. Carcinogenic risk

Both cancer risk (CR) and hazard ratios (HR) were calculated according to the USEPA (2005) and Jiang et al. (2005). The CR was calculated as:

$$CR = EDI \times CSF \quad (4)$$

where the CSF is the cancer slope factor of the congener (USEPA, 2012). If the CR is $>10^6$ it is considered 'acceptable risk', between 10^6 and 10^4 are considered 'levels of concern' and a CR smaller than 10^4 is deemed 'unacceptable risk' (USEPA, 2005). The CSFs (mg/kg per day) for ΣHCH (as γ-HCH), ΣCHL, and ΣDDT are 1.1, 0.35, and 0.34 respectively.

The hazard ratios for both non-carcinogenic and carcinogenic effects were calculated according to Jiang et al. (2005):

$$HR = EDI/BMC \quad (5)$$

where the BMC is the benchmark concentration, derived from the USEPA CSF:

$$BMC = (Risk \times BM)/(Fish\ consumption \times CSF) \quad (6)$$

where the risk is set at one in a million chance for lifetime exposure, and fish consumption is the amount of fish consumed per day relative to body mass (g/kg per day). An HR greater than one indicates a potential risk to human health (Dougherty et al., 2000).

2.4. Statistical analysis

Chemical analysis results were grouped based on the congener classes (ΣHCHs, ΣCHLs, ΣDDTs, and ΣOCPs). The data sets were tested for normality using the D'Agostino-Pearson omnibus test. The data sets were found to be non-parametric and thus significant differences were tested using the Kruskal-Wallis test with Dunn's multiple comparison-test as post-hoc test. Unpaired *t*-tests were used to compare means from literature with our results provided that results from literature were reported as means and standard deviations. Significant differences ($p < 0.05$) are indicated by common superscripts in the tables and figures.

Discriminant function analysis (DFA) is similar to multivariate ANOVAs but indicate the similarity/dissimilarity of datasets (OCP accumulation profiles). Datapoints below LOD were replaced with the frequency of detection multiplied by the LOQ (Wepener et al., 2012; Verheart et al., 2013). This DFA was performed using PASW Statistics 18. Fisher's functional coefficient was used as a posteriori test.

3. Results

3.1. OCP tissue residues

The OCP residues quantified in the muscle of *C. gariepinus* (ng/g wet mass) from the study area are reported in Table 1. Of the 22 compounds analysed two were detected in the reference fish (n = 10), 50% from fish at Orlando Dam (n = 9), 60% in fish from Lenasia Dam (n = 11), and 55% from fish at Fleurhof Dam (n = 10). The lipid content, fish mass and fish lengths are presented in Table S1. Significant differences were found between the lipid percentages ($p < 0.05$) of fish from the different sites (Table S1). However, there were no significant differences between the sizes (both mass and length) of the fish between the sites ($p > 0.05$) (Table S1). For accurate comparison, concentration in terms of wet mass were reported, however lipid mass concentrations

Table 1
Means, standard deviation, and ranges of organochlorine pesticides (ng/g wet mass) in *Clarias gariepinus* muscle tissue sampled during October 2013 from impoundments in the upper Klip River catchment, namely Orlando, Lenasia and Fleurhof Dams, and a reference group. Common superscripts within rows denote significant differences ($p < 0.05$). ND indicates that OCPs were not detected.

OCP	Reference (n = 10)	Orlando (n = 9)	Lenasia (n = 11)	Fleurhof (n = 10)
HCB	ND	22 ± 6	30 ± 19	8.2*
α-HCH	ND	ND	9	ND
γ-HCH	ND	ND	ND	6.9 ± 1.8
ΣHCHs	ND	ND	[a]9*	[a]6.9 ± 1.8
Range			ND–9	4.9–11
trans-Heptachlor-epoxide	ND	ND	10 ± 12	6.5*
trans-Chlordane	ND	20 ± 14	13 ± 5.8	17 ± 9.9
trans-Nonachlor	ND	21 ± 13	28 ± 22	15 ± 7.4
cis-Chlordane	ND	18 ± 10	19 ± 14	14 ± 9.1
cis-Nonachlor	ND	ND	8.8 ± 1.2	12 ± 6.3
ΣCHLs	ND	29 ± 39	49 ± 44	47 ± 33
Range		ND–124	ND–165	8.6–133
Dieldrin	ND	18 ± 12	13 ± 7.4	13 ± 9.4
o,p′-DDE	ND	37*	ND	ND
p,p′-DDE	5.6 ± 1.4	76 ± 73	138 ± 120	80 ± 36
o,p′-DDD	ND	19 ± 15	48 ± 45	9.4 ± 3.7
p,p′-DDD	5.0 ± 2.6	37 ± 36	55 ± 57	17 ± 10
o,p′-DDT	ND	7 ± 2.2	7.4 ± 4.0	ND
p,p′-DDT	88*	15 ± 14	7.4 ± 5.5	12 ± 5.0
ΣDDTs	[abc]12.7 ± 28	[a]145 ± 141	[b]256 ± 231	[c]117 ± 97
Range	ND–97.4	31–683	73–893	69–264
ΣDDT/ΣDDxa	0	0.13	0.06	0.11
ΣOCPs	[abc]12.7 ± 28	[a]193 ± 190	[b]335 ± 315	[c]183 ± 100
Range	ND–97.4	32–683	81–1190	105–458

* Indicates data for single fish (N = 1).

were also recorded and were only used when comparative literature lacked wet mass concentration values.

Among the DDTs, *p,p′*-DDE, *p,p′*-DDD, and *p,p′*-DDT were detected in the fish from the reference group but the ΣDDTs in these fish was significantly lower than all the environmental sites despite the unexpected high *p,p′*-DDT found in only one specimen. The ΣOCPs of the reference site were also significantly less than the other sites. The only site that had α-HCH in fish was Lenasia. Similarly, Fleurhof was the only site with fish that had γ-HCH residues. *trans*-Heptachlor epoxide was detected at Lenasia and Fleurhof only. Concentrations of ΣCHLs were similar among sites (no significant differences, $p > 0.05$). The fish from Lenasia had the widest range of ΣCHLs, ranging between ND and 165 ng/g wm. Dieldrin was the only drin detected in the fish from all the sites, with similar residue levels. The DDTs were the most prevalent class across the sites. All targeted DDTs were present at Orlando and almost all were detected at Fleurhof and Lenasia. Only *o,p′*-DDE was not detected at Fleurhof and Lenasia. The ΣDDTs were the greatest at Lenasia and ranged between 73 and 893 ng/g wm. Lenasia had the greatest ΣOCPs with a range of 81 to 1190 ng/g wm.

3.2. OCP compositions

The compositions of the different congeners per OCP class are shown in Fig. 2. The composition of ΣHCHs differed between the sites. The ΣHCH compositions were dominated by α-HCH in fish from Lenasia and γ-HCH in the fish from Fleurhof.

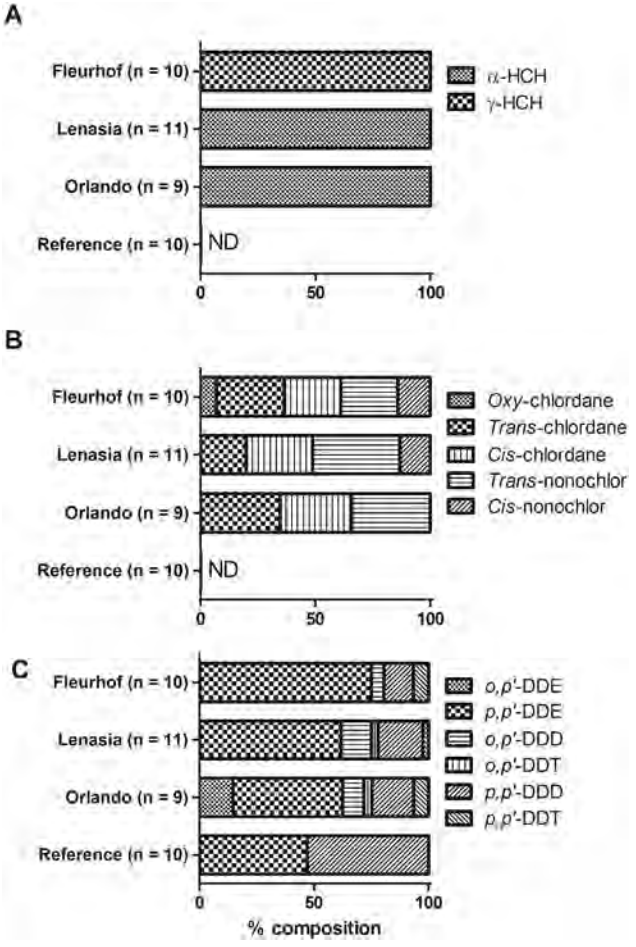

Fig. 2. Composition of organochlorine pesticides residues in *Clarias gariepinus* from a reference group and individuals sampled from three impoundments (Lenasia Dam, Fleurhof Dam and Orlando Dam) in the Klip River catchment A) hexachlorocyclohexanes (HCHs); B) chlordanes (CHLs); and C) DDTs.

The ΣCHLs at Fleurhof were divided between nonachlor (47%) and chlordane (53%). The contributions made to the ΣCHLs at Lenasia were dominated by the *trans* isomer of nonachlor and *cis* isomer of chlordane. The two chlordane isomers made up more than half of the CHLs at Orlando.

The most dominant DDT congener in the reference fish was *p,p′*-DDT. Overall, *p,p′*-DDE was the dominant congener at the environmental sites, contributing 68% at Fleurhof, 54% at Lenasia, and 40% at Orlando. *p,p′*-DDD was the second most prevalent congener at these sites.

The discriminant function analysis on OCP accumulation data explained 92.5% of the variation in the data (Fig. 3). Function 1 along the x-axis accounted for 79.4% of the total variation whilst function 2 along the y-axis accounted for 13.1%. Based on the structure matrix of the analysis (Table S2) γ-HCH and *cis*-nonachlor loads in the fish were the main factors for separation along the x-axis with dieldrin, *p,p′*-DDE and *trans*-chlordane driving y-axis separation. Reclassification of the data resulted in 100% of the data points reclassified into their respective original site classifications (Table S3). The ordination in Fig. 3 and the reclassification results indicate that the accumulated concentrations of OCPs in *C. gariepinus* from the various sites are distinct. In order to confirm site differences a discriminant function analysis (DFA) was performed on the OCP results. This analysis classifies samples based on their unique combination of variable values (in this case the combination of concentration and composition of OCPs) in order to determine statistical difference between the sample sets (sites). Fleurhof separated from all the other sites along the first function mainly in terms of γ-HCH load whereas differences between the other sites were along the y-axis attributing the separation to the driving factors along that function, i.e. Lenasia Dam had the highest OCP concentrations and greatest diversity of OCPs detected, and separated from all the other surveys along the second function.

3.3. Human health risk from consumption of fish tissue

The maximum safe consumption limit, EDI, HR and CR from fish consumption from the study sites are shown in Table 2. The maximum amount of fish that can be safely consumed per day was deemed the smallest for the ΣDDTs at all the sites, followed by that for ΣCHLs (Table 2). The HR for HCH at Fleurhof was >1 (50th percentile) but was not calculated for the other two sites because HCH was not detected

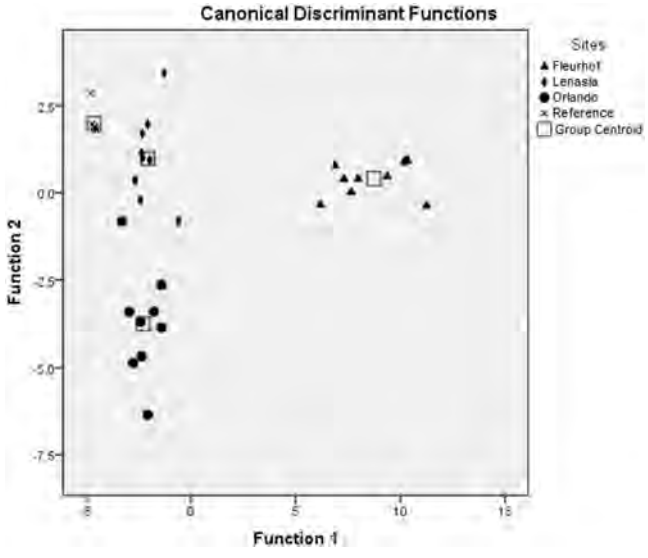

Fig. 3. Discriminant function analysis of organochlorine pesticides residues in *Clarias gariepinus* from a reference group and individuals sampled from three impoundments (Lenasia Dam, Fleurhof Dam and Orlando Dam) in the Klip River catchment. Function 1 (79.4%) and 2 (13.1%) refer to the first two canonical functions of a multivariate data set and collectively explain 92.5% of the variation in the accumulation data.

Table 2
The 50th and 95th (in parentheses) percentile wet mass OCP concentrations, estimated daily intakes, cancer hazard ratio and risks for consuming *Clarias gariepinus* from Orlando, Lenasia and Fleurhof Dams in the upper Klip River catchment compared to Yohannes et al. (2014a) and Gerber et al. (2016). Exposure parameters included in subscript.

	Orlando *Clarias gariepinus*			Lenasia *Clarias gariepinus*			Fleurhof *Clarias gariepinus*			Yohannes et al., 2014a, 2014bLake Ziway *Clarias gariepinus*			Gerber et al., 2016 Luvuvhu River *Hydrocynus vitattus*			Gerber et al., 2016 Olifants River *Hydrocynus vitattus*		
	ΣHCH	ΣCHL	ΣDDT	ΣHCH	ΣCHL	ΣDDT	ΣHCH	ΣCHL	ΣDDT	ΣHCH	ΣCHL	ΣDDT	ΣHCH	ΣCHL	ΣDDT	ΣHCH	ΣCHL	ΣDDT
50th(95th) concentrations (ng/g wm)	0 (0)	5.3 (94)	113 (367)	0 (4.6)	28 (123)	148 (650)	6.6 (10)	35 (106)	101 (211)	0.54 (1.53)	0.85 (1.41)	4.91 (21.21)	1.98 (9.73)	0.77 (9.05)	32.02 (1071)	2.25 (8.99)	0.81 (12.22)	12.34 (279.81)
50th(95th) maximum safe consumption limit (kg per day)	–	6.7 (0.4)	0.3 (0.08)	– (7.8)	1.3 (0.3)	0.2 (0.04)	5.5 (3.5)	1.0 (0.3)	0.3 (0.1)									
50th(95th) estimated daily intake(ng/kg body mass per day)	0 (0)	2.7 (47)	56 (184)	0 (2.3)	14 (62)	74 (325)	3.3 (5.1)	18 (53)	50 (106)	0.27 (0.77)	0.42 (0.72)	2.46 (10.61)	0.99 (4.86)	0.39 (4.52)	16.01 (535.26)	1.13 (4.49)	0.41 (6.11)	6.17 (139.9)
50th(95th) hazard ratio	0 (0)	64 (1119)	1379 (4500)	0 (17)	337 (1467)	1810 (7966)	25 (39)	417 (1260)	1237 (2587)				7.5 (36.8)	9.2 (107.7)	392 (13,119)	8.5 (34)	9.7 (145.4)	151 (3429)
50th(95th) cancer risk ($\times 10^4$)	0 (0)	9 (164)	191 (624)	0 (25)	50 (216)	251 (1105)	36 (56)	61 (185)	172 (359)	2.9 (8.4)	1.5 (2.5)	8.4 (36)	10.87 (53.5)	1.35 (15.83)	54.43 (1820)	12.38 (49.43)	1.43 (21.38)	20.98 (475.7)

Cancer slope factors: ΣHCH (1.1); ΣCHL (0.35); ΣDDT (0.34) [USEPA, 2000].
Benchmark concentration (μg/kg per day): ΣHCH (0.132); ΣCHL (0.042); ΣDDT (0.0408).
Allowable daily intake g/kg per day): ΣHCH (5000); ΣCHL (500); ΣDDT (10,000) (WHO, 2010).
Safety action levels: ΣCHL (300 ng/g); ΣDDT (5000 ng/g) (FDA, 2011).
Minimal risk level: ΣHCH (600); ΣCHL (600); ΣDDT (500) (ATSDR, 2017b).

Table 3
Mean ± SD of organochlorine pesticide concentrations (ng/g wet mass and ng/g lipid mass in bold) in epaxial muscle tissue of *Clarias gariepinus* from three impoundments, Orlando, Lenasia and Fleurhof, from the Klip River catchment South Africa. Results are compared to other studies across South Africa and Africa as well as compared to another apex predator.

	Sites	*trans*-Chlordane	*trans*-Nonachlor	*cis*-Chlordane	*cis*-Nonachlor	ΣCHLs	*o,p′* -DDE	*p,p′*-DDE	*o,p′* -DDD	*p,p′* -DDD	*o,p′* -DDT	*p,p′*-DDT	ΣDDTs	DDT/DDx	References
Clarias gariepinus	Orlando Dam, South Africa	20 ± 14 **49 ± 104**	21 ± 13 **42 ± 98**	18 ± 10 **35 ± 81**	–	29 ± 39 **127 ± 285**	37 **152**	76 ± 73 **345 ± 561**	19 ± 15 **75 ± 116**	37 ± 36 **176 ± 291**	7 ± 2.2 **8.2 ± 16**	15 ± 14 **57 ± 108**	145 ± 141 **680 ± 1069**	**0.13**	This study
	Lenasia Dam, South Africa	13 ± 5.8 **20 ± 42**	28 ± 22 **102 ± 138**	19 ± 14 **63 ± 90**	8.08 ± 1.2 **12 ± 28**	49 ± 44 **198 ± 268**	–	138 ± 120 **581 ± 741**	48 ± 45 **200 ± 270**	55 ± 57 **230 ± 351**	7.4 ± 4.0 **24 ± 29**	7.4 ± 5.5 **33 ± 36**	256 ± 231 **1070 ± 1423**	**0.06**	
	Fleurhof dam, South Africa	17 ± 9.9 **297 ± 189**	15 ± 7.4 **512 ± 430**	14 ± 9.1 **322 ± 158**	12 ± 6.3 **137 ± 264**	47 ± 33 **1270 ± 689**	–	80 ± 36 **3593 ± 4570**	9.4 ± 3.7 **377 ± 415**	17 ± 10 **531 ± 355**	–	12 ± 5.0 **257 ± 142**	117 ± 97 **4760 ± 5284**	**0.11**	
	Xikundu Weir, South Africa[a]	–	–	–	–	–	50	63,500	440	8500	2500	6600	81,000	1.01	Barnhoorn et al., 2009
	Nanondi Dam, South Africa[a]	–	–	–	–	–	–	2100 ± 1000	30 ± 20	500 ± 300	–	–	2600 ± 1300		Barnhoorn et al., 2009
	Roodeplaat Dam, South Africa	–	–	–	–	–	–	138 ± 95	–	113	–	168	151 ± 88	0.67	Barnhoorn et al., 2015
	Rietvlei Dam, South Africa	–	–	–	–	–	–	212 ± 13	–	127 ± 86	–	198 ± 77	336 ± 263	0.58	Barnhoorn et al., 2015
	Okavango Delta (MVC),Botswana	–	–	–	–	–	–	–	–	–	–	–	16 ± 7.2	–	Mbongwe et al., 2003
	Okavango Delta (Tsetse fly control), Botswana	–	–	–	–	–	–	–	–	–	–	–	3.0 ± 1.6	–	Mbongwe et al., 2003
	Lake Ziway, Ethiopia	0.29 ± 0.1	0.35 ± 0.23	0.16 ± 0.05	–	0.90 ± 0.25	0.1 ± 0.1	6.9 ± 11	–	0.8 ± 0.7	0.4 ± 0.1	0.6 ± 0.4	9.0 ± 11	0.13	Yohannes et al., 2014a
	Lakes Volta & Weija, Ghana	**0.63–2.7**	**0.42–1.4**	**0.62–1.6**	**0.23–0.58**	**1.9–6.28**	–	–	–	–	–	–	–	–	Adu-Kumi et al., 2010
	Mamba Weir, South Africa	–	–	–	–	<LOQ	–	–	–	–	–	–	13 ± 7.2	–	Verhaert et al., 2017
	Olifants River Gorge, South Africa	–	–	–	–	<LOQ	–	–	–	–	–	–	21 ± 17	–	Verhaert et al., 2017
Hydrocynus vittatus	Pongolapoort Dam, South Africa	–	–	–	**1.05 ± 0.65**	**3.8 ± 1.61**	**7.1 ± 2.7**	**5600 ± 2499**	**20 ± 3.5**	**245 ± 46**	**36 ± 7.9**	**536 ± 113**	**6444 ± 2635**	0.10	Wepener et al., 2012
	Olifants River, South Africa	**8 ± 3.5**	**13 ± 2.7**	**12 ± 3.4**	**5.3 ± 3.4**	**50 ± 15**	**13 ± 3.7**	**475 ± 229**	**18 ± 5.6**	**63 ± 13**	**29 ± 9.7**	**50 ± 17**	**647 ± 260**	0.14	Gerber et al., 2016
	Luvuvhu River, South Africa	**28.3 ± 11**	**4.3 ± 3.6**	**15 ± 4. 8**	**6.8 ± 2.5**	**58 ± 14**	**79 ± 16**	**2342 ± 945**	**64 ± 11**	**451 ± 171**	**122 ± 31**	**1189 ± 555**	**4249 ± 1680**	0.45	Gerber et al., 2016

[a] Study determined OCPs in fat samples only.

in fish from those sites. The greatest HR values were for the DDTs ranging from 1237 to 1810 for the 50th percentile (Table 2). Hazard risk could be determined for all 95th percentiles across all compound classes except for ΣHCHs at Orlando because they were not detected. The risk at the 95th percentile was very high for both the chlordanes and the DDTs, with maximum HR values of 1467 and 7966 respectively, both at Lenasia (Table 2). The carcinogenic risk (CR) calculated for those with detected concentrations were the greatest for DDT for both the 50th and 95th percentiles. The greatest DDT CR was at Lenasia (1105) followed by Orlando (624) (Table 2). The CR for chlordane (216) was also the greatest at Lenasia (Table 2). A Monte-Carlo simulation (Oracle Crystal Ball) with a 1000 iterations was applied to quantify the uncertainties of the effect of BM (60–80 kg) on the final CR. The results showed a maximum variation of 9% in the final cancer risk calculated.

4. Discussion

This paper reports the residue levels of DDT and other OCPs in epaxial muscle tissue of *C. gariepinus* from impoundments in an urban area where the poor and unemployed make use of fish as a source of protein. This paper further compares to levels found in other studies (Table 3) and extrapolates findings to potential human health risks from fish consumption in the study area. For accurate comparison, concentrations in terms of wet mass were used. The fact that *C. gariepinus* is the top predator in the study area, apart from piscivorous water birds, makes the species comparable to other apex predators from other African systems e.g. tigerfish (*Hydrocynus vittatus*). For those findings in literature where ng/g lipid was used, we converted our results to ng/g lipid for comparison (Table 3). The OCP concentrations in fish from the different sites were in the order of Lenasia > Orlando > Fleurhof. There were no statistical significant differences ($p > 0.05$) in composition of OCPs in the fish among the different sites (Fig. 2). This indicates towards shared sources of OCPs between the sites. Only the HCHs differed statistically ($p < 0.05$) between the sites. The dissimilarities in OCP concentrations (Table 1) supported by the DFA results (Fig. 3) indicate that the extent of OCP input, rather than the type of input, is the major difference between the sites. A study of the catchment (Fig. 1) shows different sub-catchment sizes of each impoundment, which may be the main attributing factor to the OCP input differences.

Chlordanes were one of the most prominent OCP classes in fish from the present study. Oxychlordane mostly, nonachlor, and to a lesser extent heptachlor-epoxide are all bio-accumulating metabolites of chlordane (Bondy et al., 2000). Heptachlor-epoxide, in the absence of other stable chlordane metabolites, is generally considered to have originated from heptachlor itself (ATSDR, 2007). The detection of only nonachlor and trace amounts of *trans*-heptachlor-epoxide could indicate a recent uptake and that chlordane had not been converted into oxychlordane yet. Historic exposure would only leave oxychlordane, as it is the dominant bio-accumulating metabolite (Hirasawa and Takizawa, 1989; Sasaki et al., 1992). Chlordane and its metabolites have the ability to irreversibly bind to cellular macromolecules and are considered epigenetic carcinogens, causing liver cancer in mice (ATSDR, 1994). The *trans*-isomer of both nonachlor and chlordane were higher at Fleurhof and Orlando, than its *cis*-counterpart, and so more toxic effects are expected in the fish from these sites as the *trans*-isomers are regarded as more toxic (Bondy et al., 2000). The individual CHL isomers reported by Yohannes et al. (2014a) were significantly lower ($p < 0.05$) than the lowest detected values in our study (Table 3). The ΣCHLs reported by Wepener et al. (2012) and Adu-Kumi et al. (2010) were significantly lower ($p < 0.05$) than the ΣCHLs in the fish from Fleurhof, and all our sites, respectively. Gerber et al. (2016) reported significantly lower ($p < 0.05$) ΣCHLs (in ng/g lipid) from the Olifants- and Luvuvhu Rivers during a high flow survey that was roughly half of what is reported at Orlando and Lenasia, and 20 times lower than Fleurhof (Table 3). The higher levels found in the present study, indicate a recent input event. The lack of oxychlordane indicates that the trace *trans*-heptachlor-epoxide detected might be from historic use of heptachlor only (ATSDR, 2007). However, the similar levels of both chlordane to nonachlor indicate a possible recent input event only for chlordane.

In the case of drins the expected result for historic input would be dieldrin as the major accumulating metabolite. This is because aldrin breaks down faster in the environment into dieldrin, which readily accumulates in lipid tissue where it is highly stable (ATSDR, 2002). In this study, dieldrin was the only drin detected. Therefore there is no evidence of recent drin input, except if only dieldrin itself was introduced.

As with many other studies the most prevalent congener measured was *p,p′*-DDE (Barnhoorn et al., 2009; Wepener et al., 2012; Yohannes et al., 2014a; Gerber et al., 2016). Higher metabolite levels (DDE and DDD) show historic use of DDT, but a higher *p,p′*-DDE residue level may also be indicative of internal bio-transformation of DDT ingested with prey (Ssebugere et al., 2009; Wepener et al., 2012). When compared to the ΣDDTs in *C. gariepinus* from a South African DDT sprayed area, the residue levels found in the fish from our study were considerably lower than what was quantified in *C. gariepinus* from Xikunndu Weir and Nanondi Dam (Barnhoorn et al., 2009) (Table 3). The ΣDDTs in fish from Orlando and Fleurhof were statistically lower ($p < 0.05$) than Nanondi Dam. Apart from being in an active MVC area, the ΣDDTs reported by Barnhoorn et al. (2009) were not quantified in the muscle tissue (as in the present study) but in the fat—where these lipophilic pollutants bio-accumulate (Jones and De Voogt, 1999). Mbongwe et al. (2003) reported ΣDDT values in *C. gariepinus* from areas in Botswana sprayed for mosquito and tsetse fly control. These levels were between 20 and 100 times lower than the greatest concentrations (Lenasia and Fleurhof) of the present study (Table 3). Similarly, *C. gariepinus* from Lake Ziway in Ethiopia where DDT is actively used, had ΣDDT concentrations 11 times lower (significantly, $p < 0.05$) (Yohannes et al., 2014a) (Table 3). Due to the lack of information on OCPs in *C. gariepinus* in South African systems in general, we compared our results to that of another apex predator, *H. vittatus* in South African systems. The DDT and its metabolites in *H. vittatus* from South Africa were more comparable to those found in *C. gariepinus* from Soweto and Lenasia (Table 3). The ΣDDTs in Pongolapoort Dam *H. vittatus* were greater than Lenasia (significantly, $p < 0.05$) and Fleurhof, whereas Gerber et al. (2016) reported lower values in tigerfish from the Olifants River (high flow) in the Kruger National Park—which is similar to what was found in the fish from Orlando (Table 3). However, in the same study by Gerber et al. (2016), the ΣDDTs in the *H. vittatus* from the Luvuvhu River (high flow) was 4248 ± 1680 ng/g lipid, which is similar to what was found in the Orlando fish. It must be mentioned that these authors reported ΣDDT concentrations double (Olifants River) and 6.7 times (Luvuvhu River) greater than the greatest concentrations of the current study, during the low flow season (2010). This was attributed to additional OCP inputs rather than lipid reserves (Gerber et al., 2016). In contrast to the high ΣDDTs in the tigerfish from the Olifants River, Verhaert et al. (2017) reported lower levels of ΣDDTs in *C. gariepinus* from the same study area (Olifants River). These results were 12 times lower than what was found in the fish from Lenasia (Table 3). In *C. gariepinus* from Roodeplaat and Rietvlei Dams, which are not in the South African MVC area (Barnhoorn et al., 2015), ΣDDTs levels were similar (not significantly different) to our results (Table 3).

The occurrence of OCPs in this urban area is of concern as it is not an MVC area. An explanation of possible sources could be illegal use (Rother et al., 2008) or from the historic production and formulation of these pesticides within the province/larger area surrounding the study area (DEA, 2011). The ratio between metabolites and parent compounds was calculated to indicate recent or historic use of DDT (Strandberg and Hites, 2001). DDT breaks down into DDD or DDE in the environment. The mechanisms of breakdown in different substrates are explained in the toxicological profile of DDT (ATSDR, 2002). Both DDD and DDE are more persistent in an aquatic environment (USEPA, 1979). In light of these differences in breakdown rates and differences

in metabolism and excretion rates between DDT and its metabolites in animals the ratio of DDT/DDx is used as an indication of recent DDT introduction. A ratio larger than 1 provides evidence that DDT has been recently introduced however Strandberg and Hites (2001) do not allude to a specific timeframe. This is difficult to do as breakdown can be influenced by a number of abiotic and biotic factors as evident from the ATSDR (2002) report. The ratios of ΣDDT/ΣDDx were all below one indicating historic use of DDT. Other studies in South Africa had similar results (Table 3) with the exception of Xikundu Weir, which is located in an active MVC area (Barnhoorn et al., 2009). The result of the present study is not surprising, since DDT is not actively used in the study area. The DDT inputs can only be attributed to historic use/production in the area or long range air transport from MVC areas.

Other OCP groups such as the heptachlors and chlordanes can also give an indication as to how recent inputs occurred, to a certain extent, when compared to their breakdown products as previously discussed. This is however, less accurate than for DDT, because these compounds are generally less persistent. Looking at the evidence that chlordane might be the only OCP recently introduced into the system illegal use of pesticides arises as a potential source. The applications of chlordane include termite control and as a broad spectrum agro-insecticide (Stockholm Convention, 2008). The study area is an urban area and not a prominent agricultural area. Thus illegal use in the immediate area is not likely and a more probable source would be long range transport. Barnhoorn et al. (2015) indicated the presence of OCPs in *C. gariepinus* at sites outside MVC areas also indicating long range transport possibilities. OCPs have been found in areas as far as the Arctic Circle (Halsall, 2004; Kallenborn et al., 2007). This implies that organisms from an environment with no direct input of a specific contaminant can present low- to mid-level bio-accumulation concentrations of that contaminant.

The relatively high OCP levels is of concern as one would expect the residue levels to be lower in urban areas than in areas such as actively DDT sprayed zones. This suggests major overall input in the Klip River system. The relatively high residues in the fish can also be attributed to bio-magnification through the food web. Even though it was not determined in the present study, it is an important factor to consider when making interpretations, as OCPs have been shown to bio-magnify in fish (Kidd et al., 2001; Verheart et al., 2013). *Clarias gariepinus* specifically is expected to have higher accumulation as it is a bottom-dwelling fish and associated with the sediments—where most of these lipophilic compounds accumulate in the aquatic environment (Yohannes et al., 2013a). Other than the fish, aquatic birds which are higher in the food web are also at risk. OCPs have been reported in African birds: in non-piscivorous birds such as ducks (Evans and Bouwman, 1993), egrets and ibises (Bouwman et al., 2008); small piscivorous birds like kingfishers (Evans and Bouwman, 2000) and hamerkop (Yohannes et al., 2014b, 2017); and large piscivorous birds like cormorant (Bouwman et al., 2008), and pelican (Yohannes et al., 2014b, 2017). Since this catchment is not within major agricultural land, the levels of agricultural pesticides at high enough concentrations to cause unacceptable human health risk are alarming.

Humans who are consuming contaminated fish are at risk of both acute and chronic effects health effects (Du Preez et al., 2003). The MRLs used in the maximum safe consumption limit calculations are based on non-carcinogenic effects only (ATSDR, 2017a). More specifically the MRLs of HCH, chlordane, and DDT were derived from acute (1–14 days) and intermediate (14–364 days) exposure data, which measured developmental, hepatic, and neurological end-points (ATSDR, 2017b). The maximum safe consumption limit results show that if a person (weighing 60 kg) consumes >40 g of *C. gariepinus* from Lenasia per day, they may be at risk of acute health effects associated with OCPs. Similarly, consuming 80 g and 100 g of fish from Orlando and Fleurhof respectively, persons would also be at risk for acute health effects. These maximum consuming limits are very conservative and only serve as an indication of limits not to be exceeded to prevent acute toxicity. The EDI at each site were well below the allowable daily intake set by the WHO (2010), as well as the action safety levels in edible fish by the United States Food and Drug Administration (FDA, 2011) (Table 2).

The current study used the same parameters to calculate health risk as Yohannes et al. (2014a) and Gerber et al. (2016) and therefore the EDIs and lifetime cancer risks can be compared. The EDIs of ΣHCHs for the present study were lower than literature (Table 2). In contrast, the ΣCHLs of all three sites (both 50th and 95th percentiles) were greater than EDIs reported by Yohannes et al. (2014a) and Gerber et al. (2016). For the ΣDDT 95th percentile the EDI of the Luvuvhu River (Gerber et al., 2016) was 1.6 times greater than the Lenasia EDI (Table 2). After Lenasia, the third greatest EDI was calculated for Orlando, followed by the Olifants River and finally Lake Ziway (Table 2). Based on these results it is apparent that the potential intake of OCPs in this urban study area is similar and even greater than areas where active use of pesticides occurs.

The HR and cancer risk estimates show that the OCP residues in the muscle of *C. gariepinus* pose a severe risk to human health if consumed. The threshold for allowable risk using the HR is set at one (Dougherty et al., 2000). All the calculated HR values for the present study exceeded this allowable threshold (Table 2). In most cases the HRs were in the thousands and were comparable to the HR values calculated by Gerber et al. (2016) for ΣDDTs (Table 2). Acceptable risk, when applying cancer risk estimations, is set at 1 in 10,000 (USEPA, 2005). All those sites with detected concentrations of any OCP had cancer risk. The health risk calculated by Barnhoorn et al. (2015) for fish from non-MVC areas were considerably lower than what was surmised in the present study. The most notable risks were calculated for the ΣDDTs, with an 1100 in 10,000 risk at Lenasia (95th percentile) and a 620 in 10,000 risk (95th percentile) at Orlando. These high health risks were similar to what Gerber et al. (2016) reported for the Luvuvhu River ΣDDT cancer risks. Background cancer rates for South Africa projected by the National Cancer Registry of South Africa are estimated as one in eight for men and one in nine for women (CANSA, 2015). This translates to 1250 in 10,000 for men and 1110 in 10,000 for women. The results of the present study are below this background rate, except for Lenasia where the 95th percentile value is similar to the background value for women. Although our health risk assessment was conservatively calculated for adults, it must be mentioned that infants and children are considered to be high risk groups. Because OCPs accumulate in breast milk (Bouwman and Kylin, 2009; Landigran et al., 2002), nursing infants are exposed to these pollutants and are also at risk. The USEPA (2017) reports an extra safety factor of ten (×10) when calculating risk for infants and children.

Overall, the data suggest that OCPs in fish from this area potentially make a low contribution to cancer cases in the study area. However, a few factors have to be considered when interpreting these risk values: The calculations made regarding human health risk assessments are based on assumptions regarding lifetime exposure parameters. Other toxic and carcinogenic compounds not targeted in the present study may very well be present in these fish that would also contribute to the health risk to consumers. The data arises from a model species which is not necessarily the only species of fish consumed in the area. With all of these limitations considered, the maximum safe consumption limit was calculated to be 40 g of fish per day and this would protect the consumer from acute health risks. However, the cancer risk assessment demonstrated that there is an unacceptable risk when consuming 30 g of fish per day over a lifetime.

5. Conclusion

This study found unexpected high levels of apparently redundant OCPs in a highly populated urban area. DDTs were the most detected OCP group. Their presence is most likely attributed to long distance transport and historic production and formulation of OCPs in the areas

surrounding the study site. The concentrations of OCPs in the fish pose great risk to human health, even higher than international acceptable levels using standard risk assessment parameters. With the record unemployment rate (StatsSA, 2017a) and increasing poverty among South Africans (StatsSA, 2017b) citizens resorting to urban fisheries for food may be a reality. The results obtained through the present study should be considered by national authorities to be incorporated into management plans for the Klip River, to decrease the potential risk of these pollutants to human and wildlife health.

Acknowledgements

The authors acknowledge the reviewers for their valued inputs into improving the manuscript. This study was funded by the Water Research Commission of South Africa (WRC, K2/2242/1/16), and the National Research Foundation (Innovation student bursary SF1208219521, and Grant No. 103487) with no conflict of interest. Opinions expressed and conclusions arrived at are those of the authors only, and are not necessarily to be attributed to the NRF. This work was supported by Grants-in-Aid for Scientific Research from the Ministry of Education, Culture, Sports, Science and Technology of Japan awarded to M. Ishizuka (No. 16H0177906), Y. Ikenaka (No. 26304043, 15H0282505, 15K1221305), and the Sumitomo Foundation (PK361791) and JSPS Core to Core Program (AA Science Platforms) and Bilateral Joint Research Project (PG36150002 and PG36150003). We are grateful to Natasha Vogt for generating the map and Takahiro Ichise for technical support. This is contribution number 219 from the NWU-Water Research Group.

Appendix A. Supplementary data

Supplementary data to this article can be found online at https://doi.org/10.1016/j.scitotenv.2018.02.075.

References

Adu-Kumi, S., Kawano, M., Shiki, Y., Yeboah, P.O., Carboo, D., Pwamang, J., Morita, M., Suzuki, N., 2010. Organochlorine pesticides (OCPs), dioxin-like polychlorinated biphenyls (dl-PCBs), polychlorinated dibenzo-*p*-dioxins and polychlorinated dibenzo furans (PCDD/Fs) in edible fish from Lake Volta, Lake Bosumtwi and Weija Lake in Ghana. Chemosphere 81, 675–684.

ATSDR, Agency for Toxic Substances and Disease Registry, 1994. Toxicological profile for chlordane. https://www.atsdr.cdc.gov/toxprofiles/tp31.pdf, Accessed date: 11 January 2017.

ATSDR, Agency for Toxic Substances and Disease Registry, 2002. Toxicological profile for aldrin/dieldrin. https://www.atsdr.cdc.gov/toxprofiles/tp1.pdf, Accessed date: 11 January 2017.

ATSDR, Agency for Toxic Substances and Disease Registry, 2007. Toxicological profile for heptachlor and heptachlor epoxide. https://www.atsdr.cdc.gov/toxprofiles/tp12.pdf, Accessed date: 11 January 2017.

ATSDR, Agency for Toxic Substances and Disease Registry, 2017a. Minimum risk levels (MRLs). https://www.atsdr.cdc.gov/mrls/index.asp, Accessed date: 11 January 2017.

ATSDR, Agency for Toxic Substances and Disease Registry, 2017b. Minimum risk levels (MRLs). https://www.atsdr.cdc.gov/mrls/pdfs/atsdr_mrls.pdf, Accessed date: 11 January 2017.

Barnhoorn, I.E.J., Bornman, M.S., Jansen van Rensburg, C., Bouwman, H., 2009. DDT residues in water, sediment, domestic and indigenous biota from a currently DDT-sprayed area. Chemosphere 77, 1236–1241.

Barnhoorn, I.E.J., Van Dyk, J.C., Genthe, B., Harding, W.R., Wagenaar, G.M., Bornman, M.S., 2015. Organochlorine pesticide levels in *Clarias gariepinus* from polluted freshwater impoundments in South Africa and the associated human health risks. Chemosphere 120, 391–397.

Bondy, G.S., Newsome, W.H., Armstrong, C.L., Suzuki, A.M., Doucet, J., Fernie, S., Hierlihy, S.L., Feeley, M.M., Baker, M.G., 2000. *trans*-Nonachlor and *cis*-nonachlor toxicity in Sprague-Dawley rats: comparison with technical chlordane. Toxicol. Sci. 58, 386–398.

Bouwman, H., 2004. South Africa and the Stockholm Convention on persistent organic pollutants. S. Afr. J. Sci. 100, 323–328.

Bouwman, H., Kylin, H., 2009. Malaria control insecticide residues in breast milk: the need to consider infant health risks. Environ. Health Perspect. 117, 1477–1480.

Bouwman, H., Polder, A., Venter, B., Skaare, J.U., 2008. Organochlorine contaminants in cormorant, darter, egret and ibis eggs from South Africa. Chemosphere 71, 227–241.

Brooke, B., Koekemoer, L., Kruger, P., Urbach, J., Misiani, E., Coetzee, M., 2013. Malaria vector control in South Africa. S. Afr. Med. J. 103, 784–788.

CANSA, Cancer Association of South Africa, 2015. Fact sheet on the top ten cancers per population group. http://www.cansa.org.za/files/2015/09/Fact-Sheet-Top-Ten-Cancers-per-Population-Group-Sept-2015.pdf, Accessed date: 6 May 2017.

CCAC, Canadian Council on Animal Care, 2005. Guidelines on: the care and use of fish in research, teaching and testing. http://www.ccac.ca/Documents/Standards/Guidelines/Fish.pdf, Accessed date: 5 December 2017.

DEA, Department of Environmental Affairs, 2011. National implementation plan for the Stockholm Convention in persistent organic pollutants. https://www.environment.gov.za/sites/default/files/docs/national_implementation_plaun_organic_pollutants.pdf, Accessed date: 30 March 2017.

Doong, R.-A., Sun, Y.-C., Liao, P.-L., Peng, C.-K., Wu, S.-C., 2002. Distribution and fate of organochlorine pesticide residues in sediments from selected rivers in Taiwan. Chemosphere 48, 237–246.

Dougherty, C.P., Holtz, S.H., Reinert, J.C., Panyocosit, L., Axelrad, D.A., Woodruff, T.J., 2000. Dietary exposures to food contaminants across the United States. Environ. Res. 84, 170–185.

Du Preez, H.H., Heath, R.G.M., Sandham, L.A., Genthe, B., 2003. Methodology for the assessment of human health risks associated with the consumption of chemical contaminated freshwater fish in South Africa. Water SA 29, 69–90.

DWAS, Department of Water Affairs and Sanitation, 2004. Upper Vaal Water Management Area: internal strategic perspective. https://www.dwaf.gov.za/Documents/Other/WMA/Upper_Vaal_ISP.pdf, Accessed date: 5 December 2017.

Evans, S.W., Bouwman, H., 1993. Levels of DDT in the liver tissue of two duck species from the Pongolo floodplain. Ostrich 64, 46–47.

Evans, S.W., Bouwman, H., 2000. The geographic variation and potential risk of DDT in the blood of pied kingfishers from northern KwaZulu-Natal, South Africa. Ostrich 71, 351–354.

FDA, Food and Drug Administration, 2011. FDA and EPA safety levels in regulation and guidance. Fish and Fishery Products: Hazards and Control Guidance :pp. 439–454. https://www.fda.gov/downloads/food/guidanceregulation/ucm251970.pdf, Accessed date: 10 April 2017.

Gerber, R., Smit, N.J., Van Vuren, J.H.J., Nakayama, S.M.M., Yohannes, Y.B., Ikenaka, Y., Ishizuka, M., Wepener, V., 2016. Bioaccumulation and human health risk assessment of DDT and other organochlorine pesticides in an apex aquatic predator from a premier conservation area. Sci. Total Environ. 550, 522–533.

Gong, P., Wang, X., Xue, Y., Sheng, J., Gao, S., Tian, L., Yao, T., 2015. Influence of atmospheric circulation on the long-range transport of organochlorine pesticides to the western Tibetan Plateau. Atmos. Res. 166, 157–164.

Halsall, C.J., 2004. Investigating the occurrence of persistent organic pollutants (POPs) in the arctic: their atmospheric behaviour and interaction with the seasonal snow pack. Environ. Pollut. 128, 163–175.

Hirasawa, F., Takizawa, Y., 1989. Accumulation and declination of chlordane congeners in mice. Toxicol. Lett. 47, 109–117.

Jiang, Q.T., Lee, T.K., Chen, K., Wong, H.L., Zheng, J.S., Giesy, J.P., Lo, K.K., Yamashita, N., Lam, P.K., 2005. Human health risk assessment of organochlorines associated with fish consumption in a coastal city in China. Environ. Pollut. 136, 155–165.

Jones, K.C., De Voogt, P., 1999. Persistent organic pollutants (POPs): state of the science. Environ. Pollut. 100, 209–221.

Kallenborn, R., Christensen, G., Evenset, A., Schlabach, M., Stohl, A., 2007. Atmospheric transport of persistent organic pollutants (POPs) to Bjørnøya (Bear Island). J. Environ. Monit. 9, 1082–1091.

Kidd, K.S., Bootsma, H.A., Hesslein, R.H., 2001. Biomagnification of DDT through the benthic and pelagic food webs of Lake Malawi, East Africa: importance of trophic level and carbon source. Environ. Sci. Technol. 35, 14–20.

Landigran, P.J., Sonawane, B., Mattison, D., McCally, M., Garg, A., 2002. Chemical contaminants in breast milk and their impacts on children's health: an overview. Environ. Health Perspect. 110, A313–A315.

Mbongwe, B., Legrand, M., Blais, J.M., Kimpe, L.E., Ridal, J., Lean, D.R.S., 2003. Dichlorodiphenyltrichloroethane in aquatic ecosystem of the Okavango Delta, Botswana, South Africa. Environ. Toxicol. Chem. 22, 7–19.

McHugh, K.J., Smit, N.J., Van Vuren, J.H.J., Van Dyk, J.C., Bervoets, L., Covaci, A., Wepener, V., 2011. A histology-based fish health assessment of the tigerfish, *Hydrocynus vittatus* from a DDT-affected area. Phys. Chem. Earth 36 (985-904).

Pozo, K., Harner, T., Wania, F., Muir, D.C.G., Jones, K.C., Barrie, L.A., 2006. Towards a global network for persistent organic pollutants in air: results from the GAPS study. Environ. Sci. Technol. 40, 4867–4873.

Puoane, T., Steyn, K., Bradshaw, D., Laubscher, R., Fourie, J., Lambert, V., Mbananga, N., 2002. Obesity in South Africa: the South African demographic and health survey. Obes. Res. 10, 1038–1048.

Rother, H.A., Hall, R., London, L., 2008. Pesticide use among emerging farmers in South Africa: contributing factors and stakeholder perspectives. Dev. South. Afr. 25, 399–424.

Rouhani, Q., Britz, P.J., 2011. Participatory development of provincial aquaculture programmes for improved rural food security and livelihood alternatives. Water Research Commission Report TT 502/11 (Pretoria).

Sasaki, K., Kawasaki, Y., Sekita, K., Ochiai, T., Takeda, M., Uchiyama, M., 1992. Disposition of β-hexachlorocyclohexane, *p,p′*-DDT, and *trans*-chlordane administered subcutaneously to monkeys (*Macaca fascicularis*). Arch. Environ. Contam. Toxicol. 22, 25–29.

Ssebugere, P., Kiremire, B.T., Kishimba, M., Wandiga, S.O., Nyanzi, S.A., Wasswa, J., 2009. DDT and metabolites in fish from Lake Edward, Uganda. Chemosphere 76, 212–215.

Statistics South Africa (StatsSA), 2011. Statistics by place. http://www.statssa.gov.za/?page_id=993&id=city-of-johannesburg-municipality, Accessed date: 4 December 2017.

Statistics South Africa (StatsSA), 2017. Statistical release P0211 quarterly labour force survey quarter 2: 2017. http://www.statssa.gov.za/publications/P0211/P02112ndQuarter2017.pdf, Accessed date: 4 December 2017.

Statistics South Africa (StatsSA), 2017b. Poverty trends in South Africa: an examination of absolute poverty between 2006 & 2015. http://www.statssa.gov.za/?p=10341, Accessed date: 8 August 2017.
Stockholm Convention, 2008. All POPs listed in the Stockholm Convention. http://www.pops.int/TheConvention/ThePOPs/AllPOPs/tabid/2509/Default.aspx, Accessed date: 9 December 2017.
Strandberg, B., Hites, R.A., 2001. Concentration of organochlorine pesticides in wine corks. Chemosphere 44, 729–735.
USEPA, United States Environmental Protection Agency, 1979. Water-related environmental fate of 129 priority pollutants. Introduction and Technical Background, Metals and Inorganics, Pesticides and PCBs. vol. I . https://nepis.epa.gov/EPA/html/DLwait.htm?url=/Exe/ZyPDF.cgi/P100K7FH.PDF?Dockey=P100K7FH.PDF, Accessed date: 26 January 2018.
USEPA, United States Environmental Protection Agency, 2005. Guidelines for carcinogen risk assessment. http://www.epa.gov/cancerguidelines/2005, Accessed date: 13 August 2017.
USEPA United States Environmental Protection Agency, 2000. Guidance for assessing chemical contaminant data for use in fish advisories volume 2 risk assessment and fish consumption limits third edition. https://www.epa.gov/sites/production/files/2015-06/documents/volume2.pdf, Accessed date: 8 February 2018.
USEPA, United States Environmental Protection Agency, 2012. Human health risk assessment: risk based screening table. http://www.epa.gov/reg3hwmd/risk/human/pdf/NOV_2012_FISH.pdf, Accessed date: 13 August 2017.
USEPA, United States Environmental Protection Agency, 2017. Assessing human health risk from pesticides. https://www.epa.gov/pesticide-science-and-assessing-pesticide-risks/assessing-human-health-risk-pesticides#safety, Accessed date: 12 December 2017.
Van der Oost, R., Beyer, J., Vermeulen, N.P.E., 2003. Fish bioaccumulation and biomarkers in environmental risk assessment: a review. Environ. Toxicol. Pharmacol. 13, 57–149.
Verhaert, V., Newmark, N., D'Hollander, W., Covaci, A., Vlok, W., Wepener, V., Addo-Bediako, A., Jooste, A., Teuchies, J., Blust, R., Bervoets, L., 2017. Persistent organic pollutants in the Olifants River Basin, South Africa: bioaccumulation and trophic transfer through a subtropical aquatic food web. Sci. Total Environ. 586, 792–806.
Verheart, V., Covaci, A., Bouillon, S., Abrantes, K., Musibono, D., Bervoets, L., Verheyen, E., Blust, R., 2013. Baseline levels and trophic transfer of persistent organic pollutants in sediments and biota from the Congo River Basin (DR Congo). Environ. Int. 59, 290–302.
Viljoen, I.M., Bornman, R., Bouwman, H., 2016. DDT exposure of frogs: a case study from Limpopo Province, South Africa. Chemosphere 159, 335–341.
Wepener, V., Van Dyk, C., Bervoets, L., O'Brien, G., Covaci, A., Cloete, Y., 2011. An assessment of the influence of multiple stressors on the Vaal River, South Africa. Phys. Chem. Earth 36, 949–962.
Wepener, V., Smit, N., Covaci, A., Dyke, S., Bervoets, L., 2012. Seasonal bioaccumulation of organohalogens in tigerfish *Hydrocynus vittatus* Castelnau, from Lake Pongolapoort, South Africa. Bull. Environ. Contam. Toxicol. 88, 277–282.
WHO, World Health Organisation, 2010. Human health risk assessment toolkit. World Health Organisation, Geneva, Switzerlandhttp://apps.who.int/iris/bitstream/10665/44458/1/9789241548076_eng.pdf, Accessed date: 25 October 2017.
Yohannes, Y.B., Ikenaka, Y., Saengtienchai, A., Watanabe, K.P., Nakayama, S.M.M., Ishizuka, M., 2013a. Occurrence, distribution, and ecological risk assessment of DDTs and heavy metals in surface sediments from Lake Awassa–Ethiopian Rift Valley Lake. Environ. Sci. Pollut. Res. 20, 8663–8671.
Yohannes, Y.B., Ikenaka, Y., Nakayama, S.M.M., Saengtienchai, A., Watanabe, K., Ishizuka, M., 2013b. Organochlorine pesticides and heavy metals in fish from Lake Awassa, Ethiopia: insights from stable isotope analysis. Chemosphere 91, 857–863.
Yohannes, Y.B., Ikenaka, Y., Saengtienchai, A., Watanabe, K.P., Nakayama, S.M.M., Ishizuka, M., 2014a. Concentrations and human health risk assessment of organochlorine pesticides in edible fish species from a Rift Valley Lake–Lake Ziway, Ethiopia. Ecotoxicol. Environ. Saf. 106, 95–101.
Yohannes, Y.B., Ikenaka, Y., Nakayama, S.M.M., Ishizuka, M., 2014b. Organochlorine pesticides in bird species and their prey (fish) from the Ethiopian Rift Valley region, Ethiopia. Environ. Pollut. 192, 121–128.
Yohannes, Y.B., Ikenaka, Y., Nakayama, S.M.M., Ishizuka, M., 2017. DDTs and other organochlorine pesticides in tissues of four bird species from the Rift valley region, Ethiopia. Sci. Total Environ. 574, 1389–1395.

The Journal of Veterinary Medical Science

FULL PAPER

Toxicology

Sex and site differences in urinary excretion of conjugated pyrene metabolites in the West African Shorthorn cattle

Nesta BORTEY-SAM[1)], Yoshinori IKENAKA[1,2)]*, Osei AKOTO[3)], Shouta M.M. NAKAYAMA[1)], Jemima T. MARFO[1)], Aksorn SAENGTIENCHAI[4)], Hazuki MIZUKAWA[1)] and Mayumi ISHIZUKA[1)]

[1)]Laboratory of Toxicology, Department of Environmental Veterinary Science, Graduate School of Veterinary Medicine, Hokkaido University, Kita 18, Nishi 9, Kita ku, Sapporo, Hokkaido 060-818, Japan
[2)]Water Research Group, Unit for Environmental Sciences and Management, North-West University, Potchefstroom, South Africa
[3)]Department of Chemistry, Kwame Nkrumah University of Science and Technology, Kumasi, Ghana
[4)]Department of Pharmacology, Faculty of Veterinary Medicine, Kasetsart University, Bangkok, Thailand

ABSTRACT. Industrialization, economic and population growth rates in Ghana have increased the release of contaminants including polycyclic aromatic hydrocarbons (PAHs) into the environment through which humans and animals are exposed. Cattle is reported to be exposed to high levels of PAHs through feed and inhalation. Once exposed, PAHs are metabolized and excreted in urine, feces or bile. In a previous study, cattle in Ghana was reported to excrete high levels of 1-hydroxypyrene (1-OHPyr) due to high exposure to the parent compound, pyrene. 1-OHPyr is further metabolized to glucuronide and sulfate conjugates. Thus, the aim of this study was to investigate the sex and site differences in urinary excretion of conjugated pyrene metabolites using cattle urine collected from rural and urban sites of the Ashanti region, Ghana. From the results, geometric mean concentration adjusted by specific gravity indicated that 1-OHPyreneGlucuronide (PyG) was the most abundant conjugate followed by PyrenediolSulfate (M3). The sum of conjugated pyrene metabolites and sum of both conjugated and deconjugated pyrene metabolites correlated significantly with PyG, PydiolSulfate (M2) and PydiolSulfate (M3). The study revealed no significant difference in urinary excretion of conjugated pyrene metabolites between rural and urban sites. This indicated that similar to urban sites, cattle in rural sites were exposed to high levels of pyrene. There was no significant difference in urinary concentrations of conjugated pyrene metabolites between sexes.

KEY WORDS: cattle, Kumasi, metabolites, PAHs, urine

J. Vet. Med. Sci.
80(2): 375–381, 2018
doi: 10.1292/jvms.17-0410

Received: 30 July 2017
Accepted: 6 December 2017
Published online in J-STAGE: 27 December 2017

Polycyclic aromatic hydrocarbons (PAHs), the 9th most hazardous substance based on the Agency for Toxic Substance and Disease Registry's (ATSDR) list [1], are formed during incomplete combustion of organic materials. Anthropogenic activities are the major sources of PAHs in the environment. PAHs are ubiquitous and found in vehicle exhaust, wood and cigarette smoke. Human and animal exposure to PAHs are mainly through consumption of contaminated food and water and inhalation [2, 16]. A number of PAHs gain promutagenic and procarcinogenic activities that could contribute to the incidence of cancer in humans and animals [35]. In both humans and animals, PAHs are metabolized by cytochrome P450 enzymes and excreted in urine, feces or bile [10, 26]. Pyrene, a four ring PAH, is also metabolized by cytochrome P450 enzymes to 1-hydroxypyrene (1-OHPyr) which has been suggested as a biomarker of PAHs exposure [10, 12]. Hydroxypyrene is further metabolized by phase II reactions to form conjugates, such as glucuronide and sulfate [37].

In recent years, Ghana's Kumasi region has seen tremendous increase in population, industrialization and economic activities. These activities and many more could lead to deterioration of the environment and pollution likely to reach disturbing levels [8]. Some of these activities and combustion processes have caused an increase in the levels of PAHs and its metabolites in both environmental and biological samples in Kumasi [4–8].

Cattle is reported to excrete large amount of PAH metabolites due to high intake or exposure to the parent compound [33]. In addition to inhalation, feed is one of the dominant sources of cattle's exposure to PAHs [6, 13]. In previous studies, high levels of

*Correspondence to: Ikenaka, Y.: y_ikenaka@vetmed.hokudai.ac.jp

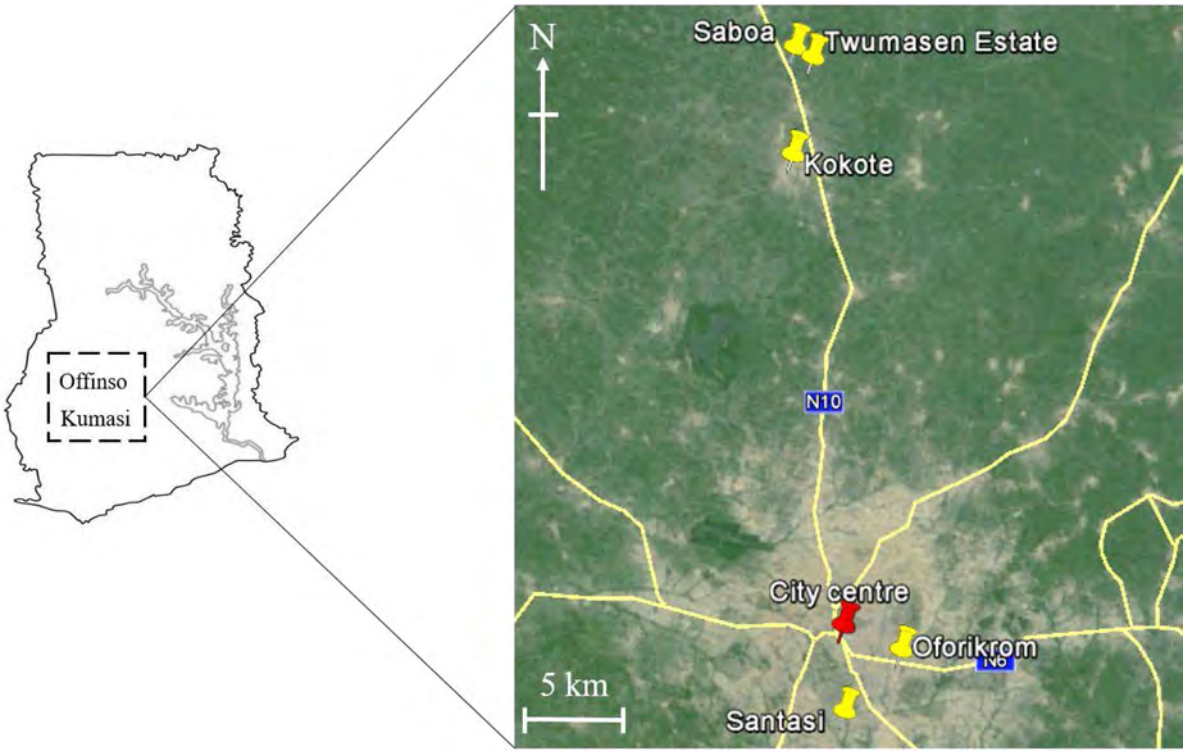

Fig. 1. Map showing cattle urine sampling locations in the Ashanti Region, Ghana (yellow pins indicate sampled locations and red pin indicates city center in Kumasi) (Obtained from Bortey-Sam *et al.* [6]).

1-OHPyr was detected in cattle urine in rural and urban sites of Ghana. Although not significant, the levels of 1-OHPyr detected in cattle urine from urban sites was higher than rural sites and vehicular traffic was the major contributing factor [6]. Bortey-Sam *et al.* [6] further highlighted that 1-OHPyr was higher (P>0.05) in female compared to male cattle. The high urinary concentrations of 1-OHPyr could be due to high exposure of cattle to PAHs including pyrene [6]. Despite this, there is limited/no study from literature that has determined the levels of conjugated pyrene metabolites in cattle urine. Based on these findings and gaps, the objectives of the current study were to: determine the concentrations of conjugated pyrene metabolites in urine of cattle that has been environmentally exposed to pyrene; and find any sex and site differences in urinary excretion of these conjugated metabolites.

MATERIALS AND METHODS

Sampling

In August 2014, urine of healthy cattle (West African Shorthorn) were randomly collected from 5 communities in Kumasi and Offinso, both in the Ashanti Region of Ghana. Offinso is about 33 km from the city centre of Kumasi (Fig. 1). In Kumasi (urban), samples were collected from Oforikrom and Santasi, which are 5.1 and 3.5 km from the city centre, respectively, where previous studies reported high concentrations of PAHs including pyrene in particulate matter with diameter 10 μm or less (PM10), soils and livers of wild rats [4, 5, 7, 8]. On the other hand, the three sites in Offinso (Twumasen Estate, Saboa and Kokote) selected for cattle urine sampling (Fig. 1) are in rural and agricultural areas.

A total of 95 spot urine (30 males and 65 females) were collected from cattle within these rural and urban sites (Fig. 1). The samples collected were transferred to labeled corning tubes (Corning Inc., Corning, NY, U.S.A.) and kept frozen at the Department of Chemistry, Kwame Nkrumah University Science and Technology (KNUST), Ghana. Only ages of cattle from two sites (Twumasen Estate and Saboa) were obtained from the herdsmen and the average ages were 2.9 ± 1.0 years (Twumasen Estate) and 4.2 ± 2.9 years (Saboa). Later, the samples collected were transported to the Laboratory of Toxicology, Graduate School of Veterinary Medicine, Hokkaido University, Japan where they were stored at −30°C until analysis (quarantine number for importing is 26 douken 383).

Extraction and analysis of conjugated pyrene metabolites

The extraction process was modified from previous protocols [32, 33]. Briefly, 5 m*l* of urine was acidified (to pH 6.8) with 1 M formic acid (Wako Pure Chemicals, Osaka, Japan) and 6-hydroxychrysene (AccuStandard Incorporation, New Haven, CT, U.S.A.) added as an internal standard. The acidified samples were loaded onto an Oasis WAX plus solid-phase extraction cartridge (50 mg; Waters) conditioned with 10 m*l* methanol and MilliQ water (10 m*l*). The loaded samples were washed with 5 m*l* each of 0.1 M

sodium hydroxide solution, 0.1 M sodium phosphate buffer (pH 7.4) and Milli Q water. Cartridges were then dried under vacuum. The target analytes were sequentially eluted with methanol/10% formic acid solution (9:1 v/v, 10 m*l*), and then with methanol/ethyl acetate/diethylamine solution (50:50:1 v/v, 2 m*l*). The eluate was reduced to 100 μl under a gentle nitrogen flow, and re-dissolved to 0.5 m*l* using methanol for LC-MS/MS analysis with an ODS-120 T column (ODS-120T 2.1 × 300 mm; Tosoh).

Samples were analyzed for 1-OHPyrene glucuronide (PyG), 1-OHPyrene sulfate (PyS) and two isomers of Pyrenedoil sulfate (M2 and M3) (represented as PydiolS, M2 and M3). Mobile phase A consisted of 10 mM ammonium acetate buffer (pH 5.0), and mobile phase B was a methanol/acetonitrile/water solution (38:57:5, v/v/v). The solvent gradient was as follows: 10% mobile phase B at the first 2 min, followed by a linear gradient to 100% mobile phase B from 2 to 35 min, and then 100% mobile phase B at 35 to 45 min. Solvent flow rate was 0.5 m*l*/min, and column temperature was 45°C. Target compounds were determined by multiple-reaction monitoring (MRM) in the negative ionization mode. A Shimadzu 8030 triple quadrupole mass spectrometer, upgraded to 8040 with UF lens, (ESI MS-MS; Shimadzu Corp., Kyoto, Japan), equipped with a Prominence UFLC system (Shimadzu Corp.) was used for analysis.

Specific gravity (SG) of cattle urine

In this study, specific gravity (SG) illustrated by Nermell *et al.* [30] was used to adjust urinary concentrations of conjugated pyrene metabolites. The mean (ranges) SG detected in cattle urine using a refractometer (ATAGO Co., Ltd., PAL-095, Tokyo, Japan) were Oforikrom (1.013; [1.004–1.029]), Santasi (1.035; [1.03–1.041]), Twumasen Estate (1.035; [1.028–1.04]), Saboa (1.036; [1.026–1.049]) and Kokote (1.037; [1.029–1.042]). The formula applied [30] to each urine concentration was as follows:

$$\text{SG\_corrected concentration} = \text{urinary OH} - \text{PAH concentration} \times \frac{(\text{SG}_{\text{target}} - 1.0)}{(\text{SG}_{\text{sample}} - 1.0)}$$

Where, $\text{SG}_{\text{target}}$ is the mean specific gravity of cattle urine per community; $\text{SG}_{\text{sample}}$ is the specific gravity of a particular sample.

Quality control and quality assurance

For measurement of conjugated pyrene metabolites, quantitation was performed using six–point calibration; 1, 5, 10, 25, 50 and 100 μg/*l*), and linearity (r^2) were all greater than 0.995. Analytical methods were checked for precision and accuracy. Limits of detection (LODs) were calculated based on 3SD/S (SD is the standard deviation of the response of seven replicate standard solution measurements and S is the slope of the calibration curve). LOD ranged from 0.57–1.70 *n*g/m*l* for PyG and PydiolS (M3), respectively and average recovery rate (%) for 6-hydroxy chrysene was 93.3 ± 10.5. For every batch of 10 samples, a solvent blank, a spiked solvent blank (internal standard spiked into solvent), and duplicate sample were analyzed. The average recovery in spiked blanks was 97 ± 9.3%. Blanks were run periodically and contained no detectable amount of target analyte. The coefficients of variation was less than 20%.

Statistical analysis

Data analysis was performed using IBM SPSS v 20 (SPSS Incorporation, Chicago, IL, U.S.A.). Kolmogorov-Smirnov (K-S) and Shapiro-Wilks (S-W) tests were used to determine the normality of data and were considered statistically significant if *P* value was less than 0.05. Concentrations of conjugated pyrene metabolites below their respective LODs were replaced with a value of LOD/2. ANOVA and Tukey analyses of log transformed data were used to compare concentrations in cattle urine from the study areas and differences were considered statistically significant with *P* value <0.05. Student's *t*-test was also used to compare concentrations between male and female cattle; and, between urban and rural sites. Pearson's correlation of log transformed data was used to determine the relationship between 1-OHPyr and conjugated pyrene metabolites. Statistical significance for the correlation analysis was at a *P* value<0.05. Data for 1-OHPyr was obtained from Bortey-Sam *et al.* [6].

RESULTS

The normality tests (K-S and S-W's tests) showed a significant variation ($P<0.01$) in the distribution of the conjugated pyrene metabolites measured. As shown in Table 1, there was no significant difference ($P>0.05$) in the levels of PyG, PyS and PydiolS (M3) excreted in cattle urine from the study areas except PydiolS (M3) which was significantly lower in cattle in Oforikrom. Moreover, PydiolS (M2) was significantly higher ($P<0.05$) in Kokote compared to Twumasen Estate and Oforikrom.

Specific gravity adjusted geometric mean concentrations (GM_{SG}) revealed PyG (4.10 ± 4.44 *n*g/m*l*) as the most dominant conjugate in cattle urine from all study sites followed by PydiolS (M3) (3.14 ± 2.96 *n*g/m*l*) >PydiolS (M2) (1.24 ± 1.68 *n*g/m*l*) and >PyS (0.424 ± 0.435 *n*g/m*l*).

With the exception of PyS, urinary concentrations of conjugated pyrene metabolites were higher ($P>0.05$) in rural sites compared to urban sites (Table 2). Moreover, no significant gender differences ($P>0.05$) were observed for the conjugated pyrene metabolites studied (Table 3).

The study revealed significant correlation ($P<0.05$) between 1-OHPyr and PydiolS (M2) (Table 4) although, there was no significant association between 1-OHPyr and the other conjugated metabolites (Table 4). The study further showed that the sum of conjugated pyrene metabolites (∑Conj Pyr met) and sum of both conjugated and deconjugated pyrene metabolites (∑Pyrene met) correlated significantly ($P<0.01$) with PyG, PydiolS (M2) and PydiolS (M3) (Table 4). Similarly, there was a significant correlation

Table 1. Specific gravity adjusted concentrations (*n*g/m*l*) of conjugated pyrene metabolites in cattle urine in the Ashanti Region of Ghana

Sample site		n	Location	PyG	PyS	PydiolS (M2)	PydiolS (M3)
Oforikrom	$GM_{SG} \pm SD$	8	urban	2.88 ± 3.58[a)]	0.684 ± 0.634[a)]	0.260 ± 0.198[c)]	1.19 ± 1.09[b)]
Santasi	$GM_{SG} \pm SD$	9	urban	4.19 ± 2.49[a)]	0.516 ± 0.365[a)]	1.66 ± 1.59[ab)]	3.29 ± 2.72[a)]
Twumasen Estate	$GM_{SG} \pm SD$	31	rural	4.33 ± 4.27[a)]	0.341 ± 0.197[a)]	1.040 ± 0.866[bc)]	2.71 ± 2.06[a)]
Saboa	$GM_{SG} \pm SD$	40	rural	4.64 ± 5.07[a)]	0.417 ± 0.497[a)]	1.51 ± 2.09[a)]	4.10 ± 3.41[a)]
Kokote	$GM_{SG} \pm SD$	7	rural	2.28 ± 1.77[a)]	0.553 ± 0.437[a)]	2.35 ± 1.31[a)]	1.810 ± 0.997[a)]

n: number of samples; different letter (a, b, c and d) within a column indicate significant difference ($P<0.05$) among communities; GM_{SG}: geometric mean concentration adjusted by specific gravity; SD: standard deviation.

Table 2. Specific gravity adjusted concentrations (*n*g/m*l*) of conjugated pyrene metabolites in cattle urine from urban and rural sites

Site		n	PyG	PyS	PydiolS (M2)	PydiolS (M3)
Urban	$GM_{SG} \pm SD$	17	3.52 ± 2.99[a)]	0.589 ± 0.514[a)]	0.793 ± 1.52[a)]	2.55 ± 2.63[a)]
Rural	$GM_{SG} \pm SD$	78	4.24 ± 4.67[a)]	0.395 ± 0.409[a)]	1.36 ± 1.71[a)]	3.24 ± 3.01[a)]

n: number of samples; GM_{SG}: geometric mean concentration adjusted by specific gravity; SD: standard deviation; different letters (a and b) within a column indicate significant differences (Student's *t*-test; $P<0.05$).

Table 3. Sex differences in urinary excretion (*n*g/m*l*) of conjugated pyrene metabolites

Sex		n	PyG	PyS	PydiolS (M2)	PydiolS (M3)
Male	$GM_{SG} \pm SD$	30	4.16 ± 3.72[a)]	0.545 ± 0.535[a)]	1.00 ± 1.17[a)]	2.71 ± 2.74[a)]
Female	$GM_{SG} \pm SD$	65	4.07 ± 4.76[a)]	0.378 ± 0.363[a)]	1.37 ± 1.86[a)]	3.31 ± 3.02[a)]

n: number of samples; GM_{SG}: geometric mean concentration adjusted by specific gravity; SD: standard deviation; different letters (a and b) within a column indicate significant differences (Student's *t*-test; $P<0.05$).

Table 4. Pearson's correlation of 1-OHPyr and conjugated pyrene metabolites in cattle urine

Variables	PyG	PyS	PydiolS (M2)	PydiolS (M3)	∑Conj Pyr met	1-OHPyr	∑Pyrene met
PyG	1						
PyS	−0.0804	1					
PydiolS (M2)	0.0520	−0.169	1				
PydiolS (M3)	0.340[b)]	0.133	0.186	1			
∑Conj Pyr met	0.796[b)]	−0.0073	0.398[b)]	0.695[b)]	1		
1-OHPyr	−0.181	−0.205	0.256[a)]	−0.135	−0.0717	1	
∑Pyrene met	0.768[b)]	−0.0445	0.436[b)]	0.678[b)]	0.986[b)]	0.0747	1

1-OHPyr: 1-hydroxy pyrene; PyG: 1-hydroxy pyrene glucuronide; PyS: 1-hydroxy pyrene sulfate; PydiolS (M2): pyrenediol sulfate (M2); PydiolS (M3): pyrenediol sulfate (M3); ∑Conjugated Pyr: sum of conjugated pyrene metabolites; ∑Pyrene met: sum of conjugated and deconjugated pyrene metabolites; a) $P<0.05$; b) $P<0.01$.

($P<0.01$) between PyG and PydiolS (M3). As shown in Table 4, there was no significant correlation between other conjugated pyrene metabolites.

DISCUSSION

Excretion of conjugated pyrene metabolites in cattle urine

The significantly higher ($P<0.05$) levels of PydiolS (M2) in Kokote compared to Twumasen Estate and Oforikrom could be due to differences in levels of exposure and/or metabolism. In a previous study, urinary concentrations of 1-OHPyr was significantly higher ($P<0.05$) in cattle in Kokote than levels in cattle in Saboa and Twumasen Estate [6].

In a study by Saengtienchai *et al.* in Japan and Thailand, PyG was the dominant conjugate excreted via urine in the majority of mammals including cattle [33]. Pyrene-1-sulfate, pyrenediol-sulfate and pyrenediol-disulfate were also detected in urine of cattle and other mammals [33]. A wide range of species including mice, rats, dogs, cattle, rabbits and pigs all have genomes containing a single SULT1A1 gene [9, 18, 27]. However, in ungulates, the UGT activities may be higher than SULT [15, 36].

Unadjusted urinary levels of PyG in cattle from this study were comparable to higher than the study conducted in Japan and Thailand [33]. The higher levels in this study could be attributed to cattle's exposure to higher levels of pyrene from the study area

[6]. Bortey-Sam *et al.* highlighted that catttle's exposure to pyrene in the Ashanti Region of Ghana could mainly be attributed to vehicular activities or traffic [6]. In Kumasi, fuel combustion was the dominant source of PAHs in PM10 and soils, and pyrene was highly abundant [7, 8]. Moreover, some farms in Ghana are located near major road with high vehicular activities or traffic and grazing animals could be exposed to pyrene through this process [40]. According to Laflamme and Hites, during vehicular emission, the high molecular weight PAHs, including pyrene, are dominant [23]. PAHs in the atmosphere are known to settle in soil [31] and this could also increase cattle's exposure, because these free-range cattle pick food and/or water from the ground.

Site differences in urinary excretions of conjugated pyrene metabolites

This study revealed that cattle in rural sites were exposed to higher levels of pyrene. In previous studies there was no significant difference (P>0.05) in urinary excretion of 1-OHPyr in cattle in rural and urban sites. In a study by Ferrari *et al.* [17], higher levels of 1-OHPyr were detected in urine of cattle in rural areas compared to urban. Ferrari *et al.* therefore suggested that there could be other sources of pyrene exposure besides traffic [17] such as barn dust, soils, indoor air and/or forage [13].

Sex differences in urinary excretions of conjugated pyrene metabolites

There are only a few studies in literature that have assessed gender differences in urinary excretion of PAH metabolites in cattle [6]. Bortey-Sam *et al.* [6] indicated that there was no significant sex difference in urinary concentrations of 1-OHPyr between male and female cattle. However, differences or similarities in urinary excretion PAH metabolite in humans have been documented [3, 11, 25, 39]. Thai *et al.* [41] revealed no differences between male and female in urinary concentrations of OHPyr in humans, which was similar to other results obtained [3, 11, 25]. On the other hand, urinary 1-OHPyr levels were higher in women than men workers [20]. The reason for these similarities and differences could be due to the fact that intake, accumulation and excretion rates of chemicals differ by sex in cattle, although information on other factors such as ADME (absorption, distribution, metabolism and excretion) would be needed to support this statement [22].

The differences or similarities in urinary excretion of conjugated pyrene metabolites between sexes could also be due to non-pharmacogenetic factors including age, species, disease factors or exposure to environmental pollutants which could contribute to the expression and regulation of hepatic P450 in these domestic animals [19, 29]. In addition, although no gender difference was observed in male and female limousin cattle, male piedmontese cattle showed significantly higher CYP3A-dependent drug metabolizing enzyme activities compared to females [14].

Correlation between 1-OHPyr and conjugated pyrene metabolites

The results obtained from this study was similar to previous studies (mammalian urine) where no significant correlations existed between 1-OHPyr and total pyrene metabolites. Moreover, 1-OHPyr did not show any significant correlation with conjugated metabolites such as PyG and PyS. Furthermore, PyS showed no association (P>0.05) with PyG and total pyrene metabolites in mammalian urine. Nonetheless, a positive association (r=0.996, P<0.05) was observed between urinary PyG and total pyrene metabolites [33]. The possible reason for these correlations, especially, between PyG and ∑Pyrene met/∑Conj Pyr met could be due to the fact that glucuronide have been shown to account for over 80% of total pyrene metabolites in human urine [34]. Moreover, in a study of healthy and non-smoking humans, Saengtienchai *et al.* [33] found that over 75% of total pyrene metabolites existed as glucuronide conjugate. This trend could be due to high activity of UGT enzymes, which have been known to be involved in glucuronidation of 1-OHPyr in human, mice and ungulates [21, 24, 28, 33, 34, 37, 38]. The UGT activity in addition to other substrates have been suggested to be higher than SULT in ungulates [15, 33, 36].

In conclusion, cattle in Kumasi and Offinso (Ghana) have been exposed to high levels of pyrene. Of the urinary concentrations of conjugated pyrene metabolites studied, PyG was the most abundant followed by PydiolS (M3). The study revealed no significant difference in urinary concentrations of conjugated pyrene metabolites between rural and urban sites, and similar to urban areas, cattle in rural sites were exposed to high levels of pyrene. From this study, there was no significant difference in urinary excretion of conjugated pyrene metabolites between sexes.

ACKNOWLEDGMENTS. This work was supported by Grants-in-Aid for Scientific Research from the Ministry of Education, Culture, Sports, Science and Technology of Japan awarded to M. Ishizuka (No. 16H0177906), Y. Ikenaka (No. 26304043, 15H0282505, 15K1221305), S. Nakayama (16K16197), and the foundations of Sumitomo and JSPS Core to Core Program (AA Science Platforms) and Bilateral Joint Research Project (PG36150002 and PG36150003). We also acknowledge the financial support by The Mitsui & Co., Ltd. Environment Fund, the Soroptimist Japan Foundation and the Nakajima Foundation. We are grateful to Mr. Takahiro Ichise for technical support.

REFERENCES

1. ATSDR 2015. Priority List of Hazardous Substances. ATSDR (Agency for Toxic Substance and Disease Registry), Division Of Toxicology & Human Health Sciences.
2. Barranco, A., Alonso-Salces, R. M., Crespo, I., Berrueta, L. A., Gallo, B., Vicente, F. and Sarobe, M. 2004. Polycyclic aromatic hydrocarbon content in commercial Spanish fatty foods. *J. Food Prot.* **67**: 2786–2791. [Medline] [CrossRef]
3. Bartolomé, M., Ramos, J. J., Cutanda, F., Huetos, O., Esteban, M., Ruiz-Moraga, M., Calvo, E., Pérez-Gómez, B., González, O., Castaño A., BIOAMBIENT.ES 2015. Urinary polycyclic aromatic hydrocarbon metabolites levels in a representative sample of the Spanish adult population:

The BIOAMBIENT.ES project. *Chemosphere* **135**: 436–446. [Medline] [CrossRef]
4. Bortey-Sam, N., Akoto, O., Ikenaka, Y., Nakayama, S. M. and Ishizuka, M. 2013. Determination of benzo[a]pyrene levels in ambient air and the source of polycyclic aromatic hydrocarbons using a diagnostic ratio method in Ghana. *Jpn. J. Vet. Res.* **61** Suppl: S72–S74. [Medline]
5. Bortey-Sam, N., Ikenaka, Y., Akoto, O., Nakayama, S., Beyene, Y., Yohannes, E. B., Saengtienchai, A., Mizukawa, H. and Ishizuka, M. 2015. Exposure levels of polycyclic aromatic hydrocarbons (PAHs) and heavy metals in wild rats in Kumasi, Ghana. 7th International Toxicology Symposium in Africa.
6. Bortey-Sam, N., Ikenaka, Y., Akoto, O., Nakayama, S. M. M., Marfo, J., Saengtienchai, A., Mizukawa, H. and Ishizuka, M. 2016. Excretion of polycyclic aromatic hydrocarbon metabolites (OH-PAHs) in cattle urine in Ghana. *Environ. Pollut.* **218**: 331–337. [Medline] [CrossRef]
7. Bortey-Sam, N., Ikenaka, Y., Akoto, O., Nakayama, S. M., Yohannes, Y. B., Baidoo, E., Mizukawa, H. and Ishizuka, M. 2015. Levels, potential sources and human health risk of polycyclic aromatic hydrocarbons (PAHs) in particulate matter (PM(10)) in Kumasi, Ghana. *Environ. Sci. Pollut. Res. Int.* **22**: 9658–9667. [Medline] [CrossRef]
8. Bortey-Sam, N., Ikenaka, Y., Nakayama, S. M. M., Akoto, O., Yohannes, Y. B., Baidoo, E., Mizukawa, H. and Ishizuka, M. 2014. Occurrence, distribution, sources and toxic potential of polycyclic aromatic hydrocarbons (PAHs) in surface soils from the Kumasi Metropolis, Ghana. *Sci. Total Environ.* **496**: 471–478. [Medline] [CrossRef]
9. Bradley, M. E. and Benner, S. A. 2005. Phylogenomic approaches to common problems encountered in the analysis of low copy repeats: the sulfotransferase 1A gene family example. *BMC Evol. Biol.* **5**: 22. [Medline] [CrossRef]
10. Burgaz, S., Borm, P. J. and Jongeneelen, F. J. 1992. Evaluation of urinary excretion of 1-hydroxypyrene and thioethers in workers exposed to bitumen fumes. *Int. Arch. Occup. Environ. Health* **63**: 397–401. [Medline] [CrossRef]
11. CDC 2005. National Center for Environmental Health. Third National Report on Human Exposure to Environmental Chemicals. NCEH Pub. No. 05-0570; 2005. Atlanta.
12. Chetiyanukornkul, T., Toriba, A., Kameda, T., Tang, N. and Hayakawa, K. 2006. Simultaneous determination of urinary hydroxylated metabolites of naphthalene, fluorene, phenanthrene, fluoranthene and pyrene as multiple biomarkers of exposure to polycyclic aromatic hydrocarbons. *Anal. Bioanal. Chem.* **386**: 712–718. [Medline] [CrossRef]
13. Ciganek, M., Ulrich, R., Neca, J. and Raszyk, J. 2002. Exposure of pig fatteners and dairy cows to polycyclic aromatic hydrocarbons. *Vet. Med. (Praha)* **47**: 137–142.
14. Dacasto, M., Eeckhoutte, C., Capolongoa, F., Dupuy, J., Carletti, M., Calléja, C., Nebbia, C., Alvinerie, M. and Galtier, P. 2005. Effect of breed and gender on bovine liver cytochrome P450 3A (CYP3A) expression and inter-species comparison with other domestic ruminants. *Vet. Res.* **36**: 179–190. [Medline] [CrossRef]
15. Darwish, W., Ikenaka, Y., Eldaly, E. and Ishizuka, M. 2010. Mutagenic activation and detoxification of benzo[a]pyrene in vitro by hepatic cytochrome P450 1A1 and phase II enzymes in three meat-producing animals. *Food Chem. Toxicol.* **48**: 2526–2531. [Medline] [CrossRef]
16. Dissanayake, A. and Galloway, T. S. 2004. Evaluation of fixed wavelength fluorescence and synchronous fluorescence spectrophotometry as a biomonitoring tool of environmental contamination. *Mar. Environ. Res.* **58**: 281–285. [Medline] [CrossRef]
17. Ferrari, S., Mandel, F. and Berset, J. D. 2002. Quantitative determination of 1 -hydroxypyrene in bovine urine samples using high-performance liquid chromatography with fluorescence and mass spectrometric detection. *Chemosphere* **47**: 173–182. [Medline] [CrossRef]
18. Gamage, N., Barnett, A., Hempel, N., Duggleby, R. G., Windmill, K. F., Martin, J. L. and McManus, M. E. 2006. Human sulfotransferases and their role in chemical metabolism. *Toxicol. Sci.* **90**: 5–22. [Medline] [CrossRef]
19. Guengerich, F. P. 2002. Cytochrome p. 450. *In*: Enzyme Systems That Metabolise Drugs and Other Xenobiotics. (Ioannides C. ed.), John Wiley & Sons Inc., New York.
20. Guo, H., Huang, K., Zhang, X., Zhang, W., Guan, L., Kuang, D., Deng, Q., Deng, H., Zhang, X., He, M., Christiani, D. and Wu, T. 2014. Women are more susceptible than men to oxidative stress and chromosome damage caused by polycyclic aromatic hydrocarbons exposure. *Environ. Mol. Mutagen.* **55**: 472–481. [Medline] [CrossRef]
21. Kakimoto, K., Toriba, A., Ohno, T., Ueno, M., Kameda, T., Tang, N. and Hayakawa, K. 2008. Direct measurement of the glucuronide conjugate of 1-hydroxypyrene in human urine by using liquid chromatography with tandem mass spectrometry. *J. Chromatogr. B Analyt. Technol. Biomed. Life Sci.* **867**: 259–263. [Medline] [CrossRef]
22. Kim, M., Kim, D. G., Bong, Y. H., Jang, J. H. and Son, S. W. 2013. Concentrations of PCDD/Fs, dioxin-like PCBs, PBDEs, and hexachlorobenzene in fat samples from cattle of different ages and gender in Korea. *Food Chem.* **138**: 1786–1791. [Medline] [CrossRef]
23. Laflamme, R. E. and Hites, R. A. 1978. The global distribution of polycyclic aromatic hydrocarbons in recent sediments. *Geochim. Cosmochim. Acta* **42**: 289–303. [CrossRef]
24. Lee, C. H., Ito, Y., Yanagiba, Y., Yamanoshita, O., Kim, H., Zhang, S. Y., Kamijima, M., Gonzalez, F. J. and Nakajima, T. 2007. Pyrene-induced CYP1A2 and SULT1A1 may be regulated by CAR and not by AhR. *Toxicology* **238**: 147–156. [Medline] [CrossRef]
25. Levine, H., Berman, T., Goldsmith, R., Göen, T., Spungen, J., Novack, L., Amitai, Y., Shohat, T. and Grotto, I. 2015. Urinary concentrations of polycyclic aromatic hydrocarbons in Israeli adults: demographic and life-style predictors. *Int. J. Hyg. Environ. Health* **218**: 123–131. [Medline] [CrossRef]
26. Li, Z., Sandau, C. D., Romanoff, L. C., Caudill, S. P., Sjodin, A., Needham, L. L. and Patterson, D. G. Jr. 2008. Concentration and profile of 22 urinary polycyclic aromatic hydrocarbon metabolites in the US population. *Environ. Res.* **107**: 320–331. [Medline] [CrossRef]
27. Lin, Z., Lou, Y. and Squires, J. E. 2004. Molecular cloning and functional analysis of porcine SULT1A1 gene and its variant: a single mutation SULT1A1 causes a significant decrease in sulfation activity. *Mamm. Genome* **15**: 218–226. [Medline] [CrossRef]
28. Luukkanen, L., Mikkola, J., Forsman, T., Taavitsainen, P., Taskinen, J. and Elovaara, E. 2001. Glucuronidation of 1-hydroxypyrene by human liver microsomes and human UDP-glucuronosyltransferases UGT1A6, UGT1A7, and UGT1A9: development of a high-sensitivity glucuronidation assay for human tissue. *Drug Metab. Dispos.* **29**: 1096–1101. [Medline]
29. Nebbia, C. 2001. Biotransformation enzymes as determinants of xenobiotic toxicity in domestic animals. *Vet. J.* **161**: 238–252. [Medline] [CrossRef]
30. Nermell, B., Lindberg, A. L., Rahman, M., Berglund, M., Persson, L. A., El Arifeen, S. and Vahter, M. 2008. Urinary arsenic concentration adjustment factors and malnutrition. *Environ. Res.* **106**: 212–218. [Medline] [CrossRef]
31. Rey-Salgueiro, L., Martinez-Carballo, E., Garcia-Falcon, M. S. and Simal-Gandara, J. 2008. Effects of a chemical company fire on the occurrence of polycyclic aromatic hydrocarbons in plant foods. *Food Chem.* **108**: 347–353. [CrossRef]
32. Saengtienchai, A., Ikenaka, Y., Bortey-Sam, N., Jermnark, U., Mizukawa, H., Kawai, Y. K., Nakayama, S. M. M. and Ishizuka, M. 2016. The African hedgehog (Atelerix albiventris): Low phase I and phase II metabolism activities. *Comp. Biochem. Physiol. C Toxicol. Pharmacol.* **190**: 38–47 [Medline]. [Medline] [CrossRef]
33. Saengtienchai, A., Ikenaka, Y., Nakayama, S. M., Mizukawa, H., Kakehi, M., Bortey-Sam, N., Darwish, W. S., Tsubota, T., Terasaki, M.,

Poapolathep, A. and Ishizuka, M. 2014. Identification of interspecific differences in phase II reactions: determination of metabolites in the urine of 16 mammalian species exposed to environmental pyrene. *Environ. Toxicol. Chem.* **33**: 2062–2069. [Medline] [CrossRef]
34. Singh, R., Tuček, M., Maxa, K., Tenglerová, J. and Weyand, E. H. 1995. A rapid and simple method for the analysis of 1-hydroxypyrene glucuronide: a potential biomarker for polycyclic aromatic hydrocarbon exposure. *Carcinogenesis* **16**: 2909–2915. [Medline] [CrossRef]
35. Sinha, R., Peters, U., Cross, A. J., Kulldorff, M., Weissfeld, J. L., Pinsky, P. F., Rothman, N. and Hayes, R. B. 2005. Meat, meat cooking methods and preservation, and risk for colorectal adenoma. *Cancer Res.* **65**: 8034–8041. [Medline] [CrossRef]
36. Smith, G. S., Watkins, J. B., Thompson, T. N., Rozman, K. and Klaassen, C. D. 1984. Oxidative and conjugative metabolism of xenobiotics by livers of cattle, sheep, swine and rats. *J. Anim. Sci.* **58**: 386–395. [Medline] [CrossRef]
37. Strickland, P. and Kang, D. 1999. Urinary 1-hydroxypyrene and other PAH metabolites as biomarkers of exposure to environmental PAH in air particulate matter. *Toxicol. Lett.* **108**: 191–199. [Medline] [CrossRef]
38. Strickland, P. T., Kang, D., Bowman, E. D., Fitzwilliam, A., Downing, T. E., Rothman, N., Groopman, J. D. and Weston, A. 1994. Identification of 1-hydroxypyrene glucuronide as a major pyrene metabolite in human urine by synchronous fluorescence spectroscopy and gas chromatography-mass spectrometry. *Carcinogenesis* **15**: 483–487. [Medline] [CrossRef]
39. Sul, D., Ahn, R., Im, H., Oh, E., Kim, J. H., Kim, J. G., Kim, P., Kim, H. A., Park, W. Y., Son, B. S., Shin, D., Shim, A. S., Yang, W., Yu, S. D., Lee, K. H., Lee, K. J., Lee, S. D., Lee, J. W., Lee, C. K., Jang, B. K., Choi, K., Han, D. H., Hwang, M. Y. and Lee, J. H. 2012. Korea National Survey for Environmental Pollutants in the human body 2008: 1-hydroxypyrene, 2-naphthol, and cotinine in urine of the Korean population. *Environ. Res.* **118**: 25–30. [Medline] [CrossRef]
40. Tay, C. K. and Biney, C. A. 2013. Levels and sources of polycyclic aromatic hydrocarbons (PAHs) in selected irrigated urban agricultural soils in Accra, Ghana. *Environ. Earth Sci.* **68**: 1773–1782. [CrossRef]
41. Thai, P. K., Heffernan, A. L., Toms, L. L., Li, Z., Calafat, A. M., Hobson, P., Broomhall, S. and Mueller, J. F. 2016. Monitoring exposure to polycyclic aromatic hydrocarbons in an Australian population using pooled urine samples. *Environ. Int.* **88**: 30–35. [Medline] [CrossRef]

Chemosphere 212 (2018) 994–1001

Contents lists available at ScienceDirect

Chemosphere

journal homepage: www.elsevier.com/locate/chemosphere

Characterization and imaging of lead distribution in bones of lead-exposed birds by ICP-MS and LA-ICP-MS

Chihiro Ishii [a], Shouta M.M. Nakayama [a], Andrew Kataba [a], Yoshinori Ikenaka [a, b], Keisuke Saito [c], Yukiko Watanabe [c], Yoshiki Makino [d], Takehisa Matsukawa [e], Ayano Kubota [e], Kazuhito Yokoyama [e], Hazuki Mizukawa [a], Takafumi Hirata [d], Mayumi Ishizuka [a, *]

[a] Laboratory of Toxicology, Department of Environmental Veterinary Sciences, School of Veterinary Medicine, Hokkaido University, Sapporo, Kita18, Nishi9, Kita-ku, Sapporo, Hokkaido 060-0818, Japan
[b] Water Research Group, Unit for Environmental Sciences and Management, North-West University, Private Bag X6001, Potchefstroom, South Africa
[c] Institute for Raptor Biomedicine Japan, 2-2101, Hokuto, Kushiro-shi, Hokkaido 084-0922, Japan
[d] Graduate School of Science, The University of Tokyo, 7-3-1 Hongo, Bunkyo-ku, Tokyo 113-0033, Japan
[e] Department of Epidemiology and Environmental Health, Juntendo University Faculty of Medicine, 2-1-1 Hongo, Bunkyo-ku, Tokyo 113-8421, Japan

HIGHLIGHTS

- Bones have differing Pb accumulation patterns depending on bone type.
- Bones consist of trabecular tissue and contain bone marrow accumulate Pb rapidly.
- Pb levels between bone and other soft tissue have the significant correlation.
- Bone tissue could be a good indicator of Pb exposure and potential avian poisoning.

GRAPHICAL ABSTRACT

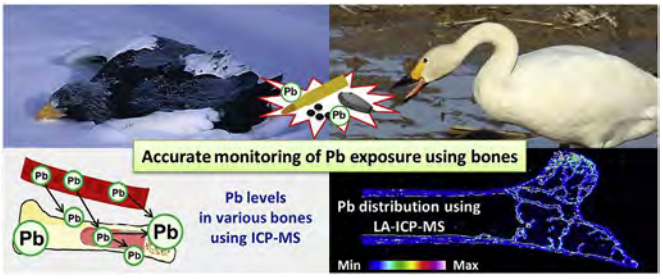

ARTICLE INFO

Article history:
Received 29 April 2018
Received in revised form
19 August 2018
Accepted 29 August 2018
Available online 31 August 2018

Handling Editor: Willie Peijnenburg

Keywords:
Pb accumulation
Trabecular bone
Bone marrow
Tissue correlation
Eagles
Swans

ABSTRACT

Lead (Pb) poisoning in raptors and water birds is a serious problem in many countries. However, only a small fraction of Pb poisoning has been detected in birds. Bone specimens may be useful indices of Pb exposure because bones contain ~90% of the total Pb body burden. The original purpose of this study was to comprehensively analyze Pb accumulation in various bone types using inductively coupled plasma-mass spectrometry (ICP-MS). Since our results showed that Pb accumulation differed greatly depending on bone type, a secondary objective was defined, aiming to investigate the fine Pb distribution and its relation to bone structure and bone marrow by using laser ablation (LA)-ICP-MS. Our findings suggested that bone samples (1) consisting of trabecular tissue and (2) those that contain bone marrow could accumulate high levels of Pb following acute exposure. The shorter turnover time of trabecular bone can cause a rapid accumulation of Pb, and bone marrow may have an important role for internal exposure of Pb to bone tissue. Pb is accumulated in bones via blood flow, and bone marrow receives blood from outside the bones. In conclusion, bone samples provide valuable information on Pb exposure and could be useful to investigate and understand mortalities related to suspected Pb poisoning.

* Corresponding author.
E-mail address: ishizum@vetmed.hokudai.ac.jp (M. Ishizuka).

https://doi.org/10.1016/j.chemosphere.2018.08.149
0045-6535/

1. Introduction

Many terrestrial and water birds die worldwide due to lead (Pb) poisoning (Andreotti and Borghesi, 2013; Berny et al., 2015; Fisher et al., 2006; Ishii et al., 2017; Kendall et al., 1996; Mateo, 2009; Scheuhammer and Norris, 1996; Whitehead and Tschirner, 1991). Pb is introduced to their habitats in the form of shotgun pellets, rifle bullets (that shatter into fragments on impact), or fishing tackles (i.e., sinkers). Raptors ingest Pb from prey that have been shot with Pb ammunition (Saito, 2009), and water birds ingest Pb fragments from shot pellets or fishing sinkers when they feed or take small stones from the sediment to act as gastroliths (Martinez-Haro et al., 2011).

Pb exposure can cause a variety of sub-lethal toxic effects and direct mortality (Kendall et al., 1996). Sub-lethal effects of Pb are exerted on the nervous system, kidney, liver, intestines and circulatory system, resulting in physiological, biological and behavioral changes (Cade, 2007; Fisher et al., 2006; Scheuhammer, 1987). Pb exposure also decrease the activity of δ-aminolevulinic acid dehydratase (ALA-d) - an enzyme of the heme biosynthesis pathway (Binkowski and Sawicka-Kapusta, 2015). As a result of these changes, birds may become increasingly susceptible to predation, starvation and infection by various diseases, increasing the probability of death from secondary causes (Fisher et al., 2006; Scheuhammer and Norris, 1996). For these reasons it is important to understand the adverse effect of Pb accumulation from the aspect of their conservation. Species with international statuses as endangered, vulnerable or threatened have been reported as ingesting and consequently being poisoned by Pb ammunition fragments, as for instance, Californian condor (*Gymnogyps californianus*), white-rumped vulture (*Gyps bengalensis*), Spanish imperial eagle (*Aquila adalberti*), whooping crane (*Grus americana*), Steller's sea eagle (*Haliaeetus pelagicus*) and white-tailed sea eagle (*Haliaeetus albicilla*) (Fisher et al., 2006). In Hokkaido, the northernmost island of Japan, many endangered Steller's sea eagles and white-tailed sea eagles are dying due to Pb toxicity despite regulations aiming to minimize the introduction of this element to their habitats (Saito, 2009). Many water birds, including swans, are also exposed to Pb in Japan (Honda et al., 1990) and around the world (Haig et al., 2014; Mateo, 2009; Rattner, 2009; Whitehead and Tschirner, 1991). However, only a fraction of Pb exposure has been identified because weak wild birds tend to hide from humans. Moreover, it is reported that the most important factor precluding the observation of Pb poisoned waterfowl is probably the rapid removal of sick and dead birds by predators and scavengers (Pain, 1991). Therefore, a greater understanding of Pb exposure in birds is necessary to improve the regulation and conservation of avian species.

Concentrations of Pb are generally highest in the blood immediately after absorption, followed by liver and kidneys within days to months, with Pb deposited in bone being able to remain for years (Fisher et al., 2006; Pain, 1996). Although liver or blood samples being traditionally used as indicators of Pb exposure, it might be difficult to obtain these specimens from the natural environment because other animals frequently consume the internal organs of carcasses. Bone specimens, on the other hand, remain in the environment, and many bones are kept in museums or universities, being available for analysis.

Bones contain 84%–90% of the total Pb body burden in raptors (García-Fernández et al., 1997), and Pb can substitute Ca in hydroxyapatite of bones (Ellis et al., 2006). Previous studies investigating Pb exposure in birds using bones have focused on the humerus or femur (Mateo et al., 2003; Pain et al., 2005), and ulna (Ethier et al., 2007). The accumulation patterns of Pb differ depending on the structure and function of the bone. Therefore, an understanding of Pb distribution in various types of bones becomes fundamental for monitoring Pb exposure in birds.

The original purpose of this study was to comprehensively analyze Pb accumulation in various bone types of birds using ICP-MS. Bone types that could potentially be used as indicators for Pb exposure were discussed. The second purpose was to analyze more detailed accumulation features of Pb in according to bone type, by element imaging using laser ablation-inductively coupled plasma-mass spectrometry (LA-ICP-MS). By revealing the detailed distribution of Pb, a conjecture upon the route of Pb accumulation in bones can be attained. For this purpose, the femur and tibiotarsus were specifically selected to understand the differences between swans and eagles based on the presence or absence of bone marrow (tibiotarsus possesses bone marrow in both species, but only swans have bone marrow in the femur). LA-ICP-MS plays a key role as a microanalytical technique, and enables multi-element analysis, and has been used to produce images of detailed, regionally-specific element distribution in thin sections of tissues (Becker et al., 2007; Limbeck et al., 2015). Other elements, such as cadmium (Cd), were also measured to compare with Pb accumulation. To our knowledge, this is the first study to perform LA-ICP-MS analysis in avian bones to investigate Pb exposure. Detailed imaging of Pb distribution and the comparison of Pb localization with other elements in bones should help us understand the accumulation mechanisms of Pb, and more accurately assess Pb exposure and mortality in birds.

2. Materials and methods

2.1. Sampling

This study analyzed carcasses of Steller's sea eagle (n = 3), white-tailed sea eagle (n = 2), whooper swan (*Cygnus cygnus*, n = 2) and an unknown species of swan (n = 2) all of which except for one swan (swan D) likely died due to Pb poisoning, according to the hepatic Pb levels. The categories used in Japan are as follows; hepatic Pb concentration in wet weight: < 0.2 mg/kg, normal range; 0.2–2 mg/kg, abnormal level of Pb exposure; and >2 mg/kg, Pb poisoning (Saito, 2009). Swan (D) also accumulated abnormal level of Pb, but not up to the lethality level. Swan (D) was included in the analysis to elucidate the effects of different levels of Pb accumulation. A mountain hawk-eagle (*Spizaetus nipalensis*, n = 1) that died due to other causes in a Pb free environment was used as a control. The Kushiro Nature Conservation Office, Ministry of the Environment, and Institute for Raptor Biomedicine Japan provided all the Steller's sea eagles, one of the white-tailed sea eagles, one of the swans and the mountain hawk-eagle. The Hokkaido Institute of Public Health provided another white-tailed sea eagle. The Ibaraki Prefectural Government, Environmental Policy Division, provided three of the swans. Bones (cranial bone, hyoid bone, atlas, axis, 3rd and 4th cervical vertebrae, notarium, scapula, sternum, keel, coracoideum, costa vertebralis, costa sternalis, ilium, pygostyle, humerus, radius, ulna, phalanx distalis digiti majoris, femur, patella, tibiotarsus, fibula, tarsometatarsus, and os digiti pedis), spinal cord specimens, and bone marrow (axis, radius, ulna, tibiotarsus, and tarsometatarsus) were collected from the birds (Fig. S1). Bone marrow from the femur was collected in all the swans. For the spinal cord, the spinous process was collected. For the long bones, diaphysis was selected. For the femur and tibiotarsus, diaphysis (proximal, medial, and distal) and epiphysis (surface and core in proximal and distal) were collected (Fig. S2). Two samples were collected from the same parts of all the bone types and the average concentration of the two samples was used. The femur and tibiotarsus were specifically selected for this study to understand the

differences between swans and eagles based on the presence or absence of bone marrow. Femur bones in swans contain bone marrow, whereas in eagles they do not. Bone marrow is present in the tibiotarsus of both birds. For the duplication of measurements, replicate sub-samples were taken from the same region of the same bone. The average concentration from each region was used for the analysis. Several bone parts could not be collected for the analysis, because they had been used for taxidermy or had already been removed. Bone samples were kept at −20 °C. All the samples used during this study were obtained either from animals involved in road-kill incidents or unsuccessful treatment of poisoning cases, being only analyzed following official approval from the Ministry of the Environment.

2.2. Analysis of element concentrations using ICP-MS

Periosteum (a specialized connective tissue covering all bones of the body) was removed from bone samples. After that, samples were washed with distilled water (Maruyama Manufacturing, Tokyo, Japan) and ultrasonicated to remove other remaining tissue before drying. The analysis of element concentrations followed the method in Yabe et al. (2015). Samples were dried for 24 h at 50 °C and digested with nitric acid (Kanto Chemical Corporation, Tokyo, Japan) and hydrogen peroxide (Kanto Chemical Corporation) in a microwave digestion system (Speedwave Two, Berghof, Germany). Concentrations of elements were measured with an inductively coupled plasma-mass spectrometer (ICP-MS; 7700 series, Agilent Technology, Tokyo, Japan). Analytical quality control was performed using Bone Ash (National Institute of Standards and Technology, Gaithersburg, MD), DOLT-4 (dogfish liver) and DORM-3 (fish protein) (National Research Council of Canada, Ottawa, Canada) certified reference materials. Replicate analyses of these reference materials showed good recoveries (80%–102%). The detection limits for Pb, iron (Fe), copper (Cu), zinc (Zn), arsenic (As), cadmium (Cd) were 0.001, 0.154, 0.007, 0.226, 0.002, and 0.001 μg/kg. RSD values were lower than 10%. More details regarding pretreatment and mass spectrometry procedures are presented in Text S2 and Table S1.

2.3. Analysis of element distribution using LA-ICP-MS

The bones were briefly washed and embedded in epoxy resin, sliced to ~40 μm sections along the transversal axis, and polished. The bone sections were systematically scanned by a focused laser beam using LA (NWR213; ESI, Portland, OR, USA)-ICP-QQQ-MS (8800 series; Agilent Technologies, Tokyo, Japan). LA-ICP-MS operating conditions were optimized using NIST 610 glass (National Institute of Standards and Technology, Gaithersburg, MD, USA). Images of LA-ICP-MS were reconstructed by iQuant2 (Suzuki et al., submitted to Journal of Mass Spectrometry Society of Japan). More details regarding pretreatment and mass spectrometry procedures are presented in Text S2 and Table S2.

2.4. Statistics

Spearman's rank correlation coefficient (ρ) was used to analyze the relationships among the bones, livers, and kidneys of eagles and swans with a significance level of $p < 0.05$. Statistical analyses were performed in JMP Pro 14 (SAS Institute, Cary, NC).

3. Results

3.1. Differences in Pb concentration depend on bone type

All data, including the concentrations of elements and replicate samples collected from each bone, is shown in Table S4 and S5. There were large differences in Pb concentration depending on bone type. In eagles, the axis, hyoid (around the greater horn), keel, pygostyle and patella accumulated higher Pb concentrations (generally exceeded 50 mg/kg and sometimes 100 mg/kg in several birds) than cortical bones (Fig. 1). In swans, the hyoid bone, scapula, keel, costa vertebralis and pygostyle had higher Pb concentrations (also over 100 mg/kg in several birds) than cortical bones (Fig. 2). Although the Pb concentration in one swan (D) was lower (<5 mg/kg) than in the other three swans, it exhibited similar Pb distribution patterns (Fig. S3). The levels of Pb in bone marrow were not high when compared to trabecular bones (highly porous or cellular form of bone). The mountain hawk-eagle used as control had low Pb concentrations in all bones (Table S4).

Steller's sea eagle (C) had higher Pb concentrations (dry weight) in the axis (127.9 mg/kg), hyoid (110.2 mg/kg), and keel (28.9 mg/kg) than the humerus (diaphysis, 3.6 mg/kg) and femur (diaphysis, 4.9 mg/kg). Hepatic Pb concentration in this eagle was very high (58.4 mg/kg, dry weight), indicating severe Pb poisoning.

Within the femur and the tibiotarsus, Pb concentrations in the epiphysis (which mainly consisted of trabecular bone) were substantially higher than the diaphysis (which mainly consisted of cortical bone) for both eagles and swans (Fig. 3-a and -b).

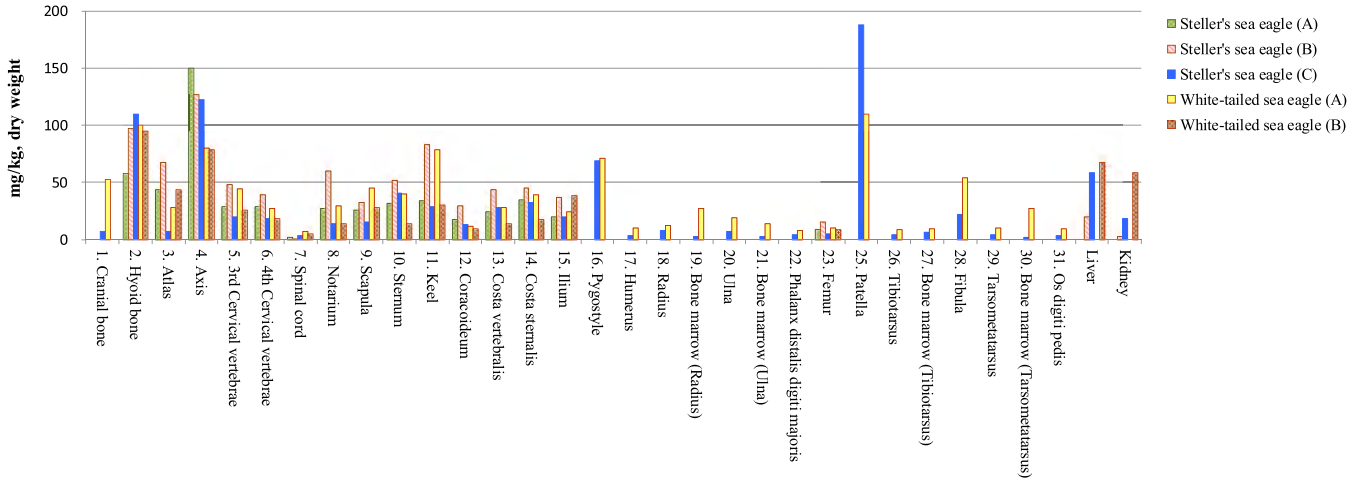

Fig. 1. Pb distribution in bone and organ tissues from Steller's sea eagle (n = 3) and white-tailed sea eagle (n = 2). The position of each bone is shown in Fig. S1.

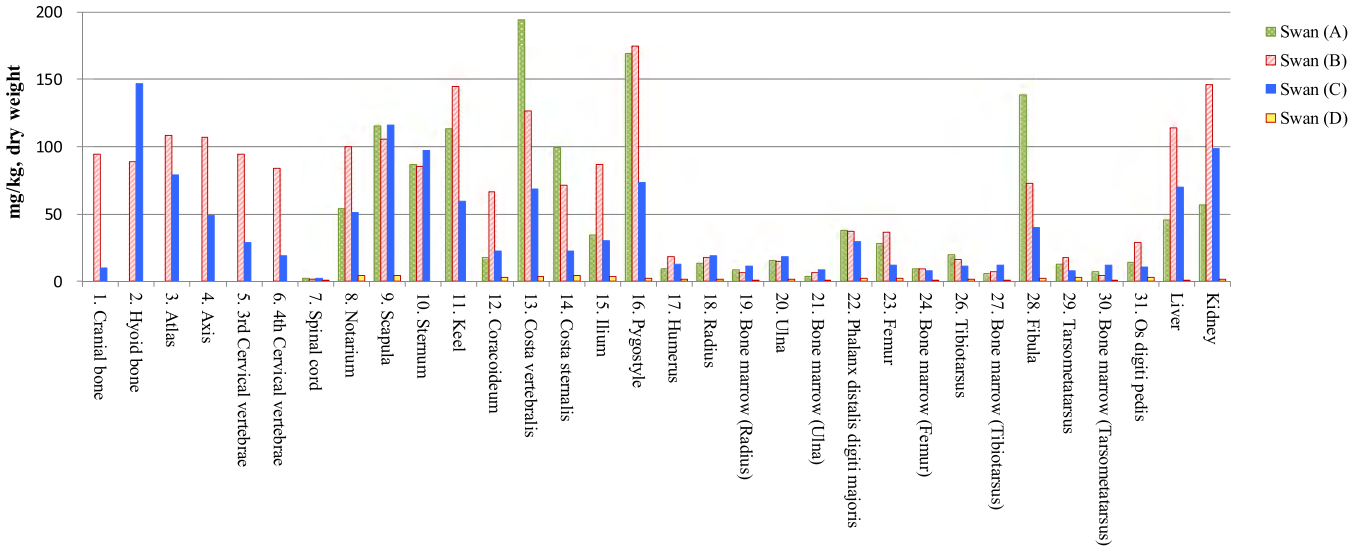

Fig. 2. Pb distribution in bone and organ tissues from swans (n = 4). Data for swan (D) was shown in Fig. S3, an expanded version of this figure. The position of each bone is shown in Fig. S1.

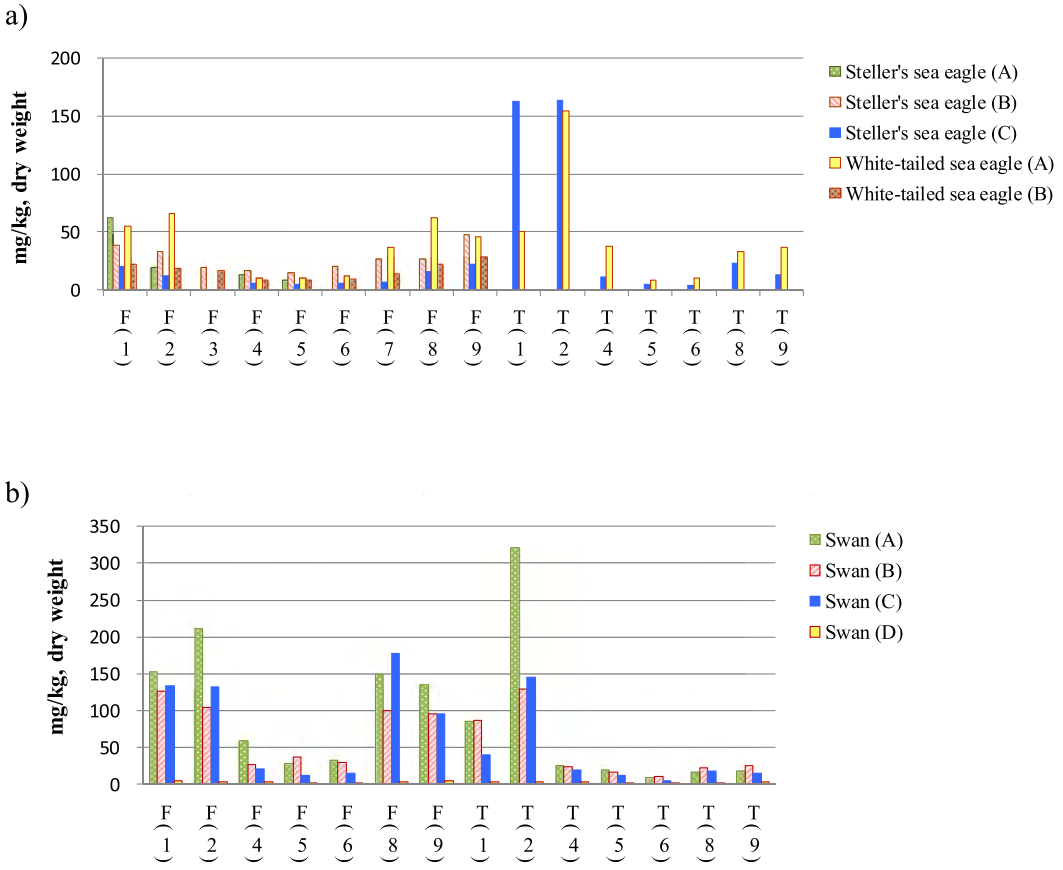

Fig. 3. Pb concentrations in the diaphysis and the epiphysis in femur (F) and tibiotarsus (T) in eagles (a) and swans (b). (1): epiphysis (proximal, surface); (2): epiphysis (proximal, core); (3): diaphysis (proximal, internal struts); (4): diaphysis (proximal); (5): diaphysis (medial); (6): diaphysis (distal); (7): diaphysis (distal, internal struts); (8): epiphysis (distal, core); and (9): epiphysis (distal, surface). The position of each part is shown in Fig. S2.

Furthermore, in the tibiotarsus, the proximal epiphysis that included bone marrow had the highest concentration. In swans, femur that included bone marrow showed higher Pb concentration than humerus devoid of bone marrow. In eagles, the femur and humerus both lacked bone marrow and showed similar Pb levels. The level of Pb in bone marrow itself sometimes differed depending on whether it was obtained from the proximal or distal part of the same bone (the average is shown in Figs. 1 and 2; data of each level

is not shown).

There were significant correlations in Pb concentrations between bones and the liver or kidney in both eagles and swans (Table S3 and Fig. S4). Correlations between humerus and kidney or liver were especially high (humerus-kidney: $\rho = 1.00$ and humerus-liver: $\rho = 0.90$, $p < 0.05$, respectively).

3.2. Detailed distribution pattern of Pb determination using LA-ICP-MS

Photomicrographs of the femur and tibiotarsus of Steller's sea eagle are shown in Fig. S5, and Pb distribution in the femur and tibiotarsus of Steller's sea eagle and whooper swan obtained by element imaging are shown in Fig. 4. The epiphysis in all four bone types had higher signal intensity - counts per second (cps) - of Pb than the diaphysis. The inner parts of the diaphysis of the bones showed high signal intensity. In the epiphysis of femur from whooper swan or tibiotarsus from Steller's sea eagle and whooper swan, the surface of the trabecular bone had high signal intensity. However, the femur of adult Steller's sea eagle differed from the other bones; Pb accumulation in the surface of the hollow epiphysis was slightly high, but the signal intensity did not differ greatly.

When compared to the accumulation of other elements, areas which revealed high Pb signal intensity showed low signal intensity for Ca (Fig. 5). Local distributions of ^{13}C, ^{25}Mg, ^{31}P, ^{55}Mn, ^{57}Fe, ^{65}Cu, ^{66}Zn, ^{206}Pb and ^{207}Pb in the femur and tibiotarsus of Steller's sea eagle and whooper swan are shown in Figs. S6–S9.

4. Discussion

4.1. Importance of trabecular bone and bone marrow in Pb accumulation

Our findings suggest that, in avian species, trabecular bone and bones with active marrow can play an important role in understanding Pb toxicity, as they tend to accumulate Pb rapidly.

The hyoid, keel and pygostyle, bones that mainly consist of trabecular bone type, had remarkably high Pb concentration in both eagles and swans (Figs. 1 and 2). In the femur and tibiotarsus, the epiphysis had a higher Pb level than the diaphysis (Fig. 3-a and

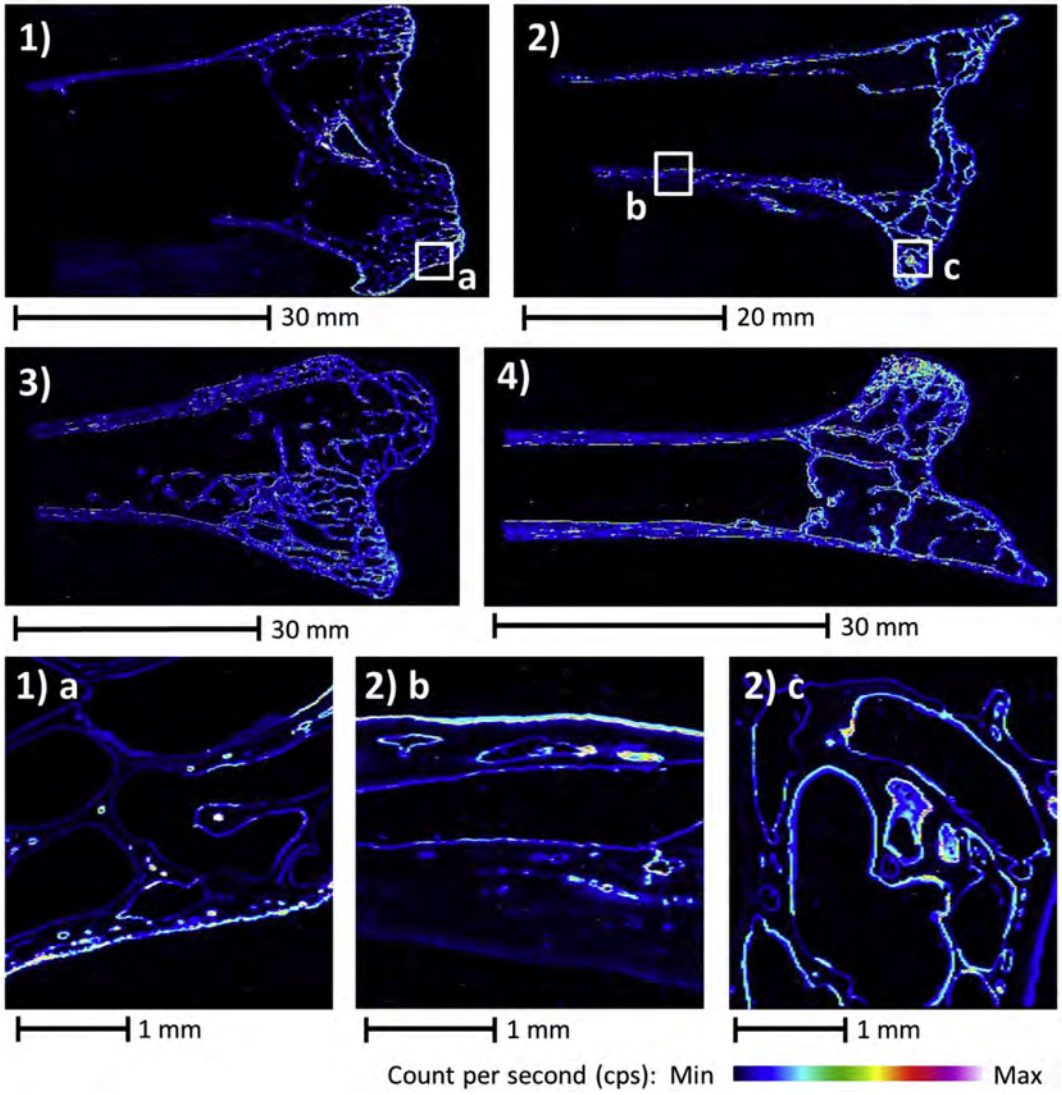

Fig. 4. Pb distribution in femur (distal) and tibiotarsus (proximal) of Steller's sea eagle and whooper swan using LA-ICP-MS. 1) femur of Steller's sea eagle, 2) tibiotarsu of Steller's sea eagle, 3) femur of whooper swan, 4) tibiotarsus of whooper swan. The figures on the bottom row are an expanded version of a, b and c in 1), and 2). Scale bars and ranges of counts per second (cps) of Pb differ between images.

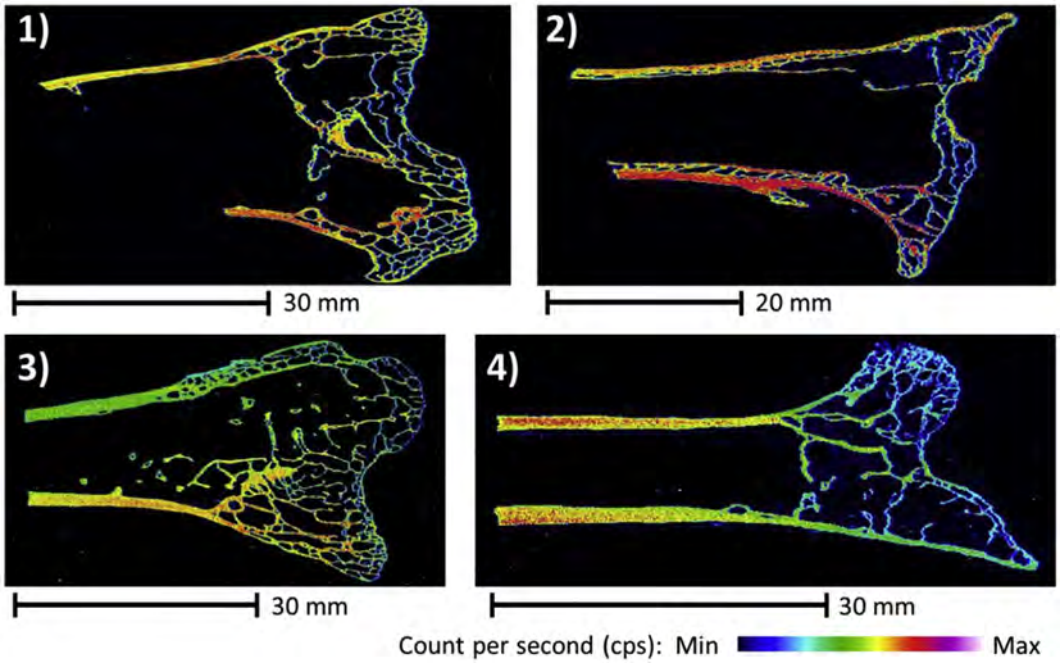

Fig. 5. Ca distribution in femur (distal) and tibiotarsus (proximal) of Steller's sea eagle and whooper swan using LA-ICP-MS. 1) Femur of Steller's sea eagle, 2) tibiotarsus of Steller's sea eagle, 3) femur of whooper swan, 4) tibiotarsus of whooper swan. Scale bars and ranges of counts per second (cps) of Ca differ between images.

-b). These levels of Pb concentration differ because the diaphysis is mainly composed of cortical bone, whereas the epiphysis is mainly composed of trabecular bone. This trend is supported by a previous study, which found that, in humans, Pb in trabecular bones is more biologically active than Pb in cortical bones (Barbosa et al., 2005). The authors of the study also reported that trabecular bone had a larger surface area and received a greater volume of blood compared to cortical bone. Moreover, the shorter turnover time of trabecular bone causes a rapid accumulation of Pb. The half-life of Pb in trabecular bone may vary from a few to 16 years in vertebrae, whereas the half-life in cortical bone often ranges from 5 to 15 years, but may exceed 25 years (Gerhardsson et al., 2005). Additionally, other trabecular bone, such as the axis, scapula, costa and patella, were found to have higher concentrations of Pb than cortical bone, such as the diaphysis of the humerus, radius, ulna and tarsometatarsus (Figs. 1 and 2).

Bones containing bone marrow are another factor determining Pb accumulation, because Pb is delivered to bone marrow by blood vessels. Avian bone marrow consists of cell rich and highly vascularized tissues (Higgins, 1999; Tavassoli and Yoffey, 1983), which may result in significant Pb accumulation. The Pb level in bone marrow was not particularly high, which may be caused by the differences of half-life of Pb in blood (about 1 month (Hu et al., 1998)) and bones (many years). The Pb level in the femur was higher in swans than that in eagles. Eagle femurs do not contain bone marrow, whereas swan femurs do. In the tibiotarsus, the proximal epiphysis that contained bone marrow had the highest concentration of Pb. The peripheral portion of the marrow cylinder is hyperplastic (a tissue or organ prone to an abnormal increase in the number of cells) in adult birds, whereas the axial portion is hypoplastic (tissue or organ that undergoes incomplete or sub development) and contains a large amount of fat (Higgins, 1999; Jordan and Robeson, 1942). These characteristics may explain the differences in Pb concentrations in bone marrow within the same bone.

Age related differences in Pb accumulation may also exist, because young and adult birds have different bone structure and functions of bone marrow. During postnatal development, a large portion of the skeleton becomes pneumatized, displacing hemopoietic bone marrow (Schepelmann, 1990). In this study, age differences were not evaluated as a factor because the sample size was limited. Further research may clarify the relationship between Pb distribution in bones and age differences.

4.2. Assessment of Pb exposure

In raptors, Pb concentrations >10 mg/kg in the humerus or femur have been considered abnormal levels of accumulation (Mateo et al., 2003). In water birds Pb concentrations of 20 mg/kg in the femur have been considered a high level of exposure (Pain et al., 2005).

This study showed that, although Pb levels in the bones of Steller's sea eagle (C) and swan (C) were lower than the reference levels described above, the concentrations in the liver and kidney were remarkably high (Figs. 1 and 2). Pb levels in the humerus were significantly correlated with liver ($\rho = 0.90$) and kidney ($\rho = 1.00$). Liver and kidney samples are widely used for the assessment of Pb exposure (Beyer et al., 1988; Guitart et al., 1994). Therefore, these results suggest that the humerus may be a good indicator of Pb exposure. However, from our results it would seem that in absolute value, Pb accumulation is lower in humerus. For the same bird, while liver concentrations would indicate high levels of exposure, the humerus concentration would be below the reference level. If humerus (or femur) are to be used for the assessment of Pb exposure, the fact that birds with abnormal levels of Pb accumulation in these bones that are below reference levels should be taken into consideration. On the other hand, trabecular bones, such as the hyoid, keel or pygostyle, may be potential indicators for acute Pb exposure in birds because they could accumulate Pb faster and at higher levels than other bones.

In avian species, acute Pb poisoning and mortality can follow the ingestion of a single Pb pellet (Fisher et al., 2006; Pain and Rattner,

1988). Based on Pb half-life in cortical bone (e.g. diaphysis of the humerus) this may be a better dosimeter of chronic Pb exposure than trabecular bone (e.g. axis) (Hu et al., 1998). In rats and humans, trabecular bone is reported to be a better indicator for acute or intermediate Pb exposure (Brito et al., 2014; Gerhardsson et al., 1993). The Pb distribution patterns in bone would be different depending on the circumstances surrounding Pb exposure. In cases of acute exposure, Pb levels in trabecular bone could be significantly higher than in cortical bone, whereas in cases of chronic exposure, the differences of concentration between trabecular and cortical bone may be lower (Hu et al., 1998).

4.3. Detailed Pb distribution patterns in femur and tibiotarsus bones using element imaging

The comparison of Pb concentrations in various bone types using ICP-MS indicated that trabecular bone and bones that contain bone marrow accumulate Pb rapidly. Therefore, further and more detailed analyses of Pb distribution using LA-ICP-MS were performed to verify this finding.

The comparison of Ca and Pb distributions also indicated that Pb accumulation may be faster in trabecular bones than in cortical bones. The regions with high Pb signal intensity showed low Ca signal intensity (Fig. 5), suggesting that the Pb accumulation may have started from bone parts with lower density. In humans, the bone density of trabecular bone is lower than that of cortical bone (Lang et al., 2004). A previous study on vultures suggested that the mineralization degree of bones decreases as Pb accumulation increases (Gangoso et al., 2009). Pb and Ca may interact when in a scenario of Pb exposure.

Bone marrow could be an important driver of the differences in Pb distribution among bones. The main difference between the femur of Steller's sea eagle and tibiotarsus of Steller's sea eagle, whooper swan, and the femur of whooper swan, was the absence or presence of bone marrow. The detailed analysis of these bones showed that bone parts in contact with bone marrow had high Pb accumulations. Conversely, the femur of adult Steller's sea eagle had slightly high Pb accumulation in the surface of the hollow epiphysis, but the level did not differ greatly from its inner side. Therefore, bone marrow plays an important role in carrying Pb into bones. Pb is accumulated into bones via blood flow, and bone marrow due to its strong vascularization, receives large amounts of blood from the systemic circulation.

Pb concentrations in bone marrow showed that bone marrow itself did not have higher Pb concentration than trabecular bone (Figs. 1 and 2). The half-life of Pb in blood is around one month (Hu et al., 1998), which is significantly shorter than in bones, resulting in lower Pb signal intensity in bone marrow.

In conclusion, Pb accumulation depends on bone type, and, as such, bones can be effectively used to understand Pb exposure in birds. In Japan, many raptors and water birds die due to Pb toxicity, despite regulations against indiscriminately introducing Pb into the environment. The results obtained in this work added by further research on Pb accumulation in bones will allow this matrix to be used as an indicator for Pb toxicity levels in avian species. The increased knowledge on birds' Pb exposure will, in turn, allow us to develop more appropriate regulations for the protection of this endangered natural resource.

Acknowledgements

This work was supported by Grants-in-Aid for Scientific Research from the Ministry of Education, Culture, Sports, Science, and Technology of Japan awarded to M. Ishizuka (No. 16H01779), Y. Ikenaka (No. 17K2003807, 18H04132), S. Nakayama (No. 16K16197, 17KK0009). This research was also supported by JST/JICA, SATREPS (Science and Technology Research Partnership for Sustainable Development) and the Environment Research and Technology Development Fund (SII-1/3-2, 4RF-1802/18949907) of the Environmental Restoration and Conservation Agency of Japan. We also acknowledge the financial support by the Nihon Seimei Foundation, the Soroptimist Japan Foundation, the foundations of Sumitomo. One of the authors (C. Ishii) was a Research Fellow of the Japan Society for the Promotion of Science (No. 15J01937). We would like to express our appreciation to Dr. Kazuo Jin (Hokkaido Institute of Public Health) and Ibaraki Prefectural Government, Environmental Policy Division for the provision of samples. We are grateful to Kosuke Nakamura and Hidehiko Nomura (Faculty of Science, Hokkaido University), Takahiro Ichise and Nagisa Hirano (Graduate School of Veterinary Medicine, Hokkaido University) for their technical support. The English in this manuscript was proofread by uni-edit.

Appendix A. Supplementary data

Supplementary data related to this article can be found at https://doi.org/10.1016/j.chemosphere.2018.08.149.

References

Andreotti, A., Borghesi, F., 2013. Embedded lead shot in European starlings Sturnus vulgaris: an underestimated hazard for humans and birds of prey. Eur. J. Wildl. Res. 59, 705–712.

Barbosa Jr., F., Tanus-Santos, J.E., Gerlach, R.F., Parsons, P.J., 2005. A critical review of biomarkers used for monitoring human exposure to lead: advantages, limitations, and future needs. Environ. Health Perspect. 1669–1674.

Becker, J.S., Zoriy, M., Becker, J.S., Dobrowolska, J., Matusch, A., 2007. Laser ablation inductively coupled plasma mass spectrometry (LA-ICP-MS) in elemental imaging of biological tissues and in proteomics. J. Anal. Atom. Spectrom. 22, 736–744.

Berny, P., Vilagines, L., Cugnasse, J.-M., Mastain, O., Chollet, J.-Y., Joncour, G., Razin, M., 2015. VIGILANCE POISON: illegal poisoning and lead intoxication are the main factors affecting avian scavenger survival in the Pyrenees (France). Ecotoxicol. Environ. Saf. 118, 71–82.

Beyer, W.N., Spann, J.W., Sileo, L., Franson, J.C., 1988. Lead poisoning in six captive avian species. Arch. Environ. Contam. Toxicol. 17, 121–130.

Binkowski, Ł.J., Sawicka-Kapusta, K., 2015. Lead poisoning and its in vivo biomarkers in mallard and coot from two hunting activity areas in Poland. Chemosphere 127, 101–108.

Brito, J.A.A., Costa, I.M., e Silva, A.M., Marques, J.M.S., Zagalo, C.M., Cavaleiro, I.I.B., Fernandes, T.A.P., Gonçalves, L.L., 2014. Changes in bone Pb accumulation: cause and effect of altered bone turnover. Bone 64, 228–234.

Cade, T.J., 2007. Exposure of California condors to lead from spent ammunition. J. Wildl. Manag. 71, 2125–2133.

Ellis, D.E., Terra, J., Warschkow, O., Jiang, M., González, G.B., Okasinski, J.S., Bedzyk, M.J., Rossi, A.M., Eon, J.-G., 2006. A theoretical and experimental study of lead substitution in calcium hydroxyapatite. Phys. Chem. Chem. Phys. 8, 967–976.

Ethier, A.L.M., Braune, B.M., Scheuhammer, A.M., Bond, D.E., 2007. Comparison of lead residues among avian bones. Environ. Pollut. 145, 915–919.

Fisher, I.J., Pain, D.J., Thomas, V.G., 2006. A review of lead poisoning from ammunition sources in terrestrial birds. Biol. Conserv. 131, 421–432. https://doi.org/10.1016/j.biocon.2006.02.018.

Gangoso, L., Álvarez-Lloret, P., Rodríguez-Navarro, A.A.B., Mateo, R., Hiraldo, F., Donázar, J.A., 2009. Long-term effects of lead poisoning on bone mineralization in vultures exposed to ammunition sources. Environ. Pollut. 157, 569–574.

García-Fernández, A.J., Motas-Guzmán, M., Navas, I., Maria-Mojica, P., Luna, A., Sánchez-García, J.A., 1997. Environmental exposure and distribution of lead in four species of raptors in southeastern Spain. Arch. Environ. Contam. Toxicol. 33, 76–82.

Gerhardsson, L., Akantis, A., Lundström, N.-G., Nordberg, G.F., Schütz, A., Skerfving, S., 2005. Lead concentrations in cortical and trabecular bones in deceased smelter workers. J. Trace Elem. Med. Biol. 19, 209–215.

Gerhardsson, L., Attewell, R., Chettle, D.R., Englyst, V., Lundström, N.G., Nordberg, G.F., Nyhlin, H., Scott, M.C., Todd, A.C., 1993. In vivo measurements of lead in bone in long-term exposed lead smelter workers. Arch. Environ. Heal. An Int. J. 48, 147–156.

Guitart, R., To-Figueras, J., Mateo, R., Bertolero, A., Cerradelo, S., Martínez-Vilalta, A., 1994. Lead poisoning in waterfowl from the Ebro Delta, Spain: calculation of lead exposure thresholds for mallards. Arch. Environ. Contam. Toxicol. 27, 289–293.

Haig, S.M., D'Elia, J., Eagles-Smith, C., Fair, J.M., Gervais, J., Herring, G., Rivers, J.W.,

Schulz, J.H., 2014. The persistent problem of lead poisoning in birds from ammunition and fishing tackle. Condor 116, 408–428. https://doi.org/10.1650/CONDOR-14-36.1.
Higgins, J., 1999. Túnel: a case study of avian zooarchaeology and taphonomy. J. Archaeol. Sci. 26, 1449–1457.
Honda, K., Lee, D.P., Tatsukawa, R., 1990. Lead poisoning in swans in Japan. Environ. Pollut. 65, 209–218.
Hu, H., Rabinowitz, M., Smith, D., 1998. Bone lead as a biological marker in epidemiologic studies of chronic toxicity: conceptual paradigms. Environ. Health Perspect. 106, 1.
Ishii, C., Nakayama, S.M.M., Ikenaka, Y., Nakata, H., Saito, K., Watanabe, Y., Mizukawa, H., Tanabe, S., Nomiyama, K., Hayashi, T., 2017. Lead exposure in raptors from Japan and source identification using Pb stable isotope ratios. Chemosphere 186, 367–373.
Jordan, H.E., Robeson, J.M., 1942. The production of lymphoid nodules in the bone marrow of the domestic pigeon, following splenectomy. Am. J. Anat. 71, 181–205.
Kendall, R.J., Lacker, T.E., Bunck, C., Daniel, B., Driver, C., Grue, C.E., Leighton, F., Stansley, W., Watanabe, P.G., Whitworth, M., 1996. An ecological risk assessment of lead shot exposure in non-waterfowl avian species: upland game birds and raptors. Environ. Toxicol. Chem. 15, 4–20. https://doi.org/10.1002/etc.5620150103.
Lang, T., LeBlanc, A., Evans, H., Lu, Y., Genant, H., Yu, A., 2004. Cortical and trabecular bone mineral loss from the spine and hip in long-duration spaceflight. J. Bone Miner. Res. 19, 1006–1012.
Limbeck, A., Galler, P., Bonta, M., Bauer, G., Nischkauer, W., Vanhaecke, F., 2015. Recent advances in quantitative LA-ICP-MS analysis: challenges and solutions in the life sciences and environmental chemistry. Anal. Bioanal. Chem. 407, 6593–6617.
Martinez-Haro, M., Taggart, M.A., Martín-Doimeadiós, R.R.C., Green, A.J., Mateo, R., 2011. Identifying sources of Pb exposure in waterbirds and effects on porphyrin metabolism using noninvasive fecal sampling. Environ. Sci. Technol. 45, 6153–6159. https://doi.org/10.1021/es2009242.
Mateo, R., 2009. Lead poisoning in wild birds in Europe and the regulations adopted by different countries. Ingestion Lead From Spent Ammunit. Implic. Wildl. humans 2009, 71–98.
Mateo, R., Taggart, M., Meharg, A.A., 2003. Lead and arsenic in bones of birds of prey from Spain. Environ. Pollut. 126, 107–114.
Pain, D.J., 1996. Lead in Waterfowl. Lewis Publishers, New York.
Pain, D.J., 1991. Why are lead-poisoned waterfowl rarely seen?: the disappearance of waterfowl carcasses in the Camargue, France. Wildfowl 42, 118–122.
Pain, D.J., Meharg, A.A., Ferrer, M., Taggart, M., Penteriani, V., 2005. Lead concentrations in bones and feathers of the globally threatened Spanish imperial eagle. Biol. Conserv. 121, 603–610.
Pain, D.J., Rattner, B.A., 1988. Mortality and hematology associated with the ingestion of one number four lead shot in black ducks, Anas rubripes. Bull. Environ. Contam. Toxicol. 40, 159–164.
Rattner, B.A., 2009. History of wildlife toxicology. Ecotoxicology 18, 773–783.
Saito, K., 2009. Lead poisoning of Steller's Sea-Eagle (Haliaeetus pelagicus) and Whitetailed Eagle (Haliaeetus albicilla) caused by the ingestion of lead bullets and slugs. Hokkaido Japan. In: Watson, R.T., Fuller, M., Pokras, M., Hunt, W.G. (Eds.), Ingestion Lead from Spent Ammunit. Implic. Wildl. Humans. Peregrine Fund, Boise, Idaho, USA.
Schepelmann, K., 1990. Erythropoietic bone marrow in the pigeon: development of its distribution and volume during growth and pneumatization of bones. J. Morphol. 203, 21–34.
Scheuhammer, A.M., 1987. The chronic toxicity of aluminium, cadmium, mercury, and lead in birds: a review. Environ. Pollut. 46, 263–295. https://doi.org/10.1016/0269-7491(87)90173-4.
Scheuhammer, A.M., Norris, S.L., 1996. The ecotoxicology of lead shot and lead fishing weights. Ecotoxicology 5, 279–295.
Tavassoli, M., Yoffey, J.M., 1983. Bone Marrow, Structure and Function. AR Liss.
Whitehead, P.J., Tschirner, K., 1991. Lead shot ingestion and lead poisoning of magpie geese Anseranas semipalmata foraging in a northern Australian hunting reserve. Biol. Conserv. 58, 99–118.
Yabe, J., Nakayama, S.M.M., Ikenaka, Y., Yohannes, Y.B., Bortey-Sam, N., Oroszlany, B., Muzandu, K., Choongo, K., Kabalo, A.N., Ntapisha, J., Mweene, A., Umemura, T., Ishizuka, M., 2015. Lead poisoning in children from townships in the vicinity of a lead-zinc mine in Kabwe, Zambia. Chemosphere 119, 941–947. https://doi.org/10.1016/j.chemosphere.2014.09.028.

Environmental Pollution 243 (2018) 713–722

Contents lists available at ScienceDirect

Environmental Pollution

journal homepage: www.elsevier.com/locate/envpol

Heavy metals in slag affect inorganic N dynamics and soil bacterial community structure and function☆

Miyuki Oka [a], Yoshitaka Uchida [b, *]

[a] School of Agriculture, Hokkaido University, Kita 9, Nishi 9, Kita-ku, Sapporo, Hokkaido, 060-8589, Japan
[b] Research Faculty of Agriculture, Hokkaido University, Kita 9, Nishi 9, Kita-ku, Sapporo, Hokkaido, 060-8589, Japan

ARTICLE INFO

Article history:
Received 20 March 2018
Received in revised form
3 September 2018
Accepted 4 September 2018
Available online 6 September 2018

Keywords:
Slag
Heavy metal
Nitrogen cycle
Bacterial community structure
Bacterial community function

ABSTRACT

Heavy metal contamination of soil in the vicinity of mining sites is a serious environmental problem around the world when mining residue (slag) is dispersed as dust. We conducted an incubation experiment to investigate the effect of a slag containing high levels of Pb and Zn (62.2 and 33.6 g kg^{-1} slag as PbO and ZnO, respectively, sampled from a site formerly used as a lead and zinc mine) on the nitrogen cycle when mixed with soil (0–0.048 g slag g^{-1} soil). The nitrogen cycle provides many life supporting-functions. To assess the quality of the soil in terms of the nitrogen cycle we focused on the dynamics of nitrate and ammonium, and bacterial community structure and functions within the soil. After two weeks of pre-incubation, ^{15}N-labeled urea (500 mg N kg^{-1}) was added to the soil. Changes in soil pH, the concentration and ^{15}N ratio of nitrate (NO_3^--N) and ammonium, and bacterial relative abundance and community structure were measured. Results indicated that increasing the ratio of slag to soil had a stronger negative effect on nitrification than ammonification, as suggested by slower nitrate accumulation rates as the slag:soil ratio increased. In the treatment with the highest amount of slag, the concentration of NO_3^--N was 50% of that in the controls at the end of the incubation. Regarding the bacterial community, *Firmicutes* had a positive and *Planctomycetes* a negative correlation with increasing slag concentration. Bacterial community functional analysis showed the proportion of bacterial DNA sequences related to nitrogen metabolism was depressed with increasing slag, from 0.68 to 0.65. We concluded that the slag impacted the soil bacterial community structure, and consequently influenced nitrogen dynamics. This study could form the basis of further investigation into the resistance of the nitrogen cycle to contamination in relation to soil bacterial community.

1. Introduction

Soil contamination caused by the slag produced during mining for metals is one of the most serious global environmental issues. The slag often contains hazardous components including heavy metals such as Pb and Zn. In contaminated sites, plant biomass and diversity decrease (Nagajyoti et al., 2010; Hernández and Pastor, 2008). When plant biomass decreases, some of the benefits provided by the plants to soils (e.g., the formation of aggregates and retention of moisture) may decline or cease. This results in reduced soil stability, and may lead to the spread of contaminated soils further into the surrounding environment through wind and water erosion (Zuazo and Pleguezuelo, 2009). In fact, around areas contaminated by heavy metals the damage caused to human health by ingestion of dust is a significant problem (Zhao et al., 2012; Taylor et al., 2014). To minimize the spread of contaminants into residential areas, the importance of plant cover has been discussed previously (Wong, 2003).

One of the reasons for the decrease in plant biomass is insufficient nutrient supply, a prime example being inorganic nitrogen (N) (Bååth, 1989). Nitrogen is a major growth-limiting factor for plants in the natural environment. Available N, including ammonium (NH_4^+) and nitrate (NO_3^-), is supplied from the residues of plants, animals, and microorganisms, or dinitrogen gas in the air. For sufficient N to be available to plants, soil microbial activities such as decomposition, ammonification, and nitrification are important. Environmental factors inhibiting soil microbial activity, such as presence of contaminants, can result in reduced plant growth and biomass production. In soils bearing a high concentration of heavy metals, the

☆ This paper has been recommended for acceptance by Prof. W. Wen-Xiong.
* Corresponding author.
E-mail address: uchiday@chem.agr.hokudai.ac.jp (Y. Uchida).

https://doi.org/10.1016/j.envpol.2018.09.024
0269-7491/

diversity and biomass of soil microorganisms is decreased (Bååth, 1989; Giller et al., 1998). Heavy metals affect the growth, morphology, and metabolism of soil microorganisms (Leita et al., 1995). This stagnates N cycling and decreases the abundance and diversity of plant species able to grow in the area (Giller et al., 1998).

Several studies have examined the N cycle and microbial activity in soils contaminated with Pb, Zn or other risk elements. Some of these have shown that contaminants influence mineralization (Vásquez-Murrieta et al., 2006), while others have shown that heavy metals had only a small effect on ammonification but a larger effect on nitrification (Rother et al., 1982; Ueda et al., 1988). Contrastingly, another report suggested that Pb and Cd contamination of soil had no effect on nitrification (Cela and Sumner, 2002).

Additionally, many studies have been conducted focusing on soil bacterial community structure and activity in contaminated sites, revealing that these parameters are changed in the presence of heavy metals (Ellis et al., 2003, Wang et al., 2007, Gołębiewski et al., 2014).

Although the effects of slag containing high levels of risk elements, including heavy metals, on the N cycle and soil microbes have been investigated, few studies have shown the relationship between them. Better understanding of the impacts of slag on soil bacterial community and function related to the N cycle will provide basic information to assist in more efficient recovery of soil N and plants as vegetation cover in the contaminated sites, which in turn will ameliorate the potential environmental risk of mining.

Our study focused on the relationship between the supply of inorganic N, bacterial abundance, and community structure and function. We evaluated the N cycle in soil contaminated with a slag containing Pb and Zn, using the nitrogen-15 (^{15}N) tracing technique. By comparing the N dynamics with the quantitative and qualitative data of microorganism populations, we attempted to link changes in biological properties of a contaminated soil with the N cycle.

2. Materials & methods

2.1. Soil sampling and physicochemical properties of soil and slag

Soil (0–10 cm depth) was collected from the experimental corn (*Zea mays*) farm of Hokkaido University, Sapporo, Japan (43°3′N, 141°20′E) in May 2017. The sampled soil was air dried and sieved through a 2 mm mesh. The pH of the soil was 5.77 ± 0.33 (s.d., $n = 3$), and total C and N were 42.3 ± 0.85 g kg^{-1} and 3.60 ± 0.21 g kg^{-1}, respectively. To measure soil pH, 3 g of dry soil was mixed with 7.5 ml Milli-Q water and shaken for 30 min, followed by pH measurement using a pH meter (AS800, AS ONE Corporation, Osaka, Japan). Total C and N content of the soil samples were determined using an elemental analyzer (EA 2400 Series; Perkin Elmer, Foster City, CA, USA).

A Zn-leaching residue (slag) was sampled in February 2017 from the surface of the former mining site in Kabwe, Zambia (14°27′19″S, 28°26′0″E) and sieved to retain particles ≤7 μm. The pH of the slag was 6.03 ± 0.04 (s.d., $n = 3$), and total C and N were 3.55 ± 0.33 g kg^{-1} and 1.68 ± 0.85 g kg^{-1} (s.d., $n = 4$), respectively. The same methods and devices as the soil samples (AS800 and EA 2400) were used to measure these slag characteristics. The chemical composition of the sieved slag was analyzed with Cartesian geometry energy dispersive X-ray fluorescence spectrometer (NEX CG; Rigaku Corporation, Tokyo, Japan). As risk elements, the slag contained 6.22% PbO, 3.36% ZnO, 0.07% As_2O_3 and 0.0003% HgO. The levels of water-soluble Pb and Zn in the slag were 0.78 and 1.18 mg g^{-1} slag (measured after 3 g of the slag was shaken in 120 ml water for 4 h). The soil collected from the farm in Hokkaido University contained no detectable Pb or Zn.

2.2. Incubation setup

To test the effect of the slag on the sampled soil, 45 g of the soil and varying amounts of the slag were mixed and packed in separate 120 ml plastic cups. Four different contamination levels for Pb and Zn were created, equating to 0, 100, 500 and 3000 mg Pb and 0, 54, 270, and 1620 mg Zn kg^{-1} dry soil, and these were designated as Control (C), and Low (L), Middle (M) and High (H) concentrations of heavy metals (Table 1). The range of slag:soil ratios was determined based on previously performed field experiments (Ikenaka et al., 2010).

Three replicates for each treatment were prepared on five sampling occasions. In total, 60 (= 4 treatments * 3 replicates * 5 sampling days) cores were arranged. The samples were compressed to 0.9 g cm^{-3}, and Milli-Q water was added to achieve a water-filled pore space (WFPS) of 60%. To avoid excess soil moisture loss the cups were closed with plastic lids into which six holes (diameter 1 mm) had been perforated. The moisture content was maintained at 60% WFPS by adding Milli-Q water every 2 days. The particle density of the soil was taken as 2.65 g cm^{-3} for the calculation of the WFPS. Thus, the soil porosity was $1 - (0.9\ \text{g cm}^{-3} / 2.65\ \text{g cm}^{-3}) = 66\%$.

The soil samples were incubated for two weeks and then three atom% ^{15}N-labeled urea was applied (500 mg N kg^{-1} dry soil–slag mixture). The soil was sampled destructively on the day of urea application (immediately after the urea application, day 0), and at 1, 6, 14 and 28 days after urea application. The samples were divided for the measurement of pH (using the method described previously), inorganic N, and bacterial DNA.

2.3. Measurement of ammonium and nitrate

For the determination of inorganic N (NO_3^--N and NH_4^+-N) concentration, 3 g of the sampled fresh soil was extracted with 2 M KCl (15 ml). After shaking the mixture for 30 min, the suspension was filtered through a filter paper (Grade 5C, <5 mm; Advantec, Tokyo, Japan). The extracted solution was stored at 4 °C until measurement. For the measurement, a colorimetric method was employed with a flow injection analyzer (AQLA-700; Aqualab, Tokyo, Japan) as described previously (Hamamoto and Uchida, 2015).

In brief the methods used were: for NO_3^--N, the cadmium reduction and *N*-(1-Naphthyl)ethylenediamine dihydrochloride method; and for NH_4^+-N, the indophenol blue method. Results are shown as mg N kg^{-1} soil.

2.4. Isotopic N measurement

To measure the ^{15}N ratio in the extracted inorganic N, the NO_3^- in the KCl solution was converted into NO_2^- using spongy cadmium and further reduced to N_2O with sodium azide in acetic acid according to methods previously described (McIlvin and Altabet,

Table 1
Incubation setup for each treatment. C, L, M and H stand for control, low, medium and high level of slag applied into the soil.

Incubation setup	C	L	M	H
Dry soil (g)	45.0	45.0	45.0	45.0
Slag (g)	0.0	0.1	0.4	2.2
Pb (mg/kg)	0.0	100.0	500.0	3000.0
Zn (mg/kg)	0.0	54.0	270.1	1620.6
Volume (cm^3)	50.0	50.1	50.4	52.4
WFPS (%)	60.0	60.0	60.0	60.0
Urea (mg)	48.2	48.3	48.6	50.5

2005). KCl solution (1 ml) was placed in a 20 ml glass vial with 4 ml buffer solution containing NaCl (final concentration 0.5 M) and $NaHCO_3$ to make the solution around pH 8. Then, 0.2 g of spongy cadmium was added and the vial was shaken for 18 h. After shaking, the supernatant was moved to another vial. The azide/acetic acid buffer was prepared on the day of use. NaN_2 (0.65 g) was dissolved in 9 ml Milli-Q water and mixed with 1 ml acetic acid. The buffer was purged with He for 20 min to remove N_2O in the solution. Using a syringe, 0.2 ml buffer solution was injected and mixed with the sample in the vial closed with a rubber and plastic lid. After 30 min shaking, 0.1 ml NaOH (ca. 6 M) was added to stop the reaction. The N_2O produced was preserved in the vial at room temperature until measurement.

The isotopic N ratio of NH_4^+-N was measured by oxidizing to N_2O using NaOBr according to the method of Laughlin et al. (1997). To prepare the NaOBr, first 50 g NaOH was dissolved in 400 ml Milli-Q water and preserved at 4 °C overnight. Then, 16 ml of Br_2 was added to the prepared NaOH solution on ice over a period of 30 min. The solution was then diluted to 500 ml total and stored at 4 °C until use. An aliquot (1 ml) of the extracted KCl solution was placed in a 20 ml vial, the vial was sealed with a rubber and plastic lid, and its headspace was replaced with He. NaOBr purged with He was then injected into the vial using a syringe and in another syringe, the produced N_2O was collected. The N_2O was preserved in a new vial at a room temperature until measurement.

The N_2O was diluted with zero air to increase the gas volume and to reduce the N_2O concentration to about 100 $\mu l\, l^{-1}$ for NH_4^+-derived N_2O, and to between 300 and 5000 $\mu l\, l^{-1}$ for NO_3^--derived N_2O. An Isotopic Nitrous Oxide Analyzer (Model 914-0027, Los Gatos Research) was used for the measurement. The ^{15}N ratio of NO_3^--N was calculated by dividing $^{14}N^{15}NO$ by total N_2O since the NO_3^--N in the original solution bonds in the middle position (α site) of the N_2O. The ^{15}N ratio of NH_4^+-N was calculated by dividing total isotopic N_2O ($^{14}N^{15}NO$ plus $^{15}N^{14}NO$) by total N_2O.

2.5. Measurement of bacterial abundance

On each sampling day, DNA was extracted from the fresh soil with PowerSoil DNA Isolation Kit (MoBio Laboratories, Carlsbad, CA, USA) according to the manufacturer's instructions. The extracted DNA was purified with Agencourt AMPure XP (Beckman Coulter) according to a predetermined protocol. The concentration of the purified DNA was measured with Qubit dsDNA HS Assay Kit (Invitrogen, USA). The purified DNA was then diluted 100 times with nuclease-free water for qPCR. A standard curve was prepared with a DNA sample from the control treatment on day 0 to determine the relative bacterial abundance among different treatments at different timings. We used the QuantiTect SYBR Green PCR kit (Qiagen, Mississauga, ON, Canada) and Mx3000P/Mx3005P QPCR Systems (Agilent). For primers, 27F/519R (Abujabhah et al., 2018) were chosen for bacterial (16S rRNA) quantitative analysis. The initial denaturation temperature was 95 °C with an annealing temperature of 95 °C, and the extension was conducted for 1 min at 58 °C for 35 cycles. The final extension was done at 72 °C for 30 s. The relative abundance was expressed based on the abundance of the 16S rRNA genes of the control treatment at day 0.

2.6. Amplification and sequencing of 16S rRNA in soil

Bacterial community analysis was performed on all DNA samples extracted from soil on day 0 and 28. The first polymerase chain reaction (PCR) was conducted using primers to amplify the V4 region of 16S rRNA (amplicon size ~250 bp, forward primer = 515F: 5′-GTGCCAGCMGCCGCGGTAA-3′, reverse primer = 806R: 5′-GGACTACHVGGGTWTCTAAT-3′). For PCR, samples were prepared with 10 μL of AmpliTaq Gold® 360 Master Mix (Applied BiosystemsTM, Foster City, U.S.A.), 0.4 μL of forward primer, 0.4 μL of reverse primer and 1–2 μL of DNA extract. Nuclease-free water was added to make up to a final volume of 20 μL. The first PCR cycle was 95 °C for 10 min, then 20 cycles at 95 °C for 30 s, 57 °C for 30 s, and 72 °C for 1 min, followed by 72 °C for 7 min. The first PCR products were then purified with Agencourt AMPure XP (Beckman Coulter) according to the given protocol.

Using the amplicon obtained from the first PCR procedure, another PCR was performed to make it Ion Torrent sequencing sample-specific. To achieve this, a forward primer of 515F attached with the sequence of Ion Xpress Barcode Adapters 19–42 Kit (Life Technologies), and reverse primer of 806F attached with the sequence of Ion P1 adaptor (Ion Torrent; Life Technologies) were used (Table S1). The PCR sample contained 10 μL of AmpliTaq Gold® 360 Master Mix (Applied BiosystemsTM, Foster City, U.S.A.), 0.4 μL of forward primer, 0.4 μL of reverse primer and 4 μL of purified first PCR product. Nuclease-free water was added to make up to a final volume of 20 μL. The second PCR cycle was 95 °C for 10 min, then 5 cycles at 95 °C for 30 s, 57 °C for 30 s, and 72 °C for 1 min, followed by 72 °C for 7 min. The second PCR products were purified with the same method as above. The concentration of purified DNA was measured using Qubit dsDNA HS Assay Kit (Invitrogen, USA). The final length and concentration of the amplicons were confirmed using a Bioanalyzer High Sensitivity DNA Kit (Agilent Technologies, Palo Alto, CA, USA).

The library was diluted to 50 pM using Low TE (Tris-EDTA; 10 mM Tris base, 0.1 mM EDTA, Ion Torrent; Life Technologies). Ion Chef Instruments (Ion Torrent Life Technologies, USA) with the Ion PGM Hi-Q Chef kit was used for the loading of the library into the Ion 318 chip (Ion Torrent Life Technologies, USA).

2.7. Analyses of the 16S rRNA based bacterial community structures

The obtained sequences were analyzed through Metagenomics 16S w1.1 in Ion Reporter. Then, to analyze the changes in microbial community structure and their interactions with soil environments, Detrended Correspondence Analysis (DCA) was conducted using the diversity data at phylum or family level and environmental factors, including slag concentration (g slag g^{-1} soil), pH, concentration of NH_4^+-N and NO_3^--N, and bacterial abundance. The importance of phyla or families that constituted <5% of each sample was down-weighted. The value of DCA1 was less than 2.0 in each case, indicating that linear relationships existed between microbial abundance and environmental factors. Based on this result, Redundancy Analysis (RDA) was conducted using the square root-converted data of species proportions. The result of RDA is shown in a tri-plot.

Heatmaps were constructed with the metagenomics data at phylum and family levels. Phyla or families whose relative abundance was <1% on average are not shown on the heatmaps.

For the functional analysis of microbiota from 16S rRNA data, Phylogenetic Investigation of Communities by Reconstruction of Unobserved States (PICRUSt) software was used (Langille et al., 2013). The analysis was conducted following the tutorial. Operational Taxonomic Units (OTUs) were prepared by eliminating all the OTUs that matched the GreenGenes 13_5 reference sequence with 97% similarity. The functions of each sample were predicted from the normalized OTU tables referencing KEGG orthology values level 3.

2.8. Statistical analysis

For the concentrations and isotopic ratios of inorganic N, and the relative amounts of soil bacterial DNA, two-way analysis of variance (ANOVA) was used to determine the effects of the amount of heavy

metal and the sampling date. One-way ANOVA and Tukey's test was performed for the analysis of significant differences among samples on each date or for each treatment. For microbial diversity analysis, the Shannon–Wiener index was calculated, and the significant effect of day and treatment was also investigated in the same way. All data are presented as mean ± s.d. Statistical analysis was performed using R ver. 3.1.2 (R Foundation for Statistical Computing, Vienna, Austria).

3. Results

3.1. Dynamics of ammonium, nitrate and pH

As shown in Fig. 1a, NH_4^+-N concentration peaked on day 6 in the control treatment and on day 14 in the slag-treated variants. By day 28, NH_4^+-N concentration had decreased to 220 mg N kg^{-1} dry soil in C and L and to around 310 mg N kg^{-1} dry soil in M and H. Statistically significant effects ($p < 0.05$) of the slag application rates were seen on all sampling days except for day 0 (Table 2). The isotopic ratios of NH_4^+-N remained constant at about 3.0 ± 0.7% in all samples and there were no significant differences throughout the incubation period (Fig. 1b).

In all treatments, the extracted NO_3^--N concentrations increased throughout the incubation period (Fig. 1c). On all sampling days, treatment C contained the highest and the treatment H contained the lowest level of NO_3^--N. In contrast, there were no clear differences in the isotopic ratios in NO_3^--N among the four treatments (Fig. 1d). However, the treatments with a higher concentration of slag (M and H) tended to have a lower ^{15}N ratio compared to the control.

No significant differences were seen in total inorganic N concentration among the four treatments on all sampling days except on days 1 and 6 (Fig. S1, Table S2). On day 14, total inorganic N concentration reached a peak at about 600 mg N kg^{-1} in all treatments. The total concentration decreased to about 440 mg N kg^{-1} on day 28. While concentrations were similar, the NO_3^--N to NH_4^+-N ratio showed significant differences on days 14 and 28.

There were no significant effects on pH from the treatments or the soil sampling times (Fig. S2), although soil pH tended to decrease with increasing slag concentration. At the beginning of the incubation, soil pH ranged from 4.1 to 4.4 in all treatments. On day 6, the effect of the slag was clearest; pH was about 5.2 in treatments C and L and 4.7 in M and H. In all treatments, pH rose to its highest on day 6 and decreased to around 4.2 by the end of the incubation.

3.2. Soil bacterial abundance

The relative abundance of soil bacteria tended to decrease with increasing slag concentration. However, this trend was only seen in the first 2 weeks and there was no difference among the treatments by day 28 (Fig. S3).

In the control treatment, on day 1, the relative abundance of bacteria was the highest among all samples, after which abundance decreased continuously until the end of the experiment. In treatment L, bacterial DNA was highest on day 0 and then decreased over time. There were peaks for treatments M and H on day 6. By day 28, the relative quantity of DNA was almost the same in all treatments.

3.3. Bacterial community structures

On average, 67,267 reads were mapped per sample for 16S rRNA. The following diversity and community analyses were conducted at phylum and family levels.

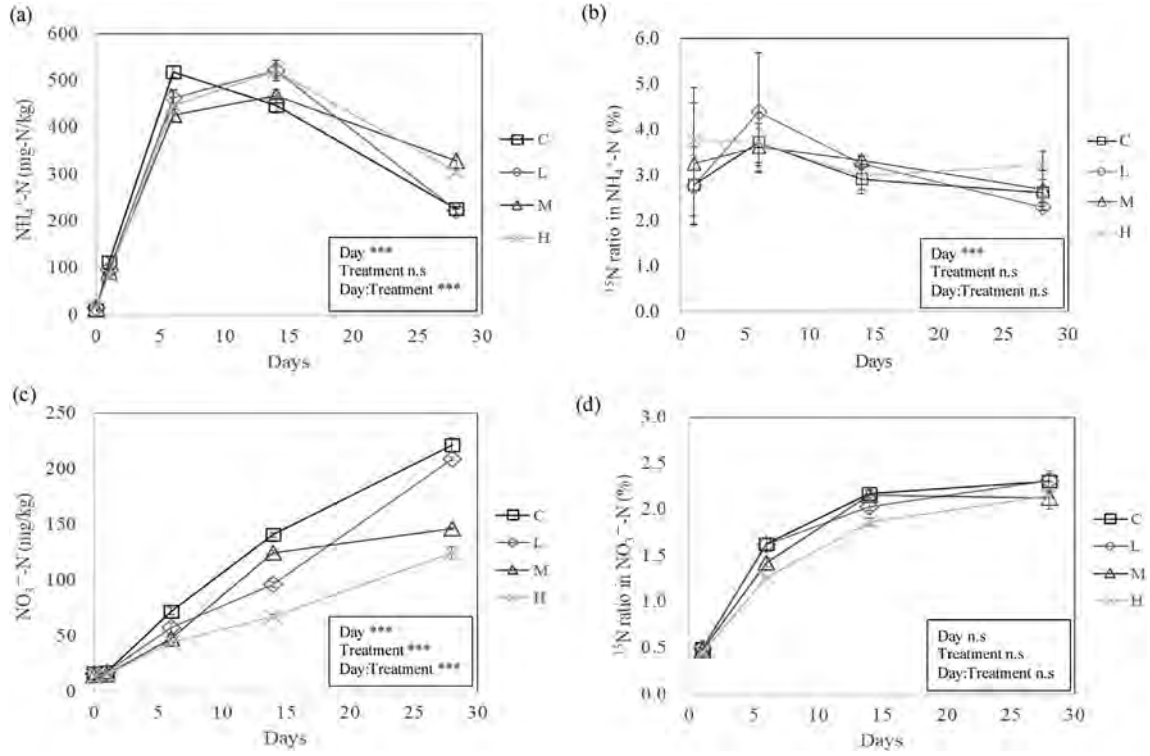

Fig. 1. The time course changes of the concentration and ^{15}N ratio of ammonium (a and b) and nitrate (c and d). The x axis represents days after the application of slag on the soil. C, L, M and H stand for the control, low, medium, high amount of slag mixed into the soils, respectively. The results from two-way ANOVA were shown on the right bottom of each figure. "***" and "n.s." stand for the significance level of $p < 0.001$ and not significant, respectively.

Table 2
The concentration (mg-N/kg) of inorganic-N. C, L, M and H stand for control, low, medium and high level of slag applied into the soil. The significance levels from ANOVA were stated below each inorganic-N type for each sampling date (n.s., *, ** and *** represent $p \geq 0.05$, $p < 0.05$, $p < 0.01$ and $p < 0.001$, respectively). The alphabets beside each number represent the results from multiple comparison for each inorganic-N type for each sampling day. The number in the brackets represent standard deviations (n = 3).

Property	Treatment	Date				
		0	1	6	14	28
NH_4^+-N	C	10.4 (0.3) a	113.2 (7.8) a	518.4 (12.3) a	446.9 (16.3) a	225.9 (0.6) a
	L	14.1 (5.5) a	95.9 (2.9) ab	462.4 (17.3) ab	522.0 (22.1) ab	222.2 (8.1) a
	M	13.4 (1.8) a	92.3 (5.4) ab	426.5 (12.5) b	467.4 (14.4) ab	328.6 (16.0) b
	H	15.6 (1.0) a	86.1 (2.4) b	446.9 (16.3) b	520.2 (9.5) b	305.8 (3.7) b
	ANOVA	n.s	*	*	*	***
NO_3^--N	C	16.4 (0.4) a	17.6 (0.5) a	72.1 (3.4) a	140.7 (2.0) a	221.0 (7.0) a
	L	16.0 (0.1) ab	17.6 (1.0) a	57.3 (4.6) ab	96.3 (2.5) b	208.7 (1.6) a
	M	14.6 (0.7) ab	15.4 (0.4) a	47.2 (3.8) b	124.8 (1.8) c	146.3 (0.7) b
	H	13.3 (0.5) b	15.1 (0.4) a	44.4 (0.5) b	67.3 (2.4) d	124.6 (5.4) c
	ANOVA	*	n.s	**	***	***

Signif. codes: 0 '***' 0.001 '**' 0.01 '*' 0.05.

The average Shannon–Wiener diversity index of each sample is shown in Table 3. No interaction effects of sampling day and treatment were seen (two-way ANOVA). There were no significant effects of slag application on diversity at either phylum level ($p > 0.05$) or family level ($p > 0.1$). Treatment H had the lowest, and L the highest, diversity indexes while treatments C and M had similar moderate levels of bacterial diversity.

3.3.1. Community structure analysis

Fig. S4 shows the percentage of each phylum in all DNA samples. *Proteobacteria* or *Firmicutes* were either the first or second largest phylum in all samples.

The result of RDA is shown in Fig. 2. The first component (RDA1) accounted for 62.7% of the variation in the data and the second (RDA2) and third component (RDA3) accounted for 15.9% and 2.5%, respectively. Overall, RDA1 was positively correlated with the amount of NH_4^+-N, and RDA2 was negatively correlated with the contamination level of slag containing heavy metals. Using RDA with stepwise regression, slag concentration, pH, and NH_4^+-N concentration were selected as significant explanatory variables.

The bacterial communities in soil contaminated with >8.0 g slag kg^{-1} dry soil (M and H) tended to have similar community structures, with relatively higher proportions of *Firmicutes* (28%–42%) and *Actinobacteria* (5.6%–9.3%), and lower percentages of *Planctomycetes* (<5.9%, except 28M2 (7.36%)). When sampling days were compared, the abundance of *Bacteroidetes* was relatively higher in samples taken on day 28. The samples lacking or with low amounts of slag (C and L) measured on day 0 were clustered into the same group (based on pH) with a dominance of *Proteobacteria*.

Heatmaps were constructed based on the relative abundance of each phylum and family (Fig. S5). Regarding community structure at phylum level, samples were clustered into three major groups; (1) C and L on day 0, (2) M and H on day 0, and (3) all groups on day 28. The patterns for each phylum indicated four major groups, with *Firmicutes* and *Proteobacteria* clustered alone. *Firmicutes* appeared more frequently in treatments M and H than in C and L. The relative abundance of *Proteobacteria* was higher in samples on day 0. Other phyla were better represented on day 28, except for *Armatimonadetes* and *Verrucomicrobia*.

At the family level, the effect of the slag was clearer than at phylum level. Treatments C and L, and M and H, were clustered together regardless of sampling day. *Thermoanaerobacteraceae* (*Firmicutes*) was the only family that showed a positive association with the M and H treatments. *Ectothiorhodospiraceae* and *Sphingomonadaceae* appeared more often on day 0 (although the proportion of the former decreased in treatments M and H on day 28). *Planctomycetaceae* was clustered as the family that showed the clearest negative correlation to slag concentration.

3.3.2. Community functional analysis

Fig. S6 shows bacterial functional features with significant differences ($p < 0.05$) between control and slag-containing treatments (those with sequence proportions <0.5% are omitted). On days 0 and 28, the functions related to bacterial motility ("Bacterial motility," "Flagellar assembly") were decreased in the slag-containing treatments. In contrast, "General functions," "Pyruvate metabolism," "Valine, leucine and isoleucine biosynthesis" and "Protein export" were increased in the slag-containing treatments. Some functions only featured in the results on days 0 and 28. For example, on day 0, "Bacterial chemotaxis" and "Two-component

Table 3
Shannon-Wiener diversity index for soil bacterial communities at the phylum and family levels for each sampling day (0 and 28) for each treatment (C, L, M and H for control, low, medium and high levels of slag applied into the soils). The alphabets beside each number represent the results from multiple comparison among the treatments for each bacterial category (phylum or family). The number in the brackets represent standard deviations (n = 3).

Shannon-Wiener diversity index (H′)					
Treatment	Phylum		Family		
	0	28	0	28	
C	1.63 (0.04)	1.80 (0.08)	3.10 (0.04)	3.21 (0.08)	ab
L	1.70 (0.03)	1.87 (0.04)	3.24 (0.02)	3.33 (0.10)	a
M	1.63 (0.02)	1.80 (0.02)	3.24 (0.02)	3.23 (0.07)	ab
H	1.56 (0.02)	1.78 (0.03)	2.97 (0.05)	3.20 (0.10)	b
Day	***		*		
Treatment	***		*		
Day:Treatment	***		*		

Signif. codes: 0 '***' 0.001 '**' 0.01 '*' 0.05.

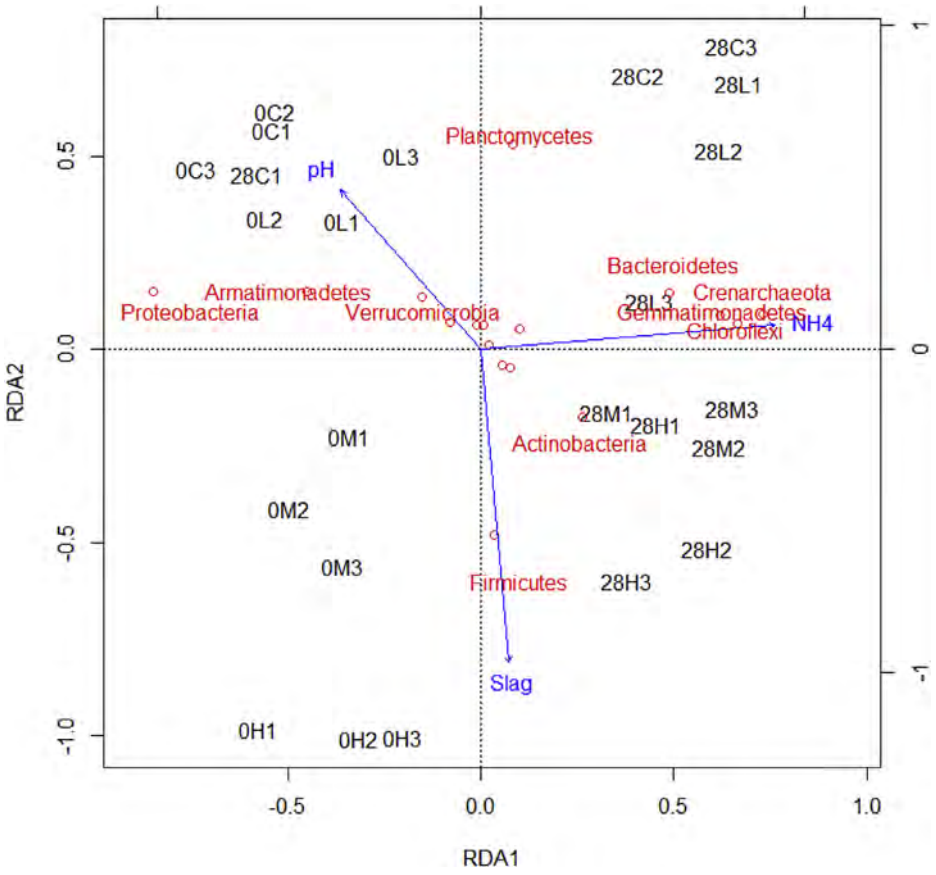

Fig. 2. RDA plot of the bacterial community structures. Blue arrows are influential environmental factors and the red letters were phylum names. The black letters were the sample names. The sample names represent sampling days, treatment, andthereplicatenumber. Forexample,"0L2" is the sample taken from the soil of replicate number 2 with low Pb concentration (100 mg-Pb/kgdrysoil) on day 0. Similarly,C,M and H represent the soil samples received control, medium and high levels of the slag, respectively.

system" were considerably lower in the contaminated samples, while the metabolism of some amino acids and sugars ("Histidine metabolism," "Starch and sucrose metabolism," "Cysteine and methionine metabolism," and "Galactose metabolism") was higher in the slag treatments. On day 28, functions related to the metabolism of carboxylic acids ("Fatty acid metabolism," "Propanoate metabolism," and "Butanoate metabolism") and carboxylates ("Glyoxylate and dicarboxylate metabolism") were high in slag-containing samples.

The proportions of sequences of N metabolism are shown in Fig. 3. Nitrogen metabolism includes dissimilatory NO_3^--N reduction, assimilatory NO_3^--N reduction, denitrification, N fixation, nitrification, and anaerobic ammonium oxidation (anammox). Both on day 0 and 28, the relative abundance of bacteria that have genes related to N metabolism tended to decrease in the slag-contaminated soil. The impact was clearer on day 0 and there was a negative correlation of relative abundance with slag concentration. On day 28, the differences between the four treatments were reduced.

4. Discussion

4.1. Slag effects on N dynamics

The appearance of the peak concentration of NH_4^+-N was delayed in the slag-containing treatments (L, M, and H) compared to the control treatment (Fig. 1a). This might be the result of the slag depressing urease activity through which NH_4^+ is released from urea added to the soil. Yang et al. (2006) investigated the effects of Cd, Zn, and Pb (in concentrations of 0–50, 0–800, and 0–1000 mg kg^{-1}, respectively) on soil urease activity and reported that these heavy metals decreased urease activity. Heavy metal ions are known to react with the sulfhydryl groups on the active site of urease (Shaw, 1954) and metal ions including Mn^{2+}, Pb^{2+}, Co^{2+}, Cd^{2+}, Ni^{2+}, and Cu^{2+} have been reported to be urease inhibitors (Upadhyay, 2012). There is a possibility that urea was adsorbed by the slag, but the slag used in the current experiment contained very low levels of C (0.36%), so the urea adsorption capacity of the slag could be considered low. It has been reported for a variety of soils that C levels positively influence urea adsorption capacity (Chin and Kroontje, 1962).

We were unable to identify the substance or element within the slag that had impacted the N cycle in the current experiment. The slag contained various metals (Section 2.1). Several preliminary experiments were performed to test the impact of pure heavy metal compounds, such as $PbNO_3$ and $Pb(CH_3COO)_2$, on N cycle activities in soils. However, we concluded that the presence of C and N in the test compounds influenced N cycle activities. Thus, the pure heavy metals were not used in the current study and this study aimed to identify the potential effect of the slag accumulating in the open air, and the mixing ratios of slag to soil were determined from these field data (Ikenaka et al., 2010).

In the current study, most of the extracted NH_4^+-N was derived from the applied urea since the isotopic ratio was constant at around 3 atom%, the same value as the ^{15}N levels of the added urea (Fig. 1b). Thus, soil N was not contributing to the soil NH_4^+-N pool,

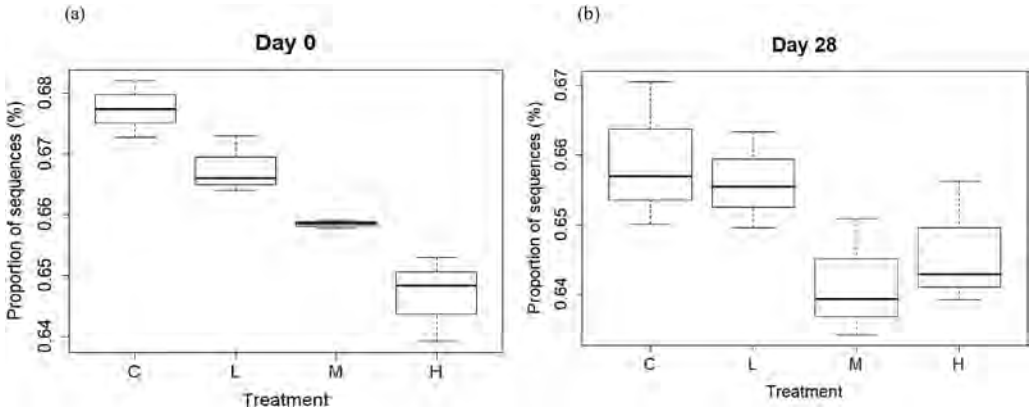

Fig. 3. The proportion of the sequences (%) of N metabolism (dissimilatory NO_3^--N reduction, assimilatory NO_3^--N reduction, denitrification, N fixation, nitrification, and anammox) within the soil bacterial community, on day 0 (a) and 28 (b). The treatment (x axis) C, L, M and H stand for the control, low, medium and high level of slag application rates to the soils, respectively.

and it was urea hydrolysis that was likely controlling the increase of NH_4^+-N. If so, urea hydrolysis might have been delayed due to inhibition of urease activity by the slag treatments in this experiment. The amount of NH_4^+-N was 200–300 mg N kg^{-1} soil even at the end of the current experiment, whereas the original concentration of soil NH_4^+-N was <20 mg N kg^{-1} soil (Table 2, day 0). The relatively constant ^{15}N ratio of NH_4^+-N in the current experiment may simply have been due to the relative excess of NH_4^+-N from the applied urea compared to NH_4^+-N from soil N. Also, the soil was pre-incubated for two weeks, and the active mineralization of soil N might have ceased before the commencement of the experiment. Previous studies have reported soil N mineralization during urea hydrolysis due to increasing soil pH (e.g., Tong and Xu, 2012) but we did not observe an increase in soil pH during the current experiment, probably due to the buffering capacity of the soil.

Increasing amounts of slag negatively influenced the accumulation of NO_3^--N in the soils (Fig. 1c, Table 2). Compared to the effects of slag on NH_4^+-N concentration, the effect on NO_3^--N was more significant, suggesting that the slag influenced nitrification more than ammonification. This inference is in agreement with the study by Rother et al. (1982) who reported that nitrification was considerably more sensitive than ammonification to Cd, Zn and Pb. They studied the effects on soil of Cd, Zn and Pb at concentrations of 1000–5000, 1000–5000 and 10,000–20,000 mg kg^{-1}, respectively. Ueda et al. (1988) investigated the effects of anionic heavy metals, such as CrO_4^{2-}, MoO_4^{2-}, WO_4^{2-}, and VO_3^-, on ammonification and nitrification and found similar tendencies. This study suggested that the different sensitivities of the two processes to heavy metals may be due to the difference in the number of reaction steps between nitrification and ammonification. One chemical reaction step is needed to convert urea to NH_4^+-N whereas two steps are required to nitrify NH_4^+-N to NO_3^--N ($NH_4^+ \rightarrow NO_2^- \rightarrow NO_3^-$). Heavy metal inhibition of nitrification in wastewater treatment plants has been well studied and it is reported that the oxidation of NH_4^+ to NO_2^- by ammonia oxidizing bacteria is thought to be the most sensitive step in the process (Epa, 1993). Stephen et al. (1999) showed ammonia and NH_4^+ accumulated in the presence of toxic metals (Cd, Co, Cs and Sr) in soil and referred to the negative influence of these metals on ammonia oxidation. Radniecki and Ely (2008) investigated both ammonia-dependent and hydrazine-dependent specific oxygen uptake rate in cell suspensions of an ammonia oxidizing bacteria species and reported that an increase in Zn^{2+} inhibited ammonia oxidation, the first step of nitrification. On this basis we concluded that the slow accumulation of NH_4^+-N and the reduced concentration of NO_3^--N in the slag-containing treatments seen in the current study were due to relatively stronger inhibition of ammonia oxidation by heavy metals compared to that of the urease activity, which converts urea to NH_4^+-N.

In the slag-contaminated soils, the ratio of NH_4^+-N to NO_3^--N rose compared to the control. However, the total amount of inorganic N decreased in all of the treatments to a similar level from day 14–28 (Fig. S1). Since the total amount of inorganic N (NO_3^--N plus NH_4^+-N) was the same in all treatments for each day (day 14 and 28), the mechanism behind the loss of inorganic N during this period was apparently different between the less contaminated soils (soil C and L) and the heavily contaminated soils (soil M and H). Processes such as denitrification and immobilization, related to the loss of inorganic N from soils, is a topic recommended for future study.

The concentration of NH_4^+-N can decrease as a result of immobilization. Yet, as described below, bacterial relative abundance decreased in the treatments with higher slag concentrations, indicating that the NH_4^+-N might not have been actively immobilized in the presence of the slag. The loss of NH_4^+-N in the slag-contaminated treatments in the current experiment was more likely due to NH_3 volatilization rather than immobilization. Kim et al. (2012) reported that nitrification inhibitor application increased the NH_3 loss from soil. It is probable that the heavy metals in slag inhibited nitrification and that accumulated NH_4^+-N volatilized as NH_3 rather than becoming NO_3^--N and remaining in the soil. From this, we conclude that the mechanism for the loss of inorganic N was different in contaminated and uncontaminated soils although further studies are needed to confirm this.

There was a tendency for the isotopic ratio of NO_3^--N to be lower in slag-treated variants (especially H), though the differences were not statistically significant (Fig. 1d). The decrease in isotopic ratio was correlated to the decrease in concentration of NO_3^--N in general. Dai et al. (2004) reported that net N mineralization was lower in the presence of elevated levels of risk elements in a pasture soil. In the current study, the contribution made by mineralized soil organic N to increase the inorganic N pool was small, even in the control soil. Thus, a negative effect of slag on soil N mineralization was not clearly demonstrated in the current study.

4.2. Slag effects on the abundance of bacterial DNA

A marked increase in the relative abundance of bacterial DNA was observed from day 0–1 only in the control treatment (Fig. S3). Thus, in the absence of slag, soil bacteria responded positively to the urea application over a short period. Previous reports have stated that the soil microbial population tends to decrease with an

increase in heavy metal concentration (Bååth, 1989). This is due to a decrease in substrate utilization efficiency as a result of a high energy cost metabolism against metal stress (Chander and Joergensen, 2001). The relatively lower abundance of bacteria in the control treatment on day 0 might be due to nutrient deficiency caused by higher microbial activity during the pre-incubation period.

4.3. The explanation from the change in bacterial community structure

4.3.1. Diversity analysis

Slag application did not change bacterial diversity significantly at either phylum or family level (Table 3). Microbial diversity in the sample with a low amount of slag (L, about 0.2% by weight) was the highest among all treatments; as the amount of slag increased in treatments M and H, the bacterial diversity tended to decrease. This result is consistent with a previous study in which a low application rate of biosolids (containing heavy metals) increased soil microbial diversity while at high rates diversity decreased (Mossa et al., 2017). This increase in microbial diversity with a low level of biosolid application was due to the high organic matter content of the biosolid. In the current study, in treatment L, the bacteria present in the applied slag might have grown in the soil to produce the relatively higher diversity compared to the control. The presence of a low level of slag might also act as a moderate environmental stress, decreasing competitive exclusion, and leading to the observed increase in diversity (Giller et al., 1998). As the concentration of heavy metals in the soil increased (treatments M and H), more bacterial species might have died due to greater stress. In the presence of an environmental stress, bacterial diversity is considered to decrease as a result of the death of some intolerant species and the prospering of more tolerant species (Atlas, 1984). This is consistent with many previous studies reporting that bacterial diversity tends to be lower in heavy metal-contaminated soil (Sandaa et al., 1999; Xie et al., 2016).

Bacterial diversity tended to be higher on day 28 than on day 0 in all treatments. The application of urea, from which NH_4^+-N is easily released, might have improved the growth of bacterial species that were depressed due to substrate depletion.

4.3.2. Community structure analysis

RDA showed that pH, the amount of NH_4^+-N, and slag concentration were the environmental factors that most influenced bacterial community structure. However, the pH fluctuation observed during the incubation period ranged from 4.1 to 5.3, thus other potential factors influenced by the addition of the slag have to be investigated in future, such as changes in physical properties of the soil. Also, it is possible that microbes were introduced with the slag, thereby influencing the microbial communities in the soil. The high levels of NH_4^+-N released from urea on day 28 might explain why all samples (except 28C1) taken on day 28 had high RDA1 values (Fig. 2). The relative increase of *Crenarchaeota*, *Chloroflexi*, *Gemmatimonadetes*, and *Bacteroidetes* on this day was due to this NH_4^+-N abundance. Among these phyla there were some containing species known to conduct ammonium oxidation (e.g., *Crenarchaeota*) (Nicol and Schleper, 2006) or nitrite oxidation (e.g., *Chloroflexi*) (Udert et al., 2005). The abundance of NH_4^+-N in the environment might have favored those species that oxidize NH_4^+ and NO_2^-.

The abundance of *Firmicutes* was positively correlated with slag concentration while that of *Planctomycetes* was negatively correlated (Fig. 2). Ellis et al. (2003) reported that *Firmicutes* (mainly *Bacillus* spp.) exhibit high relative abundance in slag-contaminated sites. Liu et al. (2018) also found that this phylum is among the five most abundant phyla in sediment polluted with heavy metals. In the current study, the high proportion of *Thermoanaerobacteraceae* (*Firmicutes*, *Clostridia*) with increasing slag concentration explains the increase in abundance of *Firmicutes* (Fig. S7a). This family is mainly isolated from hot springs and is known for its strictly anaerobic, rod-shaped, spore-forming character (Stackebrandt, 2014). There are few other studies published to date about the environments occupied by this bacterial family. The ability to form spores might be an advantage for these microbes, enabling them to survive in environments with heavy metal stress. A study by Smejkalova et al. (2003) showing an increase in spore-forming bacteria in heavy metal-contaminated soil supports this hypothesis. Another factor potentially influencing bacterial survival under heavy metal stress is sequestration ability. Previous studies suggest that in heavy metal-contaminated sites, gram-negative bacteria are more widespread than gram-positive bacteria because the cell walls of gram-positive bacteria are better able to bind metal cations (Evans and Furlong, 2003; Çolak et al., 2011). Also, *Bacillus* spp seen in metal-stressed environments can act as a biosorbent (Volesky and Holan, 1995). The mechanism of heavy metal resistance of members of the *Thermoanaerobacteraceae* requires further investigation.

The major proportion of extracted 16S rRNA originated from *Planctomycetes*, and RDA results showed that they were negatively affected by the heavy metals. Fuerst and Sagulenko (2011) reported several unique features of this phylum, such as peptidoglycan-lacking proteinaceous cell walls, and intracellular membranes that form separate compartments within the cell cytoplasm. These unique features might make this phylum especially sensitive to heavy metals. Bacterial resistance mechanisms, such as the excretion of metals out of the cell (Silver and Phung, 1996), have been previously reported, but further study is needed to understand the susceptibility of this phylum to heavy metals.

In *Planctomycetes*, there are families that conduct anaerobic NH_4^+-N oxidation (anammox) and which possess distinctive cell structure, for example *Candidatus*. Anammox is known to be inhibited in the presence of heavy metals (Jin et al., 2012). Hu et al. (2011) and Xi et al. (2016) investigated anammox bacteria in agricultural soil and forest soil, respectively, and reported *Candidatus Brocadia fulgida* and *Candidatus Jettenia asiatica* as being the dominant anammox phylotypes. In the current study, it was found that *Candidatus Brocadiaceae* tended to decrease as the proportion of slag in the soil increased (Fig. S7b). Thus, it could be expected that the presence of heavy metals decreased the proportion of this phylum and family and, although the total amount of N removed by their anammox activity would not have been large, this could have had an influence in the slag-contaminated soil.

Both environmental factors and species relationships may change the proportion of a species in the community (Perez-Garcia et al., 2016), therefore it is important to further investigate the reasons behind these changes, and to ask whether they are the direct result of the effects of the slag or are driven by microbial metabolism interactions.

4.3.3. Community function

There were influences of both the treatments and the sampling days on the bacterial community functions. Some previous studies reported that the motility of specific bacterial species was inhibited in the presence of heavy metals (Adler and Templeton, 1967; Singh et al., 2014). In their study, Singh et al. concluded that the presence of Cd^{2+} and Pb^{2+} ions prevented flagella development of a metal-resistant bacterium (strain CM100B). This agrees with the current results that showed a decrease in DNA sequences related to bacterial motility in the more slag-containing treatments (Fig. S6).

The current study demonstrated that some general metabolic functions, such as pyruvate metabolism, were relatively high in the

slag-containing samples both on day 0 and day 28 (Fig. S6). Bacteria resistant to heavy metals have various detoxification strategies, such as intra- or extracellular sequestration, export and permeability barriers (Rouch et al., 1995). These mechanisms involve special biochemical processes seen only under metal stress, for example membrane transport protein expression and increased ATP consumption (Nies, 1999). The relatively active functions seen in the contaminated treatments in this study may be related to these mechanisms.

On day 0, very significant differences between the control and the slag-treated samples were found especially in bacterial functions related to motility (such as "Bacterial chemotaxis" and "Bacterial motility proteins") and repair ("DNA repair and recombination protein"). In contrast, on day 28, the functions showing significant differences between the control and the slag-treated samples were related to fatty acid metabolism ("Fatty acid metabolism," "Butanoate metabolism," "Propanoate metabolism") (Fig. S6). One reason for the difference might be due to the application of urea. On day 28, with a high level of inorganic N, bacterial groups favoring high N conditions might have become active and the effect of the slag on these groups was different from that on microbes present at the beginning of the experiment.

The functional analysis also suggested negative impacts of the slag on N metabolism by bacteria (Fig. 3). From the results, we cannot determine which particular reaction(s) within the N cycle were more sensitive than others. Yet, the proportion of N metabolizing bacteria tended to decrease in the slag-containing treatment, even in the presence of a high level of inorganic N (day 28).

Kandeler et al. (2000) examined the impact of heavy metals on soil microbial biomass, enzyme activity (urease, alkaline phosphatase, and xylanase), and microbial community structure, concluding that microbial community structure was the least affected of the three. In our study, we found that the slag containing heavy metals influenced the bacterial community structure, as well as the N dynamics and the relative abundance of bacteria. The slag did not affect the bacterial diversity significantly, but it influenced the bacterial community structure and functions. This is consistent with the study by Li et al. (2017) that concluded long-term heavy metal (Cd, As, Pb, and Zn) contamination had a greater effect on microbial composition than on diversity, although in our study, no significant tolerance by archaea (ex. *Crenarchaeota*) was seen. Changes in bacterial community structure may influence bacterial functions in N cycling. Nutrient cycling in slag-contaminated sites may be influenced by a combination of changes in bacterial community structure and abundance.

5. Conclusion

This study suggests that slag from a mining site containing heavy metals (Pb and Zn) had a strong negative impact on nitrification, more so than on ammonification. Due to the disturbance of the nitrification process, the accumulation rate of NO_3^--N was slower in slag-contaminated soils. Slag applied to soil at 4.9% by weight caused a ~50% reduction in the accumulation of NO_3^--N compared to the control four weeks after the application of urea, an outcome that could limit the growth of plants dependent on NO_3^--N. Soil bacterial abundance tended to be lower with increasing slag concentration. Soil bacterial community structure was significantly influenced by the slag; as the slag to soil ratio increased, the relative abundance of *Firmicutes* increased and that of *Planctomycetes* decreased. Families within *Planctomycetes* that conduct anammox also considerably decreased. The change in microbial community structure affected community functions including N metabolism. Our study suggests that slag mixed with soil influences soil microbial community structure, and consequently the N cycle-related soil functions. Future research on the effect of slag on microbial community structure, the N cycle in the soil, and their relationships and mechanisms is recommended.

Acknowledgement

This work was funded by the Japan Science and Technology Agency (JST) and the Japan International Cooperation Agency (JICA), under the program Science and Technology Research Partnership for Sustainable Development (SATREPS) "Visualization of Impact of Chronic/Latent Chemical Hazard and Geo-Ecological Remediation (Grant ID: 15543708)".

Appendix A. Supplementary data

Supplementary data related to this article can be found at https://doi.org/10.1016/j.envpol.2018.09.024.

References

Abujabhah, I.S., Doyle, R.B., Bound, S.A., Bowman, J.P., 2018. Assessment of bacterial community composition, methanotrophic and nitrogen-cycling bacteria in three soils with different biochar application rates. J. Soils Sediments 18 (1), 148–158. https://doi.org/10.1007/s11368-017-1733-1.

Adler, J., Templeton, B., 1967. The effect of environmental conditions on the motility of Escherichia coli. Microbiology 46 (2), 175–184. https://doi.org/10.1099/00221287-46-2-175.

Atlas, R.N., 1984. Use of microbial diversity measurements to assess environmental stress. In: Current Perspectives in Microbial Ecology, pp. 540–545.

Bååth, E., 1989. Effects of heavy metals in soil on microbial processes and populations (a review). Water Air Soil Pollut. 47 (3–4), 335–379. https://doi.org/10.1007/BF00279331.

Cela, S., Sumner, M.E., 2002. Critical concentrations of copper, nickel, lead, and cadmium in soils based on nitrification. Commun. Soil Sci. Plant Anal. 33 (1–2), 19–30.

Çolak, F., Atar, N., Yazıcıoğlu, D., Olgun, A., 2011. Biosorption of lead from aqueous solutions by Bacillus strains possessing heavy-metal resistance. Chem. Eng. J. 173 (2), 422–428. https://doi.org/10.1016/j.cej.2011.07.084.

Chander, K., Joergensen, R.G., 2001. Decomposition of 14 C glucose in two soils with different amounts of heavy metal contamination. Soil Biol. Biochem. 33 (12), 1811–1816. https://doi.org/10.1016/s0038-0717(01)00108-0.

Chin, W.-T., Kroontje, W., 1962. Mechanisms of urea adsorption by soils. Soil Sci. Soc. Am. J. 26 (5), 479–481. https://doi:10.2136/sssaj1962.03615995002600050021x.

Dai, J., Becquer, T., Rouiller, J.H., Reversat, G., Bernhard-Reversat, F., Lavelle, P., 2004. Influence of heavy metals on C and N mineralisation and microbial biomass in Zn-, Pb-, Cu-, and Cd-contaminated soils. Appl. Soil Ecol. 25 (2), 99–109. https://doi.org/10.1016/j.apsoil.2003.09.003.

Ellis, R.J., Morgan, P., Weightman, A.J., Fry, J.C., 2003. Cultivation-dependent and-independent approaches for determining bacterial diversity in heavy-metal-contaminated soil. Appl. Environ. Microbiol. 69 (6), 3223–3230. https://doi.org/10.1128/aem.69.6.3223-3230.2003.

Epa, U.S., 1993. Process Design Manual of Nitrogen Control. EP A.

Evans, G.M., Furlong, J.C., 2003. Environmental Biotechnology: Theory and Application. IK International Pvt Ltd, p. 293.

Fuerst, J.A., Sagulenko, E., 2011. Beyond the bacterium: planctomycetes challenge our concepts of microbial structure and function. Nat. Rev. Microbiol. 9 (6), 403–413. https://doi.org/10.1038/nrmicro2578.

Giller, K.E., Witter, E., Mcgrath, S.P., 1998. Toxicity of heavy metals to microorganisms and microbial processes in agricultural soils: a review. Soil Biol. Biochem. 30 (10), 1389–1414. https://doi.org/10.1016/S0038-0717(97)00270-8.

Gołębiewski, M., Deja-Sikora, E., Cichosz, M., Tretyn, A., Wróbel, B., 2014. 16S rDNA pyrosequencing analysis of bacterial community in heavy metals polluted soils. Microb. Ecol. 67 (3), 635–647. https://doi.org/10.1007/s00248-013-0344-7.

Hamamoto, T., Uchida, Y., 2015. Sodium contents in dairy cow urine and soil aggregate sizes influence the amount of nitrogen lost from soil. In: Applied and Environmental Soil Science, 2015. https://doi.org/10.1155/2015/275985.

Hernández, A.J., Pastor, J., 2008. Relationship between plant biodiversity and heavy metal bioavailability in grasslands overlying an abandoned mine. Environ. Geochem. Health 30 (2), 127–133. https://doi.org/10.1007/s10653-008-9150-4.

Hu, B.L., Rush, D., van der Biezen, E., Zheng, P., van Mullekom, M., Schouten, S., Damsté, J.S.S., Smolders, A.J.P., Jetten, M.S.M., Kartal, B., 2011. New anaerobic, ammonium-oxidizing community enriched from peat soil. Appl. Environ. Microbiol. 77 (3), 966–971. https://doi.org/10.1128/aem.02402-10.

Ikenaka, Y., Nakayama, S.M., Muzandu, K., Choongo, K., Teraoka, H., Mizuno, N., Ishizuka, M., 2010. Heavy metal contamination of soil and sediment in Zambia. Afr. J. Environ. Sci. Technol. 4 (11), 729–739. https://doi.org/10.1201/b16566-7.

Jin, R.C., Yang, G.F., Yu, J.J., Zheng, P., 2012. The inhibition of the Anammox process: a review. Chem. Eng. J. 197, 67–79. https://doi.org/10.1016/j.cej.2012.05.014.

Kandeler, E., Tscherko, D., Bruce, K.D., Stemmer, M., Hobbs, P.J., Bardgett, R.D., Amelung, W., 2000. Structure and function of the soil microbial community in microhabitats of a heavy metal polluted soil. Biol. Fertil. Soils 32 (5), 390–400. https://doi.org/10.1007/s003740000268.

Kim, D.G., Saggar, S., Roudier, P., 2012. The effect of nitrification inhibitors on soil ammonia emissions in nitrogen managed soils: a meta-analysis. Nutrient Cycl. Agroecosyst. 93 (1), 51–64. https://doi.org/10.1007/s10705-012-9498-9.

Langille, M.G., Zaneveld, J., Caporaso, J.G., McDonald, D., Knights, D., Reyes, J.A., Clemente, J.C., Burkepile, D.E., Thurber, R.L.V., Knight, R., Beiko, R.G., Huttenhower, C., 2013. Predictive functional profiling of microbial communities using 16S rRNA marker gene sequences. Nat. Biotechnol. 31 (9), 814–821. https://doi.org/10.1038/nbt.2676.

Laughlin, R.J., Stevens, R.J., Zhuo, S., 1997. Determining nitrogen-15 in ammonium by producing nitrous oxide. Soil Sci. Soc. Am. J. 61 (2), 462–465. https://doi.org/10.2136/sssaj1997.03615995006100020013x.

Leita, L., Nobili, M.D., Muhlbachova, G., Mondini, C., Marchiol, L., Zerbi, G., 1995. Bioavailability and effects of heavy metals on soil microbial biomass survival during laboratory incubation. Biol. Fertil. Soils 19 (2–3), 103–108. https://doi.org/10.1007/BF00336144.

Li, X., Meng, D., Li, J., Yin, H., Liu, H., Liu, X., Cheng, C., Xiao, Y., Liu, Z., Yan, M., 2017. Response of soil microbial communities and microbial interactions to long-term heavy metal contamination. Environ. Pollut. 231, 908–917. https://doi.org/10.1016/j.envpol.2017.08.057.

Liu, J., Chen, X., Shu, H.Y., Lin, X.R., Zhou, Q.X., Bramryd, T., Shu, W.S., Huang, L.N., 2018. Microbial community structure and function in sediments from e-waste contaminated rivers at Guiyu area of China. Environ. Pollut. 235, 171–179. https://doi.org/10.1016/j.envpol.2017.12.008.

McIlvin, M.R., Altabet, M.A., 2005. Chemical conversion of nitrate and nitrite to nitrous oxide for nitrogen and oxygen isotopic analysis in freshwater and seawater. Anal. Chem. 77 (17), 5589–5595. https://doi.org/10.1021/ac050528s.

Mossa, A.W., Dickinson, M.J., West, H.M., Young, S.D., Crout, N.M., 2017. The response of soil microbial diversity and abundance to long-term application of biosolids. Environ. Pollut. 224, 16–25. https://doi.org/10.1016/j.envpol.2017.02.056.

Nagajyoti, P.C., Lee, K.D., Sreekanth, T.V.M., 2010. Heavy metals, occurrence and toxicity for plants: a review. Environ. Chem. Lett. 8 (3), 199–216. https://doi.org/10.1007/s10311-010-0297-8.

Nicol, G.W., Schleper, C., 2006. Ammonia-oxidising Crenarchaeota: important players in the nitrogen cycle? Trends Microbiol. 14 (5), 207–212. https://doi.org/10.1016/j.tim.2006.03.004.

Nies, D.H., 1999. Microbial heavy-metal resistance. Appl. Microbiol. Biotechnol. 51 (6), 730–750. https://doi.org/10.1007/s002530051457.

Perez-Garcia, O., Lear, G., Singhal, N., 2016. Metabolic network modeling of microbial interactions in natural and engineered environmental systems. Front. Microbiol. 7. https://doi.org/10.3389/fmicb.2016.00673.

Radniecki, T.S., Ely, R.L., 2008. Zinc chloride inhibition of Nitrosococcus mobilis. Biotechnol. Bioeng. 99 (5), 1085–1095. https://doi.org/10.1002/bit.21672.

Rother, J.A., Millbank, J.W., Thornton, I., 1982. Effects of heavy-metal additions on ammonification and nitrification in soils contaminated with cadmium, lead and zinc. Plant Soil 69 (2), 239–258. https://doi.org/10.1007/BF02374519.

Rouch, D.A., Lee, B.T., Morby, A.P., 1995. Understanding cellular responses to toxic agents: a model for mechanism-choice in bacterial metal resistance. J. Ind. Microbiol. 14 (2), 132–141. https://doi.org/10.1007/bf01569895.

Sandaa, R.A., Torsvik, V., Enger, Ø., Daae, F.L., Castberg, T., Hahn, D., 1999. Analysis of bacterial communities in heavy metal-contaminated soils at different levels of resolution. FEMS (Fed. Eur. Microbiol. Soc.) Microbiol. Ecol. 30 (3), 237–251. https://doi.org/10.1016/s0168-6496(99)00062-8.

Shaw, W.H., 1954. The inhibition of urease by various metal ions. J. Am. Chem. Soc. 76 (8), 2160–2163. https://doi.org/10.1021/ja01637a034.

Smejkalova, M., Mikanova, O., Boruvka, L., 2003. Effects of heavy metal concentrations on biological activity of soil micro-organisms. Plant Soil Environ. 49 (7), 321–326. https://doi.org/10.17221/4131-pse.

Silver, S., Phung, L.T., 1996. Bacterial heavy metal resistance: new surprises. Annu. Rev. Microbiol. 50 (1), 753–789. https://doi.org/10.1146/annurev.micro.50.1.753.

Singh, A.K., Dhanjal, S., Cameotra, S.S., 2014. Surfactin restores and enhances swarming motility under heavy metal stress. Colloids Surfaces B Biointerfaces 116, 26–31. https://doi.org/10.1016/j.colsurfb.2013.12.035.

Stackebrandt, E., 2014. The family Thermoanaerobacteraceae. In: The Prokaryotes. Springer Berlin Heidelberg, pp. 413–419. https://doi.org/10.1007/978-3-642-30120-9_367.

Stephen, J.R., Chang, Y.J., Macnaughton, S.J., Kowalchuk, G.A., Leung, K.T., Flemming, C.A., White, D.C., 1999. Effect of toxic metals on indigenous soil β-subgroup proteobacterium ammonia oxidizer community structure and protection against toxicity by inoculated metal-resistant bacteria. Appl. Environ. Microbiol. 65 (1), 95–101.

Taylor, M.P., Mould, S.A., Kristensen, L.J., Rouillon, M., 2014. Environmental arsenic, cadmium and lead dust emissions from metal mine operations: implications for environmental management, monitoring and human health. Environ. Res. 135, 296–303. https://doi.org/10.1016/j.envres.2014.08.036.

Tong, D., Xu, R., 2012. Effects of urea and $(NH_4)_2SO_4$ on nitrification and acidification of Ultisols from Southern China. J. Environ. Sci. 24, 682–689. https://doi.org/10.1016/S1001-0742(11)60832-2.

Udert, K.M., Larsen, T.A., Gujer, W., 2005. Chemical nitrite oxidation in acid solutions as a consequence of microbial ammonium oxidation. Environ. Sci. Technol. 39 (11), 4066–4075. https://doi.org/10.1021/es048422m.

Ueda, K., Kobayashi, M., Takahashi, E., 1988. Effect of anionic heavy metals on ammonification and nitrification in soil. Soil Sci. Plant Nutr. 34 (1), 139–146. https://doi.org/10.1080/00380768.1988.10415587.

Upadhyay, L.S.B., 2012. Urease inhibitors: a review. Indian J. Biotechnol. 11, 381–388.

Vásquez-Murrieta, M.S., Migueles-Garduño, I., Franco-Hernández, O., Govaerts, B., Dendooven, L., 2006. C and N mineralization and microbial biomass in heavy-metal contaminated soil. Eur. J. Soil Biol. 42 (2), 89–98. https://doi.org/10.1016/j.ejsobi.2005.10.002.

Volesky, B., Holan, Z.R., 1995. Biosorption of heavy metals. Biotechnol. Prog. 11 (3), 235–250. https://doi.org/10.1021/bp00033a001.

Wang, Y., Shi, J., Wang, H., Lin, Q., Chen, X., Chen, Y., 2007. The influence of soil heavy metals pollution on soil microbial biomass, enzyme activity, and community composition near a copper smelter. Ecotoxicol. Environ. Saf. 67 (1), 75–81. https://doi.org/10.1016/j.ecoenv.2006.03.007.

Wong, M.H., 2003. Ecological restoration of mine degraded soils, with emphasis on metal contaminated soils. Chemosphere 50 (6), 775–780. https://doi.org/10.1016/S0045-6535(02)00232-1.

Xi, D., Bai, R., Zhang, L., Fang, Y., 2016. Contribution of anammox to nitrogen removal in two temperate forest soils. Appl. Environ. Microbiol. 82 (15), 4602–4612. https://doi.org/10.1128/aem.00888-16.

Xie, Y., Fan, J., Zhu, W., Amombo, E., Lou, Y., Chen, L., Fu, J., 2016. Effect of heavy metals pollution on soil microbial diversity and bermudagrass genetic variation. Front. Plant Sci. 7. https://doi.org/10.3389/fpls.2016.00755.

Yang, Z., Liu, S., Zheng, D., Feng, S., 2006. Effects of cadmium, zinc and lead on soil enzyme activities. J. Environ. Sci. (China) 18 (6), 1135–1141. https://doi.org/10.1016/s1001-0742(06)60051-x.

Zhao, H., Xia, B., Fan, C., Zhao, P., Shen, S., 2012. Human health risk from soil heavy metal contamination under different land uses near Dabaoshan Mine, Southern China. Sci. Total Environ. 417, 45–54. https://doi.org/10.1016/j.scitotenv.2011.12.047.

Zuazo, V.H.D., Pleguezuelo, C.R.R., 2009. Soil-erosion and runoff prevention by plant covers: a review. In: Sustainable Agriculture. Springer, Dordrecht, pp. 785–811. https://doi.org/10.1007/978-90-481-2666-8_48.

PLOS ONE

RESEARCH ARTICLE

Investigation of mRNA expression changes associated with field exposure to DDTs in chickens from KwaZulu-Natal, South Africa

Lesa A. Thompson[1], Yoshinori Ikenaka[1,2], Wageh S. Darwish[1,3], Yared B. Yohannes[1,4], Johan J. van Vuren[2], Victor Wepener[2], Nico J. Smit[2], Atnafu G. Assefa[1,4], Ahmed Tharwat[1,3], Walaa Fathy Saad Eldin[5], Shouta M. M. Nakayama[1], Hazuki Mizukawa[6], Mayumi Ishizuka[1]*

1 Laboratory of Toxicology, Department of Environmental Veterinary Sciences, Graduate School of Veterinary Medicine, Hokkaido University, Sapporo, Hokkaido, Japan, **2** Water Research Group, Unit for Environmental Sciences and Management, North-West University, Potchefstroom, South Africa, **3** Food Control Department, Faculty of Veterinary Medicine, Zagazig University, Zagazig, Egypt, **4** Department of Chemistry, College of Natural and Computational Science, University of Gondar, Gondar, Ethiopia, **5** Educational Veterinary Hospital, Faculty of Veterinary Medicine, Zagazig University, Zagazig, Egypt, **6** Department of Environmental Veterinary Sciences, Graduate School of Veterinary Medicine, Hokkaido University, Sapporo, Hokkaido, Japan

* ishizum@vetmed.hokudai.ac.jp

Citation: Thompson LA, Ikenaka Y, Darwish WS, Yohannes YB, van Vuren JJ, Wepener V, et al. (2018) Investigation of mRNA expression changes associated with field exposure to DDTs in chickens from KwaZulu-Natal, South Africa. PLoS ONE 13 (10): e0204400. https://doi.org/10.1371/journal.pone.0204400

Editor: Joëlle Rüegg, Karolinska Institutet, SWEDEN

Received: October 30, 2017

Accepted: September 8, 2018

Published: October 11, 2018

Data Availability Statement: All relevant data are within the paper.

Funding: We gratefully acknowledge support from the Leading Program at Hokkaido University and the Japan Society for the Promotion of Science (JSPS KAKENHI, grant number 16J02013) to L. Thompson. Also thanks to Grants-in-Aid for Scientific Research from the Ministry of Education, Culture, Sports, Science and Technology of Japan to M. Ishizuka (number 16H0177906), Y. Ikenaka

Abstract

The objective of this study was to identify potential mRNA expression changes in chicken livers associated with environmental exposure to dichloro-diphenyl-trichloroethane (DDT) and its metabolites (DDTs). In particular, we focused on genes relating to the immune system and metabolism. We analyzed liver samples from free-ranging chickens in KwaZulu-Natal, South Africa, for contamination by DDTs. This area predominantly uses DDT in its malaria control program, and homes are sprayed annually with the pesticide. Genes relating to the immune system and metabolism were selected as potential genetic biomarkers that could be linked to higher contamination with DDTs. RT-qPCR analysis on 39 samples showed strong correlations between DDTs contamination and mRNA expression for the following genes: *AvBD1*, *AvBD2*, *AvBD6* and *AvBD7* (down-regulated), and *CYP17*, *ELOVL2* and *SQLE* (up-regulated). This study shows for the first time interesting and significant correlations between genetic material collected from environmentally-exposed chickens and mRNA expression of several genes involved in immunity and metabolism. These findings show the usefulness of analysis on field samples from a region with high levels of environmental contamination in detecting potential biomarkers of exposure. In particular, we observed clear effects from DDT contamination on mRNA expression of genes involved in immune suppression, endocrine-disrupting effects, and lipid dysregulation. These results are of interest in guiding future studies to further elucidate the pathways involved in and clinical importance of toxicity associated with DDT exposure from contaminated environments, to ascertain the health risk to livestock and any subsequent risks to food security for people.

(numbers 26304043, 15H0282505, 15K1221305, 17K2003807) and S.M.M. Nakayama (number 16K16197), the foundation of JSPS Core-to-Core Program (AA Science Platforms) and Bilateral Joint Research Project (PG36150002 and PG36150003). We also acknowledge support from the Soroptimist Japan, Nakajima, Sumitomo and Nihon Seimei Foundations, JST/JICA and SATREPS (Science and Technology Research Partnership for Sustainable Development).

Competing interests: The authors have declared that no competing interests exist.

Introduction

The KwaZulu-Natal Province of South Africa is currently considered an endemic area for malaria and the mainstay of malaria control is the use of DDT in indoor residual spraying (IRS) programs [1,2]. Under guidance from the World Health Organization (WHO), local health centers annually spray the pesticide inside homes on walls and outside under roof eaves to reduce mosquito populations which transmit the disease. DDT and its breakdown metabolites (collectively known as DDTs) enter the environment as dust contamination and are a source of contamination via inhalation, contact and ingestion [3,4]. While exposure to DDTs is primarily via dermal contact and inhalation of aerosolized spray for workers administering DDT, ingestion is thought to be a more significant exposure route for other people and non-target species such as livestock [5–7].

When DDT was initially popular as an agricultural pesticide in the 1940s, it was thought to be toxic only to insects. However, by the 1960s it became apparent that non-target species were susceptible to toxic effects, notably DDT affecting reproduction in birds of prey populations, publicized widely in Rachel Carson's book "Silent Spring" [8]. Eggshell thinning is the most well-known effect of DDT in birds, but other effects include reduced post-hatch survival, altered sexual behavior, neurotoxicity and smaller brain size [9–12]. Field sampling of avian species with lifelong environmental exposure has identified correlations between DDTs contamination and various hormonal and immune responses [13–16]. Chickens show signs of DDT toxicity, but higher levels compared to other avian species are required before clinical signs are seen [17–19]. Clinical signs reported in chickens after DDT exposure include tremors, hyperexcitability, death, and various reproductive effects (reduced egg production and hatchability, reduced perinatal survival, decreased eggshell thickness) [20–22]. The acute lethal toxicity dose in chickens is reported as >300 mg/kg [23]. Despite the growing list of toxic effects of DDTs, our understanding of the mechanisms of action is still lacking.

Xenobiotic contamination is not usually assessed in cases where an infectious agent is deemed the cause of death. Previous field studies have not investigated links between exposure with DDTs and immune function in chickens. Although reports have shown a link between DDT exposure and immunotoxicity in chickens experimentally [24–27], this study is the first to identify changes at the level of mRNA expression after environmental exposure. This evidence supports a need for further investigation of the role that DDTs may play in altering susceptibility to infectious agents. Plasma DDE levels have been linked to immune suppression in people [28]. Host defense peptides are conserved across a wide range of organisms, and play an important role in the innate immune system [29]. In birds, only beta-defensins (avian beta-defensins, AvBD, also known as gallinacins, GAL) have been described, with over 25 detected [30]. Although expressed in a wide range of tissues, expression of most *AvBD* genes is usually low in the liver [31]. Factors which affect expression include estrogen in the female reproductive tract, dietary Vitamin D_3 concentration, inflammatory stimuli, and infections such as *Salmonella spp* and viruses [31–36]. Effects seen with infections depend on the organ affected, and also the chicken breed or age. No studies have previously linked these genes to DDTs exposure. However, any resulting alteration in immune function may increase a bird's susceptibility to disease, leading to decreased productivity and also potentially an increased human health risk after consumption.

Similarly, metabolic changes caused by chemicals may also affect growth and productivity in chickens. Endocrine disrupting chemicals (EDCs) interfere with hormone systems, leading to disturbed glucose and fat metabolism [37]. Although risks have been documented in many species, understanding of the molecular mechanisms of action and involvement in metabolic disorders is still lacking. Organochlorine pesticides like DDT are known to be such EDCs, and

interfere with hormone signalling and metabolic pathways [5,38,39]. Levels of DDTs have been linked to type 2 diabetes and metabolic syndromes in people [40,41]. Involvement of the insulin-like growth factor-binding protein 1 (IGFBP1) has been demonstrated in insulin signaling in chickens [42]. DDTs are lipophilic, with highest concentrations detected in high-lipid organs such as the liver. The liver is also a key location for whole body lipid metabolism, including fatty acid metabolism. Elongation of very long chain fatty acids elongase 2 (ELOVL2) is one of the two fatty acid elongase subtypes involved in polyunsaturated fatty acid (PUFA) biosynthesis in the chicken liver [43,44]. Squalene epoxidase (SQLE) is differentially expressed in fat tissues from fast-growing versus slow-growing chickens, and is involved in endogenous cellular cholesterol synthesis [45]. DDT exposure is associated with reproductive effects and gender alteration *in ovo*, and cytochrome P450 Family 17 Subfamily A Member 1 (CYP17A1) is involved in sex differentiation [46].

Chickens are an important food source for people, and thus any clinical or subclinical toxic effects could impact food security for local people where DDT is used to control vector-borne disease such as malaria. Chickens as livestock are relatively easy to sample and may be useful as a sentinel species for contamination by DDTs in wild birds in the region. The objective of this study was therefore to investigate mRNA expression changes associated with contamination by DDTs in free-ranging chickens from environmental exposure in an area where DDT is sprayed as part of a malaria control program. A number of genes were identified as biomarkers for DDTs exposure. RT-PCR was used to confirm statistical significance of dose-related changes in mRNA expression in a large number of samples across a broad range of contamination levels.

Materials and methods

Chemicals and reagents

Test reagents (oligo(dT) primers, reverse transcriptase (RT) buffer, and RT ACE) were purchased from Toyobo Co. (Osaka, Japan), TRI reagent from Sigma Chemical Co. (St. Louis, MO, USA), dNTP mix from Takara (Takara Bio Inc Japan), primer sets from Invitrogen (Carlsbad, CA, USA), and RNAlater from Sigma-Aldrich (St Louis, MO). A standard mixture of DDTs (Dr Ehrenstorfer GmbH, Germany) was purchased. Pesticide grade organic solvents and anhydrous sodium sulfate were purchased from Kanto Chemical Corp. (Tokyo, Japan). For microarray analysis, RNeasy Mini Kit from Qiagen (Hilden, Germany) was used, and Low Input Quick Amp Labeling Kit, Gene Expression Hybrization Kit, and Chicken (v2) Gene Expression Microarray (4X44K) were purchased from Agilent Technologies (Palo Alto, CA). All other reagents were purchased from Wako Pure Chemical Industries (Tokyo, Japan).

Sampling sites and sample collection

The sampling area was within the Jozini (town location 27˚ 25' 45.7" S 32˚ 3' 54.3" E) and Umhlabuyalingana (27˚ 12' 41.8" S 32˚ 26' 48.2" E) local municipalities, in Umkhanyakude District Municipality of KwaZulu-Natal Province of South Africa (Fig 1). Samples were collected from homesteads located in the following areas: Mamfene, Shemula, Mzondi, Makanis and Ndumo. At the time of sampling in October 2014, malaria was endemic in the region and DDT applied annually to homes. Chickens live free-range in homesteads where DDT is applied. Sampling was overseen by Jozini Health Center and the local veterinary office in Ndumo. Samples were obtained from domestic chickens with agreement from each homestead owner. Chickens were slaughtered by cervical dislocation followed immediately by decapitation and exsanguination. Liver samples were collected (n = 39) immediately after slaughter

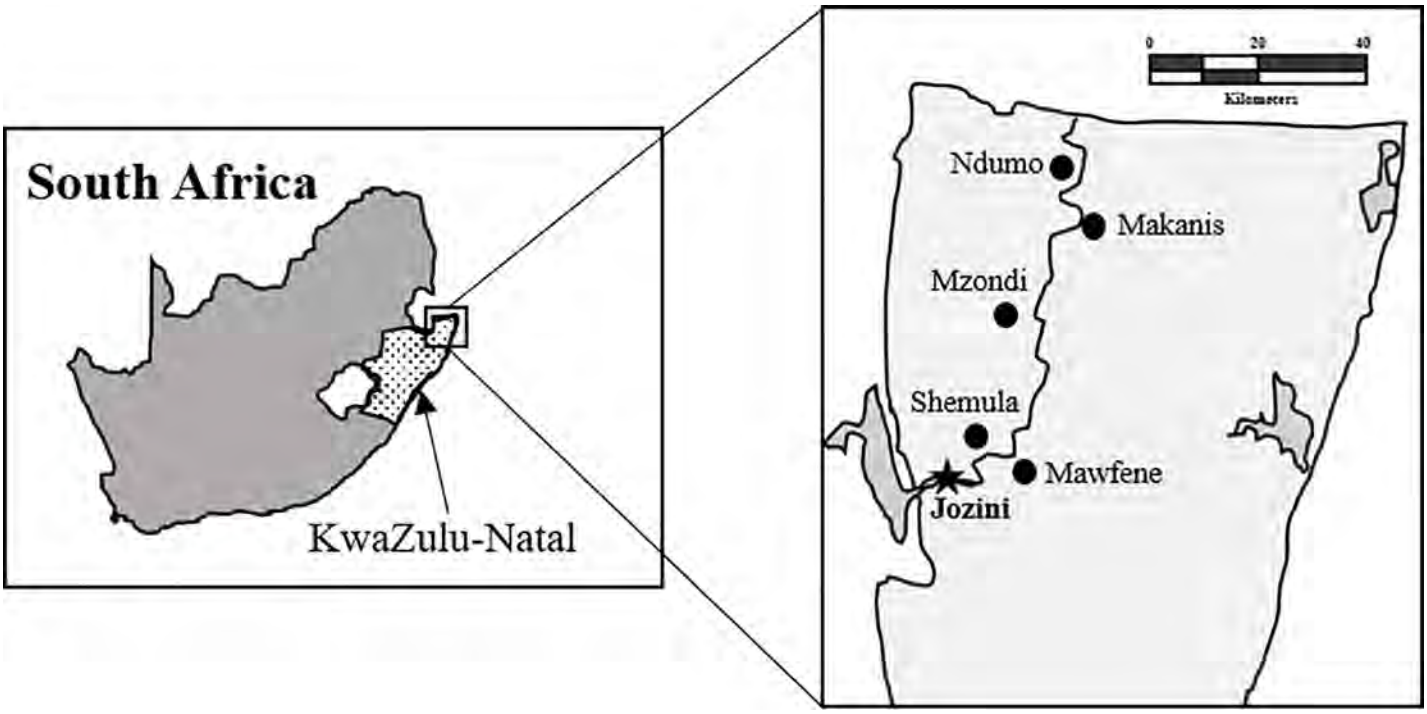

Fig 1. Map of region showing sampling sites in the northern part of KwaZulu-Natal Province, South Africa.

https://doi.org/10.1371/journal.pone.0204400.g001

and aliquots stored in clean plastic vessels (for chemical analysis) and Eppendorf tubes containing RNAlater preservative (for mRNA expression analyses) (see Table 1 for details).

This study was carried out in strict accordance with Hokkaido University guidelines, with veterinary certificates obtained from the agricultural office in Japan (Certificate number: 26 douken 523) and the veterinary office in Ndumo. Necessary approvals and international laws were adhered to regarding transfer of samples from South Africa to Japan.

Sample preparation and storage

Liver was selected as the organ of interest for two main reasons. Firstly, DDT is lipophilic and is stored in body compartments with high lipid content, such as the liver. This organ is thus a

Table 1. Biometric data for chickens sampled in KwaZulu-Natal for this study.

	Mean	Range
Estimated age (months)[1]	13 ± 7	7–30
Weight (kg)[2]	1.5 ± 0.4	0.9–2.8
Body condition score[3]	2 ± 0.7	0–3
Lipid % in liver samples	3.8 ± 2.2	0.3–7.9
Supplied diet[4]	Maize (home-grown or shop-bought), leftovers, rice, bread, fresh vegetables	
Source	Shemula (11), Makanis (9), Ndumo (8), Mzondi (6), Mamfene (5)	

N/K = not known

1. Age estimation by owner at time of purchase.
2. Body weights for chickens are ante-mortem.
3. Based on Gregory and Robins 0–3 scale for layer hens [47].
4. Diet supplied by owner in addition to chickens foraging around the homestead.

https://doi.org/10.1371/journal.pone.0204400.t001

good representation of contamination within the animal, and many studies analyze concentration of DDTs in the liver. Secondly, this organ is important in detoxification of chemicals and has many metabolic functions.

Liver samples were collected from freshly slaughtered chickens and stored via two methods. Samples for chemical analysis were frozen to -20˚C shortly after collection. Samples for mRNA analysis were placed into RNAlater tissue storage reagent to stabilize and protect cellular RNA, and frozen. Samples were then transported to the Laboratory of Toxicology in Hokkaido University, and maintained at -80˚C until analysis.

Organochlorine extraction and analysis (DDTs)

Frozen samples were defrosted and analyzed to measure levels of DDT and its metabolites (*o*,*p*'-DDT, *p*,*p*'-DDT, *o*,*p*'-DDD, *p*,*p*'-DDD, *o*,*p*'-DDE and *p*,*p*'-DDE–collectively termed "DDTs") using a slightly modified version of Yohannes et al.'s method [48]. Briefly, 1 g of liver was homogenized with anhydrous sodium sulfate before automatic extraction for 3.5 hours with a mixture of hexane:acetone (3:1 *v/v*) in a Soxhlet extractor (SOX416 macro SOXTHERM unit, Gerhardt, Germany). Each sample extract was spiked with 3,3',4,4'-tetrachlorobiphenyl (PCB 77) surrogate standard, then concentrated prior to clean-up in a glass column packed with activated florisil and eluted with hexane : dichloromethane (7 : 3 *v/v*). After further concentration, 2,4,5,6-tetrachloro-*m*-xylene (TC*m*X) was added as a syringe spike, before analysis using a gas-chromatograph with ^{63}Ni electron capture detector (GC-ECD: Shimadzu GC-2014, Kyoto, Japan). The machine condition parameters and QA/QC analysis were as in Thompson et al. [7].

RNA extraction and cDNA synthesis

Total RNA was extracted using TRI reagent from the RNAlater-preserved samples, following the manufacturer's protocol. Complementary DNA (cDNA) was synthesized according to Darwish et al.'s method [49].

Selection of genes of interest

In our ongoing efforts to investigate the crosstalk between DDTs and mRNA expression relating to immunity and metabolism, we conducted a preliminary study to investigate gene expression changes using microarray. Total RNA samples were selected from two chickens matched for gender, body weight and body condition score. Neither chicken had any signs of ill health on ante-mortem or post-mortem examination; their liver total DDTs concentrations were 1,116.0 ng/g and 1,938.0 ng/g wet weight, respectively. A spectrophotometer (Nanodrop 1000, Thermo Fisher Scientific, Waltham, MA) and 2100 BioAnalyzer series II (Agilent Technologies, Palo Alto, CA) were used to determine nucleic acid quantity, quality and purity. Low Input Quick Amp Labeling Kit was used according to manufacturer directions, and cRNA purified using RNeasy Mini spin columns before quality inspection using the Agilent 2100 BioAnalyzer series II. Gene Expression Hybrization Kit was used to hybridize cyanine3-labeled cRNA. Samples were co-hybridized to Chicken (v2) Gene Expression Microarray (4X44K, Agilent Technologies), before incubation for 17 hours at 65˚C. After washing, slides were scanned using an Agilent Technologies Microarray Scanner at 5 μm resolution. Raw data was digitized using Agilent Feature Extraction Software, version 10.7.3.1, and normalized to 75th percentile shift in GeneSpring (Agilent Technologies). The microarray dataset is accessible through ArrayExpress accession number E-MTAB-7130. This study assessed liver samples from chickens exposed environmentally to DDTs, and identified a number of functional areas and possible genes of interest. These genes fell into two categories: the innate immune system

(*AvBD*s), and metabolism of steroid hormones and lipids (*IGFBP1*, *ELOVL2*, *SQLE*, and *CYP17A1*), with fold change expression differences between low and high DDTs-contaminated samples ranging from 8.3 to 21.5 for these genes.

Quantitative real-time polymerase chain reaction

Chicken liver mRNA levels were determined by quantitative real-time RT-PCR using SYBR qPCR mix (Toyobo) and a StepOne real-time PCR system (Applied Biosystems). Primer sets for specific genes tested are described in Table 2. The method was performed according to Mureithi et al. [50]. In brief, PCRs were run with a final volume of 10 μl, containing SYBR qPCR Mix (Toyobo), 10 μM of each primer, 600 ng cDNA, 50X ROX reference dye and RNase-free water. Cycle conditions were as follows: 95˚C for 20 s initial holding stage, 40 denaturation cycles of 95˚C for 3 s and 62˚C annealing for 30 s, and 95˚C extension for 15 s. Amplification of a single amplicon of the expected size was confirmed using melting curve analysis and agarose gel electrophoresis. Experiments were repeated at least three times on different occasions. The sample containing the lowest contamination level of DDTs was assigned as a relative reference sample. In this study, two reference genes, namely *GAPDH* and *ACTB*, were used to normalize mRNA expression of target genes. Both reference gene mRNA expressions were not affected by exposure to DDT and were eventually expressed in all tested samples. Target gene expressions recorded in this study were normalized with respect to *GAPDH* mRNA expression and calculated relative to the nominal reference level using the comparative threshold cycle (Ct) method.

Statistical analysis

Amplification efficiencies for targets tested in this study ranged from 92.24% to 109.28%. These values were retrieved using slope factors from cDNA standard curves using the following formula: efficiency = -1+10(-1/slope), where efficiencies between 90 and 110% are typically

Table 2. qRT-PCR primer sequence information used in this study.

Gene		Sequence		Product size (bp)	Amplification efficiency (%)	Slope factor
	Accession number	Forward	Reverse			
AvBD1 (GAL1)	NM_204993.1	CCTGTGAAAACCCGGGACA	GCACAGAAGCCACTCTTTCG	145	92.24	-3.52
AvBD2 (GAL2)	NM_001201399.1	ACTGCCTGCCACATACATTTC	AGACAACCCTGGAGAAGCCT	127	98.76	-3.35
AvBD6 (GAL6)	NM_001001193.1	TTGCAGGTCAGCCCTACTTT	CCGGTAATATGGCCACCGAC	95	96.96	-3.40
AvBD7 (GAL7)	NM_001001194.1	ATTTCACATCCCAGCCGTGG	AGGCCTAGGAATGAAGGGCT	103	109.28	-3.12
IGFBP1	NM_001001294.1	TCACTGGATGGAGATTCCGC	AAGCTCCACAGAGAACCTGG	164	96.65	-3.41
ELOVL2	NM_001197308.1	CATGTGGGTTTCCCTTTGGC	GACTTCTGTTGTGACGGGGG	146	102.56	-3.26
SQLE	NM_001194927.1	CCATTTTTGGAGCGTCAGCC	GATGCCCAGGAAAGTCCACA	71	101.82	-3.28
CYP17A1	NM_001001901.2	CCCTACCTGGAGGCTACCAT	CGGACCAGAGGTTGATGACC	145	93.32	-3.49
ACTB (housekeeping)	L08165	CCCATCTATGAAGGCTACGC	TCCTTGATGTCACGCACAAT	152	100.59	-3.31
GAPDH (housekeeping)	NM_204305.1	ACACAGAAGACGGTGGATGG	GGCAGGTCAGGTCAACAACA	193	102.87	-3.26

https://doi.org/10.1371/journal.pone.0204400.t002

acceptable [51]. Data analysis was conducted using Microsoft Excel 2014 and JMP Pro 12 (SAS Institute Inc., Cary, NC, USA). Contamination levels of DDTs are shown as median and range values in ng/g wet weight and ng/g lipid weight of tissue. Statistical significance was calculated using multivariate Spearman's correlation analysis between mRNA expression and summed DDTs in chicken livers, by positive or negative correlation. A p-value of less than 0.05 was considered significant. Principle components analyses were used to investigate correlations of DDTs contamination, biometric data and mRNA expression. These analyses were made independently without data correction or adjustment of α value.

Results and discussion

DDTs concentrations

Contamination by DDT and its metabolites was detected in liver samples assessed (Table 3). The median of summed DDTs was 919 ng/g wet weight (ww), with a maximum of 14,398 ng/g ww. Concentrations of DDTs were comparable to those detected in chicken livers from Limpopo Province in another IRS-treated area of South Africa [52]. In the Limpopo study, the median sum of DDTs was 1,100 ng/g ww compared to 919 ng/g ww in this KwaZulu-Natal study. A study sampling chicken livers from an electrical and electronic waste (e-waste) site in China detected a much lower contamination level of 200 ng/g lw [53], compared to 29,235 ng/g lw in KwaZulu-Natal. DDT is not currently applied at the e-waste recycling area but legacy contamination is present.

The predominant congener was *p*,*p*'-DDE, and comprised approximately 75% of the DDTs. This congener has been linked to many toxic effects in birds, including eggshell thinning [54,55]. Estrogenic effects of DDTs are thought to affect avian embryos more than those of mammals, and phase I metabolites (DDE and DDD) may be more estrogenic than parent compounds [56–58].

Several factors may confound results from samples collected under field conditions–for example, difference in chicken breed, age, diet, body condition and health. As far as was possible, chickens selected from the study site were comparable. Husbandry methods resembled other households in the region. Adult birds of similar weight and body condition, without clinical signs of disease, were analyzed. No pathological conditions were detected on gross post-mortem examination of the birds. Chronicity of exposure may affect contamination levels, as bioaccumulation of DDTs occurs [59]. Comparison of DDTs concentration with biometric data (body condition score, body weight, estimated age and liver lipid percent) did not show any associations (data not shown). Statistical analysis did not show any difference in sampling location within the study area.

Table 3. Levels of DDT and metabolites detected in liver from free-ranging chickens in KwaZulu-Natal.

	ng/g wet weight		ng/g lipid weight	
	Median	Range	Median	Range
p,*p*'-DDE	692	18–10,537	20,186	289–227,891
o,*p*'-DDD	10	<LOD—166	246	<LOD—5,919
p,*p*'-DDD	89	<LOD—1,840	2,929	<LOD—47,273
o,*p*'-DDT	11	<LOD—302	458	<LOD—8,280
p,*p*'-DDT	54	<LOD—1,923	1,333	<LOD—18,756
Sum of DDTs	919	36–14,398	29,235	555–288,928

<LOD = below limit of detection

https://doi.org/10.1371/journal.pone.0204400.t003

qPCR mRNA expression results

Samples were all obtained from an area in KwaZulu-Natal Province where the Jozini Health Center administers DDT annually as part of their malaria control program. As this region is endemic for malaria, all homes are treated. In this scenario, it was not possible to obtain negative control samples from untreated homesteads and so statistical analyses were conducted by setting the reference sample for relative comparisons as that with the lowest concentration of summed DDTs.

A preliminary study using microarray analysis on samples from chickens exposed environmentally to DDTs identified a number of functional areas and possible genes of interest. Genes of interest were selected based on consideration of reported effects of DDTs and results from this microarray analysis. In particular, we focused on the innate immune system and on metabolism, particularly that of steroid hormones and lipids. A number of genes examined were significantly down-regulated (Fig 2): *AvBD1*, *AvBD2*, *AvBD6*, and *AvBD7*. Although there was a trend for down-regulation of *IGFBP1* with increasing DDTs, it was not a statistically significant association. The following genes were significantly up-regulated in samples with higher contamination levels of DDTs: *ELOVL2*, *SQLE* and *CYP17A1*. The principal components analysis plot (Fig 3) explains 71.8% of the variation between summed DDTs concentration and mRNA expression, with 58.4% on the first axis and 13.4% on the second. This plot suggests strong negative correlations between DDTs contamination and mRNA expression of avian beta-defensins assessed, and strong positive correlations with expression of *CYP17A1*, *ELOVL2* and *SQLE*.

Defensins have antimicrobial activity against many bacteria and fungi (reviewed in Cuperus et al [31]). They also play a role in immune regulation, binding to chemokine receptors, inducing pro-inflammatory cytokine expression, having anti-inflammatory properties and enhancing wound healing [60–62]. Expression of a range of *AvBD* genes showed a negative correlation with summed DDTs contamination: AvBD1 ($p = 0.0020$), *AvBD2* ($p < 0.0001$), *AvBD6* ($p = 0.0036$) and *AvBD7* ($p < 0.0001$). Reduction in expression levels of these important innate immunity genes may lead to increased susceptibility to disease with DDTs exposure. In this study, no signs of clinical disease were noted in the chickens ante-mortem or during post-mortem examination, but other investigations such as histopathology or bacterial culture were not performed.

IGFBP1 is a regulator of somatic growth and has been identified as a biomarker for visceral adiposity [63]. *IGFBP1* mRNA expression is involved in signaling between growth hormone (GH), thyroid hormone and body fat regulation in chickens but has not previously been linked to DDTs exposure [64]. Insulin signaling is affected by IGFBP1 in chickens [42]. There was a slight downward trend for *IGFBP1* expression with higher summed DDTs concentrations in the chicken livers but it was not statistically significant ($p = 0.3739$). Adipose tissue has been shown to be the primary tissue for storage of DDTs, and future work may elucidate a link between DDTs contamination and adipose production [65].

DDTs have been linked in mammalian species to obesity and metabolic syndromes [66]. Long chain PUFAs are necessary in vertebrates for normal growth and development, synthesized via either desaturation or elongation from dietary linoleic acid and a-linolenic acid. The *ELOVL2* gene plays a role in the fatty acid elongation pathway, and is essential for converting plant-derived α-linolenic acid (ALA) to eicosapentaenoic acid (EPA) and docosahexaenoic acid (DHA) [43,67]. *ELOVL2* expression was also significantly up-regulated with increasing DDTs contamination ($p < 0.0001$). There are no reports of metabolic syndromes such as diabetes occurring in birds due to DDT. However, this change in metabolism is important as

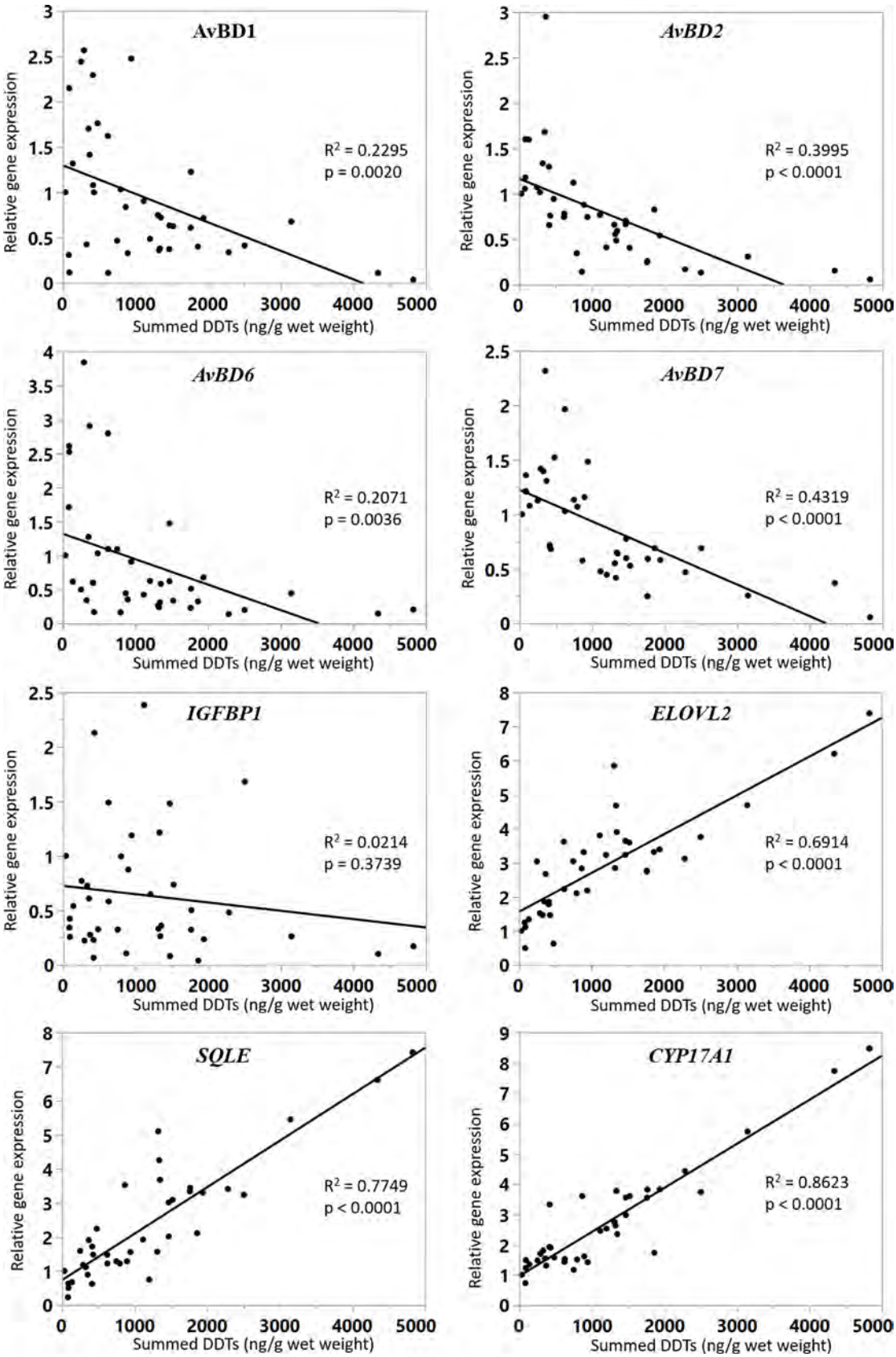
AvBD1
R² = 0.2295
p = 0.0020
AvBD2
R² = 0.3995
p < 0.0001
AvBD6
R² = 0.2071
p = 0.0036
AvBD7
R² = 0.4319
p < 0.0001
IGFBP1
R² = 0.0214
p = 0.3739
ELOVL2
R² = 0.6914
p < 0.0001
SQLE
R² = 0.7749
p < 0.0001
CYP17A1
R² = 0.8623
p < 0.0001
Relative gene expression
Summed DDTs (ng/g wet weight)

Fig 2. Correlation between mRNA expression and contamination levels (summed DDTs by wet weight). Summed DDTs (ng/g wet weight, x-axis) are plotted against relative mRNA expression (y-axis). R^2 values and *p*-values are shown.

https://doi.org/10.1371/journal.pone.0204400.g002

poultry are an important source of long-chain polyunsaturated fatty acids (PUFAs) for people, particularly in countries where fish consumption is low [67].

Little is yet known about the function of SQLE. Administration of GH in rapidly-growing chickens down regulated expression of hepatic *SQLE*, which is also involved in lipid metabolism [64]. SQLE is involved in cholesterol synthesis in cells and also peripheral clock genes (delta 2 crystallin, Cry, and aryl hydrocarbon receptor nuclear translocator-like protein, Bmal)

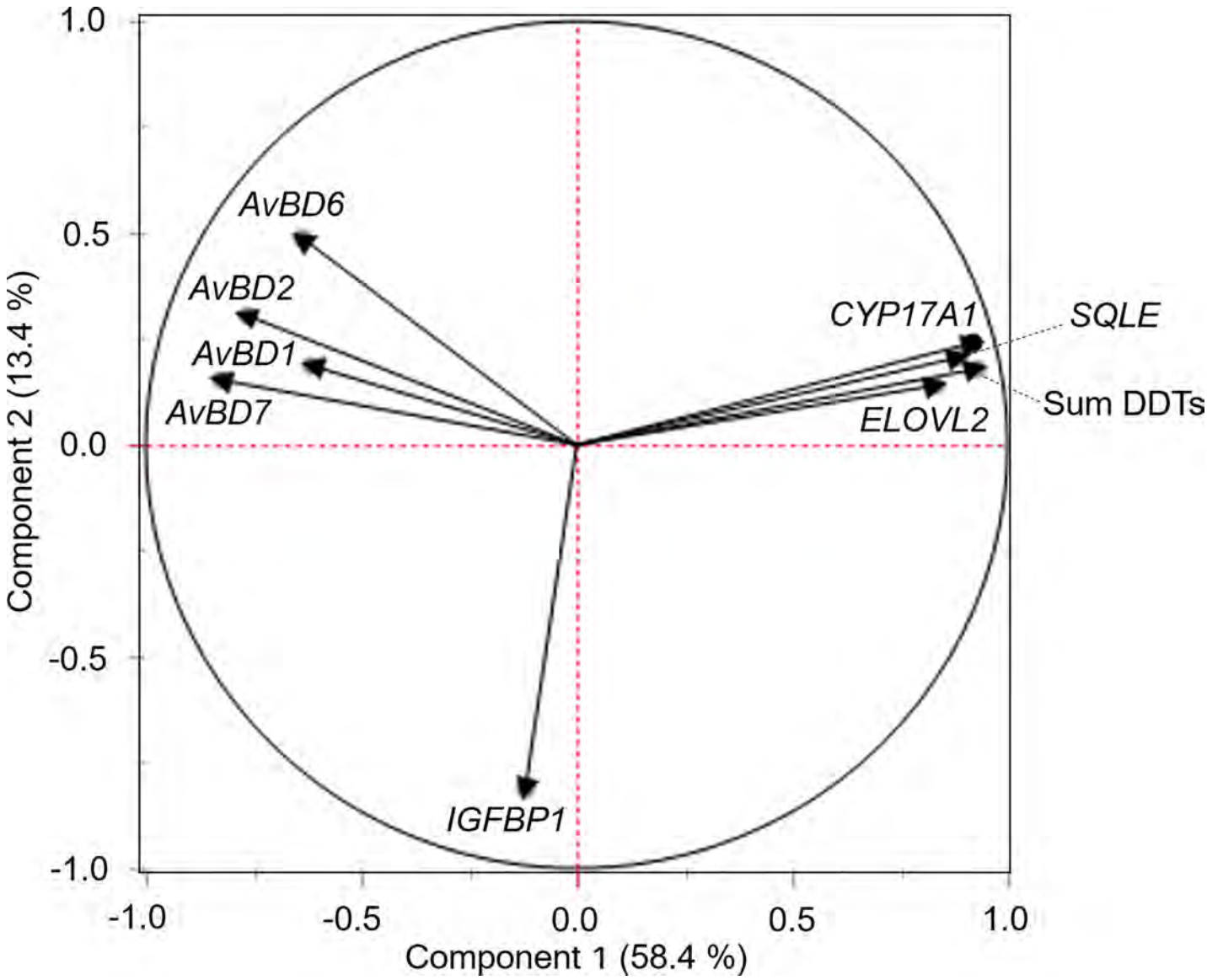

Fig 3. Principal components analysis of gene expression in chickens by summed DDTs concentrations. The first axis explains 58.4% of the variance in the data, showing strong negative correlation between DDTs contamination and beta-defensin mRNA expression, and strong positive correlation with mRNA expression relating to metabolism (*CYP17A1*, *ELOVL2* and *SQLE*). Key: *AvBD1* (avian beta-defensin 1), *AvBD2* (avian beta-defensin 2), *AvBD6* (avian beta-defensin 6), *AvBD7* (avian beta-defensin 7), *IGFBP1* (insulin-like growth factor-binding protein 1), *ELOVL2* (elongation of very long chain fatty acids elongase 2), *SQLE* (squalene epoxidase), *CYP17A1* (cytochrome P450 Family 17 Subfamily A Member 1).

https://doi.org/10.1371/journal.pone.0204400.g003

[68]. Cry and Bmal are involved in regulation of corticosteroid synthesis pathways, and their expression in broiler chicken adrenal glands is affected by ACTH treatment [69]. Again, expression of this gene, *SQLE*, was significantly up-regulated with increasing concentration of DDTs ($p < 0.0001$). Many xenobiotics are known to affect hormones, and this potential effect from DDTs on corticosteroid synthesis and cholesterol synthesis could affect many areas of metabolism. In livestock species, successful and rapid growth is particularly important, and any imbalances caused by xenobiotics are likely to affect food production. This could be significant in areas like KwaZulu-Natal where poverty and food security are problematic [70].

Studies on mammalian species have shown induction of cytochrome P450 (CYP) enzymes in rat liver microsomes after exposure with technical grade DDT [71]. CYP enzymes are important in phase I metabolism of xenobiotics [72]. Concentration responses to p,p'-DDT have been shown to vary between avian species [73]. CYP17A1 is also involved in androgen hormone synthesis and sex differentiation of birds [74–77]. The association between up-regulation of *CYP17A1* mRNA expression and DDTs concentration in sampled livers was highly significant ($p < 0.0001$). This strong correlation supports evidence linking DDTs exposure to biased sex ratios in gull embryos [46].

Regression analysis (Table 4) showed strong positive correlation between concentrations of *p,p'*-DDE, *p,p'*-DDD and *p,p'*-DDT with mRNA expression of *ELOVL2*, *SQLE* and *CYP17A1*. There was strong negative correlation between DDT congeners and expression of the *AvBD* genes assessed (*AvBD1*, *AvBD2*, *AvBD6* and *AvBD7*). For the *AvBD* genes, *p,p'*-DDE and *p,p'*-DDD were most significantly associated. *AvBD7* gene showed significant (*p*-value <0.0001–0.0391) negative correlation with all of the DDT congeners detected, and thus may be a sensitive biomarker for DDTs contamination. These data support the hypothesis that the *p,p'*-DDE congener, the most abundant contaminant and known endocrine disruptor, is the cause of many adverse effects associated with DDTs exposure. However, in light of the comparatively low concentrations of *p,p'*-DDD and *p,p'*-DDT in chickens sampled, it is interesting to note that these also significantly affect most of the genes analysed.

Conclusions

This study shows for the first time interesting and significant correlations between genetic material collected from environmentally-exposed chickens and mRNA expression of several genes involved in immunity and metabolism. During malaria control programs, DDT has been applied to the study area in KwaZulu-Natal for more than a decade. This has led to a high level of environmental contamination and a source of DDTs for local livestock. The study clearly shows a link between this contamination of free-ranging chickens and mRNA

Table 4. Correlation between DDT congeners and mRNA expression in KwaZulu-Natal chicken livers. *A *p*-value of <0.05 was considered significant.

Gene	Regression statistics (R-squared (*p*-value))				
	***p,p'*-DDE**	***o,p'*-DDD**	***p,p'*-DDD**	***o,p'*-DDT**	***p,p'*-DDT**
AvBD1	**0.2473 (0.0013*)**	0.0033 (0.7264)	0.0920 (0.0604)	0.0187 (0.4060)	0.0975 (0.0529)
AvBD2	**0.3719 (<0.0001*)**	0.1154 (0.0344)	**0.3260 (0.0001*)**	0.0550 (0.1507)	**0.1478 (0.0157*)**
AvBD6	**0.1877 (0.0059*)**	0.0522 (0.1617)	**0.1711 (0.0089*)**	0.0680 (0.1089)	0.0761 (0.0891)
AvBD7	**0.3730 (<0.0001*)**	**0.1096 (0.0395*)**	**0.3866 (<0.0001*)**	**0.1101 (0.0391*)**	**0.2197 (0.0026*)**
IGFBP1	0.0210 (0.3789)	0.0078 (0.5939)	0.0059 (0.6412)	0.0045 (0.6838)	0.0475 (0.1825)
CYP17A1	**0.8298 (<0.0001*)**	0.0589 (0.1367)	**0.4179 (<0.0001*)**	0.0420 (0.2105)	**0.6816 (<0.0001*)**
ELOVL2	**0.6495 (<0.0001*)**	0.0363 (0.2451)	**0.2654 (0.0008*)**	**0.1928 (0.0052*)**	**0.6128 (<0.0001*)**
SQLE	**0.7318 (<0.0001*)**	0.0570 (0.1432)	**0.4516 (<0.0001*)**	0.0240 (0.3464)	**0.5894 (<0.0001*)**

https://doi.org/10.1371/journal.pone.0204400.t004

expression changes that may have health impacts on both the chickens and the local human population.

Of particular interest are the genes involved in steroid synthesis, *CYP17A1* and *SQLE*. These are potential targets for the mechanism of estrogen-mimicry by DDTs. This endocrine disruption is well documented in several species. Up-regulation of the *ELOVL2* gene involved in fatty acid elongation is a strong link to lipid metabolism, and may help explain the connection between DDTs and metabolic syndromes reported in people. Down-regulation of several *AvBD* genes involved in the innate immune system are a potentially serious concern for the health of poultry livestock, where lowered immunity linked to increased infectious disease will impact not only bird health but also may be a problem for food security in people.

Ideally samples would be matched for confounding factors. It would also be useful to perform further chemical analyses to ascertain co-contamination with other xenobiotics in both the chickens and environment. An *in vivo* exposure study using environmental level concentrations of contaminants needs to be performed to remove potential confounding factors and bias such as age, breed, period of exposure, and concomitant exposure with other contaminants. It would be useful to consider DDTs across multiple generations to ascertain the full gamut of effects on the birds as embryos, developing young, and reproducing adults. Assessment of other closely related genes will also further elucidate the mechanisms involved and aid our understanding of the wide range of toxic effects and clinical importance of DDT and its metabolites.

Acknowledgments

We are indebted to contacts in the KZN region of South Africa, who assisted with collection of samples. Thanks especially to Samwel Menyuka and Nelson Nkwanyana for being guides and interpreters, and to Dr Ntantiso at Jozini Agriculture Office. Facilitation for this study was also received from Bruce Margot, Bheki Owabe and Phineas Zikhali in the KwaZula-Natal Health Department, and various guides to health camps. Takahiro Ichise and Nagisa Hirano gave laboratory support in Hokkaido University. We are grateful to Hokkaido System Science Co., Ltd. (Sapporo, Japan), who performed the microarray analysis. This is contribution number 247 from the NWU-Water Research Group.

Author Contributions

Conceptualization: Lesa A. Thompson, Johan J. van Vuren, Shouta M. M. Nakayama.

Data curation: Lesa A. Thompson, Yoshinori Ikenaka, Wageh S. Darwish.

Formal analysis: Lesa A. Thompson, Atnafu G. Assefa, Ahmed Tharwat, Walaa Fathy Saad Eldin.

Funding acquisition: Mayumi Ishizuka.

Investigation: Lesa A. Thompson, Yoshinori Ikenaka, Wageh S. Darwish, Yared B. Yohannes, Atnafu G. Assefa, Ahmed Tharwat, Walaa Fathy Saad Eldin.

Methodology: Lesa A. Thompson, Wageh S. Darwish, Yared B. Yohannes, Shouta M. M. Nakayama.

Project administration: Yoshinori Ikenaka, Mayumi Ishizuka.

Resources: Victor Wepener, Nico J. Smit, Mayumi Ishizuka.

Supervision: Yoshinori Ikenaka, Wageh S. Darwish, Johan J. van Vuren, Victor Wepener, Shouta M. M. Nakayama, Hazuki Mizukawa, Mayumi Ishizuka.

Validation: Lesa A. Thompson, Yoshinori Ikenaka, Wageh S. Darwish, Yared B. Yohannes.

Visualization: Lesa A. Thompson.

Writing – original draft: Lesa A. Thompson.

Writing – review & editing: Yoshinori Ikenaka, Wageh S. Darwish, Yared B. Yohannes, Johan J. van Vuren, Victor Wepener, Nico J. Smit, Shouta M. M. Nakayama, Hazuki Mizukawa, Mayumi Ishizuka.

References

1. Maharaj R, Morris N, Seocharan I, Kruger P, Moonasar D, Mabuza A, et al. The feasibility of malaria elimination in South Africa. Malaria Journal. 2012 Dec 19; 11(1):423.
2. Wepener V, Smit N, Covaci A, Dyke S, Bervoets L. Seasonal bioaccumulation of organohalogens in tigerfish, Hydrocynus vittatus Castelnau, from Lake Pongolapoort, South Africa. Bulletin of environmental contamination and toxicology. 2012 Feb 1; 88(2):277–82. https://doi.org/10.1007/s00128-011-0439-0 PMID: 22033654
3. Mansouri A, Cregut M, Abbes C, Durand MJ, Landoulsi A, Thouand G. The environmental issues of DDT pollution and bioremediation: a multidisciplinary review. Applied biochemistry and biotechnology. 2017 Jan 1; 181(1):309–39. https://doi.org/10.1007/s12010-016-2214-5 PMID: 27591882
4. Sereda B, Bouwman H, Kylin H. Comparing Water, Bovine Milk, and Indoor Residual Spraying as Possible Sources of DDTand Pyrethroid Residues in Breast Milk. Journal of Toxicology and Environmental Health, Part A. 2009 Jun 30; 72(13):842–51.
5. Mrema EJ, Rubino FM, Brambilla G, Moretto A, Tsatsakis AM, Colosio C. Persistent organochlorinated pesticides and mechanisms of their toxicity. Toxicology. 2013 May 10; 307:74–88. https://doi.org/10.1016/j.tox.2012.11.015 PMID: 23219589
6. Ortelee MF. Study of men with prolonged intensive occupational exposure to DDT. Arch. Indust. Health. 1958; 18(5):433–40.
7. Thompson LA, Ikenaka Y, Yohannes YB, van Vuren JJ, Wepener V, Smit NJ, et al. Concentrations and Human Health Risk Assessment of DDT and Its Metabolites in Free-range and Commercial Chicken Products from KwaZulu-Natal, South Africa. Food Additives & Contaminants: Part A. 2017 Jul 19(just-accepted).
8. Carson R. Silent Spring. Greenwich, Connecticut.
9. Gómez-Ramírez P, Martínez-López E, García-Fernández AJ, Zweers AJ, Van den Brink NW. Organohalogen exposure in a Eurasian Eagle owl (Bubo bubo) population from Southeastern Spain: Temporal–spatial trends and risk assessment. Chemosphere. 2012 Aug 31; 88(8):903–11. https://doi.org/10.1016/j.chemosphere.2012.03.014 PMID: 22503462
10. Iwaniuk AN, Koperski DT, Cheng KM, Elliott JE, Smith LK, Wilson LK, et al. The effects of environmental exposure to DDT on the brain of a songbird: changes in structures associated with mating and song. Behavioural brain research. 2006 Oct 2; 173(1):1–10. https://doi.org/10.1016/j.bbr.2006.05.026 PMID: 16828177
11. Kamata R, Shiraishi F, Takahashi S, Shimizu A, Nakajima D, Kageyama S, et al. The effects of transovarian exposure to p, p'-DDT and p, p'-DDE on avian reproduction using Japanese quails. The Journal of toxicological sciences. 2013 Dec 1; 38(6):903–12. PMID: 24213010
12. Lundholm CE. The effects of DDE, PCB and chlordane on the binding of progesterone to its cytoplasmic receptor in the eggshell gland mucosa of birds and the endometrium of mammalian uterus. Comparative Biochemistry and Physiology Part C: Comparative Pharmacology. 1988 Jan 1; 89(2):361–8.
13. Bustnes JO, Hanssen SA, Folstad I, Erikstad KE, Hasselquist D, Skaare JU. Immune function and organochlorine pollutants in arctic breeding glaucous gulls. Archives of environmental contamination and toxicology. 2004 Oct 1; 47(4):530–41. https://doi.org/10.1007/s00244-003-3203-6 PMID: 15499504
14. Verreault J, Skaare JU, Jenssen BM, Gabrielsen GW. Effects of organochlorine contaminants on thyroid hormone levels in Arctic breeding glaucous gulls, Larus hyperboreus. Environmental health perspectives. 2004 Apr; 112(5):532–7. https://doi.org/10.1289/ehp.6756 PMID: 15064156
15. Verreault J, Letcher RJ, Ropstad E, Dahl E, Gabrielsen GW. Organohalogen contaminants and reproductive hormones in incubating glaucous gulls (Larus hyperboreus) from the Norwegian Arctic. Environmental toxicology and chemistry. 2006 Nov 1; 25(11):2990–6. PMID: 17089723

16. Verreault J, Bech C, Letcher RJ, Ropstad E, Dahl E, Gabrielsen GW. Organohalogen contamination in breeding glaucous gulls from the Norwegian Arctic: Associations with basal metabolism and circulating thyroid hormones. Environmental Pollution. 2007 Jan 31; 145(1):138–45. https://doi.org/10.1016/j.envpol.2006.03.049 PMID: 16713050

17. Heath RG, Spann JW, Kreitzer JF. Marked DDE impairment of mallard reproduction in controlled studies. Nature. 1969 Oct; 224:47–8. PMID: 5822906

18. Kamata R, Shiraishi F, Takahashi S, Shimizu A, Shiraishi H. Reproductive and developmental effects of transovarian exposure to o, pN-DDT in Japanese quails. Environmental toxicology and chemistry. 2009 Apr 1; 28(4):782–90. https://doi.org/10.1897/08-218R.1 PMID: 19391684

19. Waibel GP, Speers GM, Waibel PE. Effects of DDT and Charcoal on Performance of White Leghorn Hens 1, 2. Poultry science. 1972 Nov 1; 51(6):1963–7. https://doi.org/10.3382/ps.0511963 PMID: 4660978

20. Britton WM. Toxicity of high dietary levels of DDT in laying hens. Bulletin of environmental contamination and toxicology. 1975; 13(6):703–706. PMID: 1139052

21. St Omer VV. Chronic and acute toxicity of the chlorinated hydrocarbon insecticides in mammals and birds. The Canadian Veterinary Journal. 1970; 11(11):215. PMID: 4992437

22. Weihe M. Effects of DDT on reproduction in hens. Basic & Clinical Pharmacology & Toxicology. 1967; 25(S4):54

23. Konst H, Plummer PJG. Studies on the Toxity of DDT. Canadian journal of comparative medicine and veterinary science. 1946; 10(5):128. PMID: 17648191

24. Glick B. Antibody-mediated immunity in the presence of mirex and DDT. Poultry science. 1974; 53 (4):1476–1485. https://doi.org/10.3382/ps.0531476 PMID: 4850595

25. Latimer JW, Siegel HS. Immune response in broilers fed technical grade DDT. Poultry science. 1974; 53(3):1078–1083. https://doi.org/10.3382/ps.0531078 PMID: 4841696

26. Lavoie ET, Wiley F, Grasman KA, Tillitt DE, Sikarskie JG, Bowerman WW. Effect of in ovo exposure to an organochlorine mixture extracted from double crested cormorant eggs (Phalacrocorax auritus) and PCB 126 on immune function of juvenile chickens. Archives of environmental contamination and toxicology. 2007; 53(4):655–661. https://doi.org/10.1007/s00244-006-0150-z PMID: 17882474

27. Nvota J, Horváth J, Tesarová D. Effect of DDT, intensive use of the floor surface and post-incubation stress on the development of immune response in chickens. Veterinarni medicina. 1977; 22(9):561–567. PMID: 413247

28. Vine MF, Stein L, Weigle K, Schroeder J, Degnan D, Tse CK, et al. Plasma 1, 1-dichloro-2, 2-bis (p-chlorophenyl) ethylene (DDE) levels and immune response. American journal of epidemiology. 2001 Jan 1; 153(1):53–63. PMID: 11159147

29. Lehrer RI, Ganz T. Defensins of vertebrate animals. Current opinion in immunology. 2002 Feb 1; 14 (1):96–102. PMID: 11790538

30. Hellgren O, Ekblom R. Evolution of a cluster of innate immune genes (β-defensins) along the ancestral lines of chicken and zebra finch. Immunome Research. 2010 Apr 1; 6(1):3.

31. Cuperus T, Coorens M, van Dijk A, Haagsman HP. Avian host defense peptides. Developmental & Comparative Immunology. 2013 Nov 30; 41(3):352–69.

32. Akbari MR, Haghighi HR, Chambers JR, Brisbin J, Read LR, Sharif S. Expression of antimicrobial peptides in cecal tonsils of chickens treated with probiotics and infected with Salmonella enterica serovar typhimurium. Clinical and Vaccine Immunology. 2008 Nov 1; 15(11):1689–93. https://doi.org/10.1128/CVI.00242-08 PMID: 18827189

33. Derache C, Esnault E, Bonsergent C, Le Vern Y, Quéré P, Lalmanach AC. Differential modulation of ptides in cecal tonsils of chickens treated with probiotics and infected with Salmonella enterica serovar typhimurium. Clinical and Vaccine Immunology. 2008 Noative Immunology. 2009 Sep 30; 33(9):959–66.

34. Ma D, Lin L, Zhang K, Han Z, Shao Y, Liu X, et al. Three novel Anas platyrhynchos avian ation of ptides in cecal tonsils of chickens treated with probiotics and infected with Salmonella enterica serovar typhi1 Nov 30; 49(1):84–96.

35. Subedi K, Isobe N, Nishibori M, Yoshimura Y. Changes in the expression of gallinacins, antimicrobial peptides, in ovarian follicles during follicular growth and in response to lipopolysaccharide in laying hens (Gallus domesticus). Reproduction. 2007 Jan 1; 133(1):127–33. https://doi.org/10.1530/REP-06-0083 PMID: 17244739

36. Zhang GW, Li DB, Lai SJ, Chen SY, Lei RP, Zhou DG. Effects of dietary vitamin D3 supplementation on AvBD-1 and chCATH-1 genes expression in chicken. The Journal of Poultry Science. 2011; 48(4):254–8.

37. Swedenborg E, Rüegg J, Mäkelä S, Pongratz I. Endocrine disruptive chemicals: mechanisms of action and involvement in metabolic disorders. Journal of molecular endocrinology. 2009; 43(1):1–10. https://doi.org/10.1677/JME-08-0132 PMID: 19211731

38. Bradlow HL, Davis DL, Lin G, Sepkovic D, Tiwari R. Effects of pesticides on the ratio of 16 alpha/2-hydroxyestrone: a biologic marker of breast cancer risk. Environmental Health Perspectives. 1995 Oct; 103(Suppl 7):147.

39. Hayes CL, Spink DC, Spink BC, Cao JQ, Walker NJ, Sutter TR. 17 beta-estradiol hydroxylation catalyzed by human cytochrome P450 1B1. Proceedings of the National Academy of Sciences. 1996 Sep 3; 93(18):9776–81.

40. Al-Othman AA, Abd-Alrahman SH, Al-Daghri NM. DDT and its metabolites are linked to increased risk of type 2 diabetes among Saudi adults: a cross-sectional study. Environmental Science and Pollution Research. 2015 Jan 1; 22(1):379–86. https://doi.org/10.1007/s11356-014-3371-0 PMID: 25077657

41. Lee DH, Steffes MW, Sjödin A, Jones RS, Needham LL, Jacobs DR Jr. Low dose organochlorine pesticides and polychlorinated biphenyls predict obesity, dyslipidemia, and insulin resistance among people free of diabetes. PloS one. 2011 Jan 26; 6(1):e15977. https://doi.org/10.1371/journal.pone.0015977 PMID: 21298090

42. Dupont J, Tesseraud S, Derouet M, Collin A, Rideau N, Crochet S, et al. Insulin immuno-neutralization in chicken: effects on insulin signaling and gene expression in liver and muscle. Journal of endocrinology. 2008 Jun 1; 197(3):531–42. https://doi.org/10.1677/JOE-08-0055 PMID: 18492818

43. Gregory MK, Geier MS, Gibson RA, James MJ. Functional characterization of the chicken fatty acid elongases. The Journal of nutrition. 2013 Jan 1; 143(1):12–6. https://doi.org/10.3945/jn.112.170290 PMID: 23173174

44. Jing M, Gakhar N, Gibson RA, House JD. Dietary and ontogenic regulation of fatty acid desaturase and elongase expression in broiler chickens. Prostaglandins, Leukotrienes and Essential Fatty Acids (PLEFA). 2013 Aug 31; 89(2):107–13.

45. D5Andre HC, Paul W, Shen, Jia X, Zhang R, Sun L, et al. Identification and characterization of genes that control fat deposition in chickens. Journal of animal science and biotechnology. 2013 Nov 9; 4 (1):43. https://doi.org/10.1186/2049-1891-4-43 PMID: 24206759

46. Fry DM, Toone CK. DDT-induced feminization of gull embryos. Science. 1981 Aug 21; 213(4510):922–4. PMID: 7256288

47. Gregory NG, Robins JK. A body condition scoring system for layer hens. New Zealand Journal of Agricultural Research. 1998 Dec 1; 41(4):555–9.

48. Yohannes YB, Ikenaka Y, Saengtienchai A, Watanabe KP, Nakayama SM, Ishizuka M. Concentrations and human health risk assessment of organochlorine pesticides in edible fish species from a Rift Valley lake—Lake Ziway, Ethiopia. Ecotoxicology and environmental safety. 2014 Aug 31; 106:95–101. https://doi.org/10.1016/j.ecoenv.2014.04.014 PMID: 24836883

49. Darwish WS, Ikenaka Y, Ohno M, Eldaly EA, Ishizuka M. Carotenoids as regulators for inter-species difference in cytochrome P450 1A expression and activity in ungulates and rats. Food and Chemical Toxicology. 2010 Nov 30; 48(11):3201–8. https://doi.org/10.1016/j.fct.2010.08.022 PMID: 20797421

50. Mureithi D, Darwish WS, Ikenaka Y, Kanja L, Ishizuka M. Cytochrome P450 3A mRNA expression along goat and rat gastrointestinal tracts. Japanese Journal of Veterinary Research. 2012; 60(4):205–10. PMID: 23304981

51. Agilent Technologies. Introduction to Quantitative PCR. 2012. https://www.agilent.com/cs/library/brochures/Brochure_Guide%20to%20QPCR_IN70200C.pdf Downloaded 2018/03/20.

52. Van Dyk JC, Bouwman H, Barnhoorn IE, Bornman MS. DDT contamination from indoor residual spraying for malaria control. Science of the total environment. 2010 Jun 1; 408(13):2745–52. https://doi.org/10.1016/j.scitotenv.2010.03.002 PMID: 20381127

53. Labunska I, Abdallah MA, Eulaers I, Covaci A, Tao F, Wang M, et al. Human dietary intake of organohalogen contaminants at e-waste recycling sites in Eastern China. Environment international. 2015 Jan 31; 74:209–20. https://doi.org/10.1016/j.envint.2014.10.020 PMID: 25454238

54. Lundholm CE. The distribution of calmodulin in the mucosa of the avian oviduct and the effect of p-p'-DDE on some of its metabolic parameters. Comparative Biochemistry and Physiology Part C: Comparative Pharmacology. 1990 Jan 1; 96(2):321–6.

55. Lundholm CE, Bartonek M. Effects of p, plin in the mucosa of chlorinated hydrocarbons on the formation of prostaglandins by the avian eggshell gland mucosa. Archives of toxicology. 1992 Jul 28; 66(6):387–91. PMID: 1444803

56. Bulger WH, Muccitelli RM, Kupfer D. Studies on the in vivo and in vitro estrogenic activities of methoxychlor and its metabolites. Role of hepatic mono-oxygenase in methoxychlor activation. Biochemical pharmacology. 1978 Jan 1; 27(20):2417–23. PMID: 728194

57. Fry DM. Reproductive effects in birds exposed to pesticides and industrial chemicals. Environmental Health Perspectives. 1995 Oct; 103(Suppl 7):165–71.

58. Korach KS, Sarver PA, Chae K, McLachlan JA, McKinney JD. Estrogen receptor-binding activity of polychlorinated hydroxybiphenyls: conformationally restricted structural probes. Molecular pharmacology. 1988 Jan 1; 33(1):120–6. PMID: 3122017

59. Li X, Gan Y, Yang X, Zhou J, Dai J, Xu M. Human health risk of organochlorine pesticides (OCPs) and polychlorinated biphenyls (PCBs) in edible fish from Huairou Reservoir and Gaobeidian Lake in Beijing, China. Food chemistry. 2008 Jul 15; 109(2):348–54. https://doi.org/10.1016/j.foodchem.2007.12.047 PMID: 26003357

60. Ganz T. Defensins: antimicrobial peptides of innate immunity. Nature reviews immunology. 2003 Sep 1; 3(9):710–20. https://doi.org/10.1038/nri1180 PMID: 12949495

61. Semple F, MacPherson H, Webb S, Cox SL, Mallin LJ, Tyrrell C, et al. Human s-defensin 3 affects the activity of pro-inflammatory pathways associated with MyD88 and TRIF. European journal of immunology. 2011 Nov 1; 41(11):3291–300. https://doi.org/10.1002/eji.201141648 PMID: 21809339

62. Semple F, Dorin JR. s Defensins: multifunctional modulators of infection, inflammation and more? Journal of innate immunity. 2012; 4(4):337–48. https://doi.org/10.1159/000336619 PMID: 22441423

63. Lim U, Turner SD, Franke AA, Cooney RV, Wilkens LR, Ernst T, et al. Predicting total, abdominal, visceral and hepatic adiposity with circulating biomarkers in Caucasian and Japanese American women. PloS one. 2012 Aug 17; 7(8):e43502. https://doi.org/10.1371/journal.pone.0043502 PMID: 22912885

64. Wang X, Carre W, Saxton AM, Cogburn LA. Manipulation of thyroid status and/or GH injection alters hepatic gene expression in the juvenile chicken. Cytogenetic and genome research. 2007; 117(1–4):174–88. https://doi.org/10.1159/000103178 PMID: 17675858

65. De Los Reyes MA, Mora EC. Tissue residues and ultrastructural changes induced by DDT in chickens. Poultry science. 1979 Sep 1; 58(5):1183–91. https://doi.org/10.3382/ps.0581183 PMID: 523383

66. Skinner MK, Manikkam M, Tracey R, Guerrero-Bosagna C, Haque M, Nilsson EE. Ancestral dichlorodiphenyltrichloroethane (DDT) exposure promotes epigenetic transgenerational inheritance of obesity. BMC medicine. 2013 Oct 23; 11(1):228.

67. Gregory MK, James MJ. Functional characterization of the duck and turkey fatty acyl elongase enzymes ELOVL5 and ELOVL2. The Journal of nutrition. 2014 Aug 1; 144(8):1234–9. https://doi.org/10.3945/jn.114.194159 PMID: 24919687

68. Nakamura Y, Sakakibara J, Izumi T, Shibata A, Ono T. Transcriptional regulation of squalene epoxidase by sterols and inhibitors in HeLa cells. Journal of Biological Chemistry. 1996 Apr 5; 271(14):8053–6. PMID: 8626488

69. Bureau C, Hennequet-Antier C, Couty M, Guémené D. Gene array analysis of adrenal glands in broiler chickens following ACTH treatment. BMC genomics. 2009 Sep 14; 10(1):430.

70. Morgenthal TL, Kellner K, Van Rensburg L, Newby TS, Van der Merwe JP. Vegetation and habitat types of the Umkhanyakude Node. South African Journal of Botany. 2006 Feb 28; 72(1):1–0.

71. Sierra-Santoyo A, Hernandez M, Albores A, Cebrian ME. Sex-dependent regulation of hepatic cytochrome P-450 by DDT. Toxicological Sciences. 2000 Mar 1; 54(1):81–7. PMID: 10746934

72. Kitamura S, Shimizu Y, Shiraga Y, Yoshida M, Sugihara K, Ohta S. Reductive Metabolism of p, pochrome P-450 by DDT. Toxicological Sciences. 2000 Mar 1; 54(1):81–7.6 Feb 28;72(1):1–0. Apr 5;271(:113–8. PMID: 10746934

73. Davison KL, Sell JL. Dieldrin and p, p'-DDT effects on some microsomal enzymes of livers of chickens and mallard ducks. Journal of agricultural and food chemistry. 1972 Nov; 20(6):1198–205. PMID: 5083525

74. Akazome Y, Abe T, Mori T. Differentiation of chicken gonad as an endocrine organ: expression of LH receptor, FSH receptor, cytochrome P450c17 and aromatase genes. Reproduction. 2002 May 1; 123(5):721–8. PMID: 12006100

75. Cruze L, Kohno S, McCoy MW, Guillette LJ. Towards an understanding of the evolution of the chorioallantoic placenta: steroid biosynthesis and steroid hormone signaling in the chorioallantoic membrane of an oviparous reptile. Biology of reproduction. 2012 Sep 1; 87(3).

76. Freking F, Nazairians T, Schlinger BA. The expression of the sex steroid-synthesizing enzymes CYP11A1, 3β-HSD, CYP17, and CYP19 in gonads and adrenals of adult and developing zebra finches. General and comparative endocrinology. 2000 Aug 31; 119(2):140–51. https://doi.org/10.1006/gcen.2000.7503 PMID: 10936034

77. Yoshida K, Shimada K, Saito N. Expression of P450 17ral and comparative endocrinoase genes in the chicken gonad before and after sexual differentiation. General and comparative endocrinology. 1996 May 31; 102(2):233–40. https://doi.org/10.1006/gcen.1996.0064 PMID: 8998967

Ecotoxicology (2018) 27:1203–1216
https://doi.org/10.1007/s10646-018-1972-y

Linking organochlorine exposure to biomarker response patterns in Anurans: a case study of Müller's clawed frog (*Xenopus muelleri*) from a tropical malaria vector control region

Nico J Wolmarans[1] · Louis H Du Preez[1,2] · Yared Beyene Yohannes[3] · Yoshinori Ikenaka[1,3] · Mayumi Ishizuka[3] · Nico J Smit[1] · Victor Wepener[1]

Accepted: 20 July 2018 / Published online: 1 September 2018

Abstract

Organochlorine pesticides are highly persistent in aquatic ecosystems. Amphibians, specifically anurans, play an intricate part in the aquatic food web, and have very permeable skin which makes them prone to bioaccumulation of persistent pollutants. In this study the bioaccumulation of various legacy organochlorine pesticides (OCPs)—including dichlorodiphenyltrichloroethane (DDT), currently used for malaria vector control (MVC)—was assessed along with a set of biomarker responses in Müller's clawed frog *Xenopus muelleri* collected from the lower Phongolo River floodplain in South Africa. Possible relationships between bioaccumulation and biomarkers (of exposure, oxidative stress biomarkers, and cellular energy allocation) alongside their temporal changes were investigated. The OCP concentrations showed a significant increase over time for the duration of the study. The increase correlated negatively with rainfall from the region. DDT levels were well below expected effects levels with *p,p*-DDE being the main contributing metabolite. The results of this study indicate OCPs actively accumulate at sub-lethal levels in aquatic frogs from the study area, while showing possible relations towards some of the biochemical stress responses measured. Most notable were negative relationships indicated between *p,p*-DDE and acetylcholinesterase, malondialdehyde, and carbohydrates and protein energy availability. Levels of DDT were not found to be significantly higher than other legacy pesticides in the frog tissue, although evidence of newly introduced DDT in the frog tissue was found. Further investigation about sub-lethal effects of these pesticides on anurans is required to gain better insight into their full impact on animal livelihood.

Keywords Amphibians · Bioaccumulation · Pesticides · DDT · HCH · South Africa

Introduction

Organochlorine pesticides

Due to their persistent nature and global distribution, organochlorine pesticides (OCPs) have been banned in most countries around the world (Ritter et al. 1995). While they were still in use these OCPs played a large role in agriculture for their use as insecticides (Ritter et al. 1995; UNEP 2010). South Africa is one of the few African countries where the use of dichlorodiphenyltrichloroethane (DDT) as malaria vector control (MVC) agent through controlled indoor residual spraying (IRS) is still permitted (Bouwman et al. 2011). The IRS method limits the quantity of pesticides used in MVC through only allowing application to the interior walls and ceilings, and exterior eaves of homesteads in malaria risk regions (Gaspar et al. 2016).

Electronic supplementary material The online version of this article (https://doi.org/10.1007/s10646-018-1972-y) contains supplementary material, which is available to authorized users.

✉ Nico J Wolmarans
21600600@nwu.ac.za

[1] Water Research Group, Unit for Environmental Sciences and Management, North-West University, Private Bag X6001, Potchefstroom 2520, South Africa

[2] South African Institute for Aquatic Biodiversity, Somerset Street, Grahamstown 6139, South Africa

[3] Laboratory of Toxicology, Department of Environmental Veterinary Sciences, Graduate School of Veterinary Medicine, Hokkaido University, N18, W9, Kita-ku, Sapporo 060-0818, Japan

There is however increasing evidence that DDT has still been entering the environment long after its conventional use was banned. Van Dyk et al. (2010) showed the presence of DDT in chickens and other matrices in and directly around homesteads in the Limpopo Province of South Africa. Gerber et al. (2016) and Viljoen et al. (2016) assessed DDT bioaccumulation in aquatic biota from rivers in the same region and recorded levels of 4000–32,000 (ng/g lipid weight) ∑DDTs in tigerfish (*Hydrocynus vittatus*) and 5–650 (ng/g wet weight) ∑DDTs in anurans (*Xenopus* spp.) respectively. Recently Verhaert et al. (2017) investigated trophic transfer of various persistent organic pollutants including OCPs in the aquatic food web of the Olifants River Basin in South Africa. They detected DDTs in most of the food web components analysed and showed trophic magnification of DDTs to be higher in this sub-tropical region (during winter specifically) compared to data from a tropical region. Thompson et al. (2017) and Yohannes et al. (2017) reported DDT exposure in domestic poultry and wildlife from in and around homesteads in the Phongolo floodplain region in northern KwaZulu-Natal Province of South Africa.

This region is regarded as a biodiversity hotspot for amphibians (Netherlands et al. 2015) and the risk of DDT exposure to these and other aquatic organisms is still not fully understood (Dube et al. 2016). Its use is crucial in the prevention of malaria (Bouwman et al. 2011). Despite their environmental persistence, knowledge regarding levels and effects of DDT and other OCPs in anurans are limited with most of the available toxicity data being generated in the 1970s (Pauli et al. 2000). The majority of studies on DDT bioaccumulation in anurans only report on body burdens and not concomitant biological responses (Jofré et al. 2008; Viljoen et al. 2016). According to Monastersky (2014) amphibians are currently amongst the most threatened animals on earth, that is why it is essential to evaluate exposure scenarios that could influence their populations health and fitness (Melvin et al. 2016).

Another organochlorine pesticide group of concern in the Phongolo region are the hexachlorocyclohexanes (HCHs). Buah-Kwofie and Humphries (2017) attributed the high levels of ΣHCHs in sediments from water bodies in northern KwaZulu-Natal (83–187 ng/g dry weight) to the recent agriculture application in the region. These HCHs were historically mainly used in the form of technical HCH (consisting of 55–80% α-, 5–14% β-, 8–15% γ-, 6–10% δ-, and 1–5% ε-HCH isomers) and in later years lindane (γ-HCH) as broad spectrum insecticides in agriculture (UNEP 2010). Main uses included seed treatment, ecto-parasite control on livestock, wood, and tree covering (UNEP 2010). These historical uses have relevance to the study area because of catchment land use.

Study area

The Phongolo floodplain in north eastern South Africa is a biodiversity hotspot with over 400 bird species, more than 40 fish species and 45 frog species (Mallory 2002; Du Preez and Carruthers 2017). Since the mid-1970s this large floodplain has been subjected to artificial flooding due to the construction of the Pongolapoort Dam (Wepener et al. 2012). This regulation, together with below average rain falls for the past decade, has resulted in a decline in the water quantity and quality of the Phongolo River and associated floodplain wetlands (Dube et al. 2016). Dube et al (2016) indicate that the stress of decreased water and increased levels of OCPs such as DDT and other agricultural pesticides pose a threat to the aquatic biodiversity of the floodplain. Land use in the Phongolo River catchment upstream of the floodplain mainly consists of forestry and sugarcane farming, which as stated in section 1.1 has been historically associated to HCH usage. In the floodplain itself maize farming (mostly as subsistence farming) is practiced on a smaller scale (Personal observation). Other OCPs that used to be important in these agricultural activities are Chlordane and Aldrin (Ritter et al. 1995).

Indicator species

The use of *Xenopus* as a model organism is well established in ecotoxicology with embryos commonly used to study teratogenic effects using the Frog Embryo Teratogenesis Assay – *Xenopus* (FETAX). Adult *Xenopus* are not in particular known to have high susceptibility to toxic effects of anthropogenic pollutants (*see* Pauli et al. 2000), but this can make them good indicators of bioaccumulation and good models for sub-lethal effect. Their central placement in the aquatic food web (Lindholm et al. 2007) means early response effects measured in *Xenopus* can be monitored and managed before effects reach top predator level at which point irreversible effects may have occurred throughout the rest of the food web. Their fully aquatic nature and bottom dwelling habits also make them more prone to contact with pollutants that accumulate in sediments such as OCPs and uptake is facilitated through their highly permeable skin. *Xenopus laevis* is the most commonly used model anuran from Southern Africa. The study area marks a slight overlap in the natural distribution of *X. laevis* and its sub-tropical relative *X. muelleri* (Du Preez and Carruthers 2017), but *X. laevis* is in reality quite scarce in this region (Netherlands et al. 2015) resulting *X. muelleri* as being the obvious choice for this study. Positive identification was easily made through the long (longer than the radius of the eye: distinct from *X. laevis*) sub-ocular tentacles found on *X. muelleri* (Du Preez and Carruthers 2017).

Biomarker responses

When attempting to link environmental exposure of pollutants to biological effects, biomarker responses are commonly used. An integrated biomarker response approach has recently been shown to be useful in discriminating among environmentally relevant exposure scenarios in aquatic ecosystems by Schoenaers et al. (2016). The integrated biomarker suite for this study were selected to indicate, biotransformation of xenobiotic compounds through cytochrome P450 (CYP450) activity, exposure to neurotoxic compounds through acetylcholinesterase (AChE) activity, oxidative stress through means of both antioxidant systems—superoxide dismutase (SOD) and catalase (CAT)—and oxidative damage indicators—protein carbonyls (PC) and malondialdehyde (MDA)—, and energetics though cellular energy allocation. This suite of biomarkers is considered to be indicative of anthropogenic stressors according to Gerber et al. (2018), who showed that these biomarker responses can be indicative of OCP and metal accumulation in tigerfish (*Hydrocynus vittatus*). Oxidative stress biomarkers were used by several authors (Borković-Mitić et al. 2016; Prokić et al. 2016) to determine effects of metal exposure in the marsh frog, *Pelophylax ridibundus*. The same biomarkers were applied to evaluate the effects of carbamate pesticides (Falfushinska et al. 2008) and organophosphates (Kanter and Celik 2011) to the same species. Biomarkers have also been applied in laboratory bioassays to evaluate the antioxidant responses of *X. laevis* to crude oil extracts (Eriyamremu et al. 2008). These biomarker responses are therefore also regularly used in studies on frogs and may be applied to contaminant groups such as OCPs for investigating the interactions between chemical pollution and biochemical changes. Apart from direct toxicity mechanisms expected to be activated through exposure to OCPs, the persistence of these compounds at detectable levels in an organism may decrease the cellular energy budget and increase radical oxygen species formation (Gerber et al. 2018), which could be detected through means of the measured biomarker responses in this study.

Study aims

The aims of this study were therefore to determine the extent to which amphibians from this system are exposed to DDT and other OCPs, along with the temporal variation in chemical loads, using the anuran Müller's clawed frog (*Xenopus muelleri*) as indicator organism. To evaluate the impact of continued DDT inputs through isomer ratio analysis. To compare DDT bioaccumulation in *X. muelleri* to bioaccumulation of other OCPs expected from historical use in the system. Finally, to relate the OCP exposure to biological effects in *X. muelleri* through utilisation of a suite of biomarker responses. This includes biomarkers of exposure, oxidative stress and cellular energy allocation.

Materials and methods

Ethical clearance and permits

Frogs were collected under Ezemvelo-KZN Wildlife permit numbers: OP 5139/2012 & OP 5261/2014. The study was approved by the North-West University AnimCare Ethics Committee (NWU-00095-12-A4).

Field methods: sample collection and handling

Frog sample collection was conducted during four separate surveys over a two-year period. IRS application occurs in the summer months (November to February). The November 2012 and 2013 surveys were therefore during the MVC period and are labelled D (Table 1). The two surveys after the MVC period were undertaken in April 2013 and 2014 and are labelled A (Table 1). Sampling was conducted in floodplain ponds within the Ndumo game reserve to determine the chemical loads of the floodplain frogs in the area (Fig. 1).

Xenopus muelleri collection was done through both active (night frogging by hand) and passive (commercial chicken liver baited bucket traps) sampling techniques. The animals were euthanized through double pithing as described by Amitrano and Tortora (2012) as chemical euthanasia could possibly compromise the biomarker results (Velisek et al. 2011). The liver mass and total body mass of each animal was recorded upon dissection for calculation of the hepatosomatic index (HSI), which is defined as the ratio between the two values. For biomarker analyses the liver and muscle from the right thigh was removed and placed in Hendrikson's buffer (40 mM tris-HCl, 10 nM 2-Mercaptoethanol, 1 mM 0.04% bovine serum albumin [BSA], 1 nM ethylene-diamine-tetraacetic acid [EDTA]) and flash frozen in liquid N_2. These samples were later transferred from liquid N_2 to an −80 °C freezer in the laboratory until biomarker analysis was undertaken.

Table 1 Survey labels and descriptions

Year	2012	2013	2013	2014
Month	Nov	April	Nov	April
IRS	During spraying-D	After spraying-A	During spraying-D	After spraying-A
Label	2012D	2013A	2013D	2014A

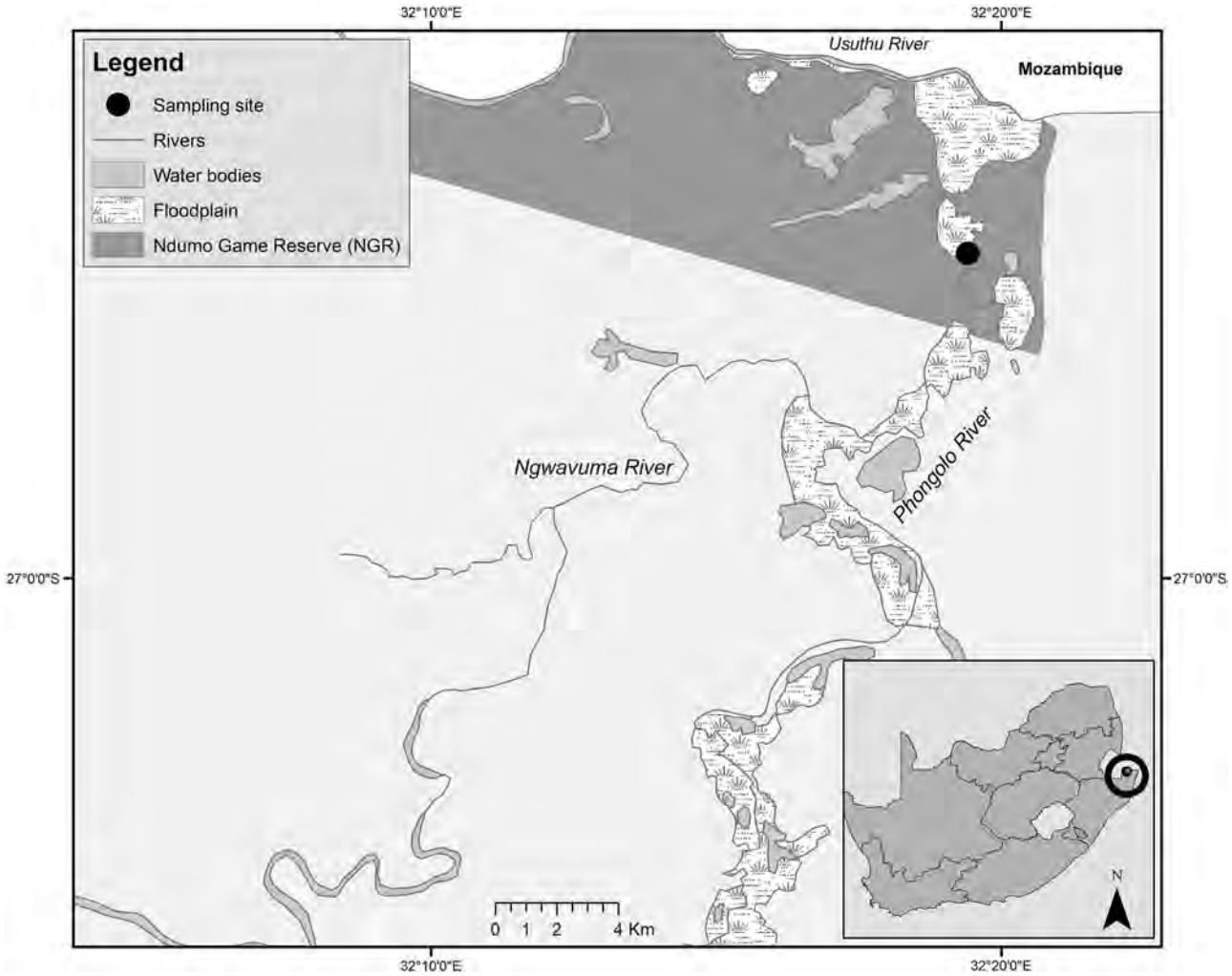

Fig. 1 Map of the study area indicating sampling area. *Xenopus muelleri* were collected from within the Ndumo Game reserve for chemical and biomarker analysis

The remaining carcass, to be used for whole body OCP bioaccumulation analysis, was wrapped in aluminium foil and frozen at −20 °C until analysis. The absence of the entire liver and a piece of muscle for the whole frog analysis was consistent throughout the study, making results from this study comparable. However, the lack of these pieces could affect comparisons with literature, as the liver is considered a major bioaccumulation organ for xenobiotics. Fagotti et al. (2005) found that DDT tissue accumulation patterns in *Rana esculenta* were that the brain contained the highest concentration, with the liver accumulating the third largest percentage of the total DDT in the body. Therefore it should be borne in mind that the absence of liver in the analysed whole specimens from this study probably result in underestimation of OCPs when compared to other studies using whole organisms in the literature.

Organochlorine pesticide analyses

The method used for chemical residue extraction and analysis was adapted from Yohannes et al. (2013). Automated hot-Soxhlet extraction using 1:3 v/v acetone:hexane was done on anhydrous $NaSO_4$ desiccated whole frog samples (5–10 g). Lipid percentage was determined gravimetrically on a dried 20% aliquot of the extract. Samples containing more than 5% lipids were subjected to gel permeation chromatography for size exclusion separation of lipids. For final clean-up, samples were filtered through 6 g of 5% deactivated Florisil and eluted with 3:7 v/v dichloromethane:hexane (100 mL). Extracts were then evaporated to dryness and reconstituted in 100 µL *n*-Decane.

Chemical analysis was performed on a gas-chromatograph with a Ni electron capture detector (GC-ECD: Shimadzu GC-2014) with Nitrogen as make-up gas

(45 mL/min flow rate). An ENV-8MS capillary column (30 m × 0.25 mm i.d., 0.25 µm film thickness) was used for separation of target compounds with He as carrier gas (1 mL/min flow rate). Splitless injection was used (1 µL injection volume; 250 °C inlet temperature). The following GC oven program was set: initial temperature of 100 °C held for 1 min, followed by 12 °C/min ramp to 180 °C, followed by 4 °C/min ramp to 240 °C, followed by 10 °C/min ramp to 270 °C held for 5 min. The detector temperature was set at 320 °C. A mixture containing 22 persistent organic pollutant (POP) pesticides (Dr Ehrenstorfer, GmbH) was used as external standard. Calibrations were done using 5-point standard curves from concentrations ranging between 10 µg/L and 500 µg/L (R^2 ranged between 0.997 and 0.999 for all compounds). Recoveries were calibrated using PCB# 77 as surrogate marker and were between 60 and 95% (mean 75.6%). The data reported were adjusted according to recovery. Standard reference material SRM 1947 (Lake Michigan Fish Tissue) analysed using the same method produced recoveries ranging from 75 to 110% with the residual standard deviation less than 12%. Limits of detection based on 3:1 signal to noise ratio (S/N) were below 0.5 ng/g for all OCPs.

Biomarker analyses

Samples were thawed and preparation was conducted at 4 °C to preserve protein stability. Three sample batches (A, B, and C) were prepared. Due to the small size of frog livers, some specimen samples were pooled to obtain sufficient sample mass for biomarker analyses. Sample pooling was done per collection site and samples below the required minimum liver mass were pooled together in equal mass at random (within each site and survey) until all samples had reached the required liver mass. Batch A consisted of 0.05 g of liver tissue in 250 µL of Tris-sucrose buffer (0.05 M Tris-HCl [pH 7.4], 0.2 M sucrose). The samples were homogenised and centrifuged at 9500 × *g* for 10 min. The supernatant was used for acetylcholinesterase (AChE) and malondialdehyde (MDA) analysis. For Batch B 0.05 g of liver tissue in 1 mL potassium phosphate buffer (0.09 M $K_2HPO_4 + KH_2PO_4$ [pH7.4]) was homogenised and centrifuged at 10,000 × *g* for 30 min. The supernatant from this batch was used for catalase (CAT), superoxide dismutase (SOD), cytochrome P450 (CYP450) and protein carbonyl (PC) analyses. The third batch (C) consisted 0.2 g muscle tissue in 400 µL of electron transport system (ETS) homogenising buffer (0.1 M Tris-HCl [pH 8.5], 0.2% v/v Triton-X, 15% m/v polyvinyl pyrolidone, 153 µM $MgSO_4$), which was then homogenised and used for the cellular energy allocation (CEA) analyses.

Acetylcholinesterase activity was determined using the assay described by Ellman et al. (1961) where thiocholine, a breakdown product of acetylcholine formed through hydrolysis by AChE, reacts with dithiobisnitro-benzoate (DTNB) to generate a 5-thio-2-nitrobenzoate anion. The product has a yellow colour which is quantified by its absorbance at 405 nm. Cytochrome P450 demethylating activity was measured using an assay kit based on formaldehyde formation (DetectX Demethylating P450 fluorescent activity kit, Arbor Assays). These two biomarkers were performed as biomarkers of exposure indicating both direct toxicant effect and xenobiotic metabolism activation. To measure oxidative stress an array of enzymatic and non-enzymatic biomarkers regarding the cellular antioxidant system were analysed. The SOD activity was determined using the assay described by Del Meastro and McDonald (1989). In this assay the inhibition of pyrogallol autoxidation is measured as a function of the rate of free radical Oxygen conversion to H_2O_2 by SOD. The CAT activity was determined by a static timed reaction between H_2O_2 and CAT enzymes. KMnO4 is added after the reaction as photometric agent which in turn reacts with residual H_2O_2. The excess $KMnO_4$ is then measured as a function of the amount of H_2O_2 breakdown by CAT in the reaction time period as described by Cohen et al. (1970). The MDA content was determined using a colorimetric assay based on thiobarbituric acid's reaction with MDA as a measurement of lipid peroxidation as described by Üner et al. (2006). Protein carbonyl content was measured through a 2,4-Dinitrophenylhydrazine (DNPH) reaction with carbonyl groups in proteins and provides a measurement of protein oxidation based on the method of Parves and Riasuddin (2005). The activity and concentrations of all the biomarkers assayed in the liver tissue are expressed in terms of mg protein which was determined using the method of Bradford (1976) for each sample after pooling of batches A and B for the assays performed within the batch.

The cellular energy allocation assay performed is based on the protocols of De Coen and Janssen (1997) and De Coen and Janssen (2003) and reflects the difference between the total energy available (in terms of carbohydrate, lipid and protein reserves) and the energy consumed (as reflected in electron transport system (ETS) activity. Total carbohydrates were determined using the GOD-PAP 1 448 668 Roche test kit. This method Lipid content was assayed according to Bligh and Dyer (1959) while the protein content was once again determined according to the method described by Bradford (1976). The above concentrations were converted into energy equivalents using the combustion enthalpy of glycogen (17,500 mJ/mg), protein (24,000 mJ/mg), and lipids (36,500 mJ/mg) to calculate the total available energy (Ea) (De Coen and Janssen 1997). The consumed energy (Ec) was determined by means of the stoichiometric relationship between formazan formation and oxygen consumption (1:2) of the ETS. The

oxygen consumption results were then converted into energy equivalents using the combustion enthalpy of O_2 (484 kJ/mol) (De Coen and Janssen 1997). An energy budget was calculated using the equation: CEA = Ea − Ec with Ea being the sum of the protein, carbohydrate and lipid energy equivalents and Ec being the ETS energy equivalents.

Statistical analyses

Prior to analysis the data were checked for normality (D'Agostino-Pearson normality test) and homogeneity of variance (Levene's test). The temporal differences in OCP bioaccumulation and biomarker responses were measured using the non-parametric Kruskal–Wallis test coupled with Dunn's post hoc test as none of the datasets conformed to normality. Significance was regarded at $p < 0.05$. For all statistical analyses non-detect chemical data were replaced with LOQ × F per compound per survey, where LOQ is the limit of quantification of the compound and F is the frequency of detection within the survey (Wepener et al. 2012; Verhaert et al. 2013). Non-detect values are however shown as ND in tables and zero values in graphs for simplified visual interpretation. Temporal correlations in OCP concentrations as well as correlations with abiotic factors were measured through means of Spearman correlations of individual frog chemical data as all data in this instance did not have Gaussian distribution. Pearson's correlation, and Log (dose) vs. response variable slope nonlinear regression analyses were performed on hepatosomatic index (HSI) values vs. individual OCP concentrations to investigate possible relationships. Generalised linear model (GLM) multiple regressions were performed in conjunction with a redundancy analysis (RDA) between individual biomarker responses and OCP accumulation data to assess relationships while accounting for the composition of the data. Forward selection of explanatory variables in the RDA was used to select significant response variables on which GLM regression was performed.

Results

Organochlorine pesticide bioaccumulation

Chemical analysis revealed the presence of 10 of the 22 analysed OCPs in *X. muelleri* tissue from the Phongolo floodplain (Table S1). All of the 51 (total number of frogs from all surveys) analysed frog samples contained detectable OCPs. Specific detection frequencies are provided in supplementary material (Table S2). Two compound groups detected with highest prevalence and at distinguishably higher concentrations than others were DDTs and HCHs,

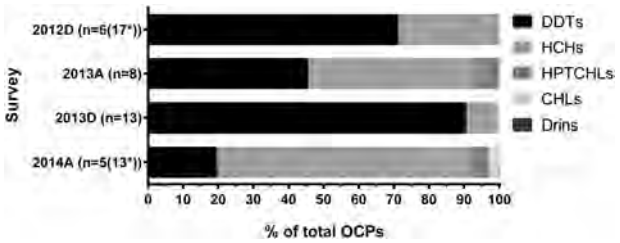

Fig. 2 Bar graph indicating the percentage composition of organochlorine pesticide (OCP) groups contributing towards total OCP accumulation for each survey (DDTs dichlorodiphenyltrichloroethane isomers and their metabolites, HCHs hexachlorocyclohexane isomers, HTPCHLs heptachlor isomers of which only trans-heptachlor epoxide was detected, CHLs chlordane isomers of which only cis-chlordane was detected, Drins Aldrin was the only detected compound from the drin group)

making up cumulatively, more than 90% of detected OCPs for all surveys (Fig. 2). Individual compounds detected at highest concentrations per single frog (before pooling) were γ-HCH, *p,p*-DDD, and *p,p*-DDE at 19,364, 7219 and 7057 ng/g lipid respectively. γ-Hexachlorocyclohexane made up the majority of the total HCH concentrations detected. Other OCPs detected at lower levels included Aldrin, *cis*-Chlordane, *trans*-Heptachlor epoxide, α-HCH, δ-HCH and *o,p*-DDT (Fig. 3a–e,Table S1).

During vs after spraying period

The highest total OCPs mean (±SE) concentration as well as the highest maximum value per frog was recorded as 8689 ± 2037 ng/g lipid and 21,399 ng/g lipid respectively, both from the 2014A survey. For the same survey γ-HCH had the highest mean for any single compound detected at 6350 ± 1803 ng/g lipid. OCP compositional changes were observed for sequential surveys per spraying season, where a decrease in total DDTs from during (D) to after (A) spraying surveys and an HCH increase over the same periods was seen (Fig. 3b). There were no significant differences in total OCP levels between this timeframe from during (D) to after (A) spraying per season. However significant differences were recorded in total OCPs between the two active spraying period surveys (2013A and 2013D; $p < 0.05$) (Fig. 4). A temporal increase in total OCPs was observed over the total period of the study (Fig. 4; Spearman $r = 0.84$ $p < 0.0001$). Significant negative correlation (Spearman $r = -0.531$, p value = 0.0004) was found between total OCP accumulation and average rainfall data from the area during survey months (Rainfall data obtained from Worldweatheronline (2016); Fig. 4, Table S3). No significant correlation was found between rainfall and animal body mass nor total OCPs and animal body mass. Furthermore there was significant negative correlation between total HCH accumulation and rainfall, but not

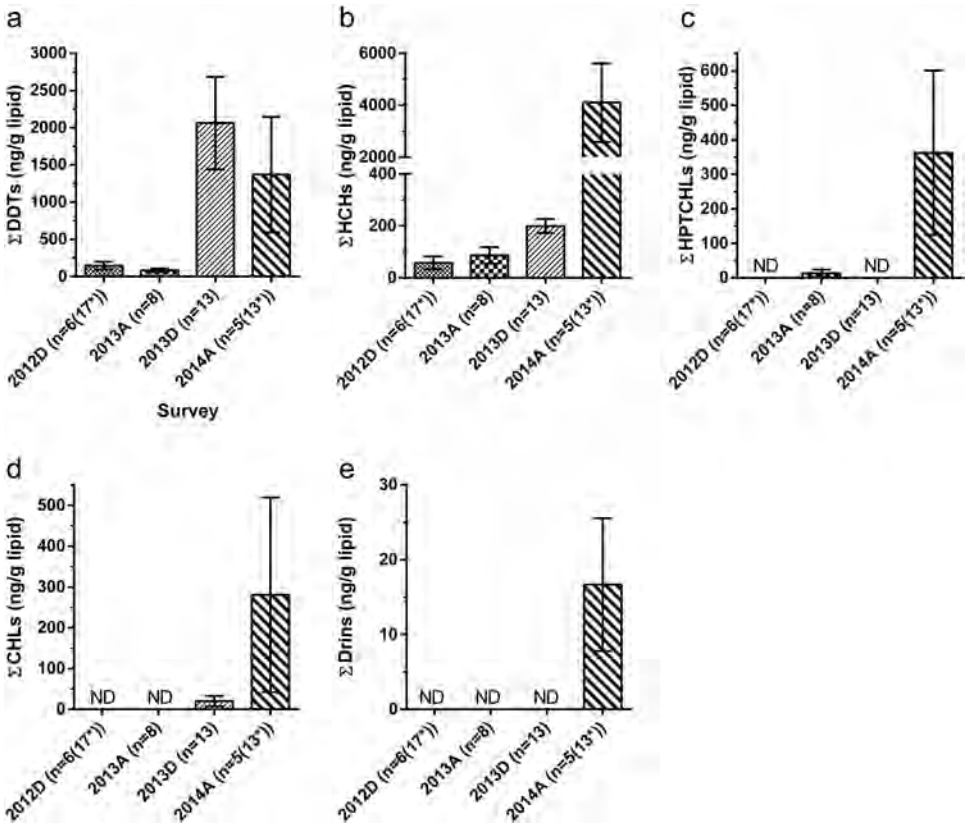

Fig. 3 Bar graphs indicating the mean (±standard error) concentrations (ng/g lipid) of the various OCP groups in Xenopus muelleri tissue across the four surveys for **a** DDTs (dichlorodiphenyltrichloroethane isomers and their metabolites), **b** HCHs (hexachlorocyclohexane isomers), **c** HTPCHLs (heptachlor isomers and metabolites) of which only trans-heptachlor epoxide was detected, **d** CHLs (chlordane isomers) of which only cis-chlordane was detected, and **e** Drins of which only Aldrin was detected. Pooled sample sizes are indicated for each survey with * marking the original number of frogs used

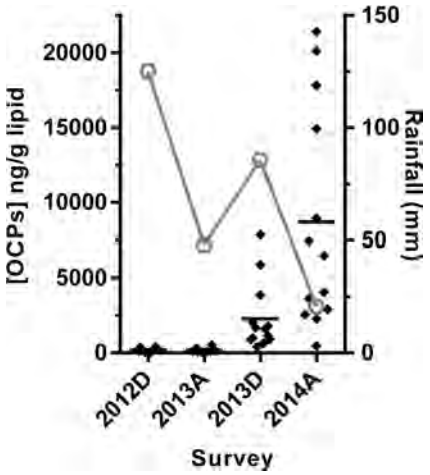

Fig. 4 Scatter plot of individual frog data points (black diamonds) and mean values (black lines) for total organochlorine pesticide (OCP) accumulation (left *y*-axis) in Xenopus muelleri for all of the surveys conducted. Overlaid on the right *y*-axis is the average rainfall in the sampling area during the month of each survey (grey circles and connecting lines). Spearman correlation indicated significant unimodal increase over time (Spearman $r = 0.84$) for total OCP concentrations. No significant correlation was found between rainfall and OCP data

between total DDT accumulation and rainfall (Table S3). The ratio between *p,p*-DDT and its metabolites (sum of *p,p*-DDD and *p,p*-DDE) was used to determine recentness of DDT exposure as described by Strandberg and Hites (2001). These ratios of the individual frogs analysed only indicated samples with recent DDT exposure (DDT/∑metabolites > 1) at the end of the 2012–2013 spraying season (2013A). There was an absence of *p,p*-DDT for the 2014A survey (Fig. 5). The HCH composition (Fig. 6) indicated γ-HCH as the main contributing isomer in all surveys making up more than 99% of the total HCHs except during the 2012 spraying season where δ-HCH was the main contributing isomer.

Biomarker responses

During vs after spraying period

All biomarker response results are given in Table 2. The CYP450 assay results indicated no significant temporal changes. Results from the AChE, PC and MDA assays indicated a significant decrease between spraying seasons from 2013A to 2013D, while SOD and CAT activity increased significantly over the same period. The CEA results for total available energy indicated no significant temporal change, however, the composition of available energy sources changed over time, from being mainly protein based to being mainly lipid based, with a subsequent decrease in carbohydrate energy storage. The energy consumption indicated a slight temporal increase. This variation

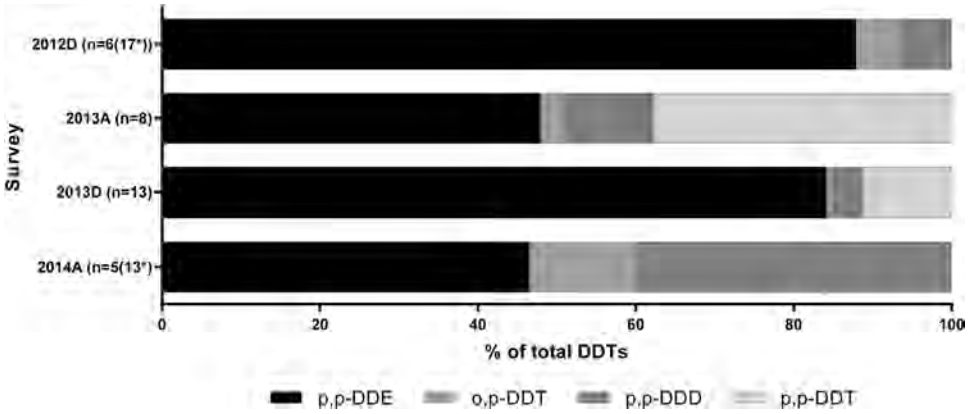

Fig. 5 Normalised bar graph indicating the percentage contribution of the different dichlorodiphenyltrichloroethane (DDT) isomers and metabolites towards the total DDTs measured during each survey

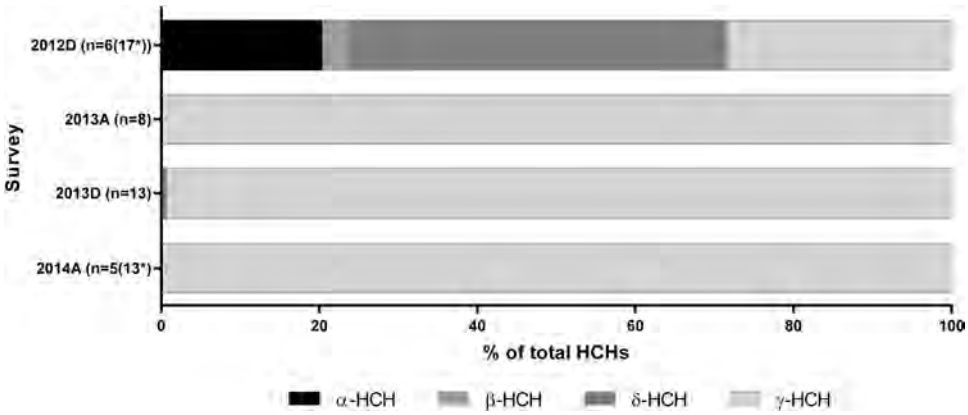

Fig. 6 Normalized bar graph indicating the percentage composition of different Hexachlorocyclohexane (HCH) isomers contributing towards the total HCH concentration for each survey

in the CEA data correspond to the changes observed in the oxidative stress biomarkers. The total CEA budget also showed no significant differences on a temporal scale.

Exposure vs biomarkers

A variable slope logarithm of dose vs response curve (Y = Bottom + (Top − Bottom)/(1 + 10^((LogIC50 − X) * HillSlope))) was fitted to bioaccumulation and corresponding HSI data. The relation between HSI values and γ-HCH was found to have a moderate fit with the regression line Y = 0,01047 + (0,02607–0,01047)/(1 + 10^((2683−X) *−2045)) ($R^2 = 0.54$; $p < 0.0001$), showing a decrease in HSI as the concentration of γ-HCH in the body increases. None of the other OCPs measured fitted dose response regressions towards HSI. In terms of correlation however, the Log values of the total OCP concentrations showed moderate negative correlation with HSI (Pearson's $r = -0.53$; $p < 0.0001$).

A redundancy analysis (RDA) was performed on pooled samples chemical data with their corresponding biomarker response. Only 49.6% of the total variation in chemical data was accounted by the biomarker responses with no clear separation of surveys through this analysis (Figure S2). Only 36.91% of the variation is described across the first two axes. Monte-Carlo permutation test indicated that explanatory variables significantly accounted for variation in the response data ($p = 0.006$). Individual axis statistics regarding the RDA are given in Table 3.

Using forward selection of explanatory variables the GLM regression of normalized responses vs individual OCP concentrations indicated some significant relationships (Table 4). The AChE, MDA, Ea-carbohydrates, and Ea-proteins values had significantly non-zero negative relationships towards *p,p*-DDE accumulation. The Ec and Ea-lipids showed significant positive relationships towards *p,p*-DDT. All of these responses were only significantly explained by a single variable. The CYP450 results showed a negative relationship towards α-HCH as the first selected variable and in conjunction with α-HCH a positive relationship towards δ-HCH as the second selected variable explaining CYP450 variation.

Discussion

Organochlorine pesticide bioaccumulation

Most compounds were only found in low ng/g lipid amounts as would be expected from legacy pesticides that

Table 2 Biomarker response assay results for *Xenopus muelleri* indicating the mean value and standard error of the mean (±SEM) for all the surveys conducted

Survey		2012D	2013A	2013D	2014A
n		6(17)*	8	13	5(13)*
	Unit	Mean	Mean	Mean	Mean
CYP450	µM/mg protein	0.71 ± 0.3	0.64 ± 0.04[a]	0.73 ± 0.04[a]	0.82 ± 0.06
AChE	Absorbance/min/mg protein	0.0015 ± 2.1E −4[a]	0.002 ± 3.85E−4[b]	3.1E−4 ± 3.82E−5[a,b]	5.09E−4 ± 1.7E−4
MDA	nmol/mg protein	2.5 ± 0.1	3.1 ± 0.3[a,b]	0.5 ± 0.04[a]	0.4 ± 0.06[b]
PC	nmol carbonyls/mg protein	49 ± 26.1	163.8 ± 40.8[a, b]	25.3 ± 3.2[a]	17.2 ± 1.2[b]
SOD	ng SOD/mg protein	0.19 ± 0.05	0.097 ± 0.076[a,b]	56.8 ± 19[a]	62.3 ± 15.7[b]
CAT	µmol H_2O_2/min/mg protein	21.4 ± 6.7	17.4 ± 1.2[a]	38.8 ± 8.3[a]	33 ± 9.1
Ea-carbohydrates	J/g	11.6 ± 1.5[a]	10.5 ± 2.5[b]	2.6 ± 0.4[a,b]	3.9 ± 0.9
Ea-lipids	J/g	44.9 ± 5.7[a]	57.1 ± 6.7[b]	279.5 ± 36.7[a,b]	178 ± 33.8
Ea-proteins	J/g	201.9 ± 6.8	221.9 ± 4.3[a,b]	122.9 ± 7.1[a]	117.7 ± 11.6[b]
Ea	J/g	258.4 ± 7.4[a]	289.5 ± 11.7	405 ± 33.4[a]	299.6 ± 44
Ec	J/g	15.1 ± 3.1[a]	34.2 ± 6.7	40 ± 3.8[a]	26.4 ± 7.2
CEA	J/g	243.3 ± 9.3	255.3 ± 11.2	365 ± 34.6	273.2 ± 46.4

[a,b] indicates significant differences ($p < 0.05$) per response (rows) between comparable surveys

**n* value in parentheses shows original number of frogs before pooling

Table 3 Results of the redundancy analysis (RDA) performed on biomarker response and OCP bioaccumulation data (bi-plot of first two axes shown in supplementary Figure S2)

	Axis 1	Axis 2	Axis 3	Axis 4
Eigenvalue	0.2380	0.1311	0.0680	0.0206
Explained variation (cumulative)	23.8	36.91	43.71	45.76
Pseudo-canonical correlation	0.7653	0.8404	0.7066	0.4915
Explained fitted variation (cumulative)	48.00	74.44	88.15	92.30

Axis one accounted for 23.80% of the total variation in the data and a further 13.11% was accounted for across the second axis. Monte-Carlo permutation test results on all axes showed a pseudo-F statistic of 2.1 ($p = 0.006$)

Table 4 Generalised linear model regression between normalized biomarker responses and organochlorine pesticide concentrations (ng/g lipid) in *Xenopus muelleri* from all surveys conducted

Compound	Biomarker assay	Response	*p*-value	R^2
p,p-DDE	AChE	↓	0.029	0.15
	MDA	↓	0.011	0.19
	Ea-carbohydrates	↓	0.038	0.13
	Ea-proteins	↓	0.015	0.18
p,p-DDT	Ea-lipids	↑	0.040	0.13
	Ec	↑	0.017	0.18
α-HCH	CYP450	↓	0.027	0.15
δ-HCH[a]	CYP450	↑	0.002	0.28

Only variables selected through forward selection were included

[a]*δ*-HCH was the second variable selected for CYP450 variance explanation through forward selection. All other response variation was only significantly explained by a single variable

have already been phased out of use for a few decades. All OCPs detected were well below known effect concentrations for amphibians reported in literature. It is noteworthy however that almost all available toxicity literature with regards to OCPs do not concern African species. A body burden as high as 110,000 ng/g lipid was reported for *p,p*-DDT with no observable effects for *Rana temporaria* tadpoles (Cooke 1979). The recent study by Viljoen et al. (2016) in another DDT-sprayed area of South Africa indicated a mean concentration of 402.1 ng/g wet mass total DDTs from lipid bodies of *Xenopus spp*. sampled in 2009. The current study analysed whole frogs with the highest wet mass mean (per survey) concentration at 16.1 ng/g and the highest lipid mass mean concentration at 2062.1 ng/g. Lipid mass concentration of the whole body would have a closer relation to wet mass concentration of lipid bodies, but an outright comparison of concentrations from the two studies cannot be made to the differences in methods used. Lambert (2001) lists a table of DDT residues in amphibians in sub-Saharan Africa, all of which are in the µg/g range in terms of wet mass, 100 times higher than values from this study. Most of these studies were during the active unregulated use of DDT. Differences in chemical levels between studies in Lambert (2001) could indicate the positive impact of strict regulations and proper IRS implementation by governments in reducing environmental DDT levels, compared to times in history when DDT use was unregulated. The recentness of exposure analysis results indicate the uptake of new DDT

from the environment by the end of the first spraying season, but not the second. The term recent in this analysis refers to the lack of time for the DDT to break down into its metabolites. This length of time varies due to a number of environmental factors that apply to the breakdown of these compounds in the environment. Recent introduction of DDT is assumed when the concentration of the parent compound is higher than that of the sum of the breakdown products. This means that there was not enough time for breakdown before uptake, as well as not enough time for biological breakdown after uptake. Even though the DDT metabolites *p,p*-DDD and *p,p*-DDE are also well documented to have both primary toxic effects as well as secondary endocrine disruption effects (Bouwman et al. 2011) this ratio is important in understanding the dynamics of the compounds within these organisms and this system as well as interpreting any possible effects observed as the different compounds have different toxicity signatures (ATSDR 2002).

The most abundant isomer of HCH was γ-HCH, which is also the most toxic isomer (ATSDR 2005). Fagotti et al. (2005) measured 2.38×10^{-3} ng/g wet mass of γ-HCH in *Rana esculenta* (now *Pelophylax esculentus*) from central Italy compared to 6.59 ng/g wet mass mean concentration in *X. muelleri* for the 2014 after spraying survey of this study. Toxicity test results on amphibians vary greatly between sources, most likely due to species differences. The lowest LC_{50} reported was for *Rana limnocharis* (now *Fejervarya limnocharis*), with the LC_{50} being 0.94 mg/L after 48 h exposure (Pan and Liang 1993). Marchal-Ségault and Ramade 1981 indicated reduced time to metamorphosis in *X. laevis* tadpoles exposed to 2 mg/L of γ-HCH. None of these studies however report body burdens in comparison to toxicity, making interpretation of field results complex. The composition of total HCHs by different HCH isomers can indicate the type of HCH used in the system so some extent. Technical grade HCH has a more balanced composition while lindane consists almost solely of γ-HCH. In this system only the first survey samples contained isomers other than γ-HCH. What is interesting is that neither α-HCH (main isomer in technical grade HCH) nor β-HCH (most persistent isomer) were the most prevalent isomers for that survey which alludes to a unique uptake or metabolic scenario for the frogs during this survey. The consistency of lindane accumulation detected throughout the other surveys of this study corresponds with historic lindane use in the area. This possibility of historic use is based on forestry land use in the upper catchment of the river and livestock dipping for ecto-parasites in the floodplain as possible sources.

The increase in total OCPs over the study period suggests recent availability of the compounds in the floodplain aquatic system. Composition changes irregularly along with the increase. There is a general decreasing trend in rainfall over the study period that shows negative correlation with total OCP accumulation. A similar correlation was found between total HCHs and rainfall, which makes sense as this compound group made up a large proportion of the total OCPs in most samples. This evidence leans toward indicating that accumulation of these compounds is driven by the rainfall dilution effect where increased rainfall (i.e. increased water volume) decreases the effective concentration of compounds in a specific water body. This is expected of historical persistent lipophilic compounds in aquatic systems because of changes in the binding to dissolved organic matter as described for b-HCH by Kalbitz et al. (1997). There was however no such correlation between total DDTs and rainfall. This lack of any relationship shows that the pattern of DDT accumulation was not significantly influenced by rainfall. If DDT in this system were mostly from historical use, one would expect negative correlation similar to that found between HCHs and rainfall. If DDT was largely from new input in surrounding areas one would on the other hand expect a positive correlation with rainfall as runoff would be the main input into a water body. The fact that there is no correlation combined with the presence of recent DDT input in some, but not all surveys, could indicate that DDT fluctuations are from specific non-rainfall related input events and that run-off is not such a major pathway for DDT, to significantly increase accumulation in the frogs. However, four surveys are not enough to make conclusive arguments regarding rainfall patterns and correlations. The question is however raised by this data is if run-off is not a major input factor for DDT in this ecosystem, what is? Illegal use or improper handling of DDT in the area has not been documented, but cannot be ruled out.

Biomarker responses

There is a reduction in oxidative damage (MDA and PC) observed in this study, as the anti-oxidant enzyme activity (SOD and CAT) increases. This indicates that the initial oxidative damage was not necessarily caused by overloading of the anti-oxidant system. This introduces the possibility that the anti-oxidant enzyme activity during the first spraying season could have been inhibited. Antioxidant enzyme inhibition has been observed in *Orechromis niloticus* in rivers associated with metal contamination by Carvalho et al. (2012), however none of the OCP concentrations measured in this study have been reported to result in such a response. Banerjee et al. (1999) reported increased SOD and CAT activity in humans with high lindane exposure. In this study however the increase in OCP accumulation between the two seasons where the oxidative stress changes were observed consisted mostly of DDTs. It

is also possible that the specific mixture of contaminants had additive or opposing effects resulting in the observed change. Mixture exposure effects on oxidative stress responses have previously been documented (Kanter and Celik 2011; Melvin et al. 2016). The changes in Ea composition observed could indicate either a dietary change, or a response towards increased stress on the organism. The increased lipid energy storage is generally considered a positive response, however as it is coupled with a decrease in both, protein and carbohydrate storage, as well as a slight increase in ETS activity, it is more likely to be considered a stress response in this instance. There is increasing evidence that persistent pollutants such as OCPs can act as obesogens. La Merrill et al. (2013) discusses the effects and influences that POPs accumulation may have on adipose tissue and vice versa. The authors state that both positive and negative correlations may exist between POPs and adipose tissue mass, but that these correlations are compound specific. La Merrill et al. (2013) also states that the obesogenic effects of contaminants may follow non-monotonic dose-response patterns. Increased body mass or adipose tissue mass might be seen at low doses of a certain compound while higher doses result in cachexia. The lipid energy response seen in the current study may well be due to obesogenic effects, but more research in this area would be needed to fully understand the mechanisms in anurans, and at these levels of accumulation. Melvin et al. (2016) indicated a decrease in glycogen levels of the striped marsh frog (*Limnodynastes peronii*) when exposed to increasing concentrations of wastewater effluent. The change from protein based energy storage to lipid based storage in the current study coincides with an increase in both protein and lipid oxidative damage. An increase in protein damage could lead to reduced protein storage. As this change occurs over the same period as the dramatic increase in lipophilic OCP accumulation, it is possible that the body could increase lipid storage in reaction to exposure to OCPs. The increase in lipid content due to persistent organic pollutant exposure has been documented in fish (Hodson et al. 1992). Even though the specific effects in anurans are not known the evidence does seem to point towards obesogenic effects as stated by La Merrill et al. (2013). All of the observed bioenergetics changes in the present study were only compositional and did not drastically affect the total CEA of *X. muelleri*. The frogs therefore were able to compensate for minor changes in their energy storage and consumption in such a way that their net energy budget remained fairly unchanged leading to the conclusion that their total fitness (as defined by their bioenergetics) was not influenced by the presence of OCPs.

The negative correlation of HSI with γ-HCH accumulation is contradictory towards the results obtained by Melvin et al. (2016) who found a positive correlation towards wastewater effluent exposure, although they also mention several references where both positive and negative trends have been found in fish exposed to wastewater treatment. An increase in HSI would be expected if there is increased xenobiotic metabolism taking place in the liver. This increase in liver mass has been associated with hypertrophy and increased detoxification enzyme activity in fish exposed to various contaminants (Andersson et al. 1987; Banaee et al. 2013) OCPs are however persistent and accumulative (Ritter et al. 1995) and high enough levels could hypothetically cause liver damage rather than being metabolised. The results observed in this study are most likely associated with liver atrophy similar to that reported in Banded Gourami (*Colisa fasciatus*, now *Trichogaster fasciatus*) exposed to γ-HCH (Verma et al. 1975). This atrophy can be the result of oxidative damage evidenced through the PC and MDA analyses results, however histological analysis would be necessary for determination of specific causes. Mchugh et al. 2011 reported histological signs of liver damage such as granular degeneration in tigerfish (*Hydrocynus vitatus*) from the Pongolapoort dam, with a maximum accumulation of 5537.41 ng/g lipid.

As this study was field based the composition of OCPs between individual frogs showed high variation along with their measured responses. The use of multivariate statistics was incorporated in order to determine at which extent each OCP individually and related to each other was correlated with the observed effects. This takes into account the possibility of multiple OCPs having similar or opposite effects within a mixture. There was no clear separation or grouping of samples based on survey through RDA analysis (Figure S2) indicating that observed relationships between any biomarker response and OCP accumulation observed were not driven by survey temporal differences, but rather by individual sample chemical load and composition. The quantification of significant correlations within the data matrix were done through GLM multiple regression (Table 4). Decreased AChE can be a result of neurotoxicity since it is known to be inhibited by pesticides such as organophosphates. The toxic effects may be enhanced for *p,p*-DDE due to its persistence in fatty tissue (Van der Oost et al. 2003), even though the toxicity is generally lower for this compound than for *p,p*-DDT. The decreased MDA response is expected to coincide with increased SOD and/or CAT, however the data suggests that the enzyme activity is not driven by a specific factor, but a combination of compounds regulate the anti-oxidant enzymes with greater variability. The resulting decrease in lipid peroxidation then being a more stable response shows relation to *p,p*-DDE levels, but is not necessarily directly decreased by *p,p*-DDE. Lipid peroxidation is not generally associated with DDE exposure

in fish, but has in some instances shown decreases related to the presence of OCPs, however it has been indicated as an important response to low level environmental toxicants in general (Van der Oost et al. 2003). As fundamental data on anurans are lacking in this regard, all possible associated responses still require investigation. The CEA components also showed relation to both *p,p*-DDT and *p,p*-DDE, which brings slight plausibility to the hypothesis that the changes observed within the CEA data itself were due to stress response. However, without solid evidence this is simply a possibility and cannot be proven. Both protein and carbohydrate energy storage showed negative relation to *p,p*-DDE, meanwhile the components, Ea-lipids and Ec, showed positive responses to *p,p*-DDT levels. Spacie and Hamelink (1982) suggested increased rate of hydrophobic chemical uptake in fish having higher lipid content. Following the logic of this idea available lipid energy storage could have led to higher *p,p*-DDT uptake rates. However, the increased Ec with higher *p,p*-DDT does rather suggest increased physiological stress on the animals due the presence of the parent DDT compound. The conclusions of Spacie and Hamelink (1982) do not account for these Ec changes and is therefore not likely to be applicable to the present study scenario.

The regression analysis results mostly concern DDT, but two low level compounds δ-HCH and α-HCH showed combined influence on the CYP450 responses. As one response was negative and one positive these results show the need for mixture exposure scenario research. Kortenkamp (2007) states that the effect of pesticides that show individual effects can be reduced when these pesticides are combined. The two opposing responses found in the present study, might very well be the case, but it would have to be confirmed through testing. Both an increase and decrease in CYP450 has been related to OCP exposure in different fish (Van der Oost et al. 2003). The δ-HCH–CYP450 response had the best fit of all regressions in the matrix and was the only variable to show significant secondary influence on a biomarker response. The overall composition of chemicals and the absence of these HCH isomers in some surveys however decrease the likelihood of causality being an accurate interpretation without more knowledge on the behaviour of these compounds in mixtures. In general deriving causality from field based observations is an arduous task due to the large number of variables in play, but the distinct correlations found within the matrix of chemical and response data from this study do suggest some form of interconnectivity in the instances described. More data would be required in order to factually attribute these responses to OCP accumulation specifically, but this study does open a line of scientific questioning to be pursued in future research.

Conclusion

There is clear evidence that anurans from the Phongolo River floodplain in South Africa do accumulate OCPs from the aquatic environment. The level of total OCP accumulation has shown an increase over the period of this study and did not correlate to seasonal trends in terms of introduction of Malaria vector control pesticides in the region. This increase did however show a negative correlation with rainfall. A 2 year study is not enough to draw conclusions regarding such a correlation, but is important for future investigations as drought has been a major issue in the region since 2015. It was shown that DDT still enters the aquatic environment and readily accumulates in *Xenopus muelleri*, however DDT accumulation was not seen to relate to rainfall. The DDT levels in the frogs also did not follow a distinct pattern relating to MVC spraying seasons in the area. There is also a strong possibility of biochemical responses towards the presence of these pesticides at sub-lethal concentrations in anurans. The results of this study show that not only the concentrations, but also the specific composition of these pesticide mixtures in the environment should be taken into account in assessing possible biochemical effects they may have on aquatic organisms such as frogs. The biochemical response effects of OCPs in anurans warrants further investigation before any attributions can be made. There is also a need for toxicity testing of these compounds on African anuran species with regards to body burdens and mixture effects. With such data available the use of biomarker responses in biomonitoring studies could prove useful as early warning indications for preventative management of chemical exposure.

Acknowledgements The Authors of this article would like to acknowledge the contributions made by the following people/entities during the course of this study. Edward Netherlands and Lizaan De Necker (sampling), Claire Edwards and Dr. Ruan Gerber (biomarker analysis), and Ichise Pappy (Chemical analysis). This study was made possible through the financial contributions of the Water Research Commission (WRC) of South Africa (Project K5-12185, N.J. Smit, PI). This contribution 203 from the NWU-Water Research Group.

Compliance with ethical standards

Conflict of interest The authors declare that they have no conflict of interest.

References

Amitrano R, Tortora G (2012) Update: anatomy & physiology laboratory manual, 8th Edition. Cengage Learning, Boston, Massachusetts, USA, p 149

Andersson T, Bengtsson BE, Förlin L, Härdig J, Larsson Â (1987) Long-term effects of bleached kraft mill effluents on carbohydrate metabolism and hepatic xenobiotic biotransformationenzymes in fish. Ecotoxocol Environ Safe 13:53–60

ATSDR (Agency for Toxic Substances and Disease Registry) (2002) Toxicological profile for DDT, DDE, and DDD. U.S. Department of Health and Human Services. Agency for Toxic Substances and Disease Registry. http://www.atsdr.cdc.gov/toxprofiles/tp35.pdf. Accessed March 2018

ATSDR (Agency for Toxic Substances and Disease Registry) (2005) Toxicological profile for alpha-, beta-, gamma-, and delta-hexachlorocyclohexane. U.S. Department of Health and Human Services. Agency for Toxic Substances and Disease Registry. http://www.atsdr.cdc.gov/toxprofiles/tp43.pdf. Accessed Feb 2018

Banaee M, Sureda A, Mirvaghefi AR, Ahmadi K (2013) Biochemical and histological changes in the liver tissue of rainbow trout (*Oncorhynchus mykiss*) exposed to sub-lethal concentrations of diazinon. Fish Physiol Biochem 39:489–501

Banerjee BD, Seth V, Bhattacharya A, Pasha ST, Chakraborty AK (1999) Biochemical effects of some pesticides on lipid peroxidation and free-radical scavengers. Toxicol Lett 107:33–47

Bligh EG, Dyer WJ (1959) A rapid method of lipid extraction and purification. Can J Physiol Pharm 37:911–917

Borković-Mitić SS, Prokić MD, Krizmanić II, Mutić J, Trifković J, Gavrić J, Despotović SG, Gavrilović BR, Radovanović TB, Pavlović SZ, Saičić ZS (2016) Biomarkers of oxidative stress and metal accumulation in marsh frog (*Pelophylax ridibundus*). Environ Sci Pollut Res 23:9649–9659

Bouwman H, Van den Berg H, Kylin H (2011) DDT and malaria prevention: addressing the paradox. Environ Health Perspect 119:744–747

Bradford MM (1976) A rapid and sensitive method for the quantitation of microgram quantities of protein utilizing the principle of protein-dye binding. Anal Biochem 72:248–254

Buah-Kwofie A, Humphries MS (2017) The distribution of organochlorine pesticides in sediments from iSimangaliso Wetland Park: ecological risks and implications for conservation in a biodiversity hotspot. Environ Pollut 229:715–723

Carvalho CD, Bernusso VA, de Araújo HSS, Espíndola ELG, Fernandes MN (2012) Biomarker responses as indication of contaminant effect in *Orechromis niloticus*. Chemosphere 89:60–69

Cohen G, Demiec D, Marcus J (1970) Measurement of catalase activity in tissue extracts. Anal Biochem 34:30–38

Cooke AS (1979) The influence of rearing density on the subsequent response to DDT dosing for tadpoles of the frog *Rana temporaria*. Bull Environm Contam Toxicol 21:837–841

De Coen WM, Janssen CR (1997) The use of biomarkers in *Daphnia magna* toxicity testing. IV. Cellular energy allocation: a new methodology to assess the energy budget of toxicant-stressed *Daphnia* populations. J Aquat Ecosyst Stress Recovery 6:43–55

De Coen WM, Janssen CR (2003) The missing biomarker link: relationships between effects on the cellular energy allocation biomarker of toxicant-stressed *Daphnia magna* and corresponding population characteristics. Environ Toxicol Chem 22:1632–1641

Del Meastro RF, McDonald W (1989) Oxidative enzymes in tissue homogenates, Chapter 4. In: Greenwald RA (Ed.) CRC handbook of methods for oxygen radical research, 3rd ed. CRC Press, Boca Raton, p 291–293

Du Preez LH, Carruthers V (2017) Frogs of Southern Africa: a complete guide. Struik Nature, Random House Struik, Cape Town

Dube T, Wepener V, Van Vuren JHJ, Smit NJ, Brendonck L (2016) The case for environmental flow determination for the Phongolo River, South Africa. Afr J Aquat Sci 40:269–276

Ellman GL, Courtney KD, Andres Jr V, Featherstone RM (1961) A new and rapid colorimetric determination of acetylcholinesterase activity. Biochem Pharmacol 7:88–95

Eriyamremu GE, Osagie VE, Omoregie SE, Omofoma CO (2008) Alterations in glutathione reductase, superoxide dismutase, and lipid peroxidation of tadpoles (*Xenopus laevis*) exposed to Bonny Light crude oil and its fractions. Ecotox Environ Safe 71:284–290

Fagotti A, Morosi L, De Rosa I, Clarioni R, Simoncelli F, Pascolini R, Pellegrino R, Guex G, Hotz H (2005) Bioaccumulation of organochlorine pesticides in frogs of the *Rana esculenta* complex in central Italy. Amphib-Reptil 26:93–104

Falfushinska HI, Romanchuk LD, Stolyar OB (2008) Different responses of biochemical markers in frogs (Rana ridibunda) from urban and rural wetlands to the effect of carbamate fungicide. Comp Biochem Physiol C 148:223–229

Gaspar FW, Chevrier J, Bornman R, Crause M, Obida M, Barr DB, Bradman A, Bouwman H, Eskenazi B (2016) Corrigendum to "Undisturbed dust as a metric of long-term indoor insecticide exposure: residential DDT contamination from indoor residual spraying and its association with serum levels in the VHEMBE cohort" [Environ. Int. 85C (2015) 163–167]. Environ Int 94:778–783

Gerber R, Smit NJ, Van Vuren JHJ, Nakayama SMM, Yohannes YB, Ikenaka Y, Ishizuka M, Wepener V (2016) Bioaccumulation and human health risk assessment of DDT and other organochlorine pesticides in an apex aquatic predator from a premier conservation area. Sci Total Environ 550:522–533

Gerber R, Smit NJ, Van Vuren JHJ, Ikenaka Y, Wepener v (2018) Biomarkers in tigerfish (*Hydrocynus vittatus*) as indicators of metal and organic pollution in ecologically sensitive subtropical rivers. Ecotox Environ Safe 157:307–317

Hodson PV, Thivierge D, Levesque M, McWhirter M, Ralph K, Gray B, Whittle DM, Carey JH, Van Der Kraak G (1992) Effects of bleached kraft mill effluent on fish in the St. Maurice River, Quebec. Environ Toxicol Chem 11:1635–1651

Jofré MB, Antón RI, Caviedes-Vidal E (2008) Organochlorine contamination in Anuran Amphibians of an artificial lake in the semiarid midwest of Argentina. Arch Environ Contam Toxicol 55:471–480

Kalbitz K, Popp P, Geyer W, Hanschmann G (1997) β-HCH mobilization in polluted wetland soils influenced by dissolved organic matter. Sci Total Environ 204:37–48

Kanter A, Celik I (2011) Acute effects of fenthion on certain oxidative stress biomarkers in various tissues of frogs (*Rana ridibunda*). Toxicol Ind Health 28:369–376

Kortenkamp A (2007) Ten years of mixing cocktails: a review of combination effects of endocrine-disrupting chemicals. Environ Health Perspect 115:98–105

Lambert MRK (2001) Residue loads in amphibians used as biomarkers of pesticide levels entering food chains in Sub-Saharan Africa. Afr J Herpetol 50:105–114

La Merrill M, Emond C, Kim MJ, Antignac J, Le Bizec B, Clément K, Birnbaum LS, Barouki R (2013) Toxicological function of adipose tissue: focus on persistent organic pollutants. Environ Health Perspect 121:162–169

Lindholm M, Hessen DO, Mosepele K, Wolski P (2007) Food webs and energy fluxes on a seasonal floodplain: the influence of flood size. Wetlands 27:775–784

Mallory S (2002) Overview of the water resources of the Usutu-Mhlathuze water management area. Final report, Department: Water Affairs and Forestry of South Africa, Pretoria

Marchal-Ségault D, Ramade F (1981) The effects of lindane, an insecticide, on hatching and postembryonic development of *Xenopus laevis* (Daudin) Anuran amphibian. Environ Res 24:250–258

Melvin SD, Lanctôt CM, Van de Merwe JP, Leusch FDL (2016) Altered bioenergetics and developmental effects in striped marsh frog (*Limnodynastes peronii*) tadpoles exposed to UV treated sewage. Aquat Toxicol 175:30–38

Monastersky R (2014) Life—a status report. Nature 516:158–161

Mchugh KJ, Smit NJ, Van Vuren JHJ, Van Dyk JC, Bervoets L, Covaci A, Wepener V (2011) A histology-based fish health assessment of the tigerfish, *Hydrocynus vittatus* from a DDT-affected area. Phys Chem Earth 36:895–904

Pan D, Liang X (1993) Safety study of pesticide on bog frog, a predatory natural enemy of pest in paddy field. J Hunan Agric Coll 19:47–54

Netherlands EC, Cook CA, Kruger DJD, Du Preez LH, Smit NJ (2015) Biodiversity of frog haemoparasites from sub-tropical northern KwaZulu-Natal, South Africa. Int J Parasitol Parasites Wildl 4:135–141

Parves S, Riasuddin S (2005) Protein carbonyls, novel biomarkers of exposure to oxidative stress inducing pesticides in freshwater fish *Channa punctata* (Bloch). Environ Toxicol Phar 20:112–117

Pauli BD, Perrault JA, Money SL (2000) RATL: a database of reptile and amphibian toxicology literature. Technical Report Series No. 357. Canadian Wildlife Service, Québec

Prokić MD, Borković-Mitić SS, Krizmanić II, Mutić JJ, Vukojević V, Mohammed Nasia M, Gavrić JP, Despotović SG, Gavrilović BR, Radovanović TB, Pavlović SZ, Saičić ZS (2016) Antioxidative responses of the tissues of two wild populations of *Pelophylax esculentus* frogs to heavy metal pollution. Ecotox Environ Safe 128:21–29

Ritter L, Solomon KR, Forget J, Stemeroff M, O'Leary C (1995) Persistent organic pollutants, an assessment report on: DDT, Aldrin, Dieldrin, Endrin, Chlordane, Heptachlor, Hexachlorobenzene, Mirex, Toxaphene, Polychlorinated Biphenyls, Dioxins, and Furans. PCS 95.39. Final Report. International Programme on Chemical Safety, Guelph

Schoenaers S, Vergauwen L, Hagenaars A, Vanhaecke L, AbdElgawad H, Asard H, Covaci A, Bervoets L, Knapen D (2016) Prioritization of contaminated watercourses using an integrated biomarker approach in caged carp. Water Res 99:129–139

Spacie A, Hamelink JL (1982) Alternative models for describing the bioconcentration of organics in fish. Environ Toxicol Chem 1:309–320

Strandberg B, Hites RA (2001) Concentration of organochlorine pesticides in Wine Corks. Chemosphere 44:729–735

Thompson LA, Ikenaka Y, Yohannes YB, Van Vuren JHJ, Wepener V, Smit NJ, Darwish WS, Nakayama SMM, Mizukawa H, Ishizuka M (2017) Concentrations and human health risk assessment of DDT and its metabolites in free-range and commercial chicken products from KwaZulu-Natal, South Africa. Food Add Contam 34:1959–1969

UNEP (2010) The 9 new POPs, an introduction to the nine chemicals added to the Stockholm Convention by the Conference of the Parties at its fourth meeting. United Nations Environment Programme (UNEP). chm.pops.int. Accessed Feb 2018

Üner N, Oruç EO, Sevgiler Y, Şahin N, Durmaz H, Usta D (2006) Effects of diazinon on acetylcholinesterase activity and lipid peroxidation of *Oreochromis niloticus*. Environ Toxicol Phar 21:241–245

Van der Oost R, Beyer J, Vermeulen NPE (2003) Fish bioaccumulation and biomarkers in environmental risk assessment: a review. Environ Toxicol Phar 13:57–149

Van Dyk JC, Bouwman H, Barnhoorn IEJ, Bornman MS (2010) DDT contamination from indoor residual spraying for malaria control. Sci Total Environ 408:2745–2752

Velisek J, Stara A, Li Z, Silovska S, Turek J (2011) Comparison of the effects of fouer anaesthetics on blood biochemical profiles and oxidative stress biomarkers in rainbow trout. Aquaculture 310:369–375

Verhaert V, Covaci A, Bouillon S, Abrantes K, Musibono D, Bervoets L, Verheyen E, Blust R (2013) Baseline levels and trophic transfer of persistent organic pollutants in sediments and biota from the Congo River Basin (DR Congo). Environ Int 59:290–302

Verhaert V, Newmark N, D'Hollander W, Covaci A, Vlok W, Wepener V, Addo-Bediako A, Jooste A, Teuchies J, Blust R, Bervoets L (2017) Persistent organic pollutants in the Olifants River Basin, South Africa: bioaccumulation and trophic transfer through a subtropical aquatic food web. Sci Total Environ 586:792–806

Verma SR, Gupta SP, Tyagi MP (1975) Studies on the toxicity of Lindane on Colisa fasciatus (part I: TLm measurements and histopathological changes in certain tissues). Gegenbaurs Morphol Jahrb 121:38–54

Viljoen IM, Bornman R, Bouwman H (2016) DDT exposure of frogs: a case study from Limpopo Province, South Africa. Chemosphere 159:335–341

Worldweatheronline (2016) Ndumo, KwaZulu-Natal Monthly Climate Average, South Africa. https://www.worldweatheronline.com/ndumo-weather-averages/kwazulu-natal/za.aspx. Accessed May 2017

Wepener V, Smit NJ, Covaci A, Dyke S, Bervoets L (2012) Seasonal bioaccumulation of organohalogens in tigerfish, hydrocynus vittatus castelnau, from Lake Pongolapoort, South Africa. Bull Environ Contam Toxicol 88:277–282

Yohannes YB, Ikenaka Y, Ito G, Nakayama SMM, Mizukawa H, Wepener V, Smit NJ, Van Vuren JHJ, Ishizuka M (2017) Assessment of DDT contamination in house rat as a possible bioindicator in DDT-sprayed areas from Ethiopia and South Africa. Environ Sci Pollut Res 24:23763–23770

Yohannes YB, Ikenaka Y, Nakayama SMM, Saengtienchai A, Watanabe K, Ishizuka M (2013) Organochlorine pesticides and heavy metals in fish from Lake Awassa, Ethiopia: insights from stable isotope analysis. Chemosphere 91:857–863

Chemosphere 225 (2019) 647–658

Contents lists available at ScienceDirect

Chemosphere

journal homepage: www.elsevier.com/locate/chemosphere

Evidence of impacts from DDT in pelican, cormorant, stork, and egret eggs from KwaZulu-Natal, South Africa

H. Bouwman [a, *, 1], Y.B. Yohannes [b, c, 1], S.M.M. Nakayama [b], K. Motohira [b], M. Ishizuka [b], M.S. Humphries [d], V. van der Schyff [a], M. du Preez [a], A. Dinkelmann [a], Y. Ikenaka [a, b]

[a] Research Unit, Environmental Sciences and Management, North-West University, Potchefstroom, 2520, South Africa
[b] Laboratory of Toxicology, Department of Environmental Veterinary Sciences, Graduate School of Veterinary Medicine, Hokkaido University, Sapporo, Hokkaido, Japan
[c] Department of Chemistry, College of Natural and Computational Science, University of Gondar, Gondar, Ethiopia
[d] Molecular Sciences Institute, School of Chemistry, University of the Witwatersrand, Johannesburg, South Africa

HIGHLIGHTS

- Eggs of four predatory aquatic bird species from KwaZulu-Natal analysed for DDTs.
- Concentrations were similar or lower in KwaZulu-Natal than in Limpopo province.
- DDT composition suggest pelicans feeding from different food web than other species.
- Strong evidence of eggshell thinning associated with DDT for pelican eggs.
- Urgent efforts to reduce or eliminate DDT for malaria control needed.

GRAPHICAL ABSTRACT

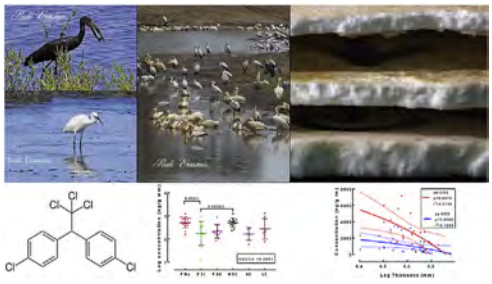

ARTICLE INFO

Article history:
Received 24 December 2018
Received in revised form
7 March 2019
Accepted 8 March 2019
Available online 12 March 2019

Handling Editor: J. de Boer

Keywords:
Eggshell thinning
DDE
DDD
DDT
Effects
Malaria control

ABSTRACT

DDT remains in use for malaria control in South Africa. We quantified DDTs in aquatic bird eggs from the highly biodiverse northern KwaZulu-Natal, a province of South Africa where DDT has been used for more than 80 years for malaria control. Pelican eggs had the highest ΣDDT concentration (7200 ng/g lipid mass; lm), Little Egret eggs had 6900 ΣDDT lm, African Openbill eggs had 3400 ng/g lm ΣDDT, and White-breasted Cormorant had 2400 ng/g lm. All species had non-significantly different mean concentrations of *o,p'*-DDT, *p,p'*-DDT, and ΣDDT, but with significant differences for *p,p*-DDE, *o,p'*-DDD, *p,p'*-DDD, %DDT, %DDD, and %lipid. The thinnest pelican eggshell (0.40 mm) had a ΣDDT concentration of 3300 ng/g lm.; the thickest shell (0.96 mm) had the lowest ΣDDT concentration at 29 ng/g lm; a 58% difference. Linear regressions of concentrations with shell thickness for the pelican eggs were significant for *p,p'*-DDE and *p,p'*-DDD, indicating risk of reproductive impairment. Compositional profiles indicate different food webs for the different species. DDT concentrations were lower than from another DDT-sprayed locality in South Africa, possible linked to differences in hydrology and rainfall. We conclude that significant ecotoxic threats associated with DDT remain in this area, and possibly threatens birds from less polluted areas. Our findings suggest continued negative human health and environmental impacts from

* Corresponding author.
E-mail address: henk.bouwman@nwu.ac.za (H. Bouwman).
[1] Both authors contributed equally.

https://doi.org/10.1016/j.chemosphere.2019.03.043

DDT. There is an urgency to move away from DDT as quickly as possible; alternatively, to implement practices that prevent emissions of DDT to the environment while protecting human life.

1. Introduction

Despite decades of continuous efforts to combat malaria using DDT in many areas of the world, remarkably little is known of its environmental impacts in such areas compared with developed countries where DDT has primarily been used in agriculture. DDT is a legacy pesticide albeit with a remaining legal use for malaria control in some African countries (Stockholm Convention, 2018). Between 2001 and 2014, South Africa reported 603 metric tons of active ingredient compared with 53,933 metric tons reported globally – the latest figure likely an underestimation due to incomplete data (Van den Berg et al., 2017). DDT use in neighbouring Mozambique was 1340 tons active ingredient between 2005 and 2011, and nothing between 2012 and 2014 (Van den Berg et al., 2017). No more recent data is publicly available, and no data at all on provincial use, including Maputo Province in Mozambique that borders KwaZulu-Natal, a province of South Africa, to the south (Fig. 1).

Intensive use of DDT to combat malaria transmission has led to widespread contamination where applied, in adjacent areas (Bouwman et al., 2015; Van Dyk et al., 2010; Barnhoorn et al., 2009), and even farther away (Garcia-Heras et al., 2018). We previously reported very high concentrations of DDT in bird eggs from the Limpopo province, South Africa, where health authorities use DDT and other insecticides as indoor residual spraying (IRS) to prevent malaria transmission (Fig. 1; Bouwman et al., 2013). Significant eggshell thinning in eggs of Cattle Egrets *Bubulcus ibis* (33% between thickest and thinnest) was associated with increasing but low concentrations of *p,p'*-DDT and *p,p'*-DDE (means between 20 and 290 ng/g wm). In addition, very high concentrations of DDT were found in eggs of Grey Heron *Ardea cinerea,* with a mean of 13,000 ng/g wm and a maximum of 24,000 ng/g wm (Bouwman et al., 2013). Within the IRS area of Limpopo, no breeding colonies of any aquatic birds could be located, a great cause of concern due to its proximity to the Kruger National Park, the largest national park in South Africa (Fig. 1). We deduced that the high DDT concentrations were likely responsible for the absence of colonially-breeding aquatic birds within the IRS area (Bouwman et al., 2013). In the same publication we predicted that similar pollution profiles would be found at other malaria areas in South Africa where DDT is sprayed (Bouwman et al., 2013), including the northern parts of KwaZulu-Natal, a province located approximately 520 km south-east of the Limpopo province (Fig. 1).

The northern regions of KwaZulu-Natal are rich in biodiversity with many nature reserves (Fig. 1). This region is the most southern part of the great Mozambique Coastal Plain, making it the southernmost distribution of many tropical animal and plant species, and is therefore of considerable scientific and conservation interest (Cooper, 1980). The Ndumo Game Reserve (NGR; Fig. 1) in particular boasts with 462 bird species (65% of the total for South Africa). Rare species such as Neergaard's Sunbird *Nectarinia neergaardi*, Saddle-billed Stork *Ephippiorhynchus senegalensis*, the African Openbill stork *Anastomus lamelligerus*, and both of Africa's pelican species (the Pink-backed Pelican *Pelecanus rufescens* and Great White Pelican *P. onocrotalus*) breed here. The iSimangaliso Wetland Park (iSWP; Fig. 1) has a bird list of 520 species (https://isimangaliso.com), including both pelican species and a variety of marine birds.

Fish collected from pans (floodplain lakes) from the Phongolo Floodplain in northern KwaZulu-Natal in 1985/86 clearly indicated bioaccumulation of DDTs (Bouwman et al., 1990). The most recent reports from KwaZulu-Natal on DDT in fish-eating birds (Evans and Bouwman, 1993, 2000) were based on Pied Kingfisher *Ceryle rudis* blood and tissues. Extrapolating from the highest blood concentrations indicated that *p, p'*-DDE concentrations in Pied Kingfisher eggs could be as high as 4200 ng/g wm. In Brown Pelican *P. occidentalis* eggs, *p,p'*-DDE concentrations of 2500–3000 ng/g wm have been associated with substantially impaired reproductive success, while 4000 ng/g wm have been linked with total reproductive failure (Blus, 1982). The highest extrapolated Pied Kingfisher egg concentrations exceeded these levels, indicating reproductive risk to Pied Kingfishers (Evans and Bouwman, 2000) and other piscivorous birds in this region. In the intervening 30 years, no work has been done on wild birds from KwaZulu-Natal.

Other work from the northern parts of KwaZulu-Natal has added to the concerns about the threats that continued use of DDT poses to wildlife. DDT has been found in high concentrations in crocodile fat (Buah-Kwofie et al., 2018a) and fish (Buah-Kwofie et al., 2018b) from the iSWP, in fish from the Phongolo River upstream and inside the NGR (Bouwman et al., 1990; Smit et al., 2016; Wepener et al., 2012), and in frogs from NGR (Wolmerans et al., 2018). High concentrations of DDT associated with malaria control in the environment and wildlife coincide with human exposures, including via locally grown food (Buah-Kwofie et al., In review). We previously reported very high DDT concentrations in breast milk from breastfeeding mothers living in areas where DDT is used for IRS in the KwaZulu-Natal and Limpopo provinces (Bouwman et al., 1994, 2012), partly mediated through consumption of free-roaming chickens and their eggs (Van Dyk et al., 2010; Gyalpo et al., 2012; Thompson et al., 2017). DDT in chickens from IRS areas in KwaZulu-Natal affected mRNA expression of genes involved in immune suppression, endocrine-disruption, and lipid dysregulation (Thompson et al., 2018). These findings confirm birds as important and relevant indicators of human and environmental health.

DDT is a well-established threat to bird reproduction (Peakall et al., 1973; Blus, 1982; Cooper, 1991; Lundholm, 1997; USDoI, 1998). Given the findings of previous studies conducted on people and biota, the lack of data on DDT in bird eggs from the biodiverse KwaZulu-Natal region where DDT is used are therefore of great concern. The aim of this study was to collect, analyse, and interpret current concentrations of DDT in colonial aquatic birds from two key breeding sites in KwaZulu-Natal; NGR, and iSWP.

2. Materials and methods

2.1. Location, egg collection, and species

We collected eggs from the north-eastern part of KwaZulu-Natal (Fig. 1), where DDT and pyrethroids are used for malaria control. More information on how DDT is applied for malaria control can be obtained from Bornman et al. (2012) and Bouwman et al. (2012).

Permissions to collect eggs in KwaZulu-Natal were obtained from Ezemvelo KZN Wildlife (OP 1186/2013 and OP 4105/2013) and iSimangaliso Wetland Park Authority. The study received ethical

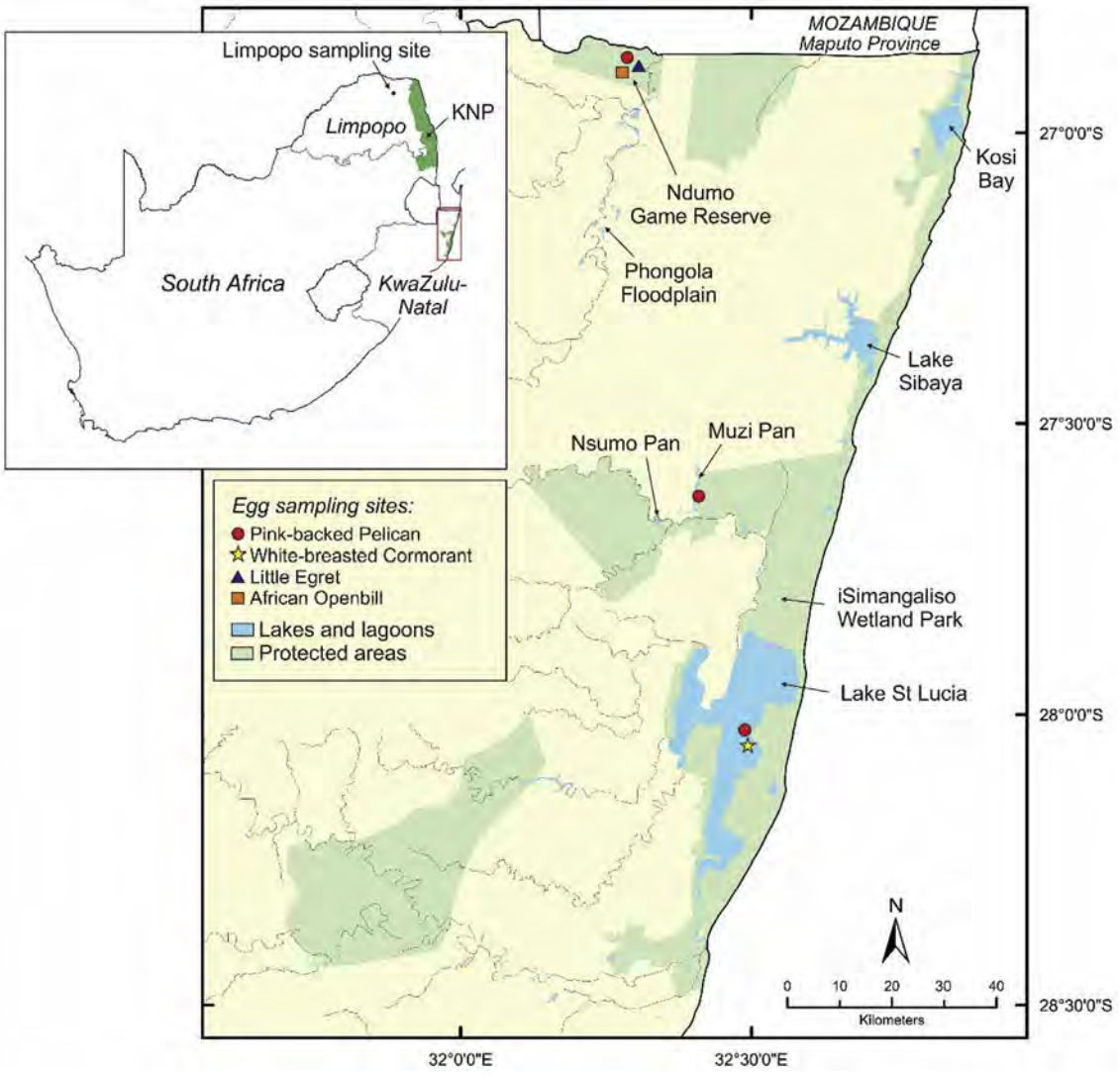

Fig. 1. Locations of sampling sites, and other sites mentioned in text.

clearance from the North-West University (NWU-00055-07-A3) and the University of the Witwatersrand (AESC-20133,201). DDT has been used in this area for malaria control since the 1950s, with an interruption between 1996 and 2000 when pyrethroids exclusively were used, and thereafter a combination of DDT and pyrethroids (Bouwman et al., 2012).

Breeding colonies were located in 2013 with the help of game wardens. We were restricted in the number of eggs we could collect due to scarcity of breeding pelicans and African Openbill *A. lamelligerus* in South Africa, and the need not to disturb the breeding of co-located species. The climbing difficulty of the trees as well as safety (crocodile and hippo) restricted access to some colonies. We collected eggs from nests by scaling trees using rock-climbing gear and a double-belay system and not disturbing other nesting birds. The eggs were wrapped in clean foil or in plastic bags, and kept on ice until frozen.

We collected 59 eggs of four different colonially-breeding aquatic bird species from three sites (Fig. 1). At NGR, we collected 11 Pink-backed Pelican *P. rufescens*, five African Openbill, and seven Little Egret *Egretta garzetta* eggs. From St. Lucia in the iMWP, we collected 11 White-breasted Cormorant *Phalacrocorax lucidus* and 10 Pink-backed Pelican eggs, and 15 Pink-backed Pelican eggs from Muzi Pan. All the bird species belong to the Order Ciconiiformes that includes grebes, herons, storks, and penguins, all of which are predatory (mostly piscivore) birds - except flamingos.

The following descriptions and dimensions (given here as means) are from Hockey et al. (2005), Tarbotton (2011), and Bowker and Downs (2012) to provide background on size, breeding, movement, and trophic levels that will be used in interpretation of the results from the present study. The information available is limited since very little biological work has been done on these species in southern Africa. There are no systematic programmes to record breeding sites and attempts for any bird species in South Africa, so the breeding site records and attempts are very likely under-reported.

- Pink-backed Pelicans are rather large birds, weighing up to 6 kg with a wingspan of up to 2.9 m. Females catch small tilapia and other small fish, with an estimated daily intake of 780 g. One to four eggs are laid per clutch. Although they are considered non-migratory, they do move roam over large distances. In northern KwaZulu-Natal, they breed irregularly, seemingly shifting between breeding sites according to conditions. There are 66 breeding records from seven sites in northern KwaZulu-Natal

between 1920 and 2010; only two records were from NGR, 25 from Nsumu Pan, near Muzi Pan, and one from iSWP.

- African Openbills (commonly called the Openbilled Stork in South Africa) have a length of 1.1 m and weighs about 1.1 kg. They have a large, vice-like bill with an opening in the middle. The bill is used to locate and catch mainly large molluscs under water. They pry open the shells and extract the flesh with their sharp lower mandible, or leave large bivalves (50–60 mm) exposed outside of water, until they open. They do not crack the shells with their bills. They lay three to four eggs per clutch. There are three breeding records from three sites in northern KwaZulu-Natal between 1920 and 2010; one record from NGR, one from Nsumu Pan, and one from iSWP. Therefore, although they are non-migratory, there does not seem to be a large degree of site-fidelity.
- Little Egrets are 65 cm long, weighs about 520 g, and catch food in shallow water, mainly fish up to 14 g per day, but also frogs, insects, worms, and crustaceans. A clutch consists of two to four eggs. There are nine breeding records from seven sites in northern KwaZulu-Natal between 1920 and 2010; no sites from NGR, three from iSWP, and the rest outside these reserves.
- The White-breasted Cormorant is very similar to the Great Cormorant *P. carbo* that has a wide distribution, including Europe. It is 90 cm long, weighs approximately 2 kg and has a wingspan of 1.9 m. Their diet consists mainly of fish, usually 10–20 g in size, which they catch while swimming underwater. The clutch size is usually between three and four. There are 49 breeding records from 18 sites in northern KwaZulu-Natal between 1920 and 2010; 1 site from NGR, 37 from iSWP, and the rest outside these reserves. As for the other species, although non-migratory, individuals breed at different sites according to conditions and opportunity.

2.2. Egg analyses

Standards of DDTs (*o,p'*-DDT, *p,p'*-DDT, *o,p'*-DDE, *p,p'*-DDE, *o,p'*-DDD and *p,p'*-DDD), surrogate standard (PCB 77), and internal standard (2,4,5,6-tetrachloro-m-xylene) were obtained from Dr. Ehrenstorfer Laboratories (Augsburg, Germany). Acetone, *n*-hexane and dichloromethane were of pesticide grade, and anhydrous sodium sulfate was specific for pesticide residue analysis (Kanto Chemical Corp, Tokyo, Japan). Florisil (60–100 mesh) (Kanto Chemical Corp, Tokyo, Japan) was activated at 130 °C overnight before use (5% deactivation with water).

Sample preparation and chemical analyses of DDTs were done in the Laboratory of Toxicology at the Hokkaido University, Graduate School of Veterinary Medicine, Japan. Determination of DDTs in egg samples was performed as described by Yohannes et al. (2017) with minor modifications. Approximately 0.5 g of egg content was homogenized with anhydrous sodium sulfate, spiked with surrogate standard (PCB 77), and Soxhlet extracted with 150 ml hexane/acetone (3:1 v/v) in hot extraction mode for 4 h. The lipid content was determined gravimetrically from an aliquot of the extract. Another aliquot of the extract used for chemical analysis was subjected to gel permeation chromatography for lipid removal. The lipid free eluate was concentrated and further purified on a column filled with 4 g Florisil (5% deactivated). The final eluate was concentrated to near dryness, reconstituted in 100 μL *n*-decane, and spiked with internal standard (2, 4, 5, 6-tetrachloro-*m*-xylene) prior to instrumental analysis.

Gas chromatographic (GC) analysis was performed using a Shimadzu 2014 gas chromatograph equipped with ^{63}Ni electron capture detector (Shimadzu, Kyoto, Japan) and ENV−8MS capillary column (30 m × 0.25 mm inner diameter, with a 0.25 μm film thickness). Helium at a flow rate of 1.0 mL/min and nitrogen at 45 mL/min were used as carrier and make-up gasses, respectively. Splitless injection of 1 μl was used with the following temperature programme: 100 °C (1 min hold time), 20 °C/min to 200 °C, 3 °C/min to 260 °C with 10 min hold time. The injection port and detector temperatures were 250 °C and 310 °C, respectively.

DDTs were identified by comparing their retention time with the corresponding standards, and multi-level calibration curves ($r^2 > 0.995$) were created for quantification. Confirmation of target residues on representative samples was performed using a Thermo Scientific DSQ II single stage quadrupole GC-MS system. The quality control and quality assurance were performed by analyses of procedural blanks, spiked blanks, and blind duplicate samples. Recovery for individual DDTs was between 90% and 105%, and average recovery for the surrogate PCB 77 standard was 90 ± 9%. The limit of detection (LOD) was set at a signal-to-noise ratio (S/N) of 3, ranged from 0.05 to 0.2 ng/g. Data are reported as ng/g wet mass (wm), and ng/g lipid mass (lm). Since embryo development affects lipid composition (Romanoff, 1932), we mainly base our discussions on wet mass.

2.3. Eggshell thickness

The possible association between DDT and eggshell thickness was investigated only for pelicans as we had more eggs of this species than the others (Table 1). The shells were gently washed, the membrane removed, and allowed to air-dry for at least three weeks. The thickness was measured at three locations on the equator with a Kroeplin electronic digital calliper (accurate to 0.01 mm) and the mean used for further calculations.

2.4. Statistics

%DDT and %DDD were calculated according to the percentage of *p,p'*-DDT and *p,p'*-DDD of the sum of all DDT compounds, for each egg. GraphPad Prism version 7.04 for Windows (www.graphpad.com) was used for descriptive data analyses per species and breeding site (three sites for pelicans collected at three different colonies, and one each for the other species). Because data were not normally distributed, log-transformed concentrations of the DDTs, ΣDDT, and %DDT were compared using ANOVA, with multiple post-test comparisons using Tukey.

To ordinate the differences and similarities of the DDT composition of each sample, species, and collection site relative to each other, we used MjM Software PC-ORD version 7.03 (www.pcord.com). We chose nonmetric multidimensional scaling (NMS) that avoids the assumption of linear relationships between variables (in this case, covariance of related compounds such as the DDTs) using ranked distances to linearise the relationships between measured distances in ordination space. Concentrations were relativised per egg to investigate pollutant profiles (fingerprints) rather than absolute concentrations. Gower-ignore-0, was used as distance measure. From random starting configurations, we allowed a maximum of six dimensions and 500 iterations, using 250 runs of real data. When the standard deviation of the stress of the last ten runs reached <0.0001, a stable ordination was assumed. Monte Carlo tests were done with 250 runs of randomised data. Convex hulls for each species were drawn to assess congruence (overlap) of proportional contributions ('fingerprints') of the analysed compounds.

Table 1
Summary statistics for DDT concentrations in eggs analysed from KwaZulu-Natal. P Mu = Pelican eggs from Muzi Pan. P St = Pelican eggs from St. Lucia. P Nd = Pelican eggs from Ndumu Game reserve. WBC = White-breasted Cormorant eggs. AO = African Openbill eggs. LE = Little Egret eggs.

n		Wet mass (ng/g)							Lipid mass (ng/g)					
		P Mu	P St	P Nd	WBC	AO	LE		P Mu	P St	P Nd	WBC	AO	LE
		15	10	11	11	5	7		15	10	11	11	5	7
p,p'-DDE	Min	160	13	84	240	60	79		650	50	1500	1200	1100	1700
	Median	510	180	190	570	170	220		1800	1000	4000	1900	2500	3000
	Max	1200	990	870	1200	300	1300		5100	4200	14,000	5700	3900	15,000
	Mean	580	290	280	570	190	450		2000	1100	4700	2220	2500	6100
	SD	270	280	230	280	93	490		1100	1200	3700	1200	1100	5400
o,p'-DDD	Min	0.074	<LOQ	3.2	0.82	7.7	3.7		0.23	11	88	4.3	120	44
	Median	1.1	12	15	1.2	12	5.8		4	43	260	4.4	150	84
	Max	11	21	25	1.5	18	14		44	83	620	6.7	290	160
	Mean	2.6	12	15	1.2	12	5.8		9	47	270	5.1	170	93
	SD	3.7	7.3	8.0	0.32	3.9	3.8		13	22	170	1.4	67	45
o,p'-DDT	Min	6.5	0.88	4.6	4.7	5.4	7.3		23	3.1	78	19	73	87
	Median	13	12	11	13	15	10		37	39	170	49	210	130
	Max	18	24	17	18	18	14		94	78	400	82	280	270
	Mean	13	12	11	13	14	10		45	43	190	49	200	160
	SD	3.8	6.2	3.7	4.7	5.2	2.3		19	24	88	20	81	76
p,p'-DDD	Min	39	14	22	<LOQ	6.1	2.7		160	50	500	<LOQ	120	34
	Median	130	130	89	5.9	12	9.4		480	500	880	22	140	170
	Max	780	1000	370	12	29	27		3200	4400	3500	71	390	390
	Mean	180	250	100	7.0	14	11		670	960	1700	30	200	180
	SD	190	300	96	3.7	8.7	8.0		790	1300	1200	22	120	130
p,p'-DDT	Min	8.3	0.85	5.0	3.1	9.7	7.4		23	3.0	94	7.8	120	95
	Median	18	32	12	15	16	20		56	107	200	49	300	260
	Max	36	70	41	31	47	46		190	280	1500	120	560	850
	Mean	19	34	16	16	22	22		71	120	320	64	300	350
	SD	9	22	12	8.7	15	15		44	83	390	39	190	270
ΣDDT	Min	230	29	120	270	100	100		940	100	2700	1400	2000	2000
	Median	670	420	330	590	240	260		2400	1800	5700	1900	3700	3500
	Max	2100	2100	1300	1300	350	1400		8400	9100	20,000	5900	4700	17,000
	Mean	800	590	420	600	250	500		2800	2200	7200	2400	3400	6900
	SD	440	600	330	280	100	500		1800	2600	5100	1300	1100	5700
%DDT	Min	0.86	3.0	2.6	0.47	2.8	3.2	%DDD	12	27	10		2.9	1.5
	Median	3.0	6.6	3.5	2.0	11	5.1		19	40	20	0.94	5.7	2.1
	Max	6	14	7.3	7.9	15	9.2		38.04	53	36	3.8	8.4	6.5
	Mean	3.0	6.8	3.9	3.1	9.5	5.7		20	40	24	1.0	5.7	3.1
	SD	1.6	3.1	1.3	2.4	5.5	2.2		8.395	10	9.0	1.1	1.9	1.8
Eggshell thickness (mm)	Min	0.61	0.69	0.40	0.39	0.32	0.24	Percentage Lipid	1.9	1.8	2.8	1.6	5.2	3.2
	Median	0.70	0.74	0.54	0.43	0.39	0.27		2.9	2.9	5.4	2.7	7.4	7.8
	Max	0.8	0.96	0.6	0.58	0.43	0.31		3.8	4.4	15	4.0	8.8	9.0
	Mean	0.70	0.78	0.53	0.46	0.37	0.27		2.9	2.8	6.6	2.7	7.2	6.9
	SD	0.065	0.09	0.055	0.060	0.044	0.024		0.51	0.71	3.8	0.71	1.5	2.4

3. Results

3.1. Analytical and statistical results

All compounds occurred at detectable quantities in all eggs, except *o,p'*-DDD in one Pink-backed Pelican egg from St. Lucia, two pelican eggs from Muzi Pan, eight White-breasted Cormorant eggs, one Little Egret egg, and *p,p'*-DDD in two White-breasted Cormorant eggs (Table 1; Fig. 2). Pelican eggs from Muzi Pan had the highest wet mass concentrations of *p,p'*-DDE and ΣDDT. Pelican eggs from St. Lucia had the highest *p,p'*-DDD and *p,p'*-DDT, pelican eggs from NGR had the highest *o,p'*-DDD. African Openbill eggs had the highest mean *o,p'*-DDT and %DDT. On a lipid mass (lm) basis, pelican eggs from NGR had the highest concentrations for *o,p'*-DDD, *p,p'*-DDD, *p,p'*-DDT and ΣDDT (Table 1). The smallest bird, the Little Egret, had the highest mean *p,p'*-DDE concentration at 6100 ng/g lm, but lower concentrations of the other compounds relative to the other birds. The data of one White-breasted Cormorant egg was excluded as an outlier from all stats, as the concentration of *p,p'*-DDE was exceedingly high at 7900 ng/g wm. The concentrations of the other compounds were <LOQ for *o,p'*-DDD and *p,p'*-DDD, 18 ng/g wm for *o,p'*-DDT, and 16 ng/g wm for *p,p'*-DDT. *o,p'*-DDE was never detected.

There were no significant differences in concentrations shown by Tukey post-tests between any of the species for log-transformed *o,p'*-DDT, *p,p'*-DDT, and ΣDDT (Fig. 2). However, differences between species and pelican collection sites, especially for *o,p'*-DDD and *p,p'*-DDD were observed (Fig. 2B and D). On a log-scale, the three non-pelican species all had significantly lower mean concentrations of *p,p'*-DDD compared with the pelicans from any site. Significant differences in %DDT (Fig. 2G) were mainly driven by differences in *p,p'*-DDE, not *p,p'*-DDT (Fig. 2G and A, respectively). %DDD was significantly higher in eggs from all pelican sites compared with the other species, but all comparisons were also different, except for the two indicated (Table 1; Fig. 2H).

Considering the three pelican sites separately (one-way ANOVA with Tukey's post-test), there were no significant differences between the sites for *o,p'*-DDT, *p,p'*-DDD, and *p,p'*-DDT. Eggs from Muzi Pan had significantly higher mean *p,p'*-DDE than eggs from the other two sites (580 ng/g wm, vs. 280 and 290 ng/g wm for the other two, Table 1). Mean *o,p'*-DDD was significantly lower in the Muzi Pan eggs than the other two sites. ΣDDT was significantly higher in Muzi Pan than NGR eggs (800 ng/g wm vs. 420 ng/g wm), while NGR eggs had significantly lower %DDT (Table 1). The mean percentage lipid composition differed significantly between the species and pelican sites (Fig. 2I), indicating the use of wet mass as a

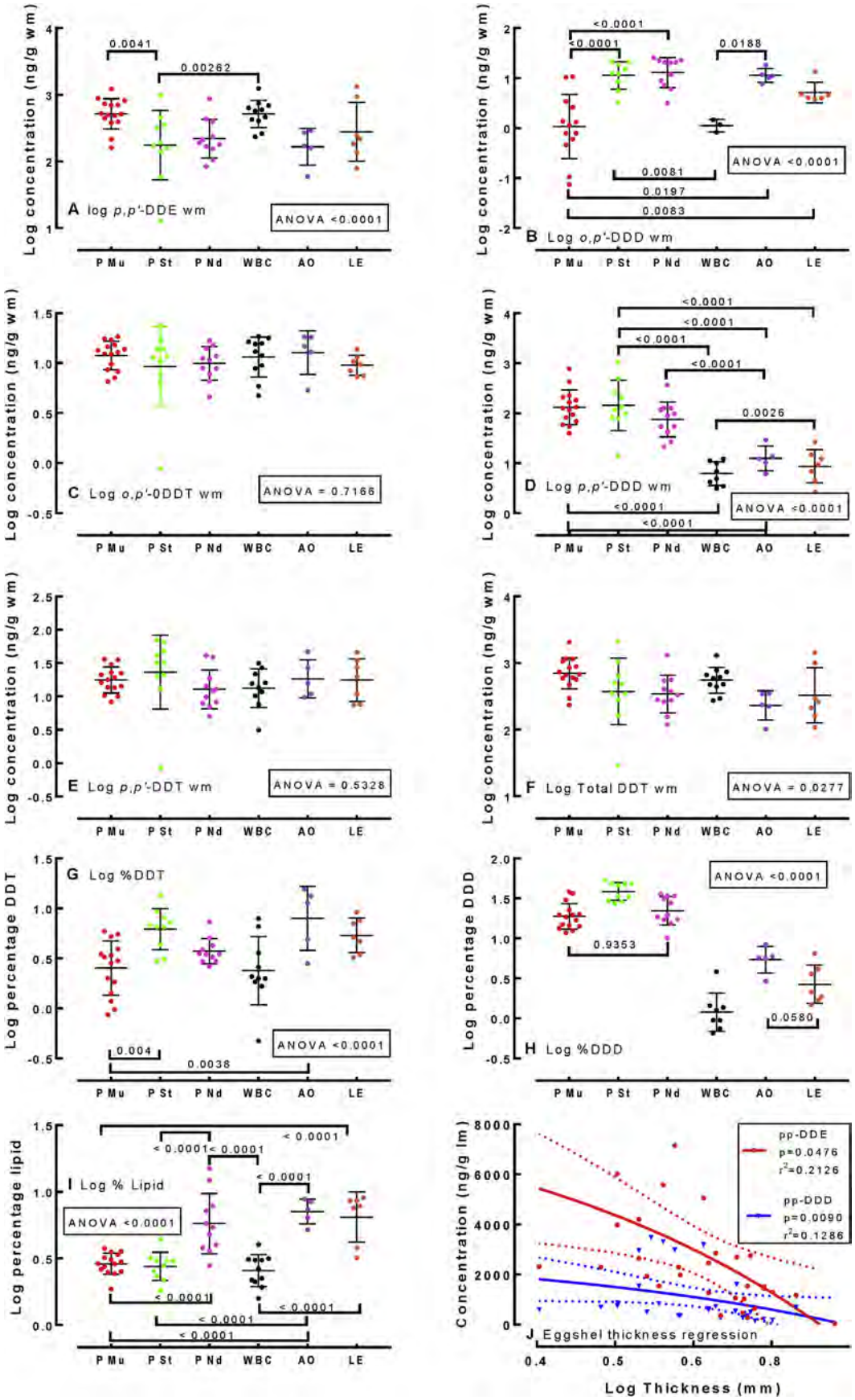

Fig. 2. Scatterplots showing mean and standard deviations of concentrations, percentages, and eggshell thickness regression. Fig. 2a–f are in ng/g wet mass. Fig. 2j is in ng/g wet mass. Results of ANOVA tests are indicated in boxes. Hooked horizontal lines and associated values indicate significant differences of Tukey post-tests in all graphs, except for 2H where all means were significantly different from each other, except the two indicated. P = Pelican eggs from Muzi Pan. P St = Pelican eggs from St. Lucia. P Nd = Pelican eggs from Ndumu Game reserve. WBC = White-breasted Cormorant eggs. AO = African Openbill eggs. LE = Little Egret eggs.

better basis for comparisons of concentrations.

The NMS ordination of relativised data needed only two dimensions (Fig. 3) and 57 iterations to reach a final instability of <0.0001 and a final stress of 10.27. A final stress between 10 and 20 indicates a satisfactory result, typical of ecological studies (McCune and Grace, 2002). Axis 1 explained 58.3% of the variations or differences between the samples, generally indicating the influence of *p,p'*-DDE, *p,p'*-DDD and *o,p'*-DDD, on the horizontal axis. The second axis explained 36.7% of the differences, marginally influenced by higher relative compositions of *p,p'*-DDT and *o,p'*-DDT. The convex hulls connecting the outer samples of each species and pelican collection site represents 'fingerprints'. Overlap indicates congruence of the 'fingerprints', while non-overlap shows differences. The egg concentrations from the three pelican collection sites overlapped with each other (associated with the *p,p'*-DDD vector), despite the differences indicated in Table 1 and Fig. 2. The relative compositions of the DDTs are therefore similar for the pelican eggs from the three sites. The three other species overlapped with each other but not with the pelicans, indicating different relative DDT isomer and congener compositions. The White-breasted Cormorant and Little Egret were associated with higher relative *p,p'*-DDE, while the African Openbill were more aligned with higher *o,p'*-DDT, *p,p'*-DDT, and to a lesser extent *o,p'*-DDT.

3.2. Eggshell thickness

Only the Pink-backed Pelican had enough samples (n = 31) to test for eggshell thinning. The mean and median thickness were both 0.66 mm (range 0.40–0.96 mm). The thinnest eggshell was about 58% thinner than the thickest. The differences in thickness is visualised in Fig. 4. The thinnest shell (0.40 mm) had ΣDDT concentrations of 118 ng/g wm and 3300 ng/g lm. The thickest shell (0.96 mm) had the lowest ΣDDT concentrations at 29 ng/g wm and 100 ng/g lm. The reduction in thickness associated with DDTs was not apparent using regressions of wet mass based data. Linear regressions on lipid mass data showed significant ($p < 0.05$) thinning of pelican eggshells associated with *p,p'*-DDE and *p,p*-DDD concentrations plotted on a log-scale (Fig. 2H).

4. Discussion

4.1. Concentrations

We expected more differentiation in concentrations between the species investigated, given their differences in sizes and trophic levels (Table 1; Fig. 2). Comparisons are confounded as the differences between species also depended on concentration basis; i.e. wet mass or lipid mass. The African Openbill eggs had the lowest mean *p,p'*-DDE and ΣDDT concentrations on a wet mass basis (190 ng/g wm and 250 ng/g wm, respectively), but third highest on a lipid mass basis (2500 ng/g and 3400 ng/g lm, respectively) (Table 1); and there are many other such instances in Table 1 and Fig. 2. These differences also hold true for medians. This probably reflects a combination of differences in normal lipid composition between eggs of different species, the stage of embryo development that may not have coincided between species and localities, and DDT compositional differences in their food items. Since embryo development affects lipid composition (Romanoff, 1932), we mainly base our discussions on wet mass, but also provide lipid mass concentrations for comparisons with other studies (Table 2).

The active ingredient portion of the 75% water wettable DDT formulation powder used for indoor malaria control consists of 72%–75% *p,p'*-DDT, with 22% made up by *o,p'*-DDT (Bouwman et al., 2005). The applied compounds (*p,p'*-DDT and *o,p'*-DDT) did not show significant differences in median concentrations between the

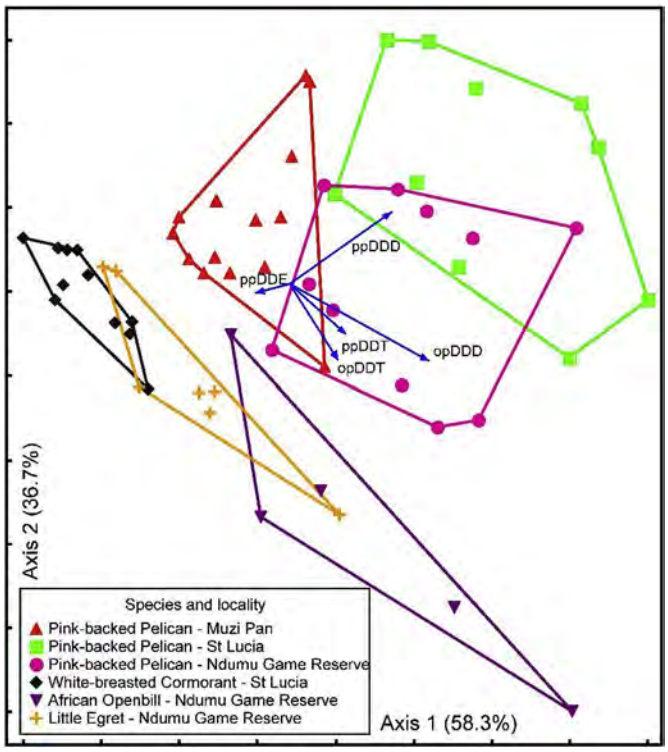

Fig. 3. Non-metric multidimensional scaled (NMS) ordination of the relative (wet-mass based) concentrations of DDTs in eggs from three different species from KwaZulu-Natal. Gower-ignore-0 was used as distance measure. Only two dimensions were needed, after 57 iterations, a final instability of 0.0000, and a final stress of 10.27. Axis 1 explained 58.3% of the variations, and second axis explained 36.7%.

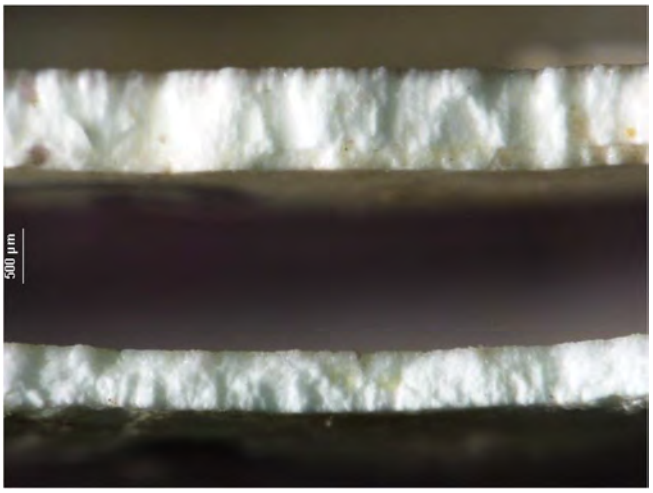

Fig. 4. Photographs illustrating the differences in eggshell thickness from Pink-Backed Pelican eggs from KwaZlulu-Natal. The thinnest eggshell (bottom) was about 58% thinner than the thickest (top). The thinnest shell (0.40 mm) had ΣDDT concentrations of 118 ng/g wet mass/3300 ng/g lipid mass. The thickest shell (0.96 mm) had the lowest ΣDDT concentrations of all Pink-backed Pelican eggs at 29 ng/g wet mass/100 ng/g lipid mass. (For interpretation of the references to colour in this figure legend, the reader is referred to the Web version of this article.)

eggs of any the species and between the different pelican collection sites (one-way ANOVA with Tukey's post-test, Fig. 2C and E). This implies that malaria control is the source of DDTs in top avian predators in the system as they have similar *p,p'*-DDT and *o,p'*-DDT concentrations (Fig. 2; Table 1), but they do not nearly reflect the

Table 2
Non-exhaustive table of concentrations (ng/g lipid mass) from comparable studies from elsewhere, and data from the present study.

No	Species	Location	Sampled	ΣDDT	Reference
1	Great Blue Heron	Canada	1994	1616	Thomas & Anthony (1999)
2	Great Blue Heron	Canada	1997	52,000	Laporte (1982)
3	Great Blue Heron	Canada	1998	3,59,000	Laporte (1982)
4	Grey Heron	Namibia	1970s	9200	Van Dyk et al. (1982)
5	Grey Heron	Limpopo Province, RSA	2009	2,30,000	Bouwman et al. (2013)
6	Night Heron	Hong Kong, PRC	2006	2500	Wang et al. (2011)
7	Great Egret	Hong Kong, PRC	2006	16,000	Wang et al. (2011)
8	Cattle Egret	India	2007	984	Malik et al. (2011)
9	Cattle Egret	Gauteng, RSA	2004/5	330	Polder et al. (2008)
10	Cattle Egret	Gauteng, RSA	2004/5	430	Polder et al. (2008)
11	Cattle Egret	Limpopo Province, RSA	2009/9	340	Bouwman et al. (2013)
12	Cattle Egret	Limpopo Province, RSA	2009/10	420	Bouwman et al. (2013)
13	Cattle Egret	Limpopo Province, RSA	2009/10	4300	Bouwman et al. (2013)
14	Little Egret	Hong Kong, PRC	2006	16,100	Wang et al. (2011)
15	Little Egret	Quanzhou, PRC	2004	58,000	Lam et al. (2008)
16	Little Egret	Ndumo Game Reserve, RSA	2012/13	6900	This study
17	European Shag	Norway	2003–04	1500	Herzke et al. (2009)
18	Double-crested Cormorants	Lake Huron, Canada	1972/73	1,96,000	Weseloh and Teeple (1983)
19	Reed Cormorant	Gauteng, RSA	2004/5	7000	Polder et al. (2008)
20	Great Cormorant	Netherlands	1988/9	1,32,000	Dirksen et al. (1995)
21	White-breasted Cormorant	Eastern Cape, RSA	1979	170[a]	De Kock and Randall, 1984
22	White-breasted Cormorant	Eastern Cape, RSA	1978	635[a]	Van Dyk et al., 1982
23	White-breasted Cormorant	St Lucia, RSA	2012/13	2400	This study
24	African Darter	Gauteng, RSA	2004/5	4400	Polder et al. (2008)
25	African Sacred Ibis	Gauteng, RSA	2004/5	1200	Polder et al. (2008)
26	Brown Pelican	San Benito, California, USA	1969–71	67,000	Jehl (1973)
27	Brown Pelican	San Martin, California, USA	1969	1,58,000	Jehl (1973)
28	Brown Pelican	Los Coronados, California, USA	1969	13,42,000	Jehl (1973)
29	Brown Pelican	Los Coronados, California, USA	1970	5,23,000	Jehl (1973)
30	Pink-backed Pelican	Muzi Pan, RSA	2012/13	2800	This study
31	Pink-backed Pelican	St. Lucia, RSA	2012/13	2200	This study
32	Pink-backed Pelican	Ndumo Game Reserve, RSA	2012/13	7200	This study
33	African Openbill	Ndumo Game Reserve, RSA	2012/13	3400	This study
34	Pied Kingfisher[b]	Ndumo Game Reserve, RSA	1993	960	Evans & Bouwman (2000)
35	Pied Kingfisher[b]	St. Lucia, RSA	1993	350	Evans & Bouwman (2000)
36	Pied Kingfisher[b]	Kosi Bay, RSA	1993	2910	Evans & Bouwman (2000)
37	Pied Kingfisher[b]	Mkuzi Nature Reserve, RSA	1993	1090	Evans & Bouwman (2000)

[a] DDE only, as wet mass.
[b] Calculated from blood concentrations.

original 5:1 composition of the active ingredient. The vapour pressure for *o,p'*-DDT is approximately five times higher than *p,p'*-DDT (55.3 and 7.26 mm x 10^{-7} Hg at 30 °C, respectively; Spencer and Cliath, 1972), implying that *o,p'*-DDT will volatilize in larger amounts and enter the environment more readily when compared with *p,p'*-DDT. This suggests that environmental sources of DDT in the eggs may have been from aerially transported DDT, post-IRS application.

Breeding Brown Pelican on the Atlantic coast of the USA fly 20–150 km from their colonies (Poli, 2015). It is therefore possible that the foraging ranges of breeding Pink-backed Pelicans from our three sites overlap since they are located within 130 km of each other (Fig. 1). Because of this, we expected a homogenous profile in concentrations and relative composition between eggs from the different breeding sites thereby allowing the pooling of data. However, there were major differences in mean and median concentrations and patterns of the breakdown products between the species and collection sites, suggesting influence from an interplay between factors such as food, location, and metabolism (Table 1). Despite no significant differences between median *o,p'*-DDT, *p,p'*-DDD, and *p,p'*-DDT egg concentrations, the median *p,p'*-DDE, *o,p'*-DDD, and ΣDDT between the breeding sites were significantly different (Fig. 2; one-way ANOVA with Tukey's post-test). It is difficult to explain this, since Pink-backed pelicans are known to roam for hundreds of kilometres (Hockey et al., 2005).

Taking into account that the IRS-applied DDT active ingredient content is 72%–75% *p,p'*-DDT, the mean percentage *p,p'*-DDT composition in the eggs for all species and pelican collection sites were low, between 3 and 9.5% (Fig. 2G; Table 1). This is to be expected due to environmental and biological breakdown of the parent compounds in various compartments. The higher %DDT in the African Openbill (9.5%) may reflect bioaccumulation that starts with the lowest trophic level organisms (in this case, molluscs that lives in sediments), with increasing transformation to other compounds in higher trophic levels. For the African Openbill, the direct food source is mainly sediment-dwelling bivalve molluscs, which bio-concentrates DDTs from filtering of DDT-containing water and bio-concentrates DDT-containing small particles including plankton. We know that sediment at Lake Sibaya (Fig. 1) is highly polluted with DDT (Humphries, 2013). For the piscivorous bird species, the food web is longer than the food web of the bivalve molluscs by at least one additional trophic level; from phytoplankton and zooplankton, to small insects, to small and larger fish (in addition to direct bio-concentration of compounds from the water by all these organisms). However, we found no significant differences in median ΣDDT concentrations in eggs of any of the four bird species. This suggests that the molluscs, although a primary consumer, contains levels of ΣDDT that causes DDT concentrations in the eggs of the African Openbill equivalent to their co-occurring piscivorous birds. This further implies that the African Openbill, presumably feeding on a lower trophic level, is as much at risk from DDT as co-occurring large piscivorous birds. Future studies examining DDT in the bivalve prey of the African Openbill, as well as looking at eggs from other openbill stork populations, is suggested.

4.2. Differences in food webs?

Despite no differences in ΣDDT concentrations between any species or pelican egg collection site, median *p,p'*-DDD and %*p,p'*-DDD was significantly higher (by an order of magnitude) in pelican eggs when compared to the other species we sampled (Fig. 2D and H; Table 1). However, there were no differences between the three sets of pelican eggs ($p = 0.5328$, one-way ANOVA).

DDT degrades to DDE mainly under aerobic conditions in the environment, and to DDD under anaerobic conditions in the presence of organic matter (Guenzi and Beard, 1967; Spencer and Cliath, 1972). Presumably, pelicans feed on fish that consume prey that accumulate *p,p'*-DDD from anaerobic sources more so than the other three species. Pelican eggs from the present study had 29% *p,p'*-DDD, while the White-breasted Cormorant, African Openbill, and Little Egret eggs had 1.0%, 5.7%, and 3.1% *p,p'*-DDD (Table 1; which did not differ significantly between them; $p = 0.1764$, one-way ANOVA), respectively. Either the latter three species have mechanisms that metabolically (and anaerobically) produces *p,p'*-DDD from *p,p'*-DDT (the concentrations of the latter did not differ between species, Fig. 2C), selectively assimilates less *p,p'*-DDD from their food, selectively deposits less *p,p'*-DDD in their eggs (all of which we doubt), or more likely, feed from a food web not directly linked to that of the pelican.

A further indication of differences in food webs can be seen in Fig. 3 where the vectors for *p,p'*-DDE and *p,p'*-DDD, both breakdown products of *p,p'*-DDT, are opposing (an increase in the concentration of one compound is associated with a decrease in the other). Fig. 3 also illustrates the differences in relative composition of the DDT compounds. The convex hulls of the Pink-backed Pelicans overlapped, showing congruence in relative composition. The other three species had convex hulls that overlapped with each other (indicating congruence in relative compositions), but not with the Pink-Backed Pelicans, indicating a major difference in relative DDT compound compositions, further supporting the possibility of different food webs. Borgå et al. (2005b) remarked that reliance should not be placed on summed congeners, as this may mask the effects of differences in physiochemical and environmental properties and behaviours, as observed in this study.

Differences in congener proportions for PCBs in birds have been linked with metabolic differences of PCBs between bird species (Borgå et al., 2005a; Quinn et al., 2013). Here, all four bird species (belonging to the same order of birds) consume prey rich in protein and fat. Therefore, major species-specific metabolic differences that may explain the differences in *p,p'*-DDD but not the near equality in ΣDDT and *p,p'*-DDT concentrations is unlikely. It would be interesting to conduct stable isotope analyses to shed more light on this conundrum. However, the different food webs need to be known as stable isotopes metabolically behave different from persistent pesticides and in different prey (Ricca et al., 2008). In addition, there are many other considerations to consider when applying stable isotope analyses to ecotoxicology (Jardine et al., 2006).

4.3. Comparisons with other data

The ΣDDT concentrations in the bird eggs of the present study seem relatively low when compared with local historic data and data from the Limpopo province and elsewhere (Table 2). Little Egret (no. 16) had much less ΣDDT than the other two reports for this species (nos. 14 and 15), as well as all other egrets and herons (nos. 1–7), but not the terrestrial Cattle Egret (nos. 9–13). All the cormorants (including shags) listed (nos. 17–22) had higher concentrations, except eggs from the Eastern Cape, RSA (nos. 21–22) where little or no DDT has presumably been used. Still, the mean ΣDDT concentration from St. Lucia is two orders of magnitude less compared with that measured in eggs of the Great Cormorant in The Netherlands (no. 20). White-breasted Cormorant eggs from St. Lucia had similar concentrations to eggs of the African Darter and African Sacred Ibis from Gauteng, South Africa (nos. 24 and 25). Here, DDT has never been used for malaria control, and is most likely due to legacy residues from agricultural use. South Africa has banned the use of DDT in agriculture since 1976 (Bouwman, 2003).

It is however, the differences between the concentrations in the pelican eggs from the present study (Nos. 30–32) with those from elsewhere (nos. 26–30) that is notable—up to three orders of magnitude. Past agricultural use of DDT as used in the USA therefore contributed much more than IRS alone. This makes sense, as agricultural use of DDT in the 60s in the USA was much more intense than for IRS (Baris et al., 1998). However, Grey Heron egg concentrations from Limpopo province (No. 5), where DDT is used under similar circumstances as in KwaZulu-Natal, were two orders of magnitude higher than the pelicans from the present study (Table 2). DDT concentrations in human breast milk were similar between the two regions (900 ng/ml wm, 750 ng/ml wm, and 490 ng/ml wm for two villages in KwaZulu-Natal and one in Limpopo province, respectively, for primiparae mothers—maximum was 6200 ng/ml; Bouwman et al., 2012), indicating no major differences in IRS application. Pelicans do not breed in the Limpopo Province, so direct comparison is not possible.

With comparable DDT data now available, a possible explanation might be that the Phongolo River, which is associated with a large floodplain and wetland system, would dilute DDT more than the drier Luvuvhu River in Limpopo with fewer floodplains, less wetlands, and a lower river flow (Luvuvhu River, mean annual flow 73.5 million m^3 vs. Phongolo River mean annual flow 463 million m^3, calculated from data since 2004). This explanation is further supported with fish data. ΣDDT in tiger fish from the Luvuvhu River (draining the malaria area in the Limpopo Province where the Limpopo bird eggs were collected) were much higher than in the Phongolo River (calculated at 310 ng/g wm (Gerber et al., 2016) vs. 21 ng/g wm (Smit et al., 2016), respectively), suggesting that differences in hydrology might be involved. The lower concentrations in bird eggs and fish from KwaZulu-Natal therefore, indicate much lower exposure and risk compared to the Limpopo Province. In section 4.3, we will discuss another possible reason for the lower concentrations in KwaZulu-Natal eggs.

4.4. Effect levels and eggshell thickness

Endocrine disrupting chemicals such as PCBs and DDE in animals have been associated with altered thyroid hormone function and neuro-endocrine systems, activation of the stress response (Dawson, 2000; Fry, 1995; Langer et al., 1998), and effects on the gonadal steroid hormones of animals (Beard et al., 2000). Delayed sexual maturation and impaired mating behaviour (Ottinger et al., 2005), thinning of eggshells, developmental effects, and embryo mortality have been associate with *p,p'*-DDE (Lundholm, 1997; Zimmermann et al., 1997).

Eggshell thinning associated with DDT have been measured in African Fish Eagle *Haliaeetus vocifer* by 11–20% (Douthwaite, 1989), and Peregrine Falcon *Falco peregrinus* in Zimbabwe by 10% (Hartley et al., 1995). In South Africa, Lanner Falcon *Falco biarmicus* and Bateleur *Terathopius ecaudatus* eggs had 8.8% and 10% thinner shells, respectively (Snelling et al., 1984), African Darters had thinner eggs by 17% (Bouwman et al., 2008), Cattle Egret by 33% (Bouwman et al., 2013), and African Penguin by 38%–40% (Bouwman et al., 2015). Eggs from the terrestrially feeding Cattle Egrets from the Limpopo Province in particular had thinner shells in three colonies from outside to inside the IRS area, at increasing levels of ΣDDT (19 ng/g wm, 92 ng/g wm, and 290 ng/g wm).

Eggshell thickness concomitantly decreased significantly from 0.23 mm, to 0.21 mm, to 0.19 mm, in the same order. Thinning associated with these low ΣDDT levels for a terrestrial bird species was unexpected and cause for concern (Bouwman et al., 2008).

Blus (1982) estimated substantial impaired reproductive success at 3000 ng/g wm ΣDDT, and failure at 4000 ng/g wm for the Brown Pelican in the USA, due to eggshell thinning. This assessment was based on the findings of DDE concentrations of 2800 ng/g wm associated with reproductive impairment of piscivore bird populations, while 1000 ng/g wm has been linked to reduced heron survival (Connell et al., 2003). The mean ΣDDT in Pink-backed Pelican eggs of this study at NGR and St. Lucia (800 ng/g wm and 590 ng/g wm, respectively; Table 1) did not exceed the "critical level for reproductive success" (3000 ng/g wm) calculated for Brown Pelicans in field studies in the USA (USDoI, 1998). They did however, exceed the non-effect level estimated at 500 ng/g wm (Cooper, 1991), which was also exceeded by the White-breasted Cormorant at 600 ng/g wm, and is equalled by the Little Egret at 500 ng/g wm (Table 1). All species and sites had eggs that exceeded the 500 ng/g wm non-effect level, except the African Openbill that was lower.

The Pink-backed Pelican eggshells had thicknesses ranging between 0.40 mm and 0.96 mm (Table 1; Fig. 4), with an overall mean and median of 0.66 mm. The thinnest shell was 58% thinner than the thickest. The eggs collected from the three sites did not show a consistent eggshell thickness pattern. Eggshells from NGR, with the lowest mean ΣDDT in wet mass also had the thinnest shells (mean 0.53). This picture, however, changes when lipid mass concentrations are considered. The thinnest mean shells (0.53 mm) at NGR had more than double the mean ΣDDT (7200 ng/g lm), and the thickest eggs from St. Lucia (mean 0.78 mm) had the lowest mean ΣDDT at 2200 ng/g lm (Table 1). Regressions of all wet mass based DDT concentrations against thickness were not significantly different from zero, but on lipid mass, *p,p'*-DDE and *p,p'*-DDD were significantly associated with thinning (Fig. 2J). We cannot explain the differences between wet and lipid based data vis-à-vis eggshell thickness, and there are many factors involved (Hernández et al., 2018). However, the large differences in eggshell thickness (Fig. 4) coupled with exceedances of known wet mass based risk levels, and biological plausibility based on many other studies, lead us to conclude that DDT is strongly associated with eggshell thinning.

The species we studied are all considered resident in the sense that they do not migrate on a seasonal basis. Pelicans and African Openbill do however roam over large distances (Hockey et al., 2005). They also seem to breed irregularly, abandoning sites and establishing new sites according to opportunity and conditions (Bowker and Downs, 2012). From the few data we have, it seems as if malaria control differs north and south of the South Africa/Mozambique border. It is possible therefore, that individuals from less contaminated areas will breed south of the border in South Africa. Less polluted individuals may therefore mask reproductive impairments in colonies, possibly explaining the large differences in eggshell thickness we observed.

4.5. Synthesis, conclusions, and recommendations

DDT continues to pollute biota such as fish and birds in the malaria-endemic areas of northern KwaZulu-Natal. Wild birds from here were last assessed 30 years ago – since then the IRS regime had changed from solely relying on DDT to a combination of DDT and pyrethroids. This may have contributed towards reduction in ΣDDT concentrations using comparable data in tiger fish over the same 30 years. Our data and findings, together with those from others, confirm that IRS continues to release DDT into local aquatic ecosystems, which have faced continuous ecotoxic stress for more than 80 years. Birds that enter the malaria-controlled areas where DDT is used from less polluted areas to breed might also mask reproductive impairment and contribute towards differences in concentrations in eggs as we have seen in eggs from the three breeding sites. Long-term studies should also be instituted to monitor hatching and fledging success of the larger aquatic birds, especially both pelican species.

Despite feeding on a lower trophic level, African Openbill eggs had concentrations equivalent to those of the other species. This implies that their molluscan prey contributes DDT to the African Openbill eggs to the same extent as the piscivorous species we studied. If such is the case, the bivalve molluscs they prey on may also face threats. Surveys of the DDT concentrations and health of these ecologically important animals need to be done. It also implies that the African Openbill face the same threats from DDT as birds feeding at higher trophic levels. The potential for eggshell thinning in this species should be investigated.

DDT concentrations in eggs of the four species of birds we analysed were difficult to interpret as wet mass and lipid mass data did not show the same relative patterns. This may reflect a combination of influence of locality, species, diet, time of laying, asynchronous embryo development in each colony, embryo development per se per egg, and maternal food. The DDT concentrations in Pink-backed Pelican eggs approach, equal, and exceed established levels of concern. Eggshell thinning (up to 58%) was significantly associated with *p,p'*-DDE and *p,p'*-DDD concentrations on a lipid mass basis.

Based on remarkably consistent relative and absolute *p,p'*-DDT and *o,p'*-DDT compositions between species and breeding sites, we suspect that aerial transport between site of application and site of uptake may play a role. If this is the case, better application methods might reduce the escape of DDT from IRS sites with a concomitant reduction in environmental pollution. The monitoring of DDT, including the use of passive air samplers, should be implemented within and adjacent to areas where DDT is used for malaria control.

There are indications that pelicans feed from a different food web route than the other species, mainly based on the concentrations and relative contributions of *p,p'*-DDD and *p,p'*-DDE. These differences need to be investigated, as *p,p'*-DDD is derived from anaerobic metabolism, and *p,p'*-DDE aerobically. If different food webs are involved, using a single top-predator species as indicator might not be enough to monitor and predict harmful effects to all bird species. More knowledge on the food webs, in conjunction with stable isotope studies, may shed more light.

DDT concentrations in eggs from KwaZulu-Natal in general were generally lower than in eggs from equivalent birds from elsewhere in the world where DDT was used mainly in agriculture. DDT concentrations in eggs were also lower than eggs from the Limpopo Province where breeding impact is suspected, and eggshell thinning associated with DDT has been detected. Differences in hydrology and rainfall may be explanations for this difference, implying that single area monitoring as well as modelling using general assumptions could supply potentially highly erroneous estimations of risk.

All species we studied seem not to have strong fidelity to their breeding localities, but move between breeding colonies according to opportunity and conditions. Reproductive impairment and failure might therefore be masked by influx of individuals from less polluted areas, and breeding success of all the larger aquatic birds should be monitored.

We conclude that significant threats to predatory birds remain in this highly bio-diverse area of KwaZulu-Natal and to birds from adjacent, less polluted areas. Taken together with other indicators, such as very high concentrations of DDT in breast milk, crocodiles,

fish and frogs, the evidence strongly suggest continuous negative human health and environmental impacts from DDT as used in IRS, more than 35 years after its use in agriculture was stopped in South Africa. Furthermore, our data and findings strongly stress the urgency to move away from DDT as quickly as possible, or, at the very least, to implement practices that reduce human exposure to DDT, protects humans from malaria, and prevents emissions of DDT to the environment (Bouwman et al., 2011). These science-based recommendations have been made repeatedly over decades of research here and elsewhere in South Africa, and urgent action is required.

Acknowledgements

We thank J.P. Huisamen for logistical support and collecting the eggs, G.R., Barnard for the photo of the eggshells, and the Persistent Organic Pollutant and Toxicant (POPT) editorial collective for many improvements to the manuscript. The iSimangaliso Wetland Park Authority granted us permission to work at Lake St Lucia and Muzi Pan. Caroline Fox and Sbu Mfeka from Ezemvelo KZN Wildlife assisted with the collection of eggs from Lake St Lucia. MH was funded by the National Research Foundation (Grant number 96296). HB was funded by the Water Research Commission (Project K5-2185), and National Research Foundation (Grant number 77197). Opinions expressed and conclusions arrived at are those of the authors and not necessarily attributed to the NRF or WRC.

References

Barnhoorn, I.E.J., Bornman, M.S., Janse van Rensburg, C.J., Bouwman, H., 2009. DDT residues in water, sediment, domestic and indigenous biota from a currently DDT-sprayed area. Chemosphere 77, 1236–1241.
Baris, D., Zahm, S.H., Cantor, K.P., Blair, A., 1998. Agricultural use of DDT and risk of non-Hodgkin's lymphoma: pooled analysis of three case-control studies in the United States. Occup. Environ. Med. 55, 522–527.
Beard, J., Marshall, S., Jong, K., Newton, R., Triplett-McBride, T., Humphries, B., Bronks, R., 2000. 1,1,1-trichloro-2,2-bis (p-chlorophenyl)-ethane (DDT) and reduced bone mineral density. Arch. Environ. Health 55, 177–180.
Blus, L.J., 1982. Further interpretation of the relation of organochlorine residues in Brown Pelican eggs to reproductive success. Environ. Pollut. Ser. A. 28, 15–33.
Borgå, K., Gabrielson, G.W., Skaare, J.U., Kleivane, L., Nortstrom, R.J., Fisk, A.T., 2005a. Why do organochlorine differences between Arctic regions vary among trophic levels? Environ. Sci. Technol. 39, 4343–4352.
Borgå, K., Hop, H., Skaare, J.U., Wolkers, H., Gabrielson, G.W., 2005b. Selective bioaccumulation of chlorinated pesticides and metabolites in Arctic seabirds. Environ. Pollut. 145, 545–553.
Bornman, M., Schlemmer, L., van der Walt, T., van Dyk, C., Bouwman, H., 2012. Implications for health education and intervention strategies arising from children's caregivers concerns following successful malaria control. Trans. R. Soc. Trop. Med. Hyg. 106, 408–414.
Bouwman, H., 2003. POPs in southern Africa. Handb. Environ. Chem. 3, 297–320. Part 0.
Bouwman, H., Becker, P.J., Schutte, C.H.J., 1994. Malaria control and longitudinal changes in levels of DDT and its metabolites in human serum from Kwazulu. Bull. WHO 72, 921–930.
Bouwman, H., Coetzee, A., Schutte, C.H.J., 1990. Environmental and health implications of DDT-contaminated fish from the Pongolo flood plain. Afr. J. Zool. 104, 275–286.
Bouwman, H., Govender, D., Underhill, L., Polder, A., 2015. Chlorinated, brominated and fluorinated organic pollutants in African Penguin eggs: 30 years since the previous assessment. Chemosphere 126, 1–10.
Bouwman, H., Kylin, H., Sereda, B., Bornman, R., 2012. High levels of DDT in breast milk: intake, risk, lactation duration, and involvement of gender. Environ. Pollut. 170, 63–70.
Bouwman, H., Polder, A., Venter, B., Skaare, J.U., 2008. Organochlorine contaminants in cormorant, darter, egret, and ibis eggs from South Africa. Chemosphere 71, 227–241.
Bouwman, H., Sereda, B., Meinhardt, H.M., 2005. Simultaneous presence of DDT and pyrethroid residues in human breast milk samples from a malaria endemic area in South Africa. Environ. Pollut. 144, 902–917.
Bouwman, H., Van den Berg, H., Kylin, H., 2011. DDT and malaria prevention: Addressing the paradox. Environ. Health Perspect. 119, 744–747.
Bouwman, H., Viljoen, I.M., Quinn, L.P., Polder, A., 2013. Halogenated pollutants in terrestrial and aquatic bird eggs: converging patterns of pollutant profiles, and impacts and risks from high levels. Environ. Res. 126, 240–253.
Bowker, M.W., Downs, C.T., 2012. Breeding of large, water-associated, colonially nesting birds of the North-eastern region of KwaZulu-Natal, South Africa. Waterbirds 35, 270–291.
Buah-Kwofie, A., Humphries, M.S., Combrink, X., Myburgh, J.G., 2018a. Accumulation of organochlorine pesticides in fat tissue of wild Nile crocodiles (*Crocodylus niloticus*) from iSimangaliso Wetland Park, South Africa. Chemosphere 195, 463–471.
Buah-Kwofie, A., Humphries, M.S., Pillay, L., 2018b. Bioaccumulation and risk assessment of organochlorine pesticides in fish from a global biodiversity hotspot: iSimangaliso Wetland Park, South Africa. Sci. Total Environ. 621, 273–281.
Buah-Kwofie, A., Humphries, M.S., Pillay, L. Dietary exposure and risk assessment of organochlorine pesticide residues in rural communities living within catchment areas of iSimangaliso World Heritage Site, South Africa. In Review: Food Additives and Contaminants: Part A.
Connell, D.W., Fung, C.N., Minh, T.B., Tanabe, S., Lam, P.K.S., Wong, B.S.F., Lam, M.H.W., Wong, L.C., Wu, R.S.S., Richardson, B.J., 2003. Risk to breeding success of fish-eating Ardeids due to persistent organic contaminants in Hong Kong: evidence from organochlorine compounds in eggs. Water Res. 37, 459–467.
Cooper, K., 1991. Effects of pesticides on wildlife. In: Hayes, W.J., Laws, E.R. (Eds.), Handbook of Pesticide Toxicology. Academic Press, San Diego, pp. 463–496.
Cooper, K.H., 1980. Bird ecology of Maputaland. In: Bruton, M.N., Cooper, K.H. (Eds.), Studies on the Ecology of Maputaland. Grahamstown. Rhodes University, pp. 300–306.
Dawson, A., 2000. Mechanisms of endocrine disruption with particular reference to occurrence in avian wildlife: a review. Ecotoxicology 9, 59–69.
Douthwaite, R.J., 1989. Effects of DDT on the fish eagle *Haliaeetus vocifer* population of Lake Kariba in Zimbabwe. Ibis 134, 250–258.
De Kock, A.C., Randall, R.M., 1984. Organochlorine insecticide and polychlorinated biphenyl residues in eggs of coastal birds from the Eastern Cape, South Africa. Environ. Pollut. Ser. B 35, 193–201.
Dirksen, S., Boudewijn, T.J., Slager, L.K., Mes, R.G., van Schaick, M.J.M., de Voogt, P., 1995. Reduced breeding success of Cormorants (*Phalacrocorax carbo sinensis*) in relation to persistent organochlorine pollution of aquatic habitats in The Netherlands. Environ. Pollut. 88, 119–132.
Evans, S.W., Bouwman, H., 1993. DDT levels in the blood of pied Kingfishers *Ceryle rudis* from KwaZulu, South Africa. Ann. Musee R. Afr. Cent. Sci. Zool.
Evans, S.W., Bouwman, H., 2000. The geographic variation and potential risk of DDT in the blood of Pied Kingfishers from northern KwaZulu-Natal, South Africa. Ostrich 71, 351–354.
Fry, D.M., 1995. Reproductive effects in birds exposed to pesticides and industrial chemicals. Environ. Health Perspect. 103, 165–171.
Garcia-Heras, M.S., Arroyo, B., Simmons, R.E., Camarero, P.R., Mateo, R., Mougeot, F., 2018. Blood concentrations of PCBs and DDTs in an avian predator endemic to southern Africa: Associations with habitat, electrical transformers and diet. Environ. Pollut. 232, 440–449.
Gerber, R., Smit, N.J., Van Vuuren, J.H.J., Nakayama, S.M.M., Yohannes, Y.B., Ikenaka, Y., Ishizuka, M., Wepener, V., 2016. Bioaccumulation and human health risk assessment of DDT and other organochlorine pesticides in an apex aquatic predator from a premier conservation area. Sci. Total. Environ. 550, 522–533.
Guenzi, W.D., Beard, W.E., 1967. Anaerobic biodegradation of DDT to DDD in soil. Science 156, 116–117.
Gyalpo, T., Fritsche, L., Bouwman, H., Bornman, R., Scheringer, M., Hungerbühler, K., 2012. Estimation of human body concentrations of DDT from indoor residual spraying for malaria control. Environ. Pollut. 169, 235–241.
Hartley, R.R., Newton, I., Robertson, M., 1995. Organochlorine residues and eggshell thinning in the Peregrine falcon *Falco peregrinus minor* in Zimbabwe. Ostrich 66, 69–73.
Hernández, M., Colomer, M.A., Pizarro, M., Margalida, A., 2018. Changes in eggshell thickness and ultrastructure in the Bearded Vulture (*Gypaetus barbatus*) Pyrenean population: a long-term analysis. Sci. Total Environ. 624, 713–721.
Herzke, D., Nygard, T., Berger, U., Huber, S., Rov, N., 2009. Perfluorinated and other persistent halogenated organic compounds in European shag (*Phalacrocorax aristotelis*) and common eider (*Somateria mollissima*) from Norway: a suburban to remote pollutant gradient. Sci. Total Environ. 408, 340–348.
Humphries, M.S., 2013. DDT residue contamination in sediments from Lake Sibaya in northern KwaZulu-Natal, South Africa: implications for conservation in a world heritage site. Chemosphere 93, 1494–1499.
Hockey, P.A.R., Dean, W.R.J., Ryan, P.G., 2005. Roberts Birds of Southern Africa. The Trustees of the John Voelcker Bird Book Fund, Cape Town.
Jardine, D.J., Kidd, K.A., Fisk, A.T., 2006. Applications, considerations, and sources of uncertainty when using stable isotope analysis in ecotoxicology. Environ. Sci. Technol. 40, 7501–7511.
Jehl, J.R., 1973. Studies in a declining population of Brown pelicans in northwestern Baja California. Condor 75, 69–79.
Lam, J.C.W., Murphy, M.B., Wang, Y., Tanabe, S., Giesy, J.P., Lam, P.K.S., 2008. Risk assessment of organohalogenated compounds in water bird eggs from South China. Environ. Sci. Technol. 42, 6296–6302.
Langer, P., Tajtakova, M., Fodor, G., Kocan, A., Bohov, P., Michalek, J., Kreze, A., 1998. Increased thyroid volume and prevalence of thyroid disorders in an area heavily polluted by polychlorinated biphenyls. Eur. J. Endocrinol. 139, 402–409.
Laporte, P., 1982. Organochlorine residues and eggshell measurements of great blue heron eggs from Quebec. Colon. Waterbirds 5, 95–103.
Lundholm, C.E., 1997. DDE-induced eggshell thinning in birds: effects of p,p'-DDE on the calcium and prostaglandin metabolism of the eggshell gland. Comp.

Biochem. Physiol. C Comp. Pharmacol. Toxicol. Endocrinol. 118, 113–128.
Malik, R.N., Rauf, S., Mohammad, A., Eqani, S.A.M.A., Ahad, K., 2011. Organochlorine residual concentrations in cattle egret from the Punjab Province, Pakistan. Environ. Monit. Assess. 173, 325–341.
McCune, B., Grace, J.B., 2002. Analysis of Ecological Communities. MjM Software Design, Gleneden Beach, Oregon.
Ottinger, M.A., Quinn, M.J., Lavoie, E., Abdelnabi, M.A., Thompson, N., Hazelton, J.L., Wu, J.M., Beavers, J., Jaber, M., 2005. Consequences of endocrine disrupting chemicals on reproductive endocrine function in birds: establishing reliable end points of exposure. Domest. Anim. Endocrinol. 29, 411–419.
Peakall, D.B., Lincer, J.L., Risebrough, R.W., Pritchard, J.B., Kinter, W.B., 1973. DDE-induced egg-shell thinning: Structural and physiological effects in three species. Comp. Gen. Pharmacol. 4, 305–313.
Polder, A., Venter, B., Skaare, J.U., Bouwman, H., 2008. Polybrominated diphenyl ethers and HBCD in bird eggs of South Africa. Chemosphere 73, 148–154.
Poli, C., 2015. Variability in Movement Patterns and Habitat Use of Two Species of Pelecaniformes. All Theses, p. 2161. https://tigerprints.clemson.edu/all_theses/2161.
Quinn, L.P., Roos, C., Pieters, R., Løkken, K., Polder, A., Skaare, J.U., Bouwman, H., 2013. Levels of PCBs in wild bird eggs: Considering toxicity through enzyme induction potential and molecular structure. Chemosphere 90, 1109–1116.
Ricca, M.A., Miles, A.K., Anthony, R.C., 2008. Sources of organochlorine contaminants and mercury in seabirds from the Aleutian archipelago of Alaska: nferences from spatial and trophic variation. Sci. Total Environ. 406, 308–323.
Romanoff, A.L., 1932. Fat metabolism of the chick embryo under standard conditions of artificial incubation. Biol. Bull. 54–62.
Smit, N.J., Vlok, W., Van Vuuren, J.H.J., Du Preez, L., Van Eeden, E., O'Brian, G.C., Wepener, V., 2016. Socio-ecological System Management of the Lower Phongolo River and Floodplain Using Relative Risk Assessment. Report to the Water Research Commission, pp. 1–417. WRC Report No. 2185/1/16.
Snelling, J.C., Kemp, A.C., Lincer, J.L., 1984. Organochlorine residues in southern African raptor eggs. In: Mendelsohn, J.M., Sapsford, C.W. (Eds.), Proceedings of the Second Symposium on African Predatory Birds. Natal Bird Club, Durban, pp. 161–168.
Spencer, W.F., Cliath, M.M., 1972. Volatility of DDT and related compounds. J. Agric. Food Chem. 20, 645–649.
Stockholm Convention, 2018. http://chm.pops.int/. (Accessed 17 February 2018).
Tarbotton, W., 2011. Robert's Nests and Birds. The Trustees of the John Voelcker Bird Book Fund, Cape Town.
Thomas, C.M., Anthony, R.G., 1999. Environmental contaminants in great blue herons (*Ardea herodias*) from the lower Columbia and Willamette rivers, Oregon and Washington, USA. Environ. Toxicol. Chem. 18, 2804–2816.
Thompson, L.A., Ikenaka, Y., Yohannes, Y.B., Van Vuren, J.J., Wepener, V., Smit, N.J., Darwish, W.S., Nakayama, S.M.M., Mizukawa, H., Ishizuka, M., 2017. Concentrations and human health risk assessment of DDT and its metabolites in free-range and commercial chicken products from KwaZulu-Natal, South Africa. Food Addit. Contam. 34, 1959–1969.
Thompson, L.A., Ikenaka, Y., Darwish, W.,S., Yohannes, Y.B., Janse van Vuuren, J., Wepener, V., Smit, N.J., Assefa, A.G., Tharwat, A., Eldin, W.F.S., Nakayama, S.M.M., Mizakuwa, H., Ishizuka, M., 2018. Investigation of mRNA expression changes associated with field exposure to DDTs in chickens from KwaZulu-Natal, South Africa. PLoS One 13 (10), e0204400. https://doi.org/10.1371/journal. pone. 0204400.
USDoI, 1998. Guidelines for Interpretation of Biological Effects of Selected Constituents in Biota, Water, and Sediment: DDT. US Department of the Interior. Contaminant guidelines, pp. 1–90.
Van den Berg, H., Manuweera, G., Konradsen, F., 2017. Global trends in the production and use of DDT for control of malaria and other vector-borne diseases. Malar. J. 16, 401. https://doi.org/10.1186/s12936-017-2050-2.
Van Dyk, J.C., Bouwman, H., Barnhoorn, I.E.J., Bornman, M.S., 2010. DDT contamination from indoor residual spraying for malaria control. Sci. Total Environ. 408, 2745–2752.
Van Dyk, L.P., Wiese, I.H., Mullen, J.E.C., 1982. Management and determination of pesticide residues in South Africa. Residue Rev. 82, 38–124.
Wang, Y., Murphy, M.B., Lam, J.C.W., Jiao, L.P., Wong, C.C.L., Yeung, L.W.Y., Lam, P.K.S., 2011. Polychlorinated biphenyls and organochlorine pesticides in local waterbird eggs from Hong Kong: risk assessment to local waterbirds. Chemosphere 83, 891–896.
Wepener, V., Smit, N., Covaci, A., Dyke, S., Bervoets, L., 2012. Seasonal bioaccumulation of organohalogens in tigerfish, *Hydrocynus vittatus* Castelnau, from Lake Pongolapoort, South Africa. Bull. Environ. Contam. Toxicol. 88, 277–282.
Weseloh, D.V., Teeple, S.M., 1983. Double-crested Cormorants of the Great Lakes: egg-laying parameters, reproductive failure, and contaminant residues in eggs, Lake Huron 1972- 1973. Can. J. Zool. 61, 427–436.
Wolmerans, N.J., Du Preez, L.H., Yohannes, Y.B., Ikenaka, Y., IshiZuka, M., Smit, N.J., Wepener, V., 2018. Linking organochlorine exposure to biomarker response patterns in Anurans: a case study of Müller's clawed frog (*Xenopus muelleri*) from a tropical malaria vector control region. Ecotoxicology 27, 1203–1216. Online, .org/10.1007/s10646-018-1972-y.
Yohannes, Y.B., Ikenaka, Y., Nakayama, S.M.M., Ishizuka, M., 2017. DDTs and other organochlorine pesticides in tissues of four bird species from the Rift Valley region, Ethiopia. Sci. Total Environ. 574, 1389–1395.
Zimmermann, G., Dietrich, D.R., Schmid, P., Schlatter, C., 1997. Congener-specific bioaccumulation of PCBs in different water bird species. Chemosphere 34, 1379–1388.

Pesticide Biochemistry and Physiology 156 (2019) 44–55

Contents lists available at ScienceDirect

Pesticide Biochemistry and Physiology

journal homepage: www.elsevier.com/locate/pest

Baseline bio-accumulation concentrations and resulting oxidative stress in *Synodontis zambezensis* after an acute laboratory exposure to 4,4′-DDT

C.M. Volschenk[a,*], Y. Ikenaka[c,d], Y.B. Yohannes[c], S.M. Nakayama[c], M. Ishizuka[c], E. Smit[b], J.H.J. van Vuren[a], R. Greenfield[a]

[a] Department of Zoology, University of Johannesburg, PO Box 524, Auckland Park, Johannesburg, South Africa
[b] Department of Chemistry, University of Johannesburg, PO Box 524, Auckland Park, Johannesburg, South Africa
[c] Laboratory of Toxicology, Department of Environmental Veterinary Sciences, Graduate School of Veterinary Medicine, Hokkaido University, N18, W9, Kita-ku, Sapporo 060-0818, Japan
[d] School of Biological Sciences, North-West University, X6001, Potchefstroom 2520, South Africa

ARTICLE INFO

Keywords:
4,4′-DDT
Synodontis zambezensis
Bioaccumulation
Acute exposure
Biomarkers
Oxidative stress

ABSTRACT

The use of 1,1′-(2,2,2-Trichloro-1,1-ethanediyl)bis(4-chlorobenzene) (DDT) as a pesticide for the control of insects vectors responsible for the spread of many life threatening diseases was officially banned in 1972 by the United States Environmental Protection Agency (USEPA). It was banned throughout the world, in most developed countries, because of the toxic effects it causes in wildlife, including birds and fish. However, DDT is still used in approximately 43 African countries, including South Africa, to control the spread of malaria. The lipophilic nature of DDT and therefore its persistence in the environment makes it extremely important for laboratory based studies to be conducted in an effort to evaluate the accumulation potential and possible physiological effects of DDT in aquatic organisms under controlled conditions. The aim of this study was to establish baseline bioaccumulation concentrations within *Synodontis zambezensis* following an acute exposure to 4,4′-DDT. The three metabolites analysed were 4,4′-DDE, 4,4′-DDD and 4,4′-DDT. None of the 2,4′-isomers were analysed in this study since the acute exposure used a solution of 98.7% pure 4,4′-DDT (Sigma-Aldrich PESTANAL®, Analytical Standard, CAS-No 50-29-3, Batch number SZBE057XV) and not a mixture of 4,4′-DDT and 2,4′-DDT as found in technical grade DDT. Soxhlet extraction of tissue samples and liquid/liquid extraction of water samples followed by analysis through Gas-chromatography mass-spectrophotometry was completed. Mean 4,4′-DDE, 4,4′-DDD and 4,4′-DDT concentrations ranged from 15.34 ng/g to 45.34 ng/g, 28.16 ng/g to 63.25 ng/g and 28.64 ng/g to 96.21 ng/g respectively. All of the accumulated concentrations fell within environmentally relevant concentrations with no input through the food web. The accumulated concentrations of 4,4′-DDT and its three metabolites resulted in oxidative stress responses within the gills and the liver tissue of *S. zambezensis*. Significant differences ($p \leq .05$) were observed between malondialdehyde (MDA) and reduced glutathione (GSH) within the liver and in superoxide dismutase (SOD), catalase (CAT) and reduced glutathione (GSH) in the gills.

1. Introduction

The control of pests through the use of pesticides is a requirement in the agricultural sector which relies on the use of herbicides, fungicides and insecticides to increase high-quality production of desired crops (Oerke, 2006; Bennett et al., 2003). Increasing populations leads to an increasing demand for products including food and clothing, inevitably leading to an increase in the production of pesticides throughout the world (van Dyk et al., 2007). Although many pesticides are designed to affect and control a specific group of organisms, many have the potential to cause harm to non-target organisms resulting in detrimental ecosystem changes (Davies et al., 2007).

1,1′-(2,2,2-Trichloro-1,1-ethanediyl)bis(4-chlorobenzene) also known more commonly as 4,4′-DDT was originally synthesised in 1874 by the Austrian chemist, Othmar Zeidler for the use of pest control on crops of corn (Zeidler, 1874). Once its insecticidal properties were discovered in 1939 it was put into large-scale synthesis and application to eradicate the spread of diseases such as malaria, typhus and the bubonic plague (World Health Organisation (WHO), 1979). Although DDT was banned in 1972 by the United States Environmental Protection Agency (USEPA) it is still used in the North Eastern parts of South Africa for the control of malaria transmission (Barnhoorn et al., 2009). DDT is applied through Indoor Residual Spraying (IRS) annually in the Limpopo Province, in particular, the Vhemba District Municipality (World Health Organisation (WHO),

* Corresponding author.
E-mail address: CVolschenk@golder.co.za (C.M. Volschenk).

https://doi.org/10.1016/j.pestbp.2019.02.005
Received 16 October 2018; Received in revised form 10 January 2019; Accepted 5 February 2019
Available online 06 February 2019
0048-3575/

2002; Barnhoorn et al., 2009). Through the movement of spray drift from sites of application, accumulation takes place in aquatic systems, as well as human and animal tissues, in areas that may not have been sprayed with 4,4′-DDT (Aneck-Hahn et al., 2006; Whitworth et al., 2014; Gaspar et al., 2015). The accumulation of organochlorine pesticides (OCP's), a group which includes 4,4′-DDT, can cause toxic effects in fish, and eventually lead to disruption on a physiological and biological level (Da Cuña et al., 2013).

Monitoring potential changes within specific organisms has become increasingly important and this can be done through various means (Dix et al., 2007). The organisms used to study the effects of chemicals will differ depending on the system that is being monitored (Smolders et al., 2003). Test organisms used in biomonitoring studies are known as biological indicators or bio-indicators (Naigaga et al., 2011) and have been defined as meeting the following criteria (Zhou et al., 2008): 1) organisms should accumulate high levels of pollutants without death, 2) organisms should represent the local population, 3) organisms should be widely distributed and have a high abundance for repetitive sampling and repetition, 4) organisms should have a long lifespan, 5) organisms should be easy to sample, 6) organisms should live in water (aquatic) and 7) organisms should occupy an important position in the food chain.

Bio-monitoring with the use of fish as a bioindicator is considered a successful means of monitoring the current state of a system as native fish species are constantly exposed to changes which occur within the system (van der Oost et al., 2003). The species used for this study is *Synodontis zambezensis*, commonly known as the brown squeaker due to the stridulatory "squeaking" noise it makes when it is stressed (Koblmüller et al., 2006). This species is an important food source for young children in the local communities surrounding the Lower Phongolo River and Floodplain (Coetzee et al., 2015). This species is known for its high-fat content and may, therefore, bio-accumulate pesticides to much higher concentrations than those seen in other fish species (Coetzee et al., 2015; Smit et al., 2016). This poses an increased threat to human populations relying on this species as a source of nourishment (Coetzee et al., 2015).

Biomarkers of effect, which reflect oxidative stress in the cells and tissue of organisms, where chosen for analysis in this study (Almroth et al., 2008). Oxidative stress as defined by Almroth et al. (2008) refers to an imbalance in pro-oxidants and antioxidants within an organism which may lead to damage. Reactive oxygen species (ROS's) form within the tissues of aquatic organisms in response to exposure to xenobiotics (Ferreira et al., 2005). The three main ROS's that form within fish species and result in oxidative stress are hydrogen peroxide, superoxide radicals and hydroxyl radicals (Atli et al., 2006). Superoxide dismutase (SOD) is an antioxidant which forms in response to the breakdown of fatty components of cell membranes by the action of ROS's (Rola et al., 2012). Catalase (CAT) works together with SOD to neutralize the resulting ROS's caused by aerobic metabolism or exposure to pollutants (Khessiba et al., 2005). The formation of the ROS malondialdehyde (MDA) following the oxidation of polyunsaturated fatty acids is an indication of oxidative stress and is measured through the biomarker MDA (Flohr et al., 2012). Structural changes, which occur in amino acid groups, result in damaged proteins known as protein carbonyls (PC) (Zusterzeel et al., 2001). The formation of PC is irreversible and is used as a biomarker of oxidative stress (Almroth et al., 2008; Almroth et al., 2005). Glutathione (GSH) acts on various ROS's to prevent damage to components present within the cell of affected organisms (Filipak Neto et al., 2008). This antioxidant acts directly on ROS's formed through lipid and protein peroxidation, forming oxidized glutathione disulphide (GSSG) (Slaninova et al., 2009).

The aim of this study was to establish baseline accumulation data within *S. zambezensis*, which may reflect the accumulation that would take place after application of 4,4′-DDT through IRS in nearby areas or after a spill event. The possible effects of such an exposure will be reflected by oxidative stress biomarkers, resulting in an assessment of the stress experienced by these individuals due to an acute exposure to 4,4′-DDT.

2. Materials and methods

2.1. Fish collection

Fish were collected from an aquaculture facility in Limpopo province and transported back to the University of Johannesburg in a 1000 L plastic transport tank. The addition of oxygen to the tank through compressed air pumps, aided in the reduction of mortality during transport (Mlambo et al., 2009).

2.2. Acclimation

At the University of Johannesburg, fish were acclimatised for two months before any exposure experiments were performed. The environmental room in which the fish were housed was kept at a constant temperature of 26 °C and a day/night cycle of 12/12.

Borehole water was circulated from the reservoir through the biological filter and pumped back into the reservoir (Mlambo et al., 2009). Feeding of the fish did not take place during the first 72 h after arrival as this can prove lethal when fish are experiencing stress (Barton, 2002).

Sufficient places of refuge were provided and shade cloth was placed over the tanks since this species is light sensitive (Sautter et al., 2007). The preferred habitat of this species requires places to hide during the day as they are nocturnal animals (Skelton, 2001). Fish were housed according to the guidelines provided in the SANS 10386 document for use of animals in research (South African National Standard (SANS), 2008).

2.3. Exposure concentrations

The stock solution used for the exposure experiments was prepared by dissolving 4,4′-DDT (98.7%, Sigma-Aldrich PESTANAL®, Analytical Standard, CAS-No 50-29-3, Batch number SZBE057XV) in ethanol (95%, Merck Millipore). Ethanol was used as the organic solvent for the 4,4′-DDT because it is insoluble in water and is therefore required to be dissolved in an organic solvent before addition to any water source (Pontolillo and Eganhouse, 2001).

One hundred milligrams 4,4′-DDT was dissolved in 1 L ethanol to make up a stock solution with a concentration of 98,700 ng/mL. From this stock solution, concentrations to be used for the 96-hour exposure period were calculated based on Toxicological information gathered from the Material Safety Data Sheet (according to regulations (EC) No. 1907/2006, Version 5.2 Revision Date 26.11.2014) and environmentally relevant concentrations (Smit et al., 2016).

The concentrations chosen were intended to correspond with environmentally relevant concentrations, but they were not intended to cause mortality in the exposed fish. The highest exposure concentration was six times higher than the LC_{50} values found in *Pimephales promelas* and *Lepomis macrochirus* juveniles (Sigma-Aldrich, 2014). This exposure was a sub lethal exposure to 4,4′-DDT and was intended to allow for the determination of baseline bioaccumulation and resulting oxidative stress biomarker concentrations. 2,4′-DDT and its degradation products were not considered in this study.

The exposure was run in duplicate rather than in triplicate because of the amount of space required for the exposure as well as the limited amount of fish available. The rest of the adult fish collected from the aquaculture unit in Limpopo were intended for experimentation in different sections of the study.

2.4. Exposure system and transfer of fish

Each of the 16 exposure tanks was 100 L in volume. Exactly 50 L of borehole water was added to each tank and allowed to stand with corner filters for two weeks. After the two weeks establishing period, five fish from the main holding tank were added to each of the 16

exposure tanks. The fish were left in the exposure tanks for a further two week acclimation period during which they were fed once every three days. Feeding stopped 24 h before the commencement of the exposure.

Day 1: 32 mL ethanol was added to the solvent control (tank 2:1 and 2:2) and the first two 4,4′-DDT volumes of stock solution were added to the respective tanks 3:1 and 3:2 = 1 mL stock solution resulting in 1.974 ng/mL concentration in exposure tanks; 4:1 and 4:2 = 2 mL stock solution resulting in 3.948 ng/mL concentration in exposure tanks.

Day 2: Volumes of the stock solution were added to the remaining eight tanks 5:1 and 5:2 = 4 mL stock solution resulting in 7.896 ng/mL concentration in the exposure tanks; 6:1 and 6:2 = 8 mL stock solution resulting in 15.792 ng/mL concentration in the exposure tanks; 7:1 and 7:2 = 16 mL stock solution resulting in 31.584 ng/mL concentration in the exposure tanks; 8:1 and 8:2 = 32 mL stock solution resulting in 63.168 ng/L concentration in the exposure tanks.

The concentrations were added one hour apart on both days to allow for adequate dissection times of five fish per hour.

2.5. Water quality

Standard in Situ water quality parameters, dissolved oxygen, oxygen percentage, Total Dissolved Solids (TDS), conductivity, temperature and pH, were measured in each tank at 24-hour intervals. The first readings were taken 20 min after the addition of the relevant concentrations to allow for a homogenous mixture of water and 4,4′-DDT stock solution or 95% ethanol in the case of the solvent control. The water parameters were measured using a Eutech Multi-Parameter (PCTestr™ 35) instrument.

2.6. Tissue sample collection

Biometric data of each fish was taken before and during dissection. The standard and total lengths were measured. Total weight, gutted weight, liver mass and gonadal mass were all recorded using a Sartorius Basic BA210S scale.

Muscle tissue was excised from the lateral side of each fish for bioaccumulation analysis. This tissue was wrapped separately in tinfoil and placed into individual zip-lock bags. Liver and gill tissue was removed from each fish and placed into separate falcon tubes containing Henriksson's Stabilising Buffer (Henriksson et al., 1986). All samples were frozen at −80 °C until further analysis.

2.7. Water sample collection

Water samples were collected in brown glass bottles from each tank at 24-hour intervals. The first water sample was collected half an hour after the addition of the 4,4′-DDT stock solution to allow for homogeneity of the water and 4,4′-DDT stock solution.

2.8. DDT analysis of tissue and water

2.8.1. Tissue extraction

The procedure of Yohannes et al. (Yohannes et al., 2013) was followed for the extraction and analysis of 4,4′-DDT and its degradation products from muscle tissue samples. One modification was made to this protocol, but the standards used remained the same as in the original extraction technique. The modification was a shorter extraction time, from 6 hours to four hours and thirty minutes. This adjustment was made with the introduction of updated system software. The organic solvents used during extraction were acetone (≥99.8%, Sigma-Aldrich, 34,850) and hexane (≥97.0%, Sigma-Aldrich, 34,859) at a ratio of 3:1 and the organic solvents used for extract clean-up were dichloromethane (DCM) (≥99.8%, Sigma-Aldrich, 34,856) and hexane at a ratio of 2:7. A wet weight of 10 g of muscle tissue was homogenised in anhydrous sodium sulphate (≥99.0%, Sigma-Aldrich, 239,313) and was placed into a pre-washed (acetone and hexane) extraction thimble. The surrogate standard 2,4,5,6-tetrachloro-m-xylene (TCmX) (200 µg/L in methanol, Sigma-Aldrich, 48,317) was added to the homogenate and the extraction thimble was placed into the extraction chamber with 150 mL of the extraction solvent. The extraction was completed with Soxtherm Apparatus (S306AK Automatic Extractor, Gerhardt Germany). The extract was concentrated to ± 2 mL using a rotary evaporator and diluted to 10 mL with hexane. Twenty percent of this mixture was used to determine the fat content of the fish through gravimetric lipid determination and the remaining 80% was dried to half of its volume with nitrogen gas and subjected to a clean-up procedure to remove excess fat. Due to the high-fat content, a double clean-up procedure was required. The first clean-up was done using Gel Permeation Chromatography (G-Prep GPC8100, GL Sciences, Japan) with a 1:1 mixture of DCM and hexane. The resulting solution was concentrated again to ± 2 mL and subjected to a second clean-up procedure. The second clean-up was done using 4 g activated Florisil® (≥80%, Sigma-Aldrich, 03286), a small amount of anhydrous sodium sulphate and glass wool (Sigma-Aldrich, 18,421). One hundred and twenty mL of a 1:1 mixture of DCM:hexane was allowed to flow through the column in a drop wise manner. The resulting solution was again concentrated with a rotary evaporator, and further dried with nitrogen gas. The final liquid was reconstituted in 100 µL of n-decane (≥95%, Sigma-Aldrich, 30,570) and analysed on a Shimadzu QP2010 GC–MS.

2.8.2. Water extraction

Extraction of 4,4′-DDT and its degradation products from the water samples taken every 24 h was done according to the extraction methods outlined in Mahugija et al. (Mahugija et al., 2015) with some modifications. The modifications included; smaller volumes of water collected for extraction and the use of clean-up with activated Florisil® instead of silica gel or alumina. Each 250 mL sample was collected in a brown glass bottle. These samples were frozen until extraction and analysis took place.

Each sample was extracted by first placing the sample into a Squibb style separating funnel and adding 60 mL DCM, the mixture was vigorously shaken for 30 s and the organic layer (bottom layer) was drained into an Erlenmeyer flask. This was done three times, resulting in 180 mL DCM extract. Anhydrous sodium sulphate was added to this extract and mixed together in order to remove any excess water from the mixture. This “dry” extract was filtered through filter paper, glass wool and more anhydrous sodium sulphate into a flat-bottomed rotary flask and concentrated to ± 0.5 mL using a rotary evaporator. The resulting evaporated sample was spiked with 100 µL of 100 ppb internal standard 3,3′,4,4′-tetrachlorobiphenyl (PCB #77, Sigma-Aldrich, 35,496) before the clean-up of the sample. The spiked samples were cleaned up through glass wool, 3 g of activated Florisil® and 1 g of anhydrous sodium sulphate after the addition of 100 mL of hexane: DCM (1:1) clean-up solvent. The solution was collected in a second flat bottomed evaporation flask and evaporated to ± 1 mL. The resulting residue was concentrated under a light stream of nitrogen gas to near dryness and finally reconstituted in 100 µL of n-decane for later analysis using a Shimadzu QP2010 GC–MS.

2.8.3. Gas chromatography-mass spectrometry

Gas chromatography-mass spectrophotometry (GC–MS) (Shimadzu QP2010 GC–MS) was used to quantify the amount of 4,4′-DDT and its degradation products in the prepared tissue and water samples. Calibration curves were used to quantify the amount of 4,4′-DDT and its potential degradation products, 4,4′-DDE and 4,4′-DDD.

A Shimadzu 2010 plus GC–MS with AOC 20i autosampler was used. Instrument parameters were based on EPA Method 8081b (United States Environmental Protection Agency (USEPA), 2007). A Zebron ZB-5Msplus capillary column (30 m × 0.25 mm i.d., 0.25 µm film thickness) was used. Splitless injections of 1 µL were performed. The temperature of the GC oven was kept constant at 60 °C for 2 min, after

which it was ramped up by 10 °C/min where it was kept constant for 2 min. The signal was detected using electron ionization mass spectrometry (EI-MS) with and interface temperature of 280 °C and ion source at 230 °C. Selected Ion Monitoring (SIM) was used for the analysis since the concentrations of 4,4′-DDT and its degradation products were very low. The following *m/z* values were selected for SIM: 246, 248, 176, 318, 235, 167. Each sample was analysed in triplicate and the average of each sample was taken as the final concentration.

In order to determine the percentage of the initial dose of 4,4′-DDT accumulated by fish and extracted from the water, the presence of degradation products had to be taken into account. During degradation/metabolisim a stoichiometric ratio of 1:1 for 4,4′-DDT and its respective degradation products exists. Therefore the masses obtained from the calibration experiments (GC–MS) were converted to moles. The moles of 4,4′-DDT, 4,4′-DDE and 4,4′-DDD were then added to get the total number of moles of 4,4′-DDT from which it originated. The total number of moles were then converted to mass to give 4,4′-DDT equivalents.

Therefore, DDT equivalents were determined using the following equation:

$$DDT\ equivalents\ in\ ng/g = \left[\left(\frac{x\ ng\ DDT}{g\ sample} \times \frac{1\ mole\ DDT}{354.48\ g\ DDT}\right) + \left(\frac{y\ ng\ DDD}{g\ sample} \times \frac{1\ mole\ DDD}{320.\ 04\ g\ DDD}\right) + \left(\frac{z\ ng\ DDE}{g\ sample} \times \frac{1\ mole\ DDE}{318.03\ g\ DDE}\right)\right] \times \frac{354.48\ g\ DDT}{1\ mole\ DDT}$$

where x, y and z represent the values obtained from calibration experiments (i.e. GC–MS) for 4,4′-DDT, 4,4′-DDD and 4,4′-DDE respectively (Table 4).

2.8.4. Quality control and quality assurance

The internal standard used for the water samples (PCB#77) was added at a volume of 100 µL and a concentration of 100 ppb before the clean-up procedure. The internal standard used for the tissue samples was TCmX. All recoveries of the internal standard were acceptable based on previous literature (Yohannes et al., 2013) and were above 85%. 4,4′-DDT and all possible degradation products were identified using Selected Ion Monitoring (SIM) and retention times were checked and assigned to each peak. Multi-level calibration curves were created for each metabolite and linearity was successfully achieved ($R^2 \geq 0.995$). Procedural and spiked blanks were analysed along with samples to assure quality control according to literature and reported results showed acceptable recoveries between 90% and 105% (Yohannes et al., 2014). The concentrations of tissue samples are expressed in lipid weight. The concentrations for water samples are however expressed in wet weight.

2.9. Biomarker analysis of muscle and gill tissue

The biomarker protocols outlined in the section to follow were all completed within standard operating guidelines outlined in the relevant literature. All protocols used a 96 well microtiter plate and protein content was determined in the tissues for each of the biomarkers according to the method of Bradford (Bradford, 1976). Absorbance was measured at 630 nm with bovine serum albumin (BSA) used as a standard. All biomarker activities are expressed per milligram protein to allow for standardisation.

2.9.1. Superoxide dismutase

The protocol applied for the analysis of SOD was adapted from Greenwald (Greenwald, 1985). Zero point two grams of liver tissue was homogenised in 200 µL General Homogenising Buffer (GHB) and the homogenate was centrifuged (High Speed Refrigerated Centrifuge: NovaFuge B113-21R, Senova Biotech Co.,Ltd) at 7393*g*. The reaction was initiated by adding 25 µL 1,2,3-Benzenetriol (Pyrogallol ≥98%, Sigma-Aldrich) solution just before analysis. The measurements were recorded for 10 mins total length with excitation readings being taken at 60 s intervals. The samples were analysed on a Multi-Detection microplate reader (FLx800 Fluorescence Microplate Reader, BioTek® Instruments, Inc.). Analysis was carried out in a dark room as pyrogallol is extremely light sensitive.

2.9.2. Catalase

The procedural methodology for CAT activity was adapted from Cohen et al. (Cohen et al., 1970). Phosphate buffer (1 mL, 0.01 M, pH 7) and 0.1 g of liver tissue were homogenised and centrifuged at 5590*g*. for 10 mins at 4 °C. The amount of unreacted $KMnO_4$ was then measured spectrophotometrically at 409 nm using an automated microplate reader (Elx800-Universal Microplate Reader, BioTek® Instruments, Inc.).

2.9.3. Malondialdehyde

Malondialdehyde (MDA) was analysed through procedures and methodologies adapted from Ohkawa et al. (Ohkawa et al., 1979) including modifications by Üner et al. (Üner et al., 2006). Homogenate was prepared by homogenising 0.05 g of liver tissue in 250 µL of Tris/Sucrose Buffer and then centrifuging at 5045*g*. for 10 min at 4 °C. The samples and blank were added in triplicate to a microtiter plate at a volume of 245 µL and analysed at 540 nm using an automated microplate reader (Elx800-Universal microplate reader, BioTek® Instruments, Inc.).

2.9.4. Protein carbonyl

Methodologies were adapted from Parvez and Raisuddin (Parvez and Raisuddin, 2005) as assayed by Levine et al. (Levine et al., 1990) and also contains modifications applied by Floor and Wetzel (Floor and Wetzel, 1998). Zero point one grams of liver tissue was homogenised in GHB and centrifuged at 10188*g*. for 30 min at 4 °C. After the above mentioned protocols were followed, 100 µL of the resulting liquid was analysed at 366 nm using an automated microplate reader (Elx800-Universal microplate reader, BioTek® Instruments, Inc.).

2.9.5. Reduced glutathione

Reduced glutathione (GSH) content was determined following the protocols outlined by Cohn and Lyle (Cohn and Lyle, 1966). A homogenate of 100 mg of tissue and 250 µL Tris/Sucrose Buffer was processed following the above mentioned protocol and 100 µL of the sample was analysed at 420 nm emission with excitation of 350 nm (Elx800-Universal microplate reader, BioTek® Instruments, Inc.).

2.10. Statistics

SPSS version 25 (IBM Software Group) was used for one-way analysis of variance (ANOVA) following log transformation of all accumulation and biomarker data to ensure homogeneity. Significant differences ($p \leq .05$) between concentrations and skewness of data were determined using the Tukey Post Hoc test (Yohannes et al., 2013). Multivariate statistics were applied to the bioaccumulation and biomarker data. Constrained redundancy analysis (RDA) was applied to determine the influence of 4,4′-DDT and its degradation products on the spread of the oxidative stress biomarkers analysed (Quinn and Keough, 2002). The constrained RDA was completed with the use of Canoco 5 software.

3. Results

3.1. Biometric data

The standard length of the exposed fish ranged from 69 mm to 106 mm with the total lengths ranging from 89 mm to 132 mm (Table 1). The total mass ranged from 7.22 g to 23.82 g with no significant differences ($p \leq .05$) seen in the lipid contents of the exposed fish. The gonadal and liver mass ranged from 0.02 g to 1.40 g and 0.06 g

Table 1
Biometric data (Mean ± SD) and range of *Synodontis zambezensis* exposed to *4,4′*-DDT during an acute exposure.

Exposure conc. (ng/mL)	Number of Fish (n)	Standard Length (mm)	Total Length (mm)	Total Mass (g)	Liver Mass (g)	Gonadal Mass (g)	Lipid %
Control	10	91.50 ± 3.07 (79–106)	112.8 ± 10.26 (96–131)	14.83 ± 3.66 (9.23–22.35)	0.139 ± 0.04 (0.07–0.19)	0.20 ± 0.25 (0.05–0.86)	7.07 ± 0.88 (4.58–10.19)
Solvent control	10	82.10 ± 7.26 (71–97)	104.90 ± 8.80 (90–121)	12.41 ± 3.27 (7.36–17.70)	0.16 ± 0.06 (0.08–0.26)	0.14 ± 0.14 (0.02–0.52)	10.25 ± 0.35 (9.22–11.51)
1.97	10	85.70 ± 6.11 (79–96)	108.10 ± 7.65 (102–124)	12.84 ± 2.97 (9.68–18.19)	0.11 ± 0.03 (0.09–0.19)	0.09 ± 0.06 (0.04–24)	9.03 ± 1.10 (6.94–11.56)
3.95	10	82.30 ± 7.62 (71–99)	104.00 ± 7.29 (92–119)	11.54 ± 3.18 (8.03–18.72)	0.10 ± 0.03 (0.06–0.16)	0.09 ± 0.11 (0.02–0.40)	6.87 ± 1.42 (2.73–10.12)
7.90	10	88.70 ± 10.12 (69–105)	113.20 ± 12.30 (89–132)	14.54 ± 4.75 (7.22–23.82)	0.14 ± 0.06 (0.06–0.24)	0.25 ± 0.28 (0.03–1.00)	4.62 ± 0.41 (3.60–6.21)
15.79	10	88.10 ± 8.12 (78–102)	110.80 ± 9.86 (98–131)	14.05 ± 3.60 (9.55–21.47)	0.15 ± 0.04 (0.10–0.24)	0.23 ± 0.18 (0.07–0.56)	5.55 ± 0.30 (5.32–6.56)
31.58	10	87.50 ± 6.10 (78–95)	113.70 ± 8.59 (101–124)	14.62 ± 3.99 (9.43–22.08)	0.17 ± 0.06 (0.07–0.27)	0.31 ± 0.42 (0.02–1.40)	4.30 ± 0.29 (3.34–5.19)
63.17	10	87.60 ± 7.77 (81–100)	107.60 ± 11.10 (99–126)	12.83 ± 3.96 (8.90–19.16)	0.16 ± 0.05 (0.12–0.24)	0.18 ± 0.24 (0.03–0.60)	5.13 ± 1.03 (1.97–8.61)

to 0.26 g respectively. These organ parameters where measured to calculate the Gonadosomatic and Hepatosomatic Indices, but these indices yielded no significant differences ($p \leq .05$) between fish in the varying exposure concentrations.

3.2. Water quality

The water quality parameters changed slightly during the acute exposure period but were fairly constant (Table 2). The mean pH readings across all 16 exposure tanks ranged from 7.45 to 7.79 which falls within the pH tolerance of *Synodontis zambezensis* (Skelton, 2001). The dissolved oxygen (D.O mg/L) and oxygen percentage (O_2%) was very low during the initial measurement taken 30 min after the addition of the concentrations and the ethanol in the case of the solvent control. The oxygen levels stabilized hereafter and resulted in a mean across all tanks ranging from 5.59 mg/L to 6.70 mg/L (D.O) and 74.50% to 84.49% (O_2%). Since the exposure tanks were kept in an environmental room maintained at a constant temperature of 26 °C, the mean temperature of the water did not fluctuate much throughout the exposure period and ranged from 25.41 °C to 26.17 °C, again falling within the temperature tolerance range of *Synodontis zambezensis* (Skelton, 2001). Increases in conductivity (EC) and total dissolved solids (TDS) are directly proportional to increases in the concentration of DDT added to the exposure tanks. The mean EC and TDS ranged from 263.10 µS/cm to 1269.40 µS/cm and 133.20 mg/L to 649.50 mg/L respectively.

3.3. Levels of DDT in Synodontis zambezensis

All three of the degradation products were found in the fish exposed to the 4,4′-DDT in all six exposure concentrations. The 4,4′-DDT used was of 98.7% purity purchased from Sigma-Aldrich PESTANAL® as an Analytical Standard (CAS-No 50-29-3, Batch number SZBE057XV). The readings are reported in lipid mass because there were no significant differences ($p \leq .05$) found in the fat content of the fish in each of the exposure tanks (Table 1). Accumulated concentrations for the control tanks are not included in the results section because, as expected, there was no 4,4′-DDT or its degradation products found in the tissue of the fish in these tanks. The *S. zambezensis* used in the exposure were bred and grown completely in captivity before the exposure took place. Accumulated concentrations varied throughout the exposure tanks and did not always reflect the nominal concentrations added at the beginning of the 96-h exposure period (Table 3). The mean 4,4′-DDE concentrations ranged from 15.35 ng/g to 45.34 ng/g. Mean 4,4′-DDD concentrations ranged from 28.16 ng/g to 63.25 ng/g and mean 4,4′-DDT concentrations ranged from 28.64 ng/g to 96.21 ng/g. Notably, 4,4′-DDE and 4,4′-DDT were accumulated to the highest concentration in the exposure tank within the highest nominal concentration (63.17 ng/mL). This was however not the case with 4,4′-DDD which was accumulated to the highest concentration in the exposure tank with the second highest nominal concentration (31.58 ng/mL).

It is clear that *S. zambezensis* accumulates 4,4′-DDT and its degradation products from its immediate environment, in this case the exposure tank water. The results listed in Table 4, show that from a nominal concentration of 1.97 ng/mL (lowest) to 63.17 ng/mL (highest) a 4,4′-DDT equivalents of 76.92 ng/g and 213.53 ng/g respectively were accumulated after the acute exposure period. Should the exposure period be increased, even larger amounts of 4,4′-DDT equivalents are expected.

The trend seen is that the accumulated concentrations of each degradation product seems to increase as the nominal concentration increases from the lowest nominal concentration (1.97 ng/mL) to the highest nominal concentration (61.17 ng/mL) (Fig. 1). The accumulated concentrations of each degradation product increases as the nominal concentration increases, however the total percentage accumulated (Table 4) of the initial dose of 4,4′-DDT decreases as the nominal concentrations increases.

Table 2
In Situ water quality parameters (Mean ± SD) and range readings taken of the exposure tanks during the course of the 96-hour *4,4′*-DDT exposure experiment. pH, Dissolved Oxygen (D.O), Oxygen percentage ($O_{2\%}$), Electrical Conductivity (EC), Temperature (°C) and Total Dissolved Solids (TDS).

Exposure conc. (ng/mL)	pH	D.O (mg/L)	O_2 (%)	EC (μS/cm)	Temp. (°C)	TDS (mg/L)
Control	7.51 ± 0.17 (6.92–7.93)	6.13 ± 0.76 (3.81–7.69)	75.51 ± 9.03 (48.20–94.60)	263.10 ± 1.63 (259.00–268)	26.04 ± 0.33 (25.40–28.50)	133.20 ± 0.69 (131.00–135.00)
Solvent control	7.59 ± 0.22 (6.61–7.98)	6.05 ± 0.80 (3.76–8.86)	74.50 ± 9.70 (46.60–108.20)	785.20 ± 17.00 (660.00–757.00)	25.78 ± 0.10 (25.3–26.1)	394.00 ± 8.14 (370.00–436.00)
1.97	7.59 ± 0.21 (6.63–7.91)	5.69 ± 0.48 (4.27–6.64)	70.31 ± 5.85 (53.10–82.30)	692.00 ± 12.19 (659.00–757.00)	25.93 ± 0.12 (25.40–26.30)	344.40 ± 6.57 (328.00–379.00)
3.95	7.45 ± 0.21 (7.12–8.03)	5.60 ± 0.57 (5.06–8.63)	69.33 ± 7.03 (61.80–105.20)	962.70 ± 14.77 (1125.00–1139.00)	26.17 ± 0.11 (25.30–25.80)	482.20 ± 7.40 (560.00–618.00)
7.90	7.64 ± 0.17 (7.12–8.03)	6.91 ± 0.55 (5.06–8.63)	84.49 ± 6.78 (61.80–105.20)	1160.20 ± 14.43 (1125.00–1235.00)	25.41 ± 0.08 (25.30–25.80)	588.80 ± 10.92 (560.00–618.00)
15.79	7.79 ± 0.12 (7.36–8.00)	6.70 ± 0.55 (4.84–8.56)	82.21 ± 6.67 (59.50–104.00)	1269.40 ± 38.97 (1113.00–1499.00)	25.67 ± 0.09 (25.20–26.10)	633.70 ± 19.66 (557.00–748.00)
31.58	7.61 ± 0.15 (7.03–7.95)	6.12 ± 0.36 (4.80–6.88)	75.39 ± 4.48 (59.20–83.70)	1300.80 ± 9.51 (1254.00–1359.00)	25.71 ± 0.18 (25.30–26.30)	649.50 ± 4.50 (629.00–678.00)
63.17	7.60 ± 0.21 (6.31–8.02)	6.19 ± 0.43 (4.72–7.39)	76.36 ± 5.19 (58.40–90.60)	1139.80 ± 10.11 (1101.00–1186.00)	26.01 ± 0.09 (25.60–26.30)	568.70 ± 5.06 (536.00–591.00)

Table 3
Levels of accumulation in *S. zambezensis* muscle tissue and concentrations in water samples of the 4,4′-DDT degradation products (Mean ± SD) and range after an acute laboratory exposure.

	Exposure Conc. (ng/mL)	4,4′-DDE (ng/g)	4,4′-DDD (ng/g)	4,4′-DDT (ng/g)		4,4′-DDE (ng/mL)	4,4′-DDD (ng/mL)	4,4′-DDT (ng/mL)
Tissue	1.97	15.34 ± 1.49 (11.18–15.52)	28.16 ± 3.92 (19.55–40.20)	28.64 ± 2.57 (22.39–36.27)	Water	0.43 ± 0.08 (0.34–1.24)	3.98 ± 0.21 (2.95–4.99)	0.75 ± 0.07 (3.40–3.46)
	3.95	35.32 ± 8.75 (11.26–80.31)	42.50 ± 4.83 (25.28–67.59)	39.90 ± 7.45 (0.98–67.94)		5.91 ± 0.63 (3.33–9.30)	7.27 ± 0.55 (4.47–9.87)	7.74 ± 0.40 (5.50–9.29)
	7.90	20.88 ± 2.18 (13.07–32.52)	43.73 ± 7.00 (17.35–74.86)	47.72 ± 7.46 (22.00–87.20)		2.51 ± 0.16 (1.71–3.32)	3.99 ± 0.14 (3.51–4.90)	5.13 ± 0.16 (4.60–6.06)
	15.79	29.43 ± 2.76 (19.59–41.18)	48.87 ± 2.62 (39.55–61.69)	54.12 ± 9.06 (1.65–87.48)		2.04 ± 0.05 (1.92–2.26)	3.80 ± 0.30 (3.26–6.81)	5.33–0.25 (4.67–7.43)
	31.58	40.70 ± 4.90 (20.89–62.78)	63.25 ± 8.50 (44.76–114.53)	75.32 ± 8.27 (52.26–124.75)		10.50 ± 2.08 (4.12–25.39)	11.19 ± 1.69 (5.83–23.42)	9.59 ± 0.71 (6.72–10.77)
	63.17	45.34 ± 5.21 (33.72–72.83)	60.29 ± 2.49 (54.63–75.88)	96.21 ± 6.41 (72.57–128.83)		2.85 ± 0.24 (1.97–4.31)	4.12 ± 0.21 (3.38–5.55)	7.38 ± 0.99 (4.84–16.34)

Table 4
Levels of accumulation of the 4,4′-DDT degradation products in *S. zambezensis* muscle tissue and extracted from the exposure tank water as well as percentage 4,4′-DDT accumulated in *S. zambezensis*. The 4,4′-DDT used was of 98.7% purity purchased from Sigma-Aldrich PESTANAL® as an Analytical Standard (CAS-No 50–29-3, Batch number SZBE057XV).

Exposure Tanks		Average accumulated by *S. zambezensis* (ng/g)					Average extracted from water after 96-h (ng/mL)				
Conc. (ng/mL)	Total DDT in tank (μg)	4,4′-DDE	4,4′-DDD	4,4′-DDT	4,4′-DDT Equivalents	% initial dose	4,4′-DDE	4,4′-DDD	4,4′-DDT	4,4′-DDT Equivalents	% initial dose
1.97	98.70	15.34	28.16	28.64	76.92	77.93	0.43	3.98	0.97	5.86	5.94
3.95	197.40	35.32	42.50	39.90	126.34	64.00	5.91	7.27	7.74	22.39	11.34
7.90	394.80	20.88	43.73	47.72	119.43	30.25	2.51	3.99	5.13	12.34	3.13
15.79	789.60	29.43	48.87	54.12	141.05	17.86	2.04	3.80	5.33	11.81	1.50
31.58	1579.20	40.70	63.25	75.32	190.75	12.08	10.50	11.19	9.59	33.69	2.13
63.17	3158.40	45.34	60.29	96.21	213.53	6.76	2.85	4.12	7.38	15.11	0.48

3.4. Levels of DDT in water samples

In the current study, the three degradation products found were 4,4′-DDE (0.34 ng/mL to 25.39 ng/mL), 4,4′-DDD (2.95 ng/mL to 23.42 ng/mL) and 4,4′-DDT (3.40 μg/L to 16.34 μg/L), and unlike in the fish tissue, 4,4′-DDD is found at the highest concentrations (Table 3). The general trend sees the constant presence of all three degradation products with the highest concentrations of the 4,4′-DDE and 4,4′-DDD being found in the second highest nominal concentration. The highest concentration of the parent compound 4,4′-DDT was however found in the highest nominal concentration.

When looking at the concentrations at 24-h intervals, there is no clear trend for the various concentrations in exposure tanks, but the duplicate tanks showed the same trend in each concentration, giving confidence that the extraction and analysis of the samples were consistent throughout. The presence of a low standard deviation (SD) is also an indication of the consistency.

Each exposure tank, regardless of the nominal concentration added,shows the presence of all 3 degradation products, with little variation between the 24-hour sample periods. The general trend was that the concentrations of each metabolite seemed to decrease over the 96-hour period. This decrease over time may be linked to increased degradation and adsorbtion to colloidal particulates within exposure tank water (Taha and Mobasser, 2014).

At the highest exposure concentration, it is notable that although all three degradation products are present, the concentrations are less than half those found in the second highest concentration. The duplicate tanks at the highest concentration contained large amounts of secreted mucus from the fish. This mucus was removed from the water samples before extraction and analysis and this may be the reason why these degradation products do not occur at these high concentrations.

The parent compound 4,4′-DDT occurs at all intervals in all tanks and indicates the “recent” nature of this exposure.

3.5. Oxidative stress biomarkers

The resulting biomarker responses in the liver and gill tissue are reported in Fig. 1A–E, with significant differences ($p \leq .05$) being indicated by common superscripts (Capital or small letters of the alphabet). Unfortunately MDA analysis could only be performed in the liver tissue as the gills were too small to allow for the analysis of MDA as well as the other oxidative stress biomarkers. The liver and the gills were used because the liver is the detoxifying organ of the organism and the gills are in direct contact with the aquatic environment and may show more advanced changes during an acute exposure (Rola et al., 2012).

The SOD analysis resulted in varied responses between tissues. The SOD response in the liver tissue ranged from a mean of 0.93 ng SOD/mg protein to 1.57 ng SOD/mg protein, while in the gills the response was much higher and ranged from a mean of 2.05 ng SOD/mg protein to 4.06 ng SOD/mg protein. There were no significant differences ($p \leq .05$) noted within the liver at the varying concentrations, but within the gills significantly higher concentrations of SOD were found at the 7.90 ng/mL and 31.50 ng/mL exposure concentration when compared to the control. A significantly higher SOD response was also noted in the gills at the 31.58 ng/mL exposure concentration when compared with the 15.79 ng/mL exposure concentration (Fig. 1A).

The MDA (nmol/mg protein) ranged from a mean of 0.11 nmol/mg protein to 0.66 nmol/mg protein and a significant difference ($p \leq .05$) is noted between the 3.95 ng/mL and 7.90 ng/mL exposure concentrations, with a significantly lower resonse in the higher exposure concentration (Fig. 1E).

Protein carbonyl responses were similar when comparing the gills and the liver and ranged from a mean of 185.07 nmol carbonyl/mg protein to 255.34 nmol carbonyl/mg protein and from 213.79 nmol carbonyl/mg protein to 272.84 nmol carbonyl/mg protein respectively. There was a significant difference ($p \leq .05$) noted only in the liver tissue with a significantly lower PC concentration in the 1.97 ng/mL exposure concentration when compared with the control (Fig. 1B).

The CAT concentrations ranged from 26.17 μmol H_2O_2/min/mg protein to 57.86 μmol H_2O_2/min/mg protein in the gills and from 150.62 μmol H_2O_2/min/mg protein to 274.01 μmol H_2O_2/min/mg protein in the liver. The response of CAT was clearly greater within the liver tissue, however there was no significant difference ($p \leq .05$) found between exposure concentrations in the liver tissue (Fig. 1C). In the gill tissue significantly lower CAT responses were noted at the 7.90 ng/mL, 31.58 ng/mL and 63.17 ng/mL exposure concentrations when compared to the control. A significantly higher response in CAT was found at the 1.97 ng/mL exposure concentration when compared with the response seen at the 7.90 ng/mL and 31.58 ng/mL exposure concentrations. The final significant difference seen in CAT was a higher response at the 3.95 ng/mL exposure concentration when compared to the 7.90 ng/mL and 31.58 ng/mL exposure concentrations.

Reduced glutathione concentrations within the gill tissue showed a significantly higher response at the 63.17 ng/mL exposure concentration when compared to all other exposure concentrations and the control (Fig. 1D). In the liver tissue a significantly higher response was seen at the 1.97 ng/mL and 3.95 ng/mL exposure concentrations when compared to the 15.79 ng/mL and the 31.58 ng/mL exposure concentrations. The GSH concentrations in the gills ranged from a mean of 1.95 μg/mg protein to 4.67 μg/mg protein. The mean range of GSH in the liver tissue was from 1.26 μg/mg protein to 2.26 μg/mg protein.

3.6. Relationship between biomarkers and bioaccumulation

In order to relate the biomarkers of oxidative stress to 4,4′-DDT and its degradation products, an RDA triplot was constructed (Fig. 2). An RDA can be considered a constrained version of a Principal Component Analysis (PCA), meaning that the responses (oxidative stress biomarkers) are constrained by the 4,4′-DDT and the degradation products

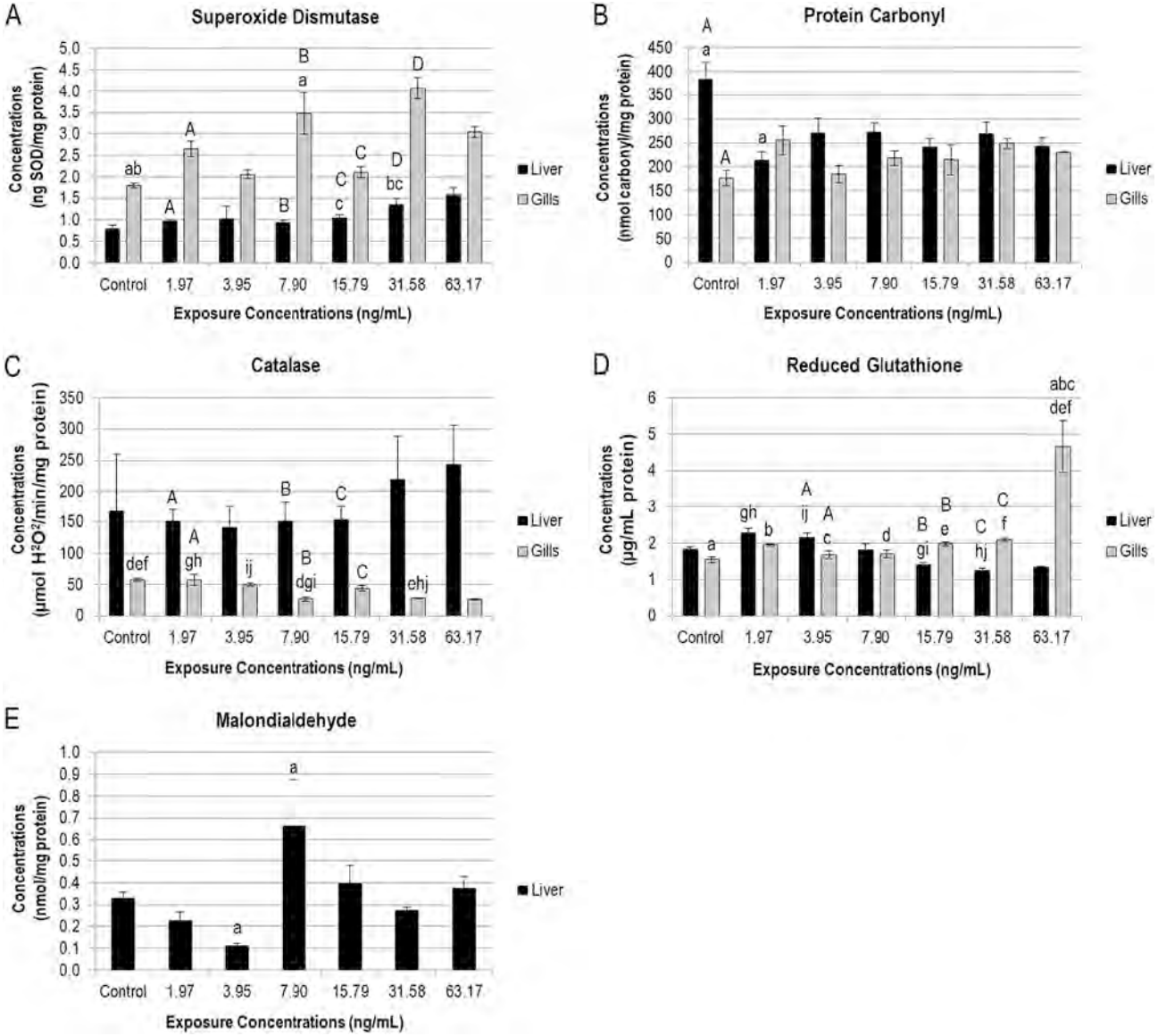

Fig. 1. Biomarkers of Oxidative stress within the liver and the gills of *Synodontis zambezensis* after an acute exposure to 4,4′-DDT. Superoxide dismutase (Fig. 1A), PC (Fig. 1B), CAT (Fig. 1C), GSH (Fig. 1D) and MDA (Fig. 1E). Significant differences ($p \leq .05$) between tissues within the same biomarker are indicated by the presence of capital letter suberscripts. Significant diffierences ($p \leq .05$) within the same tissue (liver or gills) of the same biomarker are indicated by common lower case letter suberscripts.

(Quinn and Keough, 2002). This constrained ordination gives an indication of the effect of 4,4′-DDT and its degradation products on the spread of the oxidative stress biomarkers within the two focus tissues. he angles between all vectors reflect their (linear) correlation. The correlation between the responses (oxidative stress biomarkers), the contsraining variables (4,4′-DDT and its degradation products) or any combination thereof, is equal to the cosine of the angle between vectors (arrows) (Quinn and Keough, 2002). For example, should the angle between two vectors be at an angle equal to 90°, the two vectors are uncorrelated since cos(90) = 0. However, should the angle between two vetors equal 20°, these two vectors will have a strong, positive correlation since cos(20) = 0.94 (Quinn and Keough, 2002). The length of the arrows is also an indication of the strength or influence of the vector, with longer arrows having a greater influence (Quinn and Keough, 2002).

The ordination in Fig. 2 explains 94.41% of the variance within the data. The first axis (function 1 – Horizontal axis) explains 35.77% of the variance within the data. The second axis (function 2 – Vertical axis) explains 58.64% of the variance within the data and a clear separation is seen vertically between SOD in the gills and liver, GSH in the gills, and CAT in the liver tissue when compared with the other biomarkers of oxidative stress. The arrow for 4,4′-DDT is much longer than that of its degradation products and this indicates its increased influence on the resulting biomarker excitation.

The angle between SOD in the gills and liver as well as GSH in the gills indicates a strong correlation of these biomarkers with 4,4′-DDT (≤90°). The same can be seen with 4,4′-DDD and 4,4′-DDE with the above mentioned biomarkers. The angles between 4,4′-DDT and its degradation products and MDA in the liver are ≥90°, this indicates a weak correlation between the biomarker response and 4,4′-DDT and its degradation product. This can be seen with PC and GSH in the liver, as well as CAT and PC in the gills.

The correlation coefficients glisted in Table 5, give a clearer indication of the correlations between the different oxidative stress biomarkers in the liver and gill tissues, and 4,4′-DDT and its degradation products seen in the RDA triplot. Correlation coefficients are values which range between +1.0 and − 1.0, and give an indication of the relationship between two sets of variables (Quinn and Keough, 2002),

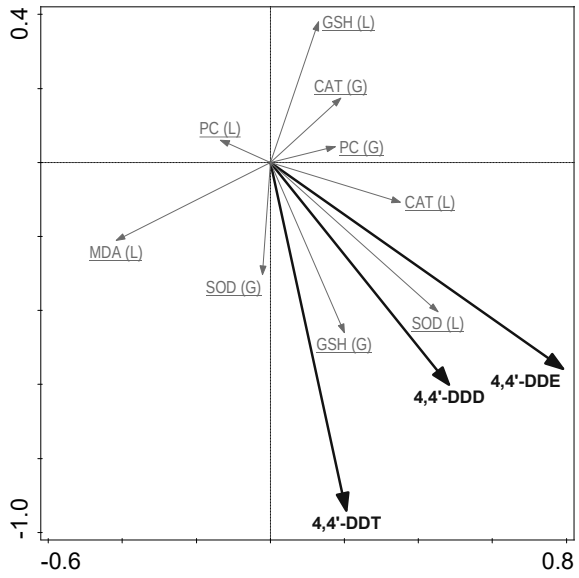

Fig. 2. RDA triplot showing resulting oxidative stress biomarker responses in *Synodontis zambezensis* following an acute exposure to varying concentrations of 4,4′-DDT. The resulting oxidative stress biomarkers are constrained in this ordination by 4,4′-DDT and its degradation products, 4,4′-DDE and 4,4′-DDD.

for example SOD in the gills and 4,4′-DDT. In this example there is a positive correlation indicated by a correlation coefficient of 0.28, and this is corroborated by the $\leq 90^{\circ}$ angle seen between these two arrows in the RDA triplot (Fig. 2). The same justification can be made by comparing the correlation coefficients listed in Table 5 and the angles between the various arrows in the RDA triplot in Fig. 2.

4. Discussion

4.1. Water quality

The TDS within aquatic systems is contributed to by both inorganic and organic dissolved salts (Thirumalini and Joseph, 2009), therefore higher dissolved salts leads to higher TDS readings. The EC of a water sample can be correlated with TDS but gives slightly different information, as it relates to the electrical nature of the dissolved salts within the water (Atekwana et al., 2004). Both the TDS and the EC readings increased as the exposure concentrations of 4,4′-DDT increased in the relevant exposure tanks. The addition of contaminants from the 4,4′-DDT may have contributed to the increase in EC (Thirumalini and Joseph, 2009), but the increases in TDS are much more significant across the exposure tanks. Since TDS readings are affected by both organic and inorganic salts, the increase in mucus secreted by the fish in the tanks containing higher 4,4′-DDT concentrations may have affected the TDS (Church et al., 2009). Fish mucus is composed mainly of large macromolecules which form a gel in water (Easy and Ross, 2009), these macromolecules may interact with dissolved ions and affect the total TDS readings (Easy and Ross, 2009).

Table 5
Tabulated correlation coefficients (factor or component loadingds) between the resulting oxidative stress biomarkers (SOD,MDA, PC, CAT and GSH) in both the liver and gill tissue of *Synodontis zambezensis* in relation to 4,4′-DDT and its degradation products 4,4′-DDE and 4,4′-DDT.

	Liver			Gills		
	4,4′-DDE	4,4′-DDD	4,4′-DDT	4,4′-DDE	4,4′-DDD	4,4′-DDT
SOD	0.57	0.50	0.49	0.15	0.18	0.28
MDA	−0.21	−0.08	0.11	NA	NA	NA
PC	−0.24	0.15	0.02	0.09	0.11	0.02
CAT	0.34	0.24	0.17	0.10	−0.12	−0.17
GSH	−0.11	−0.17	−0.33	0.46	0.27	0.43

4.2. Levels of DDT in Synodontis zambezensis

The decrease in total percentage accumulated (Table 4) as the nominal concentrations increases can be attributed to various factors that may include increased volatization through photodegradation, adsorption to the tank surfaces and sedimentation resulting in less bioavailability of the metabolites (Foght et al., 2001). Volatization of 4,4′-DDT occurs almost immediately after it enters the aquatic environment and the reported half-life for 4,4′-DDT is approximately 56 days in lakes and 28 days in riverine systems (United States Environmental Protection Agency (USEPA), 1989; Bedos et al., 2002).

The only routes of accumulation present in this study were directly through either the skin or respiration through the gills. It is, therefore, no surprise that the bioaccumulation of the parent compounds (4,4′-DDT) is much higher than that of the more degraded forms (DDE and DDD) (Yohannes et al., 2014) in all of the exposure tanks. Higher concentrations of 4,4′-DDE and 4,4′-DDD are associated with biomagnification through the food chain since they are a result of the physiological breakdown of 4,4′-DDT through animal metabolic processes (Rognerud et al., 2002). The general pattern of accumulation seen in the wild is that 4,4′-DDE is the highest, followed by 4,4′-DDD and then 4,4′-DDT (Bedos et al., 2002). There was some metabolic breakdown in this study, but since the exposure was acute, the exposed fish did not metabolize the 4,4′-DDT to the same extent as they would have over a longer period of time. A study conducted by Macek and Korn (Macek and Korn, 1970) revealed the importance that the food chain plays in the accumulation of 4,4′-DDT within fish. In the study, the results show that up to 35.5% of the 4,4′-DDT available to *Salvelinus fontinalis* (brook trout) was accumulated when it was exposed through its diet. On the other hand, only 3.55% of the total 4,4′-DDT available was accumulated when exposure took place only through the water (Kidd et al., 2001).

An observation made during the exposure period was that the higher concentrations caused the fish to secrete large quantities of mucus into the water. This mucus can be secreted as a response to pathogenic agents or xenobiotics in their environment, and the quantity and nature of the mucus they secret can vary in relation to the changes in the environment (Easy and Ross, 2009). The presence of these high volumes of mucus may have increased the surface area for adhesion of 4,4′-DDT and its degradation products, making the bioavailability lower in the tanks. This means that even though the nominal concentrations were highest in the tanks, the ability for accumulation to occur was decreased (Foght et al., 2001). Mucus has also been shown to serve a protective function in fish, creating a barrier between the fish and the external environment (Church et al., 2009), this may in turn decrease the ability for the fish to bioaccumulate toxicants. As seen in Table 4, in the lowest nominal concentration, 73.08% of the 4,4′-DDT added to the tank was accumulated by *S. zambezensis*, and this percentage decreases as the nominal concentration increases. In the highest nominal concentration, only 6.39% of the initial 4,4′-DDT was accumulated by *S. zambezensis*, another indication that although the overall accumulation increased as the nominal concentration increased, the percentage accumulated still decreases.

Synodontis sp. is known for its high tissue fat content which has been previously linked to their higher than normal buoyancy and results in their ability to achieve their well documented upside-down swimming behaviour (Lalèyè et al., 2006). Since 4,4′-DDT is lipophilic and accumulates in fatty tissues (Gaspar et al., 2015) it is expected that fish with higher fat contents will accumulate higher concentrations of 4,4′-DDT (Kidd et al., 2001). Unfortunately, the full extent of *S. zambezensis* accumulation is not clear from the results of this study since the exposure period was acute and because the addition of bio-magnification through

the food chain is not illustrated here as it was not within the scope of the study. It is clear from this study, however, that *S. zambezensis* does accumulate 4,4′-DDT and its degradation products at significant concentrations, even only after a single exposure and during a 96-hour period. The accumulated concentrations found during this study fall within the environmentally relevant concentrations found in the same species in the Lower Phongolo River and Floodplain (Smit et al., 2016). In the study by Smit et al. (Smit et al., 2016), 4,4′-DDT concentrations ranged from 0.07 ng/g to 802.17 ng/g and 4,4′-DDE concentrations ranged from 0.09 ng/g to 1208.18 ng/g. The lowest degradation product found was 4,4′-DDD and ranged from 0.07 ng/g and 567.07 ng/g. Although these concentrations were much higher than those found in the current study, the concentrations are within the environmental range of accumulation. Conversely, 4,4′-DDE in the study by Smit et al. (Smit et al., 2016) is much higher and is a clear reflection of the effect of the food chain on accumulation in this fish species (Smit et al., 2016).

4.3. Levels of DDT in water samples

A microcosm study done by the USEPA (United States Environmetnal Protection Agency (USEPA), 1979) illustrates the fate of 4,4′-DDT in the aquatic environment after 30–40 days. The 4,4′-DDT concentrations present in the water column had decreased below detectable limits and that 90% of the initial 4,4′-DDT added was not present in the fish, invertebrates, algae or sediment within the pond and was therefore presumed to have volatized during the course of the experiment. During the first 30 days, 4,4′-DDT was the main degradation product present. The results of this study reflect those found in the microcosm study (United States Environmetnal Protection Agency (USEPA), 1979).

The formation of 4,4′-DDE takes place through photochemical reactions, which require the presence of sunlight (Leaños-Castañeda et al., 2007) as well as through bacterial dehydrochlorination (Leaños-Castañeda et al., 2007) and animal dehydrochlorination (Kitamura et al., 2002). The breakdown of 4,4′-DDT after addition to the exposure tanks may have been affected by the day/night cycle present within the environmental room as well as bacteria present within the borehole water and on the skin of *S. zambezensis*. For this reason, 4,4′-DDE may not have been very high within the fish tissue, but the degradation processes within the water increased the presence of 4,4′-DDE. The presence/absence of some degradation products and not others is unclear, but the previously mentioned adhesion and adsorption properties of 4,4′-DDT and it's degradation products may be responsible for this (Pontolillo and Eganhouse, 2001). The general trend observed was that the concentrations of each metabolite decreases over the 96-hour period, and may be attributed to the degradation of 4,4′-DDT in aquatic systems into its degradation products (Taha and Mobasser, 2014). The mucal secretions could also have contained higher concentrations of the 4,4′-DDE and 4,4′-DDD than the fish tissue because they were secreted by the fish and could have been a mechanism to release 4,4′-DDT and any of its degradation products from their bodies (Church et al., 2009). Since these secretions were not tested separately, in this case, it can not be confirmed whether or not this is a valid assumption.

4.4. Oxidative stress biomarkers and the link to bioaccumulation

The formation of ROS within both the liver and the gills of *S zambezensis* is a physiological response to the exposure to 4,4′-DDT (Abdollahi et al., 2004). The formation of antioxidant species in response to exposure to various xenobiotics has been widely documented in a variety of aquatic organisms (van der Oost et al., 2003; Ferreira et al., 2005).

The constant presence of PC within the liver tissue of *S. zambezensis* from the control throughout the exposure concentrations is an indication that there may not have been high levels of protein breakdown within the organism (Parvez and Raisuddin, 2005). This does not necessarily mean that there was no potential for protein damage, but the short length of the exposure period may have reduced the physiological adaptation of PC production from taking full effect (Connell et al., 2016). There were no significant differences ($p \leq .05$) noted in PC concentrations in the gill tissue of *S. zambezensis*, which is surprising considering their proximity to the 4,4′-DDT in the exposure tank (Rola et al., 2012). The concentrations of PC reported in a study by Smit et al. (Smit et al., 2016) are similar to those found during this study. *Synodontis zambezensis* in the study by Smit et al. (Smit et al., 2016) had much higher PC concentrations than the other three fish species studied. This may be an indication that *S. zambezensis* has naturally higher PC concentrations than those found in other fish species. The RDA ordination shows a negative correlation between 4,4′-DDT and its degradation products and PC activity indicated by the $\geq 90^{\circ}$ angle.

Oxidative stress is clearly seen to occur in the liver tissue of *S. zambezensis* through the presence of higher concentrations of MDA from the control to the exposure concentrations that follow. Lipid peroxidation is often a precursor to protein damage (Traverso et al., 2004) and this could be another indication of the effect that the length of the exposure has on the formation of particular ROS's and antioxidants (Connell et al., 2016). Since MDA is a precursor to PC, the action of MDA within the liver may be preventing further damage from occurring within the proteins further down the oxidative cycle (Traverso et al., 2004).

Superoxide dismutase and CAT work together in an effort to balance out the oxidation caused by ROS's and are often referred to as the first line of defence in the presence of oxidative stress (van der Oost et al., 2003), and this can clearly be seen in the gill tissue of *S. zambezensis*. As the SOD activity increases from the control to the exposure concentrations, CAT activity decreases. This balancing effect is also clear in the RDA with increased length of SOD and CAT arrows and direct correlation ($< 90^{\circ}$ angle) with 4,4′-DDT and its degradation products. The significantly higher concentration of CAT in the gills at the lower concentration of 4,4′-DDT indicates an initial adaptive response by the fish in this concentration (Abdollahi et al., 2004).

Reduced glutathione plays an important role in both direct and enzymatic neutralization of ROS's (Giustarini et al., 2013). Its activity can be seen in both the liver and gills of *S. zambezensis*, but its effect is more apparent in the gills. At the highest exposure concentration, the GSH activity is significantly higher ($p \leq .05$) than the control and all other (lower) exposure concentrations. The RDA ordination also shows the importance of GSH activity in the gill tissue with its close proximity ($< 90^{\circ}$ angle) to 4,4′-DDT and its degradation products. A more conclusive way of measuring GSH activity within an organism is to compare the production of GSH to its oxidized form GSSG (Giustarini et al., 2013), and could be considered in future studies.

5. Conclusions and recommendations

This is the first laboratory-based study to report on accumulated concentrations of 4,4′-DDT, its degradation products and the resulting oxidative stress biomarkers within *Synodontis zambezensis*. Based on the results it is clear that even an acute exposure to relatively low concentrations of 4,4′-DDT, can result in some accumulation without the contribution of biomagnification through the food chain. Although chronic exposure periods are considered to give a more accurate indication of the physiological responses in aquatic organisms, an acute exposure such as this has proven that oxidative stress may still result after a short exposure to xenobiotics. These results reflect those which may occur during a spill event or during spray contamination of nearby water sources. The exact mechanisms of metabolism and the enzymatic systems involved in the breakdown and storage of 4,4′-DDT and its degradation products, in this fish species, have not been previously documented, and so it is recommended that further studies e.g. chronic exposure of this species to 4,4′-DDT be completed. Chronic exposure experiments may also allow for the species specific Bioconcentration

Factor (BCF) for 4,4′-DDT to be calculated (United States Environmental Protection Agency (USEPA), 1996). Since the uptake phase in this study was not 28 days and the ratio between uptake and depuration was not noted, it is not possible to calculate the species specific BCF from the current data. It is further recommended that the battery of oxidative stress biomarkers be increased to include the ratio calculation of GSSG to GSH, specifically within the gill tissue. The inclusion of gill histology studies is also recommended to determine whether structural changes have taken place within the gills since they are in direct contact with the toxicant (Rola et al., 2012). Identification of possible changes may enhance the understanding of oxydative stress within the gill tissue.

The interactions that have taken place between the 4,4′-DDT, the exposure borehole water and the conditions within the environmental room are unclear and further investigation into the partitioning, volatilization and adsorption of 4,4′-DDT needs to be investigated.

Acknowledgements

This study was supported through funding by the National Research Foundation (NRF – UID: 102440), Hokkaido University, Sapporo Japan (UID 92424 Japan/ SA Bi-lateral Programme) and the University of Johannesburg (Global Excellence Stature Scholarship). Mr. Harris and Dr. Meyer from Shimadzu South Africa are acknowledged for the use of their equipment.

References

Abdollahi, M., Ranjbar, A., Shadnia, S., Nikfar, S., Rezaie, A., 2004. Pesticides and oxidative stress: a review. Med. Sci. Monit. Int. Med. J. Exp. Clin. Res. 10, 141–147(http://www.medscimonit.com/pub/vol_10/no_6/4163.pdfwww.MEDSCIMONIT.com accessed September 17, 2018).

Almroth, B., Sturve, J., Berglund, Å., Förlin, L., 2005. Oxidative damage in eelpout (Zoarces viviparus), measured as protein carbonyls and TBARS, as biomarkers. Aquat. Toxicol. 73, 171–180. https://doi.org/10.1016/j.aquatox.2005.03.007.

Almroth, B., Sturve, J., Stephensen, E., Holth, T., Förlin, L., 2008. Protein carbonyls and antioxidant defenses in corkwing wrasse (Symphodus melops) from a heavy metal polluted and a PAH polluted site. Mar. Environ. Res. 66, 271–277. https://doi.org/10.1016/j.marenvres.2008.04.002.

Aneck-Hahn, N., Schulenburg, G., Bornman, M., Farias, P., De Jager, C., 2006. Impaired semen quality associated with environmental DDT exposure in young men living in a Malaria Area in the Limpopo Province, South Africa. J. Androl. 28, 423–434. https://doi.org/10.2164/jandrol.106.001701.

Atekwana, E., Atekwana, E., Rowe, R., Werkema, D., Legall, F., 2004. The relationship of total dissolved solids measurements to bulk electrical conductivity in an aquifer contaminated with hydrocarbon. J. Appl. Geophys. 56, 281–294. https://doi.org/10.1016/j.jappgeo.2004.08.003.

Atli, G., Alptekin, Ö., Tükel, S., Canli, M., 2006. Response of catalase activity to Ag+, Cd2+, Cr6+, Cu2+ and Zn2+ in five tissues of freshwater fish Oreochromis niloticus. Comp. Biochem. Physiol. Part C Toxicol. Pharmacol. 143, 218–224. https://doi.org/10.1016/j.cbpc.2006.02.003.

Barnhoorn, I.E.J., Bornman, M., Jansen van Rensburg, C., Bouwman, H., 2009. DDT residues in water, sediment, domestic and indigenous biota from a currently DDT-sprayed area. Chemosphere 77, 1236–1241. https://doi.org/10.1016/j.chemosphere.2009.08.045.

Barton, B., 2002. Stress in fishes: a diversity of responses with particular reference to changes in circulating corticosteroids. Integr. Comp. Biol. 42, 517–525. https://doi.org/10.1093/icb/42.3.517.

Bedos, C., Cellier, P., Calvet, R., Barriuso, E., Gabrielle, B., 2002. Mass transfer of pesticides into the atmosphere by volatilization from soils and plants: overview. Agronomie 22, 21–33. https://doi.org/10.1051/agro:2001003.

Bennett, R., Buthelezi, T., Ismael, Y., Morse, S., 2003. Bt cotton, pesticides, labour and health: a case study of smallholder farmers in the Makhathini Flats. Repub. S. Afr. Outlook Agric. 32, 123–128. https://doi.org/10.5367/000000003101294361.

Bradford, M., 1976. A rapid and sensitive method for the quantitation of microgram quantities of protein utilizing the principle of protein-dye binding. Anal. Biochem. 72, 248–254. https://doi.org/10.1016/0003-2697(76)90527-3.

Church, M.R., Ebersole, J.L., Rensmeyer, K.M., Couture, R.B., Barrows, F.T., Noakes, D.L.G., 2009. Mucus: a new tissue fraction for rapid determination of fish diet switching using stable isotope analysis. Can. J. Fish. Aquat. Sci. 66, 1–5. https://doi.org/10.1139/F08-206.

Coetzee, H., Nell, W., Van Eeden, E., De Crom, E., 2015. Artisanal fisheries in the Ndumo area of the lower Phongolo River Floodplain, South Africa. Koedoe 57, 2009–2014. https://doi.org/10.4102/koedoe.v57i1.1248.

Cohen, G., Dembiec, D., Marcus, J., 1970. Measurement of catalase activity in tissue extracts. Anal. Biochem. 34, 30–38. https://doi.org/10.1016/0003-2697(70)90083-7.

Cohn, V., Lyle, J., 1966. A fluorometric assay for glutathione. Anal. Biochem. 14, 434–440. https://doi.org/10.1016/0003-2697(66)90286-7.

Connell, D.W., Yu, Q.J., Verma, V., 2016. Influence of exposure time on toxicity—an overview. Toxicology 355–356, 49–53. https://doi.org/10.1016/j.tox.2016.05.015.

Da Cuña, R.H., Pandolfi, M., Genovese, G., Piazza, Y., Ansaldo, M., Lo Nostro, F.L., 2013. Endocrine disruptive potential of endosulfan on the reproductive axis of Cichlasoma dimerus (Perciformes, Cichlidae). Aquat. Toxicol. 126, 299–305. https://doi.org/10.1016/j.aquatox.2012.09.015.

Davies, T.G.E., Field, L.M., Usherwood, P.N.R., Williamson, M.S., 2007. DDT, pyrethrins, pyrethroids and insect sodium channels. IUBMB Life 59, 151–162. https://doi.org/10.1080/15216540701352042.

Dix, D.J., Houck, K.A., Martin, M.T., Richard, A.M., Setzer, R.W., Kavlock, R.J., 2007. The ToxCast program for prioritizing toxicity testing of environmental chemicals. Toxicol. Sci. 95, 5–12. https://doi.org/10.1093/toxsci/kfl103.

Easy, R., Ross, N., 2009. Changes in Atlantic salmon (Salmo salar) epidermal mucus protein composition profiles following infection with sea lice (Lepeophtheirus salmonis). Comp. Biochem. Physiol. Part D Genomics Proteomics. 4, 159–167. https://doi.org/10.1016/j.cbd.2009.02.001.

Ferreira, M., Moradas-Ferreira, P., Reis-Henriques, M., 2005. Oxidative stress biomarkers in two resident species, mullet (Mugil cephalus) and flounder (Platichthys flesus), from a polluted site in River Douro Estuary, Portugal. Aquat. Toxicol. 71, 39–48. https://doi.org/10.1016/j.aquatox.2004.10.009.

Filipak Neto, F., Zanata, S., Silva de Assis, H., Nakao, L., Randi, M., Oliveira Ribeiro, C., 2008. Toxic effects of DDT and methyl mercury on the hepatocytes from Hoplias malabaricus. Toxicol. Vitr. 22, 1705–1713. https://doi.org/10.1016/j.tiv.2008.07.006.

Flohr, L., Fuzinatto, C., Melegari, S., Matias, W., 2012. Effects of exposure to soluble fraction of industrial solid waste on lipid peroxidation and DNA methylation in erythrocytes of Oreochromis niloticus, as assessed by quantification of MDA and m5dC rates. Ecotoxicol. Environ. Saf. 76, 63–70. https://doi.org/10.1016/j.ecoenv.2011.10.016.

Floor, E., Wetzel, M., 1998. Increased protein oxidation in human substantia nigra pars compacta in comparison with basal ganglia and prefrontal cortex measured with an improved dinitrophenylhydrazine assay. J. Neurochem. 70, 268–275. https://doi.org/10.1046/j.1471-4159.1998.70010268.x. (accessed September 13, 2018).

Foght, J., April, T., Biggar, K., Aislabie, J., 2001. Bioremediation of DDT-contaminated soils: a review. Bioremediat. J. 5, 225–246. https://doi.org/10.1080/20018891079302.

Gaspar, F., Harley, K., Kogut, K., Chevrier, J., Mora, A., Sjödin, A., Eskenazi, B., 2015. Prenatal DDT and DDE exposure and child IQ in the CHAMACOS cohort. Environ. Int. 85, 206–212. https://doi.org/10.1016/j.envint.2015.09.004.

Giustarini, D., Dalle-Donne, I., Milzani, A., Fanti, P., Rossi, R., 2013. Analysis of GSH and GSSG after derivatization with N-ethylmaleimide. Nat. Protoc. 8, 1660–1669. https://doi.org/10.1038/nprot.2013.095.

Greenwald, R., 1985. Handbook Methods for Oxygen Radical Research, 1st ed. CRC Presshttps://doi.org/10.1201/9781351072922.

Henriksson, J., Chi, M.-Y., Hintz, C., Young, D., Kaiser, K., Salmons, S., Lowry, O., 1986. Chronic stimulation of mammalian muscle: changes in enzymes of six metabolic pathways. Am. Physiol. Soc. C251, 614–632.

Khessiba, A., Roméo, M., Aïssa, P., 2005. Effects of some environmental parameters on catalase activity measured in the mussel (Mytilus galloprovincialis) exposed to lindane. Environ. Pollut. 133, 275–281. https://doi.org/10.1016/j.envpol.2004.05.035.

Kidd, K., Bootsma, H., Hesslein, R., Muir, D., Hecky, R., 2001. Biomagnification of DDT through the Benthic and Pelagic Food Webs of Lake Malawi, East Africa: importance of trophic level and carbon source. Environ. Sci. Technol. 35, 14–20. https://doi.org/10.1021/es001119a.

Kitamura, S., Shimizu, Y., Shiraga, Y., Yoshida, M., Sugihara, K., Ohta, S., 2002. Reductive metabolism of p,p'-DDT and o,p'-DDT by rat liver cytochrome P450. Drug Metab. Dispos. 30, 113–118. https://doi.org/10.1124/dmd.30.2.113.

Koblmüller, S., Sturmbauer, C., Verheyen, E., Meyer, A., Salzburger, W., 2006. Mitochondrial phylogeny and phylogeography of East African squeaker catfishes (Siluriformes: Synodontis). BMC Evol. Biol. 6, 49. https://doi.org/10.1186/1471-2148-6-49.

Lalèyè, P., Chikou, A., Gnohossou, P., Vandewalle, P., Philippart, J., Teugels, G., 2006. Studies on the biology of two species of catfish Synodontis schall and Synodontis nigrita (Ostariophysi: Mochokidae) from the Ouémé River, Bénin. Belgian J. Zool. 136, 193–201.

Leaños-Castañeda, O., Van Der Kraak, G., Rodríguez-Canul, R., Gold, G., 2007. Endocrine disruption mechanism of o,p'-DDT in mature male tilapia (Oreochromis niloticus). Toxicol. Appl. Pharmacol. 221, 158–167. https://doi.org/10.1016/j.taap.2007.03.011.

Levine, R., Garland, D., Oliver, C., Amici, A., Climent, I., Lenz, A., Ahn, B., Shaltiel, S., Stadtman, E., 1990. Determination of carbonyl content in oxidatively modified proteins. Methods Enzymol. 186, 464–478. https://doi.org/10.1016/0076-6879(90)86141-H.

Macek, K., Korn, S., 1970. Significance of the food chain in DDT accumulation by fish. J. Fish. Res. Board Canada. 27, 1496–1498. https://doi.org/10.1139/f70-172.

Mahugija, J., Henkelmann, B., Schramm, K.-W., 2015. Levels and patterns of organochlorine pesticides and their degradation products in rainwater in Kibaha Coast Region, Tanzania. Chemosphere 118, 12–19. https://doi.org/10.1016/j.chemosphere.2014.05.051.

Mlambo, S., van Vuren, J., Barnhoorn, I.E., Bornman, M., 2009. Histopathological changes in the reproductive system (ovaries and testes) of Oreochromis mossambicus following exposure to DDT. Environ. Toxicol. Pharmacol. 28, 133–139. https://doi.org/10.1016/j.etap.2009.03.011.

Naigaga, I., Kaiser, H., Muller, W., Ojok, L., Mbabazi, D., Magezi, G., Muhumuza, E.,

2011. Fish as bioindicators in aquatic environmental pollution assessment: a case study in Lake Victoria wetlands, Uganda. Phys. Chem. Earth, Parts A/B/C. 36, 918–928. https://doi.org/10.1016/j.pce.2011.07.066.
Oerke, E.C., 2006. Crop losses to pests. J. Agric. Sci. 144, 31–43. https://doi.org/10.1017/S0021859605005708.
Ohkawa, H., Ohishi, N., Yagi, K., 1979. Assay for lipid peroxides in animal tissues by thiobarbituric acid reaction. Anal. Biochem. 95, 351–358. https://doi.org/10.1016/0003-2697(79)90738-3.
Parvez, S., Raisuddin, S., 2005. Protein carbonyls: novel biomarkers of exposure to oxidative stress-inducing pesticides in freshwater fish Channa punctata (Bloch). Environ. Toxicol. Pharmacol. 20, 112–117. https://doi.org/10.1016/j.etap.2004.11.002.
Pontolillo, J., Eganhouse, R., 2001. The Search for Reliable Aqueous Solubility (Sw) and Octanol-Water Partition Coefficient (Kow) Data for Hydrophobic Organic Compounds: DDT and DDE as a Case Study. (http://pubs.water.usgs.gov/wri01-4201/ accessed November 28, 2018).
Quinn, G., Keough, M., 2002. Experimental Design and Data Analysis for Biologists. The Press Syndicate of the University of Cambridge, Cambridge(http://www.cambridge.org accessed September 13, 2018).
Rognerud, S., Grimalt, J., Rosseland, B., Fernandez, P., Hofer, R., Lackner, R., Lauritzen, B., Lien, L., Massabuau, J., Ribes, A., 2002. Mercury and organochlorine contamination in Brown Trout (Salmo trutta) and Arctic Charr (Salvelinus alpinus) from high mountain lake in Europe and the Svalbard Archipelago. Water Air Soil Pollut. Focus. 2, 209–232. https://doi.org/10.1023/A:1020110810195.
Rola, R., Monteiro, M. da C., Reis, S. da S., Sandrini, J., 2012. Molecular and biochemical biomarkers responses in the mussel Mytilus edulis collected from Southern Brazil coast. Mar. Pollut. Bull. 64, 766–771. https://doi.org/10.1016/j.marpolbul.2012.01.004.
Sautter, J., Kaiser, H., Focken, U., Becker, K., 2007. Panagrellus redivivus (Linné) as a live food organism in the early rearing of the catfish Synodontis petricola (Matthes). Aquac. Res. 38, 653–659. https://doi.org/10.1111/j.1365-2109.2007.01714.x.
Sigma-Aldrich, 2014. Safety Data Sheet: 4,4′-DDT. (sigma-aldrich.com).
Skelton, P., 2001. A Complete Guide to Freshwater Fishes of Southern Africa, Stuik.
Slaninova, A., Smutna, M., Modra, H., Svobodova, Z., Slaninová, M., 2009. A Review: Oxidative Stress in Fish Induced by Pesticides. (www.nel.edu accessed September 17, 2018).
Smit, N., Vlok, W., van Vuren, J., Du Preez, L., Van Eeden, E., O'Brien, G., Wepener, V., 2016. Socio-ecological system management of the lower Phongolo River and Floodplain using relative risk methodology. In: Water Research Commission.
Smolders, R., Bervoets, L., Wepener, V., Blust, R., 2003. A conceptual framework for using mussels as biomonitors in whole effluent toxicity. Hum. Ecol. Risk Assess. An Int. J. 9, 741–760. https://doi.org/10.1080/713609965.
South African National Standard (SANS), 2008. SANS 10386: The Care and Use of Animals for Scientific Purposes, South African Bureau of Standards. Pretoria. .
Taha, M., Mobasser, S., 2014. Adsorption of DDT from contaminated soil using carbon nanotubes. Soil Sediment Contam. An Int. J. 23, 703–714. https://doi.org/10.1080/15320383.2014.864254.
Thirumalini, S., Joseph, K., 2009. Correlation between electrical conductivity and total dissolved solids in natural waters. Malays. J. Sci. 28, 55–61. https://doi.org/10.22452/mjs.vol28no1.7.
Traverso, N., Menini, S., Maineri, E., Patriarca, S., Odetti, P., Cottalasso, D., Marinari, U., Pronzato, M., 2004. Malondialdehyde, a lipoperoxidation-derived aldehyde, can bring about secondary oxidative damage to proteins. J. Gerontol. Ser. A Biol. Sci. Med. Sci. 59, B890–B895. https://doi.org/10.1093/gerona/59.9.B890.
Üner, N., Oruç, E., Sevgiler, Y., Şahin, N., Durmaz, H., Usta, D., 2006. Effects of diazinon on acetylcholinesterase activity and lipid peroxidation in the brain of Oreochromis niloticus. Environ. Toxicol. Pharmacol. 21, 241–245. https://doi.org/10.1016/j.etap.2005.08.007.
United States Environmental Protection Agency (USEPA), 1989. Environmental Fate and Effects Division, Pesticide Environmental Fate (DDT (p, p'), Washington DC). .
United States Environmental Protection Agency (USEPA), 1996. Ecological Effects - Test Guidelines OPPTS 850.1730 Fish BCF, Washington DC.
United States Environmental Protection Agency (USEPA), 2007. EPA Method 8081b - Organochlorine Pesticides by Gas-Chromatography. Washington DC. (http://www.caslab.com/EPA-Method-8081B/).
United States Environmetnal Protection Agency (USEPA), 1979. Methods for Chemical Analysis of Water and Wastes, Cincinatti.
van der Oost, R., Beyer, J., Vermeulen, N., 2003. Fish bioaccumulation and biomarkers in environmental risk assessment: a review. Environ. Toxicol. Pharmacol. 13, 57–149. https://doi.org/10.1016/S1382-6689(02)00126-6.
van Dyk, J., Pieterse, G., van Vuren, J., 2007. Histological changes in the liver of Oreochromis mossambicus (Cichlidae) after exposure to cadmium and zinc. Ecotoxicol. Environ. Saf. 66, 432–440. https://doi.org/10.1016/j.ecoenv.2005.10.012.
Whitworth, K., Bornman, R., Archer, J., Kudumu, M., Travlos, G., Wilson, R., Longnecker, M., 2014. Predictors of plasma DDT and DDE concentrations among women exposed to indoor residual spraying for Malaria Control in the South African Study of Women and babies (SOWB). Environ. Health Perspect. 122, 545–552. https://doi.org/10.1289/ehp.1307025.
World Health Organisation (WHO), 1979. Environmental Health Criteria 9, DDT and its Derivatives. Geneva. .
World Health Organisation (WHO), 2002. Application of Residual Sprays for Vector Control: Manual for Indoor Residual Spraying. Geneva. .
Yohannes, Y., Ikenaka, Y., Nakayama, S., Saengtienchai, A., Watanabe, K., Ishizuka, M., 2013. Organochlorine pesticides and heavy metals in fish from Lake Awassa, Ethiopia: Insights from stable isotope analysis. Chemosphere 91, 857–863. https://doi.org/10.1016/j.chemosphere.2013.01.047.
Yohannes, Y., Ikenaka, Y., Saengtienchai, A., Watanabe, K., Nakayama, S., Ishizuka, M., 2014. Concentrations and human health risk assessment of organochlorine pesticides in edible fish species from a Rift Valley lake—Lake Ziway, Ethiopia. Ecotoxicol. Environ. Saf. 106, 95–101. https://doi.org/10.1016/j.ecoenv.2014.04.014.
Zeidler, O., 1874. I. Verbindungen von Chloral mit Brom- und Chlorbenzol. Berichte Der Dtsch. Chem. Gesellschaft. 7, 1180–1181. https://doi.org/10.1002/cber.18740070278.
Zhou, Q., Zhang, J., Fu, J., Shi, J., Jiang, G., 2008. Biomonitoring: an appealing tool for assessment of metal pollution in the aquatic ecosystem. Anal. Chim. Acta 606, 135–150. https://doi.org/10.1016/j.aca.2007.11.018.
Zusterzeel, P., Peters, W., Visser, W., Hermsen, K., Roelofs, H., Steegers, E., 2001. A polymorphism in the gene for microsomal epoxide hydrolase is associated with pre-eclampsia. J. Med. Genet. 38, 234–237. https://doi.org/10.1136/jmg.38.4.234.

African Journal of Aquatic Science 2018, 43(3): 305–312

AFRICAN JOURNAL OF AQUATIC SCIENCE
ISSN 1608-5914 EISSN 1727-9364
https://doi.org/10.2989/16085914.2018.1511408

First report on OH-PAHs in South African *Clarias gariepinus* bile from an urban impacted system

W Pheiffer[1]*, N Bortey-Sam[2], Y Ikenaka[1,2], SMM Nakayama[2], H Mizukawa[3], M Ishizuka[2], NJ Smit[1] and R Pieters[1]

[1] Water Research Group, Unit for Environmental Science and Management, North-West University, Private Bag X6001, Potchefstroom 2520, South Africa
[2] Laboratory of Toxicology, Department of Environmental Veterinary Science, Hokkaido University, Kita 18, Nishi 9, Kita ku, Sapporo 060–0818, Japan
[3] Department of Environmental Veterinary Science, Graduate School of Veterinary Medicine, Hokkaido University, Kita 18, Nishi 9, Kita ku, Sapporo 060–0818, Japan
**Corresponding author, email: wihanpheiffernwu@gmail.com*

The concentrations of selected hydroxylated polycyclic aromatic hydrocarbons (OH-PAHs) were determined in the bile of the African sharptooth catfish *Clarias gariepinus* from impoundments in the urban impacted Klip River system in Soweto, South Africa. Fish were sampled from three impoundments (Lenasia, Fleurhof, and Orlando dams) during the early high-flow season (September/October) of 2013. Biliary OH-PAHs were analysed using a high-pressure liquid chromatograph coupled to a tandem mass spectrometer (HPLC-MS/MS). Seven of the thirteen targeted metabolites were present in the fish of Soweto. The ΣOH-PAHs ranged between 0.1 and 1 876 ng ml^{-1}, with greatest ΣOH-PAH mean at Orlando (947 ng ml^{-1}) followed by Fleurhof (371 ng ml^{-1}). The most dominant metabolite in the sampling area was 2–,3–OH fluorene, ranging between not detected and 1 429 ng ml^{-1}, with the greatest mean at Orlando (709 ng ml^{-1}). PAH metabolites quantified in *C. gariepinus* most likely originated from the sediments. The hepatosomatic index of the *C. gariepinus* increased proportionally with the biliary OH-PAH concentrations. To the authors' knowledge this data on biliary OH-PAH for fish is the first for South Africa.

Keywords: Freshwater toxicology, Klip River, sharptooth catfish, Soweto

Introduction

Soweto is South Africa's most densely populated area (PopulationLabs 2011) and is located in one of Africa's fifteen largest metropolitans, Johannesburg. The Klip River flows through Soweto and is considered to be among South Africa's most polluted rivers (McCarthy and Venter 2006). The area is known to have industrial pollution, specifically organic chemicals (Quinn et al. 2009; Nieuwoudt et al. 2011; Moja et al. 2013; Okedeyi et al. 2013; Bengu et al. 2017; Pheiffer et al. 2018). Polycyclic aromatic hydrocarbons (PAHs) are a group of organic contaminants that are ubiquitous in the environment (Stogiannidis and Laane 2015). These pollutants are mainly from anthropogenic origins, such as urban and industrial sources (Angerer et al. 1997; Maliszewska-Kordybach et al. 2009), which account for its constant input into the environment. Once released into the atmosphere their semi-volatile characteristics allow them to disperse among air, water, sediments and soils. PAHs that are deposited into water bind to and accumulate in the sediment, owing to their lipophilic nature (Brenner et al. 2002). These contaminated sediments are considered a major source of exposure to bottom dwelling fish (Stein et al. 1990). PAHs were chosen as indicators for organic pollutant contamination in this particular part of South Africa, because they often co-occur with other industrial pollutants, such as polychlorinated biphenyls (PCBs), polychlorinated dibenzo-*p*-dioxins and -furans (PCDD/Fs) and polybrominated diphenyl ethers (PBDEs) (Rudel et al. 2003; Vane et al. 2014).

PAHs enter benthic fish's bodies via epithelial absorption (mainly in gills) or their gut after ingestion of contaminated sediment or food (Varanasi et al. 1989). PAHs are known to be embryotoxic, teratogenic, genotoxic (Sogbanmu et al. 2016), and carcinogenic to fish (Hawkins et al. 1990). Once these contaminants enter the fish, they are transported to its liver where they are bio-transformed (Hylland 2006). Bio-transformation happens when phase I and II detoxification enzymes introduce polar conjugates to the native PAH by means of oxidative, reductive and/or hydrolytic processes. Once conjugated the PAHs become water soluble and are collected in the gall bladder (Tuvikene 1995).

Glucuronidated and sulphated metabolites increase in the bile during starvation periods (Beyer et al. 1997), but is released into the digestive tract when feeding commences. Because the fish rapidly metabolise the PAHs their muscle and liver are not ideal tissues to analyse for PAH exposure, because of low accumulation rates (van der Oost et al. 2003). However, biliary metabolites found in the bile are a useful indicator of recent PAH exposure and are a biomarker for environmental risk assessment (Tuvikene 1995; Richardson et al. 2001; Ruddock et al. 2003; van der

Published online 11 Sep 2018

Oost et al. 2003). Fish represent vertebrates of the aquatic system (Colin et al. 2016) and are an ideal biomarker for the aquatic environment. The consumption of the fish by subsistent fishermen and their families, which is a reality even for the very urban nature of the study area, might cause additional exposure to humans already exposed to the PAH in air.

Most of the literature on OH-PAHs in fish is for marine or estuarine environments (Aas et al. 2000; Richardson et al. 2001; Ruddock et al. 2003; Jonsson et al. 2004) and little is known for these compounds from freshwater fish globally, and even less for Africa. *Clarias gariepinus* (Burchell, 1822) is a bottom dwelling freshwater fish found relatively high in the food chain (and therefore a good indicator of the degree of PAH pollution in the ecosystem) and is widespread throughout Africa (Skelton 2001), making it an ideal fish species for comparative use in African studies.

The primary aim of this paper is to report on the OH-PAHs in *C. gariepinus* sampled in an urban impacted area in South Africa, and secondly, discuss its influence on the fish by comparing the hepatosomatic index (HSI) and the condition factor (CF) of the fish to that of the reference.

Material and Methods

Sites and sample collection

African sharptooth catfish, *Clarias gariepinus*, were collected in September/October 2013 from three impoundments in the urban areas of Soweto and Lenasia, Gauteng, South Africa (Figure 1). Sites were distributed over the upper catchment of the Klip River: Fleurhof Dam located in the north, Orlando Dam in the middle, and Lenasia Dam representing the most southern part of the study area. The Klip River is the largest tributary of the Vaal River and together with other sources it supplies potable water to the Gauteng Province (DWAS 2004). Ten fish from each site were collected using fyke nets. Fish were kept in aerated tanks until they were euthanized by severing the spinal cord/cervical vertebrate dislocation (NWU Ethics approval: AREC-130913–015). The CF and HSI of each fish were recorded (Pheiffer et al. 2015) by the following formulae: CF = body mass (gutted mass, g)/length^3 (total length, mm) × 100; and the HSI = liver mass (g)/body mass (gutted mass, g) × 100. The gall bladder was removed and kept at −20 °C in 4 ml amber glass vials. A reference group, consisting of fish from the Mooi River system (North West Province), approximately 100 km southwest from the study area and in a different catchment, was depurated for six months at the Water Research Group's aquarium at the North-West University (Potchefstroom Campus) under standard conditions (CCAC 2005). The reference fish were treated in the same manner as the experimental fish.

Bile deconjugation and metabolite extraction

The bile extraction method was adapted from Guo et al. (2013) and Bortey-Sam et al. (2016). A radio-labelled internal standard containing 2–OH fluorene-$^{13}C_6$ (OHFlu-$^{13}C_6$), 3–OH phenanthrene-D9 (OHPhe-D9), and 1–OH pyrene-$^{13}C_6$ (OHPyr-$^{13}C_6$) (Cambridge Isotope Laboratories Inc, USA) was added to 30 µl bile. The samples were deconjugated with 10 µl β-glucorunidase

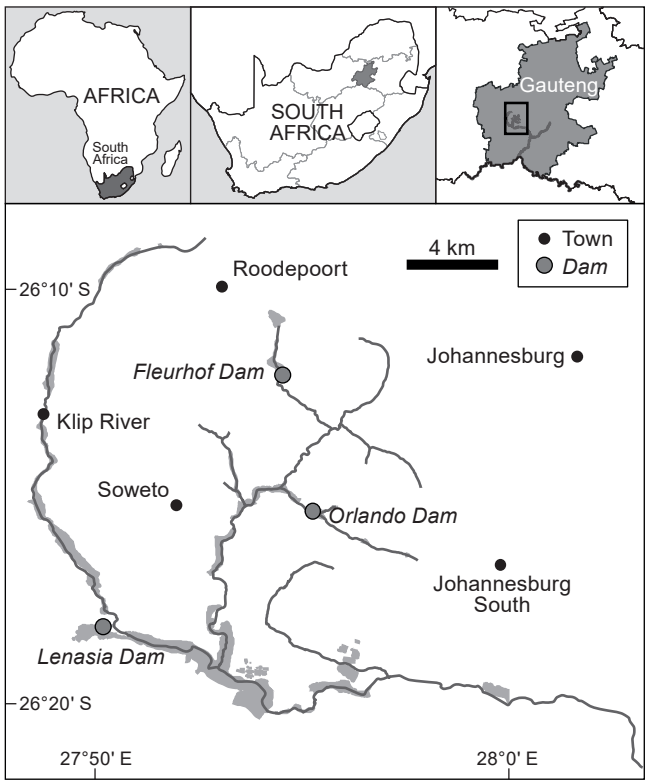

Figure 1: Map of *Clarias gariepinus* sampling sites in the urban impacted Klip River system

(bovine liver, Type B-1, 1 240 units ml^{-1}, Sigma-Aldrich) and 10 µl aryl-sulphatase (*Patella vulgata* Type V, 34 units ml^{-1}, Sigma-Aldrich) in 2 ml sodium acetate buffer (pH 5.6), incubated for 6 hours at 37 °C. The sample volume was increased with 2 ml double distilled water. Deconjugated metabolites were extracted by addition of 5 ml pentane (HPLC grade, Kanto Chemical Corp., Tokyo, Japan) and shaken for 30 minutes. Samples were centrifuged for 10 minutes at 1 600 g and the organic phase collected. The watery phase was extracted a second time and this volume of organic phase was added to the first. The collected supernatant was reduced by evaporation to 50–100 µl with a gentle nitrogen flow at 37 °C. The samples were filtered through a 0.2 µm syringe filter (ADVANTEC, Toyo Roshi Ltd, Japan) and reconstituted to 500 µl methanol and stored at 4 °C before instrumental analysis.

Quantification of deconjugated PAHs

Hydroxylated PAHs quantified included 2–OH naphthalene (2–OH Nap), 9–OH fluorene (9–OH Flu), 2–,3–OH fluorene (isomer co-elution) (2–,3–OH Flu), 2–OH phenanthrene (2–OH Phe), 1–,9–OH phenanthrene (isomer co-elution) (1–,9–OH Phe), 3–OH phenanthrene (3–OH Phe), 4–OH phenanthrene (4–OH Phe), 1–OH pyrene (1–OH Pyr), 6–OH chrysene (6–OH Chr), 3–OH benzo(e)pyrene (3–OH BeP), and 9–OH benzo(a)pyrene (9–OH BaP). Analysis was performed on a Shimadzu Triple-Quad 8040 HPLC-MS/MS with a UF lens. The standards were of high purity (≥98%) and purchased from Cambridge Isotope

Laboratories Inc. (Amdover, MA, USA). The metabolites were separated on an Agilent Eclipse PAH column (150 × 2.1 mm, 3.5 µm df). The initial mobile phase was 95% solvent A (2:3 methanol:water mixture) and 5% solvent B (methanol). After two minutes the ratio changed to 60:40 (A:B) for 23 minutes. The mobile phase composition changed to 5:95 (A:B) for five minutes and finally returned to the initial composition. The flow rate was constant at 250 µl min^{-1}. Target analytes were identified based on retention time, elution order and obtained mass spectra in the negative electrospray ionisation (ESI) mode (Bortey-Sam et al. 2016).

Quality control

A five-point non-matrix-matched calibration curve was constructed for quantification using OH-PAH standards (1–50 ng ml^{-1}) spiked with 25 ng ml^{-1} internal standard. Calibration curves were constructed for each of the 11 OH-PAH metabolites, each with R^2 values greater than 0.9. Quantification was done using peak area ratios to mass ratios (Bortey-Sam et al. 2016).

The limit of detection (LOD) and limit of quantification (LOQ) were calculated using linear regression analysis of the constructed calibration curves:

$$S_{y/x} = \sqrt{\frac{\sum_i (y_i - \hat{y}_i)^2}{n-2}}$$

where $S_{y/x}$ is the standard error of the regression (Miller and Miller 2010). The LOD was defined as three times the standard deviation of $S_{y/x}$ and the LOQ was defined as ten times the standard deviation of $S_{y/x}$.

Additionally, an internal standard blank and solvent blank were analysed between samples and retention times were confirmed throughout the course of the analysis. Recoveries of the internal standards were: 117% for OHFlu-$^{13}C_6$, 105% for OHPhe-D9, and 126% for OHPyr-$^{13}C_6$, with a mean recovery of 116% ± 10.7.

Statistical analysis

Statistical analysis was done using GraphPad Prism version 5. The D'Agostino and Pearson omnibus test was used to test for normality. One-way analysis of variance (ANOVA) was performed if the data were distributed normally followed by Tukey's multiple comparison test as a *post hoc* test. For non-parametric data the Kruskal–Wallis test was used together with Dunn's multiple comparison test as a *post hoc* test. A result of $p < 0.05$ was considered significant. Metabolite concentrations below the LODs and not detected, are reported as zero values and those below the LOQs are represented with its respective half-LOQ. The correlation between OH-PAHs and the HSI, and OH-PAHs and CF were tested with a Spearman's rank correlation.

The multivariate statistics used in the current study included principle component analysis (PCA), as well as redundancy analysis (RDA) (Canoco for Windows version 5) (Šmilauer and Lepš 2014). PCAs are based on a linear response model that explains the variation between species data and environmental variables (Scott and Clarke 2000; Van den Brink et al. 2003) to identify underlying variables that might explain the patterns observed in the PCA. An RDA allows the driving or explanatory variables to be selected, which then allows focus on the part of the variance explained by these selected external explanatory variables (Van den Brink et al. 2003). RDAs are used to determine similarities or differences between datasets, based on the selected variables. Values of samples used in the PCA below the limit of detection were replaced with half-LOD values to avoid using zero values. The dataset was log-transformed during the analysis. The OH-PAHs were used as the explanatory data in the RDA. If a metabolite was not found in any of the samples, it was excluded from a statistical analysis to prevent skewed results. The concentrations of the corresponding native PAHs in the sediment, Nap, Flu, Phe, Pyr, and BaP (Table 1) (Pheiffer et al. 2018), were used as the species variables.

The biplots (PCA) and triplots (RDA) were interpreted according to Šmilauer and Lepš (2014). The angle between the vector arrows indicates the correlation between the individual environmental variables and/or species data arrows. An angle close to 0° indicates a positive correlation between the variables; an angle closer to 90° shows no correlation; wheras an angle approaching 180° indicates negative correlation between variables. The perpendicular line between a sample symbol and a particular species arrow can be used to estimate the value of that sample in terms of the variable it is perpendicular to.

Results

There were no significant differences between the CF of male and female fish at any of the sites ($p > 0.05$), subsequently the CF reported was for both sexes. There were also no significant differences seen between the CFs of fish from different sites ($p = 0.25$) (Table 2). There were also no significant differences between both the mass and total lengths of the fish from the different sites ($p > 0.05$), indicating that the fish were all similar in size and are therefore comparable when interpreting results (Table 2). Orlando had the highest HSI, and together with Fleurhof had significantly higher HSI than the reference fish ($p < 0.0001$). The HSI of Orlando fish was also significantly higher than those of Lenasia ($p < 0.05$) (Table 2) (Pheiffer et al. 2015).

There were no significant differences between the metabolite data or the sex of the fish at any of the sites. Orlando had the highest mean ΣOH-PAHs concentration, 947 ng ml^{-1}, followed by fish from Fleurhof (371 ng ml^{-1}) and Lenasia (196 ng ml^{-1}) (Table 3). The latter two were significantly lower than the Orlando results ($p < 0.05$). The Orlando fish were the only fish that had eight of the 13 targeted hydroxyl-PAHs, whereas fish from the other impoundments had a lower number (Table 3). The metabolite(s) with the highest concentration was 2–,3–OH Flu in the bile of the Orlando fish (mean 709 ng ml^{-1}, range 172–1 429 ng ml^{-1}). The co-eluting 2–,3–OH Flu was the dominant metabolite(s) in the study area, contributing 75% to 89% of the total targeted metabolites in the fish from the study area, and 92% in the reference fish. 9–OH Flu and 1–OH Pyr were the second and third most contributing metabolites (Table 3).

Discussion

The most dominant metabolite(s) in the current study was 2–,3–OH Flu. However, 1–OH Pyr was the most prevalent in other studies (van der Oost et al. 1994; Ruddock et al.. 2003). Fluorene, the native of 2–,3–OH Flu, is a main component (but not exclusively) of petrogenic sources (Stogiannidis and Laane 2015), whereas the native form of 1–OH Pyr, pyrene, is one of the most abundant pyrogenic PAHs (Page et al. 1999; De Luca et al. 2004). The metabolites in *C. gariepinus* suggest that they possibly originated from petroleum related sources. However, source identification using native PAHs in the sediments of the same study area (Pheiffer et al. 2018) identified the biomass combustion and diesel fuel emissions as the main sources.

Spatial variations between the biliary PAHs were investigated by a PCA. Factors 1 and 2 describe 75% of the variation (Figure 2). Factor 1 (54%) distinguishes between those fish where the OH-PAHs were more abundant on the positive side (all of the Orlando fish and half of the fish from Fleurhof) and less abundant on the negative side (all of the reference fish and half of the Lenasia fish). Factor 2 (21%) shows the contrast between the most prevalent metabolites, namely the pyrene-type metabolites (positive side) and the fluorene-types (negative) (Figure 2), which mostly influenced the position of the fish with the lower OH-PAH abundance.

A redundancy analysis was completed to establish whether the PAH metabolites in the fish bile and the native compounds found in the sediments were associated with one another (Figure 3). Prior to statistical analysis metabolite data was grouped if more than one isomer was present, e.g. 2–,3–OH Flu and 9–OH Flu as ΣOH Flu, 2–OH Phe

Table 1: Concentrations of naphthalene, fluorene, phenanthrene, pyrene, and benzo(a)pyrene (ng g^{-1} dry mass, DM) in sediments of three impoundments in Soweto and Lenasia (as reported by Pheiffer et al. 2018)

Site	Nap	Flu	Phe	Pyr	BaP
Fleurhof	70	13	99	129	14
Lenasia	125	37	56	31	14
Orlando	144	53	138	120	17

Table 2: Sex ratio, mean mass and mass range, total length, condition factor and hepato-somatic index of fish from the three urban impoundments (Fleurhof, Lenasia and Orlando) and the reference. Significant difference is indicated by common superscripts

Site	F:M	Mean mass (g)	Mass range (g)			Total length(TL) range (mm)			CF	HSI%*		
Fleurhof	5:5	3 024	1 720	–	4 840	570	–	850	0.86 ± 0.1	1.5	±	0.5[a]
Lenasia	5:5	2 838	960	–	4 540	510	–	820	0.78 ± 0.1	1.2	±	0.2[b]
Orlando	6:3	2 416	1 000	–	4 270	510	–	830	0.76 ± 0.1	2.1	±	0.5[b,c]
Reference site	5:5	3 738	1 220	–	5 380	570	–	900	0.78 ± 0.1	0.7	±	0.3[a,c]

* From Pheiffer et al. 2015

Table 3: Quantified biliary OH-PAHs (ng ml^{-1}) of *Clarias gariepinus* from the three urban impoundments (Fleurhof, Lenasia and Orlando) and the reference site. Ratios represent detection frequency. Significant difference is indicated by common superscripts

	2–OH Nap	9–OH Flu	2–,3–OH Flu	2–OH Phe	4–OH Phe	1–OH Pyr	9–OH BaP	ΣOH-PAHs
Fleurhof		10/10	7/10	2/10		8/10	1/10	
Mean (SD)	ND[a]	35 (31)[a]	280 (268)[a]	1.8 (4.7)[a]	ND[a]	55 (36)[a]	0.8 (2.5)[a]	371 (323)[a]
Range		4.7–96	0–706	0–16		0–116	0–8.4	63–996
Lenasia		10/11	9/11		1/11			
Mean (SD)	ND[a]	21 (15)[b]	175 (129)[b]	ND[b]	0.3 (0.8)[b]	ND[a,b]	ND[b]	196 (143)[b]
Range		0–49	0–411		0–2.8			0–459
Orlando	4/9	9/9	9/9	6/9	6/9	9/9	7/9	
Mean (SD)	22 (35)[a]	90 (59)[c]	709 (446)[a,b,c]	20 (25)[a,b,c]	20 (26)[a,b,c]	86 (38)[b,c]	9.5 (10)[a,b,c]	947 (608)[a,b,c]
Range	0–89	21–196	172–1 429	0–84	0–84	26–146	0–34	292–1 879
Reference site	3/10		6/10			3/10		
Mean (SD)	1.8 (2.5)	ND[a,b,c]	102 (72)[c]	ND[c]	ND[c]	6.2 (10)[c]	ND[c]	99 (76)[c]
Range	0–6.1		0–187			0–33		0.1–171
LOD	0.09	0.18	0.07	0.07	0.04	0.26	0.09	
LOQ	0.3	0.6	0.25	0.23	0.15	0.87	0.32	

SD = standard deviation; ND = not detected

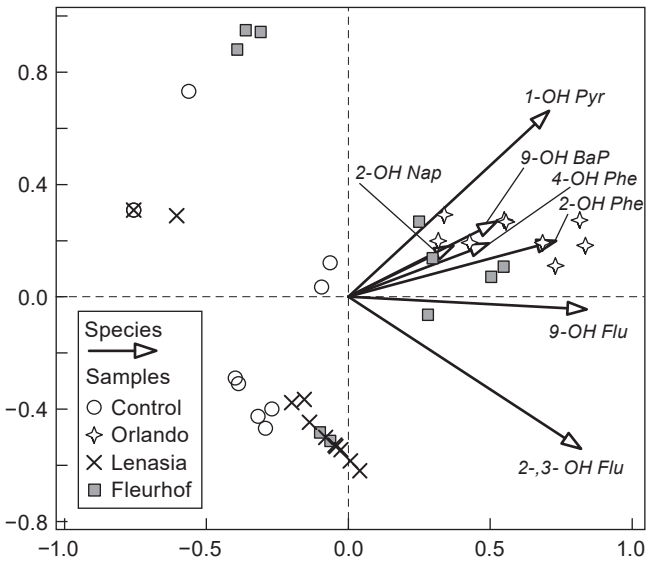

Figure 2: PCA biplot of biliary OH-PAHs of *Clarias gariepinus* from the three urban impoundments (Fleurhof, Lenasia and Orlando) and the reference site. The ordination explains 75% of the variance in the data with 53.9% by factor 1 and 21.2% by factor 2

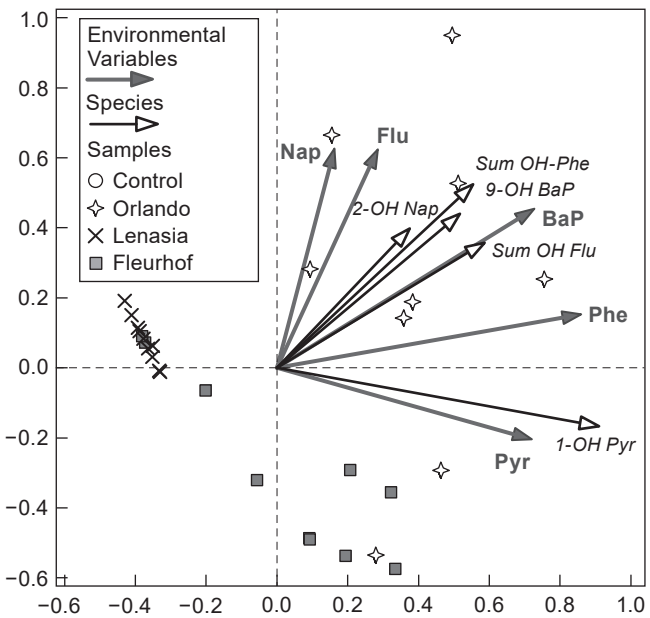

Figure 3: RDA triplot of biliary OH-PAHs of Clarias gariepinus and the native PAHs in the sediment from the three urban impoundments. The ordination explains 57.47% (p = 0.002) of the variance, 43.74% by factor 1 and 13.73% by factor 2

and 4–OH Phe as ΣOH Phe. The reference fish metabolite data was not included in this analysis, because there were no corresponding native PAH sediment values for them.

The explanatory variables, i.e. the native PAHs in the respective impound sediment, account for 58% of the variation in Figure 3. The fish from the three sites grouped separately. This pattern shows that the OH-PAHs in the individual fish differ sufficiently enough among the sites to ordinate according to their respective impoundments. Factor 1 (44%) distinguished between the fish with OH-PAHs (positive side) and those with little or no OH-PAHs (negative side). Factor 2 (14%) separated fish with more 'lighter' OH-PAHs on the positive axis from those with the 'heavier' metabolites on the negative axis (Figure 3).

For bile to be a toxicological significant indicator of contamination, it should reflect the concentrations of native PAH in the environment (Ruddock et al. 2003). However, it is often difficult to directly compare biliary PAHs levels to native PAHs in the water, sediment and muscle, owing to the fast metabolism of these contaminants. In the current study, a redundancy analysis showed that *C. gariepinus* must have been exposed to the native PAHs in the sediment, because the angles between the vector lines of the metabolites and the native PAHs were all <90° (Figure 3).

The levels of phenanthrene in the sediments of the sampling sites were slightly greater than that of fluorene (Table 1) (Pheiffer et al. 2018), but this was not reflected in the metabolite data. The only phenanthrene metabolites in the bile were 2 and 4–OH Phe, at very low levels compared with 2–,3–OH Flu (Table 3). Two possibilities could explain this. First, phenanthrene has a relatively long half-life in soil-like matrices (Leblanc 2004) and a high affinity for sediment particles (Yuan et al. 2001), decreasing its bio-availability and therefore lead to a lower concentration thereof in the fish. Second, lower molecular mass metabolites, such as those of phenanthrene are also excreted in the urine (Solbakken et al. 1980; Timbrell 2000), resulting in lower biliary concentrations of OH-Phe isomers.

Literature available on biliary PAHs for freshwater fish is limited, especially for African fish, consequently our results were also compared with laboratory exposed fish, as well as studies conducted on estuaries. The levels of 9–OH benzo(a)pyrene of the current study was lower than BaP-like metabolites quantified from laboratory exposed *Clarias gariepinus* (Mdegela et al. 2006), channel catfish (*Ictalurus punctatus*) and brown bullhead (*Ameiurus nebulosus*) (Willett et al. 2000). The latter two are catfish from the family Ictaluridae and are similar to *C. gariepinus* in the sense of habitat and feeding. *Clarias gariepinus* exposed to 18.21 ng ml^{-1} waterborne BaP, had 118 940 ± 12 670 ng ml^{-1} BaP-type fluorescent compounds (FACs) in the bile after a 6 h exposure (Mdegela et al. 2006). After a single 10 mg kg^{-1} body mass intraperitoneal injection of BaP, *I. punctatus* and *A. nebulosus* had 3 100 ± 1 400 and 9 300 ± 3 600 ng ml^{-1} total BaP metabolites in their bile respectively after the 6 hours exposure, which increased to 701 000 ± 206 000 and 616 000 ± 326 000 ng ml^{-1} after a 7 d exposure (Willett et al. 2000). Compared with the high metabolite levels reported for the laboratory exposed fish, the fish from our study area seem to be exposed less frequently and/or to a more diffuse (chronic) PAH input.

Numerous studies have been conducted on the biliary PAH of the European eel (*Anguilla anguilla*), specifically quantifying the levels of 1–OH Pyr with fluorescence (Ruddock et al. 2003; Nagel et al. 2012; Kammann et al. 2014; Wariaghli et al. 2015). The levels of 1–OH Pyr in *C. gariepinus* of the current study were notably lower than any of the mentioned *A. anguilla* studies. The mean levels

of 1–OH Pyr in the Orlando fish (highest for the current study) was 36 times lower than what was reported for eels from the Rhine River (Germany) (3 160 ng ml^{-1}) (Kammann et al. 2014) and British estuarine eels from the Tees River (3 108 ng ml^{-1}) (Ruddock et al. 2003), and 60 times lower than the Tyne River (5 150 ng ml^{-1}) (Ruddock et al. 2003). The results compared with are from the most inland sites (i.e. freshwater sites) in the respective studies.

The levels of biliary 1–OH Pyr in brown trout (*Salmo trutta*) from high altitude lakes in Norway and Austria (Escartin and Porte 1999) were 1.8 and 2.5 times (154 ng ml^{-1} and 218 ng ml^{-1}) greater than in fish from Orlando. However, the levels of 9–OH Flu in *S. trutta* (12.9 ng ml^{-1}: Norway and 7 ng ml^{-1}: Austria) (Escartin and Porte 1999) were between 3 and 13 times lower than in the *C. gariepinus* from Orlando and Fleurhof (Table 3). The ΣOH-PAHs quantified in *C. gariepinus* from Orlando was 2 and 4 times greater than in *S. trutta* from Norwegian (454.5 ng ml^{-1}) and Austrian lakes (196 ng ml^{-1}) (Escartin and Porte 1999). The ΣOH-PAHs from Fleurhof were 1.2 times lower than the Norwegian lake, but 1.9 times greater than the Austrian lake (Escartin and Porte 1999). The fact that our study area was situated in an urban area, with more regular PAH inputs, might substantiate the higher metabolite concentrations.

The ΣOH-PAHs of estuarine dab (*Limanda limanda*) from the Seine River in France, ranged between 147 and 770 ng g^{-1} bile. Comparisons with our results may be made if the units are converted to parts per billion (1 ng g^{-1} = 1 ppb = 1 ng ml^{-1}). Our range enveloped that seen for *L. limanda* (Table 3). The maximum ΣOH-PAHs at Fleurhof (996 ng ml^{-1}) and Orlando (1 879 ng ml^{-1}) were greater than the total metabolites in *L. limanda* of the Seine River estuary (Dévier et al. 2013).

The CF of *C. gariepinus* from Orlando Dam in 2015/2016 reported by Bengu et al. (2017) were lower than the current study, showing that there is potentially decline in condition of these fish in Orlando Dam. There was no correlation between the CF and biliary metabolites of the respective fish, which coincides with the findings of Tuvikene et al. (1996) and Barra et al. (2001) on rainbow trout (*Oncorhynchus mykiss*). The HSI recorded by Bengu et al. (2017) in fish from Orlando Dam were similar to the HSI of fish from Fleurhof and Lenasia in the current study and lower than fish sampled in Orlando Dam during the current study. An increase of HIS, attributable to chemical contaminant exposure, notably PAHs, has been reported in numerous studies (Everaarts et al. 1993; Pinkney et al. 2001). However, the opposite was reported for *A. nebulosus* from Lake Erie tributaries, where BaP and Nap-type metabolites negatively correlated with the HSI. This HSI decrease could be attributed to additional PCB and pesticide interactions (Yang and Baumann 2006). Tuvikene et al. (1996) and Barra et al. (2001) found no correlation between the HSI and biliary metabolites in *O. mykiss.* In the current study, the HSI of *C. gariepinus* correlates significantly with the biliary metabolites: The ΣOH-PAHs correlated strongly with the HSI (r = 0.7031, p < 0.0001), 1–OH Pyr and 2–,3–OH Flu correlated moderately (r = 0.55 p = 0.0003, and r = 0.67 p < 0.0001, respectively). The exposure to PAHs often results in the formation of tumours and lesions in the liver (Hawkins et al. 1990; Vogelbein et al. 1990) leading to an increased liver mass and therefore an increased HSI. The correlation found between the PAH metabolites and the HSI of *C. gariepinus* suggests that the PAHs are contributing to this increase in liver size, together with other xenobiotic classes bound to have been present.

The overall lower concentrations of biliary metabolites in *C. gariepinus* compared with literature could be ascribed to the lower input of native PAHs from anthropogenic sources, because South Africa is not as industrialised as the countries compared against earlier. The influence of fish species' metabolic rates might also explain the observed difference between the subtropical *C. gariepinus* and the more temperate fish species of Europe. The fact that biliary PAHs were quantified in the fish from the current study makes OH-PAHs in bile an effective indicator of PAH exposure, even in aquatic environment with low inputs.

Conclusions

The fact that *C. gariepinus* are bottom dwelling fish associated with sediments (Bruton 1988) and subsequently exposed to PAHs in the sediments, as well as their widespread distribution throughout Africa, makes it a suitable species to monitor PAH contamination in Africa. Of the 11 targeted OH-PAHs, seven metabolites were present in fish from Soweto, South Africa. The most prevalent isomers were 2–,3–OH Flu, 1–OH Pyr, and 9–OH Flu. The concentrations of biliary PAH metabolites in *C. gariepinus* were generally lower than the levels in literature for fish from European estuaries and rivers. However, the metabolites quantified have shown to be a burden on the liver, as observed by the positive correlation between the OH-PAHs and the HSI. The use of biliary PAHs has proven to be an effective biomonitoring tool to assess PAH exposures in aquatic systems and indirect human exposure. To the authors' knowledge the data on biliary PAH metabolites for *C. gariepinus* is the first for South Africa.

Acknowledgements — The current study was funded by the Water Research Commission of South Africa (WRC, K2/2242/1/16), and the National Research Foundation (Innovation student bursary SF1208219521, and Grant No. 103487). Opinions expressed and conclusions arrived at are those of the authors only, and are not necessarily to be attributed to the NRF. This work was also supported by Grants-in-Aid for Scientific Research from the Ministry of Education, Culture, Sports, Science and Technology of Japan awarded to M Ishizuka (No. 16H0177906), Y Ikenaka (No. 26304043, 15H0282505, 15K1221305), S Nakayama (No. 16K16197), and the foundations of Sumitomo and JSPS Core to Core Program (AA Science Platforms) and Bilateral Joint Research Project (PG36150002 and PG36150003). The Gauteng Department of Agriculture and Rural development, Directorate of Conservation Permit Office, is acknowledged for the issue of the sampling permit (CPE2/0097). We are grateful to Natasha Vogt for generating the map and Takahiro Ichise for technical support.

References

Aas E, Baussant T, Balk L, Liewenborg B, Anderson OK. 2000. PAH metabolites in bile, cytochrome P4501A and DNA adducts as environmental risk parameters for chronic oil exposure: A

laboratory experiment with Atlantic cod. *Aquatic Toxicology* 51: 241–258.

Angerer J, Mannschreck C, Gündel J. 1997. Biological monitoring and biochemical effect monitoring of exposure to polycyclic aromatic hydrocarbons. *International Archives of Occupational and Environmental Health* 70: 365–377.

Barra R, Sanchez-Hernandez JC, Orrego O, Parra O, Gavilan JF. 2001. Bioavailability of PAHs in Biobio River (Chile): MFO activity and biliary fluorescence in juvenile *Oncorhynchus mykiss. Chemosphere* 45: 439–444.

Bengu TS, du Plessis J, Modley LS, van Dyk JC. 2017. Health effects in fish from the polluted Orlando Dam and Klipspruit wetland system, Soweto, South Africa. *African Journal of Aquatic Science* 42: 131–141.

Beyer J, Sandvik M, Skåre JU, Egaas E, Hylland K, Waagbø R, Goksøyr A. 1997. Time- and dose-dependent biomarker responses in flounder (*Platichthys flesus* L) exposed to benzo[a]-pyrene, 2,3,3',4,4',5–hexachlorobiphenyl (PCB-156) and cadmium. *Biomarkers* 2: 35–44.

Bortey-Sam N, Ikenaka Y, Akoto O, Nakayama SMM, Marfo J, Saengtienchai A et al. 2016. Excretion of polycyclic aromatic hydrocarbon metabolites (OH-PAHs) in cattle urine in Ghana. *Environmental Pollution* 218: 331–337.

Brenner RC, Magar VS, Ickes JA, Abbott JE, Stout, S.A., Crecelius, E.A., et al. 2002. Characterization and fate of PAH-contaminated sediments at the Wyckoff/Eagle Harbor Superfund Site. *Environmental Science and Technology* 36: 2605–2613.

Bruton MN. 1988. Systematics and biology of Clariid catfish. *In* Hecht T, Uys W, Britz PJ, (Eds) *The culture of sharptooth catfish Clarias gariepinus in southern Africa*, 1st Edn. South African National Scientific Programmes Report No 153, Pretoria, pp 1–10.

CCAC (Canadian Council on Animal Care). 2005. Guidelines on: The care and use of fish in research, teaching and testing. http://www.ccac.ca/Documents/Standards/Guidelines/Fish.pdf. [Accessed 12 November 2017].

Colin N, Porte C, Fernandes D, Barata Padrós F, Carrassón M, Monroy M et al. 2016. Ecological relevance of biomarkers in monitoring studies of macro-invertebrates and fish in Mediterranean rivers. *The Science of the Total Environment* 540: 307–323.

De Luca G, Furesi A, Leardi R, Micera G, Panzanelli A, Piu PC. 2004. Polycyclic aromatic hydrocarbons assessment in the sediments of the Porto Torres Harbor (Northern Sardinia, Italy). *Marine Chemistry* 86: 15–32.

Dévier M-H, Le Dû-Lacoste M, Akcha F, Morin B, Peluhet L, Le Menach K, et al. 2013. Biliary PAH metabolites, EROD activity and DNA damage in dab (*Limanda limanda*) from Seine Estuary (France). *Environmental Science and Pollution Research International* 20: 708–722.

DWAS (Department of Water Affairs and Sanitation). 2004. Upper Vaal Water Management Area: Internal Strategic Perspective. https://www.dwaf.gov.za/ Documents/Other/WMA/Upper_Vaal_ ISP.pdf. [Accessed 12 November 2017]

Escartin E, Porte C. 1999. Biomonitoring of PAH pollution in high-altitude mountain lakes through the analysis of fish bile. *Environmental Science and Technology* 33: 406–409.

Everaarts JM, Shugart LR, Gustin MK, Hawkins WE, Walker WW. 1993. Biological markers in fish: DNA integrity, hematological parameters and liver somatic index. *Marine Environmental Research* 35: 101–107.

Guo Y, Senthilkumar K, Alomirah H, Moon HB, Minh TB, Mohd MA et al. 2013. Concentrations and profiles of urinary polycyclic aromatic hydrocarbons (OH-PAHs) in several Asian Countries. *Environmental Science and Technology* 47: 2932–2938.

Hawkins WE, Walker WW, Overstreet RM, Lytle JS, Lytle TF. 1990. Carcinogenic effects of some polycyclic aromatic hydrocarbons on the Japanese medaka and guppy in waterborne exposures. *Science of the Total Environment* 94: 155–167.

Hylland K. 2006. Polycyclic aromatic hydrocarbon (PAH) ecotoxicology in marine ecosystems. *Journal of Toxicology and Environmental Health, Part A* 69: 109–123.

Jonsson G, Bechmann RK, Bamber SD, Baussant T. 2004. Bioconcentration, biotransformation, and elimination of polycyclic aromatic hydrocarbons in sheepshead minnows (*Cyprinodon variegatus*) exposed to contaminated seawater. *Environmental Toxicology and Chemistry* 23: 1538–1548.

Kammann U, Brinkmann M, Freese M, Pohlman J-D, Stoffels S, Hollert H et al. 2014. PAH metabolites, GST, and EROD in European eel (*Anguilla anguilla*) as possible indicators for eel habitat quality in German rivers. *Environmental Science and Pollution Research International* 21: 2519–2530.

Leblanc GA. 2004. Acute Toxicity. *In* Hodgson E (Ed.). *Modern textbook of toxicology*, 3rd Edn. pp 213–224. Hoboken. John Wiley and Sons, Inc.

Maliszewska-Kordybach B, Smreczak B, Klimkowicz-Pawlas A. 2009. Concentrations, sources, and spatial distribution of individual polycyclic aromatic (PAHs) in agricultural soils in the Eastern part of the EU: Poland as a case study. *The Science of the Total Environment* 407: 3746–3753.

McCarthy TS, Venter JS. 2006. Increasing pollution levels on the Witwatersrand recorded in the peat deposits of the Klip River wetland. *South African Journal of Science* 102: 27–34.

Mdegela RH, Braathen M, Correira D, Mosha RD, Skaare JU, Sandvik M. 2006. Influence of 17α-ethynylestradiol on CYP1A, GST and biliary FACs responses in male African sharptooth catfish (*Clarias gariepinus*) exposed to waterborne Benzo[a] Pyrene. *Ecotoxicology* 15: 629–637.

Miller JN, Miller JC. 2010. Statistics and chemometrics for analytical chemistry, 6th Edn. pp 110–124. Harlow, Prentice Hall.

Moja SJ, Mtunzi F, Madlanga X. 2013. Determination of polycyclic aromatic hydrocarbons (PAHs) in river water samples from the Vaal Triangle area in South Africa. *Journal of Environmental Science and Health.* Part A*, Toxic/Hazardous Substances and Environmental Engineering* 48: 847–854.

Nagel F, Kammann U, Wagner C, Hanel R. 2012. Metabolites of polycyclic aromatic hydrocarbons (PAHs) in bile as biomarkers of pollution in European eel (*Anguilla anguilla*) from German rivers. *Archives of Environmental Contamination and Toxicology* 62: 254–263.

Nieuwoudt C, Pieters R, Quinn LP, Kylin H, Borgen AR, Bouwman H. 2011. Polycyclic aromatic hydrocarbons (PAHs) in soil and sediment from industrial, residential and agricultural areas in central South Africa: an initial assessment. *Soil and Sediment Contamination* 20: 188–204.

Okedeyi OO, Nindi MM, Dube S, Awofolu OR. 2013. Distribution and potential sources of polycyclic aromatic hydrocarbons in soils around coal-fired power plants in South Africa. *Environmental Monitoring and Assessment* 185: 2073–2082.

Page DS, Boehm PD, Douglas GS, Bence AE, Burns WA, Mankiewicz PJ. 1999. Pyrogenic polycyclic aromatic hydrocarbons in sediments record past human activity: a case study in Prince William Sound, Alaska. *Marine Pollution Bulletin* 38: 247–260.

Pheiffer W, Pieters R, Smit NJ. 2015. Health assessment and biomarker responses of *Clarias gariepinus* from impoundments in an urban area, South Africa. Peer reviewed and revised paper presented at the 7th International Toxicology Symposium in Africa (ISTA7), 31 August 2015, Johannesburg, South Africa: pp 20–21. [Date accessed 26 January 2018].

Pheiffer W, Quinn LP, Bouwman H, Smit NJ, Pieters R. 2018. Polycyclic aromatic hydrocarbons (PAHs) in sediments from a typical urban impacted river: Application of a comprehensive risk assessment. *Ecotoxicology* 27: 336–351.

Pinkney AE, Harshbarger JC, May EB, Melancon MJ. 2001. Tumor prevalence and biomarkers of exposure in brown

bullheads (*Ameiurus nebulosus*) from the tidal Potomac River, USA, watershed. *Environmental Toxicology and Chemistry* 20: 1196–1205.

Population Labs. 2011. South Africa population map. http://www.populationlabs.com/south_africa_population.asp. [Accessed 12 November 2017].

Quinn L, Pieters R, Nieuwoudt C, Borgen AR, Kylin H, Bouwman H. 2009. Distribution profiles of selected organic pollutants in soils and sediments of industrial, residential and agricultural areas of South Africa. *Journal of Environmental Monitoring* 11: 1647–1657.

Richardson DM, Davies IM, Moffat CF, Pollard P, Stag RM. 2001. Biliary PAH metabolites and EROD activity in flounder (*Platichthys flesus)* from a contaminated estuarine environment. *Journal of Environmental Monitoring* 3: 610–615.

Ruddock PJ, Bird DJ, McEvoy J, Peters LD. 2003. Bile metabolites of polycyclic aromatic hydrocarbons (PAHs) in European eels *Anguilla anguilla* from United Kingdom estuaries. *Science of the Total Environment* 301: 105–117.

Rudel RA, Camann DE, Spengler JD, Korn KR, Brody JG. 2003. Phthalates, alkylphenols, pesticides, polybrominated diphenyl ethers, and other endocrine-disrupting compounds in indoor air and dust. *Environmental Science and Technology* 37: 4543–4553.

Scott A, Clarke R. 2000. Multivariate techniques. *In* Sparks T (Ed.*) Statistics in ecotoxicology*. pp: 149–178. 1st Edn. Chichester, England. John Wiley and Sons, Inc.

Skelton P. 2001. A complete guide to the freshwater fishes of Southern Africa, pp 229–230. 2nd Edn. Cape Town. Struik Publishers.

Šmilauer P, Lepš J. 2014. Multivariate analysis of ecological data using CANOCO 5, 2nd Edn. Cambridge. Cambridge University Press.

Sogbanmu TO, Nagy E, Phillips DH, Arlt VM, Otitoloju AA, Bury NR. 2016. Lagos lagoon sediment organic extracts and polycyclic aromatic hydrocarbons induce embryotoxic, teratogenic and genotoxic effects in *Danio rerio* (zebrafish) embryos. *Environmental Science and Pollution Research International* 23: 14489–14501.

Solbakken JE, Palmork KH, Neppelberg T, Scheline RR. 1980. Urinary and biliary metabolites of phenanthrene in coalfish (*Pollachius virens*). *Acta Pharmacologica et Toxicologica* 46: 127–132.

Stein JE, Reichert WL, Nishimoto M, Varanasi U. 1990. Overview of studies on liver carcinogenesis in English sole from Puget Sound; evidence for a xenobiotic chemical etiology II: Biochemical studies. *Science of the Total Environment* 94: 51–69.

Stogiannidis E, Laane R. 2015. Source characterization of polycyclic aromatic hydrocarbons by using their molecular indices: An overview of possibilities. pp 49–133. *In* Whitacre DM (Ed.) *Reviews of Environmental Contamination and Toxicology*, Vol 234. Switzerland. Springer International Publishing.

Timbrell JA. 2000. Factors affecting toxic responses: disposition. pp 25–62. *In* Timbrell JA (Ed.) *Principles of biochemical toxicology*, 3rd Edn. London. Taylor and Francis.

Tuvikene A. 1995. Responses of fish to polycyclic aromatic hydrocarbons (PAHs). *Annales Zoologici Fennici* 32: 295–309.

Tuvikene A, Huuskonen S, Roy S, Lindström-Seppä P. 1996. Biomontoring of South Estonian waters by means of xenobiotics metabolites of rainbow trout (*Oncorhynchus mykiss*) liver. *Comparative Biochemistry and Physiology* Part C: *Pharmacology, Toxicology and Endocrinology* 114: 171–177.

Van den Brink PJ, Van den Brink NW, Ter Braak CJF. 2003. Multivariate analysis of ecotoxicological data using ordination: Demonstrations of utility on the basis of various examples. *Australian Journal of Ecotoxicology* 9: 141–156.

Van der Oost R, Beyer J, Vermeulen NPE. 2003. Fish bioaccumulation and biomarkers in environmental risk assessment: a review. *Environmental Toxicology and Pharmacology* 13: 57–149.

Van der Oost R, Van Schooten FJ, Ariese F, Heida H, Satumalay K, Vermeulen, NPE. 1994. Bioaccumulation, biotransformation and DNA binding of PAHs in feral eel (*Anguilla anguilla*) exposed to polluted sediments: A field survey. *Environmental Toxicology and Chemistry* 13: 859–870.

Vane CH, Kim AW, Beriro DJ, Cave MR, Knights K, Moss-Hayes V et al. 2014. Polycyclic aromatic hydrocarbons (PAH) and polychlorinated biphenyls (PCB) in urban soils of Greater London, UK. *Applied Geochemistry* 51: 303–314.

Varanasi U, Stein JE, Nishimoto M. 1989. Biotransformation and disposition of PAH in fish. pp 93–150. *In* Varanasi U (Ed.) *Metabolism of Polycyclic Aromatic Hydrocarbons in the Aquatic Environment*, 1st Edn. Boca Raton. CRC Press.

Vogelbein WK, Fournie JW, Van Veld PA, Huggett RJ. 1990. Hepatic neoplasms in the mummichog *Fundulus heteroclitus* from a creosote-contaminated site. *Cancer Research* 50: 5978–5986.

Wariaghli F, Kammann U, Hanel R, Yahyaoui A. 2015. PAH metabolites in bile of European eel (*Anguilla anguilla*) from Morocco. *Bulletin of Environmental Contamination and Toxicology* 95: 740–744.

Willett KL, Gardinali PR, Lienesch LA, Di Giulio RT. 2000. Comparative metabolism and excretion of benzo(a)pyrene in 2 species of ictalurid catfish. *Toxicological Sciences* 58: 68–76.

Yang X, Baumann PC. 2006. Biliary PAH metabolites and the hepatosomatic index of brown bullheads from Lake Erie tributaries. *Ecological Indicators* 6: 567–574.

Yuan SY, Chang JS, Yen JH, Chang BV. 2001. Biodegradation of phenanthrene in river sediment. *Chemosphere* 43: 273–278.

Manuscript received: 26 January 2018, revised: 09 July 2018, accepted: 10 August 2018.
Associate Editor: C van Dyk

Characterization, Spatial Variation and Risk Assessment of Heavy Metals and a Metalloid in Surface Soils in Obuasi, Ghana

Osei Akoto,[1] Nesta Bortey-Sam,[2] Shouta M.M. Nakayama,[2] Yoshinori Ikenaka,[2] Elvis Baidoo1, Joseph Apau,[1] Jemima Tiwaa Marfo,[2] Mayumi Ishizuka[2]

1 Department of Chemistry, Kwame Nkrumah University of Science and Technology, Kumasi, Ghana.
2 Laboratory of Toxicology, Graduate School of Veterinary Medicine, Hokkaido University, Kita 18, Nishi 9, Kita ku, Sapporo 060-0818, Japan

Corresponding author:
Mayumi Ishizuka

Tel. +81–11–706–6949
ishizum@vetmed.hokudai.ac.jp

Background. Soil contamination with heavy metals and metalloids has become an increasingly important issue in recent years.
Objectives. The present study examines possible contamination of the environment with metals from gold mining activities in Obuasi, Ghana.
Methods. Soil samples were collected from commercial and residential areas and tailing dams in Obuasi in order to investigate the extent of lead (Pb), cadmium (Cd), mercury (Hg), copper (Cu), zinc (Zn), cobalt (Co), chromium (Cr), nickel (Ni) and arsenic (As) pollution, create thematic maps showing the extent of heavy metals pollution, identify the sources of pollution, and to assess risks to humans and the surrounding ecological system.
Results. Mean concentrations of metals from the study were found in the order of As > Cu > Zn > Cr > Ni > Pb > Co > Hg > Cd. The results showed that all communities were severely polluted with As, and distribution maps highlighted two hot spots at the sulfite treatment plant and Pompura treatment plant tailings dams. Additionally, the levels of Pb, Cu and Zn were elevated around the city center where vehicular traffic is very dense. Principal component analysis indicated that mining activities may have significantly contributed to metal levels in Obuasi soils. The potential ecological risk (RI) indicated that soils in 41% of the communities pose very high risks to the surrounding ecological system, 50% pose considerable risk, and 9% pose a moderate risk. Arsenic and Hg contributed 73 and 15% of the RI, respectively. The average hazard quotient due to soil As exposure was 2.51 ± 1.23 and ingestion of soils in 95% of the communities in the study area could pose non-carcinogenic health risks to children. Moreover, the average cancer risk for children from the communities was 1.13×10^{-3}. Based on the United States Environmental Protection Agency (USEPA) recommendation for cancer risk of 10^{-6} to 10^{-4}, the cancer risk for children ($> 10^{-3}$) was higher in 45% of the studied communities.
Conclusions. The central part of the study area is polluted with Pb, Zn and Cu, and As pollution is severe in all of the studied communities. The RI from all study sites revealed very high risk to the ecological system, including mammals. There could be non-cancer and cancer risks to Obuasi residents due to ingestion of As-contaminated soils, and children are particularly vulnerable.
Competing Interests. The author declares no competing financial interests
Keywords: metals, mining, hazard quotient, thematic maps, ecological, cancer risk
Received March 9, 2018. Accepted May 24, 2018
J Health Pollution 19: (180902) 2018

Introduction

Soil contamination with heavy metals and metalloids has become an increasingly important issue in recent years. High concentrations of toxic metals in soil can reduce soil fertility and lead to accumulations in food and drinking water, with the potential to endanger human health through ingestion and/or inhalation.[1-5] Exposure to high concentrations of lead can affect the central nervous system and reduces intelligent quotient in humans.[4] Intake of cadmium (Cd)-contaminated food causes acute gastrointestinal effects, and kidney damage has been reported with chronic exposures.[6,7] Children are more susceptible to heavy metal poisoning because they have an active digestive system and higher rate of metal absorption.[4] In addition to these toxicities, the non-biodegradable nature and long half-lives of these metals in soil also pose risks.[8-11]

Mining, smelting, vehicular emissions, industrial waste and other related activities are some of the major sources of heavy metals soils contamination.[8,12,13] Numerous studies regarding metal contamination in mining and smelting areas have been performed in the Europe, the United States, and Africa.[12,14-19]

The mining sector in Ghana has seen extensive expansion over recent decades. This rapid development has resulted in the generation of toxic substances which pollute soil, rivers, streams and boreholes.[1,12,20] Heavy metals and arsenic pollution in soils and other environmental media in Obuasi have been previously studied.[21-24] Toxicological risks arise when soil arsenic (As) concentrations exceed 40 mg/kg.[25] Studies have shown that prolonged exposure to As could lead to cancer, diabetes, thickening of the skin, nervous system disorders, liver disease and digestive system problems.[26]

There are limited published data on the risks of metal exposure in Obuasi municipality through soil exposure, and little action has been taken over the years to deal with this problem. The objectives of the present study were to investigate the extent of heavy metals and metalloid pollution in the topsoil of communities within the Obuasi municipality, to create thematic maps of metal concentrations in the study area using geographical information systems mapping techniques, to identify possible contamination sources and relationships between metals and soil properties, and to assess the risk of these metals to humans and the surrounding ecological system.

Abbreviations

AAS	Atomic absorption spectrophotometry	*HQ*	Hazard quotient
dw	Dry weight	*RI*	Ecological risk

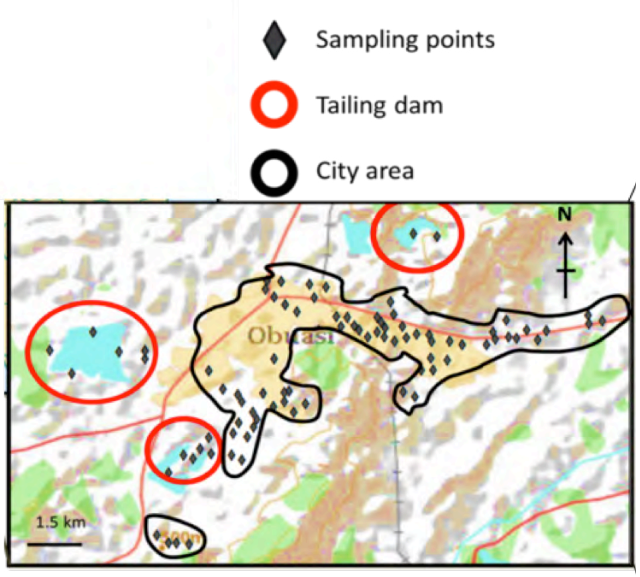

Figure 1 — Map of study area showing the sampling points

Methods

The Obuasi municipality is situated at the southern end of the Ashanti Region at 06°12'00"N 01°41'00"W. It covers a land area of 162.4 km^2, with 53 communities. Obuasi is the administrative capital where the lucrative Obuasi Gold Mine (Anglo Gold Ashanti) is also located. The municipality has an estimated resident population of 287,000.[27] The topography is undulating with a semi-equatorial climate with a double rainfall regime. Mean monthly rainfall ranges from 3.5 (January) to 283 mm (July). The average annual temperature is 25.5°C with relative humidity between 75%–80% in the wet season.[28] Obuasi has the richest gold deposits in West Africa, and mining (including artisanal and small-scale mining) began in the 17th century. Since the late 1890s, Obuasi has developed into a modern mining town and it is one of the most densely populated areas in Ghana. Due its mountainous landscape with limited flat land, many of the residential and commercial structures are constructed on hillsides and on the flat areas within mountainous areas. Communities are therefore susceptible to pollution from various sources, including mining.

Sampling, sample preparation and analysis

As shown in Figure 1, twenty communities and two tailing dams were selected for the present study. The sampling sites/points were selected to represent a wide area of the town (*Figure 1*) and geographical coordinates for each site were recorded with a Garmin (etrex) global

position system. A total of 86 surface soil samples were collected from open spaces within commercial and residential areas and tailings dams. The top soil layer was collected to a depth of about 10 cm with a stainless-steel spatula, as anthropogenic sources of pollutants usually contaminate the upper layer of soil.[29]

The collected samples were placed in labeled Corning tubes (Corning Incorporated, New York, USA) and transported to the toxicology laboratory at the Graduate School of Veterinary Medicine, Hokkaido University, Japan where they were stored at -30°C until analysis. Due to lack of background concentrations in soils in Obuasi, Ghana, data from 5 soil samples from the University of Mines and Technology campus in Tarkwa, Ghana, (Tarkwa is another mining community in Ghana) were used as reference values to evaluate the extent of metal pollution in the present study.[1] University of Mines and Technology is a public university located in Tarkwa, and because it has low vehicular and industrial (mining) activities, heavy metals and metalloids from point sources were assumed to be negligible.[1] Additionally, concentrations of metals in University of Mines and Technology were all low compared to the world range for unpolluted soils described by Kabata-Pendias and Pendias.[30]

Prior to chemical analysis, soil samples were air dried. Roots, stones and other unwanted materials were removed and remaining soil samples crushed. The homogenized samples were sieved through a 2-mm mesh. Soil samples were digested using a microwave digestion system (Speedwave MWS-2, Berghof, Germany) equipped with temperature and pressure feedback controls. Metals were digested by weighing 1 g of dried soil into pre-washed digestion vessels. Then 10.0 mL of 60% nitric acid (HNO_3) (atomic absorption spectrometry grade; Kanto Chemical Corporation, Tokyo, Japan) was added. The vessels and content were covered and placed in the microwave oven for digestion. The microwave unit was calibrated to a temperature of 200°C and digestion was allowed for 45 minutes at 180 psi. After digestion, the solutions were allowed to cool and filtered using ash-less filter paper 5B (Advantec, Tokyo, Japan) into Corning tubes. Lanthanum chloride (1 mL, atomic absorption spectrometry grade, 100 g La/L solution, Wako Pure Chemical Industries Ltd., Osaka, Japan) was added to prevent physical, chemical and ionization/interference during metal analysis with atomic absorption spectrophotometry (AAS). Samples were diluted to a volume of 50 mL with 2% HNO_3 prepared with milli-Q water. Reagent blanks were prepared using the same procedure. Concentrations of chromium (Cr), copper (Cu), As, Cd, cobalt (Co), nickel (Ni), lead (Pb) and zinc (Zn) were determined by AAS (Z-2010, Hitachi High Technologies Corporation, Tokyo, Japan) with either the acetylene flame or argon non-flame method, after preparation of calibration standards. Cadmium, Cr, Ni, Pb and As were analyzed by graphite furnace AAS with Zeeman background correction, while Cu and Zn were analyzed by flame AAS with deuterium background correction. The concentration of total mercury (Hg) was measured by thermal decomposition, gold amalgamation and AAS (Mercury Analyzer, MA–3000, Nippon Instruments Corporation, Tokyo, Japan), after preparation of calibration standards.

The water content of each soil sample was measured after 12 hours of drying in an oven at 105°C. Soil organic matter (soil organic matter) content was determined by loss of weight on ignition at an oven temperature of 600°C for 5 hours. pH was measured in a soil deionized water suspension (soil: water, 1:2.5 by volume) by a calibrated pH meter.

Quality control and quality assurance

For quality control, blanks were analyzed after analysis of every 10 samples. Soil recovery rates (%) using certified reference materials (BCR-320R and SRM 1944) were: Cr (80–115), Co (96–111), Cu (88–95), Zn (90–95), Cd (113–120), Pb (91–114), Ni (85–87) and As (113–121). The detection limits (mg/kg) were 0.5 for Cr, 0.5 for Co, 1.0 for Cu, 0.1 for Zn, 0.2 for Cd, 1.0 for Pb, 0.5 for Ni and 2.0 for As. The detection limit of Hg in soil samples was 2.0 pg total Hg. Concentrations of metals and the studied metalloid in soils were expressed in mg/kg dry weight (dw).

Data analysis

Potential ecological risk (RI) is a commonly used indicator to assess the effects of heavy metals and metalloids in the environment, including soils and sediments. The RI was calculated using Equations 1 through 4:

Equation 1

$$C^i_f = C^i/C^i_n$$

Equation 2

$$C_{deg} = \Sigma\, C^i_f$$

Equation 3

$$E^i r = T^i_r \times C^i_f$$

Equation 4

$$RI = \Sigma\, E^i_r$$

Where C^i_f is the pollution coefficient of a metal which can reflect the pollution character of the investigated region but

cannot reveal the ecological effects.[31,32] C^i is the concentration of metals in soils. C^i_n is the reference values of the heavy metals in soil/sediments. The C^i_f of each metal was calculated and classified as either low ($C^i_f \leq 1$), middle ($1 < C^i_f \leq 3$) or high ($C^i_f > 3$).[33]

C_{deg} represents the integrated pollution level in the environment and is expressed as the sum of C^i_f for all examined metals. The four pollution levels were categorized as $C_{deg} < 5$, low pollution; $5 \leq C_{deg} < 10$, medium pollution; $10 \leq C_{deg} < 20$, high pollution; and $C_{deg} \geq 20$, very high pollution.[34] E^i_r is the monomial potential ecological risk factor of the individual metal and T^i_r is the metal toxic factor (based on the standardized heavy metal toxic factor). Referring to Hakanson, we used the following T^i_r values: Hg = 40; Cd = 30; As = 10; Cu = Pb = Ni = 5, Cr = 2, and Zn = 1.[31] The RI is defined as the sum of E^i_r for all metals and has been grouped into four categories by Hakanson as shown in Table 1.[31]

E^i_r	Single factor pollution ecological risk level	RI value	General potential ecological risk level
$E^i_r < 40$	Low risk	RI ≤ 150	Low risk
$40 \leq E^i_r < 80$	Moderate risk	150 < RI ≤ 300	Moderate risk
$80 \leq E^i_r < 160$	Considerable risk	300 < RI ≤ 600	Considerable risk
$E^i_r < 320$	High risk	RI < 600	Very high risk
$E^i_r \geq 320$	Very high risk		

Abbreviations: E^i_r, monomial potential ecological risk factor; RI, potential ecological risk.
Source: Hakanson, 1980[31]

Table 1 — Single Factor and General Potential Ecological Risk Levels

Human health risk assessment

Soil ingestion is one of the most common pathways through which humans, especially children, are exposed to metals.[35] The risk due to metals was therefore assessed via oral ingestion. For incidental soil ingestion, Equation 5 were used according to the United States Environmental Protection Agency (USEPA).[36]

Equation 5

$$CDI_{metal} = (M_{soil} \times IngR \times EF \times ED \times CF)/(BW \times AT)$$

Where CDI_{metal} = metal daily intake (mg/kg/day); Msoil = average metal concentration in soil (mg/kg); IngR = ingestion rate of soil (mg/day); EF = exposure frequency (day/year); ED = exposure duration (year); BW = body weight (kg); AT = averaging time (days); and CF = conversion factor (10^{-6} kg/mg).[36] The above equation assumes 100% bioavailability of the ingested soil-borne contaminant. Carcinogenic risk was determined by Equation 6.

Equation 6

$$Cancer\ risk = CDI_{metal} \times SF$$

SF is the cancer slope factor $(mg/kg/day)^{-1}$.[36] For non-cancer risk, the hazard quotient (HQ) was calculated according to Equation 7 below, where RfD is the reference dose (mg/kg/day).[36] All parameters used in the present study have been previously described.[37]

Equation 7

$$HQ = CDI/RfD$$

For the risk assessment, an HQ value greater than 1 indicates the potential for non-carcinogenic health effects, while HQ < 1 means residents are not likely to experience any health risks as a result of exposure.[38] The acceptable or tolerable cancer risk for regulatory purposes is within the range of 10^{-6} –10^{-4}.[38]

Statistical analysis

Statistical analyses were performed using statistical analysis software (SPSS) 20.0 (IBM SPSS Inc., Chicago, USA). Kolmogorov–Smirnov (K-S) and Shapiro–Wilk's tests were used to determine the normality of data and results were considered to be statistically significant if the p value was less than 0.05. Statistical analyses were carried out after data were log transformed (normalized). Spatial distributions were performed using ArcGIS 9.3 (ESRI Co., Redlands, USA). In order to identify the important parameters affecting the chemistry of soil and to investigate the possible sources of these metals, Pearson's correlation matrix (at a significance level of $p<0.05$) and principal component analysis were used, respectively. The principal components based on log transformed data were extracted with eigenvalues >1 through a varimax rotation.

Results

Average concentrations of heavy metals and a metalloid (As) in soils in communities within the Obuasi municipality are shown in Supplemental Material 1. Mean concentrations (mg/kg dw) of metals decreased in the order As > Cu > Zn > Cr > Ni > Pb > Co > Hg > Cd (*Supplemental Material 1*). Kolmogorov–Smirnov and Shipro-Wilks statistical tests showed a significant distribution (p 0.05) of metals in the communities

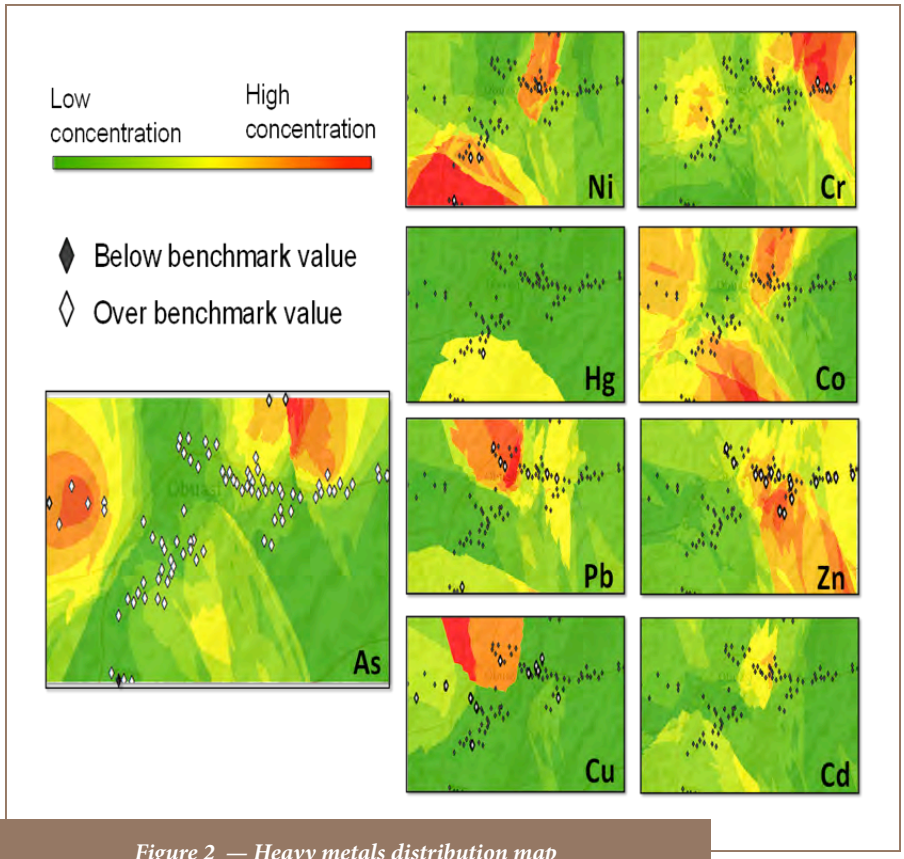

Figure 2 — Heavy metals distribution map

(*Supplemental Material 1*). Arsenic, Pb and Hg were classified as the 1st, 2nd and 3rd most hazardous substances.[39] Cadmium (7th) was excluded due to low concentrations throughout the study area.

An overall examination of As distribution in soil found that the highest mean concentration (598 ± 132 mg/kg dw) was detected in samples from the Pompura Treatment Plant tailings dam, while the lowest (89.7 ± 58.2 mg/kg dw) was detected in samples from Sanso (*Supplemental Material 1*). Levels of As throughout the entire study area were extremely high compared to the world range for unpolluted soils and USEPA recommended levels (*Supplemental Material 1*), and could pose toxicological risks in the study area.[25,30,40,41]

As shown in Supplemental Material 1, mean Pb content in soil ranged from 4.30 ± 0.719 (Danquah Estate) to 189 ± 131 (Bedieso) mg/kg dw. The highest mean concentration of Hg was recorded at Sanso (5.19 ± 7.28 mg/kg dw) and lowest was 0.05 ± 0.01 mg/kg dw in Danquah Estate. Mercury pollution could well be underestimated in this study as small-scale gold miners using amalgamation is widespread in the area and no samples were collected from small-scale mining facilities.

Distribution maps

The distribution map of As in topsoils within the Obuasi municipality showed that As is widespread throughout the communities, with the highest concentrations detected at the Pompura Treatment Plant tailings dam (*Figure 2*). Although levels exceeded recommended guidelines at all sites, the distribution of As showed two hotspots at the Sulfite Treatment Plant (Sulfite Treatment Plant) and Pompura Treatment Plant tailings dam (*Figure 2*). Nickel levels within the study area were generally low compared to recommended levels, but showed wide variation. Nickel recorded a hotspot around the tailings dams (Sulfite Treatment Plant and Pompura Treatment Plant) and Sanso (*Figures 1 and 2*). While Hg showed hotspots at Sanso, Cd did not show any appreciable variation in its distribution within the study area. As shown in Figure 2, Cu showed hotspots at Bediaso.

Relationship between heavy metals and soil properties

Soil properties, such as pH and soil organic matter, play an important role in the mobility, adsorption, desorption, movement and bioavailability of heavy metals, thus influencing their distribution and biological availability in soils.[42-44] This role is generally illustrated by good correlations between heavy metal concentrations and soil properties.[45,46] Soil pH in the samples ranged from 6.35 (Brono Estate) to 7.31 (Brahabebome), with a mean value of 6.73 ± 0.48, whereas the soil organic matter content ranged from 3.43 (Kwabrafosu) to 10.3% (Bill Huston) (*Supplemental Material 1*).

Sources of metals in soil

Three principal components (PC1, PC2, and PC3) were extracted, accounting for 66.9% of the total variance. As shown in Figure 3, PC1, the most important component, explained 35% of the total variance and was characterized by high loadings of As, Co, Cu, Zn, Cd, and Pb.

Nickel and Cr were grouped under PC2 and made up 21% of the component. PC3 explained 11.6% of the total variance and was dominated by high loading of Hg.

Soil contamination risks

Table 2 shows the C^i_f and C_{deg} of metals and their contributions to the total potential ecological risk of surface soils. The average C^i_f of Cu, Ni and As indicated high pollution (C^i_f > 3), while Hg indicated moderate pollution. The C_{deg} of metals ranged from 25.4 (Boete) - 130 (Pompura Treatment Plant), with an average of 61.9 ± 28.2. As shown in Table 2, all of the communities including the two tailing dams were very highly polluted with metals (*Tables 1 and 2*).

Human health risks

Arsenic was the most abundant metal in the present analysis. The overall average concentration of As in the study area (256 ± 135 mg/kg) was more than 14 times higher than the USEPA recommended value (18 mg/kg) (*Table 1*). Further, the calculated HQs for Cu, Zn, Pb, Ni and Co were less than 1 for both children and adults from all study sites (data not shown).

As shown in Table 3, the HQ for As ranged from 0.955 to 6.37 (children) and 0.102 to 0.683 (adults). Ingestion of soils in 95% of the communities in the study area could pose non-carcinogenic health risks to children. Some of the communities with the highest HQ were Anyinam (5.11), Bruno Estate (4.35), Kwabrafosu (4.27), and Tutuka (4.08), etc. The average HQ in the communities (without tailing dams) for both children and adults was 2.51 ± 1.23 and 0.270 ± 0.132, respectively.

The cancer risk posed by As for children ranged from 4.30×10^{-4} to

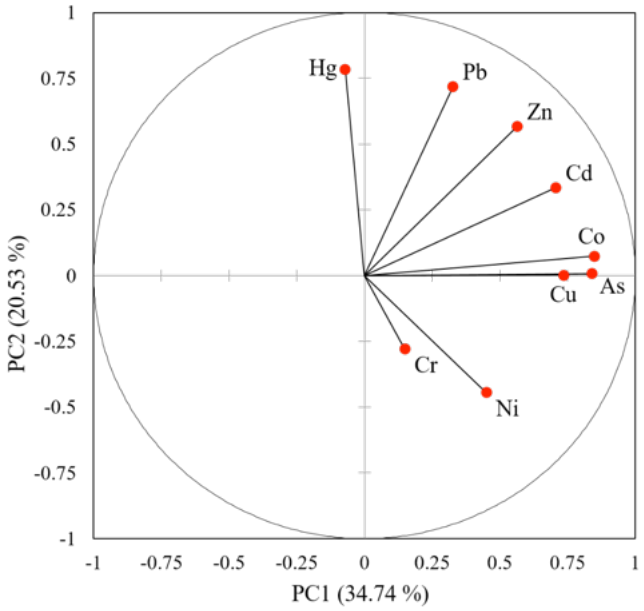

Figure 3 — Distribution of heavy metals and a metalloid in soils in Obuasi, Ghana

Sample site	Hg	Cu	Zn	Pb	Cd	Ni	As	Cr	Cdeg
PTP tailings dam	0.38	**6.67**	0.88	0.31	0.26	**16.2**	**103**	**2.61**	**130**
STP tailings dam	0.21	**1.48**	0.40	0.22	0.30	**17.1**	**54.6**	**1.02**	**75.4**
Sanso	**21.6**	**1.38**	0.87	**1.68**	0.13	**17.6**	**15.4**	0.63	**59.3**
Sam Jona Estate	0.33	**4.76**	0.73	0.35	0.10	**1.13**	**52.2**	**3.10**	**62.7**
Bruno Estate	0.29	**1.25**	0.50	0.36	0.18	**3.22**	**70.5**	**1.97**	**78.2**
Danquah	0.21	**1.09**	0.48	0.08	0.10	**9.43**	**43.9**	**1.32**	**56.6**
Anyinam	**1.29**	**1.55**	0.83	0.59	0.25	**10.7**	**82.7**	**1.55**	**99.5**
Bill Huston	0.46	0.90	0.51	0.29	0.07	**5.79**	**26.7**	0.78	**35.5**
Pomposo	0.46	0.90	**1.28**	**1.05**	0.05	**3.88**	**20.0**	**5.09**	**32.7**
Akaporiso	0.71	**1.26**	**1.83**	0.53	0.13	**3.75**	**25.3**	**1.25**	**34.8**
Bossman	0.54	**1.23**	0.55	0.13	0.08	**4.93**	**33.4**	**1.22**	**42.1**
Brahabebome	**1.57**	0.69	**1.34**	0.32	0.22	**3.07**	**29.1**	**2.36**	**38.7**
Boete	**2.44**	0.62	0.70	0.17	0.07	**2.46**	**17.7**	**1.13**	**25.4**
Ahansonyewudia	**5.09**	**2.10**	**2.31**	**1.42**	0.27	**6.12**	**31.0**	**1.84**	**50.1**
Esikafuoabantem	**1.32**	**11.2**	**2.38**	0.25	0.08	**11.5**	**63.4**	0.78	**91.0**
Tutuka	**2.38**	**2.26**	**1.68**	**2.27**	0.28	**12.9**	**66.0**	**1.23**	**89.1**
Central Market	0.75	**1.91**	**2.01**	**1.57**	0.64	**2.46**	**45.1**	0.61	**55.1**
Wawasi	**1.80**	**1.20**	**1.26**	0.33	0.28	**2.97**	**28.7**	**2.34**	**38.9**
Kwabrafosu	**3.33**	**1.46**	**1.72**	**1.28**	0.31	**1.44**	**69.1**	0.64	**79.3**
Estate	0.67	**2.80**	**1.24**	0.49	0.38	**2.25**	**23.6**	**2.32**	**33.7**
Bediaso	**4.08**	**59.6**	**1.01**	**3.63**	0.44	**2.93**	**32.2**	**1.54**	**105**
Bongobri	1.00	**1.20**	**1.54**	**1.19**	0.28	**2.55**	**38.4**	**1.86**	**48.1**
Average	2.32	4.89	1.18	0.84	0.22	6.57	44.2	1.69	61.9
SD	4.51	12.4	0.61	0.87	0.15	5.40	23.3	1.03	28.2
Minimum	0.21	0.62	0.40	0.08	0.05	1.13	15.4	0.61	25.4
Maximum	21.6	59.6	2.38	3.63	0.64	17.61	103	5.09	130

Abbreviations: C^i_f, metal pollution coefficient; C_{deg}, integrated pollution level. Bold indicates high C^i_f and C_{deg} values (i.e. middle to high pollution) based on: (a) low ($C^i_f \leq 1$), middle ($1 < C^i_f \leq 3$) or high ($C^i_f > 3$).[33] (b) $C_{deg} < 5$, low pollution; $5 \leq C_{deg} < 10$, medium pollution; $10 \leq C_{deg} < 20$, high pollution; and $C_{deg} \geq 20$, very high pollution.[34]

Table 2 — Metal Pollution Coefficient and Integrated Pollution Level of Heavy Metals and a Metalloid in Surface Soils at Obuasi, Ghana

	Hazard Quotient		Cancer risk	
Sample sites	Child (As)	Adult (As)	Child (As)	Adult (As)
PTP tailings dam	6.37	0.683	2.87E-03	3.08E-04
STP tailings dam	3.37	0.362	1.52E-03	1.63E-04
Sanso	0.955	0.102	4.30E-04	4.62E-05
Sam Jona Estate	3.22	0.346	1.45E-03	1.56E-04
Bruno Estate	4.35	0.467	1.96E-03	2.10E-04
Danquah	2.71	0.291	1.22E-03	1.31E-04
Anyinam	5.11	0.548	2.30E-03	2.47E-04
Bill Huston	1.65	0.177	7.43E-04	7.98E-05
Pomposo	1.23	0.132	5.56E-04	5.97E-05
Akaporiso	1.56	0.168	7.05E-04	7.56E-05
Bossman	2.06	0.221	9.30E-04	9.98E-05
Brahabebome	1.80	0.193	8.10E-04	8.70E-05
Boete	1.09	0.117	4.94E-04	5.30E-05
Ahansonyewudia	1.91	0.205	8.63E-04	9.26E-05
Esikafuoabantem	3.92	0.420	1.76E-03	1.89E-04
Tutuka	4.08	0.437	1.84E-03	1.97E-04
Central Market	2.79	0.299	1.26E-03	1.35E-04
Wawasi	1.77	0.190	8.01E-04	8.59E-05
Kwabrafosu	4.27	0.458	1.92E-03	2.06E-04
Estate	1.45	0.156	6.57E-04	7.05E-05
Bediaso	1.99	0.213	8.97E-04	9.62E-05
Bongobri	2.37	0.255	1.07E-03	1.15E-04
Average	2.73	0.293	1.23E-03	1.32E-04
SD	1.44	0.154	6.48E-04	6.96E-05
Median	2.22	0.238	1.00E-03	1.07E-04
Minimum	0.955	0.102	4.30E-04	4.62E-05
Maximum	6.37	0.683	2.87E-03	3.08E-04

Abbreviations: SD, standard deviation

Table 3 — Human Health Risk Characterization for Arsenic in Obuasi Soils

2.87×10^{-3} (*Table 3*). Based on the USEPA recommended range of 10^{-6} to 10^{-4}, the cancer risk for children (greater than 10^{-3}) was higher in 45% of the communities. Anyinam (2.3×10^{-3}) recorded the highest cancer risk, followed by Bruno Estate (1.96×10^{-3}), Kwabrafosu (1.92×10^{-3}), Tutuka (1.84×10^{-3}), Esikafuoanbantem (1.76×10^{-3}), Sam Jona Estate (1.45×10^{-3}), Central market (1.26×10^{-3}), Danquah (1.22×10^{-3}) and Bongobri (1.07×10^{-3}). The average cancer risk assessment based on soil ingestion in the studied communities was higher for children (1.13×10^{-3}) than adults (1.22×10^{-4}). The carcinogenic risk of As for adults through ingestion of soil in the studied communities ranged from 4.62×10^{-5} to 2.47×10^{-4} at Sanso and Anyinam, respectively (*Table 3*).

Discussion

The high levels of As in the study area could be due to the nature of the gold bearing ore which is comprised of mineralized pyrites and arsenopyrites.[47] Arsenic is a toxic substance and due to its non-biodegradable nature, it can accumulate in surface soils and lead to contamination of food crops, surface and ground water. It can also enter the food chain through plant assimilation. The concentrations of As in communities in the present study far exceeded those recorded in a previous study by Amonoo-Neizer et al. at Kwabrafoso (48.9 ± 10.9 mg/kg dw).[47]

Lead concentrations in soils were high in some communities, but compared to average concentrations in urban soils worldwide, the mean value (43.8 ± 45.2 mg/kg dw) in the present study was low compared to values reported in large and industrialized cities such as Palermo (Sicily) (202 mg/kg) and Rome (330 mg/kg).[48,49] However, compared to unpolluted soils, Pb levels were higher in 23% of the communities (*Supplemental Material 1*).[30] The presence of elevated levels of Pb in soil from some communities, including the central market, is not surprising because Pb has greater soil retention and adsorption capacity than any other metal. Lead is therefore considered immobile in sub-surface soil and generally gets accumulated in surface soils when deposited.[50]

The concentrations of soil Hg determined in some areas (Sanso and Boete) in this study were higher than those reported in previous studies, and may be due to recent Hg contamination.[47] The concentrations at some sites coupled with wide coefficients of variation (coefficients of variation of 194%; *Supplemental Material 1*) suggest anthropogenic sources, since Hg is used to amalgamate gold from ore.

Distribution maps

The high concentrations or hotspots at some sites could be attributed to artisanal and small-scale gold mining activities. Illegal mining activities are frequently practiced in some communities and this could be the source of soil heavy metals pollution. The distribution pattern of Pb and Cu showed hotspots around the city center (central market), with higher levels than recommended for Pb.

Heavy metals and soil properties

Metal mobility and availability are generally higher in acidic soil conditions. The thresholds for the solubility and uptake of metals such as Zn, Ni As and Cr occur between pH of 4.5 and 6.42. The pH of the soil within the study area (6.35 to 7.31) was above the threshold for heavy metal mobility and therefore would have no significant effect on the mobility and availability of heavy metals in soil. When metals are bound to organic matter, the toxic effects may be pronounced, because the metal becomes more bioavailable.[51] No metals in the study area showed any significant correlation with pH and soil organic matter (*Table 4*), similar to the results by Manta et al. and Al–Khashman and Shawabkeh.[48,52] This could be attributed to the narrow range of pH (near neutrality) in the samples. Additionally, lack of significant correlation between soil properties and heavy metals could be attributed to a continuous input since the release and transport of heavy metals are complex processes.[46,53,54] Another possible explanation could be variations in soil type within the sampling area.[46,54]

Source identification

Lead was highly distributed around the city center where vehicular traffic is very dense and therefore lead pollution could be related to vehicular traffic. The use of leaded fuel in the past may account for the high levels of Pb in soil in the central part of the city. Even though the use of leaded petrol has ceased in Ghana, Pb is highly immobile and could remain strongly bound to soil. Pollution with the other metals, Cu and Zn, were more likely to have come from the wear and tear of tires, engine and brakes, and therefore their concentrations are expected to increase in this area since vehicular

	Hg	Cu	Zn	Pb	Cd	Co	Ni	As	Cr	SOM	pH
Hg	1.00										
Cu	-0.05	1.00									
Zn	-0.29	0.01	1.00								
Pb	-0.12	0.68*	0.32	1.00							
Cd	0.11	0.30	0.32	0.52*	1.00						
Co	-0.05	-0.10	-0.13	0.03	0.17	1.00					
Ni	0.48	-0.09	-0.17	-0.02	-0.13	0.73*	1.00				
As	0.07	-0.02	-0.02	-0.10	0.17	0.66*	0.39	1.00			
Cr	-0.17	-0.03	-0.08	-0.10	-0.19	-0.20	-0.25	-0.07	1.00		
SOM	-0.10	-0.16	-0.13	0.06	-0.30	-0.43	-0.20	-0.39	-0.11	1.00	
pH	-0.14	-0.11	0.11	0.12	-0.16	-0.15	0.03	-0.17	0.35	0.01	1.00

*correlation is significant at the $p < 0.05$ level

Table 4 — Correlation Between Metal Concentrations, Soil Organic Matter and Soil pH

Sample site	Hg	Cu	Zn	Pb	Cd	Ni	As	Cr	RI
PTP tailings dam	15.0	33.3	0.88	1.57	7.69	**81.3**	**1031**	5.21	**1176**
STP tailings dam	8.4	7.40	0.40	1.10	8.92	**85.8**	**546**	2.03	**660**
Sanso	**865**	6.90	0.87	8.42	3.85	**88.0**	**154**	1.25	**1129**
Sam Jona Estate	13.3	23.8	0.73	1.74	3.08	5.66	**522**	6.20	**576**
Bruno Estate	11.6	6.24	0.50	1.81	5.38	16.1	**705**	3.94	**750**
Danquah	8.33	5.43	0.48	0.41	3.08	**47.1**	**439**	2.63	**507**
Anyinam	**51.6**	7.74	0.83	2.97	7.62	**53.5**	**827**	3.09	**955**
Bill Huston	18.3	4.52	0.51	1.46	2.00	28.9	**267**	1.55	**324**
Pomposo	18.3	4.48	1.28	5.26	1.54	19.4	**200**	10.2	**260**
Akaporiso	28.3	6.31	1.83	2.67	3.85	18.7	**253**	2.50	**317**
Bossman	21.6	6.14	0.55	0.67	2.31	24.6	**334**	2.43	**392**
Brahabebome	**62.8**	3.45	1.34	1.61	6.54	15.3	**291**	4.72	**387**
Boete	**97.7**	3.10	0.70	0.85	2.00	12.3	**177**	2.27	**296**
Ahansonyewudia	**203**	10.4	2.31	7.11	8.08	30.6	**310**	3.67	**576**
Esikafuoabantem	**52.6**	**56.1**	2.38	1.27	2.31	**57.6**	**634**	1.57	**808**
Tutuka	**95.1**	11.3	1.68	11.3	8.46	**64.6**	**660**	2.45	**855**
Central Market	30.0	9.57	2.01	7.85	19.2	12.3	**451**	1.23	**533**
Wawasi	**72.1**	6.02	1.26	1.63	8.46	14.8	**287**	4.68	**397**
Kwabrafosu	**133**	7.29	1.72	6.38	9.23	7.22	**691**	1.27	**857**
Estate	26.6	14.0	1.24	2.44	11.5	11.2	**236**	4.64	**308**
Bediaso	**163**	**298**	1.01	18.1	13.1	14.6	**322**	3.08	**834**
Bongobri	40.0	6.02	1.54	5.94	8.46	12.7	**384**	3.72	**462**
Average	92.6	24.4	1.18	4.21	6.67	32.8	442	3.38	607
SD	180	62.3	0.61	4.35	4.36	26.9	233	2.07	276
Minimum	8.33	3.10	0.40	0.41	1.54	5.66	154	1.23	260
Maximum	865	298	2.38	18.1	19.2	88.1	1031	10.2	1176

Bold indicates E^i_r (monomial potential ecological risk factor) and RI (potential ecological risk)

indicates moderate to high risk of heavy metals and/or metalloid.

Table 5 — Monomial Potential Ecological Risk Factor and Potential Ecological Risk of Heavy Metals and a Metalloid in Surface Soils in Obuasi, Ghana

traffic is heavy. Additionally, the presence of Zn in the environment is associated with mining and smelting, which pollutes the air, water and soil, which ultimately undergoes oxidation to release Zn^{2+} ions.[55]

Levels of As in soils could have resulted from blasting of gold bearing rock, which is the most common method of obtaining ore. Miners engage in surface and sub-surface mining.[56] Arsenic levels in soils could also be due to the nature of the gold bearing ore, which is comprised of mineralized pyrites and arsenopyrites. Processing of the ore involves roasting, and this results in the production of arsenic trioxide gas which is distributed throughout the study area by air currents.

The possible sources of Cr in soils from Obuasi could be due to weathering of the rock system. Other sources of Cr in the study area could be the occasional discharge of acid industrial wastes or mine drainage.[55]

In Ghana, amalgamation using Hg is the preferred gold recovery method employed by almost all artisanal gold miners because it is a very simple and inexpensive technique.[47] The high levels of Hg in soils could therefore be due to contamination from mining processes.

Ecological risk assessment

The very high pollution ($C_{deg} \geq 20$) found in the present study could be due to the proximity of some sample sites to the mines, as we observed very high C_{deg} values from the two tailings dams. In addition, high pollution levels could be attributed to the several artisanal and small-scale mining activities within some communities.

The E^i_r of As showed that 59% of sampled sites posed potentially high risks to the surrounding ecological system. Mercury was found to pose moderate to very high risks in 45% of the sampled sites (*Tables 1 and 5*). As shown in Table 5, the RI at all study sites ranged from 260 (Pomposi) - 1176 (Pompura Treatment Plant), with an average of 607 ± 276. According to the classification by Hakanson (*Table 1*), soils in 41% of all study sites pose very high risks to the ecological system, 50% pose considerable risk, and 9% pose moderate risks to the ecological system.[31] Arsenic and Hg on average contributed 73 and 15%, respectively (total contribution 88%), of the RI. This trend is similar to that in a study by Bortey-Sam et al., in which As and Hg contributed 85% of the total RI in agricultural soils in Tarkwa, Ghana.[12] However, in that study, the contribution from As was 10%, and 75% for Hg.[12] The average RI of heavy metals and a metalloid from all study sites in Obuasi (607 ± 276) indicated very high risk (*Tables 1 and 5*) to the ecological system, including mammals, higher than that reported by Bortey-Sam et al. in Tarkwa soils.[12]

Human health risks

The human health risk assessment for children determined HQs suggesting potential non-carcinogenic risks due to As exposure (*Table 3*). As shown in Table 3, HQs for children throughout the study area were high (average of 2.73 ± 1.44; range 0.955-6.37). In the communities without tailing dams, the average HQ ranged from 0.955 (Sanso) to 5.11 (Anyinam), with an average of 2.51 ± 1.23. Remedial action and control methods are therefore required in the communities to further avoid the deleterious effects of As exposure. However, the HQs for adults were all below 1, mainly due to behavioral differences. The high HQs detected for children could be due to their frequent hand-to-mouth or object-to-mouth activities, which could increase toxicant exposure, including As.[57,58] Previous studies have found that children typically ingest an average of 50 mg/d of soil.[59] However, in the case of pica, this amount could be higher.[60,61]

The present study further revealed that the cancer risk due to As exposure was higher for children (1.13×10^{-3}) compared to adults (1.22×10^{-4}). Based on these results, there could be potential cancer risks for Obuasi residents, especially children. The high non-cancer and cancer risks detected in the communities, particularly Anyinam, Bruno Estate, Sam Jona Estate and Danquah could be due to their proximity to the Sulfite Treatment Plant tailings dam (*Figure 1*), in addition to other artisanal and small-scale mining activities within the study areas. In Kumasi, Ghana, Darko et al. reported that the cancer risk (based on maximum exposure point concentration) for As due to soil ingestion was 3.22×10^{-5} for children and 1.73×10^{-5} for adults.[37]

Conclusions

The investigation of soil samples in the Obuasi municipality has revealed high accumulations of As in surface soils and levels exceeded background concentrations throughout the study area. Distribution maps for As highlighted two hotspots around the tailing dams, while Pb, Cu and Zn were elevated in the central area of the Obuasi municipality. Principal component analysis indicated that mining activities have played a significant role in the levels of some metals in Obuasi soils. The RI of the results showed that the investigated soils could pose very high risks to the surrounding ecological system due to metal exposure, and As and Hg contributed 88% of these risks. The current study found that ingestion of As-contaminated soils could pose both

non-cancer and cancer risks to Obuasi residents, especially children.

Funding

Grants-in-Aid for Scientific Research from the Ministry of Education, Culture, Sports, Science and Technology of Japan

Authors' contributions

All authors contributed equally to the preparation and approval of the final manuscript.

Acknowledgements

This work was supported by Grants-in-Aid for Scientific Research from the Ministry of Education, Culture, Sports, Science and Technology of Japan awarded to M. Ishizuka (No. 24405004 and No. 24248056) and Y. Ikenaka (No. 26304043, 15H0282505, 15K1221305), and the foundation of JSPS Core to Core Program (AA Science Platforms) and Bilateral Joint Research Project (PG36150002 and PG36150003). We also acknowledge the financial support by The Mitsui & Co., Ltd. Environment Fund.

References

1. **Bortey-Sam N, Nakayama SM, Ikenaka Y, Akoto O, Baidoo E, Mizukawa H, Ishizuka M.** Health risk assessment of heavy metals and metalloid in drinking water from communities near gold mines in Tarkwa, Ghana. Environ Monit Assess [Internet]. 2015 Jul [cited 2018 May 26];187(7):397. Available from: https://link.springer.com/article/10.1007%2Fs10661-015-4630-3 Subscription required to view.

2. **Bortey-Sam N, Nakayama SM, Akoto O, Ikenaka Y, Fobil JN, Baidoo E, Mizukawa H, Ishizuka M.** Accumulation of heavy metals and metalloid in foodstuffs from agricultural soils around Tarkwa area in Ghana, and associated human health risks. Int J Environ Res Public Health [Internet]. 2015 Aug [cited 2018 May 26];12(8):8811-27. Available from: https://www.ncbi.nlm.nih.gov/pmc/articles/PMC4555249/

3. **Bortey-Sam N, Nakayama SM, Ikenaka Y, Akoto O, Baidoo E, Yohannes YB, Mizukawa H, Ishizuka M.** Human health risks from metals and metalloid via consumption of food animals near gold mines in Tarkwa, Ghana: estimation of the daily intakes and target hazard quotients (THQs). Ecotoxicol Environ Saf [Internet]. 2015 Jan [cited 2018 May 26];111:160-7. Available from: https://doi.org/10.1016/j.ecoenv.2014.09.008 Subscription required to view.

4. **Carr R, Zhang C, Moles N, Harder M.** Identification and mapping of heavy metal pollution in soils of a sports ground in Galway City, Ireland, using a portable XRF analyser and GIS. Environ Geochem Health [Internet]. 2008 Feb [cited 2018 May 26];30(1):45-52. Available from: https://link.springer.com/article/10.1007%2Fs10653-007-9106-0 Subscription required to view.

5. **Lu A, Zhang S, Shan X.** Time effect on the fractionation of heavy metals in soils. Geoderma [Internet]. 2005 Apr [cited 2018 May 28];125(3-4):225-34. Available from: https://doi.org/10.1016/j.geoderma.2004.08.002 Subscription required to view.

6. **Barbier O, Jacquillet G, Tauc M, Cougnon M, Poujeol P.** Effect of heavy metals on, and handling by, the kidney. Nephron Physiol [Internet]. 2005 [cited 2018 May 26];99(4):105-10. Available from: https://doi.org/10.1159/000083981

7. **Godt J, Scheidig F, Grosse-Siestrup C, Esche V, Brandenburg P, Reich A, Groneberg DA.** The toxicity of cadmium and resulting hazards for human health. J Occup Med Toxicol [Internet]. 2006 Sep 10 [cited 2018 May 26];1:22. Available from: https://www.ncbi.nlm.nih.gov/pmc/articles/PMC1578573/

8. **Li X, Lee SL, Wong SC, Shi W, Thornton I.** The study of metal contamination in urban soils of Hong Kong using a GIS-based approach. Environ Pollut [Internet]. 2004 May [cited 2018 May 21];129(1):113-24. Available from: https://doi.org/10.1016/j.envpol.2003.09.030 Subscription required to view.

9. **Akoto O, Ephraim JH, Darko G.** Heavy metals pollution in surface soils in the vicinity of abundant railway servicing workshop in Kumasi, Ghana. Int J Environ Res [Internet]. 2008 [cited 2018 May 26];2(4):359-64. Available from: https://ijer.ut.ac.ir/article_215_0.html

10. **Urzelai A, Vega M, Angulo E.** Deriving ecological risk based soil quality values in the Barque country. Sci Total Environ [Internet]. 2000 Mar [cited 2018 May 26];247(2-3):279-84. Available from: https://doi.org/10.1016/S0048-9697(99)00497-0 Subscription required to view.

11. **Li PJ, Stagnitti F, Xiong X, Peterson J.** Temporal and spatial distribution patterns of heavy metals in soil at a long-standing sewage farm. Environ Monit Assess [Internet]. 2009 Feb [cited 2018 May 28];149(1-4):275-82. Available from: https://link.springer.com/article/10.1007%2Fs10661-008-0201-1 Subscription required to view.

12. **Bortey-Sam N, Nakayama SM, Akoto O, Ikenaka Y, Baidoo E, Mizukawa H, Ishizuka M.** Ecological risk of heavy metals and a metalloid in agricultural soils in Tarkwa, Ghana. Int J Environ Res Public Health [Internet]. 2015 Sep 11 [cited 2018 May 28];12(9):11448-65. Available from: https://www.ncbi.nlm.nih.gov/pmc/articles/PMC4586685/

13. **Surthland RA, Tolosa CA, Tack FM, Verloo MG.** Characterization of selected element concentrations and enrichment ratios in background and anthropogenically impacted roadside areas. Arch Environ Contam Toxicol [Internet]. 2000 May [cited 2018 May 28];38(4):428-38. Available from: https://link.springer.com/article/10.1007/s002440010057 Subscription required to view.

14. **Alloway BJ, Davies BE.** Trace element content of soils affected by base metal mining in Wales. Geoderma [Internet]. 1971 Apr [cited 2018 May 28];5(3):197-208. Available from: https://doi.org/10.1016/0016-7061(71)90009-7 Subscription required to view.

15. **Fuge R, Paveley CF, Holdham MT.** Heavy metal contamination in the Tanant Valley, North Wales. Environ Geochem Health [Internet]. 1989 Dec [cited 2018 May 28];11(3-4):127-35. Available from: https://link.springer.com/article/10.1007/BF01758662 Subscription required to view.

16. **Razus P, Christides A.** An investigation on heavy metals in an industrial area in Greece. Int J Environ Res [Internet]. 2010 [cited 2018 May 28];4(4):785-94. Available from: https://ijer.ut.ac.ir/article_265.html

17. **Levy DB, Barbarick KA, Siemer G, Sommers LE.** Distribution and partitioning of trace metals in contaminated soils near Leadville, Colorado. J Environ Qual [Internet]. 1991 [cited 2018 May 28];21(2):185-95. Available from: https://dl.sciencesocieties.org/publications/jeq/abstracts/21/2/JEQ0210020185 Subscription required to view.

18. **Ikenaka Y, Nakayama SM, Muzandu K, Choongo K, Teraok, H, Mizuno N, Ishizuka M.** Heavy metal contamination of soil and sediment in Zambia. Afr J Environ Sci Technol [Internet]. 2010 Nov [cited 2018

May 28];4(11):729-39. Available from: https://www.ajol.info/index.php/ajest/article/download/71339/60292

19. **Nakayama SM, Ikenaka Y, Hamada K, Muzandu K, Choongo K, Teraoka H, Mizuno N, Ishizuka M.** Metal and metalloid contamination in roadside soil and wild rats around a Pb–Zn mine in Kabwe, Zambia. Environ Pollut [Internet]. 2011 Jan [cited 2018 May 28];159(1):175-81. Available from: https://doi.org/10.1016/j.envpol.2010.09.007 Subscription required to view.

20. **Asante KA, Agusa T, Subramanian A, Ansa-Asare OD, Biney CA, Tanabe S.** Contamination status of arsenic and other trace elements in drinking water and residents from Tarkwa, a historic mining township in Ghana. Chemosphere [Internet]. 2007 Jan [cited 2018 May 28];66(8):1513-22. Available from: https://doi.org/10.1016/j.chemosphere.2006.08.022 Subscription required to view.

21. **Amonoo-Neizer EH, Amekor EM.** Determination of total arsenic in environmental samples from Kumasi and Obuasi, Ghana. Environ Health Persp [Internet]. 1993 Apr 22 [cited 2018 May 28];101(1):46-9. Available from: https://www.ncbi.nlm.nih.gov/pmc/articles/PMC1519647/

22. **Antwi-Agyei P, Hogarh JN, Foli G.** Trace elements contamination of soils around gold mine tailings dams at Obuasi, Ghana. Afr J Environ Sci Tech [Internet]. 2009 Nov [cited 2018 May 28];3(11):353-9. Available from: https://www.ajol.info/index.php/ajest/article/viewFile/56263/44708

23. **Golow AA, Laryea JN.** Levels of iron, silver, zinc, and lead in oranges and avocados from two gold-rich towns compared with levels in an adjacent gold-deficient town. Bull Environ Contam Toxicol [Internet]. 1994 Sep [cited 2018 May 28];53(3):332-6. Available from: https://link.springer.com/article/10.1007%2FBF00197222 Subscritption required to view.

24. **Kumi-Boateng B.** Assessing the special distribution of arsenic concentration from goldmine for environmental management at Obuasi, Ghana [M.Sc. thesis]. [Kumasi, Ghana]: Kwame Nkrumah University of Science and Technology; 2007 Mar. 67 p.

25. **Pendergrass A, Butcher JD.** Uptake of lead and arsenic in food plants grown in contaminated soil from Barber Orchard, NC. Microchem J [Internet]. 2006 Jun [cited 2018 May 28];83(1):14-6. Available from: https://doi.org/10.1016/j.microc.2005.12.003 Subscription required to view.

26. **Kapaj S, Peterson H, Liber K, Bhattacharya P.** Human health effects from chronic arsenic poisoning: a review. J Environ Sci Health A Tox Hazard Subst Environ Eng [Internet]. 2006 [cited 2018 May 28];41(10):2399-428. Available from: https://www.epa.gov/foia/human-health-effects-chronic-arsenic-poisoning-review

27. **2010 population and housing census: summary report of final results** [Internet]. Accra, Ghana: Ghana Statistical Service; 2012 May [cited 2013 May 12]. 117 p. Available from: http://www.statsghana.gov.gh/docfiles/2010phc/Census2010_Summary_report_of_final_results.pdf

28. **Obuasi municipal assembly development plan.** Ghana: Medium Term Development Plan; 2006. p. 24-6.

29. **Baltrenas P, Oskinis V, Ignatavicius G, Kumpiene J.** Mechanical disturbance of soils in the field of trainings in the Lithuanian central firing ground in Pabradė and possibilities of environmental protection improving. Environ Eng. 2001;9(2):103-10.

30. **Kabata-Pendias A, Pendias H.** Trace elements in soils and plants. 2nd ed. Boca Raton, FL: CRC Press; 1991. 384 p.

31. **Hakanson L.** An ecological risk index for aquatic pollution control: a sedimentological approach. Water Res [Internet]. 1980 [cited 2018 May 28];14(8):975-1001. Available from: https://doi.org/10.1016/0043-1354(80)90143-8 Subscription required to view.

32. **Zhu W, Bian B, Li L.** Heavy metal contamination of road deposited sediments in a medium size city of China. Environ Monit Assess [Internet]. 2008 Dec [cited 2018 May 28];147(1-3):171-81. Available from: https://link.springer.com/article/10.1007%2Fs10661-007-0108-2 Subscription required to view.

33. **Chen TB, Zheng YM, Lei M, Huang ZC, Wu HT, Chen H, Fan KK, Yu K, Wu X, Tian QZ.** Assessment of heavy metal pollution in surface soils of urban parks in Beijing, China. Chemosphere [Internet]. 2005 Jul [cited 2018 May 28];60(4):542-51. Available from: https://doi.org/10.1016/j.chemosphere.2004.12.072 Subscription required to view.

34. **Loska K, Weichula D.** Application of principal component analysis for the estimation of source of heavy metal contamination in surface sediments from the Rybnik Reservoir. Chemosphere [Internet]. 51(8):723-33. Available from: https://doi.org/10.1016/S0045-6535(03)00187-5 Subscription required to view.

35. **Ng JC, Juhasz A, Smith E, Naidu R.** Assessing the bioavailability and bioaccessibility of metals and metalloids. Environ Sci Pollut Res [Internet]. 2015 Jun [cited 2018 May 28];22(12):8802-25. Available from: https://link.springer.com/article/10.1007/s11356-013-1820-9 Subscription required to view.

36. **Risk assessment guidance for superfund (RAGS).** Vol. 1, Human health evaluation manual [Internet]. Washington, D.C.: US Environmental Protection Agency; 2004 [cited 2018 May 28]. Part E: Supplemental guidance for dermal risk assessment. Available from: https://www.epa.gov/risk/risk-assessment-guidance-superfund-rags-part-e

37. **Darko G, Dodd M, Nkansah MA, Ansah E, Aduse-Poku Y.** Distribution and bioaccessibility of metals in urban soils of Kumasi, Ghana. Environ Monit Assess [Internet]. 2017 Jun [cited 2018 May 28];189(6):260. Available from: https://link.springer.com/article/10.1007%2Fs10661-017-5972-9 Subscription required to view.

38. **Baseline human health risk assessment, Vasquez Boulevard and I–70 superfund site, Denver CO** [Internet]. Denver, CO: US Environmental Protection Agency; 2001 Aug [cited 2018 May 28]. 170 p. Available from: https://nepis.epa.gov/Exe/ZyPURL.cgi?Dockey=P1006STM.TXT

39. **Minimum risk levels [Internet]. Atlanta, GA: Agency for Toxic Substances and Disease Registry; 2012 Feb** [cited 2018 May 28]. 14 p. Available from: http://ulpeis.anl.gov/documents/dpeis/references/pdfs/ATSDR_2012.pdf

40. **Guidance for developing ecological soil screening levels** [Internet]. Washington, D.C.: US Environmental Protection Agency; 2003 Nov [cited 2012 Dec 10]. 87 p. OSWER-Directive 9285.7-55. Available from: https://rais.ornl.gov/documents/ecossl.pdf

41. **Framework for inorganic metals risk assessment** [Internet]. Washington, D.C.: v2004 Nov [cited 2018 May 28]. 334 p. Draft EPA/630/P-04/068B. Available from: https://nepis.epa.gov/Exe/ZyPURL.cgi?Dockey=90160D00.TXT

42. **de Matos AT, Fontes MP, da Costa LM, Martinez MA.** Mobility of heavy metals as related to soil chemical and mineralogical characteristics of Brazilian soils. Environ Pollut [Internet]. 2001 [cited 2018 May 28];111(3):429-35. Available from: https://doi.org/10.1016/S0269-7491(00)00088-9 Subscription required to view.

43. **Khan S, Cao Q, Zheng YM, Huang YZ, Zhu YG.** Health risks of heavy metals in contaminated soils and food crops irrigated with wastewater in Beijing, China. Environ Pollut [Internet]. 2008 Apr [cited 2018 May 2];152(3):686-92. Available from: https://doi.org/10.1016/j.envpol.2007.06.056 Subscription required to view.

44. **Hernandez L, Probst A, Probst JL, Ulrich E.** Heavy metal distribution in some French forest soils: evidence for atmospheric contamination. Sci Total Environ [Internet]. 2003 Aug 1 [cited 2018 May 28];312(1-3):195-219. Available from: https://doi.org/10.1016/S0048-9697(03)00223-7 Subscription required to view.

45. **Gjoka F, Felix-Henningsen P, Wegener HR, Salillari I, Beqiraj A.** Heavy metals in soils from Tirana

(Albania). Environ Monit Assess [Internet]. 2011 Jan [cited 2018 May 28];172(1-4):517-27. Available from: https://link.springer.com/article/10.1007%2Fs10661-010-1351-5 Subscription required to view.

46. **Lu A, Wang J, Qin X, Wang K, Han P, Zhang S. Multivariate and geostatistical analyses of the spatial distribution and origin of heavy metals in the agricultural soils in Shunyi, Beijing, China.** Sci Total Environ [Internet]. 2012 May [cited 2018 May 28];425:66-74. Available from: https://doi.org/10.1016/j.scitotenv.2012.03.003 Subscription required to view.

47. **Amonoo-Neizer EH, Nyamah D, Bakiamoh SB. Mercury and arsenic pollution in soil and biological samples around the mining town of Obuasi, Ghana.** Water Air Soil Pollut [Internet]. 1996 Oct [cited 2018 May 28];91(3-4):363-73. Available from: https://link.springer.com/article/10.1007/BF00666270 Subscription required to view.

48. **Manta DS, Angelone M, Bellanca A, Neri R, Sprovieri M.** Heavy metals in urban soils: a case study from the city of Palermo (Sicily), Italy. Sci Total Environ [Internet]. 2002 Dec 2 [cited 2018 May 28];300(1-3):229-43. Available from: https://doi.org/10.1016/S0048-9697(02)00273-5 Subscription required to view.

49. **Angelone M, Teofili C, Dowgiallo G.** Lead and cadmium distribution in urban soil and plants in the city of Rome: a preliminary study. Proceedings of the Third International Conference on the Biogeochemistry of Trace Elements; 1995 May 10-15; Paris. Rome: Food and Agriculture Organization of the United Nations; 1995. p. 23-4.

50. **McLean JE, Bledsoe BE.** Behavior of metals in soil. Washington, D.C.: US Environmental Protection Agency; 1992. EPA/540/S-92/018.

51. **Salim HM, Sparks DL.** Heavy metal release in soils. Boca Raton, FL: CRC Press; 2001 Jun 15. 246 p.

52. **Al-Khashman OA, Shawabkeh RA.** Metals distribution in soils around the cement factory in southern Jordan. Environ Pollut [Internet]. 2006 Apr [cited 2018 May 28];140(3):387-94. Available from: https://doi.org/10.1016/j.envpol.2005.08.023 Subscription required to view.

53. **Chen T, Liu X, Zhu M, Zhao K, Wu J, Xu J, Huang P. Identification of trace element sources and associated risk assessment in vegetable soils of the urban-rural transitional area of Hangzhou, China.** Environ Pollut [Internet]. 2008 Jan [cited 2018 May 28];151(1):67-78. Available from: https://doi.org/10.1016/j.envpol.2007.03.004 Subscription required to view.

54. **Grant C, Sheppard S.** Fertilizer impacts on cadmium availability in agricultural soils and crops. Hum Ecol Risk Assess [Internet]. 2008 [cited 2018 May 28];14(2):210-28. Available from: https://doi.org/10.1080/10807030801934895 Subscription required to view.

55. **Obiri S.** Determination of heavy metals in water from boreholes in Dumasi in the Wassa West District of western region of Republic of Ghana. Environ Monit Assess [Internet]. 2007 Jul [cited 2018 May 28];130(1-3):455-63. Available from: https://link.springer.com/article/10.1007%2Fs10661-006-9435-y Subscription required to view.

56. **Amponsah-Tawiah K, Dartey-Baah K.** 2011 The Mining Industry in Ghana: A Blessing or a Curse International Journal of Business and Social Science [Internet] 2011 Jul [cited 2018 July]: 2 (12) ; 66. Available from: https://pdfs.semanticscholar.org/23b3/41893980832be50fff5e4fd289362afed41e.pdf

57. **Yabe J, Nakayama SM, Ikenaka Y, Yohannes YB, Bortey-Sam N, Oroszlany B, Muzandu K, Choongo K, Kabalo AN, Ntapisha J, Mweene A, Umemura T, Ishizuka M.** Lead poisoning in children from townships in the vicinity of a lead-zinc mine in Kabwe, Zambia. Chemosphere [Internet]. 2015 Jan [cited 2018 May 28];119:941-7. Available from: https://doi.org/10.1016/j.chemosphere.2014.09.028 Subscription required to view.

58. **Yabe J, Nakayama SM, Ikenaka Y, Yohannes YB, Bortey-Sam N, Kabalo AN, Ntapisha J, Mizukawa H, Umemura T, Ishizuka M.** Lead and cadmium excretion in feces and urine of children from polluted townships near a lead-zinc mine in Kabwe, Zambia. Chemosphere [Internet]. 2018 Jul [cited 2018 May 28];202:48-55. Available from: https://doi.org/10.1016/j.chemosphere.2018.03.079 Subscription required to view.

59. **Stanek EJ.** 3rd, Calabrese EJ. Daily estimates of soil ingestion in children. Environ Health Perspect [Internet]. 1995 Mar [cited 2018 May 28];103(3):276-85. Available from: https://www.ncbi.nlm.nih.gov/pmc/articles/PMC1519074/

60. **Mielke HW, Reagan PL.** Soil is an important pathway of human lead exposure. Environ Health Perspect [Internet]. 1998 Feb [cited 2018 May 26];106(Suppl 1):217-29. Available from: https://www.ncbi.nlm.nih.gov/pmc/articles/PMC1533263/

61. **Calabrese EJ, Stanek EJ, James RC, Roberts SM.** Soil ingestion: a concern for acute toxicity in children. Environ Health Perspect [Internet]. 1997 Dec [cited 2018 May 28];105(12):1354-8. Available from: https://www.ncbi.nlm.nih.gov/pmc/articles/PMC1470417/

Environmental Toxicology and Chemistry

Original Article

Biotransport of Metallic Trace Elements from Marine to Terrestrial Ecosystems by Seabirds

A. Shoji, K.H. Elliott, S. Aris-Brosou, H. Mizukawa, S.M.M. Nakayama Y. Ikenaka, M. Ishizuka, T. Kuwae, K. Watanabe, J.E. Gonzalez, Y. Watanuki

Environ Toxicol Chem., **Accepted Article** • DOI: 10.1002/etc.4286

Original Article **Environmental Toxicology and Chemistry**
DOI 10.1002/etc.4286

Biotransport of Metallic Trace Elements from Marine to Terrestrial Ecosystems by Seabirds

Running head: Trans-ecosystem biotransport of contaminants

A. Shoji[a,b,*], K.H. Elliott[c], S. Aris-Brosou[d], H. Mizukawa[e], S.M.M. Nakayama[e] Y. Ikenaka[e,f], M. Ishizuka[e], T. Kuwae[g], K. Watanabe[g], J.E. Gonzalez[h], Y. Watanuki[a]

[a]Graduate School of Fisheries Sciences, Hokkaido University, 3-1-1 Minatocho, Hakodate, Hokkaido 041 8611 Japan
[b]Department of Zoology, Oxford University, Woodstock Road, Oxford OX2 6GG UK
[c]Department of Natural Resource Sciences, McGill University, 2111 Lakeshore Road, Ste. Anne de Belevue, Quebec H9X 3V9 Canada
[d]Departments of Biology / Statistics, University of Ottawa, 30 Marie Curie, Ottawa, Ontario K1N 6N5 Canada
[e]Department of Environmental Veterinary Sciences, Laboratory of Toxicology, Hokkaido University, Kita 18, Nishi 9, Kita-ku, Sapporo, Hokkaido 060-0818 Japan
[f]Water Research Group, Unit for Environmental Sciences and Management, North-West University, Potchefstroom Campus, 11 Hoffman Street, Potchefstroom 2531 South Africa.
[g]Coastal and Estuarine Environment Research Group, Port and Airport Research Institute, 3-1-1, Nagase, Yokosuka 239-0826, Japan
[h]Departament de Biologia Evolutiva, Ecologia i Ciències Ambientals, Universitat de Barcelona, Av. Diagonal, 645, 08028 Barcelona Spain

***Corresponding author:** Akiko Shoji, akikosho@gmail.com

This article contains online-only Supplemental Data

Submitted 18 July 2018; Returned for Revisions 28 September 2018; Accepted 28 September 2018

Abstract

Physical systems, such as currents and winds, have traditionally been considered responsible for transporting contaminants. While evidence is mounting that animals play a role in this process through their movements, we still know little about how such contaminant biotransport occurs, and the extent of effects at deposition sites. Here, we address this question by studying how rhinoceros auklets (*Cerorhinca monocerata*), a seabird that occurs in immense colonies (~300,000 pairs at our study site, Teuri Island), affect contaminant levels at their colony, and at nearby sites. More specifically, we hypothesize that contaminants are transported and deposited by seabirds at their colony, and that these contaminants are passed on locally to the terrestrial ecosystem. To test this hypothesis, we analyzed the concentration of nine heavy metal and metalloids, as well as $\delta^{13}C$ and $\delta^{15}N$ stable isotopes, in bird tissues, plants and soil, both within and outside of the colony. Our results show that rhinoceros auklets transport marine-derived mercury, possibly from their wintering location, and deposit mercury *via* their feces at their breeding site, thereby contaminating plants and soils within the breeding colony. Our work confirms not only that animals can transport contaminants from marine to terrestrial ecosystems, potentially over unexpectedly long distances, but also that bird tissues contribute locally to plant contamination. This article is protected by copyright. All rights reserved

Keywords: Biological transport; rhinoceros auklet; mercury; bioaccumulation; machine learning

INTRODUCTION

Migratory species, such as marine apex predators, can transport significant quantities of nutrients across ecosystem boundaries into recipient food webs (Michelutti et al., 2009). These animals often carry high contaminant loads as a result of both bioaccumulation and biomagnification through marine foodwebs (Fisk et al., 2003; Mallory and Braune, 2012). Among top predators, recent studies have highlighted a major role played by seabirds in transferring contaminants from marine to terrestrial ecosystems (Sun et al., 2004; Evenset et al., 2007; Choy et al., 2010a,b). As seabirds nest in immense colonies that can be at the same location for centuries, they can create highly concentrated contaminated sites at their breeding site through the accumulation of feces, feathers, and carcasses (Blais et al., 2005; Ellis et al., 2006; Mulder et al., 2011; Bauer and Hoye, 2014).

Among these contaminants, mercury is particularly problematic because this trace metal is a neurotoxin occurring in ecosystems throughout the world. In contrast to some organic contaminants, mercury pollution is difficult to remediate (Elliott and Elliott, 2016) because (i) mercury does not naturally degrade, and (ii) it is continually released by common industrial activities (Driscoll et al., 2013; Mason et al., 2012; Selin, 2009; Vo et al., 2011). As such, mercury levels in surface oceans have tripled since the Industrial Revolution (Driscoll et al., 2013; Lamborg et al., 2014; Poulain et al., 2015). Contaminants such as mercury are being added to recipient sites at concentrations far beyond those individually transported by physical processes (Blais et al., 2007). Yet, among these physical drivers, the relative roles of anthropogenic *vs*. biological vectors are difficult to tease apart (Lamborg et al., 2014), and, to date, received little attention. While the role of seabirds in transferring marine-derived nutrients (*e.g.*, Farina et al., 2003; Ellis et al., 2006) and contaminants (*e.g.*, Blais et al., 2007; Michelutti et al., 2010) across ecosystem boundaries is recognized, both the origin and the pathway from sea to land taken by these biotransported contaminants remains unclear.

Here, we assess the origin and pathway of allochthonous mercury transported and

deposited by seabirds at their breeding colony, and determine the impact of such biotransport on terrestrial ecosystems. To evaluate the role of seabirds as biovectors, we measured mercury concentrations in rhinoceros auklets (*Cerorhinca monocerata*) sampled at Teuri Island, in the Sea of Japan − one of the largest colonies of this species in the world, where *ca.* 300,000 pairs breed annually (Watanuki and Ito, 2012). As already advocated (Mallory et al. 2010), we simultaneously sampled multiple proxies of seabird health (tissues, feces), as well as soil and plants within and outside seabird colony to measure the impact of these sea-to-land biovectors. This allowed us to study metal biotransport in which auklets bioaccumulate mercury at sea through foraging, carry it in their tissues to their breeding site, and deposit it mainly in guano (auklets do not moult at breeding stage: Gaston and Dechesne, 1996), which degrades and is eventually transferred to plants. To characterize this biotransport process, we measured mercury concentrations in soil, plant roots and plant leaves, at both auklet-affected sites and control sites, where no seabirds have nested at least within the past 30 years (Y. Watanuki, unpublished data). Because mercury burden is often correlated with levels of other elements (Michelutti et al., 2010), we also measured levels of eight other metals and metalloids in the same samples of roots to evaluate the effects of auklets on the root metal profiles.

METHODS AND MATERIALS

Ethical note

All work was conducted under the permits of the Ministry of the Environment, the Agency of Cultural Affairs, and Hokkaido University's Ethical Review Board. To avoid bird disturbance, handling of auklets was kept to a minimum.

Study site and field collections

Teuri Island (44°24'N, 141°17'E) lies 38 km off Haborocho harbor along the northwestern coast of Hokkaido, in the northern Sea of Japan. In 2016, adult rhinoceros auklets were

caught by hand during incubation (May) and chick-provisioning (June-July) periods. Blood (1 mL) was drawn from the brachial vein using 25G syringes. Upon collection, the blood samples were immediately centrifuged to separate plasma from red blood cells, and stored in a freezer at -20°C. To collect fecal samples, birds were placed in a box before blood collection. We released the birds typically within 10 min, regardless of whether fecal samples were successfully collected. No individual was sampled more than once. Whole plants were collected during incubation and chick-provisioning periods from both the auklet affected (*i.e.*, center of the colony) and unaffected sites (*i.e.*, outside of colony; Fig 1). We set up study plots at two auklet-affected sites (approximately 100 m apart) and at three control sites to examine the effect of auklets on the entire island. We focused vegetation collection on the Scandinavian small-reed (*Calamagrostis purpurea* (Trin.) Trin. subsp. *langsdorfii* (Link) Tzvelev; *Iwanogariyasu* [イワノガリヤス] in Japanese), the dominant plant species at both the auklet-affected and control sites. Surface soil samples were simultaneously taken near the plant sample sites using a trowel. Additionally, soil core samples were taken near the plant and soil sample sites using a 4.4 cm internal diameter custom-made corer that was pushed directly into the soil to identify the longitudinal effect of auklet deposition on soil profiles. The core tubes were pushed until they met strong resistance (~9-12 cm), indicating that the entire sedimentary record was retrieved. The cores were sectioned at 1 cm intervals on site using a vertical extruder. We finally note that while the area occupied by the colony has expanded or contracted since the early 1970s, the sites that we selected remained well within or well outside of the colony (respectively) over the past ~50 years (Y. Watanuki, pers. obs.).

Laboratory analyses

All samples were shipped frozen to the Department of Environmental Veterinary Sciences, Hokkaido University. We then followed standard laboratory procedures for each analysis (see below). More specifically, for plant samples, the whole plants were rinsed in distilled water and the roots and leaves were extracted. Feces and the extracted plant samples were air-dried,

weighed, dried at 50°C in an oven for approximately 48 h, and manually homogenized prior to analysis of each sample. For animal tissues, red blood cells were analyzed as wet weight for mercury analysis, but freeze-dried for stable isotope analysis prior to the analyses. Soil and plant samples were divided in half, with one half used for measuring metal and metalloid concentrations, and the rest used for measuring stable isotope ratios of carbon ($\delta^{13}C$) and nitrogen ($\delta^{15}N$), which are proxies for feeding habitat and trophic level, respectively, and to examine the impacts of those in soil and plant samples (Newsome et al., 2007). Blood and fecal samples were analyzed separately for measuring metal and metalloid concentrations, and stable isotope ratios of carbon ($\delta^{13}C$) and nitrogen ($\delta^{15}N$), due to small quantity of samples. Sample sizes for each analysis are shown in Table S1.

Total mercury analyses

Concentrations of total mercury (denoted Hg hereafter, unless otherwise stated) in red blood cells, feces, soil, root and leaf samples were determined using a Direct Thermal Decomposition Mercury Analyzer (MA-3000, Nippon Instruments). After preparation of the calibration standards, the concentration of Hg was measured by thermal decomposition. Analytical accuracy for Hg was determined by analyzing one or two blank samples with each sample set, as well as Standard Reference Materials (SRMs): BCR-320, DOLT-4 and tomato leaves obtained from the Canadian National Research Council. Recoveries of all SRMs were within the certified range of values (BCR-320: 98 ± 4% (n = 2); DOLT-4: 101 ± 8% (n = 2); tomato leaves: 98 ± 2% (n = 12), Average ± SD). The detection limit of the analyzer was at 0.001 ng. Hg concentrations for blood are reported in μg g^{-1} wet weight (ww), and for the remaining matrices in μg g^{-1} dry weight (dw).

Extraction and analysis of heavy metals and metalloids

We measured concentrations of eight elements (Cd, Cr, Co, Ni, Cu, Zn, Pb, and As) as per Nakata et al. (2016), using an inductively coupled plasma-mass spectrometer (ICP-MS; 7700 series, Agilent technologies, Tokyo, Japan). Briefly, all laboratory materials and instruments used in the heavy metal analysis were washed with 2% nitric acid (HNO_3), and rinsed at least twice with distilled water. Samples of approximately 1.0 g of plant roots were dried for 48 h in an oven at 50°C. The dried samples were placed in pre-washed digestion vessels, followed by acid digestion using nitric acid (atomic absorption spectrometry grade, 60%, Kanto Chemical Corp., Tokyo) and hydrogen peroxide (Cica reagent, 30%, Kanto Chemical Corp.) in a microwave digestion system (Speed Wave MWS-2, Berghof, Germany). After cooling, each mixture was transferred into a plastic tube, and various elements were determined using an ICP-MS. Analytical quality control was performed using the DORM-3, and DOLT-4 certified reference materials (National Research Council of Canada, Ottawa, ON). Replicate analysis of these reference materials showed good recoveries (95–105%, n = 5, respectively). The instrument detection limits for Cd, Cr, Co, Ni, Cu, Zn, Pb and As were 0.2, 0.5, 0.5, 0.5, 1.0, 0.1, 1.0 and 2.0 μg kg^{-1}, respectively.

Stable isotope analyses

All processed and homogenized samples were shipped to the Port and Airport Research Institute in Yokosuka, Japan. To remove inorganic carbon, all samples except for blood were acidified with 1N HCl and dried at 60°C. Lipids were not removed from blood and plant samples due to expected low lipid levels. Isotopically fractionated metabolites, such as urea and ammonium as well as inorganic carbon were removed from fecal samples using a 2:1 chloroform:methanol soak and rinse (Kuwae et al., 2008). Isotope fractionation in catabolism occurs when nitrogen in amino acid is deaminated to produce metabolites depleted in ^{15}N (Fry, 2006). Thus, uric acid, which may be a major nitrogen metabolite in fecal samples, is not fractionated because uric acid is not produced through deamination. Both $\delta^{13}C$ and $\delta^{15}N$

were measured with an isotope ratio mass spectrometer (Delta Plus Advantage, Thermo Electron, Bremen, Germany) coupled with an elemental analyzer (Flash EA 1112; Thermo Electron). Results were reported in delta notation in parts per thousand (‰) relative to VPDB ($\delta^{13}C$) and Air ($\delta^{15}N$). L-Histidine ($\delta^{13}C$ –PDB (‰) = −10.18; $\delta^{15}N$ –Air (‰) = −7.81; Shoko Co., Ltd., Minato-ku, Tokyo) was included as an internal standard every 5th sample to check analytical accuracy. Based on within-run replicate measurements of multiple standards (L-Histidine; L-Alanine ($\delta^{13}C$ –VPDB (‰) = -19.6; $\delta^{15}N$ –Air (‰) = 10.1; Shoko Science Co., Ltd., Yokohama, Kanagawa); L-Alanine ($\delta^{13}C$ –VPDB (‰) = -19.6; $\delta^{15}N$ –Air (‰) = 26.1; Shoko Science Co., Ltd.), measurement precision for both $\delta^{13}C$ and $\delta^{15}N$ values was estimated to be always at or below 0.3‰.

Statistical analyses

Elemental compositions were $\log_{10}$-transformed prior to analysis. We examined the effect of site (auklet-affected *vs*. control), stage (incubation *vs*. chick-provisioning), $\delta^{15}N$, $\delta^{13}C$ in roots and an interaction term of stage × $\delta^{15}N$ on Hg in roots when using linear models. Model selection was based on Akaike's information criteria (AIC). The model that received the lowest AIC was designated as the best model. Models within 2.0 units of the best model were considered as indistinguishable from the best model (Burnham and Anderson, 2010). To account for uncertainty in the model selection process, a model averaging approach was used, in which the parameter estimates of factors included in the adequate models were weighed with the corresponding Akaike weights, and averaged. To visualize if the auklet-affected site could be teased apart from control sites, a principal component analysis (PCA) was performed with nine heavy metal (Cd, Pb, Hg, Cu, Zn, Cr, Co, Ni) and metalloid (As) concentrations in roots. To assess the predictive power of metal and metalloid concentrations on determining the presence of auklets, we employed a supervised machine-learning algorithm based on adaptive boosting (Freund et al. 1996). The classifier's accuracy was determined by 10-fold cross-validation (CV_{10}), where the algorithm is trained on nine tenths of the data and the last

decile is used to compute a confusion matrix; this process was repeated 100 times. Finally, significance between the two types of sites for nine element concentrations was assessed based on the Dunn test, and general linear models were fitted to the data. All statistical analyses were performed in R 3.4.2 (R Core Team, 2017). For comparison purposes in the Discussion, we assumed a moisture of 65% in red blood cells (Tartu et al., 2014; Bond and Robertson, 2015) and 79% in whole blood (Eagles-Smith et al., 2008), and also that red blood cells consist of 45% of the whole blood, while most mercury is accumulated in red blood cells (Bond and Robertson 2015).

RESULTS

Mercury and stable isotope ratios in red blood cells and feces

We detected quantifiable concentrations of Hg in blood and feces in all individuals. Mean [Hg] in auklet red blood cells during the study period [mean ± 1SD (range)] was 0.86 ± 0.27 (0.47-1.6) μg g^{-1} ww (Fig. 2a), and was similar between incubation and chick-provisioning periods (Table 1; $P = 0.06$). Mean [Hg] in auklet feces during the entire study period was 0.08 ± 0.10 μg g^{-1} dw and decreased from incubation to chick rearing (Table 1; $t = 2.25$, $P = 0.04$, df = 8). Stable isotope ratios, $\delta^{15}N$ ($\Delta AIC = 1.71$) or $\delta^{13}C$ ($\Delta AIC = 1.99$), varied independently of Hg in red blood cells, but were stage-dependent (Fig. S1), through time (from incubation to chick-rearing), $\delta^{15}N$ increased, while $\delta^{13}C$ decreased (Table 1, Fig. S1).

Mercury and stable isotope results in plants and soil

Mean [Hg] in roots at the auklet-affected site was higher than those at the control site ($P < 0.0001$; Fig 2d), but mean concentrations in leaves were marginally detectable and similar between the two sites ($P = 0.08$; Table 2). Thus, only roots were considered for further statistical analyses. Mean [Hg], $\delta^{15}N$ and $\delta^{13}C$ in soil were similar between auklet-affected and control sites (Table 2, Fig. 2c). We did not find any auklet effects on [Hg], $\delta^{15}N$ and $\delta^{13}C$ in soil core samples at any given depth (Table S2). Although we did not compare identical depths, because values did not vary with depth at either site, we concluded that levels were

likely similar among sites. Among root samples, the fitting of linear models explaining root [Hg] showed that site (auklet affected *vs*. control), $\delta^{15}N$ (positive), and breeding stage (incubation *vs*. chick-provisioning) were variables included in the best models (with $\Delta AIC < 2$; Table 3).

Concentration of metals and metalloids in roots

Based on a PCA, the concentrations of the nine elements (Cd, Pb, Hg, Cu, Zn, Cr, Co, Ni, and As) allow discrimination of the two types of sites, with some overlap (Fig. 3). To differentiate affected from non-affected sites based on these nine concentrations, the trained adaptive boosting classifier showed that only three of them (As, Cd, and Co) are critical (importance values > 1; CV_{10} classification success rate = 80%; Fig S2), and hence provide a distinct signature for auklet presence. Indeed, all three have significantly different concentrations among sites (at the 0.5% level) with, however, [Cd] being higher at the control site (Fig. 4). Hg is not directly a critical feature for classification for three reasons: (i) [Hg] covaries with [As] and [Co], with all three elements explaining most of the concentration variance among sites (50%; Fig. 3), (ii) [As] and [Co] are both orthogonal to (independent of) [Cd]; and (iii) all three concentrations, [As,] [Co], and [Cd], are an order of magnitude higher than [Hg], whose signal is hence overwhelmed (Fig. 4). Most remarkably, although Hg is not critical in distinguishing auklet presence at a given site, Hg is the element that, as shown above, is the most affected by auklets ($P < 10^{-3}$) at their breeding site.

DISCUSSION

Seabirds are critical biovectors in ecosystems due to their frequent commutes between sea and land during the breeding season (Blais et al., 2007; Mallory et al., 2015). Based on a quasi-experimental approach, we evaluated the possible role of seabirds as biovectors of allochthonous mercury from oceanic into terrestrial ecosystems, by focusing on a highly mobile marine top predator, the rhinoceros auklet. We show that seabirds deposited allochthonous mercury from sea to land *via* their feces, at their breeding colony, and that

allochthonous mercury was then transferred to terrestrial plants, thereby crossing ecosystem boundaries.

Hg fluxes in seabirds through their breeding season

We detected mercury in both red blood cells and feces of all individuals assayed, confirming that auklets carry detectable amounts of mercury not only in their tissues such as liver and kidney (Ishii et al., 2014), but also in their fecal matter. Average blood [Hg] measured at Teuri (2.46 ± 0.76 1SD μg g^{-1} dw, Table 1) was higher to that reported at 1.75 μg g^{-1} dw on average (note: this is measured in whole blood; Hipfner et al., 2011) in a Canadian auklet population in the eastern Pacific, or in other piscivorous species such as the Antarctic petrels (at 0.84 μg g^{-1} dw on average: *Thalassoica antarctica*; Carravieri et al., 2017). While other work reported higher concentrations in seabirds (at 8.22 μg g^{-1} dw on average in brown skuas *Stercorarius antarcticus*; Goutte et al., 2014; 2.7 μg g^{-1} dw in snow petrels *Pagodroma nivea*; Tartu et al., 2014, see also review in Ackerman et al., 2016), the lowest [Hg] that we detected in red blood cell (1.34 μg g^{-1}dw, converted from ww) still exceeds the avian affect threshold (1.20 μg g^{-1} dw; in double-crested cormorant *Phalacrocorax auratus* Gibson et al., 2014; 1.20 μg g^{-1} dw; in black-legged kittiwake *Rissa tridactyla* Tartu et al., 2015). It is however unclear whether or to what extent such elevated Hg contamination levels in Teuri auklets are possibly detrimental to their health.

Such detrimental effects potentially occur throughout the entire breeding season of auklets, as their mean blood mercury concentrations were essentially identical between the two breeding stages. The timeframe for integration of mercury into the blood system (half-life of 30-65 days reported in great skuas; Bearhop et al., 2000) and of $\delta^{15}N$ / $\delta^{13}C$ (half-life of roughly 20 days in this system; Carleton and Martinez del Rio, 2005) are roughly the same as the length of their breeding season, hereby ruling out the possibility that high tissue [Hg] and isotopic ratio changes were due to proximal (*i.e.*, at colony) causes, and suggesting that most of the Hg measured in auklets comes from their wintering grounds. While it is likely that foraging habitats and/or prey of auklets changed as breeding progressed (*i.e.*, average $\delta^{13}C$ values and $\delta^{15}N$ changed over the course of breeding; Fig S1), blood [Hg] was constant throughout the breeding season, further suggesting that either no Hg intake occurred during

breeding, or that [Hg] in auklets was at a dynamic equilibrium. However, the reason why blood [Hg] was stage-independent while blood $\delta^{13}C$ and $\delta^{15}N$ are stage-dependent is unexpected. Indeed, previous work on rhinoceros auklets at Teuri showed that, as these birds shift from smaller crustaceans such as copepods (for self-feeding during incubation) to larger fish (for chick-provisioning), their $\delta^{15}N$ values increase (Ito et al., 2010). As Hg levels in copepods are lower than in fish, this dietary shift should lead to a concomitant increase in blood Hg (Davoren and Burger, 1999), which we did not observe here. While unexpected, our results are however not unique, as Hg levels do not always systematically increase with trophic levels (Hipfner et al., 2011), and other studies also failed to show clear patterns between $\delta^{15}N$ and Hg within single seabird populations (Elliott et al., 1992, 2016; Hipfner et al., 2011; Tartu et al., 2014). These conflicting results suggest that blood [Hg] during breeding results from a dynamic equilibrium, between Hg intake and offloading, and that a lack of increase in blood [Hg] concomitant to an increase in $\delta^{15}N$ might be due to Hg contents being either higher than expected in copepods, of lower than expected in larger fish, possibly due to a shift in availability of preys that are usually harvested by auklets during chick provisioning.

However, a constant blood [Hg] may not just be due to extrinsic factors, but also result from intrinsic features such as the long-term persistence of Hg in auklets' tissues (Monteiro and Furness, 1995). Age may also be a confounding variable, since Hg may bioaccumulate in body tissues with age in marine vertebrates (Thompson, 1990 – but see Furness et al., 1990). Experimental studies showed that excretion of Hg *via* feces was about 22% of the intake in black-headed gull chicks (*Chroicocephalus ridibundus*; Lewis and Furness, 1991). While we could not control mercury intake, our recorded mean Hg levels in feces was 3% of the recorded blood Hg when data were pooled. Auklet species do not molt during the breeding phase (Pyle, 2009; Sorensen et al., 2010), and thus, biological transport by auklets occurs *via* feces and potentially carcasses and/or abandoned eggs rather than *via* feathers. However, fecal [Hg] decreased between the two breeding stages, and as we showed above that Hg in consumed prey most likely increases through breeding stages, an alternative explanation must

be sought. As sample sizes for feces analyses are quite small (see Table 2), the interpretation of these results requires caution.

Hg transfer from contaminated seabirds to plants and soil

The roots of the plants at the colony were found to have higher Hg levels than those at the control sites (Table 2), hereby suggesting that the origin of this contamination was likely to be seabirds. Although Hg levels in roots are much lower than in auklet tissues and feces, the detected Hg is likely to be organic Hg as a result of biotransport, and should not be detected under Japanese Environmental Guidelines (Ministry of Environment Japan).

In this study, we set up three control plots at Teuri where auklets or other seabirds are rarely observed flying over or perch on the sites (A. Shoji, pers. obs.). Although we did not experimentally manipulate auklet activity, or even their contamination levels, there is growing evidence supporting a causal relationship between contaminated seabirds and contaminated plants, as allochthonous inputs from seabirds significantly affect the chemical properties of both soil and flora in the proximity of their colonies (Breuning-Masden et al., 2008; Zwolicki et al., 2013, 2015; Ziolek and Melke, 2014). While seabirds can efficiently transfer heavy metals to both sediments and aquatic plants (Godzik, 1991; Blais et al., 2005; Evenset, 2007), our results are based on a novel approach that allowed us to show evidence for a direct transfer from a marine to a terrestrial ecosystem, by simultaneously collecting samples along the biotransport chain, from the biovectors to the terrestrial plants. Indeed, as our study sites are separated by at most 2 km, and are all located in similar soil, geologic, and atmospheric contexts, it is unlikely that variation in soil, geology, or atmospheric deposition rates explain the differences in [Hg] or in the other metals that we measured. Therefore, the most likely source of Hg in roots is from contaminated seabirds, which as discussed above, most likely bring Hg from outside of the colony area, from their wintering grounds.

Mercury in roots does not seem to be transferred to the leaves of contaminated plants. Indeed, while Hg in leaves was similar between auklet-affected and control sites, it was remarkably lower than in roots (Table 2). Although few studies have examined Hg uptake by plant tissues in wild populations, Tomiyasu et al. (2003) reported that Hg in leaves is lower than in roots in goldenrod (*Solidago altissima*), and showed that Hg does not seem to move from roots to leaves. While their results suggest that Hg in leaves may originate from the air, and not from the roots, it may also explain why our Hg levels in leaves are lower than in roots – and are also site-independent – if the Hg intake pathways differ in leaves and roots. We suggest that Hg in roots results from plant uptake from the soil, where Hg was deposited by contaminated seabirds *via* their fecal matter.

Under this scenario, it could be expected that Hg in the soil of auklet-affected sites would be higher than at our control sites. Contrary to this expectation however, we found that Hg in soil was not different between auklet-affected and control sites, while still being significantly higher than in contaminated roots (Fig. 2). Note that here, we measured Hg as *total mercury* concentration. A possible explanation of this counter-intuitive result is that inorganic mercury contained in the soil may have overwhelmed the signal from biovectors (Lubick and Malakoff, 2013). For instance, Asian dust storms containing Hg from China occur year round, but are more intense in the auklet's spring breeding season (Japan Meteorological Agency, 2017). Indeed, our soil Hg concentrations exceeded soil quality guidelines (Ministry of Environment Japan, 2008). We propose that organic Hg (methylmercury: the form of Hg that can pass through biological membranes; Mason et al., 1996), which is carried and deposited by auklets, is more efficiently absorbed by the roots than inorganic Hg. As no information on the efficiency of this process seems to be available, further quantification of organic Hg and tracing of Hg in soil with stable Hg isotope ratios (δ^{200}Hg; Lepak et al., 2015) would help resolve some of these issues.

While we found that biotransport significantly affected total mercury, other metals that we measured were not affected in the same way or extent. Indeed, while higher

concentrations of Hg, As, Pb, Co were found in roots at the auklet-affected site, the reverse was found for Cd. The reason why Cd concentration in roots at the control site was higher than at the auklet affected site is unclear, but may not be biologically meaningful due to the large variance at each site.

We demonstrated that the concentration profile of metal and metalloid contaminants alone creates a signature for plants impacted by seabirds, and that rhinoceros auklets act as a major biovector of such contaminants, transferring mercury and other metalloids from oceanic to terrestrial ecosystems. In theory, the source of this mercury can either be local, resulting from their foraging activity during the breeding season, or come from the distant wintering grounds. However, we provide some evidence downplaying the importance of local foraging sources of Hg transferred to local plants, suggesting instead that transferred Hg potentially resulted from their migratory behavior. Our work illustrates the importance of accounting for this source of contamination in terrestrial habitats when assessing the environmental risk of bioaccumulated contaminants.

Acknowledgement

We thank B. Rattner and two anonymous reviewers for providing us with comments that improved this work, as well as the many people who helped with fieldwork at Teuri, with special gratitude to M. Yamamoto, U. Shimabukura, N. Sato, S. Hashimoto and A. Umeyama. We would like to thank M. Aotsuka and Y. Kusakabe for logistic support during the fieldwork at Teuri Island. E. Takagi, J. Okado, N. Hirano, T. Ichise, N. Okuno helped with lab analyses, and R. Fujita for identifying the species of Poaceae. The fieldwork was conducted under the permits of the Ministry of the Environment and the Agency of Cultural Affairs. This study was supported by Grant-in-Aid for Scientific Research (AS: 20241001 520 and 24370016; MI: 16H0177906 and 16K1503406; YI: 15H0282505 and 17K2003807;

S.M.M.N: 16K16197; HM: 15K1613205), Shiseido and the Akiyama Life Science Foundation (AS), the Nihon Seimei Foundation, the Soroptimist Japan Foundation, the Nakajima Foundation, the Sumitomo Foundation, and the Natural Sciences and Engineering Research Council of Canada (KHE, SAB).

REFERENCES

Ackerman, J. T., C. A. Eagles-Smith, M. P. Herzoga, A. Hartman, A. K. Jackson, J. E. Elliott, S. S. Vander Pol, and C.E. Bryan. 2016. Avian mercury exposure and toxicological risk across western North America: A synthesis. Science of The Total Environment 568: 749-769.

Bauer, S., and B. J. Hoye. 2014. Migratory animals couple biodiversity and ecosystem functioning worldwide. Science 344: 1242552-1-8.

Bearshop, S., G. D. Ruxton, and R. W. Furness. 2000. Dynamics of mercury in feathers and blood of Great Skuas. Environmental Toxicology and Chemistry 19: 1638-1640.

Blais, J.M., L.E. Kimpe, D. McMahon, B.E. Keatley, M.L. Mallory, M.S.V. Douglas, and J.P. Smol. 2005. Arctic seabirds transport marine-derived contaminants. Science 309: 445.

Blais, J.M., R.W. Macdonald, D. Mackay, E. Webster, C. Harvey, and J. P. Smol. 2007. Biologically mediated transport of contaminants in aquatic systems. Environmental Science & Technology 41: 1075-1084.

Bond, A.L., and G.J. Robertson., 2015. Mercury concentrations in multiple tissues of Arctic Iceland Gulls (*Larus glaucoides*) wintering in Newfoundland. Arctic Science 1: 1-8.

Breuning-Masden, H., C.B. Ehlers, and O.K. Borggaad. 2008. The impact of perennial cormorant colonies on soil phosphorus status. Ceoderma 148: 51-54.

Burnham, K.P., and D.R. Anderson., 2002. Model selection and multimodel inference: A practical information-theoretic approach (2nd ed.). New York: Springer-Verlag.

Carleton, S. A., and C. Martinez del Rio. 2005. The effect of cold induced increased metabolic rate on the rate of ^{13}C and ^{15}N incorporation in house sparrows (*Passer domesticus*). Oecologia 144: 226-232.

Carravieri, A., J. Fort, A. Tarroux, Y. Cherel, O. P. Love, S. Prieur, M. Brault-Favrou, P. Bustamante, and S. Descamps. 2017. Mercury exposure and short-term consequences on physiology and reproduction in Antarctic petrels. Environmental Pollution.

Choy, E. S., L. E. Kimpe, M. L. Mallory, J. P. Smol, and J. M. Blais. 2010a. Contamination of an arctic terrestrial food web with marine-derived persistent organic pollutants transported by breeding seabirds. Environmental Pollution 158: 3431-3438.

Choy, E. S., M. Gauthier, M. L. Mallory, J. P. Smol, M.S.V. Douglas, D. Lean and J. M. Blais. 2010b. An isotopic investigation of mercury accumulation in terrestrial food webs adjacent to an Arctic seabird colony. Science of the Total Environment 408: 1858-1867.

Davoren, G., and A. Burger. 1999. Differences in prey selection and behaviour during self-feeding and chick provisioning in rhinoceros auklets. Animal Behavior 58: 853-863.

Driscoll, C. T., R. P. Mason, H. M. Chan, D. J. Jacob, and N. Pirrone. 2013. Mercury as a global pollutant: sources, pathways, and effects. Environmental Science & Technology 47: 4967−4983.

Eagles-Smith, C.A., Ackerman, J.T., Adelsbach, T.L., Takekawa, J.Y., Miles, A.K., Keister, R.A., 2008. Mercury correlations among six tissues for four waterbird species breeding in San Francisco Bay, California, USA. Environmental Toxicology and Chemistry 10, 2136-2153.

Elliott, J.E., A. M. Scheuhammer, F.A. Leighton, and P.A. Pearce. 1992. Heavy metal and metallothionein concentrations in Atlantic Canadian seabirds. Archives of Environmental Contamination and Toxicology 22: 63-73.

Elliott, K.H., and J. E. Elliott. 2016. Origin of Sulfur in diet drives spatial and temporal mercury trends in seabird eggs from Pacific Canada 1968–2015. Environmental Science & Technology 50: 13380-13386.

Ellis, J.C., J.M. Farina, and J.D. Witman. 2006. Nutrient transfer from sea to land: the case of gulls and cormorants in the Gulf of Marine. Journal of Animal Ecology 75: 565-574.

Evenset, A., J. Carroll, G.N. Christensen, R. Kallenborn, D. Gregor and G.W. Gabrielsen. 2007. Seabird guano is an efficient conveyer of persistent organic pollutants (POPs) to Arctic Lake ecosystems. Environmental Science & Technology 41: 1173-1179.

Farina, J.M., S. Salazar, K.P.Wallem, J.D. Witman, Ellis J.C. 2003. Nutrient exchanges between marine and terrestrial ecosystems: the case of the Galapagos sea lion *Zalophus wollebaecki*. Journal of Animal Ecology 72: 873-887.

Fisk, A. T., K. E. Hobbs, and D. C. Muir. 2003. Canadian Arctic Contaminants Assessment Report II Contaminant Levels, Trends and Effects in the Biological Environment. Ottawa, Northern Contaminants Program (NCP): 151.

Freund Y., R. E. Schapire. 1996. Experiments with a new boosting algorithm. *In* Proceedings of the Thirteenth International Conference on Machine Learning (ed. Kaufmann M.), pp. 148–156.

Fry, B. 2006. *Stable Isotope Ecology*. Springer, New York.

Furness, R.W., S.A. Lewis., and Mills J.A. 1990. Mercury levels in the plumage of red-billed gulls Larus novaehollandiae scopulinus of known sex and age. Environmental Pollution 63: 33-39.

Gaston, A. J. and S. B. Dechesne (1996). Rhinoceros Auklet (*Cerorhinca monocerata*), version 2.0. In The Birds of North America (A. F. Poole and F. B. Gill, Editors). Cornell Lab of Ornithology, Ithaca, NY, USA.

Gibson, L.A., R.A. Lavoie., S. Bissegger., L.M. Campbell., and V.S. Langlois. 2014. A positive correlation between mercury and oxidative stress-related gene expression (GPX3 and GSTM3) is measured in female double-crested cormorant blood. Exotoxicology 23: 1004-1014.

Godzik, B. 1991. Heavy metals and macroelements in the tundra of southern Spitsbergen: the effect of little auk *Alle alle* (L) olonies. Polar Research 9: 121-131.

Goutte, A., P. Bustamante, C. Barbraud, K. Delord, H. Weimerskirch, and O. Chastel. 2014. Demographic responses to mercury exposure in two closely related Antarctic top predators. Ecology 95: 1075-1086.

Hipfner, J.M., K.A. Hobson, and J.E. Elliott. 2011. Ecological factors differentially affect mercury levels in two species of sympatric marine birds of the North Pacific. Science of the Total Environment 409: 1328-1335.

Ishii, C., Y. Ikenaka, S. M. M. Nakayama, Y. Suzuki, Y. Watanuki, Y. Watanabe, Y. B. Yohannes, H. Mizukawa, and M. Ishizuka. 2014. Contamination status and accumulation characteristics of metals and a metalloid in birds on Teuri Island, Hokkaido, Japan. Japanese Journal of Veterinary Research 62: 143-149.

Ito, M., A. Takahashi, N. Kokubun, A. S. Kitaysky, and Y. Watanuki. 2010. Foraging behavior of incubating and chick-provisioning thick-billed murres *Uria lomvia*. Aquatic Biology 8: 279-287.

Japan Meteorological Agency. 2017. http://www.jma.go.jp/, accessed as of 29 Nov 2017 (*in* Japanese).

Kuwae, T., P. G. Beninger, P. Decottignies, K. J. Mathot, D. R. Lund, and R. W. Elner. 2008. Biofilm grazing in a higher vertebrate: the Western Sandpiper, *Calidris mauri*. Ecology 89: 599-606.

Lamborg, C.H., C. R. Hammerschmidt, K. L. Bowman, G. J. Swarr, K. M. Munson, D. C. Ohnemus, P. J. Lam, L. Heimburger, M. J. A. Rijkenberg, and M.A. Saito. 2014. A global ocean inventory of anthropogenic mercury based on water column measurements. Nature 512: 65-68.

Lepak, R.F., Y. Runsheng, P. David, J. M. Krabbenhoft, J. F. Ogorek, T. DeWild, M. Holsen, and J. P. Hurley. 2015. Use of stable isotope signatures to determine mercury sources in the Great Lakes. Environmental Science & Technology Letters 2: 335-341.

Lewis, S.A., and R.W. Furness. 1991. Mercury accumulation and excretion in laboratory reared black-headed gull *Larus ridibundus* chicks. Archives of Environmental Contamination and Toxicology 21: 316-320.

Lubick, N, and D. Malakoff. 2013. With pact's completion, the real work begins. Science 341: 1443-1445.

Mallory, M. L., S. A. Robinson, C. E. Hebert, M. R. Forbes. 2010. Seabirds as indicators of aquatic ecosystem conditions: A case for gathering multiple proxies of seabird health. Marine pollution bulletin 60: 7-12.

Mallory, M.L., and B. M. Braune, 2012. Tracking contaminants in seabirds of Arctic Canada: temporal and spatial insights. Marine pollution bulletin 64: 1475-1484.

Mallory, M. L., L. Mahon, M. D. Tomlik, C. White, G. R. Milton, and I. Spooner. 2015. Colonial marine birds influence island soil chemistry through biotransport of trace elements. Water, Air, & Soil Pollution: 226: 31.

Mason, R.P., H.R. Reinfelder, and F.M.M. Morel. 1996. Uptake, toxicity, and trophic transfer of mercury in a coastal diatom. Environmental Science & Technology 30: 1835-1845.

Mason, R. P., Choi, A. L., Sunderland, E. M. 2012. Mercury biogeochemical cycling in the ocean and policy implications. Environmental Research 119: 101-117.

Michelutti, N., J. M. Blais, M. L. Mallory, J. Brash, J. Thienpont, L. E. Kimpe, M. S. Douglas, and J. P. Smol. 2010. Trophic position influences the efficacy of seabirds as metal biovectors. Proceedings of the National Academy of Sciences: 107: 10543-10548.

Michelutti, N., B. E. Keatley, S. Brimble, J.M. Blais, H. Liu, M.S.V. Douglas, M.L. Mallory, R. W. Macdonald, and J. P. Smol. 2009. Seabird-driven shifts in Arctic pond ecosystems. Proceeding of the Royal Society B-Biological Sciences 276: 591-596.

Ministry of Environment Japan. 2008. https://www.env.go.jp/chemi/tmms/lmrm/02/ref02.pdf (*in* Japanese).

Monteiro, L.R, and R.W. Furness. 1995. Seabirds as monitors of mercury in the marine environment. Water, Air and Soil Pollution 80: 851-870.

Mulder, C.P., H. Jones, K. Kameda, C. Palmborg, S. Schmidt, J.C.Ellis, J.L. Orrock, D.A. Wait, D.A. Wardle, L. Yang, H. Young, D.A. Croll, and E. Vidal. 2011. Impacts of seabirds on plant and soil properties. *In* Mulder, C.P.H., Anderson, W.B., Towns, D.R., and Bellingham, P.J. (eds.), *Seabird Islands: Ecology, Invasion, and Restoration*, New York; Oxford University Press 135-176.

Nakata, H., S.M.M. Nakayama, J. Yabe, A. Liazambi, H. Mizukawa, W.S. Darwish, Y. Ikenaka, and M. Ishizuka. 2016. Reliability of stable Pb isotopes to identify Pb sources and verifying biological fractionation of Pb isotopes in goats and chickens. Environmental Pollution 208: 395-403.

Newsome, S.D., C. Martinez del Rio, S. Bearshop, and D.L. Phillips. 2007. A niche for isotopic ecology. Frontiers in Ecology and the Environment. 5: 429-436.

Poulain, A.J., S. Aris-Brosou, J.M. Blais, M. Brazeau, W.B. Keller, and A.M. Paterson. 2015. Microbial DNA records historical delivery of anthropogenic mercury. The ISME Journal 9: 2541-2550.

Pyle, P. 2009. Age determination and molt strategies in North American alcids. Marine Ornithology 37: 219−225.

R Core Team. 2017. R: A language and environment for statistical computing. Vienna, Austria: R Foundation for Statistical Computing Available at: https://www.R-project.org/.

Selin, N. E. 2009. Global biochemical cycling of mercury: a review. Annual Review of Environment Resources 34: 43-63.

Sorensen MC, J. M. Hipfner,T. K. Kyser, D. R. Norris. 2010. Prebreeding diet influences ornament size in the rhinoeros auklet *Cerorhinca monocerata*. Ibis 152: 29−37.

Sun, L.G., Z. Renbin, Y. Xuebin, L. Xiaodong, X. Zhouqing, and W. A. Yuhong. 2004. Geochemical method for the reconstruction of the occupation history of a penguin colony in the maritime Antarctic. Polar Biology 27: 670-678.

Tartu, S., P. Bustamante, A. Goutte, Y. Charel, H. Weimerskirch, J.O. Bustnes, and O. Chastel. 2014. Age-related mercury contamination and relationship with luteinizing hormone in a long-lived Antarctic bird. PLoS One 9: e103642.

Thompson, D.R. 1990. 'Metal levels in marine vertebrates'. *In* R.W. Furness and P.S. Ranbow (eds) Heavy Metals in the Marine Environment. CRC Press, New York.

Tomiyasu, T., T. Matsuo, J. Miyamoto, R. Imura, K. Anazawa, and H. Sakamoto. 2005. Low level mercury uptake by plants from natural environment-Mercury distribution in *Solidago altissima* L-. Environmental Sciences 12: 231-238.

Vo, A. T. E., Bank, M. S., Shine, J. P., Edwards, S. V. 2011. Temporal increase in organic mercury in an endangered pelagic seabird assessed y century-old museum specimens. Proceedings of the National Academy of Sciences of the United States of America 108: 7466-7471.

Watanuki, Y, and M. Ito. 2012. Climate effects on breeding seabirds of the northern Japan Sea. Marine Ecology-Progress Series 454: 183-196.

Zwolicki, A., K.M. Zmudczynska-Skarbek, L. Iliszko, and L. Stempnieqicz. 2013. Guano deposition and nutrient enrichment in the vicinity of planktivorous and piscivorous seabird colonies in Spitsbergen. Polar Biology 36: 363-372.

Zwolicki, A., M. Barcikowski, A. Barcikowski, M. Cymerski, L. Stempnieqicz, and P. Convey. 2015. Seabird colony effects on soil properties and vegetation zonation patterns on King George Island, Marine Antarctic. Polar Biology 38: 1645-1655.

Ziolek, M, and J. Melke. 2014. The impact of seabird on the content of various forms of phosphorus in organic soils of the Bellsund coast, western Spitsbergen. Polar Research 33: 19986.

Table 1. Total mercury concentrations (Hg in μg g^{-1}), stable isotope ratios ($\delta^{15}N$, $\delta^{13}C$ in ‰) and sample sizes (*N*) in red blood cells (RBC in ww) and fecal samples (feces in dw) during incubation and chick-provisioning periods. Assuming moisture content of 65% in RBC, converted values in RBC in dw were provided for comparable purpose.

	Sample	Incubation	converted in *dw*	*N*	Chick-provisioning	converted in *dw*	*N*
Hg	RBC	0.99 ± 0.32	≈ 2.83 ± 0.32	9	0.77 ± 0.18	≈ 2.20 ± 0.18	12
	Feces	0.22 ± 0.17		2	0.05 ± 0.01		7
$\delta^{15}N$	RBC	10.90 ± 0.30		24	11.9 ± 0.40		28
	Feces	11.60 ± 1.60		4	12.7 ± 0.60		12
$\delta^{13}C$	RBC	-19.00 ± 0.30		24	-20.00 ± 0.40		28
	Feces	-21.60 ± 1.10		4	-23.80 ± 0.60		12

Table 2. Total mercury concentration (Hg), stable isotope ratio ($\delta^{15}N$, $\delta^{13}C$), sample size (*N*) in roots and leaves of Scandinavian small-reed, and soil, at auklet-affected (affected) and control (control) sites.

		Incubation				Chick-provisioning			
	Sample	Affected	*N*	Control	*N*	Affected	*N*	Control	*N*
Hg	Roots	0.04 ± 0.01	6	0.02 ± 0.01	9	0.07 ± 0.07	7	0.02 ± 0.01	9
	Leaves	0.0077 ± 0.0023	6	0.0051 ± 0.0022	9	0.0097 ± 0.0048	6	0.0099 ± 0.0049	17
	Soil	0.06 ± 0.01	2	0.09 ± 0.07	3	0.06 ± 0.05	9	0.09 ± 0.05	7
$\delta^{15}N$	Roots	6.0 ± 1.5	8	6.15 ± 2.8	7	7.6 ± 2.3	10	7.1 ± 2.4	7
	Leaves	4.7 ± 1.9	8	4.7 ± 1.9	9	8.4 ± 3.5	6	6.7 ± 2.8	18
	Soil	10.0 ± 2.4	2	9.2 ± 2.3	3	10.5 ± 1.9	10	9.4 ± 2.0	9
$\delta^{13}C$	Roots	-27.4 ± 1.1	8	-28.0 ± 0.5	7	-27.2 ± 1.1	10	-27.3 ± 1.1	7
	Leaves	-27.5 ± 1.3	8	-28.3 ± 0.3	9	-28.3 ± 1.2	6	-28.1 ± 1.1	18
	Soil	-25.6 ± 0.2	2	-27.3 ± 0.7	3	-25.5 ± 0.3	10	-26.4 ± 1.1	9

Table 3 Model selection results by ΔAIC based on linear models explaining log_{10}-transformed Hg in roots of Scandinavian small-reed at Teuri in 2016 ($log_{10}(Hg) \sim \sum$ variables). The best model is in boldface. The number of parameters (df) and Akaike weight (w_i) are also shown. Potential factors included are Site (auklet affected *vs*. control), Stage (incubation *vs*. chick-provisioning), $\delta^{15}N$, $\delta^{13}C$ in the roots and an interaction term of Stage × $\delta^{15}N$. Models within 2 AIC units of the best model are shaded in light gray.

	Model ($\sum$ variables)	df	ΔAIC	w_i
Hg Roots	**Site + $\delta^{15}N$**	**22**	**0.00**	**0.39**
	Site + Stage + $\delta^{15}N$	21	1.07	0.23
	Site + Stage + $\delta^{13}C$	21	2.89	0.09
	Site + Stage + $\delta^{15}N$ + $\delta^{13}C$ + Stage × $\delta^{15}N$	19	3.02	0.09
	Site + Stage	27	3.03	0.09
	Site + Stage + $\delta^{15}N$ + $\delta^{13}C$	20	3.06	0.09
	Site	28	5.38	0.03
	$\delta^{15}N$	23	13.82	0.00
	Stage × $\delta^{15}N$	21	14.14	0.00
	$\delta^{13}C$	23	15.95	0.00
	Stage	28	21.06	0.00

Figure captions

Figure 1. Map showing the location of Teuri Island in the North Pacific. An unfilled square symbol indicates the location of Teuri Island. Black filled circle: auklet affected sites; gray filled circle: control sites

Figure 2. Schematic simplified mercury transfer pathway via seabirds. Mercury concentration (a) in red blood cells (ww)(n = 21), (b) in auklet feces (dw) during incubation (n = *2*) and chick-provisioning periods (n = *7*), (c) in soil (n = 10) and (d) in roots at control (n = 15) and Auklet affected sites (n = 11) collected from Teuri Island during auklet breeding season in 2016. Boxplots show the first quartile, median, third quartile, and range of $\log_{10}$-transformed concentrations.

Figure 3. A principal components analysis of nine metals (As, Cd, Pb, Hg, Cu, Zn, Cr, Co, Ni) in roots between auklet-affected and control sites. Ellipses are shown in 95% concentration of points.

Figure 4. Metal concentrations in roots (dw) at auklet-affected and control sites. The response variables are each analysed element that was $\log_{10}$ transformed. Control indicates samples collected at the control site (n = 12) and Auklet affected indicates samples collected at the auklet affected sites (n = 8). Individual values are shown as dots. Boxplots show the first quartile, median, third quartile, and range of $\log_{10}$-transformed concentrations.

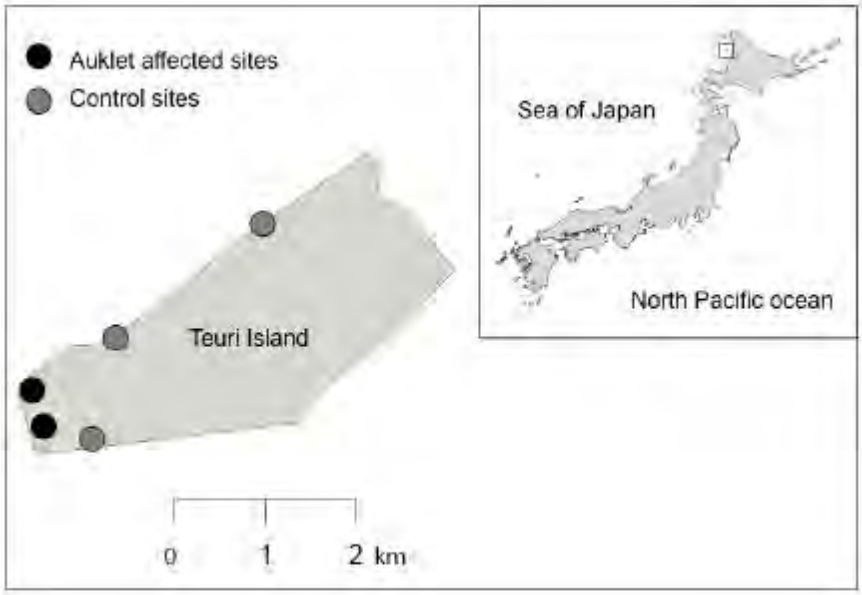

Figure 1

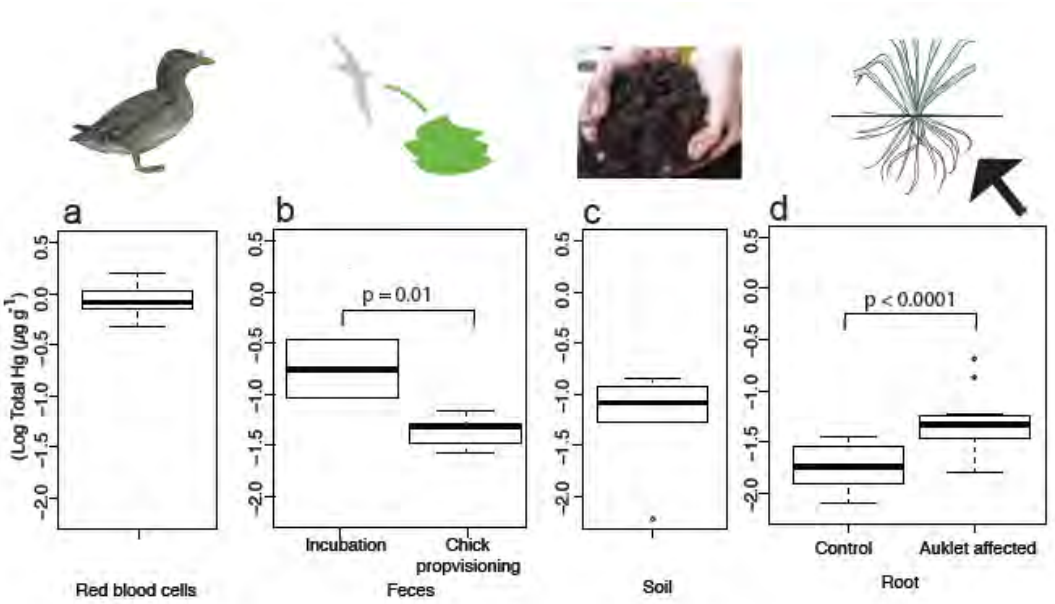

Figure 2

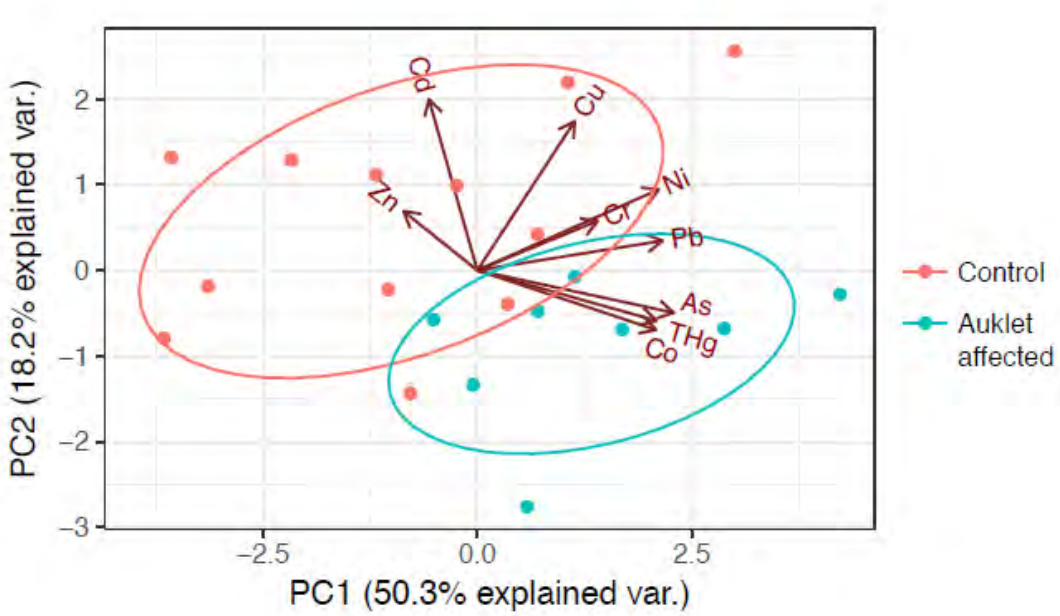

Figure 3

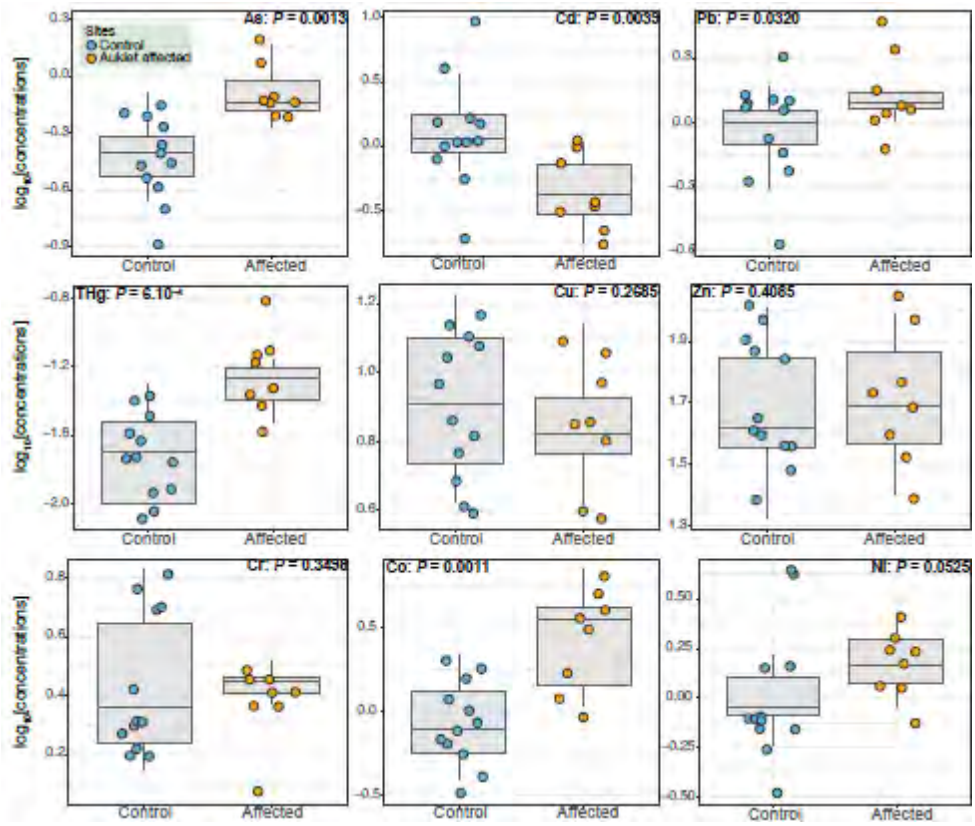

Figure 4

Chemosphere 225 (2019) 647–658

Contents lists available at ScienceDirect

Chemosphere

journal homepage: www.elsevier.com/locate/chemosphere

Evidence of impacts from DDT in pelican, cormorant, stork, and egret eggs from KwaZulu-Natal, South Africa

H. Bouwman [a, *, 1], Y.B. Yohannes [b, c, 1], S.M.M. Nakayama [b], K. Motohira [b], M. Ishizuka [b], M.S. Humphries [d], V. van der Schyff [a], M. du Preez [a], A. Dinkelmann [a], Y. Ikenaka [a, b]

[a] Research Unit, Environmental Sciences and Management, North-West University, Potchefstroom, 2520, South Africa
[b] Laboratory of Toxicology, Department of Environmental Veterinary Sciences, Graduate School of Veterinary Medicine, Hokkaido University, Sapporo, Hokkaido, Japan
[c] Department of Chemistry, College of Natural and Computational Science, University of Gondar, Gondar, Ethiopia
[d] Molecular Sciences Institute, School of Chemistry, University of the Witwatersrand, Johannesburg, South Africa

HIGHLIGHTS

- Eggs of four predatory aquatic bird species from KwaZulu-Natal analysed for DDTs.
- Concentrations were similar or lower in KwaZulu-Natal than in Limpopo province.
- DDT composition suggest pelicans feeding from different food web than other species.
- Strong evidence of eggshell thinning associated with DDT for pelican eggs.
- Urgent efforts to reduce or eliminate DDT for malaria control needed.

GRAPHICAL ABSTRACT

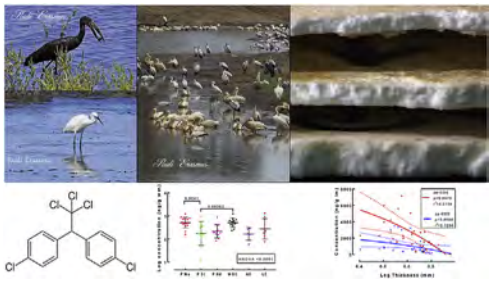

ARTICLE INFO

Article history:
Received 24 December 2018
Received in revised form
7 March 2019
Accepted 8 March 2019
Available online 12 March 2019

Handling Editor: J. de Boer

Keywords:
Eggshell thinning
DDE
DDD
DDT
Effects
Malaria control

ABSTRACT

DDT remains in use for malaria control in South Africa. We quantified DDTs in aquatic bird eggs from the highly biodiverse northern KwaZulu-Natal, a province of South Africa where DDT has been used for more than 80 years for malaria control. Pelican eggs had the highest ΣDDT concentration (7200 ng/g lipid mass; lm), Little Egret eggs had 6900 ΣDDT lm, African Openbill eggs had 3400 ng/g lm ΣDDT, and White-breasted Cormorant had 2400 ng/g lm. All species had non-significantly different mean concentrations of *o,p'*-DDT, *p,p'*-DDT, and ΣDDT, but with significant differences for *p,p*-DDE, *o,p'*-DDD, *p,p'*-DDD, %DDT, %DDD, and %lipid. The thinnest pelican eggshell (0.40 mm) had a ΣDDT concentration of 3300 ng/g lm.; the thickest shell (0.96 mm) had the lowest ΣDDT concentration at 29 ng/g lm; a 58% difference. Linear regressions of concentrations with shell thickness for the pelican eggs were significant for *p,p'*-DDE and *p,p'*-DDD, indicating risk of reproductive impairment. Compositional profiles indicate different food webs for the different species. DDT concentrations were lower than from another DDT-sprayed locality in South Africa, possible linked to differences in hydrology and rainfall. We conclude that significant ecotoxic threats associated with DDT remain in this area, and possibly threatens birds from less polluted areas. Our findings suggest continued negative human health and environmental impacts from

* Corresponding author.
E-mail address: henk.bouwman@nwu.ac.za (H. Bouwman).
[1] Both authors contributed equally.

https://doi.org/10.1016/j.chemosphere.2019.03.043

DDT. There is an urgency to move away from DDT as quickly as possible; alternatively, to implement practices that prevent emissions of DDT to the environment while protecting human life.

1. Introduction

Despite decades of continuous efforts to combat malaria using DDT in many areas of the world, remarkably little is known of its environmental impacts in such areas compared with developed countries where DDT has primarily been used in agriculture. DDT is a legacy pesticide albeit with a remaining legal use for malaria control in some African countries (Stockholm Convention, 2018). Between 2001 and 2014, South Africa reported 603 metric tons of active ingredient compared with 53,933 metric tons reported globally – the latest figure likely an underestimation due to incomplete data (Van den Berg et al., 2017). DDT use in neighbouring Mozambique was 1340 tons active ingredient between 2005 and 2011, and nothing between 2012 and 2014 (Van den Berg et al., 2017). No more recent data is publicly available, and no data at all on provincial use, including Maputo Province in Mozambique that borders KwaZulu-Natal, a province of South Africa, to the south (Fig. 1).

Intensive use of DDT to combat malaria transmission has led to widespread contamination where applied, in adjacent areas (Bouwman et al., 2015; Van Dyk et al., 2010; Barnhoorn et al., 2009), and even farther away (Garcia-Heras et al., 2018). We previously reported very high concentrations of DDT in bird eggs from the Limpopo province, South Africa, where health authorities use DDT and other insecticides as indoor residual spraying (IRS) to prevent malaria transmission (Fig. 1; Bouwman et al., 2013). Significant eggshell thinning in eggs of Cattle Egrets *Bubulcus ibis* (33% between thickest and thinnest) was associated with increasing but low concentrations of *p,p'*-DDT and *p,p'*-DDE (means between 20 and 290 ng/g wm). In addition, very high concentrations of DDT were found in eggs of Grey Heron *Ardea cinerea,* with a mean of 13,000 ng/g wm and a maximum of 24,000 ng/g wm (Bouwman et al., 2013). Within the IRS area of Limpopo, no breeding colonies of any aquatic birds could be located, a great cause of concern due to its proximity to the Kruger National Park, the largest national park in South Africa (Fig. 1). We deduced that the high DDT concentrations were likely responsible for the absence of colonially-breeding aquatic birds within the IRS area (Bouwman et al., 2013). In the same publication we predicted that similar pollution profiles would be found at other malaria areas in South Africa where DDT is sprayed (Bouwman et al., 2013), including the northern parts of KwaZulu-Natal, a province located approximately 520 km south-east of the Limpopo province (Fig. 1).

The northern regions of KwaZulu-Natal are rich in biodiversity with many nature reserves (Fig. 1). This region is the most southern part of the great Mozambique Coastal Plain, making it the southernmost distribution of many tropical animal and plant species, and is therefore of considerable scientific and conservation interest (Cooper, 1980). The Ndumo Game Reserve (NGR; Fig. 1) in particular boasts with 462 bird species (65% of the total for South Africa). Rare species such as Neergaard's Sunbird *Nectarinia neergaardi*, Saddle-billed Stork *Ephippiorhynchus senegalensis*, the African Openbill stork *Anastomus lamelligerus*, and both of Africa's pelican species (the Pink-backed Pelican *Pelecanus rufescens* and Great White Pelican *P. onocrotalus*) breed here. The iSimangaliso Wetland Park (iSWP; Fig. 1) has a bird list of 520 species (https://isimangaliso.com), including both pelican species and a variety of marine birds.

Fish collected from pans (floodplain lakes) from the Phongolo Floodplain in northern KwaZulu-Natal in 1985/86 clearly indicated bioaccumulation of DDTs (Bouwman et al., 1990). The most recent reports from KwaZulu-Natal on DDT in fish-eating birds (Evans and Bouwman, 1993, 2000) were based on Pied Kingfisher *Ceryle rudis* blood and tissues. Extrapolating from the highest blood concentrations indicated that *p, p'*-DDE concentrations in Pied Kingfisher eggs could be as high as 4200 ng/g wm. In Brown Pelican *P. occidentalis* eggs, *p,p'*-DDE concentrations of 2500–3000 ng/g wm have been associated with substantially impaired reproductive success, while 4000 ng/g wm have been linked with total reproductive failure (Blus, 1982). The highest extrapolated Pied Kingfisher egg concentrations exceeded these levels, indicating reproductive risk to Pied Kingfishers (Evans and Bouwman, 2000) and other piscivorous birds in this region. In the intervening 30 years, no work has been done on wild birds from KwaZulu-Natal.

Other work from the northern parts of KwaZulu-Natal has added to the concerns about the threats that continued use of DDT poses to wildlife. DDT has been found in high concentrations in crocodile fat (Buah-Kwofie et al., 2018a) and fish (Buah-Kwofie et al., 2018b) from the iSWP, in fish from the Phongolo River upstream and inside the NGR (Bouwman et al., 1990; Smit et al., 2016; Wepener et al., 2012), and in frogs from NGR (Wolmerans et al., 2018). High concentrations of DDT associated with malaria control in the environment and wildlife coincide with human exposures, including via locally grown food (Buah-Kwofie et al., In review). We previously reported very high DDT concentrations in breast milk from breastfeeding mothers living in areas where DDT is used for IRS in the KwaZulu-Natal and Limpopo provinces (Bouwman et al., 1994, 2012), partly mediated through consumption of free-roaming chickens and their eggs (Van Dyk et al., 2010; Gyalpo et al., 2012; Thompson et al., 2017). DDT in chickens from IRS areas in KwaZulu-Natal affected mRNA expression of genes involved in immune suppression, endocrine-disruption, and lipid dysregulation (Thompson et al., 2018). These findings confirm birds as important and relevant indicators of human and environmental health.

DDT is a well-established threat to bird reproduction (Peakall et al., 1973; Blus, 1982; Cooper, 1991; Lundholm, 1997; USDoI, 1998). Given the findings of previous studies conducted on people and biota, the lack of data on DDT in bird eggs from the biodiverse KwaZulu-Natal region where DDT is used are therefore of great concern. The aim of this study was to collect, analyse, and interpret current concentrations of DDT in colonial aquatic birds from two key breeding sites in KwaZulu-Natal; NGR, and iSWP.

2. Materials and methods

2.1. Location, egg collection, and species

We collected eggs from the north-eastern part of KwaZulu-Natal (Fig. 1), where DDT and pyrethroids are used for malaria control. More information on how DDT is applied for malaria control can be obtained from Bornman et al. (2012) and Bouwman et al. (2012).

Permissions to collect eggs in KwaZulu-Natal were obtained from Ezemvelo KZN Wildlife (OP 1186/2013 and OP 4105/2013) and iSimangaliso Wetland Park Authority. The study received ethical

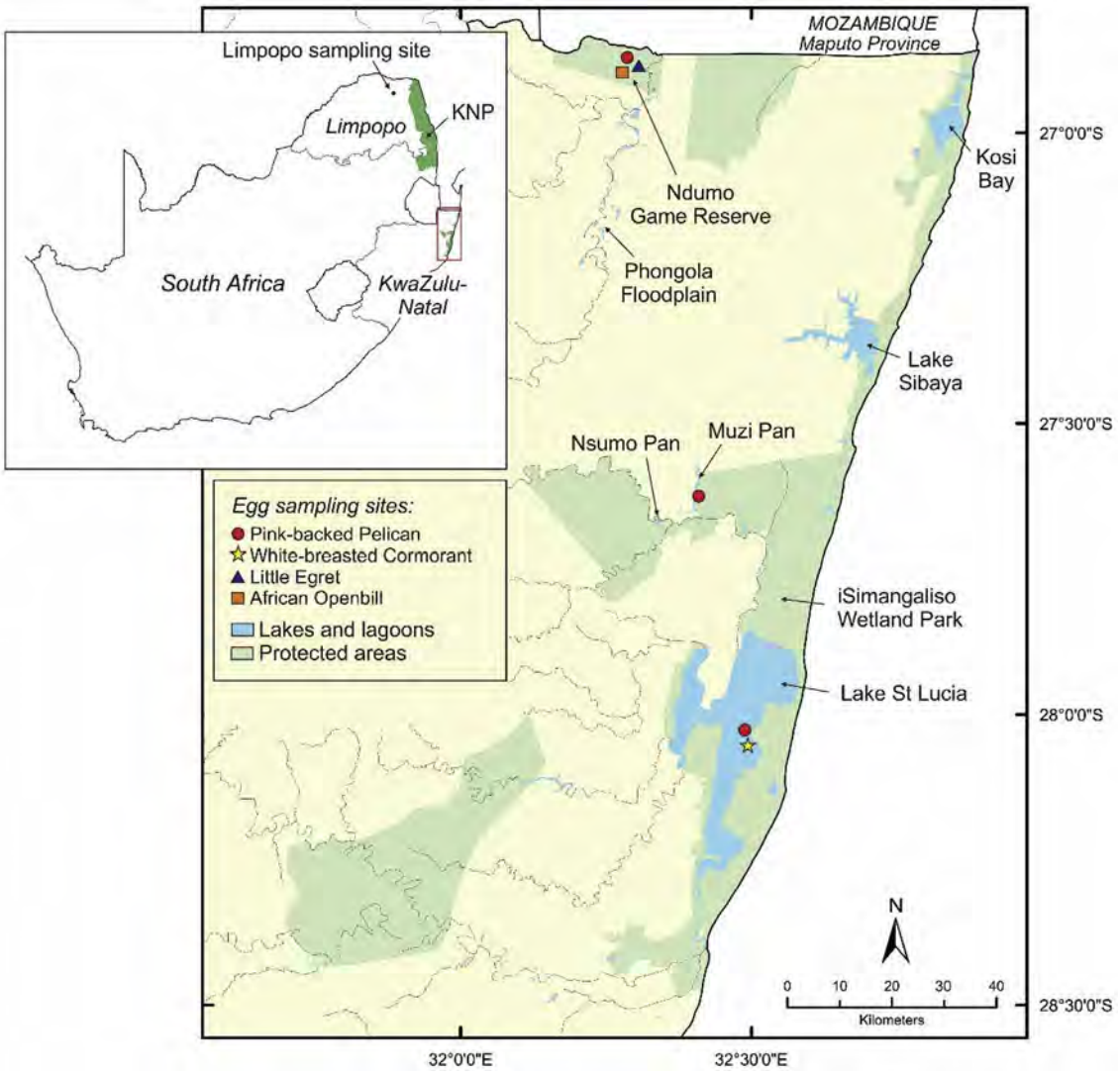

Fig. 1. Locations of sampling sites, and other sites mentioned in text.

clearance from the North-West University (NWU-00055-07-A3) and the University of the Witwatersrand (AESC-20133,201). DDT has been used in this area for malaria control since the 1950s, with an interruption between 1996 and 2000 when pyrethroids exclusively were used, and thereafter a combination of DDT and pyrethroids (Bouwman et al., 2012).

Breeding colonies were located in 2013 with the help of game wardens. We were restricted in the number of eggs we could collect due to scarcity of breeding pelicans and African Openbill *A. lamelligerus* in South Africa, and the need not to disturb the breeding of co-located species. The climbing difficulty of the trees as well as safety (crocodile and hippo) restricted access to some colonies. We collected eggs from nests by scaling trees using rock-climbing gear and a double-belay system and not disturbing other nesting birds. The eggs were wrapped in clean foil or in plastic bags, and kept on ice until frozen.

We collected 59 eggs of four different colonially-breeding aquatic bird species from three sites (Fig. 1). At NGR, we collected 11 Pink-backed Pelican *P. rufescens*, five African Openbill, and seven Little Egret *Egretta garzetta* eggs. From St. Lucia in the iMWP, we collected 11 White-breasted Cormorant *Phalacrocorax lucidus* and 10 Pink-backed Pelican eggs, and 15 Pink-backed Pelican eggs from Muzi Pan. All the bird species belong to the Order Ciconiiformes that includes grebes, herons, storks, and penguins, all of which are predatory (mostly piscivore) birds - except flamingos.

The following descriptions and dimensions (given here as means) are from Hockey et al. (2005), Tarbotton (2011), and Bowker and Downs (2012) to provide background on size, breeding, movement, and trophic levels that will be used in interpretation of the results from the present study. The information available is limited since very little biological work has been done on these species in southern Africa. There are no systematic programmes to record breeding sites and attempts for any bird species in South Africa, so the breeding site records and attempts are very likely under-reported.

- Pink-backed Pelicans are rather large birds, weighing up to 6 kg with a wingspan of up to 2.9 m. Females catch small tilapia and other small fish, with an estimated daily intake of 780 g. One to four eggs are laid per clutch. Although they are considered non-migratory, they do move roam over large distances. In northern KwaZulu-Natal, they breed irregularly, seemingly shifting between breeding sites according to conditions. There are 66 breeding records from seven sites in northern KwaZulu-Natal

between 1920 and 2010; only two records were from NGR, 25 from Nsumu Pan, near Muzi Pan, and one from iSWP.

- African Openbills (commonly called the Openbilled Stork in South Africa) have a length of 1.1 m and weighs about 1.1 kg. They have a large, vice-like bill with an opening in the middle. The bill is used to locate and catch mainly large molluscs under water. They pry open the shells and extract the flesh with their sharp lower mandible, or leave large bivalves (50–60 mm) exposed outside of water, until they open. They do not crack the shells with their bills. They lay three to four eggs per clutch. There are three breeding records from three sites in northern KwaZulu-Natal between 1920 and 2010; one record from NGR, one from Nsumu Pan, and one from iSWP. Therefore, although they are non-migratory, there does not seem to be a large degree of site-fidelity.
- Little Egrets are 65 cm long, weighs about 520 g, and catch food in shallow water, mainly fish up to 14 g per day, but also frogs, insects, worms, and crustaceans. A clutch consists of two to four eggs. There are nine breeding records from seven sites in northern KwaZulu-Natal between 1920 and 2010; no sites from NGR, three from iSWP, and the rest outside these reserves.
- The White-breasted Cormorant is very similar to the Great Cormorant *P. carbo* that has a wide distribution, including Europe. It is 90 cm long, weighs approximately 2 kg and has a wingspan of 1.9 m. Their diet consists mainly of fish, usually 10–20 g in size, which they catch while swimming underwater. The clutch size is usually between three and four. There are 49 breeding records from 18 sites in northern KwaZulu-Natal between 1920 and 2010; 1 site from NGR, 37 from iSWP, and the rest outside these reserves. As for the other species, although non-migratory, individuals breed at different sites according to conditions and opportunity.

2.2. Egg analyses

Standards of DDTs (*o,p'*-DDT, *p,p'*-DDT, *o,p'*-DDE, *p,p'*-DDE, *o,p'*-DDD and *p,p'*-DDD), surrogate standard (PCB 77), and internal standard (2,4,5,6-tetrachloro-m-xylene) were obtained from Dr. Ehrenstorfer Laboratories (Augsburg, Germany). Acetone, *n*-hexane and dichloromethane were of pesticide grade, and anhydrous sodium sulfate was specific for pesticide residue analysis (Kanto Chemical Corp, Tokyo, Japan). Florisil (60–100 mesh) (Kanto Chemical Corp, Tokyo, Japan) was activated at 130 °C overnight before use (5% deactivation with water).

Sample preparation and chemical analyses of DDTs were done in the Laboratory of Toxicology at the Hokkaido University, Graduate School of Veterinary Medicine, Japan. Determination of DDTs in egg samples was performed as described by Yohannes et al. (2017) with minor modifications. Approximately 0.5 g of egg content was homogenized with anhydrous sodium sulfate, spiked with surrogate standard (PCB 77), and Soxhlet extracted with 150 ml hexane/acetone (3:1 v/v) in hot extraction mode for 4 h. The lipid content was determined gravimetrically from an aliquot of the extract. Another aliquot of the extract used for chemical analysis was subjected to gel permeation chromatography for lipid removal. The lipid free eluate was concentrated and further purified on a column filled with 4 g Florisil (5% deactivated). The final eluate was concentrated to near dryness, reconstituted in 100 μL *n*-decane, and spiked with internal standard (2, 4, 5, 6-tetrachloro-*m*-xylene) prior to instrumental analysis.

Gas chromatographic (GC) analysis was performed using a Shimadzu 2014 gas chromatograph equipped with ^{63}Ni electron capture detector (Shimadzu, Kyoto, Japan) and ENV−8MS capillary column (30 m × 0.25 mm inner diameter, with a 0.25 μm film thickness). Helium at a flow rate of 1.0 mL/min and nitrogen at 45 mL/min were used as carrier and make-up gasses, respectively. Splitless injection of 1 μl was used with the following temperature programme: 100 °C (1 min hold time), 20 °C/min to 200 °C, 3 °C/min to 260 °C with 10 min hold time. The injection port and detector temperatures were 250 °C and 310 °C, respectively.

DDTs were identified by comparing their retention time with the corresponding standards, and multi-level calibration curves ($r^2 > 0.995$) were created for quantification. Confirmation of target residues on representative samples was performed using a Thermo Scientific DSQ II single stage quadrupole GC-MS system. The quality control and quality assurance were performed by analyses of procedural blanks, spiked blanks, and blind duplicate samples. Recovery for individual DDTs was between 90% and 105%, and average recovery for the surrogate PCB 77 standard was 90 ± 9%. The limit of detection (LOD) was set at a signal-to-noise ratio (S/N) of 3, ranged from 0.05 to 0.2 ng/g. Data are reported as ng/g wet mass (wm), and ng/g lipid mass (lm). Since embryo development affects lipid composition (Romanoff, 1932), we mainly base our discussions on wet mass.

2.3. Eggshell thickness

The possible association between DDT and eggshell thickness was investigated only for pelicans as we had more eggs of this species than the others (Table 1). The shells were gently washed, the membrane removed, and allowed to air-dry for at least three weeks. The thickness was measured at three locations on the equator with a Kroeplin electronic digital calliper (accurate to 0.01 mm) and the mean used for further calculations.

2.4. Statistics

%DDT and %DDD were calculated according to the percentage of *p,p'*-DDT and *p,p'*-DDD of the sum of all DDT compounds, for each egg. GraphPad Prism version 7.04 for Windows (www.graphpad.com) was used for descriptive data analyses per species and breeding site (three sites for pelicans collected at three different colonies, and one each for the other species). Because data were not normally distributed, log-transformed concentrations of the DDTs, ΣDDT, and %DDT were compared using ANOVA, with multiple post-test comparisons using Tukey.

To ordinate the differences and similarities of the DDT composition of each sample, species, and collection site relative to each other, we used MjM Software PC-ORD version 7.03 (www.pcord.com). We chose nonmetric multidimensional scaling (NMS) that avoids the assumption of linear relationships between variables (in this case, covariance of related compounds such as the DDTs) using ranked distances to linearise the relationships between measured distances in ordination space. Concentrations were relativised per egg to investigate pollutant profiles (fingerprints) rather than absolute concentrations. Gower-ignore-0, was used as distance measure. From random starting configurations, we allowed a maximum of six dimensions and 500 iterations, using 250 runs of real data. When the standard deviation of the stress of the last ten runs reached <0.0001, a stable ordination was assumed. Monte Carlo tests were done with 250 runs of randomised data. Convex hulls for each species were drawn to assess congruence (overlap) of proportional contributions ('fingerprints') of the analysed compounds.

Table 1
Summary statistics for DDT concentrations in eggs analysed from KwaZulu-Natal. P Mu = Pelican eggs from Muzi Pan. P St = Pelican eggs from St. Lucia. P Nd = Pelican eggs from Ndumu Game reserve. WBC = White-breasted Cormorant eggs. AO = African Openbill eggs. LE = Little Egret eggs.

n		Wet mass (ng/g)							Lipid mass (ng/g)					
		P Mu	P St	P Nd	WBC	AO	LE		P Mu	P St	P Nd	WBC	AO	LE
		15	10	11	11	5	7		15	10	11	11	5	7
p,p'-DDE	Min	160	13	84	240	60	79		650	50	1500	1200	1100	1700
	Median	510	180	190	570	170	220		1800	1000	4000	1900	2500	3000
	Max	1200	990	870	1200	300	1300		5100	4200	14,000	5700	3900	15,000
	Mean	580	290	280	570	190	450		2000	1100	4700	2220	2500	6100
	SD	270	280	230	280	93	490		1100	1200	3700	1200	1100	5400
o,p'-DDD	Min	0.074	<LOQ	3.2	0.82	7.7	3.7		0.23	11	88	4.3	120	44
	Median	1.1	12	15	1.2	12	5.8		4	43	260	4.4	150	84
	Max	11	21	25	1.5	18	14		44	83	620	6.7	290	160
	Mean	2.6	12	15	1.2	12	5.8		9	47	270	5.1	170	93
	SD	3.7	7.3	8.0	0.32	3.9	3.8		13	22	170	1.4	67	45
o,p'-DDT	Min	6.5	0.88	4.6	4.7	5.4	7.3		23	3.1	78	19	73	87
	Median	13	12	11	13	15	10		37	39	170	49	210	130
	Max	18	24	17	18	18	14		94	78	400	82	280	270
	Mean	13	12	11	13	14	10		45	43	190	49	200	160
	SD	3.8	6.2	3.7	4.7	5.2	2.3		19	24	88	20	81	76
p,p'-DDD	Min	39	14	22	<LOQ	6.1	2.7		160	50	500	<LOQ	120	34
	Median	130	130	89	5.9	12	9.4		480	500	880	22	140	170
	Max	780	1000	370	12	29	27		3200	4400	3500	71	390	390
	Mean	180	250	100	7.0	14	11		670	960	1700	30	200	180
	SD	190	300	96	3.7	8.7	8.0		790	1300	1200	22	120	130
p,p'-DDT	Min	8.3	0.85	5.0	3.1	9.7	7.4		23	3.0	94	7.8	120	95
	Median	18	32	12	15	16	20		56	107	200	49	300	260
	Max	36	70	41	31	47	46		190	280	1500	120	560	850
	Mean	19	34	16	16	22	22		71	120	320	64	300	350
	SD	9	22	12	8.7	15	15		44	83	390	39	190	270
ΣDDT	Min	230	29	120	270	100	100		940	100	2700	1400	2000	2000
	Median	670	420	330	590	240	260		2400	1800	5700	1900	3700	3500
	Max	2100	2100	1300	1300	350	1400		8400	9100	20,000	5900	4700	17,000
	Mean	800	590	420	600	250	500		2800	2200	7200	2400	3400	6900
	SD	440	600	330	280	100	500		1800	2600	5100	1300	1100	5700
%DDT	Min	0.86	3.0	2.6	0.47	2.8	3.2	%DDD	12	27	10		2.9	1.5
	Median	3.0	6.6	3.5	2.0	11	5.1		19	40	20	0.94	5.7	2.1
	Max	6	14	7.3	7.9	15	9.2		38.04	53	36	3.8	8.4	6.5
	Mean	3.0	6.8	3.9	3.1	9.5	5.7		20	40	24	1.0	5.7	3.1
	SD	1.6	3.1	1.3	2.4	5.5	2.2		8.395	10	9.0	1.1	1.9	1.8
Eggshell thickness (mm)	Min	0.61	0.69	0.40	0.39	0.32	0.24	Percentage Lipid	1.9	1.8	2.8	1.6	5.2	3.2
	Median	0.70	0.74	0.54	0.43	0.39	0.27		2.9	2.9	5.4	2.7	7.4	7.8
	Max	0.8	0.96	0.6	0.58	0.43	0.31		3.8	4.4	15	4.0	8.8	9.0
	Mean	0.70	0.78	0.53	0.46	0.37	0.27		2.9	2.8	6.6	2.7	7.2	6.9
	SD	0.065	0.09	0.055	0.060	0.044	0.024		0.51	0.71	3.8	0.71	1.5	2.4

3. Results

3.1. Analytical and statistical results

All compounds occurred at detectable quantities in all eggs, except *o,p'*-DDD in one Pink-backed Pelican egg from St. Lucia, two pelican eggs from Muzi Pan, eight White-breasted Cormorant eggs, one Little Egret egg, and *p,p'*-DDD in two White-breasted Cormorant eggs (Table 1; Fig. 2). Pelican eggs from Muzi Pan had the highest wet mass concentrations of *p,p'*-DDE and ΣDDT. Pelican eggs from St. Lucia had the highest *p,p'*-DDD and *p,p'*-DDT, pelican eggs from NGR had the highest *o,p'*-DDD. African Openbill eggs had the highest mean *o,p'*-DDT and %DDT. On a lipid mass (lm) basis, pelican eggs from NGR had the highest concentrations for *o,p'*-DDD, *p,p'*-DDD, *p,p'*-DDT and ΣDDT (Table 1). The smallest bird, the Little Egret, had the highest mean *p,p'*-DDE concentration at 6100 ng/g lm, but lower concentrations of the other compounds relative to the other birds. The data of one White-breasted Cormorant egg was excluded as an outlier from all stats, as the concentration of *p,p'*-DDE was exceedingly high at 7900 ng/g wm. The concentrations of the other compounds were <LOQ for *o,p'*-DDD and *p,p'*-DDD, 18 ng/g wm for *o,p'*-DDT, and 16 ng/g wm for *p,p'*-DDT. *o,p'*-DDE was never detected.

There were no significant differences in concentrations shown by Tukey post-tests between any of the species for log-transformed *o,p'*-DDT, *p,p'*-DDT, and ΣDDT (Fig. 2). However, differences between species and pelican collection sites, especially for *o,p'*-DDD and *p,p'*-DDD were observed (Fig. 2B and D). On a log-scale, the three non-pelican species all had significantly lower mean concentrations of *p,p'*-DDD compared with the pelicans from any site. Significant differences in %DDT (Fig. 2G) were mainly driven by differences in *p,p'*-DDE, not *p,p'*-DDT (Fig. 2G and A, respectively). %DDD was significantly higher in eggs from all pelican sites compared with the other species, but all comparisons were also different, except for the two indicated (Table 1; Fig. 2H).

Considering the three pelican sites separately (one-way ANOVA with Tukey's post-test), there were no significant differences between the sites for *o,p'*-DDT, *p,p'*-DDD, and *p,p'*-DDT. Eggs from Muzi Pan had significantly higher mean *p,p'*-DDE than eggs from the other two sites (580 ng/g wm, vs. 280 and 290 ng/g wm for the other two, Table 1). Mean *o,p'*-DDD was significantly lower in the Muzi Pan eggs than the other two sites. ΣDDT was significantly higher in Muzi Pan than NGR eggs (800 ng/g wm vs. 420 ng/g wm), while NGR eggs had significantly lower %DDT (Table 1). The mean percentage lipid composition differed significantly between the species and pelican sites (Fig. 2I), indicating the use of wet mass as a

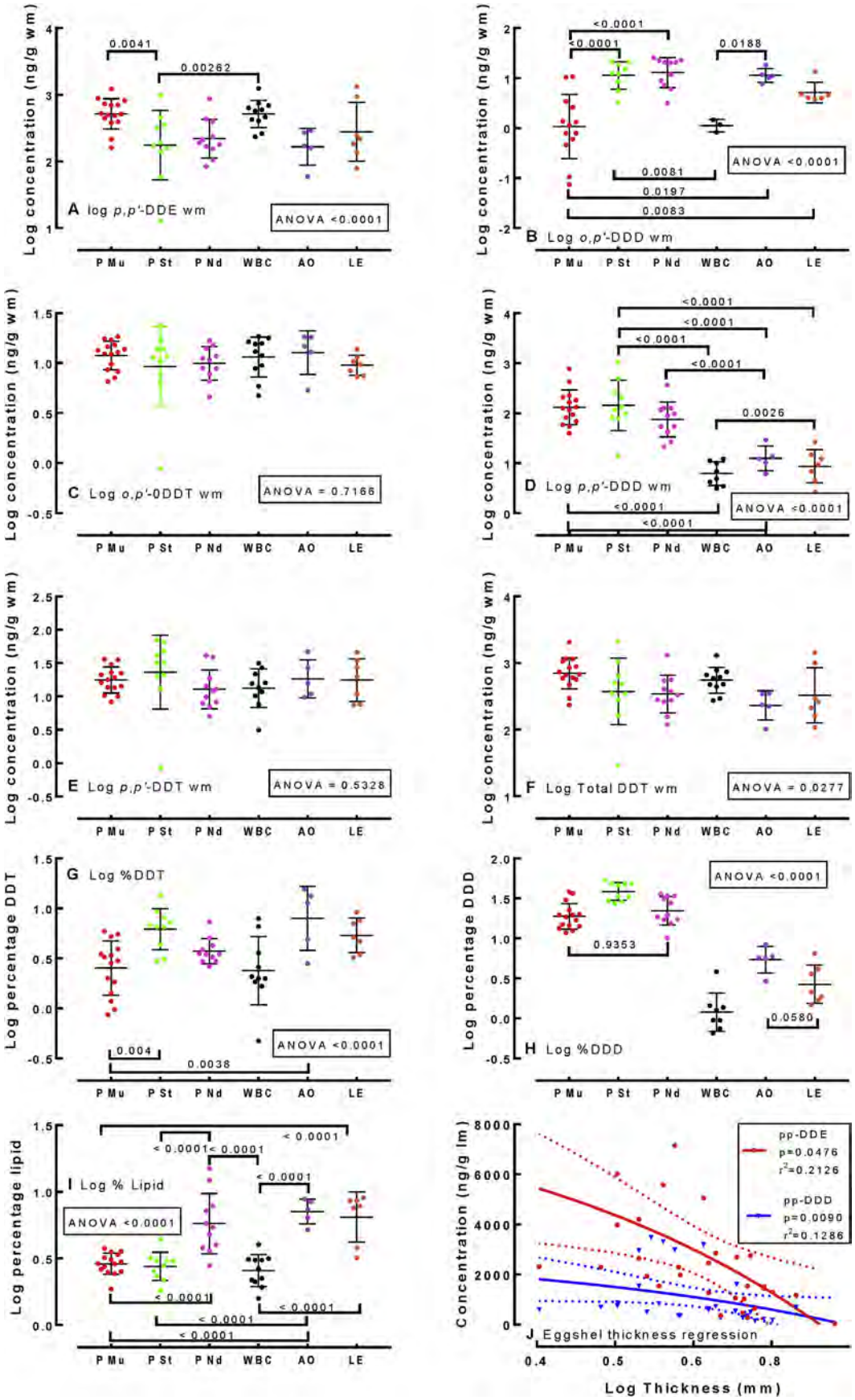

Fig. 2. Scatterplots showing mean and standard deviations of concentrations, percentages, and eggshell thickness regression. Fig. 2a–f are in ng/g wet mass. Fig. 2j is in ng/g wet mass. Results of ANOVA tests are indicated in boxes. Hooked horizontal lines and associated values indicate significant differences of Tukey post-tests in all graphs, except for 2H where all means were significantly different from each other, except the two indicated. P = Pelican eggs from Muzi Pan. P St = Pelican eggs from St. Lucia. P Nd = Pelican eggs from Ndumu Game reserve. WBC = White-breasted Cormorant eggs. AO = African Openbill eggs. LE = Little Egret eggs.

better basis for comparisons of concentrations.

The NMS ordination of relativised data needed only two dimensions (Fig. 3) and 57 iterations to reach a final instability of <0.0001 and a final stress of 10.27. A final stress between 10 and 20 indicates a satisfactory result, typical of ecological studies (McCune and Grace, 2002). Axis 1 explained 58.3% of the variations or differences between the samples, generally indicating the influence of *p,p'*-DDE, *p,p'*-DDD and *o,p'*-DDD, on the horizontal axis. The second axis explained 36.7% of the differences, marginally influenced by higher relative compositions of *p,p'*-DDT and *o,p'*-DDT. The convex hulls connecting the outer samples of each species and pelican collection site represents 'fingerprints'. Overlap indicates congruence of the 'fingerprints', while non-overlap shows differences. The egg concentrations from the three pelican collection sites overlapped with each other (associated with the *p,p'*-DDD vector), despite the differences indicated in Table 1 and Fig. 2. The relative compositions of the DDTs are therefore similar for the pelican eggs from the three sites. The three other species overlapped with each other but not with the pelicans, indicating different relative DDT isomer and congener compositions. The White-breasted Cormorant and Little Egret were associated with higher relative *p,p'*-DDE, while the African Openbill were more aligned with higher *o,p'*-DDT, *p,p'*-DDT, and to a lesser extent *o,p'*-DDT.

3.2. Eggshell thickness

Only the Pink-backed Pelican had enough samples (n = 31) to test for eggshell thinning. The mean and median thickness were both 0.66 mm (range 0.40–0.96 mm). The thinnest eggshell was about 58% thinner than the thickest. The differences in thickness is visualised in Fig. 4. The thinnest shell (0.40 mm) had ΣDDT concentrations of 118 ng/g wm and 3300 ng/g lm. The thickest shell (0.96 mm) had the lowest ΣDDT concentrations at 29 ng/g wm and 100 ng/g lm. The reduction in thickness associated with DDTs was not apparent using regressions of wet mass based data. Linear regressions on lipid mass data showed significant ($p < 0.05$) thinning of pelican eggshells associated with *p,p'*-DDE and *p,p*-DDD concentrations plotted on a log-scale (Fig. 2H).

4. Discussion

4.1. Concentrations

We expected more differentiation in concentrations between the species investigated, given their differences in sizes and trophic levels (Table 1; Fig. 2). Comparisons are confounded as the differences between species also depended on concentration basis; i.e. wet mass or lipid mass. The African Openbill eggs had the lowest mean *p,p'*-DDE and ΣDDT concentrations on a wet mass basis (190 ng/g wm and 250 ng/g wm, respectively), but third highest on a lipid mass basis (2500 ng/g and 3400 ng/g lm, respectively) (Table 1); and there are many other such instances in Table 1 and Fig. 2. These differences also hold true for medians. This probably reflects a combination of differences in normal lipid composition between eggs of different species, the stage of embryo development that may not have coincided between species and localities, and DDT compositional differences in their food items. Since embryo development affects lipid composition (Romanoff, 1932), we mainly base our discussions on wet mass, but also provide lipid mass concentrations for comparisons with other studies (Table 2).

The active ingredient portion of the 75% water wettable DDT formulation powder used for indoor malaria control consists of 72%–75% *p,p'*-DDT, with 22% made up by *o,p'*-DDT (Bouwman et al., 2005). The applied compounds (*p,p'*-DDT and *o,p'*-DDT) did not show significant differences in median concentrations between the

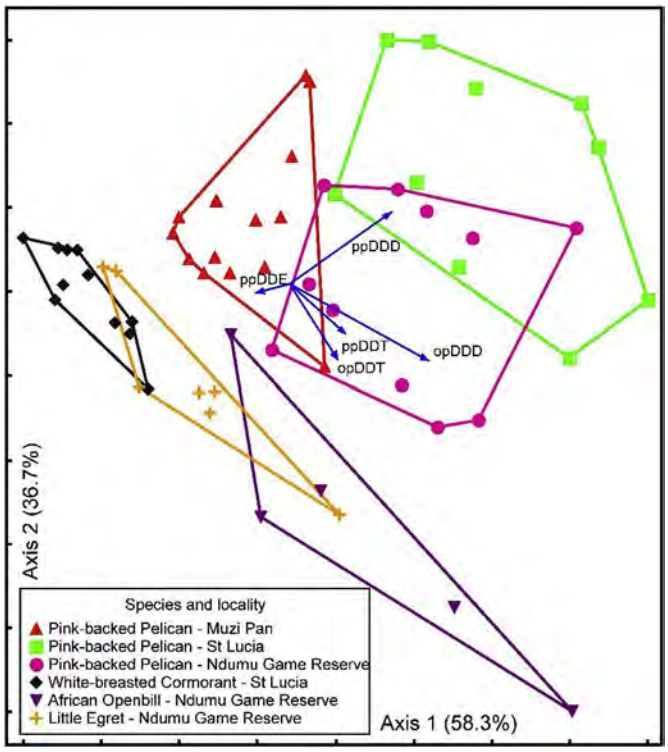

Fig. 3. Non-metric multidimensional scaled (NMS) ordination of the relative (wet-mass based) concentrations of DDTs in eggs from three different species from KwaZulu-Natal. Gower-ignore-0 was used as distance measure. Only two dimensions were needed, after 57 iterations, a final instability of 0.0000, and a final stress of 10.27. Axis 1 explained 58.3% of the variations, and second axis explained 36.7%.

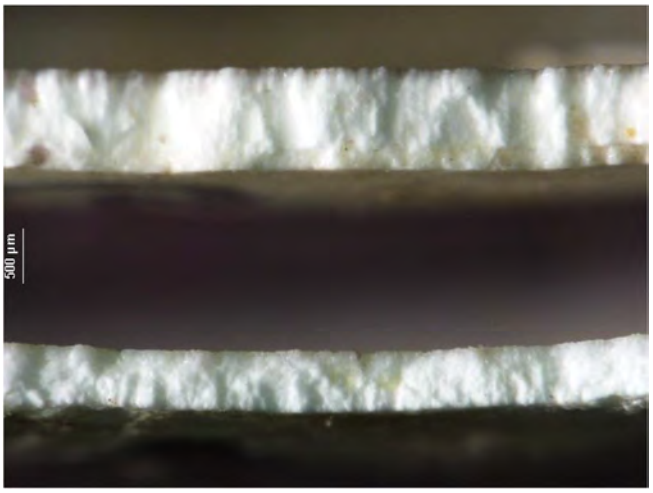

Fig. 4. Photographs illustrating the differences in eggshell thickness from Pink-Backed Pelican eggs from KwaZlulu-Natal. The thinnest eggshell (bottom) was about 58% thinner than the thickest (top). The thinnest shell (0.40 mm) had ΣDDT concentrations of 118 ng/g wet mass/3300 ng/g lipid mass. The thickest shell (0.96 mm) had the lowest ΣDDT concentrations of all Pink-backed Pelican eggs at 29 ng/g wet mass/100 ng/g lipid mass. (For interpretation of the references to colour in this figure legend, the reader is referred to the Web version of this article.)

eggs of any the species and between the different pelican collection sites (one-way ANOVA with Tukey's post-test, Fig. 2C and E). This implies that malaria control is the source of DDTs in top avian predators in the system as they have similar *p,p'*-DDT and *o,p'*-DDT concentrations (Fig. 2; Table 1), but they do not nearly reflect the

Table 2
Non-exhaustive table of concentrations (ng/g lipid mass) from comparable studies from elsewhere, and data from the present study.

No	Species	Location	Sampled	ΣDDT	Reference
1	Great Blue Heron	Canada	1994	1616	Thomas & Anthony (1999)
2	Great Blue Heron	Canada	1997	52,000	Laporte (1982)
3	Great Blue Heron	Canada	1998	3,59,000	Laporte (1982)
4	Grey Heron	Namibia	1970s	9200	Van Dyk et al. (1982)
5	Grey Heron	Limpopo Province, RSA	2009	2,30,000	Bouwman et al. (2013)
6	Night Heron	Hong Kong, PRC	2006	2500	Wang et al. (2011)
7	Great Egret	Hong Kong, PRC	2006	16,000	Wang et al. (2011)
8	Cattle Egret	India	2007	984	Malik et al. (2011)
9	Cattle Egret	Gauteng, RSA	2004/5	330	Polder et al. (2008)
10	Cattle Egret	Gauteng, RSA	2004/5	430	Polder et al. (2008)
11	Cattle Egret	Limpopo Province, RSA	2009/9	340	Bouwman et al. (2013)
12	Cattle Egret	Limpopo Province, RSA	2009/10	420	Bouwman et al. (2013)
13	Cattle Egret	Limpopo Province, RSA	2009/10	4300	Bouwman et al. (2013)
14	Little Egret	Hong Kong, PRC	2006	16,100	Wang et al. (2011)
15	Little Egret	Quanzhou, PRC	2004	58,000	Lam et al. (2008)
16	Little Egret	Ndumo Game Reserve, RSA	2012/13	6900	This study
17	European Shag	Norway	2003–04	1500	Herzke et al. (2009)
18	Double-crested Cormorants	Lake Huron, Canada	1972/73	1,96,000	Weseloh and Teeple (1983)
19	Reed Cormorant	Gauteng, RSA	2004/5	7000	Polder et al. (2008)
20	Great Cormorant	Netherlands	1988/9	1,32,000	Dirksen et al. (1995)
21	White-breasted Cormorant	Eastern Cape, RSA	1979	170[a]	De Kock and Randall, 1984
22	White-breasted Cormorant	Eastern Cape, RSA	1978	635[a]	Van Dyk et al., 1982
23	White-breasted Cormorant	St Lucia, RSA	2012/13	2400	This study
24	African Darter	Gauteng, RSA	2004/5	4400	Polder et al. (2008)
25	African Sacred Ibis	Gauteng, RSA	2004/5	1200	Polder et al. (2008)
26	Brown Pelican	San Benito, California, USA	1969–71	67,000	Jehl (1973)
27	Brown Pelican	San Martin, California, USA	1969	1,58,000	Jehl (1973)
28	Brown Pelican	Los Coronados, California, USA	1969	13,42,000	Jehl (1973)
29	Brown Pelican	Los Coronados, California, USA	1970	5,23,000	Jehl (1973)
30	Pink-backed Pelican	Muzi Pan, RSA	2012/13	2800	This study
31	Pink-backed Pelican	St. Lucia, RSA	2012/13	2200	This study
32	Pink-backed Pelican	Ndumo Game Reserve, RSA	2012/13	7200	This study
33	African Openbill	Ndumo Game Reserve, RSA	2012/13	3400	This study
34	Pied Kingfisher[b]	Ndumo Game Reserve, RSA	1993	960	Evans & Bouwman (2000)
35	Pied Kingfisher[b]	St. Lucia, RSA	1993	350	Evans & Bouwman (2000)
36	Pied Kingfisher[b]	Kosi Bay, RSA	1993	2910	Evans & Bouwman (2000)
37	Pied Kingfisher[b]	Mkuzi Nature Reserve, RSA	1993	1090	Evans & Bouwman (2000)

[a] DDE only, as wet mass.
[b] Calculated from blood concentrations.

original 5:1 composition of the active ingredient. The vapour pressure for *o,p'*-DDT is approximately five times higher than *p,p'*-DDT (55.3 and 7.26 mm x 10^{-7} Hg at 30 °C, respectively; Spencer and Cliath, 1972), implying that *o,p'*-DDT will volatilize in larger amounts and enter the environment more readily when compared with *p,p'*-DDT. This suggests that environmental sources of DDT in the eggs may have been from aerially transported DDT, post-IRS application.

Breeding Brown Pelican on the Atlantic coast of the USA fly 20–150 km from their colonies (Poli, 2015). It is therefore possible that the foraging ranges of breeding Pink-backed Pelicans from our three sites overlap since they are located within 130 km of each other (Fig. 1). Because of this, we expected a homogenous profile in concentrations and relative composition between eggs from the different breeding sites thereby allowing the pooling of data. However, there were major differences in mean and median concentrations and patterns of the breakdown products between the species and collection sites, suggesting influence from an interplay between factors such as food, location, and metabolism (Table 1). Despite no significant differences between median *o,p'*-DDT, *p,p'*-DDD, and *p,p'*-DDT egg concentrations, the median *p,p'*-DDE, *o,p'*-DDD, and ΣDDT between the breeding sites were significantly different (Fig. 2; one-way ANOVA with Tukey's post-test). It is difficult to explain this, since Pink-backed pelicans are known to roam for hundreds of kilometres (Hockey et al., 2005).

Taking into account that the IRS-applied DDT active ingredient content is 72%–75% *p,p'*-DDT, the mean percentage *p,p'*-DDT composition in the eggs for all species and pelican collection sites were low, between 3 and 9.5% (Fig. 2G; Table 1). This is to be expected due to environmental and biological breakdown of the parent compounds in various compartments. The higher %DDT in the African Openbill (9.5%) may reflect bioaccumulation that starts with the lowest trophic level organisms (in this case, molluscs that lives in sediments), with increasing transformation to other compounds in higher trophic levels. For the African Openbill, the direct food source is mainly sediment-dwelling bivalve molluscs, which bio-concentrates DDTs from filtering of DDT-containing water and bio-concentrates DDT-containing small particles including plankton. We know that sediment at Lake Sibaya (Fig. 1) is highly polluted with DDT (Humphries, 2013). For the piscivorous bird species, the food web is longer than the food web of the bivalve molluscs by at least one additional trophic level; from phytoplankton and zooplankton, to small insects, to small and larger fish (in addition to direct bio-concentration of compounds from the water by all these organisms). However, we found no significant differences in median ΣDDT concentrations in eggs of any of the four bird species. This suggests that the molluscs, although a primary consumer, contains levels of ΣDDT that causes DDT concentrations in the eggs of the African Openbill equivalent to their co-occurring piscivorous birds. This further implies that the African Openbill, presumably feeding on a lower trophic level, is as much at risk from DDT as co-occurring large piscivorous birds. Future studies examining DDT in the bivalve prey of the African Openbill, as well as looking at eggs from other openbill stork populations, is suggested.

4.2. Differences in food webs?

Despite no differences in ΣDDT concentrations between any species or pelican egg collection site, median *p,p'*-DDD and %*p,p'*-DDD was significantly higher (by an order of magnitude) in pelican eggs when compared to the other species we sampled (Fig. 2D and H; Table 1). However, there were no differences between the three sets of pelican eggs ($p = 0.5328$, one-way ANOVA).

DDT degrades to DDE mainly under aerobic conditions in the environment, and to DDD under anaerobic conditions in the presence of organic matter (Guenzi and Beard, 1967; Spencer and Cliath, 1972). Presumably, pelicans feed on fish that consume prey that accumulate *p,p'*-DDD from anaerobic sources more so than the other three species. Pelican eggs from the present study had 29% *p,p'*-DDD, while the White-breasted Cormorant, African Openbill, and Little Egret eggs had 1.0%, 5.7%, and 3.1% *p,p'*-DDD (Table 1; which did not differ significantly between them; $p = 0.1764$, one-way ANOVA), respectively. Either the latter three species have mechanisms that metabolically (and anaerobically) produces *p,p'*-DDD from *p,p'*-DDT (the concentrations of the latter did not differ between species, Fig. 2C), selectively assimilates less *p,p'*-DDD from their food, selectively deposits less *p,p'*-DDD in their eggs (all of which we doubt), or more likely, feed from a food web not directly linked to that of the pelican.

A further indication of differences in food webs can be seen in Fig. 3 where the vectors for *p,p'*-DDE and *p,p'*-DDD, both breakdown products of *p,p'*-DDT, are opposing (an increase in the concentration of one compound is associated with a decrease in the other). Fig. 3 also illustrates the differences in relative composition of the DDT compounds. The convex hulls of the Pink-backed Pelicans overlapped, showing congruence in relative composition. The other three species had convex hulls that overlapped with each other (indicating congruence in relative compositions), but not with the Pink-Backed Pelicans, indicating a major difference in relative DDT compound compositions, further supporting the possibility of different food webs. Borgå et al. (2005b) remarked that reliance should not be placed on summed congeners, as this may mask the effects of differences in physiochemical and environmental properties and behaviours, as observed in this study.

Differences in congener proportions for PCBs in birds have been linked with metabolic differences of PCBs between bird species (Borgå et al., 2005a; Quinn et al., 2013). Here, all four bird species (belonging to the same order of birds) consume prey rich in protein and fat. Therefore, major species-specific metabolic differences that may explain the differences in *p,p'*-DDD but not the near equality in ΣDDT and *p,p'*-DDT concentrations is unlikely. It would be interesting to conduct stable isotope analyses to shed more light on this conundrum. However, the different food webs need to be known as stable isotopes metabolically behave different from persistent pesticides and in different prey (Ricca et al., 2008). In addition, there are many other considerations to consider when applying stable isotope analyses to ecotoxicology (Jardine et al., 2006).

4.3. Comparisons with other data

The ΣDDT concentrations in the bird eggs of the present study seem relatively low when compared with local historic data and data from the Limpopo province and elsewhere (Table 2). Little Egret (no. 16) had much less ΣDDT than the other two reports for this species (nos. 14 and 15), as well as all other egrets and herons (nos. 1–7), but not the terrestrial Cattle Egret (nos. 9–13). All the cormorants (including shags) listed (nos. 17–22) had higher concentrations, except eggs from the Eastern Cape, RSA (nos. 21–22) where little or no DDT has presumably been used. Still, the mean ΣDDT concentration from St. Lucia is two orders of magnitude less compared with that measured in eggs of the Great Cormorant in The Netherlands (no. 20). White-breasted Cormorant eggs from St. Lucia had similar concentrations to eggs of the African Darter and African Sacred Ibis from Gauteng, South Africa (nos. 24 and 25). Here, DDT has never been used for malaria control, and is most likely due to legacy residues from agricultural use. South Africa has banned the use of DDT in agriculture since 1976 (Bouwman, 2003).

It is however, the differences between the concentrations in the pelican eggs from the present study (Nos. 30–32) with those from elsewhere (nos. 26–30) that is notable—up to three orders of magnitude. Past agricultural use of DDT as used in the USA therefore contributed much more than IRS alone. This makes sense, as agricultural use of DDT in the 60s in the USA was much more intense than for IRS (Baris et al., 1998). However, Grey Heron egg concentrations from Limpopo province (No. 5), where DDT is used under similar circumstances as in KwaZulu-Natal, were two orders of magnitude higher than the pelicans from the present study (Table 2). DDT concentrations in human breast milk were similar between the two regions (900 ng/ml wm, 750 ng/ml wm, and 490 ng/ml wm for two villages in KwaZulu-Natal and one in Limpopo province, respectively, for primiparae mothers—maximum was 6200 ng/ml; Bouwman et al., 2012), indicating no major differences in IRS application. Pelicans do not breed in the Limpopo Province, so direct comparison is not possible.

With comparable DDT data now available, a possible explanation might be that the Phongolo River, which is associated with a large floodplain and wetland system, would dilute DDT more than the drier Luvuvhu River in Limpopo with fewer floodplains, less wetlands, and a lower river flow (Luvuvhu River, mean annual flow 73.5 million m^3 vs. Phongolo River mean annual flow 463 million m^3, calculated from data since 2004). This explanation is further supported with fish data. ΣDDT in tiger fish from the Luvuvhu River (draining the malaria area in the Limpopo Province where the Limpopo bird eggs were collected) were much higher than in the Phongolo River (calculated at 310 ng/g wm (Gerber et al., 2016) vs. 21 ng/g wm (Smit et al., 2016), respectively), suggesting that differences in hydrology might be involved. The lower concentrations in bird eggs and fish from KwaZulu-Natal therefore, indicate much lower exposure and risk compared to the Limpopo Province. In section 4.3, we will discuss another possible reason for the lower concentrations in KwaZulu-Natal eggs.

4.4. Effect levels and eggshell thickness

Endocrine disrupting chemicals such as PCBs and DDE in animals have been associated with altered thyroid hormone function and neuro-endocrine systems, activation of the stress response (Dawson, 2000; Fry, 1995; Langer et al., 1998), and effects on the gonadal steroid hormones of animals (Beard et al., 2000). Delayed sexual maturation and impaired mating behaviour (Ottinger et al., 2005), thinning of eggshells, developmental effects, and embryo mortality have been associate with *p,p'*-DDE (Lundholm, 1997; Zimmermann et al., 1997).

Eggshell thinning associated with DDT have been measured in African Fish Eagle *Haliaeetus vocifer* by 11–20% (Douthwaite, 1989), and Peregrine Falcon *Falco peregrinus* in Zimbabwe by 10% (Hartley et al., 1995). In South Africa, Lanner Falcon *Falco biarmicus* and Bateleur *Terathopius ecaudatus* eggs had 8.8% and 10% thinner shells, respectively (Snelling et al., 1984), African Darters had thinner eggs by 17% (Bouwman et al., 2008), Cattle Egret by 33% (Bouwman et al., 2013), and African Penguin by 38%–40% (Bouwman et al., 2015). Eggs from the terrestrially feeding Cattle Egrets from the Limpopo Province in particular had thinner shells in three colonies from outside to inside the IRS area, at increasing levels of ΣDDT (19 ng/g wm, 92 ng/g wm, and 290 ng/g wm).

Eggshell thickness concomitantly decreased significantly from 0.23 mm, to 0.21 mm, to 0.19 mm, in the same order. Thinning associated with these low ΣDDT levels for a terrestrial bird species was unexpected and cause for concern (Bouwman et al., 2008).

Blus (1982) estimated substantial impaired reproductive success at 3000 ng/g wm ΣDDT, and failure at 4000 ng/g wm for the Brown Pelican in the USA, due to eggshell thinning. This assessment was based on the findings of DDE concentrations of 2800 ng/g wm associated with reproductive impairment of piscivore bird populations, while 1000 ng/g wm has been linked to reduced heron survival (Connell et al., 2003). The mean ΣDDT in Pink-backed Pelican eggs of this study at NGR and St. Lucia (800 ng/g wm and 590 ng/g wm, respectively; Table 1) did not exceed the "critical level for reproductive success" (3000 ng/g wm) calculated for Brown Pelicans in field studies in the USA (USDoI, 1998). They did however, exceed the non-effect level estimated at 500 ng/g wm (Cooper, 1991), which was also exceeded by the White-breasted Cormorant at 600 ng/g wm, and is equalled by the Little Egret at 500 ng/g wm (Table 1). All species and sites had eggs that exceeded the 500 ng/g wm non-effect level, except the African Openbill that was lower.

The Pink-backed Pelican eggshells had thicknesses ranging between 0.40 mm and 0.96 mm (Table 1; Fig. 4), with an overall mean and median of 0.66 mm. The thinnest shell was 58% thinner than the thickest. The eggs collected from the three sites did not show a consistent eggshell thickness pattern. Eggshells from NGR, with the lowest mean ΣDDT in wet mass also had the thinnest shells (mean 0.53). This picture, however, changes when lipid mass concentrations are considered. The thinnest mean shells (0.53 mm) at NGR had more than double the mean ΣDDT (7200 ng/g lm), and the thickest eggs from St. Lucia (mean 0.78 mm) had the lowest mean ΣDDT at 2200 ng/g lm (Table 1). Regressions of all wet mass based DDT concentrations against thickness were not significantly different from zero, but on lipid mass, *p,p'*-DDE and *p,p'*-DDD were significantly associated with thinning (Fig. 2J). We cannot explain the differences between wet and lipid based data vis-à-vis eggshell thickness, and there are many factors involved (Hernández et al., 2018). However, the large differences in eggshell thickness (Fig. 4) coupled with exceedances of known wet mass based risk levels, and biological plausibility based on many other studies, lead us to conclude that DDT is strongly associated with eggshell thinning.

The species we studied are all considered resident in the sense that they do not migrate on a seasonal basis. Pelicans and African Openbill do however roam over large distances (Hockey et al., 2005). They also seem to breed irregularly, abandoning sites and establishing new sites according to opportunity and conditions (Bowker and Downs, 2012). From the few data we have, it seems as if malaria control differs north and south of the South Africa/Mozambique border. It is possible therefore, that individuals from less contaminated areas will breed south of the border in South Africa. Less polluted individuals may therefore mask reproductive impairments in colonies, possibly explaining the large differences in eggshell thickness we observed.

4.5. Synthesis, conclusions, and recommendations

DDT continues to pollute biota such as fish and birds in the malaria-endemic areas of northern KwaZulu-Natal. Wild birds from here were last assessed 30 years ago – since then the IRS regime had changed from solely relying on DDT to a combination of DDT and pyrethroids. This may have contributed towards reduction in ΣDDT concentrations using comparable data in tiger fish over the same 30 years. Our data and findings, together with those from others, confirm that IRS continues to release DDT into local aquatic ecosystems, which have faced continuous ecotoxic stress for more than 80 years. Birds that enter the malaria-controlled areas where DDT is used from less polluted areas to breed might also mask reproductive impairment and contribute towards differences in concentrations in eggs as we have seen in eggs from the three breeding sites. Long-term studies should also be instituted to monitor hatching and fledging success of the larger aquatic birds, especially both pelican species.

Despite feeding on a lower trophic level, African Openbill eggs had concentrations equivalent to those of the other species. This implies that their molluscan prey contributes DDT to the African Openbill eggs to the same extent as the piscivorous species we studied. If such is the case, the bivalve molluscs they prey on may also face threats. Surveys of the DDT concentrations and health of these ecologically important animals need to be done. It also implies that the African Openbill face the same threats from DDT as birds feeding at higher trophic levels. The potential for eggshell thinning in this species should be investigated.

DDT concentrations in eggs of the four species of birds we analysed were difficult to interpret as wet mass and lipid mass data did not show the same relative patterns. This may reflect a combination of influence of locality, species, diet, time of laying, asynchronous embryo development in each colony, embryo development per se per egg, and maternal food. The DDT concentrations in Pink-backed Pelican eggs approach, equal, and exceed established levels of concern. Eggshell thinning (up to 58%) was significantly associated with *p,p'*-DDE and *p,p'*-DDD concentrations on a lipid mass basis.

Based on remarkably consistent relative and absolute *p,p'*-DDT and *o,p'*-DDT compositions between species and breeding sites, we suspect that aerial transport between site of application and site of uptake may play a role. If this is the case, better application methods might reduce the escape of DDT from IRS sites with a concomitant reduction in environmental pollution. The monitoring of DDT, including the use of passive air samplers, should be implemented within and adjacent to areas where DDT is used for malaria control.

There are indications that pelicans feed from a different food web route than the other species, mainly based on the concentrations and relative contributions of *p,p'*-DDD and *p,p'*-DDE. These differences need to be investigated, as *p,p'*-DDD is derived from anaerobic metabolism, and *p,p'*-DDE aerobically. If different food webs are involved, using a single top-predator species as indicator might not be enough to monitor and predict harmful effects to all bird species. More knowledge on the food webs, in conjunction with stable isotope studies, may shed more light.

DDT concentrations in eggs from KwaZulu-Natal in general were generally lower than in eggs from equivalent birds from elsewhere in the world where DDT was used mainly in agriculture. DDT concentrations in eggs were also lower than eggs from the Limpopo Province where breeding impact is suspected, and eggshell thinning associated with DDT has been detected. Differences in hydrology and rainfall may be explanations for this difference, implying that single area monitoring as well as modelling using general assumptions could supply potentially highly erroneous estimations of risk.

All species we studied seem not to have strong fidelity to their breeding localities, but move between breeding colonies according to opportunity and conditions. Reproductive impairment and failure might therefore be masked by influx of individuals from less polluted areas, and breeding success of all the larger aquatic birds should be monitored.

We conclude that significant threats to predatory birds remain in this highly bio-diverse area of KwaZulu-Natal and to birds from adjacent, less polluted areas. Taken together with other indicators, such as very high concentrations of DDT in breast milk, crocodiles,

fish and frogs, the evidence strongly suggest continuous negative human health and environmental impacts from DDT as used in IRS, more than 35 years after its use in agriculture was stopped in South Africa. Furthermore, our data and findings strongly stress the urgency to move away from DDT as quickly as possible, or, at the very least, to implement practices that reduce human exposure to DDT, protects humans from malaria, and prevents emissions of DDT to the environment (Bouwman et al., 2011). These science-based recommendations have been made repeatedly over decades of research here and elsewhere in South Africa, and urgent action is required.

Acknowledgements

We thank J.P. Huisamen for logistical support and collecting the eggs, G.R., Barnard for the photo of the eggshells, and the Persistent Organic Pollutant and Toxicant (POPT) editorial collective for many improvements to the manuscript. The iSimangaliso Wetland Park Authority granted us permission to work at Lake St Lucia and Muzi Pan. Caroline Fox and Sbu Mfeka from Ezemvelo KZN Wildlife assisted with the collection of eggs from Lake St Lucia. MH was funded by the National Research Foundation (Grant number 96296). HB was funded by the Water Research Commission (Project K5-2185), and National Research Foundation (Grant number 77197). Opinions expressed and conclusions arrived at are those of the authors and not necessarily attributed to the NRF or WRC.

References

Barnhoorn, I.E.J., Bornman, M.S., Janse van Rensburg, C.J., Bouwman, H., 2009. DDT residues in water, sediment, domestic and indigenous biota from a currently DDT-sprayed area. Chemosphere 77, 1236–1241.
Baris, D., Zahm, S.H., Cantor, K.P., Blair, A., 1998. Agricultural use of DDT and risk of non-Hodgkin's lymphoma: pooled analysis of three case-control studies in the United States. Occup. Environ. Med. 55, 522–527.
Beard, J., Marshall, S., Jong, K., Newton, R., Triplett-McBride, T., Humphries, B., Bronks, R., 2000. 1,1,1-trichloro-2,2-bis (p-chlorophenyl)-ethane (DDT) and reduced bone mineral density. Arch. Environ. Health 55, 177–180.
Blus, L.J., 1982. Further interpretation of the relation of organochlorine residues in Brown Pelican eggs to reproductive success. Environ. Pollut. Ser. A. 28, 15–33.
Borgå, K., Gabrielson, G.W., Skaare, J.U., Kleivane, L., Nortstrom, R.J., Fisk, A.T., 2005a. Why do organochlorine differences between Arctic regions vary among trophic levels? Environ. Sci. Technol. 39, 4343–4352.
Borgå, K., Hop, H., Skaare, J.U., Wolkers, H., Gabrielson, G.W., 2005b. Selective bioaccumulation of chlorinated pesticides and metabolites in Arctic seabirds. Environ. Pollut. 145, 545–553.
Bornman, M., Schlemmer, L., van der Walt, T., van Dyk, C., Bouwman, H., 2012. Implications for health education and intervention strategies arising from children's caregivers concerns following successful malaria control. Trans. R. Soc. Trop. Med. Hyg. 106, 408–414.
Bouwman, H., 2003. POPs in southern Africa. Handb. Environ. Chem. 3, 297–320. Part 0.
Bouwman, H., Becker, P.J., Schutte, C.H.J., 1994. Malaria control and longitudinal changes in levels of DDT and its metabolites in human serum from Kwazulu. Bull. WHO 72, 921–930.
Bouwman, H., Coetzee, A., Schutte, C.H.J., 1990. Environmental and health implications of DDT-contaminated fish from the Pongolo flood plain. Afr. J. Zool. 104, 275–286.
Bouwman, H., Govender, D., Underhill, L., Polder, A., 2015. Chlorinated, brominated and fluorinated organic pollutants in African Penguin eggs: 30 years since the previous assessment. Chemosphere 126, 1–10.
Bouwman, H., Kylin, H., Sereda, B., Bornman, R., 2012. High levels of DDT in breast milk: intake, risk, lactation duration, and involvement of gender. Environ. Pollut. 170, 63–70.
Bouwman, H., Polder, A., Venter, B., Skaare, J.U., 2008. Organochlorine contaminants in cormorant, darter, egret, and ibis eggs from South Africa. Chemosphere 71, 227–241.
Bouwman, H., Sereda, B., Meinhardt, H.M., 2005. Simultaneous presence of DDT and pyrethroid residues in human breast milk samples from a malaria endemic area in South Africa. Environ. Pollut. 144, 902–917.
Bouwman, H., Van den Berg, H., Kylin, H., 2011. DDT and malaria prevention: Addressing the paradox. Environ. Health Perspect. 119, 744–747.
Bouwman, H., Viljoen, I.M., Quinn, L.P., Polder, A., 2013. Halogenated pollutants in terrestrial and aquatic bird eggs: converging patterns of pollutant profiles, and impacts and risks from high levels. Environ. Res. 126, 240–253.
Bowker, M.W., Downs, C.T., 2012. Breeding of large, water-associated, colonially nesting birds of the North-eastern region of KwaZulu-Natal, South Africa. Waterbirds 35, 270–291.
Buah-Kwofie, A., Humphries, M.S., Combrink, X., Myburgh, J.G., 2018a. Accumulation of organochlorine pesticides in fat tissue of wild Nile crocodiles (*Crocodylus niloticus*) from iSimangaliso Wetland Park, South Africa. Chemosphere 195, 463–471.
Buah-Kwofie, A., Humphries, M.S., Pillay, L., 2018b. Bioaccumulation and risk assessment of organochlorine pesticides in fish from a global biodiversity hotspot: iSimangaliso Wetland Park, South Africa. Sci. Total Environ. 621, 273–281.
Buah-Kwofie, A., Humphries, M.S., Pillay, L. Dietary exposure and risk assessment of organochlorine pesticide residues in rural communities living within catchment areas of iSimangaliso World Heritage Site, South Africa. In Review: Food Additives and Contaminants: Part A.
Connell, D.W., Fung, C.N., Minh, T.B., Tanabe, S., Lam, P.K.S., Wong, B.S.F., Lam, M.H.W., Wong, L.C., Wu, R.S.S., Richardson, B.J., 2003. Risk to breeding success of fish-eating Ardeids due to persistent organic contaminants in Hong Kong: evidence from organochlorine compounds in eggs. Water Res. 37, 459–467.
Cooper, K., 1991. Effects of pesticides on wildlife. In: Hayes, W.J., Laws, E.R. (Eds.), Handbook of Pesticide Toxicology. Academic Press, San Diego, pp. 463–496.
Cooper, K.H., 1980. Bird ecology of Maputaland. In: Bruton, M.N., Cooper, K.H. (Eds.), Studies on the Ecology of Maputaland. Grahamstown. Rhodes University, pp. 300–306.
Dawson, A., 2000. Mechanisms of endocrine disruption with particular reference to occurrence in avian wildlife: a review. Ecotoxicology 9, 59–69.
Douthwaite, R.J., 1989. Effects of DDT on the fish eagle *Haliaeetus vocifer* population of Lake Kariba in Zimbabwe. Ibis 134, 250–258.
De Kock, A.C., Randall, R.M., 1984. Organochlorine insecticide and polychlorinated biphenyl residues in eggs of coastal birds from the Eastern Cape, South Africa. Environ. Pollut. Ser. B 35, 193–201.
Dirksen, S., Boudewijn, T.J., Slager, L.K., Mes, R.G., van Schaick, M.J.M., de Voogt, P., 1995. Reduced breeding success of Cormorants (*Phalacrocorax carbo sinensis*) in relation to persistent organochlorine pollution of aquatic habitats in The Netherlands. Environ. Pollut. 88, 119–132.
Evans, S.W., Bouwman, H., 1993. DDT levels in the blood of pied Kingfishers *Ceryle rudis* from KwaZulu, South Africa. Ann. Musee R. Afr. Cent. Sci. Zool.
Evans, S.W., Bouwman, H., 2000. The geographic variation and potential risk of DDT in the blood of Pied Kingfishers from northern KwaZulu-Natal, South Africa. Ostrich 71, 351–354.
Fry, D.M., 1995. Reproductive effects in birds exposed to pesticides and industrial chemicals. Environ. Health Perspect. 103, 165–171.
Garcia-Heras, M.S., Arroyo, B., Simmons, R.E., Camarero, P.R., Mateo, R., Mougeot, F., 2018. Blood concentrations of PCBs and DDTs in an avian predator endemic to southern Africa: Associations with habitat, electrical transformers and diet. Environ. Pollut. 232, 440–449.
Gerber, R., Smit, N.J., Van Vuuren, J.H.J., Nakayama, S.M.M., Yohannes, Y.B., Ikenaka, Y., Ishizuka, M., Wepener, V., 2016. Bioaccumulation and human health risk assessment of DDT and other organochlorine pesticides in an apex aquatic predator from a premier conservation area. Sci. Total. Environ. 550, 522–533.
Guenzi, W.D., Beard, W.E., 1967. Anaerobic biodegradation of DDT to DDD in soil. Science 156, 116–117.
Gyalpo, T., Fritsche, L., Bouwman, H., Bornman, R., Scheringer, M., Hungerbühler, K., 2012. Estimation of human body concentrations of DDT from indoor residual spraying for malaria control. Environ. Pollut. 169, 235–241.
Hartley, R.R., Newton, I., Robertson, M., 1995. Organochlorine residues and eggshell thinning in the Peregrine falcon *Falco peregrinus minor* in Zimbabwe. Ostrich 66, 69–73.
Hernández, M., Colomer, M.A., Pizarro, M., Margalida, A., 2018. Changes in eggshell thickness and ultrastructure in the Bearded Vulture (*Gypaetus barbatus*) Pyrenean population: a long-term analysis. Sci. Total Environ. 624, 713–721.
Herzke, D., Nygard, T., Berger, U., Huber, S., Rov, N., 2009. Perfluorinated and other persistent halogenated organic compounds in European shag (*Phalacrocorax aristotelis*) and common eider (*Somateria mollissima*) from Norway: a suburban to remote pollutant gradient. Sci. Total Environ. 408, 340–348.
Humphries, M.S., 2013. DDT residue contamination in sediments from Lake Sibaya in northern KwaZulu-Natal, South Africa: implications for conservation in a world heritage site. Chemosphere 93, 1494–1499.
Hockey, P.A.R., Dean, W.R.J., Ryan, P.G., 2005. Roberts Birds of Southern Africa. The Trustees of the John Voelcker Bird Book Fund, Cape Town.
Jardine, D.J., Kidd, K.A., Fisk, A.T., 2006. Applications, considerations, and sources of uncertainty when using stable isotope analysis in ecotoxicology. Environ. Sci. Technol. 40, 7501–7511.
Jehl, J.R., 1973. Studies in a declining population of Brown pelicans in northwestern Baja California. Condor 75, 69–79.
Lam, J.C.W., Murphy, M.B., Wang, Y., Tanabe, S., Giesy, J.P., Lam, P.K.S., 2008. Risk assessment of organohalogenated compounds in water bird eggs from South China. Environ. Sci. Technol. 42, 6296–6302.
Langer, P., Tajtakova, M., Fodor, G., Kocan, A., Bohov, P., Michalek, J., Kreze, A., 1998. Increased thyroid volume and prevalence of thyroid disorders in an area heavily polluted by polychlorinated biphenyls. Eur. J. Endocrinol. 139, 402–409.
Laporte, P., 1982. Organochlorine residues and eggshell measurements of great blue heron eggs from Quebec. Colon. Waterbirds 5, 95–103.
Lundholm, C.E., 1997. DDE-induced eggshell thinning in birds: effects of p,p'-DDE on the calcium and prostaglandin metabolism of the eggshell gland. Comp.

Biochem. Physiol. C Comp. Pharmacol. Toxicol. Endocrinol. 118, 113–128.
Malik, R.N., Rauf, S., Mohammad, A., Eqani, S.A.M.A., Ahad, K., 2011. Organochlorine residual concentrations in cattle egret from the Punjab Province, Pakistan. Environ. Monit. Assess. 173, 325–341.
McCune, B., Grace, J.B., 2002. Analysis of Ecological Communities. MjM Software Design, Gleneden Beach, Oregon.
Ottinger, M.A., Quinn, M.J., Lavoie, E., Abdelnabi, M.A., Thompson, N., Hazelton, J.L., Wu, J.M., Beavers, J., Jaber, M., 2005. Consequences of endocrine disrupting chemicals on reproductive endocrine function in birds: establishing reliable end points of exposure. Domest. Anim. Endocrinol. 29, 411–419.
Peakall, D.B., Lincer, J.L., Risebrough, R.W., Pritchard, J.B., Kinter, W.B., 1973. DDE-induced egg-shell thinning: Structural and physiological effects in three species. Comp. Gen. Pharmacol. 4, 305–313.
Polder, A., Venter, B., Skaare, J.U., Bouwman, H., 2008. Polybrominated diphenyl ethers and HBCD in bird eggs of South Africa. Chemosphere 73, 148–154.
Poli, C., 2015. Variability in Movement Patterns and Habitat Use of Two Species of Pelecaniformes. All Theses, p. 2161. https://tigerprints.clemson.edu/all_theses/2161.
Quinn, L.P., Roos, C., Pieters, R., Løkken, K., Polder, A., Skaare, J.U., Bouwman, H., 2013. Levels of PCBs in wild bird eggs: Considering toxicity through enzyme induction potential and molecular structure. Chemosphere 90, 1109–1116.
Ricca, M.A., Miles, A.K., Anthony, R.C., 2008. Sources of organochlorine contaminants and mercury in seabirds from the Aleutian archipelago of Alaska: nferences from spatial and trophic variation. Sci. Total Environ. 406, 308–323.
Romanoff, A.L., 1932. Fat metabolism of the chick embryo under standard conditions of artificial incubation. Biol. Bull. 54–62.
Smit, N.J., Vlok, W., Van Vuuren, J.H.J., Du Preez, L., Van Eeden, E., O'Brian, G.C., Wepener, V., 2016. Socio-ecological System Management of the Lower Phongolo River and Floodplain Using Relative Risk Assessment. Report to the Water Research Commission, pp. 1–417. WRC Report No. 2185/1/16.
Snelling, J.C., Kemp, A.C., Lincer, J.L., 1984. Organochlorine residues in southern African raptor eggs. In: Mendelsohn, J.M., Sapsford, C.W. (Eds.), Proceedings of the Second Symposium on African Predatory Birds. Natal Bird Club, Durban, pp. 161–168.
Spencer, W.F., Cliath, M.M., 1972. Volatility of DDT and related compounds. J. Agric. Food Chem. 20, 645–649.
Stockholm Convention, 2018. http://chm.pops.int/. (Accessed 17 February 2018).
Tarbotton, W., 2011. Robert's Nests and Birds. The Trustees of the John Voelcker Bird Book Fund, Cape Town.
Thomas, C.M., Anthony, R.G., 1999. Environmental contaminants in great blue herons (*Ardea herodias*) from the lower Columbia and Willamette rivers, Oregon and Washington, USA. Environ. Toxicol. Chem. 18, 2804–2816.
Thompson, L.A., Ikenaka, Y., Yohannes, Y.B., Van Vuren, J.J., Wepener, V., Smit, N.J., Darwish, W.S., Nakayama, S.M.M., Mizukawa, H., Ishizuka, M., 2017. Concentrations and human health risk assessment of DDT and its metabolites in free-range and commercial chicken products from KwaZulu-Natal, South Africa. Food Addit. Contam. 34, 1959–1969.
Thompson, L.A., Ikenaka, Y., Darwish, W.,S., Yohannes, Y.B., Janse van Vuuren, J., Wepener, V., Smit, N.J., Assefa, A.G., Tharwat, A., Eldin, W.F.S., Nakayama, S.M.M., Mizakuwa, H., Ishizuka, M., 2018. Investigation of mRNA expression changes associated with field exposure to DDTs in chickens from KwaZulu-Natal, South Africa. PLoS One 13 (10), e0204400. https://doi.org/10.1371/journal. pone. 0204400.
USDoI, 1998. Guidelines for Interpretation of Biological Effects of Selected Constituents in Biota, Water, and Sediment: DDT. US Department of the Interior. Contaminant guidelines, pp. 1–90.
Van den Berg, H., Manuweera, G., Konradsen, F., 2017. Global trends in the production and use of DDT for control of malaria and other vector-borne diseases. Malar. J. 16, 401. https://doi.org/10.1186/s12936-017-2050-2.
Van Dyk, J.C., Bouwman, H., Barnhoorn, I.E.J., Bornman, M.S., 2010. DDT contamination from indoor residual spraying for malaria control. Sci. Total Environ. 408, 2745–2752.
Van Dyk, L.P., Wiese, I.H., Mullen, J.E.C., 1982. Management and determination of pesticide residues in South Africa. Residue Rev. 82, 38–124.
Wang, Y., Murphy, M.B., Lam, J.C.W., Jiao, L.P., Wong, C.C.L., Yeung, L.W.Y., Lam, P.K.S., 2011. Polychlorinated biphenyls and organochlorine pesticides in local waterbird eggs from Hong Kong: risk assessment to local waterbirds. Chemosphere 83, 891–896.
Wepener, V., Smit, N., Covaci, A., Dyke, S., Bervoets, L., 2012. Seasonal bioaccumulation of organohalogens in tigerfish, *Hydrocynus vittatus* Castelnau, from Lake Pongolapoort, South Africa. Bull. Environ. Contam. Toxicol. 88, 277–282.
Weseloh, D.V., Teeple, S.M., 1983. Double-crested Cormorants of the Great Lakes: egg-laying parameters, reproductive failure, and contaminant residues in eggs, Lake Huron 1972- 1973. Can. J. Zool. 61, 427–436.
Wolmerans, N.J., Du Preez, L.H., Yohannes, Y.B., Ikenaka, Y., IshiZuka, M., Smit, N.J., Wepener, V., 2018. Linking organochlorine exposure to biomarker response patterns in Anurans: a case study of Müller's clawed frog (*Xenopus muelleri*) from a tropical malaria vector control region. Ecotoxicology 27, 1203–1216. Online, .org/10.1007/s10646-018-1972-y.
Yohannes, Y.B., Ikenaka, Y., Nakayama, S.M.M., Ishizuka, M., 2017. DDTs and other organochlorine pesticides in tissues of four bird species from the Rift Valley region, Ethiopia. Sci. Total Environ. 574, 1389–1395.
Zimmermann, G., Dietrich, D.R., Schmid, P., Schlatter, C., 1997. Congener-specific bioaccumulation of PCBs in different water bird species. Chemosphere 34, 1379–1388.

Science of the Total Environment 685 (2019) 1116–1126

Contents lists available at ScienceDirect

Science of the Total Environment

journal homepage: www.elsevier.com/locate/scitotenv

Bioaccumulation of persistent organic pollutants and their trophic transfer through the food web: Human health risks to the rural communities reliant on fish from South Africa's largest floodplain

C.M. Volschenk [a], R. Gerber [b,*], M.T. Mkhonto [a], Y. Ikenaka [b,c], Y.B. Yohannes [c,d], S. Nakayama [c], M. Ishizuka [c], J.H.J. van Vuren [a,b], V. Wepener [b,c], N.J. Smit [b]

[a] Department of Zoology, Kingsway Campus, University of Johannesburg, PO Box 524, Auckland Park 2006, South Africa
[b] Unit for Environmental Sciences and Management, Potchefstroom Campus, North-West University, X6001, Potchefstroom 2520, South Africa
[c] Laboratory of Toxicology, Department of Environmental Veterinary Sciences, Graduate School of Veterinary Medicine, Hokkaido University, N18, W9, Kita-ku, Sapporo 060-0818, Japan
[d] Department of Chemistry, College of Natural and Computational Sciences, University of Gondar, P.O. Box 196, Gondar, Ethiopia

HIGHLIGHTS

- South Africa's largest floodplain not been assessed for OCPs for three decades.
- High OCP concentration found in other aquatic ecosystems of eastern South Africa.
- OCPs and stable isotopes assessed in ecologically and economically important fishes.
- High levels of γ-HCH (Lindane) in all species sampled
- Trophic transfer of DDT demonstrated major ecological and human health risks.

GRAPHICAL ABSTRACT

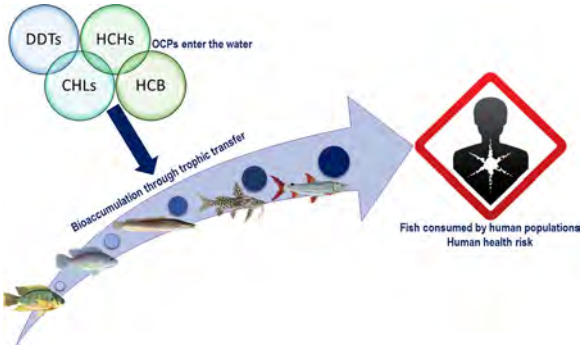

ARTICLE INFO

Article history:
Received 3 April 2019
Received in revised form 4 June 2019
Accepted 9 June 2019
Available online 14 June 2019

1. Introduction

The Phongolo River Floodplain (PRF) is South Africa's largest floodplain, unique in being the only large floodplain able to sustain permanent waters throughout the dry season (Kyle, 2002). This highly productive region contains around 90 floodplain associated pans which are rich in biodiversity and is known to be of high ecological and socio-economic importance (Dube et al., 2017). The floodplain is surrounded by informal settlements and rural communities which are reliant on these aquatic resources, not only for domestic use or agricultural purposes such as watering livestock and subsistence farming, but also for subsistence fisheries as a source of protein (Coetzee et al., 2015). A recent study by Coetzee et al. (2015) indicated that several

* Corresponding author.
E-mail address: gerberrjl@gmail.com (R. Gerber).

https://doi.org/10.1016/j.scitotenv.2019.06.144
0048-9697/

fish species in the study area are important sources of protein within artisanal fishery practices. Contamination due to the introduction of pesticides into aquatic ecosystems is of great concern, as many banned (World Health Organisation (WHO, 2002)) organochlorine pesticides (OCPs) are persistent in the environment and this is reflected by the fact that although many OCPs are no longer used, they still remain present in many, if not all aquatic ecosystems (Gerber et al., 2016). Implementation of effective long term management plans rely directly on fully understanding chemical compounds as well as their risks to both ecosystems and humans, where these aspects can be assessed using; (1) stable isotopes and trophic magnification factors (TMF's) and (2) human health risk assessments via exposure through consumption (Verhaert et al., 2013, 2017).

Studies concerning OCPs in the Southern Hemisphere are considered to be underrepresented (Verhaert et al., 2017), notably those in aquatic ecosystems. Of late, however, there has been a renewed effort in South Africa and several recent studies have examined OCP concentrations in the aquatic environment (Barnhoorn et al., 2015; Buah-Kwofie et al., 2018; Buah-Kwofie and Humphries, 2017; Gerber et al., 2015, 2016; Pheiffer et al., 2018; Verhaert et al., 2017; Wagenaar and Barnhoorn, 2018; Wepener et al., 2012). The present study focuses on OCP contamination of multiple fish species, trophic transfer and a desktop approach in determining human health risks associated with fish consumption from sub-tropical systems of the PRF. The study area is defined as an intermediate to low-risk malaria area (McHugh et al., 2011; Wepener et al., 2011). Spraying of Dichlorodiphenyltrichloroethane (DDT) in this area takes place for the purpose of malaria vector control (MVC), starting in January and extending through to the end of March (Bouwman et al., 1990). DDT has received continuous media attention since its banning (within South Africa) in 1996 and is well known for its use in the management of the spread of malaria in South Africa and many other African countries (Deribe et al., 2011). The ban of DDT led to a large decline in its overall use as a general pesticide (Van Dyk et al., 2010). Notwithstanding the spraying of DDT for MVC, illegal usage of other OCPs in subtropical and temperate regions of South Africa has been demonstrated by Gerber et al. (2016) and Pheiffer et al. (2018). Large scale agriculture is found both upstream (Wepener et al., 2012) and within the study area (Dube et al., 2017) it could therefore be expected that levels of other OCPs such as Lindane and hexachlorobenzene (HCB) can also be of environmental concern.

Close to three decades have passed since the only previous study (Bouwman et al., 1990) evaluating OCPs (DDT only) in fish from the PRF. Three economically important fish species were assessed for DDT in the previous study, where in this study five economically and ecologically important species were identified and selected for investigation of OCP contamination in the PRF. These were; *Hydrocynus vittatus* Castelnau 1861, *Synodontis zambezensis* Peters 1852, *Clarias gariepinus* (Burchell 1822), *Oreochromis mossambicus* (Peters 1852) and *Coptodon rendalli* (Boulenger 1897). For ecological purposes species were selected to represent various trophic levels and functional feeding groups; *H. vittatus* (top aquatic predator – mainly piscivore), *Cl. gariepinus* (omnivore – feeding across most trophic levels), *S. zambezensis* (invertivorous), *O. mossambicus* (detritivore), *Co. rendalli* (herbivore/invertivore) (Skelton, 2001). In terms of preference as protein source and therefore relevance to human health, Coetzee et al. (2015) found that these five species were the most consumed by the rural community in the PRF (percentages in parentheses indicate the percentage of the community which was interviewed which eat the different species), in the order of; *Co. rendalli* (89%), *O. mossambicus* (77%), *S. zambezensis* (64%), *Cl. gariepinus* (55%) and *H. vittatus* (47%).

The purpose of this study was to assess the occurrence and levels of major OCPs in ecologically and economically important fish species in the PRF. With the major foci on potential ecological and human health risks. The specific objectives identified were: 1) the production of a baseline OCP data set for fish from the PRF by assessing spatial and temporal patterns of bioaccumulation; 2) investigation of trophic transfer and biomagnification through a sub-tropical food web and 3) implementation of a desktop approach to evaluate potential human health risks by consumption of OCP contaminated fish. To our knowledge, this is the first study to present levels of various OCP compounds and their trophic transfer in fish from the PRF.

2. Materials and methods

2.1. Study area

Sites selected in this study fall within the Ndumo Game Reserve (NGR) which is situated in the PRF in Maputaland, KwaZulu-Natal. This is the only protected area on the PRF and is the most downstream section of the Phongolo River in South Africa and thus should be representative of activities occurring within the catchment. The PRF is characterised by large extensive wetlands. The Phongolo River (PR), which is one of the main tributaries to the Maputo River in Mozambique runs east through the town of Pongola and is impounded to form Lake Pongolapoort. The construction of the dam took place in 1973 with the aim to use water resources for irrigation purposes in the area. As the PR is impounded it requires a controlled flooding period for renewal of freshwater every year. Water is released from the Pongolapoort Dam which is situated upstream from the NGR. The controlled flooding regime (October/November) has been changed many times since the building of the Pongolapoort Dam and is essential for the survival of the aquatic ecosystem of the PR and the PRF (Dube et al., 2017). The sites selected are representative of the two typical habitats in the area, i.e. the river and a floodplain pan, namely; the Nyamithi Pan (NP) (Fig. 1, Site 1) and the Phongolo River (PR) (Fig. 1, Site 2).

2.2. Sample collection

Fish were collected during three surveys, firstly the end of Austral spring, in November 2012 (post controlled flooding from Lake Pongolapoort) hereafter referred to as the controlled flood (CF) survey, secondly during Austral autumn, in April 2013 (post the rainy and wet season with some natural high flows) hereafter referred to as the wet season (WS) survey and at the start of Austral spring in September 2013 hereafter referred to as the dry season (DS) survey.

A variety of sampling techniques were used, including rod and line, fyke nets, seine nets and electrofishing. Caught fish were temporarily kept in containers with battery operated air pumps to supply oxygen as they were transported to the field station for dissection. Prior to data collection all experimental procedures were ratified by the University of Johannesburg's Institutional Research Ethics Committee. Axial muscle tissue was removed from the lateral sides of the fish for the analysis of OCPs and stable isotopes, wrapped in aluminium foil and placed into individual zip-lock bags and frozen at −20 °C until further analyses. Samples were transported back to the laboratory at the University of Johannesburg for analysis.

2.3. OCPs

2.3.1. Chemicals and sample preparation

The following compounds were included in the analysis: DDT and metabolites (o,p′-DDD, o,p′-DDE, o,p′-DDT, p,p′-DDD, p,p′-DDE, and p,p′-DDT), chlordanes-CHLs (trans-chlordane and trans-nonachlor (TN)), hexachlorocyclohexanes (α-, β-, ɗ- and γ- HCHs) and hexachlorobenzene (HCB). Preparation of the samples, standards used, and analysis of samples were all done according to Yohannes et al. (2013) with some modifications. The extraction time was extended from 4 h 30 min to 6 h. Analysis of OCPs was carried out with a gas chromatograph (GC) equipped with ^{63}Ni electron capture detector (GC-ECD: Shimadzu GC-2014, Kyoto, Japan). The concentrations were expressed in wet weight (ww), with lipid weight (lw) concentrations included

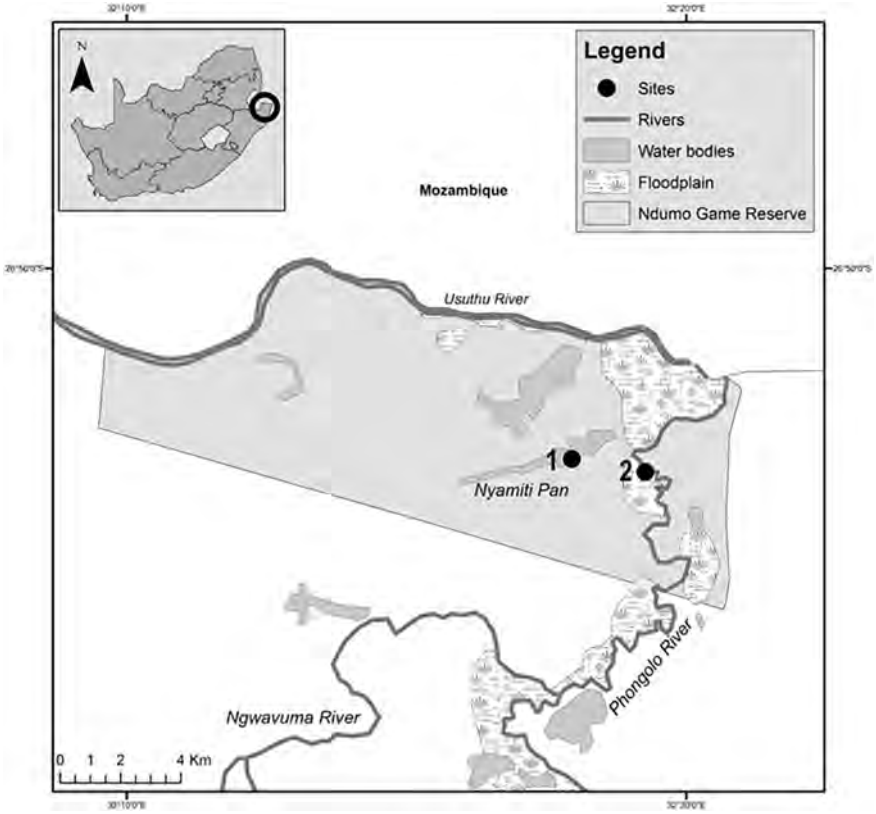

Fig. 1. Map showing sites chosen for the study within the KwaZulu-Natal Province of Southern Africa; 1) Nyamithi Pan (NP) and 2) Phongolo River (PR) within the Ndumo Game Reserve (NGR, highlighted in grey). River flow in the PR is south to north and in the Usuthu River is west to east.

and were calculated using the fat content of the fish which were calculated using gravimetric lipid determination.

2.3.2. OCP analysis

The procedures followed, with some modifications and standards (10 μg/mL mixture containing DDTs, HCHs, Chlordanes and Drins) are according to Yohannes et al. (2013). Solvents used were hexane and acetone in a 3:1 ratio (extraction solvent) and dichloromethane and hexane solution at a ratio of 2:7 (clean-up solvent). Muscle tissue (10 g wet weight) from each fish was homogenized with anhydrous sodium sulphate and spiked with a surrogate standard of 2,4,5,6-tetrachloro-m-xylene (TCmX). The surrogate standard spiked tissue mixture was placed into the extraction chamber and filled with 150 mL extraction solvent. The chambers where placed into the Soxtherm apparatus (S306AK Automatic Extractor, C. Gerhardt GmbH &Co. KG, Konigswinter, Germany) for an extraction time of 6 h, the resulting extract was concentrated to 2 mL using a rotary evaporator (rotovapor) which was diluted to 10 mL using hexane. A fraction of 20% of this dilution was used for gravimetric lipid determination and the rest was used in a clean-up process after being dried to half its volume using nitrogen gas and a heating plate. The clean-up procedure was applied in order to remove excess lipids and this was done with activated florisil (6 g) packed into a glass cylinder and topped off with 1 cm of anhydrous sodium sulphate. Dichloromethane:hexane (120 mL) was eluted through the florisil in a drip wise manner and the resulting liquid was again concentrated through the use of a rotary evaporator to 2 mL. Minimal dilution with hexane was applied and the sample was concentrated to near dryness with nitrogen gas and diluted again with 100 μL n-decane. The resulting concentrate was transferred to a Gas Chromatography (GC) vial for analysis.

2.3.3. Quality assurance/quality control (QA/QC)

All quality controls used during the analysis of OCPs was done according to Yohannes et al. (2013). A comparison between the retention times of corresponding standards was used to identify the specific OCPs found within each sample. Quantifications of OCP levels were obtained through creating multi-level calibration curves and through this linearity ($R^2 \geq 0.995$) was achieved. Procedural blanks and spiked blanks were used to perform quality control, which showed that blank samples had no presence of the target metabolites and that a recovery rate of 90 to 105% was present within the spiked samples. The surrogate samples spiked with TCmX had a recovery rate of 85 ± 11%. Standard reference material SRM 1947 (Lake Michigan Fish Tissue) was used to check the validity of the extraction and analytical methods.

2.4. Stable isotope analysis

Fish samples were weighed to 5 g and dried in an oven at 60 °C. Once dried, the samples were ground to a fine powder using a pestle and mortar. To remove the fats from the samples, a 2:1 (*v*/v) mixture of chloroform:methanol was added to each sample. Ratios of stable isotopes of Carbon ($\delta^{13}C$) and Nitrogen ($\delta^{15}N$) were measured using an isotope ratio mass spectrometer which was equipped with an elemental analyser (Fisons NA1500-Finnigan MAT 252). Replicate error within ± 0.2‰ for both $\delta^{15}N$ and $\delta^{13}C$ measurements were indicated by replicate measurements of internal laboratory standards.

Stable isotope results are expressed as the deviation from standards using the following formula:

$$\delta^{13}C;\delta^{15}N = \left[\left(R_{sample}/R_{reference}\right) - 1\right] \times 1000 \quad (1)$$

where $R = {}^{13}C/{}^{12}C$ for carbon and ${}^{15}N/{}^{14}N$ for nitrogen.

Relative trophic levels were derived from animal $\delta^{15}N$ values using the following equation (Verhaert et al., 2017).

$$TL_{consumer} = \left[\left(\delta^{15}N_{consumer} - \delta^{15}N_{primary\ consumer}\right)/\Delta\delta^{15}N\right] + 2$$

where $TL_{consumer}$ is the trophic level of the organism in question (e.g. *S. zambezensis*), $\delta^{15}N_{consumer}$ is $\delta^{15}N$ of the same organism, $\delta^{15}N_{primary\ consumer}$ is the mean $\delta^{15}N$ of a local long-lived primary consumer, 2 is the trophic level of the primary consumer and $\Delta\delta^{15}N$ is the trophic enrichment factor, or the shift in $\delta^{15}N$ between two consecutive trophic levels. In the present study, the primary consumer used as a baseline was the macrophyte species *Potamageton schweinfurthii*. A $\Delta\delta^{15}N$ trophic enrichment factor of 3‰ was used as this is the most adequate estimate for non-acid treated muscle tissue. TMF's were based on lipid normalised contaminant OCP concentrations and relative trophic levels and were calculated from the slope of the regression of the log-transformed concentrations of pollutants versus trophic level calculated based on $\delta^{15}N$ (Verhaert et al., 2017). The TMFs were only calculated for sites and surveys containing all sampled species, using the following equation:

$$\text{Log [contaminant]} = a + bTL \qquad TMF = 10^{b}$$

TMF's can be compared across systems and between chemicals to understand variations in biomagnification caused by differences in chemical properties. TMF's represent the average biomagnification through the food web, and take into consideration the bioavailable concentrations of chemicals within a system. Should the resulting TMF value be equal to one (TMF = 1), the chemical does not biomagnify on average through the food web. A TMF value higher than 1 (TMF > 1) illustrates that biomagnification of said chemical is taking place through the food web with an average factor of TMF per trophic level (TL). On the other hand, a TMF value below one (TMF < 1) indicates that the chemical is decreasing through the food web with an average factor of TMF per TL and this can be referred to as trophic dilution (Borgå et al., 2012).

2.5. Human health risk assessment

Various international organisations have established a range of standards and instructions estimating potential risks to human health from fish contaminated with environmental pollutants (USEPA, 2016). By comparing levels with laws and guidelines, straight forward risk assessments can be performed, these assessments, however, do not consider factors such as eating habits and consumption rates. Therefore the health risk assessment in this study follows that of Gerber et al. (2016) and is performed at both the 50th and 95th percentile of measured concentrations. These values in turn provide a comprehensive evaluation of potential health risks (Gerber et al., 2016; Yohannes et al., 2014) to the rural communities of the PRF through the consumption of OCP contaminated fishes.

2.5.1. Estimated daily intake (EDI)

The estimated daily dietary intakes of groups of OCPs from fish consumption were calculated as follows for each of the fish species:

$$EDI = \frac{C \times DR}{BW}$$

where *C* is the measured OCP concentration ($ng \cdot g^{-1}$ ww), DR is the estimated daily consumption rate of fish ($g \cdot d^{-1}$) and BW is the estimated average body weight (kg) of people in the area. The BW was set at 60 kg (WHO, 2002), and the estimated daily consumption rate was conservatively assumed to be 30 $g \cdot ww \cdot d^{-1}$ per person.

2.5.2. Potential carcinogenic risks

In order to assess the potential carcinogenic risks posed by OCPs through contaminated fish consumption, both cancer risk estimates and hazard ratios were calculated according to USEPA guidelines and Dougherty et al. (2000) and Jiang et al. (2005) respectively. The cancer risks (CR) associated with OCPs were estimated using the following equation:

$$CR = EDI \times CSF$$

where CSF is the cancer slope factor taken from USEPA (2012) and the equation from USEPA (2005). Results are interpreted as follows: $<10^{6}$ is considered acceptable, between 10^{6} and 10^{4} is considered to be an area of concern and carcinogenic risks $> 10^{4}$ are considered unacceptable (USEPA, 2005).

Hazard ratios (HR) for both non-carcinogenic and carcinogenic effects were calculated following Jiang et al. (2005):

$$HR = \frac{EDI}{BMC}$$

where the BMC refers to the Benchmark calculation. The BMC for cancer effects was derived from the USEPA cancer slope factor (CSF) obtained from the USEPA Integrated Risk Information System (IRIS). The BMC is calculated as follows:

$$\text{Cancer BMC} = \frac{\text{Risk} \times \text{BW}}{\text{Fish Consumption} \times \text{CSF}}$$

where the risk is set to a one in a million chance due to a lifetime of exposure and the fish consumption is the amount of fish consumed per kg body weight of the individual per day i.e. g. $kg^{-1} \cdot d^{-1}$. A hazard ratio greater than one indicates that there is a potential risk to human health (Dougherty et al., 2000).

2.6. Statistical analysis

SPSS version 21 was used for statistical analysis of bioaccumulation data, means and standard errors of the mean. A one way ANOVA was applied to the data following log transformation to ensure homogeneity. Significant differences ($p < 0.05$) between surveys and sampling periods were determined using the Tukey-Kramer post hoc test. Spearman rho ranked correlation coefficients were determined for OCP concentrations (wet weight) versus fish size and lipid content (%) of the muscle tissue.

3. Results

3.1. Temporal and spatial variation in OCP bioaccumulation in sampled fish species

Two sites, i.e. Nyamithi Pan and the Phongolo River were sampled during three surveys representing different hydrological and catchment run-off conditions. Not all species could be collected at each site and during each survey. The fish weight, length, lipid content and OCP concentrations in muscle tissue of *H. vitattus*, *S. zambezensis*, *O. mossambicus*, *Cl. gariepinus* and *Co. rendalli* are presented in Tables S1 to S5 respectively. Fish sampled from NP during the three surveys were similar in size, whereas the fish sampled during the wet season from the PR were significantly smaller (*H. vitattus* – $F = 8.687$, $df = 47$, $p = 0.001$; *S. zambezensis* – $F = 4.336$, $df = 51$, $p = 0.009$; *Cl. gariepinus* – $F = 14.188$, $df = 49$, $p = 0.00001$; *O. mossambicus* – $F = 37.91$, $df = 76$, $p < 0.00001$; *Co. rendalli* – $F = 49.644$, $df = 35$, $p < 0.00001$). The lipid content of the muscle tissue of the two predatory species, *H. vittatus* and *S. zambezensis*, was significantly higher than the other three species and also displayed the greatest variation between surveys (0.4–8%) (*H. vitattus* – $F = 5.931$, $df = 47$, $p = 0.002$; *S. zambezensis* – $F = 7.21$, $df = 51$, $p = 0.0004$; *Cl. gariepinus* – F =

0.529, df = 49, p = 0.665; *O. mossambicus* – F = 2.205, df = 76, p = 0.151; *Co. rendalli* – F = 2.135, df = 35, p = 0.134). The other three species with detritivorous/omnivorous feeding habits had fairly constant lipid content ranging between 0.2 and 1.3%. The lipid content from fish collected during the dry season was generally lower compared to the other sampling surveys.

HCHs: The average ΣHCHs varied between 0.3 and 300 ng·g lw across all sites and surveys for the five fish species. The highest concentrations were recorded in *Cl. gariepinus* (0.01–1040 $ng \cdot g^{-1}$ lw), *H. vittatus* (0.01–2210 $ng \cdot g^{-1}$ lw) and *O. mossambicus* (0.06–2111 $ng \cdot g^{-1}$ lw). The ΣHCHs were the highest during the dry season when compared to the higher flow and run-off periods (*H. vitattus* – F = 1.755, df = 47, p = 0.170; *S. zambezensis* – F = 3.222, df = 51, p = 0.031; *Cl. gariepinus* – F = 5.367, df = 49, p = 0.003; *O. mossambicus* – F = 2.859, df = 76, p = 0.029; *Co. rendalli* – F = 7.11, df = 35, p = 0.003). In general, the ΣHCHs in fish from the river site during the high flow were generally lower than the fish sampled from Nyamithi Pan. The dominant HCH congeners were α-HCH and γ-HCH with only the detritivore/herbivore species (*O. mossambicus* and *C. rendalli*) displaying bioaccumulation of the ɗ-HCH congener.

ΣCHLs: The average ΣCHLs ranged from 0.39 to 426 $ng \cdot g^{-1}$ lw with the highest levels recorded in *Co. rendalli* from the Phongolo River (0.03–953 $ng \cdot g^{-1}$ lw) during the wet season followed by *O. mossambicus* from the Nyamithi Pan (0.01–1484 $ng \cdot g^{-1}$ lw) during the controlled flood. The lowest concentrations were found in the predatory fish species (*H vittatus* and *S. zambezensis*). There were no clear spatial and temporal CHL bioaccumulation patterns (*H. vitattus* – F = 2.647, df = 47, p = 0.061; *S. zambezensis* – F = 3.084, df = 51, p = 0.036; *Cl. gariepinus* – F = 2.021, df = 49, p = 0.124; *O. mossambicus* – F = 3.04, df = 76, p = 0.023; *Co. rendalli* – F = 0.641, df = 35, p = 0.553). Only two congeners were identified of which trans-Nonachlor was most prevalent and occurred in the highest concentrations. The highest levels of the trans-Chlordane were recorded in *O. mossambicus* (7.7–45 $ng \cdot g^{-1}$ lw).

HCB: Hexachlorobenzene concentrations were recorded mostly in *S. zambezensis* and *C. rendalli*, whereas for *Cl. gariepinus* the HCBs were below detection. For the other species HCBs were only recorded during a single survey (*H. vitattus* – F = 1.969, df = 47, p = 0.132; *S. zambezensis* – F = 2.393, df = 51, p = 0.08; *Cl. gariepinus* – too few groups; *O. mossambicus* – F = 0.986, df = 76, p = 0.421; *Co. rendalli* – F = 8.929, df = 35, p = 0.001). The average HCBs in *Co. rendalli* ranged between 0.4 and 1082 $ng \cdot g^{-1}$ lw in Nyamithi Pan during the dry and wet seasons respectively. The levels in *S. zambezensis* were lower ranging between 4.2 and 2.8 $ng \cdot g^{-1}$ lw during the corresponding surveys.

DDTs: Dichlorodiphenyltrichloroethane (o,p′- and p,p′-DDE, DDD and DDT) was found in all five species at both sites during all three sampling periods, making it the most abundant OCP in the studied system. The concentrations found were also the highest of all the OCPs tested for and were significantly higher in all five species. Concentrations ranged from 22.1 to 11,576.5 $ng \cdot g^{-1}$ lw in *H. vittatus*, from 0.27 to 2721.32 $ng \cdot g^{-1}$ lw in *S. zambezensis*, from 0.06 to 4935.15 $ng \cdot g^{-1}$ lw in *O. mossambicus*, from 0.16 to 8147.31 $ng \cdot g^{-1}$ lw in *Cl. gariepinus* and from 0.06 to 1515.12 $ng \cdot g^{-1}$ lw in *Co. rendalli* (*H. vitattus* – F = 5.777, df = 47, p = 0.002; *S. zambezensis* – F = 8.407, df = 51, p = 0.0001; *Cl. gariepinus* – F = 0.752, df = 49, p = 0.527; *O. mossambicus* – F = 5.861, df = 76, p = 0.0004; *Co. rendalli* – F = 0.525, df = 35, p = 0.596). The highest concentrations were in *H. vittatus*, the species that occupies the top of the food web within this system. There were no distinct temporal and spatial ΣDDTs bioaccumulation patterns that were similar for all species. In general, ΣDDTs were higher during the dry season compared to the other surveys in *H. vittatus*, *O. mossambicus*, (PR), *Cl. gariepinus* and *C. rendalli*. Only *S. zambezensis* and *O. mossambicus* (NP) had higher ΣDDT concentrations during the wet season. On a spatial scale *S. zambezensis*, *Cl. gariepinus* and *Co. rendalli* from PR had higher ΣDDTs than from NP whereas *O. mossambicus* and *H. vitattus* had higher levels in the NP compared to the river site.

Table 1
Spearman rho ranked correlation coefficients for various organochlorine pesticide concentrations in muscle tissue of several fish species from the Phongolo River floodplain vs total lengths (mm) and lipid content of muscle tissue (%). Values in bold indicate significant correlations.

Species	Variable	HCH	DDT	CHL	HCB
Hydrocynus vittatus	Length	−0.113	**0.293***	−0.003	**−0.533****
	Lipid	**0.365***	**0.519****	**0.294***	0.244
Synodontis zambezensis	Length	**−0.387****	**−0.477****	**−0.644****	**−0.528****
	Lipid	**0.324***	**0.418****	**0.608****	**0.564****
Clarias gariepinus	Length	**−0.300***	**−0.352***	**−0.322***	–
	Lipid	0.127	**0.517****	0.080	–
Oreochromis mossambicus	Length	**−0.266***	**−0.505****	**−0.405****	**−0.514****
	Lipid	**0.404****	**0.537****	**0.272***	**0.309****
Coptodon rendalli	Length	0.249	−0.124	−0.124	−0.070
	Lipid	0.197	**0.580****	0.020	0.145

* Correlation is significant at the 0.05 level (2-tailed).
** Correlation is significant at the 0.01 level (2-tailed).

The p,p′-DDE congener was the most common followed by p,p′-DDT throughout all fish species during all of the surveys.

3.1.1. Effects of size and lipid content on OCP bioaccumulation

The correlation analysis (Spearman rho) between OCP concentrations with size and lipid content revealed that size was not a major factor in OCP bioaccumulation (Table 1). In fact, size had significant negative relationship with accumulated OCPs, this is especially true for *S. zambezensis* (HCH – $r_s = -0.387$, DDT - $r_s = -477$, CHL - $r_s = -0.644$, HCB - $r_s = -0.528$), *Cl. gariepinus* (HCH – $r_s = -0.3$, DDT - $r_s = -352$, CHL - $r_s = -0.322$, HCB – not detected) and *O. mossambicus* (HCH – $r_s = -0.266$, DDT - $r_s = -0.505$, CHL - $r_s = -0.405$, HCB - $r_s = -0.514$), whereas, *H. vitattus* only had a significant negative correlation with HCB ($r_s = -0.533$) and a significant positive correlation with DDT ($r_s = 0.293$) and OCP accumulation in *Co. rendalli* had no correlation with size. The lipid content in *H. vitattus* (HCH – $r_s = 0.365$, DDT - $r_s = 0.519$, CHL - $r_s = 0.294$, HCB - $r_s = 0.244$), *S. zambezensis* (HCH – $r_s = 0.324$, DDT - $r_s = 0.418$, CHL - $r_s = 0.608$, HCB - $r_s = 0.564$) and *O. mossambicus* (HCH – $r_s = 0.404$, DDT - $r_s = 0.537$, CHL - $r_s = 0.405$, HCB - $r_s = 0.309$) were all significantly positively correlated to all OCP groups, except for HCB in *H. vitattus*. Only DDTs were significantly positively correlated in both Cl. gariepinus ($r_s = 0.517$) and Co. rendalli ($r_s = 0.580$), while all other groups had no correlation.

3.2. Trophic magnification and transfer as indicated by stable isotopes

The trophic magnification of OCPs is based on the relationship between the trophic level (TL) and the log contaminant concentration. Resulting linear regression graphs show TMF > 1 and therefore biomagnification through the food web occurs, but this is only the case in ΣDDT (Fig. 2A, B, C and D). Trophic magnification of ΣDDT can clearly be seen in the Nyamithi Pan during all three sampling periods with TMF values ranging from 2.2 to 2.34 (Fig. 2A, B and C). Organochlorine pesticides which have a Log Kow > 5 tend to biomagnify through the food chain and Fig. 3 clearly illustrates this in the case of ΣDDTs. Compounds with lower Log Kow values tend not to biomagnify and this is the case within both the NP and the PR, with ΣHCH's (TMFs: NP-CF – 0.06, NP-WS – 0.21, NP-DS – 0.03), ΣCHL's (TMFs: NP-CF – 0.05, NP-WS – 0.09, NP-DS – 0.03, PR-WS – 0.62) and HCB (TMFs: NP-CF – 0.004, NP-DS – 0.09, PR-WS – 0.05) showing no biomagnification through the food web.

3.3. Human health risk

The 50th and 95th percentile values calculated for the EDI, HRs and the cancer risk estimates of the different OCPs in the muscle tissue of

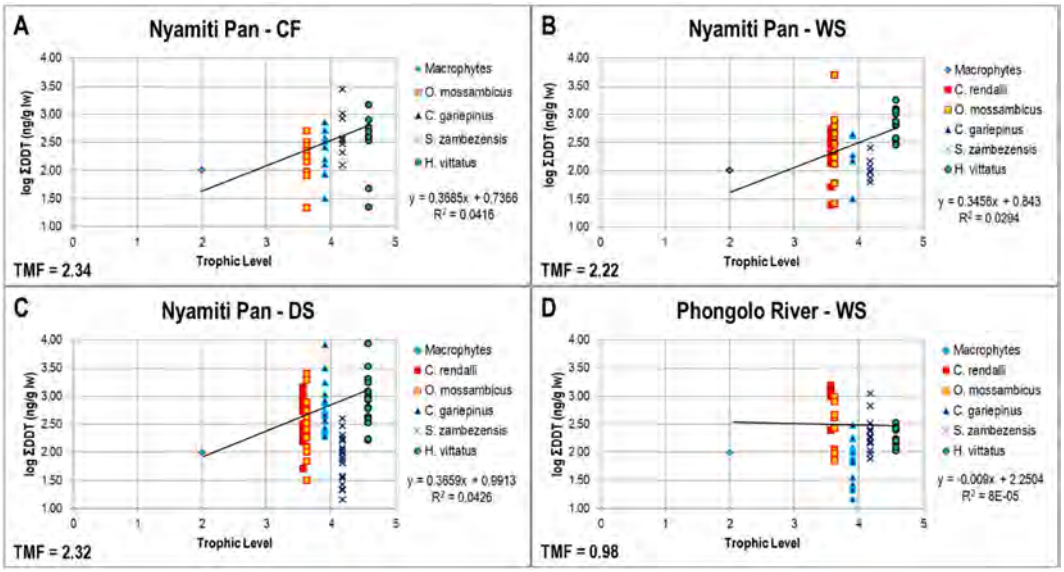

Fig. 2. Relationship between the trophic level (TL) and log concentrations of ΣDDT of food webs in the Nyamithi Pan during controlled flood (CF – panel A), wet season (WS – panel B) and dry season (DS – panel C) and the Phongolo River during the wet season (WS – panel D). The resulting trophic magnification factor (TMF) is listed in the bottom left hand corner of each corresponding graph.

the fish species sampled during this study are shown in Table 2. The calculated EDI values for all species during all surveys and sites were well below the indicated acceptable/tolerable daily intakes at both the 50th and 95th percentile (EDI Range ($ng \cdot kg^{-1} \cdot bw \cdot d^{-1}$): HCH - *H. vitattus*: 0.005–1.01, *S. zambezensis*: 0.03–3.36, *Cl. gariepinus*: 0.005–1.37, *O. mossambicus*: 0.03–0.505, *C. rendalli*: 0.015–0.765; HCB - *H. vitattus*: 0.01–0.61, *S. zambezensis*: 0.015–0.43, *Cl. gariepinus*: not detected, *O. mossambicus*: 0.005–0.03, *C. rendalli*: 0.005–16.56; CHL - *H. vitattus*: 0.005–0.53, *S. zambezensis*: 0.015–1.16, *Cl. gariepinus*: 0.005–0.1, *O. mossambicus*: 0.01–2.67, *C. rendalli*: 0.08–0.89; DDT - *H. vitattus*: 1.06–25.39, *S. zambezensis*: 1.63–15.46, *Cl. gariepinus*: 0.18–2.01, *O. mossambicus*: 0.08–3.46, *C. rendalli*: 0.44–6.88). Even so, the HRs and cancer risk estimates show that there are long term risks associated with the consumption of the studied fish species. In terms of the HRs, at the 50th percentile almost all fish and species contaminated with HCHs and DDTs during all surveys and sites showed risk while only certain fish species (*S. zambezensis* and *C. rendalli*) during select surveys indicated risk due to contamination with HCBs and CHLs (HCH - *H. vitattus:* 0.04–0.8, *S. zambezensis:* 0.23–2.2, *Cl. gariepinus*: 0.04–0.19, *O. mossambicus*: 0.23–0.7, *C. rendalli*: 0.11–1.33, HCB - *H. vitattus*: 0.01,

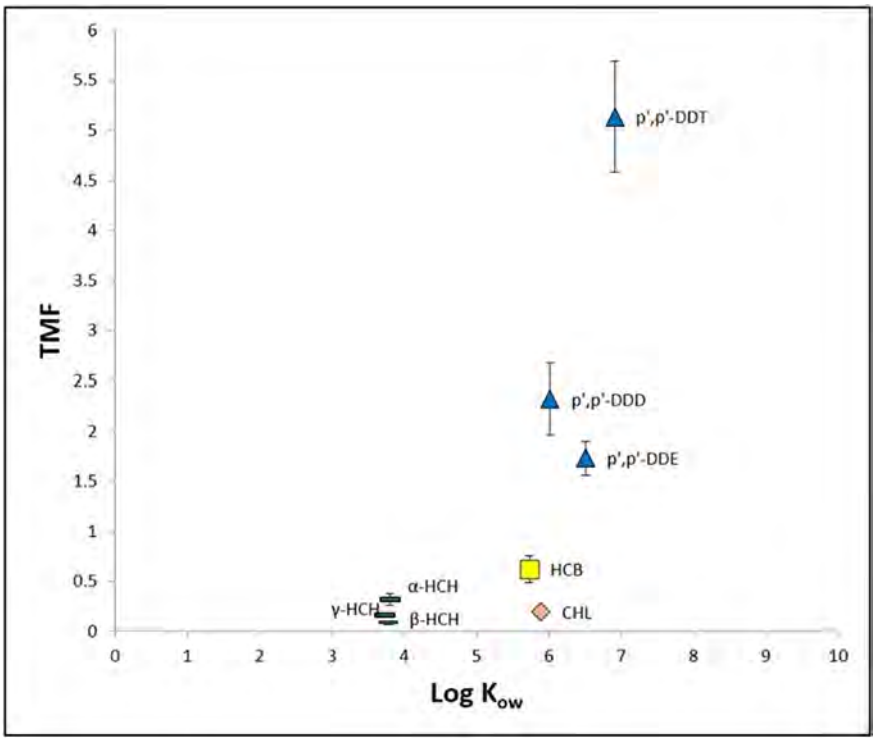

Fig. 3. Average (±1SE) trophic magnification factors (TMF) versus log Kow for the different organochlorine pesticides measured in several fish species from the Phongolo River floodplain.

Table 2

50th percentile and 95th percentile (in parentheses) concentrations (wet weight), estimated exposure, benchmark concentrations, carcinogenic hazard ratios and estimated cancer risks for several fish species consumed from the Phongolo River floodplain. BD indicates that values were below detection. BMC - Benchmark concentrations; Underlined values indicate risk.

Fish species	Site and survey	HCH				HCB				CHL			
		CSF[b] $mg\cdot kg^{-1}\cdot d^{-1}$	BMC $ug\cdot kg^{-1}\cdot d^{-1}$	ADI[c] $ng\cdot kg^{-1}\cdot bw\cdot d^{-1}$	TDI[d] $ng\cdot kg^{-1}\cdot bw\cdot d^{-1}$	CSF[b] $mg\cdot kg^{-1}\cdot d^{-1}$	BMC $ug\cdot kg^{-1}\cdot d^{-1}$	ADI[c] $ng\cdot kg^{-1}\cdot bw\cdot d^{-1}$	TDI[d] $ng\cdot kg^{-1}\cdot bw\cdot d^{-1}$	CSF[b] $mg\cdot kg^{-1}\cdot d^{-1}$	BMC $ug\cdot kg^{-1}\cdot d^{-1}$	ADI[c] $ng\cdot kg^{-1}\cdot bw\cdot d^{-1}$	TDI[d] $ng\cdot kg^{-1}\cdot bw\cdot d^{-1}$
		1.1[a]	0.132	5000[a]	3000[a]	1.6	0.192		170	0.35	0.042	500	500
		Measured concentrations $(ng\cdot g^{-1})$ ww	Estimated daily intakes $ng\cdot kg^{-1}\cdot bw\cdot d^{-1}$	Carcinogenic hazard ratios[e]	Cancer risk estimates[f] $(\times 10^4)$	Measured concentrations $(ng\cdot g^{-1})$ ww	Estimated daily intakes $ng\cdot kg^{-1}\cdot bw\cdot d^{-1}$	Carcinogenic hazard ratios[e]	Cancer risk estimates[f] $(\times 10^4)$	Measured concentrations $(ng\cdot g^{-1})$ ww	Estimated daily intakes $ng\cdot kg^{-1}\cdot bw\cdot d^{-1}$	Carcinogenic hazard ratios[e]	Cancer risk estimates[f] $(\times 10^4)$
Hydrocynus vittatus	NP CF	0.01 (0.6)	0.005 (0.3)	0.04 (2.27)	0.06 (3.3)	BD	–	–	–	0.01 (0.15)	0.005 (0.08)	0.12 (1.79)	0.018 (0.26)
	NP WS	0.1 (1.44)	0.05 (0.72)	0.37 (5.46)	0.55 (7.92)	BD	–	–	–	0.05 (1.05)	0.025 (0.53)	0.6 (12.5)	0.09 (1.84)
	NP DS	0.04 (0.92)	0.02 (0.46)	0.15 (3.49)	0.22 (5.06)	BD	–	–	–	0.03 (0.07)	0.015 (0.04)	0.36 (0.83)	0.053 (0.12)
	PR WS	0.21 (2.01)	0.105 (1.01)	0.8 (7.61)	1.2 (11.1)	0.02 (1.22)	0.01 (0.61)	0.05 (3.2)	0.16 (9.76)	0.05 (0.08)	0.025 (0.04)	0.6 (0.95)	0.088 (0.14)
Synodontis zambezensis	NP CF	0.06 (0.79)	0.03 (0.395)	0.23 (3)	0.33 (4.35)	BD	–	–	–	0.02 (0.1)	0.01 (0.05)	0.24 (1.19)	0.035 (0.18)
	NP WS	0.2 (6.72)	0.1 (3.36)	0.76 (25.5)	1.1 (37)	0.03 (0.86)	0.015 (0.43)	0.08 (2.24)	0.24 (6.88)	0.03 (2.32)	0.015 (1.16)	0.36 (27.6)	0.053 (4.06)
	NP DS	0.58 (1.32)	0.29 (0.66)	2.2 (5)	3.19 (7.26)	0.12 (0.59)	0.06 (0.295)	0.31 (1.54)	0.96 (4.72)	0.33 (0.55)	0.165 (0.28)	3.93 (6.55)	0.58 (0.96)
	PR WS	0.31 (0.74)	0.155 (0.37)	1.17 (2.8)	1.7 (4.1)	0.07 (0.19)	0.035 (0.07)	0.18 (0.49)	0.56 (1.52)	0.61 (1.16)	0.305 (0.58)	7.26 (13.81)	1.07 (2.03)
Clarias gariepinus	NP CF	0.01 (0.14)	0.005 (0.07)	0.04 (0.5)	0.06 (0.77)	BD	–	–	–	BD	–	–	–
	NP WS	0.03 (1.15)	0.015 (0.58)	0.11 (4.36)	0.17 (6.33)	BD	–	–	–	0.01 (0.04)	0.005 (0.02)	0.12 (0.48)	0.02 (0.07)
	NP DS	BD	–	–	–	BD	–	–	–	BD	–	–	–
	PR WS	0.05 (2.74)	0.025 (1.37)	0.19 (10.4)	0.28 (15.1)	BD	–	–	–	0.02 (0.2)	0.01 (0.1)	0.24 (2.38)	0.04 (0.35)
Orechromis mossambicus	NP CF	0.06 (1.01)	0.03 (0.505)	0.23 (3.83)	0.33 (5.6)	BD	–	–	–	0.01 (1.59)	0.01 (0.79)	0.12 (18.93)	0.02 (2.78)
	NP WS	0.12 (0.32)	0.06 (0.16)	0.46 (1.21)	0.7 (1.76)	BD	–	–	–	0.05 (0.15)	0.03 (0.08)	0.6 (1.79)	0.09 (0.26)
	NP DS	0.12 (0.32)	0.06 (0.16)	0.46 (1.21)	0.7 (1.76)	BD	–	–	–	0.05 (0.15)	0.03 (0.08)	0.6 (1.79)	0.09 (0.26)
	PR WS	0.18 (0.77)	0.09 (0.385)	0.7 (2.92)	0.99 (4.24)	BD	–	–	–	0.07 (0.28)	0.04 (0.14)	0.83 (3.33)	0.12 (0.49)
	PR DS	0.38 (0.83)	0.19 (0.415)	1.44 (3.14)	2.1 (4.6)	0.01 (0.05)	0.005 (0.03)	0.026 (0.13)	0.08 (0.4)	0.24 (5.34)	0.12 (2.67)	2.86 (63.6)	0.42 (9.35)
Coptodon rendalli	NP WS	0.09 (0.73)	0.045 (0.37)	0.34 (2.77)	0.5 (4.02)	5.37 (33.12)	2.69 (16.56)	13.98 (86.3)	43 (265)	0.16 (1.06)	0.08 (0.53)	1.9 (12.6)	0.28 (1.86)
	NP DS	0.35 (1.53)	0.175 (0.765)	1.33 (5.8)	1.93 (8.42)	0.01 (0.02)	0.005 (0.01)	0.03 (0.05)	0.08 (0.16)	0.25 (1.79)	0.13 (0.89)	2.98 (21.3)	0.44 (3.13)
	PR WS	0.03 (0.03)	0.015 (0.02)	0.11 (0.11)	0.17 (0.17)	0.03 (0.31)	0.015 (0.16)	0.08 (0.81)	0.24 (2.48)	0.59 (0.98)	0.3 (0.49)	7.02 (11.67)	1.03 (1.72)

[a] For γ-HCH.
[b] Cancer slope factors (CSF) from USEPA (2013).
[c] ADI — acceptable daily intake from WHO (2010).
[d] TDI — tolerable daily intake from Australian Government Department of Health Office of Chemical Safety (AGDHOCS) (2014).
[e] Any ratio > 1 indicates a risk.
[f] Risks > 1 in 10^4 are unacceptable.

S. zambezensis: 0.08–0.31, *Cl. gariepinus*: not detected, *O. mossambicus*: 0.026, *C. rendalli*: 0.03–13.98; CHL - *H. vitattus*: 0.12–0.6, *S. zambezensis*: 0.24–7.26, *Cl. gariepinus*: 0.12–0.24, *O. mossambicus*: 0.12–2.86, *C. rendalli*: 1.9–7.02; DDT - *H. vitattus*: 25.98–146.3, *S. zambezensis*: 39.8–189.5, *Cl. gariepinus*: 4.41–21.45, *O. mossambicus*: 1.96–14.34, *C. rendalli*: 10.8–21.2). At the 95th percentile (HR) all OCP groups in all fish species during the vast majority of surveys indicated risk if consumed (HCH - *H. vitattus*: 2.27–7.61, *S. zambezensis*: 2.8–25.5, *Cl. gariepinus*: 0.5–10.4, *O. mossambicus*: 1.21–3.83, *C. rendalli*: 0.11–5.8; HCB - *H. vitattus*: 3.2, *S. zambezensis*: 0.49–2.24, *Cl. gariepinus*: not detected, *O. mossambicus*: 0.13, *C. rendalli*: 0.05–86.3; CHL - *H. vitattus*: 0.93–1.79, *S. zambezensis*: 1.19–27.6, *Cl. gariepinus*: 0.48–2.38, *O. mossambicus*: 1.79–63.6, *C. rendalli*: 11.67–21.3; DDT - *H. vitattus*: 55.9–622, *S. zambezensis*: 102.6–379, *Cl. gariepinus*: 20.7–72.6, *O. mossambicus*: 7.48–84.8, *C. rendalli*: 49.3–168.6). In terms of the cancer risk estimates HCH, HCB and CHL concentrations all indicated similar trends, with estimated cancer risks at the 50th percentile indicating an area of concern (HCH (in 10^4) - *H. vitattus*: 0.06–1.2, *S. zambezensis*: 0.33–3.19, *Cl. gariepinus*: 0.06–0.28, *O. mossambicus*: 0.33–0.99, *C. rendalli*: 0.17–1.93; HCB (in 10^4) - *H. vitattus*: 0.16, *S. zambezensis*: 0.24–0.96, *Cl. gariepinus*: not detected, *O. mossambicus*: 0.08, *C. rendalli*: 0.08–43; CHL (in 10^4) - *H. vitattus*: 0.018–0.09, *S. zambezensis*: 0.035–1.07, *Cl. gariepinus*: 0.02–0.04, *O. mossambicus*: 0.02–0.42, *C. rendalli*: 0.28–1.03), while concentrations at the 95th percentile showed unacceptable cancer risks to consumers (HCH (in 10^4) - *H. vitattus*: 3.3–11.1, *S. zambezensis*: 4.1–37, *Cl. gariepinus*: 0.77–15.1, *O. mossambicus*: 1.76–5.6, *C. rendalli*: 0.17–8.42; HCB (in 10^4) - *H. vitattus*: 9.76, *S. zambezensis*: 1.52–6.88, *Cl. gariepinus*: not detected, *O. mossambicus*: 0.4, *C. rendalli*: 0.16–265; CHL (in 10^4) - *H. vitattus*: 0.12–1.84, *S. zambezensis*: 0.18–4.03, *Cl. gariepinus*: 0.07–0.35, *O. mossambicus*: 0.26–9.35, *C. rendalli*: 1.72–3.13). For DDT estimations at the 50th and the 95th percentiles indicated unacceptable cancer risks to consumers (50th (in 10^4) - *H. vitattus*: 3.6–20.3, *S. zambezensis*: 5.53–26.3, *Cl. gariepinus*: 0.61–2.98, *O. mossambicus*: 0.27–1.99, *C. rendalli*: 1.49–2.94; 95th (in 10^4) - *H. vitattus*: 7.8–86.3, *S. zambezensis*: 14.2–44.3, *Cl. gariepinus*: 2.87–10.1, *O. mossambicus*: 1.04–11.8, *C. rendalli*: 6.83–23.39).

4. Discussion

The recent focus on OCP contamination in South Africa's aquatic ecosystems have highlighted the need for more studies and monitoring efforts (Gerber et al., 2016; Pheiffer et al., 2018). This especially applies for ecologically and socio-economically sensitive areas (Buah-Kwofie and Humphries, 2017) such as the PRF and its surrounding communities. The present study aimed to determine levels of selected OCPs in several fish species and further look at biomagnification and the potential for ecological and human health related risks through TMFs and a desktop approach to assess cancer risks. Of late there has been renewed interest in persistent pollutants in the Phongolo system, with studies finding high concentrations of OCPs in fish from the Pongolapoort Dam (Wepener et al., 2012), upstream of the study site, and Maputo Bay, where the Maputo River drains into the Indian Ocean (Thompson et al., 2018). As such, this is the first study to determine OCP concentrations in the economically and ecologically sensitive PRF which is situated between the aforementioned sites. In terms of the selected species, *O. mossambicus*, *Cl. gariepinus* and *H. vittatus* have been well studied in terms of levels of pollutants and specifically persistent ones such as OCPs (Buah-Kwofie et al., 2018; Gerber et al., 2016; Pheiffer et al., 2018). Whereas, *Co. rendalli* and *S. zambezensis* are by far less studied, with this study being only the third and second record regarding OCPs in these species, respectively (Caldas et al., 1999; Govaerts et al., 2018).

4.1. Organochlorine pesticides in the Phongolo River floodplain

Residue levels of OCPs in fish from South Africa are well discussed in several recent publications, including Gerber et al. (2016), Buah-Kwofie et al. (2018), Govaerts et al. (2018) and Pheiffer et al. (2018). When considering the available literature on the floodplain, the levels of OCPs in the different fish species sampled in the present study are lower than upstream in Lake Pongolapoort (Wepener et al., 2012) and similar to levels found in marine species in Maputo Bay (Thompson et al., 2018). The only previous study (Bouwman et al., 1990) attributed this decrease along the floodplain region to photodecomposition, adsorption to the fine clay particles and organic sediment as well as biological decomposition. The same study (Bouwman et al., 1990) also found much higher concentrations of DDT in several fish species from the PR and its associated pans in the floodplain. Potentially indicating very good management practices regarding spraying for MVC and pesticide spraying from old stockpiles, and further potential run off and contamination in the Floodplain area since the banning of the measured OCPs. Of the various conservation areas assessed throughout north-eastern South Africa, where malaria vector control is practised, OCP residues of all groups were much lower in PRF fish when compared to fish from coastal areas with close proximity to the study area, i.e. Isimangiliso Wetland Park (Buah-Kwofie et al., 2018) and the Kruger National Park (Gerber et al., 2016; Verhaert et al., 2017). Surprisingly, fish from the PRF region were far less contaminated with OCPs than fish from a non-agriculture, non-MVC region in the interior of South Africa (Pheiffer et al., 2018). Among the OCPs measured, DDT and its metabolites predominated, followed by HCHs, CHLs and lastly HCB. The different DDT congener ratios (i.e. DDT:DDE + DDD and DDE:DDT) indicated that the bioaccumulation results are evidence of historical use of DDT (Gong et al., 2007; Strandberg and Hites, 2001). The dominance of α-HCH and γ-HCH congeners indicate the use of technical grade HCH in the area (Gong et al., 2007). The greater concentrations of trans-nonachlor congener is in accordance with the findings of Bondy et al. (2000), who indicated that this is the main form in which CHLs are bioaccumulated. These accumulation patterns were seen throughout the species and sites and are of a similar pattern as observed in aforementioned studies. This might be related to the predominance of DDT as the choice pesticide prior to the ban on OCPs and the continued spraying for MVC in many areas of South Africa.

4.2. Factors affecting bioaccumulation in fish species

Although no significant trends could be observed both spatially and temporally, some tendencies were evident. Fish from the river tended to have greater concentrations of OCPs than their counterparts in the floodplain pan, while the greatest accumulation was found during the dry season survey. The differences between the habitats can be ascribed to greater organic contents and thus adsorption of OCPs in the floodplain lake (NP) as opposed to the river (PR). Heath and Plater (2010) found that floodplain pans along the Phongolo River were rich in organic matter and fine sediments. Bouwman et al. (1990) argued that this is one of the main factors which decreased OCP concentrations. Gerber et al. (2016) also found concentrations to be highest in fish at the end of the dry period when flow is lowest and rain has been absent. This likely results in contaminants becoming more concentrated as water levels are lower than in other seasons and as such the OCPs are more available within the environment. Regardless of site/habitat or season, the bioaccumulation profiles (i.e. the various congeners and metabolites accumulated) within species remained fairly similar; apart from bioaccumulation profiles, large concentration variations of different OCPs occurred between species. The two species of cichlids (*O. mossambicus and C. rendalli*) not only consistently had a greater variety of OCPs but also in higher concentrations than the remaining species during the majority of the surveys. This was an unexpected result as both species are herbivorous/detritivorous, whereas the other three

species are invertivorous (*S. zambezensis*), omnivorous (*C. gariepinus*) and predatory (*H. vittatus*) (Skelton, 2001). The stable isotope results confirmed that cichlids occupied the lowest trophic levels of the different fish species. Therefore, dietary habits did not predict the accumulation patterns found by Verhaert et al. (2013, 2017) and Govaerts et al. (2018) in other tropical and subtropical areas in Africa. None of the OCP groups nor any of the metabolites biomagnified within the PR itself, whereas ΣDDTs biomagnified in the associated floodplain lake. Although *H. vittatus* occupies the highest trophic level in both systems, it did not necessarily accumulate more OCPs than the other fish species observed. This disparity compared to literature is likely a result of the size of the tigerfish caught from the PR. Tigerfish individuals were much smaller than those collected from NP and were almost certainly still feeding on insects rather than fish as their much larger counterparts in the pan (Skelton, 2001). Other biological aspects that have been reported to influence OCP accumulation are fish size and lipid content. In this study a negative relationship was generally found with size, as reported previously for two fish species (*H. vitattus* and *Labeo congoro*) from the Olifants River (Verhaert et al., 2017). In contrast, OCP accumulation increased significantly with increased lipid content in this study, while Verhaert et al. (2017) did not find such a relationship in fish species from the Olifants River. It is expected that lipid content should influence bioaccumulation, since OCPs are known to be lipophilic. The lipid content, however, only explained conspecific differences and not between individual fish species; *S. zambezensis* had the highest lipid content while the two cichlid species had the lowest, yet specimens of *O. mossambicus* and *Co. rendalli* had much higher OCP concentrations.

4.3. Trophic magnification of organochlorine pesticides in aquatic systems of the Phongolo River floodplain

The understanding of the trophic transfer of contaminants in the PRF is essential to evaluate the ecological and human health-related consequences, as the wetlands in the NGR are classified as RAMSAR sites and people in and along the PRF consume fish from the system. When the TMF is greater than one, then biomagnification of the said pollutant occurs in the food web. The results of this study clearly illustrate that TL plays an important role in the movement of specifically DDT through the food webs of the PRF. Biomagnification and trophic transfer of persistent pollutants such as OCPs have been shown in various tropical and subtropical systems (Govaerts et al., 2018; Verhaert et al., 2013, 2017). The higher Kow found in DDT and all of its degradation products means that the biomagnification of this chemical is not only aided by its presence throughout the food chain, but through its chemical characteristics. The TMFs of DDTs determined by Verhaert et al. (2013) from the Congo River basin (Tropical climate) were slightly lower than those found in this study, whereas TMFs for DDTs from other areas with sub-tropical climates in South Africa (Ga-Selati River and Olifants River) ranged between similar values (TMF = 2.4) and with the majority being several times higher (TMF = 14) (Govaerts et al., 2018; Verhaert et al., 2017). However, HCH, HCB and CHL were not found to biomagnify in the present study, whereas in the Congo River system, Olifants River and Ga-Selati River all of the aforementioned OCPs were found to biomagnify throughout the food webs, respectively. This particular finding could be explained for HCH, not however for HCB and CHL. Organic compounds with an octanol water partition coefficient ($LogK_{ow}$) lower than five (i.e. HCHs) have a decreased potential for biomagnification, whereas those with $LogK_{ow}$ higher than five (i.e. HCB, CHLs and DDTs) have the greatest potential for biomagnification (Ikemoto et al., 2008). Verhaert et al. (2017) provided a comprehensive summary of TMFs of OCPs from around the globe, with DDTs from this study being comparable to the majority of international studies. However, other international studies have also indicated biomagnification of HCHs which was not found in the present study. Previous studies have indicated that latitude may be a determining factor (as discussed in Verhaert et al., 2017), with TMFs increasing with higher latitudes. This scenario, however, does not seem to play a major role in the PRF as this system is further south and thus higher in latitude than the other aforementioned systems studied within South Africa. Although Borgå et al. (2012) stated that the various mechanisms behind TMFs increasing with latitude are not well understood, processes include biodilution, excretion rates and food web complexity. Explanations why only DDTs biomagnified may be found in Govaerts et al. (2018), where it has been contended that $\delta^{15}N$ is only an effective predictor for DDT and not for other POPs and that other POPs do not follow clear relationships with trophic level.

4.4. Ecological risks to animals reliant on the Phongolo River floodplain

The biomagnification of specifically DDTs is of concern, especially to animals at higher trophic levels and those included in specific conservation efforts or areas. The Nile crocodile (*Crocodylus niloticus*) is one of these consumers and under constant threat, although it is listed by the IUCN as a species of least concern. In KwaZulu-Natal, it is, however, considered a protected species (Calverley and Downs, 2014a). The NGR houses the third largest crocodile population in South Africa, where individuals in the NGR are already threatened by loss of reproductive habitats, illegal harvesting and snaring (Calverley and Downs, 2014a) and now have to face an additional anthropogenic threat, which in this case are OCPs. Trophic transfer in this species is highly likely as fish form a major component of the diet of individuals under 2.2 m, while larger size classes of crocodiles still continue to feed on fish although not as the main source of protein (Calverley and Downs, 2014b). As the RAMSAR designation suggests, the NGR is an important bird habitat (Malherbe, 2018). A variety of bird species (e.g. Pelicans, *Pelecanus onocrotalus*) utilise the wetlands of the NGR either as feeding or breeding grounds or a combination of both. In total, 19 species of water birds are listed as red data (NGR IMP 2009–2013, 2009).

DDT itself has been shown to have numerous deleterious effects on bird populations in South Africa (Bouwman et al., 2013), including Ndumo and surrounding areas (Bouwman et al., 2019) and elsewhere in the world (Fry, 1995). It could also be linked to egg shell thinning and resulting population declines of bird species. According to Gonzalez-Jauregui et al. (2012), endocrine disruption and thus impacts on various reproductive variables from DDT on crocodiles has been cited several times. Even though OCP concentrations in this study and within the PRF are quite low compared to other areas of the world, risks to long-lived animals such as *P. onocrotalus* (51 years) and *Cr. niloticus* (80 years) may be very real. The low concentrations of OCPs within the fish were shown to have unacceptable long-term risks to humans (see below) using very conservative estimates of only 30 g portions/person/day. These aforementioned animals consume up to 100 times the amount of fish per day; *P. onocrotalus* 1.1–1.4 kg fish/day (Whitfield and Blaber, 1978) and *C. niloticus* 0.14% of body weight/day (Hutton, 1987) with adult crocodiles weighing anywhere upwards of 220 kg. This implies that the risk to these animals is >100 times larger than for humans over their lifetimes. It is important to also remember that DDT is classified as A3 Confirmed animal carcinogen (ACGIH, 2010).

4.5. Human health risks to the communities reliant on the Phongolo River floodplain

Using the 50th and 95th percentile values of the OCPs for the desktop assessment of health risks to the communities surrounding the PRF, it was found that neither the acceptable (ADI) of the World Health organisation (WHO, 2010) nor the tolerable (TDI) (AGDHOCS, 2014) daily intakes were exceeded. Nonetheless, the HRs as well as the cancer risk estimates indicated potential long-term risks that are associated with consumption of fish tissue from the selected species. The OCPs of concern were generally in the order of DDT > HCH > CHL > HCB. While contamination of fish tissue with HCHs, CHLs and HCB only pointed

toward an area of concern at the 95th percentile and for all DDTs it indicated an unacceptable cancer risk. This is not the first study in South Africa revealing such pronounced risks to human health from fish consumption; several other studies have found much greater risks to consumers (Gerber et al., 2016; Pheiffer et al., 2018). The evaluation further indicated that the DDTs are of particular concern and follows recommendations by Gerber et al. (2016) and Pheiffer et al. (2018) to implement appropriate management strategies. Although the desktop approach utilised during this study serves as an adequate initial screening for potential risks, the approach is limited by looking at individual chemicals, whereas chemicals occur as mixtures and potentially pose an even greater risk to consumers. The analysed OCPs not only pose cancer risks to consumers but also numerous, cancer unrelated risk factors. These risks are well discussed by Barnhoorn et al. (2015) and Gerber et al. (2016) and include consequences such as central nervous system effects, liver damage and alterations, various reproductive changes as well as immune suppression; the latter being of paramount importance, especially in a community already stricken with the highest HIV infection rates in South Africa (De Wet et al., 2013).

As mentioned previously DDT is used within the area as MVC and is applied as indoor residual spraying in ≥80% of houses in the area and although oral ingestion of food is the primary exposure route, the ingestion of contaminated drinking water along with inhalation of contaminated air and dermal contact with contaminated surfaces is believed to contribute to exposure (USEPA, 2018). These last two mentioned exposure routes are highly likely as the spraying of DDT occurs inside the houses. Fish are however not the only OCP contaminated protein ingested by the rural communities on northern KwaZulu-Natal. Thompson et al. (2017) found unacceptable human health and cancer risks associated with the consumption of free range chickens and their eggs contaminated with DDTs. These authors concluded that the consumption of these free range chicken products from the area on their own posed particularly high risks to humans. With this study we have shown that consumption of contaminated fish muscle further exacerbates this problem and could potentially indicate that people from the region are at more risk than is indicated in this study or the study by Thompson et al. (2017). These results and from other studies are of real concern as DDT is now classed as a Group B2 probable human carcinogen (USEPA, 2018).

5. Conclusion

This is the first study to report OCP contaminant concentrations in the aquatic systems of the NGR and only the second from the PRF. It was demonstrated that all five of the ecologically and economically important fish species accumulated OCPs and that in the floodplain lake (NP) trophic transfer of DDT was evident. Accumulation was seasonal with the highest concentrations found at the end of the dry season, most likely as a result of highly-concentrated OCPs due to lower water levels. Although concentrations were far below other assessments done in South Africa and elsewhere in the world, these contaminants still pose ecologically-relevant risks to important consumers such as Nile crocodiles and various species of water birds. Most importantly, it was shown that these contaminants pose significant health risks to communities in and around the PRF. However, a limitation of this study is that health risks could not be evaluated for different age classes. Even more concerning are the anecdotal reports that *S. zambezensis* is used to feed babies and toddlers and therefore may pose even a larger risk than previously assumed. The fact that specifically DDTs already reached levels of concern is worrisome, since DDT is used in MVC in the area and spraying will continue for the foreseeable future. This may potentially lead to an even greater contamination of the area and accumulation within the biota, thus complicating the situation even further. We therefore recommend continuous monitoring of the aquatic ecosystems associated with the PRF and implementation and striving toward even better management and public education.

CRediT authorship contribution statement

C.M. Volschenk: Writing - original draft, Visualization, Investigation. **R. Gerber:** Writing - original draft, Visualization, Conceptualization, Writing - review & editing. **M.T. Mkhonto:** Visualization, Investigation. **Y. Ikenaka:** Funding acquisition, Conceptualization, Writing - review & editing. **Y.B. Yohannes:** Investigation, Writing - review & editing. **S. Nakayama:** Funding acquisition, Writing - review & editing. **M. Ishizuka:** Funding acquisition, Writing - review & editing. **J.H.J. van Vuren:** Supervision, Conceptualization, Writing - review & editing. **V. Wepener:** Project administration, Conceptualization, Writing - review & editing. **N.J. Smit:** Supervision, Funding acquisition, Project administration, Conceptualization, Writing - review & editing.

Acknowledgements

The authors would like to thank the Water Research Commission (WRC) of South Africa (Project K5-12185, N.J. Smit, PI) for the financial support of this study. This work is also based on the research and researchers supported in part by the National Research Foundation (NRF) of South Africa (Grant Numbers: 105979 and 85505). Opinions, findings, conclusions and recommendations expressed in this publication is that of the authors, and the NRF accepts no liability whatsoever in this regard. This study was supported in part by Grants-in-Aid for Scientific Research from the Ministry of education, Culture, Sports, Science and Technology of Japan, awarded to M. Ishizuka (No. 16H01779, 18KK028708), Y Ikenaka (No. 17K2003807, 18H04132), S Nakayama (No. 16K16197, 17KK0009). We also acknowledge Ezemvelo KZN wildlife for providing permits and provisions that allowed the completion of field sample collections within Ndumo Game Reserve and particularly to previous Conservation Manager Amos Tembe and District Ecologist uMkhanyakude Cathariné Hanekom. Also to Dr. Wynand Malherbe, North-West University, for generating the study site map. This is contribution number 350 from the NWU-Water Research Group.

Appendix A. Supplementary data

Supplementary data to this article can be found online at https://doi.org/10.1016/j.scitotenv.2019.06.144.

References

American Conference of Governmental Industrial Hygienists TLVs and BEIs, 2010. Threshold Limit Values for Chemical Substances and Physical Agents and Biological Exposure Indices. Cincinnati, OH. p. 23.

Australian Government Department of Health Office of Chemical safety (AGDHOCS), 2014. ADI List: Acceptable Daily intakes for agricultural and veterinary chemicals. Available from. http://www.health.gov.au/internet/main/publishing.nsf/content/ocs-adi-list.htm, Accessed date: December 2015.

Barnhoorn, I.E.J., van Dyk, J.C., Genthe, B., Harding, W.R., Wagenaar, G.M., Bornman, M.S., 2015. Organochlorine pesticide levels in Clarias gariepinus from polluted freshwater impoundments in South Africa and associated human health risks. Chemosphere 120, 391–397. https://doi.org/10.1016/j.chemosphere.2014.08.030.

Bondy, G.S., Newsome, W.H., Armstrong, C.L., Suzuki, C.A.M., Doucet, J., Fernie, S., Hierlihy, S.L., Feeley, M.M., Barker, M.G., 2000. Trans-nonachlor and cis-nonachlor toxicity in Sprague-Dawley rats: comparison with technical chlordane. Toxicol. Sci. 58, 386–398. https://doi.org/10.1093/toxsci/58.2.386.

Borgå, K., Kidd, K.A., Muir, D.C., Berglund, O., Conder, J.M., Gobas, F.A., Kucklick, J., Malm, O., Powell, D.E., 2012. Trophic magnification factors: considerations of ecology, ecosystems, and study design. Integr. Environ. Assess. Manag. 8, 64–84. https://doi.org/10.1002/ieam.244.

Bouwman, H., Coetzee, A., Schutte, C., 1990. Environmental and health implications of DDT-contaminated fish from the Pongolo flood plain. J. African Zool. 104, 275–286.

Bouwman, H., Viljoen, I.M., Quinn, L.P., Polder, A., 2013. Halogenated pollutants in terrestrial and aquatic bird eggs: converging patterns of pollutant profiles, and impacts and risks from high levels. Environ. Res. 126, 240–253. https://doi.org/10.1016/j.envres.2013.06.003.

Bouwman, H., Yohannes, Y.B., Nakayama, S.M.M., Motohira, K., Ishizuka, M., Humphries, M.S., van der Schyff, V., du Preez, M., Dinkelman, A., Ikenaka, Y., 2019. Evidence of Impacts From DDT in Pelican, Cormorant, Stork and Egret Eggs from KwaZulu-Natal, South Africa. (in press). https://doi.org/10.1016/j.chemosphere.2019.03.043.

Buah-Kwofie, A., Humphries, M.S., 2017. The distribution of organochlorine pesticides in sediments from iSimangaliso Wetland Park: ecological risks and implications for

conservation in a biodiversity hotspot. Environ. Pollut. 229, 715–723. https://doi.org/10.1016/j.envpol.2017.07.031.
Buah-Kwofie, A., Humphries, M.S., Pillay, L., 2018. Bioaccumulation and risk assessment of organochlorine pesticides in fish from a global biodiversity hotspot: iSimangaliso Wetland Park, South Africa. Sci. Total Environ. 621, 273–281. https://doi.org/10.1016/j.scitotenv.2017.11.212.
Caldas, E.D., Coelho, R., Souza, L.C.K.R., Silva, S.C., 1999. Organochlorine pesticides in water, sediment, and fish Paranoa Lake of Brasilia, Brazil. Bull. Environ. Contam. Toxicol. 62, 199–206. https://doi.org/10.1007/s001289900860.
Calverley, P.M., Downs, C.T., 2014a. Population status of Nile crocodiles in Ndumo Game Reserve, Kwazulu-Natal, South Africa (1971–2012). Herpetologica 70, 417–425. https://doi.org/10.1655/HERPETOLOGICA-D-13-00090.
Calverley, P.M., Downs, C.T., 2014b. Habitat use by Nile crocodiles in Ndumo Game Reserve, South Africa: a naturally patchy environment. Herpetologica 70, 426–438. https://doi.org/10.1655/HERPETOLOGICA-D-13-00088.
Coetzee, H., Nell, W., Van Eeden, E., De Crom, E., 2015. Artisanal fisheries in the Ndumo area of the lower Phongolo River Floodplain, South Africa. Koedoe 57, 2009–2014. https://doi.org/10.4102/koedoe.v57i1.1248.
De Wet, H., Nciki, S., van Vuuren, S.F., 2013. Medicinal plants used for the treatment of various skin disorders by a rural community in northern Maputaland, South Africa. J. Ethnobiol. Ethnomed. 9, 51. https://doi.org/10.1186/1746-4269-9-51.
Deribe, E., Rosseland, B., Borgstrøm, R., Salbu, B., Gebremariam, Z., Dadebo, E., Norli, H., Eklo, O., 2011. Bioaccumulation of persistent organic pollutants (POPs) in fish species from Lake Koka, Ethiopia: the influence of lipid content and trophic position. Sci. Total Environ. 410–411, 136–145. https://doi.org/10.1016/j.scitotenv.2011.09.008.
Dougherty, C.P., Holtz, S.H., Reinert, J.C., Panyacosit, L., Axelrad, D.A., Woodruff, T.J., 2000. Dietary exposures to food contaminants across the United States. Environ. Res. 84, 170–185. https://doi.org/10.1006/enrs.2000.4027.
Dube, T., DeNecker, L., van Vuren, J.H.J., Wepener, V., Smit, N.J., Brendonck, L., 2017. Spatial and temporal variation of invertebrate community structure in flood-controlled tropical floodplain wetlands. J. Freshw. Ecol. 32, 1–15. https://doi.org/10.1080/02705060.2016.1230562.
Fry, D.M., 1995. Reproductive effects in birds exposed to pesticides and industrial chemicals. Environ. Health Perspect. 103, 165–171. https://doi.org/10.1289/ehp.95103s7165.
Gerber, R., Smit, N.J., van Vuren, J.H.J., Nakayama, S.M.M., Yohannes, Y.B., Ikenaka, Y., Ishizuka, M., Wepener, V., 2015. Application of a Sediment Quality Index for the assessment and monitoring of metals and organochlorines in a premier conservation area. Environ. Sci. Pollut. Res. 22, 19971–19989. https://doi.org/10.1007/s11356-015-5206-z.
Gerber, R., Smit, N.J., Van Vuren, J.H.J., Nakayama, S.M.M., Yohannes, Y.B., Ikenaka, Y., Ishizuka, M., Wepener, V., 2016. Bioaccumulation and human health risk assessment of DDT and other organochlorine pesticides in an apex aquatic predator from a premier conservation area. Sci. Total Environ. 550, 522–533. https://doi.org/10.1016/j.scitotenv.2016.01.129.
Gong, X., Qi, S., Wang, Y., Julia, E.B., Lv, C., 2007. Historical contamination and sources of organochlorine pesticides in sediment cores from Quanzhou Bay, Southeast China. Mar. Pollut. Bull. 54, 1434–1440. https://doi.org/10.1016/j.marpolbul.2007.05.006.
Gonzalez-Jauregui, M., Valdespino, C., Salame-Mendez, A., Aguirre-Leon, G., Rendon-vonOsten, J., 2012. Persistent organic contaminants and steroid hormones levels in Morelet's crocodiles from the southern Gulf of Mexico. Arch. Environ. Contam. Toxicol. 62, 445–454.
Govaerts, A., Verhaert, V., Covaci, A., Jaspers, V.L.B., Berg, O.K., Addo-Bediako, A., Jooste, A., Bervoets, L., 2018. Distribution and bioaccumulation of POPs and mercury in the Ga-Selati River (South Africa) and the rivers Gudbrandsdalslågen and Rena (Norway). Environ. Int. 121, 1319–1330. https://doi.org/10.1016/j.envint.2018.10.058.
Heath, S.K., Plater, A.J., 2010. Records of pan (floodplain wetland) sedimentation as an approach for post-hoc investigation of the hydrological impacts of dam impoundment: the Pongolo river, KwaZulu-Natal. Water Res. 44, 4226–4240. https://doi.org/10.1016/j.watres.2010.05.026.
Hutton, J.M., 1987. Growth and feeding ecology of the Nile crocodile Crocodylus niloticus at Ngezi, Zimbabwe. J. Anim. Ecol. 56, 25–38.
Ikemoto, T., Phuc Cam Tu, N., Watanabe, M.X., Okuda, N., Omori, K., Tanabe, S., et al., 2008. Analysis of biomagnification of persistent organic pollutants in the aquatic food web of the Mekong Delta, South Vietnam using stable carbon and nitrogen isotopes. Chemosphere 72, 104–114.
Jiang, Q.T., Lee, T.K.M., Chen, K., Wong, H.L., Zheng, J.S., Giesy, J.P., Lo, K.K.W., Yamashita, N., Lam, P.K.S., 2005. Human health risk assessment of organochlorines associated with fish consumption in a coastal city in China. Environ. Pollut. 136, 155–165. https://doi.org/10.1016/j.envpol.2004.09.028.
Kyle, R., 2002. Interesting new record and further notes on the occurrence of marine fish in Nyamithi Pan, Ndumo Game Reserve, South Africa. Koedoe 45, 123–125. https://doi.org/10.4102/koedoe.v45i2.29.
Malherbe, W., 2018. Ramsar wetlands in South Africa: historic and current research. S. Afr. J. Sci. & Tech. 37 (1), 2018.
McHugh, K.J., Smit, N.J., Van Vuren, J.H.J., Van Dyk, J.C., Bervoets, L., Covaci, A., Wepener, V., 2011. A histology-based fish health assessment of the tigerfish, Hydrocynus vittatus from a DDT-affected area. Phys. Chem. Earth, Parts A/B/C 36, 895–904. https://doi.org/10.1016/J.PCE.2011.07.077.
Ndumo Game Reserve: Integrated Management Plan (NGR IMP): 2009-2013, 2009. Version 1. Ezemvelo KZN Wildlife, Pietermaritzburg, South Africa.
Pheiffer, W., Wolmarans, N.J., Gerber, R., Yohannes, Y.B., Ikenaka, Y., Ishizuka, M., Smit, N.J., Wepener, V., Pieters, R., 2018. Fish consumption from urban impoundments: what are the health risks associated with DDTs and other organochlorine pesticides in fish to township residents of a major inland city. Sci. Total Environ. 628–629, 517–527. https://doi.org/10.1016/j.scitotenv.2018.02.075.
Skelton, P., 2001. A Complete Guide to Freshwater Fishes of Southern Africa. Stuik.
Strandberg, B., Hites, R.A., 2001. Concentration of organochlorine pesticides in wine corks. Chemosphere 44, 729–735. https://doi.org/10.1016/S0045-6535(00)00262-9.
Thompson, L.A., Ikenaka, Y., Yohannes, Y.B., van Vuren, J.J., Wepener, W., Smit, N.J., Darwish, W.S., Nakayama, S.M.M., Mizukawa, H., Ishizuka, M., 2017. Food Additives and Contaminants: Part A 34, 1959–1969.
Thompson, L.A., Ikenaka, Y., Yohannes, Y.B., Ichise, T., Ito, G., Bortey-Sam, N., van Vuren, J.J., Wepener, V., Smit, N.J., Darwish, W.S., Nakayama, S.M.M., Mizukawa, H., Ishizuka, M., 2018. Human health risk from consumption of marine fish contaminated with DDT and its metabolites in Maputo Bay, Mozambique. Bull. Environ. Contam. Toxicol. 100, 672–676. https://doi.org/10.1007/s00128-018-2323-7.
United States Environmental Protection Agency (USEPA), 2005. Guidelines for Carcinogen Risk Assessment. http://www.epa.gov/cancerguidelines/2005, Accessed date: December 2015.
United States Environmental Protection Agency (USEPA), 2012. Human health risk assessment: Risk based screening table. http://www.epa.gov/reg3hwmd/risk/human/pdf/NOV_2012_FISH.pdf, Accessed date: December 2015.
United States Environmental Protection Agency (USEPA), 2013. Food Safety. http://www.epa.gov/oecaagct/tfsy.html, Accessed date: December 2015.
United States Environmental Protection Agency (USEPA), 2016. Development of National Bioaccumulation Factors: Supplemental Information for EPA's 2015 Human Health Criteria Update Office of Science and Technology. Washington DC.
United States Environmental Protection Agency (USEPA), 2018. Chemicals Evaluated for Carcinogenic Potential: Potential Annual Cancer Report.
Van Dyk, J., Bouwman, H., Barnhoorn, I., Bornman, M., 2010. DDT contamination from indoor residual spraying for malaria control. Sci. Total Environ. 408, 2745–2752. https://doi.org/10.1016/j.scitotenv.2010.03.002.
Verhaert, V., Covaci, A., Bouillon, S., Abrantes, K., Musibono, D., Bervoets, L., Verheyen, E., Blust, R., 2013. Baseline levels and trophic transfer of persistent organic pollutants in sediments and biota from the Congo River Basin (DR Congo). Environ. Int. 59, 290–302. https://doi.org/10.1016/j.envint.2013.05.015.
Verhaert, V., Newmark, N., D'Hollander, W., Covaci, A., Vlok, W., Wepener, V., Addo-Bediako, A., Jooste, A., Teuchies, J., Blust, R., Bervoets, L., 2017. Persistent organic pollutants in the Olifants River Basin, South Africa: bioaccumulation and trophic transfer through a subtropical aquatic food web. Sci. Total Environ. 586, 792–806. https://doi.org/10.1016/j.scitotenv.2017.02.057.
Wagenaar, G., Barnhoorn, I., 2018. Health and chemical burdens of fish species from polluted and hyper-eutrophic freshwater ecosystems in South Africa. African J. Aquat. Sci. 43, 271–280. https://doi.org/10.2989/16085914.2018.1490245.
Wepener, V., van Dyk, C., Bervoets, L., O'Brien, G., Covaci, A., Cloete, Y., 2011. An assessment of the influence of multiple stressors on the Vaal River, South Africa. Phys. Chem. Earth, Parts A/B/C 36, 949–962. https://doi.org/10.1016/j.pce.2011.07.075.
Wepener, V., Smit, N., Covaci, A., Dyke, S., Bervoets, L., 2012. Seasonal bioaccumulation of organohalogens in tigerfish, Hydrocynus vittatus Castelnau, from Lake Pongolapoort, South Africa. Bull. Environ. Contam. Toxicol. 88, 277–282. https://doi.org/10.1007/s00128-011-0439-0.
Whitfield, A.K., Blaber, S.J., 1978. Feeding ecology of piscivorous birds at Lake St Lucia, part 1: diving birds. Ostrich 49, 185–198.
WHO, 2002. Inventory of IPCS and Other WHO Pesticide Evaluations and Summary of Toxicological Evaluations Performed by the Joint Meeting on Pesticide Residues (JMPR).
World Health Organisation (WHO), 2010. Inventory of ICPS and Other WHO Pesticide Evaluations and Summary of Toxicological Evaluations Performed by the Joint Meeting on Pesticide Residues (JMPRs) through 2010.
Yohannes, Y., Ikenaka, Y., Nakayama, S., Saengtienchai, A., Watanabe, K., Ishizuka, M., 2013. Organochlorine pesticides and heavy metals in fish from Lake Awassa, Ethiopia: insights from stable isotope analysis. Chemosphere 91, 857–863. https://doi.org/10.1016/j.chemosphere.2013.01.047.
Yohannes, Y., Ikenaka, Y., Saengtienchai, A., Watanabe, K., Nakayama, S., Ishizuka, M., 2014. Concentrations and human health risk assessment of organochlorine pesticides in edible fish species from a Rift Valley lake—Lake Ziway, Ethiopia. Ecotoxicol. Environ. Saf. 106, 95–101. https://doi.org/10.1016/j.ecoenv.2014.04.014.

Aquatic Toxicology 215 (2019) 105287

Contents lists available at ScienceDirect

Aquatic Toxicology

journal homepage: www.elsevier.com/locate/aqtox

How toxic is a non-toxic nanomaterial: Behaviour as an indicator of effect in *Danio rerio* exposed to nanogold

Tarryn L. Botha[a,*], Sarel J. Brand[a,b], Yoshinori Ikenaka[a,c], Shouta M.M. Nakayama[c], Mayumi Ishizuka[c], Victor Wepener[a]

[a] Unit for Environmental Sciences and Management, North-West University, Private Bag X6001, Potchefstroom, 2520, South Africa
[b] South African Research Chair for Nanotechnology for Water, Department of Applied Chemistry, University of Johannesburg, South Africa
[c] Laboratory of Toxicology, Department of Environmental Veterinary Sciences, Graduate School of Veterinary Medicine, Hokkaido University, N18, W9, Kita-ku, Sapporo 060-0818, Japan

ARTICLE INFO

Keywords:
Nanogold
Zebrafish
Adverse outcomes pathway
Swimming behaviour

ABSTRACT

Gold nanoparticles are used as drug delivery vectors based on the assumption that they have low toxicity. Literature has, however, produced conflicting results over the last few years. As such, this study aimed to investigate the toxicological effects of nanogold (nAu) on several indicators that range from subcellular to whole-organism level. Gene regulation, changes in oxidative stress biomarkers and swimming performance were assessed in *Danio rerio* (zebrafish) following exposures to nAu. Adult zebrafish were exposed *in vivo* to nAu for 96 h and swimming performance measured post-exposure. Liver tissue was collected for DNA microarray and Real-Time Polymerase Chain Reactions (RT-PCR) analyses to determine changes in gene expression (catalase, superoxide dismutase and metallothioneins) and protein biomarker analyses (catalase, superoxide dismutase, acetylcholine esterase, malondialdehyde, cellular energy allocation and metallothionein) were performed on whole-body samples. Swimming behaviour was assessed in 1.1 L Tecniplast™ tanks for a period of six hours and videos were analysed using Noldus EthoVision software. Critical swimming speed was measured in a Loligo® swimming tunnel. The DNA microarray revealed that fish exposed to 20 mg/L differed most from the control group. At 20 mg/L there was a significant increase in gene expression for all genes analysed but this didn't translate to significant responses in protein biomarker levels except for an increase in protein carbonyl formation. The behaviour results demonstrated significant changes in distance moved, swimming speed, acceleration bouts, zone alterations and time spent within the top zone – responses that are usually observed in fish responding to toxicological stress. Furthermore, the critical swimming speed of exposed fish was decreased significantly compared to the control. Since swimming performance and social interaction among zebrafish is essential to their survival, whole-organism behaviour that suggests a toxicological response after exposure to nAu is in agreement with the genetic responses measured in this study.

1. Introduction

During recent decades, advances in technology and the use and production of nanomaterials (NMs) have expanded significantly (Colvin, 2003; Giese et al., 2018; Lead et al., 2018; Suh et al., 2009;). Due to the diverse structural and chemical characteristics of these materials (Colvin, 2003; Nel et al., 2006; Oberdrster et al., 2005), they are broadly applied in the fields of medicine (Zhang et al., 2016), agriculture (Khot et al., 2012) and industry (Kasukabe et al., 2016; Mura et al., 2015; Souza and Fernando, 2016). Gold nanoparticles (nAu), in particular, have been applied in a range of biomedical applications, including imaging, diagnostics and as a delivery system for transporting pharmaceutical agents into cells (Boisselier and Astruc, 2009) and more recently of the potential applications for slow release of accumulated gold nanoclusters in muscle tissue (Zhang et al., 2014). However, despite NMs displaying great potential in a range of sectors and applications, the production, use, and disposal of the products they are contained in, eventually lead to nanoparticles being present and persisting in the environment (Wiesner et al., 2006), especially in water sources like lakes and rivers (Moore, 2006) where their unique physiochemical properties may adversely affect living organisms (Lam et al., 2004; Nel et al., 2006) and the environment (Colvin, 2003; Moore, 2006; Oberdrster et al., 2005). Furthermore, nanoparticles may enter living organisms by various routes, e.g. via external epithelia,

* Corresponding author.
E-mail address: 26964546@nwu.ac.za (T.L. Botha).

https://doi.org/10.1016/j.aquatox.2019.105287
Received 3 July 2019; Received in revised form 27 August 2019; Accepted 27 August 2019
Available online 29 August 2019
0166-445X/

through direct ingestion or by direct movement across the gills in fish (Moore, 2006; Utembe et al., 2018), subsequently being internalized by internal tissues, organs and cells by means of endocytosis (Panyam and Labhasetwar, 2003; Vetten et al., 2013). Furthermore, their innate ability to interact on the cellular level, allows NMs to accumulate within cells and potentially induce toxic effects (Vetten et al., 2013; Carnovale et al., 2016), including inflammation, aberrant cellular oxidative status and cell death (Buzea et al., 2007; Choi et al., 2016). Despite this, nAu has been widely reported as non-toxic with studies reporting nAu uptake but low toxicological effects (Bar-llan et al., 2009; Fratoddi et al., 2015). Considering the presence of these particles in the environment and their ability to persist there, the caveat arises to investigate the extent to which they may affect the health of species residing in these ecosystems (Avellan et al., 2018). The survival of fish, for example, is predicated on their ability to swim. Any pollutant and/or toxicant affecting their swimming performance would, therefore, have the potential to affect the behaviour and survival of such a species due to interfering with their ability to manoeuvre their environment, feed and breed. Importantly, it has been predicted that organisms would resist swimming as a response to limit toxicant uptake (Mitzel et al., 2017).

The use of fish as an experimental model allows for assessing the toxicity of possible pollutants on aquatic organisms. In this regard, *Danio rerio* (zebrafish) has been thoroughly validated as a model in a variety of fields, including toxicology (Kalueff et al., 2016), and holds great potential as a model of behavioural ecotoxicology (Ahmad et al., 2012). Due to their sensitivity to a wide range of pollutants, zebrafish have been described as an ideal model to measure aquatic health and distinctive aberrancies in their morphology, physiology and behaviour can be utilized as biological indicators (Dai et al., 2014). The aim of this study was to determine the gene expression and biomarker response of selected genes and to link these to a whole-organism response by assessing swimming behaviour and sustained swimming speed (measured as critical swimming speed).

2. Materials and methods

2.1. Characterization

MINTEK, a minerals processing and metallurgical engineering company in South Africa, supplied the citrate-capped stock concentrations of 1 g/L gold nanoparticles (14 ± 2 nm nAu with product code TMU14 G). Exposure concentrations were made up in ISO standard fish media (OECD-203). The physicochemical parameters were measured in 24 h intervals for the duration of the test. The pH, electrical conductivity (EC), total dissolved solids (TDS), oxygen saturation (% O_2) and dissolved oxygen (DO) concentration (mg/L) were measured using a handheld Eutech pH 110 RS232C meter, Eutech CON 110 RS232C conductivity and TDS meter, and Eutech DO6 DO meter. The hydrodynamic size and zeta potential were measured using a Malvern Zetasizer Nano series, NanoZS at 0 h and 96 h. Particle shape and size were further confirmed using transmission electron microscopy (FEI Tecnai G2) where nAu in ISO medium was dropped onto a carbon-coated copper grid and allowed to settle for five minutes before excess water was removed using a filter paper by touching only the edge of the droplet. The grid was allowed to dry prior to examination at high resolution (200 kV).

2.2. Danio rerio 96 h exposures

All procedures performed in studies involving animals were approved by the AnimCare animal research ethics committee (NHREC reg. number AREC-130913-015) of the North-West University. All animals were maintained and procedures performed in accordance with the code of ethics in research, training and testing of drugs in South Africa and complied with national legislation (ethics approval number: NWU-00269-16-A5).

For this study, the exposures were conducted following the OECD-TG203 protocol using long-fin wild-type adult fish (3.65 ± 0.3 cm in total length). A concentration range of 5 mg/L to 45 mg/L was selected based on preliminary microarray findings at 20, 25 and 30 mg/L (not presented) as well as findings in Botha et al. (2015). Three replicates, consisting of five adults each, were carried out in Tecniplast 1.1 L tanks with a continuous supply of oxygen to maintain saturation above 60% for the duration of the test. The following parameters were recorded at 24 h intervals: the temperature (26.4–27.9 °C), pH (7.13–8.42), electrical conductivity (642–765 µS/cm) and oxygen saturation (65.1–98.7 %).

Subsequent to exposure, fish were stunned by applying a blow to the head and sacrificed by severing the spinal cord behind the head (according to the South African National Animal ethics guidelines). Five pooled liver samples were collected for microarray analysis and Real-time Polymerase Chain Reactions (RT-PCR). The remaining whole-body samples were frozen at −80 °C in buffers suitable for biochemical biomarker analyses.

2.3. RNA isolation and microarray analysis from Danio rerio liver samples

Liver samples were stored in RNA Later (Ambion, South Africa) at −80 °C pending analysis. An RNA isolation protocol was used where samples were homogenized in TRI Reagent® using a hand-held homogenizer; chloroform was added and samples were vortexed and then centrifuged at 12,000 *g* for twenty minutes at 4 °C to separate RNA from the sample. The top layer containing the RNA was placed on a blue ring Nucleospin RNA II kit (Macherey- Nagel, Osaka Japan) filter membrane and standard protocol provided with the kit was used to remove further DNA, salts and proteins present. The RNA was eluted from the membrane using RNase free ultrapure MilliQ water.

The RNA quality was checked using a NanoDrop 1000A Spectrophotometer (Delaware, USA) to determine the amount of aRNA to be added while examining the 260:280 absorbance ratio and gel electrophoresis. For additional confirmation, a Bioanalyzer and RNA Nano Chips (Agilent Technologies, Tokyo Japan) were employed. The isolated RNA was prepared for microarray analysis (Affymetrix GeneChip® Zebrafish Genome Array, Tokyo Japan) using standard Affymetrix protocols.

2.4. Real-time polymerase chain reaction using cDNA

Genes relating to oxidative stress were selected for quantification using RT-PCR. Primers were designed using the NCBI (National Centre for Biotechnology Information) website, Primer3 and Primer-Blast and primer sequences were confirmed using available literature (Miller et al., 2012; Lerebours et al., 2009). Forward and reverse primers (Sigma Aldrich, Tokyo Japan) were diluted from 100 µM stock solution to 10 µM using MilliQ water.

Amplification efficiency of between 80–105% was achieved, while the R^2 value was > 0.98. Gene expression was determined using a Fast SYBR Master mix (Yokohama, Japan) where Bactin was used as an endogenous control. Bactin, catalase (CAT), superoxide dismutase (SOD1) and metallothionein (MT1 and MT2) were set to an annealing temperature of 60°. The quantitation comparative Ct (ΔΔCt) advanced setup was used and gene expression was compared between concentrations using ΔCt values (Degger et al., 2015).

2.5. Biochemical biomarker analyses in Danio rerio tissue samples

Various biomarkers of exposure were analyzed to provide a better understanding of the effects of nAu and included acetylcholine esterase (AChE; an enzyme that catalyses the breakdown of the neurotransmitter, acetylcholine) and metallothionein (MT; a specific indicator of metal exposure). Biomarkers of effect explored possible

oxidative stress mechanisms by determining levels of enzymatic biomarkers, i.e. catalase (CAT) and superoxide-dismutase (SOD) and non-enzymatic biomarkers, i.e. lipid peroxidation (malondialdehyde; MDA) and protein carbonyls (PC) as measures of oxidative stress and oxidative damage, respectively. Cellular energy allocation (CEA) was also determined quantify the effect of nAu-exposure on whole-body energy reserves (Verslycke et al., 2003). The head, skin and fins were removed from ten fish and the remaining tissue (organs, skeleton and muscle with fascial sheaths) were used for analysis. All samples were homogenized on ice in their respective buffers; general phosphate homogenizing buffer (CAT, SOD, PC), tris sucrose buffer (AChE, MDA), homogenizing buffer (MT) and cold MilliQ water (CEA) and then centrifuged. Protein content in each sample was determined to express biomarker concentrations as activity per mg protein for comparative analysis. The protein content was determined for each of the different biomarkers separately using the method introduced by Bradford (1976). Detailed biomarker processing methods can be found in Gerber et al. (2018) as well as the Supplementary file. The activity of CAT (μmol H_2O_2/mg protein/minute) was determined by means of a protocol adapted from Cohen et al. (1970) while the protocol for determining SOD activity (ng SOD/mg protein) was adapted from Greenwald (1989). The AChE activity (Abs/min/mg protein) was calculated by using a standard curve as adapted from Ellman et al. (1961) and MDA (as a measure of lipid peroxidation; concentration of thiobarbituric acid reactive substances (TBARS) in nmol/mg protein) was measured according to an adapted protocol (Ohkawa et al., 1979) as modified by Üner et al. (2006). Metallothioneins (nM/mg protein; using a standard curve) was determined by using a protocol by Atli and Canli (2008) and Fernandes et al. (2008) while GSH activity was determined using a protocol by Cohn and Lyle (1966). The PC concentration (nmol carbonyls/mg protein) was determined using an adapted protocol from Parvez and Raisuddin (2005) as assayed by Levine et al. (1990) and modified by Floor and Wetzel (1998).

2.6. Swimming behaviour and performance

The above-mentioned exposure conditions were applied to control fish and fish exposed to 20 mg/L nAu. This exposure concentration was selected based on the microarray clustering results. After a 96 h exposure period, eight fish per group were randomly selected for swimming behaviour analysis and the remaining eight fish per group were used to determine the sustained swimming speed. Fish were fed TetraPRO Colour flakes (TetraGmbH, Germany) and allowed to acclimate overnight in oxygenated tanks at 27 ± 1 °C before performing the following procedures.

2.6.1. Swimming behaviour

Adult long-fin wild-type zebrafish (3.97 ± 0.27 cm in total length) were individually placed in 1.1 L Tecniplast tanks containing either fresh ISO medium (control) or exposure medium (20 mg/L nAu). In this manner, eight control and eight exposed fish were recorded using a GigE digital camera (Noldus® Information Technology, Wageningen, The Netherlands) for a period of six hours. The video files were subsequently analysed using EthoVision® XT software (Noldus® Information Technology, Wageningen, The Netherlands). Video recordings were interpreted by physically viewing them and interpolating any missing data points by placing the marker on the animal at the coordinates it appeared in the arena as well as reassigning any incorrect data points where the software had lost track of the organism. Tanks were digitally sectioned using the EthoVision® XT software into top and bottom zones; the top zone comprised the top third of the tank and the bottom zone the remaining two-thirds to the bottom of the tank. The endpoints analysed were distance travelled, swimming speed, high acceleration bouts, time spent immobile, number of zone alterations and time spent in the top zone. Data were exported to GraphPad Prism® 5 for statistical analysis.

2.6.2. Critical swimming speed

Assessment of critical swimming speed (Ucrit) was performed using a 170 mL Loligo® swim chamber (Viborg, Denmark). The swim chamber was calibrated using the digital particle tracking velocimetry (DPTV) from Loligo® Systems (Viborg, Denmark). Fresh oxygenated medium was used to fill the chamber. Control and exposed (20 mg/L) zebrafish were placed in the chamber individually to and the comparative maximum sustained swimming speed calculated for each fish.

Adult zebrafish were individually placed in the respirometer and allowed to acclimatize for twenty minutes before initiating swimming at a velocity of two body lengths per second (bl/s). The velocity was increased in increments of 0.5 bl/s in five-minute intervals (Plaut, 2000) and these step-wise increases were maintained until the fish could no longer maintain their position within the chamber. The Ucrit experiment was concluded when fatigue set in (resulting in the fish being impinged to the opposite end of the respirometer for a period of three seconds). The critical swimming speed was calculated using the following equation:

$$Ucrit = Ui + [Uii\ (Ti\ /\ Tii)]$$

where Ui represents the highest velocity maintained for the whole interval (cm/s), Uii the increase in velocity per increment (cm/s), Ti the time elapsed at fatigue velocity (min) and Tii the time elapsed per interval (min) (Plaut, 2001).

2.7. CytoViva® dark-field hyperspectral imaging

Fish were sacrificed and stored at −80 °C overnight. Whole fish samples (three per concentration) were embedded into a cryopreservative gel (Tissue-Tek® O.C.T.™ Compound, Sigma Aldrich South Africa) and stored overnight at −80 °C to harden. The cryostat (Cryocut E) was switched on two hours prior to use to ensure a temperature of −20 °C was achieved. Samples were cryomicrotomed at 7 μm and cooled between slices using cryofreeze aerosol; ribbons were lifted by touching a clean microscope slide kept at room temperature to melt the sample in place. Once on the slide, a coverslip was placed over the sample and samples could be stored at −80 °C until further analysis using an Olympus BX43 microscope integrated with CytoViva® 150 Unit (Alabama, USA). Images were captured using the Dagexcel X16 camera and DAGE Exponent software at 60x and 100x magnification.

The remaining fish muscle was rinsed three times in MilliQ water to remove any externally bound nAu and was pooled (n = 10) before being placed in a drying oven at 50 °C. A dry weight of 0.01 g was measured and placed in a microwave digestion tube. Hydrogen peroxide (30%) (1000 μL) and 65% nitric acid (7 mL) were added and samples were loaded into a microwave digestion system (Ethos, Milestone Microwave Laboratory Systems). The temperature was increased to 200 °C for 10 min and maintained for another 20 min. Once cooled, samples were analysed using inductively coupled plasma mass spectrometry to determine the concentration of accumulated gold (Baldwin et al., 1994).

2.8. Statistical analysis

The clustering and gene ontology (GO) was carried out using DNASTAR ArrayStar- Gene Expression Software. Real-time Polymerase Chain Reactions gene data were analysed by performing a one-way ANOVA (in the case of normally distributed data; Kruskal-Wallis test was performed as a non-parametric alternative) with post-hoc Tukey's multiple comparisons test. Biomarker concentrations and activity were log-transformed and grouped according to exposure concentrations and analysed using IBM SPSS Statistics for Windows, version 22 (IBM Corp., Armonk, N.Y., USA). Differences between means were determined using Multiple analysis of variance (MANOVA). Swimming performance data were analysed using unpaired t-tests (in the case of normally distributed

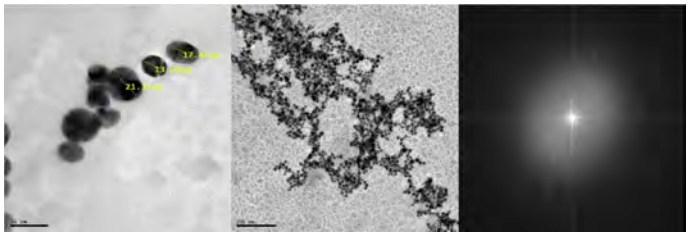

Fig. 1. The transmission electron microscopy of citrate capped spherical gold nanoparticles (14 ± 2 nm) in ISO fish medium with the associated fast fourier transform image of the nAu to confirm the presence of a crystal lattice.

data; Mann-Whitney *U*test was performed as a non-parametric alternative). The significance of results was ascertained at $p < 0.05$. The graphical representations were compiled using GraphPad Prism software (Prism 5 for Windows; Version 5.02, California USA) and data were reported as mean and SEM (standard error of the mean).

3. Results

3.1. Characterization

The physicochemical parameters remained stable over the 96 h exposure period. The pH and temperature remained constant during the exposure with an average pH of 7.88 (7.13–8.42) and temperature of 26.6 °C (25.4–26.9 °C). Oxygen levels were above 4.49 mg/L during the exposure period and EC ranged between 642–765 µS/cm while the TDS was 336 mg/L on average and ranging between 321–412 mg/L. The characterization results showed that citrate capped spherical gold nanoparticles (14 ± 2 nm) agglomerated in ISO fish medium (Fig. 1). A predominant proportion (87.8%) of the particles were 127.9 nm at 0 h while only 12.2% remained around 17.12 nm. However, after 96 h more than 60% of the materials had formed agglomerates of 121.5 nm but up to 894.5 nm in size. The zeta potential was negative (- 4.09 mV) at 96 h.

3.2. RNA isolation and microarray analysis from Danio rerio liver samples

The clustering established that the control was the least related to all nAu exposures (Fig. 2). The lowest concentrations (5, 10 and 15 mg/L) were closely related to control, while 20 mg/L differed most and was associated with the down-regulation of several genes. The GO biological process revealed genetic alterations relating to developmental processes, the establishment of localization, biogenesis, metabolic processes, locomotion, biological adhesion and response to a stimulus. The cellular component showed responses relating to the membrane part, extracellular region part, cell junctions and synapses, while molecular function showed responses relating to binding, receptor activity including steroid binding, transporter activity, structural molecule activity and enzyme regulator activity. The gene expression analysis revealed a significant increase in CAT (2.5x fold change), SOD (4x fold change), MT1 (4x fold change) and MT2 (7x fold change) activity at 20 mg/L when compared to control (Fig. 3). Even though gene expression was affected, the protein biomarker responses in whole-body fish showed no significant differences except for protein carbonyls (Fig. 4) – a response that is indicative of protein damage.

3.3. Swimming behaviour and performance

Several observations related to the swimming behaviour of zebrafish exposed to 20 mg/L nAu were affected compared to the control group (Fig. 5). After performing unpaired t-tests, it was calculated that the mean distance travelled (Control = 52,213 ± 2872 cm; exposed = 39,863 ± 8636 cm) and mean swimming speed (Control 2.42 ± 0.13 cm/s; exposed = 1.85 ± 0.40 cm/s) showed the largest variation within the nAu exposed group. This was further confirmed by a significantly higher ($p < 0.05$) total number of acceleration bouts within the exposed group (n = 212.9) vs the control group (n = 93.25). *Danio rerio* exposed to nAu were also found to remain within the bottom half of the tank and significantly alternate between the bottom and top zones (Control; n = 464; zone alterations and exposed n = 114.4. The swimming trajectories appeared jagged and erratic within the nAu exposed group as opposed to the control group which had smooth circular movements (not presented; own observations).

An unpaired t-test, t (12) = 2.20, (data distributed normally as per Shapiro-Wilk normality test) indicated that the Ucrit (Fig. 6) of the nAu-exposed group (28.5 ± 6.5 bl/s) was significantly decreased compared to the control group (35.3 ± 4.9 bl/s). Fish were, therefore, when forced to swim, physically unable to maintain the same maximum swimming speed post-exposure.

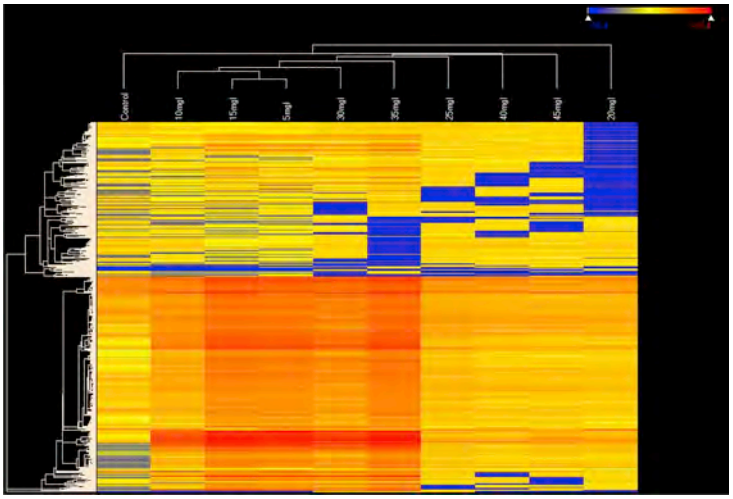

Fig. 2. Hierarchical clustering of genes in the liver of adult *Danio rerio* (up-regulation – red; down-regulation - blue) at the different nAu exposure concentrations. Only those genes with a fold change greater than 8 are represented.

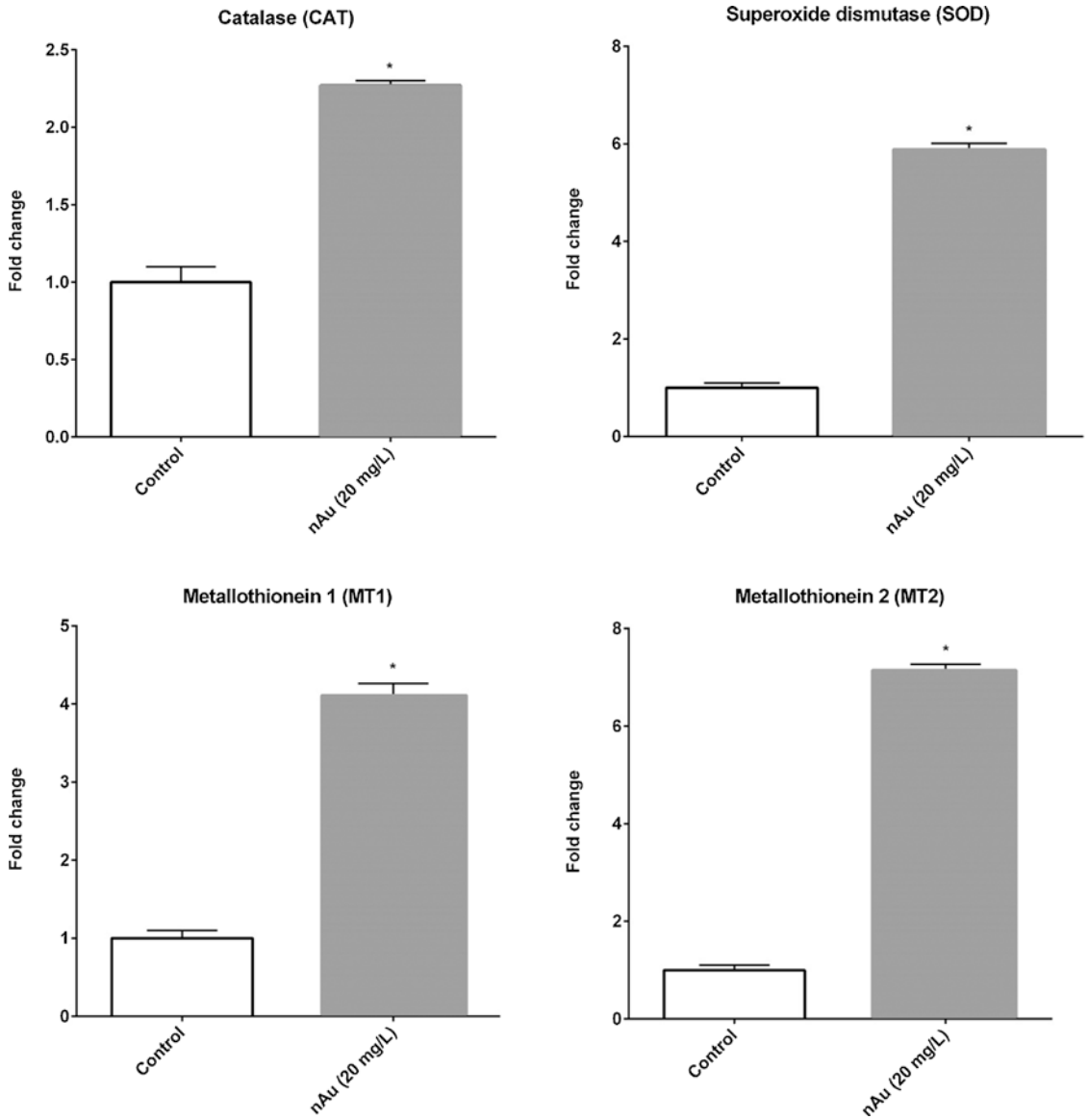

Fig. 3. Mean ± SEM representing RT-PCR fold change for CAT, SOD, and MT biomarkers in liver tissue of adult *Danio rerio* at an exposure concentration of 20 mg/L. Asterisks indicate significant differences from the control group (Dunnett T3; $p < 0.05$).

3.4. CytoViva® dark-field hyperspectral imaging

The concentration of gold in the muscle tissue in the 20 mg/L exposure was 2.07 µg/g (dry weight) in comparison to the below detection limits measured in control fish, thus indicating gold bioaccumulation. The CytoViva® dark-field hyperspectral imaging of longitudinal cryo-sections of *Danio rerio* was only undertaken on muscle tissue. Gold was confirmed in muscle tissue as nAu agglomerates, seen in Fig. 7. At higher magnification, these agglomerates were identified as pockets in muscle tissue. Primary sized nAu (14 ± 2 nm) were not visible during dark-field imaging but larger agglomerates (> 500 nm) in clusters could be identified. Whether the agglomerates were inside tissue or on top of the tissue still needs to be determined.

4. Discussion

An adverse outcomes pathway framework evaluates measurable key events over different levels of biological organization in order to predict a mode of action; subcellular interaction with a toxicant initiates a molecular event that can lead to an adverse outcome on the individual or population level (Ankley and Edwards, 2018). As such, this study indicates a clear adverse outcome pathway effect. Gene-related changes occurred after 96 h in response to nAu exposure. While this did not directly translate to alterations in protein levels, the analysis of whole-organism behaviour revealed significant aberrations compared to control, indicating that zebrafish are either directly affected by nAu uptake or try to actively avoid uptake by means of decreased active swimming within the water column.

The microarray results demonstrated a clear relationship between 20 mg/L, 25 mg/L and 40 mg/L, 45 mg/L exposure groups. It is proposed that this relationship occurs due to particle agglomeration patterns and surface charge. The 20 mg/l and 25 mg/l concentrations had a varied size distribution and particles ranged from small aggregates (17.12 nm) to large agglomerates (894.5 nm) but had an average size of 314.6 nm across both concentrations. Lapresta-Fernandez and Blasco (2012) also suggested that less particle aggregation occurs at a negative charge due to steric stabilization mechanisms making more nAu particles available for biological uptake, distribution and possible toxicity. On the other hand, in the 40 mg/L and 45 mg/L concentrations, the particle agglomerates could be observed with the naked eye and were

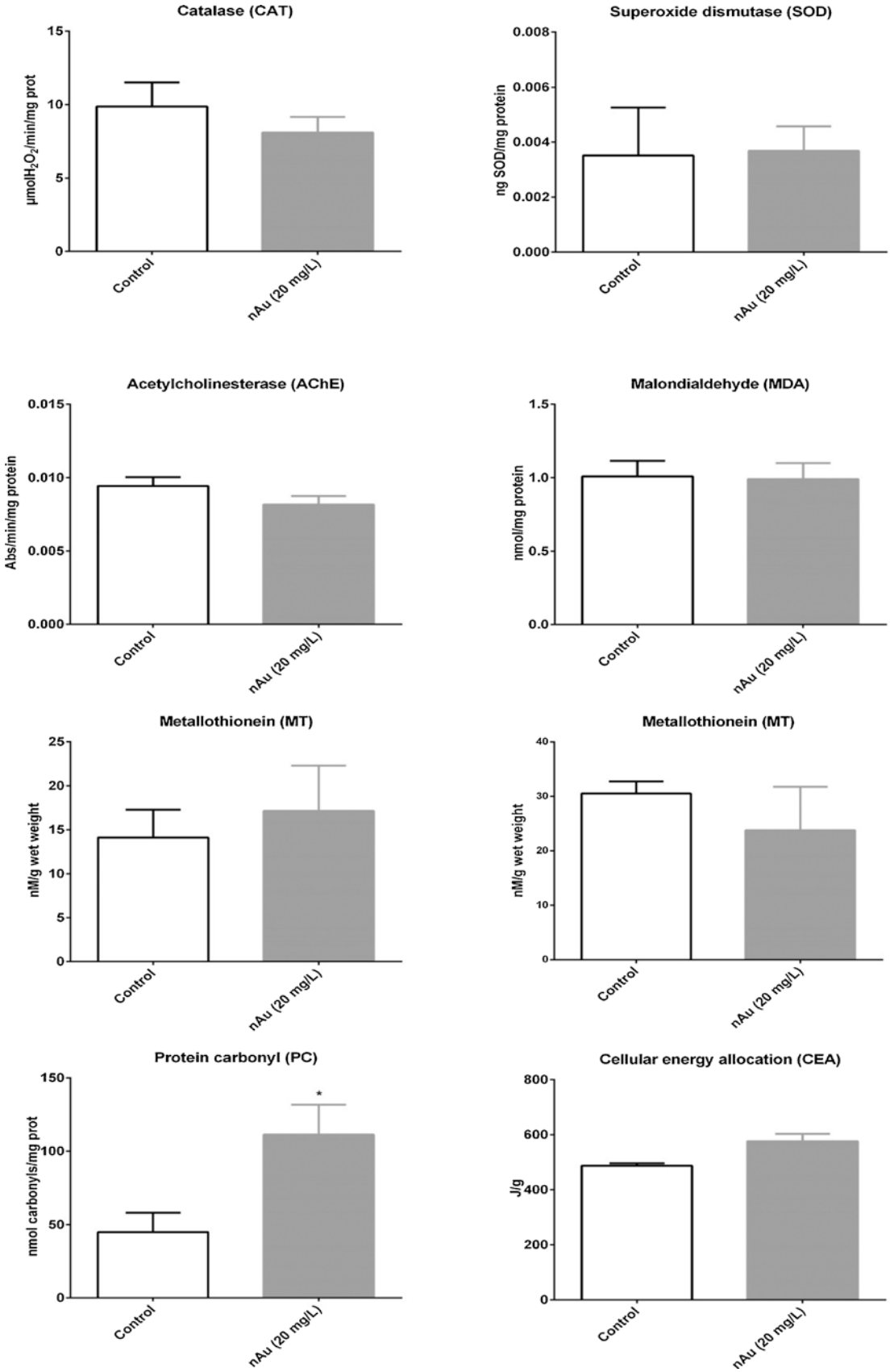

Fig. 4. Mean ± SEM activity for CAT, SOD, AChE, MDA, CEA, MT and PC biomarkers in whole-body and gill tissue of *Danio rerio* exposed to 20 mg/L nAu. Asterisks indicate significant differences from the control group (Dunnett T3; $p < 0.05$).

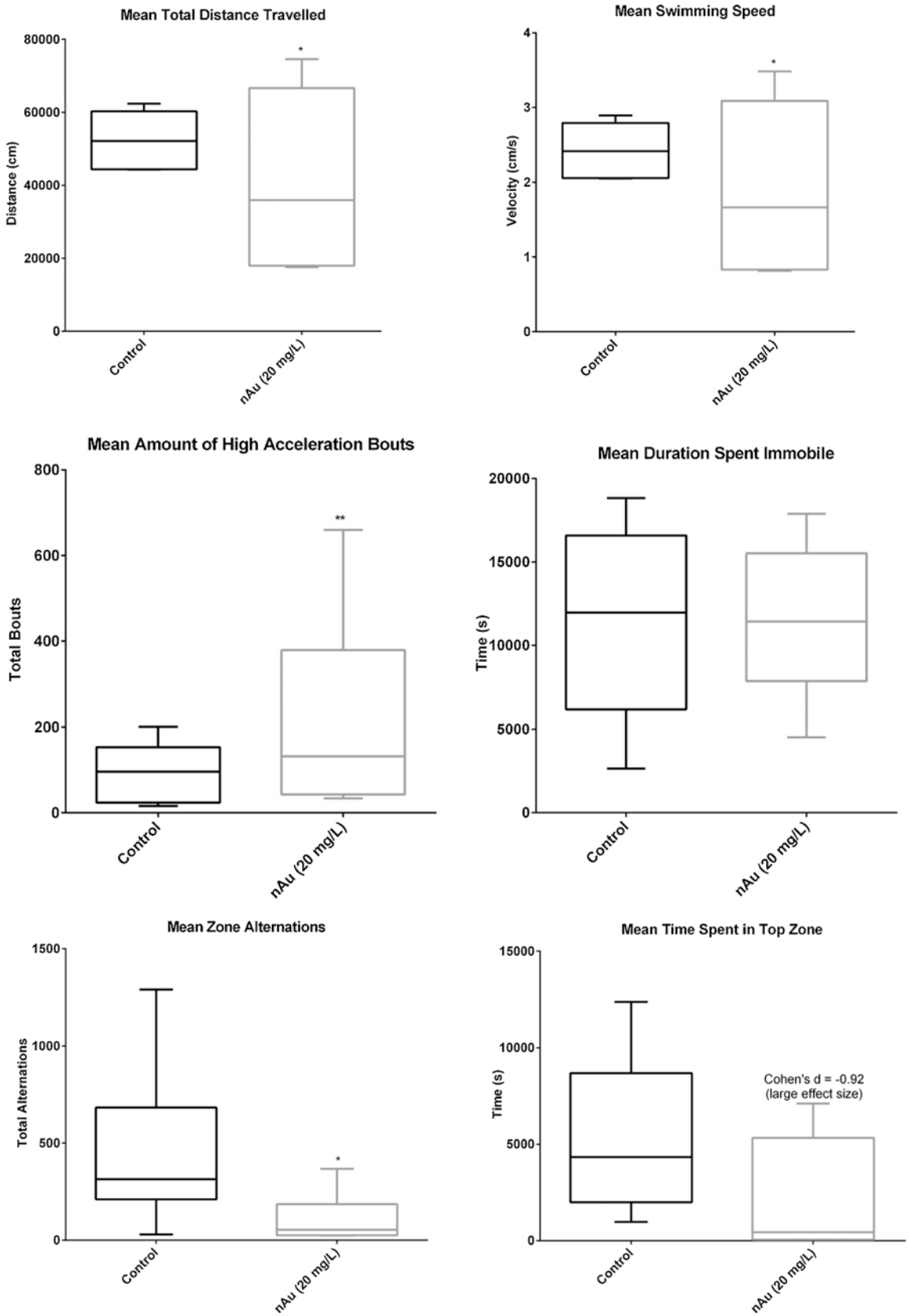

Fig. 5. The swimming behaviour of adult *Danio rerio* exposed to 20 mg/L of nAu for 96 h using swimming trajectories analysed over an additional period of six hours.

measured to be as large as 2 mm in diameter. Studies have indicated that citrate capped anionic gold is not particularly toxic (Bar-llan et al., 2009; Fratoddi et al., 2015; Michalec et al., 2017). Once added to a reconstituted water media, divalent cations such as Ca^{2+} and Mg^{2+} present in the reconstituted medium enhance the formation of aggregates in solution. In this study, we observed all nAu particles in

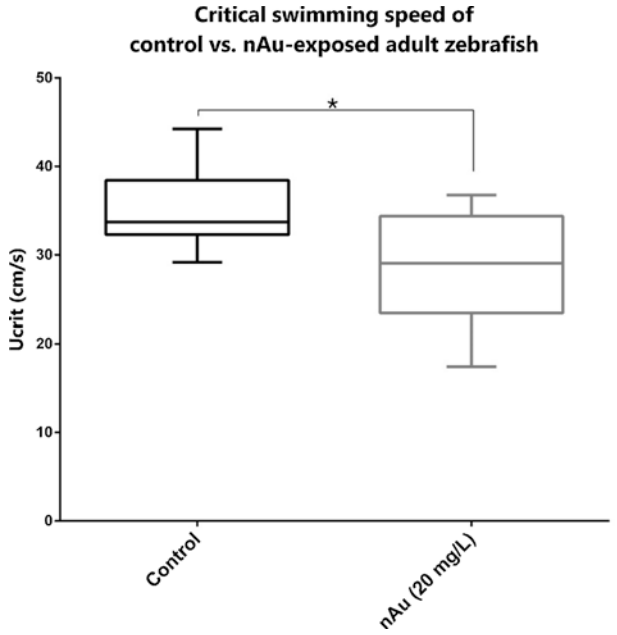

Fig. 6. The critical swimming speed of control and nAu exposed adult *Danio rerio* after a 96 h exposure.

citrate to be 14 ± 2 nm but an immediate increase occurred once added to the medium (12.2% at 17.12 nm), a trend that continued throughout the exposure duration of 96 h (35.8% at 121.5 nm). It needs to be mentioned that at 40 and 45 mg/L agglomerations could be seen macroscopically; at these concentrations fish ingested agglomerates – an observation confirmed via TEM of the intestine where agglomerates were broken into smaller sizes once again (not presented).

The microarray results confirmed that exposure to nAu initiates a cascade of reactions related to antioxidant activity in response to ROS formation in zebrafish. Considering that alterations indicated by microarray results were not reflected on protein level, it should be acknowledged that these results were measured at one point and could be representative of a transient process that is subject to homeostatic modification. Biochemical homeostasis may therefore be achieved through homeostasis-related defence mechanisms before toxic effects can become apparent on a higher level of organisation. Physical limitations imposed by homeostasis in the form of sequestration of nAu in muscle tissue can affect swimming behaviour and other traits reliant on swimming i.e. predator avoidance, foraging and social behaviour (Kasumyan, 2001; Zhang et al., 2014).

The GO pathways (Martinovic et al., 2009) that were analysed on genes with an eightfold change or higher revealed a significant response ($p < 0.05$) in genes involved in biological processes related to development (71%). Dosing of nanoparticles to cell lines leads to inflammatory/immune responses, up-regulation of antioxidants, protein expression, cell cycle responses, defence responses and detoxification of lipid metabolism (Li et al., 2010; Jovanovic et al., 2011; Roy et al., 2014). Other genes that also underwent significant regulation (74.5%) included cellular, chemical, stress and endogenous stimulus responses. Ladhar et al. (2013) showed that dietary cadmium nanoparticle exposure did not change MT2 expression after a thirty-day exposure. In this study, MT1 and MT2 gene expression increased 6-fold. In the current study, MT levels in the whole body and gills were measured and no significant differences found following exposure to nAu. The cellular component focused on the membrane part and all selected genes were involved in membrane processes (100%). The integral component, plasma membrane part, mitochondrial membrane, transmembrane transporter complex, energy-dependent (ATP and NADH) membrane transport complexes, pore complexes and ion channels were all significantly influenced ($p < 0.05$) when compared to control. The molecular functions involved several binding processes, including protein binding, organic cyclic compound binding, carbohydrate-binding, ion binding, small molecule binding and chromatin binding. Brandenberger et al. (2010) reported that no oxidative or inflammatory effects were observed due to exposure to nAu – this was mirrored in the biomarker responses measured in the current study where no significant changes were observed either. However, it has to be noted that consistent decreases in antioxidant enzymes (CAT and SOD) over time have been reported previously (Vutukuru et al., 2006), and it can, therefore, be expected that antioxidant defence mechanisms would be impaired after a period of 96 h.

A significant increase in PC further indicated damage to proteins via ROS formation that occurs when GSH, CAT and SOD are unable to decrease ROS formation. However, it could also have been caused by mechanical damage due to interactions with proteins and other cellular components (Losin et al. 2009) as indicated by the microarray analysis. Nanoparticles which are often the same size as protein molecules can interfere with cell signalling and interact directly with proteins by changing the conformation or by acting as a chaperone, which could lead to peptide aggregation and fibrillation (Elsaesser and Howard, 2012).

In fish, the gills are in direct contact with the exposure medium and under stressful circumstances (i.e. toxicant exposure) increased respiration would occur across the gill surface. While metallothionein stimulation occurs in the presence of metal exposures, the MT assay of the gills indicated no significant increase when compared to the control group thereby relating a nano-specific uptake rather than metal ion uptake. Other studies have shown that exposure to nanomaterials can

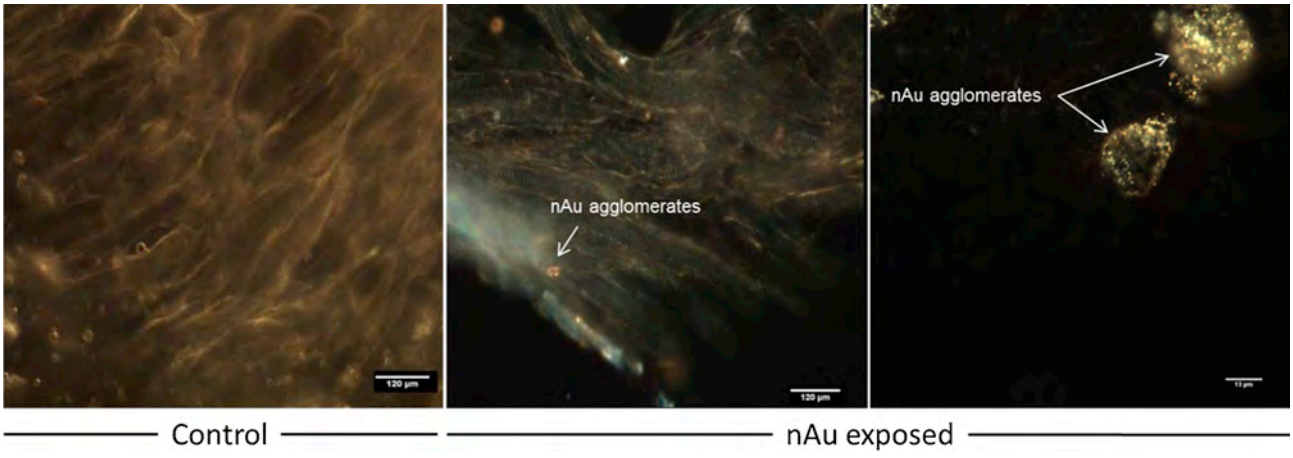

Fig. 7. CytoViva dark-field imaging of cryopreserved muscle tissue of control and nAu exposed adult Danio rerio after a 96 h exposure.

cause histological alterations such as gill filament thickening, sub-epithelial oedema, hyperplasia, lamellar fusion and telangiectasia (Griffitt et al., 2007; Pecoraro et al., 2017).

In a study by Zhang et al. (2014) using a mammalian *in vivo* model, the biphasic release of gold nanoparticles was observed after accumulation in muscle tissue. The highest accumulation in muscle occurred within seven days of exposure – a timeframe that corresponds to that of our study. Studies have reported uptake of metal-based nanomaterials into various organs and the circulation of fish species (Bar-llan et al., 2009; Zhu et al., 2010; Skjolding et al., 2017). Further investigation is needed to determine the effect of nAu accumulation in muscle.

Behavioural alterations have shown significant promise as an endpoint measurement for nanomaterials since it has been demonstrated to reflect effects related to toxicity across a range of aquatic species in different life stages at sub-lethal exposure concentrations (Holzner et al., 2017; Michalec et al., 2017). Conflicting results exist where some species show hyperactive responses as seen in our study and others show decreased movement (Ahmad et al., 2012; Sovová et al., 2014; Strungaru et al., 2018). Although a significant decrease in distance moved and swimming speed was observed there was a significant increase in acceleration bouts where fish were observed to have erratic movements, darting at the bottom of the tank. This was further confirmed by the number of zone alterations observed in our study between the top and bottom sections of the tank; fish were found to spend the majority of their time at the bottom of their tanks – identified as a behavioural stress response in fish (Kalueff et al., 2016).

Zebrafish are well adapted to fast, sustained swimming and normally hold their position against the current due to optomotor responses (Plaut, 2001, 2000). The direct interaction of nAu with gill tissue can affect respiration and oxidative stress has an effect on free radical imbalance – effects that manifest into a significant behavioural response. Gene expression showed significant increases in CAT, SOD and MTs but the biomarkers measured at the same time did not, the PC results did, however, indicate damage. By performing a forced swim test, it could be concluded that these fish are unable to maintain the same level of sustained swimming speeds measured in their control counterparts. A significant reduction in fishes' ability to maintain sustained swimming speed can manifest into an ecologically relevant ecotoxicological response and suggests that exposure to nAu may even influence the survival of free-living aquatic organisms.

5. Conclusion

In conclusion, the current study aimed to investigate the possible toxic effects of nAu in zebrafish. Subsequent to exposing fish to a range of concentrations, a concentration of 20 mg/L was found to have the largest impact on gene expression. These aberrancies did not necessarily extend to protein expression but was accompanied by a decrease in critical swimming speed and altered behaviour that suggest the presence of a stress response. Despite previously being reported to be non-toxic, results presented here suggest that nAu could, in fact, elicit a stress response and affect behaviour in zebrafish after short-term exposure. As such, further investigation is warranted in order to comprehensively characterize the extent to which nAu could possibly affect processes and biomarkers from cellular to organismic level.

Ethical standards

All procedures performed in studies involving animals were approved by the AnimCare animal research ethics committee (NHREC reg. number AREC-130913-015) of the North-West University. All animals were maintained and procedures performed in accordance with the code of ethics in research, training and testing of drugs in South Africa and complied with national legislation (ethics approval number: NWU-00269-16-A5).

Declaration of Competing Interest

The authors declare that they have no conflict of interest relating to the work presented in this manuscript.

Acknowledgements

The research is based on work supported by the Department of Science and Technology in South Africa. The authors wish to thank MINTEK for supplying the nAu stock solutions. We would like to acknowledge the financial support by Grants-in-Aid for Scientific Research from the Ministry of Education, Culture, Sports, Science and Technology of Japan awarded to M. Ishizuka (No. < GN2 > 24405004 and No. < GN2 > 24248056) < /GN2 > < /GN2 > and Y. Ikenaka (No. < GN2 > 26304043, < GN2 > 15H0282505, < GN2 > 15K1221305) < /GN2 > < /GN2 > < /GN2 > , and the foundation of JSPS Core to Core Program(AA Science Platforms) and Bilateral Joint Research Project (PG36150002 and < GN4 > PG36150003). < / GN4 > Bioassays were conducted in the National Aquatic Bioassay Facility at North-West University, South Africa (NRF EQP Grant 99024).

Appendix A. Supplementary data

Supplementary material related to this article can be found, in the online version, at doi:https://doi.org/10.1016/j.aquatox.2019.105287.

References

Ahmad, F., Noldus, L.P.J.J., Tegelenbosch, R.A.J., Richardson, M.K., 2012. Zebrafish embryos and larvae in behavioural assays. Behaviour 149 (10–12), 1241–1281. https://doi.org/10.1163/1568539X-00003020.

Ankley, G.T., Edwards, S.W., 2018. The adverse outcome pathway: a multifaceted framework supporting 21st century toxicology. Curr. Opin. Toxicol. 9, 1–7. https://doi.org/10.1016/j.cotox.2018.03.004.

Avellan, A., Simonin, M., McGivney, E., Bossa, N., Spielman-Sun, E., Rocca, J.D., et al., 2018. Gold nanoparticle biodissolution by a freshwater macrophyte and its associated microbiome. Nat. Nanotechnol. https://doi.org/10.1038/s41565-018-0231-y.

Baldwin, S., Deaker, M., Maher, W., 1994. Low volume microwave digestion of marine biological tissues for measurement of trace elements. Analyst 119, 1701–1704.

Bar-llan, O., Albrecht, R.M., Fako, V.E., Furgeson, D.Y., 2009. Toxicity assessments of multisized gold and silver nanoparticles in zebrafish embryos. Small 2222, 1897–1910. https://doi.org/10.1002/smll.200801716.

Boisselier, E., Astruc, D., 2009. Gold nanoparticles in nanomedicine: preparations, imaging, diagnostics, therapies and toxicity. Chem. Soc. Rev. 38 (6), 1759–1782. https://doi.org/10.1039/B806051G.

Buzea, C., Pacheco, I.I., Robbie, K., 2007. Nanomaterials and nanoparticles: sources and toxicity. Biointerphases 2 (4), Mr17–Mr71.

Carnovale, C., Bryant, G., Shukla, R., Bansal, V., 2016. Size, shape and surface chemistry of nano-gold dictate its cellular interactions, uptake and toxicity. Prog. Mater. Sci. 83, 152–190. https://doi.org/10.1016/j.pmatsci.2016.04.003.

Choi, J.S., Kim, R.-O., Yoon, S., Kim, W.-K., 2016. Developmental toxicity of zinc oxide nanoparticles to zebrafish (Danio rerio): a transcriptomic analysis. PLoS One 11 (8), e0160763. https://doi.org/10.1371/journal.pone.0160763.

Colvin, V.L., 2003. The potential environmental impact of engineered nanomaterials. Nat. Biotechnol. 21 (10), 1166–1170. https://doi.org/10.1038/nbt875.

Dai, Y.-J., Jia, Y.-F., Chen, N., et al., 2014. Zebrafish as a model system to study toxicology. Environ. Toxicol. Chem. 33 (1), 11–17. https://doi.org/10.1002/etc.2406.

Fratoddi, I., Venditti, I., Cametti, C., Russo, M.V., 2015. How toxic are gold nanoparticles? The state-of-the-art 8 (6), 1771–1799. https://doi.org/10.1007/s12274-014-0697-3.

Gerber, R., Smit, N.J., van Vuren, J.H.J., Ikenaka, Y., Wepener, V., 2018. Biomarkers in tigerfish (*Hydrocynus vittatus*) as indicators of metal and organic pollution in ecologically sensitive subtropical rivers. Ecotoxicol. Environ. Saf. 157, 307–317. https://doi.org/10.1016/j.ecoenv.2018.03.091.

Giese, B., Klaessig, F., Park, B., Kaegi, R., Steinfeldt, M., 2018. Risks, release and concentrations of engineered nanomaterial in the environment. Sci. Rep. (September 2017), 1–18. https://doi.org/10.1038/s41598-018-19275-4.

Griffitt, R.J., Weil, R., Hyndman, K.A., Denslow, N.D., Powers, K., Taylor, D., Barber, D.S., 2007. Exposure to copper nanoparticles causes gill injury and acute lethality in zebrafish (*Danio rerio*). Environ. Sci. Technol. 41 (23), 8178–8186. https://doi.org/10.1021/es071235e.

Holzner, M., Barras, A., Lacoste, A., 2017. Short-Term Exposure to Gold Nanoparticle Suspension Impairs Swimming Behavior in a Widespread Calanoid Copepod * François-Ga E 228. pp. 102–110. https://doi.org/10.1016/j.envpol.2017.04.084.

Kalueff, A.V., Echevarria, D.J., Homechaudhuri, S., et al., 2016. Zebrafish neurobehavioral phenomics for aquatic neuropharmacology and toxicology research. Aquat. Toxicol. 170, 297–309. https://doi.org/10.1016/j.aquatox.2015.08.007.

Kasukabe, T., Nishihara, H., Iwamura, S., Kyotani, T., 2016. Remarkable performance improvement of inexpensive ball-milled Si nanoparticles by carbon-coating for Li-ion batteries. J. Power Sources 319, 99–103. https://doi.org/10.1016/j.jpowsour.2016.04.050.

Kasumyan, A.O., 2001. Effects of chemical pollutants on foraging behavior and sensitivity of fish to food stimuli. J. Ichthyol. 41, 76–87.

Khot, L.R., Sankaran, S., Maja, J.M., Ehsani, R., Schuster, E.W., 2012. Applications of nanomaterials in agricultural production and crop protection: a review. Crop. Prot. 35, 64–70. https://doi.org/10.1016/j.cropro.2012.01.007.

Ladhar, C., Geffroy, B., Cambier, S., Treguer-Delapierre, M., Durand, E., Brèthes, D., Bourdineaud, J.-P., 2013. Impact of dietary cadmium sulphide nanoparticles on *Danio rerio* (zebrafish) at very low contamination pressure. Nanotoxicology 8 (6), 676–685. https://doi.org/10.3109/17435390.2013.822116.

Lam, C.W., James, J.T., McCluskey, R., Hunter, R.L., 2004. Pulmonary toxicity of single-wall carbon nanotubes in mice 7 and 90 days after intratracheal instillation. Toxicol. Sci. 77 (1), 126–134. https://doi.org/10.1093/toxsci/kfg243.

Lead, J.R., Batley, G.E., Alvarez, P.J.J., Handy, R.D., Mclaughlin, M.J., 2018. Nanomaterials in the environment: behavior, fate, bioavailability, and effects — an updated review. Environ. Toxicol. Chem. 37 (8), 2029–2063. https://doi.org/10.1002/etc.4147.

Michalec, F.-G., Holzner, M., Barras, A., Lacoste, A.-S., Brunet, L., Lee, J.-S., et al., 2017. Short-term exposure to gold nanoparticle suspension impairs swimming behavior in a widespread calanoid copepod. Environ. Pollut. 228, 102–110. https://doi.org/10.1016/j.envpol.2017.04.084.

Mitzel, M.R., Lin, N., Whalen, K., Tufenkji, N., 2017. Environmental Science Nano swimming response to silver nanoparticles †. Environ. Sci. Nano 4, 1328–1338. https://doi.org/10.1039/C7EN00233E.

Moore, M.N., 2006. Do nanoparticles present ecotoxicological risks for the health of the aquatic environment? Environ. Int. 32 (8), 967–976. https://doi.org/10.1016/j.envint.2006.06.014.

Mura, S., Greppi, G., Malfatti, L., et al., 2015. Multifunctionalization of wool fabrics through nanoparticles: a chemical route towards smart textiles. J. Colloid Interface Sci. 456, 85–92. https://doi.org/10.1016/j.jcis.2015.06.018.

Nel, A., Xia, T., Mädler, L., Li, N., 2006. Toxic potential of materials at the Nanolevel. Science 311 (5761), 622–627.

Oberdörster, G., Oberdörster, E., Oberdörster, J., 2005. Nanotoxicology: an emerging discipline evolving from studies of ultrafine particles. Environ. Health Perspect. 113 (7), 823–839. https://doi.org/10.1289/ehp.7339.

Panyam, J., Labhasetwar, V., 2003. Biodegradable nanoparticles for drug and gene delivery to cells and tissue. Adv. Drug Deliv. Rev. 55 (3), 329–347. https://doi.org/10.1016/S0169-409X(02)00228-4.

Pecoraro, R., Marino, F., Salvaggio, A., Capparucci, F., Di Caro, G., Iaria, C., et al., 2017. Evaluation of Chronic Nanosilver Toxicity to Adult Zebrafish. Front. Physiol. 8. https://doi.org/10.3389/fphys.2017.01011.

Plaut, I., 2000. Effects of fin size on swimming performance, behavior and routine activity of Zebrafish *Danio rerio*. J. Exp. Biol. 203, 813–820.

Plaut, I., 2001. Critical swimming speed: its ecological relevance. Comparative Biochemistry and Physiology Part A. 131 (1), 41–50 14-43.

Skjolding, L.M., Ašmonaitė, G., Jølck, R.I., Andresen, T.L., Selck, H., Baun, A., 2017. An assessment of the importance of exposure routes to the uptake and internal localisation of fluorescent nanoparticles in zebrafish (*Danio rerio*), using light sheet microscopy. Nanotoxicology 5390 (April). https://doi.org/10.1080/17435390.2017.1306128.

Souza, V.G.L., Fernando, A.L., 2016. Nanoparticles in food packaging: biodegradability and potential migration to food—a review. Food Packag. Shelf Life 8, 63–70. https://doi.org/10.1016/j.fpsl.2016.04.001.

Sovová, T., Boyle, D., Sloman, K.A., Vanegas, C., Handy, R.D., 2014. Impaired behavioural response to alarm substance in rainbow trout exposed to copper nanoparticles. Aquat. Toxicol. 152, 195–204. https://doi.org/10.1016/j.aquatox.2014.04.003.

Strungaru, S.-A., Plavan, G., Ciobica, A., Nicoara, M., Robea, M.A., Solcan, C., et al., 2018. Acute exposure to gold induces fast changes in social behavior and oxidative stress of zebrafish (*Danio rerio*). J. Trace Elem. Med. Biol. 50, 249–256. https://doi.org/10.1016/j.jtemb.2018.07.013.

Suh, W.H., Suslick, K.S., Stucky, G.D., Suh, Y.-H., 2009. Nanotechnology, nanotoxicology, and neuroscience. Prog. Neurobiol. 87 (3), 133–170. https://doi.org/10.1016/j.pneurobio.2008.09.009.

Utembe, W., Wepener, V., Yu, I.J., Gulumian, M., 2018. An assessment of applicability of existing approaches of predicting bioaccumulation of conventional substances to nanomaterials. Environ. Toxicol. Chem. 37 (12), 2972–2988.

Vetten, M.A., Tlotleng, N., Tanner Rascher, D., Skepu, A., Keter, F.K., Boodhia, K., Koekemoer, L.A., Andraos, C., Tshikhudo, R., Gulumian, M., 2013. Label-free in vitro toxicity and uptake assessment of citrate stabilised gold nanoparticles in three cell lines. Part. Fibre Toxicol. 10, 1–15. https://doi.org/10.1186/1743-8977-10-50.

Vutukuru, S.S., Chintada, S., Radha Madhavi, K., Venkateswara Rao, J., Anjaneyulu, Y., 2006. Acute effects of copper on superoxide dismutase, catalase and lipid peroxidation in the freshwater teleost fish, *Esomus danricus*. Fish Physiol. Biochem. 32 (3), 221–229. https://doi.org/10.1007/s10695-006-9004-x.

Wiesner, M.R., Lowry, G.V., Alvarez, P., Dionysiou, D., Biswas, P., 2006. Assessing the risks of manufactured nanomaterials. Environ. Sci. Technol. 40 (14), 4336–4345. https://doi.org/10.1021/es062726m.

Zhang, H., Zhai, Y., Wang, J., Zhai, G., 2016. New progress and prospects: the application of nanogel in drug delivery. Mater. Sci. Eng. C 60, 560–568. https://doi.org/10.1016/j.msec.2015.11.041.

Zhang, X.-D., Luo, Z., Chen, J., Wang, H., Song, S.-S., Shen, X., et al., 2014. Storage of Gold Nanoclusters in Muscle Leads to their Biphasic in Vivo Clearance. Small 11 (14), 1683–1690. https://doi.org/10.1002/smll.201402233.

Zhu, Z.-J., Carboni, R., Quercio, M.J., Yan, B., Miranda, O.R., Anderton, D.L., et al., 2010. Surface Properties Dictate Uptake, Distribution, Excretion, and Toxicity of Nanoparticles in Fish. Small 6 (20), 2261–2265. https://doi.org/10.1002/smll.201000989.

Chemosphere 246 (2020) 125733

Contents lists available at ScienceDirect

Chemosphere

journal homepage: www.elsevier.com/locate/chemosphere

Cellulose-metallothionein biosorbent for removal of Pb(II) and Zn(II) from polluted water

Wilson Mwandira [a], Kazunori Nakashima [b, *], Yuki Togo [a], Tsutomu Sato [b], Satoru Kawasaki [b]

[a] Graduate School of Engineering, Hokkaido University, Kita 13, Nishi 8, Kita-Ku, Sapporo, 060-8628, Japan
[b] Faculty of Engineering, Hokkaido University, Kita 13, Nishi 8, Kita-Ku, Sapporo, 060-8628, Japan

HIGHLIGHTS

- Metallothionein/cellulose biosorbent was designed for heavy metal removal.
- The biosorbents was found to be very efficient in removal of heavy metals.
- The biosorbent showed regeneration and recyclability for seven times.
- Effective metal ion removal was achieved when applied in real mine wastewater.

GRAPHICAL ABSTRACT

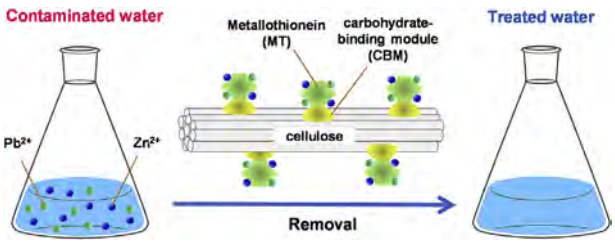

ARTICLE INFO

Article history:
Received 24 September 2019
Received in revised form
20 December 2019
Accepted 22 December 2019
Available online 26 December 2019

Handling Editor: Y Yeomin Yoon

Keywords:
Metallothionein
Cellulose
Biosorbent
Adsorption
Metal ions
Mine wastewater

ABSTRACT

Intake of toxic trace elements in drinking water can lead to adverse health effects. To remove toxic trace elements from water, we developed a novel biosorbent composed of cellulose and a fusion protein. The fusion protein was constructed from metallothionein (MT) and a carbohydrate-binding module (CBM), where CBM can bind to cellulose while MT can capture heavy metal ions in solution. In a batch experiment, the biosorbent had maximum biosorption capacities for Pb(II) and Zn(II) ions of 39.02 mg/g and 29.28 mg/g, respectively. Furthermore, the biosorbent could be used in a semi-continuous system and showed good regeneration and recyclability. Both cellulose and the MT-CBM are environmentally friendly and renewable materials, and this biosorbent has great potential for efficient removal of toxic trace elements from polluted water.

1. Introduction

Heavy metals have become a predominant contaminant of water because of constant growth in industrialization and urbanization (Chen et al., 2018). Once toxic heavy metals, such as lead (Pb) and zinc (Zn), enter the human body, they accumulate and cause various health problems. Lead has no known beneficial effects on human health, whereas Zn is essential (Zoroddu et al., 2019). However, Zn is toxic at high concentrations (Baran et al., 2018). Lead causes neurodevelopment disorders and Zn imparts an undesirable astringent taste to water, and both should be removed from drinking water (World Health Organization, 2017).

To date, toxic trace elements have been removed by

* Corresponding author.
E-mail address: nakashima@geo-er.eng.hokudai.ac.jp (K. Nakashima).

https://doi.org/10.1016/j.chemosphere.2019.125733
0045-6535/

conventional water treatment methods which include coagulation, flocculation, clarification, and filtration, and followed by disinfection (Gitis and Hankins, 2018; Singh et al., 2018). However, many of these techniques are suboptimal. Biosorption has emerged as an alternative method that is efficient, simple, and specific (Singh et al., 2018). The biosorption process involves interaction of a solid phase (biosorbent) with a liquid phase (water) containing the dissolved species to be adsorbed (metal ions). Biosorbents effectively remove heavy metals from water (Fakhre and Ibrahim, 2018). Cellulose is attractive as a biosorbent because it is stable, inert, and the most abundant polymer on Earth (Abouzeid et al., 2019). However, natural cellulose has not been used as a biosorbent because of its low metal-ion adsorption capacity (Hokkanen et al., 2016). To address this challenge, we have developed a functional cellulose modified with metallothionein (MT), which adsorbs metal ions, by using a carbohydrate-binding module (CBM) as a binder.

In this research, we constructed a biosorbent by fusion protein of MT from *Synechococcus elongatus* and CBM from *Clostridium thermocellum* (Fig. 1). MTs are a group of well-conserved proteins that act as antioxidants. They are found in all living organisms and contain a sulfhydryl group that bind to heavy metals (Chaudhary et al., 2018; Mekawy et al., 2018). However, MT would not be easy to recover after dispersion. To address this, we investigated modifying MT by fusing it with CBM. Because CBM binds to cellulose by hydrophobic interaction (Chang et al., 2018), the cellulose-MT-CBM biosorbent would be stable and easily recycled (Yunus and Tsai, 2015). Although peptide-based biosorbents have been previously suggested for water treatment (Xu et al., 2002), our biosorbent is unique in that it can be prepared in a single-step without protein purification by using cellulose-binding ability of CBM. The MT can adsorb various toxic trace elements that may be present in polluted water. We have investigated the removal of toxic metal ions, which are contained in real mine wastewater, by using a novel biosorbent.

2. Materials and methods

2.1. Plasmid construction and protein expression

The gene for MT from *S. elongatus* PCC7942 (Shi et al., 1992) was synthesized by Eurofins Genomics (Tokyo, Japan). Genomic DNA from *C. thermocellum* NBRC 103400 was obtained from NBRC (Kisarazu, Japan). The polymerase chain reaction (PCR) was performed using PrimeSTAR® HS DNA polymerase (Takara Bio Inc., Otsu, Japan) with the oligonucleotide primers (Eurofins Genomics) listed in Table S1. The gene for MT was amplified from the vector containing the synthesized MT gene using primers MT-F and MT-R.

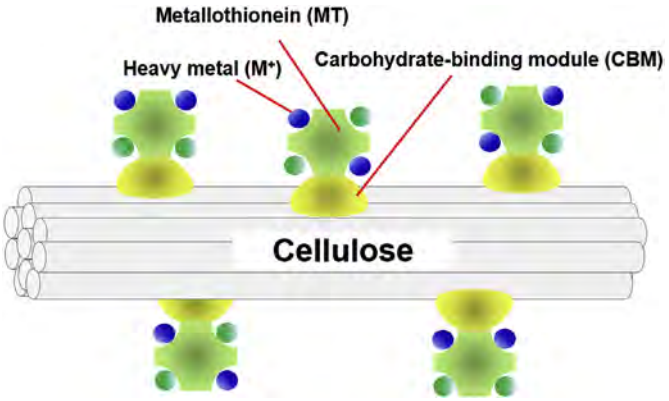

Fig. 1. Illustration of cellulose-MT-CBM.

The gene for CBM 3 (Hong et al., 2007) was cloned from genomic DNA of *C. thermocellum* using the primers CBM-F and CBM-R. The genes of MT and CBM were fused by overlap PCR using the primers OL-F, OL-R, IF-F, and IF-R. The amplified gene was inserted into pET-15b vector (Merck Biosciences GmbH, Schwalbach Ts., Germany), which was cut by *Nco* I and *Xho* I, using an In-Fusion HD Cloning Kit to obtain the pET-MT-CBM vector (Fig. S1). The nucleotide sequence of the MT-CBM fusion gene (648 bp) was verified by DNA sequencing (Eurofins Genomics).

To express the target protein, *Escherichia coli* BL21(DE3) strain (Nippon Gene Co. Ltd, Toyama, Japan) was transformed with the pET-MT-CBM vector. The transformant was grown at 37 °C in Luria-Bertani (LB) medium containing 100 μg/mL ampicillin. When the optical density of the culture medium measured at a wavelength of 600 nm (OD_{600}) reached 0.45, the expression of the protein was induced by adding isopropyl β-D-1- thiogalactopyranoside (IPTG, final concentration of 1 mM) to the medium and culturing at 15 °C for 24 h. The bacterial cells expressing the proteins were harvested by centrifugation at 8000×*g* for 10 min and lysed by ultrasonication at 30 kHz for 5 min (Vibra-Cell™ VCX 130, Sonics & Materials, Inc., Newtown, USA). After centrifugation of the cell lysate at 8000×*g* for 10 min, the supernatant was recovered and used directly in biosorption studies.

2.2. Preparation of the cellulose-MT-CBM biosorbent

Biosorption of the protein onto cellulose is illustrated in Fig. 2. To immobilize the MT-CBM fusion protein on cellulose and obtain the cellulose-MT-CBM biosorbent, Whatman filter paper No. 1 was cut into rectangular pieces (1 g) and then suspended in 5 mL of the crude protein mixture (protein concentration of 250 μg/mL) obtained in Section 2.1 for 2 h at 25 °C. The filter paper and cellulose-MT-CBM biosorbent were analyzed by using attenuated total reflectance Fourier transform infrared (ATR-FTIR) (JASCO 360 FTIR Spectrometer, JASCO, Japan). The point of zero charge (pzc) for the cellulose-MT-CBM was determined by the pH drift method (Bakatula et al., 2018).

2.3. Metal ion adsorption experiments

A metal ion stock solution was prepared using $PbCl_2$ and $ZnCl_2$ (Wako Pure Chemical Industries Ltd, Tokyo, Japan), which were dissolved in distilled water. Solutions with different final concentrations of the metal ions were obtained by dilution of the stock solution. Metal adsorption was investigated in batch experiments. The effect of pH (2.0–9.0) on the removal of Pb(II) and Zn(II) was investigated by mixing 1 g of the prepared biosorbent with 100 mL of a 20 mg/L metal solution in a 250 mL Erlenmeyer flask. Then, the flasks were placed on a shaker at 100 rpm for 1 h. The adsorbent was recovered by centrifugation at 8000×*g* for 10 min and the supernatant was filtered through a 0.45-μm filter. The metal ion concentration in the supernatant was measured by inductively coupled plasma atomic emission spectroscopy (ICP-AES) (ICPE-9820, Shimadzu Corporation, Kyoto, Japan). The effect of the contact time (0–60 min) was studied by varying this while keeping all other parameters fixed.

Biosorption was analyzed using the Langmuir isotherm model:

$$Q_{eq} = \frac{Q_{max} \cdot K \cdot C_{eq}}{1 + K \cdot C_{eq}}, \quad (1)$$

where Q_{eq} is the quantity adsorbed (mg/g), C_{eq} is the equilibrium concentration of the adsorbate (mg/L), Q_{max} is the saturation adsorption capacity (mg/g), and K is the equilibrium constant.

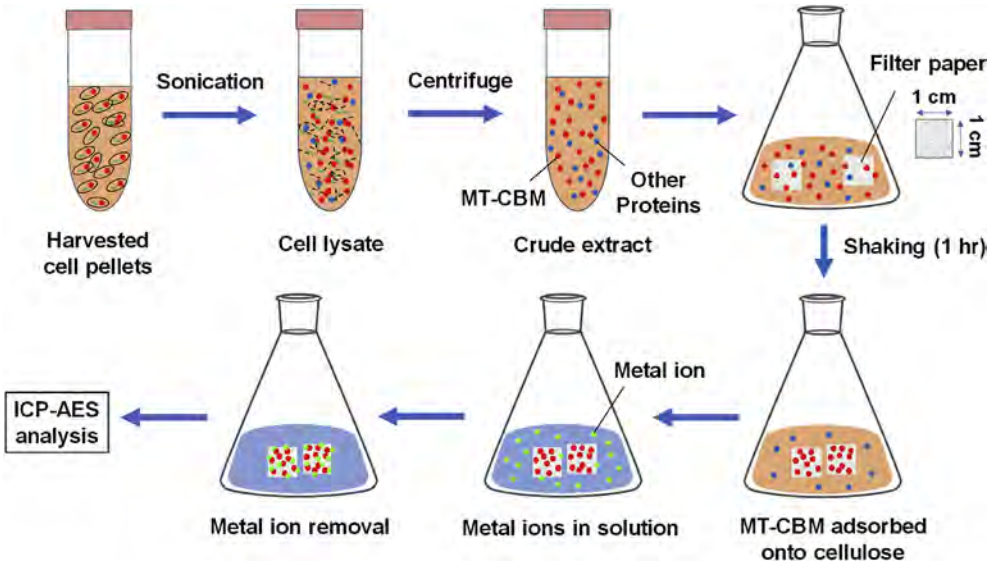

Fig. 2. The process of immobilization of the MT-CBM protein on cellulose.

2.4. Semi-continuous adsorption system and recyclability of the cellulose-MT-CBM biosorbent

The reusability of the adsorbent in a semi-continuous system was tested seven times with the experimental setup illustrated in Fig. 3. To determine the recoverability and reusability of the biosorbent, a column (syringe of mean diameter, D_{50} = 2.5 cm and height, h = 7 cm) was prepared by placing 2 g of cellulose in a 30-mL syringe. Then, 10 mL of crude extract containing overexpressed MT-CBM protein (total protein concentration: 250 μg/mL) was added to be adsorbed onto the cellulose, and the column was kept at 25 °C in an incubator for 1 h. After washing three times with deionized water, a Pb(II) or Zn(II) aqueous solution was allowed to percolate through the column. The filtrate was collected for metal analysis. A valve was used to regulate the flow rate of the filtrate from the column. To desorb the adsorbed metal ions, 10 mL of 20 mM EDTA buffer (pH 8) was added to the column. To regenerate the column, 10 mL of fresh MT-CBM protein was added. A column containing only cellulose was used for control experiments. Treatment of actual mine wastewater collected from Chingola, Copperbelt, Zambia was investigated using the column.

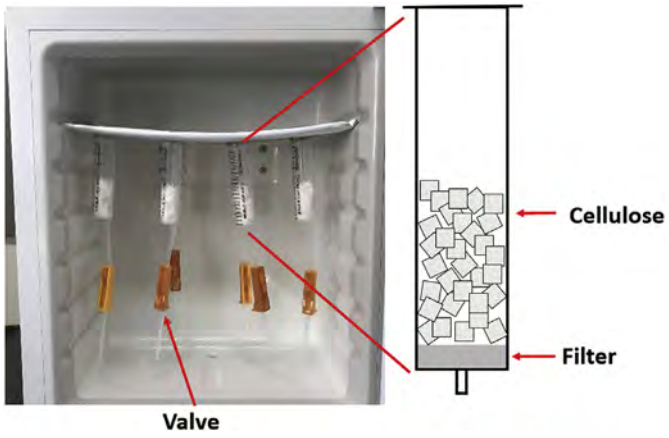

Fig. 3. Setup for the cellulose-MT-CBM biosorbent regeneration experiments.

2.5. X-ray photoelectron spectroscopy analysis

X-ray photoelectron spectroscopy (XPS) measurements were performed by using a JPS-9200 spectrometer (JEOL Ltd, Tokyo, Japan) to explore the electronic states of Pb and Zn on the biosorbent using monochromatic Mg Kα radiation. To compensate for surface charge effects, the binding energies were calibrated using C 1s at 284.80 eV.

3. Results and discussion

3.1. Verification of plasmid construction, protein expression, and protein binding ability to cellulose

Fig. 4 shows the results of SDS-PAGE analysis for the protein expressed in *E. coli* BL21(DE3) and biosorption of the protein to cellulose. Fig. 4(a) shows the supernatant of the cell lysate of *E. coli* expressing MT-CBM. We found that the MT-CBM was successfully expressed in a soluble form with a molecular weight of 23.1 kDa. To

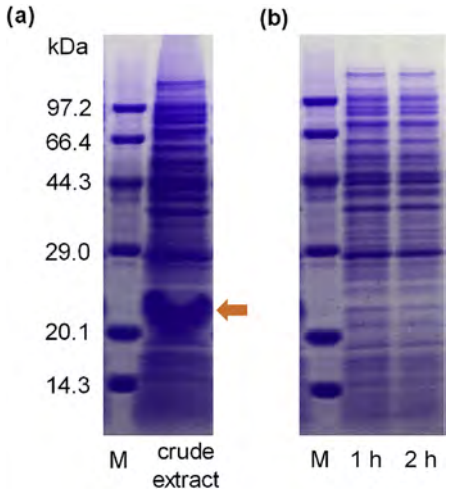

Fig. 4. SDS-PAGE of (a) crude extract after expression of MT-CBM and (b) after addition of filter paper to crude extract (1 h and 2 h). M: protein marker.

verify the binding ability of the MT-CBM on cellulose, filter papers were added to the cell lysate. After 1 h, the band for MT-CBM disappeared, indicating that the MT-CBM in the cell lysate was adsorbed on cellulose (Fig. 4(b)). This result showed that MT-CBM could be purified using cellulose in a single step. This result is consistent with previous studies where CBM was observed to bind to cellulosic material (Hong et al., 2007). We then used the cellulose-based biosorbent (cellulose-MT-CBM) for further studies. The FTIR spectra are obtained for pure cellulose and cellulose-MT-CBM (Fig. S2). The results showed that the pure cellulose had no distinguishable functional groups compared with the cellulose-MT-CBM, where broad and strong bands at 3251 cm^{-1} (amine (-NH)), 1625 cm^{-1} (amide group (C=O), and 1302 cm^{-1} (C—O stretching) confirmed the presence of bound protein on the cellulose.

3.2. Metal ion adsorption experiments

3.2.1. The effect of contact time

Contact time is an important factor affecting the efficiency of biosorption because it provides valuable information on how fast the removal process occurs. Time course of metal ion adsorption is shown in Fig. S3. Equilibrium of the biosorption of Pb(II) and Zn(II) on the cellulose-MT-CBM reached equilibrium within 10 min. This rapid metal sorption is highly desirable for biosorbents for practical applications.

3.2.2. Effect of pH on metal ion adsorption

The effect of the initial pH of the solution on metal ion adsorption on cellulose-MT-CBM and untreated cellulose (control) is shown in Fig. 5(a). The influence of pH on the biosorption of Pb(II) and Zn(II) indicated that the biosorption increased with pH. From pH 2.0 to 7.0, the percentage of Pb(II) removed increased from 0.8% to 94%, and that of Zn(II) increased from 52% to 60%. The slightly lower biosorption yield observed for Zn(II) could be attributed to the possible inert nature of one of the MT binding sites to Zn as reported previously (Harrison et al., 2002).

At lower pH values, the binding sites are protonated and the metal ions are in solution because they cannot access the binding sites on the cellulose-MT-CBM. At higher pH values, the binding sites are deprotonated, negatively charged, and more favorable for adsorption. The control had negligible biosorption capacity at all pH values because of a lack of binding ability. The percentages of Pb(II) and Zn(II) removed increased significantly at pH 6.5. This higher adsorption could be related to the pzc of the cellulose-MT-CBM (Fig. 5(b)). At pH > pzc, the biosorption of Pb(II) and Zn(II) to the biosorbent is favorable because of the presence of negatively charged functional groups of the protein (Bakatula et al., 2018). Therefore, negatively charged functional groups at pH 6.5 would be able to attract and sequester positively charged metal ions.

3.2.3. Biosorption capacity

The adsorption isotherm was studied to understand the equilibrium distribution of Pb(II) and Zn(II) between the aqueous phase and surface of the biosorbent. The Langmuir isotherm model was suitable for the experimental data as shown by a good fit with model data (Fig. S4). This indicates that the biosorption of Pb(II) and Zn(II) onto the cellulose-MT-CBM takes place via a monolayer mechanism. The maximum biosorption capacities for Pb(II) and Zn(II) were higher than those obtained with other cellulose-based biosorbents. For Pb (II), Dhir and Kumar (2010) found a Q_{max} value of 41.84 mg/g for wheat straw compared with 39.02 mg/g for the cellulose-MT-CBM in the present study. For Zn (II), Tian et al. (2017) found a Q_{max} value of 5.38 mg/g on a cellulose nanofibril aerogel compared with 29.28 mg/g on the cellulose-MT-CBM in the present study. These results indicate that the cellulose-MT-CBM biosorbent can be used for the removal of heavy metals from water.

3.3. Recyclability of the cellulose-MT-CBM biosorbent

Recyclability of the cellulose-MT-CBM biosorbent was examined because waste has a huge negative impact on the natural environment. The results for the biosorbent recyclability experiments are shown in Fig. 6. The cellulose-MT-CBM was regenerated seven times and the bound metal ion was desorbed by 20 mM EDTA. In cycle 4, the adsorption ability slightly decreased. The adsorption ability could be restored by addition of MT-CBM to the cellulose, which resulted in an increase in the metal biosorption. These results show that the biosorbent could be used for multiple metal sorption/desorption cycles without any significant loss in its efficiency.

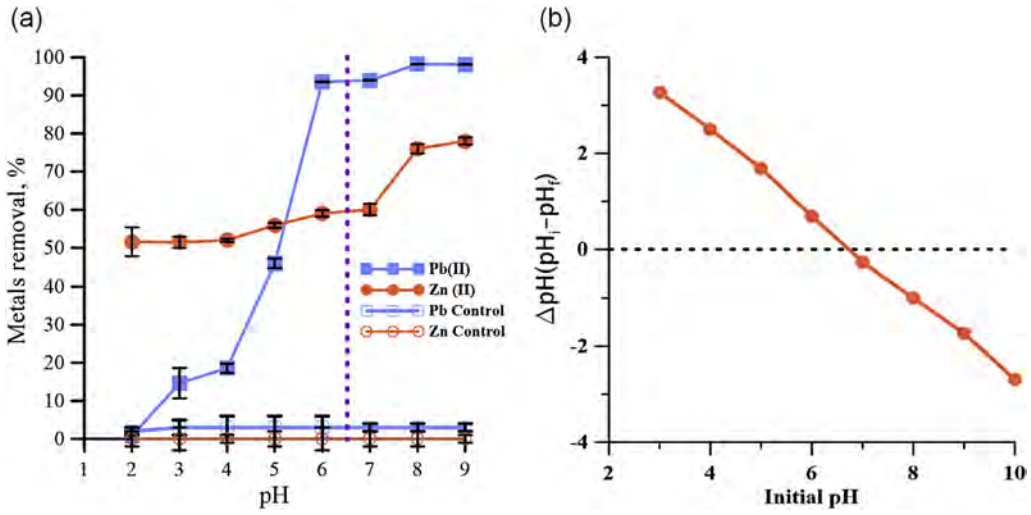

Fig. 5. (a) Effect of pH on the adsorption of Pb(II) and Zn(II) on cellulose-MT-CBM (biomass dosage: 10 g/L, initial metal ion concentration: 20 mg/L, temperature: room temperature; the purple dotted line indicates the pzc of the biosorbent) and (b) pzc of the cellulose-MT-CBM biosorbent. (For interpretation of the references to colour in this figure legend, the reader is referred to the Web version of this article.)

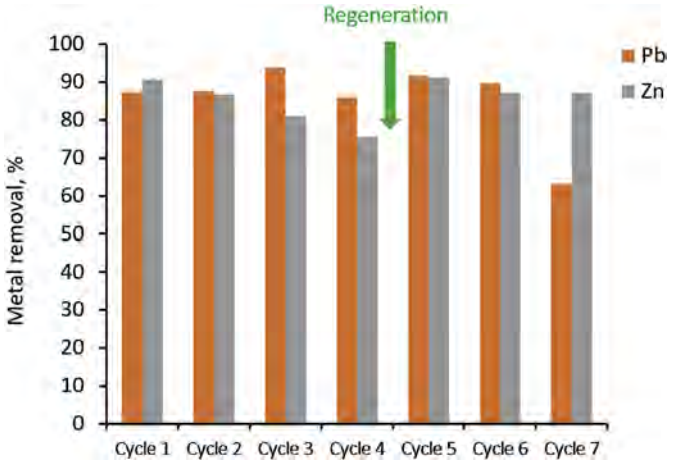

Fig. 6. Pb(II) and Zn(II) removal efficiencies of the cellulose-MT-CBM biosorbent for different cycles (initial metal ion concentration: 20 mg/L, pH: 6.5, temperature: room temperature).

3.4. XPS analysis

XPS measurements of cellulose-MT-CBM after metal adsorption were performed to confirm the electronic state(s) of Pb(II) and Zn(II) on the biosorbent. XPS wide scan spectra of cellulose-MT-CBM before and after Pb(II) and Zn(II) adsorption depicted core levels of C 1s, O 1s, N 1s, Pb 4d, and Zn 2p (Fig. 7). Two new peaks at 141 and 136 eV appeared after Pb (II) adsorption, which were attributed to the Pb 4f orbital (Qiao et al., 2019). One new peak at 1022 eV was attributed to the Zn 2p orbital (Zhou et al., 2016). These results indicate that Pb(II) and Zn(II) are adsorbed on the biosorbent. The source of N 1s is the MT-CBM protein bound on the cellulose.

Metal adsorption by cellulose-MT-CBM could be attributed to the formation of N: Pb^{2+} and N: Zn^{2+} complexes, in which a lone pair of electrons from the N atom in $-NH_2$ group is donated to a shared bond between the nitrogen atom and Pb^{2+} or Zn^{2+}. Additionally, the oxygen atom could be responsible for heavy metal removal via ionic interactions with Pb^{2+} and Zn^{2+}. The O 1s peak at 532.29 eV was modeled after curve fitting and attributed to the oxygen-rich functional groups such as −COOH group, which interact with heavy metals to form O: Pb^{2+} or O: Zn^{2+}. The XPS results confirm the FTIR data that identified organic functional groups such as $-NH_2$ and −COOH groups on the biosorbent (Fig. S2). Furthermore, the removal of heavy metals by the cellulose-MT-CBM occurs via heavy metal complexation with the thiol group of cysteine-rich MTs (Diep et al., 2018) and ion exchange with the O atom in the biosorbent as previously reported (Jana et al., 2016).

3.5. Treatment of actual mine wastewater by the cellulose-MT-CBM biosorbent

To demonstrate industrial application of the cellulose-MT-CBM, the biosorbent was used to treat contaminated surface water from an industrial source. The Mushishima stream in Chingola, Zambia, which flows into the Kafue River, is affected by effluent from the active Nchanga Mine (Sracek et al., 2012). It is essential to evaluate the performance of the biosorbent in a multi-metal system that reflects real effluent as opposed to simulated metal ion solutions. Table 1 shows the water quality data obtained before and after treatment with the cellulose-MT-CBM using the setup illustrated in

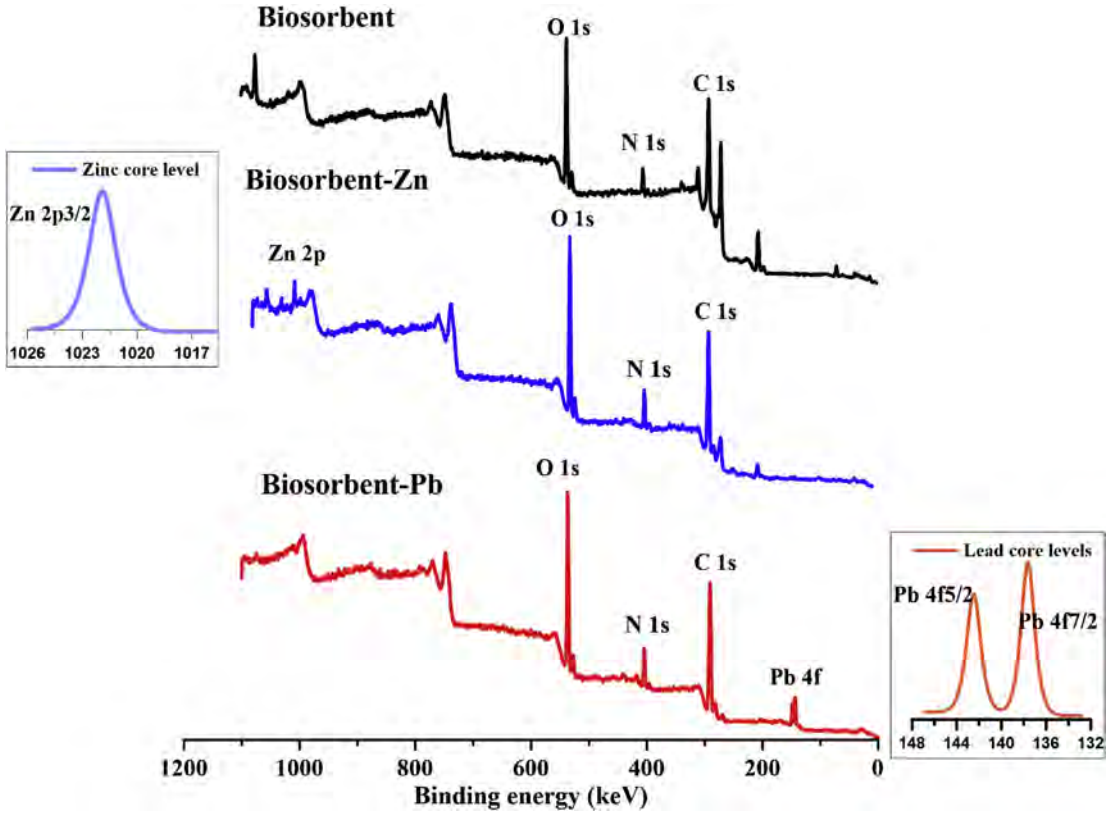

Fig. 7. Typical XPS wide scan spectra of the cellulose-MT-CBM before and after Pb(II) and Zn(II) adsorption.

Table 1
Concentrations of metal ions in mine wastewater before and after treatment with the cellulose-MT-CBM biosorbent.

Toxic trace elements of concern	Before (mg/L)	After (mg/L)	WHO acceptable Limit (mg/L)
Pb	0.19	<0.001	0.01
Cu	14.56	<0.001	2.00
Ni	7.74	<0.001	0.07
Cd	0.34	<0.001	0.10

Fig. 3. Treated water from the site showed complete removal of toxic elements with below the detection limit of ICP-AES. These results show that the cellulose-MT-CBM is effective and be applied in the mining industry as a clean-up technique.

4. Conclusion

In this study we developed a novel biosorbent composed of cellulose and a fusion protein. The fusion protein was constructed from metallothionein (MT) and a carbohydrate-binding module (CBM), where CBM binds to cellulose and MT captures heavy metal ions in solution. The biosorbent had maximum biosorption capacities of 39.02 mg/g for Pb(II) and 29.28 mg/g for Zn(II) ions. The resulted cellulose-MT-CBM biosorbent showed regeneration and reusability after repeated using seven times in a semi-continuous system. The biosorbent was applied to purify multiparameter contaminated real mining wastewater and showed complete removal of Pb(II), Cu(II), Ni(II), and Cd(II) to below detection limit. Because of these capabilities, this biosorbent has great potential for efficient removal of toxic trace elements from polluted water.

Declaration of competing interest

None.

CRediT authorship contribution statement

Wilson Mwandira: Conceptualization, Investigation, Methodology, Writing - original draft. **Kazunori Nakashima:** Conceptualization, Funding acquisition, Investigation, Methodology, Project administration, Writing - review & editing. **Yuki Togo:** Methodology, Writing - review & editing. **Tsutomu Sato:** Investigation, Writing - review & editing. **Satoru Kawasaki:** Funding acquisition, Supervision, Writing - review & editing.

Acknowledgments

This work was partly supported by Japan Society for the Promotion of Science (JSPS) KAKENHI (grant number JP18H03395) and Japan Science and Technology Agency (JST), Japan International Cooperation Agency (JICA), and Science and Technology Research Partnership for Sustainable Development (SATREPS). We thank the Laboratory of XPS analysis, Joint-use facilities, Hokkaido University, supported by the Material Analysis and Structure Analysis Open Unit (MASAOU) for XPS analysis.

Appendix A. Supplementary data

Supplementary data to this article can be found online at https://doi.org/10.1016/j.chemosphere.2019.125733.

References

Abouzeid, R.E., Khiari, R., El-Wakil, N., Dufresne, A., 2019. Current state and new trends in the use of cellulose nanomaterials for wastewater treatment. Biomacromolecules 20, 573–597. https://doi.org/10.1021/acs.biomac.8b00839.
Bakatula, E.N., Richard, D., Neculita, C.M., Zagury, G.J., 2018. Determination of point of zero charge of natural organic materials. Environ. Sci. Pollut. Res. 25, 7823–7833. https://doi.org/10.1007/s11356-017-1115-7.
Baran, A., Wieczorek, J., Mazurek, R., Urban, K., Klimkowicz-pawlas, A., 2018. Potential Ecological Risk Assessment and Predicting Zinc Accumulation in Soils, pp. 435–450. https://doi.org/10.1007/s10653-017-9924-7.
Chang, F., Xue, S., Xie, X., Fang, W., Fang, Z., Xiao, Y., 2018. Carbohydrate-binding module assisted purification and immobilization of β-glucosidase onto cellulose and application in hydrolysis of soybean isoflavone glycosides. J. Biosci. Bioeng. 125, 185–191. https://doi.org/10.1016/J.JBIOSC.2017.09.001.
Chaudhary, K., Agarwal, S., Khan, S., 2018. Role of phytochelatins (PCs), metallothioneins (MTs), and heavy metal ATPase (HMA) genes in heavy metal tolerance. In: Mycoremediation and Environmental Sustainability. Springer, Cham, pp. 39–60. https://doi.org/10.1007/978-3-319-77386-5_2.
Chen, L., Zhou, S., Shi, Y., Wang, C., Li, B., Li, Y., Wu, S., 2018. Heavy metals in food crops , soil , and water in the Lihe River Watershed of the Taihu Region and their potential health risks when ingested. Sci. Total Environ. 615, 141–149. https://doi.org/10.1016/j.scitotenv.2017.09.230.
Dhir, B., Kumar, R., 2010. Adsorption of heavy metals by salvinia biomass and agricultural residues. Int. J. Environ. Res. 4, 427–432.
Diep, P., Mahadevan, R., Yakunin, A.F., 2018. Heavy metal removal by bioaccumulation using genetically engineered microorganisms. Front. Bioeng. Biotechnol. 6, 157. https://doi.org/10.3389/fbioe.2018.00157.
Fakhre, N.A., Ibrahim, B.M., 2018. The use of new chemically modified cellulose for heavy metal ion adsorption. J. Hazard Mater. 343, 324–331. https://doi.org/10.1016/j.jhazmat.2017.08.043.
Gitis, V., Hankins, N., 2018. Water treatment chemicals. Trends and challenges 25, 34–38. https://doi.org/10.1016/j.jwpe.2018.06.003.
Harrison, M.D., Sadler, P.J., Robinson, A.K., Robinson, N.J., Parkinson, J.A., Cavet, J.S., Blindauer, C.A., 2002. A metallothionein containing a zinc finger within a four-metal cluster protects a bacterium from zinc toxicity. Proc. Natl. Acad. Sci. 98, 9593–9598. https://doi.org/10.1073/pnas.171120098.
Hokkanen, S., Bhatnagar, A., Sillanpää, M., 2016. A review on modification methods to cellulose-based adsorbents to improve adsorption capacity. Water Res. 91, 156–173. https://doi.org/10.1016/j.watres.2016.01.008.
Hong, J., Ye, X., Zhang, Y.H.P., 2007. Quantitative determination of cellulose accessibility to cellulase based on adsorption of a nonhydrolytic fusion protein containing CBM and GFP with its applications. Langmuir 23, 12535–12540. https://doi.org/10.1021/la7025686.
Jana, A., Bhattacharya, P., Sarkar, S., Majumdar, S., Ghosh, S., 2016. An ecofriendly approach towards remediation of high lead containing toxic industrial effluent by a combined biosorption and microfiltration process: a total reuse prospect. Desalin. Water Treat. 57, 5498–5513. https://doi.org/10.1080/19443994.2015.1004596.
Mekawy, A.M.M., Assaha, D.V.M., Munehiro, R., Kohnishi, E., Nagaoka, T., Ueda, A., Saneoka, H., 2018. Characterization of type 3 metallothionein-like gene (OsMT-3a) from rice, revealed its ability to confer tolerance to salinity and heavy metal stresses. Environ. Exp. Bot. 147, 157–166. https://doi.org/10.1016/j.envexpbot.2017.12.002.
Qiao, W., Zhang, Y., Xia, H., Luo, Y., Liu, S., Wang, S., Wang, W., 2019. Bioimmobilization of lead by Bacillus subtilis X3 biomass isolated from lead mine soil under promotion of multiple adsorption mechanisms. R. Soc. Open Sci. 6 https://doi.org/10.1098/rsos.181701.
Shi, J., Lindsay, W.P., Huckle, J.W., Morby, A.P., Robinson, N.J., 1992. Cyanobacterial metallothionein gene expressed in Escherichia coli Metal-binding properties of the expressed protein. FEBS Lett. 303, 159–163. https://doi.org/10.1016/0014-5793(92)80509-F.
Singh, N.B., Nagpal, G., Agrawal, S., Rachna, 2018. Water purification by using adsorbents: a review. Environ. Technol. Innov. 11, 187–240. https://doi.org/10.1016/j.eti.2018.05.006.
Sracek, O., Kříbek, B., Mihaljevič, M., Majer, V., Veselovský, F., Vencelides, Z., Nyambe, I., 2012. Mining-related contamination of surface water and sediments of the Kafue River drainage system in the Copperbelt district, Zambia: an example of a high neutralization capacity system. J. Geochem. Explor. 112, 174–188. https://doi.org/10.1016/j.gexplo.2011.08.007.
Tian, C., Qing, Y., Luo, S., Wu, Q., She, J., Wu, Y., 2017. Reusable and cross-linked cellulose nanofibrils aerogel for the removal of heavy metal ions. Polym. Compos. 39, 4442–4451. https://doi.org/10.1002/pc.24536.
World Health Organization, 2017. Guidelines for Drinking-Water Quality. https://doi.org/10.1016/S1462-0758(00)00006-6.
Xu, Z., Bae, W., Mulchandani, A., Mehra, R.K., Chen, W., 2002. Heavy metal removal by novel CBD-EC20 sorbents immobilized on cellulose. Biomacromolecules 3, 462–465. https://doi.org/10.1021/bm015631f.
Yunus, I.S., Tsai, S.-L., 2015. Designed biomolecule–cellulose complexes for

palladium recovery and detoxification. RSC Adv. 5, 20276–20282. https://doi.org/10.1039/C4RA16200E.
Zhou, Y., Zhang, Z., Zhang, J., Xia, S., 2016. New insight into adsorption characteristics and mechanisms of the biosorbent from waste activated sludge for heavy metals. J. Environ. Sci. (China) 45, 248–256. https://doi.org/10.1016/j.jes.2016.03.007.
Zoroddu, M.A., Aaseth, J., Crisponi, G., Peana, M., Nurchi, V.M., 2019. The essential metals for humans: a brief overview Maria. J. Inorg. Biochem. #pagerange#. https://doi.org/10.1016/j.jinorgbio.2019.03.013.

The Journal of Veterinary Medical Science

FULL PAPER

Toxicology

Current situation regarding lead exposure in birds in Japan (2015–2018); lead exposure is still occurring

Chihiro ISHII[1)], Yoshinori IKENAKA[1,2)], Shouta M.M. NAKAYAMA[1)], Takeshi KURITANI[3)], Mitsuhiro NAKAGAWA[3)], Keisuke SAITO[4)], Yukiko WATANABE[4)], Kohei OGASAWARA[4)], Manabu ONUMA[5)], Atsushi HAGA[5)] and Mayumi ISHIZUKA[1)]*

[1)]Laboratory of Toxicology, Department of Environmental Veterinary Sciences, School of Veterinary Medicine, Hokkaido University, Kita18, Nishi9, Kita-ku, Sapporo, Hokkaido 060-0818, Japan
[2)]Water Research Group, Unit for Environmental Sciences and Management, North-West University, 11 Hoffman Street, Potchefstroom, 2531, South Africa
[3)]Graduate School of Science, Hokkaido University, Kita10, Nishi8, Kita-ku, Sapporo, Hokkaido 060-0810, Japan
[4)]Institute for Raptor Biomedicine Japan, 2-2101 Hokuto, Kushiro-shi, Hokkaido 084-0922, Japan
[5)]National Institute for Environmental Studies, 16-2 Onogawa, Tsukuba, Ibaraki 305-8506, Japan

ABSTRACT. Birds of a number of species have died as a result of lead (Pb) poisoning, including many Steller's sea eagles (*Haliaeetus pelagicus*) and white-tailed sea eagles (*Haliaeetus albicilla*) in Hokkaido, the northernmost island of Japan. To address this issue, the use of any type of Pb ammunition for hunting of large animals was prohibited in Hokkaido in 2004. However, Pb poisoning is still being reported in this area, and there are few regulations regarding the use of Pb ammunition in other parts of Japan, where it has been reported that eagles and water birds have been exposed to Pb. This study was performed to accurately determine the current level of Pb exposure of birds found dead in the field or dead in the wild bird centers in Japan (June 2015–May 2018) and to identify the sources of Pb. Pb exposure was found to still be occurring in raptors and water birds in various parts of Japan. Twenty-six point five % and 5.9% of the recorded deaths of Steller's sea eagles and white-tailed sea eagles, respectively, were found to have been poisoned by Pb. In addition, Pb isotope ratio analysis showed that both Pb rifle bullets and Pb shot pellets cause Pb exposure in birds, and these endangered eagles are also exposed to Pb in Hokkaido due to the illegal use of Pb ammunition. Changing to Pb-free ammunition, such as copper (Cu) rifle bullets, steel shot pellets, or bismuth shot pellets, will be essential for the conservation of avian species in Japan.

KEY WORDS: Pb ammunition, Pb exposure, Pb isotope ratios, raptor, water bird

J. Vet. Med. Sci.
82(8): 1118–1123, 2020
doi: 10.1292/jvms.20-0104

Received: 28 February 2020
Accepted: 28 May 2020
Advanced Epub:
18 June 2020

Birds of a number of species have died as a result of lead (Pb) poisoning, including at least 33 raptors, 30 other terrestrial bird species, and water birds in the world [1, 23]. Furthermore, both the number of taxa affected and geographical spread of cases have increased [24]. Raptors can experience secondary Pb poisoning from feeding on animals with Pb ammunition embedded in their tissues, while water birds commonly suffer from Pb poisoning through ingestion of Pb shot pellets or sinkers lying in lakes and marshes, which they mistake for grit [2, 8, 27]. When raptors consume these water birds, they are also exposed to Pb.

Pb is an accumulative metabolic poison that produces toxic effects in a wide range of physiological and biochemical systems, including the hematopoietic, vascular, nervous, renal, immune, and reproductive systems, and elevated accumulation of Pb leads to high mortality rates [13, 24]. Sublethal doses of Pb alter movement behaviors [5] and affect sperm quality and reproductive success [29]. There is also a possibility that birds exposed to Pb cannot migrate. The ecological significance of mortalities and the effect on reproductive system associated with Pb exposure must be viewed within the context of cumulative risks to avian populations [13].

Although the use of Pb in gasoline, paints, and various household items is prohibited because of its toxicity, Pb ammunition is still widely used for hunting and shooting [1]. Non-Pb shot, such as copper (Cu) rifle bullets or iron-tungsten-nickel shot pellets, have been developed [3, 7] and their efficacy has been demonstrated [12]. However, there are few nationally regulated bans on the

*Correspondence to: Ishizuka, M.: ishizum@vetmed.hokudai.ac.jp

(Supplementary material: refer to PMC https://www.ncbi.nlm.nih.gov/pmc/journals/2350/)

use of Pb ammunition despite the scientific evidence for the risks it poses and increasing policy imperatives [1].

In Hokkaido, the northernmost island of Japan, many Steller's sea eagles (*Haliaeetus pelagicus*) and white-tailed sea eagles (*Haliaeetus albicilla*) have died from Pb poisoning after ingesting Pb fragments from sika deer (*Cervus nippon*) carcasses. The number of sika deer is increasing in Hokkaido, and hunting is needed for management of their population. Due to the toxicity of Pb, it is required to use copper (Cu) rifle bullets or slugs instead of Pb bullets for hunting sika deer. A regulation to ban the use of Pb rifle bullets for hunting sika deer was introduced in 2000, and the use of Pb shot pellets for hunting sika deer was prohibited in 2001. In addition, an extended ban was initiated in 2004, which prohibited the use of any type of Pb-containing ammunition for hunting large animal species. This regulation was enforced in 2014, prohibiting the possession of Pb rifle bullets, slugs, or large shot pellets during hunting; prior to this regulation, it was not illegal to carry Pb ammunition when hunting, but hunters were punished if they were found to have used such ammunition. However, although more than 10 years have passed since the introduction of legislation regarding Pb ammunition, Pb poisoning is still being reported in Hokkaido [10]. In other parts of Japan, both regulations and surveillance were less extensive than in Hokkaido, however, eagles and water birds were exposed to Pb [9, 11, 20].

Various thresholds for Pb toxicity in birds have been reported in the literature [6, 13, 14, 18, 26]. The background level of Pb in the liver is generally <2 mg/kg wet weight (6–7 mg/kg dry weight) or <1 mg/kg wet weight (3 mg/kg dry weight) in raptors [21]. Some authors have reported that a liver Pb concentration of >6 mg/kg dry weight in raptors indicates abnormally high exposure to Pb, while a concentration of >20 mg/kg dry weight indicates acute exposure and absorption, resulting in Pb poisoning [21, 22]. The following categories are used in Japan based on the hepatic Pb concentration in wet weight: <0.2 mg/kg, normal range; 0.2−2 mg/kg, high level of Pb exposure; and >2 mg/kg, Pb poisoning [24].

The relative abundances of the naturally occurring isotopes of Pb (^{204}Pb, ^{206}Pb, ^{207}Pb, and ^{208}Pb) vary among industrial materials, allowing the isotope ratios in organisms to be used to determine the source of Pb exposure, as reported previously in raptors [4]. The following Pb isotope ratios (^{208}Pb/^{206}Pb, ^{207}Pb/^{206}Pb) were reported for various types of Pb ammunition obtained from stores in Japan: rifle bullets, 1.90−2.10 and 0.75−0.88; shot pellets, 2.07−2.14 and 0.85−0.87; and fishing sinkers, 2.08−2.20 and 0.84−0.90. These materials had been purchased or collected from the carcasses of birds up until 2001. We confirmed that the Pb isotope ratios of Pb rifle bullets, shot pellets, and fishing sinkers used by hunters and fishermen recently were comparable to these values and the results of Pb isotope ratio in the liver of bird would reflect that in the main source of exposure [10].

This study was performed to accurately determine the current levels of Pb exposure in wild birds carried to clinics or wild bird centers in Japan (June 2015−May 2018) and to identify the sources of Pb by analyzing the Pb isotope ratios.

MATERIALS AND METHODS

Sampling

Liver specimens from the carcasses of birds were obtained from the Institute for Raptor Biomedicine Japan, National Institute for Environmental Studies, or wild bird centers for analysis of their Pb concentrations and Pb isotope ratios. Samples were collected from June 2015 to May 2018 from the following locations and species: from Hokkaido, white-tailed sea eagle (*n*=51), Steller's sea eagle (*n*=34), Blakiston's fish owl (*Ketupa blakistoni*) (*n*=7), mountain hawk eagle (*Spizaetus nipalensis*) (*n*=3), northern goshawk (*Accipiter gentilis*) (*n*=3), Eurasian hobby (*Falco subbuteo*) (*n*=2), peregrine falcon (*Falco peregrinus*) (*n*=1), sparrow hawk (*Accipiter nisus*) (*n*=1), ural owl (*Strix uralensis japonica*) (*n*=1), jungle crow (*Corvus macrorhynchos*) (*n*=2), and whooper swan (*Cygnus cygnus*) (*n*=1); from Honshu (the main island) or Kyushu (southwestern island), peregrine falcon (*n*=6), northern goshawk (*n*=5), sparrow hawk (*n*=4), ural owl (*n*=4), mountain hawk eagle (*n*=2), whooper swan (*n*=2), and greater white-fronted goose (*Anser albifrons*) (*n*=2). Swans that had died in one lake in Honshu (see Introduction) were not included in the analysis to exclude any potential sampling bias around the ratio of Pb exposure in swans. The specimens were transported to the School of Veterinary Medicine, Hokkaido University, Sapporo, Japan, where they were stored at −20°C until analysis. The ages of raptors were estimated from their morphological characteristics, such as the development of the gonads and feathers, the color of their feathers and iris, and molting condition [19]. Sampling areas are shown in Supplementary Fig. 1 and individual information is shown in Supplementary Table 3. The map information for Supplementary Fig. 1 was downloaded from Geospatial Information Authority of Japan and depicted by sf package [25] and ggplot2 [30] on R software ver. 3.5.1 [28].

Four shot pellets from the stomach of a whooper swan and fragments of Pb ammunition from the stomachs of two Steller's sea eagles were also collected to analyze the Pb isotope ratios in Pb ammunition.

Pb concentration

Pb concentrations were analyzed according to the method of Yabe *et al*. [31]. Samples of 100−300 mg of soft tissues were digested with 5 m*l* of 30% nitric acid (Kanto Chemical Corp., Tokyo, Japan) and 1 m*l* of 30% hydrogen peroxide (Kanto Chemical Corp.) in a microwave digestion system (Speedwave Two; Berghof, Eningen, Germany), after which the volume was made up to 10 m*l* by adding 2% nitric acid. Digestion was performed under the following conditions: 180°C for 15 min, 200°C for 20 min, and 100°C for 20 min. The Pb concentration and isotope ratios were then measured using an inductively coupled plasma–mass spectrometer (ICP-MS) (7700 series; Agilent Technology, Tokyo, Japan) (see Supplementary Table 1 for detailed analytical conditions), which was calibrated using ICP-MS Calibration Standards (Agilent Technology) to establish standard curves before analysis. Standard solutions (0, 10, 50, 100, 250, and 500 μg/*l* were prepared with 2% nitric acid and the standard curves had r^2 values of 0.998. All chemicals and standard stock solutions were of analytical reagent grade (Wako Pure Chemicals Industries, Osaka, Japan). Distilled and deionized water was used (Milli-Q; Merck Millipore, Billerica, MA, USA), and analytical quality

control was performed using DOLT-4 (dogfish liver) and DORM-3 (fish protein) certified reference materials (National Research Council of Canada, Ottawa, ON, Canada), which were shown to have good recoveries (95–105%) through replicate analysis. Thallium (^{205}Tl) was used as an internal standard for the Pb concentration analysis. The limit of detection for Pb was 0.001 μg/kg.

Pb isotope analysis

The chemical procedures were carried out in a clean room with a Class 1000. The sample dissolution procedure was similar to the method described by Kuritani and Nakamura [16]. The extracted solutions of liver were transferred into Teflon tubes after analysis of Pb levels. One drop (~30 μl) of 0.05 N phosphoric acid (orthophosphoric acid 85%; Merck KGaA, Darmstadt, Germany) was added to the tubes to avoid complete dryness prior to evaporation. The mixed solution was dried for 15 hr on a hotplate at 100°C. After evaporation, three drops (~90 μl) of 8 N hydrogen bromide (once distilled, Analytical Grade 48%; Kanto Chemical Corp.) was added to the tubes. The tubes were placed on a hotplate at 120°C for 1 hr for re-drying. At the final step of pre-treatment before applying to the column, 0.3 m*l* of 0.5 N hydrogen bromide was introduced into the tube to dissolve residues. A polyethylene column was charged with 0.1 m*l* of anion exchange resin (AG1-X8, analytical grade, 200–400 mesh, chloride form; Bio-Rad, Hercules, CA, USA). The resin bed was washed by flushing the column with 1.0 m*l* of 0.5 N nitric acid (EL Grade 61%; Kanto Chemical Corp.) followed by 1.0 m*l* of double distilled deionized water, at a rate of ~0.03 m*l*/min. The column was conditioned with 0.2 m*l* of 0.5 N hydrogen bromide. The sample dissolved in 0.3 m*l* of 0.5 N hydrogen bromide was loaded onto the column. To wash out residual organic compounds originally derived from liver samples, 0.3 m*l* of 0.5 N hydrogen bromide was introduced twice. Subsequently, 0.8 m*l* of 0.25 N hydrogen bromide–0.5 N nitric acid mixture was applied to the column to remove elements other than Pb. Finally, the column was washed again with 0.1 m*l* of double distilled deionized water. After all washing procedures, 1.3 m*l* of 3% nitric acid was introduced to drop Pb out from the resin. Then, 2 μl of 50 mg/*l* thallium (Tl) was added to Pb eluted solution as an external standard for the analytical procedure.

Pb isotopic ratios of ^{208}Pb/^{206}Pb and ^{207}Pb/^{206}Pb were determined on a multiple collector (MC)-ICP-MS (Neptune Plus; Thermo Finnigan, San Jose, CA, USA) in static mode with the Faraday cup configuration. Other general parameters are described in Supplementary Table 2. Mass fractionation factors for Pb were corrected using an external standard of Tl. In addition, mass-dependent inter-element fractionations were also corrected by applying a standard bracketing method using NIST SRM 981 (National Institute of Standards and Technology, Gaithersburg, MD, USA), and the data were finally normalized to ^{206}Pb/^{204}Pb=16.9424, ^{207}Pb/^{204}Pb=15.5003, and ^{208}Pb/^{204}Pb=36.7266 [17]. The 2SE values of ^{208}Pb/^{206}Pb or ^{207}Pb/^{206}Pb were <0.0002.

Statistical analysis

Differences in the Pb concentrations between Steller's sea eagles and white-tailed sea eagles were analyzed using the Mann–Whitney *U* test. Statistical analysis was performed with JMP Pro 14 (SAS Institute, Cary, NC, USA). In all analyses, $P<0.05$ was taken to indicate statistical significance.

RESULTS

In total, nine of 34 Steller's sea eagles (26.5%) and three of 51 white-tailed sea eagles (5.9%) from Hokkaido, and two whooper swans from Hokkaido or Honshu exceeded the background level of Pb poisoning (i.e., >2 mg/kg wet weight of Pb in the liver). In addition, two white-tailed sea eagles, three Steller's sea eagles, and one Eurasian hobby from Hokkaido, and one mountain hawk eagle and one greater white-fronted goose from Honshu showed high Pb exposure (0.2–2 mg/kg) (Tables 1 and 2, Supplementary Fig. 2).

As for the species difference between Steller's sea eagles and white-tailed sea eagles, statistical analysis showed that Steller's

Table 1. Hepatic Pb levels (mg/kg, wet weight, range) and the assesments of Pb exposure in birds from Hokkaido

Species	Sample size	Pb concentration in liver	Assessments		
		mg/kg, wet wt, median, (range)	Pb poisoning (>2.0 mg.kg)	High Pb exposure (0.2–2.0 mg/kg)	Non toxic (<0.2 mg/kg)
White-tailed sea eagle	51	0.068 (0.003–50.79)	3	2	46
Steller's sea eagle	34	0.082 (0.003–72.01)	9	3	22
Blakiston's fish-owl	7	0.036 (0.001–0.070)	0	0	7
Mountain hawk-eagle	3	0.095 (0.023–0.120)	0	0	3
Northern goshawk	3	0.025 (0.007–0.136)	0	0	3
Eurasian Hobby	2	(0.092, 0.278)	0	1	1
Jungle crow	2	(0.063, 0.107)	0	0	2
Peregrine falcon	1	0.093	0	0	1
Sparrow hawk	1	0.065	0	0	1
Ural owl	1	0.137	0	0	1
Whooper swan	1	19.56	1	0	0

Table 2. Hepatic Pb levels (mg/kg, wet weight, range) and the assesments of Pb exposure in birds from Honshu or Kyushu

Species	Sample size	Pb concentration in liver	Assessments		
			Pb poisoning (>2.0 mg.kg)	High Pb exposure (0.2–2.0 mg/kg)	Non toxic (<0.2 mg/kg)
Peregrine falcon	6	0.050 (0.023–0.095)	0	0	5
Northern goshawk	5	0.080 (0.032–0.157)	0	0	5
Sparrowhawk	4	0.047 (0.017–0.080)	0	0	3
Ural owl	4	0.031 (0.015–0.054)	0	0	3
Mountain hawk-eagle	2	(0.051, 0.705)	0	1	1
Whooper swan	2	(0.182, 19.58)	1	0	1
Greater white-fronted goose	2	(0.097, 0.719)	0	1	1

Table 3. Pb isotope ratios in liver and ammunition from the stomach of Steller's sea eagle and whooper swan

	Sample	Pb isotope ratios	
		208/206 Pb	207/206 Pb
Steller's sea eagle	Liver	2.05	0.84
	Ammunition from the stomach	2.06	0.84
Steller's sea eagle	Liver	2.11	0.87
	Ammunition from the stomach_1	2.11	0.87
	Ammunition from the stomach_2	2.11	0.87
	Ammunition from the stomach_3	2.11	0.87
Whooper swan	Liver	2.13	0.88
	Ammunition from the stomach_1	2.16	0.90
	Ammunition from the stomach_2	2.12	0.87
	Ammunition from the stomach_3	2.10	0.86
	Ammunition from the stomach_4	2.10	0.86
	Avarage of the above ammunition	2.12	0.87

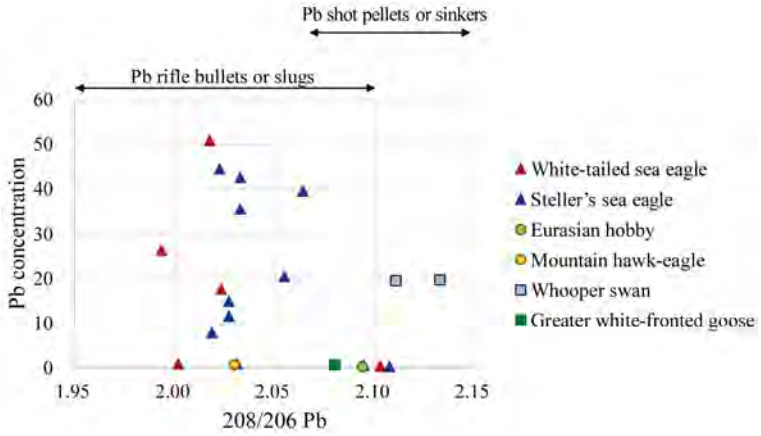

Fig. 1. Comparison of (a) Pb concentration and Pb isotope ratio ($^{208}Pb/^{206}Pb$) in the livers of birds that had high Pb concentrations (>0.2 mg/kg, wet weight).

sea eagles accumulated higher levels of Pb than white-tailed sea eagles, and there was a significant difference ($P<0.03$).

The fragments of Pb ammunition extracted from the stomachs of two Steller's sea eagles had the same isotope ratios as occurred in the livers of the same individuals. A whooper swan showed the same isotope ratios in its liver as the midrange of the isotope ratios of the four pieces of ammunition found in its stomach (Table 3).

The Pb isotope ratios of almost all of the white-tailed sea eagles and Steller's sea eagles, and one mountain hawk eagle were very similar to those of Pb rifle bullets or slugs (Fig. 1). While several sea eagles, one Eurasian hobby, whooper swans, and one greater white-fronted goose had similar Pb isotope ratios with Pb shot pellets or sinkers (Fig. 1). All data are shown in Supplementary Table 3.

DISCUSSION

Pb exposure in birds was shown to have occurred in both Hokkaido and Honshu. Despite prohibition of the use of Pb ammunition, endangered eagles were poisoned by Pb in Hokkaido. Pb poisoning has a large effect to the population of endangered eagles. Birds were also exposed to Pb in Honshu where regulation of the use of Pb ammunition is limited. As the sample number from Honshu was small, they may represent only a portion of the total number of cases.

As for the species difference between Steller's sea eagles and white-tailed sea eagles, Steller's sea eagles accumulated higher levels of Pb than white-tailed sea eagles ($P<0.03$). A previous study showed the same situation in Japan [10]. Steller's sea eagles have a higher risk of ingesting Pb from deer carcasses because their body size is larger than white-tailed sea eagles, and they regularly defeat white-tailed sea eagles to feed on deer carcasses. Furthermore, many sea eagles change their main food source from fish to deer during the hunting season. This tendency to change their diet is stronger in the Steller's sea eagle.

The Pb isotope ratios indicated that almost all of the white-tailed sea eagles and Steller's sea eagles examined were exposed to Pb from Pb rifle bullets or slugs, while several sea eagles had ingested Pb shot pellets or sinkers (Fig. 1). One mountain hawk eagle was found to contain Pb from a Pb rifle bullet, while one Eurasian hobby, whooper swans, and one greater white-fronted goose had ingested Pb shot pellets or sinkers (Fig. 1). Pb isotope ratio analysis showed that both Pb rifle bullets and Pb shot pellets cause Pb exposure in birds, and endangered eagles are also exposed to Pb in Hokkaido due to the illegal use of Pb ammunition. In addition, only limited numbers of birds were obtained from Honshu and Kyushu, but it was clear that birds here were also exposed to Pb from Pb shot pellets or sinkers. The observation that one swan contained four different Pb isotope ratios in four Pb shot pellets indicated that several types of Pb shot pellets had been used in the same area.

Previous study showed that 42% of Steller's sea eagles (18 of 43 cases) and 24% of white-tailed sea eagles (12 of 50 cases) exceeded the level of Pb poisoning (>2 mg/kg wet weight in liver) and one mountain hawk eagle exceeded the level of high Pb exposure (>0.1 mg/kg wet weight in blood) from 2004 to 2015 in Hokkaido [10]. In 2014, the regulation was enforced in Hokkaido that prohibited the possession of Pb rifle bullets, slugs, or large shot pellets for hunting. Prior to this regulation, it was not illegal for hunters to keep Pb ammunition, but they were punished if they were found to use such ammunition. This study, the ratio of Pb exposed birds in Hokkaido decreased. It would be because of the enforced regulation, however, Pb exposure still occurred in Hokkaido due to the illegal use of Pb ammunition. Previous study also showed that in Honshu and Shikoku (a southern island), threes golden eagles, one black kite, and one northern goshawk were exposed to Pb from 1993 to 2015 [10]. This study also indicated that several birds accumulated high levels of Pb in Honshu. Recent studies indicated that some partial bans on the use of lead ammunition do little to reduce lead poisoning mortality in raptors and scavengers [24]. Improvement to the regulation to prohibit the use of Pb ammunition across all parts of Japan is required to conserve avian species.

It has been demonstrated that Pb-free ammunition, such as copper (Cu) rifle bullets, steel shot pellets, and bismuth, shot pellets, have the same or even greater effectiveness as Pb ammunition for hunting, and are much less toxic to birds [12, 27]. For example, Cu toxicity was not confirmed in American kestrel (*Falco sparverius*) that had ingested Cu shot pellets [7]. However, Cu poisoning has sometimes been reported in the waterfowl [15]. Therefore, Cu rifle bullets or slugs would be useful as alternatives to the Pb ammunition that is the source of Pb poisoning in raptors. Steel shot pellets and bismuth pellets should be recommended as alternatives to Pb shot pellets to protect both raptors and waterfowl from Pb poisoning. In Hokkaido, the use of Cu rifle bullets is required instead of Pb rifle bullets and Cu rifle bullets are available at stores. Although many hunters in Hokkaido use Cu rifle bullets, some hunters prefer Pb rifle bullets to Cu ones. One of the reasons is Pb ammunition is inexpensive.

Although the fishing tackle was not found from the stomach of birds in this study, there is also a possibility that fishing sinker is one of the sources of Pb in birds. The use of all Pb fishing tackle is prohibited in Denmark, and there are some restrictions on the use of Pb fishing tackle in European countries, Canada, and the United States to conserve avian species from Pb exposure [8]. In Japan, anyone can obtain Pb-free fishing tackles at stores, however, information of Pb exposure in birds from the ingestion of Pb fishing tackles is not spread sufficiently. The consideration of the use of non-Pb fishing sinkers is also required in Japan.

Pb exposure is still occurring in raptors and water birds in various parts of Japan. In Hokkaido, both Pb rifle bullets and Pb shot pellets cause Pb exposure in birds, and endangered eagles are also exposed to Pb due to the illegal use of Pb ammunition. In Honshu and Kyushu, it was clear that birds were also exposed to Pb from Pb shot pellets or sinkers. It is clear that non-Pb ammunition needs to be used for hunting to reduce Pb exposure and conserve wild birds. In addition, continuous monitoring for Pb levels in wild birds to provide the accurate information about Pb exposure in birds would be important to improve the situation in Japan.

AKNOWLEDGMENTS. We would like to thank Yamashina Institute for Ornithology, Raptor Conservation Center, and The Miyagi Prefectural Izunuma-Uchinuma Environmental Foundation for providing samples. This work was supported by Grants-in-Aid for Scientific Research from the Ministry of Education, Culture, Sports, Science, and Technology of Japan awarded to M. Ishizuka (No. 16H01779), Y. Ikenaka (No. 17K20038, 18H04132), S. Nakayama (No. 16K16197, 17KK0009), and C. Ishii (No. 18H06028). This research was also supported by the Inui Memorial Trust for Research on Animal Science, JST/JICA, SATREPS (Science and Technology Research Partnership for Sustainable Development) and the Environment Research and Technology Development Fund (SII-1/3-2, 4RF-1802/18949907) of the Environmental Restoration and Conservation Agency of Japan. We also acknowledge the financial support by the Nihon Seimei Foundation, the Soroptimist Japan Foundation, the foundations of Sumitomo. We are grateful to Takahiro Ichise, Mai Tamba and Nagisa Hirano (School of Veterinary Medicine, Hokkaido University) for their technical support.

REFERENCES

1. Arnemo, J. M., Andersen, O., Stokke, S., Thomas, V. G., Krone, O., Pain, D. J. and Mateo, R. 2016. Health and environmental risks from lead-based ammunition: science versus socio-politics. *EcoHealth* **13**: 618–622. [Medline] [CrossRef]
2. Bellrose, F. C. 1959. Lead poisoning as a mortality factor in waterfowl populations. *Bull. Ill. Nat. Hist. Surv.* **27**: 235–288. [CrossRef]
3. Brewer, L., Fairbrother, A., Clark, J. and Amick, D. 2003. Acute toxicity of lead, steel, and an iron-tungsten-nickel shot to mallard ducks (Anas platyrhynchos). *J. Wildl. Dis.* **39**: 638–648. [Medline] [CrossRef]
4. Church, M. E., Gwiazda, R., Risebrough, R. W., Sorenson, K., Chamberlain, C. P., Farry, S., Heinrich, W., Rideout, B. A. and Smith, D. R. 2006. Ammunition is the principal source of lead accumulated by California condors re-introduced to the wild. *Environ. Sci. Technol.* **40**: 6143–6150. [Medline] [CrossRef]
5. Ecke, F., Singh, N. J., Arnemo, J. M., Bignert, A., Helander, B., Berglund, Å. M. M., Borg, H., Bröjer, C., Holm, K., Lanzone, M., Miller, T., Nordström, Å., Räikkönen, J., Rodushkin, I., Ågren, E. and Hörnfeldt, B. 2017. Sublethal lead exposure alters movement behavior in free-ranging golden eagles. *Environ. Sci. Technol.* **51**: 5729–5736. [Medline] [CrossRef]
6. Fisher, I. J., Pain, D. J. and Thomas, V. G. 2006. A review of lead poisoning from ammunition sources in terrestrial birds. *Biol. Conserv.* **131**: 421–432. [CrossRef]
7. Franson, J. C., Lahner, L. L., Meteyer, C. U. and Rattner, B. A. 2012. Copper pellets simulating oral exposure to copper ammunition: absence of toxicity in American kestrels (Falco sparverius). *Arch. Environ. Contam. Toxicol.* **62**: 145–153. [Medline] [CrossRef]
8. Haig, S. M., D'Elia, J., Eagles-Smith, C., Fair, J. M., Gervais, J., Herring, G., Rivers, J. W. and Schulz, J. H. 2014. The persistent problem of lead poisoning in birds from ammunition and fishing tackle. *Condor* **116**: 408–428. [CrossRef]
9. Honda, K., Lee, D. P. and Tatsukawa, R. 1990. Lead poisoning in swans in Japan. *Environ. Pollut.* **65**: 209–218. [Medline] [CrossRef]
10. Ishii, C., Nakayama, S. M. M., Ikenaka, Y., Nakata, H., Saito, K., Watanabe, Y., Mizukawa, H., Tanabe, S., Nomiyama, K., Hayashi, T. and Ishizuka, M. 2017. Lead exposure in raptors from Japan and source identification using Pb stable isotope ratios. *Chemosphere* **186**: 367–373. [Medline] [CrossRef]
11. Ishii, C., Nakayama, S. M. M., Kataba, A., Ikenaka, Y., Saito, K., Watanabe, Y., Makino, Y., Matsukawa, T., Kubota, A., Yokoyama, K., Mizukawa, H., Hirata, T. and Ishizuka, M. 2018. Characterization and imaging of lead distribution in bones of lead-exposed birds by ICP-MS and LA-ICP-MS. *Chemosphere* **212**: 994–1001. [Medline] [CrossRef]
12. Kanstrup, N., Balsby, T. J. S. and Thomas, V. G. 2016. Efficacy of non-lead rifle ammunition for hunting in Denmark. *Eur. J. Wildl. Res.* **62**: 333–340. [CrossRef]
13. Kendall, R. J., Lacker, T. E., Bunck, C., Daniel, B., Driver, C., Grue, C. E., Leighton, F., Stansley, W., Watanabe, P. G. and Whitworth, M. 1996. An ecological risk assessment of lead shot exposure in non-waterfowl avian species: Upland game birds and raptors. *Environ. Toxicol. Chem.* **15**: 4–20. [CrossRef]
14. Kim, E.Y., Goto, R., Iwata, H., Masuda, Y., Tanabe, S. and Fujita, S. 1999. Preliminary survey of lead poisoning of Steller's sea eagle (Haliaeetus pelagicus) and white-tailed sea eagle (Haliaeetus albicilla) in Hokkaido, Japan. *Environ. Toxicol. Chem.* **18**: 448–451. [CrossRef]
15. Kobayashi, Y., Shimada, A., Umemura, T. and Nagai, T. 1992. An outbreak of copper poisoning in Mute swans (Cygnus olor). *J. Vet. Med. Sci.* **54**: 229–233. [Medline] [CrossRef]
16. Kuritani, T. and Nakamura, E. 2002. Precise isotope analysis of nanogram-level Pb for natural rock samples without use of double spikes. *Chem. Geol.* **186**: 31–43. [CrossRef]
17. Kuritani, T. and Nakamura, E. 2003. Highly precise and accurate isotopic analysis of small amounts of Pb using 205 Pb–204 Pb and 207 Pb-204 Pb, two double spikes. *J. Anal. At. Spectrom.* **18**: 1464–1470. [CrossRef]
18. Kurosawa, N. 2000. Lead poisoning in Steller's sea eagles and white-tailed sea eagles. First symposium on Stellar's and white-tailed sea eagles in east Asia. Wild Bird Society of Japan, Tokyo.
19. Lovette, I. J. and Fitzpatrick, J. W. 2016. Avian Anatomy. Handbook of Bird Biology, 3rd ed., John Wiley & Sons. Hoboken.
20. Ochiai, K., Hoshiko, K., Jin, K., Tsuzuki, T. and Itakura, C. 1993. A survey of lead poisoning in wild waterfowl in Japan. *J. Wildl. Dis.* **29**: 349–352. [Medline] [CrossRef]
21. Pain, D. J. and Amiard-Triquet, C. 1993. Lead poisoning of raptors in France and elsewhere. *Ecotoxicol. Environ. Saf.* **25**: 183–192. [Medline] [CrossRef]
22. Pain, D. J., Sears, J. and Newton, I. 1995. Lead concentrations in birds of prey in Britain. *Environ. Pollut.* **87**: 173–180. [Medline] [CrossRef]
23. Pain, D. J., Fisher, I. J. and Thomas, V. G. 2009. A global update of lead poisoning in terrestrial birds from ammunition sources. pp. 99–118. *In*: Ingestion of Lead from Spent Ammunition: Implications for Wildlife and Humans, Peregrine Fund, Boise.
24. Pain, D. J., Mateo, R. and Green, R. E. 2019. Effects of lead from ammunition on birds and other wildlife: A review and update. *Ambio* **48**: 935–953. [Medline] [CrossRef]
25. Pebesma, E. 2018. Simple features for R: standardized support for spatial vector data. *R J.* **10**: 439–446. [CrossRef]
26. Saito, K. 2009. Lead poisoning of Steller's Sea-Eagle (*Haliaeetus pelagicus*) and Whitetailed Eagle (*Haliaeetus albicilla*) caused by the ingestion of lead bullets and slugs. Ingestion of Lead from spent Ammunition: Implications for Wildlife and Humans. pp. 302–309, Peregrine Fund, Boise.
27. Scheuhammer, A. M. and Norris, S. L. 1996. The ecotoxicology of lead shot and lead fishing weights. *Ecotoxicology* **5**: 279–295. [Medline] [CrossRef]
28. Team, R. C. R. 2013. A Language and Environment for Statistical Computing. R Foundation for Statistical Computing, Vienna.
29. Vallverdú-Coll, N., Mougeot, F., Ortiz-Santaliestra, M. E., Castaño, C., Santiago-Moreno, J. and Mateo, R. 2016. Effects of lead exposure on sperm quality and reproductive success in an avian model. *Environ. Sci. Technol.* **50**: 12484–12492. [Medline] [CrossRef]
30. Wickham, H. 2016. ggplot2: Elegant Graphics for Data Analysis. Springer-Verlag, New York.
31. Yabe, J., Nakayama, S. M. M., Ikenaka, Y., Yohannes, Y. B., Bortey-Sam, N., Oroszlany, B., Muzandu, K., Choongo, K., Kabalo, A. N., Ntapisha, J., Mweene, A., Umemura, T. and Ishizuka, M. 2015. Lead poisoning in children from townships in the vicinity of a lead-zinc mine in Kabwe, Zambia. *Chemosphere* **119**: 941–947. [Medline] [CrossRef]

The Journal of Veterinary Medical Science

NOTE

Wildlife Science

Relationship between blood test values and blood lead (Pb) levels in Black-headed gull (*Chroicocephalus ridibundus*: Laridae)

Nana USHINE[1)]*, Shouta M.M. NAKAYAMA[2)], Mayumi ISHIZUKA[2)], Tatsuo SATO[3)], Yoshihiro KURAHASHI[4)], Emu WAKAYAMA[1)], Natsuko SUGIURA[1)] and Shin-ichi HAYAMA[1)]

[1)]Laboratory of Wildlife Medicine, Nippon Veterinary and Life Science University, 1-7-1 Kyonan-cho, Musashino-shi, Tokyo 180-8602, Japan
[2)]Laboratory of Toxicology, Department of Environmental Veterinary Sciences, Faculty of Veterinary Medicine, Hokkaido University, Kita 18, Nishi 9, Kita-ku, Sapporo, Hokkaido 060-0818, Japan
[3)]The Friends of the Gyotoku Bird Observatory NPO, 4-22-11 Fukuei, Ichikawa-shi, Chiba 272-0137, Japan
[4)]Japanese Bird Banding Association, 115 Konoyama, Abiko-shi, Chiba 277-1145, Japan

J. Vet. Med. Sci.
82(8): 1124–1129, 2020
doi: 10.1292/jvms.20-0246

Received: 26 April 2020
Accepted: 7 June 2020
Advanced Epub:
19 June 2020

ABSTRACT. Few studies have evaluated immunosuppression due to lead accumulation below the overt toxicity threshold. If low levels of lead accumulation cause immunosuppression in birds, those birds could become more susceptible to pathogens. We aimed to determine if low levels of lead accumulation lead to immunosuppression in Black-headed gulls (*Chroicocephalus ridibundus*). Gulls were captured in Tokyo-bay and Mikawa-bay from January to April 2019. Their blood samples were analyzed for eight items. The data were analyzed to evaluate the correlation between lead concentrations and the variables from each bay. Lead was positively correlated with the percentage of heterophils and heterophil and lymphocyte ratio and negatively with lymphocytes. Thus, low lead accumulation levels may induce changes in percentage of the heterophils and lymphocyte.

KEY WORDS: blood status, *Chroicocephalus ridibundus*, immunosuppression, Japan, Lead accumulation

Lead is a common pollutant found in various avian species [10, 31, 32]. When birds are acutely poisoned with high lead levels, they develop lethargy, or death without clinical signs. In the chronic phase, they develop various clinical signs, such as aplastic anemia, thin eggshell, immunosuppression, and neurological symptoms (e.g., depression and torticollis) [13, 27, 30, 51, 52, 64]. Lead accumulation affects the survival of some avian species [33, 39, 45, 50], such as Common pochard (*Aythya ferina*) and California condor (*Gymnogyps californianus*) [22, 27, 47, 63].

Lead has mainly become an environmental pollutant because of its use in bullets and fishing sinkers [54, 56, 57]. Some overseas regions have banned or restricted the use of lead bullets to prevent environmental pollution and reduce their impact on wildlife [34, 57, 58]. In Japan, the use of lead bullets has only been restricted in Hokkaido since 2000 [4, 37]. Nakata *et al.* [41] reported that environmental lead pollution had mainly occurred in southern areas of Japan by assessing lead accumulation levels in wild caught two Rattus species (*Rattus norvegicus* and *Rattus rattus*). In Japan, some wild birds are affected by lead pollution, such as gooses and swans [40, 42–44]. If the birds inhabiting Japan become an immunosuppression due to a lead accumulate, they may become more susceptible to pathogens, such as highly pathogenic avian influenza virus (HPAIV).

Susceptibility (immunity) can be evaluated by calculating the ratio of heterophils and lymphocytes (H/L ratio) [21]. Heterophils and lymphocytes account for 95% of all leukocytes in avian peripheral blood [12]. Heterophils and lymphocytes are measured for avian health assessment because heterophils are involved in coping with immediate infections and lymphocytes being more consequential in communicable diseases though cellular and humoral immunity [2, 15, 31, 52]. A higher percentage of lymphocytes than heterophils reflects proper immune function in some avian species [29, 48].

Black-headed gull (*Chroicocephalus ridibundus*) is a migratory bird that are affected by lead accumulation [28, 36, 38, 46]. The gulls migrate to Japan from Russia, North China, and Mongolia [3, 5, 37], and in winter, they live in loosely knit locks [1, 19]. Although the gull is a familiar species, its population declined by approximately 45% in the European region from 1989 to 2014 [49]. There is concern about mass mortality due to oil spills or chemical accumulation [18, 36]. Additionally, they are highly susceptible to HPAIV [25, 35, 60], so if lead accumulation causes an immunosuppression regardless its accumulated level, various

*Correspondence to: Ushine, N.: noname.mj.7510@gmail.com

Table 1. Sex and age classification of Black-headed gulls (*Chroicocephalus ridibundus*) captured from January 2019 to April 2019 at two bays

Area (Bay)	Male/Adult	Female/Adult	Male/Yealing[a)]	Male/Yearling[a)]
Tokyo-bay	36	30	2	0
Mikawa-bay	5	16	2	2

a) Yearling data was not available for statistical analysis due to the small sample size.

risks may increase—such as spreading and deaths from these viruses. Therefore, we conducted this study to assess if low levels of lead accumulation cause immunosuppression by analyzing the relationship between lead accumulation level and blood parameters in the Black-headed gull.

This study was approved by the University's Laboratory Animal Ethics Committee (approval number: 30S-47), Ministry of the Environment, Chiba prefecture (approval number: 739-1568, 1667), and Aichi prefecture (approval number: 588-5). The study was conducted from January 2019 to April 2019 in the Ichikawa City, Chiba Prefecture, Japan (Tokyo-bay) and Gamagori City, Aichi prefecture, Japan (Mikawa-bay). The Black-headed gulls were captured by noose trap or whoosh net [9, 55]. Gaunt *et al.* [17] reported that ethical blood sampling requires that the collection be less than 1% of their body mass. Therefore, the captured gulls were weighed quickly, and blood of less than 0.5% of the body mass was collected from the right median metatarsal vein or posterior branch of the brachial vein using a heparinized syringe and 26G needle. After hemostasis, we placed a metal ring on its right tarsus, and released it. We evaluated the following indexes for health condition and body condition: runny nose and wheezing by inspection and auscultation; feces evaluation for green stool, bloody stool, and diarrhea; checked the keel score for nutritional status [17]; dehydration was confirmed by palpation of the conjunctiva, and a skin pinch test; assessing neurological symptoms such as torticollis, nystagmus, and dizziness by observing the captured gull's behavior.

We assessed age because lead accumulation levels are closely related to a bird's age [24, 47]. Age was evaluated using their plumage [3]; gulls that had a juvenile plumage were classified as "Yearling", and did not have a juvenile plumage were "Adult" [20]. Sex was identified using polymerase chain reaction (PCR) [7, 61]. Red blood cell (RBC; 10^6cells/μl) and leukocyte (WBC; cells/μl) were counted using a Neubauer hemocytometer after staining with Natt and Herrick's solution [8, 53]. Packed cell volume (PCV; %) was determined using the microhematocrit method [53]. Hemoglobin (Hb; g/dl) was measured as an absorbance at 540 nm (Synerger HTX, BioTek®, Chicago, IL, USA) [11]. Percentage of heterophil (Het) and lymphocyte (Lym) were evaluated using blood smears that were stained with Light-Giemsa staining solution and H/L ratio was calculated. A blood clot was used to measure the lead levels in gull's peripheral blood. Briefly, blood samples which was autoclaved beforehand were digested with 5 ml of 30% nitric acid (Kanto Chemical Corp., Tokyo, Japan) and 1 ml of 30% hydrogen peroxide (Kanto Chemical Corporation) in a microwave digestion system (Berghof, Eningen, Germany). Lead concentration were measured with an inductively coupled plasma–mass spectrometer (Agilent Technology, Tokyo, Japan) [59]. Analytical quality control was performed using the certified reference material of Seronorm™ Trace Elements Whole Blood L-2 (Sero, Billingstad, Norway). Replicate analysis of reference material showed good accuracy (relative standard deviation less than 3%) and recoveries (95–105%). Finally, the measurements were converted to the amount of lead per μl of clots (Lead).

Statistical analyses were performed with software R (ver. 3.5.0) and Stata (ver. 14.0). A Wilcoxon rank-sum test was performed to determine whether age (Yearling and Adult), sex, and area (Tokyo-bay and Mikawa-bay) were associated with the lead level. If a significant difference was found in the three indices, a Spearman's rank correlation was performed between the hematologic parameters and lead concentration for each index. For all analyses, $P<0.05$ was considered statistically significant.

A total of 93 birds (68 from Tokyo-bay, 25 from Mikawa-bay) were captured (Table 1). The sample size of the Yearling was small; therefore, only the Adult was included in the statistical analysis. Lead concentrations were significantly higher in the Tokyo-bay than in the Mikawa-bay, but there were no significant differences in lead concentrations between male and female gulls. Therefore, only area was included in the Spearman's rank correlation. The hematologic parameters from each bay are shown in Table 2. In the Tokyo-bay population, Het was significantly positively correlated with Lead ($P<0.05$; $\rho= 0.6$; Fig. 1a), and Lym was significantly negatively correlated with Lead ($P<0.05$; $\rho= -0.6$; Fig. 1b). Same trend was observed in the Mikawa-bay population ($P<0.05$; $\rho= 0.6$; Fig. 2a; and $P<0.05$; $\rho= -0.5$; Fig. 2b, respectively). Further, the H/L ratio in the gulls from each bay was significantly positively correlated with Lead ($P<0.05$; Tokyo-bay: $\rho= 0.5$, Mikawa-bay: $\rho= 0.6$; Fig. 3). The other hematologic parameters were not significantly correlated with lead concentration ($P>0.05$).

The lead levels of the gull population in each bay were classified as low-level accumulation based on previous report [62]. Although little is known about the transitions (changes) in blood concentrations following low lead accumulation, high lead accumulation has been reported in some avian species. For instance, some seagull species quickly develop many symptoms, such as anemia and neurological symptoms, following exposure to high lead concentrations [23]. On the other hand, regarding clinical symptoms related to low lead accumulation, Hollady *et al.* [23] reported that domestic pigeons (Columbidae) exposed to low lead accumulation did not exhibit any clinical signs. Therefore, we concluded that gulls were more likely to have been a steady, low lead accumulation since the beginning of exposure, than exposed to high and gradually decreasing from that levels.

Lead pollution in gulls in each bay was recognized as short-term exposure for the following two reasons. First, studies have reported that lead in the avian body is excreted into the eggshell [6], therefore, it is possible that males can be exposed to a higher level of lead accumulation than females, especially during the season after breeding. However, we did not observe any differences in lead levels

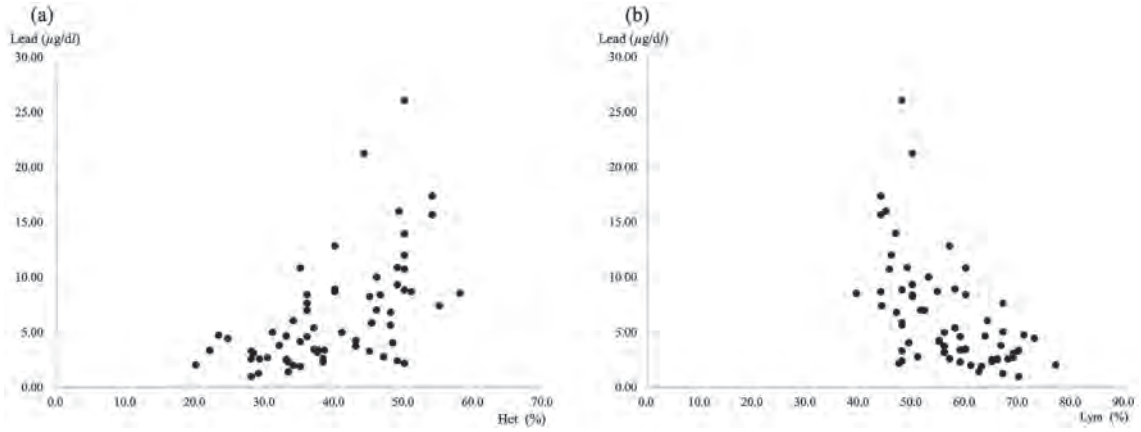

Fig. 1. Relationship between heterophils (Het; a) or lymphocytes (Lym; b) and lead concentration (Lead) in the Tokyo-bay population. The scatter diagram indicates the proportion of Het (a), and Lym (b) and is presented on the horizontal axis (unit: %). The vertical axis corresponds to the lead concentration in each diagram. In Tokyo-bay, 36 male Adults and 30 female Adults were captured from January 2019 to April 2019. Het was significantly positively correlated with lead concentration ($P<0.05$; $\rho= 0.6$), and Lym was significantly negatively correlated with lead concentration ($P<0.05$; $\rho= -0.6$).

Table 2. The values of 10 blood status items in Black-headed gulls (*Chroicocephalus ridibundus*) from two bays

a. Tokyo-bay

Item (unit)	N[a)]	Mid[b)]	Max[c)]	Min[d)]
RBC[e)] (*10^6cell/μl)	66	3.02	3.81	1.52
Hb[f)] (g/dl)	66	8.86	19.66	4.13
PCV[g)] (%)	66	39.0	55.0	30.0
WBC[h)] (cell/μl)	66	9,200	13,000	2,100
H/L ratio	66	0.65	1.47	0.26
Het[i)] (%)	66	38.4	58.0	20.0
Lym[j)] (%)	66	56.5	77.0	39.4
Mon[k)] (%)	66	2.0	6.3	0.2
Eos[l)] (%)	66	0.7	3.0	0.0
Bas[m)] (%)	66	0.0	1.0	0.0
Lead[n)] (μg/dl)	66	4.68	26.05	0.94

b. Mikawa-bay

Item (unit)	N	Mid	Max	Min
RBC (*10^6cell/μl)	21	2.06	3.23	1.76
Hb (g/dl)	21	17.50	24.39	9.56
PCV (%)	21	40.0	44.0	30.0
WBC (cell/μl)	21	4,400	9,600	2,800
H/L ratio	21	0.53	1.34	0.22
Het (%)	21	33.7	57.0	17.7
Lym (%)	21	64.0	79.0	42.5
Mon (%)	21	1.7	3.6	0.3
Eos (%)	21	0.0	2.5	0.0
Bas (%)	21	0.0	1.0	0.0
Lead (μg/dl)	21	2.73	5.92	1.50

a) Sample size, b) median value, c) maximum value, d) minimum value, e) red blood cell number, f) hemoglobin g) packed cell volume, h) white blood cell number i) percentage of heterophil, j) percentage of lymphocyte, k) percentage of monocyte, l) percentage of eosinophil m) percentage of basophil n) lead concentration.

by sex during the winter season, thus, we concluded that the gull populations were accumulated in a short time period. Second, bird banding has shown that Black-headed gulls migrate across the two bays in one day [Ushine unpublished]. Although the gulls in each bay were able to interact, there were significant differences in blood lead levels between each population. It was possible that the gulls were exposed to lead in the short term at each bay.

Although most of them are high level accumulation, there are some theories that explain the effect of lead accumulation on immunity,

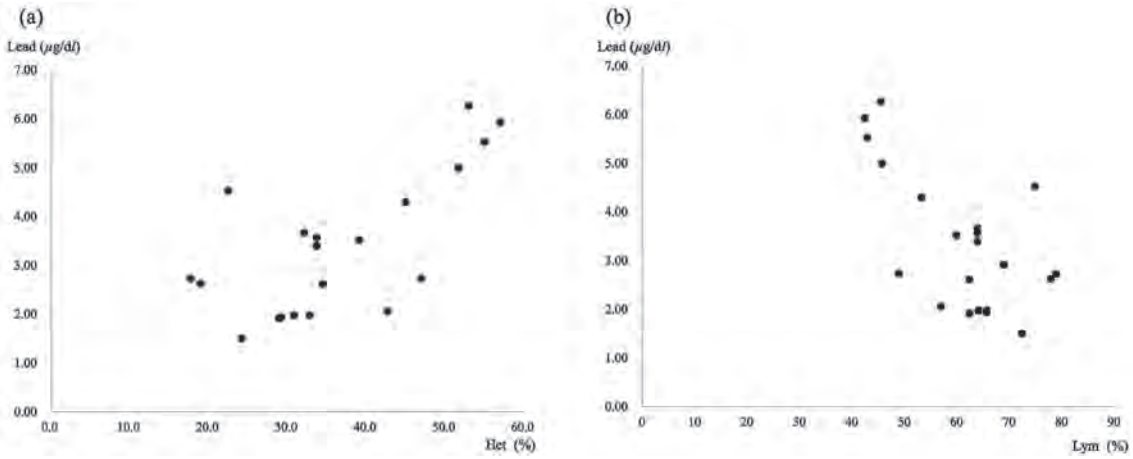

Fig. 2. Relationship between heterophils (Het; a) or lymphocytes (Lym; b) and lead concentration in the Mikawa-bay population. The scatter diagram indicates the proportion of Het (a), and Lym (b) and is presented on the horizontal axis (unit: %). The vertical axis corresponds to the lead concentration (Lead) in each diagram (unit: μg/d*l*). In Mikawa-bay, five male Adults and 16 female Adults were captured from January 2019 to April 2019. Het was significantly positively correlated with lead concentration (P<0.05; ρ= 0.6), and Lym was significantly negatively correlated with lead concentration (P<0.05; ρ= −0.5).

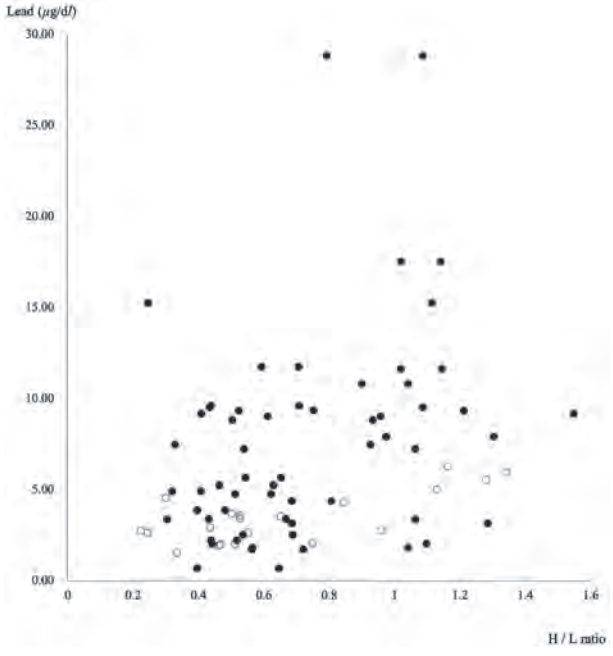

Fig. 3. Relationship between the heterophil and lymphocyte ratio (H/L ratio) and lead concentration (Lead) in each bay. The scatter diagram indicates the proportion of the H/L ratio on the horizontal axis. The vertical axis corresponds to the lead concentration in each diagram (unit: μg/d*l*). In Mikawa-bay (open circle), five male Adults and 16 female Adults were captured from January 2019 to April 2019. In Tokyo-bay (filled circle), 36 male Adults and 30 female Adults were captured from January 2019 to April 2019. H/L ratio was significantly positively correlated with lead concentration (P<0.05; Tokyo-bay: ρ= 0.5, Mikawa-bay: ρ= 0.6).

including the suppression of lymphocyte number [14, 16, 40]. In this study, the leukocyte did not change with Lead; however, there were changes in the differential blood counts. That is, lead caused to decrease the percentage of Lymphocyte and increase Heterophil, which was possibly a foreign body reaction or an inflammatory response that were targeted to lead. Increased inflammatory responses cause to the production of cytokines [26], which suppress immune function. Therefore, we hypothesized that lead accumulation has a direct immunosuppressive effect due to the decrease in lymphocytes and an indirect effect due to the increase in heterophils.

The limitations of the study were the small sample size in each bay, especially of Yearlings. Analysis stratified by age was considered important for assessing environmental pollutants that accumulate in the short and long term in the avian body. Additionally, this study was designed to be as non-invasive as possible. Using blood samples rather than necropsy precluded the kind of detailed analysis that could be performed when measuring parameters such as the lead concentration in organs.

ACKNOWLEDGMENTS. We thank all the staff of the Gyotoku Bird Observatory Society NPO. We are grateful to Ms. S. Hirota, Ms. H. Sasaki, Ms. H. Otsubo, Dr. S. Moriguchi, and Dr. T. Kato from the Department of Wildlife medicine of the Nippon veterinary and life science University of Tokyo prefecture for the great cooperation in this survey. We also thank to Mr. K. Uchida and Dr. K. Tokita for many advises. Finally, we are grateful to Ms. N. Hirano amd Mr. T. Ichise for the critical help with lead measurement. This work was supported by the Sasakawa Scientific Research Grant from The Japan Science Society and the Environment Research and Technology Development Fund (SII-1) of the Environmental Restoration and Conservation Agency of Japan. This research was also supported by JST/JICA, SATREPS (Science and Technology Research Partnership for Sustainable Development; No. JPMJSA1501) and Program for supporting introduction of the new sharing system (JPMXS0420100619).

REFERENCES

1. Andersson, M., Götmark, F. and Wiklund, C. G. 1981. Food information in the black-headed gull, *Larus ridibundus*. *Behav. Ecol. Sociobiol.* **9**: 199–202. [CrossRef]
2. Artacho, P., Soto-Gamboa, M., Verdugo, C. and Nespolo, R. F. 2007. Using haematological parameters to infer the health and nutritional status of an endangered black-necked swan population. *Comp. Biochem. Physiol. A Mol. Integr. Physiol.* **147**: 1060–1066. [Medline] [CrossRef]
3. Baker, K. 1993. Black headed gull. p. 24. *In*: Identification Guide to European Non-passerines, British Trust for Ornithology, Norfolk.
4. Berglund, Å. M., Rainio, M. J. and Eeva, T. 2015. Temporal trends in metal pollution: using bird excrement as indicator. *PLoS One* **10**: e0117071. [Medline] [CrossRef]
5. Brazil, M. 2009. Black-headed-gull. p. 210. *In*: Birds of East Asia: China, Taiwan, Korea, Japan, and Russia. A&C Black, London.
6. Burger, J. 1994. Heavy metals in avian eggshells: another excretion method. *J. Toxicol. Environ. Health* **41**: 207–220. [Medline] [CrossRef]
7. Çakmak, E., Akın Pekşen, Ç. and Bilgin, C. C. 2017. Comparison of three different primer sets for sexing birds. *J. Vet. Diagn. Invest.* **29**: 59–63. [Medline] [CrossRef]
8. Campbell, T. W. 1988. Avian Hematology and Cytology. Columbus, The Iowa State University Press, Ames.
9. Colles, F. M. 2006. Population Structure and dynamics of Campylobacter Populations Carried by Wild Birds and Chickens Reared in a Free-range Woodland Environment, University of Oxford, Oxford.
10. Cromie, R., Newth, J., Reeves, J., O'Brien, M., Beckmann, K. and Brown, M. 2014. The sociological and political aspects of reducing lead poisoning from bullet in the UK: why the transition to non-toxic bullet is so difficult. p. 104. Proceedings of the Oxford Lead Symposium, Oxford.
11. Dacie, J. and Lewis, S. 1975. Practical Haematology, 5th ed. p. 629. Churchill Living Stone, Edinburgh.
12. Davis, A., Maney, D. and Maerz, J. 2008. The use of leukocyte profiles to measure stress in vertebrates: a review for ecologists. *Funct. Ecol.* **22**: 760–772. [CrossRef]
13. Fallon, J. A., Redig, P., Miller, T. A., Lanzone, M. and Katzner, T. 2017. Guidelines for evaluation and treatment of lead poisoning of wild raptors. *Wildl.* **41**: 205–211. [CrossRef]
14. Farrer, D. G., Hueber, S., Laiosa, M. D., Eckles, K. G. and McCabe, M. J. Jr. 2008. Reduction of myeloid suppressor cell derived nitric oxide provides a mechanistic basis of lead enhancement of alloreactive $CD4^+$ T cell proliferation. *Toxicol. Appl. Pharmacol.* **229**: 135–145. [Medline] [CrossRef]
15. Fronstin, R. B., Christians, J. K. and Williams, T. D. 2016. Experimental reduction of haematocrit affects reproductive performance in European starlings. *Funct. Ecol.* **30**: 398–409. [CrossRef]
16. Gao, D., Mondal, T. K. and Lawrence, D. A. 2007. Lead effects on development and function of bone marrow-derived dendritic cells promote Th2 immune responses. *Toxicol. Appl. Pharmacol.* **222**: 69–79. [Medline] [CrossRef]
17. Gaunt, A. S., Oring, L. W., Able, K., Anderson, D., Baptista, L., Barlow, J. and Wingfield, J. 1997. Guidelines to the Use of Wild Birds in Research, The Ornithological Council, Chicago.
18. Gorski, W., Jakuczun, B., Nitecki, C. and Petryna, A. 1977. Investigation of oil pollution on the Polish Baltic coast in 1974–1975. *Przegl. Zool.* **21**: 20–23.
19. Götmark, F., Winkler, D. W. and Andersson, M. 1986. Flock-feeding on fish schools increases individual success in gulls. *Nature* **319**: 589–591. [Medline] [CrossRef]
20. Harrison, P. 1985. Seabirds. *In*: An Identification Guide, Croom Helm, London.
21. Hegemann, A., Matson, K. D., Both, C. and Tieleman, B. I. 2012. Immune function in a free-living bird varies over the annual cycle, but seasonal patterns differ between years. *Oecologia* **170**: 605–618. [Medline] [CrossRef]
22. Hernández, M. and Margalida, A. 2009. Assessing the risk of lead exposure for the conservation of the endangered Pyrenean bearded vulture (*Gypaetus barbatus*) population. *Environ. Res.* **109**: 837–842. [Medline] [CrossRef]
23. Holladay, J. P., Nisanian, M., Williams, S., Tuckfield, R. C., Kerr, R., Jarrett, T., Tannenbaum, L., Holladay, S. D., Sharma, A. and Gogal, R. M. Jr. 2012. Dosing of adult pigeons with as little as one #9 lead pellet caused severe δ-ALAD depression, suggesting potential adverse effects in wild populations. *Ecotoxicology* **21**: 2331–2337. [Medline] [CrossRef]
24. Ishii, C., Nakayama, S. M. M., Ikenaka, Y., Nakata, H., Saito, K., Watanabe, Y., Mizukawa, H., Tanabe, S., Nomiyama, K., Hayashi, T. and Ishizuka, M. 2017. Lead exposure in raptors from Japan and source identification using Pb stable isotope ratios. *Chemosphere* **186**: 367–373. [Medline] [CrossRef]
25. Jourdain, E., van Riel, D., Munster, V. J., Kuiken, T., Waldenström, J., Olsen, B. and Ellström, P. 2011. The pattern of influenza virus attachment varies among wild bird species. *PLoS One* **6**: e24155. [Medline] [CrossRef]
26. Kapcala, L. P. 1999. Inflammatory stress and the immune system. pp. 409–433. *In*: Military Strategies for Sustainment of Nutrition and Immune Function in the Field, National Academy of Medicine, Northwest.
27. Kendall, R. J., Lacker, T. E. Jr., Bunck, C., Daniel, B., Driver, C., Grue, C. E., Leighton, F., Stansley, W., Watanabe, P. G. and Whitworth, M. 1996. An ecological risk assessment of lead shot exposure in non-waterfowl avian species: upland game birds and raptors. Environmental Toxicology and Chemistry. *Int. J. Res.* **15**: 4–20.
28. Kitowski, I., Indykiewicz, P., Wiącek, D. and Jakubas, D. 2017. Intra-clutch and inter-colony variability in element concentrations in eggshells of the black-headed gull, *Chroicocephalus ridibundus*, in northern Poland. *Environ. Sci. Pollut. Res. Int.* **24**: 10341–10353. [Medline] [CrossRef]
29. Krams, I., Vrublevska, J., Cirule, D., Kivleniece, I., Krama, T., Rantala, M. J., Sild, E. and Hõrak, P. 2012. Heterophil/lymphocyte ratios predict the magnitude of humoral immune response to a novel antigen in great tits (*Parus major*). *Comp. Biochem. Physiol. A Mol. Integr. Physiol.* **161**: 422–428. [Medline] [CrossRef]
30. Krone, O. 2018. Lead Poisoning in Birds of Prey. Birds of Prey, Springer, Berlin.
31. Lobato, E., Moreno, J., Merino, S., Sanz, J. J. and Arriero, E. 2005. Hematological variables are good predictors of recruitment in nestling pied flycatchers (*Ficedula hypoleuca*). *Ecoscience* **12**: 27–34. [CrossRef]
32. Masindi, V. and Muedi, K. L. 2018. Environmental contamination by heavy metals. *Heavy Metals* **19**: 2019.
33. Mateo, R. 2009. Lead poisoning in wild birds in Europe and the regulations adopted by different countries. pp. 71–98. *In*: Ingestion of Lead from Spent Bullet: Implications for Wildlife and Humans (Watson, R. T., Fuller., Pokras, M. and Hunt, W. G. eds.), The Peregrine Fund, Boise.
34. Mateo, R. and Kanstrup, N. 2019. Regulations on lead ammunition adopted in Europe and evidence of compliance. *Ambio* **48**: 989–998. [Medline] [CrossRef]
35. Melville, D. S. and Shortridge, K. F. 2006. Migratory waterbirds and avian influenza in the East Asian–Australasian Flyway with particular reference to the 2003–2004 H5N1 outbreak. pp.432–438. *In*: Waterbirds Around the World (Boere, G., Galbraith, C. A. and Stroud, D. eds.), Stationery Office Books, London.

36. Migula, P., Augustyniak, M. and Kowalczyk, K. 2000. Heavy metals, resting metabolism rates and breeding parameters in two populations of Black-headed gull *Larus ridibundus* from the industrially Polluted areas of upper Silesia, Poland. *Acta Ornithol.* **35**: 159–172. [CrossRef]
37. Moynihan, M. 1955. Some aspects of reproductive behavior in the Black-headed Gull (*Larus ridibundus*) and related species. *Behaviour* **4** Supplement: 1–201.
38. Muller, W., Dijkstra, C. and Groothuis, T. G. G. 2003. Inter-sexual differences in T-cell-mediated immunity of Black-headed gull chicks (*Larus ridibundus*) depend on the hatching order. *Behav. Ecol. Sociobiol.* **55**: 80–86. [CrossRef]
39. Nain, S. and Smits, J. E. 2011. Subchronic lead exposure, immunotoxicology and increased disease resistance in Japanese quail (*Corturnix coturnix japonica*). *Ecotoxicol. Environ. Saf.* **74**: 787–792. [Medline] [CrossRef]
40. Nakade, T., Tomura, Y., Jin, K., Taniyama, H., Yamamoto, M., Kikkawa, A., Miyagi, K., Uchida, E., Asakawa, M., Mukai, T., Shirasawa, M. and Yamaguchi, M. 2005. Lead poisoning in whooper and tundra swans. *J. Wildl. Dis.* **41**: 253–256. [Medline] [CrossRef]
41. Nakata, H., Nakayama, S. M., Oroszlany, B., Ikenaka, Y., Mizukawa, H., Tanaka, K., Harunari, T., Tanikawa, T., Darwish, W. S., Yohannes, Y. B., Saengtienchai, A. and Ishizuka, M. 2017. Monitoring lead (Pb) pollution and identifying Pb pollution sources in Japan using stable Pb isotope analysis with kidneys of wild rats. *Int. J. Environ. Res. Public Health* **14**: 56. [Medline] [CrossRef]
42. Ochiai, K., Jin, K., Itakura, C., Goryo, M., Yamashita, K., Mizuno, N., Fujinaga, T. and Tsuzuki, T. 1992. Pathological study of lead poisoning in whooper swans (*Cygnus cygnus*) in Japan. *Avian Dis.* **36**: 313–323. [Medline] [CrossRef]
43. Ochiai, K., Hoshiko, K., Jin, K., Tsuzuki, T. and Itakura, C. 1993. A survey of lead poisoning in wild waterfowl in Japan. *J. Wildl. Dis.* **29**: 349–352. [Medline] [CrossRef]
44. Ochiai, K., Kimura, T., Uematsu, K., Umemura, T. and Itakura, C. 1999. Lead poisoning in wild waterfowl in Japan. *J. Wildl. Dis.* **35**: 766–769. [Medline] [CrossRef]
45. Oleksyn, J. and Reich, P. B. 1994. Pollution, habitat destruction, and biodiversity in Poland. *Biol. Conserv.* **8**: 943–960. [CrossRef]
46. Orlowski, G., Polechonski, R., Dobicki, W. and Zawada, Z. 2007. Heavy metal concentrations in the tissues of the Black-headed gull *Larus ridibundus* L. nesting in the dam reservoir in south-western Poland. *Pol. J. Ecol.* **55**: 783–793.
47. Pain, D. J., Mateo, R. and Green, R. E. 2019. Effects of lead from ammunition on birds and other wildlife: A review and update. *Ambio* **48**: 935–953. [Medline] [CrossRef]
48. Pap, P. L., Vágási, C. I., Tökölyi, J., Czirják, G. A. and Barta, Z. 2010. Variation in haematological indices and immune function during the annual cycle in the Great Tit *Parus major*. *Ardea* **98**: 105–112. [CrossRef]
49. Poprach, K., Machar, I. and Maton, K. 2016. Long-term decline in breeding abundance of Black-headed gull (*Chroicocephalus ridibundus*) in the Czech Republic: a case study of a population trend at the Chomoutov lake. *Ekologia (Bratisl.)* **35**: 350–358. [CrossRef]
50. Rahman, F., Ismail, A., Omar, H. and Hussin, M. Z. 2017. Exposure of the endangered Milky stork population to cadmium and lead via food and water intake in Kuala Gula Bird Sanctuary, Perak, Malaysia. *Toxicol. Rep.* **4**: 502–506. [Medline] [CrossRef]
51. Reid, C., McInnes, K., McLelland, J. M. and Gartrell, B. D. 2012. Anthropogenic lead (Pb) exposure in populations of a wild parrot (*kea Nestor notabilis*). *N. Z. J. Ecol.* **36**: 56–63.
52. Saito, K. 2009. Lead poisoning of Steller's sea-eagle (*Haliaeetus pelagicus*) and whitetailed eagle (*Haliaeetus albicilla*) caused by the ingestion of lead bullets and slugs, in Hokkaido, Japan. pp. 302–309. *In*: Ingestion of Lead from Spent Bullet: Implications for Wildlife and Humans (Watson, R. T., Fuller., Pokras, M. and Hunt, W. G. eds.),The Peregrine Fund, Boise.
53. Schalm, O., Jain, N. and Caroll, E. 1975. Veterinary Haematology, Lea and Febiger, Philadelphia.
54. Scheuhammer, A. M. and Norris, S. L. 1996. The ecotoxicology of lead shot and lead fishing weights. *Ecotoxicology* **5**: 279–295. [Medline] [CrossRef]
55. Sutherland, W. J., Newton, I. and Green, R. 2004. Bird Ecology and Conservation: A Handbook of Techniques, Oxford University Press, Oxford.
56. Thomas, V. G. 1997. Attitudes and issues preventing bans on toxic lead shot and sinkers in North America and Europe. *Environ. Values* **6**: 185–199. [CrossRef]
57. Thomas, V. G. 2010. Achieving uniform regulation of environmental lead exposure and poisoning in wildlife and humans. *Environmentalist* **30**: 206–210. [CrossRef]
58. Thomas, V. G. and Guitart, R. 2013. Transition to non-toxic gunshot use in Olympic shooting: policy implications for IOC and UNEP in resolving an environmental problem. *Ambio* **42**: 746–754. [Medline] [CrossRef]
59. Toyomaki, H., Yabe, J., Nakayama, S. M. M., Yohannes, Y. B., Muzandu, K., Liazambi, A., Ikenaka, Y., Kuritani, T., Nakagawa, M. and Ishizuka, M. 2020. Factors associated with lead (Pb) exposure on dogs around a Pb mining area, Kabwe, Zambia. *Chemosphere* **247**: 125884. [Medline] [CrossRef]
60. Tsubokura, M., Otsuki, K., Kawaoka, Y. and Yanagawa, R. 1981. Isolation of influenza A viruses from migratory waterfowls in San-in District, Western Japan in 1979–1980. *Zentralbl. Bakteriol. Mikrobiol. Hyg. B* **173**: 494–500. [Medline]
61. Ushine, N., Sato, T., Kato, T. and Hayama, S. I. 2017. Analysis of body mass changes in the Black-Headed Gull (*Larus ridibundus*) during the winter. *J. Vet. Med. Sci.* **79**: 1627–1632. [Medline] [CrossRef]
62. Vallverdú-Coll, N. 2016. Immunotoxic and reproductive effects of lead on avifauna affected by shot ingestion. Universidad de Castilla-La Mancha: Ciudad Real.
63. Wiemeyer, S. N., Scott, J. M., Anderson, M. P., Bloom, P. H. and Stafford, C. J. 1988. Environmental contaminants in California condors. *J. Wildl. Manage.* **52**: 238–247. [CrossRef]
64. Williams, R. J., Holladay, S. D., Williams, S. M. and Gogal, R. M. 2017. Environmental lead and wild birds: a review. *In*: Reviews of Environmental Contamination and Toxicology Vol. 245 (de Voogt, P. ed.), Springer, Berlin.

Environmental Pollution 283 (2021) 117086

Contents lists available at ScienceDirect

Environmental Pollution

journal homepage: www.elsevier.com/locate/envpol

Analysis of lead distribution in avian organs by LA-ICP-MS: Study of experimentally lead-exposed ducks and kites☆

Ryouta Torimoto [a], Chihiro Ishii [b], Hiroshi Sato [b], Keisuke Saito [c], Yukiko Watanabe [c], Kohei Ogasawara [c], Ayano Kubota [d], Takehisa Matsukawa [d, e], Kazuhito Yokoyama [d, f], Atsushi Kobayashi [a, *], Takashi Kimura [a], Shouta M.M. Nakayama [b], Yoshinori Ikenaka [b, g], Mayumi Ishizuka [b]

[a] Laboratory of Comparative Pathology, Faculty of Veterinary Medicine, Hokkaido University, Kita 18 Nishi 9, Kita-ku, Sapporo, Hokkaido, 060-0818, Japan
[b] Laboratory of Toxicology, Faculty of Veterinary Medicine, Hokkaido University, Kita 18 Nishi 9, Kita-ku, Sapporo, Hokkaido, 060-0818, Japan
[c] Institute for Raptor Biomedicine Japan, Hokuto 2-2101, Kushiro, Hokkaido, 084-0922, Japan
[d] Department of Epidemiology and Environmental Health, Juntendo University Faculty of Medicine, Hongo 2-1-1, Bunkyo-ku, Tokyo, 113-8421, Japan
[e] Department of Forensic Medicine, Juntendo University Faculty of Medicine, Hongo 2-1-1, Bunkyo-ku, Tokyo, 113-8421, Japan
[f] Department of Epidemiology and Social Medicine, Graduate School of Public Health, International University of Health and Welfare, Akasaka 4-1-26, Minato-ku, Tokyo, 107-8402, Japan
[g] Water Research Group, Unit for Environmental Sciences and Management, North-West University, Potchefstroom, 2531, South Africa

ARTICLE INFO

Article history:
Received 17 January 2021
Received in revised form
1 April 2021
Accepted 2 April 2021
Available online 5 April 2021

Keywords:
Lead
LA-ICP-MS
Imaging
Waterfowl
Raptor

ABSTRACT

Lead poisoning of wild birds by ingestion of lead ammunition occurs worldwide. Histopathological changes in organs of lead-intoxicated birds are widely known, and lead concentration of each organ is measurable using mass spectrometry. However, detailed lead localization at the suborgan level has remained elusive in lead-exposed birds. Here we investigated the detailed lead localization in organs of experimentally lead-exposed ducks and kites by laser ablation inductively coupled plasma mass spectrometry (LA-ICP-MS). In both the ducks and kites, lead accumulated diffusely in the liver, renal cortex, and brain. Lead accumulation was restricted to the red pulp in the spleen. With regard to species differences in lead distribution patterns, it is noteworthy that intensive lead accumulation was observed in the arterial walls only in the kites. In addition, the distribution of copper in the brain was altered in the lead-exposed ducks. Thus, the present study shows suborgan lead distribution in lead-exposed birds and its differences between avian species for the first time. These findings will provide fundamental information to understand the cellular processes of lead poisoning and the mechanisms of species differences in susceptibility to lead exposure.

1. Introduction

The use of lead shots and bullets has been regulated in many countries. However, lead poisoning of wild birds is widespread all over the world (Pain et al., 2019). In the field, the ingestion of lead ammunition and fishing sinkers causes many cases of lead poisoning in waterfowls and raptors (Scheuhammer and Norris, 1996; Fisher et al., 2006; Saito, 2009). According to recent statistics, lead poisoning is estimated to kill annually a million waterfowls in Europe (Berny et al., 2015; Pain, 2019) and three million birds in the US (De Francisco et al., 2003). Lead poisoning in avian species has been recognized in Japan since 1985 (Honda et al., 1990), and endangered raptors in Japan have also been affected since 1996 (Saito, 2009). In birds, lead exposure exerts toxicity in various organs such as the liver, kidney, cardiovascular system, brain, and bone. The common gross lesions in birds are atrophy and brownish discoloration of the liver, distended gallbladder with bile, multifocal pallor areas in the myocardium, multifocal petechial hemorrhage in the cerebellum, and hypoplasia of the bone marrow (Ochiai et al., 1993; Manning et al., 2019). The histological lesions include hepatic hemosiderosis, degeneration and necrosis of the proximal renal tubules, degeneration and necrosis of myocardium, and cerebellar perivascular hemorrhage (Ochiai et al., 1993;

☆ This paper has been recommended for acceptance by Philip N. Smith.
* Corresponding author.
E-mail address: kobayashi@vetmed.hokudai.ac.jp (A. Kobayashi).

https://doi.org/10.1016/j.envpol.2021.117086
0269-7491/

Manning et al., 2019). Lead also interferes heme biosynthesis through the inhibition of the activities of δ-aminolevulinic acid dehydratase (ALAD) and ferrochelatase (Rogan et al., 1986; Fisher, 2006; Liao et al., 2008). Therefore, the diagnosis of avian lead poisoning is usually made by the characteristic histological changes, the level of ALAD activity in blood, and the lead concentration in blood and organs.

Lead concentration in organs is measurable by inductively coupled plasma-mass spectrometry (ICP-MS) using tissue homogenates (Ishii et al., 2017; Togao et al., 2020). In addition, special staining methods for lead in tissue sections have been developed to detect gunshot residues (Neri et al., 2007; Turillazzi et al., 2013). However, the detailed lead distribution in lead-exposed animals at the suborgan level cannot be analyzed by these methods. Recently, we showed the tissue distribution of lead in lead-exposed mice using laser ablation (LA)-ICP-MS (Togao et al., 2020). LA-ICP-MS can identify metals in tissue sections and is useful to reveal the detailed tissue distribution of metals (Ek et al., 2004; Ishii et al., 2018).

In the present study, we established a model of low-dose lead exposure in waterfowls and raptors by administration of one to three lead pellets, reproducing the low-dose lead exposure found in the field. Then, we investigated the histological distribution of lead in organs of the lead-exposed birds using LA-ICP-MS. In addition, we compared the tissue distribution of lead between waterfowls and raptors because the sensitivity to lead poisoning is reported to be different among avian species (De Francisco et al., 2003).

2. Materials and methods

2.1. Animal experiments

Animal experiments were performed in strict accordance with the Regulations for Animal Experiments and Related Activities at Hokkaido University. The protocols for animal experiments were approved by the Association for the Assessment and Accreditation of Laboratory Animal Care International and the Institutional Animal Care and Use Committee of Hokkaido University (approval No. 18-0092 and No. 19-0033).

Seven, bred, eight-week-old Muscovy ducks (*Cairina moschata*; body weight, 3.3–3.8 kg) were purchased from Sankyo Labo Service. The ducks were randomly divided into two groups; untreated control (n = 3) and lead-treated (n = 4). The ducks were housed individually in cages in controlled light (12 h light/dark cycle) and constant temperature (23 ± 2 °C) with free access to food and water. All ducks were acclimated for a week before treatment and kept on a fresh diet. Lead-treated ducks were given three lead pellets (240 ± 1.7 mg) in a style of oral forced ingestion. Control and lead-treated groups were euthanized with overdose of pentobarbital sodium on 29 or 30 days after the lead treatment.

Five black kites (*Milvus migrans*; body weight, 1.0–1.1 kg) were kept in the Institute for Raptor Biomedicine Japan. All kites were unsuitable for release because most had persistent wing damages. These kites were otherwise in good condition. The kites were placed individually in outdoor cages. Each pen was furnished with a log for perching and a pan of water. All kites were acclimated to the pens for a week or more before the treatment and were kept on a diet. The kites were randomly divided into two groups; untreated control (n = 2) and lead-treated (n = 3). Lead-treated kites were given one lead pellet (77.9–88.4 mg) mixed with venison. To confirm the existence of lead pellet in the gastrointestinal tract, the kites were radiographed every day for 14 days after the lead administration. In two kites (Kite-Lead-2 and Kite-Lead-3), the lead pellet disappeared on radiographs probably due to regurgitation or excretion at 7 and 10 days after the lead administration, respectively. Therefore, these kites were dosed one lead pellet again within 24 h. Control and lead-treated groups were euthanized with overdose of pentobarbital sodium on 29 or 30 days after the first lead treatment.

2.2. Blood collection

Blood samples (5 ml and 4 ml from the ducks and kites, respectively) were obtained from the brachial veins at 28 days after the lead treatment. Blood was quickly heparinized to avoid coagulation and kept on ice until further processing within 2 h.

2.3. Tissue sample collection

Liver, spleen, kidney, heart, lung, cerebrum, midbrain, cerebellum, and bone marrow were collected from the euthanized birds and divided into three pieces. One was used for quantitative analysis of lead by ICP-MS, another was used for histopathological analysis, and the other was used for imaging analysis of lead by LA-ICP-MS.

2.4. Quantitative analysis of lead by ICP-MS

Analyses of lead concentrations in bird organs (liver, spleen, kidney, heart, cerebrum, midbrain, cerebellum, and blood) were performed as reported previously (Yabe et al., 2015). The amounts of samples analyzed are summarized in Appendix A: Table A.1 Samples were digested with nitric acid (HNO_3) and hydrogen peroxide (H_2O_2) in microwave. The concentration of lead was measured with ICP-MS 7700 series (Agilent Technology). Analytical quality control was performed using DOLT-4 (dogfish liver) and DORM-3 (fish protein) (National Research Council of Canada) certified reference materials. Replicate analyses of these reference materials showed good recoveries (95–105%); the linearity range of standard solution was 0–500 μg/L (0, 0.25, 0.5, 1, 5, 10, 25, 50, 100, 250, 500 μg/L, R^2 of standard curve was more than 0.9999); the limit of detection was 0.001 μg/kg; and the limit of quantification was 0.003 μg/kg. The limit of quantification was determined as 10 × standard deviation of the intercept/the average of the slope obtained from seven measurements of the standard solutions. For the analysis of lead concentration, Thallium (^{205}TI) was used as an internal standard for the lead concentration analysis.

2.5. Histopathological analysis

For histopathological analysis, the collected organs (liver, spleen, kidney, heart, lung, cerebrum, midbrain, cerebellum, and bone marrow) were fixed in 10% buffered formalin for 48 h at room temperature and embedded in paraffin. The embedded tissues were sectioned at a thickness of 4 μm and were stained with hematoxylin and eosin (H&E).

2.6. Lead staining

Lead staining was performed as previously reported (Turillazzi et al., 2013; Neri et al., 2007). Deparaffinized and rehydrated tissue sections were incubated with a staining solution containing 2.5 mg/ml sodium rhodizonate (FUJIFILM Wako Chemicals) and 1.67 mg/ml tartaric acid (Sigma-Aldrich) for 1 min. The sections were counterstained with hematoxylin for 30 s, washed with distilled water, dehydrated and mounted. Kidney sections were also stained with acid-fast stain to detect intranuclear lead inclusion body.

2.7. Imaging analysis of lead by LA-ICP-MS

For LA-ICP-MS, the collected organs (liver, spleen, kidney, heart, cerebrum, midbrain, and cerebellum) were washed with sterilized phosphate-buffered saline (PBS) to remove blood and then embedded in Tissue-Tek O.C.T. Compound (Sakura Finetek). The embedded tissues were frozen in isopentane, which had been cold with dry ice, allowed to dry and then stored at −80 °C. The frozen tissues were sectioned at a thickness of 15 μm using a cryostat Leica CM 3500. Some neighboring sections were cut to a thickness of 8 μm for H&E staining. The sections were analyzed using an LA system (NWR213; esi Japan, Tokyo, Japan, working at a wavelength of 213 nm, pulse duration of 4 ns, and fluence of 0.5–0.6 J cm^{-2}) associated with an ICP-MS 8800 series (Agilent Technology) and scanned by a focused laser beam. Laser spot size, scan speed line and offset between line were set at 100 μm, 100 μm s^{-1} and 100 μm, respectively. ICP-MS conditions were the following: RF plasma source, 1600 W; He carrier gas, 0.8 L min^{-1}. Measured isotope (dwell time, second) were as follows: ^{13}C (0.005), ^{25}Mg (0.005), ^{31}P (0.005), ^{43}Ca (0.005), ^{55}Mn (0.005), ^{57}Fe (0.005), ^{65}Cu (0.005), ^{66}Zn (0.005), ^{206}Pb (0.01), ^{207}Pb (0.01), ^{208}Pb (0.01). In this analysis, no quantification of Pb was conducted due to lack of suitable reference materials for calibration, however intensity of Pb (and other elements) was normalized to ^{13}C (carbon) intensity as Wu et al. (2009), Johnston et al. (2019) and others have utilized to normalize the ablation efficiency. From the continuous list of raw pixel values data, elemental images were reconstructed using LA-ICP-MS Image generator house-made software iQquant2 (Kawakami et al., 2016).

3. Results

3.1. Clinical signs

Clinical signs of the ducks are summarized in Table 1. Duck-Lead-3 showed mild anorexia and lethargy at 21 days after the lead treatment. The other ducks appeared healthy. The control group did not show any clinical signs.

Clinical signs of the kites are summarized in Table 2. Kite-Lead-2 showed moderate anorexia, lethargy and exercise intolerance at 7 days after the lead administration, and Kite-Lead 1 showed mild anorexia and lethargy at one day after the lead treatment. The other kites appeared healthy. The control group did not show any clinical signs.

3.2. Necropsy findings

Necropsy findings of the ducks are summarized in Table 1. An eroded lead pellets remained in the stomach of all the lead-treated ducks except for Duck-Lead-3. Duck-Lead-1, Duck-Lead-2 and Duck-Control-2 showed focal discolored foci on the surface of the liver. In the Duck-Lead-4, mild hepatomegaly and multifocal yellowish foci on the surface of the liver were observed. In addition, the spleen was mildly swollen, and the right metanephros was defective. Duck-Lead-3, Duck-Control-1 and Duck-Control-3 did not show any gross pathological changes.

Necropsy findings of the kites are summarized in Table 2. No lead pellet was found in the gastrointestinal tract of all the lead-

Table 1
Summary of clinical signs, necropsy findings and histopathological findings of the ducks.

Duck	Clinical signs	Necropsy findings	Histopathological findings
Lead-1	None	Liver: focal dark red foci	Liver: hydropic degeneration of hepatocytes, diffuse, moderate; subcapsular hemorrhage and edema, focal, mild Kidney: vacuolar degeneration of the renal tubules, diffuse, mild
Lead-2	None	Liver: focal yellowish-white foci	Liver: hydropic degeneration of hepatocytes, diffuse, moderate Kidney: vacuolar degeneration of the renal tubules, diffuse, mild
Lead-3	Mild anorexia and lethargy	None	Liver: vacuolar degeneration of hepatocytes, diffuse, moderate Kidney: vacuolar degeneration of the renal tubules, multifocal, mild
Lead-4	None	Liver: mild hepatomegaly and multifocal yellowish foci Spleen: mild splenomegaly Kidney: defect of the right metanephros	Liver: deposition of amyloid within the hepatic portal area, sinusoid and white pulp, diffuse, moderate; vacuolar degeneration of hepatocytes, diffuse, moderate Kidney: vacuolar degeneration of the renal tubules, diffuse, mild
Control-1	None	None	Liver: vacuolar degeneration of hepatocytes, diffuse, moderate Kidney: vacuolar degeneration of the renal tubules, multifocal, mild
Control-2	None	Liver: focal white foci	None
Control-3	None	None	Liver: vacuolar degeneration of hepatocytes, diffuse, moderate Kidney: vacuolar degeneration of the renal tubules, multifocal, mild

Table 2
Summary of clinical signs, necropsy findings and histopathological findings of the kites.

Kite	Age and sex	Clinical signs	Necropsy findings	Histopathological findings
Lead-1	6 y, female	Mild anorexia and lethargy	Liver: focal yellowish-white foci	Kidney: deposition of lipofuscin in the renal tubules, diffuse, mild; enlargement of the collecting ducts, moderate Bone marrow: hypoplasia, mild
Lead-2	2 y, female	Moderate anorexia, lethargy and exercise intolerance	Heart: mild fragileness	Kidney: deposition of lipofuscin in the renal tubules, diffuse, mild Heart: myocarditis, lymphocytic, focal, mild Lung: pulmonary congestion, diffuse, mild
Lead-3	2 y, male	None	Liver: focal yellowish-white foci	Kidney: deposition of lipofuscin in the renal tubules, diffuse, mild
Control-1	6 y, female	None	None	Kidney: deposition of lipofuscin in the renal tubules, diffuse, mild
Control-2	3 y, female	None	None	Kidney: deposition of lipofuscin in the renal tubules, diffuse, mild Spleen: deposition of amyloid within the splenic sinusoid, focal

treated kites. Kite-Lead-1 and Kite-Lead-3 showed focal yellowish-white foci on the surface of the liver. The heart of Kite-Lead-2 was mildly fragile. No gross pathological change was noted in the other organs of the lead-treated kites and the control kites.

3.3. Histopathological findings

Histopathologic findings of the ducks are summarized in Table 1. Duck-Lead-1, Duck-Lead-2 and Dcuk-Control-3 showed hydropic degeneration of hepatocytes, while Duck-Lead-3, Duck-Lead-4 and Dcuk-Control-1 showed vacuolar degeneration of hepatocytes. All ducks except Duck-Control-2 showed vacuolar degeneration of the renal tubular epithelia. Deposition of amyloid in the hepatic portal area, sinusoid of the liver, and white pulp of the spleen was noted in Duck-Lead-4.

Histopathological findings of the kites are summarized in Table 2. In Kite-Lead-1, an enlargement of the collecting ducts of the kidney and mild hypoplasia of the bone marrow were observed. Mild myocarditis and mild pulmonary congestion were noted in Kite-Lead-2. All kites showed the deposition of lipofuscin in the renal tubular epithelia. Deposition of amyloid in sinusoid of the liver was noted in Kite-Control-2.

Intranuclear lead inclusion body was not found in the acid-fast stained kidney sections of the ducks and kites (data not shown). Lead staining using the sodium rhodizonate reaction was negative in all the ducks and kites (data not shown).

3.4. ICP-MS analysis

In the quantitative analysis of lead by ICP-MS, Duck-Lead-3 and Kite-Lead-1 showed the highest lead concentrations in each group. The liver and kidneys showed higher lead concentrations compared with the other organs examined (Table 3). The lead concentrations in untreated control groups were less than 0.01 mg/L or mg/kg (data not shown).

3.5. LA-ICP-MS analysis

Tissue distributions of lead were examined in Duck-Lead-3 and Kite-Lead-1 by LA-ICP-MS, as these birds showed the highest lead concentrations. In addition, the cerebrum, midbrain, and cerebellum of Duck-Lead-1, or the cerebrum, midbrain, cerebellum, and heart of Kite-Lead-3 were also examined to confirm the characteristic patterns of lead distribution.

In the lead-exposed duck, diffuse lead accumulation except for veins was noted in the liver (Fig. 1A). Connective tissues surrounding veins showed slightly higher intensities. The lumen of the gallbladder also showed lead accumulation. In the spleen, lead accumulation was restricted to the red pulp (Fig. 1B). In the kidney, diffuse lead accumulation was observed in the cortex (Fig. 1C). The cortical areas surrounding the interlobular veins showed higher intensities compared with the areas around the central veins. Notably, the medullary cones did not show lead accumulation. In the brain, lead accumulated diffusely in the cerebrum (Fig. 1D). In the cerebellar cortex, the gray matter showed diffuse lead accumulation, with higher intensities in the Purkinje cell layer (Fig. 1E). In the midbrain, the optic tectum (stratum griseum et fibrosum superficiale, stratum griseum centrale, stratum griseum periventriculare), central gray substance, and oculomotor nerves showed intensive lead accumulation (Fig. 1F). Lead accumulation was not observed in the untreated control duck (Fig. 1G and H).

In the lead-exposed kite, intensive lead accumulation in the hepatic arterial walls was observed in addition to diffuse accumulation in hepatic parenchyma (Fig. 2A). In the spleen, the wall of splenic artery showed much higher amount of lead accumulation than those of the red pulp (Fig. 2B). In the kidney, the patterns of lead distribution were the same as those of the duck kidney (Fig. 2C). Diffuse lead accumulation was observed in the renal cortex, with higher intensities around the interlobular veins. Materials contained in dilated collecting ducts also showed lead signals. In the cerebrum, intensive lead accumulation was noted in the peripheral area of the hyperpallium, hippocampus, and hypothalamus, in addition to diffuse accumulation in parenchyma (Fig. 2D). In the cerebellum, lead accumulated diffusely in the gray matter, with higher intensities in the Purkinje cell layer (Fig. 2E). In the midbrain, the optic tectum (stratum griseum et fibrosum superficiale, stratum griseum centrale, stratum griseum periventriculare), central gray substance, nucleus mesencephalicus lateralis pars dorsalis, brachium cunjuctivum, and oculomotor nerves showed intensive lead accumulation (Fig. 2E). Lead accumulation was not observed in the untreated control kite (Fig. 2F and G). Thus, the pattens of lead accumulation in the lead-exposed kites were basically similar to those of the lead-exposed ducks, with more prominent lead accumulation in some brain regions, *e.g.*, hyperpallium, hippocampus, hypothalamus, and optic tectum. Meanwhile, the intensive lead accumulation in the arterial wall was characteristic to the lead-exposed kite. The intensive lead accumulation in the arterial wall was also confirmed in the heart of the lead-exposed kite (Fig. 2H). The walls of coronary artery and aorta showed high amount of lead accumulation in addition to those of the cardiac cartilage.

Taking advantage of LA-ICP-MS that enables to visualize the distribution of essential elements in tissue sections, we also examined localization of magnesium, phosphorus, calcium, manganese, iron, copper, zinc at the suborgan level in the lead-exposed ducks and kites. Notably, the distribution of copper was altered in the cerebrum of the lead-exposed ducks (Fig. 3). Copper accumulated in the entopallium only in the lead-exposed ducks and not in the control duck or the lead-exposed kites. Localization of the other elements in each organ was not altered by the lead administration (data not shown).

Table 3
Lead concentrations in the duck and kite organs.

Organ	Duck-Lead-3[a]	Duck-Lead-1	Kite-Lead-1	Kite-Lead-3
Blood[b]	2.95	–	0.99	–
Liver	6.18	–	1.70	–
Spleen	2.80	–	0.35	–
Pronephros	4.89	–	4.90	–
Mesonephros	5.41	–	3.04	–
Metanephros	5.80	–	4.15	–
Cerebrum	0.68	0.18	0.53	0.24
Midbrain	0.81	0.32	0.76	1.52
Cerebellum	0.93	0.73	0.63	0.69
Heart	–	–	–	0.03

[a] Data are expressed as mg/L in blood or mg/kg in wet weight in the other organs.
[b] Lead concentration in blood at 28 d after the lead administration.

4. Discussion

In the present study, lead distribution in organs of experimentally lead-exposed ducks and kites were investigated at the suborgan level by LA-ICP-MS. Although almost all of the ducks and kites lacked lead-associated pathological changes due to the low-dosage of lead administration, tissue distribution of lead could be clearly identified. In addition, species differences in lead distribution patterns were also revealed.

In the liver, lead accumulated diffusely in parenchyma in both the duck and kite. This distribution pattern is the same as those in lead-exposed mice (Togao et al., 2020). Lead-intoxicated animals

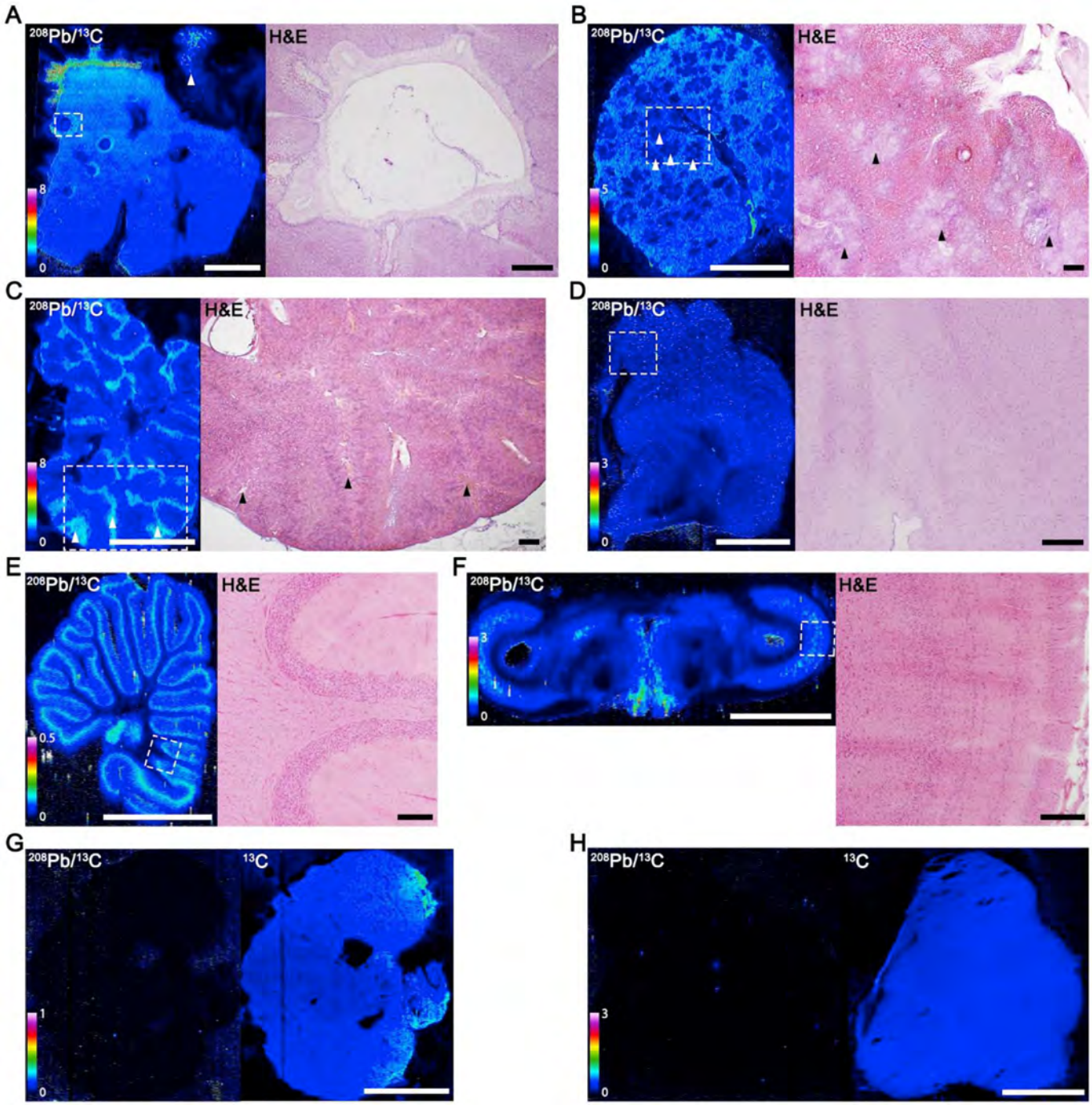

Fig. 1. Lead distribution in the duck organs. (A) Lead accumulated diffusely in the liver. Lead signals were also observed in the gallbladder (arrowhead). Duck-Lead-3. (B) Lead accumulated in the red pulp of the spleen. The white pulp (arrowheads) lacked lead accumulation. Duck-Lead-3. (C) Lead accumulated diffusely in the cortical area of the kidney, with intensive accumulation around the interlobular veins (arrowheads). Duck-Lead-3. (D–F) Lead accumulated diffusely in the cerebrum (D, Duck-Lead-3), cerebellar cortex (E, Duck-Lead-1), and midbrain (F, Duck-Lead-3). The Purkinje cell layer, optic tectum, central gray matter, and oculomotor nerves showed higher amount of lead accumulation. (G, H) Lead accumulation was not observed in the organs of the untreated control duck (G, spleen; H, cerebrum; Duck-Control-3). The areas enclosed by the dashed lines are shown in the H&E images. Scale bars: 5 mm in LA-ICP-MS images and 500 μm in H&E images.

show degeneration of hepatocytes and hemosiderosis (Ochiai et al., 1993; Jarrar and Taib, 2012; Hegazy and Fouad, 2014). Thus, the diffuse distribution of lead in hepatocytes is compatible with the histopathological changes in lead-intoxicated animals.

In the spleen, lead accumulated only in the red pulp in both the duck and kite. This finding is in line with the report that 95% of lead in blood accumulates in erythrocytes (Hernández-Avila et al., 1998). In addition, hemosiderin-laden (erythrophagocytic) macrophages increase in the red pulp in lead-intoxicated waterfowls (Ochiai et al., 1993). It has been reported that lead specifically affects macrophages in the red pulp in lead-exposed mice (Corsetti et al., 2017). Therefore, the lead accumulation in the red pulp may reflect the lead accumulation in erythrocytes and erythrophagocytic macrophages.

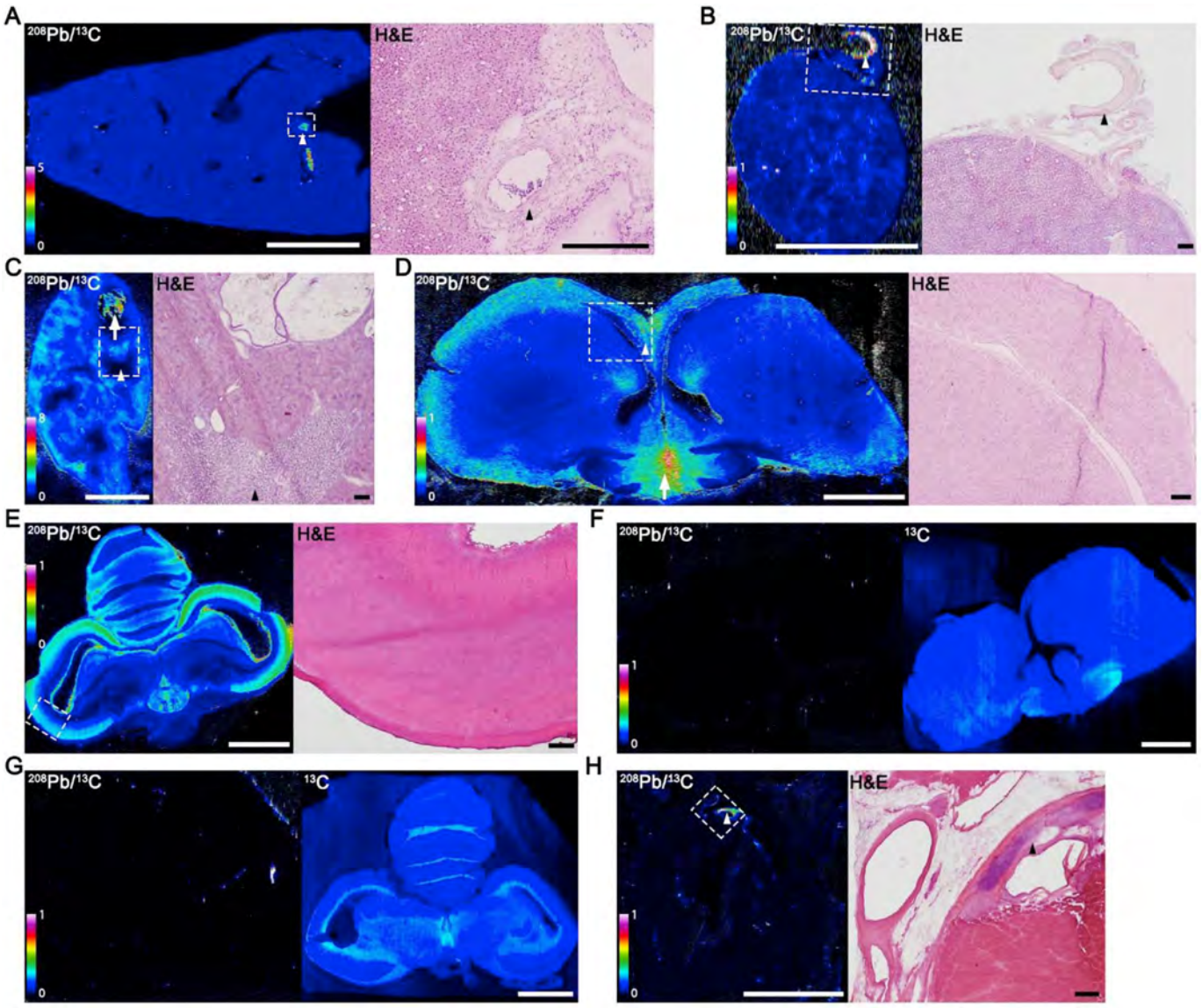

Fig. 2. Lead distribution in the kite organs. (A) Lead accumulated diffusely in the liver, with intensive accumulation in the arterial walls (arrowheads). Kite-Lead-1. (B) Lead accumulated in the red pulp of the spleen, with intensive accumulation in the arterial walls (arrowheads). Kite-Lead-1. (C) Lead accumulated diffusely in the cortical area of the kidney. Lead accumulated also in the dilated collecting ducts (arrow). The medullary cones (arrowheads) lacked lead accumulation. Kite-Lead-1. (D) Lead accumulated diffusely in the cerebrum, with intensive accumulation in the periphery of the hyperpallium, hippocampus (arrowhead), and hypothalamus (arrow). Kite-Lead-1. (E) Lead accumulated diffusely in the cerebellar cortex and midbrain, with intensive accumulation in the Purkinje cell layer, optic tectum, central gray matter, nucleus mesencephalicus lateralis pars dorsalis, brachium cunjuctivum, and oculomotor nerves. Kite-Lead-3. (F, G) Lead accumulation was not observed in the organs of the untreated control kite (F, cerebrum; G, cerebellum and midbrain; Kite-Control-2). (H) Lead accumulated in the arterial walls of the heart in addition to the cardiac cartilage (arrowheads). Kite-Lead-3. The areas enclosed by the dashed lines are shown in the H&E images. Scale bars: 5 mm in LA-ICP-MS images and 500 μm in H&E images.

In the kidneys of the duck and kite, lead accumulated diffusely in the cortical area, particularly around the interlobular veins, without accumulation in the medullary cones. These distribution patterns are different from those observed in lead-exposed mice, in which corticomedullary boundaries show higher amount of lead accumulation than the cortex (Togao et al., 2020). Birds and mammals have different kidney structures in terms of nephron, portal system, and stratified cortex and medulla (Morild et al., 1985; Harr, 2002). Thus, these structural differences may account for the different lead distribution. Meanwhile, the lack of lead accumulation in the renal medulla is common in both birds and mammals. The appearance of inclusion bodies composed of lead, α-synuclein and metallothionein in the proximal tubules is a histological hallmark of lead-intoxicated animals (Moore and Goyer, 1974; Qu et al., 2002; Zuo et al., 2009). In addition, lead-intoxicated animals show degeneration and necrosis of the proximal tubules. Therefore, the diffuse lead distribution in the cortical area is in line with the histopathological changes of the lead-intoxicated animals.

In the brain, lead accumulated diffusely in the cerebrum, cerebellar cortex, and midbrain in both the ducks and kites, with higher intensities in the Purkinje cell layer, optic tectum, central gray substance, and oculomotor nerves. In the kites, hippocampus, hyperpallium, and hypothalamus also showed higher amount of lead accumulation. These patterns of lead distribution partially overlap with those of rodents, in which lead preferentially accumulates in hippocampus and the cerebral cortex (Lefauconnier et al., 1983; Al-Shimali et al., 2016; Togao et al., 2020). In lead-exposed rodents, neuronal damages are mainly observed in

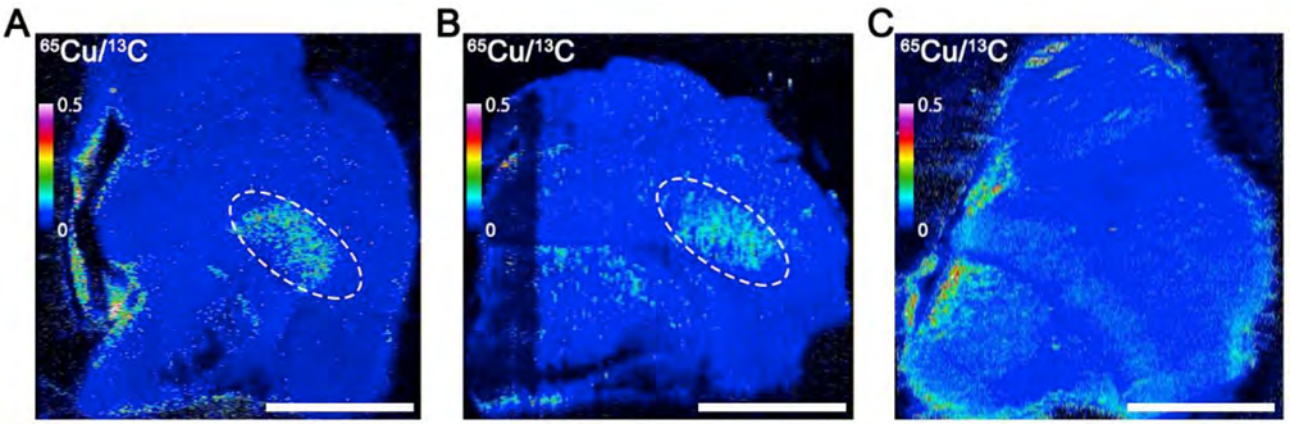

Fig. 3. Copper distribution in the duck brains. (A, B) Copper accumulated in the entopallium (encircled by the dashed lines) of the lead-exposed ducks (A, Duck-Lead-3; B, Duck-Lead1). (C) Copper accumulation in the entopallium was not observed in the untreated control duck (Duck-Control-3). Scale bars: 5 mm.

hippocampus, the parietal cortex, and Purkinje cells (Sharifi et al., 2002; Dribben et al., 2011; Gargouri et al., 2012; Owoeye and Onwuka, 2016), and lipid peroxidation is noted in thalamus, hippocampus, the parietal cortex and striatum in rats (Villeda-Hernández et al., 2001). In birds, lead exposure causes neurological dysfunction like blindness, head tilt, and seizures (Fallon et al., 2017). The intensive lead accumulation in the Purkinje cell layer and optic tectum may account for these clinical signs in birds. In addition, the lead accumulation in hippocampus of the kites may associate with the finding that lead exposure has a negative impact on learning and behavior in avian species (Burger and Gochfeld, 2005; Ecke et al., 2017). Further studies will be needed to investigate the relationship between the lead distribution in the brain and neurological signs in lead-exposed birds. In addition, the identification of brain cell types which have higher amount of lead will aid to unveil the mechanisms of lead-induced neurotoxicity. For example, astrocytes generate and store glutathione sulfhydryl enzymes that can bind lead, and the interaction between astrocytes and neurons is inhibited by lead through the prevention of glutamate and glycogen metabolisms (Strużyńska et al., 2005; Liu et al., 2015).

Meanwhile, lead exposure caused copper accumulation in the entopallium of the duck brain. It has been reported that lead administration increases copper concentrations in the brain or in cultured astrocytes (Tiffany-Castiglioni et al., 1987; Sierra et al., 1989). Lead exposure induces copper uptake by up-regulation of the expression of Cu transporter 1 (CTR1) and reduces copper efflux by down-regulation of the expression of ATPase copper transporting alpha (ATP7A) (Zheng et al., 2014). The entopallium is one of the visual centers in the bird brain and a target of the tectofugal visual pathway, *i.e.*, a visual route travels from the eyes to optic tectum to thalamus and then to the entopallium (Karten and Hodos, 1970). The clinical relevance and molecular mechanisms of the copper accumulation in the entopallium of the lead-exposed ducks needs to be investigated in the future.

The most striking difference in lead distributions between the ducks and kites was the intensive accumulation in the arterial walls of the kites. In lead-intoxicated eagles, hemorrhage and ischemia caused by fibrinoid necrosis of small and medium caliber arteries are frequently found in the heart, brain, and eyes (Manning et al., 2019). Thus, arterial walls may be one of the target organs of lead-poisoning in raptors. Lead exposure causes cardiovascular degeneration also in humans and rodents (Navas-Acien et al., 2007; Fiorim et al., 2011; Ozturk et al., 2014; Nascimento et al., 2015). In rats, lead exposure increases the activity of plasma matrix metalloproteinase 9 (MMP9) (92-kDa type IV collagenase) (Nascimento et al., 2015), which can digest type IV collagen in the basement membrane of blood vessels and elastin of the tunica media of blood vessels (Wilhelm et al., 1989; Collier et al., 1988; Yasmin et al., 2005). Further, lead exposure increases the expression of MMP2 (72-kDa type IV collagenase) and MMP9 in hippocampus and the cerebral cortex of mice, resulting in cerebral vascular lesions (Ning et al., 2016). In addition, lead-induced expression of MMP2 and MMP9 affects the blood-brain-barrier permeability through degradation of tight junction proteins (Liu et al., 2017). Although the distribution of MMPs in avian species has not been investigated, lead may bind and activate MMP2 and MMP9 in the arterial walls in raptors. The molecular mechanisms of the predisposition to the lead accumulation in the arterial walls in raptors should be investigated in the future.

Little is known about the toxicity caused by low-level lead exposure in birds. To date, lead toxicity in birds has only been investigated by high-dose lead exposure (Franson et al.,1983; Hoffman et al., 1985; Mautino and Bell, 1986; Pain, 1990; Redig et al., 1991; Rocke and Samuel, 1991; Ochiai et al., 1993; Hiraga et al., 2008). In mammals, low-dose lead exposure exerts toxic effects (Dribben et al., 2011; Flora et al., 2012; Lanphear et al., 2018; Rahman et al., 2018), and Centers for Disease Control and Prevention (CDC) suggested that the safe blood lead level in humans should be reduced from 10 μg/dL to 5 μg/dL (CDC, 2012). Thus, it is currently considered that previous effect-level 'thresholds' should be abandoned in the field of avian lead poisoning (Pain et al., 2019). To reproduce the low-dose lead exposure found in the field, we established a model of low-dose lead exposure in waterfowls and raptors in the present study. Although these birds lacked apparent lead-associated pathological changes, the imaging analysis using LA-ICP-MS clearly identified lead distribution in organs. In addition, the alteration of copper distribution in the brain was also detected by LA-ICP-MS. Thus, the present study will provide useful information to understand the mechanisms of lead poisoning in birds caused by low-level exposure in the field.

5. Conclusions

Here we demonstrate detailed lead distribution in organs of experimentally lead-exposed birds and its differences between avian species for the first time. The present study will pave the way for better understanding the cellular processes of lead poisoning and the mechanisms of species differences in susceptibility to lead exposure.

Funding

This work was supported by the Grants-in-Aid for Scientific Research from the Ministry of Education, Culture, Sports, Science and Technology of Japan awarded to T. Matsukawa (No. 19H01081), M. Ishizuka (No. 16H0177906, 18K1984708, 18KK028708 and JPMXS0420100620), Y. Ikenaka (No. 18H0413208), and S.M.M. Nakayama (No. 17KK0009, 20K20633). This work was also supported by the foundation of JSPS Bilateral Open Partnership Joint Research Projects (JPJSBP120209902) and the Environment Research and Technology Development Fund (SII-1/3-2, 4RF-1802/18949907) of the Environmental Restoration and Conservation Agency of Japan. We also acknowledge financial support from the Soroptimist Japan Foundation, the Nakajima Foundation, the Sumitomo Foundation, the Nihon Seimei Foundation, act beyond trust, the Japan Prize Foundation, and Triodos Foundation. This research was also supported by JST/JICA, SATREPS (Science and Technology Research Partnership for Sustainable Development; No. JPMJSA1501). The funders had no role in study design, data collection and analysis, decision to publish, or preparation of the manuscript.

Author statement

Ryouta Torimoto: performed experiments, wrote manuscript. Chihiro Ishii: performed experiments. Hiroshi Sato: performed experiments. Keisuke Saito: performed experiments. Yukiko Watanabe: performed experiments. Kohei Ogasawara: performed experiments. Ayano Kubota: performed experiments. Takehisa Matsukawa: performed experiments. Kazuhito Yokoyama: provided technical and editorial assistance. Atsushi Kobayashi: performed experiments, wrote manuscript. Takashi Kimura: provided technical and editorial assistance. Shouta M. M. Nakayama: conceived and designed experiments. Yoshinori Ikenaka: conceived and designed experiments. performed experiments, wrote manuscript. Mayumi Ishizuka: conceived and designed experiments. All authors critically revised the manuscript and approved the manuscript to be published.

Declaration of competing interest

The authors declare that they have no known competing financial interests or personal relationships that could have appeared to influence the work reported in this paper.

Acknowledgement

We would like to express our appreciation to all the members of Laboratory of Comparative Pathology and Laboratory of Toxicology, Faculty of Veterinary Medicine, Hokkaido University and the Institute for Raptor Biomedicine Japan for helpful discussions, encouragement and support.

Appendix A. Supplementary data

Supplementary data to this article can be found online at https://doi.org/10.1016/j.envpol.2021.117086.

References

Al-Shimali, H., Al-Musaileem, A.F., Rao, M.S., Khan, K.M., 2016. Low-dose exposure to lead during pregnancy affects spatial learning, memory and neurogenesis in hippocampus of young rats. J. Neurol. Neurosci. 7, 1–12.

Berny, P., Vilagines, L., Cugnasse, J.M., Mastain, O., Chollet, J.Y., Joncour, G., Razin, M., 2015. Vigilance POISON: illegal poisoning and lead intoxication are the main factors affecting avian scavenger survival in the Pyrenees (France). Ecotoxicol. Environ. Saf. 118, 71–82.

Burger, J., Gochfeld, M., 2005. Effects of lead on learning in herring gulls: an avian wildlife model for neurobehavioral deficits. Neurotoxicology 26, 615–624.

CDC, Advisory Committee on Childhood Lead Poisoning Prevention, 2012. Low Level Lead Exposure Harms Children: a Renewed Call for Primary Prevention. https://www.cdc.gov/nceh/lead/ACCLPP/Final_Document_030712.pdf. (Accessed 16 March 2021).

Collier, I.E., Wilhelm, S.M., Eisen, A.Z., Marmer, B.L., Grant, G.A., Seltzer, J.L., Kronberger, A., He, C.S., Bauer, E.A., Goldberg, G.I., 1988. H-ras oncogene-transformed human bronchial epithelial cells (TBE-1) secrete a single metalloprotease capable of degrading basement membrane collagen. J. Biol. Chem. 263, 6579–6587.

Corsetti, G., Romano, C., Stacchiotti, A., Pasini, E., Dioguardi, F.S., 2017. Endoplasmic reticulum stress and apoptosis triggered by sub-chronic lead exposure in mice spleen: a histopathological study. Biol. Trace Elem. Res. 178, 86–97.

De Francisco, N., Ruiz Troya, J.D., Agüera, E.I., 2003. Lead and lead toxicity in domestic and free living birds. Avian Pathol. 32, 3–13.

Dribben, W.H., Creeley, C.E., Farber, N., 2011. Low-level lead exposure triggers neuronal apoptosis in the developing mouse brain. Neurotoxicol. Teratol. 33, 473–480.

Ecke, F., Singh, N.J., Arnemo, J.M., Bignert, A., Helander, B., Berglund, Å.M.M., Borg, H., Bröjer, C., Holm, K., Lanzone, M., Miller, T., Nordström, Å., Räikkönen, J., Rodushkin, I., Ågren, E., Hörnfeldt, B., 2017. Sublethal lead exposure alters movement behavior in free-ranging golden eagles. Environ. Sci. Technol. 51, 5729–5736.

Ek, K.H., Morrison, G.M., Lindberg, P. Rauch S., 2004. Comparative tissue distribution of metals in birds in Sweden using ICP-MS and laser ablation ICP-MS. Arch. Environ. Contam. Toxicol. 47, 259–269.

Fallon, J.A., Redig, P., Miller, T., Lanzone, M., Katzner, T., 2017. Guidelines for evaluation and treatment of lead poisoning of wild raptors. Wildl. Soc. Bull. 41, 205–211.

Fiorim, J., Ribeiro, R.F., Silveira, E.A., Padilha, A.S., Vescovi, M., Vinícius, A., de Jesus, H.C., Stefanon, I., Salaices, M., Vassallo, D.V., 2011. Low-level lead exposure increases systolic arterial pressure and endothelium-derived vasodilator factors in rat aortas. PloS One 6, e17117.

Fisher, I.J., Pain, D.J., Thomas, V.G., 2006. A review of lead poisoning from ammunition sources in terrestrial birds. Biol. Conserv. 131, 421–432.

Flora, G., Gupta, D., Tiwari, A., 2012. Toxicity of lead: a review with recent updates. Interdiscipl. Toxicol. 5, 47–58.

Franson, J.C., Sileo, L., Pattee, O.H., Moore, J.F., 1983. Effects of chronic dietary lead in American kestrels (*Falco sparverius*). J. Wildl. Dis. 19, 110–113.

Gargouri, M., Ghorbel-Koubaa, F., Bonenfant-Magné, M., Magné, C., Dauvergne, X., Ksouri, R., Krichen, Y., Abdelly, C., El Feki, A., 2012. Spirulina or dandelion-enriched diet of mothers alleviates lead-induced damages in brain and cerebellum of newborn rats. Food Chem. Toxicol. 50, 2303–2310.

Harr, K.E., 2002. Clinical chemistry of companion avian species: a review. Vet. Clin. Pathol. 31, 140–151.

Hegazy, A.M.S., Fouad, U.A., 2014. Evaluation of lead hepatotoxicity, histological, histochemical and ultrastructural study. Forensic Med. Anat. Res. 2, 70–79.

Hernández-Avila, M., Smith, D., Meneses, F., Sanin, L.H., Hu, H., 1998. The influence of bone and blood lead on plasma lead levels in environmentally exposed adults. Environ. Health Perspect. 106, 473–477.

Hiraga, T., Ohyama, K., Hashigaya, A., Ishikawa, T., Muramoto, W., Kitagawa, H., Mizuno, N., Teraoka, H., 2008. Lead exposure induces pycnosis and enucleation of peripheral erythrocytes in the domestic fowl. Vet. J. 178, 109–114.

Hoffman, D.J., Christian, F.J., Pattee, O.H., Bunck, C.M., Murray, H.C., 1985. Biochemical and hematological effects of lead ingestion in nestling American kestrels (*Falco sparverius*). Comp. Biochem. Physiol. C Comp. Pharmacol. Toxicol. 80, 431–439.

Honda, K., Lee, D.P., Tatsukawa, R., 1990. Lead poisoning in swans in Japan. Environ. Pollut. 65, 209–218.

Ishii, C., Nakayama, S.M.M., Ikenaka, Y., Nakata, H., Saito, K., Watanabe, Y., Mizukawa, H., Tanabe, S., Nomiyama, K., Hayashi, T., Ishizuka, M., 2017. Lead exposure in raptors from Japan and source identification using Pb stable isotope ratios. Chemosphere 186, 367–373.

Ishii, C., Nakayama, S.M.M., Kataba, A., Ikenaka, Y., Saito, K., Watanabe, Y., Makino, Y., Matsukawa, T., Kubota, A., Yokoyama, K., Mizukawa, H., Hirata, T., Ishizuka, M., 2018. Characterization and imaging of lead distribution in bones of lead-exposed birds by ICP-MS and LA-ICP-MS. Chemosphere 212, 994–1001.

Jarrar, B.M., Taib, N.T., 2012. Histological and histochemical alterations in the liver induced by lead chronic toxicity. Saudi J. Biol. Sci. 19, 203–210.

Johnston, J.E., Franklin, M., Roh, H., Austin, C., Arora, M., 2019. Lead and arsenic in shed deciduous teeth of children living near a lead-acid battery smelter. Environ. Sci. Technol. 53, 6000–6006.

Karten, H.J., Hodos, W., 1970. Telencephalic projections of the nucleus rotundus in the pigeon (*Columba livia*). J. Comp. Neurol. 140, 35–51.

Kawakami, T., Hokada, T., Sakata, S., Hirata, T., 2016. Possible polymetamorphism and brine infiltration recorded in the garnet-sillimanite gneiss, Skallevikshalsen, Lutzow-Holm Complex, East Antarctica. J. Mineral. Petrol. Sci. 111, 129–143.

Lanphear, B.P., Rauch, S., Auinger, P., Allen, R.W., Hornung, R.W., 2018. Low-level lead exposure and mortality in US adults: a population-based cohort study. Lancet Public Health 3, e177–e184.

Lefauconnier, J.M., Bernard, G., Mellerio, F., Sebille, A., Cesarini, E., 1983. Lead distribution in the nervous system of 8-month-old rats intoxicated since birth by

lead. Experientia 39, 1030–1031.
Liao, Y., Yu, F., Jin, Y., Lu, C., Li, G., Zhi, X., An, L., Yang, J., 2008. Selection of micronutrients used along with DMSA in the treatment of moderately lead intoxicated mice. Arch. Toxicol. 82, 37–43.
Liu, J.T., Dong, M.H., Zhang, J.Q., Bai, Y., Kuang, F., Chen, L.W., 2015. Microglia and astroglia: the role of neuroinflammation in lead toxicity and neuronal injury in the brain. Neuroimmunol. Neuroinflammation 2, 131–137.
Liu, X., Su, P., Meng, S., Aschner, M., Cao, Y., Luo, W., Zheng, G., Liu, M., 2017. Role of matrix metalloproteinase-2/9 (MMP2/9) in lead-induced changes in an in vitro blood-brain barrier model. Int. J. Biol. Sci. 13, 1351–1360.
Manning, L.K., Wünschmann, A., Armién, A.G., Willette, M., MacAulay, K., Bender, J.B., Buchweitz, J.P., Redig, P., 2019. Lead intoxication in free-ranging bald eagles (*Haliaeetus leucocephalus*). Vet. Pathol. 56, 289–299.
Mautino, M., Bell, J.U., 1986. Experimental lead toxicity in the ring-necked duck. Environ. Res. 41, 538–545.
Moore, J.F., Goyer, R.A., 1974. Lead induced inclusion bodies: composition and probable role in lead metabolism. Environ. Health Perspect. 7, 121–127.
Morild, I., Bohle, A., Christensen, J.A., 1985. Structure of the avian kidney. Anat. Rec. 212, 33–40.
Nascimento, R.A., Mendes, G., Possomato-Vieira, J.S., Gonçalves-Rizzi, V.H., Kushima, H., Delella, F.K., Dias-Junior, C.A., 2015. Metalloproteinase inhibition protects against reductions in circulating adrenomedullin during lead-induced acute hypertension. Basic Clin. Pharmacol. Toxicol. 116, 508–515.
Navas-Acien, A., Guallar, E., Silbergeld, E.K., Rothenberg, S.J., 2007. Lead exposure and cardiovascular disease - a systematic review. Environ. Health Perspect. 115, 472–482.
Neri, M., Turillazzi, E., Riezzo, I., Fineschi, V., 2007. The determination of firing distance applying a microscopic quantitative method and confocal laser scanning microscopy for detection of gunshot residue particles. Int. J. Leg. Med. 121, 287–292.
Ning, L., Xing, L., Li, L., Pingan, Z., Mingwu, Q., Qiuyan, Z., Lianjun, S.Y., Zengli, Y., 2016. The expression of MMP2 and MMP9 in the hippocampus and cerebral cortex of newborn under maternal lead exposure. Exp. Biol. Med. 241, 1811–1818.
Ochiai, K., Jin, K., Goryo, M., Tsuzuki, T., Itakura, C., 1993. Pathomorphologic findings of lead poisoning in white-fronted geese (*Anser alhifrons*). Vet. Pathol. 30, 522–528.
Owoeye, O., Onwuka, S.K., 2016. Lead toxicity: effect of *Launaea taraxacifolia* on the histological and oxidative alterations in rat regio III cornu ammonis and cerebellum. Anat. J. Africa 5, 783–794.
Ozturk, M.T., Yavuz, B., Ozkan, S., Ayturk, M., Akkan, T., Ozkan, E., Tutkun, E., Yilmaz, Ö.H., 2014. Lead exposure is related to impairment of aortic elasticity parameters. J. Clin. Hypertens. 16 (11), 790–793.
Pain, D.J., 1990. Lead shot ingestion by waterbirds in the Camargue, France: an investigation of levels and interspecific differences. Environ. Pollut. 66, 273–285.
Pain, D.J., Mateo, R., Green, R.E., 2019. Effects of lead from ammunition on birds and other wildlife: a review and update. Ambio 48, 935–953.
Qu, W., Diwan, B.A., Liu, J., Goyer, R.A., Dawson, T., Horton, J.L., Cherian, M.G., Waalkes, M.P., 2002. The metallothionein-null phenotype is associated with heightened sensitivity to lead toxicity and an inability to form inclusion bodies. Am. J. Pathol. 160, 1047–1056.
Rahman, A., Khan, K.M., Rao, M.S., 2018. Exposure to low level of lead during preweaning period increases metallothionein-3 expression and dysregulates divalent cation levels in the brain of young rats. Neurotoxicology 65, 135–143.
Redig, P.T., Lawler, E.M., Schwartz, S., Dunnette, J.L., Stephenson, B., Duke, G.E., 1991. Effects of chronic exposure to sublethal concentrations of lead acetate on heme synthesis and immune function in red-tailed hawks. Arch. Environ. Contam. Toxicol. 21, 72–77.
Rocke, T.E., Samuel, M.D., 1991. Effects of lead shot ingestion on selected cells of the mallard immune system. J. Wildl. Dis. 27, 1–9.
Rogan, W.J., Reigart, J.R., Gladen, B.C., 1986. Association of amino levulinate dehydratase levels and ferrochelatase inhibition in childhood lead exposure. J. Pediatr. 109, 60–64.
Saito, K., 2009. Lead poisoning of Steller's sea eagle (*Haliaeetus pelagicus*) and White-tailed eagle (*Haliaeetus albicilla*) caused by the ingestion of lead bullets and slugs, in Hokkaido, Japan. In: Watson, R.T., Fuller, M., Pokras, M., Hunt, W.G. (Eds.), Ingestion Lead from Spent Ammunition: Implications for Wildlife and Humans. Peregrine Fund, Idaho, pp. 302–309.
Scheuhammer, A.M., Norris, S.L., 1996. The ecotoxicology of lead shot and lead fishing weights. Ecotoxicology 5, 279–295.
Sharifi, A.M., Baniasadi, S., Jorjani, M., Rahimi, F., Bakhshayesh, M., 2002. Investigation of acute lead poisoning on apoptosis in rat hippocampus in vivo. Neurosci. Lett. 329, 45–48.
Sierra, E.M., Rowles, T.K., Martin, J., Bratton, G.R., Womac, C., Tiffany-Castiglioni, E., 1989. Low level lead neurotoxicity in a pregnant Guinea pigs model: neuroglial enzyme activities and brain trace metal concentrations. Toxicology 59, 81–96.
Strużyńska, L., Chalimoniuk, M., Sulkowski, G., 2005. The role of astroglia in Pb-exposed adult rat brain with respect to glutamate toxicity. Toxicology 212, 185–194.
Tiffany-Castiglioni, E., Zmudzki, J., Wu, J.N., Bratton, G.R., 1987. Effects of lead treatment on intracellular iron and copper concentrations in cultured astroglia. Metab. Brain Dis. 2, 61–79.
Togao, M., Nakayama, S.M.M., Ikenaka, Y., Mizukawa, H., Makino, Y., Kubota, A., Matsukawa, T., Yokoyama, K., Hirata, T., Ishizuka, M., 2020. Bioimaging of Pb and STIM1 in mice liver, kidney and brain using laser ablation inductively coupled plasma mass spectrometry (LA-ICP-MS) and immunohistochemistry. Chemosphere 238, 124581.
Turillazzi, E., Di Peri, G.P., Nieddu, A., Bello, S., Monaci, F., Neri, M., Pomara, C., Rabozzi, R., Riezzo, I., Fineschi, V., 2013. Analytical and quantitative concentration of gunshot residues (Pb, Sb, Ba) to estimate entrance hole and shooting-distance using confocal laser microscopy and inductively coupled plasma atomic emission spectrometer analysis: an experimental study. Forensic Sci. Int. 231, 142–149.
Villeda-Hernández, J., Barroso-Moguel, R., Méndez-Armenta, M., Nava-Ruíz, C., Huerta-Romero, R., Ríos, C., 2001. Enhanced brain regional lipid peroxidation in developing rats exposed to low level lead acetate. Brain Res. Bull. 55, 247–251.
Wilhelm, S.M., Collier, I.E., Marmer, B.L., Eisen, A.Z., Grant, G.A., Goldberg, G.I., 1989. SV40-transformed human lung fibroblasts secrete a 92-kDa type IV collagenase which is identical to that secreted by normal human macrophages. J. Biol. Chem. 264, 17213–17221.
Wu, B., Zoriy, M., Chen, Y., Becker, J.S., 2009. Imaging of nutrient elements in the leaves of *Elsholtzia splendens* by laser ablation inductively coupled plasma mass spectrometry (LA-ICP-MS). Talanta 78, 132–137.
Yabe, J., Nakayama, S.M.M., Ikenaka, Y., Yohannes, Y.B., Bortey-Sam, N., Oroszlany, B., Muzandu, K., Choongo, K., Kabalo, A.N., Ntapisha, J., Mweene, A., Umemura, T., Ishizuka, M., 2015. Lead poisoning in children from townships in the vicinity of a lead-zinc mine in Kabwe, Zambia. Chemosphere 119, 941–947.
Yasmin, S.W., McEniery, C.M., Dakham, Z., Pusalkar, P., Maki-Petaja, K., Ashby, M.J., Cockcroft, J.R., Wilkinson, I.B., 2005. Matrix metalloproteinase-9 (MMP-9), MMP-2, and serum elastase activity are associated with systolic hypertension and arterial stiffness. Arterioscler. Thromb. Vasc. Biol. 25, 372–378.
Zheng, G., Zhang, J., Xu, Y., Shen, X., Song, H., Jing, J., Luo, W., Zheng, W., Chen, J., 2014. Involvement of CTR1 and ATP7A in lead (Pb)-induced copper (Cu) accumulation in choroidal epithelial cells. Toxicol. Lett. 225, 110–118.
Zuo, P., Qu, W., Cooper, R.N., Goyer, R.A., Diwan, B.A., Waalkes, M.P., 2009. Potential role of α-synuclein and metallothionein in lead-induced inclusion body formation. Toxicol. Sci. 111, 100–108.

February 16, 2022

Correction of Annex 4/KAMPAI Project Handover Equipment List

We notify you of the correction related to the above title.
The “Atomic Absorption Spectrometry” listed in the “KAMPAI Project Handover Equipment List/Group 2” has been deleted from the list because they were donated equipment of Hokkaido University. (see Certificate of Handover/Donated Equipment List attached)

Attachment: Certificate of Handover/Donated Equipment List attached

北海道大学・大学院獣医学研究院・獣医学部
Faculty of Veterinary Medicine, Hokkaido University

CERTIFICATE OF HANDOVER

ATTENTION : Chief Representative
JICA Zambia Office

PROJECT TITLE : The Project of Visualization of Impact of Chronic/Latent Chemical Hazard & Geo-Ecological Remediation (KAMPAI project)

This is to certify that the equipment in the attached "Donated Equipment List" for KAMPAI project has been donated properly as of 16th February 2022 from Hokkaido University to University of Zambia.

Therefore, the equipment will be deleted from "KAMPAI Project Handover Equipment List (Group 2-No17, No18)" attached to the Certificate of Handover dated February 16, 2022. (refer to the Attachment)

16th February 2022

石塚 真由美

Prof. Mayumi Ishizuka
Professor of Faculty of Veterinary Medicine
Hokkaido University

Prof. King Nalubamba
Dean of School of Veterinary Medicine
University of Zambia

Attachment: Certificate of Handover/KAMPAI project Handover Equipment List

Donated Equipment List

#	Item	Currency	Unit price	Q'ty	Total	Procurement in	Date of introduction
1	Atomic Absorption Spectrometry accessories	JPY	1,300,000	1	1,300,000	Japan	Dec 2018
2	Atomic Absorption Spectrometry with accessories	JPY	4,000,000	1	4,000,000	Japan	Dec 2018
			TOTAL		5,300,000		

NKS 石塚

Attachment

Japan International Cooperation Agency

CERTIFICATE OF HANDOVER

THE PROJECT FOR VISUALIZATION
OF
IMPACT OF CHRONIC / LATENT CHEMICAL HAZARD
AND
GEO-ECOLOGICAL REMEDIATION IN ZAMBIA

This is to certify that the equipments in the attached list for above-mentioned project have been handed over properly as of 10 February 2022 to the University of Zambia.

K. Tokuhashi

Mr. Kazuhiko Tokuhashi
Chief Representative
Japan International Cooperation Agency (JICA) Zambia Office

Prof. Luke E. Mumba
Vice Chancellor
University of Zambia

石塚 真由美

Prof. Mayumi Ishizuka
Professor of Faculty of
Veterinary Medicine
Hokkaido University

Prof. King Nalubamba
Dean of School of
Veterinary Medicine
The University of Zambia

Chishala.

Dr. Benson Chishala
Dean of School of Agricultural Sciences
The University of Zambia

Dr. Bunda Besa
Dean of School of Mines
The University of Zambia

School of Veterinary Medicine
The University of Zambia
JICA KAMPAI Project

LEM

KAMPAI Project Handover Equipment List

(More than 50,000 yen value per unit)

Group 1) Scool of Agricultural Sciences, UNZA

The exchange rate uses the JICA Monthly Transaction Rate)

#	Item	Currency	Unit price	Qty	Total	Total in Japan	Procurement in	Date of procurement
1	Spectroradiometer (FieldSpec4)	JPY	10,000,000	1	10,000,000	10,000,000	Japan	Aug 2017
2	Weather station (POTEKA)	JPY	1,250,000	2	2,500,000	2,500,000	Japan	Aug 2017
3	Weather station (SESAME)	JPY	930,000	2	1,860,000	1,860,000	Japan	Aug 2017
4	CO2 analyzer	JPY	825,000	1	825,000	825,000	Japan	Feb 2017
5	Soil respiration analyzer	JPY	745,000	1	745,000	745,000	Japan	Feb 2017
6	EC meter	JPY	98,000	1	98,000	98,000	Japan	May 2017
7	ORP meter	JPY	65,000	1	65,000	65,000	Japan	May 2017
8	Desktop pH meter with accessories	JPY	66000	1	66,000	66,000	Japan	May 2017
9	Greenhouse(8mx12m)/ HAYGROVE PIONEER 4 SERIES POLY TUNNELS	ZMK	74,358	1	74,358	610,330	Zambia	Oct 2019
					Total	16,769,330		

Group 2) School of Veterinary Medicine, UNZA

#	Item	Currency	Unit price	Qty	Total	Total in Japan	Procurement in	Date of procurement
1	TOYOTA Land Cruiser (BAE 5283)	USD	50,036	1	50,036	5,761,145	Zambia	Feb 2017
2	HP Color LaserJet Pro MFP M477fnw 4in1	ZMK	6,726	1	6,726	69,231	Zambia	Oct 2018
3	HP Personal Computer 15 Note Book	ZMK	6,586	1	6,586	75,429	Zambia	Dec 2018
4	HP Color LaserJet Pro MFP M477fdw 4in1	ZMK	22,668	1	22,668	273,921	Zambia	Sep 2017
5	40kVA Generator with shelter and fence	USD	15,866	1	15,866	1,767,429	Zambia	Sep 2018
6	Shelter and fence for 40kVA Generator	ZMK	13,650	1	13,650	149,850	Zambia	Sep 2018
7	10kVA UPS	ZMK	32,116	2	64,232	600,312	Zambia	Oct 2018
8	10kVA UPS	ZMK	82,320	1	82,320	403,533	Zambia	May 2021
9	3kVA UPS	ZMK	16,213	3	48,639	454,580	Zambia	Oct 2018
10	40 feet Container/warehouse for KAMPAI Monitoring Laboratory	ZMK	39,095	1	39,095	358,736	Zambia	Feb 2019
11	-20℃ deep freezer (vertical)	ZMK	6,919	1	6,919	86,813	Zambia	Jul 1917
12	-20℃ deep freezer (horizontal)	ZMK	9,995	1	9,995	48,906	Zambia	Jun 2021
13	-80℃ deep freezer	JPY	750,000	2	1,500,000	1,500,000	Japan	Oct 2018 Oct 2021
14	Microwave digestion system (Speed wave entry) with accessories	JPY	2,600,000	2	5,200,000	5,200,000	Japan	Oct 2018 Oct 2021
15	Microwave digestion system vessel	JPY	100,000	10	1,000,000	1,000,000	Japan	Feb 2020
16	Microwave digestion system turning table	JPY	110,000	1	110,000	110,000	Japan	Feb 2021
17	Atomic Absorption Spectrometry accessories	JPY	1,300,000	1	1,300,000	1,300,000	Japan	Dec 2018
18	Atomic Absorption Spectrometry with accessories	JPY	4,000,000	1	4,000,000	4,000,000	Japan	Dec 2018
19	Cooling water circulator (chiller)	JPY	200,000	2	400,000	400,000	Japan	Dec 2018 Oct 2021
20	Silent air compressor	JPY	260,000	1	260,000	260,000	Japan	Dec 2018
21	Draft chamber	JPY	1,700,000	1	1,700,000	1,700,000	Japan	Oct 2018
22	230V Centrifugal Fan Set CMP 514-4M/AL	JPY	160,000	1	160,000	160,000	Japan	Feb 2020
23	230V Centrifugal Fan Set CMP 616-4M/AL	JPY	180,000	1	180,000	180,000	Japan	Feb 2020
24	Speed Controller RM-01	JPY	80,000	2	160,000	160,000	Japan	Feb 2020
25	Mercury analyzer with accessories	JPY	5,000,000	1	5,000,000	5,000,000	Japan	Feb 2021
26	Air compressor	JPY	450,000	1	450,000	450,000	Japan	Feb 2021
27	Small program electric furnace	JPY	140,000	1	140,000	140,000	Japan	Feb 2021
28	Metal analyzer MP-AES Agilent 4210 with accessories	JPY	5,440,000	1	5,440,000	5,440,000	Japan	Oct 2021
29	Air/nitrogen gas generator	JPY	2,320,000	1	2,320,000	2,320,000	Japan	Oct 2021
30	Autosampler	JPY	1,400,000	1	1,400,000	1,400,000	Japan	Oct 2021
31	Sirocco fan and inverter	JPY	50,000	1	50,000	50,000	Japan	Oct 2021
32	Lab table small with wagon	JPY	130,000	2	260,000	260,000	Japan	Oct 2021
33	Lab table large	JPY	200,000	1	200,000	200,000	Japan	Dec 2018

石塚 LEM

34	Forced air flow oven and stand	JPY	160,000	2	320,000	320,000	Japan	Feb 2018
35	Down transformer	JPY	50,000	10	500,000	500,000	Japan	Oct 2016, Feb & Oct 2021
36	Lead care II Analyzer	USD	2,440	3	7,320	813,128	SOUTH AFRICA	Jun 2017
37	DW maker	JPY	620,000	1	620,000	620,000	Japan	Feb 2017
38	DDW (Milli-Q water) maker	JPY	390,000	1	390,000	390,000	Japan	Feb 2017
39	Water softening plant	JPY	130,000	1	130,000	130,000	Japan	July 2019
40	Autoclave quioment	JPY	530,000	1	530,000	530,000	Japan	Oct 2018
41	Thermal cycler	JPY	76,000	1	76,000	76,000	Japan	Feb 2018
42	Thermal cycler	JPY	350,000	1	350,000	350,000	Japan	July 2019
43	Realtime PCR with laptop computer and accessories	JPY	1,620,000	1	1,620,000	1,620,000	Japan	Oct 2018
44	DNA/RNA sequencer MinION	JPY	500,000	1	500,000	500,000	Japan	Feb 2018
45	Fluorometer	JPY	210,000	1	210,000	210,000	Japan	Feb 2018
46	Beads crusher and accessories	JPY	340,000	1	340,000	340,000	Japan	Dec 2018
47	Plate reader	JPY	500,000	1	500,000	500,000	Japan	July 2019
48	Spectrophotometer / fluorometer DS-11	JPY	1,230,000	1	1,230,000	1,230,000	Japan	Feb 2021
49	Vortex mixer	JPY	43,000	2	86,000	86,000	Japan	Feb 2021
50	Clean bench	JPY	150,000	1	150,000	150,000	Japan	Oct 2018
51	Blood biochemical analyzer	JPY	1,000,000	1	1,000,000	1,000,000	Japan	Oct 2018
52	Thermostat dry bath with accessories	JPY	70,000	1	70,000	70,000	Japan	Feb 2018
53	Desktop centrifuge A with accessories	JPY	150,000	4	600,000	600,000	Japan	May 2017
54	Desktop centrifuge B with accessories	JPY	670,000	1	670,000	670,000	Japan	Feb 2017
55	Refrigerated centrifuge with accessories	JPY	910,000	1	910,000	910,000	Japan	Dec 2018
56	Electronic balance	JPY	130,000	2	260,000	260,000	Japan	Feb 2018
57	Multi shaker with holder	JPY	300,000	1	300,000	300,000	Japan	Feb 2017
58	pH meter	JPY	70,000	1	70,000	70,000	Japan	July 2019
59	Multi function water quality meter	JPY	150,000	1	150,000	150,000	Japan	May 2017
60	Ultrasonic washing machine	JPY	136,000	1	136,000	136,000	Japan	Feb 2018
61	Low volume air sampler	JPY	800,000	1	800,000	800,000	Japan	Feb 2017
62	Agate mortar and pestle	JPY	82,000	1	82,000	82,000	Japan	May 2017
63	Hyperspectrum camera with accessories	JPY	4,670,000	1	4,670,000	4,670,000	Japan	Feb 2021
64	Cephalostat	JPY	154,000	1	154,000	154,000	Japan	Feb 2021
65	Gas cylinder stand	JPY	26,000	3	78,000	78,000	Japan	Feb 2021 Oct 2021
66	Dry shipper	JPY	630,000	1	630,000	630,000	Japan	Feb 2021
67	Ice crusher	JPY	90,000	1	90,000	90,000	Japan	Feb 2021
68	Vein viewer	JPY	80,000	3	240,000	240,000	Japan	Oct 2018
69	Dryice maker	JPY	150,000	1	150,000	150,000	Japan	May 2017
70	LED illuminators FAS-Dig	JPY	85,000	1	85,000	85,000	Japan	July 2019
71	Digital camera	JPY	78,000	1	78,000	78,000	Japan	July 2019
					Total	60,868,011		

Group 3) School of Mines, UNZA

1	Weather station	JPY	1,180,000	1	1,180,000	1,180,000	Japan	Feb 2017
2	Electronic furnace	JPY	320,000	1	320,000	320,000	Japan	Oct 2018
3	Down transformer	JPY	59,000	1	59,000	59,000	Japan	Oct 2018
4	Portable XRD/XRF equipment and accessories	JPY	10,670,000	1	10,670,000	10,670,000	Japan	Feb 2017
5	Bore hole	USD	4,778	3	14,333	1,501,570	Zambia	Nov 2016
					Total	13,730,570		

NKS

石塚 LEM